# Accepted Manuscript

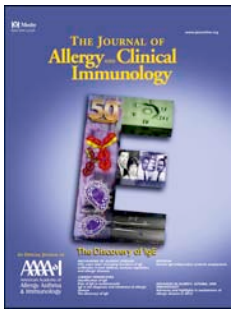


Shared genetic variants suggest common pathways in allergy and autoimmune diseases

Eskil Kreiner, MD, PhD, Johannes Waage, PhD, Marie Standl, PhD, Susanne Brix, PhD, Tune H. Pers, PhD, Alexessander Couto Alves, PhD, Nicole M. Warrington, PhD, Carla MT. Tiesler, MSc, Elaine Fuertes, PhD, Lude Franke, PhD; AAGC, Joel N. Hirschhorn, MD, PhD, Alan James, MD, Angela Simpson, MD, PhD, Joyce Y. Tung, PhD, Gerard H. Koppelman, MD, PhD, Dirkje S. Postma, MD, PhD, Craig E. Pennell, MD, PhD, Marjo-Riitta Jarvelin, MD, Adnan Custovic, MD, PhD, Nicholas Timpson, PhD, Manuel A. Ferreira, PhD, David P. Strachan, MD, John Henderson, MD, David Hinds, PhD, Hans Bisgaard, MD, DMSci, Klaus Bønnelykke, MD, PhD

PII: S0091-6749(17)30207-5

DOI: 10.1016/j.jaci.2016.10.055

Reference: YMAI 12620

To appear in: *Journal of Allergy and Clinical Immunology*

Received Date: 12 March 2016

Revised Date: 12 September 2016

Accepted Date: 11 October 2016

Please cite this article as: Kreiner E, Waage J, Standl M, Brix S, Pers TH, Couto Alves A, Warrington NM, Tiesler CM, Fuertes E, Franke L, Hirschhorn JN, James A, Simpson A, Tung JY, Koppelman GH, Postma DS, Pennell CE, Jarvelin M-R, Custovic A, Timpson N, Ferreira MA, Strachan DP, Henderson J, Hinds D, Bisgaard H, Bønnelykke K, Shared genetic variants suggest common pathways in allergy and autoimmune diseases, *Journal of Allergy and Clinical Immunology* (2017), doi: 10.1016/j.jaci.2016.10.055.

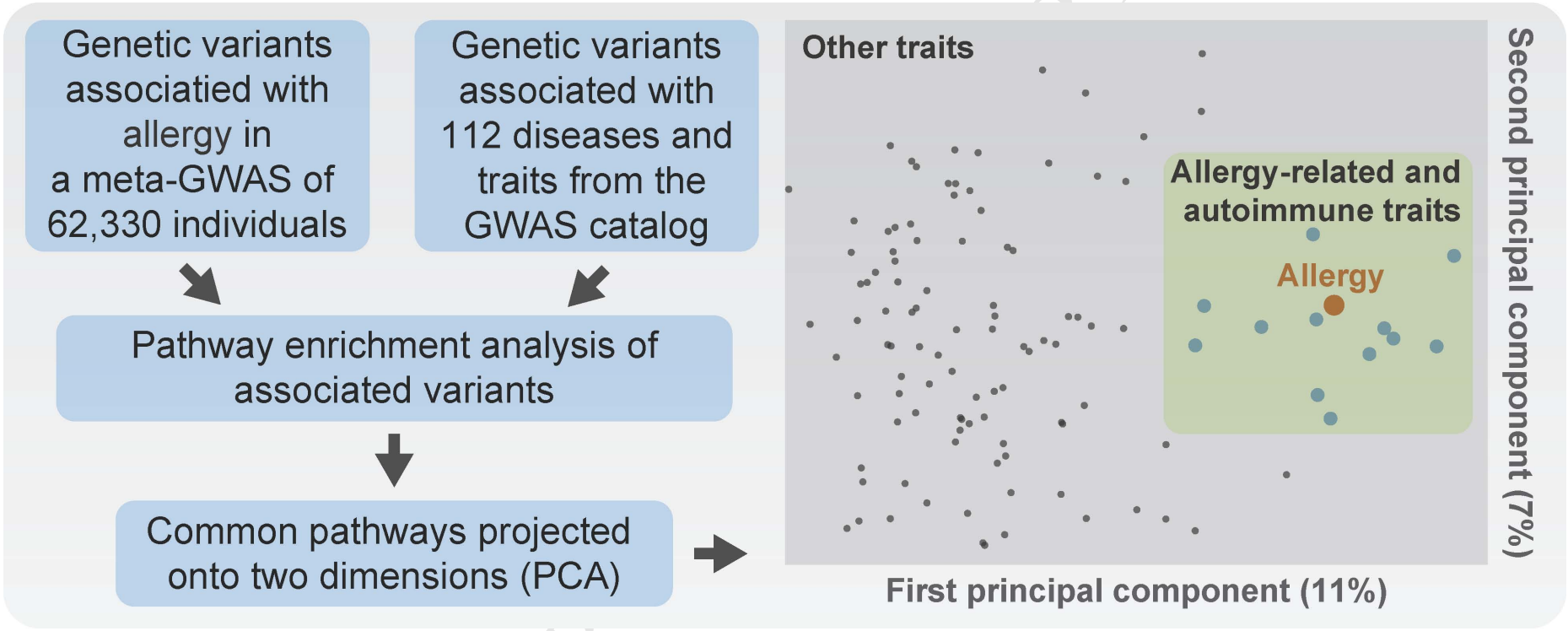

# Shared genetic variants suggest common pathways in allergy and autoimmune diseases

Eskil Kreiner, MD, PhD[1,†]; Johannes Waage, PhD[1,†]; Marie Standl, PhD[2]; Susanne Brix, PhD[3]; Tune H Pers, PhD[3-5]; Alexessander Couto Alves, PhD[6]; Nicole M Warrington, PhD[7,8]; Carla MT Tiesler, MSc[2,9]; Elaine Fuertes, PhD[2]; Lude Franke, PhD[10]; AAGC, Joel N Hirschhorn, MD, PhD[4,5,11]; Alan James, MD[12-14]; Angela Simpson, MD, PhD[15]; Joyce Y Tung, PhD[16]; Gerard H Koppelman, MD, PhD[17]; Dirkje S Postma, MD, PhD[18]; Craig E Pennell, MD, PhD[8]; Marjo-Riitta Jarvelin, MD[19-23]; Adnan Custovic, MD, PhD[24]; Nicholas Timpson, PhD[25]; Manuel A Ferreira, PhD[26]; David P Strachan, MD[27]; John Henderson, MD[28]; David Hinds, PhD[16]; Hans Bisgaard, MD, DMSci[1]; Klaus Bønnelykke, MD, PhD[1]

1: Copenhagen Prospective Studies on Asthma in Childhood, Health Sciences, University of Copenhagen, Danish Pediatric Asthma Center, Copenhagen University Hospital, Gentofte, Denmark

2: Institute of Epidemiology I, Helmholtz Zentrum München, German Research Center for Environmental Health, Neuherberg, Germany

3: Department of Biotechnology and Biomedicine, Technical University of Denmark, Lyngby, Denmark

4: Division of Endocrinology and Center for Basic and Translational Obesity Research, Boston Children's Hospital, Boston, USA

5: Medical and Population Genetics Program, Broad Institute of MIT and Harvard, Cambridge, USA

6: Department of Epidemiology and Biostatistics, School of Public Health, Imperial College London, UK

7: The University of Queensland Diamantina Institute, The University of Queensland, Translational Research Institute, Brisbane, Australia

8: School of Women's and Infants' Health, The University of Western Australia, Perth, Australia

9: Ludwig-Maximilians-University of Munich, Dr. von Hauner Children's Hospital, Munich, Germany

10: Department of Genetics, University of Groningen, University Medical Centre Groningen, Groningen, 9711, The Netherlands

11: Department of Genetics, Harvard Medical School, Boston, 02115, USA

12: Busselton Population Medical Research Foundation, Sir Charles Gairdner Hospital, Perth, Western Australia, Australia

13: School of Medicine and Pharmacology, University of WA, Nedlands, Australia

14: Department of Pulmonary Physiology, West Australian Sleep Disorders Research Institute, Nedlands, Australia

15: University of Manchester, Manchester Academic Health Science Centre, University Hospital of South Manchester NHS Foundation Trust, Manchester, UK

16: 23andMe, Mountain View, Calif.

17: Department of Pediatric Pulmonology and Pediatric Allergology, Beatrix Children's Hospital, GRIAC, University Medical Center Groningen, University of Groningen, Groningen, The Netherlands

18: University of Groningen, Department of Pulmonology, GRIAC, University Medical Center Groningen, Groningen, The Netherlands

19: Department of Epidemiology and Biostatistics, MRC Health Protection Agency (HPA) Centre for Environment and Health, School of Public Health, Imperial College London, UK

20: Center for Life Course Epidemiology, Faculty of Medicine, P.O.Box 5000, FI-90014 University of Oulu, Finland

21: Biocenter Oulu, P.O.Box 5000, Aapistie 5A, FI-90014 University of Oulu, Finland

22: Unit of Primary Care, Oulu University Hospital, Kajaanintie 50, P.O.Box 20, FI-90220 Oulu, 90029 OYS, Finland

23: Department of Children and Young People and Families, National Institute for Health and Welfare, Aapistie 1, Box 310, FI-90101 Oulu, Finland

24: University of Manchester, Manchester Academic Health Science Centre, University Hospital of South Manchester NHS Foundation Trust, Manchester, UK

25: The MRC Integrative Epidemiology Unit at the University of Bristol, UK

26: Queensland Institute of Medical Research, Brisbane, Australia

27: Population Health Research Institute, St George's, University of London, Cranmer Terrace, London SW17 0RE

28: School of Social and Community Medicine, University of Bristol, Bristol, UK

†: These authors contributed equally to this work.

**Corresponding author:**
Klaus Bønnelykke, MD, PhD
Copenhagen Prospective Studies on Asthma in Childhood, Health Sciences, University of Copenhagen, Danish Pediatric Asthma Center, Copenhagen University Hospital, Gentofte, Denmark
Email: kb@copsac.com
Phone: +1 848-525-8121
Fax: 45-3977-7129

## Abstract

**Background**

The relationship between allergy and autoimmune disorders is complex and poorly understood.

**Objective**

To investigate commonalities in genetic loci and pathways between allergy and autoimmune diseases to elucidate shared disease mechanisms.

**Methods**

We meta-analyzed two GWAS on self-reported allergy and sensitization comprising a total of 62,330 individuals. These results were used to calculate enrichment for SNPs previously associated with autoimmune diseases. Furthermore, we probed for enrichment within genetic pathways and of transcription factor binding sites, and characterized commonalities in the variant burden on tissue-specific regulatory sites by calculating the enrichment of allergy SNPs falling in gene regulatory regions in various cells using Encode Roadmap DHS data, and compared the allergy data with all known diseases.

**Results**

Among 290 loci previously associated with 16 autoimmune diseases, we found a significant enrichment of loci also associated with allergy ($p=1.4e-17$) encompassing 29 loci at a false discovery rate<0.05. Such enrichment seemed to be a general characteristic for all

autoimmune diseases. Among the common loci, 48% had the same direction of effect for allergy and autoimmune diseases. Additionally, we observed an enrichment of allergy SNPs falling within immune pathways and regions of chromatin accessible in immune cells that was also represented in autoimmune diseases, but not in other diseases.

**Conclusion**

We identified shared susceptibility loci and commonalities in pathways between allergy and autoimmune diseases, suggesting shared diseases mechanisms. Further studies of these shared genetic mechanisms might help understanding the complex relationship between these diseases, including the parallel increase in disease prevalence.

## Capsule Summary

We identified shared susceptibility loci and commonalities in pathways between allergy and autoimmune diseases. Further studies of these loci and related mechanisms might help understanding the complex relationship between allergy and autoimmunity.

## Key messages

- Allergy and autoimmune diseases share genetic susceptibility loci.
- These results indicate commonalities in gene regulation and genetic pathways between allergy and autoimmune diseases.
- Further studies of common genetic loci and the related mechanisms might help understanding the complex relationship between allergy and autoimmunity.

## Key words

Allergy, Single Nucleotide Polymorphism, Autoimmune Disease, Autoimmunity, Genetic Association Studies

## Abbreviations

DEPICT: Data-driven Expression Prioritized Integration for Complex Traits gene set enrichment method

DHS: DNase Hypersensitive Sites

GWA(S): Genome Wide Association (Studies)

PCA: Principal Component Analysis

SNP: Single Nucleotide Polymorphism

## Introduction

There has been a parallel increase in allergic and autoimmune disorders in recent decades in "westernized" countries[1] suggesting that these diseases may share disease mechanisms and etiologies. In line with this, allergy and autoimmune disorders seem to share environmental risk factors including birth by caesarian section[2]. This observation is in apparent contrast to the understanding of allergy and autoimmune diseases as representatives of distinct immunological disorders with counteracting underlying immune mechanisms. Autoimmune diseases are in general thought to act through a Th1/Th17-driven cell mediated immune response,[3] while allergy and asthma encompass a Th2-mediated response[4]. Counteracting immune mechanisms have been supported by some epidemiological studies of comorbidity suggesting a lower incidence of allergy among patients with autoimmune diseases, including rheumatoid arthritis[5,6] and multiples sclerosis[7], although the evidence of such inverse relationship is conflicting.[8]

Both allergy and autoimmune diseases are highly heritable diseases and an increasing number of susceptibility loci have been discovered.[9–11] We hypothesized that studying commonalities in the genetic architecture could provide a key to understanding the complex relationship between these diseases by pinpointing possible common disease mechanisms. In a wider perspective, this might help to explain the mechanisms and aetiologies responsible for the contemporaneous, dramatic increase in incidence of allergic and autoimmune disorders[1].

We studied commonalities between allergy and autoimmune disease in terms of susceptibility loci, genetic pathways and regulatory mechanisms. We meta-analyzed two

GWAS on allergic sensitization and allergic symptoms representing the largest GWAS on allergy to date. These data were then combined with publically available GWAS data on autoimmune diseases, as well as public data on molecular pathways, transcription factor binding sites and regulatory DNA regions. The primary analyses used a methodological approach that was agnostic to the direction of effect (including loci where the risk-allele was the same for allergy and autoimmune disease as well as loci where the risk allele for one disease was protective for the other). We hypothesized that loci with same direction of effect for different diseases might be involved in shared mechanisms and thereby help understanding the parallel epidemics of diseases, while loci with opposite direction of effect might help understanding counteracting (diverging) disease mechanisms. In analogue, gene variants in beta-adrenoreceptors are likely to show diverging effects with respect to risk of cardiac and respiratory diseases but still pinpoint an essential mechanism for both diseases. For allergy and autoimmune diseases such loci might be involved in “polarization” of the immune response. We therefore chose an approach that would capture common genetic loci with both same and opposite direction of effect since we believe that both might confer important information and thereby help to elucidate the complex mechanistic relationship between these diseases.

## Methods

### Study group

To obtain the largest possible GWAS data set for allergy, we meta-analyzed results from two recent GWAS on self-reported allergy[9] and sensitization[10], including ~2.2 million directly genotyped and imputed single nucleotide polymorphisms (SNPs), using a fixed effects model. The self-reported allergy dataset comprised 23,335 individuals with self-reported allergy for cat-, dust-mite and/or pollen-allergy and 26,311 control subjects without symptoms. The allergic sensitization dataset included 5,809 subjects with allergic sensitization defined by either skin prick test or specific IgE measurement and 9,875 control subjects without allergic sensitization with data from the following cohorts: AAGC, ALSPAC, B58C, COPSAC2000, LISA, MAAS, NFBC 1966, RAINE and PIAMA (**Supplementary Methods**).

### Common genetic loci

To identify common genetic loci, we identified all SNPs previously shown to be associated with autoimmune diseases from the NHGRI GWAS catalog[12]. From each locus defined by genetic distance (**Supplementary Methods**) the most significant SNP associated with autoimmune diseases (the index disease, one of 16 different diseases) was chosen, leaving 290 candidate SNPs which where subsequently extracted from the allergy meta-analysis results (**Supplementary Methods, Supplementary Table 1 and Supplementary Figure 1**). For each SNP, the direction of effect of the risk allele for allergy was compared with the direction of effect for the index autoimmune disease as well as for other autoimmune diseases with reported loci in high LD.

Among these autoimmune disease-associated SNPs (loci) we calculated an enrichment of significant SNPs in relation to allergy ($P<0.05$) as compared to expected under the null hypothesis. Enrichment was only calculated for diseases with at least ten loci associated with the index disease and therefore not calculated for systemic sclerosis, sarcoidosis, primary sclerosing cholangitis and myasthenia gravis. As a methodological negative control, SNPs related to two non-inflammatory phenotypes with reasonable GWA study sizes, migraine and the combination of bipolar disorder and schizophrenia from the GWAS catalog, were analyzed similarly.

**Commonalities in genetic pathways**

To investigate commonalities in functional origins, the Data-driven Expression Prioritized Integration for Complex Traits (DEPICT) gene set enrichment method[13] was applied to 123 diseases and traits in the GWAS catalog, as well as the current association data set on allergy, by analyzing gene set enrichments for 14,416 reconstituted gene sets capturing a wide spectrum of molecular pathways, functional annotations and mouse phenotypes. For visualization purposes the resulting enrichment matrix was reduced to fewer dimensions by principal component analysis (**Figure 1**, **Supplementary Methods**). Similarly, this approach was applied to the common loci between allergy and autoimmune diseases (**Figure 2**), and to allergy and Crohn's disease separately to identify common and disease specific networks (**Figure 3**, **Supplementary Methods**). Crohn's disease was used as a representative of autoimmune diseases as this represents the largest, with respect to sample size, public available GWAS dataset to date of an autoimmune disease[14]. Also, we consider this a good

representative of autoimmune diseases since it is considered to be Th1 driven immune like most autoimmune diseases.

The enrichment of transcription factor (TF) binding sites in loci common between allergy and autoimmune diseases was calculated using ENCODE data by assessing the overlap between loci and binding sites for 161 TFs compared to random expectations (**Supplementary Methods**).

**Common disease-implicated cell types**

To identify and visualize common disease-implicated cell types, the tendency of disease associated loci to fall in cell-type specific regulatory DNase Hypersensitive Sites (DHS) (a proxy for accessible and/or regulatory DNA) was calculated for all diseases in the GWAS catalog, as well as allergy based upon the current association data-set. This enrichment was computed for 168 cell types and cell lines (hereafter described as cells) from the ENCODE Roadmap repository[15]. Duplicates and directly redundant cell types were removed before analyses. As with pathway enrichments, the resulting enrichment matrix was reduced to fewer dimensions by PCA for visualization (**Supplementary Methods**). For allergy this was also compared for the full range of p-values within the allergy meta-analysis in bins of decreasing p-value thresholds, essentially as done by Maurano and colleagues[16]. This was similarly done for Crohn's disease for comparison[14] using data from a GWAS metanalysis[14] including data from 6 studies of European descent with in total 6,333 cases and 15,056 controls in the discovery imputed with Hapmap III or II with in total of 953,242 autosomal SNPs. To validate specific findings, the DHS enrichment was re-calculated for enhancer regions in data from the more conservative FANTOM5 set[17].

## Results

### Allergy meta-analysis

By use of the joint meta-analysis on combined data from allergic sensitization and self reported allergy we increased the number of allergy-associated SNPs compared to the previous GWAS (**Supplementary Figure 2**) resulting in a total number of 19 genome-wide significant loci (**Supplementary Figure 3**). One of these; rs11122898 near *ANAPC1/MERKT* (p=1.9e-8) has not previously been associated with allergy or any related trait. In addition there were 5 novel suggestive loci (p<e-5): rs7612543 near *ZBTB38* (p=1.0e-7); rs9790601 near *NFKB1* (P=7.4e-8); rs7072398 near *IL2RA* (p=5.2e-7); rs12365699 near *CXCR5* (p=6.5e-7) and rs12900122 near *RORA* (p=3.5e-7) (**Supplementary Figure 4 and Supplementary Table 2**). Notably, all of these suggestive loci have previously been described in relation to autoimmune disorders[11,18–30].

### Commonalities in genetic loci, pathways and disease implicated cell types between allergy and autoimmune diseases

There was a significant enrichment of autoimmune-associated loci with low p-values among the allergy loci from the current meta-analysis compared with expected (enrichment OR=4.36 [3.2-5.9], p=1.4e-17) (**Figure 1A, Table 1 and supplementary table 3**). A similar enrichment was seen for the two allergy phenotypes separately (self reported allergy: OR=4.1 [3.0-5.5] p=1.1e-15, and allergic sensitization: OR=2.7 [1.6-4.0] p=1.8e-5) (**Supplementary Figure 5**). This enrichment was also seen for the individual autoimmune diseases (**Figure 1A and Supplementary Figure 6**), although not statistically significant for

Systemic Lupus Erythematosus and Ankylosing Spondylitis and for Psoriasis and Graves Disease after adjusting for multiple testing (**Table 1**). We a priori chose a P-value threshold for the calculations of enrichment of <0.05. Using lower thresholds (P <0.01 or 0.001) generally resulted in higher enrichment and significant enrichment for all autoimmune diseases.

As a methodological negative control, SNPs related to two non-inflammatory phenotypes with a large number of known genome-wide significant loci, migraine and the combination of bipolar disorder and schizophrenia from the GWAS catalog were extracted from the allergy meta-analysis. These showed no significant overlap with allergy loci (**Supplementary Figures 7 and 8**).

Using DEPICT to identify significantly enriched reconstituted gene sets for allergy (**Supplementary Table 4**) and all diseases in the GWAS catalog, we identified a strong separation of autoimmune diseases, allergy and asthma from other traits on the first PCA component (Wilcoxon rank sum test $p_{PC1}$=8.142e-08, Wilcoxon rank sum test) (**Figure 1B and Supplementary Figures 9 and 10**). Notably, no other disease groups seemed to cluster strongly together (**Supplementary Figures 9 and 10**).

Analysis of all published SNP-to-trait associations and the tendency of these SNPs to fall within regions of open chromatin (represented by DHS) in specific cell types[31] likewise revealed that autoimmune diseases, allergy and asthma clustered together, and differentiated from other non-immune diseases on the first two PCA components (**Supplementary Figures 11 and 12**, $p_{PC1}$=0.0035, $p_{PC2}$=3.856e-07, Wilcoxon rank sum test). Loadings indicated that immune cells are responsible for this partitioning (**Supplementary**

**Figure 13**). Hierarchical clustering of the DHS sites within immune cells similarly showed the tendency of co-clustering of autoimmune diseases with allergy and asthma (**Supplementary Figure 14**). Specific DHS-analyses of allergy and Crohn's disease showed similar enrichment in variants falling within DHS regions of immune cells (**Supplementary Figure 15**). For allergy, these findings were validated in the FANTOM5 high confidence enhancer data set, which showed comparable enrichment among immune cells (**Supplementary Figure 16**)"

**The specific common genetic loci**

Out of the 290 autoimmune disease SNPs investigated, 29 were significantly associated with allergy at a FDR <0.05 (**Table 2**). Eleven of these common loci (*C11ORF30*, *LPP*, *PLCL1*, *HLA-B*, *SMAD3*, *IKZF3*, *MYC*, *CLEC16A, NDFIP1, BACH2* and *IL2RA/IL15RA*) were already reported to be associated with allergy[9,10,32,33] (**Table 2 and Supplementary Table 5 and 6**). The remaining 18 overlapping loci included the mapped genes: *NFKB1*, *SH2B3*, *AKAP11/TNFSF11*, *ABO*, *C12ORF30*, *CD247*, *RADSNB*, *EP300*, *RORC*, *PSMG1*, *HDAC7/VDR*, *HLA-DPB2*, *BACH2*, *TNFAIP3*, *KIF1B*, *RPS6KA4*, *ERBB3*, *THADA*, and *GLB1/CCR4*. Look up of the 29 common loci in the separate results from the 2 different allergy-phenotypes (allergic symptoms and allergic sensitization) generally showed similar results, including same direction of effect for the two allergy-phenotypes for 28 out of 29 loci (**Supplementary Table 5**). For the majority of loci the effect size was higher for allergic sensitization compared to allergic symptoms, as would be expected due to the more homogenous phenotype, and for the majority of loci with evidence of heterogeneity between phenotypes, heterogeneity was due to this. The NDFIP1 locus seemed only to be associated with self reported allergy.

Comparison of the direction of effect between allergy and autoimmune disease was possible for 27 of the 29 common loci compared with the index autoimmune disease. For 13 of these (48%), we found the same direction of effect meaning that the allele increasing the risk of allergy also increases the risk of the autoimmune disease (**Table 2**). For the remaining 14 loci (52%), we found opposite direction of effect with the risk allele for allergy being associated with reduced risk of the index autoimmune disease (**Table 2 and Supplementary Table 5**). The majority of autoimmune diseases showed examples of both same and opposite direction of effect compared to allergy. For some of the common loci where several autoimmune diseases have reported association, the different autoimmune diseases showed differences in direction of effect relative to allergy (*HLA-B*, *BACH2* and *RPS6KA4*). After gene set enrichment analyses of these 29 common loci, the resulting significant hits were all ontological terms relating to immune function, including immunoglobulin diversification and production, T-and B-cell activation, signaling by nuclear receptors and abnormal immune cell physiology. (**Figure 2**, **Supplementary Figure 17 and Supplementary Table 7**). Coloring for loci with same vs. opposite direction of effect for allergy and autoimmune diseases showed no clear systematic differences (Figure 2).

To investigate the potential enrichment for certain transcription factors in mediating the effect at common loci, public transcription factor binding data from ENCODE were analyzed for overlap within loci common between allergy and autoimmune diseases. This revealed significant enrichment for several immune related transcription factors (**Supplementary Figure 18**).

In order to investigate if the common loci seem to tag the same genetic variant, we performed regional association plots showing that, for almost all loci, the autoimmune disease tagging SNP is also within the LD-block with strongest regional association with allergy (**Supplementary Figure 19**). Tagging of the same genetic variation at common loci was further supported by paired comparison of regional association plots for Crohn's disease[14] and allergy, respectively, for the most statistically significant common loci (**Supplementary Figure 20**).

**Shared and differential genetic pathways for Allergy and Crohn's disease**

A direct comparison of pathways targeted by allergy-related loci vs. Crohn's disease loci revealed that a large proportion of shared as well as disease-specific pathways, with a strong predominance of T cell signaling modules within the shared grouping (**Figure 3**).

## Discussion

Our study demonstrated substantial commonalities between allergy and autoimmune diseases in terms of susceptibility loci, genetic pathways and genomic regulatory sites (DHS). This overlap in genetic mechanisms seemed to be a general phenomenon for allergy autoimmune diseases and distinct from other diseases. Our study identifies a substantial number of novel overlapping loci for allergy and autoimmune diseases suggesting both shared (increasing risk of both autoimmune and allergic disease) as well as diverging genetic mechanisms.

*Strengths and limitations*

By combining two GWAS on allergic sensitization and allergic symptoms respectively, we were able to obtain the most powerful GWAS dataset on allergy to date, which allowed a systematic analysis of the genetic commonalities of allergy and autoimmune diseases. The clinical phenotypes are not identical, with allergic sensitization often being present without symptoms and vice versa, which can also be seen as a limitation of the study. However, the phenotypes are closely correlated genetically as suggested from the initial publications of the individual GWAS' showing highly consistent mutual replication of top-SNPs between studies[9,10]. The improved number of significant SNPs and a higher number of genome-wide significant loci in the combined meta-analysis performed here compared with the individual GWAS results also underscores the validity of the combined meta-analysis approach. Furthermore, the common loci between allergy and autoimmunity generally showed similar results for the two allergy-related phenotypes (**Supplementary Table 5**), and

the enrichment of autoimmune loci was also similar for both phenotypes (**Supplementary Figure 5**), strongly suggesting that the conclusions of this study is not affected by the combination of allergy-related phenotypes.

In the primary analyses we combined GWAS loci from several autoimmune diseases. This was done in order to assess commonalities between allergy and autoimmune diseases in general and to obtain enough autoimmune loci and thereby statistical power to perform more systematic analyses. However, it should be noted that autoimmune diseases represent a heterogenous group of diseases, and the genetic architecture of autoimmune genes seem to include shared, but also differential and opposing genetic mechanisms[34-36]. We therefore also performed separate enrichment analyses for the different autoimmune diseases showing that enrichment for allergy-related loci seem to be the case for the majority of autoimmune diseases (**Supplementary table 8**).

It is a limitation that we did not have access to GWAS data for all autoimmune diseases. For the regional analyses of shared loci, a publicly available GWAS dataset on Crohn's disease was therefore used as a representative of autoimmune disease. It is a limitation of the analyses based on GWAS-catalog markers, that genotype chips and imputation panels and procedures differ between studies, adding marker coverage heterogeneity.

Our study is also limited by differences in study size of GWAS on autoimmune diseases, meaning that the diseases where the largest GWAS have been performed, and most loci have been discovered, will have a relatively larger impact on the results of the analysis combining all autoimmune diseases. The number of reported loci for each autoimmune disease is shown in Table 1.

*Interpretation*

We found substantial overlap of susceptibility loci for allergy and autoimmune diseases suggesting commonalities in the genetic background and hence the possibility of shared pathogenetic mechanisms. The possible common etiology of allergy and autoimmune diseases was further supported by co-clustering of autoimmune diseases, asthma and allergy in terms of genetic pathways and regulatory sites implying shared disease pathways beyond overlap of associated SNPs.

To our knowledge, no previous study has had sufficient statistical power to systematically explore commonalities in the genetic architecture between allergy and autoimmunity. One previous study found no association between susceptibility loci for type 1 diabetes and total IgE levels[37] arguing against a shared genetic background. However, that study had much lower statistical power than the present study, and the genetics of total IgE has been shown to be different from the genetics of allergen-specific IgE[10]. Another study compared results from a GWAS on asthma with published GWAS results on autoimmune diseases and found evidence of 7 overlapping susceptibility loci, both showing examples of opposite and same direction of effect for asthma and autoimmune diseases[38].

Importantly, our study demonstrates common loci with both the same and opposite direction of effects, potentially pointing towards both converging (shared) and diverging (counteracting) mechanisms, either increasing the risk of both allergy and autoimmune diseases, or increasing the risk for one of the diseases while protecting against the other. Our study thereby provides further understanding of the complex genetic relationship between allergy and autoimmune diseases. We hypothesize that the common loci with same

direction of effect may be involved in the mechanisms causing the contemporaneous epidemics of allergy and autoimmune diseases[39] by increasing the susceptibility to immune disorders in general, probably by mechanisms involving gene-environment interaction. Complementarily, common loci with opposite direction of effect may be involved in mechanisms determining the type of immune disorder developing in the individual, resulting in the inverse relationship observed between allergy and some autoimmune diseases[5–7]. Understanding the mechanisms of these common genetic loci may improve understanding of the epidemics of allergy and autoimmune diseases. It may also help predict how targeting specific disease mechanisms could have the unintended consequence of increasing the risk of other diseases. We expect the loci with *same direction of effect* to be of particular importance in the search for common mechanisms driving the parallel increases in disease incidence. Of specific interest are the loci at *C11orf30*, *PLCL1* and *SMAD3,* which were strongly associated with allergy as well as several autoimmune diseases. Of these, *C11orf30* and *SMAD3* were also identified in a previous study comparing asthma and autoimmune diseases[38]. Some of the loci with same direction of effect were linked to immune-related transcription factors (*RORC*, *SMAD3*), transcriptional co-factors (*EP300*), cell-cycle regulators (*THADA*) or regulators of transcription (*C11ORF30*, *PLCL1*, *AKAP11*, *NDFIP1*). Several are directly implicated in regulation of regulatory T cells (Treg, *SMAD3*[40], *EP300*[41]) and Th17 cells (*RORC*[42], *SMAD3*[40]), or regulation of immune activity *(IL2RA*). This supports a commonality of autoimmune and allergic diseases based on defects in immune suppressive functions. Other loci with same direction of effect included *CLEC16A*, *TNFSF11*, *CCR4* and *GLB1*, all involved in immune function by different means.

Loci with *opposite direction of effect* might be involved in "polarization" of the immune response. Since allergy is acknowledged to involve Th2-mediated pathology, while most autoimmune diseases involve Th1 cells as well as pathogenic Th17 cells, any genetic factors that perturb Th differentiation ability or the immunosuppressive Treg function could potentially influence the risk of specific disease development. The loci with opposite direction of effect included *LPP*, *NFKB1, TNFAIP3,* all involved in immune cell signaling and activation/deactivation processes. Several of the other loci with opposite direction of effect function as possible regulators of immune cell differentiation (*HDAC7*/*VDR*[43,44], *IKZF3*[45], *SH2B3*, *BACH2*, *RPS6KA4* (*MSK2*)[46]) and cell-cycle regulation (*RAD51L1*), while the remaining loci (*C12ORF30*, *PSMG1*, *HLA-DPB2*, *KIF1B*) are more general regulators of cellular function. It should however be noted that given the complexity of genetic regulation and the fact that the causal genetic variant is unknown for most susceptibility loci, the finding of common genetic loci with apparent opposite direction of effect should be interpreted with caution. It is possible that this is the result of different underlying causal variants in the region, although comparison of regional association plots suggested that the association signals for allergy and autoimmune disease did tag the same genetic variation. Potential polarizing mechanisms associated with these loci should be addressed in future studies, e.g. by demonstrating opposite disease relationships on the level of gene expression and/or protein levels.

Gene set enrichment analyses of the 29 shared loci (**Figure 2**, **Supplementary Figure 17 and Supplementary Table 7**) indicate that immune functioning and activation status specifically within T cells represents a shared focal point for allergy and autoimmune diseases.

Involvement of shared immunological paths was further supported based on the type of transcription factors found to be enriched within the common loci where generic immune regulatory transcription factors including MTA3, WRNIP1 and IKZF1 (Ikaros) turned out as central players (**Supplementary Figure 18**). MTA3 has been shown to be involved in B-cell and T helper cell differentiation[47,48] and WRNIP1 has been reported to regulate expression of transcription factors involved in Treg functioning[49]. IKZF1 activates extensive transcriptional programs involving especially regulation of T, B and NK cells with effects on differentiation, proliferation and apoptotic programs in these cell types[50]. Moreover, several other directly immune-related transcription factors were identified amongst the top 10 hits, including NFATC1, STAT2, MEF2C, RELA, SP2 and ZEB1[51–56].

The comparative pathway analysis between allergy and Crohn's disease highlights that the common pathways of these diseases are founded on (de)regulation of adaptive immune signaling, involving TCR, CD28, IL2/3/5/6, IFNg, GM-CSF, JAK/STAT and IL receptor signaling as well as of apoptosis and IgA production. The Crohn's disease-specific network primarily included pathways associated with innate immune activation involving TLR and NOD signaling, while allergy-specific pathways were associated with signaling from receptor tyrosine kinases such as EGFR. (**Figure 3**)

A strong co-clustering and separation of allergy, asthma and autoimmune diseases in terms of enrichment of SNPs in cell type specific DHS sites, points towards common immune modulatory mechanisms facilitated by the effect of the genetic SNP burden in immune cell-specific regulatory regions (**Supplementary Figures 11 and 13**). For Allergy and Crohn's disease, these related primarily to T and B cell functions (**Supplementary Figure 15**). In

accordance with our findings of coinciding immune cell involvement in several immune-mediated diseases, one previous study on Multiple Sclerosis reported several genetic markers in relevant DHS sites in immune cells.[57] Accordingly and in line with our findings a recent paper focusing on autoimmune disease variants show how these immune mediated diseases are correlated and cluster in tendency for associated variants to be enriched in specifically immune cell enhancers.[58] Moreover, the enrichment of immune-cell specific DHS sites specifically within promoter regions (**Supplementary Methods, Supplementary Figure 21**) may be a result of the adaptability and immediate early gene response requirements of the immune system, and since their positioning is essential for gene expression levels this might also explain why the identified specific SNP variants pose increased risk for disease penetrance.

In addition to pinpointing common loci between allergy and autoimmune diseases, our identification of common loci also suggests a large number of novel allergy loci; 18 of the 29 common loci have not previously been associated with allergy (**Table 2**). Our study suggests that these are all susceptibility loci for allergy that did not reach the criteria for genome-wide significance and was therefore not discovered in previous GWAS.
Furthermore, our combined meta-analysis on allergy and allergic symptoms identified suggestive allergy loci with several previously related to immune function (*NFKB1*[59] and *CXCR5*[60], **Supplementary Table 2**). One novel suggestive allergy locus was discovered at rs11122898 and reached the genome-wide significance threshold. This locus is close to *ANAPC1* but is most likely affecting the upstream *MERKT* gene (**Supplementary Figure 22**), which is involved in regulation of dendritic cells via B-cell activating factor (BAFF)[61]. One

493 additional suggestive locus was at *ZBTB38*, and genes within this family have been shown to
494 have important function in naive B-cell differentiation[62], and have been associated to
495 eczema[63] and asthma with hay fever[33] although it has not been shown that these genes are
496 the causal genes within these loci.
497
498 In conclusion, we performed the first large study on commonalities in the genetic origins of
499 allergy and autoimmune diseases and documented substantial genetic overlap between
500 these diseases. The recent availability of a vast array of genomics data from the ENCODE and
501 other consortia provides a solid foundation for systems biology analysis in disease settings.
502 Exploiting this approach, we identified common molecular pathways between allergy and
503 autoimmune diseases, identical patterns of overlaps with open chromatin specifically within
504 immune cell-specific regulatory regions, and overlap in transcription factor binding sites,
505 emphasizing common characteristics in gene regulation. Further investigation of these
506 commonalities in genetic mechanisms might improve understanding of important biological
507 pathways that increases the risk of allergy and autoimmune diseases as well as mechanisms
508 differentiating these diverse diseases. Understanding of potential shared genetic origins of
509 allergy and autoimmune diseases, maybe particularly related to the loci with the same
510 direction of effect, could point to vulnerable “hot” points in immune system pathways that
511 may also be affected by other modifiers such as epigenetics and environmental exposures.
512 This insight might provide important clues for understanding the parallel epidemics of these
513 diseases and thereby enforce future disease prevention.
514
515

**Acknowledgements and funding**

Please see supplement.

**Author Contributions**

**Statistical and functional analysis:** E.K-M., J.W., M.S, T.H.P, A.C.A, N.M.W., L.F., J.N.H, A.S., G.H.K., D.S.P., A.C., N.T., D.P.S, D.H.,

**Study design:** E.K-M., J.W., A.S., J.Y.T., G.H.K., D.S.P., A.C., N.T., M.A.F, D.P.S, A.J.H., D.H., H.B., K.B.

**Writing paper:** E.K-M., J.W., M.S, S.B., T.H.P, H.B., K.B.

**Data collection:** E.K.-M., M.S, E.F., A.J., A.S., G.H.K., D.S.P., C.E.P., A.C., D.P.S, A.J.H., H.B., K.B.

**Genotyping:** C.M.T.T., A.S., G.H.K., C.E.P., A.C., H.B.

**Revising and reviewing paper:** E.K.-M., J.W., M.S, S.B., T.H.P, A.C.A, N.M.W., C.M.T.T., E.F., L.F., J.N.H, A.J., A.S., J.Y.T., G.H.K., D.S.P., C.E.P., M.R.J., A.C., N.T., M.A.F, D.P.S, A.J.H., D.H., H.B., K.B.

**Competing financial interests**

D.H. and J.Y.T. are employees of 23andMe. The remaining authors declared no competing interests of relevance to this paper.

## Figure Legends

**Figure 1. Commonalities in susceptibility loci and genetic pathways between allergy and autoimmune diseases**

**A)** Autoimmune disease-associated loci and their association with allergy. Quantile-quantile plots representing the observed vs. expected p-values in the combined allergy GWAS for all 290 candidate autoimmune disease-associated loci (large panel), and separately for selected autoimmune diseases (smaller panels). Solid line reflects the p-value distribution under the null, while the dashed line is the distribution of all SNPs from the allergy meta-analysis. T1D: Type 1 diabetes.

**B)** Commonalities in genetic pathways. Principal component analysis of DEPICT gene set enrichment results based on trait- associated variants for 123 traits from the GWAS Catalog and allergy. The blue area represents the shared minimal ellipsoid area of allergy and autoimmune diseases.

**Figure 2. Pathway-based analysis of common loci**

Principal component analysis of DEPICT gene set enrichment results based on the 29 common loci between allergy and autoimmune diseases, with each dot representing a single enriched gene set. Loadings for the index genes are illustrated by arrows. Genes denoted in blue and orange represent same and opposite direction of effect for allergy, respectively, a*s compared to index autoimmune disease*. For genes denoted in gray, index autoimmune disease did not report effect allele. The blue areas represent cohesive clusters of gene sets

558 with similar immune function. The individual gene set names are shown in **Supplementary**
559 **Figure 15.**
560
561 **Figure 3. Common and disease-specific genetic pathways**
562 DEPICT gene-set enrichment map of common (blue), allergy-specific (red) and Crohn's
563 Disease-specific (green) pathways. The correlation between pathways is depicted by the line
564 width. Sets with a correlation < 0.4 and singletons are not shown.
565
566
567

568 **Table 1 – Enrichment of significant allergy loci among autoimmune disease-associated loci**

| Phenotype | # Loci | # Sig. Loci* | Proportion Sig. | eOR | CI | P |
|---|---|---|---|---|---|---|
| **All Autoimmune Loci** | 290 | 57 | 0.20 | 4.36 | [3.20-5.85] | **1.40E-17**§ |
| **Inflammatory Bowel Disease** | 178 | 42 | 0.24 | 5.51 | [3.80-7.84] | **2.60E-16**§ |
| **Crohn's Disease** | 97 | 26 | 0.27 | 6.53 | [4.00-10.36] | **5.00E-12**§ |
| **Ulcerative Colitis** | 60 | 16 | 0.27 | 6.48 | [3.41-11.72] | **6.40E-08**§ |
| **Multiple Sclerosis** | 54 | 12 | 0.22 | 5.09 | [2.44-9.86] | **2.10E-05**§ |
| **Type 1 Diabetes** | 43 | 8 | 0.19 | 4.07 | [1.63-8.94] | **1.70E-03**§ |
| **Arthritis** | 40 | 9 | 0.23 | 5.18 | [2.17-11.14] | **2.00E-04**§ |
| **Celiac Disease** | 36 | 11 | 0.31 | 7.85 | [3.48-16.53] | **1.70E-06**§ |
| **Systemic Lupus Erythematosus** | 27 | 4 | 0.15 | 3.10 | [0.78-9.07] | 5.30E-02 |
| **Primary Biliary Cirrosis** | 23 | 7 | 0.30 | 7.80 | [2.71-20.03] | **1.40E-04**§ |
| **Psoriasis** | 19 | 4 | 0.21 | 4.75 | [1.15-14.93] | **1.62E-02** |
| **Graves Disease** | 15 | 3 | 0.20 | 4.46 | [0.81-16.52] | **4.20E-02** |
| **Ankylosing Spondylitis** | 11 | 2 | 0.18 | 3.96 | [0.42-19.14] | 1.10E-01 |

* With P<0.05 to allergy

Bold: Nominal significant. §: Significant at Bonferroni (0.05/13)

eOR: enrichment Odds-Ratio calculated for autoimmune diseases with at least 10 loci

569

570

571

572 **Table 2 – Common loci between allergy and autoimmune diseases**

| Chr:BP | Gene | SNP | MAF* | Beta | P, FDR | Het. P** | Traits§ | Direction £ | Known allergy Locus | Other genes in LD > 0.5 |
|---|---|---|---|---|---|---|---|---|---|---|
| 11:75976842 | *C11ORF30* | rs2155219[T] | 0.47 | 0.12 | 6.10E-23 | 5.20E-03 | CrD(+), **IBD(+)**, UC(+) | Same | Yes$ | - |
| 3:189595248 | *LPP* | rs1464510[A] | 0.48 | -0.07 | 4.20E-07 | 1.40E-01 | **CeD(-)** | Opposite | Yes$ | - |
| 2:198605140 | *PLCL1* | rs6738825[A] | 0.48 | 0.06 | 9.20E-07 | 1.90E-01 | **CrD**(+) | Same | Yes$ | ANKRD44, BOLL, COQ10B, HSPD1, HSPE1, MARS2, MOB4,, RFTN2, SF3B1 |
| 6:31444079 | *HLA-B* | rs7743761[A] | 0.26 | -0.07 | 1.90E-06 | 4.00E-01 | **AS(na)**, GD(-), SLE(+), UC(+) | na | Yes$ | - |
| 15:65229650 | *SMAD3* | rs17293632[T] | 0.27 | 0.07 | 2.00E-06 | 1.90E-01 | **CrD(+)**, IBD(+) | Same | Yes$ | - |
| 17:35175785 | *IKZF3* | rs907092[A] | 0.49 | -0.06 | 4.10E-05 | 8.30E-01 | CrD(-), **IBD(-)**, PBC(-), T1D(-), UC(-) | Opposite | Yes$ | GSDMB, ORMDL3, ZPBP2 |
| 8:128884211 | *MYC* | rs4410871[T] | 0.28 | 0.06 | 4.10E-05 | 8.60E-04 | **MS(-)** | Opposite | Yes$ | - |
| 12:110368991 | *SH2B3* | rs3184504[T] | 0.45 | -0.06 | 5.30E-05 | 7.50E-02 | A(-), CeD(-), **T1D(-)** | Opposite | Novel | ACAD10, ADAM1, ALDH2, ATXN2, BRAP, C12orf47, C12orf51, ERP29, MAPKAP5, NAA25, TMEM116, TRAFD1 |
| 13:41950880 | *AKAP11, TNFSF11* | rs2062305[A] | 0.43 | -0.05 | 2.00E-03 | 8.50E-01 | **CrD(+)** | Same | Novel | - |
| 16:11087374 | *CLEC16A* | rs12708716[A] | 0.35 | 0.05 | 2.00E-03 | 8.60E-02 | MS(+), PBC(+), **T1D(+)** | Same | Yes$ | - |
| 9:135139050 | *ABO* | rs505922[T] | 0.37 | -0.05 | 2.00E-03 | 2.90E-01 | **GD(+)** | Opposite | Novel | - |
| 12:110971201 | *C12ORF30* | rs17696736[A] | 0.42 | 0.05 | 2.20E-03 | 1.50E-01 | **T1D(-)** | Opposite | Novel | - |
| 4:103770651 | *NFKB1€* | rs7665090[A] | 0.49 | 0.04 | 2.70E-03 | 7.00E-01 | **PBC(-)** | Opposite | Novel | MANBA |
| 1:165678008 | *CD247* | rs864537[A] | 0.38 | 0.04 | 4.80E-03 | 6.10E-01 | **A(+)**, CeD(+), SC(+) | Same | Novel | - |
| 14:67823346 | *RADSNB* | rs911263[T] | 0.29 | -0.04 | 6.40E-03 | 1.80E-02 | **PBC(-)** | Opposite | Novel | - |
| 22:39761288 | *EP300* | rs4820425[A] | 0.29 | 0.05 | 6.60E-03 | 8.60E-01 | **CrD**(+) | Same | Novel | CHADL, DNAJB7, L3MBTL2, RANGAP1, ST13, XPNPEP3, ZC3H7B |
| 1:150068 | *RORC* | rs484560 | 0.14 | -0.06 | 7.50E-03 | 7.40E-01 | **IBD(+)** | Same | Novel | - |

| | | | | | | | | | | |
|---|---|---|---|---|---|---|---|---|---|---|
| 304 | | 4[A] | | | | | | | | |
| 10:6109567 | *IL2RA, IL15RA* | rs12722563[A] | 0.12 | 0.06 | 7.50E-03 | 1.00E+00 | **T1D(na)** | na | Yes$$ | - |
| 21:39387404 | *PSMG1* | rs2836878[A] | 0.26 | 0.05 | 7.50E-03 | 3.10E-01 | AS(-), **IBD(-)**, UC(-) | Opposite | Novel | - |
| 12:46494635 | *HDAC7, VDR* | rs11168249[T] | 0.48 | 0.04 | 8.70E-03 | 4.60E-01 | **IBD(-)** | Opposite | Novel | - |
| 6:33168096 | *HLA-DPB2* | rs2281388[A] | 0.02 | -0.13 | 8.80E-03 | 3.10E-01 | **GD(-)** | Opposite | Novel | - |
| 6:91014952 | *BACH2* | rs11755527[C] | 0.42 | 0.04 | 8.80E-03 | 3.90E-02 | CrD(+), **T1D(-)** | Opposite | Yes$$$ | - |
| 6:138048197 | *TNFAIP3* | rs6920220[A] | 0.22 | -0.05 | 1.00E-02 | 3.20E-01 | A(-), CeD(-), **IBD(-)**, UC(-) | Opposite | Novel | - |
| 5:141493388 | *NDFIP1* | rs6863411[A] | 0.37 | -0.04 | 1.00E-02 | 4.90E-02 | **IBD(+)** | Same | Yes$$$ | - |
| 1:10275699 | *KIF1B* | rs10492972[T] | 0.34 | 0.04 | 1.40E-02 | 5.00E-01 | **MS(-)** | Opposite | Novel | PGD, UBE4B |
| 11:63864311 | *RPS6KA4* | rs663743[A] | 0.36 | 0.04 | 2.50E-02 | 2.40E-01 | CrD(-), **S(+)** | Same | Novel | CCDC88B, ESRRA, GPR137, PRDX5, TRMT112 |
| 12:56482180 | *ERBB3* | rs2292239[T] | 0.32 | 0.04 | 2.50E-02 | 2.10E-01 | **T1D(+)** | Same | Novel | IKZF4, SUOX |
| 2:43660422 | *THADA* | rs10495903[T] | 0.12 | 0.05 | 3.40E-02 | 5.50E-01 | **CrD(+)**, IBD(+) | Same | Novel | - |
| 3:32990473 | *GLB1, CCR4* | rs13314993[T] | 0.43 | -0.03 | 4.70E-02 | 8.00E-02 | **CeD(+)** | Same | Novel | - |

** As reported by Bønnelykke et al.[5]*

*** Test for heterogeneity within the allergy meta-analysis*

*§ Reported traits associated with locus ( autoimmune trait marker LD with allergy marker > 0.6 and allergy marker p < 0.05) A: Arthritis, AS: Ankylosing Spondylitis, CeD: Celiac Disease, CrD: Crohn's Disease, GD: Graves Disease, IBD: Inflammatory Bowel Disease, MS: Multiple Sclerosis, P:Psoriasis, PBC: Primary Biliary Cirrhosis, SLE: Systemic lupus erythematosus, SS: Systemic Sclerosis UC: Ulcerative Colitis, T1D: Type 1 Diabetes. The index disease used in the comparison of effect direction marked by bold and underlined. +/- denotes direction of effect for the autoimmune disease compared to the direction allergy.*

*£ As compared to index autoimmune disease (underlined and bold in the "Traits" column)-SNP effect direction. Na: Some diseases have not reported the effect allele*

*$ Genome-wide significant association to allergy/allergic sesnsitization reported by Hinds et al, and/or Bønnelykke et al.[4,5]*

*$$ Suggestive association to asthma with hayfever reported by Ferreira et al.[33]*

*$$$ Suggestive association to asthma reported by Ferreira et al.[32]*

573

## References


1. Bach J-F. The Effect of Infections on Susceptibility to Autoimmune and Allergic Diseases. N Engl J Med. 2002;347(12):911–20.
2. Sevelsted A, Stokholm J, Bønnelykke K, Bisgaard H. Cesarean section and chronic immune disorders. Pediatrics. 2015 Jan;135(1):e92–8.
3. Steinman L. A brief history of TH17, the first major revision in the TH1/TH2 hypothesis of T cell–mediated tissue damage. Nat Med. 2007 Jan;13(1):139–45.
4. Lloyd CM, Hessel EM. Functions of T cells in asthma: more than just TH2 cells. Nat Rev Immunol. 2010 Dec;10(12):838–48.
5. Rudwaleit M, Andermann B, Alten R, Sörensen H, Listing J, Zink A, et al. Atopic disorders in ankylosing spondylitis and rheumatoid arthritis. Ann Rheum Dis. 2002 Nov;61(11):968–74.
6. Verhoef CM, van Roon JA, Vianen ME, Bruijnzeel-Koomen CA, Lafeber FP, Bijlsma JW. Mutual antagonism of rheumatoid arthritis and hay fever; a role for type 1/type 2 T cell balance. Ann Rheum Dis. 1998 May;57(5):275–80.
7. Bergamaschi R, Villani S, Crabbio M, Ponzio M, Romani A, Verri A, et al. Inverse relationship between multiple sclerosis and allergic respiratory diseases. Neurol Sci Off J Ital Neurol Soc Ital Soc Clin Neurophysiol. 2009 Apr;30(2):115–8.
8. Rabin RL, Levinson AI. The nexus between atopic disease and autoimmunity: a review of the epidemiological and mechanistic literature. Clin Exp Immunol. 2008 Jul;153(1):19–30.
9. Hinds DA, McMahon G, Kiefer AK, Do CB, Eriksson N, Evans DM, et al. A genome-wide association meta-analysis of self-reported allergy identifies shared and allergy-specific susceptibility loci. Nat Genet. 2013 Aug;45(8):907–11.
10. Bønnelykke K, Matheson MC, Pers TH, Granell R, Strachan DP, Alves AC, et al. Meta-analysis of genome-wide association studies identifies ten loci influencing allergic sensitization. Nat Genet. 2013 Aug;45(8):902–6.
11. Jostins L, Ripke S, Weersma RK, Duerr RH, McGovern DP, Hui KY, et al. Host-microbe interactions have shaped the genetic architecture of inflammatory bowel disease. Nature. 2012 Nov 1;491(7422):119–24.
12. Welter D, MacArthur J, Morales J, Burdett T, Hall P, Junkins H, et al. The NHGRI GWAS Catalog, a curated resource of SNP-trait associations. Nucleic Acids Res. 2014 Jan;42(Database issue):D1001–6.
13. Pers TH, Karjalainen JM, Chan Y, Westra H-J, Wood AR, Yang J, et al. Biological interpretation of genome-wide association studies using predicted gene functions. Nat Commun. 2015;6:5890.
14. Franke A, McGovern DPB, Barrett JC, Wang K, Radford-Smith GL, Ahmad T, et al. Genome-wide meta-analysis increases to 71 the number of confirmed Crohn's disease susceptibility loci. Nat Genet. 2010 Dec;42(12):1118–25.
15. Consortium TEP. An integrated encyclopedia of DNA elements in the human genome. Nature. 2012 Sep 6;489(7414):57–74.
16. Maurano MT, Humbert R, Rynes E, Thurman RE, Haugen E, Wang H, et al. Systematic localization of common disease-associated variation in regulatory DNA. Science. 2012 Sep 7;337(6099):1190–5.
17. Andersson R, Gebhard C, Miguel-Escalada I, Hoof I, Bornholdt J, Boyd M, et al. An atlas of active enhancers across human cell types and tissues. Nature. 2014 Mar

27;507(7493):455–61.
18. Hirota T, Takahashi A, Kubo M, Tsunoda T, Tomita K, Sakashita M, et al. Genome-wide association study identifies eight new susceptibility loci for atopic dermatitis in the Japanese population. Nat Genet. 2012 Nov;44(11):1222–6.
19. Moffatt MF, Gut IG, Demenais F, Strachan DP, Bouzigon E, Heath S, et al. A large-scale, consortium-based genomewide association study of asthma. N Engl J Med. 2010 Sep 23;363(13):1211–21.
20. Gudbjartsson DF, Bjornsdottir US, Halapi E, Helgadottir A, Sulem P, Jonsdottir GM, et al. Sequence variants affecting eosinophil numbers associate with asthma and myocardial infarction. Nat Genet. 2009 Mar;41(3):342–7.
21. Nair RP, Duffin KC, Helms C, Ding J, Stuart PE, Goldgar D, et al. Genome-wide scan reveals association of psoriasis with IL-23 and NF-kappaB pathways. Nat Genet. 2009 Feb;41(2):199–204.
22. Urayama KY, Jarrett RF, Hjalgrim H, Diepstra A, Kamatani Y, Chabrier A, et al. Genome-wide association study of classical Hodgkin lymphoma and Epstein-Barr virus status-defined subgroups. J Natl Cancer Inst. 2012 Feb 8;104(3):240–53.
23. Stahl EA, Raychaudhuri S, Remmers EF, Xie G, Eyre S, Thomson BP, et al. Genome-wide association study meta-analysis identifies seven new rheumatoid arthritis risk loci. Nat Genet. 2010 Jun;42(6):508–14.
24. International Multiple Sclerosis Genetics Consortium, Wellcome Trust Case Control Consortium 2, Sawcer S, Hellenthal G, Pirinen M, Spencer CCA, et al. Genetic risk and a primary role for cell-mediated immune mechanisms in multiple sclerosis. Nature. 2011 Aug 11;476(7359):214–9.
25. Petukhova L, Duvic M, Hordinsky M, Norris D, Price V, Shimomura Y, et al. Genome-wide association study in alopecia areata implicates both innate and adaptive immunity. Nature. 2010 Jul 1;466(7302):113–7.
26. Barrett JC, Clayton DG, Concannon P, Akolkar B, Cooper JD, Erlich HA, et al. Genome-wide association study and meta-analysis find that over 40 loci affect risk of type 1 diabetes. Nat Genet. 2009 Jun;41(6):703–7.
27. Han J-W, Zheng H-F, Cui Y, Sun L-D, Ye D-Q, Hu Z, et al. Genome-wide association study in a Chinese Han population identifies nine new susceptibility loci for systemic lupus erythematosus. Nat Genet. 2009 Nov;41(11):1234–7.
28. Lango Allen H, Estrada K, Lettre G, Berndt SI, Weedon MN, Rivadeneira F, et al. Hundreds of variants clustered in genomic loci and biological pathways affect human height. Nature. 2010 Oct 14;467(7317):832–8.
29. Zhernakova A, Stahl EA, Trynka G, Raychaudhuri S, Festen EA, Franke L, et al. Meta-analysis of genome-wide association studies in celiac disease and rheumatoid arthritis identifies fourteen non-HLA shared loci. PLoS Genet. 2011 Feb;7(2):e1002004.
30. Mells GF, Floyd JAB, Morley KI, Cordell HJ, Franklin CS, Shin S-Y, et al. Genome-wide association study identifies 12 new susceptibility loci for primary biliary cirrhosis. Nat Genet. 2011 Apr;43(4):329–32.
31. Gusev A, Lee SH, Trynka G, Finucane H, Vilhjálmsson BJ, Xu H, et al. Partitioning heritability of regulatory and cell-type-specific variants across 11 common diseases. Am J Hum Genet. 2014 Nov 6;95(5):535–52.
32. Ferreira MAR, Matheson MC, Duffy DL, Marks GB, Hui J, Le Souëf P, et al. Identification of IL6R and chromosome 11q13.5 as risk loci for asthma. Lancet. 2011 Sep 10;378(9795):1006–14.

667 33. Ferreira MAR, Matheson MC, Tang CS, Granell R, Ang W, Hui J, et al. Genome-
668 wide association analysis identifies 11 risk variants associated with the asthma with hay fever
669 phenotype. J Allergy Clin Immunol. 2014 Jun;133(6):1564–71.
670 34. Cotsapas C, Voight BF, Rossin E, Lage K, Neale BM, et al. Pervasive sharing of
671 genetic effects in autoimmune disease. PLoS Genet. 2011 Aug;7(8):e1002254
672 35. Sirota M, Schaub MA, Batzoglou S, Robinson WH, Butte AJ. Autoimmune disease
673 classification by inverse association with SNP alleles. PLoS Genet. 2009 Dec;5(12):e1000792
674 36. Cotsapas C, Hafler DA. Immune-mediated disease genetics: the shared basis of
675 pathogenesis. Trends Immunol. 2013 Jan;34(1):22-6
676 37. Maier LM, Howson JMM, Walker N, Spickett GP, Jones RW, Ring SM, et al.
677 Association of IL13 with total IgE: evidence against an inverse association of atopy and
678 diabetes. J Allergy Clin Immunol. 2006 Jun;117(6):1306–13.
679 38. Li X, Ampleford EJ, Howard TD, Moore WC, Torgerson DG, et al. Genome-wide
680 association studies of asthma indicate opposite immunopathogenesis direction from
681 autoimmune diseases. J Allergy Clin Immunol. 2012 Oct;130(4):861-8.e7
682 39. Bach J-F. The effect of infections on susceptibility to autoimmune and allergic
683 diseases. N Engl J Med. 2002 Sep 19;347(12):911–20.
684 40. Takimoto T, Wakabayashi Y, Sekiya T, Inoue N, Morita R, Ichiyama K, et al. Smad2
685 and Smad3 are redundantly essential for the TGF-beta-mediated regulation of regulatory T
686 plasticity and Th1 development. J Immunol Baltim Md 1950. 2010 Jul 15;185(2):842–55.
687 41. Bhatt D, Ghosh S. Regulation of the NF-κB-Mediated Transcription of Inflammatory
688 Genes. Front Immunol. 2014;5:71.
689 42. Kofler DM, Marson A, Dominguez-Villar M, Xiao S, Kuchroo VK, Hafler DA.
690 Decreased RORC-dependent silencing of prostaglandin receptor EP2 induces autoimmune
691 Th17 cells. J Clin Invest. 2014 Jun 2;124(6):2513–22.
692 43. Jeffery LE, Burke F, Mura M, Zheng Y, Qureshi OS, Hewison M, et al. 1,25-
693 Dihydroxyvitamin D3 and IL-2 combine to inhibit T cell production of inflammatory
694 cytokines and promote development of regulatory T cells expressing CTLA-4 and FoxP3. J
695 Immunol Baltim Md 1950. 2009 Nov 1;183(9):5458–67.
696 44. Palmer MT, Lee YK, Maynard CL, Oliver JR, Bikle DD, Jetten AM, et al. Lineage-
697 specific effects of 1,25-dihydroxyvitamin D(3) on the development of effector CD4 T cells. J
698 Biol Chem. 2011 Jan 14;286(2):997–1004.
699 45. Liao W, Lin J-X, Wang L, Li P, Leonard WJ. Modulation of cytokine receptors by IL-
700 2 broadly regulates differentiation into helper T cell lineages. Nat Immunol. 2011
701 Jun;12(6):551–9.
702 46. Ananieva O, Darragh J, Johansen C, Carr JM, McIlrath J, Park JM, et al. The kinases
703 MSK1 and MSK2 act as negative regulators of Toll-like receptor signaling. Nat Immunol.
704 2008 Sep;9(9):1028–36.
705 47. Fujita N, Jaye DL, Geigerman C, Akyildiz A, Mooney MR, Boss JM, et al. MTA3 and
706 the Mi-2/NuRD complex regulate cell fate during B lymphocyte differentiation. Cell. 2004
707 Oct 1;119(1):75–86.
708 48. Chen R, Bélanger S, Frederick MA, Li B, Johnston RJ, Xiao N, et al. In vivo RNA
709 interference screens identify regulators of antiviral CD4(+) and CD8(+) T cell differentiation.
710 Immunity. 2014 Aug 21;41(2):325–38.
711 49. Du W, Wang D, Shen Y-W, Lee W-H, Riggs A, Liu C-P. WRNIP1 is a key regulator
712 of antigen-specific Treg cells. (IRC4P.480). J Immunol. 2014 May 1;192(1
713 Supplement):60.7–60.7.

50. Yoshida T, Ng SY-M, Georgopoulos K. Awakening lineage potential by Ikaros-mediated transcriptional priming. Curr Opin Immunol. 2010 Apr;22(2):154–60.
51. Koch S, Reppert S, Finotto S. NFATc1 deletion in T lymphocytes inhibits the allergic trait in a murine model of asthma. Clin Exp Allergy J Br Soc Allergy Clin Immunol. 2015 Feb 1;
52. Yan H, Krishnan K, Greenlund AC, Gupta S, Lim JT, Schreiber RD, et al. Phosphorylated interferon-alpha receptor 1 subunit (IFNaR1) acts as a docking site for the latent form of the 113 kDa STAT2 protein. EMBO J. 1996 Mar 1;15(5):1064–74.
53. Clark RI, Tan SWS, Péan CB, Roostalu U, Vivancos V, Bronda K, et al. MEF2 is an in vivo immune-metabolic switch. Cell. 2013 Oct 10;155(2):435–47.
54. Pittet LA, Quinton LJ, Yamamoto K, Robson BE, Ferrari JD, Algül H, et al. Earliest innate immune responses require macrophage RelA during pneumococcal pneumonia. Am J Respir Cell Mol Biol. 2011 Sep;45(3):573–81.
55. Terrados G, Finkernagel F, Stielow B, Sadic D, Neubert J, Herdt O, et al. Genome-wide localization and expression profiling establish Sp2 as a sequence-specific transcription factor regulating vitally important genes. Nucleic Acids Res. 2012 Sep;40(16):7844–57.
56. Wang J, Lee S, Teh CE-Y, Bunting K, Ma L, Shannon MF. The transcription repressor, ZEB1, cooperates with CtBP2 and HDAC1 to suppress IL-2 gene activation in T cells. Int Immunol. 2009 Mar;21(3):227–35.
57. Elangovan RI, Disanto G, Berlanga-Taylor AJ, Ramagopalan SV, Handunnetthi L. Regulatory genomic regions active in immune cell types explain a large proportion of the genetic risk of multiple sclerosis. J Hum Genet. 2014 Apr;59(4):211–5.
58. Farh KK-H, Marson A, Zhu J, Kleinewietfeld M, Housley WJ, Beik S, et al. Genetic and epigenetic fine mapping of causal autoimmune disease variants. Nature. 2015 Feb 19;518(7539):337–43.
59. Tak PP, Firestein GS. NF-kappaB: a key role in inflammatory diseases. J Clin Invest. 2001 Jan;107(1):7–11.
60. Chevalier N, Jarrossay D, Ho E, Avery DT, Ma CS, Yu D, et al. CXCR5 expressing human central memory CD4 T cells and their relevance for humoral immune responses. J Immunol Baltim Md 1950. 2011 May 15;186(10):5556–68.
61. Gohlke PR, Williams JC, Vilen BJ, Dillon SR, Tisch R, Matsushima GK. The receptor tyrosine kinase MerTK regulates dendritic cell production of BAFF. Autoimmunity. 2009 Mar;42(3):183–97.
62. Lee S-U, Maeda T. POK/ZBTB proteins: an emerging family of proteins that regulate lymphoid development and function. Immunol Rev. 2012 May;247(1):107–19.
63. Paternoster L, Standl M, Chen C-M, Ramasamy A, Bønnelykke K, Duijts L, et al. Meta-analysis of genome-wide association studies identifies three new risk loci for atopic dermatitis. Nat Genet. 2011 Dec 25;44(2):187–92.

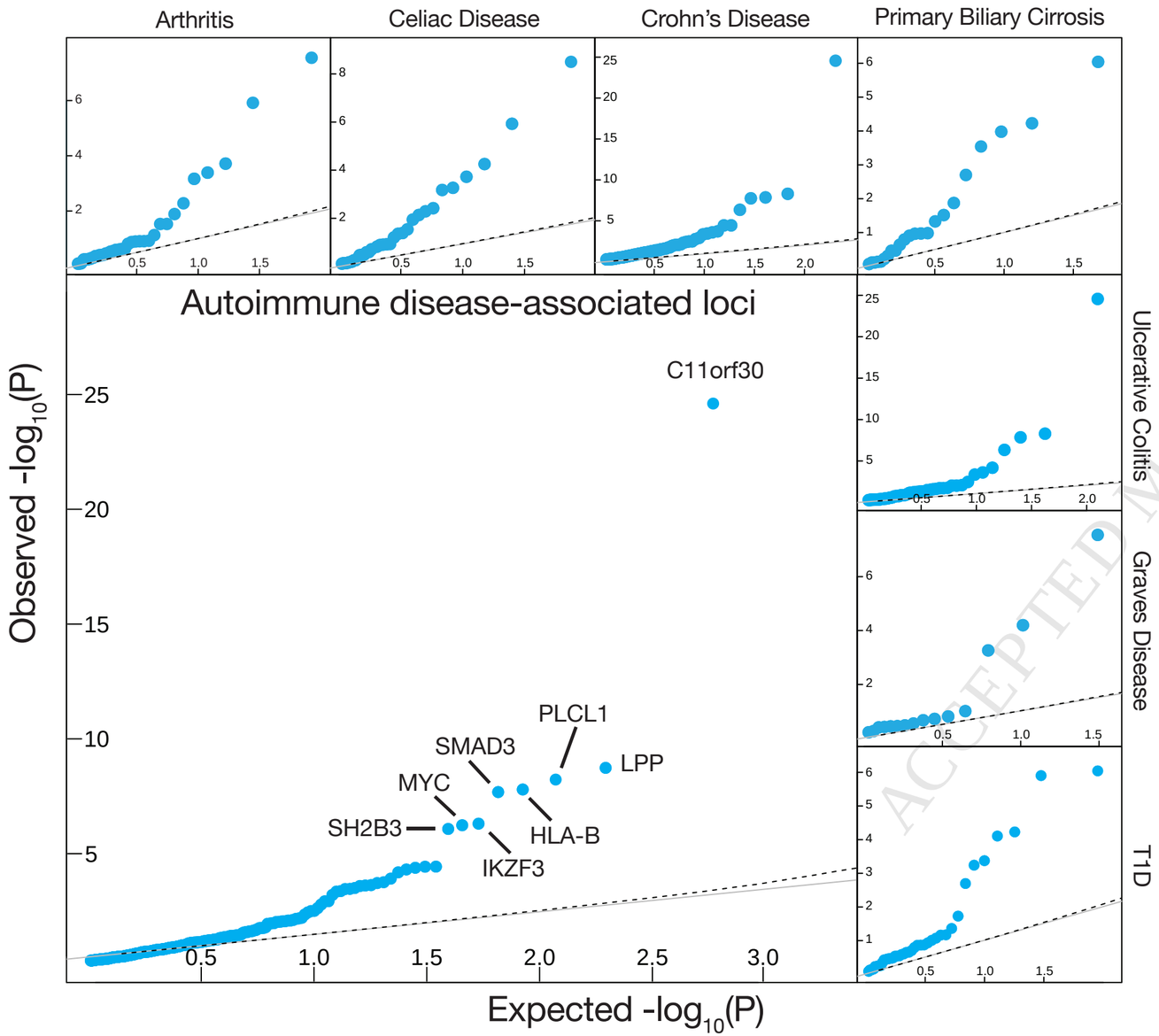


B

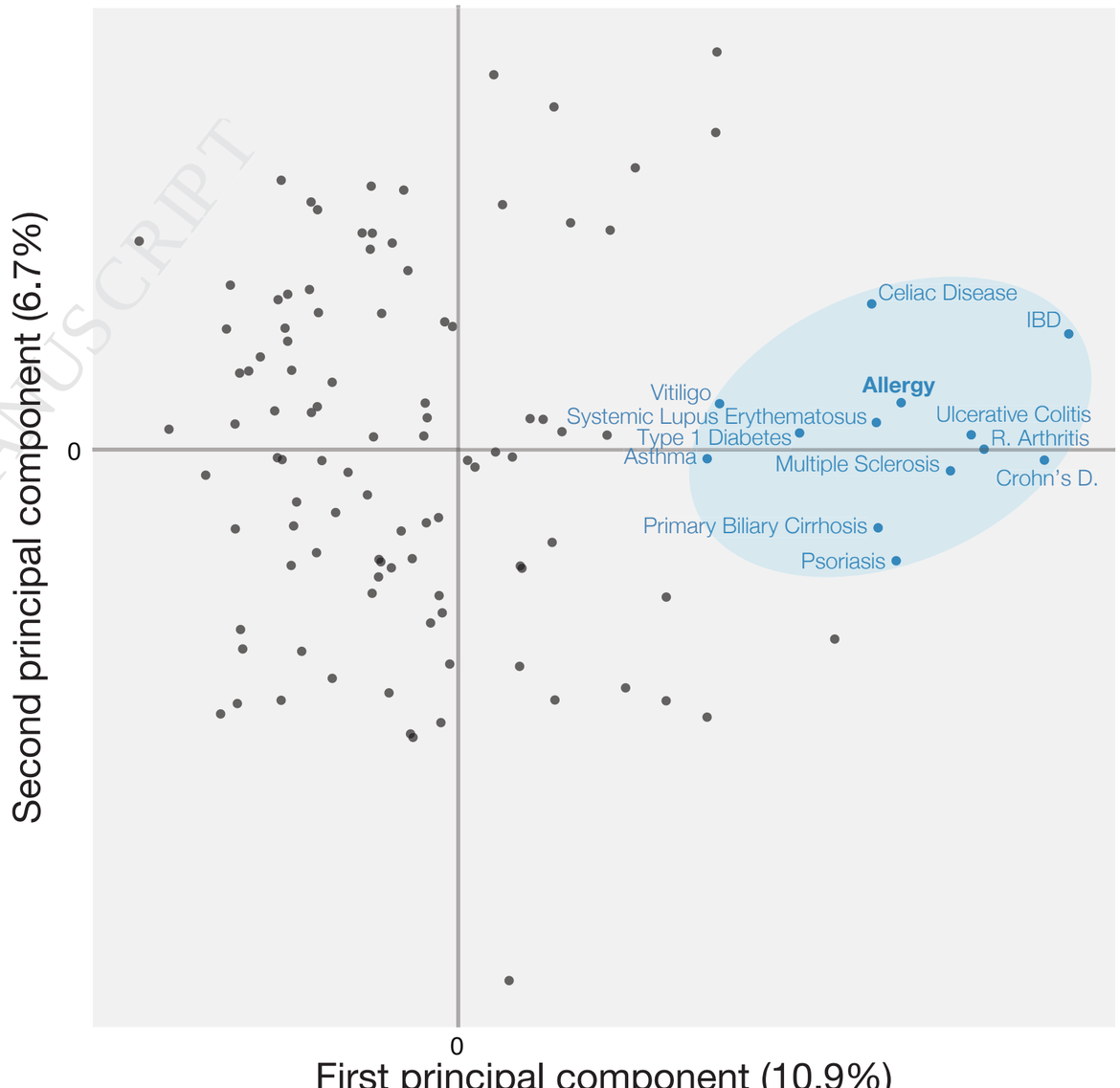

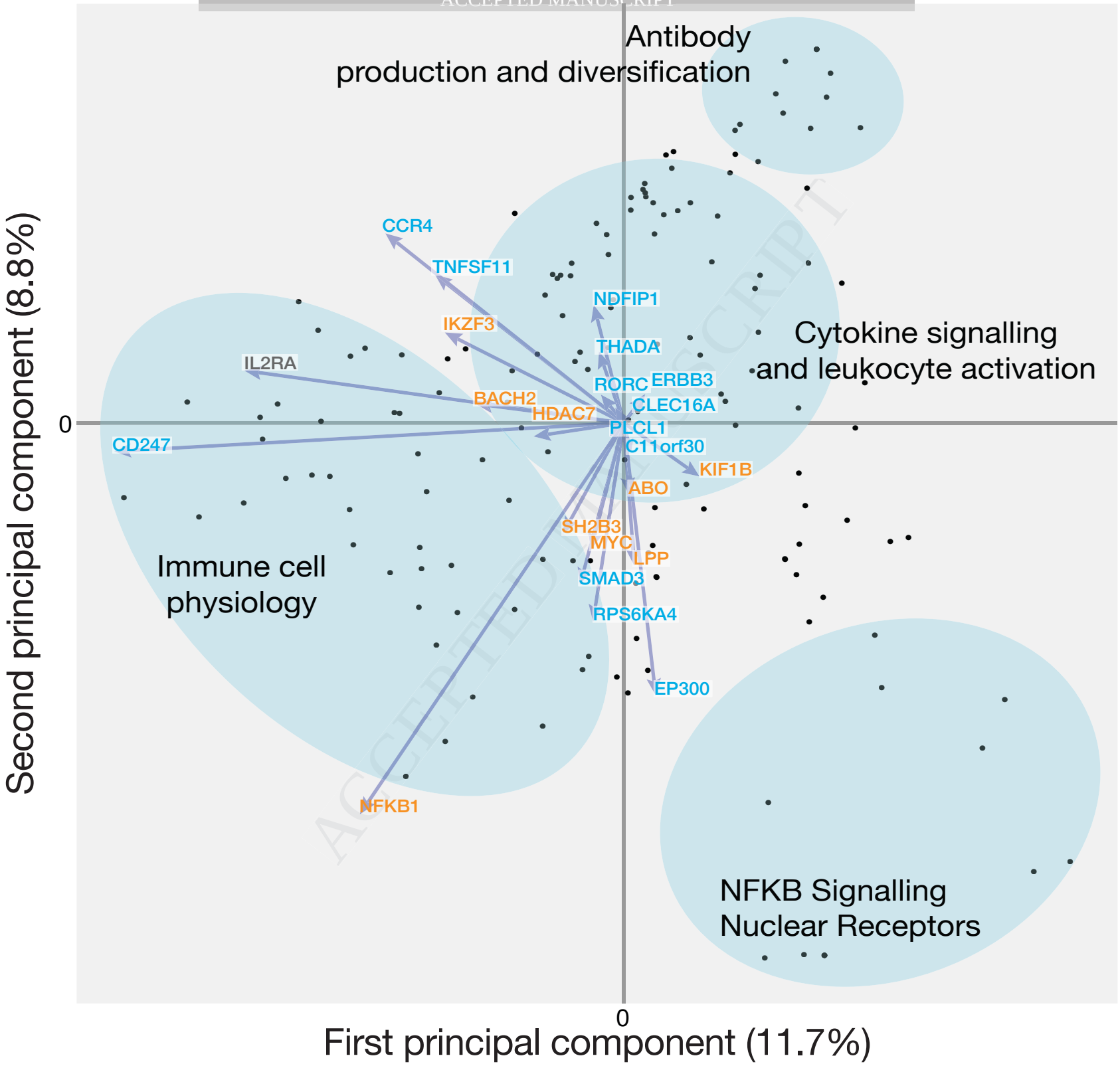

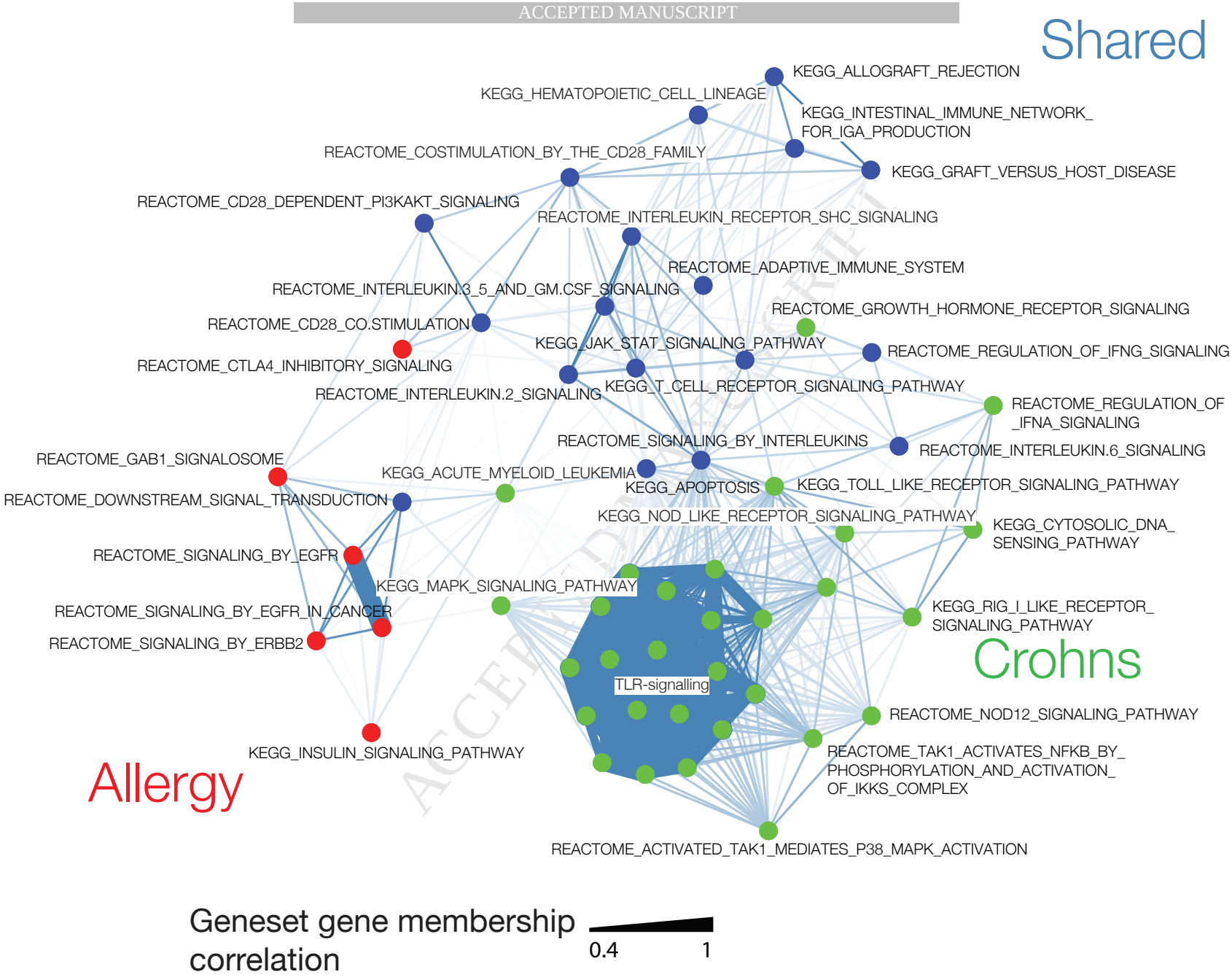

# Supplement - Shared genetic variants suggest common pathways in allergy and autoimmune diseases

# Supplementary Methods

**Discovery and meta-analysis**

Discovery results from an allergic sensitization GWAS was included as one of the datasets comprising results from 5,809 with allergic sensitization and 9,875 controls with data from the following cohorts: AAGC, ALSPAC[1], B58C, COPSAC2000, LISA, MAAS, NFBC 1966, RAINE and PIAMA. Please see discovery paper for ethical statements, cohort profiles and numbers.[2] Sensitization status was assessed objectively by either elevated levels of allergen-specific IgE (sIgE) in blood or by a positive skin reaction after skin prick test (SPT) against common food and inhalant allergens. The SPT cut off level was 3 mm larger than the negative control for cases, and below 1 mm for controls. For sIgE, cases were defined as levels at or above 3.5 IU/mL and for controls below 0.35 IU/mL. Imputation was independently conducted for each study with reference to HapMap phase 2 or 3 CEU genotypes (Central European ancestry). Study level association analysis was performed using logistic regression models based on an expected additive allelic dosage model for SNPs, adjusting for ancestry-informative principal components as necessary. SNPs with MAF <1% and/or poor imputation quality (MACH $r^2$ <0.3 or IMPUTE proper info <0.4) were excluded. After genomic control at the level of the individual studies, the summary statistics were meta-analyzed using a fixed effects model and inverse variance as weights in METAL (2010-08-01). In total 2,400,129 SNPs were available in three or more cohorts.

GWAS results from the 23andMe study were included in the present study involving 10,509 individuals with self-reported cat-allergy, 9,815 with Dust-mite allergy, 16,133 with Pollen allergy (grasses, trees or weeds) and 26,311 without symptoms in a total of 46,646 individuals. Allergy was defined as those individuals who reported a positive allergy test, difficulty in swallowing or speaking, hives, itchy mouth, itchy eyes, itchy nose or asthma in response to a particular allergen.[3] The second part of the study sample on self-reported allergy (mothers from the Alspac cohort) was not included in the present study as these individuals are related to individuals in the GWA on sensitization.

Imputation was performed in the 23andMe study using the 1000 Genomes reference (August 2010 release) in batches. SNPs with an imputed $r^2 > 0.5$ averaged across all batches and $r^2 > 0.3$ in every batch were used. SNPs were remapped to B36. A generalized estimating equation (GEE) model was applied to assess the shared genetic effects on all three phenotypes taking into account the correlations between these phenotypes.

The meta-analysis was performed using a fixed effects model using inverse variance as weights in METAL (2010-08-01)[4] after a second genomic control for the meta-analysis of the dataset on self reported allergy and sensitization.

**Enrichment of autoimmune disease-associated loci and allergy**

Candidate loci were chosen from the GWA's catalog[5] accessed 25th of November 2013 using autoimmune and inflammatory traits of interest (**Supplementary Table E1**). These reported traits were collapsed into 16 overall autoimmune disease traits. All SNP-trait associations with P<5e-8 were used. We collapsed close SNPs into loci (+/-250kb)[6] and used for each locus the SNP with lowest reported P as index SNP (**Supplementary Figure 1**). For common loci (listed in table 2), all original publications were checked for effect allele, and any discrepancies with the GWA'S catalog was corrected. After the extraction of SNP-associations, the enrichment Odds Ratio was calculated as the number of observed extracted SNPs with P<0.05 out of total extracted SNPs as compared to total number of independent SNPs with P<0.05 within the GWA discovery results using a Fisher's exact test. For this we used Hapmap, CEU panel, to define independent loci. This was performed using PLINK (--indep-pairwise 200 5 0.5) with a sliding window on 200 SNPs at steps on 5 SNPs pruning the datasets to contain only one of 2 correlated SNPs with a r^2>0.5. To plot enrichment, we equally plotted observed P-values against expected under the null hypothesis (QQ plots). Enrichment and QQ plots were plotted overall for all 290 loci and separately for each of the 16 autoimmune diseases, however only for those diseases with more than 10 loci reported in the GWA catalogue. For extracted SNPs a False Discovery Rate corrected P-value < 0.05 was considered significant. Analysis were performed in Plink[7] and R project (3.0.1)[8].

**Functional evaluation**

Enrichment of SNPs falling in DHS sites:

DHS sites were downloaded from the ENCODE project[9] and from the Epigenomics Roadmap[10] selecting only cell types (or cell lines, herefrom "cell types") with duplicates, removing transformed cell types, and removing redundant cell lines, based on manual curation. Huh7 was an outlier in all analyses, and was removed. DHS sites were set to a fixed width of 150bp from center of region for all cell types. Allergy and Crohn's Disease SNPs were split in bins of increasing p-value cutoff, starting at 1 (including all SNPs and setting baseline for enrichment) and decreasing one decimal digitor each bin (1, 0.1, 0.001 etc). Each bin was overlapped with DHS regions using bedtools v2.19.0, and enrichment for each bin was calculated for each cell type as compared to p =1. For GWAS Catalogue SNPs, SNPs were selected for traits with > 30 reported associated SNPs. For identical SNPs for the same trait, the SNP with the lowest p-value was chosen. SNPs were then overlapped with DHS regions using bedtools v2.19.0, and ratio of overlapping SNPs was calculated. To filter out non-informative cell-types, only cell-types with the highest quartile of overlap ratios was included. For immune cell hierarchical clustering the manhattan distance of square root transformed ratios were used. For PCA, log10 transformed ratios were used.

Enrichment of SNPs falling in FANTOM enhancers:

FANTOM cell specific enhancers were downloaded from 'http://enhancer.binf.ku.dk/' and were set to a fixed width of 150bp from center of region for all cell types. The ratio between overlaps of all SNPs ($p <= 1$) and SNPs at $p <= 1e-5$ was calculated, and a p-value for this ratio calculated using a binomial test with the genomic overlap frequency as null frequency, calculated as the number of total enhancers per cell type times enhancer length (150bp), divided by the total number of base pairs shown to be bound by transcription factors in the human genome across cell types in the ENCODE project (231mb)[9]. FDR values were calculated adjusting p-values with the Benjamini-Hochberg method.

Data-driven Enrichment-Prioritized Integration for Complex Traits (DEPICT):

For details of this method please refer to Pers et al.[11] . DEPICT facilitates gene set enrichment analysis by testing whether genes in associated regions enrich for reconstituted versions of known pathways, gene sets, as well as protein complexes. The gene-set enrichment analyses in DEPICT contains three steps: first a scoring step; second a bias correcting step taking into account gene density that possibly could inflate results due to gene length and finally estimating experiment-wide FDR's.

Gene set reconstitution is accomplished by identifying genes that are co-expressed with genes in a given gene set based on a panel of 77,840 gene expression microarrays; genes that co-express with genes from a given gene set are likely to be part of that gene set.[12] In DEPICT, several types of gene sets were reconstituted: 5,984 protein complexes that were derived from 169,810 high-confidence experimentally-derived protein-protein interactions[13]; 2,473 phenotypic gene sets derived from 211,882 gene-phenotype pairs from the Mouse Genetics Initiative[14]; 737 Reactome database pathways[15]; 184 KEGG database pathways[16]; and 5,083 Gene Ontology database terms[17]. In addition, the DEPICT also facilitates tissue and cell type enrichment analysis, by testing whether genes in associated regions are highly expressed in any of 209 Medical Subject Heading annotations of 37,427 microarrays from the Affymetrix U133 Plus 2.0 Array platform. We used DEPICT to test enrichment in a total of 14,461 reconstituted gene sets and enrichment of 209 tissue and cell type annotations.

For the allergy meta-analysis, and Crohns disease, DEPICT was performed on all loci P<10e-5. For PCA GWAS catalogue data, DEPICT was performed on all traits with more than 30 reported associated SNPs. For identical SNPs for the same trait, the SNP with the lowest p-value was chosen.

Pathway analysis and visualization for allergy and Crohn's disease:

To account for difference in GWAS study sizes, a linear model was fitted between logged p-values of DEPICT results for allergy and Chron's disease, and the estimator was used to adjust the p-value thresholds for the largest study, Crohn's disease. The inflation estimate for Crohn's disease was 1.21. Shared pathways were set at $p_{allergy}$ and $p_{crohns\_adjusted} < 0.001$, allergy specific pathways were set at $p_{allergy} < 0.001$ and $p_{crohns\_adjusted} > 0.05$ and Crohn's disease specific pathways were set at $p_{allergy} > 0.05$ and $p_{crohns\_adjusted} < 0.001$.

DHS genomic location:

Genomic regions for 186 cell types, of which 14 cell types (CD14_Primary_Cells, CD19_Primary_Cells_Peripheral_UW, CD20, CD3_Primary_Cells_Cord_BI, CD3_Primary_Cells_Peripheral_UW, CD34Mobilized, CD56_Primary_Cells, Th0, Th1, Th17, Th2, Treg, GM12864, and Fetal_Thymus) were annotated as immune cells, were downloaded from the ROADMAP and ENCODE tracks (June 2014) in the UCSC Genome Browser and processed by bedtools, ensuring no redundancy between exons, introns, promoters (defined as 5000 bases upstream and 200 bases downstream of transcription start sites), and intergenic sites. DHS sites were overlapped with genomic regions, requiring 1bp of overlap. Enrichment of markers in DHS regions was calculated for GWAS catalog traits with 30 or more reported variants, and was normalized by trait SNP count and cell type specific DNAse sequence lenghts.

The uneven distribution of cell types within the Roadmap ENCODE dataset could possibly contribute to the separation of immune-mediated diseases from other diseases. However, repeated iterative removal of ¼ of cell types continuously produced a statistical significant separation of autoimmune diseases, allergy and asthma vs. other traits (results not shown), hence supporting the finding of common SNPs and cell types to congregate in allergy and autoimmune diseases. In addition, hierarchical clustering was performed on the full ENCODE Roadmap set to investigate if this clustering was facilitated by similar DHS-profiles in different immune cells, basically representing a single "immune-system-footprint", but this was not the case, as different immune cell types also separated internally, comparable to other non-immune cell types (**Supplementary Figure 18**).

A further cluster analysis of the cell-type specific genomic DHS location in all cells (intronic, exonic, intergenic, promotor) was performed revealing that the DHS sites in immune cells tend to fall within promotor and exonic regions (**Supplementary Figure 19**).

Transcription factor binding sites:

Transcription factor binding sites for 161 transcription sites were downloaded in BED format from ENCODE for the hg19 build, and were intersected with 28 independent shared loci, expanded to included markers with r2>= 0.5 in the 1000g CEU panel, using BedTools. Enrichment and one-sided p-values were calculated in relation to an empirical null distribution of loci overlap for each TF, generated by 10,000 random permutations of random genomic loci with the same length characteristics as the 28 LD-expanded shared loci**.** Random locus LD-structure was assumed to have no effect on TF-binding probability as a function of locus length.

## Acknowledgements and funding

**23andMe:** We thank the customers of 23andMe who answered surveys, as well as the employees of 23andMe, who together made the 23andMe research possible. This work was supported in part by the National Heart, Lung, and Blood Institute of the US National Institutes of Health under grant 1R43HL115873-01.

**AAGC:** QIMR: We thank the twins and their families for their participation; Dixie Statham, Ann Eldridge, Marlene Grace, Kerrie McAloney (sample collection); Lisa Bowdler, Steven Crooks (DNA processing); David Smyth, Harry Beeby, Daniel Park (IT support). Busselton: The Busselton Health Study acknowledges the numerous Busselton community volunteers who assisted with data collection and the study participants from the Shire of Busselton.

The NHMRC (including grants 613627 and 1036550), Asthma Foundations in Tasmania, Queensland and Victoria, The Clifford Craig Trust in Northern Tasmania, Lew Carty Foundation, Royal Hobart Research Foundation and the University of Melbourne, Cooperative Research Centre for Asthma, New South Wales Department of Health, Children's Hospital Westmead, University of Sydney. Contributions of goods and services were made to the CAPS study by Allergopharma Joachim Ganzer KG Germany, John Sands Australia, Hasbro, Toll refrigerated, AstraZeneca Australia, and Nu-Mega Ingredients Pty Ltd. Goods were provided at reduced cost to the CAPS study by Auspharm, Allersearch and Goodman Fielder Foods. MCM, SCD and MAB are supported by the NHMRC Fellowship Scheme. The Busselton Health Study acknowledges the generous support for the 1994/5 follow-up study from Healthway, Western Australia.

**ALSPAC:** We are extremely grateful to all the families who took part in this study, the midwives for their help in recruiting them, and the whole ALSPAC team, which includes interviewers, computer and laboratory technicians, clerical workers, research scientists, volunteers, managers, receptionists and

nurses. The UK Medical Research Council and the Wellcome Trust (Grant ref: 102215/2/13/2) and the University of Bristol provide core support for ALSPAC. This publication is the work of the authors Nicholas Timpson and John Henderson will serve as guarantors for the contents of this paper. This research was specifically funded by The MRC Centre for Causal Analyses in Translational Medicine (grant G0600705) provided funding for N Timpson.

GWAS data was generated by Sample Logistics and Genotyping Facilities at the Wellcome Trust Sanger Institute and LabCorp (Laboratory Corportation of America) using support from 23andMe.

**B58C:** We acknowledge use of phenotype and genotype data from the British 1958 Birth Cohort DNA collection, funded by the Medical Research Council grant G0000934 and the Wellcome Trust grant 068545/Z/02. (http://www.b58cgene.sgul.ac.uk/). Genotyping for the B58C-WTCCC subset was funded by the Wellcome Trust grant 076113/B/04/Z. The B58C-T1DGC genotyping utilized resources provided by the Type 1 Diabetes Genetics Consortium, a collaborative clinical study sponsored by the National Institute of Diabetes and Digestive and Kidney Diseases (NIDDK), National Institute of Allergy and Infectious Diseases (NIAID), National Human Genome Research Institute (NHGRI), National Institute of Child Health and Human Development (NICHD), and Juvenile Diabetes Research Foundation International (JDRF) and supported by U01 DK062418. B58C-T1DGC GWAS data were deposited by the Diabetes and Inflammation Laboratory, Cambridge Institute for Medical Research (CIMR), University of Cambridge, which is funded by Juvenile Diabetes Research Foundation International, the Wellcome Trust and the National Institute for Health Research Cambridge Biomedical Research Centre; the CIMR is in receipt of a Wellcome Trust Strategic Award (079895). The B58C-GABRIEL genotyping was supported by a contract from the European Commission Framework Programme 6 (018996) and grants from the French Ministry of Research.

**COPSAC2000:** We thank all the families participating in the COPSAC cohort for their effort and commitment; and the whole COPSAC study team including computer and laboratory technicians,

research scientists, managers, receptionists, and nurses. We also wish to thank Bjarne Kristensen and Inger Pedersen (Phadia Denmark) for their dedicated work with the IgE-analyses.

COPSAC is funded by: the Lundbeck Foundation, the Danish Council for Strategic Research, ,the Pharmacy Foundation, the Danish Agency for Science, Technology and Innovation, the EU Seventh Framework Programme, Ronald McDonald House Charities, the Global Excellence in Health award Programme, the Danish Medical Research Council, the Director K. GAD and family Foundation, the A. P. Møller og Hustru Chastine Mc-Kinney Møller General Purpose Foundation, the Aage Bang Foundation, the Health Insurance Foundation, the East Danish Medical Research Council, the Copenhagen City Council Research Foundation, the Kai and Gunhild Lange Foundation, the Dagmar Marshall Foundation, the Ville Heise legacy, the Region of Copenhagen, the Ib Henriksen foundation, the Birgit and Svend Pock-Steen foundation, the Danish Ministry of the Interior and Health's Research Centre for Environmental Health, the Gerda and Aage Hensch foundation, the Rosalie Petersens Foundation, the Hans and Nora Buchard Foundation, the Gangsted Foundation, the Danish Medical Association, Asthma-Allergy Denmark, the Danish Otolaryngology Association, the Oda Pedersen legacy, the Højmosegaard Legacy, the A. P. Møller og Hustru Chastine Mc-Kinney Møller Foundation for the advancement of Medical Knowledge, the Jacob and Olga Madsen Foundation, the Aase and Einar Danielsen Foundation, and Queen Louise's Children's' Hospital Research Foundation.

The IgE analyses were sponsored by Phadia ApS.

The funding agencies did not have any role in study design, data collection and analysis, decision to publish, or preparation of the manuscript.

**LISA/GINI:** The authors thank all the families for their participation in the GINIplus and LISAplus studies. Furthermore, we thank all members of the GINIplus and LISAplus Study Groups for their excellent work. The LISAplus Study Group consists of the following: The study team wishes to acknowledge the following: Helmholtz Zentrum Muenchen - German Research Center for Environment and Health, Institute of Epidemiology I, Neuherberg (Heinrich J, Wichmann HE,

Sausenthaler S, Chen C-M); University of Leipzig, Department of Pediatrics (Borte M), Department of Environmental Medicine and Hygiene (Herbarth O); Department of Pediatrics, Marien-Hospital, Wesel (von Berg A); Bad Honnef (Schaaf B); UFZ-Centre for Environmental Research Leipzig-Halle, Department of Environmental Immunology (Lehmann I); IUF – Leibniz Research Institute for Environmental Medicine, Düsseldorf (Krämer U); Department of Pediatrics, Technical University, Munich (Bauer CP, Hoffman U); Centre for Allergy and Environment, Technical University, Munich (Behrendt H).

The GINIplus Study Group consists of the following: The study team wishes to acknowledge the following: Helmholtz Zentrum Muenchen - German Research Center for Environmental Health, Institute of Epidemiology I, Munich (Heinrich J, Wichmann HE, Sausenthaler S, Chen C-M, Thiering E, Tiesler C, Standl M, Schnappinger M, Rzehak P); Department of Pediatrics, Marien-Hospital, Wesel (Berdel D, von Berg A, Beckmann C, Groß I); Department of Pediatrics, Ludwig Maximilians University, Munich (Koletzko S, Reinhardt D, Krauss-Etschmann S); Department of Pediatrics, Technical University, Munich (Bauer CP, Brockow I, Grübl A, Hoffmann U); IUF – Leibniz Research Institute for Environmental Medicine, Düsseldorf (Krämer U, Link E, Cramer C); Centre for Allergy and Environment, Technical University, Munich (Behrendt H).

Personal and financial support by the Munich Center of Health Sciences (MCHEALTH) as part of the Ludwig-Maximilians University Munich LMU innovative is gratefully acknowledged.

**Manchester Asthma and Allergy Study (MAAS):** We would like to thank the children and their parents for their continued support and enthusiasm. We greatly appreciate the commitment they have given to the project. We would also like to acknowledge the hard work and dedication of the study team (post-doctoral scientists, research fellows, nurses, physiologists, technicians and clerical staff).

MAAS was supported by the Asthma UK Grants No 301 (1995-1998), No 362 (1998-2001), No 01/012 (2001-2004), No 04/014 (2004-2007) and The Moulton Charitable Foundation (2004-current); age 11 years clinical follow-up is funded by the Medical Research Council (MRC) Grant G0601361.

**NFBC 1966:** We thank Professor Paula Rantakallio (launch of NFBC 1966 and 1986), Ms Outi Tornwall and Ms Minttu Jussila (DNA biobanking).

Financial support was received from the Academy of Finland (project grants 104781, 120315 and Center of Excellence in Complex Disease Genetics), University Hospital Oulu, Biocenter, University of Oulu, Finland, the European Commission (EURO-BLCS, Framework 5 award QLG1-CT-2000-01643), NHLBI grant 5R01HL087679-02 through the STAMPEED program (1RL1MH083268-01), NIH/NIMH (5R01MH63706:02), ENGAGE project and grant agreement HEALTH-F4-2007-201413, and the Medical Research Council (G0500539, PrevMetSyn/SALVE). The DNA extractions, sample quality controls, biobank up-keeping and aliquotting was performed in the National Public Health Institute, Biomedicum Helsinki, Finland and supported financially by the Academy of Finland and Biocentrum Helsinki. A. Couto Alves acknowledges the European Commission, Framework 7, grant number 223367. Jess L Buxton acknowledges the Wellcome Trust fellowship grant, number WT088431MA.

**RAINE:** The authors are grateful to the Raine Study participants, their families, and to the Raine Study research staff for cohort coordination and data collection. The authors gratefully acknowledge the assistance of the Western Australian DNA Bank (National Health and Medical Research Council of Australia National Enabling Facility). The following Institutions provide funding for Core Management of the Raine Study: The University of Western Australia (UWA), Raine Medical Research Foundation, UWA Faculty of Medicine, Dentistry and Health Sciences, The Telethon Institute for Child Health Research, Curtin University, Edith Cowan University and Women and Infants Research Foundation. This study was supported by project grants from the National Health and Medical Research Council of

Australia (Grant ID 403981 and ID 003209; http://www.nhmrc.gov.au/) and the Canadian Institutes of Health Research (Grant ID MOP-82893; http://www.cihr-irsc.gc.ca/e/193.html).

**PIAMA:** The PIAMA study would like to thank all participants, and co-investigators of the study.

The PIAMA study is supported by the Dutch Asthma Foundation (grant 3.4.01.26, 3.2.06.022, 3.4.09.081 and 3.2.10.085CO), the ZonMw (a Dutch organization for health research and development; grant 912-03-031), and the ministry of the environment.

Genome-wide genotyping was funded by the European Commission as part of GABRIEL (A multidisciplinary study to identify the genetic and environmental causes of asthma in the European Community) contract number 018996 under the Integrated Program LSH-2004-1.2.5-1 Post genomic approaches to understand the molecular basis of asthma aiming at a preventive or therapeutic control.

## Supplementary Figure 1

Flowchart of the selected known autoimmune disease associated SNPs/loci for lookup in the allergy GWAS identified within the GWA's catalog (accessed 25th of November 2013). Please also see methods section here in the supplement. A detailed description for each step in the flow chart:
1) The GWA's catalog[5] were accessed 25th of November 2013.
2) All autoimmune diseases and associations to SNPs were selected with p<5*10^-8. The chosen traits were collapsed into 16 overall autoimmune disease categories (see supplemental table 1)
3) We collapsed close SNPs into loci (+/-250kb)[6] and used for each locus only the SNP with lowest reported P as index SNP and as representative for the specific locus.
4) For several of the SNPs we had to use a proxy SNP as the index SNP were not present within the allergy GWAS. Proxy SNPs were chosen on highest r2 to index SNP and if two or more proxies had the same r2 the SNP closest in physical distance to the index SNP were chosen. In total 290 SNPs were available for look up/extraction within the allergy GWAS.

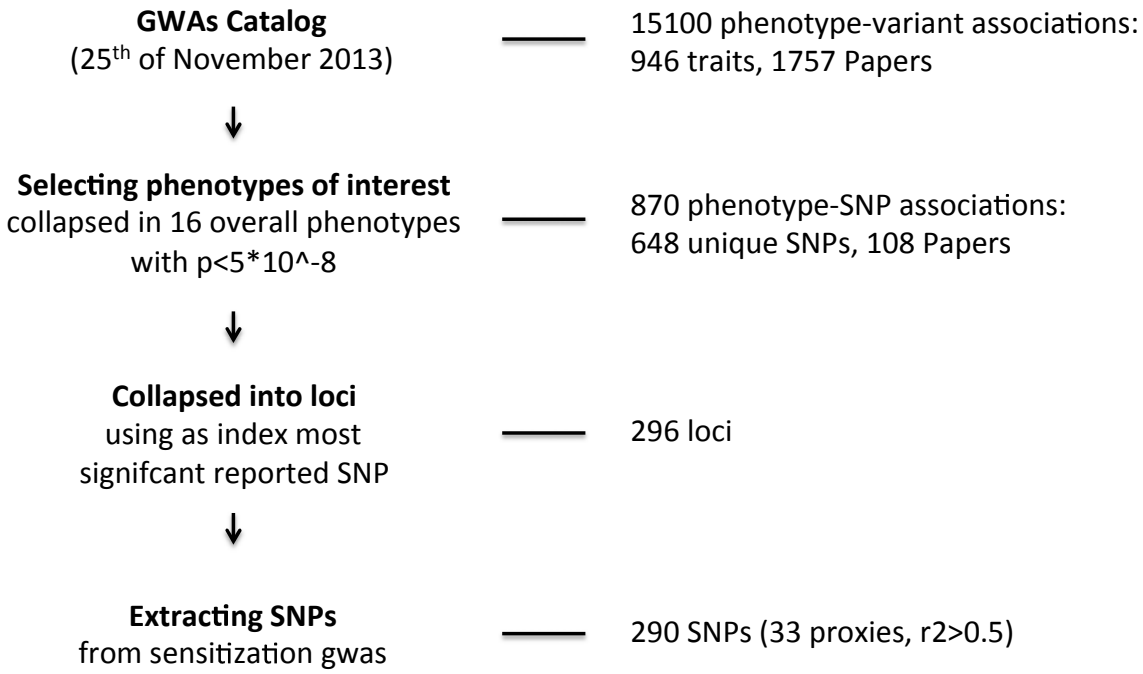

## Supplementary Figure 2

QQ plot of the of the meta-analysed 2,284,215 SNPs and association to 1) Sensitization[2] 2) Self-reported allergy[3] 3) These two data-sets meta-analysed and 4) Without reported known loci

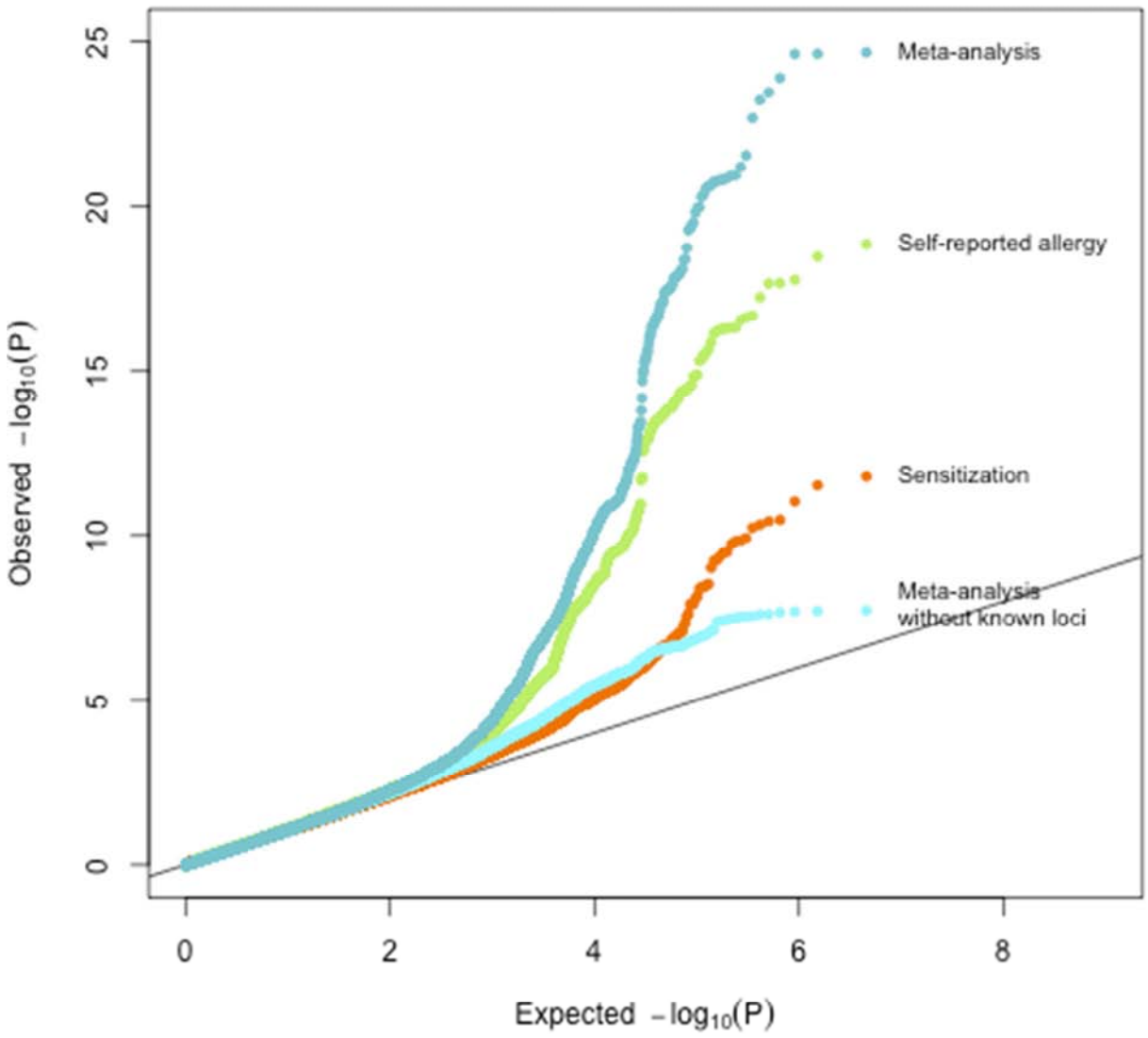

## Supplementary Figure 3

Manhattan plot of the of the meta-analysed 2,284,215 SNPs and association to allergy. Red dots indicate novel loci not described in the discovery papers (grey)[2,3], with p<5*10e-6. Dashed line: 10e-6. Solid line: 5e-8.

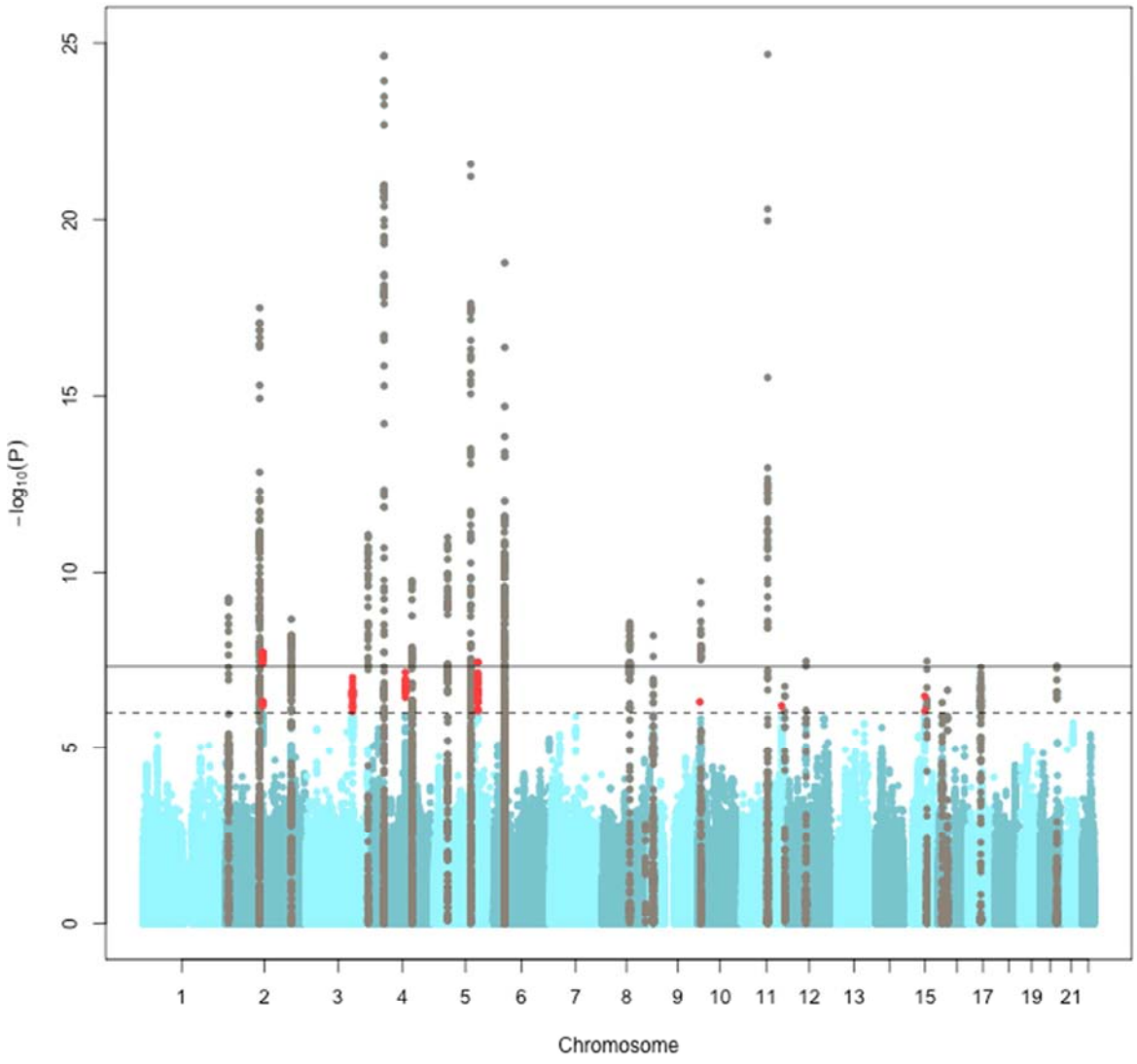

## Supplementary Figure 4

LocusZoom plots of the suggestive novel loci from the allergy meta-analyses

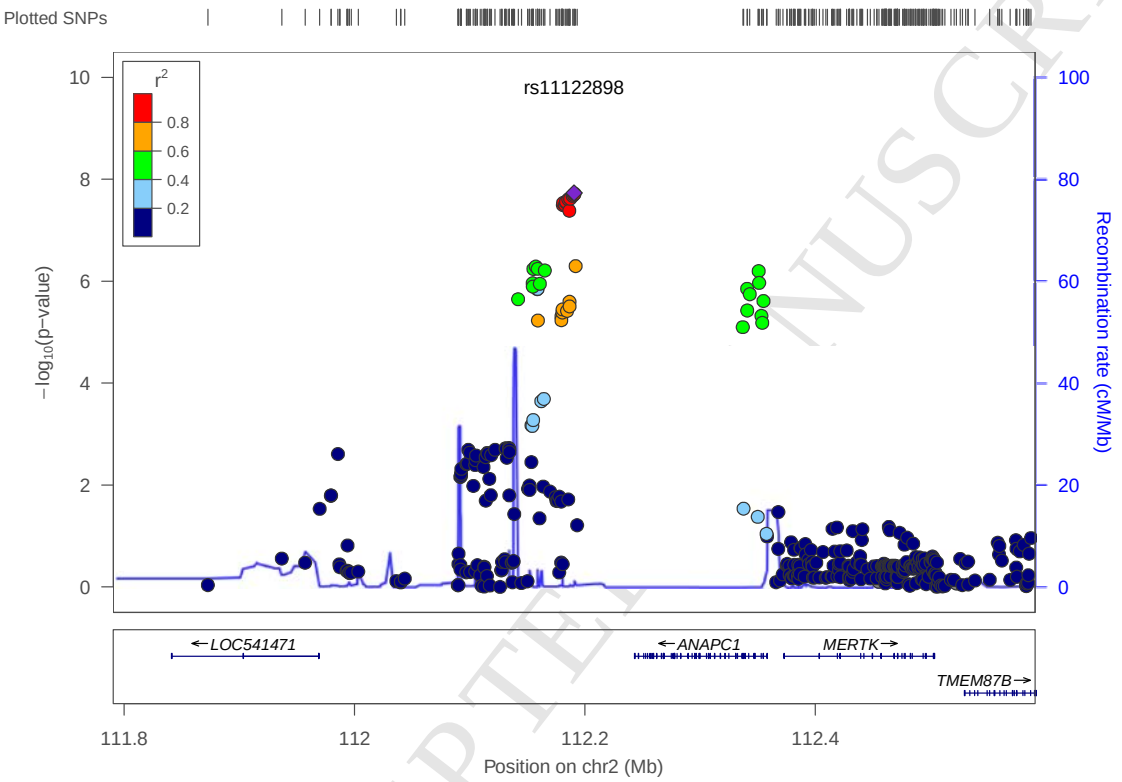

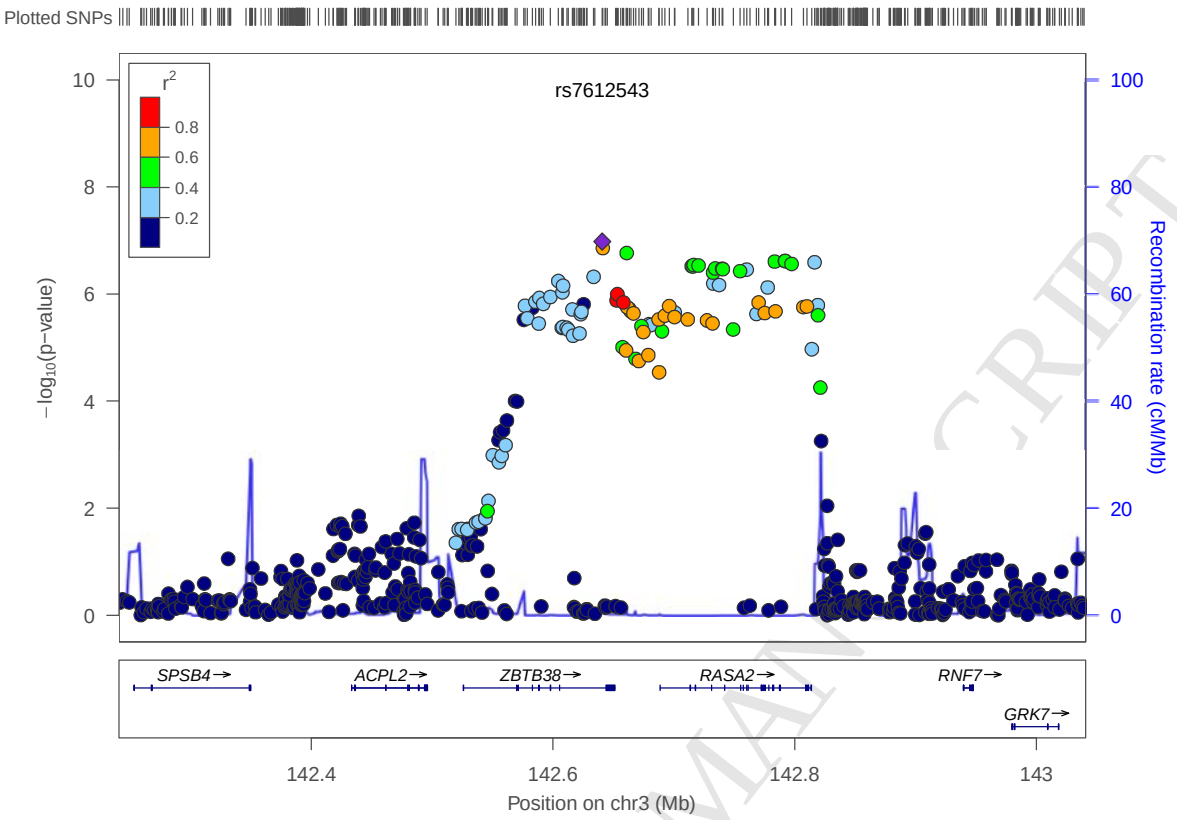

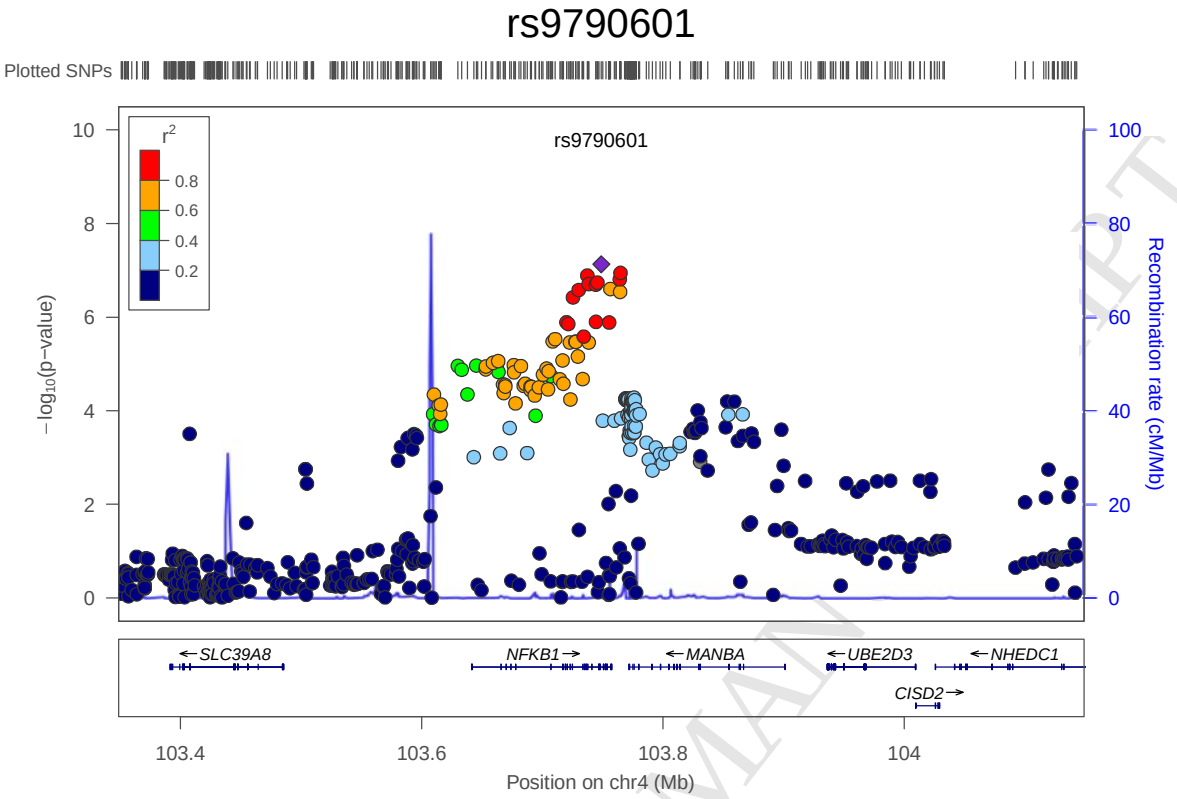

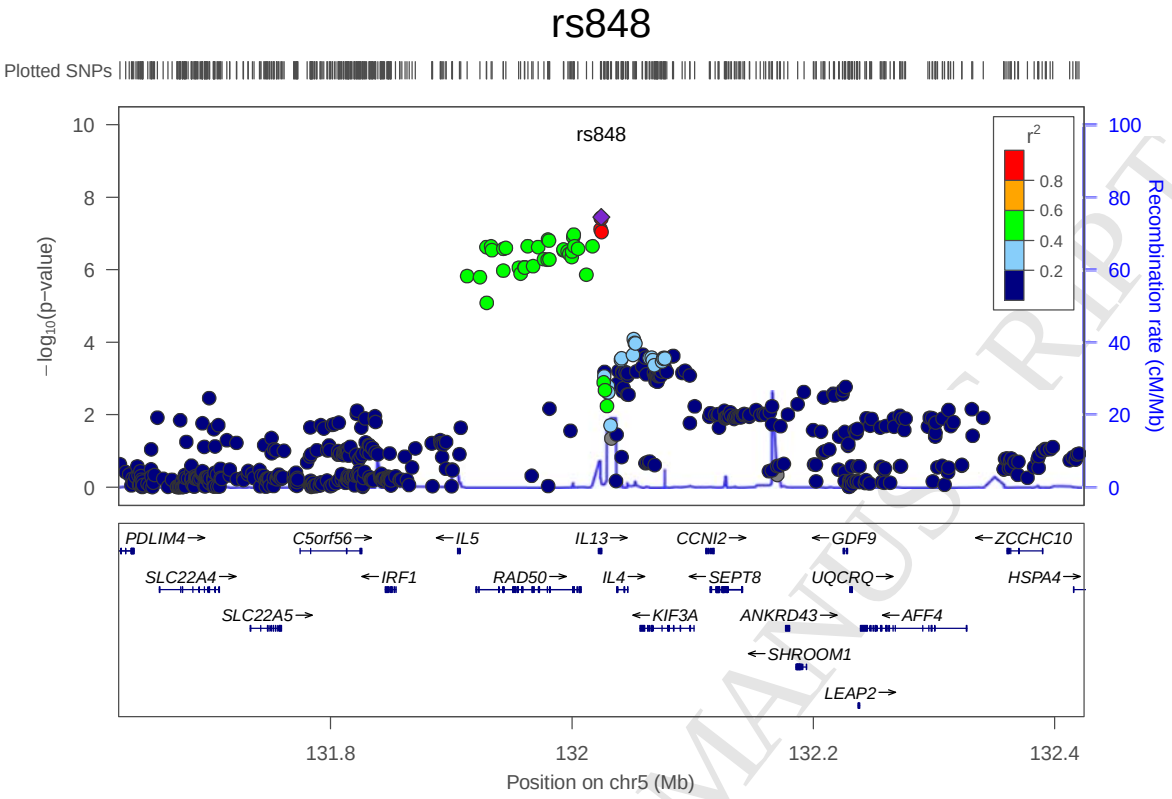

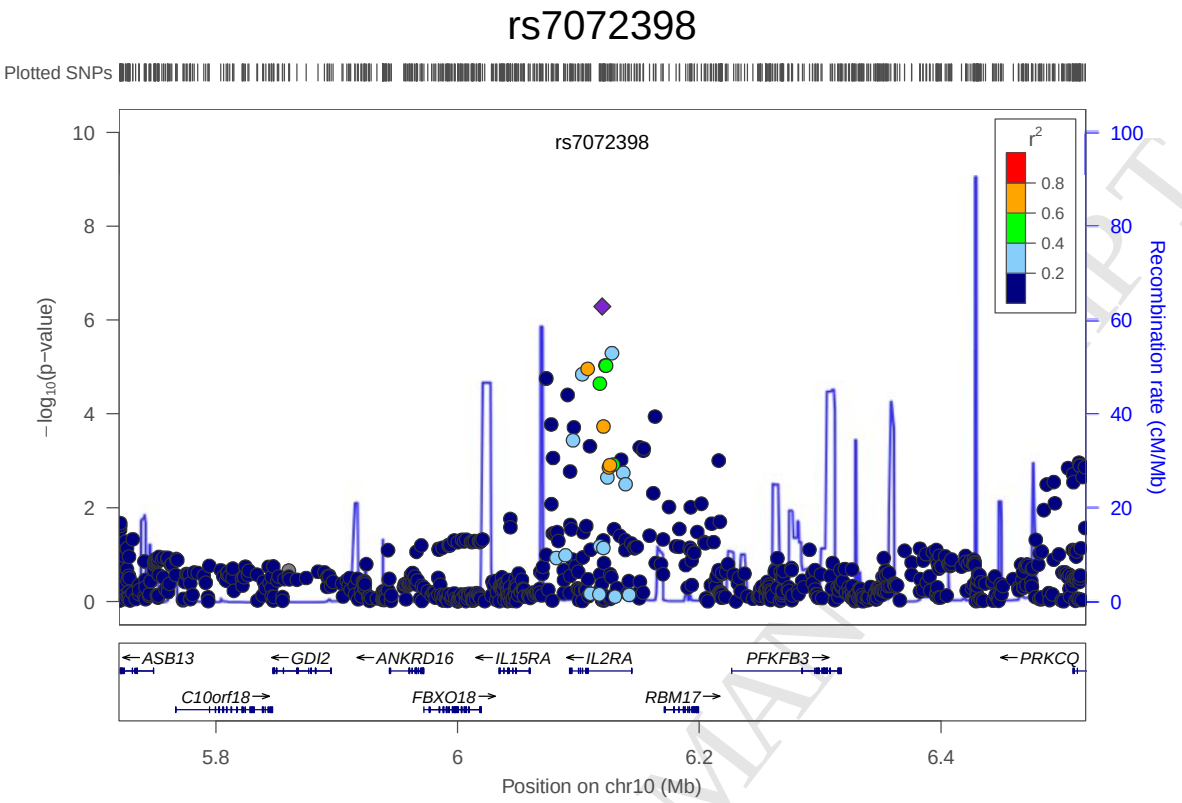

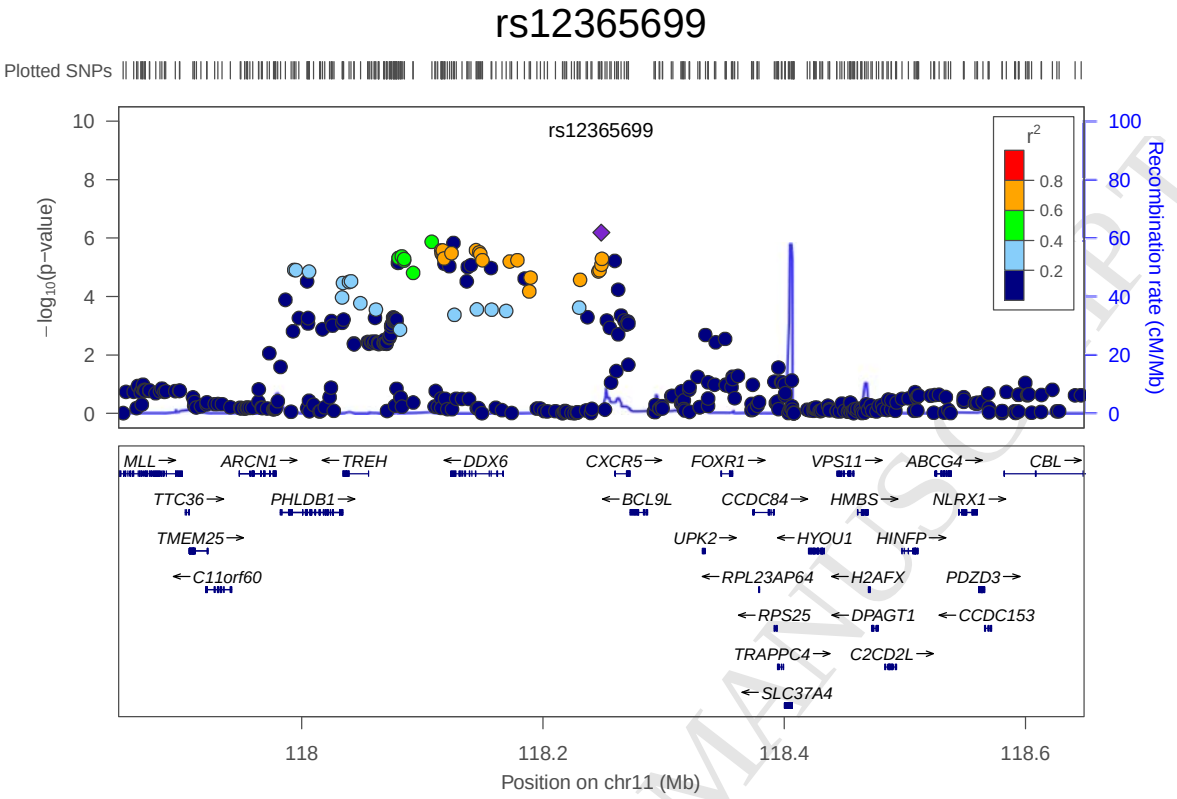

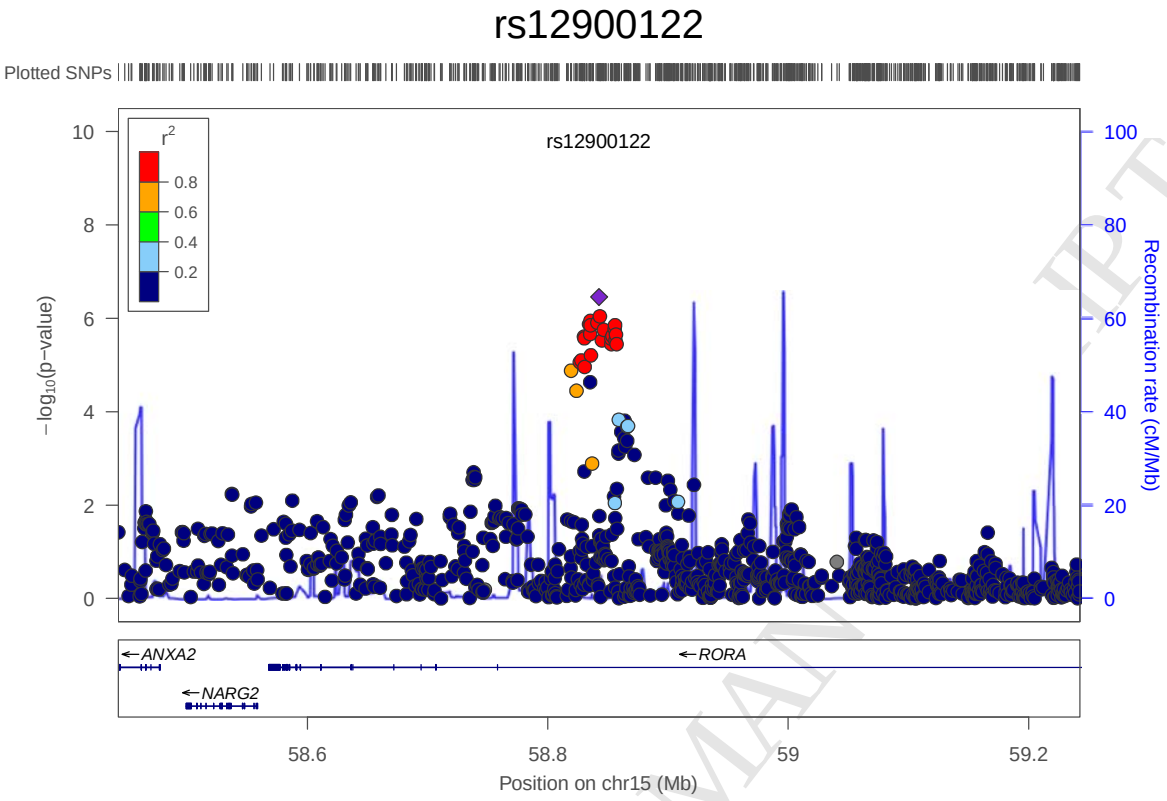

## Supplementary Figure 5

QQ plots of the autoimmune disease associated loci within the combined allergy meta-analysis as well as allergic sensitization and self-reported allergy separately. The numbers in the figures show enrichment Odds Ratio and P-value for enrichment.

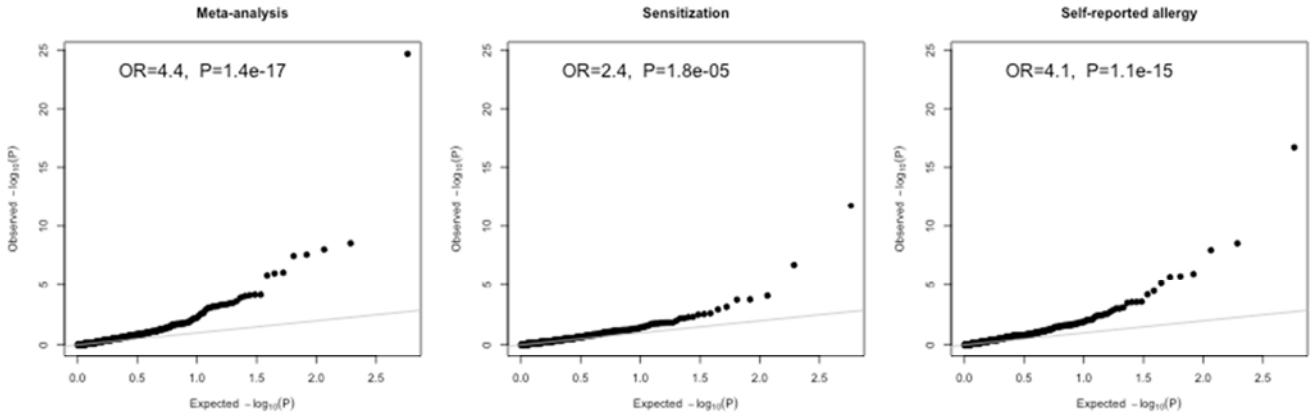

## Supplementary Figure 6

Separate QQ plots of the autoimmune disease associated loci within the allergy meta-analysis with printed calculated enrichment Odds Ratio and P-value for enrichment. Only plotted for autoimmune diseases with at least 10 loci associated. Solid line reflects the P-value distribution under the null while the dashed is the distribution of all SNPs from the allergy meta-analysis.

**Ankylosing Spondylitis:**

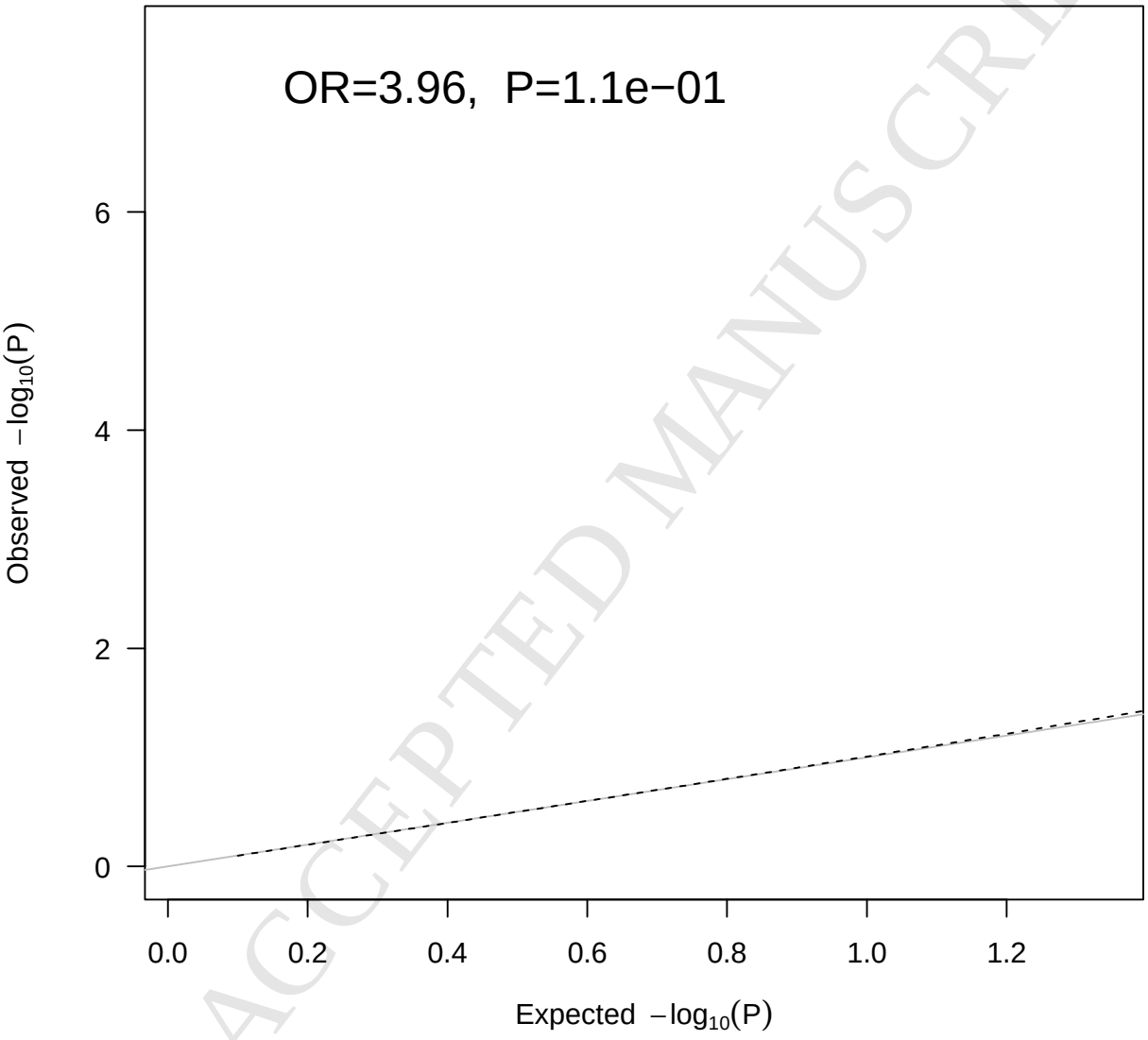

**Psoriasis:**

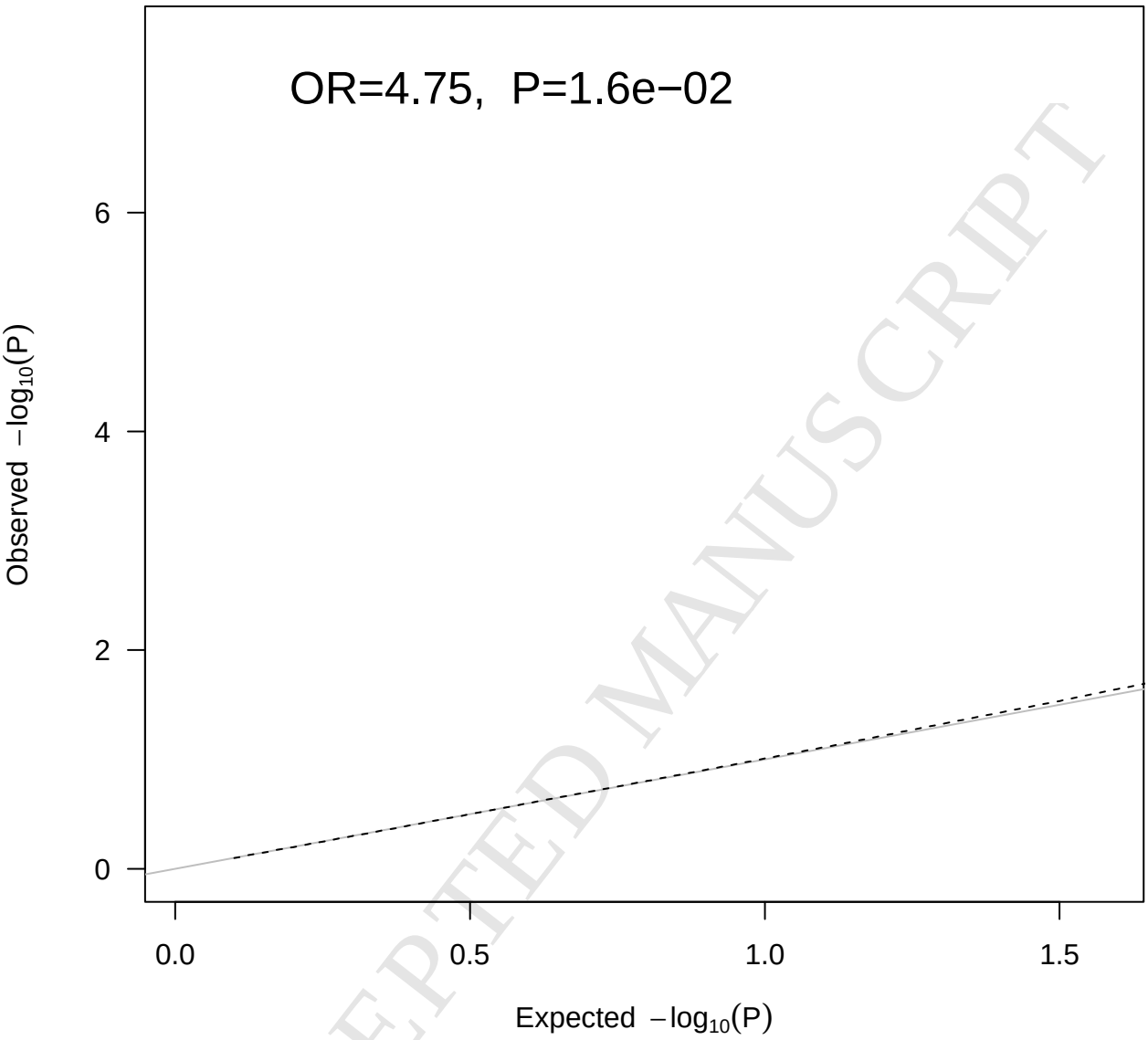

**Arthirits:**

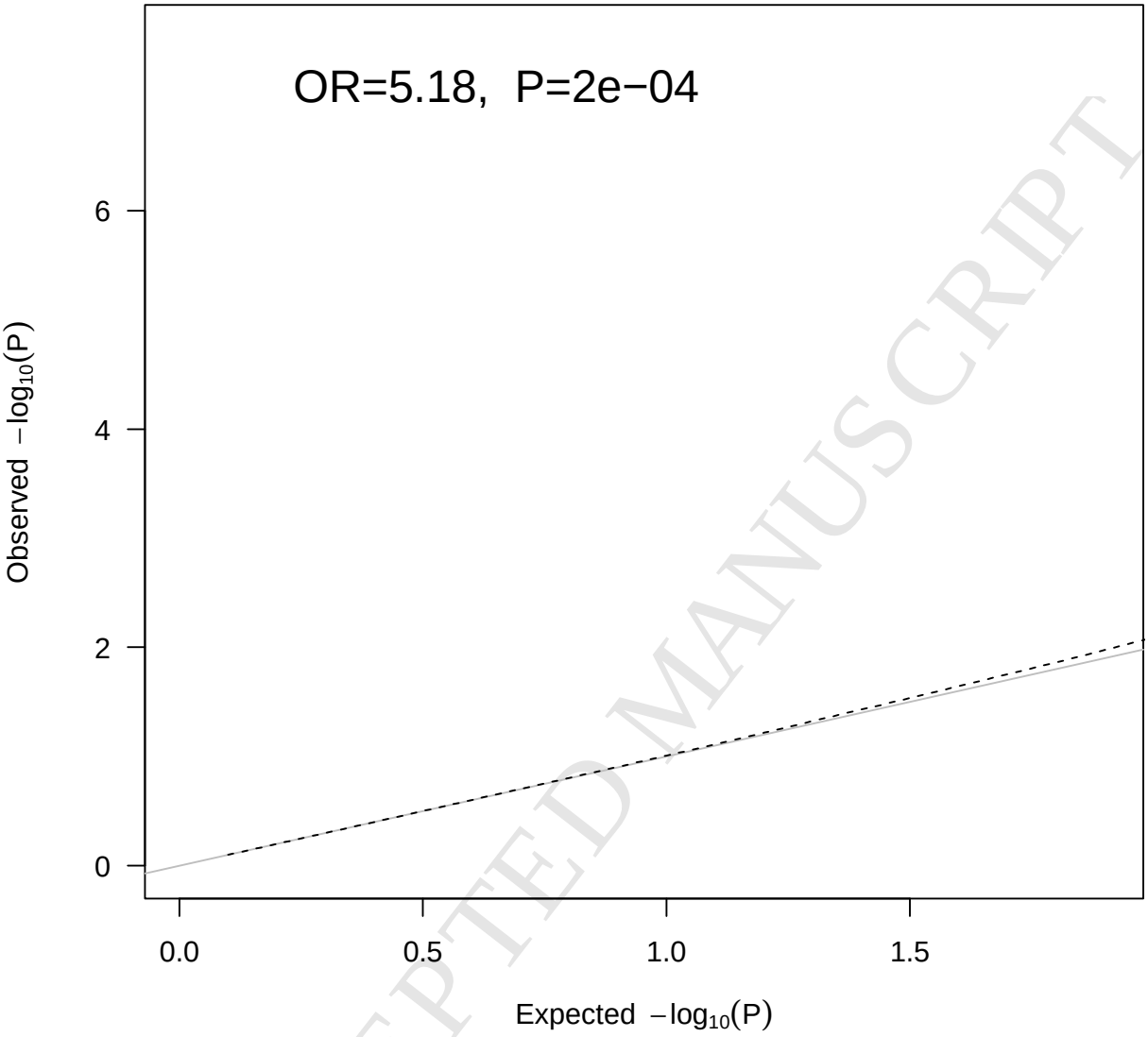

**Celiac Disease:**

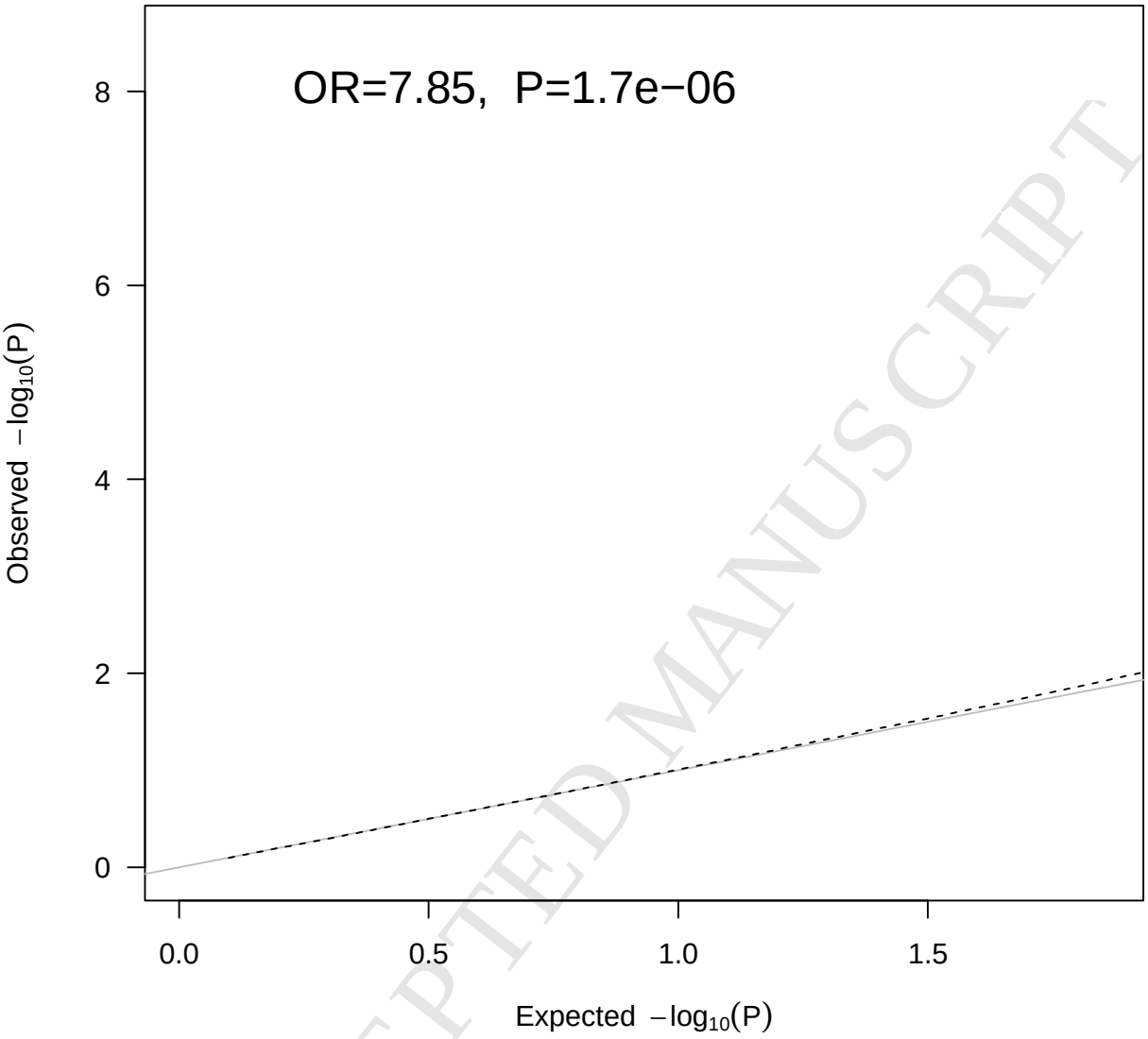

**Primary Biliary Cirrhosis:**

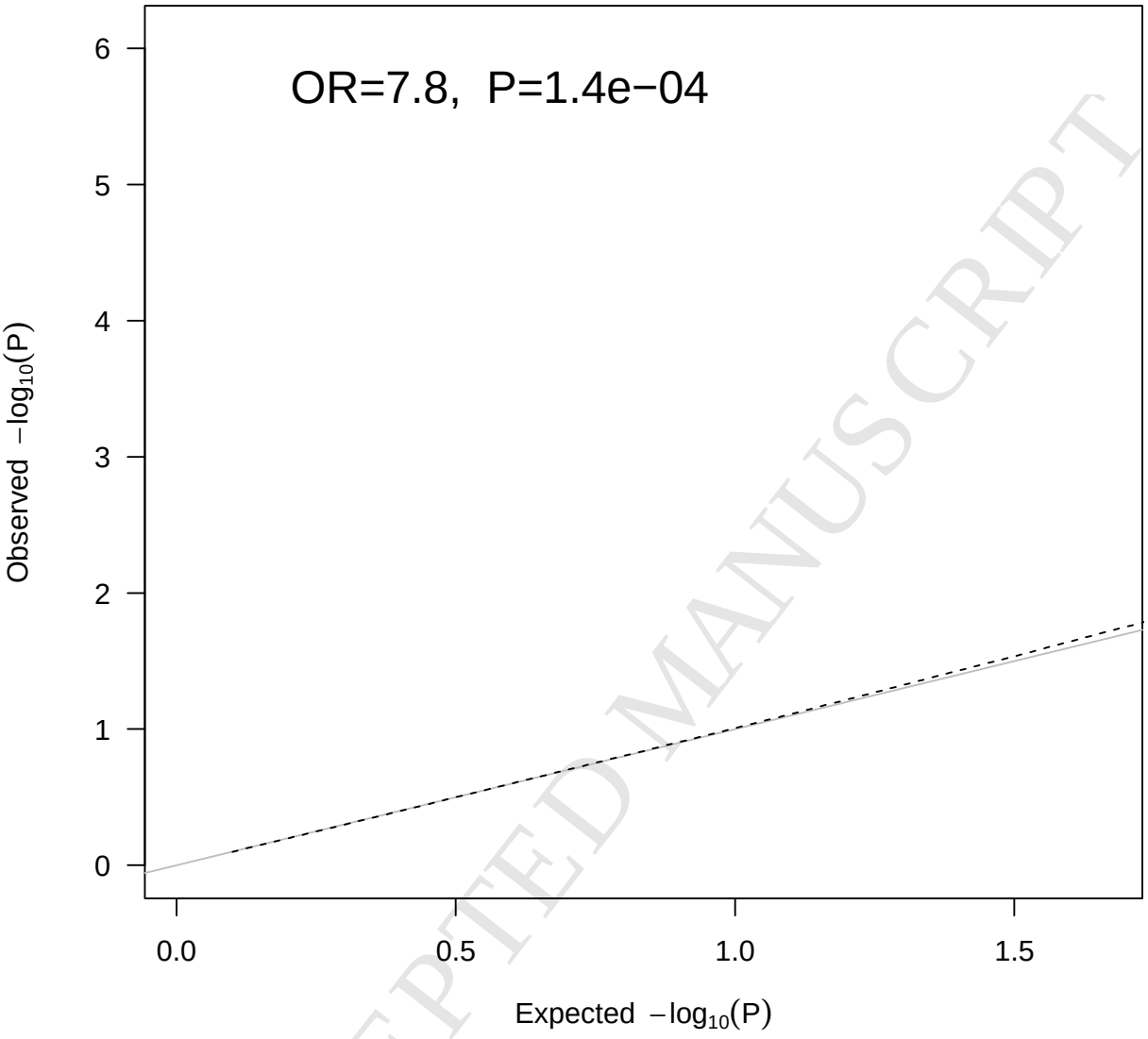

**Ulcerative colitis:**

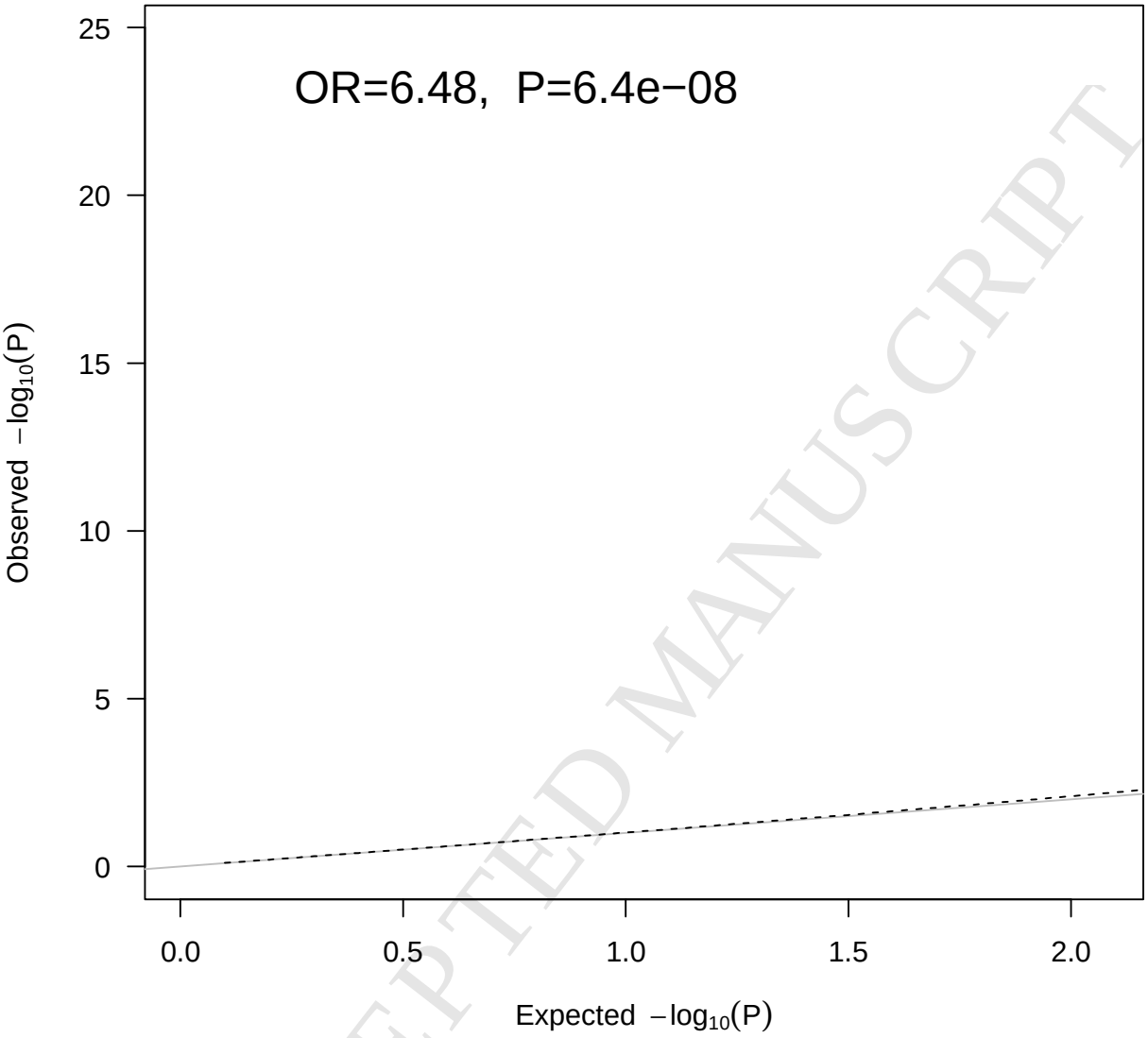

**Crohn's Disease:**

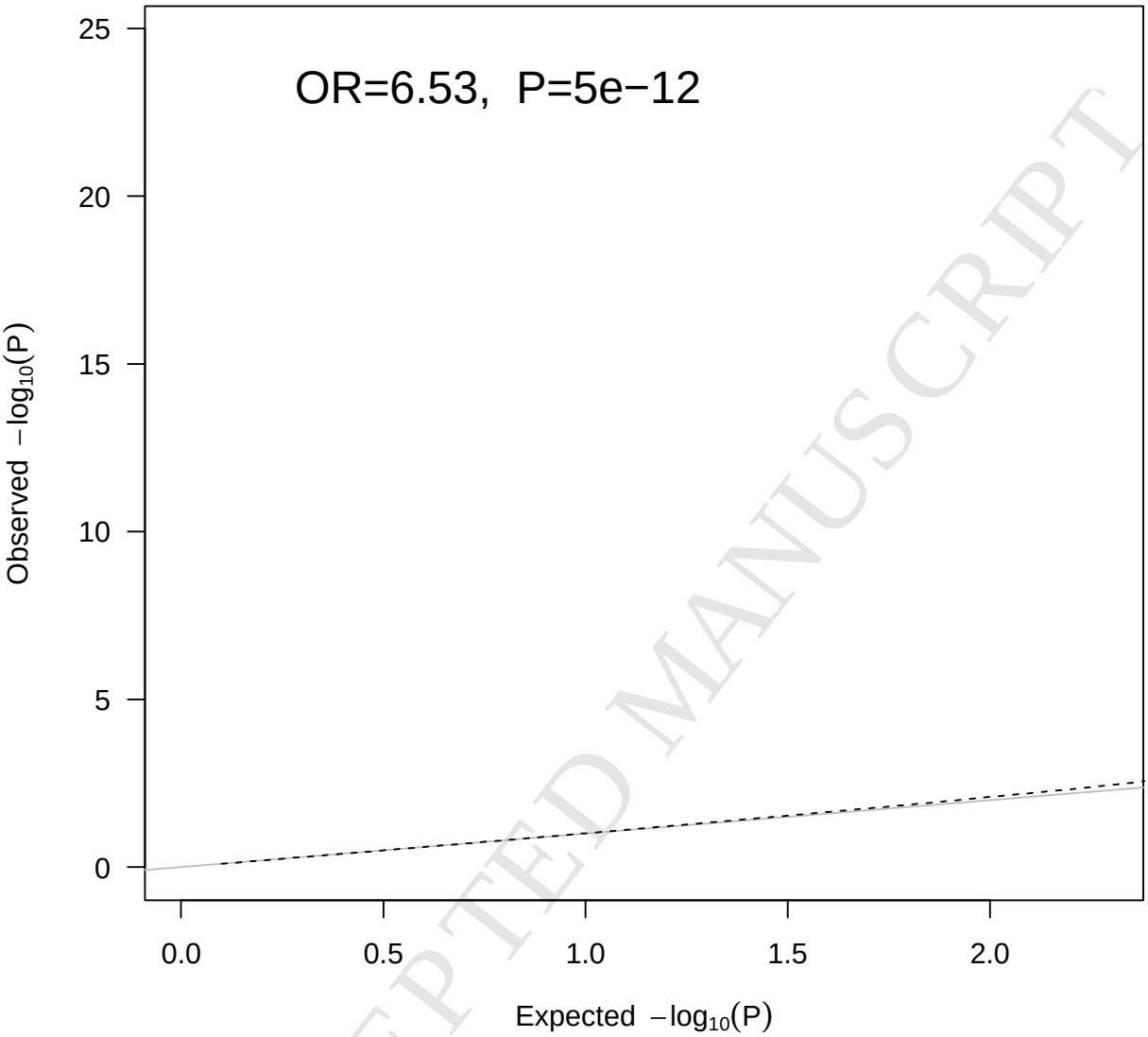

**Graves Disease:**

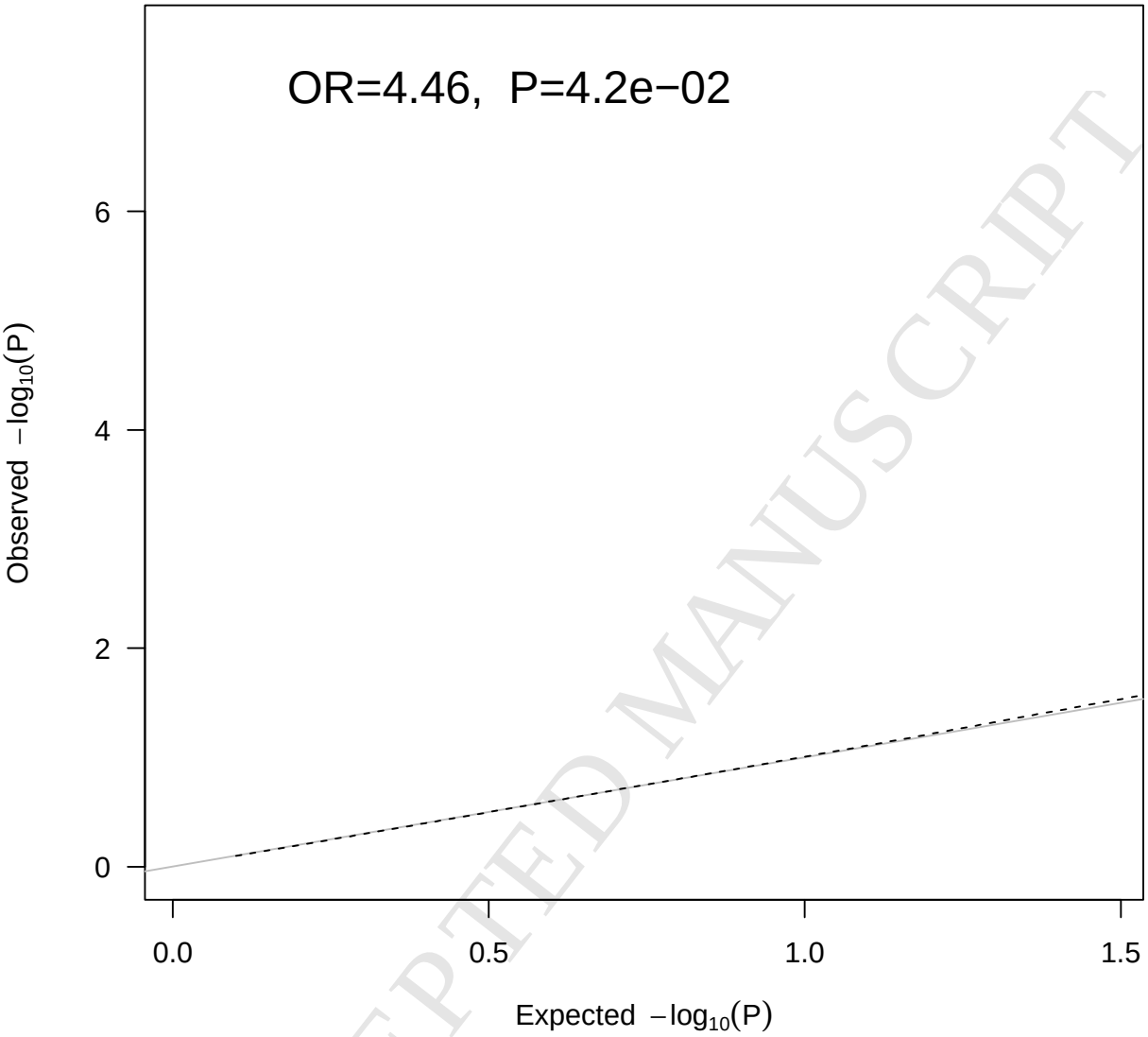

**Inflammatory Bowel Disease:**

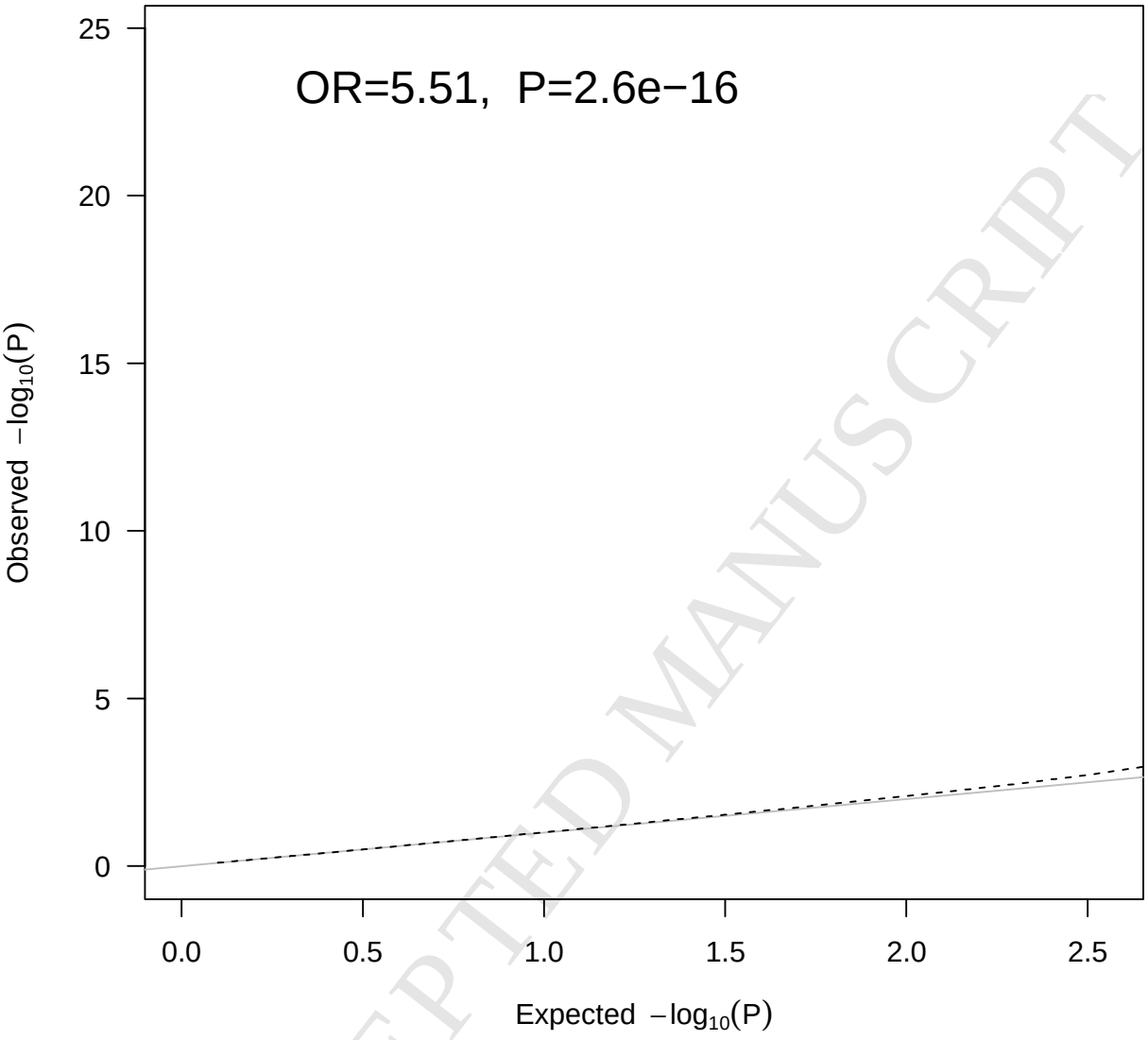

**Systemic Lupus Erythematosus:**

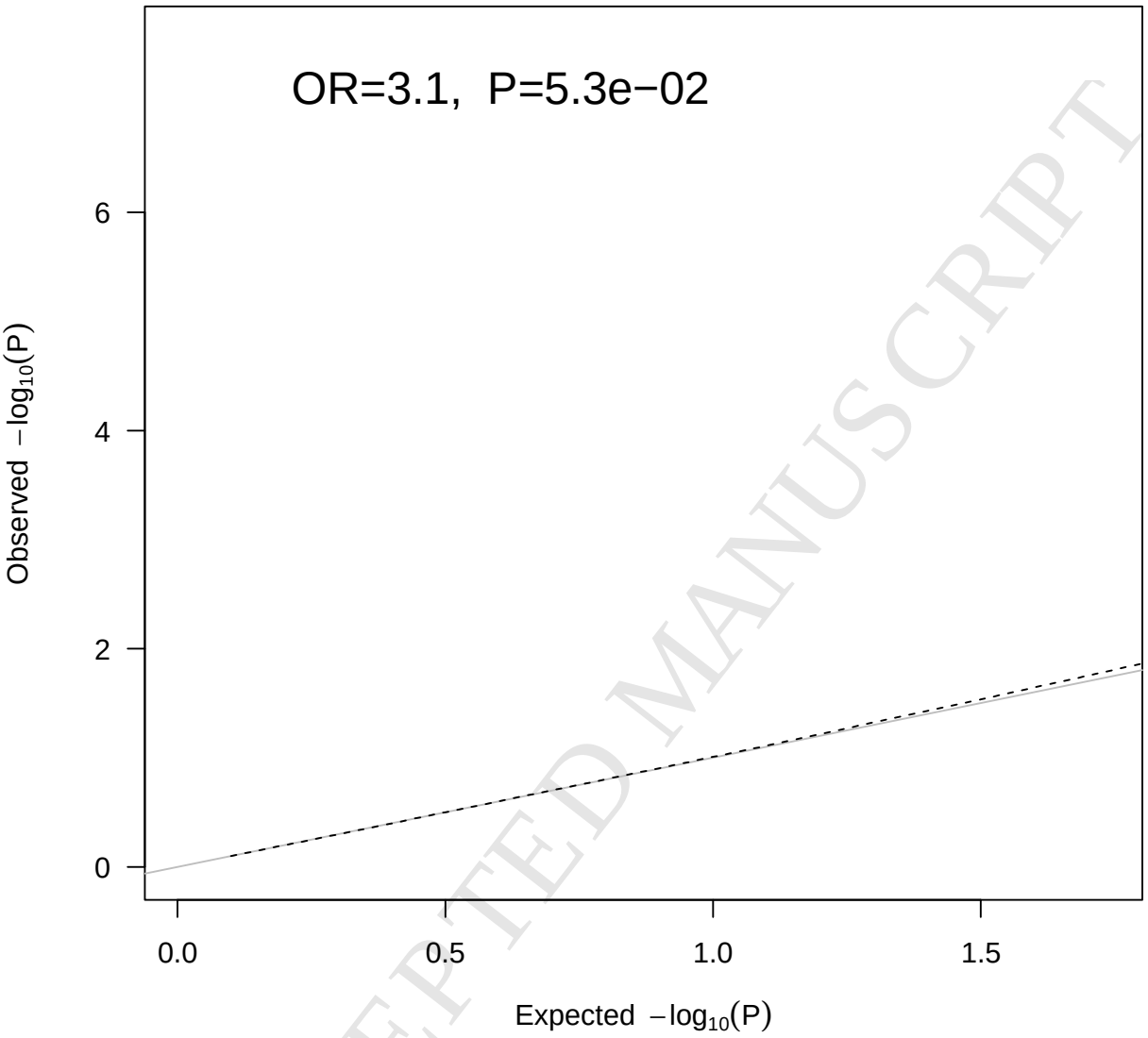

**Multiple Sclerosis:**

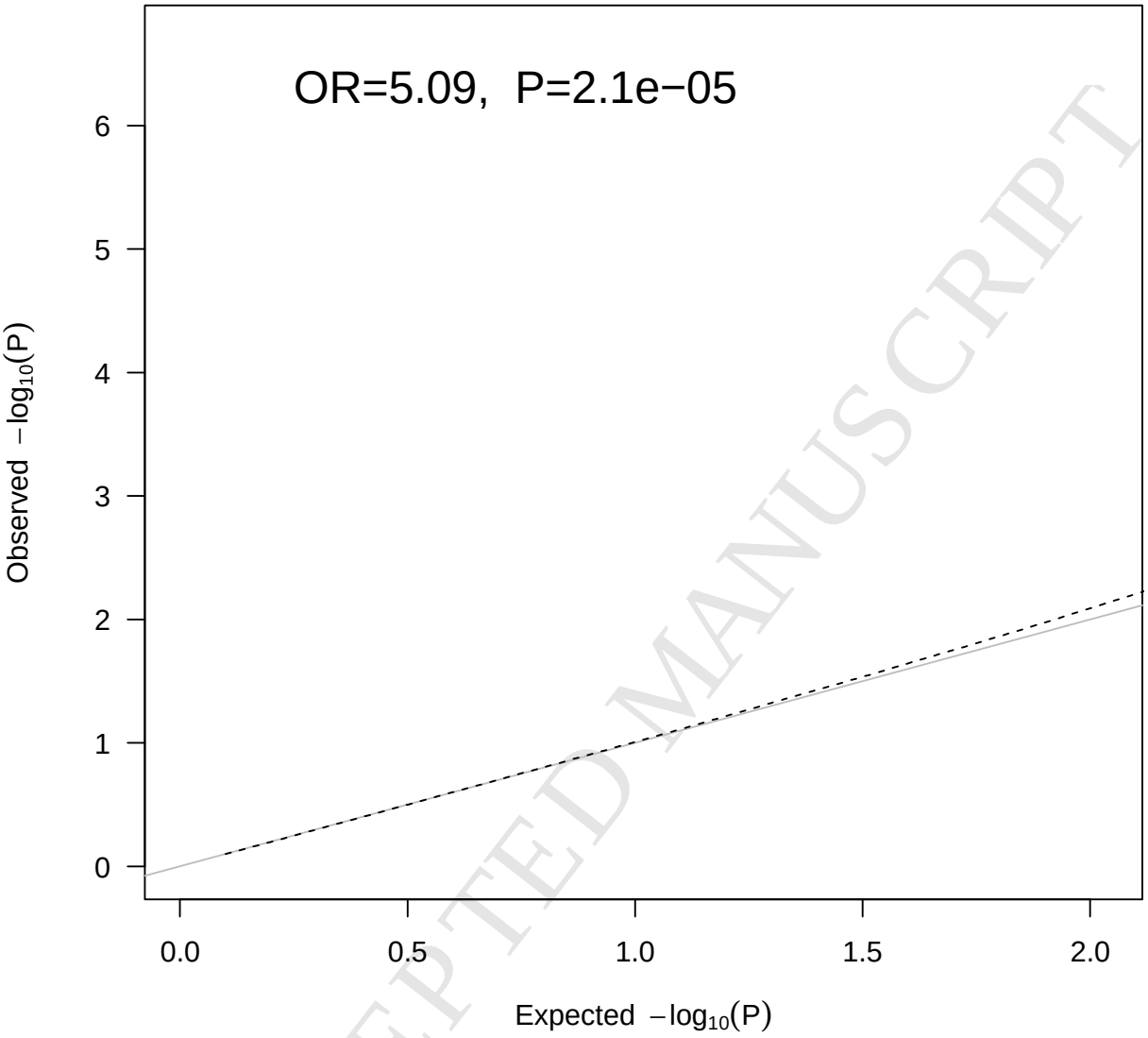

**Type-1 Diabetes:**

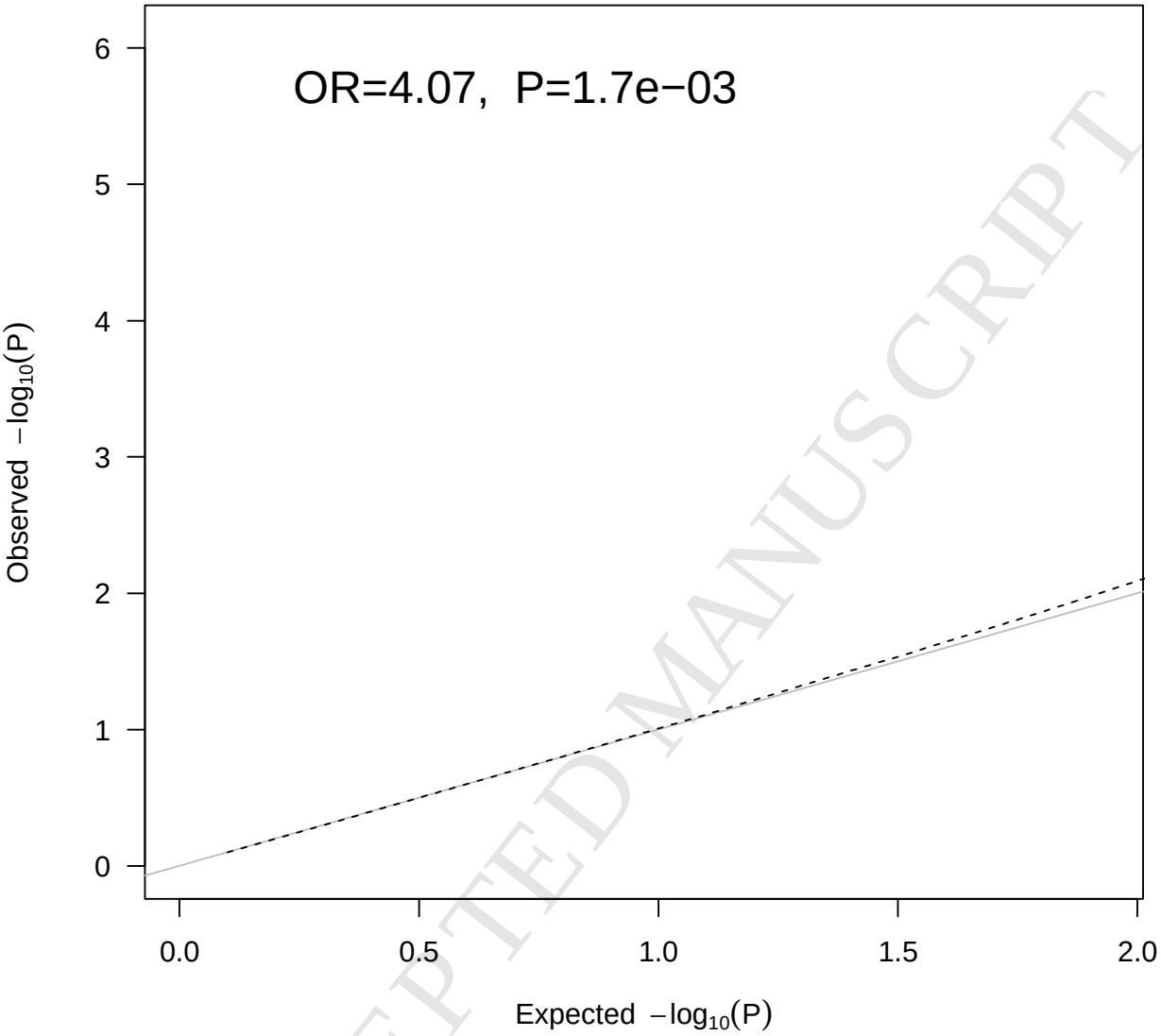

## Supplementary Figure 7

QQ plot of 57 Migraine loci extracted from the allergy meta-analysis results.

**Migraine:**

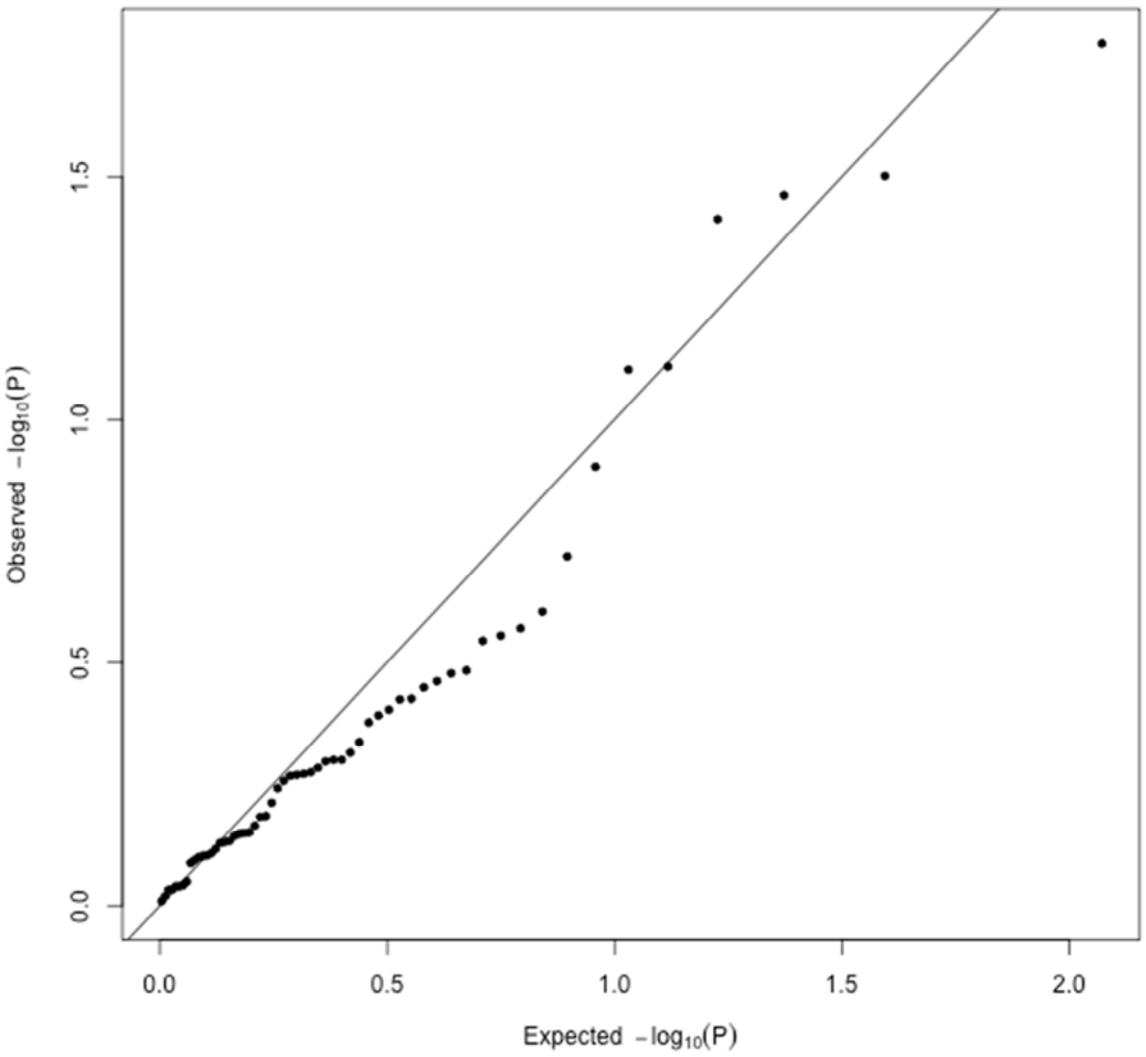

## Supplementary Figure 8

QQ plot of 77 loci associated with the combined phenotype of schizophrenia and bipolar disorder extracted from the allergy meta-analysis results.

**Bipolar disorder and schizophrenia:**

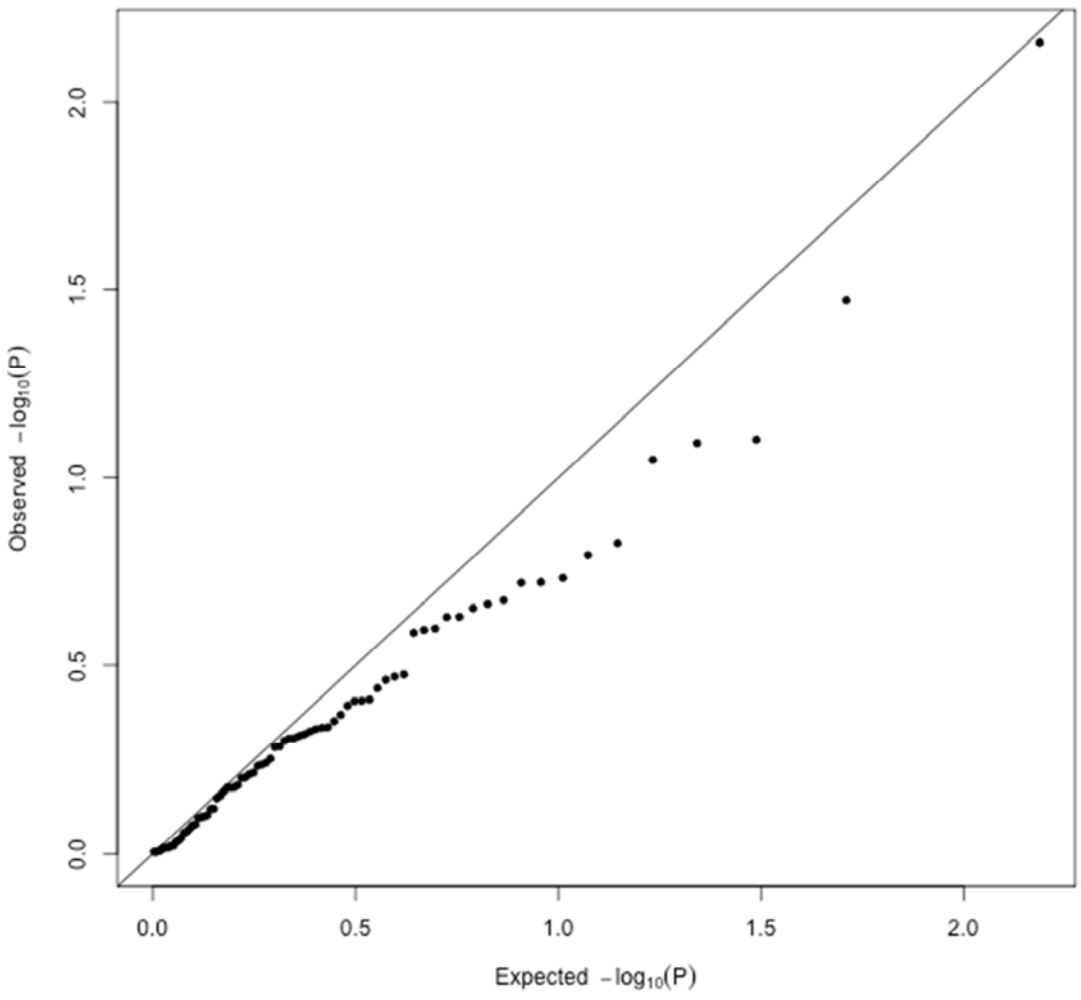

## Supplementary Figure 9

Principal component plot of GWAS Catalogue SNPs' perturbation of gene networks, based on the DEPICT tool, PC1 vs PC3

(PLEASE SEE SEPARATE FILE)

## Supplementary Figure 10

Principal component plot of GWAS Catalogue SNPs' perturbation of gene networks, based on the DEPICT tool, PC1 vs PC2, all trait names.

(PLEASE SEE SEPARATE FILE)

## Supplementary Figure 11

Allergy related loci and their resemblance to autoimmune disease and other types of disease loci were assessed by principal component analysis by analyzing the tendency of each trait-locus to fall in DHS sites in specific cell lines. This plot shows PC1 vs. PC2 and has the outlier “lipid metabolism phenotypes” omitted, and only names for autoimmune diseases, asthma and allergy are printed. The blue area represents the shared minimal ellipsoid area of immune-mediated diseases.

(PLEASE SEE SEPARATE FILE)

## Supplementary Figure 12

Allergy related loci and their resemblance to autoimmune disease and other types of disease loci were assessed by principal component analysis by analyzing the tendency of each trait-locus to fall in DHS sites in specific cell lines. This plot shows PC1 vs. PC2 for the full data set.

(PLEASE SEE SEPARATE FILE)

## Supplementary Figure 13

Allergy related loci and their resemblance to autoimmune disease and other types of disease loci were assessed by principal component analysis by analyzing the tendency of each trait-locus to fall in DHS sites in specific cell lines. This plot shows PC1 vs. PC2 overlayed with cell- and tissue type loadings.

(PLEASE SEE SEPARATE FILE)

## Supplementary Figure 14

Hierarchical clustering of all NHRGI GWAS catalog diseases' associated SNPs' tendency to fall within DHS sites for immune cell types within the Encode data set.

(PLEASE SEE SEPARATE FILE)

## Supplementary Figure 15

Enrichment of DHS sites in SNPs associated to allergy and Crohn's disease.
X-axis denominates all SNPs associated to the given trait at –log10(p) <= x, and y gives the enrichment of DHS sites for a given cell/tissue-type for those SNPs, as compared to all SNPs (x=0). Immune cells are indicated in blue.

(PLEASE SEE SEPARATE FILE)

## Supplementary Figure 16

Enrichment of SNPs falling in FANTOM enhancers

(PLEASE SEE SEPARATE FILE)

## Supplementary Figure 17

PCA plot of DEPICT pathway perturbation analysis, showing names for all gene sets.

(PLEASE SEE SEPARATE FILE)

## Supplementary Figure 18

Enrichment of shared loci with ENCODE ChIP-seq based transcription factor binding sites. Green line indicates FDR < 0.05. Transcription factors in blue have FDR < 0.05 and enrichment >= 3.

(PLEASE SEE SEPARATE FILE)

## Supplementary Figure 19

LocusZoom plots of the autoimmune disease associated loci within the allergy meta-analysis. Each dot represents the association between allergy and the particular SNP. The purple SNP is the index SNP for which the remaining SNPs are colored with respect to the r2 value to the index SNP. The position on the Y-axis represents the P-value (left handside Y-axis). The blue line represents recombination rates (righ handside Y-axis)

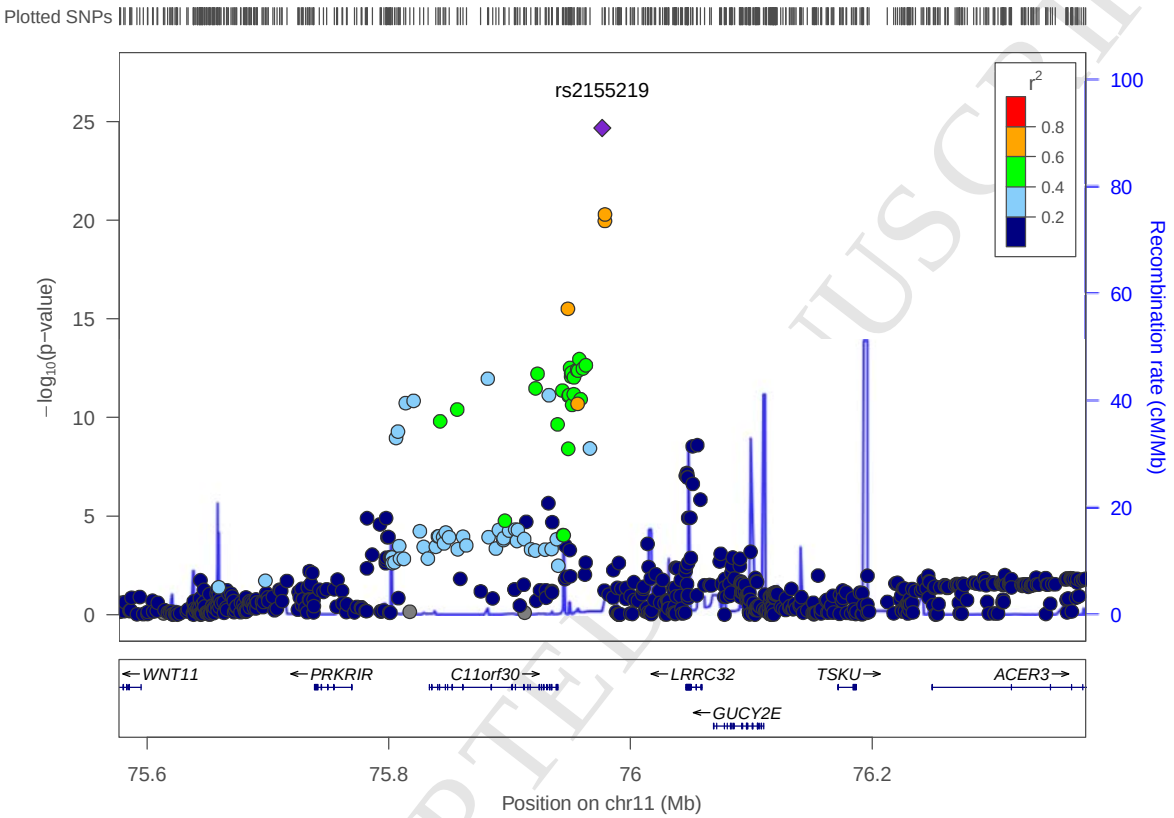

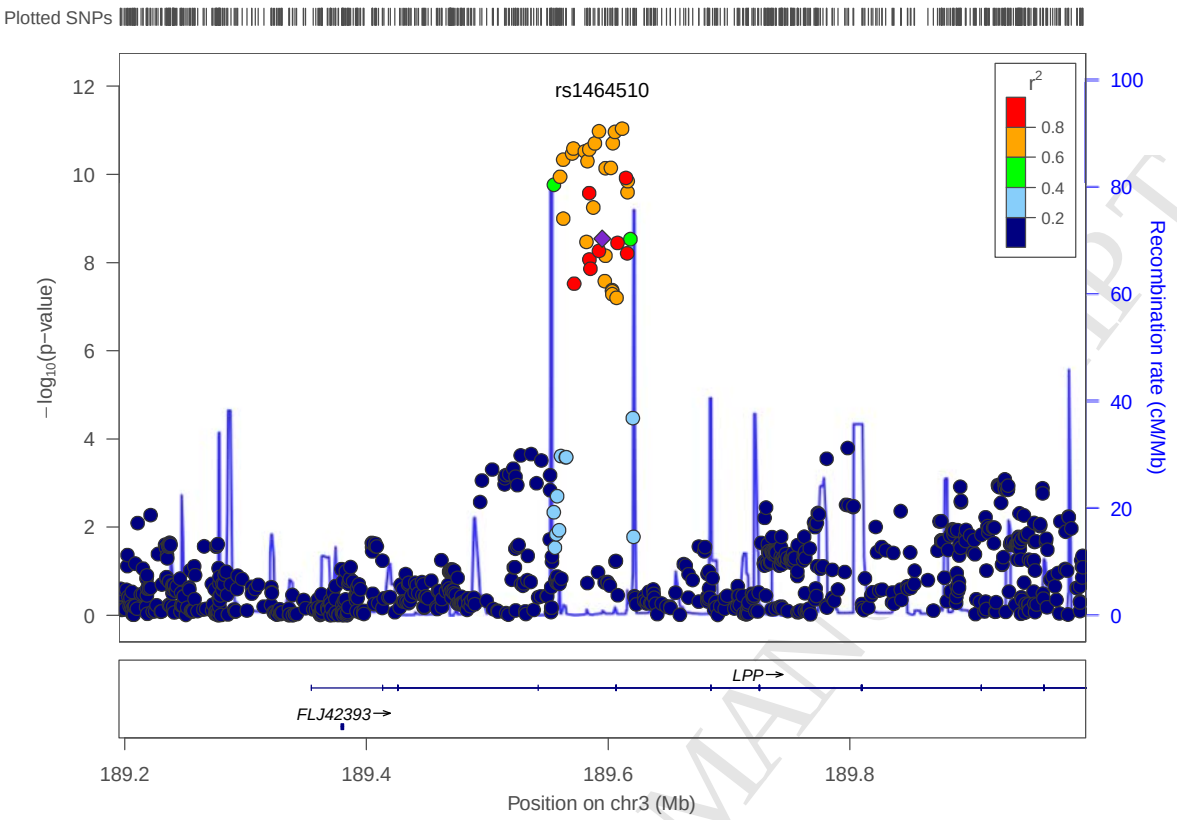

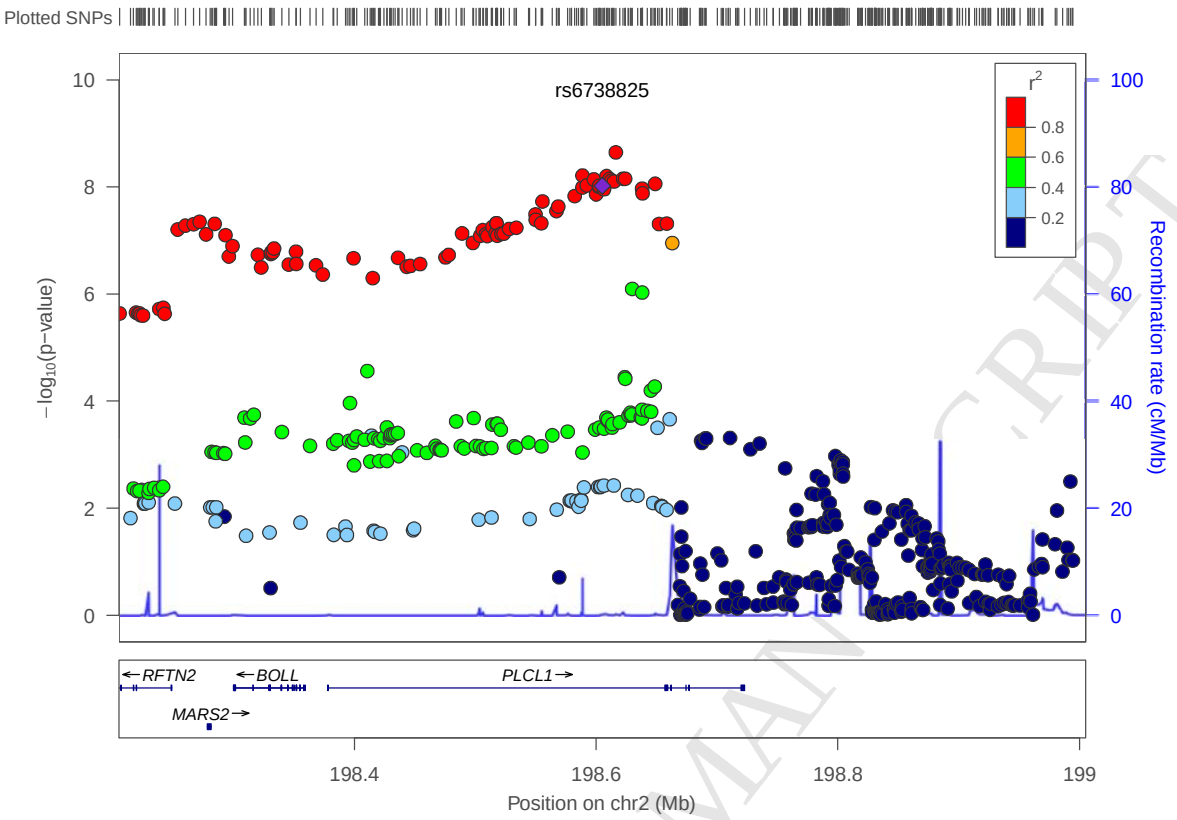

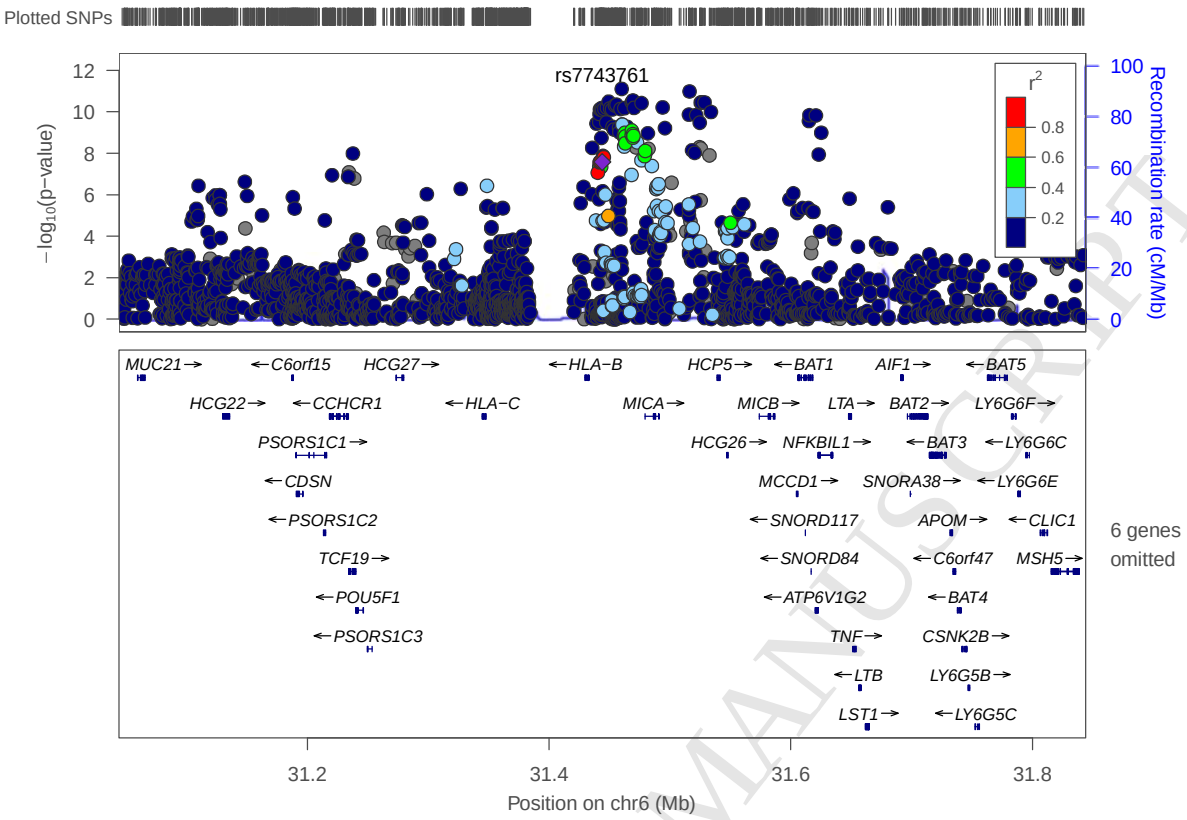

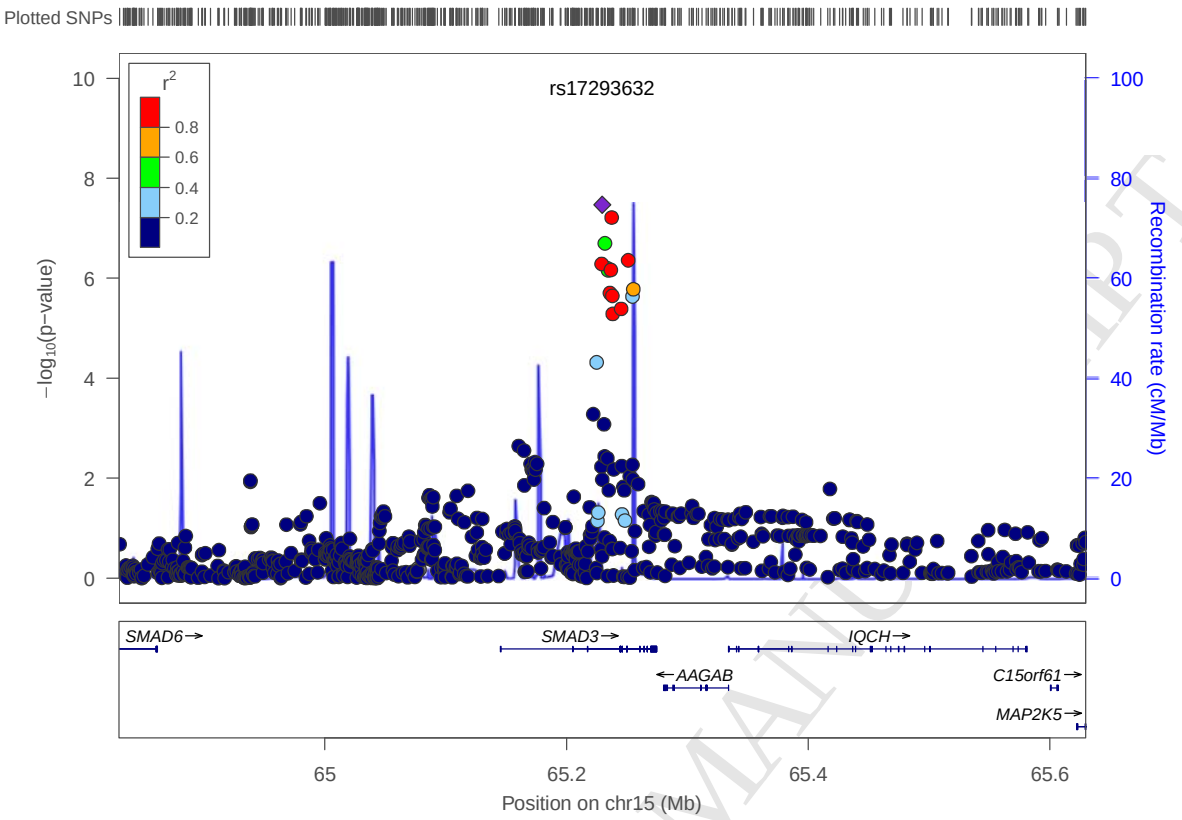

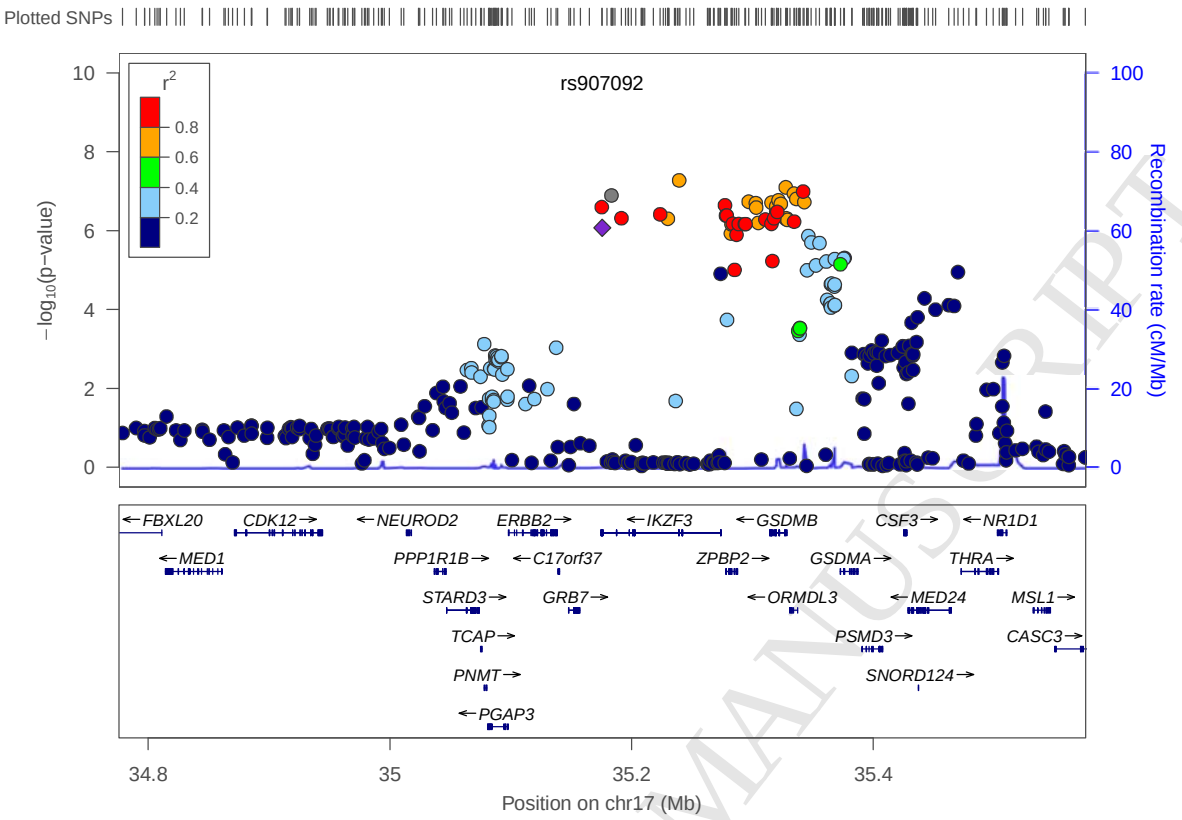

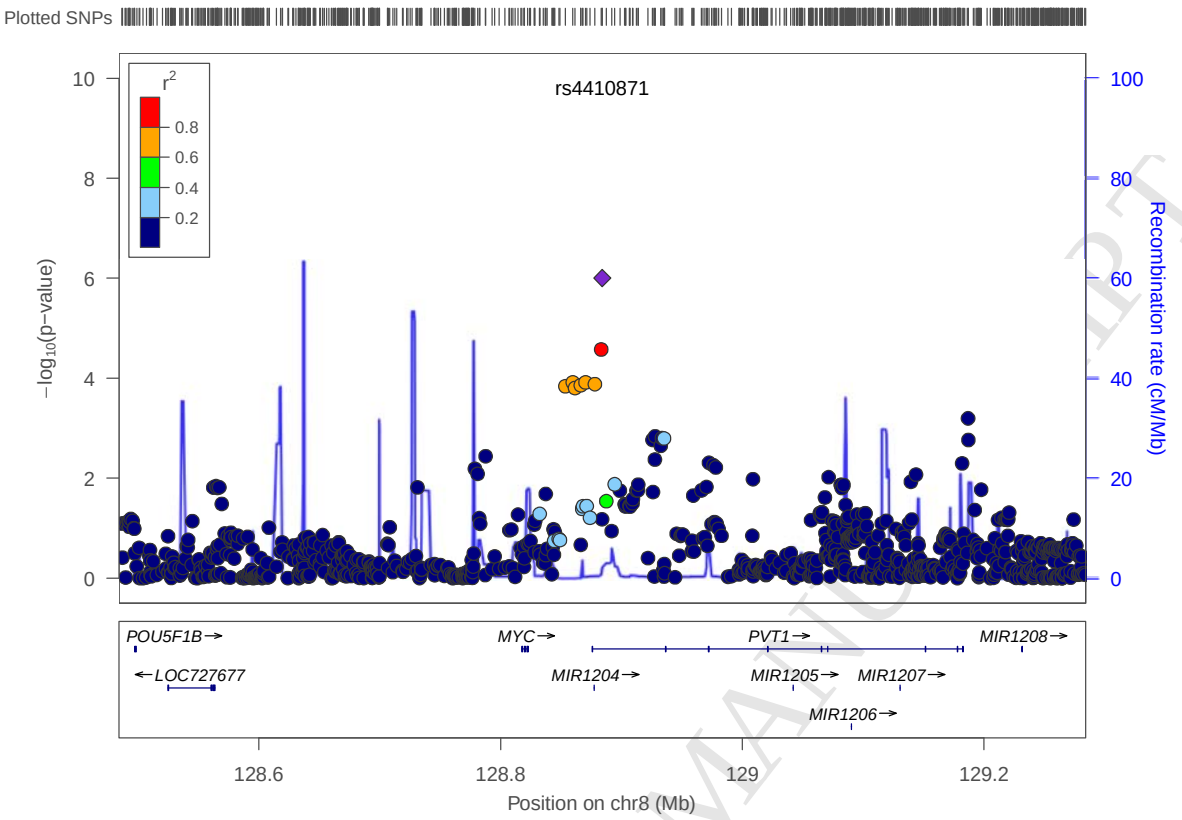

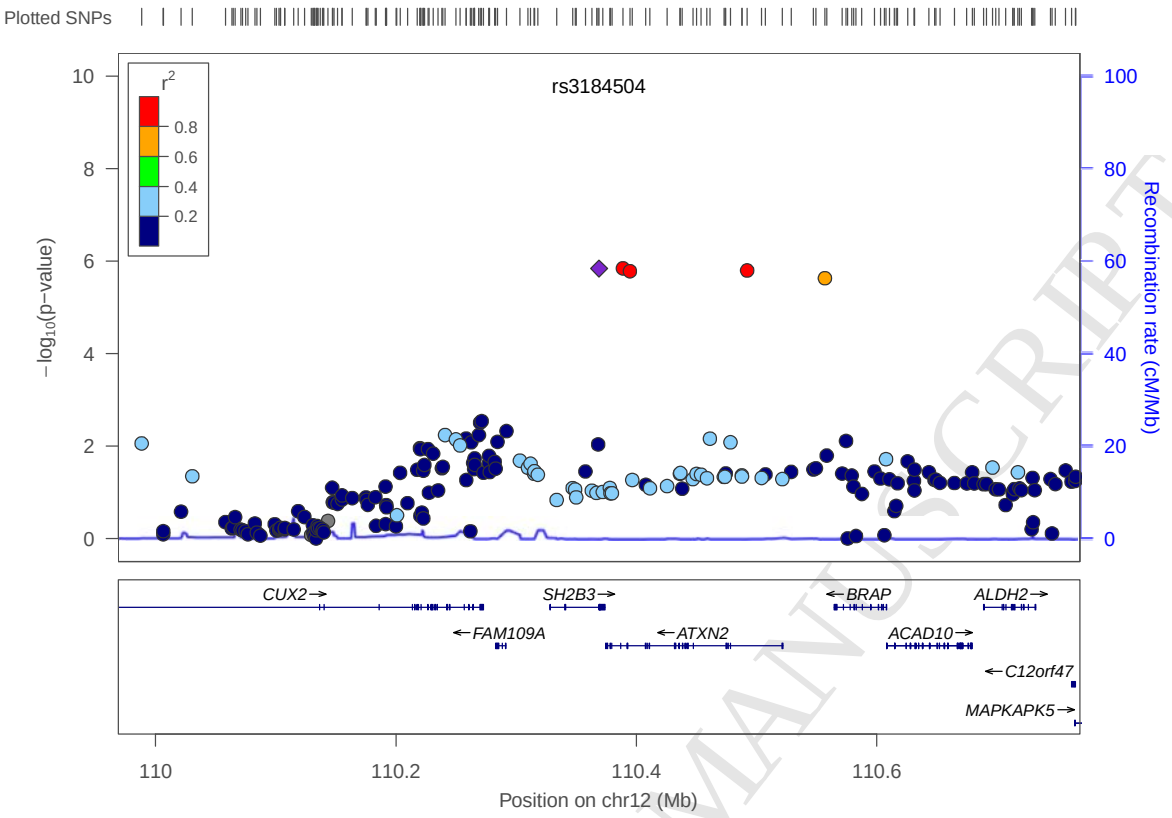

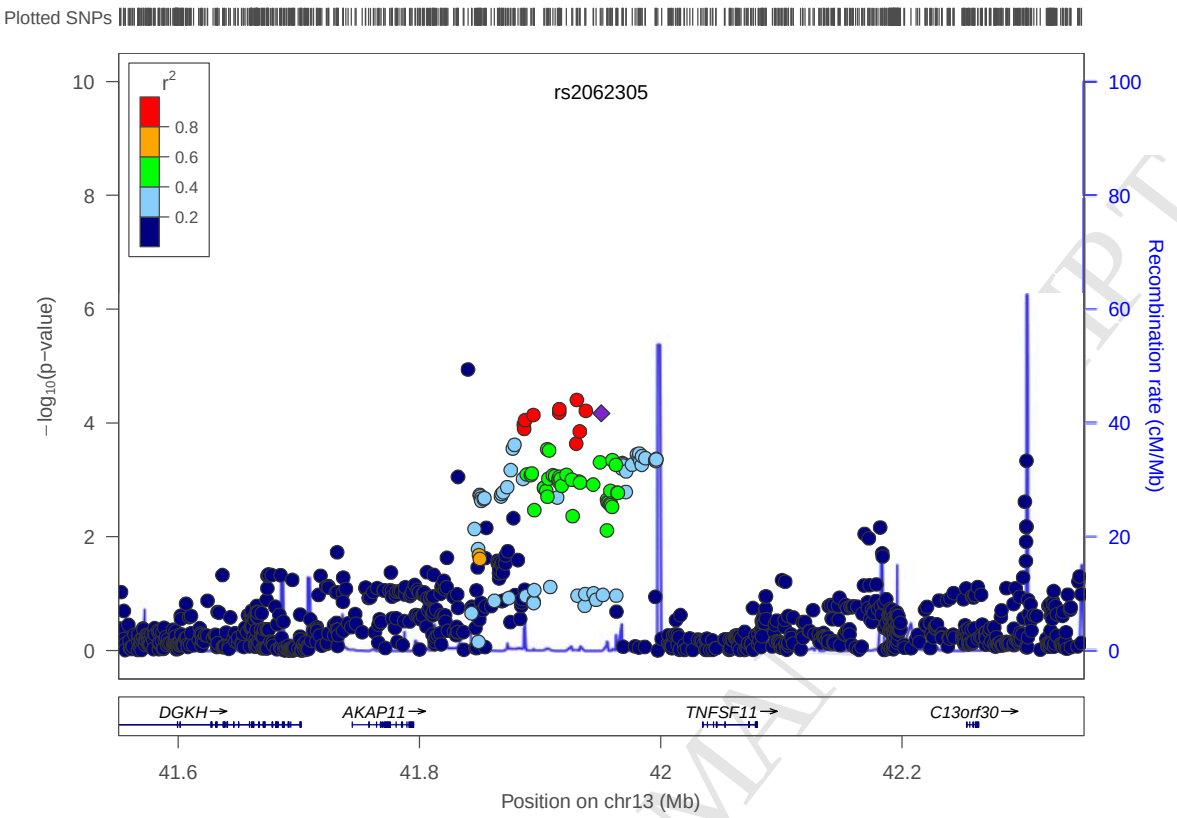

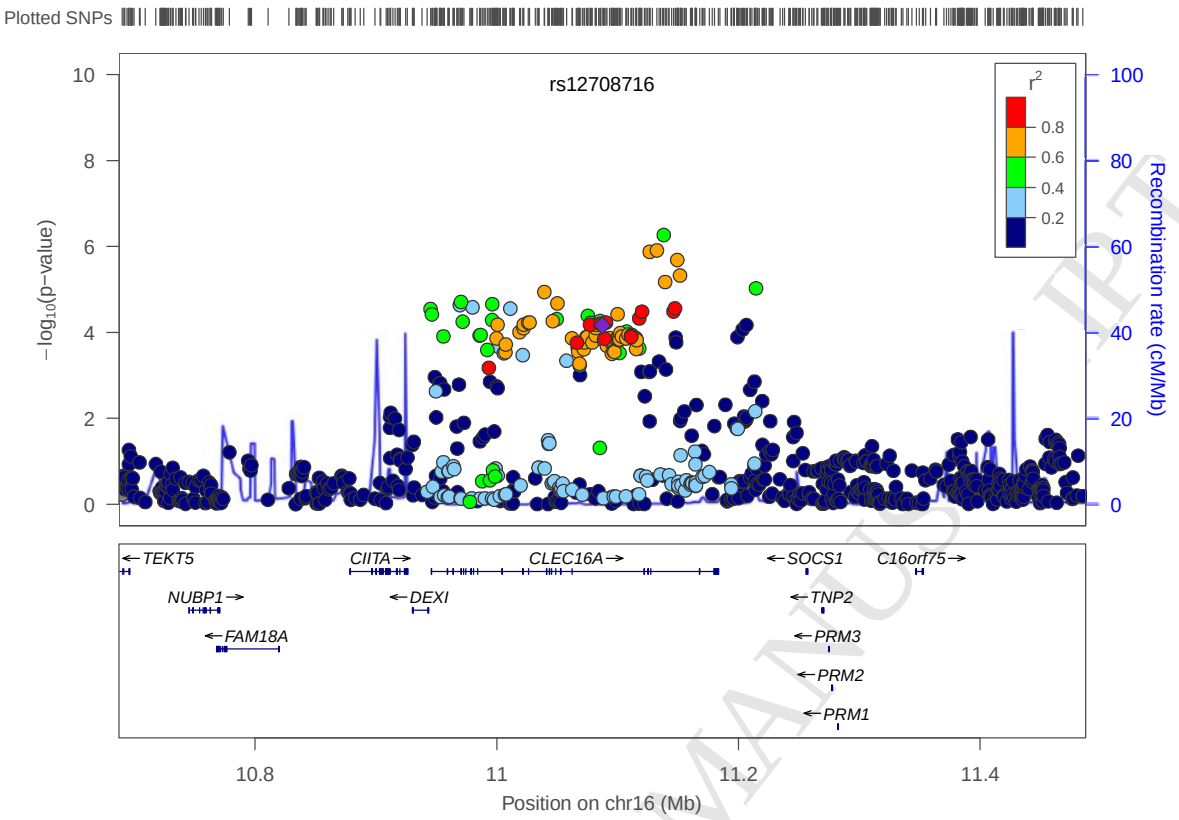

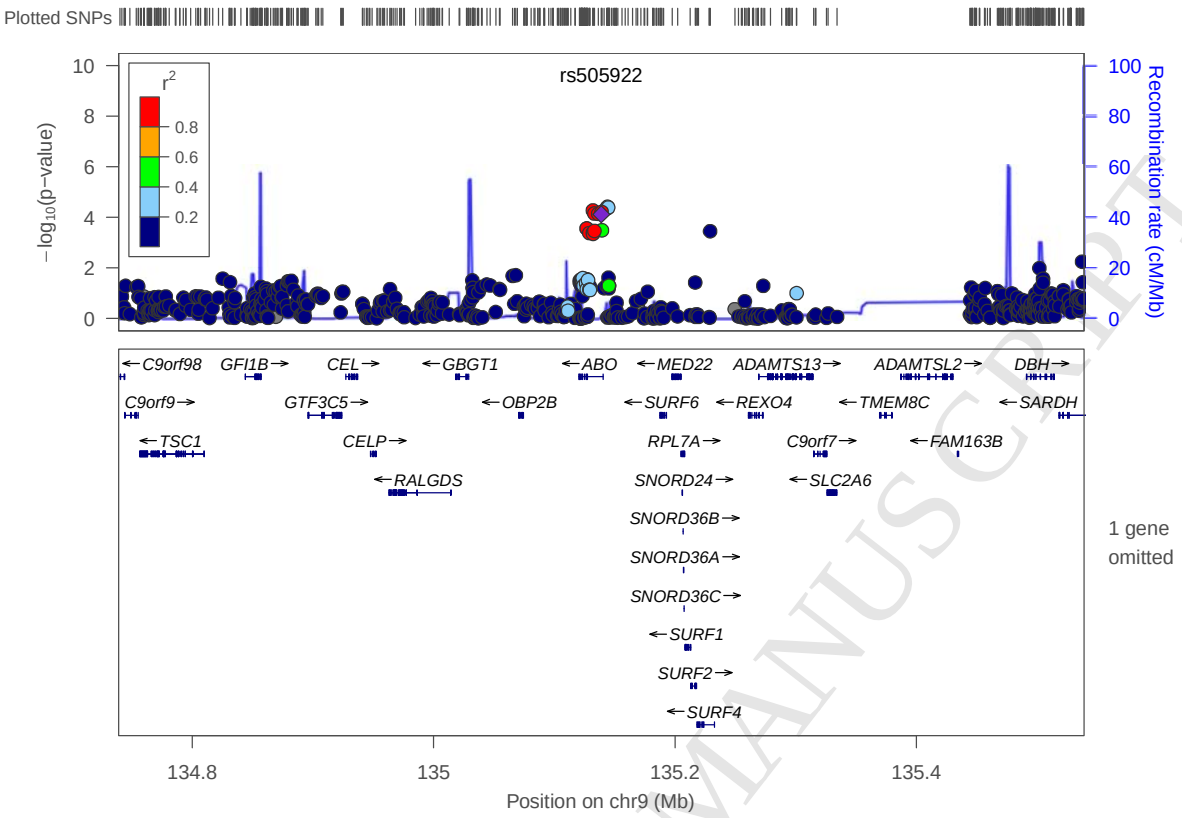

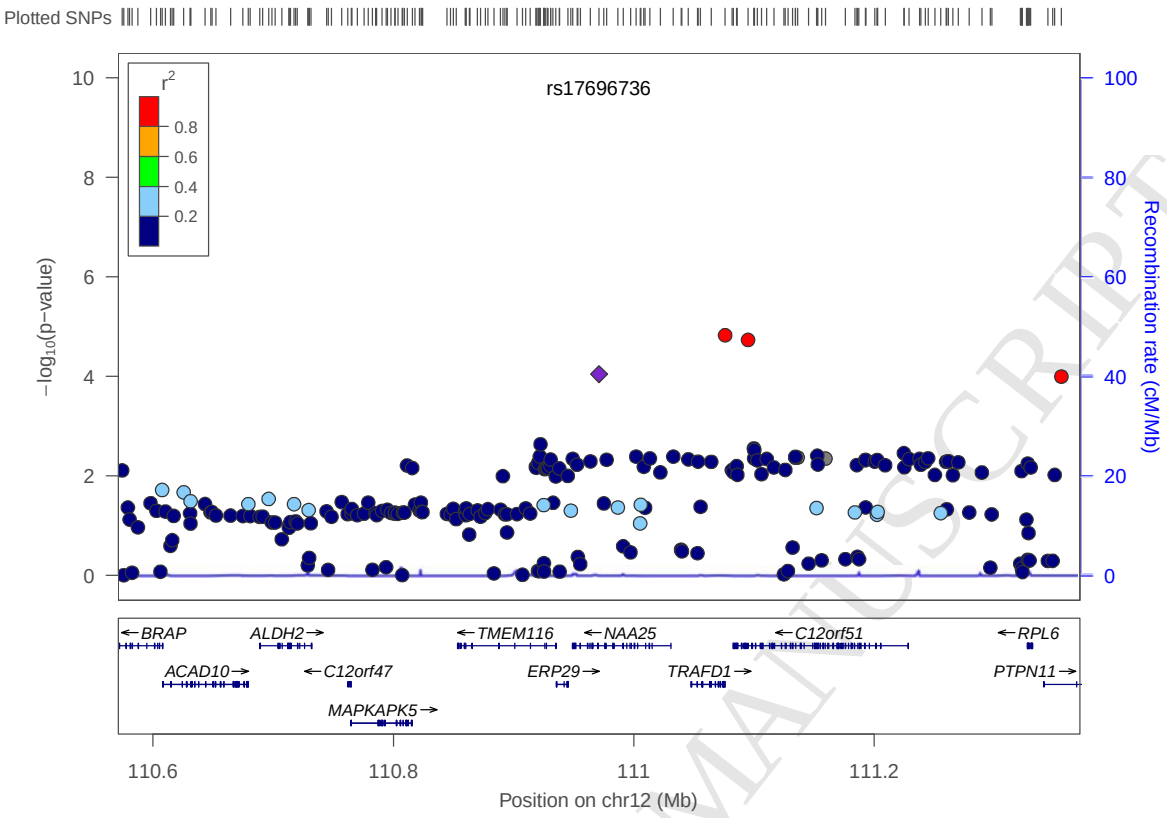

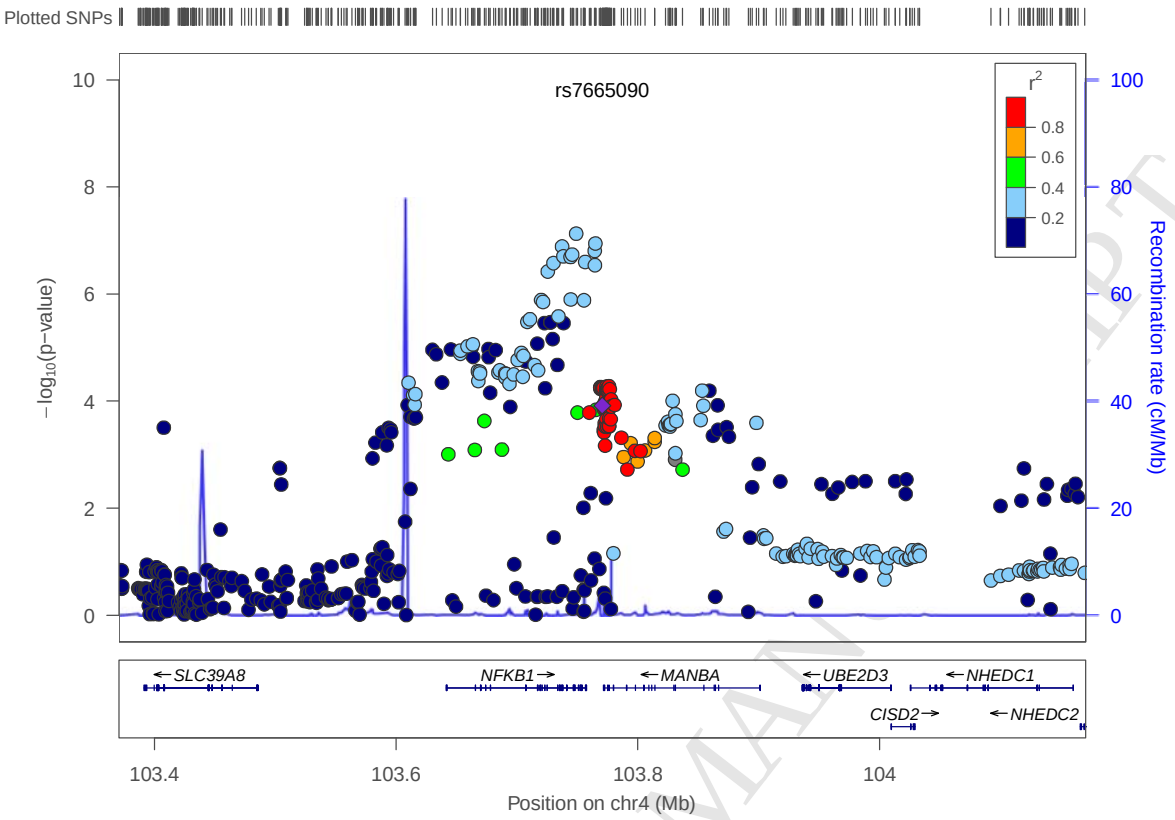

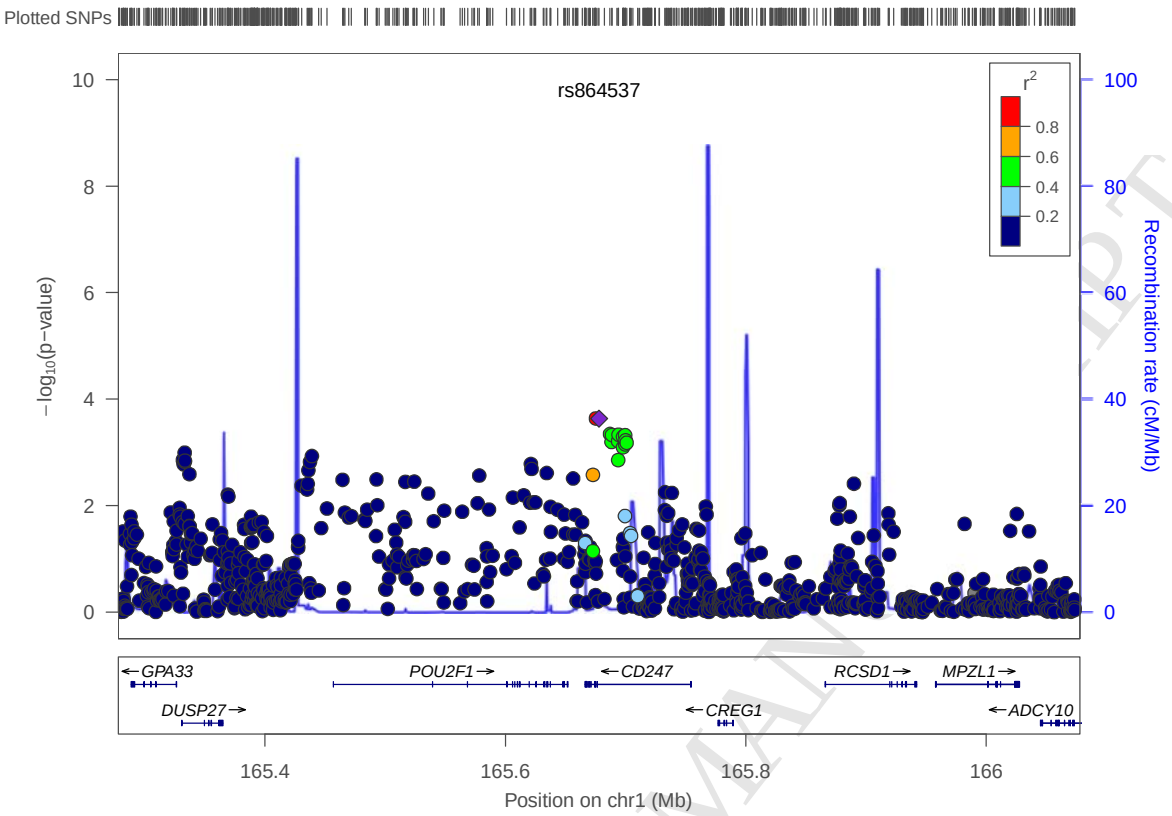

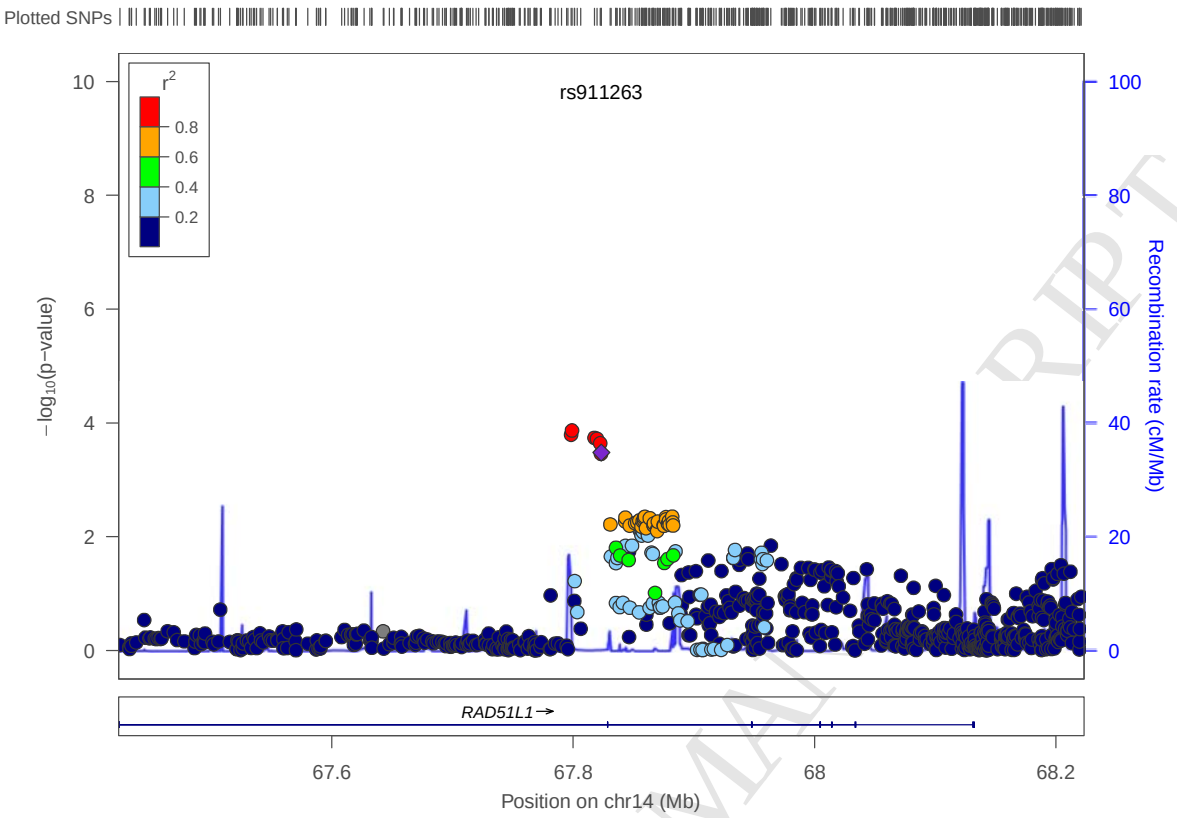

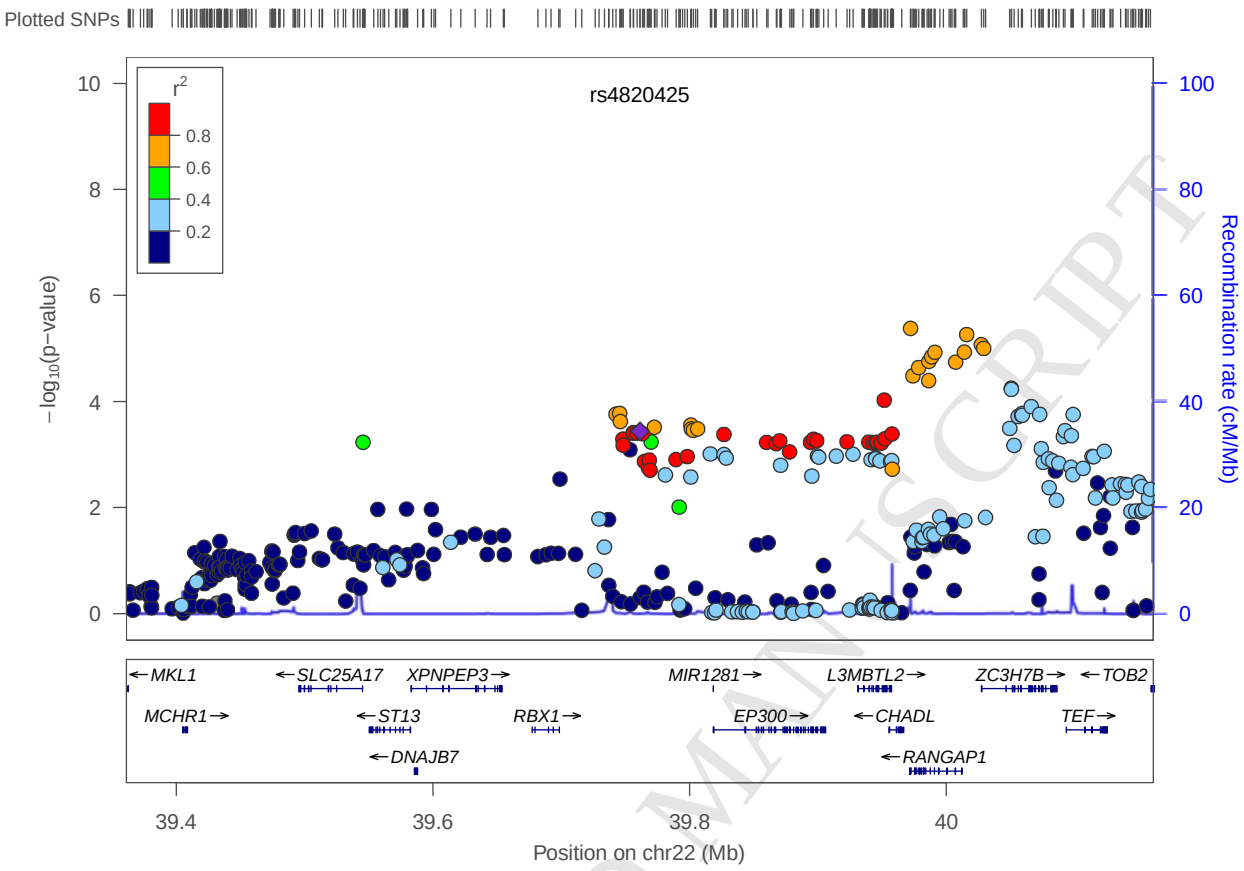

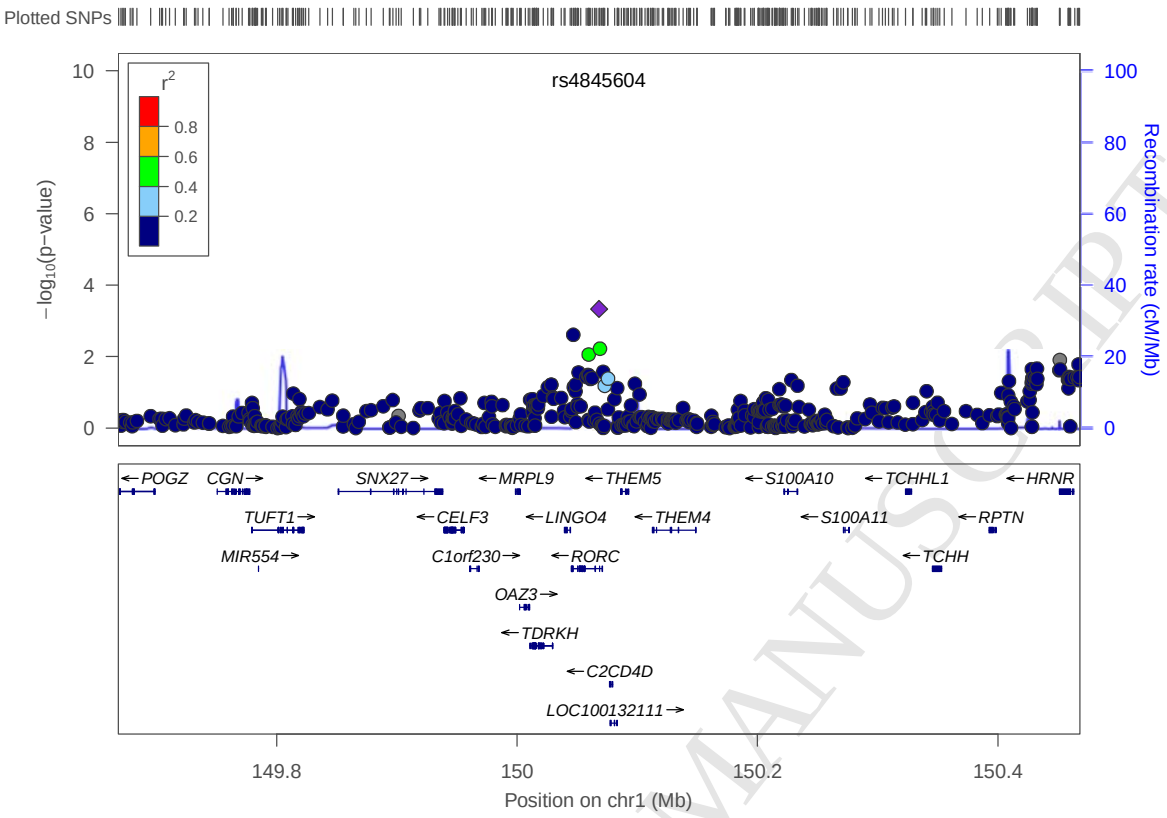

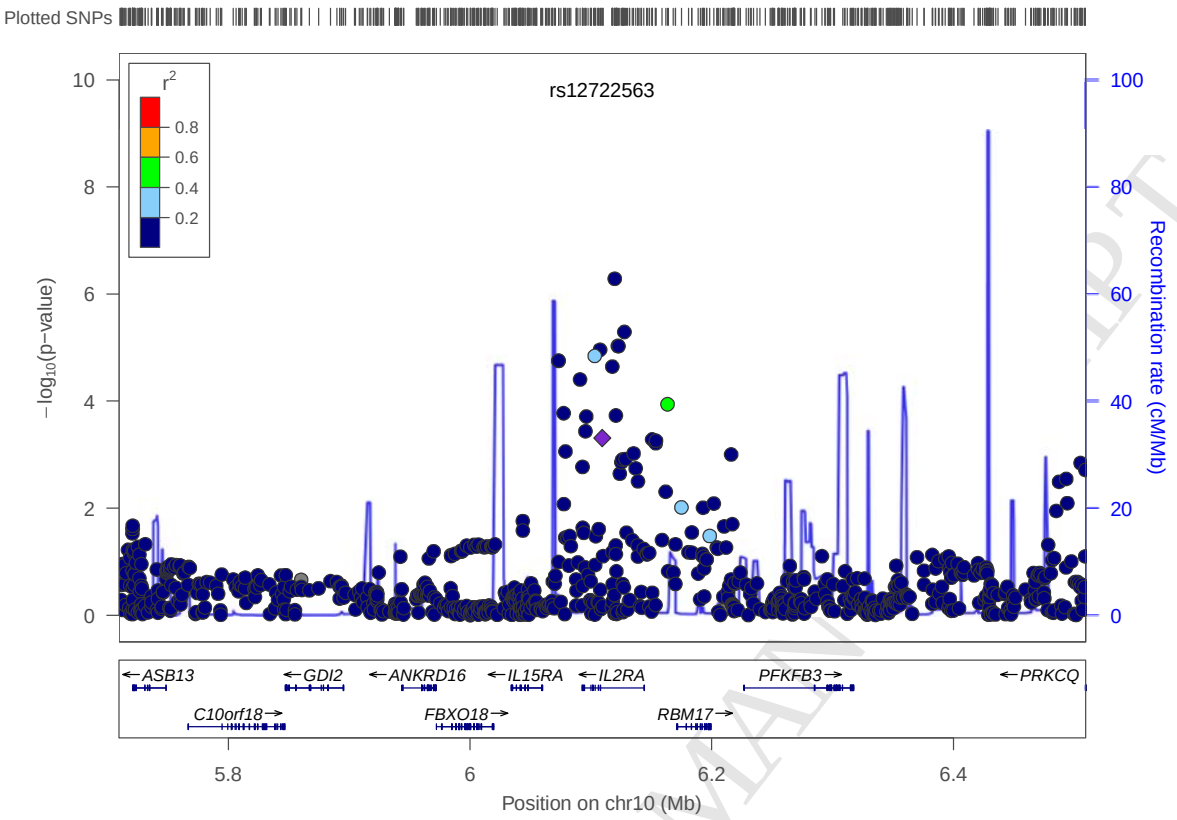

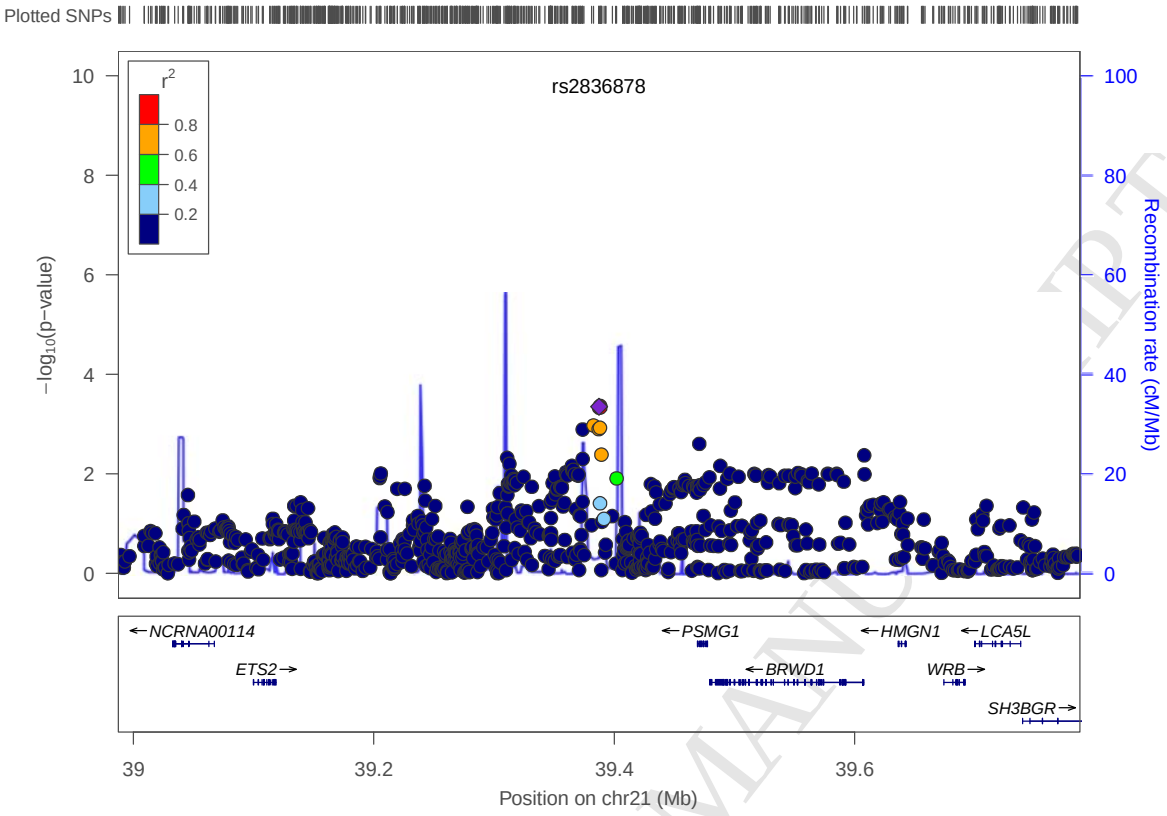

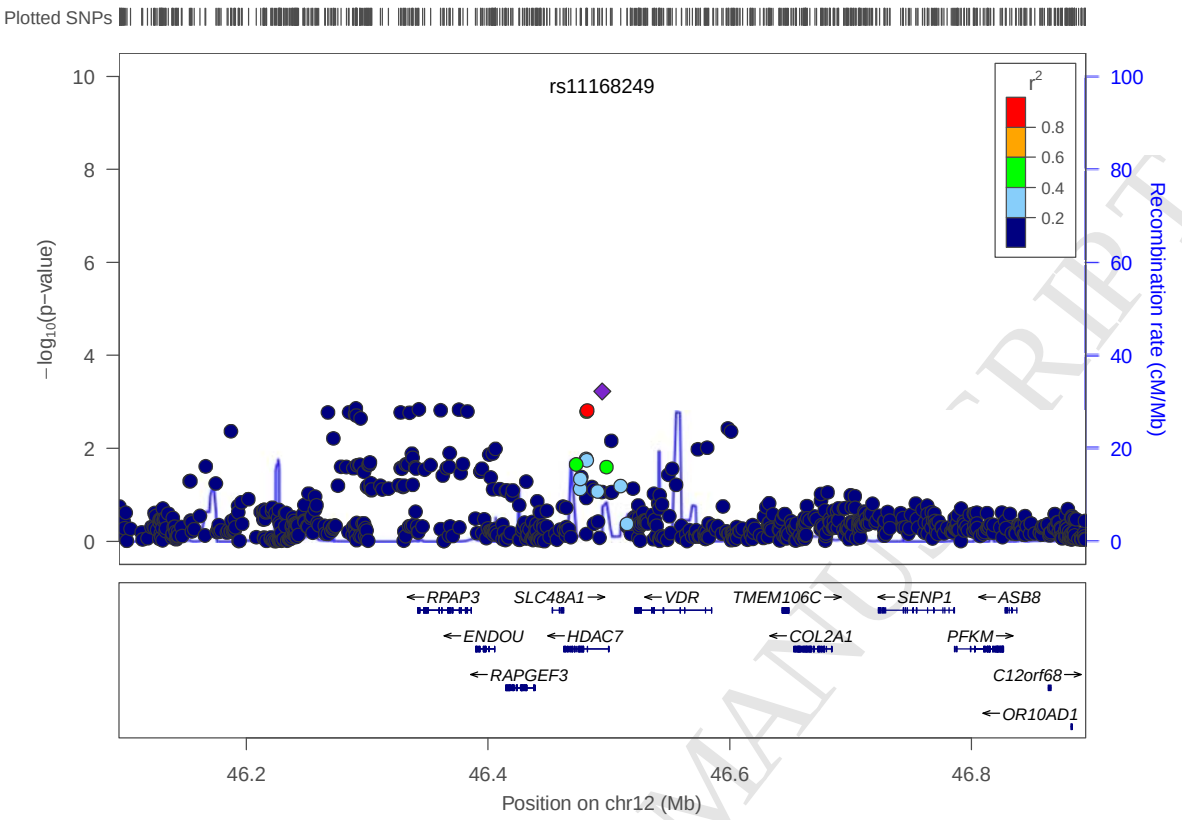

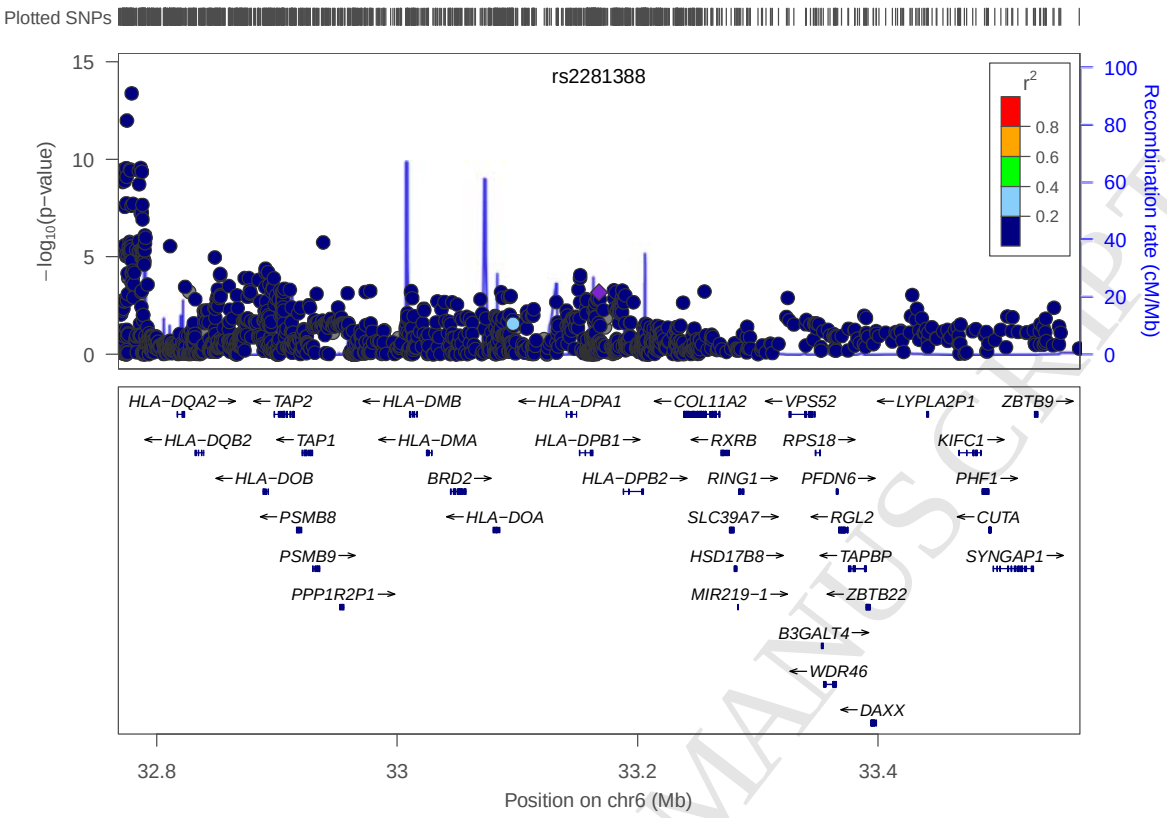

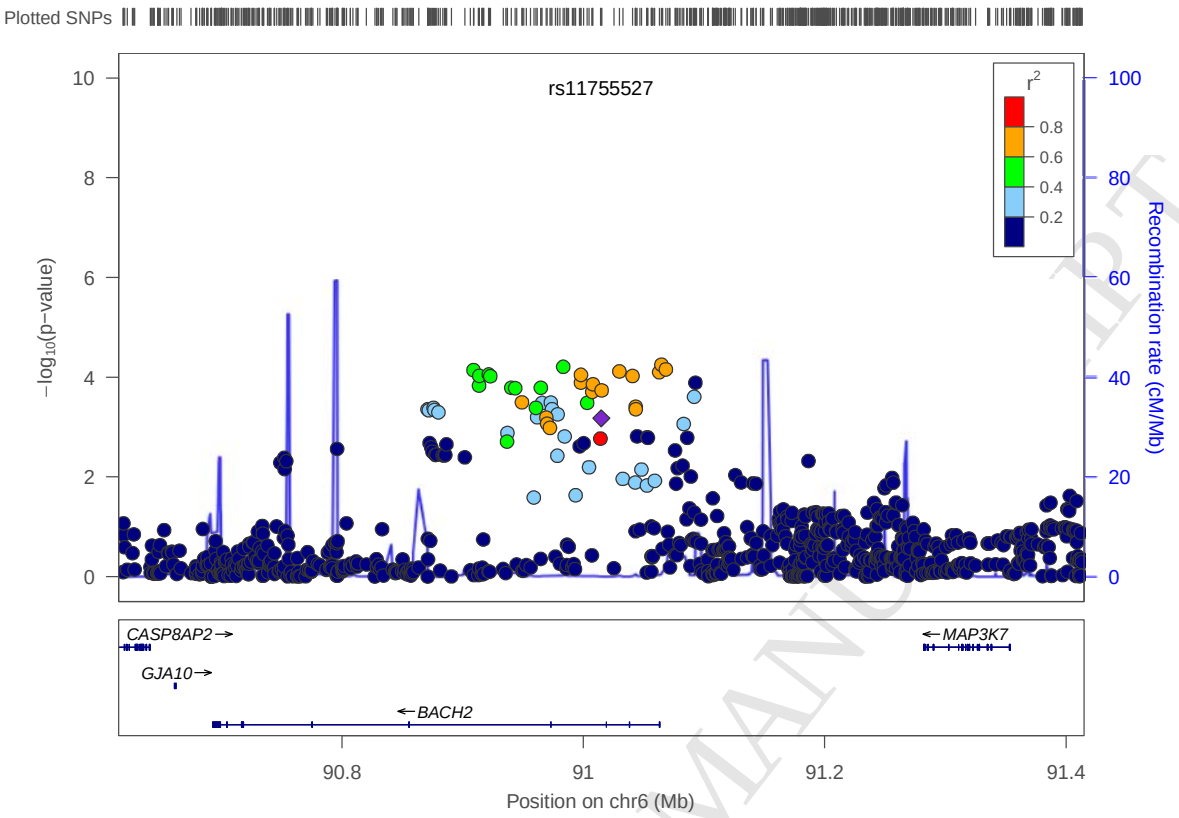

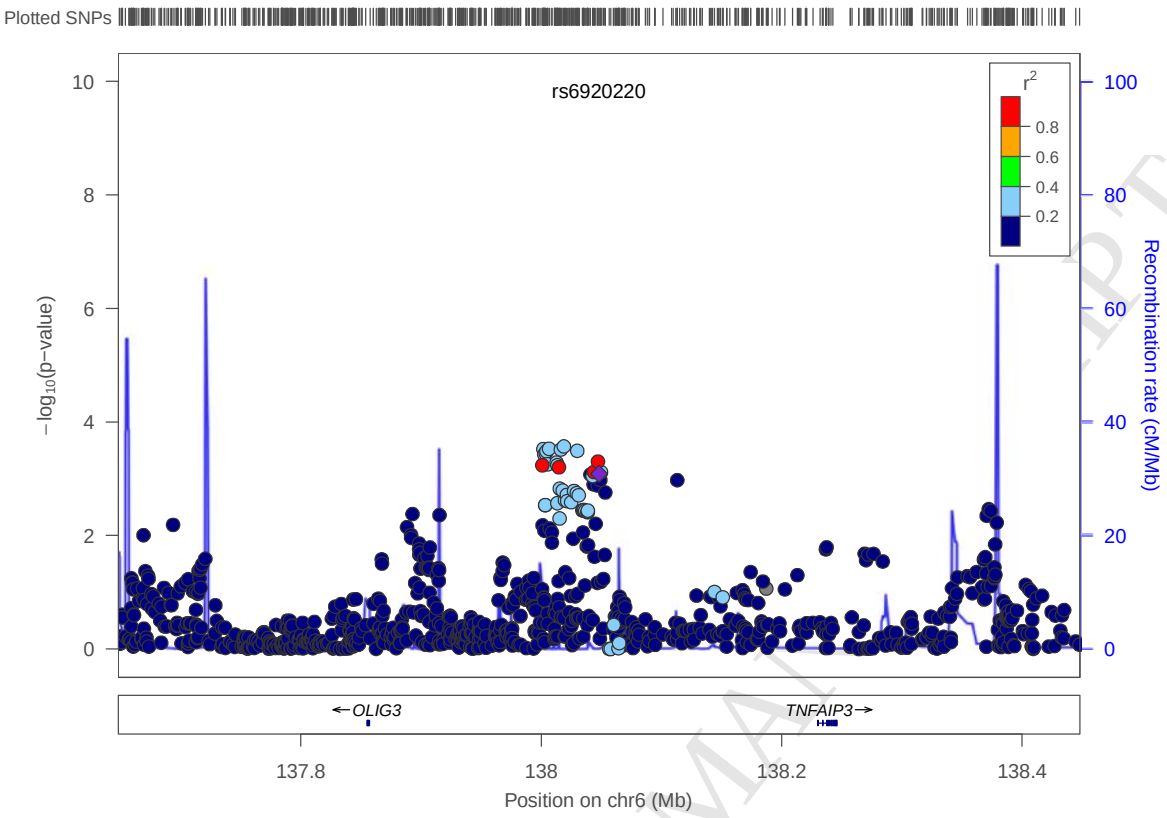

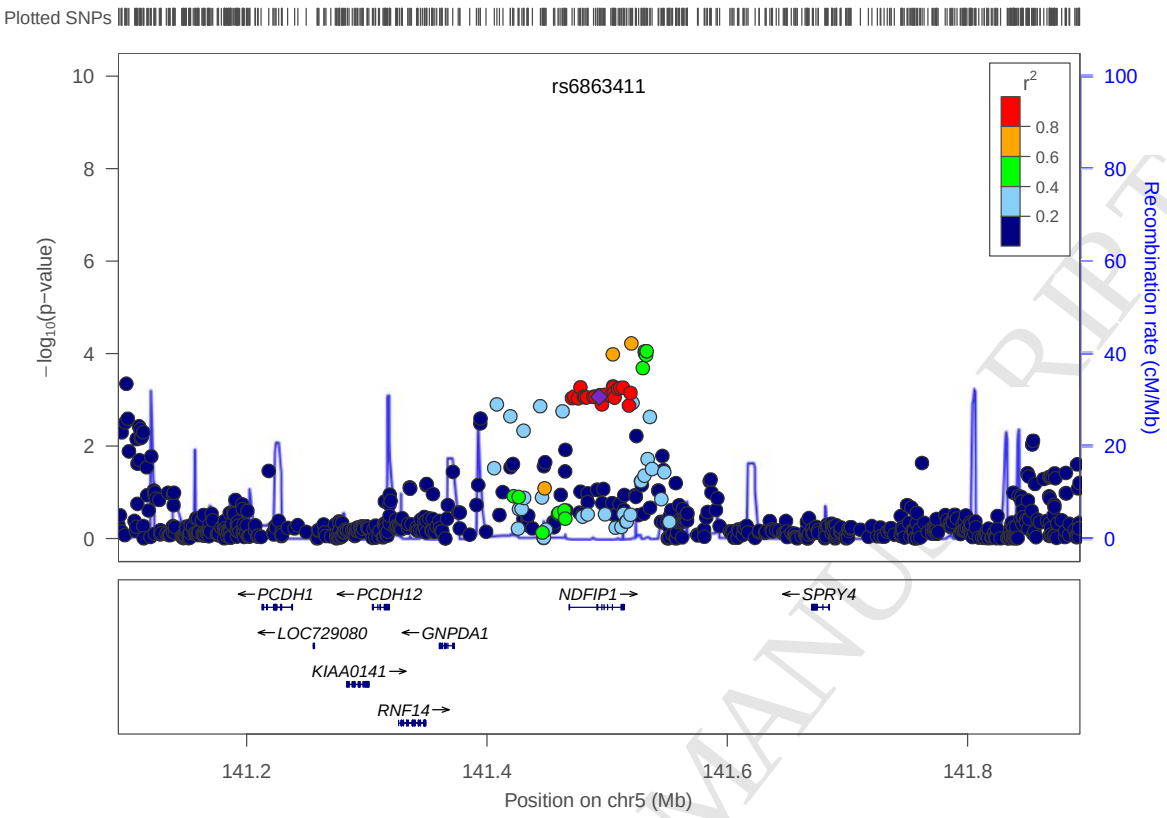

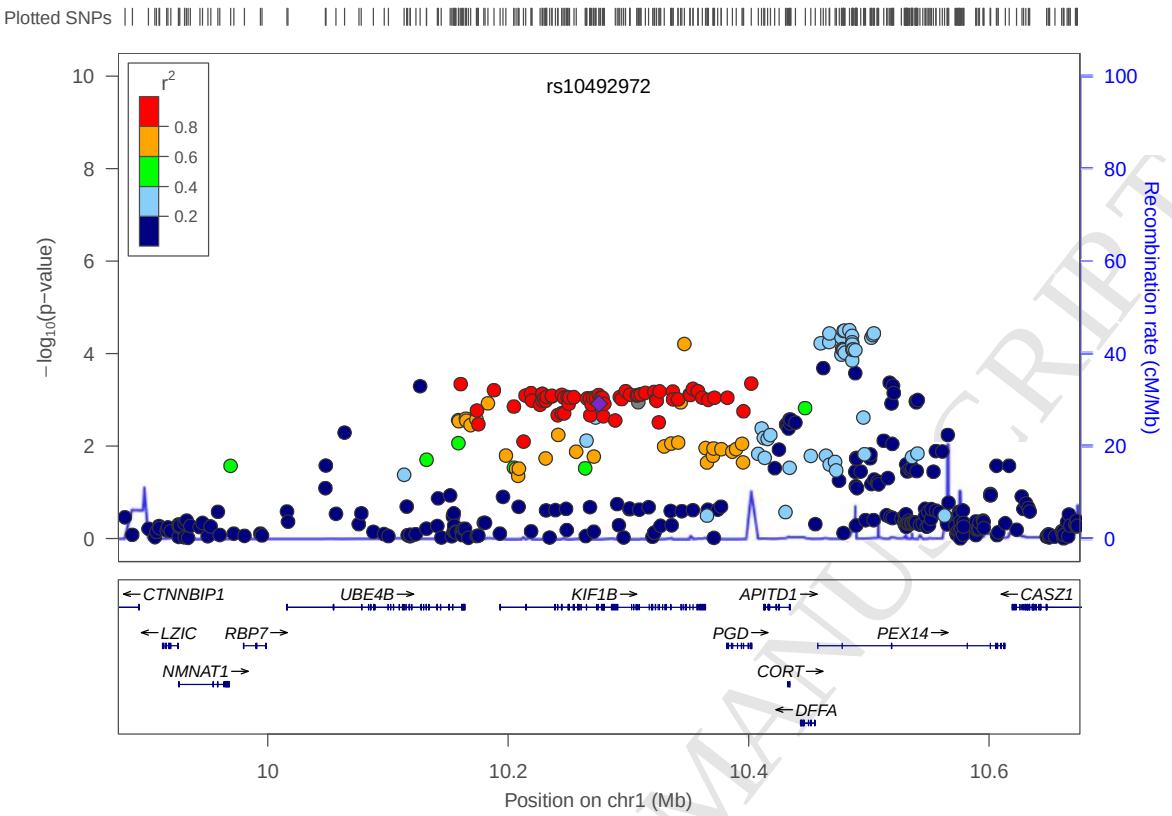

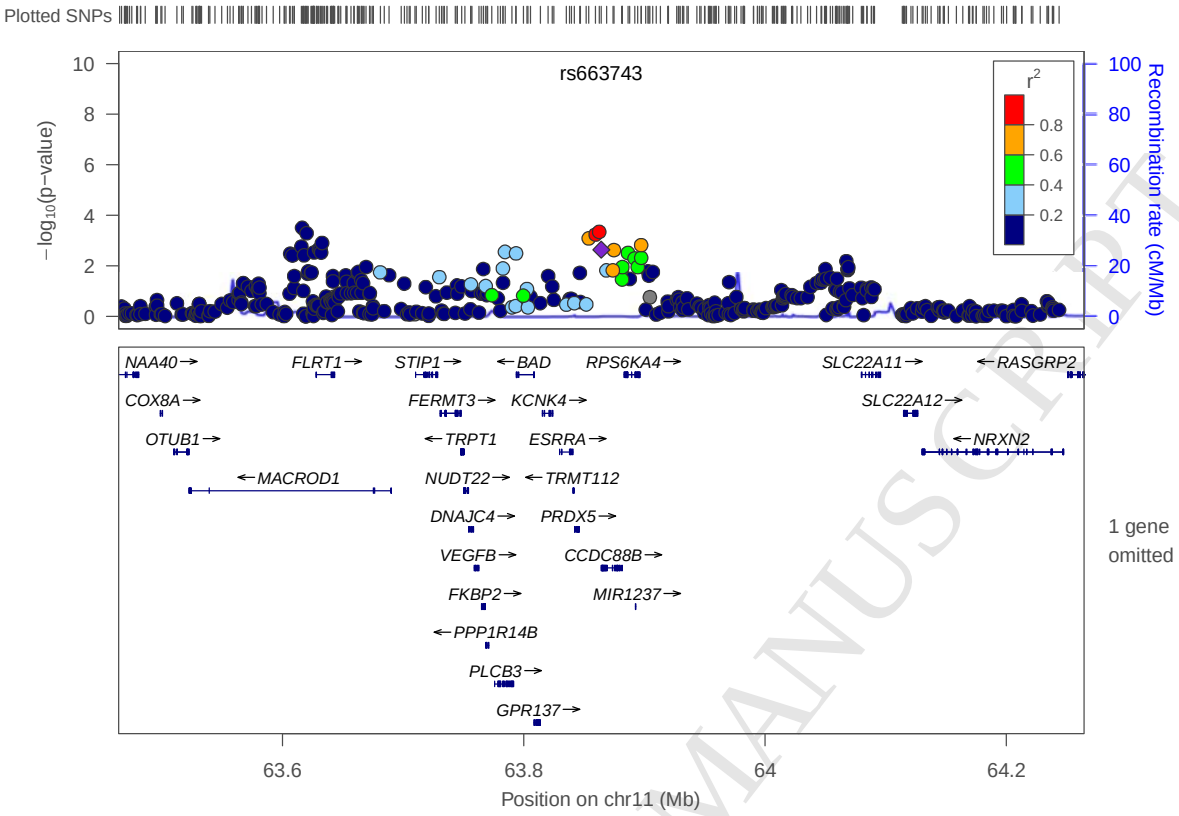

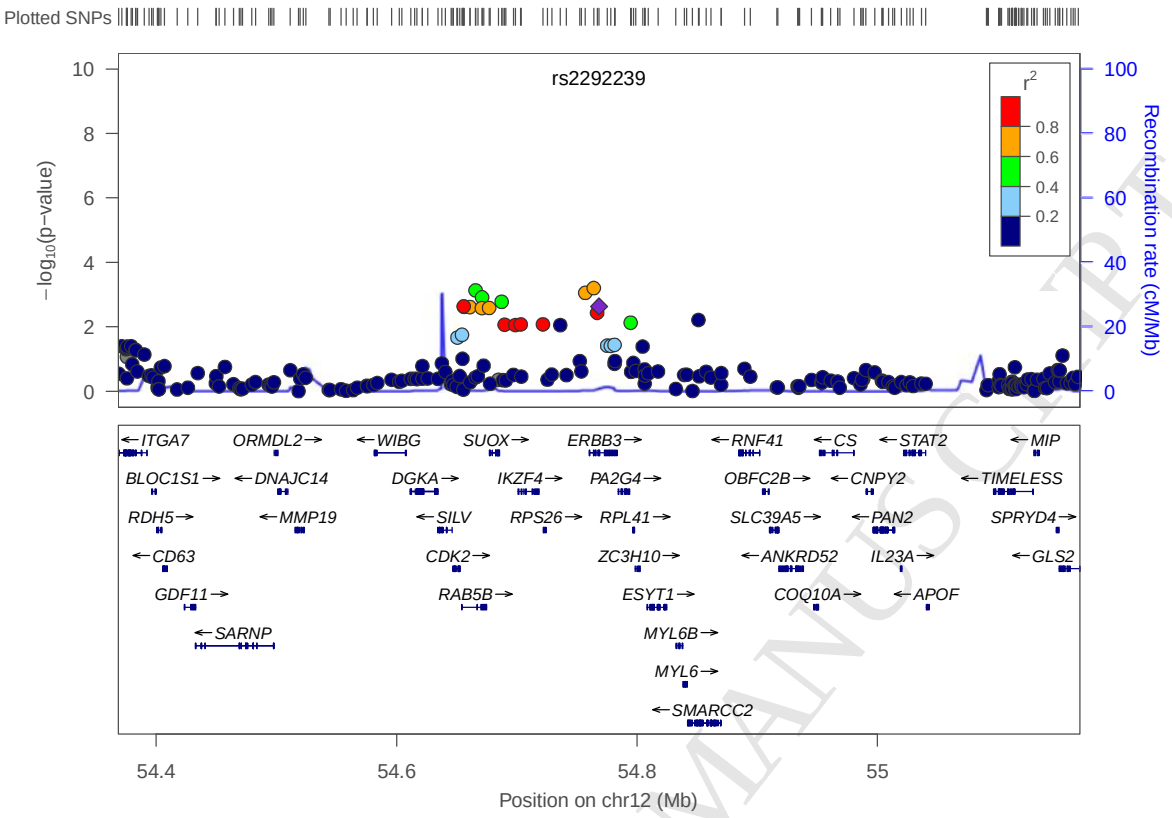

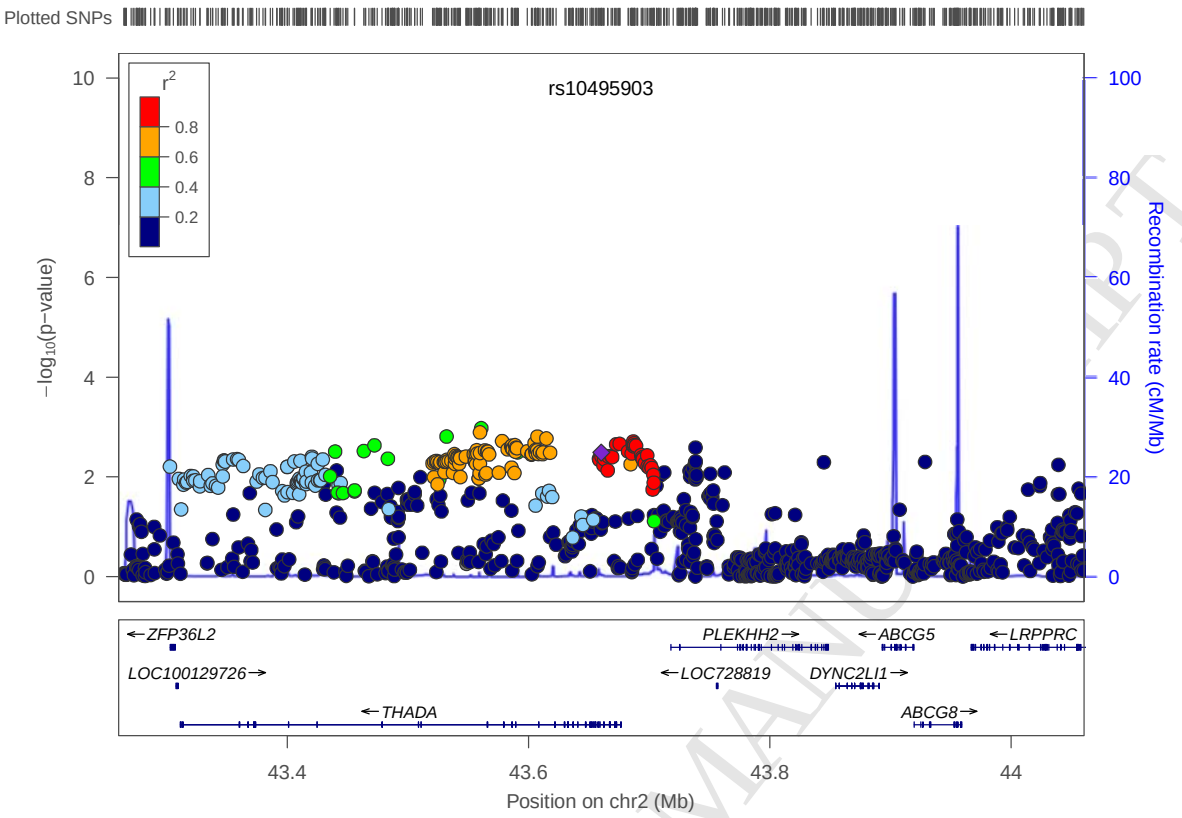

## Supplementary Figure 20

Paired LocusZoom plots within a Crohn's data[17] meta-analysis (top panel) and the allergy meta-analysis (bottom panel) for the 5 most significant shared loci.

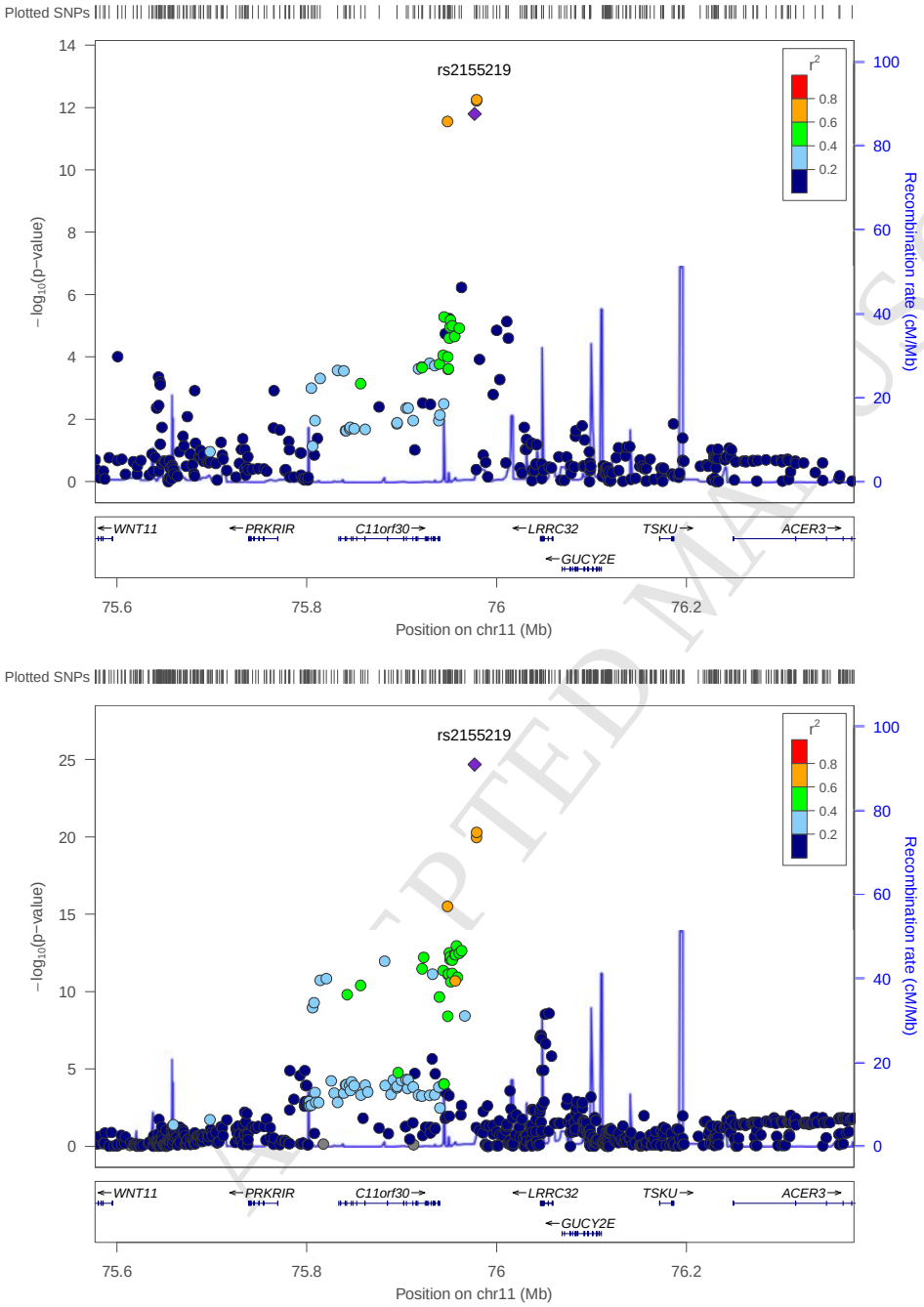

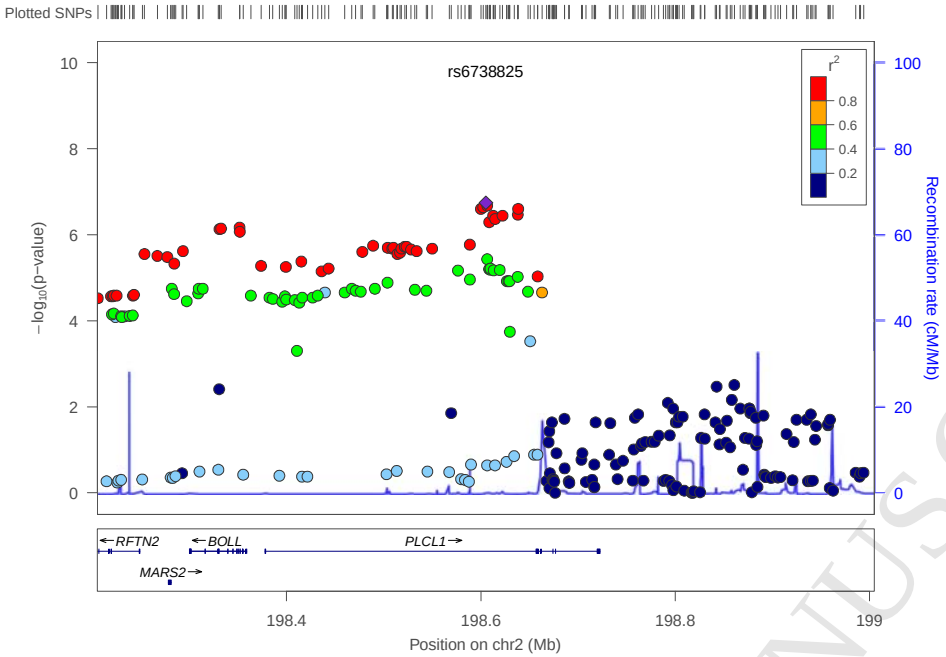


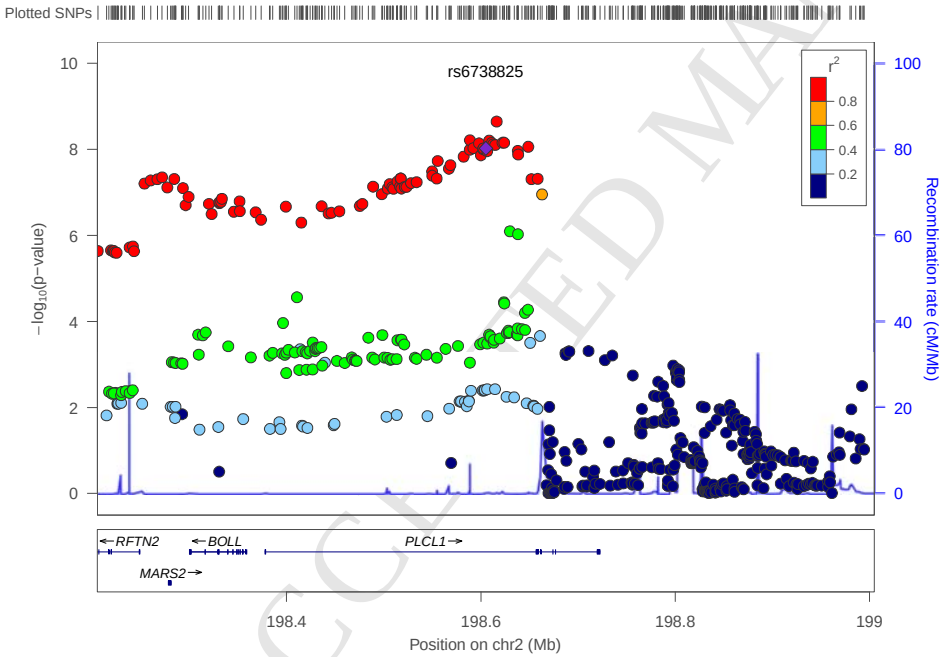

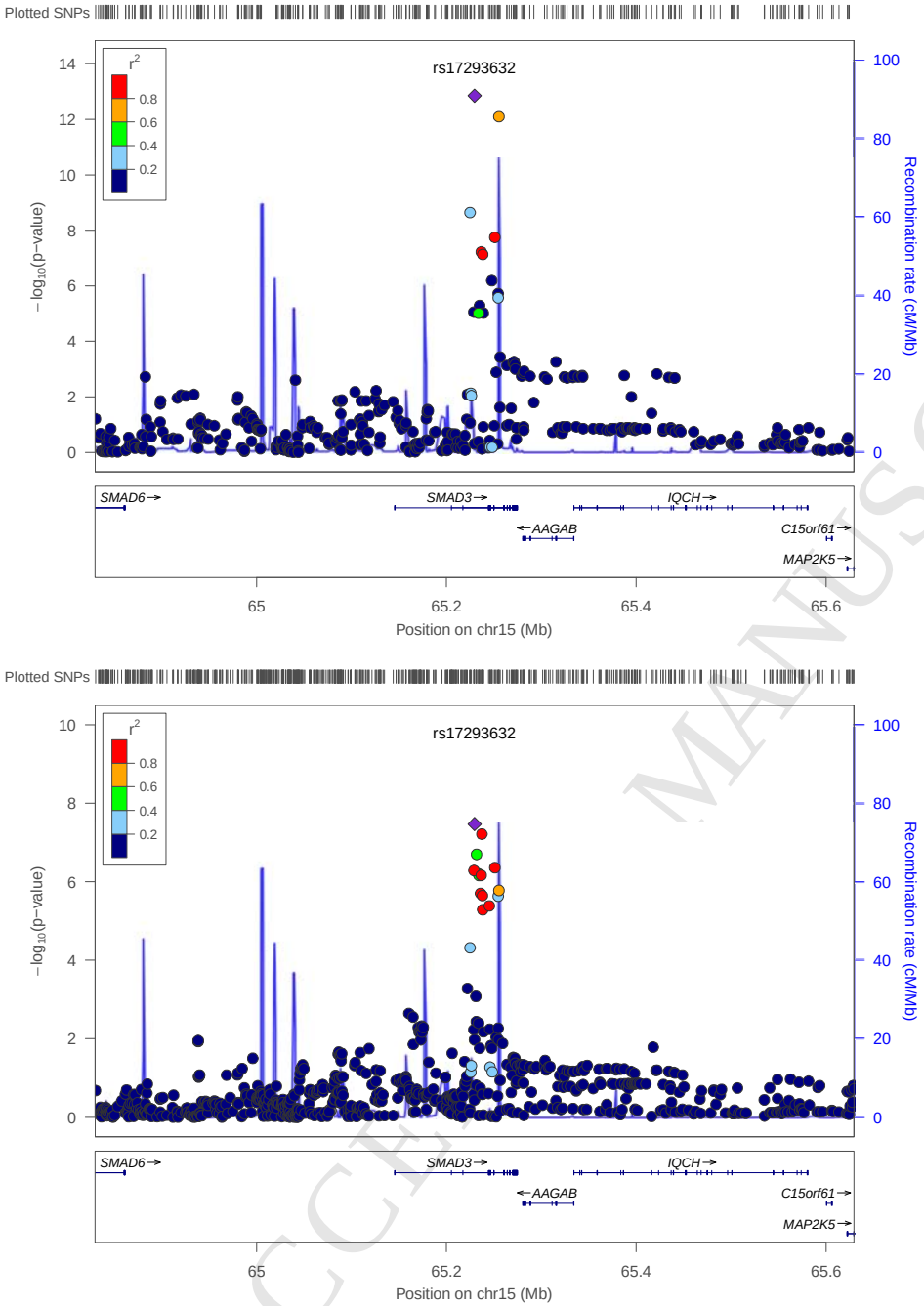

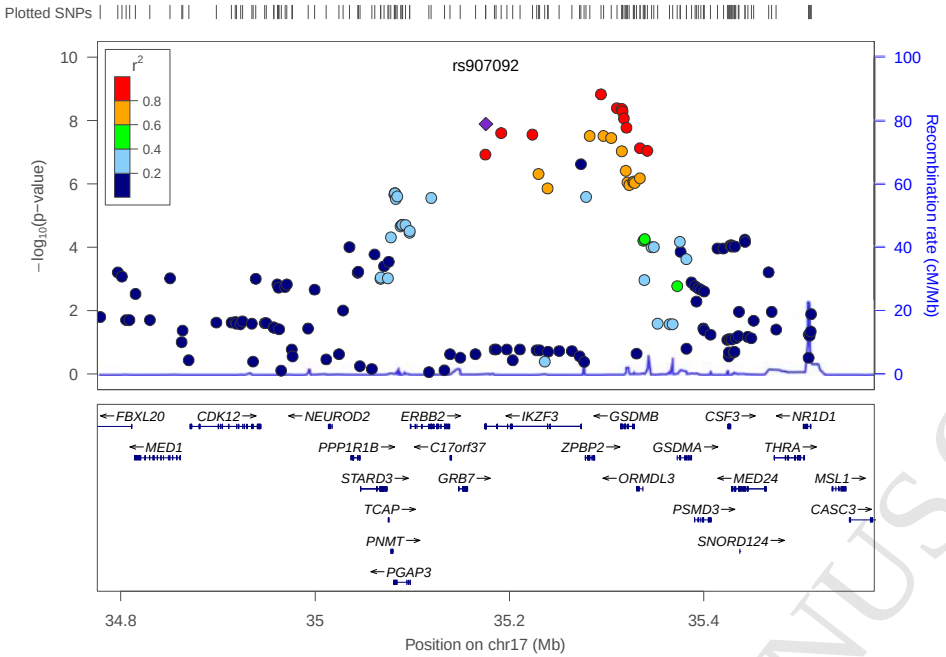


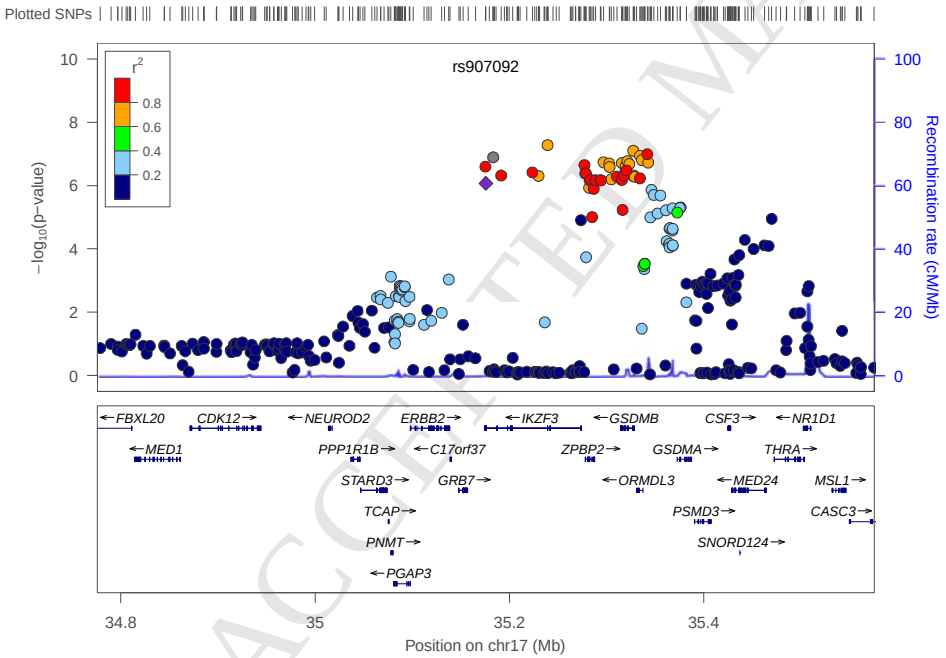

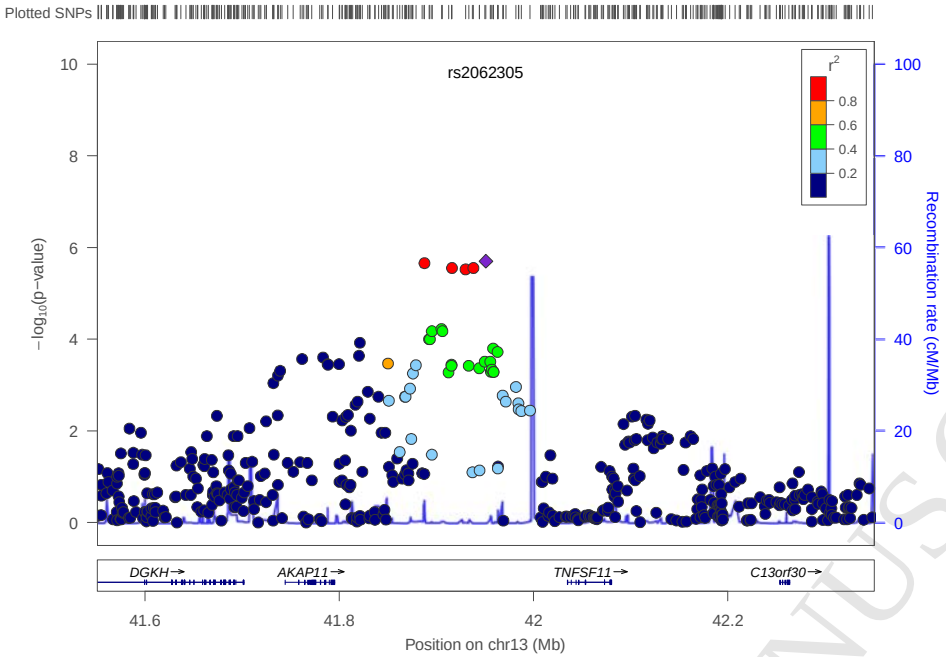


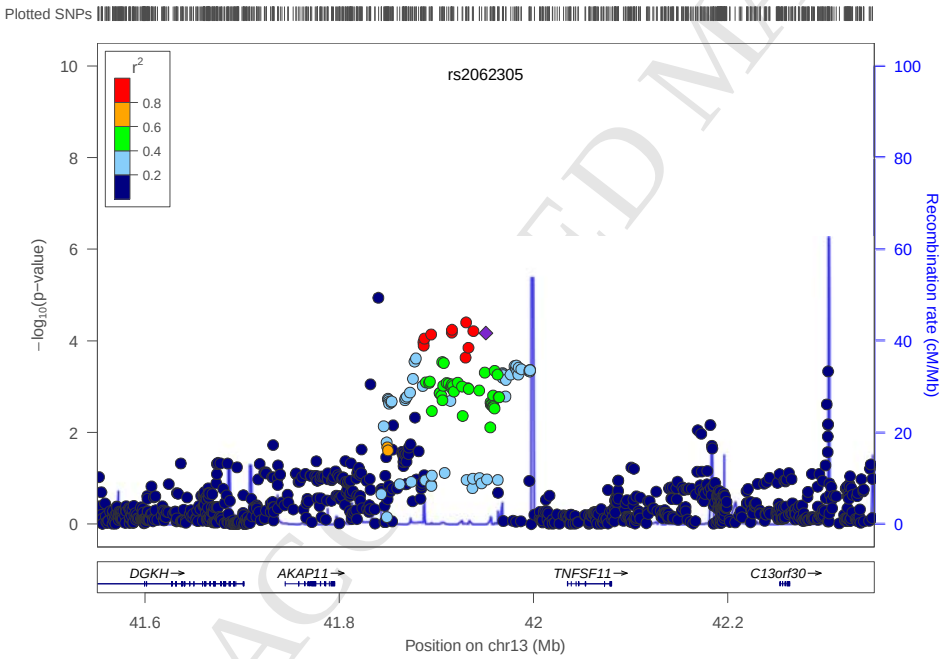

## Supplementary Figure 21

ENCODE Roadmap DHS region overlap with genomic features. DHS regions for each cell type (vertical lines) were overlapped with genomic features (exons, introns, promoters, and intergenic (remaining)) (horizontal lines). Overlaps were z-scaled within each feature, and a heatmap was generated after hierarchical clustering. Immune cells are marked in red at bottom.

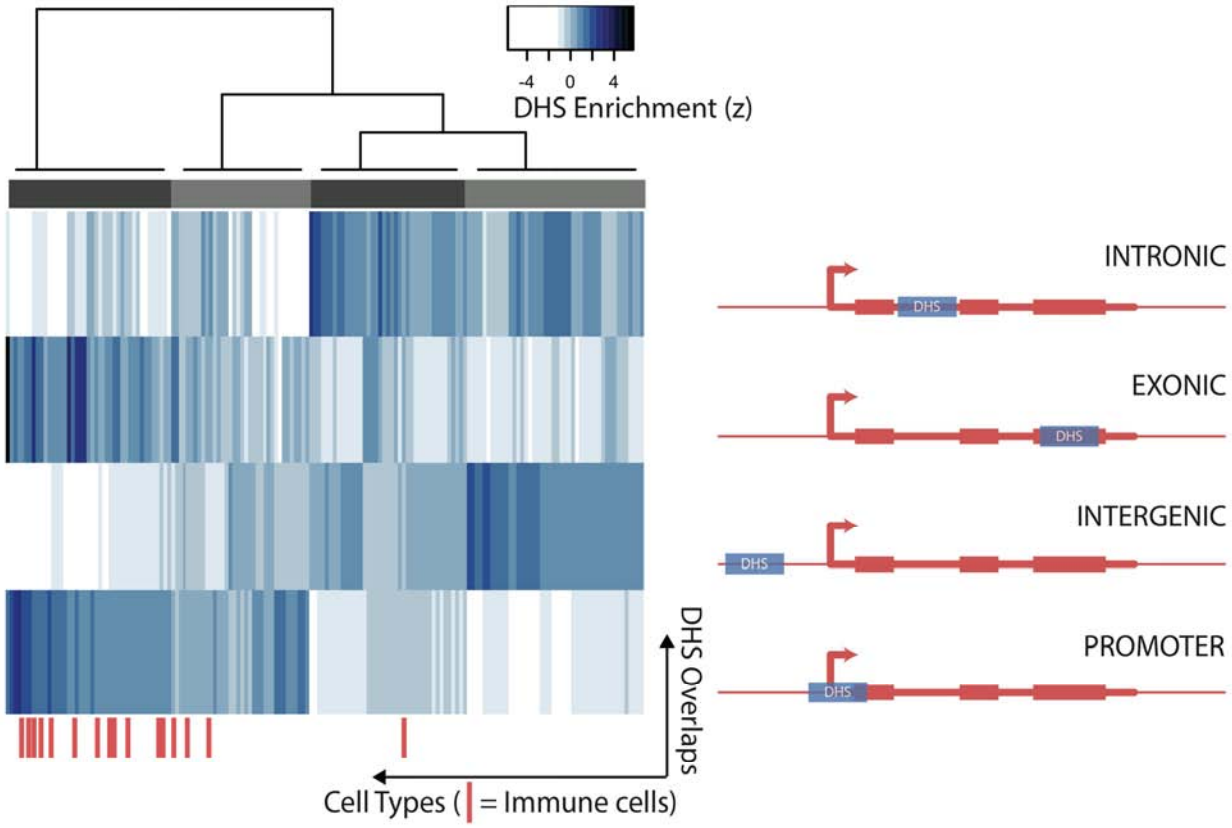

## Supplementary Figure 22

Association plot for rs11122898 with added enhancer regions for four cell types, as well as enhancer-to gene regulatory associations, from the FANTOM5 data repository[19].

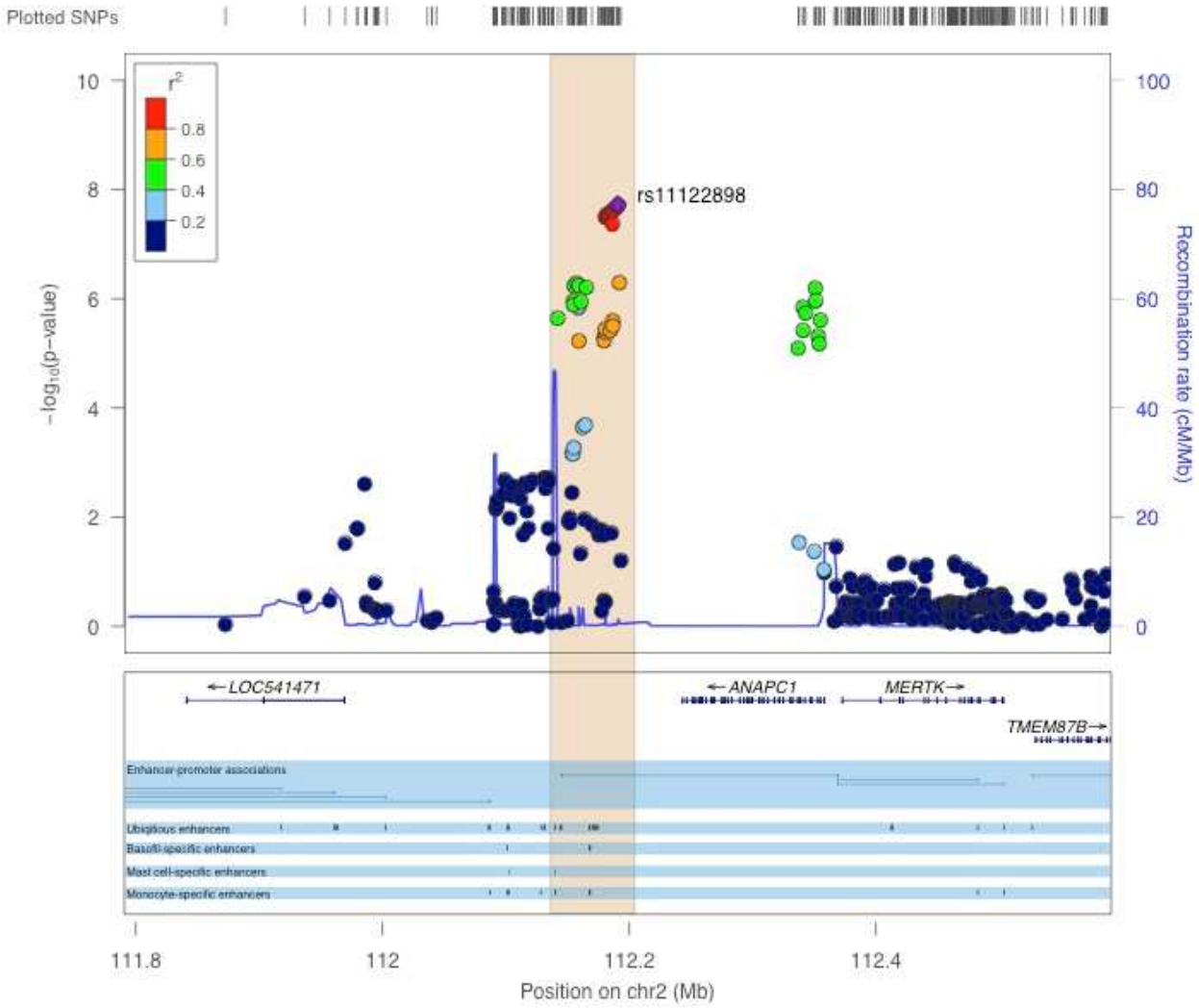

## Supplement references

1. Boyd A, Golding J, Macleod J, Lawlor DA, Fraser A, Henderson J, et al. Cohort Profile: the "children of the 90s"--the index offspring of the Avon Longitudinal Study of Parents and Children. Int J Epidemiol. 2013 Feb;42(1):111–27.
2. Bønnelykke K, Matheson MC, Pers TH, Granell R, Strachan DP, Alves AC, et al. Meta-analysis of genome-wide association studies identifies ten loci influencing allergic sensitization. Nat Genet. 2013 Aug;45(8):902–6.
3. Hinds DA, McMahon G, Kiefer AK, Do CB, Eriksson N, Evans DM, et al. A genome-wide association meta-analysis of self-reported allergy identifies shared and allergy-specific susceptibility loci. Nat Genet. 2013 Aug;45(8):907–11.
4. Willer CJ, Li Y, Abecasis GR. METAL: fast and efficient meta-analysis of genomewide association scans. Bioinforma Oxf Engl. 2010 Sep 1;26(17):2190–1.
5. Hindorff L, Junkins H, Hall P, Metha J, Manolio T. A Catalog of Published Genome-Wide Association Studies [Internet]. [cited 2011 Sep 22]. Available from: www.genome.gov/gwastudies/
6. Parkes M, Cortes A, van Heel DA, Brown MA. Genetic insights into common pathways and complex relationships among immune-mediated diseases. Nat Rev Genet [Internet]. 2013 Aug 6 [cited 2013 Aug 12];advance online publication. Available from: http://www.nature.com.ep.fjernadgang.kb.dk/nrg/journal/vaop/ncurrent/abs/nrg3502.html
7. Purcell S, Neale B, Todd-Brown K, Thomas L, Ferreira MAR, Bender D, et al. PLINK: a tool set for whole-genome association and population-based linkage analyses. Am J Hum Genet. 2007 Sep;81(3):559–75.
8. R Core Team. R: A language and environment for statistical computing. Vienna, Austria: R Foundation for Statistical Computing; 2014.
9. Consortium TEP. An integrated encyclopedia of DNA elements in the human genome. Nature. 2012 Sep 6;489(7414):57–74.
10. Bernstein BE, Stamatoyannopoulos JA, Costello JF, Ren B, Milosavljevic A, Meissner A, et al. The NIH Roadmap Epigenomics Mapping Consortium. Nat Biotechnol. 2010 Oct;28(10):1045–8.
11. Pers TH, Karjalainen JM, Chan Y, Westra HJ, Wood AR, Yang J, et al. Biological interpretation of genome-wide association studies using predicted gene functions. Nat Commun. 2015 Jan 19;6:5890.
12. Cvejic A, Haer-Wigman L, Stephens JC, Kostadima M, Smethurst PA, Frontini M, et al. SMIM1 underlies the Vel blood group and influences red blood cell traits. Nat Genet. 2013 May;45(5):542–5.
13. Lage K, Karlberg EO, Størling ZM, Olason PI, Pedersen AG, Rigina O, et al. A human phenome-interactome network of protein complexes implicated in genetic disorders. Nat Biotechnol. 2007 Mar;25(3):309–16.
14. Bult CJ, Richardson JE, Blake JA, Kadin JA, Ringwald M, Eppig JT, et al. Mouse genome informatics in a new age of biological inquiry. IEEE International Symposium on Bio-Informatics and Biomedical Engineering, 2000 Proceedings. 2000. p. 29–32.

15. Croft D, O'Kelly G, Wu G, Haw R, Gillespie M, Matthews L, et al. Reactome: a database of reactions, pathways and biological processes. Nucleic Acids Res. 2011 Jan;39(Database issue):D691–7.
16. Kanehisa M, Goto S, Sato Y, Furumichi M, Tanabe M. KEGG for integration and interpretation of large-scale molecular data sets. Nucleic Acids Res. 2012 Jan;40(Database issue):D109–14.
17. Ashburner M, Ball CA, Blake JA, Botstein D, Butler H, Cherry JM, et al. Gene ontology: tool for the unification of biology. The Gene Ontology Consortium. Nat Genet. 2000 May;25(1):25–9.
18. Franke A, McGovern DPB, Barrett JC, Wang K, Radford-Smith GL, Ahmad T, et al. Genome-wide meta-analysis increases to 71 the number of confirmed Crohn's disease susceptibility loci. Nat Genet. 2010 Dec;42(12):1118–25.
19. Andersson R, Gebhard C, Miguel-Escalada I, Hoof I, Bornholdt J, Boyd M, et al. An atlas of active enhancers across human cell types and tissues. Nature. 2014 Mar 27;507(7493):455–61.

## Traits for lookup within the GWA catalog

*Trait name within the GWA'catalog collapsed to 16 overall traits*

| COLLAPSED | GWAS CATALOG TRAIT NAME(S) |
|---|---|
| Ankylosing spondylitis | Ankylosing spondylitis |
| Arthritis | Arthritis (juvenile idiopathic), Celiac disease and Rheumatoid arthritis, Psoriatic arthritis, Rheumatoid arthritis |
| Celiac Disease | Celiac disease, Celiac disease and Rheumatoid arthritis, Crohn's disease and celiac disease |
| Crohn's Disease | Crohn's disease, Crohn's disease and celiac disease, Crohn's disease and psoriasis, Crohn's disease and sarcoidosis (combined) |
| Graves' Disease | Graves' disease |
| Inflammatory Bowel Disease | Crohn's disease, Crohn's disease and celiac disease, Crohn's disease and psoriasis, Crohn's disease and sarcoidosis (combined), Inflammatory bowel disease, Inflammatory bowel disease (early onset), Ulcerative colitis |
| Multiple Sclerosis | Multiple sclerosis, Multiple sclerosis (age of onset), Multiple sclerosis (severity), Multiple sclerosis--Brain Glutamate Levels |
| Myasthenia Gravis | Myasthenia gravis |
| Primary Biliary Cirrhosis | Primary biliary cirrhosis |
| Primary Sclerosing Cholangitis | Primary sclerosing cholangitis |
| Psoriasis | Crohn's disease and psoriasis, Psoriasis |
| Sarcoidosis | Crohn's disease and sarcoidosis (combined), Sarcoidosis |
| Systemic Lupus Erythematosus | Systemic lupus erythematosus |
| Systemic Sclerosis | Systemic sclerosis |
| Type 1 Diabetes | Diabetes (incident), Type 1 diabetes, Type 1 diabetes autoantibodies, Type 1 diabetes nephropathy |
| Ulcerative Colitis | Ulcerative colitis |

# The two trait strata used in figure 1

**Allergy-related and auto-immune traits**

Allergy
Asthma
Celiac disease
Crohns
Inflammatory bowel disease
Multiple sclerosis
Primary biliary cirrhosis
Psoriasis
Rheumatoid arthritis
Systemic lupus erythematosus
Type 1 diabetes
Ulcerative colitis
Vitiligo

**Other traits**

Acute lymphoblastic leukemia -childhood-
Adiponectin levels
Age-related macular degeneration
Airflow obstruction
Alcohol dependence
Amyotrophic lateral sclerosis
Attention deficit hyperactivity disorder
Autism spectrum disorder, attention deficit-hyperactivity disorder, bipolar disorder, major depressive disorder, and schizophrenia -combined-
Bilirubin levels
Bipolar disorder
Bipolar disorder and schizophrenia
Bladder cancer
Blood pressure
Body mass index
Bone mineral density
Bone mineral density -spine-
Breast cancer
Breast size
C-reactive protein
Cardiovascular disease risk factors
Cholesterol, total
Chronic kidney disease

Chronic lymphocytic leukemia
Chronic obstructive pulmonary disease-related biomarkers
Cognitive performance
Colorectal cancer
Corneal astigmatism
Corneal structure
Coronary artery calcification
Coronary heart disease
Dental caries
Diastolic blood pressure
Disc degeneration -lumbar-
Fasting glucose-related traits
Fasting glucose-related traits -interaction with BMI-
Fibrinogen
HDL cholesterol
Heart rate
Hippocampal atrophy
HIV-1 control
Hypertension
Immune reponse to smallpox -secreted IFN-alpha-
Immune response to smallpox vaccine -IL-6-
Iron status biomarkers
LDL cholesterol
Lipid metabolism phenotypes
Longevity
Lung cancer
Major depressive disorder
Mean corpuscular hemoglobin
Mean corpuscular volume
Mean platelet volume
Menarche -age at onset-
Menopause -age at onset-
Metabolic syndrome
Metabolic traits
Metabolite levels
Migraine
Migraine - clinic-based
Migraine without aura
Myopia -pathological-
Obesity
Orofacial clefts

Pancreatic cancer
Periodontitis -Mean PAL-
Personality dimensions
Phospholipid levels -plasma-
Platelet counts
Prostate cancer
Prostate cancer -gene x gene interaction-
Protein quantitative trait loci
Pulmonary function
Pulmonary function -interaction-
Pulmonary function decline
QT interval
Quantitative traits
Red blood cell traits
Response to amphetamines
Response to antipsychotic treatment
Response to statin therapy
Response to tocilizumab in rheumatoid arthritis
Schizophrenia
Sex hormone-binding globulin levels
Smoking behavior
Subcutaneous adipose tissue
Sudden cardiac arrest
Systolic blood pressure
Testicular germ cell tumor
Thiazide-induced adverse metabolic effects in hypertensive patients
Thyroid hormone levels
Triglycerides
Tuberculosis
Type 2 diabetes
Urate levels
Uric acid levels
Visceral adipose tissue adjusted for BMI
Visceral adipose tissue-subcutaneous adipose tissue ratio
Visceral fat
Weight

## Top loci allergy meta-analysis

| Chr:BP | Gene | SNP | Effect Allele | Beta | P | I^2 | Het. P | Beta, 23andMe | Beta, Eagle | Effect Allele Freq. Eagle | Previous associations with allergy or related traits |
|---|---|---|---|---|---|---|---|---|---|---|---|
| 2:198616285 | PLCL1 | rs745899 | a | 0.07 | 2.3E-09 | 0 | 3.9E-01 | 0.07 | 0.05 | 0.52 | Hinds et al. |
| 2:8359186 | | rs13416555 | c | 0.08 | 5.9E-10 | -45.7 | 1.5E-01 | 0.07 | 0.11 | 0.69 | Hinds et al. |
| 2:102280646 | IL1RL1,IL18R1 | rs11690644 | a | 0.15 | 3.3E-18 | 0 | 7.3E-01 | 0.14 | 0.16 | 0.86 | Bønnelykke et al + Hinds et al |
| 3:189611673 | LPP | rs9860547 | a | 0.08 | 9.2E-12 | -43.5 | 1.5E-01 | 0.07 | 0.11 | 0.43 | Bønnelykke et al + Hinds et al |
| 4:38476105 | FAM114A1, TLR1, TLR10 | rs4833095 | t | 0.14 | 2.3E-25 | 49.8 | 1.5E-02 | 0.12 | 0.21 | 0.80 | Bønnelykke et al + Hinds et al |
| 4:123548812 | ADAD1 | rs17388568 | a | 0.08 | 1.7E-10 | -89.6 | 2.1E-01 | 0.07 | 0.11 | 0.32 | Bønnelykke et al + Hinds et al |
| 5:40522653 | PTGER4 | rs7720838 | t | 0.08 | 1.1E-11 | 0 | 3.3E-01 | 0.08 | 0.05 | 0.58 | Hinds et al. |
| 5:110495398 | WDR36 | rs1438673 | t | -0.11 | 2.8E-22 | 0 | 9.5E-01 | -0.11 | -0.11 | 0.51 | Bønnelykke et al + Hinds et al |
| 6:31460092 | HLA-B … | rs9266772 | t | -0.10 | 7.8E-12 | 0 | 6.7E-01 | -0.10 | -0.11 | 0.81 | Bønnelykke et al + Hinds et al |
| 6:32734289 | HLA-DCB1 … | rs6906021 | t | -0.10 | 1.8E-19 | 14.3 | 6.1E-02 | -0.09 | -0.15 | 0.56 | Bønnelykke et al + Hinds et al |
| 8:81452180 | ZBTB10 | rs4739737 | t | -0.07 | 2.8E-09 | -12.4 | 1.0E-01 | -0.06 | -0.11 | 0.65 | Hinds et al. |
| 8:128884211 | MYC | rs4410871 | t | 0.06 | 1E-06 | 73 | 8.6E-04 | 0.04 | 0.15 | 0.28 | Bønnelykke et al + Hinds et al |
| 9:6209176 | IL33 | rs2066362 | t | 0.09 | 6.4E-09 | 0 | 3.5E-01 | 0.10 | 0.06 | 0.16 | Hinds et al. |
| 10:8971799 | | rs11255965 | a | -0.22 | 1.8E-10 | 0 | 3.3E-01 | -0.20 | -0.30 | 0.03 | Hinds et al. |
| 11:75976842 | C11ORF30 | rs2155219 | t | 0.12 | 2.1E-25 | 61.5 | 5.2E-03 | 0.10 | 0.18 | 0.47 | Bønnelykke et al + Hinds et al |
| 11:127693112 | ETS1 | rs970924 | a | -0.06 | 1.9E-07 | 0 | 6.2E-01 | -0.06 | -0.05 | 0.53 | Hinds et al. |
| 12:55775976 | STAT6, LRP1 | rs1059513 | t | 0.10 | 3.4E-08 | 85.3 | 6.3E-06 | 0.07 | 0.29 | 0.90 | Bønnelykke et al. |
| 15:65229650 | SMAD3 | rs17293632 | t | 0.07 | 3.4E-08 | -75.5 | 1.9E-01 | 0.08 | 0.04 | 0.27 | Hinds et al. |
| 16:11138204 | CLEC16A | rs7203459 | t | 0.07 | 5.4E-07 | -157.7 | 2.8E-01 | 0.07 | 0.03 | 0.75 | Hinds et al. |
| 16:27318330 | IL21R | rs2107357 | a | 0.09 | 2.4E-07 | 0 | 8.1E-01 | 0.09 | 0.08 | 0.12 | Hinds et al. |
| 17:35239327 | IKZF3, ZPBP2 | rs3816470 | a | 0.06 | 5.3E-08 | 0 | 1.0E+00 | 0.06 | 0.06 | 0.46 | Hinds et al. |
| 20:49576030 | NFATC2 | rs6126249 | a | -0.14 | 4.7E-08 | -99.6 | 2.2E-01 | -0.15 | -0.06 | 0.06 | Hinds et al. |
| 2:112190645 | ANAPC1 | rs11122898 | a | -0.07 | 1.90E-08 | 22.5 | 4.9E-02 | -0.06 | -0.11 | 0.53 | **Novel** |
| 3:142640902 | ZBTB38 | rs7612543 | t | 0.06 | 1.00E-07 | -46.6 | 1.5E-01 | 0.05 | 0.10 | 0.43 | **Novel (1)** |
| 4:103749001 | NFKB1 | rs9790601 | a | 0.07 | 7.40E-08 | -10 | 9.9E-02 | 0.06 | 0.11 | 0.67 | **Novel (2,3)** |
| 5:132024399 | IL4, IL13, RAD50 | rs848 | a | 0.08 | 3.50E-08 | -167.3 | 2.9E-01 | 0.07 | 0.11 | 0.27 | 4-8 |
| 10:6119852 | IL2RA, IL15RA | rs7072398 | a | -0.06 | 5.20E-07 | 0 | 7.5E-01 | -0.06 | -0.05 | 0.45 | 9-14 |

| | | | | | | | | | | | |
|---|---|---|---|---|---|---|---|---|---|---|---|
| 11:118248496 | CXCR5 | rs12365699 | a | -0.08 | 6.50E-07 | -93.4 | 2.1E-01 | -0.07 | -0.12 | 0.17 | **Novel (15-19)** |
| 15:58842703 | RORA | rs12900122 | t | -0.09 | 3.50E-07 | 28.2 | 4.1E-02 | -0.07 | -0.15 | 0.15 | 5 |

1: Height (Gudbjartsson DF, Nat Genet, 2008)
2: Schizophrenia (Liou YJ, Plos One, 2012)
3: IBD (Jostins L, Nature, 2012)
4: Eczema (Hirota, Nat Genet, 2012)
5: Asthma (Moffatt, NEJM, 2010)
6: Eosinophil counts (Gudbjartsson DF, Nat Genet, 2009)
7: Psoriases (Nair RP, Nat Genet, 2009)
8: Hodgkin's lymphoma (Urayama KY, J Natl Cancer Inst, 2012)
9: IBD (Jostins L, Nature, 2012)
10: Rheumatoid arthritis (Stahl EA, Nat Genet, 2010)
11: Multiple sclerosis (Sawcer S, Nature, 2011)
12: Alopecia areata (Petukhova L, Nature, 2010)
13: Type 1 diabetes (Barrett JC, Nat Genet, 2009)
14: Asthma and hayfever (Ferreira, JACI 2014)
15: Systemic lupus erythematosus (Han JW, Nat Genet, 2009)
16: Height (Lango Allen H, Nature, 2010)
17: Celiac disease and Rheumatoid arthritis (Zhernakova A, PloS Genet, 2011)
18: Vitiligo (Tang XF, J Invest Dermatol, 2012)
19: Primary biliary cirrhosis (Mells GF, Nat Genet, 2011)

**Enrichment analyses for various P thresholds**

| | | P<0.05 | | | | | | P<0.01 | | | | | | P<0.001 | | | | | |
|---|---|---|---|---|---|---|---|---|---|---|---|---|---|---|---|---|---|---|---|
| Phenotype | # Loci | # Sig Loci | Prop. Sig | eOR | OR low. | OR up. | P | # Sig Loci | Prop. Sig | eOR | OR low. | OR up. | P | # Sig Loci | Prop. Sig | eOR | OR low. | OR up. | P |
| All Autoimmune Loci | 290 | 57 | 0.20 | 4.36 | 3.20 | 5.85 | 1.4E-17 | 33 | 0.11 | 10.12 | 6.81 | 14.60 | 2.6E-21 | 24 | 0.08 | 34.35 | 21.51 | 52.55 | 5.9E-28 |
| Inflammatory Bowel Disease | 178 | 42 | 0.24 | 5.51 | 3.80 | 7.84 | 2.6E-16 | 22 | 0.12 | 11.12 | 6.76 | 17.47 | 1.7E-15 | 16 | 0.09 | 37.61 | 20.90 | 63.30 | 9.3E-20 |
| Crohn's Disease | 97 | 26 | 0.27 | 6.53 | 4.00 | 10.36 | 5.0E-12 | 17 | 0.18 | 16.75 | 9.29 | 28.56 | 7.0E-15 | 11 | 0.11 | 48.67 | 23.34 | 92.03 | 3.5E-15 |
| Ulcerative Colitis | 60 | 16 | 0.27 | 6.48 | 3.41 | 11.72 | 6.4E-08 | 8 | 0.13 | 12.13 | 4.97 | 25.72 | 8.7E-07 | 7 | 0.12 | 50.25 | 19.24 | 111.30 | 3.0E-10 |
| Multiple Sclerosis | 54 | 12 | 0.22 | 5.09 | 2.44 | 9.86 | 2.1E-05 | 7 | 0.13 | 11.74 | 4.47 | 26.16 | 5.1E-06 | 5 | 0.09 | 38.86 | 12.05 | 97.56 | 3.6E-07 |
| Type 1 Diabetes | 43 | 8 | 0.19 | 4.07 | 1.63 | 8.94 | 1.7E-03 | 7 | 0.16 | 15.33 | 5.75 | 34.95 | 1.1E-06 | 6 | 0.14 | 61.76 | 21.25 | 148.72 | 1.9E-09 |
| Arthritis | 40 | 9 | 0.23 | 5.18 | 2.17 | 11.14 | 2.0E-04 | 6 | 0.15 | 13.91 | 4.77 | 33.58 | 1.0E-05 | 5 | 0.13 | 54.43 | 16.60 | 140.44 | 7.6E-08 |
| Celiac Disease | 36 | 11 | 0.31 | 7.85 | 3.48 | 16.53 | 1.7E-06 | 9 | 0.25 | 26.26 | 10.87 | 57.63 | 5.3E-10 | 6 | 0.17 | 76.15 | 25.85 | 186.24 | 6.0E-10 |
| Systemic Lupus Erythematosus | 27 | 4 | 0.15 | 3.10 | 0.78 | 9.07 | 5.3E-02 | 2 | 0.07 | 6.31 | 0.72 | 25.30 | 4.5E-02 | 2 | 0.07 | 30.47 | 3.49 | 122.65 | 2.3E-03 |
| Primary Biliary Cirrosis | 23 | 7 | 0.30 | 7.80 | 2.71 | 20.03 | 1.4E-04 | 5 | 0.22 | 21.89 | 6.35 | 61.23 | 8.6E-06 | 4 | 0.17 | 80.09 | 19.79 | 241.44 | 4.0E-07 |
| Psoriasis | 19 | 4 | 0.21 | 4.75 | 1.15 | 14.93 | 1.6E-02 | 4 | 0.21 | 21.02 | 5.08 | 65.99 | 8.2E-05 | 3 | 0.16 | 71.24 | 13.31 | 249.62 | 1.7E-05 |
| Graves Disease | 15 | 3 | 0.20 | 4.46 | 0.81 | 16.52 | 4.2E-02 | 3 | 0.20 | 19.71 | 3.57 | 72.90 | 8.0E-04 | 3 | 0.20 | 95.24 | 17.21 | 355.76 | 8.0E-06 |
| Ankylosing Spondylitis | 11 | 2 | 0.18 | 3.96 | 0.42 | 19.14 | 1.1E-01 | 2 | 0.18 | 17.52 | 1.84 | 84.71 | 8.0E-03 | 2 | 0.18 | 84.66 | 8.88 | 406.25 | 3.7E-04 |

## DEPICT gene set enrichment analysis for allergy

| Original gene set ID | Original gene set description | Nominal P value | False discovery rate |
|---|---|---|---|
| MP:0002362 | abnormal spleen marginal zone morphology | 1.44E-08 | 0 |
| MP:0002743 | glomerulonephritis | 2.04E-08 | 0 |
| ENSG00000142208 | AKT1 subnetwork | 6.22E-08 | 0 |
| GO:0030097 | hemopoiesis | 1.77E-07 | 0 |
| GO:0048534 | hemopoietic or lymphoid organ development | 3.01E-07 | 0 |
| MP:0000693 | spleen hyperplasia | 3.03E-07 | 0 |
| MP:0001823 | thymus hypoplasia | 3.26E-07 | 0 |
| MP:0000703 | abnormal thymus morphology | 4.04E-07 | 0 |
| MP:0001859 | kidney inflammation | 7.05E-07 | 0 |
| GO:0051251 | positive regulation of lymphocyte activation | 7.17E-07 | 0 |
| MP:0008482 | decreased spleen germinal center number | 8.67E-07 | 0 |
| GO:0012502 | induction of programmed cell death | 2.72E-06 | 0.001923077 |
| GO:0002696 | positive regulation of leukocyte activation | 2.59E-06 | 0.002 |
| GO:0032943 | mononuclear cell proliferation | 8.63E-06 | 0.002 |
| MP:0010766 | abnormal NK cell physiology | 8.04E-06 | 0.002040816 |
| GO:0046649 | lymphocyte activation | 2.57E-06 | 0.002083333 |
| MP:0002391 | abnormal Peyer's patch germinal center morphology | 7.76E-06 | 0.002083333 |
| GO:0002521 | leukocyte differentiation | 7.74E-06 | 0.00212766 |
| MP:0004794 | increased anti-nuclear antigen antibody level | 2.43E-06 | 0.002173913 |
| MP:0008102 | lymph node hyperplasia | 7.51E-06 | 0.002173913 |
| GO:0042113 | B cell activation | 7.12E-06 | 0.002222222 |
| MP:0008209 | decreased pre-B cell number | 1.79E-05 | 0.002238806 |
| MP:0000691 | enlarged spleen | 2.21E-06 | 0.002272727 |
| MP:0008082 | increased single-positive T cell number | 7.02E-06 | 0.002272727 |
| ENSG00000091831 | ESR1 subnetwork | 1.78E-05 | 0.002272727 |
| ENSG00000015475 | BID subnetwork | 1.75E-05 | 0.002307692 |
| GO:0050670 | regulation of lymphocyte proliferation | 6.32E-06 | 0.002325581 |
| ENSG00000105639 | JAK3 subnetwork | 1.67E-05 | 0.00234375 |
| GO:0050863 | regulation of T cell activation | 2.19E-06 | 0.002380952 |
| ENSG00000171150 | SOCS5 subnetwork | 6.12E-06 | 0.002380952 |
| ENSG00000198646 | NCOA6 subnetwork | 1.52E-05 | 0.002380952 |
| REACTOME_CD28_CO:STIMULATI | REACTOME_CD28_CO:STIMULATION | 1.50E-05 | 0.002419355 |
| GO:0050870 | positive regulation of T cell activation | 6.03E-06 | 0.002439024 |
| GO:0030099 | myeloid cell differentiation | 1.42E-05 | 0.002459016 |
| MP:0002722 | abnormal immune system organ morphology | 2.11E-06 | 0.0025 |
| GO:0046651 | lymphocyte proliferation | 5.91E-06 | 0.0025 |
| GO:0031295 | T cell costimulation | 1.33E-05 | 0.0025 |
| GO:0031294 | lymphocyte costimulation | 1.33E-05 | 0.002542373 |
| GO:0070661 | leukocyte proliferation | 5.80E-06 | 0.002564103 |
| MP:0005027 | increased susceptibility to parasitic infection | 1.33E-05 | 0.002586207 |
| ENSG00000003400 | CASP10 subnetwork | 1.80E-06 | 0.002631579 |
| MP:0002123 | abnormal hematopoiesis | 5.61E-06 | 0.002631579 |
| MP:0005150 | cachexia | 1.33E-05 | 0.002631579 |
| MP:0002619 | abnormal lymphocyte morphology | 1.26E-05 | 0.002678571 |
| GO:0050865 | regulation of cell activation | 5.60E-06 | 0.002702703 |
| GO:0046631 | alpha-beta T cell activation | 1.05E-05 | 0.002727273 |
| MP:0008215 | decreased immature B cell number | 1.51E-06 | 0.002777778 |
| MP:0006414 | decreased T cell apoptosis | 5.02E-06 | 0.002777778 |
| GO:0042110 | T cell activation | 9.94E-06 | 0.002777778 |
| GO:0032944 | regulation of mononuclear cell proliferation | 9.40E-06 | 0.002830189 |
| MP:0003304 | large intestinal inflammation | 4.82E-06 | 0.002857143 |

| | | | |
|---|---|---|---|
| GO:0070663 | regulation of leukocyte proliferation | 9.34E-06 | 0.002884615 |
| ENSG00000186350 | RXRA subnetwork | 1.41E-06 | 0.002941176 |
| ENSG00000138378 | STAT4 subnetwork | 4.53E-06 | 0.002941176 |
| MP:0002145 | abnormal T cell differentiation | 8.88E-06 | 0.002941176 |
| GO:0050867 | positive regulation of cell activation | 3.75E-06 | 0.003030303 |
| GO:0045321 | leukocyte activation | 1.29E-06 | 0.003125 |
| MP:0000706 | small thymus | 3.67E-06 | 0.003125 |
| MP:0005017 | decreased B cell number | 3.48E-06 | 0.003225806 |
| MP:0005091 | increased double-positive T cell number | 1.28E-06 | 0.003333333 |
| ENSG00000185507 | IRF7 subnetwork | 3.42E-06 | 0.003333333 |
| MP:0008470 | abnormal spleen B cell follicle morphology | 3.38E-06 | 0.003448276 |
| GO:0002694 | regulation of leukocyte activation | 1.25E-06 | 0.003571429 |
| GO:0006917 | induction of apoptosis | 3.34E-06 | 0.003571429 |
| MP:0005463 | abnormal CD4-positive T cell physiology | 1.94E-05 | 0.003676471 |
| MP:0000711 | thymus cortex hypoplasia | 3.30E-06 | 0.003703704 |
| MP:0008553 | increased circulating tumor necrosis factor level | 1.15E-06 | 0.003846154 |
| GO:0051249 | regulation of lymphocyte activation | 9.01E-07 | 0.004166667 |
| MP:0000688 | lymphoid hyperplasia | 1.97E-05 | 0.004347826 |
| MP:0008497 | decreased IgG2b level | 2.12E-05 | 0.005 |
| ENSG00000111537 | IFNG subnetwork | 2.26E-05 | 0.005633803 |
| GO:0042098 | T cell proliferation | 2.49E-05 | 0.005844156 |
| ENSG00000105397 | TYK2 subnetwork | 6.67E-05 | 0.005882353 |
| GO:0030183 | B cell differentiation | 7.80E-05 | 0.005902778 |
| MP:0005348 | increased T cell proliferation | 2.47E-05 | 0.005921053 |
| ENSG00000111679 | PTPN6 subnetwork | 6.59E-05 | 0.005925926 |
| MP:0008474 | absent spleen germinal center | 7.74E-05 | 0.005944056 |
| GO:0002684 | positive regulation of immune system process | 6.59E-05 | 0.005970149 |
| GO:0050864 | regulation of B cell activation | 5.35E-05 | 0.005982906 |
| ENSG00000180008 | SOCS4 subnetwork | 7.17E-05 | 0.005985915 |
| ENSG00000166888 | STAT6 subnetwork | 2.44E-05 | 0.006 |
| MP:0000221 | decreased leukocyte cell number | 8.46E-05 | 0.006 |
| MP:0002459 | abnormal B cell physiology | 6.39E-05 | 0.006015038 |
| MP:0002401 | abnormal lymphopoiesis | 3.02E-05 | 0.006024096 |
| ENSG00000175505 | CLCF1 subnetwork | 7.16E-05 | 0.006028369 |
| ENSG00000172216 | CEBPB subnetwork | 5.34E-05 | 0.006034483 |
| GO:0042100 | B cell proliferation | 8.46E-05 | 0.006040268 |
| MP:0001800 | abnormal humoral immune response | 6.37E-05 | 0.006060606 |
| REACTOME_SIGNALING_BY_EGFR | REACTOME_SIGNALING_BY_EGFR | 7.14E-05 | 0.006071429 |
| MP:0008578 | decreased circulating interferon-gamma level | 2.40E-05 | 0.006081081 |
| MP:0001806 | decreased IgM level | 8.42E-05 | 0.006081081 |
| MP:0004796 | increased anti-histone antibody level | 5.25E-05 | 0.006086957 |
| MP:0001861 | lung inflammation | 2.82E-05 | 0.006097561 |
| ENSG00000177606 | JUN subnetwork | 6.35E-05 | 0.00610687 |
| GO:0050671 | positive regulation of lymphocyte proliferation | 7.14E-05 | 0.006115108 |
| ENSG00000120738 | EGR1 subnetwork | 8.35E-05 | 0.006122449 |
| ENSG00000170345 | FOS subnetwork | 9.20E-05 | 0.006129032 |
| REACTOME_SIGNALING_BY_INTE | REACTOME_SIGNALING_BY_INTERLEUKINS | 4.95E-05 | 0.006140351 |
| MP:0008537 | increased susceptibility to induced colitis | 6.04E-05 | 0.006147541 |
| ENSG00000146904 | EPHA1 subnetwork | 6.24E-05 | 0.006153846 |
| MP:0001873 | stomach inflammation | 6.90E-05 | 0.00615942 |
| GO:0002287 | alpha-beta T cell activation involved in immune response | 2.36E-05 | 0.006164384 |
| ENSG00000030110 | BAK1 subnetwork | 8.04E-05 | 0.006164384 |
| MP:0005014 | increased B cell number | 9.15E-05 | 0.006168831 |
| REACTOME_CD28_DEPENDENT_P | REACTOME_CD28_DEPENDENT_PI3KAKT_SIGNALING | 2.79E-05 | 0.00617284 |

| | | | |
|---|---|---|---|
| MP:0002497 | increased IgE level | 4.94E-05 | 0.00619469 |
| MP:0004762 | increased anti-double stranded DNA antibody level | 5.98E-05 | 0.006198347 |
| ENSG00000096717 | SIRT1 subnetwork | 6.18E-05 | 0.00620155 |
| MP:0008499 | increased IgG1 level | 6.76E-05 | 0.00620438 |
| ENSG00000127191 | TRAF2 subnetwork | 7.95E-05 | 0.006206897 |
| ENSG00000107581 | EIF3A subnetwork | 9.01E-05 | 0.00620915 |
| GO:0002294 | CD4-positive, alpha-beta T cell differentiation involved in | 1.04E-04 | 0.006213018 |
| MP:0008568 | abnormal interleukin secretion | 4.82E-05 | 0.00625 |
| GO:0007260 | tyrosine phosphorylation of STAT protein | 8.71E-05 | 0.00625 |
| GO:0002293 | alpha-beta T cell differentiation involved in immune resp | 2.36E-05 | 0.00625 |
| MP:0008495 | decreased IgG1 level | 2.75E-05 | 0.00625 |
| MP:0003945 | abnormal lymphocyte physiology | 5.98E-05 | 0.00625 |
| MP:0002189 | abnormal myocardial trabeculae morphology | 6.17E-05 | 0.00625 |
| GO:0042093 | T-helper cell differentiation | 1.04E-04 | 0.00625 |
| MP:0005095 | decreased T cell proliferation | 1.02E-04 | 0.006287425 |
| MP:0001805 | decreased IgG level | 8.58E-05 | 0.006291391 |
| ENSG00000084774 | CAD subnetwork | 6.14E-05 | 0.006299213 |
| MP:0005018 | decreased T cell number | 5.86E-05 | 0.006302521 |
| GO:0046634 | regulation of alpha-beta T cell activation | 4.74E-05 | 0.006306306 |
| ENSG00000136488 | CSH1 subnetwork | 1.02E-04 | 0.006325301 |
| ENSG00000064012 | CASP8 subnetwork | 2.72E-05 | 0.006329114 |
| ENSG00000120833 | SOCS2 subnetwork | 6.14E-05 | 0.006349206 |
| MP:0003725 | increased autoantibody level | 5.67E-05 | 0.006355932 |
| ENSG00000168811 | IL12A subnetwork | 4.59E-05 | 0.006363636 |
| MP:0002490 | abnormal immunoglobulin level | 9.96E-05 | 0.006363636 |
| MP:0004816 | abnormal class switch recombination | 9.28E-05 | 0.006369427 |
| ENSG00000131788 | PIAS3 subnetwork | 6.12E-05 | 0.0064 |
| MP:0004804 | decreased susceptibility to autoimmune diabetes | 9.94E-05 | 0.006402439 |
| MP:0001790 | abnormal immune system physiology | 2.72E-05 | 0.006410256 |
| ENSG00000141968 | VAV1 subnetwork | 9.25E-05 | 0.006410256 |
| GO:0035710 | CD4-positive, alpha-beta T cell activation | 4.56E-05 | 0.006422018 |
| REACTOME_SIGNALING_BY_EGFR | REACTOME_SIGNALING_BY_EGFR_IN_CANCER | 1.05E-04 | 0.006432749 |
| GO:0032946 | positive regulation of mononuclear cell proliferation | 9.93E-05 | 0.006441718 |
| MP:0000714 | increased thymocyte number | 6.12E-05 | 0.006451613 |
| MP:0008641 | increased circulating interleukin-1 beta level | 3.15E-05 | 0.006470588 |
| GO:0042509 | regulation of tyrosine phosphorylation of STAT protein | 1.05E-04 | 0.006470588 |
| KEGG_T_CELL_RECEPTOR_SIGNAL | KEGG_T_CELL_RECEPTOR_SIGNALING_PATHWAY | 1.28E-04 | 0.006476684 |
| MP:0002023 | B cell derived lymphoma | 4.47E-05 | 0.006481481 |
| GO:0030888 | regulation of B cell proliferation | 9.84E-05 | 0.006481481 |
| MP:0008083 | decreased single-positive T cell number | 1.36E-04 | 0.0065 |
| ENSG00000100393 | EP300 subnetwork | 6.10E-05 | 0.006504065 |
| GO:0070665 | positive regulation of leukocyte proliferation | 1.22E-04 | 0.006510417 |
| ENSG00000173757 | STAT5B subnetwork | 9.81E-05 | 0.006521739 |
| MP:0001577 | anemia | 1.33E-04 | 0.006532663 |
| MP:0005466 | abnormal T-helper 2 physiology | 4.39E-05 | 0.006542056 |
| MP:0002494 | increased IgM level | 1.22E-04 | 0.006544503 |
| MP:0008475 | intermingled spleen red and white pulp | 3.10E-05 | 0.006547619 |
| MP:0000218 | increased leukocyte cell number | 1.46E-04 | 0.006553398 |
| MP:0005092 | decreased double-positive T cell number | 9.74E-05 | 0.0065625 |
| MP:0002444 | abnormal T cell physiology | 1.33E-04 | 0.006565657 |
| ENSG00000136634 | IL10 subnetwork | 1.21E-04 | 0.006578947 |
| MP:0008075 | decreased CD4-positive T cell number | 1.46E-04 | 0.006585366 |
| MP:0000702 | enlarged lymph nodes | 1.32E-04 | 0.006598985 |
| GO:0046632 | alpha-beta T cell differentiation | 4.34E-05 | 0.006603774 |

| | | | |
|---|---|---|---|
| ENSG00000113302 | IL12B subnetwork | 9.43E-05 | 0.006603774 |
| ENSG00000142273 | CBLC subnetwork | 1.21E-04 | 0.006613757 |
| MP:0006413 | increased T cell apoptosis | 1.44E-04 | 0.006617647 |
| MP:0002371 | abnormal thymus cortex morphology | 1.32E-04 | 0.006632653 |
| MP:0008603 | decreased circulating interleukin-4 level | 9.35E-05 | 0.00664557 |
| ENSG00000184557 | SOCS3 subnetwork | 1.21E-04 | 0.006648936 |
| MP:0008751 | abnormal interleukin level | 1.42E-04 | 0.006650246 |
| MP:0001858 | intestinal inflammation | 4.29E-05 | 0.006666667 |
| MP:0008500 | increased IgG2a level | 1.31E-04 | 0.006666667 |
| ENSG00000110944 | IL23A subnetwork | 1.40E-04 | 0.006683168 |
| MP:0002442 | abnormal leukocyte physiology | 1.20E-04 | 0.006684492 |
| ENSG00000084676 | NCOA1 subnetwork | 1.08E-04 | 0.006686047 |
| MP:0000709 | enlarged thymus | 1.29E-04 | 0.006701031 |
| ENSG00000127318 | IL22 subnetwork | 1.40E-04 | 0.006716418 |
| ENSG00000147873 | IFNA5 subnetwork | 1.19E-04 | 0.00672043 |
| GO:0048872 | homeostasis of number of cells | 4.24E-05 | 0.006730769 |
| MP:0008496 | decreased IgG2a level | 3.32E-05 | 0.006741573 |
| ENSG00000120242 | IFNA8 subnetwork | 1.19E-04 | 0.006756757 |
| MP:0005070 | impaired NK cell cytolysis | 1.49E-04 | 0.006763285 |
| ENSG00000188379 | IFNA2 subnetwork | 1.19E-04 | 0.006793478 |
| MP:0002460 | decreased immunoglobulin level | 4.23E-05 | 0.006796117 |
| MP:0003643 | spleen atrophy | 3.32E-05 | 0.006818182 |
| ENSG00000186803 | IFNA10 subnetwork | 1.19E-04 | 0.006830601 |
| ENSG00000185338 | SOCS1 subnetwork | 4.04E-05 | 0.006862745 |
| ENSG00000147877 | ENSG00000147877 subnetwork | 1.19E-04 | 0.006868132 |
| GO:0043367 | CD4-positive, alpha-beta T cell differentiation | 3.25E-05 | 0.006896552 |
| ENSG00000186809 | ENSG00000186809 subnetwork | 1.19E-04 | 0.006906077 |
| GO:0002285 | lymphocyte activation involved in immune response | 4.03E-05 | 0.006930693 |
| MP:0008049 | increased memory T cell number | 1.12E-04 | 0.006936416 |
| ENSG00000120247 | ENSG00000120247 subnetwork | 1.19E-04 | 0.006944444 |
| MP:0008498 | decreased IgG3 level | 3.23E-05 | 0.006976744 |
| ENSG00000137080 | IFNA21 subnetwork | 1.19E-04 | 0.00698324 |
| ENSG00000164399 | IL3 subnetwork | 3.52E-05 | 0.006989247 |
| MP:0002432 | abnormal CD4-positive T cell morphology | 3.97E-05 | 0.007 |
| ENSG00000147885 | IFNA16 subnetwork | 1.19E-04 | 0.007022472 |
| MP:0001807 | decreased IgA level | 1.18E-04 | 0.007062147 |
| ENSG00000143207 | RFWD2 subnetwork | 3.49E-05 | 0.007065217 |
| ENSG00000132170 | PPARG subnetwork | 3.88E-05 | 0.007070707 |
| GO:0002286 | T cell activation involved in immune response | 1.18E-04 | 0.007102273 |
| GO:0042129 | regulation of T cell proliferation | 3.44E-05 | 0.007142857 |
| MP:0008040 | decreased NK T cell number | 3.75E-05 | 0.007142857 |
| REACTOME_COSTIMULATION_BY | REACTOME_COSTIMULATION_BY_THE_CD28_FAMILY | 1.17E-04 | 0.007142857 |
| MP:0002495 | increased IgA level | 1.16E-04 | 0.007183908 |
| MP:0002492 | decreased IgE level | 1.52E-04 | 0.007211538 |
| GO:0030098 | lymphocyte differentiation | 3.75E-05 | 0.007216495 |
| MP:0008700 | decreased interleukin-4 secretion | 3.39E-05 | 0.007222222 |
| MP:0000715 | decreased thymocyte number | 3.73E-05 | 0.007291667 |
| GO:0046636 | negative regulation of alpha-beta T cell activation | 3.70E-05 | 0.007368421 |
| GO:0002292 | T cell differentiation involved in immune response | 3.69E-05 | 0.007446809 |
| KEGG_INSULIN_SIGNALING_PATH | KEGG_INSULIN_SIGNALING_PATHWAY | 1.60E-04 | 0.007619048 |
| ENSG00000113525 | IL5 subnetwork | 1.56E-04 | 0.007655502 |
| REACTOME_INTERLEUKIN:3_5_AI | REACTOME_INTERLEUKIN:3_5_AND_GM:CSF_SIGNALIN( | 1.63E-04 | 0.007819905 |
| ENSG00000164305 | CASP3 subnetwork | 1.68E-04 | 0.007981221 |
| MP:0008045 | decreased NK cell number | 1.68E-04 | 0.008018868 |

| | | | |
|---|---|---|---|
| ENSG00000101096 | NFATC2 subnetwork | 1.74E-04 | 0.008064516 |
| GO:0045191 | regulation of isotype switching | 1.72E-04 | 0.008101852 |
| MP:0002144 | abnormal B cell differentiation | 1.77E-04 | 0.008108108 |
| ENSG00000072274 | TFRC subnetwork | 1.71E-04 | 0.008139535 |
| MP:0000219 | increased neutrophil cell number | 1.76E-04 | 0.008144796 |
| GO:0051250 | negative regulation of lymphocyte activation | 1.69E-04 | 0.00817757 |
| GO:0050776 | regulation of immune response | 1.76E-04 | 0.008181818 |
| ENSG00000215769 | ENSG00000215769 subnetwork | 1.76E-04 | 0.008219178 |
| ENSG00000182481 | KPNA2 subnetwork | 1.76E-04 | 0.008256881 |
| MP:0001601 | abnormal myelopoiesis | 1.78E-04 | 0.008295964 |
| MP:0004800 | decreased susceptibility to experimental autoimmune er | 2.35E-04 | 0.0086 |
| GO:0045911 | positive regulation of DNA recombination | 2.16E-04 | 0.008606557 |
| ENSG00000134954 | ETS1 subnetwork | 2.32E-04 | 0.008634538 |
| ENSG00000115705 | TPO subnetwork | 2.14E-04 | 0.008641975 |
| ENSG00000186660 | ZFP91 subnetwork | 2.39E-04 | 0.008661417 |
| GO:0042102 | positive regulation of T cell proliferation | 1.85E-04 | 0.008666667 |
| ENSG00000130427 | EPO subnetwork | 2.28E-04 | 0.008669355 |
| ENSG00000142224 | IL19 subnetwork | 2.46E-04 | 0.008671587 |
| ENSG00000105193 | RPS16 subnetwork | 2.12E-04 | 0.008677686 |
| ENSG00000131323 | TRAF3 subnetwork | 2.04E-04 | 0.008686441 |
| MP:0008596 | increased circulating interleukin-6 level | 1.94E-04 | 0.008695652 |
| ENSG00000172179 | PRL subnetwork | 2.39E-04 | 0.008695652 |
| ENSG00000145839 | IL9 subnetwork | 2.46E-04 | 0.008703704 |
| KEGG_HEMATOPOIETIC_CELL_LIN | KEGG_HEMATOPOIETIC_CELL_LINEAGE | 2.24E-04 | 0.008704453 |
| ENSG00000120235 | IFNA6 subnetwork | 1.83E-04 | 0.008705357 |
| GO:0001772 | immunological synapse | 2.10E-04 | 0.008713693 |
| ENSG00000114127 | XRN1 subnetwork | 1.99E-04 | 0.008723404 |
| GO:0000060 | protein import into nucleus, translocation | 2.38E-04 | 0.008730159 |
| ENSG00000113263 | ITK subnetwork | 1.90E-04 | 0.008733624 |
| ENSG00000111536 | IL26 subnetwork | 2.46E-04 | 0.008736059 |
| REACTOME_REGULATION_OF_IFN | REACTOME_REGULATION_OF_IFNG_SIGNALING | 2.23E-04 | 0.008739837 |
| ENSG00000054267 | ARID4B subnetwork | 2.10E-04 | 0.00875 |
| ENSG00000117020 | AKT3 subnetwork | 1.98E-04 | 0.008760684 |
| ENSG00000120210 | INSL6 subnetwork | 2.37E-04 | 0.00876494 |
| ENSG00000177047 | IFNW1 subnetwork | 2.46E-04 | 0.008768657 |
| REACTOME_ZINC_INFLUX_INTO_( | REACTOME_ZINC_INFLUX_INTO_CELLS_BY_THE_SLC39_ | 1.89E-04 | 0.00877193 |
| MP:0008088 | abnormal T-helper 1 cell differentiation | 2.21E-04 | 0.00877551 |
| MP:0008476 | increased spleen red pulp amount | 2.07E-04 | 0.008786611 |
| ENSG00000150281 | CTF1 subnetwork | 1.97E-04 | 0.008798283 |
| ENSG00000183709 | IL28A subnetwork | 2.46E-04 | 0.008801498 |
| ENSG00000118260 | CREB1 subnetwork | 1.88E-04 | 0.008810573 |
| MP:0000689 | abnormal spleen morphology | 2.07E-04 | 0.008823529 |
| KEGG_GRAFT_VERSUS_HOST_DIS | KEGG_GRAFT_VERSUS_HOST_DISEASE | 2.49E-04 | 0.008823529 |
| ENSG00000128342 | LIF subnetwork | 2.46E-04 | 0.008834586 |
| REACTOME_SIGNALING_BY_SCF:K | REACTOME_SIGNALING_BY_SCF:KIT | 1.97E-04 | 0.008836207 |
| GO:0050871 | positive regulation of B cell activation | 1.88E-04 | 0.008849558 |
| ENSG00000164400 | CSF2 subnetwork | 2.05E-04 | 0.008860759 |
| ENSG00000197110 | IL28B subnetwork | 2.46E-04 | 0.008867925 |
| MP:0001952 | increased airway responsiveness | 1.96E-04 | 0.008874459 |
| ENSG00000164136 | IL15 subnetwork | 2.46E-04 | 0.008901515 |
| ENSG00000138684 | IL21 subnetwork | 2.46E-04 | 0.008935361 |
| ENSG00000147896 | IFNK subnetwork | 2.46E-04 | 0.008969466 |
| ENSG00000184995 | IFNE subnetwork | 2.46E-04 | 0.009003831 |
| MP:0001828 | abnormal T cell activation | 2.43E-04 | 0.009019608 |

| | | | |
|---|---|---|---|
| ENSG00000104432 | IL7 subnetwork | 2.46E-04 | 0.009038462 |
| ENSG00000162892 | IL24 subnetwork | 2.46E-04 | 0.009073359 |
| ENSG00000182393 | IL29 subnetwork | 2.46E-04 | 0.009108527 |
| GO:0043370 | regulation of CD4-positive, alpha-beta T cell differentiati | 2.44E-04 | 0.009143969 |
| GO:0045619 | regulation of lymphocyte differentiation | 2.43E-04 | 0.009179688 |
| ENSG00000171855 | IFNB1 subnetwork | 2.74E-04 | 0.00923913 |
| MP:0005671 | abnormal response to transplant | 2.72E-04 | 0.009272727 |
| MP:0005016 | decreased lymphocyte cell number | 2.70E-04 | 0.009306569 |
| ENSG00000113520 | IL4 subnetwork | 2.69E-04 | 0.009340659 |
| MP:0002493 | increased IgG level | 2.97E-04 | 0.009649123 |
| MP:0000708 | thymus hyperplasia | 2.93E-04 | 0.009683099 |
| MP:0004799 | increased susceptibility to experimental autoimmune en | 2.87E-04 | 0.009717314 |
| MP:0008078 | increased CD8-positive T cell number | 2.82E-04 | 0.009747292 |
| GO:0005031 | tumor necrosis factor-activated receptor activity | 2.87E-04 | 0.009751773 |
| MP:0008211 | decreased mature B cell number | 2.86E-04 | 0.009786477 |
| GO:0002637 | regulation of immunoglobulin production | 2.86E-04 | 0.009821429 |
| MP:0000685 | abnormal immune system morphology | 2.85E-04 | 0.009856631 |
| MP:0005013 | increased lymphocyte cell number | 3.09E-04 | 0.009861592 |
| ENSG00000170677 | SOCS6 subnetwork | 3.17E-04 | 0.009863946 |
| ENSG00000005339 | CREBBP subnetwork | 2.83E-04 | 0.009892086 |
| GO:0032880 | regulation of protein localization | 3.09E-04 | 0.009895833 |
| KEGG_INTESTINAL_IMMUNE_NET | KEGG_INTESTINAL_IMMUNE_NETWORK_FOR_IGA_PRO | 3.16E-04 | 0.009897611 |
| MP:0009790 | decreased susceptibility to viral infection induced morbi | 3.04E-04 | 0.009930314 |
| GO:0008285 | negative regulation of cell proliferation | 3.16E-04 | 0.009931507 |
| ENSG00000133704 | IPO8 subnetwork | 3.04E-04 | 0.009965035 |
| REACTOME_INTERLEUKIN:2_SIGN | REACTOME_INTERLEUKIN:2_SIGNALING | 3.14E-04 | 0.009965636 |
| ENSG00000109471 | IL2 subnetwork | 3.28E-04 | 0.009966216 |
| ENSG00000103723 | AP3B2 subnetwork | 3.12E-04 | 0.01 |
| ENSG00000160185 | UBASH3A subnetwork | 3.23E-04 | 0.01 |
| ENSG00000136244 | IL6 subnetwork | 3.38E-04 | 0.010367893 |
| ENSG00000095752 | IL11 subnetwork | 3.37E-04 | 0.010402685 |
| GO:2000514 | regulation of CD4-positive, alpha-beta T cell activation | 3.36E-04 | 0.01043771 |
| ENSG00000162434 | JAK1 subnetwork | 3.46E-04 | 0.010726073 |
| MP:0008567 | decreased interferon-gamma secretion | 3.46E-04 | 0.010761589 |
| GO:0060334 | regulation of interferon-gamma-mediated signaling path | 3.44E-04 | 0.010797342 |
| GO:0060330 | regulation of response to interferon-gamma | 3.44E-04 | 0.010833333 |
| MP:0000694 | spleen hypoplasia | 3.46E-04 | 0.010855263 |
| ENSG00000108342 | CSF3 subnetwork | 3.54E-04 | 0.011074919 |
| GO:0001773 | myeloid dendritic cell activation | 3.53E-04 | 0.011111111 |
| GO:0042531 | positive regulation of tyrosine phosphorylation of STAT p | 3.51E-04 | 0.011147541 |
| ENSG00000167363 | FN3K subnetwork | 3.57E-04 | 0.011201299 |
| ENSG00000138095 | LRPPRC subnetwork | 3.64E-04 | 0.011217949 |
| MP:0008566 | increased interferon-gamma secretion | 3.60E-04 | 0.011254019 |
| GO:0002250 | adaptive immune response | 3.58E-04 | 0.011290323 |
| MP:0004771 | increased anti-single stranded DNA antibody level | 3.58E-04 | 0.011326861 |
| MP:0001860 | liver inflammation | 3.73E-04 | 0.011464968 |
| ENSG00000145777 | TSLP subnetwork | 3.68E-04 | 0.011501597 |
| ENSG00000126561 | STAT5A subnetwork | 3.94E-04 | 0.0115625 |
| MP:0008101 | lymph node hypoplasia | 3.94E-04 | 0.011598746 |
| MP:0008074 | increased CD4-positive T cell number | 3.92E-04 | 0.01163522 |
| MP:0004809 | increased hematopoietic stem cell number | 4.29E-04 | 0.011641791 |
| MP:0002871 | albuminuria | 4.21E-04 | 0.011666667 |
| MP:0008097 | increased plasma cell number | 3.86E-04 | 0.011671924 |
| GO:0005035 | death receptor activity | 4.29E-04 | 0.011676647 |

| | | | |
|---|---|---|---|
| GO:0002312 | B cell activation involved in immune response | 4.17E-04 | 0.011702128 |
| GO:0045086 | positive regulation of interleukin-2 biosynthetic process | 3.81E-04 | 0.011708861 |
| ENSG00000168610 | STAT3 subnetwork | 4.28E-04 | 0.011711712 |
| ENSG00000065609 | SNAP91 subnetwork | 4.16E-04 | 0.011737805 |
| ENSG00000162891 | IL20 subnetwork | 3.75E-04 | 0.011746032 |
| GO:0030217 | T cell differentiation | 4.27E-04 | 0.011746988 |
| MP:0005093 | decreased B cell proliferation | 4.14E-04 | 0.0117737 |
| ENSG00000116030 | SUMO1 subnetwork | 4.27E-04 | 0.011782477 |
| KEGG_VEGF_SIGNALING_PATHW/ | KEGG_VEGF_SIGNALING_PATHWAY | 4.06E-04 | 0.011801242 |
| MP:0008688 | decreased interleukin-2 secretion | 4.14E-04 | 0.011809816 |
| MP:0003957 | abnormal nitric oxide homeostasis | 4.37E-04 | 0.01183432 |
| GO:0002695 | negative regulation of leukocyte activation | 4.02E-04 | 0.011838006 |
| ENSG00000176177 | ENTHD1 subnetwork | 4.13E-04 | 0.011846154 |
| GO:0045580 | regulation of T cell differentiation | 4.35E-04 | 0.011869436 |
| GO:0042092 | type 2 immune response | 4.12E-04 | 0.011882716 |
| REACTOME_SIGNALING_BY_ERBB | REACTOME_SIGNALING_BY_ERBB2 | 4.35E-04 | 0.011904762 |
| ENSG00000169194 | IL13 subnetwork | 4.10E-04 | 0.011919505 |
| MP:0005088 | increased acute inflammation | 4.76E-04 | 0.011925287 |
| GO:0002683 | negative regulation of immune system process | 4.75E-04 | 0.011959654 |
| MP:0002891 | increased insulin sensitivity | 4.53E-04 | 0.011988304 |
| GO:0045830 | positive regulation of isotype switching | 4.73E-04 | 0.01199422 |
| ENSG00000035115 | SH3YL1 subnetwork | 4.50E-04 | 0.01202346 |
| ENSG00000105221 | AKT2 subnetwork | 4.69E-04 | 0.012028986 |
| MP:0002398 | abnormal bone marrow cell morphology/development | 4.50E-04 | 0.012058824 |
| GO:0001816 | cytokine production | 4.59E-04 | 0.012063953 |
| REACTOME_INTERLEUKIN:6_SIGN | REACTOME_INTERLEUKIN:6_SIGNALING | 4.49E-04 | 0.012094395 |
| MP:0008173 | increased follicular B cell number | 4.57E-04 | 0.012099125 |
| ENSG00000198791 | CNOT7 subnetwork | 4.83E-04 | 0.01260745 |
| GO:0045885 | positive regulation of survival gene product expression | 4.90E-04 | 0.012784091 |
| GO:0000018 | regulation of DNA recombination | 5.03E-04 | 0.01281337 |
| ENSG00000099985 | OSM subnetwork | 4.88E-04 | 0.012820513 |
| KEGG_TGF_BETA_SIGNALING_PA | KEGG_TGF_BETA_SIGNALING_PATHWAY | 5.02E-04 | 0.012849162 |
| ENSG00000147168 | IL2RG subnetwork | 4.87E-04 | 0.012857143 |
| MP:0002344 | abnormal lymph node B cell domain morphology | 5.02E-04 | 0.012885154 |
| ENSG00000118495 | PLAGL1 subnetwork | 4.99E-04 | 0.012921348 |
| MP:0008484 | decreased spleen germinal center size | 4.93E-04 | 0.012957746 |
| MP:0008660 | increased interleukin-10 secretion | 4.93E-04 | 0.01299435 |
| GO:0002263 | cell activation involved in immune response | 5.05E-04 | 0.013019391 |
| ENSG00000170484 | KRT74 subnetwork | 4.91E-04 | 0.013031161 |
| GO:0002366 | leukocyte activation involved in immune response | 5.05E-04 | 0.013055556 |
| REACTOME_CD28_DEPENDENT_V | REACTOME_CD28_DEPENDENT_VAV1_PATHWAY | 5.10E-04 | 0.013259669 |
| MP:0005015 | increased T cell number | 5.13E-04 | 0.013498623 |
| ENSG00000003402 | CFLAR subnetwork | 5.32E-04 | 0.01352459 |
| ENSG00000111145 | ELK3 subnetwork | 5.25E-04 | 0.013561644 |
| KEGG_AMYOTROPHIC_LATERAL_S | KEGG_AMYOTROPHIC_LATERAL_SCLEROSIS_ALS | 5.38E-04 | 0.013586957 |
| MP:0005465 | abnormal T-helper 1 physiology | 5.17E-04 | 0.013598901 |
| MP:0005090 | increased double-negative T cell number | 5.38E-04 | 0.013623978 |
| GO:0002697 | regulation of immune effector process | 5.48E-04 | 0.01395664 |
| MP:0008501 | increased IgG2b level | 5.63E-04 | 0.014189189 |
| MP:0002499 | chronic inflammation | 5.65E-04 | 0.014285714 |
| MP:0001792 | impaired wound healing | 5.99E-04 | 0.015425532 |
| GO:0031334 | positive regulation of protein complex assembly | 6.17E-04 | 0.015445026 |
| ENSG00000143621 | ILF2 subnetwork | 5.98E-04 | 0.015466667 |
| REACTOME_DOWNSTREAM_SIGN | REACTOME_DOWNSTREAM_SIGNAL_TRANSDUCTION | 6.16E-04 | 0.015485564 |

| | | | |
|---|---|---|---|
| MP:0005078 | abnormal cytotoxic T cell physiology | 5.96E-04 | 0.015508021 |
| ENSG00000124813 | RUNX2 subnetwork | 6.12E-04 | 0.015526316 |
| GO:0051043 | regulation of membrane protein ectodomain proteolysis | 5.91E-04 | 0.015549598 |
| REACTOME_INTERLEUKIN_RECEP | REACTOME_INTERLEUKIN_RECEPTOR_SHC_SIGNALING | 6.07E-04 | 0.015567282 |
| MP:0004392 | abnormal CD8-positive T cell physiology | 5.88E-04 | 0.015591398 |
| GO:0002819 | regulation of adaptive immune response | 6.04E-04 | 0.015608466 |
| ENSG00000189162 | ENSG00000189162 subnetwork | 6.04E-04 | 0.015649867 |
| ENSG00000185104 | FAF1 subnetwork | 6.20E-04 | 0.015665796 |
| MP:0008682 | decreased interleukin-17 secretion | 6.32E-04 | 0.015673575 |
| MP:0005079 | defective cytotoxic T cell cytolysis | 6.31E-04 | 0.015714286 |
| GO:0005126 | cytokine receptor binding | 6.30E-04 | 0.015755208 |
| ENSG00000168040 | FADD subnetwork | 6.40E-04 | 0.015769231 |
| MP:0000696 | abnormal Peyer's patch morphology | 6.38E-04 | 0.015809769 |
| MP:0008255 | decreased megakaryocyte cell number | 6.37E-04 | 0.015850515 |
| GO:0019221 | cytokine-mediated signaling pathway | 6.35E-04 | 0.015891473 |
| MP:0008713 | abnormal cytokine level | 6.50E-04 | 0.015943878 |
| MP:0000716 | abnormal immune system cell morphology | 6.46E-04 | 0.015984655 |
| GO:0045637 | regulation of myeloid cell differentiation | 6.58E-04 | 0.016157761 |
| ENSG00000076984 | MAP2K7 subnetwork | 6.62E-04 | 0.016202532 |
| MP:0002831 | absent Peyer's patches | 6.62E-04 | 0.016243655 |
| ENSG00000096968 | JAK2 subnetwork | 6.79E-04 | 0.016460396 |
| MP:0005011 | increased eosinophil cell number | 6.79E-04 | 0.016501241 |
| REACTOME_CTLA4_INHIBITORY_S | REACTOME_CTLA4_INHIBITORY_SIGNALING | 6.67E-04 | 0.016540404 |
| GO:0002889 | regulation of immunoglobulin mediated immune respon | 6.75E-04 | 0.016542289 |
| MP:0008699 | increased interleukin-4 secretion | 6.81E-04 | 0.01654321 |
| ENSG00000161326 | DUSP14 subnetwork | 6.74E-04 | 0.016583541 |
| ENSG00000104833 | TUBB4A subnetwork | 6.69E-04 | 0.016624685 |
| ENSG00000081237 | PTPRC subnetwork | 6.73E-04 | 0.016625 |
| GO:0050868 | negative regulation of T cell activation | 6.72E-04 | 0.016666667 |
| ENSG00000065559 | MAP2K4 subnetwork | 6.71E-04 | 0.016708543 |
| MP:0000322 | increased granulocyte number | 6.88E-04 | 0.017076167 |
| ENSG00000117632 | STMN1 subnetwork | 6.87E-04 | 0.017118227 |
| ENSG00000064835 | POU1F1 subnetwork | 7.07E-04 | 0.017149758 |
| MP:0001881 | abnormal mammary gland physiology | 7.04E-04 | 0.017191283 |
| ENSG00000182866 | LCK subnetwork | 7.03E-04 | 0.01723301 |
| ENSG00000108924 | HLF subnetwork | 7.02E-04 | 0.017274939 |
| MP:0003009 | abnormal cytokine secretion | 6.93E-04 | 0.017279412 |
| ENSG00000116824 | CD2 subnetwork | 7.01E-04 | 0.017317073 |
| ENSG00000097033 | SH3GLB1 subnetwork | 7.01E-04 | 0.017359413 |
| ENSG00000173273 | TNKS subnetwork | 7.21E-04 | 0.017590361 |
| MP:0005010 | abnormal CD8-positive T cell morphology | 7.26E-04 | 0.017668269 |
| GO:0003712 | transcription cofactor activity | 7.36E-04 | 0.017822967 |
| GO:0006509 | membrane protein ectodomain proteolysis | 7.35E-04 | 0.017865707 |
| GO:0032609 | interferon-gamma production | 7.55E-04 | 0.018095238 |
| KEGG_ALLOGRAFT_REJECTION | KEGG_ALLOGRAFT_REJECTION | 7.54E-04 | 0.018138425 |
| ENSG00000107643 | MAPK8 subnetwork | 7.62E-04 | 0.018364929 |
| MP:0005154 | increased B cell proliferation | 7.70E-04 | 0.018396226 |
| KEGG_JAK_STAT_SIGNALING_PAT | KEGG_JAK_STAT_SIGNALING_PATHWAY | 7.60E-04 | 0.018408551 |
| ENSG00000165732 | DDX21 subnetwork | 7.66E-04 | 0.018439716 |
| ENSG00000160712 | IL6R subnetwork | 7.75E-04 | 0.018588235 |
| ENSG00000159388 | BTG2 subnetwork | 7.85E-04 | 0.018691589 |
| ENSG00000117091 | CD48 subnetwork | 7.84E-04 | 0.018735363 |
| REACTOME_ADAPTIVE_IMMUNE_ | REACTOME_ADAPTIVE_IMMUNE_SYSTEM | 7.83E-04 | 0.018779343 |
| GO:0001817 | regulation of cytokine production | 7.96E-04 | 0.018997669 |

| | | | |
|---|---|---|---|
| MP:0008752 | abnormal tumor necrosis factor level | 7.97E-04 | 0.019069767 |
| REACTOME_GAB1_SIGNALOSOMI | REACTOME_GAB1_SIGNALOSOME | 8.06E-04 | 0.019212963 |
| MP:0000495 | abnormal colon morphology | 8.00E-04 | 0.019257541 |
| ENSG00000112033 | PPARD subnetwork | 8.55E-04 | 0.019748858 |
| ENSG00000145675 | PIK3R1 subnetwork | 8.51E-04 | 0.01979405 |
| MP:0008050 | decreased memory T cell number | 8.57E-04 | 0.019817768 |
| ENSG00000101017 | CD40 subnetwork | 8.47E-04 | 0.01983945 |
| MP:0008560 | increased tumor necrosis factor secretion | 8.41E-04 | 0.019885057 |
| MP:0005232 | abnormal mesenteric lymph node morphology | 8.37E-04 | 0.019930876 |
| GO:0002764 | immune response-regulating signaling pathway | 8.30E-04 | 0.019976905 |
| MP:0000717 | abnormal lymphocyte cell number | 9.09E-04 | 0.020267261 |
| GO:0070201 | regulation of establishment of protein localization | 8.75E-04 | 0.020294785 |
| ENSG00000049618 | ARID1B subnetwork | 9.08E-04 | 0.0203125 |
| MP:0004974 | decreased regulatory T cell number | 8.74E-04 | 0.020340909 |
| MP:0001829 | increased activated T cell number | 8.95E-04 | 0.020357942 |
| KEGG_APOPTOSIS | KEGG_APOPTOSIS | 8.79E-04 | 0.020361991 |
| MP:0009543 | abnormal thymus corticomedullary boundary morpholog | 8.93E-04 | 0.020403587 |
| MP:0001194 | dermatitis | 8.90E-04 | 0.020449438 |
| GO:0045622 | regulation of T-helper cell differentiation | 8.89E-04 | 0.020495495 |
| MP:0005596 | increased susceptibility to type I hypersensitivity reactio | 8.86E-04 | 0.020541761 |
| MP:0002875 | decreased erythrocyte cell number | 9.17E-04 | 0.020555556 |
| ENSG00000137275 | RIPK1 subnetwork | 9.20E-04 | 0.020620843 |
| GO:0042035 | regulation of cytokine biosynthetic process | 9.22E-04 | 0.020685841 |
| GO:0002712 | regulation of B cell mediated immunity | 9.32E-04 | 0.020723684 |
| MP:0002052 | decreased tumor incidence | 9.47E-04 | 0.02076087 |
| ENSG00000085760 | MTIF2 subnetwork | 9.32E-04 | 0.020769231 |
| GO:0032649 | regulation of interferon-gamma production | 9.41E-04 | 0.020787746 |
| ENSG00000178363 | CALML3 subnetwork | 9.46E-04 | 0.0208061 |
| ENSG00000137834 | SMAD6 subnetwork | 9.28E-04 | 0.020814978 |
| ENSG00000123268 | ATF1 subnetwork | 9.44E-04 | 0.020851528 |
| GO:0050730 | regulation of peptidyl-tyrosine phosphorylation | 9.25E-04 | 0.020860927 |
| MP:0001845 | abnormal inflammatory response | 9.50E-04 | 0.020932755 |
| ENSG00000174697 | LEP subnetwork | 9.56E-04 | 0.021166307 |
| MP:0004939 | abnormal B cell morphology | 9.56E-04 | 0.021212121 |
| ENSG00000074966 | TXK subnetwork | 9.62E-04 | 0.021290323 |
| MP:0002357 | abnormal spleen white pulp morphology | 9.61E-04 | 0.021336207 |
| ENSG00000077238 | IL4R subnetwork | 9.74E-04 | 0.021351931 |
| GO:0042108 | positive regulation of cytokine biosynthetic process | 9.84E-04 | 0.021474359 |
| ENSG00000012048 | BRCA1 subnetwork | 9.82E-04 | 0.021520343 |
| GO:0050731 | positive regulation of peptidyl-tyrosine phosphorylation | 0.00100585 | 0.021641791 |
| MP:0008826 | abnormal splenic cell ratio | 0.001013025 | 0.021656051 |
| GO:0046637 | regulation of alpha-beta T cell differentiation | 0.001009887 | 0.021702128 |
| MP:0002412 | increased susceptibility to bacterial infection | 0.001015669 | 0.021716102 |
| ENSG00000125691 | RPL23 subnetwork | 0.001021808 | 0.021775899 |
| REACTOME_DOWNSTREAM_TCR_ | REACTOME_DOWNSTREAM_TCR_SIGNALING | 0.001029263 | 0.021940928 |
| KEGG_LEISHMANIA_INFECTION | KEGG_LEISHMANIA_INFECTION | 0.001033612 | 0.022 |
| ENSG00000215301 | DDX3X subnetwork | 0.001041585 | 0.0221174 |
| GO:0032813 | tumor necrosis factor receptor superfamily binding | 0.00103925 | 0.022163866 |
| GO:0009897 | external side of plasma membrane | 0.001046818 | 0.022280335 |
| GO:0071345 | cellular response to cytokine stimulus | 0.001052788 | 0.022442589 |
| ENSG00000156587 | UBE2L6 subnetwork | 0.001063371 | 0.022708333 |
| REACTOME_PIP3_ACTIVATES_AKT | REACTOME_PIP3_ACTIVATES_AKT_SIGNALING | 0.001076098 | 0.023076923 |
| MP:0011353 | expanded mesangial matrix | 0.001120198 | 0.02311609 |
| ENSG00000108175 | ZMIZ1 subnetwork | 0.001080487 | 0.02313278 |

| | | | |
|---|---|---|---|
| GO:0002757 | immune response-activating signal transduction | 0.001112978 | 0.023163265 |
| ENSG00000101210 | EEF1A2 subnetwork | 0.001109745 | 0.023210634 |
| ENSG00000203879 | GDI1 subnetwork | 0.001108868 | 0.023258197 |
| ENSG00000171094 | ALK subnetwork | 0.001105904 | 0.023305955 |
| MP:0008044 | increased NK cell number | 0.001102851 | 0.023353909 |
| ENSG00000134460 | IL2RA subnetwork | 0.001102796 | 0.023402062 |
| GO:0033365 | protein localization to organelle | 0.00110215 | 0.023450413 |
| GO:0042094 | interleukin-2 biosynthetic process | 0.00109777 | 0.023498965 |
| MP:0008466 | enlarged mesenteric lymph nodes | 0.001129562 | 0.023529412 |
| GO:0046425 | regulation of JAK-STAT cascade | 0.001127107 | 0.023577236 |
| ENSG00000134001 | EIF2S1 subnetwork | 0.001153625 | 0.023742455 |
| GO:0002460 | adaptive immune response based on somatic recombina | 0.001152277 | 0.023790323 |
| ENSG00000170581 | STAT2 subnetwork | 0.001147935 | 0.023838384 |
| MP:0000479 | abnormal enterocyte morphology | 0.001145598 | 0.02388664 |
| ENSG00000147403 | RPL10 subnetwork | 0.001166015 | 0.024096386 |
| ENSG00000169083 | AR subnetwork | 0.001178903 | 0.024348697 |
| ENSG00000113594 | LIFR subnetwork | 0.001192671 | 0.0247 |
| REACTOME_TCR_SIGNALING | REACTOME_TCR_SIGNALING | 0.001201636 | 0.024701195 |
| ENSG00000114423 | CBLB subnetwork | 0.001201078 | 0.024750499 |
| GO:0033209 | tumor necrosis factor-mediated signaling pathway | 0.001204393 | 0.024751491 |
| MP:0000220 | increased monocyte cell number | 0.001219359 | 0.024753452 |
| GO:0000989 | transcription factor binding transcription factor activity | 0.001214392 | 0.024802372 |
| MP:0009788 | increased susceptibility to bacterial infection induced mo | 0.001224854 | 0.02480315 |
| ENSG00000112214 | FHL5 subnetwork | 0.001214084 | 0.024851485 |
| ENSG00000122756 | CNTFR subnetwork | 0.001228883 | 0.024852652 |
| GO:0016447 | somatic recombination of immunoglobulin gene segmen | 0.001239408 | 0.024853229 |
| MP:0004946 | abnormal regulatory T cell physiology | 0.001242869 | 0.024853801 |
| ENSG00000142166 | IFNAR1 subnetwork | 0.001208172 | 0.024900794 |
| ENSG00000115085 | ZAP70 subnetwork | 0.001233967 | 0.024901961 |
| ENSG00000140443 | IGF1R subnetwork | 0.001240897 | 0.024902344 |
| ENSG00000165806 | CASP7 subnetwork | 0.001251669 | 0.025193798 |
| MP:0008208 | decreased pro-B cell number | 0.001247944 | 0.025194553 |
| ENSG00000204628 | GNB2L1 subnetwork | 0.001248827 | 0.025242718 |
| ENSG00000129473 | BCL2L2 subnetwork | 0.001295254 | 0.025673077 |
| GO:0034612 | response to tumor necrosis factor | 0.001321798 | 0.025717017 |
| ENSG00000137193 | PIM1 subnetwork | 0.001293902 | 0.025722543 |
| MP:0002217 | small lymph nodes | 0.001325766 | 0.025763359 |
| MP:0002359 | abnormal spleen germinal center morphology | 0.001319861 | 0.025766284 |
| GO:0042826 | histone deacetylase binding | 0.001292417 | 0.025772201 |
| ENSG00000172939 | OXSR1 subnetwork | 0.001330106 | 0.025809524 |
| ENSG00000187840 | EIF4EBP1 subnetwork | 0.001319099 | 0.025815739 |
| ENSG00000177600 | RPLP2 subnetwork | 0.001288138 | 0.02582205 |
| ENSG00000140395 | WDR61 subnetwork | 0.001354944 | 0.025901328 |
| GO:0002020 | protease binding | 0.001341683 | 0.02595057 |
| MP:0001870 | salivary gland inflammation | 0.001386615 | 0.026132075 |
| MP:0008079 | decreased CD8-positive T cell number | 0.001365812 | 0.026136364 |
| ENSG00000106682 | EIF4H subnetwork | 0.0013884 | 0.026177024 |
| GO:0004896 | cytokine receptor activity | 0.001381244 | 0.026181474 |
| MP:0002022 | increased lymphoma incidence | 0.001410967 | 0.026454034 |
| ENSG00000101076 | HNF4A subnetwork | 0.001405276 | 0.026503759 |
| MP:0003799 | impaired macrophage chemotaxis | 0.001413489 | 0.026685393 |
| GO:0050866 | negative regulation of cell activation | 0.001428801 | 0.02682243 |
| KEGG_CYTOKINE_CYTOKINE_RECI | KEGG_CYTOKINE_CYTOKINE_RECEPTOR_INTERACTION | 0.001443766 | 0.026951673 |
| ENSG00000110395 | CBL subnetwork | 0.001436858 | 0.026958955 |

| | | | |
|---|---|---|---|
| REACTOME_CYTOKINE_SIGNALIN | REACTOME_CYTOKINE_SIGNALING_IN_IMMUNE_SYSTEI | 0.001442542 | 0.027001862 |
| GO:0051170 | nuclear import | 0.001455987 | 0.027179963 |
| GO:0015026 | coreceptor activity | 0.00146037 | 0.027222222 |
| ENSG00000168685 | IL7R subnetwork | 0.001477848 | 0.027306273 |
| ENSG00000082512 | TRAF5 subnetwork | 0.001474287 | 0.027356747 |
| ENSG00000113580 | NR3C1 subnetwork | 0.001485073 | 0.027481618 |
| ENSG00000169047 | IRS1 subnetwork | 0.001483371 | 0.027532228 |
| ENSG00000134470 | IL15RA subnetwork | 0.001500929 | 0.028062157 |
| MP:0005042 | abnormal level of surface class II molecules | 0.001495057 | 0.028073394 |
| ENSG00000123329 | ARHGAP9 subnetwork | 0.001499429 | 0.028113553 |
| ENSG00000073584 | SMARCE1 subnetwork | 0.001525127 | 0.02831216 |
| ENSG00000140009 | ESR2 subnetwork | 0.001528574 | 0.028351449 |
| GO:0016444 | somatic cell DNA recombination | 0.001524098 | 0.028363636 |
| GO:0002562 | somatic diversification of immune receptors via germline | 0.001524098 | 0.028415301 |
| ENSG00000149269 | PAK1 subnetwork | 0.001536448 | 0.028429603 |
| GO:0002706 | regulation of lymphocyte mediated immunity | 0.001516689 | 0.028467153 |
| ENSG00000112658 | SRF subnetwork | 0.001535827 | 0.028481013 |
| ENSG00000175197 | DDIT3 subnetwork | 0.00154455 | 0.028558559 |
| GO:0045076 | regulation of interleukin-2 biosynthetic process | 0.001556326 | 0.028815081 |
| GO:0001819 | positive regulation of cytokine production | 0.001554597 | 0.028866906 |
| MP:0009542 | decreased thymocyte apoptosis | 0.001589153 | 0.028914591 |
| ENSG00000134352 | IL6ST subnetwork | 0.001577354 | 0.028928571 |
| MP:0001802 | arrested B cell differentiation | 0.001588109 | 0.028966132 |
| ENSG00000160014 | CALM3 subnetwork | 0.001606842 | 0.028975265 |
| ENSG00000171720 | HDAC3 subnetwork | 0.001575754 | 0.028980322 |
| ENSG00000143933 | CALM2 subnetwork | 0.001606842 | 0.029026549 |
| ENSG00000105976 | MET subnetwork | 0.001568842 | 0.029032258 |
| ENSG00000198087 | CD2AP subnetwork | 0.001603558 | 0.029040853 |
| ENSG00000198668 | CALM1 subnetwork | 0.001606842 | 0.029078014 |
| ENSG00000137070 | IL11RA subnetwork | 0.001622674 | 0.029210526 |
| ENSG00000206452 | HLA-C subnetwork | 0.001616349 | 0.029225352 |
| ENSG00000145623 | OSMR subnetwork | 0.001622674 | 0.029261863 |
| GO:0051052 | regulation of DNA metabolic process | 0.001614083 | 0.029276896 |
| ENSG00000010610 | CD4 subnetwork | 0.00163543 | 0.029422067 |
| GO:0018108 | peptidyl-tyrosine phosphorylation | 0.001644246 | 0.02972028 |
| ENSG00000141510 | TP53 subnetwork | 0.001662151 | 0.02973913 |
| MP:0000488 | abnormal intestinal epithelium morphology | 0.001659955 | 0.029790941 |
| MP:0002420 | abnormal adaptive immunity | 0.001658336 | 0.029842932 |
| MP:0008735 | increased susceptibility to endotoxin shock | 0.00166543 | 0.029861111 |
| GO:0050688 | regulation of defense response to virus | 0.001694184 | 0.029896907 |
| ENSG00000131724 | IL13RA1 subnetwork | 0.001695745 | 0.029931389 |
| ENSG00000206328 | ENSG00000206328 subnetwork | 0.001692082 | 0.029948365 |
| MP:0001718 | abnormal visceral yolk sac morphology | 0.001697943 | 0.029965753 |
| ENSG00000206439 | TNF subnetwork | 0.001692082 | 0.03 |
| ENSG00000204490 | TNF subnetwork | 0.001692082 | 0.030051813 |
| MP:0002375 | abnormal thymus medulla morphology | 0.001711589 | 0.030068143 |
| ENSG00000107175 | CREB3 subnetwork | 0.001683703 | 0.030103806 |
| ENSG00000197063 | MAFG subnetwork | 0.001708544 | 0.030119454 |
| GO:0046427 | positive regulation of JAK-STAT cascade | 0.001676183 | 0.030155979 |
| MP:0003850 | abnormal thymocyte activation | 0.00170342 | 0.03017094 |
| MP:0002339 | abnormal lymph node morphology | 0.001721904 | 0.030272109 |
| GO:0005164 | tumor necrosis factor receptor binding | 0.001726868 | 0.030390492 |
| GO:0001783 | B cell apoptotic process | 0.001732424 | 0.030626058 |
| GO:0045621 | positive regulation of lymphocyte differentiation | 0.00173199 | 0.030677966 |

| | | | |
|---|---|---|---|
| GO:0003713 | transcription coactivator activity | 0.001751704 | 0.030775717 |
| ENSG00000140396 | NCOA2 subnetwork | 0.001750821 | 0.030827703 |
| GO:0042107 | cytokine metabolic process | 0.001769304 | 0.030976431 |
| ENSG00000141736 | ERBB2 subnetwork | 0.001777224 | 0.031008403 |
| ENSG00000162594 | IL23R subnetwork | 0.001819507 | 0.031666667 |
| GO:0016922 | ligand-dependent nuclear receptor binding | 0.001797823 | 0.031711409 |
| ENSG00000163599 | CTLA4 subnetwork | 0.00181723 | 0.031719533 |
| ENSG00000114391 | RPL24 subnetwork | 0.001815338 | 0.031772575 |
| GO:0002822 | regulation of adaptive immune response based on soma | 0.001811883 | 0.031825796 |
| GO:0042089 | cytokine biosynthetic process | 0.001837897 | 0.031946755 |
| GO:0002252 | immune effector process | 0.001848732 | 0.03230897 |
| ENSG00000124334 | IL9R subnetwork | 0.001863319 | 0.032504146 |
| ENSG00000096996 | IL12RB1 subnetwork | 0.001886619 | 0.032590759 |
| GO:0050869 | negative regulation of B cell activation | 0.001883541 | 0.032644628 |
| GO:0006606 | protein import into nucleus | 0.001876838 | 0.032698675 |
| GO:0002573 | myeloid leukocyte differentiation | 0.001896466 | 0.032976974 |
| ENSG00000081985 | IL12RB2 subnetwork | 0.001891037 | 0.033031301 |
| GO:0034097 | response to cytokine stimulus | 0.001899985 | 0.03316913 |
| ENSG00000080824 | HSP90AA1 subnetwork | 0.001938956 | 0.033770492 |
| GO:0002449 | lymphocyte mediated immunity | 0.001942445 | 0.033797054 |
| GO:0001934 | positive regulation of protein phosphorylation | 0.001949276 | 0.033905229 |
| ENSG00000112208 | BAG2 subnetwork | 0.001968696 | 0.034257749 |
| ENSG00000163932 | PRKCD subnetwork | 0.001977579 | 0.034446254 |
| GO:0051019 | mitogen-activated protein kinase binding | 0.001980839 | 0.034471545 |
| ENSG00000198576 | ARC subnetwork | 0.001993753 | 0.034577922 |
| MP:0008135 | small Peyer's patches | 0.001998426 | 0.034683955 |
| MP:0005343 | increased circulating aspartate transaminase level | 0.002007392 | 0.034708738 |
| ENSG00000206218 | ENSG00000206218 subnetwork | 0.002027995 | 0.035048232 |
| ENSG00000100385 | IL2RB subnetwork | 0.002022527 | 0.035056543 |
| ENSG00000206289 | RXRB subnetwork | 0.002027995 | 0.03510467 |
| ENSG00000204231 | RXRB subnetwork | 0.002027995 | 0.03516129 |
| GO:0031347 | regulation of defense response | 0.002038876 | 0.035232745 |
| ENSG00000169682 | SPNS1 subnetwork | 0.002057824 | 0.035303514 |
| ENSG00000117400 | MPL subnetwork | 0.002051969 | 0.03536 |
| ENSG00000115053 | NCL subnetwork | 0.002063456 | 0.035406699 |
| GO:0002700 | regulation of production of molecular mediator of immu | 0.002047039 | 0.035416667 |
| GO:0002377 | immunoglobulin production | 0.002070725 | 0.035509554 |
| ENSG00000056972 | TRAF3IP2 subnetwork | 0.002105457 | 0.035759494 |
| KEGG_CHRONIC_MYELOID_LEUKE | KEGG_CHRONIC_MYELOID_LEUKEMIA | 0.002111547 | 0.035781991 |
| ENSG00000170889 | RPS9 subnetwork | 0.002099789 | 0.035816165 |
| ENSG00000112290 | WASF1 subnetwork | 0.002124986 | 0.035849057 |
| ENSG00000159128 | IFNGR2 subnetwork | 0.002096552 | 0.035850556 |
| MP:0008661 | decreased interleukin-10 secretion | 0.00209965 | 0.035873016 |
| REACTOME_INTERLEUKIN:7_SIGN | REACTOME_INTERLEUKIN:7_SIGNALING | 0.002122713 | 0.035905512 |
| ENSG00000126934 | MAP2K2 subnetwork | 0.002122553 | 0.035962145 |
| ENSG00000109320 | NFKB1 subnetwork | 0.0021382 | 0.036263736 |
| KEGG_DORSO_VENTRAL_AXIS_FC | KEGG_DORSO_VENTRAL_AXIS_FORMATION | 0.002144587 | 0.036442006 |
| GO:0002703 | regulation of leukocyte mediated immunity | 0.002153759 | 0.036619718 |
| GO:0000988 | protein binding transcription factor activity | 0.002164508 | 0.036640625 |
| GO:0022415 | viral reproductive process | 0.002172641 | 0.036682243 |
| ENSG00000159110 | IFNAR2 subnetwork | 0.002169893 | 0.03673947 |
| ENSG00000078900 | TP73 subnetwork | 0.002200723 | 0.036858476 |
| GO:0018212 | peptidyl-tyrosine modification | 0.002203554 | 0.036956522 |
| ENSG00000110324 | IL10RA subnetwork | 0.002227659 | 0.037171561 |

| | | | |
|---|---|---|---|
| ENSG00000185291 | IL3RA subnetwork | 0.00223223 | 0.037211094 |
| ENSG00000159113 | ENSG00000159113 subnetwork | 0.00222641 | 0.037229102 |
| ENSG00000168884 | TNIP2 subnetwork | 0.002231611 | 0.037268519 |
| GO:0051054 | positive regulation of DNA metabolic process | 0.002215848 | 0.037286822 |
| ENSG00000108773 | KAT2A subnetwork | 0.002248501 | 0.037615385 |
| MP:0000208 | decreased hematocrit | 0.002260364 | 0.037941628 |
| GO:0008234 | cysteine-type peptidase activity | 0.002279069 | 0.038190184 |
| GO:0045334 | clathrin-coated endocytic vesicle | 0.002291464 | 0.03820827 |
| GO:0002208 | somatic diversification of immunoglobulins involved in ir | 0.002316191 | 0.038328313 |
| GO:0005125 | cytokine activity | 0.002321839 | 0.038345865 |
| ENSG00000215292 | ENSG00000215292 subnetwork | 0.002314565 | 0.038350983 |
| MP:0003156 | abnormal leukocyte migration | 0.002297859 | 0.038379205 |
| GO:0045190 | isotype switching | 0.002316191 | 0.038386124 |
| ENSG00000204389 | HSPA1A subnetwork | 0.002314565 | 0.038409091 |
| GO:0002204 | somatic recombination of immunoglobulin genes involve | 0.002316191 | 0.038444109 |
| ENSG00000204388 | HSPA1B subnetwork | 0.002314565 | 0.038467375 |
| GO:0046635 | positive regulation of alpha-beta T cell activation | 0.002307067 | 0.038473282 |
| ENSG00000212860 | ENSG00000212860 subnetwork | 0.002314565 | 0.038525836 |
| ENSG00000212866 | HSPA1B subnetwork | 0.002314565 | 0.038584475 |
| ENSG00000141655 | TNFRSF11A subnetwork | 0.002341034 | 0.038588589 |
| ENSG00000112964 | GHR subnetwork | 0.002310308 | 0.038643293 |
| MP:0008479 | decreased spleen white pulp amount | 0.002372376 | 0.038673621 |
| MP:0009503 | abnormal mammary gland duct morphology | 0.002367407 | 0.038731343 |
| REACTOME_DEATH_RECEPTOR__ | REACTOME_DEATH_RECEPTOR__SIGNALLING | 0.002364447 | 0.038789238 |
| ENSG00000185436 | IL28RA subnetwork | 0.002395376 | 0.038831361 |
| REACTOME_EXTRINSIC_PATHWA | REACTOME_EXTRINSIC_PATHWAY_FOR_APOPTOSIS | 0.002364447 | 0.038847305 |
| GO:0002831 | regulation of response to biotic stimulus | 0.002390618 | 0.038872404 |
| GO:0045620 | negative regulation of lymphocyte differentiation | 0.002392702 | 0.038888889 |
| ENSG00000005007 | UPF1 subnetwork | 0.002360781 | 0.038905547 |
| GO:0004713 | protein tyrosine kinase activity | 0.002389246 | 0.038930163 |
| MP:0005026 | decreased susceptibility to parasitic infection | 0.002387799 | 0.038988095 |
| ENSG00000185651 | UBE2L3 subnetwork | 0.002407768 | 0.039069424 |
| ENSG00000138814 | PPP3CA subnetwork | 0.002477044 | 0.039809384 |
| GO:0051223 | regulation of protein transport | 0.002452338 | 0.039823009 |
| ENSG00000156482 | RPL30 subnetwork | 0.002472855 | 0.039867841 |
| MP:0001846 | increased inflammatory response | 0.002503636 | 0.039883552 |
| GO:0045121 | membrane raft | 0.002467557 | 0.039911635 |
| REACTOME_INTRINSIC_PATHWA | REACTOME_INTRINSIC_PATHWAY_FOR_APOPTOSIS | 0.002530989 | 0.039912917 |
| MP:0001246 | mixed cellular infiltration to dermis | 0.002471124 | 0.039926471 |
| ENSG00000184779 | RPS17 subnetwork | 0.002496578 | 0.039941691 |
| MP:0004969 | pale kidney | 0.002515884 | 0.03997093 |
| MP:0002024 | T cell derived lymphoma | 0.002485774 | 0.03998538 |
| ENSG00000182774 | RPS17L subnetwork | 0.002496578 | 0.04 |
| REACTOME_THE_ROLE_OF_NEF_I | REACTOME_THE_ROLE_OF_NEF_IN_HIV:1_REPLICATION | 0.002484023 | 0.040043924 |
| ENSG00000025800 | KPNA6 subnetwork | 0.002549877 | 0.040289855 |
| GO:0050778 | positive regulation of immune response | 0.002583363 | 0.040359712 |
| ENSG00000123496 | IL13RA2 subnetwork | 0.002582358 | 0.040417867 |
| GO:0051247 | positive regulation of protein metabolic process | 0.002576073 | 0.040448625 |
| ENSG00000103522 | IL21R subnetwork | 0.002582358 | 0.04047619 |
| ENSG00000164485 | IL22RA2 subnetwork | 0.002582358 | 0.040534682 |
| ENSG00000185950 | IRS2 subnetwork | 0.002601971 | 0.041104735 |
| MP:0004992 | increased bone resorption | 0.002601334 | 0.041163793 |
| ENSG00000016402 | IL20RA subnetwork | 0.00261819 | 0.041260745 |
| GO:0034504 | protein localization to nucleus | 0.002626602 | 0.041273247 |

| | | | |
|---|---|---|---|
| ENSG00000110330 | BIRC2 subnetwork | 0.002695777 | 0.041430595 |
| ENSG00000067606 | PRKCZ subnetwork | 0.00268215 | 0.041465149 |
| MP:0001847 | brain inflammation | 0.002692713 | 0.041489362 |
| ENSG00000115953 | ENSG00000115953 subnetwork | 0.002654346 | 0.0415 |
| ENSG00000107968 | MAP3K8 subnetwork | 0.002660791 | 0.041512126 |
| ENSG00000066336 | SPI1 subnetwork | 0.002674244 | 0.041524217 |
| ENSG00000165025 | SYK subnetwork | 0.002691033 | 0.041548295 |
| ENSG00000065883 | CDK13 subnetwork | 0.002714842 | 0.04165488 |
| GO:0019900 | kinase binding | 0.002726596 | 0.04180791 |
| MP:0004076 | abnormal vitelline vascular remodeling | 0.002735218 | 0.041819464 |
| MP:0004185 | abnormal adipocyte glucose uptake | 0.002780103 | 0.042237762 |
| ENSG00000142677 | IL22RA1 subnetwork | 0.002764709 | 0.042264416 |
| MP:0002406 | increased susceptibility to infection | 0.002779891 | 0.042296919 |
| GO:0002200 | somatic diversification of immune receptors | 0.002763632 | 0.042323944 |
| ENSG00000027697 | IFNGR1 subnetwork | 0.002789713 | 0.042329149 |
| MP:0005089 | decreased double-negative T cell number | 0.002798287 | 0.042339833 |
| REACTOME_MTOR_SIGNALLING | REACTOME_MTOR_SIGNALLING | 0.002776377 | 0.042356241 |
| ENSG00000100351 | GRAP2 subnetwork | 0.002787333 | 0.042388268 |
| GO:0004709 | MAP kinase kinase kinase activity | 0.002774072 | 0.04241573 |
| MP:0002723 | abnormal immune serum protein physiology | 0.002833012 | 0.042628651 |
| ENSG00000163823 | CCR1 subnetwork | 0.002851502 | 0.042916667 |
| ENSG00000130255 | RPL36 subnetwork | 0.002864084 | 0.043065187 |
| ENSG00000151846 | PABPC3 subnetwork | 0.002884879 | 0.043767313 |
| ENSG00000102882 | MAPK3 subnetwork | 0.002901131 | 0.043775934 |
| ENSG00000113494 | PRLR subnetwork | 0.002914107 | 0.044060773 |
| ENSG00000110700 | RPS13 subnetwork | 0.002930823 | 0.044077135 |
| GO:0051169 | nuclear transport | 0.002958022 | 0.044109589 |
| GO:0006913 | nucleocytoplasmic transport | 0.002921755 | 0.044137931 |
| REACTOME_PI3K_EVENTS_IN_ERI | REACTOME_PI3K_EVENTS_IN_ERBB4_SIGNALING | 0.002952633 | 0.044170096 |
| ENSG00000212981 | ENSG00000212981 subnetwork | 0.002943291 | 0.044222834 |
| ENSG00000101665 | SMAD7 subnetwork | 0.002951987 | 0.044230769 |
| MP:0008024 | absent lymph nodes | 0.002978903 | 0.044254446 |
| MP:0010026 | decreased liver cholesterol level | 0.002986913 | 0.044467213 |
| GO:0004197 | cysteine-type endopeptidase activity | 0.00300094 | 0.044815825 |
| MP:0005659 | decreased susceptibility to diet-induced obesity | 0.003041882 | 0.045034014 |
| REACTOME_DARPP:32_EVENTS | REACTOME_DARPP:32_EVENTS | 0.003037227 | 0.045095368 |
| ENSG00000186951 | PPARA subnetwork | 0.003047564 | 0.04517663 |
| REACTOME_PI3K_EVENTS_IN_ERI | REACTOME_PI3K_EVENTS_IN_ERBB2_SIGNALING | 0.003067533 | 0.045725916 |
| ENSG00000077097 | TOP2B subnetwork | 0.003070201 | 0.045731707 |
| GO:0030155 | regulation of cell adhesion | 0.003114822 | 0.045872801 |
| ENSG00000185591 | SP1 subnetwork | 0.003131315 | 0.046153846 |
| KEGG_TYPE_I_DIABETES_MELLITU | KEGG_TYPE_I_DIABETES_MELLITUS | 0.003147623 | 0.04615903 |
| ENSG00000143384 | MCL1 subnetwork | 0.003128601 | 0.046216216 |
| MP:0003333 | liver fibrosis | 0.003163665 | 0.046567968 |
| GO:0002443 | leukocyte mediated immunity | 0.003191921 | 0.046639785 |
| ENSG00000173039 | RELA subnetwork | 0.003206985 | 0.046711409 |
| GO:0045727 | positive regulation of translation | 0.003259425 | 0.047520107 |
| GO:0045582 | positive regulation of T cell differentiation | 0.003263857 | 0.047523427 |
| MP:0003179 | decreased platelet cell number | 0.003293572 | 0.047666667 |
| MP:0008687 | increased interleukin-2 secretion | 0.003285993 | 0.047727273 |
| ENSG00000023445 | BIRC3 subnetwork | 0.003289397 | 0.047730307 |
| MP:0008703 | decreased interleukin-5 secretion | 0.003321743 | 0.047869507 |
| ENSG00000168310 | IRF2 subnetwork | 0.003381515 | 0.048470745 |
| ENSG00000088367 | EPB41L1 subnetwork | 0.003396101 | 0.048541114 |

| | | | |
|---|---|---|---|
| GO:0001782 | B cell homeostasis | 0.003393759 | 0.048605578 |
| GO:0019058 | viral infectious cycle | 0.003404747 | 0.048675497 |
| ENSG00000049283 | EPN3 subnetwork | 0.0034253 | 0.048677249 |
| GO:0007259 | JAK-STAT cascade | 0.003436803 | 0.048745046 |
| ENSG00000213341 | CHUK subnetwork | 0.003469403 | 0.048878628 |
| REACTOME_DEADENYLATION_OF | REACTOME_DEADENYLATION_OF_MRNA | 0.003478213 | 0.048880105 |
| ENSG00000082074 | FYB subnetwork | 0.003510415 | 0.049210526 |
| ENSG00000187555 | USP7 subnetwork | 0.003522492 | 0.04934297 |
| MP:0000333 | decreased bone marrow cell number | 0.003542333 | 0.049737533 |
| MP:0001120 | abnormal uterus morphology | 0.003559883 | 0.049803922 |
| REACTOME_NGF_SIGNALLING_VI | REACTOME_NGF_SIGNALLING_VIA_TRKA_FROM_THE_P | 0.003571959 | 0.049804433 |
| ENSG00000123411 | IKZF4 subnetwork | 0.003551717 | 0.049868938 |
| ENSG00000165030 | NFIL3 subnetwork | 0.003557542 | 0.04986911 |
| MP:0002455 | abnormal dendritic cell antigen presentation | 0.003567512 | 0.049869452 |
| MP:0002396 | abnormal hematopoietic system morphology/developm | 0.003614081 | 0.050260078 |
| ENSG00000167601 | AXL subnetwork | 0.00361075 | 0.050325521 |
| ENSG00000056558 | TRAF1 subnetwork | 0.003678622 | 0.051232166 |
| ENSG00000137841 | PLCB2 subnetwork | 0.003677118 | 0.051233766 |
| GO:0060055 | angiogenesis involved in wound healing | 0.003696406 | 0.05142487 |
| ENSG00000173153 | ESRRA subnetwork | 0.003761445 | 0.051732991 |
| MP:0008597 | decreased circulating interleukin-6 level | 0.003750113 | 0.051737452 |
| GO:0070664 | negative regulation of leukocyte proliferation | 0.003745369 | 0.051739691 |
| ENSG00000101109 | STK4 subnetwork | 0.003743548 | 0.051741935 |
| ENSG00000066027 | PPP2R5A subnetwork | 0.003735785 | 0.051746442 |
| MP:0002418 | increased susceptibility to viral infection | 0.003756988 | 0.051799486 |
| ENSG00000128656 | CHN1 subnetwork | 0.003742145 | 0.051808786 |
| ENSG00000038358 | EDC4 subnetwork | 0.003806167 | 0.052046036 |
| REACTOME_SIGNALING_BY_ERBB | REACTOME_SIGNALING_BY_ERBB4 | 0.003801989 | 0.052051282 |
| ENSG00000130811 | EIF3G subnetwork | 0.003804652 | 0.052112676 |
| GO:0002253 | activation of immune response | 0.003825233 | 0.052295918 |
| ENSG00000132382 | MYBBP1A subnetwork | 0.003823096 | 0.052298851 |
| MP:0009347 | increased trabecular bone thickness | 0.003849894 | 0.052484076 |
| MP:0004803 | increased susceptibility to autoimmune diabetes | 0.003861423 | 0.052608142 |
| GO:0002381 | immunoglobulin production involved in immunoglobulin | 0.00387776 | 0.052728426 |
| ENSG00000072062 | PRKACA subnetwork | 0.003873865 | 0.052731893 |
| MP:0002419 | abnormal innate immunity | 0.003908998 | 0.053231939 |
| ENSG00000160691 | SHC1 subnetwork | 0.003962455 | 0.053860759 |
| ENSG00000125686 | MED1 subnetwork | 0.003991029 | 0.054292929 |
| ENSG00000178982 | EIF3K subnetwork | 0.003988374 | 0.054298357 |
| MP:0001928 | abnormal ovulation | 0.003995514 | 0.054350567 |
| MP:0004787 | abnormal dorsal aorta morphology | 0.004017181 | 0.054722922 |
| ENSG00000119535 | CSF3R subnetwork | 0.004049854 | 0.055345912 |
| ENSG00000198223 | CSF2RA subnetwork | 0.004083158 | 0.055897114 |
| ENSG00000091181 | IL5RA subnetwork | 0.004081748 | 0.055967337 |
| MP:0008664 | decreased interleukin-12 secretion | 0.004116956 | 0.056758448 |
| ENSG00000116560 | SFPQ subnetwork | 0.004109708 | 0.056766917 |
| ENSG00000100368 | CSF2RB subnetwork | 0.004126787 | 0.0569375 |
| ENSG00000162290 | ENSG00000162290 subnetwork | 0.004169537 | 0.057285181 |
| ENSG00000169062 | UPF3A subnetwork | 0.004168227 | 0.057356608 |
| ENSG00000166170 | BAG5 subnetwork | 0.004193683 | 0.057382134 |
| ENSG00000083845 | RPS5 subnetwork | 0.004186716 | 0.057391304 |
| GO:0032633 | interleukin-4 production | 0.004158777 | 0.057428215 |
| ENSG00000116678 | LEPR subnetwork | 0.004186332 | 0.057462687 |
| ENSG00000140464 | PML subnetwork | 0.004279036 | 0.058281829 |

| | | | |
|---|---|---|---|
| GO:0051222 | positive regulation of protein transport | 0.004272429 | 0.05835396 |
| GO:0030890 | positive regulation of B cell proliferation | 0.00427045 | 0.05842627 |
| ENSG00000137379 | ENSG00000137379 subnetwork | 0.00430557 | 0.058435961 |
| ENSG00000196230 | TUBB subnetwork | 0.00430557 | 0.058508015 |
| ENSG00000183311 | TUBB subnetwork | 0.00430557 | 0.058580247 |
| GO:0042088 | T-helper 1 type immune response | 0.004390912 | 0.058834356 |
| MP:0002078 | abnormal glucose homeostasis | 0.004426832 | 0.058852259 |
| MP:0008750 | abnormal interferon level | 0.004367679 | 0.058856089 |
| MP:0002032 | sarcoma | 0.004387567 | 0.058906634 |
| MP:0002389 | abnormal Peyer's patch follicle morphology | 0.004425526 | 0.058924205 |
| ENSG00000206088 | ENSG00000206088 subnetwork | 0.004446104 | 0.058963415 |
| ENSG00000150455 | TIRAP subnetwork | 0.004421714 | 0.058996328 |
| ENSG00000121774 | KHDRBS1 subnetwork | 0.004417735 | 0.059068627 |
| GO:0045639 | positive regulation of myeloid cell differentiation | 0.004474935 | 0.0590743 |
| MP:0008076 | abnormal CD4-positive T cell differentiation | 0.004512129 | 0.059428224 |
| ENSG00000147677 | EIF3H subnetwork | 0.004517638 | 0.059538275 |
| ENSG00000100906 | NFKBIA subnetwork | 0.004524208 | 0.059587379 |
| ENSG00000206279 | DAXX subnetwork | 0.004620392 | 0.060288809 |
| ENSG00000198033 | TUBA3C subnetwork | 0.004581051 | 0.060290557 |
| GO:0046640 | regulation of alpha-beta T cell proliferation | 0.00458958 | 0.060338573 |
| ENSG00000206206 | DAXX subnetwork | 0.004620392 | 0.060361446 |
| ENSG00000075886 | TUBA3D subnetwork | 0.004581051 | 0.060363636 |
| ENSG00000204209 | DAXX subnetwork | 0.004620392 | 0.060434258 |
| MP:0001770 | abnormal iron level | 0.004617488 | 0.060507246 |
| GO:0071356 | cellular response to tumor necrosis factor | 0.004648544 | 0.060637019 |
| ENSG00000134242 | PTPN22 subnetwork | 0.00466028 | 0.060744298 |
| ENSG00000186879 | ENSG00000186879 subnetwork | 0.004694688 | 0.061270983 |
| ENSG00000183763 | TRAIP subnetwork | 0.004717284 | 0.06135006 |
| ENSG00000153827 | TRIP12 subnetwork | 0.004708221 | 0.061363636 |
| GO:0046777 | protein autophosphorylation | 0.004704167 | 0.061377246 |
| GO:0048535 | lymph node development | 0.004748722 | 0.061382598 |
| MP:0005554 | decreased circulating creatinine level | 0.004728808 | 0.061396181 |
| KEGG_CHEMOKINE_SIGNALING_P | KEGG_CHEMOKINE_SIGNALING_PATHWAY | 0.004765279 | 0.06172619 |
| ENSG00000100030 | MAPK1 subnetwork | 0.004802224 | 0.062187872 |
| ENSG00000105447 | GRWD1 subnetwork | 0.004833012 | 0.062529691 |
| MP:0009339 | decreased splenocyte number | 0.004852193 | 0.062618483 |
| MP:0004919 | abnormal positive T cell selection | 0.004882296 | 0.062676887 |
| ENSG00000145715 | RASA1 subnetwork | 0.00487711 | 0.062691854 |
| REACTOME_PI3KAKT_ACTIVATION | REACTOME_PI3KAKT_ACTIVATION | 0.004850794 | 0.062692764 |
| GO:0048302 | regulation of isotype switching to IgG isotypes | 0.004866339 | 0.062706856 |
| MP:0009763 | increased sensitivity to induced morbidity/mortality | 0.004864633 | 0.062781065 |
| ENSG00000135930 | EIF4E2 subnetwork | 0.004912176 | 0.063117647 |
| ENSG00000134419 | RPS15A subnetwork | 0.004912169 | 0.063191991 |
| MP:0002452 | abnormal antigen presenting cell physiology | 0.004932516 | 0.063396005 |
| GO:0070851 | growth factor receptor binding | 0.004986063 | 0.063668224 |
| ENSG00000127314 | RAP1B subnetwork | 0.004982456 | 0.063684211 |
| MP:0005153 | abnormal B cell proliferation | 0.004970717 | 0.063716295 |
| MP:0005312 | pericardial effusion | 0.004981913 | 0.063758782 |
| ENSG00000011260 | UTP18 subnetwork | 0.004969611 | 0.06379108 |
| MP:0008037 | abnormal T cell morphology | 0.005006552 | 0.064760793 |
| GO:0033619 | membrane protein proteolysis | 0.005021457 | 0.06497669 |
| ENSG00000115145 | STAM2 subnetwork | 0.005040168 | 0.065075669 |
| MP:0008182 | decreased marginal zone B cell number | 0.00511 | 0.065872093 |
| MP:0000493 | rectal prolapse | 0.005124718 | 0.065893271 |

| | | | |
|---|---|---|---|
| MP:0009336 | increased splenocyte proliferation | 0.005122604 | 0.065969803 |
| MP:0011427 | mesangial cell hyperplasia | 0.005137271 | 0.066048667 |
| REACTOME_NEF:MEDIATES_DOW | REACTOME_NEF:MEDIATES_DOWN_MODULATION_OF_ | 0.005153873 | 0.066203704 |
| ENSG00000089009 | RPL6 subnetwork | 0.0051828 | 0.066339492 |
| GO:0071214 | cellular response to abiotic stimulus | 0.005200461 | 0.066378316 |
| ENSG00000180733 | ENSG00000180733 subnetwork | 0.005180047 | 0.066416185 |
| ENSG00000174444 | RPL4 subnetwork | 0.005208802 | 0.066417051 |
| ENSG00000136156 | ITM2B subnetwork | 0.005245076 | 0.066685846 |
| ENSG00000087088 | BAX subnetwork | 0.005261334 | 0.066704937 |
| ENSG00000052723 | SIKE1 subnetwork | 0.005250993 | 0.066724138 |
| MP:0004751 | increased length of allograft survival | 0.005272604 | 0.066800459 |
| MP:0009006 | prolonged estrous cycle | 0.005290895 | 0.066953036 |
| ENSG00000173848 | NET1 subnetwork | 0.00532498 | 0.067371429 |
| GO:0032663 | regulation of interleukin-2 production | 0.005312911 | 0.067391304 |
| ENSG00000187266 | EPOR subnetwork | 0.005348922 | 0.067522831 |
| GO:0002768 | immune response-regulating cell surface receptor signali | 0.005382293 | 0.067613636 |
| GO:0042327 | positive regulation of phosphorylation | 0.005369612 | 0.067653759 |
| MP:0001219 | thick epidermis | 0.005379517 | 0.067690557 |
| MP:0004151 | decreased circulating iron level | 0.0053688 | 0.067730901 |
| MP:0001272 | increased metastatic potential | 0.005407028 | 0.067913832 |
| ENSG00000141480 | ARRB2 subnetwork | 0.005402862 | 0.067990919 |
| ENSG00000198911 | SREBF2 subnetwork | 0.00542706 | 0.068006795 |
| KEGG_ERBB_SIGNALING_PATHW | KEGG_ERBB_SIGNALING_PATHWAY | 0.005479898 | 0.068700565 |
| ENSG00000138385 | SSB subnetwork | 0.005478223 | 0.068778281 |
| ENSG00000105851 | PIK3CG subnetwork | 0.005487984 | 0.068792325 |
| GO:0002440 | production of molecular mediator of immune response | 0.005523508 | 0.069222097 |
| MP:0001793 | altered susceptibility to infection | 0.005536049 | 0.069313063 |
| ENSG00000159692 | CTBP1 subnetwork | 0.005563581 | 0.069606742 |
| MP:0008181 | increased marginal zone B cell number | 0.005567405 | 0.069640853 |
| ENSG00000142534 | RPS11 subnetwork | 0.005563249 | 0.069685039 |
| ENSG00000112062 | MAPK14 subnetwork | 0.005593471 | 0.069820829 |
| ENSG00000103197 | TSC2 subnetwork | 0.005590856 | 0.069899103 |
| GO:0002467 | germinal center formation | 0.005651784 | 0.070134228 |
| GO:0017038 | protein import | 0.0056615 | 0.070223464 |
| GO:0016445 | somatic diversification of immunoglobulins | 0.005687666 | 0.070591518 |
| GO:0045581 | negative regulation of T cell differentiation | 0.005704502 | 0.070680045 |
| ENSG00000196911 | KPNA5 subnetwork | 0.005734738 | 0.070935412 |
| ENSG00000110931 | CAMKK2 subnetwork | 0.005746499 | 0.071078977 |
| ENSG00000173486 | FKBP2 subnetwork | 0.005751782 | 0.071166667 |
| MP:0002705 | dilated renal tubules | 0.005760662 | 0.071198668 |
| MP:0000240 | extramedullary hematopoiesis | 0.005898194 | 0.072560976 |
| ENSG00000206294 | ENSG00000206294 subnetwork | 0.005931453 | 0.072646733 |
| GO:0050852 | T cell receptor signaling pathway | 0.005956989 | 0.073064159 |
| ENSG00000108561 | C1QBP subnetwork | 0.005995508 | 0.073480663 |
| MP:0003644 | thymus atrophy | 0.006018874 | 0.07384106 |
| GO:0042974 | retinoic acid receptor binding | 0.006027703 | 0.074035281 |
| ENSG00000154582 | TCEB1 subnetwork | 0.006034605 | 0.074063877 |
| ENSG00000196313 | POM121 subnetwork | 0.006087653 | 0.07469747 |
| ENSG00000157168 | NRG1 subnetwork | 0.006099412 | 0.07478022 |
| MP:0001869 | pancreas inflammation | 0.006145634 | 0.074917673 |
| GO:0050792 | regulation of viral reproduction | 0.006148765 | 0.075 |
| ENSG00000152689 | RASGRP3 subnetwork | 0.006167163 | 0.075136911 |
| REACTOME_CIRCADIAN_CLOCK | REACTOME_CIRCADIAN_CLOCK | 0.006182968 | 0.075492341 |
| GO:0042516 | regulation of tyrosine phosphorylation of Stat3 protein | 0.006240831 | 0.075846995 |

| | | | |
|---|---|---|---|
| MP:0000628 | abnormal mammary gland development | 0.006272629 | 0.076091703 |
| KEGG_PRIMARY_IMMUNODEFICI | KEGG_PRIMARY_IMMUNODEFICIENCY | 0.006292383 | 0.076117775 |
| MP:0001245 | thick dermal layer | 0.006330932 | 0.076605005 |
| ENSG00000131759 | RARA subnetwork | 0.006329747 | 0.076688453 |
| KEGG_MTOR_SIGNALING_PATHW | KEGG_MTOR_SIGNALING_PATHWAY | 0.006397122 | 0.077361564 |
| ENSG00000123908 | EIF2C2 subnetwork | 0.006391782 | 0.077445652 |
| ENSG00000129460 | NGDN subnetwork | 0.006418433 | 0.077603037 |
| REACTOME_PD:1_SIGNALING | REACTOME_PD:1_SIGNALING | 0.006503195 | 0.078216216 |
| MP:0003449 | abnormal intestinal goblet cell morphology | 0.006480572 | 0.078223185 |
| GO:0051427 | hormone receptor binding | 0.006501816 | 0.078300866 |
| MP:0005416 | abnormal circulating protein level | 0.006517014 | 0.078725702 |
| ENSG00000122025 | FLT3 subnetwork | 0.006556476 | 0.078856526 |
| REACTOME_DOWNSTREAM_SIGN | REACTOME_DOWNSTREAM_SIGNALING_OF_ACTIVATED | 0.006566772 | 0.078987069 |
| ENSG00000138794 | CASP6 subnetwork | 0.006598702 | 0.079547901 |
| ENSG00000146648 | EGFR subnetwork | 0.006655927 | 0.080268817 |
| MP:0003718 | maternal effect | 0.006695153 | 0.080827068 |
| ENSG00000118513 | MYB subnetwork | 0.00673056 | 0.080975348 |
| KEGG_NATURAL_KILLER_CELL_MI | KEGG_NATURAL_KILLER_CELL_MEDIATED_CYTOTOXICIT | 0.006711824 | 0.081062232 |
| MP:0008217 | abnormal B cell activation | 0.00678853 | 0.081798715 |
| GO:0002902 | regulation of B cell apoptotic process | 0.00683697 | 0.082264957 |
| ENSG00000096060 | FKBP5 subnetwork | 0.006850838 | 0.082302772 |
| ENSG00000153879 | CEBPG subnetwork | 0.006829643 | 0.082352941 |
| ENSG00000206293 | ENSG00000206293 subnetwork | 0.006878298 | 0.082359192 |
| GO:0044419 | interspecies interaction between organisms | 0.006847792 | 0.082390608 |
| ENSG00000206229 | ENSG00000206229 subnetwork | 0.006878298 | 0.082446809 |
| GO:0008134 | transcription factor binding | 0.006909575 | 0.082449629 |
| GO:0042503 | tyrosine phosphorylation of Stat3 protein | 0.00690583 | 0.082484076 |
| ENSG00000204257 | HLA-DMA subnetwork | 0.006878298 | 0.082534611 |
| GO:0051607 | defense response to virus | 0.00694538 | 0.082838983 |
| KEGG_PROSTATE_CANCER | KEGG_PROSTATE_CANCER | 0.007051574 | 0.083526927 |
| GO:0002429 | immune response-activating cell surface receptor signali | 0.007048249 | 0.083562368 |
| ENSG00000142539 | SPIB subnetwork | 0.007045165 | 0.083650794 |
| MP:0005152 | pancytopenia | 0.007079722 | 0.084124473 |
| MP:0002461 | increased immunoglobulin level | 0.007107038 | 0.084263158 |
| ENSG00000142937 | RPS8 subnetwork | 0.007102403 | 0.084299262 |
| MP:0005025 | abnormal response to infection | 0.007128851 | 0.084384858 |
| MP:0001505 | hunched posture | 0.007149663 | 0.084417629 |
| GO:0009896 | positive regulation of catabolic process | 0.007149619 | 0.084506303 |
| MP:0003944 | abnormal T cell subpopulation ratio | 0.007202073 | 0.084853249 |
| MP:0005553 | increased circulating creatinine level | 0.007221516 | 0.084921466 |
| MP:0001716 | abnormal placenta labyrinth morphology | 0.00726362 | 0.085198745 |
| ENSG00000111802 | TDP2 subnetwork | 0.007279442 | 0.085370951 |
| ENSG00000145425 | RPS3A subnetwork | 0.007304963 | 0.08546875 |
| ENSG00000101773 | RBBP8 subnetwork | 0.007297727 | 0.085557873 |
| GO:0002699 | positive regulation of immune effector process | 0.007295036 | 0.08559499 |
| MP:0008098 | decreased plasma cell number | 0.00733289 | 0.085639958 |
| MP:0008723 | impaired eosinophil recruitment | 0.00737179 | 0.086070686 |
| MP:0002962 | increased urine protein level | 0.007412216 | 0.086604361 |
| ENSG00000198821 | CD247 subnetwork | 0.00744905 | 0.086749482 |
| ENSG00000116478 | HDAC1 subnetwork | 0.007420618 | 0.086773859 |
| ENSG00000117560 | FASLG subnetwork | 0.007448271 | 0.086839378 |
| ENSG00000161570 | CCL5 subnetwork | 0.007476417 | 0.086983471 |
| REACTOME_PHOSPHORYLATION_ | REACTOME_PHOSPHORYLATION_OF_CD3_AND_TCR_ZE | 0.007488894 | 0.086996904 |
| ENSG00000203283 | ENSG00000203283 subnetwork | 0.007476417 | 0.087073423 |

| | | | |
|---|---|---|---|
| MP:0005166 | decreased susceptibility to injury | 0.007524675 | 0.087525773 |
| ENSG00000075415 | SLC25A3 subnetwork | 0.007561862 | 0.087808642 |
| ENSG00000175354 | PTPN2 subnetwork | 0.007556618 | 0.08784758 |
| GO:0046633 | alpha-beta T cell proliferation | 0.007600285 | 0.088090349 |
| MP:0003628 | abnormal leukocyte adhesion | 0.007586996 | 0.088129496 |
| GO:0048291 | isotype switching to IgG isotypes | 0.007719202 | 0.088809766 |
| ENSG00000138326 | RPS24 subnetwork | 0.007714359 | 0.088900204 |
| ENSG00000152422 | XRCC4 subnetwork | 0.007691714 | 0.088928571 |
| MP:0008127 | decreased dendritic cell number | 0.007710944 | 0.088939857 |
| KEGG_AUTOIMMUNE_THYROID_I | KEGG_AUTOIMMUNE_THYROID_DISEASE | 0.007670614 | 0.088957055 |
| KEGG_SMALL_CELL_LUNG_CANCI | KEGG_SMALL_CELL_LUNG_CANCER | 0.007685716 | 0.088968335 |
| ENSG00000115641 | FHL2 subnetwork | 0.007659641 | 0.088996929 |
| ENSG00000124214 | STAU1 subnetwork | 0.007657425 | 0.089036885 |
| ENSG00000162227 | TAF6L subnetwork | 0.007744762 | 0.089086294 |
| ENSG00000171608 | PIK3CD subnetwork | 0.007742275 | 0.089126016 |
| GO:0000956 | nuclear-transcribed mRNA catabolic process | 0.007657269 | 0.089128205 |
| GO:0010608 | posttranscriptional regulation of gene expression | 0.007794867 | 0.089401623 |
| GO:0006605 | protein targeting | 0.007825919 | 0.089817629 |
| ENSG00000026103 | FAS subnetwork | 0.007871008 | 0.089818548 |
| MP:0001853 | heart inflammation | 0.007840944 | 0.089827935 |
| ENSG00000106299 | WASL subnetwork | 0.00786968 | 0.089909183 |
| GO:0031341 | regulation of cell killing | 0.007884852 | 0.089979859 |
| ENSG00000105197 | TIMM50 subnetwork | 0.007866396 | 0.09 |
| ENSG00000187899 | ENSG00000187899 subnetwork | 0.007865271 | 0.090091001 |
| MP:0008481 | increased spleen germinal center number | 0.007977446 | 0.090822467 |
| GO:0032623 | interleukin-2 production | 0.007953444 | 0.09084507 |
| ENSG00000171490 | RSL1D1 subnetwork | 0.007969782 | 0.090913655 |
| ENSG00000184047 | DIABLO subnetwork | 0.007968481 | 0.090954774 |
| REACTOME_PKB:MEDIATED_EVEI | REACTOME_PKB:MEDIATED_EVENTS | 0.008062846 | 0.091683367 |
| MP:0005616 | decreased susceptibility to type IV hypersensitivity react | 0.008110607 | 0.092192192 |
| GO:0070227 | lymphocyte apoptotic process | 0.008153094 | 0.09245 |
| ENSG00000115415 | STAT1 subnetwork | 0.008214474 | 0.092807193 |
| ENSG00000085511 | MAP3K4 subnetwork | 0.008227181 | 0.092914172 |
| REACTOME_VIRAL_DSRNATLR3TR | REACTOME_VIRAL_DSRNATLR3TRIF_COMPLEX_ACTIVAT | 0.008229687 | 0.092921236 |
| ENSG00000213923 | CSNK1E subnetwork | 0.008248019 | 0.092978088 |
| MP:0005566 | decreased blood urea nitrogen level | 0.008256877 | 0.092985075 |
| GO:0004702 | receptor signaling protein serine/threonine kinase activi | 0.008303551 | 0.093389662 |
| GO:0018024 | histone-lysine N-methyltransferase activity | 0.00833754 | 0.093694141 |
| GO:0019901 | protein kinase binding | 0.008360417 | 0.09389881 |
| MP:0003721 | increased tumor growth/size | 0.008372743 | 0.09395441 |
| ENSG00000069399 | BCL3 subnetwork | 0.008387221 | 0.093960396 |
| GO:0032729 | positive regulation of interferon-gamma production | 0.008402957 | 0.094015826 |
| MP:0000512 | intestinal ulcer | 0.008409972 | 0.094021739 |
| ENSG00000103275 | UBE2I subnetwork | 0.008472768 | 0.094471866 |
| GO:0051044 | positive regulation of membrane protein ectodomain pr | 0.008473266 | 0.094477318 |
| MP:0008828 | abnormal lymph node cell ratio | 0.008563643 | 0.095427729 |
| GO:0050851 | antigen receptor-mediated signaling pathway | 0.0085489 | 0.095517241 |
| ENSG00000118503 | TNFAIP3 subnetwork | 0.008562025 | 0.095521654 |
| GO:0046625 | sphingolipid binding | 0.008611456 | 0.095776031 |
| ENSG00000130382 | MLLT1 subnetwork | 0.008633576 | 0.095829244 |
| ENSG00000159216 | RUNX1 subnetwork | 0.008651234 | 0.095833333 |
| GO:0045937 | positive regulation of phosphate metabolic process | 0.008664437 | 0.095890411 |
| GO:0010562 | positive regulation of phosphorus metabolic process | 0.008664437 | 0.095984329 |
| MP:0002376 | abnormal dendritic cell physiology | 0.008705436 | 0.096187683 |

| | | | |
|---|---|---|---|
| REACTOME_INTERFERON_GAMM | REACTOME_INTERFERON_GAMMA_SIGNALING | 0.008722318 | 0.096240234 |
| ENSG00000132676 | DAP3 subnetwork | 0.008733734 | 0.096341463 |
| GO:0042508 | tyrosine phosphorylation of Stat1 protein | 0.008738378 | 0.096345029 |
| ENSG00000146232 | NFKBIE subnetwork | 0.008799837 | 0.096890185 |
| GO:0034101 | erythrocyte homeostasis | 0.008799602 | 0.096984436 |
| ENSG00000134107 | BHLHE40 subnetwork | 0.008795364 | 0.097030185 |
| MP:0004031 | insulitis | 0.008837825 | 0.097038835 |
| ENSG00000144713 | RPL32 subnetwork | 0.008850326 | 0.0971387 |
| GO:0002437 | inflammatory response to antigenic stimulus | 0.008904194 | 0.097674419 |
| GO:0031349 | positive regulation of defense response | 0.008926838 | 0.097773475 |
| GO:0043900 | regulation of multi-organism process | 0.008981162 | 0.098115942 |
| GO:0030101 | natural killer cell activation | 0.008978446 | 0.098162476 |
| ENSG00000131982 | ENSG00000131982 subnetwork | 0.008991288 | 0.098262548 |
| ENSG00000108946 | PRKAR1A subnetwork | 0.00905159 | 0.098413462 |
| ENSG00000179295 | PTPN11 subnetwork | 0.009010311 | 0.098457088 |
| ENSG00000001167 | NFYA subnetwork | 0.009037836 | 0.098460058 |
| ENSG00000106052 | TAX1BP1 subnetwork | 0.009065838 | 0.098463016 |
| ENSG00000110448 | CD5 subnetwork | 0.00903084 | 0.098506744 |
| MP:0005036 | diarrhea | 0.009092858 | 0.098992322 |
| REACTOME_SIGNALING_BY_FGFR | REACTOME_SIGNALING_BY_FGFR | 0.009132591 | 0.099568966 |
| GO:0002832 | negative regulation of response to biotic stimulus | 0.009128612 | 0.099616491 |
| ENSG00000125952 | MAX subnetwork | 0.009142522 | 0.099617225 |
| REACTOME_SIGNALING_BY_PDGF | REACTOME_SIGNALING_BY_PDGF | 0.009264381 | 0.10081262 |
| REACTOME_IMMUNOREGULATOI | REACTOME_IMMUNOREGULATORY_INTERACTIONS_BET | 0.009316896 | 0.101098376 |
| ENSG00000063761 | ADCK1 subnetwork | 0.009391896 | 0.102051527 |
| MP:0004810 | decreased hematopoietic stem cell number | 0.00944295 | 0.102235966 |
| GO:0032945 | negative regulation of mononuclear cell proliferation | 0.009483448 | 0.10227704 |
| GO:0019955 | cytokine binding | 0.009440297 | 0.102333333 |
| GO:0050672 | negative regulation of lymphocyte proliferation | 0.009483448 | 0.102374169 |
| ENSG00000169967 | MAP3K2 subnetwork | 0.009463151 | 0.102376426 |
| ENSG00000164050 | PLXNB1 subnetwork | 0.009436647 | 0.102383222 |
| ENSG00000198851 | CD3E subnetwork | 0.009517534 | 0.10250947 |
| MP:0002074 | abnormal hair texture | 0.009516638 | 0.102606635 |
| ENSG00000171148 | TADA3 subnetwork | 0.00957861 | 0.102882798 |
| GO:0072160 | nephron tubule epithelial cell differentiation | 0.00955404 | 0.102885525 |
| MP:0003699 | abnormal female reproductive system physiology | 0.009638317 | 0.103201507 |
| ENSG00000154016 | GRAP subnetwork | 0.009618185 | 0.103207547 |
| REACTOME_BMAL1CLOCKNPAS2_ | REACTOME_BMAL1CLOCKNPAS2_ACTIVATES_GENE_EXF | 0.009606585 | 0.10325779 |
| ENSG00000106992 | AK1 subnetwork | 0.009636672 | 0.103298775 |
| ENSG00000204390 | HSPA1L subnetwork | 0.009656927 | 0.103339605 |
| REACTOME_EFFECTS_OF_PIP2_H | REACTOME_EFFECTS_OF_PIP2_HYDROLYSIS | 0.009683918 | 0.103618421 |
| MP:0006043 | decreased apoptosis | 0.009714416 | 0.103849765 |
| ENSG00000215778 | ENSG00000215778 subnetwork | 0.009730942 | 0.10393627 |
| ENSG00000160791 | CCR5 subnetwork | 0.009730942 | 0.104033771 |
| ENSG00000106144 | CASP2 subnetwork | 0.009814657 | 0.104634831 |
| GO:0016064 | immunoglobulin mediated immune response | 0.009888307 | 0.10505145 |
| GO:0008633 | activation of pro-apoptotic gene products | 0.00992291 | 0.105560748 |
| ENSG00000119383 | PPP2R4 subnetwork | 0.009948837 | 0.105783582 |
| GO:0045070 | positive regulation of viral genome replication | 0.009947972 | 0.105882353 |
| GO:0050714 | positive regulation of protein secretion | 0.009993921 | 0.105959032 |
| ENSG00000077150 | NFKB2 subnetwork | 0.009979876 | 0.105964585 |
| GO:0044403 | symbiosis, encompassing mutualism through parasitism | 0.010065971 | 0.106651163 |
| ENSG00000095794 | CREM subnetwork | 0.010079658 | 0.106737918 |
| ENSG00000107338 | SHB subnetwork | 0.010127822 | 0.106963788 |

| | | | |
|---|---|---|---|
| ENSG00000010810 | FYN subnetwork | 0.010261719 | 0.107770583 |
| MP:0003045 | fibrosis | 0.010256521 | 0.107824074 |
| MP:0009583 | increased keratinocyte proliferation | 0.010249538 | 0.107831325 |
| ENSG00000099804 | CDC34 subnetwork | 0.010231487 | 0.107931354 |
| ENSG00000158517 | NCF1 subnetwork | 0.010334346 | 0.108548983 |
| MP:0002332 | abnormal exercise endurance | 0.010353813 | 0.108679594 |
| GO:0030218 | erythrocyte differentiation | 0.010403811 | 0.108894009 |
| ENSG00000060138 | CSDA subnetwork | 0.010400438 | 0.108948339 |
| ENSG00000136942 | RPL35 subnetwork | 0.010477192 | 0.109668508 |
| ENSG00000124151 | NCOA3 subnetwork | 0.0105561 | 0.110809568 |
| ENSG00000137285 | TUBB2B subnetwork | 0.01058676 | 0.110983456 |
| ENSG00000063177 | RPL18 subnetwork | 0.010596036 | 0.111019284 |
| MP:0001585 | hemolytic anemia | 0.010634022 | 0.111330275 |
| REACTOME_DEADENYLATION:DEI | REACTOME_DEADENYLATION:DEPENDENT_MRNA_DEC/ | 0.010730934 | 0.111563071 |
| GO:0071887 | leukocyte apoptotic process | 0.010680163 | 0.111640697 |
| MP:0008577 | increased circulating interferon-gamma level | 0.010711657 | 0.111665142 |
| MP:0002018 | malignant tumors | 0.010707764 | 0.111721612 |
| ENSG00000105887 | MTPN subnetwork | 0.010770887 | 0.11173516 |
| GO:0043011 | myeloid dendritic cell differentiation | 0.010823732 | 0.112226277 |
| KEGG_RENAL_CELL_CARCINOMA | KEGG_RENAL_CELL_CARCINOMA | 0.010830562 | 0.11230629 |
| REACTOME_NF:KB_ACTIVATION_ | REACTOME_NF:KB_ACTIVATION_THROUGH_FADDRIP:1_ | 0.010860184 | 0.112613843 |
| ENSG00000104365 | IKBKB subnetwork | 0.010924199 | 0.112647325 |
| ENSG00000105640 | RPL18A subnetwork | 0.010914441 | 0.112658802 |
| GO:0071634 | regulation of transforming growth factor beta productio | 0.010911018 | 0.112715713 |
| GO:0019724 | B cell mediated immunity | 0.010896239 | 0.112784349 |
| GO:0071604 | transforming growth factor beta production | 0.010911018 | 0.112818182 |
| ENSG00000204273 | ENSG00000204273 subnetwork | 0.010971594 | 0.112986425 |
| GO:0006968 | cellular defense response | 0.010988061 | 0.113019892 |
| ENSG00000168399 | ENSG00000168399 subnetwork | 0.010971594 | 0.113088768 |
| MP:0005339 | increased susceptibility to atherosclerosis | 0.011082345 | 0.11361587 |
| GO:0032673 | regulation of interleukin-4 production | 0.011091611 | 0.113636364 |
| ENSG00000073009 | IKBKG subnetwork | 0.0111104 | 0.113669065 |
| ENSG00000131469 | RPL27 subnetwork | 0.011057534 | 0.113673285 |
| GO:0008287 | protein serine/threonine phosphatase complex | 0.011090249 | 0.113738739 |
| GO:0035257 | nuclear hormone receptor binding | 0.011052015 | 0.113775971 |
| ENSG00000133124 | IRS4 subnetwork | 0.011182508 | 0.11381932 |
| KEGG_TYROSINE_METABOLISM | KEGG_TYROSINE_METABOLISM | 0.011146543 | 0.113868941 |
| GO:0016278 | lysine N-methyltransferase activity | 0.011181408 | 0.113921218 |
| ENSG00000111615 | KRR1 subnetwork | 0.011157351 | 0.113946188 |
| ENSG00000170365 | SMAD1 subnetwork | 0.01124644 | 0.113960749 |
| ENSG00000066117 | SMARCD1 subnetwork | 0.011142917 | 0.113971249 |
| ENSG00000169220 | RGS14 subnetwork | 0.011234041 | 0.114017857 |
| GO:0016279 | protein-lysine N-methyltransferase activity | 0.011181408 | 0.114023297 |
| ENSG00000139515 | PDX1 subnetwork | 0.011265266 | 0.114024933 |
| MP:0003091 | abnormal cell migration | 0.011217008 | 0.114030384 |
| ENSG00000107566 | ERLIN1 subnetwork | 0.011260716 | 0.114081996 |
| ENSG00000090863 | GLG1 subnetwork | 0.011298066 | 0.114323843 |
| MP:0004842 | abnormal large intestine crypts of Lieberkuhn morpholo | 0.011334909 | 0.114653641 |
| GO:0030159 | receptor signaling complex scaffold activity | 0.01132912 | 0.114711111 |
| ENSG00000100603 | SNW1 subnetwork | 0.011391747 | 0.114849291 |
| GO:0005070 | SH3/SH2 adaptor activity | 0.011389067 | 0.114862467 |
| MP:0009766 | increased sensitivity to xenobiotic induced morbidity/m | 0.011408109 | 0.115057573 |
| MP:0005325 | abnormal renal glomerulus morphology | 0.011428481 | 0.115132743 |
| MP:0008115 | abnormal dendritic cell differentiation | 0.011481895 | 0.115649867 |

| | | | |
|---|---|---|---|
| ENSG00000169750 | RAC3 subnetwork | 0.011637642 | 0.117137809 |
| MP:0008502 | increased IgG3 level | 0.011675014 | 0.117210944 |
| ENSG00000012124 | CD22 subnetwork | 0.011757299 | 0.117665198 |
| ENSG00000005022 | SLC25A5 subnetwork | 0.011751583 | 0.117768959 |
| ENSG00000095585 | BLNK subnetwork | 0.011784257 | 0.117825704 |
| GO:0002763 | positive regulation of myeloid leukocyte differentiation | 0.011845285 | 0.11814587 |
| ENSG00000100181 | ENSG00000100181 subnetwork | 0.011840341 | 0.118161829 |
| MP:0002816 | colitis | 0.011894665 | 0.118464912 |
| ENSG00000105376 | ICAM5 subnetwork | 0.011887383 | 0.118525022 |
| MP:0002356 | abnormal spleen red pulp morphology | 0.011944601 | 0.118591426 |
| ENSG00000089351 | GRAMD1A subnetwork | 0.011935702 | 0.118607706 |
| MP:0008522 | abnormal lymph node germinal center morphology | 0.011926009 | 0.118624014 |
| ENSG00000182578 | CSF1R subnetwork | 0.012055283 | 0.119667832 |
| ENSG00000173163 | COMMD1 subnetwork | 0.012079032 | 0.119694323 |
| GO:0003690 | double-stranded DNA binding | 0.012177982 | 0.120767888 |
| ENSG00000106263 | EIF3B subnetwork | 0.012185432 | 0.120775261 |
| ENSG00000152495 | CAMK4 subnetwork | 0.012184812 | 0.120880558 |
| GO:0001776 | leukocyte homeostasis | 0.012237341 | 0.121018277 |
| MP:0002928 | abnormal bile duct morphology | 0.012251548 | 0.121043478 |
| ENSG00000213658 | LAT subnetwork | 0.012343012 | 0.121807124 |
| MP:0010308 | decreased tumor latency | 0.01239992 | 0.122309028 |
| MP:0000490 | abnormal crypts of Lieberkuhn morphology | 0.012521968 | 0.123330442 |
| ENSG00000092098 | RNF31 subnetwork | 0.012548524 | 0.123570191 |
| KEGG_ASTHMA | KEGG_ASTHMA | 0.012556532 | 0.123593074 |
| ENSG00000180353 | HCLS1 subnetwork | 0.012614269 | 0.124178201 |
| MP:0006345 | absent second branchial arch | 0.012657342 | 0.124697755 |
| MP:0005350 | increased susceptibility to autoimmune disorder | 0.012654391 | 0.124762316 |
| MP:0004189 | abnormal alveolar process morphology | 0.012677503 | 0.124805867 |
| ENSG00000167286 | CD3D subnetwork | 0.012710256 | 0.125086207 |
| ENSG00000100294 | MCAT subnetwork | 0.012719633 | 0.125150732 |
| MP:0006387 | abnormal T cell number | 0.012738162 | 0.125301205 |
| ENSG00000141027 | NCOR1 subnetwork | 0.01280179 | 0.125515464 |
| MP:0005094 | abnormal T cell proliferation | 0.012780182 | 0.125537403 |
| GO:0002507 | tolerance induction | 0.012813832 | 0.125579399 |
| ENSG00000127616 | SMARCA4 subnetwork | 0.012963289 | 0.126237201 |
| GO:0050798 | activated T cell proliferation | 0.012872775 | 0.126286449 |
| MP:0008190 | decreased transitional stage B cell number | 0.012954826 | 0.126302306 |
| MP:0008721 | abnormal chemokine level | 0.012892034 | 0.126306769 |
| ENSG00000105204 | DYRK1B subnetwork | 0.012990461 | 0.126342711 |
| ENSG00000141646 | SMAD4 subnetwork | 0.012917336 | 0.126369863 |
| GO:0002761 | regulation of myeloid leukocyte differentiation | 0.012948385 | 0.126410256 |
| KEGG_VIRAL_MYOCARDITIS | KEGG_VIRAL_MYOCARDITIS | 0.01293498 | 0.126432849 |
| ENSG00000121966 | CXCR4 subnetwork | 0.013024066 | 0.126448041 |
| GO:0050727 | regulation of inflammatory response | 0.01305834 | 0.126573129 |
| ENSG00000113721 | PDGFRB subnetwork | 0.013067198 | 0.126593033 |
| ENSG00000204104 | TRAF3IP1 subnetwork | 0.013036482 | 0.126595745 |
| MP:0005031 | abnormal trophoblast layer morphology | 0.013155025 | 0.127589134 |
| ENSG00000161203 | AP2M1 subnetwork | 0.013201406 | 0.128050847 |
| GO:0001906 | cell killing | 0.013192314 | 0.12807464 |
| ENSG00000163811 | WDR43 subnetwork | 0.013245162 | 0.128238781 |
| MP:0003229 | abnormal vitelline vasculature morphology | 0.013310337 | 0.128637902 |
| ENSG00000151247 | EIF4E subnetwork | 0.013365347 | 0.129078614 |
| GO:0018105 | peptidyl-serine phosphorylation | 0.013444981 | 0.129898649 |
| ENSG00000130165 | ELOF1 subnetwork | 0.013472787 | 0.130168776 |

| | | | |
|---|---|---|---|
| MP:0006269 | abnormal mammary gland growth during pregnancy | 0.013516485 | 0.130454928 |
| MP:0000352 | decreased cell proliferation | 0.013507276 | 0.130564924 |
| ENSG00000015285 | WAS subnetwork | 0.013598145 | 0.131102694 |
| GO:0001818 | negative regulation of cytokine production | 0.013640389 | 0.131202691 |
| ENSG00000139323 | POC1B subnetwork | 0.013737613 | 0.131821998 |
| MP:0005289 | increased oxygen consumption | 0.013732949 | 0.131932773 |
| ENSG00000151849 | CENPJ subnetwork | 0.013746849 | 0.131963087 |
| REACTOME_TRANSLOCATION_OF | REACTOME_TRANSLOCATION_OF_ZAP:70_TO_IMMUNC | 0.013784764 | 0.132187762 |
| ENSG00000206306 | HLA-DRB1 subnetwork | 0.013815407 | 0.132217573 |
| ENSG00000126767 | ELK1 subnetwork | 0.013825279 | 0.132232441 |
| ENSG00000188846 | RPL14 subnetwork | 0.013834237 | 0.132247285 |
| ENSG00000206240 | HLA-DRB1 subnetwork | 0.013815407 | 0.132328308 |
| MP:0008554 | decreased circulating tumor necrosis factor level | 0.013928133 | 0.133096828 |
| MP:0001377 | abnormal mating frequency | 0.013970201 | 0.133402836 |
| GO:0002274 | myeloid leukocyte activation | 0.013986192 | 0.133458333 |
| GO:0018209 | peptidyl-serine modification | 0.014068338 | 0.134151414 |
| ENSG00000205517 | RGL3 subnetwork | 0.014045027 | 0.13417985 |
| GO:0048524 | positive regulation of viral reproduction | 0.014144568 | 0.134338843 |
| ENSG00000136286 | MYO1G subnetwork | 0.014156751 | 0.134393064 |
| KEGG_ADIPOCYTOKINE_SIGNALIN | KEGG_ADIPOCYTOKINE_SIGNALING_PATHWAY | 0.014144049 | 0.134408602 |
| GO:0042510 | regulation of tyrosine phosphorylation of Stat1 protein | 0.01408137 | 0.134413965 |
| ENSG00000147853 | AK3 subnetwork | 0.01413683 | 0.134478477 |
| MP:0001844 | autoimmune response | 0.014132864 | 0.134548467 |
| KEGG_B_CELL_RECEPTOR_SIGNAI | KEGG_B_CELL_RECEPTOR_SIGNALING_PATHWAY | 0.014125759 | 0.134618574 |
| ENSG00000151065 | DCP1B subnetwork | 0.014121846 | 0.134688797 |
| ENSG00000198626 | RYR2 subnetwork | 0.014115133 | 0.134759136 |
| ENSG00000110092 | CCND1 subnetwork | 0.014227194 | 0.13490099 |
| ENSG00000198053 | SIRPA subnetwork | 0.014260226 | 0.135284419 |
| GO:0007249 | I-kappaB kinase/NF-kappaB cascade | 0.014320139 | 0.135538209 |
| ENSG00000206450 | HLA-B subnetwork | 0.014309109 | 0.135608553 |
| GO:0032613 | interleukin-10 production | 0.014306311 | 0.135720165 |
| GO:0050900 | leukocyte migration | 0.014306084 | 0.13583196 |
| GO:0002260 | lymphocyte homeostasis | 0.014372639 | 0.135878489 |
| REACTOME_TRAF6_MEDIATED_N | REACTOME_TRAF6_MEDIATED_NF:KB_ACTIVATION | 0.014429834 | 0.135995086 |
| ENSG00000125503 | PPP1R12C subnetwork | 0.014400732 | 0.136013126 |
| MP:0000291 | enlarged pericardium | 0.014421852 | 0.136106557 |
| GO:0032615 | interleukin-12 production | 0.014486461 | 0.136415712 |
| ENSG00000143768 | LEFTY2 subnetwork | 0.014564746 | 0.137080948 |
| MP:0003492 | abnormal involuntary movement | 0.014591278 | 0.137091503 |
| MP:0008681 | increased interleukin-17 secretion | 0.014710693 | 0.137510171 |
| ENSG00000105647 | PIK3R2 subnetwork | 0.01472051 | 0.137560976 |
| GO:0004715 | non-membrane spanning protein tyrosine kinase activity | 0.014663413 | 0.137591837 |
| GO:0043122 | regulation of I-kappaB kinase/NF-kappaB cascade | 0.014706057 | 0.13762215 |
| GO:0045061 | thymic T cell selection | 0.014697614 | 0.137693562 |
| MP:0000496 | abnormal small intestine morphology | 0.014690318 | 0.137724307 |
| KEGG_PANCREATIC_CANCER | KEGG_PANCREATIC_CANCER | 0.014770553 | 0.137855402 |
| ENSG00000162772 | ATF3 subnetwork | 0.01479101 | 0.137905844 |
| ENSG00000172809 | RPL38 subnetwork | 0.01489184 | 0.138520614 |
| GO:0060333 | interferon-gamma-mediated signaling pathway | 0.014846263 | 0.138523925 |
| ENSG00000152518 | ZFP36L2 subnetwork | 0.014885441 | 0.13855178 |
| ENSG00000114737 | CISH subnetwork | 0.014914624 | 0.138570275 |
| REACTOME_GENERATION_OF_SE | REACTOME_GENERATION_OF_SECOND_MESSENGER_M | 0.014861174 | 0.138573744 |
| ENSG00000100239 | PPP6R2 subnetwork | 0.014869468 | 0.138582996 |
| GO:0033158 | regulation of protein import into nucleus, translocation | 0.014936993 | 0.138700565 |

| | | | |
|---|---|---|---|
| ENSG00000091127 | PUS7 subnetwork | 0.014978712 | 0.139112903 |
| MP:0004953 | decreased spleen weight | 0.015035908 | 0.139452496 |
| ENSG00000171552 | BCL2L1 subnetwork | 0.015028406 | 0.139524577 |
| MP:0006380 | abnormal spermatid morphology | 0.015087492 | 0.139903459 |
| MP:0001732 | postnatal growth retardation | 0.015160725 | 0.140353698 |
| ENSG00000108861 | DUSP3 subnetwork | 0.015329793 | 0.140764331 |
| ENSG00000107562 | CXCL12 subnetwork | 0.01532553 | 0.140796813 |
| ENSG00000103671 | TRIP4 subnetwork | 0.015342987 | 0.140811456 |
| GO:0050708 | regulation of protein secretion | 0.015323242 | 0.140869219 |
| ENSG00000149273 | RPS3 subnetwork | 0.015320159 | 0.140981644 |
| ENSG00000184863 | RBM33 subnetwork | 0.015231227 | 0.141004016 |
| MP:0000217 | abnormal leukocyte cell number | 0.015240133 | 0.141011236 |
| ENSG00000183520 | UTP11L subnetwork | 0.015305116 | 0.141014377 |
| GO:0006916 | anti-apoptosis | 0.015266967 | 0.141032826 |
| ENSG00000104856 | RELB subnetwork | 0.015293496 | 0.141047162 |
| ENSG00000105429 | MEGF8 subnetwork | 0.015258649 | 0.141065705 |
| ENSG00000171223 | JUNB subnetwork | 0.015285859 | 0.14108 |
| GO:0003707 | steroid hormone receptor activity | 0.01538453 | 0.141096979 |
| ENSG00000147439 | BIN3 subnetwork | 0.015250823 | 0.141098637 |
| ENSG00000184967 | NOC4L subnetwork | 0.015464253 | 0.141620334 |
| ENSG00000157557 | ETS2 subnetwork | 0.015488542 | 0.141666667 |
| ENSG00000198793 | MTOR subnetwork | 0.015500027 | 0.141673275 |
| ENSG00000211790 | ENSG00000211790 subnetwork | 0.015551248 | 0.14207607 |
| ENSG00000102010 | BMX subnetwork | 0.015580685 | 0.142359462 |
| ENSG00000125977 | EIF2S2 subnetwork | 0.015668007 | 0.142648221 |
| MP:0008133 | decreased Peyer's patch number | 0.015660191 | 0.142721519 |
| MP:0001919 | abnormal reproductive system physiology | 0.015716974 | 0.142969984 |
| ENSG00000182718 | ANXA2 subnetwork | 0.01574091 | 0.143014996 |
| ENSG00000118922 | KLF12 subnetwork | 0.015853379 | 0.143769716 |
| GO:0051059 | NF-kappaB binding | 0.01587726 | 0.144050433 |
| ENSG00000158042 | MRPL17 subnetwork | 0.015900012 | 0.144094488 |
| ENSG00000005175 | RPAP3 subnetwork | 0.016023744 | 0.145125786 |
| GO:0010761 | fibroblast migration | 0.016018993 | 0.14516129 |
| GO:0032386 | regulation of intracellular transport | 0.016050091 | 0.14520817 |
| ENSG00000103342 | GSPT1 subnetwork | 0.016174102 | 0.146075353 |
| GO:0033138 | positive regulation of peptidyl-serine phosphorylation | 0.016212165 | 0.146235294 |
| GO:0045672 | positive regulation of osteoclast differentiation | 0.016245008 | 0.14624119 |
| ENSG00000125912 | NCLN subnetwork | 0.016240537 | 0.146355799 |
| ENSG00000100815 | TRIP11 subnetwork | 0.016292039 | 0.146713615 |
| MP:0000604 | amyloidosis | 0.016432282 | 0.147849883 |
| MP:0008714 | lung carcinoma | 0.016443657 | 0.147851563 |
| GO:0022627 | cytosolic small ribosomal subunit | 0.016529271 | 0.148207327 |
| ENSG00000111424 | VDR subnetwork | 0.016515263 | 0.148283931 |
| GO:0071260 | cellular response to mechanical stimulus | 0.016506726 | 0.148399688 |
| MP:0001273 | decreased metastatic potential | 0.016581343 | 0.148753894 |
| ENSG00000163512 | AZI2 subnetwork | 0.016607642 | 0.149027237 |
| GO:0043123 | positive regulation of I-kappaB kinase/NF-kappaB cascad | 0.016734371 | 0.15 |
| ENSG00000006075 | CCL3 subnetwork | 0.016773529 | 0.15042735 |
| MP:0008108 | abnormal small intestinal villus morphology | 0.016845344 | 0.150737005 |
| GO:0046639 | negative regulation of alpha-beta T cell differentiation | 0.016837859 | 0.150815217 |
| ENSG00000105401 | CDC37 subnetwork | 0.016976971 | 0.151627907 |
| ENSG00000178950 | GAK subnetwork | 0.017046231 | 0.152246321 |
| GO:0046822 | regulation of nucleocytoplasmic transport | 0.017124042 | 0.152472952 |
| GO:0046677 | response to antibiotic | 0.017097855 | 0.152513534 |

| | | | |
|---|---|---|---|
| ENSG00000099308 | MAST3 subnetwork | 0.017089941 | 0.152592879 |
| ENSG00000132471 | WBP2 subnetwork | 0.017170384 | 0.152700617 |
| ENSG00000198755 | RPL10A subnetwork | 0.017214646 | 0.152775636 |
| ENSG00000157077 | ZFYVE9 subnetwork | 0.017169761 | 0.152779923 |
| ENSG00000081189 | MEF2C subnetwork | 0.017267267 | 0.152966102 |
| ENSG00000145907 | G3BP1 subnetwork | 0.017280006 | 0.153040801 |
| GO:0046006 | regulation of activated T cell proliferation | 0.017323648 | 0.153384615 |
| ENSG00000004478 | FKBP4 subnetwork | 0.017426239 | 0.154688701 |
| GO:0070228 | regulation of lymphocyte apoptotic process | 0.017473165 | 0.155069124 |
| ENSG00000136518 | ACTL6A subnetwork | 0.017493563 | 0.15514198 |
| ENSG00000198265 | HELZ subnetwork | 0.017722837 | 0.156940184 |
| MP:0000599 | enlarged liver | 0.017761079 | 0.157318008 |
| GO:0031343 | positive regulation of cell killing | 0.017778926 | 0.157388974 |
| MP:0009133 | decreased white fat cell size | 0.017836203 | 0.157727621 |
| MP:0005666 | abnormal adipose tissue physiology | 0.017867309 | 0.157912844 |
| ENSG00000054796 | SPO11 subnetwork | 0.017895819 | 0.158097785 |
| ENSG00000211735 | ENSG00000211735 subnetwork | 0.017965743 | 0.158174905 |
| MP:0003627 | abnormal leukocyte tethering or rolling | 0.017981556 | 0.158282675 |
| ENSG00000211810 | ENSG00000211810 subnetwork | 0.017965743 | 0.158295282 |
| MP:0002335 | decreased airway responsiveness | 0.017913694 | 0.158320611 |
| ENSG00000211799 | ENSG00000211799 subnetwork | 0.017965743 | 0.158415842 |
| ENSG00000211739 | ENSG00000211739 subnetwork | 0.017965743 | 0.158536585 |
| MP:0006271 | abnormal involution of the mammary gland | 0.017963339 | 0.158619375 |
| GO:0008629 | induction of apoptosis by intracellular signals | 0.018024914 | 0.158731967 |
| ENSG00000211762 | ENSG00000211762 subnetwork | 0.018096528 | 0.159294385 |
| ENSG00000198324 | FAM109A subnetwork | 0.018170127 | 0.159855951 |
| GO:0032655 | regulation of interleukin-12 production | 0.018199176 | 0.159924242 |
| MP:0003793 | abnormal submandibular gland morphology | 0.018228267 | 0.160060514 |
| ENSG00000163486 | SRGAP2 subnetwork | 0.018226145 | 0.160181681 |
| ENSG00000139722 | VPS37B subnetwork | 0.0182925 | 0.160582011 |
| REACTOME_CHEMOKINE_RECEPT | REACTOME_CHEMOKINE_RECEPTORS_BIND_CHEMOKIN | 0.018314249 | 0.160649547 |
| ENSG00000162692 | VCAM1 subnetwork | 0.018391621 | 0.161283019 |
| GO:0035591 | signaling adaptor activity | 0.018409386 | 0.161387632 |
| MP:0001614 | abnormal blood vessel morphology | 0.018522217 | 0.161402851 |
| ENSG00000133026 | MYH10 subnetwork | 0.018463877 | 0.161454408 |
| MP:0002358 | abnormal spleen periarteriolar lymphoid sheath morpho | 0.018521224 | 0.161524024 |
| ENSG00000175104 | TRAF6 subnetwork | 0.018538128 | 0.161544228 |
| ENSG00000151498 | ACAD8 subnetwork | 0.01847542 | 0.161558735 |
| ENSG00000135605 | TEC subnetwork | 0.018516749 | 0.161645379 |
| ENSG00000197373 | ENSG00000197373 subnetwork | 0.01851591 | 0.161729323 |
| ENSG00000168255 | POLR2J3 subnetwork | 0.01851591 | 0.161851016 |
| MP:0006341 | small first branchial arch | 0.018602955 | 0.161872659 |
| ENSG00000050748 | MAPK9 subnetwork | 0.018626255 | 0.161901198 |
| ENSG00000100365 | NCF4 subnetwork | 0.018708129 | 0.162752431 |
| ENSG00000198618 | ENSG00000198618 subnetwork | 0.018796338 | 0.163077496 |
| MP:0004947 | skin inflammation | 0.018779155 | 0.163097015 |
| GO:0003714 | transcription corepressor activity | 0.01876614 | 0.163106796 |
| GO:0030674 | protein binding, bridging | 0.018878115 | 0.163187221 |
| ENSG00000148303 | RPL7A subnetwork | 0.018755644 | 0.16319133 |
| ENSG00000196262 | PPIA subnetwork | 0.018796338 | 0.163199105 |
| ENSG00000157456 | CCNB2 subnetwork | 0.018910063 | 0.163214551 |
| MP:0002088 | abnormal embryonic growth/weight/body size | 0.018865842 | 0.163271375 |
| MP:0009338 | increased splenocyte number | 0.018838623 | 0.163291139 |
| MP:0001851 | eye inflammation | 0.018943744 | 0.163316024 |

| | | | |
|---|---|---|---|
| ENSG00000100266 | PACSIN2 subnetwork | 0.018854141 | 0.163355655 |
| MP:0003724 | increased susceptibility to induced arthritis | 0.018998538 | 0.163676798 |
| GO:0010740 | positive regulation of intracellular protein kinase cascade | 0.019035627 | 0.163962963 |
| MP:0005362 | abnormal Langerhans cell physiology | 0.019070406 | 0.164016272 |
| ENSG00000180182 | MED14 subnetwork | 0.019055759 | 0.164063657 |
| GO:0031331 | positive regulation of cellular catabolic process | 0.019139725 | 0.164412417 |
| ENSG00000156127 | BATF subnetwork | 0.019181369 | 0.164623338 |
| ENSG00000135341 | MAP3K7 subnetwork | 0.019227884 | 0.164749263 |
| GO:0004879 | ligand-activated sequence-specific DNA binding RNA poly | 0.019208086 | 0.164833948 |
| ENSG00000100784 | RPS6KA5 subnetwork | 0.019275423 | 0.165070007 |
| ENSG00000055732 | MCOLN3 subnetwork | 0.019357295 | 0.165135929 |
| MP:0000295 | trabecula carnea hypoplasia | 0.01934771 | 0.165194996 |
| ENSG00000108679 | LGALS3BP subnetwork | 0.019311812 | 0.165206186 |
| ENSG00000124614 | RPS10 subnetwork | 0.019356005 | 0.165257353 |
| ENSG00000119414 | PPP6C subnetwork | 0.019417759 | 0.165418502 |
| ENSG00000121440 | PDZRN3 subnetwork | 0.019588656 | 0.166544387 |
| ENSG00000123416 | TUBA1B subnetwork | 0.019627177 | 0.166788856 |
| ENSG00000123643 | SLC36A1 subnetwork | 0.019651314 | 0.166813187 |
| GO:0042176 | regulation of protein catabolic process | 0.01977288 | 0.167862372 |
| ENSG00000161405 | IKZF3 subnetwork | 0.01978599 | 0.167922458 |
| ENSG00000070759 | TESK2 subnetwork | 0.019868221 | 0.168494152 |
| GO:0046641 | positive regulation of alpha-beta T cell proliferation | 0.01989497 | 0.168722628 |
| ENSG00000182093 | WRB subnetwork | 0.019894122 | 0.168845873 |
| MP:0000280 | thin ventricular wall | 0.02003116 | 0.169418182 |
| ENSG00000143398 | PIP5K1A subnetwork | 0.019976477 | 0.169438366 |
| GO:0032800 | receptor biosynthetic process | 0.020052536 | 0.169440407 |
| GO:0048305 | immunoglobulin secretion | 0.020030904 | 0.169541485 |
| ENSG00000148737 | TCF7L2 subnetwork | 0.020004359 | 0.169569971 |
| MP:0001926 | female infertility | 0.020026044 | 0.169664967 |
| ENSG00000134987 | WDR36 subnetwork | 0.020173597 | 0.170174165 |
| GO:0050690 | regulation of defense response to virus by virus | 0.020169123 | 0.170261438 |
| ENSG00000139514 | SLC7A1 subnetwork | 0.02021882 | 0.170377085 |
| ENSG00000068615 | REEP1 subnetwork | 0.020317898 | 0.170628613 |
| ENSG00000120910 | PPP3CC subnetwork | 0.02031469 | 0.170751988 |
| ENSG00000123091 | RNF11 subnetwork | 0.020313924 | 0.170875543 |
| MP:0001825 | arrested T cell differentiation | 0.020276011 | 0.170942029 |
| ENSG00000183034 | OTOP2 subnetwork | 0.020310855 | 0.17096307 |
| ENSG00000112249 | ASCC3 subnetwork | 0.020445705 | 0.171407942 |
| MP:0008803 | abnormal placental labyrinth vasculature morphology | 0.020479641 | 0.171449171 |
| ENSG00000172116 | CD8B subnetwork | 0.020460699 | 0.171464646 |
| GO:0010627 | regulation of intracellular protein kinase cascade | 0.020502331 | 0.171469741 |
| ENSG00000177463 | NR2C2 subnetwork | 0.020514955 | 0.171490281 |
| ENSG00000181163 | NPM1 subnetwork | 0.020581397 | 0.171942446 |
| GO:0001910 | regulation of leukocyte mediated cytotoxicity | 0.020749841 | 0.173616104 |
| ENSG00000204221 | WDR46 subnetwork | 0.02079276 | 0.173833453 |
| ENSG00000089022 | MAPKAPK5 subnetwork | 0.020834635 | 0.17390681 |
| ENSG00000206284 | WDR46 subnetwork | 0.02079276 | 0.173958333 |
| ENSG00000108055 | SMC3 subnetwork | 0.02083297 | 0.173995696 |
| ENSG00000164587 | RPS14 subnetwork | 0.02089599 | 0.174266285 |
| MP:0008973 | decreased erythroid progenitor cell number | 0.020879272 | 0.174391117 |
| MP:0004905 | decreased uterus weight | 0.021005213 | 0.17498213 |
| MP:0004955 | increased thymus weight | 0.02099781 | 0.175071531 |
| ENSG00000166402 | TUB subnetwork | 0.02105352 | 0.175285714 |
| GO:0008170 | N-methyltransferase activity | 0.021119188 | 0.17551675 |

| | | | |
|---|---|---|---|
| GO:0004177 | aminopeptidase activity | 0.021108702 | 0.175606277 |
| ENSG00000172115 | CYCS subnetwork | 0.021102525 | 0.175624554 |
| MP:0005033 | abnormal trophoblast giant cells | 0.0212214 | 0.176068376 |
| MP:0005331 | insulin resistance | 0.021377457 | 0.176865672 |
| GO:0032653 | regulation of interleukin-10 production | 0.021361182 | 0.17688478 |
| MP:0000596 | abnormal liver development | 0.021354167 | 0.176903915 |
| GO:0050707 | regulation of cytokine secretion | 0.021443246 | 0.177166193 |
| ENSG00000119616 | FCF1 subnetwork | 0.021463647 | 0.177217885 |
| GO:0000288 | nuclear-transcribed mRNA catabolic process, deadenylat | 0.021510327 | 0.17751773 |
| ENSG00000033800 | PIAS1 subnetwork | 0.02153731 | 0.177604536 |
| MP:0001212 | skin lesions | 0.021589171 | 0.178045326 |
| GO:0043383 | negative T cell selection | 0.02166969 | 0.178591649 |
| ENSG00000142453 | CARM1 subnetwork | 0.021802377 | 0.179110797 |
| ENSG00000211889 | ENSG00000211889 subnetwork | 0.021832538 | 0.17914024 |
| MP:0003795 | abnormal bone structure | 0.021822484 | 0.179196051 |
| GO:0043372 | positive regulation of CD4-positive, alpha-beta T cell diff | 0.021801388 | 0.179237288 |
| ENSG00000153233 | PTPRR subnetwork | 0.021773771 | 0.179349364 |
| GO:2000516 | positive regulation of CD4-positive, alpha-beta T cell acti | 0.021801388 | 0.179363958 |
| ENSG00000137713 | PPP2R1B subnetwork | 0.02193512 | 0.180246479 |
| ENSG00000156675 | RAB11FIP1 subnetwork | 0.022002491 | 0.180788177 |
| ENSG00000122691 | TWIST1 subnetwork | 0.022092154 | 0.181131413 |
| ENSG00000106546 | AHR subnetwork | 0.02213809 | 0.181144663 |
| MP:0000704 | abnormal thymus development | 0.022090975 | 0.181223629 |
| GO:0061008 | hepaticobiliary system development | 0.022216935 | 0.181438596 |
| ENSG00000105216 | ENSG00000105216 subnetwork | 0.02230724 | 0.181757703 |
| MP:0004808 | abnormal hematopoietic stem cell morphology | 0.022285551 | 0.181779958 |
| ENSG00000065183 | WDR3 subnetwork | 0.022267847 | 0.181802244 |
| ENSG00000144668 | ITGA9 subnetwork | 0.022351375 | 0.182155353 |
| MP:0008702 | increased interleukin-5 secretion | 0.022416148 | 0.182424878 |
| MP:0002411 | decreased susceptibility to bacterial infection | 0.022402557 | 0.182482517 |
| ENSG00000026508 | CD44 subnetwork | 0.022483725 | 0.182751397 |
| MP:0004876 | decreased mean systemic arterial blood pressure | 0.022625417 | 0.183879972 |
| MP:0010875 | increased bone volume | 0.022702359 | 0.184553696 |
| GO:0001909 | leukocyte mediated cytotoxicity | 0.02272624 | 0.18456446 |
| ENSG00000057657 | PRDM1 subnetwork | 0.022804879 | 0.184700974 |
| ENSG00000198933 | TBKBP1 subnetwork | 0.022827142 | 0.184746352 |
| ENSG00000100644 | HIF1A subnetwork | 0.022779957 | 0.184759916 |
| ENSG00000213625 | LEPROT subnetwork | 0.022769088 | 0.184818942 |
| ENSG00000179583 | CIITA subnetwork | 0.022886781 | 0.184906315 |
| ENSG00000133740 | E2F5 subnetwork | 0.022874733 | 0.184930556 |
| MP:0008827 | abnormal thymus cell ratio | 0.022911276 | 0.184951456 |
| ENSG00000123685 | BATF3 subnetwork | 0.023048132 | 0.185511757 |
| ENSG00000126749 | ENSG00000126749 subnetwork | 0.023060895 | 0.185521769 |
| MP:0001222 | epidermal hyperplasia | 0.022998309 | 0.185585586 |
| ENSG00000075391 | RASAL2 subnetwork | 0.023036745 | 0.185640138 |
| ENSG00000121022 | COPS5 subnetwork | 0.023012086 | 0.18566482 |
| ENSG00000127666 | TICAM1 subnetwork | 0.023132572 | 0.185946133 |
| ENSG00000188404 | SELL subnetwork | 0.023192774 | 0.186103448 |
| MP:0003710 | abnormal physiological neovascularization | 0.0231893 | 0.186197378 |
| MP:0009395 | increased nucleated erythrocyte cell number | 0.023317044 | 0.186519945 |
| ENSG00000132964 | CDK8 subnetwork | 0.023306553 | 0.186545079 |
| GO:2000106 | regulation of leukocyte apoptotic process | 0.02333765 | 0.186563574 |
| ENSG00000177169 | ULK1 subnetwork | 0.023296412 | 0.186604683 |
| ENSG00000142676 | RPL11 subnetwork | 0.023289098 | 0.186664369 |

| | | | |
|---|---|---|---|
| MP:0010144 | abnormal tumor vascularization | 0.023431131 | 0.186831276 |
| MP:0000609 | abnormal liver physiology | 0.023415574 | 0.186890872 |
| ENSG00000139318 | DUSP6 subnetwork | 0.02340568 | 0.18698489 |
| ENSG00000173110 | HSPA6 subnetwork | 0.02357548 | 0.187021858 |
| REACTOME_ACTIVATION_OF_BH3 | REACTOME_ACTIVATION_OF_BH3:ONLY_PROTEINS | 0.023574047 | 0.187149692 |
| ENSG00000101966 | XIAP subnetwork | 0.023497689 | 0.187217272 |
| ENSG00000204120 | GIGYF2 subnetwork | 0.023562977 | 0.187243502 |
| ENSG00000160654 | CD3G subnetwork | 0.023512077 | 0.187260274 |
| MP:0009858 | abnormal cellular extravasation | 0.023543955 | 0.187268994 |
| ENSG00000160220 | ENSG00000160220 subnetwork | 0.023670942 | 0.187849829 |
| GO:0004003 | ATP-dependent DNA helicase activity | 0.023753115 | 0.188335607 |
| ENSG00000108256 | NUFIP2 subnetwork | 0.023799247 | 0.188479891 |
| GO:0045785 | positive regulation of cell adhesion | 0.023975119 | 0.189713896 |
| KEGG_PATHWAYS_IN_CANCER | KEGG_PATHWAYS_IN_CANCER | 0.024090985 | 0.189850645 |
| ENSG00000147689 | FAM83A subnetwork | 0.024073992 | 0.189877717 |
| ENSG00000175390 | EIF3F subnetwork | 0.024107068 | 0.189891452 |
| ENSG00000148843 | PDCD11 subnetwork | 0.024068871 | 0.189972808 |
| ENSG00000165704 | HPRT1 subnetwork | 0.024039347 | 0.190027229 |
| ENSG00000139687 | RB1 subnetwork | 0.024054064 | 0.190034014 |
| ENSG00000137574 | TGS1 subnetwork | 0.024168714 | 0.190176152 |
| ENSG00000126261 | UBA2 subnetwork | 0.024164599 | 0.190305085 |
| ENSG00000119812 | FAM98A subnetwork | 0.024192415 | 0.190385917 |
| ENSG00000130522 | JUND subnetwork | 0.024226636 | 0.19056157 |
| REACTOME_TERMINATION_OF_O | REACTOME_TERMINATION_OF_O:GLYCAN_BIOSYNTHES | 0.024348225 | 0.190633423 |
| REACTOME_SEMA4D_INDUCED_( | REACTOME_SEMA4D_INDUCED_CELL_MIGRATION_AND | 0.024342399 | 0.190728254 |
| ENSG00000124181 | PLCG1 subnetwork | 0.0242481 | 0.190736984 |
| ENSG00000120156 | TEK subnetwork | 0.024336796 | 0.190823212 |
| ENSG00000122026 | RPL21 subnetwork | 0.024408246 | 0.190942761 |
| MP:0002500 | granulomatous inflammation | 0.024329035 | 0.190952059 |
| GO:0050699 | WW domain binding | 0.024563111 | 0.190997323 |
| ENSG00000120709 | FAM53C subnetwork | 0.024489353 | 0.191006711 |
| ENSG00000110492 | MDK subnetwork | 0.02453476 | 0.191024782 |
| ENSG00000177879 | AP3S1 subnetwork | 0.024478168 | 0.191034251 |
| MP:0011402 | renal cast | 0.024320924 | 0.191081081 |
| GO:0050710 | negative regulation of cytokine secretion | 0.024471188 | 0.19109543 |
| GO:0030889 | negative regulation of B cell proliferation | 0.024531404 | 0.191119303 |
| ENSG00000171863 | RPS7 subnetwork | 0.024513082 | 0.19121395 |
| ENSG00000110987 | BCL7A subnetwork | 0.024468222 | 0.191223941 |
| GO:0035850 | epithelial cell differentiation involved in kidney developn | 0.02445575 | 0.191251682 |
| GO:0045136 | development of secondary sexual characteristics | 0.024660898 | 0.191644385 |
| ENSG00000141522 | ARHGDIA subnetwork | 0.024632556 | 0.191672241 |
| MP:0008189 | increased transitional stage B cell number | 0.024700785 | 0.191883768 |
| ENSG00000055208 | TAB2 subnetwork | 0.024748531 | 0.192189586 |
| REACTOME_NUCLEAR_RECEPTOR | REACTOME_NUCLEAR_RECEPTOR_TRANSCRIPTION_PAT | 0.024844126 | 0.192861908 |
| GO:0042104 | positive regulation of activated T cell proliferation | 0.024871086 | 0.192866667 |
| ENSG00000065675 | PRKCQ subnetwork | 0.02492125 | 0.193009321 |
| ENSG00000129250 | KIF1C subnetwork | 0.02491394 | 0.193071286 |
| MP:0008254 | increased megakaryocyte cell number | 0.024969036 | 0.19334664 |
| MP:0005425 | increased macrophage cell number | 0.025016229 | 0.193716755 |
| ENSG00000130479 | MAP1S subnetwork | 0.025101152 | 0.194156707 |
| ENSG00000070756 | PABPC1 subnetwork | 0.025099565 | 0.194252492 |
| ENSG00000168488 | ATXN2L subnetwork | 0.02518203 | 0.194757797 |
| GO:0033157 | regulation of intracellular protein transport | 0.025225314 | 0.194893899 |
| GO:0010212 | response to ionizing radiation | 0.025251814 | 0.19509609 |

| | | | |
|---|---|---|---|
| GO:0030522 | intracellular receptor mediated signaling pathway | 0.025283297 | 0.195331126 |
| ENSG00000130312 | MRPL34 subnetwork | 0.025313137 | 0.195433488 |
| MP:0000737 | abnormal myotome development | 0.025370601 | 0.196097884 |
| MP:0005461 | abnormal dendritic cell morphology | 0.025433345 | 0.196532365 |
| ENSG00000211455 | STK38L subnetwork | 0.025432858 | 0.19666226 |
| ENSG00000164342 | TLR3 subnetwork | 0.025542833 | 0.19690178 |
| ENSG00000143119 | CD53 subnetwork | 0.025536894 | 0.196998681 |
| ENSG00000169375 | SIN3A subnetwork | 0.025523935 | 0.19709571 |
| ENSG00000112576 | CCND3 subnetwork | 0.025639597 | 0.197891963 |
| GO:0045346 | regulation of MHC class II biosynthetic process | 0.025698396 | 0.198123766 |
| ENSG00000206308 | HLA-DRA subnetwork | 0.025790777 | 0.198783695 |
| REACTOME_SEMA4D_IN_SEMAPI | REACTOME_SEMA4D_IN_SEMAPHORIN_SIGNALING | 0.025782281 | 0.198881579 |
| ENSG00000196083 | IL1RAP subnetwork | 0.02583406 | 0.198981603 |
| ENSG00000118046 | STK11 subnetwork | 0.025868525 | 0.199212081 |
| ENSG00000198034 | RPS4X subnetwork | 0.025930209 | 0.199606299 |
| ENSG00000164889 | SLC4A2 subnetwork | 0.026070727 | 0.200819672 |
| ENSG00000132153 | DHX30 subnetwork | 0.026120032 | 0.200883508 |
| MP:0006410 | abnormal common myeloid progenitor cell morphology | 0.026118806 | 0.200982318 |
| ENSG00000141543 | EIF4A3 subnetwork | 0.026111871 | 0.201048493 |
| ENSG00000078142 | PIK3C3 subnetwork | 0.026206144 | 0.201308044 |
| ENSG00000138293 | NCOA4 subnetwork | 0.026288758 | 0.201764706 |
| ENSG00000058668 | ATP2B4 subnetwork | 0.026360181 | 0.202088773 |
| GO:0046209 | nitric oxide metabolic process | 0.02634496 | 0.202090137 |
| ENSG00000149923 | PPP4C subnetwork | 0.026413545 | 0.202149837 |
| ENSG00000115904 | SOS1 subnetwork | 0.026400895 | 0.202151239 |
| MP:0008092 | abnormal T-helper 2 cell differentiation | 0.026386749 | 0.202185258 |
| MP:0000602 | enlarged liver sinusoidal spaces | 0.026533781 | 0.20263329 |
| ENSG00000198734 | F5 subnetwork | 0.026491602 | 0.202734375 |
| REACTOME_HEMOSTASIS | REACTOME_HEMOSTASIS | 0.026531799 | 0.202765127 |
| GO:0033077 | T cell differentiation in thymus | 0.026593793 | 0.202956465 |
| ENSG00000128829 | EIF2AK4 subnetwork | 0.026601649 | 0.202987013 |
| REACTOME_NOD12_SIGNALING_ | REACTOME_NOD12_SIGNALING_PATHWAY | 0.026722461 | 0.203926022 |
| ENSG00000012223 | LTF subnetwork | 0.026855742 | 0.20460441 |
| ENSG00000105173 | CCNE1 subnetwork | 0.026985756 | 0.204680439 |
| GO:2000116 | regulation of cysteine-type endopeptidase activity | 0.02697464 | 0.204780362 |
| ENSG00000065361 | ERBB3 subnetwork | 0.026950723 | 0.204883571 |
| MP:0008539 | decreased susceptibility to induced colitis | 0.026945952 | 0.204886731 |
| MP:0003132 | increased pre-B cell number | 0.026961976 | 0.204912734 |
| MP:0001824 | abnormal thymus involution | 0.026939239 | 0.20501943 |
| ENSG00000169429 | IL8 subnetwork | 0.026937797 | 0.205119896 |
| MP:0006270 | abnormal mammary gland growth during lactation | 0.027229639 | 0.206354839 |
| MP:0000511 | abnormal intestinal mucosa morphology | 0.027345609 | 0.206954282 |
| MP:0002993 | arthritis | 0.027305907 | 0.20696325 |
| GO:0045884 | regulation of survival gene product expression | 0.027336924 | 0.206990979 |
| GO:0001889 | liver development | 0.027394617 | 0.207271557 |
| ENSG00000107485 | GATA3 subnetwork | 0.027504257 | 0.208135048 |
| ENSG00000102001 | CACNA1F subnetwork | 0.027600351 | 0.208611825 |
| GO:0000289 | nuclear-transcribed mRNA poly(A) tail shortening | 0.027700071 | 0.209242619 |
| GO:0002718 | regulation of cytokine production involved in immune re | 0.027699179 | 0.209344894 |
| ENSG00000147507 | ENSG00000147507 subnetwork | 0.027730729 | 0.209364978 |
| ENSG00000169439 | SDC2 subnetwork | 0.027801401 | 0.209615385 |
| GO:0009986 | cell surface | 0.027835013 | 0.209801409 |
| GO:0042130 | negative regulation of T cell proliferation | 0.027867894 | 0.209980806 |
| ENSG00000206505 | HLA-A subnetwork | 0.027847441 | 0.209987196 |

| | | | |
|---|---|---|---|
| ENSG00000136448 | NMT1 subnetwork | 0.028096063 | 0.211413043 |
| REACTOME_NEPHRIN_INTERACTI | REACTOME_NEPHRIN_INTERACTIONS | 0.028121789 | 0.212108626 |
| GO:0070064 | proline-rich region binding | 0.028179732 | 0.212220804 |
| MP:0008210 | increased mature B cell number | 0.028163725 | 0.212292465 |
| ENSG00000148400 | NOTCH1 subnetwork | 0.028501777 | 0.214490446 |
| ENSG00000160633 | SAFB subnetwork | 0.028532697 | 0.214535623 |
| ENSG00000166167 | BTRC subnetwork | 0.028499282 | 0.214595284 |
| ENSG00000105141 | CASP14 subnetwork | 0.028531506 | 0.214640356 |
| ENSG00000004059 | ARF5 subnetwork | 0.028496657 | 0.214732143 |
| ENSG00000108604 | SMARCD2 subnetwork | 0.0286187 | 0.215416402 |
| ENSG00000206267 | ENSG00000206267 subnetwork | 0.028857809 | 0.21634981 |
| GO:0042054 | histone methyltransferase activity | 0.028796871 | 0.216412698 |
| ENSG00000153563 | CD8A subnetwork | 0.028833364 | 0.216465736 |
| GO:0017053 | transcriptional repressor complex | 0.02878992 | 0.216486658 |
| ENSG00000204351 | SKIV2L subnetwork | 0.028857809 | 0.216487001 |
| MP:0005419 | hypoalbuminemia | 0.028966058 | 0.21685642 |
| ENSG00000152894 | PTPRK subnetwork | 0.028960085 | 0.216898734 |
| MP:0002727 | decreased circulating insulin level | 0.028959084 | 0.217036099 |
| ENSG00000137154 | RPS6 subnetwork | 0.029035922 | 0.217045455 |
| ENSG00000173473 | SMARCC1 subnetwork | 0.029032183 | 0.217087808 |
| GO:0032270 | positive regulation of cellular protein metabolic process | 0.029029077 | 0.217225032 |
| ENSG00000185551 | NR2F2 subnetwork | 0.029140776 | 0.217665615 |
| MP:0009321 | increased histiocytic sarcoma incidence | 0.029162837 | 0.21778058 |
| GO:0043028 | cysteine-type endopeptidase regulator activity involved i | 0.029269366 | 0.218261965 |
| ENSG00000083520 | DIS3 subnetwork | 0.029258577 | 0.218273472 |
| ENSG00000147010 | SH3KBP1 subnetwork | 0.029408363 | 0.218561558 |
| ENSG00000092470 | WDR76 subnetwork | 0.029342936 | 0.218565135 |
| ENSG00000179335 | CLK3 subnetwork | 0.02943587 | 0.218601004 |
| ENSG00000143514 | TP53BP2 subnetwork | 0.029390375 | 0.218604651 |
| ENSG00000061273 | HDAC7 subnetwork | 0.02936128 | 0.218616352 |
| MP:0002161 | abnormal fertility/fecundity | 0.02948831 | 0.218640351 |
| ENSG00000147604 | RPL7 subnetwork | 0.029426552 | 0.218644068 |
| ENSG00000164951 | PDP1 subnetwork | 0.029519265 | 0.218659987 |
| ENSG00000006062 | MAP3K14 subnetwork | 0.029474482 | 0.218714734 |
| ENSG00000178562 | CD28 subnetwork | 0.029568031 | 0.218804756 |
| GO:0033135 | regulation of peptidyl-serine phosphorylation | 0.029798473 | 0.220419012 |
| ENSG00000065717 | TLE2 subnetwork | 0.029843676 | 0.22053125 |
| ENSG00000165699 | TSC1 subnetwork | 0.029867829 | 0.220549656 |
| GO:0072676 | lymphocyte migration | 0.029908491 | 0.220755306 |
| ENSG00000100354 | TNRC6B subnetwork | 0.029956573 | 0.220760599 |
| ENSG00000150907 | FOXO1 subnetwork | 0.029946809 | 0.220867124 |
| ENSG00000186575 | NF2 subnetwork | 0.030114926 | 0.221344119 |
| MP:0008734 | decreased susceptibility to endotoxin shock | 0.030108029 | 0.221419676 |
| ENSG00000080503 | SMARCA2 subnetwork | 0.030102364 | 0.22152648 |
| ENSG00000055130 | CUL1 subnetwork | 0.030273273 | 0.222008679 |
| ENSG00000008735 | MAPK8IP2 subnetwork | 0.030269813 | 0.222115385 |
| MP:0001622 | abnormal vasculogenesis | 0.030268909 | 0.222253259 |
| ENSG00000196735 | HLA-DQA1 subnetwork | 0.03022682 | 0.222263682 |
| MP:0002874 | decreased hemoglobin content | 0.030302456 | 0.222273854 |
| GO:0042101 | T cell receptor complex | 0.030240063 | 0.222311995 |
| REACTOME_TRANSCRIPTIONAL_R | REACTOME_TRANSCRIPTIONAL_REGULATION_OF_WHIT | 0.030345785 | 0.222352941 |
| MP:0003352 | increased circulating renin level | 0.030268772 | 0.222391304 |
| ENSG00000116604 | MEF2D subnetwork | 0.03041584 | 0.222603587 |
| ENSG00000121753 | BAI2 subnetwork | 0.030404787 | 0.222679455 |

| | | | |
|---|---|---|---|
| MP:0006050 | pulmonary fibrosis | 0.030484613 | 0.22302225 |
| GO:0071346 | cellular response to interferon-gamma | 0.030625539 | 0.223703704 |
| MP:0005399 | increased susceptibility to fungal infection | 0.030580816 | 0.223749228 |
| MP:0008782 | increased B cell apoptosis | 0.030725888 | 0.2245219 |
| GO:0030332 | cyclin binding | 0.030806564 | 0.224984596 |
| MP:0008186 | increased pro-B cell number | 0.030840337 | 0.224984615 |
| ENSG00000196236 | XPNPEP3 subnetwork | 0.030825734 | 0.225 |
| GO:0043281 | regulation of cysteine-type endopeptidase activity involv | 0.030794496 | 0.225 |
| GO:0043368 | positive T cell selection | 0.030871719 | 0.225092251 |
| MP:0004841 | abnormal small intestine crypts of Lieberkuhn morpholo | 0.030914813 | 0.225337838 |
| GO:0045670 | regulation of osteoclast differentiation | 0.030910568 | 0.225414874 |
| GO:0060090 | binding, bridging | 0.030975992 | 0.225721301 |
| ENSG00000115946 | PNO1 subnetwork | 0.031128397 | 0.226348039 |
| GO:0002708 | positive regulation of lymphocyte mediated immunity | 0.031110742 | 0.226364194 |
| GO:0002705 | positive regulation of leukocyte mediated immunity | 0.031110742 | 0.226503067 |
| ENSG00000179344 | HLA-DQB1 subnetwork | 0.031248973 | 0.226819572 |
| ENSG00000186468 | RPS23 subnetwork | 0.031269745 | 0.226833741 |
| ENSG00000126001 | CEP250 subnetwork | 0.031237742 | 0.226927785 |
| KEGG_ACUTE_MYELOID_LEUKEM | KEGG_ACUTE_MYELOID_LEUKEMIA | 0.031225984 | 0.226944274 |
| MP:0000266 | abnormal heart morphology | 0.031412237 | 0.227286585 |
| ENSG00000089157 | RPLP0 subnetwork | 0.031374671 | 0.227289377 |
| ENSG00000149554 | CHEK1 subnetwork | 0.03138977 | 0.227303234 |
| ENSG00000182568 | SATB1 subnetwork | 0.031441285 | 0.227330896 |
| ENSG00000121067 | SPOP subnetwork | 0.031369784 | 0.227397679 |
| ENSG00000006712 | PAF1 subnetwork | 0.031478044 | 0.227496955 |
| MP:0002416 | abnormal proerythroblast morphology | 0.031577484 | 0.227889294 |
| ENSG00000118689 | FOXO3 subnetwork | 0.031571317 | 0.227967133 |
| MP:0011501 | increased glomerular capsule space | 0.031669476 | 0.227973301 |
| ENSG00000130713 | EXOSC2 subnetwork | 0.031686836 | 0.22801698 |
| ENSG00000151090 | THRB subnetwork | 0.031646539 | 0.228020644 |
| ENSG00000108094 | CUL2 subnetwork | 0.031634045 | 0.228145897 |
| ENSG00000198604 | BAZ1A subnetwork | 0.031645102 | 0.228159174 |
| MP:0003383 | abnormal gluconeogenesis | 0.031798255 | 0.228757576 |
| MP:0002190 | disorganized myocardium | 0.03181139 | 0.228800727 |
| ENSG00000043462 | LCP2 subnetwork | 0.031998391 | 0.230217786 |
| MP:0001712 | abnormal placenta development | 0.031995375 | 0.230326877 |
| ENSG00000116918 | TSNAX subnetwork | 0.032067486 | 0.230574018 |
| ENSG00000124762 | CDKN1A subnetwork | 0.032109445 | 0.230597465 |
| MP:0003884 | decreased macrophage cell number | 0.032086769 | 0.230615942 |
| ENSG00000103152 | MPG subnetwork | 0.032057011 | 0.230622733 |
| ENSG00000135090 | TAOK3 subnetwork | 0.032137297 | 0.230729795 |
| ENSG00000124198 | ARFGEF2 subnetwork | 0.032275288 | 0.231445783 |
| ENSG00000063046 | EIF4B subnetwork | 0.032253675 | 0.231464738 |
| ENSG00000163517 | HDAC11 subnetwork | 0.032308185 | 0.231517158 |
| ENSG00000128272 | ATF4 subnetwork | 0.032340327 | 0.231558363 |
| MP:0001874 | acanthosis | 0.032414753 | 0.23190018 |
| REACTOME_NUCLEOTIDE:BINDIN | REACTOME_NUCLEOTIDE:BINDING_DOMAIN_LEUCINE_I | 0.032494247 | 0.232241587 |
| GO:0045178 | basal part of cell | 0.032640796 | 0.233333333 |
| REACTOME_TRANSLATION_INITIA | REACTOME_TRANSLATION_INITIATION_COMPLEX_FORM | 0.032691171 | 0.233673469 |
| MP:0011098 | complete embryonic lethality during organogenesis | 0.0327344 | 0.234013197 |
| ENSG00000172175 | MALT1 subnetwork | 0.032904946 | 0.234931096 |
| MP:0004856 | decreased ovary weight | 0.032884542 | 0.234982014 |
| GO:0043566 | structure-specific DNA binding | 0.032934119 | 0.23502994 |
| GO:0030684 | preribosome | 0.032957879 | 0.23518851 |

| | | | |
|---|---|---|---|
| GO:0035967 | cellular response to topologically incorrect protein | 0.033094196 | 0.236124402 |
| ENSG00000196981 | WDR5B subnetwork | 0.033196318 | 0.236293206 |
| ENSG00000065833 | ME1 subnetwork | 0.033134383 | 0.236341901 |
| ENSG00000117266 | CDK18 subnetwork | 0.033193337 | 0.236374478 |
| GO:2000108 | positive regulation of leukocyte apoptotic process | 0.033182471 | 0.236426014 |
| ENSG00000136383 | ALPK3 subnetwork | 0.033180841 | 0.236477612 |
| GO:0006111 | regulation of gluconeogenesis | 0.033172847 | 0.23655914 |
| REACTOME_OPIOID_SIGNALLING | REACTOME_OPIOID_SIGNALLING | 0.033277671 | 0.23707564 |
| REACTOME_RIBOSOMAL_SCANNI | REACTOME_RIBOSOMAL_SCANNING_AND_START_COD( | 0.033331643 | 0.23718025 |
| MP:0000607 | abnormal hepatocyte morphology | 0.03332458 | 0.237202381 |
| ENSG00000100353 | EIF3D subnetwork | 0.033373486 | 0.237336504 |
| REACTOME_TOLL_LIKE_RECEPTOI | REACTOME_TOLL_LIKE_RECEPTOR_3_TLR3_CASCADE | 0.033517474 | 0.237551867 |
| REACTOME_GROWTH_HORMONI | REACTOME_GROWTH_HORMONE_RECEPTOR_SIGNALIN | 0.033449175 | 0.237648456 |
| REACTOME_TRIF_MEDIATED_TLR | REACTOME_TRIF_MEDIATED_TLR3_SIGNALING | 0.033517474 | 0.237692764 |
| ENSG00000013297 | CLDN11 subnetwork | 0.033556026 | 0.237766588 |
| GO:0001666 | response to hypoxia | 0.033513738 | 0.237774481 |
| GO:0051092 | positive regulation of NF-kappaB transcription factor acti | 0.033441725 | 0.237789661 |
| ENSG00000058404 | CAMK2B subnetwork | 0.033868889 | 0.239197166 |
| ENSG00000166046 | TCP11L2 subnetwork | 0.033806179 | 0.239266706 |
| ENSG00000120659 | TNFSF11 subnetwork | 0.033851606 | 0.239279386 |
| GO:0006402 | mRNA catabolic process | 0.033890163 | 0.239292035 |
| MP:0008813 | decreased common myeloid progenitor cell number | 0.033797328 | 0.239319527 |
| ENSG00000114867 | EIF4G1 subnetwork | 0.033922179 | 0.239357311 |
| MP:0003448 | altered tumor morphology | 0.033837142 | 0.239361702 |
| MP:0006082 | CNS inflammation | 0.033787742 | 0.239402013 |
| MP:0001654 | hepatic necrosis | 0.034012498 | 0.239687684 |
| ENSG00000140600 | SH3GL3 subnetwork | 0.034104537 | 0.2401649 |
| KEGG_PHOSPHATIDYLINOSITOL_S | KEGG_PHOSPHATIDYLINOSITOL_SIGNALING_SYSTEM | 0.034148444 | 0.240523838 |
| GO:0050810 | regulation of steroid biosynthetic process | 0.034206683 | 0.240617647 |
| ENSG00000166441 | RPL27A subnetwork | 0.034245408 | 0.240628672 |
| MP:0005621 | abnormal cell physiology | 0.034237655 | 0.240652557 |
| MP:0002446 | abnormal macrophage morphology | 0.034280896 | 0.240669014 |
| ENSG00000070159 | PTPN3 subnetwork | 0.034279212 | 0.240810335 |
| ENSG00000086189 | DIMT1 subnetwork | 0.034484695 | 0.242228739 |
| GO:0042517 | positive regulation of tyrosine phosphorylation of Stat3 p | 0.034547681 | 0.242819461 |
| ENSG00000146950 | SHROOM2 subnetwork | 0.034612188 | 0.243292326 |
| GO:0043560 | insulin receptor substrate binding | 0.034710368 | 0.244145199 |
| ENSG00000155506 | LARP1 subnetwork | 0.03476518 | 0.244558221 |
| ENSG00000168542 | COL3A1 subnetwork | 0.034949027 | 0.24619883 |
| ENSG00000171105 | INSR subnetwork | 0.035099626 | 0.247223846 |
| REACTOME_MYD88_CASCADE_IN | REACTOME_MYD88_CASCADE_INITIATED_ON_PLASMA_ | 0.03521243 | 0.247466511 |
| ENSG00000182511 | FES subnetwork | 0.035143757 | 0.247488318 |
| MP:0005012 | decreased eosinophil cell number | 0.035164635 | 0.24757735 |
| REACTOME_TOLL_LIKE_RECEPTOI | REACTOME_TOLL_LIKE_RECEPTOR_5_TLR5_CASCADE | 0.03521243 | 0.247610723 |
| ENSG00000168477 | TNXB subnetwork | 0.035190993 | 0.247666278 |
| REACTOME_TOLL_LIKE_RECEPTOI | REACTOME_TOLL_LIKE_RECEPTOR_10_TLR10_CASCADE | 0.03521243 | 0.247755102 |
| ENSG00000168918 | INPP5D subnetwork | 0.03532893 | 0.248195576 |
| KEGG_FC_EPSILON_RI_SIGNALIN( | KEGG_FC_EPSILON_RI_SIGNALING_PATHWAY | 0.035407239 | 0.248545666 |
| MP:0001190 | reddish skin | 0.035465067 | 0.24875 |
| ENSG00000170260 | ZNF212 subnetwork | 0.035502487 | 0.248925044 |
| REACTOME_MYD88:INDEPENDEN | REACTOME_MYD88:INDEPENDENT_CASCADE_INITIATED | 0.035626355 | 0.249448956 |
| ENSG00000179409 | GEMIN4 subnetwork | 0.035616745 | 0.249506674 |
| ENSG00000067182 | TNFRSF1A subnetwork | 0.035590319 | 0.24956446 |
| KEGG_CELL_ADHESION_MOLECUI | KEGG_CELL_ADHESION_MOLECULES_CAMS | 0.03567273 | 0.249710145 |

| | | | |
|---|---|---|---|
| ENSG00000087250 | MT3 subnetwork | 0.035702556 | 0.249797219 |
| MP:0010373 | myeloid hyperplasia | 0.035824622 | 0.250144592 |
| REACTOME_ENERGY_DEPENDENT | REACTOME_ENERGY_DEPENDENT_REGULATION_OF_MT | 0.035809871 | 0.250260417 |
| MP:0003025 | increased vasoconstriction | 0.035781244 | 0.250289519 |
| ENSG00000114125 | RNF7 subnetwork | 0.035909759 | 0.250722543 |
| ENSG00000212695 | ENSG00000212695 subnetwork | 0.036134993 | 0.252019619 |
| GO:0034976 | response to endoplasmic reticulum stress | 0.036110227 | 0.252020785 |
| GO:0035258 | steroid hormone receptor binding | 0.036095099 | 0.252108608 |
| GO:0050663 | cytokine secretion | 0.036326863 | 0.253344867 |
| GO:0045060 | negative thymic T cell selection | 0.036378964 | 0.253542627 |
| ENSG00000128594 | LRRC4 subnetwork | 0.036371316 | 0.253573487 |
| GO:0045089 | positive regulation of innate immune response | 0.036502615 | 0.254202648 |
| GO:0002861 | regulation of inflammatory response to antigenic stimulu | 0.036588881 | 0.254482759 |
| ENSG00000162419 | GMEB1 subnetwork | 0.036578771 | 0.254542841 |
| ENSG00000130340 | SNX9 subnetwork | 0.036561503 | 0.254574223 |
| ENSG00000169372 | CRADD subnetwork | 0.036704074 | 0.255112005 |
| ENSG00000120509 | PDZD11 subnetwork | 0.036885834 | 0.256483075 |
| ENSG00000140350 | ANP32A subnetwork | 0.03688332 | 0.25663031 |
| ENSG00000126070 | EIF2C3 subnetwork | 0.036951088 | 0.256737385 |
| ENSG00000206353 | SKIV2L subnetwork | 0.037000771 | 0.256905444 |
| ENSG00000102096 | PIM2 subnetwork | 0.037173425 | 0.256938892 |
| REACTOME_PLATELET_HOMEOST | REACTOME_PLATELET_HOMEOSTASIS | 0.037114878 | 0.257065217 |
| ENSG00000163877 | SNIP1 subnetwork | 0.037167161 | 0.257085714 |
| REACTOME_INTERLEUKIN:1_SIGN | REACTOME_INTERLEUKIN:1_SIGNALING | 0.037106986 | 0.257126503 |
| KEGG_NEUROTROPHIN_SIGNALIN | KEGG_NEUROTROPHIN_SIGNALING_PATHWAY | 0.037081163 | 0.257130584 |
| ENSG00000079335 | CDC14A subnetwork | 0.037235916 | 0.257130633 |
| GO:0031968 | organelle outer membrane | 0.037150685 | 0.257146941 |
| MP:0002027 | lung adenocarcinoma | 0.037223048 | 0.257191781 |
| ENSG00000114686 | MRPL3 subnetwork | 0.037333184 | 0.257264957 |
| ENSG00000161016 | RPL8 subnetwork | 0.037314624 | 0.257354618 |
| GO:0005160 | transforming growth factor beta receptor binding | 0.037435103 | 0.258058087 |
| MP:0009356 | decreased liver triglyceride level | 0.037595097 | 0.259191804 |
| ENSG00000055332 | EIF2AK2 subnetwork | 0.03772195 | 0.259829545 |
| REACTOME_ACTIVATED_TLR4_SIG | REACTOME_ACTIVATED_TLR4_SIGNALLING | 0.037714376 | 0.259835134 |
| GO:0045732 | positive regulation of protein catabolic process | 0.037710809 | 0.259982935 |
| GO:0046638 | positive regulation of alpha-beta T cell differentiation | 0.037797286 | 0.260221465 |
| ENSG00000166164 | BRD7 subnetwork | 0.037945137 | 0.261435868 |
| ENSG00000173917 | HOXB2 subnetwork | 0.038144528 | 0.262563812 |
| MP:0010769 | abnormal survival | 0.03822364 | 0.263002833 |
| ENSG00000153922 | CHD1 subnetwork | 0.038214242 | 0.263038549 |
| ENSG00000173011 | TADA2B subnetwork | 0.038390696 | 0.263865308 |
| ENSG00000156802 | ATAD2 subnetwork | 0.038387691 | 0.264014723 |
| ENSG00000108984 | MAP2K6 subnetwork | 0.038535132 | 0.264612776 |
| ENSG00000120699 | EXOSC8 subnetwork | 0.038524453 | 0.264762443 |
| MP:0004510 | myositis | 0.038597583 | 0.264858757 |
| ENSG00000099875 | MKNK2 subnetwork | 0.038646069 | 0.265019763 |
| ENSG00000115738 | ID2 subnetwork | 0.038698112 | 0.265208804 |
| ENSG00000063438 | AHRR subnetwork | 0.038713291 | 0.265228426 |
| ENSG00000131503 | ANKHD1 subnetwork | 0.038764442 | 0.265549296 |
| MP:0005670 | abnormal white adipose tissue physiology | 0.038755661 | 0.265586246 |
| GO:0051023 | regulation of immunoglobulin secretion | 0.039052523 | 0.266863406 |
| REACTOME_NFKB_AND_MAP_KIN | REACTOME_NFKB_AND_MAP_KINASES_ACTIVATION_M | 0.039039352 | 0.266929134 |
| ENSG00000149948 | HMGA2 subnetwork | 0.039024279 | 0.266966798 |
| ENSG00000177426 | TGIF1 subnetwork | 0.039165917 | 0.266993831 |

| | | | |
|---|---|---|---|
| MP:0002451 | abnormal macrophage physiology | 0.039007263 | 0.267004505 |
| ENSG00000183405 | ENSG00000183405 subnetwork | 0.039500691 | 0.267093541 |
| GO:0019079 | viral genome replication | 0.03915913 | 0.267143659 |
| MP:0005565 | increased blood urea nitrogen level | 0.039106948 | 0.267162921 |
| ENSG00000156976 | EIF4A2 subnetwork | 0.039495087 | 0.26718663 |
| KEGG_NOD_LIKE_RECEPTOR_SIGI | KEGG_NOD_LIKE_RECEPTOR_SIGNALING_PATHWAY | 0.03915258 | 0.267293655 |
| MP:0008080 | abnormal CD8-positive T cell differentiation | 0.039553405 | 0.267306622 |
| MP:0000600 | liver hypoplasia | 0.039479053 | 0.267307692 |
| REACTOME_EICOSANOID_LIGANI | REACTOME_EICOSANOID_LIGAND:BINDING_RECEPTORS | 0.039465995 | 0.267373118 |
| ENSG00000198286 | CARD11 subnetwork | 0.039308195 | 0.267469205 |
| ENSG00000124588 | NQO2 subnetwork | 0.039589828 | 0.267509728 |
| ENSG00000135968 | GCC2 subnetwork | 0.039462277 | 0.267522321 |
| ENSG00000143851 | PTPN7 subnetwork | 0.039254957 | 0.267544843 |
| GO:0004428 | inositol or phosphatidylinositol kinase activity | 0.039572298 | 0.267547275 |
| ENSG00000179071 | CCDC89 subnetwork | 0.039608273 | 0.267555556 |
| GO:0042493 | response to drug | 0.039303978 | 0.267591036 |
| ENSG00000206560 | ANKRD28 subnetwork | 0.039441695 | 0.267615857 |
| ENSG00000105229 | PIAS4 subnetwork | 0.039431465 | 0.26773743 |
| ENSG00000100968 | NFATC4 subnetwork | 0.039427495 | 0.267859139 |
| REACTOME_NONSENSE_MEDIATI | REACTOME_NONSENSE_MEDIATED_DECAY_ENHANCED | 0.039415497 | 0.267897092 |
| MP:0003984 | embryonic growth retardation | 0.039747605 | 0.267914587 |
| REACTOME_NONSENSE:MEDIATE | REACTOME_NONSENSE:MEDIATED_DECAY | 0.039415497 | 0.268047006 |
| ENSG00000113387 | SUB1 subnetwork | 0.039739154 | 0.268063263 |
| GO:0050691 | regulation of defense response to virus by host | 0.039719857 | 0.26815658 |
| ENSG00000165943 | MOAP1 subnetwork | 0.039833245 | 0.268486696 |
| GO:0019783 | small conjugating protein-specific protease activity | 0.039943317 | 0.268826135 |
| ENSG00000182953 | ENSG00000182953 subnetwork | 0.039917912 | 0.268864266 |
| GO:0032770 | positive regulation of monooxygenase activity | 0.039988064 | 0.268898727 |
| ENSG00000167526 | RPL13 subnetwork | 0.040030908 | 0.269109513 |
| MP:0005181 | decreased circulating estradiol level | 0.040112979 | 0.269679381 |
| ENSG00000139613 | SMARCC2 subnetwork | 0.040208426 | 0.270331492 |
| REACTOME_SIGNALLING_BY_NGF | REACTOME_SIGNALLING_BY_NGF | 0.040270043 | 0.270734401 |
| MP:0002740 | heart hypoplasia | 0.040362498 | 0.271109272 |
| GO:0048146 | positive regulation of fibroblast proliferation | 0.040429184 | 0.271251378 |
| GO:0030838 | positive regulation of actin filament polymerization | 0.040423032 | 0.271345836 |
| ENSG00000102387 | TAF7L subnetwork | 0.040529346 | 0.271751101 |
| MP:0004950 | abnormal brain vasculature morphology | 0.04051515 | 0.271790634 |
| ENSG00000166681 | NGFRAP1 subnetwork | 0.040575608 | 0.27187672 |
| MP:0000359 | abnormal mast cell morphology | 0.04059864 | 0.271892189 |
| GO:0046965 | retinoid X receptor binding | 0.04069069 | 0.272374931 |
| GO:0006954 | inflammatory response | 0.040713061 | 0.272417582 |
| ENSG00000198824 | CHAMP1 subnetwork | 0.041135078 | 0.274712329 |
| REACTOME_TOLL_RECEPTOR_CA | REACTOME_TOLL_RECEPTOR_CASCADES | 0.041121824 | 0.274780702 |
| ENSG00000204103 | MAFB subnetwork | 0.041109643 | 0.274794295 |
| MP:0005185 | decreased circulating progesterone level | 0.041097021 | 0.274890231 |
| ENSG00000162924 | REL subnetwork | 0.041076052 | 0.274903899 |
| MP:0005517 | decreased liver regeneration | 0.041491286 | 0.276725082 |
| GO:0045577 | regulation of B cell differentiation | 0.041616733 | 0.277285167 |
| ENSG00000109475 | RPL34 subnetwork | 0.04173099 | 0.277759563 |
| ENSG00000105662 | CRTC1 subnetwork | 0.041738472 | 0.277799017 |
| ENSG00000140575 | IQGAP1 subnetwork | 0.041765962 | 0.277811135 |
| GO:0051260 | protein homooligomerization | 0.041722568 | 0.27788409 |
| ENSG00000116095 | PLEKHA3 subnetwork | 0.041717587 | 0.278008753 |
| ENSG00000107625 | DDX50 subnetwork | 0.041892281 | 0.278587016 |

| | | | |
|---|---|---|---|
| ENSG00000121892 | PDS5A subnetwork | 0.041927526 | 0.278625954 |
| GO:0004402 | histone acetyltransferase activity | 0.04200861 | 0.278991826 |
| GO:0045646 | regulation of erythrocyte differentiation | 0.042088672 | 0.279411765 |
| REACTOME_CREB_PHOSPHORYLA | REACTOME_CREB_PHOSPHORYLATION_THROUGH_THE_ | 0.042160297 | 0.279472539 |
| ENSG00000107882 | SUFU subnetwork | 0.042136721 | 0.279488575 |
| ENSG00000125733 | TRIP10 subnetwork | 0.042108483 | 0.279504627 |
| GO:0045428 | regulation of nitric oxide biosynthetic process | 0.042183272 | 0.279538043 |
| MP:0005076 | abnormal cell differentiation | 0.042228869 | 0.279766431 |
| GO:0032965 | regulation of collagen biosynthetic process | 0.042275264 | 0.280157438 |
| MP:0003887 | increased hepatocyte apoptosis | 0.042350106 | 0.28049376 |
| ENSG00000137996 | RTCD1 subnetwork | 0.04243374 | 0.281182213 |
| ENSG00000006715 | VPS41 subnetwork | 0.0425614 | 0.28200542 |
| MP:0008174 | decreased follicular B cell number | 0.042584394 | 0.282042254 |
| ENSG00000072195 | SPEG subnetwork | 0.042735291 | 0.282531098 |
| GO:0033993 | response to lipid | 0.04268812 | 0.282539253 |
| MP:0002080 | prenatal lethality | 0.042732292 | 0.282683983 |
| ENSG00000130520 | LSM4 subnetwork | 0.042856643 | 0.28327027 |
| ENSG00000188386 | PPP3R2 subnetwork | 0.042919597 | 0.283576445 |
| KEGG_MAPK_SIGNALING_PATHW | KEGG_MAPK_SIGNALING_PATHWAY | 0.04299072 | 0.283675121 |
| MP:0010900 | abnormal pulmonary interalveolar septum morphology | 0.042980284 | 0.283774298 |
| ENSG00000115616 | SLC9A2 subnetwork | 0.043139884 | 0.284213362 |
| GO:0007292 | female gamete generation | 0.043105578 | 0.28425027 |
| ENSG00000169136 | ATF5 subnetwork | 0.043130946 | 0.284339623 |
| GO:0033613 | activating transcription factor binding | 0.043452649 | 0.284413498 |
| REACTOME_IRAK2_MEDIATED_A | REACTOME_IRAK2_MEDIATED_ACTIVATION_OF_TAK1_( | 0.043350014 | 0.284541063 |
| ENSG00000124486 | USP9X subnetwork | 0.043448526 | 0.284565916 |
| MP:0004952 | increased spleen weight | 0.043496994 | 0.284582441 |
| ENSG00000182621 | PLCB1 subnetwork | 0.043417573 | 0.284603004 |
| ENSG00000124788 | ATXN1 subnetwork | 0.043246263 | 0.284607104 |
| GO:0001912 | positive regulation of leukocyte mediated cytotoxicity | 0.043433714 | 0.28463807 |
| REACTOME_TRAF6_MEDIATED_I | REACTOME_TRAF6_MEDIATED_INDUCTION_OF_TAK1_( | 0.043350014 | 0.284693878 |
| MP:0005251 | blepharitis | 0.043281267 | 0.284696073 |
| MP:0009346 | decreased trabecular bone thickness | 0.043301276 | 0.284704301 |
| ENSG00000122965 | RBM19 subnetwork | 0.043239288 | 0.284706516 |
| REACTOME_RESPONSE_TO_ELEV | REACTOME_RESPONSE_TO_ELEVATED_PLATELET_CYTOS | 0.043348766 | 0.284846857 |
| MP:0001787 | pericardial edema | 0.043698686 | 0.285721925 |
| MP:0001655 | multifocal hepatic necrosis | 0.043682649 | 0.285794543 |
| GO:0045954 | positive regulation of natural killer cell mediated cytotox | 0.043769799 | 0.286171917 |
| GO:0002717 | positive regulation of natural killer cell mediated immuni | 0.043769799 | 0.286324786 |
| ENSG00000133703 | KRAS subnetwork | 0.043817329 | 0.286339381 |
| KEGG_COLORECTAL_CANCER | KEGG_COLORECTAL_CANCER | 0.043755404 | 0.286370925 |
| ENSG00000147140 | NONO subnetwork | 0.043849425 | 0.2864 |
| MP:0008246 | abnormal leukocyte morphology | 0.043914145 | 0.286600959 |
| ENSG00000069667 | RORA subnetwork | 0.043892174 | 0.286620469 |
| GO:0052548 | regulation of endopeptidase activity | 0.044006805 | 0.287040979 |
| ENSG00000136352 | NKX2-1 subnetwork | 0.043995986 | 0.287087327 |
| ENSG00000161970 | RPL26 subnetwork | 0.044072734 | 0.287367021 |
| ENSG00000127388 | ENSG00000127388 subnetwork | 0.044156982 | 0.287672689 |
| MP:0008673 | decreased interleukin-13 secretion | 0.04418023 | 0.287679235 |
| ENSG00000197558 | ENSG00000197558 subnetwork | 0.044156982 | 0.287825625 |
| MP:0003606 | kidney failure | 0.044294374 | 0.288428875 |
| ENSG00000090659 | CD209 subnetwork | 0.044378385 | 0.288779841 |
| ENSG00000120333 | MRPS14 subnetwork | 0.044419643 | 0.288944857 |
| GO:0004843 | ubiquitin-specific protease activity | 0.044572029 | 0.289285714 |

| | | | |
|---|---|---|---|
| MP:0009230 | abnormal sperm head morphology | 0.044619249 | 0.289323467 |
| ENSG00000196498 | NCOR2 subnetwork | 0.044521404 | 0.289327331 |
| ENSG00000132109 | TRIM21 subnetwork | 0.044658582 | 0.289408347 |
| ENSG00000206258 | TNXB subnetwork | 0.044614466 | 0.289423585 |
| ENSG00000087266 | SH3BP2 subnetwork | 0.044565855 | 0.289438857 |
| ENSG00000163558 | PRKCI subnetwork | 0.044514412 | 0.28945416 |
| ENSG00000120798 | NR2C1 subnetwork | 0.044947029 | 0.291420275 |
| GO:0051353 | positive regulation of oxidoreductase activity | 0.045098762 | 0.291442865 |
| MP:0004130 | abnormal muscle cell glucose uptake | 0.045034287 | 0.291486558 |
| GO:0030120 | vesicle coat | 0.045089303 | 0.291517387 |
| ENSG00000147905 | ZCCHC7 subnetwork | 0.045027056 | 0.291561181 |
| ENSG00000073756 | PTGS2 subnetwork | 0.045147661 | 0.291657895 |
| ENSG00000143093 | FAM40A subnetwork | 0.045019579 | 0.291688654 |
| ENSG00000086065 | CHMP5 subnetwork | 0.045229284 | 0.291899001 |
| GO:0032507 | maintenance of protein location in cell | 0.045389458 | 0.292981073 |
| ENSG00000100316 | RPL3 subnetwork | 0.045523057 | 0.293363064 |
| REACTOME_PLATELET_ACTIVATIC | REACTOME_PLATELET_ACTIVATION_SIGNALING_AND_A | 0.045450557 | 0.29340515 |
| GO:0043901 | negative regulation of multi-organism process | 0.045513481 | 0.293490814 |
| ENSG00000117450 | PRDX1 subnetwork | 0.045495053 | 0.293539916 |
| GO:0042306 | regulation of protein import into nucleus | 0.045579051 | 0.293654955 |
| MP:0001715 | placental labyrinth hypoplasia | 0.045626536 | 0.293867925 |
| ENSG00000082701 | GSK3B subnetwork | 0.045943977 | 0.294548774 |
| GO:0045058 | T cell selection | 0.045989318 | 0.294551616 |
| GO:0042267 | natural killer cell mediated cytotoxicity | 0.045785353 | 0.294659686 |
| REACTOME_TOLL_LIKE_RECEPTOI | REACTOME_TOLL_LIKE_RECEPTOR_TLR6TLR2_CASCADE | 0.045940262 | 0.294702505 |
| GO:0002228 | natural killer cell mediated immunity | 0.045785353 | 0.294814039 |
| REACTOME_TOLL_LIKE_RECEPTOI | REACTOME_TOLL_LIKE_RECEPTOR_2_TLR2_CASCADE | 0.045940262 | 0.294856397 |
| REACTOME_MYD88MAL_CASCAD | REACTOME_MYD88MAL_CASCADE_INITIATED_ON_PLAS | 0.045940262 | 0.295010449 |
| GO:0034105 | positive regulation of tissue remodeling | 0.045874283 | 0.295133438 |
| REACTOME_TOLL_LIKE_RECEPTOI | REACTOME_TOLL_LIKE_RECEPTOR_TLR1TLR2_CASCADE | 0.045940262 | 0.295164663 |
| MP:0003658 | abnormal capillary morphology | 0.046117711 | 0.295205836 |
| ENSG00000144852 | NR1I2 subnetwork | 0.046140878 | 0.295234375 |
| REACTOME_TRAF3:DEPENDENT_I | REACTOME_TRAF3:DEPENDENT_IRF_ACTIVATION_PATH | 0.045931944 | 0.295292887 |
| GO:0045342 | MHC class II biosynthetic process | 0.046221787 | 0.295679334 |
| ENSG00000078304 | PPP2R5C subnetwork | 0.046308277 | 0.295688312 |
| ENSG00000082175 | PGR subnetwork | 0.04633835 | 0.295716511 |
| ENSG00000177106 | EPS8L2 subnetwork | 0.046302064 | 0.295841996 |
| ENSG00000160293 | VAV2 subnetwork | 0.046287256 | 0.295865835 |
| MP:0002672 | abnormal branchial arch artery morphology | 0.046284078 | 0.295967742 |
| ENSG00000179271 | GADD45GIP1 subnetwork | 0.046393013 | 0.296133887 |
| ENSG00000206305 | HLA-DQA1 subnetwork | 0.046537959 | 0.296630378 |
| ENSG00000206413 | ENSG00000206413 subnetwork | 0.046595984 | 0.296633868 |
| ENSG00000206239 | ENSG00000206239 subnetwork | 0.046537959 | 0.296784232 |
| ENSG00000206493 | HLA-E subnetwork | 0.046595984 | 0.296787565 |
| ENSG00000169031 | COL4A3 subnetwork | 0.046742722 | 0.297490947 |
| ENSG00000118194 | TNNT2 subnetwork | 0.046736194 | 0.297619048 |
| GO:0042506 | tyrosine phosphorylation of Stat5 protein | 0.046972811 | 0.298296335 |
| ENSG00000086015 | MAST2 subnetwork | 0.046904678 | 0.298319545 |
| ENSG00000174748 | RPL15 subnetwork | 0.046953723 | 0.298321281 |
| ENSG00000000938 | FGR subnetwork | 0.04694486 | 0.298397933 |
| ENSG00000143155 | TIPRL subnetwork | 0.047087127 | 0.298506694 |
| ENSG00000092820 | EZR subnetwork | 0.047046052 | 0.298581743 |
| ENSG00000120693 | SMAD9 subnetwork | 0.047080786 | 0.298583205 |
| ENSG00000052749 | RRP12 subnetwork | 0.047223532 | 0.298587571 |

| | | | |
|---|---|---|---|
| ENSG00000069431 | ABCC9 subnetwork | 0.047033067 | 0.298684211 |
| KEGG_ENDOMETRIAL_CANCER | KEGG_ENDOMETRIAL_CANCER | 0.04722101 | 0.29868962 |
| GO:0051707 | response to other organism | 0.047080321 | 0.298737113 |
| GO:0051235 | maintenance of location | 0.047189858 | 0.29874036 |
| ENSG00000023171 | GRAMD1B subnetwork | 0.047182825 | 0.298791152 |
| ENSG00000137547 | MRPL15 subnetwork | 0.047177146 | 0.298919197 |
| MP:0010377 | abnormal gut flora balance | 0.047524546 | 0.300564392 |
| ENSG00000136485 | DCAF7 subnetwork | 0.04751436 | 0.300667351 |
| ENSG00000120889 | TNFRSF10B subnetwork | 0.047565564 | 0.300769231 |
| ENSG00000115325 | DOK1 subnetwork | 0.047752143 | 0.301099182 |
| ENSG00000086061 | DNAJA1 subnetwork | 0.047734698 | 0.301099744 |
| ENSG00000158796 | DEDD subnetwork | 0.047703911 | 0.301126472 |
| GO:0042379 | chemokine receptor binding | 0.047696264 | 0.301178279 |
| MP:0000465 | gastrointestinal hemorrhage | 0.04772736 | 0.301202661 |
| ENSG00000015171 | ZMYND11 subnetwork | 0.047668283 | 0.301230138 |
| GO:0090311 | regulation of protein deacetylation | 0.047850534 | 0.301325854 |
| ENSG00000182498 | ENSG00000182498 subnetwork | 0.04783347 | 0.301377551 |
| ENSG00000096150 | RPS18 subnetwork | 0.04783347 | 0.301531394 |
| MP:0008168 | decreased B-1a cell number | 0.047934768 | 0.301605505 |
| ENSG00000206212 | ENSG00000206212 subnetwork | 0.04783347 | 0.301685393 |
| KEGG_LONG_TERM_POTENTIATIC | KEGG_LONG_TERM_POTENTIATION | 0.047826713 | 0.30183955 |
| ENSG00000213741 | RPS29 subnetwork | 0.048075256 | 0.302343352 |
| ENSG00000125447 | GGA3 subnetwork | 0.048129339 | 0.302647658 |
| GO:0030968 | endoplasmic reticulum unfolded protein response | 0.048276244 | 0.302845528 |
| MP:0008617 | increased circulating interleukin-12 level | 0.048233454 | 0.30292472 |
| GO:0009615 | response to virus | 0.048320379 | 0.302996445 |
| GO:0034620 | cellular response to unfolded protein | 0.048276244 | 0.302999492 |
| ENSG00000177728 | KIAA0195 subnetwork | 0.048214533 | 0.303002545 |
| GO:0031663 | lipopolysaccharide-mediated signaling pathway | 0.048365563 | 0.303071066 |
| ENSG00000157933 | SKI subnetwork | 0.048438212 | 0.303247083 |
| ENSG00000029725 | RABEP1 subnetwork | 0.048602542 | 0.304054739 |
| ENSG00000067048 | DDX3Y subnetwork | 0.048602331 | 0.304208925 |
| GO:0051090 | regulation of sequence-specific DNA binding transcriptio | 0.048738043 | 0.305015198 |
| ENSG00000103994 | ZFP106 subnetwork | 0.048772485 | 0.305086032 |
| ENSG00000104825 | NFKBIB subnetwork | 0.048755806 | 0.305088608 |
| ENSG00000185630 | PBX1 subnetwork | 0.04883062 | 0.305260496 |
| ENSG00000132906 | CASP9 subnetwork | 0.048925626 | 0.306016178 |
| GO:0031625 | ubiquitin protein ligase binding | 0.049047233 | 0.306619505 |
| GO:0030125 | clathrin vesicle coat | 0.049243741 | 0.307329975 |
| ENSG00000137171 | KLC4 subnetwork | 0.049151273 | 0.30739899 |
| ENSG00000182899 | RPL35A subnetwork | 0.049171194 | 0.307420495 |
| GO:0032496 | response to lipopolysaccharide | 0.049238175 | 0.307484879 |
| MP:0010180 | increased susceptibility to weight loss | 0.049218649 | 0.307513868 |
| REACTOME_TOLL_LIKE_RECEPTOI | REACTOME_TOLL_LIKE_RECEPTOR_4_TLR4_CASCADE | 0.04928976 | 0.307527694 |
| MP:0004201 | fetal growth retardation | 0.049208242 | 0.307618567 |
| ENSG00000165912 | PACSIN3 subnetwork | 0.049322809 | 0.307674887 |
| MP:0009335 | decreased splenocyte proliferation | 0.049415557 | 0.308249497 |
| MP:0005559 | increased circulating glucose level | 0.049656532 | 0.309417378 |
| GO:0002544 | chronic inflammatory response | 0.049624279 | 0.309451986 |
| ENSG00000132970 | WASF3 subnetwork | 0.04968821 | 0.309462851 |
| ENSG00000197943 | PLCG2 subnetwork | 0.049643116 | 0.309472362 |
| ENSG00000156136 | DCK subnetwork | 0.049729647 | 0.309483191 |
| MP:0002590 | increased mean corpuscular volume | 0.049838598 | 0.309854564 |
| ENSG00000131043 | C20orf4 subnetwork | 0.04988718 | 0.30994489 |

| | | | |
|---|---|---|---|
| GO:0000123 | histone acetyltransferase complex | 0.049864415 | 0.309949875 |
| GO:0009607 | response to biotic stimulus | 0.049974713 | 0.310290436 |
| GO:0019218 | regulation of steroid metabolic process | 0.050052249 | 0.310705353 |
| ENSG00000121031 | ENSG00000121031 subnetwork | 0.050046841 | 0.310835836 |
| ENSG00000065243 | PKN2 subnetwork | 0.050099019 | 0.3109 |
| MP:0001719 | absent vitelline blood vessels | 0.050171672 | 0.311169415 |
| ENSG00000146109 | ABT1 subnetwork | 0.050337114 | 0.312112887 |
| ENSG00000149016 | TUT1 subnetwork | 0.050510478 | 0.313354968 |
| REACTOME_MTORC1:MEDIATED_ | REACTOME_MTORC1:MEDIATED_SIGNALLING | 0.050570663 | 0.313622754 |
| ENSG00000133056 | PIK3C2B subnetwork | 0.050675466 | 0.314214464 |
| ENSG00000105810 | CDK6 subnetwork | 0.050733815 | 0.314581256 |
| ENSG00000135932 | CAB39 subnetwork | 0.050780561 | 0.314598904 |
| GO:0005901 | caveola | 0.050937702 | 0.315231458 |
| ENSG00000141052 | MYOCD subnetwork | 0.050922094 | 0.315338645 |
| ENSG00000130726 | TRIM28 subnetwork | 0.051139682 | 0.316517413 |
| MP:0005617 | increased susceptibility to type IV hypersensitivity reacti | 0.051239288 | 0.31661699 |
| MP:0000603 | pale liver | 0.051207662 | 0.316625249 |
| ENSG00000090989 | EXOC1 subnetwork | 0.051192594 | 0.316708105 |
| ENSG00000149806 | FAU subnetwork | 0.051294401 | 0.316832175 |
| ENSG00000163519 | TRAT1 subnetwork | 0.051385478 | 0.317270471 |
| GO:0070035 | purine NTP-dependent helicase activity | 0.051559181 | 0.31817055 |
| GO:0008026 | ATP-dependent helicase activity | 0.051559181 | 0.318328373 |
| GO:0051861 | glycolipid binding | 0.051590841 | 0.318359762 |
| ENSG00000211899 | ENSG00000211899 subnetwork | 0.051680019 | 0.318514851 |
| GO:0002828 | regulation of type 2 immune response | 0.051675765 | 0.31867261 |
| ENSG00000007908 | SELE subnetwork | 0.051851181 | 0.318864198 |
| REACTOME_NF:KB_IS_ACTIVATED | REACTOME_NF:KB_IS_ACTIVATED_AND_SIGNALS_SURV | 0.051833627 | 0.318898221 |
| MP:0006143 | increased systemic arterial diastolic blood pressure | 0.051817839 | 0.318932279 |
| ENSG00000065882 | TBC1D1 subnetwork | 0.051891826 | 0.318978282 |
| ENSG00000163466 | ARPC2 subnetwork | 0.051808795 | 0.319040554 |
| ENSG00000160808 | MYL3 subnetwork | 0.052022268 | 0.31910389 |
| GO:0005057 | receptor signaling protein activity | 0.05192365 | 0.319141589 |
| ENSG00000175793 | SFN subnetwork | 0.051805135 | 0.319148936 |
| GO:0000299 | integral to membrane of membrane fraction | 0.051989802 | 0.319230769 |
| ENSG00000129347 | KRI1 subnetwork | 0.052019659 | 0.319236453 |
| GO:0050729 | positive regulation of inflammatory response | 0.05201027 | 0.319344505 |
| ENSG00000114491 | UMPS subnetwork | 0.052160637 | 0.319419862 |
| GO:0043027 | cysteine-type endopeptidase inhibitor activity involved i | 0.052124669 | 0.319478603 |
| ENSG00000065989 | PDE4A subnetwork | 0.05210845 | 0.319512795 |
| ENSG00000170027 | YWHAG subnetwork | 0.052229927 | 0.319523576 |
| ENSG00000197958 | RPL12 subnetwork | 0.052216504 | 0.31968059 |
| MP:0003103 | liver degeneration | 0.052463748 | 0.321035837 |
| MP:0002702 | decreased circulating free fatty acid level | 0.052551958 | 0.32124632 |
| GO:0008009 | chemokine activity | 0.052624228 | 0.321456596 |
| GO:0050728 | negative regulation of inflammatory response | 0.052700823 | 0.321960784 |
| MP:0003936 | abnormal reproductive system development | 0.052858324 | 0.323027927 |
| MP:0005464 | abnormal platelet physiology | 0.052963568 | 0.323056235 |
| REACTOME_NICD_TRAFFICS_TO_ | REACTOME_NICD_TRAFFICS_TO_NUCLEUS | 0.052962631 | 0.323214286 |
| ENSG00000138709 | LARP1B subnetwork | 0.052920984 | 0.323237023 |
| REACTOME_NOTCH:HLH_TRANSC | REACTOME_NOTCH:HLH_TRANSCRIPTION_PATHWAY | 0.052962631 | 0.323372491 |
| ENSG00000120899 | PTK2B subnetwork | 0.053161425 | 0.324023438 |
| GO:0001562 | response to protozoan | 0.05313602 | 0.324035173 |
| ENSG00000134717 | BTF3L4 subnetwork | 0.053125215 | 0.324144673 |
| ENSG00000183751 | TBL3 subnetwork | 0.053252983 | 0.32442655 |

| | | | |
|---|---|---|---|
| REACTOME_TRAF6_MEDIATED_IN | REACTOME_TRAF6_MEDIATED_INDUCTION_OF_NFKB_A | 0.053414898 | 0.325536585 |
| ENSG00000101266 | CSNK2A1 subnetwork | 0.053486428 | 0.32588981 |
| MP:0006042 | increased apoptosis | 0.053615251 | 0.326046738 |
| GO:0045063 | T-helper 1 cell differentiation | 0.053583744 | 0.32608378 |
| MP:0002724 | enhanced wound healing | 0.053569808 | 0.326145224 |
| ENSG00000164742 | ADCY1 subnetwork | 0.053758141 | 0.326861314 |
| ENSG00000197122 | SRC subnetwork | 0.053968277 | 0.327063107 |
| ENSG00000094631 | HDAC6 subnetwork | 0.053951958 | 0.327124818 |
| ENSG00000143190 | POU2F1 subnetwork | 0.05384071 | 0.327213035 |
| MP:0000416 | sparse hair | 0.053945192 | 0.32723518 |
| ENSG00000083544 | TDRD3 subnetwork | 0.053920886 | 0.327297035 |
| GO:0010332 | response to gamma radiation | 0.054022547 | 0.327341097 |
| MP:0001613 | abnormal vasodilation | 0.054263036 | 0.328540252 |
| ENSG00000105618 | PRPF31 subnetwork | 0.054296919 | 0.328599127 |
| ENSG00000213281 | NRAS subnetwork | 0.054339487 | 0.328609496 |
| MP:0000274 | enlarged heart | 0.054702553 | 0.330823245 |
| ENSG00000135679 | MDM2 subnetwork | 0.054727507 | 0.330880929 |
| ENSG00000126226 | PCID2 subnetwork | 0.05491788 | 0.331497585 |
| ENSG00000007171 | NOS2 subnetwork | 0.054955035 | 0.331554804 |
| ENSG00000084623 | EIF3I subnetwork | 0.054893663 | 0.33160058 |
| ENSG00000064300 | NGFR subnetwork | 0.054916316 | 0.331657806 |
| ENSG00000011405 | PIK3C2A subnetwork | 0.054885438 | 0.331712627 |
| MP:0001130 | abnormal ovarian folliculogenesis | 0.055224741 | 0.333132239 |
| REACTOME_AKT_PHOSPHORYLAT | REACTOME_AKT_PHOSPHORYLATES_TARGETS_IN_THE_ | 0.055283834 | 0.333188616 |
| ENSG00000121879 | PIK3CA subnetwork | 0.055320574 | 0.333341369 |
| ENSG00000121858 | TNFSF10 subnetwork | 0.055445204 | 0.333903614 |
| ENSG00000143476 | DTL subnetwork | 0.055586531 | 0.334223184 |
| MP:0006117 | aortic valve stenosis | 0.05563928 | 0.334278846 |
| ENSG00000130338 | TULP4 subnetwork | 0.055583615 | 0.334359962 |
| KEGG_OOCYTE_MEIOSIS | KEGG_OOCYTE_MEIOSIS | 0.055690685 | 0.334382508 |
| GO:0045069 | regulation of viral genome replication | 0.055551267 | 0.334441233 |
| ENSG00000101336 | HCK subnetwork | 0.055572517 | 0.334448724 |
| REACTOME_REGULATION_OF_AM | REACTOME_REGULATION_OF_AMPK_ACTIVITY_VIA_LKB | 0.055782032 | 0.334726225 |
| GO:0032814 | regulation of natural killer cell activation | 0.055913984 | 0.335285646 |
| REACTOME_TOLL_LIKE_RECEPTOI | REACTOME_TOLL_LIKE_RECEPTOR_9_TLR9_CASCADE | 0.055950316 | 0.335292706 |
| ENSG00000153187 | HNRNPU subnetwork | 0.056078265 | 0.335827338 |
| ENSG00000166949 | SMAD3 subnetwork | 0.056135102 | 0.335953979 |
| ENSG00000144895 | EIF2A subnetwork | 0.056237144 | 0.336320077 |
| ENSG00000108298 | RPL19 subnetwork | 0.056289734 | 0.336566092 |
| GO:0045088 | regulation of innate immune response | 0.056407089 | 0.33709369 |
| MP:0008126 | increased dendritic cell number | 0.056453427 | 0.337099857 |
| ENSG00000136997 | MYC subnetwork | 0.0563521 | 0.33715311 |
| GO:0002702 | positive regulation of production of molecular mediator | 0.056348368 | 0.3372427 |
| ENSG00000162616 | DNAJB4 subnetwork | 0.05640303 | 0.337254902 |
| REACTOME_METABOLISM_OF_M | REACTOME_METABOLISM_OF_MRNA | 0.056557171 | 0.337535817 |
| ENSG00000163554 | SPTA1 subnetwork | 0.056756237 | 0.338400955 |
| MP:0000642 | enlarged adrenal glands | 0.056971233 | 0.339037178 |
| ENSG00000112578 | BYSL subnetwork | 0.056964793 | 0.339198856 |
| MP:0001958 | emphysema | 0.056944333 | 0.339289122 |
| MP:0002136 | abnormal kidney physiology | 0.057090586 | 0.339661744 |
| ENSG00000105202 | FBL subnetwork | 0.057143662 | 0.339785714 |
| ENSG00000119139 | TJP2 subnetwork | 0.057299987 | 0.340304183 |
| ENSG00000123358 | NR4A1 subnetwork | 0.057258712 | 0.340433127 |
| ENSG00000085276 | MECOM subnetwork | 0.057279957 | 0.340461465 |

| | | | |
|---|---|---|---|
| MP:0008965 | increased basal metabolism | 0.057297919 | 0.340466001 |
| GO:0042800 | histone methyltransferase activity (H3-K4 specific) | 0.057637388 | 0.341169508 |
| MP:0008140 | podocyte foot process effacement | 0.057636241 | 0.341307437 |
| GO:0002715 | regulation of natural killer cell mediated immunity | 0.057629407 | 0.341469194 |
| GO:0042269 | regulation of natural killer cell mediated cytotoxicity | 0.057629407 | 0.341631105 |
| ENSG00000135801 | TAF5L subnetwork | 0.057495572 | 0.341638955 |
| MP:0002270 | abnormal pulmonary alveolus morphology | 0.057562269 | 0.341646891 |
| ENSG00000169756 | LIMS1 subnetwork | 0.057599935 | 0.341674573 |
| ENSG00000148798 | INA subnetwork | 0.057759675 | 0.341694274 |
| ENSG00000144935 | TRPC1 subnetwork | 0.057553626 | 0.341785375 |
| ENSG00000137177 | KIF13A subnetwork | 0.057867462 | 0.342336802 |
| ENSG00000164244 | PRRC1 subnetwork | 0.057935124 | 0.342364066 |
| ENSG00000164167 | LSM6 subnetwork | 0.058000538 | 0.34251299 |
| REACTOME_PLATELET_DEGRANU | REACTOME_PLATELET_DEGRANULATION | 0.057993417 | 0.342627599 |
| GO:0005667 | transcription factor complex | 0.058163235 | 0.343578848 |
| ENSG00000095015 | MAP3K1 subnetwork | 0.058299941 | 0.344218971 |
| GO:0032350 | regulation of hormone metabolic process | 0.058471943 | 0.344813767 |
| KEGG_PRION_DISEASES | KEGG_PRION_DISEASES | 0.058455351 | 0.34490566 |
| MP:0000136 | abnormal microglial cell morphology | 0.058568285 | 0.345311027 |
| MP:0008070 | absent T cells | 0.058724781 | 0.346021657 |
| ENSG00000166793 | YPEL4 subnetwork | 0.058700558 | 0.346043335 |
| ENSG00000185057 | ENSG00000185057 subnetwork | 0.058840417 | 0.346217105 |
| ENSG00000198518 | HIST1H4E subnetwork | 0.059863411 | 0.346260388 |
| GO:0010893 | positive regulation of steroid biosynthetic process | 0.058824147 | 0.346285849 |
| ENSG00000182247 | UBE2E2 subnetwork | 0.058896709 | 0.346359793 |
| ENSG00000182217 | HIST2H4B subnetwork | 0.059863411 | 0.346420323 |
| ENSG00000154415 | PPP1R3A subnetwork | 0.058822984 | 0.34644873 |
| ENSG00000111731 | KIAA0528 subnetwork | 0.058815852 | 0.346517647 |
| MP:0003231 | abnormal placenta vasculature | 0.058931043 | 0.346525822 |
| ENSG00000198558 | HIST1H4L subnetwork | 0.059863411 | 0.346580407 |
| ENSG00000153094 | BCL2L11 subnetwork | 0.059949554 | 0.346723581 |
| ENSG00000183941 | HIST2H4A subnetwork | 0.059863411 | 0.346740638 |
| MP:0009660 | abnormal induced retinal neovascularization | 0.059024245 | 0.346855936 |
| ENSG00000197238 | HIST1H4J subnetwork | 0.059863411 | 0.346901018 |
| REACTOME_TRAF6_MEDIATED_IN | REACTOME_TRAF6_MEDIATED_INDUCTION_OF_PROINF | 0.059067128 | 0.346927767 |
| ENSG00000197914 | HIST1H4K subnetwork | 0.059863411 | 0.347061546 |
| ENSG00000197837 | HIST4H4 subnetwork | 0.059863411 | 0.347222222 |
| ENSG00000124529 | HIST1H4B subnetwork | 0.059863411 | 0.347383048 |
| ENSG00000071462 | WBSCR22 subnetwork | 0.060094936 | 0.347416974 |
| MP:0000010 | abnormal abdominal fat pad morphology | 0.059233781 | 0.347469541 |
| ENSG00000103363 | TCEB2 subnetwork | 0.059216999 | 0.347538678 |
| ENSG00000198327 | HIST1H4F subnetwork | 0.059863411 | 0.347544022 |
| ENSG00000119698 | PPP4R4 subnetwork | 0.059296969 | 0.347681499 |
| ENSG00000087269 | NOP14 subnetwork | 0.060208005 | 0.347695853 |
| ENSG00000158406 | HIST1H4H subnetwork | 0.059863411 | 0.347705146 |
| ENSG00000204673 | AKT1S1 subnetwork | 0.060253169 | 0.347719945 |
| ENSG00000137807 | KIF23 subnetwork | 0.059332182 | 0.347776217 |
| ENSG00000115966 | ATF2 subnetwork | 0.060206846 | 0.347786999 |
| MP:0006344 | small second branchial arch | 0.059416377 | 0.347803738 |
| ENSG00000197061 | HIST1H4C subnetwork | 0.059863411 | 0.347866419 |
| ENSG00000170315 | UBB subnetwork | 0.059400436 | 0.347872838 |
| ENSG00000111530 | CAND1 subnetwork | 0.059367538 | 0.347917642 |
| ENSG00000188987 | HIST1H4D subnetwork | 0.059863411 | 0.348027842 |
| ENSG00000099901 | RANBP1 subnetwork | 0.059400114 | 0.348035547 |

| | | | |
|---|---|---|---|
| ENSG00000198339 | HIST1H4I subnetwork | 0.059863411 | 0.348189415 |
| GO:0045185 | maintenance of protein location | 0.059529694 | 0.348341896 |
| ENSG00000196176 | HIST1H4A subnetwork | 0.059863411 | 0.348351138 |
| ENSG00000115234 | SNX17 subnetwork | 0.059858795 | 0.348466543 |
| MP:0008477 | decreased spleen red pulp amount | 0.05983363 | 0.348489075 |
| ENSG00000165280 | VCP subnetwork | 0.059829291 | 0.348604651 |
| ENSG00000117222 | RBBP5 subnetwork | 0.05978036 | 0.348626629 |
| ENSG00000170035 | UBE2E3 subnetwork | 0.05981929 | 0.348673802 |
| ENSG00000171791 | BCL2 subnetwork | 0.059762622 | 0.348695855 |
| GO:0004950 | chemokine receptor activity | 0.059737241 | 0.348765144 |
| GO:0001637 | G-protein coupled chemoattractant receptor activity | 0.059737241 | 0.348927739 |
| GO:0006417 | regulation of translation | 0.059727769 | 0.348997201 |
| MP:0002407 | abnormal double-negative T cell morphology | 0.059693374 | 0.349089636 |
| ENSG00000147889 | CDKN2A subnetwork | 0.05970689 | 0.349090061 |
| ENSG00000112592 | TBP subnetwork | 0.060525317 | 0.349585635 |
| ENSG00000183735 | TBK1 subnetwork | 0.060794874 | 0.351127474 |
| MP:0001698 | decreased embryo size | 0.060889013 | 0.351448942 |
| ENSG00000008988 | RPS20 subnetwork | 0.060976272 | 0.352 |
| ENSG00000085365 | ENSG00000085365 subnetwork | 0.061036454 | 0.35222886 |
| MP:0008057 | abnormal DNA replication | 0.061070741 | 0.352342673 |
| ENSG00000126351 | THRA subnetwork | 0.061145999 | 0.352571166 |
| GO:0048643 | positive regulation of skeletal muscle tissue developmen | 0.061294173 | 0.352980284 |
| ENSG00000196365 | LONP1 subnetwork | 0.061341354 | 0.353116407 |
| GO:0002698 | negative regulation of immune effector process | 0.061284115 | 0.353119266 |
| GO:0008624 | induction of apoptosis by extracellular signals | 0.061260389 | 0.35316659 |
| ENSG00000138685 | FGF2 subnetwork | 0.061454481 | 0.353573065 |
| GO:0052547 | regulation of peptidase activity | 0.061495853 | 0.353638444 |
| GO:0031100 | organ regeneration | 0.061479118 | 0.35364011 |
| ENSG00000010671 | BTK subnetwork | 0.061507458 | 0.353682525 |
| ENSG00000121274 | PAPD5 subnetwork | 0.061905814 | 0.35571037 |
| ENSG00000165556 | CDX2 subnetwork | 0.061905676 | 0.355872943 |
| MP:0011090 | partial perinatal lethality | 0.061898353 | 0.355921353 |
| GO:0014896 | muscle hypertrophy | 0.061967402 | 0.355981735 |
| ENSG00000141506 | PIK3R5 subnetwork | 0.062217211 | 0.356697039 |
| ENSG00000104892 | KLC3 subnetwork | 0.0622055 | 0.356859617 |
| KEGG_NON_SMALL_CELL_LUNG_ | KEGG_NON_SMALL_CELL_LUNG_CANCER | 0.062186452 | 0.356908345 |
| GO:0003300 | cardiac muscle hypertrophy | 0.062360215 | 0.356912233 |
| MP:0000598 | abnormal liver morphology | 0.062122587 | 0.356960292 |
| MP:0001722 | pale yolk sac | 0.062176773 | 0.357071168 |
| GO:0014897 | striated muscle hypertrophy | 0.062360215 | 0.357074613 |
| GO:0019838 | growth factor binding | 0.062357755 | 0.357214383 |
| REACTOME_INNATE_IMMUNE_S\ | REACTOME_INNATE_IMMUNE_SYSTEM | 0.062331033 | 0.357240437 |
| ENSG00000144908 | ALDH1L1 subnetwork | 0.062538017 | 0.357659091 |
| MP:0003037 | increased infarction size | 0.062671371 | 0.358242507 |
| GO:0005640 | nuclear outer membrane | 0.062667877 | 0.358382553 |
| ENSG00000148296 | SURF6 subnetwork | 0.062850961 | 0.359097096 |
| ENSG00000157625 | TAB3 subnetwork | 0.06281936 | 0.359123922 |
| ENSG00000138193 | PLCE1 subnetwork | 0.062889269 | 0.359206349 |
| GO:0010745 | negative regulation of macrophage derived foam cell diff | 0.063068922 | 0.359551833 |
| REACTOME_PI:3K_CASCADE | REACTOME_PI:3K_CASCADE | 0.063021928 | 0.359560489 |
| ENSG00000196455 | PIK3R4 subnetwork | 0.063000761 | 0.359610154 |
| GO:0050777 | negative regulation of immune response | 0.063066098 | 0.359692029 |
| ENSG00000136279 | DBNL subnetwork | 0.06310281 | 0.359751131 |
| ENSG00000157106 | SMG1 subnetwork | 0.063406144 | 0.361261872 |

| | | | |
|---|---|---|---|
| MP:0008478 | increased spleen white pulp amount | 0.063526946 | 0.361776673 |
| ENSG00000119638 | NEK9 subnetwork | 0.063569705 | 0.361929507 |
| ENSG00000066777 | ARFGEF1 subnetwork | 0.063669705 | 0.36241535 |
| GO:0004869 | cysteine-type endopeptidase inhibitor activity | 0.063668473 | 0.362579042 |
| ENSG00000129282 | MRM1 subnetwork | 0.063802343 | 0.363199458 |
| ENSG00000183207 | RUVBL2 subnetwork | 0.063850941 | 0.363373929 |
| ENSG00000135829 | DHX9 subnetwork | 0.06389124 | 0.363435528 |
| GO:0042522 | regulation of tyrosine phosphorylation of Stat5 protein | 0.064002589 | 0.363963964 |
| GO:0046966 | thyroid hormone receptor binding | 0.063983677 | 0.36399279 |
| ENSG00000142867 | BCL10 subnetwork | 0.064171322 | 0.364790635 |
| ENSG00000078043 | PIAS2 subnetwork | 0.064271774 | 0.365211521 |
| GO:0043525 | positive regulation of neuron apoptotic process | 0.06431239 | 0.365317139 |
| ENSG00000211460 | TSN subnetwork | 0.064345008 | 0.365377698 |
| REACTOME_P75NTR_SIGNALS_VI | REACTOME_P75NTR_SIGNALS_VIA_NF:KB | 0.064412997 | 0.365573034 |
| GO:0032602 | chemokine production | 0.064508106 | 0.365880503 |
| GO:0050856 | regulation of T cell receptor signaling pathway | 0.064566776 | 0.366052986 |
| ENSG00000076944 | STXBP2 subnetwork | 0.064619525 | 0.366165919 |
| GO:0043235 | receptor complex | 0.064594417 | 0.366270197 |
| ENSG00000145592 | RPL37 subnetwork | 0.064619062 | 0.366330193 |
| ENSG00000112306 | RPS12 subnetwork | 0.065086268 | 0.367172845 |
| ENSG00000154727 | GABPA subnetwork | 0.065085108 | 0.367314567 |
| MP:0000048 | abnormal stria vascularis morphology | 0.065007371 | 0.367352415 |
| ENSG00000096433 | ITPR3 subnetwork | 0.065066393 | 0.367478766 |
| GO:0002262 | myeloid cell homeostasis | 0.065001331 | 0.367494407 |
| MP:0005408 | hypopigmentation | 0.064995785 | 0.367614145 |
| REACTOME_RIG:IMDA5_MEDIATE | REACTOME_RIG:IMDA5_MEDIATED_INDUCTION_OF_IFN | 0.064985771 | 0.36773399 |
| ENSG00000166333 | ILK subnetwork | 0.064952017 | 0.367741935 |
| KEGG_PHENYLALANINE_METABO | KEGG_PHENYLALANINE_METABOLISM | 0.06494202 | 0.367884357 |
| GO:0004691 | cAMP-dependent protein kinase activity | 0.065268419 | 0.368013393 |
| ENSG00000108270 | AATF subnetwork | 0.065351307 | 0.368451584 |
| ENSG00000088247 | KHSRP subnetwork | 0.06551094 | 0.369014712 |
| GO:0043029 | T cell homeostasis | 0.065578986 | 0.36902852 |
| ENSG00000134440 | NARS subnetwork | 0.065482908 | 0.369090098 |
| ENSG00000099622 | CIRBP subnetwork | 0.065711405 | 0.369643653 |
| GO:0031594 | neuromuscular junction | 0.065784926 | 0.369692924 |
| ENSG00000124383 | MPHOSPH10 subnetwork | 0.065743028 | 0.369701692 |
| MP:0003356 | impaired luteinization | 0.065813355 | 0.36975089 |
| ENSG00000133818 | RRAS2 subnetwork | 0.065884872 | 0.370008893 |
| REACTOME_MYD88_DEPENDENT | REACTOME_MYD88_DEPENDENT_CASCADE_INITIATED_ | 0.065964891 | 0.370213239 |
| REACTOME_TOLL_LIKE_RECEPTOI | REACTOME_TOLL_LIKE_RECEPTOR_78_TLR78_CASCADE | 0.065964891 | 0.370377778 |
| ENSG00000158092 | NCK1 subnetwork | 0.066006373 | 0.370492895 |
| GO:0048660 | regulation of smooth muscle cell proliferation | 0.066077489 | 0.370705726 |
| KEGG_WNT_SIGNALING_PATHW/ | KEGG_WNT_SIGNALING_PATHWAY | 0.066288833 | 0.370995575 |
| GO:0008276 | protein methyltransferase activity | 0.066148322 | 0.370997783 |
| ENSG00000165219 | GAPVD1 subnetwork | 0.066265422 | 0.371004869 |
| MP:0003961 | decreased lean body mass | 0.066146103 | 0.371118012 |
| ENSG00000131236 | CAP1 subnetwork | 0.066258081 | 0.371147033 |
| ENSG00000115232 | ITGA4 subnetwork | 0.066215455 | 0.37116578 |
| ENSG00000167549 | CORO6 subnetwork | 0.066254864 | 0.371289322 |
| ENSG00000029363 | BCLAF1 subnetwork | 0.06645313 | 0.371649713 |
| MP:0003814 | vascular smooth muscle cell hypoplasia | 0.066549258 | 0.372116659 |
| ENSG00000178913 | TAF7 subnetwork | 0.06660887 | 0.372119205 |
| ENSG00000105699 | LSR subnetwork | 0.066540953 | 0.372126437 |
| GO:0032689 | negative regulation of interferon-gamma production | 0.066580507 | 0.372128975 |

| | | | |
|---|---|---|---|
| ENSG00000198517 | MAFK subnetwork | 0.066755843 | 0.372859665 |
| ENSG00000158186 | MRAS subnetwork | 0.066808092 | 0.37300397 |
| ENSG00000203747 | FCGR3A subnetwork | 0.066882357 | 0.373170194 |
| ENSG00000115290 | GRB14 subnetwork | 0.066989512 | 0.373534597 |
| ENSG00000159593 | NAE1 subnetwork | 0.067147239 | 0.374008811 |
| ENSG00000175467 | SART1 subnetwork | 0.067246567 | 0.374548657 |
| REACTOME_NEGATIVE_REGULAT | REACTOME_NEGATIVE_REGULATORS_OF_RIG:IMDA5_S | 0.067312131 | 0.374801937 |
| ENSG00000096238 | ENSG00000096238 subnetwork | 0.067724099 | 0.376701801 |
| ENSG00000206394 | CLIC1 subnetwork | 0.067724099 | 0.376867311 |
| GO:0042347 | negative regulation of NF-kappaB import into nucleus | 0.067702369 | 0.377022867 |
| ENSG00000213719 | CLIC1 subnetwork | 0.067724099 | 0.377032967 |
| GO:0030879 | mammary gland development | 0.067699244 | 0.37716674 |
| GO:0030532 | small nuclear ribonucleoprotein complex | 0.067962247 | 0.378050922 |
| ENSG00000104852 | SNRNP70 subnetwork | 0.068145573 | 0.37898201 |
| GO:0032388 | positive regulation of intracellular transport | 0.068287206 | 0.379517544 |
| ENSG00000185811 | IKZF1 subnetwork | 0.068347432 | 0.379811486 |
| ENSG00000115594 | IL1R1 subnetwork | 0.068414467 | 0.379951797 |
| GO:0048659 | smooth muscle cell proliferation | 0.068482901 | 0.380332895 |
| ENSG00000122406 | RPL5 subnetwork | 0.068527722 | 0.380385289 |
| ENSG00000206503 | HLA-A subnetwork | 0.06872247 | 0.381342957 |
| ENSG00000162704 | ARPC5 subnetwork | 0.068698587 | 0.381400438 |
| GO:2000696 | regulation of epithelial cell differentiation involved in kid | 0.068823855 | 0.381424825 |
| GO:0070229 | negative regulation of lymphocyte apoptotic process | 0.068776504 | 0.381460429 |
| ENSG00000157388 | CACNA1D subnetwork | 0.068899793 | 0.381681223 |
| GO:0032964 | collagen biosynthetic process | 0.068883117 | 0.381760594 |
| MP:0002644 | decreased circulating triglyceride level | 0.068975423 | 0.381994762 |
| GO:0017127 | cholesterol transporter activity | 0.069079324 | 0.382569808 |
| ENSG00000174485 | DENND4A subnetwork | 0.069182103 | 0.38325338 |
| ENSG00000198900 | TOP1 subnetwork | 0.069321662 | 0.383529412 |
| GO:0015278 | calcium-release channel activity | 0.069295129 | 0.383565824 |
| GO:0032611 | interleukin-1 beta production | 0.069487031 | 0.384320557 |
| MP:0005508 | abnormal skeleton morphology | 0.069570407 | 0.384588594 |
| ENSG00000123094 | RASSF8 subnetwork | 0.069642673 | 0.385030461 |
| MP:0003026 | decreased vasoconstriction | 0.06971046 | 0.385254458 |
| ENSG00000138757 | G3BP2 subnetwork | 0.069793681 | 0.385586957 |
| ENSG00000164754 | RAD21 subnetwork | 0.069849758 | 0.385599479 |
| ENSG00000102309 | PIN4 subnetwork | 0.069848553 | 0.385767058 |
| REACTOME_ACTIVATION_OF_THE | REACTOME_ACTIVATION_OF_THE_MRNA_UPON_BINDI | 0.069952326 | 0.385953105 |
| GO:0045624 | positive regulation of T-helper cell differentiation | 0.070014248 | 0.386284722 |
| MP:0009640 | abnormal renal tubule epithelium morphology | 0.070037708 | 0.386355748 |
| ENSG00000163624 | CDS1 subnetwork | 0.070090921 | 0.386491761 |
| MP:0001914 | hemorrhage | 0.070324624 | 0.388036411 |
| MP:0009541 | increased thymocyte apoptosis | 0.070361166 | 0.388214905 |
| GO:0046890 | regulation of lipid biosynthetic process | 0.070428048 | 0.388436553 |
| MP:0008561 | decreased tumor necrosis factor secretion | 0.070458594 | 0.388593074 |
| ENSG00000106355 | LSM5 subnetwork | 0.070599012 | 0.38929035 |
| MP:0001119 | abnormal female reproductive system morphology | 0.070646633 | 0.389338235 |
| ENSG00000145741 | BTF3 subnetwork | 0.070733546 | 0.389481641 |
| ENSG00000112186 | CAP2 subnetwork | 0.070756424 | 0.389507772 |
| MP:0000754 | paresis | 0.07071312 | 0.389585134 |
| GO:0018205 | peptidyl-lysine modification | 0.070689119 | 0.389602248 |
| GO:0019216 | regulation of lipid metabolic process | 0.070912963 | 0.390120794 |
| ENSG00000175745 | NR2F1 subnetwork | 0.070977182 | 0.390172414 |
| REACTOME_EARLY_PHASE_OF_HI | REACTOME_EARLY_PHASE_OF_HIV_LIFE_CYCLE | 0.070899941 | 0.390224428 |

| | | | |
|---|---|---|---|
| ENSG00000117461 | PIK3R3 subnetwork | 0.070970337 | 0.390275981 |
| REACTOME_REGULATION_OF_LIP | REACTOME_REGULATION_OF_LIPID_METABOLISM_BY_I | 0.071037046 | 0.390542869 |
| REACTOME_NUCLEAR_EVENTS_K | REACTOME_NUCLEAR_EVENTS_KINASE_AND_TRANSCRI | 0.071137339 | 0.390913006 |
| MP:0004982 | abnormal osteoclast morphology | 0.071231859 | 0.390942341 |
| MP:0011108 | partial embryonic lethality during organogenesis | 0.071210798 | 0.391024537 |
| GO:0010506 | regulation of autophagy | 0.071324705 | 0.391268817 |
| ENSG00000164605 | ENSG00000164605 subnetwork | 0.071421959 | 0.391938951 |
| GO:0042613 | MHC class II protein complex | 0.07160758 | 0.392844865 |
| ENSG00000141644 | MBD1 subnetwork | 0.071694808 | 0.393148625 |
| ENSG00000162624 | LHX8 subnetwork | 0.071758592 | 0.393261803 |
| ENSG00000154556 | SORBS2 subnetwork | 0.071756423 | 0.393430657 |
| GO:0045767 | regulation of anti-apoptosis | 0.072315771 | 0.394807692 |
| ENSG00000141551 | CSNK1D subnetwork | 0.072348047 | 0.39480991 |
| ENSG00000105364 | MRPL4 subnetwork | 0.072064949 | 0.39487784 |
| ENSG00000133794 | ARNTL subnetwork | 0.072194456 | 0.394905822 |
| ENSG00000184634 | MED12 subnetwork | 0.072302748 | 0.394955109 |
| GO:0070670 | response to interleukin-4 | 0.07203153 | 0.395002145 |
| GO:0035097 | histone methyltransferase complex | 0.07217434 | 0.395010707 |
| GO:0051224 | negative regulation of protein transport | 0.072061966 | 0.39504717 |
| ENSG00000138190 | EXOC6 subnetwork | 0.072290391 | 0.395081266 |
| GO:0034708 | methyltransferase complex | 0.07217434 | 0.395179949 |
| GO:0043621 | protein self-association | 0.072282791 | 0.395250321 |
| GO:0051091 | positive regulation of sequence-specific DNA binding tra | 0.072513546 | 0.395518566 |
| ENSG00000115718 | PROC subnetwork | 0.07250439 | 0.395666097 |
| GO:0006473 | protein acetylation | 0.072566739 | 0.395755119 |
| GO:0022407 | regulation of cell-cell adhesion | 0.072806443 | 0.39657155 |
| MP:0010763 | abnormal hematopoietic stem cell physiology | 0.072770291 | 0.396591393 |
| GO:0032642 | regulation of chemokine production | 0.072729033 | 0.396609808 |
| ENSG00000156374 | PCGF6 subnetwork | 0.072763563 | 0.396653879 |
| REACTOME_PLCG1_EVENTS_IN_E | REACTOME_PLCG1_EVENTS_IN_ERBB2_SIGNALING | 0.072988179 | 0.396896259 |
| KEGG_UBIQUITIN_MEDIATED_PR | KEGG_UBIQUITIN_MEDIATED_PROTEOLYSIS | 0.072913422 | 0.396914894 |
| GO:0010712 | regulation of collagen metabolic process | 0.072965119 | 0.396916206 |
| ENSG00000151461 | UPF2 subnetwork | 0.072889956 | 0.396934866 |
| ENSG00000215120 | ENSG00000215120 subnetwork | 0.073055783 | 0.396941376 |
| MP:0000364 | abnormal vascular regression | 0.073038855 | 0.396961326 |
| ENSG00000142541 | RPL13A subnetwork | 0.073149834 | 0.397197452 |
| ENSG00000155508 | CNOT8 subnetwork | 0.073523476 | 0.397970402 |
| ENSG00000175333 | ENSG00000175333 subnetwork | 0.073332455 | 0.397984726 |
| ENSG00000060140 | STYK1 subnetwork | 0.073464254 | 0.398010161 |
| ENSG00000188191 | PRKAR1B subnetwork | 0.073557069 | 0.398034658 |
| ENSG00000170145 | SIK2 subnetwork | 0.073431564 | 0.398050847 |
| GO:0035035 | histone acetyltransferase binding | 0.073414678 | 0.398092412 |
| ENSG00000157873 | TNFRSF14 subnetwork | 0.073510683 | 0.398096447 |
| GO:0006475 | internal protein amino acid acetylation | 0.073673309 | 0.398100464 |
| GO:0070482 | response to oxygen levels | 0.073499858 | 0.39813796 |
| KEGG_RIG_I_LIKE_RECEPTOR_SIG | KEGG_RIG_I_LIKE_RECEPTOR_SIGNALING_PATHWAY | 0.07360855 | 0.398141107 |
| ENSG00000163029 | SMC6 subnetwork | 0.073324626 | 0.39815365 |
| ENSG00000125968 | ID1 subnetwork | 0.073402576 | 0.398176421 |
| ENSG00000125508 | SRMS subnetwork | 0.073464254 | 0.398178738 |
| ENSG00000184009 | ACTG1 subnetwork | 0.073657316 | 0.398226351 |
| ENSG00000163283 | ALPP subnetwork | 0.073818182 | 0.399008439 |
| ENSG00000151693 | ASAP2 subnetwork | 0.074055333 | 0.399473241 |
| ENSG00000145349 | CAMK2D subnetwork | 0.073957769 | 0.399493884 |
| GO:0032816 | positive regulation of natural killer cell activation | 0.074093417 | 0.399557709 |

| | | | |
|---|---|---|---|
| GO:0001779 | natural killer cell differentiation | 0.074036349 | 0.399599494 |
| ENSG00000138767 | CNOT6L subnetwork | 0.074134623 | 0.399621053 |
| ENSG00000167085 | PHB subnetwork | 0.074190782 | 0.399852694 |
| ENSG00000087077 | TRIP6 subnetwork | 0.074248764 | 0.39995793 |
| ENSG00000140992 | PDPK1 subnetwork | 0.074356725 | 0.4004836 |
| MP:0005501 | abnormal skin physiology | 0.07441506 | 0.400672551 |
| ENSG00000060069 | CTDP1 subnetwork | 0.074506479 | 0.401071429 |
| MP:0001711 | abnormal placenta morphology | 0.074677294 | 0.401826196 |
| GO:0051272 | positive regulation of cellular component movement | 0.074667714 | 0.401973961 |
| REACTOME_TAK1_ACTIVATES_NF | REACTOME_TAK1_ACTIVATES_NFKB_BY_PHOSPHORYLA | 0.074780222 | 0.402161141 |
| GO:2000241 | regulation of reproductive process | 0.074813749 | 0.40232802 |
| ENSG00000141959 | PFKL subnetwork | 0.07503058 | 0.403140704 |
| ENSG00000197303 | ENSG00000197303 subnetwork | 0.074950896 | 0.403207547 |
| MP:0000692 | small spleen | 0.075029956 | 0.403288647 |
| MP:0002458 | abnormal B cell number | 0.075091232 | 0.403348681 |
| ENSG00000042980 | ADAM28 subnetwork | 0.075015897 | 0.403436714 |
| MP:0002423 | abnormal mast cell physiology | 0.075282602 | 0.404013378 |
| ENSG00000108654 | DDX5 subnetwork | 0.075265334 | 0.404077792 |
| GO:0050715 | positive regulation of cytokine secretion | 0.075250593 | 0.404142259 |
| ENSG00000197471 | SPN subnetwork | 0.075365532 | 0.404262432 |
| MP:0002276 | abnormal lung interstitium morphology | 0.07558581 | 0.404904007 |
| MP:0004566 | myocardial fiber degeneration | 0.075627169 | 0.404964539 |
| ENSG00000157344 | ENSG00000157344 subnetwork | 0.075569759 | 0.405010438 |
| KEGG_ANTIGEN_PROCESSING_AN | KEGG_ANTIGEN_PROCESSING_AND_PRESENTATION | 0.075560182 | 0.405116959 |
| ENSG00000115761 | NOL10 subnetwork | 0.075692587 | 0.405150125 |
| ENSG00000152942 | RAD17 subnetwork | 0.075884863 | 0.405578684 |
| ENSG00000159840 | ZYX subnetwork | 0.075911002 | 0.405617978 |
| ENSG00000172795 | DCP2 subnetwork | 0.075821568 | 0.405666667 |
| ENSG00000099917 | MED15 subnetwork | 0.075875957 | 0.405726781 |
| ENSG00000101224 | CDC25B subnetwork | 0.075802041 | 0.405731555 |
| ENSG00000133657 | ATP13A3 subnetwork | 0.076399576 | 0.405764463 |
| GO:0030140 | trans-Golgi network transport vesicle | 0.075973092 | 0.405779626 |
| ENSG00000111252 | SH2B3 subnetwork | 0.07631822 | 0.405789909 |
| MP:0004984 | increased osteoclast cell number | 0.075961697 | 0.405865225 |
| MP:0000750 | abnormal muscle regeneration | 0.076390327 | 0.405890864 |
| ENSG00000109606 | DHX15 subnetwork | 0.076134531 | 0.405892116 |
| MP:0002417 | abnormal megakaryocyte morphology | 0.076071221 | 0.40589946 |
| ENSG00000118007 | STAG1 subnetwork | 0.076303306 | 0.405937112 |
| ENSG00000136718 | IMP4 subnetwork | 0.076279661 | 0.40598096 |
| ENSG00000142494 | SLC47A1 subnetwork | 0.076106164 | 0.406000831 |
| GO:0042611 | MHC protein complex | 0.076268214 | 0.406004141 |
| GO:0004386 | helicase activity | 0.07604542 | 0.406005819 |
| GO:0051220 | cytoplasmic sequestering of protein | 0.076126457 | 0.406019095 |
| ENSG00000096171 | VARS subnetwork | 0.076248035 | 0.406027341 |
| ENSG00000204394 | VARS subnetwork | 0.076248035 | 0.406195607 |
| GO:0046885 | regulation of hormone biosynthetic process | 0.076238477 | 0.406343284 |
| GO:0016581 | NuRD complex | 0.076219397 | 0.406428868 |
| ENSG00000099964 | ENSG00000099964 subnetwork | 0.076647618 | 0.406833196 |
| ENSG00000144744 | UBA3 subnetwork | 0.076657726 | 0.406892282 |
| GO:0030275 | LRR domain binding | 0.076640593 | 0.407001239 |
| GO:0032675 | regulation of interleukin-6 production | 0.076844179 | 0.407838284 |
| MP:0001290 | delayed eyelid opening | 0.077113232 | 0.408920478 |
| ENSG00000109618 | SEPSECS subnetwork | 0.077107047 | 0.409047815 |
| GO:0042991 | transcription factor import into nucleus | 0.07723727 | 0.409122735 |

| | | | |
|---|---|---|---|
| ENSG00000104689 | TNFRSF10A subnetwork | 0.077106297 | 0.409216495 |
| ENSG00000176444 | CLK2 subnetwork | 0.077271509 | 0.409242487 |
| ENSG00000164934 | DCAF13 subnetwork | 0.077362905 | 0.409354441 |
| GO:0090316 | positive regulation of intracellular protein transport | 0.07736143 | 0.40952283 |
| REACTOME_CGMP_EFFECTS | REACTOME_CGMP_EFFECTS | 0.077332306 | 0.409547325 |
| ENSG00000198909 | MAP3K3 subnetwork | 0.077443096 | 0.409576654 |
| ENSG00000137947 | GTF2B subnetwork | 0.077510033 | 0.409737058 |
| GO:0044445 | cytosolic part | 0.077670018 | 0.410328542 |
| GO:0003746 | translation elongation factor activity | 0.077739831 | 0.410488506 |
| ENSG00000206406 | CSNK2B subnetwork | 0.078027882 | 0.411229508 |
| ENSG00000196591 | HDAC2 subnetwork | 0.077954675 | 0.411366434 |
| ENSG00000204435 | CSNK2B subnetwork | 0.078027882 | 0.411398114 |
| ENSG00000163050 | ADCK3 subnetwork | 0.078099817 | 0.411552642 |
| ENSG00000206300 | ENSG00000206300 subnetwork | 0.078027882 | 0.411566858 |
| MP:0003303 | peritoneal inflammation | 0.078284111 | 0.411947627 |
| ENSG00000162244 | RPL29 subnetwork | 0.078280217 | 0.412095784 |
| ENSG00000061938 | TNK2 subnetwork | 0.078466905 | 0.412111928 |
| ENSG00000082641 | NFE2L1 subnetwork | 0.078245166 | 0.412141687 |
| ENSG00000106443 | PHF14 subnetwork | 0.078452434 | 0.41225991 |
| ENSG00000090020 | SLC9A1 subnetwork | 0.078387769 | 0.412310838 |
| KEGG_P53_SIGNALING_PATHWA\ | KEGG_P53_SIGNALING_PATHWAY | 0.078438951 | 0.41236713 |
| MP:0000245 | abnormal erythropoiesis | 0.078687764 | 0.413250306 |
| GO:0032844 | regulation of homeostatic process | 0.078760975 | 0.413280294 |
| ENSG00000204217 | BMPR2 subnetwork | 0.078736802 | 0.413346939 |
| ENSG00000125347 | IRF1 subnetwork | 0.078893059 | 0.413743883 |
| MP:0008214 | increased immature B cell number | 0.079147498 | 0.415124338 |
| GO:0052742 | phosphatidylinositol kinase activity | 0.079179565 | 0.415158924 |
| ENSG00000010818 | HIVEP2 subnetwork | 0.0793209 | 0.415723014 |
| MP:0001132 | absent mature ovarian follicles | 0.079435271 | 0.416266287 |
| MP:0010869 | decreased bone trabecula number | 0.079686646 | 0.417127746 |
| MP:0000066 | osteoporosis | 0.079661466 | 0.417216117 |
| ENSG00000088356 | PDRG1 subnetwork | 0.079927501 | 0.418117121 |
| GO:0032620 | interleukin-17 production | 0.080130662 | 0.418323864 |
| ENSG00000118520 | ARG1 subnetwork | 0.080059425 | 0.418386835 |
| ENSG00000128340 | RAC2 subnetwork | 0.080037527 | 0.418455285 |
| GO:0032660 | regulation of interleukin-17 production | 0.080130662 | 0.418493707 |
| MP:0003567 | abnormal fetal cardiomyocyte proliferation | 0.08012343 | 0.418643379 |
| ENSG00000051382 | PIK3CB subnetwork | 0.080345248 | 0.419208925 |
| ENSG00000167508 | MVD subnetwork | 0.080507727 | 0.419408428 |
| GO:0001727 | lipid kinase activity | 0.080439384 | 0.419424169 |
| ENSG00000117877 | CD3EAP subnetwork | 0.080561582 | 0.419433198 |
| MP:0010209 | abnormal circulating chemokine level | 0.080529666 | 0.419441069 |
| ENSG00000105963 | ADAP1 subnetwork | 0.080505529 | 0.419578435 |
| GO:0004721 | phosphoprotein phosphatase activity | 0.080715536 | 0.419923139 |
| GO:0042036 | negative regulation of cytokine biosynthetic process | 0.080753637 | 0.420056611 |
| ENSG00000120158 | RCL1 subnetwork | 0.080712984 | 0.42009308 |
| ENSG00000175866 | BAIAP2 subnetwork | 0.080821684 | 0.420129345 |
| GO:0070646 | protein modification by small protein removal | 0.081220653 | 0.421391129 |
| MP:0008279 | arrest of spermiogenesis | 0.081215586 | 0.421540944 |
| ENSG00000125731 | SH2D3A subnetwork | 0.081073711 | 0.421555556 |
| ENSG00000198802 | ENSG00000198802 subnetwork | 0.081123658 | 0.421607431 |
| ENSG00000156299 | TIAM1 subnetwork | 0.081202403 | 0.421670702 |
| GO:0061005 | cell differentiation involved in kidney development | 0.081195785 | 0.421800565 |
| GO:0033002 | muscle cell proliferation | 0.081520915 | 0.422654048 |

| | | | |
|---|---|---|---|
| GO:0090030 | regulation of steroid hormone biosynthetic process | 0.081448694 | 0.422712616 |
| ENSG00000103194 | USP10 subnetwork | 0.0815053 | 0.42272361 |
| GO:0051259 | protein oligomerization | 0.081570188 | 0.4227657 |
| GO:0045429 | positive regulation of nitric oxide biosynthetic process | 0.081762974 | 0.423641851 |
| ENSG00000188620 | HMX3 subnetwork | 0.081871236 | 0.423823884 |
| ENSG00000150991 | UBC subnetwork | 0.081832465 | 0.42385358 |
| ENSG00000172349 | IL16 subnetwork | 0.082041966 | 0.424517685 |
| GO:0002687 | positive regulation of leukocyte migration | 0.082148825 | 0.425090398 |
| ENSG00000100985 | MMP9 subnetwork | 0.082216006 | 0.425110397 |
| ENSG00000115317 | HTRA2 subnetwork | 0.082210163 | 0.425180723 |
| GO:0071560 | cellular response to transforming growth factor beta stin | 0.082296257 | 0.425290814 |
| ENSG00000111816 | FRK subnetwork | 0.082279116 | 0.42538122 |
| ENSG00000103423 | DNAJA3 subnetwork | 0.082622922 | 0.4258 |
| MP:0002223 | lymphoid hypoplasia | 0.082601464 | 0.42585034 |
| GO:0031641 | regulation of myelination | 0.082600052 | 0.426020817 |
| ENSG00000085224 | ATRX subnetwork | 0.082784464 | 0.426067864 |
| ENSG00000089094 | KDM2B subnetwork | 0.082766617 | 0.426138179 |
| ENSG00000135372 | NAT10 subnetwork | 0.08249222 | 0.426142743 |
| MP:0009791 | increased susceptibility to viral infection induced morbid | 0.08257849 | 0.426151382 |
| GO:0045815 | positive regulation of gene expression, epigenetic | 0.082711659 | 0.4262495 |
| GO:0043502 | regulation of muscle adaptation | 0.082569508 | 0.426262019 |
| ENSG00000108826 | MRPL27 subnetwork | 0.082761818 | 0.426288454 |
| REACTOME_NONSENSE_MEDIATE | REACTOME_NONSENSE_MEDIATED_DECAY_INDEPENDE | 0.083006146 | 0.426314741 |
| ENSG00000138031 | ADCY3 subnetwork | 0.082946486 | 0.426335726 |
| ENSG00000169710 | FASN subnetwork | 0.082975653 | 0.426365086 |
| ENSG00000196961 | AP2A1 subnetwork | 0.08256772 | 0.426432866 |
| MP:0010792 | abnormal stomach mucosa morphology | 0.082760696 | 0.426438849 |
| ENSG00000115677 | HDLBP subnetwork | 0.082896363 | 0.426476457 |
| MP:0009789 | decreased susceptibility to bacterial infection induced m | 0.082925422 | 0.42648584 |
| GO:0042523 | positive regulation of tyrosine phosphorylation of Stat5 p | 0.083137948 | 0.426691879 |
| ENSG00000143771 | CNIH4 subnetwork | 0.083134717 | 0.426841896 |
| GO:0009898 | internal side of plasma membrane | 0.083345211 | 0.427616395 |
| ENSG00000180209 | MYLPF subnetwork | 0.083444483 | 0.427673956 |
| ENSG00000124587 | PEX6 subnetwork | 0.083430522 | 0.42774463 |
| ENSG00000104814 | MAP4K1 subnetwork | 0.083760641 | 0.42945151 |
| ENSG00000162367 | TAL1 subnetwork | 0.084064633 | 0.430949543 |
| ENSG00000058729 | RIOK2 subnetwork | 0.084243542 | 0.43112609 |
| ENSG00000212645 | ENSG00000212645 subnetwork | 0.084173666 | 0.431183009 |
| ENSG00000153317 | ASAP1 subnetwork | 0.084146487 | 0.431254964 |
| ENSG00000111775 | COX6A1 subnetwork | 0.084233307 | 0.431257438 |
| ENSG00000153914 | SREK1 subnetwork | 0.084215782 | 0.431369048 |
| ENSG00000101213 | PTK6 subnetwork | 0.084341313 | 0.431609195 |
| ENSG00000114062 | UBE3A subnetwork | 0.084543325 | 0.432158416 |
| ENSG00000132394 | EEFSEC subnetwork | 0.084530971 | 0.432270206 |
| MP:0005165 | increased susceptibility to injury | 0.084722435 | 0.432305259 |
| MP:0002007 | increased cellular sensitivity to gamma-irradiation | 0.084624225 | 0.43236342 |
| MP:0000250 | abnormal vasoconstriction | 0.084659141 | 0.4323704 |
| MP:0011086 | partial postnatal lethality | 0.084720122 | 0.432476266 |
| ENSG00000033327 | GAB2 subnetwork | 0.084904866 | 0.432589814 |
| GO:0010906 | regulation of glucose metabolic process | 0.084890553 | 0.43264218 |
| ENSG00000139132 | FGD4 subnetwork | 0.084838239 | 0.432687747 |
| MP:0000639 | abnormal adrenal gland morphology | 0.084873718 | 0.432734097 |
| ENSG00000175792 | RUVBL1 subnetwork | 0.085025552 | 0.432951855 |
| ENSG00000186868 | MAPT subnetwork | 0.08512083 | 0.433293886 |

| | | | |
|---|---|---|---|
| ENSG00000196459 | TRAPPC2 subnetwork | 0.085251032 | 0.433884949 |
| ENSG00000148660 | CAMK2G subnetwork | 0.085277241 | 0.433910989 |
| ENSG00000111653 | ING4 subnetwork | 0.085303232 | 0.433917323 |
| ENSG00000165516 | KLHDC2 subnetwork | 0.08522295 | 0.434010252 |
| ENSG00000213764 | ENSG00000213764 subnetwork | 0.085251032 | 0.434055972 |
| ENSG00000174307 | PHLDA3 subnetwork | 0.085417364 | 0.434336875 |
| ENSG00000082014 | SMARCD3 subnetwork | 0.085572504 | 0.435031471 |
| ENSG00000132142 | ACACA subnetwork | 0.085597188 | 0.435076681 |
| GO:0009314 | response to radiation | 0.085861308 | 0.435714286 |
| MP:0001192 | scaly skin | 0.085727962 | 0.435731132 |
| ENSG00000140368 | PSTPIP1 subnetwork | 0.085846716 | 0.435747939 |
| ENSG00000081248 | CACNA1S subnetwork | 0.085810386 | 0.435776031 |
| ENSG00000213639 | PPP1CB subnetwork | 0.08584143 | 0.43589945 |
| ENSG00000007816 | ENSG00000007816 subnetwork | 0.085947624 | 0.435955277 |
| REACTOME_FORMATION_OF_THI | REACTOME_FORMATION_OF_THE_TERNARY_COMPLEX_ | 0.086126866 | 0.436153545 |
| MP:0001191 | abnormal skin condition | 0.086123271 | 0.436285266 |
| ENSG00000110651 | CD81 subnetwork | 0.086122936 | 0.436456292 |
| GO:0002825 | regulation of T-helper 1 type immune response | 0.086106296 | 0.436588235 |
| ENSG00000196681 | ENSG00000196681 subnetwork | 0.08630937 | 0.436664059 |
| ENSG00000176534 | ENSG00000176534 subnetwork | 0.08630937 | 0.436834898 |
| ENSG00000124208 | TMEM189-UBE2V1 subnetwork | 0.086386956 | 0.436845192 |
| ENSG00000198637 | ENSG00000198637 subnetwork | 0.08630937 | 0.437005871 |
| GO:0042326 | negative regulation of phosphorylation | 0.086476491 | 0.437045721 |
| ENSG00000007866 | TEAD3 subnetwork | 0.086292066 | 0.437059514 |
| MP:0010279 | increased gastrointestinal tumor incidence | 0.086556083 | 0.437265625 |
| MP:0000259 | abnormal vascular development | 0.08671348 | 0.437836783 |
| ENSG00000198918 | RPL39 subnetwork | 0.086911865 | 0.438089669 |
| GO:0033598 | mammary gland epithelial cell proliferation | 0.086810044 | 0.438095238 |
| GO:0032103 | positive regulation of response to external stimulus | 0.086823845 | 0.438099883 |
| MP:0001544 | abnormal cardiovascular system physiology | 0.086910767 | 0.43824103 |
| ENSG00000135655 | USP15 subnetwork | 0.087151849 | 0.439072848 |
| ENSG00000137497 | NUMA1 subnetwork | 0.087132659 | 0.439224474 |
| GO:0043967 | histone H4 acetylation | 0.087239927 | 0.439661215 |
| ENSG00000114767 | RRP9 subnetwork | 0.087361393 | 0.44 |
| ENSG00000132361 | KIAA0664 subnetwork | 0.087391614 | 0.440062233 |
| MP:0000379 | decreased hair follicle number | 0.087421178 | 0.440124417 |
| ENSG00000132005 | RFX1 subnetwork | 0.087360352 | 0.440171273 |
| ENSG00000196504 | PRPF40A subnetwork | 0.087525906 | 0.440271845 |
| GO:0060749 | mammary gland alveolus development | 0.087523028 | 0.440423465 |
| GO:0061377 | mammary gland lobule development | 0.087523028 | 0.440594637 |
| GO:0032273 | positive regulation of protein polymerization | 0.087793014 | 0.441559953 |
| ENSG00000165688 | PMPCA subnetwork | 0.087776125 | 0.441634317 |
| ENSG00000178409 | BEND3 subnetwork | 0.087857814 | 0.441679597 |
| MP:0003667 | hemangiosarcoma | 0.08820116 | 0.442987214 |
| MP:0003427 | parakeratosis | 0.088131347 | 0.443039938 |
| MP:0001545 | abnormal hematopoietic system physiology | 0.088184014 | 0.443100775 |
| ENSG00000167004 | PDIA3 subnetwork | 0.088498918 | 0.444616576 |
| GO:0006809 | nitric oxide biosynthetic process | 0.088679142 | 0.445394737 |
| ENSG00000151239 | TWF1 subnetwork | 0.088788532 | 0.445419405 |
| GO:0003706 | ligand-regulated transcription factor activity | 0.088754929 | 0.445456303 |
| ENSG00000106070 | GRB10 subnetwork | 0.08866339 | 0.445528455 |
| GO:0030521 | androgen receptor signaling pathway | 0.088753501 | 0.445628627 |
| ENSG00000102572 | STK24 subnetwork | 0.089057353 | 0.446101891 |
| ENSG00000139144 | PIK3C2G subnetwork | 0.088941822 | 0.446116692 |

| | | | |
|---|---|---|---|
| ENSG00000172340 | SUCLG2 subnetwork | 0.088973885 | 0.446137505 |
| GO:0008080 | N-acetyltransferase activity | 0.089043725 | 0.446235521 |
| GO:0004114 | 3',5'-cyclic-nucleotide phosphodiesterase activity | 0.0892536 | 0.447164352 |
| ENSG00000173511 | VEGFB subnetwork | 0.089511475 | 0.448592907 |
| ENSG00000114166 | KAT2B subnetwork | 0.089504137 | 0.448688777 |
| GO:0032635 | interleukin-6 production | 0.089615529 | 0.448709553 |
| ENSG00000130592 | LSP1 subnetwork | 0.089585496 | 0.448786127 |
| MP:0008705 | increased interleukin-6 secretion | 0.089731381 | 0.449075857 |
| GO:0030335 | positive regulation of cell migration | 0.089816187 | 0.449326405 |
| GO:0003724 | RNA helicase activity | 0.089856774 | 0.449326664 |
| MP:0004505 | decreased renal glomerulus number | 0.089980202 | 0.449846213 |
| ENSG00000105610 | KLF1 subnetwork | 0.089977227 | 0.450019231 |
| ENSG00000168036 | CTNNB1 subnetwork | 0.090088866 | 0.450230592 |
| GO:0005099 | Ras GTPase activator activity | 0.0901364 | 0.450403381 |
| ENSG00000103319 | EEF2K subnetwork | 0.090212683 | 0.450556622 |
| GO:0010575 | positive regulation vascular endothelial growth factor pr | 0.090252693 | 0.450613968 |
| ENSG00000129521 | EGLN3 subnetwork | 0.090210658 | 0.450710445 |
| MP:0004883 | abnormal vascular wound healing | 0.090319716 | 0.450786344 |
| GO:0045787 | positive regulation of cell cycle | 0.090395996 | 0.450977386 |
| ENSG00000140988 | RPS2 subnetwork | 0.090373037 | 0.451016104 |
| GO:0004198 | calcium-dependent cysteine-type endopeptidase activity | 0.090445509 | 0.451168582 |
| GO:0004112 | cyclic-nucleotide phosphodiesterase activity | 0.090641304 | 0.451991574 |
| ENSG00000073614 | KDM5A subnetwork | 0.090751769 | 0.452431087 |
| ENSG00000214026 | MRPL23 subnetwork | 0.09082326 | 0.452698048 |
| GO:0016790 | thiolester hydrolase activity | 0.090902676 | 0.452792655 |
| REACTOME_GTP_HYDROLYSIS_AN | REACTOME_GTP_HYDROLYSIS_AND_JOINING_OF_THE_( | 0.0909982 | 0.452924312 |
| GO:0009925 | basal plasma membrane | 0.090995261 | 0.453078394 |
| GO:0001067 | regulatory region nucleic acid binding | 0.091090297 | 0.453093965 |
| GO:0000975 | regulatory region DNA binding | 0.091090297 | 0.4532671 |
| ENSG00000145216 | FIP1L1 subnetwork | 0.091207027 | 0.453398244 |
| REACTOME_INTERFERON_SIGNAL | REACTOME_INTERFERON_SIGNALING | 0.091391515 | 0.453831491 |
| ENSG00000111276 | CDKN1B subnetwork | 0.091372978 | 0.453852021 |
| ENSG00000123836 | PFKFB2 subnetwork | 0.091360492 | 0.453910721 |
| GO:0051240 | positive regulation of multicellular organismal process | 0.091357978 | 0.454064885 |
| ENSG00000158711 | ELK4 subnetwork | 0.091703614 | 0.455449695 |
| ENSG00000100949 | RABGGTA subnetwork | 0.092082502 | 0.456811263 |
| GO:0016407 | acetyltransferase activity | 0.092165183 | 0.456882129 |
| GO:0048771 | tissue remodeling | 0.092080068 | 0.456966121 |
| ENSG00000204301 | NOTCH4 subnetwork | 0.092052598 | 0.457025895 |
| ENSG00000173674 | EIF1AX subnetwork | 0.092161144 | 0.457036896 |
| GO:0070231 | T cell apoptotic process | 0.092033027 | 0.457047619 |
| GO:0019210 | kinase inhibitor activity | 0.092471681 | 0.457164519 |
| GO:0004690 | cyclic nucleotide-dependent protein kinase activity | 0.092436521 | 0.457205157 |
| GO:0003725 | double-stranded RNA binding | 0.092411918 | 0.457286528 |
| ENSG00000137992 | DBT subnetwork | 0.092430408 | 0.457340668 |
| GO:0048732 | gland development | 0.092405389 | 0.457384207 |
| ENSG00000196084 | ENSG00000196084 subnetwork | 0.09231008 | 0.457449639 |
| ENSG00000143947 | RPS27A subnetwork | 0.092345161 | 0.457465805 |
| GO:0004221 | ubiquitin thiolesterase activity | 0.092393895 | 0.457538929 |
| REACTOME_PPARA_ACTIVATES_G | REACTOME_PPARA_ACTIVATES_GENE_EXPRESSION | 0.092777742 | 0.458582797 |
| ENSG00000143375 | CGN subnetwork | 0.09292121 | 0.458996212 |
| ENSG00000141141 | DDX52 subnetwork | 0.093158544 | 0.459863688 |
| ENSG00000123405 | NFE2 subnetwork | 0.09319308 | 0.459897805 |
| ENSG00000141076 | CIRH1A subnetwork | 0.093299078 | 0.460098336 |

| | | | |
|---|---|---|---|
| ENSG00000177200 | CHD9 subnetwork | 0.093259151 | 0.460121075 |
| GO:0018393 | internal peptidyl-lysine acetylation | 0.093467535 | 0.460808768 |
| REACTOME_MRNA_DECAY_BY_5_ | REACTOME_MRNA_DECAY_BY_5_TO_3_EXORIBONUCLE | 0.093448201 | 0.460964083 |
| ENSG00000131652 | THOC6 subnetwork | 0.093566802 | 0.461291541 |
| REACTOME_IRAK2_MEDIATED_A( | REACTOME_IRAK2_MEDIATED_ACTIVATION_OF_TAK1_( | 0.093524687 | 0.461314696 |
| MP:0003057 | abnormal epicardium morphology | 0.093837938 | 0.462627407 |
| ENSG00000136628 | EPRS subnetwork | 0.094055706 | 0.463428895 |
| KEGG_LEUKOCYTE_TRANSENDOT | KEGG_LEUKOCYTE_TRANSENDOTHELIAL_MIGRATION | 0.094051903 | 0.46354717 |
| ENSG00000039987 | BEST2 subnetwork | 0.09447006 | 0.465346908 |
| GO:0043548 | phosphatidylinositol 3-kinase binding | 0.09451731 | 0.465454203 |
| ENSG00000165197 | FIGF subnetwork | 0.094585615 | 0.465617935 |
| MP:0008396 | abnormal osteoclast differentiation | 0.094787338 | 0.466208584 |
| MP:0001541 | abnormal osteoclast physiology | 0.094763092 | 0.466271186 |
| ENSG00000115484 | CCT4 subnetwork | 0.094849553 | 0.466371848 |
| GO:0008625 | induction of apoptosis via death domain receptors | 0.095112209 | 0.467318541 |
| MP:0000952 | abnormal CNS glial cell morphology | 0.095080549 | 0.467419112 |
| MP:0001125 | abnormal oocyte morphology | 0.095226737 | 0.46768797 |
| GO:0048661 | positive regulation of smooth muscle cell proliferation | 0.095332008 | 0.467731029 |
| GO:0005996 | monosaccharide metabolic process | 0.09526507 | 0.467737693 |
| ENSG00000186230 | ZNF749 subnetwork | 0.095402776 | 0.467949681 |
| ENSG00000186654 | PRR5 subnetwork | 0.09550079 | 0.468355856 |
| GO:0034754 | cellular hormone metabolic process | 0.095745767 | 0.468909295 |
| ENSG00000143669 | LYST subnetwork | 0.095699419 | 0.46896099 |
| ENSG00000174775 | HRAS subnetwork | 0.095735065 | 0.469010124 |
| MP:0001201 | translucent skin | 0.095685603 | 0.469118199 |
| ENSG00000186115 | CYP4F2 subnetwork | 0.095935616 | 0.469670288 |
| ENSG00000178105 | DDX10 subnetwork | 0.096015884 | 0.470037453 |
| ENSG00000100292 | HMOX1 subnetwork | 0.096331862 | 0.471201347 |
| ENSG00000109339 | MAPK10 subnetwork | 0.096286041 | 0.471246724 |
| GO:0070742 | C2H2 zinc finger domain binding | 0.096557499 | 0.472446689 |
| ENSG00000137757 | CASP5 subnetwork | 0.096648699 | 0.472812266 |
| ENSG00000087157 | PGS1 subnetwork | 0.096705654 | 0.473028037 |
| GO:0045736 | negative regulation of cyclin-dependent protein kinase a | 0.097012457 | 0.473192996 |
| KEGG_TOLL_LIKE_RECEPTOR_SIGI | KEGG_TOLL_LIKE_RECEPTOR_SIGNALING_PATHWAY | 0.096789547 | 0.473206278 |
| ENSG00000102606 | ARHGEF7 subnetwork | 0.096976017 | 0.473276183 |
| ENSG00000152944 | MED21 subnetwork | 0.096953229 | 0.473442745 |
| ENSG00000109971 | HSPA8 subnetwork | 0.096972796 | 0.473452647 |
| GO:0042169 | SH2 domain binding | 0.096952035 | 0.473619403 |
| ENSG00000101361 | NOP56 subnetwork | 0.096929571 | 0.473646883 |
| ENSG00000175826 | CTDNEP1 subnetwork | 0.096890184 | 0.473683227 |
| MP:0001929 | abnormal gametogenesis | 0.096923127 | 0.473786408 |
| ENSG00000161204 | ABCF3 subnetwork | 0.097402578 | 0.475018615 |
| GO:0048545 | response to steroid hormone stimulus | 0.097379105 | 0.475046555 |
| GO:0020027 | hemoglobin metabolic process | 0.097640553 | 0.476311872 |
| MP:0008410 | increased cellular sensitivity to ultraviolet irradiation | 0.097719977 | 0.476525298 |
| KEGG_CYTOSOLIC_DNA_SENSING | KEGG_CYTOSOLIC_DNA_SENSING_PATHWAY | 0.097807586 | 0.476701376 |
| ENSG00000111245 | MYL2 subnetwork | 0.097838051 | 0.476728625 |
| ENSG00000115977 | AAK1 subnetwork | 0.09788551 | 0.476923077 |
| ENSG00000197157 | SND1 subnetwork | 0.097973356 | 0.477181582 |
| MP:0004988 | increased osteoblast cell number | 0.097947583 | 0.477191679 |
| GO:0006401 | RNA catabolic process | 0.098092887 | 0.477598367 |
| ENSG00000175220 | ARHGAP1 subnetwork | 0.098211471 | 0.477940631 |
| ENSG00000160613 | PCSK7 subnetwork | 0.098247724 | 0.478041543 |
| ENSG00000129559 | NEDD8 subnetwork | 0.098342962 | 0.47836485 |

| | | | |
|---|---|---|---|
| KEGG_RNA_DEGRADATION | KEGG_RNA_DEGRADATION | 0.098459512 | 0.478817643 |
| ENSG00000162409 | PRKAA2 subnetwork | 0.098573687 | 0.479277778 |
| ENSG00000105974 | CAV1 subnetwork | 0.098572421 | 0.479455354 |
| ENSG00000116001 | TIA1 subnetwork | 0.098711719 | 0.479607698 |
| GO:0002367 | cytokine production involved in immune response | 0.098692227 | 0.479674195 |
| GO:0051050 | positive regulation of transport | 0.098816377 | 0.479874214 |
| ENSG00000169032 | MAP2K1 subnetwork | 0.099133982 | 0.481067603 |
| ENSG00000174292 | TNK1 subnetwork | 0.099099301 | 0.481146026 |
| MP:0004502 | decreased incidence of chemically-induced tumors | 0.099126088 | 0.481152993 |
| MP:0001240 | abnormal epidermis stratum corneum morphology | 0.09907333 | 0.481157544 |
| ENSG00000130826 | DKC1 subnetwork | 0.099221616 | 0.481462334 |
| GO:0007595 | lactation | 0.099303572 | 0.481875231 |
| MP:0008873 | increased physiological sensitivity to xenobiotic | 0.099519941 | 0.482436417 |
| GO:0006109 | regulation of carbohydrate metabolic process | 0.099507452 | 0.482503687 |
| ENSG00000147065 | MSN subnetwork | 0.099450215 | 0.482509225 |
| ENSG00000092529 | CAPN3 subnetwork | 0.099500864 | 0.482663224 |
| GO:0009306 | protein secretion | 0.099734151 | 0.483548268 |
| ENSG00000127334 | DYRK2 subnetwork | 0.099806444 | 0.483793738 |
| ENSG00000073050 | XRCC1 subnetwork | 0.09995673 | 0.484278351 |
| REACTOME_REGULATION_OF_KIT | REACTOME_REGULATION_OF_KIT_SIGNALING | 0.100047885 | 0.484578579 |
| ENSG00000185619 | PCGF3 subnetwork | 0.100159091 | 0.484797794 |
| GO:0030331 | estrogen receptor binding | 0.100115393 | 0.484841795 |
| ENSG00000079102 | RUNX1T1 subnetwork | 0.100132495 | 0.48484737 |
| GO:0043254 | regulation of protein complex assembly | 0.100373577 | 0.485176341 |
| ENSG00000008838 | MED24 subnetwork | 0.100313845 | 0.485244395 |
| GO:0060760 | positive regulation of response to cytokine stimulus | 0.10044007 | 0.485347044 |
| ENSG00000115268 | RPS15 subnetwork | 0.100627627 | 0.485625229 |
| ENSG00000168118 | RAB4A subnetwork | 0.100594297 | 0.485669725 |
| KEGG_INOSITOL_PHOSPHATE_ME | KEGG_INOSITOL_PHOSPHATE_METABOLISM | 0.100614772 | 0.485674982 |
| ENSG00000104131 | EIF3J subnetwork | 0.100589658 | 0.485829662 |
| MP:0005578 | teratozoospermia | 0.100894406 | 0.48686332 |
| GO:2000147 | positive regulation of cell motility | 0.10089139 | 0.48702346 |
| GO:0010494 | cytoplasmic stress granule | 0.101192354 | 0.488103953 |
| ENSG00000149311 | ATM subnetwork | 0.101141969 | 0.488186813 |
| GO:0002224 | toll-like receptor signaling pathway | 0.101187157 | 0.488264372 |
| ENSG00000168264 | IRF2BP2 subnetwork | 0.101614964 | 0.490193926 |
| ENSG00000080819 | CPOX subnetwork | 0.101662195 | 0.490288954 |
| ENSG00000136573 | BLK subnetwork | 0.101723295 | 0.490420475 |
| MP:0005630 | increased lung weight | 0.101852932 | 0.490844298 |
| ENSG00000163510 | CWC22 subnetwork | 0.102069256 | 0.491672754 |
| ENSG00000099389 | ENSG00000099389 subnetwork | 0.102055409 | 0.491761052 |
| GO:0005605 | basal lamina | 0.10230425 | 0.492387733 |
| ENSG00000163737 | PF4 subnetwork | 0.102380566 | 0.492755474 |
| GO:0090023 | positive regulation of neutrophil chemotaxis | 0.102557673 | 0.493305363 |
| ENSG00000080839 | RBL1 subnetwork | 0.102632276 | 0.493563093 |
| ENSG00000117751 | PPP1R8 subnetwork | 0.102867117 | 0.494153005 |
| ENSG00000171365 | CLCN5 subnetwork | 0.102795999 | 0.49416697 |
| GO:0002218 | activation of innate immune response | 0.102914734 | 0.494227968 |
| MP:0001176 | abnormal lung development | 0.102858686 | 0.494314869 |
| ENSG00000173267 | SNCG subnetwork | 0.103046894 | 0.494776119 |
| ENSG00000105063 | PPP6R1 subnetwork | 0.103139274 | 0.495105531 |
| GO:0016514 | SWI/SNF complex | 0.103255977 | 0.495743907 |
| ENSG00000131467 | PSME3 subnetwork | 0.103413941 | 0.496418182 |
| ENSG00000165288 | BRWD3 subnetwork | 0.103547646 | 0.497073791 |

| | | | |
|---|---|---|---|
| GO:0031072 | heat shock protein binding | 0.103733013 | 0.497693425 |
| GO:0002237 | response to molecule of bacterial origin | 0.103694467 | 0.497747093 |
| GO:0010563 | negative regulation of phosphorus metabolic process | 0.104048422 | 0.497971014 |
| ENSG00000151320 | AKAP6 subnetwork | 0.104253126 | 0.498047722 |
| ENSG00000140319 | SRP14 subnetwork | 0.104173286 | 0.498099891 |
| GO:0042345 | regulation of NF-kappaB import into nucleus | 0.10424595 | 0.498119349 |
| ENSG00000196656 | ENSG00000196656 subnetwork | 0.103882256 | 0.498130672 |
| GO:0045936 | negative regulation of phosphate metabolic process | 0.104048422 | 0.498151504 |
| ENSG00000109458 | GAB1 subnetwork | 0.10394018 | 0.498185776 |
| GO:0070461 | SAGA-type complex | 0.104132998 | 0.498207171 |
| ENSG00000163464 | CXCR1 subnetwork | 0.104157954 | 0.498225923 |
| ENSG00000173530 | TNFRSF10D subnetwork | 0.104319077 | 0.498229129 |
| GO:0042348 | NF-kappaB import into nucleus | 0.10424595 | 0.498299566 |
| ENSG00000197728 | RPS26 subnetwork | 0.103882256 | 0.498311547 |
| ENSG00000089220 | PEBP1 subnetwork | 0.104038714 | 0.498332125 |
| MP:0003717 | pallor | 0.104016445 | 0.498404062 |
| ENSG00000071242 | RPS6KA2 subnetwork | 0.104448081 | 0.498428468 |
| ENSG00000116473 | RAP1A subnetwork | 0.104655362 | 0.498503426 |
| ENSG00000115548 | KDM3A subnetwork | 0.104514511 | 0.498555435 |
| GO:0051651 | maintenance of location in cell | 0.104569507 | 0.498610108 |
| GO:0034103 | regulation of tissue remodeling | 0.104648647 | 0.498665224 |
| ENSG00000071082 | RPL31 subnetwork | 0.104646265 | 0.498845182 |
| ENSG00000137309 | HMGA1 subnetwork | 0.104834897 | 0.499099099 |
| GO:0030316 | osteoclast differentiation | 0.104786067 | 0.499134823 |
| GO:0019835 | cytolysis | 0.104920948 | 0.499207493 |
| ENSG00000179958 | DCTPP1 subnetwork | 0.105167756 | 0.500234066 |
| GO:0030518 | intracellular steroid hormone receptor signaling pathway | 0.105402023 | 0.501547876 |
| MP:0003447 | decreased tumor growth/size | 0.105447307 | 0.501673264 |
| ENSG00000100749 | VRK1 subnetwork | 0.105519775 | 0.501852518 |
| GO:0008301 | DNA binding, bending | 0.105664479 | 0.502409205 |
| ENSG00000184922 | FMNL1 subnetwork | 0.10615637 | 0.504455623 |
| GO:0030852 | regulation of granulocyte differentiation | 0.106154287 | 0.504618979 |
| ENSG00000089154 | GCN1L1 subnetwork | 0.106237093 | 0.504741379 |
| GO:2000107 | negative regulation of leukocyte apoptotic process | 0.106414599 | 0.505691203 |
| GO:0005024 | transforming growth factor beta-activated receptor activ | 0.1068042 | 0.507663317 |
| GO:0030669 | clathrin-coated endocytic vesicle membrane | 0.107028972 | 0.508736993 |
| GO:0050681 | androgen receptor binding | 0.107166529 | 0.50945122 |
| GO:0042274 | ribosomal small subunit biogenesis | 0.107286637 | 0.50989602 |
| REACTOME_FATTY_ACID_TRIACYI | REACTOME_FATTY_ACID_TRIACYLGLYCEROL_AND_KETC | 0.107327105 | 0.509942673 |
| GO:0006984 | ER-nucleus signaling pathway | 0.107374522 | 0.509953455 |
| ENSG00000110958 | PTGES3 subnetwork | 0.107450873 | 0.509982111 |
| ENSG00000064393 | HIPK2 subnetwork | 0.107318285 | 0.510017921 |
| MP:0005668 | decreased circulating leptin level | 0.10736753 | 0.510100287 |
| MP:0004978 | decreased B-1 B cell number | 0.107443023 | 0.510146743 |
| ENSG00000117318 | ID3 subnetwork | 0.107644988 | 0.510779407 |
| ENSG00000186716 | BCR subnetwork | 0.107623683 | 0.510783262 |
| ENSG00000129152 | MYOD1 subnetwork | 0.107762976 | 0.511079342 |
| ENSG00000129824 | RPS4Y1 subnetwork | 0.107888977 | 0.511117059 |
| ENSG00000140682 | TGFB1I1 subnetwork | 0.107876163 | 0.511228133 |
| ENSG00000136045 | PWP1 subnetwork | 0.107844778 | 0.511232143 |
| MP:0003215 | renal interstitial fibrosis | 0.107841521 | 0.511414791 |
| ENSG00000206506 | HLA-G subnetwork | 0.108069837 | 0.51152476 |
| MP:0005030 | absent amnion | 0.108132784 | 0.511534354 |
| ENSG00000136021 | SCYL2 subnetwork | 0.108179287 | 0.511654804 |

| | | | |
|---|---|---|---|
| ENSG00000112651 | MRPL2 subnetwork | 0.108130256 | 0.511680912 |
| ENSG00000105953 | OGDH subnetwork | 0.107993813 | 0.511701748 |
| ENSG00000206443 | ENSG00000206443 subnetwork | 0.108069837 | 0.511707056 |
| ENSG00000180530 | NRIP1 subnetwork | 0.10802354 | 0.511733238 |
| ENSG00000204632 | HLA-G subnetwork | 0.108069837 | 0.511889483 |
| ENSG00000119285 | HEATR1 subnetwork | 0.108288038 | 0.512024191 |
| ENSG00000152484 | USP12 subnetwork | 0.108395489 | 0.51230441 |
| ENSG00000131747 | TOP2A subnetwork | 0.108562799 | 0.512753108 |
| MP:0008866 | chromosomal instability | 0.108522457 | 0.512904373 |
| KEGG_TYPE_II_DIABETES_MELLIT | KEGG_TYPE_II_DIABETES_MELLITUS | 0.108554457 | 0.512935323 |
| ENSG00000054611 | TBC1D22A subnetwork | 0.108693982 | 0.513103693 |
| REACTOME_MAPK_TARGETS_NU | REACTOME_MAPK_TARGETS_NUCLEAR_EVENTS_MEDIA | 0.108873308 | 0.513809017 |
| MP:0002652 | thin myocardium | 0.109103388 | 0.51469127 |
| ENSG00000073282 | TP63 subnetwork | 0.10941974 | 0.515208924 |
| ENSG00000102755 | FLT1 subnetwork | 0.109496482 | 0.515256637 |
| ENSG00000147443 | DOK2 subnetwork | 0.109343933 | 0.515349167 |
| GO:0090079 | translation regulator activity, nucleic acid binding | 0.109276539 | 0.515360057 |
| ENSG00000137486 | ARRB1 subnetwork | 0.10941004 | 0.515373716 |
| GO:0051087 | chaperone binding | 0.109387631 | 0.515379164 |
| MP:0001780 | decreased brown adipose tissue amount | 0.109322046 | 0.515460993 |
| ENSG00000145781 | COMMD10 subnetwork | 0.109557016 | 0.515516631 |
| ENSG00000122778 | KIAA1549 subnetwork | 0.109708971 | 0.515823904 |
| MP:0004181 | abnormal carotid artery morphology | 0.109793695 | 0.515995051 |
| ENSG00000120129 | DUSP1 subnetwork | 0.109708243 | 0.516006367 |
| MP:0001263 | weight loss | 0.109924508 | 0.51608404 |
| GO:0031401 | positive regulation of protein modification process | 0.109900039 | 0.516142706 |
| ENSG00000108587 | GOSR1 subnetwork | 0.109857703 | 0.516166078 |
| GO:0032393 | MHC class I receptor activity | 0.109997092 | 0.516166608 |
| ENSG00000164078 | MST1R subnetwork | 0.110101041 | 0.516707833 |
| ENSG00000184886 | PIGW subnetwork | 0.11018501 | 0.517054674 |
| MP:0004188 | delayed embryo turning | 0.110227254 | 0.517136812 |
| REACTOME_NITRIC_OXIDE_STIMU | REACTOME_NITRIC_OXIDE_STIMULATES_GUANYLATE_C | 0.110563687 | 0.518380282 |
| ENSG00000101558 | VAPA subnetwork | 0.110545797 | 0.518492427 |
| GO:0042162 | telomeric DNA binding | 0.110538068 | 0.518604651 |
| ENSG00000139835 | GRTP1 subnetwork | 0.11051672 | 0.518646458 |
| GO:0071495 | cellular response to endogenous stimulus | 0.110684939 | 0.518831397 |
| GO:0008135 | translation factor activity, nucleic acid binding | 0.110725424 | 0.518947924 |
| ENSG00000163346 | PBXIP1 subnetwork | 0.111339253 | 0.520814321 |
| MP:0002947 | hemangioma | 0.111312968 | 0.520839185 |
| ENSG00000155660 | PDIA4 subnetwork | 0.111403537 | 0.520964912 |
| ENSG00000156261 | CCT8 subnetwork | 0.111307886 | 0.521004566 |
| GO:0005858 | axonemal dynein complex | 0.11148272 | 0.521020337 |
| ENSG00000138029 | HADHB subnetwork | 0.111472334 | 0.521062785 |
| ENSG00000165271 | NOL6 subnetwork | 0.111304546 | 0.521187632 |
| ENSG00000122140 | MRPS2 subnetwork | 0.11129414 | 0.521265378 |
| ENSG00000187109 | NAP1L1 subnetwork | 0.111211702 | 0.521280338 |
| GO:0019319 | hexose biosynthetic process | 0.111269086 | 0.521360759 |
| GO:0031958 | corticosteroid receptor signaling pathway | 0.111742172 | 0.522169646 |
| ENSG00000092067 | CEBPE subnetwork | 0.111825024 | 0.522372109 |
| ENSG00000175416 | CLTB subnetwork | 0.111938451 | 0.522994746 |
| ENSG00000100206 | DMC1 subnetwork | 0.112203261 | 0.523444056 |
| REACTOME_ACTIVATION_OF_THI | REACTOME_ACTIVATION_OF_THE_AP:1_FAMILY_OF_TR | 0.112064238 | 0.523476891 |
| ENSG00000108107 | RPL28 subnetwork | 0.112186845 | 0.523522211 |
| ENSG00000006125 | AP2B1 subnetwork | 0.112151872 | 0.523547936 |

| | | | |
|---|---|---|---|
| MP:0002410 | decreased susceptibility to viral infection | 0.112248268 | 0.523610626 |
| ENSG00000161618 | ALDH16A1 subnetwork | 0.11214366 | 0.523678684 |
| GO:0001913 | T cell mediated cytotoxicity | 0.112326536 | 0.52382949 |
| ENSG00000070882 | OSBPL3 subnetwork | 0.112359148 | 0.523873559 |
| ENSG00000105849 | TWISTNB subnetwork | 0.112667327 | 0.524642483 |
| MP:0011109 | partial lethality throughout fetal growth and developmer | 0.112533229 | 0.524650838 |
| ENSG00000112078 | KCTD20 subnetwork | 0.112648526 | 0.524773203 |
| ENSG00000157404 | KIT subnetwork | 0.112618062 | 0.524816754 |
| ENSG00000134853 | PDGFRA subnetwork | 0.112755223 | 0.524982566 |
| MP:0008395 | abnormal osteoblast differentiation | 0.113003882 | 0.525200139 |
| KEGG_GNRH_SIGNALING_PATHW | KEGG_GNRH_SIGNALING_PATHWAY | 0.112974513 | 0.525278552 |
| GO:0035004 | phosphatidylinositol 3-kinase activity | 0.112961365 | 0.52539185 |
| ENSG00000119699 | TGFB3 subnetwork | 0.112901296 | 0.525566399 |
| GO:0016303 | 1-phosphatidylinositol-3-kinase activity | 0.112961365 | 0.525574913 |
| ENSG00000114942 | EEF1B2 subnetwork | 0.113129638 | 0.525765484 |
| MP:0008663 | increased interleukin-12 secretion | 0.11326754 | 0.526313043 |
| GO:0046982 | protein heterodimerization activity | 0.113506215 | 0.5274244 |
| GO:0045597 | positive regulation of cell differentiation | 0.113471306 | 0.527468707 |
| ENSG00000196975 | ANXA4 subnetwork | 0.113681953 | 0.528204238 |
| GO:0050755 | chemokine metabolic process | 0.113674289 | 0.52833565 |
| MP:0011101 | partial prenatal lethality | 0.113764479 | 0.528358209 |
| ENSG00000013455 | ENSG00000013455 subnetwork | 0.113745388 | 0.5284375 |
| MP:0002664 | decreased circulating adrenocorticotropin level | 0.114037958 | 0.529528105 |
| MP:0003227 | abnormal vascular branching morphogenesis | 0.114205547 | 0.53012487 |
| ENSG00000118094 | TREH subnetwork | 0.11424868 | 0.530166436 |
| ENSG00000148408 | CACNA1B subnetwork | 0.114404993 | 0.530561331 |
| GO:0050854 | regulation of antigen receptor-mediated signaling pathw | 0.114379445 | 0.53067591 |
| MP:0003562 | abnormal pancreatic beta cell physiology | 0.114658268 | 0.531446867 |
| ENSG00000137054 | POLR1E subnetwork | 0.114619663 | 0.531475069 |
| ENSG00000165525 | NEMF subnetwork | 0.114735387 | 0.531476998 |
| ENSG00000166710 | B2M subnetwork | 0.114695654 | 0.531522491 |
| ENSG00000137818 | RPLP1 subnetwork | 0.114582801 | 0.531537929 |
| ENSG00000113319 | RASGRF2 subnetwork | 0.11492598 | 0.532129278 |
| MP:0002182 | abnormal astrocyte morphology | 0.114913673 | 0.532192254 |
| GO:0050431 | transforming growth factor beta binding | 0.115084911 | 0.532326545 |
| ENSG00000043093 | DCUN1D1 subnetwork | 0.115034842 | 0.53238342 |
| ENSG00000163682 | RPL9 subnetwork | 0.115218346 | 0.532385384 |
| GO:0034341 | response to interferon-gamma | 0.115121147 | 0.532401656 |
| ENSG00000118515 | SGK1 subnetwork | 0.115016592 | 0.532463718 |
| GO:0030595 | leukocyte chemotaxis | 0.115080576 | 0.532493094 |
| GO:0016573 | histone acetylation | 0.11537 | 0.53255854 |
| GO:0043966 | histone H3 acetylation | 0.115291485 | 0.532563749 |
| ENSG00000182754 | ENSG00000182754 subnetwork | 0.115218346 | 0.532568966 |
| ENSG00000134215 | VAV3 subnetwork | 0.115316384 | 0.532604203 |
| ENSG00000167721 | TSR1 subnetwork | 0.115205317 | 0.532666437 |
| ENSG00000151422 | FER subnetwork | 0.115530938 | 0.532782938 |
| MP:0000292 | distended pericardium | 0.115523613 | 0.532931865 |
| GO:0042362 | fat-soluble vitamin biosynthetic process | 0.115520399 | 0.533063683 |
| ENSG00000140326 | CDAN1 subnetwork | 0.115826118 | 0.534009629 |
| ENSG00000154001 | PPP2R5E subnetwork | 0.116020322 | 0.534232223 |
| GO:0008083 | growth factor activity | 0.115941887 | 0.53432451 |
| MP:0008898 | abnormal acrosome morphology | 0.116006008 | 0.534347079 |
| MP:0003719 | abnormal pericyte morphology | 0.11615064 | 0.534769918 |
| ENSG00000150990 | DHX37 subnetwork | 0.116186503 | 0.534809475 |

| | | | |
|---|---|---|---|
| ENSG00000171858 | RPS21 subnetwork | 0.116434942 | 0.535574614 |
| GO:0018394 | peptidyl-lysine acetylation | 0.116418795 | 0.535741249 |
| GO:0032007 | negative regulation of TOR signaling cascade | 0.116575362 | 0.536042524 |
| GO:0002758 | innate immune response-activating signal transduction | 0.116663128 | 0.536544395 |
| GO:0048145 | regulation of fibroblast proliferation | 0.116864617 | 0.536888052 |
| GO:0046688 | response to copper ion | 0.116840312 | 0.536952055 |
| ENSG00000176165 | FOXG1 subnetwork | 0.11683838 | 0.537101747 |
| GO:0032722 | positive regulation of chemokine production | 0.116831456 | 0.537268677 |
| GO:0070741 | response to interleukin-6 | 0.117097404 | 0.537786521 |
| ENSG00000118971 | CCND2 subnetwork | 0.117157094 | 0.537927497 |
| GO:0000784 | nuclear chromosome, telomeric region | 0.117082806 | 0.537953457 |
| GO:0032469 | endoplasmic reticulum calcium ion homeostasis | 0.117382723 | 0.538957265 |
| ENSG00000055044 | NOP58 subnetwork | 0.117760464 | 0.540533151 |
| ENSG00000111737 | RAB35 subnetwork | 0.117951474 | 0.540719891 |
| KEGG_THYROID_CANCER | KEGG_THYROID_CANCER | 0.117989959 | 0.540757162 |
| ENSG00000038427 | VCAN subnetwork | 0.117834378 | 0.540843867 |
| REACTOME_L13A:MEDIATED_TRA | REACTOME_L13A:MEDIATED_TRANSLATIONAL_SILENCIN | 0.117941606 | 0.540887372 |
| REACTOME_3_:UTR:MEDIATED_T | REACTOME_3_:UTR:MEDIATED_TRANSLATIONAL_REGUI | 0.117941606 | 0.541072038 |
| ENSG00000057608 | GDI2 subnetwork | 0.117937809 | 0.541205601 |
| ENSG00000115661 | STK16 subnetwork | 0.118312084 | 0.541802999 |
| ENSG00000173867 | ENSG00000173867 subnetwork | 0.118342481 | 0.541805792 |
| MP:0008944 | decreased sensitivity to induced cell death | 0.118309116 | 0.541987726 |
| ENSG00000114857 | NKTR subnetwork | 0.118433459 | 0.542012943 |
| MP:0000270 | abnormal heart tube morphology | 0.118494343 | 0.542100783 |
| ENSG00000101343 | CRNKL1 subnetwork | 0.118567426 | 0.542256637 |
| ENSG00000163453 | IGFBP7 subnetwork | 0.118636296 | 0.54244641 |
| ENSG00000069956 | MAPK6 subnetwork | 0.11871027 | 0.54255102 |
| ENSG00000158769 | F11R subnetwork | 0.118905492 | 0.543471608 |
| ENSG00000146007 | ZMAT2 subnetwork | 0.119019619 | 0.543796737 |
| ENSG00000157326 | DHRS4 subnetwork | 0.119125729 | 0.543887946 |
| ENSG00000132842 | AP3B1 subnetwork | 0.119101979 | 0.543953804 |
| ENSG00000107560 | RAB11FIP2 subnetwork | 0.119081589 | 0.544053687 |
| GO:0032947 | protein complex scaffold | 0.119349864 | 0.544184469 |
| REACTOME_SIGNALING_BY_CONS | REACTOME_SIGNALING_BY_CONSTITUTIVELY_ACTIVE_E | 0.119348784 | 0.544369064 |
| ENSG00000189037 | DUSP21 subnetwork | 0.119284033 | 0.544467074 |
| GO:0006278 | RNA-dependent DNA replication | 0.1193452 | 0.544519851 |
| GO:0042033 | chemokine biosynthetic process | 0.119559327 | 0.545067797 |
| ENSG00000157514 | TSC22D3 subnetwork | 0.11960862 | 0.545205015 |
| GO:0006310 | DNA recombination | 0.119658132 | 0.545342141 |
| ENSG00000104946 | TBC1D17 subnetwork | 0.11971658 | 0.545411446 |
| ENSG00000196235 | SUPT5H subnetwork | 0.119760771 | 0.545599188 |
| KEGG_EPITHELIAL_CELL_SIGNALIN | KEGG_EPITHELIAL_CELL_SIGNALING_IN_HELICOBACTER_ | 0.11992987 | 0.546226734 |
| MP:0005601 | increased angiogenesis | 0.120028045 | 0.546414073 |
| GO:0000184 | nuclear-transcribed mRNA catabolic process, nonsense-r | 0.120269293 | 0.547075727 |
| MP:0008808 | decreased spleen iron level | 0.120235967 | 0.547091647 |
| ENSG00000145348 | TBCK subnetwork | 0.120392801 | 0.547112462 |
| ENSG00000126458 | RRAS subnetwork | 0.12033963 | 0.547194998 |
| ENSG00000110768 | GTF2H1 subnetwork | 0.120367892 | 0.547195946 |
| ENSG00000106245 | BUD31 subnetwork | 0.120836604 | 0.549172856 |
| ENSG00000113758 | DBN1 subnetwork | 0.12091126 | 0.549308134 |
| MP:0010760 | abnormal macrophage chemotaxis | 0.121000546 | 0.549510796 |
| GO:0045120 | pronucleus | 0.121137839 | 0.549831423 |
| ENSG00000111348 | ARHGDIB subnetwork | 0.121129179 | 0.549966273 |
| ENSG00000129315 | CCNT1 subnetwork | 0.121181761 | 0.550016852 |

| | | | |
|---|---|---|---|
| GO:0060205 | cytoplasmic membrane-bounded vesicle lumen | 0.121413072 | 0.550909704 |
| MP:0010264 | increased hepatoma incidence | 0.121484698 | 0.551111485 |
| MP:0008719 | impaired neutrophil recruitment | 0.121603768 | 0.551363177 |
| ENSG00000159217 | IGF2BP1 subnetwork | 0.121580726 | 0.551414141 |
| MP:0011092 | complete embryonic lethality | 0.121925527 | 0.552674966 |
| ENSG00000165416 | SUGT1 subnetwork | 0.122181181 | 0.553985873 |
| MP:0000606 | decreased hepatocyte number | 0.12221903 | 0.554102219 |
| ENSG00000166197 | NOLC1 subnetwork | 0.122388683 | 0.554771505 |
| ENSG00000108469 | RECQL5 subnetwork | 0.122523953 | 0.554885829 |
| KEGG_FC_GAMMA_R_MEDIATED | KEGG_FC_GAMMA_R_MEDIATED_PHAGOCYTOSIS | 0.122384731 | 0.554957983 |
| ENSG00000007392 | LUC7L subnetwork | 0.122517826 | 0.555055425 |
| ENSG00000109929 | SC5DL subnetwork | 0.122672027 | 0.555421282 |
| GO:0010675 | regulation of cellular carbohydrate metabolic process | 0.122735326 | 0.555637584 |
| ENSG00000161217 | PCYT1A subnetwork | 0.122874523 | 0.556222744 |
| GO:0042976 | activation of Janus kinase activity | 0.123028403 | 0.556247906 |
| GO:0019867 | outer membrane | 0.123027693 | 0.556434316 |
| GO:2000117 | negative regulation of cysteine-type endopeptidase activ | 0.122984887 | 0.556486758 |
| ENSG00000197971 | MBP subnetwork | 0.122949477 | 0.556522468 |
| GO:0002456 | T cell mediated immunity | 0.123246481 | 0.557401206 |
| ENSG00000136653 | RASSF5 subnetwork | 0.123285995 | 0.557415467 |
| ENSG00000080845 | DLGAP4 subnetwork | 0.123383339 | 0.557527601 |
| ENSG00000152234 | ATP5A1 subnetwork | 0.123348859 | 0.55753012 |
| GO:0044212 | transcription regulatory region DNA binding | 0.123500159 | 0.557976589 |
| ENSG00000206557 | TRIM71 subnetwork | 0.12364825 | 0.558205214 |
| ENSG00000166889 | PATL1 subnetwork | 0.123614167 | 0.558207957 |
| ENSG00000150687 | PRSS23 subnetwork | 0.123787645 | 0.558837287 |
| ENSG00000090339 | ICAM1 subnetwork | 0.12402965 | 0.559749583 |
| GO:0008207 | C21-steroid hormone metabolic process | 0.123999603 | 0.559769539 |
| GO:0007163 | establishment or maintenance of cell polarity | 0.12425888 | 0.560353451 |
| ENSG00000173542 | MOB1B subnetwork | 0.124303463 | 0.5604 |
| MP:0000321 | increased bone marrow cell number | 0.12425669 | 0.560523682 |
| MP:0004056 | abnormal myocardium compact layer morphology | 0.124247788 | 0.560694027 |
| ENSG00000175029 | CTBP2 subnetwork | 0.124234802 | 0.560847797 |
| MP:0004805 | absent oocytes | 0.124433311 | 0.560879707 |
| ENSG00000174233 | ADCY6 subnetwork | 0.124670524 | 0.562075283 |
| MP:0004499 | increased incidence of chemically-induced tumors | 0.124784944 | 0.562366844 |
| ENSG00000011052 | NME2 subnetwork | 0.124861372 | 0.562408516 |
| ENSG00000134574 | DDB2 subnetwork | 0.124761883 | 0.562437562 |
| ENSG00000119689 | DLST subnetwork | 0.124857079 | 0.562595674 |
| GO:0045768 | positive regulation of anti-apoptosis | 0.125119344 | 0.563214761 |
| GO:0040008 | regulation of growth | 0.125097941 | 0.56333555 |
| GO:0000781 | chromosome, telomeric region | 0.125274805 | 0.563887043 |
| ENSG00000184110 | EIF3C subnetwork | 0.125255159 | 0.563958126 |
| ENSG00000205937 | RNPS1 subnetwork | 0.125341023 | 0.564164729 |
| ENSG00000140538 | NTRK3 subnetwork | 0.125649731 | 0.564953581 |
| GO:0090312 | positive regulation of protein deacetylation | 0.125568551 | 0.565051444 |
| ENSG00000166266 | CUL5 subnetwork | 0.1256456 | 0.565107794 |
| GO:0009894 | regulation of catabolic process | 0.125615776 | 0.565129396 |
| ENSG00000151150 | ANK3 subnetwork | 0.125560427 | 0.565205843 |
| ENSG00000172572 | PDE3A subnetwork | 0.125778814 | 0.56528008 |
| MP:0004875 | increased mean systemic arterial blood pressure | 0.12583706 | 0.56530308 |
| ENSG00000123609 | NMI subnetwork | 0.125940609 | 0.565359153 |
| GO:0043491 | protein kinase B signaling cascade | 0.125818176 | 0.565424122 |
| GO:0016579 | protein deubiquitination | 0.125923709 | 0.565480132 |

| | | | |
|---|---|---|---|
| ENSG00000171862 | PTEN subnetwork | 0.126092196 | 0.565982793 |
| ENSG00000165630 | PRPF18 subnetwork | 0.126318787 | 0.567036057 |
| ENSG00000079435 | LIPE subnetwork | 0.126382891 | 0.567080026 |
| MP:0002408 | abnormal double-positive T cell morphology | 0.126468835 | 0.567355372 |
| REACTOME_EGFR_INTERACTS_W | REACTOME_EGFR_INTERACTS_WITH_PHOSPHOLIPASE_( | 0.12651443 | 0.567465301 |
| ENSG00000072135 | PTPN18 subnetwork | 0.126558927 | 0.567525603 |
| GO:0031348 | negative regulation of defense response | 0.126660394 | 0.567651915 |
| GO:0045408 | regulation of interleukin-6 biosynthetic process | 0.12674546 | 0.567992737 |
| ENSG00000163781 | TOPBP1 subnetwork | 0.126859096 | 0.568168317 |
| GO:0045444 | fat cell differentiation | 0.126960806 | 0.568304749 |
| ENSG00000115808 | STRN subnetwork | 0.126932492 | 0.568327285 |
| MP:0001179 | thick pulmonary interalveolar septum | 0.127148786 | 0.568951879 |
| ENSG00000069869 | NEDD4 subnetwork | 0.127109904 | 0.569007583 |
| ENSG00000119335 | SET subnetwork | 0.127334294 | 0.569637562 |
| MP:0001658 | increased mortality induced by gamma-irradiation | 0.127486878 | 0.569881501 |
| GO:0005083 | small GTPase regulator activity | 0.127478951 | 0.570052684 |
| ENSG00000112685 | EXOC2 subnetwork | 0.127564666 | 0.570065789 |
| ENSG00000031544 | ENSG00000031544 subnetwork | 0.127539192 | 0.570088845 |
| ENSG00000141101 | NOB1 subnetwork | 0.127462137 | 0.57020751 |
| GO:0051270 | regulation of cellular component movement | 0.127713439 | 0.570430638 |
| ENSG00000085117 | CD82 subnetwork | 0.127702888 | 0.57055245 |
| GO:0040017 | positive regulation of locomotion | 0.128027537 | 0.571119134 |
| MP:0010876 | decreased bone volume | 0.12800182 | 0.571208142 |
| MP:0011290 | decreased nephron number | 0.127975836 | 0.571297209 |
| MP:0008008 | early cellular replicative senescence | 0.127964871 | 0.571386334 |
| ENSG00000161021 | MAML1 subnetwork | 0.12793941 | 0.571409793 |
| ENSG00000158987 | RAPGEF6 subnetwork | 0.128298123 | 0.57234252 |
| ENSG00000184451 | CCR10 subnetwork | 0.128380551 | 0.572377049 |
| ENSG00000134046 | MBD2 subnetwork | 0.128426599 | 0.572386103 |
| KEGG_RIBOSOME | KEGG_RIBOSOME | 0.128355062 | 0.572466382 |
| ENSG00000051180 | RAD51 subnetwork | 0.128535556 | 0.572903014 |
| ENSG00000102871 | TRADD subnetwork | 0.128607483 | 0.572977399 |
| MP:0000334 | decreased granulocyte number | 0.128715786 | 0.573191489 |
| GO:0042095 | interferon-gamma biosynthetic process | 0.128686396 | 0.573248199 |
| ENSG00000188170 | ENSG00000188170 subnetwork | 0.12895456 | 0.573797841 |
| ENSG00000065485 | PDIA5 subnetwork | 0.128993185 | 0.573806409 |
| ENSG00000077809 | GTF2I subnetwork | 0.128909109 | 0.573871073 |
| ENSG00000165637 | VDAC2 subnetwork | 0.129206745 | 0.574273113 |
| GO:0005161 | platelet-derived growth factor receptor binding | 0.12918276 | 0.574444444 |
| ENSG00000178568 | ERBB4 subnetwork | 0.12917955 | 0.574566852 |
| MP:0002118 | abnormal lipid homeostasis | 0.129332627 | 0.574640758 |
| MP:0005277 | abnormal brainstem morphology | 0.129408859 | 0.574763304 |
| ENSG00000204348 | DOM3Z subnetwork | 0.13010725 | 0.575251869 |
| ENSG00000206266 | ENSG00000206266 subnetwork | 0.13010725 | 0.575438882 |
| ENSG00000104938 | CLEC4M subnetwork | 0.129975237 | 0.575504557 |
| ENSG00000198211 | TUBB3 subnetwork | 0.129817708 | 0.57553781 |
| GO:0003950 | NAD+ ADP-ribosyltransferase activity | 0.129861668 | 0.57554578 |
| ENSG00000100302 | RASD2 subnetwork | 0.12967626 | 0.575562806 |
| GO:0006959 | humoral immune response | 0.130069383 | 0.575569291 |
| MP:0005164 | abnormal response to injury | 0.12989787 | 0.575570033 |
| GO:0046332 | SMAD binding | 0.130032393 | 0.575593882 |
| GO:0033017 | sarcoplasmic reticulum membrane | 0.129636102 | 0.575603786 |
| ENSG00000206346 | DOM3Z subnetwork | 0.13010725 | 0.575626016 |
| ENSG00000138642 | HERC6 subnetwork | 0.129963005 | 0.575643113 |

| | | | |
|---|---|---|---|
| ENSG00000101204 | CHRNA4 subnetwork | 0.129813 | 0.575692859 |
| ENSG00000130332 | LSM7 subnetwork | 0.12981292 | 0.575880626 |
| GO:0034694 | response to prostaglandin stimulus | 0.130334324 | 0.576267057 |
| ENSG00000100097 | LGALS1 subnetwork | 0.130629677 | 0.577182733 |
| GO:0003823 | antigen binding | 0.130526098 | 0.57720039 |
| ENSG00000070770 | CSNK2A2 subnetwork | 0.13071011 | 0.577255029 |
| ENSG00000114302 | PRKAR2A subnetwork | 0.130601469 | 0.577288961 |
| ENSG00000204642 | HLA-F subnetwork | 0.131216551 | 0.579066753 |
| ENSG00000184304 | PRKD1 subnetwork | 0.131121381 | 0.579111255 |
| ENSG00000169714 | CNBP subnetwork | 0.131186839 | 0.579124797 |
| ENSG00000197879 | MYO1C subnetwork | 0.131161702 | 0.579166667 |
| ENSG00000120094 | HOXB1 subnetwork | 0.131571036 | 0.580709427 |
| MP:0004889 | increased energy expenditure | 0.131918639 | 0.582399611 |
| MP:0011294 | renal glomerulus hypertrophy | 0.131986135 | 0.58263192 |
| ENSG00000136731 | UGGT1 subnetwork | 0.132183346 | 0.582751374 |
| MP:0002183 | gliosis | 0.132180064 | 0.582923674 |
| ENSG00000130699 | TAF4 subnetwork | 0.132178693 | 0.583096085 |
| ENSG00000129351 | ILF3 subnetwork | 0.132142949 | 0.583171521 |
| ENSG00000182367 | ENSG00000182367 subnetwork | 0.132963724 | 0.583210035 |
| ENSG00000099860 | GADD45B subnetwork | 0.132310436 | 0.583290239 |
| GO:0002690 | positive regulation of leukocyte chemotaxis | 0.132937727 | 0.583333333 |
| ENSG00000067208 | EVI5 subnetwork | 0.133044472 | 0.583440514 |
| GO:0031233 | intrinsic to external side of plasma membrane | 0.133240135 | 0.583461785 |
| GO:0034774 | secretory granule lumen | 0.133330596 | 0.583488447 |
| GO:0071559 | response to transforming growth factor beta stimulus | 0.132934546 | 0.583504989 |
| ENSG00000008130 | NADK subnetwork | 0.133223292 | 0.58352072 |
| GO:0044130 | negative regulation of growth of symbiont in host | 0.132907422 | 0.58356407 |
| ENSG00000113643 | RARS subnetwork | 0.133191185 | 0.583627892 |
| ENSG00000108443 | RPS6KB1 subnetwork | 0.133329319 | 0.583675762 |
| MP:0003670 | dilated renal glomerular capsule | 0.132475033 | 0.58371567 |
| GO:0012510 | trans-Golgi network transport vesicle membrane | 0.133179952 | 0.583735133 |
| GO:0044126 | regulation of growth of symbiont in host | 0.132907422 | 0.583752013 |
| ENSG00000002330 | BAD subnetwork | 0.133788821 | 0.583808 |
| ENSG00000023734 | STRAP subnetwork | 0.133646323 | 0.583936579 |
| GO:0044110 | growth involved in symbiotic interaction | 0.132907422 | 0.583940077 |
| GO:0032733 | positive regulation of interleukin-10 production | 0.133782593 | 0.583994878 |
| MP:0001175 | abnormal lung morphology | 0.133854789 | 0.584005118 |
| GO:0000783 | nuclear telomere cap complex | 0.133570605 | 0.584022436 |
| ENSG00000143799 | PARP1 subnetwork | 0.13347337 | 0.584087263 |
| ENSG00000109819 | PPARGC1A subnetwork | 0.133763226 | 0.584101825 |
| ENSG00000167553 | TUBA1C subnetwork | 0.133636601 | 0.584107658 |
| GO:0044116 | growth of symbiont involved in interaction with host | 0.132907422 | 0.584128263 |
| GO:0031000 | response to caffeine | 0.133540216 | 0.584172547 |
| GO:0000782 | telomere cap complex | 0.133570605 | 0.584209683 |
| GO:0044117 | growth of symbiont in host | 0.132907422 | 0.58431657 |
| ENSG00000215328 | HSPA1A subnetwork | 0.13395532 | 0.584351023 |
| MP:0002429 | abnormal blood cell morphology/development | 0.133935511 | 0.584409978 |
| MP:0003634 | abnormal glial cell morphology | 0.132699706 | 0.584463824 |
| GO:0044146 | negative regulation of growth of symbiont involved in int | 0.132907422 | 0.584504998 |
| ENSG00000167670 | CHAF1A subnetwork | 0.132840663 | 0.584559535 |
| MP:0011186 | abnormal visceral endoderm morphology | 0.132828125 | 0.584635249 |
| GO:0045926 | negative regulation of growth | 0.134263211 | 0.584652202 |
| GO:0044144 | modulation of growth of symbiont involved in interactio | 0.132907422 | 0.584693548 |
| ENSG00000149091 | DGKZ subnetwork | 0.132804791 | 0.584711011 |

| | | | |
|---|---|---|---|
| MP:0002929 | abnormal bile duct development | 0.134253748 | 0.584806894 |
| REACTOME_PAUSING_AND_RECC | REACTOME_PAUSING_AND_RECOVERY_OF_ELONGATIO | 0.134228326 | 0.584897829 |
| GO:0031647 | regulation of protein stability | 0.134361771 | 0.58492823 |
| REACTOME_HIV:1_ELONGATION_ | REACTOME_HIV:1_ELONGATION_ARREST_AND_RECOVE | 0.134228326 | 0.585084637 |
| GO:0004675 | transmembrane receptor protein serine/threonine kinas | 0.134439119 | 0.585108418 |
| REACTOME_PAUSING_AND_RECC | REACTOME_PAUSING_AND_RECOVERY_OF_HIV:1_ELON | 0.134228326 | 0.585271565 |
| REACTOME_ELONGATION_ARRES | REACTOME_ELONGATION_ARREST_AND_RECOVERY | 0.134228326 | 0.585458613 |
| ENSG00000079277 | MKNK1 subnetwork | 0.134727021 | 0.586121734 |
| ENSG00000161955 | TNFSF13 subnetwork | 0.134880192 | 0.586123488 |
| MP:0000414 | alopecia | 0.134840464 | 0.586150907 |
| GO:0048015 | phosphatidylinositol-mediated signaling | 0.134804115 | 0.58616242 |
| GO:0042542 | response to hydrogen peroxide | 0.134722515 | 0.586292636 |
| GO:0048017 | inositol lipid-mediated signaling | 0.134804115 | 0.586349156 |
| MP:0001209 | spontaneous skin ulceration | 0.134974364 | 0.586446071 |
| ENSG00000169398 | PTK2 subnetwork | 0.13516168 | 0.586963434 |
| GO:0005741 | mitochondrial outer membrane | 0.1352031 | 0.586967578 |
| ENSG00000008294 | SPAG9 subnetwork | 0.13513673 | 0.587070611 |
| MP:0003566 | abnormal cell adhesion | 0.135582071 | 0.587321712 |
| GO:0022626 | cytosolic ribosome | 0.135560499 | 0.587428662 |
| REACTOME_ACTIVATED_TAK1_M | REACTOME_ACTIVATED_TAK1_MEDIATES_P38_MAPK_A | 0.135555732 | 0.58761497 |
| ENSG00000145723 | GIN1 subnetwork | 0.135543571 | 0.587722081 |
| GO:0031093 | platelet alpha granule lumen | 0.135537206 | 0.587829261 |
| ENSG00000168078 | PBK subnetwork | 0.135494196 | 0.587948555 |
| MP:0001121 | uterus hypoplasia | 0.135516588 | 0.587968254 |
| ENSG00000136717 | BIN1 subnetwork | 0.135732178 | 0.588038657 |
| GO:0043500 | muscle adaptation | 0.135489978 | 0.588103558 |
| MP:0006094 | increased fat cell size | 0.135777106 | 0.588137472 |
| MP:0002957 | intestinal adenocarcinoma | 0.135486329 | 0.588290435 |
| GO:0002221 | pattern recognition receptor signaling pathway | 0.13601833 | 0.588449367 |
| ENSG00000019991 | HGF subnetwork | 0.136006524 | 0.588588161 |
| ENSG00000214485 | ENSG00000214485 subnetwork | 0.135972816 | 0.588679544 |
| MP:0004893 | decreased adiponectin level | 0.136134685 | 0.58881683 |
| GO:0007004 | telomere maintenance via telomerase | 0.136309527 | 0.589563567 |
| ENSG00000164338 | UTP15 subnetwork | 0.136377445 | 0.589709137 |
| ENSG00000159251 | ACTC1 subnetwork | 0.136526533 | 0.590107459 |
| GO:0016641 | oxidoreductase activity, acting on the CH-NH2 group of c | 0.137058602 | 0.592432859 |
| ENSG00000160087 | UBE2J2 subnetwork | 0.13711966 | 0.592514214 |
| ENSG00000087303 | NID2 subnetwork | 0.137399579 | 0.593341748 |
| ENSG00000197757 | HOXC6 subnetwork | 0.137319974 | 0.593369119 |
| ENSG00000137324 | ENSG00000137324 subnetwork | 0.137513713 | 0.593379571 |
| GO:0003705 | RNA polymerase II distal enhancer sequence-specific DN | 0.137560654 | 0.593381658 |
| GO:0034142 | toll-like receptor 4 signaling pathway | 0.137385129 | 0.593450126 |
| ENSG00000206376 | EHMT2 subnetwork | 0.137513713 | 0.593566698 |
| ENSG00000204371 | EHMT2 subnetwork | 0.137513713 | 0.593753943 |
| KEGG_CIRCADIAN_RHYTHM_MAI | KEGG_CIRCADIAN_RHYTHM_MAMMAL | 0.137878753 | 0.594833018 |
| ENSG00000131504 | DIAPH1 subnetwork | 0.137921014 | 0.59488189 |
| GO:0051879 | Hsp90 protein binding | 0.138458312 | 0.596164728 |
| ENSG00000115590 | IL1R2 subnetwork | 0.138300249 | 0.596175637 |
| ENSG00000089159 | PXN subnetwork | 0.138427698 | 0.596194969 |
| ENSG00000105671 | DDX49 subnetwork | 0.138408438 | 0.5962095 |
| MP:0000336 | decreased mast cell number | 0.138280428 | 0.596268892 |
| MP:0002079 | increased circulating insulin level | 0.138583958 | 0.596324222 |
| GO:0051347 | positive regulation of transferase activity | 0.138402698 | 0.596381372 |
| GO:0002360 | T cell lineage commitment | 0.138561753 | 0.596464488 |

| | | | |
|---|---|---|---|
| GO:0003678 | DNA helicase activity | 0.138766857 | 0.59648462 |
| ENSG00000113916 | BCL6 subnetwork | 0.138695099 | 0.59656093 |
| GO:0030529 | ribonucleoprotein complex | 0.138824661 | 0.596642611 |
| REACTOME_MAP_KINASE_ACTIV/ | REACTOME_MAP_KINASE_ACTIVATION_IN_TLR_CASCAI | 0.13875797 | 0.596656201 |
| REACTOME_SIGNALING_BY_TGF_ | REACTOME_SIGNALING_BY_TGF_BETA | 0.139169477 | 0.597663844 |
| ENSG00000104408 | EIF3E subnetwork | 0.139143811 | 0.597788582 |
| MP:0005264 | glomerulosclerosis | 0.139255142 | 0.597962382 |
| GO:0015248 | sterol transporter activity | 0.139393047 | 0.598167293 |
| GO:0044454 | nuclear chromosome part | 0.13935019 | 0.598198057 |
| ENSG00000178951 | ZBTB7A subnetwork | 0.139548896 | 0.598512371 |
| ENSG00000119630 | PGF subnetwork | 0.139695983 | 0.599076393 |
| ENSG00000077420 | APBB1IP subnetwork | 0.139791184 | 0.599139549 |
| GO:0005942 | phosphatidylinositol 3-kinase complex | 0.139764699 | 0.599217527 |
| ENSG00000100387 | RBX1 subnetwork | 0.139856623 | 0.599280576 |
| GO:0045648 | positive regulation of erythrocyte differentiation | 0.139964225 | 0.599546592 |
| ENSG00000145192 | AHSG subnetwork | 0.140101145 | 0.599828071 |
| GO:0032451 | demethylase activity | 0.140210788 | 0.6000625 |
| GO:0004860 | protein kinase inhibitor activity | 0.140730278 | 0.601669267 |
| ENSG00000162889 | MAPKAPK2 subnetwork | 0.14060392 | 0.601686446 |
| ENSG00000099956 | SMARCB1 subnetwork | 0.140558155 | 0.601702593 |
| GO:0051721 | protein phosphatase 2A binding | 0.140778142 | 0.601715533 |
| GO:0030162 | regulation of proteolysis | 0.140826964 | 0.60173005 |
| ENSG00000014216 | CAPN1 subnetwork | 0.14080878 | 0.601761771 |
| ENSG00000160447 | PKN3 subnetwork | 0.140714834 | 0.601825843 |
| ENSG00000099942 | CRKL subnetwork | 0.140675051 | 0.601857633 |
| ENSG00000139546 | TARBP2 subnetwork | 0.141080945 | 0.602445483 |
| ENSG00000100867 | DHRS2 subnetwork | 0.141034218 | 0.602446245 |
| ENSG00000077549 | CAPZB subnetwork | 0.141371984 | 0.603565867 |
| ENSG00000061936 | SFSWAP subnetwork | 0.141557946 | 0.604374222 |
| ENSG00000196954 | CASP4 subnetwork | 0.141667984 | 0.604777467 |
| GO:0032616 | interleukin-13 production | 0.14181245 | 0.60503888 |
| ENSG00000103126 | AXIN1 subnetwork | 0.141783134 | 0.605102676 |
| GO:0008757 | S-adenosylmethionine-dependent methyltransferase act | 0.142131072 | 0.605748912 |
| ENSG00000140379 | BCL2A1 subnetwork | 0.142100377 | 0.605859496 |
| ENSG00000092969 | TGFB2 subnetwork | 0.142062483 | 0.605923507 |
| KEGG_GLIOMA | KEGG_GLIOMA | 0.142200801 | 0.60593352 |
| ENSG00000138756 | BMP2K subnetwork | 0.142375201 | 0.606380006 |
| ENSG00000028839 | TBPL1 subnetwork | 0.142351165 | 0.606459627 |
| GO:0042226 | interleukin-6 biosynthetic process | 0.142501587 | 0.606562209 |
| ENSG00000105372 | RPS19 subnetwork | 0.142533655 | 0.6066067 |
| ENSG00000121057 | AKAP1 subnetwork | 0.142460316 | 0.606657356 |
| GO:0022409 | positive regulation of cell-cell adhesion | 0.143785342 | 0.60683984 |
| GO:2001056 | positive regulation of cysteine-type endopeptidase activi | 0.143924804 | 0.606879607 |
| ENSG00000179151 | EDC3 subnetwork | 0.143850121 | 0.606914567 |
| GO:0048144 | fibroblast proliferation | 0.143770999 | 0.606964945 |
| GO:0048520 | positive regulation of behavior | 0.143712344 | 0.606982467 |
| ENSG00000160282 | FTCD subnetwork | 0.143651176 | 0.607032933 |
| GO:0043130 | ubiquitin binding | 0.142655558 | 0.60703876 |
| ENSG00000175221 | MED16 subnetwork | 0.144015089 | 0.607046362 |
| GO:0043280 | positive regulation of cysteine-type endopeptidase activi | 0.143924804 | 0.607066052 |
| REACTOME_COMMON_PATHWA' | REACTOME_COMMON_PATHWAY | 0.143623437 | 0.607096675 |
| GO:0032101 | regulation of response to external stimulus | 0.144073306 | 0.607105586 |
| ENSG00000143632 | ACTA1 subnetwork | 0.143699332 | 0.607107692 |
| ENSG00000108504 | ENSG00000108504 subnetwork | 0.144104828 | 0.607118748 |

| | | | |
|---|---|---|---|
| ENSG00000120008 | WDR11 subnetwork | 0.1436085 | 0.607175855 |
| GO:0032612 | interleukin-1 production | 0.143607572 | 0.607362908 |
| ENSG00000167815 | PRDX2 subnetwork | 0.142929177 | 0.607510065 |
| REACTOME_TAT:MEDIATED_HIV:: | REACTOME_TAT:MEDIATED_HIV:1_ELONGATION_ARRES | 0.143587533 | 0.60751926 |
| GO:0043487 | regulation of RNA stability | 0.144249684 | 0.60756135 |
| GO:0048636 | positive regulation of muscle organ development | 0.142892847 | 0.607589839 |
| REACTOME_PAUSING_AND_RECC | REACTOME_PAUSING_AND_RECOVERY_OF_TAT:MEDIAT | 0.143587533 | 0.607706535 |
| ENSG00000197694 | SPTAN1 subnetwork | 0.142835432 | 0.607749535 |
| GO:0045844 | positive regulation of striated muscle tissue developmen | 0.142892847 | 0.607778122 |
| MP:0005592 | abnormal vascular smooth muscle morphology | 0.143576535 | 0.607816836 |
| GO:0019207 | kinase regulator activity | 0.144348116 | 0.607881018 |
| ENSG00000136111 | TBC1D4 subnetwork | 0.143026051 | 0.607894737 |
| ENSG00000182287 | AP1S2 subnetwork | 0.14352249 | 0.607914224 |
| ENSG00000128692 | ENSG00000128692 subnetwork | 0.143564099 | 0.607942628 |
| ENSG00000143171 | RXRG subnetwork | 0.143327575 | 0.607972806 |
| MP:0000420 | ruffled hair | 0.143500468 | 0.608009259 |
| KEGG_SYSTEMIC_LUPUS_ERYTHE | KEGG_SYSTEMIC_LUPUS_ERYTHEMATOSUS | 0.1433731 | 0.608047575 |
| ENSG00000149480 | MTA2 subnetwork | 0.143320686 | 0.608145286 |
| ENSG00000144061 | NPHP1 subnetwork | 0.143488192 | 0.608150664 |
| ENSG00000213949 | ITGA1 subnetwork | 0.143293471 | 0.608163265 |
| ENSG00000099991 | CABIN1 subnetwork | 0.143152485 | 0.608232745 |
| GO:0032715 | negative regulation of interleukin-6 production | 0.143462228 | 0.608261272 |
| MP:0005023 | abnormal wound healing | 0.14327947 | 0.60830498 |
| ENSG00000145833 | DDX46 subnetwork | 0.143279366 | 0.608493193 |
| ENSG00000145414 | NAF1 subnetwork | 0.144990855 | 0.610940852 |
| ENSG00000078401 | EDN1 subnetwork | 0.144980729 | 0.611112814 |
| GO:0010950 | positive regulation of endopeptidase activity | 0.145067662 | 0.611121324 |
| MP:0000601 | small liver | 0.14547945 | 0.612492345 |
| GO:0002230 | positive regulation of defense response to virus by host | 0.145438006 | 0.612511485 |
| ENSG00000163938 | GNL3 subnetwork | 0.145581262 | 0.612687481 |
| ENSG00000107341 | UBE2R2 subnetwork | 0.145890597 | 0.613604402 |
| MP:0001145 | abnormal male reproductive system morphology | 0.145949708 | 0.613661369 |
| GO:0032411 | positive regulation of transporter activity | 0.145886988 | 0.613761468 |
| GO:0042308 | negative regulation of protein import into nucleus | 0.145847133 | 0.613796268 |
| ENSG00000162869 | PPP1R21 subnetwork | 0.145813461 | 0.613846389 |
| GO:0032182 | small conjugating protein binding | 0.146376411 | 0.614876411 |
| ENSG00000198380 | GFPT1 subnetwork | 0.146351037 | 0.614972527 |
| ENSG00000144158 | ENSG00000144158 subnetwork | 0.146475828 | 0.615054912 |
| MP:0003459 | increased fear-related response | 0.146272288 | 0.61507791 |
| ENSG00000140750 | ARHGAP17 subnetwork | 0.146344886 | 0.615099237 |
| ENSG00000164362 | TERT subnetwork | 0.147040768 | 0.615202189 |
| ENSG00000141434 | MEP1B subnetwork | 0.146558968 | 0.615202806 |
| ENSG00000115685 | PPP1R7 subnetwork | 0.146330252 | 0.615210751 |
| MP:0010948 | abnormal double-strand DNA break repair | 0.147038617 | 0.615374088 |
| ENSG00000140986 | RPL3L subnetwork | 0.146926654 | 0.615525114 |
| ENSG00000175387 | SMAD2 subnetwork | 0.147034104 | 0.615546091 |
| ENSG00000005194 | CIAPIN1 subnetwork | 0.147169312 | 0.615592705 |
| GO:0031063 | regulation of histone deacetylation | 0.14701503 | 0.61559647 |
| ENSG00000088826 | SMOX subnetwork | 0.146670978 | 0.615625 |
| ENSG00000054523 | KIF1B subnetwork | 0.146925403 | 0.615712546 |
| KEGG_VASCULAR_SMOOTH_MUS | KEGG_VASCULAR_SMOOTH_MUSCLE_CONTRACTION | 0.146806355 | 0.61575259 |
| MP:0004256 | abnormal maternal decidual layer morphology | 0.146906987 | 0.615854401 |
| ENSG00000167971 | CASKIN1 subnetwork | 0.146780577 | 0.615909784 |
| ENSG00000141068 | KSR1 subnetwork | 0.147524208 | 0.615928398 |

| | | | |
|---|---|---|---|
| GO:0043543 | protein acylation | 0.147495521 | 0.61599393 |
| ENSG00000143878 | RHOB subnetwork | 0.147614988 | 0.615999393 |
| GO:0000228 | nuclear chromosome | 0.147476146 | 0.616150577 |
| MP:0008720 | impaired neutrophil chemotaxis | 0.147452195 | 0.616276951 |
| KEGG_ASCORBATE_AND_ALDARA | KEGG_ASCORBATE_AND_ALDARATE_METABOLISM | 0.147432603 | 0.616403402 |
| ENSG00000067596 | DHX8 subnetwork | 0.147396923 | 0.616408387 |
| ENSG00000205726 | ITSN1 subnetwork | 0.147744026 | 0.616616131 |
| GO:0030130 | clathrin coat of trans-Golgi network vesicle | 0.147986106 | 0.617414368 |
| ENSG00000132646 | PCNA subnetwork | 0.148130571 | 0.617909091 |
| GO:0032731 | positive regulation of interleukin-1 beta production | 0.148393263 | 0.618791641 |
| GO:0042990 | regulation of transcription factor import into nucleus | 0.148362484 | 0.618812481 |
| GO:0061180 | mammary gland epithelium development | 0.148513744 | 0.619013018 |
| ENSG00000078061 | ARAF subnetwork | 0.148558444 | 0.61903753 |
| MP:0000382 | underdeveloped hair follicles | 0.148619704 | 0.619122542 |
| GO:0032735 | positive regulation of interleukin-12 production | 0.148702393 | 0.619434362 |
| MP:0008706 | decreased interleukin-6 secretion | 0.148812961 | 0.619655277 |
| ENSG00000100079 | LGALS2 subnetwork | 0.148877619 | 0.619709794 |
| ENSG00000152270 | PDE3B subnetwork | 0.14896298 | 0.619990934 |
| ENSG00000078399 | HOXA9 subnetwork | 0.149086399 | 0.620543807 |
| ENSG00000115694 | STK25 subnetwork | 0.149322123 | 0.621467391 |
| GO:0033028 | myeloid cell apoptotic process | 0.149285913 | 0.621473875 |
| GO:0043627 | response to estrogen stimulus | 0.149667701 | 0.622955026 |
| MP:0000249 | abnormal blood vessel physiology | 0.149743103 | 0.623129149 |
| ENSG00000114739 | ACVR2B subnetwork | 0.149809493 | 0.623167421 |
| GO:0032870 | cellular response to hormone stimulus | 0.149967166 | 0.623349412 |
| GO:0005802 | trans-Golgi network | 0.149944836 | 0.623446924 |
| GO:0046782 | regulation of viral transcription | 0.15016967 | 0.623869801 |
| ENSG00000115274 | INO80B subnetwork | 0.150442196 | 0.6243528 |
| ENSG00000137752 | CASP1 subnetwork | 0.150425587 | 0.624465522 |
| ENSG00000100364 | KIAA0930 subnetwork | 0.150398779 | 0.624578313 |
| GO:0042287 | MHC protein binding | 0.150393641 | 0.624751431 |
| MP:0006355 | abnormal sixth branchial arch artery morphology | 0.150786221 | 0.625511432 |
| ENSG00000151694 | ADAM17 subnetwork | 0.150760896 | 0.625624436 |
| ENSG00000183093 | ENSG00000183093 subnetwork | 0.151583928 | 0.625988616 |
| ENSG00000157540 | DYRK1A subnetwork | 0.150949717 | 0.626015038 |
| ENSG00000129219 | PLD2 subnetwork | 0.151546491 | 0.626026371 |
| ENSG00000148396 | SEC16A subnetwork | 0.151059759 | 0.626044485 |
| GO:0019080 | viral genome expression | 0.151514068 | 0.626094125 |
| GO:0004683 | calmodulin-dependent protein kinase activity | 0.151027043 | 0.626112447 |
| ENSG00000125991 | ERGIC3 subnetwork | 0.151203154 | 0.626239111 |
| MP:0002640 | reticulocytosis | 0.151154111 | 0.626246995 |
| GO:0019083 | viral transcription | 0.151514068 | 0.626281859 |
| GO:0010952 | positive regulation of peptidase activity | 0.151336248 | 0.626448514 |
| ENSG00000176406 | RIMS2 subnetwork | 0.151513138 | 0.626469706 |
| ENSG00000071655 | MBD3 subnetwork | 0.151325275 | 0.626591592 |
| MP:0008058 | abnormal DNA repair | 0.151501526 | 0.626627663 |
| ENSG00000120837 | NFYB subnetwork | 0.151500518 | 0.626815726 |
| ENSG00000110367 | DDX6 subnetwork | 0.151826399 | 0.626819407 |
| ENSG00000111961 | SASH1 subnetwork | 0.15194474 | 0.627125749 |
| REACTOME_SIGNAL_TRANSDUCT | REACTOME_SIGNAL_TRANSDUCTION_BY_L1 | 0.151993469 | 0.627192457 |
| ENSG00000185825 | BCAP31 subnetwork | 0.152341248 | 0.628231598 |
| ENSG00000205918 | ENSG00000205918 subnetwork | 0.152525751 | 0.628430493 |
| GO:0009988 | cell-cell recognition | 0.152432632 | 0.628507329 |
| ENSG00000116161 | CACYBP subnetwork | 0.152511336 | 0.628588517 |

| | | | |
|---|---|---|---|
| ENSG00000117242 | ENSG00000117242 subnetwork | 0.152706891 | 0.628816851 |
| ENSG00000089693 | MLF2 subnetwork | 0.152694769 | 0.628974895 |
| GO:0021854 | hypothalamus development | 0.152785133 | 0.629077061 |
| ENSG00000106571 | GLI3 subnetwork | 0.152825108 | 0.629083308 |
| ENSG00000177971 | IMP3 subnetwork | 0.152958066 | 0.629295943 |
| ENSG00000181555 | SETD2 subnetwork | 0.152926942 | 0.62941791 |
| GO:0034138 | toll-like receptor 3 signaling pathway | 0.152954078 | 0.629453894 |
| ENSG00000110237 | ARHGEF17 subnetwork | 0.153109674 | 0.629674918 |
| GO:0009617 | response to bacterium | 0.153186413 | 0.629815146 |
| ENSG00000111652 | COPS7A subnetwork | 0.153447912 | 0.630789866 |
| GO:0045080 | positive regulation of chemokine biosynthetic process | 0.153655179 | 0.631451132 |
| GO:0019318 | hexose metabolic process | 0.153709345 | 0.631560917 |
| ENSG00000141232 | TOB1 subnetwork | 0.153793624 | 0.631571896 |
| ENSG00000155926 | SLA subnetwork | 0.15376135 | 0.631715307 |
| ENSG00000172062 | SMN1 subnetwork | 0.154098099 | 0.631857355 |
| ENSG00000205571 | SMN2 subnetwork | 0.154098099 | 0.632045184 |
| ENSG00000168538 | TRAPPC11 subnetwork | 0.154020726 | 0.632108864 |
| ENSG00000118181 | RPS25 subnetwork | 0.154089234 | 0.632158787 |
| ENSG00000068024 | HDAC4 subnetwork | 0.154014842 | 0.632282059 |
| ENSG00000198805 | PNP subnetwork | 0.154011137 | 0.632440476 |
| ENSG00000149930 | TAOK2 subnetwork | 0.154323263 | 0.632714583 |
| MP:0001691 | abnormal somite shape | 0.154317625 | 0.632902555 |
| GO:0015935 | small ribosomal subunit | 0.154437157 | 0.633061164 |
| ENSG00000155959 | VBP1 subnetwork | 0.154514917 | 0.63317008 |
| GO:0008186 | RNA-dependent ATPase activity | 0.154698905 | 0.633827893 |
| GO:0005072 | transforming growth factor beta receptor, cytoplasmic m | 0.154769021 | 0.633921685 |
| GO:0046834 | lipid phosphorylation | 0.155017751 | 0.634578885 |
| REACTOME_VIRAL_MRNA_TRANS | REACTOME_VIRAL_MRNA_TRANSLATION | 0.155300795 | 0.63526971 |
| ENSG00000072518 | MARK2 subnetwork | 0.155285843 | 0.635443226 |
| MP:0002768 | small adrenal glands | 0.155400735 | 0.6356 |
| ENSG00000166913 | YWHAB subnetwork | 0.155631543 | 0.636467279 |
| MP:0003209 | abnormal pulmonary elastic fiber morphology | 0.155588112 | 0.636492891 |
| ENSG00000198130 | HIBCH subnetwork | 0.155788984 | 0.636900533 |
| MP:0005179 | decreased circulating cholesterol level | 0.155847606 | 0.63706718 |
| ENSG00000111716 | LDHB subnetwork | 0.155970059 | 0.637089618 |
| ENSG00000131023 | LATS1 subnetwork | 0.155959525 | 0.637278107 |
| ENSG00000164924 | YWHAZ subnetwork | 0.156070475 | 0.637448255 |
| ENSG00000076555 | ACACB subnetwork | 0.156383774 | 0.63764758 |
| GO:0016607 | nuclear speck | 0.156548537 | 0.637687998 |
| ENSG00000124207 | CSE1L subnetwork | 0.156348973 | 0.637732507 |
| GO:0034968 | histone lysine methylation | 0.15661358 | 0.63776533 |
| ENSG00000159461 | AMFR subnetwork | 0.156532276 | 0.637772861 |
| REACTOME_FORMATION_OF_A_I | REACTOME_FORMATION_OF_A_POOL_OF_FREE_40S_SI | 0.156683901 | 0.637827881 |
| ENSG00000115020 | PIKFYVE subnetwork | 0.156340942 | 0.637891317 |
| ENSG00000116044 | NFE2L2 subnetwork | 0.156530485 | 0.63796105 |
| ENSG00000099783 | HNRNPM subnetwork | 0.156338771 | 0.638079764 |
| GO:0045087 | innate immune response | 0.156291093 | 0.638091017 |
| GO:0016493 | C-C chemokine receptor activity | 0.156288522 | 0.638264854 |
| ENSG00000135503 | ACVR1B subnetwork | 0.156982874 | 0.638457008 |
| ENSG00000142611 | PRDM16 subnetwork | 0.156951147 | 0.638497791 |
| ENSG00000211456 | SACM1L subnetwork | 0.156931221 | 0.638612257 |
| GO:0001914 | regulation of T cell mediated cytotoxicity | 0.157122749 | 0.638743378 |
| ENSG00000172172 | MRPL13 subnetwork | 0.157180915 | 0.638849662 |
| GO:0016605 | PML body | 0.157102383 | 0.638872535 |

| | | | |
|---|---|---|---|
| MP:0003909 | increased eating behavior | 0.157235886 | 0.639 |
| ENSG00000166484 | MAPK7 subnetwork | 0.157461211 | 0.639900029 |
| ENSG00000183918 | SH2D1A subnetwork | 0.15755625 | 0.639964737 |
| ENSG00000120265 | PCMT1 subnetwork | 0.157523676 | 0.639991182 |
| ENSG00000132825 | PPP1R3D subnetwork | 0.157711184 | 0.640320212 |
| ENSG00000163513 | TGFBR2 subnetwork | 0.157895141 | 0.640402113 |
| ENSG00000113460 | BRIX1 subnetwork | 0.157869295 | 0.640502055 |
| ENSG00000140382 | HMG20A subnetwork | 0.158182166 | 0.640624084 |
| ENSG00000163017 | ACTG2 subnetwork | 0.158115844 | 0.640650645 |
| ENSG00000116062 | MSH6 subnetwork | 0.158230223 | 0.640656122 |
| ENSG00000108840 | HDAC5 subnetwork | 0.157853007 | 0.640660793 |
| MP:0010903 | abnormal pulmonary alveolus wall morphology | 0.158353513 | 0.640693591 |
| ENSG00000186446 | ZNF501 subnetwork | 0.158391176 | 0.640696314 |
| ENSG00000102024 | PLS3 subnetwork | 0.158046637 | 0.640762463 |
| ENSG00000189229 | ENSG00000189229 subnetwork | 0.158090183 | 0.640765172 |
| ENSG00000170727 | BOP1 subnetwork | 0.158337391 | 0.640778689 |
| GO:0001961 | positive regulation of cytokine-mediated signaling pathw | 0.158483785 | 0.640830652 |
| KEGG_PATHOGENIC_ESCHERICHI/ | KEGG_PATHOGENIC_ESCHERICHIA_COLI_INFECTION | 0.158635579 | 0.640838691 |
| ENSG00000099246 | RAB18 subnetwork | 0.158037766 | 0.640921091 |
| MP:0009643 | abnormal urine homeostasis | 0.158333368 | 0.640951684 |
| ENSG00000171219 | CDC42BPG subnetwork | 0.158625273 | 0.640996785 |
| ENSG00000113575 | PPP2CA subnetwork | 0.158020744 | 0.641006455 |
| ENSG00000213585 | VDAC1 subnetwork | 0.158739213 | 0.64107508 |
| GO:0002685 | regulation of leukocyte migration | 0.158608458 | 0.641140351 |
| KEGG_ADHERENS_JUNCTION | KEGG_ADHERENS_JUNCTION | 0.158879852 | 0.641182482 |
| GO:0004115 | 3',5'-cyclic-AMP phosphodiesterase activity | 0.158945346 | 0.641185055 |
| GO:0000245 | spliceosomal complex assembly | 0.158849036 | 0.641252921 |
| ENSG00000088205 | DDX18 subnetwork | 0.159044786 | 0.641348118 |
| ENSG00000154710 | RABGEF1 subnetwork | 0.159369104 | 0.641727352 |
| ENSG00000180628 | PCGF5 subnetwork | 0.159268573 | 0.641737103 |
| ENSG00000072310 | SREBF1 subnetwork | 0.159178304 | 0.641746865 |
| MP:0000260 | abnormal angiogenesis | 0.159148116 | 0.641759043 |
| ENSG00000119408 | NEK6 subnetwork | 0.159424069 | 0.641817123 |
| REACTOME_ETHANOL_OXIDATIOI | REACTOME_ETHANOL_OXIDATION | 0.159240198 | 0.641822157 |
| MP:0005048 | thrombosis | 0.159362161 | 0.641885198 |
| MP:0002680 | decreased corpora lutea number | 0.159561526 | 0.64209607 |
| MP:0005595 | abnormal vascular smooth muscle physiology | 0.159702289 | 0.642505821 |
| ENSG00000164708 | PGAM2 subnetwork | 0.159790699 | 0.64275531 |
| ENSG00000115963 | RND3 subnetwork | 0.159833456 | 0.642830134 |
| REACTOME_PURINE_RIBONUCLEC | REACTOME_PURINE_RIBONUCLEOSIDE_MONOPHOSPHA | 0.159959472 | 0.643195696 |
| ENSG00000196924 | FLNA subnetwork | 0.160520947 | 0.645377907 |
| ENSG00000138771 | SHROOM3 subnetwork | 0.160560243 | 0.645408312 |
| GO:0006094 | gluconeogenesis | 0.160789088 | 0.646179547 |
| ENSG00000172613 | RAD9A subnetwork | 0.160831327 | 0.646180656 |
| MP:0000188 | abnormal circulating glucose level | 0.161071035 | 0.647139954 |
| ENSG00000141378 | PTRH2 subnetwork | 0.161124473 | 0.647155298 |
| ENSG00000174547 | MRPL11 subnetwork | 0.161220501 | 0.647504353 |
| REACTOME_CAP:DEPENDENT_TR/ | REACTOME_CAP:DEPENDENT_TRANSLATION_INITIATION | 0.161462316 | 0.648013917 |
| ENSG00000173327 | MAP3K11 subnetwork | 0.161402606 | 0.648085292 |
| REACTOME_EUKARYOTIC_TRANSI | REACTOME_EUKARYOTIC_TRANSLATION_INITIATION | 0.161462316 | 0.648201856 |
| GO:0051241 | negative regulation of multicellular organismal process | 0.161576502 | 0.648289855 |
| ENSG00000111266 | DUSP16 subnetwork | 0.161685153 | 0.648406721 |
| ENSG00000116288 | PARK7 subnetwork | 0.161647689 | 0.648464213 |
| ENSG00000133511 | ENSG00000133511 subnetwork | 0.161860285 | 0.64881297 |

| | | | |
|---|---|---|---|
| ENSG00000131374 | TBC1D5 subnetwork | 0.161959285 | 0.648900463 |
| MP:0010418 | perimembraneous ventricular septal defect | 0.161849552 | 0.648928468 |
| ENSG00000102241 | HTATSF1 subnetwork | 0.161927885 | 0.648986975 |
| ENSG00000120437 | ACAT2 subnetwork | 0.162295569 | 0.650216951 |
| GO:0030914 | STAGA complex | 0.162345561 | 0.650303644 |
| ENSG00000117000 | RLF subnetwork | 0.162545874 | 0.650505634 |
| ENSG00000156273 | BACH1 subnetwork | 0.162508928 | 0.650578035 |
| ENSG00000131196 | NFATC1 subnetwork | 0.162489671 | 0.650693842 |
| ENSG00000102753 | KPNA3 subnetwork | 0.162692511 | 0.651083189 |
| ENSG00000148175 | STOM subnetwork | 0.162810425 | 0.651270575 |
| ENSG00000100150 | DEPDC5 subnetwork | 0.162903366 | 0.651356813 |
| ENSG00000022267 | FHL1 subnetwork | 0.163023749 | 0.65170225 |
| ENSG00000174231 | PRPF8 subnetwork | 0.163018742 | 0.651890332 |
| MP:0011320 | abnormal glomerular capillary morphology | 0.163157768 | 0.652018454 |
| ENSG00000142675 | CNKSR1 subnetwork | 0.163143363 | 0.652148832 |
| ENSG00000111605 | CPSF6 subnetwork | 0.163249601 | 0.652205246 |
| GO:0071478 | cellular response to radiation | 0.163534208 | 0.652216465 |
| GO:0002821 | positive regulation of adaptive immune response | 0.163520745 | 0.652346674 |
| MP:0004001 | decreased hepatocyte proliferation | 0.163366913 | 0.652463977 |
| GO:0005730 | nucleolus | 0.163509203 | 0.65250576 |
| ENSG00000160049 | DFFA subnetwork | 0.163491298 | 0.652650533 |
| REACTOME_EUKARYOTIC_TRANSI | REACTOME_EUKARYOTIC_TRANSLATION_ELONGATION | 0.163764736 | 0.653021583 |
| ENSG00000129354 | AP1M2 subnetwork | 0.163916351 | 0.653322785 |
| MP:0005220 | abnormal exocrine pancreas morphology | 0.164008808 | 0.653738855 |
| MP:0008869 | anovulation | 0.164180454 | 0.654067261 |
| ENSG00000168066 | SF1 subnetwork | 0.164135875 | 0.65406843 |
| ENSG00000151067 | CACNA1C subnetwork | 0.164373221 | 0.65466954 |
| ENSG00000172936 | MYD88 subnetwork | 0.164629681 | 0.654806313 |
| ENSG00000100697 | DICER1 subnetwork | 0.164433395 | 0.654811836 |
| MP:0008000 | increased ovary tumor incidence | 0.164673762 | 0.654819277 |
| GO:0006469 | negative regulation of protein kinase activity | 0.164528022 | 0.654895205 |
| ENSG00000175899 | A2M subnetwork | 0.164498782 | 0.654910971 |
| MP:0001501 | abnormal sleep pattern | 0.164740029 | 0.654918268 |
| REACTOME_DAG_AND_IP3_SIGN/ | REACTOME_DAG_AND_IP3_SIGNALING | 0.164614817 | 0.654936854 |
| GO:0043154 | negative regulation of cysteine-type endopeptidase activ | 0.164783877 | 0.654959862 |
| ENSG00000106617 | PRKAG2 subnetwork | 0.16494434 | 0.655574663 |
| GO:0031983 | vesicle lumen | 0.165282864 | 0.656500573 |
| ENSG00000148516 | ZEB1 subnetwork | 0.165269045 | 0.656631338 |
| ENSG00000119760 | SUPT7L subnetwork | 0.165218953 | 0.656633238 |
| ENSG00000111087 | GLI1 subnetwork | 0.165520271 | 0.657386201 |
| ENSG00000133895 | MEN1 subnetwork | 0.165822029 | 0.657937643 |
| ENSG00000174780 | SRP72 subnetwork | 0.16577995 | 0.657939914 |
| MP:0004207 | squamous cell carcinoma | 0.165727828 | 0.657985117 |
| ENSG00000013364 | MVP subnetwork | 0.166116981 | 0.658009709 |
| GO:0071013 | catalytic step 2 spliceosome | 0.165958406 | 0.658147513 |
| MP:0005318 | decreased triglyceride level | 0.166098556 | 0.658154813 |
| GO:0005217 | intracellular ligand-gated ion channel activity | 0.165905098 | 0.658207035 |
| ENSG00000170962 | PDGFD subnetwork | 0.166095361 | 0.658314286 |
| ENSG00000145431 | PDGFC subnetwork | 0.166095361 | 0.658502429 |
| ENSG00000042429 | MED17 subnetwork | 0.166341842 | 0.658721096 |
| REACTOME_P75NTR_RECRUITS_S | REACTOME_P75NTR_RECRUITS_SIGNALLING_COMPLEXI | 0.166506403 | 0.659160959 |
| ENSG00000107937 | GTPBP4 subnetwork | 0.166668961 | 0.659743224 |
| MP:0004560 | abnormal chorionic plate morphology | 0.16680049 | 0.659908754 |
| GO:0060389 | pathway-restricted SMAD protein phosphorylation | 0.167521398 | 0.6599631 |

| | | | |
|---|---|---|---|
| MP:0001862 | interstitial pneumonia | 0.166778518 | 0.659997148 |
| GO:0017124 | SH3 domain binding | 0.167594737 | 0.660045403 |
| ENSG00000108395 | TRIM37 subnetwork | 0.167259481 | 0.66008248 |
| KEGG_TIGHT_JUNCTION | KEGG_TIGHT_JUNCTION | 0.166907989 | 0.660102593 |
| GO:0032651 | regulation of interleukin-1 beta production | 0.167331012 | 0.660122263 |
| MP:0000367 | abnormal coat/ hair morphology | 0.16751783 | 0.660136286 |
| ENSG00000076641 | PAG1 subnetwork | 0.167062744 | 0.660165148 |
| GO:0048475 | coated membrane | 0.167014785 | 0.660168043 |
| ENSG00000147649 | MTDH subnetwork | 0.167440507 | 0.660184659 |
| ENSG00000130779 | CLIP1 subnetwork | 0.167222276 | 0.660199147 |
| ENSG00000109906 | ZBTB16 subnetwork | 0.167380065 | 0.660204662 |
| GO:2000243 | positive regulation of reproductive process | 0.166884687 | 0.660233751 |
| ENSG00000163931 | TKT subnetwork | 0.167177541 | 0.660273193 |
| MP:0010249 | lactation failure | 0.167807046 | 0.660292033 |
| REACTOME_O:LINKED_GLYCOSYL | REACTOME_O:LINKED_GLYCOSYLATION_OF_MUCINS | 0.167512643 | 0.660309571 |
| ENSG00000065534 | MYLK subnetwork | 0.167141045 | 0.660318816 |
| ENSG00000175054 | ATR subnetwork | 0.167434432 | 0.660343848 |
| GO:0030117 | membrane coat | 0.167014785 | 0.660356125 |
| GO:0014823 | response to activity | 0.167779566 | 0.660380034 |
| GO:0070603 | SWI/SNF-type complex | 0.167909226 | 0.660416667 |
| ENSG00000159131 | GART subnetwork | 0.167738088 | 0.660496454 |
| MP:0001923 | reduced female fertility | 0.168065864 | 0.660782091 |
| GO:0030374 | ligand-dependent nuclear receptor transcription coactiva | 0.168198344 | 0.660843715 |
| GO:0001892 | embryonic placenta development | 0.168165935 | 0.660903427 |
| GO:0032006 | regulation of TOR signaling cascade | 0.168131403 | 0.660963173 |
| GO:0047485 | protein N-terminus binding | 0.168460704 | 0.661202263 |
| ENSG00000110711 | AIP subnetwork | 0.168437892 | 0.661375212 |
| MP:0008874 | decreased physiological sensitivity to xenobiotic | 0.168412923 | 0.661435041 |
| MP:0001726 | abnormal allantois morphology | 0.168683194 | 0.661863688 |
| REACTOME_METABOLISM_OF_RI | REACTOME_METABOLISM_OF_RNA | 0.168795357 | 0.662044105 |
| ENSG00000152382 | TADA1 subnetwork | 0.169003666 | 0.662644815 |
| MP:0009011 | prolonged diestrus | 0.16896012 | 0.662662521 |
| ENSG00000122870 | BICC1 subnetwork | 0.16924844 | 0.663319209 |
| GO:0050702 | interleukin-1 beta secretion | 0.169374752 | 0.663438735 |
| GO:0016568 | chromatin modification | 0.16935725 | 0.663513132 |
| ENSG00000185499 | MUC1 subnetwork | 0.169589746 | 0.663729913 |
| ENSG00000133313 | CNDP2 subnetwork | 0.16955768 | 0.663733785 |
| GO:0002820 | negative regulation of adaptive immune response | 0.169481599 | 0.66378775 |
| ENSG00000100888 | CHD8 subnetwork | 0.169548563 | 0.663836389 |
| ENSG00000134759 | ELP2 subnetwork | 0.169530932 | 0.663854402 |
| ENSG00000135972 | MRPS9 subnetwork | 0.169705801 | 0.663965614 |
| ENSG00000008128 | CDK11A subnetwork | 0.169840916 | 0.664169014 |
| ENSG00000138768 | USO1 subnetwork | 0.169793457 | 0.664201183 |
| ENSG00000106976 | DNM1 subnetwork | 0.170089412 | 0.664738176 |
| REACTOME_PROLACTIN_RECEPTO | REACTOME_PROLACTIN_RECEPTOR_SIGNALING | 0.17015806 | 0.664776245 |
| ENSG00000089048 | ESF1 subnetwork | 0.170089329 | 0.664925373 |
| MP:0004964 | absent inner cell mass | 0.17035375 | 0.665101237 |
| ENSG00000100485 | SOS2 subnetwork | 0.170275903 | 0.665222285 |
| ENSG00000166025 | AMOTL1 subnetwork | 0.170349086 | 0.665288326 |
| MP:0001155 | arrest of spermatogenesis | 0.170607061 | 0.665538072 |
| REACTOME_ACTIVATED_AMPK_S | REACTOME_ACTIVATED_AMPK_STIMULATES_FATTY:ACI | 0.170580422 | 0.665612704 |
| ENSG00000117322 | CR2 subnetwork | 0.170537225 | 0.665645207 |
| MP:0010909 | pulmonary alveolar hemorrhage | 0.170779598 | 0.666207865 |
| ENSG00000168530 | MYL1 subnetwork | 0.17112867 | 0.667874193 |

| | | | |
|---|---|---|---|
| ENSG00000186416 | NKRF subnetwork | 0.171163698 | 0.667925323 |
| ENSG00000120656 | TAF12 subnetwork | 0.171440563 | 0.668541374 |
| MP:0010810 | increased type II pneumocyte number | 0.171541561 | 0.668573031 |
| GO:0003785 | actin monomer binding | 0.171409272 | 0.668588664 |
| ENSG00000113240 | CLK4 subnetwork | 0.171369886 | 0.668635981 |
| ENSG00000083168 | KAT6A subnetwork | 0.171522841 | 0.668662367 |
| GO:0050709 | negative regulation of protein secretion | 0.171810484 | 0.669408632 |
| MP:0002792 | abnormal retinal vasculature morphology | 0.171862469 | 0.669431213 |
| MP:0011099 | complete lethality throughout fetal growth and develop | 0.17190251 | 0.669495798 |
| ENSG00000163902 | RPN1 subnetwork | 0.172099339 | 0.670022403 |
| ENSG00000138798 | EGF subnetwork | 0.172144457 | 0.670030795 |
| MP:0002884 | abnormal branchial arch morphology | 0.172338075 | 0.670752869 |
| ENSG00000100726 | TELO2 subnetwork | 0.172441633 | 0.67106883 |
| REACTOME_PLATELET_SENSITIZA | REACTOME_PLATELET_SENSITIZATION_BY_LDL | 0.172587422 | 0.671149008 |
| GO:0002755 | MyD88-dependent toll-like receptor signaling pathway | 0.172562294 | 0.671182886 |
| ENSG00000115935 | WIPF1 subnetwork | 0.1725396 | 0.671258741 |
| MP:0003084 | abnormal skeletal muscle fiber morphology | 0.172846487 | 0.671897708 |
| GO:0009225 | nucleotide-sugar metabolic process | 0.173053774 | 0.672701872 |
| MP:0004991 | decreased bone strength | 0.173198065 | 0.672982407 |
| MP:0005319 | abnormal enzyme/ coenzyme level | 0.173178947 | 0.673072626 |
| ENSG00000134318 | ROCK2 subnetwork | 0.173423191 | 0.67361809 |
| ENSG00000189091 | SF3B3 subnetwork | 0.173527646 | 0.673792911 |
| GO:0060396 | growth hormone receptor signaling pathway | 0.17400551 | 0.673900334 |
| ENSG00000083896 | YTHDC1 subnetwork | 0.174065763 | 0.67393543 |
| GO:0071378 | cellular response to growth hormone stimulus | 0.17400551 | 0.674087998 |
| ENSG00000111641 | NOP2 subnetwork | 0.173837176 | 0.674170616 |
| REACTOME_ERKMAPK_TARGETS | REACTOME_ERKMAPK_TARGETS | 0.173641536 | 0.674176897 |
| ENSG00000145604 | SKP2 subnetwork | 0.173928053 | 0.67418501 |
| GO:0034502 | protein localization to chromosome | 0.17399235 | 0.674247911 |
| ENSG00000164609 | SLU7 subnetwork | 0.174170796 | 0.674248748 |
| GO:0034134 | toll-like receptor 2 signaling pathway | 0.173802639 | 0.674274958 |
| ENSG00000075151 | EIF4G3 subnetwork | 0.173925939 | 0.674345039 |
| GO:0000790 | nuclear chromatin | 0.174247222 | 0.674381085 |
| GO:0044246 | regulation of multicellular organismal metabolic process | 0.173798098 | 0.67446304 |
| GO:0010921 | regulation of phosphatase activity | 0.174445122 | 0.674583102 |
| GO:0016866 | intramolecular transferase activity | 0.174388541 | 0.674589936 |
| GO:0033574 | response to testosterone stimulus | 0.174380257 | 0.674763626 |
| GO:0033276 | transcription factor TFTC complex | 0.174789373 | 0.676104473 |
| ENSG00000113013 | HSPA9 subnetwork | 0.174919582 | 0.676541667 |
| ENSG00000015479 | MATR3 subnetwork | 0.175183892 | 0.676859046 |
| MP:0003089 | decreased skin tensile strength | 0.175152674 | 0.676908132 |
| MP:0002861 | abnormal tail bud morphology | 0.175062133 | 0.677006387 |
| ENSG00000129048 | CCRL1 subnetwork | 0.17513429 | 0.677054414 |
| REACTOME_N:GLYCAN_ANTENNA | REACTOME_N:GLYCAN_ANTENNAE_ELONGATION_IN_TI | 0.175405547 | 0.677503467 |
| ENSG00000168028 | RPSA subnetwork | 0.1756148 | 0.677813193 |
| MP:0009406 | decreased skeletal muscle fiber number | 0.175740194 | 0.677839335 |
| ENSG00000116761 | CTH subnetwork | 0.175702091 | 0.677902466 |
| MP:0001552 | increased circulating triglyceride level | 0.175604105 | 0.677945661 |
| MP:0002687 | oligozoospermia | 0.175572955 | 0.678008874 |
| ENSG00000166228 | PCBD1 subnetwork | 0.175822552 | 0.678039324 |
| ENSG00000079432 | CIC subnetwork | 0.176125606 | 0.678867977 |
| ENSG00000102391 | ENSG00000102391 subnetwork | 0.17618975 | 0.678984505 |
| MP:0010182 | decreased susceptibility to weight gain | 0.176120581 | 0.679042082 |
| GO:0071216 | cellular response to biotic stimulus | 0.176764006 | 0.681244813 |

| | | | |
|---|---|---|---|
| ENSG00000009954 | BAZ1B subnetwork | 0.177143706 | 0.682743363 |
| GO:0035303 | regulation of dephosphorylation | 0.177504478 | 0.684051962 |
| ENSG00000144029 | MRPS5 subnetwork | 0.177492333 | 0.684213437 |
| GO:0016638 | oxidoreductase activity, acting on the CH-NH2 group of c | 0.177783705 | 0.685262431 |
| ENSG00000119953 | SMNDC1 subnetwork | 0.177748818 | 0.685299807 |
| MP:0001200 | thick skin | 0.17791008 | 0.685708368 |
| ENSG00000158941 | KIAA1967 subnetwork | 0.178004043 | 0.685854264 |
| ENSG00000126777 | KTN1 subnetwork | 0.177980055 | 0.685891773 |
| ENSG00000156453 | PCDH1 subnetwork | 0.178118236 | 0.6861617 |
| ENSG00000102054 | RBBP7 subnetwork | 0.17842485 | 0.686438809 |
| ENSG00000101945 | SUV39H1 subnetwork | 0.178264227 | 0.686482759 |
| ENSG00000171824 | EXOSC10 subnetwork | 0.178411367 | 0.686572925 |
| ENSG00000181222 | POLR2A subnetwork | 0.178559664 | 0.686759438 |
| ENSG00000178607 | ERN1 subnetwork | 0.178398177 | 0.686762272 |
| ENSG00000198961 | PJA2 subnetwork | 0.178679601 | 0.687121212 |
| ENSG00000105176 | URI1 subnetwork | 0.178786249 | 0.687427706 |
| ENSG00000115756 | HPCAL1 subnetwork | 0.179092762 | 0.688329205 |
| ENSG00000007312 | CD79B subnetwork | 0.17913451 | 0.688332416 |
| ENSG00000160469 | BRSK1 subnetwork | 0.179184756 | 0.688390646 |
| ENSG00000109111 | SUPT6H subnetwork | 0.179063427 | 0.68844989 |
| ENSG00000075785 | RAB7A subnetwork | 0.179391034 | 0.688943894 |
| ENSG00000169598 | DFFB subnetwork | 0.179900349 | 0.689837957 |
| ENSG00000137764 | MAP2K5 subnetwork | 0.17981008 | 0.689846112 |
| ENSG00000125954 | CHURC1-FNTB subnetwork | 0.179942814 | 0.689854476 |
| GO:0061134 | peptidase regulator activity | 0.180184198 | 0.689882095 |
| GO:2000145 | regulation of cell motility | 0.179784699 | 0.689925783 |
| MP:0001177 | atelectasis | 0.179892218 | 0.689986264 |
| ENSG00000177189 | RPS6KA3 subnetwork | 0.180170392 | 0.690043884 |
| GO:0016763 | transferase activity, transferring pentosyl groups | 0.179767893 | 0.690046742 |
| GO:0050732 | negative regulation of peptidyl-tyrosine phosphorylation | 0.180021651 | 0.69007686 |
| ENSG00000132155 | RAF1 subnetwork | 0.18033347 | 0.690079474 |
| ENSG00000106991 | ENG subnetwork | 0.180123696 | 0.690082305 |
| ENSG00000205302 | SNX2 subnetwork | 0.18028726 | 0.690090461 |
| ENSG00000115919 | KYNU subnetwork | 0.180113689 | 0.690244237 |
| GO:0070723 | response to cholesterol | 0.18044878 | 0.690520548 |
| ENSG00000110680 | CALCA subnetwork | 0.180543991 | 0.690580504 |
| MP:0003641 | small lung | 0.18053849 | 0.690728568 |
| MP:0001182 | lung hemorrhage | 0.180679261 | 0.69091158 |
| ENSG00000067900 | ROCK1 subnetwork | 0.180868298 | 0.691625616 |
| ENSG00000197461 | PDGFA subnetwork | 0.181339804 | 0.693296854 |
| GO:0071222 | cellular response to lipopolysaccharide | 0.181748195 | 0.693797814 |
| ENSG00000126602 | TRAP1 subnetwork | 0.181800795 | 0.693840481 |
| ENSG00000138363 | ATIC subnetwork | 0.181552651 | 0.693886761 |
| GO:0030118 | clathrin coat | 0.181725924 | 0.693919104 |
| ENSG00000172780 | RAB43 subnetwork | 0.18165454 | 0.69393111 |
| MP:0004255 | abnormal spongiotrophoblast layer morphology | 0.181644785 | 0.694093519 |
| ENSG00000010017 | RANBP9 subnetwork | 0.18194351 | 0.694374659 |
| MP:0001759 | increased urine glucose level | 0.181989726 | 0.694403494 |
| ENSG00000173726 | TOMM20 subnetwork | 0.182096843 | 0.694582424 |
| GO:0004857 | enzyme inhibitor activity | 0.18226197 | 0.694939989 |
| ENSG00000114670 | NEK11 subnetwork | 0.182455158 | 0.694959128 |
| GO:0016569 | covalent chromatin modification | 0.182482997 | 0.694974121 |
| ENSG00000215692 | ENSG00000215692 subnetwork | 0.182429044 | 0.694998637 |
| ENSG00000078579 | FGF20 subnetwork | 0.18224527 | 0.695020464 |

| | | | |
|---|---|---|---|
| ENSG00000162734 | PEA15 subnetwork | 0.182549498 | 0.695125272 |
| GO:0045822 | negative regulation of heart contraction | 0.182386263 | 0.695132261 |
| ENSG00000180902 | D2HGDH subnetwork | 0.182429044 | 0.695188113 |
| GO:0071636 | positive regulation of transforming growth factor beta pı | 0.182839179 | 0.696256466 |
| ENSG00000120800 | UTP20 subnetwork | 0.183037107 | 0.696843537 |
| ENSG00000120256 | LRP11 subnetwork | 0.18306866 | 0.6968716 |
| MP:0000921 | demyelination | 0.182993653 | 0.696883506 |
| GO:0045072 | regulation of interferon-gamma biosynthetic process | 0.183414147 | 0.697284085 |
| GO:0070925 | organelle assembly | 0.183245454 | 0.69742997 |
| GO:0090109 | regulation of cell-substrate junction assembly | 0.183413308 | 0.697473513 |
| REACTOME_ENOS_ACTIVATION_A | REACTOME_ENOS_ACTIVATION_AND_REGULATION | 0.183566399 | 0.697529859 |
| GO:0002576 | platelet degranulation | 0.183629052 | 0.697584803 |
| GO:0051893 | regulation of focal adhesion assembly | 0.183413308 | 0.697663043 |
| REACTOME_METABOLISM_OF_NI | REACTOME_METABOLISM_OF_NITRIC_OXIDE | 0.183566399 | 0.697719251 |
| ENSG00000120705 | ETF1 subnetwork | 0.183407543 | 0.697825496 |
| ENSG00000111269 | CREBL2 subnetwork | 0.183378898 | 0.697974443 |
| GO:0042809 | vitamin D receptor binding | 0.183765858 | 0.697978839 |
| GO:0045766 | positive regulation of angiogenesis | 0.183836776 | 0.698060754 |
| GO:0016570 | histone modification | 0.18399278 | 0.698427332 |
| ENSG00000104823 | ECH1 subnetwork | 0.184123216 | 0.698997018 |
| GO:0034698 | response to gonadotropin stimulus | 0.184236756 | 0.699011108 |
| MP:0011096 | complete embryonic lethality before somite formation | 0.184227335 | 0.699173442 |
| GO:0030131 | clathrin adaptor complex | 0.184329088 | 0.699309317 |
| ENSG00000196782 | MAML3 subnetwork | 0.184463893 | 0.699323227 |
| GO:0035770 | ribonucleoprotein granule | 0.184416486 | 0.699363661 |
| GO:0010611 | regulation of cardiac muscle hypertrophy | 0.184917892 | 0.701014885 |
| GO:0010888 | negative regulation of lipid storage | 0.185008616 | 0.701298701 |
| ENSG00000111328 | CDK2AP1 subnetwork | 0.185220232 | 0.70208277 |
| ENSG00000180871 | CXCR2 subnetwork | 0.185568247 | 0.703217086 |
| ENSG00000091073 | ENSG00000091073 subnetwork | 0.18565512 | 0.703351351 |
| GO:0042994 | cytoplasmic sequestering of transcription factor | 0.185549355 | 0.703353164 |
| MP:0001078 | abnormal phrenic nerve morphology | 0.185967415 | 0.704471764 |
| ENSG00000079785 | DDX1 subnetwork | 0.186081064 | 0.704808212 |
| ENSG00000109046 | WSB1 subnetwork | 0.186336855 | 0.705357625 |
| MP:0001783 | decreased white adipose tissue amount | 0.186296833 | 0.70537257 |
| ENSG00000092841 | MYL6 subnetwork | 0.186406417 | 0.705423637 |
| GO:0031330 | negative regulation of cellular catabolic process | 0.186276638 | 0.705482042 |
| GO:0045940 | positive regulation of steroid metabolic process | 0.186712868 | 0.706051213 |
| ENSG00000164707 | SLC13A4 subnetwork | 0.186694825 | 0.706187652 |
| ENSG00000081800 | SLC13A1 subnetwork | 0.186694825 | 0.706378101 |
| ENSG00000010030 | ETV7 subnetwork | 0.186864876 | 0.706467259 |
| GO:0019059 | initiation of viral infection | 0.186677822 | 0.706487726 |
| ENSG00000138448 | ITGAV subnetwork | 0.187057067 | 0.707246767 |
| MP:0005334 | abnormal fat pad morphology | 0.187321898 | 0.707983306 |
| ENSG00000068366 | ACSL4 subnetwork | 0.187416672 | 0.708019376 |
| ENSG00000130985 | UBA1 subnetwork | 0.187398364 | 0.708115747 |
| GO:0033081 | regulation of T cell differentiation in thymus | 0.187308602 | 0.708120119 |
| MP:0011143 | thick lung-associated mesenchyme | 0.187654774 | 0.709187517 |
| ENSG00000198730 | CTR9 subnetwork | 0.187754367 | 0.709290132 |
| ENSG00000115221 | ITGB6 subnetwork | 0.187827361 | 0.709314516 |
| ENSG00000112237 | CCNC subnetwork | 0.187727925 | 0.709359871 |
| MP:0003204 | decreased neuron apoptosis | 0.18863396 | 0.712187584 |
| ENSG00000157191 | NECAP2 subnetwork | 0.188867906 | 0.71268797 |
| ENSG00000075539 | FRYL subnetwork | 0.188957058 | 0.712748256 |

| | | | |
|---|---|---|---|
| MP:0001547 | abnormal lipid level | 0.188928033 | 0.712751678 |
| GO:0060326 | cell chemotaxis | 0.188845829 | 0.712771958 |
| ENSG00000144648 | CCBP2 subnetwork | 0.188837815 | 0.712936593 |
| ENSG00000174405 | LIG4 subnetwork | 0.189219569 | 0.713710759 |
| GO:0046849 | bone remodeling | 0.189468829 | 0.713763066 |
| ENSG00000166582 | CENPV subnetwork | 0.189300128 | 0.713841202 |
| MP:0001636 | irregular heartbeat | 0.189457828 | 0.713914209 |
| ENSG00000198523 | PLN subnetwork | 0.189433253 | 0.714038616 |
| GO:0061135 | endopeptidase regulator activity | 0.18983765 | 0.71414236 |
| GO:0006694 | steroid biosynthetic process | 0.189885838 | 0.714178705 |
| ENSG00000118058 | MLL subnetwork | 0.189682209 | 0.714318243 |
| ENSG00000168274 | HIST1H2AE subnetwork | 0.189835237 | 0.714333512 |
| ENSG00000167658 | EEF2 subnetwork | 0.189651362 | 0.714402465 |
| ENSG00000172757 | CFL1 subnetwork | 0.189785331 | 0.714408141 |
| ENSG00000137259 | HIST1H2AB subnetwork | 0.189835237 | 0.714524766 |
| GO:0031929 | TOR signaling cascade | 0.190020622 | 0.714562717 |
| GO:0002756 | MyD88-independent toll-like receptor signaling pathway | 0.190087483 | 0.714665775 |
| ENSG00000125538 | IL1B subnetwork | 0.190440576 | 0.715944935 |
| GO:0071706 | tumor necrosis factor superfamily cytokine production | 0.190551796 | 0.716194548 |
| ENSG00000113368 | LMNB1 subnetwork | 0.191092846 | 0.716711123 |
| GO:0032352 | positive regulation of hormone metabolic process | 0.191163221 | 0.71676 |
| MP:0004187 | cardia bifida | 0.191064147 | 0.716848986 |
| ENSG00000139719 | VPS33A subnetwork | 0.190987091 | 0.716964762 |
| ENSG00000136931 | NR5A1 subnetwork | 0.190841636 | 0.716991718 |
| GO:0019209 | kinase activator activity | 0.191057529 | 0.717026955 |
| ENSG00000070831 | CDC42 subnetwork | 0.190925083 | 0.717120726 |
| MP:0002310 | decreased susceptibility to hepatic steatosis | 0.190980558 | 0.717129506 |
| ENSG00000196363 | WDR5 subnetwork | 0.191463593 | 0.717341502 |
| MP:0008844 | decreased subcutaneous adipose tissue amount | 0.191336817 | 0.717395361 |
| KEGG_RETINOL_METABOLISM | KEGG_RETINOL_METABOLISM | 0.191461407 | 0.717505995 |
| ENSG00000075884 | ARHGAP15 subnetwork | 0.191441727 | 0.717590618 |
| GO:0090317 | negative regulation of intracellular protein transport | 0.191640641 | 0.717842876 |
| ENSG00000100612 | DHRS7 subnetwork | 0.191813394 | 0.718477103 |
| ENSG00000178921 | PFAS subnetwork | 0.191867641 | 0.718512111 |
| GO:0003743 | translation initiation factor activity | 0.192053431 | 0.719026078 |
| REACTOME_PECAM1_INTERACTIO | REACTOME_PECAM1_INTERACTIONS | 0.192299216 | 0.719739292 |
| ENSG00000136807 | CDK9 subnetwork | 0.19253942 | 0.720744681 |
| KEGG_NON_HOMOLOGOUS_END | KEGG_NON_HOMOLOGOUS_END_JOINING | 0.192624894 | 0.720911991 |
| GO:0043189 | H4/H2A histone acetyltransferase complex | 0.192727544 | 0.721132376 |
| MP:0001533 | abnormal skeleton physiology | 0.192825251 | 0.721365931 |
| ENSG00000164070 | HSPA4L subnetwork | 0.192955195 | 0.721758767 |
| MP:0000613 | abnormal salivary gland morphology | 0.193157671 | 0.722390438 |
| ENSG00000164867 | NOS3 subnetwork | 0.193329979 | 0.72295539 |
| MP:0001984 | abnormal olfaction | 0.19381135 | 0.723667462 |
| ENSG00000075945 | KIFAP3 subnetwork | 0.193657321 | 0.723733086 |
| ENSG00000188153 | COL4A5 subnetwork | 0.19375485 | 0.723779841 |
| GO:0016835 | carbon-oxygen lyase activity | 0.193646769 | 0.723872081 |
| GO:0008063 | Toll signaling pathway | 0.193590075 | 0.723904964 |
| GO:0042116 | macrophage activation | 0.194247782 | 0.725145811 |
| ENSG00000118785 | SPP1 subnetwork | 0.194660909 | 0.726444091 |
| ENSG00000166592 | RRAD subnetwork | 0.194822027 | 0.726455797 |
| ENSG00000139372 | TDG subnetwork | 0.194718841 | 0.726529801 |
| MP:0002421 | abnormal cell-mediated immunity | 0.194648783 | 0.726610125 |
| ENSG00000170860 | LSM3 subnetwork | 0.194814534 | 0.726621657 |

| | | | |
|---|---|---|---|
| ENSG00000145901 | TNIP1 subnetwork | 0.19478151 | 0.726681674 |
| GO:0045309 | protein phosphorylated amino acid binding | 0.194973406 | 0.72701773 |
| MP:0001882 | abnormal lactation | 0.195253799 | 0.728346561 |
| ENSG00000164111 | ANXA5 subnetwork | 0.195441499 | 0.729013488 |
| GO:0035088 | establishment or maintenance of apical/basal cell polarit | 0.195778482 | 0.729271191 |
| GO:0046823 | negative regulation of nucleocytoplasmic transport | 0.19554657 | 0.729309889 |
| ENSG00000153774 | CFDP1 subnetwork | 0.195857295 | 0.729435058 |
| GO:0061245 | establishment or maintenance of bipolar cell polarity | 0.195778482 | 0.729463814 |
| GO:0042588 | zymogen granule | 0.19573111 | 0.729637949 |
| MP:0006356 | abnormal third branchial arch artery morphology | 0.195776098 | 0.729656539 |
| ENSG00000068971 | PPP2R5B subnetwork | 0.195695077 | 0.72975152 |
| ENSG00000163528 | CHCHD4 subnetwork | 0.196100808 | 0.7304038 |
| MP:0003917 | increased kidney weight | 0.196408531 | 0.731210443 |
| MP:0005222 | abnormal somite size | 0.196400162 | 0.731390135 |
| ENSG00000111049 | MYF5 subnetwork | 0.196369928 | 0.731437995 |
| REACTOME_CHOLESTEROL_BIOSY | REACTOME_CHOLESTEROL_BIOSYNTHESIS | 0.196816785 | 0.73197261 |
| ENSG00000197386 | HTT subnetwork | 0.196908077 | 0.73209584 |
| REACTOME_PEPTIDE_CHAIN_ELO | REACTOME_PEPTIDE_CHAIN_ELONGATION | 0.196803044 | 0.73211275 |
| GO:0010559 | regulation of glycoprotein biosynthetic process | 0.196782687 | 0.732252964 |
| GO:0031434 | mitogen-activated protein kinase kinase binding | 0.196762078 | 0.732353716 |
| ENSG00000071051 | NCK2 subnetwork | 0.196757867 | 0.732533615 |
| GO:0004004 | ATP-dependent RNA helicase activity | 0.197094561 | 0.732578947 |
| GO:0030216 | keratinocyte differentiation | 0.197082389 | 0.732719137 |
| ENSG00000212664 | ENSG00000212664 subnetwork | 0.197255267 | 0.733017627 |
| ENSG00000066136 | NFYC subnetwork | 0.197456976 | 0.733403472 |
| REACTOME_METABOLISM_OF_LI | REACTOME_METABOLISM_OF_LIPIDS_AND_LIPOPROTEI | 0.197580565 | 0.733438486 |
| ENSG00000087074 | PPP1R15A subnetwork | 0.197722232 | 0.733565423 |
| ENSG00000101246 | ARFRP1 subnetwork | 0.197573411 | 0.733578754 |
| ENSG00000105509 | HAS1 subnetwork | 0.197692747 | 0.73370565 |
| MP:0008392 | decreased primordial germ cell number | 0.197874683 | 0.733771008 |
| GO:0005149 | interleukin-1 receptor binding | 0.197810358 | 0.733779879 |
| ENSG00000158710 | TAGLN2 subnetwork | 0.197968813 | 0.733880284 |
| GO:0033673 | negative regulation of kinase activity | 0.198169145 | 0.734233998 |
| ENSG00000181031 | RPH3AL subnetwork | 0.198220342 | 0.734251246 |
| GO:0072202 | cell differentiation involved in metanephros developmer | 0.198163929 | 0.73440042 |
| ENSG00000211896 | ENSG00000211896 subnetwork | 0.198147968 | 0.734514436 |
| ENSG00000185532 | PRKG1 subnetwork | 0.198416815 | 0.734805978 |
| MP:0010025 | decreased total body fat amount | 0.198482869 | 0.734888598 |
| ENSG00000009307 | CSDE1 subnetwork | 0.198734892 | 0.735757338 |
| ENSG00000215021 | PHB2 subnetwork | 0.19915479 | 0.735874967 |
| REACTOME_NRAGE_SIGNALS_DE | REACTOME_NRAGE_SIGNALS_DEATH_THROUGH_JNK | 0.199329741 | 0.735964454 |
| ENSG00000185697 | MYBL1 subnetwork | 0.199366895 | 0.735968121 |
| ENSG00000115816 | CEBPZ subnetwork | 0.199239099 | 0.735983264 |
| GO:0030334 | regulation of cell migration | 0.199067743 | 0.73599843 |
| ENSG00000127948 | POR subnetwork | 0.199139782 | 0.736028257 |
| GO:0050850 | positive regulation of calcium-mediated signaling | 0.199045622 | 0.736112565 |
| GO:0001784 | phosphotyrosine binding | 0.199328886 | 0.736143791 |
| ENSG00000110880 | CORO1C subnetwork | 0.198904278 | 0.736154048 |
| ENSG00000099399 | MAGEB2 subnetwork | 0.19904198 | 0.736292223 |
| ENSG00000102974 | CTCF subnetwork | 0.199040853 | 0.736485071 |
| ENSG00000130758 | MAP3K10 subnetwork | 0.199849288 | 0.737594672 |
| ENSG00000155438 | MKI67IP subnetwork | 0.199818285 | 0.737617555 |
| KEGG_PORPHYRIN_AND_CHLORC | KEGG_PORPHYRIN_AND_CHLOROPHYLL_METABOLISM | 0.200148008 | 0.738077224 |
| ENSG00000185386 | MAPK11 subnetwork | 0.200069092 | 0.738188463 |

| | | | |
|---|---|---|---|
| ENSG00000163882 | POLR2H subnetwork | 0.200223765 | 0.738223787 |
| ENSG00000102226 | USP11 subnetwork | 0.200137775 | 0.738243737 |
| KEGG_FOCAL_ADHESION | KEGG_FOCAL_ADHESION | 0.200060716 | 0.738368146 |
| GO:0004866 | endopeptidase inhibitor activity | 0.200608884 | 0.739674055 |
| GO:0014743 | regulation of muscle hypertrophy | 0.200816523 | 0.740289364 |
| ENSG00000129083 | COPB1 subnetwork | 0.200967479 | 0.74074798 |
| GO:0018904 | organic ether metabolic process | 0.20102423 | 0.740815529 |
| ENSG00000095002 | MSH2 subnetwork | 0.201156198 | 0.740898438 |
| MP:0000932 | absent notochord | 0.201205097 | 0.740952877 |
| GO:0051098 | regulation of binding | 0.201145543 | 0.741052357 |
| MP:0002060 | abnormal skin morphology | 0.20145241 | 0.741788131 |
| ENSG00000186810 | CXCR3 subnetwork | 0.201558235 | 0.741959407 |
| GO:0051348 | negative regulation of transferase activity | 0.201918502 | 0.742344684 |
| ENSG00000064313 | TAF2 subnetwork | 0.202098695 | 0.742428571 |
| ENSG00000139921 | TMX1 subnetwork | 0.201900886 | 0.742485699 |
| ENSG00000132196 | HSD17B7 subnetwork | 0.201855428 | 0.742522757 |
| GO:0051341 | regulation of oxidoreductase activity | 0.202085534 | 0.742543518 |
| ENSG00000197312 | DDI2 subnetwork | 0.201825449 | 0.742598855 |
| ENSG00000061987 | MON2 subnetwork | 0.202059605 | 0.74264553 |
| MP:0000428 | abnormal craniofacial morphology | 0.202542376 | 0.74407946 |
| GO:0044447 | axoneme part | 0.202747615 | 0.744588632 |
| REACTOME_G:PROTEIN_MEDIATE | REACTOME_G:PROTEIN_MEDIATED_EVENTS | 0.202743325 | 0.744768951 |
| MP:0003077 | abnormal cell cycle | 0.202854406 | 0.744849507 |
| MP:0003503 | decreased activity of thyroid | 0.202940931 | 0.745032425 |
| MP:0009504 | abnormal mammary gland epithelium morphology | 0.202994298 | 0.745111515 |
| ENSG00000148468 | FAM171A1 subnetwork | 0.203180226 | 0.745580612 |
| MP:0004229 | abnormal embryonic erythropoiesis | 0.20315838 | 0.745683173 |
| GO:0031329 | regulation of cellular catabolic process | 0.203266704 | 0.745685411 |
| REACTOME_APOPTOSIS | REACTOME_APOPTOSIS | 0.203396463 | 0.745984456 |
| MP:0004404 | cochlear outer hair cell degeneration | 0.203505165 | 0.746270396 |
| GO:0006541 | glutamine metabolic process | 0.203856876 | 0.747476055 |
| MP:0000351 | increased cell proliferation | 0.203839015 | 0.747591921 |
| ENSG00000163586 | FABP1 subnetwork | 0.204072994 | 0.748033126 |
| ENSG00000205246 | RPSAP58 subnetwork | 0.204387551 | 0.748474269 |
| ENSG00000005156 | LIG3 subnetwork | 0.204286529 | 0.748499353 |
| ENSG00000069702 | TGFBR3 subnetwork | 0.204363613 | 0.748525608 |
| ENSG00000171311 | EXOSC1 subnetwork | 0.204855474 | 0.749728612 |
| ENSG00000092439 | TRPM7 subnetwork | 0.204839555 | 0.749896587 |
| GO:0050891 | multicellular organismal water homeostasis | 0.205024425 | 0.750129199 |
| ENSG00000141738 | GRB7 subnetwork | 0.205304517 | 0.750878099 |
| ENSG00000183684 | ALYREF subnetwork | 0.205288309 | 0.750955825 |
| GO:0055037 | recycling endosome | 0.205873745 | 0.752541935 |
| ENSG00000174953 | DHX36 subnetwork | 0.205866997 | 0.752684564 |
| ENSG00000136149 | ENSG00000136149 subnetwork | 0.20584292 | 0.752711077 |
| ENSG00000114209 | PDCD10 subnetwork | 0.206159829 | 0.753482972 |
| ENSG00000008405 | CRY1 subnetwork | 0.206288769 | 0.753740005 |
| MP:0002908 | delayed wound healing | 0.206395682 | 0.753971119 |
| GO:0032452 | histone demethylase activity | 0.206791908 | 0.755349317 |
| GO:0032740 | positive regulation of interleukin-17 production | 0.206832168 | 0.755373711 |
| ENSG00000105821 | DNAJC2 subnetwork | 0.206934105 | 0.755591342 |
| REACTOME_PLC:GAMMA1_SIGNA | REACTOME_PLC:GAMMA1_SIGNALLING | 0.207007975 | 0.755731582 |
| GO:0045073 | regulation of chemokine biosynthetic process | 0.207580523 | 0.756103829 |
| MP:0003396 | abnormal embryonic hematopoiesis | 0.207528515 | 0.756169666 |
| ENSG00000153208 | MERTK subnetwork | 0.207515343 | 0.75629982 |

| | | | |
|---|---|---|---|
| KEGG_ABC_TRANSPORTERS | KEGG_ABC_TRANSPORTERS | 0.2075122 | 0.756468621 |
| GO:0035329 | hippo signaling cascade | 0.207504333 | 0.75663751 |
| ENSG00000153071 | DAB2 subnetwork | 0.207460775 | 0.756664951 |
| ENSG00000101182 | PSMA7 subnetwork | 0.207329871 | 0.756773114 |
| GO:0043903 | regulation of symbiosis, encompassing mutualism throug | 0.207444991 | 0.756808237 |
| GO:0005507 | copper ion binding | 0.20743182 | 0.756951596 |
| ENSG00000115289 | PCGF1 subnetwork | 0.208209934 | 0.758260534 |
| REACTOME_N:GLYCAN_ANTENNA | REACTOME_N:GLYCAN_ANTENNAE_ELONGATION | 0.208329784 | 0.758528127 |
| GO:0030856 | regulation of epithelial cell differentiation | 0.208701394 | 0.758679487 |
| ENSG00000134982 | APC subnetwork | 0.208430226 | 0.758718541 |
| ENSG00000100105 | PATZ1 subnetwork | 0.208540479 | 0.758803901 |
| ENSG00000065000 | AP3D1 subnetwork | 0.208587091 | 0.758840133 |
| GO:0006953 | acute-phase response | 0.208845952 | 0.758854434 |
| MP:0009719 | reduced cerebellar foliation | 0.208692037 | 0.758861246 |
| ENSG00000106244 | PDAP1 subnetwork | 0.208906438 | 0.758877786 |
| ENSG00000213246 | SUPT4H1 subnetwork | 0.208509207 | 0.758883184 |
| ENSG00000111300 | NAA25 subnetwork | 0.208673716 | 0.758940482 |
| ENSG00000188986 | COBRA1 subnetwork | 0.208823323 | 0.758959241 |
| MP:0009657 | failure of chorioallantoic fusion | 0.20902418 | 0.75908043 |
| ENSG00000012983 | MAP4K5 subnetwork | 0.209259853 | 0.759769526 |
| ENSG00000168148 | HIST3H3 subnetwork | 0.20939231 | 0.759854108 |
| GO:0034130 | toll-like receptor 1 signaling pathway | 0.20945723 | 0.759889969 |
| MP:0004007 | abnormal lung vasculature morphology | 0.209372863 | 0.760035842 |
| ENSG00000110075 | PPP6R3 subnetwork | 0.209697632 | 0.760616526 |
| GO:0005657 | replication fork | 0.209926864 | 0.761163683 |
| ENSG00000137831 | UACA subnetwork | 0.210376672 | 0.762525562 |
| ENSG00000160584 | SIK3 subnetwork | 0.210348996 | 0.762592687 |
| ENSG00000011422 | PLAUR subnetwork | 0.210488617 | 0.762688474 |
| ENSG00000056661 | PCGF2 subnetwork | 0.210869447 | 0.763796627 |
| ENSG00000105329 | TGFB1 subnetwork | 0.211134467 | 0.76433495 |
| GO:0030851 | granulocyte differentiation | 0.211110628 | 0.764466292 |
| GO:0016032 | viral reproduction | 0.211082953 | 0.764546616 |
| ENSG00000165733 | BMS1 subnetwork | 0.211475732 | 0.764644405 |
| ENSG00000169895 | SYAP1 subnetwork | 0.211281119 | 0.76471414 |
| MP:0000662 | abnormal branching of the mammary ductal tree | 0.211348731 | 0.764812452 |
| ENSG00000076043 | REXO2 subnetwork | 0.211439979 | 0.764817649 |
| ENSG00000138698 | RAP1GDS1 subnetwork | 0.211473188 | 0.764839368 |
| ENSG00000114030 | KPNA1 subnetwork | 0.211422486 | 0.76494898 |
| GO:0006919 | activation of cysteine-type endopeptidase activity involv | 0.2117998 | 0.765100586 |
| ENSG00000183337 | BCOR subnetwork | 0.211761975 | 0.765142639 |
| MP:0008439 | abnormal cortical plate morphology | 0.211752868 | 0.765299363 |
| GO:0008060 | ARF GTPase activator activity | 0.211687989 | 0.765328746 |
| REACTOME_CASPASE:MEDIATED_ | REACTOME_CASPASE:MEDIATED_CLEAVAGE_OF_CYTOS | 0.211961955 | 0.765385594 |
| ENSG00000196136 | SERPINA3 subnetwork | 0.211940713 | 0.76540224 |
| GO:0045910 | negative regulation of DNA recombination | 0.212106517 | 0.765492241 |
| ENSG00000197586 | ENTPD6 subnetwork | 0.212205855 | 0.765522502 |
| ENSG00000136068 | FLNB subnetwork | 0.212160282 | 0.765539166 |
| MP:0006354 | abnormal fourth branchial arch artery morphology | 0.212077875 | 0.76562341 |
| MP:0001195 | flaky skin | 0.212345115 | 0.76581088 |
| MP:0005620 | abnormal muscle contractility | 0.212390848 | 0.765832274 |
| GO:0033630 | positive regulation of cell adhesion mediated by integrin | 0.212556914 | 0.765997969 |
| MP:0001764 | abnormal homeostasis | 0.212488407 | 0.766031504 |
| GO:0002711 | positive regulation of T cell mediated immunity | 0.212803253 | 0.766057839 |
| GO:0031519 | PcG protein complex | 0.212526031 | 0.766078232 |

| | | | |
|---|---|---|---|
| ENSG00000136950 | ARPC5L subnetwork | 0.213057077 | 0.766206285 |
| GO:0048008 | platelet-derived growth factor receptor signaling pathwa | 0.212789674 | 0.766214159 |
| ENSG00000132467 | UTP3 subnetwork | 0.212728927 | 0.766218274 |
| ENSG00000163166 | IWS1 subnetwork | 0.212925992 | 0.766345422 |
| ENSG00000182533 | CAV3 subnetwork | 0.213041729 | 0.76634981 |
| GO:0048662 | negative regulation of smooth muscle cell proliferation | 0.212720013 | 0.766362021 |
| ENSG00000092621 | PHGDH subnetwork | 0.213018614 | 0.766442698 |
| ENSG00000113712 | CSNK1A1 subnetwork | 0.213338405 | 0.766599139 |
| MP:0004047 | abnormal milk composition | 0.213297405 | 0.766734229 |
| GO:0042612 | MHC class I protein complex | 0.213336041 | 0.766767984 |
| ENSG00000027075 | PRKCH subnetwork | 0.213769768 | 0.767155499 |
| GO:0051489 | regulation of filopodium assembly | 0.213864851 | 0.767235279 |
| ENSG00000135046 | ANXA1 subnetwork | 0.213617676 | 0.767261453 |
| MP:0002989 | small kidney | 0.21366043 | 0.767282389 |
| ENSG00000133107 | TRPC4 subnetwork | 0.213704671 | 0.767290665 |
| MP:0001388 | abnormal stationary movement | 0.213748667 | 0.767311583 |
| ENSG00000144674 | GOLGA4 subnetwork | 0.213570578 | 0.767316456 |
| GO:0010632 | regulation of epithelial cell migration | 0.213946736 | 0.767344618 |
| REACTOME_STEROID_HORMONE | REACTOME_STEROID_HORMONES | 0.213847424 | 0.767353387 |
| ENSG00000150630 | VEGFC subnetwork | 0.214087057 | 0.767630715 |
| GO:0030139 | endocytic vesicle | 0.214148391 | 0.767727273 |
| GO:0007159 | leukocyte cell-cell adhesion | 0.21455377 | 0.767809428 |
| MP:0005292 | improved glucose tolerance | 0.214502483 | 0.767826525 |
| ENSG00000170847 | ENSG00000170847 subnetwork | 0.21435874 | 0.767953571 |
| GO:0010907 | positive regulation of glucose metabolic process | 0.214477306 | 0.767957125 |
| MP:0000417 | short hair | 0.21426286 | 0.767975259 |
| MP:0004784 | abnormal anterior cardinal vein morphology | 0.214467697 | 0.768138244 |
| ENSG00000173534 | ENSG00000173534 subnetwork | 0.21435874 | 0.7681474 |
| GO:0042578 | phosphoric ester hydrolase activity | 0.214701967 | 0.768258569 |
| ENSG00000189060 | H1F0 subnetwork | 0.214933252 | 0.768858655 |
| MP:0005582 | increased renin activity | 0.215084269 | 0.769282116 |
| ENSG00000146535 | GNA12 subnetwork | 0.215227498 | 0.769629816 |
| GO:0017069 | snRNA binding | 0.215294988 | 0.769725579 |
| GO:0022612 | gland morphogenesis | 0.215347508 | 0.769758369 |
| ENSG00000183558 | HIST2H2AA3 subnetwork | 0.215476783 | 0.769781187 |
| ENSG00000034152 | MAP2K3 subnetwork | 0.215391358 | 0.769791142 |
| ENSG00000203812 | HIST2H2AA4 subnetwork | 0.215476783 | 0.769974843 |
| MP:0004701 | decreased circulating insulin-like growth factor I level | 0.215649405 | 0.770266533 |
| MP:0011260 | abnormal head mesenchyme morphology | 0.215772863 | 0.77036944 |
| MP:0004567 | decreased myocardial fiber number | 0.215739398 | 0.770462544 |
| ENSG00000143575 | HAX1 subnetwork | 0.21611131 | 0.771019588 |
| ENSG00000143256 | PFDN2 subnetwork | 0.216166109 | 0.771039418 |
| ENSG00000134313 | KIDINS220 subnetwork | 0.216028966 | 0.771067839 |
| GO:0019902 | phosphatase binding | 0.216082818 | 0.771112786 |
| ENSG00000147883 | CDKN2B subnetwork | 0.216333262 | 0.771536145 |
| ENSG00000126785 | RHOJ subnetwork | 0.216526275 | 0.771595184 |
| ENSG00000185621 | LMLN subnetwork | 0.216482346 | 0.771613146 |
| ENSG00000084073 | ZMPSTE24 subnetwork | 0.216441939 | 0.771718946 |
| ENSG00000136875 | PRPF4 subnetwork | 0.216739104 | 0.772191575 |
| GO:0070232 | regulation of T cell apoptotic process | 0.217191709 | 0.772734101 |
| GO:0071496 | cellular response to external stimulus | 0.217004328 | 0.772794486 |
| ENSG00000047315 | POLR2B subnetwork | 0.217191404 | 0.772915101 |
| ENSG00000160075 | SSU72 subnetwork | 0.216976255 | 0.772950614 |
| ENSG00000147669 | POLR2K subnetwork | 0.217165487 | 0.773033567 |

| | | | |
|---|---|---|---|
| GO:0032732 | positive regulation of interleukin-1 production | 0.217120674 | 0.773089451 |
| ENSG00000125740 | FOSB subnetwork | 0.217480405 | 0.773373373 |
| ENSG00000122641 | INHBA subnetwork | 0.21743549 | 0.773416771 |
| REACTOME_HORMONE:SENSITIVI | REACTOME_HORMONE:SENSITIVE_LIPASE_HSL:MEDIATI | 0.217548936 | 0.773442582 |
| MP:0011506 | glomerular crescent | 0.217739332 | 0.773830958 |
| ENSG00000067533 | RRP15 subnetwork | 0.217722819 | 0.773949475 |
| GO:0030544 | Hsp70 protein binding | 0.217849075 | 0.7740375 |
| ENSG00000182255 | KCNA4 subnetwork | 0.218556848 | 0.776593352 |
| ENSG00000110107 | PRPF19 subnetwork | 0.218603877 | 0.776636682 |
| MP:0001426 | polydipsia | 0.21881244 | 0.776697454 |
| GO:0016307 | phosphatidylinositol phosphate kinase activity | 0.218712444 | 0.776760739 |
| ENSG00000206156 | ENSG00000206156 subnetwork | 0.2187878 | 0.776803995 |
| GO:0033674 | positive regulation of kinase activity | 0.218711236 | 0.776954784 |
| MP:0002463 | abnormal neutrophil physiology | 0.2190646 | 0.777439481 |
| ENSG00000085231 | TAF9 subnetwork | 0.219143233 | 0.777507485 |
| GO:0032354 | response to follicle-stimulating hormone stimulus | 0.219187239 | 0.777662759 |
| ENSG00000139239 | ENSG00000139239 subnetwork | 0.219430674 | 0.777928714 |
| ENSG00000132698 | RAB25 subnetwork | 0.219547341 | 0.77797708 |
| ENSG00000090060 | PAPOLA subnetwork | 0.219391717 | 0.77798554 |
| GO:0046364 | monosaccharide biosynthetic process | 0.219381966 | 0.778154613 |
| ENSG00000116717 | GADD45A subnetwork | 0.219543213 | 0.778158485 |
| ENSG00000165409 | TSHR subnetwork | 0.219756815 | 0.778237052 |
| MP:0005597 | decreased susceptibility to type I hypersensitivity reactio | 0.219831997 | 0.778304705 |
| ENSG00000130669 | PAK4 subnetwork | 0.219713831 | 0.778306351 |
| GO:0001541 | ovarian follicle development | 0.219893434 | 0.778484321 |
| GO:0045740 | positive regulation of DNA replication | 0.219965475 | 0.778514556 |
| ENSG00000172943 | PHF8 subnetwork | 0.220117065 | 0.778662024 |
| MP:0008280 | male germ cell apoptosis | 0.220089502 | 0.778768657 |
| MP:0006262 | testis tumor | 0.220192477 | 0.778816509 |
| ENSG00000165309 | ARMC3 subnetwork | 0.220735745 | 0.778876209 |
| ENSG00000120688 | WBP4 subnetwork | 0.220675275 | 0.778933002 |
| ENSG00000113070 | HBEGF subnetwork | 0.220634685 | 0.778965004 |
| ENSG00000150459 | SAP18 subnetwork | 0.220373458 | 0.779144917 |
| MP:0010868 | increased bone trabecula number | 0.220632416 | 0.779145978 |
| MP:0004028 | chromosome breakage | 0.220594998 | 0.779215297 |
| GO:0016571 | histone methylation | 0.220462848 | 0.779286779 |
| MP:0004851 | increased testis weight | 0.220589425 | 0.779359165 |
| ENSG00000169696 | ASPSCR1 subnetwork | 0.221006459 | 0.779394991 |
| MP:0005438 | abnormal glycogen homeostasis | 0.220578707 | 0.779515528 |
| MP:0003983 | decreased cholesterol level | 0.220986784 | 0.77952629 |
| ENSG00000036672 | USP2 subnetwork | 0.221150754 | 0.779615861 |
| ENSG00000139567 | ACVRL1 subnetwork | 0.221115299 | 0.779697571 |
| GO:0044452 | nucleolar part | 0.221387998 | 0.780064388 |
| GO:0045834 | positive regulation of lipid metabolic process | 0.221374675 | 0.780208075 |
| ENSG00000128052 | KDR subnetwork | 0.221362212 | 0.780339445 |
| ENSG00000070423 | RNF126 subnetwork | 0.221543298 | 0.780391186 |
| ENSG00000183283 | DAZAP2 subnetwork | 0.221748073 | 0.781076733 |
| ENSG00000127947 | PTPN12 subnetwork | 0.221827517 | 0.781229894 |
| MP:0005344 | increased circulating bilirubin level | 0.221894358 | 0.781284018 |
| ENSG00000134697 | GNL2 subnetwork | 0.222016516 | 0.781367458 |
| ENSG00000103365 | GGA2 subnetwork | 0.221998747 | 0.781535988 |
| ENSG00000163349 | HIPK1 subnetwork | 0.222265515 | 0.782254078 |
| GO:0042056 | chemoattractant activity | 0.222334174 | 0.782394366 |
| ENSG00000117713 | ARID1A subnetwork | 0.222255163 | 0.782435105 |

| | | | |
|---|---|---|---|
| ENSG00000165458 | INPPL1 subnetwork | 0.222642314 | 0.782859965 |
| ENSG00000104312 | RIPK2 subnetwork | 0.222776214 | 0.783012346 |
| GO:0030728 | ovulation | 0.222629644 | 0.783028656 |
| MP:0004852 | decreased testis weight | 0.223089077 | 0.784020237 |
| MP:0010254 | nuclear cataracts | 0.223069367 | 0.784127376 |
| ENSG00000075089 | ACTR6 subnetwork | 0.223140485 | 0.784221564 |
| GO:0043022 | ribosome binding | 0.223453072 | 0.785104809 |
| GO:0005548 | phospholipid transporter activity | 0.223426087 | 0.785125802 |
| ENSG00000138592 | USP8 subnetwork | 0.223645722 | 0.785564596 |
| ENSG00000138081 | FBXO11 subnetwork | 0.223736896 | 0.785777668 |
| MP:0003085 | abnormal egg cylinder morphology | 0.224079658 | 0.786511456 |
| ENSG00000148773 | MKI67 subnetwork | 0.224043367 | 0.786594381 |
| ENSG00000197045 | GMFB subnetwork | 0.224185149 | 0.786748768 |
| GO:0051225 | spindle assembly | 0.224668723 | 0.78688867 |
| MP:0009434 | paraparesis | 0.224260129 | 0.786949027 |
| ENSG00000116489 | CAPZA1 subnetwork | 0.224658453 | 0.787020649 |
| ENSG00000132522 | GPS2 subnetwork | 0.224622233 | 0.787091222 |
| GO:0051701 | interaction with host | 0.224603562 | 0.787260207 |
| MP:0004696 | abnormal thyroid follicle morphology | 0.224562902 | 0.787269373 |
| ENSG00000197043 | ANXA6 subnetwork | 0.224536788 | 0.787340059 |
| GO:0000981 | sequence-specific DNA binding RNA polymerase II transc | 0.224473181 | 0.787349249 |
| ENSG00000184371 | CSF1 subnetwork | 0.224450423 | 0.787518464 |
| ENSG00000168522 | FNTA subnetwork | 0.225036238 | 0.788058968 |
| GO:0010573 | vascular endothelial growth factor production | 0.225262687 | 0.788555992 |
| GO:0002709 | regulation of T cell mediated immunity | 0.225324372 | 0.788558802 |
| GO:0010574 | regulation of vascular endothelial growth factor producti | 0.225262687 | 0.788749693 |
| GO:0008094 | DNA-dependent ATPase activity | 0.225442153 | 0.788905253 |
| ENSG00000100448 | CTSG subnetwork | 0.225980281 | 0.78922097 |
| ENSG00000083857 | FAT1 subnetwork | 0.225671927 | 0.789266438 |
| ENSG00000130429 | ARPC1B subnetwork | 0.225630862 | 0.789349693 |
| REACTOME_LIPID_DIGESTION_MO | REACTOME_LIPID_DIGESTION_MOBILIZATION_AND_TRA | 0.226080876 | 0.789358315 |
| KEGG_STEROID_BIOSYNTHESIS | KEGG_STEROID_BIOSYNTHESIS | 0.22597726 | 0.789402107 |
| GO:0005844 | polysome | 0.22593286 | 0.789460784 |
| GO:0035162 | embryonic hemopoiesis | 0.225876204 | 0.789602746 |
| ENSG00000197498 | RPF2 subnetwork | 0.225922271 | 0.789629811 |
| ENSG00000168092 | PAFAH1B2 subnetwork | 0.225868773 | 0.789747363 |
| ENSG00000090382 | LYZ subnetwork | 0.226244467 | 0.789777179 |
| ENSG00000104221 | BRF2 subnetwork | 0.226317811 | 0.78996328 |
| ENSG00000185722 | ANKFY1 subnetwork | 0.226378801 | 0.789965737 |
| ENSG00000139436 | GIT2 subnetwork | 0.226889714 | 0.790752504 |
| ENSG00000141367 | CLTC subnetwork | 0.226819341 | 0.790796871 |
| ENSG00000108510 | MED13 subnetwork | 0.226859685 | 0.790823558 |
| ENSG00000104960 | PTOV1 subnetwork | 0.226802147 | 0.790953545 |
| ENSG00000031823 | RANBP3 subnetwork | 0.226699644 | 0.791020308 |
| MP:0001126 | abnormal ovary morphology | 0.226797078 | 0.791122524 |
| ENSG00000124160 | NCOA5 subnetwork | 0.226786134 | 0.7912182 |
| ENSG00000120438 | TCP1 subnetwork | 0.227086293 | 0.791316561 |
| ENSG00000113048 | MRPS27 subnetwork | 0.227237346 | 0.791442871 |
| GO:0000460 | maturation of 5.8S rRNA | 0.227218385 | 0.791599512 |
| GO:0043414 | macromolecule methylation | 0.227346424 | 0.791615816 |
| ENSG00000152291 | TGOLN2 subnetwork | 0.227471779 | 0.791971694 |
| GO:0050880 | regulation of blood vessel size | 0.227773496 | 0.793083679 |
| KEGG_LYSINE_DEGRADATION | KEGG_LYSINE_DEGRADATION | 0.228202649 | 0.793919084 |
| REACTOME_EUKARYOTIC_TRANSL | REACTOME_EUKARYOTIC_TRANSLATION_TERMINATION | 0.228198505 | 0.79407606 |

| | | | |
|---|---|---|---|
| GO:0006970 | response to osmotic stress | 0.228106729 | 0.794146341 |
| GO:0051403 | stress-activated MAPK cascade | 0.228187391 | 0.794233114 |
| obsolete_molecular_function | obsolete_molecular_function | 0.228308233 | 0.794273879 |
| ENSG00000099864 | PALM subnetwork | 0.228479898 | 0.79462981 |
| GO:0030119 | AP-type membrane coat adaptor complex | 0.228658084 | 0.794635036 |
| GO:0032652 | regulation of interleukin-1 production | 0.228447434 | 0.794640682 |
| ENSG00000131018 | SYNE1 subnetwork | 0.228546716 | 0.794704164 |
| ENSG00000102978 | POLR2C subnetwork | 0.228638856 | 0.794755415 |
| ENSG00000196700 | ZNF512B subnetwork | 0.228594062 | 0.794778481 |
| MP:0008585 | absent photoreceptor outer segment | 0.228825927 | 0.795183654 |
| REACTOME_HOST_INTERACTIONS | REACTOME_HOST_INTERACTIONS_OF_HIV_FACTORS | 0.228880238 | 0.795184825 |
| ENSG00000005844 | ITGAL subnetwork | 0.229122895 | 0.795818138 |
| ENSG00000104375 | STK3 subnetwork | 0.229322675 | 0.796451142 |
| GO:0042310 | vasoconstriction | 0.229798976 | 0.798226002 |
| GO:0006730 | one-carbon metabolic process | 0.229986565 | 0.798760933 |
| ENSG00000106367 | AP1S1 subnetwork | 0.230022887 | 0.798846247 |
| ENSG00000114503 | NCBP2 subnetwork | 0.230176587 | 0.798907502 |
| ENSG00000103942 | HOMER2 subnetwork | 0.230501572 | 0.79900582 |
| MP:0002656 | abnormal keratinocyte differentiation | 0.230148522 | 0.799028655 |
| ENSG00000140694 | PARN subnetwork | 0.230352718 | 0.79910216 |
| ENSG00000100346 | CACNA1I subnetwork | 0.230482463 | 0.799138976 |
| ENSG00000105698 | USF2 subnetwork | 0.230442015 | 0.799199418 |
| ENSG00000166908 | PIP4K2C subnetwork | 0.230300661 | 0.799235437 |
| ENSG00000166947 | EPB42 subnetwork | 0.231160908 | 0.801272727 |
| ENSG00000132470 | ITGB4 subnetwork | 0.2312524 | 0.80140572 |
| GO:0035264 | multicellular organism growth | 0.231386209 | 0.801526163 |
| ENSG00000100324 | TAB1 subnetwork | 0.231329261 | 0.801526533 |
| GO:0071396 | cellular response to lipid | 0.231511932 | 0.801562122 |
| ENSG00000089737 | DDX24 subnetwork | 0.232093306 | 0.802224371 |
| ENSG00000161513 | FDXR subnetwork | 0.232031872 | 0.802273277 |
| ENSG00000134058 | CDK7 subnetwork | 0.23202894 | 0.802443154 |
| ENSG00000179348 | GATA2 subnetwork | 0.231805265 | 0.80248184 |
| ENSG00000140564 | FURIN subnetwork | 0.232256246 | 0.802525985 |
| ENSG00000158290 | CUL4B subnetwork | 0.231992432 | 0.802552625 |
| ENSG00000138101 | DTNB subnetwork | 0.231947927 | 0.802589545 |
| ENSG00000196557 | CACNA1H subnetwork | 0.231940507 | 0.802771726 |
| ENSG00000106541 | AGR2 subnetwork | 0.232534726 | 0.803262446 |
| GO:0004707 | MAP kinase activity | 0.23269856 | 0.803344603 |
| ENSG00000179094 | PER1 subnetwork | 0.232689959 | 0.803429952 |
| ENSG00000101161 | PRPF6 subnetwork | 0.232683181 | 0.803587823 |
| ENSG00000204434 | ENSG00000204434 subnetwork | 0.23283171 | 0.803730082 |
| GO:0005227 | calcium activated cation channel activity | 0.23297162 | 0.803823884 |
| REACTOME_INTEGRIN_CELL_SUR | REACTOME_INTEGRIN_CELL_SURFACE_INTERACTIONS | 0.232948732 | 0.803957529 |
| ENSG00000189319 | FAM53B subnetwork | 0.232916358 | 0.803982621 |
| ENSG00000143942 | CHAC2 subnetwork | 0.233186517 | 0.804413893 |
| MP:0001876 | decreased inflammatory response | 0.233282667 | 0.804702194 |
| ENSG00000198925 | ATG9A subnetwork | 0.233367971 | 0.804881871 |
| ENSG00000100902 | PSMA6 subnetwork | 0.234041729 | 0.807192771 |
| ENSG00000164104 | HMGB2 subnetwork | 0.234012832 | 0.807206556 |
| KEGG_GLYCOSAMINOGLYCAN_BI | KEGG_GLYCOSAMINOGLYCAN_BIOSYNTHESIS_KERATAN | 0.234385902 | 0.807861787 |
| ENSG00000104973 | MED25 subnetwork | 0.234460859 | 0.807883967 |
| ENSG00000185736 | ADARB2 subnetwork | 0.234283151 | 0.807889665 |
| REACTOME_RAP1_SIGNALLING | REACTOME_RAP1_SIGNALLING | 0.234379432 | 0.808044316 |
| MP:0003866 | abnormal defecation | 0.234709986 | 0.808880866 |

| | | | |
|---|---|---|---|
| KEGG_COMPLEMENT_AND_COAG | KEGG_COMPLEMENT_AND_COAGULATION_CASCADES | 0.234958244 | 0.809151034 |
| ENSG00000163909 | HEYL subnetwork | 0.234916618 | 0.809225403 |
| ENSG00000165782 | TMEM55B subnetwork | 0.235031316 | 0.809232989 |
| MP:0001596 | hypotension | 0.234898232 | 0.809323869 |
| ENSG00000104812 | GYS1 subnetwork | 0.235424517 | 0.810564904 |
| ENSG00000124145 | SDC4 subnetwork | 0.235553153 | 0.810838741 |
| ENSG00000137561 | TTPA subnetwork | 0.235941688 | 0.811965401 |
| GO:0002714 | positive regulation of B cell mediated immunity | 0.236240784 | 0.811987041 |
| GO:0002891 | positive regulation of immunoglobulin mediated immune | 0.236240784 | 0.812181949 |
| GO:0090066 | regulation of anatomical structure size | 0.236197648 | 0.812256903 |
| GO:0043030 | regulation of macrophage activation | 0.236147043 | 0.81244295 |
| ENSG00000147162 | OGT subnetwork | 0.236197156 | 0.812451969 |
| GO:0034695 | response to prostaglandin E stimulus | 0.236532826 | 0.812532982 |
| ENSG00000092203 | TOX4 subnetwork | 0.236478162 | 0.812607965 |
| ENSG00000141759 | TXNL4A subnetwork | 0.236622949 | 0.812625899 |
| GO:0004697 | protein kinase C activity | 0.236697249 | 0.812754735 |
| GO:0048536 | spleen development | 0.237003814 | 0.813260661 |
| GO:0016585 | chromatin remodeling complex | 0.236977366 | 0.813287803 |
| ENSG00000130159 | ECSIT subnetwork | 0.236942723 | 0.813410834 |
| ENSG00000182606 | TRAK1 subnetwork | 0.23712862 | 0.81360479 |
| GO:0017017 | MAP kinase tyrosine/serine/threonine phosphatase activ | 0.237463328 | 0.814523467 |
| GO:0051010 | microtubule plus-end binding | 0.237506143 | 0.814555901 |
| MP:0005281 | increased fatty acid level | 0.237820774 | 0.815557683 |
| GO:0071371 | cellular response to gonadotropin stimulus | 0.237950609 | 0.815865039 |
| MP:0008071 | absent B cells | 0.238022027 | 0.815921053 |
| MP:0002048 | increased lung adenoma incidence | 0.238119648 | 0.816132504 |
| MP:0000460 | mandible hypoplasia | 0.238297413 | 0.816618843 |
| MP:0005439 | decreased glycogen level | 0.238448948 | 0.81667065 |
| ENSG00000198478 | SH3BGRL2 subnetwork | 0.238412142 | 0.816746354 |
| GO:0031091 | platelet alpha granule | 0.238678587 | 0.817359618 |
| ENSG00000184216 | IRAK1 subnetwork | 0.238735811 | 0.817462972 |
| MP:0003964 | abnormal noradrenaline level | 0.238800062 | 0.817482684 |
| ENSG00000104872 | PIH1D1 subnetwork | 0.238876787 | 0.817562082 |
| ENSG00000005810 | MYCBP2 subnetwork | 0.23909391 | 0.817628817 |
| ENSG00000103769 | RAB11A subnetwork | 0.239054257 | 0.817680744 |
| ENSG00000173575 | CHD2 subnetwork | 0.238969451 | 0.817689186 |
| GO:0035150 | regulation of tube size | 0.239021058 | 0.817732697 |
| MP:0005217 | abnormal pancreatic beta cell morphology | 0.239320994 | 0.818280467 |
| GO:0016575 | histone deacetylation | 0.239513756 | 0.818688915 |
| ENSG00000124571 | XPO5 subnetwork | 0.239473328 | 0.81875298 |
| GO:0060135 | maternal process involved in female pregnancy | 0.240084912 | 0.819830872 |
| GO:0000302 | response to reactive oxygen species | 0.240053813 | 0.819907076 |
| GO:0016741 | transferase activity, transferring one-carbon groups | 0.240034081 | 0.820030982 |
| ENSG00000129988 | LBP subnetwork | 0.240413836 | 0.820180866 |
| ENSG00000039537 | C6 subnetwork | 0.240364252 | 0.820257082 |
| GO:0014911 | positive regulation of smooth muscle cell migration | 0.24032596 | 0.820357143 |
| ENSG00000188313 | PLSCR1 subnetwork | 0.240833261 | 0.820401616 |
| GO:0006479 | protein methylation | 0.240670375 | 0.820439952 |
| GO:0002347 | response to tumor cell | 0.240307039 | 0.820445344 |
| MP:0001695 | abnormal gastrulation | 0.240726826 | 0.820482644 |
| MP:0011100 | complete preweaning lethality | 0.24057677 | 0.82050916 |
| MP:0003542 | abnormal vascular endothelial cell development | 0.24082883 | 0.82058474 |
| GO:0008213 | protein alkylation | 0.240670375 | 0.820635109 |
| ENSG00000114346 | ECT2 subnetwork | 0.240993511 | 0.82071751 |

| | | | |
|---|---|---|---|
| ENSG00000125630 | POLR1B subnetwork | 0.241048781 | 0.820771971 |
| MP:0002168 | other aberrant phenotype | 0.241504452 | 0.821777831 |
| ENSG00000068781 | STON1-GTF2A1L subnetwork | 0.241584454 | 0.821879449 |
| MP:0004933 | abnormal epididymis epithelium morphology | 0.241408035 | 0.82190691 |
| MP:0000230 | abnormal systemic arterial blood pressure | 0.241503852 | 0.821961064 |
| ENSG00000150093 | ITGB1 subnetwork | 0.242275896 | 0.822059172 |
| ENSG00000119772 | DNMT3A subnetwork | 0.242210367 | 0.822064394 |
| MP:0000172 | abnormal bone marrow cell number | 0.242177252 | 0.822105139 |
| GO:0071564 | npBAF complex | 0.242171656 | 0.822276172 |
| ENSG00000079385 | CEACAM1 subnetwork | 0.242124906 | 0.82228145 |
| MP:0008563 | decreased interferon-alpha secretion | 0.241778574 | 0.82232503 |
| ENSG00000204898 | ENSG00000204898 subnetwork | 0.242124906 | 0.822476303 |
| GO:0034762 | regulation of transmembrane transport | 0.242014554 | 0.8226055 |
| ENSG00000141867 | BRD4 subnetwork | 0.242111635 | 0.822611993 |
| ENSG00000161270 | NPHS1 subnetwork | 0.241887674 | 0.822628083 |
| GO:0009982 | pseudouridine synthase activity | 0.241983588 | 0.822670145 |
| GO:0019722 | calcium-mediated signaling | 0.242612809 | 0.822847682 |
| GO:0045862 | positive regulation of proteolysis | 0.242591278 | 0.822983203 |
| ENSG00000123838 | C4BPA subnetwork | 0.242690544 | 0.82299598 |
| ENSG00000116251 | RPL22 subnetwork | 0.242547248 | 0.823000473 |
| GO:0016791 | phosphatase activity | 0.242944098 | 0.823717797 |
| GO:0016887 | ATPase activity | 0.24299541 | 0.823771267 |
| GO:0000118 | histone deacetylase complex | 0.242924025 | 0.823829787 |
| MP:0000440 | domed cranium | 0.243871081 | 0.824781994 |
| ENSG00000148942 | SLC5A12 subnetwork | 0.243830649 | 0.824823197 |
| GO:0006446 | regulation of translational initiation | 0.243374291 | 0.824828727 |
| GO:0070423 | nucleotide-binding oligomerization domain containing si | 0.24382204 | 0.824970526 |
| GO:0035872 | nucleotide-binding domain, leucine rich repeat containin | 0.24382204 | 0.825165094 |
| MP:0001570 | abnormal circulating enzyme level | 0.243552721 | 0.825236183 |
| ENSG00000159186 | ENSG00000159186 subnetwork | 0.244061978 | 0.825329877 |
| ENSG00000117245 | KIF17 subnetwork | 0.243720478 | 0.825348124 |
| GO:0003018 | vascular process in circulatory system | 0.243781656 | 0.825353941 |
| GO:0002753 | cytoplasmic pattern recognition receptor signaling pathv | 0.24382204 | 0.825359755 |
| MP:0002665 | decreased circulating corticosterone level | 0.243646475 | 0.825395514 |
| GO:0071479 | cellular response to ionizing radiation | 0.243694664 | 0.825413126 |
| GO:0008278 | cohesin complex | 0.244204085 | 0.825583039 |
| MP:0002026 | leukemia | 0.244350473 | 0.82589496 |
| ENSG00000024422 | EHD2 subnetwork | 0.24476301 | 0.827024482 |
| GO:0001954 | positive regulation of cell-matrix adhesion | 0.244817378 | 0.827053424 |
| ENSG00000039319 | ZFYVE16 subnetwork | 0.24475927 | 0.827207441 |
| ENSG00000136754 | ABI1 subnetwork | 0.245352478 | 0.827661575 |
| ENSG00000139842 | CUL4A subnetwork | 0.245048647 | 0.827705882 |
| ENSG00000182541 | LIMK2 subnetwork | 0.245272729 | 0.827709852 |
| REACTOME_SIGNALING_BY_NOT( | REACTOME_SIGNALING_BY_NOTCH | 0.245328812 | 0.827715092 |
| ENSG00000075426 | FOSL2 subnetwork | 0.245127703 | 0.827769936 |
| ENSG00000105369 | CD79A subnetwork | 0.245219932 | 0.82784572 |
| GO:0008209 | androgen metabolic process | 0.245656054 | 0.828064819 |
| GO:0010676 | positive regulation of cellular carbohydrate metabolic pr | 0.24564806 | 0.828200611 |
| ENSG00000147955 | SIGMAR1 subnetwork | 0.245740047 | 0.828304766 |
| MP:0008294 | abnormal zona fasciculata morphology | 0.245792295 | 0.82834507 |
| GO:0001952 | regulation of cell-matrix adhesion | 0.245841661 | 0.828361887 |
| GO:0045913 | positive regulation of carbohydrate metabolic process | 0.24564806 | 0.828395207 |
| ENSG00000171681 | ATF7IP subnetwork | 0.246072984 | 0.828817734 |
| ENSG00000205250 | E2F4 subnetwork | 0.246066431 | 0.829012201 |

| | | | |
|---|---|---|---|
| ENSG00000102554 | KLF5 subnetwork | 0.246293712 | 0.829420732 |
| ENSG00000112029 | FBXO5 subnetwork | 0.246750398 | 0.830506092 |
| ENSG00000206407 | ENSG00000206407 subnetwork | 0.246710854 | 0.830524959 |
| ENSG00000206489 | PPP1R10 subnetwork | 0.246710854 | 0.830719644 |
| ENSG00000204569 | PPP1R10 subnetwork | 0.246710854 | 0.83091442 |
| ENSG00000185129 | PURA subnetwork | 0.247074472 | 0.83102318 |
| REACTOME_PERK_REGULATED_G | REACTOME_PERK_REGULATED_GENE_EXPRESSION | 0.246981641 | 0.831026001 |
| MP:0011368 | increased kidney apoptosis | 0.247150005 | 0.831086142 |
| ENSG00000180573 | HIST1H2AC subnetwork | 0.247055881 | 0.831135831 |
| GO:0005516 | calmodulin binding | 0.24727174 | 0.831277791 |
| ENSG00000111640 | GAPDH subnetwork | 0.24752803 | 0.83152479 |
| GO:0016604 | nuclear body | 0.24749432 | 0.831567251 |
| GO:0045638 | negative regulation of myeloid cell differentiation | 0.247611762 | 0.831599252 |
| ENSG00000011600 | TYROBP subnetwork | 0.247453247 | 0.831609733 |
| GO:0050434 | positive regulation of viral transcription | 0.247717056 | 0.831767181 |
| ENSG00000130119 | GNL3L subnetwork | 0.247809408 | 0.831876607 |
| GO:0046854 | phosphatidylinositol phosphorylation | 0.248163585 | 0.832721963 |
| MP:0001239 | abnormal epidermis stratum granulosum morphology | 0.248498537 | 0.83302217 |
| MP:0001261 | obese | 0.24860386 | 0.833030091 |
| GO:0010922 | positive regulation of phosphatase activity | 0.248332556 | 0.83306866 |
| GO:0071219 | cellular response to molecule of bacterial origin | 0.248292254 | 0.833111423 |
| ENSG00000047849 | MAP4 subnetwork | 0.248486834 | 0.833158263 |
| ENSG00000149177 | PTPRJ subnetwork | 0.248590589 | 0.833177788 |
| GO:0046886 | positive regulation of hormone biosynthetic process | 0.248484104 | 0.833329442 |
| ENSG00000173876 | TUBB8 subnetwork | 0.248789564 | 0.833523787 |
| ENSG00000103490 | PYCARD subnetwork | 0.248844784 | 0.833585917 |
| GO:0072332 | signal transduction by p53 class mediator resulting in ind | 0.249247037 | 0.834494408 |
| GO:0004954 | prostanoid receptor activity | 0.249339381 | 0.834524918 |
| ENSG00000198836 | OPA1 subnetwork | 0.249205252 | 0.834525752 |
| MP:0008111 | abnormal granulocyte differentiation | 0.249183293 | 0.834638695 |
| GO:0004953 | icosanoid receptor activity | 0.249339381 | 0.834719311 |
| ENSG00000197822 | OCLN subnetwork | 0.249555683 | 0.834881285 |
| ENSG00000079841 | RIMS1 subnetwork | 0.249912069 | 0.834910486 |
| ENSG00000162614 | NEXN subnetwork | 0.249555072 | 0.835075669 |
| ENSG00000167548 | MLL2 subnetwork | 0.249907063 | 0.835104651 |
| GO:0045907 | positive regulation of vasoconstriction | 0.249797088 | 0.835120987 |
| MP:0002654 | spongiform encephalopathy | 0.249743489 | 0.835210612 |
| ENSG00000100453 | GZMB subnetwork | 0.249896885 | 0.835287276 |
| ENSG00000169057 | MECP2 subnetwork | 0.250217518 | 0.835681079 |
| ENSG00000181690 | PLAG1 subnetwork | 0.250495392 | 0.835744137 |
| ENSG00000111725 | PRKAB1 subnetwork | 0.250551058 | 0.835747447 |
| ENSG00000181218 | HIST3H2A subnetwork | 0.250479873 | 0.835845332 |
| ENSG00000214826 | ENSG00000214826 subnetwork | 0.250385552 | 0.835873606 |
| ENSG00000101306 | MYLK2 subnetwork | 0.250437449 | 0.835876887 |
| ENSG00000111788 | ENSG00000111788 subnetwork | 0.250385552 | 0.83606786 |
| ENSG00000070061 | IKBKAP subnetwork | 0.250707102 | 0.836307728 |
| ENSG00000071894 | CPSF1 subnetwork | 0.250821983 | 0.836461717 |
| ENSG00000057468 | MSH4 subnetwork | 0.250986671 | 0.836471134 |
| MP:0005584 | abnormal enzyme/coenzyme activity | 0.250966388 | 0.836583952 |
| GO:0071383 | cellular response to steroid hormone stimulus | 0.250943191 | 0.836720019 |
| GO:0050853 | B cell receptor signaling pathway | 0.251780162 | 0.837994906 |
| MP:0011204 | abnormal visceral yolk sac blood island morphology | 0.251731731 | 0.838026864 |
| GO:0010181 | FMN binding | 0.251704331 | 0.838163076 |
| ENSG00000137710 | RDX subnetwork | 0.251600812 | 0.838180765 |

| | | | |
|---|---|---|---|
| GO:0035267 | NuA4 histone acetyltransferase complex | 0.251674772 | 0.838276182 |
| MP:0001713 | decreased trophoblast giant cell number | 0.251594818 | 0.838351878 |
| MP:0001786 | skin edema | 0.252147128 | 0.838775746 |
| GO:0002675 | positive regulation of acute inflammatory response | 0.252104111 | 0.838819444 |
| MP:0005065 | abnormal neutrophil morphology | 0.252743977 | 0.840654638 |
| ENSG00000100345 | MYH9 subnetwork | 0.252716894 | 0.840745025 |
| MP:0003406 | failure of zygotic cell division | 0.252851937 | 0.84093432 |
| ENSG00000188486 | H2AFX subnetwork | 0.253011591 | 0.841375723 |
| ENSG00000127445 | PIN1 subnetwork | 0.253041709 | 0.841377716 |
| GO:0042177 | negative regulation of protein catabolic process | 0.253163217 | 0.841622371 |
| GO:0060759 | regulation of response to cytokine stimulus | 0.253430536 | 0.842421442 |
| ENSG00000131746 | TNS4 subnetwork | 0.253934485 | 0.842893401 |
| ENSG00000125107 | CNOT1 subnetwork | 0.253672706 | 0.842966043 |
| ENSG00000135097 | MSI1 subnetwork | 0.253894105 | 0.842995615 |
| ENSG00000123737 | EXOSC9 subnetwork | 0.254036612 | 0.843091119 |
| ENSG00000004700 | RECQL subnetwork | 0.253814066 | 0.843107827 |
| GO:0071826 | ribonucleoprotein complex subunit organization | 0.253771186 | 0.843140878 |
| GO:0040029 | regulation of gene expression, epigenetic | 0.253882992 | 0.843144044 |
| GO:0002824 | positive regulation of adaptive immune response based ( | 0.254138503 | 0.843231089 |
| ENSG00000171566 | PLRG1 subnetwork | 0.254529486 | 0.844258704 |
| GO:0006997 | nucleus organization | 0.254730641 | 0.844423963 |
| GO:0032355 | response to estradiol stimulus | 0.254707269 | 0.844526389 |
| GO:0003993 | acid phosphatase activity | 0.254701006 | 0.844686491 |
| ENSG00000180228 | PRKRA subnetwork | 0.254892085 | 0.844759272 |
| ENSG00000106344 | RBM28 subnetwork | 0.255120988 | 0.845244127 |
| ENSG00000044574 | HSPA5 subnetwork | 0.255198703 | 0.845371863 |
| ENSG00000101680 | LAMA1 subnetwork | 0.255440722 | 0.84554763 |
| GO:0022618 | ribonucleoprotein complex assembly | 0.255346644 | 0.845614641 |
| REACTOME_PLC_BETA_MEDIATEI | REACTOME_PLC_BETA_MEDIATED_EVENTS | 0.255521021 | 0.845617667 |
| GO:0043021 | ribonucleoprotein complex binding | 0.255594396 | 0.845699172 |
| MP:0002413 | abnormal megakaryocyte progenitor cell morphology | 0.255433459 | 0.845742232 |
| ENSG00000118898 | PPL subnetwork | 0.255907491 | 0.846608416 |
| ENSG00000185634 | SHC4 subnetwork | 0.256107431 | 0.847046656 |
| GO:0042992 | negative regulation of transcription factor import into nu | 0.256068055 | 0.847114943 |
| ENSG00000101412 | E2F1 subnetwork | 0.25627375 | 0.847277739 |
| ENSG00000130193 | C8orf55 subnetwork | 0.256319476 | 0.847278365 |
| ENSG00000105281 | SLC1A5 subnetwork | 0.256231539 | 0.847300092 |
| GO:0019903 | protein phosphatase binding | 0.256471277 | 0.847600459 |
| ENSG00000139726 | DENR subnetwork | 0.256731625 | 0.847808628 |
| ENSG00000097007 | ABL1 subnetwork | 0.25669054 | 0.847888455 |
| GO:0045684 | positive regulation of epidermis development | 0.256673378 | 0.847979798 |
| GO:0000794 | condensed nuclear chromosome | 0.256847512 | 0.848118835 |
| GO:0001916 | positive regulation of T cell mediated cytotoxicity | 0.256963701 | 0.848142628 |
| GO:0034637 | cellular carbohydrate biosynthetic process | 0.256952963 | 0.84831422 |
| ENSG00000215694 | ENSG00000215694 subnetwork | 0.25729185 | 0.849049038 |
| GO:0018210 | peptidyl-threonine modification | 0.257355338 | 0.849072165 |
| ENSG00000168393 | DTYMK subnetwork | 0.25729185 | 0.84924364 |
| ENSG00000069424 | KCNAB2 subnetwork | 0.257591461 | 0.849358974 |
| MP:0008658 | decreased interleukin-1 beta secretion | 0.257290097 | 0.849438331 |
| ENSG00000133121 | STARD13 subnetwork | 0.257574077 | 0.849484772 |
| REACTOME_PROSTANOID_METAI | REACTOME_PROSTANOID_METABOLISM | 0.257539393 | 0.849507558 |
| MP:0001943 | abnormal respiration | 0.257717535 | 0.849553674 |
| REACTOME_BETA:CATENIN_PHOS | REACTOME_BETA:CATENIN_PHOSPHORYLATION_CASCA | 0.257830964 | 0.849576756 |
| ENSG00000188739 | RBM34 subnetwork | 0.257802148 | 0.849691076 |

| | | | |
|---|---|---|---|
| GO:0030414 | peptidase inhibitor activity | 0.258006849 | 0.849942831 |
| GO:0043401 | steroid hormone mediated signaling pathway | 0.257978424 | 0.850068618 |
| GO:0046930 | pore complex | 0.258307017 | 0.85056 |
| ENSG00000087111 | PIGS subnetwork | 0.258291817 | 0.850697302 |
| GO:0042803 | protein homodimerization activity | 0.258596518 | 0.851565356 |
| ENSG00000140848 | CPNE2 subnetwork | 0.258914507 | 0.85252456 |
| ENSG00000145692 | BHMT subnetwork | 0.259468297 | 0.853331052 |
| MP:0008809 | increased spleen iron level | 0.259420663 | 0.853354633 |
| ENSG00000068394 | GPKOW subnetwork | 0.259306797 | 0.85336758 |
| GO:0019825 | oxygen binding | 0.259363749 | 0.853423876 |
| GO:0019208 | phosphatase regulator activity | 0.25965269 | 0.853443558 |
| GO:0048747 | muscle fiber development | 0.259295023 | 0.853516785 |
| ENSG00000204361 | FAM55B subnetwork | 0.259646391 | 0.853626825 |
| ENSG00000099995 | SF3A1 subnetwork | 0.259288949 | 0.853688899 |
| GO:0005086 | ARF guanyl-nucleotide exchange factor activity | 0.259857588 | 0.854138167 |
| MP:0006301 | abnormal mesenchyme morphology | 0.259958852 | 0.854251197 |
| ENSG00000100836 | PABPN1 subnetwork | 0.26024124 | 0.854452289 |
| GO:0006704 | glucocorticoid biosynthetic process | 0.260198288 | 0.85453303 |
| ENSG00000178952 | TUFM subnetwork | 0.260150848 | 0.854556847 |
| MP:0001931 | abnormal oogenesis | 0.260116765 | 0.854603464 |
| ENSG00000017427 | IGF1 subnetwork | 0.260355347 | 0.854610656 |
| ENSG00000168502 | CCDC165 subnetwork | 0.260422503 | 0.854666515 |
| MP:0005293 | impaired glucose tolerance | 0.260679876 | 0.855257169 |
| REACTOME_SHC1_EVENTS_IN_ER | REACTOME_SHC1_EVENTS_IN_ERBB2_SIGNALING | 0.260947457 | 0.855823476 |
| ENSG00000116830 | TTF2 subnetwork | 0.260997157 | 0.855867637 |
| ENSG00000060688 | SNRNP40 subnetwork | 0.260924887 | 0.85592719 |
| ENSG00000143013 | LMO4 subnetwork | 0.26113321 | 0.856343793 |
| ENSG00000136560 | TANK subnetwork | 0.26131694 | 0.856568182 |
| MP:0010123 | increased bone mineral content | 0.261264234 | 0.856671971 |
| ENSG00000184226 | PCDH9 subnetwork | 0.261490434 | 0.857021132 |
| MP:0008892 | abnormal sperm flagellum morphology | 0.261600259 | 0.857167197 |
| ENSG00000137936 | BCAR3 subnetwork | 0.262089924 | 0.857714999 |
| ENSG00000122966 | CIT subnetwork | 0.26204129 | 0.857762143 |
| ENSG00000176974 | SHMT1 subnetwork | 0.261971622 | 0.857763905 |
| ENSG00000196839 | ADA subnetwork | 0.262191632 | 0.85779265 |
| ENSG00000204592 | HLA-E subnetwork | 0.26193689 | 0.857856494 |
| GO:0005319 | lipid transporter activity | 0.261927214 | 0.858017261 |
| ENSG00000008083 | JARID2 subnetwork | 0.262383548 | 0.858391926 |
| ENSG00000137815 | RTF1 subnetwork | 0.262814332 | 0.859693878 |
| ENSG00000138443 | ABI2 subnetwork | 0.263205668 | 0.861085922 |
| ENSG00000169567 | HINT1 subnetwork | 0.263389982 | 0.861650045 |
| ENSG00000165392 | WRN subnetwork | 0.263601788 | 0.862165836 |
| ENSG00000049246 | PER3 subnetwork | 0.263702141 | 0.862298981 |
| ENSG00000173175 | ADCY5 subnetwork | 0.26359531 | 0.862349875 |
| ENSG00000133961 | NUMB subnetwork | 0.2643231 | 0.862567812 |
| GO:0044448 | cell cortex part | 0.264014914 | 0.862698053 |
| MP:0001932 | abnormal spermiogenesis | 0.263966217 | 0.862723568 |
| ENSG00000058272 | PPP1R12A subnetwork | 0.264311867 | 0.862728917 |
| ENSG00000172534 | HCFC1 subnetwork | 0.264067448 | 0.862729124 |
| MP:0004956 | decreased thymus weight | 0.264409765 | 0.862734463 |
| ENSG00000181929 | PRKAG1 subnetwork | 0.264290331 | 0.862833559 |
| GO:0045860 | positive regulation of protein kinase activity | 0.264226781 | 0.862836462 |
| ENSG00000134684 | YARS subnetwork | 0.26396567 | 0.862918931 |
| ENSG00000110321 | EIF4G2 subnetwork | 0.264198665 | 0.862929864 |

| | | | |
|---|---|---|---|
| ENSG00000177700 | POLR2L subnetwork | 0.264518039 | 0.86293493 |
| ENSG00000107223 | EDF1 subnetwork | 0.264829547 | 0.863445473 |
| ENSG00000144231 | POLR2D subnetwork | 0.264880861 | 0.863487585 |
| ENSG00000124641 | MED20 subnetwork | 0.264828525 | 0.86364047 |
| GO:0009895 | negative regulation of catabolic process | 0.264988023 | 0.863687655 |
| GO:0001933 | negative regulation of protein phosphorylation | 0.264777574 | 0.863733906 |
| GO:0050673 | epithelial cell proliferation | 0.265157771 | 0.864090704 |
| GO:0000175 | 3'-5'-exoribonuclease activity | 0.265620862 | 0.864686655 |
| ENSG00000188342 | GTF2F2 subnetwork | 0.265604321 | 0.864847802 |
| REACTOME_PHASE_1_:_FUNCTIO | REACTOME_PHASE_1_:_FUNCTIONALIZATION_OF_COM | 0.26581024 | 0.864868214 |
| ENSG00000100142 | POLR2F subnetwork | 0.265901658 | 0.864898649 |
| ENSG00000074370 | ATP2A3 subnetwork | 0.265786983 | 0.864995493 |
| ENSG00000169189 | NSMCE1 subnetwork | 0.265596567 | 0.865020298 |
| ENSG00000123576 | ESX1 subnetwork | 0.265772285 | 0.865111562 |
| ENSG00000170759 | KIF5B subnetwork | 0.26557058 | 0.865159035 |
| GO:0048511 | rhythmic process | 0.266320039 | 0.865698852 |
| ENSG00000136937 | NCBP1 subnetwork | 0.266221695 | 0.86572844 |
| GO:0019048 | virus-host interaction | 0.266282573 | 0.865736155 |
| GO:0006412 | translation | 0.266451725 | 0.865987849 |
| ENSG00000174437 | ATP2A2 subnetwork | 0.266683526 | 0.8663481 |
| GO:0001890 | placenta development | 0.266671852 | 0.86648673 |
| ENSG00000005075 | POLR2J subnetwork | 0.266669562 | 0.866670416 |
| GO:0045471 | response to ethanol | 0.266875974 | 0.866734098 |
| GO:0002823 | negative regulation of adaptive immune response based | 0.266803067 | 0.86673786 |
| GO:0031593 | polyubiquitin binding | 0.267282257 | 0.866887343 |
| ENSG00000079246 | XRCC5 subnetwork | 0.267069737 | 0.866924978 |
| ENSG00000072501 | SMC1A subnetwork | 0.267197694 | 0.866939829 |
| ENSG00000146677 | ENSG00000146677 subnetwork | 0.267163338 | 0.866999775 |
| ENSG00000163362 | C1orf106 subnetwork | 0.266969002 | 0.867 |
| ENSG00000181856 | SLC2A4 subnetwork | 0.267027909 | 0.867052348 |
| ENSG00000196415 | PRTN3 subnetwork | 0.26728078 | 0.86708193 |
| ENSG00000148672 | GLUD1 subnetwork | 0.267507954 | 0.867126514 |
| ENSG00000183072 | NKX2-5 subnetwork | 0.267460093 | 0.867220103 |
| ENSG00000134086 | VHL subnetwork | 0.267866744 | 0.868019735 |
| ENSG00000166501 | PRKCB subnetwork | 0.268062404 | 0.868142089 |
| ENSG00000127688 | GAN subnetwork | 0.267990072 | 0.868262332 |
| REACTOME_REGULATION_OF_PY | REACTOME_REGULATION_OF_PYRUVATE_DEHYDROGEN | 0.268048086 | 0.868291863 |
| GO:0008430 | selenium binding | 0.268223656 | 0.868346774 |
| GO:0005952 | cAMP-dependent protein kinase complex | 0.268183591 | 0.868373292 |
| GO:0052745 | inositol phosphate phosphatase activity | 0.268547091 | 0.868449318 |
| ENSG00000215305 | VPS16 subnetwork | 0.268984481 | 0.86849866 |
| ENSG00000108854 | SMURF2 subnetwork | 0.268498086 | 0.8685094 |
| MP:0001701 | incomplete embryo turning | 0.26847806 | 0.868636669 |
| GO:0002039 | p53 binding | 0.269095717 | 0.868639714 |
| ENSG00000137672 | TRPC6 subnetwork | 0.268697434 | 0.868642362 |
| ENSG00000131899 | LLGL1 subnetwork | 0.268973043 | 0.868659218 |
| MP:0004774 | abnormal bile salt level | 0.268389041 | 0.868701008 |
| MP:0008722 | abnormal chemokine secretion | 0.268924882 | 0.868741618 |
| ENSG00000009413 | REV3L subnetwork | 0.268802953 | 0.868761181 |
| ENSG00000067560 | RHOA subnetwork | 0.268874859 | 0.868801699 |
| GO:0046165 | alcohol biosynthetic process | 0.268476233 | 0.868831169 |
| REACTOME_METABOLISM_OF_PO | REACTOME_METABOLISM_OF_PORPHYRINS | 0.268696305 | 0.868836689 |
| MP:0004500 | increased incidence of ionizing radiation-induced tumors | 0.269261674 | 0.868899308 |
| GO:0060341 | regulation of cellular localization | 0.269202731 | 0.868959357 |

| | | | |
|---|---|---|---|
| ENSG00000105855 | ITGB8 subnetwork | 0.269383603 | 0.869095982 |
| ENSG00000143772 | ITPKB subnetwork | 0.269474438 | 0.869243641 |
| REACTOME_DEFENSINS | REACTOME_DEFENSINS | 0.269438295 | 0.869247936 |
| ENSG00000185214 | ENSG00000185214 subnetwork | 0.269685136 | 0.869808164 |
| ENSG00000124642 | ENSG00000124642 subnetwork | 0.269937993 | 0.870278707 |
| ENSG00000133101 | CCNA1 subnetwork | 0.270027381 | 0.870407936 |
| ENSG00000184825 | HIST1H2AH subnetwork | 0.269937993 | 0.870472792 |
| GO:0046660 | female sex differentiation | 0.270275685 | 0.870982839 |
| GO:0008168 | methyltransferase activity | 0.270499072 | 0.871390374 |
| ENSG00000168135 | KCNJ4 subnetwork | 0.270658537 | 0.871447661 |
| ENSG00000168495 | POLR3D subnetwork | 0.270641627 | 0.871608376 |
| MP:0004957 | abnormal blastocyst morphology | 0.27092864 | 0.871617713 |
| ENSG00000107758 | PPP3CB subnetwork | 0.270996771 | 0.871646274 |
| GO:0016410 | N-acyltransferase activity | 0.270839338 | 0.871649599 |
| GO:0043393 | regulation of protein binding | 0.270816669 | 0.871732354 |
| ENSG00000076242 | MLH1 subnetwork | 0.27092071 | 0.871744937 |
| MP:0005342 | abnormal intestinal lipid absorption | 0.271164293 | 0.872030694 |
| MP:0001260 | increased body weight | 0.271312574 | 0.872198755 |
| GO:0010869 | regulation of receptor biosynthetic process | 0.271416516 | 0.872304957 |
| MP:0002643 | poikilocytosis | 0.271311777 | 0.872392706 |
| ENSG00000143702 | CEP170 subnetwork | 0.271636219 | 0.872412261 |
| ENSG00000143569 | UBAP2L subnetwork | 0.271814397 | 0.872508324 |
| ENSG00000101158 | TH1L subnetwork | 0.271618435 | 0.872539436 |
| GO:0051099 | positive regulation of binding | 0.271529307 | 0.872544444 |
| ENSG00000165632 | TAF3 subnetwork | 0.271730176 | 0.872607151 |
| REACTOME_INTERFERON_ALPHA | REACTOME_INTERFERON_ALPHABETA_SIGNALING | 0.271811623 | 0.87267984 |
| ENSG00000182319 | SGK223 subnetwork | 0.272149774 | 0.873302264 |
| ENSG00000115008 | IL1A subnetwork | 0.273548048 | 0.874359258 |
| ENSG00000134882 | UBAC2 subnetwork | 0.273517436 | 0.874486188 |
| GO:0032403 | protein complex binding | 0.272536922 | 0.874517417 |
| ENSG00000198677 | TTC37 subnetwork | 0.27340661 | 0.874541234 |
| ENSG00000172915 | NBEA subnetwork | 0.273473399 | 0.874568966 |
| MP:0001284 | absent vibrissae | 0.272625479 | 0.874622893 |
| GO:0004385 | guanylate kinase activity | 0.272895656 | 0.874673166 |
| ENSG00000125398 | SOX9 subnetwork | 0.27338069 | 0.874679345 |
| GO:0051345 | positive regulation of hydrolase activity | 0.272941887 | 0.87470093 |
| ENSG00000141696 | LEPREL4 subnetwork | 0.273144909 | 0.874756529 |
| ENSG00000130041 | ENSG00000130041 subnetwork | 0.272814023 | 0.874772778 |
| ENSG00000215440 | NPEPL1 subnetwork | 0.273195497 | 0.874784244 |
| REACTOME_CREB_PHOSPHORYLA | REACTOME_CREB_PHOSPHORYLATION_THROUGH_THE_ | 0.273359844 | 0.874795399 |
| MP:0002020 | increased tumor incidence | 0.273905087 | 0.874828956 |
| REACTOME_DEVELOPMENTAL_BI | REACTOME_DEVELOPMENTAL_BIOLOGY | 0.272893184 | 0.874844858 |
| GO:0043209 | myelin sheath | 0.273298886 | 0.874845133 |
| MP:0000187 | abnormal triglyceride level | 0.273866558 | 0.87486755 |
| ENSG00000076928 | ARHGEF1 subnetwork | 0.273141404 | 0.87492805 |
| ENSG00000011451 | WIZ subnetwork | 0.273838567 | 0.87493928 |
| ENSG00000184787 | UBE2G2 subnetwork | 0.273738657 | 0.874961343 |
| ENSG00000177954 | RPS27 subnetwork | 0.272814023 | 0.874966741 |
| ENSG00000130956 | HABP4 subnetwork | 0.274078969 | 0.874972424 |
| GO:0048038 | quinone binding | 0.274013555 | 0.875 |
| ENSG00000180900 | SCRIB subnetwork | 0.272765046 | 0.875005544 |
| ENSG00000105245 | NUMBL subnetwork | 0.273131386 | 0.875011072 |
| MP:0011091 | complete prenatal lethality | 0.273816709 | 0.875066254 |
| MP:0000296 | absent trabeculae carneae | 0.274239443 | 0.875093716 |

| | | | |
|---|---|---|---|
| ENSG00000178573 | MAF subnetwork | 0.273103017 | 0.875149502 |
| ENSG00000119203 | CPSF3 subnetwork | 0.274227818 | 0.875242611 |
| ENSG00000198612 | COPS8 subnetwork | 0.274371596 | 0.87526455 |
| ENSG00000180581 | ENSG00000180581 subnetwork | 0.274795875 | 0.87540731 |
| ENSG00000125868 | DSTN subnetwork | 0.274501284 | 0.875424289 |
| ENSG00000136986 | DERL1 subnetwork | 0.274905714 | 0.875506162 |
| ENSG00000030304 | MUSK subnetwork | 0.27467827 | 0.875567306 |
| ENSG00000143742 | SRP9 subnetwork | 0.274795875 | 0.875600088 |
| ENSG00000171241 | SHCBP1 subnetwork | 0.274650985 | 0.875617012 |
| ENSG00000170653 | ATF7 subnetwork | 0.274770105 | 0.875671806 |
| GO:0000287 | magnesium ion binding | 0.274896925 | 0.875676866 |
| ENSG00000159346 | ADIPOR1 subnetwork | 0.27502254 | 0.875687569 |
| ENSG00000158560 | DYNC1I1 subnetwork | 0.275183285 | 0.876044875 |
| ENSG00000157764 | BRAF subnetwork | 0.275325959 | 0.876303057 |
| ENSG00000117533 | VAMP4 subnetwork | 0.275417977 | 0.876495163 |
| ENSG00000169306 | IL1RAPL1 subnetwork | 0.275843014 | 0.877676412 |
| GO:0001047 | core promoter binding | 0.275970644 | 0.878021978 |
| MP:0001819 | abnormal immune cell physiology | 0.276402617 | 0.878358209 |
| ENSG00000183574 | RNF5 subnetwork | 0.276391566 | 0.878507135 |
| ENSG00000204308 | RNF5 subnetwork | 0.276391566 | 0.878700044 |
| ENSG00000126945 | HNRNPH2 subnetwork | 0.276331244 | 0.878877417 |
| ENSG00000206254 | ENSG00000206254 subnetwork | 0.276391566 | 0.878893038 |
| MP:0002747 | abnormal aortic valve morphology | 0.276281573 | 0.878960668 |
| ENSG00000177455 | CD19 subnetwork | 0.276758415 | 0.879135586 |
| ENSG00000131037 | EPS8L1 subnetwork | 0.276715235 | 0.879185868 |
| ENSG00000100138 | NHP2L1 subnetwork | 0.276998763 | 0.87988594 |
| GO:0046824 | positive regulation of nucleocytoplasmic transport | 0.277410459 | 0.881260965 |
| ENSG00000158773 | USF1 subnetwork | 0.277740908 | 0.881832128 |
| GO:0031018 | endocrine pancreas development | 0.277727879 | 0.881959667 |
| ENSG00000100280 | AP1B1 subnetwork | 0.277693733 | 0.882065337 |
| ENSG00000163960 | UBXN7 subnetwork | 0.27788576 | 0.882131902 |
| ENSG00000133997 | MED6 subnetwork | 0.278076695 | 0.882347788 |
| ENSG00000166135 | HIF1AN subnetwork | 0.278036358 | 0.88237678 |
| ENSG00000132326 | PER2 subnetwork | 0.278375691 | 0.882786168 |
| ENSG00000168496 | FEN1 subnetwork | 0.278338416 | 0.882891856 |
| ENSG00000138696 | BMPR1B subnetwork | 0.278289553 | 0.882964747 |
| ENSG00000004455 | AK2 subnetwork | 0.278690299 | 0.883676149 |
| GO:0032387 | negative regulation of intracellular transport | 0.278922576 | 0.88373415 |
| ENSG00000085662 | AKR1B1 subnetwork | 0.278815995 | 0.883792651 |
| MP:0002840 | abnormal lens fiber morphology | 0.278864024 | 0.883796195 |
| GO:0045861 | negative regulation of proteolysis | 0.278772906 | 0.883843798 |
| ENSG00000105669 | COPE subnetwork | 0.279237831 | 0.884666667 |
| MP:0005100 | abnormal choroid pigmentation | 0.279377787 | 0.884673367 |
| GO:0045078 | positive regulation of interferon-gamma biosynthetic pr | 0.279469665 | 0.884731324 |
| GO:0008211 | glucocorticoid metabolic process | 0.279618064 | 0.884759825 |
| ENSG00000178035 | IMPDH2 subnetwork | 0.279374362 | 0.884855769 |
| ENSG00000131791 | PRKAB2 subnetwork | 0.279596991 | 0.884931208 |
| REACTOME_INFLUENZA_VIRAL_R | REACTOME_INFLUENZA_VIRAL_RNA_TRANSCRIPTION_A | 0.280062053 | 0.885598953 |
| ENSG00000138032 | PPM1B subnetwork | 0.280002588 | 0.885639459 |
| GO:0010743 | regulation of macrophage derived foam cell differentiati | 0.27992376 | 0.885658153 |
| ENSG00000135486 | HNRNPA1 subnetwork | 0.280450632 | 0.886780105 |
| GO:0002922 | positive regulation of humoral immune response | 0.280684237 | 0.886857018 |
| ENSG00000118579 | MED28 subnetwork | 0.280818867 | 0.886906318 |
| ENSG00000161960 | EIF4A1 subnetwork | 0.280660499 | 0.886941356 |

| | | | |
|---|---|---|---|
| ENSG00000063244 | U2AF2 subnetwork | 0.280787387 | 0.886979734 |
| ENSG00000105085 | MED26 subnetwork | 0.280558178 | 0.887044711 |
| GO:0051568 | histone H3-K4 methylation | 0.280628544 | 0.887047536 |
| GO:0005840 | ribosome | 0.280932587 | 0.887148769 |
| MP:0000371 | diluted coat color | 0.281206471 | 0.887192601 |
| ENSG00000213920 | MDP1 subnetwork | 0.281035008 | 0.88720601 |
| ENSG00000072694 | FCGR2B subnetwork | 0.281096414 | 0.887219682 |
| ENSG00000197785 | ATAD3A subnetwork | 0.281201729 | 0.887385721 |
| ENSG00000176170 | SPHK1 subnetwork | 0.281359579 | 0.887456484 |
| MP:0003853 | dry skin | 0.281606512 | 0.887926909 |
| GO:0043274 | phospholipase binding | 0.281868202 | 0.888163043 |
| ENSG00000147536 | GINS4 subnetwork | 0.281937012 | 0.888241687 |
| GO:0004725 | protein tyrosine phosphatase activity | 0.281744785 | 0.888255763 |
| GO:0061039 | ovum-producing ovary development | 0.281840029 | 0.888323549 |
| ENSG00000197343 | ZNF655 subnetwork | 0.282249075 | 0.888961321 |
| GO:0090132 | epithelium migration | 0.282591719 | 0.889824066 |
| GO:0048020 | CCR chemokine receptor binding | 0.282652392 | 0.889837134 |
| GO:0010631 | epithelial cell migration | 0.282591719 | 0.89001738 |
| ENSG00000130176 | CNN1 subnetwork | 0.282842832 | 0.890197568 |
| ENSG00000065427 | KARS subnetwork | 0.283160457 | 0.890991969 |
| GO:0035825 | reciprocal DNA recombination | 0.283414694 | 0.891034258 |
| GO:2000242 | negative regulation of reproductive process | 0.28321571 | 0.891037326 |
| KEGG_GLYCOSYLPHOSPHATIDYLIN | KEGG_GLYCOSYLPHOSPHATIDYLINOSITOL_GPI_ANCHOR | 0.283265885 | 0.891060968 |
| GO:0007131 | reciprocal meiotic recombination | 0.283414694 | 0.891227499 |
| GO:0014074 | response to purine-containing compound | 0.283353101 | 0.891247289 |
| ENSG00000215719 | ENSG00000215719 subnetwork | 0.283879852 | 0.891809317 |
| ENSG00000163162 | RNF149 subnetwork | 0.283761177 | 0.891881639 |
| ENSG00000169016 | E2F6 subnetwork | 0.283853428 | 0.891970091 |
| ENSG00000196284 | SUPT3H subnetwork | 0.284482303 | 0.892815408 |
| ENSG00000127511 | SIN3B subnetwork | 0.284409211 | 0.89295302 |
| MP:0010124 | decreased bone mineral content | 0.284475392 | 0.89297619 |
| ENSG00000140262 | TCF12 subnetwork | 0.284652411 | 0.893130679 |
| ENSG00000181991 | MRPS11 subnetwork | 0.284406837 | 0.893135557 |
| MP:0003572 | abnormal uterus development | 0.284358799 | 0.89317591 |
| ENSG00000134602 | ENSG00000134602 subnetwork | 0.28438513 | 0.893231536 |
| ENSG00000196405 | EVL subnetwork | 0.284916834 | 0.893643243 |
| ENSG00000137076 | TLN1 subnetwork | 0.284848943 | 0.893662124 |
| GO:0032259 | methylation | 0.285004592 | 0.893677043 |
| ENSG00000167641 | PPP1R14A subnetwork | 0.284905628 | 0.893717561 |
| ENSG00000173744 | AGFG1 subnetwork | 0.285125028 | 0.89387292 |
| ENSG00000015153 | YAF2 subnetwork | 0.285369042 | 0.894028078 |
| REACTOME_METABOLISM_OF_PF | REACTOME_METABOLISM_OF_PROTEINS | 0.285459839 | 0.894126539 |
| GO:0015085 | calcium ion transmembrane transporter activity | 0.285361721 | 0.894178008 |
| ENSG00000135269 | TES subnetwork | 0.28533374 | 0.894273984 |
| ENSG00000181817 | LSM10 subnetwork | 0.286077996 | 0.894588185 |
| GO:0090068 | positive regulation of cell cycle process | 0.286042638 | 0.894619366 |
| GO:0030132 | clathrin coat of coated pit | 0.286143644 | 0.894675577 |
| GO:0005158 | insulin receptor binding | 0.2859295 | 0.894703344 |
| REACTOME_TRANSLATION | REACTOME_TRANSLATION | 0.285976484 | 0.894704487 |
| MP:0002833 | increased heart weight | 0.286231759 | 0.894795259 |
| MP:0002133 | abnormal respiratory system physiology | 0.285883011 | 0.894799309 |
| ENSG00000073910 | FRY subnetwork | 0.28574053 | 0.894851036 |
| ENSG00000172845 | SP3 subnetwork | 0.285853458 | 0.8949169 |
| ENSG00000198924 | DCLRE1A subnetwork | 0.286655844 | 0.896326223 |

| | | | |
|---|---|---|---|
| MP:0004045 | abnormal cell cycle checkpoint function | 0.286754485 | 0.896456269 |
| GO:0008630 | DNA damage response, signal transduction resulting in ir | 0.287101814 | 0.897287406 |
| ENSG00000108798 | ABI3 subnetwork | 0.287052102 | 0.897351421 |
| MP:0002216 | abnormal seminiferous tubule morphology | 0.287045889 | 0.897480078 |
| GO:0035586 | purinergic receptor activity | 0.287403476 | 0.897901872 |
| ENSG00000120087 | HOXB7 subnetwork | 0.287398877 | 0.89806285 |
| ENSG00000063978 | RNF4 subnetwork | 0.287558378 | 0.898300344 |
| ENSG00000122257 | RBBP6 subnetwork | 0.287622578 | 0.898311465 |
| ENSG00000196092 | PAX5 subnetwork | 0.287694648 | 0.898344086 |
| ENSG00000141026 | MED9 subnetwork | 0.288159646 | 0.899119037 |
| MP:0001011 | abnormal superior cervical ganglion morphology | 0.288136009 | 0.899269289 |
| GO:0051896 | regulation of protein kinase B signaling cascade | 0.288248405 | 0.899344791 |
| REACTOME_GRB2_EVENTS_IN_EF | REACTOME_GRB2_EVENTS_IN_ERBB2_SIGNALING | 0.28804928 | 0.899354977 |
| GO:0005247 | voltage-gated chloride channel activity | 0.28811211 | 0.899376612 |
| GO:0050701 | interleukin-1 secretion | 0.288383831 | 0.899591924 |
| ENSG00000039123 | SKIV2L2 subnetwork | 0.288585244 | 0.900118102 |
| ENSG00000158417 | EIF5B subnetwork | 0.288777486 | 0.900429277 |
| MP:0004618 | thoracic vertebral transformation | 0.288745476 | 0.900525977 |
| KEGG_BLADDER_CANCER | KEGG_BLADDER_CANCER | 0.289285387 | 0.901984979 |
| MP:0009050 | dilated proximal convoluted tubules | 0.289774857 | 0.903475649 |
| ENSG00000151729 | SLC25A4 subnetwork | 0.289944449 | 0.903527015 |
| MP:0000358 | abnormal cell morphology | 0.290531689 | 0.903540107 |
| GO:0010038 | response to metal ion | 0.289851281 | 0.903549979 |
| GO:0050921 | positive regulation of chemotaxis | 0.290594715 | 0.903571429 |
| ENSG00000147145 | LPAR4 subnetwork | 0.290490317 | 0.903605049 |
| ENSG00000153807 | ENSG00000153807 subnetwork | 0.290190943 | 0.903609683 |
| ENSG00000171453 | POLR1C subnetwork | 0.289925157 | 0.903645722 |
| GO:0000979 | RNA polymerase II core promoter sequence-specific DNA | 0.290465999 | 0.903691419 |
| ENSG00000156697 | UTP14A subnetwork | 0.290145629 | 0.903696165 |
| GO:0033599 | regulation of mammary gland epithelial cell proliferation | 0.290286846 | 0.903758835 |
| MP:0000383 | abnormal hair follicle orientation | 0.290087483 | 0.903762058 |
| GO:0007569 | cell aging | 0.290438055 | 0.903831336 |
| ENSG00000146963 | LUC7L2 subnetwork | 0.290132685 | 0.903836262 |
| ENSG00000028137 | TNFRSF1B subnetwork | 0.290420918 | 0.903896382 |
| ENSG00000196396 | PTPN1 subnetwork | 0.290367111 | 0.903972163 |
| REACTOME_TRIGLYCERIDE_BIOSY | REACTOME_TRIGLYCERIDE_BIOSYNTHESIS | 0.291566886 | 0.904790866 |
| REACTOME_HIV_INFECTION | REACTOME_HIV_INFECTION | 0.291051292 | 0.904810776 |
| REACTOME_POST_NMDA_RECEP | REACTOME_POST_NMDA_RECEPTOR_ACTIVATION_EVE | 0.291367203 | 0.904816318 |
| GO:0016209 | antioxidant activity | 0.291151448 | 0.904905943 |
| ENSG00000174371 | EXO1 subnetwork | 0.291890959 | 0.904924323 |
| ENSG00000100056 | DGCR14 subnetwork | 0.291473229 | 0.904932735 |
| ENSG00000151224 | MAT1A subnetwork | 0.29122824 | 0.904936952 |
| ENSG00000144891 | AGTR1 subnetwork | 0.29155965 | 0.904941302 |
| GO:0060260 | regulation of transcription initiation from RNA polymera | 0.29199702 | 0.904954187 |
| MP:0004200 | decreased fetal size | 0.291288421 | 0.904957265 |
| ENSG00000129465 | RIPK3 subnetwork | 0.291526655 | 0.904974381 |
| REACTOME_G_ALPHA_1213_SIGN | REACTOME_G_ALPHA_1213_SIGNALLING_EVENTS | 0.291365049 | 0.904977569 |
| GO:0033549 | MAP kinase phosphatase activity | 0.292154607 | 0.905015974 |
| GO:0048185 | activin binding | 0.292109479 | 0.905017043 |
| ENSG00000196419 | XRCC6 subnetwork | 0.292327307 | 0.905077709 |
| ENSG00000182180 | MRPS16 subnetwork | 0.291869902 | 0.905085288 |
| ENSG00000183117 | CSMD1 subnetwork | 0.291720366 | 0.905088543 |
| GO:2000142 | regulation of transcription initiation, DNA-dependent | 0.29199702 | 0.905147059 |
| ENSG00000196611 | MMP1 subnetwork | 0.291832461 | 0.905161015 |

| | | | |
|---|---|---|---|
| ENSG00000134202 | GSTM3 subnetwork | 0.291801805 | 0.90524744 |
| GO:0005768 | endosome | 0.292323418 | 0.905259796 |
| ENSG00000171475 | WIPF2 subnetwork | 0.292716603 | 0.905990636 |
| GO:0042168 | heme metabolic process | 0.292666077 | 0.905991911 |
| ENSG00000206340 | C4A subnetwork | 0.293134473 | 0.906568878 |
| GO:0019003 | GDP binding | 0.293106344 | 0.906602169 |
| ENSG00000102145 | GATA1 subnetwork | 0.292933448 | 0.906606383 |
| MP:0006398 | increased long bone epiphyseal plate size | 0.293077572 | 0.906656742 |
| ENSG00000115091 | ACTR3 subnetwork | 0.293049093 | 0.906764518 |
| ENSG00000169100 | SLC25A6 subnetwork | 0.293461094 | 0.90703208 |
| ENSG00000159082 | SYNJ1 subnetwork | 0.293454935 | 0.907214195 |
| ENSG00000182957 | SPATA13 subnetwork | 0.29368378 | 0.907283924 |
| MP:0008019 | increased liver tumor incidence | 0.293411162 | 0.907311371 |
| REACTOME_LIPOPROTEIN_METAI | REACTOME_LIPOPROTEIN_METABOLISM | 0.293762228 | 0.907367304 |
| ENSG00000107263 | RAPGEF1 subnetwork | 0.293660066 | 0.907391674 |
| ENSG00000166930 | MS4A5 subnetwork | 0.293878063 | 0.907406621 |
| ENSG00000130939 | UBE4B subnetwork | 0.293840771 | 0.907503715 |
| GO:0005044 | scavenger receptor activity | 0.294090383 | 0.907583793 |
| ENSG00000132561 | MATN2 subnetwork | 0.294086986 | 0.907776363 |
| ENSG00000184678 | HIST2H2BE subnetwork | 0.29427662 | 0.908091198 |
| ENSG00000104921 | FCER2 subnetwork | 0.294806411 | 0.908697034 |
| GO:0045124 | regulation of bone resorption | 0.294786284 | 0.908794236 |
| ENSG00000013561 | RNF14 subnetwork | 0.294776829 | 0.908976261 |
| ENSG00000111540 | RAB5B subnetwork | 0.294639747 | 0.909043681 |
| ENSG00000153162 | BMP6 subnetwork | 0.294745237 | 0.909115964 |
| GO:0034339 | regulation of transcription from RNA polymerase II prom | 0.294997923 | 0.909140013 |
| ENSG00000162909 | CAPN2 subnetwork | 0.295245645 | 0.909731046 |
| ENSG00000070808 | CAMK2A subnetwork | 0.295539661 | 0.910533559 |
| KEGG_HEDGEHOG_SIGNALING_P/ | KEGG_HEDGEHOG_SIGNALING_PATHWAY | 0.295672266 | 0.910592593 |
| GO:0051972 | regulation of telomerase activity | 0.295660637 | 0.910774767 |
| REACTOME_ACTIVATION_OF_RAC | REACTOME_ACTIVATION_OF_RAC | 0.296028682 | 0.910956007 |
| ENSG00000213397 | HAUS7 subnetwork | 0.295940452 | 0.91110876 |
| MP:0000470 | abnormal stomach morphology | 0.296022003 | 0.91114872 |
| GO:0010042 | response to manganese ion | 0.296459893 | 0.911857958 |
| GO:0031490 | chromatin DNA binding | 0.296434612 | 0.911997886 |
| ENSG00000168002 | POLR2G subnetwork | 0.296699701 | 0.912085358 |
| GO:0005852 | eukaryotic translation initiation factor 3 complex | 0.29663376 | 0.91215131 |
| GO:0043256 | laminin complex | 0.296431717 | 0.912180165 |
| MP:0008974 | proportional dwarf | 0.296995592 | 0.912727081 |
| GO:0010035 | response to inorganic substance | 0.297180965 | 0.912901182 |
| GO:0032570 | response to progesterone stimulus | 0.297365272 | 0.913075137 |
| ENSG00000116459 | ATP5F1 subnetwork | 0.297168806 | 0.913083421 |
| ENSG00000125249 | RAP2A subnetwork | 0.297358644 | 0.913236225 |
| GO:0043488 | regulation of mRNA stability | 0.297514441 | 0.913238397 |
| MP:0002642 | anisocytosis | 0.297684734 | 0.913251107 |
| ENSG00000120949 | TNFRSF8 subnetwork | 0.297479462 | 0.913304495 |
| GO:0004467 | long-chain fatty acid-CoA ligase activity | 0.297880653 | 0.913358618 |
| MP:0002904 | increased circulating parathyroid hormone level | 0.297661461 | 0.913412062 |
| ENSG00000077063 | CTTNBP2 subnetwork | 0.297876638 | 0.913551106 |
| MP:0006055 | abnormal vascular endothelial cell morphology | 0.297640038 | 0.91356254 |
| ENSG00000004660 | CAMKK1 subnetwork | 0.297864993 | 0.913733137 |
| MP:0002041 | increased pituitary adenoma incidence | 0.298034561 | 0.913756056 |
| MP:0005505 | increased platelet cell number | 0.298226425 | 0.914097705 |
| ENSG00000196218 | RYR1 subnetwork | 0.298435595 | 0.914183502 |

| | | | |
|---|---|---|---|
| ENSG00000197915 | HRNR subnetwork | 0.298215338 | 0.914248104 |
| ENSG00000105220 | GPI subnetwork | 0.298489338 | 0.914275195 |
| ENSG00000148218 | ALAD subnetwork | 0.298427435 | 0.914344349 |
| ENSG00000169957 | ZNF768 subnetwork | 0.29837891 | 0.914347368 |
| MP:0002264 | abnormal bronchus morphology | 0.299033822 | 0.914455175 |
| MP:0005168 | abnormal female meiosis | 0.298986873 | 0.91448971 |
| ENSG00000103507 | BCKDK subnetwork | 0.298696735 | 0.91450799 |
| ENSG00000086619 | ERO1LB subnetwork | 0.298822118 | 0.914554435 |
| MP:0000828 | abnormal fourth ventricle morphology | 0.298665001 | 0.914595163 |
| REACTOME_IRS:RELATED_EVENTS | REACTOME_IRS:RELATED_EVENTS | 0.298975443 | 0.914608276 |
| ENSG00000136738 | STAM subnetwork | 0.298648702 | 0.914713925 |
| ENSG00000120690 | ELF1 subnetwork | 0.29881618 | 0.914715157 |
| REACTOME_IRS:MEDIATED_SIGN/ | REACTOME_IRS:MEDIATED_SIGNALLING | 0.298975443 | 0.91480042 |
| MP:0001413 | abnormal response to new environment | 0.298969165 | 0.91495062 |
| ENSG00000108424 | KPNB1 subnetwork | 0.29930362 | 0.91498426 |
| ENSG00000100083 | GGA1 subnetwork | 0.299299745 | 0.915155332 |
| ENSG00000125944 | HNRNPR subnetwork | 0.299617756 | 0.915935795 |
| REACTOME_ANTIGEN_PROCESSIN | REACTOME_ANTIGEN_PROCESSING_UBIQUITINATION__ | 0.299823239 | 0.916362492 |
| ENSG00000139496 | NUPL1 subnetwork | 0.299949416 | 0.916547819 |
| GO:0005815 | microtubule organizing center | 0.300107369 | 0.916890333 |
| REACTOME_SIGNALING_BY_NOD/ | REACTOME_SIGNALING_BY_NODAL | 0.30043252 | 0.917050691 |
| GO:0055001 | muscle cell development | 0.300357884 | 0.917075215 |
| GO:0071407 | cellular response to organic cyclic compound | 0.300716559 | 0.917176052 |
| GO:0042771 | DNA damage response, signal transduction by p53 class I | 0.300350325 | 0.917215004 |
| ENSG00000183765 | CHEK2 subnetwork | 0.30069572 | 0.917305276 |
| GO:0090130 | tissue migration | 0.300624004 | 0.917350785 |
| GO:0008641 | small protein activating enzyme activity | 0.30030333 | 0.917389937 |
| ENSG00000170820 | FSHR subnetwork | 0.300344924 | 0.917396772 |
| ENSG00000078902 | TOLLIP subnetwork | 0.300923031 | 0.917507325 |
| ENSG00000198689 | SLC9A6 subnetwork | 0.30143613 | 0.918782681 |
| GO:0045786 | negative regulation of cell cycle | 0.301414632 | 0.918891213 |
| ENSG00000050820 | BCAR1 subnetwork | 0.301410125 | 0.91908349 |
| GO:0032320 | positive regulation of Ras GTPase activity | 0.301600065 | 0.919144709 |
| ENSG00000118523 | CTGF subnetwork | 0.301912485 | 0.919763796 |
| MP:0008347 | decreased gamma-delta T cell number | 0.301870671 | 0.919788835 |
| REACTOME_ASSOCIATION_OF_TF | REACTOME_ASSOCIATION_OF_TRICCCT_WITH_TARGET_ | 0.302418864 | 0.920317394 |
| MP:0000003 | abnormal adipose tissue morphology | 0.302165787 | 0.920344828 |
| ENSG00000107949 | BCCIP subnetwork | 0.302392723 | 0.920436508 |
| GO:0050848 | regulation of calcium-mediated signaling | 0.302564376 | 0.920553236 |
| ENSG00000137642 | SORL1 subnetwork | 0.302637166 | 0.920601127 |
| MP:0006319 | abnormal epididymal fat pad morphology | 0.302384694 | 0.920618341 |
| ENSG00000148848 | ADAM12 subnetwork | 0.303200571 | 0.920639717 |
| KEGG_CALCIUM_SIGNALING_PAT | KEGG_CALCIUM_SIGNALING_PATHWAY | 0.30281225 | 0.92064469 |
| ENSG00000161547 | SRSF2 subnetwork | 0.302949149 | 0.920646507 |
| ENSG00000116711 | PLA2G4A subnetwork | 0.30234751 | 0.920664438 |
| ENSG00000141030 | COPS3 subnetwork | 0.303174397 | 0.920716965 |
| ENSG00000174791 | RIN1 subnetwork | 0.303111281 | 0.9207734 |
| GO:0006304 | DNA modification | 0.302927914 | 0.920807259 |
| ENSG00000065057 | NTHL1 subnetwork | 0.302800311 | 0.920815943 |
| GO:0046626 | regulation of insulin receptor signaling pathway | 0.303080417 | 0.92087156 |
| ENSG00000136810 | TXN subnetwork | 0.303443544 | 0.9211875 |
| ENSG00000148180 | GSN subnetwork | 0.303545756 | 0.921412206 |
| ENSG00000121671 | CRY2 subnetwork | 0.303745035 | 0.921855477 |
| GO:0071902 | positive regulation of protein serine/threonine kinase ac | 0.303979259 | 0.921883455 |

| | | | |
|---|---|---|---|
| MP:0002132 | abnormal respiratory system morphology | 0.303846579 | 0.921923798 |
| ENSG00000100395 | L3MBTL2 subnetwork | 0.303945621 | 0.921981682 |
| GO:0006611 | protein export from nucleus | 0.304278773 | 0.922679983 |
| ENSG00000198742 | SMURF1 subnetwork | 0.304402228 | 0.922831288 |
| ENSG00000116898 | MRPS15 subnetwork | 0.304860862 | 0.923498233 |
| GO:0043550 | regulation of lipid kinase activity | 0.30496499 | 0.923659601 |
| MP:0002447 | abnormal erythrocyte morphology | 0.304859925 | 0.923690229 |
| ENSG00000121807 | CCR2 subnetwork | 0.304803433 | 0.923715949 |
| ENSG00000215782 | ENSG00000215782 subnetwork | 0.304803433 | 0.92390807 |
| ENSG00000116962 | NID1 subnetwork | 0.305447164 | 0.924237077 |
| GO:0009612 | response to mechanical stimulus | 0.305411999 | 0.924377076 |
| ENSG00000144218 | AFF3 subnetwork | 0.305379522 | 0.924454829 |
| ENSG00000165476 | REEP3 subnetwork | 0.305295912 | 0.924506545 |
| GO:0019887 | protein kinase regulator activity | 0.30537503 | 0.924636477 |
| GO:0008601 | protein phosphatase type 2A regulator activity | 0.305804602 | 0.924948111 |
| ENSG00000105568 | PPP2R1A subnetwork | 0.305978989 | 0.925378709 |
| MP:0003420 | delayed intramembranous bone ossification | 0.306181846 | 0.925923237 |
| ENSG00000097046 | CDC7 subnetwork | 0.30620389 | 0.925959345 |
| ENSG00000149357 | LAMTOR1 subnetwork | 0.306650628 | 0.927140784 |
| ENSG00000150760 | DOCK1 subnetwork | 0.306642486 | 0.927281211 |
| ENSG00000184900 | SUMO3 subnetwork | 0.306964041 | 0.927813472 |
| GO:0060644 | mammary gland epithelial cell differentiation | 0.306927585 | 0.927839967 |
| GO:0040012 | regulation of locomotion | 0.307148318 | 0.928180688 |
| MP:0002784 | abnormal Sertoli cell morphology | 0.307256878 | 0.928350943 |
| MP:0005244 | hemopericardium | 0.307689119 | 0.92961889 |
| MP:0010383 | increased adenoma incidence | 0.30801596 | 0.930389315 |
| ENSG00000112242 | E2F3 subnetwork | 0.308123624 | 0.930569358 |
| REACTOME_SIGNALING_BY_ROBO | REACTOME_SIGNALING_BY_ROBO_RECEPTOR | 0.308266125 | 0.930821776 |
| ENSG00000116285 | ERRFI1 subnetwork | 0.308470723 | 0.931109042 |
| ENSG00000166337 | TAF10 subnetwork | 0.308437033 | 0.931198262 |
| GO:0050860 | negative regulation of T cell receptor signaling pathway | 0.309083774 | 0.931237092 |
| ENSG00000126218 | F10 subnetwork | 0.309353967 | 0.931262897 |
| MP:0001380 | reduced male mating frequency | 0.309324449 | 0.931372549 |
| GO:0043388 | positive regulation of DNA binding | 0.309248348 | 0.931379026 |
| GO:0050858 | negative regulation of antigen receptor-mediated signali | 0.309083774 | 0.931429457 |
| GO:0018107 | peptidyl-threonine phosphorylation | 0.309246213 | 0.931561016 |
| GO:0042446 | hormone biosynthetic process | 0.309080446 | 0.931590909 |
| ENSG00000148143 | ZNF462 subnetwork | 0.308895329 | 0.931724209 |
| MP:0010825 | abnormal lung saccule morphology | 0.309057325 | 0.931731763 |
| GO:0022602 | ovulation cycle process | 0.309056123 | 0.931914014 |
| ENSG00000132300 | PTCD3 subnetwork | 0.308892989 | 0.931916873 |
| MP:0005169 | abnormal male meiosis | 0.308788537 | 0.931940422 |
| ENSG00000149532 | CPSF7 subnetwork | 0.308850826 | 0.932006205 |
| GO:0006110 | regulation of glycolysis | 0.310216486 | 0.932248094 |
| ENSG00000131368 | MRPS25 subnetwork | 0.310166032 | 0.93231657 |
| ENSG00000172058 | SERF1A subnetwork | 0.310090593 | 0.932323232 |
| ENSG00000205572 | SERF1B subnetwork | 0.310090593 | 0.932515464 |
| ENSG00000132341 | RAN subnetwork | 0.309834189 | 0.932535589 |
| ENSG00000034971 | MYOC subnetwork | 0.310028751 | 0.932604661 |
| ENSG00000007968 | E2F2 subnetwork | 0.31035498 | 0.932612279 |
| GO:0070193 | synaptonemal complex organization | 0.310000173 | 0.932724835 |
| GO:0000159 | protein phosphatase type 2A complex | 0.31057468 | 0.932907743 |
| ENSG00000064703 | DDX20 subnetwork | 0.310516631 | 0.932955716 |
| ENSG00000170608 | FOXA3 subnetwork | 0.310703457 | 0.933127445 |

| | | | |
|---|---|---|---|
| GO:0046825 | regulation of protein export from nucleus | 0.310865725 | 0.93313786 |
| ENSG00000196305 | IARS subnetwork | 0.310826922 | 0.933185841 |
| ENSG00000088035 | ALG6 subnetwork | 0.31100898 | 0.933347048 |
| ENSG00000130772 | MED18 subnetwork | 0.310804844 | 0.933347056 |
| ENSG00000184083 | FAM120C subnetwork | 0.311191942 | 0.933669272 |
| MP:0000826 | abnormal third ventricle morphology | 0.311489676 | 0.933867653 |
| GO:0004842 | ubiquitin-protein ligase activity | 0.311488438 | 0.934049332 |
| ENSG00000172006 | ZNF554 subnetwork | 0.311433643 | 0.934066612 |
| GO:0030260 | entry into host cell | 0.312339578 | 0.934163592 |
| MP:0009115 | abnormal fat cell morphology | 0.31141517 | 0.934176434 |
| ENSG00000074181 | NOTCH3 subnetwork | 0.312467266 | 0.934289813 |
| MP:0006304 | abnormal seminiferous epithelium morphology | 0.312556062 | 0.934344262 |
| GO:0051828 | entry into other organism involved in symbiotic interacti | 0.312339578 | 0.934355136 |
| ENSG00000028277 | POU2F2 subnetwork | 0.311774825 | 0.934364085 |
| MP:0000611 | jaundice | 0.312728832 | 0.934381401 |
| MP:0002932 | abnormal joint morphology | 0.312830508 | 0.934425558 |
| ENSG00000168005 | C11orf84 subnetwork | 0.312717296 | 0.934511371 |
| ENSG00000081019 | RSBN1 subnetwork | 0.312895092 | 0.934520885 |
| GO:0051806 | entry into cell of other organism involved in symbiotic in | 0.312339578 | 0.93454676 |
| ENSG00000107796 | ACTA2 subnetwork | 0.312019762 | 0.934579055 |
| ENSG00000143373 | ZNF687 subnetwork | 0.31188984 | 0.934582991 |
| REACTOME_CLASS_I_MHC_MEDI | REACTOME_CLASS_I_MHC_MEDIATED_ANTIGEN_PROCE | 0.312095862 | 0.934654075 |
| GO:0051539 | 4 iron, 4 sulfur cluster binding | 0.311973022 | 0.934658041 |
| GO:0052192 | movement in environment of other organism involved in | 0.312339578 | 0.934738462 |
| GO:0044409 | entry into host | 0.312339578 | 0.934930242 |
| ENSG00000020922 | MRE11A subnetwork | 0.312267107 | 0.935067734 |
| GO:0052126 | movement in host environment | 0.312339578 | 0.935122101 |
| MP:0008593 | increased circulating interleukin-10 level | 0.313288956 | 0.935509619 |
| ENSG00000160255 | ITGB2 subnetwork | 0.313363346 | 0.935584203 |
| ENSG00000111229 | ARPC3 subnetwork | 0.313246008 | 0.935609007 |
| ENSG00000117133 | RPF1 subnetwork | 0.313510333 | 0.935761047 |
| ENSG00000197442 | MAP3K5 subnetwork | 0.313832912 | 0.93577269 |
| MP:0003453 | abnormal keratinocyte physiology | 0.313808004 | 0.935902678 |
| ENSG00000143537 | ADAM15 subnetwork | 0.31367496 | 0.935958274 |
| MP:0001486 | abnormal startle reflex | 0.313778437 | 0.936063395 |
| ENSG00000071626 | DAZAP1 subnetwork | 0.314130679 | 0.936460249 |
| ENSG00000186153 | WWOX subnetwork | 0.314262732 | 0.936646915 |
| ENSG00000146587 | RBAK subnetwork | 0.314327666 | 0.936741573 |
| GO:0060443 | mammary gland morphogenesis | 0.314424193 | 0.936785131 |
| GO:0090398 | cellular senescence | 0.314505839 | 0.936889933 |
| ENSG00000048052 | HDAC9 subnetwork | 0.314728806 | 0.936938776 |
| MP:0000183 | decreased circulating LDL cholesterol level | 0.314709803 | 0.937099408 |
| ENSG00000104081 | BMF subnetwork | 0.314696596 | 0.937229481 |
| ENSG00000074590 | NUAK1 subnetwork | 0.315409067 | 0.938961436 |
| GO:0010677 | negative regulation of cellular carbohydrate metabolic p | 0.315859095 | 0.939482267 |
| MP:0010019 | liver vascular congestion | 0.315956611 | 0.939545547 |
| GO:0045912 | negative regulation of carbohydrate metabolic process | 0.315859095 | 0.939673802 |
| GO:0004527 | exonuclease activity | 0.315848947 | 0.939834829 |
| REACTOME_TIE2_SIGNALING | REACTOME_TIE2_SIGNALING | 0.315723227 | 0.939881681 |
| ENSG00000120696 | KBTBD7 subnetwork | 0.316150106 | 0.939914425 |
| ENSG00000151322 | NPAS3 subnetwork | 0.31583763 | 0.939995921 |
| ENSG00000100299 | ARSA subnetwork | 0.316247501 | 0.940069261 |
| MP:0004737 | absent distortion product otoacoustic emissions | 0.31632419 | 0.940152749 |
| ENSG00000173402 | DAG1 subnetwork | 0.31658736 | 0.94069436 |

| | | | |
|---|---|---|---|
| GO:0005798 | Golgi-associated vesicle | 0.31676004 | 0.940738856 |
| MP:0009548 | abnormal platelet aggregation | 0.316669458 | 0.940757329 |
| GO:0051168 | nuclear export | 0.317235034 | 0.941187233 |
| ENSG00000155966 | AFF2 subnetwork | 0.317152108 | 0.941285337 |
| GO:0060393 | regulation of pathway-restricted SMAD protein phospho | 0.317209375 | 0.941297275 |
| GO:0005527 | macrolide binding | 0.317046208 | 0.941373347 |
| ENSG00000136603 | SKIL subnetwork | 0.317105738 | 0.941375102 |
| GO:0005528 | FK506 binding | 0.317046208 | 0.941564917 |
| ENSG00000070814 | TCOF1 subnetwork | 0.31744792 | 0.941595528 |
| GO:0016836 | hydro-lyase activity | 0.317577114 | 0.941932534 |
| ENSG00000161956 | SENP3 subnetwork | 0.31789907 | 0.942443632 |
| ENSG00000168067 | MAP4K2 subnetwork | 0.317870109 | 0.942574157 |
| ENSG00000116544 | DLGAP3 subnetwork | 0.318305772 | 0.943338749 |
| MP:0003436 | decreased susceptibility to induced arthritis | 0.318706709 | 0.94336714 |
| ENSG00000186867 | QRFPR subnetwork | 0.318775957 | 0.943378625 |
| MP:0010179 | rough coat | 0.318648233 | 0.943396226 |
| GO:0046456 | icosanoid biosynthetic process | 0.318636352 | 0.94356737 |
| ENSG00000083290 | ULK2 subnetwork | 0.31854853 | 0.943576213 |
| ENSG00000198231 | DDX42 subnetwork | 0.318521455 | 0.943676411 |
| GO:0006641 | triglyceride metabolic process | 0.318500561 | 0.943827411 |
| GO:0007143 | female meiosis | 0.319201169 | 0.943981763 |
| GO:0050918 | positive chemotaxis | 0.319028094 | 0.944028792 |
| GO:0010638 | positive regulation of organelle organization | 0.319196491 | 0.944142683 |
| MP:0004772 | abnormal bile secretion | 0.319185993 | 0.944293533 |
| ENSG00000047249 | ATP6V1H subnetwork | 0.319506262 | 0.94440956 |
| GO:0060444 | branching involved in mammary gland duct morphogene | 0.319499724 | 0.944590762 |
| GO:0006305 | DNA alkylation | 0.319979087 | 0.945171087 |
| GO:0006306 | DNA methylation | 0.319979087 | 0.945362495 |
| GO:0090307 | spindle assembly involved in mitosis | 0.320811314 | 0.946642395 |
| MP:0006027 | impaired lung alveolus development | 0.321637636 | 0.946691547 |
| KEGG_CELL_CYCLE | KEGG_CELL_CYCLE | 0.320637316 | 0.946701073 |
| ENSG00000057593 | F7 subnetwork | 0.320605777 | 0.946761134 |
| ENSG00000196943 | C14orf21 subnetwork | 0.321482362 | 0.946770287 |
| ENSG00000197555 | SIPA1L1 subnetwork | 0.32072706 | 0.946792796 |
| ENSG00000115524 | SF3B1 subnetwork | 0.32154599 | 0.946801211 |
| ENSG00000104067 | TJP1 subnetwork | 0.320795226 | 0.946803561 |
| ENSG00000071054 | MAP4K4 subnetwork | 0.321815748 | 0.946813874 |
| MP:0001849 | ear inflammation | 0.321754666 | 0.946833401 |
| GO:0048610 | cellular process involved in reproduction | 0.321624695 | 0.946842211 |
| GO:0007596 | blood coagulation | 0.32145527 | 0.946870583 |
| MP:0002667 | decreased circulating aldosterone level | 0.321415979 | 0.946970921 |
| ENSG00000143322 | ABL2 subnetwork | 0.321322376 | 0.947010101 |
| ENSG00000205339 | IPO7 subnetwork | 0.321387273 | 0.947101596 |
| MP:0004838 | abnormal neural fold elevation formation | 0.321182507 | 0.947129573 |
| KEGG_ALANINE_ASPARTATE_ANI | KEGG_ALANINE_ASPARTATE_AND_GLUTAMATE_METAB | 0.322009508 | 0.947157258 |
| ENSG00000165916 | PSMC3 subnetwork | 0.321121412 | 0.947159321 |
| ENSG00000123700 | KCNJ2 subnetwork | 0.32123404 | 0.947160469 |
| GO:0032147 | activation of protein kinase activity | 0.321314776 | 0.947191352 |
| ENSG00000113161 | HMGCR subnetwork | 0.321120613 | 0.947340748 |
| ENSG00000130803 | ZNF317 subnetwork | 0.322338695 | 0.947451652 |
| ENSG00000135845 | PIGC subnetwork | 0.322312785 | 0.947551884 |
| ENSG00000179632 | MAF1 subnetwork | 0.322273261 | 0.947591697 |
| ENSG00000132432 | SEC61G subnetwork | 0.322218326 | 0.947641605 |
| MP:0005159 | azoospermia | 0.322483356 | 0.947653575 |

| | | | |
|---|---|---|---|
| ENSG00000074047 | GLI2 subnetwork | 0.322796922 | 0.948318905 |
| ENSG00000156603 | MED19 subnetwork | 0.32277469 | 0.948449456 |
| ENSG00000171444 | MCC subnetwork | 0.322976509 | 0.948752013 |
| ENSG00000128245 | YWHAH subnetwork | 0.323512645 | 0.950020125 |
| GO:0008194 | UDP-glycosyltransferase activity | 0.323777725 | 0.950040217 |
| ENSG00000137074 | APTX subnetwork | 0.323601676 | 0.950160966 |
| MP:0002810 | microcytic anemia | 0.323766411 | 0.950201126 |
| MP:0005533 | increased body temperature | 0.323706241 | 0.950221283 |
| ENSG00000106615 | RHEB subnetwork | 0.324118803 | 0.951055489 |
| ENSG00000156313 | RPGR subnetwork | 0.324190091 | 0.951165829 |
| GO:0010742 | macrophage derived foam cell differentiation | 0.324661746 | 0.951284625 |
| ENSG00000168476 | REEP4 subnetwork | 0.324777378 | 0.951384708 |
| GO:0090077 | foam cell differentiation | 0.324661746 | 0.951475607 |
| ENSG00000100311 | PDGFB subnetwork | 0.324660178 | 0.951656627 |
| KEGG_MELANOMA | KEGG_MELANOMA | 0.324641946 | 0.951777465 |
| ENSG00000089289 | IGBP1 subnetwork | 0.324572148 | 0.951787867 |
| REACTOME_MICRORNA_MIRNA_ | REACTOME_MICRORNA_MIRNA_BIOGENESIS | 0.324506971 | 0.951828411 |
| ENSG00000163347 | CLDN1 subnetwork | 0.325033837 | 0.951976324 |
| REACTOME_REGULATORY_RNA_F | REACTOME_REGULATORY_RNA_PATHWAYS | 0.324506971 | 0.952019695 |
| GO:0030855 | epithelial cell differentiation | 0.32520326 | 0.952095868 |
| ENSG00000164045 | CDC25A subnetwork | 0.325192654 | 0.95225677 |
| ENSG00000153147 | SMARCA5 subnetwork | 0.325539097 | 0.95295769 |
| MP:0000273 | overriding aorta | 0.325640537 | 0.953067362 |
| REACTOME_METABOLISM_OF_PO | REACTOME_METABOLISM_OF_POLYAMINES | 0.325888133 | 0.953315969 |
| GO:0046627 | negative regulation of insulin receptor signaling pathway | 0.325874991 | 0.953446894 |
| GO:0032835 | glomerulus development | 0.325844222 | 0.953517739 |
| REACTOME_ERKS_ARE_INACTIVA | REACTOME_ERKS_ARE_INACTIVATED | 0.32605775 | 0.953595753 |
| REACTOME_FRS2:MEDIATED_ACT | REACTOME_FRS2:MEDIATED_ACTIVATION | 0.326158176 | 0.953725215 |
| GO:0033627 | cell adhesion mediated by integrin | 0.326504417 | 0.954665599 |
| ENSG00000197448 | GSTK1 subnetwork | 0.326810631 | 0.954842906 |
| GO:0008138 | protein tyrosine/serine/threonine phosphatase activity | 0.326655554 | 0.954874875 |
| ENSG00000111142 | METAP2 subnetwork | 0.326944461 | 0.95490098 |
| MP:0004890 | decreased energy expenditure | 0.326780384 | 0.954993995 |
| ENSG00000160973 | FOXH1 subnetwork | 0.327214225 | 0.955046972 |
| GO:0007568 | aging | 0.326934365 | 0.955062025 |
| ENSG00000071909 | MYO3B subnetwork | 0.327133494 | 0.95519896 |
| ENSG00000133935 | C14orf1 subnetwork | 0.327211799 | 0.955237905 |
| GO:0005665 | DNA-directed RNA polymerase II, core complex | 0.32735339 | 0.955275779 |
| ENSG00000136869 | TLR4 subnetwork | 0.327109382 | 0.9553 |
| GO:0034644 | cellular response to UV | 0.327449433 | 0.955364635 |
| GO:0017002 | activin-activated receptor activity | 0.327679252 | 0.955501198 |
| MP:0005032 | abnormal ectoplacental cone morphology | 0.327879135 | 0.955577729 |
| ENSG00000160307 | S100B subnetwork | 0.327652108 | 0.955602157 |
| REACTOME_RNA_POLYMERASE_I | REACTOME_RNA_POLYMERASE_III_TRANSCRIPTION | 0.327808389 | 0.955608782 |
| ENSG00000100941 | PNN subnetwork | 0.327643894 | 0.95578306 |
| REACTOME_RNA_POLYMERASE_I | REACTOME_RNA_POLYMERASE_III_ABORTIVE_AND_RET | 0.327808389 | 0.955799561 |
| ENSG00000056678 | ENSG00000056678 subnetwork | 0.328306188 | 0.956122856 |
| ENSG00000157500 | APPL1 subnetwork | 0.328209004 | 0.95627494 |
| ENSG00000204197 | KIFC1 subnetwork | 0.328306188 | 0.956313585 |
| MP:0003135 | increased erythroid progenitor cell number | 0.329129778 | 0.958464606 |
| ENSG00000171885 | AQP4 subnetwork | 0.329258023 | 0.958592504 |
| MP:0001131 | abnormal ovarian follicle morphology | 0.329708465 | 0.959002191 |
| MP:0009399 | increased skeletal muscle fiber size | 0.329692506 | 0.959123506 |
| GO:0051897 | positive regulation of protein kinase B signaling cascade | 0.329582978 | 0.959137106 |

| | | | |
|---|---|---|---|
| GO:0022829 | wide pore channel activity | 0.329570346 | 0.959278453 |
| ENSG00000173230 | GOLGB1 subnetwork | 0.329683715 | 0.959284718 |
| ENSG00000107130 | NCS1 subnetwork | 0.330016342 | 0.959695401 |
| ENSG00000215467 | ENSG00000215467 subnetwork | 0.329997104 | 0.95980685 |
| GO:0000795 | synaptonemal complex | 0.330192253 | 0.959850746 |
| ENSG00000111361 | EIF2B1 subnetwork | 0.33016119 | 0.960021895 |
| GO:0008585 | female gonad development | 0.330397353 | 0.960115377 |
| ENSG00000184845 | DRD1 subnetwork | 0.330351057 | 0.960167131 |
| ENSG00000176273 | SLC35G1 subnetwork | 0.330573505 | 0.960491249 |
| ENSG00000115875 | SRSF7 subnetwork | 0.33062605 | 0.960499105 |
| ENSG00000103653 | CSK subnetwork | 0.330902507 | 0.960631955 |
| GO:0050817 | coagulation | 0.330732637 | 0.960636183 |
| ENSG00000181656 | GPR88 subnetwork | 0.330817407 | 0.960653946 |
| ENSG00000196411 | EPHB4 subnetwork | 0.331019061 | 0.960788794 |
| GO:0045028 | G-protein coupled purinergic nucleotide receptor activity | 0.331300375 | 0.961290963 |
| GO:0001608 | G-protein coupled nucleotide receptor activity | 0.331300375 | 0.961481923 |
| ENSG00000115461 | IGFBP5 subnetwork | 0.332067557 | 0.962046401 |
| ENSG00000132664 | POLR3F subnetwork | 0.332000037 | 0.96204879 |
| ENSG00000144118 | RALB subnetwork | 0.331657909 | 0.962142573 |
| GO:0005762 | mitochondrial large ribosomal subunit | 0.331879949 | 0.962152778 |
| ENSG00000133627 | ACTR3B subnetwork | 0.331998046 | 0.962239635 |
| ENSG00000108515 | ENO3 subnetwork | 0.331828376 | 0.962306471 |
| GO:0000315 | organellar large ribosomal subunit | 0.331879949 | 0.962343719 |
| ENSG00000100852 | ARHGAP5 subnetwork | 0.332247699 | 0.962440523 |
| ENSG00000136631 | VPS45 subnetwork | 0.331824151 | 0.962487592 |
| ENSG00000144580 | RQCD1 subnetwork | 0.332321359 | 0.962517344 |
| ENSG00000121068 | TBX2 subnetwork | 0.332475784 | 0.962732858 |
| ENSG00000171421 | MRPL36 subnetwork | 0.332673375 | 0.962814419 |
| ENSG00000104529 | EEF1D subnetwork | 0.332839523 | 0.962848941 |
| ENSG00000120533 | ENY2 subnetwork | 0.332541301 | 0.962849217 |
| ENSG00000069275 | NUCKS1 subnetwork | 0.332633332 | 0.962925911 |
| GO:0000186 | activation of MAPKK activity | 0.332962508 | 0.962955265 |
| ENSG00000013275 | PSMC4 subnetwork | 0.332813519 | 0.962960396 |
| GO:0030133 | transport vesicle | 0.333202865 | 0.96368494 |
| GO:0072215 | regulation of metanephros development | 0.333500048 | 0.964174085 |
| GO:0007051 | spindle organization | 0.333424236 | 0.964196676 |
| ENSG00000196712 | NF1 subnetwork | 0.333583633 | 0.964240506 |
| GO:0006979 | response to oxidative stress | 0.333846336 | 0.964949575 |
| ENSG00000196866 | HIST1H2AD subnetwork | 0.334520949 | 0.965025651 |
| ENSG00000112081 | SRSF3 subnetwork | 0.334560792 | 0.965062142 |
| ENSG00000198374 | HIST1H2AL subnetwork | 0.334520949 | 0.965216104 |
| GO:0035173 | histone kinase activity | 0.33422722 | 0.965382336 |
| ENSG00000196787 | HIST1H2AG subnetwork | 0.334520949 | 0.965406632 |
| GO:0006006 | glucose metabolic process | 0.334908309 | 0.965424798 |
| ENSG00000174227 | PIGG subnetwork | 0.334978713 | 0.965441466 |
| GO:0007599 | hemostasis | 0.334813668 | 0.965450601 |
| ENSG00000183020 | AP2A2 subnetwork | 0.334743945 | 0.965473373 |
| GO:0045197 | establishment or maintenance of epithelial cell apical/ba | 0.334206076 | 0.965503953 |
| ENSG00000177485 | ZBTB33 subnetwork | 0.334884101 | 0.965536278 |
| ENSG00000184348 | HIST1H2AK subnetwork | 0.334520949 | 0.965597236 |
| ENSG00000139343 | SNRPF subnetwork | 0.334165709 | 0.965635501 |
| ENSG00000134216 | CHIA subnetwork | 0.334377389 | 0.965754642 |
| ENSG00000196747 | HIST1H2AI subnetwork | 0.334520949 | 0.965787915 |
| ENSG00000108518 | PFN1 subnetwork | 0.334156979 | 0.965816528 |

| | | | |
|---|---|---|---|
| MP:0002637 | small uterus | 0.335168106 | 0.965871921 |
| GO:0046850 | regulation of bone remodeling | 0.334504117 | 0.965939167 |
| ENSG00000113282 | CLINT1 subnetwork | 0.335342203 | 0.966272656 |
| GO:0055002 | striated muscle cell development | 0.335393779 | 0.966298995 |
| GO:0009651 | response to salt stress | 0.335512468 | 0.9663418 |
| MP:0002424 | abnormal reticulocyte morphology | 0.33548525 | 0.966374557 |
| MP:0008565 | decreased interferon-beta secretion | 0.335652213 | 0.966535433 |
| ENSG00000063176 | SPHK2 subnetwork | 0.335741961 | 0.966660106 |
| ENSG00000183305 | MAGEA2B subnetwork | 0.335942725 | 0.966928979 |
| ENSG00000148719 | DNAJB12 subnetwork | 0.335902323 | 0.967040535 |
| GO:0005689 | U12-type spliceosomal complex | 0.336193336 | 0.967387884 |
| MP:0001729 | impaired embryo implantation | 0.336512115 | 0.967652841 |
| MP:0009655 | abnormal secondary palate development | 0.336578418 | 0.967698506 |
| ENSG00000141380 | SS18 subnetwork | 0.336505548 | 0.967813606 |
| ENSG00000117676 | RPS6KA1 subnetwork | 0.336462028 | 0.967866273 |
| ENSG00000105258 | POLR2I subnetwork | 0.336757517 | 0.967989782 |
| ENSG00000161980 | POLR3K subnetwork | 0.337265194 | 0.968259419 |
| GO:0032768 | regulation of monooxygenase activity | 0.337246449 | 0.968390579 |
| GO:0030833 | regulation of actin filament polymerization | 0.33722661 | 0.968541421 |
| ENSG00000176102 | CSTF3 subnetwork | 0.337165419 | 0.968545062 |
| GO:0030867 | rough endoplasmic reticulum membrane | 0.337444499 | 0.968550128 |
| ENSG00000163939 | PBRM1 subnetwork | 0.337155477 | 0.968725452 |
| MP:0011405 | tubulointerstitial nephritis | 0.33705031 | 0.968752456 |
| GO:0016180 | snRNA processing | 0.337629826 | 0.968840722 |
| ENSG00000197530 | MIB2 subnetwork | 0.337155359 | 0.968915734 |
| GO:0060068 | vagina development | 0.337757731 | 0.968974309 |
| GO:0004143 | diacylglycerol kinase activity | 0.337909369 | 0.969186275 |
| ENSG00000165059 | PRKACG subnetwork | 0.338300011 | 0.969314398 |
| GO:0006700 | C21-steroid hormone biosynthetic process | 0.338124965 | 0.969364955 |
| MP:0000166 | abnormal chondrocyte morphology | 0.338079763 | 0.969388355 |
| ENSG00000164344 | KLKB1 subnetwork | 0.338282107 | 0.969435737 |
| ENSG00000183943 | PRKX subnetwork | 0.338241583 | 0.969498334 |
| GO:0003735 | structural constituent of ribosome | 0.338483961 | 0.969633764 |
| KEGG_HUNTINGTONS_DISEASE | KEGG_HUNTINGTONS_DISEASE | 0.33857154 | 0.969786567 |
| MP:0004532 | abnormal inner hair cell stereociliary bundle morphology | 0.338691375 | 0.969870791 |
| ENSG00000117480 | FAAH subnetwork | 0.338811973 | 0.970121354 |
| GO:0001959 | regulation of cytokine-mediated signaling pathway | 0.33891339 | 0.970215264 |
| ENSG00000160094 | ZNF362 subnetwork | 0.339040856 | 0.970338486 |
| GO:0006607 | NLS-bearing substrate import into nucleus | 0.339251949 | 0.970453657 |
| ENSG00000068323 | TFE3 subnetwork | 0.339115161 | 0.970500782 |
| ENSG00000172977 | KAT5 subnetwork | 0.339206704 | 0.970516331 |
| ENSG00000173567 | GPR113 subnetwork | 0.339758453 | 0.971321087 |
| GO:0055029 | nuclear DNA-directed RNA polymerase complex | 0.339893586 | 0.971371362 |
| MP:0005452 | abnormal adipose tissue amount | 0.339746573 | 0.97146208 |
| MP:0005560 | decreased circulating glucose level | 0.340082788 | 0.97148018 |
| GO:0000428 | DNA-directed RNA polymerase complex | 0.339893586 | 0.971561157 |
| ENSG00000130024 | PHF10 subnetwork | 0.339723165 | 0.971593353 |
| GO:0003887 | DNA-directed DNA polymerase activity | 0.340038373 | 0.971601563 |
| GO:0010951 | negative regulation of endopeptidase activity | 0.340583554 | 0.971729382 |
| MP:0001449 | abnormal learning/ memory | 0.340228761 | 0.971754831 |
| ENSG00000143727 | ACP1 subnetwork | 0.340544221 | 0.971821373 |
| GO:0032039 | integrator complex | 0.341663223 | 0.971827017 |
| MP:0003786 | premature aging | 0.341627788 | 0.97187014 |
| MP:0000233 | abnormal blood flow velocity | 0.341586778 | 0.971874392 |

| | | | |
|---|---|---|---|
| ENSG00000130147 | SH3BP4 subnetwork | 0.340213581 | 0.971905506 |
| ENSG00000118640 | VAMP8 subnetwork | 0.340743042 | 0.971910331 |
| ENSG00000074211 | PPP2R2C subnetwork | 0.340462846 | 0.971917675 |
| MP:0009292 | increased inguinal fat pad weight | 0.340540799 | 0.97200117 |
| ENSG00000100129 | EIF3L subnetwork | 0.341560239 | 0.972024504 |
| GO:0005637 | nuclear inner membrane | 0.340392461 | 0.972053084 |
| ENSG00000135213 | POM121C subnetwork | 0.340447702 | 0.972078049 |
| ENSG00000160741 | CRTC2 subnetwork | 0.341523631 | 0.972135771 |
| ENSG00000105856 | HBP1 subnetwork | 0.341507678 | 0.972208171 |
| ENSG00000100568 | VTI1B subnetwork | 0.341376012 | 0.97236714 |
| MP:0000523 | cortical renal glomerulopathies | 0.341507594 | 0.972397354 |
| MP:0000013 | abnormal adipose tissue distribution | 0.341430928 | 0.972401713 |
| MP:0001395 | bidirectional circling | 0.341369198 | 0.972527259 |
| GO:0032784 | regulation of transcription elongation, DNA-dependent | 0.341350332 | 0.972648491 |
| ENSG00000164220 | F2RL2 subnetwork | 0.341180168 | 0.97266173 |
| ENSG00000159228 | CBR1 subnetwork | 0.342048369 | 0.972697241 |
| ENSG00000159348 | CYB5R1 subnetwork | 0.34134608 | 0.972828204 |
| ENSG00000106400 | ZNHIT1 subnetwork | 0.341176128 | 0.972841551 |
| ENSG00000143437 | ARNT subnetwork | 0.34131554 | 0.972959283 |
| ENSG00000168439 | STIP1 subnetwork | 0.342318868 | 0.973411696 |
| MP:0001606 | impaired hematopoiesis | 0.3425361 | 0.973941336 |
| ENSG00000154143 | PANX3 subnetwork | 0.343526154 | 0.974186677 |
| ENSG00000178177 | LCORL subnetwork | 0.34346445 | 0.97421073 |
| ENSG00000163520 | FBLN2 subnetwork | 0.34341316 | 0.97421542 |
| GO:0016502 | nucleotide receptor activity | 0.343371169 | 0.974278241 |
| ENSG00000132356 | PRKAA1 subnetwork | 0.343668908 | 0.974303136 |
| REACTOME_ABC:FAMILY_PROTEI | REACTOME_ABC:FAMILY_PROTEINS_MEDIATED_TRANSI | 0.343228916 | 0.974311749 |
| MP:0002675 | asthenozoospermia | 0.34364132 | 0.974404647 |
| MP:0000484 | abnormal pulmonary artery morphology | 0.342732119 | 0.974412507 |
| ENSG00000172725 | CORO1B subnetwork | 0.343212432 | 0.97443281 |
| GO:0001614 | purinergic nucleotide receptor activity | 0.343371169 | 0.974467054 |
| GO:0008212 | mineralocorticoid metabolic process | 0.343168869 | 0.974486036 |
| ENSG00000148158 | SNX30 subnetwork | 0.343329177 | 0.97449118 |
| ENSG00000116191 | RALGPS2 subnetwork | 0.342918822 | 0.974597166 |
| MP:0005311 | abnormal circulating amino acid level | 0.343830408 | 0.974627443 |
| ENSG00000120875 | DUSP4 subnetwork | 0.343007913 | 0.974650621 |
| ENSG00000197969 | VPS13A subnetwork | 0.343152691 | 0.974655674 |
| GO:0048041 | focal adhesion assembly | 0.342874348 | 0.97468932 |
| ENSG00000128591 | FLNC subnetwork | 0.343914505 | 0.974690402 |
| GO:0042753 | positive regulation of circadian rhythm | 0.343139201 | 0.974796275 |
| GO:0030128 | clathrin coat of endocytic vesicle | 0.343101365 | 0.974839899 |
| MP:0008872 | abnormal physiological response to xenobiotic | 0.344049619 | 0.975062875 |
| GO:0051785 | positive regulation of nuclear division | 0.344607646 | 0.975178675 |
| GO:0045840 | positive regulation of mitosis | 0.344607646 | 0.975367079 |
| ENSG00000165029 | ABCA1 subnetwork | 0.344805581 | 0.975371693 |
| MP:0005122 | increased circulating thyroid-stimulating hormone level | 0.344534199 | 0.975371981 |
| ENSG00000197635 | DPP4 subnetwork | 0.344719488 | 0.975395906 |
| GO:0010510 | regulation of acetyl-CoA biosynthetic process from pyruv | 0.345114315 | 0.975424383 |
| ENSG00000206274 | ENSG00000206274 subnetwork | 0.344325723 | 0.975439954 |
| GO:0004175 | endopeptidase activity | 0.34452145 | 0.975541167 |
| ENSG00000179364 | PACS2 subnetwork | 0.345204584 | 0.97557377 |
| GO:0006086 | acetyl-CoA biosynthetic process from pyruvate | 0.345114315 | 0.97561258 |
| GO:0005525 | GTP binding | 0.344476851 | 0.975613764 |
| ENSG00000206383 | HSPA1L subnetwork | 0.344325723 | 0.975628627 |

| | | | |
|---|---|---|---|
| GO:0060056 | mammary gland involution | 0.345070175 | 0.975656117 |
| GO:0032414 | positive regulation of ion transmembrane transporter ac | 0.344945802 | 0.975694981 |
| ENSG00000198625 | MDM4 subnetwork | 0.345018635 | 0.975709323 |
| ENSG00000132139 | GAS2L2 subnetwork | 0.344470023 | 0.975783063 |
| ENSG00000134852 | CLOCK subnetwork | 0.345449626 | 0.975882013 |
| ENSG00000188021 | UBQLN2 subnetwork | 0.345409835 | 0.975964134 |
| MP:0005006 | abnormal osteoblast physiology | 0.34670586 | 0.976888334 |
| GO:0045182 | translation regulator activity | 0.346686973 | 0.977018454 |
| ENSG00000172850 | LSM2 subnetwork | 0.346187561 | 0.977103794 |
| ENSG00000109133 | TMEM33 subnetwork | 0.346673887 | 0.977196693 |
| ENSG00000011007 | TCEB3 subnetwork | 0.346283457 | 0.977204467 |
| ENSG00000111987 | ENSG00000111987 subnetwork | 0.346187561 | 0.977291988 |
| ENSG00000090615 | GOLGA3 subnetwork | 0.346917485 | 0.977315527 |
| GO:0030971 | receptor tyrosine kinase binding | 0.346649123 | 0.977346154 |
| ENSG00000125170 | DOK4 subnetwork | 0.346997774 | 0.977358309 |
| MP:0005418 | abnormal circulating hormone level | 0.346402744 | 0.977410972 |
| ENSG00000204392 | LSM2 subnetwork | 0.346187561 | 0.977480254 |
| GO:0043470 | regulation of carbohydrate catabolic process | 0.346647787 | 0.977534141 |
| ENSG00000167258 | CDK12 subnetwork | 0.346046504 | 0.977534695 |
| GO:0046889 | positive regulation of lipid biosynthetic process | 0.346591086 | 0.977650568 |
| GO:0030168 | platelet activation | 0.346185425 | 0.97765896 |
| GO:0004437 | inositol or phosphatidylinositol phosphatase activity | 0.346146981 | 0.977673926 |
| GO:0043471 | regulation of cellular carbohydrate catabolic process | 0.346647787 | 0.977722201 |
| ENSG00000072958 | AP1M1 subnetwork | 0.34656548 | 0.97776174 |
| ENSG00000163430 | FSTL1 subnetwork | 0.347269864 | 0.978044564 |
| MP:0000288 | abnormal pericardium morphology | 0.347482076 | 0.978452084 |
| REACTOME_CELL_SURFACE_INTE | REACTOME_CELL_SURFACE_INTERACTIONS_AT_THE_VA | 0.347748723 | 0.978738721 |
| GO:0060669 | embryonic placenta morphogenesis | 0.347730791 | 0.978888249 |
| MP:0011095 | complete embryonic lethality between implantation and | 0.348129315 | 0.979138692 |
| ENSG00000088179 | PTPN4 subnetwork | 0.348086985 | 0.979230622 |
| GO:0019229 | regulation of vasoconstriction | 0.348034791 | 0.979274611 |
| GO:0009755 | hormone-mediated signaling pathway | 0.347990637 | 0.979299424 |
| ENSG00000211614 | ENSG00000211614 subnetwork | 0.348798501 | 0.979429228 |
| ENSG00000091428 | RAPGEF4 subnetwork | 0.348292815 | 0.97943038 |
| ENSG00000132589 | FLOT2 subnetwork | 0.348842188 | 0.979433167 |
| MP:0011094 | complete embryonic lethality before implantation | 0.34873171 | 0.979444444 |
| ENSG00000101331 | C20orf160 subnetwork | 0.348618802 | 0.97945573 |
| REACTOME_SHC1_EVENTS_IN_ER | REACTOME_SHC1_EVENTS_IN_ERBB4_SIGNALING | 0.348674432 | 0.979459667 |
| ENSG00000087008 | ACOX3 subnetwork | 0.348606538 | 0.979595553 |
| ENSG00000196776 | CD47 subnetwork | 0.348976632 | 0.979628566 |
| GO:0006639 | acylglycerol metabolic process | 0.348559214 | 0.979677914 |
| ENSG00000169813 | HNRNPF subnetwork | 0.348531518 | 0.979798658 |
| ENSG00000143368 | SF3B4 subnetwork | 0.349189738 | 0.979967458 |
| GO:0032986 | protein-DNA complex disassembly | 0.349391531 | 0.980112875 |
| GO:0006337 | nucleosome disassembly | 0.349391531 | 0.980300421 |
| ENSG00000075413 | MARK3 subnetwork | 0.349572288 | 0.98036534 |
| ENSG00000125743 | SNRPD2 subnetwork | 0.349693277 | 0.98040153 |
| GO:0031498 | chromatin disassembly | 0.349391531 | 0.980488038 |
| GO:0070717 | poly-purine tract binding | 0.349800711 | 0.980529535 |
| MP:0001675 | abnormal ectoderm development | 0.349680287 | 0.98053165 |
| ENSG00000135903 | PAX3 subnetwork | 0.350001967 | 0.980925076 |
| ENSG00000092199 | HNRNPC subnetwork | 0.350499376 | 0.982336645 |
| GO:0030658 | transport vesicle membrane | 0.350602282 | 0.982445081 |
| ENSG00000183023 | SLC8A1 subnetwork | 0.350491937 | 0.982486146 |

| | | | |
|---|---|---|---|
| ENSG00000158792 | SPATA2L subnetwork | 0.350760923 | 0.982677617 |
| ENSG00000154188 | ANGPT1 subnetwork | 0.350936824 | 0.983091465 |
| ENSG00000124155 | PIGT subnetwork | 0.351235802 | 0.983361954 |
| ENSG00000108465 | CDK5RAP3 subnetwork | 0.351293777 | 0.983384205 |
| ENSG00000132669 | RIN2 subnetwork | 0.351208915 | 0.983435115 |
| ENSG00000160967 | ENSG00000160967 subnetwork | 0.351075266 | 0.983466972 |
| GO:0030880 | RNA polymerase complex | 0.351178168 | 0.983556022 |
| ENSG00000163083 | INHBB subnetwork | 0.351710461 | 0.984197978 |
| ENSG00000148082 | SHC3 subnetwork | 0.351925487 | 0.984658658 |
| ENSG00000106804 | C5 subnetwork | 0.352006358 | 0.984709247 |
| ENSG00000105327 | BBC3 subnetwork | 0.35209635 | 0.984807472 |
| MP:0001723 | disorganized yolk sac vascular plexus | 0.352227476 | 0.984899009 |
| MP:0004779 | abnormal production of surfactant | 0.352206092 | 0.985000953 |
| GO:0002688 | regulation of leukocyte chemotaxis | 0.352398674 | 0.985101924 |
| MP:0005182 | increased circulating estradiol level | 0.35300371 | 0.986048725 |
| ENSG00000123612 | ACVR1C subnetwork | 0.352999129 | 0.986226918 |
| ENSG00000167088 | SNRPD1 subnetwork | 0.352951149 | 0.986243336 |
| REACTOME_TRAF6_MEDIATED_IF | REACTOME_TRAF6_MEDIATED_IRF7_ACTIVATION | 0.352888163 | 0.986250238 |
| ENSG00000104320 | NBN subnetwork | 0.352881858 | 0.986438095 |
| ENSG00000134184 | GSTM1 subnetwork | 0.35329653 | 0.986510654 |
| GO:0060402 | calcium ion transport into cytosol | 0.353355624 | 0.98651322 |
| ENSG00000095637 | SORBS1 subnetwork | 0.353437051 | 0.986515785 |
| GO:0008408 | 3'-5' exonuclease activity | 0.353564709 | 0.986584902 |
| ENSG00000113595 | TRIM23 subnetwork | 0.353290028 | 0.986679353 |
| MP:0000239 | absent common myeloid progenitor cells | 0.354231463 | 0.98781832 |
| GO:0070330 | aromatase activity | 0.354436899 | 0.987901235 |
| ENSG00000087365 | SF3B2 subnetwork | 0.354182422 | 0.98790154 |
| ENSG00000112742 | TTK subnetwork | 0.354342028 | 0.987963139 |
| GO:0001741 | XY body | 0.354405437 | 0.987965426 |
| MP:0002467 | impaired neutrophil phagocytosis | 0.354167531 | 0.988060837 |
| GO:0042634 | regulation of hair cycle | 0.354563158 | 0.988159894 |
| MP:0001762 | polyuria | 0.354632448 | 0.9882191 |
| MP:0004057 | thin myocardium compact layer | 0.354729366 | 0.988287775 |
| ENSG00000164086 | DUSP7 subnetwork | 0.355113548 | 0.988994307 |
| KEGG_REGULATION_OF_ACTIN_C | KEGG_REGULATION_OF_ACTIN_CYTOSKELETON | 0.355102791 | 0.989163029 |
| ENSG00000153989 | NUS1 subnetwork | 0.355644504 | 0.989727066 |
| REACTOME_FACILITATIVE_NA:INI | REACTOME_FACILITATIVE_NA:INDEPENDENT_GLUCOSE_ | 0.35532824 | 0.989755265 |
| ENSG00000197561 | ELANE subnetwork | 0.355562351 | 0.989817975 |
| ENSG00000135074 | ADAM19 subnetwork | 0.355631213 | 0.989886256 |
| MP:0005039 | hypoxia | 0.355525537 | 0.989929831 |
| GO:0048286 | lung alveolus development | 0.355467204 | 0.990003794 |
| MP:0002796 | impaired skin barrier function | 0.355860971 | 0.990212242 |
| ENSG00000110244 | APOA4 subnetwork | 0.35647742 | 0.990876396 |
| GO:0070076 | histone lysine demethylation | 0.356677459 | 0.990921127 |
| ENSG00000189369 | GSPT2 subnetwork | 0.356451473 | 0.99096933 |
| GO:0001046 | core promoter sequence-specific DNA binding | 0.3563857 | 0.990977088 |
| MP:0005266 | abnormal metabolism | 0.356218676 | 0.991019326 |
| GO:0030010 | establishment of cell polarity | 0.356657405 | 0.991042376 |
| MP:0006317 | decreased urine sodium level | 0.356621969 | 0.991059603 |
| ENSG00000197756 | RPL37A subnetwork | 0.357126365 | 0.991082562 |
| MP:0002703 | abnormal renal tubule morphology | 0.356366474 | 0.991126894 |
| GO:0020037 | heme binding | 0.35660813 | 0.991228236 |
| GO:0016863 | intramolecular oxidoreductase activity, transposing C=C | 0.356964408 | 0.991257089 |
| MP:0002160 | abnormal reproductive system morphology | 0.357121689 | 0.991260393 |

| | | | |
|---|---|---|---|
| GO:0014909 | smooth muscle cell migration | 0.357067427 | 0.991305991 |
| ENSG00000166986 | MARS subnetwork | 0.356362075 | 0.991314643 |
| MP:0004924 | abnormal behavior | 0.357266419 | 0.991329807 |
| ENSG00000116353 | MECR subnetwork | 0.357345359 | 0.991378659 |
| ENSG00000104497 | SNX16 subnetwork | 0.3568936 | 0.991386157 |
| ENSG00000146674 | IGFBP3 subnetwork | 0.356964401 | 0.991444507 |
| GO:0004532 | exoribonuclease activity | 0.357547558 | 0.991459041 |
| ENSG00000074696 | PTPLAD1 subnetwork | 0.357511834 | 0.991504625 |
| GO:0060761 | negative regulation of response to cytokine stimulus | 0.357454108 | 0.991521903 |
| MP:0001633 | poor circulation | 0.357733644 | 0.991556604 |
| ENSG00000165934 | CPSF2 subnetwork | 0.357708971 | 0.991658804 |
| MP:0002073 | abnormal hair growth | 0.357984758 | 0.992105263 |
| ENSG00000113356 | POLR3G subnetwork | 0.358378722 | 0.99270362 |
| ENSG00000083642 | PDS5B subnetwork | 0.358361648 | 0.992805959 |
| GO:0005159 | insulin-like growth factor receptor binding | 0.358341531 | 0.992917767 |
| ENSG00000100028 | SNRPD3 subnetwork | 0.358588604 | 0.993213949 |
| ENSG00000008300 | CELSR3 subnetwork | 0.358958282 | 0.993258004 |
| MP:0001183 | overexpanded pulmonary alveoli | 0.358672377 | 0.993281191 |
| MP:0003172 | abnormal lysosome physiology | 0.359103457 | 0.993298193 |
| GO:0051053 | negative regulation of DNA metabolic process | 0.3590521 | 0.993362832 |
| MP:0000091 | short premaxilla | 0.359761423 | 0.993394099 |
| MP:0001346 | abnormal lacrimal gland morphology | 0.358952986 | 0.993445093 |
| ENSG00000159352 | PSMD4 subnetwork | 0.358833522 | 0.993499152 |
| GO:0030041 | actin filament polymerization | 0.35974745 | 0.993533835 |
| ENSG00000184489 | PTP4A3 subnetwork | 0.360010011 | 0.993546872 |
| REACTOME_MEIOSIS | REACTOME_MEIOSIS | 0.358914238 | 0.993547476 |
| ENSG00000085063 | CD59 subnetwork | 0.360131536 | 0.993577465 |
| ENSG00000117395 | EBNA1BP2 subnetwork | 0.359704778 | 0.993617221 |
| ENSG00000187446 | ENSG00000187446 subnetwork | 0.359953257 | 0.993639609 |
| GO:0032677 | regulation of interleukin-8 production | 0.359561726 | 0.993643032 |
| ENSG00000132383 | RPA1 subnetwork | 0.359367613 | 0.993658261 |
| ENSG00000105726 | ATP13A1 subnetwork | 0.35966611 | 0.993710041 |
| ENSG00000147202 | DIAPH2 subnetwork | 0.359324755 | 0.993732355 |
| GO:0004693 | cyclin-dependent protein kinase activity | 0.360126299 | 0.993735913 |
| ENSG00000134070 | IRAK2 subnetwork | 0.359558675 | 0.993820542 |
| ENSG00000089234 | BRAP subnetwork | 0.359507621 | 0.993838194 |
| GO:0005881 | cytoplasmic microtubule | 0.36027498 | 0.993879084 |
| ENSG00000185721 | DRG1 subnetwork | 0.36048324 | 0.99413476 |
| GO:0031098 | stress-activated protein kinase signaling cascade | 0.36054298 | 0.994182774 |
| KEGG_BASE_EXCISION_REPAIR | KEGG_BASE_EXCISION_REPAIR | 0.360448185 | 0.994218134 |
| ENSG00000136715 | SAP130 subnetwork | 0.360691289 | 0.994502814 |
| GO:0032092 | positive regulation of protein binding | 0.361025934 | 0.994582943 |
| ENSG00000123064 | DDX54 subnetwork | 0.360927222 | 0.994693418 |
| ENSG00000127481 | UBR4 subnetwork | 0.360899621 | 0.994748687 |
| GO:0031965 | nuclear membrane | 0.36101084 | 0.99476003 |
| ENSG00000162129 | CLPB subnetwork | 0.360877368 | 0.994841493 |
| GO:0031435 | mitogen-activated protein kinase kinase kinase binding | 0.361184735 | 0.994883808 |
| ENSG00000181852 | RNF41 subnetwork | 0.361453025 | 0.995428143 |
| MP:0009264 | failure of eyelid fusion | 0.362147778 | 0.996397155 |
| ENSG00000111596 | CNOT2 subnetwork | 0.362126741 | 0.996499438 |
| ENSG00000085274 | MYNN subnetwork | 0.362246232 | 0.996500749 |
| GO:0070192 | chromosome organization involved in meiosis | 0.362362144 | 0.996538821 |
| MP:0000427 | abnormal hair cycle | 0.362094691 | 0.996629845 |
| ENSG00000206385 | ENSG00000206385 subnetwork | 0.362086088 | 0.996779026 |

| | | | |
|---|---|---|---|
| ENSG00000137337 | MDC1 subnetwork | 0.362086088 | 0.996965724 |
| ENSG00000163950 | SLBP subnetwork | 0.362037573 | 0.996983889 |
| MP:0003157 | impaired muscle relaxation | 0.362793979 | 0.997149 |
| GO:0006325 | chromatin organization | 0.362754907 | 0.997176515 |
| GO:0045987 | positive regulation of smooth muscle contraction | 0.362710483 | 0.997288199 |
| GO:0006662 | glycerol ether metabolic process | 0.362687567 | 0.99738122 |
| GO:0070988 | demethylation | 0.363121723 | 0.997533632 |
| ENSG00000037241 | RPL26L1 subnetwork | 0.363006596 | 0.997542056 |
| ENSG00000185024 | BRF1 subnetwork | 0.363077896 | 0.997607924 |
| GO:0004252 | serine-type endopeptidase activity | 0.363364862 | 0.997703081 |
| MP:0002599 | increased mean platelet volume | 0.36324389 | 0.997720904 |
| ENSG00000120549 | KIAA1217 subnetwork | 0.363422727 | 0.997750187 |
| GO:0051017 | actin filament bundle assembly | 0.363354373 | 0.997833396 |
| ENSG00000134398 | ERN2 subnetwork | 0.363548033 | 0.998030614 |
| GO:0001935 | endothelial cell proliferation | 0.364098797 | 0.999197611 |
| GO:0043405 | regulation of MAP kinase activity | 0.364355655 | 0.999300634 |
| ENSG00000165119 | HNRNPK subnetwork | 0.364229956 | 0.99931903 |
| ENSG00000100462 | PRMT5 subnetwork | 0.364314552 | 0.999356463 |
| ENSG00000125753 | VASP subnetwork | 0.36409622 | 0.999374767 |
| REACTOME_SYNTHESIS_OF_SUBS | REACTOME_SYNTHESIS_OF_SUBSTRATES_IN_N:GLYCAN | 0.364941629 | 0.999748557 |
| ENSG00000104915 | STX10 subnetwork | 0.364748137 | 0.999916123 |
| GO:0032872 | regulation of stress-activated MAPK cascade | 0.364937586 | 0.999925484 |
| ENSG00000140264 | SERF2 subnetwork | 0.364713815 | 0.999953393 |
| ENSG00000180176 | TH subnetwork | 0.364673816 | 0.999981354 |
| MP:0005599 | increased cardiac muscle contractility | 0.365285068 | 1 |
| GO:0031280 | negative regulation of cyclase activity | 1 | 1 |
| MP:0009764 | decreased sensitivity to induced morbidity/mortality | 0.365344124 | 1.000027917 |
| ENSG00000197003 | ENSG00000197003 subnetwork | 0.364916645 | 1.000065213 |
| GO:0007194 | negative regulation of adenylate cyclase activity | 1 | 1.000069152 |
| ENSG00000184708 | EIF4ENIF1 subnetwork | 0.365256939 | 1.00012102 |
| GO:0051350 | negative regulation of lyase activity | 1 | 1.000138313 |
| REACTOME_INTEGRIN_ALPHAIIB_ | REACTOME_INTEGRIN_ALPHAIIB_BETA3_SIGNALING | 0.365181294 | 1.000148976 |
| REACTOME_ADHERENS_JUNCTIO | REACTOME_ADHERENS_JUNCTIONS_INTERACTIONS | 0.999999998 | 1.000207483 |
| ENSG00000197369 | ENSG00000197369 subnetwork | 0.364916645 | 1.000251584 |
| GO:0021953 | central nervous system neuron differentiation | 0.999999996 | 1.000276663 |
| GO:0043092 | L-amino acid import | 0.999999996 | 1.000345853 |
| GO:0007193 | adenylate cyclase-inhibiting G-protein coupled receptor | 0.999999993 | 1.000415053 |
| GO:0051960 | regulation of nervous system development | 0.999999992 | 1.000484262 |
| GO:0030815 | negative regulation of cAMP metabolic process | 0.999999992 | 1.00055348 |
| GO:0030818 | negative regulation of cAMP biosynthetic process | 0.999999992 | 1.000622708 |
| MP:0003484 | abnormal channel response | 0.999999989 | 1.000691946 |
| ENSG00000198954 | KIAA1279 subnetwork | 0.365650307 | 1.000725716 |
| GO:0042471 | ear morphogenesis | 0.999999985 | 1.000761193 |
| GO:0030803 | negative regulation of cyclic nucleotide biosynthetic pro | 0.999999983 | 1.00083045 |
| GO:0030809 | negative regulation of nucleotide biosynthetic process | 0.999999983 | 1.000899716 |
| MP:0006144 | increased systemic arterial systolic blood pressure | 0.365791302 | 1.000911628 |
| GO:0030800 | negative regulation of cyclic nucleotide metabolic proces | 0.999999983 | 1.000968992 |
| GO:0045980 | negative regulation of nucleotide metabolic process | 0.999999981 | 1.001038278 |
| GO:0008343 | adult feeding behavior | 0.999999975 | 1.001107573 |
| MP:0008536 | enlarged third ventricle | 0.999999972 | 1.001176878 |
| GO:0050767 | regulation of neurogenesis | 0.999999958 | 1.001246192 |
| GO:0021510 | spinal cord development | 0.999999953 | 1.001315516 |
| GO:0045664 | regulation of neuron differentiation | 0.999999949 | 1.00138485 |
| MP:0009293 | decreased inguinal fat pad weight | 0.366042744 | 1.001432292 |

| | | | |
|---|---|---|---|
| ENSG00000151835 | SACS subnetwork | 0.366097895 | 1.001441324 |
| GO:0032281 | alpha-amino-3-hydroxy-5-methyl-4-isoxazolepropionic a | 0.999999925 | 1.001454193 |
| GO:0021517 | ventral spinal cord development | 0.999999888 | 1.001523546 |
| GO:0045686 | negative regulation of glial cell differentiation | 0.999999879 | 1.001592908 |
| GO:0004497 | monooxygenase activity | 0.3663168 | 1.001608106 |
| MP:0004753 | abnormal miniature excitatory postsynaptic currents | 0.999999858 | 1.00166228 |
| MP:0006060 | increased cerebral infarction size | 0.366279805 | 1.001710673 |
| GO:0030534 | adult behavior | 0.999999854 | 1.001728198 |
| GO:0006817 | phosphate ion transport | 0.99999985 | 1.001797589 |
| GO:0043090 | amino acid import | 0.999999821 | 1.00186699 |
| GO:0032279 | asymmetric synapse | 0.999999814 | 1.0019364 |
| GO:0072079 | nephron tubule formation | 0.999999794 | 1.00200582 |
| MP:0002882 | abnormal neuron morphology | 0.999999759 | 1.002075249 |
| REACTOME_NEUROTRANSMITTEF | REACTOME_NEUROTRANSMITTER_RELEASE_CYCLE | 0.999999731 | 1.002144689 |
| GO:0006814 | sodium ion transport | 0.999999724 | 1.002214137 |
| GO:0014014 | negative regulation of gliogenesis | 0.999999712 | 1.002283596 |
| GO:0014013 | regulation of gliogenesis | 0.999999683 | 1.002349598 |
| GO:0021954 | central nervous system neuron development | 0.999999674 | 1.002419075 |
| GO:0045599 | negative regulation of fat cell differentiation | 0.366867911 | 1.002452164 |
| GO:0042472 | inner ear morphogenesis | 0.999999658 | 1.002488562 |
| ENSG00000131437 | KIF3A subnetwork | 0.366957009 | 1.002516716 |
| GO:0033013 | tetrapyrrole metabolic process | 0.366820142 | 1.002517651 |
| REACTOME_TRANSMISSION_ACR | REACTOME_TRANSMISSION_ACROSS_CHEMICAL_SYNAF | 0.999999656 | 1.002558059 |
| GO:0050885 | neuromuscular process controlling balance | 0.999999499 | 1.002627565 |
| GO:0021846 | cell proliferation in forebrain | 0.999999496 | 1.002697081 |
| GO:0006778 | porphyrin-containing compound metabolic process | 0.366820142 | 1.002703958 |
| GO:0034332 | adherens junction organization | 0.999999457 | 1.002766607 |
| GO:0003309 | type B pancreatic cell differentiation | 0.366789006 | 1.002788104 |
| GO:0007420 | brain development | 0.999999445 | 1.002836142 |
| ENSG00000145191 | EIF2B5 subnetwork | 0.367344218 | 1.002848924 |
| ENSG00000077782 | FGFR1 subnetwork | 0.367115009 | 1.002869081 |
| MP:0006074 | abnormal retinal rod bipolar cell morphology | 0.999999397 | 1.002902219 |
| GO:0015672 | monovalent inorganic cation transport | 0.999999386 | 1.002971773 |
| MP:0008014 | increased lung tumor incidence | 0.367331956 | 1.003035084 |
| GO:0007605 | sensory perception of sound | 0.999999296 | 1.003041337 |
| MP:0003461 | abnormal response to novel object | 0.999999257 | 1.003110911 |
| ENSG00000171942 | OR10H2 subnetwork | 0.367552331 | 1.00312616 |
| MP:0003312 | abnormal locomotor coordination | 0.367823164 | 1.003161506 |
| ENSG00000168497 | SDPR subnetwork | 0.36751101 | 1.00317313 |
| ENSG00000113739 | STC2 subnetwork | 0.999999174 | 1.003180494 |
| ENSG00000173540 | GMPPB subnetwork | 0.367303523 | 1.003193465 |
| MP:0008547 | abnormal neocortex morphology | 0.999999066 | 1.003250087 |
| ENSG00000118705 | RPN2 subnetwork | 0.367814271 | 1.00331046 |
| GO:0035249 | synaptic transmission, glutamatergic | 0.999999008 | 1.00331622 |
| ENSG00000137843 | PAK6 subnetwork | 0.367711222 | 1.003320349 |
| GO:0072078 | nephron tubule morphogenesis | 0.999998938 | 1.003382363 |
| ENSG00000075340 | ADD2 subnetwork | 0.367979698 | 1.003411198 |
| MP:0004100 | abnormal spinal cord interneuron morphology | 0.99999891 | 1.003451984 |
| GO:0043025 | neuronal cell body | 0.999998658 | 1.003518146 |
| GO:0043406 | positive regulation of MAP kinase activity | 0.368168548 | 1.003557532 |
| GO:0007156 | homophilic cell adhesion | 0.999998642 | 1.003587786 |
| ENSG00000180855 | ZNF443 subnetwork | 0.368078726 | 1.00360519 |
| GO:0048741 | skeletal muscle fiber development | 0.36825099 | 1.003630974 |
| GO:0003229 | ventricular cardiac muscle tissue development | 0.999998566 | 1.003657436 |

| | | | |
|---|---|---|---|
| GO:0061384 | heart trabecula morphogenesis | 0.368146255 | 1.003669385 |
| GO:0021515 | cell differentiation in spinal cord | 0.999998498 | 1.003727096 |
| MP:0000467 | abnormal esophagus morphology | 0.999998461 | 1.003796765 |
| GO:0030425 | dendrite | 0.999998391 | 1.003866445 |
| GO:0007270 | neuron-neuron synaptic transmission | 0.999998263 | 1.003936133 |
| GO:0044297 | cell body | 0.99999823 | 1.004005832 |
| GO:0090103 | cochlea morphogenesis | 0.999998182 | 1.00407554 |
| MP:0005272 | abnormal temporal bone morphology | 0.999997934 | 1.004145258 |
| MP:0001363 | increased anxiety-related response | 0.999997844 | 1.004214985 |
| GO:0060174 | limb bud formation | 0.999997738 | 1.004284722 |
| GO:0003208 | cardiac ventricle morphogenesis | 0.999997732 | 1.004354469 |
| ENSG00000198898 | CAPZA2 subnetwork | 0.36860529 | 1.004361111 |
| GO:0048839 | inner ear development | 0.999997731 | 1.004424226 |
| GO:0043112 | receptor metabolic process | 0.368584807 | 1.00446379 |
| GO:0007269 | neurotransmitter secretion | 0.999997687 | 1.004493992 |
| ENSG00000198929 | NOS1AP subnetwork | 0.999997147 | 1.004556821 |
| MP:0001488 | increased startle reflex | 0.999996378 | 1.004616186 |
| REACTOME_SEROTONIN_NEUROT | REACTOME_SEROTONIN_NEUROTRANSMITTER_RELEASI | 0.999995819 | 1.004679033 |
| REACTOME_DOPAMINE_NEUROT | REACTOME_DOPAMINE_NEUROTRANSMITTER_RELEASE | 0.999995819 | 1.004748836 |
| GO:0015077 | monovalent inorganic cation transmembrane transporte | 0.99999529 | 1.004818649 |
| GO:0030900 | forebrain development | 0.999995095 | 1.004888472 |
| GO:0002052 | positive regulation of neuroblast proliferation | 0.999994984 | 1.004958304 |
| GO:0043583 | ear development | 0.999994426 | 1.005024672 |
| GO:0007212 | dopamine receptor signaling pathway | 0.999994257 | 1.005094523 |
| GO:0030672 | synaptic vesicle membrane | 0.999994088 | 1.005164385 |
| GO:0051952 | regulation of amine transport | 0.999993834 | 1.005234256 |
| MP:0002805 | abnormal conditioned taste aversion behavior | 0.999993568 | 1.005293709 |
| GO:0050905 | neuromuscular process | 0.999993533 | 1.005363598 |
| GO:0072175 | epithelial tube formation | 0.999993301 | 1.005433498 |
| GO:0051101 | regulation of DNA binding | 0.369039851 | 1.005489724 |
| ENSG00000155363 | MOV10 subnetwork | 0.999993106 | 1.00549993 |
| GO:0097060 | synaptic membrane | 0.999992694 | 1.005562895 |
| GO:0007618 | mating | 0.999992564 | 1.005632823 |
| MP:0005270 | abnormal zygomatic bone morphology | 0.999992184 | 1.005702761 |
| ENSG00000152601 | MBNL1 subnetwork | 0.999991255 | 1.005758798 |
| REACTOME_NEURONAL_SYSTEM | REACTOME_NEURONAL_SYSTEM | 0.999991173 | 1.005828754 |
| ENSG00000086589 | RBM22 subnetwork | 0.369248191 | 1.005858941 |
| MP:0002945 | abnormal inhibitory postsynaptic currents | 0.999990784 | 1.00589872 |
| MP:0009747 | impaired behavioral response to xenobiotic | 0.999990727 | 1.005965217 |
| GO:0050954 | sensory perception of mechanical stimulus | 0.999990634 | 1.006035202 |
| GO:0021781 | glial cell fate commitment | 0.999990324 | 1.006101718 |
| ENSG00000012660 | ELOVL5 subnetwork | 0.999989935 | 1.006171723 |
| MP:0005106 | abnormal incus morphology | 0.999989018 | 1.006238258 |
| GO:0044319 | wound healing, spreading of cells | 0.999988871 | 1.006308281 |
| ENSG00000003393 | ALS2 subnetwork | 0.369536401 | 1.006366833 |
| GO:0001505 | regulation of neurotransmitter levels | 0.999988582 | 1.006378314 |
| GO:0055010 | ventricular cardiac muscle tissue morphogenesis | 0.999988097 | 1.006448357 |
| ENSG00000137709 | POU2F3 subnetwork | 0.369711539 | 1.006456984 |
| MP:0004725 | decreased platelet serotonin level | 0.369654936 | 1.006476684 |
| GO:0035313 | wound healing, spreading of epidermal cells | 0.999988044 | 1.00651493 |
| MP:0002272 | abnormal nervous system electrophysiology | 0.999987695 | 1.006584992 |
| MP:0003235 | abnormal alisphenoid bone morphology | 0.999987355 | 1.006651584 |
| MP:0000937 | abnormal motor neuron morphology | 0.999986951 | 1.006718184 |
| GO:0060560 | developmental growth involved in morphogenesis | 0.999986937 | 1.006788275 |

| | | | |
|---|---|---|---|
| GO:0001838 | embryonic epithelial tube formation | 0.999986554 | 1.006858376 |
| GO:0016358 | dendrite development | 0.999986461 | 1.006928487 |
| ENSG00000157193 | LRP8 subnetwork | 0.999986365 | 1.006998607 |
| GO:0006750 | glutathione biosynthetic process | 0.999985573 | 1.007058291 |
| GO:0007416 | synapse assembly | 0.999985292 | 1.00712843 |
| GO:0010975 | regulation of neuron projection development | 0.999984969 | 1.007198579 |
| GO:0015800 | acidic amino acid transport | 0.999984953 | 1.007268738 |
| GO:0045211 | postsynaptic membrane | 0.999984721 | 1.00733194 |
| GO:0005925 | focal adhesion | 0.370148007 | 1.007340976 |
| ENSG00000124217 | MOCS3 subnetwork | 0.370028956 | 1.00736219 |
| ENSG00000067715 | SYT1 subnetwork | 0.999984616 | 1.007402118 |
| REACTOME_NOREPINEPHRINE_N | REACTOME_NOREPINEPHRINE_NEUROTRANSMITTER_RI | 0.999984314 | 1.007468822 |
| GO:0006939 | smooth muscle contraction | 0.370518693 | 1.007491225 |
| MP:0001152 | Leydig cell hyperplasia | 0.370147335 | 1.007527279 |
| ENSG00000106638 | TBL2 subnetwork | 0.999984149 | 1.007535535 |
| MP:0011348 | abnormal renal glomerulus basement membrane morph | 0.370290907 | 1.007579959 |
| GO:0022890 | inorganic cation transmembrane transporter activity | 0.999983649 | 1.007602258 |
| MP:0004132 | absent embryonic cilia | 0.370513455 | 1.007668145 |
| GO:0042490 | mechanoreceptor differentiation | 0.999983636 | 1.007672474 |
| MP:0009712 | impaired conditioned place preference behavior | 0.999983106 | 1.0077427 |
| GO:0034067 | protein localization in Golgi apparatus | 0.370485668 | 1.007798928 |
| GO:0006836 | neurotransmitter transport | 0.999983027 | 1.007812936 |
| GO:0007339 | binding of sperm to zona pellucida | 0.370450841 | 1.00784658 |
| GO:0015813 | L-glutamate transport | 0.999983004 | 1.007883181 |
| GO:0050884 | neuromuscular process controlling posture | 0.999982836 | 1.007953436 |
| ENSG00000144596 | ENSG00000144596 subnetwork | 0.999981678 | 1.008023702 |
| GO:0007218 | neuropeptide signaling pathway | 0.999981219 | 1.008090491 |
| ENSG00000158169 | FANCC subnetwork | 0.999980911 | 1.008153803 |
| ENSG00000173113 | TRMT112 subnetwork | 0.370798193 | 1.008154784 |
| GO:0015812 | gamma-aminobutyric acid transport | 0.999979364 | 1.008213638 |
| GO:0015837 | amine transport | 0.999979237 | 1.008283941 |
| GO:0001764 | neuron migration | 0.999978688 | 1.008354254 |
| ENSG00000089041 | P2RX7 subnetwork | 0.370961047 | 1.008411819 |
| MP:0005132 | decreased luteinizing hormone level | 0.999978163 | 1.008424576 |
| GO:0021872 | forebrain generation of neurons | 0.999975581 | 1.00848096 |
| GO:0010092 | specification of organ identity | 0.999975401 | 1.008551301 |
| MP:0003056 | abnormal hyoid bone morphology | 0.999974936 | 1.008621652 |
| GO:2000677 | regulation of transcription regulatory region DNA bindin | 0.999974539 | 1.008688525 |
| GO:0043094 | cellular metabolic compound salvage | 0.999973663 | 1.008751919 |
| GO:0021889 | olfactory bulb interneuron differentiation | 0.999972821 | 1.008822298 |
| MP:0000458 | abnormal mandible morphology | 0.99997282 | 1.008892688 |
| GO:0060284 | regulation of cell development | 0.999971885 | 1.008959598 |
| MP:0000851 | cerebellum hypoplasia | 0.999970951 | 1.009019539 |
| GO:0045761 | regulation of adenylate cyclase activity | 0.999970147 | 1.009086468 |
| GO:0014048 | regulation of glutamate secretion | 0.999967897 | 1.009153406 |
| GO:0021522 | spinal cord motor neuron differentiation | 0.999967834 | 1.009223843 |
| GO:0006695 | cholesterol biosynthetic process | 0.371334523 | 1.009268833 |
| GO:0032480 | negative regulation of type I interferon production | 0.371462665 | 1.009283869 |
| MP:0005107 | abnormal stapes morphology | 0.999967455 | 1.0092908 |
| GO:0043202 | lysosomal lumen | 0.371403876 | 1.009322503 |
| ENSG00000065268 | WDR18 subnetwork | 0.999967437 | 1.009361257 |
| GO:0050807 | regulation of synapse organization | 0.99996729 | 1.009431723 |
| GO:0061333 | renal tubule morphogenesis | 0.99996668 | 1.009502199 |
| ENSG00000084234 | APLP2 subnetwork | 0.999966367 | 1.009572685 |

| | | | |
|---|---|---|---|
| MP:0003635 | abnormal synaptic transmission | 0.999966334 | 1.009643181 |
| GO:0003002 | regionalization | 0.999965989 | 1.009713687 |
| GO:0051588 | regulation of neurotransmitter transport | 0.999965013 | 1.009777219 |
| MP:0002998 | abnormal bone remodeling | 0.371781486 | 1.009797048 |
| GO:0019787 | small conjugating protein ligase activity | 0.371731589 | 1.009817309 |
| GO:0002089 | lens morphogenesis in camera-type eye | 0.999964432 | 1.009847744 |
| GO:0048713 | regulation of oligodendrocyte differentiation | 0.999964395 | 1.009918279 |
| MP:0003008 | enhanced long term potentiation | 0.999963149 | 1.009985331 |
| GO:0050750 | low-density lipoprotein particle receptor binding | 0.999962076 | 1.010038421 |
| ENSG00000153487 | ING1 subnetwork | 0.372394675 | 1.010058954 |
| GO:0034763 | negative regulation of transmembrane transport | 0.372344949 | 1.010088447 |
| GO:0046928 | regulation of neurotransmitter secretion | 0.999960651 | 1.010105491 |
| ENSG00000163629 | PTPN13 subnetwork | 0.372054121 | 1.010134637 |
| GO:0034654 | nucleobase-containing compound biosynthetic process | 0.99996017 | 1.010176064 |
| MP:0008657 | increased interleukin-1 beta secretion | 0.372010252 | 1.010237963 |
| GO:0014047 | glutamate secretion | 0.99995873 | 1.010246646 |
| ENSG00000141447 | OSBPL1A subnetwork | 0.372332456 | 1.010256174 |
| ENSG00000162337 | LRP5 subnetwork | 0.99995765 | 1.010317238 |
| GO:0002053 | positive regulation of mesenchymal cell proliferation | 0.372191736 | 1.010372488 |
| MP:0008283 | small hippocampus | 0.999956158 | 1.010384347 |
| ENSG00000143867 | OSR1 subnetwork | 0.372332456 | 1.010442396 |
| GO:0016331 | morphogenesis of embryonic epithelium | 0.99995394 | 1.01044797 |
| GO:0030660 | Golgi-associated vesicle membrane | 0.372555573 | 1.010453122 |
| GO:0021511 | spinal cord patterning | 0.999953795 | 1.010518591 |
| REACTOME_JNK_C:JUN_KINASES_ | REACTOME_JNK_C:JUN_KINASES_PHOSPHORYLATION_A | 0.372287837 | 1.010527286 |
| GO:0035148 | tube formation | 0.999952016 | 1.010585727 |
| MP:0001905 | abnormal dopamine level | 0.37267611 | 1.010589319 |
| REACTOME_HDL:MEDIATED_LIPI | REACTOME_HDL:MEDIATED_LIPID_TRANSPORT | 0.372798404 | 1.010622239 |
| GO:0005938 | cell cortex | 0.372749555 | 1.010633401 |
| MP:0001900 | impaired synaptic plasticity | 0.999950851 | 1.010649378 |
| MP:0004091 | abnormal Z lines | 0.999950195 | 1.010716533 |
| GO:0002369 | T cell cytokine production | 0.373019855 | 1.010737946 |
| GO:0072522 | purine-containing compound biosynthetic process | 0.9999488 | 1.010783697 |
| GO:0017016 | Ras GTPase binding | 0.372973019 | 1.010785938 |
| ENSG00000107187 | LHX3 subnetwork | 0.999947845 | 1.010854366 |
| ENSG00000136531 | SCN2A subnetwork | 0.99994708 | 1.010921549 |
| GO:0051339 | regulation of lyase activity | 0.999945673 | 1.010988742 |
| GO:0048709 | oligodendrocyte differentiation | 0.999945083 | 1.011059441 |
| GO:0050808 | synapse organization | 0.99994409 | 1.011126652 |
| MP:0011448 | decreased dopaminergic neuron number | 0.999943166 | 1.011193873 |
| GO:0061351 | neural precursor cell proliferation | 0.999942094 | 1.011257606 |
| GO:0021537 | telencephalon development | 0.999940363 | 1.011321349 |
| GO:0032769 | negative regulation of monooxygenase activity | 0.999940132 | 1.011388597 |
| MP:0002196 | absent corpus callosum | 0.999939755 | 1.011459354 |
| GO:0021795 | cerebral cortex cell migration | 0.999938794 | 1.01153012 |
| GO:0007610 | behavior | 0.999938363 | 1.011600896 |
| GO:0003401 | axis elongation | 0.999938234 | 1.011668183 |
| MP:0002206 | abnormal CNS synaptic transmission | 0.999937964 | 1.011738978 |
| GO:0071599 | otic vesicle development | 0.999936872 | 1.011806285 |
| GO:0005230 | extracellular ligand-gated ion channel activity | 0.999936796 | 1.0118771 |
| MP:0002594 | low mean erythrocyte cell number | 0.373500598 | 1.011922723 |
| MP:0008911 | induced hyperactivity | 0.99993606 | 1.011947925 |
| MP:0003996 | clonic seizures | 0.999933946 | 1.01200826 |
| GO:0019935 | cyclic-nucleotide-mediated signaling | 0.999932414 | 1.012075604 |

| | | | |
|---|---|---|---|
| ENSG00000105649 | RAB3A subnetwork | 0.999932091 | 1.012142957 |
| GO:0031344 | regulation of cell projection organization | 0.999931505 | 1.01221032 |
| MP:0008267 | abnormal hippocampus CA3 region morphology | 0.99993073 | 1.012277692 |
| ENSG00000113140 | SPARC subnetwork | 0.373689791 | 1.012325239 |
| MP:0001415 | increased exploration in new environment | 0.999928132 | 1.012338072 |
| GO:2000311 | regulation of alpha-amino-3-hydroxy-5-methyl-4-isoxazo | 0.999928119 | 1.012408964 |
| GO:0005216 | ion channel activity | 0.999928092 | 1.012479866 |
| GO:0007626 | locomotory behavior | 0.999927117 | 1.012550777 |
| GO:0031279 | regulation of cyclase activity | 0.999925753 | 1.012618197 |
| GO:0022843 | voltage-gated cation channel activity | 0.999925223 | 1.012689129 |
| GO:0061311 | cell surface receptor signaling pathway involved in heart | 0.999924351 | 1.012753065 |
| GO:0048935 | peripheral nervous system neuron development | 0.999924315 | 1.012824016 |
| GO:0048934 | peripheral nervous system neuron differentiation | 0.999924315 | 1.012894977 |
| GO:0045879 | negative regulation of smoothened signaling pathway | 0.99992335 | 1.012962444 |
| ENSG00000174996 | KLC2 subnetwork | 0.373981113 | 1.013003495 |
| GO:2000826 | regulation of heart morphogenesis | 0.999923212 | 1.013033424 |
| MP:0001364 | decreased anxiety-related response | 0.99992273 | 1.013100911 |
| GO:0048715 | negative regulation of oligodendrocyte differentiation | 0.999921475 | 1.013164903 |
| GO:0007379 | segment specification | 0.999921284 | 1.013235913 |
| GO:0045666 | positive regulation of neuron differentiation | 0.999921148 | 1.013306932 |
| ENSG00000166747 | AP1G1 subnetwork | 0.374134596 | 1.013313718 |
| GO:0007409 | axonogenesis | 0.999920028 | 1.013377962 |
| GO:0001755 | neural crest cell migration | 0.999917816 | 1.013431476 |
| REACTOME_ACETYLCHOLINE_NEU | REACTOME_ACETYLCHOLINE_NEUROTRANSMITTER_REL | 0.999917412 | 1.013492008 |
| GO:0045296 | cadherin binding | 0.999915128 | 1.013563065 |
| GO:0060113 | inner ear receptor cell differentiation | 0.999913902 | 1.013634133 |
| REACTOME_TRANSPORT_OF_INO | REACTOME_TRANSPORT_OF_INORGANIC_CATIONSANIC | 0.999913601 | 1.01370521 |
| GO:0043587 | tongue morphogenesis | 0.999912137 | 1.013776297 |
| GO:0050804 | regulation of synaptic transmission | 0.999911423 | 1.013843888 |
| GO:0032640 | tumor necrosis factor production | 0.374556977 | 1.013866936 |
| GO:0042249 | establishment of planar polarity of embryonic epithelium | 0.999911385 | 1.013914995 |
| GO:0034702 | ion channel complex | 0.999910492 | 1.013986112 |
| GO:0045685 | regulation of glial cell differentiation | 0.999909205 | 1.014050224 |
| GO:0032680 | regulation of tumor necrosis factor production | 0.374556977 | 1.014053309 |
| MP:0001704 | abnormal dorsal-ventral axis patterning | 0.374468199 | 1.014055893 |
| GO:0046873 | metal ion transmembrane transporter activity | 0.999909198 | 1.014121361 |
| MP:0002774 | small prostate gland | 0.374819295 | 1.014155796 |
| MP:0005498 | hyporesponsive to tactile stimuli | 0.9999057 | 1.014174968 |
| ENSG00000081052 | COL4A4 subnetwork | 0.375602371 | 1.014218922 |
| MP:0003637 | cochlear ganglion hypoplasia | 0.999904293 | 1.014239108 |
| ENSG00000072803 | FBXW11 subnetwork | 0.37479165 | 1.014287027 |
| GO:0051414 | response to cortisol stimulus | 0.999903628 | 1.014303256 |
| GO:0001759 | organ induction | 0.999902184 | 1.014363904 |
| MP:0002038 | carcinoma | 0.375592183 | 1.014377407 |
| ENSG00000115266 | APC2 subnetwork | 0.999901775 | 1.014435088 |
| KEGG_HISTIDINE_METABOLISM | KEGG_HISTIDINE_METABOLISM | 0.375872009 | 1.014504306 |
| GO:0022838 | substrate-specific channel activity | 0.99990074 | 1.014506281 |
| MP:0008029 | abnormal paraxial mesoderm morphology | 0.375766664 | 1.014537122 |
| GO:0050706 | regulation of interleukin-1 beta secretion | 0.37558827 | 1.014563463 |
| GO:2000179 | positive regulation of neural precursor cell proliferation | 0.999900673 | 1.014577485 |
| ENSG00000136574 | GATA4 subnetwork | 0.37584601 | 1.0146261 |
| GO:0006813 | potassium ion transport | 0.999900433 | 1.014648698 |
| GO:0051966 | regulation of synaptic transmission, glutamatergic | 0.999900159 | 1.014719921 |
| GO:0050704 | regulation of interleukin-1 secretion | 0.37558827 | 1.014749587 |

| | | | |
|---|---|---|---|
| GO:0009953 | dorsal/ventral pattern formation | 0.999900065 | 1.014791155 |
| REACTOME_AMYLOIDS | REACTOME_AMYLOIDS | 0.999895081 | 1.014851867 |
| ENSG00000174851 | YIF1A subnetwork | 0.375570871 | 1.014899083 |
| GO:0043954 | cellular component maintenance | 0.999894799 | 1.01491961 |
| MP:0005329 | abnormal myocardium layer morphology | 0.376175437 | 1.01494137 |
| REACTOME_HIV_LIFE_CYCLE | REACTOME_HIV_LIFE_CYCLE | 0.375273391 | 1.01494675 |
| GO:0043198 | dendritic shaft | 0.999892934 | 1.014983851 |
| GO:0030295 | protein kinase activator activity | 0.37538241 | 1.015008261 |
| GO:0010883 | regulation of lipid storage | 0.375240218 | 1.015013774 |
| GO:0042698 | ovulation cycle | 0.375557698 | 1.015039457 |
| GO:0005313 | L-glutamate transmembrane transporter activity | 0.999892075 | 1.015041079 |
| ENSG00000154429 | C1orf96 subnetwork | 0.375497618 | 1.015060573 |
| GO:0032204 | regulation of telomere maintenance | 0.375193999 | 1.015099192 |
| GO:0021516 | dorsal spinal cord development | 0.99989116 | 1.01511236 |
| ENSG00000067369 | TP53BP1 subnetwork | 0.376410239 | 1.015116279 |
| ENSG00000124193 | SRSF6 subnetwork | 0.376713368 | 1.015141812 |
| GO:0009163 | nucleoside biosynthetic process | 0.999890039 | 1.015176628 |
| ENSG00000198373 | WWP2 subnetwork | 0.376492459 | 1.015195899 |
| ENSG00000058335 | RASGRF1 subnetwork | 0.376367058 | 1.015228938 |
| GO:0021895 | cerebral cortex neuron differentiation | 0.999887891 | 1.015230369 |
| ENSG00000135446 | CDK4 subnetwork | 0.376690945 | 1.015281845 |
| ENSG00000143507 | DUSP10 subnetwork | 0.376627321 | 1.015284642 |
| GO:2001022 | positive regulation of response to DNA damage stimulus | 0.99988718 | 1.015301679 |
| GO:0048675 | axon extension | 0.999885644 | 1.015365974 |
| GO:0005088 | Ras guanyl-nucleotide exchange factor activity | 0.376901088 | 1.015376875 |
| ENSG00000131370 | SH3BP5 subnetwork | 0.376367022 | 1.015414911 |
| GO:0050432 | catecholamine secretion | 0.999883785 | 1.01541974 |
| GO:0002016 | regulation of blood volume by renin-angiotensin | 0.999882622 | 1.015487565 |
| GO:0003156 | regulation of organ formation | 0.999881798 | 1.015558912 |
| GO:0051969 | regulation of transmission of nerve impulse | 0.999880548 | 1.015626757 |
| GO:0000096 | sulfur amino acid metabolic process | 0.999879814 | 1.015698124 |
| ENSG00000196914 | ARHGEF12 subnetwork | 0.377119947 | 1.015739894 |
| GO:0048663 | neuron fate commitment | 0.999879065 | 1.015765987 |
| GO:0060538 | skeletal muscle organ development | 0.377760223 | 1.015771689 |
| MP:0005606 | increased bleeding time | 0.377205164 | 1.015782736 |
| ENSG00000188976 | NOC2L subnetwork | 0.377340901 | 1.015813528 |
| ENSG00000084674 | APOB subnetwork | 0.999878673 | 1.01583386 |
| GO:0030530 | heterogeneous nuclear ribonucleoprotein complex | 0.377292035 | 1.015889559 |
| ENSG00000162613 | FUBP1 subnetwork | 0.999876433 | 1.015905257 |
| GO:0009913 | epidermal cell differentiation | 0.377866851 | 1.015951424 |
| ENSG00000198838 | RYR3 subnetwork | 0.377757764 | 1.015957252 |
| GO:0042391 | regulation of membrane potential | 0.999875342 | 1.015976664 |
| ENSG00000040199 | PHLPP2 subnetwork | 0.377701825 | 1.016005847 |
| ENSG00000176894 | PXMP2 subnetwork | 0.999874745 | 1.016044566 |
| MP:0006009 | abnormal neuronal migration | 0.999873636 | 1.016112478 |
| MP:0000788 | abnormal cerebral cortex morphology | 0.999871133 | 1.016180399 |
| ENSG00000164252 | AGGF1 subnetwork | 0.377687851 | 1.016182383 |
| ENSG00000152056 | AP1S3 subnetwork | 0.377642264 | 1.016240175 |
| MP:0005105 | abnormal middle ear ossicle morphology | 0.999867374 | 1.016241299 |
| ENSG00000198932 | GPRASP1 subnetwork | 0.999866853 | 1.016312755 |
| MP:0009142 | decreased prepulse inhibition | 0.999864194 | 1.016384221 |
| GO:0048562 | embryonic organ morphogenesis | 0.999862395 | 1.016448664 |
| GO:0007214 | gamma-aminobutyric acid signaling pathway | 0.999860479 | 1.016499051 |
| GO:0034220 | ion transmembrane transport | 0.999860315 | 1.016570544 |

| | | | |
|---|---|---|---|
| MP:0002058 | neonatal lethality | 0.999859125 | 1.016642048 |
| ENSG00000125351 | UPF3B subnetwork | 0.378206321 | 1.016642322 |
| GO:0005231 | excitatory extracellular ligand-gated ion channel activity | 0.999858932 | 1.016713562 |
| ENSG00000119392 | GLE1 subnetwork | 0.379112013 | 1.016754738 |
| ENSG00000170017 | ALCAM subnetwork | 0.379174901 | 1.016760794 |
| ENSG00000069329 | VPS35 subnetwork | 0.378895253 | 1.016782133 |
| REACTOME_GABA_RECEPTOR_AC | REACTOME_GABA_RECEPTOR_ACTIVATION | 0.999858896 | 1.016785086 |
| GO:0000307 | cyclin-dependent protein kinase holoenzyme complex | 0.378970448 | 1.01681553 |
| GO:0015114 | phosphate ion transmembrane transporter activity | 0.999858422 | 1.016853103 |
| MP:0003409 | decreased width of hypertrophic chondrocyte zone | 0.379609097 | 1.016872952 |
| MP:0004929 | decreased epididymis weight | 0.379069123 | 1.016885365 |
| ENSG00000144028 | SNRNP200 subnetwork | 0.378875271 | 1.016912837 |
| GO:0007628 | adult walking behavior | 0.999853946 | 1.016921129 |
| REACTOME_P75_NTR_RECEPTOR | REACTOME_P75_NTR_RECEPTOR:MEDIATED_SIGNALLIN | 0.378732389 | 1.016937249 |
| GO:0030126 | COPI vesicle coat | 0.379562634 | 1.016976151 |
| MP:0004610 | small vertebrae | 0.379473345 | 1.016979243 |
| GO:0014032 | neural crest cell development | 0.99985242 | 1.016985646 |
| REACTOME_INFLAMMASOMES | REACTOME_INFLAMMASOMES | 0.378674007 | 1.016985951 |
| KEGG_METABOLISM_OF_XENOBI | KEGG_METABOLISM_OF_XENOBIOTICS_BY_CYTOCHROM | 0.378838004 | 1.016988875 |
| ENSG00000197081 | IGF2R subnetwork | 0.378607498 | 1.016998175 |
| GO:0045843 | negative regulation of striated muscle tissue developmer | 0.9998425 | 1.017036099 |
| MP:0009749 | enhanced behavioral response to addictive substance | 0.999840597 | 1.017097115 |
| MP:0009278 | abnormal bone marrow cell physiology | 0.379463398 | 1.017146239 |
| GO:0002455 | humoral immune response mediated by circulating immı | 0.378585644 | 1.01714729 |
| GO:0032958 | inositol phosphate biosynthetic process | 0.999840022 | 1.017168696 |
| GO:0016577 | histone demethylation | 0.379871024 | 1.017176128 |
| MP:0001798 | impaired macrophage phagocytosis | 0.378537261 | 1.017177802 |
| GO:0090407 | organophosphate biosynthetic process | 0.999840022 | 1.017240287 |
| ENSG00000058799 | YIPF1 subnetwork | 0.379422386 | 1.017249545 |
| ENSG00000130589 | RP4-697K14.7 subnetwork | 0.379820355 | 1.017252047 |
| GO:0005244 | voltage-gated ion channel activity | 0.999838261 | 1.01730133 |
| GO:0015020 | glucuronosyltransferase activity | 0.380015546 | 1.017354921 |
| GO:0022832 | voltage-gated channel activity | 0.999838261 | 1.017372941 |
| MP:0002066 | abnormal motor capabilities/coordination/movement | 0.99983655 | 1.017430482 |
| MP:0002916 | increased synaptic depression | 0.999830972 | 1.017480991 |
| MP:0009456 | impaired cued conditioning behavior | 0.999826833 | 1.017545589 |
| GO:0015698 | inorganic anion transport | 0.999826476 | 1.017617237 |
| GO:0071600 | otic vesicle morphogenesis | 0.999824983 | 1.017685374 |
| ENSG00000085741 | WNT11 subnetwork | 0.999822989 | 1.017746479 |
| ENSG00000169884 | WNT10B subnetwork | 0.999822989 | 1.017818156 |
| ENSG00000105989 | WNT2 subnetwork | 0.999822989 | 1.017889844 |
| ENSG00000135925 | WNT10A subnetwork | 0.999822989 | 1.017961541 |
| ENSG00000143816 | WNT9A subnetwork | 0.999822989 | 1.018033249 |
| ENSG00000082516 | GEMIN5 subnetwork | 0.380378435 | 1.018042925 |
| ENSG00000158955 | WNT9B subnetwork | 0.999822989 | 1.018104967 |
| ENSG00000061492 | WNT8A subnetwork | 0.999822989 | 1.018176694 |
| ENSG00000075290 | WNT8B subnetwork | 0.999822989 | 1.018248432 |
| MP:0001463 | abnormal spatial learning | 0.999821727 | 1.018316657 |
| MP:0005193 | abnormal anterior eye segment morphology | 0.999813619 | 1.018374322 |
| GO:0007224 | smoothened signaling pathway | 0.999811386 | 1.018439042 |
| ENSG00000172794 | RAB37 subnetwork | 0.999807543 | 1.018500247 |
| GO:0030163 | protein catabolic process | 0.381091102 | 1.018552488 |
| ENSG00000154764 | WNT7A subnetwork | 0.999806355 | 1.018572033 |
| GO:0048813 | dendrite morphogenesis | 0.999805342 | 1.018640305 |

| | | | |
|---|---|---|---|
| ENSG00000122484 | RPAP2 subnetwork | 0.381049545 | 1.018646685 |
| MP:0000812 | abnormal dentate gyrus morphology | 0.99980487 | 1.018712111 |
| REACTOME_NEF_MEDIATED_DO\ | REACTOME_NEF_MEDIATED_DOWNREGULATION_OF_M | 0.381208237 | 1.018730706 |
| ENSG00000128016 | ZFP36 subnetwork | 0.381296431 | 1.018745461 |
| KEGG_RIBOFLAVIN_METABOLISM | KEGG_RIBOFLAVIN_METABOLISM | 0.381018019 | 1.018759084 |
| GO:0031397 | negative regulation of protein ubiquitination | 0.99980064 | 1.018766302 |
| GO:0043240 | Fanconi anaemia nuclear complex | 0.99979721 | 1.018831077 |
| ENSG00000163956 | LRPAP1 subnetwork | 0.38140975 | 1.018887275 |
| GO:0034703 | cation channel complex | 0.99979548 | 1.018899387 |
| GO:0006275 | regulation of DNA replication | 0.381002417 | 1.01892604 |
| MP:0001071 | abnormal facial nerve morphology | 0.999794978 | 1.018971231 |
| ENSG00000174720 | LARP7 subnetwork | 0.381604065 | 1.018989294 |
| ENSG00000136231 | IGF2BP3 subnetwork | 0.999793311 | 1.019043086 |
| ENSG00000188488 | SERPINA5 subnetwork | 0.380773831 | 1.019085288 |
| GO:0007015 | actin filament organization | 0.381001469 | 1.019111232 |
| MP:0004077 | abnormal striatum morphology | 0.999791406 | 1.019114951 |
| REACTOME_CELL_DEATH_SIGNAL | REACTOME_CELL_DEATH_SIGNALLING_VIA_NRAGE_NRI | 0.381594089 | 1.019165154 |
| GO:0045453 | bone resorption | 0.380887893 | 1.019172727 |
| GO:0022836 | gated channel activity | 0.999786872 | 1.019176247 |
| ENSG00000215760 | ENSG00000215760 subnetwork | 0.381901419 | 1.01924193 |
| ENSG00000167306 | MYO5B subnetwork | 0.38099272 | 1.019241956 |
| GO:0015081 | sodium ion transmembrane transporter activity | 0.99978583 | 1.019244604 |
| MP:0000031 | abnormal cochlea morphology | 0.999785029 | 1.019316499 |
| GO:0015079 | potassium ion transmembrane transporter activity | 0.99978421 | 1.019384876 |
| ENSG00000187325 | TAF9B subnetwork | 0.381901419 | 1.019426809 |
| GO:0035567 | non-canonical Wnt receptor signaling pathway | 0.999783265 | 1.01945679 |
| GO:0072009 | nephron epithelium development | 0.999782508 | 1.019528715 |
| REACTOME_CLASS_A1_RHODOPS | REACTOME_CLASS_A1_RHODOPSIN:LIKE_RECEPTORS | 0.381861429 | 1.019539187 |
| GO:0090189 | regulation of branching involved in ureteric bud morpho | 0.99977914 | 1.019600649 |
| ENSG00000170606 | HSPA4 subnetwork | 0.382298082 | 1.01963218 |
| GO:0008239 | dipeptidyl-peptidase activity | 0.382150811 | 1.019651922 |
| GO:0048265 | response to pain | 0.999778645 | 1.019672594 |
| REACTOME_SMOOTH_MUSCLE_C | REACTOME_SMOOTH_MUSCLE_CONTRACTION | 0.38210623 | 1.019718948 |
| GO:0009084 | glutamine family amino acid biosynthetic process | 0.999773282 | 1.019730435 |
| GO:0045351 | type I interferon biosynthetic process | 0.382279713 | 1.019771656 |
| GO:0006164 | purine nucleotide biosynthetic process | 0.999769534 | 1.019802399 |
| ENSG00000067704 | IARS2 subnetwork | 0.382238114 | 1.019811492 |
| GO:0030424 | axon | 0.999766962 | 1.019867316 |
| GO:0021879 | forebrain neuron differentiation | 0.999760327 | 1.019925184 |
| GO:0045165 | cell fate commitment | 0.999756444 | 1.01997953 |
| GO:0007597 | blood coagulation, intrinsic pathway | 0.99975567 | 1.020048002 |
| GO:0045931 | positive regulation of mitotic cell cycle | 0.382597743 | 1.020086941 |
| ENSG00000134245 | WNT2B subnetwork | 0.999753987 | 1.020120014 |
| GO:0044462 | external encapsulating structure part | 0.999748131 | 1.020167326 |
| GO:0005811 | lipid particle | 0.382573885 | 1.020217391 |
| GO:0030313 | cell envelope | 0.999748131 | 1.020239356 |
| ENSG00000186834 | HEXIM1 subnetwork | 0.382882873 | 1.020275163 |
| ENSG00000047621 | C12orf4 subnetwork | 0.999747746 | 1.020311397 |
| ENSG00000107789 | MINPP1 subnetwork | 0.999744384 | 1.020372855 |
| MP:0001417 | decreased exploration in new environment | 0.999743811 | 1.020444915 |
| ENSG00000128487 | SPECC1 subnetwork | 0.382872774 | 1.020450842 |
| ENSG00000107201 | DDX58 subnetwork | 0.382980557 | 1.020461538 |
| GO:0061326 | renal tubule development | 0.999741741 | 1.020513454 |
| GO:0015267 | channel activity | 0.999740838 | 1.020585535 |

| | | | |
|---|---|---|---|
| GO:0005681 | spliceosomal complex | 0.38286988 | 1.020626585 |
| GO:0022803 | passive transmembrane transporter activity | 0.999740838 | 1.020657625 |
| MP:0002906 | increased susceptibility to pharmacologically induced sei | 0.999740769 | 1.020729726 |
| GO:0030594 | neurotransmitter receptor activity | 0.999740519 | 1.020801837 |
| GO:0010977 | negative regulation of neuron projection development | 0.999740284 | 1.020873958 |
| GO:0051932 | synaptic transmission, GABAergic | 0.999738429 | 1.020939024 |
| MP:0002067 | abnormal sensory capabilities/reflexes/nociception | 0.999728788 | 1.020989966 |
| ENSG00000135940 | COX5B subnetwork | 0.383335832 | 1.021042157 |
| GO:0008038 | neuron recognition | 0.999727965 | 1.021062116 |
| GO:0060986 | endocrine hormone secretion | 0.383277882 | 1.021100253 |
| ENSG00000136854 | STXBP1 subnetwork | 0.999727958 | 1.021134276 |
| ENSG00000188064 | WNT7B subnetwork | 0.999727684 | 1.021202912 |
| ENSG00000175224 | ATG13 subnetwork | 0.383520727 | 1.02121541 |
| GO:0050433 | regulation of catecholamine secretion | 0.999726739 | 1.021271558 |
| GO:0001673 | male germ cell nucleus | 0.383495333 | 1.021318741 |
| GO:0051954 | positive regulation of amine transport | 0.999725086 | 1.021340213 |
| GO:0048167 | regulation of synaptic plasticity | 0.999724635 | 1.021408879 |
| GO:0019933 | cAMP-mediated signaling | 0.999723211 | 1.021481089 |
| ENSG00000185236 | RAB11B subnetwork | 0.383689372 | 1.021491863 |
| MP:0006309 | decreased retinal ganglion cell number | 0.999718398 | 1.021542704 |
| ENSG00000169242 | EFNA1 subnetwork | 0.999718234 | 1.021614933 |
| GO:0030261 | chromosome condensation | 0.999717905 | 1.021687173 |
| ENSG00000003096 | KLHL13 subnetwork | 0.383839683 | 1.021723016 |
| MP:0004739 | conductive hearing loss | 0.999714874 | 1.021755887 |
| GO:0046686 | response to cadmium ion | 0.999713864 | 1.021824611 |
| GO:0008344 | adult locomotory behavior | 0.999710373 | 1.021889808 |
| MP:0000087 | absent mandible | 0.999709205 | 1.021962088 |
| GO:0021514 | ventral spinal cord interneuron differentiation | 0.999708808 | 1.022034378 |
| ENSG00000180817 | PPA1 subnetwork | 0.384802238 | 1.022049802 |
| GO:0071549 | cellular response to dexamethasone stimulus | 0.999707681 | 1.022103141 |
| GO:0090022 | regulation of neutrophil chemotaxis | 0.384774041 | 1.022107923 |
| MP:0005587 | abnormal Meckel's cartilage morphology | 0.999706357 | 1.022175451 |
| ENSG00000065548 | ZC3H15 subnetwork | 0.384183799 | 1.02219812 |
| GO:0042659 | regulation of cell fate specification | 0.999704826 | 1.022247771 |
| ENSG00000211660 | ENSG00000211660 subnetwork | 0.384336744 | 1.022271413 |
| GO:0071248 | cellular response to metal ion | 0.384771171 | 1.022292419 |
| ENSG00000099817 | POLR2E subnetwork | 0.384627079 | 1.022318527 |
| ENSG00000093100 | ENSG00000093100 subnetwork | 0.999704306 | 1.022320102 |
| ENSG00000106258 | CYP3A5 subnetwork | 0.384491341 | 1.02232659 |
| MP:0010053 | decreased grip strength | 0.999701912 | 1.022385367 |
| ENSG00000104517 | UBR5 subnetwork | 0.384576923 | 1.022403829 |
| ENSG00000204983 | PRSS1 subnetwork | 0.384758851 | 1.022440874 |
| GO:0050982 | detection of mechanical stimulus | 0.999698663 | 1.022443564 |
| ENSG00000211653 | ENSG00000211653 subnetwork | 0.384336744 | 1.022456172 |
| ENSG00000115596 | WNT6 subnetwork | 0.99969479 | 1.022501769 |
| ENSG00000021461 | CYP3A43 subnetwork | 0.384491341 | 1.022511292 |
| GO:0000768 | syncytium formation by plasma membrane fusion | 0.385059842 | 1.022523904 |
| GO:0003001 | generation of a signal involved in cell-cell signaling | 0.999693657 | 1.022574138 |
| GO:0023061 | signal release | 0.999693657 | 1.022646518 |
| MP:0009750 | impaired behavioral response to addictive substance | 0.999687944 | 1.022708289 |
| GO:0072080 | nephron tubule development | 0.999686718 | 1.022780688 |
| GO:0006206 | pyrimidine base metabolic process | 0.999684145 | 1.022849558 |
| ENSG00000108379 | WNT3 subnetwork | 0.999683913 | 1.022921977 |
| GO:0008589 | regulation of smoothened signaling pathway | 0.99968275 | 1.022994406 |

| | | | |
|---|---|---|---|
| GO:0006820 | anion transport | 0.999677132 | 1.023045603 |
| MP:0006000 | abnormal corneal epithelium morphology | 0.999676824 | 1.023118051 |
| GO:0051963 | regulation of synapse assembly | 0.999676462 | 1.02319051 |
| GO:0021675 | nerve development | 0.999674398 | 1.023255896 |
| GO:0030104 | water homeostasis | 0.385594309 | 1.023323116 |
| MP:0000034 | abnormal vestibule morphology | 0.999670965 | 1.023324834 |
| ENSG00000099800 | TIMM13 subnetwork | 0.385514924 | 1.023327322 |
| MP:0001890 | anencephaly | 0.999668147 | 1.023390239 |
| GO:0035116 | embryonic hindlimb morphogenesis | 0.999663207 | 1.023445027 |
| MP:0008642 | decreased circulating interleukin-1 beta level | 0.385486065 | 1.023466811 |
| ENSG00000121058 | COIL subnetwork | 0.385709402 | 1.023472147 |
| GO:0015844 | monoamine transport | 0.9996627 | 1.023517535 |
| ENSG00000138722 | MMRN1 subnetwork | 0.385851931 | 1.023553793 |
| ENSG00000120254 | MTHFD1L subnetwork | 0.99965626 | 1.02358651 |
| ENSG00000176476 | ENSG00000176476 | 0.385824011 | 1.023639149 |
| MP:0002885 | abnormal AMPA-mediated synaptic currents | 0.999652636 | 1.023651952 |
| ENSG00000184117 | NIPSNAP1 subnetwork | 0.999647437 | 1.023720947 |
| GO:0051928 | positive regulation of calcium ion transport | 0.387277829 | 1.023738553 |
| MP:0001510 | abnormal coat appearance | 0.387764663 | 1.023740362 |
| GO:0005635 | nuclear envelope | 0.386960073 | 1.023741912 |
| GO:0008831 | dTDP-4-dehydrorhamnose reductase activity | 0.387537926 | 1.02374843 |
| GO:0021513 | spinal cord dorsal/ventral patterning | 0.999643243 | 1.023782864 |
| REACTOME_ZINC_TRANSPORTERS | REACTOME_ZINC_TRANSPORTERS | 0.387047858 | 1.023809524 |
| REACTOME_CELL:CELL_JUNCTION | REACTOME_CELL:CELL_JUNCTION_ORGANIZATION | 0.999641132 | 1.023848335 |
| GO:0031365 | N-terminal protein amino acid modification | 0.387118464 | 1.023850162 |
| ENSG00000185658 | BRWD1 subnetwork | 0.386251042 | 1.023878984 |
| GO:0046906 | tetrapyrrole binding | 0.387267714 | 1.023886494 |
| GO:0008154 | actin polymerization or depolymerization | 0.389495007 | 1.023888591 |
| ENSG00000182636 | NDN subnetwork | 0.387209384 | 1.023890785 |
| GO:0005537 | mannose binding | 0.388822437 | 1.023891273 |
| MP:0002465 | abnormal eosinophil physiology | 0.388916224 | 1.023904881 |
| GO:0060401 | cytosolic calcium ion transport | 0.38753468 | 1.023914214 |
| ENSG00000178184 | PARD6G subnetwork | 0.387746565 | 1.023914993 |
| MP:0002689 | abnormal molar morphology | 0.999635562 | 1.023917358 |
| ENSG00000070371 | CLTCL1 subnetwork | 0.388772373 | 1.023922375 |
| ENSG00000122861 | PLAU subnetwork | 0.386958484 | 1.023925939 |
| ENSG00000137693 | YAP1 subnetwork | 0.389442196 | 1.0239375 |
| ENSG00000169371 | SNUPN subnetwork | 0.389197129 | 1.023941397 |
| MP:0010867 | abnormal bone trabecula morphology | 0.387405606 | 1.023958707 |
| GO:0001917 | photoreceptor inner segment | 0.386089718 | 1.023963964 |
| MP:0005087 | decreased acute inflammation | 0.387925887 | 1.023964868 |
| ENSG00000109846 | CRYAB subnetwork | 0.387658372 | 1.023977395 |
| ENSG00000197459 | HIST1H2BH subnetwork | 0.386155436 | 1.023977662 |
| GO:0015172 | acidic amino acid transmembrane transporter activity | 0.999634943 | 1.023989935 |
| ENSG00000189079 | ARID2 subnetwork | 0.388112373 | 1.023992116 |
| MP:0004131 | abnormal embryonic cilium morphology | 0.387721383 | 1.024 |
| GO:0030135 | coated vesicle | 0.386239636 | 1.024018372 |
| MP:0005323 | dystonia | 0.387502584 | 1.024026207 |
| GO:0050662 | coenzyme binding | 0.999633593 | 1.024062522 |
| GO:0019433 | triglyceride catabolic process | 0.386940126 | 1.024074074 |
| GO:0019915 | lipid storage | 0.388756027 | 1.024078712 |
| MP:0002953 | thick ventricular wall | 0.389191232 | 1.024106505 |
| ENSG00000164985 | PSIP1 subnetwork | 0.389116024 | 1.024110813 |
| GO:0019888 | protein phosphatase regulator activity | 0.388584489 | 1.024118489 |

| | | | |
|---|---|---|---|
| GO:0044060 | regulation of endocrine process | 0.389440189 | 1.024120379 |
| ENSG00000198400 | NTRK1 subnetwork | 0.389343304 | 1.024124687 |
| GO:0014046 | dopamine secretion | 0.999631466 | 1.024131575 |
| GO:0034061 | DNA polymerase activity | 0.387918772 | 1.024139477 |
| GO:0015030 | Cajal body | 0.388475647 | 1.024145031 |
| ENSG00000095485 | CWF19L1 subnetwork | 0.38905858 | 1.024150876 |
| MP:0001917 | intraventricular hemorrhage | 0.388100584 | 1.024157706 |
| ENSG00000138162 | TACC2 subnetwork | 0.388729216 | 1.024172482 |
| GO:0014059 | regulation of dopamine secretion | 0.999631466 | 1.024204183 |
| MP:0005562 | decreased mean corpuscular hemoglobin | 0.388433053 | 1.024229943 |
| ENSG00000148377 | IDI2 subnetwork | 0.388557587 | 1.024230218 |
| REACTOME_INFLUENZA_LIFE_CYC | REACTOME_INFLUENZA_LIFE_CYCLE | 0.388359356 | 1.024243238 |
| GO:0046058 | cAMP metabolic process | 0.999618452 | 1.02424844 |
| MP:0000433 | microcephaly | 0.38693641 | 1.024258227 |
| GO:0070059 | intrinsic apoptotic signaling pathway in response to endo | 0.388283556 | 1.024265496 |
| GO:0022408 | negative regulation of cell-cell adhesion | 0.388699177 | 1.024293128 |
| GO:0016339 | calcium-dependent cell-cell adhesion | 0.999618247 | 1.024321066 |
| ENSG00000214122 | ENSG00000214122 subnetwork | 0.389754038 | 1.024357372 |
| GO:0002076 | osteoblast development | 0.999618117 | 1.024393703 |
| GO:0048247 | lymphocyte chemotaxis | 0.389842447 | 1.024406568 |
| GO:0019001 | guanyl nucleotide binding | 0.386933079 | 1.024442446 |
| GO:0001708 | cell fate specification | 0.999617939 | 1.02446635 |
| GO:0007179 | transforming growth factor beta receptor signaling pathv | 0.389917978 | 1.02447359 |
| GO:0005249 | voltage-gated potassium channel activity | 0.999613575 | 1.024531915 |
| GO:0008536 | Ran GTPase binding | 0.390054902 | 1.024603033 |
| GO:0051340 | regulation of ligase activity | 0.999608244 | 1.024604582 |
| GO:0032561 | guanyl ribonucleotide binding | 0.386933079 | 1.024626731 |
| GO:0042475 | odontogenesis of dentin-containing tooth | 0.999604759 | 1.024673713 |
| REACTOME_PTM_GAMMA_CARB | REACTOME_PTM_GAMMA_CARBOXYLATION_HYPUSINE | 0.386678031 | 1.024725473 |
| GO:0044272 | sulfur compound biosynthetic process | 0.999604596 | 1.0247464 |
| GO:0009411 | response to UV | 0.386899782 | 1.024766103 |
| GO:0008047 | enzyme activator activity | 0.386647098 | 1.024774937 |
| GO:0009165 | nucleotide biosynthetic process | 0.999603531 | 1.024819098 |
| GO:0030426 | growth cone | 0.999600087 | 1.024888258 |
| GO:0032231 | regulation of actin filament bundle assembly | 0.386875809 | 1.024914522 |
| GO:0007340 | acrosome reaction | 0.999595811 | 1.024950333 |
| GO:0070301 | cellular response to hydrogen peroxide | 0.386806984 | 1.024964003 |
| GO:0070325 | lipoprotein particle receptor binding | 0.999586479 | 1.025019513 |
| GO:0071705 | nitrogen compound transport | 0.999585434 | 1.025088703 |
| ENSG00000092964 | DPYSL2 subnetwork | 0.999584353 | 1.025157902 |
| GO:0042069 | regulation of catecholamine metabolic process | 0.99958367 | 1.025227111 |
| GO:0019934 | cGMP-mediated signaling | 0.999570592 | 1.025275037 |
| ENSG00000206480 | FLOT1 subnetwork | 0.391304349 | 1.025333689 |
| ENSG00000166925 | TSC22D4 subnetwork | 0.999566915 | 1.025337166 |
| GO:0071695 | anatomical structure maturation | 0.999565902 | 1.025409952 |
| MP:0004452 | abnormal pterygoid process morphology | 0.999563698 | 1.025479199 |
| MP:0000471 | abnormal stomach epithelium morphology | 0.391616904 | 1.025498043 |
| REACTOME_ISG15_ANTIVIRAL_M | REACTOME_ISG15_ANTIVIRAL_MECHANISM | 0.39105225 | 1.025498753 |
| ENSG00000137312 | FLOT1 subnetwork | 0.391304349 | 1.025516198 |
| MP:0004860 | dilated kidney collecting duct | 0.390614382 | 1.025548422 |
| GO:0006171 | cAMP biosynthetic process | 0.999562682 | 1.025548456 |
| ENSG00000161920 | MED11 subnetwork | 0.39174065 | 1.025555753 |
| ENSG00000123106 | CCDC91 subnetwork | 0.391989616 | 1.025613224 |
| GO:0042734 | presynaptic membrane | 0.999561991 | 1.025617722 |

| | | | |
|---|---|---|---|
| REACTOME_NETRIN:1_SIGNALINC | REACTOME_NETRIN:1_SIGNALING | 0.391612316 | 1.025662693 |
| REACTOME_ANTIVIRAL_MECHAN | REACTOME_ANTIVIRAL_MECHANISM_BY_IFN:STIMULAT | 0.39105225 | 1.025681454 |
| GO:0051282 | regulation of sequestering of calcium ion | 0.390905149 | 1.025681697 |
| ENSG00000164171 | ITGA2 subnetwork | 0.391834474 | 1.025684566 |
| MP:0003702 | abnormal chromosome morphology | 0.391228586 | 1.025685541 |
| GO:0030799 | regulation of cyclic nucleotide metabolic process | 0.999560339 | 1.025690549 |
| ENSG00000206379 | FLOT1 subnetwork | 0.391304349 | 1.025698772 |
| ENSG00000134308 | YWHAQ subnetwork | 0.390611037 | 1.025731359 |
| MP:0006337 | abnormal first branchial arch morphology | 0.999558565 | 1.025745633 |
| ENSG00000100811 | YY1 subnetwork | 0.391980442 | 1.025751111 |
| ENSG00000058866 | DGKG subnetwork | 0.391208356 | 1.025788068 |
| MP:0001243 | abnormal dermal layer morphology | 0.391588821 | 1.025800712 |
| GO:0009190 | cyclic nucleotide biosynthetic process | 0.99955596 | 1.025814928 |
| MP:0002690 | akinesia | 0.391031049 | 1.025819672 |
| GO:0051283 | negative regulation of sequestering of calcium ion | 0.390905149 | 1.025864528 |
| GO:0090177 | establishment of planar polarity involved in neural tube ( | 0.999554805 | 1.025880682 |
| GO:0021799 | cerebral cortex radially oriented cell migration | 0.999550566 | 1.025946445 |
| GO:0016701 | oxidoreductase activity, acting on single donors with inc | 0.392198246 | 1.02600853 |
| GO:0048588 | developmental cell growth | 0.999548734 | 1.026019321 |
| ENSG00000100664 | EIF5 subnetwork | 0.390831815 | 1.026025321 |
| GO:0051209 | release of sequestered calcium ion into cytosol | 0.390905149 | 1.026047424 |
| GO:0021543 | pallium development | 0.999548662 | 1.026092207 |
| ENSG00000106105 | GARS subnetwork | 0.392537482 | 1.026141005 |
| GO:0008556 | potassium-transporting ATPase activity | 0.99954837 | 1.026165104 |
| GO:0007389 | pattern specification process | 0.999535926 | 1.026220249 |
| ENSG00000119401 | TRIM32 subnetwork | 0.39243917 | 1.026239119 |
| ENSG00000106459 | NRF1 subnetwork | 0.39252067 | 1.026278863 |
| GO:0050773 | regulation of dendrite development | 0.9995316 | 1.026289612 |
| GO:0022411 | cellular component disassembly | 0.392409679 | 1.026332623 |
| MP:0003402 | decreased liver weight | 0.393079858 | 1.026339127 |
| GO:0005720 | nuclear heterochromatin | 0.393023691 | 1.02636154 |
| MP:0009754 | enhanced behavioral response to cocaine | 0.999531593 | 1.026362538 |
| GO:0001937 | negative regulation of endothelial cell proliferation | 0.999527859 | 1.026431922 |
| GO:0045202 | synapse | 0.999527652 | 1.026504868 |
| MP:0002941 | increased circulating alanine transaminase level | 0.393017605 | 1.026525905 |
| ENSG00000214114 | MYCBP subnetwork | 0.392798173 | 1.026531156 |
| ENSG00000172893 | DHCR7 subnetwork | 0.392733106 | 1.026535866 |
| REACTOME_TRANSMEMBRANE_T | REACTOME_TRANSMEMBRANE_TRANSPORT_OF_SMALL | 0.999526109 | 1.026567164 |
| ENSG00000136891 | TEX10 subnetwork | 0.392958145 | 1.026601597 |
| MP:0001399 | hyperactivity | 0.999521468 | 1.026636577 |
| GO:0050829 | defense response to Gram-negative bacterium | 0.392942589 | 1.026695066 |
| GO:0046415 | urate metabolic process | 0.999520997 | 1.026705999 |
| GO:0045176 | apical protein localization | 0.99952059 | 1.026778986 |
| MP:0008284 | abnormal hippocampus pyramidal cell layer | 0.999520453 | 1.026851984 |
| MP:0002243 | abnormal vomeronasal organ morphology | 0.99951691 | 1.026917881 |
| GO:0071804 | cellular potassium ion transport | 0.999516068 | 1.026990899 |
| GO:0071805 | potassium ion transmembrane transport | 0.999516068 | 1.027063927 |
| ENSG00000166206 | GABRB3 subnetwork | 0.999513679 | 1.027133409 |
| ENSG00000115806 | GORASP2 subnetwork | 0.393560156 | 1.02714539 |
| MP:0009355 | increased liver triglyceride level | 0.393521406 | 1.027176804 |
| MP:0003460 | decreased fear-related response | 0.999513649 | 1.027206458 |
| GO:0018345 | protein palmitoylation | 0.99950653 | 1.027258179 |
| MP:0005407 | hyperalgesia | 0.99950217 | 1.027324134 |
| ENSG00000171603 | CLSTN1 subnetwork | 0.999497119 | 1.027390098 |

| | | | |
|---|---|---|---|
| GO:0051352 | negative regulation of ligase activity | 0.999494381 | 1.027463186 |
| GO:0051444 | negative regulation of ubiquitin-protein ligase activity | 0.999494381 | 1.027536283 |
| ENSG00000137699 | TRIM29 subnetwork | 0.999487772 | 1.027602277 |
| GO:0033293 | monocarboxylic acid binding | 0.999485706 | 1.027675395 |
| GO:0090190 | positive regulation of branching involved in ureteric bud | 0.999484919 | 1.027748523 |
| GO:0022029 | telencephalon cell migration | 0.999468153 | 1.027800313 |
| ENSG00000149295 | DRD2 subnetwork | 0.999466502 | 1.027873461 |
| GO:0008328 | ionotropic glutamate receptor complex | 0.999465545 | 1.027946619 |
| GO:0030808 | regulation of nucleotide biosynthetic process | 0.999461549 | 1.028009111 |
| GO:0030802 | regulation of cyclic nucleotide biosynthetic process | 0.999461549 | 1.028082289 |
| ENSG00000122566 | HNRNPA2B1 subnetwork | 0.393995008 | 1.028124446 |
| GO:0030513 | positive regulation of BMP signaling pathway | 0.999456306 | 1.028148359 |
| ENSG00000204967 | PCDHA4 subnetwork | 0.999455051 | 1.028214438 |
| GO:0060078 | regulation of postsynaptic membrane potential | 0.999448814 | 1.028276967 |
| MP:0000746 | weakness | 0.999446601 | 1.028350185 |
| MP:0000061 | fragile skeleton | 0.99943643 | 1.028416293 |
| REACTOME_GABA_SYNTHESIS_RE | REACTOME_GABA_SYNTHESIS_RELEASE_REUPTAKE_ANI | 0.999432719 | 1.028478849 |
| GO:0015293 | symporter activity | 0.999432179 | 1.028552097 |
| GO:0060998 | regulation of dendritic spine development | 0.999431435 | 1.028625356 |
| GO:0002407 | dendritic cell chemotaxis | 0.394201312 | 1.02866005 |
| GO:0050769 | positive regulation of neurogenesis | 0.999427723 | 1.028691502 |
| GO:0007187 | G-protein coupled receptor signaling pathway, coupled t | 0.999424087 | 1.028746973 |
| ENSG00000166407 | LMO1 subnetwork | 0.999423526 | 1.028820261 |
| MP:0003131 | increased erythrocyte cell number | 0.394468443 | 1.028830824 |
| MP:0001511 | disheveled coat | 0.394353371 | 1.028841042 |
| MP:0000036 | absent semicircular canals | 0.999421507 | 1.028889997 |
| ENSG00000179950 | PUF60 subnetwork | 0.394774214 | 1.028916622 |
| GO:0006790 | sulfur compound metabolic process | 0.999418154 | 1.028963306 |
| GO:0030850 | prostate gland development | 0.39457809 | 1.028993978 |
| MP:0004247 | small pancreas | 0.394464603 | 1.029013111 |
| GO:0030178 | negative regulation of Wnt receptor signaling pathway | 0.999409223 | 1.029018811 |
| ENSG00000167005 | NUDT21 subnetwork | 0.394756155 | 1.029072238 |
| GO:0032228 | regulation of synaptic transmission, GABAergic | 0.999404125 | 1.029088577 |
| ENSG00000172500 | FIBP subnetwork | 0.394927181 | 1.029106195 |
| GO:0035115 | embryonic forelimb morphogenesis | 0.999396068 | 1.029151226 |
| GO:0046520 | sphingoid biosynthetic process | 0.99939048 | 1.029213884 |
| GO:0016702 | oxidoreductase activity, acting on single donors with inc | 0.394749418 | 1.029245617 |
| GO:0007405 | neuroblast proliferation | 0.999387809 | 1.029280114 |
| REACTOME_AMINO_ACID_AND_( | REACTOME_AMINO_ACID_AND_OLIGOPEPTIDE_SLC_TR | 0.999385091 | 1.029353482 |
| ENSG00000173786 | CNP subnetwork | 0.999383339 | 1.029426861 |
| GO:0043101 | purine-containing compound salvage | 0.999382601 | 1.02950025 |
| GO:0042063 | gliogenesis | 0.999376515 | 1.029562955 |
| ENSG00000081479 | LRP2 subnetwork | 0.999368788 | 1.029611408 |
| GO:0031145 | anaphase-promoting complex-dependent proteasomal u | 0.999367076 | 1.029681261 |
| GO:0015291 | secondary active transmembrane transporter activity | 0.999364935 | 1.029751123 |
| GO:0048665 | neuron fate specification | 0.999359234 | 1.029799601 |
| MP:0005445 | abnormal neurotransmitter secretion | 0.999355482 | 1.029873048 |
| GO:0051436 | negative regulation of ubiquitin-protein ligase activity in | 0.99934574 | 1.029942939 |
| GO:0071436 | sodium ion export | 0.999344997 | 1.030016406 |
| GO:0030002 | cellular anion homeostasis | 0.999342914 | 1.030079184 |
| GO:0006525 | arginine metabolic process | 0.999334346 | 1.030120568 |
| MP:0000029 | abnormal malleus morphology | 0.999331073 | 1.030190497 |
| GO:0002087 | regulation of respiratory gaseous exchange by neurologi | 0.999327062 | 1.030260435 |
| GO:0044065 | regulation of respiratory system process | 0.999327062 | 1.030333952 |

| | | | |
|---|---|---|---|
| GO:0005272 | sodium channel activity | 0.999325488 | 1.030407479 |
| ENSG00000047932 | GOPC subnetwork | 0.395602857 | 1.030470547 |
| ENSG00000111186 | WNT5B subnetwork | 0.999323409 | 1.03047388 |
| GO:0000785 | chromatin | 0.395666324 | 1.030491687 |
| GO:0001786 | phosphatidylserine binding | 0.395556552 | 1.030502477 |
| MP:0004393 | abnormal cochlear inner hair cell morphology | 0.395775522 | 1.030539346 |
| GO:0016799 | hydrolase activity, hydrolyzing N-glycosyl compounds | 0.395506413 | 1.030543267 |
| GO:0051890 | regulation of cardioblast differentiation | 0.999322766 | 1.030543858 |
| MP:0004068 | dilated dorsal aorta | 0.999321023 | 1.030613847 |
| GO:0031128 | developmental induction | 0.999318694 | 1.030673139 |
| REACTOME_INFLUENZA_INFECTIC | REACTOME_INFLUENZA_INFECTION | 0.395913921 | 1.03071959 |
| GO:0006821 | chloride transport | 0.99931647 | 1.030743147 |
| GO:0043174 | nucleoside salvage | 0.999310641 | 1.030816734 |
| MP:0006020 | decreased tympanic ring size | 0.999310277 | 1.030890333 |
| GO:0030427 | site of polarized growth | 0.999309955 | 1.030963941 |
| GO:0051439 | regulation of ubiquitin-protein ligase activity involved in | 0.99929055 | 1.031019709 |
| GO:0033238 | regulation of cellular amine metabolic process | 0.999289291 | 1.031089766 |
| GO:0070570 | regulation of neuron projection regeneration | 0.999275569 | 1.031127696 |
| GO:0048679 | regulation of axon regeneration | 0.999275569 | 1.031201343 |
| GO:0001841 | neural tube formation | 0.99927209 | 1.031264286 |
| ENSG00000198010 | DLGAP2 subnetwork | 0.396192882 | 1.031297508 |
| GO:0060602 | branch elongation of an epithelium | 0.999250543 | 1.031312951 |
| GO:0021527 | spinal cord association neuron differentiation | 0.999249865 | 1.031383055 |
| GO:0005267 | potassium channel activity | 0.999249359 | 1.031456741 |
| MP:0001602 | impaired myelopoiesis | 0.396341157 | 1.031468717 |
| GO:0048704 | embryonic skeletal system morphogenesis | 0.99924408 | 1.03151972 |
| MP:0006033 | abnormal external auditory canal morphology | 0.999239403 | 1.031593426 |
| ENSG00000168539 | CHRM1 subnetwork | 0.999221991 | 1.031627841 |
| ENSG00000137500 | CCDC90B subnetwork | 0.999221749 | 1.031701565 |
| ENSG00000162302 | RPS6KA4 subnetwork | 0.397039412 | 1.031768443 |
| GO:0043043 | peptide biosynthetic process | 0.999221042 | 1.0317753 |
| GO:0008289 | lipid binding | 0.396894239 | 1.031797316 |
| GO:0071621 | granulocyte chemotaxis | 0.39669306 | 1.031831832 |
| ENSG00000163531 | NFASC subnetwork | 0.999220567 | 1.031849046 |
| ENSG00000111859 | NEDD9 subnetwork | 0.396764489 | 1.031861533 |
| ENSG00000197711 | ENSG00000197711 subnetwork | 0.397016598 | 1.031897617 |
| GO:0003197 | endocardial cushion development | 0.999213481 | 1.03191208 |
| GO:0010466 | negative regulation of peptidase activity | 0.396887057 | 1.031944199 |
| REACTOME_ACTIVATION_OF_GEI | REACTOME_ACTIVATION_OF_GENES_BY_ATF4 | 0.396604429 | 1.031949108 |
| GO:0022834 | ligand-gated channel activity | 0.999211768 | 1.031982272 |
| GO:0071622 | regulation of granulocyte chemotaxis | 0.39669306 | 1.032014134 |
| GO:0015276 | ligand-gated ion channel activity | 0.999211768 | 1.032056048 |
| ENSG00000168172 | HOOK3 subnetwork | 0.999209405 | 1.032129835 |
| ENSG00000133083 | DCLK1 subnetwork | 0.999207569 | 1.032200057 |
| GO:0051129 | negative regulation of cellular component organization | 0.999204596 | 1.032273865 |
| ENSG00000187672 | ERC2 subnetwork | 0.999203181 | 1.032344108 |
| MP:0000762 | abnormal tongue morphology | 0.999203012 | 1.032417936 |
| GO:0005680 | anaphase-promoting complex | 0.999202593 | 1.032491775 |
| GO:0005178 | integrin binding | 0.397404197 | 1.032539262 |
| GO:0044456 | synapse part | 0.999201943 | 1.032565625 |
| GO:0043113 | receptor clustering | 0.999199708 | 1.032639485 |
| ENSG00000196367 | TRRAP subnetwork | 0.397541836 | 1.032657022 |
| MP:0003123 | paternal imprinting | 0.999196995 | 1.032709779 |
| GO:0035725 | sodium ion transmembrane transport | 0.999190219 | 1.032772929 |

| | | | |
|---|---|---|---|
| MP:0008948 | decreased neuron number | 0.999181798 | 1.032843242 |
| GO:0001736 | establishment of planar polarity | 0.999181462 | 1.032917144 |
| GO:0032094 | response to food | 0.999155432 | 1.032958855 |
| MP:0001447 | abnormal nest building behavior | 0.999149763 | 1.033022041 |
| MP:0008023 | abnormal styloid process morphology | 0.999133168 | 1.033049453 |
| GO:0051321 | meiotic cell cycle | 0.39775389 | 1.033056977 |
| GO:0021988 | olfactory lobe development | 0.99913289 | 1.033116232 |
| GO:0042445 | hormone metabolic process | 0.397893703 | 1.033124669 |
| ENSG00000183431 | SF3A3 subnetwork | 0.397830106 | 1.03313933 |
| GO:0021772 | olfactory bulb development | 0.99913289 | 1.03319018 |
| GO:0070403 | NAD+ binding | 0.999129371 | 1.033260558 |
| ENSG00000070501 | POLB subnetwork | 0.99912456 | 1.033327368 |
| GO:0008066 | glutamate receptor activity | 0.999112254 | 1.033369129 |
| ENSG00000159023 | EPB41 subnetwork | 0.398027384 | 1.033400917 |
| REACTOME_CLASS_C3_METABOT | REACTOME_CLASS_C3_METABOTROPIC_GLUTAMATEPH | 0.999102511 | 1.033428796 |
| GO:0051351 | positive regulation of ligase activity | 0.99910144 | 1.033502792 |
| GO:0018130 | heterocycle biosynthetic process | 0.999100557 | 1.033576799 |
| GO:0030814 | regulation of cAMP metabolic process | 0.999092725 | 1.033632913 |
| ENSG00000180879 | SSR4 subnetwork | 0.39815396 | 1.033641812 |
| GO:0051437 | positive regulation of ubiquitin-protein ligase activity inv | 0.999088434 | 1.033699778 |
| GO:0048821 | erythrocyte development | 0.398483577 | 1.033759028 |
| GO:0030817 | regulation of cAMP biosynthetic process | 0.999086999 | 1.033773815 |
| GO:0046852 | positive regulation of bone remodeling | 0.399265394 | 1.033831546 |
| ENSG00000114251 | WNT5A subnetwork | 0.999084168 | 1.033847862 |
| GO:0005003 | ephrin receptor activity | 0.999074848 | 1.033911175 |
| ENSG00000198176 | TFDP1 subnetwork | 0.398483378 | 1.033941156 |
| GO:0017156 | calcium ion-dependent exocytosis | 0.999063599 | 1.033967333 |
| ENSG00000108883 | EFTUD2 subnetwork | 0.399617235 | 1.033992268 |
| ENSG00000198788 | MUC2 subnetwork | 0.398451031 | 1.034008811 |
| GO:0045780 | positive regulation of bone resorption | 0.399265394 | 1.034013366 |
| MP:0002021 | increased incidence of induced tumors | 0.398381008 | 1.034023616 |
| GO:0031644 | regulation of neurological system process | 0.999054894 | 1.034027081 |
| GO:0051495 | positive regulation of cytoskeleton organization | 0.399205419 | 1.034045734 |
| ENSG00000124194 | GDAP1L1 subnetwork | 0.399521559 | 1.034083319 |
| ENSG00000144285 | SCN1A subnetwork | 0.398723438 | 1.034096513 |
| ENSG00000132334 | PTPRE subnetwork | 0.999053778 | 1.034097585 |
| GO:0005246 | calcium channel regulator activity | 0.99903834 | 1.034143021 |
| GO:0007126 | meiosis | 0.39910908 | 1.034163294 |
| GO:0007184 | SMAD protein import into nucleus | 0.399615992 | 1.034173989 |
| ENSG00000079739 | PGM1 subnetwork | 0.3991858 | 1.034183673 |
| ENSG00000038002 | AGA subnetwork | 0.399490425 | 1.034186006 |
| ENSG00000070366 | SMG6 subnetwork | 0.398819497 | 1.034187357 |
| MP:0005167 | abnormal blood-brain barrier function | 0.399763117 | 1.034188335 |
| GO:0007631 | feeding behavior | 0.999028698 | 1.034213544 |
| MP:0005306 | abnormal phalanx morphology | 0.999019693 | 1.03426616 |
| MP:0002912 | abnormal excitatory postsynaptic potential | 0.999016711 | 1.034322368 |
| GO:0051327 | M phase of meiotic cell cycle | 0.39910908 | 1.034345301 |
| ENSG00000160062 | ZBTB8A subnetwork | 0.999012262 | 1.034392919 |
| GO:0009063 | cellular amino acid catabolic process | 0.999011757 | 1.034467063 |
| GO:0042359 | vitamin D metabolic process | 0.399092059 | 1.034500968 |
| ENSG00000168906 | MAT2A subnetwork | 0.399943679 | 1.03450729 |
| GO:0044349 | DNA excision | 0.999005733 | 1.034541219 |
| ENSG00000139668 | WDFY2 subnetwork | 0.399022588 | 1.034559859 |
| GO:0000718 | nucleotide-excision repair, DNA damage removal | 0.999005733 | 1.034615385 |

| | | | |
|---|---|---|---|
| GO:0007188 | adenylate cyclase-modulating G-protein coupled receptc | 0.99900256 | 1.034682392 |
| GO:0070979 | protein K11-linked ubiquitination | 0.999002032 | 1.034756578 |
| REACTOME_INTERACTION_BETW | REACTOME_INTERACTION_BETWEEN_L1_AND_ANKYRIN | 0.999001693 | 1.034830776 |
| GO:0021885 | forebrain cell migration | 0.998997416 | 1.034897813 |
| GO:0045216 | cell-cell junction organization | 0.998992446 | 1.034961274 |
| ENSG00000139083 | ETV6 subnetwork | 0.998985725 | 1.035021158 |
| GO:0090175 | regulation of establishment of planar polarity | 0.99898435 | 1.035095395 |
| GO:0060071 | Wnt receptor signaling pathway, planar cell polarity path | 0.99898435 | 1.035169643 |
| GO:0003231 | cardiac ventricle development | 0.998981531 | 1.035240316 |
| MP:0002765 | short fibula | 0.998980975 | 1.035314585 |
| GO:0044282 | small molecule catabolic process | 0.998975311 | 1.035385278 |
| MP:0001473 | reduced long term potentiation | 0.99896794 | 1.03544163 |
| MP:0002797 | increased thigmotaxis | 0.998964862 | 1.035508754 |
| GO:0048706 | embryonic skeletal system development | 0.998957558 | 1.035579476 |
| ENSG00000090273 | NUDC subnetwork | 0.998954972 | 1.035650208 |
| ENSG00000114315 | HES1 subnetwork | 0.400472238 | 1.035677907 |
| MP:0006065 | abnormal heart position or orientation | 0.998944949 | 1.035703007 |
| ENSG00000139505 | MTMR6 subnetwork | 0.400560908 | 1.035776997 |
| GO:0048013 | ephrin receptor signaling pathway | 0.998943083 | 1.035777347 |
| ENSG00000086205 | FOLH1 subnetwork | 0.401138674 | 1.035814484 |
| REACTOME_TANDEM_PORE_DOM | REACTOME_TANDEM_PORE_DOMAIN_POTASSIUM_CHA | 0.998942503 | 1.035851698 |
| REACTOME_MITOTIC_SPINDLE_C | REACTOME_MITOTIC_SPINDLE_CHECKPOINT | 0.998925149 | 1.035882986 |
| ENSG00000104695 | PPP2CB subnetwork | 0.400981752 | 1.035894737 |
| ENSG00000007174 | DNAH9 subnetwork | 0.401039939 | 1.035923522 |
| GO:0035036 | sperm-egg recognition | 0.401102602 | 1.035925991 |
| ENSG00000169213 | RAB3B subnetwork | 0.998921075 | 1.035935817 |
| GO:0007274 | neuromuscular synaptic transmission | 0.998911132 | 1.035999426 |
| MP:0000186 | decreased circulating HDL cholesterol level | 0.400974583 | 1.036058958 |
| MP:0004097 | abnormal cerebellar cortex morphology | 0.998910114 | 1.036073813 |
| ENSG00000147383 | NSDHL subnetwork | 0.400924257 | 1.036082836 |
| REACTOME_PI3K_CASCADE | REACTOME_PI3K_CASCADE | 0.400850902 | 1.03608917 |
| ENSG00000205155 | PSENEN subnetwork | 0.99890352 | 1.036141031 |
| ENSG00000123562 | MORF4L2 subnetwork | 0.401427816 | 1.036170026 |
| MP:0005618 | decreased urine potassium level | 0.400812907 | 1.036209621 |
| GO:0006865 | amino acid transport | 0.998902236 | 1.03621544 |
| ENSG00000135047 | CTSL1 subnetwork | 0.401379123 | 1.036228962 |
| GO:0001658 | branching involved in ureteric bud morphogenesis | 0.998892287 | 1.036282677 |
| GO:0048712 | negative regulation of astrocyte differentiation | 0.998889885 | 1.036357107 |
| MP:0009757 | impaired behavioral response to morphine | 0.998887448 | 1.036424364 |
| GO:0017134 | fibroblast growth factor binding | 0.40177637 | 1.036468734 |
| MP:0003076 | increased susceptibility to ischemic brain injury | 0.998874828 | 1.036470081 |
| GO:0006891 | intra-Golgi vesicle-mediated transport | 0.401606139 | 1.036470382 |
| GO:0032266 | phosphatidylinositol-3-phosphate binding | 0.998872448 | 1.03654454 |
| MP:0004086 | absent heartbeat | 0.401731537 | 1.0365452 |
| GO:0060606 | tube closure | 0.998867347 | 1.036608233 |
| ENSG00000150768 | DLAT subnetwork | 0.401694316 | 1.036621693 |
| ENSG00000154608 | ENSG00000154608 subnetwork | 0.998866677 | 1.036682713 |
| GO:0072088 | nephron epithelium morphogenesis | 0.99885749 | 1.036742833 |
| ENSG00000105737 | GRIK5 subnetwork | 0.998856691 | 1.036817333 |
| ENSG00000120251 | GRIA2 subnetwork | 0.99885281 | 1.036884657 |
| ENSG00000114554 | PLXNA1 subnetwork | 0.998846291 | 1.036948397 |
| MP:0001442 | decreased grooming behavior | 0.998842358 | 1.037022928 |
| ENSG00000150753 | CCT5 subnetwork | 0.402284083 | 1.037029582 |
| ENSG00000082805 | ERC1 subnetwork | 0.402150473 | 1.037068815 |

| | | | |
|---|---|---|---|
| GO:0051953 | negative regulation of amine transport | 0.998837763 | 1.037093876 |
| ENSG00000159479 | MED8 subnetwork | 0.402098362 | 1.037110333 |
| ENSG00000107807 | TLX1 subnetwork | 0.402238277 | 1.037114846 |
| MP:0003148 | decreased cochlear coiling | 0.998836464 | 1.037168428 |
| ENSG00000170743 | SYT9 subnetwork | 0.998830688 | 1.037242991 |
| GO:0032589 | neuron projection membrane | 0.998828392 | 1.037313969 |
| MP:0001393 | ataxia | 0.998823335 | 1.037374173 |
| GO:0015294 | solute:cation symporter activity | 0.998820329 | 1.037441576 |
| GO:0006379 | mRNA cleavage | 0.998818029 | 1.037508989 |
| MP:0001330 | abnormal optic nerve morphology | 0.998793127 | 1.037554836 |
| ENSG00000025772 | TOMM34 subnetwork | 0.998780156 | 1.037607883 |
| REACTOME_DEPOLARIZATION_OI | REACTOME_DEPOLARIZATION_OF_THE_PRESYNAPTIC_T | 0.99878014 | 1.037682515 |
| GO:0046513 | ceramide biosynthetic process | 0.998756877 | 1.037706805 |
| GO:0045168 | cell-cell signaling involved in cell fate commitment | 0.998750361 | 1.037770664 |
| ENSG00000172164 | SNTB1 subnetwork | 0.40261544 | 1.037819391 |
| MP:0002739 | abnormal olfactory bulb development | 0.998747585 | 1.037823741 |
| REACTOME_SULFUR_AMINO_ACI | REACTOME_SULFUR_AMINO_ACID_METABOLISM | 0.998745247 | 1.037891215 |
| ENSG00000016490 | CLCA1 subnetwork | 0.402837318 | 1.03795697 |
| GO:0010001 | glial cell differentiation | 0.998741028 | 1.037962297 |
| ENSG00000106004 | HOXA5 subnetwork | 0.402795291 | 1.038024843 |
| GO:0019827 | stem cell maintenance | 0.998740133 | 1.038033389 |
| GO:0032154 | cleavage furrow | 0.403109943 | 1.038068182 |
| GO:0070265 | necrotic cell death | 0.402764058 | 1.03808399 |
| GO:0046496 | nicotinamide nucleotide metabolic process | 0.998739912 | 1.038104491 |
| ENSG00000185745 | IFIT1 subnetwork | 0.402979838 | 1.038116474 |
| ENSG00000134072 | CAMK1 subnetwork | 0.998733936 | 1.038175603 |
| GO:0005261 | cation channel activity | 0.998713016 | 1.038225133 |
| ENSG00000101082 | SLA2 subnetwork | 0.403107116 | 1.038249694 |
| GO:0001573 | ganglioside metabolic process | 0.99871295 | 1.038299863 |
| GO:0042733 | embryonic digit morphogenesis | 0.998712367 | 1.038374604 |
| GO:0048103 | somatic stem cell division | 0.99870604 | 1.038445756 |
| GO:0006282 | regulation of DNA repair | 0.998704436 | 1.038516919 |
| GO:2001020 | regulation of response to DNA damage stimulus | 0.998702974 | 1.038584491 |
| GO:0072028 | nephron morphogenesis | 0.998695206 | 1.038641273 |
| MP:0000830 | abnormal diencephalon morphology | 0.998691705 | 1.038712465 |
| ENSG00000198001 | IRAK4 subnetwork | 0.403506751 | 1.038727718 |
| MP:0009888 | palatal shelves fail to meet at midline | 0.998688149 | 1.038787268 |
| GO:0009187 | cyclic nucleotide metabolic process | 0.998661729 | 1.038815268 |
| GO:0006638 | neutral lipid metabolic process | 0.403479822 | 1.038830624 |
| GO:0032098 | regulation of appetite | 0.998652664 | 1.038857678 |
| REACTOME_ENDOSOMAL_SORTI | REACTOME_ENDOSOMAL_SORTING_COMPLEX_REQUIR | 0.998650091 | 1.038921703 |
| MP:0000430 | absent maxillary shelf | 0.998649178 | 1.038996542 |
| GO:0060198 | clathrin sculpted vesicle | 0.998642239 | 1.039067791 |
| GO:0042474 | middle ear morphogenesis | 0.99863231 | 1.03912464 |
| REACTOME_LIGAND:GATED_ION_ | REACTOME_LIGAND:GATED_ION_CHANNEL_TRANSPOR | 0.998628744 | 1.039177895 |
| GO:0048168 | regulation of neuronal synaptic plasticity | 0.998628436 | 1.039252774 |
| MP:0002546 | mydriasis | 0.998616852 | 1.039302443 |
| GO:0022604 | regulation of cell morphogenesis | 0.998609777 | 1.039373739 |
| MP:0002199 | abnormal brain commissure morphology | 0.998608681 | 1.039441441 |
| ENSG00000173210 | ABLIM3 subnetwork | 0.403834894 | 1.039463568 |
| GO:0001738 | morphogenesis of a polarized epithelium | 0.998605816 | 1.039516362 |
| GO:0060896 | neural plate pattern specification | 0.403909926 | 1.03951782 |
| MP:0002207 | abnormal long term potentiation | 0.998591762 | 1.039569668 |
| MP:0001961 | abnormal reflex | 0.998575258 | 1.039622982 |

| | | | |
|---|---|---|---|
| ENSG00000177283 | FZD8 subnetwork | 0.405909898 | 1.039650678 |
| MP:0002699 | abnormal vitreous body morphology | 0.99856497 | 1.039651071 |
| GO:0007223 | Wnt receptor signaling pathway, calcium modulating pat | 0.998560869 | 1.039726027 |
| GO:0046464 | acylglycerol catabolic process | 0.405875377 | 1.039727099 |
| GO:0044106 | cellular amine metabolic process | 0.998560573 | 1.039800995 |
| MP:0001404 | no spontaneous movement | 0.998553673 | 1.039872368 |
| GO:0034599 | cellular response to oxidative stress | 0.406069252 | 1.039887055 |
| GO:0044269 | glycerol ether catabolic process | 0.405875377 | 1.039907858 |
| ENSG00000100599 | RIN3 subnetwork | 0.404117231 | 1.039912664 |
| GO:0005342 | organic acid transmembrane transporter activity | 0.998551418 | 1.039943751 |
| ENSG00000115840 | SLC25A12 subnetwork | 0.998546836 | 1.040015145 |
| GO:0008146 | sulfotransferase activity | 0.99854177 | 1.040086549 |
| GO:0046461 | neutral lipid catabolic process | 0.405875377 | 1.04008868 |
| ENSG00000135316 | SYNCRIP subnetwork | 0.404259036 | 1.040089067 |
| GO:0034705 | potassium channel complex | 0.998533261 | 1.040154357 |
| ENSG00000133958 | UNC79 subnetwork | 0.405846842 | 1.040173913 |
| GO:0060765 | regulation of androgen receptor signaling pathway | 0.406462012 | 1.040189269 |
| GO:0008076 | voltage-gated potassium channel complex | 0.998533261 | 1.040229388 |
| GO:0051926 | negative regulation of calcium ion transport | 0.405815068 | 1.040233084 |
| GO:0048608 | reproductive structure development | 0.406333312 | 1.040272711 |
| GO:0043523 | regulation of neuron apoptotic process | 0.405097392 | 1.040273662 |
| ENSG00000179915 | NRXN1 subnetwork | 0.998516145 | 1.040275574 |
| ENSG00000163440 | PDCL2 subnetwork | 0.405736456 | 1.040283577 |
| ENSG00000135144 | DTX1 subnetwork | 0.405696854 | 1.040307987 |
| REACTOME_BIOLOGICAL_OXIDAT | REACTOME_BIOLOGICAL_OXIDATIONS | 0.406261806 | 1.040314454 |
| MP:0001242 | hyperkeratosis | 0.405596829 | 1.040322019 |
| ENSG00000213555 | ENSG00000213555 subnetwork | 0.406451936 | 1.040343869 |
| ENSG00000163132 | MSX1 subnetwork | 0.998515814 | 1.040350624 |
| GO:0009416 | response to light stimulus | 0.405268635 | 1.040364175 |
| GO:2000021 | regulation of ion homeostasis | 0.405203153 | 1.040371209 |
| MP:0004279 | abnormal rostral migratory stream morphology | 0.99850949 | 1.04041847 |
| GO:0000188 | inactivation of MAPK activity | 0.405580641 | 1.040433496 |
| ENSG00000180185 | FAHD1 subnetwork | 0.405070881 | 1.040437587 |
| GO:0015093 | ferrous iron transmembrane transporter activity | 0.40494206 | 1.040460412 |
| GO:0017171 | serine hydrolase activity | 0.405691291 | 1.040471632 |
| GO:0007608 | sensory perception of smell | 0.99849546 | 1.040475503 |
| ENSG00000108039 | XPNPEP1 subnetwork | 0.404892306 | 1.040484912 |
| ENSG00000185787 | MORF4L1 subnetwork | 0.405504643 | 1.040517241 |
| GO:0033628 | regulation of cell adhesion mediated by integrin | 0.405536311 | 1.040527599 |
| GO:0001542 | ovulation from ovarian follicle | 0.405049566 | 1.040531822 |
| ENSG00000113068 | PFDN1 subnetwork | 0.998489674 | 1.040543368 |
| GO:0051654 | establishment of mitochondrion localization | 0.998477412 | 1.040593202 |
| GO:0033014 | tetrapyrrole biosynthetic process | 0.405460984 | 1.040602682 |
| ENSG00000143858 | SYT2 subnetwork | 0.998465169 | 1.04065026 |
| ENSG00000152455 | SUV39H2 subnetwork | 0.404891192 | 1.040666434 |
| GO:0035176 | social behavior | 0.998460957 | 1.040718152 |
| GO:0006779 | porphyrin-containing compound biosynthetic process | 0.405460984 | 1.040783972 |
| GO:0060291 | long-term synaptic potentiation | 0.998460902 | 1.040793273 |
| ENSG00000162298 | SYVN1 subnetwork | 0.404646083 | 1.040799581 |
| ENSG00000168003 | SLC3A2 subnetwork | 0.40487282 | 1.040830571 |
| ENSG00000138442 | WDR12 subnetwork | 0.404600564 | 1.040841627 |
| MP:0003861 | abnormal nervous system development | 0.998452015 | 1.040853967 |
| GO:0051438 | regulation of ubiquitin-protein ligase activity | 0.99845162 | 1.040929108 |
| GO:0050873 | brown fat cell differentiation | 0.407808818 | 1.040957908 |

| | | | |
|---|---|---|---|
| ENSG00000163399 | ATP1A1 subnetwork | 0.407421056 | 1.040967406 |
| ENSG00000105438 | KDELR1 subnetwork | 0.407493956 | 1.040968972 |
| GO:0048641 | regulation of skeletal muscle tissue development | 0.404864516 | 1.040994764 |
| MP:0009940 | abnormal hippocampus pyramidal cell morphology | 0.998448152 | 1.04100065 |
| ENSG00000136146 | MED4 subnetwork | 0.407579344 | 1.041005199 |
| ENSG00000126214 | KLC1 subnetwork | 0.407746922 | 1.041016979 |
| GO:0005523 | tropomyosin binding | 0.998432873 | 1.041043321 |
| ENSG00000103426 | CORO7 subnetwork | 0.407386148 | 1.04106121 |
| GO:2000177 | regulation of neural precursor cell proliferation | 0.998417612 | 1.041089609 |
| ENSG00000124299 | PEPD subnetwork | 0.407671924 | 1.041093398 |
| ENSG00000102780 | DGKH subnetwork | 0.404838883 | 1.041097923 |
| ENSG00000150995 | ITPR1 subnetwork | 0.407990752 | 1.041099567 |
| ENSG00000138071 | ACTR2 subnetwork | 0.408272467 | 1.041107266 |
| ENSG00000090861 | AARS subnetwork | 0.40725856 | 1.041136167 |
| GO:0048037 | cofactor binding | 0.998392571 | 1.041146736 |
| ENSG00000089280 | FUS subnetwork | 0.407944838 | 1.041167302 |
| KEGG_SPLICEOSOME | KEGG_SPLICEOSOME | 0.407353842 | 1.04117239 |
| GO:0030312 | external encapsulating structure | 0.99838885 | 1.041214704 |
| ENSG00000054118 | THRAP3 subnetwork | 0.408247018 | 1.041218204 |
| GO:0042533 | tumor necrosis factor biosynthetic process | 0.407252003 | 1.041282096 |
| GO:0055008 | cardiac muscle tissue morphogenesis | 0.998388724 | 1.041289903 |
| ENSG00000138668 | HNRNPD subnetwork | 0.408205747 | 1.041320526 |
| MP:0005223 | abnormal anterior-posterior polarity of the somites | 0.406991925 | 1.041336806 |
| GO:0014033 | neural crest cell differentiation | 0.998386811 | 1.041361502 |
| REACTOME_SRP:DEPENDENT_CO | REACTOME_SRP:DEPENDENT_COTRANSLATIONAL_PROT | 0.407166274 | 1.041391878 |
| ENSG00000163602 | RYBP subnetwork | 0.408510081 | 1.041395711 |
| GO:0005543 | phospholipid binding | 0.407073827 | 1.041407742 |
| MP:0006316 | increased urine sodium level | 0.408188886 | 1.041422884 |
| GO:0090179 | planar cell polarity pathway involved in neural tube closu | 0.99838678 | 1.041436723 |
| GO:0042534 | regulation of tumor necrosis factor biosynthetic process | 0.407252003 | 1.04146278 |
| GO:0090178 | regulation of establishment of planar polarity involved in | 0.99838678 | 1.041511956 |
| MP:0009289 | decreased epididymal fat pad weight | 0.408492534 | 1.041523958 |
| GO:0006415 | translational termination | 0.408157387 | 1.041533934 |
| GO:0035136 | forelimb morphogenesis | 0.998378829 | 1.041576362 |
| MP:0003078 | aphakia | 0.998366114 | 1.041633552 |
| ENSG00000008196 | TFAP2B subnetwork | 0.998364589 | 1.041708815 |
| GO:0001843 | neural tube closure | 0.998353293 | 1.041769637 |
| ENSG00000123384 | LRP1 subnetwork | 0.998352883 | 1.04184492 |
| MP:0000516 | abnormal renal/urinary system morphology | 0.998350062 | 1.0419166 |
| ENSG00000079819 | EPB41L2 subnetwork | 0.998349339 | 1.041991905 |
| GO:0060026 | convergent extension | 0.998346469 | 1.042063607 |
| ENSG00000131876 | SNRPA1 subnetwork | 0.40892468 | 1.042064315 |
| REACTOME_MRNA_SPLICING_:_M | REACTOME_MRNA_SPLICING_:_MINOR_PATHWAY | 0.408848929 | 1.042071589 |
| GO:0042813 | Wnt-activated receptor activity | 0.998343125 | 1.042131704 |
| GO:0060079 | regulation of excitatory postsynaptic membrane potenti | 0.998335099 | 1.042203427 |
| GO:0050803 | regulation of synapse structure and activity | 0.998334164 | 1.042278774 |
| MP:0002110 | abnormal digit morphology | 0.998333137 | 1.042354132 |
| GO:0030510 | regulation of BMP signaling pathway | 0.998305667 | 1.042378886 |
| GO:0019439 | aromatic compound catabolic process | 0.998301707 | 1.042450647 |
| ENSG00000092108 | SCFD1 subnetwork | 0.409141947 | 1.042480553 |
| GO:0008509 | anion transmembrane transporter activity | 0.998299884 | 1.042526034 |
| ENSG00000166411 | IDH3A subnetwork | 0.409389557 | 1.042544921 |
| ENSG00000174622 | ENSG00000174622 subnetwork | 0.998288635 | 1.042586968 |
| ENSG00000198728 | LDB1 subnetwork | 0.998284825 | 1.042655142 |

| | | | |
|---|---|---|---|
| GO:0031589 | cell-substrate adhesion | 0.409377661 | 1.042707793 |
| ENSG00000007372 | PAX6 subnetwork | 0.998282169 | 1.042726944 |
| GO:0008235 | metalloexopeptidase activity | 0.409317313 | 1.042732458 |
| MP:0000438 | abnormal cranium morphology | 0.998272435 | 1.042787905 |
| GO:0010765 | positive regulation of sodium ion transport | 0.998272252 | 1.042863344 |
| GO:0031406 | carboxylic acid binding | 0.998272213 | 1.042938793 |
| GO:0045739 | positive regulation of DNA repair | 0.998263987 | 1.043010636 |
| GO:0031345 | negative regulation of cell projection organization | 0.998254653 | 1.043075253 |
| REACTOME_POST:TRANSLATIONA | REACTOME_POST:TRANSLATIONAL_PROTEIN_MODIFICA | 0.409654514 | 1.043090344 |
| MP:0009453 | enhanced contextual conditioning behavior | 0.998245909 | 1.04313988 |
| ENSG00000032742 | IFT88 subnetwork | 0.998239218 | 1.043208134 |
| GO:0014020 | primary neural tube formation | 0.998236621 | 1.043283636 |
| GO:0046134 | pyrimidine nucleoside biosynthetic process | 0.998226873 | 1.043337435 |
| MP:0005205 | abnormal eye anterior chamber morphology | 0.998223197 | 1.043412957 |
| GO:0030902 | hindbrain development | 0.998222569 | 1.04348487 |
| GO:0009954 | proximal/distal pattern formation | 0.998208206 | 1.043545935 |
| GO:0007158 | neuron cell-cell adhesion | 0.998207873 | 1.043621489 |
| GO:0021545 | cranial nerve development | 0.998206792 | 1.043693433 |
| ENSG00000213023 | SYT3 subnetwork | 0.998205288 | 1.043769008 |
| ENSG00000158691 | ZSCAN12 subnetwork | 0.410148123 | 1.043776972 |
| ENSG00000206380 | C6orf48 subnetwork | 0.410095469 | 1.04378453 |
| ENSG00000137474 | MYO7A subnetwork | 0.998194207 | 1.043833732 |
| ENSG00000141279 | NPEPPS subnetwork | 0.410297683 | 1.043839517 |
| GO:0030832 | regulation of actin filament length | 0.410234804 | 1.043847083 |
| GO:0002526 | acute inflammatory response | 0.410389904 | 1.04386646 |
| GO:0009070 | serine family amino acid biosynthetic process | 0.998193034 | 1.043909328 |
| MP:0000130 | abnormal trabecular bone morphology | 0.410612313 | 1.043955854 |
| ENSG00000204387 | C6orf48 subnetwork | 0.410095469 | 1.043964773 |
| GO:0009124 | nucleoside monophosphate biosynthetic process | 0.998192831 | 1.043984935 |
| ENSG00000088833 | NSFL1C subnetwork | 0.410494977 | 1.04400552 |
| GO:0007519 | skeletal muscle tissue development | 0.410550762 | 1.044015178 |
| GO:0007512 | adult heart development | 0.998192753 | 1.044060553 |
| GO:0015179 | L-amino acid transmembrane transporter activity | 0.998189113 | 1.044132561 |
| ENSG00000206271 | ENSG00000206271 subnetwork | 0.410095469 | 1.044145078 |
| GO:0031290 | retinal ganglion cell axon guidance | 0.998183485 | 1.044197334 |
| GO:0044089 | positive regulation of cellular component biogenesis | 0.998171158 | 1.044247627 |
| ENSG00000170043 | TRAPPC1 subnetwork | 0.410813925 | 1.044301724 |
| MP:0004726 | abnormal nasal capsule morphology | 0.998155751 | 1.044305173 |
| ENSG00000168615 | ADAM9 subnetwork | 0.410891008 | 1.044354422 |
| GO:0010659 | cardiac muscle cell apoptotic process | 0.998151658 | 1.044369973 |
| GO:0001158 | enhancer sequence-specific DNA binding | 0.998147378 | 1.044442029 |
| GO:0070411 | I-SMAD binding | 0.411461262 | 1.04447314 |
| GO:0005245 | voltage-gated calcium channel activity | 0.998142629 | 1.044510472 |
| ENSG00000204523 | ENSG00000204523 subnetwork | 0.411077319 | 1.044553602 |
| GO:0008214 | protein dealkylation | 0.411396847 | 1.044558292 |
| MP:0000564 | syndactyly | 0.998136918 | 1.044571677 |
| ENSG00000116171 | SCP2 subnetwork | 0.411166749 | 1.044632087 |
| GO:0022804 | active transmembrane transporter activity | 0.998133606 | 1.044636515 |
| ENSG00000169251 | NMD3 subnetwork | 0.41169602 | 1.044690189 |
| GO:0015909 | long-chain fatty acid transport | 0.998128987 | 1.044712235 |
| GO:0006482 | protein demethylation | 0.411396847 | 1.044738202 |
| ENSG00000165494 | PCF11 subnetwork | 0.411640453 | 1.044766741 |
| REACTOME_GABA_A_RECEPTOR_ | REACTOME_GABA_A_RECEPTOR_ACTIVATION | 0.998126505 | 1.044787967 |
| ENSG00000125675 | GRIA3 subnetwork | 0.998122031 | 1.044863709 |

| | | | |
|---|---|---|---|
| ENSG00000110876 | SELPLG subnetwork | 0.411304938 | 1.04486561 |
| GO:0071339 | MLL1 complex | 0.411388826 | 1.044909561 |
| GO:0030148 | sphingolipid biosynthetic process | 0.998121294 | 1.044932212 |
| ENSG00000163634 | THOC7 subnetwork | 0.411856116 | 1.044983652 |
| GO:0034374 | low-density lipoprotein particle remodeling | 0.998117237 | 1.0449971 |
| MP:0000781 | decreased corpus callosum size | 0.998108477 | 1.045069248 |
| GO:0009069 | serine family amino acid metabolic process | 0.998089272 | 1.045123278 |
| REACTOME_REGULATION_OF_IFN | REACTOME_REGULATION_OF_IFNA_SIGNALING | 0.41198039 | 1.045182381 |
| GO:0007164 | establishment of tissue polarity | 0.998082879 | 1.04519182 |
| GO:0015807 | L-amino acid transport | 0.998082476 | 1.045267624 |
| KEGG_GLYCOSAMINOGLYCAN_BI | KEGG_GLYCOSAMINOGLYCAN_BIOSYNTHESIS_HEPARAN | 0.998078652 | 1.045343439 |
| ENSG00000166401 | SERPINB8 subnetwork | 0.412674998 | 1.045344443 |
| GO:0051955 | regulation of amino acid transport | 0.998065497 | 1.045404758 |
| ENSG00000204580 | DDR1 subnetwork | 0.412635472 | 1.045429553 |
| GO:0022839 | ion gated channel activity | 0.412149706 | 1.045449854 |
| GO:0016853 | isomerase activity | 0.412215645 | 1.045450636 |
| ENSG00000169992 | NLGN2 subnetwork | 0.99805765 | 1.045476968 |
| GO:0007160 | cell-matrix adhesion | 0.412380887 | 1.045520206 |
| MP:0000195 | hypocalcemia | 0.4132415 | 1.04552162 |
| MP:0001360 | abnormal social investigation | 0.998054276 | 1.045549187 |
| GO:0051931 | regulation of sensory perception | 0.412921403 | 1.04557864 |
| GO:0060603 | mammary gland duct morphogenesis | 0.412825353 | 1.045594297 |
| GO:0071774 | response to fibroblast growth factor stimulus | 0.413208992 | 1.045606659 |
| ENSG00000137332 | DDR1 subnetwork | 0.412635472 | 1.045609211 |
| MP:0000554 | abnormal carpal bone morphology | 0.998047865 | 1.045610535 |
| REACTOME_PHOSPHOLIPASE_C:M | REACTOME_PHOSPHOLIPASE_C:MEDIATED_CASCADE | 0.412488194 | 1.045632737 |
| ENSG00000172057 | ORMDL3 subnetwork | 0.998047043 | 1.045679147 |
| GO:0032846 | positive regulation of homeostatic process | 0.413054691 | 1.045690987 |
| ENSG00000114019 | AMOTL2 subnetwork | 0.998032203 | 1.045729628 |
| GO:0051930 | regulation of sensory perception of pain | 0.412921403 | 1.0457582 |
| GO:0044344 | cellular response to fibroblast growth factor stimulus | 0.413208992 | 1.045786131 |
| ENSG00000215522 | DDR1 subnetwork | 0.412635472 | 1.045788931 |
| ENSG00000171564 | FGB subnetwork | 0.413444664 | 1.045789022 |
| GO:0043555 | regulation of translation in response to stress | 0.412588201 | 1.045796802 |
| GO:0031012 | extracellular matrix | 0.998031864 | 1.045805515 |
| GO:0007620 | copulation | 0.99802947 | 1.045881414 |
| ENSG00000147601 | TERF1 subnetwork | 0.413415859 | 1.045891233 |
| ENSG00000128050 | PAICS subnetwork | 0.998015106 | 1.045910147 |
| GO:0031396 | regulation of protein ubiquitination | 0.998005321 | 1.045975176 |
| GO:0007589 | body fluid secretion | 0.413800452 | 1.045981148 |
| REACTOME_TRAFFICKING_OF_GL | REACTOME_TRAFFICKING_OF_GLUR2:CONTAINING_AM | 0.99800242 | 1.046051103 |
| ENSG00000001630 | CYP51A1 subnetwork | 0.41377651 | 1.046100446 |
| MP:0004792 | abnormal synaptic vesicle number | 0.997994228 | 1.046116152 |
| MP:0000298 | absent atrioventricular cushions | 0.413734033 | 1.046176924 |
| GO:0021871 | forebrain regionalization | 0.997991279 | 1.046184841 |
| MP:0005178 | increased circulating cholesterol level | 0.414126226 | 1.046231586 |
| GO:0042598 | vesicular fraction | 0.414036767 | 1.046239507 |
| GO:0003207 | cardiac chamber formation | 0.997987328 | 1.046249909 |
| MP:0004722 | abnormal platelet dense granule number | 0.413976212 | 1.0462817 |
| GO:0004016 | adenylate cyclase activity | 0.997946267 | 1.046293204 |
| ENSG00000160310 | PRMT2 subnetwork | 0.413715428 | 1.046313443 |
| GO:0003206 | cardiac chamber morphogenesis | 0.997936172 | 1.046354658 |
| GO:0045494 | photoreceptor cell maintenance | 0.997929943 | 1.046430646 |
| GO:0035809 | regulation of urine volume | 0.414308372 | 1.046489125 |

| | | | |
|---|---|---|---|
| ENSG00000159166 | LAD1 subnetwork | 0.413713289 | 1.046492883 |
| GO:0005242 | inward rectifier potassium channel activity | 0.997926222 | 1.046506645 |
| MP:0001327 | decreased retinal photoreceptor cell number | 0.414471106 | 1.046524568 |
| ENSG00000161647 | MPP3 subnetwork | 0.997919946 | 1.046571761 |
| ENSG00000120948 | TARDBP subnetwork | 0.414436259 | 1.046618151 |
| GO:0005758 | mitochondrial intermembrane space | 0.414649343 | 1.046629021 |
| MP:0008143 | abnormal dendrite morphology | 0.997916929 | 1.046647781 |
| REACTOME_PHOSPHORYLATION_ | REACTOME_PHOSPHORYLATION_OF_THE_APCC | 0.997905516 | 1.046709284 |
| REACTOME_GPVI:MEDIATED_ACT | REACTOME_GPVI:MEDIATED_ACTIVATION_CASCADE | 0.414635017 | 1.046739689 |
| GO:0046943 | carboxylic acid transmembrane transporter activity | 0.997899889 | 1.04677806 |
| MP:0000049 | abnormal middle ear morphology | 0.997847926 | 1.046839352 |
| GO:0043084 | penile erection | 0.9978918 | 1.046846847 |
| ENSG00000113312 | TTC1 subnetwork | 0.997823126 | 1.046857288 |
| ENSG00000132780 | NASP subnetwork | 0.414623595 | 1.046884629 |
| GO:0045880 | positive regulation of smoothened signaling pathway | 0.997808247 | 1.046889761 |
| GO:0050686 | negative regulation of mRNA processing | 0.997794723 | 1.046940407 |
| GO:0050819 | negative regulation of coagulation | 0.997787005 | 1.047012864 |
| GO:0006749 | glutathione metabolic process | 0.997780112 | 1.047085332 |
| ENSG00000170486 | KRT72 subnetwork | 0.415120689 | 1.047161423 |
| GO:0046467 | membrane lipid biosynthetic process | 0.997778269 | 1.047161445 |
| ENSG00000026025 | VIM subnetwork | 0.415185651 | 1.047179005 |
| GO:0009799 | specification of symmetry | 0.997746821 | 1.047190317 |
| GO:0002028 | regulation of sodium ion transport | 0.997719757 | 1.047211923 |
| GO:0032095 | regulation of response to food | 0.997682724 | 1.047218991 |
| ENSG00000077264 | PAK3 subnetwork | 0.415067729 | 1.047246451 |
| GO:0015849 | organic acid transport | 0.997650103 | 1.047255144 |
| GO:0005234 | extracellular-glutamate-gated ion channel activity | 0.997634082 | 1.047298575 |
| GO:0060996 | dendritic spine development | 0.997616567 | 1.047345648 |
| MP:0008788 | abnormal fetal cardiomyocyte morphology | 0.414963587 | 1.047348161 |
| GO:0032868 | response to insulin stimulus | 0.415058352 | 1.047417037 |
| GO:0005578 | proteinaceous extracellular matrix | 0.997614658 | 1.047421818 |
| REACTOME_APC:CDC20_MEDIATI | REACTOME_APC:CDC20_MEDIATED_DEGRADATION_OF | 0.997605719 | 1.04748709 |
| GO:0035510 | DNA dealkylation | 0.415338523 | 1.047538462 |
| GO:0021700 | developmental maturation | 0.99760369 | 1.047559645 |
| GO:0072073 | kidney epithelium development | 0.997592774 | 1.047624936 |
| ENSG00000158445 | KCNB1 subnetwork | 0.997589658 | 1.047693875 |
| MP:0010404 | ostium primum atrial septal defect | 0.997581252 | 1.047759185 |
| GO:0035019 | somatic stem cell maintenance | 0.997556437 | 1.047806315 |
| MP:0006142 | abnormal sinoatrial node conduction | 0.997540908 | 1.04787892 |
| ENSG00000140939 | NOL3 subnetwork | 0.415527065 | 1.04788925 |
| GO:0070566 | adenylyltransferase activity | 0.997517867 | 1.047936982 |
| GO:0051000 | positive regulation of nitric-oxide synthase activity | 0.415620388 | 1.047957963 |
| ENSG00000183598 | HIST2H3D subnetwork | 0.415932282 | 1.047967896 |
| ENSG00000067836 | ROGDI subnetwork | 0.997508676 | 1.047980496 |
| REACTOME_CHAPERONIN:MEDIA | REACTOME_CHAPERONIN:MEDIATED_PROTEIN_FOLDIN | 0.415797404 | 1.048001367 |
| ENSG00000136636 | KCTD3 subnetwork | 0.415719099 | 1.048009568 |
| MP:0000531 | right pulmonary isomerism | 0.997487818 | 1.0480131 |
| GO:0005095 | GTPase inhibitor activity | 0.415995996 | 1.048028001 |
| ENSG00000109472 | CPE subnetwork | 0.997487301 | 1.048089381 |
| GO:0070838 | divalent metal ion transport | 0.416049168 | 1.04809662 |
| ENSG00000203811 | HIST2H3C subnetwork | 0.415932282 | 1.048146883 |
| GO:0001891 | phagocytic cup | 0.416155007 | 1.048156682 |
| GO:0030195 | negative regulation of blood coagulation | 0.997483922 | 1.048162032 |
| ENSG00000109917 | ZNF259 subnetwork | 0.997469246 | 1.048220135 |

| | | | |
|---|---|---|---|
| REACTOME_INACTIVATION_OF_A | REACTOME_INACTIVATION_OF_APCC_VIA_DIRECT_INHI | 0.997458806 | 1.048285527 |
| REACTOME_INHIBITION_OF_THE_ | REACTOME_INHIBITION_OF_THE_PROTEOLYTIC_ACTIVI | 0.997458806 | 1.048361849 |
| GO:0007600 | sensory perception | 0.99744572 | 1.04842362 |
| GO:0003205 | cardiac chamber development | 0.997438083 | 1.048496323 |
| KEGG_RNA_POLYMERASE | KEGG_RNA_POLYMERASE | 0.416385828 | 1.048523891 |
| GO:0050768 | negative regulation of neurogenesis | 0.997428948 | 1.048565395 |
| GO:0008203 | cholesterol metabolic process | 0.41656646 | 1.04860116 |
| MP:0002988 | decreased urine osmolality | 0.416625806 | 1.048601399 |
| GO:0051937 | catecholamine transport | 0.997426015 | 1.04864176 |
| ENSG00000198822 | GRM3 subnetwork | 0.997425968 | 1.048718135 |
| GO:0042623 | ATPase activity, coupled | 0.416556636 | 1.048737417 |
| MP:0000373 | belly spot | 0.997425791 | 1.048794523 |
| ENSG00000035403 | VCL subnetwork | 0.416984856 | 1.048815408 |
| GO:0050661 | NADP binding | 0.997419497 | 1.048867279 |
| ENSG00000141456 | ENSG00000141456 subnetwork | 0.416952172 | 1.048900443 |
| ENSG00000099365 | STX1B subnetwork | 0.997406966 | 1.048929118 |
| MP:0002641 | anisopoikilocytosis | 0.416862018 | 1.048959754 |
| MP:0002736 | abnormal nociception after inflammation | 0.997405749 | 1.049005537 |
| ENSG00000135698 | MPHOSPH6 subnetwork | 0.416925989 | 1.049028133 |
| REACTOME_ANTIGEN_PRESENTA | REACTOME_ANTIGEN_PRESENTATION_FOLDING_ASSEM | 0.417259829 | 1.049045997 |
| MP:0001489 | decreased startle reflex | 0.997394926 | 1.049078324 |
| ENSG00000113569 | NUP155 subnetwork | 0.417419873 | 1.049097411 |
| ENSG00000169347 | GP2 subnetwork | 0.417371818 | 1.049122807 |
| GO:0046395 | carboxylic acid catabolic process | 0.997390642 | 1.049151122 |
| ENSG00000188529 | SRSF10 subnetwork | 0.417257937 | 1.04922474 |
| GO:0016054 | organic acid catabolic process | 0.997390642 | 1.049227574 |
| ENSG00000184702 | SEPT5 subnetwork | 0.997390591 | 1.049304037 |
| GO:0042053 | regulation of dopamine metabolic process | 0.997360582 | 1.049311275 |
| GO:0070410 | co-SMAD binding | 0.417236882 | 1.04935242 |
| GO:0045601 | regulation of endothelial cell differentiation | 0.997357543 | 1.049384111 |
| MP:0000854 | abnormal cerebellum development | 0.997348663 | 1.049460602 |
| GO:0008652 | cellular amino acid biosynthetic process | 0.997347609 | 1.049537105 |
| GO:0016917 | GABA receptor activity | 0.997322961 | 1.049584457 |
| GO:0021987 | cerebral cortex development | 0.997314121 | 1.049646398 |
| GO:0017147 | Wnt-protein binding | 0.997301163 | 1.049711994 |
| ENSG00000184486 | POU3F2 subnetwork | 0.997300995 | 1.049788537 |
| GO:0042476 | odontogenesis | 0.997297976 | 1.049861445 |
| GO:0007219 | Notch signaling pathway | 0.997296685 | 1.049938011 |
| ENSG00000133112 | TPT1 subnetwork | 0.997286686 | 1.050003647 |
| GO:0045598 | regulation of fat cell differentiation | 0.417855167 | 1.050025541 |
| REACTOME_CLASS_B2_SECRETIN_ | REACTOME_CLASS_B2_SECRETIN_FAMILY_RECEPTORS | 0.997265971 | 1.050054705 |
| KEGG_LYSOSOME | KEGG_LYSOSOME | 0.997255361 | 1.050120359 |
| GO:0044309 | neuron spine | 0.997237237 | 1.050164138 |
| GO:0043197 | dendritic spine | 0.997237237 | 1.050240753 |
| ENSG00000100109 | TFIP11 subnetwork | 0.417998541 | 1.050289411 |
| MP:0001384 | abnormal pup retrieval | 0.997236618 | 1.050317379 |
| MP:0003787 | abnormal imprinting | 0.997235501 | 1.050394017 |
| GO:0050995 | negative regulation of lipid catabolic process | 0.997230592 | 1.05045972 |
| GO:0008202 | steroid metabolic process | 0.418136835 | 1.050468085 |
| MP:0002682 | decreased mature ovarian follicle number | 0.418254796 | 1.050518972 |
| GO:0032489 | regulation of Cdc42 protein signal transduction | 0.997227224 | 1.050529081 |
| ENSG00000150086 | GRIN2B subnetwork | 0.418189259 | 1.050536079 |
| GO:0043088 | regulation of Cdc42 GTPase activity | 0.997227224 | 1.050605751 |
| GO:0051443 | positive regulation of ubiquitin-protein ligase activity | 0.997224403 | 1.050678783 |

| | | | |
|---|---|---|---|
| GO:0002720 | positive regulation of cytokine production involved in im | 0.419207207 | 1.050687606 |
| GO:0000079 | regulation of cyclin-dependent protein kinase activity | 0.997210296 | 1.050737226 |
| GO:0007050 | cell cycle arrest | 0.418521933 | 1.050765306 |
| MP:0008260 | abnormal autophagy | 0.997209509 | 1.050802978 |
| MP:0005130 | decreased follicle stimulating hormone level | 0.997140324 | 1.050810337 |
| ENSG00000145794 | MEGF10 subnetwork | 0.419186533 | 1.05083206 |
| ENSG00000133937 | GSC subnetwork | 0.419133639 | 1.050840693 |
| REACTOME_ROLE_OF_DCC_IN_RI | REACTOME_ROLE_OF_DCC_IN_REGULATING_APOPTOSI | 0.997098704 | 1.050850551 |
| MP:0009831 | abnormal sperm midpiece morphology | 0.418482409 | 1.050884504 |
| REACTOME_APCCCDC20_MEDIAT | REACTOME_APCCCDC20_MEDIATED_DEGRADATION_OF | 0.997093917 | 1.050909025 |
| GO:0001960 | negative regulation of cytokine-mediated signaling pathv | 0.419115517 | 1.050959742 |
| MP:0001322 | abnormal iris morphology | 0.997080896 | 1.050967506 |
| GO:0032312 | regulation of ARF GTPase activity | 0.418997016 | 1.050994053 |
| GO:0006413 | translational initiation | 0.418938749 | 1.050994222 |
| MP:0000807 | abnormal hippocampus morphology | 0.997064585 | 1.051022346 |
| ENSG00000160789 | LMNA subnetwork | 0.419072238 | 1.051027863 |
| GO:0045649 | regulation of macrophage differentiation | 0.418471258 | 1.051037768 |
| MP:0002229 | neurodegeneration | 0.418735794 | 1.051054242 |
| ENSG00000013441 | CLK1 subnetwork | 0.419650995 | 1.051068884 |
| MP:0005602 | decreased angiogenesis | 0.419579744 | 1.05107755 |
| MP:0002938 | white spotting | 0.997062657 | 1.051099102 |
| ENSG00000053372 | MRTO4 subnetwork | 0.419458072 | 1.051111866 |
| GO:0000217 | DNA secondary structure binding | 0.418931441 | 1.051130376 |
| GO:0051354 | negative regulation of oxidoreductase activity | 0.997035815 | 1.051139351 |
| GO:0010623 | developmental programmed cell death | 0.418860057 | 1.05116457 |
| ENSG00000147382 | FAM58A subnetwork | 0.419767145 | 1.051170483 |
| ENSG00000106278 | PTPRZ1 subnetwork | 0.997030953 | 1.051212475 |
| GO:0016126 | sterol biosynthetic process | 0.419566703 | 1.051221996 |
| GO:0031998 | regulation of fatty acid beta-oxidation | 0.997016465 | 1.051267348 |
| GO:0006520 | cellular amino acid metabolic process | 0.997009164 | 1.051333187 |
| GO:0040036 | regulation of fibroblast growth factor receptor signaling | 0.99699532 | 1.051388077 |
| ENSG00000145819 | ARHGAP26 subnetwork | 0.419951997 | 1.051450136 |
| ENSG00000162735 | PEX19 subnetwork | 0.996976062 | 1.051457587 |
| GO:0016705 | oxidoreductase activity, acting on paired donors, with in | 0.420111995 | 1.051492031 |
| ENSG00000143753 | DEGS1 subnetwork | 0.420020866 | 1.051492284 |
| ENSG00000169188 | APEX2 subnetwork | 0.996957405 | 1.051508841 |
| GO:0016504 | peptidase activator activity | 0.420257941 | 1.051525424 |
| ENSG00000157152 | ENSG00000157152 subnetwork | 0.996946832 | 1.051560102 |
| KEGG_NEUROACTIVE_LIGAND_RE | KEGG_NEUROACTIVE_LIGAND_RECEPTOR_INTERACTION | 0.996943487 | 1.051625987 |
| ENSG00000013573 | DDX11 subnetwork | 0.420367625 | 1.051669209 |
| GO:0008308 | voltage-gated anion channel activity | 0.420242561 | 1.051678251 |
| GO:0007216 | G-protein coupled glutamate receptor signaling pathway | 0.99694185 | 1.051702843 |
| ENSG00000169744 | LDB2 subnetwork | 0.996933601 | 1.051768747 |
| GO:0001656 | metanephros development | 0.996922322 | 1.051823697 |
| GO:0031111 | negative regulation of microtubule polymerization or de | 0.996916922 | 1.051875 |
| GO:0031683 | G-protein beta/gamma-subunit complex binding | 0.996899567 | 1.051929966 |
| GO:0006740 | NADPH regeneration | 0.996898634 | 1.052006872 |
| MP:0000890 | thin cerebellar molecular layer | 0.420646149 | 1.052050152 |
| ENSG00000142230 | SAE1 subnetwork | 0.996893378 | 1.052076479 |
| GO:0017145 | stem cell division | 0.99687474 | 1.052138783 |
| MP:0004136 | abnormal tongue muscle morphology | 0.996870549 | 1.052212066 |
| GO:0001709 | cell fate determination | 0.996867976 | 1.052289016 |
| GO:0048635 | negative regulation of muscle organ development | 0.996862388 | 1.052355006 |
| MP:0002761 | abnormal hippocampal mossy fiber morphology | 0.99685935 | 1.052428321 |

| | | | |
|---|---|---|---|
| GO:0043176 | amine binding | 0.996858712 | 1.052505303 |
| REACTOME_ACTIVATION_OF_GAI | REACTOME_ACTIVATION_OF_GABAB_RECEPTORS | 0.996853556 | 1.052574982 |
| REACTOME_GABA_B_RECEPTOR_ | REACTOME_GABA_B_RECEPTOR_ACTIVATION | 0.996853556 | 1.052651986 |
| GO:0010720 | positive regulation of cell development | 0.99679102 | 1.052692617 |
| GO:0005253 | anion channel activity | 0.996845685 | 1.052703395 |
| GO:0050770 | regulation of axonogenesis | 0.996765455 | 1.052740378 |
| ENSG00000170296 | GABARAP subnetwork | 0.99676242 | 1.052802781 |
| ENSG00000170445 | HARS subnetwork | 0.421031364 | 1.05282907 |
| REACTOME_NEUROTRANSMITTEF | REACTOME_NEUROTRANSMITTER_RECEPTOR_BINDING_ | 0.996752708 | 1.052872512 |
| GO:0051647 | nucleus localization | 0.421534353 | 1.052876967 |
| GO:0030276 | clathrin binding | 0.421495526 | 1.052911307 |
| ENSG00000145375 | SPATA5 subnetwork | 0.4213545 | 1.052929225 |
| ENSG00000125651 | GTF2F1 subnetwork | 0.421690641 | 1.052935206 |
| GO:0009855 | determination of bilateral symmetry | 0.99674835 | 1.052942253 |
| ENSG00000174177 | CTU2 subnetwork | 0.421620391 | 1.052961083 |
| GO:0009798 | axis specification | 0.996742377 | 1.053012004 |
| MP:0008022 | dilated heart ventricle | 0.421460713 | 1.053038768 |
| ENSG00000101144 | BMP7 subnetwork | 0.421313074 | 1.053048264 |
| GO:0001823 | mesonephros development | 0.996733841 | 1.053078106 |
| GO:0006739 | NADP metabolic process | 0.996733789 | 1.053155198 |
| MP:0001469 | abnormal contextual conditioning behavior | 0.996715018 | 1.053192035 |
| GO:0001948 | glycoprotein binding | 0.422198095 | 1.053220081 |
| MP:0003657 | abnormal erythrocyte osmotic lysis | 0.421312568 | 1.053226626 |
| GO:0046942 | carboxylic acid transport | 0.996695173 | 1.053236199 |
| ENSG00000212802 | ENSG00000212802 subnetwork | 0.422062283 | 1.053246534 |
| KEGG_GLYCOSPHINGOLIPID_BIOS | KEGG_GLYCOSPHINGOLIPID_BIOSYNTHESIS_GLOBO_SER | 0.996670021 | 1.053280369 |
| GO:0060997 | dendritic spine morphogenesis | 0.996652173 | 1.053331869 |
| GO:0048009 | insulin-like growth factor receptor signaling pathway | 0.422278328 | 1.05333784 |
| GO:0008022 | protein C-terminus binding | 0.422192066 | 1.053372781 |
| GO:0097061 | dendritic spine organization | 0.996652173 | 1.053409008 |
| GO:0007141 | male meiosis I | 0.421979198 | 1.053416779 |
| ENSG00000174766 | ENSG00000174766 subnetwork | 0.422062283 | 1.053424658 |
| MP:0004765 | decreased brainstem auditory evoked potential | 0.996651138 | 1.053486158 |
| ENSG00000125354 | SEPT6 subnetwork | 0.996641978 | 1.053559657 |
| MP:0005294 | abnormal heart ventricle morphology | 0.422426021 | 1.053573843 |
| GO:0034435 | cholesterol esterification | 0.996638496 | 1.053629505 |
| ENSG00000135823 | STX6 subnetwork | 0.422549871 | 1.053649265 |
| GO:0034433 | steroid esterification | 0.996638496 | 1.053706688 |
| GO:0051018 | protein kinase A binding | 0.422709947 | 1.053749367 |
| ENSG00000124006 | OBSL1 subnetwork | 0.422669974 | 1.053775338 |
| GO:0034434 | sterol esterification | 0.996638496 | 1.053783883 |
| MP:0004830 | short incisors | 0.996631256 | 1.053857425 |
| GO:0016409 | palmitoyltransferase activity | 0.996625776 | 1.053927315 |
| GO:0009112 | nucleobase metabolic process | 0.996567152 | 1.053934931 |
| REACTOME_AMINE_COMPOUND_ | REACTOME_AMINE_COMPOUND_SLC_TRANSPORTERS | 0.996551223 | 1.05399018 |
| MP:0009546 | absent gastric milk in neonates | 0.996550401 | 1.054067424 |
| GO:0050974 | detection of mechanical stimulus involved in sensory per | 0.996484599 | 1.054075051 |
| REACTOME_REDUCTION_OF_CYT | REACTOME_REDUCTION_OF_CYTOSOLIC_CA_LEVELS | 0.423247948 | 1.054133626 |
| GO:0048521 | negative regulation of behavior | 0.996410054 | 1.054137956 |
| ENSG00000129245 | FXR2 subnetwork | 0.996461363 | 1.054141318 |
| MP:0003408 | increased width of hypertrophic chondrocyte zone | 0.424761218 | 1.054170871 |
| MP:0000243 | myoclonus | 0.996406255 | 1.054215233 |
| ENSG00000171992 | SYNPO subnetwork | 0.423231102 | 1.054269322 |
| MP:0003425 | abnormal optic vesicle formation | 0.996403824 | 1.054285191 |

| | | | |
|---|---|---|---|
| MP:0009862 | abnormal aorta elastic tissue morphology | 0.42474338 | 1.05432296 |
| GO:0006013 | mannose metabolic process | 0.423504829 | 1.05434306 |
| MP:0002919 | enhanced paired-pulse facilitation | 0.996399224 | 1.054355158 |
| REACTOME_SHC1_EVENTS_IN_EC | REACTOME_SHC1_EVENTS_IN_EGFR_SIGNALING | 0.424906946 | 1.054371952 |
| ENSG00000167325 | RRM1 subnetwork | 0.422994738 | 1.054373522 |
| ENSG00000131242 | RAB11FIP4 subnetwork | 0.423454037 | 1.054385965 |
| MP:0001354 | increased aggression towards males | 0.424713604 | 1.054416218 |
| GO:0008656 | cysteine-type endopeptidase activator activity involved i | 0.423228649 | 1.054421941 |
| GO:0001964 | startle response | 0.996397591 | 1.054432468 |
| ENSG00000165996 | PTPLA subnetwork | 0.425040338 | 1.054446125 |
| ENSG00000166866 | MYO1A subnetwork | 0.423112164 | 1.054448759 |
| REACTOME_SLC:MEDIATED_TRAN | REACTOME_SLC:MEDIATED_TRANSMEMBRANE_TRANSF | 0.996393504 | 1.054502457 |
| GO:2000191 | regulation of fatty acid transport | 0.423797187 | 1.054526298 |
| ENSG00000051128 | HOMER3 subnetwork | 0.424689622 | 1.054534747 |
| ENSG00000132872 | SYT4 subnetwork | 0.996389321 | 1.054565122 |
| ENSG00000104980 | TIMM44 subnetwork | 0.423226574 | 1.054591492 |
| ENSG00000086232 | EIF2AK1 subnetwork | 0.425030428 | 1.054614997 |
| MP:0003243 | abnormal dopaminergic neuron morphology | 0.996380131 | 1.054627796 |
| REACTOME_METABOLISM_OF_ST | REACTOME_METABOLISM_OF_STEROID_HORMONES_A | 0.423769901 | 1.054653515 |
| GO:0006414 | translational elongation | 0.42548811 | 1.054686713 |
| ENSG00000133816 | MICAL2 subnetwork | 0.996377059 | 1.054694147 |
| ENSG00000068976 | PYGM subnetwork | 0.42467205 | 1.054695389 |
| ENSG00000148297 | MED22 subnetwork | 0.425960881 | 1.054715556 |
| MP:0003912 | decreased drinking behavior | 0.996353476 | 1.054760508 |
| ENSG00000105486 | LIG1 subnetwork | 0.423747453 | 1.054763912 |
| KEGG_ALZHEIMERS_DISEASE | KEGG_ALZHEIMERS_DISEASE | 0.425422079 | 1.054771505 |
| ENSG00000072315 | TRPC5 subnetwork | 0.424445177 | 1.054773531 |
| GO:0071363 | cellular response to growth factor stimulus | 0.424635941 | 1.054805588 |
| ENSG00000147416 | ATP6V1B2 subnetwork | 0.425372777 | 1.054822719 |
| ENSG00000125814 | NAPB subnetwork | 0.996337728 | 1.054830546 |
| ENSG00000105373 | GLTSCR2 subnetwork | 0.424304545 | 1.054867778 |
| MP:0008528 | polycystic kidney | 0.425952688 | 1.054884189 |
| MP:0003924 | herniated diaphragm | 0.424601935 | 1.054890572 |
| GO:0004970 | ionotropic glutamate receptor activity | 0.996322912 | 1.054893258 |
| ENSG00000105323 | HNRNPUL1 subnetwork | 0.424421476 | 1.05490064 |
| ENSG00000058091 | CDK14 subnetwork | 0.42532116 | 1.054907563 |
| MP:0000157 | abnormal sternum morphology | 0.426301568 | 1.054939618 |
| ENSG00000198242 | RPL23A subnetwork | 0.426242986 | 1.054940446 |
| ENSG00000175906 | ARL4D subnetwork | 0.425874733 | 1.054943764 |
| MP:0000864 | abnormal cerebellum vermis morphology | 0.996308822 | 1.054959648 |
| ENSG00000145782 | ATG12 subnetwork | 0.424284503 | 1.055003369 |
| ENSG00000155111 | CDK19 subnetwork | 0.42579405 | 1.055011753 |
| GO:0016805 | dipeptidase activity | 0.99629335 | 1.055022379 |
| MP:0003830 | abnormal testis development | 0.426180773 | 1.055025168 |
| GO:0030286 | dynein complex | 0.425656194 | 1.055047027 |
| GO:0033119 | negative regulation of RNA splicing | 0.99629164 | 1.055099795 |
| ENSG00000137673 | MMP7 subnetwork | 0.425763859 | 1.055130143 |
| ENSG00000104897 | SF3A2 subnetwork | 0.424277561 | 1.055155855 |
| MP:0002910 | abnormal excitatory postsynaptic currents | 0.996286179 | 1.055173553 |
| MP:0001935 | decreased litter size | 0.426549994 | 1.055196982 |
| GO:0010800 | positive regulation of peptidyl-threonine phosphorylatio | 0.424229332 | 1.055232558 |
| ENSG00000035862 | TIMP2 subnetwork | 0.996283698 | 1.055247321 |
| MP:0003271 | abnormal duodenum morphology | 0.426513779 | 1.055298457 |
| GO:0090102 | cochlea development | 0.996269243 | 1.055313761 |

| | | | |
|---|---|---|---|
| ENSG00000151292 | CSNK1G3 subnetwork | 0.42646374 | 1.055332886 |
| ENSG00000073711 | PPP2R3A subnetwork | 0.424221027 | 1.055376707 |
| GO:0016042 | lipid catabolic process | 0.996268185 | 1.055387551 |
| ENSG00000130638 | ATXN10 subnetwork | 0.996240685 | 1.055439331 |
| GO:0004065 | arylsulfatase activity | 0.996239665 | 1.055516811 |
| ENSG00000155130 | MARCKS subnetwork | 0.996205607 | 1.055550253 |
| MP:0008918 | microgliosis | 0.427257318 | 1.055575088 |
| MP:0005358 | abnormal incisor morphology | 0.99619866 | 1.055620411 |
| GO:0000723 | telomere maintenance | 0.42705645 | 1.055628141 |
| ENSG00000135100 | HNF1A subnetwork | 0.426900926 | 1.055630027 |
| MP:0006298 | abnormal platelet activation | 0.426838019 | 1.055647729 |
| ENSG00000108387 | SEPT4 subnetwork | 0.996184284 | 1.055668551 |
| ENSG00000184313 | HEATR8 subnetwork | 0.427399803 | 1.055682959 |
| GO:0005048 | signal sequence binding | 0.427253329 | 1.05574347 |
| GO:0045103 | intermediate filament-based process | 0.996183735 | 1.055746071 |
| ENSG00000130733 | YIPF2 subnetwork | 0.426815246 | 1.055757627 |
| MP:0002095 | abnormal skin pigmentation | 0.427033488 | 1.055771486 |
| ENSG00000152661 | GJA1 subnetwork | 0.427505965 | 1.055799163 |
| MP:0000279 | ventricular hypoplasia | 0.427165164 | 1.055803048 |
| GO:0042133 | neurotransmitter metabolic process | 0.996177288 | 1.055812587 |
| ENSG00000198641 | ENSG00000198641 subnetwork | 0.42761285 | 1.05583905 |
| GO:0006029 | proteoglycan metabolic process | 0.996176798 | 1.055890129 |
| ENSG00000141570 | CBX8 subnetwork | 0.427605559 | 1.055898594 |
| ENSG00000183508 | FAM46C subnetwork | 0.996158758 | 1.055930959 |
| GO:0042481 | regulation of odontogenesis | 0.996157399 | 1.056001175 |
| GO:0060993 | kidney morphogenesis | 0.996146777 | 1.056075075 |
| GO:0051899 | membrane depolarization | 0.996143784 | 1.056148986 |
| GO:0030204 | chondroitin sulfate metabolic process | 0.427798382 | 1.056214453 |
| GO:0072528 | pyrimidine-containing compound biosynthetic process | 0.996133885 | 1.056222908 |
| GO:0046129 | purine ribonucleoside biosynthetic process | 0.996120872 | 1.056278472 |
| ENSG00000148925 | BTBD10 subnetwork | 0.429255672 | 1.05630105 |
| ENSG00000163288 | GABRB1 subnetwork | 0.427894706 | 1.056338853 |
| GO:0042455 | ribonucleoside biosynthetic process | 0.996120872 | 1.056356088 |
| GO:0042451 | purine nucleoside biosynthetic process | 0.996120872 | 1.056433715 |
| ENSG00000126883 | NUP214 subnetwork | 0.42924009 | 1.056452151 |
| GO:0006369 | termination of RNA polymerase II transcription | 0.99610541 | 1.056496656 |
| GO:0030539 | male genitalia development | 0.996082441 | 1.056548582 |
| MP:0006089 | abnormal vestibular saccule morphology | 0.996081282 | 1.056622565 |
| ENSG00000156508 | EEF1A1 subnetwork | 0.429238994 | 1.056628314 |
| ENSG00000197279 | ZNF165 subnetwork | 0.996076911 | 1.056692884 |
| ENSG00000105248 | CCDC94 subnetwork | 0.42921333 | 1.056721147 |
| MP:0001634 | internal hemorrhage | 0.428200176 | 1.056746363 |
| GO:0048266 | behavioral response to pain | 0.996070902 | 1.056755863 |
| GO:0045335 | phagocytic vesicle | 0.428139381 | 1.056780936 |
| ENSG00000078018 | MAP2 subnetwork | 0.996046265 | 1.056796795 |
| GO:0005275 | amine transmembrane transporter activity | 0.996046008 | 1.056874495 |
| GO:0046545 | development of primary female sexual characteristics | 0.429204698 | 1.056897415 |
| GO:0051962 | positive regulation of nervous system development | 0.996040174 | 1.056944853 |
| GO:0051965 | positive regulation of synapse assembly | 0.996040174 | 1.057022575 |
| ENSG00000112526 | ENSG00000112526 subnetwork | 0.42917448 | 1.05702369 |
| GO:0043266 | regulation of potassium ion transport | 0.996019555 | 1.057085601 |
| GO:0016896 | exoribonuclease activity, producing 5'-phosphomonoest | 0.428428893 | 1.057154798 |
| MP:0000848 | abnormal pons morphology | 0.996016576 | 1.057159668 |
| ENSG00000215077 | BRD2 subnetwork | 0.42917448 | 1.057200067 |

| | | | |
|---|---|---|---|
| ENSG00000085563 | ABCB1 subnetwork | 0.428505804 | 1.057203744 |
| GO:0048854 | brain morphogenesis | 0.996008569 | 1.057219035 |
| MP:0004227 | increased cellular sensitivity to ionizing radiation | 0.429662368 | 1.057258333 |
| KEGG_GLUTATHIONE_METABOLI | KEGG_GLUTATHIONE_METABOLISM | 0.996003621 | 1.057285767 |
| ENSG00000162368 | CMPK1 subnetwork | 0.428588062 | 1.057286096 |
| GO:0016486 | peptide hormone processing | 0.995978418 | 1.057315728 |
| ENSG00000128641 | MYO1B subnetwork | 0.429870602 | 1.057321339 |
| ENSG00000126821 | SGPP1 subnetwork | 0.428687973 | 1.05732665 |
| GO:0005792 | microsome | 0.430504619 | 1.057344868 |
| ENSG00000204256 | BRD2 subnetwork | 0.42917448 | 1.057376502 |
| GO:0071901 | negative regulation of protein serine/threonine kinase a | 0.430103319 | 1.057385512 |
| GO:0008188 | neuropeptide receptor activity | 0.995929086 | 1.057390377 |
| REACTOME_VOLTAGE_GATED_PC | REACTOME_VOLTAGE_GATED_POTASSIUM_CHANNELS | 0.995975963 | 1.057393511 |
| MP:0005478 | decreased circulating thyroxine level | 0.430036417 | 1.057411726 |
| GO:0021915 | neural tube development | 0.995928176 | 1.057464499 |
| ENSG00000041357 | PSMA4 subnetwork | 0.429129114 | 1.057477883 |
| GO:0005506 | iron ion binding | 0.429868228 | 1.057497501 |
| GO:0045123 | cellular extravasation | 0.429808151 | 1.057507082 |
| MP:0004003 | abnormal vascular endothelial cell physiology | 0.430636156 | 1.057518297 |
| KEGG_STEROID_HORMONE_BIOS | KEGG_STEROID_HORMONE_BIOSYNTHESIS | 0.430496582 | 1.057520799 |
| GO:0019370 | leukotriene biosynthetic process | 0.429085735 | 1.057520868 |
| GO:0006521 | regulation of cellular amino acid metabolic process | 0.995899765 | 1.057523915 |
| GO:0021955 | central nervous system neuron axonogenesis | 0.995878827 | 1.057575981 |
| ENSG00000065978 | YBX1 subnetwork | 0.430453439 | 1.057588617 |
| GO:0007423 | sensory organ development | 0.995868172 | 1.057642773 |
| ENSG00000066032 | CTNNA2 subnetwork | 0.430411356 | 1.057648136 |
| GO:0043450 | alkene biosynthetic process | 0.429085735 | 1.057697445 |
| ENSG00000090621 | PABPC4 subnetwork | 0.99585757 | 1.057705895 |
| GO:0007140 | male meiosis | 0.43037679 | 1.057749292 |
| GO:0035020 | regulation of Rac protein signal transduction | 0.995852881 | 1.057765347 |
| REACTOME_SOS:MEDIATED_SIGN | REACTOME_SOS:MEDIATED_SIGNALLING | 0.429048293 | 1.057765531 |
| GO:0060992 | response to fungicide | 0.995841096 | 1.057828487 |
| GO:0008064 | regulation of actin polymerization or depolymerization | 0.430828046 | 1.057833028 |
| GO:0072378 | blood coagulation, fibrin clot formation | 0.995817838 | 1.057884276 |
| MP:0002089 | abnormal postnatal growth/weight/body size | 0.430372678 | 1.057908758 |
| GO:0015171 | amino acid transmembrane transporter activity | 0.995779408 | 1.057914305 |
| ENSG00000143079 | CTTNBP2NL subnetwork | 0.429046458 | 1.057942208 |
| GO:0006885 | regulation of pH | 0.995739682 | 1.057951701 |
| GO:0010498 | proteasomal protein catabolic process | 0.9957375 | 1.058025919 |
| ENSG00000151623 | NR3C2 subnetwork | 0.431464613 | 1.058038532 |
| ENSG00000099882 | ENSG00000099882 subnetwork | 0.428998396 | 1.058043769 |
| GO:0051705 | behavioral interaction between organisms | 0.995726964 | 1.058096465 |
| GO:0071456 | cellular response to hypoxia | 0.431136585 | 1.058120013 |
| ENSG00000100304 | TTLL12 subnetwork | 0.431621839 | 1.058136832 |
| MP:0005435 | hemoperitoneum | 0.431009132 | 1.058155969 |
| MP:0011346 | renal tubule atrophy | 0.431440939 | 1.058164452 |
| ENSG00000149294 | NCAM1 subnetwork | 0.995714892 | 1.058167023 |
| GO:0007130 | synaptonemal complex assembly | 0.431062181 | 1.058171239 |
| GO:0009311 | oligosaccharide metabolic process | 0.995708423 | 1.058241273 |
| MP:0009538 | abnormal synapse morphology | 0.995696814 | 1.058311851 |
| ENSG00000084463 | WBP11 subnetwork | 0.431438113 | 1.058331949 |
| GO:0048339 | paraxial mesoderm development | 0.431318485 | 1.058351338 |
| MP:0011106 | partial embryonic lethality before somite formation | 0.431783971 | 1.058359621 |
| MP:0000852 | small cerebellum | 0.995678022 | 1.058371391 |

| | | | |
|---|---|---|---|
| ENSG00000142657 | PGD subnetwork | 0.431417335 | 1.058433034 |
| GO:0003016 | respiratory system process | 0.995677538 | 1.058445672 |
| ENSG00000196220 | SRGAP3 subnetwork | 0.995669902 | 1.058512598 |
| GO:0048532 | anatomical structure arrangement | 0.995632541 | 1.058531644 |
| GO:0042737 | drug catabolic process | 0.995619823 | 1.058580165 |
| GO:0001649 | osteoblast differentiation | 0.995608425 | 1.058647115 |
| GO:0007215 | glutamate receptor signaling pathway | 0.995603953 | 1.05871776 |
| ENSG00000075624 | ACTB subnetwork | 0.432258094 | 1.058742535 |
| ENSG00000121957 | GPSM2 subnetwork | 0.995597112 | 1.0587921 |
| ENSG00000105613 | MAST1 subnetwork | 0.432220023 | 1.058793761 |
| ENSG00000169045 | HNRNPH1 subnetwork | 0.43209593 | 1.058829876 |
| MP:0009171 | enlarged pancreatic islets | 0.995595291 | 1.05886645 |
| GO:0060081 | membrane hyperpolarization | 0.995565911 | 1.058907644 |
| GO:0031952 | regulation of protein autophosphorylation | 0.432070964 | 1.058939243 |
| ENSG00000138083 | SIX3 subnetwork | 0.432213474 | 1.058961168 |
| MP:0002566 | abnormal sexual interaction | 0.995530245 | 1.058967271 |
| GO:0016597 | amino acid binding | 0.995507599 | 1.059026907 |
| GO:0042551 | neuron maturation | 0.995503045 | 1.059101298 |
| GO:0016594 | glycine binding | 0.995484996 | 1.059172012 |
| ENSG00000112448 | ENSG00000112448 subnetwork | 0.995454286 | 1.059202183 |
| ENSG00000204713 | TRIM27 subnetwork | 0.995454286 | 1.059280289 |
| MP:0011102 | partial embryonic lethality | 0.432606343 | 1.059311774 |
| ENSG00000166716 | ZNF592 subnetwork | 0.432840537 | 1.059315432 |
| ENSG00000215641 | TRIM27 subnetwork | 0.995454286 | 1.059358407 |
| ENSG00000091436 | ENSG00000091436 subnetwork | 0.432569794 | 1.059363078 |
| ENSG00000188459 | ENSG00000188459 subnetwork | 0.432788929 | 1.059375 |
| GO:0030055 | cell-substrate junction | 0.432716651 | 1.059393135 |
| ENSG00000151834 | GABRA2 subnetwork | 0.995447325 | 1.059432849 |
| GO:0030166 | proteoglycan biosynthetic process | 0.995420369 | 1.059481487 |
| GO:0030916 | otic vesicle formation | 0.995408074 | 1.059559637 |
| ENSG00000181790 | BAI1 subnetwork | 0.995397232 | 1.059630422 |
| GO:0003211 | cardiac ventricle formation | 0.995389961 | 1.059697529 |
| ENSG00000125730 | C3 subnetwork | 0.433092806 | 1.05974478 |
| MP:0000571 | interdigital webbing | 0.995384291 | 1.059772023 |
| ENSG00000206466 | GABBR1 subnetwork | 0.995380948 | 1.059846528 |
| ENSG00000204681 | GABBR1 subnetwork | 0.995380948 | 1.059924734 |
| ENSG00000149503 | INCENP subnetwork | 0.433245752 | 1.05996686 |
| ENSG00000206511 | GABBR1 subnetwork | 0.995380948 | 1.060002952 |
| MP:0000180 | abnormal circulating cholesterol level | 0.433347152 | 1.060023194 |
| MP:0005241 | abnormal retinal ganglion layer morphology | 0.995343277 | 1.06002952 |
| MP:0003073 | abnormal metacarpal bone morphology | 0.995342293 | 1.060107757 |
| GO:0035145 | exon-exon junction complex | 0.433563295 | 1.060127526 |
| ENSG00000087263 | OGFOD1 subnetwork | 0.433625935 | 1.060134128 |
| GO:0031076 | embryonic camera-type eye development | 0.995315275 | 1.060156481 |
| GO:0048814 | regulation of dendrite morphogenesis | 0.995253871 | 1.060186757 |
| ENSG00000141582 | CBX4 subnetwork | 0.434071489 | 1.060198511 |
| GO:0016578 | histone deubiquitination | 0.433514588 | 1.060203744 |
| ENSG00000147246 | HTR2C subnetwork | 0.995242062 | 1.06025395 |
| MP:0002001 | blindness | 0.995192435 | 1.060262089 |
| MP:0001148 | enlarged testis | 0.433758919 | 1.060289735 |
| ENSG00000185432 | METTL7A subnetwork | 0.434530033 | 1.060305785 |
| REACTOME_NACL:_DEPENDENT_I | REACTOME_NACL:_DEPENDENT_NEUROTRANSMITTER_ | 0.995182814 | 1.060332989 |
| GO:0001974 | blood vessel remodeling | 0.434063642 | 1.060373925 |
| REACTOME_GAMMA:CARBOXYLA | REACTOME_GAMMA:CARBOXYLATION_TRANSPORT_AN | 0.43421654 | 1.060378763 |

| | | | |
|---|---|---|---|
| MP:0001915 | intracranial hemorrhage | 0.43396885 | 1.060402185 |
| MP:0001516 | abnormal motor coordination/ balance | 0.995174818 | 1.060403899 |
| MP:0004148 | increased compact bone thickness | 0.434319108 | 1.060434926 |
| MP:0002920 | decreased paired-pulse facilitation | 0.995150641 | 1.060448974 |
| REACTOME_TRANSPORT_TO_THE | REACTOME_TRANSPORT_TO_THE_GOLGI_AND_SUBSEQ | 0.433930155 | 1.060470121 |
| GO:0007368 | determination of left/right symmetry | 0.995129373 | 1.060475593 |
| REACTOME_PEPTIDE_LIGAND:BIN | REACTOME_PEPTIDE_LIGAND:BINDING_RECEPTORS | 0.434522269 | 1.060481071 |
| MP:0005044 | sepsis | 0.434061346 | 1.060541122 |
| ENSG00000137575 | SDCBP subnetwork | 0.995129147 | 1.060553914 |
| REACTOME_METAL_ION_SLC_TR/ | REACTOME_METAL_ION_SLC_TRANSPORTERS | 0.43445009 | 1.060565476 |
| GO:0034707 | chloride channel complex | 0.995100754 | 1.060610089 |
| ENSG00000117650 | NEK2 subnetwork | 0.995051242 | 1.060636726 |
| MP:0002856 | abnormal vestibular ganglion morphology | 0.995047925 | 1.060715077 |
| GO:0043496 | regulation of protein homodimerization activity | 0.434748429 | 1.060766815 |
| GO:0051925 | regulation of calcium ion transport via voltage-gated calc | 0.995036043 | 1.060786052 |
| GO:0007350 | blastoderm segmentation | 0.995019995 | 1.060831178 |
| MP:0000813 | abnormal hippocampus layer morphology | 0.995013396 | 1.060902172 |
| GO:0001945 | lymph vessel development | 0.995010078 | 1.060980566 |
| ENSG00000176903 | PNMA1 subnetwork | 0.995005743 | 1.061055276 |
| ENSG00000168924 | LETM1 subnetwork | 0.43490454 | 1.061087244 |
| ENSG00000117528 | ABCD3 subnetwork | 0.994981755 | 1.061107826 |
| MP:0005403 | abnormal nerve conduction | 0.99497848 | 1.061182557 |
| ENSG00000010278 | CD9 subnetwork | 0.43557617 | 1.061202772 |
| GO:0033275 | actin-myosin filament sliding | 0.994974536 | 1.061253603 |
| GO:0010522 | regulation of calcium ion transport into cytosol | 0.435518824 | 1.061270627 |
| ENSG00000137955 | RABGGTB subnetwork | 0.435060858 | 1.061275401 |
| ENSG00000107447 | DNTT subnetwork | 0.436257572 | 1.061293245 |
| REACTOME_SIGNALLING_TO_ERK | REACTOME_SIGNALLING_TO_ERKS | 0.436486639 | 1.0612959 |
| ENSG00000139618 | BRCA2 subnetwork | 0.436416016 | 1.061305995 |
| GO:0030049 | muscle filament sliding | 0.994974536 | 1.061332052 |
| ENSG00000143466 | IKBKE subnetwork | 0.436350283 | 1.061340801 |
| ENSG00000113141 | IK subnetwork | 0.435710474 | 1.061357638 |
| ENSG00000131941 | RHPN2 subnetwork | 0.435370524 | 1.061367013 |
| GO:0032720 | negative regulation of tumor necrosis factor production | 0.435496946 | 1.061388018 |
| GO:0060688 | regulation of morphogenesis of a branching structure | 0.99497361 | 1.061410512 |
| GO:0031099 | regeneration | 0.436155248 | 1.061420567 |
| REACTOME_ION_TRANSPORT_BY | REACTOME_ION_TRANSPORT_BY_P:TYPE_ATPASES | 0.435191467 | 1.0614222 |
| GO:0015269 | calcium-activated potassium channel activity | 0.435436243 | 1.061422912 |
| ENSG00000160201 | U2AF1 subnetwork | 0.43524045 | 1.061445087 |
| ENSG00000104637 | ENSG00000104637 subnetwork | 0.436256086 | 1.061459878 |
| GO:0051213 | dioxygenase activity | 0.436119663 | 1.061463656 |
| ENSG00000198569 | SLC34A3 subnetwork | 0.435349178 | 1.061467966 |
| GO:0003924 | GTPase activity | 0.436589796 | 1.06147514 |
| GO:0007076 | mitotic chromosome condensation | 0.994971244 | 1.061488984 |
| ENSG00000176386 | CDC26 subnetwork | 0.994964796 | 1.061545287 |
| GO:0019206 | nucleoside kinase activity | 0.99493273 | 1.061586809 |
| ENSG00000112335 | SNX3 subnetwork | 0.435975691 | 1.061609499 |
| MP:0004616 | lumbar vertebral transformation | 0.436118857 | 1.061630399 |
| GO:0048701 | embryonic cranial skeleton morphogenesis | 0.994932136 | 1.061665311 |
| ENSG00000203852 | HIST2H3A subnetwork | 0.435924193 | 1.061669141 |
| GO:0051047 | positive regulation of secretion | 0.436059571 | 1.061673537 |
| GO:0034505 | tooth mineralization | 0.994923187 | 1.061725336 |
| MP:0002862 | altered righting response | 0.994918804 | 1.061789069 |
| MP:0003137 | abnormal impulse conducting system conduction | 0.994901345 | 1.061849112 |

| | | | |
|---|---|---|---|
| GO:0019717 | synaptosome | 0.994898547 | 1.061923959 |
| GO:0007611 | learning or memory | 0.994891664 | 1.061995118 |
| MP:0008540 | abnormal cerebrum morphology | 0.994869463 | 1.062040394 |
| MP:0002059 | abnormal seminal vesicle morphology | 0.994834573 | 1.062074578 |
| MP:0003921 | abnormal heart left ventricle morphology | 0.43761091 | 1.062095316 |
| ENSG00000205420 | KRT6A subnetwork | 0.994819141 | 1.062123566 |
| GO:0009310 | amine catabolic process | 0.994811064 | 1.062187361 |
| GO:0032392 | DNA geometric change | 0.437593853 | 1.062220579 |
| GO:0046486 | glycerolipid metabolic process | 0.437401078 | 1.062251274 |
| MP:0008947 | increased neuron number | 0.994807849 | 1.062258566 |
| GO:0021983 | pituitary gland development | 0.994792662 | 1.062311279 |
| GO:0001504 | neurotransmitter uptake | 0.994785047 | 1.062382503 |
| MP:0000410 | waved hair | 0.437378348 | 1.062393092 |
| GO:0032508 | DNA duplex unwinding | 0.437593853 | 1.0623952 |
| ENSG00000133318 | RTN3 subnetwork | 0.994752032 | 1.062438934 |
| ENSG00000164597 | COG5 subnetwork | 0.437552278 | 1.062454785 |
| ENSG00000108590 | MED31 subnetwork | 0.437345497 | 1.062460931 |
| MP:0005195 | abnormal posterior eye segment morphology | 0.994734511 | 1.06248427 |
| MP:0005114 | premature hair loss | 0.437217422 | 1.062489715 |
| ENSG00000134333 | LDHA subnetwork | 0.437301383 | 1.062504113 |
| MP:0001093 | small trigeminal ganglion | 0.994725618 | 1.062537015 |
| MP:0009593 | absent chorion | 0.437164608 | 1.062549375 |
| MP:0005236 | abnormal olfactory nerve morphology | 0.99469082 | 1.062563856 |
| ENSG00000064999 | ANKS1A subnetwork | 0.438669554 | 1.06260456 |
| MP:0000832 | abnormal thalamus morphology | 0.994678615 | 1.062627721 |
| GO:0005254 | chloride channel activity | 0.994632207 | 1.062654572 |
| GO:0030325 | adrenal gland development | 0.437136578 | 1.062658436 |
| ENSG00000197766 | CFD subnetwork | 0.438610631 | 1.062680446 |
| ENSG00000135744 | AGT subnetwork | 0.437969454 | 1.062690981 |
| GO:0060119 | inner ear receptor cell development | 0.994608029 | 1.062711049 |
| MP:0000951 | sporadic seizures | 0.994592174 | 1.062774939 |
| GO:0061077 | chaperone-mediated protein folding | 0.438579544 | 1.062789171 |
| GO:0035270 | endocrine system development | 0.437948888 | 1.062824515 |
| ENSG00000105048 | TNNT1 subnetwork | 0.994564625 | 1.062835136 |
| GO:0016053 | organic acid biosynthetic process | 0.99450987 | 1.062843493 |
| ENSG00000108312 | UBTF subnetwork | 0.438811788 | 1.062848475 |
| MP:0001927 | abnormal estrous cycle | 0.438200502 | 1.062892101 |
| GO:0045495 | pole plasm | 0.438395454 | 1.062902167 |
| ENSG00000049759 | NEDD4L subnetwork | 0.438552242 | 1.062906137 |
| GO:0046394 | carboxylic acid biosynthetic process | 0.99450987 | 1.062922222 |
| ENSG00000167083 | GNGT2 subnetwork | 0.99449156 | 1.062986147 |
| ENSG00000115170 | ACVR1 subnetwork | 0.438157815 | 1.063000986 |
| ENSG00000163879 | DNALI1 subnetwork | 0.438526892 | 1.063055966 |
| ENSG00000139970 | RTN1 subnetwork | 0.994490248 | 1.063061194 |
| GO:0060293 | germ plasm | 0.438395454 | 1.06307667 |
| GO:0008514 | organic anion transmembrane transporter activity | 0.994483176 | 1.063128843 |
| GO:0005310 | dicarboxylic acid transmembrane transporter activity | 0.994476707 | 1.063192798 |
| ENSG00000103187 | COTL1 subnetwork | 0.994458947 | 1.063245647 |
| GO:0043186 | P granule | 0.438395454 | 1.063251232 |
| ENSG00000164758 | MED30 subnetwork | 0.438991367 | 1.063297262 |
| MP:0004402 | decreased cochlear outer hair cell number | 0.994443085 | 1.063313324 |
| ENSG00000176658 | MYO1D subnetwork | 0.439368511 | 1.063325143 |
| ENSG00000168961 | LGALS9 subnetwork | 0.994426023 | 1.063358779 |
| GO:0002793 | positive regulation of peptide secretion | 0.994361734 | 1.063359769 |

| | | | |
|---|---|---|---|
| ENSG00000131153 | GINS2 subnetwork | 0.439252712 | 1.063395052 |
| GO:0004806 | triglyceride lipase activity | 0.994344948 | 1.063405233 |
| GO:0006873 | cellular ion homeostasis | 0.994314117 | 1.063439585 |
| MP:0000223 | decreased monocyte cell number | 0.439159297 | 1.06345681 |
| ENSG00000066044 | ELAVL1 subnetwork | 0.439344778 | 1.063466579 |
| REACTOME_CYCLIN_AB1_ASSOCI | REACTOME_CYCLIN_AB1_ASSOCIATED_EVENTS_DURINC | 0.994281674 | 1.063499889 |
| ENSG00000106799 | TGFBR1 subnetwork | 0.439600251 | 1.063500901 |
| ENSG00000197892 | KIF13B subnetwork | 0.439122908 | 1.063532787 |
| MP:0005156 | bradykinesia | 0.439229369 | 1.063536545 |
| GO:0048598 | embryonic morphogenesis | 0.99427038 | 1.063560202 |
| GO:0004722 | protein serine/threonine phosphatase activity | 0.439715288 | 1.06358055 |
| ENSG00000053900 | ANAPC4 subnetwork | 0.994251425 | 1.063613109 |
| GO:0043467 | regulation of generation of precursor metabolites and er | 0.440182874 | 1.06361629 |
| MP:0002978 | absent otoliths | 0.439558397 | 1.063625942 |
| MP:0001731 | abnormal postnatal growth | 0.440362355 | 1.063628188 |
| MP:0005590 | increased vasodilation | 0.994235091 | 1.063669732 |
| ENSG00000143379 | SETDB1 subnetwork | 0.994223878 | 1.063737486 |
| GO:0005884 | actin filament | 0.44033455 | 1.063753066 |
| MP:0005192 | increased motor neuron number | 0.994174785 | 1.063753337 |
| GO:0032330 | regulation of chondrocyte differentiation | 0.440181973 | 1.063790283 |
| GO:0032024 | positive regulation of insulin secretion | 0.994173652 | 1.063828525 |
| ENSG00000136238 | RAC1 subnetwork | 0.440135992 | 1.063898887 |
| ENSG00000162664 | ZNF326 subnetwork | 0.994166286 | 1.063900015 |
| MP:0005104 | abnormal tarsal bone morphology | 0.994153248 | 1.06395668 |
| MP:0000753 | paralysis | 0.994136063 | 1.064005935 |
| GO:0032462 | regulation of protein homooligomerization | 0.440828286 | 1.064019608 |
| MP:0009703 | decreased birth body size | 0.440595292 | 1.064026484 |
| GO:0043394 | proteoglycan binding | 0.994117538 | 1.064047778 |
| ENSG00000172053 | QARS subnetwork | 0.44011483 | 1.064048437 |
| MP:0003068 | enlarged kidney | 0.440042362 | 1.064091653 |
| MP:0000947 | convulsive seizures | 0.994090471 | 1.064093337 |
| ENSG00000103343 | ZNF174 subnetwork | 0.440776198 | 1.064103612 |
| ENSG00000184185 | KCNJ12 subnetwork | 0.440717611 | 1.064138607 |
| GO:0042136 | neurotransmitter biosynthetic process | 0.994084251 | 1.064168584 |
| ENSG00000101608 | MYL12A subnetwork | 0.440020222 | 1.064208545 |
| GO:0031398 | positive regulation of protein ubiquitination | 0.994054327 | 1.064210448 |
| GO:0006098 | pentose-phosphate shunt | 0.994044301 | 1.064270872 |
| MP:0009758 | impaired behavioral response to cocaine | 0.994039484 | 1.064346148 |
| GO:0005581 | collagen | 0.993999917 | 1.064376902 |
| GO:0071377 | cellular response to glucagon stimulus | 0.99398628 | 1.064452197 |
| GO:0015295 | solute:hydrogen symporter activity | 0.993965643 | 1.064508945 |
| GO:0005248 | voltage-gated sodium channel activity | 0.993947924 | 1.06456199 |
| GO:0000062 | fatty-acyl-CoA binding | 0.993922338 | 1.06461133 |
| ENSG00000171208 | NETO2 subnetwork | 0.441173709 | 1.064643907 |
| GO:0030433 | ER-associated protein catabolic process | 0.99392113 | 1.064686665 |
| ENSG00000185479 | KRT6B subnetwork | 0.441246678 | 1.064706843 |
| REACTOME_CRMPS_IN_SEMA3A_ | REACTOME_CRMPS_IN_SEMA3A_SIGNALING | 0.993914923 | 1.064758298 |
| ENSG00000141564 | RPTOR subnetwork | 0.441142302 | 1.06476066 |
| MP:0000026 | abnormal inner ear morphology | 0.993909114 | 1.064837368 |
| GO:0016782 | transferase activity, transferring sulfur-containing groups | 0.993892232 | 1.064897883 |
| GO:0032897 | negative regulation of viral transcription | 0.442804509 | 1.064905568 |
| ENSG00000177733 | HNRNPA0 subnetwork | 0.442273094 | 1.064922575 |
| GO:0080008 | CUL4 RING ubiquitin ligase complex | 0.442436299 | 1.06492586 |
| MP:0002972 | abnormal cardiac muscle contractility | 0.442549766 | 1.064956012 |

| | | | |
|---|---|---|---|
| GO:0043161 | proteasomal ubiquitin-dependent protein catabolic proc | 0.993878131 | 1.064958408 |
| ENSG00000104964 | AES subnetwork | 0.442132014 | 1.064976357 |
| MP:0002397 | abnormal bone marrow morphology | 0.442778313 | 1.064981273 |
| ENSG00000215754 | ENSG00000215754 subnetwork | 0.442377594 | 1.064985332 |
| ENSG00000113558 | SKP1 subnetwork | 0.442719986 | 1.064991857 |
| ENSG00000181029 | TRAPPC5 subnetwork | 0.44262563 | 1.064994299 |
| GO:0005089 | Rho guanyl-nucleotide exchange factor activity | 0.442037773 | 1.065003262 |
| ENSG00000077312 | SNRPA subnetwork | 0.441487642 | 1.065022861 |
| GO:0060134 | prepulse inhibition | 0.993873108 | 1.065033796 |
| ENSG00000099725 | ENSG00000099725 subnetwork | 0.442016513 | 1.065087261 |
| ENSG00000167751 | KLK2 subnetwork | 0.442265822 | 1.065088034 |
| GO:0014075 | response to amine stimulus | 0.993860098 | 1.06509434 |
| MP:0003755 | abnormal palate morphology | 0.993759287 | 1.065130015 |
| ENSG00000184357 | HIST1H1B subnetwork | 0.993833246 | 1.06513632 |
| ENSG00000145147 | SLIT2 subnetwork | 0.993744331 | 1.065186864 |
| ENSG00000102981 | PARD6A subnetwork | 0.442005613 | 1.065261011 |
| MP:0001077 | abnormal spinal nerve morphology | 0.993741443 | 1.065262298 |
| GO:0060736 | prostate gland growth | 0.443393229 | 1.065292012 |
| ENSG00000006747 | SCIN subnetwork | 0.441655647 | 1.065297959 |
| GO:0007168 | receptor guanylyl cyclase signaling pathway | 0.993707747 | 1.065308018 |
| ENSG00000140451 | PIF1 subnetwork | 0.443167451 | 1.065332031 |
| ENSG00000108592 | FTSJ3 subnetwork | 0.443500156 | 1.065346454 |
| GO:0051208 | sequestering of calcium ion | 0.441752718 | 1.065368919 |
| ENSG00000103479 | RBL2 subnetwork | 0.993703737 | 1.065383472 |
| ENSG00000115750 | TAF1B subnetwork | 0.441986219 | 1.065394028 |
| ENSG00000128951 | DUT subnetwork | 0.443364942 | 1.065408396 |
| ENSG00000125970 | RALY subnetwork | 0.443146066 | 1.065432199 |
| MP:0003111 | abnormal cell nucleus morphology | 0.443327871 | 1.065435313 |
| ENSG00000112305 | SMAP1 subnetwork | 0.441942398 | 1.065437337 |
| GO:0001518 | voltage-gated sodium channel complex | 0.993693152 | 1.065447789 |
| GO:0032200 | telomere organization | 0.441871136 | 1.065448017 |
| GO:0015103 | inorganic anion transmembrane transporter activity | 0.993670276 | 1.065493534 |
| ENSG00000135862 | LAMC1 subnetwork | 0.443806872 | 1.065499025 |
| ENSG00000204319 | ENSG00000204319 subnetwork | 0.444043898 | 1.065556458 |
| ENSG00000117360 | PRPF3 subnetwork | 0.443696721 | 1.065560976 |
| MP:0002741 | small olfactory bulb | 0.993667475 | 1.065572735 |
| GO:0042640 | anagen | 0.993645813 | 1.065607345 |
| GO:0048477 | oogenesis | 0.443942497 | 1.065642776 |
| GO:0015297 | antiporter activity | 0.993594499 | 1.065649394 |
| ENSG00000134014 | ELP3 subnetwork | 0.443804406 | 1.065672248 |
| ENSG00000078747 | ITCH subnetwork | 0.443688042 | 1.065709872 |
| ENSG00000138495 | COX17 subnetwork | 0.444019372 | 1.065713357 |
| ENSG00000151332 | MBIP subnetwork | 0.993590398 | 1.065724907 |
| REACTOME_POTASSIUM_CHANN | REACTOME_POTASSIUM_CHANNELS | 0.993569013 | 1.06578556 |
| ENSG00000130294 | KIF1A subnetwork | 0.993567012 | 1.065864813 |
| GO:0030823 | regulation of cGMP metabolic process | 0.993533143 | 1.065903175 |
| ENSG00000125166 | GOT2 subnetwork | 0.993526513 | 1.06597873 |
| ENSG00000037749 | MFAP3 subnetwork | 0.444271255 | 1.06600065 |
| ENSG00000087460 | GNAS subnetwork | 0.993524043 | 1.066054295 |
| MP:0001970 | abnormal pain threshold | 0.993506616 | 1.066118715 |
| ENSG00000171346 | KRT15 subnetwork | 0.993505079 | 1.066198021 |
| MP:0001650 | abnormal seizure response to electrical stimulation | 0.993498674 | 1.066266181 |
| GO:0010658 | striated muscle cell apoptotic process | 0.993480086 | 1.06632691 |
| MP:0004608 | abnormal cervical axis morphology | 0.99344779 | 1.066380208 |

| | | | |
|---|---|---|---|
| GO:0009123 | nucleoside monophosphate metabolic process | 0.99340161 | 1.066396309 |
| ENSG00000183155 | RABIF subnetwork | 0.993371579 | 1.066457062 |
| GO:0030826 | regulation of cGMP biosynthetic process | 0.993356027 | 1.066525266 |
| MP:0002733 | abnormal thermal nociception | 0.993326294 | 1.066582316 |
| MP:0000759 | abnormal skeletal muscle morphology | 0.993292793 | 1.066613323 |
| ENSG00000180210 | F2 subnetwork | 0.444590337 | 1.066639597 |
| GO:0038024 | cargo receptor activity | 0.444651764 | 1.066653134 |
| MP:0009845 | abnormal neural crest cell morphology | 0.993286236 | 1.066685276 |
| GO:0001885 | endothelial cell development | 0.993245183 | 1.066716296 |
| ENSG00000170178 | HOXD12 subnetwork | 0.44487537 | 1.066769481 |
| ENSG00000176749 | CDK5R1 subnetwork | 0.993234786 | 1.066784544 |
| REACTOME_APOPTOTIC_EXECUTI | REACTOME_APOPTOTIC_EXECUTION__PHASE | 0.44498526 | 1.066815452 |
| GO:0032272 | negative regulation of protein polymerization | 0.993233841 | 1.066863971 |
| ENSG00000183791 | TCEB3C subnetwork | 0.444874326 | 1.066934567 |
| ENSG00000152583 | SPARCL1 subnetwork | 0.993219628 | 1.066935964 |
| ENSG00000100321 | SYNGR1 subnetwork | 0.993203016 | 1.066996798 |
| ENSG00000140941 | MAP1LC3B subnetwork | 0.993187738 | 1.06704647 |
| MP:0005650 | abnormal limb bud morphology | 0.993174463 | 1.067114769 |
| MP:0002128 | abnormal blood circulation | 0.445169874 | 1.067129179 |
| GO:0031143 | pseudopodium | 0.993147527 | 1.067179353 |
| ENSG00000145423 | SFRP2 subnetwork | 0.993120162 | 1.067225326 |
| GO:0030073 | insulin secretion | 0.99310913 | 1.067289928 |
| GO:0045922 | negative regulation of fatty acid metabolic process | 0.993098242 | 1.067365716 |
| REACTOME_GLUCAGON:TYPE_LIC | REACTOME_GLUCAGON:TYPE_LIGAND_RECEPTORS | 0.993082807 | 1.067419163 |
| MP:0001539 | decreased caudal vertebrae number | 0.993075781 | 1.06748752 |
| GO:0001540 | beta-amyloid binding | 0.99307545 | 1.067567064 |
| GO:0043531 | ADP binding | 0.99302997 | 1.067575825 |
| MP:0000150 | abnormal rib morphology | 0.993008812 | 1.067644209 |
| MP:0002114 | abnormal axial skeleton morphology | 0.992988117 | 1.06770515 |
| ENSG00000174903 | RAB1B subnetwork | 0.992950073 | 1.067751193 |
| GO:0032982 | myosin filament | 0.992949919 | 1.067830786 |
| GO:0044087 | regulation of cellular component biogenesis | 0.445511745 | 1.067832225 |
| ENSG00000100151 | PICK1 subnetwork | 0.99291286 | 1.067861935 |
| MP:0001944 | abnormal pancreas morphology | 0.992909483 | 1.067941549 |
| GO:0000242 | pericentriolar material | 0.445664296 | 1.067959117 |
| ENSG00000096467 | ENSG00000096467 subnetwork | 0.446046805 | 1.067976982 |
| ENSG00000100503 | NIN subnetwork | 0.992885923 | 1.067998807 |
| ENSG00000155380 | SLC16A1 subnetwork | 0.446190409 | 1.068044077 |
| GO:0008021 | synaptic vesicle | 0.992865449 | 1.068052345 |
| REACTOME_MEIOTIC_SYNAPSIS | REACTOME_MEIOTIC_SYNAPSIS | 0.446136557 | 1.068063209 |
| MP:0000528 | delayed kidney development | 0.992841055 | 1.068098434 |
| ENSG00000206403 | ABHD16A subnetwork | 0.446046805 | 1.06815013 |
| MP:0009114 | decreased pancreatic beta cell mass | 0.446443045 | 1.068156787 |
| ENSG00000175895 | PLEKHF2 subnetwork | 0.992836101 | 1.068174361 |
| MP:0002812 | spherocytosis | 0.445858551 | 1.068183293 |
| MP:0004275 | abnormal postnatal subventricular zone morphology | 0.992799334 | 1.068194362 |
| ENSG00000115561 | CHMP3 subnetwork | 0.446536374 | 1.068218623 |
| GO:0070098 | chemokine-mediated signaling pathway | 0.992776708 | 1.068255389 |
| MP:0003049 | abnormal lumbar vertebrae morphology | 0.992749905 | 1.068301507 |
| MP:0003993 | abnormal ventral spinal root morphology | 0.44643277 | 1.068313624 |
| ENSG00000100519 | PSMC6 subnetwork | 0.446347397 | 1.068316591 |
| ENSG00000204427 | ABHD16A subnetwork | 0.446046805 | 1.068323334 |
| GO:0004890 | GABA-A receptor activity | 0.992715943 | 1.068340172 |
| ENSG00000164109 | MAD2L1 subnetwork | 0.992715564 | 1.068419875 |

| | | | |
|---|---|---|---|
| GO:0006636 | unsaturated fatty acid biosynthetic process | 0.446021675 | 1.068439831 |
| REACTOME_PROLONGED_ERK_A( | REACTOME_PROLONGED_ERK_ACTIVATION_EVENTS | 0.446947764 | 1.068454693 |
| ENSG00000112773 | FAM46A subnetwork | 0.44685599 | 1.068460667 |
| GO:0001882 | nucleoside binding | 0.446738765 | 1.068482837 |
| MP:0005631 | decreased lung weight | 0.446920296 | 1.068490047 |
| GO:0043062 | extracellular structure organization | 0.992712469 | 1.06849959 |
| GO:0030198 | extracellular matrix organization | 0.992712469 | 1.068579317 |
| ENSG00000101333 | PLCB4 subnetwork | 0.446841086 | 1.068617452 |
| MP:0003722 | absent ureter | 0.992697323 | 1.068644131 |
| GO:0072511 | divalent inorganic cation transport | 0.447238621 | 1.068667098 |
| GO:0045749 | negative regulation of S phase of mitotic cell cycle | 0.992688456 | 1.068712687 |
| ENSG00000042753 | AP2S1 subnetwork | 0.44718404 | 1.068718654 |
| ENSG00000183049 | CAMK1D subnetwork | 0.992666869 | 1.068770057 |
| GO:0015850 | organic alcohol transport | 0.99265502 | 1.068842365 |
| GO:0002504 | antigen processing and presentation of peptide or polysa | 0.447699654 | 1.068873262 |
| MP:0008943 | increased sensitivity to induced cell death | 0.447774025 | 1.068910619 |
| GO:0006941 | striated muscle contraction | 0.992649011 | 1.06891095 |
| ENSG00000153107 | ANAPC1 subnetwork | 0.99264383 | 1.068987011 |
| MP:0003207 | decreased cellular sensitivity to gamma-irradiation | 0.447900636 | 1.069004525 |
| GO:0030225 | macrophage differentiation | 0.447522667 | 1.06902798 |
| REACTOME_ACTIVATION_OF_DN/ | REACTOME_ACTIVATION_OF_DNA_FRAGMENTATION_F | 0.447678886 | 1.069029911 |
| MP:0002237 | abnormal nasal cavity morphology | 0.992614732 | 1.069051885 |
| ENSG00000162511 | LAPTM5 subnetwork | 0.992574465 | 1.069086905 |
| ENSG00000163539 | CLASP2 subnetwork | 0.992568321 | 1.069166729 |
| GO:0000152 | nuclear ubiquitin ligase complex | 0.992499993 | 1.069190562 |
| ENSG00000100413 | POLR3H subnetwork | 0.448484866 | 1.069192897 |
| REACTOME_APOPTOSIS_INDUCEI | REACTOME_APOPTOSIS_INDUCED_DNA_FRAGMENTATI | 0.447678886 | 1.069202781 |
| MP:0000968 | abnormal sensory neuron innervation pattern | 0.992479065 | 1.069248002 |
| MP:0002591 | decreased mean corpuscular volume | 0.448446237 | 1.069284792 |
| ENSG00000128266 | GNAZ subnetwork | 0.992463256 | 1.069320388 |
| GO:0060249 | anatomical structure homeostasis | 0.448400859 | 1.069376716 |
| ENSG00000135506 | OS9 subnetwork | 0.448338683 | 1.069395995 |
| GO:0002011 | morphogenesis of an epithelial sheet | 0.992460358 | 1.069400254 |
| GO:0043403 | skeletal muscle tissue regeneration | 0.992453921 | 1.069472662 |
| ENSG00000196150 | ZNF250 subnetwork | 0.992441952 | 1.069541346 |
| ENSG00000180104 | EXOC3 subnetwork | 0.448334331 | 1.069560653 |
| REACTOME_INHIBITION_OF_REPL | REACTOME_INHIBITION_OF_REPLICATION_INITIATION_( | 0.448220151 | 1.069607368 |
| ENSG00000183048 | SLC25A10 subnetwork | 0.992440249 | 1.069621246 |
| REACTOME_INTERACTIONS_OF_R | REACTOME_INTERACTIONS_OF_REV_WITH_HOST_CELLI | 0.44830379 | 1.069636511 |
| GO:0045104 | intermediate filament cytoskeleton organization | 0.992391503 | 1.069652596 |
| MP:0000585 | kinked tail | 0.992368655 | 1.069717573 |
| GO:0019359 | nicotinamide nucleotide biosynthetic process | 0.992365597 | 1.069793768 |
| ENSG00000129993 | CBFA2T3 subnetwork | 0.992330457 | 1.069828875 |
| GO:0005865 | striated muscle thin filament | 0.99232527 | 1.069901353 |
| ENSG00000137267 | TUBB2A subnetwork | 0.992299399 | 1.069936472 |
| GO:0006835 | dicarboxylic acid transport | 0.992298788 | 1.070016444 |
| ENSG00000008311 | AASS subnetwork | 0.992288673 | 1.070085215 |
| GO:0021766 | hippocampus development | 0.992278361 | 1.070157733 |
| GO:0016460 | myosin II complex | 0.99226456 | 1.070226525 |
| KEGG_DRUG_METABOLISM_CYTC | KEGG_DRUG_METABOLISM_CYTOCHROME_P450 | 0.449097893 | 1.070243666 |
| MP:0001899 | absent long term depression | 0.992238422 | 1.070257944 |
| GO:0017158 | regulation of calcium ion-dependent exocytosis | 0.99220974 | 1.070300583 |
| ENSG00000048540 | LMO3 subnetwork | 0.992200422 | 1.07037314 |
| GO:0030175 | filopodium | 0.449066295 | 1.070376049 |

| | | | |
|---|---|---|---|
| GO:0034605 | cellular response to heat | 0.992187418 | 1.070438229 |
| GO:0016055 | Wnt receptor signaling pathway | 0.992180434 | 1.070507068 |
| GO:0030072 | peptide hormone secretion | 0.992167691 | 1.070557218 |
| MP:0002948 | abnormal neuron specification | 0.992165905 | 1.070637295 |
| MP:0001433 | polyphagia | 0.992145207 | 1.070702424 |
| GO:0071941 | nitrogen cycle metabolic process | 0.992111955 | 1.07075634 |
| ENSG00000160199 | PKNOX1 subnetwork | 0.449395227 | 1.0708293 |
| GO:0055081 | anion homeostasis | 0.992105131 | 1.070836451 |
| MP:0000039 | abnormal otic capsule morphology | 0.992103171 | 1.070916573 |
| ENSG00000120057 | SFRP5 subnetwork | 0.992072142 | 1.070989225 |
| ENSG00000106483 | SFRP4 subnetwork | 0.992072142 | 1.071069371 |
| ENSG00000104332 | SFRP1 subnetwork | 0.992072142 | 1.071149529 |
| GO:0000187 | activation of MAPK activity | 0.449822028 | 1.071154466 |
| GO:0070848 | response to growth factor stimulus | 0.449603684 | 1.071196967 |
| MP:0004462 | small basisphenoid bone | 0.44976565 | 1.07121432 |
| ENSG00000176697 | BDNF subnetwork | 0.992065555 | 1.071222214 |
| REACTOME_CONVERSION_FROM | REACTOME_CONVERSION_FROM_APCCDC20_TO_APC | 0.991997412 | 1.071227545 |
| ENSG00000101146 | RAE1 subnetwork | 0.450084761 | 1.071273167 |
| GO:0001706 | endoderm formation | 0.991979262 | 1.071292761 |
| GO:0015872 | dopamine transport | 0.991915296 | 1.071328043 |
| ENSG00000170876 | TMEM43 subnetwork | 0.991867849 | 1.071355843 |
| ENSG00000169641 | LUZP1 subnetwork | 0.450065967 | 1.071373308 |
| ENSG00000171557 | FGG subnetwork | 0.449764707 | 1.071387097 |
| ENSG00000120088 | CRHR1 subnetwork | 0.991858921 | 1.071428571 |
| GO:0005876 | spindle microtubule | 0.450249927 | 1.07148727 |
| ENSG00000135900 | MRPL44 subnetwork | 0.450044395 | 1.071489602 |
| ENSG00000163814 | CDCP1 subnetwork | 0.991845745 | 1.07150131 |
| ENSG00000213416 | KRTAP4-12 subnetwork | 0.991826874 | 1.071547851 |
| ENSG00000174744 | BRMS1 subnetwork | 0.450348747 | 1.071564363 |
| GO:0030111 | regulation of Wnt receptor signaling pathway | 0.991737528 | 1.071581037 |
| ENSG00000212908 | ENSG00000212908 subnetwork | 0.991826874 | 1.071628099 |
| MP:0010519 | atrioventricular block | 0.991722987 | 1.071638829 |
| ENSG00000164080 | RAD54L2 subnetwork | 0.991689098 | 1.071674157 |
| MP:0004994 | abnormal brain wave pattern | 0.991630389 | 1.071683272 |
| MP:0000752 | dystrophic muscle | 0.991621549 | 1.071759814 |
| MP:0000030 | abnormal tympanic ring morphology | 0.991598407 | 1.071825129 |
| GO:0071702 | organic substance transport | 0.991595901 | 1.071901693 |
| GO:0038032 | termination of G-protein coupled receptor signaling path | 0.991573554 | 1.071937055 |
| ENSG00000068793 | CYFIP1 subnetwork | 0.991487224 | 1.071977816 |
| REACTOME_G1S:SPECIFIC_TRANS | REACTOME_G1S:SPECIFIC_TRANSCRIPTION | 0.991556812 | 1.072002398 |
| MP:0003817 | abnormal pituitary diverticulum morphology | 0.991463395 | 1.072039424 |
| GO:0005179 | hormone activity | 0.991454331 | 1.072097294 |
| MP:0002551 | abnormal blood coagulation | 0.450652314 | 1.072113062 |
| ENSG00000175602 | CCDC85B subnetwork | 0.991372418 | 1.07214184 |
| GO:0007411 | axon guidance | 0.991450017 | 1.072177661 |
| GO:0042755 | eating behavior | 0.991352518 | 1.072207227 |
| GO:0043551 | regulation of phosphatidylinositol 3-kinase activity | 0.45064373 | 1.072229381 |
| GO:0010002 | cardioblast differentiation | 0.991350272 | 1.072283872 |
| GO:0060070 | canonical Wnt receptor signaling pathway | 0.991319214 | 1.072326785 |
| GO:0006140 | regulation of nucleotide metabolic process | 0.991309792 | 1.07240345 |
| ENSG00000089818 | NECAP1 subnetwork | 0.450845918 | 1.072447665 |
| GO:0072529 | pyrimidine-containing compound catabolic process | 0.991300948 | 1.072453877 |
| ENSG00000181789 | COPG subnetwork | 0.450923155 | 1.072500403 |
| MP:0002090 | abnormal vision | 0.991294984 | 1.072526813 |

| | | | |
|---|---|---|---|
| ENSG00000105894 | PTN subnetwork | 0.99127079 | 1.072581008 |
| GO:0014003 | oligodendrocyte development | 0.991249202 | 1.072631461 |
| GO:0050890 | cognition | 0.991247208 | 1.072708177 |
| ENSG00000135480 | KRT7 subnetwork | 0.991242674 | 1.072784905 |
| GO:0042220 | response to cocaine | 0.991220425 | 1.072842887 |
| GO:0014073 | response to tropane | 0.991220425 | 1.072923389 |
| GO:0003203 | endocardial cushion morphogenesis | 0.991203523 | 1.072996398 |
| MP:0006379 | abnormal spermatocyte morphology | 0.451243993 | 1.073060206 |
| ENSG00000105514 | RAB3D subnetwork | 0.991200787 | 1.073073171 |
| GO:0035108 | limb morphogenesis | 0.991182775 | 1.073089913 |
| GO:0035107 | appendage morphogenesis | 0.991182775 | 1.073170457 |
| ENSG00000094880 | CDC23 subnetwork | 0.991172352 | 1.073243507 |
| KEGG_CARDIAC_MUSCLE_CONTR | KEGG_CARDIAC_MUSCLE_CONTRACTION | 0.991169902 | 1.073320321 |
| ENSG00000186469 | GNG2 subnetwork | 0.991127518 | 1.073363363 |
| GO:0034381 | plasma lipoprotein particle clearance | 0.991119177 | 1.073440198 |
| GO:0007020 | microtubule nucleation | 0.99111305 | 1.07351329 |
| MP:0000536 | hydroureter | 0.991066611 | 1.073541338 |
| GO:0010769 | regulation of cell morphogenesis involved in differentiati | 0.991051531 | 1.073606939 |
| ENSG00000160299 | PCNT subnetwork | 0.991050968 | 1.07368757 |
| ENSG00000102893 | PHKB subnetwork | 0.991032386 | 1.073753192 |
| GO:0050879 | multicellular organismal movement | 0.99101339 | 1.073822579 |
| GO:0034312 | diol biosynthetic process | 0.451999459 | 1.07389836 |
| GO:0050881 | musculoskeletal movement | 0.99101339 | 1.073903245 |
| ENSG00000092054 | MYH7 subnetwork | 0.990991751 | 1.073953873 |
| GO:0010543 | regulation of platelet activation | 0.990980506 | 1.074027047 |
| ENSG00000184575 | XPOT subnetwork | 0.451728327 | 1.074030259 |
| GO:0042423 | catecholamine biosynthetic process | 0.451999459 | 1.074071095 |
| MP:0003938 | abnormal ear development | 0.990956827 | 1.074077692 |
| MP:0000897 | abnormal midbrain morphology | 0.990941398 | 1.07412083 |
| ENSG00000154978 | VOPP1 subnetwork | 0.990904845 | 1.074156459 |
| ENSG00000120907 | ADRA1A subnetwork | 0.990902147 | 1.074233429 |
| GO:0009713 | catechol-containing compound biosynthetic process | 0.451999459 | 1.074243887 |
| GO:0042439 | ethanolamine-containing compound metabolic process | 0.99088594 | 1.074302894 |
| GO:0021952 | central nervous system projection neuron axonogenesis | 0.990844807 | 1.07432727 |
| ENSG00000185615 | PDIA2 subnetwork | 0.451983206 | 1.074368463 |
| GO:0060123 | regulation of growth hormone secretion | 0.99083797 | 1.074400511 |
| GO:0034483 | heparan sulfate sulfotransferase activity | 0.990819391 | 1.074462487 |
| GO:0070252 | actin-mediated cell contraction | 0.990788748 | 1.07449064 |
| GO:0016755 | transferase activity, transferring amino-acyl groups | 0.451968744 | 1.074509173 |
| GO:0042166 | acetylcholine binding | 0.990774289 | 1.074552632 |
| ENSG00000101160 | CTSZ subnetwork | 0.452335259 | 1.074593986 |
| MP:0003311 | aminoaciduria | 0.990766823 | 1.074633431 |
| GO:0019098 | reproductive behavior | 0.990728193 | 1.074676643 |
| ENSG00000101150 | TPD52L2 subnetwork | 0.990688832 | 1.07470106 |
| MP:0001092 | abnormal trigeminal ganglion morphology | 0.990674119 | 1.074770608 |
| MP:0006358 | absent pinna reflex | 0.990670511 | 1.074851448 |
| MP:0004113 | abnormal aortic arch morphology | 0.990668705 | 1.0749323 |
| GO:0090276 | regulation of peptide hormone secretion | 0.990668072 | 1.075013165 |
| GO:0051646 | mitochondrion localization | 0.990658569 | 1.075086518 |
| GO:0005980 | glycogen catabolic process | 0.990621886 | 1.075129787 |
| MP:0002639 | micrognathia | 0.990621193 | 1.075210685 |
| GO:0010976 | positive regulation of neuron projection development | 0.990605187 | 1.075280307 |
| ENSG00000108823 | SGCA subnetwork | 0.990563444 | 1.075316075 |
| GO:0019362 | pyridine nucleotide metabolic process | 0.990550511 | 1.075385715 |

| | | | |
|---|---|---|---|
| REACTOME_INSULIN_RECEPTOR_ | REACTOME_INSULIN_RECEPTOR_SIGNALLING_CASCADE | 0.452735874 | 1.075409968 |
| GO:0072524 | pyridine-containing compound metabolic process | 0.990550511 | 1.075466657 |
| GO:0060675 | ureteric bud morphogenesis | 0.990547388 | 1.075540083 |
| GO:0061001 | regulation of dendritic spine morphogenesis | 0.990543983 | 1.075609756 |
| GO:0046717 | acid secretion | 0.990523017 | 1.075638034 |
| GO:0048306 | calcium-dependent protein binding | 0.990475413 | 1.07567008 |
| GO:0090277 | positive regulation of peptide hormone secretion | 0.990454062 | 1.075713425 |
| GO:0033044 | regulation of chromosome organization | 0.453499409 | 1.075742495 |
| REACTOME_FACTORS_INVOLVED_ | REACTOME_FACTORS_INVOLVED_IN_MEGAKARYOCYTE_ | 0.45293641 | 1.075759524 |
| GO:0001657 | ureteric bud development | 0.990449576 | 1.075790663 |
| ENSG00000113456 | RAD1 subnetwork | 0.453467747 | 1.075859024 |
| MP:0003633 | abnormal nervous system physiology | 0.990444929 | 1.075871677 |
| ENSG00000136944 | LMX1B subnetwork | 0.990428804 | 1.075941407 |
| ENSG00000001626 | CFTR subnetwork | 0.453404027 | 1.075951502 |
| REACTOME_FORMATION_OF_INC | REACTOME_FORMATION_OF_INCISION_COMPLEX_IN_G | 0.990407888 | 1.076007381 |
| GO:0051457 | maintenance of protein location in nucleus | 0.453361092 | 1.076011886 |
| ENSG00000136110 | LECT1 subnetwork | 0.454035604 | 1.076026628 |
| REACTOME_DUAL_INCISION_REA | REACTOME_DUAL_INCISION_REACTION_IN_GG:NER | 0.990407888 | 1.07608843 |
| GO:0030137 | COPI-coated vesicle | 0.453747031 | 1.076091493 |
| ENSG00000148053 | NTRK2 subnetwork | 0.45332801 | 1.076104418 |
| ENSG00000151748 | SAV1 subnetwork | 0.45318486 | 1.076104773 |
| MP:0001852 | conjunctivitis | 0.454025688 | 1.076143109 |
| ENSG00000123131 | PRDX4 subnetwork | 0.453919783 | 1.076147304 |
| REACTOME_REGULATION_OF_AP | REACTOME_REGULATION_OF_APOPTOSIS | 0.990399221 | 1.076161959 |
| GO:0006725 | cellular aromatic compound metabolic process | 0.990324431 | 1.07617523 |
| GO:0044427 | chromosomal part | 0.453889041 | 1.07622372 |
| GO:0016798 | hydrolase activity, acting on glycosyl bonds | 0.990312193 | 1.076233708 |
| GO:0004745 | retinol dehydrogenase activity | 0.453321881 | 1.07626928 |
| MP:0001728 | failure of embryo implantation | 0.45419818 | 1.076271051 |
| ENSG00000112936 | C7 subnetwork | 0.453181616 | 1.076277724 |
| GO:0060716 | labyrinthine layer blood vessel development | 0.990296273 | 1.076295961 |
| GO:0002791 | regulation of peptide secretion | 0.990282828 | 1.076373295 |
| GO:0070555 | response to interleukin-1 | 0.454709287 | 1.076377764 |
| MP:0000454 | abnormal jaw morphology | 0.990114383 | 1.076390564 |
| ENSG00000047579 | DTNBP1 subnetwork | 0.454409167 | 1.076406926 |
| GO:0033555 | multicellular organismal response to stress | 0.990213477 | 1.076445098 |
| GO:0060173 | limb development | 0.990095675 | 1.076449084 |
| GO:0090087 | regulation of peptide transport | 0.990282828 | 1.076454408 |
| GO:0006816 | calcium ion transport | 0.45435275 | 1.076467287 |
| GO:0031424 | keratinization | 0.454688738 | 1.076478129 |
| GO:0060039 | pericardium development | 0.454894867 | 1.07648943 |
| ENSG00000141956 | PRDM15 subnetwork | 0.454558981 | 1.076494631 |
| ENSG00000168412 | MTNR1A subnetwork | 0.454638948 | 1.076522436 |
| GO:0048736 | appendage development | 0.990095675 | 1.076530228 |
| ENSG00000008277 | ADAM22 subnetwork | 0.990079891 | 1.076592537 |
| MP:0008544 | impaired olfaction | 0.99003048 | 1.07661339 |
| ENSG00000104824 | HNRNPL subnetwork | 0.45488264 | 1.076613807 |
| ENSG00000107819 | SFXN3 subnetwork | 0.989991767 | 1.076626706 |
| ENSG00000104549 | SQLE subnetwork | 0.454550388 | 1.076667201 |
| GO:0042436 | indole-containing compound catabolic process | 0.98998605 | 1.076707887 |
| GO:0006569 | tryptophan catabolic process | 0.98998605 | 1.076789081 |
| GO:0046218 | indolalkylamine catabolic process | 0.98998605 | 1.076870287 |
| ENSG00000135052 | GOLM1 subnetwork | 0.989972163 | 1.076947734 |
| GO:0007200 | phospholipase C-activating G-protein coupled receptor s | 0.989950868 | 1.077006336 |

| | | | |
|---|---|---|---|
| GO:0051784 | negative regulation of nuclear division | 0.989935814 | 1.077061175 |
| ENSG00000137203 | TFAP2A subnetwork | 0.455197285 | 1.077117694 |
| GO:0045839 | negative regulation of mitosis | 0.989935814 | 1.077142426 |
| ENSG00000164093 | PITX2 subnetwork | 0.989898492 | 1.077178423 |
| MP:0001968 | abnormal touch/ nociception | 0.989880985 | 1.077244605 |
| GO:0071845 | cellular component disassembly at cellular level | 0.456047076 | 1.077290168 |
| GO:0003416 | endochondral bone growth | 0.98987978 | 1.077325888 |
| GO:0044243 | multicellular organismal catabolic process | 0.989846393 | 1.077354362 |
| MP:0003355 | decreased ovulation rate | 0.456007698 | 1.077430445 |
| GO:0002790 | peptide secretion | 0.989841004 | 1.077431892 |
| ENSG00000109272 | PF4V1 subnetwork | 0.455696306 | 1.077468395 |
| ENSG00000073578 | SDHA subnetwork | 0.455824928 | 1.077491601 |
| GO:0022603 | regulation of anatomical structure morphogenesis | 0.989814054 | 1.07749434 |
| ENSG00000151576 | QTRTD1 subnetwork | 0.455779177 | 1.077528 |
| GO:0035137 | hindlimb morphogenesis | 0.98977348 | 1.077534154 |
| MP:0001134 | absent corpus luteum | 0.455486363 | 1.077537624 |
| GO:0034706 | sodium channel complex | 0.989736545 | 1.077570199 |
| ENSG00000107854 | TNKS2 subnetwork | 0.456277442 | 1.077581522 |
| GO:0005671 | Ada2/Gcn5/Ada3 transcription activator complex | 0.456005674 | 1.077602751 |
| ENSG00000034713 | GABARAPL2 subnetwork | 0.455615233 | 1.077637266 |
| ENSG00000205813 | ENSG00000205813 subnetwork | 0.455696306 | 1.077640845 |
| MP:0005274 | abnormal viscerocranium morphology | 0.989730372 | 1.077643995 |
| ENSG00000115306 | SPTBN1 subnetwork | 0.455982766 | 1.077703135 |
| REACTOME_STRIATED_MUSCLE_( | REACTOME_STRIATED_MUSCLE_CONTRACTION | 0.98972528 | 1.077717802 |
| GO:0034330 | cell junction organization | 0.989715157 | 1.077787844 |
| GO:0009952 | anterior/posterior pattern specification | 0.989701893 | 1.077857898 |
| ENSG00000134809 | TIMM10 subnetwork | 0.989701151 | 1.077939289 |
| GO:0008236 | serine-type peptidase activity | 0.456591925 | 1.078004155 |
| GO:0019932 | second-messenger-mediated signaling | 0.989697083 | 1.078020692 |
| GO:0023019 | signal transduction involved in regulation of gene expres | 0.989652835 | 1.078037913 |
| GO:0032781 | positive regulation of ATPase activity | 0.989625288 | 1.078066465 |
| GO:0005813 | centrosome | 0.456562588 | 1.078112514 |
| REACTOME_G_PROTEIN_GATED_ | REACTOME_G_PROTEIN_GATED_POTASSIUM_CHANNEL | 0.989609557 | 1.078132789 |
| ENSG00000156711 | MAPK13 subnetwork | 0.456730426 | 1.078135485 |
| REACTOME_INHIBITION__OF_VO | REACTOME_INHIBITION__OF_VOLTAGE_GATED_CA2_CH | 0.989609557 | 1.078214232 |
| ENSG00000126522 | ASL subnetwork | 0.457013545 | 1.078270244 |
| MP:0002062 | abnormal associative learning | 0.989535162 | 1.078286491 |
| REACTOME_ACTIVATION_OF_G_I | REACTOME_ACTIVATION_OF_G_PROTEIN_GATED_POTA | 0.989609557 | 1.078295686 |
| MP:0003232 | abnormal forebrain development | 0.989514634 | 1.078326407 |
| GO:0005643 | nuclear pore | 0.456941576 | 1.078354633 |
| MP:0002574 | increased vertical activity | 0.989506681 | 1.078400332 |
| ENSG00000121152 | NCAPH subnetwork | 0.989482534 | 1.078455377 |
| GO:0035113 | embryonic appendage morphogenesis | 0.989456877 | 1.078510429 |
| MP:0002825 | abnormal notochord morphology | 0.989382484 | 1.078548753 |
| GO:0030326 | embryonic limb morphogenesis | 0.989456877 | 1.078591943 |
| GO:0004835 | tubulin-tyrosine ligase activity | 0.989380817 | 1.078618943 |
| KEGG_ARRHYTHMOGENIC_RIGHT | KEGG_ARRHYTHMOGENIC_RIGHT_VENTRICULAR_CARDI | 0.989364702 | 1.078658905 |
| MP:0000077 | abnormal interparietal bone morphology | 0.989288727 | 1.078708604 |
| ENSG00000104863 | LIN7B subnetwork | 0.989342984 | 1.078713994 |
| GO:0045502 | dynein binding | 0.989285835 | 1.078778828 |
| ENSG00000163637 | PRICKLE2 subnetwork | 0.98928441 | 1.078860405 |
| GO:0008360 | regulation of cell shape | 0.989274333 | 1.078930651 |
| GO:0060411 | cardiac septum morphogenesis | 0.989270821 | 1.079008471 |
| MP:0000792 | abnormal cortical marginal zone morphology | 0.989205967 | 1.079025792 |

| | | | |
|---|---|---|---|
| REACTOME_CELL_JUNCTION_ORG | REACTOME_CELL_JUNCTION_ORGANIZATION | 0.989199369 | 1.079103631 |
| GO:0031333 | negative regulation of protein complex assembly | 0.989175137 | 1.079143657 |
| GO:0030675 | Rac GTPase activator activity | 0.4576453 | 1.07915403 |
| ENSG00000110721 | CHKA subnetwork | 0.457738777 | 1.079189275 |
| GO:0006699 | bile acid biosynthetic process | 0.989172237 | 1.079225299 |
| ENSG00000150787 | PTS subnetwork | 0.457624814 | 1.07925447 |
| ENSG00000164611 | PTTG1 subnetwork | 0.989144368 | 1.079272906 |
| GO:0034614 | cellular response to reactive oxygen species | 0.457468347 | 1.079279783 |
| MP:0002843 | decreased systemic arterial blood pressure | 0.457576125 | 1.079315025 |
| GO:0030551 | cyclic nucleotide binding | 0.989143484 | 1.07935457 |
| ENSG00000105607 | GCDH subnetwork | 0.9891246 | 1.079356792 |
| GO:0060045 | positive regulation of cardiac muscle cell proliferation | 0.989101204 | 1.079419555 |
| GO:0007567 | parturition | 0.989097855 | 1.079501249 |
| MP:0001406 | abnormal gait | 0.989077082 | 1.079567817 |
| ENSG00000204218 | ENSG00000204218 subnetwork | 0.98906132 | 1.07963818 |
| GO:0043596 | nuclear replication fork | 0.458001407 | 1.079671294 |
| MP:0000255 | vasculature congestion | 0.458061045 | 1.079674537 |
| GO:0006353 | transcription termination, DNA-dependent | 0.989054914 | 1.079708554 |
| ENSG00000105972 | ENSG00000105972 subnetwork | 0.989032859 | 1.079782724 |
| GO:0070509 | calcium ion import | 0.989021057 | 1.079849334 |
| ENSG00000087274 | ADD1 subnetwork | 0.988997436 | 1.07991974 |
| ENSG00000104835 | FBXO17 subnetwork | 0.988988153 | 1.079993942 |
| MP:0000819 | abnormal olfactory bulb morphology | 0.98897807 | 1.080071942 |
| MP:0008531 | increased chemical nociceptive threshold | 0.988962338 | 1.080131021 |
| GO:0048705 | skeletal system morphogenesis | 0.988961856 | 1.08021283 |
| GO:0032526 | response to retinoic acid | 0.988842039 | 1.080259071 |
| GO:0015300 | solute:solute antiporter activity | 0.988960251 | 1.080290865 |
| ENSG00000138039 | LHCGR subnetwork | 0.988819745 | 1.080299242 |
| GO:0009074 | aromatic amino acid family catabolic process | 0.988792376 | 1.080350784 |
| GO:0005916 | fascia adherens | 0.988773099 | 1.080413699 |
| ENSG00000165156 | ZHX1 subnetwork | 0.458477886 | 1.080443452 |
| MP:0004542 | impaired acrosome reaction | 0.988753729 | 1.080480412 |
| GO:0045665 | negative regulation of neuron differentiation | 0.98875024 | 1.080558503 |
| GO:0048853 | forebrain morphogenesis | 0.988737648 | 1.080617658 |
| REACTOME_PYRIMIDINE_METABO | REACTOME_PYRIMIDINE_METABOLISM | 0.988730694 | 1.080688192 |
| GO:0003007 | heart morphogenesis | 0.988668868 | 1.080698097 |
| ENSG00000110318 | KIAA1377 subnetwork | 0.988661352 | 1.080757277 |
| GO:0043586 | tongue development | 0.98850679 | 1.080794602 |
| ENSG00000004975 | DVL2 subnetwork | 0.98864816 | 1.080805094 |
| GO:0048703 | embryonic viscerocranium morphogenesis | 0.988610745 | 1.080826384 |
| GO:0055003 | cardiac myofibril assembly | 0.988472738 | 1.080853806 |
| GO:0008272 | sulfate transport | 0.988432266 | 1.080886479 |
| GO:0043462 | regulation of ATPase activity | 0.988399512 | 1.080930532 |
| GO:0060914 | heart formation | 0.988385748 | 1.081001138 |
| GO:0015851 | nucleobase transport | 0.988383385 | 1.081083131 |
| GO:0070936 | protein K48-linked ubiquitination | 0.458777816 | 1.081092504 |
| MP:0005176 | eyelids fail to open | 0.988378389 | 1.081161344 |
| GO:0004407 | histone deacetylase activity | 0.988373464 | 1.081243362 |
| GO:0033558 | protein deacetylase activity | 0.988373464 | 1.081325393 |
| GO:0032314 | regulation of Rac GTPase activity | 0.988363301 | 1.081399848 |
| MP:0003054 | spina bifida | 0.988294032 | 1.081406025 |
| GO:0060343 | trabecula formation | 0.988288559 | 1.081484292 |
| ENSG00000131095 | GFAP subnetwork | 0.988258872 | 1.081539804 |
| ENSG00000137726 | FXYD6 subnetwork | 0.988250083 | 1.081610504 |

| | | | |
|---|---|---|---|
| ENSG00000075651 | PLD1 subnetwork | 0.461321296 | 1.081635729 |
| ENSG00000061676 | NCKAP1 subnetwork | 0.988246243 | 1.081688805 |
| MP:0008411 | decreased cellular sensitivity to ultraviolet irradiation | 0.461290738 | 1.081735957 |
| GO:0031400 | negative regulation of protein modification process | 0.988209694 | 1.081736754 |
| ENSG00000182934 | SRPR subnetwork | 0.988171025 | 1.081765733 |
| ENSG00000198216 | CACNA1E subnetwork | 0.461746632 | 1.081777108 |
| MP:0009642 | abnormal blood homeostasis | 0.463031969 | 1.081821056 |
| ENSG00000168827 | GFM1 subnetwork | 0.461700842 | 1.081829713 |
| GO:0060216 | definitive hemopoiesis | 0.463208786 | 1.081842604 |
| MP:0004491 | abnormal orientation of outer hair cell stereociliary bunc | 0.988170957 | 1.081847859 |
| ENSG00000139269 | INHBE subnetwork | 0.463154861 | 1.081879248 |
| MP:0000125 | absent incisors | 0.461576419 | 1.081887391 |
| ENSG00000197249 | SERPINA1 subnetwork | 0.98814874 | 1.081888239 |
| ENSG00000150527 | CTAGE5 subnetwork | 0.46128566 | 1.081891763 |
| MP:0001289 | persistence of hyaloid vascular system | 0.463402283 | 1.081911532 |
| ENSG00000131183 | SLC34A1 subnetwork | 0.4629912 | 1.081913043 |
| GO:0071900 | regulation of protein serine/threonine kinase activity | 0.463484403 | 1.08191439 |
| GO:0030552 | cAMP binding | 0.988118268 | 1.081921033 |
| MP:0002799 | abnormal passive avoidance behavior | 0.987806164 | 1.081969766 |
| MP:0002674 | abnormal sperm motility | 0.988092545 | 1.081972815 |
| ENSG00000152520 | PAN3 subnetwork | 0.461690389 | 1.081985411 |
| ENSG00000124092 | CTCFL subnetwork | 0.459223339 | 1.081996492 |
| ENSG00000175189 | INHBC subnetwork | 0.461258364 | 1.082007937 |
| GO:0004553 | hydrolase activity, hydrolyzing O-glycosyl compounds | 0.987857601 | 1.082009115 |
| ENSG00000018236 | CNTN1 subnetwork | 0.988064251 | 1.082009417 |
| GO:0003006 | developmental process involved in reproduction | 0.463354813 | 1.082011376 |
| MP:0008321 | small adenohypophysis | 0.987930484 | 1.082014279 |
| GO:0042693 | muscle cell fate commitment | 0.987792443 | 1.082032971 |
| MP:0004485 | increased response of heart to induced stress | 0.46156438 | 1.082035216 |
| ENSG00000172531 | PPP1CA subnetwork | 0.462975151 | 1.082036686 |
| GO:0005924 | cell-substrate adherens junction | 0.460162719 | 1.082038835 |
| GO:0032155 | cell division site part | 0.461155878 | 1.082049857 |
| GO:0045933 | positive regulation of muscle contraction | 0.460076297 | 1.082083731 |
| GO:0010390 | histone monoubiquitination | 0.988034344 | 1.082087795 |
| GO:0005123 | death receptor binding | 0.46122643 | 1.082092396 |
| ENSG00000116741 | RGS2 subnetwork | 0.987777353 | 1.082107582 |
| ENSG00000123338 | NCKAP1L subnetwork | 0.464291366 | 1.082137224 |
| ENSG00000196792 | STRN3 subnetwork | 0.459614083 | 1.082143426 |
| GO:0000301 | retrograde transport, vesicle recycling within Golgi | 0.462963284 | 1.082144552 |
| GO:0001938 | positive regulation of endothelial cell proliferation | 0.462556466 | 1.082175083 |
| MP:0008535 | enlarged lateral ventricles | 0.987774749 | 1.082186004 |
| ENSG00000035928 | RFC1 subnetwork | 0.462012515 | 1.082207957 |
| GO:0032153 | cell division site | 0.461155878 | 1.082221693 |
| ENSG00000168385 | SEPT2 subnetwork | 0.462928428 | 1.082244543 |
| REACTOME_RNA_POLYMERASE_I | REACTOME_RNA_POLYMERASE_III_TRANSCRIPTION_INI | 0.45944423 | 1.082246492 |
| ENSG00000206247 | ENSG00000206247 subnetwork | 0.460023278 | 1.082253185 |
| MP:0005191 | head tilt | 0.460074777 | 1.08225601 |
| GO:0005891 | voltage-gated calcium channel complex | 0.98776173 | 1.082260638 |
| GO:0000303 | response to superoxide | 0.460609379 | 1.082275763 |
| REACTOME_RNA_POLYMERASE_I | REACTOME_RNA_POLYMERASE_III_TRANSCRIPTION_TEI | 0.462547607 | 1.08230684 |
| ENSG00000078295 | ADCY2 subnetwork | 0.464291049 | 1.082307935 |
| MP:0002636 | delayed vaginal opening | 0.459610646 | 1.082307938 |
| ENSG00000213024 | NUP62 subnetwork | 0.462881504 | 1.082312925 |
| ENSG00000049541 | RFC2 subnetwork | 0.46443698 | 1.0823214 |

| | | | |
|---|---|---|---|
| GO:0016052 | carbohydrate catabolic process | 0.987745386 | 1.082323885 |
| REACTOME_BRANCHED:CHAIN_A | REACTOME_BRANCHED:CHAIN_AMINO_ACID_CATABOL | 0.460390618 | 1.082344048 |
| GO:0016525 | negative regulation of angiogenesis | 0.987709183 | 1.082360541 |
| ENSG00000188428 | MUTED subnetwork | 0.460490228 | 1.082362768 |
| ENSG00000021488 | SLC7A9 subnetwork | 0.460705376 | 1.082366036 |
| GO:0045109 | intermediate filament organization | 0.987679146 | 1.082366801 |
| GO:0043499 | eukaryotic cell surface binding | 0.461146253 | 1.082369759 |
| GO:0003682 | chromatin binding | 0.459575124 | 1.082392795 |
| MP:0004966 | abnormal inner cell mass proliferation | 0.462518762 | 1.082414885 |
| ENSG00000145703 | IQGAP2 subnetwork | 0.464533865 | 1.082418795 |
| GO:0097094 | craniofacial suture morphogenesis | 0.98764036 | 1.082422469 |
| ENSG00000204304 | PBX2 subnetwork | 0.460023278 | 1.082425545 |
| MP:0002764 | short tibia | 0.461061436 | 1.082427709 |
| ENSG00000158528 | PPP1R9A subnetwork | 0.46395524 | 1.082428165 |
| MP:0000281 | abnormal interventricular septum morphology | 0.46286601 | 1.082428797 |
| ENSG00000135750 | KCNK1 subnetwork | 0.460569019 | 1.082437162 |
| ENSG00000118965 | WDR35 subnetwork | 0.462714532 | 1.082439063 |
| ENSG00000085733 | CTTN subnetwork | 0.464270117 | 1.082447144 |
| GO:0000305 | response to oxygen radical | 0.460609379 | 1.082447908 |
| MP:0003564 | abnormal insulin secretion | 0.462453913 | 1.082459614 |
| REACTOME_CYCLIN_D_ASSOCIAT | REACTOME_CYCLIN_D_ASSOCIATED_EVENTS_IN_G1 | 0.464192147 | 1.082460155 |
| ENSG00000005884 | ITGA3 subnetwork | 0.462814754 | 1.082481405 |
| GO:0060363 | cranial suture morphogenesis | 0.98764036 | 1.082504751 |
| ENSG00000173366 | ENSG00000173366 subnetwork | 0.461142437 | 1.082525814 |
| MP:0008146 | asymmetric rib-sternum attachment | 0.461030792 | 1.082544097 |
| ENSG00000135249 | RINT1 subnetwork | 0.459921466 | 1.082547395 |
| ENSG00000167711 | SERPINF2 subnetwork | 0.463930153 | 1.082551713 |
| ENSG00000159259 | CHAF1B subnetwork | 0.462425569 | 1.082551877 |
| ENSG00000100994 | PYGB subnetwork | 0.462293082 | 1.08255427 |
| ENSG00000175445 | LPL subnetwork | 0.460957016 | 1.082573109 |
| GO:0008201 | heparin binding | 0.987637651 | 1.082587046 |
| ENSG00000206315 | PBX2 subnetwork | 0.460023278 | 1.082597961 |
| REACTOME_G1_PHASE | REACTOME_G1_PHASE | 0.464192147 | 1.082630997 |
| GO:0003407 | neural retina development | 0.98762782 | 1.082650346 |
| ENSG00000169180 | XPO6 subnetwork | 0.462279491 | 1.082654517 |
| ENSG00000078808 | SDF4 subnetwork | 0.463897952 | 1.082667404 |
| ENSG00000140374 | ETFA subnetwork | 0.459912892 | 1.082695985 |
| GO:0008277 | regulation of G-protein coupled receptor protein signalir | 0.987601137 | 1.082709854 |
| MP:0002269 | muscular atrophy | 0.460952895 | 1.0827134 |
| ENSG00000169217 | CD2BP2 subnetwork | 0.462421707 | 1.082723384 |
| GO:0050771 | negative regulation of axonogenesis | 0.987571994 | 1.082757965 |
| GO:0016888 | endodeoxyribonuclease activity, producing 5'-phosphom | 0.46418115 | 1.082786109 |
| MP:0004274 | abnormal embryonic/fetal subventricular zone morpholc | 0.987538077 | 1.082813688 |
| ENSG00000048828 | FAM120A subnetwork | 0.987505116 | 1.082854209 |
| GO:0042982 | amyloid precursor protein metabolic process | 0.460950403 | 1.082877583 |
| MP:0000966 | decreased sensory neuron number | 0.987504289 | 1.082936568 |
| GO:0051971 | positive regulation of transmission of nerve impulse | 0.987458282 | 1.082961892 |
| GO:0016079 | synaptic vesicle exocytosis | 0.987437424 | 1.083013845 |
| GO:0007625 | grooming behavior | 0.987403328 | 1.083065804 |
| GO:0019321 | pentose metabolic process | 0.987385198 | 1.083102556 |
| MP:0002260 | abnormal thyroid cartilage morphology | 0.987374402 | 1.083165944 |
| REACTOME_PYRIMIDINE_CATABC | REACTOME_PYRIMIDINE_CATABOLISM | 0.987373306 | 1.083248364 |
| ENSG00000157483 | MYO1E subnetwork | 0.464980212 | 1.083312313 |
| GO:0005504 | fatty acid binding | 0.987368782 | 1.083326992 |

| | | | |
|---|---|---|---|
| GO:0009064 | glutamine family amino acid metabolic process | 0.987364832 | 1.083405632 |
| GO:0023021 | termination of signal transduction | 0.987292383 | 1.08341198 |
| ENSG00000138750 | NUP54 subnetwork | 0.465104017 | 1.083425284 |
| ENSG00000167460 | TPM4 subnetwork | 0.987231937 | 1.083429746 |
| GO:0050775 | positive regulation of dendrite morphogenesis | 0.987223459 | 1.083500799 |
| ENSG00000182923 | CEP63 subnetwork | 0.465307115 | 1.083525055 |
| MP:0002014 | increased papilloma incidence | 0.98720151 | 1.083564251 |
| MP:0003998 | decreased thermal nociceptive threshold | 0.987168534 | 1.083593453 |
| ENSG00000171530 | TBCA subnetwork | 0.465278076 | 1.083640662 |
| GO:0001501 | skeletal system development | 0.987073882 | 1.083655677 |
| GO:0035815 | positive regulation of renal sodium excretion | 0.987146603 | 1.083656921 |
| GO:0035282 | segmentation | 0.987051636 | 1.083734389 |
| GO:0043124 | negative regulation of I-kappaB kinase/NF-kappaB casca | 0.465686119 | 1.083740157 |
| GO:0060349 | bone morphogenesis | 0.986944465 | 1.083789033 |
| ENSG00000163485 | ADORA1 subnetwork | 0.987049012 | 1.083816922 |
| GO:0007096 | regulation of exit from mitosis | 0.986942997 | 1.083871582 |
| ENSG00000149782 | PLCB3 subnetwork | 0.465677748 | 1.083879351 |
| GO:0043330 | response to exogenous dsRNA | 0.46555704 | 1.083921538 |
| ENSG00000115760 | BIRC6 subnetwork | 0.986939288 | 1.083954144 |
| ENSG00000084754 | HADHA subnetwork | 0.465631469 | 1.083963453 |
| ENSG00000111364 | DDX55 subnetwork | 0.465853459 | 1.083971028 |
| ENSG00000100227 | POLDIP3 subnetwork | 0.466000524 | 1.083976074 |
| ENSG00000102898 | NUTF2 subnetwork | 0.466067096 | 1.084017941 |
| GO:0007173 | epidermal growth factor receptor signaling pathway | 0.465941257 | 1.084028652 |
| MP:0002887 | decreased susceptibility to pharmacologically induced se | 0.986939277 | 1.084036718 |
| ENSG00000138376 | BARD1 subnetwork | 0.466199785 | 1.08407017 |
| MP:0001325 | abnormal retina morphology | 0.986937508 | 1.084115496 |
| GO:0016712 | oxidoreductase activity, acting on paired donors, with in | 0.466179089 | 1.084154209 |
| GO:0034329 | cell junction assembly | 0.986934473 | 1.084194286 |
| GO:0003279 | cardiac septum development | 0.986907596 | 1.084250229 |
| GO:0017157 | regulation of exocytosis | 0.986897825 | 1.084329041 |
| ENSG00000133773 | CCDC59 subnetwork | 0.986889309 | 1.084404054 |
| ENSG00000122545 | SEPT7 subnetwork | 0.986861321 | 1.084460026 |
| GO:0009268 | response to pH | 0.986844513 | 1.084523628 |
| GO:0006672 | ceramide metabolic process | 0.986823165 | 1.084583429 |
| GO:0021549 | cerebellum development | 0.986805456 | 1.08464705 |
| REACTOME_NCAM1_INTERACTIO | REACTOME_NCAM1_INTERACTIONS | 0.986701564 | 1.084694267 |
| GO:0010721 | negative regulation of cell development | 0.986782745 | 1.084710681 |
| ENSG00000160678 | S100A1 subnetwork | 0.986686561 | 1.084761723 |
| GO:0072527 | pyrimidine-containing compound metabolic process | 0.986676059 | 1.084836816 |
| MP:0002557 | abnormal social/conspecific interaction | 0.986649482 | 1.084911919 |
| GO:0070307 | lens fiber cell development | 0.98660905 | 1.084937462 |
| GO:0015833 | peptide transport | 0.986589058 | 1.084989703 |
| ENSG00000041982 | TNC subnetwork | 0.46690461 | 1.085031447 |
| ENSG00000197321 | SVIL subnetwork | 0.466774027 | 1.085042466 |
| MP:0011093 | complete embryonic lethality at implantation | 0.986552726 | 1.085045767 |
| GO:0043691 | reverse cholesterol transport | 0.466717499 | 1.085110901 |
| GO:0009110 | vitamin biosynthetic process | 0.466879378 | 1.085123447 |
| MP:0000846 | abnormal medulla oblongata morphology | 0.986548056 | 1.085124723 |
| MP:0000886 | abnormal cerebellar granule layer | 0.986532222 | 1.085192249 |
| GO:0030288 | outer membrane-bounded periplasmic space | 0.986510477 | 1.085248341 |
| MP:0004324 | vestibular hair cell degeneration | 0.986322958 | 1.085285812 |
| MP:0003932 | abnormal molar crown morphology | 0.986446284 | 1.085291873 |
| GO:0015370 | solute:sodium symporter activity | 0.986405338 | 1.085306013 |

| | | | |
|---|---|---|---|
| ENSG00000103742 | IGDCC4 subnetwork | 0.468477057 | 1.085316714 |
| GO:0042597 | periplasmic space | 0.986510477 | 1.085331146 |
| MP:0002584 | small ectoplacental cone | 0.468337847 | 1.085343476 |
| GO:0044247 | cellular polysaccharide catabolic process | 0.986312006 | 1.085349565 |
| GO:0031267 | small GTPase binding | 0.468431487 | 1.085424181 |
| GO:0009251 | glucan catabolic process | 0.986312006 | 1.08543241 |
| MP:0009238 | coiled sperm flagellum | 0.468299613 | 1.085490196 |
| GO:0030199 | collagen fibril organization | 0.986289627 | 1.085492366 |
| ENSG00000145365 | TIFA subnetwork | 0.468149499 | 1.085509179 |
| MP:0001502 | abnormal circadian rhythm | 0.468675882 | 1.085530647 |
| MP:0000088 | short mandible | 0.986192259 | 1.08553596 |
| ENSG00000114850 | SSR3 subnetwork | 0.986260738 | 1.085540881 |
| ENSG00000105880 | DLX5 subnetwork | 0.986169461 | 1.085607391 |
| KEGG_GLYCOSPHINGOLIPID_BIOS | KEGG_GLYCOSPHINGOLIPID_BIOSYNTHESIS_LACTO_AND | 0.468111915 | 1.085608914 |
| GO:0010810 | regulation of cell-substrate adhesion | 0.468284645 | 1.08561343 |
| KEGG_FATTY_ACID_METABOLISM | KEGG_FATTY_ACID_METABOLISM | 0.467295256 | 1.085654771 |
| ENSG00000120149 | MSX2 subnetwork | 0.98607436 | 1.085685376 |
| ENSG00000168421 | RHOH subnetwork | 0.986162865 | 1.085686469 |
| ENSG00000140678 | ITGAX subnetwork | 0.467820035 | 1.085691849 |
| GO:0060537 | muscle tissue development | 0.467582236 | 1.085724387 |
| MP:0005410 | abnormal fertilization | 0.46809622 | 1.08574792 |
| ENSG00000082898 | XPO1 subnetwork | 0.467679142 | 1.085765907 |
| ENSG00000100170 | SLC5A1 subnetwork | 0.986069848 | 1.085768291 |
| GO:0014009 | glial cell proliferation | 0.986017129 | 1.085797755 |
| ENSG00000182004 | SNRPE subnetwork | 0.467782533 | 1.08579956 |
| GO:0015923 | mannosidase activity | 0.985978181 | 1.085823404 |
| ENSG00000130653 | PNPLA7 subnetwork | 0.467452832 | 1.085845646 |
| MP:0001313 | increased incidence of corneal inflammation | 0.467555905 | 1.085871444 |
| GO:0046839 | phospholipid dephosphorylation | 0.985956224 | 1.085879612 |
| MP:0009414 | skeletal muscle fiber necrosis | 0.98589923 | 1.085912911 |
| ENSG00000005961 | ITGA2B subnetwork | 0.46809576 | 1.085918367 |
| REACTOME_REV:MEDIATED_NUC | REACTOME_REV:MEDIATED_NUCLEAR_EXPORT_OF_HIV | 0.468044703 | 1.085955409 |
| GO:0048820 | hair follicle maturation | 0.985770691 | 1.085964242 |
| GO:0007494 | midgut development | 0.985877295 | 1.085969134 |
| ENSG00000178896 | EXOSC4 subnetwork | 0.468005793 | 1.086031721 |
| GO:0048864 | stem cell development | 0.985765823 | 1.086035761 |
| ENSG00000163828 | ENSG00000163828 subnetwork | 0.468951421 | 1.08604232 |
| GO:0010634 | positive regulation of epithelial cell migration | 0.469071472 | 1.086115029 |
| GO:0048645 | organ formation | 0.985762334 | 1.086118753 |
| GO:0000272 | polysaccharide catabolic process | 0.985753506 | 1.086197937 |
| GO:0042752 | regulation of circadian rhythm | 0.46954731 | 1.086198528 |
| KEGG_ENDOCYTOSIS | KEGG_ENDOCYTOSIS | 0.469809019 | 1.086199343 |
| MP:0002940 | variable body spotting | 0.985740484 | 1.086273311 |
| GO:0032012 | regulation of ARF protein signal transduction | 0.469958437 | 1.086311014 |
| MP:0001216 | abnormal epidermal layer morphology | 0.46972386 | 1.08633589 |
| MP:0010879 | decreased trabecular bone volume | 0.469525609 | 1.0863373 |
| GO:0032580 | Golgi cisterna membrane | 0.46979939 | 1.086338028 |
| GO:0015491 | cation:cation antiporter activity | 0.98574045 | 1.08635634 |
| ENSG00000166855 | CLPX subnetwork | 0.46925422 | 1.086360075 |
| ENSG00000129255 | MPDU1 subnetwork | 0.469671047 | 1.086380714 |
| ENSG00000182326 | C1S subnetwork | 0.469489504 | 1.086389977 |
| GO:0001702 | gastrulation with mouth forming second | 0.985618036 | 1.086407767 |
| GO:0005834 | heterotrimeric G-protein complex | 0.985574616 | 1.086433486 |
| ENSG00000171867 | PRNP subnetwork | 0.985736061 | 1.08643556 |

| | | | |
|---|---|---|---|
| ENSG00000107862 | GBF1 subnetwork | 0.469386469 | 1.086503212 |
| ENSG00000020426 | MNAT1 subnetwork | 0.46946018 | 1.086505326 |
| ENSG00000128683 | GAD1 subnetwork | 0.985573733 | 1.086508907 |
| ENSG00000091536 | MYO15A subnetwork | 0.985551479 | 1.086557578 |
| MP:0000111 | cleft palate | 0.985526108 | 1.086583314 |
| ENSG00000160803 | UBQLN4 subnetwork | 0.985510685 | 1.086658764 |
| GO:0001570 | vasculogenesis | 0.985442047 | 1.086702616 |
| ENSG00000140105 | WARS subnetwork | 0.985497443 | 1.086730402 |
| ENSG00000101004 | NINL subnetwork | 0.985426867 | 1.086774268 |
| GO:0010822 | positive regulation of mitochondrion organization | 0.985421482 | 1.086849755 |
| ENSG00000154342 | WNT3A subnetwork | 0.985408797 | 1.086917604 |
| ENSG00000130254 | SAFB2 subnetwork | 0.985401273 | 1.086989288 |
| GO:0072089 | stem cell proliferation | 0.985364019 | 1.087045681 |
| ENSG00000183395 | PMCH subnetwork | 0.985261665 | 1.08706283 |
| ENSG00000112559 | MDFI subnetwork | 0.985338423 | 1.087086777 |
| REACTOME_ADENYLATE_CYCLASE | REACTOME_ADENYLATE_CYCLASE_ACTIVATING_PATHW | 0.985241158 | 1.087103934 |
| GO:0006112 | energy reserve metabolic process | 0.985230143 | 1.087171833 |
| GO:0050953 | sensory perception of light stimulus | 0.985198393 | 1.087228261 |
| ENSG00000187239 | FNBP1 subnetwork | 0.985191067 | 1.087303835 |
| ENSG00000087586 | AURKA subnetwork | 0.985159844 | 1.087367938 |
| GO:0060415 | muscle tissue morphogenesis | 0.985156148 | 1.087447362 |
| GO:0007019 | microtubule depolymerization | 0.985089791 | 1.087480858 |
| GO:0006760 | folic acid-containing compound metabolic process | 0.984973214 | 1.087505744 |
| ENSG00000145864 | GABRB2 subnetwork | 0.985056157 | 1.087514358 |
| GO:0007129 | synapsis | 0.470477605 | 1.087572345 |
| MP:0006325 | impaired hearing | 0.984957314 | 1.087581374 |
| MP:0001300 | ocular hypertelorism | 0.984937151 | 1.087641697 |
| GO:0061371 | determination of heart left/right asymmetry | 0.984676876 | 1.087657064 |
| ENSG00000043591 | ADRB1 subnetwork | 0.984899366 | 1.08767905 |
| GO:0060674 | placenta blood vessel development | 0.984866664 | 1.087701088 |
| GO:0072006 | nephron development | 0.98477225 | 1.087703976 |
| GO:0001947 | heart looping | 0.984676876 | 1.087740403 |
| GO:0016861 | intramolecular oxidoreductase activity, interconverting a | 0.470645423 | 1.087785424 |
| MP:0005262 | coloboma | 0.984673689 | 1.087819923 |
| GO:0016775 | phosphotransferase activity, nitrogenous group as accep | 0.984670013 | 1.087899456 |
| GO:0009975 | cyclase activity | 0.984646353 | 1.087956009 |
| ENSG00000172020 | GAP43 subnetwork | 0.984641016 | 1.088035564 |
| ENSG00000175063 | UBE2C subnetwork | 0.9846289 | 1.088095968 |
| GO:0002090 | regulation of receptor internalization | 0.984510854 | 1.088132475 |
| ENSG00000214717 | ZBED1 subnetwork | 0.984470298 | 1.088162233 |
| MP:0002065 | abnormal fear/anxiety-related behavior | 0.984610326 | 1.088171713 |
| MP:0001129 | impaired ovarian folliculogenesis | 0.470958503 | 1.08818793 |
| ENSG00000125084 | WNT1 subnetwork | 0.984463919 | 1.088230333 |
| ENSG00000138396 | ENSG00000138396 subnetwork | 0.470929646 | 1.088272088 |
| GO:0032963 | collagen metabolic process | 0.471190767 | 1.088287232 |
| GO:0051180 | vitamin transport | 0.984450947 | 1.088290775 |
| GO:0035813 | regulation of renal sodium excretion | 0.984404699 | 1.088324387 |
| ENSG00000011275 | RNF216 subnetwork | 0.471154962 | 1.088332291 |
| GO:0035812 | renal sodium excretion | 0.984404699 | 1.088407853 |
| ENSG00000162521 | RBBP4 subnetwork | 0.471139141 | 1.088455526 |
| GO:0072163 | mesonephric epithelium development | 0.984387679 | 1.088475993 |
| MP:0003691 | abnormal microglial cell physiology | 0.471348291 | 1.0885 |
| REACTOME_REGULATION_OF_INS | REACTOME_REGULATION_OF_INSULIN_SECRETION_BY_ | 0.47140738 | 1.088501797 |
| GO:0072164 | mesonephric tubule development | 0.984387679 | 1.088559485 |

| | | | |
|---|---|---|---|
| ENSG00000171533 | MAP6 subnetwork | 0.984370251 | 1.088619975 |
| GO:0007613 | memory | 0.984331882 | 1.088657461 |
| GO:0043204 | perikaryon | 0.984316896 | 1.088733313 |
| ENSG00000169155 | ZBTB43 subnetwork | 0.984277636 | 1.088747794 |
| GO:0015669 | gas transport | 0.471580066 | 1.088753515 |
| ENSG00000087095 | NLK subnetwork | 0.472292908 | 1.088753705 |
| ENSG00000129625 | REEP5 subnetwork | 0.471669326 | 1.088778697 |
| GO:0003777 | microtubule motor activity | 0.472078625 | 1.088810861 |
| REACTOME_CHYLOMICRON:MED | REACTOME_CHYLOMICRON:MEDIATED_LIPID_TRANSPO | 0.471900292 | 1.088815173 |
| GO:0033003 | regulation of mast cell activation | 0.984276794 | 1.088823665 |
| MP:0001515 | abnormal grip strength | 0.472017436 | 1.088848135 |
| GO:0051281 | positive regulation of release of sequestered calcium ion | 0.472252828 | 1.088868955 |
| MP:0009237 | kinked sperm flagellum | 0.984264737 | 1.08889571 |
| ENSG00000141503 | MINK1 subnetwork | 0.472431309 | 1.08893481 |
| GO:0007127 | meiosis I | 0.471810102 | 1.088952217 |
| MP:0001353 | increased aggression towards mice | 0.984247994 | 1.088963929 |
| MP:0003659 | abnormal lymph circulation | 0.471893656 | 1.088977361 |
| GO:0019432 | triglyceride biosynthetic process | 0.472247785 | 1.08903105 |
| MP:0000751 | myopathy | 0.984247807 | 1.089047509 |
| GO:0005849 | mRNA cleavage factor complex | 0.472584289 | 1.089100265 |
| GO:0043325 | phosphatidylinositol-3,4-bisphosphate binding | 0.984245436 | 1.089131102 |
| GO:0016780 | phosphotransferase activity, for other substituted phosp | 0.984216144 | 1.089176326 |
| ENSG00000184588 | PDE4B subnetwork | 0.984108644 | 1.089216891 |
| GO:0000216 | M/G1 transition of mitotic cell cycle | 0.984180663 | 1.089221557 |
| ENSG00000197579 | TOPORS subnetwork | 0.47288101 | 1.089253429 |
| MP:0009936 | abnormal dendritic spine morphology | 0.984096681 | 1.089281327 |
| ENSG00000090006 | LTBP4 subnetwork | 0.472832112 | 1.08933749 |
| MP:0000964 | small dorsal root ganglion | 0.984085062 | 1.089341934 |
| ENSG00000158195 | WASF2 subnetwork | 0.472773191 | 1.089359214 |
| MP:0008412 | increased cellular sensitivity to oxidative stress | 0.984064572 | 1.089406389 |
| REACTOME_IRON_UPTAKE_AND_ | REACTOME_IRON_UPTAKE_AND_TRANSPORT | 0.984026538 | 1.089467015 |
| GO:0006688 | glycosphingolipid biosynthetic process | 0.983964764 | 1.089512289 |
| REACTOME_CDC20PHOSPHO:APC | REACTOME_CDC20PHOSPHO:APCC_MEDIATED_DEGRAD | 0.983935033 | 1.08955757 |
| MP:0000572 | abnormal autopod morphology | 0.98391769 | 1.089637425 |
| GO:0060795 | cell fate commitment involved in formation of primary g | 0.98389676 | 1.089701928 |
| ENSG00000204655 | MOG subnetwork | 0.983894803 | 1.089785648 |
| ENSG00000204590 | GNL1 subnetwork | 0.475675558 | 1.089786113 |
| ENSG00000135424 | ITGA7 subnetwork | 0.475892802 | 1.089837335 |
| ENSG00000101138 | CSTF1 subnetwork | 0.475763333 | 1.089857431 |
| ENSG00000137345 | MOG subnetwork | 0.983894803 | 1.089869381 |
| GO:0046689 | response to mercury ion | 0.47583066 | 1.089882244 |
| ENSG00000206456 | ENSG00000206456 subnetwork | 0.983894803 | 1.089953127 |
| ENSG00000206412 | GNL1 subnetwork | 0.475675558 | 1.089955046 |
| ENSG00000130741 | EIF2S3 subnetwork | 0.476008809 | 1.08997057 |
| GO:0001710 | mesodermal cell fate commitment | 0.983865587 | 1.089998463 |
| ENSG00000173702 | MUC13 subnetwork | 0.473291954 | 1.090065451 |
| GO:0009452 | RNA capping | 0.983856788 | 1.090070704 |
| ENSG00000206492 | GNL1 subnetwork | 0.475675558 | 1.090124031 |
| MP:0009743 | preaxial polydactyly | 0.983840279 | 1.090127584 |
| ENSG00000160145 | KALRN subnetwork | 0.983793165 | 1.090146042 |
| ENSG00000133398 | MED10 subnetwork | 0.475472348 | 1.090150458 |
| ENSG00000078269 | SYNJ2 subnetwork | 0.475620995 | 1.090153512 |
| GO:0043535 | regulation of blood vessel endothelial cell migration | 0.983702381 | 1.090213715 |
| REACTOME_SIGNALLING_TO_RAS | REACTOME_SIGNALLING_TO_RAS | 0.475424081 | 1.09021874 |

| | | | |
|---|---|---|---|
| ENSG00000163806 | SPDYA subnetwork | 0.476254996 | 1.090221431 |
| GO:0048486 | parasympathetic nervous system development | 0.983786202 | 1.090222154 |
| MP:0004179 | transmission ratio distortion | 0.473433459 | 1.090230601 |
| GO:0048634 | regulation of muscle organ development | 0.47620323 | 1.090243147 |
| ENSG00000174446 | SNAPC5 subnetwork | 0.475256296 | 1.090245227 |
| ENSG00000128731 | HERC2 subnetwork | 0.983682714 | 1.090278312 |
| ENSG00000121989 | ACVR2A subnetwork | 0.475181599 | 1.090282521 |
| GO:0003085 | negative regulation of systemic arterial blood pressure | 0.475612574 | 1.090291563 |
| GO:0030136 | clathrin-coated vesicle | 0.475320594 | 1.090293296 |
| ENSG00000135723 | FHOD1 subnetwork | 0.473498283 | 1.090302228 |
| GO:0072509 | divalent inorganic cation transmembrane transporter act | 0.476788433 | 1.09031859 |
| ENSG00000181019 | NQO1 subnetwork | 0.983653485 | 1.090327541 |
| REACTOME_PLATELET_CALCIUM_ | REACTOME_PLATELET_CALCIUM_HOMEOSTASIS | 0.475396435 | 1.09034135 |
| GO:0071548 | response to dexamethasone stimulus | 0.983419692 | 1.09038994 |
| MP:0009760 | abnormal mitotic spindle morphology | 0.983498444 | 1.090390679 |
| ENSG00000070785 | EIF2B3 subnetwork | 0.983649985 | 1.09041138 |
| GO:0007220 | Notch receptor processing | 0.983390425 | 1.090427659 |
| GO:0001516 | prostaglandin biosynthetic process | 0.475172525 | 1.090428505 |
| ENSG00000116350 | SRSF4 subnetwork | 0.476686175 | 1.090462562 |
| ENSG00000125378 | BMP4 subnetwork | 0.476779552 | 1.090464037 |
| GO:0070613 | regulation of protein processing | 0.983629994 | 1.090468317 |
| GO:0034704 | calcium channel complex | 0.983368529 | 1.090488462 |
| GO:0016646 | oxidoreductase activity, acting on the CH-NH group of do | 0.983356126 | 1.090572352 |
| GO:0035085 | cilium axoneme | 0.476602377 | 1.090583411 |
| REACTOME_CLASSICAL_ANTIBOD | REACTOME_CLASSICAL_ANTIBODY:MEDIATED_COMPLEI | 0.477102768 | 1.090584416 |
| ENSG00000075673 | ATP12A subnetwork | 0.476669823 | 1.090584868 |
| GO:0043666 | regulation of phosphoprotein phosphatase activity | 0.476474153 | 1.090595975 |
| GO:0046457 | prostanoid biosynthetic process | 0.475172525 | 1.090597826 |
| GO:0007601 | visual perception | 0.983338729 | 1.090644715 |
| ENSG00000175166 | PSMD2 subnetwork | 0.474829216 | 1.090644911 |
| ENSG00000188687 | SLC4A5 subnetwork | 0.474896975 | 1.090654133 |
| REACTOME_DSCAM_INTERACTIO | REACTOME_DSCAM_INTERACTIONS | 0.4765552 | 1.090659341 |
| ENSG00000182752 | PAPPA subnetwork | 0.474698644 | 1.090673092 |
| GO:0042393 | histone binding | 0.475070916 | 1.090680336 |
| ENSG00000138741 | TRPC3 subnetwork | 0.477074108 | 1.09068347 |
| ENSG00000091129 | NRCAM subnetwork | 0.474770068 | 1.090690084 |
| GO:0015718 | monocarboxylic acid transport | 0.983324539 | 1.090713242 |
| GO:0001530 | lipopolysaccharide binding | 0.474205728 | 1.090725179 |
| REACTOME_BILE_SALT_AND_ORG | REACTOME_BILE_SALT_AND_ORGANIC_ANION_SLC_TR/ | 0.475005 | 1.090725493 |
| ENSG00000133706 | LARS subnetwork | 0.476461193 | 1.090741601 |
| ENSG00000103510 | KAT8 subnetwork | 0.477342029 | 1.090741886 |
| GO:0035091 | phosphatidylinositol binding | 0.475160552 | 1.090743904 |
| MP:0005326 | abnormal podocyte morphology | 0.474401728 | 1.0907514 |
| MP:0002823 | abnormal rib development | 0.474121914 | 1.090785992 |
| ENSG00000115541 | HSPE1 subnetwork | 0.474324771 | 1.090788859 |
| MP:0004220 | abnormal peripheral nervous system regeneration | 0.983315536 | 1.090789474 |
| ENSG00000066427 | ATXN3 subnetwork | 0.983253059 | 1.090811851 |
| MP:0002864 | abnormal ocular fundus morphology | 0.474694321 | 1.090827114 |
| MP:0000434 | megacephaly | 0.474632155 | 1.090880112 |
| ENSG00000133116 | KL subnetwork | 0.477325219 | 1.090887309 |
| MP:0004409 | abnormal crista ampullaris neuroepithelium morphology | 0.983247063 | 1.090895798 |
| ENSG00000160202 | CRYAA subnetwork | 0.474535813 | 1.090908384 |
| GO:0004622 | lysophospholipase activity | 0.474115746 | 1.090948007 |
| ENSG00000167996 | FTH1 subnetwork | 0.983231412 | 1.090968214 |

| | | | |
|---|---|---|---|
| MP:0003949 | abnormal circulating lipid level | 0.474620511 | 1.09100311 |
| MP:0005404 | abnormal axon morphology | 0.983188137 | 1.091009852 |
| REACTOME_RAFMAP_KINASE_CA | REACTOME_RAFMAP_KINASE_CASCADE | 0.473926247 | 1.091021648 |
| MP:0009331 | absent primitive node | 0.474004821 | 1.091054189 |
| ENSG00000148200 | NR6A1 subnetwork | 0.474071381 | 1.091071151 |
| GO:0001824 | blastocyst development | 0.983184501 | 1.091093834 |
| REACTOME_MEMBRANE_BINDIN | REACTOME_MEMBRANE_BINDING_AND_TARGETTING_( | 0.983169666 | 1.091158584 |
| GO:0000932 | cytoplasmic mRNA processing body | 0.473919927 | 1.091191589 |
| ENSG00000184672 | RALYL subnetwork | 0.983121787 | 1.091192548 |
| GO:0015711 | organic anion transport | 0.983113393 | 1.091272713 |
| GO:0001190 | RNA polymerase II transcription factor binding transcript | 0.98310945 | 1.091349041 |
| GO:0001105 | RNA polymerase II transcription coactivator activity | 0.98310945 | 1.091433082 |
| ENSG00000165775 | FUNDC2 subnetwork | 0.983095387 | 1.091509434 |
| GO:0031532 | actin cytoskeleton reorganization | 0.983038749 | 1.09155114 |
| GO:0048489 | synaptic vesicle transport | 0.982998745 | 1.091592852 |
| KEGG_FRUCTOSE_AND_MANNOS | KEGG_FRUCTOSE_AND_MANNOSE_METABOLISM | 0.477797518 | 1.091624169 |
| GO:0045995 | regulation of embryonic development | 0.982998246 | 1.091676937 |
| ENSG00000168765 | GSTM4 subnetwork | 0.982971003 | 1.091737925 |
| ENSG00000155974 | GRIP1 subnetwork | 0.982964439 | 1.091818182 |
| ENSG00000134287 | ARF3 subnetwork | 0.982835361 | 1.091847742 |
| ENSG00000139182 | CLSTN3 subnetwork | 0.982663948 | 1.091854192 |
| ENSG00000169509 | CRCT1 subnetwork | 0.982496394 | 1.091867725 |
| ENSG00000101439 | CST3 subnetwork | 0.98278507 | 1.091885644 |
| ENSG00000167136 | ENDOG subnetwork | 0.982958861 | 1.091898451 |
| GO:0030858 | positive regulation of epithelial cell differentiation | 0.982460305 | 1.091901788 |
| ENSG00000166887 | VPS39 subnetwork | 0.982655316 | 1.091926782 |
| GO:0000038 | very long-chain fatty acid metabolic process | 0.982622069 | 1.09197626 |
| ENSG00000182492 | BGN subnetwork | 0.982450692 | 1.091978259 |
| GO:0009247 | glycolipid biosynthetic process | 0.98240585 | 1.092000771 |
| REACTOME_REGULATION_OF_AP | REACTOME_REGULATION_OF_APCC_ACTIVATORS_BETV | 0.982401899 | 1.092084972 |
| GO:0060840 | artery development | 0.982359285 | 1.092130629 |
| ENSG00000185883 | ATP6V0C subnetwork | 0.98235906 | 1.092214853 |
| MP:0011104 | partial embryonic lethality before implantation | 0.982327767 | 1.092283665 |
| MP:0004989 | decreased osteoblast cell number | 0.982324331 | 1.092360201 |
| GO:0045921 | positive regulation of exocytosis | 0.982317584 | 1.092432891 |
| GO:0071108 | protein K48-linked deubiquitination | 0.478268625 | 1.092490729 |
| MP:0002757 | decreased vertical activity | 0.982310209 | 1.092513307 |
| MP:0005633 | increased circulating sodium level | 0.982292218 | 1.092582163 |
| ENSG00000131100 | ATP6V1E1 subnetwork | 0.478720067 | 1.092598024 |
| GO:0050796 | regulation of insulin secretion | 0.982280218 | 1.092647172 |
| MP:0003063 | increased coping response | 0.982259344 | 1.092696759 |
| GO:0048169 | regulation of long-term neuronal synaptic plasticity | 0.98221663 | 1.092719346 |
| ENSG00000198681 | MAGEA1 subnetwork | 0.478704672 | 1.092751274 |
| GO:0008603 | cAMP-dependent protein kinase regulator activity | 0.982188424 | 1.09275737 |
| GO:0016272 | prefoldin complex | 0.478449438 | 1.092769968 |
| ENSG00000168907 | PLA2G4F subnetwork | 0.478671332 | 1.092819642 |
| ENSG00000133710 | SPINK5 subnetwork | 0.982173758 | 1.092826272 |
| GO:0055062 | phosphate ion homeostasis | 0.982118872 | 1.092833436 |
| GO:0003158 | endothelium development | 0.982031194 | 1.092917246 |
| GO:0072506 | trivalent inorganic anion homeostasis | 0.982118872 | 1.092917792 |
| ENSG00000186831 | ENSG00000186831 subnetwork | 0.478649819 | 1.092934363 |
| GO:0032102 | negative regulation of response to external stimulus | 0.481287409 | 1.092941628 |
| GO:0060445 | branching involved in salivary gland morphogenesis | 0.479059733 | 1.092962963 |
| ENSG00000168090 | COPS6 subnetwork | 0.480327959 | 1.092989072 |

| | | | |
|---|---|---|---|
| ENSG00000164402 | SEPT8 subnetwork | 0.982026918 | 1.092997761 |
| ENSG00000214869 | ENSG00000214869 subnetwork | 0.478624732 | 1.093018227 |
| MP:0003728 | abnormal retinal photoreceptor layer morphology | 0.982010548 | 1.093066708 |
| GO:0042440 | pigment metabolic process | 0.47946111 | 1.09308404 |
| GO:0005721 | centromeric heterochromatin | 0.479526724 | 1.093085106 |
| MP:0001153 | small seminiferous tubules | 0.481263331 | 1.093086496 |
| ENSG00000111642 | CHD4 subnetwork | 0.480043144 | 1.093092561 |
| ENSG00000075891 | PAX2 subnetwork | 0.479044702 | 1.09309307 |
| GO:0007520 | myoblast fusion | 0.479396318 | 1.093098396 |
| MP:0000930 | wavy neural tube | 0.479345239 | 1.093128181 |
| ENSG00000113522 | RAD50 subnetwork | 0.479171672 | 1.093133776 |
| GO:0015296 | anion:cation symporter activity | 0.981990363 | 1.093139526 |
| GO:0010524 | positive regulation of calcium ion transport into cytosol | 0.480221342 | 1.093148576 |
| ENSG00000183741 | CBX6 subnetwork | 0.480323156 | 1.093149631 |
| ENSG00000198300 | ZIM2 subnetwork | 0.480018898 | 1.093183919 |
| MP:0008263 | abnormal hippocampus CA1 region morphology | 0.981959261 | 1.093185328 |
| GO:0005604 | basement membrane | 0.481251935 | 1.09323909 |
| GO:0016234 | inclusion body | 0.480203048 | 1.093263012 |
| ENSG00000153944 | MSI2 subnetwork | 0.479320545 | 1.093265967 |
| MP:0001065 | abnormal trigeminal nerve morphology | 0.981955518 | 1.093269751 |
| MP:0001438 | aphagia | 0.981903632 | 1.0932924 |
| ENSG00000064995 | TAF11 subnetwork | 0.480545567 | 1.093305633 |
| GO:0051702 | interaction with symbiont | 0.479994224 | 1.093313819 |
| ENSG00000113658 | SMAD5 subnetwork | 0.481197983 | 1.093314892 |
| ENSG00000124782 | RREB1 subnetwork | 0.479720495 | 1.093317404 |
| ENSG00000171403 | KRT9 subnetwork | 0.98188932 | 1.093357535 |
| GO:0070160 | occluding junction | 0.479961969 | 1.093412943 |
| ENSG00000160844 | GATS subnetwork | 0.481104527 | 1.093435819 |
| REACTOME_APCCCDH1_MEDIATE | REACTOME_APCCCDH1_MEDIATED_DEGRADATION_OF_ | 0.981886253 | 1.09344199 |
| ENSG00000154447 | SH3RF1 subnetwork | 0.481183391 | 1.093452198 |
| ENSG00000170312 | CDK1 subnetwork | 0.480686333 | 1.093483613 |
| MP:0002855 | abnormal cochlear ganglion morphology | 0.981844293 | 1.093483971 |
| GO:0035914 | skeletal muscle cell differentiation | 0.480975373 | 1.09349531 |
| GO:0033605 | positive regulation of catecholamine secretion | 0.981815879 | 1.093541409 |
| ENSG00000124535 | WRNIP1 subnetwork | 0.481087051 | 1.093550123 |
| GO:0005923 | tight junction | 0.479961969 | 1.093581446 |
| GO:0031102 | neuron projection regeneration | 0.981748133 | 1.093583404 |
| ENSG00000176095 | IP6K1 subnetwork | 0.480944679 | 1.093586589 |
| ENSG00000076924 | XAB2 subnetwork | 0.480894847 | 1.093631749 |
| GO:0005913 | cell-cell adherens junction | 0.981739029 | 1.093652449 |
| ENSG00000150337 | FCGR1A subnetwork | 0.981700249 | 1.093679005 |
| MP:0004768 | abnormal axonal transport | 0.479944656 | 1.093719174 |
| MP:0002913 | abnormal PNS synaptic transmission | 0.981698535 | 1.093755796 |
| GO:0031970 | organelle envelope lumen | 0.480881463 | 1.093769231 |
| GO:0015929 | hexosaminidase activity | 0.981679222 | 1.093805549 |
| GO:0035326 | enhancer binding | 0.981625153 | 1.093820529 |
| GO:0001508 | regulation of action potential | 0.981619692 | 1.093897349 |
| GO:0005892 | acetylcholine-gated channel complex | 0.981613399 | 1.093970315 |
| REACTOME_INSULIN_RECEPTOR_ | REACTOME_INSULIN_RECEPTOR_RECYCLING | 0.981522106 | 1.094046699 |
| GO:0006909 | phagocytosis | 0.9816128 | 1.09405489 |
| MP:0009890 | cleft secondary palate | 0.9814839 | 1.094100363 |
| ENSG00000007168 | PAFAH1B1 subnetwork | 0.981423019 | 1.094172918 |
| GO:0015464 | acetylcholine receptor activity | 0.981475336 | 1.094181101 |
| REACTOME_ADENYLATE_CYCLASE | REACTOME_ADENYLATE_CYCLASE_INHIBITORY_PATHW/ | 0.981351358 | 1.094257096 |

| | | | |
|---|---|---|---|
| GO:0010469 | regulation of receptor activity | 0.981422422 | 1.094257541 |
| GO:0048599 | oocyte development | 0.481966593 | 1.094294271 |
| ENSG00000163743 | RCHY1 subnetwork | 0.482116305 | 1.094296023 |
| REACTOME_INHIBITION_OF_ADEI | REACTOME_INHIBITION_OF_ADENYLATE_CYCLASE_PATI | 0.981351358 | 1.094341739 |
| GO:2000756 | regulation of peptidyl-lysine acetylation | 0.981324167 | 1.094391584 |
| ENSG00000099139 | PCSK5 subnetwork | 0.482071814 | 1.094410319 |
| GO:0043195 | terminal button | 0.981290795 | 1.094445304 |
| GO:0052689 | carboxylic ester hydrolase activity | 0.981268915 | 1.094510638 |
| ENSG00000111199 | TRPV4 subnetwork | 0.482317707 | 1.094511821 |
| GO:0030665 | clathrin coated vesicle membrane | 0.981170443 | 1.094540741 |
| GO:0032288 | myelin assembly | 0.981263371 | 1.094591458 |
| GO:0017075 | syntaxin-1 binding | 0.981169195 | 1.094625445 |
| GO:0010662 | regulation of striated muscle cell apoptotic process | 0.981167914 | 1.094706292 |
| ENSG00000107611 | CUBN subnetwork | 0.980941628 | 1.094716674 |
| ENSG00000156970 | BUB1B subnetwork | 0.980882774 | 1.094724007 |
| GO:0006911 | phagocytosis, engulfment | 0.981121902 | 1.094729102 |
| GO:0003151 | outflow tract morphogenesis | 0.981039232 | 1.094736435 |
| GO:0008156 | negative regulation of DNA replication | 0.482526813 | 1.094781274 |
| GO:0009065 | glutamine family amino acid catabolic process | 0.980863851 | 1.09479328 |
| ENSG00000154928 | EPHB1 subnetwork | 0.980852285 | 1.094847077 |
| GO:0035253 | ciliary rootlet | 0.980820432 | 1.094889267 |
| ENSG00000070018 | LRP6 subnetwork | 0.980800312 | 1.094931464 |
| ENSG00000116670 | MAD2L2 subnetwork | 0.980789296 | 1.094981413 |
| ENSG00000183092 | BEGAIN subnetwork | 0.980784196 | 1.09506235 |
| GO:0003417 | growth plate cartilage development | 0.980499916 | 1.09511118 |
| GO:0031109 | microtubule polymerization or depolymerization | 0.98077497 | 1.0951433 |
| GO:0090199 | regulation of release of cytochrome c from mitochondria | 0.980475477 | 1.095161165 |
| MP:0008148 | abnormal rib-sternum attachment | 0.980602955 | 1.095173536 |
| ENSG00000178028 | DMAP1 subnetwork | 0.980771248 | 1.095224262 |
| GO:0006825 | copper ion transport | 0.980463118 | 1.095242154 |
| GO:0008028 | monocarboxylic acid transmembrane transporter activity | 0.980434206 | 1.095292157 |
| ENSG00000133265 | HSPBP1 subnetwork | 0.48285233 | 1.095326888 |
| GO:0006370 | mRNA capping | 0.980403822 | 1.095349919 |
| GO:0033762 | response to glucagon stimulus | 0.980297411 | 1.095403457 |
| GO:0003338 | metanephros morphogenesis | 0.980383196 | 1.095403813 |
| GO:0044420 | extracellular matrix part | 0.980265627 | 1.095465116 |
| REACTOME_PURINE_SALVAGE | REACTOME_PURINE_SALVAGE | 0.980243613 | 1.095530661 |
| GO:0033108 | mitochondrial respiratory chain complex assembly | 0.980238534 | 1.09560397 |
| ENSG00000175213 | ZNF408 subnetwork | 0.980198023 | 1.09562689 |
| GO:0008210 | estrogen metabolic process | 0.483307173 | 1.095690184 |
| GO:0000097 | sulfur amino acid biosynthetic process | 0.980174085 | 1.095692463 |
| ENSG00000163462 | TRIM46 subnetwork | 0.98014483 | 1.095742536 |
| GO:0030004 | cellular monovalent inorganic cation homeostasis | 0.483184386 | 1.095742559 |
| GO:0050996 | positive regulation of lipid catabolic process | 0.485340468 | 1.095746143 |
| GO:0010811 | positive regulation of cell-substrate adhesion | 0.483853679 | 1.095794393 |
| ENSG00000197858 | GPAA1 subnetwork | 0.485618247 | 1.095801527 |
| GO:0016500 | protein-hormone receptor activity | 0.980137316 | 1.095827517 |
| GO:0005930 | axoneme | 0.483286901 | 1.095842921 |
| ENSG00000165629 | ATP5C1 subnetwork | 0.48375851 | 1.095862069 |
| GO:0042993 | positive regulation of transcription factor import into nu | 0.485318864 | 1.095867705 |
| GO:0007617 | mating behavior | 0.980129036 | 1.095900876 |
| GO:0016814 | hydrolase activity, acting on carbon-nitrogen (but not pe | 0.483179588 | 1.095910695 |
| ENSG00000177425 | PAWR subnetwork | 0.485515786 | 1.095937691 |
| GO:0006733 | oxidoreduction coenzyme metabolic process | 0.980108036 | 1.095939342 |

| | | | |
|---|---|---|---|
| GO:0051117 | ATPase binding | 0.485947778 | 1.095948421 |
| ENSG00000153006 | SREK1IP1 subnetwork | 0.485609056 | 1.095953581 |
| ENSG00000100926 | TM9SF1 subnetwork | 0.483852295 | 1.095962305 |
| ENSG00000128578 | FAM40B subnetwork | 0.485848305 | 1.095963065 |
| ENSG00000143761 | ARF1 subnetwork | 0.485295595 | 1.095974026 |
| GO:0031016 | pancreas development | 0.483728837 | 1.095976395 |
| MP:0003797 | abnormal compact bone morphology | 0.486032955 | 1.096002441 |
| ENSG00000167645 | YIF1B subnetwork | 0.485787583 | 1.096008243 |
| GO:0042742 | defense response to bacterium | 0.486302955 | 1.096011896 |
| GO:0046933 | hydrogen ion transporting ATP synthase activity, rotatior | 0.980096393 | 1.096012722 |
| GO:0042470 | melanosome | 0.484060699 | 1.096017767 |
| ENSG00000169282 | KCNAB1 subnetwork | 0.98003531 | 1.096043445 |
| ENSG00000101003 | GINS1 subnetwork | 0.486469401 | 1.09605885 |
| GO:0006839 | mitochondrial transport | 0.484156533 | 1.096071975 |
| MP:0002267 | abnormal bronchiole morphology | 0.483685494 | 1.096075425 |
| ENSG00000120500 | ARR3 subnetwork | 0.485277608 | 1.096103301 |
| GO:0042246 | tissue regeneration | 0.980030096 | 1.096128482 |
| REACTOME_CELL:EXTRACELLULAF | REACTOME_CELL:EXTRACELLULAR_MATRIX_INTERACTIC | 0.485170551 | 1.096133272 |
| ENSG00000203813 | HIST1H3H subnetwork | 0.486280151 | 1.096148566 |
| GO:0048770 | pigment granule | 0.484060699 | 1.096185662 |
| MP:0000934 | abnormal telencephalon development | 0.980009669 | 1.096198014 |
| GO:0060541 | respiratory system development | 0.486453635 | 1.096203111 |
| ENSG00000136273 | HUS1 subnetwork | 0.484963042 | 1.096207951 |
| ENSG00000145242 | EPHA5 subnetwork | 0.483680987 | 1.096212818 |
| ENSG00000156973 | PDE6D subnetwork | 0.486217162 | 1.096216629 |
| MP:0003953 | abnormal hormone level | 0.48426428 | 1.096218037 |
| GO:0050919 | negative chemotaxis | 0.979956261 | 1.096220998 |
| ENSG00000135916 | ITM2C subnetwork | 0.484337327 | 1.096233925 |
| MP:0000153 | rib bifurcation | 0.9799255 | 1.096271147 |
| MP:0004938 | dilated vasculature | 0.485157556 | 1.09628554 |
| MP:0000550 | abnormal forelimb morphology | 0.979857923 | 1.09629026 |
| MP:0003560 | osteoarthritis | 0.483642898 | 1.096304248 |
| ENSG00000088320 | REM1 subnetwork | 0.484813138 | 1.096344448 |
| ENSG00000132535 | DLG4 subnetwork | 0.979842155 | 1.096352065 |
| ENSG00000131795 | RBM8A subnetwork | 0.484939814 | 1.096352653 |
| ENSG00000173465 | SSSCA1 subnetwork | 0.484447493 | 1.09636461 |
| MP:0005282 | decreased fatty acid level | 0.979818204 | 1.096402236 |
| ENSG00000133805 | AMPD3 subnetwork | 0.485125502 | 1.096414921 |
| GO:0030224 | monocyte differentiation | 0.484557968 | 1.096418733 |
| GO:0060485 | mesenchyme development | 0.979767784 | 1.096429126 |
| MP:0001504 | abnormal posture | 0.979702968 | 1.09645602 |
| REACTOME_TETRAHYDROBIOPTE | REACTOME_TETRAHYDROBIOPTERIN_BH4_SYNTHESIS_F | 0.484700022 | 1.096458078 |
| GO:0002065 | columnar/cuboidal epithelial cell differentiation | 0.486747763 | 1.096471037 |
| MP:0002175 | decreased brain weight | 0.484789127 | 1.096473918 |
| GO:0002886 | regulation of myeloid leukocyte mediated immunity | 0.979664586 | 1.096490683 |
| ENSG00000160972 | PPP1R16A subnetwork | 0.979398893 | 1.096540075 |
| ENSG00000170604 | IRF2BP1 subnetwork | 0.979563557 | 1.096563907 |
| ENSG00000184916 | JAG2 subnetwork | 0.979656047 | 1.096568057 |
| MP:0000534 | abnormal ureter morphology | 0.979511451 | 1.096594704 |
| GO:0051279 | regulation of release of sequestered calcium ion into cyt | 0.484686238 | 1.096602907 |
| GO:0004930 | G-protein coupled receptor activity | 0.979385955 | 1.096609709 |
| ENSG00000156052 | GNAQ subnetwork | 0.487096002 | 1.096609782 |
| ENSG00000144867 | SRPRB subnetwork | 0.979371915 | 1.096683238 |
| MP:0009866 | abnormal aorta wall morphology | 0.487032102 | 1.096693081 |

| | | | |
|---|---|---|---|
| GO:0006783 | heme biosynthetic process | 0.487296922 | 1.096709825 |
| ENSG00000125482 | TTF1 subnetwork | 0.487004409 | 1.096753544 |
| GO:0018022 | peptidyl-lysine methylation | 0.487247323 | 1.096755027 |
| ENSG00000152578 | GRIA4 subnetwork | 0.979369969 | 1.09676843 |
| ENSG00000102781 | KATNAL1 subnetwork | 0.979361916 | 1.096841983 |
| GO:0050806 | positive regulation of synaptic transmission | 0.979321506 | 1.0968767 |
| GO:0048708 | astrocyte differentiation | 0.979260254 | 1.096899767 |
| MP:0001178 | pulmonary hypoplasia | 0.979243769 | 1.096969461 |
| GO:0006103 | 2-oxoglutarate metabolic process | 0.979241999 | 1.097054709 |
| ENSG00000106305 | AIMP2 subnetwork | 0.979167403 | 1.097124203 |
| ENSG00000167768 | KRT1 subnetwork | 0.979233551 | 1.097132199 |
| GO:2000273 | positive regulation of receptor activity | 0.979052394 | 1.097154851 |
| ENSG00000086827 | ZW10 subnetwork | 0.978995926 | 1.097174065 |
| GO:0005416 | cation:amino acid symporter activity | 0.97895261 | 1.09718162 |
| MP:0002544 | brachydactyly | 0.97916642 | 1.097205597 |
| GO:0050922 | negative regulation of chemotaxis | 0.978942325 | 1.097255268 |
| ENSG00000105290 | APLP1 subnetwork | 0.978926077 | 1.097336703 |
| GO:0006220 | pyrimidine nucleotide metabolic process | 0.978915849 | 1.097390932 |
| ENSG00000105464 | GRIN2D subnetwork | 0.978899202 | 1.09744517 |
| GO:0005539 | glycosaminoglycan binding | 0.978872116 | 1.097511083 |
| MP:0004355 | short radius | 0.978823179 | 1.097542004 |
| MP:0004748 | increased susceptibility to age-related hearing loss | 0.978790098 | 1.097592377 |
| GO:2000027 | regulation of organ morphogenesis | 0.978787243 | 1.097673876 |
| MP:0000455 | abnormal maxilla morphology | 0.978747787 | 1.097712596 |
| REACTOME_ASSEMBLY_OF_HIV_\ | REACTOME_ASSEMBLY_OF_HIV_VIRION | 0.978733701 | 1.097778556 |
| ENSG00000172466 | ZNF24 subnetwork | 0.97870295 | 1.097852307 |
| ENSG00000062725 | APPBP2 subnetwork | 0.978698567 | 1.097922179 |
| GO:0043086 | negative regulation of catalytic activity | 0.978671429 | 1.097960931 |
| ENSG00000109065 | NAT9 subnetwork | 0.48809206 | 1.097982643 |
| MP:0004111 | abnormal coronary artery morphology | 0.488049551 | 1.098005177 |
| ENSG00000006740 | ARHGAP44 subnetwork | 0.978669472 | 1.098046389 |
| GO:0030496 | midbody | 0.978656808 | 1.098108508 |
| ENSG00000011465 | DCN subnetwork | 0.488044579 | 1.098172403 |
| ENSG00000107537 | PHYH subnetwork | 0.978646499 | 1.098190098 |
| GO:0043647 | inositol phosphate metabolic process | 0.978612853 | 1.098252238 |
| ENSG00000169783 | LINGO1 subnetwork | 0.978565905 | 1.098271566 |
| GO:0031646 | positive regulation of neurological system process | 0.978564192 | 1.098349295 |
| GO:0009066 | aspartate family amino acid metabolic process | 0.978529813 | 1.098419249 |
| GO:0021587 | cerebellum morphogenesis | 0.978526735 | 1.098500896 |
| GO:0051349 | positive regulation of lyase activity | 0.978524481 | 1.098586449 |
| GO:0060441 | epithelial tube branching involved in lung morphogenesi | 0.978485791 | 1.098636965 |
| MP:0004921 | decreased placenta weight | 0.978465681 | 1.09868749 |
| ENSG00000071994 | PDCD2 subnetwork | 0.488655815 | 1.098698828 |
| GO:0032637 | interleukin-8 production | 0.488600885 | 1.098729072 |
| GO:0030177 | positive regulation of Wnt receptor signaling pathway | 0.978430584 | 1.098734128 |
| MP:0001436 | abnormal suckling behavior | 0.97831759 | 1.098753409 |
| MP:0001274 | curly vibrissae | 0.488775299 | 1.098790323 |
| GO:0042312 | regulation of vasodilation | 0.978418411 | 1.098800249 |
| GO:0045446 | endothelial cell differentiation | 0.978229273 | 1.098827242 |
| ENSG00000168487 | BMP1 subnetwork | 0.488837439 | 1.098836148 |
| ENSG00000049540 | ELN subnetwork | 0.978316569 | 1.098839021 |
| ENSG00000184481 | FOXO4 subnetwork | 0.488577308 | 1.098858274 |
| MP:0011386 | increased metanephric mesenchyme apoptosis | 0.978222005 | 1.098905081 |
| ENSG00000169139 | UBE2V2 subnetwork | 0.978216961 | 1.098990726 |

| | | | |
|---|---|---|---|
| ENSG00000084733 | RAB10 subnetwork | 0.978210134 | 1.099068589 |
| GO:0061387 | regulation of extent of cell growth | 0.978189799 | 1.09913867 |
| ENSG00000108010 | GLRX3 subnetwork | 0.978183075 | 1.09921266 |
| ENSG00000126803 | HSPA2 subnetwork | 0.489096381 | 1.099224217 |
| GO:0050839 | cell adhesion molecule binding | 0.978071169 | 1.099263215 |
| MP:0003313 | abnormal locomotor activation | 0.978175533 | 1.099294457 |
| GO:0016337 | cell-cell adhesion | 0.978049321 | 1.099341131 |
| GO:0051015 | actin filament binding | 0.977850224 | 1.099348776 |
| GO:0045746 | negative regulation of Notch signaling pathway | 0.977986475 | 1.099364473 |
| ENSG00000099937 | SERPIND1 subnetwork | 0.97794345 | 1.099395617 |
| REACTOME_RECRUITMENT_OF_N | REACTOME_RECRUITMENT_OF_NUMA_TO_MITOTIC_CE | 0.977849672 | 1.099430622 |
| GO:0004889 | acetylcholine-activated cation-selective channel activity | 0.977794859 | 1.099481279 |
| GO:0090200 | positive regulation of release of cytochrome c from mito | 0.977788113 | 1.099539746 |
| GO:0031114 | regulation of microtubule depolymerization | 0.977770995 | 1.099609924 |
| GO:0015874 | norepinephrine transport | 0.977764393 | 1.099691816 |
| GO:0031281 | positive regulation of cyclase activity | 0.97774507 | 1.099742509 |
| ENSG00000102977 | ACD subnetwork | 0.489392539 | 1.099802281 |
| ENSG00000139549 | DHH subnetwork | 0.489455794 | 1.099817518 |
| GO:0045762 | positive regulation of adenylate cyclase activity | 0.97774507 | 1.099828326 |
| MP:0003954 | abnormal Reichert's membrane morphology | 0.977739202 | 1.099906352 |
| GO:0060042 | retina morphogenesis in camera-type eye | 0.977722453 | 1.099980489 |
| ENSG00000108264 | TADA2A subnetwork | 0.490122481 | 1.1 |
| ENSG00000151743 | AMN1 subnetwork | 0.489981362 | 1.100015193 |
| GO:0010771 | negative regulation of cell morphogenesis involved in dif | 0.489899191 | 1.100037988 |
| GO:0046785 | microtubule polymerization | 0.977704912 | 1.100046831 |
| REACTOME_SEMAPHORIN_INTER | REACTOME_SEMAPHORIN_INTERACTIONS | 0.490207713 | 1.100060744 |
| ENSG00000136450 | SRSF1 subnetwork | 0.490074188 | 1.100106334 |
| GO:0048863 | stem cell differentiation | 0.97770341 | 1.100132698 |
| ENSG00000137413 | TAF8 subnetwork | 0.489884699 | 1.100136778 |
| ENSG00000105379 | ETFB subnetwork | 0.489648629 | 1.100136841 |
| GO:0070647 | protein modification by small protein conjugation or rem | 0.490741685 | 1.100144136 |
| ENSG00000166595 | FAM96B subnetwork | 0.489742788 | 1.100152022 |
| ENSG00000182359 | KBTBD3 subnetwork | 0.490667618 | 1.100159332 |
| GO:0048593 | camera-type eye morphogenesis | 0.977480288 | 1.100160056 |
| MP:0003892 | abnormal gastric gland morphology | 0.977550622 | 1.100167851 |
| ENSG00000124783 | SSR1 subnetwork | 0.977648609 | 1.100179547 |
| MP:0008235 | increased susceptibility to neuronal excitotoxicity | 0.977424316 | 1.100183493 |
| GO:0001076 | RNA polymerase II transcription factor binding transcript | 0.489845164 | 1.100235598 |
| MP:0002115 | abnormal limb bone morphology | 0.97708384 | 1.10024215 |
| GO:0043526 | neuroprotection | 0.490471379 | 1.100242903 |
| GO:0045841 | negative regulation of mitotic metaphase/anaphase tran | 0.977411349 | 1.100261596 |
| ENSG00000101189 | C20orf20 subnetwork | 0.977033716 | 1.100277322 |
| ENSG00000134371 | CDC73 subnetwork | 0.977369211 | 1.100300664 |
| ENSG00000135018 | UBQLN1 subnetwork | 0.976969418 | 1.100300781 |
| GO:0016796 | exonuclease activity, active with either ribo- or deoxyribo | 0.49065573 | 1.100303536 |
| REACTOME_GRB2_EVENTS_IN_EC | REACTOME_GRB2_EVENTS_IN_EGFR_SIGNALING | 0.490576607 | 1.100311172 |
| MP:0008997 | increased blood osmolality | 0.490420972 | 1.100334042 |
| ENSG00000152268 | ENSG00000152268 subnetwork | 0.9773156 | 1.100335833 |
| GO:0060562 | epithelial tube morphogenesis | 0.977243659 | 1.100335859 |
| ENSG00000143382 | ADAMTSL4 subnetwork | 0.976968561 | 1.100386749 |
| GO:0060841 | venous blood vessel development | 0.976946579 | 1.100441475 |
| MP:0004418 | small parietal bone | 0.976924237 | 1.100507932 |
| MP:0009832 | abnormal sperm mitochondrial sheath morphology | 0.976908685 | 1.100582213 |
| ENSG00000158022 | TRIM63 subnetwork | 0.976904477 | 1.100664322 |

| | | | |
|---|---|---|---|
| GO:0016998 | cell wall macromolecule catabolic process | 0.976847905 | 1.100687822 |
| GO:0090278 | negative regulation of peptide hormone secretion | 0.976812233 | 1.100723052 |
| MP:0001259 | abnormal body weight | 0.490969151 | 1.100743325 |
| ENSG00000141198 | TOM1L1 subnetwork | 0.97669666 | 1.100797436 |
| GO:0045723 | positive regulation of fatty acid biosynthetic process | 0.976793142 | 1.100801282 |
| GO:0048484 | enteric nervous system development | 0.976635058 | 1.100801407 |
| MP:0002100 | abnormal tooth morphology | 0.976623458 | 1.100871843 |
| GO:0016208 | AMP binding | 0.976615928 | 1.100957929 |
| ENSG00000135828 | RNASEL subnetwork | 0.976610197 | 1.101040119 |
| GO:0044042 | glucan metabolic process | 0.976608018 | 1.101126232 |
| GO:0006073 | cellular glucan metabolic process | 0.976608018 | 1.101212358 |
| MP:0000857 | abnormal cerebellar foliation | 0.976603467 | 1.101294587 |
| GO:0008484 | sulfuric ester hydrolase activity | 0.976597663 | 1.101376829 |
| REACTOME_POST:TRANSLATIONA | REACTOME_POST:TRANSLATIONAL_MODIFICATION_SYN | 0.491557337 | 1.101387204 |
| ENSG00000166848 | TERF2IP subnetwork | 0.491619412 | 1.101394573 |
| MP:0005450 | abnormal energy expenditure | 0.976591081 | 1.101459083 |
| MP:0009661 | abnormal pregnancy | 0.491460874 | 1.101478617 |
| ENSG00000177542 | SLC25A22 subnetwork | 0.976581919 | 1.101537438 |
| MP:0009885 | abnormal palatal shelf elevation | 0.491545834 | 1.101539045 |
| GO:0005085 | guanyl-nucleotide exchange factor activity | 0.493332134 | 1.101556126 |
| ENSG00000100167 | SEPT3 subnetwork | 0.976541341 | 1.101576682 |
| ENSG00000170004 | CHD3 subnetwork | 0.491441319 | 1.101585014 |
| GO:0005100 | Rho GTPase activator activity | 0.493508541 | 1.101600967 |
| GO:0048024 | regulation of nuclear mRNA splicing, via spliceosome | 0.976524775 | 1.101647234 |
| GO:0033143 | regulation of intracellular steroid hormone receptor sign | 0.493482034 | 1.101691843 |
| ENSG00000174243 | DDX23 subnetwork | 0.493319185 | 1.101699909 |
| ENSG00000033011 | ALG1 subnetwork | 0.97652064 | 1.101729535 |
| GO:0032456 | endocytic recycling | 0.493269465 | 1.101745504 |
| ENSG00000186395 | KRT10 subnetwork | 0.493213581 | 1.101753325 |
| GO:0043433 | negative regulation of sequence-specific DNA binding tra | 0.491860769 | 1.101795999 |
| REACTOME_GLUCAGON_SIGNALI | REACTOME_GLUCAGON_SIGNALING_IN_METABOLIC_RE | 0.976517357 | 1.101815763 |
| GO:0055038 | recycling endosome membrane | 0.491971539 | 1.101863919 |
| GO:0045773 | positive regulation of axon extension | 0.976478026 | 1.101866781 |
| ENSG00000063322 | MED29 subnetwork | 0.493197196 | 1.101904762 |
| ENSG00000124164 | VAPB subnetwork | 0.49273513 | 1.101936753 |
| ENSG00000161202 | DVL3 subnetwork | 0.976472429 | 1.101945205 |
| ENSG00000114742 | WDR48 subnetwork | 0.493121792 | 1.101965528 |
| ENSG00000100522 | GNPNAT1 subnetwork | 0.492597895 | 1.101997881 |
| GO:0031346 | positive regulation of cell projection organization | 0.97637092 | 1.102012057 |
| GO:0007213 | G-protein coupled acetylcholine receptor signaling pathv | 0.976469953 | 1.102023642 |
| GO:0048844 | artery morphogenesis | 0.976290981 | 1.102027873 |
| GO:0010821 | regulation of mitochondrion organization | 0.976235497 | 1.102035863 |
| ENSG00000145736 | GTF2H2 subnetwork | 0.492532162 | 1.102051166 |
| ENSG00000072133 | RPS6KA6 subnetwork | 0.492705297 | 1.102058111 |
| GO:0016311 | dephosphorylation | 0.492480401 | 1.102089326 |
| GO:0051183 | vitamin transporter activity | 0.976194956 | 1.102094753 |
| GO:0032461 | positive regulation of protein oligomerization | 0.493855661 | 1.102106296 |
| ENSG00000173207 | CKS1B subnetwork | 0.493116074 | 1.102124603 |
| ENSG00000070367 | EXOC5 subnetwork | 0.492414114 | 1.102142641 |
| GO:0060828 | regulation of canonical Wnt receptor signaling pathway | 0.976184708 | 1.102165401 |
| REACTOME_EGFR_DOWNREGULA | REACTOME_EGFR_DOWNREGULATION | 0.493036927 | 1.102170296 |
| ENSG00000104419 | NDRG1 subnetwork | 0.493823963 | 1.102204772 |
| ENSG00000002822 | MAD1L1 subnetwork | 0.976064095 | 1.102204903 |
| GO:0019897 | extrinsic to plasma membrane | 0.97615768 | 1.102216479 |

| | | | |
|---|---|---|---|
| ENSG00000181467 | RAP2B subnetwork | 0.492906439 | 1.102239032 |
| ENSG00000055957 | ITIH1 subnetwork | 0.492319482 | 1.102256892 |
| GO:0051301 | cell division | 0.976039982 | 1.102271659 |
| ENSG00000150347 | ARID5B subnetwork | 0.492398943 | 1.102286839 |
| GO:0009880 | embryonic pattern specification | 0.975980682 | 1.102287505 |
| GO:0031514 | motile cilium | 0.493019103 | 1.102306761 |
| ENSG00000130787 | HIP1R subnetwork | 0.49218684 | 1.102310606 |
| ENSG00000171549 | ENSG00000171549 subnetwork | 0.975969108 | 1.10235036 |
| ENSG00000164091 | WDR82 subnetwork | 0.492288201 | 1.102355704 |
| ENSG00000182520 | ENSG00000182520 subnetwork | 0.975969108 | 1.102436731 |
| GO:0030509 | BMP signaling pathway | 0.975955474 | 1.10249569 |
| GO:0001832 | blastocyst growth | 0.975898514 | 1.102515477 |
| ENSG00000114354 | TFG subnetwork | 0.494216826 | 1.102535849 |
| GO:0097031 | mitochondrial respiratory chain complex I biogenesis | 0.975890377 | 1.102594044 |
| ENSG00000092531 | SNAP23 subnetwork | 0.494196297 | 1.102641908 |
| GO:0010257 | NADH dehydrogenase complex assembly | 0.975890377 | 1.102680461 |
| MP:0001402 | hypoactivity | 0.975727997 | 1.102739887 |
| GO:0032981 | mitochondrial respiratory chain complex I assembly | 0.975890377 | 1.102766891 |
| GO:0033189 | response to vitamin A | 0.975677189 | 1.102791062 |
| GO:0014704 | intercalated disc | 0.975888263 | 1.102849416 |
| GO:0009435 | NAD biosynthetic process | 0.97566839 | 1.102877529 |
| MP:0005298 | abnormal clavicle morphology | 0.975662813 | 1.102960088 |
| ENSG00000172660 | TAF15 subnetwork | 0.494495001 | 1.103018412 |
| ENSG00000120860 | CCDC53 subnetwork | 0.975654979 | 1.103034818 |
| ENSG00000186847 | KRT14 subnetwork | 0.494740147 | 1.103069845 |
| GO:0050821 | protein stabilization | 0.494682848 | 1.103092939 |
| ENSG00000112739 | PRPF4B subnetwork | 0.975649665 | 1.103117403 |
| REACTOME_GLUTATHIONE_SYNT | REACTOME_GLUTATHIONE_SYNTHESIS_AND_RECYCLIN( | 0.975632668 | 1.103156863 |
| GO:0005859 | muscle myosin complex | 0.975555317 | 1.103168876 |
| GO:0042491 | auditory receptor cell differentiation | 0.975482271 | 1.103204424 |
| ENSG00000166579 | NDEL1 subnetwork | 0.975293871 | 1.10323264 |
| MP:0000441 | increased cranium width | 0.494680017 | 1.103251848 |
| GO:0032481 | positive regulation of type I interferon production | 0.97547668 | 1.103287048 |
| GO:0010639 | negative regulation of organelle organization | 0.975267699 | 1.103287822 |
| ENSG00000166603 | MC4R subnetwork | 0.975433923 | 1.103334379 |
| GO:0015298 | solute:cation antiporter activity | 0.975232998 | 1.103339088 |
| MP:0004359 | short ulna | 0.975214933 | 1.103413907 |
| ENSG00000109501 | WFS1 subnetwork | 0.494965518 | 1.103431373 |
| REACTOME_REGULATION_OF_MI | REACTOME_REGULATION_OF_MITOTIC_CELL_CYCLE | 0.975196981 | 1.103476964 |
| REACTOME_APCC:MEDIATED_DE | REACTOME_APCC:MEDIATED_DEGRADATION_OF_CELL_ | 0.975196981 | 1.103563579 |
| ENSG00000104643 | MTMR9 subnetwork | 0.975191924 | 1.103642358 |
| ENSG00000104388 | RAB2A subnetwork | 0.975158384 | 1.103685822 |
| GO:0046879 | hormone secretion | 0.975089443 | 1.103686111 |
| ENSG00000158301 | GPRASP2 subnetwork | 0.975049663 | 1.103698178 |
| GO:0018214 | protein carboxylation | 0.495307976 | 1.103701191 |
| ENSG00000144381 | HSPD1 subnetwork | 0.495974216 | 1.103734377 |
| ENSG00000119729 | RHOQ subnetwork | 0.495188633 | 1.103740009 |
| REACTOME_AUTODEGRADATION | REACTOME_AUTODEGRADATION_OF_CDH1_BY_CDH1A | 0.97502678 | 1.103765214 |
| MP:0004310 | small otic vesicle | 0.97494975 | 1.103800848 |
| MP:0004742 | abnormal vestibular system physiology | 0.495942742 | 1.103862952 |
| GO:0017187 | peptidyl-glutamic acid carboxylation | 0.495307976 | 1.103867612 |
| GO:0045667 | regulation of osteoblast differentiation | 0.974941773 | 1.10388361 |
| GO:0070491 | repressing transcription factor binding | 0.495891442 | 1.103923784 |
| MP:0002069 | abnormal eating/drinking behavior | 0.974909007 | 1.103927113 |

| | | | |
|---|---|---|---|
| GO:0044259 | multicellular organismal macromolecule metabolic proce | 0.495849054 | 1.10393944 |
| GO:0000930 | gamma-tubulin complex | 0.974842257 | 1.103950986 |
| MP:0004025 | polyploidy | 0.495655048 | 1.1039789 |
| GO:0035051 | cardiac cell differentiation | 0.974799239 | 1.103998429 |
| MP:0004008 | abnormal GABA-mediated receptor currents | 0.97475066 | 1.104038023 |
| GO:0004629 | phospholipase C activity | 0.974675331 | 1.104042269 |
| ENSG00000105723 | GSK3A subnetwork | 0.495826569 | 1.104045502 |
| ENSG00000171401 | KRT13 subnetwork | 0.495629275 | 1.104085017 |
| GO:0010324 | membrane invagination | 0.974654293 | 1.104109374 |
| ENSG00000108296 | CWC25 subnetwork | 0.495793335 | 1.104151597 |
| GO:0006897 | endocytosis | 0.974654293 | 1.104196134 |
| GO:0005977 | glycogen metabolic process | 0.974626054 | 1.104247544 |
| ENSG00000161542 | PRPSAP1 subnetwork | 0.496297775 | 1.104260765 |
| ENSG00000151617 | EDNRA subnetwork | 0.974625721 | 1.104334329 |
| MP:0008789 | abnormal olfactory epithelium morphology | 0.974614138 | 1.104413267 |
| ENSG00000164506 | STXBP5 subnetwork | 0.496434351 | 1.104418185 |
| ENSG00000105443 | CYTH2 subnetwork | 0.974569866 | 1.104452916 |
| ENSG00000147852 | VLDLR subnetwork | 0.974555027 | 1.104516154 |
| GO:0003179 | heart valve morphogenesis | 0.974494195 | 1.104540094 |
| MP:0004769 | abnormal synaptic vesicle morphology | 0.97447745 | 1.10460728 |
| ENSG00000082458 | DLG3 subnetwork | 0.97446057 | 1.104678409 |
| ENSG00000130724 | CHMP2A subnetwork | 0.974429067 | 1.104714162 |
| GO:0009914 | hormone transport | 0.974403173 | 1.10478531 |
| GO:0032465 | regulation of cytokinesis | 0.974395381 | 1.104860401 |
| MP:0004770 | abnormal synaptic vesicle recycling | 0.974375621 | 1.104931571 |
| MP:0004016 | decreased bone mass | 0.496732902 | 1.104951836 |
| ENSG00000127993 | RBM48 subnetwork | 0.97431414 | 1.104987021 |
| ENSG00000076864 | RAP1GAP subnetwork | 0.974275535 | 1.10501888 |
| REACTOME_APCCCDC20_MEDIAT | REACTOME_APCCCDC20_MEDIATED_DEGRADATION_OF | 0.974262054 | 1.105097947 |
| KEGG_BIOSYNTHESIS_OF_UNSATI | KEGG_BIOSYNTHESIS_OF_UNSATURATED_FATTY_ACIDS | 0.974211334 | 1.105141621 |
| MP:0004184 | abnormal baroreceptor physiology | 0.496954031 | 1.105153476 |
| ENSG00000008869 | HEATR5B subnetwork | 0.974183245 | 1.105204973 |
| MP:0008587 | short photoreceptor outer segment | 0.496912956 | 1.105206922 |
| REACTOME_ACTIVATION_OF_APC | REACTOME_ACTIVATION_OF_APCC_AND_APCCCDC20_M | 0.974123996 | 1.105217186 |
| GO:0090100 | positive regulation of transmembrane receptor protein s | 0.974118097 | 1.105296293 |
| MP:0001008 | abnormal sympathetic ganglion morphology | 0.974114826 | 1.105383283 |
| ENSG00000116957 | TBCE subnetwork | 0.974069305 | 1.105399449 |
| MP:0006395 | abnormal epiphyseal plate morphology | 0.974034025 | 1.105462846 |
| ENSG00000133226 | SRRM1 subnetwork | 0.497218769 | 1.105482852 |
| GO:0001525 | angiogenesis | 0.497147715 | 1.105513766 |
| ENSG00000164692 | COL1A2 subnetwork | 0.974030049 | 1.105545934 |
| REACTOME_APCCCDC20_MEDIAT | REACTOME_APCCCDC20_MEDIATED_DEGRADATION_OF | 0.973997464 | 1.10560148 |
| ENSG00000180616 | SSTR2 subnetwork | 0.973943269 | 1.105645225 |
| ENSG00000120658 | ENOX1 subnetwork | 0.973928194 | 1.105720472 |
| ENSG00000111358 | GTF2H3 subnetwork | 0.497935556 | 1.105731671 |
| ENSG00000109670 | FBXW7 subnetwork | 0.497909725 | 1.105762585 |
| ENSG00000125818 | PSMF1 subnetwork | 0.973916337 | 1.105795732 |
| ENSG00000129514 | FOXA1 subnetwork | 0.49769472 | 1.105825316 |
| GO:0061053 | somite development | 0.973899553 | 1.105863128 |
| GO:0010972 | negative regulation of G2/M transition of mitotic cell cyc | 0.497887087 | 1.105876165 |
| ENSG00000037042 | TUBG2 subnetwork | 0.497814634 | 1.105892079 |
| GO:0060428 | lung epithelium development | 0.49766225 | 1.105908886 |
| GO:0030801 | positive regulation of cyclic nucleotide metabolic proces | 0.973881329 | 1.105930535 |
| GO:0007052 | mitotic spindle organization | 0.497598798 | 1.105932331 |

| | | | |
|---|---|---|---|
| GO:0048762 | mesenchymal cell differentiation | 0.973844698 | 1.105970384 |
| ENSG00000116903 | EXOC8 subnetwork | 0.497555579 | 1.106008422 |
| ENSG00000042832 | TG subnetwork | 0.973803191 | 1.106018117 |
| GO:0005793 | endoplasmic reticulum-Golgi intermediate compartment | 0.973745502 | 1.106034347 |
| REACTOME_GLUTAMATE_NEURO | REACTOME_GLUTAMATE_NEUROTRANSMITTER_RELEAS | 0.9730926 | 1.106053918 |
| ENSG00000164076 | CAMKV subnetwork | 0.973694285 | 1.106078153 |
| ENSG00000170276 | ENSG00000170276 subnetwork | 0.973069977 | 1.10611352 |
| GO:0072530 | purine-containing compound transmembrane transport | 0.973274651 | 1.106132261 |
| MP:0001386 | abnormal maternal nurturing | 0.973671839 | 1.106145604 |
| GO:0048568 | embryonic organ development | 0.97335888 | 1.106147541 |
| ENSG00000119318 | RAD23B subnetwork | 0.973055168 | 1.106184957 |
| GO:0015802 | basic amino acid transport | 0.973623879 | 1.106193365 |
| MP:0002063 | abnormal learning/memory/conditioning | 0.973595243 | 1.106241135 |
| ENSG00000171703 | TCEA2 subnetwork | 0.973053471 | 1.106272175 |
| ENSG00000072864 | NDE1 subnetwork | 0.972982413 | 1.106292383 |
| ENSG00000119929 | CUTC subnetwork | 0.973583815 | 1.106316495 |
| ENSG00000167977 | KCTD5 subnetwork | 0.972971363 | 1.106359909 |
| GO:0005201 | extracellular matrix structural constituent | 0.972965584 | 1.106447161 |
| ENSG00000038274 | MAT2B subnetwork | 0.97294841 | 1.106510766 |
| GO:0016247 | channel regulator activity | 0.972937232 | 1.1065941 |
| REACTOME_SYNTHESIS_OF_BILE_ | REACTOME_SYNTHESIS_OF_BILE_ACIDS_AND_BILE_SAL | 0.972920767 | 1.106657727 |
| GO:0019905 | syntaxin binding | 0.97290455 | 1.106737141 |
| GO:0051482 | elevation of cytosolic calcium ion concentration involved | 0.972904517 | 1.106824458 |
| MP:0003727 | abnormal retinal layer morphology | 0.972835407 | 1.106836831 |
| MP:0001440 | abnormal grooming behavior | 0.972821045 | 1.106904443 |
| ENSG00000134597 | RBMX2 subnetwork | 0.498652015 | 1.10694653 |
| GO:0031225 | anchored to membrane | 0.972794607 | 1.106960227 |
| ENSG00000160917 | CPSF4 subnetwork | 0.498855306 | 1.106996997 |
| GO:0031577 | spindle checkpoint | 0.972770482 | 1.107019967 |
| ENSG00000105926 | MPP6 subnetwork | 0.498634834 | 1.107097792 |
| GO:0010833 | telomere maintenance via telomere lengthening | 0.498791881 | 1.107103169 |
| MP:0003733 | abnormal retinal inner nuclear layer morphology | 0.972760028 | 1.107103394 |
| MP:0009454 | impaired contextual conditioning behavior | 0.972746843 | 1.107178941 |
| ENSG00000034053 | APBA2 subnetwork | 0.972706617 | 1.107218977 |
| ENSG00000076554 | TPD52 subnetwork | 0.972673304 | 1.107262967 |
| GO:0034035 | purine ribonucleoside bisphosphate metabolic process | 0.972660306 | 1.107342492 |
| GO:0050427 | 3'-phosphoadenosine 5'-phosphosulfate metabolic proce | 0.972660306 | 1.107429925 |
| GO:0005545 | 1-phosphatidylinositol binding | 0.4991882 | 1.107453836 |
| GO:0009994 | oocyte differentiation | 0.499481202 | 1.107516879 |
| GO:0034032 | purine nucleoside bisphosphate metabolic process | 0.972660306 | 1.107517372 |
| REACTOME_MRNA_PROCESSING | REACTOME_MRNA_PROCESSING | 0.499436858 | 1.107570528 |
| GO:0009072 | aromatic amino acid family metabolic process | 0.972534703 | 1.107577792 |
| GO:0033875 | ribonucleoside bisphosphate metabolic process | 0.972660306 | 1.107604833 |
| GO:0042165 | neurotransmitter binding | 0.972534074 | 1.107665271 |
| GO:0045682 | regulation of epidermis development | 0.499424274 | 1.107684226 |
| GO:0007190 | activation of adenylate cyclase activity | 0.972526508 | 1.107736967 |
| GO:0072498 | embryonic skeletal joint development | 0.97243848 | 1.107753377 |
| ENSG00000168438 | CDC40 subnetwork | 0.499652913 | 1.107763276 |
| REACTOME_GRB2SOS_PROVIDES_ | REACTOME_GRB2SOS_PROVIDES_LINKAGE_TO_MAPK_S | 0.500059766 | 1.107772448 |
| MP:0001556 | increased circulating HDL cholesterol level | 0.499391927 | 1.107782948 |
| ENSG00000198467 | TPM2 subnetwork | 0.49974375 | 1.10779211 |
| GO:0045744 | negative regulation of G-protein coupled receptor protei | 0.972410178 | 1.107813241 |
| MP:0005352 | small cranium | 0.972408387 | 1.107900766 |
| ENSG00000106290 | TAF6 subnetwork | 0.500048472 | 1.107923538 |

| | | | |
|---|---|---|---|
| ENSG00000163918 | RFC4 subnetwork | 0.499988249 | 1.107954716 |
| MP:0005643 | decreased dopamine level | 0.972378127 | 1.107972503 |
| ENSG00000188130 | MAPK12 subnetwork | 0.499939858 | 1.108015897 |
| GO:0043009 | chordate embryonic development | 0.972369929 | 1.108052153 |
| GO:0051238 | sequestering of metal ion | 0.50033135 | 1.108062341 |
| ENSG00000115844 | DLX2 subnetwork | 0.972352492 | 1.108123913 |
| GO:0016125 | sterol metabolic process | 0.500298181 | 1.108153477 |
| REACTOME_METABOLISM_OF_AI | REACTOME_METABOLISM_OF_AMINO_ACIDS_AND_DEI | 0.972132442 | 1.108205534 |
| GO:0060076 | excitatory synapse | 0.972344793 | 1.10820754 |
| ENSG00000139998 | RAB15 subnetwork | 0.971944115 | 1.108211434 |
| ENSG00000143499 | SMYD2 subnetwork | 0.971866173 | 1.108212083 |
| GO:0090090 | negative regulation of canonical Wnt receptor signaling p | 0.972278708 | 1.1082319 |
| MP:0000120 | malocclusion | 0.972091936 | 1.108253617 |
| ENSG00000171848 | RRM2 subnetwork | 0.500572478 | 1.108254682 |
| GO:0005775 | vacuolar lumen | 0.500643827 | 1.108275914 |
| MP:0002745 | abnormal atrioventricular valve morphology | 0.972266192 | 1.108276026 |
| GO:0008088 | axon cargo transport | 0.972052876 | 1.108297755 |
| MP:0000967 | abnormal sensory neuron projections | 0.971866014 | 1.108299723 |
| REACTOME_GLUTATHIONE_CONJ | REACTOME_GLUTATHIONE_CONJUGATION | 0.971825617 | 1.108351787 |
| REACTOME_ABCA_TRANSPORTER | REACTOME_ABCA_TRANSPORTERS_IN_LIPID_HOMEOST | 0.50057156 | 1.108420737 |
| ENSG00000111344 | RASAL1 subnetwork | 0.971812276 | 1.108431543 |
| MP:0008406 | increased cellular sensitivity to hydrogen peroxide | 0.971772313 | 1.108455941 |
| ENSG00000196285 | ENSG00000196285 subnetwork | 0.5014156 | 1.108466717 |
| ENSG00000004948 | CALCR subnetwork | 0.50092793 | 1.108542977 |
| ENSG00000163875 | MEAF6 subnetwork | 0.971767232 | 1.108543628 |
| ENSG00000119917 | IFIT3 subnetwork | 0.501677417 | 1.108567584 |
| ENSG00000129675 | ARHGEF6 subnetwork | 0.500887439 | 1.108589187 |
| GO:0046658 | anchored to plasma membrane | 0.501014565 | 1.108594101 |
| MP:0005423 | abnormal somatic nervous system physiology | 0.971717749 | 1.108595728 |
| ENSG00000132475 | H3F3B subnetwork | 0.5014156 | 1.108632555 |
| ENSG00000135409 | AMHR2 subnetwork | 0.501105314 | 1.10864521 |
| ENSG00000034693 | PEX3 subnetwork | 0.502212528 | 1.108649537 |
| GO:0006085 | acetyl-CoA biosynthetic process | 0.502470593 | 1.108674231 |
| ENSG00000138778 | CENPE subnetwork | 0.97171247 | 1.108679484 |
| GO:0033631 | cell-cell adhesion mediated by integrin | 0.502101839 | 1.108711895 |
| GO:0003906 | DNA-(apurinic or apyrimidinic site) lyase activity | 0.501675872 | 1.108718409 |
| ENSG00000188994 | ZNF292 subnetwork | 0.502298264 | 1.108730396 |
| GO:0005773 | vacuole | 0.971711197 | 1.10876721 |
| ENSG00000163041 | H3F3A subnetwork | 0.5014156 | 1.108798444 |
| ENSG00000108848 | LUC7L3 subnetwork | 0.502458738 | 1.108809915 |
| ENSG00000196584 | XRCC2 subnetwork | 0.502211211 | 1.10881518 |
| MP:0004358 | bowed tibia | 0.501641584 | 1.108824409 |
| ENSG00000110169 | HPX subnetwork | 0.501974995 | 1.108826607 |
| ENSG00000113645 | WWC1 subnetwork | 0.97169139 | 1.10883121 |
| MP:0000521 | abnormal kidney cortex morphology | 0.502061103 | 1.10883276 |
| ENSG00000172379 | ARNT2 subnetwork | 0.501360563 | 1.10885214 |
| ENSG00000133316 | WDR74 subnetwork | 0.502412366 | 1.108885902 |
| GO:0048332 | mesoderm morphogenesis | 0.501300468 | 1.108898369 |
| REACTOME_GLYCOGEN_BREAKDO | REACTOME_GLYCOGEN_BREAKDOWN_GLYCOGENOLYSI | 0.971673913 | 1.108899177 |
| ENSG00000153395 | LPCAT1 subnetwork | 0.501940397 | 1.108910151 |
| MP:0003072 | abnormal metatarsal bone morphology | 0.971651663 | 1.108963197 |
| ENSG00000101365 | IDH3B subnetwork | 0.971632376 | 1.109031186 |
| GO:0007040 | lysosome organization | 0.971604185 | 1.109079395 |
| ENSG00000127946 | HIP1 subnetwork | 0.971525243 | 1.109099905 |

| | | | |
|---|---|---|---|
| MP:0004859 | abnormal synaptic plasticity | 0.97150835 | 1.10916792 |
| MP:0002781 | increased circulating testosterone level | 0.502794048 | 1.109186567 |
| GO:0051781 | positive regulation of cell division | 0.502979721 | 1.109198747 |
| ENSG00000069011 | PITX1 subnetwork | 0.971507212 | 1.10925574 |
| REACTOME_P38MAPK_EVENTS | REACTOME_P38MAPK_EVENTS | 0.502778566 | 1.109292432 |
| MP:0002572 | abnormal emotion/affect behavior | 0.971480553 | 1.109311901 |
| ENSG00000173598 | NUDT4 subnetwork | 0.502949479 | 1.109312043 |
| GO:0051093 | negative regulation of developmental process | 0.97146589 | 1.109387868 |
| GO:0006942 | regulation of striated muscle contraction | 0.971463062 | 1.109467807 |
| MP:0001385 | pup cannibalization | 0.971333226 | 1.109473267 |
| ENSG00000089199 | CHGB subnetwork | 0.971445551 | 1.109527958 |
| GO:0045668 | negative regulation of osteoblast differentiation | 0.971324171 | 1.109553232 |
| ENSG00000148943 | LIN7C subnetwork | 0.971297799 | 1.109605482 |
| ENSG00000022355 | GABRA1 subnetwork | 0.971279895 | 1.109669624 |
| REACTOME_RESOLUTION_OF_AP | REACTOME_RESOLUTION_OF_AP_SITES_VIA_THE_MULT | 0.503574431 | 1.109683912 |
| GO:0071299 | cellular response to vitamin A | 0.971265241 | 1.109733777 |
| ENSG00000108001 | EBF3 subnetwork | 0.503412905 | 1.109800119 |
| GO:0071300 | cellular response to retinoic acid | 0.971265241 | 1.109821712 |
| REACTOME_REMOVAL_OF_DNA_ | REACTOME_REMOVAL_OF_DNA_PATCH_CONTAINING_ | 0.503574431 | 1.109849389 |
| MP:0003849 | greasy coat | 0.503711635 | 1.109853906 |
| REACTOME_REGULATION_OF_INS | REACTOME_REGULATION_OF_INSULIN_SECRETION_BY_ | 0.971237096 | 1.109881924 |
| ENSG00000132357 | CARD6 subnetwork | 0.503369786 | 1.109891094 |
| ENSG00000101811 | CSTF2 subnetwork | 0.50354846 | 1.109917972 |
| ENSG00000149970 | CNKSR2 subnetwork | 0.971078398 | 1.109919943 |
| REACTOME_BASIGIN_INTERACTIC | REACTOME_BASIGIN_INTERACTIONS | 0.971208335 | 1.109934221 |
| MP:0001777 | abnormal body temperature homeostasis | 0.971072857 | 1.109992073 |
| GO:0006283 | transcription-coupled nucleotide-excision repair | 0.971203231 | 1.110018229 |
| ENSG00000197451 | HNRNPAB subnetwork | 0.504373731 | 1.110020846 |
| ENSG00000079805 | DNM2 subnetwork | 0.503971654 | 1.110074516 |
| GO:0048333 | mesodermal cell differentiation | 0.971062382 | 1.11008007 |
| GO:0006266 | DNA ligation | 0.503905054 | 1.110090923 |
| GO:0006664 | glycolipid metabolic process | 0.971040352 | 1.110140331 |
| GO:0030323 | respiratory tube development | 0.504481839 | 1.110153342 |
| ENSG00000114982 | KANSL3 subnetwork | 0.504363086 | 1.110163812 |
| MP:0002686 | globozoospermia | 0.504301277 | 1.110187668 |
| GO:0045981 | positive regulation of nucleotide metabolic process | 0.971036705 | 1.110220425 |
| GO:0032967 | positive regulation of collagen biosynthetic process | 0.504235397 | 1.110233875 |
| ENSG00000086758 | HUWE1 subnetwork | 0.505025454 | 1.110270712 |
| GO:0030574 | collagen catabolic process | 0.971021189 | 1.110288637 |
| MP:0003545 | increased alcohol consumption | 0.970919914 | 1.110301348 |
| MP:0005459 | decreased percent body fat | 0.504915604 | 1.110340723 |
| ENSG00000183785 | TUBA8 subnetwork | 0.504160741 | 1.110348681 |
| GO:0030165 | PDZ domain binding | 0.970891337 | 1.110361646 |
| GO:0010714 | positive regulation of collagen metabolic process | 0.504235397 | 1.110399285 |
| GO:0001726 | ruffle | 0.504845621 | 1.110401786 |
| KEGG_O_GLYCAN_BIOSYNTHESIS | KEGG_O_GLYCAN_BIOSYNTHESIS | 0.505014836 | 1.110428444 |
| GO:0021575 | hindbrain morphogenesis | 0.970882201 | 1.110445749 |
| GO:0048589 | developmental growth | 0.970517396 | 1.110460965 |
| GO:0009950 | dorsal/ventral axis specification | 0.970710551 | 1.110467238 |
| ENSG00000115163 | CENPA subnetwork | 0.97079605 | 1.110470374 |
| ENSG00000125352 | RNF113A subnetwork | 0.504826782 | 1.110514958 |
| MP:0003960 | increased lean body mass | 0.970693841 | 1.110539468 |
| GO:0031110 | regulation of microtubule polymerization or depolymeriz | 0.970511333 | 1.110549076 |
| MP:0004423 | abnormal squamosal bone morphology | 0.970486757 | 1.110633233 |

| | | | |
|---|---|---|---|
| ENSG00000168556 | ING2 subnetwork | 0.504818568 | 1.110680262 |
| ENSG00000141985 | SH3GL1 subnetwork | 0.970366429 | 1.11068254 |
| ENSG00000100505 | TRIM9 subnetwork | 0.50528761 | 1.110685604 |
| GO:0060395 | SMAD protein signal transduction | 0.970451734 | 1.11068566 |
| GO:0032420 | stereocilium | 0.970363011 | 1.110770696 |
| GO:0043300 | regulation of leukocyte degranulation | 0.970348462 | 1.110835053 |
| GO:0050766 | positive regulation of phagocytosis | 0.970323784 | 1.110895451 |
| ENSG00000123159 | GIPC1 subnetwork | 0.970299946 | 1.110971737 |
| GO:0090184 | positive regulation of kidney development | 0.970281966 | 1.111024216 |
| GO:0045055 | regulated secretory pathway | 0.970269313 | 1.111084643 |
| GO:0031080 | Nup107-160 complex | 0.970262074 | 1.111172874 |
| GO:0051491 | positive regulation of filopodium assembly | 0.505538773 | 1.111182156 |
| ENSG00000145321 | GC subnetwork | 0.970223036 | 1.11122141 |
| ENSG00000102109 | PCSK1N subnetwork | 0.970188971 | 1.111285839 |
| KEGG_PENTOSE_AND_GLUCUROI | KEGG_PENTOSE_AND_GLUCURONATE_INTERCONVERSIC | 0.505667734 | 1.111351472 |
| ENSG00000116954 | RRAGC subnetwork | 0.970172256 | 1.111354249 |
| GO:0030017 | sarcomere | 0.970142564 | 1.111402812 |
| REACTOME_SIGNAL_ATTENUATIC | REACTOME_SIGNAL_ATTENUATION | 0.970104222 | 1.111423578 |
| REACTOME_MITOCHONDRIAL_FA | REACTOME_MITOCHONDRIAL_FATTY_ACID_BETA:OXIDA | 0.970084657 | 1.111495988 |
| ENSG00000139116 | KIF21A subnetwork | 0.970064273 | 1.111568409 |
| ENSG00000115507 | OTX1 subnetwork | 0.970026567 | 1.111605085 |
| ENSG00000182901 | RGS7 subnetwork | 0.96999302 | 1.111645741 |
| ENSG00000181072 | CHRM2 subnetwork | 0.969969412 | 1.11170627 |
| GO:0017136 | NAD-dependent histone deacetylase activity | 0.96991968 | 1.11176681 |
| GO:0034979 | NAD-dependent protein deacetylase activity | 0.96991968 | 1.111855178 |
| ENSG00000179041 | RRS1 subnetwork | 0.508837636 | 1.111873799 |
| GO:0009792 | embryo development ending in birth or egg hatching | 0.969894374 | 1.111911765 |
| GO:0000149 | SNARE binding | 0.969808927 | 1.111912712 |
| ENSG00000184408 | KCND2 subnetwork | 0.969633161 | 1.111971215 |
| GO:0000070 | mitotic sister chromatid segregation | 0.969779676 | 1.111977262 |
| ENSG00000100380 | ST13 subnetwork | 0.969610419 | 1.112011928 |
| MP:0004613 | fusion of vertebral arches | 0.969451052 | 1.112013839 |
| ENSG00000136999 | NOV subnetwork | 0.508825152 | 1.112015962 |
| MP:0008877 | abnormal DNA methylation | 0.969744772 | 1.112021945 |
| KEGG_GLYCOSAMINOGLYCAN_DE | KEGG_GLYCOSAMINOGLYCAN_DEGRADATION | 0.969344307 | 1.112075412 |
| GO:0046519 | sphingoid metabolic process | 0.969606182 | 1.112080484 |
| GO:0006536 | glutamate metabolic process | 0.969443679 | 1.112102291 |
| ENSG00000173991 | TCAP subnetwork | 0.508804179 | 1.11210643 |
| MP:0000343 | altered response to myocardial infarction | 0.509066185 | 1.112106663 |
| GO:0001676 | long-chain fatty acid metabolic process | 0.969316684 | 1.11213206 |
| ENSG00000087903 | RFX2 subnetwork | 0.506416838 | 1.112149116 |
| MP:0003071 | decreased vascular permeability | 0.508771022 | 1.112167357 |
| ENSG00000189308 | LIN54 subnetwork | 0.508727699 | 1.112176549 |
| MP:0010029 | abnormal basicranium morphology | 0.969271898 | 1.11218474 |
| ENSG00000158486 | DNAH3 subnetwork | 0.50904983 | 1.112211879 |
| ENSG00000100813 | ACIN1 subnetwork | 0.50638244 | 1.112240048 |
| MP:0004395 | increased cochlear inner hair cell number | 0.969254759 | 1.112249363 |
| GO:0003081 | regulation of systemic arterial blood pressure by renin-a | 0.969213955 | 1.112310018 |
| ENSG00000206502 | ZNRD1 subnetwork | 0.508726893 | 1.112333629 |
| ENSG00000172380 | GNG12 subnetwork | 0.506374259 | 1.112383004 |
| GO:0016616 | oxidoreductase activity, acting on the CH-OH group of dc | 0.506596514 | 1.112384912 |
| ENSG00000159164 | SV2A subnetwork | 0.969210319 | 1.112398536 |
| GO:0022010 | central nervous system myelination | 0.506325657 | 1.112444279 |
| ENSG00000180914 | OXTR subnetwork | 0.969199341 | 1.112463191 |

| | | | |
|---|---|---|---|
| ENSG00000206429 | ENSG00000206429 subnetwork | 0.508726893 | 1.112498151 |
| ENSG00000182580 | EPHB3 subnetwork | 0.508556897 | 1.112509247 |
| GO:0046939 | nucleotide phosphorylation | 0.508268476 | 1.112531458 |
| GO:0060065 | uterus development | 0.5081849 | 1.112533314 |
| GO:0006687 | glycosphingolipid metabolic process | 0.96918937 | 1.112543776 |
| GO:0017137 | Rab GTPase binding | 0.508490753 | 1.11255549 |
| GO:0034062 | RNA polymerase activity | 0.508077058 | 1.112559242 |
| MP:0006279 | abnormal limb development | 0.969052709 | 1.112565674 |
| GO:0000578 | embryonic axis specification | 0.969147778 | 1.112588554 |
| ENSG00000149257 | SERPINH1 subnetwork | 0.506780184 | 1.112590943 |
| GO:0017048 | Rho GTPase binding | 0.507767459 | 1.112603734 |
| GO:0032291 | axon ensheathment in central nervous system | 0.506325657 | 1.1126096 |
| ENSG00000130725 | UBE2M subnetwork | 0.507917244 | 1.112614815 |
| ENSG00000164815 | ORC5 subnetwork | 0.969017742 | 1.112618422 |
| MP:0000350 | abnormal cell proliferation | 0.506225496 | 1.112657946 |
| ENSG00000112941 | PAPD7 subnetwork | 0.508457643 | 1.112660944 |
| ENSG00000066379 | ZNRD1 subnetwork | 0.508726893 | 1.112662722 |
| ENSG00000105705 | SUGP1 subnetwork | 0.508176998 | 1.112675848 |
| GO:0030593 | neutrophil chemotaxis | 0.507862164 | 1.112690769 |
| ENSG00000114854 | TNNC1 subnetwork | 0.968998897 | 1.112699045 |
| MP:0001005 | abnormal retinal rod cell morphology | 0.507752542 | 1.112709352 |
| GO:0003899 | DNA-directed RNA polymerase activity | 0.508077058 | 1.112724041 |
| ENSG00000143748 | NVL subnetwork | 0.506308867 | 1.112752675 |
| MP:0010701 | fusion of atlas and odontoid process | 0.507665375 | 1.112755707 |
| ENSG00000198062 | POTEH subnetwork | 0.508423921 | 1.112759029 |
| ENSG00000164494 | PDSS2 subnetwork | 0.968982369 | 1.112767736 |
| GO:0035065 | regulation of histone acetylation | 0.968610652 | 1.112805704 |
| ENSG00000182400 | TRAPPC6B subnetwork | 0.507608529 | 1.112809489 |
| MP:0008450 | retinal photoreceptor degeneration | 0.968965032 | 1.112824494 |
| GO:0031060 | regulation of histone methylation | 0.509500811 | 1.112843427 |
| ENSG00000188223 | LIN37 subnetwork | 0.507561566 | 1.112855872 |
| ENSG00000155868 | MED7 subnetwork | 0.507148792 | 1.112859899 |
| ENSG00000128534 | NAA38 subnetwork | 0.968598233 | 1.112882409 |
| GO:0051216 | cartilage development | 0.96895607 | 1.112901171 |
| ENSG00000186340 | THBS2 subnetwork | 0.507441704 | 1.112904183 |
| GO:0005385 | zinc ion transmembrane transporter activity | 0.507067834 | 1.112906338 |
| ENSG00000107281 | NPDC1 subnetwork | 0.507383768 | 1.112920932 |
| GO:0030324 | lung development | 0.507510106 | 1.112931929 |
| GO:0000146 | microfilament motor activity | 0.96891943 | 1.11294202 |
| GO:0031672 | A band | 0.968586779 | 1.112967094 |
| ENSG00000109107 | ALDOC subnetwork | 0.968803032 | 1.112971961 |
| GO:0014812 | muscle cell migration | 0.507035502 | 1.112975059 |
| ENSG00000044115 | CTNNA1 subnetwork | 0.968894992 | 1.112998805 |
| MP:0001529 | abnormal vocalization | 0.968560339 | 1.113003984 |
| ENSG00000180370 | PAK2 subnetwork | 0.507357141 | 1.113004451 |
| GO:0007026 | negative regulation of microtubule depolymerization | 0.968531186 | 1.113064786 |
| ENSG00000170542 | SERPINB9 subnetwork | 0.50734427 | 1.113139932 |
| ENSG00000178999 | AURKB subnetwork | 0.968512953 | 1.113141536 |
| GO:0051640 | organelle localization | 0.968510345 | 1.113226269 |
| ENSG00000102218 | RP2 subnetwork | 0.968508334 | 1.113315001 |
| REACTOME_CALNEXINCALRETICU | REACTOME_CALNEXINCALRETICULIN_CYCLE | 0.968446274 | 1.113316062 |
| ENSG00000144191 | CNGA3 subnetwork | 0.968440079 | 1.113396843 |
| GO:0000910 | cytokinesis | 0.968409747 | 1.113449733 |
| GO:0044062 | regulation of excretion | 0.96838755 | 1.113522564 |

| | | | |
|---|---|---|---|
| GO:0001503 | ossification | 0.96830531 | 1.113527629 |
| GO:0044275 | cellular carbohydrate catabolic process | 0.968303854 | 1.113616427 |
| GO:0045111 | intermediate filament cytoskeleton | 0.968274625 | 1.113669352 |
| MP:0001721 | absent visceral yolk sac blood islands | 0.51016107 | 1.113716226 |
| ENSG00000149968 | MMP3 subnetwork | 0.510005376 | 1.113727662 |
| REACTOME_INTRINSIC_PATHWAY | REACTOME_INTRINSIC_PATHWAY | 0.968260626 | 1.113742224 |
| MP:0008288 | abnormal adrenal cortex morphology | 0.968243756 | 1.113803143 |
| REACTOME_TRANSCRIPTION_OF_ | REACTOME_TRANSCRIPTION_OF_THE_HIV_GENOME | 0.510124842 | 1.113821618 |
| ENSG00000100650 | SRSF5 subnetwork | 0.510396094 | 1.113859779 |
| ENSG00000171723 | GPHN subnetwork | 0.968227705 | 1.113864071 |
| ENSG00000164168 | TMEM184C subnetwork | 0.968183284 | 1.113881133 |
| ENSG00000154473 | BUB3 subnetwork | 0.96818022 | 1.113970002 |
| ENSG00000102003 | SYP subnetwork | 0.510372471 | 1.114016829 |
| REACTOME_APOPTOTIC_CLEAVA | REACTOME_APOPTOTIC_CLEAVAGE_OF_CELLULAR_PRO | 0.510585691 | 1.114032758 |
| MP:0001392 | abnormal locomotor behavior | 0.968175984 | 1.114058885 |
| GO:0060348 | bone development | 0.968153811 | 1.114143792 |
| GO:0007250 | activation of NF-kappaB-inducing kinase activity | 0.510570406 | 1.114160272 |
| GO:0022037 | metencephalon development | 0.968028766 | 1.114169992 |
| GO:0050906 | detection of stimulus involved in sensory perception | 0.968123482 | 1.114176841 |
| GO:0043299 | leukocyte degranulation | 0.968021155 | 1.114258919 |
| MP:0003224 | neuron degeneration | 0.968014567 | 1.11434387 |
| GO:0070412 | R-SMAD binding | 0.511559164 | 1.114363583 |
| ENSG00000164270 | HTR4 subnetwork | 0.967959841 | 1.114376946 |
| ENSG00000150672 | DLG2 subnetwork | 0.967891616 | 1.114382085 |
| GO:0072077 | renal vesicle morphogenesis | 0.967779808 | 1.114428298 |
| REACTOME_TRANSFERRIN_ENDO | REACTOME_TRANSFERRIN_ENDOCYTOSIS_AND_RECYCL | 0.967872283 | 1.11445509 |
| GO:0046527 | glucosyltransferase activity | 0.511679742 | 1.114464575 |
| MP:0011024 | abnormal branching involved in lung morphogenesis | 0.511541824 | 1.114490939 |
| GO:0021904 | dorsal/ventral neural tube patterning | 0.96777528 | 1.114513296 |
| GO:0030857 | negative regulation of epithelial cell differentiation | 0.511790686 | 1.114536082 |
| GO:0048011 | nerve growth factor receptor signaling pathway | 0.511515596 | 1.114581491 |
| ENSG00000134365 | CFHR4 subnetwork | 0.511400721 | 1.11458364 |
| ENSG00000163810 | TGM4 subnetwork | 0.96777233 | 1.1146023 |
| ENSG00000176108 | CHMP6 subnetwork | 0.511914558 | 1.11466647 |
| ENSG00000179588 | ZFPM1 subnetwork | 0.967770741 | 1.114687325 |
| ENSG00000138795 | LEF1 subnetwork | 0.511370219 | 1.114733196 |
| GO:0051602 | response to electrical stimulus | 0.967756912 | 1.114768371 |
| MP:0001304 | cataracts | 0.967689418 | 1.114797508 |
| GO:0014902 | myotube differentiation | 0.511331982 | 1.114816453 |
| ENSG00000139220 | PPFIA2 subnetwork | 0.967676545 | 1.114870586 |
| ENSG00000087338 | GMCL1 subnetwork | 0.512122524 | 1.114877797 |
| GO:0060350 | endochondral bone morphogenesis | 0.967676225 | 1.11495566 |
| GO:0045806 | negative regulation of endocytosis | 0.511067354 | 1.114960165 |
| GO:0003755 | peptidyl-prolyl cis-trans isomerase activity | 0.511202684 | 1.114970501 |
| ENSG00000161638 | ITGA5 subnetwork | 0.511330609 | 1.114973459 |
| ENSG00000164885 | CDK5 subnetwork | 0.967660801 | 1.115032758 |
| MP:0006054 | spinal hemorrhage | 0.511285886 | 1.115042029 |
| MP:0005619 | increased urine potassium level | 0.511167565 | 1.115061218 |
| ENSG00000114978 | MOB1A subnetwork | 0.512265125 | 1.115066981 |
| GO:0009309 | amine biosynthetic process | 0.967644804 | 1.115097883 |
| ENSG00000047056 | WDR37 subnetwork | 0.967639999 | 1.115179 |
| GO:0002474 | antigen processing and presentation of peptide antigen | 0.96763054 | 1.115252138 |
| GO:0007606 | sensory perception of chemical stimulus | 0.967607988 | 1.115321292 |
| ENSG00000132639 | SNAP25 subnetwork | 0.967568238 | 1.115354488 |

| | | | |
|---|---|---|---|
| GO:0012507 | ER to Golgi transport vesicle membrane | 0.512557993 | 1.11535688 |
| ENSG00000176986 | SEC24C subnetwork | 0.967461342 | 1.115412903 |
| ENSG00000124610 | HIST1H1A subnetwork | 0.967554004 | 1.115435651 |
| ENSG00000183873 | SCN5A subnetwork | 0.512518619 | 1.115462173 |
| GO:0030804 | positive regulation of cyclic nucleotide biosynthetic proc | 0.967449488 | 1.115482091 |
| ENSG00000206282 | RGL2 subnetwork | 0.967228531 | 1.115555022 |
| GO:0030810 | positive regulation of nucleotide biosynthetic process | 0.967449488 | 1.11557128 |
| MP:0008519 | thin retinal outer plexiform layer | 0.967360351 | 1.115601759 |
| ENSG00000111275 | ALDH2 subnetwork | 0.967422355 | 1.11560451 |
| ENSG00000206210 | ENSG00000206210 subnetwork | 0.967228531 | 1.115644245 |
| GO:0072087 | renal vesicle development | 0.967198922 | 1.115713486 |
| ENSG00000100325 | ASCC2 subnetwork | 0.967070936 | 1.115744 |
| ENSG00000186051 | TAL2 subnetwork | 0.96717715 | 1.115786737 |
| MP:0000623 | decreased salivation | 0.967062119 | 1.115817265 |
| MP:0005574 | decreased pulmonary respiratory rate | 0.966955037 | 1.115830533 |
| MP:0008415 | abnormal neurite morphology | 0.966931358 | 1.115887813 |
| ENSG00000109911 | ELP4 subnetwork | 0.966881631 | 1.115917093 |
| GO:0044291 | cell-cell contact zone | 0.966870452 | 1.115990396 |
| ENSG00000138411 | HECW2 subnetwork | 0.966847941 | 1.116035697 |
| MP:0003384 | abnormal ventral body wall morphology | 0.966786248 | 1.116040983 |
| ENSG00000142871 | CYR61 subnetwork | 0.966766594 | 1.116110311 |
| MP:0002064 | seizures | 0.966667094 | 1.116160929 |
| ENSG00000116750 | UCHL5 subnetwork | 0.966746619 | 1.116171644 |
| ENSG00000053918 | KCNQ1 subnetwork | 0.96635557 | 1.116182124 |
| GO:0070972 | protein localization in endoplasmic reticulum | 0.966628589 | 1.116198254 |
| REACTOME_ACTIVATION_OF_CH/ | REACTOME_ACTIVATION_OF_CHAPERONE_GENES_BY_X | 0.966585797 | 1.116251602 |
| GO:0006754 | ATP biosynthetic process | 0.966350438 | 1.116263516 |
| GO:0060572 | morphogenesis of an epithelial bud | 0.966525894 | 1.116284936 |
| GO:0035383 | thioester metabolic process | 0.966341233 | 1.116348927 |
| GO:0006637 | acyl-CoA metabolic process | 0.966341233 | 1.116438356 |
| GO:0015450 | P-P-bond-hydrolysis-driven protein transmembrane tran | 0.966292255 | 1.11645169 |
| ENSG00000214655 | KIAA0913 subnetwork | 0.966246127 | 1.116497076 |
| GO:0051320 | S phase | 0.966136746 | 1.11653578 |
| ENSG00000188312 | CENPP subnetwork | 0.966080487 | 1.116553134 |
| GO:0042354 | L-fucose metabolic process | 0.966011281 | 1.116558468 |
| GO:0033267 | axon part | 0.966224076 | 1.116574519 |
| GO:0042772 | DNA damage response, signal transduction resulting in t | 0.965990163 | 1.11661991 |
| GO:0003281 | ventricular septum development | 0.965945783 | 1.116681363 |
| GO:0046887 | positive regulation of hormone secretion | 0.965943985 | 1.116770883 |
| ENSG00000129990 | SYT5 subnetwork | 0.965732935 | 1.116782936 |
| ENSG00000211895 | ENSG00000211895 subnetwork | 0.965911388 | 1.116836367 |
| GO:0051494 | negative regulation of cytoskeleton organization | 0.965699286 | 1.116844427 |
| ENSG00000170734 | POLH subnetwork | 0.965843477 | 1.116869788 |
| GO:0006767 | water-soluble vitamin metabolic process | 0.965660308 | 1.116901917 |
| GO:0032728 | positive regulation of interferon-beta production | 0.965609844 | 1.116915303 |
| REACTOME_DEPOSITION_OF_NE\ | REACTOME_DEPOSITION_OF_NEW_CENPA:CONTAINING | 0.965579184 | 1.11698484 |
| REACTOME_NUCLEOSOME_ASSEI | REACTOME_NUCLEOSOME_ASSEMBLY | 0.965579184 | 1.117074442 |
| MP:0008584 | photoreceptor outer segment degeneration | 0.513478804 | 1.117090936 |
| GO:0007029 | endoplasmic reticulum organization | 0.965522999 | 1.117107902 |
| MP:0004704 | short vertebral column | 0.965501852 | 1.117177471 |
| GO:0042277 | peptide binding | 0.513626623 | 1.117213477 |
| MP:0008725 | enlarged heart atrium | 0.965337378 | 1.117221732 |
| GO:0031581 | hemidesmosome assembly | 0.965469373 | 1.117231004 |
| ENSG00000139197 | PEX5 subnetwork | 0.965302001 | 1.117247191 |

| | | | |
|---|---|---|---|
| MP:0003698 | abnormal male reproductive system physiology | 0.965433464 | 1.117268496 |
| GO:0003254 | regulation of membrane depolarization | 0.965260077 | 1.117296733 |
| GO:0005801 | cis-Golgi network | 0.965253949 | 1.117382405 |
| ENSG00000128595 | CALU subnetwork | 0.965097827 | 1.11743878 |
| ENSG00000130164 | LDLR subnetwork | 0.965242435 | 1.11746809 |
| REACTOME_POSTSYNAPTIC_NICO | REACTOME_POSTSYNAPTIC_NICOTINIC_ACETYLCHOLINE | 0.965076464 | 1.117496387 |
| ENSG00000141552 | ANAPC11 subnetwork | 0.965217882 | 1.117521676 |
| ENSG00000165417 | GTF2A1 subnetwork | 0.514492389 | 1.117550691 |
| REACTOME_ACTIVATION_OF_NIC | REACTOME_ACTIVATION_OF_NICOTINIC_ACETYLCHOLIN | 0.965076464 | 1.117586124 |
| GO:0005770 | late endosome | 0.514703873 | 1.117641011 |
| ENSG00000112159 | MDN1 subnetwork | 0.51447048 | 1.117663483 |
| REACTOME_ACETYLCHOLINE_BIN | REACTOME_ACETYLCHOLINE_BINDING_AND_DOWNSTR | 0.965076464 | 1.117675875 |
| ENSG00000140416 | TPM1 subnetwork | 0.514644064 | 1.117680329 |
| GO:0004576 | oligosaccharyl transferase activity | 0.965061886 | 1.117753594 |
| GO:0032535 | regulation of cellular component size | 0.514425424 | 1.117761611 |
| ENSG00000160783 | PMF1 subnetwork | 0.964953707 | 1.117804643 |
| GO:0006656 | phosphatidylcholine biosynthetic process | 0.965055892 | 1.117835341 |
| GO:0002438 | acute inflammatory response to antigenic stimulus | 0.964892153 | 1.117842224 |
| ENSG00000119866 | BCL11A subnetwork | 0.514121982 | 1.117860294 |
| GO:0043034 | costamere | 0.514406311 | 1.117911216 |
| ENSG00000165178 | ENSG00000165178 subnetwork | 0.514061043 | 1.117914399 |
| ENSG00000115128 | ENSG00000115128 subnetwork | 0.51433309 | 1.1179212 |
| GO:0060351 | cartilage development involved in endochondral bone m | 0.964884031 | 1.117932032 |
| ENSG00000099810 | MTAP subnetwork | 0.513996063 | 1.1179391 |
| ENSG00000107282 | APBA1 subnetwork | 0.964877692 | 1.11801382 |
| ENSG00000068654 | POLR1A subnetwork | 0.514305191 | 1.118041464 |
| ENSG00000176788 | BASP1 subnetwork | 0.9648554 | 1.11807955 |
| MP:0001156 | abnormal spermatogenesis | 0.515209488 | 1.118103069 |
| GO:0002792 | negative regulation of peptide secretion | 0.964843998 | 1.118153327 |
| ENSG00000112992 | NNT subnetwork | 0.515145406 | 1.118157122 |
| REACTOME_NUCLEAR_SIGNALINC | REACTOME_NUCLEAR_SIGNALING_BY_ERBB4 | 0.515079478 | 1.118211191 |
| GO:0050994 | regulation of lipid catabolic process | 0.964833462 | 1.118235152 |
| ENSG00000169067 | ACTBL2 subnetwork | 0.515685467 | 1.118243838 |
| MP:0001422 | abnormal drinking behavior | 0.515595668 | 1.118246515 |
| GO:0035112 | genitalia morphogenesis | 0.51580789 | 1.118277835 |
| GO:0006878 | cellular copper ion homeostasis | 0.515545081 | 1.118278544 |
| MP:0000520 | absent kidney | 0.964819654 | 1.118308954 |
| ENSG00000124688 | MAD2L1BP subnetwork | 0.964782732 | 1.118346596 |
| GO:0090263 | positive regulation of canonical Wnt receptor signaling p | 0.964569197 | 1.11839926 |
| GO:0003382 | epithelial cell morphogenesis | 0.964683893 | 1.118421899 |
| GO:0032400 | melanosome localization | 0.964767 | 1.118424437 |
| ENSG00000169249 | ZRSR2 subnetwork | 0.515537275 | 1.118428005 |
| GO:0007094 | mitotic cell cycle spindle assembly checkpoint | 0.964554843 | 1.118485165 |
| ENSG00000185624 | P4HB subnetwork | 0.515497002 | 1.11848943 |
| ENSG00000166900 | STX3 subnetwork | 0.964535712 | 1.118550981 |
| GO:0045725 | positive regulation of glycogen biosynthetic process | 0.964510114 | 1.11858464 |
| ENSG00000126215 | XRCC3 subnetwork | 0.96450796 | 1.118674602 |
| MP:0003920 | abnormal heart right ventricle morphology | 0.964462709 | 1.118720341 |
| ENSG00000162928 | PEX13 subnetwork | 0.964451867 | 1.118786197 |
| ENSG00000101751 | POLI subnetwork | 0.516966285 | 1.118790275 |
| ENSG00000127884 | ECHS1 subnetwork | 0.516164202 | 1.118810502 |
| ENSG00000100162 | CENPM subnetwork | 0.964408347 | 1.118819886 |
| ENSG00000047457 | CP subnetwork | 0.964397757 | 1.11890185 |
| GO:0014015 | positive regulation of gliogenesis | 0.964330845 | 1.118923485 |

| | | | |
|---|---|---|---|
| GO:0043506 | regulation of JUN kinase activity | 0.964252702 | 1.118941101 |
| ENSG00000198000 | NOL8 subnetwork | 0.516807426 | 1.118945055 |
| GO:0010259 | multicellular organismal aging | 0.517085985 | 1.118948602 |
| MP:0009429 | decreased embryo weight | 0.516960716 | 1.118954153 |
| ENSG00000124228 | DDX27 subnetwork | 0.516541364 | 1.118960715 |
| ENSG00000167840 | ZNF232 subnetwork | 0.516461934 | 1.118963495 |
| GO:0016859 | cis-trans isomerase activity | 0.516389508 | 1.118966276 |
| ENSG00000055609 | MLL3 subnetwork | 0.516670215 | 1.118987249 |
| GO:0072341 | modified amino acid binding | 0.964228311 | 1.119002977 |
| GO:0004867 | serine-type endopeptidase inhibitor activity | 0.516767089 | 1.119065064 |
| ENSG00000124074 | C16orf48 subnetwork | 0.964217503 | 1.119072912 |
| REACTOME_CITRIC_ACID_CYCLE_ | REACTOME_CITRIC_ACID_CYCLE_TCA_CYCLE | 0.516954542 | 1.119118078 |
| ENSG00000162191 | UBXN1 subnetwork | 0.516354472 | 1.119130371 |
| ENSG00000165588 | OTX2 subnetwork | 0.964213964 | 1.119158954 |
| GO:0006635 | fatty acid beta-oxidation | 0.964197773 | 1.11924501 |
| MP:0003161 | absent lateral semicircular canal | 0.96414523 | 1.119278757 |
| ENSG00000180198 | RCC1 subnetwork | 0.964118722 | 1.119344711 |
| GO:0051318 | G1 phase | 0.964023762 | 1.119370421 |
| REACTOME_INTEGRATION_OF_EI | REACTOME_INTEGRATION_OF_ENERGY_METABOLISM | 0.96379442 | 1.119433035 |
| GO:0004620 | phospholipase activity | 0.963717191 | 1.119442655 |
| GO:0007263 | nitric oxide mediated signal transduction | 0.964008775 | 1.119444444 |
| GO:0060536 | cartilage morphogenesis | 0.963970006 | 1.119490297 |
| ENSG00000110148 | CCKBR subnetwork | 0.963713823 | 1.119524768 |
| MP:0008511 | thin retinal inner nuclear layer | 0.963929938 | 1.119560316 |
| GO:0016846 | carbon-sulfur lyase activity | 0.963682317 | 1.119594812 |
| ENSG00000185049 | WHSC2 subnetwork | 0.517430464 | 1.119677892 |
| GO:0015643 | toxin binding | 0.963681063 | 1.119685008 |
| GO:0051900 | regulation of mitochondrial depolarization | 0.963503242 | 1.11975423 |
| GO:0032862 | activation of Rho GTPase activity | 0.963671827 | 1.119771189 |
| GO:0010165 | response to X-ray | 0.963479523 | 1.119812233 |
| GO:0001655 | urogenital system development | 0.517569575 | 1.119836042 |
| GO:0046470 | phosphatidylcholine metabolic process | 0.963642547 | 1.119837241 |
| GO:0003215 | cardiac right ventricle morphogenesis | 0.963471843 | 1.119886364 |
| MP:0001362 | abnormal anxiety-related response | 0.963441074 | 1.119948416 |
| GO:0071897 | DNA biosynthetic process | 0.517860892 | 1.120002927 |
| MP:0000116 | abnormal tooth development | 0.963420649 | 1.120018539 |
| ENSG00000198835 | GJC2 subnetwork | 0.517814994 | 1.120086346 |
| GO:0070279 | vitamin B6 binding | 0.963399675 | 1.120092705 |
| ENSG00000071537 | SEL1L subnetwork | 0.518135081 | 1.120103847 |
| ENSG00000100410 | PHF5A subnetwork | 0.518013264 | 1.120153621 |
| GO:0030170 | pyridoxal phosphate binding | 0.963399675 | 1.120183005 |
| ENSG00000131462 | TUBG1 subnetwork | 0.517794397 | 1.120206382 |
| GO:0032370 | positive regulation of lipid transport | 0.51811143 | 1.120223815 |
| GO:0046459 | short-chain fatty acid metabolic process | 0.963397399 | 1.120273321 |
| GO:0019898 | extrinsic to membrane | 0.963366806 | 1.120331398 |
| ENSG00000125885 | MCM8 subnetwork | 0.963165514 | 1.12034035 |
| GO:0019842 | vitamin binding | 0.963336723 | 1.120365293 |
| GO:0043168 | anion binding | 0.963137544 | 1.120402484 |
| ENSG00000069966 | GNB5 subnetwork | 0.963066752 | 1.120424296 |
| MP:0000755 | hindlimb paralysis | 0.963335459 | 1.120455645 |
| ENSG00000177469 | PTRF subnetwork | 0.518353106 | 1.120488447 |
| GO:0010656 | negative regulation of muscle cell apoptotic process | 0.9630649 | 1.120514682 |
| GO:0048483 | autonomic nervous system development | 0.963021481 | 1.120580879 |
| MP:0002673 | abnormal sperm number | 0.963016551 | 1.120667258 |

| | | | |
|---|---|---|---|
| GO:0017153 | sodium:dicarboxylate symporter activity | 0.963014438 | 1.120749617 |
| GO:0005328 | neurotransmitter:sodium symporter activity | 0.962815065 | 1.120782889 |
| GO:0032459 | regulation of protein oligomerization | 0.518573178 | 1.120814447 |
| ENSG00000197223 | C1D subnetwork | 0.96299727 | 1.120831988 |
| GO:0030837 | negative regulation of actin filament polymerization | 0.962779826 | 1.120853176 |
| MP:0008670 | decreased interleukin-12b secretion | 0.518692638 | 1.120891813 |
| MP:0005269 | abnormal occipital bone morphology | 0.962987841 | 1.120914373 |
| GO:0002062 | chondrocyte differentiation | 0.962769638 | 1.120935583 |
| GO:0030134 | ER to Golgi transport vesicle | 0.519029865 | 1.120967271 |
| ENSG00000164944 | KIAA1429 subnetwork | 0.962705436 | 1.120993784 |
| GO:0016574 | histone ubiquitination | 0.962687481 | 1.121064105 |
| ENSG00000117500 | TMED5 subnetwork | 0.518831478 | 1.121064172 |
| GO:0001568 | blood vessel development | 0.519008357 | 1.121101856 |
| ENSG00000142039 | CCDC97 subnetwork | 0.519555723 | 1.12110219 |
| ENSG00000033627 | ATP6V0A1 subnetwork | 0.962656497 | 1.121118288 |
| ENSG00000164687 | FABP5 subnetwork | 0.518964506 | 1.121163403 |
| MP:0002655 | abnormal keratinocyte morphology | 0.519626564 | 1.121172092 |
| GO:0006898 | receptor-mediated endocytosis | 0.96262446 | 1.121172481 |
| REACTOME_BIOSYNTHESIS_OF_TI | REACTOME_BIOSYNTHESIS_OF_THE_N:GLYCAN_PRECUF | 0.519521686 | 1.121200175 |
| MP:0010301 | increased stomach tumor incidence | 0.519284092 | 1.121209465 |
| ENSG00000172315 | TP53RK subnetwork | 0.962615892 | 1.121250909 |
| ENSG00000163110 | PDLIM5 subnetwork | 0.519221695 | 1.121256392 |
| ENSG00000170632 | ARMC10 subnetwork | 0.519477994 | 1.121283586 |
| ENSG00000215756 | ENSG00000215756 subnetwork | 0.962592003 | 1.121317235 |
| GO:0043434 | response to peptide hormone stimulus | 0.519455631 | 1.121403534 |
| ENSG00000118137 | APOA1 subnetwork | 0.962592003 | 1.121407802 |
| MP:0004158 | right aortic arch | 0.96255941 | 1.121457997 |
| ENSG00000117399 | CDC20 subnetwork | 0.962554878 | 1.12154859 |
| MP:0000159 | abnormal xiphoid process morphology | 0.962477983 | 1.121620748 |
| GO:0007501 | mesodermal cell fate specification | 0.962552242 | 1.12163112 |
| MP:0001566 | hyperphosphatemia | 0.962455576 | 1.121675016 |
| ENSG00000161888 | SPC24 subnetwork | 0.962408735 | 1.121733333 |
| GO:0031122 | cytoplasmic microtubule organization | 0.962383691 | 1.121799741 |
| GO:0014031 | mesenchymal cell development | 0.962350259 | 1.121858078 |
| MP:0009886 | failure of palatal shelf elevation | 0.962314094 | 1.121912383 |
| ENSG00000169727 | GPS1 subnetwork | 0.520183107 | 1.121946593 |
| GO:0031047 | gene silencing by RNA | 0.520274776 | 1.121950686 |
| GO:0001669 | acrosomal vesicle | 0.962271708 | 1.121958613 |
| REACTOME_ION_CHANNEL_TRAN | REACTOME_ION_CHANNEL_TRANSPORT | 0.962242206 | 1.122008892 |
| ENSG00000145041 | VPRBP subnetwork | 0.520151004 | 1.122037361 |
| REACTOME_GAP_JUNCTION_DEG | REACTOME_GAP_JUNCTION_DEGRADATION | 0.96224107 | 1.122095561 |
| ENSG00000172137 | CALB2 subnetwork | 0.962193832 | 1.122125647 |
| MP:0011097 | complete embryonic lethality before turning of embryo | 0.962189842 | 1.122212339 |
| MP:0004615 | cervical vertebral transformation | 0.520632936 | 1.122240047 |
| ENSG00000118491 | C6orf94 subnetwork | 0.962132865 | 1.122246482 |
| ENSG00000112715 | VEGFA subnetwork | 0.520554187 | 1.122294341 |
| MP:0005542 | corneal vascularization | 0.52049847 | 1.122297593 |
| ENSG00000163785 | RYK subnetwork | 0.962118877 | 1.122325111 |
| GO:0051882 | mitochondrial depolarization | 0.961710752 | 1.122358414 |
| ENSG00000173372 | C1QA subnetwork | 0.961669663 | 1.122380451 |
| GO:0008250 | oligosaccharyltransferase complex | 0.962097965 | 1.122395665 |
| ENSG00000112379 | KIAA1244 subnetwork | 0.961812414 | 1.1224011 |
| GO:0060251 | regulation of glial cell proliferation | 0.961636521 | 1.12243486 |
| MP:0003723 | abnormal long bone morphology | 0.961948101 | 1.122443779 |

| | | | |
|---|---|---|---|
| MP:0009450 | abnormal axon fasiculation | 0.962076673 | 1.12246623 |
| ENSG00000161533 | ACOX1 subnetwork | 0.961315628 | 1.122466408 |
| GO:0009071 | serine family amino acid catabolic process | 0.961273947 | 1.122492512 |
| MP:0000876 | Purkinje cell degeneration | 0.961622721 | 1.122513555 |
| REACTOME_MITOTIC_G2:G2M_P | REACTOME_MITOTIC_G2:G2M_PHASES | 0.961229148 | 1.122522668 |
| MP:0003052 | omphalocele | 0.961151994 | 1.122524492 |
| ENSG00000149636 | DSN1 subnetwork | 0.961105837 | 1.122538462 |
| MP:0000933 | abnormal rhombomere morphology | 0.96158949 | 1.122580123 |
| ENSG00000167842 | MIS12 subnetwork | 0.961105837 | 1.122629363 |
| GO:0048644 | muscle organ morphogenesis | 0.961585671 | 1.122666936 |
| GO:0021782 | glial cell development | 0.961092109 | 1.122700032 |
| GO:0060416 | response to growth hormone stimulus | 0.520895493 | 1.122739866 |
| GO:0001502 | cartilage condensation | 0.961068945 | 1.122770714 |
| GO:0060219 | camera-type eye photoreceptor cell differentiation | 0.961048539 | 1.122837356 |
| GO:0019213 | deacetylase activity | 0.960848655 | 1.122911772 |
| ENSG00000139112 | GABARAPL1 subnetwork | 0.961043668 | 1.122928311 |
| REACTOME_SPRY_REGULATION_( | REACTOME_SPRY_REGULATION_OF_FGF_SIGNALING | 0.521078494 | 1.122940662 |
| ENSG00000138092 | CENPO subnetwork | 0.960714057 | 1.122972206 |
| GO:0034446 | substrate adhesion-dependent cell spreading | 0.960841252 | 1.122994652 |
| MP:0003604 | single kidney | 0.961014856 | 1.122994977 |
| GO:0043395 | heparan sulfate proteoglycan binding | 0.960686876 | 1.123038898 |
| ENSG00000116852 | KIF21B subnetwork | 0.960674624 | 1.123113705 |
| GO:0030016 | myofibril | 0.960667868 | 1.123200681 |
| ENSG00000170144 | HNRNPA3 subnetwork | 0.521411544 | 1.123229379 |
| GO:0009062 | fatty acid catabolic process | 0.960614703 | 1.12324309 |
| KEGG_BASAL_CELL_CARCINOMA | KEGG_BASAL_CELL_CARCINOMA | 0.960580386 | 1.123305772 |
| MP:0003203 | increased neuron apoptosis | 0.521633482 | 1.123339161 |
| GO:0001953 | negative regulation of cell-matrix adhesion | 0.521954109 | 1.123340128 |
| REACTOME_G2M_TRANSITION | REACTOME_G2M_TRANSITION | 0.96053368 | 1.123344143 |
| ENSG00000160224 | AIRE subnetwork | 0.521400835 | 1.123349366 |
| GO:0044327 | dendritic spine head | 0.960455856 | 1.123350089 |
| MP:0004110 | transposition of great arteries | 0.521347212 | 1.123367347 |
| GO:0014069 | postsynaptic density | 0.960455856 | 1.123441174 |
| GO:0043547 | positive regulation of GTPase activity | 0.521602063 | 1.123451843 |
| ENSG00000131459 | GFPT2 subnetwork | 0.522111704 | 1.123467754 |
| GO:0071359 | cellular response to dsRNA | 0.521851812 | 1.123492572 |
| ENSG00000215320 | ENSG00000215320 subnetwork | 0.521949377 | 1.123496432 |
| ENSG00000165023 | DIRAS2 subnetwork | 0.960440349 | 1.123512001 |
| GO:0051592 | response to calcium ion | 0.522309467 | 1.123555523 |
| ENSG00000100288 | CHKB subnetwork | 0.522231903 | 1.12356623 |
| GO:0045132 | meiotic chromosome segregation | 0.960425971 | 1.123603114 |
| GO:0010579 | positive regulation of adenylate cyclase activity involved | 0.960396742 | 1.12363747 |
| GO:0010564 | regulation of cell cycle process | 0.521843974 | 1.123648944 |
| GO:0007189 | adenylate cyclase-activating G-protein coupled receptor | 0.960396742 | 1.123728607 |
| MP:0001524 | impaired limb coordination | 0.523107027 | 1.12380814 |
| GO:0010578 | regulation of adenylate cyclase activity involved in G-pro | 0.960396742 | 1.12381976 |
| MP:0003141 | cardiac fibrosis | 0.522982627 | 1.123822332 |
| GO:0005154 | epidermal growth factor receptor binding | 0.523058208 | 1.123877017 |
| GO:0005882 | intermediate filament | 0.960369986 | 1.123890647 |
| ENSG00000163605 | PPP4R2 subnetwork | 0.522928381 | 1.123891232 |
| ENSG00000085832 | EPS15 subnetwork | 0.52263711 | 1.123905136 |
| ENSG00000111707 | SUDS3 subnetwork | 0.522721497 | 1.123938027 |
| MP:0000880 | decreased Purkinje cell number | 0.524297133 | 1.123952139 |
| ENSG00000173599 | PC subnetwork | 0.522842678 | 1.123963636 |

| | | | |
|---|---|---|---|
| GO:0016829 | lyase activity | 0.960357891 | 1.123973714 |
| ENSG00000103415 | HMOX2 subnetwork | 0.522899759 | 1.123981966 |
| ENSG00000215902 | ENSG00000215902 subnetwork | 0.522609833 | 1.123995925 |
| GO:0072273 | metanephric nephron morphogenesis | 0.96031297 | 1.124 |
| ENSG00000130414 | NDUFA10 subnetwork | 0.523424658 | 1.124022955 |
| GO:0001701 | in utero embryonic development | 0.523355941 | 1.124026446 |
| GO:0030176 | integral to endoplasmic reticulum membrane | 0.524266115 | 1.124049898 |
| GO:0006706 | steroid catabolic process | 0.960301443 | 1.124070919 |
| ENSG00000123240 | OPTN subnetwork | 0.5237915 | 1.124074343 |
| GO:0034383 | low-density lipoprotein particle clearance | 0.523333189 | 1.124117134 |
| GO:0042375 | quinone cofactor metabolic process | 0.960260238 | 1.124117504 |
| ENSG00000105289 | TJP3 subnetwork | 0.524473654 | 1.124137181 |
| ENSG00000120708 | TGFBI subnetwork | 0.523743102 | 1.124164972 |
| ENSG00000120334 | CENPL subnetwork | 0.960241429 | 1.12417627 |
| ENSG00000161040 | FBXL13 subnetwork | 0.524153779 | 1.124180209 |
| GO:0014910 | regulation of smooth muscle cell migration | 0.524248982 | 1.124198462 |
| ENSG00000010256 | UQCRC1 subnetwork | 0.960189995 | 1.124214755 |
| ENSG00000108468 | CBX1 subnetwork | 0.52411678 | 1.124263532 |
| GO:0009126 | purine nucleoside monophosphate metabolic process | 0.523703644 | 1.124277415 |
| ENSG00000168702 | LRP1B subnetwork | 0.96002097 | 1.124281539 |
| ENSG00000197429 | IPP subnetwork | 0.959948708 | 1.124283511 |
| ENSG00000181061 | HIGD1A subnetwork | 0.960162081 | 1.124289773 |
| GO:0030516 | regulation of axon extension | 0.960096684 | 1.124291744 |
| MP:0001196 | shiny skin | 0.523955184 | 1.124303136 |
| ENSG00000162946 | DISC1 subnetwork | 0.524623971 | 1.12431492 |
| GO:0002920 | regulation of humoral immune response | 0.524702214 | 1.124347637 |
| ENSG00000173805 | HAP1 subnetwork | 0.959920446 | 1.124354498 |
| GO:0005372 | water transmembrane transporter activity | 0.524098549 | 1.124397678 |
| GO:0009167 | purine ribonucleoside monophosphate metabolic proces | 0.523703644 | 1.124440732 |
| REACTOME_MRNA_3:END_PROCI | REACTOME_MRNA_3:END_PROCESSING | 0.959917245 | 1.124445798 |
| MP:0010378 | increased respiratory quotient | 0.524071858 | 1.124502831 |
| REACTOME_POST:ELONGATION_I | REACTOME_POST:ELONGATION_PROCESSING_OF_INTR( | 0.959917245 | 1.124537112 |
| REACTOME_ADP_SIGNALLING_TH | REACTOME_ADP_SIGNALLING_THROUGH_P2Y_PURINO( | 0.959914469 | 1.124624381 |
| ENSG00000064961 | HMG20B subnetwork | 0.959844141 | 1.124642625 |
| GO:0006957 | complement activation, alternative pathway | 0.959839475 | 1.124721794 |
| MP:0009745 | abnormal behavioral response to xenobiotic | 0.525105917 | 1.124775362 |
| MP:0000277 | abnormal heart shape | 0.959812144 | 1.12478879 |
| ENSG00000147082 | CCNB3 subnetwork | 0.525028633 | 1.12484418 |
| GO:0060004 | reflex | 0.959809025 | 1.124876107 |
| GO:0051187 | cofactor catabolic process | 0.959773556 | 1.124939064 |
| ENSG00000198301 | SDAD1 subnetwork | 0.525356181 | 1.12494929 |
| GO:0046530 | photoreceptor cell differentiation | 0.959700204 | 1.124987811 |
| ENSG00000162552 | WNT4 subnetwork | 0.959753883 | 1.124989843 |
| ENSG00000105695 | MAG subnetwork | 0.959683718 | 1.125050792 |
| ENSG00000126583 | PRKCG subnetwork | 0.525352224 | 1.125097812 |
| MP:0000556 | abnormal hindlimb morphology | 0.959667158 | 1.125125975 |
| REACTOME_COOPERATION_OF_P | REACTOME_COOPERATION_OF_PREFOLDIN_AND_TRICC | 0.526063992 | 1.125130246 |
| GO:0050772 | positive regulation of axonogenesis | 0.959636813 | 1.125193042 |
| ENSG00000073921 | PICALM subnetwork | 0.525962604 | 1.125246091 |
| GO:0060601 | lateral sprouting from an epithelium | 0.959625708 | 1.12526012 |
| ENSG00000055163 | CYFIP2 subnetwork | 0.525696961 | 1.125282445 |
| REACTOME_PREFOLDIN_MEDIATI | REACTOME_PREFOLDIN_MEDIATED_TRANSFER_OF_SUB | 0.526063992 | 1.125293096 |
| ENSG00000158828 | PINK1 subnetwork | 0.525627564 | 1.125329567 |
| REACTOME_FORMATION_OF_THI | REACTOME_FORMATION_OF_THE_EARLY_ELONGATION | 0.95960482 | 1.125335339 |

| | | | |
|---|---|---|---|
| GO:0016235 | aggresome | 0.525926125 | 1.125351093 |
| ENSG00000167930 | ITFG3 subnetwork | 0.525825833 | 1.1253874 |
| REACTOME_FORMATION_OF_THI | REACTOME_FORMATION_OF_THE_HIV:1_EARLY_ELONG | 0.95960482 | 1.125426829 |
| GO:0010885 | regulation of cholesterol storage | 0.525910866 | 1.125477845 |
| GO:0046969 | NAD-dependent histone deacetylase activity (H3-K9 spec | 0.959574087 | 1.125493943 |
| GO:0032129 | histone deacetylase activity (H3-K9 specific) | 0.959574087 | 1.125585461 |
| ENSG00000101132 | PFDN4 subnetwork | 0.526294106 | 1.12558964 |
| ENSG00000152253 | SPC25 subnetwork | 0.95943009 | 1.125597755 |
| ENSG00000134690 | CDCA8 subnetwork | 0.959519398 | 1.1256404 |
| ENSG00000140463 | BBS4 subnetwork | 0.959388469 | 1.125644571 |
| GO:0010464 | regulation of mesenchymal cell proliferation | 0.526430045 | 1.125665509 |
| GO:0008105 | asymmetric protein localization | 0.959282914 | 1.125681282 |
| ENSG00000115947 | ORC4 subnetwork | 0.959352561 | 1.125691394 |
| ENSG00000171873 | ADRA1D subnetwork | 0.959231052 | 1.125732184 |
| MP:0002944 | increased lactate dehydrogenase level | 0.959178914 | 1.125774957 |
| MP:0000749 | muscle degeneration | 0.959095924 | 1.125809601 |
| ENSG00000138433 | CIR1 subnetwork | 0.959056256 | 1.125860526 |
| GO:0046463 | acylglycerol biosynthetic process | 0.526666322 | 1.125875036 |
| MP:0004736 | abnormal distortion product otoacoustic emission | 0.959039497 | 1.125948079 |
| REACTOME_POST:CHAPERONIN_T | REACTOME_POST:CHAPERONIN_TUBULIN_FOLDING_PA | 0.95902549 | 1.126027509 |
| GO:0046460 | neutral lipid biosynthetic process | 0.526666322 | 1.1260379 |
| MP:0003205 | testicular atrophy | 0.958964323 | 1.126066254 |
| GO:0003071 | renal system process involved in regulation of systemic a | 0.958956464 | 1.126145706 |
| ENSG00000136982 | DSCC1 subnetwork | 0.95895103 | 1.126233312 |
| GO:0005184 | neuropeptide hormone activity | 0.95883556 | 1.12626608 |
| GO:0021695 | cerebellar cortex development | 0.958949587 | 1.126325002 |
| ENSG00000011243 | AKAP8L subnetwork | 0.527010753 | 1.126355748 |
| MP:0001526 | abnormal placing response | 0.958833069 | 1.126357788 |
| GO:0005112 | Notch binding | 0.958820739 | 1.126429153 |
| ENSG00000137812 | CASC5 subnetwork | 0.958819346 | 1.126508673 |
| MP:0009814 | increased prostaglandin level | 0.52733923 | 1.1265756 |
| ENSG00000175279 | APITD1 subnetwork | 0.958796878 | 1.126588207 |
| REACTOME_KINESINS | REACTOME_KINESINS | 0.527387666 | 1.126615118 |
| ENSG00000182973 | CNOT10 subnetwork | 0.527543245 | 1.1266291 |
| ENSG00000126217 | MCF2L subnetwork | 0.958788792 | 1.126671825 |
| GO:0043073 | germ cell nucleus | 0.527313293 | 1.126709556 |
| REACTOME_COMPLEMENT_CASC | REACTOME_COMPLEMENT_CASCADE | 0.527234681 | 1.126713418 |
| GO:0033178 | proton-transporting two-sector ATPase complex, catalyti | 0.958687924 | 1.126729124 |
| GO:0090192 | regulation of glomerulus development | 0.958760645 | 1.12673102 |
| GO:0030897 | HOPS complex | 0.958671827 | 1.126784259 |
| MP:0004042 | decreased susceptibility to kidney reperfusion injury | 0.527539249 | 1.126791908 |
| ENSG00000117592 | PRDX6 subnetwork | 0.958548549 | 1.126870111 |
| ENSG00000149084 | HSD17B12 subnetwork | 0.958667897 | 1.126871995 |
| ENSG00000155097 | ATP6V1C1 subnetwork | 0.958480822 | 1.126884524 |
| ENSG00000204133 | ENSG00000204133 subnetwork | 0.958427289 | 1.12691524 |
| GO:0030247 | polysaccharide binding | 0.958413298 | 1.12699894 |
| GO:0001871 | pattern binding | 0.958413298 | 1.127090805 |
| MP:0001046 | abnormal enteric neuron morphology | 0.958222905 | 1.127170811 |
| GO:0006385 | transcription elongation from RNA polymerase III promo | 0.958411452 | 1.127178609 |
| ENSG00000122786 | CALD1 subnetwork | 0.958194563 | 1.127234181 |
| GO:0006386 | termination of RNA polymerase III transcription | 0.958411452 | 1.127270504 |
| ENSG00000014138 | POLA2 subnetwork | 0.958177894 | 1.127301639 |
| GO:0030057 | desmosome | 0.958157701 | 1.127377263 |
| MP:0000269 | abnormal heart looping | 0.958066755 | 1.127387652 |

| | | | |
|---|---|---|---|
| ENSG00000138758 | SEPT11 subnetwork | 0.958062773 | 1.127471452 |
| GO:0050482 | arachidonic acid secretion | 0.958048911 | 1.127538951 |
| MP:0008261 | arrest of male meiosis | 0.528984003 | 1.127574272 |
| GO:0005583 | fibrillar collagen | 0.958045488 | 1.127630935 |
| GO:0046164 | alcohol catabolic process | 0.958040165 | 1.127722934 |
| ENSG00000149100 | EIF3M subnetwork | 0.528975004 | 1.12773691 |
| ENSG00000169592 | INO80E subnetwork | 0.528114099 | 1.127744871 |
| GO:0042417 | dopamine metabolic process | 0.957933936 | 1.127760098 |
| ENSG00000088926 | F11 subnetwork | 0.528262523 | 1.127787406 |
| GO:0003729 | mRNA binding | 0.529137205 | 1.1277938 |
| ENSG00000060339 | CCAR1 subnetwork | 0.528216937 | 1.127798642 |
| ENSG00000108828 | VAT1 subnetwork | 0.958038347 | 1.127810868 |
| ENSG00000133812 | SBF2 subnetwork | 0.957925262 | 1.127839889 |
| GO:0032869 | cellular response to insulin stimulus | 0.528969838 | 1.127877957 |
| GO:0051287 | NAD binding | 0.957881854 | 1.127903371 |
| MP:0008762 | embryonic lethality | 0.957829954 | 1.127938296 |
| GO:0007062 | sister chromatid cohesion | 0.529339595 | 1.127955594 |
| ENSG00000135999 | EPC2 subnetwork | 0.528922675 | 1.127975761 |
| GO:0016505 | apoptotic protease activator activity | 0.528441322 | 1.12799278 |
| MP:0000562 | polydactyly | 0.957827583 | 1.128030365 |
| GO:0070243 | regulation of thymocyte apoptotic process | 0.528876308 | 1.128051948 |
| ENSG00000092847 | EIF2C1 subnetwork | 0.528599851 | 1.128056879 |
| ENSG00000213066 | FGFR1OP subnetwork | 0.52856845 | 1.128097026 |
| ENSG00000102580 | DNAJC3 subnetwork | 0.957826555 | 1.128122449 |
| REACTOME_DESTABILIZATION_OF | REACTOME_DESTABILIZATION_OF_MRNA_BY_TRISTETR | 0.528860761 | 1.128171453 |
| ENSG00000179889 | PDXDC1 subnetwork | 0.528746582 | 1.12817552 |
| GO:0034109 | homotypic cell-cell adhesion | 0.957823284 | 1.128210466 |
| ENSG00000144283 | PKP4 subnetwork | 0.957528875 | 1.128275074 |
| ENSG00000065665 | SEC61A2 subnetwork | 0.957813072 | 1.128286251 |
| MP:0010386 | abnormal urinary bladder physiology | 0.957752206 | 1.128300808 |
| MP:0005309 | increased circulating ammonia level | 0.529547077 | 1.12831195 |
| MP:0000786 | abnormal embryonic neuroepithelial layer differentiation | 0.957693171 | 1.128315368 |
| MP:0006069 | abnormal retinal neuronal layer morphology | 0.957626903 | 1.128317681 |
| ENSG00000143870 | PDIA6 subnetwork | 0.957452349 | 1.128326391 |
| GO:0030252 | growth hormone secretion | 0.957450958 | 1.128418559 |
| ENSG00000162374 | ELAVL4 subnetwork | 0.957418768 | 1.12848215 |
| GO:0032421 | stereocilium bundle | 0.95741469 | 1.128574346 |
| GO:0001990 | regulation of systemic arterial blood pressure by hormor | 0.957330405 | 1.128580766 |
| ENSG00000198951 | NAGA subnetwork | 0.957323514 | 1.128664815 |
| ENSG00000165868 | HSPA12A subnetwork | 0.95731027 | 1.128740704 |
| ENSG00000145391 | SETD7 subnetwork | 0.957308724 | 1.128824779 |
| GO:0061383 | trabecula morphogenesis | 0.957245263 | 1.128835309 |
| ENSG00000171362 | ENSG00000171362 subnetwork | 0.957242312 | 1.128923492 |
| ENSG00000166451 | CENPN subnetwork | 0.957209866 | 1.128987166 |
| ENSG00000100253 | MIOX subnetwork | 0.529939931 | 1.129064572 |
| ENSG00000066654 | THUMPD1 subnetwork | 0.957203358 | 1.129075376 |
| GO:0007413 | axonal fasciculation | 0.957167305 | 1.129110457 |
| GO:0015749 | monosaccharide transport | 0.957158887 | 1.129190515 |
| GO:0016197 | endosomal transport | 0.957139339 | 1.12925832 |
| ENSG00000142892 | PIGK subnetwork | 0.956987312 | 1.129259017 |
| ENSG00000117697 | NSL1 subnetwork | 0.956939286 | 1.129302307 |
| MP:0001431 | abnormal eating behavior | 0.957116624 | 1.129330226 |
| MP:0001297 | microphthalmia | 0.95693417 | 1.129386503 |
| GO:0000819 | sister chromatid segregation | 0.956928392 | 1.129478894 |

| | | | |
|---|---|---|---|
| GO:0044264 | cellular polysaccharide metabolic process | 0.956896054 | 1.12950585 |
| ENSG00000023318 | ERP44 subnetwork | 0.956856829 | 1.12957372 |
| GO:0043516 | regulation of DNA damage response, signal transduction | 0.956805891 | 1.129604779 |
| GO:0021761 | limbic system development | 0.956768493 | 1.129639935 |
| GO:0010591 | regulation of lamellipodium assembly | 0.956618103 | 1.129652971 |
| ENSG00000186871 | ERCC6L subnetwork | 0.956700796 | 1.129658728 |
| GO:0019363 | pyridine nucleotide biosynthetic process | 0.956459413 | 1.129686477 |
| GO:0002021 | response to dietary excess | 0.956614854 | 1.129737251 |
| GO:0072525 | pyridine-containing compound biosynthetic process | 0.956459413 | 1.12977896 |
| ENSG00000129810 | SGOL1 subnetwork | 0.956304793 | 1.129804307 |
| GO:0019320 | hexose catabolic process | 0.956211557 | 1.129810842 |
| ENSG00000102225 | CDK16 subnetwork | 0.956186274 | 1.12985423 |
| MP:0005564 | increased hemoglobin content | 0.956431971 | 1.129859178 |
| ENSG00000169252 | ADRB2 subnetwork | 0.956155436 | 1.1299181 |
| GO:0055067 | monovalent inorganic cation homeostasis | 0.956124471 | 1.129957408 |
| MP:0003731 | abnormal retinal outer nuclear layer morphology | 0.955860069 | 1.129959033 |
| ENSG00000111674 | ENO2 subnetwork | 0.530507957 | 1.130007205 |
| GO:0050684 | regulation of mRNA processing | 0.956104891 | 1.130021298 |
| GO:0048742 | regulation of skeletal muscle fiber development | 0.530443592 | 1.130033146 |
| ENSG00000163191 | S100A11 subnetwork | 0.955848802 | 1.130035234 |
| GO:0006575 | cellular modified amino acid metabolic process | 0.955792171 | 1.130066377 |
| GO:0071174 | mitotic cell cycle spindle checkpoint | 0.956099926 | 1.130109773 |
| GO:0005326 | neurotransmitter transporter activity | 0.95604061 | 1.130124529 |
| MP:0003058 | increased insulin secretion | 0.955785082 | 1.130154893 |
| ENSG00000163681 | SLMAP subnetwork | 0.530915802 | 1.130177131 |
| MP:0010412 | atrioventricular septal defect | 0.955656257 | 1.130213115 |
| ENSG00000117385 | LEPRE1 subnetwork | 0.530781671 | 1.130236243 |
| MP:0010956 | abnormal mitochondrial ATP synthesis coupled electron | 0.955784461 | 1.130243423 |
| ENSG00000105325 | FZR1 subnetwork | 0.530719093 | 1.130247803 |
| MP:0001475 | reduced long term depression | 0.955632364 | 1.130272973 |
| GO:0004708 | MAP kinase kinase activity | 0.530910876 | 1.130325508 |
| GO:0006892 | post-Golgi vesicle-mediated transport | 0.955607759 | 1.13033694 |
| ENSG00000163904 | SENP2 subnetwork | 0.531096422 | 1.130338373 |
| ENSG00000154839 | SKA1 subnetwork | 0.955592997 | 1.130409117 |
| MP:0003878 | abnormal ear physiology | 0.955549527 | 1.130460807 |
| GO:0007398 | ectoderm development | 0.95532976 | 1.130464201 |
| MP:0000480 | increased rib number | 0.954905059 | 1.130475096 |
| ENSG00000198399 | ITSN2 subnetwork | 0.954989728 | 1.130505415 |
| ENSG00000172602 | RND1 subnetwork | 0.531231235 | 1.130521163 |
| REACTOME_BOTULINUM_NEURO | REACTOME_BOTULINUM_NEUROTOXICITY | 0.955534364 | 1.130528905 |
| ENSG00000129170 | CSRP3 subnetwork | 0.955309553 | 1.130540518 |
| GO:0015116 | sulfate transmembrane transporter activity | 0.954896329 | 1.130551452 |
| ENSG00000075239 | ACAT1 subnetwork | 0.954833993 | 1.130562167 |
| ENSG00000178585 | CTNNBIP1 subnetwork | 0.95524631 | 1.130575835 |
| ENSG00000117758 | STX12 subnetwork | 0.955527744 | 1.130621617 |
| ENSG00000117118 | SDHB subnetwork | 0.954811367 | 1.130626231 |
| ENSG00000064490 | RFXANK subnetwork | 0.955217134 | 1.130631665 |
| MP:0004096 | abnormal midbrain-hindbrain boundary development | 0.955167939 | 1.130642382 |
| GO:0046883 | regulation of hormone secretion | 0.954751824 | 1.130669786 |
| MP:0002650 | abnormal ameloblast morphology | 0.954691178 | 1.130684617 |
| ENSG00000156873 | PHKG2 subnetwork | 0.954641083 | 1.130732288 |
| GO:0033865 | nucleoside bisphosphate metabolic process | 0.954589177 | 1.130763547 |
| ENSG00000012211 | PRICKLE3 subnetwork | 0.954551749 | 1.130811232 |
| ENSG00000173406 | DAB1 subnetwork | 0.95452274 | 1.130858926 |

| | | | |
|---|---|---|---|
| ENSG00000126067 | PSMB2 subnetwork | 0.954447394 | 1.130881991 |
| ENSG00000139433 | GLTP subnetwork | 0.954446407 | 1.130974869 |
| ENSG00000072952 | MRVI1 subnetwork | 0.531989383 | 1.130986624 |
| MP:0008025 | brain vacuoles | 0.954402028 | 1.130997947 |
| GO:0043010 | camera-type eye development | 0.95438757 | 1.131074421 |
| ENSG00000072110 | ACTN1 subnetwork | 0.531977008 | 1.131120541 |
| ENSG00000129991 | TNNI3 subnetwork | 0.954376886 | 1.13116323 |
| GO:0046365 | monosaccharide catabolic process | 0.954371756 | 1.131252054 |
| ENSG00000196923 | PDLIM7 subnetwork | 0.531942307 | 1.131254496 |
| REACTOME_DESTABILIZATION_OI | REACTOME_DESTABILIZATION_OF_MRNA_BY_BUTYRAT | 0.531699501 | 1.131296776 |
| GO:0046068 | cGMP metabolic process | 0.954348926 | 1.131320352 |
| GO:0016849 | phosphorus-oxygen lyase activity | 0.954280472 | 1.131322925 |
| ENSG00000113889 | KNG1 subnetwork | 0.531645288 | 1.131337268 |
| ENSG00000139352 | ASCL1 subnetwork | 0.532534415 | 1.131345214 |
| REACTOME_REGULATION_OF_IN | REACTOME_REGULATION_OF_INSULIN_SECRETION | 0.954217151 | 1.131350152 |
| ENSG00000136243 | NUPL2 subnetwork | 0.531897445 | 1.131359712 |
| MP:0004543 | abnormal sperm physiology | 0.531814752 | 1.131378616 |
| GO:0060487 | lung epithelial cell differentiation | 0.53262996 | 1.13138382 |
| GO:0032587 | ruffle membrane | 0.532694858 | 1.131400862 |
| GO:0022624 | proteasome accessory complex | 0.954184954 | 1.131402038 |
| ENSG00000155657 | TTN subnetwork | 0.532488277 | 1.13142159 |
| ENSG00000162105 | SHANK2 subnetwork | 0.954136475 | 1.131425166 |
| ENSG00000111786 | SRSF9 subnetwork | 0.53235763 | 1.131466571 |
| MP:0010736 | abnormal extraembryonic ectoderm morphology | 0.954100798 | 1.131493506 |
| GO:0016881 | acid-amino acid ligase activity | 0.532319928 | 1.131542997 |
| GO:0048246 | macrophage chemotaxis | 0.532476769 | 1.131548304 |
| GO:0030901 | midbrain development | 0.954089489 | 1.131561858 |
| REACTOME_G_ALPHA_Z_SIGNALI | REACTOME_G_ALPHA_Z_SIGNALLING_EVENTS | 0.954079473 | 1.13162611 |
| MP:0001312 | abnormal cornea morphology | 0.954052532 | 1.131686262 |
| GO:0043269 | regulation of ion transport | 0.954007885 | 1.131721756 |
| GO:0048002 | antigen processing and presentation of peptide antigen | 0.953977547 | 1.131761368 |
| ENSG00000140829 | DHX38 subnetwork | 0.53352304 | 1.13184558 |
| ENSG00000031691 | CENPQ subnetwork | 0.953966638 | 1.131850329 |
| ENSG00000009790 | TRAF3IP3 subnetwork | 0.533218234 | 1.13189977 |
| KEGG_LINOLEIC_ACID_METABOLI | KEGG_LINOLEIC_ACID_METABOLISM | 0.533689282 | 1.131915352 |
| MP:0000588 | thick tail | 0.953950948 | 1.131939304 |
| GO:0006281 | DNA repair | 0.533005493 | 1.13194225 |
| ENSG00000074319 | TSG101 subnetwork | 0.53347515 | 1.131943448 |
| MP:0009232 | abnormal sperm nucleus morphology | 0.533125408 | 1.131995116 |
| GO:0045616 | regulation of keratinocyte differentiation | 0.533649545 | 1.132006027 |
| MP:0000042 | abnormal organ of Corti morphology | 0.953928524 | 1.132011844 |
| ENSG00000130175 | PRKCSH subnetwork | 0.533194547 | 1.132019245 |
| ENSG00000142731 | PLK4 subnetwork | 0.533374585 | 1.132045944 |
| ENSG00000185247 | MAGEA11 subnetwork | 0.533472358 | 1.132091588 |
| GO:0007492 | endoderm development | 0.953926954 | 1.13210496 |
| ENSG00000183091 | NEB subnetwork | 0.953890381 | 1.132136394 |
| ENSG00000102189 | EEA1 subnetwork | 0.533874488 | 1.132168986 |
| MP:0008456 | abnormal retinal rod cell outer segment morphology | 0.953872219 | 1.132213081 |
| GO:0048488 | synaptic vesicle endocytosis | 0.953869821 | 1.132298009 |
| GO:0042402 | cellular biogenic amine catabolic process | 0.953869203 | 1.132391179 |
| GO:0021602 | cranial nerve morphogenesis | 0.953868766 | 1.132484365 |
| GO:0030048 | actin filament-based movement | 0.953853359 | 1.132552876 |
| GO:0008353 | RNA polymerase II carboxy-terminal domain kinase activ | 0.953796067 | 1.132567901 |
| GO:0008320 | protein transmembrane transporter activity | 0.953772965 | 1.132640547 |

| | | | |
|---|---|---|---|
| GO:0022884 | macromolecule transmembrane transporter activity | 0.953772965 | 1.132733783 |
| GO:0007422 | peripheral nervous system development | 0.953314114 | 1.132793839 |
| ENSG00000173482 | PTPRM subnetwork | 0.953753623 | 1.132802338 |
| MP:0001293 | anophthalmia | 0.953555357 | 1.132855731 |
| ENSG00000114812 | VIPR1 subnetwork | 0.95330006 | 1.132878913 |
| ENSG00000123360 | PDE1B subnetwork | 0.953739238 | 1.132879137 |
| GO:0015924 | mannosyl-oligosaccharide mannosidase activity | 0.953236229 | 1.132881621 |
| GO:0016903 | oxidoreductase activity, acting on the aldehyde or oxo gr | 0.9535026 | 1.132907848 |
| GO:0009068 | aspartate family amino acid catabolic process | 0.953708562 | 1.132935364 |
| GO:0019748 | secondary metabolic process | 0.953477296 | 1.132959974 |
| ENSG00000173581 | CCDC106 subnetwork | 0.953227673 | 1.132966716 |
| ENSG00000155366 | RHOC subnetwork | 0.535053071 | 1.132991979 |
| ENSG00000179841 | AKAP5 subnetwork | 0.534896446 | 1.132994269 |
| MP:0004970 | kidney atrophy | 0.535122884 | 1.133030216 |
| GO:0071173 | spindle assembly checkpoint | 0.953202824 | 1.133031227 |
| GO:0006895 | Golgi to endosome transport | 0.953137321 | 1.133046309 |
| ENSG00000002834 | LASP1 subnetwork | 0.534867749 | 1.133084969 |
| MP:0002258 | abnormal cricoid cartilage morphology | 0.953086532 | 1.133090235 |
| ENSG00000165731 | RET subnetwork | 0.535796081 | 1.133092548 |
| ENSG00000181085 | MAPK15 subnetwork | 0.535046753 | 1.133139951 |
| GO:0042645 | mitochondrial nucleoid | 0.535266826 | 1.133154353 |
| ENSG00000147130 | ZMYM3 subnetwork | 0.953057616 | 1.133158892 |
| ENSG00000143801 | PSEN2 subnetwork | 0.535762037 | 1.133168813 |
| MP:0003896 | prolonged PR interval | 0.953016997 | 1.133198714 |
| KEGG_GLYOXYLATE_AND_DICARE | KEGG_GLYOXYLATE_AND_DICARBOXYLATE_METABOLISI | 0.535462705 | 1.133230747 |
| ENSG00000182473 | EXOC7 subnetwork | 0.534865061 | 1.133247349 |
| GO:0051146 | striated muscle cell differentiation | 0.536063468 | 1.133249929 |
| REACTOME_CREATION_OF_C4_A | REACTOME_CREATION_OF_C4_AND_C2_ACTIVATORS | 0.53572427 | 1.133259408 |
| ENSG00000170624 | SGCD subnetwork | 0.9529979 | 1.133279756 |
| GO:0042572 | retinol metabolic process | 0.535423531 | 1.133299928 |
| ENSG00000050405 | LIMA1 subnetwork | 0.952959677 | 1.133323716 |
| ENSG00000122692 | SMU1 subnetwork | 0.535679693 | 1.133335718 |
| ENSG00000130560 | UBAC1 subnetwork | 0.952923146 | 1.133375927 |
| ENSG00000126461 | SCAF1 subnetwork | 0.53561305 | 1.133390583 |
| ENSG00000173545 | ZNF622 subnetwork | 0.53485477 | 1.133402609 |
| GO:0031258 | lamellipodium membrane | 0.53606212 | 1.133404833 |
| ENSG00000100241 | SBF1 subnetwork | 0.952899794 | 1.133448759 |
| ENSG00000131238 | PPT1 subnetwork | 0.952831145 | 1.133451517 |
| MP:0002075 | abnormal coat/hair pigmentation | 0.534800689 | 1.133457569 |
| GO:0002448 | mast cell mediated immunity | 0.952797843 | 1.133516121 |
| GO:0014070 | response to organic cyclic compound | 0.536035528 | 1.13353833 |
| MP:0003662 | abnormal long bone epiphyseal plate proliferative zone | 0.534789031 | 1.133591398 |
| GO:0009116 | nucleoside metabolic process | 0.95278734 | 1.133609599 |
| ENSG00000119138 | KLF9 subnetwork | 0.534735027 | 1.133617723 |
| GO:0071813 | lipoprotein particle binding | 0.952722821 | 1.133645361 |
| ENSG00000116016 | EPAS1 subnetwork | 0.53461228 | 1.133670396 |
| ENSG00000133477 | FAM83F subnetwork | 0.536324636 | 1.133724089 |
| ENSG00000159086 | GCFC1 subnetwork | 0.534713437 | 1.133737272 |
| GO:0071814 | protein-lipid complex binding | 0.952722821 | 1.133738865 |
| ENSG00000005882 | PDK2 subnetwork | 0.952675572 | 1.133754021 |
| GO:0008593 | regulation of Notch signaling pathway | 0.952621307 | 1.133756806 |
| MP:0001967 | deafness | 0.952528498 | 1.133780216 |
| ENSG00000141200 | KIF2B subnetwork | 0.952504264 | 1.133853135 |
| ENSG00000151702 | FLI1 subnetwork | 0.536682059 | 1.133873964 |

| | | | |
|---|---|---|---|
| ENSG00000126756 | UXT subnetwork | 0.5365999 | 1.133885951 |
| ENSG00000104722 | NEFM subnetwork | 0.952488983 | 1.13394257 |
| GO:0070207 | protein homotrimerization | 0.536564947 | 1.133983705 |
| ENSG00000063601 | MTMR1 subnetwork | 0.952459667 | 1.134015514 |
| ENSG00000136842 | TMOD1 subnetwork | 0.952430525 | 1.134080218 |
| GO:0032225 | regulation of synaptic transmission, dopaminergic | 0.952385209 | 1.134116045 |
| ENSG00000090539 | CHRD subnetwork | 0.952311634 | 1.134160132 |
| GO:0015399 | primary active transmembrane transporter activity | 0.952304711 | 1.134249629 |
| GO:0048730 | epidermis morphogenesis | 0.952095828 | 1.134266369 |
| GO:0034394 | protein localization at cell surface | 0.95203728 | 1.134327002 |
| GO:0015405 | P-P-bond-hydrolysis-driven transmembrane transporter | 0.952304711 | 1.134343268 |
| GO:0005520 | insulin-like growth factor binding | 0.537000834 | 1.134354908 |
| GO:0003333 | amino acid transmembrane transport | 0.952255585 | 1.134383256 |
| REACTOME_THROMBIN_SIGNALL | REACTOME_THROMBIN_SIGNALLING_THROUGH_PROTE | 0.95203336 | 1.134420679 |
| GO:0060048 | cardiac muscle contraction | 0.952024216 | 1.134501982 |
| ENSG00000099797 | TECR subnetwork | 0.951984456 | 1.134542 |
| ENSG00000183856 | IQGAP3 subnetwork | 0.951952196 | 1.134582025 |
| GO:0060122 | inner ear receptor stereocilium organization | 0.951912644 | 1.13464271 |
| ENSG00000088038 | CNOT3 subnetwork | 0.951912271 | 1.134736451 |
| MP:0006400 | decreased molar number | 0.951908321 | 1.134826076 |
| GO:0001976 | neurological system process involved in regulation of sys | 0.951896279 | 1.134907453 |
| GO:0080025 | phosphatidylinositol-3,5-bisphosphate binding | 0.951889378 | 1.13500124 |
| REACTOME_ANDROGEN_BIOSYN | REACTOME_ANDROGEN_BIOSYNTHESIS | 0.951859332 | 1.135061983 |
| ENSG00000145335 | SNCA subnetwork | 0.537385926 | 1.135078571 |
| ENSG00000095261 | PSMD5 subnetwork | 0.951857587 | 1.135155798 |
| GO:0005976 | polysaccharide metabolic process | 0.951806744 | 1.135204166 |
| ENSG00000198722 | UNC13B subnetwork | 0.951801865 | 1.135298008 |
| ENSG00000134444 | KIAA1468 subnetwork | 0.951745141 | 1.135350529 |
| MP:0000644 | dextrocardia | 0.951695611 | 1.135369988 |
| GO:0072170 | metanephric tubule development | 0.951654282 | 1.135410121 |
| ENSG00000173171 | MTX1 subnetwork | 0.951632643 | 1.135479203 |
| GO:0003337 | mesenchymal to epithelial transition involved in metane | 0.951562724 | 1.135506947 |
| MP:0000841 | abnormal hindbrain morphology | 0.951484126 | 1.135518154 |
| ENSG00000127922 | SHFM1 subnetwork | 0.951323282 | 1.13554471 |
| ENSG00000163235 | TGFA subnetwork | 0.951250886 | 1.135547651 |
| GO:0007320 | insemination | 0.951441947 | 1.135562448 |
| GO:0017085 | response to insecticide | 0.951225525 | 1.135612642 |
| KEGG_N_GLYCAN_BIOSYNTHESIS | KEGG_N_GLYCAN_BIOSYNTHESIS | 0.53786713 | 1.135654099 |
| GO:0006400 | tRNA modification | 0.951193093 | 1.135661095 |
| GO:0009201 | ribonucleoside triphosphate biosynthetic process | 0.951099996 | 1.135729063 |
| ENSG00000196872 | C2orf55 subnetwork | 0.951182385 | 1.135734381 |
| ENSG00000116833 | NR5A2 subnetwork | 0.951061559 | 1.135773401 |
| GO:0006182 | cGMP biosynthetic process | 0.950992957 | 1.1357805 |
| MP:0010819 | primary atelectasis | 0.537852476 | 1.135787745 |
| ENSG00000172354 | GNB2 subnetwork | 0.950969043 | 1.13585382 |
| ENSG00000112851 | ERBB2IP subnetwork | 0.950937082 | 1.135914735 |
| ENSG00000102384 | CENPI subnetwork | 0.950917006 | 1.13597566 |
| GO:0010876 | lipid localization | 0.538387965 | 1.135978307 |
| ENSG00000171759 | PAH subnetwork | 0.950910332 | 1.136061434 |
| REACTOME_RNA_POLYMERASE_I | REACTOME_RNA_POLYMERASE_III_TRANSCRIPTION_INI | 0.538361321 | 1.136061947 |
| ENSG00000066248 | NGEF subnetwork | 0.950871026 | 1.136097541 |
| GO:0009948 | anterior/posterior axis specification | 0.950682984 | 1.136172768 |
| GO:0005547 | phosphatidylinositol-3,4,5-trisphosphate binding | 0.950861019 | 1.136175058 |
| MP:0006396 | decreased long bone epiphyseal plate size | 0.538353458 | 1.136216988 |

| | | | |
|---|---|---|---|
| GO:0072234 | metanephric nephron tubule development | 0.950651057 | 1.136225462 |
| GO:0031105 | septin complex | 0.540502273 | 1.136227247 |
| GO:0042787 | protein ubiquitination involved in ubiquitin-dependent p | 0.540872711 | 1.136237033 |
| MP:0008249 | abnormal common lymphocyte progenitor cell morpholc | 0.540595085 | 1.136243424 |
| ENSG00000153140 | CETN3 subnetwork | 0.950825521 | 1.136244306 |
| ENSG00000062485 | CS subnetwork | 0.538307357 | 1.136314963 |
| GO:0072243 | metanephric nephron epithelium development | 0.950651057 | 1.136319583 |
| ENSG00000101442 | ACTR5 subnetwork | 0.540832069 | 1.136320352 |
| ENSG00000198804 | MT-CO1 subnetwork | 0.540760382 | 1.136361052 |
| GO:0032156 | septin cytoskeleton | 0.540502273 | 1.136388849 |
| ENSG00000143228 | NUF2 subnetwork | 0.950636236 | 1.136393008 |
| GO:0044433 | cytoplasmic vesicle part | 0.540069957 | 1.136393396 |
| ENSG00000143995 | MEIS1 subnetwork | 0.538276377 | 1.136398686 |
| ENSG00000088538 | DOCK3 subnetwork | 0.540372819 | 1.13643477 |
| GO:0008375 | acetylglucosaminyltransferase activity | 0.541070458 | 1.136437908 |
| REACTOME_ARMS:MEDIATED_AC | REACTOME_ARMS:MEDIATED_ACTIVATION | 0.540281285 | 1.136439954 |
| ENSG00000151725 | MLF1IP subnetwork | 0.950606472 | 1.136441591 |
| ENSG00000129691 | ASH2L subnetwork | 0.540215805 | 1.136480717 |
| ENSG00000135775 | COG2 subnetwork | 0.540471982 | 1.136493599 |
| ENSG00000135597 | REPS1 subnetwork | 0.950528244 | 1.136513921 |
| ENSG00000123080 | CDKN2C subnetwork | 0.950603306 | 1.136519181 |
| REACTOME_MRNA_SPLICING | REACTOME_MRNA_SPLICING | 0.540052123 | 1.136519573 |
| ENSG00000212875 | ENSG00000212875 subnetwork | 0.540760382 | 1.136522604 |
| GO:0060589 | nucleoside-triphosphatase regulator activity | 0.538837816 | 1.136553003 |
| GO:0021984 | adenohypophysis development | 0.9505219 | 1.136599818 |
| ENSG00000067842 | ATP2B3 subnetwork | 0.538799093 | 1.13666524 |
| KEGG_GLYCOSPHINGOLIPID_BIOS | KEGG_GLYCOSPHINGOLIPID_BIOSYNTHESIS_GANGLIO_S | 0.950507847 | 1.136673297 |
| REACTOME_MRNA_SPLICING_:_M | REACTOME_MRNA_SPLICING_:_MAJOR_PATHWAY | 0.540052123 | 1.136681378 |
| ENSG00000126247 | CAPNS1 subnetwork | 0.539158084 | 1.136744153 |
| GO:0009886 | post-embryonic morphogenesis | 0.95050546 | 1.136767509 |
| GO:0032934 | sterol binding | 0.539896088 | 1.136789631 |
| ENSG00000141837 | CACNA1A subnetwork | 0.539824711 | 1.136794872 |
| MP:0001147 | small testis | 0.539632752 | 1.136824854 |
| ENSG00000122705 | CLTA subnetwork | 0.539763188 | 1.136828608 |
| ENSG00000136108 | CKAP2 subnetwork | 0.540051583 | 1.136843229 |
| REACTOME_RNA_POLYMERASE_I | REACTOME_RNA_POLYMERASE_II_TRANSCRIPTION_PRE | 0.950484534 | 1.136853448 |
| ENSG00000100614 | PPM1A subnetwork | 0.540006112 | 1.136884079 |
| MP:0002051 | skin papilloma | 0.539145888 | 1.136884895 |
| ENSG00000187323 | DCC subnetwork | 0.539299403 | 1.136910024 |
| REACTOME_HIV:1_TRANSCRIPTIO | REACTOME_HIV:1_TRANSCRIPTION_INITIATION | 0.950484534 | 1.136947691 |
| GO:0005381 | iron ion transmembrane transporter activity | 0.539421887 | 1.136954662 |
| ENSG00000109072 | SEBOX subnetwork | 0.539601257 | 1.136958381 |
| ENSG00000138297 | TIMM23 subnetwork | 0.53975258 | 1.136983471 |
| ENSG00000101350 | KIF3B subnetwork | 0.539120095 | 1.137025678 |
| REACTOME_RNA_POLYMERASE_I | REACTOME_RNA_POLYMERASE_II_HIV:1_PROMOTER_E | 0.950484534 | 1.13704195 |
| ENSG00000135069 | PSAT1 subnetwork | 0.539593629 | 1.137120456 |
| REACTOME_RNA_POLYMERASE_I | REACTOME_RNA_POLYMERASE_II_TRANSCRIPTION_INIT | 0.950484534 | 1.137136224 |
| REACTOME_RNA_POLYMERASE_I | REACTOME_RNA_POLYMERASE_II_TRANSCRIPTION_INIT | 0.950484534 | 1.137230514 |
| REACTOME_RNA_POLYMERASE_I | REACTOME_RNA_POLYMERASE_II_PROMOTER_ESCAPE | 0.950484534 | 1.13732482 |
| GO:0042461 | photoreceptor cell development | 0.950460758 | 1.137381821 |
| MP:0000913 | abnormal brain development | 0.950459705 | 1.137476155 |
| ENSG00000185518 | SV2B subnetwork | 0.950430962 | 1.137549768 |
| REACTOME_RNA_POL_II_CTD_PH | REACTOME_RNA_POL_II_CTD_PHOSPHORYLATION_AND | 0.950401794 | 1.137615097 |
| GO:0030878 | thyroid gland development | 0.950339853 | 1.13763481 |

| | | | |
|---|---|---|---|
| ENSG00000113196 | HAND1 subnetwork | 0.950289305 | 1.137671119 |
| GO:0043243 | positive regulation of protein complex disassembly | 0.950220494 | 1.13769084 |
| ENSG00000143153 | ATP1B1 subnetwork | 0.950195092 | 1.137760352 |
| MP:0004251 | failure of heart looping | 0.541865129 | 1.137810769 |
| ENSG00000049167 | ERCC8 subnetwork | 0.950166666 | 1.137813278 |
| GO:0016830 | carbon-carbon lyase activity | 0.95011479 | 1.137853764 |
| MP:0000764 | abnormal tongue epithelium morphology | 0.950055968 | 1.137869356 |
| ENSG00000100554 | ATP6V1D subnetwork | 0.950035965 | 1.137959658 |
| ENSG00000108819 | ENSG00000108819 subnetwork | 0.949967701 | 1.13796696 |
| KEGG_TASTE_TRANSDUCTION | KEGG_TASTE_TRANSDUCTION | 0.949955594 | 1.138057285 |
| MP:0011228 | abnormal vitamin D level | 0.949840553 | 1.138117579 |
| ENSG00000142949 | PTPRF subnetwork | 0.949954813 | 1.138151777 |
| GO:0043015 | gamma-tubulin binding | 0.949821136 | 1.13819133 |
| ENSG00000151929 | BAG3 subnetwork | 0.949749074 | 1.138272425 |
| ENSG00000104805 | NUCB1 subnetwork | 0.949818517 | 1.138277552 |
| MP:0005551 | abnormal eye electrophysiology | 0.949742248 | 1.138358668 |
| ENSG00000117425 | PTCH2 subnetwork | 0.949737626 | 1.138449078 |
| ENSG00000115514 | TXNDC9 subnetwork | 0.949731309 | 1.138535349 |
| GO:0044306 | neuron projection terminus | 0.949689769 | 1.138580093 |
| GO:0031113 | regulation of microtubule polymerization | 0.949628742 | 1.138628999 |
| ENSG00000009335 | UBE3C subnetwork | 0.949590164 | 1.138690377 |
| ENSG00000171724 | VAT1L subnetwork | 0.949519354 | 1.138701903 |
| GO:0002275 | myeloid cell activation involved in immune response | 0.949446769 | 1.138713431 |
| MP:0003222 | increased cardiomyocyte apoptosis | 0.542442347 | 1.138721591 |
| ENSG00000134686 | PHC2 subnetwork | 0.949433856 | 1.138799767 |
| REACTOME_RNA_POLYMERASE_I | REACTOME_RNA_POLYMERASE_II_PRE:TRANSCRIPTION_ | 0.543529502 | 1.138829033 |
| GO:0044003 | modification by symbiont of host morphology or physiol | 0.543600958 | 1.138830617 |
| GO:0002279 | mast cell activation involved in immune response | 0.949417804 | 1.138877805 |
| ENSG00000110713 | NUP98 subnetwork | 0.543348512 | 1.138916466 |
| ENSG00000114520 | SNX4 subnetwork | 0.543484375 | 1.138919609 |
| ENSG00000185737 | NRG3 subnetwork | 0.543166232 | 1.138947219 |
| MP:0003055 | abnormal long bone epiphyseal plate morphology | 0.949406073 | 1.13896417 |
| ENSG00000168309 | FAM107A subnetwork | 0.949299038 | 1.138984037 |
| MP:0005669 | increased circulating leptin level | 0.543324898 | 1.139007092 |
| MP:0001680 | abnormal mesoderm development | 0.542665348 | 1.139014345 |
| ENSG00000205609 | EIF3CL subnetwork | 0.543461635 | 1.13902439 |
| ENSG00000206476 | ENSG00000206476 subnetwork | 0.54401256 | 1.139042357 |
| MP:0001491 | unresponsive to tactile stimuli | 0.949292644 | 1.13907874 |
| REACTOME_G_ALPHA_I_SIGNALL | REACTOME_G_ALPHA_I_SIGNALLING_EVENTS | 0.543158495 | 1.13908046 |
| ENSG00000187735 | TCEA1 subnetwork | 0.542775791 | 1.139094007 |
| ENSG00000134109 | EDEM1 subnetwork | 0.949204583 | 1.139102777 |
| MP:0009838 | abnormal sperm axoneme morphology | 0.54292545 | 1.1391113 |
| ENSG00000119938 | PPP1R3C subnetwork | 0.949114688 | 1.139114345 |
| GO:0031227 | intrinsic to endoplasmic reticulum membrane | 0.543307531 | 1.139126117 |
| GO:0030695 | GTPase regulator activity | 0.542854474 | 1.139138151 |
| GO:0035272 | exocrine system development | 0.543117419 | 1.139171161 |
| GO:0006576 | cellular biogenic amine metabolic process | 0.949095686 | 1.139179973 |
| ENSG00000213780 | GTF2H4 subnetwork | 0.54401256 | 1.13920374 |
| ENSG00000136270 | TBRG4 subnetwork | 0.948592756 | 1.139219439 |
| REACTOME_NRIF_SIGNALS_CELL_ | REACTOME_NRIF_SIGNALS_CELL_DEATH_FROM_THE_N | 0.948671331 | 1.139232817 |
| GO:0009145 | purine nucleoside triphosphate biosynthetic process | 0.94897878 | 1.139240559 |
| MP:0004522 | abnormal orientation of cochlear hair cell stereociliary b | 0.948824103 | 1.139242928 |
| GO:0000002 | mitochondrial genome maintenance | 0.948914502 | 1.139247983 |
| MP:0003393 | decreased cardiac output | 0.949053438 | 1.139249771 |

| | | | |
|---|---|---|---|
| GO:0010878 | cholesterol storage | 0.543098515 | 1.139290277 |
| GO:0016879 | ligase activity, forming carbon-nitrogen bonds | 0.543879751 | 1.1392928 |
| GO:0010453 | regulation of cell fate commitment | 0.948791979 | 1.139300275 |
| ENSG00000178252 | WDR6 subnetwork | 0.948591671 | 1.139314248 |
| ENSG00000215476 | ENSG00000215476 subnetwork | 0.54401256 | 1.139365169 |
| MP:0000106 | abnormal basisphenoid bone morphology | 0.948583891 | 1.139392426 |
| GO:0004033 | aldo-keto reductase (NADP) activity | 0.545951905 | 1.139445072 |
| GO:0034764 | positive regulation of transmembrane transport | 0.545676326 | 1.1394603 |
| MP:0001689 | incomplete somite formation | 0.546185822 | 1.139470713 |
| ENSG00000149428 | HYOU1 subnetwork | 0.948570426 | 1.139478941 |
| ENSG00000179091 | CYC1 subnetwork | 0.546364296 | 1.139487795 |
| ENSG00000089902 | RCOR1 subnetwork | 0.544660609 | 1.139499009 |
| GO:0031527 | filopodium membrane | 0.546037107 | 1.139524213 |
| GO:0051055 | negative regulation of lipid biosynthetic process | 0.546294559 | 1.139535704 |
| GO:0071285 | cellular response to lithium ion | 0.544280411 | 1.13953966 |
| ENSG00000105971 | CAV2 subnetwork | 0.544752434 | 1.139542946 |
| ENSG00000157985 | AGAP1 subnetwork | 0.948529413 | 1.139552984 |
| ENSG00000136003 | ISCU subnetwork | 0.546145913 | 1.139582157 |
| ENSG00000100029 | PES1 subnetwork | 0.545941478 | 1.139598927 |
| ENSG00000130288 | ENSG00000130288 subnetwork | 0.544642816 | 1.13960368 |
| ENSG00000166598 | HSP90B1 subnetwork | 0.545670099 | 1.139614243 |
| REACTOME_RNA_POLYMERASE_I | REACTOME_RNA_POLYMERASE_I_CHAIN_ELONGATION | 0.948529126 | 1.139647852 |
| MP:0001973 | increased thermal nociceptive threshold | 0.948467621 | 1.139671967 |
| GO:0070242 | thymocyte apoptotic process | 0.54461051 | 1.13967299 |
| GO:0033043 | regulation of organelle organization | 0.545638928 | 1.139683437 |
| ENSG00000145912 | NHP2 subnetwork | 0.545441746 | 1.139687588 |
| ENSG00000100714 | MTHFD1 subnetwork | 0.544420986 | 1.139689846 |
| ENSG00000100490 | CDKL1 subnetwork | 0.544547192 | 1.139692765 |
| GO:0046685 | response to arsenic-containing substance | 0.54556842 | 1.13970318 |
| ENSG00000123728 | RAP2C subnetwork | 0.545859413 | 1.139708998 |
| ENSG00000105656 | ELL subnetwork | 0.545923659 | 1.139710452 |
| GO:0090257 | regulation of muscle system process | 0.544508941 | 1.139712546 |
| ENSG00000070950 | RAD18 subnetwork | 0.545103892 | 1.139738331 |
| GO:0018198 | peptidyl-cysteine modification | 0.94846265 | 1.139762698 |
| GO:0030173 | integral to Golgi membrane | 0.544965779 | 1.139806169 |
| ENSG00000142528 | ZNF473 subnetwork | 0.545435153 | 1.139827513 |
| MP:0005058 | abnormal lysosome morphology | 0.948423512 | 1.139832626 |
| GO:0007435 | salivary gland morphogenesis | 0.546781905 | 1.1398378 |
| ENSG00000102900 | NUP93 subnetwork | 0.545080753 | 1.13985005 |
| MP:0010831 | partial lethality | 0.948395806 | 1.139873418 |
| MP:0003883 | enlarged stomach | 0.545291692 | 1.139895347 |
| ENSG00000108231 | LGI1 subnetwork | 0.948340851 | 1.139901724 |
| ENSG00000159189 | C1QC subnetwork | 0.545412575 | 1.139917986 |
| ENSG00000119048 | UBE2B subnetwork | 0.948109828 | 1.139982506 |
| GO:0031055 | chromatin remodeling at centromere | 0.948330007 | 1.139984175 |
| ENSG00000100034 | PPM1F subnetwork | 0.546769316 | 1.139991536 |
| GO:0007043 | cell-cell junction assembly | 0.948274941 | 1.140045814 |
| ENSG00000160801 | PTH1R subnetwork | 0.948107212 | 1.140073315 |
| ENSG00000177565 | TBL1XR1 subnetwork | 0.546766787 | 1.140138262 |
| GO:0034369 | plasma lipoprotein particle remodeling | 0.948084618 | 1.140151641 |
| ENSG00000105939 | ZC3HAV1 subnetwork | 0.547015855 | 1.140219997 |
| GO:0034368 | protein-lipid complex remodeling | 0.948084618 | 1.140246646 |
| GO:0034367 | macromolecular complex remodeling | 0.948084618 | 1.140341667 |
| MP:0002663 | failure to form blastocele | 0.94795084 | 1.140369228 |

| | | | |
|---|---|---|---|
| GO:0009109 | coenzyme catabolic process | 0.948054874 | 1.140395033 |
| GO:0004180 | carboxypeptidase activity | 0.947918817 | 1.140439276 |
| GO:0005097 | Rab GTPase activator activity | 0.547282803 | 1.140448329 |
| MP:0001850 | increased susceptibility to otitis media | 0.947723195 | 1.140457729 |
| REACTOME_OTHER_SEMAPHORII | REACTOME_OTHER_SEMAPHORIN_INTERACTIONS | 0.947913738 | 1.140530177 |
| GO:0032026 | response to magnesium ion | 0.547249077 | 1.140531585 |
| GO:0034121 | regulation of toll-like receptor signaling pathway | 0.94787156 | 1.140541892 |
| ENSG00000153207 | AHCTF1 subnetwork | 0.947715736 | 1.140544484 |
| GO:0048368 | lateral mesoderm development | 0.547415941 | 1.14059064 |
| ENSG00000023287 | RB1CC1 subnetwork | 0.547927457 | 1.140612676 |
| REACTOME_TRAFFICKING_OF_AM | REACTOME_TRAFFICKING_OF_AMPA_RECEPTORS | 0.947711617 | 1.140639593 |
| MP:0004486 | decreased response of heart to induced stress | 0.547878888 | 1.14064657 |
| GO:0008565 | protein transporter activity | 0.548051396 | 1.140712576 |
| ENSG00000092208 | GEMIN2 subnetwork | 0.947648338 | 1.140733945 |
| REACTOME_GLUTAMATE_BINDIN | REACTOME_GLUTAMATE_BINDING_ACTIVATION_OF_AI | 0.947711617 | 1.140734718 |
| GO:0016469 | proton-transporting two-sector ATPase complex | 0.94748767 | 1.140761595 |
| GO:0032647 | regulation of interferon-alpha production | 0.547841332 | 1.140772048 |
| ENSG00000164776 | PHKG1 subnetwork | 0.947602004 | 1.140787388 |
| MP:0002204 | abnormal neurotransmitter level | 0.947398397 | 1.140801769 |
| MP:0009937 | abnormal neuron differentiation | 0.947484887 | 1.140856761 |
| ENSG00000087302 | C14orf166 subnetwork | 0.947374728 | 1.140859408 |
| ENSG00000081026 | MAGI3 subnetwork | 0.947359973 | 1.140925401 |
| GO:0032607 | interferon-alpha production | 0.547841332 | 1.140932789 |
| MP:0005656 | decreased aggression | 0.54778571 | 1.140952649 |
| ENSG00000213465 | ARL2 subnetwork | 0.547715559 | 1.140979563 |
| ENSG00000177301 | KCNA2 subnetwork | 0.947352314 | 1.141003922 |
| MP:0000787 | abnormal telencephalon morphology | 0.947336448 | 1.141074111 |
| GO:0044242 | cellular lipid catabolic process | 0.947311751 | 1.141135965 |
| GO:0072283 | metanephric renal vesicle morphogenesis | 0.947261903 | 1.141176962 |
| MP:0010263 | total cataracts | 0.947237303 | 1.141243009 |
| MP:0005545 | abnormal lens development | 0.947214317 | 1.141313241 |
| ENSG00000100284 | TOM1 subnetwork | 0.548433802 | 1.141327608 |
| GO:0030670 | phagocytic vesicle membrane | 0.947210031 | 1.141408533 |
| ENSG00000059728 | MXD1 subnetwork | 0.548414122 | 1.141453112 |
| MP:0004249 | abnormal crista ampullaris morphology | 0.94718332 | 1.141474616 |
| ENSG00000135338 | LCA5 subnetwork | 0.947183252 | 1.141569937 |
| GO:0005625 | soluble fraction | 0.548831984 | 1.141605685 |
| KEGG_AMINO_SUGAR_AND_NUC | KEGG_AMINO_SUGAR_AND_NUCLEOTIDE_SUGAR_MET | 0.548668516 | 1.14165259 |
| GO:0007041 | lysosomal transport | 0.947178282 | 1.141656923 |
| MP:0003360 | abnormal depression-related behavior | 0.548774242 | 1.141660802 |
| GO:0030318 | melanocyte differentiation | 0.94712809 | 1.141685459 |
| GO:0000041 | transition metal ion transport | 0.947087802 | 1.141718176 |
| ENSG00000076321 | KLHL20 subnetwork | 0.946996515 | 1.141800334 |
| ENSG00000123219 | CENPK subnetwork | 0.947079724 | 1.141801019 |
| GO:0001085 | RNA polymerase II transcription factor binding | 0.549012 | 1.141810891 |
| REACTOME_MRNA_CAPPING | REACTOME_MRNA_CAPPING | 0.946960881 | 1.141849779 |
| GO:0033006 | regulation of mast cell activation involved in immune res | 0.946917932 | 1.141907587 |
| ENSG00000066933 | MYO9A subnetwork | 0.94690242 | 1.141982117 |
| ENSG00000110801 | PSMD9 subnetwork | 0.94688761 | 1.142069196 |
| ENSG00000166794 | PPIB subnetwork | 0.946843387 | 1.142131216 |
| KEGG_SULFUR_METABOLISM | KEGG_SULFUR_METABOLISM | 0.94682836 | 1.142205784 |
| MP:0002780 | decreased circulating testosterone level | 0.549425297 | 1.142256295 |
| GO:0006308 | DNA catabolic process | 0.946800864 | 1.142263646 |
| ENSG00000133275 | CSNK1G2 subnetwork | 0.946717191 | 1.142304799 |

| | | | |
|---|---|---|---|
| MP:0002209 | decreased germ cell number | 0.549375034 | 1.14231148 |
| ENSG00000188612 | SUMO2 subnetwork | 0.946666532 | 1.142358498 |
| MP:0009305 | decreased retroperitoneal fat pad weight | 0.94665066 | 1.142437291 |
| GO:0006027 | glycosaminoglycan catabolic process | 0.946632138 | 1.142520278 |
| GO:0030201 | heparan sulfate proteoglycan metabolic process | 0.946565982 | 1.14254474 |
| REACTOME_G:PROTEIN_ACTIVAT | REACTOME_G:PROTEIN_ACTIVATION | 0.946527987 | 1.142590115 |
| GO:0033176 | proton-transporting V-type ATPase complex | 0.946512122 | 1.142664771 |
| ENSG00000162645 | GBP2 subnetwork | 0.946455919 | 1.142689251 |
| ENSG00000049323 | LTBP1 subnetwork | 0.550955268 | 1.142715789 |
| ENSG00000185989 | RASA3 subnetwork | 0.551582877 | 1.142731988 |
| MP:0000418 | focal hair loss | 0.551377691 | 1.142749965 |
| GO:0042346 | positive regulation of NF-kappaB import into nucleus | 0.551480468 | 1.142779024 |
| GO:0009206 | purine ribonucleoside triphosphate biosynthetic process | 0.946429973 | 1.142780659 |
| ENSG00000128881 | TTBK2 subnetwork | 0.551319948 | 1.142798036 |
| MP:0000108 | midline facial cleft | 0.551548367 | 1.142829104 |
| ENSG00000091136 | LAMB1 subnetwork | 0.550925024 | 1.142848119 |
| ENSG00000091651 | ORC6 subnetwork | 0.9464155 | 1.142851167 |
| MP:0004087 | abnormal muscle fiber morphology | 0.549961106 | 1.142857143 |
| MP:0002950 | abnormal neural crest cell migration | 0.946377923 | 1.142921687 |
| MP:0000530 | abnormal kidney blood vessel morphology | 0.55115807 | 1.142928301 |
| GO:0001664 | G-protein coupled receptor binding | 0.551312233 | 1.142944312 |
| GO:0005795 | Golgi stack | 0.551115105 | 1.142962391 |
| ENSG00000108852 | MPP2 subnetwork | 0.946349368 | 1.142975483 |
| GO:0045909 | positive regulation of vasodilation | 0.551256645 | 1.142978395 |
| ENSG00000149131 | SERPING1 subnetwork | 0.55092362 | 1.143008564 |
| GO:0009161 | ribonucleoside monophosphate metabolic process | 0.549953954 | 1.143010828 |
| MP:0000102 | abnormal nasal bone morphology | 0.946336181 | 1.143058577 |
| MP:0002628 | hepatic steatosis | 0.549918874 | 1.143066104 |
| ENSG00000070087 | PFN2 subnetwork | 0.550188199 | 1.143105145 |
| GO:0045776 | negative regulation of blood pressure | 0.550141541 | 1.143118234 |
| GO:0031570 | DNA integrity checkpoint | 0.550900199 | 1.143126931 |
| ENSG00000095139 | ARCN1 subnetwork | 0.550264983 | 1.143127196 |
| REACTOME_GAP_JUNCTION_TRA | REACTOME_GAP_JUNCTION_TRAFFICKING | 0.946309659 | 1.143137501 |
| ENSG00000176248 | ANAPC2 subnetwork | 0.946242222 | 1.143153666 |
| REACTOME_FGFR1_LIGAND_BINI | REACTOME_FGFR1_LIGAND_BINDING_AND_ACTIVATIOI | 0.946219401 | 1.143240981 |
| GO:0016860 | intramolecular oxidoreductase activity | 0.550877596 | 1.143259374 |
| REACTOME_RNA_POLYMERASE_I | REACTOME_RNA_POLYMERASE_III_TRANSCRIPTION_INI | 0.550813979 | 1.143307584 |
| ENSG00000126581 | BECN1 subnetwork | 0.550426551 | 1.143310849 |
| GO:0033180 | proton-transporting V-type ATPase, V1 domain | 0.946207799 | 1.143328311 |
| GO:0003727 | single-stranded RNA binding | 0.550564452 | 1.143346916 |
| GO:0031228 | intrinsic to Golgi membrane | 0.552030988 | 1.14336463 |
| ENSG00000166508 | MCM7 subnetwork | 0.551982251 | 1.143398739 |
| GO:0071616 | acyl-CoA biosynthetic process | 0.946206376 | 1.143424027 |
| GO:0008252 | nucleotidase activity | 0.550787146 | 1.143426043 |
| GO:0035384 | thioester biosynthetic process | 0.946206376 | 1.143519759 |
| ENSG00000112282 | MED23 subnetwork | 0.550785004 | 1.143572633 |
| MP:0001394 | circling | 0.946198101 | 1.143607134 |
| ENSG00000126858 | RHOT1 subnetwork | 0.55227528 | 1.143680818 |
| ENSG00000146729 | GBAS subnetwork | 0.946195718 | 1.143702897 |
| GO:0034765 | regulation of ion transmembrane transport | 0.946051849 | 1.14377251 |
| GO:0006470 | protein dephosphorylation | 0.552454851 | 1.143773638 |
| GO:0050931 | pigment cell differentiation | 0.946194833 | 1.143798677 |
| MP:0008489 | slow postnatal weight gain | 0.552531492 | 1.143802521 |
| MP:0000965 | abnormal sensory neuron morphology | 0.552603159 | 1.1438454 |

| | | | |
|---|---|---|---|
| ENSG00000180190 | C8orf42 subnetwork | 0.946043256 | 1.143851566 |
| GO:0006940 | regulation of smooth muscle contraction | 0.552432831 | 1.143877837 |
| GO:0031497 | chromatin assembly | 0.946185999 | 1.14388191 |
| ENSG00000170214 | ADRA1B subnetwork | 0.945991745 | 1.143901315 |
| GO:0043631 | RNA polyadenylation | 0.945940792 | 1.143942694 |
| GO:0005343 | organic acid:sodium symporter activity | 0.945933551 | 1.144034353 |
| MP:0001236 | abnormal epidermis stratum spinosum morphology | 0.552777297 | 1.144105293 |
| GO:0004091 | carboxylesterase activity | 0.945923605 | 1.144113457 |
| ENSG00000166226 | CCT2 subnetwork | 0.5542566 | 1.144142698 |
| GO:0032892 | positive regulation of organic acid transport | 0.945795977 | 1.144192089 |
| MP:0000825 | dilated lateral ventricles | 0.945905436 | 1.144200955 |
| ENSG00000164163 | ABCE1 subnetwork | 0.554356702 | 1.144220299 |
| GO:0006775 | fat-soluble vitamin metabolic process | 0.554411871 | 1.144249023 |
| GO:0006107 | oxaloacetate metabolic process | 0.554684467 | 1.144252232 |
| MP:0008840 | abnormal spike wave discharge | 0.554241293 | 1.14426756 |
| GO:0016459 | myosin complex | 0.945766407 | 1.144271226 |
| GO:0035821 | modification of morphology or physiology of other orgar | 0.554635057 | 1.144272359 |
| MP:0000154 | rib fusion | 0.553300967 | 1.14432009 |
| ENSG00000067334 | DNTTIP2 subnetwork | 0.554191683 | 1.144322626 |
| GO:0019840 | isoprenoid binding | 0.55345144 | 1.144335664 |
| GO:0006978 | DNA damage response, signal transduction by p53 class I | 0.945734684 | 1.144346186 |
| GO:0010894 | negative regulation of steroid biosynthetic process | 0.554171032 | 1.144391675 |
| ENSG00000160213 | CSTB subnetwork | 0.553407527 | 1.144397818 |
| REACTOME_SIGNALING_BY_VEGF | REACTOME_SIGNALING_BY_VEGF | 0.553040691 | 1.144400896 |
| ENSG00000128524 | ATP6V1F subnetwork | 0.94572202 | 1.144429541 |
| GO:0051817 | modification of morphology or physiology of other orgar | 0.554635057 | 1.14443204 |
| MP:0003992 | increased mortality induced by ionizing radiation | 0.553295938 | 1.144480201 |
| GO:0031984 | organelle subcompartment | 0.55402895 | 1.144487144 |
| MP:0000955 | abnormal spinal cord morphology | 0.945721155 | 1.144525486 |
| REACTOME_ADVANCED_GLYCOSY | REACTOME_ADVANCED_GLYCOSYLATION_ENDPRODUCT | 0.554606935 | 1.144535939 |
| GO:0050926 | regulation of positive chemotaxis | 0.553267088 | 1.144549398 |
| GO:0045939 | negative regulation of steroid metabolic process | 0.554171032 | 1.144551551 |
| REACTOME_VEGF_LIGAND:RECEP | REACTOME_VEGF_LIGAND:RECEPTOR_INTERACTIONS | 0.553040691 | 1.144561109 |
| ENSG00000113578 | FGF1 subnetwork | 0.553690677 | 1.144616138 |
| GO:0007091 | mitotic metaphase/anaphase transition | 0.945715254 | 1.144617255 |
| ENSG00000198104 | OR2T6 subnetwork | 0.554016304 | 1.144619147 |
| ENSG00000078674 | PCM1 subnetwork | 0.553239362 | 1.1446676 |
| MP:0004448 | abnormal presphenoid bone morphology | 0.554164126 | 1.14467654 |
| MP:0002621 | delayed neural tube closure | 0.945688245 | 1.144688076 |
| ENSG00000154310 | TNIK subnetwork | 0.945635568 | 1.144712788 |
| GO:0042044 | fluid transport | 0.553972543 | 1.144716243 |
| REACTOME_FORMATION_OF_RN | REACTOME_FORMATION_OF_RNA_POL_II_ELONGATION | 0.555107122 | 1.144749686 |
| GO:0008333 | endosome to lysosome transport | 0.94559989 | 1.144762664 |
| GO:0030662 | coated vesicle membrane | 0.945574347 | 1.144825128 |
| GO:0034362 | low-density lipoprotein particle | 0.55396199 | 1.144862296 |
| GO:0004435 | phosphatidylinositol phospholipase C activity | 0.945542037 | 1.144887603 |
| ENSG00000173020 | ADRBK1 subnetwork | 0.55391496 | 1.144903523 |
| REACTOME_RNA_POLYMERASE_I | REACTOME_RNA_POLYMERASE_II_TRANSCRIPTION_ELC | 0.555107122 | 1.144909344 |
| MP:0002818 | abnormal dentin morphology | 0.945519369 | 1.144954282 |
| MP:0000477 | abnormal intestine morphology | 0.555349197 | 1.144966537 |
| GO:0009262 | deoxyribonucleotide metabolic process | 0.945502232 | 1.145033557 |
| ENSG00000214528 | ENSG00000214528 subnetwork | 0.555463037 | 1.145043915 |
| REACTOME_FORMATION_OF_HIV | REACTOME_FORMATION_OF_HIV:1_ELONGATION_COM | 0.555107122 | 1.145069047 |
| ENSG00000064692 | SNCAIP subnetwork | 0.555552812 | 1.145093393 |

| | | | |
|---|---|---|---|
| ENSG00000105968 | H2AFV subnetwork | 0.945487128 | 1.14510865 |
| ENSG00000213782 | DDX47 subnetwork | 0.945470822 | 1.145192146 |
| GO:0006363 | termination of RNA polymerase I transcription | 0.94543333 | 1.145242091 |
| MP:0003703 | abnormal vestibulocochlear ganglion morphology | 0.945355966 | 1.14527526 |
| GO:0019233 | sensory perception of pain | 0.945353328 | 1.145367184 |
| GO:0008645 | hexose transport | 0.945319112 | 1.14541296 |
| GO:0015758 | glucose transport | 0.945319112 | 1.145509108 |
| MP:0000873 | thin external granule cell layer | 0.555885851 | 1.145567944 |
| GO:0010517 | regulation of phospholipase activity | 0.945305011 | 1.14559268 |
| GO:0031103 | axon regeneration | 0.945273295 | 1.145663672 |
| ENSG00000136026 | CKAP4 subnetwork | 0.556075323 | 1.14569398 |
| GO:0060429 | epithelium development | 0.559549656 | 1.145713296 |
| KEGG_ALDOSTERONE_REGULATE | KEGG_ALDOSTERONE_REGULATED_SODIUM_REABSORP | 0.556210701 | 1.145729413 |
| GO:0021532 | neural tube patterning | 0.945259033 | 1.145734677 |
| GO:0030282 | bone mineralization | 0.559523467 | 1.145802743 |
| GO:0048016 | inositol phosphate-mediated signaling | 0.945253242 | 1.14581409 |
| REACTOME_TRANSPORT_OF_ORG | REACTOME_TRANSPORT_OF_ORGANIC_ANIONS | 0.559755406 | 1.145887566 |
| MP:0002712 | increased circulating glucagon level | 0.559682364 | 1.145893921 |
| ENSG00000163703 | CRELD1 subnetwork | 0.945251926 | 1.145910312 |
| GO:0048284 | organelle fusion | 0.559499439 | 1.145919922 |
| MP:0006035 | abnormal mitochondrial morphology | 0.559384236 | 1.14593265 |
| ENSG00000170522 | ELOVL6 subnetwork | 0.94511437 | 1.145947421 |
| KEGG_GALACTOSE_METABOLISM | KEGG_GALACTOSE_METABOLISM | 0.55908302 | 1.145958125 |
| ENSG00000042088 | TDP1 subnetwork | 0.55926469 | 1.145973108 |
| ENSG00000068305 | MEF2A subnetwork | 0.559340297 | 1.145980596 |
| ENSG00000139219 | COL2A1 subnetwork | 0.945231024 | 1.145989754 |
| ENSG00000118271 | TTR subnetwork | 0.945091883 | 1.14601848 |
| ENSG00000185046 | ANKS1B subnetwork | 0.556867014 | 1.146018931 |
| GO:0031985 | Golgi cisterna | 0.559489179 | 1.146057919 |
| ENSG00000065526 | SPEN subnetwork | 0.559226024 | 1.146069597 |
| ENSG00000183625 | CCR3 subnetwork | 0.559921256 | 1.14608196 |
| ENSG00000079462 | PAFAH1B3 subnetwork | 0.945056336 | 1.146085349 |
| ENSG00000174175 | SELP subnetwork | 0.559073278 | 1.146089308 |
| GO:0045947 | negative regulation of translational initiation | 0.556854669 | 1.146150633 |
| ENSG00000173692 | PSMD1 subnetwork | 0.558387061 | 1.146153846 |
| ENSG00000149187 | CELF1 subnetwork | 0.945033929 | 1.146156431 |
| ENSG00000103740 | ACSBG1 subnetwork | 0.944981253 | 1.14620652 |
| GO:0018202 | peptidyl-histidine modification | 0.559051958 | 1.146213592 |
| MP:0009172 | small pancreatic islets | 0.558792692 | 1.146218954 |
| ENSG00000104884 | ERCC2 subnetwork | 0.558901054 | 1.146247225 |
| ENSG00000140474 | ULK3 subnetwork | 0.556824009 | 1.146254525 |
| GO:0032271 | regulation of protein polymerization | 0.556761694 | 1.146267929 |
| ENSG00000100347 | SAMM50 subnetwork | 0.944968445 | 1.146286026 |
| GO:0019953 | sexual reproduction | 0.5601672 | 1.146297578 |
| GO:0042593 | glucose homeostasis | 0.558371214 | 1.146299125 |
| ENSG00000143553 | SNAPIN subnetwork | 0.944936595 | 1.146327731 |
| ENSG00000103089 | FA2H subnetwork | 0.560119775 | 1.146331672 |
| ENSG00000186193 | C9orf140 subnetwork | 0.558539431 | 1.146341802 |
| GO:0046902 | regulation of mitochondrial membrane permeability | 0.556725943 | 1.146344011 |
| GO:0051196 | regulation of coenzyme metabolic process | 0.558783693 | 1.146350264 |
| ENSG00000105829 | BET1 subnetwork | 0.559039346 | 1.146358718 |
| GO:0048243 | norepinephrine secretion | 0.944934345 | 1.146419867 |
| ENSG00000071127 | WDR1 subnetwork | 0.557988708 | 1.146421623 |
| MP:0004993 | decreased bone resorption | 0.560397862 | 1.146436479 |

| | | | |
|---|---|---|---|
| ENSG00000077942 | FBLN1 subnetwork | 0.557589176 | 1.146439499 |
| GO:0033500 | carbohydrate homeostasis | 0.558371214 | 1.146458333 |
| ENSG00000132604 | TERF2 subnetwork | 0.557671134 | 1.146460854 |
| MP:0004527 | abnormal outer hair cell stereociliary bundle morphology | 0.557800254 | 1.146482692 |
| ENSG00000167657 | DAPK3 subnetwork | 0.558283532 | 1.146485623 |
| ENSG00000144021 | CIAO1 subnetwork | 0.557952279 | 1.146490618 |
| ENSG00000110042 | DTX4 subnetwork | 0.556715291 | 1.146496727 |
| GO:0051193 | regulation of cofactor metabolic process | 0.558783693 | 1.146509368 |
| GO:0006323 | DNA packaging | 0.944932935 | 1.146516221 |
| ENSG00000108821 | COL1A1 subnetwork | 0.557892734 | 1.146517932 |
| MP:0000811 | hippocampal neuron degeneration | 0.944059335 | 1.146525616 |
| REACTOME_ENDOGENOUS_STER | REACTOME_ENDOGENOUS_STEROLS | 0.558719048 | 1.146536646 |
| ENSG00000163993 | S100P subnetwork | 0.944144037 | 1.146542732 |
| ENSG00000029534 | ANK1 subnetwork | 0.557307082 | 1.146562761 |
| ENSG00000154229 | PRKCA subnetwork | 0.557395558 | 1.146570196 |
| KEGG_PURINE_METABOLISM | KEGG_PURINE_METABOLISM | 0.557478919 | 1.146577629 |
| GO:0051058 | negative regulation of small GTPase mediated signal trar | 0.944908036 | 1.146578969 |
| ENSG00000133030 | MPRIP subnetwork | 0.557543164 | 1.146585061 |
| ENSG00000115138 | POMC subnetwork | 0.558254005 | 1.14658933 |
| GO:0005243 | gap junction channel activity | 0.556690172 | 1.146593759 |
| MP:0006059 | decreased susceptibility to ischemic brain injury | 0.9447428 | 1.146595208 |
| ENSG00000018699 | TTC27 subnetwork | 0.557778472 | 1.146600389 |
| GO:0071577 | zinc ion transmembrane transport | 0.944038578 | 1.146601043 |
| ENSG00000101901 | ALG13 subnetwork | 0.944644306 | 1.146607533 |
| GO:0007440 | foregut morphogenesis | 0.943981715 | 1.146647034 |
| ENSG00000047936 | ROS1 subnetwork | 0.944588546 | 1.146649289 |
| MP:0006267 | abnormal intercalated disc morphology | 0.944885139 | 1.146650134 |
| ENSG00000174442 | ZWILCH subnetwork | 0.944296954 | 1.146652368 |
| ENSG00000106803 | SEC61B subnetwork | 0.558215672 | 1.146672225 |
| ENSG00000165917 | RAPSN subnetwork | 0.944541198 | 1.146678439 |
| GO:0005452 | inorganic anion exchanger activity | 0.557275181 | 1.146687543 |
| GO:0070875 | positive regulation of glycogen metabolic process | 0.944474681 | 1.146724413 |
| MP:0002098 | abnormal vibrissa morphology | 0.943975986 | 1.146726691 |
| REACTOME_MEMBRANE_TRAFFI | REACTOME_MEMBRANE_TRAFFICKING | 0.94439007 | 1.146728343 |
| GO:0006818 | hydrogen transport | 0.943921609 | 1.14675587 |
| GO:0060193 | positive regulation of lipase activity | 0.943920376 | 1.146852382 |
| MP:0001458 | abnormal object recognition memory | 0.943871448 | 1.146911034 |
| ENSG00000168374 | ARF4 subnetwork | 0.943869354 | 1.147003367 |
| GO:0016229 | steroid dehydrogenase activity | 0.943833923 | 1.147045206 |
| GO:0006568 | tryptophan metabolic process | 0.943808974 | 1.147108099 |
| GO:0040037 | negative regulation of fibroblast growth factor receptor s | 0.943647575 | 1.147141293 |
| ENSG00000153044 | CENPH subnetwork | 0.943761039 | 1.147154164 |
| GO:0031902 | late endosome membrane | 0.943549663 | 1.147187132 |
| ENSG00000077721 | UBE2A subnetwork | 0.943644636 | 1.147233684 |
| MP:0003130 | anal atresia | 0.943537428 | 1.147271119 |
| ENSG00000171357 | C1orf190 subnetwork | 0.943423568 | 1.147300143 |
| GO:0009152 | purine ribonucleotide biosynthetic process | 0.943492715 | 1.147313005 |
| ENSG00000166851 | PLK1 subnetwork | 0.943423452 | 1.147396799 |
| MP:0004564 | enlarged myocardial fiber | 0.56123399 | 1.14742047 |
| REACTOME_LATE_PHASE_OF_HIV | REACTOME_LATE_PHASE_OF_HIV_LIFE_CYCLE | 0.561075505 | 1.147447427 |
| GO:0016363 | nuclear matrix | 0.56097541 | 1.14746091 |
| ENSG00000154767 | XPC subnetwork | 0.943380706 | 1.147463982 |
| MP:0005112 | abnormal spinal cord ventral horn morphology | 0.943161185 | 1.147492837 |
| GO:2000379 | positive regulation of reactive oxygen species metabolic | 0.561189848 | 1.147510029 |

| | | | |
|---|---|---|---|
| REACTOME_CROSS:PRESENTATIO | REACTOME_CROSS:PRESENTATION_OF_SOLUBLE_EXOG | 0.942695158 | 1.147542159 |
| REACTOME_PEROXISOMAL_LIPID | REACTOME_PEROXISOMAL_LIPID_METABOLISM | 0.942755271 | 1.147542366 |
| MP:0003806 | abnormal nucleotide metabolism | 0.943121784 | 1.147543194 |
| GO:0006378 | mRNA polyadenylation | 0.943363613 | 1.147543815 |
| ENSG00000152137 | HSPB8 subnetwork | 0.942949399 | 1.147572284 |
| GO:0031214 | biomineral tissue development | 0.943072996 | 1.14759356 |
| MP:0001954 | respiratory distress | 0.943343804 | 1.147619449 |
| GO:0003009 | skeletal muscle contraction | 0.942693338 | 1.147630492 |
| ENSG00000179562 | GCC1 subnetwork | 0.942945067 | 1.147664812 |
| GO:0004714 | transmembrane receptor protein tyrosine kinase activity | 0.942638538 | 1.147668241 |
| ENSG00000168397 | ATG4B subnetwork | 0.942635923 | 1.147765033 |
| ENSG00000215697 | ENSG00000215697 subnetwork | 0.942635923 | 1.147861842 |
| GO:0042558 | pteridine-containing compound metabolic process | 0.942471909 | 1.147874135 |
| ENSG00000100014 | SPECC1L subnetwork | 0.56230556 | 1.14788674 |
| MP:0000836 | abnormal substantia nigra morphology | 0.562355303 | 1.147887032 |
| MP:0002834 | decreased heart weight | 0.562246278 | 1.147914077 |
| GO:0016645 | oxidoreductase activity, acting on the CH-NH group of dc | 0.942603082 | 1.147916491 |
| ENSG00000134480 | CCNH subnetwork | 0.561932144 | 1.147933656 |
| GO:0035909 | aorta morphogenesis | 0.942454207 | 1.147941449 |
| ENSG00000176601 | YSK4 subnetwork | 0.561581663 | 1.147953257 |
| MP:0004703 | abnormal vertebral column morphology | 0.561676973 | 1.147967367 |
| REACTOME_FORMATION_OF_TR/ | REACTOME_FORMATION_OF_TRANSCRIPTION:COUPLED | 0.942128608 | 1.147982782 |
| ENSG00000153391 | INO80C subnetwork | 0.562454646 | 1.147997791 |
| ENSG00000197283 | SYNGAP1 subnetwork | 0.942313825 | 1.148025316 |
| GO:0030330 | DNA damage response, signal transduction by p53 class I | 0.942255708 | 1.148033589 |
| ENSG00000166285 | ENSG00000166285 subnetwork | 0.562221644 | 1.148038132 |
| GO:0035904 | aorta development | 0.942454207 | 1.148038306 |
| MP:0010856 | dilated respiratory conducting tubes | 0.561905817 | 1.148050871 |
| MP:0003704 | abnormal hair follicle development | 0.562683841 | 1.14805383 |
| REACTOME_DUAL_INCISION_REA | REACTOME_DUAL_INCISION_REACTION_IN_TC:NER | 0.942128608 | 1.148079683 |
| ENSG00000115252 | PDE1A subnetwork | 0.941969973 | 1.14808358 |
| MP:0001696 | failure to gastrulate | 0.563319019 | 1.148090445 |
| GO:0007034 | vacuolar transport | 0.942438564 | 1.148114083 |
| ENSG00000140553 | UNC45A subnetwork | 0.941915475 | 1.148125633 |
| ENSG00000162385 | MAGOH subnetwork | 0.561873804 | 1.148126642 |
| ENSG00000196998 | WDR45 subnetwork | 0.941307434 | 1.148128749 |
| ENSG00000186676 | ENSG00000186676 subnetwork | 0.942104493 | 1.148130171 |
| MP:0011087 | complete neonatal lethality | 0.941841165 | 1.148142363 |
| ENSG00000093217 | XYLB subnetwork | 0.941397393 | 1.148145802 |
| ENSG00000149136 | SSRP1 subnetwork | 0.562964012 | 1.148158113 |
| GO:0050678 | regulation of epithelial cell proliferation | 0.564499716 | 1.14819045 |
| ENSG00000204359 | CFB subnetwork | 0.562221644 | 1.148196767 |
| GO:0030071 | regulation of mitotic metaphase/anaphase transition | 0.941689345 | 1.148205388 |
| GO:0072594 | establishment of protein localization to organelle | 0.562682644 | 1.148205411 |
| ENSG00000116747 | TROVE2 subnetwork | 0.941293943 | 1.148221528 |
| ENSG00000198712 | MT-CO2 subnetwork | 0.563312667 | 1.148228075 |
| REACTOME_PYRUVATE_METABO | REACTOME_PYRUVATE_METABOLISM | 0.562630863 | 1.148232776 |
| MP:0000822 | abnormal brain ventricle morphology | 0.564256385 | 1.148237885 |
| MP:0002679 | abnormal corpus luteum morphology | 0.562172685 | 1.148237977 |
| GO:0031432 | titin binding | 0.941825962 | 1.148239318 |
| ENSG00000180098 | TRNAU1AP subnetwork | 0.563531329 | 1.148283706 |
| ENSG00000118402 | ELOVL4 subnetwork | 0.941669653 | 1.148298142 |
| GO:0009164 | nucleoside catabolic process | 0.941285839 | 1.148314322 |
| ENSG00000196497 | IPO4 subnetwork | 0.562962021 | 1.148316545 |

| | | | |
|---|---|---|---|
| REACTOME_PYRUVATE_METABO | REACTOME_PYRUVATE_METABOLISM_AND_CITRIC_ACI | 0.564385998 | 1.148320716 |
| ENSG00000197780 | TAF13 subnetwork | 0.564480976 | 1.148327828 |
| GO:0001958 | endochondral ossification | 0.941647856 | 1.148369795 |
| ENSG00000121542 | SEC22A subnetwork | 0.563857972 | 1.148374208 |
| KEGG_VALINE_LEUCINE_AND_ISC | KEGG_VALINE_LEUCINE_AND_ISOLEUCINE_BIOSYNTHES | 0.564241063 | 1.148375327 |
| ENSG00000212874 | ENSG00000212874 subnetwork | 0.563312667 | 1.148386429 |
| MP:0004433 | abnormal cochlear inner hair cell physiology | 0.563648969 | 1.148394211 |
| GO:0001662 | behavioral fear response | 0.941285778 | 1.148411357 |
| GO:0017148 | negative regulation of translation | 0.563838533 | 1.148456663 |
| GO:0016202 | regulation of striated muscle tissue development | 0.562954112 | 1.14846122 |
| ENSG00000112144 | ICK subnetwork | 0.941226795 | 1.14847883 |
| ENSG00000204175 | GPRIN2 subnetwork | 0.563756627 | 1.148484013 |
| ENSG00000152147 | GEMIN6 subnetwork | 0.564012895 | 1.148505304 |
| GO:0016298 | lipase activity | 0.941091505 | 1.148508157 |
| ENSG00000144848 | ATG3 subnetwork | 0.564231135 | 1.148526577 |
| GO:0006362 | transcription elongation from RNA polymerase I promote | 0.941009149 | 1.14853339 |
| MP:0002896 | abnormal bone mineralization | 0.563310168 | 1.148537931 |
| ENSG00000163161 | ERCC3 subnetwork | 0.564163193 | 1.148547032 |
| GO:0051261 | protein depolymerization | 0.940694389 | 1.148549806 |
| GO:0004716 | receptor signaling protein tyrosine kinase activity | 0.941203952 | 1.148554767 |
| GO:0048638 | regulation of developmental growth | 0.940973459 | 1.148596669 |
| MP:0001286 | abnormal eye development | 0.940673991 | 1.148613108 |
| MP:0011110 | partial preweaning lethality | 0.56329562 | 1.148661884 |
| GO:0015992 | proton transport | 0.940880865 | 1.148668301 |
| MP:0002782 | abnormal testes secretion | 0.940969996 | 1.148693777 |
| ENSG00000096063 | SRPK1 subnetwork | 0.564157268 | 1.148698347 |
| GO:0006471 | protein ADP-ribosylation | 0.940669599 | 1.14871025 |
| MP:0004556 | enlarged allantois | 0.940662369 | 1.148794722 |
| GO:0043574 | peroxisomal transport | 0.940651766 | 1.148883438 |
| MP:0001127 | small ovary | 0.565162007 | 1.148927245 |
| ENSG00000102901 | CENPT subnetwork | 0.940594031 | 1.1489341 |
| GO:0014068 | positive regulation of phosphatidylinositol 3-kinase casca | 0.565261522 | 1.148934268 |
| ENSG00000132002 | DNAJB1 subnetwork | 0.565023771 | 1.148954464 |
| REACTOME_INSULIN_SYNTHESIS_ | REACTOME_INSULIN_SYNTHESIS_AND_PROCESSING | 0.564966115 | 1.149002477 |
| ENSG00000120802 | TMPO subnetwork | 0.565139384 | 1.149009629 |
| ENSG00000137767 | SQRDL subnetwork | 0.940584302 | 1.149022843 |
| GO:0045576 | mast cell activation | 0.940532965 | 1.149086217 |
| GO:0015074 | DNA integration | 0.940492485 | 1.149124217 |
| GO:0033280 | response to vitamin D | 0.940422783 | 1.149141068 |
| ENSG00000116754 | SRSF11 subnetwork | 0.565431896 | 1.149168156 |
| GO:0050818 | regulation of coagulation | 0.9403973 | 1.149229858 |
| GO:0043603 | cellular amide metabolic process | 0.93941151 | 1.14930532 |
| MP:0005480 | increased circulating triiodothyronine level | 0.940381201 | 1.149314431 |
| ENSG00000104879 | CKM subnetwork | 0.939384009 | 1.149343387 |
| GO:0044036 | cell wall macromolecule metabolic process | 0.939343995 | 1.149368751 |
| ENSG00000145362 | ANK2 subnetwork | 0.940359353 | 1.149369392 |
| ENSG00000177791 | MYOZ1 subnetwork | 0.939851143 | 1.149402947 |
| ENSG00000167414 | GNG8 subnetwork | 0.940309741 | 1.14942013 |
| GO:0044057 | regulation of system process | 0.940245874 | 1.149441246 |
| GO:0006298 | mismatch repair | 0.939794391 | 1.149449479 |
| ENSG00000143556 | S100A7 subnetwork | 0.939210455 | 1.149466056 |
| GO:0071554 | cell wall organization or biogenesis | 0.939343995 | 1.149466147 |
| ENSG00000142192 | APP subnetwork | 0.939989104 | 1.149483445 |
| GO:0002444 | myeloid leukocyte mediated immunity | 0.940077345 | 1.149500423 |

| | | | |
|---|---|---|---|
| GO:0051875 | pigment granule localization | 0.94019038 | 1.149504699 |
| GO:0051668 | localization within membrane | 0.93918034 | 1.149521105 |
| GO:0035239 | tube morphogenesis | 0.939318694 | 1.149542373 |
| ENSG00000164022 | AIMP1 subnetwork | 0.939794256 | 1.149546841 |
| MP:0001625 | cardiac hypertrophy | 0.939714136 | 1.149576451 |
| ENSG00000078053 | AMPH subnetwork | 0.93917999 | 1.149614309 |
| MP:0003059 | decreased insulin secretion | 0.938928564 | 1.149648126 |
| GO:0046135 | pyrimidine nucleoside catabolic process | 0.939142726 | 1.149686334 |
| GO:0050832 | defense response to fungus | 0.939054741 | 1.149703264 |
| GO:0014829 | vascular smooth muscle contraction | 0.938866146 | 1.149711693 |
| GO:0043679 | axon terminus | 0.938847194 | 1.149792232 |
| MP:0004073 | caudal body truncation | 0.938843038 | 1.149889746 |
| GO:0006493 | protein O-linked glycosylation | 0.565948265 | 1.149910653 |
| GO:0006595 | polyamine metabolic process | 0.56607062 | 1.14996564 |
| GO:0055015 | ventricular cardiac muscle cell development | 0.938839546 | 1.149978796 |
| ENSG00000143614 | GATAD2B subnetwork | 0.938587567 | 1.149995758 |
| MP:0002582 | disorganized extraembryonic tissue | 0.938689093 | 1.150021208 |
| GO:0007099 | centriole replication | 0.938793336 | 1.15003393 |
| ENSG00000106006 | HOXA6 subnetwork | 0.938556058 | 1.150050908 |
| ENSG00000003756 | RBM5 subnetwork | 0.565936558 | 1.150068738 |
| MP:0000131 | abnormal long bone epiphysis morphology | 0.938519713 | 1.150097582 |
| GO:0046426 | negative regulation of JAK-STAT cascade | 0.938516157 | 1.15019518 |
| GO:0050000 | chromosome localization | 0.938370702 | 1.150254626 |
| MP:0001739 | abnormal adrenal gland secretion | 0.938465878 | 1.150263091 |
| GO:0051303 | establishment of chromosome localization | 0.938370702 | 1.150352262 |
| MP:0003675 | kidney cysts | 0.938302894 | 1.150365025 |
| ENSG00000151148 | UBE3B subnetwork | 0.938279072 | 1.150428729 |
| MP:0003645 | increased pancreatic beta cell number | 0.566353136 | 1.150432871 |
| GO:0047555 | 3',5'-cyclic-GMP phosphodiesterase activity | 0.566795871 | 1.150446306 |
| GO:0061035 | regulation of cartilage development | 0.566889752 | 1.150487436 |
| MP:0009404 | centrally nucleated skeletal muscle fibers | 0.938259294 | 1.150509424 |
| GO:0005819 | spindle | 0.568925597 | 1.150540652 |
| MP:0004814 | reduced linear vestibular evoked potential | 0.938231981 | 1.15056466 |
| ENSG00000205307 | SAP25 subnetwork | 0.566777137 | 1.150583711 |
| KEGG_PANTOTHENATE_AND_CO/ | KEGG_PANTOTHENATE_AND_COA_BIOSYNTHESIS | 0.568826771 | 1.150609172 |
| MP:0005458 | increased percent body fat | 0.56963979 | 1.150615174 |
| MP:0000885 | ectopic Purkinje cell | 0.568766082 | 1.150636637 |
| GO:0002673 | regulation of acute inflammatory response | 0.568708006 | 1.150657264 |
| GO:0015934 | large ribosomal subunit | 0.567935196 | 1.150658075 |
| ENSG00000172680 | MOS subnetwork | 0.938226381 | 1.150662364 |
| KEGG_HOMOLOGOUS_RECOMBI | KEGG_HOMOLOGOUS_RECOMBINATION | 0.566643951 | 1.150673169 |
| MP:0004901 | decreased male germ cell number | 0.566589305 | 1.150687002 |
| ENSG00000126778 | SIX1 subnetwork | 0.568650449 | 1.150725829 |
| ENSG00000076604 | TRAF4 subnetwork | 0.567806296 | 1.150726824 |
| ENSG00000077454 | LRCH4 subnetwork | 0.566777137 | 1.150741758 |
| REACTOME_GLUCONEOGENESIS | REACTOME_GLUCONEOGENESIS | 0.569621846 | 1.150745146 |
| KEGG_MATURITY_ONSET_DIABET | KEGG_MATURITY_ONSET_DIABETES_OF_THE_YOUNG | 0.938224863 | 1.150751592 |
| ENSG00000173369 | C1QB subnetwork | 0.567908887 | 1.15076786 |
| GO:0044449 | contractile fiber part | 0.938076411 | 1.15079419 |
| ENSG00000128708 | HAT1 subnetwork | 0.937902237 | 1.150798573 |
| ENSG00000091483 | FH subnetwork | 0.568579863 | 1.15080126 |
| ENSG00000143977 | SNRPG subnetwork | 0.56777899 | 1.150816075 |
| MP:0004157 | interrupted aortic arch | 0.569592891 | 1.150820457 |
| ENSG00000173281 | PPP1R3B subnetwork | 0.938213832 | 1.150832342 |

| | | | |
|---|---|---|---|
| ENSG00000148356 | LRSAM1 subnetwork | 0.567142379 | 1.150837452 |
| REACTOME_FGFR4_LIGAND_BIND | REACTOME_FGFR4_LIGAND_BINDING_AND_ACTIVATION | 0.938052185 | 1.150853721 |
| GO:0003779 | actin binding | 0.567724742 | 1.150857339 |
| GO:0031418 | L-ascorbic acid binding | 0.567451302 | 1.150864553 |
| GO:0044058 | regulation of digestive system process | 0.93786916 | 1.150870858 |
| ENSG00000179218 | CALR subnetwork | 0.569271321 | 1.150889436 |
| GO:0006397 | mRNA processing | 0.568125227 | 1.150897875 |
| ENSG00000010244 | ZNF207 subnetwork | 0.568286693 | 1.150911333 |
| GO:0019198 | transmembrane receptor protein phosphatase activity | 0.567365582 | 1.150940159 |
| GO:0009142 | nucleoside triphosphate biosynthetic process | 0.937842327 | 1.150943156 |
| GO:0051480 | cytosolic calcium ion homeostasis | 0.569569424 | 1.150950492 |
| ENSG00000132703 | APCS subnetwork | 0.568578512 | 1.150958904 |
| ENSG00000141446 | ESCO1 subnetwork | 0.567705321 | 1.150994649 |
| GO:0007623 | circadian rhythm | 0.568519625 | 1.151000137 |
| ENSG00000102103 | PQBP1 subnetwork | 0.569259438 | 1.151012728 |
| MP:0004174 | abnormal spine curvature | 0.568432306 | 1.151013976 |
| MP:0004362 | cochlear hair cell degeneration | 0.569967256 | 1.15102501 |
| ENSG00000173566 | NUDT18 subnetwork | 0.937836574 | 1.151028212 |
| ENSG00000147854 | UHRF2 subnetwork | 0.567650143 | 1.15104281 |
| GO:0051384 | response to glucocorticoid stimulus | 0.569891735 | 1.151045653 |
| ENSG00000105997 | HOXA3 subnetwork | 0.568285856 | 1.151069079 |
| MP:0002865 | increased growth rate | 0.569563769 | 1.151094242 |
| GO:0005001 | transmembrane receptor protein tyrosine phosphatase a | 0.567365582 | 1.151098147 |
| MP:0000194 | hypercalcemia | 0.937783816 | 1.151100535 |
| GO:0006720 | isoprenoid metabolic process | 0.937750691 | 1.151168621 |
| ENSG00000102158 | MAGT1 subnetwork | 0.937596732 | 1.151181571 |
| MP:0009403 | increased variability of skeletal muscle fiber size | 0.93771719 | 1.151223969 |
| ENSG00000164061 | BSN subnetwork | 0.569536428 | 1.15122435 |
| MP:0003789 | osteosarcoma | 0.937576255 | 1.151236929 |
| ENSG00000185633 | NDUFA4L2 subnetwork | 0.93752829 | 1.151271042 |
| GO:0016248 | channel inhibitor activity | 0.937513118 | 1.151347675 |
| ENSG00000039560 | RAI14 subnetwork | 0.569532695 | 1.151368176 |
| MP:0009379 | abnormal foot pigmentation | 0.57025138 | 1.151393823 |
| GO:0008200 | ion channel inhibitor activity | 0.937513118 | 1.151445578 |
| ENSG00000196531 | NACA subnetwork | 0.937503789 | 1.15152649 |
| ENSG00000163516 | ANKZF1 subnetwork | 0.570400536 | 1.151543927 |
| ENSG00000177084 | POLE subnetwork | 0.570528508 | 1.151563994 |
| REACTOME_PROCESSING_OF_CAI | REACTOME_PROCESSING_OF_CAPPED_INTRON:CONTAI | 0.570492326 | 1.151584699 |
| MP:0008272 | abnormal endochondral bone ossification | 0.937499918 | 1.151615921 |
| ENSG00000160285 | LSS subnetwork | 0.570709998 | 1.151652328 |
| MP:0005330 | cardiomyopathy | 0.937487041 | 1.151688356 |
| GO:0010799 | regulation of peptidyl-threonine phosphorylation | 0.570681574 | 1.151754985 |
| GO:0007032 | endosome organization | 0.937474336 | 1.151765056 |
| ENSG00000163069 | SGCB subnetwork | 0.937407823 | 1.151803488 |
| GO:0051310 | metaphase plate congression | 0.937288343 | 1.151867608 |
| GO:0043425 | bHLH transcription factor binding | 0.937383913 | 1.151880211 |
| ENSG00000204264 | PSMB8 subnetwork | 0.937199939 | 1.151880531 |
| ENSG00000206298 | PSMB8 subnetwork | 0.937199939 | 1.151978555 |
| GO:0008093 | cytoskeletal adaptor activity | 0.571048014 | 1.15203413 |
| REACTOME_RNA_POLYMERASE_I | REACTOME_RNA_POLYMERASE_II_TRANSCRIPTION_TER | 0.937131376 | 1.152072517 |
| ENSG00000206234 | ENSG00000206234 subnetwork | 0.937199939 | 1.152076596 |
| ENSG00000103266 | STUB1 subnetwork | 0.57116669 | 1.152102102 |
| REACTOME_POST:ELONGATION_I | REACTOME_POST:ELONGATION_PROCESSING_OF_THE_ | 0.937131376 | 1.152170582 |
| GO:0005669 | transcription factor TFIID complex | 0.571036932 | 1.152184599 |

| | | | |
|---|---|---|---|
| GO:0000314 | organellar small ribosomal subunit | 0.572101065 | 1.152262505 |
| REACTOME_CLEAVAGE_OF_GROV | REACTOME_CLEAVAGE_OF_GROWING_TRANSCRIPT_IN_ | 0.937131376 | 1.152268664 |
| ENSG00000184445 | KNTC1 subnetwork | 0.937088358 | 1.152324195 |
| MP:0005170 | cleft lip | 0.93706316 | 1.152371222 |
| GO:0046504 | glycerol ether biosynthetic process | 0.571610646 | 1.15239427 |
| ENSG00000137462 | TLR2 subnetwork | 0.572268598 | 1.152412101 |
| GO:0005763 | mitochondrial small ribosomal subunit | 0.572101065 | 1.152419575 |
| ENSG00000052802 | MSMO1 subnetwork | 0.571550719 | 1.152428708 |
| GO:0003143 | embryonic heart tube morphogenesis | 0.937055763 | 1.152469346 |
| MP:0005421 | loose skin | 0.571753027 | 1.152503069 |
| GO:0048514 | blood vessel morphogenesis | 0.571504592 | 1.152504094 |
| GO:0005790 | smooth endoplasmic reticulum | 0.572446147 | 1.152520436 |
| ENSG00000020577 | SAMD4A subnetwork | 0.572050974 | 1.152528971 |
| MP:0010375 | increased kidney iron level | 0.571842998 | 1.152536825 |
| ENSG00000196277 | GRM7 subnetwork | 0.937053081 | 1.152554713 |
| GO:0033273 | response to vitamin | 0.937027494 | 1.152610288 |
| ENSG00000060237 | WNK1 subnetwork | 0.572429161 | 1.15261616 |
| ENSG00000125810 | CD93 subnetwork | 0.572014755 | 1.152617944 |
| ENSG00000134588 | USP26 subnetwork | 0.571483746 | 1.152640917 |
| GO:0071241 | cellular response to inorganic substance | 0.575708505 | 1.152668653 |
| ENSG00000187391 | MAGI2 subnetwork | 0.936987519 | 1.15267013 |
| GO:0000940 | condensed chromosome outer kinetochore | 0.571998046 | 1.152720578 |
| GO:0016045 | detection of bacterium | 0.936967531 | 1.152759796 |
| ENSG00000157227 | MMP14 subnetwork | 0.936930681 | 1.152811142 |
| ENSG00000123143 | PKN1 subnetwork | 0.575708174 | 1.152818046 |
| ENSG00000107863 | ARHGAP21 subnetwork | 0.575656794 | 1.152872629 |
| GO:0009260 | ribonucleotide biosynthetic process | 0.936930554 | 1.152909354 |
| ENSG00000142856 | ITGB3BP subnetwork | 0.936834741 | 1.152913862 |
| MP:0003809 | abnormal hair shaft morphology | 0.575619914 | 1.15295433 |
| MP:0004000 | impaired passive avoidance behavior | 0.936817729 | 1.152990798 |
| ENSG00000157601 | MX1 subnetwork | 0.572749672 | 1.153024111 |
| GO:0050927 | positive regulation of positive chemotaxis | 0.575576465 | 1.153029276 |
| MP:0003843 | abnormal sagittal suture morphology | 0.572880485 | 1.15308499 |
| ENSG00000197616 | MYH6 subnetwork | 0.936813894 | 1.15308905 |
| ENSG00000126768 | TIMM17B subnetwork | 0.575553986 | 1.153111021 |
| GO:0000323 | lytic vacuole | 0.936765199 | 1.153123402 |
| ENSG00000163714 | U2SURP subnetwork | 0.575457116 | 1.153186441 |
| ENSG00000120868 | APAF1 subnetwork | 0.936652394 | 1.153196386 |
| MP:0002795 | dilated cardiomyopathy | 0.936575696 | 1.153196658 |
| GO:0005764 | lysosome | 0.936765199 | 1.153221682 |
| GO:0016010 | dystrophin-associated glycoprotein complex | 0.575552813 | 1.153267354 |
| ENSG00000142599 | RERE subnetwork | 0.936558049 | 1.153273657 |
| ENSG00000138764 | CCNG2 subnetwork | 0.573631911 | 1.153292517 |
| GO:0031461 | cullin-RING ubiquitin ligase complex | 0.93649362 | 1.15330804 |
| ENSG00000082146 | STRADB subnetwork | 0.575456899 | 1.153342826 |
| GO:0032368 | regulation of lipid transport | 0.573081602 | 1.153370557 |
| MP:0003048 | abnormal cervical vertebrae morphology | 0.936458302 | 1.153372271 |
| MP:0002857 | cochlear ganglion degeneration | 0.573604393 | 1.153381412 |
| ENSG00000168490 | PHYHIP subnetwork | 0.574698027 | 1.153402146 |
| ENSG00000113194 | FAF2 subnetwork | 0.573349105 | 1.153403213 |
| ENSG00000110717 | NDUFS8 subnetwork | 0.57326245 | 1.153403676 |
| ENSG00000198692 | EIF1AY subnetwork | 0.573172249 | 1.153404139 |
| ENSG00000115866 | DARS subnetwork | 0.575409582 | 1.153424658 |
| GO:0008017 | microtubule binding | 0.936428385 | 1.153453569 |

| | | | |
|---|---|---|---|
| GO:0001077 | RNA polymerase II core promoter proximal region seque | 0.573980323 | 1.153453903 |
| GO:0016236 | macroautophagy | 0.575231824 | 1.153459973 |
| ENSG00000106211 | HSPB1 subnetwork | 0.573837629 | 1.153475245 |
| GO:0006998 | nuclear envelope organization | 0.575363606 | 1.153479381 |
| REACTOME_BILE_ACID_AND_BILE | REACTOME_BILE_ACID_AND_BILE_SALT_METABOLISM | 0.936357402 | 1.153483711 |
| GO:0060191 | regulation of lipase activity | 0.936287708 | 1.153484009 |
| ENSG00000100504 | PYGL subnetwork | 0.573565736 | 1.153504355 |
| MP:0001676 | abnormal apical ectodermal ridge morphology | 0.936252725 | 1.153531218 |
| GO:0030315 | T-tubule | 0.936193925 | 1.153535784 |
| REACTOME_CYTOCHROME_P450_ | REACTOME_CYTOCHROME_P450_:_ARRANGED_BY_SUB | 0.574695873 | 1.153552024 |
| ENSG00000175324 | LSM1 subnetwork | 0.573955002 | 1.153556372 |
| GO:0004012 | phospholipid-translocating ATPase activity | 0.57532994 | 1.153568037 |
| ENSG00000013293 | SLC7A14 subnetwork | 0.575207991 | 1.153569005 |
| GO:0043498 | cell surface binding | 0.574995448 | 1.153577247 |
| ENSG00000101199 | ARFGAP1 subnetwork | 0.573806578 | 1.153577745 |
| ENSG00000165304 | MELK subnetwork | 0.573524067 | 1.153586498 |
| MP:0003862 | decreased aggression towards males | 0.936134343 | 1.153595803 |
| ENSG00000164683 | HEY1 subnetwork | 0.574928666 | 1.153611677 |
| MP:0002894 | abnormal otolith morphology | 0.575087963 | 1.153658206 |
| ENSG00000117906 | RCN2 subnetwork | 0.574166646 | 1.153684568 |
| GO:0046718 | viral entry into host cell | 0.574688157 | 1.153688358 |
| GO:0001756 | somitogenesis | 0.936133787 | 1.153694224 |
| MP:0002184 | abnormal innervation | 0.93605477 | 1.153703072 |
| ENSG00000099960 | SLC7A4 subnetwork | 0.575207991 | 1.15372557 |
| ENSG00000141384 | TAF4B subnetwork | 0.574257455 | 1.153752039 |
| MP:0001938 | delayed sexual maturation | 0.574914668 | 1.153754753 |
| ENSG00000197265 | GTF2E2 subnetwork | 0.936050461 | 1.153797252 |
| GO:0032845 | negative regulation of homeostatic process | 0.574668289 | 1.153797554 |
| MP:0000161 | scoliosis | 0.574514458 | 1.153859744 |
| ENSG00000169976 | SF3B5 subnetwork | 0.574435128 | 1.153887454 |
| ENSG00000138308 | PLA2G12B subnetwork | 0.936049575 | 1.153895716 |
| MP:0001264 | increased body size | 0.574665813 | 1.153954342 |
| MP:0003918 | decreased kidney weight | 0.576487817 | 1.153982121 |
| ENSG00000172594 | SMPDL3A subnetwork | 0.936048995 | 1.153994196 |
| GO:0016725 | oxidoreductase activity, acting on CH or CH2 groups | 0.936046524 | 1.154088426 |
| GO:0009100 | glycoprotein metabolic process | 0.935883589 | 1.154101929 |
| GO:0006334 | nucleosome assembly | 0.935987722 | 1.154110115 |
| ENSG00000122952 | ZWINT subnetwork | 0.935837895 | 1.154166311 |
| MP:0003237 | abnormal lens epithelium morphology | 0.935402261 | 1.154172361 |
| GO:0006487 | protein N-linked glycosylation | 0.935376713 | 1.154219698 |
| MP:0002961 | abnormal axon guidance | 0.935535589 | 1.154223247 |
| MP:0000285 | abnormal heart valve morphology | 0.93582167 | 1.154252049 |
| MP:0003044 | impaired basement membrane formation | 0.935736295 | 1.154252412 |
| GO:0072132 | mesenchyme morphogenesis | 0.935374373 | 1.154318298 |
| MP:0002746 | abnormal semilunar valve morphology | 0.935725397 | 1.154329633 |
| MP:0008042 | abnormal NK T cell physiology | 0.935345418 | 1.154387014 |
| ENSG00000023191 | RNH1 subnetwork | 0.9352971 | 1.154442925 |
| GO:0005096 | GTPase activator activity | 0.576787744 | 1.154475894 |
| GO:0006721 | terpenoid metabolic process | 0.935290199 | 1.154528753 |
| MP:0001523 | impaired righting response | 0.935165979 | 1.154597898 |
| ENSG00000141404 | GNAL subnetwork | 0.935250986 | 1.154601777 |
| ENSG00000018408 | WWTR1 subnetwork | 0.935142346 | 1.154675214 |
| ENSG00000068028 | RASSF1 subnetwork | 0.57802991 | 1.15469785 |
| ENSG00000087191 | PSMC5 subnetwork | 0.578149622 | 1.154751284 |

| | | | |
|---|---|---|---|
| ENSG00000179899 | ENSG00000179899 subnetwork | 0.57793595 | 1.15476609 |
| MP:0002786 | abnormal Leydig cell morphology | 0.935135365 | 1.154769638 |
| KEGG_GAP_JUNCTION | KEGG_GAP_JUNCTION | 0.577899871 | 1.154834348 |
| GO:0005283 | sodium:amino acid symporter activity | 0.935121703 | 1.154859805 |
| GO:0031235 | intrinsic to internal side of plasma membrane | 0.577118658 | 1.154915369 |
| ENSG00000132963 | POMP subnetwork | 0.934989976 | 1.154920486 |
| REACTOME_SIGNALING_BY_BMP | REACTOME_SIGNALING_BY_BMP | 0.577877447 | 1.154936435 |
| GO:0001881 | receptor recycling | 0.935111236 | 1.154945713 |
| KEGG_PYRIMIDINE_METABOLISM | KEGG_PYRIMIDINE_METABOLISM | 0.577212154 | 1.15497563 |
| GO:0032956 | regulation of actin cytoskeleton organization | 0.577665885 | 1.155006088 |
| MP:0000272 | abnormal aorta morphology | 0.577583359 | 1.155013532 |
| ENSG00000100146 | SOX10 subnetwork | 0.934982382 | 1.155014964 |
| GO:0042307 | positive regulation of protein import into nucleus | 0.577856693 | 1.155045313 |
| ENSG00000078668 | VDAC3 subnetwork | 0.934913385 | 1.155053874 |
| GO:0001539 | ciliary or flagellar motility | 0.577819932 | 1.155140693 |
| REACTOME_HORMONE_LIGAND:I | REACTOME_HORMONE_LIGAND:BINDING_RECEPTORS | 0.934908228 | 1.155148379 |
| ENSG00000168298 | HIST1H1E subnetwork | 0.577572499 | 1.155156313 |
| ENSG00000179776 | CDH5 subnetwork | 0.57857106 | 1.155161465 |
| ENSG00000144597 | EAF1 subnetwork | 0.578530935 | 1.155168919 |
| REACTOME_TRANSPORT_OF_RIB | REACTOME_TRANSPORT_OF_RIBONUCLEOPROTEINS_IN | 0.579100851 | 1.155190335 |
| ENSG00000166147 | FBN1 subnetwork | 0.579198418 | 1.15520988 |
| GO:0000084 | S phase of mitotic cell cycle | 0.934878157 | 1.155217243 |
| MP:0000740 | impaired smooth muscle contractility | 0.577505247 | 1.155224689 |
| ENSG00000100201 | DDX17 subnetwork | 0.934565082 | 1.155231862 |
| ENSG00000163527 | STT3B subnetwork | 0.934733906 | 1.15525663 |
| MP:0000538 | abnormal urinary bladder morphology | 0.934650567 | 1.155265634 |
| ENSG00000172201 | ID4 subnetwork | 0.578502484 | 1.155270983 |
| REACTOME_SCF:BETA:TRCP_MED | REACTOME_SCF:BETA:TRCP_MEDIATED_DEGRADATION_ | 0.934834601 | 1.155273287 |
| GO:0006000 | fructose metabolic process | 0.578685257 | 1.155275601 |
| MP:0000231 | hypertension | 0.578938322 | 1.155300473 |
| GO:0060021 | palate development | 0.934474774 | 1.155309772 |
| MP:0006107 | abnormal fetal atrioventricular canal morphology | 0.934555633 | 1.155317875 |
| ENSG00000031698 | SARS subnetwork | 0.579079536 | 1.155319293 |
| MP:0004609 | vertebral fusion | 0.9343831 | 1.155323064 |
| REACTOME_CELL_CYCLE_CHECKP | REACTOME_CELL_CYCLE_CHECKPOINTS | 0.934226922 | 1.155328255 |
| ENSG00000108651 | UTP6 subnetwork | 0.577493722 | 1.155333694 |
| GO:0071482 | cellular response to light stimulus | 0.579029115 | 1.155380772 |
| MP:0008277 | abnormal sternum ossification | 0.934354828 | 1.155400548 |
| ENSG00000179222 | MAGED1 subnetwork | 0.934221139 | 1.155427153 |
| ENSG00000000971 | CFH subnetwork | 0.578927416 | 1.155443004 |
| GO:0006665 | sphingolipid metabolic process | 0.934085016 | 1.155483733 |
| ENSG00000164107 | HAND2 subnetwork | 0.934211655 | 1.155521788 |
| GO:0031293 | membrane protein intracellular domain proteolysis | 0.934074841 | 1.155569826 |
| GO:0014706 | striated muscle tissue development | 0.57892535 | 1.155585573 |
| GO:0046676 | negative regulation of insulin secretion | 0.934056084 | 1.155647371 |
| GO:0030864 | cortical actin cytoskeleton | 0.933980208 | 1.155673546 |
| MP:0005140 | decreased cardiac muscle contractility | 0.93383409 | 1.155704497 |
| REACTOME_FGFR1C_LIGAND_BIN | REACTOME_FGFR1C_LIGAND_BINDING_AND_ACTIVATIC | 0.933940747 | 1.155733984 |
| ENSG00000106089 | STX1A subnetwork | 0.93380462 | 1.155773514 |
| REACTOME_PRESYNAPTIC_NICOT | REACTOME_PRESYNAPTIC_NICOTINIC_ACETYLCHOLINE_ | 0.933789993 | 1.155855393 |
| GO:0016572 | histone phosphorylation | 0.933687114 | 1.155929226 |
| GO:0005911 | cell-cell junction | 0.933776031 | 1.155950137 |
| MP:0000778 | abnormal nervous system tract morphology | 0.933666856 | 1.156006855 |
| GO:0060425 | lung morphogenesis | 0.933600326 | 1.156063073 |

| | | | |
|---|---|---|---|
| ENSG00000114573 | ATP6V1A subnetwork | 0.580071261 | 1.156082266 |
| GO:0033005 | positive regulation of mast cell activation | 0.933548662 | 1.156115015 |
| ENSG00000146425 | DYNLT1 subnetwork | 0.93352898 | 1.156184109 |
| ENSG00000074800 | ENO1 subnetwork | 0.580030411 | 1.156184246 |
| ENSG00000131187 | F12 subnetwork | 0.933250785 | 1.156207665 |
| GO:0048738 | cardiac muscle tissue development | 0.933474453 | 1.156231785 |
| ENSG00000163736 | PPBP subnetwork | 0.579918215 | 1.156246627 |
| ENSG00000128602 | SMO subnetwork | 0.579863796 | 1.156260963 |
| MP:0003451 | absent olfactory bulb | 0.933196322 | 1.156268222 |
| GO:0043576 | regulation of respiratory gaseous exchange | 0.933422187 | 1.156270896 |
| MP:0004986 | abnormal osteoblast morphology | 0.579791899 | 1.156295547 |
| GO:0072657 | protein localization in membrane | 0.933374258 | 1.156297154 |
| MP:0000681 | abnormal thyroid gland morphology | 0.580025335 | 1.156326723 |
| ENSG00000145649 | GZMA subnetwork | 0.93318752 | 1.156354515 |
| ENSG00000121621 | KIF18A subnetwork | 0.933179973 | 1.1564494 |
| ENSG00000162736 | NCSTN subnetwork | 0.932965082 | 1.156485374 |
| GO:0009595 | detection of biotic stimulus | 0.933159532 | 1.156509992 |
| ENSG00000049449 | RCN1 subnetwork | 0.933148937 | 1.156579173 |
| GO:0003170 | heart valve development | 0.932956786 | 1.156584592 |
| REACTOME_PLATELET_ADHESION | REACTOME_PLATELET_ADHESION_TO_EXPOSED_COLLA | 0.93295583 | 1.156683827 |
| GO:0061036 | positive regulation of cartilage development | 0.932950165 | 1.156778788 |
| MP:0000652 | enlarged sebaceous gland | 0.932910154 | 1.156813696 |
| ENSG00000170458 | CD14 subnetwork | 0.932879794 | 1.156891521 |
| ENSG00000073792 | IGF2BP2 subnetwork | 0.580564396 | 1.156910734 |
| GO:0006890 | retrograde vesicle-mediated transport, Golgi to ER | 0.932845615 | 1.156960776 |
| GO:0010959 | regulation of metal ion transport | 0.932706507 | 1.15697914 |
| MP:0001405 | impaired coordination | 0.932832175 | 1.157030043 |
| GO:0032874 | positive regulation of stress-activated MAPK cascade | 0.932697819 | 1.157069883 |
| GO:0060442 | branching involved in prostate gland morphogenesis | 0.932691005 | 1.157156349 |
| GO:0046961 | proton-transporting ATPase activity, rotational mechanis | 0.932602902 | 1.157187017 |
| MP:0010392 | prolonged QRS complex duration | 0.93254338 | 1.15721769 |
| REACTOME_PKA_ACTIVATION_IN | REACTOME_PKA_ACTIVATION_IN_GLUCAGON_SIGNALL | 0.932351629 | 1.157223224 |
| REACTOME_REGULATED_PROTEC | REACTOME_REGULATED_PROTEOLYSIS_OF_P75NTR | 0.581078502 | 1.15722372 |
| GO:0007128 | meiotic prophase I | 0.581162804 | 1.157229484 |
| ENSG00000155463 | OXA1L subnetwork | 0.580838052 | 1.157233383 |
| GO:0010039 | response to iron ion | 0.581024998 | 1.157292088 |
| MP:0005121 | decreased circulating prolactin level | 0.93250484 | 1.157299897 |
| MP:0001982 | decreased chemically-elicited antinociception | 0.932333968 | 1.157301151 |
| REACTOME_NUCLEAR_IMPORT_C | REACTOME_NUCLEAR_IMPORT_OF_REV_PROTEIN | 0.58095782 | 1.157320032 |
| MP:0000849 | abnormal cerebellum morphology | 0.932305464 | 1.157370501 |
| GO:0035235 | ionotropic glutamate receptor signaling pathway | 0.932065284 | 1.157446077 |
| ENSG00000111752 | PHC1 subnetwork | 0.932229569 | 1.157466277 |
| REACTOME_DOWNREGULATION_ | REACTOME_DOWNREGULATION_OF_ERRB2ERBB3_SIGN | 0.932157902 | 1.157466919 |
| GO:0043292 | contractile fiber | 0.932300943 | 1.157469931 |
| GO:0005902 | microvillus | 0.932008996 | 1.157476796 |
| GO:0015078 | hydrogen ion transmembrane transporter activity | 0.931976576 | 1.157533305 |
| MP:0000297 | abnormal atrioventricular cushion morphology | 0.931890769 | 1.15753825 |
| ENSG00000164751 | PEX2 subnetwork | 0.93186983 | 1.157594773 |
| ENSG00000071243 | ING3 subnetwork | 0.581432049 | 1.157646187 |
| MP:0001916 | intracerebral hemorrhage | 0.931254625 | 1.157660215 |
| ENSG00000033050 | ABCF2 subnetwork | 0.931326884 | 1.15768536 |
| GO:0050912 | detection of chemical stimulus involved in sensory perce | 0.931868716 | 1.157694292 |
| MP:0000627 | abnormal mammary gland morphology | 0.58236877 | 1.157695412 |
| GO:0034622 | cellular macromolecular complex assembly | 0.582487696 | 1.157721281 |

| | | | |
|---|---|---|---|
| GO:2000736 | regulation of stem cell differentiation | 0.931645803 | 1.157734973 |
| GO:0014061 | regulation of norepinephrine secretion | 0.931163853 | 1.157738966 |
| ENSG00000134871 | COL4A2 subnetwork | 0.582142228 | 1.157745626 |
| MP:0008329 | decreased somatotroph cell number | 0.931251112 | 1.157755506 |
| ENSG00000136271 | DDX56 subnetwork | 0.582313413 | 1.15777718 |
| ENSG00000197535 | MYO5A subnetwork | 0.931864951 | 1.157785229 |
| ENSG00000108061 | SHOC2 subnetwork | 0.93159436 | 1.157795838 |
| ENSG00000140307 | GTF2A2 subnetwork | 0.931039346 | 1.157800534 |
| GO:0001654 | eye development | 0.93061682 | 1.157803891 |
| ENSG00000075292 | ZNF638 subnetwork | 0.931121644 | 1.157804165 |
| REACTOME_GLYCOLYSIS | REACTOME_GLYCOLYSIS | 0.582255169 | 1.157805141 |
| GO:0015980 | energy derivation by oxidation of organic compounds | 0.931530158 | 1.15782661 |
| REACTOME_RECYCLING_OF_BILE_ | REACTOME_RECYCLING_OF_BILE_ACIDS_AND_SALTS | 0.930984606 | 1.157827022 |
| ENSG00000011304 | PTBP1 subnetwork | 0.581612379 | 1.15783376 |
| ENSG00000163530 | DPPA2 subnetwork | 0.930943383 | 1.157844909 |
| MP:0000820 | abnormal choroid plexus morphology | 0.930562087 | 1.15785622 |
| ENSG00000204086 | RPA4 subnetwork | 0.931857328 | 1.157880482 |
| GO:0006643 | membrane lipid metabolic process | 0.930906893 | 1.157888621 |
| ENSG00000085721 | RRN3 subnetwork | 0.582138236 | 1.157901467 |
| ENSG00000134248 | HBXIP subnetwork | 0.930543599 | 1.157943 |
| GO:0004861 | cyclin-dependent protein kinase inhibitor activity | 0.582082157 | 1.157963113 |
| GO:0015988 | energy coupled proton transport, against electrochemica | 0.930477197 | 1.157965211 |
| GO:0006766 | vitamin metabolic process | 0.930883869 | 1.157975381 |
| ENSG00000112304 | ACOT13 subnetwork | 0.582040056 | 1.158058435 |
| GO:0015991 | ATP hydrolysis coupled proton transport | 0.930477197 | 1.158064933 |
| ENSG00000132694 | ARHGEF11 subnetwork | 0.58187821 | 1.158080808 |
| GO:0046128 | purine ribonucleoside metabolic process | 0.930440019 | 1.158112996 |
| ENSG00000168243 | GNG4 subnetwork | 0.930385853 | 1.158173988 |
| GO:0000077 | DNA damage checkpoint | 0.581856135 | 1.158189655 |
| ENSG00000137403 | HLA-F subnetwork | 0.582030544 | 1.158200916 |
| MP:0004754 | abnormal kidney collecting duct morphology | 0.930314481 | 1.158257236 |
| ENSG00000008056 | SYN1 subnetwork | 0.930376733 | 1.158265139 |
| ENSG00000068796 | KIF2A subnetwork | 0.930311342 | 1.158352718 |
| GO:0006297 | nucleotide-excision repair, DNA gap filling | 0.930277204 | 1.158379287 |
| MP:0000189 | hypoglycemia | 0.582862013 | 1.158399462 |
| GO:0007157 | heterophilic cell-cell adhesion | 0.930222231 | 1.158436019 |
| ENSG00000101557 | USP14 subnetwork | 0.930137684 | 1.158471217 |
| MP:0003934 | abnormal pancreas development | 0.930082517 | 1.15851073 |
| GO:0010741 | negative regulation of intracellular protein kinase cascad | 0.58323764 | 1.158529372 |
| ENSG00000100242 | SUN2 subnetwork | 0.929980524 | 1.158550987 |
| MP:0002754 | dilated heart right ventricle | 0.930034549 | 1.158567488 |
| ENSG00000105371 | ICAM4 subnetwork | 0.583056997 | 1.158586606 |
| MP:0009285 | increased gonadal fat pad weight | 0.583374592 | 1.158622312 |
| GO:0001975 | response to amphetamine | 0.929962083 | 1.158637931 |
| MP:0004892 | increased adiponectin level | 0.583225 | 1.158638075 |
| ENSG00000184985 | SORCS2 subnetwork | 0.583479621 | 1.158708507 |
| MP:0004756 | abnormal proximal convoluted tubule morphology | 0.583554844 | 1.158727493 |
| GO:0021680 | cerebellar Purkinje cell layer development | 0.92995079 | 1.158729201 |
| ENSG00000164164 | OTUD4 subnetwork | 0.929868498 | 1.158734265 |
| GO:0005903 | brush border | 0.583215221 | 1.158773699 |
| MP:0001714 | absent trophoblast giant cells | 0.929805272 | 1.158782444 |
| ENSG00000177156 | TALDO1 subnetwork | 0.583654007 | 1.158800215 |
| ENSG00000085840 | ORC1 subnetwork | 0.929765586 | 1.158847879 |
| GO:0030816 | positive regulation of cAMP metabolic process | 0.929747212 | 1.158926261 |

| | | | |
|---|---|---|---|
| ENSG00000132603 | NIP7 subnetwork | 0.58385372 | 1.159020688 |
| GO:0030819 | positive regulation of cAMP biosynthetic process | 0.929747212 | 1.15902622 |
| ENSG00000146457 | WTAP subnetwork | 0.583921367 | 1.159032908 |
| ENSG00000112096 | SOD2 subnetwork | 0.929707279 | 1.159091693 |
| ENSG00000162992 | NEUROD1 subnetwork | 0.929704104 | 1.159183057 |
| GO:0030705 | cytoskeleton-dependent intracellular transport | 0.928309351 | 1.159213823 |
| ENSG00000136504 | KAT7 subnetwork | 0.929665481 | 1.159239928 |
| GO:0009312 | oligosaccharide biosynthetic process | 0.928475882 | 1.159290774 |
| MP:0004139 | abnormal gastric parietal cell morphology | 0.928284128 | 1.159292379 |
| GO:0008144 | drug binding | 0.929628534 | 1.159296808 |
| GO:0006732 | coenzyme metabolic process | 0.928696923 | 1.15934531 |
| ENSG00000205560 | CPT1B subnetwork | 0.929181167 | 1.159366367 |
| GO:0016894 | endonuclease activity, active with either ribo- or deoxyri | 0.929139957 | 1.159380126 |
| GO:0046326 | positive regulation of glucose import | 0.929410897 | 1.159381203 |
| ENSG00000163220 | S100A9 subnetwork | 0.929355642 | 1.159382013 |
| GO:0090287 | regulation of cellular response to growth factor stimulus | 0.929613856 | 1.159392527 |
| REACTOME_MG1_TRANSITION | REACTOME_MG1_TRANSITION | 0.928281589 | 1.159392552 |
| ENSG00000178127 | NDUFV2 subnetwork | 0.928669419 | 1.159402263 |
| ENSG00000167965 | MLST8 subnetwork | 0.929295469 | 1.15941735 |
| ENSG00000183691 | NOG subnetwork | 0.92956903 | 1.159432171 |
| ENSG00000205220 | PSMB10 subnetwork | 0.928924984 | 1.15943437 |
| GO:0005779 | integral to peroxisomal membrane | 0.927992865 | 1.159439018 |
| MP:0004981 | decreased neuronal precursor cell number | 0.929116849 | 1.159450009 |
| REACTOME_DNA_REPLICATION_F | REACTOME_DNA_REPLICATION_PRE:INITIATION | 0.928281589 | 1.159492741 |
| GO:0005251 | delayed rectifier potassium channel activity | 0.929069854 | 1.159498316 |
| ENSG00000153234 | NR4A2 subnetwork | 0.928900158 | 1.159512911 |
| GO:0031231 | intrinsic to peroxisomal membrane | 0.927992865 | 1.159539246 |
| ENSG00000183779 | ZNF703 subnetwork | 0.927939023 | 1.15958762 |
| GO:0007616 | long-term memory | 0.928278514 | 1.159592948 |
| KEGG_VIBRIO_CHOLERAE_INFECT | KEGG_VIBRIO_CHOLERAE_INFECTION | 0.92789707 | 1.159653294 |
| MP:0010413 | complete atrioventricular septal defect | 0.9282746 | 1.159680207 |
| ENSG00000137055 | PLAA subnetwork | 0.92786564 | 1.159714656 |
| ENSG00000065135 | GNAI3 subnetwork | 0.927785835 | 1.159741439 |
| GO:0007276 | gamete generation | 0.584367227 | 1.159750201 |
| GO:0043200 | response to amino acid stimulus | 0.927743013 | 1.159807143 |
| MP:0004022 | abnormal cone electrophysiology | 0.927635997 | 1.159816641 |
| MP:0005598 | decreased ventricle muscle contractility | 0.584578701 | 1.159854995 |
| GO:0051048 | negative regulation of secretion | 0.927585539 | 1.159865064 |
| ENSG00000099331 | MYO9B subnetwork | 0.927567052 | 1.159943772 |
| ENSG00000132507 | EIF5A subnetwork | 0.92750035 | 1.159961934 |
| MP:0005123 | increased circulating growth hormone level | 0.585029056 | 1.159995975 |
| REACTOME_THE_CITRIC_ACID_TC | REACTOME_THE_CITRIC_ACID_TCA_CYCLE_AND_RESPIR | 0.584572556 | 1.160004028 |
| GO:0016776 | phosphotransferase activity, phosphate group as accept | 0.58470547 | 1.160008055 |
| ENSG00000172766 | NAA16 subnetwork | 0.927488813 | 1.160040664 |
| GO:0008610 | lipid biosynthetic process | 0.58488684 | 1.160045631 |
| ENSG00000107779 | BMPR1A subnetwork | 0.600183775 | 1.160060178 |
| ENSG00000105298 | C19orf29 subnetwork | 0.584805254 | 1.160060403 |
| ENSG00000206286 | VPS52 subnetwork | 0.600100199 | 1.160061494 |
| MP:0002163 | abnormal gland morphology | 0.585219857 | 1.160080483 |
| ENSG00000100401 | RANGAP1 subnetwork | 0.5849907 | 1.160118089 |
| MP:0003194 | abnormal frequency of paradoxical sleep | 0.92746964 | 1.160119408 |
| ENSG00000170421 | KRT8 subnetwork | 0.585164088 | 1.160135498 |
| REACTOME_GLOBAL_GENOMIC_I | REACTOME_GLOBAL_GENOMIC_NER_GG:NER | 0.927417818 | 1.160176532 |
| ENSG00000206214 | ENSG00000206214 subnetwork | 0.600100199 | 1.160213295 |

| | | | |
|---|---|---|---|
| ENSG00000163535 | SGOL2 subnetwork | 0.92741708 | 1.160276936 |
| MP:0002759 | abnormal caudal vertebrae morphology | 0.92714355 | 1.160332439 |
| ENSG00000112478 | ENSG00000112478 subnetwork | 0.600100199 | 1.160365135 |
| GO:0006518 | peptide metabolic process | 0.927414796 | 1.160377358 |
| GO:0001754 | eye photoreceptor cell differentiation | 0.927367252 | 1.160417208 |
| ENSG00000173889 | PHC3 subnetwork | 0.927129665 | 1.160419913 |
| ENSG00000187741 | FANCA subnetwork | 0.927088203 | 1.160477098 |
| GO:0001968 | fibronectin binding | 0.600071785 | 1.160477749 |
| ENSG00000158869 | FCER1G subnetwork | 0.927366229 | 1.160517659 |
| GO:0060347 | heart trabecula formation | 0.58561638 | 1.160527022 |
| GO:0072210 | metanephric nephron development | 0.926862889 | 1.160527455 |
| MP:0002651 | abnormal sciatic nerve morphology | 0.600583883 | 1.160562459 |
| ENSG00000107404 | DVL1 subnetwork | 0.926742141 | 1.160563929 |
| ENSG00000157087 | ATP2B2 subnetwork | 0.927077988 | 1.16056893 |
| GO:0010863 | positive regulation of phospholipase C activity | 0.926818643 | 1.160576007 |
| GO:0004364 | glutathione transferase activity | 0.585855401 | 1.160576408 |
| REACTOME_ACTIVATION_OF_CH/ | REACTOME_ACTIVATION_OF_CHAPERONES_BY_IRE1ALF | 0.927002823 | 1.160587165 |
| GO:0006349 | regulation of gene expression by genetic imprinting | 0.60006943 | 1.160623118 |
| GO:0001619 | lysosphingolipid and lysophosphatidic acid receptor activ | 0.599988041 | 1.160637601 |
| ENSG00000067082 | KLF6 subnetwork | 0.58557746 | 1.160642436 |
| GO:0033327 | Leydig cell differentiation | 0.926718606 | 1.16066014 |
| ENSG00000091592 | NLRP1 subnetwork | 0.600833799 | 1.160669456 |
| ENSG00000106683 | LIMK1 subnetwork | 0.600689694 | 1.160672247 |
| ENSG00000143520 | FLG2 subnetwork | 0.926560997 | 1.160674985 |
| GO:0043623 | cellular protein complex assembly | 0.585821843 | 1.160718595 |
| GO:0048596 | embryonic camera-type eye morphogenesis | 0.926689679 | 1.160734708 |
| MP:0000920 | abnormal myelination | 0.926525157 | 1.160749567 |
| GO:0000793 | condensed chromosome | 0.585773898 | 1.160753553 |
| ENSG00000136011 | STAB2 subnetwork | 0.599982998 | 1.160769936 |
| MP:0001053 | abnormal neuromuscular synapse morphology | 0.600826204 | 1.160788545 |
| ENSG00000174989 | FBXW8 subnetwork | 0.926492674 | 1.160828495 |
| GO:0010470 | regulation of gastrulation | 0.926429743 | 1.160855434 |
| REACTOME_RNA_POLYMERASE_I | REACTOME_RNA_POLYMERASE_I_TRANSCRIPTION_INIT | 0.599750562 | 1.160867287 |
| ENSG00000204843 | DCTN1 subnetwork | 0.598956368 | 1.16088953 |
| REACTOME_GOLGI_TO_ER_RETR( | REACTOME_GOLGI_TO_ER_RETROGRADE_TRANSPORT | 0.593389109 | 1.160893448 |
| GO:0050997 | quaternary ammonium group binding | 0.599980094 | 1.160902305 |
| GO:0051028 | mRNA transport | 0.593636084 | 1.160908971 |
| ENSG00000125450 | NUP85 subnetwork | 0.593576862 | 1.160910414 |
| ENSG00000103549 | RNF40 subnetwork | 0.599627636 | 1.160916001 |
| ENSG00000127603 | MACF1 subnetwork | 0.599564671 | 1.16093709 |
| ENSG00000148688 | RPP30 subnetwork | 0.926426525 | 1.160951721 |
| REACTOME_RAS_ACTIVATION_U( | REACTOME_RAS_ACTIVATION_UOPN_CA2_INFUX_THRO | 0.593307055 | 1.160955912 |
| GO:0071103 | DNA conformation change | 0.926327211 | 1.160957004 |
| GO:0051219 | phosphoprotein binding | 0.599722367 | 1.16096043 |
| GO:0015684 | ferrous iron transport | 0.601052943 | 1.160962217 |
| GO:0009295 | nucleoid | 0.593715149 | 1.160967059 |
| ENSG00000101654 | RNMT subnetwork | 0.599948276 | 1.160969221 |
| GO:0031960 | response to corticosteroid stimulus | 0.598788656 | 1.160972569 |
| GO:0030667 | secretory granule membrane | 0.598918142 | 1.160982811 |
| GO:0006338 | chromatin remodeling | 0.594086372 | 1.161000926 |
| ENSG00000164077 | MON1A subnetwork | 0.593835461 | 1.161005291 |
| MP:0005226 | abnormal vertebral arch development | 0.926301018 | 1.161027308 |
| REACTOME_COPI_MEDIATED_TR/ | REACTOME_COPI_MEDIATED_TRANSPORT | 0.593389109 | 1.161047127 |
| MP:0000060 | delayed bone ossification | 0.599174704 | 1.16105063 |

| | | | |
|---|---|---|---|
| GO:0018410 | C-terminal protein amino acid modification | 0.593571485 | 1.161050821 |
| GO:0016591 | DNA-directed RNA polymerase II, holoenzyme | 0.599370714 | 1.161059394 |
| ENSG00000005249 | PRKAR2B subnetwork | 0.926252082 | 1.161071614 |
| MP:0004030 | induced chromosome breakage | 0.594220022 | 1.161072184 |
| ENSG00000004799 | PDK4 subnetwork | 0.594030683 | 1.161075112 |
| REACTOME_PROTEIN_FOLDING | REACTOME_PROTEIN_FOLDING | 0.599558325 | 1.161076157 |
| ENSG00000099795 | NDUFB7 subnetwork | 0.586481277 | 1.161078366 |
| REACTOME_DCC_MEDIATED_ATT | REACTOME_DCC_MEDIATED_ATTRACTIVE_SIGNALING | 0.599236584 | 1.161095082 |
| ENSG00000168807 | SNTB2 subnetwork | 0.599943401 | 1.161095101 |
| GO:0031650 | regulation of heat generation | 0.593299222 | 1.161096398 |
| GO:0032494 | response to peptidoglycan | 0.598907574 | 1.161102362 |
| ENSG00000056345 | ENSG00000056345 subnetwork | 0.594343033 | 1.161103767 |
| ENSG00000171786 | NHLH1 subnetwork | 0.598764423 | 1.16111184 |
| MP:0002575 | increased circulating ketone body level | 0.586416734 | 1.161113344 |
| GO:0005769 | early endosome | 0.601271033 | 1.161122729 |
| ENSG00000156304 | SCAF4 subnetwork | 0.599329711 | 1.16112641 |
| GO:0001660 | fever generation | 0.594535407 | 1.161147086 |
| GO:0016667 | oxidoreductase activity, acting on a sulfur group of dono | 0.92623035 | 1.161154947 |
| GO:0045745 | positive regulation of G-protein coupled receptor protein | 0.586565492 | 1.161157246 |
| ENSG00000171195 | MUC7 subnetwork | 0.593993486 | 1.161162545 |
| MP:0003985 | renal fibrosis | 0.599512647 | 1.161162821 |
| ENSG00000101349 | PAK7 subnetwork | 0.601233556 | 1.161169935 |
| ENSG00000170871 | KIAA0232 subnetwork | 0.598620737 | 1.161173845 |
| GO:0051188 | cofactor biosynthetic process | 0.586259368 | 1.161176628 |
| GO:0030259 | lipid glycosylation | 0.586368028 | 1.16118853 |
| GO:0000178 | exosome (RNase complex) | 0.5991737 | 1.161202938 |
| ENSG00000134243 | SORT1 subnetwork | 0.598576418 | 1.161214708 |
| GO:0071453 | cellular response to oxygen levels | 0.598727582 | 1.161218327 |
| ENSG00000166200 | COPS2 subnetwork | 0.594473323 | 1.161221253 |
| GO:0000045 | autophagic vacuole assembly | 0.605501235 | 1.161229391 |
| GO:0050830 | defense response to Gram-positive bacterium | 0.60557223 | 1.161240914 |
| ENSG00000143815 | LBR subnetwork | 0.586756579 | 1.161241296 |
| GO:0031652 | positive regulation of heat generation | 0.593299222 | 1.161250166 |
| GO:0045026 | plasma membrane fusion | 0.926226739 | 1.161255636 |
| ENSG00000122565 | CBX3 subnetwork | 0.60544129 | 1.161256816 |
| ENSG00000204310 | AGPAT1 subnetwork | 0.605044067 | 1.161259096 |
| GO:0006302 | double-strand break repair | 0.605370922 | 1.161264771 |
| ENSG00000152464 | RPP38 subnetwork | 0.605331595 | 1.161272727 |
| REACTOME_GLYCOSPHINGOLIPID | REACTOME_GLYCOSPHINGOLIPID_METABOLISM | 0.926135988 | 1.161299974 |
| GO:0032970 | regulation of actin filament-based process | 0.605274833 | 1.161300169 |
| GO:0050886 | endocrine process | 0.586251688 | 1.161318858 |
| GO:0001707 | mesoderm formation | 0.593263473 | 1.161324503 |
| ENSG00000099940 | SNAP29 subnetwork | 0.586720058 | 1.161329851 |
| REACTOME_TAT:MEDIATED_ELOI | REACTOME_TAT:MEDIATED_ELONGATION_OF_THE_HIV | 0.587317467 | 1.16133262 |
| ENSG00000068903 | SIRT2 subnetwork | 0.92608558 | 1.161335646 |
| ENSG00000146047 | HIST1H2BA subnetwork | 0.926002589 | 1.161353977 |
| ENSG00000143546 | S100A8 subnetwork | 0.590015988 | 1.161359702 |
| ENSG00000123374 | CDK2 subnetwork | 0.598572495 | 1.161360651 |
| GO:0042692 | muscle cell differentiation | 0.59812283 | 1.161361546 |
| GO:0017119 | Golgi transport complex | 0.590120456 | 1.161371505 |
| ENSG00000114480 | GBE1 subnetwork | 0.592312465 | 1.161375696 |
| GO:0006949 | syncytium formation | 0.589953069 | 1.161387853 |
| KEGG_VASOPRESSIN_REGULATED | KEGG_VASOPRESSIN_REGULATED_WATER_REABSORPTI | 0.592172237 | 1.161405255 |
| ENSG00000078967 | UBE2D4 subnetwork | 0.605236331 | 1.16140556 |

| | | | |
|---|---|---|---|
| ENSG00000206255 | ENSG00000206255 subnetwork | 0.605044067 | 1.161410006 |
| GO:0018208 | peptidyl-proline modification | 0.592247139 | 1.161417009 |
| MP:0002691 | small stomach | 0.598531829 | 1.161427821 |
| MP:0009009 | absent estrous cycle | 0.592942815 | 1.161431412 |
| ENSG00000109805 | NCAPG subnetwork | 0.601494696 | 1.161434919 |
| GO:0000976 | transcription regulatory region sequence-specific DNA bi | 0.925975707 | 1.161441707 |
| ENSG00000175550 | DRAP1 subnetwork | 0.597995613 | 1.161443407 |
| ENSG00000114698 | PLSCR4 subnetwork | 0.592870444 | 1.16145281 |
| GO:0048407 | platelet-derived growth factor binding | 0.592781347 | 1.161467586 |
| GO:0030145 | manganese ion binding | 0.594931061 | 1.161467829 |
| ENSG00000142875 | PRKACB subnetwork | 0.593262029 | 1.161471718 |
| MP:0005287 | narrow eye opening | 0.589922574 | 1.161482616 |
| REACTOME_HIV:1_TRANSCRIPTIO | REACTOME_HIV:1_TRANSCRIPTION_ELONGATION | 0.587317467 | 1.161488024 |
| GO:0004181 | metallocarboxypeptidase activity | 0.602013506 | 1.161492752 |
| ENSG00000102878 | HSF4 subnetwork | 0.587087373 | 1.161497791 |
| GO:0071391 | cellular response to estrogen stimulus | 0.593191148 | 1.161506359 |
| ENSG00000159459 | UBR1 subnetwork | 0.601930738 | 1.161507315 |
| ENSG00000184897 | H1FX subnetwork | 0.598116904 | 1.161507624 |
| REACTOME_INCRETIN_SYNTHESIS | REACTOME_INCRETIN_SYNTHESIS_SECRETION_AND_IN/ | 0.925941876 | 1.16151644 |
| GO:0030663 | COPI coated vesicle membrane | 0.605220761 | 1.16152397 |
| GO:0043279 | response to alkaloid | 0.59215087 | 1.161526211 |
| MP:0004024 | aneuploidy | 0.602171771 | 1.161535448 |
| ENSG00000120896 | SORBS3 subnetwork | 0.593068083 | 1.161535913 |
| ENSG00000171431 | KRT20 subnetwork | 0.592075219 | 1.161541014 |
| GO:0005200 | structural constituent of cytoskeleton | 0.590594951 | 1.16154358 |
| MP:0005441 | increased urine calcium level | 0.598506581 | 1.161547556 |
| ENSG00000166477 | LEO1 subnetwork | 0.601858311 | 1.161548008 |
| GO:0005921 | gap junction | 0.598424886 | 1.161555643 |
| ENSG00000206324 | AGPAT1 subnetwork | 0.605044067 | 1.161560957 |
| GO:0002548 | monocyte chemotaxis | 0.591022532 | 1.1615625 |
| REACTOME_NEPNS2_INTERACTS_ | REACTOME_NEPNS2_INTERACTS_WITH_THE_CELLULAR_ | 0.597958517 | 1.161569813 |
| ENSG00000126698 | DNAJC8 subnetwork | 0.587048145 | 1.161579652 |
| ENSG00000127526 | SLC35E1 subnetwork | 0.605832379 | 1.161583387 |
| ENSG00000138346 | DNA2 subnetwork | 0.58989626 | 1.161584066 |
| ENSG00000163435 | ELF3 subnetwork | 0.59054094 | 1.161591696 |
| GO:0051085 | chaperone mediated protein folding requiring cofactor | 0.590440213 | 1.161593238 |
| ENSG00000184363 | PKP3 subnetwork | 0.594916553 | 1.161594873 |
| GO:0051130 | positive regulation of cellular component organization | 0.592761272 | 1.161595068 |
| GO:0035966 | response to topologically incorrect protein | 0.593163146 | 1.161613886 |
| GO:0016624 | oxidoreductase activity, acting on the aldehyde or oxo gr | 0.92594184 | 1.161617213 |
| ENSG00000196628 | TCF4 subnetwork | 0.925824626 | 1.161635575 |
| MP:0001270 | distended abdomen | 0.590328025 | 1.161636267 |
| ENSG00000198042 | MAK16 subnetwork | 0.590401031 | 1.161641374 |
| ENSG00000106125 | FAM188B subnetwork | 0.601709098 | 1.161642493 |
| REACTOME_FORMATION_OF_HIV | REACTOME_FORMATION_OF_HIV:1_ELONGATION_COM | 0.587317467 | 1.161643469 |
| GO:0006303 | double-strand break repair via nonhomologous end joini | 0.589771117 | 1.161647122 |
| ENSG00000135821 | GLUL subnetwork | 0.59098645 | 1.161650485 |
| MP:0005440 | increased glycogen level | 0.602923893 | 1.161666884 |
| ENSG00000155957 | TMBIM4 subnetwork | 0.597922628 | 1.161669954 |
| MP:0009780 | abnormal chondrocyte physiology | 0.605020359 | 1.161672949 |
| GO:0070008 | serine-type exopeptidase activity | 0.602167735 | 1.161674066 |
| GO:0032984 | macromolecular complex disassembly | 0.5876375 | 1.161684056 |
| REACTOME_G:PROTEIN_BETAGAI | REACTOME_G:PROTEIN_BETAGAMMA_SIGNALLING | 0.598410246 | 1.161688568 |
| ENSG00000072134 | EPN2 subnetwork | 0.592069197 | 1.16168857 |

| | | | |
|---|---|---|---|
| MP:0001939 | secondary sex reversal | 0.589882996 | 1.161692205 |
| MP:0000729 | abnormal myogenesis | 0.587573534 | 1.161692308 |
| ENSG00000102804 | TSC22D1 subnetwork | 0.592582021 | 1.161692532 |
| MP:0002666 | increased circulating aldosterone level | 0.6018574 | 1.161693232 |
| ENSG00000151923 | TIAL1 subnetwork | 0.925800625 | 1.161701666 |
| ENSG00000127329 | PTPRB subnetwork | 0.587039711 | 1.1617017 |
| ENSG00000170275 | CRTAP subnetwork | 0.592744701 | 1.161702692 |
| ENSG00000094804 | CDC6 subnetwork | 0.925735042 | 1.16171136 |
| ENSG00000198947 | DMD subnetwork | 0.591345968 | 1.161715843 |
| GO:0018149 | peptide cross-linking | 0.602578809 | 1.161731698 |
| ENSG00000149182 | ARFGAP2 subnetwork | 0.597281281 | 1.161734895 |
| GO:0030742 | GTP-dependent protein binding | 0.602800702 | 1.161741683 |
| GO:0006260 | DNA replication | 0.604981467 | 1.16174597 |
| GO:0043303 | mast cell degranulation | 0.925678698 | 1.161755772 |
| GO:0016614 | oxidoreductase activity, acting on CH-OH group of donor | 0.603078106 | 1.161756651 |
| GO:0045017 | glycerolipid biosynthetic process | 0.58974714 | 1.161761962 |
| MP:0002135 | abnormal kidney morphology | 0.602710556 | 1.161762787 |
| MP:0008227 | absent anterior commissure | 0.597693884 | 1.16176664 |
| ENSG00000069974 | RAB27A subnetwork | 0.592017763 | 1.161776421 |
| GO:0030308 | negative regulation of cell growth | 0.590976305 | 1.1617917 |
| ENSG00000108829 | LRRC59 subnetwork | 0.602553816 | 1.16179196 |
| ENSG00000211973 | ENSG00000211973 subnetwork | 0.597632494 | 1.161794501 |
| ENSG00000109332 | UBE2D3 subnetwork | 0.5978175 | 1.161797974 |
| MP:0002230 | abnormal primitive streak formation | 0.59117672 | 1.161800293 |
| ENSG00000168214 | RBPJ subnetwork | 0.591466842 | 1.161800664 |
| MP:0000063 | decreased bone mineral density | 0.590801167 | 1.16180149 |
| ENSG00000140284 | SLC27A2 subnetwork | 0.597895729 | 1.161802998 |
| GO:0016458 | gene silencing | 0.602467184 | 1.161806553 |
| GO:0005932 | microtubule basal body | 0.595298216 | 1.161806656 |
| ENSG00000184270 | HIST2H2AB subnetwork | 0.597472917 | 1.161810765 |
| ENSG00000160208 | RRP1B subnetwork | 0.602919476 | 1.161811897 |
| GO:0006869 | lipid transport | 0.591653963 | 1.161817457 |
| GO:0034508 | centromere complex assembly | 0.591261525 | 1.161818665 |
| GO:0046323 | glucose import | 0.925667833 | 1.16183057 |
| ENSG00000037280 | FLT4 subnetwork | 0.588031299 | 1.161838235 |
| GO:0071326 | cellular response to monosaccharide stimulus | 0.60496104 | 1.161838513 |
| REACTOME_SHC:MEDIATED_SIGN | REACTOME_SHC:MEDIATED_SIGNALLING | 0.592744293 | 1.161843501 |
| GO:0010595 | positive regulation of endothelial cell migration | 0.595425099 | 1.161851314 |
| MP:0006280 | abnormal digit development | 0.597264157 | 1.161861506 |
| ENSG00000134363 | FST subnetwork | 0.603209576 | 1.161865954 |
| ENSG00000077522 | ACTN2 subnetwork | 0.591345919 | 1.161870265 |
| ENSG00000082258 | CCNT2 subnetwork | 0.59515495 | 1.161875826 |
| MP:0004471 | short nasal bone | 0.603356928 | 1.161875896 |
| GO:0005529 | GO:0005529 | 0.588277496 | 1.161880262 |
| MP:0005479 | decreased circulating triiodothyronine level | 0.588378585 | 1.161885355 |
| GO:0004518 | nuclease activity | 0.591591939 | 1.161892107 |
| ENSG00000159377 | PSMB4 subnetwork | 0.925649715 | 1.161901042 |
| ENSG00000086102 | NFX1 subnetwork | 0.589744886 | 1.161910157 |
| ENSG00000067829 | IDH3G subnetwork | 0.602452267 | 1.16191906 |
| ENSG00000072210 | ALDH3A2 subnetwork | 0.592007252 | 1.161924047 |
| ENSG00000112182 | BACH2 subnetwork | 0.590957701 | 1.161932952 |
| ENSG00000139625 | MAP3K12 subnetwork | 0.591852517 | 1.161933856 |
| REACTOME_INITIAL_TRIGGERING | REACTOME_INITIAL_TRIGGERING_OF_COMPLEMENT | 0.59745707 | 1.161937352 |
| MP:0006386 | absent somites | 0.595286098 | 1.161940299 |

| | | | |
|---|---|---|---|
| GO:0060590 | ATPase regulator activity | 0.587999119 | 1.161946784 |
| ENSG00000211979 | ENSG00000211979 subnetwork | 0.597632494 | 1.161947368 |
| GO:0032799 | low-density lipoprotein receptor particle metabolic proc | 0.588250011 | 1.161975408 |
| GO:0048846 | axon extension involved in axon guidance | 0.925600986 | 1.161980207 |
| ENSG00000182185 | RAD51B subnetwork | 0.924152008 | 1.161980525 |
| ENSG00000156709 | AIFM1 subnetwork | 0.603320137 | 1.161981747 |
| ENSG00000196532 | HIST1H3C subnetwork | 0.597231324 | 1.16198815 |
| GO:0071331 | cellular response to hexose stimulus | 0.60496104 | 1.161989597 |
| ENSG00000162923 | WDR26 subnetwork | 0.591797913 | 1.161995218 |
| GO:0032479 | regulation of type I interferon production | 0.588197367 | 1.161997059 |
| GO:0016706 | oxidoreductase activity, acting on paired donors, with in | 0.589575868 | 1.162008268 |
| ENSG00000168061 | SAC3D1 subnetwork | 0.58858562 | 1.162014158 |
| ENSG00000068438 | FTSJ1 subnetwork | 0.58795359 | 1.162021931 |
| MP:0009907 | decreased tongue size | 0.925557889 | 1.162028998 |
| GO:0008329 | pattern recognition receptor activity | 0.589721245 | 1.162031729 |
| GO:0007431 | salivary gland development | 0.588525955 | 1.162049158 |
| ENSG00000123975 | CKS2 subnetwork | 0.588489444 | 1.162057448 |
| GO:0070001 | aspartic-type peptidase activity | 0.925509322 | 1.162073457 |
| MP:0001096 | abnormal glossopharyngeal ganglion morphology | 0.924149564 | 1.162077211 |
| ENSG00000130702 | LAMA5 subnetwork | 0.59200237 | 1.162078353 |
| ENSG00000172071 | EIF2AK3 subnetwork | 0.589529417 | 1.162116564 |
| ENSG00000196331 | HIST1H2BO subnetwork | 0.589696722 | 1.162126667 |
| GO:0071333 | cellular response to glucose stimulus | 0.60496104 | 1.162140721 |
| ENSG00000197153 | HIST1H3J subnetwork | 0.597231324 | 1.162141164 |
| MP:0004399 | abnormal cochlear outer hair cell morphology | 0.607423755 | 1.162148685 |
| ENSG00000133119 | RFC3 subnetwork | 0.587943182 | 1.16216397 |
| ENSG00000162236 | STX5 subnetwork | 0.589050639 | 1.162166311 |
| GO:0021591 | ventricular system development | 0.924711779 | 1.162166507 |
| GO:0004190 | aspartic-type endopeptidase activity | 0.925509322 | 1.162174366 |
| MP:0001522 | impaired swimming | 0.924145808 | 1.162178261 |
| ENSG00000163002 | NUP35 subnetwork | 0.606449024 | 1.16219354 |
| ENSG00000124507 | PACSIN1 subnetwork | 0.606337736 | 1.16220968 |
| GO:0060317 | cardiac epithelial to mesenchymal transition | 0.924668611 | 1.162219711 |
| MP:0008518 | retinal outer nuclear layer degeneration | 0.603600134 | 1.162226277 |
| ENSG00000196781 | TLE1 subnetwork | 0.604913311 | 1.162226847 |
| ENSG00000158402 | CDC25C subnetwork | 0.606417493 | 1.162234043 |
| ENSG00000068400 | GRIPAP1 subnetwork | 0.607385952 | 1.162234456 |
| GO:0005761 | mitochondrial ribosome | 0.589516691 | 1.162238229 |
| ENSG00000160868 | CYP3A4 subnetwork | 0.603701824 | 1.162250749 |
| ENSG00000166165 | CKB subnetwork | 0.604865487 | 1.162254456 |
| ENSG00000105426 | PTPRS subnetwork | 0.588767802 | 1.162259615 |
| GO:0010948 | negative regulation of cell cycle process | 0.924137167 | 1.162270632 |
| ENSG00000151746 | BICD1 subnetwork | 0.92549941 | 1.162270951 |
| REACTOME_SYNTHESIS_SECRETIC | REACTOME_SYNTHESIS_SECRETION_AND_DEACYLATION | 0.924884013 | 1.16227407 |
| MP:0004484 | altered response of heart to induced stress | 0.925441797 | 1.162276359 |
| ENSG00000124789 | NUP153 subnetwork | 0.589201345 | 1.162278126 |
| GO:0031112 | positive regulation of microtubule polymerization or dep | 0.924604987 | 1.162285963 |
| ENSG00000124693 | HIST1H3B subnetwork | 0.597231324 | 1.162294218 |
| ENSG00000152700 | SAR1B subnetwork | 0.589031711 | 1.162294754 |
| GO:0045540 | regulation of cholesterol biosynthetic process | 0.604127182 | 1.162301381 |
| GO:0043508 | negative regulation of JUN kinase activity | 0.92409107 | 1.162306488 |
| ENSG00000127564 | PKMYT1 subnetwork | 0.607358974 | 1.162307294 |
| ENSG00000125835 | SNRPB subnetwork | 0.606588652 | 1.162315175 |
| ENSG00000168286 | THAP11 subnetwork | 0.604000785 | 1.162330641 |

| | | | |
|---|---|---|---|
| ENSG00000119541 | VPS4B subnetwork | 0.606331915 | 1.162347521 |
| ENSG00000167193 | CRK subnetwork | 0.604079126 | 1.162348574 |
| REACTOME_NCAM_SIGNALING_F | REACTOME_NCAM_SIGNALING_FOR_NEURITE_OUT:GR( | 0.925413018 | 1.162355598 |
| MP:0004837 | abnormal neural fold formation | 0.92459061 | 1.162365264 |
| MP:0002573 | behavioral despair | 0.92448769 | 1.162366339 |
| MP:0000837 | abnormal hypothalamus morphology | 0.924070459 | 1.162381491 |
| MP:0008533 | abnormal anterior visceral endoderm morphology | 0.604849404 | 1.162386157 |
| GO:0000313 | organellar ribosome | 0.589516691 | 1.162393276 |
| GO:0033540 | fatty acid beta-oxidation using acyl-CoA oxidase | 0.925375156 | 1.162395761 |
| KEGG_NOTCH_SIGNALING_PATH\ | KEGG_NOTCH_SIGNALING_PATHWAY | 0.589442751 | 1.162414943 |
| ENSG00000137845 | ADAM10 subnetwork | 0.607337184 | 1.162425499 |
| ENSG00000164258 | NDUFS4 subnetwork | 0.589014395 | 1.162436582 |
| MP:0005322 | abnormal serotonin level | 0.925327598 | 1.162440275 |
| ENSG00000198366 | HIST1H3A subnetwork | 0.597231324 | 1.162447313 |
| ENSG00000103035 | PSMD7 subnetwork | 0.603986564 | 1.162456026 |
| MP:0003038 | decreased infarction size | 0.588922666 | 1.162458272 |
| MP:0003270 | intestinal obstruction | 0.925144142 | 1.162459814 |
| GO:0019200 | carbohydrate kinase activity | 0.924050089 | 1.162465205 |
| ENSG00000185043 | CIB1 subnetwork | 0.604820329 | 1.162465843 |
| GO:0051020 | GTPase binding | 0.589363245 | 1.16248332 |
| ENSG00000107371 | EXOSC3 subnetwork | 0.607303863 | 1.16249838 |
| ENSG00000078699 | CBFA2T2 subnetwork | 0.595936325 | 1.162508251 |
| MP:0000558 | abnormal tibia morphology | 0.925312163 | 1.162523892 |
| MP:0004180 | failure of initiation of embryo turning | 0.604364839 | 1.162553718 |
| GO:0072074 | kidney mesenchyme development | 0.924027173 | 1.162557634 |
| ENSG00000164330 | EBF1 subnetwork | 0.60480596 | 1.16256507 |
| GO:0002209 | behavioral defense response | 0.923789937 | 1.162569614 |
| GO:0005518 | collagen binding | 0.604465562 | 1.162571615 |
| ENSG00000122126 | OCRL subnetwork | 0.603966394 | 1.162574928 |
| MP:0005534 | decreased body temperature | 0.596137695 | 1.162584136 |
| ENSG00000130227 | XPO7 subnetwork | 0.607268233 | 1.162590721 |
| ENSG00000155229 | MMS19 subnetwork | 0.596067227 | 1.162592397 |
| ENSG00000112727 | ENSG00000112727 subnetwork | 0.597231324 | 1.162600448 |
| MP:0005365 | abnormal bile salt homeostasis | 0.923990936 | 1.162623978 |
| GO:0006501 | C-terminal protein lipidation | 0.595929554 | 1.162635331 |
| ENSG00000104267 | CA2 subnetwork | 0.923921286 | 1.162642478 |
| GO:0007080 | mitotic metaphase plate congression | 0.92376628 | 1.16264903 |
| GO:0045765 | regulation of angiogenesis | 0.604676867 | 1.162665972 |
| REACTOME_REGULATION_OF_SIC | REACTOME_REGULATION_OF_SIGNALING_BY_CBL | 0.60721835 | 1.162670123 |
| ENSG00000164346 | NSA2 subnetwork | 0.596859774 | 1.162694437 |
| ENSG00000177105 | RHOG subnetwork | 0.604803753 | 1.162716387 |
| ENSG00000101856 | PGRMC1 subnetwork | 0.607767514 | 1.162723388 |
| MP:0005097 | polychromatophilia | 0.607093199 | 1.162725269 |
| MP:0009397 | increased trophoblast giant cell number | 0.604621522 | 1.162732717 |
| ENSG00000012963 | UBR7 subnetwork | 0.606994037 | 1.162733402 |
| GO:0009267 | cellular response to starvation | 0.607178803 | 1.162743065 |
| GO:0006040 | amino sugar metabolic process | 0.596646476 | 1.162745615 |
| GO:0051181 | cofactor transport | 0.923765719 | 1.162750218 |
| ENSG00000197409 | HIST1H3D subnetwork | 0.597231324 | 1.162753623 |
| GO:0021536 | diencephalon development | 0.923702654 | 1.162764383 |
| ENSG00000129562 | DAD1 subnetwork | 0.596835344 | 1.162801582 |
| GO:0035587 | purinergic receptor signaling pathway | 0.923691263 | 1.162843837 |
| ENSG00000148835 | TAF5 subnetwork | 0.606975618 | 1.162845286 |
| ENSG00000090061 | CCNK subnetwork | 0.596498358 | 1.162856201 |

| | | | |
|---|---|---|---|
| GO:0043149 | stress fiber assembly | 0.596788209 | 1.162875791 |
| GO:0033344 | cholesterol efflux | 0.596640403 | 1.162898971 |
| ENSG00000182572 | HIST1H3I subnetwork | 0.597231324 | 1.162906839 |
| MP:0001951 | abnormal breathing pattern | 0.923661998 | 1.16293201 |
| MP:0004154 | renal tubular necrosis | 0.596472824 | 1.162963452 |
| ENSG00000106633 | GCK subnetwork | 0.596427257 | 1.163024545 |
| GO:0072395 | signal transduction involved in cell cycle checkpoint | 0.923654387 | 1.163024552 |
| MP:0004930 | small epididymis | 0.596635954 | 1.163045772 |
| ENSG00000178458 | ENSG00000178458 subnetwork | 0.597231324 | 1.163060095 |
| GO:0072404 | signal transduction involved in G1/S transition checkpoir | 0.923654387 | 1.163125816 |
| GO:0072329 | monocarboxylic acid catabolic process | 0.923612325 | 1.16318356 |
| GO:0010962 | regulation of glucan biosynthetic process | 0.923437243 | 1.163207629 |
| ENSG00000196966 | HIST1H3E subnetwork | 0.597231324 | 1.163213391 |
| GO:0048592 | eye morphogenesis | 0.923574512 | 1.163241313 |
| GO:0005979 | regulation of glycogen biosynthetic process | 0.923437243 | 1.163308945 |
| MP:0001257 | increased body length | 0.923305458 | 1.163337399 |
| GO:0032885 | regulation of polysaccharide biosynthetic process | 0.923437243 | 1.163410279 |
| ENSG00000078403 | MLLT10 subnetwork | 0.923289711 | 1.16343004 |
| REACTOME_RECRUITMENT_OF_M | REACTOME_RECRUITMENT_OF_MITOTIC_CENTROSOME | 0.923239022 | 1.163461706 |
| GO:0042625 | ATPase activity, coupled to transmembrane movement c | 0.92308604 | 1.163490196 |
| GO:0060713 | labyrinthine layer morphogenesis | 0.923059115 | 1.163552379 |
| ENSG00000137825 | ITPKA subnetwork | 0.922972984 | 1.163562277 |
| REACTOME_CENTROSOME_MATU | REACTOME_CENTROSOME_MATURATION | 0.923239022 | 1.163563088 |
| GO:0060968 | regulation of gene silencing | 0.922931836 | 1.163633194 |
| GO:0007272 | ensheathment of neurons | 0.922867295 | 1.1636431 |
| ENSG00000095319 | NUP188 subnetwork | 0.608354318 | 1.163686391 |
| ENSG00000111052 | LIN7A subnetwork | 0.922475268 | 1.163718821 |
| GO:0019438 | aromatic compound biosynthetic process | 0.922421287 | 1.163737462 |
| GO:0008366 | axon ensheathment | 0.922867295 | 1.163744551 |
| MP:0006254 | thin cerebral cortex | 0.9228225 | 1.163819862 |
| ENSG00000215425 | DDX39B subnetwork | 0.922391312 | 1.163821528 |
| ENSG00000175115 | PACS1 subnetwork | 0.922700632 | 1.163861516 |
| ENSG00000168546 | GFRA2 subnetwork | 0.608491211 | 1.163865873 |
| GO:0010596 | negative regulation of endothelial cell migration | 0.922811841 | 1.163912626 |
| ENSG00000215412 | ENSG00000215412 subnetwork | 0.922391312 | 1.163923057 |
| ENSG00000152413 | HOMER1 subnetwork | 0.60872195 | 1.163978773 |
| ENSG00000094796 | KRT31 subnetwork | 0.608622973 | 1.163980583 |
| ENSG00000198563 | DDX39B subnetwork | 0.922391312 | 1.164024603 |
| ENSG00000131473 | ACLY subnetwork | 0.608799779 | 1.164041672 |
| ENSG00000164032 | H2AFZ subnetwork | 0.922348742 | 1.164086903 |
| MP:0001683 | absent mesoderm | 0.608912194 | 1.164104555 |
| GO:0042770 | signal transduction in response to DNA damage | 0.922203669 | 1.164106816 |
| ENSG00000151532 | VTI1A subnetwork | 0.92232844 | 1.164166667 |
| MP:0002750 | exophthalmos | 0.609005021 | 1.164167421 |
| GO:0071837 | HMG box domain binding | 0.9221842 | 1.164186595 |
| MP:0001629 | abnormal heart rate | 0.92216312 | 1.164253295 |
| ENSG00000132464 | ENAM subnetwork | 0.922126321 | 1.164306913 |
| REACTOME_E2F_MEDIATED_REG | REACTOME_E2F_MEDIATED_REGULATION_OF_DNA_REI | 0.921867129 | 1.164333741 |
| KEGG_CYSTEINE_AND_METHIONI | KEGG_CYSTEINE_AND_METHIONINE_METABOLISM | 0.922125419 | 1.164408555 |
| GO:0030193 | regulation of blood coagulation | 0.921844616 | 1.164417955 |
| GO:0032331 | negative regulation of chondrocyte differentiation | 0.922107429 | 1.164479658 |
| GO:0022011 | myelination in peripheral nervous system | 0.921702692 | 1.164481614 |
| ENSG00000115211 | EIF2B4 subnetwork | 0.92181048 | 1.164510917 |
| GO:0010828 | positive regulation of glucose transport | 0.922099099 | 1.164550773 |

| | | | |
|---|---|---|---|
| GO:0032292 | peripheral nervous system axon ensheathment | 0.921702692 | 1.164583333 |
| MP:0000024 | lowered ear position | 0.921677501 | 1.164637023 |
| ENSG00000064601 | CTSA subnetwork | 0.921585859 | 1.164647038 |
| KEGG_GLYCOLYSIS_GLUCONEOGE | KEGG_GLYCOLYSIS_GLUCONEOGENESIS | 0.60944955 | 1.164719959 |
| GO:0006555 | methionine metabolic process | 0.921582146 | 1.16474443 |
| GO:0004520 | endodeoxyribonuclease activity | 0.60957717 | 1.164763321 |
| MP:0010872 | increased trabecular bone mass | 0.609390539 | 1.164767141 |
| MP:0000790 | abnormal stratification in cerebral cortex | 0.921559862 | 1.1648331 |
| ENSG00000198356 | ASNA1 subnetwork | 0.92126583 | 1.164842657 |
| ENSG00000167491 | GATAD2A subnetwork | 0.921518279 | 1.164869352 |
| ENSG00000168259 | DNAJC7 subnetwork | 0.921469761 | 1.164918721 |
| GO:0009113 | purine base biosynthetic process | 0.921252618 | 1.164922633 |
| GO:0010518 | positive regulation of phospholipase activity | 0.921419768 | 1.164946246 |
| KEGG_ETHER_LIPID_METABOLISM | KEGG_ETHER_LIPID_METABOLISM | 0.92124637 | 1.16502448 |
| MP:0002731 | megacolon | 0.921243985 | 1.165121973 |
| GO:0015301 | anion:anion antiporter activity | 0.921218923 | 1.165184505 |
| ENSG00000101152 | DNAJC5 subnetwork | 0.92087069 | 1.165283002 |
| ENSG00000169862 | CTNND2 subnetwork | 0.921209495 | 1.165286401 |
| GO:0033116 | endoplasmic reticulum-Golgi intermediate compartment | 0.921125597 | 1.16530523 |
| ENSG00000130707 | ASS1 subnetwork | 0.921075415 | 1.165345928 |
| ENSG00000133103 | COG6 subnetwork | 0.611072644 | 1.165354331 |
| MP:0003732 | abnormal retinal outer plexiform layer morphology | 0.920849898 | 1.165367454 |
| MP:0002280 | abnormal intercostal muscle morphology | 0.920671072 | 1.165370144 |
| REACTOME_CYTOSOLIC_SULFONA | REACTOME_CYTOSOLIC_SULFONATION_OF_SMALL_MO | 0.920771892 | 1.165373174 |
| GO:0001578 | microtubule bundle formation | 0.920493355 | 1.16537721 |
| ENSG00000178209 | PLEC subnetwork | 0.610048354 | 1.165412464 |
| ENSG00000154174 | TOMM70A subnetwork | 0.920448274 | 1.165422319 |
| ENSG00000143006 | DMRTB1 subnetwork | 0.609982381 | 1.165427389 |
| GO:0004623 | phospholipase A2 activity | 0.920632851 | 1.165432747 |
| GO:0022613 | ribonucleoprotein complex biogenesis | 0.610316551 | 1.165445263 |
| GO:0042026 | protein refolding | 0.92107462 | 1.165447866 |
| ENSG00000169891 | REPS2 subnetwork | 0.917630377 | 1.165459573 |
| GO:0005753 | mitochondrial proton-transporting ATP synthase comple | 0.611048524 | 1.165459592 |
| ENSG00000135333 | EPHA7 subnetwork | 0.917772814 | 1.165502107 |
| GO:0007351 | tripartite regional subdivision | 0.920442955 | 1.165519958 |
| MP:0002790 | decreased circulating follicle stimulating hormone level | 0.917529105 | 1.165523751 |
| ENSG00000178741 | COX5A subnetwork | 0.91738443 | 1.165526478 |
| GO:0072376 | protein activation cascade | 0.917608556 | 1.165535558 |
| GO:0006684 | sphingomyelin metabolic process | 0.611000995 | 1.165551969 |
| GO:0051056 | regulation of small GTPase mediated signal transduction | 0.610291895 | 1.165557135 |
| ENSG00000189283 | FHIT subnetwork | 0.917496737 | 1.165577801 |
| GO:0070168 | negative regulation of biomineral tissue development | 0.610242118 | 1.165597931 |
| MP:0000633 | abnormal pituitary gland morphology | 0.917357503 | 1.165602494 |
| GO:0030299 | intestinal cholesterol absorption | 0.610662716 | 1.165620155 |
| GO:0008595 | anterior/posterior axis specification, embryo | 0.920442955 | 1.165621991 |
| REACTOME_RHO_GTPASE_CYCLE | REACTOME_RHO_GTPASE_CYCLE | 0.610581564 | 1.165622173 |
| ENSG00000118762 | PKD2 subnetwork | 0.918768658 | 1.165623082 |
| MP:0009887 | abnormal palatal shelf fusion at midline | 0.917317394 | 1.165638999 |
| ENSG00000136861 | CDK5RAP2 subnetwork | 0.920205554 | 1.165656743 |
| MP:0003638 | abnormal response/metabolism to endogenous compou | 0.611427297 | 1.165658065 |
| MP:0003043 | hypoalgesia | 0.918649482 | 1.165660907 |
| ENSG00000197860 | SGTB subnetwork | 0.918745451 | 1.16569023 |
| REACTOME_INWARDLY_RECTIFYI | REACTOME_INWARDLY_RECTIFYING_K_CHANNELS | 0.920329326 | 1.165694773 |
| GO:0046620 | regulation of organ growth | 0.61099644 | 1.165702479 |

| | | | |
|---|---|---|---|
| ENSG00000078369 | GNB1 subnetwork | 0.917290619 | 1.165710647 |
| GO:0055013 | cardiac muscle cell development | 0.918995746 | 1.165712407 |
| GO:0051322 | anaphase | 0.920433218 | 1.165715286 |
| ENSG00000134899 | ERCC5 subnetwork | 0.918488159 | 1.165726443 |
| MP:0005202 | lethargy | 0.611306056 | 1.165726639 |
| GO:0048640 | negative regulation of developmental growth | 0.92018291 | 1.165728172 |
| REACTOME_PROCESSING_OF_INT | REACTOME_PROCESSING_OF_INTRONLESS_PRE:MRNAS | 0.919909073 | 1.165736685 |
| REACTOME_SEMA3A:PLEXIN_REP | REACTOME_SEMA3A:PLEXIN_REPULSION_SIGNALING_B | 0.918641299 | 1.16575 |
| ENSG00000077080 | ACTL6B subnetwork | 0.918452769 | 1.165771694 |
| REACTOME_SIGNALING_BY_RHO_ | REACTOME_SIGNALING_BY_RHO_GTPASES | 0.610581564 | 1.16577281 |
| GO:0072663 | establishment of protein localization to peroxisome | 0.917009498 | 1.165773286 |
| MP:0004046 | abnormal mitosis | 0.918567746 | 1.165782086 |
| MP:0005409 | darkened coat color | 0.919870214 | 1.165786246 |
| REACTOME_RNA_POLYMERASE_I | REACTOME_RNA_POLYMERASE_I_TRANSCRIPTION | 0.91978579 | 1.16579201 |
| ENSG00000185008 | ROBO2 subnetwork | 0.917269128 | 1.16580427 |
| KEGG_OLFACTORY_TRANSDUCTIC | KEGG_OLFACTORY_TRANSDUCTION | 0.917110089 | 1.165807047 |
| ENSG00000148606 | POLR3A subnetwork | 0.611426922 | 1.165808491 |
| GO:0055006 | cardiac cell development | 0.918995746 | 1.165814626 |
| GO:0018958 | phenol-containing compound metabolic process | 0.917226352 | 1.16582323 |
| ENSG00000161939 | C17orf49 subnetwork | 0.611919825 | 1.165824091 |
| GO:0034377 | plasma lipoprotein particle assembly | 0.61098644 | 1.165827199 |
| MP:0009247 | meteorism | 0.920181964 | 1.165830268 |
| ENSG00000167900 | TK1 subnetwork | 0.919366109 | 1.165857293 |
| GO:0071855 | neuropeptide receptor binding | 0.916839593 | 1.165865342 |
| GO:0007612 | learning | 0.919769945 | 1.16586787 |
| GO:0032838 | cell projection cytoplasm | 0.919438648 | 1.165869051 |
| ENSG00000016082 | ISL1 subnetwork | 0.918452595 | 1.165873991 |
| GO:0006625 | protein targeting to peroxisome | 0.917009498 | 1.165875736 |
| MP:0002837 | dystrophic cardiac calcinosis | 0.918322956 | 1.165903107 |
| GO:0042149 | cellular response to glucose starvation | 0.611873634 | 1.16590997 |
| ENSG00000189285 | ENSG00000189285 subnetwork | 0.920166953 | 1.165914864 |
| GO:0031069 | hair follicle morphogenesis | 0.918416121 | 1.165914875 |
| ENSG00000100632 | ERH subnetwork | 0.916804289 | 1.165915084 |
| GO:0060412 | ventricular septum morphogenesis | 0.919753769 | 1.165948125 |
| GO:0051604 | protein maturation | 0.919361937 | 1.165955115 |
| REACTOME_TRANSPORT_OF_VIT/ | REACTOME_TRANSPORT_OF_VITAMINS_NUCLEOSIDES_ | 0.919292407 | 1.165974049 |
| GO:0065005 | protein-lipid complex assembly | 0.61098644 | 1.165977784 |
| GO:0072662 | protein localization to peroxisome | 0.917009498 | 1.165978204 |
| ENSG00000117601 | SERPINC1 subnetwork | 0.916778307 | 1.166 |
| GO:0072207 | metanephric epithelium development | 0.918318584 | 1.166001053 |
| GO:0000279 | M phase | 0.611831033 | 1.166002322 |
| ENSG00000144182 | LIPT1 subnetwork | 0.916677082 | 1.166005803 |
| ENSG00000103326 | SOLH subnetwork | 0.919731077 | 1.166024012 |
| GO:0008180 | signalosome | 0.613305656 | 1.166044536 |
| ENSG00000087258 | GNAO1 subnetwork | 0.916641084 | 1.166064363 |
| GO:0021533 | cell differentiation in hindbrain | 0.919672192 | 1.16607362 |
| REACTOME_POLYMERASE_SWITC | REACTOME_POLYMERASE_SWITCHING | 0.613136131 | 1.166074417 |
| GO:0051302 | regulation of cell division | 0.611794394 | 1.166094697 |
| GO:0060561 | apoptotic process involved in morphogenesis | 0.613238022 | 1.166110968 |
| REACTOME_G1S_TRANSITION | REACTOME_G1S_TRANSITION | 0.916587275 | 1.16611414 |
| ENSG00000198055 | GRK6 subnetwork | 0.613479994 | 1.166117617 |
| MP:0002086 | abnormal extraembryonic tissue morphology | 0.610979715 | 1.166121948 |
| GO:0042462 | eye photoreceptor cell development | 0.916456027 | 1.166138962 |
| ENSG00000175073 | VCPIP1 subnetwork | 0.916544401 | 1.166150734 |

| | | | |
|---|---|---|---|
| MP:0008546 | abnormal vesicle-mediated transport | 0.61342706 | 1.166164736 |
| ENSG00000140650 | PMM2 subnetwork | 0.61359328 | 1.166173443 |
| GO:0072331 | signal transduction by p53 class mediator | 0.916402657 | 1.166175565 |
| REACTOME_LEADING_STRAND_S | REACTOME_LEADING_STRAND_SYNTHESIS | 0.613136131 | 1.166224569 |
| ENSG00000131931 | THAP1 subnetwork | 0.916255814 | 1.166226797 |
| ENSG00000170348 | TMED10 subnetwork | 0.916395422 | 1.166260556 |
| MP:0005296 | abnormal humerus morphology | 0.916121391 | 1.166273647 |
| ENSG00000127184 | COX7C subnetwork | 0.916229336 | 1.166294211 |
| GO:0043489 | RNA stabilization | 0.612925019 | 1.16632101 |
| GO:0048617 | embryonic foregut morphogenesis | 0.916117562 | 1.166371876 |
| REACTOME_POLYMERASE_SWITC | REACTOME_POLYMERASE_SWITCHING_ON_THE_C:STRA | 0.613136131 | 1.166374759 |
| ENSG00000137876 | RSL24D1 subnetwork | 0.613790658 | 1.166415798 |
| GO:0009263 | deoxyribonucleotide biosynthetic process | 0.916069598 | 1.166417319 |
| GO:0005109 | frizzled binding | 0.613102912 | 1.166454147 |
| GO:0048255 | mRNA stabilization | 0.612925019 | 1.16647127 |
| ENSG00000159176 | CSRP1 subnetwork | 0.914605609 | 1.166472766 |
| ENSG00000039650 | PNKP subnetwork | 0.915949061 | 1.166477423 |
| GO:0042288 | MHC class I protein binding | 0.61398514 | 1.166482315 |
| REACTOME_G0_AND_EARLY_G1 | REACTOME_G0_AND_EARLY_G1 | 0.914701056 | 1.166493346 |
| ENSG00000105135 | ILVBL subnetwork | 0.614663815 | 1.166497495 |
| ENSG00000105185 | PDCD5 subnetwork | 0.915287671 | 1.166497842 |
| GO:0048010 | vascular endothelial growth factor receptor signaling pat | 0.916044745 | 1.166497976 |
| ENSG00000111790 | FGFR1OP2 subnetwork | 0.613901515 | 1.166523025 |
| ENSG00000165606 | DRGX subnetwork | 0.914580087 | 1.166544733 |
| ENSG00000167565 | SERTAD3 subnetwork | 0.915769425 | 1.166547808 |
| GO:0043304 | regulation of mast cell degranulation | 0.915918827 | 1.166549296 |
| ENSG00000111057 | KRT18 subnetwork | 0.614332795 | 1.166550971 |
| GO:0045730 | respiratory burst | 0.914958982 | 1.16656093 |
| ENSG00000025434 | NR1H3 subnetwork | 0.614611331 | 1.166563865 |
| REACTOME_ASPARAGINE_N:LINK | REACTOME_ASPARAGINE_N:LINKED_GLYCOSYLATION | 0.612891168 | 1.166576472 |
| GO:0051606 | detection of stimulus | 0.915270765 | 1.166578576 |
| MP:0004509 | abnormal pelvic girdle bone morphology | 0.91590273 | 1.166603574 |
| MP:0004965 | inner cell mass degeneration | 0.614286931 | 1.166610954 |
| GO:0032319 | regulation of Rho GTPase activity | 0.91489384 | 1.166619669 |
| GO:0009220 | pyrimidine ribonucleotide biosynthetic process | 0.915731923 | 1.166619706 |
| GO:0051970 | negative regulation of transmission of nerve impulse | 0.914561815 | 1.166625529 |
| ENSG00000147044 | CASK subnetwork | 0.915648459 | 1.166629975 |
| GO:0071843 | cellular component biogenesis at cellular level | 0.612472261 | 1.166634429 |
| GO:0008543 | fibroblast growth factor receptor signaling pathway | 0.614586547 | 1.166643105 |
| MP:0010090 | increased circulating creatine kinase level | 0.915575338 | 1.16665786 |
| GO:0031369 | translation initiation factor binding | 0.915479735 | 1.166663731 |
| ENSG00000110841 | PPFIBP1 subnetwork | 0.914372435 | 1.166669606 |
| ENSG00000104435 | STMN2 subnetwork | 0.614243174 | 1.166670953 |
| GO:0006826 | iron ion transport | 0.915267743 | 1.166676945 |
| GO:0050840 | extracellular matrix binding | 0.914536563 | 1.166693115 |
| ENSG00000117594 | HSD11B1 subnetwork | 0.915201966 | 1.166718062 |
| GO:0006516 | glycoprotein catabolic process | 0.914482923 | 1.166721037 |
| ENSG00000182979 | MTA1 subnetwork | 0.612890576 | 1.166726804 |
| ENSG00000106588 | PSMA2 subnetwork | 0.914350895 | 1.16675485 |
| ENSG00000006451 | RALA subnetwork | 0.614566225 | 1.166760925 |
| GO:0000076 | DNA replication checkpoint | 0.614213645 | 1.166769547 |
| REACTOME_TRANSCRIPTION:COU | REACTOME_TRANSCRIPTION:COUPLED_NER_TC:NER | 0.914211299 | 1.166815135 |
| GO:0051291 | protein heterooligomerization | 0.612618611 | 1.166819237 |
| GO:0021696 | cerebellar cortex morphogenesis | 0.914319633 | 1.1668357 |

| | | | |
|---|---|---|---|
| ENSG00000156049 | GNA14 subnetwork | 0.612862489 | 1.166844954 |
| REACTOME_RESPIRATORY_ELECT | REACTOME_RESPIRATORY_ELECTRON_TRANSPORT_ATP | 0.612787499 | 1.166847126 |
| GO:0042304 | regulation of fatty acid biosynthetic process | 0.914166825 | 1.166873953 |
| ENSG00000161634 | DCD subnetwork | 0.612766889 | 1.166920201 |
| ENSG00000108433 | GOSR2 subnetwork | 0.914146726 | 1.166946013 |
| ENSG00000172399 | MYOZ2 subnetwork | 0.914049359 | 1.166969563 |
| ENSG00000171916 | LGALS9C subnetwork | 0.914043242 | 1.167054879 |
| MP:0000808 | abnormal hippocampus development | 0.615046057 | 1.167092754 |
| GO:0030834 | regulation of actin filament depolymerization | 0.913939635 | 1.167110837 |
| ENSG00000170298 | LGALS9B subnetwork | 0.914043242 | 1.167157858 |
| REACTOME_CDK:MEDIATED_PHO | REACTOME_CDK:MEDIATED_PHOSPHORYLATION_AND_ | 0.913933283 | 1.167209425 |
| MP:0000539 | distended urinary bladder | 0.615196698 | 1.167212588 |
| GO:0002320 | lymphoid progenitor cell differentiation | 0.913921029 | 1.167299206 |
| ENSG00000090104 | RGS1 subnetwork | 0.913887614 | 1.167358108 |
| MP:0005543 | corneal thinning | 0.912962581 | 1.167383813 |
| ENSG00000176124 | DLEU1 subnetwork | 0.912896939 | 1.167425113 |
| ENSG00000146731 | CCT6A subnetwork | 0.61534798 | 1.16743514 |
| MP:0009304 | increased retroperitoneal fat pad weight | 0.913868681 | 1.167439089 |
| GO:0051205 | protein insertion into membrane | 0.912858928 | 1.167466419 |
| GO:0045177 | apical part of cell | 0.913423599 | 1.167499779 |
| GO:0042562 | hormone binding | 0.913817449 | 1.167511256 |
| GO:0030278 | regulation of ossification | 0.912803673 | 1.167516571 |
| ENSG00000148334 | PTGES2 subnetwork | 0.913530335 | 1.167520311 |
| GO:0019005 | SCF ubiquitin ligase complex | 0.615523374 | 1.167520544 |
| GO:0006026 | aminoglycan catabolic process | 0.913711597 | 1.167521632 |
| GO:0016485 | protein processing | 0.91339744 | 1.167554319 |
| ENSG00000112818 | MEP1A subnetwork | 0.913262417 | 1.167566254 |
| GO:0043524 | negative regulation of neuron apoptotic process | 0.913180201 | 1.167576641 |
| MP:0008027 | abnormal spinal cord white matter morphology | 0.91365566 | 1.167593819 |
| GO:0016101 | diterpenoid metabolic process | 0.913347838 | 1.167600035 |
| GO:0015697 | quaternary ammonium group transport | 0.912782432 | 1.167606505 |
| REACTOME_ORGANIC_CATIONAN | REACTOME_ORGANIC_CATIONANIONZWITTERION_TRAI | 0.910752821 | 1.167626218 |
| ENSG00000065613 | SLK subnetwork | 0.615511826 | 1.167651214 |
| ENSG00000094914 | AAAS subnetwork | 0.615926051 | 1.167652721 |
| ENSG00000007237 | GAS7 subnetwork | 0.61586552 | 1.16767424 |
| GO:0051004 | regulation of lipoprotein lipase activity | 0.910739459 | 1.167698645 |
| ENSG00000177889 | UBE2N subnetwork | 0.912777505 | 1.167705295 |
| GO:0000722 | telomere maintenance via recombination | 0.912647169 | 1.167712846 |
| ENSG00000101413 | RPRD1B subnetwork | 0.615797736 | 1.167715019 |
| REACTOME_TRANSPORT_OF_GLU | REACTOME_TRANSPORT_OF_GLUCOSE_AND_OTHER_SU | 0.911808035 | 1.167746217 |
| MP:0002286 | cryptorchism | 0.912626218 | 1.167780725 |
| GO:0031268 | pseudopodium organization | 0.910734782 | 1.167793232 |
| ENSG00000188843 | ENSG00000188843 subnetwork | 0.911982177 | 1.167805008 |
| ENSG00000116329 | OPRD1 subnetwork | 0.912774342 | 1.167808522 |
| MP:0003105 | abnormal heart atrium morphology | 0.910480506 | 1.167815685 |
| GO:0051797 | regulation of hair follicle development | 0.615773003 | 1.167820003 |
| ENSG00000070961 | ATP2B1 subnetwork | 0.911793041 | 1.167831858 |
| REACTOME_AMINO_ACID_TRANS | REACTOME_AMINO_ACID_TRANSPORT_ACROSS_THE_P | 0.912323675 | 1.167844507 |
| MP:0003666 | impaired sperm capacitation | 0.910315718 | 1.167849863 |
| ENSG00000008952 | SEC62 subnetwork | 0.912610853 | 1.167866301 |
| ENSG00000074071 | MRPS34 subnetwork | 0.910592551 | 1.167867269 |
| MP:0003911 | increased drinking behavior | 0.911971329 | 1.167886215 |
| GO:0031649 | heat generation | 0.616108068 | 1.167887848 |
| ENSG00000065150 | IPO5 subnetwork | 0.911376287 | 1.167888446 |

| | | | |
|---|---|---|---|
| ENSG00000089169 | RPH3A subnetwork | 0.911478896 | 1.167895715 |
| ENSG00000132424 | PNISR subnetwork | 0.910729784 | 1.167896695 |
| GO:0005546 | phosphatidylinositol-4,5-bisphosphate binding | 0.910449274 | 1.167901453 |
| GO:0030514 | negative regulation of BMP signaling pathway | 0.911330493 | 1.167912166 |
| ENSG00000133019 | CHRM3 subnetwork | 0.912291433 | 1.167912428 |
| ENSG00000136938 | ANP32B subnetwork | 0.910267527 | 1.167931218 |
| GO:0003044 | regulation of systemic arterial blood pressure mediated l | 0.911789992 | 1.167935216 |
| GO:0042398 | cellular modified amino acid biosynthetic process | 0.912217196 | 1.167958245 |
| ENSG00000131069 | ACSS2 subnetwork | 0.911112956 | 1.167965636 |
| MP:0001891 | hydroencephaly | 0.912610827 | 1.167969579 |
| ENSG00000181827 | RFX7 subnetwork | 0.911296432 | 1.16797131 |
| ENSG00000100911 | PSME2 subnetwork | 0.911222563 | 1.167990613 |
| GO:0060338 | regulation of type I interferon-mediated signaling pathw | 0.910245152 | 1.167994859 |
| MP:0001661 | extended life span | 0.911772574 | 1.168007612 |
| KEGG_DILATED_CARDIOMYOPATI | KEGG_DILATED_CARDIOMYOPATHY | 0.911703191 | 1.168022484 |
| MP:0005103 | abnormal retinal pigmentation | 0.910123269 | 1.168051246 |
| MP:0001957 | apnea | 0.909453279 | 1.168055186 |
| MP:0001408 | stereotypic behavior | 0.910217985 | 1.168058511 |
| ENSG00000174125 | TLR1 subnetwork | 0.912592512 | 1.168068453 |
| GO:0007507 | heart development | 0.909916691 | 1.168078219 |
| GO:0035195 | gene silencing by miRNA | 0.909710102 | 1.168085861 |
| GO:0008227 | G-protein coupled amine receptor activity | 0.90961664 | 1.168100772 |
| GO:0042730 | fibrinolysis | 0.909553775 | 1.168106813 |
| GO:0070373 | negative regulation of ERK1 and ERK2 cascade | 0.910100509 | 1.168114914 |
| MP:0001144 | vagina atresia | 0.909438302 | 1.168145519 |
| ENSG00000022840 | RNF10 subnetwork | 0.909355182 | 1.168151566 |
| ENSG00000182132 | KCNIP1 subnetwork | 0.909888587 | 1.168172949 |
| ENSG00000013375 | PGM3 subnetwork | 0.910087478 | 1.168205196 |
| ENSG00000174483 | BBS1 subnetwork | 0.90935498 | 1.168255236 |
| ENSG00000007402 | CACNA2D2 subnetwork | 0.909343115 | 1.168350049 |
| ENSG00000119888 | EPCAM subnetwork | 0.616506768 | 1.168389994 |
| GO:0009409 | response to cold | 0.909332147 | 1.16844044 |
| REACTOME_P2Y_RECEPTORS | REACTOME_P2Y_RECEPTORS | 0.909306556 | 1.168513094 |
| ENSG00000102362 | SYTL4 subnetwork | 0.616502408 | 1.168533487 |
| GO:0019637 | organophosphate metabolic process | 0.90924725 | 1.168554688 |
| ENSG00000075711 | DLG1 subnetwork | 0.90904944 | 1.168557983 |
| ENSG00000089685 | BIRC5 subnetwork | 0.909171336 | 1.168591849 |
| ENSG00000168447 | SCNN1B subnetwork | 0.909037267 | 1.168652873 |
| MP:0003694 | failure to hatch from the zona pellucida | 0.908994081 | 1.168707815 |
| KEGG_PPAR_SIGNALING_PATHW | KEGG_PPAR_SIGNALING_PATHWAY | 0.908913478 | 1.168713918 |
| ENSG00000215612 | HMX1 subnetwork | 0.616996122 | 1.168729161 |
| ENSG00000196510 | ANAPC7 subnetwork | 0.908907441 | 1.16881773 |
| ENSG00000126562 | WNK4 subnetwork | 0.616952901 | 1.168821342 |
| MP:0003087 | absent allantois | 0.616890533 | 1.168875064 |
| ENSG00000135336 | ORC3 subnetwork | 0.90887593 | 1.168886026 |
| GO:0019674 | NAD metabolic process | 0.908778982 | 1.168901031 |
| ENSG00000182872 | RBM10 subnetwork | 0.617216806 | 1.168925503 |
| GO:0006333 | chromatin assembly or disassembly | 0.908733665 | 1.168969347 |
| ENSG00000211949 | ENSG00000211949 subnetwork | 0.908689334 | 1.169015461 |
| ENSG00000134769 | DTNA subnetwork | 0.908255359 | 1.169016714 |
| ENSG00000131626 | PPFIA1 subnetwork | 0.90853377 | 1.169032172 |
| ENSG00000164818 | HEATR2 subnetwork | 0.908376257 | 1.16904 |
| ENSG00000171914 | TLN2 subnetwork | 0.908208251 | 1.169076198 |
| MP:0003169 | abnormal scala media morphology | 0.9084812 | 1.169091636 |

| | | | |
|---|---|---|---|
| GO:0042228 | interleukin-8 biosynthetic process | 0.617705427 | 1.169105587 |
| ENSG00000125124 | BBS2 subnetwork | 0.908360966 | 1.16911281 |
| GO:0008195 | phosphatidate phosphatase activity | 0.908687179 | 1.169119346 |
| ENSG00000081014 | AP4E1 subnetwork | 0.908061576 | 1.169128502 |
| REACTOME_UNWINDING_OF_DN | REACTOME_UNWINDING_OF_DNA | 0.617502486 | 1.169170619 |
| GO:0015012 | heparan sulfate proteoglycan biosynthetic process | 0.908200138 | 1.169175707 |
| GO:0044437 | vacuolar part | 0.908010606 | 1.169192458 |
| MP:0000135 | decreased compact bone thickness | 0.617703872 | 1.169255415 |
| ENSG00000214078 | CPNE1 subnetwork | 0.617628248 | 1.169257883 |
| MP:0010380 | inner cell mass apoptosis | 0.617486885 | 1.169275641 |
| ENSG00000148229 | POLE3 subnetwork | 0.907985305 | 1.169287557 |
| ENSG00000215104 | ENSG00000215104 subnetwork | 0.618044068 | 1.169345543 |
| MP:0005300 | abnormal corneal stroma morphology | 0.907953971 | 1.169378225 |
| GO:0008217 | regulation of blood pressure | 0.907616655 | 1.169385122 |
| GO:0008354 | germ cell migration | 0.618007318 | 1.169399257 |
| GO:0008158 | hedgehog receptor activity | 0.61788768 | 1.169404228 |
| GO:0006221 | pyrimidine nucleotide biosynthetic process | 0.907889828 | 1.16941998 |
| GO:0031056 | regulation of histone modification | 0.618203973 | 1.169439109 |
| ENSG00000149557 | FEZ1 subnetwork | 0.907835697 | 1.169439502 |
| ENSG00000159200 | RCAN1 subnetwork | 0.907544322 | 1.169444692 |
| ENSG00000170558 | CDH2 subnetwork | 0.617939913 | 1.16944658 |
| GO:0030835 | negative regulation of actin filament depolymerization | 0.907763037 | 1.169454578 |
| GO:0009250 | glucan biosynthetic process | 0.907534006 | 1.169544322 |
| ENSG00000164404 | GDF9 subnetwork | 0.90726725 | 1.169635862 |
| ENSG00000108179 | PPIF subnetwork | 0.618515402 | 1.169638971 |
| GO:0005978 | glycogen biosynthetic process | 0.907534006 | 1.16964842 |
| ENSG00000164919 | COX6C subnetwork | 0.907468286 | 1.169663521 |
| MP:0005627 | increased circulating potassium level | 0.618461369 | 1.169667093 |
| GO:0010970 | microtubule-based transport | 0.907349702 | 1.169674174 |
| GO:0000266 | mitochondrial fission | 0.90724575 | 1.169726649 |
| ENSG00000167461 | RAB8A subnetwork | 0.907199565 | 1.169741763 |
| ENSG00000138041 | SMEK2 subnetwork | 0.906406959 | 1.169784333 |
| ENSG00000117154 | IGSF21 subnetwork | 0.906599286 | 1.169803083 |
| GO:0001942 | hair follicle development | 0.907168466 | 1.169814765 |
| ENSG00000166128 | RAB8B subnetwork | 0.906360397 | 1.16983066 |
| ENSG00000100297 | MCM5 subnetwork | 0.906540624 | 1.169840492 |
| GO:0022405 | hair cycle process | 0.907168466 | 1.169918953 |
| GO:0070169 | positive regulation of biomineral tissue development | 0.906074927 | 1.16992689 |
| REACTOME_ACTIVATION_OF_THE | REACTOME_ACTIVATION_OF_THE_PRE:REPLICATIVE_CO | 0.906351162 | 1.169934932 |
| GO:0031272 | regulation of pseudopodium assembly | 0.906861963 | 1.16995278 |
| GO:0019228 | regulation of action potential in neuron | 0.906215918 | 1.169978604 |
| GO:0000049 | tRNA binding | 0.906315376 | 1.170003566 |
| GO:0006081 | cellular aldehyde metabolic process | 0.907080647 | 1.17001158 |
| MP:0000097 | short maxilla | 0.906073078 | 1.170022292 |
| GO:0022404 | molting cycle process | 0.907168466 | 1.170023158 |
| REACTOME_CELL_CYCLE_MITOTI | REACTOME_CELL_CYCLE_MITOTIC | 0.907024905 | 1.170075724 |
| MP:0009969 | abnormal cerebral cortex pyramidal cell morphology | 0.906070534 | 1.170126627 |
| ENSG00000136250 | AOAH subnetwork | 0.906036831 | 1.17019085 |
| GO:0006486 | protein glycosylation | 0.905998612 | 1.170255084 |
| ENSG00000197930 | ERO1L subnetwork | 0.905865951 | 1.170330062 |
| GO:0043413 | macromolecule glycosylation | 0.905998612 | 1.170359468 |
| GO:0045747 | positive regulation of Notch signaling pathway | 0.905841142 | 1.17042109 |
| GO:0055024 | regulation of cardiac muscle tissue development | 0.905810468 | 1.170476445 |
| MP:0005637 | abnormal iron homeostasis | 0.905554082 | 1.170546233 |

| | | | |
|---|---|---|---|
| ENSG00000004939 | SLC4A1 subnetwork | 0.905446433 | 1.170556994 |
| GO:0035924 | cellular response to vascular endothelial growth factor st | 0.905713059 | 1.170578262 |
| GO:0051057 | positive regulation of small GTPase mediated signal trans | 0.905803488 | 1.170580887 |
| ENSG00000122490 | PQLC1 subnetwork | 0.90566441 | 1.17060241 |
| GO:0004984 | olfactory receptor activity | 0.905309494 | 1.170609767 |
| GO:0060627 | regulation of vesicle-mediated transport | 0.905429938 | 1.170657026 |
| GO:0070542 | response to fatty acid | 0.905262214 | 1.170683036 |
| GO:0007016 | cytoskeletal anchoring at plasma membrane | 0.904990194 | 1.170684112 |
| GO:0010458 | exit from mitosis | 0.905227374 | 1.170729529 |
| MP:0001690 | failure of somite differentiation | 0.905129146 | 1.170740311 |
| ENSG00000181191 | PJA1 subnetwork | 0.904978954 | 1.170788675 |
| ENSG00000073969 | NSF subnetwork | 0.90492076 | 1.170839661 |
| MP:0001525 | impaired balance | 0.904895744 | 1.170917456 |
| GO:0048147 | negative regulation of fibroblast proliferation | 0.904820981 | 1.170919325 |
| ENSG00000103460 | TOX3 subnetwork | 0.904734019 | 1.170947999 |
| ENSG00000198846 | TOX subnetwork | 0.904734019 | 1.171052632 |
| ENSG00000124097 | ENSG00000124097 subnetwork | 0.904734019 | 1.171157283 |
| GO:0006091 | generation of precursor metabolites and energy | 0.904690845 | 1.171226204 |
| GO:0043584 | nose development | 0.904665099 | 1.171272792 |
| MP:0004599 | abnormal vertebral arch morphology | 0.904658412 | 1.171359614 |
| GO:0060325 | face morphogenesis | 0.904642108 | 1.171450921 |
| GO:0030673 | axolemma | 0.904629599 | 1.171542244 |
| ENSG00000187837 | HIST1H1C subnetwork | 0.620941029 | 1.17154809 |
| GO:0051346 | negative regulation of hydrolase activity | 0.620870797 | 1.171589167 |
| MP:0003178 | left pulmonary isomerism | 0.90460049 | 1.171593348 |
| GO:0006702 | androgen biosynthetic process | 0.621037666 | 1.171666667 |
| GO:0072655 | establishment of protein localization in mitochondrion | 0.620826626 | 1.171681359 |
| GO:0015701 | bicarbonate transport | 0.904592974 | 1.1716847 |
| MP:0001548 | hyperlipidemia | 0.619699411 | 1.171729391 |
| GO:0097006 | regulation of plasma lipoprotein particle levels | 0.904587625 | 1.171789483 |
| ENSG00000184979 | USP18 subnetwork | 0.6208096 | 1.171792742 |
| ENSG00000165672 | PRDX3 subnetwork | 0.621652489 | 1.17181679 |
| GO:0008584 | male gonad development | 0.621179964 | 1.171817137 |
| ENSG00000197111 | PCBP2 subnetwork | 0.619958674 | 1.171829814 |
| GO:0006612 | protein targeting to membrane | 0.904581147 | 1.171894285 |
| ENSG00000088256 | GNA11 subnetwork | 0.620794011 | 1.171904153 |
| KEGG_TERPENOID_BACKBONE_BI | KEGG_TERPENOID_BACKBONE_BIOSYNTHESIS | 0.621627066 | 1.171928034 |
| ENSG00000151491 | EPS8 subnetwork | 0.619952746 | 1.17197978 |
| ENSG00000167110 | GOLGA2 subnetwork | 0.621594396 | 1.171981879 |
| MP:0002777 | absent ovarian follicles | 0.904573003 | 1.171985689 |
| GO:0005484 | SNAP receptor activity | 0.620777885 | 1.172028374 |
| REACTOME_RNA_POLYMERASE_I | REACTOME_RNA_POLYMERASE_III_TRANSCRIPTION_INI | 0.621561948 | 1.172042119 |
| GO:0016746 | transferase activity, transferring acyl groups | 0.619914178 | 1.172059388 |
| GO:0001725 | stress fiber | 0.621496132 | 1.17206408 |
| REACTOME_MITOTIC_M:MG1_PH | REACTOME_MITOTIC_M:MG1_PHASES | 0.904564057 | 1.172068164 |
| ENSG00000002016 | RAD52 subnetwork | 0.621363328 | 1.17209525 |
| ENSG00000186081 | KRT5 subnetwork | 0.904518621 | 1.172132761 |
| GO:0030238 | male sex determination | 0.620751317 | 1.172139844 |
| GO:0002704 | negative regulation of leukocyte mediated immunity | 0.620672446 | 1.172142675 |
| ENSG00000173914 | RBM4B subnetwork | 0.621487751 | 1.172213711 |
| ENSG00000130640 | TUBGCP2 subnetwork | 0.904503372 | 1.172215263 |
| GO:0008286 | insulin receptor signaling pathway | 0.620234492 | 1.172230041 |
| ENSG00000114270 | COL7A1 subnetwork | 0.622047135 | 1.172232143 |
| GO:0050718 | positive regulation of interleukin-1 beta secretion | 0.622215286 | 1.172271104 |

| | | | |
|---|---|---|---|
| ENSG00000147684 | NDUFB9 subnetwork | 0.904455752 | 1.172279885 |
| GO:0002707 | negative regulation of lymphocyte mediated immunity | 0.620672446 | 1.172292546 |
| ENSG00000105357 | MYH14 subnetwork | 0.620536794 | 1.172298248 |
| MP:0005536 | Leydig cell hypoplasia | 0.622019811 | 1.172330654 |
| GO:0060479 | lung cell differentiation | 0.620490883 | 1.17237145 |
| ENSG00000138018 | EPT1 subnetwork | 0.62041361 | 1.172374312 |
| GO:0006284 | base-excision repair | 0.904445203 | 1.172375839 |
| GO:0051492 | regulation of stress fiber assembly | 0.620645167 | 1.17238491 |
| GO:0050716 | positive regulation of interleukin-1 secretion | 0.622215286 | 1.17242061 |
| ENSG00000129757 | CDKN1C subnetwork | 0.904394012 | 1.172431537 |
| GO:0071384 | cellular response to corticosteroid stimulus | 0.903833869 | 1.172483883 |
| GO:0007093 | mitotic cell cycle checkpoint | 0.90439059 | 1.172536472 |
| GO:0035250 | UDP-galactosyltransferase activity | 0.903999125 | 1.172571403 |
| GO:0071385 | cellular response to glucocorticoid stimulus | 0.903833869 | 1.172588878 |
| ENSG00000188229 | TUBB4B subnetwork | 0.622583213 | 1.172600382 |
| ENSG00000173894 | CBX2 subnetwork | 0.622678705 | 1.172610247 |
| ENSG00000214021 | TTLL3 subnetwork | 0.622444418 | 1.172618896 |
| ENSG00000189367 | KIAA0408 subnetwork | 0.904373757 | 1.172623523 |
| ENSG00000142515 | KLK3 subnetwork | 0.903781479 | 1.172640158 |
| GO:0008406 | gonad development | 0.622539346 | 1.172660632 |
| GO:0043588 | skin development | 0.904334048 | 1.172692686 |
| GO:0033197 | response to vitamin E | 0.903778336 | 1.172745186 |
| GO:0006213 | pyrimidine nucleoside metabolic process | 0.904296006 | 1.172766338 |
| ENSG00000104064 | GABPB1 subnetwork | 0.903758547 | 1.172827839 |
| MP:0005332 | abnormal amino acid level | 0.903727758 | 1.172897071 |
| GO:0010770 | positive regulation of cell morphogenesis involved in diff | 0.622885321 | 1.172938703 |
| GO:0048199 | vesicle targeting, to, from or within Golgi | 0.903697467 | 1.172975273 |
| GO:0021697 | cerebellar cortex formation | 0.903660147 | 1.17304453 |
| REACTOME_SCFSKP2:MEDIATED_ | REACTOME_SCFSKP2:MEDIATED_DEGRADATION_OF_P2 | 0.903615181 | 1.173113799 |
| MP:0000783 | abnormal forebrain morphology | 0.90356413 | 1.173147235 |
| ENSG00000112312 | GMNN subnetwork | 0.903539277 | 1.173216526 |
| GO:0060037 | pharyngeal system development | 0.90349649 | 1.173267904 |
| MP:0008545 | absent sperm flagellum | 0.903471969 | 1.173359627 |
| MP:0010067 | increased red blood cell distribution width | 0.623221667 | 1.173413609 |
| GO:0000080 | G1 phase of mitotic cell cycle | 0.903458534 | 1.173455849 |
| GO:0008033 | tRNA processing | 0.903332207 | 1.173504887 |
| GO:0018195 | peptidyl-arginine modification | 0.903422257 | 1.17352071 |
| GO:0003854 | 3-beta-hydroxy-delta5-steroid dehydrogenase activity | 0.903311215 | 1.173551829 |
| ENSG00000092853 | CLSPN subnetwork | 0.623472729 | 1.173601733 |
| GO:0042987 | amyloid precursor protein catabolic process | 0.903286807 | 1.1736212 |
| ENSG00000113555 | PCDH12 subnetwork | 0.903278253 | 1.173726457 |
| MP:0000133 | abnormal long bone metaphysis morphology | 0.903251363 | 1.173786887 |
| ENSG00000077514 | POLD3 subnetwork | 0.903175453 | 1.173820416 |
| ENSG00000142945 | KIF2C subnetwork | 0.903138747 | 1.173858437 |
| GO:0015631 | tubulin binding | 0.903073747 | 1.173887493 |
| GO:0002478 | antigen processing and presentation of exogenous pepti | 0.623824371 | 1.173895045 |
| MP:0001559 | hyperglycemia | 0.623780573 | 1.173968153 |
| MP:0001326 | retinal degeneration | 0.903067813 | 1.173979363 |
| GO:0006879 | cellular iron ion homeostasis | 0.903040003 | 1.174066762 |
| GO:0005774 | vacuolar membrane | 0.902959509 | 1.174068922 |
| GO:0009968 | negative regulation of signal transduction | 0.624076103 | 1.17415945 |
| MP:0000925 | abnormal floor plate morphology | 0.902955364 | 1.174174295 |
| GO:0051923 | sulfation | 0.902938527 | 1.174270712 |
| ENSG00000213123 | TCTEX1D2 subnetwork | 0.902877639 | 1.174331239 |

| | | | |
|---|---|---|---|
| GO:0045652 | regulation of megakaryocyte differentiation | 0.902823044 | 1.174364844 |
| GO:0016338 | calcium-independent cell-cell adhesion | 0.902691017 | 1.174405136 |
| GO:0043492 | ATPase activity, coupled to movement of substances | 0.902785092 | 1.174407434 |
| ENSG00000134138 | MEIS2 subnetwork | 0.6260563 | 1.174450794 |
| REACTOME_BASE:FREE_SUGAR:P | REACTOME_BASE:FREE_SUGAR:PHOSPHATE_REMOVAL_ | 0.625759647 | 1.174456867 |
| GO:0044440 | endosomal part | 0.626155283 | 1.174479431 |
| GO:0004303 | estradiol 17-beta-dehydrogenase activity | 0.902685766 | 1.174510596 |
| MP:0000780 | abnormal corpus callosum morphology | 0.902386905 | 1.174532878 |
| MP:0010379 | decreased respiratory quotient | 0.626035717 | 1.174549149 |
| GO:0072595 | maintenance of protein localization to organelle | 0.625726475 | 1.17456798 |
| MP:0003070 | increased vascular permeability | 0.625884179 | 1.174568089 |
| MP:0002878 | abnormal corticospinal tract morphology | 0.902482589 | 1.174571095 |
| ENSG00000135945 | REV1 subnetwork | 0.902667782 | 1.174593624 |
| GO:0090136 | epithelial cell-cell adhesion | 0.625652295 | 1.174596518 |
| REACTOME_RNA_POLYMERASE_I | REACTOME_RNA_POLYMERASE_I_PROMOTER_CLEARAN | 0.902590292 | 1.174600323 |
| GO:0009303 | rRNA transcription | 0.625988058 | 1.174609425 |
| GO:0006921 | cellular component disassembly involved in apoptotic pr | 0.627442008 | 1.174622988 |
| ENSG00000108100 | CCNY subnetwork | 0.902377517 | 1.174629413 |
| ENSG00000160752 | FDPS subnetwork | 0.626273281 | 1.174660404 |
| GO:0001522 | pseudouridine synthesis | 0.627388597 | 1.174683143 |
| ENSG00000175305 | CCNE2 subnetwork | 0.625109743 | 1.174694734 |
| ENSG00000111907 | TPD52L1 subnetwork | 0.627342355 | 1.174711624 |
| MP:0008028 | pregnancy-related premature death | 0.625642213 | 1.174726741 |
| GO:0006144 | purine base metabolic process | 0.902375861 | 1.174734951 |
| ENSG00000170142 | UBE2E1 subnetwork | 0.62730193 | 1.174765467 |
| MP:0004521 | abnormal cochlear hair cell stereociliary bundle morphol | 0.625340353 | 1.174802899 |
| GO:0032606 | type I interferon production | 0.625508821 | 1.174815662 |
| REACTOME_CA:DEPENDENT_EVE | REACTOME_CA:DEPENDENT_EVENTS | 0.6251033 | 1.174825086 |
| MP:0008883 | abnormal enterocyte proliferation | 0.624434147 | 1.174831275 |
| GO:0017144 | drug metabolic process | 0.902361098 | 1.174836014 |
| ENSG00000109193 | SULT1E1 subnetwork | 0.625421221 | 1.174837889 |
| GO:0070997 | neuron death | 0.626729257 | 1.174844563 |
| MP:0003988 | disorganized embryonic tissue | 0.627267009 | 1.174844681 |
| GO:0043046 | DNA methylation involved in gamete generation | 0.626503582 | 1.174854024 |
| ENSG00000175592 | FOSL1 subnetwork | 0.625613943 | 1.174856998 |
| ENSG00000130810 | PPAN subnetwork | 0.62530055 | 1.174901437 |
| GO:0071375 | cellular response to peptide hormone stimulus | 0.627071445 | 1.174930238 |
| ENSG00000001497 | LAS1L subnetwork | 0.627226798 | 1.174930256 |
| MP:0003119 | abnormal digestive system development | 0.902342864 | 1.174937096 |
| GO:0048569 | post-embryonic organ development | 0.625081832 | 1.174955471 |
| GO:0002827 | positive regulation of T-helper 1 type immune response | 0.62671707 | 1.174955584 |
| MP:0003656 | abnormal erythrocyte physiology | 0.626672408 | 1.174971443 |
| MP:0008451 | retinal rod cell degeneration | 0.627972538 | 1.174984167 |
| ENSG00000105701 | FKBP8 subnetwork | 0.62464963 | 1.174996817 |
| ENSG00000147869 | CER1 subnetwork | 0.627021391 | 1.175009514 |
| REACTOME_GAP_JUNCTION_TRA | REACTOME_GAP_JUNCTION_TRAFFICKING_AND_REGUL | 0.902325 | 1.175024715 |
| ENSG00000160563 | MED27 subnetwork | 0.626940625 | 1.175050749 |
| GO:0001678 | cellular glucose homeostasis | 0.625052373 | 1.175054078 |
| ENSG00000165966 | PDZRN4 subnetwork | 0.6272149 | 1.175066582 |
| GO:0050802 | circadian sleep/wake cycle, sleep | 0.902281261 | 1.175098868 |
| REACTOME_FATTY_ACYL:COA_BI | REACTOME_FATTY_ACYL:COA_BIOSYNTHESIS | 0.624625556 | 1.175101859 |
| ENSG00000059378 | PARP12 subnetwork | 0.627959703 | 1.175120345 |
| MP:0001435 | no suckling reflex | 0.627840996 | 1.175196401 |
| GO:0032369 | negative regulation of lipid transport | 0.625043279 | 1.175203614 |

| | | | |
|---|---|---|---|
| GO:0022410 | circadian sleep/wake cycle process | 0.902281261 | 1.175204494 |
| ENSG00000080802 | CNOT4 subnetwork | 0.624946166 | 1.175225913 |
| ENSG00000101868 | POLA1 subnetwork | 0.628175182 | 1.175240628 |
| MP:0001554 | increased circulating free fatty acid level | 0.627947259 | 1.175250222 |
| GO:0051648 | vesicle localization | 0.902253813 | 1.175278677 |
| ENSG00000144048 | DUSP11 subnetwork | 0.628311309 | 1.175284882 |
| ENSG00000156467 | UQCRB subnetwork | 0.62827226 | 1.175307079 |
| MP:0002971 | abnormal brown adipose tissue morphology | 0.6249309 | 1.175356415 |
| GO:0090342 | regulation of cell aging | 0.902241791 | 1.175370853 |
| GO:0042626 | ATPase activity, coupled to transmembrane movement c | 0.902185396 | 1.175409099 |
| ENSG00000159788 | RGS12 subnetwork | 0.902142728 | 1.175474328 |
| ENSG00000067066 | SP100 subnetwork | 0.628816108 | 1.175493546 |
| MP:0006397 | disorganized long bone epiphyseal plate | 0.628721376 | 1.175503101 |
| ENSG00000066735 | KIF26A subnetwork | 0.901679277 | 1.175526268 |
| GO:0009791 | post-embryonic development | 0.902087609 | 1.175535072 |
| MP:0005537 | abnormal cerebral aqueduct morphology | 0.628555268 | 1.175547538 |
| MP:0003886 | abnormal embryonic epiblast morphology | 0.628666332 | 1.175594937 |
| GO:0016813 | hydrolase activity, acting on carbon-nitrogen (but not pe | 0.901660386 | 1.175609537 |
| GO:0031057 | negative regulation of histone modification | 0.902062312 | 1.175622808 |
| GO:0040001 | establishment of mitotic spindle localization | 0.901580342 | 1.175629836 |
| GO:0007271 | synaptic transmission, cholinergic | 0.628980199 | 1.175648488 |
| ENSG00000137124 | ALDH1B1 subnetwork | 0.901988405 | 1.175674582 |
| ENSG00000105409 | ATP1A3 subnetwork | 0.90153366 | 1.175695132 |
| MP:0000137 | abnormal vertebrae morphology | 0.901958666 | 1.175744355 |
| REACTOME_G2M_CHECKPOINTS | REACTOME_G2M_CHECKPOINTS | 0.901521594 | 1.175787437 |
| GO:0031123 | RNA 3'-end processing | 0.901490285 | 1.175870759 |
| GO:0051656 | establishment of organelle localization | 0.901481401 | 1.175972097 |
| GO:0030917 | midbrain-hindbrain boundary development | 0.62933037 | 1.17598988 |
| GO:0050650 | chondroitin sulfate proteoglycan biosynthetic process | 0.901420287 | 1.175992439 |
| ENSG00000122367 | LDB3 subnetwork | 0.629400765 | 1.175992917 |
| ENSG00000092094 | OSGEP subnetwork | 0.90137974 | 1.176044292 |
| MP:0005120 | decreased circulating growth hormone level | 0.90088425 | 1.17604936 |
| GO:0000030 | mannosyltransferase activity | 0.901269674 | 1.176084999 |
| ENSG00000105011 | ASF1B subnetwork | 0.629297758 | 1.176088057 |
| GO:0001963 | synaptic transmission, dopaminergic | 0.900848582 | 1.176119269 |
| MP:0004835 | abnormal miniature endplate potential | 0.90136717 | 1.176127667 |
| GO:0007266 | Rho protein signal transduction | 0.901202467 | 1.176136875 |
| ENSG00000156795 | WDYHV1 subnetwork | 0.90109007 | 1.176204629 |
| GO:0050780 | dopamine receptor binding | 0.901177802 | 1.176206772 |
| ENSG00000181788 | SIAH2 subnetwork | 0.900847964 | 1.176225225 |
| GO:0045814 | negative regulation of gene expression, epigenetic | 0.90078917 | 1.176250113 |
| MP:0004322 | abnormal sternebra morphology | 0.900774844 | 1.176333574 |
| ENSG00000171735 | CAMTA1 subnetwork | 0.629946985 | 1.176362372 |
| MP:0004067 | abnormal trabecula carnea morphology | 0.629880103 | 1.176372028 |
| GO:0051155 | positive regulation of striated muscle cell differentiation | 0.900727466 | 1.176381004 |
| ENSG00000075914 | EXOSC7 subnetwork | 0.62981178 | 1.176413305 |
| ENSG00000151914 | DST subnetwork | 0.900719361 | 1.176464492 |
| GO:0090329 | regulation of DNA-dependent DNA replication | 0.900662185 | 1.176507436 |
| ENSG00000089053 | ANAPC5 subnetwork | 0.900337205 | 1.176512488 |
| GO:0046580 | negative regulation of Ras protein signal transduction | 0.900582572 | 1.17653236 |
| GO:0016328 | lateral plasma membrane | 0.900519363 | 1.176552781 |
| MP:0002092 | abnormal eye morphology | 0.90027879 | 1.176559964 |
| ENSG00000185245 | GP1BA subnetwork | 0.900449777 | 1.176586729 |
| ENSG00000156735 | BAG4 subnetwork | 0.900084977 | 1.176621268 |

| | | | |
|---|---|---|---|
| GO:0042552 | myelination | 0.90026907 | 1.176657048 |
| ENSG00000152582 | SPEF2 subnetwork | 0.900069914 | 1.176691322 |
| GO:0007586 | digestion | 0.900224285 | 1.176704545 |
| ENSG00000085872 | CHERP subnetwork | 0.630252376 | 1.176734926 |
| GO:0032881 | regulation of polysaccharide metabolic process | 0.900048602 | 1.176774921 |
| ENSG00000143549 | TPM3 subnetwork | 0.630382394 | 1.176845298 |
| ENSG00000198719 | DLL1 subnetwork | 0.630246562 | 1.17687737 |
| GO:0070873 | regulation of glycogen metabolic process | 0.900048602 | 1.17688109 |
| GO:0008037 | cell recognition | 0.630716954 | 1.176898294 |
| ENSG00000170927 | PKHD1 subnetwork | 0.899933015 | 1.176949107 |
| MP:0004678 | split xiphoid process | 0.900029351 | 1.176964721 |
| GO:0010824 | regulation of centrosome duplication | 0.630689502 | 1.177015416 |
| GO:0014044 | Schwann cell development | 0.899880323 | 1.177032759 |
| ENSG00000081377 | CDC14B subnetwork | 0.630940699 | 1.177043072 |
| ENSG00000197548 | ATG7 subnetwork | 0.899877522 | 1.177125451 |
| GO:0008081 | phosphoric diester hydrolase activity | 0.630657832 | 1.177132567 |
| GO:0030512 | negative regulation of transforming growth factor beta r | 0.632002786 | 1.177159793 |
| ENSG00000153113 | CAST subnetwork | 0.630912546 | 1.177166498 |
| GO:0008171 | O-methyltransferase activity | 0.632314359 | 1.177190218 |
| MP:0001255 | decreased body height | 0.899857986 | 1.177209134 |
| ENSG00000160867 | FGFR4 subnetwork | 0.632405427 | 1.177211999 |
| GO:0046148 | pigment biosynthetic process | 0.632262749 | 1.177225164 |
| ENSG00000211662 | ENSG00000211662 subnetwork | 0.89979546 | 1.177247698 |
| REACTOME_MRNA_DECAY_BY_3_ | REACTOME_MRNA_DECAY_BY_3_TO_5_EXORIBONUCLE | 0.631983965 | 1.177270434 |
| GO:0030894 | replisome | 0.632205076 | 1.177285336 |
| GO:0032467 | positive regulation of cytokinesis | 0.899758597 | 1.177331407 |
| GO:0046847 | filopodium assembly | 0.899692128 | 1.177360961 |
| ENSG00000071794 | HLTF subnetwork | 0.631977651 | 1.177400025 |
| KEGG_NICOTINATE_AND_NICOTII | KEGG_NICOTINATE_AND_NICOTINAMIDE_METABOLISM | 0.899658187 | 1.177417607 |
| GO:0043601 | nuclear replisome | 0.632205076 | 1.177433796 |
| ENSG00000122194 | PLG subnetwork | 0.631222539 | 1.177469058 |
| ENSG00000151164 | RAD9B subnetwork | 0.899583171 | 1.177474264 |
| ENSG00000108578 | BLMH subnetwork | 0.899518327 | 1.177481261 |
| ENSG00000204469 | PRRC2A subnetwork | 0.89759723 | 1.177527378 |
| MP:0004783 | abnormal cardinal vein morphology | 0.631964078 | 1.177529649 |
| ENSG00000133059 | DSTYK subnetwork | 0.632750222 | 1.177532762 |
| GO:0008198 | ferrous iron binding | 0.631506128 | 1.177553339 |
| ENSG00000005513 | SOX8 subnetwork | 0.899484953 | 1.177565029 |
| GO:0043014 | alpha-tubulin binding | 0.631586928 | 1.177568796 |
| ENSG00000161654 | LSM12 subnetwork | 0.898324937 | 1.177575292 |
| GO:0035196 | production of miRNAs involved in gene silencing by miRN | 0.898260958 | 1.177586831 |
| GO:0005740 | mitochondrial envelope | 0.631435499 | 1.177588384 |
| REACTOME_N:GLYCAN_TRIMMIN | REACTOME_N:GLYCAN_TRIMMING_IN_THE_ER_AND_C/ | 0.897688244 | 1.17759276 |
| GO:0034739 | histone deacetylase activity (H4-K16 specific) | 0.897574722 | 1.177602281 |
| GO:0000086 | G2/M transition of mitotic cell cycle | 0.898192048 | 1.177602895 |
| GO:0030863 | cortical cytoskeleton | 0.631917708 | 1.177615142 |
| MP:0000422 | delayed hair appearance | 0.899444353 | 1.177617198 |
| GO:0032105 | negative regulation of response to extracellular stimulus | 0.898961718 | 1.177634671 |
| ENSG00000186141 | POLR3C subnetwork | 0.898804325 | 1.177635147 |
| MP:0000519 | hydronephrosis | 0.631390366 | 1.177642379 |
| GO:0051881 | regulation of mitochondrial membrane potential | 0.632725494 | 1.177649653 |
| ENSG00000154889 | MPPE1 subnetwork | 0.898130174 | 1.177655147 |
| ENSG00000206296 | ENSG00000206296 subnetwork | 0.898016147 | 1.17765765 |
| GO:0072384 | organelle transport along microtubule | 0.898586066 | 1.17766525 |

| | | | |
|---|---|---|---|
| GO:0006631 | fatty acid metabolic process | 0.898512231 | 1.177685838 |
| GO:0033522 | histone H2A ubiquitination | 0.898658321 | 1.177689873 |
| REACTOME_REGULATION_OF_AC | REACTOME_REGULATION_OF_ACTIVATED_PAK:2P34_BY | 0.89940555 | 1.17769196 |
| ENSG00000125845 | BMP2 subnetwork | 0.631896991 | 1.177706966 |
| GO:0032041 | NAD-dependent histone deacetylase activity (H3-K14 spe | 0.897574722 | 1.17770888 |
| ENSG00000172301 | C17orf79 subnetwork | 0.631814796 | 1.177735706 |
| GO:0060231 | mesenchymal to epithelial transition | 0.898794331 | 1.177737094 |
| GO:0032108 | negative regulation of response to nutrient levels | 0.898961718 | 1.177741119 |
| ENSG00000206232 | ENSG00000206232 subnetwork | 0.898016147 | 1.177764206 |
| REACTOME_P53:INDEPENDENT_D | REACTOME_P53:INDEPENDENT_DNA_DAMAGE_RESPON | 0.899395397 | 1.177789322 |
| GO:0046970 | NAD-dependent histone deacetylase activity (H4-K16 spe | 0.897574722 | 1.177815499 |
| ENSG00000214265 | SNURF subnetwork | 0.633486723 | 1.177826744 |
| ENSG00000118690 | ARMC2 subnetwork | 0.89922818 | 1.177860112 |
| ENSG00000204261 | ENSG00000204261 subnetwork | 0.898016147 | 1.177870781 |
| GO:0009185 | ribonucleoside diphosphate metabolic process | 0.633685069 | 1.177876385 |
| REACTOME_P53:INDEPENDENT_G | REACTOME_P53:INDEPENDENT_G1S_DNA_DAMAGE_CH | 0.899395397 | 1.177895735 |
| GO:0031078 | histone deacetylase activity (H3-K14 specific) | 0.897574722 | 1.177922137 |
| ENSG00000106723 | SPIN1 subnetwork | 0.899217474 | 1.17793493 |
| ENSG00000071539 | TRIP13 subnetwork | 0.633472734 | 1.17796877 |
| REACTOME_FORMATION_OF_FIB | REACTOME_FORMATION_OF_FIBRIN_CLOT_CLOTTING_( | 0.63365336 | 1.177974317 |
| GO:0048873 | homeostasis of number of cells within a tissue | 0.897526105 | 1.177978993 |
| ENSG00000171861 | RNMTL1 subnetwork | 0.633195046 | 1.177998236 |
| REACTOME_UBIQUITIN_MEDIATE | REACTOME_UBIQUITIN_MEDIATED_DEGRADATION_OF_ | 0.899395397 | 1.178002169 |
| MP:0002211 | abnormal primary sex determination | 0.634195527 | 1.178041263 |
| MP:0000748 | progressive muscle weakness | 0.897370632 | 1.178056512 |
| ENSG00000163251 | FZD5 subnetwork | 0.633444516 | 1.178085642 |
| MP:0004401 | increased cochlear outer hair cell number | 0.897517125 | 1.178085665 |
| KEGG_ARACHIDONIC_ACID_MET | KEGG_ARACHIDONIC_ACID_METABOLISM | 0.633147772 | 1.178089958 |
| ENSG00000121083 | DYNLL2 subnetwork | 0.634143785 | 1.178113991 |
| MP:0009402 | decreased skeletal muscle fiber diameter | 0.897351397 | 1.178136038 |
| ENSG00000131979 | GCH1 subnetwork | 0.634020462 | 1.178171407 |
| ENSG00000084207 | GSTP1 subnetwork | 0.63410183 | 1.17819932 |
| GO:2000058 | regulation of protein ubiquitination involved in ubiquitin | 0.897335716 | 1.178224638 |
| MP:0010024 | increased total body fat amount | 0.633437271 | 1.178227736 |
| GO:0009395 | phospholipid catabolic process | 0.897288741 | 1.178267959 |
| ENSG00000104969 | SGTA subnetwork | 0.634000385 | 1.178288232 |
| GO:0001667 | ameboidal cell migration | 0.634428175 | 1.178295597 |
| MP:0001441 | increased grooming behavior | 0.897266518 | 1.178333937 |
| ENSG00000127914 | AKAP9 subnetwork | 0.634551022 | 1.178367501 |
| GO:0031623 | receptor internalization | 0.896307671 | 1.178382913 |
| ENSG00000183570 | PCBP3 subnetwork | 0.89715764 | 1.178416093 |
| REACTOME_CYCLIN_ACDK2:ASSO | REACTOME_CYCLIN_ACDK2:ASSOCIATED_EVENTS_AT_S_ | 0.89724966 | 1.178440699 |
| GO:0015936 | coenzyme A metabolic process | 0.896303985 | 1.178485261 |
| ENSG00000165684 | SNAPC4 subnetwork | 0.89702301 | 1.178491797 |
| GO:0035194 | posttranscriptional gene silencing by RNA | 0.897155638 | 1.178522882 |
| ENSG00000117408 | IPO13 subnetwork | 0.896963953 | 1.17853517 |
| ENSG00000082397 | EPB41L3 subnetwork | 0.896523452 | 1.178543575 |
| GO:0070918 | production of small RNA involved in gene silencing by RN | 0.896278291 | 1.17857402 |
| ENSG00000175110 | MRPS22 subnetwork | 0.89682807 | 1.178603808 |
| MP:0001081 | abnormal cranial ganglia morphology | 0.896658467 | 1.178618063 |
| KEGG_GLYCOSAMINOGLYCAN_BI | KEGG_GLYCOSAMINOGLYCAN_BIOSYNTHESIS_CHONDR( | 0.896946185 | 1.178623878 |
| GO:0016441 | posttranscriptional gene silencing | 0.897155638 | 1.17862969 |
| MP:0004144 | hypotonia | 0.896180596 | 1.178656324 |
| GO:0001829 | trophectodermal cell differentiation | 0.635111131 | 1.17867379 |

| | | | |
|---|---|---|---|
| GO:0031050 | dsRNA fragmentation | 0.896278291 | 1.17868094 |
| GO:0046546 | development of primary male sexual characteristics | 0.896128413 | 1.178686145 |
| MP:0000592 | short tail | 0.896825865 | 1.178710672 |
| MP:0001146 | abnormal testis morphology | 0.635058109 | 1.178721398 |
| ENSG00000124120 | TTPAL subnetwork | 0.89611774 | 1.178788566 |
| ENSG00000122585 | NPY subnetwork | 0.896058273 | 1.178822942 |
| GO:0016854 | racemase and epimerase activity | 0.635056803 | 1.178869609 |
| GO:0004659 | prenyltransferase activity | 0.895822084 | 1.178874262 |
| GO:0007566 | embryo implantation | 0.896055786 | 1.178929933 |
| MP:0001258 | decreased body length | 0.635006248 | 1.178936117 |
| ENSG00000112983 | BRD8 subnetwork | 0.895799999 | 1.178949519 |
| GO:0005262 | calcium channel activity | 0.635347943 | 1.17897813 |
| GO:0006977 | DNA damage response, signal transduction by p53 class | 0.895740726 | 1.178983928 |
| ENSG00000111669 | TPI1 subnetwork | 0.89602326 | 1.179009712 |
| GO:0072431 | signal transduction involved in mitotic cell cycle G1/S tra | 0.895740726 | 1.179090992 |
| GO:0010827 | regulation of glucose transport | 0.896002097 | 1.179094045 |
| ENSG00000165527 | ARF6 subnetwork | 0.637382739 | 1.179097744 |
| ENSG00000140022 | STON2 subnetwork | 0.637329021 | 1.179126457 |
| GO:0072413 | signal transduction involved in mitotic cell cycle checkpo | 0.895740726 | 1.179198075 |
| ENSG00000100764 | PSMC1 subnetwork | 0.637591476 | 1.179234528 |
| ENSG00000117410 | ATP6V0B subnetwork | 0.63765907 | 1.179237129 |
| GO:0031362 | anchored to external side of plasma membrane | 0.637318016 | 1.179255452 |
| MP:0008438 | abnormal cutaneous collagen fibril morphology | 0.637760429 | 1.179283567 |
| GO:0072401 | signal transduction involved in DNA integrity checkpoint | 0.895740726 | 1.179305177 |
| REACTOME_REGULATION_OF_MI | REACTOME_REGULATION_OF_MRNA_STABILITY_BY_PR | 0.635637693 | 1.179338947 |
| MP:0002980 | abnormal postural reflex | 0.637590171 | 1.179382283 |
| GO:0016323 | basolateral plasma membrane | 0.637300129 | 1.17938448 |
| GO:0072422 | signal transduction involved in DNA damage checkpoint | 0.895740726 | 1.179412299 |
| MP:0001785 | edema | 0.635763829 | 1.179486052 |
| GO:0072474 | signal transduction involved in mitotic cell cycle G1/S ch | 0.895740726 | 1.17951944 |
| GO:0007565 | female pregnancy | 0.637297148 | 1.179532347 |
| GO:0046622 | positive regulation of organ growth | 0.895710004 | 1.179590261 |
| GO:0006903 | vesicle targeting | 0.895532145 | 1.179595638 |
| GO:0043484 | regulation of RNA splicing | 0.895645148 | 1.17962475 |
| ENSG00000137801 | THBS1 subnetwork | 0.63592586 | 1.179626838 |
| GO:0034623 | cellular macromolecular complex disassembly | 0.63727985 | 1.179642633 |
| ENSG00000131558 | EXOC4 subnetwork | 0.63638794 | 1.179658463 |
| ENSG00000132016 | C19orf57 subnetwork | 0.895514322 | 1.179675573 |
| ENSG00000143401 | ANP32E subnetwork | 0.636241047 | 1.179691032 |
| ENSG00000101400 | SNTA1 subnetwork | 0.637118698 | 1.179700238 |
| ENSG00000143622 | RIT1 subnetwork | 0.895470788 | 1.179714623 |
| ENSG00000152214 | RIT2 subnetwork | 0.63608292 | 1.179717337 |
| ENSG00000108344 | PSMD3 subnetwork | 0.637235588 | 1.179721595 |
| ENSG00000163207 | IVL subnetwork | 0.638217501 | 1.179732098 |
| REACTOME_VPR:MEDIATED_NUC | REACTOME_VPR:MEDIATED_NUCLEAR_IMPORT_OF_PIC | 0.636359619 | 1.179743815 |
| GO:0032318 | regulation of Ras GTPase activity | 0.637090199 | 1.179772955 |
| ENSG00000088930 | XRN2 subnetwork | 0.636845792 | 1.179777889 |
| ENSG00000128739 | SNRPN subnetwork | 0.636907457 | 1.179799247 |
| GO:0031011 | Ino80 complex | 0.638869285 | 1.179808654 |
| ENSG00000197102 | DYNC1H1 subnetwork | 0.636523152 | 1.179811676 |
| GO:0046578 | regulation of Ras protein signal transduction | 0.636218885 | 1.179814094 |
| GO:0000236 | mitotic prometaphase | 0.89547077 | 1.179821851 |
| ENSG00000150938 | CRIM1 subnetwork | 0.636817099 | 1.179844378 |
| MP:0009873 | abnormal aorta tunica media morphology | 0.637052225 | 1.179864509 |

| | | | |
|---|---|---|---|
| MP:0003139 | patent ductus arteriosus | 0.638211724 | 1.179873545 |
| GO:0008608 | attachment of spindle microtubules to kinetochore | 0.895193394 | 1.179896345 |
| MP:0008976 | delayed female fertility | 0.895023801 | 1.17990633 |
| ENSG00000154162 | CDH12 subnetwork | 0.895448893 | 1.179906372 |
| GO:0006022 | aminoglycan metabolic process | 0.895379114 | 1.179927273 |
| GO:0007530 | sex determination | 0.636783068 | 1.179942262 |
| GO:0009593 | detection of chemical stimulus | 0.894986669 | 1.179954525 |
| GO:0033202 | DNA helicase complex | 0.638869285 | 1.179956223 |
| MP:0004090 | abnormal sarcomere morphology | 0.638417539 | 1.179959945 |
| GO:0006198 | cAMP catabolic process | 0.895159705 | 1.179962717 |
| ENSG00000196154 | S100A4 subnetwork | 0.636701162 | 1.179977404 |
| GO:0048546 | digestive tract morphogenesis | 0.89492848 | 1.179984537 |
| ENSG00000184343 | SRPK3 subnetwork | 0.895339132 | 1.17998909 |
| GO:0006476 | protein deacetylation | 0.638825558 | 1.179997498 |
| GO:0000165 | MAPK cascade | 0.638209201 | 1.180008765 |
| ENSG00000165410 | CFL2 subnetwork | 0.638750705 | 1.180020018 |
| ENSG00000130204 | TOMM40 subnetwork | 0.638168085 | 1.180031309 |
| GO:0050907 | detection of chemical stimulus involved in sensory perce | 0.894864173 | 1.180041845 |
| GO:0035412 | regulation of catenin import into nucleus | 0.894832887 | 1.180090066 |
| ENSG00000215727 | ENSG00000215727 subnetwork | 0.638656169 | 1.180121387 |
| ENSG00000156931 | VPS8 subnetwork | 0.638736678 | 1.180136386 |
| REACTOME_AQUAPORIN:MEDIAT | REACTOME_AQUAPORIN:MEDIATED_TRANSPORT | 0.894832152 | 1.180197434 |
| ENSG00000096696 | DSP subnetwork | 0.639241969 | 1.180255096 |
| ENSG00000065518 | NDUFB4 subnetwork | 0.638656169 | 1.180269086 |
| ENSG00000198700 | IPO9 subnetwork | 0.894824089 | 1.180291174 |
| MP:0011089 | complete perinatal lethality | 0.894615255 | 1.180344953 |
| MP:0003140 | dilated heart atrium | 0.894709012 | 1.180360393 |
| REACTOME_ACTIVATION_OF_ATF | REACTOME_ACTIVATION_OF_ATR_IN_RESPONSE_TO_RI | 0.893348032 | 1.180363653 |
| GO:0000291 | nuclear-transcribed mRNA catabolic process, exonucleol | 0.640330907 | 1.180375874 |
| MP:0002718 | abnormal inner cell mass morphology | 0.894563959 | 1.180379574 |
| GO:0043242 | negative regulation of protein complex disassembly | 0.894822976 | 1.18039858 |
| GO:0006691 | leukotriene metabolic process | 0.640477929 | 1.180411985 |
| ENSG00000145241 | CENPC1 subnetwork | 0.892791482 | 1.180412183 |
| ENSG00000105991 | HOXA1 subnetwork | 0.893295379 | 1.18042111 |
| KEGG_PROGESTERONE_MEDIATE | KEGG_PROGESTERONE_MEDIATED_OOCYTE_MATURATI | 0.893195715 | 1.180423883 |
| ENSG00000004487 | KDM1A subnetwork | 0.892715155 | 1.180433197 |
| GO:0000978 | RNA polymerase II core promoter proximal region seque | 0.892537839 | 1.180434188 |
| ENSG00000142507 | PSMB6 subnetwork | 0.894523175 | 1.180441511 |
| GO:0071779 | G1/S transition checkpoint | 0.894481834 | 1.18050346 |
| GO:0051428 | peptide hormone receptor binding | 0.892501159 | 1.180505382 |
| ENSG00000113812 | ACTR8 subnetwork | 0.894219345 | 1.18050724 |
| MP:0003051 | curly tail | 0.892687186 | 1.180508938 |
| GO:0042383 | sarcolemma | 0.893161363 | 1.180517823 |
| GO:0043928 | exonucleolytic nuclear-transcribed mRNA catabolic proc | 0.640330907 | 1.180523292 |
| MP:0000167 | decreased chondrocyte cell number | 0.893818311 | 1.180530248 |
| REACTOME_TELOMERE_MAINTEN | REACTOME_TELOMERE_MAINTENANCE | 0.894413635 | 1.180538104 |
| MP:0008128 | abnormal brain internal capsule morphology | 0.894313436 | 1.180540885 |
| MP:0004204 | absent stapes | 0.893088219 | 1.180543399 |
| GO:0060711 | labyrinthine layer development | 0.892467617 | 1.18054922 |
| GO:0043449 | cellular alkene metabolic process | 0.640477929 | 1.180559371 |
| ENSG00000127955 | GNAI1 subnetwork | 0.894023973 | 1.180561122 |
| GO:0048639 | positive regulation of developmental growth | 0.894089043 | 1.180562893 |
| ENSG00000177951 | BET1L subnetwork | 0.640252139 | 1.180564577 |
| MP:0001513 | limb grasping | 0.892052939 | 1.180567725 |

| | | | |
|---|---|---|---|
| MP:0004021 | abnormal rod electrophysiology | 0.894205735 | 1.180591985 |
| MP:0000069 | kyphoscoliosis | 0.640193458 | 1.180593379 |
| ENSG00000166863 | TAC3 subnetwork | 0.639998617 | 1.180594777 |
| ENSG00000167863 | ATP5H subnetwork | 0.892268443 | 1.180603212 |
| GO:0016765 | transferase activity, transferring alkyl or aryl (other than | 0.893784213 | 1.180605923 |
| GO:0016558 | protein import into peroxisome matrix | 0.892015651 | 1.180607029 |
| GO:0032088 | negative regulation of NF-kappaB transcription factor act | 0.892163852 | 1.180615132 |
| ENSG00000133243 | BTBD2 subnetwork | 0.893720705 | 1.180631493 |
| ENSG00000104626 | ERI1 subnetwork | 0.892452716 | 1.180634124 |
| MP:0001116 | small gonad | 0.893642066 | 1.180634284 |
| ENSG00000106397 | PLOD3 subnetwork | 0.893078168 | 1.180641926 |
| ENSG00000138430 | OLA1 subnetwork | 0.894022023 | 1.180668671 |
| GO:0006584 | catecholamine metabolic process | 0.891989129 | 1.180696549 |
| GO:0016634 | oxidoreductase activity, acting on the CH-CH group of do | 0.892421941 | 1.180700794 |
| GO:0044304 | main axon | 0.640156479 | 1.180703398 |
| GO:0001944 | vasculature development | 0.639868403 | 1.180714911 |
| GO:0016073 | snRNA metabolic process | 0.639981244 | 1.180729818 |
| GO:0031640 | killing of cells of other organism | 0.639787744 | 1.1807625 |
| GO:0044236 | multicellular organismal metabolic process | 0.639722929 | 1.180766346 |
| ENSG00000164134 | NAA15 subnetwork | 0.64087855 | 1.180803794 |
| GO:0034311 | diol metabolic process | 0.891989129 | 1.180804346 |
| GO:0033559 | unsaturated fatty acid metabolic process | 0.888509566 | 1.18083761 |
| ENSG00000170515 | PA2G4 subnetwork | 0.640787764 | 1.180838847 |
| GO:0030545 | receptor regulator activity | 0.891687001 | 1.180852133 |
| GO:0003015 | heart process | 0.887029978 | 1.180865614 |
| GO:0021756 | striatum development | 0.887190837 | 1.180878304 |
| KEGG_AXON_GUIDANCE | KEGG_AXON_GUIDANCE | 0.891898397 | 1.180896722 |
| MP:0001391 | abnormal tail movements | 0.891500799 | 1.180898876 |
| MP:0001314 | corneal opacity | 0.639715018 | 1.180901475 |
| ENSG00000080986 | NDC80 subnetwork | 0.887314869 | 1.180909341 |
| GO:0009712 | catechol-containing compound metabolic process | 0.891989129 | 1.180912162 |
| ENSG00000067191 | CACNB1 subnetwork | 0.888458534 | 1.180918339 |
| GO:0043473 | pigmentation | 0.891656652 | 1.180923456 |
| ENSG00000007264 | MATK subnetwork | 0.887289136 | 1.180948885 |
| REACTOME_RNA_POLYMERASE_I | REACTOME_RNA_POLYMERASE_I_RNA_POLYMERASE_II | 0.887181226 | 1.180949977 |
| MP:0002543 | brachyphalangia | 0.89119842 | 1.180955862 |
| ENSG00000140740 | UQCRC2 subnetwork | 0.890773167 | 1.180970013 |
| MP:0001006 | abnormal retinal cone cell morphology | 0.887532236 | 1.180972477 |
| MP:0009967 | abnormal neuron proliferation | 0.887024807 | 1.18097402 |
| GO:0035337 | fatty-acyl-CoA metabolic process | 0.888434028 | 1.180980752 |
| GO:0071295 | cellular response to vitamin | 0.886933773 | 1.180981454 |
| REACTOME_CDT1_ASSOCIATION_ | REACTOME_CDT1_ASSOCIATION_WITH_THE_CDC6ORC( | 0.891484104 | 1.180983921 |
| ENSG00000185313 | SCN10A subnetwork | 0.891148253 | 1.180999817 |
| GO:0006801 | superoxide metabolic process | 0.891895297 | 1.181004566 |
| MP:0003672 | abnormal ureter development | 0.887478498 | 1.181012019 |
| GO:0000381 | regulation of alternative nuclear mRNA splicing, via splic | 0.888999118 | 1.181015847 |
| REACTOME_CDO_IN_MYOGENESI | REACTOME_CDO_IN_MYOGENESIS | 0.886441452 | 1.181021495 |
| REACTOME_UBIQUITIN:DEPENDE | REACTOME_UBIQUITIN:DEPENDENT_DEGRADATION_OF | 0.887945091 | 1.181025312 |
| REACTOME_THROMBOXANE_SIG | REACTOME_THROMBOXANE_SIGNALLING_THROUGH_T | 0.891343021 | 1.181026133 |
| GO:0032856 | activation of Ras GTPase activity | 0.890739857 | 1.181032276 |
| MP:0002925 | abnormal cardiovascular development | 0.88878796 | 1.181038116 |
| GO:0006289 | nucleotide-excision repair | 0.88828374 | 1.181046021 |
| GO:0048538 | thymus development | 0.891443729 | 1.18104614 |
| ENSG00000131773 | KHDRBS3 subnetwork | 0.891092828 | 1.18106206 |

| | | | |
|---|---|---|---|
| MP:0004833 | ovary atrophy | 0.888023552 | 1.181063732 |
| MP:0004215 | abnormal myocardial fiber physiology | 0.890999641 | 1.18107404 |
| ENSG00000164056 | SPRY1 subnetwork | 0.886911389 | 1.181080709 |
| REACTOME_G_ALPHA_S_SIGNALI | REACTOME_G_ALPHA_S_SIGNALLING_EVENTS | 0.888961805 | 1.181087395 |
| GO:0046949 | fatty-acyl-CoA biosynthetic process | 0.888434028 | 1.181089009 |
| GO:0009264 | deoxyribonucleotide catabolic process | 0.888132144 | 1.181097561 |
| ENSG00000102007 | PLP2 subnetwork | 0.889598806 | 1.181099515 |
| GO:0048806 | genitalia development | 0.89092982 | 1.181099735 |
| ENSG00000134508 | CABLES1 subnetwork | 0.88890722 | 1.181103985 |
| REACTOME_HIGHLY_CALCIUM_PI | REACTOME_HIGHLY_CALCIUM_PERMEABLE_POSTSYNAI | 0.888770168 | 1.181109686 |
| ENSG00000120616 | EPC1 subnetwork | 0.886844661 | 1.181120294 |
| GO:0000959 | mitochondrial RNA metabolic process | 0.887830621 | 1.18112273 |
| REACTOME_MYOGENESIS | REACTOME_MYOGENESIS | 0.886441452 | 1.181129995 |
| ENSG00000117152 | RGS4 subnetwork | 0.890734564 | 1.181131127 |
| GO:0019865 | immunoglobulin binding | 0.888255772 | 1.181131384 |
| REACTOME_UBIQUITIN:DEPENDE | REACTOME_UBIQUITIN:DEPENDENT_DEGRADATION_OF | 0.887945091 | 1.181133633 |
| GO:0016820 | hydrolase activity, acting on acid anhydrides, catalyzing t | 0.889549275 | 1.181134408 |
| MP:0003997 | tonic-clonic seizures | 0.88678395 | 1.181141519 |
| REACTOME_TRYPTOPHAN_CATAE | REACTOME_TRYPTOPHAN_CATABOLISM | 0.886369742 | 1.181146637 |
| GO:0034199 | activation of protein kinase A activity | 0.88774893 | 1.181157692 |
| GO:0048754 | branching morphogenesis of a tube | 0.890243176 | 1.181171089 |
| ENSG00000087470 | DNM1L subnetwork | 0.890324829 | 1.181172811 |
| GO:0030947 | regulation of vascular endothelial growth factor recepto | 0.889499003 | 1.181192199 |
| GO:0006336 | DNA replication-independent nucleosome assembly | 0.886325745 | 1.181204631 |
| MP:0004098 | abnormal cerebellar granule cell morphology | 0.890543206 | 1.181217415 |
| REACTOME_DESTABILIZATION_OI | REACTOME_DESTABILIZATION_OF_MRNA_BY_AUF1_HN | 0.89009654 | 1.181217972 |
| GO:0031269 | pseudopodium assembly | 0.889254694 | 1.181228247 |
| MP:0003990 | decreased neurotransmitter release | 0.890732986 | 1.18123914 |
| REACTOME_ASSEMBLY_OF_THE_ | REACTOME_ASSEMBLY_OF_THE_PRE:REPLICATIVE_COM | 0.890213723 | 1.181247141 |
| MP:0002275 | abnormal type II pneumocyte morphology | 0.886782041 | 1.18125 |
| ENSG00000119421 | NDUFA8 subnetwork | 0.889975869 | 1.181251144 |
| ENSG00000122877 | EGR2 subnetwork | 0.890454531 | 1.181252287 |
| MP:0009748 | abnormal behavioral response to addictive substance | 0.886703891 | 1.181262056 |
| GO:0006342 | chromatin silencing | 0.889891824 | 1.181267735 |
| ENSG00000158623 | COPG2 subnetwork | 0.889459756 | 1.181268315 |
| GO:0006405 | RNA export from nucleus | 0.641191184 | 1.181292899 |
| GO:0043968 | histone H2A acetylation | 0.641251122 | 1.181295233 |
| ENSG00000131711 | MAP1B subnetwork | 0.890077052 | 1.181298618 |
| GO:0034080 | CenH3-containing nucleosome assembly at centromere | 0.886325745 | 1.181313178 |
| MP:0003031 | acidosis | 0.889864283 | 1.181339253 |
| MP:0006007 | abnormal basal ganglion morphology | 0.890718657 | 1.181342601 |
| ENSG00000214133 | ENSG00000214133 subnetwork | 0.889459756 | 1.1813765 |
| GO:0034724 | DNA replication-independent nucleosome organization | 0.886325745 | 1.181421744 |
| GO:0046324 | regulation of glucose import | 0.886086736 | 1.181480971 |
| ENSG00000132688 | NES subnetwork | 0.886278677 | 1.181484375 |
| MP:0004740 | sensorineural hearing loss | 0.641841277 | 1.181496259 |
| GO:0070302 | regulation of stress-activated protein kinase signaling ca | 0.641770766 | 1.181525128 |
| MP:0003463 | abnormal single cell response | 0.886046602 | 1.181543624 |
| GO:0071305 | cellular response to vitamin D | 0.641952908 | 1.181554669 |
| ENSG00000167674 | ENSG00000167674 subnetwork | 0.886264027 | 1.181583785 |
| MP:0001898 | abnormal long term depression | 0.886015362 | 1.181620081 |
| GO:0004601 | peroxidase activity | 0.642383448 | 1.181622228 |
| ENSG00000074054 | CLASP1 subnetwork | 0.642086505 | 1.181650461 |
| GO:0051313 | attachment of spindle microtubules to chromosome | 0.885948222 | 1.181655172 |

| | | | |
|---|---|---|---|
| ENSG00000054356 | PTPRN subnetwork | 0.642483375 | 1.181655662 |
| MP:0001211 | wrinkled skin | 0.641766408 | 1.181666251 |
| MP:0002968 | increased circulating alkaline phosphatase level | 0.642297639 | 1.181698654 |
| ENSG00000188985 | ENSG00000188985 subnetwork | 0.642608328 | 1.181707773 |
| GO:0035023 | regulation of Rho protein signal transduction | 0.885894597 | 1.181717859 |
| ENSG00000075856 | SART3 subnetwork | 0.885830578 | 1.181748368 |
| GO:0016684 | oxidoreductase activity, acting on peroxide as acceptor | 0.642383448 | 1.18176947 |
| ENSG00000137656 | BUD13 subnetwork | 0.64166303 | 1.181773952 |
| ENSG00000077348 | EXOSC5 subnetwork | 0.885758881 | 1.181778882 |
| GO:0050872 | white fat cell differentiation | 0.641738399 | 1.181782462 |
| ENSG00000137822 | TUBGCP4 subnetwork | 0.642278013 | 1.181821015 |
| GO:0009636 | response to toxin | 0.885755615 | 1.181887591 |
| MP:0001684 | abnormal axial mesoderm | 0.641658982 | 1.181921397 |
| GO:0032755 | positive regulation of interleukin-6 production | 0.643355057 | 1.181957929 |
| GO:0000398 | nuclear mRNA splicing, via spliceosome | 0.643236823 | 1.181968131 |
| REACTOME_AUTODEGRADATION | REACTOME_AUTODEGRADATION_OF_THE_E3_UBIQUITI | 0.885755551 | 1.18199632 |
| ENSG00000017797 | RALBP1 subnetwork | 0.643506032 | 1.181999751 |
| KEGG_PEROXISOME | KEGG_PEROXISOME | 0.885752796 | 1.182105069 |
| ENSG00000111481 | COPZ1 subnetwork | 0.643484777 | 1.182109521 |
| GO:0000377 | RNA splicing, via transesterification reactions with bulge | 0.643236823 | 1.182115289 |
| MP:0004163 | abnormal adenohypophysis morphology | 0.643160386 | 1.182137965 |
| ENSG00000197903 | HIST1H2BK subnetwork | 0.64306289 | 1.182166874 |
| ENSG00000110799 | VWF subnetwork | 0.885737117 | 1.182200037 |
| GO:0046875 | ephrin receptor binding | 0.642974918 | 1.182208245 |
| ENSG00000173546 | CSPG4 subnetwork | 0.885736578 | 1.182308825 |
| ENSG00000136436 | CALCOCO2 subnetwork | 0.885731658 | 1.182394625 |
| MP:0003730 | abnormal photoreceptor inner segment morphology | 0.885730755 | 1.182503451 |
| ENSG00000153707 | PTPRD subnetwork | 0.885629541 | 1.182587683 |
| REACTOME_RNA_POLYMERASE_I | REACTOME_RNA_POLYMERASE_I_PROMOTER_OPENING | 0.885715967 | 1.182593888 |
| MP:0000747 | muscle weakness | 0.885603809 | 1.182682747 |
| ENSG00000104325 | DECR1 subnetwork | 0.885530808 | 1.182722585 |
| GO:0032401 | establishment of melanosome localization | 0.885479962 | 1.182794659 |
| MP:0002769 | abnormal vas deferens morphology | 0.885428292 | 1.182843724 |
| MP:0001407 | short stride length | 0.885043045 | 1.182886493 |
| ENSG00000124802 | EEF1E1 subnetwork | 0.885145102 | 1.182906495 |
| GO:0007202 | activation of phospholipase C activity | 0.885400957 | 1.182906613 |
| ENSG00000117748 | RPA2 subnetwork | 0.884891774 | 1.182975488 |
| KEGG_PENTOSE_PHOSPHATE_PA | KEGG_PENTOSE_PHOSPHATE_PATHWAY | 0.885368634 | 1.182978723 |
| ENSG00000114745 | GORASP1 subnetwork | 0.88502271 | 1.182986271 |
| MP:0000242 | impaired fertilization | 0.884675426 | 1.183 |
| ENSG00000107438 | PDLIM1 subnetwork | 0.885307477 | 1.183018607 |
| GO:0010008 | endosome membrane | 0.644155331 | 1.183028493 |
| GO:0009119 | ribonucleoside metabolic process | 0.884863592 | 1.183066077 |
| MP:0005341 | decreased susceptibility to atherosclerosis | 0.884656688 | 1.183095216 |
| GO:0034440 | lipid oxidation | 0.884601121 | 1.183121313 |
| GO:0042278 | purine nucleoside metabolic process | 0.884468461 | 1.18313203 |
| GO:0060491 | regulation of cell projection assembly | 0.884566954 | 1.1831889 |
| GO:0009218 | pyrimidine ribonucleotide metabolic process | 0.884442233 | 1.183208852 |
| GO:0016840 | carbon-nitrogen lyase activity | 0.884304795 | 1.183247256 |
| GO:0045005 | maintenance of fidelity involved in DNA-dependent DNA | 0.884410769 | 1.183262634 |
| GO:0045669 | positive regulation of osteoblast differentiation | 0.884270405 | 1.183319498 |
| ENSG00000157916 | RER1 subnetwork | 0.884008619 | 1.183333333 |
| ENSG00000144642 | RBMS3 subnetwork | 0.884228538 | 1.183359469 |
| REACTOME_FGFR_LIGAND_BINDI | REACTOME_FGFR_LIGAND_BINDING_AND_ACTIVATION | 0.884142871 | 1.183362546 |

| | | | |
|---|---|---|---|
| MP:0000462 | abnormal digestive system morphology | 0.88392776 | 1.183382543 |
| GO:0008643 | carbohydrate transport | 0.88389403 | 1.183440989 |
| MP:0000293 | absent myocardial trabeculae | 0.646449899 | 1.183451185 |
| ENSG00000166478 | ZNF143 subnetwork | 0.883845641 | 1.183467147 |
| REACTOME_G_BETAGAMMA_SIG | REACTOME_G_BETAGAMMA_SIGNALLING_THROUGH_P | 0.646892214 | 1.183467642 |
| GO:0070536 | protein K63-linked deubiquitination | 0.644725652 | 1.183490859 |
| ENSG00000034677 | RNF19A subnetwork | 0.64466327 | 1.183495025 |
| ENSG00000177731 | FLII subnetwork | 0.644810512 | 1.183530216 |
| MP:0008753 | abnormal osteocyte morphology | 0.6446105 | 1.18353651 |
| ENSG00000096155 | BAG6 subnetwork | 0.883815794 | 1.183539455 |
| GO:0033688 | regulation of osteoblast proliferation | 0.644540929 | 1.183584225 |
| ENSG00000140525 | FANCI subnetwork | 0.64644361 | 1.183598015 |
| ENSG00000117724 | CENPF subnetwork | 0.646888778 | 1.183601984 |
| ENSG00000206313 | ENSG00000206313 subnetwork | 0.883815794 | 1.183648699 |
| ENSG00000100931 | ENSG00000100931 subnetwork | 0.64664832 | 1.183651699 |
| REACTOME_TRANSPORT_OF_THE | REACTOME_TRANSPORT_OF_THE_SLBP_INDEPENDENT_ | 0.646848389 | 1.183668155 |
| REACTOME_NUCLEOTIDE_EXCISIO | REACTOME_NUCLEOTIDE_EXCISION_REPAIR | 0.883079604 | 1.183684405 |
| REACTOME_METABOLISM_OF_NO | REACTOME_METABOLISM_OF_NON:CODING_RNA | 0.646308063 | 1.183687019 |
| ENSG00000128626 | MRPS12 subnetwork | 0.883471923 | 1.183691938 |
| MP:0002231 | abnormal primitive streak morphology | 0.647213964 | 1.183694844 |
| ENSG00000151577 | DRD3 subnetwork | 0.646003896 | 1.183697542 |
| GO:0060047 | heart contraction | 0.88332349 | 1.183707398 |
| MP:0000018 | small ears | 0.883418996 | 1.183718138 |
| GO:0051084 | 'de novo' posttranslational protein folding | 0.646430326 | 1.183720065 |
| REACTOME_CYCLIN_E_ASSOCIATI | REACTOME_CYCLIN_E_ASSOCIATED_EVENTS_DURING_C | 0.883642376 | 1.183727264 |
| ENSG00000107186 | MPDZ subnetwork | 0.883288451 | 1.183733604 |
| ENSG00000213588 | ZBTB9 subnetwork | 0.646807879 | 1.183734342 |
| GO:0040013 | negative regulation of locomotion | 0.883038918 | 1.183756814 |
| ENSG00000204463 | BAG6 subnetwork | 0.883815794 | 1.183757962 |
| GO:0033177 | proton-transporting two-sector ATPase complex, proton | 0.883609536 | 1.183781163 |
| KEGG_GLYCINE_SERINE_AND_THI | KEGG_GLYCINE_SERINE_AND_THREONINE_METABOLISM | 0.883234644 | 1.18378291 |
| GO:0032107 | regulation of response to nutrient levels | 0.646214047 | 1.183788481 |
| MP:0002970 | abnormal white adipose tissue morphology | 0.883771247 | 1.18379339 |
| GO:0048365 | Rac GTPase binding | 0.647541977 | 1.18379383 |
| ENSG00000173156 | RHOD subnetwork | 0.64748143 | 1.183804213 |
| GO:0008299 | isoprenoid biosynthetic process | 0.647184244 | 1.183804388 |
| GO:0046503 | glycerolipid catabolic process | 0.645993701 | 1.183825903 |
| REACTOME_SNRNP_ASSEMBLY | REACTOME_SNRNP_ASSEMBLY | 0.646308063 | 1.183833933 |
| GO:0042605 | peptide antigen binding | 0.645180384 | 1.183838886 |
| MP:0000162 | lordosis | 0.883019826 | 1.183852338 |
| REACTOME_PACKAGING_OF_TEL | REACTOME_PACKAGING_OF_TELOMERE_ENDS | 0.882991025 | 1.183901673 |
| ENSG00000105127 | AKAP8 subnetwork | 0.647471929 | 1.183913744 |
| GO:0031669 | cellular response to nutrient levels | 0.64779958 | 1.183921714 |
| GO:0032104 | regulation of response to extracellular stimulus | 0.646214047 | 1.183935444 |
| REACTOME_RNA_POLYMERASE_I | REACTOME_RNA_POLYMERASE_I_PROMOTER_ESCAPE | 0.645985147 | 1.183941878 |
| ENSG00000131381 | ZFYVE20 subnetwork | 0.645130979 | 1.183942559 |
| GO:0002088 | lens development in camera-type eye | 0.882891724 | 1.183958776 |
| ENSG00000136205 | TNS3 subnetwork | 0.882974947 | 1.184001848 |
| GO:0000982 | RNA polymerase II core promoter proximal region seque | 0.647751099 | 1.184006442 |
| ENSG00000136152 | COG3 subnetwork | 0.645684062 | 1.184020875 |
| ENSG00000100722 | ZC3H14 subnetwork | 0.645887067 | 1.184031056 |
| ENSG00000127588 | GNG13 subnetwork | 0.882854077 | 1.184035866 |
| ENSG00000179051 | RCC2 subnetwork | 0.882783004 | 1.184066747 |
| MP:0002657 | chondrodystrophy | 0.645811957 | 1.184072556 |

| | | | |
|---|---|---|---|
| ENSG00000118985 | ELL2 subnetwork | 0.645982855 | 1.184082723 |
| ENSG00000005469 | CROT subnetwork | 0.882728656 | 1.184088388 |
| ENSG00000169021 | UQCRFS1 subnetwork | 0.882557006 | 1.184094692 |
| GO:0090004 | positive regulation of establishment of protein localizatic | 0.645671926 | 1.184143159 |
| GO:0043408 | regulation of MAPK cascade | 0.882538857 | 1.184153334 |
| ENSG00000132612 | VPS4A subnetwork | 0.882196379 | 1.184161347 |
| MP:0006346 | small branchial arch | 0.88242732 | 1.184165742 |
| MP:0002282 | abnormal trachea morphology | 0.645584958 | 1.184166045 |
| GO:0016918 | retinal binding | 0.882707305 | 1.184170134 |
| GO:0001159 | core promoter proximal region DNA binding | 0.882292946 | 1.184172063 |
| GO:0030553 | cGMP binding | 0.882130612 | 1.184192265 |
| MP:0004597 | increased susceptibility to noise-induced hearing loss | 0.882382806 | 1.184196652 |
| GO:0016884 | carbon-nitrogen ligase activity, with glutamine as amido- | 0.64550912 | 1.184213797 |
| ENSG00000213512 | GBP7 subnetwork | 0.882002855 | 1.184230983 |
| REACTOME_METABOLISM_OF_W | REACTOME_METABOLISM_OF_WATER:SOLUBLE_VITAM | 0.881735657 | 1.184245117 |
| ENSG00000183474 | GTF2H2C subnetwork | 0.882103637 | 1.184246322 |
| GO:0043038 | amino acid activation | 0.881950544 | 1.184271171 |
| ENSG00000162512 | SDC3 subnetwork | 0.648228762 | 1.184303406 |
| GO:0007006 | mitochondrial membrane organization | 0.881234602 | 1.184319718 |
| REACTOME_METABOLISM_OF_VI | REACTOME_METABOLISM_OF_VITAMINS_AND_COFACT | 0.881735657 | 1.184354749 |
| ENSG00000108306 | FBXL20 subnetwork | 0.64836139 | 1.18436107 |
| ENSG00000139626 | ITGB7 subnetwork | 0.881463148 | 1.184368923 |
| GO:0043039 | tRNA aminoacylation | 0.881950544 | 1.184380785 |
| GO:0005874 | microtubule | 0.88138591 | 1.184385997 |
| ENSG00000104164 | PLDN subnetwork | 0.648166224 | 1.184394352 |
| ENSG00000101452 | DHX35 subnetwork | 0.881233568 | 1.184429418 |
| GO:0000226 | microtubule cytoskeleton organization | 0.881722738 | 1.184455143 |
| GO:0032438 | melanosome organization | 0.881151965 | 1.184460398 |
| GO:0004859 | phospholipase inhibitor activity | 0.880671156 | 1.184484197 |
| ENSG00000159720 | ATP6V0D1 subnetwork | 0.8816727 | 1.184513889 |
| MP:0005136 | decreased growth hormone level | 0.881128413 | 1.184528442 |
| ENSG00000163754 | GYG1 subnetwork | 0.880666658 | 1.184584724 |
| GO:0032412 | regulation of ion transmembrane transporter activity | 0.881101129 | 1.184587232 |
| ENSG00000100883 | SRP54 subnetwork | 0.880903176 | 1.184589009 |
| GO:0030934 | anchoring collagen | 0.649075694 | 1.184640604 |
| MP:0004252 | abnormal direction of heart looping | 0.880623973 | 1.184643552 |
| ENSG00000064547 | LPAR2 subnetwork | 0.649017688 | 1.184651076 |
| GO:0046379 | extracellular polysaccharide metabolic process | 0.648763173 | 1.184651566 |
| MP:0001409 | increased stereotypic behavior | 0.881067105 | 1.184659933 |
| ENSG00000155760 | FZD7 subnetwork | 0.6486135 | 1.184672527 |
| ENSG00000115540 | MOB4 subnetwork | 0.880884363 | 1.184675626 |
| ENSG00000116337 | AMPD2 subnetwork | 0.649241875 | 1.184706246 |
| GO:0043542 | endothelial cell migration | 0.648989441 | 1.184711051 |
| GO:0006354 | transcription elongation, DNA-dependent | 0.880573608 | 1.184716299 |
| ENSG00000198899 | MT-ATP6 subnetwork | 0.650849265 | 1.18474022 |
| MP:0002314 | abnormal respiratory mechanics | 0.650735766 | 1.184750679 |
| MP:0008843 | absent subcutaneous adipose tissue | 0.64918615 | 1.184778575 |
| GO:0045226 | extracellular polysaccharide biosynthetic process | 0.648763173 | 1.184798217 |
| MP:0000926 | absent floor plate | 0.880564921 | 1.184812239 |
| ENSG00000150867 | PIP4K2A subnetwork | 0.650711142 | 1.184853722 |
| GO:0001078 | RNA polymerase II core promoter proximal region seque | 0.648987527 | 1.184857673 |
| ENSG00000185637 | ENSG00000185637 subnetwork | 0.880533302 | 1.184889651 |
| ENSG00000154096 | THY1 subnetwork | 0.880472967 | 1.184934619 |
| ENSG00000099341 | PSMD8 subnetwork | 0.649698364 | 1.184971563 |

| | | | |
|---|---|---|---|
| MP:0008114 | abnormal Kupffer cell morphology | 0.649622361 | 1.184975887 |
| REACTOME_G_ALPHA_Q_SIGNAL | REACTOME_G_ALPHA_Q_SIGNALLING_EVENTS | 0.650693313 | 1.184987654 |
| REACTOME_PKA_ACTIVATION | REACTOME_PKA_ACTIVATION | 0.880453311 | 1.185030607 |
| ENSG00000198786 | MT-ND5 subnetwork | 0.650630481 | 1.185047537 |
| MP:0006359 | absent startle reflex | 0.650335619 | 1.185058678 |
| ENSG00000101473 | ACOT8 subnetwork | 0.880370436 | 1.185061683 |
| REACTOME_GLUCOSE_METABOLI | REACTOME_GLUCOSE_METABOLISM | 0.650262057 | 1.185093897 |
| REACTOME_CHROMOSOME_MAI | REACTOME_CHROMOSOME_MAINTENANCE | 0.649599443 | 1.185110067 |
| ENSG00000010803 | SCMH1 subnetwork | 0.651484125 | 1.185119635 |
| GO:0051051 | negative regulation of transport | 0.6514059 | 1.185142469 |
| ENSG00000108272 | DHRS11 subnetwork | 0.880358091 | 1.185157699 |
| ENSG00000077943 | ITGA8 subnetwork | 0.650553961 | 1.185161171 |
| ENSG00000212870 | ENSG00000212870 subnetwork | 0.650630481 | 1.185193875 |
| REACTOME_VIF:MEDIATED_DEGR | REACTOME_VIF:MEDIATED_DEGRADATION_OF_APOBEC | 0.880320555 | 1.185202709 |
| ENSG00000142627 | EPHA2 subnetwork | 0.650235455 | 1.185215618 |
| ENSG00000139180 | NDUFA9 subnetwork | 0.650498005 | 1.185251976 |
| GO:0031253 | cell projection membrane | 0.880008673 | 1.185266821 |
| GO:0032757 | positive regulation of interleukin-8 production | 0.879906125 | 1.185270095 |
| GO:0006506 | GPI anchor biosynthetic process | 0.650162491 | 1.185275581 |
| GO:0051653 | spindle localization | 0.87982007 | 1.185282651 |
| ENSG00000127022 | CANX subnetwork | 0.651405768 | 1.185288675 |
| GO:0022412 | cellular process involved in reproduction in multicellular | 0.880314828 | 1.185294118 |
| GO:0005868 | cytoplasmic dynein complex | 0.880251348 | 1.185343788 |
| GO:0051898 | negative regulation of protein kinase B signaling cascade | 0.651701579 | 1.185355778 |
| GO:0051293 | establishment of spindle localization | 0.87982007 | 1.185392685 |
| ENSG00000102119 | EMD subnetwork | 0.651303987 | 1.18540227 |
| MP:0006072 | abnormal retinal apoptosis | 0.651393542 | 1.185410241 |
| GO:0006376 | mRNA splice site selection | 0.6500725 | 1.185420272 |
| GO:0001012 | RNA polymerase II regulatory region DNA binding | 0.650145278 | 1.185422074 |
| REACTOME_INHIBITION_OF_INSU | REACTOME_INHIBITION_OF_INSULIN_SECRETION_BY_A | 0.880217684 | 1.185435226 |
| GO:0005080 | protein kinase C binding | 0.649992157 | 1.185455557 |
| ENSG00000161835 | GRASP subnetwork | 0.879636453 | 1.185481475 |
| GO:0030500 | regulation of bone mineralization | 0.652576067 | 1.185484666 |
| ENSG00000105993 | DNAJB6 subnetwork | 0.879807402 | 1.185493455 |
| MP:0003109 | short femur | 0.652673674 | 1.185541872 |
| GO:0060008 | Sertoli cell differentiation | 0.879760143 | 1.185547818 |
| ENSG00000119487 | MAPKAP1 subnetwork | 0.879604019 | 1.185572994 |
| GO:0042401 | cellular biogenic amine biosynthetic process | 0.652531961 | 1.185587583 |
| ENSG00000133027 | PEMT subnetwork | 0.65277307 | 1.185599064 |
| REACTOME_LOSS_OF_NLP_FROM | REACTOME_LOSS_OF_NLP_FROM_MITOTIC_CENTROSO | 0.879394837 | 1.185633999 |
| GO:0004602 | glutathione peroxidase activity | 0.879572541 | 1.185636668 |
| GO:0006488 | dolichol-linked oligosaccharide biosynthetic process | 0.879481103 | 1.185639978 |
| GO:0030866 | cortical actin cytoskeleton organization | 0.652913705 | 1.185662398 |
| GO:0034728 | nucleosome organization | 0.879011421 | 1.185697026 |
| ENSG00000211679 | ENSG00000211679 subnetwork | 0.652516372 | 1.185709006 |
| ENSG00000113407 | TARS subnetwork | 0.652059808 | 1.185716928 |
| MP:0005189 | abnormal anogenital distance | 0.878569279 | 1.185732218 |
| REACTOME_LOSS_OF_PROTEINS_ | REACTOME_LOSS_OF_PROTEINS_REQUIRED_FOR_INTER | 0.879394837 | 1.185744147 |
| GO:0042301 | phosphate ion binding | 0.878804077 | 1.185744167 |
| ENSG00000178053 | MLF1 subnetwork | 0.878880116 | 1.185750139 |
| ENSG00000131508 | UBE2D2 subnetwork | 0.878486672 | 1.185763437 |
| ENSG00000109519 | GRPEL1 subnetwork | 0.652014697 | 1.185764488 |
| ENSG00000156475 | PPP2R2B subnetwork | 0.652273385 | 1.185765344 |
| ENSG00000130177 | CDC16 subnetwork | 0.878974466 | 1.185765406 |

| | | | |
|---|---|---|---|
| ENSG00000100796 | SMEK1 subnetwork | 0.878743057 | 1.185789327 |
| ENSG00000171621 | SPSB1 subnetwork | 0.879375612 | 1.185826442 |
| ENSG00000187558 | ENSG00000187558 subnetwork | 0.878467275 | 1.185841161 |
| ENSG00000211677 | ENSG00000211677 subnetwork | 0.652516372 | 1.185855101 |
| MP:0000222 | decreased neutrophil cell number | 0.652448632 | 1.185884165 |
| MP:0006032 | abnormal ureteric bud morphology | 0.652219621 | 1.185891272 |
| GO:0006406 | mRNA export from nucleus | 0.652272057 | 1.185905337 |
| MP:0004811 | abnormal neuron physiology | 0.879369725 | 1.185936629 |
| ENSG00000184203 | PPP1R2 subnetwork | 0.878467275 | 1.185951451 |
| REACTOME_REGULATION_OF_IN | REACTOME_REGULATION_OF_INSULIN:LIKE_GROWTH_F | 0.87927439 | 1.185953908 |
| GO:0006586 | indolalkylamine metabolic process | 0.878407528 | 1.185964096 |
| GO:0016324 | apical plasma membrane | 0.878104391 | 1.185977482 |
| GO:0030036 | actin cytoskeleton organization | 0.663251459 | 1.186010677 |
| MP:0008271 | abnormal bone ossification | 0.878206269 | 1.186048567 |
| ENSG00000131263 | RLIM subnetwork | 0.873697192 | 1.186052164 |
| ENSG00000131149 | KIAA0182 subnetwork | 0.873645296 | 1.186074233 |
| GO:0042430 | indole-containing compound metabolic process | 0.878407528 | 1.186074419 |
| MP:0002578 | impaired ability to fire action potentials | 0.878087206 | 1.186078541 |
| GO:0045687 | positive regulation of glial cell differentiation | 0.663350966 | 1.186079097 |
| MP:0000267 | abnormal heart development | 0.663432854 | 1.186098981 |
| ENSG00000167552 | TUBA1A subnetwork | 0.663218948 | 1.186106055 |
| GO:0090092 | regulation of transmembrane receptor protein serine/th | 0.878354433 | 1.186128942 |
| GO:0050805 | negative regulation of synaptic transmission | 0.873878618 | 1.186132922 |
| GO:2000758 | positive regulation of peptidyl-lysine acetylation | 0.87803333 | 1.186133085 |
| GO:0008361 | regulation of cell size | 0.877956809 | 1.186141102 |
| REACTOME_CELL_CYCLE | REACTOME_CELL_CYCLE | 0.8736181 | 1.186161758 |
| ENSG00000113360 | DROSHA subnetwork | 0.663659331 | 1.186169052 |
| KEGG_TRYPTOPHAN_METABOLIS | KEGG_TRYPTOPHAN_METABOLISM | 0.874108272 | 1.186205607 |
| ENSG00000169271 | HSPB3 subnetwork | 0.875722322 | 1.186210114 |
| ENSG00000184937 | WT1 subnetwork | 0.873549245 | 1.186211895 |
| GO:0032890 | regulation of organic acid transport | 0.877924121 | 1.186214279 |
| GO:0016877 | ligase activity, forming carbon-sulfur bonds | 0.663218634 | 1.18625 |
| MP:0006378 | abnormal spermatogonia morphology | 0.874050916 | 1.186255725 |
| ENSG00000173636 | ENSG00000173636 subnetwork | 0.875675947 | 1.186264813 |
| ENSG00000091704 | CPA1 subnetwork | 0.874702495 | 1.186283392 |
| ENSG00000164442 | CITED2 subnetwork | 0.663643024 | 1.186300788 |
| GO:0009101 | glycoprotein biosynthetic process | 0.874618416 | 1.186300794 |
| GO:0051149 | positive regulation of muscle cell differentiation | 0.873534967 | 1.186318152 |
| MP:0004672 | short ribs | 0.877915667 | 1.186320052 |
| GO:0030141 | secretory granule | 0.877509788 | 1.186324269 |
| MP:0003036 | vertebral transformation | 0.664901224 | 1.186333374 |
| MP:0003122 | maternal imprinting | 0.875140396 | 1.186353875 |
| GO:0032435 | negative regulation of proteasomal ubiquitin-dependent | 0.875663479 | 1.186366181 |
| REACTOME_ABORTIVE_ELONGAT | REACTOME_ABORTIVE_ELONGATION_OF_HIV:1_TRANS( | 0.663204275 | 1.186369705 |
| GO:0009125 | nucleoside monophosphate catabolic process | 0.87764104 | 1.186372102 |
| ENSG00000187790 | FANCM subnetwork | 0.877771687 | 1.186382682 |
| MP:0002893 | ketoaciduria | 0.874599581 | 1.186388266 |
| GO:0000407 | pre-autophagosomal structure | 0.87349894 | 1.186396371 |
| ENSG00000131051 | RBM39 subnetwork | 0.664845556 | 1.186398305 |
| ENSG00000103051 | COG4 subnetwork | 0.877892276 | 1.18640257 |
| ENSG00000102683 | SGCG subnetwork | 0.874546149 | 1.186419695 |
| ENSG00000047410 | TPR subnetwork | 0.877496524 | 1.186420788 |
| GO:0032703 | negative regulation of interleukin-2 production | 0.663129583 | 1.186428745 |
| GO:0070328 | triglyceride homeostasis | 0.875621055 | 1.186430238 |

| | | | |
|---|---|---|---|
| ENSG00000121931 | LRIF1 subnetwork | 0.875111084 | 1.186431973 |
| GO:0016050 | vesicle organization | 0.873442609 | 1.186455897 |
| MP:0005157 | holoprosencephaly | 0.876361467 | 1.186459013 |
| MP:0002835 | abnormal cranial suture morphology | 0.663879538 | 1.186461744 |
| ENSG00000089250 | NOS1 subnetwork | 0.876226167 | 1.186465815 |
| ENSG00000161011 | SQSTM1 subnetwork | 0.875553821 | 1.186475639 |
| GO:0033057 | multicellular organismal reproductive behavior | 0.875337024 | 1.186485856 |
| GO:0051148 | negative regulation of muscle cell differentiation | 0.874954076 | 1.186490147 |
| ENSG00000137878 | GCOM1 subnetwork | 0.664788014 | 1.186493522 |
| ENSG00000198785 | GRIN3A subnetwork | 0.87748161 | 1.186503353 |
| MP:0003915 | increased left ventricle weight | 0.875420076 | 1.186505788 |
| MP:0004620 | cervical vertebral fusion | 0.874529997 | 1.186507195 |
| ENSG00000030066 | NUP160 subnetwork | 0.875087529 | 1.186510086 |
| GO:0000087 | M phase of mitotic cell cycle | 0.874461715 | 1.186515279 |
| ENSG00000152684 | PELO subnetwork | 0.656978857 | 1.186517267 |
| GO:0035094 | response to nicotine | 0.873394908 | 1.18652479 |
| MP:0001953 | respiratory failure | 0.877213845 | 1.186541508 |
| GO:0031256 | leading edge membrane | 0.877330813 | 1.186542761 |
| ENSG00000163159 | VPS72 subnetwork | 0.876210785 | 1.186553172 |
| ENSG00000187498 | COL4A1 subnetwork | 0.663120249 | 1.186554571 |
| ENSG00000095066 | HOOK2 subnetwork | 0.876117454 | 1.186561246 |
| GO:0042596 | fear response | 0.876360889 | 1.18656967 |
| ENSG00000178188 | SH2B1 subnetwork | 0.665206772 | 1.186584776 |
| ENSG00000072832 | CRMP1 subnetwork | 0.875551218 | 1.18658639 |
| GO:0031116 | positive regulation of microtubule polymerization | 0.663067527 | 1.186589364 |
| MP:0004145 | abnormal muscle electrophysiology | 0.873151701 | 1.186591186 |
| REACTOME_RNA_POLYMERASE_I | REACTOME_RNA_POLYMERASE_III_CHAIN_ELONGATION | 0.657133117 | 1.186598506 |
| ENSG00000175575 | PAAF1 subnetwork | 0.877111361 | 1.18660889 |
| GO:0048259 | regulation of receptor-mediated endocytosis | 0.877474471 | 1.186609222 |
| GO:0015459 | potassium channel regulator activity | 0.873390645 | 1.186621761 |
| MP:0000559 | abnormal femur morphology | 0.664782491 | 1.186625091 |
| ENSG00000108559 | NUP88 subnetwork | 0.87720342 | 1.186638092 |
| GO:0008380 | RNA splicing | 0.656971354 | 1.186650337 |
| ENSG00000196540 | ENSG00000196540 subnetwork | 0.656714318 | 1.186651556 |
| ENSG00000114126 | TFDP2 subnetwork | 0.873300577 | 1.186657934 |
| ENSG00000160695 | ENSG00000160695 subnetwork | 0.873122812 | 1.186660116 |
| GO:0006359 | regulation of transcription from RNA polymerase III pron | 0.657347299 | 1.186662994 |
| REACTOME_TRANSPORT_OF_THE | REACTOME_TRANSPORT_OF_THE_SLBP_DEPENDANT_M | 0.663027627 | 1.186666667 |
| ENSG00000060558 | GNA15 subnetwork | 0.665170283 | 1.186667877 |
| ENSG00000166313 | APBB1 subnetwork | 0.665327409 | 1.186671104 |
| GO:0045454 | cell redox homeostasis | 0.876728611 | 1.186671329 |
| REACTOME_SEMA3A_PAK_DEPEN | REACTOME_SEMA3A_PAK_DEPENDENT_AXON_REPULSI | 0.87678453 | 1.186672571 |
| GO:0014065 | phosphatidylinositol 3-kinase cascade | 0.656792013 | 1.186677692 |
| GO:0008306 | associative learning | 0.873082808 | 1.186686944 |
| ENSG00000175334 | BANF1 subnetwork | 0.664411686 | 1.186689689 |
| ENSG00000136930 | PSMB7 subnetwork | 0.87662788 | 1.186693398 |
| GO:0035690 | cellular response to drug | 0.8770031 | 1.186694939 |
| KEGG_MELANOGENESIS | KEGG_MELANOGENESIS | 0.877088609 | 1.186696179 |
| ENSG00000073536 | NLE1 subnetwork | 0.656904709 | 1.186697697 |
| GO:0022625 | cytosolic large ribosomal subunit | 0.664638517 | 1.186729255 |
| GO:0000375 | RNA splicing, via transesterification reactions | 0.664080225 | 1.186736178 |
| ENSG00000196655 | TRAPPC4 subnetwork | 0.656678911 | 1.186741821 |
| GO:0043331 | response to dsRNA | 0.657313712 | 1.186747062 |
| MP:0002914 | abnormal endplate potential | 0.664780405 | 1.186756691 |

| | | | |
|---|---|---|---|
| GO:0044241 | lipid digestion | 0.876988109 | 1.18676827 |
| ENSG00000174827 | PDZK1 subnetwork | 0.664721803 | 1.186773256 |
| GO:2000178 | negative regulation of neural precursor cell proliferation | 0.873065762 | 1.186783976 |
| GO:0043407 | negative regulation of MAP kinase activity | 0.653688857 | 1.186802905 |
| ENSG00000183454 | GRIN2A subnetwork | 0.663009936 | 1.186804712 |
| ENSG00000136527 | TRA2B subnetwork | 0.656516857 | 1.186805981 |
| ENSG00000125695 | STRADA subnetwork | 0.664592253 | 1.186812455 |
| REACTOME_ACTIVATION_OF_NM | REACTOME_ACTIVATION_OF_NMDA_RECEPTOR_UPON_ | 0.664406822 | 1.186821377 |
| MP:0002177 | abnormal outer ear morphology | 0.876939649 | 1.18682297 |
| ENSG00000164251 | F2RL1 subnetwork | 0.656644419 | 1.186832108 |
| GO:0008191 | metalloendopeptidase inhibitor activity | 0.656436062 | 1.186841138 |
| GO:0035064 | methylated histone residue binding | 0.664350782 | 1.186844019 |
| MP:0004173 | abnormal intervertebral disk morphology | 0.872973495 | 1.186861075 |
| KEGG_SELENOAMINO_ACID_MET | KEGG_SELENOAMINO_ACID_METABOLISM | 0.873054404 | 1.186881026 |
| MP:0003014 | abnormal kidney medulla morphology | 0.664238881 | 1.18688932 |
| ENSG00000142684 | ZNF593 subnetwork | 0.87292393 | 1.186906657 |
| ENSG00000213044 | ENSG00000213044 subnetwork | 0.662995847 | 1.186918499 |
| GO:0055117 | regulation of cardiac muscle contraction | 0.653837847 | 1.186933776 |
| ENSG00000135441 | BLOC1S1 subnetwork | 0.872870415 | 1.18696161 |
| GO:0051593 | response to folic acid | 0.872797332 | 1.186969754 |
| MP:0008388 | hypochromic microcytic anemia | 0.664346867 | 1.186975758 |
| GO:0007210 | serotonin receptor signaling pathway | 0.872469254 | 1.186978923 |
| GO:0008305 | integrin complex | 0.661778098 | 1.186985885 |
| GO:0048551 | metalloenzyme inhibitor activity | 0.656436062 | 1.186986637 |
| GO:0019203 | carbohydrate phosphatase activity | 0.657855566 | 1.187005995 |
| GO:0031670 | cellular response to nutrient | 0.872751012 | 1.187010676 |
| ENSG00000123136 | DDX39A subnetwork | 0.662968925 | 1.187014091 |
| MP:0001664 | abnormal digestion | 0.665594324 | 1.187017544 |
| MP:0000939 | decreased motor neuron number | 0.872318476 | 1.187046753 |
| GO:0009583 | detection of light stimulus | 0.661732402 | 1.187051235 |
| MP:0010878 | increased trabecular bone volume | 0.656375115 | 1.187052477 |
| MP:0002631 | abnormal epididymis morphology | 0.661662776 | 1.187055745 |
| ENSG00000126456 | IRF3 subnetwork | 0.654134642 | 1.187061646 |
| REACTOME_TRANS:GOLGI_NETW | REACTOME_TRANS:GOLGI_NETWORK_VESICLE_BUDDIN | 0.660820984 | 1.187065919 |
| ENSG00000157110 | RBPMS subnetwork | 0.872451471 | 1.187066704 |
| GO:0046328 | regulation of JNK cascade | 0.872237399 | 1.187078336 |
| ENSG00000146463 | ZMYM4 subnetwork | 0.659616697 | 1.187091064 |
| ENSG00000204271 | SPIN3 subnetwork | 0.872734499 | 1.187098436 |
| ENSG00000124575 | HIST1H1D subnetwork | 0.871948261 | 1.187101612 |
| REACTOME_AXON_GUIDANCE | REACTOME_AXON_GUIDANCE | 0.656337808 | 1.18710607 |
| ENSG00000100567 | PSMA3 subnetwork | 0.659851928 | 1.187107993 |
| ENSG00000179036 | ENSG00000179036 subnetwork | 0.872145799 | 1.18711461 |
| MP:0002102 | abnormal ear morphology | 0.871667798 | 1.187121425 |
| GO:0015149 | hexose transmembrane transporter activity | 0.661970948 | 1.187139555 |
| ENSG00000172432 | GTPBP2 subnetwork | 0.658131479 | 1.187143731 |
| ENSG00000104765 | BNIP3L subnetwork | 0.661624771 | 1.187145466 |
| GO:0050308 | sugar-phosphatase activity | 0.657855566 | 1.187151248 |
| MP:0001883 | mammary adenocarcinoma | 0.66296605 | 1.187158304 |
| MP:0004261 | abnormal embryonic neuroepithelium morphology | 0.871921911 | 1.187166026 |
| ENSG00000106636 | YKT6 subnetwork | 0.658044983 | 1.187166626 |
| ENSG00000140612 | SEC11A subnetwork | 0.662891396 | 1.187168894 |
| GO:0006361 | transcription initiation from RNA polymerase I promoter | 0.87211401 | 1.187169634 |
| GO:0034185 | apolipoprotein binding | 0.660645092 | 1.187170892 |
| GO:0015485 | cholesterol binding | 0.654091084 | 1.187176963 |

| | | | |
|---|---|---|---|
| GO:0006352 | transcription initiation, DNA-dependent | 0.660386008 | 1.187178393 |
| ENSG00000074201 | CLNS1A subnetwork | 0.661550697 | 1.187186511 |
| ENSG00000211893 | ENSG00000211893 subnetwork | 0.654016387 | 1.187193846 |
| GO:0008307 | structural constituent of muscle | 0.871831443 | 1.187207013 |
| ENSG00000187778 | MCRS1 subnetwork | 0.661492412 | 1.187209302 |
| ENSG00000186787 | SPIN2B subnetwork | 0.872734499 | 1.187209629 |
| REACTOME_CLATHRIN_DERIVED_ | REACTOME_CLATHRIN_DERIVED_VESICLE_BUDDING | 0.660820984 | 1.187210578 |
| GO:0014037 | Schwann cell differentiation | 0.660578899 | 1.187211996 |
| ENSG00000138398 | PPIG subnetwork | 0.661318874 | 1.187212276 |
| ENSG00000119718 | EIF2B2 subnetwork | 0.871638331 | 1.187213991 |
| ENSG00000177602 | GSG2 subnetwork | 0.660728621 | 1.187215113 |
| GO:0001894 | tissue homeostasis | 0.659844572 | 1.187216256 |
| GO:0031966 | mitochondrial membrane | 0.657786189 | 1.187216987 |
| GO:0010463 | mesenchymal cell proliferation | 0.659595038 | 1.187217678 |
| MP:0001651 | necrosis | 0.656165254 | 1.187223994 |
| ENSG00000185627 | PSMD13 subnetwork | 0.655935115 | 1.187231562 |
| ENSG00000009844 | VTA1 subnetwork | 0.658743548 | 1.187244836 |
| MP:0000121 | failure of tooth eruption | 0.656327906 | 1.187251656 |
| ENSG00000198910 | L1CAM subnetwork | 0.657695952 | 1.187258262 |
| ENSG00000132305 | IMMT subnetwork | 0.871598381 | 1.187269061 |
| GO:0045821 | positive regulation of glycolysis | 0.662558109 | 1.187270517 |
| ENSG00000206211 | ENSG00000206211 subnetwork | 0.655179526 | 1.187271164 |
| ENSG00000189403 | HMGB1 subnetwork | 0.660349151 | 1.18727439 |
| ENSG00000104613 | INTS10 subnetwork | 0.872110099 | 1.187276221 |
| GO:0003697 | single-stranded DNA binding | 0.655259727 | 1.18727887 |
| ENSG00000166530 | ENSG00000166530 subnetwork | 0.66238974 | 1.187285662 |
| GO:0090218 | positive regulation of lipid kinase activity | 0.665989312 | 1.187288341 |
| ENSG00000120885 | CLU subnetwork | 0.666194675 | 1.187291415 |
| GO:0010719 | negative regulation of epithelial to mesenchymal transiti | 0.662506976 | 1.187293288 |
| MP:0001656 | focal hepatic necrosis | 0.66633493 | 1.187294487 |
| MP:0005029 | abnormal amnion morphology | 0.662865423 | 1.187294933 |
| ENSG00000087245 | MMP2 subnetwork | 0.66019664 | 1.187295682 |
| GO:0032365 | intracellular lipid transport | 0.658674905 | 1.187310513 |
| ENSG00000167244 | IGF2 subnetwork | 0.659573273 | 1.187313797 |
| ENSG00000090470 | PDCD7 subnetwork | 0.660557994 | 1.187320166 |
| ENSG00000205659 | LIN52 subnetwork | 0.661458351 | 1.187323429 |
| MP:0001218 | thin epidermis | 0.661287496 | 1.187326431 |
| MP:0011088 | partial neonatal lethality | 0.662645366 | 1.187326769 |
| GO:0006986 | response to unfolded protein | 0.659828563 | 1.187330648 |
| GO:0060438 | trachea development | 0.662315806 | 1.187332766 |
| ENSG00000123066 | MED13L subnetwork | 0.656146084 | 1.187345111 |
| GO:0007204 | elevation of cytosolic calcium ion concentration | 0.6658582 | 1.187345754 |
| GO:0030219 | megakaryocyte differentiation | 0.660313286 | 1.187352116 |
| ENSG00000136521 | NDUFB5 subnetwork | 0.661103814 | 1.187359893 |
| ENSG00000116141 | MARK1 subnetwork | 0.665945365 | 1.187365429 |
| MP:0001044 | abnormal enteric nervous system morphology | 0.655928932 | 1.187371134 |
| ENSG00000152822 | GRM1 subnetwork | 0.659540867 | 1.187379411 |
| MP:0009358 | environmentally induced seizures | 0.871595447 | 1.187380416 |
| MP:0008995 | early reproductive senescence | 0.656091655 | 1.187386503 |
| ENSG00000164438 | TLX3 subnetwork | 0.65901977 | 1.187388488 |
| ENSG00000119041 | GTF3C3 subnetwork | 0.661237895 | 1.187391887 |
| ENSG00000112079 | STK38 subnetwork | 0.656320565 | 1.187397277 |
| MP:0003324 | increased liver adenoma incidence | 0.655461646 | 1.187404815 |
| ENSG00000062038 | CDH3 subnetwork | 0.666166379 | 1.187410811 |

| | | | |
|---|---|---|---|
| ENSG00000023608 | SNAPC1 subnetwork | 0.666307984 | 1.187413856 |
| ENSG00000085999 | RAD54L subnetwork | 0.662842631 | 1.187414925 |
| MP:0003871 | abnormal myelin sheath morphology | 0.660176827 | 1.187416128 |
| ENSG00000204220 | PFDN6 subnetwork | 0.655179526 | 1.187417056 |
| ENSG00000132692 | BCAN subnetwork | 0.662279198 | 1.187422455 |
| GO:0031058 | positive regulation of histone modification | 0.654888095 | 1.187429309 |
| GO:0008340 | determination of adult lifespan | 0.658663017 | 1.18743734 |
| ENSG00000100075 | SLC25A1 subnetwork | 0.659139807 | 1.187445015 |
| ENSG00000127527 | EPS15L1 subnetwork | 0.658403332 | 1.187451076 |
| GO:0040018 | positive regulation of multicellular organism growth | 0.655835409 | 1.187453965 |
| ENSG00000004897 | CDC27 subnetwork | 0.87157405 | 1.187454273 |
| ENSG00000036257 | CUL3 subnetwork | 0.658987488 | 1.187478612 |
| ENSG00000198336 | MYL4 subnetwork | 0.655917837 | 1.187486191 |
| GO:0043410 | positive regulation of MAPK cascade | 0.871408062 | 1.187489446 |
| ENSG00000163468 | CCT3 subnetwork | 0.659519356 | 1.1875 |
| ENSG00000185963 | BICD2 subnetwork | 0.658533243 | 1.187501529 |
| REACTOME_DNA_STRAND_ELON | REACTOME_DNA_STRAND_ELONGATION | 0.660162324 | 1.187512201 |
| MP:0005402 | abnormal action potential | 0.871533148 | 1.187518762 |
| GO:0045214 | sarcomere organization | 0.655778839 | 1.187519951 |
| ENSG00000134453 | RBM17 subnetwork | 0.654998762 | 1.187523049 |
| GO:0019201 | nucleotide kinase activity | 0.654871147 | 1.187526128 |
| ENSG00000154518 | ATP5G3 subnetwork | 0.655448307 | 1.187532244 |
| GO:0004536 | deoxyribonuclease activity | 0.659338473 | 1.187533594 |
| REACTOME_TRANSPORT_OF_MA | REACTOME_TRANSPORT_OF_MATURE_MRNA_DERIVED | 0.659438523 | 1.187535117 |
| MP:0003890 | abnormal embryonic-extraembryonic boundary morphol | 0.655068915 | 1.187543019 |
| GO:0005041 | low-density lipoprotein receptor activity | 0.654422998 | 1.187543061 |
| MP:0004607 | abnormal cervical atlas morphology | 0.66283962 | 1.187559256 |
| ENSG00000206283 | PFDN6 subnetwork | 0.655179526 | 1.187562984 |
| ENSG00000090487 | SPG21 subnetwork | 0.871380656 | 1.187563333 |
| GO:0016592 | mediator complex | 0.658654902 | 1.187564197 |
| ENSG00000101444 | AHCY subnetwork | 0.662278987 | 1.18756691 |
| ENSG00000125775 | SDCBP2 subnetwork | 0.674873887 | 1.187592548 |
| ENSG00000049245 | VAMP3 subnetwork | 0.654727392 | 1.187603001 |
| GO:0060117 | auditory receptor cell development | 0.871343851 | 1.187604391 |
| ENSG00000136695 | IL36RN subnetwork | 0.655750565 | 1.187610511 |
| ENSG00000086475 | SEPHS1 subnetwork | 0.65930708 | 1.187617593 |
| GO:0007632 | visual behavior | 0.667036392 | 1.187641942 |
| GO:0051865 | protein autoubiquitination | 0.654864307 | 1.187653714 |
| GO:0043409 | negative regulation of MAPK cascade | 0.654590152 | 1.187655308 |
| ENSG00000138180 | CEP55 subnetwork | 0.871295364 | 1.187659535 |
| MP:0005503 | abnormal tendon morphology | 0.655694362 | 1.187664252 |
| GO:0090207 | regulation of triglyceride metabolic process | 0.666880081 | 1.187675205 |
| ENSG00000113272 | THG1L subnetwork | 0.674847719 | 1.18768064 |
| MP:0003828 | pulmonary edema | 0.871235161 | 1.187695917 |
| MP:0008056 | abnormal retinal ganglion cell morphology | 0.67476564 | 1.18770903 |
| GO:0043567 | regulation of insulin-like growth factor receptor signaling | 0.666755011 | 1.187726613 |
| GO:0055070 | copper ion homeostasis | 0.666995358 | 1.187731062 |
| ENSG00000013583 | HEBP1 subnetwork | 0.65472392 | 1.187742927 |
| GO:0010874 | regulation of cholesterol efflux | 0.666685048 | 1.187743261 |
| MP:0000313 | abnormal cell death | 0.674629448 | 1.18776583 |
| ENSG00000185420 | SMYD3 subnetwork | 0.871221096 | 1.187788624 |
| REACTOME_DNA_REPAIR | REACTOME_DNA_REPAIR | 0.666850026 | 1.187800604 |
| REACTOME_RESPIRATORY_ELECT | REACTOME_RESPIRATORY_ELECTRON_TRANSPORT | 0.674736337 | 1.187809103 |
| MP:0004384 | small interparietal bone | 0.667218672 | 1.187818577 |

| | | | |
|---|---|---|---|
| ENSG00000159210 | SNF8 subnetwork | 0.674592696 | 1.187842036 |
| GO:0009743 | response to carbohydrate stimulus | 0.871150411 | 1.1878438 |
| ENSG00000100842 | EFS subnetwork | 0.667456459 | 1.187881898 |
| ENSG00000166862 | CACNG2 subnetwork | 0.87109238 | 1.187884904 |
| ENSG00000169925 | BRD3 subnetwork | 0.673278541 | 1.187919061 |
| ENSG00000006744 | ELAC2 subnetwork | 0.667383673 | 1.187934783 |
| ENSG00000115884 | SDC1 subnetwork | 0.67457321 | 1.187936185 |
| ENSG00000143850 | PLEKHA6 subnetwork | 0.667579934 | 1.187949771 |
| ENSG00000143106 | PSMA5 subnetwork | 0.871046227 | 1.187954183 |
| ENSG00000103154 | NECAB2 subnetwork | 0.667823085 | 1.187973691 |
| GO:0005839 | proteasome core complex | 0.86671627 | 1.187989248 |
| REACTOME_REPAIR_SYNTHESIS_( | REACTOME_REPAIR_SYNTHESIS_OF_PATCH_27:30_BASE | 0.871008766 | 1.188018779 |
| GO:0070633 | transepithelial transport | 0.668085407 | 1.188020268 |
| GO:0002577 | regulation of antigen processing and presentation | 0.673258856 | 1.188031373 |
| ENSG00000206297 | TAP1 subnetwork | 0.674565499 | 1.188048285 |
| GO:0030042 | actin filament depolymerization | 0.866673308 | 1.188063573 |
| ENSG00000111445 | RFC5 subnetwork | 0.667700225 | 1.188065918 |
| MP:0011495 | abnormal head shape | 0.667952747 | 1.188077712 |
| GO:0008653 | lipopolysaccharide metabolic process | 0.673519909 | 1.188083553 |
| GO:0051119 | sugar transmembrane transporter activity | 0.676592265 | 1.188088428 |
| ENSG00000161395 | PGAP3 subnetwork | 0.866593014 | 1.188090746 |
| ENSG00000135387 | CAPRIN1 subnetwork | 0.675276874 | 1.188095522 |
| MP:0005455 | increased susceptibility to weight gain | 0.667819945 | 1.188111044 |
| REACTOME_REPAIR_SYNTHESIS_F | REACTOME_REPAIR_SYNTHESIS_FOR_GAP:FILLING_BY_I | 0.871008766 | 1.188130341 |
| ENSG00000111845 | PAK1IP1 subnetwork | 0.668073504 | 1.188133446 |
| ENSG00000157240 | FZD1 subnetwork | 0.673120069 | 1.188142292 |
| GO:0048515 | spermatid differentiation | 0.667787446 | 1.188145823 |
| GO:0004540 | ribonuclease activity | 0.675456324 | 1.188146114 |
| ENSG00000065328 | MCM10 subnetwork | 0.676551901 | 1.188146603 |
| GO:0005501 | retinoid binding | 0.67323228 | 1.188149701 |
| MP:0002279 | abnormal diaphragm morphology | 0.86657811 | 1.188179245 |
| MP:0003354 | astrocytosis | 0.870961765 | 1.188180879 |
| MP:0008236 | decreased susceptibility to neuronal excitotoxicity | 0.675406985 | 1.188186485 |
| GO:0051402 | neuron apoptotic process | 0.673497413 | 1.188189872 |
| ENSG00000206233 | ENSG00000206233 subnetwork | 0.674565499 | 1.188190294 |
| GO:0010718 | positive regulation of epithelial to mesenchymal transitic | 0.673064381 | 1.188194777 |
| GO:0042454 | ribonucleoside catabolic process | 0.673670072 | 1.188204668 |
| GO:0034660 | ncRNA metabolic process | 0.676856789 | 1.188210413 |
| GO:0015932 | nucleobase-containing compound transmembrane trans | 0.865841068 | 1.188211689 |
| ENSG00000067225 | PKM2 subnetwork | 0.668268589 | 1.188214717 |
| MP:0002622 | abnormal cochlear hair cell morphology | 0.676495295 | 1.188216712 |
| ENSG00000116106 | EPHA4 subnetwork | 0.865783094 | 1.188238905 |
| ENSG00000065618 | COL17A1 subnetwork | 0.677840285 | 1.188254195 |
| ENSG00000174021 | GNG5 subnetwork | 0.865632163 | 1.188269739 |
| MP:0005424 | jerky movement | 0.673033416 | 1.188271235 |
| REACTOME_SYNTHESIS_SECRETIC | REACTOME_SYNTHESIS_SECRETION_AND_INACTIVATIOI | 0.87095304 | 1.188278388 |
| MP:0004101 | abnormal brain interneuron morphology | 0.866571545 | 1.188286631 |
| GO:0051693 | actin filament capping | 0.865719016 | 1.188289735 |
| ENSG00000196549 | MME subnetwork | 0.866098806 | 1.188295261 |
| ENSG00000186979 | ENSG00000186979 subnetwork | 0.864051782 | 1.188297067 |
| ENSG00000206172 | HBA1 subnetwork | 0.677787161 | 1.188300405 |
| KEGG_OXIDATIVE_PHOSPHORYLA | KEGG_OXIDATIVE_PHOSPHORYLATION | 0.866206245 | 1.188301085 |
| ENSG00000182010 | RTKN2 subnetwork | 0.866038384 | 1.188313037 |
| ENSG00000083093 | PALB2 subnetwork | 0.86599016 | 1.188321375 |

| | | | |
|---|---|---|---|
| GO:0007067 | mitosis | 0.863995199 | 1.188329076 |
| ENSG00000168394 | TAP1 subnetwork | 0.674565499 | 1.188332337 |
| ENSG00000099250 | NRP1 subnetwork | 0.866528071 | 1.188332704 |
| REACTOME_DOUBLE:STRAND_BR | REACTOME_DOUBLE:STRAND_BREAK_REPAIR | 0.67683829 | 1.188334128 |
| GO:0050680 | negative regulation of epithelial cell proliferation | 0.672902267 | 1.188340324 |
| GO:0015838 | betaine transport | 0.676066316 | 1.188345461 |
| ENSG00000136153 | LMO7 subnetwork | 0.676492398 | 1.188358369 |
| GO:0009394 | 2'-deoxyribonucleotide metabolic process | 0.865609686 | 1.188363087 |
| ENSG00000197299 | BLM subnetwork | 0.675838109 | 1.188365155 |
| GO:0015101 | organic cation transmembrane transporter activity | 0.673010009 | 1.188377666 |
| MP:0003888 | liver hemorrhage | 0.870930954 | 1.188380612 |
| ENSG00000084092 | NOA1 subnetwork | 0.672841556 | 1.188380872 |
| GO:0008635 | activation of cysteine-type endopeptidase activity involv | 0.674499127 | 1.188384744 |
| MP:0001693 | failure of primitive streak formation | 0.867311556 | 1.188388648 |
| MP:0000565 | oligodactyly | 0.867405469 | 1.188403884 |
| GO:0031903 | microbody membrane | 0.870896407 | 1.188421794 |
| GO:0009103 | lipopolysaccharide biosynthetic process | 0.677022526 | 1.188426257 |
| ENSG00000206357 | RDBP subnetwork | 0.678612093 | 1.188431815 |
| GO:0052312 | modulation of transcription in other organism involved i | 0.6776657 | 1.188434524 |
| MP:0001922 | reduced male fertility | 0.866506678 | 1.188435406 |
| GO:0000280 | nuclear division | 0.863995199 | 1.188441522 |
| ENSG00000188536 | HBA2 subnetwork | 0.677787161 | 1.188441852 |
| GO:0018196 | peptidyl-asparagine modification | 0.870334699 | 1.188442376 |
| GO:0007602 | phototransduction | 0.669673642 | 1.188446719 |
| MP:0002886 | abnormal glutamate-mediated receptor currents | 0.675809712 | 1.188447309 |
| GO:0071158 | positive regulation of cell cycle arrest | 0.866420781 | 1.188448471 |
| GO:0046697 | decidualization | 0.870503208 | 1.188449248 |
| GO:0030666 | endocytic vesicle membrane | 0.675960401 | 1.188450066 |
| ENSG00000111664 | GNB3 subnetwork | 0.673856228 | 1.188451412 |
| GO:0051233 | spindle midzone | 0.870773691 | 1.188457202 |
| GO:0019884 | antigen processing and presentation of exogenous antig | 0.670003135 | 1.188458298 |
| GO:0034593 | phosphatidylinositol bisphosphate phosphatase activity | 0.674466942 | 1.188467057 |
| ENSG00000163104 | SMARCAD1 subnetwork | 0.677503229 | 1.188467492 |
| ENSG00000164162 | ANAPC10 subnetwork | 0.67646212 | 1.188470252 |
| ENSG00000124357 | NAGK subnetwork | 0.865600262 | 1.188475345 |
| GO:0055102 | lipase inhibitor activity | 0.8672682 | 1.188477133 |
| GO:0007338 | single fertilization | 0.870699359 | 1.188484307 |
| GO:0015879 | carnitine transport | 0.676066316 | 1.188487235 |
| ENSG00000132485 | ZRANB2 subnetwork | 0.864289882 | 1.188492101 |
| GO:0043255 | regulation of carbohydrate biosynthetic process | 0.668796899 | 1.188503738 |
| ENSG00000166225 | FRS2 subnetwork | 0.672821633 | 1.188505334 |
| GO:0032434 | regulation of proteasomal ubiquitin-dependent protein c | 0.675746389 | 1.18850561 |
| MP:0001745 | increased circulating corticosterone level | 0.865551604 | 1.188507322 |
| ENSG00000152795 | HNRPDL subnetwork | 0.669787049 | 1.188514327 |
| ENSG00000093000 | NUP50 subnetwork | 0.669543832 | 1.188528243 |
| MP:0000160 | kyphosis | 0.864598819 | 1.188528466 |
| GO:0033146 | regulation of intracellular estrogen receptor signaling pa | 0.669640266 | 1.188529624 |
| GO:0022600 | digestive system process | 0.870644917 | 1.188530213 |
| MP:0000008 | increased white adipose tissue amount | 0.867217262 | 1.188532629 |
| GO:0005778 | peroxisomal membrane | 0.870896407 | 1.188533446 |
| REACTOME_METABOLISM_OF_NI | REACTOME_METABOLISM_OF_NUCLEOTIDES | 0.870485994 | 1.188537457 |
| ENSG00000072415 | MPP5 subnetwork | 0.863988205 | 1.188549257 |
| GO:0018279 | protein N-linked glycosylation via asparagine | 0.870334699 | 1.188554104 |
| MP:0010420 | muscular ventricular septal defect | 0.678092334 | 1.188564969 |

| | | | |
|---|---|---|---|
| GO:0000421 | autophagic vacuole membrane | 0.86381978 | 1.18856602 |
| GO:0007498 | mesoderm development | 0.669900541 | 1.188569881 |
| ENSG00000138468 | SENP7 subnetwork | 0.863491846 | 1.18857224 |
| ENSG00000175595 | ERCC4 subnetwork | 0.865516529 | 1.188572373 |
| MP:0002824 | abnormal chorioallantoic fusion | 0.674038244 | 1.188572454 |
| ENSG00000206268 | RDBP subnetwork | 0.678612093 | 1.188573127 |
| GO:0019829 | cation-transporting ATPase activity | 0.863732228 | 1.188574404 |
| MP:0002842 | increased systemic arterial blood pressure | 0.677663246 | 1.188576021 |
| GO:0021794 | thalamus development | 0.863075721 | 1.1885763 |
| GO:0001965 | G-protein alpha-subunit binding | 0.668682385 | 1.188579354 |
| ENSG00000160746 | ANO10 subnetwork | 0.870271412 | 1.188581234 |
| GO:0045661 | regulation of myoblast differentiation | 0.863927987 | 1.188581299 |
| ENSG00000080603 | SRCAP subnetwork | 0.669990474 | 1.188583293 |
| GO:0042573 | retinoic acid metabolic process | 0.670416801 | 1.188584145 |
| ENSG00000157020 | SEC13 subnetwork | 0.864714878 | 1.188586288 |
| ENSG00000151366 | NDUFC2 subnetwork | 0.668765391 | 1.18858676 |
| ENSG00000203814 | HIST2H2BF subnetwork | 0.670362312 | 1.188588787 |
| GO:0044253 | positive regulation of multicellular organismal metabolic | 0.674204496 | 1.188593133 |
| MP:0002685 | abnormal spermatogonia proliferation | 0.861389134 | 1.188593661 |
| GO:0006633 | fatty acid biosynthetic process | 0.674297992 | 1.188594498 |
| GO:0032008 | positive regulation of TOR signaling cascade | 0.672608437 | 1.188597122 |
| MP:0003400 | kinked neural tube | 0.67278208 | 1.188599856 |
| MP:0008428 | abnormal spatial working memory | 0.677491893 | 1.188609027 |
| MP:0000372 | irregular coat pigmentation | 0.674464307 | 1.188609184 |
| MP:0003648 | abnormal radial glial cell morphology | 0.863633674 | 1.18861119 |
| ENSG00000162407 | PPAP2B subnetwork | 0.68080027 | 1.188611572 |
| MP:0002625 | heart left ventricle hypertrophy | 0.676461501 | 1.188611972 |
| KEGG_BUTANOATE_METABOLISM | KEGG_BUTANOATE_METABOLISM | 0.870119974 | 1.188616701 |
| ENSG00000078140 | UBE2K subnetwork | 0.669524139 | 1.188617201 |
| ENSG00000106462 | EZH2 subnetwork | 0.668623223 | 1.188626221 |
| GO:0001523 | retinoid metabolic process | 0.870210445 | 1.188627174 |
| GO:0017022 | myosin binding | 0.861165297 | 1.188628382 |
| ENSG00000112640 | PPP2R5D subnetwork | 0.864582192 | 1.18863142 |
| MP:0004738 | abnormal brainstem auditory evoked potential | 0.863433041 | 1.188642174 |
| MP:0008151 | increased diameter of long bones | 0.861516249 | 1.18864693 |
| ENSG00000110436 | SLC1A2 subnetwork | 0.86329594 | 1.188649493 |
| GO:0001104 | RNA polymerase II transcription cofactor activity | 0.669467491 | 1.18865197 |
| GO:0060600 | dichotomous subdivision of an epithelial terminal unit | 0.865480352 | 1.188656336 |
| ENSG00000143418 | CERS2 subnetwork | 0.864861416 | 1.188658283 |
| MP:0002404 | increased intestinal adenoma incidence | 0.864484847 | 1.188658721 |
| MP:0003868 | abnormal feces composition | 0.86334363 | 1.188664773 |
| ENSG00000197746 | PSAP subnetwork | 0.86305316 | 1.188665214 |
| ENSG00000173349 | SFT2D3 subnetwork | 0.670334334 | 1.188665624 |
| GO:0002762 | negative regulation of myeloid leukocyte differentiation | 0.672569292 | 1.188667706 |
| MP:0002954 | abnormal aerobic energy metabolism | 0.861351058 | 1.188673247 |
| MP:0005449 | abnormal food intake | 0.861084637 | 1.188679514 |
| MP:0001045 | abnormal enteric ganglia morphology | 0.870078081 | 1.188681463 |
| ENSG00000106392 | C1GALT1 subnetwork | 0.67023591 | 1.188694344 |
| GO:0007098 | centrosome cycle | 0.669414466 | 1.188698795 |
| REACTOME_ACTIVATION_OF_KAI | REACTOME_ACTIVATION_OF_KAINATE_RECEPTORS_UP( | 0.676426376 | 1.18870006 |
| ENSG00000155980 | KIF5A subnetwork | 0.672757148 | 1.188712385 |
| ENSG00000108774 | RAB5C subnetwork | 0.678909553 | 1.188712553 |
| ENSG00000204356 | RDBP subnetwork | 0.678612093 | 1.188714473 |
| GO:0046112 | nucleobase biosynthetic process | 0.8632518 | 1.188714719 |

| | | | |
|---|---|---|---|
| ENSG00000070010 | UFD1L subnetwork | 0.668992009 | 1.188716094 |
| ENSG00000175216 | CKAP5 subnetwork | 0.672180933 | 1.188720902 |
| ENSG00000123124 | WWP1 subnetwork | 0.679076751 | 1.188721179 |
| ENSG00000137975 | CLCA2 subnetwork | 0.67419311 | 1.188723379 |
| REACTOME_A_THIRD_PROTEOLY | REACTOME_A_THIRD_PROTEOLYTIC_CLEAVAGE_RELEAS | 0.861303848 | 1.188724374 |
| REACTOME_PASSIVE_TRANSPORT | REACTOME_PASSIVE_TRANSPORT_BY_AQUAPORINS | 0.672508119 | 1.188726313 |
| ENSG00000173801 | JUP subnetwork | 0.669355971 | 1.188727558 |
| ENSG00000156076 | WIF1 subnetwork | 0.680786133 | 1.188728804 |
| ENSG00000108963 | DPH1 subnetwork | 0.676366062 | 1.188734494 |
| MP:0010103 | small thoracic cage | 0.865004693 | 1.188734991 |
| REACTOME_SYNTHESIS_AND_INT | REACTOME_SYNTHESIS_AND_INTERCONVERSION_OF_N | 0.677483777 | 1.188738685 |
| GO:0046661 | male sex differentiation | 0.865467016 | 1.188740314 |
| GO:0065004 | protein-DNA complex assembly | 0.867838343 | 1.188740692 |
| MP:0009288 | increased epididymal fat pad weight | 0.67446053 | 1.188745365 |
| MP:0003308 | abnormal cochlear sensory epithelium morphology | 0.863043468 | 1.188749408 |
| GO:0060041 | retina development in camera-type eye | 0.865091974 | 1.188754963 |
| ENSG00000109534 | GAR1 subnetwork | 0.677389263 | 1.188761167 |
| ENSG00000122180 | MYOG subnetwork | 0.670606501 | 1.188765937 |
| GO:0032543 | mitochondrial translation | 0.861073115 | 1.188773379 |
| ENSG00000158373 | HIST1H2BD subnetwork | 0.680983686 | 1.188778897 |
| REACTOME_FORMATION_OF_TUI | REACTOME_FORMATION_OF_TUBULIN_FOLDING_INTEF | 0.669309315 | 1.188780429 |
| REACTOME_TRANSPORT_OF_MA | REACTOME_TRANSPORT_OF_MATURE_MRNAS_DERIVEI | 0.672308215 | 1.188782244 |
| GO:0001833 | inner cell mass cell proliferation | 0.861895965 | 1.188782963 |
| GO:0007031 | peroxisome organization | 0.865434816 | 1.188786504 |
| ENSG00000104177 | MYEF2 subnetwork | 0.870077911 | 1.188793266 |
| ENSG00000152556 | PFKM subnetwork | 0.863014337 | 1.188800455 |
| MP:0006126 | abnormal outflow tract development | 0.867804299 | 1.188805618 |
| MP:0002192 | hydrops fetalis | 0.671133704 | 1.188811441 |
| GO:0016891 | endoribonuclease activity, producing 5'-phosphomonoes | 0.679197577 | 1.188811646 |
| ENSG00000132182 | NUP210 subnetwork | 0.669121835 | 1.188813886 |
| ENSG00000130402 | ACTN4 subnetwork | 0.862844855 | 1.188817286 |
| ENSG00000115275 | MOGS subnetwork | 0.862932931 | 1.188818345 |
| GO:0007257 | activation of JUN kinase activity | 0.87001005 | 1.188825134 |
| ENSG00000206208 | TAPBP subnetwork | 0.678587 | 1.188832065 |
| GO:0046329 | negative regulation of JNK cascade | 0.861032644 | 1.188838777 |
| ENSG00000182809 | CRIP2 subnetwork | 0.681107662 | 1.188839497 |
| GO:0010812 | negative regulation of cell-substrate adhesion | 0.672159054 | 1.188845554 |
| GO:0070303 | negative regulation of stress-activated protein kinase sig | 0.679067383 | 1.188850588 |
| GO:0043552 | positive regulation of phosphatidylinositol 3-kinase activ | 0.672498196 | 1.188850906 |
| ENSG00000179715 | FAM113B subnetwork | 0.669251119 | 1.188851392 |
| GO:0035240 | dopamine binding | 0.86538088 | 1.188856333 |
| GO:0046888 | negative regulation of hormone secretion | 0.869603539 | 1.188858568 |
| ENSG00000197961 | ZNF121 subnetwork | 0.680776271 | 1.188869782 |
| MP:0004773 | abnormal bile composition | 0.6812306 | 1.188870452 |
| ENSG00000096401 | CDC5L subnetwork | 0.869946733 | 1.188871119 |
| GO:0009620 | response to fungus | 0.861886849 | 1.188886254 |
| GO:0006271 | DNA strand elongation involved in DNA replication | 0.860349457 | 1.188895752 |
| ENSG00000073111 | MCM2 subnetwork | 0.861793283 | 1.188899431 |
| GO:0031571 | mitotic cell cycle G1/S transition DNA damage checkpoin | 0.862834858 | 1.188906265 |
| ENSG00000160957 | RECQL4 subnetwork | 0.869869276 | 1.188907705 |
| ENSG00000072778 | ACADVL subnetwork | 0.869225876 | 1.18890981 |
| ENSG00000064419 | TNPO3 subnetwork | 0.868049982 | 1.188925542 |
| GO:0032321 | positive regulation of Rho GTPase activity | 0.671299785 | 1.188926941 |
| REACTOME_OLFACTORY_SIGNALI | REACTOME_OLFACTORY_SIGNALING_PATHWAY | 0.862752287 | 1.188933649 |

| | | | |
|---|---|---|---|
| ENSG00000185359 | HGS subnetwork | 0.860316788 | 1.188937464 |
| GO:0006418 | tRNA aminoacylation for protein translation | 0.865342455 | 1.188940354 |
| GO:0001558 | regulation of cell growth | 0.672473698 | 1.188945537 |
| ENSG00000072682 | P4HA2 subnetwork | 0.672139204 | 1.188946231 |
| GO:0010243 | response to organic nitrogen | 0.861031152 | 1.188946919 |
| ENSG00000125798 | FOXA2 subnetwork | 0.869585598 | 1.188946923 |
| GO:0006888 | ER to Golgi vesicle-mediated transport | 0.868171283 | 1.188950146 |
| ENSG00000185130 | HIST1H2BL subnetwork | 0.671133319 | 1.188954327 |
| MP:0003690 | abnormal glial cell physiology | 0.869441519 | 1.188963667 |
| ENSG00000212789 | ENSG00000212789 subnetwork | 0.86899072 | 1.188972596 |
| ENSG00000112493 | TAPBP subnetwork | 0.678587 | 1.188973474 |
| MP:0002696 | decreased circulating glucagon level | 0.869198688 | 1.188974673 |
| ENSG00000151348 | EXT2 subnetwork | 0.672103222 | 1.188974913 |
| GO:0031668 | cellular response to extracellular stimulus | 0.680401306 | 1.188981844 |
| GO:0007528 | neuromuscular junction development | 0.671069267 | 1.188983051 |
| ENSG00000141034 | C17orf39 subnetwork | 0.680746345 | 1.188987072 |
| MP:0005317 | increased triglyceride level | 0.869837596 | 1.188991344 |
| ENSG00000148248 | SURF4 subnetwork | 0.862352562 | 1.188999526 |
| GO:0060571 | morphogenesis of an epithelial fold | 0.869386159 | 1.189000282 |
| GO:0032313 | regulation of Rab GTPase activity | 0.860280449 | 1.189002946 |
| ENSG00000122779 | TRIM24 subnetwork | 0.670866372 | 1.189009139 |
| MP:0005225 | abnormal vertebrae development | 0.679787244 | 1.189014252 |
| ENSG00000115361 | ACADL subnetwork | 0.671432296 | 1.189018383 |
| REACTOME_PROSTACYCLIN_SIGN | REACTOME_PROSTACYCLIN_SIGNALLING_THROUGH_PR | 0.868605369 | 1.189020254 |
| MP:0004819 | decreased skeletal muscle mass | 0.862476398 | 1.189029016 |
| GO:0031529 | ruffle organization | 0.86955522 | 1.189030588 |
| GO:0051150 | regulation of smooth muscle cell differentiation | 0.869150182 | 1.18903484 |
| KEGG_OTHER_GLYCAN_DEGRADA | KEGG_OTHER_GLYCAN_DEGRADATION | 0.862648146 | 1.189035836 |
| GO:0042537 | benzene-containing compound metabolic process | 0.670925498 | 1.189040519 |
| GO:0006936 | muscle contraction | 0.86275149 | 1.189041615 |
| ENSG00000133392 | MYH11 subnetwork | 0.679894017 | 1.189057119 |
| ENSG00000181610 | MRPS23 subnetwork | 0.861029689 | 1.189059829 |
| MP:0011423 | kidney cortex atrophy | 0.679742907 | 1.189060458 |
| ENSG00000186842 | ENSG00000186842 subnetwork | 0.680346041 | 1.189063613 |
| ENSG00000078328 | RBFOX1 subnetwork | 0.868382103 | 1.18907369 |
| ENSG00000076248 | UNG subnetwork | 0.868984212 | 1.189079864 |
| GO:0004712 | protein serine/threonine/tyrosine kinase activity | 0.67082038 | 1.189079976 |
| MP:0000035 | abnormal membranous labyrinth morphology | 0.868553689 | 1.18908046 |
| ENSG00000186318 | BACE1 subnetwork | 0.862314665 | 1.189083839 |
| GO:0017025 | TBP-class protein binding | 0.678474801 | 1.189089827 |
| MP:0005290 | decreased oxygen consumption | 0.671033022 | 1.189089925 |
| ENSG00000077157 | PPP1R12B subnetwork | 0.681442237 | 1.189091017 |
| MP:0010465 | aberrant origin of the right subclavian artery | 0.672089716 | 1.18909964 |
| ENSG00000103496 | STX4 subnetwork | 0.6796438 | 1.189100737 |
| GO:0070585 | protein localization in mitochondrion | 0.679542037 | 1.189111322 |
| ENSG00000206281 | TAPBP subnetwork | 0.678587 | 1.189114918 |
| GO:0032483 | regulation of Rab protein signal transduction | 0.860280449 | 1.18911597 |
| ENSG00000160271 | RALGDS subnetwork | 0.862244755 | 1.189116001 |
| REACTOME_RESOLUTION_OF_AB | REACTOME_RESOLUTION_OF_ABASIC_SITES_AP_SITES | 0.680741411 | 1.189116251 |
| GO:0031201 | SNARE complex | 0.862613601 | 1.189120129 |
| ENSG00000107614 | TRDMT1 subnetwork | 0.860634938 | 1.18912114 |
| ENSG00000126457 | PRMT1 subnetwork | 0.680198291 | 1.189126306 |
| REACTOME_MITOTIC_G1:G1S_PH | REACTOME_MITOTIC_G1:G1S_PHASES | 0.868508391 | 1.189126543 |
| GO:0019841 | retinol binding | 0.680312548 | 1.189145401 |

| | | | |
|---|---|---|---|
| ENSG00000137944 | CCBL2 subnetwork | 0.860220511 | 1.189152961 |
| ENSG00000183963 | SMTN subnetwork | 0.679486181 | 1.189157557 |
| MP:0003446 | renal hypoplasia | 0.671584567 | 1.189157857 |
| GO:0014002 | astrocyte development | 0.868835888 | 1.189157875 |
| GO:0048070 | regulation of developmental pigmentation | 0.860585709 | 1.189162866 |
| GO:0001893 | maternal placenta development | 0.868941898 | 1.189163606 |
| REACTOME_VIRAL_MESSENGER_I | REACTOME_VIRAL_MESSENGER_RNA_SYNTHESIS | 0.861026455 | 1.189168012 |
| GO:0051412 | response to corticosterone stimulus | 0.859151314 | 1.189172854 |
| GO:0032648 | regulation of interferon-beta production | 0.858978537 | 1.189175552 |
| ENSG00000196226 | HIST1H2BB subnetwork | 0.671969147 | 1.189199087 |
| ENSG00000117335 | CD46 subnetwork | 0.8590841 | 1.1892099 |
| GO:0051147 | regulation of muscle cell differentiation | 0.672078506 | 1.1892304 |
| ENSG00000100591 | AHSA1 subnetwork | 0.680064543 | 1.189236523 |
| GO:0002026 | regulation of the force of heart contraction | 0.671716137 | 1.189237237 |
| GO:0009582 | detection of abiotic stimulus | 0.860887535 | 1.189241949 |
| REACTOME_BASE_EXCISION_REP | REACTOME_BASE_EXCISION_REPAIR | 0.680741411 | 1.189257326 |
| GO:0001822 | kidney development | 0.860219411 | 1.189261266 |
| ENSG00000166963 | MAP1A subnetwork | 0.680197402 | 1.189267482 |
| GO:0045778 | positive regulation of ossification | 0.680657441 | 1.189273849 |
| ENSG00000186298 | PPP1CC subnetwork | 0.861020286 | 1.189276216 |
| GO:0005540 | hyaluronic acid binding | 0.858975254 | 1.189288775 |
| ENSG00000168593 | ENSG00000168593 subnetwork | 0.859396479 | 1.189289113 |
| MP:0002907 | abnormal parturition | 0.671870457 | 1.189304588 |
| MP:0005333 | decreased heart rate | 0.671949151 | 1.189311877 |
| GO:0045920 | negative regulation of exocytosis | 0.860868721 | 1.18933118 |
| ENSG00000010438 | PRSS3 subnetwork | 0.860214982 | 1.189374346 |
| GO:0033764 | steroid dehydrogenase activity, acting on the CH-OH gro | 0.858973204 | 1.189402019 |
| ENSG00000206440 | NFKBIL1 subnetwork | 0.859396479 | 1.189402303 |
| GO:0007059 | chromosome segregation | 0.860208674 | 1.189473184 |
| GO:0008334 | histone mRNA metabolic process | 0.858959393 | 1.189501 |
| ENSG00000138069 | RAB1A subnetwork | 0.859826449 | 1.189506232 |
| ENSG00000164327 | RICTOR subnetwork | 0.859626958 | 1.189518508 |
| ENSG00000113448 | PDE4D subnetwork | 0.859734044 | 1.18952902 |
| GO:0042074 | cell migration involved in gastrulation | 0.858922433 | 1.189566667 |
| ENSG00000123992 | DNPEP subnetwork | 0.860196118 | 1.189567285 |
| GO:0004993 | serotonin receptor activity | 0.859916475 | 1.189583333 |
| GO:0045596 | negative regulation of cell differentiation | 0.858656204 | 1.189597028 |
| MP:0008770 | decreased survivor rate | 0.860150401 | 1.189637626 |
| GO:0055007 | cardiac muscle cell differentiation | 0.858588862 | 1.189662729 |
| ENSG00000068878 | PSME4 subnetwork | 0.858922192 | 1.18967997 |
| GO:0005814 | centriole | 0.858854183 | 1.189688512 |
| GO:0021544 | subpallium development | 0.860147282 | 1.189746029 |
| MP:0010724 | thick interventricular septum | 0.682097681 | 1.189752399 |
| ENSG00000111602 | TIMELESS subnetwork | 0.682022425 | 1.189763033 |
| ENSG00000164053 | ATRIP subnetwork | 0.858583978 | 1.18977132 |
| GO:0032409 | regulation of transporter activity | 0.68197079 | 1.189838843 |
| GO:0034385 | triglyceride-rich lipoprotein particle | 0.85857345 | 1.189875167 |
| REACTOME_AMINE_LIGAND:BIND | REACTOME_AMINE_LIGAND:BINDING_RECEPTORS | 0.858311021 | 1.189881803 |
| KEGG_PROTEASOME | KEGG_PROTEASOME | 0.682256011 | 1.189925373 |
| MP:0002127 | abnormal cardiovascular system morphology | 0.857883913 | 1.189938966 |
| GO:0042303 | molting cycle | 0.858280805 | 1.189961868 |
| GO:0034361 | very-low-density lipoprotein particle | 0.85857345 | 1.189988564 |
| GO:0007090 | regulation of S phase of mitotic cell cycle | 0.85801783 | 1.189997139 |
| ENSG00000176884 | GRIN1 subnetwork | 0.68239128 | 1.190045008 |

| | | | |
|---|---|---|---|
| GO:0042403 | thyroid hormone metabolic process | 0.857880744 | 1.190052456 |
| MP:0001154 | seminiferous tubule degeneration | 0.858189664 | 1.190064836 |
| GO:0042633 | hair cycle | 0.858280805 | 1.190075317 |
| ENSG00000169896 | ITGAM subnetwork | 0.682517593 | 1.190081715 |
| GO:0030511 | positive regulation of transforming growth factor beta re | 0.858563233 | 1.190092451 |
| MP:0006011 | abnormal endolymphatic duct morphology | 0.857848044 | 1.190108737 |
| ENSG00000115254 | ENSG00000115254 subnetwork | 0.857785778 | 1.190136411 |
| ENSG00000166033 | HTRA1 subnetwork | 0.857779793 | 1.190245182 |
| MP:0009435 | abnormal miniature inhibitory postsynaptic currents | 0.857564653 | 1.190252863 |
| ENSG00000197976 | AKAP17A subnetwork | 0.857680245 | 1.190263334 |
| ENSG00000175482 | POLD4 subnetwork | 0.857508469 | 1.190323504 |
| GO:0044439 | peroxisomal part | 0.857318897 | 1.190340746 |
| GO:0019217 | regulation of fatty acid metabolic process | 0.857431714 | 1.190341668 |
| GO:0044438 | microbody part | 0.857318897 | 1.190454372 |
| ENSG00000174804 | FZD4 subnetwork | 0.857272054 | 1.19049642 |
| GO:2001252 | positive regulation of chromosome organization | 0.684326796 | 1.190541179 |
| GO:0061041 | regulation of wound healing | 0.857154295 | 1.190570992 |
| MP:0003120 | abnormal tracheal cartilage morphology | 0.857248218 | 1.190590987 |
| GO:0016651 | oxidoreductase activity, acting on NADH or NADPH | 0.857119663 | 1.190656035 |
| MP:0000432 | abnormal head morphology | 0.684321448 | 1.190670054 |
| ENSG00000168280 | KIF5C subnetwork | 0.682933861 | 1.190674956 |
| ENSG00000145817 | YIPF5 subnetwork | 0.856747886 | 1.190718448 |
| ENSG00000121552 | CSTA subnetwork | 0.857108452 | 1.19075542 |
| GO:0050657 | nucleic acid transport | 0.684316288 | 1.19079896 |
| GO:0006805 | xenobiotic metabolic process | 0.85674486 | 1.190832219 |
| GO:0006944 | cellular membrane fusion | 0.684606206 | 1.190843573 |
| ENSG00000083750 | RRAGB subnetwork | 0.857104945 | 1.190854823 |
| GO:0003995 | acyl-CoA dehydrogenase activity | 0.857054094 | 1.19087783 |
| ENSG00000169131 | ZNF354A subnetwork | 0.856982473 | 1.190886511 |
| ENSG00000149925 | ALDOA subnetwork | 0.683520959 | 1.190894569 |
| GO:0046034 | ATP metabolic process | 0.856718506 | 1.19090301 |
| ENSG00000167880 | EVPL subnetwork | 0.683385698 | 1.190910167 |
| GO:0050658 | RNA transport | 0.684316288 | 1.190939716 |
| GO:0043296 | apical junction complex | 0.683327793 | 1.190962358 |
| ENSG00000135390 | ATP5G2 subnetwork | 0.856498441 | 1.190962531 |
| ENSG00000214517 | PPME1 subnetwork | 0.683976271 | 1.190964995 |
| REACTOME_PEPTIDE_HORMONE_ | REACTOME_PEPTIDE_HORMONE_BIOSYNTHESIS | 0.68388617 | 1.19096984 |
| ENSG00000099204 | ABLIM1 subnetwork | 0.85667903 | 1.190973815 |
| GO:0006099 | tricarboxylic acid cycle | 0.856599372 | 1.190992067 |
| GO:0032432 | actin filament bundle | 0.683516638 | 1.191023669 |
| ENSG00000139117 | CPNE8 subnetwork | 0.856475257 | 1.191038142 |
| MP:0005547 | abnormal Muller cell morphology | 0.684796366 | 1.191045481 |
| GO:0051236 | establishment of RNA localization | 0.684316288 | 1.191080506 |
| ENSG00000115233 | PSMD14 subnetwork | 0.685358683 | 1.191081336 |
| ENSG00000068354 | TBC1D25 subnetwork | 0.683250846 | 1.191096377 |
| ENSG00000168398 | BDKRB2 subnetwork | 0.683327157 | 1.19110335 |
| KEGG_NUCLEOTIDE_EXCISION_RE | KEGG_NUCLEOTIDE_EXCISION_REPAIR | 0.856441846 | 1.191104207 |
| ENSG00000157927 | RADIL subnetwork | 0.683880209 | 1.191110717 |
| ENSG00000167978 | SRRM2 subnetwork | 0.685303482 | 1.191133412 |
| ENSG00000171793 | CTPS subnetwork | 0.683738082 | 1.191155939 |
| MP:0006303 | abnormal retinal nerve fiber layer morphology | 0.683809793 | 1.191156986 |
| GO:0031023 | microtubule organizing center organization | 0.684181327 | 1.191172993 |
| ENSG00000037965 | HOXC8 subnetwork | 0.685048096 | 1.191189323 |
| MP:0002191 | abnormal artery morphology | 0.685149081 | 1.191190364 |

| | | | |
|---|---|---|---|
| MP:0006092 | abnormal olfactory neuron morphology | 0.68637617 | 1.191193115 |
| GO:0042119 | neutrophil activation | 0.856432466 | 1.191203748 |
| GO:0061025 | membrane fusion | 0.684300246 | 1.191209506 |
| MP:0000435 | shortened head | 0.684961225 | 1.191211906 |
| ENSG00000079950 | STX7 subnetwork | 0.685275531 | 1.191220923 |
| ENSG00000172409 | CLP1 subnetwork | 0.685813329 | 1.191221239 |
| MP:0001344 | blepharoptosis | 0.686498903 | 1.191270777 |
| ENSG00000105287 | PRKD2 subnetwork | 0.685760933 | 1.191285107 |
| ENSG00000166086 | JAM3 subnetwork | 0.856388958 | 1.191288965 |
| GO:0032091 | negative regulation of protein binding | 0.686156172 | 1.191296143 |
| GO:0007265 | Ras protein signal transduction | 0.686361037 | 1.191321778 |
| GO:0007548 | sex differentiation | 0.688095226 | 1.191336313 |
| GO:0061178 | regulation of insulin secretion involved in cellular respon | 0.856278752 | 1.191359028 |
| GO:0032332 | positive regulation of chondrocyte differentiation | 0.686310603 | 1.191367925 |
| MP:0008212 | absent mature B cells | 0.685718808 | 1.191372595 |
| ENSG00000128609 | NDUFA5 subnetwork | 0.856374898 | 1.191398107 |
| ENSG00000091513 | TF subnetwork | 0.687960183 | 1.191398988 |
| MP:0000823 | abnormal lateral ventricle morphology | 0.687669479 | 1.191401836 |
| MP:0004029 | spontaneous chromosome breakage | 0.6856312 | 1.191418791 |
| MP:0002084 | abnormal developmental patterning | 0.686150837 | 1.191424864 |
| GO:0001101 | response to acid | 0.68831228 | 1.191455957 |
| MP:0001750 | increased circulating follicle stimulating hormone level | 0.688080582 | 1.191464706 |
| GO:0035773 | insulin secretion involved in cellular response to glucose | 0.856278752 | 1.191472979 |
| GO:0031528 | microvillus membrane | 0.855871942 | 1.191473684 |
| REACTOME_FORMATION_OF_ATI | REACTOME_FORMATION_OF_ATP_BY_CHEMIOSMOTIC_ | 0.688431014 | 1.1914746 |
| GO:0005614 | interstitial matrix | 0.855518055 | 1.191484779 |
| ENSG00000138594 | TMOD3 subnetwork | 0.686005198 | 1.19148773 |
| GO:0016049 | cell growth | 0.687939561 | 1.191503883 |
| ENSG00000100320 | RBFOX2 subnetwork | 0.686747035 | 1.191507544 |
| GO:0003013 | circulatory system process | 0.68765949 | 1.191530312 |
| GO:0016327 | apicolateral plasma membrane | 0.687493315 | 1.191540092 |
| GO:0031300 | intrinsic to organelle membrane | 0.687570749 | 1.191541088 |
| ENSG00000128908 | INO80 subnetwork | 0.687872502 | 1.191549959 |
| MP:0000198 | hypophosphatemia | 0.855469511 | 1.191555768 |
| GO:0042311 | vasodilation | 0.856267857 | 1.191563038 |
| ENSG00000128833 | MYO5C subnetwork | 0.686149172 | 1.191565412 |
| ENSG00000080608 | KIAA0020 subnetwork | 0.688297991 | 1.191578452 |
| GO:0046356 | acetyl-CoA catabolic process | 0.855867052 | 1.191582927 |
| REACTOME_REGULATION_OF_GL | REACTOME_REGULATION_OF_GLUCOKINASE_BY_GLUC( | 0.688617361 | 1.19159318 |
| GO:0061098 | positive regulation of protein tyrosine kinase activity | 0.855399315 | 1.191598047 |
| GO:0032069 | regulation of nuclease activity | 0.687469186 | 1.19163919 |
| ENSG00000106829 | TLE4 subnetwork | 0.68872164 | 1.191641194 |
| GO:0006914 | autophagy | 0.687411107 | 1.191655871 |
| GO:0000132 | establishment of mitotic spindle orientation | 0.856261583 | 1.191677031 |
| MP:0006264 | decreased systemic arterial systolic blood pressure | 0.687321671 | 1.191678445 |
| MP:0006138 | congestive heart failure | 0.855843137 | 1.191682619 |
| MP:0001292 | abnormal lens vesicle development | 0.856106844 | 1.19168979 |
| ENSG00000142168 | SOD1 subnetwork | 0.687151752 | 1.191694156 |
| MP:0008332 | decreased lactotroph cell number | 0.855388664 | 1.191697788 |
| ENSG00000101745 | ANKRD12 subnetwork | 0.687079879 | 1.191704961 |
| GO:0043616 | keratinocyte proliferation | 0.687267965 | 1.191730475 |
| REACTOME_SPHINGOLIPID_DE_N | REACTOME_SPHINGOLIPID_DE_NOVO_BIOSYNTHESIS | 0.687025363 | 1.191762904 |
| ENSG00000105223 | PLD3 subnetwork | 0.855343944 | 1.191778395 |
| GO:0051294 | establishment of spindle orientation | 0.856261583 | 1.191791045 |

| | | | |
|---|---|---|---|
| REACTOME_REGULATION_OF_W/ | REACTOME_REGULATION_OF_WATER_BALANCE_BY_RE | 0.855841439 | 1.191796688 |
| GO:0004222 | metalloendopeptidase activity | 0.855301644 | 1.191839862 |
| ENSG00000138835 | RGS3 subnetwork | 0.689014284 | 1.191842971 |
| GO:0070374 | positive regulation of ERK1 and ERK2 cascade | 0.687023834 | 1.191903359 |
| ENSG00000136888 | ATP6V1G1 subnetwork | 0.855260478 | 1.19190613 |
| MP:0004405 | absent cochlear hair cells | 0.689011495 | 1.19196544 |
| ENSG00000185122 | HSF1 subnetwork | 0.690508091 | 1.192005865 |
| ENSG00000198886 | MT-ND4 subnetwork | 0.690026568 | 1.192012911 |
| GO:0010927 | cellular component assembly involved in morphogenesis | 0.855257402 | 1.192020308 |
| ENSG00000159199 | ATP5G1 subnetwork | 0.690367991 | 1.19202839 |
| ENSG00000197697 | HIST1H2BE subnetwork | 0.689219468 | 1.192049595 |
| MP:0008586 | disorganized photoreceptor outer segment | 0.690833429 | 1.192049719 |
| GO:0051635 | bacterial cell surface binding | 0.85519923 | 1.192077026 |
| MP:0006362 | abnormal male germ cell morphology | 0.691349566 | 1.192090462 |
| MP:0003233 | prolonged QT interval | 0.689993989 | 1.192100012 |
| GO:0045777 | positive regulation of blood pressure | 0.689393955 | 1.192104336 |
| ENSG00000170917 | NUDT6 subnetwork | 0.690709285 | 1.192124091 |
| MP:0008515 | thin retinal outer nuclear layer | 0.690804779 | 1.192130878 |
| GO:0007289 | spermatid nucleus differentiation | 0.690352797 | 1.192150651 |
| ENSG00000167881 | SRP68 subnetwork | 0.689955407 | 1.192151914 |
| GO:0009214 | cyclic nucleotide catabolic process | 0.855189194 | 1.192167289 |
| ENSG00000140795 | MYLK3 subnetwork | 0.691327479 | 1.192195008 |
| GO:0022401 | negative adaptation of signaling pathway | 0.691274006 | 1.192205813 |
| MP:0002113 | abnormal skeleton development | 0.689926021 | 1.19222731 |
| GO:0022406 | membrane docking | 0.689777578 | 1.192231356 |
| GO:0044455 | mitochondrial membrane part | 0.689380603 | 1.192232667 |
| GO:0000775 | chromosome, centromeric region | 0.689848435 | 1.192249883 |
| ENSG00000086598 | TMED2 subnetwork | 0.691026853 | 1.192267558 |
| MP:0010027 | increased liver cholesterol level | 0.855187022 | 1.192281525 |
| ENSG00000117394 | SLC2A1 subnetwork | 0.690347078 | 1.192284675 |
| ENSG00000177302 | TOP3A subnetwork | 0.689581948 | 1.192299107 |
| GO:0023058 | adaptation of signaling pathway | 0.691274006 | 1.192345563 |
| ENSG00000182117 | NOP10 subnetwork | 0.689774554 | 1.192359643 |
| ENSG00000168646 | AXIN2 subnetwork | 0.691782123 | 1.192362657 |
| GO:0046915 | transition metal ion transmembrane transporter activity | 0.689687277 | 1.192364619 |
| GO:0070085 | glycosylation | 0.855160844 | 1.192371826 |
| ENSG00000138439 | FAM117B subnetwork | 0.85508143 | 1.192375887 |
| MP:0000043 | organ of Corti degeneration | 0.690314896 | 1.192383523 |
| MP:0001575 | cyanosis | 0.691610294 | 1.192407733 |
| GO:0070507 | regulation of microtubule cytoskeleton organization | 0.855029288 | 1.192437458 |
| MP:0006030 | abnormal otic vesicle development | 0.691753717 | 1.192449625 |
| ENSG00000109061 | MYH1 subnetwork | 0.854786 | 1.192473634 |
| MP:0001052 | abnormal muscle innervation | 0.854969189 | 1.192475077 |
| GO:0002029 | desensitization of G-protein coupled receptor protein sig | 0.691274006 | 1.192485346 |
| KEGG_PRIMARY_BILE_ACID_BIOS | KEGG_PRIMARY_BILE_ACID_BIOSYNTHESIS | 0.854930527 | 1.192517496 |
| GO:0008015 | blood circulation | 0.692618609 | 1.192545348 |
| GO:0016779 | nucleotidyltransferase activity | 0.854777934 | 1.192568799 |
| ENSG00000164331 | ANKRA2 subnetwork | 0.854726697 | 1.192611239 |
| GO:0006661 | phosphatidylinositol biosynthetic process | 0.692572114 | 1.192632257 |
| GO:0004673 | protein histidine kinase activity | 0.692103005 | 1.192639653 |
| ENSG00000135218 | CD36 subnetwork | 0.692490088 | 1.192648952 |
| REACTOME_GPCR_LIGAND_BINDI | REACTOME_GPCR_LIGAND_BINDING | 0.692749779 | 1.192669085 |
| ENSG00000109103 | UNC119 subnetwork | 0.854703921 | 1.19270164 |
| MP:0002081 | perinatal lethality | 0.854346257 | 1.192732419 |

| | | | |
|---|---|---|---|
| ENSG00000105088 | OLFM2 subnetwork | 0.854652066 | 1.192748897 |
| GO:0000155 | two-component sensor activity | 0.692103005 | 1.192779339 |
| ENSG00000177688 | SUMO4 subnetwork | 0.692480155 | 1.192782721 |
| ENSG00000175084 | DES subnetwork | 0.693118592 | 1.192817873 |
| MP:0001724 | abnormal extraembryonic endoderm formation | 0.854310606 | 1.192822875 |
| REACTOME_MEIOTIC_RECOMBIN | REACTOME_MEIOTIC_RECOMBINATION | 0.694479264 | 1.19284213 |
| GO:0034375 | high-density lipoprotein particle remodeling | 0.854646647 | 1.192863309 |
| ENSG00000173218 | VANGL1 subnetwork | 0.692463665 | 1.192898958 |
| GO:0034405 | response to fluid shear stress | 0.69346539 | 1.192902245 |
| MP:0002608 | increased hematocrit | 0.693351365 | 1.19291311 |
| REACTOME_REGULATION_OF_OR | REACTOME_REGULATION_OF_ORNITHINE_DECARBOXYL | 0.854279704 | 1.192918146 |
| ENSG00000121486 | TRMT1L subnetwork | 0.69310731 | 1.192922321 |
| REACTOME_SIGNALING_BY_INSU | REACTOME_SIGNALING_BY_INSULIN_RECEPTOR | 0.854603455 | 1.192939371 |
| ENSG00000145386 | CCNA2 subnetwork | 0.694339121 | 1.192945573 |
| MP:0005146 | decreased circulating VLDL cholesterol level | 0.697072862 | 1.192949389 |
| ENSG00000061337 | LZTS1 subnetwork | 0.694475645 | 1.192981432 |
| ENSG00000175536 | LIPT2 subnetwork | 0.692426547 | 1.192985948 |
| ENSG00000197170 | PSMD12 subnetwork | 0.697021438 | 1.192989295 |
| ENSG00000006638 | TBXA2R subnetwork | 0.693061162 | 1.192991693 |
| MP:0003864 | abnormal midbrain development | 0.854274335 | 1.193013436 |
| MP:0005172 | reduced eye pigmentation | 0.693692013 | 1.193014964 |
| GO:0002495 | antigen processing and presentation of peptide antigen v | 0.693323143 | 1.193017544 |
| ENSG00000115307 | AUP1 subnetwork | 0.694307456 | 1.193032356 |
| MP:0000141 | abnormal vertebral body morphology | 0.693799953 | 1.193045003 |
| GO:0051100 | negative regulation of binding | 0.697595683 | 1.193046512 |
| ENSG00000101040 | ZMYND8 subnetwork | 0.693625434 | 1.193055068 |
| GO:0016757 | transferase activity, transferring glycosyl groups | 0.69406779 | 1.193059126 |
| ENSG00000104290 | FZD3 subnetwork | 0.852954526 | 1.193070639 |
| ENSG00000206181 | TCEB3B subnetwork | 0.854227222 | 1.193075151 |
| GO:0006505 | GPI anchor metabolic process | 0.696785737 | 1.193079967 |
| GO:0015926 | glucosidase activity | 0.694265426 | 1.193084112 |
| GO:0061082 | myeloid leukocyte cytokine production | 0.69753179 | 1.193103849 |
| GO:0030149 | sphingolipid catabolic process | 0.697017597 | 1.19311649 |
| GO:0045095 | keratin filament | 0.852913577 | 1.193122837 |
| GO:0006084 | acetyl-CoA metabolic process | 0.694034587 | 1.193134276 |
| GO:0051082 | unfolded protein binding | 0.697446397 | 1.193137939 |
| ENSG00000088305 | DNMT3B subnetwork | 0.693954695 | 1.193139317 |
| MP:0004259 | small placenta | 0.694205076 | 1.193141722 |
| GO:0050920 | regulation of chemotaxis | 0.697275754 | 1.193147976 |
| GO:0071156 | regulation of cell cycle arrest | 0.852845999 | 1.19315582 |
| KEGG_FOLATE_BIOSYNTHESIS | KEGG_FOLATE_BIOSYNTHESIS | 0.85319208 | 1.19316806 |
| MP:0000149 | abnormal scapula morphology | 0.852736746 | 1.193168926 |
| ENSG00000154723 | ATP5J subnetwork | 0.694819327 | 1.193182349 |
| GO:0009067 | aspartate family amino acid biosynthetic process | 0.697383866 | 1.193189485 |
| ENSG00000107290 | SETX subnetwork | 0.85422627 | 1.193189672 |
| GO:0052472 | modulation by host of symbiont transcription | 0.696684614 | 1.193194784 |
| ENSG00000213672 | NCKIPSD subnetwork | 0.696764284 | 1.193195576 |
| GO:0055080 | cation homeostasis | 0.852684267 | 1.193201923 |
| MP:0002725 | abnormal vein morphology | 0.853385973 | 1.193202997 |
| REACTOME_REGULATION_OF_GE | REACTOME_REGULATION_OF_GENE_EXPRESSION_IN_B | 0.85279506 | 1.19320323 |
| ENSG00000198938 | MT-CO3 subnetwork | 0.852220814 | 1.19321243 |
| MP:0000827 | dilated third ventricle | 0.853470408 | 1.193213256 |
| GO:0016709 | oxidoreductase activity, acting on paired donors, with in | 0.853602693 | 1.193213908 |
| ENSG00000198056 | PRIM1 subnetwork | 0.695239343 | 1.193238829 |

| | | | |
|---|---|---|---|
| GO:0007254 | JNK cascade | 0.694795807 | 1.193245768 |
| GO:0055072 | iron ion homeostasis | 0.852309315 | 1.193251563 |
| MP:0009243 | hairpin sperm flagellum | 0.694927803 | 1.193253181 |
| GO:0046466 | membrane lipid catabolic process | 0.697017597 | 1.193255354 |
| ENSG00000066468 | FGFR2 subnetwork | 0.69532837 | 1.193268782 |
| ENSG00000152818 | UTRN subnetwork | 0.852420795 | 1.19327626 |
| GO:0005765 | lysosomal membrane | 0.852653202 | 1.1932782 |
| GO:0045263 | proton-transporting ATP synthase complex, coupling fact | 0.696115329 | 1.193281669 |
| MP:0005253 | abnormal eye physiology | 0.853190579 | 1.193282722 |
| ENSG00000120498 | TEX11 subnetwork | 0.696290969 | 1.193283234 |
| GO:0048285 | organelle fission | 0.853365872 | 1.193284012 |
| GO:0030641 | regulation of cellular pH | 0.8513842 | 1.193287104 |
| MP:0001306 | small lens | 0.85420347 | 1.193289815 |
| GO:0016471 | vacuolar proton-transporting V-type ATPase complex | 0.853753546 | 1.193296197 |
| ENSG00000112118 | MCM3 subnetwork | 0.695441261 | 1.193298729 |
| MP:0005491 | pancreatic islet hyperplasia | 0.695209244 | 1.193308051 |
| MP:0000284 | double outlet heart right ventricle | 0.850285722 | 1.193317261 |
| GO:0033144 | negative regulation of intracellular steroid hormone rece | 0.852214885 | 1.193317618 |
| REACTOME_EXPORT_OF_VIRAL_F | REACTOME_EXPORT_OF_VIRAL_RIBONUCLEOPROTEINS_ | 0.695053548 | 1.193318161 |
| GO:0060043 | regulation of cardiac muscle cell proliferation | 0.850218609 | 1.193326261 |
| GO:0043921 | modulation by host of viral transcription | 0.696684614 | 1.193333721 |
| GO:0071466 | cellular response to xenobiotic stimulus | 0.852622767 | 1.193344874 |
| GO:0001750 | photoreceptor outer segment | 0.695975524 | 1.193350041 |
| GO:0050654 | chondroitin sulfate proteoglycan metabolic process | 0.849540931 | 1.193350063 |
| GO:0045600 | positive regulation of fat cell differentiation | 0.849734049 | 1.193356171 |
| GO:0006956 | complement activation | 0.84989124 | 1.193362277 |
| GO:2001251 | negative regulation of chromosome organization | 0.851363781 | 1.193373146 |
| GO:0042953 | lipoprotein transport | 0.849666041 | 1.193379656 |
| MP:0003729 | abnormal photoreceptor outer segment morphology | 0.696065704 | 1.193379953 |
| GO:0000090 | mitotic anaphase | 0.854197794 | 1.193389977 |
| REACTOME_P130CAS_LINKAGE_T | REACTOME_P130CAS_LINKAGE_TO_MAPK_SIGNALING_ | 0.695585128 | 1.193392815 |
| GO:0006007 | glucose catabolic process | 0.849852738 | 1.193400232 |
| ENSG00000105402 | NAPA subnetwork | 0.852199107 | 1.193418014 |
| ENSG00000196072 | BLOC1S2 subnetwork | 0.695916825 | 1.193419212 |
| KEGG_ALPHA_LINOLENIC_ACID_M | KEGG_ALPHA_LINOLENIC_ACID_METABOLISM | 0.696289901 | 1.193422279 |
| ENSG00000096746 | HNRNPH3 subnetwork | 0.695195592 | 1.19342397 |
| MP:0001410 | head bobbing | 0.850199137 | 1.19342689 |
| GO:0015908 | fatty acid transport | 0.850593296 | 1.193430059 |
| MP:0000928 | incomplete cephalic closure | 0.854147379 | 1.193442151 |
| GO:0009410 | response to xenobiotic stimulus | 0.852622767 | 1.193459652 |
| ENSG00000136002 | ARHGEF4 subnetwork | 0.695869682 | 1.193465081 |
| REACTOME_REGULATION_OF_DN | REACTOME_REGULATION_OF_DNA_REPLICATION | 0.84953691 | 1.193465251 |
| ENSG00000118680 | MYL12B subnetwork | 0.696680722 | 1.193466869 |
| ENSG00000188157 | AGRN subnetwork | 0.851325302 | 1.193468837 |
| GO:0046851 | negative regulation of bone remodeling | 0.696623502 | 1.193483578 |
| ENSG00000163631 | ALB subnetwork | 0.854106916 | 1.193494335 |
| MP:0003720 | abnormal neural tube closure | 0.852158195 | 1.19349437 |
| REACTOME_ER:PHAGOSOME_PA | REACTOME_ER:PHAGOSOME_PATHWAY | 0.854008675 | 1.193498511 |
| MP:0005431 | decreased oocyte number | 0.850181168 | 1.19351307 |
| ENSG00000142252 | GEMIN7 subnetwork | 0.851158677 | 1.193525388 |
| ENSG00000104313 | EYA1 subnetwork | 0.850578046 | 1.193525839 |
| GO:0045930 | negative regulation of mitotic cell cycle | 0.702289234 | 1.19352676 |
| MP:0002828 | abnormal renal glomerular capsule morphology | 0.695818 | 1.193528451 |
| MP:0001963 | abnormal hearing physiology | 0.850766443 | 1.193541546 |

| | | | |
|---|---|---|---|
| GO:0010576 | metalloenzyme regulator activity | 0.70222934 | 1.193543353 |
| ENSG00000072401 | UBE2D1 subnetwork | 0.851067781 | 1.193544035 |
| GO:0032410 | negative regulation of transporter activity | 0.849514674 | 1.193551501 |
| GO:0071451 | cellular response to superoxide | 0.700079566 | 1.193565217 |
| GO:0060766 | negative regulation of androgen receptor signaling pathv | 0.850864226 | 1.193580723 |
| MP:0006036 | abnormal mitochondrial physiology | 0.850985121 | 1.19358196 |
| GO:0043536 | positive regulation of blood vessel endothelial cell migra | 0.851325156 | 1.193583815 |
| GO:0042559 | pteridine-containing compound biosynthetic process | 0.852003278 | 1.193583943 |
| GO:0051597 | response to methylmercury | 0.85174106 | 1.193586904 |
| ENSG00000136824 | SMC2 subnetwork | 0.696608052 | 1.193587653 |
| GO:0033059 | cellular pigmentation | 0.851850287 | 1.193601964 |
| ENSG00000155561 | NUP205 subnetwork | 0.848834382 | 1.1936051 |
| REACTOME_XENOBIOTICS | REACTOME_XENOBIOTICS | 0.852155055 | 1.19360924 |
| GO:0015914 | phospholipid transport | 0.69945239 | 1.193611466 |
| GO:0055012 | ventricular cardiac muscle cell differentiation | 0.851953704 | 1.193621835 |
| ENSG00000154262 | ABCA6 subnetwork | 0.849467898 | 1.193623286 |
| GO:0016528 | sarcoplasm | 0.850179256 | 1.193623384 |
| ENSG00000023228 | NDUFS1 subnetwork | 0.700190993 | 1.193623928 |
| GO:0051493 | regulation of cytoskeleton organization | 0.699627434 | 1.193630352 |
| ENSG00000162402 | USP24 subnetwork | 0.850945855 | 1.193634348 |
| GO:0006693 | prostaglandin metabolic process | 0.850567076 | 1.193636101 |
| GO:0009584 | detection of visible light | 0.847828467 | 1.193636979 |
| GO:0000075 | cell cycle checkpoint | 0.849409614 | 1.193646809 |
| MP:0010300 | increased skin tumor incidence | 0.702204421 | 1.193652445 |
| ENSG00000043355 | ZIC2 subnetwork | 0.852104101 | 1.193656752 |
| ENSG00000184432 | COPB2 subnetwork | 0.695817225 | 1.193667638 |
| ENSG00000144736 | SHQ1 subnetwork | 0.85171402 | 1.193668143 |
| ENSG00000198554 | WDHD1 subnetwork | 0.849006085 | 1.193673331 |
| MP:0000733 | abnormal muscle development | 0.849113506 | 1.193673942 |
| GO:0006544 | glycine metabolic process | 0.849319892 | 1.19368482 |
| REACTOME_BETA_DEFENSINS | REACTOME_BETA_DEFENSINS | 0.700294636 | 1.19368842 |
| ENSG00000213699 | C2orf18 subnetwork | 0.847934995 | 1.193690775 |
| ENSG00000206287 | RING1 subnetwork | 0.848806784 | 1.193691431 |
| ENSG00000101255 | TRIB3 subnetwork | 0.699427033 | 1.193703575 |
| GO:0019430 | removal of superoxide radicals | 0.700079566 | 1.193703618 |
| GO:0022904 | respiratory electron transport chain | 0.699779976 | 1.193706497 |
| ENSG00000166483 | WEE1 subnetwork | 0.696607071 | 1.193726701 |
| ENSG00000135624 | CCT7 subnetwork | 0.702175491 | 1.193726873 |
| ENSG00000205022 | PABPN1L subnetwork | 0.700767782 | 1.193738415 |
| GO:0005542 | folic acid binding | 0.847825099 | 1.193752418 |
| ENSG00000147274 | RBMX subnetwork | 0.699611586 | 1.193757252 |
| MP:0005297 | spina bifida occulta | 0.847770682 | 1.193785666 |
| GO:0009378 | four-way junction helicase activity | 0.704215122 | 1.193789644 |
| ENSG00000135404 | CD63 subnetwork | 0.849310572 | 1.193790439 |
| ENSG00000125965 | GDF5 subnetwork | 0.702124997 | 1.193795536 |
| ENSG00000120694 | HSPH1 subnetwork | 0.699312805 | 1.193800789 |
| ENSG00000204227 | RING1 subnetwork | 0.848806784 | 1.193806763 |
| ENSG00000100823 | APEX1 subnetwork | 0.699118087 | 1.193810961 |
| MP:0005102 | abnormal iris pigmentation | 0.699401922 | 1.193813117 |
| GO:0019866 | organelle inner membrane | 0.700738187 | 1.193818793 |
| ENSG00000104976 | SNAPC2 subnetwork | 0.848317511 | 1.193823103 |
| ENSG00000092850 | TEKT2 subnetwork | 0.699904905 | 1.193823222 |
| KEGG_PROXIMAL_TUBULE_BICAR | KEGG_PROXIMAL_TUBULE_BICARBONATE_RECLAMATIC | 0.698970143 | 1.193832753 |
| ENSG00000186111 | PIP5K1C subnetwork | 0.700872211 | 1.1938376 |

| | | | |
|---|---|---|---|
| GO:0071450 | cellular response to oxygen radical | 0.700079566 | 1.19384205 |
| ENSG00000102081 | FMR1 subnetwork | 0.848125556 | 1.193846079 |
| ENSG00000080815 | PSEN1 subnetwork | 0.699989378 | 1.193847135 |
| MP:0002233 | abnormal nose morphology | 0.848248498 | 1.193851508 |
| ENSG00000104142 | VPS18 subnetwork | 0.699232487 | 1.193852316 |
| ENSG00000183814 | LIN9 subnetwork | 0.700663489 | 1.193852839 |
| MP:0004624 | abnormal thoracic cage morphology | 0.8477322 | 1.193867286 |
| ENSG00000134255 | CEPT1 subnetwork | 0.699091981 | 1.193885728 |
| KEGG_SNARE_INTERACTIONS_IN_ | KEGG_SNARE_INTERACTIONS_IN_VESICULAR_TRANSPOI | 0.700604849 | 1.193898482 |
| GO:0060740 | prostate gland epithelium morphogenesis | 0.704205456 | 1.193910035 |
| GO:0033572 | transferrin transport | 0.847672349 | 1.193910225 |
| ENSG00000206215 | ENSG00000206215 subnetwork | 0.848806784 | 1.193922118 |
| ENSG00000106028 | SSBP1 subnetwork | 0.701380719 | 1.193927993 |
| ENSG00000145220 | LYAR subnetwork | 0.698941288 | 1.19393077 |
| MP:0010299 | increased mammary gland tumor incidence | 0.70212221 | 1.193933611 |
| ENSG00000146143 | ENSG00000146143 subnetwork | 0.843857621 | 1.193934538 |
| MP:0006382 | abnormal lung epithelium morphology | 0.700554844 | 1.19393834 |
| GO:0010884 | positive regulation of lipid storage | 0.844458822 | 1.193942924 |
| ENSG00000013503 | POLR3B subnetwork | 0.701928098 | 1.193943776 |
| ENSG00000115414 | FN1 subnetwork | 0.701333631 | 1.193944657 |
| ENSG00000108528 | SLC25A11 subnetwork | 0.698867084 | 1.193953299 |
| MP:0005658 | increased susceptibility to diet-induced obesity | 0.698168752 | 1.193954191 |
| MP:0001382 | abnormal nursing | 0.701239879 | 1.193978694 |
| REACTOME_FGFR2C_LIGAND_BIN | REACTOME_FGFR2C_LIGAND_BINDING_AND_ACTIVATIC | 0.843830845 | 1.193997086 |
| ENSG00000080345 | RIF1 subnetwork | 0.70185768 | 1.194000926 |
| ENSG00000172732 | MUS81 subnetwork | 0.846855593 | 1.194006004 |
| ENSG00000187079 | TEAD1 subnetwork | 0.702076606 | 1.194008097 |
| GO:0035121 | tail morphogenesis | 0.848783785 | 1.194008504 |
| GO:0007033 | vacuole organization | 0.848556012 | 1.194012179 |
| ENSG00000094916 | CBX5 subnetwork | 0.701056424 | 1.194017836 |
| ENSG00000030582 | GRN subnetwork | 0.84444874 | 1.194019998 |
| GO:0015682 | ferric iron transport | 0.847672349 | 1.194025735 |
| MP:0002766 | situs inversus | 0.704414826 | 1.194026753 |
| ENSG00000167986 | DDB1 subnetwork | 0.704184272 | 1.194030453 |
| ENSG00000145555 | MYO10 subnetwork | 0.844599418 | 1.194030865 |
| ENSG00000134640 | MTNR1B subnetwork | 0.701517425 | 1.194032874 |
| ENSG00000006634 | DBF4 subnetwork | 0.847591155 | 1.194044509 |
| ENSG00000213463 | SYNJ2BP subnetwork | 0.84406169 | 1.19404681 |
| GO:0033692 | cellular polysaccharide biosynthetic process | 0.698833533 | 1.194057163 |
| MP:0000774 | decreased brain size | 0.847306722 | 1.194057298 |
| ENSG00000136936 | XPA subnetwork | 0.698769848 | 1.194068092 |
| ENSG00000136169 | SETDB2 subnetwork | 0.84379591 | 1.194069361 |
| ENSG00000106665 | CLIP2 subnetwork | 0.842434976 | 1.194070435 |
| GO:0051918 | negative regulation of fibrinolysis | 0.847534746 | 1.194072963 |
| GO:0061099 | negative regulation of protein tyrosine kinase activity | 0.701787069 | 1.194075445 |
| GO:0042745 | circadian sleep/wake cycle | 0.848731202 | 1.19408041 |
| GO:0016627 | oxidoreductase activity, acting on the CH-CH group of do | 0.842570725 | 1.194085603 |
| REACTOME_EXTENSION_OF_TELC | REACTOME_EXTENSION_OF_TELOMERES | 0.70122426 | 1.194093804 |
| ENSG00000169679 | BUB1 subnetwork | 0.846811126 | 1.194097424 |
| ENSG00000174123 | TLR10 subnetwork | 0.70407482 | 1.194104073 |
| MP:0002762 | ectopic cerebellar granule cells | 0.844714007 | 1.194109084 |
| REACTOME_SIGNAL_AMPLIFICATI | REACTOME_SIGNAL_AMPLIFICATION | 0.843297774 | 1.194109642 |
| ENSG00000136709 | WDR33 subnetwork | 0.701719695 | 1.194115264 |
| MP:0004066 | abnormal primitive node morphology | 0.698450472 | 1.194118331 |

| | | | |
|---|---|---|---|
| ENSG00000204842 | ATXN2 subnetwork | 0.702822925 | 1.194123425 |
| ENSG00000006468 | ETV1 subnetwork | 0.698570708 | 1.194124826 |
| ENSG00000116455 | WDR77 subnetwork | 0.703887287 | 1.194125793 |
| ENSG00000206509 | HLA-F subnetwork | 0.844446644 | 1.194131068 |
| REACTOME_DNA_REPLICATION | REACTOME_DNA_REPLICATION | 0.847455766 | 1.194135295 |
| GO:0015662 | ATPase activity, coupled to transmembrane movement c | 0.843762859 | 1.194136792 |
| ENSG00000141556 | TBCD subnetwork | 0.704173924 | 1.1941509 |
| ENSG00000013374 | NUB1 subnetwork | 0.846774499 | 1.194154964 |
| ENSG00000174197 | MGA subnetwork | 0.846563752 | 1.194158675 |
| GO:0006692 | prostanoid metabolic process | 0.847300511 | 1.194163198 |
| GO:0048710 | regulation of astrocyte differentiation | 0.84241759 | 1.194167153 |
| GO:0031674 | I band | 0.839626635 | 1.194173336 |
| GO:0042641 | actomyosin | 0.7016744 | 1.194178241 |
| REACTOME_INTERACTIONS_OF_V | REACTOME_INTERACTIONS_OF_VPR_WITH_HOST_CELLI | 0.703836072 | 1.194182825 |
| ENSG00000125998 | FAM83C subnetwork | 0.843277921 | 1.194186838 |
| ENSG00000141720 | PIP4K2B subnetwork | 0.698751678 | 1.194189425 |
| ENSG00000186852 | ENSG00000186852 subnetwork | 0.843445526 | 1.194192827 |
| MP:0001879 | abnormal lymphatic vessel morphology | 0.847227109 | 1.194196515 |
| GO:0014855 | striated muscle cell proliferation | 0.842928626 | 1.194204026 |
| GO:0048048 | embryonic eye morphogenesis | 0.843718646 | 1.194204236 |
| MP:0000938 | motor neuron degeneration | 0.702783684 | 1.194209431 |
| GO:0019104 | DNA N-glycosylase activity | 0.698418869 | 1.194222274 |
| ENSG00000102678 | FGF9 subnetwork | 0.844318528 | 1.19423189 |
| GO:0031234 | extrinsic to internal side of plasma membrane | 0.844402809 | 1.19423245 |
| MP:0008572 | abnormal Purkinje cell dendrite morphology | 0.702988052 | 1.19423388 |
| GO:0002532 | production of molecular mediator involved in inflammat | 0.70375654 | 1.194234099 |
| ENSG00000104725 | ENSG00000104725 subnetwork | 0.84238684 | 1.194239564 |
| GO:0045742 | positive regulation of epidermal growth factor receptor s | 0.84675686 | 1.194241573 |
| MP:0001751 | increased circulating luteinizing hormone level | 0.704070512 | 1.194241865 |
| ENSG00000125676 | THOC2 subnetwork | 0.846540747 | 1.194245301 |
| MP:0001303 | abnormal lens morphology | 0.839775481 | 1.194261735 |
| GO:0019400 | alditol metabolic process | 0.847177714 | 1.194273405 |
| ENSG00000154380 | ENAH subnetwork | 0.843261847 | 1.194283492 |
| MP:0005171 | absent coat pigmentation | 0.844996079 | 1.194284328 |
| MP:0004190 | abnormal direction of embryo turning | 0.8436302 | 1.194285714 |
| MP:0003403 | absent placental labyrinth | 0.839624028 | 1.194289898 |
| MP:0001940 | testis hypoplasia | 0.843697131 | 1.194295987 |
| ENSG00000100285 | NEFH subnetwork | 0.842253954 | 1.194301703 |
| GO:0009147 | pyrimidine nucleoside triphosphate metabolic process | 0.704629196 | 1.194304162 |
| GO:0048841 | regulation of axon extension involved in axon guidance | 0.842907912 | 1.194315308 |
| REACTOME_SIGNALING_BY_WNT | REACTOME_SIGNALING_BY_WNT | 0.841998751 | 1.194319509 |
| GO:0046579 | positive regulation of Ras protein signal transduction | 0.839912347 | 1.194320843 |
| ENSG00000114353 | GNAI2 subnetwork | 0.703730977 | 1.194331563 |
| GO:0007176 | regulation of epidermal growth factor-activated recepto | 0.842369406 | 1.194341183 |
| GO:0030546 | receptor activator activity | 0.846512987 | 1.194341634 |
| MP:0005075 | abnormal melanosome morphology | 0.703659151 | 1.194354001 |
| MP:0004084 | abnormal cardiac muscle relaxation | 0.843114378 | 1.194355309 |
| GO:0022616 | DNA strand elongation | 0.842200758 | 1.194359548 |
| ENSG00000142186 | SCYL1 subnetwork | 0.846431032 | 1.19436531 |
| GO:0010171 | body morphogenesis | 0.843238203 | 1.194365581 |
| ENSG00000138175 | ARL3 subnetwork | 0.847162229 | 1.194374516 |
| GO:0035265 | organ growth | 0.839583091 | 1.194386958 |
| ENSG00000162188 | GNG3 subnetwork | 0.704998158 | 1.194392577 |
| MP:0000552 | abnormal radius morphology | 0.842883797 | 1.194397432 |

| | | | |
|---|---|---|---|
| ENSG00000109814 | UGDH subnetwork | 0.842147376 | 1.194397936 |
| MP:0003632 | abnormal nervous system morphology | 0.839505497 | 1.194401054 |
| ENSG00000002745 | WNT16 subnetwork | 0.846197445 | 1.194407289 |
| GO:0007009 | plasma membrane organization | 0.84638061 | 1.194413218 |
| MP:0003935 | abnormal craniofacial development | 0.839368683 | 1.19441949 |
| GO:0002579 | positive regulation of antigen processing and presentatic | 0.704802718 | 1.194431635 |
| ENSG00000162231 | NXF1 subnetwork | 0.70492679 | 1.194432277 |
| REACTOME_DEGRADATION_OF_E | REACTOME_DEGRADATION_OF_BETA:CATENIN_BY_THE | 0.841998751 | 1.19443579 |
| GO:0000151 | ubiquitin ligase complex | 0.715622848 | 1.194444444 |
| ENSG00000130706 | ADRM1 subnetwork | 0.83945071 | 1.194463972 |
| MP:0004411 | decreased endocochlear potential | 0.846322857 | 1.194465982 |
| GO:0019751 | polyol metabolic process | 0.70364569 | 1.194468822 |
| GO:0045671 | negative regulation of osteoclast differentiation | 0.715826829 | 1.19449114 |
| ENSG00000100767 | PAPLN subnetwork | 0.715399583 | 1.194493692 |
| GO:0000987 | core promoter proximal region sequence-specific DNA bi | 0.703319918 | 1.194495148 |
| GO:0031513 | nonmotile primary cilium | 0.703479408 | 1.194496419 |
| ENSG00000177479 | ARIH2 subnetwork | 0.839338948 | 1.19449707 |
| GO:0003084 | positive regulation of systemic arterial blood pressure | 0.840112611 | 1.194516538 |
| ENSG00000153201 | RANBP2 subnetwork | 0.84619662 | 1.194523071 |
| GO:0071825 | protein-lipid complex subunit organization | 0.8376281 | 1.194527047 |
| ENSG00000100342 | APOL1 subnetwork | 0.71490769 | 1.19452974 |
| GO:0046488 | phosphatidylinositol metabolic process | 0.703599334 | 1.194537475 |
| MP:0001328 | disorganized retinal layers | 0.841987018 | 1.194537488 |
| MP:0010551 | abnormal coronary vessel morphology | 0.715596822 | 1.194540393 |
| ENSG00000180596 | HIST1H2BC subnetwork | 0.712893626 | 1.194549601 |
| MP:0011084 | partial lethality at weaning | 0.712992827 | 1.194567324 |
| GO:0030865 | cortical cytoskeleton organization | 0.70327186 | 1.194569613 |
| KEGG_NITROGEN_METABOLISM | KEGG_NITROGEN_METABOLISM | 0.715798827 | 1.194581393 |
| GO:0043392 | negative regulation of DNA binding | 0.840336856 | 1.194585894 |
| GO:0016675 | oxidoreductase activity, acting on a heme group of dono | 0.715287579 | 1.194594748 |
| GO:0042575 | DNA polymerase complex | 0.845294046 | 1.194600233 |
| GO:0003209 | cardiac atrium morphogenesis | 0.703461484 | 1.194605522 |
| GO:0016862 | intramolecular oxidoreductase activity, interconverting k | 0.839337198 | 1.194608849 |
| GO:0017015 | regulation of transforming growth factor beta receptor s | 0.711994415 | 1.194610642 |
| GO:0071418 | cellular response to amine stimulus | 0.846176348 | 1.194614639 |
| REACTOME_HOMOLOGOUS_REC | REACTOME_HOMOLOGOUS_RECOMBINATION_REPAIR | 0.845477155 | 1.194615832 |
| ENSG00000138030 | KHK subnetwork | 0.840471845 | 1.194620562 |
| GO:0031576 | G2/M transition checkpoint | 0.715397881 | 1.194629461 |
| ENSG00000186895 | FGF3 subnetwork | 0.71358037 | 1.194633702 |
| GO:0055065 | metal ion homeostasis | 0.840721448 | 1.194636763 |
| GO:0006582 | melanin metabolic process | 0.839248005 | 1.194642508 |
| GO:0071827 | plasma lipoprotein particle organization | 0.8376281 | 1.194643905 |
| MP:0004398 | cochlear inner hair cell degeneration | 0.841979212 | 1.194648943 |
| ENSG00000134250 | NOTCH2 subnetwork | 0.71367338 | 1.194651401 |
| GO:0005922 | connexon complex | 0.71558527 | 1.194653409 |
| GO:0042632 | cholesterol homeostasis | 0.714903599 | 1.194659918 |
| ENSG00000075188 | NUP37 subnetwork | 0.838392509 | 1.194662757 |
| GO:0006399 | tRNA metabolic process | 0.846099737 | 1.194667442 |
| REACTOME_STABILIZATION_OF_P | REACTOME_STABILIZATION_OF_P53 | 0.840319494 | 1.194668293 |
| GO:0032233 | positive regulation of actin filament bundle assembly | 0.71377619 | 1.194669097 |
| MP:0000961 | abnormal dorsal root ganglion morphology | 0.715242927 | 1.194673715 |
| ENSG00000197846 | HIST1H2BF subnetwork | 0.712893626 | 1.194685825 |
| GO:0048469 | cell maturation | 0.83820497 | 1.194700303 |
| GO:0007044 | cell-substrate junction assembly | 0.713461261 | 1.194700855 |

| | | | |
|---|---|---|---|
| MP:0010107 | abnormal renal reabsorbtion | 0.845657406 | 1.194703657 |
| ENSG00000077380 | DYNC1I2 subnetwork | 0.711881012 | 1.194712197 |
| GO:0031572 | G2/M transition DNA damage checkpoint | 0.837166145 | 1.194714691 |
| GO:0019212 | phosphatase inhibitor activity | 0.70525273 | 1.194715916 |
| GO:0048200 | Golgi transport vesicle coating | 0.839231054 | 1.194725017 |
| MP:0005353 | abnormal patella morphology | 0.83761032 | 1.194726543 |
| MP:0001765 | abnormal ion homeostasis | 0.836993011 | 1.194728341 |
| ENSG00000134376 | CRB1 subnetwork | 0.838366782 | 1.194730668 |
| REACTOME_HOMOLOGOUS_REC | REACTOME_HOMOLOGOUS_RECOMBINATION_REPAIR_ | 0.845477155 | 1.194731736 |
| GO:0006096 | glycolysis | 0.841942257 | 1.194736073 |
| ENSG00000147133 | TAF1 subnetwork | 0.714641042 | 1.194737142 |
| GO:0004864 | protein phosphatase inhibitor activity | 0.837069877 | 1.194738645 |
| ENSG00000105664 | COMP subnetwork | 0.838625943 | 1.194741472 |
| GO:0042744 | hydrogen peroxide catabolic process | 0.840715339 | 1.194743515 |
| ENSG00000154134 | ROBO3 subnetwork | 0.711994352 | 1.194747059 |
| GO:0007585 | respiratory gaseous exchange | 0.837425886 | 1.194749976 |
| GO:0006458 | 'de novo' protein folding | 0.711742152 | 1.194756683 |
| MP:0006029 | abnormal sclerotome morphology | 0.841078101 | 1.194760187 |
| REACTOME_RESOLUTION_OF_AP | REACTOME_RESOLUTION_OF_AP_SITES_VIA_THE_SINGI | 0.841180135 | 1.194760698 |
| ENSG00000166136 | NDUFB8 subnetwork | 0.713923394 | 1.19476082 |
| GO:0006644 | phospholipid metabolic process | 0.838055825 | 1.194767726 |
| ENSG00000091409 | ITGA6 subnetwork | 0.713576287 | 1.194769827 |
| ENSG00000196470 | SIAH1 subnetwork | 0.84592134 | 1.194772573 |
| ENSG00000183336 | BOLA2 subnetwork | 0.714576963 | 1.194776374 |
| GO:0030031 | cell projection assembly | 0.846091533 | 1.194783283 |
| GO:0032933 | SREBP-mediated signaling pathway | 0.715238152 | 1.194792496 |
| GO:0006833 | water transport | 0.838336912 | 1.194793704 |
| GO:0055092 | sterol homeostasis | 0.714903599 | 1.194795814 |
| GO:0005732 | small nucleolar ribonucleoprotein complex | 0.836969034 | 1.194796358 |
| REACTOME_SPHINGOLIPID_META | REACTOME_SPHINGOLIPID_METABOLISM | 0.840664822 | 1.194796645 |
| MP:0008525 | decreased cranium height | 0.711836773 | 1.194797259 |
| MP:0000745 | tremors | 0.713238436 | 1.194807342 |
| ENSG00000099381 | SETD1A subnetwork | 0.837379585 | 1.194813075 |
| REACTOME_UNBLOCKING_OF_NI | REACTOME_UNBLOCKING_OF_NMDA_RECEPTOR_GLUT | 0.838203663 | 1.194817133 |
| GO:0009408 | response to heat | 0.838007864 | 1.194821009 |
| ENSG00000032514 | ENSG00000032514 subnetwork | 0.841547764 | 1.194821202 |
| ENSG00000168242 | HIST1H2BI subnetwork | 0.712893626 | 1.19482208 |
| GO:0009581 | detection of external stimulus | 0.845859568 | 1.194825412 |
| ENSG00000044446 | PHKA2 subnetwork | 0.837598042 | 1.194828767 |
| ENSG00000123349 | PFDN5 subnetwork | 0.714833677 | 1.194829352 |
| GO:0048384 | retinoic acid receptor signaling pathway | 0.836926572 | 1.194830118 |
| GO:0035295 | tube development | 0.707677873 | 1.194831151 |
| GO:0001191 | RNA polymerase II transcription factor binding transcript | 0.713455928 | 1.19483132 |
| GO:0000777 | condensed chromosome kinetochore | 0.841660723 | 1.19483145 |
| ENSG00000163032 | VSNL1 subnetwork | 0.714450216 | 1.194837792 |
| GO:0035964 | COPI-coated vesicle budding | 0.839231054 | 1.194841735 |
| GO:0090181 | regulation of cholesterol metabolic process | 0.841849036 | 1.194842198 |
| GO:0003684 | damaged DNA binding | 0.841922336 | 1.1948427 |
| GO:0019395 | fatty acid oxidation | 0.839060763 | 1.194850498 |
| GO:0050660 | flavin adenine dinucleotide binding | 0.846077761 | 1.194860357 |
| GO:0033124 | regulation of GTP catabolic process | 0.717664788 | 1.194866274 |
| ENSG00000058600 | POLR3E subnetwork | 0.71410945 | 1.194875299 |
| MP:0011083 | complete lethality at weaning | 0.841074971 | 1.19487667 |
| ENSG00000166233 | ARIH1 subnetwork | 0.716063503 | 1.19487791 |

| | | | |
|---|---|---|---|
| GO:0030279 | negative regulation of ossification | 0.714758794 | 1.194885653 |
| GO:0090003 | regulation of establishment of protein localization in pla | 0.705637663 | 1.194891142 |
| ENSG00000105663 | ENSG00000105663 subnetwork | 0.711740392 | 1.194893179 |
| KEGG_BASAL_TRANSCRIPTION_FA | KEGG_BASAL_TRANSCRIPTION_FACTORS | 0.838899798 | 1.194893471 |
| ENSG00000126432 | PRDX5 subnetwork | 0.714233024 | 1.19490435 |
| GO:0008378 | galactosyltransferase activity | 0.841799534 | 1.194909888 |
| ENSG00000169627 | BOLA2B subnetwork | 0.714576963 | 1.194912361 |
| GO:0051905 | establishment of pigment granule localization | 0.836893284 | 1.194912848 |
| GO:0002064 | epithelial cell development | 0.84151035 | 1.194913272 |
| GO:0009749 | response to glucose stimulus | 0.839015765 | 1.194918401 |
| MP:0005221 | abnormal rostral-caudal axis patterning | 0.70551348 | 1.194918769 |
| MP:0004231 | abnormal calcium ion homeostasis | 0.841358613 | 1.194922027 |
| ENSG00000128408 | RIBC2 subnetwork | 0.715233474 | 1.194922675 |
| GO:0072224 | metanephric glomerulus development | 0.705579107 | 1.194930876 |
| MP:0001906 | increased dopamine level | 0.836837915 | 1.194936833 |
| MP:0000914 | exencephaly | 0.714426411 | 1.194939663 |
| ENSG00000145494 | NDUFS6 subnetwork | 0.707648643 | 1.19493969 |
| MP:0000078 | abnormal supraoccipital bone morphology | 0.84104861 | 1.194944423 |
| ENSG00000187990 | HIST1H2BG subnetwork | 0.712893626 | 1.194958367 |
| GO:0048205 | COPI coating of Golgi vesicle | 0.839231054 | 1.194958476 |
| GO:0001106 | RNA polymerase II transcription corepressor activity | 0.713455928 | 1.194967514 |
| GO:0031645 | negative regulation of neurological system process | 0.712332508 | 1.194982877 |
| ENSG00000059769 | DNAJC25 subnetwork | 0.836703047 | 1.194984817 |
| ENSG00000131981 | LGALS3 subnetwork | 0.836803927 | 1.194985309 |
| GO:0030239 | myofibril assembly | 0.833588192 | 1.194985744 |
| ENSG00000137218 | FRS3 subnetwork | 0.717643286 | 1.194990366 |
| MP:0003845 | abnormal decidualization | 0.717964767 | 1.194992636 |
| MP:0003674 | oxidative stress | 0.708019425 | 1.194998852 |
| GO:0001653 | peptide receptor activity | 0.83619822 | 1.19500098 |
| GO:0051271 | negative regulation of cellular component movement | 0.711733009 | 1.195001143 |
| ENSG00000112038 | OPRM1 subnetwork | 0.841487603 | 1.19500536 |
| GO:0055074 | calcium ion homeostasis | 0.712271587 | 1.195027971 |
| GO:0015145 | monosaccharide transmembrane transporter activity | 0.836654164 | 1.195028409 |
| GO:0045932 | negative regulation of muscle contraction | 0.836049398 | 1.195029412 |
| GO:0060419 | heart growth | 0.705499688 | 1.195033418 |
| MP:0004813 | absent linear vestibular evoked potential | 0.833801746 | 1.195040794 |
| ENSG00000173418 | NAA20 subnetwork | 0.714402037 | 1.195041558 |
| ENSG00000111875 | ASF1A subnetwork | 0.836153266 | 1.195044603 |
| ENSG00000087086 | FTL subnetwork | 0.83283816 | 1.195055107 |
| ENSG00000129682 | FGF13 subnetwork | 0.832485523 | 1.195057596 |
| GO:0008238 | exopeptidase activity | 0.716296423 | 1.195060747 |
| GO:0004653 | polypeptide N-acetylgalactosaminyltransferase activity | 0.707645501 | 1.195071232 |
| GO:0019205 | nucleobase-containing compound kinase activity | 0.712862101 | 1.195071869 |
| ENSG00000151208 | DLG5 subnetwork | 0.832541534 | 1.195077771 |
| ENSG00000155329 | ZCCHC10 subnetwork | 0.833434499 | 1.195078179 |
| ENSG00000116584 | ARHGEF2 subnetwork | 0.716233041 | 1.195082898 |
| GO:0000725 | recombinational repair | 0.707967508 | 1.195084415 |
| ENSG00000129084 | PSMA1 subnetwork | 0.832948 | 1.195085113 |
| GO:0008016 | regulation of heart contraction | 0.805559293 | 1.195089875 |
| MP:0000547 | short limbs | 0.717538232 | 1.195091259 |
| ENSG00000170579 | DLGAP1 subnetwork | 0.711694068 | 1.195091989 |
| ENSG00000113810 | SMC4 subnetwork | 0.706932262 | 1.195094882 |
| GO:0060706 | cell differentiation involved in embryonic placenta devel | 0.833365907 | 1.195097364 |
| ENSG00000111880 | RNGTT subnetwork | 0.833579398 | 1.195098328 |

| | | | |
|---|---|---|---|
| MP:0005405 | axon degeneration | 0.833768528 | 1.195099292 |
| ENSG00000164329 | PAPD4 subnetwork | 0.717946689 | 1.195099705 |
| ENSG00000215639 | ENSG00000215639 subnetwork | 0.717631977 | 1.195114487 |
| ENSG00000106399 | RPA3 subnetwork | 0.833326818 | 1.195116554 |
| GO:0006312 | mitotic recombination | 0.804248677 | 1.195117982 |
| ENSG00000164975 | SNAPC3 subnetwork | 0.805513501 | 1.195124924 |
| GO:0016655 | oxidoreductase activity, acting on NADH or NADPH, quin | 0.836644926 | 1.195125894 |
| GO:0071347 | cellular response to interleukin-1 | 0.83602979 | 1.195126973 |
| ENSG00000092010 | PSME1 subnetwork | 0.833061392 | 1.19512987 |
| ENSG00000129965 | INS-IGF2 subnetwork | 0.71787421 | 1.195133144 |
| ENSG00000198018 | ENTPD7 subnetwork | 0.832471945 | 1.195155573 |
| MP:0002773 | decreased circulating luteinizing hormone level | 0.71283446 | 1.195156874 |
| GO:0008206 | bile acid metabolic process | 0.832752901 | 1.19515748 |
| GO:0030547 | receptor inhibitor activity | 0.711648584 | 1.19516 |
| GO:0031575 | mitotic cell cycle G1/S transition checkpoint | 0.832680684 | 1.195161925 |
| GO:0015108 | chloride transmembrane transporter activity | 0.832821805 | 1.195162878 |
| ENSG00000076053 | RBM7 subnetwork | 0.706671634 | 1.195167415 |
| GO:0032446 | protein modification by small protein conjugation | 0.707620971 | 1.195168333 |
| ENSG00000169020 | ATP5I subnetwork | 0.835791505 | 1.195174578 |
| ENSG00000000419 | DPM1 subnetwork | 0.833281171 | 1.195180012 |
| GO:0009060 | aerobic respiration | 0.836386857 | 1.195182789 |
| GO:0030903 | notochord development | 0.835877822 | 1.195184858 |
| REACTOME_PROCESSING_OF_CAI | REACTOME_PROCESSING_OF_CAPPED_INTRONLESS_PRI | 0.805476273 | 1.195190452 |
| MP:0000377 | abnormal hair follicle morphology | 0.706915177 | 1.195192086 |
| ENSG00000138675 | FGF5 subnetwork | 0.709250333 | 1.195195505 |
| GO:0005912 | adherens junction | 0.717085587 | 1.195195689 |
| ENSG00000138663 | COPS4 subnetwork | 0.717512262 | 1.195198413 |
| ENSG00000112049 | ENSG00000112049 subnetwork | 0.804229444 | 1.195209033 |
| MP:0005558 | decreased creatinine clearance | 0.706786387 | 1.19521399 |
| ENSG00000140481 | CCDC33 subnetwork | 0.805698876 | 1.195217303 |
| GO:0009219 | pyrimidine deoxyribonucleotide metabolic process | 0.836628636 | 1.195218499 |
| ENSG00000095380 | NANS subnetwork | 0.711349604 | 1.195220126 |
| MP:0002798 | abnormal active avoidance behavior | 0.70901906 | 1.195228263 |
| GO:0043178 | alcohol binding | 0.707575816 | 1.195230981 |
| GO:0071715 | icosanoid transport | 0.707087087 | 1.195233441 |
| MP:0002804 | abnormal motor learning | 0.83323813 | 1.195233645 |
| ENSG00000012061 | ERCC1 subnetwork | 0.832439926 | 1.195243722 |
| GO:0072012 | glomerulus vasculature development | 0.836025425 | 1.195244166 |
| GO:0061138 | morphogenesis of a branching epithelium | 0.706875743 | 1.195254803 |
| GO:0034284 | response to monosaccharide stimulus | 0.836486611 | 1.195256762 |
| GO:0043270 | positive regulation of ion transport | 0.71744826 | 1.195260234 |
| GO:0009635 | response to herbicide | 0.804643466 | 1.19526182 |
| GO:0019239 | deaminase activity | 0.716793223 | 1.19526728 |
| REACTOME_SYNTHESIS_SECRETIC | REACTOME_SYNTHESIS_SECRETION_AND_INACTIVATION | 0.804186562 | 1.195269583 |
| GO:0032376 | positive regulation of cholesterol transport | 0.706651739 | 1.195270426 |
| ENSG00000162517 | PEF1 subnetwork | 0.804470079 | 1.195271026 |
| ENSG00000122218 | COPA subnetwork | 0.711212825 | 1.195276221 |
| ENSG00000108294 | PSMB3 subnetwork | 0.804557926 | 1.195276591 |
| ENSG00000091106 | NLRC4 subnetwork | 0.836576871 | 1.195276825 |
| GO:0032592 | integral to mitochondrial membrane | 0.707530332 | 1.195282151 |
| GO:0007588 | excretion | 0.708498606 | 1.195282369 |
| ENSG00000211592 | ENSG00000211592 subnetwork | 0.716717941 | 1.195283768 |
| GO:0018200 | peptidyl-glutamic acid modification | 0.83239425 | 1.195287571 |
| ENSG00000165659 | DACH1 subnetwork | 0.711301759 | 1.195288198 |

| | | | |
|---|---|---|---|
| GO:0044460 | flagellum part | 0.835790942 | 1.19529181 |
| GO:0070161 | anchoring junction | 0.712833411 | 1.195293245 |
| GO:0042254 | ribosome biogenesis | 0.718556378 | 1.195295516 |
| GO:0048019 | receptor antagonist activity | 0.711648584 | 1.195296605 |
| ENSG00000102144 | PGK1 subnetwork | 0.709235478 | 1.195298165 |
| GO:0000413 | protein peptidyl-prolyl isomerization | 0.71154369 | 1.195301246 |
| ENSG00000158161 | EYA3 subnetwork | 0.709161182 | 1.195309095 |
| REACTOME_POST:ELONGATION_I | REACTOME_POST:ELONGATION_PROCESSING_OF_INTR( | 0.805476273 | 1.195311865 |
| MP:0009413 | skeletal muscle fiber atrophy | 0.717071574 | 1.195319946 |
| MP:0004363 | stria vascularis degeneration | 0.717419162 | 1.195327739 |
| MP:0001282 | short vibrissae | 0.804156546 | 1.195330145 |
| ENSG00000103502 | CDIPT subnetwork | 0.706261447 | 1.195331031 |
| GO:0005496 | steroid binding | 0.706079817 | 1.195335713 |
| ENSG00000103351 | CLUAP1 subnetwork | 0.83451346 | 1.195338442 |
| GO:0034104 | negative regulation of tissue remodeling | 0.835409121 | 1.195338567 |
| GO:0048678 | response to axon injury | 0.835674258 | 1.19534975 |
| GO:0000122 | negative regulation of transcription from RNA polymeras | 0.712772509 | 1.195349766 |
| GO:0030983 | mismatched DNA binding | 0.709013566 | 1.195353906 |
| GO:0032839 | dendrite cytoplasm | 0.830512898 | 1.195356297 |
| ENSG00000130307 | USHBP1 subnetwork | 0.805439936 | 1.195357107 |
| ENSG00000111450 | STX2 subnetwork | 0.806311662 | 1.195357215 |
| GO:0000082 | G1/S transition of mitotic cell cycle | 0.711618599 | 1.195358939 |
| GO:0010269 | response to selenium ion | 0.71258946 | 1.195365826 |
| GO:0007229 | integrin-mediated signaling pathway | 0.717372314 | 1.195372576 |
| REACTOME_PKA:MEDIATED_PHO | REACTOME_PKA:MEDIATED_PHOSPHORYLATION_OF_CI | 0.718525083 | 1.19537425 |
| MP:0000084 | abnormal fontanelle morphology | 0.708477018 | 1.195379405 |
| MP:0004014 | abnormal uterine environment | 0.832375187 | 1.1953856 |
| GO:0050930 | induction of positive chemotaxis | 0.711205143 | 1.19539579 |
| REACTOME_LAGGING_STRAND_S | REACTOME_LAGGING_STRAND_SYNTHESIS | 0.716632843 | 1.195396231 |
| GO:0051324 | prophase | 0.707514714 | 1.195396552 |
| MP:0002111 | abnormal tail morphology | 0.716704756 | 1.195402429 |
| MP:0000229 | abnormal megakaryocyte differentiation | 0.706212742 | 1.195405343 |
| GO:0032373 | positive regulation of sterol transport | 0.706651739 | 1.195407987 |
| GO:0044442 | microtubule-based flagellum part | 0.835790942 | 1.195409064 |
| GO:0006900 | membrane budding | 0.805391389 | 1.195412518 |
| ENSG00000102312 | PORCN subnetwork | 0.709567472 | 1.195420154 |
| ENSG00000141622 | RNF165 subnetwork | 0.716953709 | 1.195421017 |
| ENSG00000143226 | FCGR2A subnetwork | 0.718668243 | 1.195426242 |
| ENSG00000164105 | SAP30 subnetwork | 0.834488875 | 1.19542641 |
| GO:0016874 | ligase activity | 0.712743227 | 1.195429126 |
| GO:0048729 | tissue morphogenesis | 0.830400976 | 1.195429418 |
| GO:0035411 | catenin import into nucleus | 0.830484636 | 1.195429869 |
| MP:0000062 | increased bone mineral density | 0.711542428 | 1.195437914 |
| REACTOME_S_PHASE | REACTOME_S_PHASE | 0.83115438 | 1.195438406 |
| GO:0055017 | cardiac muscle tissue growth | 0.717055028 | 1.195438557 |
| ENSG00000138674 | SEC31A subnetwork | 0.831413042 | 1.195444236 |
| MP:0000690 | absent spleen | 0.804148684 | 1.195446683 |
| ENSG00000198807 | PAX9 subnetwork | 0.834174539 | 1.195449184 |
| ENSG00000116641 | DOCK7 subnetwork | 0.717334313 | 1.195451452 |
| GO:0035254 | glutamate receptor binding | 0.835642206 | 1.195452316 |
| ENSG00000163541 | SUCLG1 subnetwork | 0.80618627 | 1.1954527 |
| GO:0045833 | negative regulation of lipid metabolic process | 0.832336761 | 1.195454098 |
| ENSG00000065154 | OAT subnetwork | 0.835406964 | 1.195455884 |
| GO:0016226 | iron-sulfur cluster assembly | 0.831733774 | 1.19545589 |

| | | | |
|---|---|---|---|
| ENSG00000147050 | KDM6A subnetwork | 0.711158758 | 1.195458186 |
| GO:0000779 | condensed chromosome, centromeric region | 0.832257311 | 1.195458576 |
| GO:0043277 | apoptotic cell clearance | 0.831322408 | 1.195468442 |
| MP:0009767 | decreased sensitivity to xenobiotic induced morbidity/m | 0.834268066 | 1.195469287 |
| GO:0080111 | DNA demethylation | 0.718490948 | 1.195469989 |
| MP:0003331 | hepatocellular carcinoma | 0.70607696 | 1.195473393 |
| GO:0008376 | acetylgalactosaminyltransferase activity | 0.830363635 | 1.195473393 |
| ENSG00000197275 | RAD54B subnetwork | 0.804110336 | 1.195476748 |
| GO:0030291 | protein serine/threonine kinase inhibitor activity | 0.806308998 | 1.195478534 |
| REACTOME_GAP:FILLING_DNA_R | REACTOME_GAP:FILLING_DNA_REPAIR_SYNTHESIS_AND | 0.834458992 | 1.195480004 |
| ENSG00000111581 | NUP107 subnetwork | 0.804892001 | 1.195480887 |
| ENSG00000108797 | CNTNAP1 subnetwork | 0.830290629 | 1.19548282 |
| ENSG00000092330 | TINF2 subnetwork | 0.709002435 | 1.195485314 |
| REACTOME_TRANSCRIPTION | REACTOME_TRANSCRIPTION | 0.831131011 | 1.195487276 |
| ENSG00000121653 | MAPK8IP1 subnetwork | 0.708354507 | 1.195487427 |
| ENSG00000124356 | STAMBP subnetwork | 0.832179179 | 1.195487685 |
| GO:0010594 | regulation of endothelial cell migration | 0.707486714 | 1.195487987 |
| MP:0004263 | abnormal limb posture | 0.832106546 | 1.195492167 |
| GO:0051603 | proteolysis involved in cellular protein catabolic process | 0.707396525 | 1.195493217 |
| GO:0010226 | response to lithium ion | 0.708710635 | 1.195495237 |
| ENSG00000128654 | MTX2 subnetwork | 0.831028563 | 1.195496695 |
| ENSG00000164403 | SHROOM1 subnetwork | 0.835235759 | 1.195499166 |
| GO:0032201 | telomere maintenance via semi-conservative replication | 0.831598681 | 1.195504289 |
| GO:0005487 | nucleocytoplasmic transporter activity | 0.708465947 | 1.195505166 |
| GO:0002446 | neutrophil mediated immunity | 0.834709573 | 1.195505894 |
| GO:0051453 | regulation of intracellular pH | 0.830951114 | 1.195506117 |
| ENSG00000162688 | AGL subnetwork | 0.718430305 | 1.195509118 |
| ENSG00000127920 | GNG11 subnetwork | 0.709543159 | 1.195511351 |
| ENSG00000100596 | SPTLC2 subnetwork | 0.803915357 | 1.195516083 |
| GO:0045737 | positive regulation of cyclin-dependent protein kinase ac | 0.708942193 | 1.19551922 |
| GO:0033205 | cell cycle cytokinesis | 0.835355629 | 1.195524146 |
| MP:0002082 | postnatal lethality | 0.835622364 | 1.19553037 |
| REACTOME_SWITCHING_OF_ORI | REACTOME_SWITCHING_OF_ORIGINS_TO_A_POST:REPL | 0.804037434 | 1.195532261 |
| MP:0004221 | abnormal iridocorneal angle | 0.80538914 | 1.19553399 |
| ENSG00000110955 | ATP5B subnetwork | 0.708848387 | 1.195535919 |
| GO:0000271 | polysaccharide biosynthetic process | 0.706649373 | 1.195539825 |
| REACTOME_FGFR3_LIGAND_BIN | REACTOME_FGFR3_LIGAND_BINDING_AND_ACTIVATION | 0.806170477 | 1.195548675 |
| ENSG00000158864 | NDUFS2 subnetwork | 0.831900697 | 1.195559827 |
| ENSG00000125870 | SNRPB2 subnetwork | 0.718402584 | 1.195570911 |
| ENSG00000076003 | MCM6 subnetwork | 0.83515512 | 1.195571919 |
| GO:0031163 | metallo-sulfur cluster assembly | 0.831733774 | 1.195573738 |
| GO:0060612 | adipose tissue development | 0.711135583 | 1.195577803 |
| ENSG00000171747 | LGALS4 subnetwork | 0.707363979 | 1.195578935 |
| ENSG00000164418 | GRIK2 subnetwork | 0.830912897 | 1.195584608 |
| ENSG00000115310 | RTN4 subnetwork | 0.83201984 | 1.195584902 |
| MP:0005215 | abnormal pancreatic islet morphology | 0.832087741 | 1.195590264 |
| REACTOME_GAP:FILLING_DNA_R | REACTOME_GAP:FILLING_DNA_REPAIR_SYNTHESIS_AND | 0.834458992 | 1.195597484 |
| MP:0002801 | abnormal long term object recognition memory | 0.709773413 | 1.195598349 |
| GO:0008528 | G-protein coupled peptide receptor activity | 0.830289974 | 1.195600869 |
| ENSG00000128709 | HOXD9 subnetwork | 0.831572077 | 1.195602445 |
| GO:0042554 | superoxide anion generation | 0.835223878 | 1.195611624 |
| GO:0034285 | response to disaccharide stimulus | 0.706607307 | 1.195625648 |
| ENSG00000147509 | RGS20 subnetwork | 0.803895686 | 1.195627609 |
| ENSG00000173660 | UQCRH subnetwork | 0.835115214 | 1.195630401 |

| | | | |
|---|---|---|---|
| GO:0070003 | threonine-type peptidase activity | 0.803641204 | 1.195631365 |
| ENSG00000172638 | EFEMP2 subnetwork | 0.830242291 | 1.195644875 |
| REACTOME_ORC1_REMOVAL_FR( | REACTOME_ORC1_REMOVAL_FROM_CHROMATIN | 0.804037434 | 1.195653944 |
| ENSG00000090372 | STRN4 subnetwork | 0.830146074 | 1.195654321 |
| ENSG00000089597 | GANAB subnetwork | 0.805374159 | 1.195655488 |
| GO:0050679 | positive regulation of epithelial cell proliferation | 0.803519154 | 1.195661031 |
| GO:0006901 | vesicle coating | 0.83490431 | 1.195663491 |
| ENSG00000212915 | ENSG00000212915 subnetwork | 0.803857783 | 1.195667888 |
| REACTOME_FGFR3C_LIGAND_BIN | REACTOME_FGFR3C_LIGAND_BINDING_AND_ACTIVATIC | 0.806170477 | 1.195670051 |
| GO:0033687 | osteoblast proliferation | 0.803448924 | 1.195670775 |
| MP:0002626 | increased heart rate | 0.709927758 | 1.195673848 |
| GO:0051496 | positive regulation of stress fiber assembly | 0.805111059 | 1.19568466 |
| ENSG00000171314 | PGAM1 subnetwork | 0.711126333 | 1.195686005 |
| GO:0034470 | ncRNA processing | 0.805222316 | 1.195695263 |
| GO:0010830 | regulation of myotube differentiation | 0.830908332 | 1.195702585 |
| ENSG00000196730 | DAPK1 subnetwork | 0.709880699 | 1.195707736 |
| GO:0034661 | ncRNA catabolic process | 0.803783477 | 1.195708176 |
| ENSG00000164733 | CTSB subnetwork | 0.829965833 | 1.195717673 |
| ENSG00000136044 | APPL2 subnetwork | 0.806130855 | 1.195725454 |
| GO:0048566 | embryonic digestive tract development | 0.829867897 | 1.195737008 |
| ENSG00000057294 | PKP2 subnetwork | 0.711059757 | 1.195742733 |
| ENSG00000152256 | PDK1 subnetwork | 0.835113691 | 1.195747815 |
| GO:0048066 | developmental pigmentation | 0.83086574 | 1.195751505 |
| ENSG00000197818 | SLC9A8 subnetwork | 0.830127522 | 1.195752667 |
| GO:0004298 | threonine-type endopeptidase activity | 0.803641204 | 1.195753132 |
| GO:0006364 | rRNA processing | 0.805359025 | 1.195761764 |
| REACTOME_ADP_SIGNALLING_TH | REACTOME_ADP_SIGNALLING_THROUGH_P2Y_PURINO( | 0.720283899 | 1.195762233 |
| GO:0009744 | response to sucrose stimulus | 0.706607307 | 1.195763297 |
| GO:0008013 | beta-catenin binding | 0.710860738 | 1.195764652 |
| GO:0015721 | bile acid and bile salt transport | 0.803436154 | 1.195767115 |
| GO:0030301 | cholesterol transport | 0.807463653 | 1.195767437 |
| ENSG00000164695 | CHMP4C subnetwork | 0.720488875 | 1.195785787 |
| GO:0070306 | lens fiber cell differentiation | 0.710087316 | 1.195788931 |
| GO:0030501 | positive regulation of bone mineralization | 0.829700143 | 1.195805336 |
| ENSG00000141252 | VPS53 subnetwork | 0.829844836 | 1.195825511 |
| MP:0004321 | short sternum | 0.807422536 | 1.195832911 |
| KEGG_ECM_RECEPTOR_INTERACT | KEGG_ECM_RECEPTOR_INTERACTION | 0.8075974 | 1.195833756 |
| GO:0051248 | negative regulation of protein metabolic process | 0.711039641 | 1.19583381 |
| GO:0001774 | microglial cell activation | 0.829646618 | 1.19583951 |
| ENSG00000184895 | SRY subnetwork | 0.835101718 | 1.195840699 |
| ENSG00000132693 | CRP subnetwork | 0.803385705 | 1.195843097 |
| ENSG00000117707 | PROX1 subnetwork | 0.719870328 | 1.19584464 |
| ENSG00000131475 | VPS25 subnetwork | 0.806892378 | 1.195850244 |
| GO:0030336 | negative regulation of cell migration | 0.807352284 | 1.195852768 |
| MP:0011107 | partial embryonic lethality before turning of embryo | 0.710266909 | 1.195852904 |
| ENSG00000148308 | GTF3C5 subnetwork | 0.720444911 | 1.195858757 |
| GO:0034364 | high-density lipoprotein particle | 0.719015119 | 1.195862576 |
| MP:0009431 | decreased fetal weight | 0.719802618 | 1.195872441 |
| GO:0006403 | RNA localization | 0.710836714 | 1.195878649 |
| GO:0033137 | negative regulation of peptidyl-serine phosphorylation | 0.806989546 | 1.195886172 |
| GO:0008542 | visual learning | 0.720273773 | 1.195891727 |
| GO:0007264 | small GTPase mediated signal transduction | 0.720065927 | 1.19589645 |
| ENSG00000198780 | FAM169A subnetwork | 0.719995519 | 1.195907292 |
| ENSG00000132773 | TOE1 subnetwork | 0.710590265 | 1.195928768 |

| | | | |
|---|---|---|---|
| GO:0019861 | flagellum | 0.71924133 | 1.195931417 |
| MP:0009549 | decreased platelet aggregation | 0.829613383 | 1.195932991 |
| GO:0032924 | activin receptor signaling pathway | 0.803366958 | 1.195934379 |
| KEGG_VALINE_LEUCINE_AND_ISC | KEGG_VALINE_LEUCINE_AND_ISOLEUCINE_DEGRADATIC | 0.806877768 | 1.195941147 |
| GO:0071230 | cellular response to amino acid stimulus | 0.710790969 | 1.195952599 |
| GO:0009991 | response to extracellular stimulus | 0.807340901 | 1.195958828 |
| GO:0031032 | actomyosin structure organization | 0.828995227 | 1.195959446 |
| GO:0030246 | carbohydrate binding | 0.827157382 | 1.195971259 |
| GO:0035601 | protein deacylation | 0.710261449 | 1.19597846 |
| GO:0030262 | apoptotic nuclear change | 0.829336023 | 1.195980819 |
| MP:0001560 | abnormal circulating insulin level | 0.827611515 | 1.195982762 |
| KEGG_SPHINGOLIPID_METABOLIS | KEGG_SPHINGOLIPID_METABOLISM | 0.812806056 | 1.195984482 |
| ENSG00000131910 | NR0B2 subnetwork | 0.829254632 | 1.195995254 |
| GO:0071824 | protein-DNA complex subunit organization | 0.803318149 | 1.196000204 |
| MP:0001700 | abnormal embryo turning | 0.710430634 | 1.196002291 |
| GO:0050321 | tau-protein kinase activity | 0.721364912 | 1.196004064 |
| ENSG00000143627 | PKLR subnetwork | 0.72024274 | 1.196004295 |
| ENSG00000171560 | FGA subnetwork | 0.71979277 | 1.196007691 |
| GO:0002244 | hemopoietic progenitor cell differentiation | 0.82920162 | 1.196009691 |
| GO:0008417 | fucosyltransferase activity | 0.827332613 | 1.196011297 |
| MP:0003743 | abnormal facial morphology | 0.71946929 | 1.196011541 |
| GO:0051298 | centrosome duplication | 0.720691042 | 1.196012201 |
| GO:0008483 | transaminase activity | 0.829599657 | 1.196016606 |
| MP:0005591 | decreased vasodilation | 0.710561496 | 1.196025656 |
| ENSG00000107554 | DNMBP subnetwork | 0.828965887 | 1.196028292 |
| MP:0001340 | abnormal eyelid morphology | 0.721276687 | 1.196031836 |
| MP:0001730 | embryonic growth arrest | 0.719221785 | 1.196032824 |
| GO:0008637 | apoptotic mitochondrial changes | 0.827465117 | 1.196036465 |
| ENSG00000120071 | KIAA1267 subnetwork | 0.710759618 | 1.196038017 |
| MP:0001921 | reduced fertility | 0.828885534 | 1.196042738 |
| ENSG00000119969 | HELLS subnetwork | 0.807334771 | 1.196054767 |
| ENSG00000185973 | TMLHE subnetwork | 0.801076276 | 1.19605559 |
| GO:0015986 | ATP synthesis coupled proton transport | 0.803277398 | 1.19605585 |
| REACTOME_E2F:ENABLED_INHIBI | REACTOME_E2F:ENABLED_INHIBITION_OF_PRE:REPLICA | 0.827131208 | 1.196060065 |
| ENSG00000159063 | ALG8 subnetwork | 0.719644631 | 1.196063348 |
| ENSG00000104368 | PLAT subnetwork | 0.829157459 | 1.196068638 |
| REACTOME_DESTABILIZATION_OI | REACTOME_DESTABILIZATION_OF_MRNA_BY_KSRP | 0.71974606 | 1.196069449 |
| GO:0045851 | pH reduction | 0.828509475 | 1.196070474 |
| GO:0055088 | lipid homeostasis | 0.719412376 | 1.196073328 |
| ENSG00000130203 | APOE subnetwork | 0.812784129 | 1.196074776 |
| MP:0002188 | small heart | 0.812951875 | 1.196075567 |
| MP:0000445 | short snout | 0.813037316 | 1.196075962 |
| MP:0002730 | head shaking | 0.827608685 | 1.196076489 |
| ENSG00000162961 | DPY30 subnetwork | 0.72148665 | 1.196077878 |
| ENSG00000121741 | ZMYM2 subnetwork | 0.719572136 | 1.196079873 |
| GO:0008023 | transcription elongation factor complex | 0.721060977 | 1.196086957 |
| ENSG00000009830 | POMT2 subnetwork | 0.828147123 | 1.196098624 |
| ENSG00000091140 | DLD subnetwork | 0.812696526 | 1.196109655 |
| ENSG00000142655 | PEX14 subnetwork | 0.829590084 | 1.196110123 |
| GO:0010669 | epithelial structure maintenance | 0.828870609 | 1.196116553 |
| GO:0048471 | perinuclear region of cytoplasm | 0.720983612 | 1.196126045 |
| MP:0003858 | enhanced coordination | 0.826878313 | 1.196127913 |
| ENSG00000175634 | RPS6KB2 subnetwork | 0.827096229 | 1.196129064 |
| MP:0003290 | intestinal hypoperistalsis | 0.803179069 | 1.196131498 |

| | | | |
|---|---|---|---|
| GO:0032608 | interferon-beta production | 0.828456981 | 1.196134429 |
| GO:0051851 | modification by host of symbiont morphology or physiol | 0.721184476 | 1.196138211 |
| MP:0002647 | decreased intestinal cholesterol absorption | 0.812557603 | 1.196144153 |
| GO:0042594 | response to starvation | 0.807320991 | 1.196155797 |
| ENSG00000111711 | GOLT1B subnetwork | 0.72093093 | 1.196159494 |
| MP:0004351 | short humerus | 0.828726999 | 1.196160317 |
| MP:0008221 | abnormal hippocampal commissure morphology | 0.721276354 | 1.196161228 |
| MP:0009254 | disorganized pancreatic islets | 0.82811016 | 1.196167558 |
| MP:0002187 | abnormal fibula morphology | 0.828822552 | 1.196175539 |
| GO:0015985 | energy coupled proton transport, down electrochemical | 0.803277398 | 1.19617776 |
| ENSG00000165702 | GFI1B subnetwork | 0.80107532 | 1.196177823 |
| GO:0032269 | negative regulation of cellular protein metabolic process | 0.829506577 | 1.196178942 |
| MP:0004763 | absent brainstem auditory evoked potential | 0.812485781 | 1.196189132 |
| MP:0000164 | abnormal cartilage development | 0.802671492 | 1.19619543 |
| MP:0008034 | enhanced lipolysis | 0.827841672 | 1.196196137 |
| GO:0000083 | regulation of transcription involved in G1/S phase of mit | 0.813258532 | 1.19619724 |
| MP:0004214 | abnormal long bone diaphysis morphology | 0.826851271 | 1.196206862 |
| ENSG00000116213 | WRAP73 subnetwork | 0.812681491 | 1.196210059 |
| MP:0002176 | increased brain weight | 0.807269526 | 1.196221343 |
| REACTOME_PROTEOLYTIC_CLEAV | REACTOME_PROTEOLYTIC_CLEAVAGE_OF_SNARE_COM | 0.82868635 | 1.196224268 |
| GO:0016254 | preassembly of GPI anchor in ER membrane | 0.809735882 | 1.196227369 |
| REACTOME_M_PHASE | REACTOME_M_PHASE | 0.826567321 | 1.196230533 |
| ENSG00000044524 | EPHA3 subnetwork | 0.827088625 | 1.196232775 |
| GO:0030730 | sequestering of triglyceride | 0.803151598 | 1.196233051 |
| ENSG00000003436 | TFPI subnetwork | 0.812418276 | 1.196249244 |
| GO:0006875 | cellular metal ion homeostasis | 0.828456739 | 1.196252846 |
| ENSG00000025796 | SEC63 subnetwork | 0.813382002 | 1.196253022 |
| ENSG00000105700 | KXD1 subnetwork | 0.826511467 | 1.19625496 |
| GO:0001659 | temperature homeostasis | 0.809813616 | 1.196258091 |
| MP:0002813 | microcytosis | 0.813485066 | 1.196268506 |
| GO:0006120 | mitochondrial electron transport, NADH to ubiquinone | 0.827052718 | 1.19627206 |
| GO:0040014 | regulation of multicellular organism growth | 0.828108613 | 1.196281074 |
| GO:0001836 | release of cytochrome c from mitochondria | 0.828395664 | 1.196292079 |
| MP:0000877 | abnormal Purkinje cell morphology | 0.802802778 | 1.196292708 |
| ENSG00000161681 | SHANK1 subnetwork | 0.803087481 | 1.196293842 |
| GO:0005788 | endoplasmic reticulum lumen | 0.801070768 | 1.196300082 |
| ENSG00000197263 | OR8D2 subnetwork | 0.80266359 | 1.196307253 |
| ENSG00000134909 | ARHGAP32 subnetwork | 0.826762856 | 1.196310256 |
| GO:0006004 | fucose metabolic process | 0.826834269 | 1.196315581 |
| MP:0001157 | small seminal vesicle | 0.809613468 | 1.196322711 |
| ENSG00000175582 | RAB6A subnetwork | 0.809719442 | 1.196328141 |
| GO:0005104 | fibroblast growth factor receptor binding | 0.826483832 | 1.196333962 |
| ENSG00000171700 | RGS19 subnetwork | 0.801576968 | 1.196343207 |
| GO:0051650 | establishment of vesicle localization | 0.811362576 | 1.196355008 |
| ENSG00000196586 | MYO6 subnetwork | 0.80167807 | 1.196358901 |
| GO:0080135 | regulation of cellular response to stress | 0.828076054 | 1.196359945 |
| ENSG00000148965 | SAA4 subnetwork | 0.81241403 | 1.196364828 |
| GO:0009629 | response to gravity | 0.826322996 | 1.19637789 |
| MP:0008026 | abnormal brain white matter morphology | 0.809543461 | 1.196377985 |
| ENSG00000177963 | RIC8A subnetwork | 0.801039501 | 1.196381478 |
| KEGG_GLYCEROLIPID_METABOLIS | KEGG_GLYCEROLIPID_METABOLISM | 0.810940309 | 1.196383838 |
| GO:0031638 | zymogen activation | 0.813665002 | 1.196389728 |
| GO:0019882 | antigen processing and presentation | 0.809177797 | 1.196396761 |
| GO:0030018 | Z disc | 0.808907486 | 1.196400365 |

| | | | |
|---|---|---|---|
| ENSG00000180818 | HOXC10 subnetwork | 0.802641198 | 1.196403795 |
| GO:0016628 | oxidoreductase activity, acting on the CH-CH group of do | 0.80300579 | 1.196405262 |
| ENSG00000136813 | KIAA0368 subnetwork | 0.80308059 | 1.196405629 |
| GO:0072075 | metanephric mesenchyme development | 0.810789777 | 1.196408365 |
| MP:0001199 | thin skin | 0.802576787 | 1.19640853 |
| GO:0008173 | RNA methyltransferase activity | 0.811184627 | 1.196414866 |
| ENSG00000067057 | PFKP subnetwork | 0.81235524 | 1.196414885 |
| GO:0035102 | PRC1 complex | 0.826466963 | 1.19641794 |
| GO:0002009 | morphogenesis of an epithelium | 0.826280146 | 1.196432116 |
| MP:0004948 | abnormal neuronal precursor proliferation | 0.801564052 | 1.196434774 |
| GO:0007369 | gastrulation | 0.809139152 | 1.196441948 |
| MP:0009674 | decreased birth weight | 0.801998618 | 1.196457014 |
| REACTOME_NEGATIVE_REGULATI | REACTOME_NEGATIVE_REGULATION_OF_FGFR_SIGNALI | 0.802362297 | 1.196458461 |
| MP:0004434 | abnormal cochlear outer hair cell physiology | 0.801925052 | 1.196461758 |
| GO:0007005 | mitochondrion organization | 0.810910712 | 1.196464289 |
| GO:0045295 | gamma-catenin binding | 0.811346745 | 1.196465717 |
| GO:0006904 | vesicle docking involved in exocytosis | 0.811115045 | 1.196470054 |
| GO:0015918 | sterol transport | 0.811511614 | 1.196471479 |
| GO:0015299 | solute:hydrogen antiporter activity | 0.80208509 | 1.19647269 |
| GO:0030032 | lamellipodium assembly | 0.801013674 | 1.196473114 |
| GO:0001919 | regulation of receptor recycling | 0.802545115 | 1.196479592 |
| MP:0006108 | abnormal hindbrain development | 0.810577219 | 1.196483072 |
| ENSG00000139637 | C12orf10 subnetwork | 0.809539756 | 1.19648892 |
| GO:0009746 | response to hexose stimulus | 0.826229429 | 1.196491315 |
| ENSG00000136160 | EDNRB subnetwork | 0.800966421 | 1.196493201 |
| ENSG00000111667 | USP5 subnetwork | 0.81232923 | 1.196495209 |
| GO:0005771 | multivesicular body | 0.808879075 | 1.196506329 |
| GO:0043114 | regulation of vascular permeability | 0.810775575 | 1.196509043 |
| ENSG00000095564 | BTAF1 subnetwork | 0.802451484 | 1.196514951 |
| GO:0055021 | regulation of cardiac muscle tissue growth | 0.812254655 | 1.196515029 |
| MP:0002428 | abnormal semicircular canal morphology | 0.813825366 | 1.19651596 |
| GO:0042158 | lipoprotein biosynthetic process | 0.810296759 | 1.196517036 |
| ENSG00000126267 | COX6B1 subnetwork | 0.809122446 | 1.196527637 |
| MP:0006085 | myocardial necrosis | 0.72356773 | 1.196537162 |
| KEGG_AMINOACYL_TRNA_BIOSYI | KEGG_AMINOACYL_TRNA_BIOSYNTHESIS | 0.811657278 | 1.196537802 |
| ENSG00000113318 | MSH3 subnetwork | 0.825770099 | 1.196544191 |
| KEGG_ARGININE_AND_PROLINE_ | KEGG_ARGININE_AND_PROLINE_METABOLISM | 0.811986698 | 1.196544244 |
| GO:0009083 | branched chain family amino acid catabolic process | 0.800931234 | 1.19654908 |
| ENSG00000179801 | ENSG00000179801 subnetwork | 0.80156044 | 1.1965519 |
| MP:0001056 | abnormal cranial nerve morphology | 0.802340009 | 1.196555068 |
| REACTOME_ANTIGEN_PROCESSIN | REACTOME_ANTIGEN_PROCESSING:CROSS_PRESENTATI | 0.810212388 | 1.196557128 |
| ENSG00000149743 | TRPT1 subnetwork | 0.800777163 | 1.196563714 |
| ENSG00000101849 | TBL1X subnetwork | 0.799565951 | 1.196563908 |
| GO:0007517 | muscle organ development | 0.811616238 | 1.196567737 |
| GO:0006367 | transcription initiation from RNA polymerase II promote | 0.801918545 | 1.196568627 |
| GO:0033121 | regulation of purine nucleotide catabolic process | 0.809497344 | 1.19656952 |
| ENSG00000135604 | STX11 subnetwork | 0.825705801 | 1.196578608 |
| GO:0030964 | NADH dehydrogenase complex | 0.799464502 | 1.19657892 |
| GO:0000780 | condensed nuclear chromosome, centromeric region | 0.810472149 | 1.196583443 |
| ENSG00000173120 | KDM2A subnetwork | 0.826211041 | 1.196590232 |
| GO:0040020 | regulation of meiosis | 0.812217191 | 1.196590336 |
| GO:0010737 | protein kinase A signaling cascade | 0.808860946 | 1.19659206 |
| MP:0009746 | enhanced behavioral response to xenobiotic | 0.810570732 | 1.196593895 |
| MP:0001244 | thin dermal layer | 0.808271523 | 1.196594364 |

| | | | |
|---|---|---|---|
| GO:0014821 | phasic smooth muscle contraction | 0.825535043 | 1.196597795 |
| GO:0050764 | regulation of phagocytosis | 0.808389278 | 1.196600122 |
| GO:0050909 | sensory perception of taste | 0.808712815 | 1.196601499 |
| GO:0016769 | transferase activity, transferring nitrogenous groups | 0.723735587 | 1.196605112 |
| GO:0035050 | embryonic heart tube development | 0.809100037 | 1.196608282 |
| GO:0031667 | response to nutrient levels | 0.800857437 | 1.196610083 |
| GO:0044070 | regulation of anion transport | 0.808804245 | 1.196611972 |
| GO:0000139 | Golgi membrane | 0.810755177 | 1.196614794 |
| ENSG00000103043 | VAC14 subnetwork | 0.812138506 | 1.196615214 |
| ENSG00000124702 | KLHDC3 subnetwork | 0.811769028 | 1.196628987 |
| ENSG00000188763 | FZD9 subnetwork | 0.825478174 | 1.196632227 |
| GO:0045807 | positive regulation of endocytosis | 0.810175357 | 1.196637678 |
| ENSG00000011485 | PPP5C subnetwork | 0.825301333 | 1.196646463 |
| GO:0051917 | regulation of fibrinolysis | 0.801515015 | 1.196648616 |
| ENSG00000136158 | SPRY2 subnetwork | 0.800735797 | 1.196650302 |
| ENSG00000120805 | ARL1 subnetwork | 0.802304559 | 1.196651695 |
| ENSG00000063245 | EPN1 subnetwork | 0.81197175 | 1.196654894 |
| MP:0003225 | axonal dystrophy | 0.723564565 | 1.19666066 |
| GO:0032925 | regulation of activin receptor signaling pathway | 0.724434408 | 1.196664792 |
| ENSG00000072849 | DERL2 subnetwork | 0.800667924 | 1.196670417 |
| GO:0015629 | actin cytoskeleton | 0.825137075 | 1.196670642 |
| ENSG00000008853 | RHOBTB2 subnetwork | 0.808672269 | 1.19667207 |
| ENSG00000198561 | CTNND1 subnetwork | 0.825682386 | 1.196672626 |
| GO:0090183 | regulation of kidney development | 0.810465488 | 1.196684189 |
| REACTOME_NUCLEOTIDE:LIKE_PU | REACTOME_NUCLEOTIDE:LIKE_PURINERGIC_RECEPTORS | 0.811891868 | 1.196684832 |
| GO:0030811 | regulation of nucleotide catabolic process | 0.809497344 | 1.196690618 |
| GO:0061136 | regulation of proteasomal protein catabolic process | 0.825046718 | 1.19669516 |
| GO:0005747 | mitochondrial respiratory chain complex I | 0.799464502 | 1.196701496 |
| GO:0051184 | cofactor transporter activity | 0.784169841 | 1.196703526 |
| GO:0002080 | acrosomal membrane | 0.826210728 | 1.196709024 |
| GO:0051924 | regulation of calcium ion transport | 0.824979136 | 1.196709742 |
| ENSG00000120253 | NUP43 subnetwork | 0.808547174 | 1.196711926 |
| REACTOME_ACTIVATION_OF_CA: | REACTOME_ACTIVATION_OF_CA:PERMEABLE_KAINATE_ | 0.723910152 | 1.196712822 |
| ENSG00000196517 | SLC6A9 subnetwork | 0.800613303 | 1.196721228 |
| GO:0051297 | centrosome organization | 0.808388856 | 1.196721395 |
| ENSG00000179262 | RAD23A subnetwork | 0.783990962 | 1.196723706 |
| ENSG00000106123 | EPHB6 subnetwork | 0.724329755 | 1.196737174 |
| GO:0005776 | autophagic vacuole | 0.724761343 | 1.196744631 |
| GO:0000803 | sex chromosome | 0.82527747 | 1.196750472 |
| ENSG00000116984 | MTR subnetwork | 0.825476586 | 1.196751118 |
| REACTOME_SIGNAL_REGULATOR | REACTOME_SIGNAL_REGULATORY_PROTEIN_SIRP_FAM | 0.724179943 | 1.19675332 |
| GO:0042157 | lipoprotein metabolic process | 0.784122555 | 1.196755347 |
| MP:0005605 | increased bone mass | 0.724260882 | 1.196759311 |
| GO:0016411 | acylglycerol O-acyltransferase activity | 0.723545982 | 1.196761658 |
| ENSG00000057663 | ATG5 subnetwork | 0.722240361 | 1.19676746 |
| GO:0009108 | coenzyme biosynthetic process | 0.808654384 | 1.196767984 |
| GO:0010043 | response to zinc ion | 0.824318515 | 1.196771787 |
| GO:0015893 | drug transport | 0.826058599 | 1.196772912 |
| ENSG00000122122 | SASH3 subnetwork | 0.72442413 | 1.19678254 |
| MP:0009146 | abnormal pancreatic acinar cell morphology | 0.82617874 | 1.196783161 |
| GO:0060768 | regulation of epithelial cell proliferation involved in pros | 0.773868444 | 1.196788845 |
| ENSG00000110422 | HIPK3 subnetwork | 0.724598861 | 1.196788888 |
| ENSG00000021574 | SPAST subnetwork | 0.824264979 | 1.196791364 |
| ENSG00000206349 | ENSG00000206349 subnetwork | 0.723363825 | 1.196800361 |

| | | | |
|---|---|---|---|
| MP:0002108 | abnormal muscle morphology | 0.824108003 | 1.196800677 |
| GO:0042147 | retrograde transport, endosome to Golgi | 0.797760027 | 1.196807309 |
| MP:0003620 | oliguria | 0.824958879 | 1.196808828 |
| MP:0009400 | decreased skeletal muscle fiber size | 0.722158247 | 1.196812232 |
| ENSG00000168454 | TXNDC2 subnetwork | 0.814104988 | 1.196818365 |
| GO:0045271 | respiratory chain complex I | 0.799464502 | 1.196824096 |
| REACTOME_DIABETES_PATHWAY | REACTOME_DIABETES_PATHWAYS | 0.725057259 | 1.196835656 |
| GO:0001837 | epithelial to mesenchymal transition | 0.724137362 | 1.196837366 |
| ENSG00000124422 | USP22 subnetwork | 0.783982496 | 1.196838151 |
| ENSG00000198888 | MT-ND1 subnetwork | 0.800606325 | 1.196838551 |
| ENSG00000122679 | RAMP3 subnetwork | 0.822889995 | 1.196840741 |
| GO:0008527 | taste receptor activity | 0.724734803 | 1.196845479 |
| REACTOME_IONOTROPIC_ACTIVI | REACTOME_IONOTROPIC_ACTIVITY_OF_KAINATE_RECEI | 0.723910152 | 1.196847557 |
| ENSG00000075142 | SRI subnetwork | 0.79745095 | 1.196862483 |
| ENSG00000168872 | DDX19A subnetwork | 0.822513252 | 1.196864094 |
| ENSG00000134259 | NGF subnetwork | 0.728138309 | 1.196865204 |
| ENSG00000211619 | ENSG00000211619 subnetwork | 0.798919077 | 1.196868273 |
| ENSG00000113300 | CNOT6 subnetwork | 0.773828319 | 1.196873019 |
| ENSG00000130066 | SAT1 subnetwork | 0.824068625 | 1.196875 |
| MP:0008825 | abnormal cardiac epithelial to mesenchymal transition | 0.823950616 | 1.196884642 |
| GO:0043001 | Golgi to plasma membrane protein transport | 0.823668644 | 1.19688869 |
| ENSG00000124795 | DEK subnetwork | 0.82425112 | 1.196890547 |
| GO:0047496 | vesicle transport along microtubule | 0.824913839 | 1.19689302 |
| MP:0000276 | heart right ventricle hypertrophy | 0.723544335 | 1.196896474 |
| ENSG00000181104 | F2R subnetwork | 0.799901451 | 1.196897081 |
| ENSG00000122034 | GTF3A subnetwork | 0.797718294 | 1.196899384 |
| GO:0045823 | positive regulation of heart contraction | 0.722398968 | 1.196903204 |
| GO:0006457 | protein folding | 0.724074518 | 1.196904548 |
| MP:0002239 | abnormal nasal septum morphology | 0.799410327 | 1.196905738 |
| GO:0016529 | sarcoplasmic reticulum | 0.797565438 | 1.196909016 |
| ENSG00000135631 | RAB11FIP5 subnetwork | 0.822200934 | 1.196922693 |
| ENSG00000213905 | ENSG00000213905 subnetwork | 0.722137614 | 1.196924726 |
| ENSG00000139190 | VAMP1 subnetwork | 0.823096282 | 1.196926066 |
| GO:0072203 | cell proliferation involved in metanephros development | 0.728079801 | 1.196926436 |
| GO:0006023 | aminoglycan biosynthetic process | 0.800020783 | 1.196933238 |
| GO:2000104 | negative regulation of DNA-dependent DNA replication | 0.784431312 | 1.196933347 |
| GO:0071674 | mononuclear cell migration | 0.800406063 | 1.196934807 |
| ENSG00000206454 | POU5F1 subnetwork | 0.723363825 | 1.196935211 |
| GO:0018298 | protein-chromophore linkage | 0.823629809 | 1.196938166 |
| GO:0001936 | regulation of endothelial cell proliferation | 0.783963689 | 1.196942183 |
| ENSG00000197621 | ENSG00000197621 subnetwork | 0.725050259 | 1.196947723 |
| REACTOME_CELL:CELL_COMMUN | REACTOME_CELL:CELL_COMMUNICATION | 0.823892719 | 1.196949034 |
| ENSG00000108262 | GIT1 subnetwork | 0.797669134 | 1.196950406 |
| ENSG00000004779 | NDUFAB1 subnetwork | 0.800596321 | 1.196950783 |
| REACTOME_REMOVAL_OF_LICEN | REACTOME_REMOVAL_OF_LICENSING_FACTORS_FROM | 0.822884418 | 1.196955048 |
| GO:0002042 | cell migration involved in sprouting angiogenesis | 0.728269188 | 1.19695511 |
| GO:0006360 | transcription from RNA polymerase I promoter | 0.784749314 | 1.196955479 |
| ENSG00000156110 | ADK subnetwork | 0.799076248 | 1.19695572 |
| REACTOME_MITOTIC_PROMETAP | REACTOME_MITOTIC_PROMETAPHASE | 0.727142731 | 1.196956278 |
| MP:0006086 | decreased body mass index | 0.797360919 | 1.196959425 |
| GO:2000377 | regulation of reactive oxygen species metabolic process | 0.79884166 | 1.196965036 |
| MP:0000443 | abnormal snout morphology | 0.798898583 | 1.196965348 |
| ENSG00000102468 | HTR2A subnetwork | 0.822489221 | 1.196968488 |
| GO:0045137 | development of primary sexual characteristics | 0.81452302 | 1.196970612 |

| | | | |
|---|---|---|---|
| GO:0007622 | rhythmic behavior | 0.728034958 | 1.196976484 |
| GO:0032371 | regulation of sterol transport | 0.773809344 | 1.196978341 |
| ENSG00000108953 | YWHAE subnetwork | 0.774080657 | 1.196979299 |
| GO:0032011 | ARF protein signal transduction | 0.799376995 | 1.196982273 |
| GO:0001825 | blastocyst formation | 0.797447122 | 1.196985415 |
| ENSG00000100412 | ACO2 subnetwork | 0.824909269 | 1.196987173 |
| GO:0043486 | histone exchange | 0.815782869 | 1.196990252 |
| GO:0032148 | activation of protein kinase B activity | 0.815886849 | 1.196995579 |
| REACTOME_TRANSPORT_OF_MA | REACTOME_TRANSPORT_OF_MATURE_TRANSCRIPT_TO | 0.800533755 | 1.196996521 |
| GO:0048194 | Golgi vesicle budding | 0.784673559 | 1.196996872 |
| GO:0072593 | reactive oxygen species metabolic process | 0.785253394 | 1.196999062 |
| GO:0048193 | Golgi vesicle transport | 0.78534502 | 1.196999375 |
| ENSG00000132670 | PTPRA subnetwork | 0.814683962 | 1.197001409 |
| REACTOME_L1CAM_INTERACTIOI | REACTOME_L1CAM_INTERACTIONS | 0.799298814 | 1.19700246 |
| GO:0060322 | head development | 0.82235472 | 1.197002793 |
| ENSG00000183648 | NDUFB1 subnetwork | 0.727956455 | 1.197004144 |
| ENSG00000130561 | SAG subnetwork | 0.823070165 | 1.197010463 |
| GO:0070304 | positive regulation of stress-activated protein kinase sigr | 0.823582065 | 1.197012547 |
| REACTOME_CDC6_ASSOCIATION_ | REACTOME_CDC6_ASSOCIATION_WITH_THE_ORCORIGI | 0.823523111 | 1.197017229 |
| MP:0002563 | shortened circadian period | 0.797324734 | 1.197025889 |
| ENSG00000028528 | SNX1 subnetwork | 0.798049478 | 1.197028331 |
| ENSG00000090776 | EFNB1 subnetwork | 0.773113945 | 1.197028656 |
| MP:0002826 | tonic seizures | 0.800400528 | 1.19703173 |
| GO:0071417 | cellular response to organic nitrogen | 0.774179762 | 1.197037702 |
| GO:0005929 | cilium | 0.822199808 | 1.197042099 |
| GO:0034453 | microtubule anchoring | 0.815037947 | 1.197042849 |
| ENSG00000196290 | NIF3L1 subnetwork | 0.798137632 | 1.197044032 |
| GO:0070534 | protein K63-linked ubiquitination | 0.727114672 | 1.197045633 |
| GO:0044283 | small molecule biosynthetic process | 0.798709613 | 1.197046154 |
| GO:0051145 | smooth muscle cell differentiation | 0.783942807 | 1.197046237 |
| REACTOME_REMOVAL_OF_THE_I | REACTOME_REMOVAL_OF_THE_FLAP_INTERMEDIATE | 0.785175018 | 1.197050855 |
| ENSG00000125266 | EFNB2 subnetwork | 0.816177508 | 1.197051733 |
| GO:0000922 | spindle pole | 0.823885565 | 1.19705326 |
| GO:0016620 | oxidoreductase activity, acting on the aldehyde or oxo gr | 0.82468334 | 1.197055898 |
| GO:0009881 | photoreceptor activity | 0.722646532 | 1.19705617 |
| ENSG00000108688 | CCL7 subnetwork | 0.798823378 | 1.197057014 |
| GO:0000737 | DNA catabolic process, endonucleolytic | 0.814497725 | 1.197060896 |
| MP:0002016 | ovary cysts | 0.824878636 | 1.197061456 |
| GO:0046330 | positive regulation of JNK cascade | 0.814795091 | 1.197067109 |
| GO:0043244 | regulation of protein complex disassembly | 0.80034907 | 1.197067254 |
| ENSG00000204531 | POU5F1 subnetwork | 0.723363825 | 1.197070092 |
| ENSG00000198841 | KTI12 subnetwork | 0.822876431 | 1.197074362 |
| ENSG00000189043 | NDUFA4 subnetwork | 0.784654677 | 1.197074773 |
| MP:0001231 | abnormal epidermis stratum basale morphology | 0.725043609 | 1.197076681 |
| GO:0031146 | SCF-dependent proteasomal ubiquitin-dependent protei | 0.799240662 | 1.19707902 |
| GO:0006513 | protein monoubiquitination | 0.784596934 | 1.197079683 |
| ENSG00000169621 | APLF subnetwork | 0.774471668 | 1.19708087 |
| ENSG00000174111 | SOCS7 subnetwork | 0.800227021 | 1.197082011 |
| GO:2001014 | regulation of skeletal muscle cell differentiation | 0.822488964 | 1.197082876 |
| ENSG00000101084 | C20orf24 subnetwork | 0.815757718 | 1.197085427 |
| ENSG00000138107 | ACTR1A subnetwork | 0.723286792 | 1.197086667 |
| GO:0008395 | steroid hydroxylase activity | 0.773257625 | 1.197087122 |
| ENSG00000170776 | AKAP13 subnetwork | 0.816373254 | 1.197087476 |
| ENSG00000100479 | POLE2 subnetwork | 0.727834726 | 1.197087487 |

| | | | |
|---|---|---|---|
| ENSG00000132824 | SERINC3 subnetwork | 0.814985168 | 1.197087818 |
| GO:0043271 | negative regulation of ion transport | 0.816268941 | 1.197092206 |
| ENSG00000160200 | CBS subnetwork | 0.823411682 | 1.197096324 |
| GO:0051262 | protein tetramerization | 0.798687929 | 1.197097138 |
| GO:0006626 | protein targeting to mitochondrion | 0.727942273 | 1.197104615 |
| GO:0032374 | regulation of cholesterol transport | 0.773809344 | 1.197104818 |
| MP:0005608 | cardiac interstitial fibrosis | 0.815675184 | 1.197110262 |
| GO:0007017 | microtubule-based process | 0.800312092 | 1.197118141 |
| ENSG00000108691 | CCL2 subnetwork | 0.815254896 | 1.197118866 |
| MP:0003047 | abnormal thoracic vertebrae morphology | 0.824625071 | 1.197120263 |
| REACTOME_SYNTHESIS_OF_BILE_ | REACTOME_SYNTHESIS_OF_BILE_ACIDS_AND_BILE_SAL | 0.814678574 | 1.197121868 |
| GO:0005746 | mitochondrial respiratory chain | 0.772731651 | 1.197122302 |
| REACTOME_ASSOCIATION_OF_LI | REACTOME_ASSOCIATION_OF_LICENSING_FACTORS_WI | 0.722611809 | 1.197123519 |
| MP:0001666 | abnormal intestinal absorption | 0.727074227 | 1.197123795 |
| GO:0060271 | cilium morphogenesis | 0.822111102 | 1.197126322 |
| MP:0000953 | abnormal oligodendrocyte morphology | 0.823509602 | 1.197126494 |
| ENSG00000133104 | SPG20 subnetwork | 0.816154118 | 1.197126783 |
| ENSG00000075388 | FGF4 subnetwork | 0.798449211 | 1.197127026 |
| GO:0043252 | sodium-independent organic anion transport | 0.797317464 | 1.197128326 |
| REACTOME_MITOCHONDRIAL_TR | REACTOME_MITOCHONDRIAL_TRNA_AMINOACYLATION | 0.773102295 | 1.197128807 |
| ENSG00000142864 | SERBP1 subnetwork | 0.824834394 | 1.197130781 |
| ENSG00000153767 | GTF2E1 subnetwork | 0.773001989 | 1.197133792 |
| GO:0032391 | photoreceptor connecting cilium | 0.783907674 | 1.197134656 |
| ENSG00000116266 | STXBP3 subnetwork | 0.771925283 | 1.197135141 |
| GO:0010657 | muscle cell apoptotic process | 0.816068146 | 1.197136542 |
| ENSG00000103168 | TAF1C subnetwork | 0.727792465 | 1.197137576 |
| ENSG00000160916 | ENSG00000160916 subnetwork | 0.798650463 | 1.197137874 |
| ENSG00000039068 | CDH1 subnetwork | 0.77434604 | 1.197138332 |
| MP:0010018 | pulmonary vascular congestion | 0.798807507 | 1.197138755 |
| MP:0002633 | persistent truncus arteriosis | 0.82218164 | 1.197141574 |
| ENSG00000131143 | COX4I1 subnetwork | 0.785065454 | 1.197144048 |
| ENSG00000176732 | PFN4 subnetwork | 0.785561696 | 1.197145536 |
| MP:0002152 | abnormal brain morphology | 0.823270701 | 1.197150543 |
| REACTOME_SHC:MEDIATED_CAS | REACTOME_SHC:MEDIATED_CASCADE | 0.814943172 | 1.197152918 |
| MP:0003212 | increased susceptibility to age related obesity | 0.773578185 | 1.197156749 |
| GO:0022898 | regulation of transmembrane transporter activity | 0.815189736 | 1.197163834 |
| ENSG00000069248 | NUP133 subnetwork | 0.785151057 | 1.19716519 |
| KEGG_LONG_TERM_DEPRESSION | KEGG_LONG_TERM_DEPRESSION | 0.785008108 | 1.197169811 |
| ENSG00000110786 | PTPN5 subnetwork | 0.772038037 | 1.197172509 |
| ENSG00000144837 | PLA1A subnetwork | 0.772820684 | 1.1971755 |
| ENSG00000175203 | DCTN2 subnetwork | 0.81438591 | 1.19717608 |
| REACTOME_APOPTOTIC_CLEAVA | REACTOME_APOPTOTIC_CLEAVAGE_OF_CELL_ADHESIOI | 0.816522444 | 1.197178148 |
| REACTOME_PHASE_II_CONJUGAT | REACTOME_PHASE_II_CONJUGATION | 0.773783617 | 1.197178485 |
| MP:0001924 | infertility | 0.822863737 | 1.197178746 |
| GO:0006309 | apoptotic DNA fragmentation | 0.814497725 | 1.197181397 |
| GO:2000146 | negative regulation of cell motility | 0.773672119 | 1.197183471 |
| ENSG00000143498 | TAF1A subnetwork | 0.772677985 | 1.197185483 |
| KEGG_CITRATE_CYCLE_TCA_CYCL | KEGG_CITRATE_CYCLE_TCA_CYCLE | 0.723260567 | 1.197187782 |
| MP:0002693 | abnormal pancreas physiology | 0.815483917 | 1.197189825 |
| ENSG00000082781 | ITGB5 subnetwork | 0.725453894 | 1.19719038 |
| ENSG00000147123 | NDUFB11 subnetwork | 0.7714074 | 1.197191607 |
| REACTOME_RNA_POLYMERASE_I | REACTOME_RNA_POLYMERASE_II_TRANSCRIPTION | 0.798322907 | 1.197198276 |
| ENSG00000120697 | ALG5 subnetwork | 0.822053023 | 1.197200878 |
| GO:0007018 | microtubule-based movement | 0.798416197 | 1.197203694 |

| | | | |
|---|---|---|---|
| MP:0002752 | abnormal somatic nervous system morphology | 0.82340031 | 1.197205619 |
| ENSG00000106628 | POLD2 subnetwork | 0.774469906 | 1.197207264 |
| GO:0010717 | regulation of epithelial to mesenchymal transition | 0.773539457 | 1.197209302 |
| ENSG00000079459 | FDFT1 subnetwork | 0.727043258 | 1.197213188 |
| MP:0010402 | ventricular septal defect | 0.727431085 | 1.19721475 |
| ENSG00000099624 | ATP5D subnetwork | 0.772607634 | 1.197216931 |
| ENSG00000171843 | MLLT3 subnetwork | 0.772954427 | 1.197218109 |
| ENSG00000142156 | COL6A1 subnetwork | 0.798618997 | 1.197224787 |
| GO:0060324 | face development | 0.771347671 | 1.197228405 |
| GO:0005759 | mitochondrial matrix | 0.725401313 | 1.197229403 |
| MP:0001454 | abnormal cued conditioning behavior | 0.815422411 | 1.197229764 |
| GO:0009266 | response to temperature stimulus | 0.815672843 | 1.197230599 |
| ENSG00000118972 | FGF23 subnetwork | 0.783890051 | 1.197233532 |
| ENSG00000182944 | EWSR1 subnetwork | 0.797301601 | 1.197235923 |
| ENSG00000020633 | RUNX3 subnetwork | 0.727555942 | 1.197237476 |
| MP:0004937 | dilated heart | 0.822828447 | 1.197238285 |
| GO:0090009 | primitive streak formation | 0.772162908 | 1.197246929 |
| ENSG00000183386 | FHL3 subnetwork | 0.784970721 | 1.197247706 |
| ENSG00000109680 | TBC1D19 subnetwork | 0.772406258 | 1.197247804 |
| ENSG00000004864 | SLC25A13 subnetwork | 0.771918141 | 1.19725135 |
| ENSG00000113327 | GABRG2 subnetwork | 0.816681057 | 1.197258761 |
| MP:0001299 | abnormal eye distance/ position | 0.783838426 | 1.197259344 |
| GO:0048745 | smooth muscle tissue development | 0.727777953 | 1.197260504 |
| ENSG00000171132 | PRKCE subnetwork | 0.723197515 | 1.197260737 |
| ENSG00000127337 | YEATS4 subnetwork | 0.816764651 | 1.197264056 |
| GO:0009156 | ribonucleoside monophosphate biosynthetic process | 0.727387987 | 1.197270485 |
| REACTOME_PRESYNAPTIC_FUNCT | REACTOME_PRESYNAPTIC_FUNCTION_OF_KAINATE_REC | 0.822028172 | 1.197285429 |
| GO:0072111 | cell proliferation involved in kidney development | 0.815627316 | 1.19729064 |
| GO:0048565 | digestive tract development | 0.771304911 | 1.197291711 |
| ENSG00000120053 | GOT1 subnetwork | 0.723153949 | 1.197299887 |
| GO:0051153 | regulation of striated muscle cell differentiation | 0.796885959 | 1.197301049 |
| GO:0006613 | cotranslational protein targeting to membrane | 0.797132115 | 1.19730702 |
| ENSG00000101843 | PSMD10 subnetwork | 0.773510019 | 1.197314727 |
| MP:0004632 | abnormal cochlear OHC efferent innervation pattern | 0.783798415 | 1.197316487 |
| GO:0045604 | regulation of epidermal cell differentiation | 0.797067744 | 1.197322163 |
| GO:0004519 | endonuclease activity | 0.725594949 | 1.197325542 |
| ENSG00000108813 | DLX4 subnetwork | 0.772310624 | 1.197337215 |
| REACTOME_SYNTHESIS_OF_DNA | REACTOME_SYNTHESIS_OF_DNA | 0.797009663 | 1.197337309 |
| ENSG00000127586 | CHTF18 subnetwork | 0.727041362 | 1.197341857 |
| ENSG00000152804 | HHEX subnetwork | 0.797283707 | 1.197343541 |
| REACTOME_G1S_DNA_DAMAGE_ | REACTOME_G1S_DNA_DAMAGE_CHECKPOINTS | 0.772603567 | 1.197343634 |
| ENSG00000121691 | CAT subnetwork | 0.771895963 | 1.197351695 |
| MP:0001694 | failure to form egg cylinders | 0.771235798 | 1.197360331 |
| ENSG00000076356 | PLXNA2 subnetwork | 0.727744512 | 1.197366652 |
| GO:0000380 | alternative nuclear mRNA splicing, via spliceosome | 0.772397089 | 1.197369257 |
| ENSG00000107816 | LZTS2 subnetwork | 0.796845508 | 1.197377892 |
| ENSG00000059573 | ALDH18A1 subnetwork | 0.726888136 | 1.197380525 |
| ENSG00000120063 | GNA13 subnetwork | 0.783765304 | 1.197384085 |
| GO:0030194 | positive regulation of blood coagulation | 0.726981167 | 1.197386427 |
| GO:0005782 | peroxisomal matrix | 0.822013976 | 1.197389959 |
| ENSG00000165140 | FBP1 subnetwork | 0.785838593 | 1.197390625 |
| GO:0003073 | regulation of systemic arterial blood pressure | 0.786054055 | 1.19740679 |
| GO:0008237 | metallopeptidase activity | 0.771632649 | 1.197414433 |
| ENSG00000146733 | PSPH subnetwork | 0.786288448 | 1.197418011 |

| | | | |
|---|---|---|---|
| GO:0050664 | oxidoreductase activity, acting on NADH or NADPH, oxyg | 0.728595278 | 1.197419969 |
| ENSG00000153933 | DGKE subnetwork | 0.723146651 | 1.197429248 |
| ENSG00000117984 | CTSD subnetwork | 0.797264731 | 1.197430627 |
| MP:0002836 | abnormal chorion morphology | 0.771836572 | 1.197430872 |
| GO:0042384 | cilium assembly | 0.783699273 | 1.197436031 |
| GO:0006184 | GTP catabolic process | 0.783319043 | 1.197440184 |
| GO:0032993 | protein-DNA complex | 0.772554021 | 1.197443903 |
| MP:0005642 | decreased mean corpuscular hemoglobin concentration | 0.817113938 | 1.197460859 |
| GO:0022900 | electron transport chain | 0.723092282 | 1.197462788 |
| MP:0005216 | abnormal pancreatic alpha cell morphology | 0.785977144 | 1.197463806 |
| MP:0000079 | abnormal basioccipital bone morphology | 0.786235241 | 1.197464598 |
| GO:0030203 | glycosaminoglycan metabolic process | 0.796813721 | 1.197470177 |
| GO:0019894 | kinesin binding | 0.816961135 | 1.197470387 |
| GO:0051904 | pigment granule transport | 0.728704218 | 1.197476217 |
| GO:0048525 | negative regulation of viral reproduction | 0.783229833 | 1.197476489 |
| ENSG00000107623 | GDF10 subnetwork | 0.783549017 | 1.19747728 |
| ENSG00000172270 | BSG subnetwork | 0.783640441 | 1.197477543 |
| ENSG00000162702 | ZNF281 subnetwork | 0.722989023 | 1.197479418 |
| GO:0048487 | beta-tubulin binding | 0.783464556 | 1.19748224 |
| ENSG00000140285 | FGF7 subnetwork | 0.771235795 | 1.197487277 |
| GO:0006261 | DNA-dependent DNA replication | 0.786429013 | 1.197491151 |
| GO:0006071 | glycerol metabolic process | 0.771762729 | 1.197504768 |
| ENSG00000188878 | FBF1 subnetwork | 0.821637816 | 1.197508488 |
| GO:0031907 | microbody lumen | 0.822013976 | 1.197509483 |
| ENSG00000181090 | EHMT1 subnetwork | 0.72688584 | 1.197514866 |
| GO:0015036 | disulfide oxidoreductase activity | 0.796775604 | 1.197536768 |
| GO:0046605 | regulation of centrosome cycle | 0.786215159 | 1.197542435 |
| REACTOME_CALCITONIN:LIKE_LIC | REACTOME_CALCITONIN:LIKE_LIGAND_RECEPTORS | 0.817081681 | 1.19754592 |
| ENSG00000188419 | CHM subnetwork | 0.771190987 | 1.197550631 |
| GO:0000786 | nucleosome | 0.821882334 | 1.197553914 |
| GO:0016051 | carbohydrate biosynthetic process | 0.816946289 | 1.197560486 |
| MP:0010984 | abnormal metanephric mesenchyme morphology | 0.817266147 | 1.197561465 |
| GO:0042743 | hydrogen peroxide metabolic process | 0.821484573 | 1.197567918 |
| ENSG00000070182 | SPTB subnetwork | 0.821779987 | 1.197578632 |
| ENSG00000072201 | LNX1 subnetwork | 0.818464159 | 1.197579675 |
| ENSG00000131721 | RHOXF2 subnetwork | 0.820688643 | 1.197580726 |
| ENSG00000100934 | SEC23A subnetwork | 0.821171863 | 1.197581934 |
| ENSG00000198873 | GRK5 subnetwork | 0.796737215 | 1.197593088 |
| MP:0001208 | blistering | 0.796352567 | 1.197596995 |
| REACTOME_FANCONI_ANEMIA_P | REACTOME_FANCONI_ANEMIA_PATHWAY | 0.821613219 | 1.197598122 |
| GO:0045071 | negative regulation of viral genome replication | 0.783229833 | 1.19760163 |
| GO:0008242 | omega peptidase activity | 0.771049419 | 1.197608442 |
| MP:0002273 | abnormal pulmonary alveolus epithelial cell morphology | 0.725835856 | 1.19761236 |
| ENSG00000077235 | GTF3C1 subnetwork | 0.72666401 | 1.197615039 |
| REACTOME_GAP_JUNCTION_ASSI | REACTOME_GAP_JUNCTION_ASSEMBLY | 0.822007373 | 1.197619048 |
| GO:0006893 | Golgi to plasma membrane transport | 0.786867529 | 1.197622268 |
| ENSG00000115392 | FANCL subnetwork | 0.776518413 | 1.197624065 |
| MP:0004777 | abnormal phospholipid level | 0.783073707 | 1.19762726 |
| GO:0005905 | coated pit | 0.81842211 | 1.197629548 |
| MP:0000757 | herniated abdominal wall | 0.770888136 | 1.197634454 |
| ENSG00000054116 | TRAPPC3 subnetwork | 0.820510407 | 1.197635 |
| MP:0001073 | abnormal glossopharyngeal nerve morphology | 0.726875465 | 1.197643627 |
| GO:0001556 | oocyte maturation | 0.771170541 | 1.197645811 |
| ENSG00000174469 | CNTNAP2 subnetwork | 0.820921107 | 1.197646177 |

| | | | |
|---|---|---|---|
| GO:0030258 | lipid modification | 0.821017055 | 1.197646412 |
| ENSG00000160551 | TAOK1 subnetwork | 0.821406386 | 1.197647353 |
| ENSG00000116809 | ZBTB17 subnetwork | 0.818903044 | 1.19765578 |
| ENSG00000130762 | ARHGEF16 subnetwork | 0.821475582 | 1.197657577 |
| KEGG_ONE_CARBON_POOL_BY_F | KEGG_ONE_CARBON_POOL_BY_FOLATE | 0.770839218 | 1.19766603 |
| GO:0072001 | renal system development | 0.819231265 | 1.197671507 |
| ENSG00000135363 | LMO2 subnetwork | 0.765639909 | 1.197672432 |
| MP:0000182 | increased circulating LDL cholesterol level | 0.728959663 | 1.197677932 |
| MP:0002576 | abnormal enamel morphology | 0.786828152 | 1.197679259 |
| GO:0001967 | suckling behavior | 0.82082787 | 1.197680928 |
| GO:0006906 | vesicle fusion | 0.821145254 | 1.197681623 |
| GO:0016758 | transferase activity, transferring hexosyl groups | 0.77100444 | 1.197682435 |
| MP:0004182 | abnormal spermiation | 0.767336483 | 1.197682472 |
| MP:0004985 | decreased osteoclast cell number | 0.729050893 | 1.197683787 |
| GO:0043534 | blood vessel endothelial cell migration | 0.765967353 | 1.197683851 |
| ENSG00000106554 | CHCHD3 subnetwork | 0.78301048 | 1.197684508 |
| GO:0016810 | hydrolase activity, acting on carbon-nitrogen (but not pe | 0.820457113 | 1.197684768 |
| ENSG00000205531 | NAP1L4 subnetwork | 0.796724961 | 1.197685423 |
| GO:0019002 | GMP binding | 0.820680569 | 1.197685463 |
| MP:0010954 | abnormal cellular respiration | 0.767823089 | 1.197689277 |
| GO:0031901 | early endosome membrane | 0.796619492 | 1.197690329 |
| ENSG00000111237 | VPS29 subnetwork | 0.820622312 | 1.19770023 |
| MP:0003982 | increased cholesterol level | 0.821341575 | 1.197702068 |
| GO:0016127 | sterol catabolic process | 0.819702969 | 1.197702703 |
| ENSG00000151552 | QDPR subnetwork | 0.776473612 | 1.197702845 |
| MP:0011049 | impaired adaptive thermogenesis | 0.76578792 | 1.197704708 |
| ENSG00000038382 | TRIO subnetwork | 0.796345588 | 1.197704817 |
| MP:0005278 | abnormal cholesterol homeostasis | 0.78322113 | 1.197705895 |
| MP:0005238 | increased brain size | 0.796245376 | 1.197709727 |
| ENSG00000180340 | FZD2 subnetwork | 0.726631915 | 1.197710181 |
| MP:0010403 | atrial septal defect | 0.818658787 | 1.197710191 |
| GO:0030949 | positive regulation of vascular endothelial growth factor | 0.81750939 | 1.197712222 |
| ENSG00000206427 | PRRC2A subnetwork | 0.770775718 | 1.197724138 |
| GO:0055093 | response to hyperoxia | 0.819185512 | 1.197726362 |
| GO:0034340 | response to type I interferon | 0.767280005 | 1.197730179 |
| ENSG00000093167 | LRRFIP2 subnetwork | 0.7867759 | 1.197736261 |
| GO:0005796 | Golgi lumen | 0.818419174 | 1.197739575 |
| ENSG00000115942 | ORC2 subnetwork | 0.819332484 | 1.197741839 |
| ENSG00000127554 | GFER subnetwork | 0.726564891 | 1.197743601 |
| GO:0009055 | electron carrier activity | 0.726850299 | 1.197744361 |
| REACTOME_SHC:RELATED_EVENT | REACTOME_SHC:RELATED_EVENTS | 0.767779118 | 1.197747604 |
| MP:0003910 | decreased eating behavior | 0.818892165 | 1.197755736 |
| MP:0005028 | abnormal trophectoderm morphology | 0.765595306 | 1.197757608 |
| GO:0048278 | vesicle docking | 0.796191476 | 1.197776405 |
| ENSG00000127824 | TUBA4A subnetwork | 0.782830537 | 1.197777894 |
| REACTOME_SIGNALLING_TO_P38 | REACTOME_SIGNALLING_TO_P38_VIA_RIT_AND_RIN | 0.766293483 | 1.197780623 |
| ENSG00000154277 | UCHL1 subnetwork | 0.78672129 | 1.197782867 |
| ENSG00000143333 | RGS16 subnetwork | 0.791593501 | 1.197785367 |
| ENSG00000066926 | FECH subnetwork | 0.796542582 | 1.197787611 |
| GO:0051325 | interphase | 0.820018152 | 1.197788452 |
| ENSG00000167283 | ATP5L subnetwork | 0.782916843 | 1.197788582 |
| MP:0000492 | abnormal rectum morphology | 0.820452608 | 1.197794559 |
| ENSG00000213611 | ENSG00000213611 subnetwork | 0.818001487 | 1.197798616 |
| ENSG00000197959 | DNM3 subnetwork | 0.765951294 | 1.197801025 |

| | | | |
|---|---|---|---|
| ENSG00000167792 | NDUFV1 subnetwork | 0.783006966 | 1.197804496 |
| GO:0060038 | cardiac muscle cell proliferation | 0.796614735 | 1.197808417 |
| ENSG00000126005 | ENSG00000126005 subnetwork | 0.77069297 | 1.197808554 |
| ENSG00000114784 | EIF1B subnetwork | 0.776710554 | 1.197808681 |
| GO:0070206 | protein trimerization | 0.795944519 | 1.19781176 |
| REACTOME_VPU_MEDIATED_DEC | REACTOME_VPU_MEDIATED_DEGRADATION_OF_CD4 | 0.819153854 | 1.197816288 |
| MP:0000067 | osteopetrosis | 0.765560944 | 1.197821444 |
| GO:0006707 | cholesterol catabolic process | 0.819702969 | 1.197822605 |
| GO:0006497 | protein lipidation | 0.817698093 | 1.197822815 |
| ENSG00000085415 | SEH1L subnetwork | 0.776470007 | 1.197823796 |
| ENSG00000196890 | HIST3H2BB subnetwork | 0.76726673 | 1.197825855 |
| GO:0002070 | epithelial cell maturation | 0.796136344 | 1.197827654 |
| GO:0006650 | glycerophospholipid metabolic process | 0.818334345 | 1.197829356 |
| MP:0002841 | impaired skeletal muscle contractility | 0.767732148 | 1.19783257 |
| ENSG00000101057 | MYBL2 subnetwork | 0.7408434 | 1.197834472 |
| ENSG00000153046 | CDYL subnetwork | 0.740910773 | 1.197834711 |
| MP:0003149 | abnormal tectorial membrane morphology | 0.767488436 | 1.197842531 |
| GO:0043624 | cellular protein complex disassembly | 0.817820775 | 1.197843098 |
| ENSG00000206318 | ENSG00000206318 subnetwork | 0.770775718 | 1.197851231 |
| GO:0030520 | intracellular estrogen receptor signaling pathway | 0.765499862 | 1.197853252 |
| GO:0010389 | regulation of G2/M transition of mitotic cell cycle | 0.767581905 | 1.197853414 |
| GO:0017091 | AU-rich element binding | 0.818410339 | 1.197854637 |
| GO:0070888 | E-box binding | 0.766233181 | 1.19786042 |
| MP:0008875 | abnormal xenobiotic pharmacokinetics | 0.770645486 | 1.197861388 |
| GO:0000726 | non-recombinational repair | 0.791563564 | 1.197862761 |
| MP:0003419 | delayed endochondral bone ossification | 0.817962832 | 1.197863591 |
| GO:0072372 | primary cilium | 0.766156517 | 1.197865528 |
| MP:0000278 | abnormal myocardial fiber morphology | 0.819629479 | 1.197867441 |
| ENSG00000168283 | BMI1 subnetwork | 0.81888764 | 1.197875752 |
| MP:0008033 | impaired lipolysis | 0.726564876 | 1.197878073 |
| ENSG00000151276 | MAGI1 subnetwork | 0.796063675 | 1.197878913 |
| GO:0043241 | protein complex disassembly | 0.765321277 | 1.1978795 |
| GO:0031301 | integral to organelle membrane | 0.791740384 | 1.197883899 |
| GO:0031124 | mRNA 3'-end processing | 0.820253057 | 1.197883942 |
| GO:0014066 | regulation of phosphatidylinositol 3-kinase cascade | 0.765410377 | 1.197885067 |
| MP:0002981 | increased liver weight | 0.819999868 | 1.197888311 |
| GO:0007584 | response to nutrient | 0.820424693 | 1.197889367 |
| ENSG00000083312 | TNPO1 subnetwork | 0.819553173 | 1.197897266 |
| ENSG00000114416 | FXR1 subnetwork | 0.795397442 | 1.197897991 |
| GO:0070469 | respiratory chain | 0.770438872 | 1.197898089 |
| GO:0042773 | ATP synthesis coupled electron transport | 0.78282526 | 1.197903158 |
| ENSG00000075618 | FSCN1 subnetwork | 0.770360458 | 1.197903174 |
| GO:0045445 | myoblast differentiation | 0.790922929 | 1.197912998 |
| REACTOME_PLATELET_AGGREGA | REACTOME_PLATELET_AGGREGATION_PLUG_FORMATI | 0.767075826 | 1.197915778 |
| GO:0007281 | germ cell development | 0.726242255 | 1.197916433 |
| GO:0071514 | genetic imprinting | 0.776438885 | 1.197918423 |
| ENSG00000122884 | P4HA1 subnetwork | 0.817930953 | 1.197918547 |
| ENSG00000128322 | IGLL1 subnetwork | 0.775279878 | 1.197920625 |
| GO:0043044 | ATP-dependent chromatin remodeling | 0.767703325 | 1.19792288 |
| GO:0005875 | microtubule associated complex | 0.795940673 | 1.19792482 |
| ENSG00000143033 | MTF2 subnetwork | 0.793582419 | 1.197929575 |
| ENSG00000138802 | SEC24B subnetwork | 0.767255615 | 1.197932211 |
| MP:0000192 | abnormal mineral level | 0.818314111 | 1.197934423 |
| MP:0008807 | increased liver iron level | 0.760480233 | 1.197941524 |

| | | | |
|---|---|---|---|
| GO:0016878 | acid-thiol ligase activity | 0.726357136 | 1.197944744 |
| ENSG00000140990 | NDUFB10 subnetwork | 0.820362154 | 1.19794918 |
| REACTOME_AMINE:DERIVED_HO | REACTOME_AMINE:DERIVED_HORMONES | 0.776388562 | 1.197949826 |
| REACTOME_AMINO_ACID_SYNTH | REACTOME_AMINO_ACID_SYNTHESIS_AND_INTERCONV | 0.726419673 | 1.19795059 |
| GO:0002063 | chondrocyte development | 0.792454085 | 1.197952642 |
| MP:0003339 | decreased pancreatic beta cell number | 0.792655203 | 1.197953065 |
| GO:0046320 | regulation of fatty acid oxidation | 0.740834299 | 1.197955472 |
| GO:0003774 | motor activity | 0.726544717 | 1.197956434 |
| GO:0090101 | negative regulation of transmembrane receptor protein | 0.791857246 | 1.197956544 |
| GO:0090002 | establishment of protein localization in plasma membrar | 0.775178641 | 1.197957352 |
| GO:0005544 | calcium-dependent phospholipid binding | 0.765290846 | 1.197964744 |
| GO:0006690 | icosanoid metabolic process | 0.795376084 | 1.197969909 |
| GO:0035335 | peptidyl-tyrosine dephosphorylation | 0.760421087 | 1.197973554 |
| ENSG00000168291 | PDHB subnetwork | 0.793698276 | 1.197976252 |
| GO:0033151 | V(D)J recombination | 0.791547439 | 1.1979764 |
| REACTOME_MUSCLE_CONTRACTI | REACTOME_MUSCLE_CONTRACTION | 0.770630872 | 1.197977922 |
| GO:0051445 | regulation of meiotic cell cycle | 0.819979539 | 1.197983185 |
| MP:0001074 | abnormal vagus nerve morphology | 0.820236032 | 1.19798379 |
| GO:0015238 | drug transmembrane transporter activity | 0.790767564 | 1.197985082 |
| KEGG_STARCH_AND_SUCROSE_M | KEGG_STARCH_AND_SUCROSE_METABOLISM | 0.792792488 | 1.197989456 |
| GO:0000977 | RNA polymerase II regulatory region sequence-specific D | 0.767017051 | 1.197995522 |
| REACTOME_METABOLISM_OF_CA | REACTOME_METABOLISM_OF_CARBOHYDRATES | 0.770351949 | 1.197998513 |
| ENSG00000174718 | C12orf35 subnetwork | 0.795787603 | 1.198001648 |
| ENSG00000197747 | S100A10 subnetwork | 0.790891006 | 1.198006008 |
| GO:0072503 | cellular divalent inorganic cation homeostasis | 0.765233495 | 1.198007266 |
| ENSG00000131269 | ABCB7 subnetwork | 0.818276637 | 1.198009426 |
| ENSG00000124333 | VAMP7 subnetwork | 0.792101094 | 1.198013862 |
| MP:0001496 | audiogenic seizures | 0.729352301 | 1.198014097 |
| MP:0011085 | complete postnatal lethality | 0.795909661 | 1.198022453 |
| ENSG00000127928 | GNGT1 subnetwork | 0.765160454 | 1.198023082 |
| GO:0008654 | phospholipid biosynthetic process | 0.795632844 | 1.198026994 |
| GO:0090150 | establishment of protein localization in membrane | 0.793489541 | 1.198027267 |
| ENSG00000101265 | RASSF2 subnetwork | 0.741084305 | 1.198027766 |
| GO:0042775 | mitochondrial ATP synthesis coupled electron transport | 0.78282526 | 1.198028449 |
| ENSG00000144554 | FANCD2 subnetwork | 0.79412192 | 1.198028896 |
| GO:0001840 | neural plate development | 0.790711411 | 1.198031496 |
| ENSG00000033122 | LRRC7 subnetwork | 0.792623771 | 1.198035567 |
| ENSG00000122133 | PAEP subnetwork | 0.72622422 | 1.198039766 |
| GO:0051385 | response to mineralocorticoid stimulus | 0.793564673 | 1.198042962 |
| MP:0008414 | abnormal spatial reference memory | 0.767237034 | 1.198043919 |
| MP:0005201 | abnormal retinal pigment epithelium morphology | 0.792424262 | 1.198045502 |
| GO:0005355 | glucose transmembrane transporter activity | 0.766650202 | 1.198053126 |
| GO:0055123 | digestive system development | 0.776915607 | 1.198056463 |
| MP:0004592 | small mandible | 0.782765898 | 1.198059623 |
| GO:0014888 | striated muscle adaptation | 0.740786921 | 1.198059965 |
| ENSG00000112531 | QKI subnetwork | 0.761140225 | 1.198061224 |
| GO:0030003 | cellular cation homeostasis | 0.7770086 | 1.198061934 |
| GO:0012506 | vesicle membrane | 0.792987198 | 1.198062216 |
| ENSG00000005189 | ENSG00000005189 subnetwork | 0.77637155 | 1.19806557 |
| GO:0071697 | ectodermal placode morphogenesis | 0.795287948 | 1.198067409 |
| GO:0006511 | ubiquitin-dependent protein catabolic process | 0.726156095 | 1.198067633 |
| GO:0045927 | positive regulation of growth | 0.791502672 | 1.198069358 |
| MP:0008582 | short photoreceptor inner segment | 0.790667206 | 1.198072739 |
| GO:0045333 | cellular respiration | 0.765108382 | 1.198076307 |

| | | | |
|---|---|---|---|
| REACTOME_SEROTONIN_RECEPT | REACTOME_SEROTONIN_RECEPTORS | 0.795357776 | 1.198077914 |
| ENSG00000182149 | IST1 subnetwork | 0.792046087 | 1.198080902 |
| GO:0002027 | regulation of heart rate | 0.792352819 | 1.198081498 |
| ENSG00000109062 | SLC9A3R1 subnetwork | 0.791097571 | 1.198084093 |
| REACTOME_GENERIC_TRANSCRIP | REACTOME_GENERIC_TRANSCRIPTION_PATHWAY | 0.766602542 | 1.198090259 |
| MP:0001158 | abnormal prostate gland morphology | 0.795762047 | 1.198094159 |
| GO:0016925 | protein sumoylation | 0.793431746 | 1.19809937 |
| ENSG00000014641 | MDH1 subnetwork | 0.760418445 | 1.198102355 |
| ENSG00000184640 | SEPT9 subnetwork | 0.787359448 | 1.198106533 |
| GO:0000724 | double-strand break repair via homologous recombinatio | 0.740741038 | 1.198109359 |
| ENSG00000180138 | CSNK1A1L subnetwork | 0.777101377 | 1.198109531 |
| MP:0001302 | eyelids open at birth | 0.791324829 | 1.198110375 |
| GO:0007603 | phototransduction, visible light | 0.793099042 | 1.198114085 |
| GO:0004549 | tRNA-specific ribonuclease activity | 0.761017053 | 1.198114525 |
| MP:0000522 | kidney cortex cysts | 0.791441253 | 1.198115747 |
| ENSG00000163635 | ATXN7 subnetwork | 0.782724428 | 1.198116958 |
| GO:0030228 | lipoprotein particle receptor activity | 0.767010828 | 1.198117936 |
| ENSG00000157766 | ACAN subnetwork | 0.761102888 | 1.19812547 |
| GO:0032886 | regulation of microtubule-based process | 0.770344015 | 1.19812573 |
| REACTOME_THE_NLRP3_INFLAM | REACTOME_THE_NLRP3_INFLAMMASOME | 0.787439283 | 1.198127536 |
| GO:0034358 | plasma lipoprotein particle | 0.790550847 | 1.19812934 |
| REACTOME_PROCESSIVE_SYNTHE | REACTOME_PROCESSIVE_SYNTHESIS_ON_THE_C:STRAN | 0.775544682 | 1.198131926 |
| ENSG00000108669 | CYTH1 subnetwork | 0.794113293 | 1.198142223 |
| GO:0006270 | DNA-dependent DNA replication initiation | 0.793370645 | 1.198145661 |
| MP:0000527 | abnormal kidney development | 0.79297319 | 1.198155039 |
| KEGG_REGULATION_OF_AUTOPH | KEGG_REGULATION_OF_AUTOPHAGY | 0.793218857 | 1.198155611 |
| ENSG00000124406 | ATP8A1 subnetwork | 0.777362847 | 1.198157507 |
| GO:0060976 | coronary vasculature development | 0.792302254 | 1.198158875 |
| MP:0008814 | reduced nerve conduction velocity | 0.77745163 | 1.198162965 |
| MP:0003827 | abnormal Wolffian duct morphology | 0.760833096 | 1.198173025 |
| MP:0000875 | abnormal cerebellar Purkinje cell layer | 0.775708991 | 1.198174528 |
| ENSG00000111262 | KCNA1 subnetwork | 0.768222237 | 1.198179302 |
| ENSG00000176105 | YES1 subnetwork | 0.741259715 | 1.198182219 |
| GO:0021903 | rostrocaudal neural tube patterning | 0.77631527 | 1.198186419 |
| GO:0051329 | interphase of mitotic cell cycle | 0.776366081 | 1.19818661 |
| MP:0006058 | decreased cerebral infarction size | 0.770130564 | 1.198188868 |
| GO:0043087 | regulation of GTPase activity | 0.729981247 | 1.198188932 |
| MP:0006090 | abnormal utricle morphology | 0.787327812 | 1.198189574 |
| GO:0071696 | ectodermal placode development | 0.795287948 | 1.198190908 |
| MP:0005657 | abnormal neural plate morphology | 0.790662891 | 1.19819171 |
| GO:0048029 | monosaccharide binding | 0.7669791 | 1.198192386 |
| GO:0006958 | complement activation, classical pathway | 0.729506819 | 1.19819331 |
| GO:0051258 | protein polymerization | 0.777291832 | 1.198194167 |
| ENSG00000168653 | NDUFS5 subnetwork | 0.760751918 | 1.198194325 |
| ENSG00000008018 | PSMB1 subnetwork | 0.770230975 | 1.198194371 |
| GO:2001021 | negative regulation of response to DNA damage stimulu | 0.760388324 | 1.198198925 |
| ENSG00000198727 | MT-CYB subnetwork | 0.765099901 | 1.198199017 |
| MP:0001648 | abnormal apoptosis | 0.729574396 | 1.198199105 |
| MP:0001706 | abnormal left-right axis patterning | 0.761000741 | 1.198205652 |
| GO:0051983 | regulation of chromosome segregation | 0.766901716 | 1.198208191 |
| ENSG00000129214 | SHBG subnetwork | 0.740730118 | 1.198208379 |
| ENSG00000101997 | CCDC22 subnetwork | 0.775832452 | 1.198211648 |
| REACTOME_GLUCOSE_TRANSPOF | REACTOME_GLUCOSE_TRANSPORT | 0.768326372 | 1.198216757 |
| GO:0030027 | lamellipodium | 0.791315017 | 1.198218909 |

| | | | |
|---|---|---|---|
| ENSG00000121390 | PSPC1 subnetwork | 0.77033115 | 1.198226423 |
| ENSG00000101977 | MCF2 subnetwork | 0.777230248 | 1.198230834 |
| ENSG00000130222 | GADD45G subnetwork | 0.760319001 | 1.19823637 |
| GO:0006972 | hyperosmotic response | 0.78271977 | 1.19824231 |
| MP:0003345 | decreased rib number | 0.776262356 | 1.198244227 |
| ENSG00000092201 | SUPT16H subnetwork | 0.760973776 | 1.198248442 |
| GO:0032436 | positive regulation of proteasomal ubiquitin-dependent | 0.794094745 | 1.198250413 |
| MP:0003216 | absence seizures | 0.781992652 | 1.198251309 |
| GO:0015175 | neutral amino acid transmembrane transporter activity | 0.775681347 | 1.198253482 |
| GO:0032994 | protein-lipid complex | 0.790550847 | 1.198253524 |
| ENSG00000184983 | NDUFA6 subnetwork | 0.793349741 | 1.198253952 |
| GO:0005212 | structural constituent of eye lens | 0.775944967 | 1.19825931 |
| ENSG00000198695 | MT-ND6 subnetwork | 0.746280142 | 1.198259442 |
| REACTOME_SYNTHESIS_OF_GLYC | REACTOME_SYNTHESIS_OF_GLYCOSYLPHOSPHATIDYLIN | 0.72983561 | 1.19826121 |
| MP:0000065 | abnormal bone marrow cavity morphology | 0.777701707 | 1.198268421 |
| GO:0015035 | protein disulfide oxidoreductase activity | 0.790480727 | 1.198268892 |
| GO:0032309 | icosanoid secretion | 0.794040166 | 1.198291525 |
| MP:0003651 | abnormal axon outgrowth | 0.769055177 | 1.198292735 |
| ENSG00000112769 | LAMA4 subnetwork | 0.72994639 | 1.198294946 |
| MP:0005324 | ascites | 0.781502729 | 1.198302421 |
| KEGG_DNA_REPLICATION | KEGG_DNA_REPLICATION | 0.74639218 | 1.198303415 |
| KEGG_GLYCEROPHOSPHOLIPID_M | KEGG_GLYCEROPHOSPHOLIPID_METABOLISM | 0.770109279 | 1.198305535 |
| MP:0002427 | disproportionate dwarf | 0.768960628 | 1.198308511 |
| GO:0060788 | ectodermal placode formation | 0.795287948 | 1.198314433 |
| MP:0000761 | thin diaphragm muscle | 0.741495453 | 1.198314792 |
| GO:0006884 | cell volume homeostasis | 0.76328425 | 1.198317797 |
| MP:0004272 | abnormal basement membrane morphology | 0.760303784 | 1.19832222 |
| MP:0002085 | abnormal embryonic tissue morphology | 0.795020283 | 1.198324224 |
| GO:0051186 | cofactor metabolic process | 0.790423054 | 1.198325731 |
| ENSG00000215693 | ENSG00000215693 subnetwork | 0.782693383 | 1.198325834 |
| ENSG00000212868 | ENSG00000212868 subnetwork | 0.765099901 | 1.198327098 |
| GO:0044450 | microtubule organizing center part | 0.776154891 | 1.198328235 |
| MP:0001324 | abnormal eye pigmentation | 0.794474408 | 1.198328346 |
| ENSG00000130299 | GTPBP3 subnetwork | 0.795117827 | 1.198329552 |
| MP:0002116 | abnormal craniofacial bone morphology | 0.794969216 | 1.198334365 |
| GO:0010565 | regulation of cellular ketone metabolic process | 0.740725249 | 1.198334987 |
| GO:0051046 | regulation of secretion | 0.766900477 | 1.198336 |
| GO:0071322 | cellular response to carbohydrate stimulus | 0.781354256 | 1.198338749 |
| ENSG00000104738 | MCM4 subnetwork | 0.729796497 | 1.198339298 |
| MP:0000286 | abnormal mitral valve morphology | 0.730173646 | 1.19834004 |
| GO:0061097 | regulation of protein tyrosine kinase activity | 0.768890419 | 1.198350888 |
| MP:0000163 | abnormal cartilage morphology | 0.782229112 | 1.198351131 |
| ENSG00000140400 | MAN2C1 subnetwork | 0.759946798 | 1.198359156 |
| ENSG00000112357 | PEX7 subnetwork | 0.781287782 | 1.198359539 |
| ENSG00000213380 | COG8 subnetwork | 0.776084025 | 1.198364979 |
| GO:0035304 | regulation of protein dephosphorylation | 0.795241953 | 1.198365811 |
| MP:0008908 | increased total fat pad weight | 0.741454653 | 1.198369685 |
| GO:0019941 | modification-dependent protein catabolic process | 0.776255445 | 1.198370597 |
| GO:0042805 | actinin binding | 0.741703169 | 1.19837573 |
| GO:0060323 | head morphogenesis | 0.781627632 | 1.198375943 |
| ENSG00000100084 | HIRA subnetwork | 0.781985988 | 1.198376793 |
| REACTOME_REGULATION_OF_BE | REACTOME_REGULATION_OF_BETA:CELL_DEVELOPMEN | 0.769179457 | 1.198378005 |
| MP:0000165 | abnormal long bone hypertrophic chondrocyte zone | 0.761774774 | 1.198384326 |
| GO:0071277 | cellular response to calcium ion | 0.746548896 | 1.198385685 |

| | | | |
|---|---|---|---|
| ENSG00000212869 | ENSG00000212869 subnetwork | 0.746280142 | 1.198390628 |
| GO:0071320 | cellular response to cAMP | 0.760259215 | 1.198391954 |
| REACTOME_TRANSPORT_OF_MA | REACTOME_TRANSPORT_OF_MATURE_MRNA_DERIVED | 0.782194103 | 1.198392838 |
| KEGG_PARKINSONS_DISEASE | KEGG_PARKINSONS_DISEASE | 0.794023137 | 1.19839459 |
| ENSG00000062822 | POLD1 subnetwork | 0.764541624 | 1.198395379 |
| GO:0000776 | kinetochore | 0.763149786 | 1.198397814 |
| GO:0010660 | regulation of muscle cell apoptotic process | 0.768835902 | 1.198398595 |
| ENSG00000113649 | TCERG1 subnetwork | 0.745462182 | 1.1984 |
| ENSG00000186432 | KPNA4 subnetwork | 0.790404825 | 1.198408502 |
| REACTOME_UNFOLDED_PROTEIN | REACTOME_UNFOLDED_PROTEIN_RESPONSE | 0.770008991 | 1.198411433 |
| ENSG00000114450 | GNB4 subnetwork | 0.782481984 | 1.198414277 |
| MP:0005145 | increased circulating VLDL cholesterol level | 0.763589102 | 1.198414739 |
| ENSG00000090266 | NDUFB2 subnetwork | 0.770097792 | 1.198416915 |
| ENSG00000215699 | ENSG00000215699 subnetwork | 0.778004009 | 1.198421385 |
| GO:0043278 | response to morphine | 0.79493743 | 1.198421867 |
| GO:0070167 | regulation of biomineral tissue development | 0.763260859 | 1.198424775 |
| GO:0033198 | response to ATP | 0.769883973 | 1.198427038 |
| ENSG00000134057 | CCNB1 subnetwork | 0.781500408 | 1.198428003 |
| GO:0003730 | mRNA 3'-UTR binding | 0.740696986 | 1.19842854 |
| REACTOME_FRS2:MEDIATED_CAS | REACTOME_FRS2:MEDIATED_CASCADE | 0.759923953 | 1.198428925 |
| MP:0000784 | forebrain hypoplasia | 0.730346434 | 1.19843523 |
| MP:0004374 | bowed radius | 0.741658144 | 1.198436123 |
| ENSG00000169564 | PCBP1 subnetwork | 0.763101886 | 1.198440514 |
| ENSG00000171634 | BPTF subnetwork | 0.763897442 | 1.198442017 |
| ENSG00000167513 | CDT1 subnetwork | 0.765096511 | 1.198444516 |
| GO:0005743 | mitochondrial inner membrane | 0.746116043 | 1.198450504 |
| GO:0030517 | negative regulation of axon extension | 0.746219676 | 1.198450673 |
| ENSG00000168395 | ING5 subnetwork | 0.782693383 | 1.198451235 |
| ENSG00000172352 | CDY1B subnetwork | 0.762306853 | 1.198455101 |
| GO:0070371 | ERK1 and ERK2 cascade | 0.763454883 | 1.198457253 |
| GO:0007030 | Golgi organization | 0.764645755 | 1.198465076 |
| ENSG00000090520 | DNAJB11 subnetwork | 0.729787736 | 1.198467733 |
| GO:0005871 | kinesin complex | 0.761746326 | 1.198475413 |
| GO:0016289 | CoA hydrolase activity | 0.782414853 | 1.198476918 |
| GO:0060053 | neurofilament cytoskeleton | 0.763807661 | 1.198479332 |
| ENSG00000122512 | PMS2 subnetwork | 0.781282522 | 1.198479925 |
| ENSG00000135365 | PHF21A subnetwork | 0.769972935 | 1.19848034 |
| ENSG00000125356 | NDUFA1 subnetwork | 0.730597316 | 1.198480447 |
| MP:0001688 | abnormal somite development | 0.782603144 | 1.19848247 |
| ENSG00000106348 | IMPDH1 subnetwork | 0.761576644 | 1.198485825 |
| GO:0005777 | peroxisome | 0.740655409 | 1.198489026 |
| KEGG_HYPERTROPHIC_CARDIOM | KEGG_HYPERTROPHIC_CARDIOMYOPATHY_HCM | 0.763559076 | 1.198489555 |
| GO:0048512 | circadian behavior | 0.777960049 | 1.198489633 |
| ENSG00000100804 | PSMB5 subnetwork | 0.769342148 | 1.198495161 |
| GO:0050892 | intestinal absorption | 0.761687046 | 1.198496725 |
| ENSG00000196535 | MYO18A subnetwork | 0.781981658 | 1.198497067 |
| GO:0051537 | 2 iron, 2 sulfur cluster binding | 0.763729753 | 1.198500589 |
| ENSG00000160007 | ARHGAP35 subnetwork | 0.790399212 | 1.198501659 |
| GO:0001763 | morphogenesis of a branching structure | 0.764528471 | 1.198507543 |
| GO:0046039 | GTP metabolic process | 0.762409304 | 1.198508904 |
| GO:0016893 | endonuclease activity, active with either ribo- or deoxyri | 0.745794503 | 1.198510079 |
| GO:0070528 | protein kinase C signaling cascade | 0.760243409 | 1.198510112 |
| GO:0051452 | intracellular pH reduction | 0.790133022 | 1.198511565 |
| ENSG00000134490 | TMEM241 subnetwork | 0.768756922 | 1.198515326 |

| | | | |
|---|---|---|---|
| ENSG00000125484 | GTF3C4 subnetwork | 0.745453293 | 1.198520386 |
| ENSG00000115207 | GTF3C2 subnetwork | 0.778123183 | 1.19852152 |
| ENSG00000175137 | SH3BP5L subnetwork | 0.76883335 | 1.198526125 |
| GO:0015645 | fatty acid ligase activity | 0.759910787 | 1.198530994 |
| ENSG00000197905 | TEAD4 subnetwork | 0.764887679 | 1.198534916 |
| MP:0009038 | decreased inferior colliculus size | 0.794817742 | 1.198535025 |
| GO:0055078 | sodium ion homeostasis | 0.765090351 | 1.198535229 |
| ENSG00000116701 | NCF2 subnetwork | 0.745631256 | 1.198537147 |
| ENSG00000144566 | RAB5A subnetwork | 0.781155204 | 1.198537276 |
| GO:2000045 | regulation of G1/S transition of mitotic cell cycle | 0.769871098 | 1.198538478 |
| GO:0043687 | post-translational protein modification | 0.781933779 | 1.198538808 |
| ENSG00000114107 | CEP70 subnetwork | 0.764464592 | 1.198539482 |
| ENSG00000154917 | RAB6B subnetwork | 0.730537928 | 1.198541737 |
| GO:0006368 | transcription elongation from RNA polymerase II promot | 0.789623772 | 1.198541775 |
| ENSG00000213199 | ACCN3 subnetwork | 0.790329208 | 1.198542985 |
| GO:0007162 | negative regulation of cell adhesion | 0.764081983 | 1.198543897 |
| ENSG00000156113 | KCNMA1 subnetwork | 0.761535647 | 1.198544732 |
| GO:0014072 | response to isoquinoline alkaloid | 0.79493743 | 1.198545492 |
| ENSG00000100461 | RBM23 subnetwork | 0.764981177 | 1.198551112 |
| GO:0002040 | sprouting angiogenesis | 0.764797868 | 1.19855615 |
| GO:0016676 | oxidoreductase activity, acting on a heme group of dono | 0.763084172 | 1.198563619 |
| ENSG00000117153 | KLHL12 subnetwork | 0.790085092 | 1.198578838 |
| ENSG00000007047 | MARK4 subnetwork | 0.760207691 | 1.198579882 |
| ENSG00000105404 | RABAC1 subnetwork | 0.746107308 | 1.198581754 |
| ENSG00000172288 | CDY1 subnetwork | 0.762306853 | 1.198583691 |
| ENSG00000168959 | GRM5 subnetwork | 0.759795088 | 1.198584499 |
| ENSG00000058262 | SEC61A1 subnetwork | 0.781808313 | 1.198590885 |
| MP:0000929 | open neural tube | 0.745769954 | 1.198592089 |
| ENSG00000143393 | PI4KB subnetwork | 0.730510464 | 1.198597452 |
| MP:0000743 | muscle spasm | 0.745936421 | 1.198597875 |
| ENSG00000069345 | DNAJA2 subnetwork | 0.768636945 | 1.19860017 |
| ENSG00000187953 | ENSG00000187953 subnetwork | 0.781282522 | 1.198605578 |
| ENSG00000163636 | PSMD6 subnetwork | 0.789471606 | 1.198608948 |
| ENSG00000017260 | ATP2C1 subnetwork | 0.730934047 | 1.198609405 |
| GO:0000502 | proteasome complex | 0.789597656 | 1.198619473 |
| ENSG00000170310 | STX8 subnetwork | 0.790297762 | 1.198620618 |
| GO:0042579 | microbody | 0.740655409 | 1.198621222 |
| ENSG00000068078 | FGFR3 subnetwork | 0.778479061 | 1.198621923 |
| MP:0000248 | macrocytosis | 0.7644502 | 1.198624933 |
| ENSG00000102030 | NAA10 subnetwork | 0.781901972 | 1.198632935 |
| ENSG00000138413 | IDH1 subnetwork | 0.74604818 | 1.198636364 |
| REACTOME_VITAMIN_B5_PANTO | REACTOME_VITAMIN_B5_PANTOTHENATE_METABOLISI | 0.768754594 | 1.198642895 |
| GO:0006119 | oxidative phosphorylation | 0.745193598 | 1.198645833 |
| GO:0072507 | divalent inorganic cation homeostasis | 0.745360935 | 1.198651611 |
| MP:0000473 | abnormal stomach glandular epithelium morphology | 0.745452175 | 1.198651759 |
| GO:0008374 | O-acyltransferase activity | 0.780759712 | 1.198651909 |
| GO:0030100 | regulation of endocytosis | 0.780840201 | 1.198652051 |
| ENSG00000074266 | EED subnetwork | 0.73105212 | 1.198654233 |
| REACTOME_HEXOSE_TRANSPORT | REACTOME_HEXOSE_TRANSPORT | 0.781132463 | 1.198657718 |
| GO:0035255 | ionotropic glutamate receptor binding | 0.739815445 | 1.198658348 |
| ENSG00000187098 | MITF subnetwork | 0.794816532 | 1.198658688 |
| GO:0001704 | formation of primary germ layer | 0.740594137 | 1.19865968 |
| KEGG_PROTEIN_EXPORT | KEGG_PROTEIN_EXPORT | 0.759910299 | 1.198659994 |
| GO:0051540 | metal cluster binding | 0.730859795 | 1.198665103 |

| | | | |
|---|---|---|---|
| KEGG_MISMATCH_REPAIR | KEGG_MISMATCH_REPAIR | 0.76986854 | 1.198665887 |
| ENSG00000087152 | ATXN7L3 subnetwork | 0.742268354 | 1.198668281 |
| GO:0007183 | SMAD protein complex assembly | 0.740523883 | 1.198670565 |
| GO:0006887 | exocytosis | 0.790074134 | 1.198672061 |
| GO:0051289 | protein homotetramerization | 0.739307335 | 1.198673887 |
| GO:0006929 | substrate-dependent cell migration | 0.762025723 | 1.198674324 |
| ENSG00000131495 | NDUFA2 subnetwork | 0.764345084 | 1.198678155 |
| ENSG00000025293 | PHF20 subnetwork | 0.76262412 | 1.198686045 |
| GO:0004129 | cytochrome-c oxidase activity | 0.763084172 | 1.19869211 |
| MP:0002734 | abnormal mechanical nociception | 0.764409155 | 1.198694349 |
| ENSG00000171345 | KRT19 subnetwork | 0.762134592 | 1.198695932 |
| GO:0048753 | pigment granule organization | 0.790002588 | 1.198697863 |
| GO:0032413 | negative regulation of ion transmembrane transporter a | 0.734086986 | 1.198698409 |
| MP:0001685 | abnormal endoderm development | 0.743855192 | 1.198698517 |
| GO:0042059 | negative regulation of epidermal growth factor receptor | 0.762301096 | 1.198701577 |
| REACTOME_RETROGRADE_NEUR | REACTOME_RETROGRADE_NEUROTROPHIN_SIGNALLIN | 0.764289078 | 1.198704774 |
| ENSG00000140403 | DNAJA4 subnetwork | 0.759794179 | 1.198708149 |
| ENSG00000140332 | TLE3 subnetwork | 0.740468954 | 1.198709037 |
| ENSG00000177380 | PPFIA3 subnetwork | 0.733991342 | 1.19870939 |
| MP:0005108 | abnormal ulna morphology | 0.769583721 | 1.198713313 |
| ENSG00000101367 | MAPRE1 subnetwork | 0.734382832 | 1.198715525 |
| GO:0015695 | organic cation transport | 0.745309211 | 1.198717246 |
| ENSG00000146276 | GABRR1 subnetwork | 0.762742157 | 1.198718361 |
| GO:0061061 | muscle structure development | 0.740384054 | 1.198719929 |
| ENSG00000130816 | DNMT1 subnetwork | 0.764242161 | 1.198720694 |
| ENSG00000213496 | ENSG00000213496 subnetwork | 0.762931187 | 1.198723997 |
| GO:0015939 | pantothenate metabolic process | 0.780732094 | 1.198725212 |
| ENSG00000185345 | PARK2 subnetwork | 0.77844706 | 1.198726986 |
| GO:0051567 | histone H3-K9 methylation | 0.789469732 | 1.198728198 |
| ENSG00000088832 | FKBP1A subnetwork | 0.780634455 | 1.198730325 |
| REACTOME_TELOMERE_C:STRAN | REACTOME_TELOMERE_C:STRAND_LAGGING_STRAND_ | 0.734468847 | 1.198732347 |
| GO:0010862 | positive regulation of pathway-restricted SMAD protein | 0.731209448 | 1.198738135 |
| GO:0008045 | motor axon guidance | 0.740021192 | 1.198746964 |
| ENSG00000110245 | APOC3 subnetwork | 0.769840482 | 1.198750797 |
| ENSG00000161800 | RACGAP1 subnetwork | 0.739255109 | 1.198751105 |
| ENSG00000105819 | PMPCB subnetwork | 0.739655879 | 1.198751795 |
| ENSG00000186908 | ZDHHC17 subnetwork | 0.789956396 | 1.198754799 |
| GO:0030431 | sleep | 0.742074727 | 1.198755918 |
| ENSG00000106366 | SERPINE1 subnetwork | 0.743710952 | 1.198758651 |
| ENSG00000166971 | AKTIP subnetwork | 0.781026881 | 1.198767569 |
| ENSG00000196501 | ENSG00000196501 subnetwork | 0.742251094 | 1.198772702 |
| ENSG00000197956 | S100A6 subnetwork | 0.788722976 | 1.198773771 |
| GO:0035066 | positive regulation of histone acetylation | 0.789843508 | 1.198775425 |
| GO:0007286 | spermatid development | 0.745192833 | 1.198777278 |
| GO:0044257 | cellular protein catabolic process | 0.739812172 | 1.19877968 |
| ENSG00000184381 | PLA2G6 subnetwork | 0.739971898 | 1.198779949 |
| KEGG_PYRUVATE_METABOLISM | KEGG_PYRUVATE_METABOLISM | 0.781127587 | 1.198783429 |
| ENSG00000135547 | HEY2 subnetwork | 0.762892268 | 1.198793566 |
| ENSG00000114054 | PCCB subnetwork | 0.7326538 | 1.198796255 |
| ENSG00000198648 | STK39 subnetwork | 0.743804713 | 1.198797232 |
| ENSG00000147099 | HDAC8 subnetwork | 0.734360007 | 1.198798799 |
| GO:0051536 | iron-sulfur cluster binding | 0.730859795 | 1.198799017 |
| GO:0003230 | cardiac atrium development | 0.759760734 | 1.198799526 |
| ENSG00000093009 | CDC45 subnetwork | 0.733965853 | 1.198803828 |

| | | | |
|---|---|---|---|
| ENSG00000115286 | NDUFS7 subnetwork | 0.742175248 | 1.198805592 |
| ENSG00000129515 | SNX6 subnetwork | 0.734899056 | 1.198810847 |
| ENSG00000153561 | RMND5A subnetwork | 0.762291291 | 1.198814123 |
| REACTOME_G_BETAGAMMA_SIG | REACTOME_G_BETAGAMMA_SIGNALLING_THROUGH_P | 0.759664265 | 1.198815549 |
| GO:0015002 | heme-copper terminal oxidase activity | 0.763084172 | 1.198820628 |
| ENSG00000090054 | SPTLC1 subnetwork | 0.779270057 | 1.198822787 |
| GO:0071229 | cellular response to acid | 0.742028406 | 1.198827351 |
| GO:0032760 | positive regulation of tumor necrosis factor production | 0.739193915 | 1.198828341 |
| ENSG00000111676 | ATN1 subnetwork | 0.74326898 | 1.198829284 |
| GO:0050999 | regulation of nitric-oxide synthase activity | 0.778414769 | 1.198832071 |
| GO:0070498 | interleukin-1-mediated signaling pathway | 0.77875366 | 1.198832562 |
| GO:0008373 | sialyltransferase activity | 0.739634207 | 1.198834512 |
| ENSG00000128513 | POT1 subnetwork | 0.743184831 | 1.19884015 |
| MP:0009409 | abnormal skeletal muscle fiber type ratio | 0.740379772 | 1.198841188 |
| MP:0010363 | increased fibrosarcoma incidence | 0.788823374 | 1.198841438 |
| MP:0002753 | dilated heart left ventricle | 0.743691719 | 1.198846407 |
| ENSG00000206495 | TRIM39 subnetwork | 0.789462545 | 1.198847472 |
| GO:0043568 | positive regulation of insulin-like growth factor receptor | 0.780632978 | 1.198850876 |
| GO:0019199 | transmembrane receptor protein kinase activity | 0.743057616 | 1.198850891 |
| GO:0048260 | positive regulation of receptor-mediated endocytosis | 0.759590052 | 1.198853112 |
| ENSG00000155511 | GRIA1 subnetwork | 0.779094988 | 1.198859336 |
| MP:0000872 | abnormal cerebellum external granule cell layer morpho | 0.733904014 | 1.198859337 |
| MP:0010099 | abnormal thoracic cage shape | 0.745157712 | 1.198859399 |
| ENSG00000164118 | CEP44 subnetwork | 0.734849785 | 1.198860731 |
| GO:0051591 | response to cAMP | 0.778694696 | 1.198863995 |
| MP:0004568 | fusion of glossopharyngeal and vagus nerve | 0.732629778 | 1.19887415 |
| GO:0031941 | filamentous actin | 0.779851804 | 1.19887605 |
| ENSG00000215755 | ENSG00000215755 subnetwork | 0.769840482 | 1.198878256 |
| ENSG00000173145 | NOC3L subnetwork | 0.739789709 | 1.198878949 |
| MP:0004910 | decreased seminal vesicle weight | 0.780588493 | 1.198882242 |
| GO:0043632 | modification-dependent macromolecule catabolic proce | 0.78871246 | 1.198882769 |
| GO:0006383 | transcription from RNA polymerase III promoter | 0.742722084 | 1.198883265 |
| ENSG00000137601 | NEK1 subnetwork | 0.750046558 | 1.19888792 |
| GO:0016876 | ligase activity, forming aminoacyl-tRNA and related com | 0.745075955 | 1.198892179 |
| MP:0001925 | male infertility | 0.734326879 | 1.198893215 |
| REACTOME_TIGHT_JUNCTION_IN | REACTOME_TIGHT_JUNCTION_INTERACTIONS | 0.743647785 | 1.198895726 |
| ENSG00000133216 | EPHB2 subnetwork | 0.779244625 | 1.198901503 |
| REACTOME_CALMODULIN_INDUC | REACTOME_CALMODULIN_INDUCED_EVENTS | 0.733663825 | 1.198903484 |
| GO:0003012 | muscle system process | 0.747369575 | 1.198906147 |
| GO:0033261 | regulation of S phase | 0.743578637 | 1.198906593 |
| ENSG00000106100 | NOD1 subnetwork | 0.742811358 | 1.198910891 |
| GO:0034399 | nuclear periphery | 0.735309723 | 1.198911232 |
| GO:0006874 | cellular calcium ion homeostasis | 0.735125912 | 1.198916546 |
| GO:0060420 | regulation of heart growth | 0.75953105 | 1.198939149 |
| ENSG00000152104 | PTPN14 subnetwork | 0.780535727 | 1.198939855 |
| ENSG00000008710 | PKD1 subnetwork | 0.778873188 | 1.198943107 |
| MP:0002561 | abnormal circadian phase | 0.73917931 | 1.198944285 |
| ENSG00000108671 | PSMD11 subnetwork | 0.733864356 | 1.198948247 |
| GO:0001569 | patterning of blood vessels | 0.734809949 | 1.198949533 |
| GO:0032855 | positive regulation of Rac GTPase activity | 0.739623573 | 1.198950392 |
| GO:0010817 | regulation of hormone levels | 0.749982735 | 1.198953222 |
| MP:0005307 | head tossing | 0.733020194 | 1.198958217 |
| MP:0001784 | abnormal fluid regulation | 0.779601668 | 1.19896501 |
| ENSG00000115241 | PPM1G subnetwork | 0.747331227 | 1.198966196 |

| | | | |
|---|---|---|---|
| GO:0030029 | actin filament-based process | 0.743180629 | 1.198966465 |
| ENSG00000155897 | ADCY8 subnetwork | 0.740374041 | 1.198967991 |
| GO:0044441 | cilium part | 0.733142008 | 1.198969474 |
| GO:0042058 | regulation of epidermal growth factor receptor signaling | 0.734747767 | 1.198971651 |
| GO:0043648 | dicarboxylic acid metabolic process | 0.7430522 | 1.198971737 |
| ENSG00000206419 | ENSG00000206419 subnetwork | 0.789462545 | 1.198971963 |
| ENSG00000185010 | F8 subnetwork | 0.779392028 | 1.198975302 |
| GO:0016831 | carboxy-lyase activity | 0.732608794 | 1.198979933 |
| REACTOME_TRNA_AMINOACYLAT | REACTOME_TRNA_AMINOACYLATION | 0.732862677 | 1.198980274 |
| ENSG00000025770 | NCAPH2 subnetwork | 0.742709864 | 1.198982174 |
| ENSG00000182446 | NPLOC4 subnetwork | 0.779085906 | 1.198985385 |
| REACTOME_LYSOSOME_VESICLE_ | REACTOME_LYSOSOME_VESICLE_BIOGENESIS | 0.788999343 | 1.198987013 |
| GO:0031954 | positive regulation of protein autophosphorylation | 0.789075519 | 1.198987118 |
| GO:0008544 | epidermis development | 0.743465713 | 1.198988789 |
| ENSG00000135250 | SRPK2 subnetwork | 0.743534298 | 1.1989889 |
| ENSG00000157349 | DDX19B subnetwork | 0.74750826 | 1.198993766 |
| ENSG00000109220 | CHIC2 subnetwork | 0.739567081 | 1.199 |
| MP:0001429 | dehydration | 0.788088046 | 1.199001456 |
| MP:0000889 | abnormal cerebellar molecular layer | 0.779843695 | 1.199001996 |
| ENSG00000169118 | CSNK1G1 subnetwork | 0.78048111 | 1.199002729 |
| ENSG00000185513 | L3MBTL1 subnetwork | 0.759476913 | 1.199003662 |
| GO:0016567 | protein ubiquitination | 0.788712148 | 1.19900738 |
| GO:0030317 | sperm motility | 0.779017296 | 1.199011567 |
| ENSG00000130208 | APOC1 subnetwork | 0.779742656 | 1.199012398 |
| GO:0070372 | regulation of ERK1 and ERK2 cascade | 0.733423383 | 1.199019935 |
| MP:0000107 | abnormal frontal bone morphology | 0.733816711 | 1.199020481 |
| GO:0016875 | ligase activity, forming carbon-oxygen bonds | 0.745075955 | 1.199023695 |
| ENSG00000213619 | NDUFS3 subnetwork | 0.735303085 | 1.199027778 |
| GO:0009434 | microtubule-based flagellum | 0.733246057 | 1.199030857 |
| REACTOME_CAM_PATHWAY | REACTOME_CAM_PATHWAY | 0.733663825 | 1.199036963 |
| MP:0001106 | abnormal Schwann cell morphology | 0.747298595 | 1.199037199 |
| GO:0070588 | calcium ion transmembrane transport | 0.739068738 | 1.199038036 |
| GO:0006200 | ATP catabolic process | 0.743027825 | 1.199048614 |
| GO:0033032 | regulation of myeloid cell apoptotic process | 0.779571624 | 1.19904897 |
| GO:0016538 | cyclin-dependent protein kinase regulator activity | 0.780240111 | 1.19905492 |
| ENSG00000164930 | FZD6 subnetwork | 0.747209771 | 1.199058978 |
| GO:0010460 | positive regulation of heart rate | 0.733568492 | 1.199064692 |
| GO:0007178 | transmembrane receptor protein serine/threonine kinas | 0.739171729 | 1.199065782 |
| ENSG00000182054 | IDH2 subnetwork | 0.73150012 | 1.199067664 |
| ENSG00000071564 | TCF3 subnetwork | 0.742952326 | 1.199070509 |
| MP:0001004 | abnormal retinal photoreceptor morphology | 0.740355157 | 1.199072745 |
| ENSG00000198868 | ENSG00000198868 subnetwork | 0.749975682 | 1.199078517 |
| GO:0045259 | proton-transporting ATP synthase complex | 0.759438932 | 1.199084348 |
| GO:0032787 | monocarboxylic acid metabolic process | 0.742682143 | 1.199086607 |
| MP:0000109 | abnormal parietal bone morphology | 0.780454991 | 1.199086614 |
| ENSG00000185324 | CDK10 subnetwork | 0.739027448 | 1.199087692 |
| GO:0006937 | regulation of muscle contraction | 0.78938199 | 1.199091192 |
| REACTOME_PROCESSIVE_SYNTHE | REACTOME_PROCESSIVE_SYNTHESIS_ON_THE_LAGGING | 0.733018261 | 1.199091821 |
| ENSG00000204599 | TRIM39 subnetwork | 0.789462545 | 1.199096479 |
| GO:0043297 | apical junction assembly | 0.733392009 | 1.199097795 |
| ENSG00000024048 | UBR2 subnetwork | 0.732605121 | 1.199102464 |
| KEGG_RENIN_ANGIOTENSIN_SYS | KEGG_RENIN_ANGIOTENSIN_SYSTEM | 0.733522372 | 1.199103563 |
| ENSG00000107295 | SH3GL2 subnetwork | 0.734745095 | 1.199104959 |
| GO:0006677 | glycosylceramide metabolic process | 0.789274688 | 1.199106679 |

| | | | |
|---|---|---|---|
| GO:0006829 | zinc ion transport | 0.780398872 | 1.199112768 |
| GO:0060525 | prostate glandular acinus development | 0.788700257 | 1.199121622 |
| KEGG_BETA_ALANINE_METABOLI | KEGG_BETA_ALANINE_METABOLISM | 0.788608166 | 1.199142322 |
| GO:0070830 | tight junction assembly | 0.732559127 | 1.199146967 |
| ENSG00000099194 | SCD subnetwork | 0.780145214 | 1.199149249 |
| GO:0004812 | aminoacyl-tRNA ligase activity | 0.745075955 | 1.199155239 |
| ENSG00000165264 | NDUFB6 subnetwork | 0.747692196 | 1.19917979 |
| GO:0046474 | glycerophospholipid biosynthetic process | 0.780232599 | 1.199180844 |
| ENSG00000179603 | GRM8 subnetwork | 0.738997598 | 1.199187127 |
| ENSG00000111432 | FZD10 subnetwork | 0.747209771 | 1.199190195 |
| GO:0009127 | purine nucleoside monophosphate biosynthetic process | 0.735864655 | 1.199200444 |
| MP:0008006 | increased stomach pH | 0.737483076 | 1.199202128 |
| ENSG00000169018 | FEM1B subnetwork | 0.73593424 | 1.199206085 |
| GO:0072531 | pyrimidine-containing compound transmembrane transp | 0.736739203 | 1.199206877 |
| ENSG00000198840 | MT-ND3 subnetwork | 0.749975682 | 1.199209292 |
| GO:0015144 | carbohydrate transmembrane transporter activity | 0.731750266 | 1.199212994 |
| GO:0016072 | rRNA metabolic process | 0.759434687 | 1.199213532 |
| REACTOME_ROLE_OF_SECOND_M | REACTOME_ROLE_OF_SECOND_MESSENGERS_IN_NETR | 0.737639468 | 1.199230002 |
| ENSG00000196353 | CPNE4 subnetwork | 0.745038083 | 1.199231951 |
| GO:0030659 | cytoplasmic vesicle membrane | 0.731855957 | 1.199235406 |
| ENSG00000160948 | VPS28 subnetwork | 0.759393023 | 1.199240384 |
| ENSG00000183495 | EP400 subnetwork | 0.731940148 | 1.199246652 |
| ENSG00000119013 | NDUFB3 subnetwork | 0.788305893 | 1.19925117 |
| ENSG00000182199 | SHMT2 subnetwork | 0.731675633 | 1.199251982 |
| ENSG00000171497 | PPID subnetwork | 0.744361503 | 1.199258731 |
| GO:0046131 | pyrimidine ribonucleoside metabolic process | 0.744946141 | 1.1992593 |
| GO:0045187 | regulation of circadian sleep/wake cycle, sleep | 0.737336589 | 1.199262913 |
| GO:0015949 | nucleobase-containing small molecule interconversion | 0.788607625 | 1.199266999 |
| MP:0000474 | abnormal foregut morphology | 0.759344633 | 1.199267241 |
| MP:0000940 | abnormal motor neuron innervation | 0.744450688 | 1.199269792 |
| MP:0000005 | increased brown adipose tissue amount | 0.732558026 | 1.199280696 |
| MP:0009417 | skeletal muscle atrophy | 0.737436934 | 1.19928516 |
| GO:0046716 | muscle cell homeostasis | 0.737601753 | 1.199301939 |
| GO:0009148 | pyrimidine nucleoside triphosphate biosynthetic process | 0.73898342 | 1.199303174 |
| REACTOME_SYNTHESIS_OF_VERY | REACTOME_SYNTHESIS_OF_VERY_LONG:CHAIN_FATTY_ | 0.736706249 | 1.199312181 |
| KEGG_DRUG_METABOLISM_OTH | KEGG_DRUG_METABOLISM_OTHER_ENZYMES | 0.737797543 | 1.199313172 |
| GO:0035338 | long-chain fatty-acyl-CoA biosynthetic process | 0.788545638 | 1.199313715 |
| GO:0003014 | renal system process | 0.737899765 | 1.199318786 |
| ENSG00000125485 | DDX31 subnetwork | 0.744888177 | 1.199319579 |
| GO:0046434 | organophosphate catabolic process | 0.736230246 | 1.199322824 |
| GO:0030502 | negative regulation of bone mineralization | 0.744820282 | 1.19933048 |
| GO:0009168 | purine ribonucleoside monophosphate biosynthetic proc | 0.735864655 | 1.199333629 |
| GO:0031526 | brush border membrane | 0.738888857 | 1.199336283 |
| ENSG00000212871 | ENSG00000212871 subnetwork | 0.749975682 | 1.199340096 |
| ENSG00000184752 | NDUFA12 subnetwork | 0.738773054 | 1.199341741 |
| ENSG00000085978 | ATG16L1 subnetwork | 0.735796655 | 1.199344663 |
| GO:0048232 | male gamete generation | 0.738182538 | 1.199346695 |
| GO:0015804 | neutral amino acid transport | 0.7370858 | 1.199362386 |
| GO:0004089 | carbonate dehydratase activity | 0.737155282 | 1.199373545 |
| ENSG00000186832 | KRT16 subnetwork | 0.74475789 | 1.199374314 |
| GO:0006024 | glycosaminoglycan biosynthetic process | 0.759326985 | 1.199374933 |
| ENSG00000127831 | VIL1 subnetwork | 0.736168027 | 1.199383813 |
| ENSG00000138834 | MAPK8IP3 subnetwork | 0.738491669 | 1.199391256 |
| MP:0000936 | small telencephalic vesicles | 0.73237355 | 1.199392012 |

| | | | |
|---|---|---|---|
| GO:0042749 | regulation of circadian sleep/wake cycle | 0.737336589 | 1.199395854 |
| GO:0051569 | regulation of histone H3-K4 methylation | 0.73229768 | 1.199414259 |
| GO:0042776 | mitochondrial ATP synthesis coupled proton transport | 0.732558007 | 1.199414455 |
| GO:0009086 | methionine biosynthetic process | 0.737024488 | 1.199423312 |
| ENSG00000114841 | DNAH1 subnetwork | 0.732141174 | 1.199425287 |
| GO:0031252 | cell leading edge | 0.736701194 | 1.199434151 |
| GO:0072659 | protein localization in plasma membrane | 0.736939614 | 1.199434339 |
| GO:0035336 | long-chain fatty-acyl-CoA metabolic process | 0.788545638 | 1.199438436 |
| MP:0008225 | abnormal anterior commissure morphology | 0.759306721 | 1.19946648 |
| GO:0010744 | positive regulation of macrophage derived foam cell diff | 0.737283699 | 1.199467849 |
| ENSG00000107242 | PIP5K1B subnetwork | 0.73225585 | 1.199469984 |
| ENSG00000212872 | ENSG00000212872 subnetwork | 0.749975682 | 1.199470928 |
| GO:0055069 | zinc ion homeostasis | 0.738461899 | 1.199474209 |
| GO:0045923 | positive regulation of fatty acid metabolic process | 0.738694699 | 1.199474383 |
| GO:0030169 | low-density lipoprotein particle binding | 0.738769805 | 1.199474441 |
| ENSG00000124172 | ATP5E subnetwork | 0.748069937 | 1.19947518 |
| ENSG00000185920 | PTCH1 subnetwork | 0.735795491 | 1.199477894 |
| GO:0007283 | spermatogenesis | 0.738182538 | 1.199479513 |
| GO:0060767 | epithelial cell proliferation involved in prostate gland dev | 0.73657343 | 1.199489513 |
| MP:0002151 | abnormal neural tube morphology/development | 0.74474513 | 1.199495005 |
| ENSG00000105655 | ISYNA1 subnetwork | 0.744674987 | 1.199516908 |
| GO:0001533 | cornified envelope | 0.736437954 | 1.19951715 |
| GO:0008175 | tRNA methyltransferase activity | 0.732537155 | 1.199520357 |
| MP:0003974 | abnormal endocardium morphology | 0.736676238 | 1.199528407 |
| MP:0004686 | decreased length of long bones | 0.738317942 | 1.199546058 |
| GO:0043218 | compact myelin | 0.736540218 | 1.199550499 |
| REACTOME_PURINE_METABOLISI | REACTOME_PURINE_METABOLISM | 0.759273928 | 1.199558047 |
| ENSG00000070193 | FGF10 subnetwork | 0.748039052 | 1.19956807 |
| ENSG00000170248 | PDCD6IP subnetwork | 0.749968171 | 1.199579969 |
| ENSG00000111241 | FGF6 subnetwork | 0.759159468 | 1.199584906 |
| ENSG00000167774 | NDUFA7 subnetwork | 0.738684421 | 1.199584993 |
| GO:0060512 | prostate gland morphogenesis | 0.738169324 | 1.199590209 |
| GO:0006882 | cellular zinc ion homeostasis | 0.738461899 | 1.199606997 |
| GO:0010288 | response to lead ion | 0.749930484 | 1.199618112 |
| GO:0009451 | RNA modification | 0.74828851 | 1.199628293 |
| GO:0022617 | extracellular matrix disassembly | 0.750676481 | 1.199645738 |
| GO:0016601 | Rac protein signal transduction | 0.759264278 | 1.199660414 |
| MP:0004734 | small thoracic cavity | 0.750575044 | 1.199672953 |
| ENSG00000134025 | ENSG00000134025 subnetwork | 0.75417116 | 1.199674479 |
| GO:0017046 | peptide hormone binding | 0.74986019 | 1.199678088 |
| GO:0031648 | protein destabilization | 0.749766462 | 1.199694423 |
| ENSG00000187514 | PTMA subnetwork | 0.754396868 | 1.199701671 |
| MP:0001674 | abnormal triploblastic development | 0.75428768 | 1.199707063 |
| ENSG00000107831 | FGF8 subnetwork | 0.759159468 | 1.199714255 |
| GO:0050962 | detection of light stimulus involved in sensory perceptio | 0.748724029 | 1.19973227 |
| GO:0001510 | RNA methylation | 0.754526159 | 1.199734244 |
| REACTOME_FGFR2_LIGAND_BINI | REACTOME_FGFR2_LIGAND_BINDING_AND_ACTIVATIO | 0.752953823 | 1.19976087 |
| GO:0007088 | regulation of mitosis | 0.753460039 | 1.19978275 |
| ENSG00000148498 | PARD3 subnetwork | 0.754166903 | 1.19979924 |
| ENSG00000088986 | DYNLL1 subnetwork | 0.748610468 | 1.199814187 |
| GO:0045022 | early endosome to late endosome transport | 0.749224846 | 1.19981979 |
| ENSG00000186184 | POLR1D subnetwork | 0.749763927 | 1.199819908 |
| GO:0008137 | NADH dehydrogenase (ubiquinone) activity | 0.752915515 | 1.199831503 |
| GO:0009132 | nucleoside diphosphate metabolic process | 0.754128586 | 1.199831778 |

| | | | |
|---|---|---|---|
| GO:0050820 | positive regulation of coagulation | 0.749172891 | 1.199836155 |
| ENSG00000205542 | TMSB4X subnetwork | 0.753557798 | 1.19983708 |
| ENSG00000158815 | FGF17 subnetwork | 0.759159468 | 1.199843632 |
| REACTOME_RECYCLING_PATHWA | REACTOME_RECYCLING_PATHWAY_OF_L1 | 0.753311982 | 1.199847892 |
| GO:0050908 | detection of light stimulus involved in visual perception | 0.748724029 | 1.199863388 |
| MP:0004936 | impaired branching involved in ureteric bud morphogen | 0.753164533 | 1.199869594 |
| GO:0043507 | positive regulation of JUN kinase activity | 0.749648911 | 1.199885371 |
| GO:0000387 | spliceosomal snRNP assembly | 0.751189643 | 1.199885596 |
| GO:0015931 | nucleobase-containing compound transport | 0.749744732 | 1.199890842 |
| REACTOME_GOLGI_ASSOCIATED_ | REACTOME_GOLGI_ASSOCIATED_VESICLE_BIOGENESIS | 0.751268753 | 1.199896503 |
| ENSG00000142798 | HSPG2 subnetwork | 0.748581189 | 1.199901618 |
| MP:0006113 | abnormal heart septum morphology | 0.748954994 | 1.199901661 |
| GO:0051783 | regulation of nuclear division | 0.753460039 | 1.199913091 |
| ENSG00000067177 | PHKA1 subnetwork | 0.753131502 | 1.199923921 |
| MP:0001663 | abnormal digestive system physiology | 0.749129046 | 1.199928993 |
| MP:0009283 | decreased gonadal fat pad weight | 0.75142104 | 1.199956427 |
| GO:0016408 | C-acyltransferase activity | 0.754109457 | 1.199956583 |
| MP:0001672 | abnormal embryogenesis/ development | 0.749067335 | 1.199961761 |
| GO:0003954 | NADH dehydrogenase activity | 0.752915515 | 1.199961948 |
| GO:0006090 | pyruvate metabolic process | 0.752680382 | 1.199972811 |
| ENSG00000162344 | FGF19 subnetwork | 0.759159468 | 1.199973037 |
| GO:0007346 | regulation of mitotic cell cycle | 0.753309739 | 1.199978268 |
| ENSG00000158874 | APOA2 subnetwork | 0.749553346 | 1.199983621 |
| ENSG00000145332 | KLHL8 subnetwork | 0.750948338 | 1.199983651 |
| GO:0007205 | protein kinase C-activating G-protein coupled receptor si | 0.749639009 | 1.199989082 |
| GO:0048485 | sympathetic nervous system development | 0.753906026 | 1.199994571 |
| GO:0030296 | protein tyrosine kinase activator activity | 0.751175853 | 1.200005448 |
| ENSG00000124171 | PARD6B subnetwork | 0.751075877 | 1.200005449 |
| ENSG00000101421 | CHMP4B subnetwork | 0.753990548 | 1.200021713 |
| GO:0051131 | chaperone-mediated protein complex assembly | 0.753773388 | 1.20004344 |
| ENSG00000198959 | TGM2 subnetwork | 0.74951394 | 1.200049143 |
| MP:0000074 | abnormal neurocranium morphology | 0.754086876 | 1.200054277 |
| GO:0050136 | NADH dehydrogenase (quinone) activity | 0.752915515 | 1.200092421 |
| GO:0016747 | transferase activity, transferring acyl groups other than a | 0.75266614 | 1.200092452 |
| ENSG00000156427 | FGF18 subnetwork | 0.759159468 | 1.20010247 |
| ENSG00000075643 | MOCOS subnetwork | 0.752594986 | 1.200119656 |
| GO:0006776 | vitamin A metabolic process | 0.753905544 | 1.200124878 |
| GO:0060742 | epithelial cell differentiation involved in prostate gland d | 0.752843691 | 1.200130492 |
| GO:0050911 | detection of chemical stimulus involved in sensory perce | 0.75222276 | 1.200212233 |
| MP:0002109 | abnormal limb morphology | 0.752582658 | 1.20022846 |
| ENSG00000070388 | FGF22 subnetwork | 0.759159468 | 1.200231931 |
| GO:0071357 | cellular response to type I interferon | 0.758960253 | 1.200231981 |
| MP:0002106 | abnormal muscle physiology | 0.751847297 | 1.200239573 |
| GO:0051378 | serotonin binding | 0.75232426 | 1.200244858 |
| GO:0000209 | protein polyubiquitination | 0.751902585 | 1.200244991 |
| GO:0050795 | regulation of behavior | 0.756303664 | 1.200249026 |
| GO:0048557 | embryonic digestive tract morphogenesis | 0.751761579 | 1.20025049 |
| ENSG00000152208 | GRID2 subnetwork | 0.754968893 | 1.200265727 |
| REACTOME_ACTIVATION_OF_CH/ | REACTOME_ACTIVATION_OF_CHAPERONES_BY_ATF6:AI | 0.752175938 | 1.200277566 |
| ENSG00000160999 | SH2B2 subnetwork | 0.752088222 | 1.200293926 |
| REACTOME_P53:DEPENDENT_G1 | REACTOME_P53:DEPENDENT_G1S_DNA_DAMAGE_CHE | 0.758870107 | 1.20030218 |
| GO:0006301 | postreplication repair | 0.752453793 | 1.20031012 |
| ENSG00000161057 | PSMC2 subnetwork | 0.759124541 | 1.20032366 |
| MP:0004617 | sacral vertebral transformation | 0.752566017 | 1.200331846 |

| | | | |
|---|---|---|---|
| GO:0030307 | positive regulation of cell growth | 0.756108729 | 1.200341168 |
| ENSG00000065054 | SLC9A3R2 subnetwork | 0.756281853 | 1.200346508 |
| KEGG_PROPANOATE_METABOLIS | KEGG_PROPANOATE_METABOLISM | 0.751747914 | 1.200359438 |
| GO:0060337 | type I interferon-mediated signaling pathway | 0.758960253 | 1.200361498 |
| GO:0000792 | heterochromatin | 0.752087323 | 1.200424605 |
| REACTOME_P53:DEPENDENT_G1_ | REACTOME_P53:DEPENDENT_G1_DNA_DAMAGE_RESPO | 0.758870107 | 1.200431732 |
| ENSG00000130396 | MLLT4 subnetwork | 0.756259838 | 1.200444011 |
| ENSG00000124222 | STX16 subnetwork | 0.75610341 | 1.200460355 |
| GO:0048871 | multicellular organismal homeostasis | 0.756044573 | 1.200487488 |
| MP:0010454 | abnormal truncus arteriosus septation | 0.755637041 | 1.200487752 |
| GO:0019843 | rRNA binding | 0.758840292 | 1.200528929 |
| ENSG00000107262 | BAG1 subnetwork | 0.756711837 | 1.200562892 |
| ENSG00000109390 | NDUFC1 subnetwork | 0.756024665 | 1.200579632 |
| GO:0005791 | rough endoplasmic reticulum | 0.755607464 | 1.200585366 |
| ENSG00000212876 | ENSG00000212876 subnetwork | 0.758818464 | 1.200609954 |
| ENSG00000121481 | RNF2 subnetwork | 0.755275293 | 1.200618154 |
| ENSG00000163082 | SGPP2 subnetwork | 0.758482122 | 1.200626418 |
| ENSG00000160194 | NDUFV3 subnetwork | 0.756684998 | 1.200660388 |
| GO:0090305 | nucleic acid phosphodiester bond hydrolysis | 0.756016118 | 1.200688049 |
| ENSG00000124635 | HIST1H2BJ subnetwork | 0.755946764 | 1.20069896 |
| GO:0016540 | protein autoprocessing | 0.755864378 | 1.200699035 |
| GO:0043236 | laminin binding | 0.756914982 | 1.200703539 |
| ENSG00000197597 | ENSG00000197597 subnetwork | 0.758352788 | 1.200707573 |
| ENSG00000170906 | NDUFA3 subnetwork | 0.755602545 | 1.200715525 |
| ENSG00000100038 | TOP3B subnetwork | 0.757040467 | 1.200735931 |
| ENSG00000198763 | MT-ND2 subnetwork | 0.758818464 | 1.200739581 |
| GO:0009081 | branched chain family amino acid metabolic process | 0.758463373 | 1.200739901 |
| ENSG00000143344 | RGL1 subnetwork | 0.757204535 | 1.200752002 |
| ENSG00000115350 | POLE4 subnetwork | 0.755463157 | 1.200764476 |
| ENSG00000114026 | OGG1 subnetwork | 0.758722963 | 1.200766656 |
| GO:0016811 | hydrolase activity, acting on carbon-nitrogen (but not pe | 0.758667422 | 1.200782937 |
| GO:0006041 | glucosamine metabolic process | 0.758331556 | 1.200810285 |
| GO:0071565 | nBAF complex | 0.755582213 | 1.200818606 |
| REACTOME_RNA_POLYMERASE_I | REACTOME_RNA_POLYMERASE_I_TRANSCRIPTION_TERI | 0.757200747 | 1.200881939 |
| GO:0006044 | N-acetylglucosamine metabolic process | 0.758331556 | 1.200940032 |
| ENSG00000198744 | ENSG00000198744 subnetwork | 0.757554247 | 1.200957274 |
| GO:0004521 | endoribonuclease activity | 0.758277033 | 1.200994165 |
| MP:0003050 | abnormal sacral vertebrae morphology | 0.75751933 | 1.201027694 |
| ENSG00000131828 | PDHA1 subnetwork | 0.757479827 | 1.20107649 |
| GO:0009566 | fertilization | 0.758263164 | 1.201096942 |
| ENSG00000125755 | SYMPK subnetwork | 0.758210425 | 1.20109706 |
| ENSG00000196374 | HIST1H2BM subnetwork | 0.758198616 | 1.20121068 |
| GO:2000602 | regulation of interphase of mitotic cell cycle | 0.758113225 | 1.201227027 |
| ENSG00000146701 | MDH2 subnetwork | 0.758109791 | 1.201356903 |
| REACTOME_CYTOSOLIC_TRNA_AI | REACTOME_CYTOSOLIC_TRNA_AMINOACYLATION | 0.757879303 | 1.201368159 |
| ENSG00000182195 | LDOC1 subnetwork | 0.758083274 | 1.201411116 |
| ENSG00000132849 | INADL subnetwork | 0.758073418 | 1.201514005 |

**Function of mapped genes at autoimmune disease associated loci with evidence for association to allergy and heterogeneity between self reported allergy and sensitization**

| | | | | | | | Meta-analysis | Fixed effects meta-analysis | | | Random effects meta-analysis | | Self reported allergy | | | Sensitization | | |
|---|---|---|---|---|---|---|---|---|---|---|---|---|---|---|---|---|---|---|
| Chr:BP | Gene | Traits§ | Direction£ | Allergy Locus$ | Function | References [PUBMEDID] | Effect | SE | P | Het P | SE | P | Effect | SE | P | Effect | SE | P |
| 11:75976842 | C11ORF30 | CrD, **IBD**, UC | Same | Yes$ | Repress transcription, possibly via its interaction with a multiprotein chromatin remodeling complex that modifies the chromatin | | 0.12 | 0.01 | 2.1E-25 | 5.2E-03 | 0.04 | 5.4E-04 | 0.10 | 0.01 | 2.1E-17 | 0.18 | 0.03 | 1.6E-12 |
| 3:189595248 | LPP | **CeD** | Opposite | Yes$ | Cell signalling | | -0.07 | 0.01 | 2.9E-09 | 0.14 | 0.02 | 2.5E-04 | -0.06 | 0.01 | 1.1E-06 | -0.10 | 0.03 | 7.8E-05 |
| 2:198605140 | PLCL1 | **CrD**, IBD, UC | Same | Yes$ | Signal transduction, negative regulation (of bone formation) | | 0.06 | 0.01 | 9.5E-09 | 0.19 | 0.02 | 6.1E-04 | 0.07 | 0.01 | 2.9E-09 | 0.03 | 0.03 | 1.7E-01 |
| 6:31444079 | HLA-B | A, **AS**, CrD, GD, IBD, P, SLE, SS, UC | na | Yes$ | Cell surface antigen (MHC class I) presenting peptides | | -0.07 | 0.01 | 2.6E-08 | 0.40 | 0.01 | 1.1E-08 | -0.07 | 0.01 | 1.8E-06 | -0.10 | 0.03 | 1.1E-03 |
| 15:65229650 | SMAD3 | **CrD**, IBD | Same | Yes$ | Affects TGFbeta pathway involved in Th17 and Treg responses | 22913656 | 0.07 | 0.01 | 3.4E-08 | 0.19 | 0.02 | 7.6E-04 | 0.08 | 0.01 | 1.1E-08 | 0.04 | 0.03 | 1.8E-01 |
| 17:35175785 | IKZF3 | CrD, **IBD**, PBC, T1D, UC | Opposite | Yes | Many genes in window, proliferation and differentiation of lymphocytes | | -0.06 | 0.01 | 8.5E-07 | 0.83 | 0.01 | 3.8E-07 | -0.06 | 0.01 | 2.1E-06 | -0.05 | 0.03 | 6.8E-02 |
| 8:128884211 | MYC$ | **MS** | Opposite | Yes$ | Transcription factor involved in the TGFbeta pathway - corepressor | 16064138 | 0.06 | 0.01 | 1.0E-06 | 8.6E-04 | 0.05 | 8.5E-02 | 0.04 | 0.01 | 2.8E-03 | 0.15 | 0.03 | 1.8E-07 |
| 12:110368991 | SH2B3 | A, CeD, **T1D** | Opposite | Novel | Key negative regulator of cytokine signaling and involved in Jak-Stat signaling | | -0.06 | 0.01 | 1.5E-06 | 0.08 | 0.03 | 8.8E-03 | -0.05 | 0.01 | 2.7E-04 | -0.10 | 0.03 | 1.6E-04 |
| 13:41950880 | AKAP11 | **CrD**, IBD | Same | Novel | Key regulator of protein kinase A | 15494034 | -0.05 | 0.01 | 6.8E-05 | 0.85 | 0.01 | 4.1E-05 | -0.05 | 0.01 | 3.2E-04 | -0.05 | 0.03 | 4.8E-02 |
| 16:11087374 | CLEC16A | CeD, CrD, IBS, MS, P, PBC, **T1D** | Same | Yes$ | Unknwon function, but exclusively expressed in immune cells, perhaps a glycan-binding receptor | 17632545 | 0.05 | 0.01 | 6.9E-05 | 0.09 | 0.02 | 1.4E-01 | 0.06 | 0.01 | 7.3E-06 | 0.01 | 0.03 | 8.1E-01 |
| 9:135139050 | ABO | **GD** | na | Novel | Glycosyltranferase involved in modification of blood type antigens (ABO), Cell surface proteins related to the ABO blood groups | | -0.05 | 0.01 | 7.6E-05 | 0.29 | 0.01 | 6.6E-04 | -0.05 | 0.01 | 3.2E-05 | -0.02 | 0.03 | 4.1E-01 |
| 12:110971201 | C12ORF30 | **T1D** | Opposite | Novel | This gene encodes the auxiliary subunit of the heteromeric N-terminal acetyltransferase B complex. Acetylation of methionine. | | 0.05 | 0.01 | 9.1E-05 | 0.15 | 0.02 | 1.0E-02 | 0.04 | 0.01 | 2.8E-03 | 0.08 | 0.03 | 2.3E-03 |
| 4:103770651 | NFKB1 | IBD, **PBC**, UC | Opposite | Novel | Major transcription factor for activation of inflammation, immunity, differentiation, cell growth, tumorigenesis and apoptosis. Encodes the p50 subunit. | | 0.04 | 0.01 | 1.2E-04 | 0.70 | 0.01 | 7.8E-05 | 0.04 | 0.01 | 7.8E-04 | 0.05 | 0.03 | 3.4E-02 |
| 1:165678008 | CD247 | **A**, CeD, SC | na | Novel | CD3 zeta chain involved in TCR assembly and activation. Low expression of the zeta chain results in impaired immune response. | | 0.04 | 0.01 | 2.3E-04 | 0.61 | 0.01 | 1.4E-04 | 0.05 | 0.01 | 2.6E-04 | 0.03 | 0.03 | 2.4E-01 |
| 14:67823346 | RAD51L1 | **PBC** | Opposite | Novel | DNA repair. Involved in cell-cycle and has been shown related to different cancer types | | -0.04 | 0.01 | 3.3E-04 | 0.02 | 0.04 | 8.6E-02 | -0.03 | 0.01 | 2.6E-02 | -0.10 | 0.03 | 1.7E-04 |
| 22:39761288 | EP300 | **CrD**, IBD | Same | Novel | Encodes p300. Transcriptional co-activator binding to CREB in the NFKB pathway | 24338025 | 0.05 | 0.01 | 3.6E-04 | 0.86 | 0.01 | 2.4E-04 | 0.04 | 0.01 | 1.3E-03 | 0.05 | 0.03 | 7.4E-02 |
| 1:150068304 | RORC | **IBD** | Same | Novel | Invovled in the cell differentiation of Th17 cells | | -0.06 | 0.02 | 4.7E-04 | 0.74 | 0.02 | 3.2E-04 | -0.05 | 0.02 | 1.9E-03 | -0.07 | 0.04 | 6.6E-02 |
| 10:6109567 | IL2RA, IL15RA | A, CrD, IBD, MS, **T1D** | Same | Yes$$ | Subunit of the IL2 receptor, can also be secreted as a soluble form (due to extracellular proteolysis) | | 0.06 | 0.02 | 4.9E-04 | 1.00 | 0.02 | 3.2E-04 | 0.06 | 0.02 | 9.5E-04 | 0.07 | 0.05 | 1.6E-01 |
| 21:39387404 | PSMG1 | AS, **IBD**, UC | Opposite | Novel | Proteasome 20S subunit | 16251969 | 0.05 | 0.01 | 4.5E-04 | 0.31 | 0.01 | 5.8E-04 | 0.04 | 0.01 | 3.8E-03 | 0.08 | 0.03 | 1.8E-02 |

| | | | | | | | | | | | | | | | | | |
|---|---|---|---|---|---|---|---|---|---|---|---|---|---|---|---|---|---|
| 12:46494635 | HDAC7, VDR | **IBD** | Opposite | Novel | Histone deacetylase 7 (interacts eg with IKZF1), Vitamin D receptor with possible effects on many immune cells | 24761763 | 0.04 | 0.01 | 6.0E-04 | 0.46 | 0.01 | 4.3E-04 | 0.04 | 0.01 | 4.7E-03 | 0.06 | 0.03 | 2.6E-02 |
| 6:33168096 | HLA-DPB2 | **GD**, SS | Opposite | Novel | Pseudogene, lncRNA gene | | -0.13 | 0.04 | 6.6E-04 | 0.31 | 0.04 | 8.2E-04 | -0.15 | 0.04 | 2.8E-04 | -0.05 | 0.09 | 5.7E-01 |
| 6:91014952 | BACH2 | CeD, CrD, IBD, MS, **T1D** | Opposite | Yes$$$ | B-cell specific transcriptional regulator | | 0.04 | 0.01 | 6.7E-04 | 0.04 | 0.03 | 7.3E-02 | 0.03 | 0.01 | 2.7E-02 | 0.09 | 0.03 | 6.8E-04 |
| 6:138048197 | TNFAIP3 | A, CeD, **IBD**, MS, P, SLE, UC | Opposite | Novel | Ubiquitin-editing enzyme. Terminating NFKB activity. | | -0.05 | 0.01 | 8.2E-04 | 0.32 | 0.01 | 6.8E-04 | -0.04 | 0.02 | 8.3E-03 | -0.07 | 0.03 | 1.6E-02 |
| 5:141493388 | NDFIP1 | CrD, **IBD** | Same | Yes$$$ | Controls suppression of inflammation (via activation of ubiquitin-protein ligase). Involved in RIG-1 regulation | 23087404 | -0.04 | 0.01 | 8.7E-04 | 0.05 | 0.03 | 3.6E-01 | -0.05 | 0.01 | 6.5E-05 | 0.01 | 0.03 | 7.8E-01 |
| 1:10275699 | KIF1B | **MS** | Opposite | Novel | Intracellular transport of organelles | 15501445 | 0.04 | 0.01 | 1.2E-03 | 0.50 | 0.01 | 8.2E-04 | 0.04 | 0.01 | 9.5E-04 | 0.02 | 0.03 | 3.9E-01 |
| 11:63864311 | RPS6KA4 | CrD, IBD, PBC, **S** | na | Novel | Limits pro-inflammation. Transcriptional co-activator binding to CREB in the NFKB pathway | | 0.04 | 0.01 | 2.3E-03 | 0.24 | 0.02 | 1.2E-02 | 0.03 | 0.01 | 2.4E-02 | 0.07 | 0.03 | 1.4E-02 |
| 12:54768447 | PA2G4 | **T1D** | Same | Novel | Co-repressor of androgen receptor. RNA binding protein regulating different genes incl. HLA-DRA, HLA-DRB1 and HLA-DQA1 expression | 21624892 | 0.04 | 0.01 | 2.3E-03 | 0.21 | 0.02 | 2.0E-02 | 0.03 | 0.01 | 2.2E-02 | 0.07 | 0.03 | 1.4E-02 |
| 2:43660422 | THADA | **CrD**, IBD | Same | Novel | Possibly involved in death receptor pathway (altered apoptosis rate) | | 0.05 | 0.02 | 3.3E-03 | 0.55 | 0.02 | 2.5E-03 | 0.05 | 0.02 | 1.3E-02 | 0.07 | 0.04 | 6.8E-02 |
| 3:32990473 | GLB1 | **CeD** | Same | Novel | Encodes beta-galactosidase-1 in ganglioside GM1 (removes b-galactose). GM1 is an innate immune regulator. | | -0.03 | 0.01 | 4.7E-03 | 0.08 | 0.03 | 8.7E-02 | -0.02 | 0.01 | 6.0E-02 | -0.08 | 0.03 | 5.0E-03 |

**As reported by Bønnelykke et al.*

*§: Reported traits associated with locus A: Arthiritis, AS: Ankylosing Spondylitis, CeD: Celiac Disease, CrD: Crohn's Disease, GD: Graves Disease, IBD: Inflammatory Bowel*

*§: Index disease used in the comparison of effect direction marked by bold and underlined*

*£: As compared to index autoimmune disease-SNP effect direcetion. Na: Some diseases have not reported the effect allele*

*$: Known associated to allergy from Hinds et al, and Bønnelykke et al. (PMID: 23817569 & 23817571)*

*$$ Suggestive association to asthma with hayfever reported by Ferreira et al. (PMID:24388013)*

*$$$ Suggestive association to asthma reported by Ferreira et al. (PMID: 21907864)*

*€: Suggestive in current meta-analysis*

**The 290 autoimmune disease associated loci and relationship to allergy**

| Chr:Bp | SNP | MAF* | BETA | P | Het.P | Autoimmune disease paper | |
|---|---|---|---|---|---|---|---|
| | | | | | | PMID | Traits for each PMID |
| 11:75976842 | rs2155219[T] | 0.4656 | 0.1177 | 2.107E-25 | 0.005227 | 21297633,23 | Inflammatory bowel disease,Ulcerative colitis,Crohn's disease,Crohn's disease |
| 3:189595248 | rs1464510[A] | 0.4824 | -0.0688 | 2.874E-09 | 0.1418 | 18311140,20 | Celiac disease,Celiac disease |
| 2:198605140 | rs6738825[A] | 0.4819 | 0.0643 | 9.472E-09 | 0.1902 | 21102463,23 | Crohn's disease,Ulcerative colitis |
| 6:31444079 | rs7743761[A] | 0.2613 | -0.0732 | 2.605E-08 | 0.3985 | 20062062,18 | Ankylosing spondylitis,Psoriasis,Psoriasis,Ankylosing spondylitis,Psoriasis,Psoriasis,Myasthenia gravis ,Psoriatic arthritis,Ulcerative colitis,Graves' disease,S |
| 15:65229650 | rs17293632[T] | 0.2695 | 0.0722 | 3.39E-08 | 0.1911 | 23128233,21 | Crohn's disease,Inflammatory bowel disease |
| 17:35175785 | rs12946510[A] | 0.4948 | -0.0564 | 8.502E-07 | 0.8262 | 23128233,19 | Inflammatory bowel disease,Type 1 diabetes,Crohn's disease,Crohn's disease,Ulcerative colitis,Primary biliary cirrhosis,Primary biliary cirrhosis,Ulcerative |
| 8:128884211 | rs4410871[T] | 0.2756 | 0.0621 | 9.973E-07 | 0.000863 | 21833088 | Multiple sclerosis |
| 12:110368991 | rs3184504[T] | 0.4541 | -0.0555 | 1.457E-06 | 0.07481 | 19430480,21 | Type 1 diabetes autoantibodies,Type 1 diabetes,Celiac disease and Rheumatoid arthritis,Celiac disease,Type 1 diabetes |
| 13:41950880 | rs2062305[A] | 0.4279 | -0.0468 | 0.00006792 | 0.8473 | 21102463 | Crohn's disease |
| 16:11087374 | rs12708716[A] | 0.3526 | 0.047 | 0.00006862 | 0.08552 | 17554260,18 | Type 1 diabetes autoantibodies,Type 1 diabetes,Type 1 diabetes,Type 1 diabetes,Multiple sclerosis,Inflammatory bowel disease,Crohn's disease and psori |
| 9:135139050 | rs505922[T] | 0.3651 | -0.0475 | 0.00007643 | 0.2859 | 23612905 | Graves' disease |
| 12:110971201 | rs17696736[A] | 0.4192 | 0.0453 | 0.00009085 | 0.1477 | 17554260,17 | Type 1 diabetes,Type 1 diabetes,Type 1 diabetes |
| 4:103770651 | rs7665090[A] | 0.4923 | 0.0443 | 0.0001218 | 0.6961 | 21399635,23 | Primary biliary cirrhosis,Ulcerative colitis |
| 1:165678008 | rs864537[A] | 0.381 | 0.0431 | 0.0002317 | 0.6093 | 21383967,20 | Celiac disease and Rheumatoid arthritis,Systemic sclerosis |
| 14:67823346 | rs911263[T] | 0.2912 | -0.0448 | 0.0003329 | 0.01792 | 21399635 | Primary biliary cirrhosis |
| 22:39761288 | rs4820425[A] | 0.2927 | 0.0451 | 0.0003634 | 0.864 | 22936669 | Crohn's disease |
| 21:39387404 | rs2836878[A] | 0.2621 | 0.0462 | 0.0004479 | 0.3133 | 21297633,18 | Inflammatory bowel disease,Inflammatory bowel disease,Ulcerative colitis,Ankylosing spondylitis,Ankylosing spondylitis |
| 1:150068304 | rs4845604[A] | 0.1443 | -0.0564 | 0.0004665 | 0.7356 | 23128233 | Inflammatory bowel disease |
| 10:6109567 | rs12722495[A] | 0.1183 | 0.0648 | 0.0004902 | 0.9971 | 21829393,21 | Type 1 diabetes autoantibodies,Multiple sclerosis,Type 1 diabetes,Rheumatoid arthritis,Multiple sclerosis,Inflammatory bowel disease,Crohn's disease,Mu |
| 12:46494635 | rs11168249[T] | 0.4785 | 0.0396 | 0.0006015 | 0.4641 | 23128233 | Inflammatory bowel disease |
| 6:33168096 | rs2281388[A] | 0.0216 | -0.1305 | 0.0006586 | 0.3146 | 21841780,21 | Graves' disease,Systemic sclerosis |
| 6:91014952 | rs11755527[C] | 0.4238 | 0.0394 | 0.0006667 | 0.03903 | 18978792,21 | Type 1 diabetes autoantibodies,Type 1 diabetes,Crohn's disease,Inflammatory bowel disease,Celiac disease,Multiple sclerosis |
| 6:138048197 | rs6920220[A] | 0.2187 | -0.0466 | 0.0008211 | 0.3216 | 21297633,18 | Inflammatory bowel disease,Rheumatoid arthritis,Rheumatoid arthritis,Ulcerative colitis,Celiac disease,Systemic lupus erythematosus,Systemic lupus eryt |
| 5:141493388 | rs6863411[A] | 0.3667 | -0.0391 | 0.0008655 | 0.04932 | 23128233,21 | Inflammatory bowel disease,Crohn's disease |
| 1:10275699 | rs10492972[T] | 0.3382 | 0.0392 | 0.001218 | 0.5009 | 18997785 | Multiple sclerosis |
| 11:63864311 | rs479777[A] | 0.3563 | 0.0381 | 0.002309 | 0.2402 | 22837380,23 | Sarcoidosis,Inflammatory bowel disease,Primary biliary cirrhosis,Crohn's disease |
| 12:54768447 | rs2292239[T] | 0.317 | 0.0371 | 0.00234 | 0.214 | 17554260,18 | Type 1 diabetes autoantibodies,Type 1 diabetes,Type 1 diabetes,Type 1 diabetes,Type 1 diabetes autoantibodies,Type 1 diabetes,Type 1 diabetes |
| 2:43660422 | rs10495903[T] | 0.123 | 0.0505 | 0.00325 | 0.5529 | 23128233,21 | Crohn's disease,Inflammatory bowel disease |
| 3:32990473 | rs13314993[T] | 0.4339 | -0.0332 | 0.00469 | 0.08012 | 20190752 | Celiac disease |
| 7:28147081 | rs864745[T] | 0.4982 | 0.0314 | 0.006176 | 0.4767 | 23128233 | Crohn's disease |
| 2:61040333 | rs7608910[A] | 0.3767 | -0.0322 | 0.006316 | 0.7635 | 21297633,23 | Inflammatory bowel disease,Ulcerative colitis,Celiac disease,Crohn's disease,Ulcerative colitis,Psoriatic arthritis,Rheumatoid arthritis,Crohn's disease and |
| 11:61320875 | rs4246215[T] | 0.3858 | -0.0324 | 0.007264 | 0.5014 | 23128233,21 | Inflammatory bowel disease,Crohn's disease |
| 6:128287458 | rs13204742[T] | 0.1303 | -0.0441 | 0.009016 | 0.2872 | 23128233,21 | Crohn's disease,Celiac disease,Multiple sclerosis |
| 16:23761361 | rs7404095[A] | 0.4325 | -0.0289 | 0.01253 | 0.4538 | 23128233 | Inflammatory bowel disease |
| 2:28468298 | rs925255[T] | 0.4589 | -0.0288 | 0.01332 | 0.743 | 23128233 | Inflammatory bowel disease |
| 6:159385965 | rs1738074[T] | 0.4396 | 0.029 | 0.01393 | 0.6404 | 21833088,20 | Celiac disease,Multiple sclerosis,Crohn's disease,Crohn's disease and celiac disease,Crohn's disease |
| 7:128505142 | rs12537284[A] | 0.1472 | -0.0394 | 0.01552 | 0.6468 | 18204446,21 | Systemic lupus erythematosus,Systemic lupus erythematosus,Ulcerative colitis,Ulcerative colitis,Primary biliary cirrhosis,Rheumatoid arthritis,Systemic lup |
| 19:1075031 | rs2024092[A] | 0.2228 | 0.033 | 0.01648 | 0.1496 | 23128233,21 | Crohn's disease,Crohn's disease |
| 1:171128857 | rs9286879[A] | 0.2602 | 0.0313 | 0.01658 | 0.3769 | 18587394,23 | Crohn's disease,Crohn's disease,Crohn's disease |
| 15:39345329 | rs28374715[A] | 0.2485 | -0.0313 | 0.0176 | 0.4917 | 23128233 | Ulcerative colitis |
| 16:67148731 | rs1728785[A] | 0.2197 | -0.0321 | 0.01777 | 0.3571 | 19915572,23 | Ulcerative colitis,Ulcerative colitis,Ulcerative colitis |
| 2:27584444 | rs1728918[T] | 0.3836 | 0.0279 | 0.01856 | 0.1102 | 23128233,21 | Crohn's disease,Crohn's disease |
| 7:116680082 | rs38904[T] | 0.446 | 0.0276 | 0.01889 | 0.1079 | 23128233 | Inflammatory bowel disease |
| 9:92968237 | rs4743820[T] | 0.3034 | -0.0295 | 0.01923 | 0.129 | 23128233 | Inflammatory bowel disease |
| 6:126740412 | rs9388489[A] | 0.4538 | -0.0265 | 0.0217 | 0.9805 | 19430480 | Type 1 diabetes |
| 6:135781048 | rs11154801[A] | 0.3507 | 0.0272 | 0.02203 | 0.1193 | 21833088 | Multiple sclerosis |
| 13:43355925 | rs3764147[A] | 0.2081 | -0.0308 | 0.0226 | 0.8101 | 18587394,21 | Crohn's disease,Crohn's disease,Crohn's disease |
| 3:103231328 | rs771767[A] | 0.2562 | 0.0296 | 0.02313 | 0.7649 | 21833088 | Multiple sclerosis |
| 10:35335437 | rs11010067[C] | 0.3543 | -0.0256 | 0.03289 | 0.973 | 23128233,21 | Inflammatory bowel disease,Ulcerative colitis,Crohn's disease,Crohn's disease |
| 5:35978799 | rs860413[A] | 0.2966 | 0.0267 | 0.03529 | 0.4051 | 21399635,21 | Primary biliary cirrhosis,Multiple sclerosis,Ulcerative colitis,Primary biliary cirrhosis |
| 20:44175471 | rs1569723[A] | 0.2546 | 0.0272 | 0.03541 | 0.1781 | 23128233,21 | Inflammatory bowel disease,Multiple sclerosis,Rheumatoid arthritis,Rheumatoid arthritis |
| 21:44440169 | rs7282490[A] | 0.4018 | 0.0244 | 0.0355 | 0.7213 | 23128233,21 | Inflammatory bowel disease,Crohn's disease,Ulcerative colitis,Crohn's disease,Celiac disease,Rheumatoid arthritis |

## DEPICT gene set enrichment analysis for shared loci

| Original gene set ID | Original gene set description | Nominal P va | False discovery rate |
|---|---|---|---|
| ENSG00000127191 | TRAF2 subnetwork | 4.57E-10 | 0 |
| ENSG00000123411 | IKZF4 subnetwork | 5.68E-10 | 0 |
| MP:0008088 | abnormal T-helper 1 cell differentiation | 4.77E-09 | 0 |
| GO:0006917 | induction of apoptosis | 5.36E-08 | 0 |
| GO:0048872 | homeostasis of number of cells | 8.25E-08 | 0 |
| GO:0012502 | induction of programmed cell death | 1.49E-07 | 0 |
| ENSG00000115415 | STAT1 subnetwork | 1.53E-06 | 0.0025 |
| GO:0030099 | myeloid cell differentiation | 1.44E-06 | 0.002631579 |
| ENSG00000171150 | SOCS5 subnetwork | 1.44E-06 | 0.002777778 |
| MP:0008470 | abnormal spleen B cell follicle morphology | 1.36E-06 | 0.002941176 |
| MP:0005091 | increased double-positive T cell number | 1.27E-06 | 0.003125 |
| MP:0006387 | abnormal T cell number | 1.20E-06 | 0.003333333 |
| ENSG00000132676 | DAP3 subnetwork | 8.71E-07 | 0.003571429 |
| MP:0005011 | increased eosinophil cell number | 5.33E-06 | 0.00375 |
| MP:0000221 | decreased leukocyte cell number | 8.67E-07 | 0.003846154 |
| GO:0002285 | lymphocyte activation involved in immune response | 5.11E-06 | 0.003846154 |
| GO:0008624 | induction of apoptosis by extracellular signals | 4.50E-06 | 0.003947368 |
| ENSG00000078043 | PIAS2 subnetwork | 4.23E-06 | 0.004054054 |
| ENSG00000100906 | NFKBIA subnetwork | 7.60E-07 | 0.004166667 |
| GO:0030097 | hemopoiesis | 4.20E-06 | 0.004166667 |
| GO:0002697 | regulation of immune effector process | 4.11E-06 | 0.004285714 |
| ENSG00000175505 | CLCF1 subnetwork | 3.65E-06 | 0.004411765 |
| ENSG00000165806 | CASP7 subnetwork | 7.23E-07 | 0.004545455 |
| ENSG00000180008 | SOCS4 subnetwork | 3.33E-06 | 0.004545455 |
| MP:0008255 | decreased megakaryocyte cell number | 3.28E-06 | 0.0046875 |
| GO:0050798 | activated T cell proliferation | 3.24E-06 | 0.00483871 |
| MP:0008474 | absent spleen germinal center | 5.59E-06 | 0.004878049 |
| ENSG00000091831 | ESR1 subnetwork | 5.13E-07 | 0.005 |
| GO:0051223 | regulation of protein transport | 3.08E-06 | 0.005 |
| ENSG00000120833 | SOCS2 subnetwork | 3.03E-06 | 0.005172414 |
| MP:0001858 | intestinal inflammation | 2.66E-06 | 0.005357143 |
| MP:0002490 | abnormal immunoglobulin level | 4.42E-07 | 0.005555556 |
| MP:0008082 | increased single-positive T cell number | 2.65E-06 | 0.005555556 |
| GO:0042110 | T cell activation | 2.56E-06 | 0.005769231 |
| ENSG00000080824 | HSP90AA1 subnetwork | 2.34E-06 | 0.006 |
| ENSG00000186660 | ZFP91 subnetwork | 2.31E-06 | 0.00625 |
| MP:0000696 | abnormal Peyer's patch morphology | 2.87E-07 | 0.00625 |
| ENSG00000170677 | SOCS6 subnetwork | 2.20E-06 | 0.006521739 |
| GO:0048534 | hemopoietic or lymphoid organ development | 2.14E-06 | 0.006818182 |
| ENSG00000168610 | STAT3 subnetwork | 2.28E-07 | 0.007142857 |
| MP:0000322 | increased granulocyte number | 2.00E-06 | 0.007142857 |
| GO:0032946 | positive regulation of mononuclear cell proliferation | 1.46E-05 | 0.00754717 |
| ENSG00000169194 | IL13 subnetwork | 1.61E-05 | 0.007589286 |
| ENSG00000124151 | NCOA3 subnetwork | 1.45E-05 | 0.007619048 |
| ENSG00000096968 | JAK2 subnetwork | 1.75E-05 | 0.007627119 |
| MP:0004804 | decreased susceptibility to autoimmune diabetes | 1.60E-05 | 0.007657658 |
| GO:0002377 | immunoglobulin production | 1.44E-05 | 0.007692308 |
| ENSG00000105639 | JAK3 subnetwork | 1.72E-05 | 0.007692308 |
| ENSG00000095752 | IL11 subnetwork | 3.31E-05 | 0.007692308 |
| ENSG00000162891 | IL20 subnetwork | 1.55E-05 | 0.007727273 |

| | | | |
|---|---|---|---|
| ENSG00000196455 | PIK3R4 subnetwork | 3.30E-05 | 0.007738095 |
| GO:0002286 | T cell activation involved in immune response | 1.71E-05 | 0.007758621 |
| GO:0030217 | T cell differentiation | 1.42E-05 | 0.00776699 |
| MP:0004974 | decreased regulatory T cell number | 6.56E-06 | 0.007777778 |
| MP:0002389 | abnormal Peyer's patch follicle morphology | 3.27E-05 | 0.007784431 |
| ENSG00000150281 | CTF1 subnetwork | 1.55E-05 | 0.007798165 |
| ENSG00000171855 | IFNB1 subnetwork | 1.31E-05 | 0.0078125 |
| ENSG00000130427 | EPO subnetwork | 1.68E-05 | 0.007826087 |
| GO:0045076 | regulation of interleukin-2 biosynthetic process | 3.24E-05 | 0.007831325 |
| MP:0001873 | stomach inflammation | 1.42E-05 | 0.007843137 |
| MP:0002495 | increased IgA level | 1.53E-05 | 0.00787037 |
| ENSG00000136488 | CSH1 subnetwork | 3.23E-05 | 0.007878788 |
| MP:0008700 | decreased interleukin-4 secretion | 1.31E-05 | 0.007894737 |
| ENSG00000113580 | NR3C1 subnetwork | 1.66E-05 | 0.007894737 |
| GO:0042098 | T cell proliferation | 2.77E-05 | 0.007894737 |
| ENSG00000131788 | PIAS3 subnetwork | 1.41E-05 | 0.007920792 |
| MP:0002619 | abnormal lymphocyte morphology | 3.22E-05 | 0.007926829 |
| GO:0045321 | leukocyte activation | 2.53E-05 | 0.007931034 |
| ENSG00000106546 | AHR subnetwork | 1.50E-05 | 0.007943925 |
| ENSG00000174697 | LEP subnetwork | 2.75E-05 | 0.00794702 |
| GO:0002637 | regulation of immunoglobulin production | 6.48E-06 | 0.007954545 |
| GO:0070227 | lymphocyte apoptotic process | 1.64E-05 | 0.007964602 |
| GO:0005164 | tumor necrosis factor receptor binding | 3.20E-05 | 0.00797546 |
| ENSG00000162892 | IL24 subnetwork | 1.29E-05 | 0.007978723 |
| MP:0006413 | increased T cell apoptosis | 2.49E-05 | 0.007986111 |
| MP:0002391 | abnormal Peyer's patch germinal center morphology | 1.40E-05 | 0.008 |
| MP:0000715 | decreased thymocyte number | 2.73E-05 | 0.008 |
| GO:0043367 | CD4-positive, alpha-beta T cell differentiation | 3.15E-05 | 0.008024691 |
| GO:0042102 | positive regulation of T cell proliferation | 2.47E-05 | 0.008041958 |
| MP:0008751 | abnormal interleukin level | 2.61E-05 | 0.008053691 |
| ENSG00000184995 | IFNE subnetwork | 1.29E-05 | 0.008064516 |
| ENSG00000172179 | PRL subnetwork | 3.02E-05 | 0.008074534 |
| ENSG00000162434 | JAK1 subnetwork | 1.40E-05 | 0.008080808 |
| ENSG00000168811 | IL12A subnetwork | 2.45E-05 | 0.008098592 |
| MP:0005078 | abnormal cytotoxic T cell physiology | 2.61E-05 | 0.008108108 |
| GO:0002706 | regulation of lymphocyte mediated immunity | 3.00E-05 | 0.008125 |
| MP:0001805 | decreased IgG level | 6.39E-06 | 0.008139535 |
| ENSG00000114737 | CISH subnetwork | 3.40E-05 | 0.008139535 |
| ENSG00000164136 | IL15 subnetwork | 1.29E-05 | 0.008152174 |
| GO:0001933 | negative regulation of protein phosphorylation | 2.37E-05 | 0.008156028 |
| GO:0001776 | leukocyte homeostasis | 2.60E-05 | 0.008163265 |
| ENSG00000196498 | NCOR2 subnetwork | 1.39E-05 | 0.008163265 |
| ENSG00000104365 | IKBKB subnetwork | 2.79E-05 | 0.008169935 |
| ENSG00000113525 | IL5 subnetwork | 2.97E-05 | 0.008176101 |
| MP:0000218 | increased leukocyte cell number | 3.38E-05 | 0.008187135 |
| ENSG00000113520 | IL4 subnetwork | 2.34E-05 | 0.008214286 |
| GO:0046636 | negative regulation of alpha-beta T cell activation | 2.60E-05 | 0.008219178 |
| GO:0045191 | regulation of isotype switching | 2.96E-05 | 0.008227848 |
| MP:0008482 | decreased spleen germinal center number | 3.35E-05 | 0.008235294 |
| ENSG00000142224 | IL19 subnetwork | 1.29E-05 | 0.008241758 |
| ENSG00000100393 | EP300 subnetwork | 1.33E-05 | 0.008247423 |
| ENSG00000136634 | IL10 subnetwork | 1.90E-05 | 0.008264463 |
| GO:0070665 | positive regulation of leukocyte proliferation | 2.32E-05 | 0.008273381 |

| | | | |
|---|---|---|---|
| MP:0001246 | mixed cellular infiltration to dermis | 2.93E-05 | 0.008280255 |
| ENSG00000115705 | TPO subnetwork | 6.09E-06 | 0.008333333 |
| ENSG00000128342 | LIF subnetwork | 1.29E-05 | 0.008333333 |
| GO:0019900 | kinase binding | 1.87E-05 | 0.008333333 |
| ENSG00000096717 | SIRT1 subnetwork | 2.30E-05 | 0.008333333 |
| GO:0002312 | B cell activation involved in immune response | 2.92E-05 | 0.008333333 |
| MP:0001194 | dermatitis | 3.52E-05 | 0.008333333 |
| ENSG00000109471 | IL2 subnetwork | 3.45E-05 | 0.008381503 |
| GO:0002684 | positive regulation of immune system process | 2.91E-05 | 0.008387097 |
| ENSG00000136244 | IL6 subnetwork | 2.26E-05 | 0.008394161 |
| GO:0046649 | lymphocyte activation | 1.87E-05 | 0.008403361 |
| ENSG00000182393 | IL29 subnetwork | 1.29E-05 | 0.008426966 |
| ENSG00000099985 | OSM subnetwork | 2.84E-05 | 0.008441558 |
| REACTOME_BMAL1CLOCKNPA | REACTOME_BMAL1CLOCKNPAS2_ACTIVATES_GENE_EXPRE | 2.25E-05 | 0.008455882 |
| GO:0051059 | NF-kappaB binding | 2.23E-05 | 0.008518519 |
| ENSG00000111536 | IL26 subnetwork | 1.29E-05 | 0.008522727 |
| ENSG00000105851 | PIK3CG subnetwork | 3.74E-05 | 0.008522727 |
| GO:0045190 | isotype switching | 2.02E-05 | 0.008527132 |
| ENSG00000146904 | EPHA1 subnetwork | 3.70E-05 | 0.008571429 |
| ENSG00000108342 | CSF3 subnetwork | 2.21E-05 | 0.00858209 |
| GO:0002208 | somatic diversification of immunoglobulins involved in imm | 2.02E-05 | 0.00859375 |
| ENSG00000147896 | IFNK subnetwork | 1.29E-05 | 0.00862069 |
| ENSG00000166888 | STAT6 subnetwork | 2.19E-05 | 0.008646617 |
| GO:0002204 | somatic recombination of immunoglobulin genes involved i | 2.02E-05 | 0.008661417 |
| GO:0002381 | immunoglobulin production involved in immunoglobulin m | 6.61E-06 | 0.008695652 |
| ENSG00000164399 | IL3 subnetwork | 2.16E-05 | 0.008712121 |
| ENSG00000145839 | IL9 subnetwork | 1.29E-05 | 0.00872093 |
| GO:0050671 | positive regulation of lymphocyte proliferation | 2.00E-05 | 0.008730159 |
| ENSG00000110944 | IL23A subnetwork | 3.87E-05 | 0.008757062 |
| MP:0000512 | intestinal ulcer | 2.05E-05 | 0.008778626 |
| MP:0008476 | increased spleen red pulp amount | 4.14E-05 | 0.008791209 |
| ENSG00000113302 | IL12B subnetwork | 2.00E-05 | 0.0088 |
| ENSG00000138684 | IL21 subnetwork | 1.29E-05 | 0.008823529 |
| ENSG00000105647 | PIK3R2 subnetwork | 4.13E-05 | 0.008839779 |
| GO:0046631 | alpha-beta T cell activation | 2.04E-05 | 0.008846154 |
| MP:0000628 | abnormal mammary gland development | 1.95E-05 | 0.008870968 |
| GO:0000018 | regulation of DNA recombination | 4.10E-05 | 0.008888889 |
| ENSG00000104432 | IL7 subnetwork | 1.29E-05 | 0.008928571 |
| ENSG00000120235 | IFNA6 subnetwork | 4.05E-05 | 0.008938547 |
| ENSG00000100030 | MAPK1 subnetwork | 1.94E-05 | 0.008943089 |
| MP:0008499 | increased IgG1 level | 4.01E-05 | 0.008988764 |
| ENSG00000131759 | RARA subnetwork | 1.94E-05 | 0.009016393 |
| ENSG00000197110 | IL28B subnetwork | 1.29E-05 | 0.009036145 |
| ENSG00000177047 | IFNW1 subnetwork | 1.29E-05 | 0.009146341 |
| GO:0030098 | lymphocyte differentiation | 4.69E-05 | 0.009162304 |
| ENSG00000105397 | TYK2 subnetwork | 4.65E-05 | 0.009210526 |
| ENSG00000164400 | CSF2 subnetwork | 5.38E-05 | 0.00925 |
| ENSG00000183709 | IL28A subnetwork | 1.29E-05 | 0.009259259 |
| GO:0050863 | regulation of T cell activation | 4.65E-05 | 0.009259259 |
| GO:0032613 | interleukin-10 production | 4.35E-05 | 0.009289617 |
| ENSG00000065883 | CDK13 subnetwork | 5.35E-05 | 0.009296482 |
| GO:0002252 | immune effector process | 4.62E-05 | 0.009308511 |
| GO:0051249 | regulation of lymphocyte activation | 5.34E-05 | 0.009343434 |

| | | | |
|---|---|---|---|
| ENSG00000108840 | HDAC5 subnetwork | 8.22E-05 | 0.009347826 |
| GO:0001816 | cytokine production | 4.59E-05 | 0.009358289 |
| GO:0001773 | myeloid dendritic cell activation | 1.29E-05 | 0.009375 |
| GO:0070661 | leukocyte proliferation | 8.11E-05 | 0.009388646 |
| GO:0033619 | membrane protein proteolysis | 5.30E-05 | 0.009390863 |
| GO:0006509 | membrane protein ectodomain proteolysis | 4.54E-05 | 0.009408602 |
| GO:0002694 | regulation of leukocyte activation | 7.67E-05 | 0.009429825 |
| GO:0032663 | regulation of interleukin-2 production | 5.21E-05 | 0.009438776 |
| GO:0032944 | regulation of mononuclear cell proliferation | 8.30E-05 | 0.00944206 |
| GO:0050864 | regulation of B cell activation | 4.45E-05 | 0.009459459 |
| GO:0050871 | positive regulation of B cell activation | 7.66E-05 | 0.009471366 |
| GO:0032633 | interleukin-4 production | 8.29E-05 | 0.009482759 |
| REACTOME_TOLL_LIKE_RECEP | REACTOME_TOLL_LIKE_RECEPTOR_10_TLR10_CASCADE | 9.70E-05 | 0.009486166 |
| GO:0016445 | somatic diversification of immunoglobulins | 5.20E-05 | 0.009487179 |
| ENSG00000142273 | CBLC subnetwork | 1.28E-05 | 0.009493671 |
| GO:0051427 | hormone receptor binding | 4.42E-05 | 0.00951087 |
| GO:0033077 | T cell differentiation in thymus | 7.57E-05 | 0.009513274 |
| REACTOME_INTERLEUKIN:2_SI | REACTOME_INTERLEUKIN:2_SIGNALING | 8.24E-05 | 0.00952381 |
| REACTOME_MYD88_CASCADE_ | REACTOME_MYD88_CASCADE_INITIATED_ON_PLASMA_M | 9.70E-05 | 0.00952381 |
| GO:0016447 | somatic recombination of immunoglobulin gene segments | 5.13E-05 | 0.009536082 |
| GO:0002703 | regulation of leukocyte mediated immunity | 6.83E-05 | 0.009545455 |
| MP:0008173 | increased follicular B cell number | 7.28E-05 | 0.009555556 |
| GO:0001817 | regulation of cytokine production | 5.66E-05 | 0.009558824 |
| REACTOME_TOLL_LIKE_RECEP | REACTOME_TOLL_LIKE_RECEPTOR_5_TLR5_CASCADE | 9.70E-05 | 0.009561753 |
| MP:0002460 | decreased immunoglobulin level | 6.16E-05 | 0.009569378 |
| GO:0046632 | alpha-beta T cell differentiation | 4.95E-05 | 0.009585492 |
| MP:0003945 | abnormal lymphocyte physiology | 6.78E-05 | 0.009589041 |
| GO:0032653 | regulation of interleukin-10 production | 7.24E-05 | 0.009598214 |
| GO:0035257 | nuclear hormone receptor binding | 9.65E-05 | 0.0096 |
| MP:0000711 | thymus cortex hypoplasia | 5.63E-05 | 0.009605911 |
| GO:0042974 | retinoic acid receptor binding | 1.27E-05 | 0.009615385 |
| MP:0005232 | abnormal mesenteric lymph node morphology | 5.99E-05 | 0.009615385 |
| MP:0005466 | abnormal T-helper 2 physiology | 8.80E-05 | 0.009623431 |
| GO:0070201 | regulation of establishment of protein localization | 6.72E-05 | 0.009633028 |
| ENSG00000120659 | TNFSF11 subnetwork | 4.88E-05 | 0.009635417 |
| GO:0070229 | negative regulation of lymphocyte apoptotic process | 9.63E-05 | 0.009638554 |
| GO:0019901 | protein kinase binding | 7.14E-05 | 0.009641256 |
| MP:0008102 | lymph node hyperplasia | 5.61E-05 | 0.009653465 |
| MP:0005092 | decreased double-positive T cell number | 5.99E-05 | 0.009661836 |
| GO:0032813 | tumor necrosis factor receptor superfamily binding | 8.70E-05 | 0.009663866 |
| ENSG00000084676 | NCOA1 subnetwork | 6.69E-05 | 0.009677419 |
| ENSG00000112208 | BAG2 subnetwork | 9.55E-05 | 0.009677419 |
| GO:0051023 | regulation of immunoglobulin secretion | 7.10E-05 | 0.009684685 |
| GO:0070663 | regulation of leukocyte proliferation | 5.56E-05 | 0.009701493 |
| ENSG00000163599 | CTLA4 subnetwork | 8.69E-05 | 0.009704641 |
| MP:0005463 | abnormal CD4-positive T cell physiology | 5.96E-05 | 0.009708738 |
| MP:0008040 | decreased NK T cell number | 9.45E-05 | 0.009716599 |
| GO:0051251 | positive regulation of lymphocyte activation | 6.65E-05 | 0.009722222 |
| MP:0003643 | spleen atrophy | 7.07E-05 | 0.009728507 |
| MP:0000689 | abnormal spleen morphology | 1.21E-05 | 0.00974026 |
| GO:0002702 | positive regulation of production of molecular mediator of | 8.52E-05 | 0.009745763 |
| MP:0003009 | abnormal cytokine secretion | 5.86E-05 | 0.009756098 |
| ENSG00000168310 | IRF2 subnetwork | 9.41E-05 | 0.009756098 |

| | | | |
|---|---|---|---|
| ENSG00000138794 | CASP6 subnetwork | 1.00E-04 | 0.009765625 |
| GO:0050870 | positive regulation of T cell activation | 6.61E-05 | 0.009767442 |
| MP:0002356 | abnormal spleen red pulp morphology | 8.49E-05 | 0.009787234 |
| MP:0001790 | abnormal immune system physiology | 9.31E-05 | 0.009795918 |
| MP:0005095 | decreased T cell proliferation | 1.00E-04 | 0.009803922 |
| MP:0001806 | decreased IgM level | 6.55E-05 | 0.009813084 |
| GO:0050778 | positive regulation of immune response | 1.23E-04 | 0.009821429 |
| ENSG00000109320 | NFKB1 subnetwork | 8.49E-05 | 0.00982906 |
| MP:0004803 | increased susceptibility to autoimmune diabetes | 9.27E-05 | 0.009836066 |
| MP:0002344 | abnormal lymph node B cell domain morphology | 9.99E-05 | 0.00984252 |
| ENSG00000198791 | CNOT7 subnetwork | 1.22E-04 | 0.009856631 |
| GO:0002260 | lymphocyte homeostasis | 6.42E-05 | 0.009859155 |
| ENSG00000147873 | IFNA5 subnetwork | 1.15E-05 | 0.009868421 |
| GO:0002507 | tolerance induction | 9.10E-05 | 0.009876543 |
| GO:0046651 | lymphocyte proliferation | 1.22E-04 | 0.009892086 |
| MP:0004393 | abnormal cochlear inner hair cell morphology | 6.41E-05 | 0.00990566 |
| MP:0002401 | abnormal lymphopoiesis | 9.04E-05 | 0.009917355 |
| GO:0042129 | regulation of T cell proliferation | 1.02E-04 | 0.009922179 |
| ENSG00000141506 | PIK3R5 subnetwork | 1.10E-04 | 0.009925094 |
| GO:0002699 | positive regulation of immune effector process | 1.22E-04 | 0.009927798 |
| MP:0001829 | increased activated T cell number | 1.25E-04 | 0.009929078 |
| REACTOME_TRAF6_MEDIATED | REACTOME_TRAF6_MEDIATED_NF:KB_ACTIVATION | 6.37E-05 | 0.009952607 |
| GO:0002696 | positive regulation of leukocyte activation | 9.00E-05 | 0.009958506 |
| MP:0008567 | decreased interferon-gamma secretion | 1.09E-04 | 0.009962406 |
| GO:0002200 | somatic diversification of immune receptors | 1.21E-04 | 0.009963768 |
| MP:0000717 | abnormal lymphocyte cell number | 1.23E-04 | 0.009964413 |
| ENSG00000147885 | IFNA16 subnetwork | 1.15E-05 | 0.01 |
| MP:0001853 | heart inflammation | 6.27E-05 | 0.01 |
| MP:0002432 | abnormal CD4-positive T cell morphology | 8.92E-05 | 0.01 |
| ENSG00000075391 | RASAL2 subnetwork | 1.09E-04 | 0.01 |
| MP:0005015 | increased T cell number | 1.18E-04 | 0.01 |
| MP:0008078 | increased CD8-positive T cell number | 1.16E-04 | 0.010036496 |
| MP:0002493 | increased IgG level | 1.09E-04 | 0.010037879 |
| GO:0071887 | leukocyte apoptotic process | 1.03E-04 | 0.01003861 |
| GO:0002449 | lymphocyte mediated immunity | 1.15E-04 | 0.01007326 |
| GO:0002700 | regulation of production of molecular mediator of immune | 1.11E-04 | 0.010074627 |
| GO:0050670 | regulation of lymphocyte proliferation | 1.08E-04 | 0.010076046 |
| MP:0005042 | abnormal level of surface class II molecules | 1.03E-04 | 0.010077519 |
| ENSG00000185811 | IKZF1 subnetwork | 1.14E-04 | 0.010110294 |
| MP:0001844 | autoimmune response | 1.08E-04 | 0.010114504 |
| ENSG00000147877 | ENSG00000147877 subnetwork | 1.15E-05 | 0.010135135 |
| GO:0001783 | B cell apoptotic process | 1.13E-04 | 0.010147601 |
| ENSG00000130522 | JUND subnetwork | 1.06E-04 | 0.010153257 |
| ENSG00000111679 | PTPN6 subnetwork | 1.13E-04 | 0.010185185 |
| GO:0002889 | regulation of immunoglobulin mediated immune response | 1.04E-04 | 0.010192308 |
| GO:0002712 | regulation of B cell mediated immunity | 1.12E-04 | 0.010223048 |
| ENSG00000188379 | IFNA2 subnetwork | 1.15E-05 | 0.010273973 |
| MP:0005089 | decreased double-negative T cell number | 1.28E-04 | 0.010314685 |
| ENSG00000171608 | PIK3CD subnetwork | 9.01E-06 | 0.010344828 |
| MP:0000691 | enlarged spleen | 1.28E-04 | 0.010350877 |
| MP:0008075 | decreased CD4-positive T cell number | 1.28E-04 | 0.010387324 |
| ENSG00000184557 | SOCS3 subnetwork | 7.19E-06 | 0.010416667 |
| ENSG00000137080 | IFNA21 subnetwork | 1.15E-05 | 0.010416667 |

| | | | |
|---|---|---|---|
| GO:0006417 | regulation of translation | 1.26E-04 | 0.010424028 |
| MP:0002497 | increased IgE level | 8.30E-06 | 0.010526316 |
| ENSG00000120242 | IFNA8 subnetwork | 1.15E-05 | 0.01056338 |
| MP:0001828 | abnormal T cell activation | 1.29E-04 | 0.010627178 |
| ENSG00000145777 | TSLP subnetwork | 7.16E-06 | 0.010638298 |
| GO:0046006 | regulation of activated T cell proliferation | 8.26E-06 | 0.010714286 |
| ENSG00000120247 | ENSG00000120247 subnetwork | 1.15E-05 | 0.010714286 |
| GO:0050776 | regulation of immune response | 1.31E-04 | 0.010726644 |
| MP:0002492 | decreased IgE level | 1.31E-04 | 0.010763889 |
| ENSG00000186809 | ENSG00000186809 subnetwork | 1.15E-05 | 0.010869565 |
| MP:0008568 | abnormal interleukin secretion | 8.12E-06 | 0.010909091 |
| ENSG00000186803 | IFNA10 subnetwork | 1.15E-05 | 0.011029412 |
| MP:0008135 | small Peyer's patches | 1.51E-04 | 0.011056106 |
| GO:0050688 | regulation of defense response to virus | 1.50E-04 | 0.011092715 |
| ENSG00000005339 | CREBBP subnetwork | 8.10E-06 | 0.011111111 |
| GO:0032880 | regulation of protein localization | 1.44E-04 | 0.011111111 |
| MP:0001870 | salivary gland inflammation | 1.50E-04 | 0.011129568 |
| MP:0008496 | decreased IgG2a level | 1.40E-04 | 0.011130137 |
| ENSG00000139546 | TARBP2 subnetwork | 1.42E-04 | 0.011148649 |
| GO:0032943 | mononuclear cell proliferation | 1.49E-04 | 0.011166667 |
| KEGG_T_CELL_RECEPTOR_SIGN | KEGG_T_CELL_RECEPTOR_SIGNALING_PATHWAY | 1.38E-04 | 0.011168385 |
| GO:0045086 | positive regulation of interleukin-2 biosynthetic process | 1.42E-04 | 0.011186441 |
| ENSG00000127318 | IL22 subnetwork | 1.12E-05 | 0.01119403 |
| GO:0048291 | isotype switching to IgG isotypes | 1.66E-04 | 0.011201299 |
| MP:0008500 | increased IgG2a level | 1.48E-04 | 0.011204013 |
| ENSG00000165280 | VCP subnetwork | 1.37E-04 | 0.011206897 |
| GO:0002562 | somatic diversification of immune receptors via germline re | 1.41E-04 | 0.01122449 |
| ENSG00000068024 | HDAC4 subnetwork | 1.64E-04 | 0.011237785 |
| MP:0000703 | abnormal thymus morphology | 1.48E-04 | 0.011241611 |
| GO:0016444 | somatic cell DNA recombination | 1.41E-04 | 0.011262799 |
| MP:0005027 | increased susceptibility to parasitic infection | 1.62E-04 | 0.01127451 |
| ENSG00000186350 | RXRA subnetwork | 1.09E-05 | 0.011290323 |
| GO:0002250 | adaptive immune response | 1.61E-04 | 0.011311475 |
| MP:0002722 | abnormal immune system organ morphology | 8.09E-06 | 0.011320755 |
| GO:0050852 | T cell receptor signaling pathway | 1.67E-04 | 0.011326861 |
| GO:0048305 | immunoglobulin secretion | 1.56E-04 | 0.011348684 |
| ENSG00000213341 | CHUK subnetwork | 1.11E-05 | 0.011363636 |
| GO:0002521 | leukocyte differentiation | 1.08E-05 | 0.01147541 |
| MP:0001881 | abnormal mammary gland physiology | 8.00E-06 | 0.011538462 |
| ENSG00000092098 | RNF31 subnetwork | 1.10E-05 | 0.011538462 |
| GO:0002708 | positive regulation of lymphocyte mediated immunity | 1.73E-04 | 0.011587302 |
| GO:0002705 | positive regulation of leukocyte mediated immunity | 1.73E-04 | 0.011624204 |
| GO:0070228 | regulation of lymphocyte apoptotic process | 1.72E-04 | 0.011661342 |
| ENSG00000185338 | SOCS1 subnetwork | 1.05E-05 | 0.011666667 |
| GO:0042094 | interleukin-2 biosynthetic process | 1.70E-04 | 0.011698718 |
| ENSG00000072274 | TFRC subnetwork | 1.10E-05 | 0.01171875 |
| MP:0008074 | increased CD4-positive T cell number | 1.70E-04 | 0.011736334 |
| GO:0035710 | CD4-positive, alpha-beta T cell activation | 7.97E-06 | 0.011764706 |
| MP:0005348 | increased T cell proliferation | 1.68E-04 | 0.011774194 |
| MP:0002339 | abnormal lymph node morphology | 1.02E-05 | 0.011864407 |
| GO:0042104 | positive regulation of activated T cell proliferation | 1.10E-05 | 0.011904762 |
| ENSG00000111537 | IFNG subnetwork | 7.62E-06 | 0.012 |
| GO:0050867 | positive regulation of cell activation | 1.75E-04 | 0.012183544 |

| | | | |
|---|---|---|---|
| ENSG00000167363 | FN3K subnetwork | 1.78E-04 | 0.0121875 |
| MP:0006270 | abnormal mammary gland growth during lactation | 1.78E-04 | 0.012225705 |
| MP:0005013 | increased lymphocyte cell number | 7.47E-06 | 0.012244898 |
| MP:0001222 | epidermal hyperplasia | 1.77E-04 | 0.012264151 |
| KEGG_DORSO_VENTRAL_AXIS_ | KEGG_DORSO_VENTRAL_AXIS_FORMATION | 1.77E-04 | 0.012302839 |
| GO:0005035 | death receptor activity | 1.81E-04 | 0.012305296 |
| ENSG00000121966 | CXCR4 subnetwork | 1.82E-04 | 0.01242236 |
| ENSG00000105810 | CDK6 subnetwork | 1.87E-04 | 0.0125387 |
| MP:0005090 | increased double-negative T cell number | 1.89E-04 | 0.012808642 |
| MP:0003449 | abnormal intestinal goblet cell morphology | 1.93E-04 | 0.013076923 |
| MP:0008661 | decreased interleukin-10 secretion | 1.99E-04 | 0.013190184 |
| GO:0005031 | tumor necrosis factor-activated receptor activity | 2.02E-04 | 0.013871951 |
| ENSG00000170484 | KRT74 subnetwork | 2.01E-04 | 0.013914373 |
| MP:0008024 | absent lymph nodes | 2.04E-04 | 0.014090909 |
| GO:0050865 | regulation of cell activation | 2.31E-04 | 0.014121037 |
| MP:0003957 | abnormal nitric oxide homeostasis | 2.04E-04 | 0.014133739 |
| MP:0009335 | decreased splenocyte proliferation | 2.31E-04 | 0.01416185 |
| MP:0005025 | abnormal response to infection | 2.30E-04 | 0.014202899 |
| GO:2000514 | regulation of CD4-positive, alpha-beta T cell activation | 2.29E-04 | 0.014244186 |
| GO:0046965 | retinoid X receptor binding | 2.17E-04 | 0.014264264 |
| ENSG00000212860 | ENSG00000212860 subnetwork | 2.23E-04 | 0.014264706 |
| REACTOME_PLCG1_EVENTS_IN | REACTOME_PLCG1_EVENTS_IN_ERBB2_SIGNALING | 2.29E-04 | 0.014285714 |
| MP:0008097 | increased plasma cell number | 2.41E-04 | 0.014285714 |
| ENSG00000204389 | HSPA1A subnetwork | 2.23E-04 | 0.014306785 |
| MP:0008501 | increased IgG2b level | 2.16E-04 | 0.014307229 |
| ENSG00000204231 | RXRB subnetwork | 2.40E-04 | 0.014325843 |
| GO:0002440 | production of molecular mediator of immune response | 2.27E-04 | 0.014327485 |
| ENSG00000212866 | HSPA1B subnetwork | 2.23E-04 | 0.014349112 |
| ENSG00000131323 | TRAF3 subnetwork | 2.14E-04 | 0.014350453 |
| ENSG00000206289 | RXRB subnetwork | 2.40E-04 | 0.014366197 |
| ENSG00000073584 | SMARCE1 subnetwork | 2.27E-04 | 0.014369501 |
| ENSG00000215292 | ENSG00000215292 subnetwork | 2.23E-04 | 0.014391691 |
| ENSG00000206218 | ENSG00000206218 subnetwork | 2.40E-04 | 0.01440678 |
| ENSG00000173757 | STAT5B subnetwork | 2.36E-04 | 0.014428571 |
| ENSG00000204388 | HSPA1B subnetwork | 2.23E-04 | 0.014434524 |
| ENSG00000184047 | DIABLO subnetwork | 2.40E-04 | 0.014447592 |
| ENSG00000116478 | HDAC1 subnetwork | 2.34E-04 | 0.014469914 |
| GO:0032623 | interleukin-2 production | 2.22E-04 | 0.014477612 |
| ENSG00000164305 | CASP3 subnetwork | 2.39E-04 | 0.014488636 |
| MP:0002455 | abnormal dendritic cell antigen presentation | 2.31E-04 | 0.014511494 |
| ENSG00000115641 | FHL2 subnetwork | 2.20E-04 | 0.014520958 |
| ENSG00000168884 | TNIP2 subnetwork | 2.38E-04 | 0.014529915 |
| REACTOME_GROWTH_HORMO | REACTOME_GROWTH_HORMONE_RECEPTOR_SIGNALING | 2.52E-04 | 0.014583333 |
| MP:0006269 | abnormal mammary gland growth during pregnancy | 2.51E-04 | 0.014623955 |
| ENSG00000141655 | TNFRSF11A subnetwork | 2.49E-04 | 0.014664804 |
| ENSG00000120210 | INSL6 subnetwork | 2.58E-04 | 0.014819945 |
| ENSG00000125686 | MED1 subnetwork | 2.62E-04 | 0.01489071 |
| MP:0000688 | lymphoid hyperplasia | 2.61E-04 | 0.014931507 |
| MP:0003156 | abnormal leukocyte migration | 2.60E-04 | 0.014972527 |
| ENSG00000137275 | RIPK1 subnetwork | 2.60E-04 | 0.015013774 |
| MP:0002217 | small lymph nodes | 2.60E-04 | 0.015055249 |
| MP:0005018 | decreased T cell number | 2.66E-04 | 0.015081522 |
| MP:0000716 | abnormal immune system cell morphology | 2.64E-04 | 0.015122616 |

| | | | |
|---|---|---|---|
| MP:0005616 | decreased susceptibility to type IV hypersensitivity reaction | 2.76E-04 | 0.015240642 |
| MP:0001807 | decreased IgA level | 2.75E-04 | 0.015281501 |
| MP:0003725 | increased autoantibody level | 2.74E-04 | 0.015322581 |
| MP:0002123 | abnormal hematopoiesis | 2.74E-04 | 0.015363881 |
| ENSG00000064012 | CASP8 subnetwork | 2.70E-04 | 0.015405405 |
| MP:0003850 | abnormal thymocyte activation | 2.67E-04 | 0.015447154 |
| REACTOME_DOWNSTREAM_SI | REACTOME_DOWNSTREAM_SIGNAL_TRANSDUCTION | 2.80E-04 | 0.015466667 |
| GO:0048302 | regulation of isotype switching to IgG isotypes | 2.90E-04 | 0.01547619 |
| ENSG00000102226 | USP11 subnetwork | 2.90E-04 | 0.015517241 |
| MP:0001577 | anemia | 2.89E-04 | 0.015558511 |
| MP:0001860 | liver inflammation | 2.97E-04 | 0.015616798 |
| ENSG00000165219 | GAPVD1 subnetwork | 2.97E-04 | 0.015657895 |
| GO:0002263 | cell activation involved in immune response | 3.01E-04 | 0.015665796 |
| MP:0002816 | colitis | 3.09E-04 | 0.015673575 |
| ENSG00000179295 | PTPN11 subnetwork | 2.96E-04 | 0.015699208 |
| GO:0002366 | leukocyte activation involved in immune response | 3.01E-04 | 0.015706806 |
| GO:0045580 | regulation of T cell differentiation | 3.05E-04 | 0.015714286 |
| MP:0008479 | decreased spleen white pulp amount | 3.12E-04 | 0.015721649 |
| MP:0008577 | increased circulating interferon-gamma level | 3.04E-04 | 0.015755208 |
| GO:0002573 | myeloid leukocyte differentiation | 3.10E-04 | 0.015762274 |
| MP:0002145 | abnormal T cell differentiation | 3.14E-04 | 0.015809769 |
| ENSG00000110395 | CBL subnetwork | 3.19E-04 | 0.015984655 |
| ENSG00000198033 | TUBA3C subnetwork | 3.29E-04 | 0.015989848 |
| MP:0005026 | decreased susceptibility to parasitic infection | 3.15E-04 | 0.016025641 |
| ENSG00000075886 | TUBA3D subnetwork | 3.29E-04 | 0.016030534 |
| MP:0000219 | increased neutrophil cell number | 3.24E-04 | 0.016071429 |
| MP:0000414 | alopecia | 3.32E-04 | 0.016329114 |
| ENSG00000196363 | WDR5 subnetwork | 3.41E-04 | 0.016583541 |
| GO:0002831 | regulation of response to biotic stimulus | 3.41E-04 | 0.016625 |
| REACTOME_EGFR_INTERACTS_ | REACTOME_EGFR_INTERACTS_WITH_PHOSPHOLIPASE_C:G | 3.39E-04 | 0.016666667 |
| GO:0045830 | positive regulation of isotype switching | 3.38E-04 | 0.016708543 |
| MP:0002088 | abnormal embryonic growth/weight/body size | 3.37E-04 | 0.01675063 |
| MP:0001861 | lung inflammation | 3.37E-04 | 0.016792929 |
| MP:0005329 | abnormal myocardium layer morphology | 3.48E-04 | 0.017910448 |
| MP:0000220 | increased monocyte cell number | 3.54E-04 | 0.017990074 |
| REACTOME_COSTIMULATION_ | REACTOME_COSTIMULATION_BY_THE_CD28_FAMILY | 3.55E-04 | 0.018069307 |
| MP:0001823 | thymus hypoplasia | 3.67E-04 | 0.018170732 |
| ENSG00000107566 | ERLIN1 subnetwork | 3.93E-04 | 0.018171021 |
| ENSG00000102882 | MAPK3 subnetwork | 4.07E-04 | 0.018192488 |
| MP:0000706 | small thymus | 3.97E-04 | 0.01820331 |
| GO:0018212 | peptidyl-tyrosine modification | 3.89E-04 | 0.018214286 |
| ENSG00000123329 | ARHGAP9 subnetwork | 3.66E-04 | 0.018215159 |
| ENSG00000141968 | VAV1 subnetwork | 3.61E-04 | 0.018226601 |
| MP:0002743 | glomerulonephritis | 4.05E-04 | 0.018235294 |
| ENSG00000116824 | CD2 subnetwork | 3.96E-04 | 0.018246445 |
| GO:0002460 | adaptive immune response based on somatic recombinatio | 3.87E-04 | 0.018257757 |
| MP:0008603 | decreased circulating interleukin-4 level | 3.63E-04 | 0.018259804 |
| ENSG00000066336 | SPI1 subnetwork | 3.60E-04 | 0.018271605 |
| GO:0002253 | activation of immune response | 4.03E-04 | 0.018278302 |
| GO:0002287 | alpha-beta T cell activation involved in immune response | 3.87E-04 | 0.018301435 |
| MP:0005014 | increased B cell number | 3.61E-04 | 0.018304668 |
| MP:0004800 | decreased susceptibility to experimental autoimmune ence | 3.78E-04 | 0.018313253 |
| GO:0002293 | alpha-beta T cell differentiation involved in immune respon | 3.87E-04 | 0.018345324 |

| | | | |
|---|---|---|---|
| MP:0002371 | abnormal thymus cortex morphology | 3.76E-04 | 0.018357488 |
| ENSG00000182866 | LCK subnetwork | 3.83E-04 | 0.018389423 |
| MP:0000702 | enlarged lymph nodes | 4.24E-04 | 0.018390805 |
| MP:0002871 | albuminuria | 3.75E-04 | 0.018401937 |
| GO:0043029 | T cell homeostasis | 4.23E-04 | 0.01843318 |
| GO:0002902 | regulation of B cell apoptotic process | 3.75E-04 | 0.018446602 |
| GO:0032673 | regulation of interleukin-4 production | 4.29E-04 | 0.018463303 |
| GO:0045885 | positive regulation of survival gene product expression | 4.21E-04 | 0.018475751 |
| GO:0033209 | tumor necrosis factor-mediated signaling pathway | 3.74E-04 | 0.018491484 |
| MP:0000708 | thymus hyperplasia | 4.20E-04 | 0.018518519 |
| GO:0032729 | positive regulation of interferon-gamma production | 4.34E-04 | 0.018535469 |
| ENSG00000169375 | SIN3A subnetwork | 4.15E-04 | 0.018561485 |
| MP:0005016 | decreased lymphocyte cell number | 4.14E-04 | 0.018604651 |
| MP:0002442 | abnormal leukocyte physiology | 4.13E-04 | 0.018648019 |
| MP:0008688 | decreased interleukin-2 secretion | 4.13E-04 | 0.018691589 |
| GO:0000060 | protein import into nucleus, translocation | 4.12E-04 | 0.018735363 |
| ENSG00000077097 | TOP2B subnetwork | 4.52E-04 | 0.019134396 |
| GO:0003712 | transcription cofactor activity | 4.51E-04 | 0.019178082 |
| MP:0000488 | abnormal intestinal epithelium morphology | 4.53E-04 | 0.019318182 |
| MP:0008115 | abnormal dendritic cell differentiation | 4.66E-04 | 0.019570136 |
| ENSG00000175354 | PTPN2 subnetwork | 4.66E-04 | 0.019614512 |
| MP:0001846 | increased inflammatory response | 4.77E-04 | 0.01986456 |
| REACTOME_SIGNALING_BY_IN | REACTOME_SIGNALING_BY_INTERLEUKINS | 4.82E-04 | 0.01988764 |
| MP:0000240 | extramedullary hematopoiesis | 4.81E-04 | 0.019932432 |
| MP:0005671 | abnormal response to transplant | 4.87E-04 | 0.019955157 |
| KEGG_JAK_STAT_SIGNALING_I | KEGG_JAK_STAT_SIGNALING_PATHWAY | 5.01E-04 | 0.020155902 |
| ENSG00000196591 | HDAC2 subnetwork | 4.95E-04 | 0.020200893 |
| MP:0008037 | abnormal T cell morphology | 5.05E-04 | 0.020222222 |
| GO:0002763 | positive regulation of myeloid leukocyte differentiation | 4.95E-04 | 0.020246085 |
| MP:0000692 | small spleen | 5.07E-04 | 0.020399113 |
| REACTOME_TRAF6_MEDIATED | REACTOME_TRAF6_MEDIATED_INDUCTION_OF_NFKB_ANI | 5.13E-04 | 0.020419426 |
| ENSG00000172216 | CEBPB subnetwork | 5.19E-04 | 0.02043956 |
| GO:0016064 | immunoglobulin mediated immune response | 5.10E-04 | 0.020464602 |
| GO:0001819 | positive regulation of cytokine production | 5.16E-04 | 0.020484581 |
| MP:0002444 | abnormal T cell physiology | 5.23E-04 | 0.020504386 |
| ENSG00000171094 | ALK subnetwork | 5.41E-04 | 0.020652174 |
| MP:0002189 | abnormal myocardial trabeculae morphology | 5.36E-04 | 0.020697168 |
| MP:0008660 | increased interleukin-10 secretion | 5.36E-04 | 0.020742358 |
| MP:0001793 | altered susceptibility to infection | 5.36E-04 | 0.020787746 |
| GO:0002443 | leukocyte mediated immunity | 5.56E-04 | 0.020932755 |
| GO:0031347 | regulation of defense response | 5.64E-04 | 0.020950324 |
| REACTOME_INTERLEUKIN_REC | REACTOME_INTERLEUKIN_RECEPTOR_SHC_SIGNALING | 5.63E-04 | 0.020995671 |
| GO:0019724 | B cell mediated immunity | 5.94E-04 | 0.021382979 |
| GO:0045911 | positive regulation of DNA recombination | 6.00E-04 | 0.021398305 |
| REACTOME_TOLL_LIKE_RECEP | REACTOME_TOLL_LIKE_RECEPTOR_TLR1TLR2_CASCADE | 6.14E-04 | 0.021398747 |
| REACTOME_NOTCH:HLH_TRAN | REACTOME_NOTCH:HLH_TRANSCRIPTION_PATHWAY | 5.85E-04 | 0.021413276 |
| MP:0008049 | increased memory T cell number | 5.92E-04 | 0.021428571 |
| REACTOME_MYD88MAL_CASC | REACTOME_MYD88MAL_CASCADE_INITIATED_ON_PLASM/ | 6.14E-04 | 0.021443515 |
| GO:0070670 | response to interleukin-4 | 5.99E-04 | 0.021443737 |
| GO:0002698 | negative regulation of immune effector process | 5.74E-04 | 0.021443966 |
| ENSG00000126561 | STAT5A subnetwork | 6.17E-04 | 0.021458333 |
| REACTOME_NICD_TRAFFICS_T | REACTOME_NICD_TRAFFICS_TO_NUCLEUS | 5.85E-04 | 0.021459227 |
| ENSG00000118260 | CREB1 subnetwork | 5.89E-04 | 0.021474359 |

| | | | |
|---|---|---|---|
| REACTOME_TOLL_LIKE_RECEP | REACTOME_TOLL_LIKE_RECEPTOR_TLR6TLR2_CASCADE | 6.14E-04 | 0.02148847 |
| ENSG00000127511 | SIN3B subnetwork | 5.79E-04 | 0.021505376 |
| KEGG_CYTOKINE_CYTOKINE_R | KEGG_CYTOKINE_CYTOKINE_RECEPTOR_INTERACTION | 6.30E-04 | 0.021517672 |
| GO:0005126 | cytokine receptor binding | 6.06E-04 | 0.021518987 |
| REACTOME_TOLL_LIKE_RECEP | REACTOME_TOLL_LIKE_RECEPTOR_2_TLR2_CASCADE | 6.14E-04 | 0.021533613 |
| MP:0001800 | abnormal humoral immune response | 6.06E-04 | 0.021564482 |
| MP:0009336 | increased splenocyte proliferation | 6.33E-04 | 0.021576763 |
| GO:0043011 | myeloid dendritic cell differentiation | 6.11E-04 | 0.021578947 |
| ENSG00000171720 | HDAC3 subnetwork | 6.39E-04 | 0.022153209 |
| GO:0018108 | peptidyl-tyrosine phosphorylation | 6.44E-04 | 0.022210744 |
| MP:0003944 | abnormal T cell subpopulation ratio | 6.47E-04 | 0.022233607 |
| REACTOME_TCR_SIGNALING | REACTOME_TCR_SIGNALING | 6.52E-04 | 0.022244898 |
| MP:0008092 | abnormal T-helper 2 cell differentiation | 6.46E-04 | 0.022268041 |
| GO:0031295 | T cell costimulation | 6.46E-04 | 0.022279261 |
| GO:0045639 | positive regulation of myeloid cell differentiation | 6.50E-04 | 0.022290389 |
| GO:0031294 | lymphocyte costimulation | 6.46E-04 | 0.022325103 |
| GO:0008134 | transcription factor binding | 6.79E-04 | 0.022434608 |
| MP:0006410 | abnormal common myeloid progenitor cell morphology | 6.77E-04 | 0.022479839 |
| REACTOME_SIGNALING_BY_SC | REACTOME_SIGNALING_BY_SCF:KIT | 6.81E-04 | 0.02248996 |
| ENSG00000160691 | SHC1 subnetwork | 6.86E-04 | 0.0225 |
| MP:0005017 | decreased B cell number | 6.73E-04 | 0.022525253 |
| MP:0002375 | abnormal thymus medulla morphology | 6.84E-04 | 0.02254509 |
| GO:0046634 | regulation of alpha-beta T cell activation | 6.91E-04 | 0.02255489 |
| MP:0001192 | scaly skin | 6.65E-04 | 0.022560976 |
| MP:0005070 | impaired NK cell cytolysis | 6.70E-04 | 0.02257085 |
| ENSG00000141027 | NCOR1 subnetwork | 6.65E-04 | 0.022606925 |
| GO:0000989 | transcription factor binding transcription factor activity | 6.68E-04 | 0.022616633 |
| ENSG00000145675 | PIK3R1 subnetwork | 6.97E-04 | 0.022709163 |
| GO:0002292 | T cell differentiation involved in immune response | 7.21E-04 | 0.022826087 |
| MP:0008127 | decreased dendritic cell number | 7.12E-04 | 0.022871287 |
| ENSG00000145907 | G3BP1 subnetwork | 7.12E-04 | 0.022916667 |
| KEGG_FC_EPSILON_RI_SIGNAL | KEGG_FC_EPSILON_RI_SIGNALING_PATHWAY | 7.09E-04 | 0.022962227 |
| GO:0042093 | T-helper cell differentiation | 7.24E-04 | 0.022986248 |
| GO:0002294 | CD4-positive, alpha-beta T cell differentiation involved in in | 7.24E-04 | 0.023031496 |
| GO:0032609 | interferon-gamma production | 7.23E-04 | 0.023076923 |
| MP:0004956 | decreased thymus weight | 7.34E-04 | 0.023385519 |
| ENSG00000084774 | CAD subnetwork | 7.30E-04 | 0.023431373 |
| ENSG00000158517 | NCF1 subnetwork | 7.44E-04 | 0.023535156 |
| MP:0008475 | intermingled spleen red and white pulp | 7.49E-04 | 0.023540856 |
| GO:0002819 | regulation of adaptive immune response | 7.46E-04 | 0.023586745 |
| GO:0071356 | cellular response to tumor necrosis factor | 7.70E-04 | 0.023694391 |
| ENSG00000056558 | TRAF1 subnetwork | 7.65E-04 | 0.02374031 |
| MP:0008702 | increased interleukin-5 secretion | 7.64E-04 | 0.023786408 |
| ENSG00000114423 | CBLB subnetwork | 7.72E-04 | 0.023938224 |
| MP:0004946 | abnormal regulatory T cell physiology | 7.93E-04 | 0.024277457 |
| ENSG00000026103 | FAS subnetwork | 8.08E-04 | 0.0243762 |
| ENSG00000048052 | HDAC9 subnetwork | 7.94E-04 | 0.024423077 |
| MP:0004816 | abnormal class switch recombination | 8.27E-04 | 0.02447619 |
| ENSG00000169967 | MAP3K2 subnetwork | 8.26E-04 | 0.024522901 |
| GO:0003713 | transcription coactivator activity | 8.24E-04 | 0.02456979 |
| MP:0008083 | decreased single-positive T cell number | 8.22E-04 | 0.024616858 |
| KEGG_CHEMOKINE_SIGNALIN | KEGG_CHEMOKINE_SIGNALING_PATHWAY | 8.41E-04 | 0.024904943 |
| GO:0002757 | immune response-activating signal transduction | 8.51E-04 | 0.025 |

| | | | |
|---|---|---|---|
| MP:0000599 | enlarged liver | 8.53E-04 | 0.025047259 |
| GO:0001910 | regulation of leukocyte mediated cytotoxicity | 8.45E-04 | 0.025047438 |
| MP:0008497 | decreased IgG2b level | 9.04E-04 | 0.025929368 |
| MP:0000693 | spleen hyperplasia | 9.14E-04 | 0.025974026 |
| MP:0005666 | abnormal adipose tissue physiology | 9.00E-04 | 0.025977654 |
| MP:0003644 | thymus atrophy | 8.99E-04 | 0.026026119 |
| ENSG00000056972 | TRAF3IP2 subnetwork | 8.96E-04 | 0.026074766 |
| REACTOME_CIRCADIAN_CLOCI | REACTOME_CIRCADIAN_CLOCK | 8.94E-04 | 0.026123596 |
| GO:0042113 | B cell activation | 8.91E-04 | 0.02612782 |
| MP:0009503 | abnormal mammary gland duct morphology | 8.88E-04 | 0.026132075 |
| ENSG00000134460 | IL2RA subnetwork | 8.94E-04 | 0.026172608 |
| MP:0000694 | spleen hypoplasia | 8.90E-04 | 0.026177024 |
| MP:0005289 | increased oxygen consumption | 9.21E-04 | 0.026296296 |
| MP:0002500 | granulomatous inflammation | 9.38E-04 | 0.026432532 |
| GO:0031341 | regulation of cell killing | 9.41E-04 | 0.026476015 |
| ENSG00000124813 | RUNX2 subnetwork | 9.73E-04 | 0.027056673 |
| MP:0000379 | decreased hair follicle number | 9.70E-04 | 0.027106227 |
| ENSG00000206088 | ENSG00000206088 subnetwork | 9.69E-04 | 0.027155963 |
| MP:0004939 | abnormal B cell morphology | 9.76E-04 | 0.027189781 |
| MP:0000685 | abnormal immune system morphology | 0.00102303 | 0.027191413 |
| MP:0008495 | decreased IgG1 level | 0.00100921 | 0.027199282 |
| GO:0043370 | regulation of CD4-positive, alpha-beta T cell differentiation | 9.68E-04 | 0.027205882 |
| MP:0002362 | abnormal spleen marginal zone morphology | 9.95E-04 | 0.02722323 |
| ENSG00000065559 | MAP2K4 subnetwork | 0.00102537 | 0.027232143 |
| REACTOME_INTERLEUKIN:3_5_ | REACTOME_INTERLEUKIN:3_5_AND_GM:CSF_SIGNALING | 0.0010166 | 0.027240143 |
| MP:0002357 | abnormal spleen white pulp morphology | 0.00100781 | 0.027248201 |
| ENSG00000082512 | TRAF5 subnetwork | 9.66E-04 | 0.027255985 |
| REACTOME_DOWNSTREAM_T( | REACTOME_DOWNSTREAM_TCR_SIGNALING | 9.96E-04 | 0.027264493 |
| KEGG_ADIPOCYTOKINE_SIGNA | KEGG_ADIPOCYTOKINE_SIGNALING_PATHWAY | 9.93E-04 | 0.027272727 |
| ENSG00000110330 | BIRC2 subnetwork | 0.0010075 | 0.027297297 |
| ENSG00000133704 | IPO8 subnetwork | 1.00E-03 | 0.027305606 |
| GO:0002437 | inflammatory response to antigenic stimulus | 9.91E-04 | 0.027322404 |
| GO:0051250 | negative regulation of lymphocyte activation | 0.00104453 | 0.027336861 |
| MP:0001928 | abnormal ovulation | 0.00100577 | 0.02734657 |
| MP:0008217 | abnormal B cell activation | 0.00104715 | 0.027376761 |
| REACTOME_PROLACTIN_RECEI | REACTOME_PROLACTIN_RECEPTOR_SIGNALING | 0.00104242 | 0.027385159 |
| GO:0002369 | T cell cytokine production | 0.00105374 | 0.027408056 |
| MP:0002358 | abnormal spleen periarteriolar lymphoid sheath morpholog | 0.00105063 | 0.02741652 |
| MP:0008553 | increased circulating tumor necrosis factor level | 0.00104025 | 0.027433628 |
| ENSG00000206560 | ANKRD28 subnetwork | 0.00103119 | 0.02745098 |
| GO:0045582 | positive regulation of T cell differentiation | 0.00105342 | 0.02745614 |
| GO:0060396 | growth hormone receptor signaling pathway | 0.00103954 | 0.02748227 |
| GO:0045672 | positive regulation of osteoclast differentiation | 0.0010382 | 0.027491103 |
| GO:0071378 | cellular response to growth hormone stimulus | 0.00103954 | 0.027531083 |
| ENSG00000143119 | CD53 subnetwork | 0.0010698 | 0.027622378 |
| ENSG00000134954 | ETS1 subnetwork | 0.00109242 | 0.02804878 |
| GO:0032649 | regulation of interferon-gamma production | 0.00109227 | 0.028097731 |
| ENSG00000100385 | IL2RB subnetwork | 0.00109907 | 0.028173913 |
| MP:0000709 | enlarged thymus | 0.0011034 | 0.028298611 |
| ENSG00000197122 | SRC subnetwork | 0.00111316 | 0.028336222 |
| ENSG00000138378 | STAT4 subnetwork | 0.00111826 | 0.028373702 |
| ENSG00000140396 | NCOA2 subnetwork | 0.00113764 | 0.028399312 |
| GO:0002764 | immune response-regulating signaling pathway | 0.00114184 | 0.028436426 |

| | | | |
|---|---|---|---|
| GO:0042506 | tyrosine phosphorylation of Stat5 protein | 0.00113245 | 0.028448276 |
| REACTOME_ADAPTIVE_IMMUI | REACTOME_ADAPTIVE_IMMUNE_SYSTEM | 0.00112908 | 0.028497409 |
| MP:0003304 | large intestinal inflammation | 0.00115691 | 0.028559177 |
| REACTOME_DAG_AND_IP3_SI | REACTOME_DAG_AND_IP3_SIGNALING | 0.00116693 | 0.029023973 |
| REACTOME_NEF:MEDIATES_D | REACTOME_NEF:MEDIATES_DOWN_MODULATION_OF_CE | 0.00117885 | 0.029145299 |
| MP:0008566 | increased interferon-gamma secretion | 0.00119897 | 0.029607509 |
| MP:0000714 | increased thymocyte number | 0.00120748 | 0.029727428 |
| MP:0000217 | abnormal leukocyte cell number | 0.0012327 | 0.029864636 |
| REACTOME_NFKB_AND_MAP_ | REACTOME_NFKB_AND_MAP_KINASES_ACTIVATION_MED | 0.00123268 | 0.029915254 |
| MP:0001825 | arrested T cell differentiation | 0.00125657 | 0.029915966 |
| GO:0003714 | transcription corepressor activity | 0.00123004 | 0.029966044 |
| ENSG00000162924 | REL subnetwork | 0.00125538 | 0.02996633 |
| ENSG00000123609 | NMI subnetwork | 0.00125529 | 0.030016863 |
| GO:0045619 | regulation of lymphocyte differentiation | 0.00122259 | 0.030017007 |
| MP:0008703 | decreased interleukin-5 secretion | 0.00127415 | 0.030033557 |
| MP:0008664 | decreased interleukin-12 secretion | 0.00128069 | 0.030067002 |
| MP:0009338 | increased splenocyte number | 0.0012474 | 0.030067568 |
| KEGG_ASTHMA | KEGG_ASTHMA | 0.00129205 | 0.030116473 |
| ENSG00000115085 | ZAP70 subnetwork | 0.00130121 | 0.030149502 |
| ENSG00000113263 | ITK subnetwork | 0.00129033 | 0.030166667 |
| GO:0002367 | cytokine production involved in immune response | 0.00130242 | 0.030182421 |
| MP:0002052 | decreased tumor incidence | 0.00130635 | 0.030215232 |
| ENSG00000051382 | PIK3CB subnetwork | 0.00128958 | 0.030217028 |
| MP:0004947 | skin inflammation | 0.00128387 | 0.030267559 |
| GO:0050851 | antigen receptor-mediated signaling pathway | 0.00131546 | 0.030280528 |
| ENSG00000050748 | MAPK9 subnetwork | 0.00131515 | 0.030330579 |
| ENSG00000055332 | EIF2AK2 subnetwork | 0.00132553 | 0.030345395 |
| GO:0002822 | regulation of adaptive immune response based on somatic | 0.00132385 | 0.030395387 |
| GO:0034612 | response to tumor necrosis factor | 0.00133443 | 0.030541872 |
| MP:0004988 | increased osteoblast cell number | 0.00134507 | 0.030737705 |
| MP:0002494 | increased IgM level | 0.00136582 | 0.030851064 |
| MP:0004392 | abnormal CD8-positive T cell physiology | 0.00138191 | 0.031158238 |
| GO:0045058 | T cell selection | 0.00137834 | 0.03120915 |
| MP:0008617 | increased circulating interleukin-12 level | 0.00139409 | 0.031351792 |
| GO:0032269 | negative regulation of cellular protein metabolic process | 0.00140302 | 0.031412338 |
| ENSG00000116918 | TSNAX subnetwork | 0.00140079 | 0.031463415 |
| MP:0005154 | increased B cell proliferation | 0.00141054 | 0.031685575 |
| GO:0001818 | negative regulation of cytokine production | 0.00141747 | 0.031693548 |
| REACTOME_NF:KB_IS_ACTIVAT | REACTOME_NF:KB_IS_ACTIVATED_AND_SIGNALS_SURVIVA | 0.0014139 | 0.03171521 |
| ENSG00000157625 | TAB3 subnetwork | 0.00141762 | 0.031723027 |
| MP:0002359 | abnormal spleen germinal center morphology | 0.00141597 | 0.03174475 |
| GO:0050731 | positive regulation of peptidyl-tyrosine phosphorylation | 0.00143999 | 0.031818182 |
| REACTOME_TRAF6_MEDIATED | REACTOME_TRAF6_MEDIATED_INDUCTION_OF_PROINFLA | 0.00143107 | 0.03184 |
| ENSG00000124588 | NQO2 subnetwork | 0.00143939 | 0.03186901 |
| MP:0002418 | increased susceptibility to viral infection | 0.00143093 | 0.031891026 |
| MP:0008498 | decreased IgG3 level | 0.00142917 | 0.031942215 |
| ENSG00000185950 | IRS2 subnetwork | 0.0014246 | 0.031993569 |
| MP:0002723 | abnormal immune serum protein physiology | 0.00146674 | 0.032324841 |
| GO:0002718 | regulation of cytokine production involved in immune resp | 0.00150461 | 0.032413249 |
| ENSG00000147168 | IL2RG subnetwork | 0.0014792 | 0.032432432 |
| ENSG00000179271 | GADD45GIP1 subnetwork | 0.00148608 | 0.032460317 |
| GO:2000107 | negative regulation of leukocyte apoptotic process | 0.00149812 | 0.032464455 |
| ENSG00000206294 | ENSG00000206294 subnetwork | 0.00149569 | 0.032488114 |

| | | | |
|---|---|---|---|
| ENSG00000159388 | BTG2 subnetwork | 0.00149792 | 0.032515823 |
| ENSG00000173473 | SMARCC1 subnetwork | 0.00151919 | 0.032598425 |
| MP:0003884 | decreased macrophage cell number | 0.00152647 | 0.032625786 |
| ENSG00000089220 | PEBP1 subnetwork | 0.00153194 | 0.032810047 |
| MP:0004955 | increased thymus weight | 0.00155974 | 0.03338558 |
| ENSG00000081237 | PTPRC subnetwork | 0.00160744 | 0.033984375 |
| KEGG_APOPTOSIS | KEGG_APOPTOSIS | 0.00160459 | 0.034037559 |
| MP:0001845 | abnormal inflammatory response | 0.00163639 | 0.034711388 |
| GO:0031593 | polyubiquitin binding | 0.00164079 | 0.034735202 |
| MP:0004799 | increased susceptibility to experimental autoimmune ence | 0.00165042 | 0.034758942 |
| ENSG00000173163 | COMMD1 subnetwork | 0.00166603 | 0.034937888 |
| ENSG00000134759 | ELP2 subnetwork | 0.00170535 | 0.035139319 |
| GO:0050868 | negative regulation of T cell activation | 0.00168678 | 0.035193798 |
| GO:0042522 | regulation of tyrosine phosphorylation of Stat5 protein | 0.00171335 | 0.035316847 |
| REACTOME_INTERLEUKIN:6_SI | REACTOME_INTERLEUKIN:6_SIGNALING | 0.0017196 | 0.035493827 |
| ENSG00000160185 | UBASH3A subnetwork | 0.00174072 | 0.035615385 |
| MP:0008079 | decreased CD8-positive T cell number | 0.00173752 | 0.035670262 |
| GO:0016922 | ligand-dependent nuclear receptor binding | 0.00174446 | 0.035714286 |
| GO:0042092 | type 2 immune response | 0.00179576 | 0.035866261 |
| KEGG_INTESTINAL_IMMUNE_N | KEGG_INTESTINAL_IMMUNE_NETWORK_FOR_IGA_PRODU | 0.00177309 | 0.035889571 |
| ENSG00000142166 | IFNAR1 subnetwork | 0.00180404 | 0.035909091 |
| MP:0001849 | ear inflammation | 0.00178797 | 0.035920852 |
| ENSG00000121031 | ENSG00000121031 subnetwork | 0.00178427 | 0.035954198 |
| REACTOME_THE_ROLE_OF_NE | REACTOME_THE_ROLE_OF_NEF_IN_HIV:1_REPLICATION_A | 0.00180393 | 0.035963581 |
| MP:0005350 | increased susceptibility to autoimmune disorder | 0.00178607 | 0.03597561 |
| REACTOME_TOLL_LIKE_RECEP | REACTOME_TOLL_LIKE_RECEPTOR_78_TLR78_CASCADE | 0.001781 | 0.036009174 |
| ENSG00000111642 | CHD4 subnetwork | 0.00182461 | 0.03602719 |
| REACTOME_MYD88_DEPENDE | REACTOME_MYD88_DEPENDENT_CASCADE_INITIATED_ON | 0.001781 | 0.036064319 |
| GO:0051224 | negative regulation of protein transport | 0.00182107 | 0.036081694 |
| MP:0002499 | chronic inflammation | 0.00183093 | 0.03612368 |
| ENSG00000206206 | DAXX subnetwork | 0.00186305 | 0.036452096 |
| ENSG00000204209 | DAXX subnetwork | 0.00186305 | 0.036506747 |
| ENSG00000206279 | DAXX subnetwork | 0.00186305 | 0.036561562 |
| ENSG00000179409 | GEMIN4 subnetwork | 0.00185592 | 0.036596386 |
| ENSG00000139144 | PIK3C2G subnetwork | 0.00186183 | 0.036616541 |
| ENSG00000198286 | CARD11 subnetwork | 0.00186979 | 0.036621824 |
| GO:0002456 | T cell mediated immunity | 0.00188638 | 0.036791045 |
| GO:0002695 | negative regulation of leukocyte activation | 0.00193788 | 0.037075332 |
| REACTOME_DEATH_RECEPTOR | REACTOME_DEATH_RECEPTOR__SIGNALLING | 0.00193115 | 0.037130178 |
| GO:0010563 | negative regulation of phosphorus metabolic process | 0.00192051 | 0.037147103 |
| REACTOME_EXTRINSIC_PATHV | REACTOME_EXTRINSIC_PATHWAY_FOR_APOPTOSIS | 0.00193115 | 0.037185185 |
| GO:0045936 | negative regulation of phosphate metabolic process | 0.00192051 | 0.037202381 |
| ENSG00000165025 | SYK subnetwork | 0.00192961 | 0.037240356 |
| ENSG00000077238 | IL4R subnetwork | 0.00191924 | 0.037257824 |
| ENSG00000198821 | CD247 subnetwork | 0.00194869 | 0.037315634 |
| ENSG00000134352 | IL6ST subnetwork | 0.00195038 | 0.037334315 |
| ENSG00000206229 | ENSG00000206229 subnetwork | 0.00197236 | 0.037335286 |
| ENSG00000204257 | HLA-DMA subnetwork | 0.00197236 | 0.037390029 |
| GO:0042100 | B cell proliferation | 0.0019643 | 0.037426471 |
| MP:0002831 | absent Peyer's patches | 0.00199234 | 0.037426901 |
| ENSG00000206293 | ENSG00000206293 subnetwork | 0.00197236 | 0.037444934 |
| MP:0001874 | acanthosis | 0.00200158 | 0.037664234 |
| GO:0045815 | positive regulation of gene expression, epigenetic | 0.00200457 | 0.037682216 |

| | | | |
|---|---|---|---|
| ENSG00000105229 | PIAS4 subnetwork | 0.00204066 | 0.038282387 |
| GO:0046425 | regulation of JAK-STAT cascade | 0.00204896 | 0.038372093 |
| ENSG00000168685 | IL7R subnetwork | 0.00207475 | 0.038405797 |
| MP:0002459 | abnormal B cell physiology | 0.0020623 | 0.038461538 |
| ENSG00000113594 | LIFR subnetwork | 0.00207966 | 0.038567294 |
| ENSG00000178950 | GAK subnetwork | 0.00210627 | 0.038920863 |
| GO:0042035 | regulation of cytokine biosynthetic process | 0.00210334 | 0.038976945 |
| ENSG00000189162 | ENSG00000189162 subnetwork | 0.00210296 | 0.039033189 |
| GO:0000988 | protein binding transcription factor activity | 0.00212311 | 0.03908046 |
| ENSG00000187266 | EPOR subnetwork | 0.00210258 | 0.039089595 |
| MP:0008752 | abnormal tumor necrosis factor level | 0.00213391 | 0.039167862 |
| GO:0046639 | negative regulation of alpha-beta T cell differentiation | 0.0021356 | 0.039183381 |
| KEGG_HEMATOPOIETIC_CELL_ | KEGG_HEMATOPOIETIC_CELL_LINEAGE | 0.00214397 | 0.039270386 |
| GO:2000106 | regulation of leukocyte apoptotic process | 0.00214502 | 0.039285714 |
| GO:0002683 | negative regulation of immune system process | 0.00217946 | 0.039800285 |
| GO:0045637 | regulation of myeloid cell differentiation | 0.00219235 | 0.04002849 |
| MP:0002423 | abnormal mast cell physiology | 0.00221942 | 0.040327169 |
| ENSG00000004059 | ARF5 subnetwork | 0.00223499 | 0.040638298 |
| ENSG00000120949 | TNFRSF8 subnetwork | 0.00223003 | 0.040696023 |
| ENSG00000112033 | PPARD subnetwork | 0.00224423 | 0.04072238 |
| GO:0043383 | negative T cell selection | 0.00225125 | 0.041018388 |
| ENSG00000173039 | RELA subnetwork | 0.00228749 | 0.041596045 |
| ENSG00000140009 | ESR2 subnetwork | 0.00229989 | 0.041607898 |
| REACTOME_PD:1_SIGNALING | REACTOME_PD:1_SIGNALING | 0.00230983 | 0.041690141 |
| ENSG00000011405 | PIK3C2A subnetwork | 0.00231935 | 0.041701828 |
| MP:0004953 | decreased spleen weight | 0.00232818 | 0.041713483 |
| ENSG00000168040 | FADD subnetwork | 0.0023463 | 0.041865358 |
| GO:0050708 | regulation of protein secretion | 0.00235067 | 0.041876751 |
| MP:0008682 | decreased interleukin-17 secretion | 0.00236625 | 0.042039106 |
| ENSG00000105197 | TIMM50 subnetwork | 0.00236385 | 0.042097902 |
| REACTOME_SIGNALING_BY_EF | REACTOME_SIGNALING_BY_ERBB4 | 0.00238921 | 0.042398884 |
| ENSG00000204273 | ENSG00000204273 subnetwork | 0.00241589 | 0.042698192 |
| ENSG00000168399 | ENSG00000168399 subnetwork | 0.00241589 | 0.04275766 |
| ENSG00000102871 | TRADD subnetwork | 0.00244638 | 0.043194444 |
| GO:0051090 | regulation of sequence-specific DNA binding transcription f | 0.0024647 | 0.043481276 |
| MP:0005334 | abnormal fat pad morphology | 0.00249523 | 0.043517241 |
| ENSG00000117461 | PIK3R3 subnetwork | 0.00251052 | 0.043552812 |
| MP:0008478 | increased spleen white pulp amount | 0.00248974 | 0.043568465 |
| GO:0009306 | protein secretion | 0.00249454 | 0.043577348 |
| GO:0010627 | regulation of intracellular protein kinase cascade | 0.00250854 | 0.043612637 |
| ENSG00000215301 | DDX3X subnetwork | 0.00248687 | 0.043628809 |
| GO:0050730 | regulation of peptidyl-tyrosine phosphorylation | 0.00251937 | 0.043630137 |
| MP:0001245 | thick dermal layer | 0.00250824 | 0.043672627 |
| GO:0030890 | positive regulation of B cell proliferation | 0.002504 | 0.043732782 |
| GO:0030888 | regulation of B cell proliferation | 0.00253607 | 0.043980848 |
| ENSG00000073009 | IKBKG subnetwork | 0.00254803 | 0.044193989 |
| MP:0000333 | decreased bone marrow cell number | 0.00258887 | 0.044550409 |
| MP:0008022 | dilated heart ventricle | 0.00257943 | 0.044611187 |
| GO:0042326 | negative regulation of phosphorylation | 0.00262322 | 0.044829932 |
| MP:0008101 | lymph node hypoplasia | 0.00262914 | 0.044836957 |
| MP:0005079 | defective cytotoxic T cell cytolysis | 0.00264567 | 0.045115332 |
| ENSG00000160712 | IL6R subnetwork | 0.00266163 | 0.045392954 |
| MP:0005465 | abnormal T-helper 1 physiology | 0.00266595 | 0.045466847 |

| | | | |
|---|---|---|---|
| GO:0002020 | protease binding | 0.00267717 | 0.045675676 |
| REACTOME_ACTIVATED_TLR4_ | REACTOME_ACTIVATED_TLR4_SIGNALLING | 0.00269777 | 0.045760431 |
| ENSG00000069399 | BCL3 subnetwork | 0.00269541 | 0.045822102 |
| GO:0045428 | regulation of nitric oxide biosynthetic process | 0.00269453 | 0.045883941 |
| GO:0045136 | development of secondary sexual characteristics | 0.00271491 | 0.045967742 |
| MP:0000359 | abnormal mast cell morphology | 0.00271904 | 0.046040268 |
| GO:0042108 | positive regulation of cytokine biosynthetic process | 0.00273762 | 0.046179625 |
| GO:0007259 | JAK-STAT cascade | 0.00274739 | 0.046251673 |
| MP:0006271 | abnormal involution of the mammary gland | 0.00275512 | 0.046256684 |
| ENSG00000077549 | CAPZB subnetwork | 0.00277378 | 0.046595461 |
| ENSG00000114030 | KPNA1 subnetwork | 0.00277957 | 0.046733333 |
| ENSG00000054267 | ARID4B subnetwork | 0.00278163 | 0.046804261 |
| KEGG_ALLOGRAFT_REJECTION | KEGG_ALLOGRAFT_REJECTION | 0.00279087 | 0.04687915 |
| GO:0001772 | immunological synapse | 0.00278888 | 0.046941489 |
| MP:0000198 | hypophosphatemia | 0.00282332 | 0.047480106 |
| ENSG00000161203 | AP2M1 subnetwork | 0.002834 | 0.047483444 |
| MP:0008522 | abnormal lymph node germinal center morphology | 0.00284187 | 0.047685185 |
| MP:0008673 | decreased interleukin-13 secretion | 0.00285556 | 0.047886394 |
| ENSG00000085760 | MTIF2 subnetwork | 0.00286787 | 0.047894737 |
| MP:0002941 | increased circulating alanine transaminase level | 0.00286172 | 0.047957839 |
| ENSG00000146232 | NFKBIE subnetwork | 0.0028595 | 0.048021108 |
| MP:0004794 | increased anti-nuclear antigen antibody level | 0.00290929 | 0.048357424 |
| ENSG00000143190 | POU2F1 subnetwork | 0.00294954 | 0.048368146 |
| ENSG00000182481 | KPNA2 subnetwork | 0.0029489 | 0.048431373 |
| ENSG00000159110 | IFNAR2 subnetwork | 0.00295465 | 0.048435463 |
| ENSG00000215769 | ENSG00000215769 subnetwork | 0.0029489 | 0.048494764 |
| ENSG00000142453 | CARM1 subnetwork | 0.00294275 | 0.04855643 |
| MP:0008254 | increased megakaryocyte cell number | 0.00294829 | 0.048558322 |
| ENSG00000111802 | TDP2 subnetwork | 0.00299696 | 0.048636364 |
| MP:0006414 | decreased T cell apoptosis | 0.00300362 | 0.048638132 |
| MP:0008827 | abnormal thymus cell ratio | 0.00299083 | 0.04869961 |
| ENSG00000116678 | LEPR subnetwork | 0.00301173 | 0.048704663 |
| MP:0005425 | increased macrophage cell number | 0.00299038 | 0.048763021 |
| ENSG00000124587 | PEX6 subnetwork | 0.00303212 | 0.048900388 |
| ENSG00000161955 | TNFSF13 subnetwork | 0.00303811 | 0.048966408 |
| ENSG00000134470 | IL15RA subnetwork | 0.00306914 | 0.048971722 |
| REACTOME_REGULATED_PROT | REACTOME_REGULATED_PROTEOLYSIS_OF_P75NTR | 0.0030689 | 0.049034749 |
| ENSG00000148737 | TCF7L2 subnetwork | 0.00305906 | 0.049096774 |
| ENSG00000003400 | CASP10 subnetwork | 0.00306871 | 0.049097938 |
| GO:0043900 | regulation of multi-organism process | 0.00307598 | 0.049101412 |
| ENSG00000113494 | PRLR subnetwork | 0.0031155 | 0.049615385 |
| GO:0045621 | positive regulation of lymphocyte differentiation | 0.00313466 | 0.049807939 |
| ENSG00000127616 | SMARCA4 subnetwork | 0.0031473 | 0.050063939 |
| ENSG00000033800 | PIAS1 subnetwork | 0.00316014 | 0.050127551 |
| GO:0070231 | T cell apoptotic process | 0.00315775 | 0.050191571 |
| GO:0042107 | cytokine metabolic process | 0.00317647 | 0.050254777 |
| MP:0008044 | increased NK cell number | 0.00318618 | 0.050445293 |
| ENSG00000185291 | IL3RA subnetwork | 0.00323788 | 0.050886076 |
| GO:0042523 | positive regulation of tyrosine phosphorylation of Stat5 pro | 0.00321941 | 0.05095057 |
| MP:0008186 | increased pro-B cell number | 0.00321248 | 0.050951777 |
| GO:0032689 | negative regulation of interferon-gamma production | 0.00320558 | 0.050952986 |
| GO:0043566 | structure-specific DNA binding | 0.00325001 | 0.051011378 |
| MP:0008050 | decreased memory T cell number | 0.00326101 | 0.051073232 |

| | | | |
|---|---|---|---|
| ENSG00000101017 | CD40 subnetwork | 0.00328713 | 0.051259446 |
| REACTOME_VIRAL_DSRNATLR3 | REACTOME_VIRAL_DSRNATLR3TRIF_COMPLEX_ACTIVATES | 0.00330006 | 0.051320755 |
| GO:0045061 | thymic T cell selection | 0.00328677 | 0.051324086 |
| ENSG00000121879 | PIK3CA subnetwork | 0.00333285 | 0.051378446 |
| GO:0004896 | cytokine receptor activity | 0.00331209 | 0.051380176 |
| ENSG00000213625 | LEPROT subnetwork | 0.00330998 | 0.051444724 |
| REACTOME_TOLL_LIKE_RECEP | REACTOME_TOLL_LIKE_RECEPTOR_9_TLR9_CASCADE | 0.0033704 | 0.05175 |
| REACTOME_MYD88:INDEPEND | REACTOME_MYD88:INDEPENDENT_CASCADE_INITIATED_C | 0.00335324 | 0.051814768 |
| MP:0008045 | decreased NK cell number | 0.00337991 | 0.051935081 |
| ENSG00000117400 | MPL subnetwork | 0.00339476 | 0.052244389 |
| GO:0005125 | cytokine activity | 0.00346773 | 0.053175592 |
| ENSG00000170260 | ZNF212 subnetwork | 0.0035211 | 0.053390875 |
| ENSG00000145623 | OSMR subnetwork | 0.0035158 | 0.053399258 |
| ENSG00000112964 | GHR subnetwork | 0.00349502 | 0.053411911 |
| MP:0000604 | amyloidosis | 0.00349439 | 0.053416149 |
| GO:0002429 | immune response-activating cell surface receptor signaling | 0.00348557 | 0.053420398 |
| REACTOME_PLC:GAMMA1_SIG | REACTOME_PLC:GAMMA1_SIGNALLING | 0.00352063 | 0.05345679 |
| ENSG00000137070 | IL11RA subnetwork | 0.0035158 | 0.053465347 |
| ENSG00000107643 | MAPK8 subnetwork | 0.00350876 | 0.053469641 |
| ENSG00000108861 | DUSP3 subnetwork | 0.00352557 | 0.053509852 |
| REACTOME_TOLL_LIKE_RECEP | REACTOME_TOLL_LIKE_RECEPTOR_3_TLR3_CASCADE | 0.00354373 | 0.053558282 |
| REACTOME_TRIF_MEDIATED_T | REACTOME_TRIF_MEDIATED_TLR3_SIGNALING | 0.00354373 | 0.053624079 |
| MP:0002407 | abnormal double-negative T cell morphology | 0.0035364 | 0.053628536 |
| ENSG00000106367 | AP1S1 subnetwork | 0.00359107 | 0.053850856 |
| ENSG00000151849 | CENPJ subnetwork | 0.00358411 | 0.053916769 |
| GO:0009897 | external side of plasma membrane | 0.00357757 | 0.053982843 |
| GO:0002711 | positive regulation of T cell mediated immunity | 0.00364746 | 0.054121212 |
| ENSG00000162594 | IL23R subnetwork | 0.00363058 | 0.054136253 |
| ENSG00000119535 | CSF3R subnetwork | 0.00362572 | 0.054141291 |
| REACTOME_GENERATION_OF_ | REACTOME_GENERATION_OF_SECOND_MESSENGER_MOL | 0.00368214 | 0.054151625 |
| ENSG00000114166 | KAT2B subnetwork | 0.0036474 | 0.054186893 |
| GO:0031343 | positive regulation of cell killing | 0.00362569 | 0.054207317 |
| MP:0004742 | abnormal vestibular system physiology | 0.00368136 | 0.054216867 |
| ENSG00000183763 | TRAIP subnetwork | 0.00367136 | 0.054227053 |
| ENSG00000179344 | HLA-DQB1 subnetwork | 0.00364608 | 0.054252734 |
| MP:0002412 | increased susceptibility to bacterial infection | 0.00362503 | 0.054273504 |
| ENSG00000166681 | NGFRAP1 subnetwork | 0.00368102 | 0.054282268 |
| GO:0051222 | positive regulation of protein transport | 0.00366665 | 0.054292624 |
| ENSG00000139613 | SMARCC2 subnetwork | 0.00366506 | 0.054358354 |
| GO:0050866 | negative regulation of cell activation | 0.00374396 | 0.054491018 |
| GO:0051248 | negative regulation of protein metabolic process | 0.00373504 | 0.054496403 |
| REACTOME_TAK1_ACTIVATES_ | REACTOME_TAK1_ACTIVATES_NFKB_BY_PHOSPHORYLATIC | 0.00372409 | 0.054501801 |
| ENSG00000104856 | RELB subnetwork | 0.00372231 | 0.054567308 |
| MP:0008681 | increased interleukin-17 secretion | 0.00377255 | 0.054784689 |
| ENSG00000126562 | WNK4 subnetwork | 0.00385245 | 0.054976303 |
| ENSG00000110324 | IL10RA subnetwork | 0.00384545 | 0.054982206 |
| MP:0008723 | impaired eosinophil recruitment | 0.00380942 | 0.055017921 |
| MP:0010766 | abnormal NK cell physiology | 0.00384495 | 0.055047506 |
| ENSG00000004478 | FKBP4 subnetwork | 0.00382089 | 0.055065554 |
| ENSG00000131724 | IL13RA1 subnetwork | 0.00381857 | 0.055071599 |
| ENSG00000010610 | CD4 subnetwork | 0.00384034 | 0.055112961 |
| GO:0050714 | positive regulation of protein secretion | 0.00382703 | 0.055119048 |
| ENSG00000081985 | IL12RB2 subnetwork | 0.00386554 | 0.055147929 |

| | | | |
|---|---|---|---|
| MP:0008699 | increased interleukin-4 secretion | 0.00390071 | 0.055378251 |
| MP:0002664 | decreased circulating adrenocorticotropin level | 0.00390989 | 0.055430933 |
| REACTOME_CD28_CO:STIMUL | REACTOME_CD28_CO:STIMULATION | 0.00394006 | 0.05571934 |
| GO:0031435 | mitogen-activated protein kinase kinase kinase binding | 0.00395404 | 0.055948174 |
| MP:0005166 | decreased susceptibility to injury | 0.00396555 | 0.056058824 |
| GO:0032655 | regulation of interleukin-12 production | 0.00398571 | 0.056286722 |
| ENSG00000124334 | IL9R subnetwork | 0.00399747 | 0.056330598 |
| GO:0042509 | regulation of tyrosine phosphorylation of STAT protein | 0.00399092 | 0.056396714 |
| GO:0032615 | interleukin-12 production | 0.00403594 | 0.056425234 |
| ENSG00000122756 | CNTFR subnetwork | 0.0040256 | 0.056432749 |
| GO:0034097 | response to cytokine stimulus | 0.00402007 | 0.056440281 |
| ENSG00000170345 | FOS subnetwork | 0.00405973 | 0.056592765 |
| ENSG00000135341 | MAP3K7 subnetwork | 0.004081 | 0.056686047 |
| REACTOME_SIGNALING_BY_N | REACTOME_SIGNALING_BY_NOTCH | 0.00407641 | 0.05669383 |
| ENSG00000171791 | BCL2 subnetwork | 0.00407524 | 0.056759907 |
| MP:0008466 | enlarged mesenteric lymph nodes | 0.00415995 | 0.057589803 |
| ENSG00000172175 | MALT1 subnetwork | 0.00415173 | 0.057656613 |
| GO:0048535 | lymph node development | 0.00414423 | 0.057665505 |
| ENSG00000206240 | HLA-DRB1 subnetwork | 0.00420593 | 0.057997699 |
| MP:0000172 | abnormal bone marrow cell number | 0.00418743 | 0.058034682 |
| MP:0009543 | abnormal thymus corticomedullary boundary morphology | 0.00421182 | 0.058045977 |
| ENSG00000206306 | HLA-DRB1 subnetwork | 0.00420593 | 0.058064516 |
| ENSG00000160791 | CCR5 subnetwork | 0.00420127 | 0.058073818 |
| MP:0005010 | abnormal CD8-positive T cell morphology | 0.00418604 | 0.058101852 |
| ENSG00000215778 | ENSG00000215778 subnetwork | 0.00420127 | 0.058140878 |
| MP:0004185 | abnormal adipocyte glucose uptake | 0.00424752 | 0.058295195 |
| ENSG00000064835 | POU1F1 subnetwork | 0.00425666 | 0.058342857 |
| ENSG00000203747 | FCGR3A subnetwork | 0.00424398 | 0.05836197 |
| GO:0001912 | positive regulation of leukocyte mediated cytotoxicity | 0.00424364 | 0.058428899 |
| GO:0030218 | erythrocyte differentiation | 0.00426362 | 0.058447489 |
| ENSG00000078142 | PIK3C3 subnetwork | 0.00424315 | 0.058495982 |
| MP:0004751 | increased length of allograft survival | 0.00430347 | 0.058779932 |
| GO:0034105 | positive regulation of tissue remodeling | 0.00430961 | 0.058826879 |
| ENSG00000102554 | KLF5 subnetwork | 0.00432739 | 0.058987486 |
| MP:0005012 | decreased eosinophil cell number | 0.004393 | 0.059410431 |
| ENSG00000159128 | IFNGR2 subnetwork | 0.00438073 | 0.059421112 |
| MP:0004151 | decreased circulating iron level | 0.00437908 | 0.059488636 |
| GO:0005070 | SH3/SH2 adaptor activity | 0.00440836 | 0.059569649 |
| GO:0008757 | S-adenosylmethionine-dependent methyltransferase activit | 0.00441094 | 0.059728507 |
| ENSG00000100603 | SNW1 subnetwork | 0.00446507 | 0.060112994 |
| GO:0004879 | ligand-activated sequence-specific DNA binding RNA polym | 0.00448771 | 0.060383747 |
| MP:0005312 | pericardial effusion | 0.00450353 | 0.06048478 |
| MP:0002446 | abnormal macrophage morphology | 0.00453096 | 0.061011236 |
| GO:0006310 | DNA recombination | 0.00452188 | 0.061036036 |
| MP:0004905 | decreased uterus weight | 0.00452726 | 0.061079865 |
| ENSG00000185247 | MAGEA11 subnetwork | 0.00457402 | 0.061086226 |
| GO:0071345 | cellular response to cytokine stimulus | 0.0045398 | 0.061111111 |
| ENSG00000138095 | LRPPRC subnetwork | 0.00455722 | 0.061154709 |
| ENSG00000137074 | APTX subnetwork | 0.00463276 | 0.061620112 |
| MP:0010308 | decreased tumor latency | 0.00463085 | 0.061689038 |
| GO:0046637 | regulation of alpha-beta T cell differentiation | 0.00464742 | 0.061830357 |
| ENSG00000197045 | GMFB subnetwork | 0.00466918 | 0.06187291 |
| ENSG00000115290 | GRB14 subnetwork | 0.00470837 | 0.062055556 |

| | | | |
|---|---|---|---|
| ENSG00000016402 | IL20RA subnetwork | 0.00470434 | 0.062068966 |
| KEGG_LEUKOCYTE_TRANSEND | KEGG_LEUKOCYTE_TRANSENDOTHELIAL_MIGRATION | 0.00468528 | 0.062138085 |
| MP:0010249 | lactation failure | 0.0047419 | 0.062208657 |
| GO:0001954 | positive regulation of cell-matrix adhesion | 0.00476475 | 0.062236988 |
| ENSG00000115317 | HTRA2 subnetwork | 0.00475816 | 0.062305987 |
| GO:0002768 | immune response-regulating cell surface receptor signaling | 0.00478479 | 0.06244469 |
| ENSG00000100368 | CSF2RB subnetwork | 0.00478901 | 0.062486188 |
| ENSG00000123496 | IL13RA2 subnetwork | 0.00484396 | 0.062871287 |
| ENSG00000164485 | IL22RA2 subnetwork | 0.00484396 | 0.062940529 |
| ENSG00000103522 | IL21R subnetwork | 0.00484396 | 0.063009923 |
| GO:0051052 | regulation of DNA metabolic process | 0.004841 | 0.06307947 |
| MP:0001869 | pancreas inflammation | 0.00487687 | 0.063186813 |
| ENSG00000135972 | MRPS9 subnetwork | 0.00491215 | 0.063307777 |
| ENSG00000027697 | IFNGR1 subnetwork | 0.00492224 | 0.063318777 |
| ENSG00000185436 | IL28RA subnetwork | 0.00488929 | 0.063336992 |
| REACTOME_CTLA4_INHIBITOR | REACTOME_CTLA4_INHIBITORY_SIGNALING | 0.00494917 | 0.063344227 |
| ENSG00000186416 | NKRF subnetwork | 0.00491675 | 0.063347921 |
| GO:0010608 | posttranscriptional regulation of gene expression | 0.00493721 | 0.063358779 |
| MP:0003721 | increased tumor growth/size | 0.00490951 | 0.063377193 |
| MP:0001952 | increased airway responsiveness | 0.0049199 | 0.063387978 |
| GO:0042169 | SH2 domain binding | 0.00502699 | 0.064332248 |
| ENSG00000196735 | HLA-DQA1 subnetwork | 0.00505107 | 0.064355363 |
| GO:0016791 | phosphatase activity | 0.00502317 | 0.064402174 |
| REACTOME_PHOSPHORYLATIO | REACTOME_PHOSPHORYLATION_OF_CD3_AND_TCR_ZETA | 0.0050459 | 0.064425163 |
| ENSG00000142677 | IL22RA1 subnetwork | 0.00501873 | 0.064472252 |
| GO:0007595 | lactation | 0.00509701 | 0.065313853 |
| MP:0009763 | increased sensitivity to induced morbidity/mortality | 0.00512492 | 0.065567568 |
| ENSG00000167670 | CHAF1A subnetwork | 0.00516842 | 0.066019417 |
| ENSG00000102606 | ARHGEF7 subnetwork | 0.00516697 | 0.066036717 |
| ENSG00000204390 | HSPA1L subnetwork | 0.00517735 | 0.066056034 |
| GO:0043966 | histone H3 acetylation | 0.00519681 | 0.066146394 |
| REACTOME_CD28_DEPENDENT | REACTOME_CD28_DEPENDENT_VAV1_PATHWAY | 0.00521875 | 0.066165414 |
| ENSG00000100266 | PACSIN2 subnetwork | 0.00521081 | 0.066236559 |
| ENSG00000137841 | PLCB2 subnetwork | 0.00533926 | 0.066666667 |
| ENSG00000108604 | SMARCD2 subnetwork | 0.00530935 | 0.066720257 |
| ENSG00000198954 | KIAA1279 subnetwork | 0.00533343 | 0.066737968 |
| GO:0032703 | negative regulation of interleukin-2 production | 0.00535151 | 0.066755603 |
| ENSG00000159113 | ENSG00000159113 subnetwork | 0.00532072 | 0.066755889 |
| GO:0007260 | tyrosine phosphorylation of STAT protein | 0.00529921 | 0.066791845 |
| ENSG00000110492 | MDK subnetwork | 0.0053982 | 0.067004264 |
| ENSG00000104825 | NFKBIB subnetwork | 0.00543143 | 0.067412141 |
| REACTOME_TRANSLOCATION_ | REACTOME_TRANSLOCATION_OF_ZAP:70_TO_IMMUNOLC | 0.00548905 | 0.067819149 |
| MP:0005036 | diarrhea | 0.00549929 | 0.067993631 |
| GO:0008301 | DNA binding, bending | 0.0054969 | 0.068065887 |
| MP:0008182 | decreased marginal zone B cell number | 0.00551992 | 0.068273305 |
| REACTOME_A_THIRD_PROTEO | REACTOME_A_THIRD_PROTEOLYTIC_CLEAVAGE_RELEASES | 0.00551802 | 0.068292683 |
| GO:0046625 | sphingolipid binding | 0.00556425 | 0.068783069 |
| ENSG00000049618 | ARID1B subnetwork | 0.00561472 | 0.06906019 |
| ENSG00000071539 | TRIP13 subnetwork | 0.00559451 | 0.069133192 |
| GO:0002720 | positive regulation of cytokine production involved in immu | 0.0056688 | 0.069222689 |
| ENSG00000206308 | HLA-DRA subnetwork | 0.00563339 | 0.069230769 |
| REACTOME_REGULATION_OF_ | REACTOME_REGULATION_OF_IFNG_SIGNALING | 0.00565111 | 0.069242902 |
| GO:0042089 | cytokine biosynthetic process | 0.00563032 | 0.069251055 |

| | | | |
|---|---|---|---|
| ENSG00000185591 | SP1 subnetwork | 0.00564785 | 0.069263158 |
| GO:0032616 | interleukin-13 production | 0.00570463 | 0.069832109 |
| ENSG00000012048 | BRCA1 subnetwork | 0.00575884 | 0.070230608 |
| MP:0008502 | increased IgG3 level | 0.00582802 | 0.070890052 |
| REACTOME_CYTOKINE_SIGNAI | REACTOME_CYTOKINE_SIGNALING_IN_IMMUNE_SYSTEM | 0.00595128 | 0.07248954 |
| MP:0002424 | abnormal reticulocyte morphology | 0.00596071 | 0.072727273 |
| ENSG00000157557 | ETS2 subnetwork | 0.00598505 | 0.072912317 |
| KEGG_AUTOIMMUNE_THYROI | KEGG_AUTOIMMUNE_THYROID_DISEASE | 0.00600463 | 0.073096976 |
| KEGG_GRAFT_VERSUS_HOST_I | KEGG_GRAFT_VERSUS_HOST_DISEASE | 0.00610289 | 0.07359375 |
| ENSG00000103275 | UBE2I subnetwork | 0.0061195 | 0.073673257 |
| MP:0001691 | abnormal somite shape | 0.00617962 | 0.073733195 |
| GO:0001906 | cell killing | 0.00617883 | 0.073809524 |
| MP:0008721 | abnormal chemokine level | 0.00618524 | 0.073811983 |
| ENSG00000151729 | SLC25A4 subnetwork | 0.00614803 | 0.073831776 |
| ENSG00000104833 | TUBB4A subnetwork | 0.00617217 | 0.07388601 |
| GO:0043122 | regulation of I-kappaB kinase/NF-kappaB cascade | 0.00614486 | 0.073908524 |
| ENSG00000112062 | MAPK14 subnetwork | 0.0061635 | 0.073910788 |
| ENSG00000083168 | KAT6A subnetwork | 0.00627009 | 0.075051546 |
| GO:0042826 | histone deacetylase binding | 0.00626867 | 0.075128999 |
| REACTOME_MAPK_TARGETS_I | REACTOME_MAPK_TARGETS_NUCLEAR_EVENTS_MEDIATE | 0.00629034 | 0.075283213 |
| REACTOME_SIGNALING_BY_PI | REACTOME_SIGNALING_BY_PDGF | 0.0062976 | 0.075360082 |
| ENSG00000146950 | SHROOM2 subnetwork | 0.00636702 | 0.076180698 |
| ENSG00000075539 | FRYL subnetwork | 0.00636624 | 0.076207605 |
| GO:0003690 | double-stranded DNA binding | 0.00641186 | 0.076820513 |
| ENSG00000158941 | KIAA1967 subnetwork | 0.00646119 | 0.07694274 |
| ENSG00000130382 | MLLT1 subnetwork | 0.00645617 | 0.076970317 |
| GO:0003707 | steroid hormone receptor activity | 0.00645152 | 0.07704918 |
| GO:0035264 | multicellular organism growth | 0.00647967 | 0.07711951 |
| GO:0002709 | regulation of T cell mediated immunity | 0.00651478 | 0.077217125 |
| ENSG00000091181 | IL5RA subnetwork | 0.00650038 | 0.077244898 |
| ENSG00000072958 | AP1M1 subnetwork | 0.00653552 | 0.077342159 |
| GO:0031348 | negative regulation of defense response | 0.00654667 | 0.077466938 |
| MP:0008484 | decreased spleen germinal center size | 0.00656785 | 0.077489837 |
| GO:0046427 | positive regulation of JAK-STAT cascade | 0.00657212 | 0.07751269 |
| GO:0035591 | signaling adaptor activity | 0.00659627 | 0.078194726 |
| GO:0004697 | protein kinase C activity | 0.0066086 | 0.078216819 |
| MP:0001145 | abnormal male reproductive system morphology | 0.00664302 | 0.078564206 |
| MP:0001212 | skin lesions | 0.00664271 | 0.078643725 |
| ENSG00000137713 | PPP2R1B subnetwork | 0.00667931 | 0.079191919 |
| ENSG00000159216 | RUNX1 subnetwork | 0.00670419 | 0.079465187 |
| ENSG00000126261 | UBA2 subnetwork | 0.00671057 | 0.079485887 |
| ENSG00000159692 | CTBP1 subnetwork | 0.00671338 | 0.079506546 |
| ENSG00000152894 | PTPRK subnetwork | 0.00672108 | 0.079527163 |
| ENSG00000061273 | HDAC7 subnetwork | 0.00676649 | 0.079759519 |
| ENSG00000087095 | NLK subnetwork | 0.0067654 | 0.079839519 |
| REACTOME_NUCLEAR_RECEPT | REACTOME_NUCLEAR_RECEPTOR_TRANSCRIPTION_PATHV | 0.0067577 | 0.079899497 |
| ENSG00000179958 | DCTPP1 subnetwork | 0.00676313 | 0.079919679 |
| ENSG00000206239 | ENSG00000206239 subnetwork | 0.00682238 | 0.07997003 |
| MP:0001132 | absent mature ovarian follicles | 0.00680876 | 0.07997998 |
| GO:0072160 | nephron tubule epithelial cell differentiation | 0.00685219 | 0.07999002 |
| ENSG00000206305 | HLA-DQA1 subnetwork | 0.00682238 | 0.08005 |
| ENSG00000096996 | IL12RB1 subnetwork | 0.00687101 | 0.080209372 |
| GO:0002262 | myeloid cell homeostasis | 0.00689087 | 0.080577689 |

| | | | |
|---|---|---|---|
| ENSG00000169047 | IRS1 subnetwork | 0.00695997 | 0.081013917 |
| ENSG00000168214 | RBPJ subnetwork | 0.00695118 | 0.081044776 |
| MP:0008181 | increased marginal zone B cell number | 0.00697078 | 0.081181728 |
| ENSG00000147145 | LPAR4 subnetwork | 0.00704025 | 0.082029703 |
| ENSG00000188404 | SELL subnetwork | 0.00703077 | 0.082061447 |
| MP:0004992 | increased bone resorption | 0.00702967 | 0.082142857 |
| ENSG00000142208 | AKT1 subnetwork | 0.00709801 | 0.082344214 |
| MP:0000208 | decreased hematocrit | 0.00711783 | 0.082411067 |
| ENSG00000196700 | ZNF512B subnetwork | 0.00715775 | 0.082593688 |
| ENSG00000065361 | ERBB3 subnetwork | 0.00714315 | 0.082625864 |
| ENSG00000172115 | CYCS subnetwork | 0.00723386 | 0.08320197 |
| ENSG00000082074 | FYB subnetwork | 0.0072628 | 0.083366142 |
| ENSG00000197943 | PLCG2 subnetwork | 0.0073083 | 0.08387414 |
| MP:0002420 | abnormal adaptive immunity | 0.00732418 | 0.084086444 |
| MP:0000611 | jaundice | 0.00742485 | 0.085574092 |
| ENSG00000198380 | GFPT1 subnetwork | 0.00744891 | 0.085798237 |
| ENSG00000170365 | SMAD1 subnetwork | 0.00744277 | 0.085833333 |
| MP:0005362 | abnormal Langerhans cell physiology | 0.00749484 | 0.08630137 |
| MP:0000511 | abnormal intestinal mucosa morphology | 0.00751125 | 0.086363636 |
| GO:0031349 | positive regulation of defense response | 0.00754481 | 0.086669922 |
| ENSG00000089693 | MLF2 subnetwork | 0.00758426 | 0.086878049 |
| ENSG00000149177 | PTPRJ subnetwork | 0.00763202 | 0.087341772 |
| ENSG00000198223 | CSF2RA subnetwork | 0.00762934 | 0.087426901 |
| ENSG00000145715 | RASA1 subnetwork | 0.00770981 | 0.087887597 |
| ENSG00000105401 | CDC37 subnetwork | 0.00770694 | 0.087972842 |
| GO:0002861 | regulation of inflammatory response to antigenic stimulus | 0.00768195 | 0.087986381 |
| ENSG00000101096 | NFATC2 subnetwork | 0.00773877 | 0.08804453 |
| GO:0045060 | negative thymic T cell selection | 0.00770635 | 0.088058252 |
| ENSG00000152382 | TADA1 subnetwork | 0.00775541 | 0.088067633 |
| GO:0051220 | cytoplasmic sequestering of protein | 0.00770523 | 0.088143829 |
| MP:0000321 | increased bone marrow cell number | 0.00775254 | 0.088152805 |
| GO:0000790 | nuclear chromatin | 0.00782063 | 0.088706564 |
| GO:0035258 | steroid hormone receptor binding | 0.00783812 | 0.088717454 |
| MP:0008826 | abnormal splenic cell ratio | 0.00784737 | 0.088776493 |
| ENSG00000153563 | CD8A subnetwork | 0.00788107 | 0.089124158 |
| GO:0019838 | growth factor binding | 0.00797046 | 0.089759615 |
| MP:0008560 | increased tumor necrosis factor secretion | 0.00802789 | 0.090047847 |
| GO:0002761 | regulation of myeloid leukocyte differentiation | 0.00799594 | 0.090057637 |
| ENSG00000127314 | RAP1B subnetwork | 0.00802439 | 0.090086207 |
| MP:0001601 | abnormal myelopoiesis | 0.00800774 | 0.090163148 |
| ENSG00000103342 | GSPT1 subnetwork | 0.00802418 | 0.090172579 |
| GO:0045622 | regulation of T-helper cell differentiation | 0.00804574 | 0.090200765 |
| GO:0034101 | erythrocyte homeostasis | 0.00811124 | 0.090544413 |
| ENSG00000138385 | SSB subnetwork | 0.00814404 | 0.09056244 |
| ENSG00000154016 | GRAP subnetwork | 0.00813711 | 0.090648855 |
| GO:0051054 | positive regulation of DNA metabolic process | 0.00822555 | 0.091207224 |
| ENSG00000149923 | PPP4C subnetwork | 0.00821688 | 0.091285714 |
| MP:0002417 | abnormal megakaryocyte morphology | 0.00822402 | 0.091294006 |
| GO:0003746 | translation elongation factor activity | 0.00826892 | 0.091500475 |
| KEGG_PRIMARY_IMMUNODEF | KEGG_PRIMARY_IMMUNODEFICIENCY | 0.00828759 | 0.091650854 |
| ENSG00000127947 | PTPN12 subnetwork | 0.0083043 | 0.091706161 |
| ENSG00000147202 | DIAPH2 subnetwork | 0.00832778 | 0.091729679 |
| GO:0071634 | regulation of transforming growth factor beta production | 0.0083254 | 0.091816462 |

| | | | |
|---|---|---|---|
| MP:0000377 | abnormal hair follicle morphology | 0.00835274 | 0.091879131 |
| GO:0071604 | transforming growth factor beta production | 0.0083254 | 0.091903409 |
| MP:0008214 | increased immature B cell number | 0.00838298 | 0.092169811 |
| MP:0005150 | cachexia | 0.00841172 | 0.092318567 |
| MP:0005093 | decreased B cell proliferation | 0.00844591 | 0.092467043 |
| ENSG00000186951 | PPARA subnetwork | 0.00845361 | 0.092521167 |
| GO:0030316 | osteoclast differentiation | 0.00853429 | 0.093327068 |
| GO:0070664 | negative regulation of leukocyte proliferation | 0.00855515 | 0.093615023 |
| ENSG00000101210 | EEF1A2 subnetwork | 0.0085989 | 0.093949343 |
| GO:0007249 | I-kappaB kinase/NF-kappaB cascade | 0.00862708 | 0.093960674 |
| KEGG_TYPE_I_DIABETES_MELL | KEGG_TYPE_I_DIABETES_MELLITUS | 0.00861865 | 0.094001874 |
| MP:0004993 | decreased bone resorption | 0.00867014 | 0.094293732 |
| MP:0001802 | arrested B cell differentiation | 0.00869807 | 0.094351074 |
| ENSG00000065989 | PDE4A subnetwork | 0.00867993 | 0.094439252 |
| ENSG00000076984 | MAP2K7 subnetwork | 0.00874029 | 0.094599628 |
| MP:0002673 | abnormal sperm number | 0.00872698 | 0.094636194 |
| ENSG00000157168 | NRG1 subnetwork | 0.00873784 | 0.094687791 |
| REACTOME_TOLL_LIKE_RECEP | REACTOME_TOLL_LIKE_RECEPTOR_4_TLR4_CASCADE | 0.0088369 | 0.09572093 |
| GO:0006730 | one-carbon metabolic process | 0.00886964 | 0.095868152 |
| GO:0043030 | regulation of macrophage activation | 0.00886748 | 0.095910781 |
| MP:0002891 | increased insulin sensitivity | 0.00895468 | 0.097356215 |
| GO:0006809 | nitric oxide biosynthetic process | 0.00897545 | 0.097405005 |
| MP:0008828 | abnormal lymph node cell ratio | 0.00901024 | 0.097685185 |
| REACTOME_CHEMOKINE_RECI | REACTOME_CHEMOKINE_RECEPTORS_BIND_CHEMOKINES | 0.00902184 | 0.09773358 |
| ENSG00000170581 | STAT2 subnetwork | 0.00904185 | 0.098151571 |
| ENSG00000163823 | CCR1 subnetwork | 0.00906696 | 0.098153278 |
| GO:0016568 | chromatin modification | 0.00911101 | 0.098293358 |
| ENSG00000091127 | PUS7 subnetwork | 0.00912414 | 0.098294931 |
| GO:0032154 | cleavage furrow | 0.00913382 | 0.098296501 |
| ENSG00000123908 | EIF2C2 subnetwork | 0.00920295 | 0.098850046 |
| KEGG_LEISHMANIA_INFECTION | KEGG_LEISHMANIA_INFECTION | 0.00932778 | 0.100275735 |
| ENSG00000166167 | BTRC subnetwork | 0.00940654 | 0.101101928 |
| MP:0005659 | decreased susceptibility to diet-induced obesity | 0.00942418 | 0.101146789 |
| ENSG00000160014 | CALM3 subnetwork | 0.00955121 | 0.10209854 |
| GO:0008170 | N-methyltransferase activity | 0.00951072 | 0.102108158 |
| ENSG00000147065 | MSN subnetwork | 0.00959936 | 0.102185792 |
| MP:0002408 | abnormal double-positive T cell morphology | 0.00958193 | 0.102187785 |
| ENSG00000198668 | CALM1 subnetwork | 0.00955121 | 0.102191781 |
| ENSG00000143933 | CALM2 subnetwork | 0.00955121 | 0.102285192 |
| ENSG00000206505 | HLA-A subnetwork | 0.00954648 | 0.102333028 |
| ENSG00000110448 | CD5 subnetwork | 0.0095354 | 0.102380952 |
| ENSG00000180176 | TH subnetwork | 0.0096936 | 0.103184713 |
| GO:0016569 | covalent chromatin modification | 0.00977638 | 0.10417802 |
| GO:0016493 | C-C chemokine receptor activity | 0.00977069 | 0.104227273 |
| MP:0002680 | decreased corpora lutea number | 0.0098005 | 0.104261106 |
| KEGG_TYPE_II_DIABETES_MEL | KEGG_TYPE_II_DIABETES_MELLITUS | 0.00979591 | 0.104310345 |
| MP:0008537 | increased susceptibility to induced colitis | 0.00984486 | 0.104574275 |
| MP:0008596 | increased circulating interleukin-6 level | 0.00990431 | 0.105113122 |
| GO:0017148 | negative regulation of translation | 0.00991493 | 0.105198915 |
| REACTOME_EFFECTS_OF_PIP2 | REACTOME_EFFECTS_OF_PIP2_HYDROLYSIS | 0.00993975 | 0.105420054 |
| ENSG00000096060 | FKBP5 subnetwork | 0.00999202 | 0.106272563 |
| MP:0004808 | abnormal hematopoietic stem cell morphology | 0.01009081 | 0.107303877 |
| GO:0040029 | regulation of gene expression, epigenetic | 0.01015461 | 0.107927928 |

| | | | |
|---|---|---|---|
| ENSG00000166949 | SMAD3 subnetwork | 0.01026494 | 0.108910891 |
| GO:0019221 | cytokine-mediated signaling pathway | 0.01030463 | 0.108939802 |
| REACTOME_NUCLEAR_EVENTS | REACTOME_NUCLEAR_EVENTS_KINASE_AND_TRANSCRIPT | 0.01028857 | 0.108992806 |
| GO:0030522 | intracellular receptor mediated signaling pathway | 0.01036025 | 0.109058296 |
| ENSG00000141736 | ERBB2 subnetwork | 0.01035271 | 0.109111311 |
| ENSG00000161021 | MAML1 subnetwork | 0.01039696 | 0.109408602 |
| ENSG00000017797 | RALBP1 subnetwork | 0.01041375 | 0.109444942 |
| ENSG00000102241 | HTATSF1 subnetwork | 0.01051635 | 0.110644007 |
| ENSG00000074211 | PPP2R2C subnetwork | 0.01053849 | 0.110723861 |
| GO:0002755 | MyD88-dependent toll-like receptor signaling pathway | 0.01056679 | 0.1109375 |
| ENSG00000156587 | UBE2L6 subnetwork | 0.01059873 | 0.111284567 |
| GO:0034103 | regulation of tissue remodeling | 0.01062551 | 0.111398041 |
| GO:0050777 | negative regulation of immune response | 0.01067067 | 0.111476868 |
| GO:0051861 | glycolipid binding | 0.01062127 | 0.111497326 |
| GO:0050728 | negative regulation of inflammatory response | 0.01068585 | 0.111555556 |
| REACTOME_CD28_DEPENDENT | REACTOME_CD28_DEPENDENT_PI3KAKT_SIGNALING | 0.01069305 | 0.111589698 |
| MP:0004919 | abnormal positive T cell selection | 0.01070549 | 0.111801242 |
| ENSG00000198851 | CD3E subnetwork | 0.01074325 | 0.112278369 |
| ENSG00000120910 | PPP3CC subnetwork | 0.01077691 | 0.112666076 |
| MP:0009583 | increased keratinocyte proliferation | 0.01080448 | 0.112876106 |
| MP:0002655 | abnormal keratinocyte morphology | 0.0108763 | 0.112951542 |
| GO:0004721 | phosphoprotein phosphatase activity | 0.01082085 | 0.112953139 |
| GO:0034134 | toll-like receptor 2 signaling pathway | 0.01084725 | 0.112985866 |
| ENSG00000107338 | SHB subnetwork | 0.01086851 | 0.113007055 |
| ENSG00000169750 | RAC3 subnetwork | 0.01086571 | 0.113018535 |
| MP:0008076 | abnormal CD4-positive T cell differentiation | 0.01095878 | 0.113512324 |
| ENSG00000164362 | TERT subnetwork | 0.01099201 | 0.113764292 |
| MP:0002458 | abnormal B cell number | 0.01104235 | 0.113859649 |
| MP:0005094 | abnormal T cell proliferation | 0.01103405 | 0.113871817 |
| MP:0011353 | expanded mesangial matrix | 0.01103118 | 0.11397188 |
| ENSG00000116560 | SFPQ subnetwork | 0.01106375 | 0.114022787 |
| ENSG00000126785 | RHOJ subnetwork | 0.01111086 | 0.114304462 |
| GO:0034130 | toll-like receptor 1 signaling pathway | 0.01110971 | 0.114360771 |
| ENSG00000132906 | CASP9 subnetwork | 0.01120178 | 0.115078671 |
| MP:0001346 | abnormal lacrimal gland morphology | 0.01124548 | 0.115327511 |
| ENSG00000143171 | RXRG subnetwork | 0.01126072 | 0.115357766 |
| ENSG00000152234 | ATP5A1 subnetwork | 0.01131273 | 0.11586748 |
| GO:0005720 | nuclear heterochromatin | 0.01134021 | 0.115897213 |
| ENSG00000064300 | NGFR subnetwork | 0.01137478 | 0.116 |
| MP:0005578 | teratozoospermia | 0.01136414 | 0.116057441 |
| ENSG00000166484 | MAPK7 subnetwork | 0.01139435 | 0.116246742 |
| ENSG00000080503 | SMARCA2 subnetwork | 0.01140993 | 0.116276042 |
| ENSG00000153827 | TRIP12 subnetwork | 0.01143505 | 0.116392021 |
| MP:0003333 | liver fibrosis | 0.01145244 | 0.116464471 |
| GO:0004709 | MAP kinase kinase kinase activity | 0.01155651 | 0.117272727 |
| ENSG00000101040 | ZMYND8 subnetwork | 0.01157746 | 0.117301038 |
| ENSG00000157106 | SMG1 subnetwork | 0.01164393 | 0.117934313 |
| ENSG00000012124 | CD22 subnetwork | 0.01169136 | 0.117989646 |
| MP:0002461 | increased immunoglobulin level | 0.01167652 | 0.118005181 |
| ENSG00000196504 | PRPF40A subnetwork | 0.01179084 | 0.118283262 |
| MP:0002144 | abnormal B cell differentiation | 0.01181139 | 0.118310463 |
| GO:0045910 | negative regulation of DNA recombination | 0.0117459 | 0.118346253 |
| ENSG00000125347 | IRF1 subnetwork | 0.01183416 | 0.118380463 |

| | | | |
|---|---|---|---|
| ENSG00000171223 | JUNB subnetwork | 0.01177965 | 0.11838488 |
| GO:0019955 | cytokine binding | 0.01173124 | 0.118405172 |
| ENSG00000158769 | F11R subnetwork | 0.0117777 | 0.118486672 |
| ENSG00000160584 | SIK3 subnetwork | 0.01177721 | 0.11858864 |
| ENSG00000094631 | HDAC6 subnetwork | 0.01191494 | 0.119092466 |
| GO:0001067 | regulatory region nucleic acid binding | 0.01198283 | 0.119276596 |
| MP:0004774 | abnormal bile salt level | 0.01193605 | 0.119289991 |
| GO:0050710 | negative regulation of cytokine secretion | 0.01195414 | 0.119299744 |
| ENSG00000172379 | ARNT2 subnetwork | 0.01197264 | 0.119309463 |
| MP:0001116 | small gonad | 0.01200785 | 0.119312394 |
| GO:0043560 | insulin receptor substrate binding | 0.0120057 | 0.119371283 |
| GO:0000975 | regulatory region DNA binding | 0.01198283 | 0.119378194 |
| ENSG00000134242 | PTPN22 subnetwork | 0.01202779 | 0.119380831 |
| GO:0032733 | positive regulation of interleukin-10 production | 0.01195403 | 0.119401709 |
| MP:0005343 | increased circulating aspartate transaminase level | 0.01197082 | 0.119411263 |
| ENSG00000177463 | NR2C2 subnetwork | 0.0120038 | 0.119430272 |
| ENSG00000149091 | DGKZ subnetwork | 0.01216929 | 0.120914479 |
| ENSG00000152518 | ZFP36L2 subnetwork | 0.01216662 | 0.120974576 |
| ENSG00000079246 | XRCC5 subnetwork | 0.01220473 | 0.121090448 |
| GO:0045727 | positive regulation of translation | 0.01219847 | 0.121150592 |
| ENSG00000133124 | IRS4 subnetwork | 0.01222922 | 0.121283784 |
| ENSG00000110987 | BCL7A subnetwork | 0.01226512 | 0.121290051 |
| ENSG00000067606 | PRKCZ subnetwork | 0.012253 | 0.121308017 |
| ENSG00000211790 | ENSG00000211790 subnetwork | 0.01233124 | 0.121590909 |
| ENSG00000123416 | TUBA1B subnetwork | 0.0123168 | 0.121693345 |
| ENSG00000171148 | TADA3 subnetwork | 0.01238153 | 0.121728188 |
| MP:0009321 | increased histiocytic sarcoma incidence | 0.01235794 | 0.121764706 |
| REACTOME_SIGNALING_BY_EF | REACTOME_SIGNALING_BY_ERBB2 | 0.01238133 | 0.121830395 |
| MP:0008687 | increased interleukin-2 secretion | 0.01235687 | 0.121867115 |
| ENSG00000009954 | BAZ1B subnetwork | 0.01245293 | 0.122045264 |
| ENSG00000153147 | SMARCA5 subnetwork | 0.01260941 | 0.123263598 |
| GO:0051019 | mitogen-activated protein kinase binding | 0.01260229 | 0.123324958 |
| ENSG00000177565 | TBL1XR1 subnetwork | 0.01265684 | 0.123642439 |
| GO:2000696 | regulation of epithelial cell differentiation involved in kidne | 0.01264875 | 0.123745819 |
| ENSG00000185507 | IRF7 subnetwork | 0.01269449 | 0.123914858 |
| MP:0004031 | insulitis | 0.01273336 | 0.124186822 |
| MP:0003853 | dry skin | 0.01286082 | 0.1255 |
| ENSG00000095015 | MAP3K1 subnetwork | 0.01289907 | 0.125770192 |
| GO:0050690 | regulation of defense response to virus by virus | 0.01297145 | 0.126289517 |
| ENSG00000104938 | CLEC4M subnetwork | 0.01300686 | 0.126910299 |
| GO:0016570 | histone modification | 0.01300565 | 0.127015794 |
| ENSG00000185104 | FAF1 subnetwork | 0.013121 | 0.127860697 |
| MP:0001929 | abnormal gametogenesis | 0.01310906 | 0.127883817 |
| ENSG00000198933 | TBKBP1 subnetwork | 0.01315648 | 0.128169014 |
| ENSG00000211799 | ENSG00000211799 subnetwork | 0.01326268 | 0.128171334 |
| ENSG00000211739 | ENSG00000211739 subnetwork | 0.01326268 | 0.128276999 |
| ENSG00000130589 | RP4-697K14.7 subnetwork | 0.01323096 | 0.128305785 |
| ENSG00000211735 | ENSG00000211735 subnetwork | 0.01326268 | 0.128382838 |
| GO:0031334 | positive regulation of protein complex assembly | 0.01322363 | 0.128411911 |
| REACTOME_ACTIVATED_TAK1_ | REACTOME_ACTIVATED_TAK1_MEDIATES_P38_MAPK_ACT | 0.01320444 | 0.12843543 |
| ENSG00000211810 | ENSG00000211810 subnetwork | 0.01326268 | 0.128488852 |
| GO:0010740 | positive regulation of intracellular protein kinase cascade | 0.0133784 | 0.128888889 |
| MP:0002376 | abnormal dendritic cell physiology | 0.01349326 | 0.1296875 |

| | | | |
|---|---|---|---|
| GO:0045884 | regulation of survival gene product expression | 0.0135619 | 0.13032046 |
| ENSG00000196230 | TUBB subnetwork | 0.01363488 | 0.130753481 |
| GO:0043901 | negative regulation of multi-organism process | 0.01365166 | 0.130851064 |
| ENSG00000183311 | TUBB subnetwork | 0.01363488 | 0.130860656 |
| ENSG00000137379 | ENSG00000137379 subnetwork | 0.01363488 | 0.130968007 |
| ENSG00000084463 | WBP11 subnetwork | 0.01361767 | 0.130993432 |
| ENSG00000167601 | AXL subnetwork | 0.01372556 | 0.131602617 |
| GO:0061180 | mammary gland epithelium development | 0.01376133 | 0.131673469 |
| ENSG00000100351 | GRAP2 subnetwork | 0.0137587 | 0.131740196 |
| MP:0006397 | disorganized long bone epiphyseal plate | 0.01392117 | 0.132750203 |
| ENSG00000120709 | FAM53C subnetwork | 0.01391376 | 0.132844336 |
| MP:0005342 | abnormal intestinal lipid absorption | 0.01391893 | 0.132858306 |
| ENSG00000178562 | CD28 subnetwork | 0.01391248 | 0.132911909 |
| ENSG00000022267 | FHL1 subnetwork | 0.01398912 | 0.132954545 |
| MP:0008735 | increased susceptibility to endotoxin shock | 0.01398302 | 0.133021933 |
| ENSG00000100815 | TRIP11 subnetwork | 0.01397665 | 0.13304878 |
| ENSG00000166793 | YPEL4 subnetwork | 0.01406583 | 0.133306321 |
| REACTOME_SIGNALLING_BY_N | REACTOME_SIGNALLING_BY_NGF | 0.01406471 | 0.133414436 |
| MP:0008133 | decreased Peyer's patch number | 0.01413446 | 0.133576052 |
| ENSG00000169682 | SPNS1 subnetwork | 0.01412502 | 0.133684211 |
| ENSG00000160310 | PRMT2 subnetwork | 0.01418753 | 0.134074373 |
| MP:0001121 | uterus hypoplasia | 0.01426737 | 0.13457189 |
| ENSG00000163029 | SMC6 subnetwork | 0.01439165 | 0.1354318 |
| MP:0008396 | abnormal osteoclast differentiation | 0.01442324 | 0.135806452 |
| ENSG00000189060 | H1F0 subnetwork | 0.01445206 | 0.136019339 |
| GO:0060135 | maternal process involved in female pregnancy | 0.01447954 | 0.136392915 |
| ENSG00000160654 | CD3G subnetwork | 0.01450307 | 0.136524537 |
| GO:0001909 | leukocyte mediated cytotoxicity | 0.01454426 | 0.136856913 |
| ENSG00000103723 | AP3B2 subnetwork | 0.01456139 | 0.137068273 |
| ENSG00000105887 | MTPN subnetwork | 0.01463066 | 0.137700321 |
| GO:0051092 | positive regulation of NF-kappaB transcription factor activit | 0.01461913 | 0.137760835 |
| MP:0002702 | decreased circulating free fatty acid level | 0.0146295 | 0.13777065 |
| ENSG00000163512 | AZI2 subnetwork | 0.01466923 | 0.13796 |
| MP:0000496 | abnormal small intestine morphology | 0.01466797 | 0.138070456 |
| ENSG00000196396 | PTPN1 subnetwork | 0.01471857 | 0.138808953 |
| GO:0030914 | STAGA complex | 0.01476281 | 0.138977636 |
| GO:0003706 | ligand-regulated transcription factor activity | 0.01481675 | 0.139146049 |
| MP:0003667 | hemangiosarcoma | 0.01483722 | 0.139282869 |
| ENSG00000108773 | KAT2A subnetwork | 0.01483489 | 0.139354067 |
| ENSG00000156273 | BACH1 subnetwork | 0.0148828 | 0.139419252 |
| ENSG00000158711 | ELK4 subnetwork | 0.01488109 | 0.139450637 |
| GO:0045121 | membrane raft | 0.01492503 | 0.139745628 |
| ENSG00000113916 | BCL6 subnetwork | 0.01497449 | 0.14 |
| MP:0009339 | decreased splenocyte number | 0.01496305 | 0.140031771 |
| ENSG00000198909 | MAP3K3 subnetwork | 0.01512139 | 0.141244057 |
| ENSG00000134058 | CDK7 subnetwork | 0.0151612 | 0.141257911 |
| MP:0003699 | abnormal female reproductive system physiology | 0.01511811 | 0.141276764 |
| GO:0030879 | mammary gland development | 0.01516092 | 0.141369755 |
| ENSG00000132669 | RIN2 subnetwork | 0.01522844 | 0.141501976 |
| ENSG00000030110 | BAK1 subnetwork | 0.01525856 | 0.141627172 |
| ENSG00000067560 | RHOA subnetwork | 0.01532067 | 0.14210734 |
| ENSG00000086061 | DNAJA1 subnetwork | 0.01534976 | 0.142350158 |
| ENSG00000068615 | REEP1 subnetwork | 0.01537854 | 0.142474389 |

| | | | |
|---|---|---|---|
| ENSG00000067182 | TNFRSF1A subnetwork | 0.01541997 | 0.142604249 |
| ENSG00000108561 | C1QBP subnetwork | 0.01541698 | 0.142677165 |
| ENSG00000156136 | DCK subnetwork | 0.01547781 | 0.142857143 |
| MP:0004930 | small epididymis | 0.01550079 | 0.142941176 |
| ENSG00000108984 | MAP2K6 subnetwork | 0.01547066 | 0.142969364 |
| ENSG00000136352 | NKX2-1 subnetwork | 0.01546613 | 0.143081761 |
| ENSG00000090863 | GLG1 subnetwork | 0.01551621 | 0.143181818 |
| ENSG00000078140 | UBE2K subnetwork | 0.01552564 | 0.143187157 |
| ENSG00000111252 | SH2B3 subnetwork | 0.01558776 | 0.143320313 |
| ENSG00000146648 | EGFR subnetwork | 0.01557036 | 0.143354183 |
| ENSG00000170145 | SIK2 subnetwork | 0.01560098 | 0.143364559 |
| GO:0032452 | histone demethylase activity | 0.01561854 | 0.143369735 |
| ENSG00000148200 | NR6A1 subnetwork | 0.01556995 | 0.14342723 |
| GO:0032153 | cell division site | 0.01573066 | 0.143847352 |
| GO:0032155 | cell division site part | 0.01573066 | 0.14395947 |
| GO:0042531 | positive regulation of tyrosine phosphorylation of STAT pro | 0.0157427 | 0.144007782 |
| GO:0002821 | positive regulation of adaptive immune response | 0.01589642 | 0.145341615 |
| ENSG00000161513 | FDXR subnetwork | 0.01590744 | 0.145384019 |
| ENSG00000182287 | AP1S2 subnetwork | 0.0158878 | 0.145412131 |
| ENSG00000211889 | ENSG00000211889 subnetwork | 0.01589151 | 0.145415695 |
| ENSG00000099308 | MAST3 subnetwork | 0.01592596 | 0.145426357 |
| REACTOME_NUCLEAR_SIGNAL | REACTOME_NUCLEAR_SIGNALING_BY_ERBB4 | 0.01599469 | 0.145859133 |
| MP:0000490 | abnormal crypts of Lieberkuhn morphology | 0.01598927 | 0.145933385 |
| GO:0030101 | natural killer cell activation | 0.01601775 | 0.146017015 |
| MP:0010378 | increased respiratory quotient | 0.01621896 | 0.147720247 |
| ENSG00000099942 | CRKL subnetwork | 0.01629775 | 0.148571429 |
| MP:0001932 | abnormal spermiogenesis | 0.01635027 | 0.148996914 |
| ENSG00000147010 | SH3KBP1 subnetwork | 0.01643578 | 0.149922899 |
| GO:0042269 | regulation of natural killer cell mediated cytotoxicity | 0.01650966 | 0.150423077 |
| GO:0002715 | regulation of natural killer cell mediated immunity | 0.01650966 | 0.150538876 |
| ENSG00000169083 | AR subnetwork | 0.01649555 | 0.150539291 |
| MP:0004969 | pale kidney | 0.01659917 | 0.151037663 |
| GO:0060416 | response to growth hormone stimulus | 0.01663846 | 0.151304682 |
| GO:0060090 | binding, bridging | 0.01662812 | 0.151344086 |
| ENSG00000177606 | JUN subnetwork | 0.0167133 | 0.152185583 |
| MP:0001847 | brain inflammation | 0.01679109 | 0.153141762 |
| ENSG00000171552 | BCL2L1 subnetwork | 0.01688937 | 0.153790199 |
| GO:0051247 | positive regulation of protein metabolic process | 0.01697471 | 0.153896104 |
| MP:0008246 | abnormal leukocyte morphology | 0.01699422 | 0.153931298 |
| MP:0004762 | increased anti-double stranded DNA antibody level | 0.01697457 | 0.154013761 |
| GO:0005097 | Rab GTPase activator activity | 0.01695732 | 0.154016832 |
| ENSG00000105662 | CRTC1 subnetwork | 0.01702095 | 0.154042715 |
| ENSG00000101665 | SMAD7 subnetwork | 0.01710443 | 0.154916159 |
| MP:0000195 | hypocalcemia | 0.01715079 | 0.155331302 |
| GO:0008009 | chemokine activity | 0.01716493 | 0.155365297 |
| REACTOME_NOD12_SIGNALIN | REACTOME_NOD12_SIGNALING_PATHWAY | 0.01724895 | 0.155922551 |
| GO:0043254 | regulation of protein complex assembly | 0.01723309 | 0.155927052 |
| ENSG00000069424 | KCNAB2 subnetwork | 0.01721495 | 0.155931559 |
| ENSG00000134107 | BHLHE40 subnetwork | 0.01727901 | 0.155951478 |
| ENSG00000121774 | KHDRBS1 subnetwork | 0.01726048 | 0.15599393 |
| MP:0008189 | increased transitional stage B cell number | 0.01734828 | 0.15658592 |
| ENSG00000126001 | CEP250 subnetwork | 0.01734314 | 0.156628788 |
| ENSG00000155926 | SLA subnetwork | 0.01744492 | 0.157223903 |

| | | | |
|---|---|---|---|
| ENSG00000139921 | TMX1 subnetwork | 0.01750823 | 0.157396226 |
| ENSG00000173153 | ESRRA subnetwork | 0.01751998 | 0.157503771 |
| GO:0006476 | protein deacetylation | 0.01749606 | 0.157515106 |
| GO:0006107 | oxaloacetate metabolic process | 0.01749224 | 0.157596372 |
| GO:0043123 | positive regulation of I-kappaB kinase/NF-kappaB cascade | 0.01766988 | 0.158854559 |
| ENSG00000137193 | PIM1 subnetwork | 0.01772673 | 0.159255079 |
| ENSG00000213923 | CSNK1E subnetwork | 0.01771218 | 0.159337349 |
| MP:0008663 | increased interleukin-12 secretion | 0.01778154 | 0.159398496 |
| ENSG00000165732 | DDX21 subnetwork | 0.01789962 | 0.160255447 |
| MP:0008098 | decreased plasma cell number | 0.01792129 | 0.160285285 |
| KEGG_MAPK_SIGNALING_PATI | KEGG_MAPK_SIGNALING_PATHWAY | 0.01804185 | 0.160727682 |
| MP:0001119 | abnormal female reproductive system morphology | 0.01806315 | 0.160794603 |
| ENSG00000206503 | HLA-A subnetwork | 0.01807591 | 0.16093633 |
| GO:0044212 | transcription regulatory region DNA binding | 0.0181313 | 0.161152695 |
| ENSG00000167286 | CD3D subnetwork | 0.01822927 | 0.1617713 |
| REACTOME_INTERLEUKIN:7_SI | REACTOME_INTERLEUKIN:7_SIGNALING | 0.01821894 | 0.161817502 |
| ENSG00000188386 | PPP3R2 subnetwork | 0.01827595 | 0.162098581 |
| ENSG00000117560 | FASLG subnetwork | 0.01838736 | 0.162788963 |
| ENSG00000109339 | MAPK10 subnetwork | 0.01838188 | 0.162910448 |
| ENSG00000092820 | EZR subnetwork | 0.01851641 | 0.164157973 |
| ENSG00000135930 | EIF4E2 subnetwork | 0.01855998 | 0.164631422 |
| ENSG00000140538 | NTRK3 subnetwork | 0.01864996 | 0.16577381 |
| ENSG00000168066 | SF1 subnetwork | 0.01867676 | 0.165787519 |
| ENSG00000074966 | TXK subnetwork | 0.01866796 | 0.165799257 |
| MP:0006398 | increased long bone epiphyseal plate size | 0.01875632 | 0.16644395 |
| GO:0002891 | positive regulation of immunoglobulin mediated immune re | 0.01884333 | 0.166678994 |
| ENSG00000112214 | FHL5 subnetwork | 0.0188058 | 0.166765579 |
| GO:0002714 | positive regulation of B cell mediated immunity | 0.01884333 | 0.166802369 |
| ENSG00000147439 | BIN3 subnetwork | 0.01882675 | 0.166814815 |
| GO:0042101 | T cell receptor complex | 0.0188168 | 0.166827279 |
| ENSG00000184226 | PCDH9 subnetwork | 0.01888163 | 0.166962306 |
| ENSG00000137834 | SMAD6 subnetwork | 0.01888856 | 0.167023634 |
| ENSG00000066027 | PPP2R5A subnetwork | 0.01897688 | 0.168081181 |
| MP:0000121 | failure of tooth eruption | 0.01900496 | 0.16810472 |
| ENSG00000198646 | NCOA6 subnetwork | 0.0191014 | 0.168754606 |
| ENSG00000099956 | SMARCB1 subnetwork | 0.01912001 | 0.168888071 |
| ENSG00000198604 | BAZ1A subnetwork | 0.01913383 | 0.168910964 |
| ENSG00000180209 | MYLPF subnetwork | 0.01938462 | 0.171433824 |
| GO:0042994 | cytoplasmic sequestering of transcription factor | 0.01941289 | 0.17143906 |
| GO:0045346 | regulation of MHC class II biosynthetic process | 0.019406 | 0.17149155 |
| ENSG00000144061 | NPHP1 subnetwork | 0.01947116 | 0.171973588 |
| ENSG00000100239 | PPP6R2 subnetwork | 0.01951743 | 0.172397361 |
| REACTOME_NUCLEOTIDE:BIND | REACTOME_NUCLEOTIDE:BINDING_DOMAIN_LEUCINE_RIC | 0.01958384 | 0.172693997 |
| ENSG00000211762 | ENSG00000211762 subnetwork | 0.01956457 | 0.172710623 |
| GO:0051607 | defense response to virus | 0.01960797 | 0.172750549 |
| MP:0005088 | increased acute inflammation | 0.01967093 | 0.173282164 |
| MP:0001787 | pericardial edema | 0.01970907 | 0.173304158 |
| ENSG00000072803 | FBXW11 subnetwork | 0.01969765 | 0.173357664 |
| REACTOME_P75NTR_SIGNALS_ | REACTOME_P75NTR_SIGNALS_VIA_NF:KB | 0.01968861 | 0.173484295 |
| MP:0008215 | decreased immature B cell number | 0.01981721 | 0.174052478 |
| MP:0010872 | increased trabecular bone mass | 0.01984923 | 0.174326293 |
| MP:0008347 | decreased gamma-delta T cell number | 0.01988738 | 0.174672489 |
| ENSG00000105699 | LSR subnetwork | 0.01994853 | 0.175272727 |

| | | | |
|---|---|---|---|
| REACTOME_MAP_KINASE_ACT | REACTOME_MAP_KINASE_ACTIVATION_IN_TLR_CASCADE | 0.0199791 | 0.175327035 |
| ENSG00000136997 | MYC subnetwork | 0.02011718 | 0.176506899 |
| GO:0005527 | macrolide binding | 0.02017602 | 0.176630435 |
| ENSG00000185697 | MYBL1 subnetwork | 0.02014687 | 0.176632801 |
| ENSG00000100811 | YY1 subnetwork | 0.02021331 | 0.176755974 |
| GO:0005528 | FK506 binding | 0.02017602 | 0.176758521 |
| ENSG00000070061 | IKBKAP subnetwork | 0.02025531 | 0.176917511 |
| MP:0005331 | insulin resistance | 0.02027785 | 0.176934201 |
| ENSG00000180855 | ZNF443 subnetwork | 0.02035537 | 0.17703677 |
| MP:0003408 | increased width of hypertrophic chondrocyte zone | 0.02033338 | 0.177056277 |
| MP:0005621 | abnormal cell physiology | 0.02032434 | 0.177075812 |
| ENSG00000162227 | TAF6L subnetwork | 0.02032388 | 0.17716763 |
| ENSG00000111605 | CPSF6 subnetwork | 0.02038822 | 0.177341499 |
| GO:0016575 | histone deacetylation | 0.02042489 | 0.177482014 |
| ENSG00000100181 | ENSG00000100181 subnetwork | 0.02045188 | 0.177534148 |
| GO:0004715 | non-membrane spanning protein tyrosine kinase activity | 0.02042355 | 0.177609791 |
| GO:0017038 | protein import | 0.02048103 | 0.177837644 |
| MP:0008211 | decreased mature B cell number | 0.0205016 | 0.177853553 |
| ENSG00000164597 | COG5 subnetwork | 0.02058342 | 0.178151862 |
| ENSG00000137171 | KLC4 subnetwork | 0.02056788 | 0.178228121 |
| MP:0002740 | heart hypoplasia | 0.0205819 | 0.178243728 |
| ENSG00000108924 | HLF subnetwork | 0.02063835 | 0.178505007 |
| MP:0010903 | abnormal pulmonary alveolus wall morphology | 0.02061992 | 0.178561203 |
| ENSG00000111424 | VDR subnetwork | 0.02083339 | 0.179914224 |
| GO:0005671 | Ada2/Gcn5/Ada3 transcription activator complex | 0.0208848 | 0.180214286 |
| GO:0043130 | ubiquitin binding | 0.02094999 | 0.180977873 |
| MP:0010875 | increased bone volume | 0.0209699 | 0.180991441 |
| ENSG00000111731 | KIAA0528 subnetwork | 0.02105558 | 0.181281139 |
| ENSG00000111737 | RAB35 subnetwork | 0.02103639 | 0.181290093 |
| ENSG00000179583 | CIITA subnetwork | 0.02112175 | 0.181321023 |
| MP:0009766 | increased sensitivity to xenobiotic induced morbidity/mort | 0.02105044 | 0.181410256 |
| REACTOME_SEMA4D_IN_SEM | REACTOME_SEMA4D_IN_SEMAPHORIN_SIGNALING | 0.02111883 | 0.181449893 |
| GO:0001782 | B cell homeostasis | 0.02108571 | 0.181472262 |
| ENSG00000108175 | ZMIZ1 subnetwork | 0.02114148 | 0.18151171 |
| ENSG00000134717 | BTF3L4 subnetwork | 0.0211876 | 0.181666667 |
| MP:0003204 | decreased neuron apoptosis | 0.02120472 | 0.18167966 |
| GO:0045429 | positive regulation of nitric oxide biosynthetic process | 0.0212358 | 0.181798867 |
| ENSG00000167548 | MLL2 subnetwork | 0.02128928 | 0.182094834 |
| ENSG00000137709 | POU2F3 subnetwork | 0.02131216 | 0.182120141 |
| ENSG00000169598 | DFFB subnetwork | 0.02129777 | 0.182142857 |
| ENSG00000012223 | LTF subnetwork | 0.02135914 | 0.18220339 |
| GO:0018024 | histone-lysine N-methyltransferase activity | 0.02142057 | 0.182498236 |
| MP:0004399 | abnormal cochlear outer hair cell morphology | 0.02147226 | 0.18255814 |
| REACTOME_TRANSCRIPTIONAI | REACTOME_TRANSCRIPTIONAL_REGULATION_OF_WHITE_ | 0.02146612 | 0.1825811 |
| MP:0008174 | decreased follicular B cell number | 0.02153392 | 0.182793807 |
| ENSG00000101076 | HNF4A subnetwork | 0.021513 | 0.182852113 |
| ENSG00000151090 | THRB subnetwork | 0.02163806 | 0.183684951 |
| MP:0005281 | increased fatty acid level | 0.02170656 | 0.183964912 |
| ENSG00000175387 | SMAD2 subnetwork | 0.02170627 | 0.184094101 |
| ENSG00000007174 | DNAH9 subnetwork | 0.02168601 | 0.18411806 |
| ENSG00000171530 | TBCA subnetwork | 0.0217992 | 0.184653118 |
| ENSG00000143768 | LEFTY2 subnetwork | 0.02179422 | 0.184712482 |
| ENSG00000101901 | ALG13 subnetwork | 0.02183661 | 0.184768908 |

| | | | |
|---|---|---|---|
| ENSG00000148377 | IDI2 subnetwork | 0.02192219 | 0.185514346 |
| GO:0060330 | regulation of response to interferon-gamma | 0.02201978 | 0.185998603 |
| MP:0002335 | decreased airway responsiveness | 0.0220597 | 0.186078158 |
| GO:0060334 | regulation of interferon-gamma-mediated signaling pathwa | 0.02201978 | 0.186128581 |
| ENSG00000197757 | HOXC6 subnetwork | 0.02200739 | 0.186223776 |
| GO:0070076 | histone lysine demethylation | 0.0221338 | 0.186715481 |
| ENSG00000124788 | ATXN1 subnetwork | 0.0221556 | 0.186864111 |
| ENSG00000111707 | SUDS3 subnetwork | 0.02228832 | 0.187848189 |
| ENSG00000132170 | PPARG subnetwork | 0.02237049 | 0.188343772 |
| MP:0003567 | abnormal fetal cardiomyocyte proliferation | 0.02241051 | 0.188630042 |
| MP:0005165 | increased susceptibility to injury | 0.02244628 | 0.188637943 |
| ENSG00000133895 | MEN1 subnetwork | 0.02252463 | 0.189305556 |
| ENSG00000103671 | TRIP4 subnetwork | 0.02269854 | 0.18982699 |
| GO:0032451 | demethylase activity | 0.02265306 | 0.18991684 |
| MP:0008190 | decreased transitional stage B cell number | 0.02264911 | 0.189944521 |
| GO:0001779 | natural killer cell differentiation | 0.02268983 | 0.189958449 |
| ENSG00000171453 | POLR1C subnetwork | 0.02261754 | 0.19000694 |
| GO:0006325 | chromatin organization | 0.02280066 | 0.19049101 |
| GO:0032945 | negative regulation of mononuclear cell proliferation | 0.02293728 | 0.191332873 |
| GO:0050672 | negative regulation of lymphocyte proliferation | 0.02293728 | 0.1914651 |
| MP:0000245 | abnormal erythropoiesis | 0.02298596 | 0.191476881 |
| MP:0000108 | midline facial cleft | 0.02301045 | 0.191689655 |
| ENSG00000178573 | MAF subnetwork | 0.02326401 | 0.194004135 |
| ENSG00000177169 | ULK1 subnetwork | 0.02329129 | 0.194008264 |
| GO:0015026 | coreceptor activity | 0.02329935 | 0.194012388 |
| ENSG00000139505 | MTMR6 subnetwork | 0.02336763 | 0.19443299 |
| GO:0004198 | calcium-dependent cysteine-type endopeptidase activity | 0.02336154 | 0.194463549 |
| ENSG00000196092 | PAX5 subnetwork | 0.02346648 | 0.195089286 |
| GO:0045670 | regulation of osteoclast differentiation | 0.02352391 | 0.195813315 |
| GO:0034061 | DNA polymerase activity | 0.02360805 | 0.196433471 |
| REACTOME_ERKMAPK_TARGE | REACTOME_ERKMAPK_TARGETS | 0.0236262 | 0.196504455 |
| GO:0042508 | tyrosine phosphorylation of Stat1 protein | 0.02368562 | 0.196952055 |
| REACTOME_INTERFERON_GAN | REACTOME_INTERFERON_GAMMA_SIGNALING | 0.02370522 | 0.197091034 |
| GO:0051091 | positive regulation of sequence-specific DNA binding transc | 0.02376486 | 0.197435021 |
| KEGG_ACUTE_MYELOID_LEUKI | KEGG_ACUTE_MYELOID_LEUKEMIA | 0.02385492 | 0.197643443 |
| ENSG00000124486 | USP9X subnetwork | 0.0238499 | 0.197778537 |
| MP:0000938 | motor neuron degeneration | 0.0241058 | 0.199351978 |
| MP:0004771 | increased anti-single stranded DNA antibody level | 0.02413016 | 0.19935242 |
| ENSG00000129250 | KIF1C subnetwork | 0.02410048 | 0.199488055 |
| ENSG00000141068 | KSR1 subnetwork | 0.02417337 | 0.199557221 |
| GO:0030183 | B cell differentiation | 0.02422668 | 0.200034037 |
| ENSG00000033327 | GAB2 subnetwork | 0.02428868 | 0.200510204 |
| GO:0051492 | regulation of stress fiber assembly | 0.02436825 | 0.201087695 |
| ENSG00000119760 | SUPT7L subnetwork | 0.02439058 | 0.201256793 |
| ENSG00000125952 | MAX subnetwork | 0.02453476 | 0.201966102 |
| ENSG00000120690 | ELF1 subnetwork | 0.02453324 | 0.202069199 |
| ENSG00000172977 | KAT5 subnetwork | 0.02451991 | 0.202138493 |
| ENSG00000198176 | TFDP1 subnetwork | 0.02462513 | 0.202777778 |
| GO:0002922 | positive regulation of humoral immune response | 0.02471844 | 0.203588355 |
| ENSG00000118965 | WDR35 subnetwork | 0.02485827 | 0.204668471 |
| ENSG00000007312 | CD79B subnetwork | 0.02492717 | 0.205037187 |
| ENSG00000163519 | TRAT1 subnetwork | 0.02497506 | 0.205236486 |
| MP:0008578 | decreased circulating interferon-gamma level | 0.02508569 | 0.205319865 |

| | | | |
|---|---|---|---|
| ENSG00000139372 | TDG subnetwork | 0.02498555 | 0.205334234 |
| GO:0042054 | histone methyltransferase activity | 0.02501289 | 0.205398111 |
| GO:0035035 | histone acetyltransferase binding | 0.02506151 | 0.205424528 |
| ENSG00000160447 | PKN3 subnetwork | 0.02505179 | 0.205495617 |
| GO:0016458 | gene silencing | 0.02537669 | 0.207416107 |
| GO:0030331 | estrogen receptor binding | 0.02534485 | 0.207459677 |
| ENSG00000071794 | HLTF subnetwork | 0.02537602 | 0.207488247 |
| ENSG00000107562 | CXCL12 subnetwork | 0.02534329 | 0.207599193 |
| GO:0050869 | negative regulation of B cell activation | 0.02533602 | 0.207705249 |
| ENSG00000163399 | ATP1A1 subnetwork | 0.02543239 | 0.207780013 |
| GO:0032182 | small conjugating protein binding | 0.02549365 | 0.208176944 |
| GO:0034339 | regulation of transcription from RNA polymerase II promote | 0.02561347 | 0.209002677 |
| ENSG00000110711 | AIP subnetwork | 0.02557952 | 0.209008707 |
| ENSG00000143867 | OSR1 subnetwork | 0.02585561 | 0.21019385 |
| GO:0072676 | lymphocyte migration | 0.02589528 | 0.210287241 |
| ENSG00000141447 | OSBPL1A subnetwork | 0.02585561 | 0.210334448 |
| ENSG00000188130 | MAPK12 subnetwork | 0.02593942 | 0.210413885 |
| ENSG00000100320 | RBFOX2 subnetwork | 0.02598819 | 0.210473649 |
| MP:0008070 | absent T cells | 0.02603973 | 0.211 |
| ENSG00000197461 | PDGFA subnetwork | 0.02605735 | 0.211192538 |
| ENSG00000158092 | NCK1 subnetwork | 0.02624286 | 0.211663353 |
| ENSG00000166747 | AP1G1 subnetwork | 0.02612796 | 0.211668883 |
| GO:0030674 | protein binding, bridging | 0.02622641 | 0.211671088 |
| KEGG_TIGHT_JUNCTION | KEGG_TIGHT_JUNCTION | 0.02614636 | 0.211694352 |
| GO:0060444 | branching involved in mammary gland duct morphogenesis | 0.02611853 | 0.211709914 |
| GO:0042379 | chemokine receptor binding | 0.02620826 | 0.211712011 |
| MP:0004255 | abnormal spongiotrophoblast layer morphology | 0.02609897 | 0.21171771 |
| MP:0005344 | increased circulating bilirubin level | 0.02619615 | 0.211819389 |
| ENSG00000107560 | RAB11FIP2 subnetwork | 0.02630459 | 0.212152318 |
| GO:0008060 | ARF GTPase activator activity | 0.02636783 | 0.212706817 |
| ENSG00000206450 | HLA-B subnetwork | 0.02665549 | 0.214781746 |
| ENSG00000197892 | KIF13B subnetwork | 0.02669298 | 0.21483807 |
| MP:0006341 | small first branchial arch | 0.02676783 | 0.215214521 |
| ENSG00000147507 | ENSG00000147507 subnetwork | 0.02675558 | 0.215224571 |
| MP:0003132 | increased pre-B cell number | 0.02683413 | 0.215699208 |
| GO:0051044 | positive regulation of membrane protein ectodomain prote | 0.02685475 | 0.215721819 |
| ENSG00000026508 | CD44 subnetwork | 0.02691898 | 0.216063199 |
| ENSG00000099964 | ENSG00000099964 subnetwork | 0.02690049 | 0.216073781 |
| ENSG00000107882 | SUFU subnetwork | 0.02702114 | 0.21648063 |
| ENSG00000163486 | SRGAP2 subnetwork | 0.02700254 | 0.216491459 |
| MP:0010179 | rough coat | 0.02699475 | 0.216568047 |
| MP:0001654 | hepatic necrosis | 0.02699121 | 0.216644737 |
| ENSG00000152689 | RASGRP3 subnetwork | 0.02710487 | 0.216918033 |
| ENSG00000203283 | ENSG00000203283 subnetwork | 0.02713408 | 0.216994106 |
| ENSG00000117877 | CD3EAP subnetwork | 0.02709289 | 0.217027559 |
| ENSG00000135090 | TAOK3 subnetwork | 0.02717224 | 0.217113874 |
| ENSG00000161570 | CCL5 subnetwork | 0.02713408 | 0.217136304 |
| GO:0050707 | regulation of cytokine secretion | 0.02722489 | 0.217495095 |
| ENSG00000130159 | ECSIT subnetwork | 0.0272764 | 0.217679739 |
| GO:0032720 | negative regulation of tumor necrosis factor production | 0.02732698 | 0.218256042 |
| ENSG00000183117 | CSMD1 subnetwork | 0.02739449 | 0.218448501 |
| GO:0002717 | positive regulation of natural killer cell mediated immunity | 0.02738403 | 0.218460535 |
| GO:0045954 | positive regulation of natural killer cell mediated cytotoxicit | 0.02738403 | 0.218603133 |

| | | | |
|---|---|---|---|
| ENSG00000082701 | GSK3B subnetwork | 0.0275234 | 0.219543974 |
| MP:0008714 | lung carcinoma | 0.02759182 | 0.219921875 |
| GO:0006338 | chromatin remodeling | 0.02762786 | 0.219973975 |
| ENSG00000165197 | FIGF subnetwork | 0.0277024 | 0.220416125 |
| ENSG00000120156 | TEK subnetwork | 0.02779655 | 0.221312541 |
| MP:0000609 | abnormal liver physiology | 0.02781994 | 0.221331169 |
| MP:0005597 | decreased susceptibility to type I hypersensitivity reaction | 0.0278515 | 0.221414666 |
| ENSG00000137601 | NEK1 subnetwork | 0.02789786 | 0.221562905 |
| ENSG00000163166 | IWS1 subnetwork | 0.02811523 | 0.223525599 |
| REACTOME_IMMUNOREGULA | REACTOME_IMMUNOREGULATORY_INTERACTIONS_BETW | 0.02816996 | 0.223639896 |
| GO:0090311 | regulation of protein deacetylation | 0.0281968 | 0.223721683 |
| GO:0035601 | protein deacylation | 0.02822654 | 0.223771022 |
| MP:0002904 | increased circulating parathyroid hormone level | 0.02828554 | 0.224111183 |
| ENSG00000118513 | MYB subnetwork | 0.02833675 | 0.224273725 |
| ENSG00000124208 | TMEM189-UBE2V1 subnetwork | 0.02833473 | 0.224418605 |
| ENSG00000136518 | ACTL6A subnetwork | 0.02839066 | 0.224709677 |
| ENSG00000116288 | PARK7 subnetwork | 0.02847546 | 0.225274017 |
| GO:0016884 | carbon-nitrogen ligase activity, with glutamine as amido-N- | 0.02854771 | 0.226127577 |
| GO:0002824 | positive regulation of adaptive immune response based on | 0.02856737 | 0.226142949 |
| ENSG00000143207 | RFWD2 subnetwork | 0.02883415 | 0.228507079 |
| GO:0006954 | inflammatory response | 0.02896638 | 0.229485531 |
| ENSG00000179094 | PER1 subnetwork | 0.02905429 | 0.229762668 |
| ENSG00000003402 | CFLAR subnetwork | 0.02898546 | 0.229787918 |
| ENSG00000100056 | DGCR14 subnetwork | 0.02908693 | 0.229807692 |
| MP:0005251 | blepharitis | 0.02905034 | 0.229878049 |
| MP:0008209 | decreased pre-B cell number | 0.0291191 | 0.22991672 |
| ENSG00000168918 | INPP5D subnetwork | 0.02903973 | 0.229993577 |
| REACTOME_ERKS_ARE_INACTI | REACTOME_ERKS_ARE_INACTIVATED | 0.0293711 | 0.231413948 |
| MP:0005277 | abnormal brainstem morphology | 0.02934752 | 0.23153009 |
| ENSG00000165030 | NFIL3 subnetwork | 0.02943159 | 0.231649616 |
| ENSG00000132005 | RFX1 subnetwork | 0.02957246 | 0.232758621 |
| REACTOME_SIGNALING_BY_EC | REACTOME_SIGNALING_BY_EGFR | 0.02956549 | 0.232811502 |
| MP:0008080 | abnormal CD8-positive T cell differentiation | 0.02961433 | 0.232929164 |
| ENSG00000164889 | SLC4A2 subnetwork | 0.029643 | 0.233195153 |
| MP:0009346 | decreased trabecular bone thickness | 0.02965895 | 0.233269598 |
| ENSG00000205302 | SNX2 subnetwork | 0.02986838 | 0.234904459 |
| ENSG00000112242 | E2F3 subnetwork | 0.02994576 | 0.235614258 |
| ENSG00000161634 | DCD subnetwork | 0.03001791 | 0.235641677 |
| REACTOME_SIGNALING_BY_EC | REACTOME_SIGNALING_BY_EGFR_IN_CANCER | 0.03002557 | 0.235650794 |
| ENSG00000131095 | GFAP subnetwork | 0.02999634 | 0.23571883 |
| GO:0008276 | protein methyltransferase activity | 0.03000795 | 0.235727908 |
| ENSG00000117713 | ARID1A subnetwork | 0.03008765 | 0.235945431 |
| ENSG00000148400 | NOTCH1 subnetwork | 0.03009804 | 0.235954344 |
| MP:0009230 | abnormal sperm head morphology | 0.03019817 | 0.236139241 |
| ENSG00000206413 | ENSG00000206413 subnetwork | 0.03018953 | 0.236257125 |
| ENSG00000206493 | HLA-E subnetwork | 0.03018953 | 0.236406844 |
| REACTOME_GAB1_SIGNALOSC | REACTOME_GAB1_SIGNALOSOME | 0.03026331 | 0.23655914 |
| ENSG00000115904 | SOS1 subnetwork | 0.03034732 | 0.236946903 |
| MP:0000493 | rectal prolapse | 0.03053528 | 0.238099747 |
| MP:0001585 | hemolytic anemia | 0.03053441 | 0.238250158 |
| ENSG00000065882 | TBC1D1 subnetwork | 0.03068466 | 0.239116719 |
| ENSG00000071537 | SEL1L subnetwork | 0.03072545 | 0.239407314 |
| MP:0000188 | abnormal circulating glucose level | 0.03081454 | 0.239521712 |

| | | | |
|---|---|---|---|
| ENSG00000135801 | TAF5L subnetwork | 0.03077349 | 0.239634531 |
| MP:0008705 | increased interleukin-6 secretion | 0.03079906 | 0.239641058 |
| MP:0008641 | increased circulating interleukin-1 beta level | 0.03091177 | 0.240037712 |
| KEGG_BASE_EXCISION_REPAIR | KEGG_BASE_EXCISION_REPAIR | 0.03089286 | 0.24009434 |
| MP:0005441 | increased urine calcium level | 0.0312187 | 0.241036852 |
| ENSG00000166164 | BRD7 subnetwork | 0.03121074 | 0.241125 |
| GO:0043149 | stress fiber assembly | 0.03118737 | 0.241181989 |
| GO:0022408 | negative regulation of cell-cell adhesion | 0.03117885 | 0.24120776 |
| MP:0003448 | altered tumor morphology | 0.03129834 | 0.241292135 |
| ENSG00000116353 | MECR subnetwork | 0.03116894 | 0.24129618 |
| MP:0009967 | abnormal neuron proliferation | 0.03116655 | 0.241384712 |
| GO:0034142 | toll-like receptor 4 signaling pathway | 0.03111637 | 0.241462649 |
| ENSG00000170962 | PDGFD subnetwork | 0.03115735 | 0.241473354 |
| ENSG00000206156 | ENSG00000206156 subnetwork | 0.03111456 | 0.241614322 |
| ENSG00000145431 | PDGFC subnetwork | 0.03115735 | 0.241624843 |
| ENSG00000103197 | TSC2 subnetwork | 0.03148109 | 0.24238927 |
| ENSG00000104689 | TNFRSF10A subnetwork | 0.03157729 | 0.243173317 |
| REACTOME_APOPTOSIS | REACTOME_APOPTOSIS | 0.03173889 | 0.244049844 |
| ENSG00000065534 | MYLK subnetwork | 0.03184871 | 0.244679527 |
| ENSG00000119866 | BCL11A subnetwork | 0.03184198 | 0.244769614 |
| MP:0002928 | abnormal bile duct morphology | 0.03190439 | 0.244962687 |
| GO:0003823 | antigen binding | 0.03214975 | 0.246737104 |
| ENSG00000107223 | EDF1 subnetwork | 0.0322331 | 0.247173913 |
| GO:0034138 | toll-like receptor 3 signaling pathway | 0.03227597 | 0.247177419 |
| ENSG00000211899 | ENSG00000211899 subnetwork | 0.03228991 | 0.247210167 |
| ENSG00000077150 | NFKB2 subnetwork | 0.03226035 | 0.247268777 |
| ENSG00000123836 | PFKFB2 subnetwork | 0.03232984 | 0.247335812 |
| MP:0002022 | increased lymphoma incidence | 0.0327317 | 0.250464396 |
| GO:0002274 | myeloid leukocyte activation | 0.03283964 | 0.251082251 |
| ENSG00000152942 | RAD17 subnetwork | 0.03280965 | 0.251082921 |
| ENSG00000144852 | NR1I2 subnetwork | 0.03291913 | 0.251172116 |
| ENSG00000154143 | PANX3 subnetwork | 0.03291413 | 0.251265432 |
| ENSG00000122512 | PMS2 subnetwork | 0.03291335 | 0.251389747 |
| ENSG00000187953 | ENSG00000187953 subnetwork | 0.03291335 | 0.251545117 |
| ENSG00000117676 | RPS6KA1 subnetwork | 0.03303965 | 0.252127004 |
| KEGG_NATURAL_KILLER_CELL_ | KEGG_NATURAL_KILLER_CELL_MEDIATED_CYTOTOXICITY | 0.03309047 | 0.2525878 |
| GO:0030032 | lamellipodium assembly | 0.03313209 | 0.252801724 |
| GO:0071383 | cellular response to steroid hormone stimulus | 0.03322053 | 0.253323077 |
| MP:0002032 | sarcoma | 0.0332658 | 0.253382534 |
| ENSG00000151292 | CSNK1G3 subnetwork | 0.0333053 | 0.253534112 |
| MP:0004809 | increased hematopoietic stem cell number | 0.0334596 | 0.25485258 |
| ENSG00000106244 | PDAP1 subnetwork | 0.03348268 | 0.254910988 |
| MP:0008388 | hypochromic microcytic anemia | 0.03350257 | 0.25493865 |
| GO:0034708 | methyltransferase complex | 0.03364482 | 0.256035539 |
| GO:0035097 | histone methyltransferase complex | 0.03364482 | 0.25619252 |
| MP:0001426 | polydipsia | 0.03372209 | 0.256368647 |
| KEGG_NON_HOMOLOGOUS_E | KEGG_NON_HOMOLOGOUS_END_JOINING | 0.03384105 | 0.257435741 |
| MP:0002406 | increased susceptibility to infection | 0.03392465 | 0.257828746 |
| ENSG00000131899 | LLGL1 subnetwork | 0.03398262 | 0.258037897 |
| GO:0050663 | cytokine secretion | 0.03401276 | 0.258094075 |
| ENSG00000114062 | UBE3A subnetwork | 0.03405956 | 0.258180708 |
| ENSG00000197822 | OCLN subnetwork | 0.03422609 | 0.25945122 |
| ENSG00000163050 | ADCK3 subnetwork | 0.03421315 | 0.259517999 |

| | | | |
|---|---|---|---|
| MP:0004982 | abnormal osteoclast morphology | 0.03431872 | 0.259932968 |
| ENSG00000174485 | DENND4A subnetwork | 0.03443793 | 0.260688185 |
| ENSG00000166135 | HIF1AN subnetwork | 0.03450878 | 0.261229458 |
| MP:0002451 | abnormal macrophage physiology | 0.03462387 | 0.262043796 |
| ENSG00000113360 | DROSHA subnetwork | 0.03469779 | 0.262522796 |
| GO:0031072 | heat shock protein binding | 0.03494901 | 0.2643898 |
| GO:0031231 | intrinsic to peroxisomal membrane | 0.03500078 | 0.264484848 |
| ENSG00000110931 | CAMKK2 subnetwork | 0.0349438 | 0.264520049 |
| GO:0046633 | alpha-beta T cell proliferation | 0.0349848 | 0.264532767 |
| ENSG00000203879 | GDI1 subnetwork | 0.03501889 | 0.264566929 |
| GO:0005779 | integral to peroxisomal membrane | 0.03500078 | 0.26464524 |
| ENSG00000173011 | TADA2B subnetwork | 0.03513027 | 0.265284504 |
| ENSG00000136485 | DCAF7 subnetwork | 0.03533911 | 0.266908651 |
| ENSG00000157404 | KIT subnetwork | 0.0354973 | 0.26786578 |
| ENSG00000198961 | PJA2 subnetwork | 0.03560807 | 0.26897281 |
| ENSG00000043462 | LCP2 subnetwork | 0.03575434 | 0.269897343 |
| ENSG00000183034 | OTOP2 subnetwork | 0.03599139 | 0.270367028 |
| GO:0000979 | RNA polymerase II core promoter sequence-specific DNA bi | 0.03598905 | 0.270529801 |
| MP:0002398 | abnormal bone marrow cell morphology/development | 0.03602438 | 0.270565244 |
| MP:0000295 | trabecula carnea hypoplasia | 0.03598169 | 0.270662651 |
| MP:0001655 | multifocal hepatic necrosis | 0.03594558 | 0.270675105 |
| ENSG00000155506 | LARP1 subnetwork | 0.03593835 | 0.270778046 |
| GO:0051043 | regulation of membrane protein ectodomain proteolysis | 0.0359338 | 0.270911285 |
| ENSG00000138798 | EGF subnetwork | 0.03615946 | 0.271351351 |
| GO:0031400 | negative regulation of protein modification process | 0.03615584 | 0.271484375 |
| ENSG00000143772 | ITPKB subnetwork | 0.03622804 | 0.271728691 |
| MP:0004130 | abnormal muscle cell glucose uptake | 0.03630861 | 0.272075585 |
| ENSG00000117266 | CDK18 subnetwork | 0.03635247 | 0.272109047 |
| ENSG00000036672 | USP2 subnetwork | 0.03634481 | 0.27221223 |
| GO:0043368 | positive T cell selection | 0.03646576 | 0.2722189 |
| MP:0004737 | absent distortion product otoacoustic emissions | 0.03641575 | 0.272365269 |
| GO:0045088 | regulation of innate immune response | 0.03645361 | 0.272381807 |
| ENSG00000163517 | HDAC11 subnetwork | 0.03669019 | 0.274267782 |
| ENSG00000069956 | MAPK6 subnetwork | 0.03692104 | 0.274910714 |
| ENSG00000007908 | SELE subnetwork | 0.03692 | 0.275074449 |
| ENSG00000185386 | MAPK11 subnetwork | 0.0368229 | 0.275134328 |
| MP:0003179 | decreased platelet cell number | 0.03702482 | 0.275163399 |
| MP:0000495 | abnormal colon morphology | 0.03705325 | 0.275178147 |
| KEGG_SMALL_CELL_LUNG_CAI | KEGG_SMALL_CELL_LUNG_CANCER | 0.03691587 | 0.275178784 |
| GO:0070411 | I-SMAD binding | 0.03701906 | 0.275208086 |
| REACTOME_EARLY_PHASE_OF | REACTOME_EARLY_PHASE_OF_HIV_LIFE_CYCLE | 0.03687713 | 0.275298329 |
| ENSG00000125398 | SOX9 subnetwork | 0.03682179 | 0.275298686 |
| ENSG00000057657 | PRDM1 subnetwork | 0.03690807 | 0.275313059 |
| ENSG00000102878 | HSF4 subnetwork | 0.03700687 | 0.275342058 |
| ENSG00000092529 | CAPN3 subnetwork | 0.03714471 | 0.275622776 |
| GO:0030159 | receptor signaling complex scaffold activity | 0.03712465 | 0.275727003 |
| MP:0005439 | decreased glycogen level | 0.03727288 | 0.276585655 |
| ENSG00000184863 | RBM33 subnetwork | 0.03734003 | 0.277191943 |
| ENSG00000198265 | HELZ subnetwork | 0.03743875 | 0.277797513 |
| MP:0000266 | abnormal heart morphology | 0.03758451 | 0.278503844 |
| MP:0001413 | abnormal response to new environment | 0.0375636 | 0.27852071 |
| ENSG00000108256 | NUFIP2 subnetwork | 0.03765487 | 0.278812057 |
| ENSG00000072310 | SREBF1 subnetwork | 0.03770409 | 0.279001772 |

| | | | |
|---|---|---|---|
| ENSG00000076242 | MLH1 subnetwork | 0.03776751 | 0.279456907 |
| ENSG00000100784 | RPS6KA5 subnetwork | 0.03792443 | 0.280707965 |
| GO:0000785 | chromatin | 0.03798873 | 0.281338443 |
| GO:0043414 | macromolecule methylation | 0.03815431 | 0.282763701 |
| GO:0000792 | heterochromatin | 0.03829341 | 0.283009994 |
| GO:0046209 | nitric oxide metabolic process | 0.03828944 | 0.283117647 |
| GO:0008168 | methyltransferase activity | 0.03824395 | 0.283156655 |
| GO:0060561 | apoptotic process involved in morphogenesis | 0.03826653 | 0.283166569 |
| REACTOME_TOLL_RECEPTOR_( | REACTOME_TOLL_RECEPTOR_CASCADES | 0.03837694 | 0.283578143 |
| GO:0006482 | protein demethylation | 0.03850619 | 0.284184272 |
| GO:0008214 | protein dealkylation | 0.03850619 | 0.284351145 |
| MP:0010144 | abnormal tumor vascularization | 0.03873024 | 0.28542522 |
| GO:0005159 | insulin-like growth factor receptor binding | 0.03876327 | 0.28549238 |
| ENSG00000162692 | VCAM1 subnetwork | 0.03882602 | 0.285509368 |
| GO:0008285 | negative regulation of cell proliferation | 0.03888651 | 0.285584795 |
| ENSG00000087266 | SH3BP2 subnetwork | 0.03881394 | 0.285588752 |
| ENSG00000139515 | PDX1 subnetwork | 0.03887765 | 0.285693388 |
| GO:0016585 | chromatin remodeling complex | 0.0390379 | 0.286265342 |
| REACTOME_COOPERATION_OI | REACTOME_COOPERATION_OF_PREFOLDIN_AND_TRICCCT | 0.03914261 | 0.286697783 |
| ENSG00000166592 | RRAD subnetwork | 0.03910559 | 0.286740654 |
| REACTOME_PREFOLDIN_MEDI | REACTOME_PREFOLDIN_MEDIATED_TRANSFER_OF_SUBST | 0.03914261 | 0.286865149 |
| ENSG00000166710 | B2M subnetwork | 0.03942939 | 0.288862974 |
| ENSG00000156675 | RAB11FIP1 subnetwork | 0.03953043 | 0.289481352 |
| ENSG00000135046 | ANXA1 subnetwork | 0.03961682 | 0.289836925 |
| REACTOME_ZINC_INFLUX_INT( | REACTOME_ZINC_INFLUX_INTO_CELLS_BY_THE_SLC39_GE | 0.03964367 | 0.289871944 |
| KEGG_PEROXISOME | KEGG_PEROXISOME | 0.04007954 | 0.290051903 |
| MP:0001859 | kidney inflammation | 0.0401049 | 0.290057637 |
| ENSG00000163554 | SPTA1 subnetwork | 0.04006104 | 0.290075014 |
| MP:0002416 | abnormal proerythroblast morphology | 0.03976626 | 0.290197789 |
| GO:0002707 | negative regulation of lymphocyte mediated immunity | 0.04005543 | 0.290213626 |
| ENSG00000163932 | PRKCD subnetwork | 0.0398623 | 0.290226218 |
| ENSG00000065675 | PRKCQ subnetwork | 0.03978931 | 0.290261628 |
| GO:0016577 | histone demethylation | 0.04016292 | 0.290270581 |
| ENSG00000143753 | DEGS1 subnetwork | 0.03985155 | 0.290336622 |
| GO:0006916 | anti-apoptosis | 0.04014948 | 0.290380184 |
| GO:0002704 | negative regulation of leukocyte mediated immunity | 0.04005543 | 0.290381282 |
| REACTOME_INNATE_IMMUNE | REACTOME_INNATE_IMMUNE_SYSTEM | 0.03989745 | 0.290405797 |
| ENSG00000008294 | SPAG9 subnetwork | 0.0398502 | 0.290505226 |
| GO:0016278 | lysine N-methyltransferase activity | 0.04002379 | 0.290514748 |
| GO:0031293 | membrane protein intracellular domain proteolysis | 0.04005128 | 0.290520231 |
| GO:0031063 | regulation of histone deacetylation | 0.03983825 | 0.290557815 |
| MP:0002447 | abnormal erythrocyte morphology | 0.04022317 | 0.290678941 |
| GO:0016279 | protein-lysine N-methyltransferase activity | 0.04002379 | 0.29068287 |
| ENSG00000064393 | HIPK2 subnetwork | 0.04025196 | 0.290684301 |
| GO:0050729 | positive regulation of inflammatory response | 0.04000662 | 0.290793283 |
| MP:0002397 | abnormal bone marrow morphology | 0.03997354 | 0.290816918 |
| GO:0008063 | Toll signaling pathway | 0.04029042 | 0.290833333 |
| MP:0005031 | abnormal trophoblast layer morphology | 0.04064801 | 0.293566916 |
| ENSG00000099389 | ENSG00000099389 subnetwork | 0.040777 | 0.294144661 |
| MP:0003799 | impaired macrophage chemotaxis | 0.04083114 | 0.294434882 |
| ENSG00000086598 | TMED2 subnetwork | 0.04093559 | 0.29504298 |
| ENSG00000109971 | HSPA8 subnetwork | 0.04097212 | 0.295074456 |
| GO:0002832 | negative regulation of response to biotic stimulus | 0.04100503 | 0.295077275 |

| | | | |
|---|---|---|---|
| GO:0005925 | focal adhesion | 0.04091525 | 0.295097477 |
| GO:0032947 | protein complex scaffold | 0.04102068 | 0.295251716 |
| MP:0004842 | abnormal large intestine crypts of Lieberkuhn morphology | 0.04115 | 0.296112064 |
| GO:0001046 | core promoter sequence-specific DNA binding | 0.04121511 | 0.296371429 |
| GO:0042578 | phosphoric ester hydrolase activity | 0.0412878 | 0.296858938 |
| GO:0042992 | negative regulation of transcription factor import into nucle | 0.0413617 | 0.297374429 |
| ENSG00000114026 | OGG1 subnetwork | 0.04151228 | 0.298060468 |
| ENSG00000140464 | PML subnetwork | 0.04157972 | 0.298346636 |
| ENSG00000085511 | MAP3K4 subnetwork | 0.04166069 | 0.298661731 |
| ENSG00000141837 | CACNA1A subnetwork | 0.04163571 | 0.298746439 |
| ENSG00000138376 | BARD1 subnetwork | 0.04170203 | 0.299032442 |
| ENSG00000110651 | CD81 subnetwork | 0.04191459 | 0.300682594 |
| ENSG00000145425 | RPS3A subnetwork | 0.04197854 | 0.300938033 |
| MP:0004189 | abnormal alveolar process morphology | 0.04206987 | 0.301505682 |
| ENSG00000157933 | SKI subnetwork | 0.04211576 | 0.30153322 |
| ENSG00000103423 | DNAJA3 subnetwork | 0.04226051 | 0.302270148 |
| ENSG00000072135 | PTPN18 subnetwork | 0.04246004 | 0.303828701 |
| ENSG00000123131 | PRDX4 subnetwork | 0.04248636 | 0.303939909 |
| MP:0004893 | decreased adiponectin level | 0.04254048 | 0.304133635 |
| REACTOME_NGF_SIGNALLING_ | REACTOME_NGF_SIGNALLING_VIA_TRKA_FROM_THE_PLA | 0.04252257 | 0.304135977 |
| ENSG00000188459 | ENSG00000188459 subnetwork | 0.04259748 | 0.304385965 |
| ENSG00000135100 | HNF1A subnetwork | 0.04265667 | 0.304435028 |
| REACTOME_PIP3_ACTIVATES_/ | REACTOME_PIP3_ACTIVATES_AKT_SIGNALING | 0.04265396 | 0.304578858 |
| ENSG00000211456 | SACM1L subnetwork | 0.0426334 | 0.30469457 |
| ENSG00000100644 | HIF1A subnetwork | 0.04299274 | 0.30728402 |
| ENSG00000162407 | PPAP2B subnetwork | 0.04308383 | 0.307529611 |
| MP:0000602 | enlarged liver sinusoidal spaces | 0.04305115 | 0.30753386 |
| ENSG00000115935 | WIPF1 subnetwork | 0.04316699 | 0.308032694 |
| ENSG00000179335 | CLK3 subnetwork | 0.04325954 | 0.308366197 |
| ENSG00000060138 | CSDA subnetwork | 0.04332552 | 0.308811937 |
| GO:0044454 | nuclear chromosome part | 0.04335586 | 0.30889139 |
| ENSG00000176165 | FOXG1 subnetwork | 0.0433837 | 0.308998875 |
| MP:0008892 | abnormal sperm flagellum morphology | 0.04352068 | 0.309893198 |
| KEGG_NOTCH_SIGNALING_PA | KEGG_NOTCH_SIGNALING_PATHWAY | 0.04355863 | 0.310365169 |
| MP:0001377 | abnormal mating frequency | 0.0436505 | 0.310752386 |
| ENSG00000157764 | BRAF subnetwork | 0.04371177 | 0.310790359 |
| ENSG00000198087 | CD2AP subnetwork | 0.04367753 | 0.310802469 |
| ENSG00000107807 | TLX1 subnetwork | 0.04370949 | 0.310964666 |
| ENSG00000142867 | BCL10 subnetwork | 0.04389041 | 0.311758119 |
| ENSG00000119812 | FAM98A subnetwork | 0.04385719 | 0.311764706 |
| ENSG00000171195 | MUC7 subnetwork | 0.04394674 | 0.311975378 |
| ENSG00000156709 | AIFM1 subnetwork | 0.04405461 | 0.312583893 |
| ENSG00000076928 | ARHGEF1 subnetwork | 0.04415144 | 0.313024036 |
| ENSG00000182195 | LDOC1 subnetwork | 0.04462389 | 0.316424581 |
| ENSG00000119138 | KLF9 subnetwork | 0.04467044 | 0.316666667 |
| MP:0002023 | B cell derived lymphoma | 0.04469907 | 0.316741071 |
| GO:0071495 | cellular response to endogenous stimulus | 0.04482857 | 0.317791411 |
| ENSG00000112290 | WASF1 subnetwork | 0.04488104 | 0.31803233 |
| ENSG00000007866 | TEAD3 subnetwork | 0.04490008 | 0.318189415 |
| GO:0048011 | nerve growth factor receptor signaling pathway | 0.04501687 | 0.318538077 |
| GO:0060055 | angiogenesis involved in wound healing | 0.04497571 | 0.318558709 |
| ENSG00000130956 | HABP4 subnetwork | 0.04500717 | 0.318604004 |
| GO:0005083 | small GTPase regulator activity | 0.04496319 | 0.318624722 |

| | | | |
|---|---|---|---|
| ENSG00000165637 | VDAC2 subnetwork | 0.04504597 | 0.318638889 |
| MP:0002828 | abnormal renal glomerular capsule morphology | 0.04525901 | 0.320460855 |
| ENSG00000163811 | WDR43 subnetwork | 0.04536424 | 0.3208264 |
| GO:0045342 | MHC class II biosynthetic process | 0.04534224 | 0.320865705 |
| ENSG00000117222 | RBBP5 subnetwork | 0.04543049 | 0.321092018 |
| MP:0004985 | decreased osteoclast cell number | 0.04546253 | 0.321191136 |
| ENSG00000065526 | SPEN subnetwork | 0.04552819 | 0.321456257 |
| ENSG00000181555 | SETD2 subnetwork | 0.04557023 | 0.321460177 |
| GO:0008175 | tRNA methyltransferase activity | 0.04555698 | 0.321610404 |
| ENSG00000198793 | MTOR subnetwork | 0.04563285 | 0.321835268 |
| ENSG00000136731 | UGGT1 subnetwork | 0.04574428 | 0.32184225 |
| ENSG00000101306 | MYLK2 subnetwork | 0.04568106 | 0.321933702 |
| ENSG00000010810 | FYN subnetwork | 0.04573751 | 0.32196468 |
| ENSG00000162772 | ATF3 subnetwork | 0.04580925 | 0.322050717 |
| ENSG00000140395 | WDR61 subnetwork | 0.0457241 | 0.322059636 |
| GO:0003705 | RNA polymerase II distal enhancer sequence-specific DNA b | 0.04585959 | 0.322203857 |
| ENSG00000213658 | LAT subnetwork | 0.0459294 | 0.322742291 |
| ENSG00000164924 | YWHAZ subnetwork | 0.04612923 | 0.323708791 |
| MP:0004950 | abnormal brain vasculature morphology | 0.04611968 | 0.323831776 |
| GO:0002544 | chronic inflammatory response | 0.04609248 | 0.323885526 |
| ENSG00000174405 | LIG4 subnetwork | 0.04611088 | 0.323982398 |
| MP:0009790 | decreased susceptibility to viral infection induced morbidity | 0.04643016 | 0.325782537 |
| ENSG00000173327 | MAP3K11 subnetwork | 0.04644813 | 0.325795829 |
| ENSG00000162735 | PEX19 subnetwork | 0.04649465 | 0.326055952 |
| MP:0005287 | narrow eye opening | 0.04654713 | 0.326233553 |
| ENSG00000184922 | FMNL1 subnetwork | 0.04663169 | 0.326684932 |
| ENSG00000097007 | ABL1 subnetwork | 0.04667574 | 0.326752464 |
| ENSG00000167258 | CDK12 subnetwork | 0.04688579 | 0.327156114 |
| ENSG00000179262 | RAD23A subnetwork | 0.04679956 | 0.327173319 |
| GO:0050727 | regulation of inflammatory response | 0.04682618 | 0.327213115 |
| MP:0000603 | pale liver | 0.046921 | 0.327250409 |
| MP:0005185 | decreased circulating progesterone level | 0.04686945 | 0.327280175 |
| ENSG00000120738 | EGR1 subnetwork | 0.04679309 | 0.327324945 |
| GO:0043543 | protein acylation | 0.04678675 | 0.327422003 |
| ENSG00000138029 | HADHB subnetwork | 0.04705998 | 0.328189749 |
| ENSG00000182578 | CSF1R subnetwork | 0.04718074 | 0.328910082 |
| ENSG00000116473 | RAP1A subnetwork | 0.04727604 | 0.32954793 |
| MP:0001272 | increased metastatic potential | 0.04734504 | 0.329749592 |
| MP:0009788 | increased susceptibility to bacterial infection induced morb | 0.04763055 | 0.330510315 |
| GO:0016741 | transferase activity, transferring one-carbon groups | 0.04757862 | 0.330570652 |
| MP:0006301 | abnormal mesenchyme morphology | 0.04750278 | 0.330576714 |
| GO:0042287 | MHC protein binding | 0.04761549 | 0.330608365 |
| ENSG00000141551 | CSNK1D subnetwork | 0.04757759 | 0.330750408 |
| ENSG00000103769 | RAB11A subnetwork | 0.0477214 | 0.331063483 |
| ENSG00000206452 | HLA-C subnetwork | 0.0477761 | 0.331344902 |
| ENSG00000126777 | KTN1 subnetwork | 0.04782978 | 0.331517615 |
| ENSG00000184451 | CCR10 subnetwork | 0.04787386 | 0.331554713 |
| ENSG00000140992 | PDPK1 subnetwork | 0.04805281 | 0.332972388 |
| ENSG00000042980 | ADAM28 subnetwork | 0.04821538 | 0.334036797 |
| ENSG00000099917 | MED15 subnetwork | 0.04833054 | 0.334883721 |
| GO:0002455 | humoral immune response mediated by circulating immun | 0.04870333 | 0.337405405 |
| MP:0003383 | abnormal gluconeogenesis | 0.04874268 | 0.337493247 |
| ENSG00000182718 | ANXA2 subnetwork | 0.04882926 | 0.338282937 |

| | | | |
|---|---|---|---|
| ENSG00000120509 | PDZD11 subnetwork | 0.04901176 | 0.339314625 |
| ENSG00000129521 | EGLN3 subnetwork | 0.04903587 | 0.339347357 |
| GO:0003993 | acid phosphatase activity | 0.04921932 | 0.340781671 |
| ENSG00000100697 | DICER1 subnetwork | 0.04936137 | 0.341864224 |
| GO:0004702 | receptor signaling protein serine/threonine kinase activity | 0.0495333 | 0.34273021 |
| ENSG00000159840 | ZYX subnetwork | 0.04956794 | 0.342734123 |
| GO:0006359 | regulation of transcription from RNA polymerase III promot | 0.04966455 | 0.342772703 |
| ENSG00000169016 | E2F6 subnetwork | 0.04964803 | 0.342795699 |
| ENSG00000154001 | PPP2R5E subnetwork | 0.04964088 | 0.342953201 |
| REACTOME_P75_NTR_RECEPT | REACTOME_P75_NTR_RECEPTOR:MEDIATED_SIGNALLING | 0.04990462 | 0.344334049 |
| ENSG00000143878 | RHOB subnetwork | 0.05002259 | 0.344635193 |
| ENSG00000157873 | TNFRSF14 subnetwork | 0.05001635 | 0.344766506 |
| ENSG00000131504 | DIAPH1 subnetwork | 0.05010198 | 0.345040214 |
| ENSG00000166197 | NOLC1 subnetwork | 0.05034272 | 0.346757771 |
| ENSG00000006075 | CCL3 subnetwork | 0.0504711 | 0.347348688 |
| ENSG00000106052 | TAX1BP1 subnetwork | 0.05062127 | 0.348367238 |
| ENSG00000172116 | CD8B subnetwork | 0.05067851 | 0.348555377 |
| ENSG00000215320 | ENSG00000215320 subnetwork | 0.0507111 | 0.348609626 |
| ENSG00000183072 | NKX2-5 subnetwork | 0.05081437 | 0.348665955 |
| ENSG00000177728 | KIAA0195 subnetwork | 0.05078135 | 0.348718633 |
| ENSG00000183305 | MAGEA2B subnetwork | 0.050759 | 0.348798077 |
| ENSG00000129473 | BCL2L2 subnetwork | 0.05074888 | 0.348824158 |
| ENSG00000130699 | TAF4 subnetwork | 0.05088327 | 0.348986667 |
| ENSG00000070882 | OSBPL3 subnetwork | 0.05107264 | 0.349813433 |
| ENSG00000133026 | MYH10 subnetwork | 0.05111998 | 0.350026638 |
| ENSG00000103266 | STUB1 subnetwork | 0.05129878 | 0.350478469 |
| GO:0032620 | interleukin-17 production | 0.05129036 | 0.350558511 |
| GO:0005667 | transcription factor complex | 0.05124048 | 0.35071885 |
| GO:0032660 | regulation of interleukin-17 production | 0.05129036 | 0.350745077 |
| MP:0003724 | increased susceptibility to induced arthritis | 0.05152283 | 0.350821845 |
| ENSG00000108651 | UTP6 subnetwork | 0.05139106 | 0.350850159 |
| REACTOME_SEMA4D_INDUCEI | REACTOME_SEMA4D_INDUCED_CELL_MIGRATION_AND_G | 0.05142807 | 0.350876261 |
| ENSG00000111653 | ING4 subnetwork | 0.05146312 | 0.350902335 |
| ENSG00000118503 | TNFAIP3 subnetwork | 0.0515147 | 0.350954907 |
| REACTOME_NRIF_SIGNALS_CE | REACTOME_NRIF_SIGNALS_CELL_DEATH_FROM_THE_NUC | 0.05157423 | 0.351059883 |
| MP:0008111 | abnormal granulocyte differentiation | 0.05164762 | 0.351721398 |
| MP:0003645 | increased pancreatic beta cell number | 0.05181809 | 0.352620434 |
| ENSG00000166313 | APBB1 subnetwork | 0.05192423 | 0.353412698 |
| ENSG00000095002 | MSH2 subnetwork | 0.05196225 | 0.353463776 |
| GO:0022407 | regulation of cell-cell adhesion | 0.05200067 | 0.353541226 |
| ENSG00000168092 | PAFAH1B2 subnetwork | 0.05208942 | 0.353882726 |
| ENSG00000105216 | ENSG00000105216 subnetwork | 0.05213939 | 0.354012672 |
| GO:0045089 | positive regulation of innate immune response | 0.05224081 | 0.354081095 |
| GO:0031331 | positive regulation of cellular catabolic process | 0.05217458 | 0.35414248 |
| ENSG00000072518 | MARK2 subnetwork | 0.05220298 | 0.354190828 |
| MP:0009006 | prolonged estrous cycle | 0.05224046 | 0.354214963 |
| GO:0042162 | telomeric DNA binding | 0.05229232 | 0.354263158 |
| MP:0001759 | increased urine glucose level | 0.05219541 | 0.354324895 |
| ENSG00000002330 | BAD subnetwork | 0.05240432 | 0.354918464 |
| GO:0031330 | negative regulation of cellular catabolic process | 0.05244882 | 0.35502103 |
| GO:0008625 | induction of apoptosis via death domain receptors | 0.05249057 | 0.355070941 |
| ENSG00000165178 | ENSG00000165178 subnetwork | 0.05284863 | 0.357484244 |
| MP:0000826 | abnormal third ventricle morphology | 0.05297066 | 0.358136483 |

| | | | |
|---|---|---|---|
| REACTOME_PI3KAKT_ACTIVAT | REACTOME_PI3KAKT_ACTIVATION | 0.05301843 | 0.358315845 |
| MP:0001219 | thick epidermis | 0.05317651 | 0.359071841 |
| GO:0010623 | developmental programmed cell death | 0.05329027 | 0.359958071 |
| ENSG00000075785 | RAB7A subnetwork | 0.05337805 | 0.360371922 |
| MP:0004952 | increased spleen weight | 0.05346573 | 0.360942408 |
| MP:0000066 | osteoporosis | 0.05356822 | 0.361564626 |
| ENSG00000185634 | SHC4 subnetwork | 0.05364617 | 0.362029289 |
| ENSG00000073614 | KDM5A subnetwork | 0.05382511 | 0.363120753 |
| GO:0032270 | positive regulation of cellular protein metabolic process | 0.05388543 | 0.363133159 |
| GO:0000217 | DNA secondary structure binding | 0.05386181 | 0.363140021 |
| MP:0000465 | gastrointestinal hemorrhage | 0.05418069 | 0.363846955 |
| GO:0051353 | positive regulation of oxidoreductase activity | 0.05399978 | 0.363935282 |
| ENSG00000104892 | KLC3 subnetwork | 0.05416667 | 0.363958333 |
| GO:2000516 | positive regulation of CD4-positive, alpha-beta T cell activat | 0.05409413 | 0.364025026 |
| ENSG00000156711 | MAPK13 subnetwork | 0.05414349 | 0.364043773 |
| GO:0043372 | positive regulation of CD4-positive, alpha-beta T cell differe | 0.05409413 | 0.364214919 |
| REACTOME_DEADENYLATION_ | REACTOME_DEADENYLATION_OF_MRNA | 0.05434692 | 0.365140479 |
| GO:0071564 | npBAF complex | 0.05448723 | 0.365618503 |
| GO:0032715 | negative regulation of interleukin-6 production | 0.05447364 | 0.365730629 |
| MP:0002136 | abnormal kidney physiology | 0.0545336 | 0.365818182 |
| ENSG00000141367 | CLTC subnetwork | 0.05464667 | 0.366225337 |
| MP:0002757 | decreased vertical activity | 0.05467379 | 0.366320706 |
| ENSG00000090487 | SPG21 subnetwork | 0.05490988 | 0.367512953 |
| GO:0051235 | maintenance of location | 0.05489849 | 0.367599793 |
| MP:0005582 | increased renin activity | 0.05488497 | 0.367660788 |
| GO:0051403 | stress-activated MAPK cascade | 0.05504402 | 0.368038302 |
| GO:0005924 | cell-substrate adherens junction | 0.05504075 | 0.368228897 |
| ENSG00000196262 | PPIA subnetwork | 0.05532645 | 0.369534884 |
| ENSG00000198618 | ENSG00000198618 subnetwork | 0.05532645 | 0.369725957 |
| ENSG00000180182 | MED14 subnetwork | 0.05532282 | 0.369917227 |
| ENSG00000104312 | RIPK2 subnetwork | 0.0554007 | 0.369963843 |
| ENSG00000135074 | ADAM19 subnetwork | 0.05553481 | 0.370676304 |
| ENSG00000109046 | WSB1 subnetwork | 0.05561078 | 0.371181631 |
| ENSG00000008735 | MAPK8IP2 subnetwork | 0.05568667 | 0.371325425 |
| ENSG00000163530 | DPPA2 subnetwork | 0.05593409 | 0.372668727 |
| GO:0042088 | T-helper 1 type immune response | 0.05590046 | 0.372706186 |
| ENSG00000105963 | ADAP1 subnetwork | 0.05606079 | 0.373377961 |
| ENSG00000100302 | RASD2 subnetwork | 0.05612375 | 0.373468863 |
| GO:0070603 | SWI/SNF-type complex | 0.05614793 | 0.37348251 |
| REACTOME_PI3K_EVENTS_IN_ | REACTOME_PI3K_EVENTS_IN_ERBB2_SIGNALING | 0.05643943 | 0.375321337 |
| ENSG00000170776 | AKAP13 subnetwork | 0.05648979 | 0.37561665 |
| MP:0008713 | abnormal cytokine level | 0.0567799 | 0.376950719 |
| ENSG00000212645 | ENSG00000212645 subnetwork | 0.0567644 | 0.377067283 |
| GO:0042393 | histone binding | 0.0569204 | 0.377088672 |
| ENSG00000134852 | CLOCK subnetwork | 0.0568913 | 0.377230769 |
| REACTOME_PI3K_EVENTS_IN_ | REACTOME_PI3K_EVENTS_IN_ERBB4_SIGNALING | 0.05688885 | 0.37742432 |
| GO:0003887 | DNA-directed DNA polymerase activity | 0.0570123 | 0.377843238 |
| ENSG00000150459 | SAP18 subnetwork | 0.05707812 | 0.378070624 |
| ENSG00000123094 | RASSF8 subnetwork | 0.05707386 | 0.378238607 |
| ENSG00000150753 | CCT5 subnetwork | 0.0571791 | 0.378374233 |
| MP:0002644 | decreased circulating triglyceride level | 0.05716041 | 0.378439898 |
| GO:0031258 | lamellipodium membrane | 0.05721091 | 0.37851303 |
| ENSG00000123268 | ATF1 subnetwork | 0.05739237 | 0.379468846 |

| | | | |
|---|---|---|---|
| GO:0001891 | phagocytic cup | 0.05765266 | 0.379898219 |
| ENSG00000129691 | ASH2L subnetwork | 0.05750819 | 0.379989791 |
| GO:0000123 | histone acetyltransferase complex | 0.05758828 | 0.379994903 |
| ENSG00000109819 | PPARGC1A subnetwork | 0.0576234 | 0.380056037 |
| ENSG00000086015 | MAST2 subnetwork | 0.05757879 | 0.380061193 |
| ENSG00000075945 | KIFAP3 subnetwork | 0.05764442 | 0.380066191 |
| ENSG00000139318 | DUSP6 subnetwork | 0.0575465 | 0.380102041 |
| ENSG00000139197 | PEX5 subnetwork | 0.05774538 | 0.380315361 |
| MP:0002396 | abnormal hematopoietic system morphology/development | 0.05807566 | 0.381180344 |
| ENSG00000100490 | CDKL1 subnetwork | 0.05805154 | 0.381196148 |
| ENSG00000113643 | RARS subnetwork | 0.0579724 | 0.381227803 |
| ENSG00000082805 | ERC1 subnetwork | 0.05803019 | 0.381288032 |
| GO:0001666 | response to hypoxia | 0.05791679 | 0.381300813 |
| MP:0004047 | abnormal milk composition | 0.05793452 | 0.381335703 |
| GO:0006605 | protein targeting | 0.05790093 | 0.381367565 |
| ENSG00000113356 | POLR3G subnetwork | 0.05796184 | 0.381395939 |
| ENSG00000126767 | ELK1 subnetwork | 0.05824304 | 0.382126582 |
| ENSG00000124181 | PLCG1 subnetwork | 0.05838764 | 0.382692308 |
| GO:0005777 | peroxisome | 0.05854009 | 0.383291203 |
| GO:0042579 | microbody | 0.05854009 | 0.383485078 |
| MP:0001764 | abnormal homeostasis | 0.05883487 | 0.38489899 |
| ENSG00000144891 | AGTR1 subnetwork | 0.05895895 | 0.385030242 |
| ENSG00000101849 | TBL1X subnetwork | 0.05894282 | 0.385047907 |
| MP:0002993 | arthritis | 0.05889891 | 0.385058051 |
| ENSG00000092094 | OSGEP subnetwork | 0.05882892 | 0.385068216 |
| ENSG00000186716 | BCR subnetwork | 0.05893492 | 0.385166498 |
| ENSG00000155366 | RHOC subnetwork | 0.05929066 | 0.385398896 |
| ENSG00000129219 | PLD2 subnetwork | 0.05910308 | 0.38545546 |
| MP:0008750 | abnormal interferon level | 0.059288 | 0.385592369 |
| MP:0001819 | abnormal immune cell physiology | 0.05909408 | 0.385624371 |
| ENSG00000034693 | PEX3 subnetwork | 0.0590604 | 0.385642317 |
| ENSG00000159348 | CYB5R1 subnetwork | 0.05924631 | 0.385653266 |
| GO:0002756 | MyD88-independent toll-like receptor signaling pathway | 0.05926705 | 0.385660472 |
| ENSG00000055208 | TAB2 subnetwork | 0.05922296 | 0.385771745 |
| MP:0002675 | asthenozoospermia | 0.05920414 | 0.385865191 |
| ENSG00000180900 | SCRIB subnetwork | 0.05940536 | 0.385907723 |
| MP:0004187 | cardia bifida | 0.0595054 | 0.386441103 |
| GO:0044419 | interspecies interaction between organisms | 0.0596402 | 0.387224449 |
| ENSG00000152137 | HSPB8 subnetwork | 0.05971908 | 0.387531297 |
| KEGG_PANCREATIC_CANCER | KEGG_PANCREATIC_CANCER | 0.05991408 | 0.38811906 |
| ENSG00000087088 | BAX subnetwork | 0.0599069 | 0.388288288 |
| GO:0070988 | demethylation | 0.05997583 | 0.388475 |
| GO:0045581 | negative regulation of T cell differentiation | 0.060104 | 0.389230385 |
| ENSG00000160007 | ARHGAP35 subnetwork | 0.06017638 | 0.389266101 |
| GO:0003697 | single-stranded DNA binding | 0.060151 | 0.389310689 |
| MP:0003795 | abnormal bone structure | 0.06049138 | 0.389324727 |
| ENSG00000073050 | XRCC1 subnetwork | 0.06047654 | 0.389468455 |
| ENSG00000138722 | MMRN1 subnetwork | 0.06023243 | 0.389496008 |
| ENSG00000145781 | COMMD10 subnetwork | 0.06043836 | 0.389607161 |
| GO:0042800 | histone methyltransferase activity (H3-K4 specific) | 0.06046105 | 0.389612326 |
| ENSG00000188313 | PLSCR1 subnetwork | 0.06042008 | 0.389701493 |
| ENSG00000126070 | EIF2C3 subnetwork | 0.06031183 | 0.389750623 |
| ENSG00000019991 | HGF subnetwork | 0.06035765 | 0.38978575 |

| | | | |
|---|---|---|---|
| ENSG00000113387 | SUB1 subnetwork | 0.06041958 | 0.38989547 |
| MP:0008126 | increased dendritic cell number | 0.06035111 | 0.389955135 |
| REACTOME_O:LINKED_GLYCOS | REACTOME_O:LINKED_GLYCOSYLATION_OF_MUCINS | 0.0604127 | 0.39001494 |
| GO:0070851 | growth factor receptor binding | 0.06073985 | 0.390769231 |
| ENSG00000147689 | FAM83A subnetwork | 0.06087007 | 0.391253717 |
| ENSG00000132326 | PER2 subnetwork | 0.06083754 | 0.391294643 |
| GO:0010741 | negative regulation of intracellular protein kinase cascade | 0.06085657 | 0.391373327 |
| MP:0005559 | increased circulating glucose level | 0.06101011 | 0.392223873 |
| ENSG00000124092 | CTCFL subnetwork | 0.06107861 | 0.39235527 |
| ENSG00000180185 | FAHD1 subnetwork | 0.06107075 | 0.392475248 |
| ENSG00000122870 | BICC1 subnetwork | 0.06145966 | 0.394609298 |
| ENSG00000158195 | WASF2 subnetwork | 0.06154845 | 0.394762846 |
| ENSG00000123091 | RNF11 subnetwork | 0.06153555 | 0.39485912 |
| REACTOME_NEF_MEDIATED_D | REACTOME_NEF_MEDIATED_DOWNREGULATION_OF_MH( | 0.06165777 | 0.395160494 |
| GO:0006304 | DNA modification | 0.06170336 | 0.39523692 |
| ENSG00000064547 | LPAR2 subnetwork | 0.0617997 | 0.39573261 |
| GO:0042613 | MHC class II protein complex | 0.06188499 | 0.396057171 |
| ENSG00000125630 | POLR1B subnetwork | 0.06187812 | 0.396203156 |
| GO:0009986 | cell surface | 0.06207782 | 0.396679784 |
| ENSG00000115053 | NCL subnetwork | 0.06205441 | 0.396776575 |
| GO:0070461 | SAGA-type complex | 0.06213532 | 0.396902655 |
| ENSG00000106299 | WASL subnetwork | 0.06205388 | 0.396971935 |
| ENSG00000090659 | CD209 subnetwork | 0.06205274 | 0.397167488 |
| GO:0045185 | maintenance of protein location | 0.06222905 | 0.397469287 |
| ENSG00000131051 | RBM39 subnetwork | 0.06242621 | 0.398501965 |
| GO:0031519 | PcG protein complex | 0.06246223 | 0.398576338 |
| GO:0006301 | postreplication repair | 0.06252921 | 0.398969578 |
| ENSG00000025800 | KPNA6 subnetwork | 0.06272673 | 0.39907045 |
| ENSG00000136383 | ALPK3 subnetwork | 0.06256678 | 0.39919078 |
| ENSG00000144674 | GOLGA4 subnetwork | 0.062709 | 0.399216838 |
| MP:0002161 | abnormal fertility/fecundity | 0.06276616 | 0.399217604 |
| ENSG00000128594 | LRRC4 subnetwork | 0.06269606 | 0.399338883 |
| GO:0002820 | negative regulation of adaptive immune response | 0.06265214 | 0.399363057 |
| ENSG00000006712 | PAF1 subnetwork | 0.06262951 | 0.399411765 |
| MP:0004201 | fetal growth retardation | 0.06296527 | 0.400244379 |
| ENSG00000108510 | MED13 subnetwork | 0.06301529 | 0.400464094 |
| REACTOME_CELL_DEATH_SIGN | REACTOME_CELL_DEATH_SIGNALLING_VIA_NRAGE_NRIF_ | 0.06320956 | 0.400901999 |
| GO:0033276 | transcription factor TFTC complex | 0.06314648 | 0.400976086 |
| ENSG00000122691 | TWIST1 subnetwork | 0.0631139 | 0.400976563 |
| GO:0006402 | mRNA catabolic process | 0.06318969 | 0.401 |
| ENSG00000178607 | ERN1 subnetwork | 0.06325738 | 0.401023392 |
| ENSG00000162521 | RBBP4 subnetwork | 0.06337629 | 0.401557936 |
| ENSG00000136754 | ABI1 subnetwork | 0.0633631 | 0.401704822 |
| ENSG00000054796 | SPO11 subnetwork | 0.0634394 | 0.401776156 |
| REACTOME_DEFENSINS | REACTOME_DEFENSINS | 0.06365694 | 0.402795333 |
| ENSG00000129675 | ARHGEF6 subnetwork | 0.06364611 | 0.402918288 |
| ENSG00000169710 | FASN subnetwork | 0.0637182 | 0.403182702 |
| GO:0006959 | humoral immune response | 0.0638399 | 0.403691112 |
| MP:0002652 | thin myocardium | 0.06390333 | 0.403808831 |
| ENSG00000071051 | NCK2 subnetwork | 0.06389891 | 0.403956311 |
| ENSG00000131374 | TBC1D5 subnetwork | 0.06406945 | 0.404631426 |
| ENSG00000119630 | PGF subnetwork | 0.0641207 | 0.404823073 |
| GO:0048732 | gland development | 0.06413898 | 0.404893411 |

| | | | |
|---|---|---|---|
| GO:0035162 | embryonic hemopoiesis | 0.06421657 | 0.40527845 |
| GO:0006342 | chromatin silencing | 0.06430856 | 0.40571152 |
| ENSG00000149480 | MTA2 subnetwork | 0.06441907 | 0.406265119 |
| GO:0060333 | interferon-gamma-mediated signaling pathway | 0.0646302 | 0.40705314 |
| MP:0008597 | decreased circulating interleukin-6 level | 0.06466465 | 0.407073877 |
| GO:0043621 | protein self-association | 0.0646159 | 0.407080715 |
| MP:0001120 | abnormal uterus morphology | 0.0647305 | 0.407239382 |
| GO:0032507 | maintenance of protein location in cell | 0.06460659 | 0.407253385 |
| GO:0032259 | methylation | 0.06484609 | 0.407863 |
| GO:0019209 | kinase activator activity | 0.06511972 | 0.408786712 |
| MP:0001926 | female infertility | 0.06511385 | 0.408887283 |
| ENSG00000178913 | TAF7 subnetwork | 0.0650187 | 0.408895853 |
| ENSG00000166165 | CKB subnetwork | 0.06507628 | 0.408939759 |
| KEGG_PROPANOATE_METABO | KEGG_PROPANOATE_METABOLISM | 0.06519991 | 0.409143407 |
| GO:0008173 | RNA methyltransferase activity | 0.06529633 | 0.409475709 |
| ENSG00000142675 | CNKSR1 subnetwork | 0.06539762 | 0.409879808 |
| GO:0005048 | signal sequence binding | 0.06558048 | 0.411124459 |
| KEGG_NOD_LIKE_RECEPTOR_S | KEGG_NOD_LIKE_RECEPTOR_SIGNALING_PATHWAY | 0.0656116 | 0.411167147 |
| GO:0043967 | histone H4 acetylation | 0.06566796 | 0.411281805 |
| ENSG00000148356 | LRSAM1 subnetwork | 0.06573828 | 0.411414868 |
| ENSG00000137673 | MMP7 subnetwork | 0.06571644 | 0.411516315 |
| ENSG00000155508 | CNOT8 subnetwork | 0.06579159 | 0.411571634 |
| ENSG00000009413 | REV3L subnetwork | 0.06577423 | 0.411577181 |
| ENSG00000133703 | KRAS subnetwork | 0.06583658 | 0.411590038 |
| MP:0000067 | osteopetrosis | 0.06597901 | 0.412422212 |
| ENSG00000166402 | TUB subnetwork | 0.06605776 | 0.412625538 |
| ENSG00000180530 | NRIP1 subnetwork | 0.06604651 | 0.412799043 |
| ENSG00000105723 | GSK3A subnetwork | 0.06622742 | 0.413401816 |
| GO:0016514 | SWI/SNF complex | 0.06622634 | 0.413575526 |
| GO:0050699 | WW domain binding | 0.06644636 | 0.414589303 |
| GO:0016605 | PML body | 0.06655653 | 0.415107399 |
| ENSG00000175866 | BAIAP2 subnetwork | 0.066614 | 0.415267176 |
| KEGG_SYSTEMIC_LUPUS_ERYT | KEGG_SYSTEMIC_LUPUS_ERYTHEMATOSUS | 0.06692619 | 0.41647619 |
| ENSG00000205250 | E2F4 subnetwork | 0.06691513 | 0.416626965 |
| ENSG00000141646 | SMAD4 subnetwork | 0.0668796 | 0.41663489 |
| ENSG00000009790 | TRAF3IP3 subnetwork | 0.06686757 | 0.416809728 |
| ENSG00000182568 | SATB1 subnetwork | 0.06704396 | 0.416825321 |
| ENSG00000006125 | AP2B1 subnetwork | 0.06719165 | 0.417173397 |
| MP:0008481 | increased spleen germinal center number | 0.06715117 | 0.417284831 |
| MP:0004856 | decreased ovary weight | 0.06711829 | 0.417293054 |
| ENSG00000132964 | CDK8 subnetwork | 0.06718948 | 0.417371673 |
| ENSG00000185122 | HSF1 subnetwork | 0.06747194 | 0.419135802 |
| ENSG00000102974 | CTCF subnetwork | 0.06752645 | 0.419269103 |
| MP:0000358 | abnormal cell morphology | 0.0676754 | 0.419606449 |
| ENSG00000163629 | PTPN13 subnetwork | 0.06765219 | 0.419710626 |
| GO:0030055 | cell-substrate junction | 0.06794238 | 0.420141844 |
| ENSG00000133961 | NUMB subnetwork | 0.06792161 | 0.420175024 |
| ENSG00000023445 | BIRC3 subnetwork | 0.06790625 | 0.420231898 |
| GO:0044087 | regulation of cellular component biogenesis | 0.06784148 | 0.420274751 |
| GO:0005099 | Ras GTPase activator activity | 0.06788767 | 0.4203125 |
| KEGG_VEGF_SIGNALING_PATH | KEGG_VEGF_SIGNALING_PATHWAY | 0.06782744 | 0.420473934 |
| ENSG00000111199 | TRPV4 subnetwork | 0.06830093 | 0.422448015 |
| REACTOME_HOST_INTERACTIC | REACTOME_HOST_INTERACTIONS_OF_HIV_FACTORS | 0.06839498 | 0.423098725 |

| | | | |
|---|---|---|---|
| ENSG00000206429 | ENSG00000206429 subnetwork | 0.06866318 | 0.424033019 |
| ENSG00000011422 | PLAUR subnetwork | 0.06870226 | 0.424210278 |
| ENSG00000206502 | ZNRD1 subnetwork | 0.06866318 | 0.424233129 |
| ENSG00000066379 | ZNRD1 subnetwork | 0.06866318 | 0.424433428 |
| GO:0000228 | nuclear chromosome | 0.06884465 | 0.424740811 |
| ENSG00000175104 | TRAF6 subnetwork | 0.06897929 | 0.425765426 |
| GO:0002823 | negative regulation of adaptive immune response based on | 0.06904468 | 0.42594162 |
| GO:0043401 | steroid hormone mediated signaling pathway | 0.06911722 | 0.426282353 |
| ENSG00000107968 | MAP3K8 subnetwork | 0.06917094 | 0.426293509 |
| ENSG00000088035 | ALG6 subnetwork | 0.06968728 | 0.429689704 |
| ENSG00000108055 | SMC3 subnetwork | 0.06996016 | 0.431367481 |
| KEGG_NEUROTROPHIN_SIGNA | KEGG_NEUROTROPHIN_SIGNALING_PATHWAY | 0.07004746 | 0.431611085 |
| ENSG00000204642 | HLA-F subnetwork | 0.07009827 | 0.431901408 |
| ENSG00000076641 | PAG1 subnetwork | 0.07026634 | 0.432395687 |
| ENSG00000168439 | STIP1 subnetwork | 0.0702525 | 0.432481238 |
| ENSG00000172602 | RND1 subnetwork | 0.07024093 | 0.432660723 |
| ENSG00000189403 | HMGB1 subnetwork | 0.07040697 | 0.4329274 |
| MP:0003403 | absent placental labyrinth | 0.07039754 | 0.432989691 |
| ENSG00000157388 | CACNA1D subnetwork | 0.07061395 | 0.434019654 |
| ENSG00000100294 | MCAT subnetwork | 0.07061171 | 0.434199438 |
| ENSG00000179632 | MAF1 subnetwork | 0.07069831 | 0.434448082 |
| ENSG00000105369 | CD79A subnetwork | 0.07073457 | 0.434712482 |
| ENSG00000005022 | SLC25A5 subnetwork | 0.0708398 | 0.435280374 |
| MP:0005223 | abnormal anterior-posterior polarity of the somites | 0.0709999 | 0.435847735 |
| GO:0032740 | positive regulation of interleukin-17 production | 0.07114387 | 0.436601307 |
| GO:0070193 | synaptonemal complex organization | 0.07126272 | 0.437470835 |
| GO:0008213 | protein alkylation | 0.07137753 | 0.437855478 |
| GO:0006479 | protein methylation | 0.07137753 | 0.438059701 |
| ENSG00000118495 | PLAGL1 subnetwork | 0.07150868 | 0.438560112 |
| ENSG00000167815 | PRDX2 subnetwork | 0.07156138 | 0.438658593 |
| GO:0008135 | translation factor activity, nucleic acid binding | 0.07172797 | 0.438906977 |
| ENSG00000123358 | NR4A1 subnetwork | 0.07172346 | 0.439087948 |
| GO:0006473 | protein acetylation | 0.07171957 | 0.439269088 |
| ENSG00000004799 | PDK4 subnetwork | 0.07187053 | 0.439586239 |
| GO:0016234 | inclusion body | 0.07196011 | 0.440032528 |
| GO:0035145 | exon-exon junction complex | 0.07213834 | 0.4408732 |
| ENSG00000188620 | HMX3 subnetwork | 0.07236734 | 0.441786543 |
| GO:0031958 | corticosteroid receptor signaling pathway | 0.07235309 | 0.441968431 |
| ENSG00000054523 | KIF1B subnetwork | 0.07270816 | 0.443947124 |
| MP:0008561 | decreased tumor necrosis factor secretion | 0.07294545 | 0.444858731 |
| ENSG00000144158 | ENSG00000144158 subnetwork | 0.07300209 | 0.444861111 |
| ENSG00000156697 | UTP14A subnetwork | 0.0730311 | 0.444863489 |
| KEGG_CHRONIC_MYELOID_LEU | KEGG_CHRONIC_MYELOID_LEUKEMIA | 0.07289703 | 0.444993046 |
| GO:0042176 | regulation of protein catabolic process | 0.07293664 | 0.444995366 |
| ENSG00000068971 | PPP2R5B subnetwork | 0.07308592 | 0.445004625 |
| ENSG00000071462 | WBSCR22 subnetwork | 0.07317432 | 0.445376791 |
| MP:0011260 | abnormal head mesenchyme morphology | 0.07329353 | 0.445590951 |
| ENSG00000049246 | PER3 subnetwork | 0.07328598 | 0.445750577 |
| GO:0009894 | regulation of catabolic process | 0.07325969 | 0.445887246 |
| ENSG00000143384 | MCL1 subnetwork | 0.07347344 | 0.446492847 |
| ENSG00000198518 | HIST1H4E subnetwork | 0.07405289 | 0.446706313 |
| ENSG00000128602 | SMO subnetwork | 0.07408264 | 0.446753544 |
| MP:0002665 | decreased circulating corticosterone level | 0.07411805 | 0.446846435 |

| | | | |
|---|---|---|---|
| ENSG00000158406 | HIST1H4H subnetwork | 0.07405289 | 0.446910755 |
| ENSG00000183941 | HIST2H4A subnetwork | 0.07405289 | 0.447115385 |
| ENSG00000086205 | FOLH1 subnetwork | 0.07421898 | 0.447304705 |
| ENSG00000198558 | HIST1H4L subnetwork | 0.07405289 | 0.447320202 |
| ENSG00000135900 | MRPL44 subnetwork | 0.07367122 | 0.447395113 |
| ENSG00000110042 | DTX4 subnetwork | 0.07365538 | 0.4474631 |
| ENSG00000197238 | HIST1H4J subnetwork | 0.07405289 | 0.447525206 |
| ENSG00000197914 | HIST1H4K subnetwork | 0.07405289 | 0.447730399 |
| MP:0001732 | postnatal growth retardation | 0.07434633 | 0.447899543 |
| GO:0005815 | microtubule organizing center | 0.07442531 | 0.44790146 |
| ENSG00000197061 | HIST1H4C subnetwork | 0.07405289 | 0.44793578 |
| ENSG00000198641 | ENSG00000198641 subnetwork | 0.0743951 | 0.447968964 |
| ENSG00000198339 | HIST1H4I subnetwork | 0.07405289 | 0.448141349 |
| ENSG00000197837 | HIST4H4 subnetwork | 0.07405289 | 0.448347107 |
| ENSG00000124529 | HIST1H4B subnetwork | 0.07405289 | 0.448553055 |
| ENSG00000182217 | HIST2H4B subnetwork | 0.07405289 | 0.448759191 |
| GO:0007130 | synaptonemal complex assembly | 0.0739034 | 0.448894009 |
| ENSG00000188987 | HIST1H4D subnetwork | 0.07405289 | 0.448965517 |
| GO:0001637 | G-protein coupled chemoattractant receptor activity | 0.07401158 | 0.44914825 |
| ENSG00000196176 | HIST1H4A subnetwork | 0.07405289 | 0.449172033 |
| GO:0004950 | chemokine receptor activity | 0.07401158 | 0.449355136 |
| ENSG00000198327 | HIST1H4F subnetwork | 0.07405289 | 0.449378739 |
| MP:0011228 | abnormal vitamin D level | 0.07475185 | 0.449863263 |
| KEGG_ANTIGEN_PROCESSING_ | KEGG_ANTIGEN_PROCESSING_AND_PRESENTATION | 0.0748102 | 0.449954442 |
| ENSG00000139436 | GIT2 subnetwork | 0.07474061 | 0.45 |
| REACTOME_PECAM1_INTERAC | REACTOME_PECAM1_INTERACTIONS | 0.07504952 | 0.450318182 |
| ENSG00000175029 | CTBP2 subnetwork | 0.07501804 | 0.450409277 |
| ENSG00000116062 | MSH6 subnetwork | 0.0749801 | 0.450454959 |
| ENSG00000180353 | HCLS1 subnetwork | 0.07497285 | 0.450637233 |
| GO:0042267 | natural killer cell mediated cytotoxicity | 0.07518349 | 0.450681199 |
| ENSG00000069667 | RORA subnetwork | 0.07496869 | 0.450819672 |
| GO:0040018 | positive regulation of multicellular organism growth | 0.07523296 | 0.450839764 |
| GO:0002228 | natural killer cell mediated immunity | 0.07518349 | 0.450885961 |
| ENSG00000103510 | KAT8 subnetwork | 0.07528458 | 0.451020871 |
| GO:0045063 | T-helper 1 cell differentiation | 0.07548215 | 0.451903898 |
| MP:0004851 | increased testis weight | 0.07547268 | 0.452018141 |
| ENSG00000173511 | VEGFB subnetwork | 0.07561709 | 0.452695967 |
| ENSG00000169567 | HINT1 subnetwork | 0.07608998 | 0.455545496 |
| GO:0002224 | toll-like receptor signaling pathway | 0.07608255 | 0.455548007 |
| ENSG00000156482 | RPL30 subnetwork | 0.07614988 | 0.455769231 |
| ENSG00000105379 | ETFB subnetwork | 0.07621425 | 0.455786618 |
| MP:0002024 | T cell derived lymphoma | 0.07620016 | 0.455879692 |
| ENSG00000166530 | ENSG00000166530 subnetwork | 0.07651365 | 0.457162223 |
| ENSG00000116830 | TTF2 subnetwork | 0.07664021 | 0.457562077 |
| ENSG00000079102 | RUNX1T1 subnetwork | 0.07663508 | 0.457746161 |
| GO:0000981 | sequence-specific DNA binding RNA polymerase II transcrip | 0.07674935 | 0.45823556 |
| KEGG_GNRH_SIGNALING_PATI | KEGG_GNRH_SIGNALING_PATHWAY | 0.07686234 | 0.45879567 |
| ENSG00000106006 | HOXA6 subnetwork | 0.07715429 | 0.460045045 |
| GO:0005814 | centriole | 0.07713985 | 0.46011717 |
| ENSG00000159259 | CHAF1B subnetwork | 0.07712656 | 0.460234445 |
| ENSG00000183735 | TBK1 subnetwork | 0.07737135 | 0.461458802 |
| ENSG00000187555 | USP7 subnetwork | 0.07751592 | 0.46194332 |
| ENSG00000103319 | EEF2K subnetwork | 0.07750874 | 0.462128713 |

| | | | |
|---|---|---|---|
| ENSG00000012983 | MAP4K5 subnetwork | 0.07760184 | 0.46227518 |
| ENSG00000006062 | MAP3K14 subnetwork | 0.07768786 | 0.462348451 |
| GO:0035064 | methylated histone residue binding | 0.07764919 | 0.462382022 |
| ENSG00000163624 | CDS1 subnetwork | 0.07768462 | 0.462556155 |
| REACTOME_BILE_SALT_AND_C | REACTOME_BILE_SALT_AND_ORGANIC_ANION_SLC_TRAN | 0.07786131 | 0.463263016 |
| ENSG00000116489 | CAPZA1 subnetwork | 0.07790198 | 0.463324361 |
| GO:0042990 | regulation of transcription factor import into nucleus | 0.07801168 | 0.463744395 |
| ENSG00000161980 | POLR3K subnetwork | 0.07811835 | 0.464141641 |
| ENSG00000169429 | IL8 subnetwork | 0.0783273 | 0.464717742 |
| ENSG00000150630 | VEGFC subnetwork | 0.07837004 | 0.464845499 |
| ENSG00000070423 | RNF126 subnetwork | 0.07846853 | 0.465219338 |
| ENSG00000196557 | CACNA1H subnetwork | 0.07867151 | 0.466144902 |
| ENSG00000085224 | ATRX subnetwork | 0.07869879 | 0.466182387 |
| MP:0001505 | hunched posture | 0.07881157 | 0.466205357 |
| ENSG00000117020 | AKT3 subnetwork | 0.07880142 | 0.466324252 |
| MP:0000274 | enlarged heart | 0.07865868 | 0.466331096 |
| ENSG00000110092 | CCND1 subnetwork | 0.07878855 | 0.466510277 |
| ENSG00000128829 | EIF2AK4 subnetwork | 0.07891597 | 0.466733601 |
| GO:0006475 | internal protein amino acid acetylation | 0.07906175 | 0.467216771 |
| ENSG00000105618 | PRPF31 subnetwork | 0.0792383 | 0.467602496 |
| ENSG00000170653 | ATF7 subnetwork | 0.07921611 | 0.46769951 |
| ENSG00000114686 | MRPL3 subnetwork | 0.07939661 | 0.468121104 |
| REACTOME_IRAK2_MEDIATED | REACTOME_IRAK2_MEDIATED_ACTIVATION_OF_TAK1_COI | 0.07937326 | 0.468195991 |
| ENSG00000212981 | ENSG00000212981 subnetwork | 0.07949151 | 0.468460854 |
| MP:0003704 | abnormal hair follicle development | 0.07948611 | 0.468647085 |
| ENSG00000087077 | TRIP6 subnetwork | 0.08002676 | 0.469525709 |
| ENSG00000143799 | PARP1 subnetwork | 0.07986685 | 0.469529516 |
| ENSG00000157514 | TSC22D3 subnetwork | 0.07979525 | 0.469538188 |
| MP:0003936 | abnormal reproductive system development | 0.07973265 | 0.469577778 |
| ENSG00000128654 | MTX2 subnetwork | 0.07999551 | 0.469600887 |
| REACTOME_POST:TRANSLATIC | REACTOME_POST:TRANSLATIONAL_PROTEIN_MODIFICATI | 0.07978543 | 0.469613505 |
| ENSG00000173110 | HSPA6 subnetwork | 0.07970673 | 0.469697643 |
| ENSG00000101945 | SUV39H1 subnetwork | 0.07998677 | 0.469787045 |
| GO:0016799 | hydrolase activity, hydrolyzing N-glycosyl compounds | 0.08044351 | 0.470079435 |
| ENSG00000120656 | TAF12 subnetwork | 0.08014183 | 0.470093044 |
| ENSG00000204632 | HLA-G subnetwork | 0.08035349 | 0.470128148 |
| ENSG00000135605 | TEC subnetwork | 0.08018501 | 0.470172719 |
| ENSG00000085662 | AKR1B1 subnetwork | 0.08039805 | 0.470229682 |
| ENSG00000183779 | ZNF703 subnetwork | 0.08028597 | 0.470243363 |
| ENSG00000118689 | FOXO3 subnetwork | 0.08044136 | 0.470286976 |
| ENSG00000206506 | HLA-G subnetwork | 0.08035349 | 0.470335986 |
| ENSG00000101751 | POLI subnetwork | 0.08028369 | 0.470451527 |
| ENSG00000206443 | ENSG00000206443 subnetwork | 0.08035349 | 0.470544007 |
| MP:0008000 | increased ovary tumor incidence | 0.08078932 | 0.471835024 |
| GO:0030296 | protein tyrosine kinase activator activity | 0.08081482 | 0.471891534 |
| ENSG00000166266 | CUL5 subnetwork | 0.08091523 | 0.472344645 |
| ENSG00000148773 | MKI67 subnetwork | 0.08106671 | 0.472929515 |
| ENSG00000130024 | PHF10 subnetwork | 0.08118418 | 0.473425804 |
| ENSG00000185432 | METTL7A subnetwork | 0.08137474 | 0.473594025 |
| MP:0008813 | decreased common myeloid progenitor cell number | 0.08134933 | 0.473604396 |
| GO:0045646 | regulation of erythrocyte differentiation | 0.08133689 | 0.473790677 |
| ENSG00000163904 | SENP2 subnetwork | 0.08133186 | 0.473867136 |
| ENSG00000099246 | RAB18 subnetwork | 0.08130166 | 0.473921655 |

| | | | |
|---|---|---|---|
| ENSG00000112249 | ASCC3 subnetwork | 0.08157159 | 0.474769433 |
| GO:0016877 | ligase activity, forming carbon-sulfur bonds | 0.08171284 | 0.475460931 |
| GO:0043235 | receptor complex | 0.08180148 | 0.476107942 |
| GO:0000299 | integral to membrane of membrane fraction | 0.08202105 | 0.477005699 |
| ENSG00000133056 | PIK3C2B subnetwork | 0.08205119 | 0.477059597 |
| ENSG00000204673 | AKT1S1 subnetwork | 0.08201932 | 0.477214912 |
| MP:0004462 | small basisphenoid bone | 0.08217456 | 0.477332457 |
| ENSG00000205155 | PSENEN subnetwork | 0.08232827 | 0.477734033 |
| ENSG00000117242 | ENSG00000117242 subnetwork | 0.08228045 | 0.47778021 |
| ENSG00000182367 | ENSG00000182367 subnetwork | 0.08232398 | 0.477921225 |
| ENSG00000186575 | NF2 subnetwork | 0.08248182 | 0.478452797 |
| KEGG_GLYOXYLATE_AND_DIC/ | KEGG_GLYOXYLATE_AND_DICARBOXYLATE_METABOLISM | 0.08259774 | 0.478459188 |
| ENSG00000168255 | POLR2J3 subnetwork | 0.08256811 | 0.478471616 |
| ENSG00000119335 | SET subnetwork | 0.08246512 | 0.478552689 |
| ENSG00000197373 | ENSG00000197373 subnetwork | 0.08256811 | 0.478680647 |
| ENSG00000078328 | RBFOX1 subnetwork | 0.08268777 | 0.478861257 |
| ENSG00000161654 | LSM12 subnetwork | 0.08314752 | 0.481045752 |
| ENSG00000121390 | PSPC1 subnetwork | 0.08307214 | 0.481051025 |
| MP:0001876 | decreased inflammatory response | 0.08310582 | 0.481081081 |
| MP:0001882 | abnormal lactation | 0.08324328 | 0.481315331 |
| ENSG00000161405 | IKZF3 subnetwork | 0.08330026 | 0.481562908 |
| ENSG00000120693 | SMAD9 subnetwork | 0.08337848 | 0.48181027 |
| MP:0005452 | abnormal adipose tissue amount | 0.0834334 | 0.482013919 |
| MP:0002687 | oligozoospermia | 0.08370528 | 0.482971329 |
| MP:0011501 | increased glomerular capsule space | 0.08368308 | 0.483007388 |
| REACTOME_GPVI:MEDIATED_/ | REACTOME_GPVI:MEDIATED_ACTIVATION_CASCADE | 0.08366487 | 0.483043478 |
| GO:0001934 | positive regulation of protein phosphorylation | 0.08388879 | 0.483890578 |
| ENSG00000070950 | RAD18 subnetwork | 0.08397031 | 0.483984375 |
| MP:0002875 | decreased erythrocyte cell number | 0.08408412 | 0.484533623 |
| MP:0002833 | increased heart weight | 0.08416758 | 0.485060711 |
| ENSG00000197442 | MAP3K5 subnetwork | 0.08419697 | 0.485110533 |
| ENSG00000161395 | PGAP3 subnetwork | 0.08435029 | 0.486070191 |
| GO:0032387 | negative regulation of intracellular transport | 0.08438713 | 0.486119532 |
| ENSG00000163466 | ARPC2 subnetwork | 0.08450252 | 0.486493506 |
| ENSG00000109906 | ZBTB16 subnetwork | 0.08452954 | 0.486542622 |
| GO:0017017 | MAP kinase tyrosine/serine/threonine phosphatase activity | 0.08478612 | 0.487743191 |
| MP:0010876 | decreased bone volume | 0.08477072 | 0.487867647 |
| ENSG00000120889 | TNFRSF10B subnetwork | 0.08499827 | 0.488915298 |
| GO:0016878 | acid-thiol ligase activity | 0.08519434 | 0.489848812 |
| ENSG00000111348 | ARHGDIB subnetwork | 0.08523793 | 0.489917962 |
| MP:0002637 | small uterus | 0.08533744 | 0.490418645 |
| GO:0048524 | positive regulation of viral reproduction | 0.08566908 | 0.491451335 |
| MP:0001231 | abnormal epidermis stratum basale morphology | 0.08557011 | 0.491461837 |
| ENSG00000115953 | ENSG00000115953 subnetwork | 0.08564006 | 0.491490737 |
| ENSG00000114857 | NKTR subnetwork | 0.08561256 | 0.491508621 |
| ENSG00000138293 | NCOA4 subnetwork | 0.08554344 | 0.491587575 |
| MP:0003718 | maternal effect | 0.08583651 | 0.492362306 |
| MP:0004256 | abnormal maternal decidual layer morphology | 0.08580774 | 0.492380542 |
| ENSG00000132522 | GPS2 subnetwork | 0.0858675 | 0.492387097 |
| MP:0000136 | abnormal microglial cell morphology | 0.0859296 | 0.492583835 |
| MP:0004796 | increased anti-histone antibody level | 0.0861804 | 0.49370434 |
| ENSG00000135679 | MDM2 subnetwork | 0.08630312 | 0.494308419 |
| ENSG00000145901 | TNIP1 subnetwork | 0.08643531 | 0.494592275 |

| | | | |
|---|---|---|---|
| ENSG00000115661 | STK16 subnetwork | 0.08641823 | 0.494654358 |
| REACTOME_REGULATION_OF_ | REACTOME_REGULATION_OF_KIT_SIGNALING | 0.08675768 | 0.495289079 |
| ENSG00000172288 | CDY1 subnetwork | 0.0867162 | 0.495351328 |
| ENSG00000172352 | CDY1B subnetwork | 0.0867162 | 0.495563652 |
| GO:0050691 | regulation of defense response to virus by host | 0.08666601 | 0.495688546 |
| ENSG00000111674 | ENO2 subnetwork | 0.08688838 | 0.495719178 |
| ENSG00000196419 | XRCC6 subnetwork | 0.08670376 | 0.495754717 |
| GO:0032231 | regulation of actin filament bundle assembly | 0.08695645 | 0.496041934 |
| ENSG00000168298 | HIST1H1E subnetwork | 0.08713551 | 0.497027374 |
| GO:0046782 | regulation of viral transcription | 0.08756101 | 0.497169008 |
| ENSG00000125695 | STRADA subnetwork | 0.08752338 | 0.497189097 |
| ENSG00000119383 | PPP2R4 subnetwork | 0.08736038 | 0.497288642 |
| MP:0002599 | increased mean platelet volume | 0.0873835 | 0.497289799 |
| ENSG00000100097 | LGALS1 subnetwork | 0.087264 | 0.497370671 |
| GO:0001047 | core promoter binding | 0.08751764 | 0.497400937 |
| GO:0032870 | cellular response to hormone stimulus | 0.08748608 | 0.497421142 |
| ENSG00000167004 | PDIA3 subnetwork | 0.08735052 | 0.497436993 |
| MP:0002594 | low mean erythrocyte cell number | 0.08746659 | 0.49750533 |
| ENSG00000028277 | POU2F2 subnetwork | 0.08744971 | 0.497610922 |
| GO:0006913 | nucleocytoplasmic transport | 0.08734659 | 0.497649573 |
| GO:0046640 | regulation of alpha-beta T cell proliferation | 0.08772621 | 0.498191489 |
| ENSG00000147140 | NONO subnetwork | 0.08779483 | 0.498319864 |
| MP:0001200 | thick skin | 0.08795497 | 0.49914966 |
| GO:0045471 | response to ethanol | 0.08806596 | 0.499490013 |
| MP:0008019 | increased liver tumor incidence | 0.0881282 | 0.499553951 |
| GO:0002828 | regulation of type 2 immune response | 0.08822696 | 0.499745223 |
| MP:0011348 | abnormal renal glomerulus basement membrane morpholc | 0.08830302 | 0.5 |
| ENSG00000184634 | MED12 subnetwork | 0.08836626 | 0.500530335 |
| ENSG00000197312 | DDI2 subnetwork | 0.08856653 | 0.501292373 |
| REACTOME_IRAK2_MEDIATED_ | REACTOME_IRAK2_MEDIATED_ACTIVATION_OF_TAK1_COI | 0.08856637 | 0.501504875 |
| MP:0008294 | abnormal zona fasciculata morphology | 0.0886297 | 0.501545955 |
| GO:0031903 | microbody membrane | 0.08870987 | 0.501650444 |
| REACTOME_TRAF6_MEDIATED | REACTOME_TRAF6_MEDIATED_INDUCTION_OF_TAK1_COI | 0.08856637 | 0.501717557 |
| GO:0005778 | peroxisomal membrane | 0.08870987 | 0.501862828 |
| GO:0042510 | regulation of tyrosine phosphorylation of Stat1 protein | 0.08885672 | 0.50251692 |
| MP:0000154 | rib fusion | 0.08892476 | 0.502748414 |
| ENSG00000005175 | RPAP3 subnetwork | 0.08935736 | 0.504898649 |
| MP:0000601 | small liver | 0.08928634 | 0.505029586 |
| GO:0010638 | positive regulation of organelle organization | 0.08935102 | 0.505069708 |
| ENSG00000130338 | TULP4 subnetwork | 0.08950057 | 0.505593077 |
| ENSG00000171475 | WIPF2 subnetwork | 0.08957815 | 0.505607083 |
| ENSG00000160972 | PPP1R16A subnetwork | 0.089529 | 0.505654008 |
| GO:0042130 | negative regulation of T cell proliferation | 0.08956947 | 0.505757065 |
| ENSG00000105221 | AKT2 subnetwork | 0.08966357 | 0.505941846 |
| MP:0000062 | increased bone mineral density | 0.09007842 | 0.507873684 |
| MP:0002642 | anisocytosis | 0.09007288 | 0.508066554 |
| ENSG00000153774 | CFDP1 subnetwork | 0.09021866 | 0.50848064 |
| GO:0031965 | nuclear membrane | 0.09029143 | 0.508876735 |
| ENSG00000067334 | DNTTIP2 subnetwork | 0.09091611 | 0.511680672 |
| ENSG00000077809 | GTF2I subnetwork | 0.09086495 | 0.511732548 |
| ENSG00000213246 | SUPT4H1 subnetwork | 0.09090026 | 0.511790668 |
| GO:0070482 | response to oxygen levels | 0.09110099 | 0.512258606 |
| ENSG00000130175 | PRKCSH subnetwork | 0.09121688 | 0.512285115 |

| | | | |
|---|---|---|---|
| ENSG00000177889 | UBE2N subnetwork | 0.09113644 | 0.512316408 |
| ENSG00000169398 | PTK2 subnetwork | 0.09109155 | 0.512431751 |
| ENSG00000196277 | GRM7 subnetwork | 0.09119865 | 0.512458054 |
| MP:0001824 | abnormal thymus involution | 0.09155645 | 0.514312657 |
| ENSG00000004700 | RECQL subnetwork | 0.09180154 | 0.515347571 |
| ENSG00000166200 | COPS2 subnetwork | 0.09180056 | 0.515542522 |
| ENSG00000164111 | ANXA5 subnetwork | 0.09188401 | 0.515780661 |
| ENSG00000092470 | WDR76 subnetwork | 0.09196945 | 0.516087866 |
| ENSG00000010278 | CD9 subnetwork | 0.09201912 | 0.51622752 |
| ENSG00000169756 | LIMS1 subnetwork | 0.09211714 | 0.516346154 |
| ENSG00000100206 | DMC1 subnetwork | 0.09233092 | 0.517467614 |
| GO:0004713 | protein tyrosine kinase activity | 0.09251651 | 0.518400167 |
| MP:0000890 | thin cerebellar molecular layer | 0.09255735 | 0.518413361 |
| ENSG00000198216 | CACNA1E subnetwork | 0.09269954 | 0.519198664 |
| GO:0032312 | regulation of ARF GTPase activity | 0.09286544 | 0.520254485 |
| REACTOME_TERMINATION_OF | REACTOME_TERMINATION_OF_O:GLYCAN_BIOSYNTHESIS | 0.09294618 | 0.520391993 |
| KEGG_VALINE_LEUCINE_AND_ | KEGG_VALINE_LEUCINE_AND_ISOLEUCINE_DEGRADATION | 0.09313405 | 0.520545379 |
| ENSG00000197081 | IGF2R subnetwork | 0.09301966 | 0.520654439 |
| ENSG00000120087 | HOXB7 subnetwork | 0.09311634 | 0.520699708 |
| MP:0001190 | reddish skin | 0.09310315 | 0.520854167 |
| ENSG00000117984 | CTSD subnetwork | 0.09327275 | 0.521348315 |
| ENSG00000008405 | CRY1 subnetwork | 0.09332272 | 0.52140183 |
| MP:0005566 | decreased blood urea nitrogen level | 0.09358417 | 0.522765073 |
| GO:0051879 | Hsp90 protein binding | 0.09362732 | 0.522880299 |
| ENSG00000075884 | ARHGAP15 subnetwork | 0.09370633 | 0.522902824 |
| ENSG00000017427 | IGF1 subnetwork | 0.09368122 | 0.522912339 |
| ENSG00000133794 | ARNTL subnetwork | 0.09376462 | 0.523059361 |
| GO:0044439 | peroxisomal part | 0.09383427 | 0.52330983 |
| GO:0072329 | monocarboxylic acid catabolic process | 0.09387213 | 0.523320896 |
| ENSG00000165912 | PACSIN3 subnetwork | 0.09391887 | 0.523331952 |
| GO:0042359 | vitamin D metabolic process | 0.09402162 | 0.523436853 |
| GO:0044438 | microbody part | 0.09383427 | 0.523526971 |
| GO:0030983 | mismatched DNA binding | 0.09400408 | 0.523612262 |
| GO:0046635 | positive regulation of alpha-beta T cell activation | 0.09413973 | 0.523861755 |
| ENSG00000102054 | RBBP7 subnetwork | 0.09421983 | 0.524141498 |
| ENSG00000167721 | TSR1 subnetwork | 0.0943385 | 0.524545079 |
| KEGG_PATHOGENIC_ESCHERIC | KEGG_PATHOGENIC_ESCHERICHIA_COLI_INFECTION | 0.09442725 | 0.524948326 |
| MP:0002060 | abnormal skin morphology | 0.09465714 | 0.525815779 |
| REACTOME_HIV_INFECTION | REACTOME_HIV_INFECTION | 0.09465508 | 0.526033058 |
| ENSG00000134480 | CCNH subnetwork | 0.09472308 | 0.526114781 |
| GO:0016571 | histone methylation | 0.09518099 | 0.528403465 |
| GO:0017124 | SH3 domain binding | 0.09520761 | 0.528453608 |
| GO:0004622 | lysophospholipase activity | 0.09517846 | 0.528600908 |
| GO:0002920 | regulation of humoral immune response | 0.09528939 | 0.528751031 |
| GO:0050709 | negative regulation of protein secretion | 0.09530993 | 0.528800989 |
| MP:0002575 | increased circulating ketone body level | 0.09557211 | 0.530313015 |
| MP:0004404 | cochlear outer hair cell degeneration | 0.09565196 | 0.530390947 |
| GO:0000781 | chromosome, telomeric region | 0.0956404 | 0.530568135 |
| GO:0000242 | pericentriolar material | 0.09583951 | 0.531283422 |
| ENSG00000140319 | SRP14 subnetwork | 0.09606034 | 0.531350021 |
| GO:0001741 | XY body | 0.09609593 | 0.531378179 |
| ENSG00000090060 | PAPOLA subnetwork | 0.0960033 | 0.531437372 |
| ENSG00000126602 | TRAP1 subnetwork | 0.09603995 | 0.531444992 |

| | | | |
|---|---|---|---|
| REACTOME_BRANCHED:CHAIN | REACTOME_BRANCHED:CHAIN_AMINO_ACID_CATABOLISM | 0.09597132 | 0.531491372 |
| ENSG00000172893 | DHCR7 subnetwork | 0.09594839 | 0.531586519 |
| MP:0010264 | increased hepatoma incidence | 0.09593936 | 0.53176398 |
| GO:0090317 | negative regulation of intracellular protein transport | 0.096271 | 0.532123821 |
| MP:0003451 | absent olfactory bulb | 0.09633521 | 0.532213115 |
| MP:0008539 | decreased susceptibility to induced colitis | 0.09648283 | 0.53269152 |
| ENSG00000165704 | HPRT1 subnetwork | 0.09657619 | 0.532964783 |
| ENSG00000132646 | PCNA subnetwork | 0.09695969 | 0.534916087 |
| MP:0004805 | absent oocytes | 0.09708562 | 0.535071575 |
| GO:0042991 | transcription factor import into nucleus | 0.09706123 | 0.5351473 |
| GO:0005912 | adherens junction | 0.09731198 | 0.535504287 |
| GO:0006305 | DNA alkylation | 0.09729532 | 0.535661765 |
| GO:0006266 | DNA ligation | 0.09723594 | 0.535752249 |
| GO:0006306 | DNA methylation | 0.09729532 | 0.53588067 |
| GO:0033081 | regulation of T cell differentiation in thymus | 0.09744353 | 0.536020408 |
| GO:0032041 | NAD-dependent histone deacetylase activity (H3-K14 specif | 0.09762383 | 0.53610998 |
| GO:0009081 | branched chain family amino acid metabolic process | 0.09765425 | 0.536217427 |
| GO:0046970 | NAD-dependent histone deacetylase activity (H4-K16 specif | 0.09762383 | 0.536328443 |
| MP:0004978 | decreased B-1 B cell number | 0.09754365 | 0.536515708 |
| GO:0031078 | histone deacetylase activity (H3-K14 specific) | 0.09762383 | 0.536547085 |
| GO:0034739 | histone deacetylase activity (H4-K16 specific) | 0.09762383 | 0.536765905 |
| ENSG00000213281 | NRAS subnetwork | 0.09798573 | 0.53751525 |
| GO:0071826 | ribonucleoprotein complex subunit organization | 0.09798181 | 0.537713588 |
| ENSG00000113758 | DBN1 subnetwork | 0.09794207 | 0.537769638 |
| ENSG00000164605 | ENSG00000164605 subnetwork | 0.09811746 | 0.53800813 |
| ENSG00000171105 | INSR subnetwork | 0.09819666 | 0.538419342 |
| ENSG00000151846 | PABPC3 subnetwork | 0.09843208 | 0.53954527 |
| ENSG00000142039 | CCDC97 subnetwork | 0.09848989 | 0.539650974 |
| MP:0003203 | increased neuron apoptosis | 0.09840719 | 0.539662876 |
| ENSG00000167971 | CASKIN1 subnetwork | 0.09863746 | 0.540365112 |
| ENSG00000100079 | LGALS2 subnetwork | 0.09879353 | 0.541038118 |
| ENSG00000163956 | LRPAP1 subnetwork | 0.09905896 | 0.542359141 |
| MP:0002223 | lymphoid hypoplasia | 0.09910198 | 0.542443274 |
| ENSG00000066926 | FECH subnetwork | 0.09919896 | 0.542689348 |
| GO:0051169 | nuclear transport | 0.09931905 | 0.542938082 |
| MP:0000334 | decreased granulocyte number | 0.09930484 | 0.543117409 |
| ENSG00000072195 | SPEG subnetwork | 0.09948647 | 0.543270008 |
| ENSG00000165943 | MOAP1 subnetwork | 0.09946489 | 0.543327942 |
| ENSG00000133657 | ATP13A3 subnetwork | 0.09940804 | 0.543365696 |
| ENSG00000174547 | MRPL11 subnetwork | 0.09957887 | 0.543555556 |
| ENSG00000132382 | MYBBP1A subnetwork | 0.09966873 | 0.543820679 |
| ENSG00000168118 | RAB4A subnetwork | 0.09974073 | 0.543964473 |
| GO:0050792 | regulation of viral reproduction | 0.09984237 | 0.544249395 |
| MP:0003077 | abnormal cell cycle | 0.10010359 | 0.545663574 |
| GO:0016573 | histone acetylation | 0.10024987 | 0.546350806 |
| ENSG00000196782 | MAML3 subnetwork | 0.10034911 | 0.546434327 |
| ENSG00000102753 | KPNA3 subnetwork | 0.10033288 | 0.546513503 |
| MP:0002419 | abnormal innate immunity | 0.10040072 | 0.546536448 |
| MP:0004532 | abnormal inner hair cell stereociliary bundle morphology | 0.10060479 | 0.547162978 |
| MP:0005605 | increased bone mass | 0.10059024 | 0.547242351 |
| GO:0016604 | nuclear body | 0.10084362 | 0.54800965 |
| ENSG00000105953 | OGDH subnetwork | 0.10084112 | 0.548230088 |
| MP:0001541 | abnormal osteoclast physiology | 0.10117967 | 0.549678457 |

| | | | |
|---|---|---|---|
| ENSG00000148408 | CACNA1B subnetwork | 0.10143727 | 0.550481734 |
| ENSG00000143851 | PTPN7 subnetwork | 0.10133966 | 0.550542387 |
| ENSG00000143155 | TIPRL subnetwork | 0.10152816 | 0.55062199 |
| KEGG_GLYCEROLIPID_METABC | KEGG_GLYCEROLIPID_METABOLISM | 0.10141317 | 0.55064257 |
| GO:0042503 | tyrosine phosphorylation of Stat3 protein | 0.10157144 | 0.550681909 |
| GO:0021591 | ventricular system development | 0.10168579 | 0.551182839 |
| ENSG00000100354 | TNRC6B subnetwork | 0.10172554 | 0.551302605 |
| ENSG00000126457 | PRMT1 subnetwork | 0.10187844 | 0.552103365 |
| GO:0032784 | regulation of transcription elongation, DNA-dependent | 0.10193942 | 0.552202643 |
| ENSG00000173465 | SSSCA1 subnetwork | 0.10198811 | 0.552281825 |
| REACTOME_EICOSANOID_LIGA | REACTOME_EICOSANOID_LIGAND:BINDING_RECEPTORS | 0.10236619 | 0.553154952 |
| MP:0005097 | polychromatophilia | 0.1021801 | 0.553161265 |
| ENSG00000058729 | RIOK2 subnetwork | 0.10233033 | 0.553236117 |
| GO:0043433 | negative regulation of sequence-specific DNA binding trans | 0.10229103 | 0.55333733 |
| ENSG00000204628 | GNB2L1 subnetwork | 0.10224015 | 0.55336 |
| GO:0043507 | positive regulation of JUN kinase activity | 0.10228703 | 0.553518593 |
| ENSG00000183337 | BCOR subnetwork | 0.10272439 | 0.55430622 |
| ENSG00000115145 | STAM2 subnetwork | 0.10257422 | 0.554331337 |
| MP:0008722 | abnormal chemokine secretion | 0.10271869 | 0.554527323 |
| ENSG00000110768 | GTF2H1 subnetwork | 0.10267254 | 0.554569034 |
| ENSG00000113522 | RAD50 subnetwork | 0.10313597 | 0.555069583 |
| KEGG_PHOSPHATIDYLINOSITO | KEGG_PHOSPHATIDYLINOSITOL_SIGNALING_SYSTEM | 0.10312271 | 0.555290374 |
| KEGG_ERBB_SIGNALING_PATH | KEGG_ERBB_SIGNALING_PATHWAY | 0.10311796 | 0.555491444 |
| ENSG00000162736 | NCSTN subnetwork | 0.10307833 | 0.555493631 |
| ENSG00000081377 | CDC14B subnetwork | 0.10303779 | 0.555535643 |
| ENSG00000117091 | CD48 subnetwork | 0.10300581 | 0.55563745 |
| ENSG00000140264 | SERF2 subnetwork | 0.10298455 | 0.55571941 |
| MP:0005596 | increased susceptibility to type I hypersensitivity reaction | 0.10342281 | 0.556173085 |
| GO:0030140 | trans-Golgi network transport vesicle | 0.10356932 | 0.556185567 |
| ENSG00000211460 | TSN subnetwork | 0.10353899 | 0.556267354 |
| ENSG00000176974 | SHMT1 subnetwork | 0.10341608 | 0.556374106 |
| REACTOME_TAT:MEDIATED_H | REACTOME_TAT:MEDIATED_HIV:1_ELONGATION_ARREST_ | 0.10340345 | 0.556475963 |
| GO:0007589 | body fluid secretion | 0.10353466 | 0.556488095 |
| REACTOME_PAUSING_AND_RE | REACTOME_PAUSING_AND_RECOVERY_OF_TAT:MEDIATEI | 0.10340345 | 0.556697138 |
| MP:0003149 | abnormal tectorial membrane morphology | 0.10378476 | 0.557230586 |
| ENSG00000065243 | PKN2 subnetwork | 0.10387707 | 0.557405941 |
| MP:0002972 | abnormal cardiac muscle contractility | 0.10376529 | 0.557431629 |
| GO:0033158 | regulation of protein import into nucleus, translocation | 0.10395205 | 0.557439652 |
| ENSG00000102001 | CACNA1F subnetwork | 0.1039456 | 0.557660333 |
| ENSG00000111615 | KRR1 subnetwork | 0.10426442 | 0.559018987 |
| KEGG_O_GLYCAN_BIOSYNTHES | KEGG_O_GLYCAN_BIOSYNTHESIS | 0.10457194 | 0.559033531 |
| GO:0032816 | positive regulation of natural killer cell activation | 0.10449263 | 0.559040663 |
| ENSG00000070159 | PTPN3 subnetwork | 0.10453978 | 0.559076559 |
| ENSG00000103653 | CSK subnetwork | 0.10449053 | 0.559261453 |
| ENSG00000104884 | ERCC2 subnetwork | 0.10448552 | 0.559482418 |
| KEGG_INSULIN_SIGNALING_PA | KEGG_INSULIN_SIGNALING_PATHWAY | 0.10440444 | 0.559489917 |
| ENSG00000105849 | TWISTNB subnetwork | 0.10445929 | 0.559525692 |
| ENSG00000078304 | PPP2R5C subnetwork | 0.10469979 | 0.559582019 |
| ENSG00000198719 | DLL1 subnetwork | 0.10482346 | 0.559712372 |
| ENSG00000122140 | MRPS2 subnetwork | 0.10481678 | 0.559913283 |
| MP:0006262 | testis tumor | 0.10504334 | 0.559968541 |
| GO:0070232 | regulation of T cell apoptotic process | 0.1050146 | 0.560011802 |
| ENSG00000136628 | EPRS subnetwork | 0.10492699 | 0.560019685 |

| | | | |
|---|---|---|---|
| MP:0000367 | abnormal coat/ hair morphology | 0.10491083 | 0.560200866 |
| ENSG00000109606 | DHX15 subnetwork | 0.10500561 | 0.560212515 |
| ENSG00000186446 | ZNF501 subnetwork | 0.10517632 | 0.560573899 |
| REACTOME_NF:KB_ACTIVATIO | REACTOME_NF:KB_ACTIVATION_THROUGH_FADDRIP:1_PA | 0.10543537 | 0.561567164 |
| ENSG00000148719 | DNAJB12 subnetwork | 0.10541603 | 0.561689587 |
| ENSG00000151929 | BAG3 subnetwork | 0.10555902 | 0.561896349 |
| MP:0008168 | decreased B-1a cell number | 0.10559673 | 0.561989796 |
| ENSG00000215902 | ENSG00000215902 subnetwork | 0.10574771 | 0.562691251 |
| MP:0001201 | translucent skin | 0.10598033 | 0.564117647 |
| ENSG00000090339 | ICAM1 subnetwork | 0.10630829 | 0.56586369 |
| REACTOME_CREB_PHOSPHOR | REACTOME_CREB_PHOSPHORYLATION_THROUGH_THE_AC | 0.1062891 | 0.566007053 |
| GO:0051496 | positive regulation of stress fiber assembly | 0.10628684 | 0.56622893 |
| MP:0000607 | abnormal hepatocyte morphology | 0.10638793 | 0.566229444 |
| GO:0009062 | fatty acid catabolic process | 0.10660952 | 0.567312207 |
| ENSG00000088247 | KHSRP subnetwork | 0.10660253 | 0.567514677 |
| MP:0000823 | abnormal lateral ventricle morphology | 0.10679584 | 0.567970278 |
| GO:0031968 | organelle outer membrane | 0.1069429 | 0.568666927 |
| GO:0018394 | peptidyl-lysine acetylation | 0.10704964 | 0.569030871 |
| GO:0019104 | DNA N-glycosylase activity | 0.10721775 | 0.569367435 |
| ENSG00000132475 | H3F3B subnetwork | 0.10739854 | 0.569368667 |
| ENSG00000121057 | AKAP1 subnetwork | 0.10716466 | 0.569394531 |
| ENSG00000163041 | H3F3A subnetwork | 0.10739854 | 0.569590643 |
| ENSG00000196285 | ENSG00000196285 subnetwork | 0.10739854 | 0.569812793 |
| ENSG00000105443 | CYTH2 subnetwork | 0.10732857 | 0.569828259 |
| MP:0000930 | wavy neural tube | 0.10738925 | 0.569996098 |
| GO:0018393 | internal peptidyl-lysine acetylation | 0.10765284 | 0.570802493 |
| ENSG00000136436 | CALCOCO2 subnetwork | 0.10782106 | 0.571397975 |
| ENSG00000136448 | NMT1 subnetwork | 0.10789698 | 0.571701051 |
| ENSG00000147099 | HDAC8 subnetwork | 0.10794749 | 0.571964981 |
| GO:0046930 | pore complex | 0.10806626 | 0.572500972 |
| ENSG00000162734 | PEA15 subnetwork | 0.10817793 | 0.572881026 |
| ENSG00000173894 | CBX2 subnetwork | 0.10833694 | 0.573493976 |
| GO:0060603 | mammary gland duct morphogenesis | 0.10865042 | 0.5747669 |
| KEGG_CELL_ADHESION_MOLE | KEGG_CELL_ADHESION_MOLECULES_CAMS | 0.10892087 | 0.576174757 |
| GO:0046578 | regulation of Ras protein signal transduction | 0.10896905 | 0.576242236 |
| ENSG00000076043 | REXO2 subnetwork | 0.10906262 | 0.576338247 |
| GO:0042516 | regulation of tyrosine phosphorylation of Stat3 protein | 0.10904048 | 0.576503686 |
| ENSG00000173418 | NAA20 subnetwork | 0.10968768 | 0.57937185 |
| GO:0009896 | positive regulation of catabolic process | 0.11003824 | 0.579744878 |
| ENSG00000079432 | CIC subnetwork | 0.11013658 | 0.579760525 |
| REACTOME_PAUSING_AND_RE | REACTOME_PAUSING_AND_RECOVERY_OF_HIV:1_ELONGA | 0.10999601 | 0.579775715 |
| ENSG00000095794 | CREM subnetwork | 0.11019927 | 0.579826255 |
| GO:0031300 | intrinsic to organelle membrane | 0.11010474 | 0.579868624 |
| REACTOME_HIV:1_ELONGATIC | REACTOME_HIV:1_ELONGATION_ARREST_AND_RECOVERY | 0.10999601 | 0.58 |
| ENSG00000165288 | BRWD3 subnetwork | 0.11033383 | 0.580042422 |
| ENSG00000166986 | MARS subnetwork | 0.11031028 | 0.580073302 |
| ENSG00000072694 | FCGR2B subnetwork | 0.10983654 | 0.580077519 |
| REACTOME_ELONGATION_ARI | REACTOME_ELONGATION_ARREST_AND_RECOVERY | 0.10999601 | 0.580224458 |
| GO:0035173 | histone kinase activity | 0.11030827 | 0.580297183 |
| ENSG00000182093 | WRB subnetwork | 0.10992687 | 0.580337079 |
| ENSG00000129460 | NGDN subnetwork | 0.11042177 | 0.580339244 |
| ENSG00000151067 | CACNA1C subnetwork | 0.1099725 | 0.580422153 |
| REACTOME_PAUSING_AND_RE | REACTOME_PAUSING_AND_RECOVERY_OF_ELONGATION | 0.10999601 | 0.58044909 |

| | | | |
|---|---|---|---|
| ENSG00000140443 | IGF1R subnetwork | 0.11052286 | 0.580674374 |
| MP:0000223 | decreased monocyte cell number | 0.11054476 | 0.580701079 |
| ENSG00000183520 | UTP11L subnetwork | 0.1106844 | 0.581382364 |
| GO:0008022 | protein C-terminus binding | 0.11076791 | 0.581620477 |
| MP:0006380 | abnormal spermatid morphology | 0.11081591 | 0.581704502 |
| ENSG00000039123 | SKIV2L2 subnetwork | 0.11111149 | 0.583019231 |
| KEGG_VIRAL_MYOCARDITIS | KEGG_VIRAL_MYOCARDITIS | 0.11153673 | 0.585409458 |
| ENSG00000204490 | TNF subnetwork | 0.11195535 | 0.585914143 |
| ENSG00000137574 | TGS1 subnetwork | 0.1116736 | 0.586010761 |
| ENSG00000206328 | ENSG00000206328 subnetwork | 0.11195535 | 0.586138804 |
| ENSG00000142655 | PEX14 subnetwork | 0.11181307 | 0.586199616 |
| ENSG00000137285 | TUBB2B subnetwork | 0.11178131 | 0.586271121 |
| ENSG00000181467 | RAP2B subnetwork | 0.11174404 | 0.586304264 |
| MP:0002411 | decreased susceptibility to bacterial infection | 0.11191233 | 0.586320031 |
| ENSG00000206439 | TNF subnetwork | 0.11195535 | 0.586363636 |
| ENSG00000114315 | HES1 subnetwork | 0.1123008 | 0.587758621 |
| ENSG00000100324 | TAB1 subnetwork | 0.11286436 | 0.58970532 |
| ENSG00000006468 | ETV1 subnetwork | 0.11277195 | 0.589735733 |
| MP:0005222 | abnormal somite size | 0.11281635 | 0.589758806 |
| ENSG00000147649 | MTDH subnetwork | 0.11301242 | 0.590187452 |
| ENSG00000214122 | ENSG00000214122 subnetwork | 0.11308046 | 0.590458891 |
| ENSG00000143669 | LYST subnetwork | 0.11345641 | 0.591676212 |
| ENSG00000187109 | NAP1L1 subnetwork | 0.11344251 | 0.59184492 |
| GO:0050431 | transforming growth factor beta binding | 0.11341773 | 0.591899121 |
| ENSG00000204104 | TRAF3IP1 subnetwork | 0.11341622 | 0.592125382 |
| ENSG00000008838 | MED24 subnetwork | 0.11369005 | 0.592671756 |
| ENSG00000082146 | STRADB subnetwork | 0.11400133 | 0.592675038 |
| GO:0022409 | positive regulation of cell-cell adhesion | 0.11396724 | 0.592729349 |
| GO:0051170 | nuclear import | 0.11409234 | 0.592813688 |
| ENSG00000166908 | PIP4K2C subnetwork | 0.11406304 | 0.592848992 |
| ENSG00000066117 | SMARCD1 subnetwork | 0.11395475 | 0.592916984 |
| GO:0043574 | peroxisomal transport | 0.11390847 | 0.593121189 |
| GO:0016311 | dephosphorylation | 0.11395129 | 0.593142857 |
| ENSG00000137547 | MRPL15 subnetwork | 0.11389106 | 0.593252002 |
| ENSG00000109618 | SEPSECS subnetwork | 0.11384281 | 0.593399466 |
| GO:0044450 | microtubule organizing center part | 0.11387377 | 0.593401983 |
| MP:0004510 | myositis | 0.11425472 | 0.593405549 |
| GO:0006606 | protein import into nucleus | 0.1143776 | 0.594034954 |
| GO:0005635 | nuclear envelope | 0.1145731 | 0.594552012 |
| ENSG00000141141 | DDX52 subnetwork | 0.114532 | 0.594587923 |
| ENSG00000148082 | SHC3 subnetwork | 0.11468322 | 0.595047438 |
| GO:0071214 | cellular response to abiotic stimulus | 0.11505427 | 0.595138101 |
| MP:0008008 | early cellular replicative senescence | 0.11473495 | 0.595201062 |
| ENSG00000108774 | RAB5C subnetwork | 0.11482399 | 0.595278726 |
| ENSG00000070759 | TESK2 subnetwork | 0.11505134 | 0.595325511 |
| GO:0048145 | regulation of fibroblast proliferation | 0.11487849 | 0.595413192 |
| MP:0003427 | parakeratosis | 0.11494175 | 0.595509663 |
| ENSG00000044574 | HSPA5 subnetwork | 0.11505028 | 0.595550928 |
| ENSG00000175054 | ATR subnetwork | 0.11503855 | 0.595681818 |
| GO:0050715 | positive regulation of cytokine secretion | 0.11528407 | 0.595935728 |
| GO:0007129 | synapsis | 0.11526053 | 0.596028744 |
| ENSG00000163346 | PBXIP1 subnetwork | 0.11566475 | 0.597336607 |
| ENSG00000117450 | PRDX1 subnetwork | 0.11563215 | 0.597411187 |

| | | | |
|---|---|---|---|
| GO:0031641 | regulation of myelination | 0.11579043 | 0.597565119 |
| GO:0035850 | epithelial cell differentiation involved in kidney developmer | 0.11578383 | 0.597753021 |
| MP:0003135 | increased erythroid progenitor cell number | 0.11592281 | 0.598226415 |
| MP:0006400 | decreased molar number | 0.11613324 | 0.598868778 |
| ENSG00000134588 | USP26 subnetwork | 0.11611871 | 0.599000377 |
| ENSG00000152422 | XRCC4 subnetwork | 0.11620977 | 0.599076517 |
| ENSG00000165392 | WRN subnetwork | 0.11630383 | 0.599359457 |
| ENSG00000067048 | DDX3Y subnetwork | 0.1163997 | 0.599435241 |
| GO:0015278 | calcium-release channel activity | 0.11637609 | 0.599491525 |
| ENSG00000104852 | SNRNP70 subnetwork | 0.11657979 | 0.600451637 |
| MP:0008872 | abnormal physiological response to xenobiotic | 0.11674782 | 0.601071832 |
| MP:0006094 | increased fat cell size | 0.11681665 | 0.60112782 |
| ENSG00000092203 | TOX4 subnetwork | 0.11670656 | 0.601128668 |
| REACTOME_MICRORNA_MIRN | REACTOME_MICRORNA_MIRNA_BIOGENESIS | 0.11694122 | 0.601145325 |
| GO:0003684 | damaged DNA binding | 0.11685899 | 0.601164976 |
| GO:0042308 | negative regulation of protein import into nucleus | 0.11700808 | 0.601201201 |
| REACTOME_REGULATORY_RN/ | REACTOME_REGULATORY_RNA_PATHWAYS | 0.11694122 | 0.60137115 |
| ENSG00000132002 | DNAJB1 subnetwork | 0.11728916 | 0.602532833 |
| ENSG00000112658 | SRF subnetwork | 0.1173705 | 0.602831958 |
| ENSG00000064703 | DDX20 subnetwork | 0.1175751 | 0.603259648 |
| MP:0000440 | domed cranium | 0.11762947 | 0.60340824 |
| MP:0004984 | increased osteoclast cell number | 0.11757155 | 0.603429535 |
| GO:0032469 | endoplasmic reticulum calcium ion homeostasis | 0.11756692 | 0.603637045 |
| ENSG00000114127 | XRN1 subnetwork | 0.11783622 | 0.604361662 |
| ENSG00000106211 | HSPB1 subnetwork | 0.11792099 | 0.604545455 |
| REACTOME_ACTIVATION_OF_I | REACTOME_ACTIVATION_OF_RAC | 0.11789545 | 0.604603293 |
| ENSG00000110880 | CORO1C subnetwork | 0.11804254 | 0.605011219 |
| GO:0003682 | chromatin binding | 0.11812176 | 0.605102804 |
| ENSG00000110958 | PTGES3 subnetwork | 0.11818322 | 0.60519432 |
| MP:0001209 | spontaneous skin ulceration | 0.1182685 | 0.605397833 |
| ENSG00000134398 | ERN2 subnetwork | 0.1184973 | 0.605767077 |
| GO:0042116 | macrophage activation | 0.11848331 | 0.605993279 |
| ENSG00000173020 | ADRBK1 subnetwork | 0.11867207 | 0.606133482 |
| MP:0001199 | thin skin | 0.11866388 | 0.606266319 |
| ENSG00000166913 | YWHAB subnetwork | 0.11863543 | 0.606287313 |
| MP:0003091 | abnormal cell migration | 0.11889874 | 0.607283905 |
| ENSG00000186395 | KRT10 subnetwork | 0.11895719 | 0.607411546 |
| ENSG00000120533 | ENY2 subnetwork | 0.11889146 | 0.607472978 |
| GO:0045814 | negative regulation of gene expression, epigenetic | 0.11902967 | 0.607517678 |
| GO:0008536 | Ran GTPase binding | 0.11902266 | 0.607706627 |
| GO:0032147 | activation of protein kinase activity | 0.11921237 | 0.607971014 |
| ENSG00000140382 | HMG20A subnetwork | 0.11917511 | 0.607973978 |
| GO:0042327 | positive regulation of phosphorylation | 0.11911152 | 0.608035714 |
| ENSG00000107262 | BAG1 subnetwork | 0.11916608 | 0.608144292 |
| KEGG_RIG_I_LIKE_RECEPTOR_S | KEGG_RIG_I_LIKE_RECEPTOR_SIGNALING_PATHWAY | 0.11938657 | 0.608543834 |
| ENSG00000101333 | PLCB4 subnetwork | 0.11945052 | 0.608559228 |
| GO:0000956 | nuclear-transcribed mRNA catabolic process | 0.11971626 | 0.608654559 |
| ENSG00000101255 | TRIB3 subnetwork | 0.11977895 | 0.608725454 |
| ENSG00000135968 | GCC2 subnetwork | 0.11968448 | 0.608769003 |
| GO:0008171 | O-methyltransferase activity | 0.11957765 | 0.608908686 |
| MP:0005153 | abnormal B cell proliferation | 0.11966317 | 0.608920623 |
| KEGG_TYROSINE_METABOLISM | KEGG_TYROSINE_METABOLISM | 0.11986206 | 0.608962963 |
| KEGG_PATHWAYS_IN_CANCER | KEGG_PATHWAYS_IN_CANCER | 0.1196485 | 0.609053803 |

| | | | |
|---|---|---|---|
| ENSG00000121653 | MAPK8IP1 subnetwork | 0.1199907 | 0.609311366 |
| ENSG00000074181 | NOTCH3 subnetwork | 0.12032457 | 0.609608278 |
| GO:0001510 | RNA methylation | 0.12014604 | 0.609715026 |
| REACTOME_MTORC1:MEDIATE | REACTOME_MTORC1:MEDIATED_SIGNALLING | 0.12031177 | 0.609778189 |
| MP:0001939 | secondary sex reversal | 0.12022457 | 0.609859415 |
| REACTOME_ACTIVATION_OF_T | REACTOME_ACTIVATION_OF_THE_AP:1_FAMILY_OF_TRAN | 0.12030955 | 0.610003698 |
| MP:0002429 | abnormal blood cell morphology/development | 0.12051497 | 0.610491319 |
| ENSG00000130726 | TRIM28 subnetwork | 0.12060451 | 0.610801329 |
| ENSG00000101266 | CSNK2A1 subnetwork | 0.12067605 | 0.611184939 |
| ENSG00000042088 | TDP1 subnetwork | 0.12079213 | 0.611398008 |
| GO:0042362 | fat-soluble vitamin biosynthetic process | 0.12075488 | 0.611402214 |
| MP:0005152 | pancytopenia | 0.12083414 | 0.611412242 |
| GO:0005813 | centrosome | 0.1211206 | 0.612265193 |
| ENSG00000157456 | CCNB2 subnetwork | 0.12101197 | 0.612274235 |
| ENSG00000130939 | UBE4B subnetwork | 0.12110638 | 0.612453943 |
| MP:0001239 | abnormal epidermis stratum granulosum morphology | 0.12126548 | 0.612849779 |
| ENSG00000133997 | MED6 subnetwork | 0.12166842 | 0.613988971 |
| GO:0030225 | macrophage differentiation | 0.12164614 | 0.614122839 |
| MP:0005419 | hypoalbuminemia | 0.12160647 | 0.614183223 |
| GO:0033157 | regulation of intracellular protein transport | 0.1215747 | 0.614262054 |
| ENSG00000177302 | TOP3A subnetwork | 0.12181537 | 0.6146086 |
| ENSG00000085999 | RAD54L subnetwork | 0.12191669 | 0.614823659 |
| ENSG00000151498 | ACAD8 subnetwork | 0.12239129 | 0.616263293 |
| ENSG00000089289 | IGBP1 subnetwork | 0.12236567 | 0.616342627 |
| ENSG00000140612 | SEC11A subnetwork | 0.12225657 | 0.616415718 |
| ENSG00000160282 | FTCD subnetwork | 0.12230918 | 0.616519824 |
| ENSG00000142539 | SPIB subnetwork | 0.12235699 | 0.616568807 |
| GO:0005057 | receptor signaling protein activity | 0.12257104 | 0.617302053 |
| ENSG00000111300 | NAA25 subnetwork | 0.12265849 | 0.617643826 |
| MP:0001943 | abnormal respiration | 0.12279482 | 0.618131868 |
| GO:0045087 | innate immune response | 0.12291449 | 0.618637862 |
| ENSG00000142611 | PRDM16 subnetwork | 0.12317475 | 0.619374314 |
| ENSG00000115541 | HSPE1 subnetwork | 0.12324549 | 0.619495245 |
| MP:0004509 | abnormal pelvic girdle bone morphology | 0.12316038 | 0.619582723 |
| ENSG00000153391 | INO80C subnetwork | 0.12337988 | 0.619780622 |
| ENSG00000134440 | NARS subnetwork | 0.1237723 | 0.621600877 |
| GO:0050434 | positive regulation of viral transcription | 0.12392317 | 0.622122762 |
| ENSG00000198211 | TUBB3 subnetwork | 0.12405215 | 0.62257122 |
| ENSG00000102030 | NAA10 subnetwork | 0.12430623 | 0.623448905 |
| ENSG00000113048 | MRPS27 subnetwork | 0.12428884 | 0.623658269 |
| ENSG00000170315 | UBB subnetwork | 0.12450356 | 0.624352426 |
| GO:0045620 | negative regulation of lymphocyte differentiation | 0.12462021 | 0.624690007 |
| REACTOME_PRESYNAPTIC_NIC | REACTOME_PRESYNAPTIC_NICOTINIC_ACETYLCHOLINE_RE | 0.12469935 | 0.624936201 |
| ENSG00000116741 | RGS2 subnetwork | 0.12485297 | 0.625437318 |
| ENSG00000147443 | DOK2 subnetwork | 0.1249232 | 0.625555556 |
| MP:0002773 | decreased circulating luteinizing hormone level | 0.12503638 | 0.626019665 |
| ENSG00000163939 | PBRM1 subnetwork | 0.12528749 | 0.626454545 |
| ENSG00000119953 | SMNDC1 subnetwork | 0.12517861 | 0.626556243 |
| GO:0018105 | peptidyl-serine phosphorylation | 0.1252704 | 0.626573299 |
| ENSG00000073282 | TP63 subnetwork | 0.12524125 | 0.62669214 |
| GO:0043409 | negative regulation of MAPK cascade | 0.12538464 | 0.626753908 |
| ENSG00000120333 | MRPS14 subnetwork | 0.12554691 | 0.626870007 |
| GO:0032386 | regulation of intracellular transport | 0.12545781 | 0.626944041 |

| | | | |
|---|---|---|---|
| ENSG00000075089 | ACTR6 subnetwork | 0.12552109 | 0.626970578 |
| MP:0008014 | increased lung tumor incidence | 0.12585064 | 0.628239564 |
| ENSG00000178105 | DDX10 subnetwork | 0.12598893 | 0.62854552 |
| ENSG00000081189 | MEF2C subnetwork | 0.12595485 | 0.628664731 |
| ENSG00000086189 | DIMT1 subnetwork | 0.12621698 | 0.629622915 |
| GO:0022618 | ribonucleoprotein complex assembly | 0.12638957 | 0.630300834 |
| GO:0033017 | sarcoplasmic reticulum membrane | 0.12654153 | 0.630887681 |
| MP:0010724 | thick interventricular septum | 0.12716328 | 0.632935647 |
| MP:0004207 | squamous cell carcinoma | 0.12714029 | 0.633056058 |
| GO:0010743 | regulation of macrophage derived foam cell differentiation | 0.12697267 | 0.633085838 |
| MP:0004810 | decreased hematopoietic stem cell number | 0.12700834 | 0.633091962 |
| MP:0005601 | increased angiogenesis | 0.12708972 | 0.633279045 |
| GO:0031329 | regulation of cellular catabolic process | 0.12713803 | 0.633285094 |
| GO:0035303 | regulation of dephosphorylation | 0.1273053 | 0.633447777 |
| GO:0006281 | DNA repair | 0.12738001 | 0.633760838 |
| GO:0072202 | cell differentiation involved in metanephros development | 0.12751091 | 0.634163958 |
| ENSG00000111145 | ELK3 subnetwork | 0.12837682 | 0.634949713 |
| GO:0070161 | anchoring junction | 0.12835853 | 0.635070068 |
| REACTOME_PKB:MEDIATED_E' | REACTOME_PKB:MEDIATED_EVENTS | 0.12844227 | 0.635098743 |
| ENSG00000114670 | NEK11 subnetwork | 0.12790053 | 0.635106383 |
| GO:0018205 | peptidyl-lysine modification | 0.12795587 | 0.635129776 |
| MP:0009395 | increased nucleated erythrocyte cell number | 0.12805596 | 0.635176513 |
| MP:0011320 | abnormal glomerular capillary morphology | 0.12835327 | 0.635280374 |
| GO:0045822 | negative regulation of heart contraction | 0.12803724 | 0.635333333 |
| MP:0006138 | congestive heart failure | 0.12789622 | 0.635335498 |
| ENSG00000140400 | MAN2C1 subnetwork | 0.12781125 | 0.635469314 |
| REACTOME_CAM_PATHWAY | REACTOME_CAM_PATHWAY | 0.12834564 | 0.635490831 |
| MP:0005617 | increased susceptibility to type IV hypersensitivity reaction | 0.12788086 | 0.635510646 |
| ENSG00000186193 | C9orf140 subnetwork | 0.12817901 | 0.635523947 |
| ENSG00000156374 | PCGF6 subnetwork | 0.12824235 | 0.63561915 |
| ENSG00000215328 | HSPA1A subnetwork | 0.12830938 | 0.635660309 |
| ENSG00000205918 | ENSG00000205918 subnetwork | 0.12861643 | 0.635696339 |
| REACTOME_CALMODULIN_IND | REACTOME_CALMODULIN_INDUCED_EVENTS | 0.12834564 | 0.635719424 |
| MP:0000613 | abnormal salivary gland morphology | 0.12885748 | 0.636921421 |
| ENSG00000015285 | WAS subnetwork | 0.12892885 | 0.637087518 |
| ENSG00000006715 | VPS41 subnetwork | 0.12914143 | 0.637123926 |
| GO:0033549 | MAP kinase phosphatase activity | 0.12899571 | 0.637199713 |
| GO:0032543 | mitochondrial translation | 0.12913931 | 0.637334289 |
| GO:0042605 | peptide antigen binding | 0.12909895 | 0.637365591 |
| MP:0002027 | lung adenocarcinoma | 0.12932648 | 0.637898317 |
| GO:0048771 | tissue remodeling | 0.12948911 | 0.638018598 |
| ENSG00000015475 | BID subnetwork | 0.12962993 | 0.638170122 |
| ENSG00000156735 | BAG4 subnetwork | 0.12958801 | 0.638237397 |
| GO:0045937 | positive regulation of phosphate metabolic process | 0.12948863 | 0.638246869 |
| ENSG00000082175 | PGR subnetwork | 0.12973634 | 0.638352983 |
| GO:0010562 | positive regulation of phosphorus metabolic process | 0.12948863 | 0.638475304 |
| ENSG00000138663 | COPS4 subnetwork | 0.12996207 | 0.638865096 |
| MP:0004616 | lumbar vertebral transformation | 0.13000178 | 0.638904745 |
| GO:0003730 | mRNA 3'-UTR binding | 0.12995148 | 0.639039629 |
| ENSG00000115020 | PIKFYVE subnetwork | 0.12994143 | 0.639196429 |
| ENSG00000124299 | PEPD subnetwork | 0.13022985 | 0.639621969 |
| GO:0007127 | meiosis I | 0.13041469 | 0.640374332 |
| ENSG00000108424 | KPNB1 subnetwork | 0.13046783 | 0.640555952 |

| | | | |
|---|---|---|---|
| GO:0042611 | MHC protein complex | 0.13060563 | 0.64086213 |
| ENSG00000125447 | GGA3 subnetwork | 0.13067712 | 0.641150285 |
| MP:0001127 | small ovary | 0.13101738 | 0.642239231 |
| ENSG00000007392 | LUC7L subnetwork | 0.13113056 | 0.642298115 |
| ENSG00000136111 | TBC1D4 subnetwork | 0.13112082 | 0.642455516 |
| ENSG00000184009 | ACTG1 subnetwork | 0.13132433 | 0.643154339 |
| ENSG00000154582 | TCEB1 subnetwork | 0.13143809 | 0.643319119 |
| MP:0000280 | thin ventricular wall | 0.13141723 | 0.643476715 |
| GO:0043022 | ribosome binding | 0.13158307 | 0.643696733 |
| ENSG00000153561 | RMND5A subnetwork | 0.13155686 | 0.643730018 |
| ENSG00000177426 | TGIF1 subnetwork | 0.13177234 | 0.644249201 |
| ENSG00000122025 | FLT3 subnetwork | 0.13186356 | 0.644446416 |
| MP:0000897 | abnormal midbrain morphology | 0.1319942 | 0.645051437 |
| ENSG00000108946 | PRKAR1A subnetwork | 0.13204357 | 0.645106383 |
| ENSG00000204580 | DDR1 subnetwork | 0.13225673 | 0.645414306 |
| MP:0008071 | absent B cells | 0.13214519 | 0.645462602 |
| ENSG00000122565 | CBX3 subnetwork | 0.13249477 | 0.6456345 |
| ENSG00000137332 | DDR1 subnetwork | 0.13225673 | 0.645642933 |
| GO:0035872 | nucleotide-binding domain, leucine rich repeat containing r | 0.13249008 | 0.64584512 |
| ENSG00000140379 | BCL2A1 subnetwork | 0.13236315 | 0.645858407 |
| ENSG00000215522 | DDR1 subnetwork | 0.13225673 | 0.645871722 |
| GO:0002753 | cytoplasmic pattern recognition receptor signaling pathway | 0.13249008 | 0.646073576 |
| GO:0070423 | nucleotide-binding oligomerization domain containing signa | 0.13249008 | 0.646302194 |
| ENSG00000136738 | STAM subnetwork | 0.13295306 | 0.64714084 |
| ENSG00000173876 | TUBB8 subnetwork | 0.13291686 | 0.647175141 |
| GO:0030742 | GTP-dependent protein binding | 0.13289273 | 0.647262451 |
| ENSG00000160293 | VAV2 subnetwork | 0.13286362 | 0.647420495 |
| GO:0046823 | negative regulation of nucleocytoplasmic transport | 0.13308764 | 0.647653493 |
| ENSG00000165140 | FBP1 subnetwork | 0.13312429 | 0.647689594 |
| ENSG00000141456 | ENSG00000141456 subnetwork | 0.13331672 | 0.648378569 |
| MP:0000291 | enlarged pericardium | 0.13330846 | 0.648554302 |
| ENSG00000198911 | SREBF2 subnetwork | 0.13364787 | 0.648944777 |
| KEGG_LYSINE_DEGRADATION | KEGG_LYSINE_DEGRADATION | 0.13349011 | 0.648978514 |
| ENSG00000162928 | PEX13 subnetwork | 0.13355384 | 0.648979233 |
| MP:0003402 | decreased liver weight | 0.13362243 | 0.649067558 |
| ENSG00000152484 | USP12 subnetwork | 0.13347033 | 0.64910148 |
| GO:0030155 | regulation of cell adhesion | 0.13353348 | 0.649119718 |
| MP:0000416 | sparse hair | 0.1339024 | 0.649560787 |
| GO:0005932 | microtubule basal body | 0.13380034 | 0.649630802 |
| ENSG00000105202 | FBL subnetwork | 0.13388496 | 0.649753954 |
| KEGG_MTOR_SIGNALING_PAT | KEGG_MTOR_SIGNALING_PATHWAY | 0.13402842 | 0.649929751 |
| ENSG00000138757 | G3BP2 subnetwork | 0.13409513 | 0.650140449 |
| ENSG00000172780 | RAB43 subnetwork | 0.13431031 | 0.65022791 |
| ENSG00000025434 | NR1H3 subnetwork | 0.13427232 | 0.650245528 |
| ENSG00000187790 | FANCM subnetwork | 0.13420244 | 0.65033345 |
| ENSG00000117000 | RLF subnetwork | 0.13426706 | 0.650438596 |
| ENSG00000143226 | FCGR2A subnetwork | 0.13440464 | 0.650718542 |
| GO:0016307 | phosphatidylinositol phosphate kinase activity | 0.13447633 | 0.650823406 |
| ENSG00000165782 | TMEM55B subnetwork | 0.13463193 | 0.651471103 |
| ENSG00000165699 | TSC1 subnetwork | 0.13480255 | 0.652188375 |
| ENSG00000002016 | RAD52 subnetwork | 0.1349593 | 0.652747637 |
| ENSG00000196924 | FLNA subnetwork | 0.13502617 | 0.653026592 |
| MP:0001711 | abnormal placenta morphology | 0.13511035 | 0.653515215 |

| | | | |
|---|---|---|---|
| GO:0050775 | positive regulation of dendrite morphogenesis | 0.135297 | 0.654353147 |
| ENSG00000023734 | STRAP subnetwork | 0.1356963 | 0.654532775 |
| ENSG00000173175 | ADCY5 subnetwork | 0.1356942 | 0.654726195 |
| MP:0002724 | enhanced wound healing | 0.13562468 | 0.65486911 |
| ENSG00000145192 | AHSG subnetwork | 0.13567701 | 0.654902303 |
| ENSG00000105610 | KLF1 subnetwork | 0.13558052 | 0.654923184 |
| ENSG00000128340 | RAC2 subnetwork | 0.13583753 | 0.65494946 |
| GO:0043202 | lysosomal lumen | 0.13590367 | 0.654982578 |
| ENSG00000130520 | LSM4 subnetwork | 0.13557447 | 0.655134474 |
| MP:0004029 | spontaneous chromosome breakage | 0.13548649 | 0.65515554 |
| ENSG00000184575 | XPOT subnetwork | 0.13555446 | 0.655293501 |
| ENSG00000120688 | WBP4 subnetwork | 0.13610812 | 0.65585162 |
| ENSG00000110700 | RPS13 subnetwork | 0.13634961 | 0.656963788 |
| REACTOME_REGULATION_OF_ | REACTOME_REGULATION_OF_MRNA_STABILITY_BY_PROTI | 0.13642989 | 0.657048381 |
| ENSG00000152944 | MED21 subnetwork | 0.13649815 | 0.6572373 |
| ENSG00000175792 | RUVBL1 subnetwork | 0.13685583 | 0.658339124 |
| GO:0009615 | response to virus | 0.13684008 | 0.658463677 |
| MP:0010373 | myeloid hyperplasia | 0.13682933 | 0.658605702 |
| ENSG00000187840 | EIF4EBP1 subnetwork | 0.13678807 | 0.658678261 |
| MP:0005416 | abnormal circulating protein level | 0.13718213 | 0.659621396 |
| ENSG00000099783 | HNRNPM subnetwork | 0.13758474 | 0.661107254 |
| ENSG00000135316 | SYNCRIP subnetwork | 0.13867634 | 0.661143645 |
| GO:0000303 | response to superoxide | 0.13843958 | 0.66115902 |
| ENSG00000105173 | CCNE1 subnetwork | 0.13752579 | 0.661163194 |
| ENSG00000111596 | CNOT2 subnetwork | 0.13866979 | 0.661354238 |
| GO:0000305 | response to oxygen radical | 0.13843958 | 0.661387164 |
| ENSG00000124145 | SDC4 subnetwork | 0.13841349 | 0.66149465 |
| GO:0045597 | positive regulation of cell differentiation | 0.13839118 | 0.661515884 |
| GO:0032483 | regulation of Rab protein signal transduction | 0.13830026 | 0.661523842 |
| ENSG00000157326 | DHRS4 subnetwork | 0.13866114 | 0.661547742 |
| ENSG00000177600 | RPLP2 subnetwork | 0.13837099 | 0.661588946 |
| GO:0016032 | viral reproduction | 0.13864025 | 0.661724138 |
| GO:0032313 | regulation of Rab GTPase activity | 0.13830026 | 0.661752506 |
| GO:0010824 | regulation of centrosome duplication | 0.13791984 | 0.661810614 |
| GO:0044130 | negative regulation of growth of symbiont in host | 0.13829157 | 0.661894882 |
| ENSG00000125733 | TRIP10 subnetwork | 0.13787694 | 0.661901457 |
| ENSG00000177485 | ZBTB33 subnetwork | 0.13802194 | 0.662118585 |
| GO:0044146 | negative regulation of growth of symbiont involved in inter | 0.13829157 | 0.662123833 |
| MP:0005065 | abnormal neutrophil morphology | 0.13894133 | 0.662276171 |
| GO:0044117 | growth of symbiont in host | 0.13829157 | 0.662352941 |
| GO:0044116 | growth of symbiont involved in interaction with host | 0.13829157 | 0.662582208 |
| ENSG00000197635 | DPP4 subnetwork | 0.13912309 | 0.662710698 |
| GO:0044144 | modulation of growth of symbiont involved in interaction w | 0.13829157 | 0.662811634 |
| GO:0002221 | pattern recognition receptor signaling pathway | 0.13923141 | 0.66287384 |
| ENSG00000181163 | NPM1 subnetwork | 0.1391223 | 0.662921542 |
| ENSG00000185989 | RASA3 subnetwork | 0.13907866 | 0.662943201 |
| GO:0044110 | growth involved in symbiotic interaction | 0.13829157 | 0.663041219 |
| MP:0008995 | early reproductive senescence | 0.13922842 | 0.663084594 |
| REACTOME_MTOR_SIGNALLIN | REACTOME_MTOR_SIGNALLING | 0.13823745 | 0.663206239 |
| GO:0044126 | regulation of growth of symbiont in host | 0.13829157 | 0.663270963 |
| MP:0002774 | small prostate gland | 0.13948705 | 0.66356456 |
| ENSG00000204120 | GIGYF2 subnetwork | 0.13941448 | 0.66362543 |
| ENSG00000132471 | WBP2 subnetwork | 0.13947525 | 0.663758159 |

| | | | |
|---|---|---|---|
| ENSG00000113013 | HSPA9 subnetwork | 0.13961494 | 0.66412633 |
| ENSG00000186153 | WWOX subnetwork | 0.1398555 | 0.664449777 |
| GO:0048144 | fibroblast proliferation | 0.13985419 | 0.664660494 |
| ENSG00000162869 | PPP1R21 subnetwork | 0.1398435 | 0.664871355 |
| ENSG00000121274 | PAPD5 subnetwork | 0.14002049 | 0.665061686 |
| MP:0000822 | abnormal brain ventricle morphology | 0.1398318 | 0.66509952 |
| GO:0032352 | positive regulation of hormone metabolic process | 0.14097003 | 0.666201022 |
| ENSG00000121671 | CRY2 subnetwork | 0.1409405 | 0.666257669 |
| ENSG00000112357 | PEX7 subnetwork | 0.14092413 | 0.666399591 |
| ENSG00000139722 | VPS37B subnetwork | 0.14111263 | 0.66649081 |
| ENSG00000137259 | HIST1H2AB subnetwork | 0.140901 | 0.666524557 |
| REACTOME_INTRINSIC_PATHW | REACTOME_INTRINSIC_PATHWAY_FOR_APOPTOSIS | 0.14107462 | 0.666530473 |
| ENSG00000158186 | MRAS subnetwork | 0.14105567 | 0.666723433 |
| GO:0051897 | positive regulation of protein kinase B signaling cascade | 0.14035407 | 0.666729452 |
| ENSG00000168274 | HIST1H2AE subnetwork | 0.140901 | 0.666751962 |
| GO:0046627 | negative regulation of insulin receptor signaling pathway | 0.1403177 | 0.666820829 |
| GO:0030852 | regulation of granulocyte differentiation | 0.14123893 | 0.666859476 |
| ENSG00000101331 | C20orf160 subnetwork | 0.140859 | 0.666877133 |
| GO:0032103 | positive regulation of response to external stimulus | 0.14049167 | 0.66692334 |
| ENSG00000185214 | ENSG00000185214 subnetwork | 0.14082196 | 0.666951178 |
| ENSG00000183207 | RUVBL2 subnetwork | 0.14048023 | 0.667117426 |
| ENSG00000165416 | SUGT1 subnetwork | 0.14081103 | 0.667144809 |
| ENSG00000132109 | TRIM21 subnetwork | 0.14065042 | 0.667162393 |
| MP:0005440 | increased glycogen level | 0.14062872 | 0.667270862 |
| GO:0031098 | stress-activated protein kinase signaling cascade | 0.14081065 | 0.667372737 |
| GO:0045787 | positive regulation of cell cycle | 0.14146846 | 0.667392044 |
| MP:0006011 | abnormal endolymphatic duct morphology | 0.14059748 | 0.667413616 |
| GO:0046626 | regulation of insulin receptor signaling pathway | 0.14142821 | 0.667465986 |
| GO:0042645 | mitochondrial nucleoid | 0.14079242 | 0.667515379 |
| ENSG00000115325 | DOK1 subnetwork | 0.14214948 | 0.668214165 |
| GO:0030041 | actin filament polymerization | 0.14211867 | 0.668237288 |
| ENSG00000162909 | CAPN2 subnetwork | 0.14185087 | 0.668416582 |
| REACTOME_DARPP:32_EVENT | REACTOME_DARPP:32_EVENTS | 0.14211545 | 0.668463886 |
| GO:0070192 | chromosome organization involved in meiosis | 0.14226873 | 0.668495935 |
| ENSG00000115548 | KDM3A subnetwork | 0.1419245 | 0.668529212 |
| MP:0002421 | abnormal cell-mediated immunity | 0.14208861 | 0.668571913 |
| ENSG00000073711 | PPP2R3A subnetwork | 0.14184903 | 0.66864378 |
| ENSG00000086758 | HUWE1 subnetwork | 0.1424016 | 0.668703453 |
| ENSG00000167641 | PPP1R14A subnetwork | 0.14206441 | 0.668713946 |
| MP:0010792 | abnormal stomach mucosa morphology | 0.14204296 | 0.668771215 |
| ENSG00000137831 | UACA subnetwork | 0.14236044 | 0.668794446 |
| REACTOME_PURINE_RIBONUC | REACTOME_PURINE_RIBONUCLEOSIDE_MONOPHOSPHATE | 0.14202282 | 0.668811545 |
| REACTOME_VPU_MEDIATED_I | REACTOME_VPU_MEDIATED_DEGRADATION_OF_CD4 | 0.14296983 | 0.671404399 |
| GO:0035253 | ciliary rootlet | 0.14303297 | 0.671414073 |
| ENSG00000119698 | PPP4R4 subnetwork | 0.14308683 | 0.671508285 |
| ENSG00000135750 | KCNK1 subnetwork | 0.14313817 | 0.671585531 |
| MP:0001422 | abnormal drinking behavior | 0.14319488 | 0.671662724 |
| ENSG00000131652 | THOC6 subnetwork | 0.14344766 | 0.672089099 |
| MP:0009719 | reduced cerebellar foliation | 0.14333794 | 0.672104019 |
| MP:0002118 | abnormal lipid homeostasis | 0.14332934 | 0.672179054 |
| ENSG00000138814 | PPP3CA subnetwork | 0.14343503 | 0.672282242 |
| MP:0003909 | increased eating behavior | 0.14357786 | 0.672284076 |
| MP:0008410 | increased cellular sensitivity to ultraviolet irradiation | 0.14364821 | 0.672445194 |

| | | | |
|---|---|---|---|
| MP:0002643 | poikilocytosis | 0.14379774 | 0.672960216 |
| ENSG00000124207 | CSE1L subnetwork | 0.14407582 | 0.673913043 |
| ENSG00000114520 | SNX4 subnetwork | 0.14413098 | 0.674039757 |
| ENSG00000112578 | BYSL subnetwork | 0.14423211 | 0.674057239 |
| MP:0000914 | exencephaly | 0.14427133 | 0.674065971 |
| MP:0002074 | abnormal hair texture | 0.14421791 | 0.674233749 |
| ENSG00000087111 | PIGS subnetwork | 0.14440355 | 0.674327052 |
| ENSG00000029363 | BCLAF1 subnetwork | 0.14445919 | 0.674335688 |
| MP:0000187 | abnormal triglyceride level | 0.14463486 | 0.675117687 |
| MP:0002229 | neurodegeneration | 0.14482587 | 0.676 |
| ENSG00000076555 | ACACB subnetwork | 0.14522262 | 0.677527712 |
| GO:0005844 | polysome | 0.14519485 | 0.677570565 |
| MP:0002051 | skin papilloma | 0.14545992 | 0.678003356 |
| GO:0060056 | mammary gland involution | 0.14551043 | 0.678010735 |
| ENSG00000153487 | ING1 subnetwork | 0.14545972 | 0.67823095 |
| GO:0000030 | mannosyltransferase activity | 0.14544934 | 0.678408328 |
| ENSG00000095585 | BLNK subnetwork | 0.14580134 | 0.678609715 |
| MP:0001931 | abnormal oogenesis | 0.1457758 | 0.678803619 |
| ENSG00000020922 | MRE11A subnetwork | 0.14575305 | 0.678913845 |
| MP:0005408 | hypopigmentation | 0.1457343 | 0.679057679 |
| ENSG00000116604 | MEF2D subnetwork | 0.14609155 | 0.679140181 |
| REACTOME_METABOLISM_OF_ | REACTOME_METABOLISM_OF_RNA | 0.14601766 | 0.679276866 |
| MP:0001927 | abnormal estrous cycle | 0.14607099 | 0.679283802 |
| ENSG00000160049 | DFFA subnetwork | 0.14597769 | 0.679370395 |
| GO:0033151 | V(D)J recombination | 0.14634905 | 0.679806085 |
| GO:0002467 | germinal center formation | 0.14630351 | 0.679866221 |
| ENSG00000198836 | OPA1 subnetwork | 0.14653316 | 0.680464572 |
| ENSG00000173120 | KDM2A subnetwork | 0.14673382 | 0.680757677 |
| REACTOME_RIG:IMDA5_MEDI | REACTOME_RIG:IMDA5_MEDIATED_INDUCTION_OF_IFN:A | 0.14667456 | 0.680845023 |
| GO:0006111 | regulation of gluconeogenesis | 0.14665387 | 0.680922152 |
| ENSG00000166848 | TERF2IP subnetwork | 0.14673064 | 0.68096828 |
| ENSG00000008130 | NADK subnetwork | 0.146871 | 0.681154103 |
| MP:0008208 | decreased pro-B cell number | 0.14683439 | 0.681197865 |
| MP:0005220 | abnormal exocrine pancreas morphology | 0.14706622 | 0.682110704 |
| ENSG00000198802 | ENSG00000198802 subnetwork | 0.14710908 | 0.682116667 |
| ENSG00000110680 | CALCA subnetwork | 0.14742812 | 0.683738754 |
| ENSG00000125868 | DSTN subnetwork | 0.14764313 | 0.684576949 |
| MP:0003983 | decreased cholesterol level | 0.14801543 | 0.685412508 |
| GO:0002218 | activation of innate immune response | 0.14796452 | 0.685457571 |
| MP:0000662 | abnormal branching of the mammary ductal tree | 0.14795976 | 0.685652463 |
| ENSG00000141522 | ARHGDIA subnetwork | 0.14793882 | 0.685730936 |
| ENSG00000136937 | NCBP1 subnetwork | 0.14833794 | 0.685996678 |
| ENSG00000068976 | PYGM subnetwork | 0.14843528 | 0.686167386 |
| ENSG00000125912 | NCLN subnetwork | 0.14832479 | 0.686191426 |
| ENSG00000134318 | ROCK2 subnetwork | 0.1482436 | 0.686282009 |
| MP:0002654 | spongiform encephalopathy | 0.14831245 | 0.686369681 |
| ENSG00000170860 | LSM3 subnetwork | 0.1485751 | 0.686487384 |
| MP:0002962 | increased urine protein level | 0.14870902 | 0.6867076 |
| GO:0004623 | phospholipase A2 activity | 0.1487922 | 0.686828135 |
| MP:0009831 | abnormal sperm midpiece morphology | 0.14904436 | 0.687748674 |
| ENSG00000126458 | RRAS subnetwork | 0.1490104 | 0.687777778 |
| ENSG00000134215 | VAV3 subnetwork | 0.14917119 | 0.688133908 |
| ENSG00000164078 | MST1R subnetwork | 0.14933453 | 0.688783963 |

| | | | |
|---|---|---|---|
| ENSG00000172071 | EIF2AK3 subnetwork | 0.14939829 | 0.688837363 |
| MP:0001891 | hydroencephaly | 0.14952905 | 0.689139073 |
| ENSG00000148218 | ALAD subnetwork | 0.1497591 | 0.690052963 |
| GO:0001916 | positive regulation of T cell mediated cytotoxicity | 0.14984243 | 0.690205162 |
| MP:0000559 | abnormal femur morphology | 0.15016594 | 0.691548131 |
| ENSG00000112651 | MRPL2 subnetwork | 0.1503405 | 0.691639128 |
| ENSG00000170027 | YWHAG subnetwork | 0.15042835 | 0.691658408 |
| GO:0042803 | protein homodimerization activity | 0.15027256 | 0.691765873 |
| ENSG00000163960 | UBXN7 subnetwork | 0.15032479 | 0.691768595 |
| ENSG00000148672 | GLUD1 subnetwork | 0.15072739 | 0.692949141 |
| GO:0031490 | chromatin DNA binding | 0.1512755 | 0.69539452 |
| ENSG00000128016 | ZFP36 subnetwork | 0.15151878 | 0.696205873 |
| ENSG00000088826 | SMOX subnetwork | 0.15147728 | 0.69630363 |
| KEGG_CIRCADIAN_RHYTHM_M | KEGG_CIRCADIAN_RHYTHM_MAMMAL | 0.15161628 | 0.69633905 |
| ENSG00000170889 | RPS9 subnetwork | 0.15189864 | 0.697840422 |
| ENSG00000134453 | RBM17 subnetwork | 0.15197621 | 0.698071852 |
| ENSG00000153233 | PTPRR subnetwork | 0.15207265 | 0.698385502 |
| ENSG00000127445 | PIN1 subnetwork | 0.15212134 | 0.698402503 |
| MP:0002896 | abnormal bone mineralization | 0.1522577 | 0.698929865 |
| ENSG00000185619 | PCGF3 subnetwork | 0.15243267 | 0.699654378 |
| ENSG00000100726 | TELO2 subnetwork | 0.1527925 | 0.701250411 |
| KEGG_GLYCEROPHOSPHOLIPID | KEGG_GLYCEROPHOSPHOLIPID_METABOLISM | 0.1528672 | 0.701381579 |
| ENSG00000148053 | NTRK2 subnetwork | 0.15360702 | 0.704585799 |
| GO:0045197 | establishment or maintenance of epithelial cell apical/basal | 0.15366971 | 0.704650016 |
| KEGG_TGF_BETA_SIGNALING_ | KEGG_TGF_BETA_SIGNALING_PATHWAY | 0.15358302 | 0.704669517 |
| GO:0008633 | activation of pro-apoptotic gene products | 0.15411883 | 0.706650246 |
| MP:0000642 | enlarged adrenal glands | 0.15409176 | 0.706652431 |
| GO:0048185 | activin binding | 0.15433126 | 0.707518056 |
| MP:0002018 | malignant tumors | 0.15442106 | 0.707677165 |
| ENSG00000198324 | FAM109A subnetwork | 0.15440446 | 0.707712504 |
| GO:0051056 | regulation of small GTPase mediated signal transduction | 0.15449691 | 0.707756642 |
| ENSG00000101204 | CHRNA4 subnetwork | 0.15459652 | 0.707983607 |
| ENSG00000073578 | SDHA subnetwork | 0.15489378 | 0.708346972 |
| MP:0002467 | impaired neutrophil phagocytosis | 0.15516862 | 0.708379615 |
| ENSG00000083520 | DIS3 subnetwork | 0.15487382 | 0.708447937 |
| GO:0022415 | viral reproductive process | 0.15474343 | 0.708456244 |
| ENSG00000137947 | GTF2B subnetwork | 0.15480806 | 0.708551769 |
| ENSG00000111229 | ARPC3 subnetwork | 0.15516715 | 0.708611111 |
| GO:0006412 | translation | 0.15486979 | 0.708647232 |
| ENSG00000109670 | FBXW7 subnetwork | 0.15499045 | 0.708687827 |
| ENSG00000147382 | FAM58A subnetwork | 0.15504024 | 0.708717697 |
| ENSG00000011007 | TCEB3 subnetwork | 0.15515254 | 0.708842759 |
| MP:0005562 | decreased mean corpuscular hemoglobin | 0.15510547 | 0.708894702 |
| GO:0016558 | protein import into peroxisome matrix | 0.15536589 | 0.709177008 |
| ENSG00000149269 | PAK1 subnetwork | 0.15549489 | 0.709467842 |
| KEGG_PROTEASOME | KEGG_PROTEASOME | 0.15580636 | 0.711031332 |
| ENSG00000173486 | FKBP2 subnetwork | 0.15592187 | 0.711598695 |
| ENSG00000132394 | EEFSEC subnetwork | 0.15600362 | 0.711823222 |
| MP:0008973 | decreased erythroid progenitor cell number | 0.15607572 | 0.71183567 |
| ENSG00000116670 | MAD2L2 subnetwork | 0.15619891 | 0.711844249 |
| ENSG00000100567 | PSMA3 subnetwork | 0.15624407 | 0.711954397 |
| MP:0009347 | increased trabecular bone thickness | 0.15617617 | 0.711978488 |
| GO:0033365 | protein localization to organelle | 0.15644188 | 0.712239583 |

| | | | |
|---|---|---|---|
| REACTOME_DOWNSTREAM_SI | REACTOME_DOWNSTREAM_SIGNALING_OF_ACTIVATED_F | 0.15643243 | 0.712455226 |
| ENSG00000149948 | HMGA2 subnetwork | 0.15685991 | 0.713349593 |
| MP:0006082 | CNS inflammation | 0.15683442 | 0.713467794 |
| ENSG00000138764 | CCNG2 subnetwork | 0.15677696 | 0.713569801 |
| GO:0043506 | regulation of JUN kinase activity | 0.15709437 | 0.71400715 |
| ENSG00000111328 | CDK2AP1 subnetwork | 0.15707592 | 0.714141743 |
| ENSG00000112592 | TBP subnetwork | 0.15720616 | 0.714506173 |
| MP:0006043 | decreased apoptosis | 0.15737826 | 0.715264696 |
| ENSG00000137807 | KIF23 subnetwork | 0.15756059 | 0.715455725 |
| MP:0000417 | short hair | 0.15762949 | 0.71554799 |
| ENSG00000108443 | RPS6KB1 subnetwork | 0.15745587 | 0.715551948 |
| ENSG00000196730 | DAPK1 subnetwork | 0.15754948 | 0.715671642 |
| GO:0051119 | sugar transmembrane transporter activity | 0.15751034 | 0.715709185 |
| ENSG00000104695 | PPP2CB subnetwork | 0.15781703 | 0.71573234 |
| ENSG00000176102 | CSTF3 subnetwork | 0.15779987 | 0.715883306 |
| ENSG00000163635 | ATXN7 subnetwork | 0.15791428 | 0.715937804 |
| GO:0008013 | beta-catenin binding | 0.15798765 | 0.716110751 |
| GO:0002758 | innate immune response-activating signal transduction | 0.15809451 | 0.716380706 |
| ENSG00000189079 | ARID2 subnetwork | 0.15817779 | 0.716553398 |
| MP:0009133 | decreased white fat cell size | 0.15826949 | 0.716612747 |
| GO:0002039 | p53 binding | 0.15843843 | 0.716989977 |
| MP:0003103 | liver degeneration | 0.15843044 | 0.717173351 |
| ENSG00000164609 | SLU7 subnetwork | 0.15920939 | 0.719022265 |
| MP:0008808 | decreased spleen iron level | 0.15919364 | 0.719125242 |
| MP:0003037 | increased infarction size | 0.15938492 | 0.719148936 |
| ENSG00000182872 | RBM10 subnetwork | 0.15930978 | 0.719155111 |
| GO:0042347 | negative regulation of NF-kappaB import into nucleus | 0.15898133 | 0.719198449 |
| GO:0034968 | histone lysine methylation | 0.15927766 | 0.719209677 |
| GO:0033674 | positive regulation of kinase activity | 0.15917754 | 0.719260575 |
| ENSG00000213639 | PPP1CB subnetwork | 0.15915544 | 0.719460594 |
| MP:0002647 | decreased intestinal cholesterol absorption | 0.15911626 | 0.719531502 |
| MP:0010279 | increased gastrointestinal tumor incidence | 0.15956534 | 0.719674509 |
| GO:0032735 | positive regulation of interleukin-12 production | 0.15966531 | 0.72003866 |
| MP:0005341 | decreased susceptibility to atherosclerosis | 0.15994298 | 0.720575933 |
| MP:0004964 | absent inner cell mass | 0.1598318 | 0.720724638 |
| ENSG00000085117 | CD82 subnetwork | 0.15993826 | 0.720775668 |
| MP:0003984 | embryonic growth retardation | 0.15993305 | 0.720975531 |
| ENSG00000143621 | ILF2 subnetwork | 0.16012523 | 0.721028939 |
| ENSG00000087191 | PSMC5 subnetwork | 0.16011533 | 0.721196526 |
| GO:0007015 | actin filament organization | 0.1603207 | 0.721873995 |
| GO:0030838 | positive regulation of actin filament polymerization | 0.16054195 | 0.722670308 |
| GO:0010907 | positive regulation of glucose metabolic process | 0.16066815 | 0.72298426 |
| GO:0009295 | nucleoid | 0.16072679 | 0.722992935 |
| GO:0070555 | response to interleukin-1 | 0.16077893 | 0.723065811 |
| GO:0030856 | regulation of epithelial cell differentiation | 0.16085182 | 0.723122593 |
| ENSG00000116030 | SUMO1 subnetwork | 0.16131318 | 0.724487179 |
| ENSG00000104814 | MAP4K1 subnetwork | 0.16128896 | 0.724623277 |
| GO:0005721 | centromeric heterochromatin | 0.16137786 | 0.724655559 |
| ENSG00000185651 | UBE2L3 subnetwork | 0.16127101 | 0.724759461 |
| GO:0043548 | phosphatidylinositol 3-kinase binding | 0.16146618 | 0.724871877 |
| GO:0046641 | positive regulation of alpha-beta T cell proliferation | 0.1612497 | 0.724927815 |
| ENSG00000137815 | RTF1 subnetwork | 0.16160672 | 0.72532821 |
| ENSG00000100311 | PDGFB subnetwork | 0.16164391 | 0.725352113 |

| | | | |
|---|---|---|---|
| ENSG00000063046 | EIF4B subnetwork | 0.16173826 | 0.725552 |
| MP:0002264 | abnormal bronchus morphology | 0.16189891 | 0.726055662 |
| ENSG00000061936 | SFSWAP subnetwork | 0.16198214 | 0.726063319 |
| ENSG00000184216 | IRAK1 subnetwork | 0.16248816 | 0.728548593 |
| ENSG00000114126 | TFDP2 subnetwork | 0.16260599 | 0.728906999 |
| MP:0008866 | chromosomal instability | 0.16264909 | 0.728913738 |
| GO:0051321 | meiotic cell cycle | 0.16284265 | 0.729358238 |
| ENSG00000184985 | SORCS2 subnetwork | 0.16280999 | 0.7294794 |
| GO:0032814 | regulation of natural killer cell activation | 0.16293002 | 0.729652091 |
| ENSG00000015479 | MATR3 subnetwork | 0.16300736 | 0.72980217 |
| ENSG00000142252 | GEMIN7 subnetwork | 0.16307259 | 0.729936204 |
| MP:0006317 | decreased urine sodium level | 0.16337627 | 0.731106505 |
| GO:0008186 | RNA-dependent ATPase activity | 0.16354141 | 0.731431304 |
| GO:0030833 | regulation of actin filament polymerization | 0.16364954 | 0.73151689 |
| ENSG00000124160 | NCOA5 subnetwork | 0.16372077 | 0.731570564 |
| ENSG00000099139 | PCSK5 subnetwork | 0.16394724 | 0.732420382 |
| MP:0004076 | abnormal vitelline vascular remodeling | 0.16408869 | 0.73272843 |
| ENSG00000133103 | COG6 subnetwork | 0.16424844 | 0.733450032 |
| KEGG_RIBOFLAVIN_METABOLI | KEGG_RIBOFLAVIN_METABOLISM | 0.16439776 | 0.733932549 |
| MP:0011204 | abnormal visceral yolk sac blood island morphology | 0.16485453 | 0.734116154 |
| ENSG00000116809 | ZBTB17 subnetwork | 0.16470045 | 0.734132783 |
| ENSG00000051180 | RAD51 subnetwork | 0.16490258 | 0.734152919 |
| GO:0004402 | histone acetyltransferase activity | 0.16477044 | 0.7341537 |
| ENSG00000105663 | ENSG00000105663 subnetwork | 0.1648294 | 0.734190476 |
| ENSG00000175110 | MRPS22 subnetwork | 0.16452099 | 0.734223919 |
| GO:0000184 | nuclear-transcribed mRNA catabolic process, nonsense-me | 0.16460438 | 0.734324324 |
| GO:0016790 | thiolester hydrolase activity | 0.16469404 | 0.734334287 |
| ENSG00000196367 | TRRAP subnetwork | 0.1646616 | 0.734424666 |
| GO:0030934 | anchoring collagen | 0.16503397 | 0.734617824 |
| ENSG00000028839 | TBPL1 subnetwork | 0.16524439 | 0.735367787 |
| GO:0008094 | DNA-dependent ATPase activity | 0.16537149 | 0.735594295 |
| GO:0005775 | vacuolar lumen | 0.16550036 | 0.736026616 |
| ENSG00000137337 | MDC1 subnetwork | 0.16619007 | 0.736246057 |
| ENSG00000075673 | ATP12A subnetwork | 0.16623145 | 0.736297698 |
| ENSG00000110799 | VWF subnetwork | 0.16626009 | 0.736317781 |
| ENSG00000180581 | ENSG00000180581 subnetwork | 0.1659518 | 0.736452735 |
| ENSG00000206385 | ENSG00000206385 subnetwork | 0.16619007 | 0.736478384 |
| GO:0003724 | RNA helicase activity | 0.16569286 | 0.736601204 |
| MP:0001218 | thin epidermis | 0.16617429 | 0.736616162 |
| ENSG00000143742 | SRP9 subnetwork | 0.1659518 | 0.736685642 |
| REACTOME_ACETYLCHOLINE_B | REACTOME_ACETYLCHOLINE_BINDING_AND_DOWNSTREA | 0.16617408 | 0.736848753 |
| MP:0003447 | decreased tumor growth/size | 0.1659491 | 0.736918697 |
| ENSG00000154556 | SORBS2 subnetwork | 0.16581515 | 0.736937935 |
| ENSG00000112144 | ICK subnetwork | 0.16588256 | 0.737037037 |
| GO:0060443 | mammary gland morphogenesis | 0.16593188 | 0.737041139 |
| REACTOME_POSTSYNAPTIC_NI | REACTOME_POSTSYNAPTIC_NICOTINIC_ACETYLCHOLINE_R | 0.16617408 | 0.737081491 |
| KEGG_PROSTATE_CANCER | KEGG_PROSTATE_CANCER | 0.16608248 | 0.737120733 |
| REACTOME_ACTIVATION_OF_I | REACTOME_ACTIVATION_OF_NICOTINIC_ACETYLCHOLINE_ | 0.16617408 | 0.737314376 |
| ENSG00000010671 | BTK subnetwork | 0.1664902 | 0.737362118 |
| ENSG00000189037 | DUSP21 subnetwork | 0.16663263 | 0.73779143 |
| MP:0002079 | increased circulating insulin level | 0.16679722 | 0.737834435 |
| ENSG00000181222 | POLR2A subnetwork | 0.16678856 | 0.738035264 |
| MP:0003231 | abnormal placenta vasculature | 0.16678647 | 0.73823622 |

| | | | |
|---|---|---|---|
| KEGG_ABC_TRANSPORTERS | KEGG_ABC_TRANSPORTERS | 0.16702137 | 0.73876652 |
| GO:0030175 | filopodium | 0.1674055 | 0.739641622 |
| ENSG00000017260 | ATP2C1 subnetwork | 0.16744272 | 0.739660591 |
| ENSG00000096150 | RPS18 subnetwork | 0.16845397 | 0.739828125 |
| MP:0000737 | abnormal myotome development | 0.16851839 | 0.739846923 |
| ENSG00000100345 | MYH9 subnetwork | 0.16740526 | 0.739874214 |
| KEGG_EPITHELIAL_CELL_SIGNA | KEGG_EPITHELIAL_CELL_SIGNALING_IN_HELICOBACTER_PY | 0.16773547 | 0.739880766 |
| ENSG00000092201 | SUPT16H subnetwork | 0.16755811 | 0.739946591 |
| ENSG00000175221 | MED16 subnetwork | 0.16821477 | 0.739981215 |
| ENSG00000180573 | HIST1H2AC subnetwork | 0.16770736 | 0.739987445 |
| ENSG00000178188 | SH2B1 subnetwork | 0.16737413 | 0.740028311 |
| MP:0000141 | abnormal vertebral body morphology | 0.16825999 | 0.740031299 |
| ENSG00000182498 | ENSG00000182498 subnetwork | 0.16845397 | 0.740059394 |
| MP:0009548 | abnormal platelet aggregation | 0.16767654 | 0.740094192 |
| MP:0002682 | decreased mature ovarian follicle number | 0.16799374 | 0.740109718 |
| ENSG00000181090 | EHMT1 subnetwork | 0.16811577 | 0.740115915 |
| MP:0000336 | decreased mast cell number | 0.16793086 | 0.740137974 |
| MP:0006042 | increased apoptosis | 0.16762261 | 0.740138191 |
| ENSG00000134243 | SORT1 subnetwork | 0.16819625 | 0.740165988 |
| ENSG00000185658 | BRWD1 subnetwork | 0.16809591 | 0.740285177 |
| ENSG00000206212 | ENSG00000206212 subnetwork | 0.16845397 | 0.740290807 |
| ENSG00000111775 | COX6A1 subnetwork | 0.16792903 | 0.740370138 |
| ENSG00000068366 | ACSL4 subnetwork | 0.16837371 | 0.740394243 |
| ENSG00000181218 | HIST3H2A subnetwork | 0.1684346 | 0.740444166 |
| MP:0000470 | abnormal stomach morphology | 0.16888428 | 0.741708307 |
| MP:0003436 | decreased susceptibility to induced arthritis | 0.16902913 | 0.741794072 |
| ENSG00000116898 | MRPS15 subnetwork | 0.16919199 | 0.741955098 |
| GO:0003678 | DNA helicase activity | 0.16914282 | 0.74198378 |
| REACTOME_MEIOSIS | REACTOME_MEIOSIS | 0.1690289 | 0.742025593 |
| ENSG00000099901 | RANBP1 subnetwork | 0.16898159 | 0.742038714 |
| ENSG00000158560 | DYNC1I1 subnetwork | 0.16953464 | 0.743500623 |
| ENSG00000142676 | RPL11 subnetwork | 0.16962117 | 0.743596136 |
| ENSG00000086232 | EIF2AK1 subnetwork | 0.16970345 | 0.743707165 |
| ENSG00000141076 | CIRH1A subnetwork | 0.1698589 | 0.743853097 |
| ENSG00000174371 | EXO1 subnetwork | 0.16983097 | 0.743882316 |
| ENSG00000084073 | ZMPSTE24 subnetwork | 0.16980879 | 0.743958268 |
| ENSG00000196923 | PDLIM7 subnetwork | 0.17001693 | 0.744043546 |
| MP:0005657 | abnormal neural plate morphology | 0.17000261 | 0.744228376 |
| GO:0017053 | transcriptional repressor complex | 0.17011793 | 0.744231965 |
| GO:0009607 | response to biotic stimulus | 0.17052334 | 0.745865713 |
| MP:0003717 | pallor | 0.17089222 | 0.747327533 |
| ENSG00000174775 | HRAS subnetwork | 0.17104427 | 0.747468944 |
| ENSG00000132341 | RAN subnetwork | 0.17109516 | 0.747547346 |
| REACTOME_MEIOTIC_RECOMI | REACTOME_MEIOTIC_RECOMBINATION | 0.17103796 | 0.747685617 |
| MP:0005418 | abnormal circulating hormone level | 0.1712714 | 0.748137803 |
| ENSG00000165630 | PRPF18 subnetwork | 0.17140384 | 0.74844865 |
| GO:0010332 | response to gamma radiation | 0.17146387 | 0.748495658 |
| ENSG00000063978 | RNF4 subnetwork | 0.17152051 | 0.748573643 |
| ENSG00000112304 | ACOT13 subnetwork | 0.17177001 | 0.74916331 |
| ENSG00000113721 | PDGFRB subnetwork | 0.17185665 | 0.749256506 |
| MP:0005266 | abnormal metabolism | 0.17173699 | 0.749302542 |
| ENSG00000102387 | TAF7L subnetwork | 0.17258607 | 0.749722308 |
| MP:0002590 | increased mean corpuscular volume | 0.17256856 | 0.749861111 |

| | | | |
|---|---|---|---|
| MP:0001698 | decreased embryo size | 0.17243286 | 0.749876429 |
| GO:0070302 | regulation of stress-activated protein kinase signaling casca | 0.17280495 | 0.750030836 |
| ENSG00000100365 | NCF4 subnetwork | 0.17255529 | 0.750030874 |
| GO:0043627 | response to estrogen stimulus | 0.17275704 | 0.750046268 |
| ENSG00000068654 | POLR1A subnetwork | 0.17240578 | 0.750046354 |
| GO:0051707 | response to other organism | 0.1723698 | 0.750061824 |
| ENSG00000129354 | AP1M2 subnetwork | 0.17252155 | 0.75009265 |
| GO:0046777 | protein autophosphorylation | 0.17234639 | 0.750200989 |
| GO:0007565 | female pregnancy | 0.17213769 | 0.750216785 |
| GO:0005640 | nuclear outer membrane | 0.17220238 | 0.750340557 |
| ENSG00000058272 | PPP1R12A subnetwork | 0.17232006 | 0.750355707 |
| MP:0002095 | abnormal skin pigmentation | 0.17292856 | 0.750416153 |
| GO:0004386 | helicase activity | 0.1722587 | 0.750510678 |
| MP:0001715 | placental labyrinth hypoplasia | 0.17231417 | 0.750556931 |
| GO:0001914 | regulation of T cell mediated cytotoxicity | 0.17327004 | 0.750815636 |
| ENSG00000150455 | TIRAP subnetwork | 0.17325179 | 0.750939039 |
| ENSG00000169439 | SDC2 subnetwork | 0.17321536 | 0.751016323 |
| ENSG00000108654 | DDX5 subnetwork | 0.17312013 | 0.751093991 |
| ENSG00000182541 | LIMK2 subnetwork | 0.17321452 | 0.751247689 |
| GO:0001913 | T cell mediated cytotoxicity | 0.17344406 | 0.751307692 |
| ENSG00000136936 | XPA subnetwork | 0.17351812 | 0.751414949 |
| ENSG00000184825 | HIST1H2AH subnetwork | 0.17392243 | 0.75174954 |
| ENSG00000141582 | CBX4 subnetwork | 0.17377871 | 0.751766513 |
| MP:0009542 | decreased thymocyte apoptosis | 0.17404286 | 0.751794479 |
| ENSG00000115718 | PROC subnetwork | 0.17399699 | 0.751795029 |
| ENSG00000076604 | TRAF4 subnetwork | 0.17374883 | 0.751889982 |
| ENSG00000126214 | KLC1 subnetwork | 0.17385735 | 0.751904177 |
| ENSG00000134371 | CDC73 subnetwork | 0.17372593 | 0.751952044 |
| ENSG00000070366 | SMG6 subnetwork | 0.17368656 | 0.75196802 |
| ENSG00000124642 | ENSG00000124642 subnetwork | 0.17392243 | 0.75198035 |
| ENSG00000169067 | ACTBL2 subnetwork | 0.17437355 | 0.752113323 |
| MP:0002410 | decreased susceptibility to viral infection | 0.17435995 | 0.752328431 |
| GO:0051347 | positive regulation of transferase activity | 0.17420712 | 0.752330573 |
| ENSG00000108953 | YWHAE subnetwork | 0.17435299 | 0.752513025 |
| ENSG00000106443 | PHF14 subnetwork | 0.17433094 | 0.752667075 |
| ENSG00000119616 | FCF1 subnetwork | 0.17454929 | 0.752770974 |
| ENSG00000160917 | CPSF4 subnetwork | 0.1746579 | 0.753168044 |
| GO:0007131 | reciprocal meiotic recombination | 0.17488483 | 0.753455657 |
| ENSG00000108465 | CDK5RAP3 subnetwork | 0.1749379 | 0.753469887 |
| GO:0031401 | positive regulation of protein modification process | 0.17482066 | 0.753671971 |
| GO:0046966 | thyroid hormone receptor binding | 0.17506264 | 0.753681638 |
| MP:0002998 | abnormal bone remodeling | 0.17501913 | 0.753682763 |
| GO:0035825 | reciprocal DNA recombination | 0.17488483 | 0.753686143 |
| GO:0031498 | chromatin disassembly | 0.17527211 | 0.753707659 |
| ENSG00000106004 | HOXA5 subnetwork | 0.17514576 | 0.753787416 |
| GO:0006337 | nucleosome disassembly | 0.17527211 | 0.753937729 |
| GO:0032986 | protein-DNA complex disassembly | 0.17527211 | 0.754167939 |
| MP:0003628 | abnormal leukocyte adhesion | 0.17555553 | 0.754682733 |
| ENSG00000122257 | RBBP6 subnetwork | 0.17586969 | 0.755348979 |
| GO:0016363 | nuclear matrix | 0.17577609 | 0.755352242 |
| MP:0001792 | impaired wound healing | 0.17584424 | 0.755442073 |
| ENSG00000138468 | SENP7 subnetwork | 0.17623378 | 0.755613021 |
| GO:0051327 | M phase of meiotic cell cycle | 0.1760676 | 0.75571124 |

| | | | |
|---|---|---|---|
| MP:0008706 | decreased interleukin-6 secretion | 0.17628595 | 0.755732968 |
| ENSG00000070831 | CDC42 subnetwork | 0.17622215 | 0.755751674 |
| ENSG00000056661 | PCGF2 subnetwork | 0.17639252 | 0.755822438 |
| ENSG00000124571 | XPO5 subnetwork | 0.1764419 | 0.755881459 |
| GO:0030374 | ligand-dependent nuclear receptor transcription coactivato | 0.17620741 | 0.755905632 |
| GO:0007126 | meiosis | 0.1760676 | 0.755941499 |
| MP:0003627 | abnormal leukocyte tethering or rolling | 0.1761759 | 0.756059683 |
| GO:0042987 | amyloid precursor protein catabolic process | 0.17660644 | 0.756136087 |
| ENSG00000153807 | ENSG00000153807 subnetwork | 0.1769316 | 0.75624621 |
| ENSG00000105245 | NUMBL subnetwork | 0.17677051 | 0.756282246 |
| GO:0004003 | ATP-dependent DNA helicase activity | 0.17672865 | 0.756299332 |
| ENSG00000168036 | CTNNB1 subnetwork | 0.17659871 | 0.756320267 |
| MP:0002078 | abnormal glucose homeostasis | 0.17670428 | 0.756407531 |
| ENSG00000147536 | GINS4 subnetwork | 0.17691188 | 0.756445253 |
| ENSG00000186842 | ENSG00000186842 subnetwork | 0.1768764 | 0.756568568 |
| GO:0031056 | regulation of histone modification | 0.17708612 | 0.756896029 |
| GO:0070265 | necrotic cell death | 0.17716822 | 0.757090909 |
| MP:0009429 | decreased embryo weight | 0.17754265 | 0.758694335 |
| ENSG00000091436 | ENSG00000091436 subnetwork | 0.17763685 | 0.758843125 |
| ENSG00000189283 | FHIT subnetwork | 0.17771552 | 0.758991826 |
| ENSG00000198374 | HIST1H2AL subnetwork | 0.17845205 | 0.759656005 |
| ENSG00000196747 | HIST1H2AI subnetwork | 0.17845205 | 0.7598853 |
| ENSG00000196787 | HIST1H2AG subnetwork | 0.17845205 | 0.760114734 |
| GO:0016338 | calcium-independent cell-cell adhesion | 0.17832166 | 0.760169235 |
| ENSG00000100395 | L3MBTL2 subnetwork | 0.17827825 | 0.760217654 |
| ENSG00000196866 | HIST1H2AD subnetwork | 0.17845205 | 0.760344307 |
| ENSG00000059728 | MXD1 subnetwork | 0.17810379 | 0.760411622 |
| MP:0002168 | other aberrant phenotype | 0.17827481 | 0.760432416 |
| ENSG00000184348 | HIST1H2AK subnetwork | 0.17845205 | 0.760574018 |
| ENSG00000058335 | RASGRF1 subnetwork | 0.17874415 | 0.760603318 |
| ENSG00000007816 | ENSG00000007816 subnetwork | 0.17826702 | 0.760647308 |
| ENSG00000124783 | SSR1 subnetwork | 0.17821504 | 0.760726172 |
| ENSG00000149311 | ATM subnetwork | 0.17891878 | 0.760962002 |
| ENSG00000105376 | ICAM5 subnetwork | 0.17921371 | 0.761889693 |
| ENSG00000152147 | GEMIN6 subnetwork | 0.17916841 | 0.761923425 |
| ENSG00000143507 | DUSP10 subnetwork | 0.17931189 | 0.762172341 |
| ENSG00000157110 | RBPMS subnetwork | 0.17937934 | 0.762364458 |
| ENSG00000215305 | VPS16 subnetwork | 0.17995504 | 0.763465585 |
| MP:0001273 | decreased metastatic potential | 0.17989479 | 0.763514732 |
| GO:0008026 | ATP-dependent helicase activity | 0.17986277 | 0.763533835 |
| ENSG00000110422 | HIPK3 subnetwork | 0.17976297 | 0.763557027 |
| ENSG00000204898 | ENSG00000204898 subnetwork | 0.17975069 | 0.763741722 |
| GO:0070035 | purine NTP-dependent helicase activity | 0.17986277 | 0.763763538 |
| ENSG00000079385 | CEACAM1 subnetwork | 0.17975069 | 0.763971695 |
| GO:0030684 | preribosome | 0.18026077 | 0.764663462 |
| GO:0034504 | protein localization to nucleus | 0.18043953 | 0.76512012 |
| ENSG00000089094 | KDM2B subnetwork | 0.18042532 | 0.765259838 |
| ENSG00000168259 | DNAJC7 subnetwork | 0.1807553 | 0.766496548 |
| GO:0000795 | synaptonemal complex | 0.18135849 | 0.767680551 |
| ENSG00000165606 | DRGX subnetwork | 0.18116807 | 0.767767107 |
| ENSG00000106070 | GRB10 subnetwork | 0.18135505 | 0.767895683 |
| ENSG00000131437 | KIF3A subnetwork | 0.18151617 | 0.767989814 |
| GO:0044427 | chromosomal part | 0.1816107 | 0.768059299 |

| | | | |
|---|---|---|---|
| GO:0030593 | neutrophil chemotaxis | 0.18134672 | 0.768110945 |
| MP:0000043 | organ of Corti degeneration | 0.18130291 | 0.768331833 |
| ENSG00000183918 | SH2D1A subnetwork | 0.18134396 | 0.768341332 |
| MP:0005668 | decreased circulating leptin level | 0.18185471 | 0.768662077 |
| ENSG00000204361 | FAM55B subnetwork | 0.18180981 | 0.768712575 |
| REACTOME_HIGHLY_CALCIUM | REACTOME_HIGHLY_CALCIUM_PERMEABLE_POSTSYNAPTI | 0.18192102 | 0.768821065 |
| ENSG00000184900 | SUMO3 subnetwork | 0.181972 | 0.768890218 |
| ENSG00000175582 | RAB6A subnetwork | 0.18240104 | 0.769173381 |
| MP:0005033 | abnormal trophoblast giant cells | 0.18240023 | 0.769402985 |
| obsolete_molecular_function | obsolete_molecular_function | 0.18232368 | 0.769408779 |
| MP:0011049 | impaired adaptive thermogenesis | 0.18221469 | 0.769530783 |
| MP:0008288 | abnormal adrenal cortex morphology | 0.18218834 | 0.769626308 |
| MP:0009541 | increased thymocyte apoptosis | 0.18232313 | 0.76963859 |
| REACTOME_SIGNALING_BY_TC | REACTOME_SIGNALING_BY_TGF_BETA | 0.18215416 | 0.769662081 |
| ENSG00000117318 | ID3 subnetwork | 0.18229726 | 0.769808784 |
| ENSG00000135144 | DTX1 subnetwork | 0.18272202 | 0.770346062 |
| GO:0031301 | integral to organelle membrane | 0.18288984 | 0.77068297 |
| ENSG00000100462 | PRMT5 subnetwork | 0.18320195 | 0.771728763 |
| GO:0045860 | positive regulation of protein kinase activity | 0.18319626 | 0.77192904 |
| MP:0009789 | decreased susceptibility to bacterial infection induced mort | 0.18355591 | 0.772238762 |
| GO:0017136 | NAD-dependent histone deacetylase activity | 0.18345758 | 0.772415847 |
| ENSG00000135363 | LMO2 subnetwork | 0.1835543 | 0.772453842 |
| GO:0034979 | NAD-dependent protein deacetylase activity | 0.18345758 | 0.772646007 |
| ENSG00000035115 | SH3YL1 subnetwork | 0.18387372 | 0.773333333 |
| KEGG_ALANINE_ASPARTATE_A | KEGG_ALANINE_ASPARTATE_AND_GLUTAMATE_METABOL | 0.18394178 | 0.773400774 |
| REACTOME_METABOLISM_OF_ | REACTOME_METABOLISM_OF_MRNA | 0.18411517 | 0.774107674 |
| ENSG00000087903 | RFX2 subnetwork | 0.18424681 | 0.774227111 |
| GO:0061377 | mammary gland lobule development | 0.18435302 | 0.774242424 |
| MP:0001148 | enlarged testis | 0.18424116 | 0.774412727 |
| GO:0060749 | mammary gland alveolus development | 0.18435302 | 0.774472511 |
| GO:0035770 | ribonucleoprotein granule | 0.1847247 | 0.774873925 |
| ENSG00000149357 | LAMTOR1 subnetwork | 0.18481573 | 0.774940688 |
| ENSG00000120008 | WDR11 subnetwork | 0.18488306 | 0.774955542 |
| MP:0005542 | corneal vascularization | 0.18491698 | 0.774977778 |
| GO:0019867 | outer membrane | 0.18486014 | 0.775051883 |
| ENSG00000213585 | VDAC1 subnetwork | 0.18470045 | 0.775059347 |
| ENSG00000188986 | COBRA1 subnetwork | 0.18465528 | 0.775155833 |
| ENSG00000182953 | ENSG00000182953 subnetwork | 0.1846475 | 0.775341449 |
| ENSG00000186318 | BACE1 subnetwork | 0.1846181 | 0.775393525 |
| MP:0005461 | abnormal dendritic cell morphology | 0.18551074 | 0.776412304 |
| GO:0009755 | hormone-mediated signaling pathway | 0.18529325 | 0.776413977 |
| GO:0046822 | regulation of nucleocytoplasmic transport | 0.18523752 | 0.776436611 |
| GO:0051272 | positive regulation of cellular component movement | 0.18550139 | 0.77658284 |
| GO:0007568 | aging | 0.18547834 | 0.776694288 |
| ENSG00000188486 | H2AFX subnetwork | 0.1854349 | 0.776761397 |
| GO:0030134 | ER to Golgi transport vesicle | 0.1858175 | 0.777460834 |
| ENSG00000155380 | SLC16A1 subnetwork | 0.18588979 | 0.777541371 |
| GO:0030544 | Hsp70 protein binding | 0.18578658 | 0.777557658 |
| ENSG00000145349 | CAMK2D subnetwork | 0.18612953 | 0.777812223 |
| ENSG00000108395 | TRIM37 subnetwork | 0.18601127 | 0.777858198 |
| ENSG00000182180 | MRPS16 subnetwork | 0.18610203 | 0.777982871 |
| ENSG00000141232 | TOB1 subnetwork | 0.18620163 | 0.777995868 |
| ENSG00000125482 | TTF1 subnetwork | 0.18635253 | 0.778503983 |

| | | | |
|---|---|---|---|
| GO:0005158 | insulin receptor binding | 0.18656825 | 0.779129794 |
| GO:0006953 | acute-phase response | 0.18663298 | 0.779165438 |
| MP:0002182 | abnormal astrocyte morphology | 0.18688746 | 0.77995283 |
| ENSG00000152270 | PDE3B subnetwork | 0.18697091 | 0.780061892 |
| ENSG00000067596 | DHX8 subnetwork | 0.18728743 | 0.78111013 |
| ENSG00000185499 | MUC1 subnetwork | 0.18725573 | 0.781237113 |
| GO:0031434 | mitogen-activated protein kinase kinase binding | 0.18723114 | 0.78134944 |
| ENSG00000164951 | PDP1 subnetwork | 0.18768848 | 0.782513983 |
| ENSG00000078808 | SDF4 subnetwork | 0.1877699 | 0.782710418 |
| KEGG_RNA_POLYMERASE | KEGG_RNA_POLYMERASE | 0.18789186 | 0.782950868 |
| MP:0011098 | complete embryonic lethality during organogenesis | 0.18801752 | 0.783264706 |
| GO:0030145 | manganese ion binding | 0.18814865 | 0.783607762 |
| ENSG00000140682 | TGFB1I1 subnetwork | 0.18842497 | 0.7844402 |
| REACTOME_FORMATION_OF_T | REACTOME_FORMATION_OF_TUBULIN_FOLDING_INTERM | 0.18841766 | 0.784641387 |
| ENSG00000083544 | TDRD3 subnetwork | 0.18861605 | 0.784900118 |
| ENSG00000104872 | PIH1D1 subnetwork | 0.18880885 | 0.785217264 |
| GO:0031625 | ubiquitin protein ligase binding | 0.18896708 | 0.785372653 |
| ENSG00000130758 | MAP3K10 subnetwork | 0.18880322 | 0.785418502 |
| ENSG00000075415 | SLC25A3 subnetwork | 0.18895264 | 0.785544467 |
| ENSG00000130479 | MAP1S subnetwork | 0.18936328 | 0.787078322 |
| MP:0002038 | carcinoma | 0.18961915 | 0.787727273 |
| REACTOME_TIGHT_JUNCTION_ | REACTOME_TIGHT_JUNCTION_INTERACTIONS | 0.18995575 | 0.78925535 |
| ENSG00000160202 | CRYAA subnetwork | 0.19007171 | 0.78968347 |
| KEGG_N_GLYCAN_BIOSYNTHES | KEGG_N_GLYCAN_BIOSYNTHESIS | 0.19029838 | 0.790624084 |
| ENSG00000124383 | MPHOSPH10 subnetwork | 0.19067239 | 0.792311072 |
| MP:0000471 | abnormal stomach epithelium morphology | 0.19097935 | 0.792698273 |
| MP:0004434 | abnormal cochlear outer hair cell physiology | 0.19121402 | 0.792781999 |
| MP:0008782 | increased B cell apoptosis | 0.19093477 | 0.792783958 |
| ENSG00000162367 | TAL1 subnetwork | 0.19103166 | 0.792875951 |
| ENSG00000140848 | CPNE2 subnetwork | 0.19112083 | 0.792938596 |
| ENSG00000099804 | CDC34 subnetwork | 0.19092486 | 0.79295754 |
| ENSG00000005156 | LIG3 subnetwork | 0.19120433 | 0.792984507 |
| GO:0071565 | nBAF complex | 0.19111037 | 0.793068149 |
| ENSG00000025293 | PHF20 subnetwork | 0.1919698 | 0.794067055 |
| ENSG00000204221 | WDR46 subnetwork | 0.19209998 | 0.794143357 |
| MP:0001130 | abnormal ovarian folliculogenesis | 0.19189306 | 0.794238623 |
| ENSG00000134250 | NOTCH2 subnetwork | 0.19195044 | 0.794240303 |
| ENSG00000206284 | WDR46 subnetwork | 0.19209998 | 0.794374818 |
| MP:0002968 | increased circulating alkaline phosphatase level | 0.1918695 | 0.794382842 |
| ENSG00000131467 | PSME3 subnetwork | 0.19185761 | 0.794570928 |
| ENSG00000146109 | ABT1 subnetwork | 0.19228247 | 0.794596563 |
| ENSG00000162191 | UBXN1 subnetwork | 0.1918525 | 0.79480292 |
| ENSG00000185973 | TMLHE subnetwork | 0.19242413 | 0.794874782 |
| GO:0016835 | carbon-oxygen lyase activity | 0.19184875 | 0.795020444 |
| ENSG00000115170 | ACVR1 subnetwork | 0.19180661 | 0.795077417 |
| GO:0045120 | pronucleus | 0.1925783 | 0.795110594 |
| ENSG00000138767 | CNOT6L subnetwork | 0.19276488 | 0.795129398 |
| ENSG00000105976 | MET subnetwork | 0.19264581 | 0.795170207 |
| GO:0045638 | negative regulation of myeloid cell differentiation | 0.19273852 | 0.795273415 |
| ENSG00000100926 | TM9SF1 subnetwork | 0.1925658 | 0.795327511 |
| ENSG00000148843 | PDCD11 subnetwork | 0.1929168 | 0.795537791 |
| ENSG00000163541 | SUCLG1 subnetwork | 0.19321048 | 0.796498111 |
| GO:0016641 | oxidoreductase activity, acting on the CH-NH2 group of don | 0.19349697 | 0.796719884 |

| | | | |
|---|---|---|---|
| ENSG00000102780 | DGKH subnetwork | 0.19346902 | 0.796864111 |
| GO:0018209 | peptidyl-serine modification | 0.19338951 | 0.796949448 |
| ENSG00000108270 | AATF subnetwork | 0.19345499 | 0.796979378 |
| MP:0002672 | abnormal branchial arch artery morphology | 0.19397005 | 0.797334106 |
| GO:0043491 | protein kinase B signaling cascade | 0.19393378 | 0.797434783 |
| ENSG00000204301 | NOTCH4 subnetwork | 0.19417666 | 0.79763905 |
| ENSG00000139117 | CPNE8 subnetwork | 0.19393372 | 0.79766599 |
| ENSG00000070501 | POLB subnetwork | 0.19377992 | 0.797692977 |
| MP:0002160 | abnormal reproductive system morphology | 0.19387927 | 0.797766821 |
| ENSG00000131626 | PPFIA1 subnetwork | 0.19384586 | 0.797795184 |
| ENSG00000069431 | ABCC9 subnetwork | 0.19435448 | 0.79806022 |
| MP:0002190 | disorganized myocardium | 0.19475157 | 0.798150289 |
| GO:0019218 | regulation of steroid metabolic process | 0.194331 | 0.798161019 |
| GO:0019915 | lipid storage | 0.19464476 | 0.798192597 |
| MP:0001147 | small testis | 0.19481235 | 0.79820861 |
| GO:0004725 | protein tyrosine phosphatase activity | 0.19471467 | 0.798236485 |
| GO:0090077 | foam cell differentiation | 0.19493512 | 0.79825296 |
| GO:2000058 | regulation of protein ubiquitination involved in ubiquitin-de | 0.19462941 | 0.798409025 |
| GO:0010742 | macrophage derived foam cell differentiation | 0.19493512 | 0.798483536 |
| GO:0002526 | acute inflammatory response | 0.19506243 | 0.798614319 |
| GO:0071636 | positive regulation of transforming growth factor beta prod | 0.1946284 | 0.798640046 |
| ENSG00000119699 | TGFB3 subnetwork | 0.19458967 | 0.798726483 |
| GO:0046395 | carboxylic acid catabolic process | 0.19532233 | 0.799120277 |
| ENSG00000151065 | DCP1B subnetwork | 0.19521323 | 0.799134199 |
| GO:0016054 | organic acid catabolic process | 0.19532233 | 0.799350837 |
| ENSG00000187899 | ENSG00000187899 subnetwork | 0.19567458 | 0.800576701 |
| ENSG00000077312 | SNRPA subnetwork | 0.19594794 | 0.801686365 |
| ENSG00000204103 | MAFB subnetwork | 0.19609884 | 0.801988473 |
| ENSG00000167193 | CRK subnetwork | 0.19643059 | 0.803182604 |
| ENSG00000134014 | ELP3 subnetwork | 0.19659744 | 0.803309353 |
| ENSG00000070770 | CSNK2A2 subnetwork | 0.1964136 | 0.803341976 |
| ENSG00000112576 | CCND3 subnetwork | 0.1965345 | 0.803412036 |
| GO:0004143 | diacylglycerol kinase activity | 0.19658924 | 0.803511802 |
| GO:0050681 | androgen receptor binding | 0.1966932 | 0.803567319 |
| GO:0022612 | gland morphogenesis | 0.19697316 | 0.80439908 |
| GO:0031594 | neuromuscular junction | 0.19694937 | 0.804501007 |
| MP:0005508 | abnormal skeleton morphology | 0.19738444 | 0.804520666 |
| ENSG00000130985 | UBA1 subnetwork | 0.19716645 | 0.804683908 |
| ENSG00000183558 | HIST2H2AA3 subnetwork | 0.19735443 | 0.804708585 |
| ENSG00000133511 | ENSG00000133511 subnetwork | 0.19714013 | 0.804785858 |
| ENSG00000116001 | TIA1 subnetwork | 0.19726693 | 0.804840563 |
| ENSG00000126749 | ENSG00000126749 subnetwork | 0.19756281 | 0.804919679 |
| ENSG00000203812 | HIST2H2AA4 subnetwork | 0.19735443 | 0.80493969 |
| ENSG00000015153 | YAF2 subnetwork | 0.19754128 | 0.805021521 |
| ENSG00000117335 | CD46 subnetwork | 0.19761833 | 0.80503298 |
| MP:0001284 | absent vibrissae | 0.19828087 | 0.80530303 |
| ENSG00000129347 | KRI1 subnetwork | 0.19812708 | 0.805350501 |
| GO:0007205 | protein kinase C-activating G-protein coupled receptor sign | 0.19784944 | 0.805358166 |
| REACTOME_REGULATION_OF_ | REACTOME_REGULATION_OF_IFNA_SIGNALING | 0.19841243 | 0.805385714 |
| ENSG00000113448 | PDE4D subnetwork | 0.19835067 | 0.805387254 |
| ENSG00000167930 | ITFG3 subnetwork | 0.198186 | 0.805391876 |
| ENSG00000144668 | ITGA9 subnetwork | 0.19810761 | 0.805466514 |
| GO:0046638 | positive regulation of alpha-beta T cell differentiation | 0.19826098 | 0.805476122 |

| | | | |
|---|---|---|---|
| ENSG00000101132 | PFDN4 subnetwork | 0.19783798 | 0.805574663 |
| GO:0010874 | regulation of cholesterol efflux | 0.1980838 | 0.805611222 |
| ENSG00000083290 | ULK2 subnetwork | 0.1979526 | 0.805643082 |
| ENSG00000163017 | ACTG2 subnetwork | 0.19782418 | 0.80574828 |
| ENSG00000115685 | PPP1R7 subnetwork | 0.1980563 | 0.805756014 |
| GO:0070001 | aspartic-type peptidase activity | 0.19928534 | 0.808416548 |
| GO:0004722 | protein serine/threonine phosphatase activity | 0.19918012 | 0.808537978 |
| ENSG00000081248 | CACNA1S subnetwork | 0.19915995 | 0.808640388 |
| GO:0004190 | aspartic-type endopeptidase activity | 0.19928534 | 0.80864726 |
| ENSG00000196084 | ENSG00000196084 subnetwork | 0.19940059 | 0.80867085 |
| ENSG00000130165 | ELOF1 subnetwork | 0.19926489 | 0.808806737 |
| GO:0035102 | PRC1 complex | 0.19963622 | 0.80926718 |
| MP:0000130 | abnormal trabecular bone morphology | 0.19972248 | 0.809307298 |
| MP:0004433 | abnormal cochlear inner hair cell physiology | 0.20004066 | 0.81045882 |
| ENSG00000100867 | DHRS2 subnetwork | 0.20057784 | 0.812692308 |
| ENSG00000128487 | SPECC1 subnetwork | 0.20082666 | 0.813226082 |
| ENSG00000119414 | PPP6C subnetwork | 0.20076078 | 0.813258331 |
| GO:0016702 | oxidoreductase activity, acting on single donors with incorp | 0.20102138 | 0.813645418 |
| ENSG00000179899 | ENSG00000179899 subnetwork | 0.20101378 | 0.813820097 |
| GO:0009103 | lipopolysaccharide biosynthetic process | 0.20155975 | 0.814204545 |
| ENSG00000163882 | POLR2H subnetwork | 0.20153747 | 0.814379085 |
| GO:0051651 | maintenance of location in cell | 0.20151122 | 0.814567936 |
| ENSG00000176095 | IP6K1 subnetwork | 0.20148355 | 0.814671595 |
| ENSG00000141101 | NOB1 subnetwork | 0.20134669 | 0.814679943 |
| GO:0046332 | SMAD binding | 0.2014754 | 0.814874858 |
| ENSG00000101773 | RBBP8 subnetwork | 0.20176936 | 0.814882136 |
| REACTOME_RNA_POLYMERAS | REACTOME_RNA_POLYMERASE_I_TRANSCRIPTION_INITIAT | 0.20193998 | 0.815271076 |
| ENSG00000175906 | ARL4D subnetwork | 0.20189118 | 0.815289608 |
| ENSG00000185043 | CIB1 subnetwork | 0.20206212 | 0.815607264 |
| ENSG00000106344 | RBM28 subnetwork | 0.2022149 | 0.815985816 |
| GO:0005776 | autophagic vacuole | 0.20226835 | 0.816023823 |
| ENSG00000133937 | GSC subnetwork | 0.2023107 | 0.816104338 |
| ENSG00000162614 | NEXN subnetwork | 0.20253428 | 0.816666667 |
| ENSG00000144029 | MRPS5 subnetwork | 0.20273191 | 0.816666667 |
| ENSG00000177479 | ARIH2 subnetwork | 0.20269543 | 0.816770538 |
| ENSG00000072952 | MRVI1 subnetwork | 0.20268374 | 0.81694531 |
| GO:0010883 | regulation of lipid storage | 0.20302829 | 0.817161856 |
| ENSG00000101350 | KIF3B subnetwork | 0.20311359 | 0.817199434 |
| GO:0004653 | polypeptide N-acetylgalactosaminyltransferase activity | 0.20319249 | 0.817279412 |
| GO:0006470 | protein dephosphorylation | 0.20296047 | 0.817327293 |
| ENSG00000121022 | COPS5 subnetwork | 0.20302387 | 0.817350693 |
| ENSG00000031698 | SARS subnetwork | 0.20372075 | 0.819522194 |
| ENSG00000115808 | STRN subnetwork | 0.2039859 | 0.820330602 |
| ENSG00000180733 | ENSG00000180733 subnetwork | 0.20408317 | 0.820466102 |
| ENSG00000011260 | UTP18 subnetwork | 0.20397362 | 0.820505936 |
| GO:0001881 | receptor recycling | 0.20419216 | 0.820799209 |
| ENSG00000084754 | HADHA subnetwork | 0.20428586 | 0.82085803 |
| MP:0001240 | abnormal epidermis stratum corneum morphology | 0.20427321 | 0.820990966 |
| ENSG00000105671 | DDX49 subnetwork | 0.20442394 | 0.82131772 |
| ENSG00000034971 | MYOC subnetwork | 0.20453515 | 0.821565585 |
| ENSG00000133818 | RRAS2 subnetwork | 0.20483407 | 0.821788732 |
| GO:0008154 | actin polymerization or depolymerization | 0.20482216 | 0.821978022 |
| MP:0002865 | increased growth rate | 0.20492999 | 0.822007885 |

| | | | |
|---|---|---|---|
| ENSG00000148158 | SNX30 subnetwork | 0.20475144 | 0.822012401 |
| ENSG00000170820 | FSHR subnetwork | 0.2046546 | 0.822053017 |
| GO:0044448 | cell cortex part | 0.2056124 | 0.822108366 |
| ENSG00000101608 | MYL12A subnetwork | 0.20537471 | 0.822189432 |
| MP:0008210 | increased mature B cell number | 0.20556647 | 0.822212862 |
| GO:0051324 | prophase | 0.20474689 | 0.822215957 |
| GO:0010611 | regulation of cardiac muscle hypertrophy | 0.20530522 | 0.822237841 |
| ENSG00000131196 | NFATC1 subnetwork | 0.20544839 | 0.822267491 |
| GO:0006260 | DNA replication | 0.20553536 | 0.822303371 |
| ENSG00000163938 | GNL3 subnetwork | 0.20526035 | 0.822328459 |
| GO:0033135 | regulation of peptidyl-serine phosphorylation | 0.20507005 | 0.822339527 |
| ENSG00000123576 | ESX1 subnetwork | 0.20523909 | 0.822405063 |
| KEGG_PRION_DISEASES | KEGG_PRION_DISEASES | 0.20575397 | 0.822509122 |
| MP:0004486 | decreased response of heart to induced stress | 0.20520791 | 0.822566123 |
| ENSG00000173530 | TNFRSF10D subnetwork | 0.2051694 | 0.822600619 |
| GO:0061099 | negative regulation of protein tyrosine kinase activity | 0.20590226 | 0.823007856 |
| ENSG00000132383 | RPA1 subnetwork | 0.20608383 | 0.823100645 |
| REACTOME_DNA_REPAIR | REACTOME_DNA_REPAIR | 0.20600126 | 0.823169705 |
| MP:0000820 | abnormal choroid plexus morphology | 0.20608146 | 0.823317443 |
| GO:0005452 | inorganic anion exchanger activity | 0.2062486 | 0.823353881 |
| ENSG00000143942 | CHAC2 subnetwork | 0.20622956 | 0.823556614 |
| GO:0001961 | positive regulation of cytokine-mediated signaling pathway | 0.2067678 | 0.825133016 |
| GO:0006625 | protein targeting to peroxisome | 0.20697931 | 0.825237829 |
| ENSG00000092330 | TINF2 subnetwork | 0.20674711 | 0.825308123 |
| ENSG00000183023 | SLC8A1 subnetwork | 0.20716863 | 0.825447427 |
| GO:0072662 | protein localization to peroxisome | 0.20697931 | 0.825468794 |
| ENSG00000065485 | PDIA5 subnetwork | 0.20716651 | 0.825678322 |
| GO:0072663 | establishment of protein localization to peroxisome | 0.20697931 | 0.825699888 |
| ENSG00000150991 | UBC subnetwork | 0.20738056 | 0.826062046 |
| GO:0046660 | female sex differentiation | 0.2073481 | 0.826139223 |
| MP:0002857 | cochlear ganglion degeneration | 0.20779565 | 0.82650014 |
| ENSG00000173210 | ABLIM3 subnetwork | 0.20777774 | 0.826647125 |
| ENSG00000130561 | SAG subnetwork | 0.20763385 | 0.826795194 |
| REACTOME_FATTY_ACID_TRIA | REACTOME_FATTY_ACID_TRIACYLGLYCEROL_AND_KETONE | 0.20769478 | 0.826829609 |
| GO:0007569 | cell aging | 0.20777104 | 0.826877967 |
| ENSG00000159023 | EPB41 subnetwork | 0.20812256 | 0.827007808 |
| ENSG00000166333 | ILK subnetwork | 0.20804969 | 0.827022879 |
| GO:0034622 | cellular macromolecular complex assembly | 0.20810105 | 0.827140865 |
| ENSG00000120800 | UTP20 subnetwork | 0.20884999 | 0.827153974 |
| KEGG_B_CELL_RECEPTOR_SIGI | KEGG_B_CELL_RECEPTOR_SIGNALING_PATHWAY | 0.2083508 | 0.82718663 |
| MP:0005670 | abnormal white adipose tissue physiology | 0.20824718 | 0.827215719 |
| GO:0030902 | hindbrain development | 0.20840832 | 0.82722083 |
| ENSG00000085872 | CHERP subnetwork | 0.20858353 | 0.827225932 |
| ENSG00000132300 | PTCD3 subnetwork | 0.20867215 | 0.827246175 |
| ENSG00000153879 | CEBPG subnetwork | 0.20875116 | 0.82730812 |
| ENSG00000004660 | CAMKK1 subnetwork | 0.20883027 | 0.827328329 |
| GO:0000118 | histone deacetylase complex | 0.20822243 | 0.82733482 |
| ENSG00000117533 | VAMP4 subnetwork | 0.20854156 | 0.827400501 |
| MP:0000598 | abnormal liver morphology | 0.20834201 | 0.827403176 |
| ENSG00000100448 | CTSG subnetwork | 0.20853979 | 0.827630846 |
| ENSG00000099399 | MAGEB2 subnetwork | 0.2090221 | 0.827632676 |
| REACTOME_ENDOGENOUS_ST | REACTOME_ENDOGENOUS_STEROLS | 0.20921227 | 0.828291667 |
| ENSG00000168496 | FEN1 subnetwork | 0.21007903 | 0.828514112 |

| | | | |
|---|---|---|---|
| ENSG00000161326 | DUSP14 subnetwork | 0.20991557 | 0.828551648 |
| MP:0002041 | increased pituitary adenoma incidence | 0.2099928 | 0.8286268 |
| ENSG00000132432 | SEC61G subnetwork | 0.21017049 | 0.828658368 |
| MP:0003215 | renal interstitial fibrosis | 0.21057324 | 0.828664091 |
| GO:0052548 | regulation of endopeptidase activity | 0.21006135 | 0.82870191 |
| ENSG00000072501 | SMC1A subnetwork | 0.20991486 | 0.828781163 |
| GO:0032872 | regulation of stress-activated MAPK cascade | 0.21055792 | 0.82881005 |
| ENSG00000142534 | RPS11 subnetwork | 0.20939953 | 0.828880866 |
| ENSG00000176105 | YES1 subnetwork | 0.20989841 | 0.828913827 |
| ENSG00000112335 | SNX3 subnetwork | 0.21054094 | 0.828956089 |
| ENSG00000169641 | LUZP1 subnetwork | 0.21026139 | 0.828968473 |
| MP:0001718 | abnormal visceral yolk sac morphology | 0.21070184 | 0.828987307 |
| GO:0004954 | prostanoid receptor activity | 0.20987951 | 0.829046563 |
| ENSG00000106991 | ENG subnetwork | 0.21041945 | 0.829104478 |
| ENSG00000089902 | RCOR1 subnetwork | 0.21053166 | 0.829157459 |
| ENSG00000140575 | IQGAP1 subnetwork | 0.21049177 | 0.829165515 |
| GO:0004953 | icosanoid receptor activity | 0.20987951 | 0.829276407 |
| MP:0003025 | increased vasoconstriction | 0.21041643 | 0.829319878 |
| ENSG00000206286 | VPS52 subnetwork | 0.20985 | 0.829381586 |
| ENSG00000060069 | CTDP1 subnetwork | 0.21088404 | 0.82942069 |
| ENSG00000168488 | ATXN2L subnetwork | 0.2109941 | 0.82953668 |
| ENSG00000112478 | ENSG00000112478 subnetwork | 0.20985 | 0.82961165 |
| MP:0000255 | vasculature congestion | 0.21106973 | 0.829625034 |
| MP:0005353 | abnormal patella morphology | 0.2111636 | 0.829837376 |
| ENSG00000206214 | ENSG00000206214 subnetwork | 0.20985 | 0.829841842 |
| ENSG00000166508 | MCM7 subnetwork | 0.2113084 | 0.829917355 |
| ENSG00000087157 | PGS1 subnetwork | 0.21127667 | 0.830022045 |
| MP:0004860 | dilated kidney collecting duct | 0.20984879 | 0.830058285 |
| MP:0003045 | fibrosis | 0.20984443 | 0.830288728 |
| GO:0048017 | inositol lipid-mediated signaling | 0.2115594 | 0.830429397 |
| GO:0048015 | phosphatidylinositol-mediated signaling | 0.2115594 | 0.83065804 |
| MP:0000157 | abnormal sternum morphology | 0.21167434 | 0.830737479 |
| ENSG00000134574 | DDB2 subnetwork | 0.21152261 | 0.830776646 |
| ENSG00000114107 | CEP70 subnetwork | 0.21191692 | 0.831636864 |
| ENSG00000029534 | ANK1 subnetwork | 0.21224239 | 0.832755776 |
| MP:0001614 | abnormal blood vessel morphology | 0.21229564 | 0.832788012 |
| GO:0060445 | branching involved in salivary gland morphogenesis | 0.21239772 | 0.833095107 |
| GO:0031058 | positive regulation of histone modification | 0.2124563 | 0.833140973 |
| MP:0003312 | abnormal locomotor coordination | 0.21258017 | 0.833365385 |
| ENSG00000186115 | CYP4F2 subnetwork | 0.21276562 | 0.834111508 |
| ENSG00000138032 | PPM1B subnetwork | 0.21304414 | 0.834700878 |
| MP:0000259 | abnormal vascular development | 0.2130268 | 0.834833928 |
| ENSG00000198062 | POTEH subnetwork | 0.2132199 | 0.834942403 |
| MP:0008212 | absent mature B cells | 0.21302227 | 0.835063152 |
| ENSG00000142937 | RPS8 subnetwork | 0.21331859 | 0.83512476 |
| ENSG00000041357 | PSMA4 subnetwork | 0.2132098 | 0.83515775 |
| GO:0009110 | vitamin biosynthetic process | 0.21356851 | 0.835786732 |
| GO:0030031 | cell projection assembly | 0.21366445 | 0.835955056 |
| MP:0000827 | dilated third ventricle | 0.2137547 | 0.836013699 |
| GO:0048146 | positive regulation of fibroblast proliferation | 0.21397989 | 0.836120996 |
| REACTOME_BIOSYNTHESIS_OF | REACTOME_BIOSYNTHESIS_OF_THE_N:GLYCAN_PRECURSC | 0.21397025 | 0.836295181 |
| ENSG00000135018 | UBQLN1 subnetwork | 0.21393429 | 0.836414681 |
| ENSG00000029725 | RABEP1 subnetwork | 0.21418191 | 0.836648427 |

| | | | |
|---|---|---|---|
| GO:0004004 | ATP-dependent RNA helicase activity | 0.21429035 | 0.836843545 |
| GO:0051130 | positive regulation of cellular component organization | 0.21417439 | 0.836850027 |
| GO:0016706 | oxidoreductase activity, acting on paired donors, with incor | 0.21451664 | 0.837544435 |
| GO:0055074 | calcium ion homeostasis | 0.21465149 | 0.837725533 |
| ENSG00000071894 | CPSF1 subnetwork | 0.21483963 | 0.83826182 |
| ENSG00000175793 | SFN subnetwork | 0.21545265 | 0.840396175 |
| ENSG00000117724 | CENPF subnetwork | 0.21554876 | 0.8404944 |
| GO:0060249 | anatomical structure homeostasis | 0.21591779 | 0.840509954 |
| GO:0043124 | negative regulation of I-kappaB kinase/NF-kappaB cascade | 0.21595412 | 0.840526172 |
| ENSG00000164506 | STXBP5 subnetwork | 0.21580119 | 0.840600273 |
| GO:0005741 | mitochondrial outer membrane | 0.21589343 | 0.840657392 |
| GO:0012507 | ER to Golgi transport vesicle membrane | 0.21575558 | 0.840665939 |
| GO:0015299 | solute:hydrogen antiporter activity | 0.21569292 | 0.840677041 |
| ENSG00000135269 | TES subnetwork | 0.21601834 | 0.840678659 |
| ENSG00000136021 | SCYL2 subnetwork | 0.21630913 | 0.84068881 |
| ENSG00000112186 | CAP2 subnetwork | 0.21624483 | 0.840767974 |
| ENSG00000136504 | KAT7 subnetwork | 0.21566479 | 0.840770071 |
| ENSG00000010803 | SCMH1 subnetwork | 0.21613969 | 0.840871935 |
| ENSG00000111358 | GTF2H3 subnetwork | 0.21621572 | 0.840928902 |
| ENSG00000115977 | AAK1 subnetwork | 0.21653662 | 0.840954842 |
| ENSG00000100105 | PATZ1 subnetwork | 0.21659497 | 0.840984498 |
| ENSG00000144580 | RQCD1 subnetwork | 0.21649301 | 0.841006803 |
| GO:0005089 | Rho guanyl-nucleotide exchange factor activity | 0.21643235 | 0.841072401 |
| ENSG00000115091 | ACTR3 subnetwork | 0.21683411 | 0.841277174 |
| GO:0051099 | positive regulation of binding | 0.2168003 | 0.841410709 |
| MP:0003057 | abnormal epicardium morphology | 0.21675258 | 0.841476346 |
| ENSG00000133627 | ACTR3B subnetwork | 0.21693508 | 0.841496876 |
| ENSG00000172053 | QARS subnetwork | 0.21708845 | 0.841730038 |
| MP:0000364 | abnormal vascular regression | 0.21725758 | 0.842316047 |
| ENSG00000182511 | FES subnetwork | 0.21770271 | 0.843054802 |
| ENSG00000156802 | ATAD2 subnetwork | 0.21767345 | 0.843188602 |
| REACTOME_CITRIC_ACID_CYCL | REACTOME_CITRIC_ACID_CYCLE_TCA_CYCLE | 0.21797098 | 0.843306233 |
| MP:0002413 | abnormal megakaryocyte progenitor cell morphology | 0.21761656 | 0.843308903 |
| ENSG00000150990 | DHX37 subnetwork | 0.21788814 | 0.843356833 |
| ENSG00000151835 | SACS subnetwork | 0.21795128 | 0.843426403 |
| GO:0046470 | phosphatidylcholine metabolic process | 0.21786731 | 0.843531326 |
| ENSG00000134982 | APC subnetwork | 0.2182881 | 0.84444595 |
| MP:0004251 | failure of heart looping | 0.21835465 | 0.844515168 |
| MP:0004597 | increased susceptibility to noise-induced hearing loss | 0.21844332 | 0.844584349 |
| GO:0015101 | organic cation transmembrane transporter activity | 0.21865274 | 0.844844384 |
| ENSG00000132970 | WASF3 subnetwork | 0.21859 | 0.844883595 |
| ENSG00000120798 | NR2C1 subnetwork | 0.21896407 | 0.845752165 |
| ENSG00000114767 | RRP9 subnetwork | 0.21914676 | 0.846145523 |
| GO:0048660 | regulation of smooth muscle cell proliferation | 0.21923902 | 0.846268253 |
| ENSG00000171208 | NETO2 subnetwork | 0.21942078 | 0.846836983 |
| ENSG00000113649 | TCERG1 subnetwork | 0.21963933 | 0.847042139 |
| MP:0001648 | abnormal apoptosis | 0.21973904 | 0.847043737 |
| ENSG00000163602 | RYBP subnetwork | 0.21960948 | 0.847149419 |
| ENSG00000175550 | DRAP1 subnetwork | 0.21972348 | 0.847191466 |
| ENSG00000155130 | MARCKS subnetwork | 0.21958873 | 0.847283784 |
| GO:0008289 | lipid binding | 0.22004573 | 0.848164642 |
| ENSG00000100599 | RIN3 subnetwork | 0.22023665 | 0.848300971 |
| GO:0008138 | protein tyrosine/serine/threonine phosphatase activity | 0.22019356 | 0.848354465 |

| | | | |
|---|---|---|---|
| ENSG00000160199 | PKNOX1 subnetwork | 0.22017549 | 0.848448462 |
| MP:0001596 | hypotension | 0.22045053 | 0.849218118 |
| GO:0042634 | regulation of hair cycle | 0.22054719 | 0.849433962 |
| GO:0005385 | zinc ion transmembrane transporter activity | 0.22064597 | 0.849555376 |
| ENSG00000173801 | JUP subnetwork | 0.22113308 | 0.849677246 |
| GO:0010591 | regulation of lamellipodium assembly | 0.22111736 | 0.849865483 |
| ENSG00000181656 | GPR88 subnetwork | 0.22086708 | 0.850067349 |
| ENSG00000034053 | APBA2 subnetwork | 0.22111657 | 0.850094187 |
| ENSG00000197711 | ENSG00000197711 subnetwork | 0.22127886 | 0.850134445 |
| GO:0008180 | signalosome | 0.22103258 | 0.850242326 |
| ENSG00000197971 | MBP subnetwork | 0.221101 | 0.850269179 |
| ENSG00000067704 | IARS2 subnetwork | 0.22151387 | 0.850416443 |
| GO:0045862 | positive regulation of proteolysis | 0.22102456 | 0.850430918 |
| ENSG00000100485 | SOS2 subnetwork | 0.22148002 | 0.850497178 |
| ENSG00000143727 | ACP1 subnetwork | 0.22145979 | 0.850685484 |
| ENSG00000102010 | BMX subnetwork | 0.22167652 | 0.850698362 |
| ENSG00000149273 | RPS3 subnetwork | 0.22178517 | 0.850980129 |
| MP:0003120 | abnormal tracheal cartilage morphology | 0.22184648 | 0.85104698 |
| GO:0021854 | hypothalamus development | 0.22277362 | 0.851483957 |
| ENSG00000168906 | MAT2A subnetwork | 0.22271955 | 0.851577962 |
| ENSG00000164134 | NAA15 subnetwork | 0.22266316 | 0.851618513 |
| ENSG00000141434 | MEP1B subnetwork | 0.22208251 | 0.851650121 |
| ENSG00000129152 | MYOD1 subnetwork | 0.22206506 | 0.851784756 |
| REACTOME_NEPHRIN_INTERA | REACTOME_NEPHRIN_INTERACTIONS | 0.22235092 | 0.851795284 |
| MP:0005326 | abnormal podocyte morphology | 0.22265981 | 0.851819641 |
| ENSG00000102978 | POLR2C subnetwork | 0.2222734 | 0.851849866 |
| ENSG00000147403 | RPL10 subnetwork | 0.22243758 | 0.851861773 |
| GO:0000122 | negative regulation of transcription from RNA polymerase I | 0.22249924 | 0.851914837 |
| ENSG00000167088 | SNRPD1 subnetwork | 0.22233424 | 0.851929778 |
| ENSG00000113161 | HMGCR subnetwork | 0.22262695 | 0.851953961 |
| MP:0000382 | underdeveloped hair follicles | 0.22225163 | 0.851997855 |
| GO:0010575 | positive regulation vascular endothelial growth factor prod | 0.22259253 | 0.852021419 |
| ENSG00000198373 | WWP2 subnetwork | 0.2229719 | 0.8521251 |
| KEGG_BETA_ALANINE_METAB | KEGG_BETA_ALANINE_METABOLISM | 0.22224308 | 0.852186159 |
| ENSG00000153094 | BCL2L11 subnetwork | 0.2232858 | 0.853113308 |
| ENSG00000117322 | CR2 subnetwork | 0.22343466 | 0.853218483 |
| GO:0030971 | receptor tyrosine kinase binding | 0.22342356 | 0.853419717 |
| ENSG00000165494 | PCF11 subnetwork | 0.22372506 | 0.854325768 |
| GO:0005643 | nuclear pore | 0.22381238 | 0.854471436 |
| ENSG00000174827 | PDZK1 subnetwork | 0.22415706 | 0.855189434 |
| ENSG00000141510 | TP53 subnetwork | 0.22411273 | 0.855310915 |
| ENSG00000088356 | PDRG1 subnetwork | 0.22428215 | 0.85532 |
| MP:0000932 | absent notochord | 0.22422686 | 0.855334756 |
| GO:0048661 | positive regulation of smooth muscle cell proliferation | 0.22453512 | 0.856158358 |
| KEGG_HISTIDINE_METABOLISM | KEGG_HISTIDINE_METABOLISM | 0.22483034 | 0.856566329 |
| ENSG00000110955 | ATP5B subnetwork | 0.22479091 | 0.856661338 |
| ENSG00000123338 | NCKAP1L subnetwork | 0.22492472 | 0.856724368 |
| ENSG00000173273 | TNKS subnetwork | 0.22478823 | 0.85684968 |
| GO:0031527 | filopodium membrane | 0.22510193 | 0.857188498 |
| MP:0000065 | abnormal bone marrow cavity morphology | 0.2254115 | 0.858089409 |
| ENSG00000124356 | STAMBP subnetwork | 0.22555954 | 0.858111702 |
| ENSG00000197471 | SPN subnetwork | 0.22538776 | 0.858211339 |
| ENSG00000089048 | ESF1 subnetwork | 0.22552108 | 0.858246874 |

| | | | |
|---|---|---|---|
| ENSG00000055130 | CUL1 subnetwork | 0.2258532 | 0.858838384 |
| ENSG00000153922 | CHD1 subnetwork | 0.22581605 | 0.858893911 |
| GO:0032129 | histone deacetylase activity (H3-K9 specific) | 0.22674858 | 0.859538951 |
| GO:0016607 | nuclear speck | 0.22629221 | 0.859585767 |
| GO:0032350 | regulation of hormone metabolic process | 0.2271365 | 0.859587411 |
| ENSG00000213066 | FGFR1OP subnetwork | 0.22721642 | 0.859637758 |
| ENSG00000139719 | VPS33A subnetwork | 0.22613723 | 0.859699708 |
| GO:0006635 | fatty acid beta-oxidation | 0.22712406 | 0.859748677 |
| GO:0046969 | NAD-dependent histone deacetylase activity (H3-K9 specifi | 0.22674858 | 0.859766764 |
| MP:0009285 | increased gonadal fat pad weight | 0.2265742 | 0.859774536 |
| GO:0004889 | acetylcholine-activated cation-selective channel activity | 0.22628884 | 0.859800797 |
| ENSG00000131747 | TOP2A subnetwork | 0.22653301 | 0.859816928 |
| ENSG00000205339 | IPO7 subnetwork | 0.22670094 | 0.859862142 |
| MP:0003710 | abnormal physiological neovascularization | 0.2270892 | 0.859870336 |
| GO:0005520 | insulin-like growth factor binding | 0.22667236 | 0.859904535 |
| ENSG00000120094 | HOXB1 subnetwork | 0.22649958 | 0.85991242 |
| ENSG00000167674 | ENSG00000167674 subnetwork | 0.22625741 | 0.859989373 |
| GO:0035088 | establishment or maintenance of apical/basal cell polarity | 0.22701434 | 0.859994705 |
| ENSG00000138802 | SEC24B subnetwork | 0.22706549 | 0.860005294 |
| ENSG00000174744 | BRMS1 subnetwork | 0.2264884 | 0.860140696 |
| GO:0061245 | establishment or maintenance of bipolar cell polarity | 0.22701434 | 0.860222458 |
| MP:0005491 | pancreatic islet hyperplasia | 0.2269614 | 0.860238411 |
| ENSG00000090020 | SLC9A1 subnetwork | 0.22764914 | 0.860705789 |
| GO:0006469 | negative regulation of protein kinase activity | 0.22775928 | 0.860954017 |
| ENSG00000206232 | ENSG00000206232 subnetwork | 0.22801168 | 0.860955649 |
| ENSG00000204261 | ENSG00000204261 subnetwork | 0.22801168 | 0.861182994 |
| ENSG00000158869 | FCER1G subnetwork | 0.22826108 | 0.861316275 |
| GO:0003906 | DNA-(apurinic or apyrimidinic site) lyase activity | 0.2283877 | 0.861363037 |
| ENSG00000206296 | ENSG00000206296 subnetwork | 0.22801168 | 0.86141046 |
| GO:0005759 | mitochondrial matrix | 0.22797316 | 0.861466314 |
| ENSG00000132356 | PRKAA1 subnetwork | 0.22833812 | 0.861471519 |
| ENSG00000161956 | SENP3 subnetwork | 0.22825149 | 0.861530343 |
| ENSG00000087074 | PPP1R15A subnetwork | 0.22821484 | 0.861546582 |
| MP:0004837 | abnormal neural fold formation | 0.22852819 | 0.861646904 |
| ENSG00000136807 | CDK9 subnetwork | 0.22849505 | 0.861729046 |
| ENSG00000138795 | LEF1 subnetwork | 0.22869377 | 0.862223393 |
| ENSG00000115289 | PCGF1 subnetwork | 0.22984142 | 0.862303459 |
| GO:0040008 | regulation of growth | 0.22970596 | 0.862313139 |
| ENSG00000151461 | UPF2 subnetwork | 0.22978484 | 0.862375459 |
| ENSG00000163161 | ERCC3 subnetwork | 0.22984082 | 0.862529489 |
| ENSG00000105821 | DNAJC2 subnetwork | 0.2297045 | 0.862539349 |
| REACTOME_MITOCHONDRIAL_ | REACTOME_MITOCHONDRIAL_FATTY_ACID_BETA:OXIDATI | 0.22970336 | 0.862765678 |
| GO:0005160 | transforming growth factor beta receptor binding | 0.2296426 | 0.862795276 |
| ENSG00000124507 | PACSIN1 subnetwork | 0.22958976 | 0.862890522 |
| ENSG00000005075 | POLR2J subnetwork | 0.23015152 | 0.863043478 |
| ENSG00000106615 | RHEB subnetwork | 0.2295864 | 0.863077731 |
| MP:0000830 | abnormal diencephalon morphology | 0.23014547 | 0.863217186 |
| ENSG00000080815 | PSEN1 subnetwork | 0.22957797 | 0.863304439 |
| ENSG00000072210 | ALDH3A2 subnetwork | 0.22900455 | 0.863339479 |
| MP:0010868 | increased bone trabecula number | 0.22947632 | 0.863455979 |
| ENSG00000110075 | PPP6R3 subnetwork | 0.22957313 | 0.863504992 |
| MP:0004889 | increased energy expenditure | 0.22944047 | 0.863590957 |
| ENSG00000204256 | BRD2 subnetwork | 0.23058245 | 0.863710099 |

| | | | |
|---|---|---|---|
| ENSG00000178921 | PFAS subnetwork | 0.23072106 | 0.863794456 |
| ENSG00000143375 | CGN subnetwork | 0.22938423 | 0.863795371 |
| ENSG00000000971 | CFH subnetwork | 0.2292467 | 0.863802632 |
| MP:0001261 | obese | 0.22943141 | 0.863804891 |
| ENSG00000108528 | SLC25A11 subnetwork | 0.23065833 | 0.863850379 |
| ENSG00000112526 | ENSG00000112526 subnetwork | 0.23058245 | 0.863936142 |
| ENSG00000144231 | POLR2D subnetwork | 0.229239 | 0.86395104 |
| ENSG00000104320 | NBN subnetwork | 0.2291821 | 0.863954713 |
| ENSG00000162946 | DISC1 subnetwork | 0.22937954 | 0.864022626 |
| ENSG00000050820 | BCAR1 subnetwork | 0.23103485 | 0.864145768 |
| ENSG00000215077 | BRD2 subnetwork | 0.23058245 | 0.864162304 |
| ENSG00000141378 | PTRH2 subnetwork | 0.23052159 | 0.864192197 |
| ENSG00000187735 | TCEA1 subnetwork | 0.23101209 | 0.864201725 |
| ENSG00000100413 | POLR3H subnetwork | 0.23112808 | 0.864285714 |
| ENSG00000164934 | DCAF13 subnetwork | 0.23100161 | 0.864362258 |
| ENSG00000020426 | MNAT1 subnetwork | 0.23124398 | 0.864438642 |
| ENSG00000109458 | GAB1 subnetwork | 0.23097052 | 0.864457516 |
| GO:0030027 | lamellipodium | 0.2314927 | 0.865283216 |
| MP:0011402 | renal cast | 0.23238547 | 0.866310857 |
| ENSG00000184489 | PTP4A3 subnetwork | 0.23204206 | 0.866336375 |
| REACTOME_INTERFERON_SIGN | REACTOME_INTERFERON_SIGNALING | 0.23216053 | 0.866340891 |
| REACTOME_SULFUR_AMINO_A | REACTOME_SULFUR_AMINO_ACID_METABOLISM | 0.23186943 | 0.866362213 |
| GO:0008565 | protein transporter activity | 0.23224643 | 0.866401772 |
| ENSG00000113318 | MSH3 subnetwork | 0.2321352 | 0.866436392 |
| ENSG00000163528 | CHCHD4 subnetwork | 0.23236163 | 0.866458333 |
| GO:0051213 | dioxygenase activity | 0.23197045 | 0.86648839 |
| ENSG00000198824 | CHAMP1 subnetwork | 0.23203282 | 0.866523213 |
| MP:0002465 | abnormal eosinophil physiology | 0.23235957 | 0.866684032 |
| ENSG00000083845 | RPS5 subnetwork | 0.23270335 | 0.867647059 |
| ENSG00000153317 | ASAP1 subnetwork | 0.2328693 | 0.868045798 |
| ENSG00000085063 | CD59 subnetwork | 0.23300095 | 0.868127438 |
| ENSG00000162704 | ARPC5 subnetwork | 0.23335462 | 0.868233766 |
| ENSG00000131043 | C20orf4 subnetwork | 0.23297401 | 0.868275234 |
| ENSG00000129315 | CCNT1 subnetwork | 0.23335175 | 0.86845934 |
| GO:0050853 | B cell receptor signaling pathway | 0.23325704 | 0.868572914 |
| MP:0004096 | abnormal midbrain-hindbrain boundary development | 0.23356672 | 0.868582922 |
| ENSG00000013275 | PSMC4 subnetwork | 0.2333266 | 0.868594075 |
| ENSG00000164053 | ATRIP subnetwork | 0.23319695 | 0.868629745 |
| ENSG00000204592 | HLA-E subnetwork | 0.23370037 | 0.868638132 |
| ENSG00000198900 | TOP1 subnetwork | 0.2334828 | 0.868644508 |
| GO:0043297 | apical junction assembly | 0.23356393 | 0.868795431 |
| ENSG00000104946 | TBC1D17 subnetwork | 0.233675 | 0.868811624 |
| ENSG00000137054 | POLR1E subnetwork | 0.23426473 | 0.86889234 |
| ENSG00000106245 | BUD31 subnetwork | 0.234161 | 0.86891507 |
| ENSG00000156313 | RPGR subnetwork | 0.23411923 | 0.868919969 |
| ENSG00000113141 | IK subnetwork | 0.23395221 | 0.868986522 |
| ENSG00000145736 | GTF2H2 subnetwork | 0.23389842 | 0.868991444 |
| ENSG00000160469 | BRSK1 subnetwork | 0.23434997 | 0.869016818 |
| REACTOME_ABORTIVE_ELONG | REACTOME_ABORTIVE_ELONGATION_OF_HIV:1_TRANSCRI | 0.23408798 | 0.869067358 |
| ENSG00000196911 | KPNA5 subnetwork | 0.23425505 | 0.869078436 |
| GO:0032635 | interleukin-6 production | 0.23403333 | 0.869085255 |
| ENSG00000054611 | TBC1D22A subnetwork | 0.23388914 | 0.869164938 |
| ENSG00000109103 | UNC119 subnetwork | 0.23481467 | 0.869253616 |

| | | | |
|---|---|---|---|
| GO:0031060 | regulation of histone methylation | 0.23447748 | 0.869283497 |
| GO:0051494 | negative regulation of cytoskeleton organization | 0.23476533 | 0.869323172 |
| ENSG00000129625 | REEP5 subnetwork | 0.23455616 | 0.86933023 |
| ENSG00000130669 | PAK4 subnetwork | 0.23459934 | 0.869364012 |
| ENSG00000157540 | DYRK1A subnetwork | 0.2347555 | 0.869509044 |
| ENSG00000132153 | DHX30 subnetwork | 0.23506211 | 0.869535484 |
| GO:0000062 | fatty-acyl-CoA binding | 0.23501619 | 0.869617966 |
| ENSG00000188878 | FBF1 subnetwork | 0.23472154 | 0.869630395 |
| REACTOME_DOUBLE:STRAND_ | REACTOME_DOUBLE:STRAND_BREAK_REPAIR | 0.23498262 | 0.86975213 |
| GO:0030889 | negative regulation of B cell proliferation | 0.23525334 | 0.869834924 |
| ENSG00000198130 | HIBCH subnetwork | 0.23522732 | 0.87000774 |
| ENSG00000196405 | EVL subnetwork | 0.23566535 | 0.871196493 |
| MP:0002874 | decreased hemoglobin content | 0.23622437 | 0.872429786 |
| ENSG00000132467 | UTP3 subnetwork | 0.23622433 | 0.872654639 |
| ENSG00000089737 | DDX24 subnetwork | 0.23618735 | 0.872763599 |
| GO:0048147 | negative regulation of fibroblast proliferation | 0.2364045 | 0.872771767 |
| REACTOME_RESOLUTION_OF_ | REACTOME_RESOLUTION_OF_ABASIC_SITES_AP_SITES | 0.23655407 | 0.872875901 |
| REACTOME_BASE_EXCISION_R | REACTOME_BASE_EXCISION_REPAIR | 0.23655407 | 0.873100695 |
| GO:0022624 | proteasome accessory complex | 0.23679866 | 0.873340196 |
| MP:0008540 | abnormal cerebrum morphology | 0.23675277 | 0.873359073 |
| MP:0002310 | decreased susceptibility to hepatic steatosis | 0.23691267 | 0.873604322 |
| GO:0032461 | positive regulation of protein oligomerization | 0.23709551 | 0.874189815 |
| GO:0040014 | regulation of multicellular organism growth | 0.23717665 | 0.874196452 |
| ENSG00000128626 | MRPS12 subnetwork | 0.23819792 | 0.876218574 |
| ENSG00000116266 | STXBP3 subnetwork | 0.23792286 | 0.876239404 |
| ENSG00000101361 | NOP56 subnetwork | 0.23817748 | 0.876430588 |
| ENSG00000079841 | RIMS1 subnetwork | 0.23790932 | 0.876464543 |
| MP:0000873 | thin external granule cell layer | 0.23817054 | 0.87664271 |
| ENSG00000111057 | KRT18 subnetwork | 0.23785345 | 0.876658098 |
| GO:0010669 | epithelial structure maintenance | 0.23790467 | 0.876676947 |
| ENSG00000103194 | USP10 subnetwork | 0.23816041 | 0.876842105 |
| ENSG00000160220 | ENSG00000160220 subnetwork | 0.23813987 | 0.877028762 |
| GO:0010745 | negative regulation of macrophage derived foam cell differ | 0.23927975 | 0.877115827 |
| ENSG00000134882 | UBAC2 subnetwork | 0.23944957 | 0.877133367 |
| ENSG00000115946 | PNO1 subnetwork | 0.23938457 | 0.877300613 |
| MP:0002747 | abnormal aortic valve morphology | 0.23927326 | 0.877314578 |
| ENSG00000112992 | NNT subnetwork | 0.23900722 | 0.877316948 |
| ENSG00000174231 | PRPF8 subnetwork | 0.23943964 | 0.877319192 |
| ENSG00000184787 | UBE2G2 subnetwork | 0.23894796 | 0.877323944 |
| ENSG00000079335 | CDC14A subnetwork | 0.23921157 | 0.877436685 |
| GO:0008653 | lipopolysaccharide metabolic process | 0.23961112 | 0.877445722 |
| ENSG00000113300 | CNOT6 subnetwork | 0.23892159 | 0.877471824 |
| MP:0000260 | abnormal angiogenesis | 0.23916329 | 0.877494882 |
| ENSG00000166603 | MC4R subnetwork | 0.23912259 | 0.877591502 |
| GO:0005849 | mRNA cleavage factor complex | 0.23883194 | 0.877626858 |
| ENSG00000136931 | NR5A1 subnetwork | 0.23877551 | 0.877646757 |
| MP:0009504 | abnormal mammary gland epithelium morphology | 0.2389215 | 0.877696644 |
| ENSG00000169062 | UPF3A subnetwork | 0.23876719 | 0.877846154 |
| GO:0032844 | regulation of homeostatic process | 0.23978649 | 0.877885598 |
| MP:0003109 | short femur | 0.23875776 | 0.878058477 |
| GO:0042026 | protein refolding | 0.24047545 | 0.878702524 |
| REACTOME_SIGNALING_BY_N | REACTOME_SIGNALING_BY_NODAL | 0.24041392 | 0.878722591 |
| ENSG00000099194 | SCD subnetwork | 0.24055664 | 0.878809888 |

| | | | |
|---|---|---|---|
| ENSG00000180879 | SSR4 subnetwork | 0.24041387 | 0.878946697 |
| ENSG00000113712 | CSNK1A1 subnetwork | 0.24037963 | 0.879094388 |
| MP:0006316 | increased urine sodium level | 0.24036038 | 0.879280429 |
| ENSG00000005844 | ITGAL subnetwork | 0.24035366 | 0.879492088 |
| ENSG00000123106 | CCDC91 subnetwork | 0.24031342 | 0.879588971 |
| ENSG00000144381 | HSPD1 subnetwork | 0.24092027 | 0.879801325 |
| ENSG00000150337 | FCGR1A subnetwork | 0.24088897 | 0.879872611 |
| ENSG00000106123 | EPHB6 subnetwork | 0.24105848 | 0.880264833 |
| GO:0032675 | regulation of interleukin-6 production | 0.24120089 | 0.88042759 |
| ENSG00000182359 | KBTBD3 subnetwork | 0.24118655 | 0.880588086 |
| GO:0045408 | regulation of interleukin-6 biosynthetic process | 0.24141915 | 0.881094148 |
| ENSG00000198677 | TTC37 subnetwork | 0.24156893 | 0.881141913 |
| ENSG00000196998 | WDR45 subnetwork | 0.24163704 | 0.88115942 |
| ENSG00000100129 | EIF3L subnetwork | 0.24197142 | 0.881170645 |
| GO:0018107 | peptidyl-threonine phosphorylation | 0.24155889 | 0.881315187 |
| GO:0032496 | response to lipopolysaccharide | 0.24196019 | 0.881369063 |
| ENSG00000141622 | RNF165 subnetwork | 0.24181224 | 0.881423126 |
| MP:0005537 | abnormal cerebral aqueduct morphology | 0.24193016 | 0.881478659 |
| REACTOME_PYRUVATE_METAI | REACTOME_PYRUVATE_METABOLISM_AND_CITRIC_ACID_ | 0.24180591 | 0.88158363 |
| GO:0010888 | negative regulation of lipid storage | 0.24219026 | 0.881827411 |
| ENSG00000116761 | CTH subnetwork | 0.242261 | 0.881895458 |
| GO:0005044 | scavenger receptor activity | 0.2423285 | 0.881900051 |
| ENSG00000141380 | SS18 subnetwork | 0.24237685 | 0.881917322 |
| GO:0043405 | regulation of MAP kinase activity | 0.24250617 | 0.881926489 |
| ENSG00000135775 | COG2 subnetwork | 0.24246286 | 0.882036004 |
| ENSG00000175197 | DDIT3 subnetwork | 0.24218861 | 0.882051282 |
| REACTOME_TRANSPORT_TO_T | REACTOME_TRANSPORT_TO_THE_GOLGI_AND_SUBSEQUE | 0.24259703 | 0.882095793 |
| MP:0000825 | dilated lateral ventricles | 0.24294038 | 0.882409517 |
| ENSG00000139220 | PPFIA2 subnetwork | 0.24274293 | 0.882429693 |
| ENSG00000205937 | RNPS1 subnetwork | 0.24304159 | 0.882527834 |
| ENSG00000156603 | MED19 subnetwork | 0.24311739 | 0.882582848 |
| GO:0033673 | negative regulation of kinase activity | 0.24292752 | 0.882594937 |
| MP:0005339 | increased susceptibility to atherosclerosis | 0.2431788 | 0.882599899 |
| GO:0004675 | transmembrane receptor protein serine/threonine kinase a | 0.24290405 | 0.882717144 |
| ENSG00000186654 | PRR5 subnetwork | 0.2428892 | 0.882877406 |
| GO:0005217 | intracellular ligand-gated ion channel activity | 0.24346303 | 0.88357775 |
| ENSG00000196981 | WDR5B subnetwork | 0.24417536 | 0.885130018 |
| ENSG00000122965 | RBM19 subnetwork | 0.24413709 | 0.885176768 |
| ENSG00000152291 | TGOLN2 subnetwork | 0.24397535 | 0.885279252 |
| ENSG00000125107 | CNOT1 subnetwork | 0.24403963 | 0.885295604 |
| ENSG00000118058 | MLL subnetwork | 0.2439326 | 0.885300809 |
| ENSG00000155957 | TMBIM4 subnetwork | 0.24411198 | 0.885324577 |
| ENSG00000075340 | ADD2 subnetwork | 0.24444583 | 0.885654807 |
| GO:0000302 | response to reactive oxygen species | 0.24464443 | 0.885678265 |
| ENSG00000177688 | SUMO4 subnetwork | 0.24438799 | 0.885726906 |
| ENSG00000197386 | HTT subnetwork | 0.24453215 | 0.88574672 |
| REACTOME_PLATELET_ACTIVA | REACTOME_PLATELET_ACTIVATION_SIGNALING_AND_AGG | 0.24471496 | 0.885757499 |
| ENSG00000160255 | ITGB2 subnetwork | 0.24460963 | 0.885775536 |
| REACTOME_INTERLEUKIN:1_SI | REACTOME_INTERLEUKIN:1_SIGNALING | 0.24491324 | 0.886365927 |
| REACTOME_SNRNP_ASSEMBL\ | REACTOME_SNRNP_ASSEMBLY | 0.24511747 | 0.886404834 |
| MP:0010363 | increased fibrosarcoma incidence | 0.24501252 | 0.886507937 |
| REACTOME_METABOLISM_OF_ | REACTOME_METABOLISM_OF_NON:CODING_RNA | 0.24511747 | 0.886628053 |
| ENSG00000172349 | IL16 subnetwork | 0.24509267 | 0.88675063 |

| | | | |
|---|---|---|---|
| MP:0009791 | increased susceptibility to viral infection induced morbidity | 0.24559751 | 0.888220488 |
| MP:0004024 | aneuploidy | 0.24597355 | 0.888800905 |
| MP:0002086 | abnormal extraembryonic tissue morphology | 0.24588841 | 0.888820423 |
| ENSG00000101336 | HCK subnetwork | 0.24580415 | 0.888827378 |
| MP:0008249 | abnormal common lymphocyte progenitor cell morphology | 0.24586547 | 0.888930818 |
| ENSG00000178568 | ERBB4 subnetwork | 0.24607838 | 0.888954511 |
| GO:0042226 | interleukin-6 biosynthetic process | 0.24596081 | 0.888961529 |
| ENSG00000021488 | SLC7A9 subnetwork | 0.24652247 | 0.890703518 |
| GO:0005839 | proteasome core complex | 0.24668799 | 0.89074818 |
| ENSG00000120948 | TARDBP subnetwork | 0.24660151 | 0.890756091 |
| GO:0007265 | Ras protein signal transduction | 0.2467743 | 0.890825803 |
| ENSG00000166794 | PPIB subnetwork | 0.24666116 | 0.890833752 |
| GO:0016614 | oxidoreductase activity, acting on CH-OH group of donors | 0.2469565 | 0.891166876 |
| MP:0009643 | abnormal urine homeostasis | 0.24702775 | 0.891206724 |
| ENSG00000134899 | ERCC5 subnetwork | 0.2470864 | 0.891259092 |
| GO:0033014 | tetrapyrrole biosynthetic process | 0.24746014 | 0.891994488 |
| MP:0005365 | abnormal bile salt homeostasis | 0.24731721 | 0.892138917 |
| GO:0006779 | porphyrin-containing compound biosynthetic process | 0.24746014 | 0.892218045 |
| ENSG00000212695 | ENSG00000212695 subnetwork | 0.24741809 | 0.89231637 |
| GO:0005765 | lysosomal membrane | 0.24764942 | 0.89251002 |
| GO:0048821 | erythrocyte development | 0.24786697 | 0.893075382 |
| GO:0048659 | smooth muscle cell proliferation | 0.24797979 | 0.893128911 |
| MP:0005560 | decreased circulating glucose level | 0.24813507 | 0.893282462 |
| ENSG00000138674 | SEC31A subnetwork | 0.24797715 | 0.893352529 |
| MP:0001656 | focal hepatic necrosis | 0.24810702 | 0.893355856 |
| MP:0005169 | abnormal male meiosis | 0.24836388 | 0.893871936 |
| GO:0016811 | hydrolase activity, acting on carbon-nitrogen (but not pepti | 0.24869871 | 0.8948625 |
| GO:0006968 | cellular defense response | 0.24869409 | 0.895061265 |
| GO:0030832 | regulation of actin filament length | 0.24885767 | 0.895176206 |
| MP:0011099 | complete lethality throughout fetal growth and developme | 0.24896264 | 0.895452274 |
| ENSG00000136279 | DBNL subnetwork | 0.24912668 | 0.895865601 |
| GO:0016701 | oxidoreductase activity, acting on single donors with incorp | 0.24937021 | 0.896441948 |
| GO:0005625 | soluble fraction | 0.24934978 | 0.896540959 |
| ENSG00000116213 | WRAP73 subnetwork | 0.24964113 | 0.897416375 |
| ENSG00000136068 | FLNB subnetwork | 0.24980005 | 0.897791365 |
| GO:0032800 | receptor biosynthetic process | 0.25003096 | 0.898154153 |
| ENSG00000144118 | RALB subnetwork | 0.2499926 | 0.898340818 |
| REACTOME_JNK_C:JUN_KINAS | REACTOME_JNK_C:JUN_KINASES_PHOSPHORYLATION_ANI | 0.25038434 | 0.899226933 |
| MP:0002209 | decreased germ cell number | 0.25054404 | 0.89965096 |
| ENSG00000132470 | ITGB4 subnetwork | 0.2508102 | 0.900099676 |
| MP:0001770 | abnormal iron level | 0.25074894 | 0.900149551 |
| GO:0051341 | regulation of oxidoreductase activity | 0.25105806 | 0.900784753 |
| ENSG00000115761 | NOL10 subnetwork | 0.25163825 | 0.901817277 |
| MP:0001613 | abnormal vasodilation | 0.25162901 | 0.901979582 |
| MP:0002628 | hepatic steatosis | 0.25183187 | 0.902077114 |
| ENSG00000168502 | CCDC165 subnetwork | 0.25159375 | 0.902079701 |
| GO:0051017 | actin filament bundle assembly | 0.25179946 | 0.902102513 |
| ENSG00000057608 | GDI2 subnetwork | 0.25176149 | 0.9021777 |
| ENSG00000043093 | DCUN1D1 subnetwork | 0.25206239 | 0.902498757 |
| GO:0060760 | positive regulation of response to cytokine stimulus | 0.2520393 | 0.902698334 |
| ENSG00000134597 | RBMX2 subnetwork | 0.25215291 | 0.902709421 |
| ENSG00000075413 | MARK3 subnetwork | 0.25242167 | 0.903367296 |
| ENSG00000162129 | CLPB subnetwork | 0.25325157 | 0.903368838 |

| | | | |
|---|---|---|---|
| ENSG00000118515 | SGK1 subnetwork | 0.25319303 | 0.903468781 |
| GO:0007128 | meiotic prophase I | 0.25313875 | 0.903630731 |
| GO:0071706 | tumor necrosis factor superfamily cytokine production | 0.25269563 | 0.903649454 |
| ENSG00000133740 | E2F5 subnetwork | 0.25397852 | 0.903718804 |
| GO:0000502 | proteasome complex | 0.25391947 | 0.903781513 |
| ENSG00000165934 | CPSF2 subnetwork | 0.2526821 | 0.903811771 |
| ENSG00000182621 | PLCB1 subnetwork | 0.25298828 | 0.903831845 |
| ENSG00000107758 | PPP3CB subnetwork | 0.25312876 | 0.90384234 |
| ENSG00000065833 | ME1 subnetwork | 0.25258462 | 0.903850932 |
| ENSG00000109133 | TMEM33 subnetwork | 0.25352318 | 0.903862342 |
| ENSG00000213465 | ARL2 subnetwork | 0.2535887 | 0.903873762 |
| GO:0030518 | intracellular steroid hormone receptor signaling pathway | 0.25345679 | 0.903888063 |
| ENSG00000198734 | F5 subnetwork | 0.25295628 | 0.903894815 |
| ENSG00000099817 | POLR2E subnetwork | 0.25389266 | 0.90394314 |
| MP:0009642 | abnormal blood homeostasis | 0.25266129 | 0.903961749 |
| GO:0051568 | histone H3-K4 methylation | 0.25293151 | 0.904019851 |
| MP:0008280 | male germ cell apoptosis | 0.25312646 | 0.904066452 |
| ENSG00000185787 | MORF4L1 subnetwork | 0.25389233 | 0.904166667 |
| ENSG00000136003 | ISCU subnetwork | 0.2529169 | 0.904182179 |
| ENSG00000115221 | ITGB6 subnetwork | 0.25416148 | 0.904323123 |
| ENSG00000198034 | RPS4X subnetwork | 0.2538821 | 0.90436557 |
| ENSG00000103426 | CORO7 subnetwork | 0.25383168 | 0.904416131 |
| ENSG00000111269 | CREBL2 subnetwork | 0.25378883 | 0.904466716 |
| ENSG00000039537 | C6 subnetwork | 0.2544226 | 0.904814815 |
| MP:0002152 | abnormal brain morphology | 0.25468923 | 0.904834731 |
| GO:0008023 | transcription elongation factor complex | 0.25465809 | 0.904909943 |
| ENSG00000167508 | MVD subnetwork | 0.25440207 | 0.904939491 |
| ENSG00000183741 | CBX6 subnetwork | 0.25463916 | 0.905096249 |
| ENSG00000107554 | DNMBP subnetwork | 0.25463472 | 0.905319674 |
| GO:0072507 | divalent inorganic cation homeostasis | 0.25492263 | 0.905536375 |
| GO:0005892 | acetylcholine-gated channel complex | 0.25497481 | 0.905547337 |
| GO:0006874 | cellular calcium ion homeostasis | 0.25512694 | 0.905928026 |
| GO:0032012 | regulation of ARF protein signal transduction | 0.25526617 | 0.906172992 |
| GO:0010893 | positive regulation of steroid biosynthetic process | 0.25547771 | 0.906279242 |
| ENSG00000159251 | ACTC1 subnetwork | 0.25546599 | 0.906465517 |
| GO:0008064 | regulation of actin polymerization or depolymerization | 0.25545722 | 0.906664203 |
| GO:0032370 | positive regulation of lipid transport | 0.25571942 | 0.907151649 |
| MP:0004986 | abnormal osteoblast morphology | 0.25581793 | 0.907186808 |
| ENSG00000143947 | RPS27A subnetwork | 0.25615553 | 0.908439961 |
| GO:0016861 | intramolecular oxidoreductase activity, interconverting ald | 0.25626678 | 0.908484998 |
| ENSG00000156261 | CCT8 subnetwork | 0.25624334 | 0.908646986 |
| GO:0010906 | regulation of glucose metabolic process | 0.2566677 | 0.908843036 |
| ENSG00000134248 | HBXIP subnetwork | 0.25657722 | 0.908845209 |
| ENSG00000147604 | RPL7 subnetwork | 0.25656375 | 0.908982551 |
| ENSG00000180628 | PCGF5 subnetwork | 0.25651149 | 0.909021632 |
| ENSG00000141959 | PFKL subnetwork | 0.25648067 | 0.909048439 |
| ENSG00000156299 | TIAM1 subnetwork | 0.25702145 | 0.909102061 |
| GO:0005923 | tight junction | 0.25696588 | 0.909141104 |
| ENSG00000070087 | PFN2 subnetwork | 0.25680608 | 0.909160118 |
| ENSG00000164105 | SAP30 subnetwork | 0.2568567 | 0.909170145 |
| GO:0070160 | occluding junction | 0.25696588 | 0.909364261 |
| ENSG00000067066 | SP100 subnetwork | 0.2574772 | 0.909458466 |
| ENSG00000215760 | ENSG00000215760 subnetwork | 0.25735904 | 0.909561167 |

| | | | |
|---|---|---|---|
| ENSG00000115392 | FANCL subnetwork | 0.25744414 | 0.909583333 |
| GO:0010494 | cytoplasmic stress granule | 0.25814526 | 0.909604106 |
| GO:0016747 | transferase activity, transferring acyl groups other than ami | 0.25820394 | 0.909662839 |
| ENSG00000169621 | APLF subnetwork | 0.25725511 | 0.909725288 |
| ENSG00000187325 | TAF9B subnetwork | 0.25735904 | 0.909784208 |
| ENSG00000114270 | COL7A1 subnetwork | 0.2581427 | 0.909826448 |
| MP:0000828 | abnormal fourth ventricle morphology | 0.25811652 | 0.909889976 |
| ENSG00000132361 | KIAA0664 subnetwork | 0.2576233 | 0.909897109 |
| ENSG00000132664 | POLR3F subnetwork | 0.25810417 | 0.910051357 |
| GO:0004428 | inositol or phosphatidylinositol kinase activity | 0.25808616 | 0.910225049 |
| REACTOME_REMOVAL_OF_DN | REACTOME_REMOVAL_OF_DNA_PATCH_CONTAINING_AB/ | 0.25802462 | 0.910276486 |
| GO:0004519 | endonuclease activity | 0.25864608 | 0.910324628 |
| ENSG00000140564 | FURIN subnetwork | 0.25779725 | 0.910347783 |
| REACTOME_RESOLUTION_OF_ | REACTOME_RESOLUTION_OF_AP_SITES_VIA_THE_MULTIPI | 0.25802462 | 0.910499266 |
| MP:0003658 | abnormal capillary morphology | 0.25882053 | 0.91051476 |
| MP:0004756 | abnormal proximal convoluted tubule morphology | 0.25864394 | 0.910546875 |
| ENSG00000119139 | TJP2 subnetwork | 0.25790862 | 0.910553379 |
| REACTOME_ANTIGEN_PROCES | REACTOME_ANTIGEN_PROCESSING:CROSS_PRESENTATION | 0.25862095 | 0.910683761 |
| ENSG00000120694 | HSPH1 subnetwork | 0.25879932 | 0.910688141 |
| GO:0044403 | symbiosis, encompassing mutualism through parasitism | 0.25801937 | 0.910722154 |
| ENSG00000186831 | ENSG00000186831 subnetwork | 0.25894496 | 0.910804878 |
| ENSG00000108039 | XPNPEP1 subnetwork | 0.25857566 | 0.910893991 |
| ENSG00000112118 | MCM3 subnetwork | 0.25922244 | 0.911335934 |
| ENSG00000183508 | FAM46C subnetwork | 0.25930941 | 0.911369729 |
| ENSG00000072062 | PRKACA subnetwork | 0.25921137 | 0.911533772 |
| ENSG00000113070 | HBEGF subnetwork | 0.25975854 | 0.911988802 |
| GO:0000723 | telomere maintenance | 0.25972676 | 0.912064767 |
| GO:0045732 | positive regulation of protein catabolic process | 0.25952273 | 0.912110136 |
| ENSG00000134419 | RPS15A subnetwork | 0.25989118 | 0.912229253 |
| REACTOME_DESTABILIZATION_ | REACTOME_DESTABILIZATION_OF_MRNA_BY_AUF1_HNRN | 0.25971201 | 0.912238188 |
| GO:0010212 | response to ionizing radiation | 0.25969833 | 0.912387333 |
| KEGG_NON_SMALL_CELL_LUN | KEGG_NON_SMALL_CELL_LUNG_CANCER | 0.26096101 | 0.912781955 |
| ENSG00000151322 | NPAS3 subnetwork | 0.26089658 | 0.912797186 |
| ENSG00000126226 | PCID2 subnetwork | 0.26079274 | 0.912864078 |
| MP:0000125 | absent incisors | 0.26027747 | 0.912953053 |
| ENSG00000203811 | HIST2H3C subnetwork | 0.26076782 | 0.912976451 |
| ENSG00000080603 | SRCAP subnetwork | 0.26024517 | 0.913017032 |
| MP:0008554 | decreased circulating tumor necrosis factor level | 0.26089241 | 0.913018685 |
| ENSG00000183598 | HIST2H3D subnetwork | 0.26076782 | 0.913198154 |
| ENSG00000100902 | PSMA6 subnetwork | 0.26058346 | 0.913304982 |
| GO:0044282 | small molecule catabolic process | 0.26075056 | 0.913371387 |
| MP:0008477 | decreased spleen red pulp amount | 0.26069558 | 0.913386783 |
| GO:0005637 | nuclear inner membrane | 0.26055777 | 0.913429752 |
| MP:0011427 | mesangial cell hyperplasia | 0.26051442 | 0.913542426 |
| GO:0032320 | positive regulation of Ras GTPase activity | 0.26043867 | 0.913582198 |
| KEGG_FOCAL_ADHESION | KEGG_FOCAL_ADHESION | 0.26137706 | 0.914051891 |
| ENSG00000182533 | CAV3 subnetwork | 0.26197346 | 0.91482333 |
| ENSG00000182774 | RPS17L subnetwork | 0.26176956 | 0.914898256 |
| ENSG00000175536 | LIPT2 subnetwork | 0.26185937 | 0.914991523 |
| GO:0033627 | cell adhesion mediated by integrin | 0.26169129 | 0.915002424 |
| ENSG00000136950 | ARPC5L subnetwork | 0.26196267 | 0.91503268 |
| ENSG00000184779 | RPS17 subnetwork | 0.26176956 | 0.915119942 |
| GO:0002825 | regulation of T-helper 1 type immune response | 0.26165472 | 0.915127273 |

| | | | |
|---|---|---|---|
| GO:0009451 | RNA modification | 0.26193296 | 0.915157385 |
| ENSG00000186868 | MAPT subnetwork | 0.26232043 | 0.915232108 |
| GO:0046580 | negative regulation of Ras protein signal transduction | 0.26229169 | 0.915405079 |
| GO:0006354 | transcription elongation, DNA-dependent | 0.26246133 | 0.915445975 |
| ENSG00000211455 | STK38L subnetwork | 0.26229065 | 0.915626512 |
| GO:0032787 | monocarboxylic acid metabolic process | 0.26224171 | 0.915666586 |
| ENSG00000169372 | CRADD subnetwork | 0.26298851 | 0.916698865 |
| GO:0032200 | telomere organization | 0.26298725 | 0.91692029 |
| ENSG00000169696 | ASPSCR1 subnetwork | 0.26292314 | 0.916924378 |
| ENSG00000057468 | MSH4 subnetwork | 0.26289849 | 0.917049299 |
| ENSG00000185621 | LMLN subnetwork | 0.26329614 | 0.917181467 |
| ENSG00000149100 | EIF3M subnetwork | 0.26329283 | 0.917402848 |
| GO:0016616 | oxidoreductase activity, acting on the CH-OH group of donc | 0.26325203 | 0.917455336 |
| ENSG00000173889 | PHC3 subnetwork | 0.26355333 | 0.918287093 |
| GO:0043903 | regulation of symbiosis, encompassing mutualism through p | 0.2637748 | 0.918801254 |
| ENSG00000170632 | ARMC10 subnetwork | 0.26399724 | 0.919165863 |
| GO:0071346 | cellular response to interferon-gamma | 0.26394305 | 0.919254883 |
| MP:0003352 | increased circulating renin level | 0.2642978 | 0.919795181 |
| ENSG00000124228 | DDX27 subnetwork | 0.26429595 | 0.920016872 |
| GO:0008080 | N-acetyltransferase activity | 0.26446594 | 0.920284269 |
| ENSG00000117632 | STMN1 subnetwork | 0.26464273 | 0.920797206 |
| GO:0030529 | ribonucleoprotein complex | 0.26488299 | 0.921478449 |
| ENSG00000197157 | SND1 subnetwork | 0.26507314 | 0.921918633 |
| ENSG00000186810 | CXCR3 subnetwork | 0.26549275 | 0.922811448 |
| GO:0016289 | CoA hydrolase activity | 0.26547988 | 0.92302141 |
| GO:0004407 | histone deacetylase activity | 0.26545672 | 0.923159288 |
| GO:0033558 | protein deacetylase activity | 0.26545672 | 0.923381468 |
| ENSG00000165516 | KLHDC2 subnetwork | 0.26584784 | 0.923533654 |
| GO:0070925 | organelle assembly | 0.26580028 | 0.923671556 |
| ENSG00000168556 | ING2 subnetwork | 0.26600145 | 0.924032684 |
| GO:0051240 | positive regulation of multicellular organismal process | 0.26619459 | 0.924123439 |
| MP:0008058 | abnormal DNA repair | 0.26616583 | 0.92426135 |
| ENSG00000171992 | SYNPO subnetwork | 0.26616559 | 0.924483421 |
| ENSG00000204523 | ENSG00000204523 subnetwork | 0.26643773 | 0.924507921 |
| GO:0000784 | nuclear chromosome, telomeric region | 0.26649896 | 0.924550036 |
| GO:0043393 | regulation of protein binding | 0.26641328 | 0.924657863 |
| ENSG00000161939 | C17orf49 subnetwork | 0.26662898 | 0.924682178 |
| REACTOME_NRAGE_SIGNALS_ | REACTOME_NRAGE_SIGNALS_DEATH_THROUGH_JNK | 0.26661855 | 0.924868042 |
| GO:0051058 | negative regulation of small GTPase mediated signal transd | 0.26678862 | 0.925047962 |
| ENSG00000166226 | CCT2 subnetwork | 0.26706814 | 0.925665308 |
| ENSG00000182247 | UBE2E2 subnetwork | 0.2677085 | 0.925920612 |
| ENSG00000182326 | C1S subnetwork | 0.26720213 | 0.925982742 |
| ENSG00000163781 | TOPBP1 subnetwork | 0.26760962 | 0.926004785 |
| MP:0002894 | abnormal otolith morphology | 0.26731328 | 0.926018208 |
| ENSG00000125755 | SYMPK subnetwork | 0.26726864 | 0.926036425 |
| ENSG00000039987 | BEST2 subnetwork | 0.2676878 | 0.926058359 |
| GO:0032007 | negative regulation of TOR signaling cascade | 0.267399 | 0.92605988 |
| GO:0042158 | lipoprotein biosynthetic process | 0.26760166 | 0.926166547 |
| GO:0007204 | elevation of cytosolic calcium ion concentration | 0.26750989 | 0.926179076 |
| GO:0090079 | translation regulator activity, nucleic acid binding | 0.26759379 | 0.926352322 |
| MP:0004560 | abnormal chorionic plate morphology | 0.26750734 | 0.926364943 |
| GO:0032640 | tumor necrosis factor production | 0.26803484 | 0.926523297 |
| GO:0032680 | regulation of tumor necrosis factor production | 0.26803484 | 0.926744742 |

| | | | |
|---|---|---|---|
| ENSG00000164338 | UTP15 subnetwork | 0.26883274 | 0.926757208 |
| ENSG00000147853 | AK3 subnetwork | 0.26881976 | 0.926823165 |
| GO:0004536 | deoxyribonuclease activity | 0.26836249 | 0.926856052 |
| MP:0002790 | decreased circulating follicle stimulating hormone level | 0.26800919 | 0.926858714 |
| ENSG00000163516 | ANKZF1 subnetwork | 0.2689749 | 0.926899262 |
| ENSG00000147669 | POLR2K subnetwork | 0.26877311 | 0.926948749 |
| ENSG00000140368 | PSTPIP1 subnetwork | 0.26832105 | 0.926969914 |
| GO:0043603 | cellular amide metabolic process | 0.26822166 | 0.927042523 |
| ENSG00000105135 | ILVBL subnetwork | 0.26853692 | 0.927046051 |
| ENSG00000108344 | PSMD3 subnetwork | 0.26907046 | 0.927059524 |
| MP:0002824 | abnormal chorioallantoic fusion | 0.26827611 | 0.927059947 |
| ENSG00000102145 | GATA1 subnetwork | 0.26913388 | 0.927064985 |
| GO:0019216 | regulation of lipid metabolic process | 0.26895269 | 0.927072415 |
| GO:0019058 | viral infectious cycle | 0.26874647 | 0.927110157 |
| ENSG00000062485 | CS subnetwork | 0.26934838 | 0.927176499 |
| REACTOME_STABILIZATION_O | REACTOME_STABILIZATION_OF_P53 | 0.26853016 | 0.927231504 |
| MP:0004227 | increased cellular sensitivity to ionizing radiation | 0.2693097 | 0.927242446 |
| ENSG00000135829 | DHX9 subnetwork | 0.26874389 | 0.927319342 |
| ENSG00000105404 | RABAC1 subnetwork | 0.26869173 | 0.927325859 |
| GO:0005024 | transforming growth factor beta-activated receptor activity | 0.2693048 | 0.927439315 |
| ENSG00000163110 | PDLIM5 subnetwork | 0.26952675 | 0.927621879 |
| MP:0004030 | induced chromosome breakage | 0.26976467 | 0.928197813 |
| ENSG00000132604 | TERF2 subnetwork | 0.27000484 | 0.928856667 |
| ENSG00000215120 | ENSG00000215120 subnetwork | 0.27018869 | 0.929194392 |
| ENSG00000120158 | RCL1 subnetwork | 0.27026767 | 0.929246852 |
| MP:0000116 | abnormal tooth development | 0.27034845 | 0.929251781 |
| ENSG00000196284 | SUPT3H subnetwork | 0.27052728 | 0.929707908 |
| ENSG00000168495 | POLR3D subnetwork | 0.27067923 | 0.929817276 |
| ENSG00000172172 | MRPL13 subnetwork | 0.27060884 | 0.929855176 |
| GO:0043281 | regulation of cysteine-type endopeptidase activity involved | 0.2706692 | 0.929978638 |
| MP:0010701 | fusion of atlas and odontoid process | 0.27106786 | 0.930925267 |
| ENSG00000204319 | ENSG00000204319 subnetwork | 0.27156242 | 0.931851588 |
| ENSG00000137055 | PLAA subnetwork | 0.27165397 | 0.931915146 |
| GO:0051298 | centrosome duplication | 0.27175949 | 0.932026066 |
| GO:0051693 | actin filament capping | 0.27155288 | 0.93204885 |
| GO:0005730 | nucleolus | 0.27151458 | 0.932222486 |
| ENSG00000154917 | RAB6B subnetwork | 0.27191572 | 0.932224064 |
| ENSG00000136715 | SAP130 subnetwork | 0.27185887 | 0.932243544 |
| MP:0000596 | abnormal liver development | 0.27219197 | 0.932402367 |
| ENSG00000159461 | AMFR subnetwork | 0.27217237 | 0.93256392 |
| ENSG00000140474 | ULK3 subnetwork | 0.27215686 | 0.93276107 |
| GO:0006607 | NLS-bearing substrate import into nucleus | 0.27248009 | 0.933073101 |
| ENSG00000206300 | ENSG00000206300 subnetwork | 0.27288277 | 0.933266415 |
| MP:0000222 | decreased neutrophil cell number | 0.27294949 | 0.933270366 |
| GO:0019200 | carbohydrate kinase activity | 0.27246272 | 0.933282063 |
| ENSG00000167085 | PHB subnetwork | 0.27259183 | 0.933337275 |
| ENSG00000108312 | UBTF subnetwork | 0.27269976 | 0.933404255 |
| MP:0000133 | abnormal long bone metaphysis morphology | 0.27266433 | 0.93347127 |
| ENSG00000206406 | CSNK2B subnetwork | 0.27288277 | 0.933486889 |
| MP:0008411 | decreased cellular sensitivity to ultraviolet irradiation | 0.27276744 | 0.9334909 |
| ENSG00000204435 | CSNK2B subnetwork | 0.27288277 | 0.933707467 |
| ENSG00000089157 | RPLP0 subnetwork | 0.27314597 | 0.933911709 |
| MP:0011186 | abnormal visceral endoderm morphology | 0.27330304 | 0.934198726 |

| | | | |
|---|---|---|---|
| REACTOME_ETHANOL_OXIDAT | REACTOME_ETHANOL_OXIDATION | 0.27360378 | 0.934969325 |
| MP:0008762 | embryonic lethality | 0.27398041 | 0.93522272 |
| REACTOME_CROSS:PRESENTAT | REACTOME_CROSS:PRESENTATION_OF_SOLUBLE_EXOGEN | 0.27414986 | 0.935265018 |
| ENSG00000138190 | EXOC6 subnetwork | 0.27386182 | 0.935310068 |
| REACTOME_HIV_LIFE_CYCLE | REACTOME_HIV_LIFE_CYCLE | 0.27372702 | 0.935314933 |
| ENSG00000172943 | PHF8 subnetwork | 0.27410828 | 0.935320452 |
| ENSG00000101811 | CSTF2 subnetwork | 0.27393454 | 0.935360679 |
| MP:0008412 | increased cellular sensitivity to oxidative stress | 0.27431161 | 0.935472098 |
| ENSG00000103365 | GGA2 subnetwork | 0.27384397 | 0.935483491 |
| GO:0045649 | regulation of macrophage differentiation | 0.27459356 | 0.935532816 |
| ENSG00000205246 | RPSAP58 subnetwork | 0.27429711 | 0.935657089 |
| ENSG00000177380 | PPFIA3 subnetwork | 0.27470373 | 0.935712606 |
| MP:0006264 | decreased systemic arterial systolic blood pressure | 0.2745835 | 0.935729412 |
| ENSG00000163785 | RYK subnetwork | 0.27456411 | 0.9359261 |
| ENSG00000196792 | STRN3 subnetwork | 0.27482036 | 0.936080414 |
| GO:0000314 | organellar small ribosomal subunit | 0.27522225 | 0.936131987 |
| GO:0043027 | cysteine-type endopeptidase inhibitor activity involved in a | 0.27455751 | 0.936146422 |
| ENSG00000089351 | GRAMD1A subnetwork | 0.27493109 | 0.936177715 |
| GO:0005763 | mitochondrial small ribosomal subunit | 0.27522225 | 0.936351891 |
| GO:0007031 | peroxisome organization | 0.27549871 | 0.936356171 |
| ENSG00000141556 | TBCD subnetwork | 0.27510785 | 0.936498237 |
| REACTOME_TRANSPORT_OF_V | REACTOME_TRANSPORT_OF_VITAMINS_NUCLEOSIDES_AN | 0.27544851 | 0.936517249 |
| ENSG00000166411 | IDH3A subnetwork | 0.27519544 | 0.936536654 |
| ENSG00000183093 | ENSG00000183093 subnetwork | 0.27536085 | 0.936557877 |
| ENSG00000004455 | AK2 subnetwork | 0.27541741 | 0.936619718 |
| ENSG00000129465 | RIPK3 subnetwork | 0.27570823 | 0.937004457 |
| ENSG00000105640 | RPL18A subnetwork | 0.27597511 | 0.937593809 |
| GO:0051087 | chaperone binding | 0.276159 | 0.938007034 |
| ENSG00000145741 | BTF3 subnetwork | 0.27628054 | 0.938150492 |
| GO:0015144 | carbohydrate transmembrane transporter activity | 0.2771099 | 0.93893826 |
| ENSG00000146701 | MDH2 subnetwork | 0.27708492 | 0.939040936 |
| MP:0009657 | failure of chorioallantoic fusion | 0.27698866 | 0.939141119 |
| ENSG00000115816 | CEBPZ subnetwork | 0.27694575 | 0.939173689 |
| ENSG00000168421 | RHOH subnetwork | 0.27705821 | 0.939178755 |
| GO:0033628 | regulation of cell adhesion mediated by integrin | 0.27690712 | 0.939253102 |
| ENSG00000122779 | TRIM24 subnetwork | 0.27733685 | 0.939259 |
| ENSG00000102158 | MAGT1 subnetwork | 0.27730657 | 0.939385083 |
| ENSG00000175467 | SART1 subnetwork | 0.27688999 | 0.93941452 |
| ENSG00000103126 | AXIN1 subnetwork | 0.27682359 | 0.939435465 |
| ENSG00000160213 | CSTB subnetwork | 0.27673385 | 0.939524256 |
| REACTOME_RNA_POLYMERAS | REACTOME_RNA_POLYMERASE_III_TRANSCRIPTION_TERM | 0.27681509 | 0.939597001 |
| ENSG00000130429 | ARPC1B subnetwork | 0.27838653 | 0.939634288 |
| MP:0008056 | abnormal retinal ganglion cell morphology | 0.27836175 | 0.939783318 |
| ENSG00000057593 | F7 subnetwork | 0.27756009 | 0.939869128 |
| ENSG00000047315 | POLR2B subnetwork | 0.27822486 | 0.93988345 |
| GO:0004520 | endodeoxyribonuclease activity | 0.2788875 | 0.939906977 |
| ENSG00000077420 | APBB1IP subnetwork | 0.27880199 | 0.93993718 |
| ENSG00000168393 | DTYMK subnetwork | 0.27817708 | 0.93993938 |
| ENSG00000164070 | HSPA4L subnetwork | 0.27885597 | 0.939951151 |
| GO:0018210 | peptidyl-threonine modification | 0.27833777 | 0.939979026 |
| ENSG00000055163 | CYFIP2 subnetwork | 0.2787665 | 0.940027926 |
| ENSG00000116459 | ATP5F1 subnetwork | 0.27772814 | 0.940037374 |
| MP:0010383 | increased adenoma incidence | 0.27796032 | 0.940058343 |

| | | | |
|---|---|---|---|
| ENSG00000094916 | CBX5 subnetwork | 0.27783925 | 0.940065375 |
| ENSG00000080608 | KIAA0020 subnetwork | 0.27804826 | 0.94009566 |
| ENSG00000136718 | IMP4 subnetwork | 0.27811997 | 0.940109634 |
| ENSG00000008710 | PKD1 subnetwork | 0.27767705 | 0.940140187 |
| ENSG00000100142 | POLR2F subnetwork | 0.2787501 | 0.940153631 |
| ENSG00000215694 | ENSG00000215694 subnetwork | 0.27817708 | 0.940158582 |
| ENSG00000175115 | PACS1 subnetwork | 0.2779349 | 0.940231092 |
| ENSG00000112078 | KCTD20 subnetwork | 0.27782615 | 0.940273237 |
| ENSG00000164330 | EBF1 subnetwork | 0.2787152 | 0.940291036 |
| ENSG00000142494 | SLC47A1 subnetwork | 0.27868419 | 0.940440149 |
| MP:0004948 | abnormal neuronal precursor proliferation | 0.27932752 | 0.941085542 |
| ENSG00000131370 | SH3BP5 subnetwork | 0.27927861 | 0.94112997 |
| ENSG00000145703 | IQGAP2 subnetwork | 0.27953348 | 0.941184669 |
| ENSG00000002745 | WNT16 subnetwork | 0.27961828 | 0.94122359 |
| MP:0001263 | weight loss | 0.27941161 | 0.941227051 |
| REACTOME_ZINC_TRANSPORT | REACTOME_ZINC_TRANSPORTERS | 0.27950397 | 0.941287175 |
| ENSG00000196305 | IARS subnetwork | 0.27961372 | 0.941430562 |
| GO:0045624 | positive regulation of T-helper cell differentiation | 0.27974966 | 0.941538997 |
| MP:0001216 | abnormal epidermal layer morphology | 0.27979421 | 0.941552564 |
| GO:0043244 | regulation of protein complex disassembly | 0.28010943 | 0.941884999 |
| GO:0005096 | GTPase activator activity | 0.28004268 | 0.941906308 |
| MP:0002128 | abnormal blood circulation | 0.27999436 | 0.941939225 |
| ENSG00000067208 | EVI5 subnetwork | 0.27994668 | 0.941983759 |
| ENSG00000092847 | EIF2C1 subnetwork | 0.28024332 | 0.942072323 |
| GO:0032770 | positive regulation of monooxygenase activity | 0.28077465 | 0.942341509 |
| MP:0004748 | increased susceptibility to age-related hearing loss | 0.28086481 | 0.94240111 |
| ENSG00000075914 | EXOSC7 subnetwork | 0.28069174 | 0.942430556 |
| REACTOME_REGULATION_OF_ | REACTOME_REGULATION_OF_ORNITHINE_DECARBOXYLAS | 0.28075048 | 0.942467022 |
| GO:0045740 | positive regulation of DNA replication | 0.28067209 | 0.942556147 |
| MP:0001257 | increased body length | 0.28065566 | 0.942670218 |
| ENSG00000096238 | ENSG00000096238 subnetwork | 0.28061186 | 0.94272643 |
| ENSG00000206394 | CLIC1 subnetwork | 0.28061186 | 0.942944856 |
| ENSG00000177700 | POLR2L subnetwork | 0.28124849 | 0.942962792 |
| GO:0015645 | fatty acid ligase activity | 0.28115666 | 0.943075145 |
| GO:0003950 | NAD+ ADP-ribosyltransferase activity | 0.28110155 | 0.943085106 |
| GO:0005657 | replication fork | 0.28140835 | 0.943093093 |
| ENSG00000177455 | CD19 subnetwork | 0.28124312 | 0.943157651 |
| ENSG00000213719 | CLIC1 subnetwork | 0.28061186 | 0.943163384 |
| ENSG00000121858 | TNFSF10 subnetwork | 0.28139528 | 0.943264787 |
| ENSG00000133477 | FAM83F subnetwork | 0.28159726 | 0.943442623 |
| ENSG00000116191 | RALGPS2 subnetwork | 0.28175488 | 0.943537964 |
| ENSG00000143514 | TP53BP2 subnetwork | 0.28170129 | 0.943582641 |
| REACTOME_STEROID_HORMO | REACTOME_STEROID_HORMONES | 0.2815834 | 0.943648961 |
| ENSG00000105371 | ICAM4 subnetwork | 0.28225465 | 0.944076976 |
| GO:0007159 | leukocyte cell-cell adhesion | 0.28221184 | 0.944179345 |
| MP:0005554 | decreased circulating creatinine level | 0.28274839 | 0.944352427 |
| MP:0006298 | abnormal platelet activation | 0.28248039 | 0.944368954 |
| GO:0034399 | nuclear periphery | 0.2822023 | 0.94438552 |
| ENSG00000131368 | MRPS25 subnetwork | 0.28212491 | 0.944429066 |
| ENSG00000152495 | CAMK4 subnetwork | 0.28217426 | 0.944488007 |
| ENSG00000110367 | DDX6 subnetwork | 0.28239697 | 0.94452765 |
| GO:0000803 | sex chromosome | 0.28246603 | 0.94452891 |
| ENSG00000131876 | SNRPA1 subnetwork | 0.28208812 | 0.944531611 |

| | | | |
|---|---|---|---|
| ENSG00000107175 | CREB3 subnetwork | 0.28274467 | 0.944535205 |
| ENSG00000171490 | RSL1D1 subnetwork | 0.28260263 | 0.944588994 |
| ENSG00000166025 | AMOTL1 subnetwork | 0.28273149 | 0.944695052 |
| MP:0005325 | abnormal renal glomerulus morphology | 0.28271707 | 0.944808932 |
| ENSG00000165916 | PSMC3 subnetwork | 0.28316513 | 0.945480681 |
| ENSG00000186184 | POLR1D subnetwork | 0.28357638 | 0.945977936 |
| GO:0071514 | genetic imprinting | 0.28342875 | 0.946033571 |
| GO:0009895 | negative regulation of catabolic process | 0.28372595 | 0.946037216 |
| ENSG00000196365 | LONP1 subnetwork | 0.2835585 | 0.946114943 |
| MP:0005311 | abnormal circulating amino acid level | 0.2837111 | 0.946197151 |
| GO:0008374 | O-acyltransferase activity | 0.2839798 | 0.946692696 |
| MP:0000186 | decreased circulating HDL cholesterol level | 0.28452054 | 0.948243398 |
| ENSG00000163558 | PRKCI subnetwork | 0.28475847 | 0.948542575 |
| GO:0030335 | positive regulation of cell migration | 0.28469661 | 0.948588154 |
| ENSG00000177971 | IMP3 subnetwork | 0.28487591 | 0.948646168 |
| GO:0016272 | prefoldin complex | 0.2850646 | 0.949059417 |
| MP:0005565 | increased blood urea nitrogen level | 0.28522964 | 0.949311927 |
| ENSG00000171861 | RNMTL1 subnetwork | 0.28562335 | 0.9501146 |
| REACTOME_APOPTOTIC_EXECI | REACTOME_APOPTOTIC_EXECUTION__PHASE | 0.285608 | 0.950320954 |
| ENSG00000101109 | STK4 subnetwork | 0.28554691 | 0.950366888 |
| ENSG00000103035 | PSMD7 subnetwork | 0.28587917 | 0.950847846 |
| ENSG00000106125 | FAM188B subnetwork | 0.28610004 | 0.951466208 |
| ENSG00000140350 | ANP32A subnetwork | 0.2863727 | 0.952290426 |
| ENSG00000105258 | POLR2I subnetwork | 0.2864938 | 0.952530341 |
| ENSG00000108798 | ABI3 subnetwork | 0.28663526 | 0.952563516 |
| MP:0001684 | abnormal axial mesoderm | 0.28676128 | 0.95271167 |
| ENSG00000197621 | ENSG00000197621 subnetwork | 0.28659803 | 0.952712912 |
| MP:0003051 | curly tail | 0.286874 | 0.952939831 |
| GO:0030532 | small nuclear ribonucleoprotein complex | 0.28707273 | 0.953144295 |
| ENSG00000133027 | PEMT subnetwork | 0.28718113 | 0.953177869 |
| ENSG00000170759 | KIF5B subnetwork | 0.28706527 | 0.953350869 |
| GO:0043388 | positive regulation of DNA binding | 0.28756904 | 0.953459694 |
| ENSG00000197063 | MAFG subnetwork | 0.28752469 | 0.953529009 |
| GO:0051539 | 4 iron, 4 sulfur cluster binding | 0.28750013 | 0.953678318 |
| ENSG00000164244 | PRRC1 subnetwork | 0.28740639 | 0.95376 |
| GO:0005802 | trans-Golgi network | 0.28749656 | 0.953896252 |
| GO:0043296 | apical junction complex | 0.28783619 | 0.954166667 |
| GO:0070741 | response to interleukin-6 | 0.28797969 | 0.9544168 |
| MP:0000165 | abnormal long bone hypertrophic chondrocyte zone | 0.28809275 | 0.954643998 |
| ENSG00000169895 | SYAP1 subnetwork | 0.28833021 | 0.955179101 |
| ENSG00000143437 | ARNT subnetwork | 0.28969906 | 0.956089525 |
| GO:0045913 | positive regulation of carbohydrate metabolic process | 0.28965932 | 0.956136364 |
| ENSG00000198924 | DCLRE1A subnetwork | 0.28940128 | 0.956211604 |
| REACTOME_RESOLUTION_OF_ | REACTOME_RESOLUTION_OF_AP_SITES_VIA_THE_SINGLE:I | 0.28954816 | 0.956265636 |
| GO:0010676 | positive regulation of cellular carbohydrate metabolic proce | 0.28965932 | 0.956353717 |
| GO:0051797 | regulation of hair follicle development | 0.28937867 | 0.956360947 |
| REACTOME_REGULATION_OF_ | REACTOME_REGULATION_OF_ACTIVATED_PAK:2P34_BY_P | 0.28952565 | 0.956449045 |
| ENSG00000143569 | UBAP2L subnetwork | 0.28993108 | 0.956506927 |
| GO:0043209 | myelin sheath | 0.28998935 | 0.956528156 |
| GO:0008610 | lipid biosynthetic process | 0.28937147 | 0.956544503 |
| REACTOME_TRIGLYCERIDE_BIC | REACTOME_TRIGLYCERIDE_BIOSYNTHESIS | 0.28965659 | 0.956571169 |
| MP:0000783 | abnormal forebrain morphology | 0.28990321 | 0.956656065 |
| MP:0003420 | delayed intramembranous bone ossification | 0.28937047 | 0.956750911 |

| | | | |
|---|---|---|---|
| REACTOME_AUTODEGRADATI | REACTOME_AUTODEGRADATION_OF_THE_E3_UBIQUITIN_ | 0.29015974 | 0.956833144 |
| ENSG00000130713 | EXOSC2 subnetwork | 0.28932679 | 0.956877704 |
| ENSG00000121067 | SPOP subnetwork | 0.28928378 | 0.956947608 |
| ENSG00000102003 | SYP subnetwork | 0.28918614 | 0.957019143 |
| GO:0000188 | inactivation of MAPK activity | 0.28924844 | 0.95705172 |
| ENSG00000164104 | HMGB2 subnetwork | 0.28907977 | 0.957090743 |
| ENSG00000115966 | ATF2 subnetwork | 0.28918399 | 0.957237292 |
| ENSG00000099381 | SETD1A subnetwork | 0.28907719 | 0.957297605 |
| REACTOME_METABOLISM_OF_ | REACTOME_METABOLISM_OF_LIPIDS_AND_LIPOPROTEINS | 0.29055593 | 0.957327586 |
| ENSG00000111602 | TIMELESS subnetwork | 0.29049553 | 0.957329249 |
| ENSG00000088205 | DDX18 subnetwork | 0.29043136 | 0.957399001 |
| ENSG00000100453 | GZMB subnetwork | 0.29071728 | 0.957505669 |
| ENSG00000175073 | VCPIP1 subnetwork | 0.28907629 | 0.957515967 |
| ENSG00000182979 | MTA1 subnetwork | 0.29065369 | 0.957518712 |
| REACTOME_SIGNALING_BY_FG | REACTOME_SIGNALING_BY_FGFR | 0.29110528 | 0.95830689 |
| MP:0006029 | abnormal sclerotome morphology | 0.29107793 | 0.958422127 |
| ENSG00000139625 | MAP3K12 subnetwork | 0.29146899 | 0.959483345 |
| GO:0051186 | cofactor metabolic process | 0.29172446 | 0.9598641 |
| GO:0006284 | base-excision repair | 0.29177316 | 0.959929801 |
| GO:0006611 | protein export from nucleus | 0.29170556 | 0.959990938 |
| GO:0019894 | kinesin binding | 0.29198276 | 0.960606747 |
| GO:0016769 | transferase activity, transferring nitrogenous groups | 0.29206524 | 0.960694885 |
| MP:0000420 | ruffled hair | 0.29249782 | 0.961021931 |
| ENSG00000052723 | SIKE1 subnetwork | 0.29244709 | 0.96111488 |
| GO:0051348 | negative regulation of transferase activity | 0.29237652 | 0.961140014 |
| ENSG00000105855 | ITGB8 subnetwork | 0.29234283 | 0.961199095 |
| ENSG00000183405 | ENSG00000183405 subnetwork | 0.29230668 | 0.961314777 |
| ENSG00000145817 | YIPF5 subnetwork | 0.29293452 | 0.962206148 |
| GO:0071013 | catalytic step 2 spliceosome | 0.29366825 | 0.962435175 |
| GO:0045927 | positive regulation of growth | 0.29352001 | 0.962556408 |
| GO:0005858 | axonemal dynein complex | 0.29361645 | 0.962632529 |
| GO:0008203 | cholesterol metabolic process | 0.29366726 | 0.962652233 |
| ENSG00000082516 | GEMIN5 subnetwork | 0.29379893 | 0.9626578 |
| ENSG00000085721 | RRN3 subnetwork | 0.29348922 | 0.962672083 |
| ENSG00000198231 | DDX42 subnetwork | 0.29330482 | 0.962759711 |
| ENSG00000160808 | MYL3 subnetwork | 0.29325841 | 0.962796476 |
| MP:0001354 | increased aggression towards males | 0.29348103 | 0.962866817 |
| GO:0016323 | basolateral plasma membrane | 0.29322785 | 0.962889742 |
| ENSG00000138758 | SEPT11 subnetwork | 0.29317294 | 0.962960452 |
| REACTOME_GAMMA:CARBOXY | REACTOME_GAMMA:CARBOXYLATION_TRANSPORT_AND_ | 0.2934592 | 0.96305035 |
| ENSG00000105248 | CCDC94 subnetwork | 0.29481415 | 0.963511691 |
| ENSG00000136636 | KCTD3 subnetwork | 0.29456061 | 0.963681368 |
| GO:0090312 | positive regulation of protein deacetylation | 0.29465578 | 0.963712036 |
| ENSG00000164050 | PLXNB1 subnetwork | 0.294811 | 0.963728356 |
| GO:0042384 | cilium assembly | 0.29414094 | 0.963736759 |
| MP:0006345 | absent second branchial arch | 0.29473634 | 0.96374269 |
| ENSG00000010244 | ZNF207 subnetwork | 0.29585138 | 0.963746359 |
| MP:0008151 | increased diameter of long bones | 0.29455909 | 0.963887013 |
| GO:0072503 | cellular divalent inorganic cation homeostasis | 0.29583731 | 0.963928732 |
| ENSG00000136560 | TANK subnetwork | 0.29440363 | 0.963941441 |
| ENSG00000132155 | RAF1 subnetwork | 0.29579843 | 0.964010312 |
| ENSG00000117528 | ABCD3 subnetwork | 0.29454761 | 0.964058982 |
| ENSG00000105011 | ASF1B subnetwork | 0.29430602 | 0.964139252 |

| | | | |
|---|---|---|---|
| MP:0011109 | partial lethality throughout fetal growth and development | 0.29440028 | 0.964158594 |
| ENSG00000177469 | PTRF subnetwork | 0.29579677 | 0.964226457 |
| MP:0004045 | abnormal cell cycle checkpoint function | 0.29553651 | 0.964228007 |
| ENSG00000054118 | THRAP3 subnetwork | 0.2945358 | 0.964253546 |
| REACTOME_RAP1_SIGNALLING | REACTOME_RAP1_SIGNALLING | 0.29565251 | 0.964359435 |
| ENSG00000024048 | UBR2 subnetwork | 0.29643332 | 0.964370387 |
| GO:0016410 | N-acyltransferase activity | 0.29578119 | 0.964397847 |
| REACTOME_CASPASE:MEDIATI | REACTOME_CASPASE:MEDIATED_CLEAVAGE_OF_CYTOSKE | 0.29552511 | 0.964444444 |
| ENSG00000143815 | LBR subnetwork | 0.29651263 | 0.964445438 |
| ENSG00000101246 | ARFRP1 subnetwork | 0.29547276 | 0.964492591 |
| ENSG00000196535 | MYO18A subnetwork | 0.29615748 | 0.964512878 |
| GO:0016887 | ATPase activity | 0.2960986 | 0.96453853 |
| ENSG00000163349 | HIPK1 subnetwork | 0.29575379 | 0.964546882 |
| GO:0071843 | cellular component biogenesis at cellular level | 0.29642873 | 0.964563758 |
| MP:0000180 | abnormal circulating cholesterol level | 0.29538122 | 0.964588949 |
| GO:0051896 | regulation of protein kinase B signaling cascade | 0.29631612 | 0.964637422 |
| MP:0000558 | abnormal tibia morphology | 0.29546028 | 0.964653043 |
| MP:0004362 | cochlear hair cell degeneration | 0.29525127 | 0.964696629 |
| GO:2001252 | positive regulation of chromosome organization | 0.29628206 | 0.964696664 |
| ENSG00000170522 | ELOVL6 subnetwork | 0.29519131 | 0.964699933 |
| ENSG00000104823 | ECH1 subnetwork | 0.29534163 | 0.964715794 |
| GO:0022613 | ribonucleoprotein complex biogenesis | 0.29641059 | 0.964723652 |
| GO:0000289 | nuclear-transcribed mRNA poly(A) tail shortening | 0.29624916 | 0.964823108 |
| MP:0003743 | abnormal facial morphology | 0.29684009 | 0.96560474 |
| MP:0001786 | skin edema | 0.29697784 | 0.965664804 |
| ENSG00000087269 | NOP14 subnetwork | 0.29695759 | 0.965780063 |
| GO:0030695 | GTPase regulator activity | 0.29744452 | 0.965945102 |
| ENSG00000185963 | BICD2 subnetwork | 0.29732697 | 0.965985711 |
| MP:0004499 | increased incidence of chemically-induced tumors | 0.29730579 | 0.966112104 |
| REACTOME_UBIQUITIN:DEPEN | REACTOME_UBIQUITIN:DEPENDENT_DEGRADATION_OF_C | 0.29726081 | 0.966138039 |
| ENSG00000150760 | DOCK1 subnetwork | 0.29743362 | 0.966149554 |
| REACTOME_UBIQUITIN:DEPEN | REACTOME_UBIQUITIN:DEPENDENT_DEGRADATION_OF_C | 0.29726081 | 0.966353887 |
| ENSG00000113460 | BRIX1 subnetwork | 0.29765325 | 0.966398929 |
| GO:0061039 | ovum-producing ovary development | 0.29778995 | 0.966514273 |
| ENSG00000138069 | RAB1A subnetwork | 0.29778227 | 0.966685255 |
| ENSG00000117751 | PPP1R8 subnetwork | 0.29798851 | 0.966740972 |
| ENSG00000121753 | BAI2 subnetwork | 0.29817172 | 0.966822638 |
| GO:2000116 | regulation of cysteine-type endopeptidase activity | 0.29810492 | 0.966882104 |
| ENSG00000158402 | CDC25C subnetwork | 0.29797631 | 0.966911929 |
| ENSG00000101868 | POLA1 subnetwork | 0.29854331 | 0.967776788 |
| ENSG00000100028 | SNRPD3 subnetwork | 0.29934496 | 0.968188889 |
| ENSG00000163714 | U2SURP subnetwork | 0.29932961 | 0.968270727 |
| ENSG00000135372 | NAT10 subnetwork | 0.29895711 | 0.968283997 |
| ENSG00000160916 | ENSG00000160916 subnetwork | 0.29909173 | 0.968331479 |
| ENSG00000204434 | ENSG00000204434 subnetwork | 0.29891258 | 0.968343722 |
| ENSG00000104221 | BRF2 subnetwork | 0.29903836 | 0.968402314 |
| MP:0000928 | incomplete cephalic closure | 0.29924749 | 0.968412275 |
| ENSG00000007264 | MATK subnetwork | 0.29932277 | 0.968463762 |
| REACTOME_RNA_POLYMERASI | REACTOME_RNA_POLYMERASE_I_TRANSCRIPTION_TERMII | 0.29888666 | 0.968470274 |
| GO:0019059 | initiation of viral infection | 0.29882917 | 0.968518931 |
| MP:0008261 | arrest of male meiosis | 0.29962216 | 0.968576505 |
| ENSG00000175634 | RPS6KB2 subnetwork | 0.29924467 | 0.968616548 |
| MP:0003648 | abnormal radial glial cell morphology | 0.29969193 | 0.968627886 |

| | | | |
|---|---|---|---|
| ENSG00000105974 | CAV1 subnetwork | 0.29954899 | 0.968729171 |
| GO:0032318 | regulation of Ras GTPase activity | 0.29961975 | 0.968780542 |
| MP:0004527 | abnormal outer hair cell stereociliary bundle morphology | 0.29989787 | 0.969156493 |
| ENSG00000155463 | OXA1L subnetwork | 0.30052419 | 0.970144124 |
| ENSG00000141644 | MBD1 subnetwork | 0.30051995 | 0.970348193 |
| ENSG00000145604 | SKP2 subnetwork | 0.30032892 | 0.970372836 |
| GO:0020027 | hemoglobin metabolic process | 0.30047544 | 0.970452529 |
| ENSG00000211896 | ENSG00000211896 subnetwork | 0.30071659 | 0.970527599 |
| ENSG00000205517 | RGL3 subnetwork | 0.30101368 | 0.970564784 |
| MP:0001270 | distended abdomen | 0.30046341 | 0.97066785 |
| GO:0006875 | cellular metal ion homeostasis | 0.30114548 | 0.970710649 |
| MP:0002705 | dilated renal tubules | 0.30099598 | 0.970746566 |
| REACTOME_ER:PHAGOSOME_ | REACTOME_ER:PHAGOSOME_PATHWAY | 0.30124298 | 0.970816733 |
| ENSG00000212915 | ENSG00000212915 subnetwork | 0.30112892 | 0.970881311 |
| KEGG_CITRATE_CYCLE_TCA_CY | KEGG_CITRATE_CYCLE_TCA_CYCLE | 0.30088136 | 0.970888741 |
| ENSG00000121481 | RNF2 subnetwork | 0.30097616 | 0.97091735 |
| ENSG00000105063 | PPP6R1 subnetwork | 0.30141492 | 0.971166187 |
| MP:0000352 | decreased cell proliferation | 0.30152121 | 0.971261062 |
| ENSG00000001167 | NFYA subnetwork | 0.30201109 | 0.971564295 |
| ENSG00000013293 | SLC7A14 subnetwork | 0.3019312 | 0.97158011 |
| ENSG00000099960 | SLC7A4 subnetwork | 0.3019312 | 0.971794872 |
| MP:0008140 | podocyte foot process effacement | 0.30189596 | 0.971888127 |
| ENSG00000168959 | GRM5 subnetwork | 0.30217089 | 0.971924011 |
| ENSG00000106633 | GCK subnetwork | 0.30224122 | 0.971930212 |
| GO:0006446 | regulation of translational initiation | 0.3018675 | 0.971992481 |
| GO:0004683 | calmodulin-dependent protein kinase activity | 0.30234527 | 0.97202473 |
| GO:0010884 | positive regulation of lipid storage | 0.30245491 | 0.97218543 |
| ENSG00000159352 | PSMD4 subnetwork | 0.30186579 | 0.972207476 |
| ENSG00000132305 | IMMT subnetwork | 0.30257005 | 0.97234606 |
| GO:0007140 | male meiosis | 0.30263306 | 0.972374228 |
| MP:0008869 | anovulation | 0.30294586 | 0.973306861 |
| MP:0001552 | increased circulating triglyceride level | 0.30315714 | 0.973875165 |
| ENSG00000108264 | TADA2A subnetwork | 0.30337755 | 0.974355017 |
| ENSG00000105287 | PRKD2 subnetwork | 0.30381323 | 0.97494491 |
| MP:0010026 | decreased liver cholesterol level | 0.30368258 | 0.974966931 |
| ENSG00000150907 | FOXO1 subnetwork | 0.30379894 | 0.975126736 |
| GO:0071897 | DNA biosynthetic process | 0.30395072 | 0.975137696 |
| GO:0016779 | nucleotidyltransferase activity | 0.304119 | 0.975192689 |
| REACTOME_NEGATIVE_REGUL | REACTOME_NEGATIVE_REGULATORS_OF_RIG:IMDA5_SIGN | 0.30421746 | 0.975297226 |
| ENSG00000153989 | NUS1 subnetwork | 0.30411666 | 0.975407489 |
| ENSG00000090382 | LYZ subnetwork | 0.30517242 | 0.975565313 |
| MP:0008734 | decreased susceptibility to endotoxin shock | 0.30438292 | 0.975577812 |
| GO:0030003 | cellular cation homeostasis | 0.30515268 | 0.975647782 |
| ENSG00000174953 | DHX36 subnetwork | 0.30444075 | 0.975660211 |
| GO:0019207 | kinase regulator activity | 0.30502433 | 0.975702988 |
| ENSG00000130227 | XPO7 subnetwork | 0.30513454 | 0.975796178 |
| GO:0070830 | tight junction assembly | 0.30500719 | 0.975873434 |
| MP:0002231 | abnormal primitive streak morphology | 0.30460725 | 0.975984598 |
| ENSG00000182446 | NPLOC4 subnetwork | 0.30496583 | 0.975989011 |
| KEGG_ONE_CARBON_POOL_BY | KEGG_ONE_CARBON_POOL_BY_FOLATE | 0.30476591 | 0.97602815 |
| KEGG_GLYCOSYLPHOSPHATIDY | KEGG_GLYCOSYLPHOSPHATIDYLINOSITOL_GPI_ANCHOR_B | 0.30494254 | 0.97611563 |
| ENSG00000070756 | PABPC1 subnetwork | 0.30488196 | 0.976154354 |
| ENSG00000120802 | TMPO subnetwork | 0.30473884 | 0.976187857 |

| | | | |
|---|---|---|---|
| ENSG00000115350 | POLE4 subnetwork | 0.30577202 | 0.976633772 |
| GO:0004298 | threonine-type endopeptidase activity | 0.30567349 | 0.976656428 |
| MP:0010760 | abnormal macrophage chemotaxis | 0.30576712 | 0.976847993 |
| GO:0070003 | threonine-type peptidase activity | 0.30567349 | 0.976870748 |
| ENSG00000183091 | NEB subnetwork | 0.30616822 | 0.977021696 |
| ENSG00000113194 | FAF2 subnetwork | 0.30566635 | 0.977063213 |
| ENSG00000047849 | MAP4 subnetwork | 0.3060374 | 0.977121245 |
| GO:0034341 | response to interferon-gamma | 0.30686883 | 0.977137546 |
| ENSG00000103363 | TCEB2 subnetwork | 0.30614922 | 0.977181061 |
| GO:0001889 | liver development | 0.30683607 | 0.977241907 |
| REACTOME_ANTIGEN_PRESEN | REACTOME_ANTIGEN_PRESENTATION_FOLDING_ASSEMBL | 0.30683579 | 0.977455699 |
| ENSG00000162512 | SDC3 subnetwork | 0.30658454 | 0.977501642 |
| GO:0080025 | phosphatidylinositol-3,5-bisphosphate binding | 0.30678278 | 0.977527352 |
| ENSG00000182473 | EXOC7 subnetwork | 0.30635046 | 0.977530675 |
| MP:0004592 | small mandible | 0.3065166 | 0.977562418 |
| GO:0006978 | DNA damage response, signal transduction by p53 class me | 0.30669327 | 0.977648862 |
| ENSG00000197694 | SPTAN1 subnetwork | 0.30649601 | 0.977688938 |
| ENSG00000134255 | CEPT1 subnetwork | 0.30676553 | 0.977697527 |
| ENSG00000174720 | LARP7 subnetwork | 0.30732399 | 0.977972028 |
| REACTOME_HORMONE_LIGAN | REACTOME_HORMONE_LIGAND:BINDING_RECEPTORS | 0.30739708 | 0.977987765 |
| GO:0016235 | aggresome | 0.30726982 | 0.977989071 |
| ENSG00000172939 | OXSR1 subnetwork | 0.30806659 | 0.978074575 |
| ENSG00000130816 | DNMT1 subnetwork | 0.30813117 | 0.978079355 |
| GO:0045080 | positive regulation of chemokine biosynthetic process | 0.30722982 | 0.978126366 |
| GO:0060589 | nucleoside-triphosphatase regulator activity | 0.30758594 | 0.978128412 |
| ENSG00000105193 | RPS16 subnetwork | 0.30752318 | 0.9781564 |
| ENSG00000213780 | GTF2H4 subnetwork | 0.30804375 | 0.978222465 |
| ENSG00000206476 | ENSG00000206476 subnetwork | 0.30804375 | 0.978435864 |
| ENSG00000213764 | ENSG00000213764 subnetwork | 0.30786289 | 0.978552718 |
| ENSG00000215476 | ENSG00000215476 subnetwork | 0.30804375 | 0.978649356 |
| ENSG00000141570 | CBX8 subnetwork | 0.30801708 | 0.978764732 |
| ENSG00000196459 | TRAPPC2 subnetwork | 0.30786289 | 0.978766376 |
| ENSG00000149016 | TUT1 subnetwork | 0.30842753 | 0.978846992 |
| ENSG00000100084 | HIRA subnetwork | 0.30863991 | 0.979309218 |
| MP:0008586 | disorganized photoreceptor outer segment | 0.30880209 | 0.97954694 |
| GO:0000932 | cytoplasmic mRNA processing body | 0.30877431 | 0.97962963 |
| ENSG00000149532 | CPSF7 subnetwork | 0.30897758 | 0.980008711 |
| GO:0005938 | cell cortex | 0.30912895 | 0.980187241 |
| ENSG00000130826 | DKC1 subnetwork | 0.30941955 | 0.980761697 |
| ENSG00000186867 | QRFPR subnetwork | 0.30939941 | 0.980953418 |
| ENSG00000096746 | HNRNPH3 subnetwork | 0.30961138 | 0.981266319 |
| GO:0017016 | Ras GTPase binding | 0.3107671 | 0.982935302 |
| GO:0031929 | TOR signaling cascade | 0.31073924 | 0.983018458 |
| ENSG00000155229 | MMS19 subnetwork | 0.31069758 | 0.983090791 |
| REACTOME_METABOLISM_OF | REACTOME_METABOLISM_OF_AMINO_ACIDS_AND_DERIV | 0.31096846 | 0.983116319 |
| ENSG00000167005 | NUDT21 subnetwork | 0.31111493 | 0.98313449 |
| ENSG00000118762 | PKD2 subnetwork | 0.3109204 | 0.983188626 |
| REACTOME_CDK:MEDIATED_P | REACTOME_CDK:MEDIATED_PHOSPHORYLATION_AND_RE | 0.31067927 | 0.983250054 |
| GO:0071902 | positive regulation of protein serine/threonine kinase activi | 0.31110167 | 0.983304404 |
| REACTOME_METABOLISM_OF | REACTOME_METABOLISM_OF_PROTEINS | 0.31067432 | 0.983463711 |
| GO:0009791 | post-embryonic development | 0.31131716 | 0.983495988 |
| ENSG00000185513 | L3MBTL1 subnetwork | 0.3106402 | 0.983568789 |
| GO:0021794 | thalamus development | 0.31145083 | 0.983597138 |

| | | | |
|---|---|---|---|
| ENSG00000135069 | PSAT1 subnetwork | 0.31058522 | 0.983652174 |
| ENSG00000197003 | ENSG00000197003 subnetwork | 0.31043397 | 0.983655937 |
| ENSG00000042429 | MED17 subnetwork | 0.31053833 | 0.983681235 |
| ENSG00000197369 | ENSG00000197369 subnetwork | 0.31043397 | 0.983869915 |
| GO:0005547 | phosphatidylinositol-3,4,5-trisphosphate binding | 0.31203928 | 0.984372969 |
| ENSG00000120438 | TCP1 subnetwork | 0.31196951 | 0.984380416 |
| ENSG00000123136 | DDX39A subnetwork | 0.31229458 | 0.984408137 |
| GO:0032233 | positive regulation of actin filament bundle assembly | 0.31185428 | 0.984500325 |
| GO:0022037 | metencephalon development | 0.31190217 | 0.984514521 |
| ENSG00000139219 | COL2A1 subnetwork | 0.31195598 | 0.984550379 |
| ENSG00000167658 | EEF2 subnetwork | 0.31227505 | 0.98461039 |
| ENSG00000053372 | MRTO4 subnetwork | 0.31219268 | 0.984733651 |
| ENSG00000163510 | CWC22 subnetwork | 0.3122629 | 0.98479108 |
| GO:0031057 | negative regulation of histone modification | 0.31256963 | 0.985168758 |
| MP:0011143 | thick lung-associated mesenchyme | 0.31265123 | 0.985280121 |
| ENSG00000124217 | MOCS3 subnetwork | 0.31286078 | 0.985300476 |
| REACTOME_DEGRADATION_O | REACTOME_DEGRADATION_OF_BETA:CATENIN_BY_THE_D | 0.31323109 | 0.985391924 |
| MP:0002768 | small adrenal glands | 0.31283873 | 0.985416216 |
| ENSG00000165271 | NOL6 subnetwork | 0.31280247 | 0.985532007 |
| ENSG00000166337 | TAF10 subnetwork | 0.31334436 | 0.9855462 |
| REACTOME_SIGNALING_BY_W | REACTOME_SIGNALING_BY_WNT | 0.31323109 | 0.985604752 |
| ENSG00000065154 | OAT subnetwork | 0.31317782 | 0.985666451 |
| ENSG00000197451 | HNRNPAB subnetwork | 0.31343555 | 0.985743579 |
| ENSG00000153187 | HNRNPU subnetwork | 0.31308211 | 0.985822347 |
| ENSG00000153046 | CDYL subnetwork | 0.31315034 | 0.985836214 |
| GO:0016888 | endodeoxyribonuclease activity, producing 5'-phosphomon | 0.31380314 | 0.985974558 |
| MP:0004686 | decreased length of long bones | 0.31359064 | 0.98607035 |
| GO:0010744 | positive regulation of macrophage derived foam cell differe | 0.31379711 | 0.986165624 |
| MP:0004991 | decreased bone strength | 0.31373205 | 0.986194996 |
| ENSG00000163877 | SNIP1 subnetwork | 0.3136984 | 0.986299892 |
| MP:0002084 | abnormal developmental patterning | 0.31408809 | 0.986328378 |
| ENSG00000133243 | BTBD2 subnetwork | 0.3140689 | 0.986476293 |
| MP:0001533 | abnormal skeleton physiology | 0.31399996 | 0.986516491 |
| MP:0000351 | increased cell proliferation | 0.31421932 | 0.986654459 |
| MP:0000003 | abnormal adipose tissue morphology | 0.31447692 | 0.987037037 |
| GO:0006497 | protein lipidation | 0.31440608 | 0.987077321 |
| ENSG00000049541 | RFC2 subnetwork | 0.31466565 | 0.987481163 |
| ENSG00000088833 | NSFL1C subnetwork | 0.31527256 | 0.988225806 |
| GO:0035329 | hippo signaling cascade | 0.31498532 | 0.988355575 |
| MP:0000249 | abnormal blood vessel physiology | 0.31526517 | 0.988406109 |
| ENSG00000155660 | PDIA4 subnetwork | 0.31523618 | 0.988489673 |
| ENSG00000187446 | ENSG00000187446 subnetwork | 0.31516867 | 0.988551754 |
| ENSG00000064961 | HMG20B subnetwork | 0.31554689 | 0.988566516 |
| GO:2000147 | positive regulation of cell motility | 0.3155999 | 0.98859046 |
| MP:0005438 | abnormal glycogen homeostasis | 0.31552685 | 0.988703783 |
| ENSG00000092853 | CLSPN subnetwork | 0.31550169 | 0.988830359 |
| ENSG00000172795 | DCP2 subnetwork | 0.31586066 | 0.98943072 |
| ENSG00000196961 | AP2A1 subnetwork | 0.31592778 | 0.989465206 |
| MP:0010180 | increased susceptibility to weight loss | 0.31603505 | 0.989607043 |
| ENSG00000112282 | MED23 subnetwork | 0.3160995 | 0.989662945 |
| GO:0005080 | protein kinase C binding | 0.31625947 | 0.989933462 |
| GO:0070008 | serine-type exopeptidase activity | 0.31643042 | 0.990085837 |
| ENSG00000160633 | SAFB subnetwork | 0.31673661 | 0.99047619 |

| | | | |
|---|---|---|---|
| MP:0000422 | delayed hair appearance | 0.31669426 | 0.990592148 |
| ENSG00000185551 | NR2F2 subnetwork | 0.31692511 | 0.990960755 |
| ENSG00000146729 | GBAS subnetwork | 0.31707362 | 0.991295026 |
| ENSG00000143093 | FAM40A subnetwork | 0.31715007 | 0.9913612 |
| ENSG00000140939 | NOL3 subnetwork | 0.31730163 | 0.991568459 |
| ENSG00000145819 | ARHGAP26 subnetwork | 0.31724035 | 0.991577368 |
| ENSG00000107796 | ACTA2 subnetwork | 0.3174252 | 0.991677378 |
| ENSG00000169045 | HNRNPH1 subnetwork | 0.31752829 | 0.991796959 |
| ENSG00000157240 | FZD1 subnetwork | 0.31895082 | 0.992723005 |
| ENSG00000177602 | GSG2 subnetwork | 0.31889335 | 0.99280683 |
| REACTOME_HOMOLOGOUS_R | REACTOME_HOMOLOGOUS_RECOMBINATION_REPAIR_OF | 0.31823959 | 0.992823529 |
| ENSG00000147050 | KDM6A subnetwork | 0.31787982 | 0.992826552 |
| GO:0031227 | intrinsic to endoplasmic reticulum membrane | 0.31836557 | 0.992901433 |
| GO:0006631 | fatty acid metabolic process | 0.31888178 | 0.992976089 |
| ENSG00000139687 | RB1 subnetwork | 0.31801423 | 0.992977949 |
| GO:0051131 | chaperone-mediated protein complex assembly | 0.31834404 | 0.993006843 |
| REACTOME_HOMOLOGOUS_R | REACTOME_HOMOLOGOUS_RECOMBINATION_REPAIR | 0.31823959 | 0.993035944 |
| GO:0008831 | dTDP-4-dehydrorhamnose reductase activity | 0.31850775 | 0.993052587 |
| ENSG00000205659 | LIN52 subnetwork | 0.31813601 | 0.993086473 |
| ENSG00000134909 | ARHGAP32 subnetwork | 0.31821453 | 0.993130751 |
| GO:0007099 | centriole replication | 0.31887859 | 0.99317745 |
| ENSG00000100804 | PSMB5 subnetwork | 0.31975914 | 0.993281516 |
| MP:0004231 | abnormal calcium ion homeostasis | 0.31877408 | 0.993292032 |
| GO:0006360 | transcription from RNA polymerase I promoter | 0.31887688 | 0.993389577 |
| GO:0019210 | kinase inhibitor activity | 0.31868768 | 0.993406711 |
| ENSG00000100014 | SPECC1L subnetwork | 0.31974178 | 0.99341853 |
| GO:0030130 | clathrin coat of trans-Golgi network vesicle | 0.31943326 | 0.993422175 |
| ENSG00000136891 | TEX10 subnetwork | 0.3194906 | 0.993423577 |
| ENSG00000141034 | C17orf39 subnetwork | 0.31874593 | 0.993440171 |
| ENSG00000028137 | TNFRSF1B subnetwork | 0.31965548 | 0.99355423 |
| ENSG00000198517 | MAFK subnetwork | 0.31971937 | 0.993555603 |
| ENSG00000026025 | VIM subnetwork | 0.31935959 | 0.993579352 |
| ENSG00000125970 | RALY subnetwork | 0.31962147 | 0.993616795 |
| ENSG00000109065 | NAT9 subnetwork | 0.31942868 | 0.993623374 |
| GO:0071560 | cellular response to transforming growth factor beta stimul | 0.31932279 | 0.993663324 |
| ENSG00000086619 | ERO1LB subnetwork | 0.32039402 | 0.994087622 |
| ENSG00000174444 | RPL4 subnetwork | 0.32014165 | 0.994114517 |
| GO:0051480 | cytosolic calcium ion homeostasis | 0.32027535 | 0.99412766 |
| ENSG00000122861 | PLAU subnetwork | 0.32033573 | 0.994128909 |
| MP:0001690 | failure of somite differentiation | 0.32020973 | 0.994147691 |
| MP:0005290 | decreased oxygen consumption | 0.32007713 | 0.994177134 |
| MP:0008753 | abnormal osteocyte morphology | 0.32072021 | 0.994252019 |
| MP:0001919 | abnormal reproductive system physiology | 0.32067916 | 0.994335813 |
| ENSG00000139112 | GABARAPL1 subnetwork | 0.32065707 | 0.994515306 |
| MP:0000808 | abnormal hippocampus development | 0.32064288 | 0.99465235 |
| ENSG00000178952 | TUFM subnetwork | 0.32136455 | 0.994747453 |
| ENSG00000173575 | CHD2 subnetwork | 0.32133912 | 0.99490554 |
| GO:0033692 | cellular polysaccharide biosynthetic process | 0.32130008 | 0.994957537 |
| ENSG00000168283 | BMI1 subnetwork | 0.32108354 | 0.995028681 |
| GO:0004866 | endopeptidase inhibitor activity | 0.32123908 | 0.995062646 |
| MP:0008489 | slow postnatal weight gain | 0.32168475 | 0.995206787 |
| ENSG00000129988 | LBP subnetwork | 0.32121289 | 0.99521028 |
| ENSG00000120696 | KBTBD7 subnetwork | 0.32158118 | 0.995342669 |

| | | | |
|---|---|---|---|
| ENSG00000174177 | CTU2 subnetwork | 0.32167255 | 0.995386084 |
| MP:0006060 | increased cerebral infarction size | 0.3218916 | 0.995716709 |
| ENSG00000058091 | CDK14 subnetwork | 0.3220001 | 0.995887216 |
| REACTOME_CA:DEPENDENT_E | REACTOME_CA:DEPENDENT_EVENTS | 0.32386768 | 0.99630137 |
| GO:0051053 | negative regulation of DNA metabolic process | 0.32381887 | 0.996384907 |
| ENSG00000128272 | ATF4 subnetwork | 0.32380719 | 0.996573898 |
| REACTOME_TAT:MEDIATED_EI | REACTOME_TAT:MEDIATED_ELONGATION_OF_THE_HIV:1_ | 0.32367686 | 0.996656823 |
| GO:0014743 | regulation of muscle hypertrophy | 0.3237699 | 0.996689161 |
| ENSG00000092439 | TRPM7 subnetwork | 0.32294263 | 0.996732234 |
| ENSG00000124198 | ARFGEF2 subnetwork | 0.32243512 | 0.996822034 |
| REACTOME_HIV:1_TRANSCRIP | REACTOME_HIV:1_TRANSCRIPTION_ELONGATION | 0.32367686 | 0.996867089 |
| MP:0002932 | abnormal joint morphology | 0.32240227 | 0.996884933 |
| GO:0035272 | exocrine system development | 0.32293935 | 0.996900783 |
| ENSG00000052749 | RRP12 subnetwork | 0.32236727 | 0.996979652 |
| ENSG00000058799 | YIPF1 subnetwork | 0.32410709 | 0.996986936 |
| MP:0010769 | abnormal survival | 0.32436929 | 0.997073684 |
| REACTOME_FORMATION_OF_I | REACTOME_FORMATION_OF_HIV:1_ELONGATION_COMPL | 0.32367686 | 0.997077442 |
| GO:0034062 | RNA polymerase activity | 0.32292696 | 0.997079983 |
| ENSG00000162517 | PEF1 subnetwork | 0.32313555 | 0.997093023 |
| ENSG00000100888 | CHD8 subnetwork | 0.32431291 | 0.997115182 |
| ENSG00000065057 | NTHL1 subnetwork | 0.32419854 | 0.997135033 |
| MP:0002048 | increased lung adenoma incidence | 0.32425961 | 0.997135636 |
| ENSG00000104921 | FCER2 subnetwork | 0.32310354 | 0.997145274 |
| REACTOME_INTEGRIN_CELL_SI | REACTOME_INTEGRIN_CELL_SURFACE_INTERACTIONS | 0.32460867 | 0.997253788 |
| MP:0002089 | abnormal postnatal growth/weight/body size | 0.324506 | 0.997274258 |
| REACTOME_P53:DEPENDENT_( | REACTOME_P53:DEPENDENT_G1S_DNA_DAMAGE_CHECKI | 0.32367343 | 0.997287885 |
| GO:0003899 | DNA-directed RNA polymerase activity | 0.32292696 | 0.997291005 |
| GO:0001919 | regulation of receptor recycling | 0.32342201 | 0.997327841 |
| GO:0071559 | response to transforming growth factor beta stimulus | 0.32331882 | 0.997368977 |
| ENSG00000148606 | POLR3A subnetwork | 0.32337549 | 0.997369533 |
| GO:0006783 | heme biosynthetic process | 0.32327001 | 0.997442401 |
| GO:0019370 | leukotriene biosynthetic process | 0.32291815 | 0.997470364 |
| GO:0080135 | regulation of cellular response to stress | 0.32350725 | 0.997476241 |
| ENSG00000112182 | BACH2 subnetwork | 0.32356608 | 0.997487331 |
| ENSG00000028528 | SNX1 subnetwork | 0.32272861 | 0.997489939 |
| REACTOME_P53:DEPENDENT_( | REACTOME_P53:DEPENDENT_G1_DNA_DAMAGE_RESPON | 0.32367343 | 0.997498417 |
| GO:0043450 | alkene biosynthetic process | 0.32291815 | 0.997681558 |
| GO:0071339 | MLL1 complex | 0.32286763 | 0.997712834 |
| ENSG00000138297 | TIMM23 subnetwork | 0.32529332 | 0.998276949 |
| ENSG00000128833 | MYO5C subnetwork | 0.32528691 | 0.998444725 |
| ENSG00000134376 | CRB1 subnetwork | 0.32525574 | 0.998570528 |
| GO:0043112 | receptor metabolic process | 0.32522209 | 0.99868587 |
| MP:0004876 | decreased mean systemic arterial blood pressure | 0.32553362 | 0.998728992 |
| GO:0009617 | response to bacterium | 0.32505519 | 0.998769198 |
| GO:0046915 | transition metal ion transmembrane transporter activity | 0.32519703 | 0.998832808 |
| ENSG00000170214 | ADRA1B subnetwork | 0.32514945 | 0.998885149 |
| ENSG00000145216 | FIP1L1 subnetwork | 0.32563673 | 0.998918294 |
| GO:0043325 | phosphatidylinositol-3,4-bisphosphate binding | 0.32579299 | 0.999034222 |
| GO:0060491 | regulation of cell projection assembly | 0.32571669 | 0.999076018 |
| ENSG00000068878 | PSME4 subnetwork | 0.32671642 | 0.999340452 |
| ENSG00000168148 | HIST3H3 subnetwork | 0.32680789 | 0.999361524 |
| ENSG00000106105 | GARS subnetwork | 0.32657786 | 0.999403016 |
| ENSG00000197961 | ZNF121 subnetwork | 0.32666778 | 0.999403141 |

| | | | |
|---|---|---|---|
| ENSG00000072133 | RPS6KA6 subnetwork | 0.32594265 | 0.999412259 |
| ENSG00000138709 | LARP1B subnetwork | 0.3265555 | 0.999497172 |
| ENSG00000082014 | SMARCD3 subnetwork | 0.32653269 | 0.999612322 |
| MP:0004521 | abnormal cochlear hair cell stereociliary bundle morpholog | 0.32647468 | 0.99971704 |
| MP:0006378 | abnormal spermatogonia morphology | 0.32704061 | 0.999780289 |
| GO:0004467 | long-chain fatty acid-CoA ligase activity | 0.32696649 | 0.999811637 |
| ENSG00000172613 | RAD9A subnetwork | 0.32643698 | 0.999832285 |
| GO:0043189 | H4/H2A histone acetyltransferase complex | 0.32641489 | 0.999884672 |
| GO:0015932 | nucleobase-containing compound transmembrane transpo | 0.32637053 | 0.999958054 |
| MP:0002906 | increased susceptibility to pharmacologically induced seizu | 1 | 1 |
| GO:0007200 | phospholipase C-activating G-protein coupled receptor sign | 1 | 1.000069152 |
| ENSG00000197265 | GTF2E2 subnetwork | 0.32632139 | 1.000073421 |
| ENSG00000101745 | ANKRD12 subnetwork | 0.32627596 | 1.000094419 |
| MP:0004784 | abnormal anterior cardinal vein morphology | 0.32620597 | 1.000094439 |
| REACTOME_GABA_RECEPTOR_ | REACTOME_GABA_RECEPTOR_ACTIVATION | 1 | 1.000138313 |
| MP:0008593 | increased circulating interleukin-10 level | 0.32740504 | 1.000177713 |
| MP:0003635 | abnormal synaptic transmission | 0.99999999 | 1.000207483 |
| REACTOME_METABOLISM_OF_ | REACTOME_METABOLISM_OF_STEROID_HORMONES_AND | 0.32738138 | 1.000240485 |
| GO:0034654 | nucleobase-containing compound biosynthetic process | 0.99999997 | 1.000276663 |
| MP:0002938 | white spotting | 0.99999997 | 1.000345853 |
| GO:0070064 | proline-rich region binding | 0.32842517 | 1.000375235 |
| MP:0002929 | abnormal bile duct development | 0.32753398 | 1.000397157 |
| MP:0003270 | intestinal obstruction | 0.99999996 | 1.000415053 |
| ENSG00000182004 | SNRPE subnetwork | 0.32836166 | 1.000437865 |
| KEGG_HOMOLOGOUS_RECOM | KEGG_HOMOLOGOUS_RECOMBINATION | 0.32737853 | 1.000439239 |
| KEGG_UBIQUITIN_MEDIATED_ | KEGG_UBIQUITIN_MEDIATED_PROTEOLYSIS | 0.32829484 | 1.000458811 |
| GO:0019935 | cyclic-nucleotide-mediated signaling | 0.99999995 | 1.000484262 |
| ENSG00000010030 | ETV7 subnetwork | 0.32734413 | 1.000512552 |
| REACTOME_CLASS_I_MHC_ME | REACTOME_CLASS_I_MHC_MEDIATED_ANTIGEN_PROCESS | 0.32824167 | 1.000542345 |
| GO:0001012 | RNA polymerase II regulatory region DNA binding | 0.32796324 | 1.000553351 |
| MP:0001322 | abnormal iris morphology | 0.99999994 | 1.00055348 |
| GO:0071478 | cellular response to radiation | 0.32774705 | 1.000564145 |
| GO:0005583 | fibrillar collagen | 0.32791211 | 1.000605681 |
| GO:0048521 | negative regulation of behavior | 0.99999993 | 1.000622708 |
| GO:0002209 | behavioral defense response | 0.99999993 | 1.000691946 |
| MP:0009011 | prolonged diestrus | 0.32786886 | 1.000699812 |
| GO:0042623 | ATPase activity, coupled | 0.32816046 | 1.000709516 |
| ENSG00000099875 | MKNK2 subnetwork | 0.3288485 | 1.000718451 |
| GO:0032602 | chemokine production | 0.32823176 | 1.0007198 |
| ENSG00000087460 | GNAS subnetwork | 0.99999992 | 1.000761193 |
| ENSG00000196411 | EPHB4 subnetwork | 0.32773939 | 1.0007628 |
| GO:0006110 | regulation of glycolysis | 0.32865446 | 1.00080225 |
| GO:0009165 | nucleotide biosynthetic process | 0.99999989 | 1.00083045 |
| ENSG00000055044 | NOP58 subnetwork | 0.32883034 | 1.000895647 |
| ENSG00000169242 | EFNA1 subnetwork | 0.99999984 | 1.000899716 |
| ENSG00000168002 | POLR2G subnetwork | 0.32874613 | 1.00090625 |
| ENSG00000142230 | SAE1 subnetwork | 0.3281585 | 1.000907952 |
| ENSG00000156467 | UQCRB subnetwork | 0.32862539 | 1.000937891 |
| GO:0071347 | cellular response to interleukin-1 | 0.32812112 | 1.000949896 |
| GO:0072522 | purine-containing compound biosynthetic process | 0.99999983 | 1.000968992 |
| GO:0008038 | neuron recognition | 0.99999981 | 1.001038278 |
| GO:0097060 | synaptic membrane | 0.99999973 | 1.001107573 |
| ENSG00000204351 | SKIV2L subnetwork | 0.32961507 | 1.001121961 |

| | | | |
|---|---|---|---|
| ENSG00000125124 | BBS2 subnetwork | 0.32907798 | 1.001165695 |
| GO:0030425 | dendrite | 0.9999997 | 1.001176878 |
| ENSG00000163069 | SGCB subnetwork | 0.99999968 | 1.001242731 |
| MP:0005553 | increased circulating creatinine level | 0.32975156 | 1.001277524 |
| GO:0060113 | inner ear receptor cell differentiation | 0.99999967 | 1.001312054 |
| ENSG00000206267 | ENSG00000206267 subnetwork | 0.32961507 | 1.001330008 |
| GO:0001890 | placenta development | 0.32906391 | 1.001353321 |
| MP:0000951 | sporadic seizures | 0.9999996 | 1.001377925 |
| ENSG00000127666 | TICAM1 subnetwork | 0.32920451 | 1.001425598 |
| MP:0008911 | induced hyperactivity | 0.99999952 | 1.001443806 |
| GO:0007187 | G-protein coupled receptor signaling pathway, coupled to c | 0.99999952 | 1.001513158 |
| ENSG00000138326 | RPS24 subnetwork | 0.32960833 | 1.001538142 |
| GO:0048169 | regulation of long-term neuronal synaptic plasticity | 0.99999951 | 1.001579057 |
| ENSG00000214265 | SNURF subnetwork | 0.32955143 | 1.001600832 |
| ENSG00000072849 | DERL2 subnetwork | 0.32952471 | 1.001642753 |
| GO:0034702 | ion channel complex | 0.99999951 | 1.001648428 |
| ENSG00000206297 | TAP1 subnetwork | 0.32945601 | 1.001663894 |
| GO:0006813 | potassium ion transport | 0.9999995 | 1.001717808 |
| REACTOME_LIGAND:GATED_IC | REACTOME_LIGAND:GATED_ION_CHANNEL_TRANSPORT | 0.9999994 | 1.001787199 |
| ENSG00000214485 | ENSG00000214485 subnetwork | 0.32999299 | 1.001796469 |
| GO:0001662 | behavioral fear response | 0.99999933 | 1.001846207 |
| ENSG00000206233 | ENSG00000206233 subnetwork | 0.32945601 | 1.00187227 |
| GO:0019933 | cAMP-mediated signaling | 0.99999922 | 1.001912152 |
| GO:0007501 | mesodermal cell fate specification | 0.99999917 | 1.00198157 |
| GO:0034703 | cation channel complex | 0.99999916 | 1.002050998 |
| ENSG00000168394 | TAP1 subnetwork | 0.32945601 | 1.002080732 |
| GO:0005249 | voltage-gated potassium channel activity | 0.99999912 | 1.002120435 |
| GO:0016247 | channel regulator activity | 0.99999895 | 1.002186417 |
| ENSG00000102103 | PQBP1 subnetwork | 0.33022823 | 1.002232143 |
| GO:0042490 | mechanoreceptor differentiation | 0.99999891 | 1.002255874 |
| GO:0007156 | homophilic cell adhesion | 0.99999887 | 1.00232534 |
| ENSG00000167986 | DDB1 subnetwork | 0.33052086 | 1.00235526 |
| GO:0006164 | purine nucleotide biosynthetic process | 0.99999886 | 1.002394815 |
| GO:0030176 | integral to endoplasmic reticulum membrane | 0.33144857 | 1.002451893 |
| ENSG00000167083 | GNGT2 subnetwork | 0.99999879 | 1.002464301 |
| ENSG00000112079 | STK38 subnetwork | 0.33041129 | 1.002480797 |
| REACTOME_INWARDLY_RECTI | REACTOME_INWARDLY_RECTIFYING_K_CHANNELS | 0.99999858 | 1.002526863 |
| ENSG00000154767 | XPC subnetwork | 0.33050535 | 1.002542549 |
| GO:0016572 | histone phosphorylation | 0.33155906 | 1.002544477 |
| GO:0009187 | cyclic nucleotide metabolic process | 0.99999855 | 1.002596367 |
| MP:0004768 | abnormal axonal transport | 0.33143501 | 1.002597268 |
| GO:0031346 | positive regulation of cell projection organization | 0.33068751 | 1.002603734 |
| ENSG00000090861 | AARS subnetwork | 0.33164244 | 1.00262668 |
| GO:0031279 | regulation of cyclase activity | 0.99999851 | 1.002665881 |
| GO:0050732 | negative regulation of peptidyl-tyrosine phosphorylation | 0.33133369 | 1.002692069 |
| GO:0070646 | protein modification by small protein removal | 0.33141561 | 1.002711654 |
| GO:0005254 | chloride channel activity | 0.99999837 | 1.002731937 |
| GO:0009190 | cyclic nucleotide biosynthetic process | 0.99999816 | 1.00280147 |
| ENSG00000106144 | CASP2 subnetwork | 0.33084269 | 1.00281062 |
| GO:0050856 | regulation of T cell receptor signaling pathway | 0.33140065 | 1.002846791 |
| ENSG00000206266 | ENSG00000206266 subnetwork | 0.33131617 | 1.002868683 |
| ENSG00000108823 | SGCA subnetwork | 0.99999804 | 1.002871012 |
| ENSG00000162337 | LRP5 subnetwork | 0.99999786 | 1.002933629 |

| | | | |
|---|---|---|---|
| GO:0005253 | anion channel activity | 0.99999783 | 1.00300319 |
| GO:0090068 | positive regulation of cell cycle process | 0.33181918 | 1.003050041 |
| GO:0060914 | heart formation | 0.99999781 | 1.003072761 |
| ENSG00000206346 | DOM3Z subnetwork | 0.33131617 | 1.003076445 |
| ENSG00000167553 | TUBA1C subnetwork | 0.33098533 | 1.003079635 |
| GO:0030165 | PDZ domain binding | 0.99999776 | 1.003142342 |
| ENSG00000173848 | NET1 subnetwork | 0.33122949 | 1.003202073 |
| GO:0022843 | voltage-gated cation channel activity | 0.99999768 | 1.003211932 |
| GO:0043092 | L-amino acid import | 0.99999748 | 1.003274594 |
| ENSG00000204348 | DOM3Z subnetwork | 0.33131617 | 1.003284293 |
| GO:0051339 | regulation of lyase activity | 0.99999724 | 1.003337265 |
| ENSG00000116754 | SRSF11 subnetwork | 0.331956 | 1.003349183 |
| ENSG00000112715 | VEGFA subnetwork | 0.33122131 | 1.003389303 |
| GO:0046068 | cGMP metabolic process | 0.9999972 | 1.003406883 |
| ENSG00000111266 | DUSP16 subnetwork | 0.33115957 | 1.003431474 |
| MP:0002940 | variable body spotting | 0.99999704 | 1.003473041 |
| GO:0022836 | gated channel activity | 0.99999596 | 1.00352533 |
| MP:0001360 | abnormal social investigation | 0.99999595 | 1.003594975 |
| GO:0005996 | monosaccharide metabolic process | 0.33211799 | 1.003658537 |
| MP:0001469 | abnormal contextual conditioning behavior | 0.99999576 | 1.003664631 |
| GO:0005244 | voltage-gated ion channel activity | 0.99999566 | 1.003734296 |
| ENSG00000099797 | TECR subnetwork | 0.33221142 | 1.003750775 |
| GO:0022832 | voltage-gated channel activity | 0.99999566 | 1.003803971 |
| ENSG00000070961 | ATP2B1 subnetwork | 0.33237551 | 1.003831853 |
| ENSG00000114491 | UMPS subnetwork | 0.33230944 | 1.003863636 |
| MP:0008027 | abnormal spinal cord white matter morphology | 0.9999956 | 1.003873655 |
| GO:0042734 | presynaptic membrane | 0.99999546 | 1.003943349 |
| GO:0046058 | cAMP metabolic process | 0.99999544 | 1.004013053 |
| MP:0001961 | abnormal reflex | 0.99999528 | 1.004082766 |
| GO:0045211 | postsynaptic membrane | 0.99999504 | 1.004152489 |
| GO:0032279 | asymmetric synapse | 0.999995 | 1.00421875 |
| MP:0008414 | abnormal spatial reference memory | 0.9999948 | 1.004288492 |
| MP:0003604 | single kidney | 0.9999947 | 1.004358244 |
| GO:0043197 | dendritic spine | 0.99999466 | 1.004428006 |
| GO:0044309 | neuron spine | 0.99999466 | 1.004497777 |
| GO:0034707 | chloride channel complex | 0.99999434 | 1.004564085 |
| GO:0007340 | acrosome reaction | 0.99999423 | 1.004633875 |
| GO:0051932 | synaptic transmission, GABAergic | 0.99999421 | 1.004703675 |
| GO:0045761 | regulation of adenylate cyclase activity | 0.99999402 | 1.004773485 |
| GO:0051969 | regulation of transmission of nerve impulse | 0.99999379 | 1.004843305 |
| ENSG00000188064 | WNT7B subnetwork | 0.99999332 | 1.004913134 |
| GO:0032228 | regulation of synaptic transmission, GABAergic | 0.99999245 | 1.004982973 |
| GO:0007494 | midgut development | 0.99999238 | 1.005052822 |
| GO:0030799 | regulation of cyclic nucleotide metabolic process | 0.99999193 | 1.005112254 |
| GO:0015459 | potassium channel regulator activity | 0.99999139 | 1.005178646 |
| MP:0002272 | abnormal nervous system electrophysiology | 0.99999127 | 1.005248523 |
| GO:0048168 | regulation of neuronal synaptic plasticity | 0.99999106 | 1.005318409 |
| GO:0006171 | cAMP biosynthetic process | 0.99999104 | 1.005388306 |
| MP:0003463 | abnormal single cell response | 0.99999078 | 1.005458212 |
| MP:0004618 | thoracic vertebral transformation | 0.33306286 | 1.005461491 |
| MP:0003789 | osteosarcoma | 0.33298963 | 1.005462619 |
| MP:0001650 | abnormal seizure response to electrical stimulation | 0.99999045 | 1.005528127 |
| ENSG00000138346 | DNA2 subnetwork | 0.33312651 | 1.00554294 |

| | | | |
|---|---|---|---|
| GO:0009124 | nucleoside monophosphate biosynthetic process | 0.99999023 | 1.005594576 |
| GO:0043090 | amino acid import | 0.99999005 | 1.005664511 |
| MP:0001900 | impaired synaptic plasticity | 0.9999893 | 1.005730978 |
| GO:0048167 | regulation of synaptic plasticity | 0.99998899 | 1.005800932 |
| GO:0034705 | potassium channel complex | 0.99998875 | 1.005870896 |
| GO:0008076 | voltage-gated potassium channel complex | 0.99998875 | 1.00594087 |
| GO:0003211 | cardiac ventricle formation | 0.99998761 | 1.006003896 |
| ENSG00000102977 | ACD subnetwork | 0.33425997 | 1.006040338 |
| REACTOME_ACTIVATION_OF_( | REACTOME_ACTIVATION_OF_G_PROTEIN_GATED_POTASS | 0.99998712 | 1.006073889 |
| REACTOME_INHIBITION__OF_' | REACTOME_INHIBITION__OF_VOLTAGE_GATED_CA2_CHAI | 0.99998712 | 1.006143891 |
| MP:0005157 | holoprosencephaly | 0.33424685 | 1.006165089 |
| REACTOME_G_PROTEIN_GATE | REACTOME_G_PROTEIN_GATED_POTASSIUM_CHANNELS | 0.99998712 | 1.006213903 |
| GO:0007212 | dopamine receptor signaling pathway | 0.99998463 | 1.006266527 |
| ENSG00000066044 | ELAVL1 subnetwork | 0.33443314 | 1.006316872 |
| GO:0014048 | regulation of glutamate secretion | 0.99998458 | 1.006336558 |
| ENSG00000138018 | EPT1 subnetwork | 0.3342397 | 1.006361952 |
| GO:0001959 | regulation of cytokine-mediated signaling pathway | 0.33458619 | 1.006396545 |
| GO:0003207 | cardiac chamber formation | 0.99998427 | 1.006406598 |
| REACTOME_RNA_POLYMERAS | REACTOME_RNA_POLYMERASE_II_TRANSCRIPTION_ELONG | 0.33418861 | 1.006476524 |
| GO:0051971 | positive regulation of transmission of nerve impulse | 0.99998424 | 1.006476648 |
| ENSG00000184967 | NOC4L subnetwork | 0.33455763 | 1.00650072 |
| ENSG00000158955 | WNT9B subnetwork | 0.9999841 | 1.006546708 |
| ENSG00000100150 | DEPDC5 subnetwork | 0.33388409 | 1.006608247 |
| ENSG00000061492 | WNT8A subnetwork | 0.9999841 | 1.006616777 |
| GO:0035094 | response to nicotine | 0.33473529 | 1.006621427 |
| REACTOME_FORMATION_OF_I | REACTOME_FORMATION_OF_RNA_POL_II_ELONGATION_( | 0.33418861 | 1.006683831 |
| ENSG00000075290 | WNT8B subnetwork | 0.9999841 | 1.006686856 |
| KEGG_GLIOMA | KEGG_GLIOMA | 0.33384498 | 1.006702413 |
| ENSG00000143816 | WNT9A subnetwork | 0.9999841 | 1.006756945 |
| ENSG00000105989 | WNT2 subnetwork | 0.9999841 | 1.006827044 |
| MP:0005181 | decreased circulating estradiol level | 0.33362673 | 1.006830376 |
| GO:0019395 | fatty acid oxidation | 0.33357221 | 1.006842105 |
| ENSG00000141384 | TAF4B subnetwork | 0.33380961 | 1.006858498 |
| REACTOME_FORMATION_OF_I | REACTOME_FORMATION_OF_HIV:1_ELONGATION_COMPL | 0.33418861 | 1.006891224 |
| ENSG00000169884 | WNT10B subnetwork | 0.9999841 | 1.006897152 |
| ENSG00000101412 | E2F1 subnetwork | 0.33496039 | 1.006937307 |
| ENSG00000111640 | GAPDH subnetwork | 0.33492737 | 1.006959293 |
| ENSG00000085741 | WNT11 subnetwork | 0.9999841 | 1.00696727 |
| ENSG00000135925 | WNT10A subnetwork | 0.9999841 | 1.007037398 |
| ENSG00000166947 | EPB42 subnetwork | 0.33417019 | 1.007047187 |
| GO:0051047 | positive regulation of secretion | 0.33380764 | 1.007066227 |
| GO:0019932 | second-messenger-mediated signaling | 0.99998357 | 1.007107536 |
| MP:0000940 | abnormal motor neuron innervation | 0.99998277 | 1.007170718 |
| ENSG00000143748 | NVL subnetwork | 0.33415268 | 1.007223825 |
| GO:0007194 | negative regulation of adenylate cyclase activity | 0.99998244 | 1.007240875 |
| GO:0006958 | complement activation, classical pathway | 0.33526143 | 1.007261709 |
| ENSG00000143977 | SNRPG subnetwork | 0.33520794 | 1.007304294 |
| GO:0005871 | kinesin complex | 0.33411863 | 1.007307772 |
| GO:0031280 | negative regulation of cyclase activity | 0.99998244 | 1.007311041 |
| ENSG00000102096 | PIM2 subnetwork | 0.33516407 | 1.007377723 |
| MP:0000029 | abnormal malleus morphology | 0.99998231 | 1.007381218 |
| MP:0006074 | abnormal retinal rod bipolar cell morphology | 0.99998189 | 1.007451404 |
| ENSG00000114251 | WNT5A subnetwork | 0.99998142 | 1.0075216 |

| | | | |
|---|---|---|---|
| GO:0051313 | attachment of spindle microtubules to chromosome | 0.99998126 | 1.007591805 |
| GO:0050804 | regulation of synaptic transmission | 0.99998115 | 1.007662021 |
| GO:0007188 | adenylate cyclase-modulating G-protein coupled receptor s | 0.99998084 | 1.007732246 |
| GO:0030814 | regulation of cAMP metabolic process | 0.99998055 | 1.007802481 |
| REACTOME_POST:CHAPERONI | REACTOME_POST:CHAPERONIN_TUBULIN_FOLDING_PATH | 0.335484 | 1.007835284 |
| GO:0017147 | Wnt-protein binding | 0.99997975 | 1.007869241 |
| ENSG00000149295 | DRD2 subnetwork | 0.99997899 | 1.007939495 |
| REACTOME_NEURONAL_SYSTE | REACTOME_NEURONAL_SYSTEM | 0.99997833 | 1.008002788 |
| GO:0051350 | negative regulation of lyase activity | 0.99997797 | 1.008073062 |
| ENSG00000176884 | GRIN1 subnetwork | 0.99997779 | 1.008143345 |
| ENSG00000022355 | GABRA1 subnetwork | 0.99997777 | 1.008213638 |
| MP:0002572 | abnormal emotion/affect behavior | 0.99997649 | 1.008280455 |
| GO:0030823 | regulation of cGMP metabolic process | 0.99997558 | 1.008350767 |
| MP:0004056 | abnormal myocardium compact layer morphology | 0.33570441 | 1.008367556 |
| ENSG00000143771 | CNIH4 subnetwork | 0.3357796 | 1.008406898 |
| GO:0031644 | regulation of neurological system process | 0.99997545 | 1.008421089 |
| GO:0043266 | regulation of potassium ion transport | 0.99997485 | 1.00848096 |
| MP:0008944 | decreased sensitivity to induced cell death | 0.3365149 | 1.0085126 |
| MP:0005591 | decreased vasodilation | 0.99997477 | 1.008547813 |
| ENSG00000119285 | HEATR1 subnetwork | 0.33642399 | 1.008608321 |
| GO:0005267 | potassium channel activity | 0.9999741 | 1.008618164 |
| GO:0008287 | protein serine/threonine phosphatase complex | 0.33597043 | 1.008618921 |
| ENSG00000164754 | RAD21 subnetwork | 0.336496 | 1.008637295 |
| ENSG00000185057 | ENSG00000185057 subnetwork | 0.33637773 | 1.008651087 |
| ENSG00000100836 | PABPN1 subnetwork | 0.33593616 | 1.008661741 |
| GO:0007413 | axonal fasciculation | 0.99997399 | 1.008688525 |
| GO:0051569 | regulation of histone H3-K4 methylation | 0.33604865 | 1.008688962 |
| GO:0045947 | negative regulation of translational initiation | 0.33625203 | 1.008746924 |
| MP:0000564 | syndactyly | 0.99997363 | 1.008758895 |
| GO:0001882 | nucleoside binding | 0.33619249 | 1.008810256 |
| GO:0009263 | deoxyribonucleotide biosynthetic process | 0.99997247 | 1.008825787 |
| ENSG00000186468 | RPS23 subnetwork | 0.33637217 | 1.0088374 |
| GO:0001958 | endochondral ossification | 0.99997118 | 1.008896176 |
| GO:0031646 | positive regulation of neurological system process | 0.99997111 | 1.008966576 |
| ENSG00000158445 | KCNB1 subnetwork | 0.9999711 | 1.009036985 |
| KEGG_COLORECTAL_CANCER | KEGG_COLORECTAL_CANCER | 0.33676308 | 1.009063908 |
| MP:0004994 | abnormal brain wave pattern | 0.99997045 | 1.009103915 |
| GO:0030802 | regulation of cyclic nucleotide biosynthetic process | 0.99997035 | 1.009174344 |
| GO:0030808 | regulation of nucleotide biosynthetic process | 0.99997035 | 1.009244783 |
| GO:0006182 | cGMP biosynthetic process | 0.9999695 | 1.009315231 |
| GO:0051966 | regulation of synaptic transmission, glutamatergic | 0.99996916 | 1.009385689 |
| ENSG00000197915 | HRNR subnetwork | 0.33688761 | 1.009389719 |
| GO:0006458 | 'de novo' protein folding | 0.33700529 | 1.009428747 |
| GO:0060627 | regulation of vesicle-mediated transport | 0.99996893 | 1.009452667 |
| GO:0007628 | adult walking behavior | 0.9999689 | 1.009523145 |
| MP:0001363 | increased anxiety-related response | 0.99996867 | 1.009593632 |
| MP:0008725 | enlarged heart atrium | 0.99996739 | 1.00966413 |
| GO:0045686 | negative regulation of glial cell differentiation | 0.99996696 | 1.009731145 |
| GO:0030817 | regulation of cAMP biosynthetic process | 0.99996446 | 1.00979817 |
| ENSG00000115596 | WNT6 subnetwork | 0.99996438 | 1.009868697 |
| GO:0009123 | nucleoside monophosphate metabolic process | 0.99996418 | 1.009939233 |
| GO:0043021 | ribonucleoprotein complex binding | 0.33739328 | 1.009965214 |
| GO:0042474 | middle ear morphogenesis | 0.99996206 | 1.010002794 |

| | | | |
|---|---|---|---|
| ENSG00000102804 | TSC22D1 subnetwork | 0.33760578 | 1.010010225 |
| GO:0004707 | MAP kinase activity | 0.3372637 | 1.010030706 |
| GO:0004175 | endopeptidase activity | 0.33734876 | 1.01004912 |
| GO:0048016 | inositol phosphate-mediated signaling | 0.99996078 | 1.010069857 |
| KEGG_FATTY_ACID_METABOLI | KEGG_FATTY_ACID_METABOLISM | 0.33768736 | 1.01012063 |
| GO:0048839 | inner ear development | 0.9999599 | 1.010140422 |
| ENSG00000101343 | CRNKL1 subnetwork | 0.33758859 | 1.010186132 |
| GO:0048638 | regulation of developmental growth | 0.9999593 | 1.01020401 |
| GO:0015267 | channel activity | 0.99995841 | 1.010271101 |
| GO:0022803 | passive transmembrane transporter activity | 0.99995841 | 1.010341695 |
| ENSG00000154447 | SH3RF1 subnetwork | 0.33757879 | 1.010362111 |
| GO:0043583 | ear development | 0.9999583 | 1.010412299 |
| GO:0030162 | regulation of proteolysis | 0.33842422 | 1.010477454 |
| MP:0000049 | abnormal middle ear morphology | 0.99995816 | 1.010482913 |
| REACTOME_ACTIVATION_OF_( | REACTOME_ACTIVATION_OF_GABAB_RECEPTORS | 0.99995798 | 1.010553536 |
| REACTOME_REGULATION_OF_ | REACTOME_REGULATION_OF_LIPID_METABOLISM_BY_PEI | 0.33838187 | 1.010602041 |
| REACTOME_GABA_B_RECEPTC | REACTOME_GABA_B_RECEPTOR_ACTIVATION | 0.99995798 | 1.01062417 |
| GO:0045821 | positive regulation of glycolysis | 0.33824759 | 1.010677828 |
| ENSG00000153107 | ANAPC1 subnetwork | 0.99995792 | 1.010694813 |
| GO:0017156 | calcium ion-dependent exocytosis | 0.99995735 | 1.010765467 |
| ENSG00000166086 | JAM3 subnetwork | 0.33836028 | 1.01077771 |
| ENSG00000137656 | BUD13 subnetwork | 0.33870149 | 1.010830104 |
| GO:0043084 | penile erection | 0.99995633 | 1.010832634 |
| MP:0008057 | abnormal DNA replication | 0.3382432 | 1.010874004 |
| MP:0009747 | impaired behavioral response to xenobiotic | 0.99995565 | 1.010899811 |
| ENSG00000158710 | TAGLN2 subnetwork | 0.33801739 | 1.010954425 |
| GO:0001755 | neural crest cell migration | 0.99995558 | 1.010970494 |
| ENSG00000118640 | VAMP8 subnetwork | 0.33869166 | 1.010975112 |
| ENSG00000105364 | MRPL4 subnetwork | 0.33814232 | 1.010990807 |
| GO:0022838 | substrate-specific channel activity | 0.99995435 | 1.011030697 |
| ENSG00000135945 | REV1 subnetwork | 0.33823078 | 1.011039624 |
| ENSG00000154764 | WNT7A subnetwork | 0.99995389 | 1.011101399 |
| MP:0002691 | small stomach | 0.33813744 | 1.011105435 |
| ENSG00000085231 | TAF9 subnetwork | 0.33885973 | 1.011143964 |
| ENSG00000182973 | CNOT10 subnetwork | 0.33801371 | 1.011150859 |
| MP:0005292 | improved glucose tolerance | 0.33892995 | 1.011151886 |
| ENSG00000172020 | GAP43 subnetwork | 0.99995134 | 1.01116162 |
| ENSG00000108679 | LGALS3BP subnetwork | 0.33930016 | 1.011191446 |
| REACTOME_TRANSPORT_OF_( | REACTOME_TRANSPORT_OF_GLUCOSE_AND_OTHER_SUG/ | 0.33906914 | 1.011208478 |
| MP:0002206 | abnormal CNS synaptic transmission | 0.99995118 | 1.01123234 |
| REACTOME_AKT_PHOSPHORYI | REACTOME_AKT_PHOSPHORYLATES_TARGETS_IN_THE_CY | 0.33940638 | 1.011240073 |
| ENSG00000122406 | RPL5 subnetwork | 0.33924304 | 1.011275209 |
| ENSG00000137497 | NUMA1 subnetwork | 0.33902527 | 1.011282104 |
| GO:0031281 | positive regulation of cyclase activity | 0.99995084 | 1.011303071 |
| GO:0045762 | positive regulation of adenylate cyclase activity | 0.99995084 | 1.011373811 |
| MP:0003172 | abnormal lysosome physiology | 0.33921516 | 1.011389568 |
| GO:0030815 | negative regulation of cAMP metabolic process | 0.99995049 | 1.011444561 |
| GO:0030818 | negative regulation of cAMP biosynthetic process | 0.99995049 | 1.011515321 |
| GO:0033119 | negative regulation of RNA splicing | 0.99994962 | 1.011582593 |
| ENSG00000185745 | IFIT1 subnetwork | 0.3396117 | 1.011634772 |
| MP:0002826 | tonic seizures | 0.99994946 | 1.011649874 |
| GO:0005216 | ion channel activity | 0.99994687 | 1.011699671 |
| REACTOME_APCCCDC20_MED | REACTOME_APCCCDC20_MEDIATED_DEGRADATION_OF_C | 0.99994662 | 1.011770469 |

| | | | |
|---|---|---|---|
| GO:0050686 | negative regulation of mRNA processing | 0.99994636 | 1.011841277 |
| ENSG00000100321 | SYNGR1 subnetwork | 0.99994556 | 1.011908595 |
| GO:0035267 | NuA4 histone acetyltransferase complex | 0.33991526 | 1.01197355 |
| REACTOME_ION_CHANNEL_TR | REACTOME_ION_CHANNEL_TRANSPORT | 0.999945 | 1.011979422 |
| GO:0042471 | ear morphogenesis | 0.9999441 | 1.012050259 |
| ENSG00000137413 | TAF8 subnetwork | 0.33989354 | 1.012098087 |
| GO:0007218 | neuropeptide signaling pathway | 0.99994386 | 1.012121106 |
| ENSG00000183684 | ALYREF subnetwork | 0.34020956 | 1.012172056 |
| GO:0044247 | cellular polysaccharide catabolic process | 0.99994146 | 1.012188463 |
| REACTOME_RNA_POLYMERASI | REACTOME_RNA_POLYMERASE_I_PROMOTER_CLEARANCE | 0.3398529 | 1.012212497 |
| ENSG00000151693 | ASAP2 subnetwork | 0.34012805 | 1.012235557 |
| GO:0009251 | glucan catabolic process | 0.99994146 | 1.012259329 |
| ENSG00000108379 | WNT3 subnetwork | 0.99994136 | 1.012330206 |
| GO:0044456 | synapse part | 0.99993821 | 1.012383587 |
| MP:0000373 | belly spot | 0.99993591 | 1.012447479 |
| GO:0007190 | activation of adenylate cyclase activity | 0.99993365 | 1.012518384 |
| GO:0002090 | regulation of receptor internalization | 0.99993252 | 1.012585796 |
| REACTOME_TRANSMISSION_A | REACTOME_TRANSMISSION_ACROSS_CHEMICAL_SYNAPSE | 0.99993149 | 1.012649716 |
| ENSG00000134245 | WNT2B subnetwork | 0.99993097 | 1.01272065 |
| GO:0007215 | glutamate receptor signaling pathway | 0.99993021 | 1.012788091 |
| MP:0002573 | behavioral despair | 0.99993006 | 1.012859044 |
| ENSG00000161204 | ABCF3 subnetwork | 0.34189389 | 1.012887224 |
| MP:0000087 | absent mandible | 0.99992807 | 1.012919498 |
| GO:0071479 | cellular response to ionizing radiation | 0.34086269 | 1.012959577 |
| REACTOME_VIF:MEDIATED_DE | REACTOME_VIF:MEDIATED_DEGRADATION_OF_APOBEC3G | 0.34096389 | 1.012987409 |
| GO:0061008 | hepaticobiliary system development | 0.34056006 | 1.012990445 |
| GO:0048712 | negative regulation of astrocyte differentiation | 0.99992802 | 1.012990471 |
| ENSG00000119689 | DLST subnetwork | 0.34068106 | 1.01304878 |
| ENSG00000164985 | PSIP1 subnetwork | 0.34188264 | 1.013051843 |
| GO:0042596 | fear response | 0.99992654 | 1.013054446 |
| GO:0006919 | activation of cysteine-type endopeptidase activity involved | 0.34126728 | 1.013058036 |
| KEGG_P53_SIGNALING_PATHV | KEGG_P53_SIGNALING_PATHWAY | 0.34052358 | 1.01307442 |
| GO:0090023 | positive regulation of neutrophil chemotaxis | 0.34118022 | 1.013080982 |
| GO:0000077 | DNA damage checkpoint | 0.3408402 | 1.013124746 |
| GO:0015079 | potassium ion transmembrane transporter activity | 0.99992572 | 1.013125438 |
| ENSG00000117480 | FAAH subnetwork | 0.34135399 | 1.013126395 |
| MP:0001696 | failure to gastrulate | 0.34106994 | 1.013137056 |
| GO:0014047 | glutamate secretion | 0.99992555 | 1.01319644 |
| MP:0004617 | sacral vertebral transformation | 0.34216243 | 1.013205829 |
| MP:0000286 | abnormal mitral valve morphology | 0.34081735 | 1.013239179 |
| ENSG00000008952 | SEC62 subnetwork | 0.34187612 | 1.013257039 |
| GO:0007610 | behavior | 0.99992221 | 1.013263947 |
| ENSG00000143466 | IKBKE subnetwork | 0.34117712 | 1.013266342 |
| ENSG00000214026 | MRPL23 subnetwork | 0.3421123 | 1.013269231 |
| MP:0004188 | delayed embryo turning | 0.34166237 | 1.013275233 |
| ENSG00000185630 | PBX1 subnetwork | 0.34174731 | 1.013333333 |
| ENSG00000174804 | FZD4 subnetwork | 0.3414598 | 1.013334009 |
| GO:0043587 | tongue morphogenesis | 0.99992164 | 1.013334969 |
| REACTOME_GABA_A_RECEPTC | REACTOME_GABA_A_RECEPTOR_ACTIVATION | 0.9999211 | 1.013406 |
| GO:0055065 | metal ion homeostasis | 0.34184833 | 1.013411669 |
| ENSG00000119203 | CPSF3 subnetwork | 0.34143991 | 1.013458418 |
| GO:0051349 | positive regulation of lyase activity | 0.9999207 | 1.013477042 |
| ENSG00000114867 | EIF4G1 subnetwork | 0.34166076 | 1.013480641 |

| | | | |
|---|---|---|---|
| ENSG00000130299 | GTPBP3 subnetwork | 0.34161221 | 1.013513788 |
| MP:0005407 | hyperalgesia | 0.99991232 | 1.013530566 |
| ENSG00000137944 | CCBL2 subnetwork | 0.9999094 | 1.01359111 |
| ENSG00000126934 | MAP2K2 subnetwork | 0.3424427 | 1.013645559 |
| ENSG00000198932 | GPRASP1 subnetwork | 0.9999064 | 1.013658673 |
| MP:0001750 | increased circulating follicle stimulating hormone level | 0.999906 | 1.013729752 |
| GO:0051205 | protein insertion into membrane | 0.99990592 | 1.013797335 |
| ENSG00000163586 | FABP1 subnetwork | 0.34255505 | 1.013804612 |
| ENSG00000090776 | EFNB1 subnetwork | 0.3424298 | 1.013820316 |
| GO:0045980 | negative regulation of nucleotide metabolic process | 0.99990467 | 1.013868434 |
| ENSG00000120658 | ENOX1 subnetwork | 0.99990397 | 1.013939543 |
| ENSG00000082641 | NFE2L1 subnetwork | 0.34276555 | 1.013950667 |
| REACTOME_ORGANIC_CATION | REACTOME_ORGANIC_CATIONANIONZWITTERION_TRANSI | 0.34270948 | 1.013983822 |
| MP:0008536 | enlarged third ventricle | 0.99990304 | 1.014007154 |
| MP:0001077 | abnormal spinal nerve morphology | 0.99990227 | 1.014078283 |
| ENSG00000145864 | GABRB2 subnetwork | 0.99990129 | 1.014149421 |
| GO:0003208 | cardiac ventricle morphogenesis | 0.99990052 | 1.014217062 |
| ENSG00000147852 | VLDLR subnetwork | 0.99990039 | 1.01428822 |
| MP:0002108 | abnormal muscle morphology | 0.99989957 | 1.014352372 |
| GO:0008328 | ionotropic glutamate receptor complex | 0.9998971 | 1.014416532 |
| GO:0030424 | axon | 0.99989633 | 1.014487719 |
| MP:0001523 | impaired righting response | 0.99989584 | 1.014558916 |
| ENSG00000154608 | ENSG00000154608 subnetwork | 0.99989502 | 1.014626614 |
| REACTOME_GLUCAGON:TYPE_ | REACTOME_GLUCAGON:TYPE_LIGAND_RECEPTORS | 0.99989222 | 1.014690812 |
| MP:0004672 | short ribs | 0.99989144 | 1.014758529 |
| MP:0000008 | increased white adipose tissue amount | 0.99988956 | 1.014826255 |
| MP:0000030 | abnormal tympanic ring morphology | 0.99988847 | 1.014897501 |
| GO:0060045 | positive regulation of cardiac muscle cell proliferation | 0.9998875 | 1.014968757 |
| GO:0030332 | cyclin binding | 0.34321189 | 1.01503334 |
| GO:0005980 | glycogen catabolic process | 0.99988685 | 1.015036512 |
| GO:0006979 | response to oxidative stress | 0.34331375 | 1.015090909 |
| MP:0006337 | abnormal first branchial arch morphology | 0.99988567 | 1.015107787 |
| GO:0030809 | negative regulation of nucleotide biosynthetic process | 0.99988488 | 1.015179073 |
| GO:0031235 | intrinsic to internal side of plasma membrane | 0.3432067 | 1.015187955 |
| ENSG00000125691 | RPL23 subnetwork | 0.34341799 | 1.015188851 |
| GO:0042772 | DNA damage response, signal transduction resulting in tran | 0.34314576 | 1.015221346 |
| GO:0030800 | negative regulation of cyclic nucleotide metabolic process | 0.99988488 | 1.015250369 |
| GO:0030803 | negative regulation of cyclic nucleotide biosynthetic proces | 0.99988488 | 1.015321674 |
| ENSG00000040199 | PHLPP2 subnetwork | 0.34355786 | 1.015357431 |
| MP:0002862 | altered righting response | 0.99988302 | 1.015385966 |
| MP:0003920 | abnormal heart right ventricle morphology | 0.99988282 | 1.015457291 |
| GO:0031638 | zymogen activation | 0.99988213 | 1.015525114 |
| GO:0007270 | neuron-neuron synaptic transmission | 0.99988171 | 1.015596459 |
| MP:0001046 | abnormal enteric neuron morphology | 0.99988154 | 1.015667814 |
| GO:0051925 | regulation of calcium ion transport via voltage-gated calciu | 0.99987863 | 1.01572864 |
| ENSG00000176894 | PXMP2 subnetwork | 0.99987735 | 1.015796501 |
| REACTOME_PHOSPHOLIPASE_ | REACTOME_PHOSPHOLIPASE_C:MEDIATED_CASCADE | 0.34374662 | 1.015808601 |
| ENSG00000111186 | WNT5B subnetwork | 0.99987438 | 1.015867885 |
| GO:0042491 | auditory receptor cell differentiation | 0.99987346 | 1.015935765 |
| MP:0006142 | abnormal sinoatrial node conduction | 0.99987066 | 1.015996626 |
| GO:0050922 | negative regulation of chemotaxis | 0.99986627 | 1.016057496 |
| MP:0009379 | abnormal foot pigmentation | 0.99985608 | 1.016111345 |
| MP:0001629 | abnormal heart rate | 0.99985605 | 1.016182777 |

| | | | |
|---|---|---|---|
| ENSG00000064419 | TNPO3 subnetwork | 0.9998536 | 1.016240157 |
| GO:0042461 | photoreceptor cell development | 0.99985317 | 1.016308093 |
| GO:0008234 | cysteine-type peptidase activity | 0.34397369 | 1.016310052 |
| GO:0005184 | neuropeptide hormone activity | 0.99985278 | 1.016379553 |
| GO:0071174 | mitotic cell cycle spindle checkpoint | 0.99985195 | 1.016447507 |
| GO:0045187 | regulation of circadian sleep/wake cycle, sleep | 0.9998506 | 1.016511955 |
| ENSG00000099204 | ABLIM1 subnetwork | 0.34413032 | 1.01653885 |
| GO:0042749 | regulation of circadian sleep/wake cycle | 0.9998506 | 1.016583445 |
| GO:0019717 | synaptosome | 0.99984805 | 1.016647911 |
| GO:0007613 | memory | 0.99984705 | 1.016715903 |
| GO:0048333 | mesodermal cell differentiation | 0.9998413 | 1.016780388 |
| GO:0030801 | positive regulation of cyclic nucleotide metabolic process | 0.9998393 | 1.016851917 |
| REACTOME_APC:CDC20_MEDI | REACTOME_APC:CDC20_MEDIATED_DEGRADATION_OF_N | 0.99983888 | 1.016923456 |
| GO:0051302 | regulation of cell division | 0.99983271 | 1.016987969 |
| GO:0014014 | negative regulation of gliogenesis | 0.99982496 | 1.0170349 |
| ENSG00000148296 | SURF6 subnetwork | 0.34473267 | 1.017079807 |
| GO:0016327 | apicolateral plasma membrane | 0.34502851 | 1.017106323 |
| ENSG00000134508 | CABLES1 subnetwork | 0.99982487 | 1.017106467 |
| ENSG00000198689 | SLC9A6 subnetwork | 0.34494142 | 1.01713998 |
| GO:0014032 | neural crest cell development | 0.99982137 | 1.017174525 |
| ENSG00000131979 | GCH1 subnetwork | 0.34471935 | 1.017214271 |
| REACTOME_GAP_JUNCTION_T | REACTOME_GAP_JUNCTION_TRAFFICKING_AND_REGULAT | 0.99982132 | 1.017246112 |
| REACTOME_NETRIN:1_SIGNAL | REACTOME_NETRIN:1_SIGNALING | 0.34491848 | 1.017274376 |
| ENSG00000168615 | ADAM9 subnetwork | 0.34449086 | 1.017288683 |
| ENSG00000198576 | ARC subnetwork | 0.34485205 | 1.017298005 |
| ENSG00000053900 | ANAPC4 subnetwork | 0.99981667 | 1.017317708 |
| GO:0032462 | regulation of protein homooligomerization | 0.34465022 | 1.017362371 |
| ENSG00000166170 | BAG5 subnetwork | 0.34469491 | 1.017368952 |
| MP:0001449 | abnormal learning/ memory | 0.99981224 | 1.017382276 |
| GO:0032993 | protein-DNA complex | 0.34518807 | 1.017425005 |
| GO:0045202 | synapse | 0.99980686 | 1.017443334 |
| MP:0005501 | abnormal skin physiology | 0.34447605 | 1.017453592 |
| GO:0050885 | neuromuscular process controlling balance | 0.99980567 | 1.01751496 |
| MP:0003225 | axonal dystrophy | 0.34462587 | 1.017517144 |
| MP:0003059 | decreased insulin secretion | 0.99980471 | 1.017579555 |
| GO:0021510 | spinal cord development | 0.99980326 | 1.01764768 |
| MP:0000947 | convulsive seizures | 0.99980272 | 1.017719335 |
| GO:0050919 | negative chemotaxis | 0.99980025 | 1.017791001 |
| GO:0051301 | cell division | 0.99979737 | 1.017862676 |
| ENSG00000139083 | ETV6 subnetwork | 0.34534519 | 1.017874396 |
| GO:0060795 | cell fate commitment involved in formation of primary gerr | 0.99979556 | 1.017927319 |
| GO:0050795 | regulation of behavior | 0.99979463 | 1.017995492 |
| MP:0008565 | decreased interferon-beta secretion | 0.34545567 | 1.018051922 |
| GO:0043954 | cellular component maintenance | 0.99979355 | 1.018060154 |
| ENSG00000092850 | TEKT2 subnetwork | 0.3458006 | 1.018080402 |
| GO:0014069 | postsynaptic density | 0.99979228 | 1.018124824 |
| GO:0044327 | dendritic spine head | 0.99979228 | 1.018196548 |
| GO:0000079 | regulation of cyclin-dependent protein kinase activity | 0.99978483 | 1.018254192 |
| GO:0009083 | branched chain family amino acid catabolic process | 0.34579465 | 1.018264978 |
| MP:0004726 | abnormal nasal capsule morphology | 0.9997839 | 1.018325935 |
| REACTOME_PTM_GAMMA_CA | REACTOME_PTM_GAMMA_CARBOXYLATION_HYPUSINE_F | 0.34576404 | 1.018339031 |
| MP:0001883 | mammary adenocarcinoma | 0.99978312 | 1.018397689 |
| ENSG00000116717 | GADD45A subnetwork | 0.3456608 | 1.018436934 |

| | | | |
|---|---|---|---|
| MP:0006059 | decreased susceptibility to ischemic brain injury | 0.9997827 | 1.018469452 |
| ENSG00000008083 | JARID2 subnetwork | 0.34573375 | 1.018473451 |
| MP:0004452 | abnormal pterygoid process morphology | 0.99978145 | 1.018541226 |
| GO:0048610 | cellular process involved in reproduction | 0.34564311 | 1.018581489 |
| GO:0007214 | gamma-aminobutyric acid signaling pathway | 0.99977841 | 1.018609486 |
| GO:0045823 | positive regulation of heart contraction | 0.9997784 | 1.01868128 |
| GO:0031577 | spindle checkpoint | 0.99977651 | 1.018749559 |
| GO:0042551 | neuron maturation | 0.99977477 | 1.018821373 |
| ENSG00000176386 | CDC26 subnetwork | 0.99977214 | 1.018886147 |
| GO:0042733 | embryonic digit morphogenesis | 0.999772 | 1.018954456 |
| REACTOME_PHOSPHORYLATIO | REACTOME_PHOSPHORYLATION_OF_THE_APCC | 0.99976832 | 1.019022774 |
| GO:0051960 | regulation of nervous system development | 0.99976824 | 1.019094627 |
| GO:0009799 | specification of symmetry | 0.99976665 | 1.019162965 |
| GO:0007625 | grooming behavior | 0.99976561 | 1.019231312 |
| GO:0050767 | regulation of neurogenesis | 0.99976104 | 1.019303195 |
| GO:0090189 | regulation of branching involved in ureteric bud morphoger | 0.99976065 | 1.019375088 |
| ENSG00000102683 | SGCG subnetwork | 0.9997535 | 1.019439938 |
| GO:0050806 | positive regulation of synaptic transmission | 0.99975341 | 1.019511851 |
| MP:0003949 | abnormal circulating lipid level | 0.34639622 | 1.019519791 |
| GO:0043113 | receptor clustering | 0.9997532 | 1.019583774 |
| ENSG00000064313 | TAF2 subnetwork | 0.34693378 | 1.019608826 |
| ENSG00000121486 | TRMT1L subnetwork | 0.34671982 | 1.019610598 |
| ENSG00000116957 | TBCE subnetwork | 0.34664809 | 1.019654688 |
| GO:0016358 | dendrite development | 0.99975312 | 1.019655708 |
| GO:0060742 | epithelial cell differentiation involved in prostate gland dev | 0.34639273 | 1.01971463 |
| GO:0005242 | inward rectifier potassium channel activity | 0.99975146 | 1.019727651 |
| ENSG00000013561 | RNF14 subnetwork | 0.34662328 | 1.019728916 |
| ENSG00000137154 | RPS6 subnetwork | 0.34656551 | 1.019732878 |
| MP:0003222 | increased cardiomyocyte apoptosis | 0.34653633 | 1.019797107 |
| ENSG00000130254 | SAFB2 subnetwork | 0.99975051 | 1.019799605 |
| GO:0031570 | DNA integrity checkpoint | 0.34693247 | 1.019813403 |
| GO:0031012 | extracellular matrix | 0.99974877 | 1.019871569 |
| MP:0003997 | tonic-clonic seizures | 0.99974772 | 1.019940014 |
| GO:0042306 | regulation of protein import into nucleus | 0.34690559 | 1.019957857 |
| GO:0016594 | glycine binding | 0.99974755 | 1.020011998 |
| MP:0001489 | decreased startle reflex | 0.99974702 | 1.020083992 |
| ENSG00000132016 | C19orf57 subnetwork | 0.99974671 | 1.020152467 |
| MP:0005270 | abnormal zygomatic bone morphology | 0.99974521 | 1.020224481 |
| MP:0004014 | abnormal uterine environment | 0.34747719 | 1.020270541 |
| REACTOME_POTASSIUM_CHAI | REACTOME_POTASSIUM_CHANNELS | 0.99974362 | 1.020292976 |
| GO:0035020 | regulation of Rac protein signal transduction | 0.9997392 | 1.020340299 |
| GO:0042745 | circadian sleep/wake cycle | 0.99973117 | 1.02039469 |
| ENSG00000198626 | RYR2 subnetwork | 0.34761959 | 1.02041675 |
| REACTOME_P53:INDEPENDEN | REACTOME_P53:INDEPENDENT_DNA_DAMAGE_RESPONSE | 0.34747132 | 1.020444979 |
| ENSG00000133816 | MICAL2 subnetwork | 0.99972461 | 1.020445559 |
| ENSG00000081026 | MAGI3 subnetwork | 0.99972435 | 1.020517619 |
| ENSG00000132589 | FLOT2 subnetwork | 0.34773187 | 1.020562901 |
| MP:0004279 | abnormal rostral migratory stream morphology | 0.99972347 | 1.020589689 |
| REACTOME_P53:INDEPENDEN | REACTOME_P53:INDEPENDENT_G1S_DNA_DAMAGE_CHEC | 0.34747132 | 1.020649559 |
| MP:0011386 | increased metanephric mesenchyme apoptosis | 0.9997229 | 1.02066177 |
| REACTOME_NEUROTRANSMIT | REACTOME_NEUROTRANSMITTER_RECEPTOR_BINDING_AI | 0.99972072 | 1.020723266 |
| GO:0043204 | perikaryon | 0.99971955 | 1.020784771 |
| MP:0002741 | small olfactory bulb | 0.99971532 | 1.020853348 |

| | | | |
|---|---|---|---|
| REACTOME_UBIQUITIN_MEDI/ | REACTOME_UBIQUITIN_MEDIATED_DEGRADATION_OF_PH | 0.34747132 | 1.020854221 |
| GO:0007062 | sister chromatid cohesion | 0.3482973 | 1.020904181 |
| ENSG00000175745 | NR2F1 subnetwork | 0.34812647 | 1.020906725 |
| GO:0002021 | response to dietary excess | 0.99971497 | 1.020925468 |
| GO:0030071 | regulation of mitotic metaphase/anaphase transition | 0.99971487 | 1.020994065 |
| KEGG_AMYOTROPHIC_LATERA | KEGG_AMYOTROPHIC_LATERAL_SCLEROSIS_ALS | 0.3474527 | 1.020998797 |
| GO:0048701 | embryonic cranial skeleton morphogenesis | 0.99970966 | 1.021048541 |
| MP:0001917 | intraventricular hemorrhage | 0.34803673 | 1.021055266 |
| ENSG00000172732 | MUS81 subnetwork | 0.34828912 | 1.021088435 |
| ENSG00000004487 | KDM1A subnetwork | 0.3481259 | 1.021111111 |
| ENSG00000172270 | BSG subnetwork | 0.34823912 | 1.021112668 |
| GO:0007094 | mitotic cell cycle spindle assembly checkpoint | 0.99970678 | 1.021113624 |
| GO:0009975 | cyclase activity | 0.99970604 | 1.021185782 |
| ENSG00000173917 | HOXB2 subnetwork | 0.34800543 | 1.021189666 |
| GO:0090407 | organophosphate biosynthetic process | 0.9997056 | 1.021254417 |
| GO:0016638 | oxidoreductase activity, acting on the CH-NH2 group of don | 0.34877387 | 1.021307216 |
| GO:0032958 | inositol phosphate biosynthetic process | 0.9997056 | 1.021326596 |
| GO:0042659 | regulation of cell fate specification | 0.99969847 | 1.02137758 |
| GO:0048532 | anatomical structure arrangement | 0.99969623 | 1.021449777 |
| ENSG00000088538 | DOCK3 subnetwork | 0.34876184 | 1.021471411 |
| ENSG00000134987 | WDR36 subnetwork | 0.34865207 | 1.021475705 |
| ENSG00000108294 | PSMB3 subnetwork | 0.34858766 | 1.0215 |
| GO:0045981 | positive regulation of nucleotide metabolic process | 0.99969414 | 1.02151845 |
| MP:0009760 | abnormal mitotic spindle morphology | 0.9996852 | 1.021572994 |
| ENSG00000130177 | CDC16 subnetwork | 0.99968297 | 1.02163108 |
| REACTOME_CYCLIN_AB1_ASSC | REACTOME_CYCLIN_AB1_ASSOCIATED_EVENTS_DURING_C | 0.99968195 | 1.021703316 |
| ENSG00000104643 | MTMR9 subnetwork | 0.99967637 | 1.02176142 |
| MP:0002805 | abnormal conditioned taste aversion behavior | 0.99967045 | 1.021815996 |
| GO:0030826 | regulation of cGMP biosynthetic process | 0.99966821 | 1.02188826 |
| GO:0006887 | exocytosis | 0.99965401 | 1.021939317 |
| MP:0002919 | enhanced paired-pulse facilitation | 0.9996534 | 1.022008063 |
| GO:0005246 | calcium channel regulator activity | 0.99965249 | 1.022080357 |
| GO:0030819 | positive regulation of cAMP biosynthetic process | 0.99964796 | 1.022142049 |
| GO:0030816 | positive regulation of cAMP metabolic process | 0.99964796 | 1.022214362 |
| GO:0042693 | muscle cell fate commitment | 0.99964749 | 1.022286685 |
| GO:0030804 | positive regulation of cyclic nucleotide biosynthetic process | 0.99964662 | 1.02235548 |
| GO:0071456 | cellular response to hypoxia | 0.34933524 | 1.022393128 |
| GO:0030810 | positive regulation of nucleotide biosynthetic process | 0.99964662 | 1.022427823 |
| GO:0090190 | positive regulation of branching involved in ureteric bud mo | 0.99964316 | 1.022496639 |
| ENSG00000145833 | DDX46 subnetwork | 0.34932527 | 1.022547453 |
| GO:0007091 | mitotic metaphase/anaphase transition | 0.99964276 | 1.022569002 |
| GO:0007422 | peripheral nervous system development | 0.99963205 | 1.022609527 |
| ENSG00000078902 | TOLLIP subnetwork | 0.34929411 | 1.022651878 |
| GO:0045807 | positive regulation of endocytosis | 0.99963164 | 1.022681908 |
| GO:0030551 | cyclic nucleotide binding | 0.9996307 | 1.022750761 |
| GO:0030553 | cGMP binding | 0.99962653 | 1.022809005 |
| GO:0001708 | cell fate specification | 0.99962212 | 1.022874336 |
| ENSG00000132535 | DLG4 subnetwork | 0.99961993 | 1.022929057 |
| MP:0001661 | extended life span | 0.99961934 | 1.023001487 |
| GO:0051954 | positive regulation of amine transport | 0.99961281 | 1.023049143 |
| GO:0040013 | negative regulation of locomotion | 0.9996126 | 1.023121592 |
| MP:0004739 | conductive hearing loss | 0.99961243 | 1.023194051 |
| GO:0032964 | collagen biosynthetic process | 0.99960872 | 1.023262979 |

| | | | |
|---|---|---|---|
| GO:0043025 | neuronal cell body | 0.99960847 | 1.023335458 |
| MP:0001441 | increased grooming behavior | 0.99960446 | 1.023400864 |
| GO:0007193 | adenylate cyclase-inhibiting G-protein coupled receptor sig | 0.99959651 | 1.023469821 |
| GO:0030837 | negative regulation of actin filament polymerization | 0.35017818 | 1.023513567 |
| GO:0048484 | enteric nervous system development | 0.99959192 | 1.023535246 |
| ENSG00000170624 | SGCD subnetwork | 0.99959065 | 1.02360068 |
| MP:0000077 | abnormal interparietal bone morphology | 0.99959033 | 1.023673209 |
| ENSG00000174437 | ATP2A2 subnetwork | 0.3501652 | 1.023717821 |
| GO:0051536 | iron-sulfur cluster binding | 0.35008593 | 1.023722555 |
| GO:0017158 | regulation of calcium ion-dependent exocytosis | 0.99958958 | 1.023742205 |
| GO:0001710 | mesodermal cell fate commitment | 0.99958734 | 1.023807668 |
| GO:0005112 | Notch binding | 0.9995859 | 1.023880227 |
| GO:0051540 | metal cluster binding | 0.35008593 | 1.023926932 |
| MP:0001380 | reduced male mating frequency | 0.35041633 | 1.023937762 |
| GO:0007611 | learning or memory | 0.99958494 | 1.023952796 |
| GO:0007223 | Wnt receptor signaling pathway, calcium modulating pathw | 0.99958303 | 1.024025376 |
| ENSG00000184304 | PRKD1 subnetwork | 0.35003214 | 1.02403155 |
| ENSG00000092067 | CEBPE subnetwork | 0.349988 | 1.024076293 |
| ENSG00000067715 | SYT1 subnetwork | 0.99957996 | 1.024090877 |
| GO:0035313 | wound healing, spreading of epidermal cells | 0.99957968 | 1.024163477 |
| REACTOME_GAP_JUNCTION_T | REACTOME_GAP_JUNCTION_TRAFFICKING | 0.99957153 | 1.024221907 |
| GO:0010092 | specification of organ identity | 0.99956551 | 1.024290981 |
| REACTOME_INHIBITION_OF_TI | REACTOME_INHIBITION_OF_THE_PROTEOLYTIC_ACTIVITY_ | 0.99956389 | 1.024360065 |
| REACTOME_INACTIVATION_OF | REACTOME_INACTIVATION_OF_APCC_VIA_DIRECT_INHIBIT | 0.99956389 | 1.024432705 |
| ENSG00000075711 | DLG1 subnetwork | 0.99956381 | 1.024505354 |
| MP:0005105 | abnormal middle ear ossicle morphology | 0.99955825 | 1.024556738 |
| GO:0050906 | detection of stimulus involved in sensory perception | 0.99955396 | 1.024608128 |
| GO:0018130 | heterocycle biosynthetic process | 0.99954634 | 1.024680806 |
| GO:0032768 | regulation of monooxygenase activity | 0.35072387 | 1.024700838 |
| REACTOME_MITOTIC_SPINDLE | REACTOME_MITOTIC_SPINDLE_CHECKPOINT | 0.99953926 | 1.0247464 |
| GO:2000677 | regulation of transcription regulatory region DNA binding | 0.99953906 | 1.024819098 |
| ENSG00000118922 | KLF12 subnetwork | 0.3508161 | 1.024845464 |
| REACTOME_G:PROTEIN_ACTIV | REACTOME_G:PROTEIN_ACTIVATION | 0.99953479 | 1.024891806 |
| REACTOME_CLASS_B2_SECRET | REACTOME_CLASS_B2_SECRETIN_FAMILY_RECEPTORS | 0.99953006 | 1.024946786 |
| MP:0002566 | abnormal sexual interaction | 0.99952998 | 1.025015965 |
| MP:0005333 | decreased heart rate | 0.9995296 | 1.025088703 |
| MP:0010380 | inner cell mass apoptosis | 0.99952829 | 1.025154354 |
| GO:0051482 | elevation of cytosolic calcium ion concentration involved in | 0.9995149 | 1.025195174 |
| ENSG00000117650 | NEK2 subnetwork | 0.99951154 | 1.025264391 |
| GO:0006941 | striated muscle contraction | 0.99950093 | 1.025312323 |
| MP:0004066 | abnormal primitive node morphology | 0.99949722 | 1.025378008 |
| ENSG00000088256 | GNA11 subnetwork | 0.99949665 | 1.025450802 |
| GO:0042462 | eye photoreceptor cell development | 0.99949438 | 1.025516507 |
| GO:0032281 | alpha-amino-3-hydroxy-5-methyl-4-isoxazolepropionic acid | 0.99949011 | 1.025578671 |
| ENSG00000124422 | USP22 subnetwork | 0.35132838 | 1.025647668 |
| GO:0071674 | mononuclear cell migration | 0.99948881 | 1.025647944 |
| GO:0021675 | nerve development | 0.99947856 | 1.025706576 |
| ENSG00000131018 | SYNE1 subnetwork | 0.35130791 | 1.025772374 |
| GO:0071173 | spindle assembly checkpoint | 0.99947781 | 1.025779419 |
| GO:0010771 | negative regulation of cell morphogenesis involved in differ | 0.35123355 | 1.025837321 |
| MP:0001890 | anencephaly | 0.99947759 | 1.025852273 |
| GO:0007601 | visual perception | 0.99947745 | 1.025925137 |
| ENSG00000157193 | LRP8 subnetwork | 0.99947561 | 1.025987356 |

| | | | |
|---|---|---|---|
| GO:0048024 | regulation of nuclear mRNA splicing, via spliceosome | 0.99945973 | 1.026021169 |
| MP:0000848 | abnormal pons morphology | 0.99945593 | 1.026079852 |
| MP:0001399 | hyperactivity | 0.99945467 | 1.026149201 |
| GO:0042472 | inner ear morphogenesis | 0.99944541 | 1.026211454 |
| GO:0060291 | long-term synaptic potentiation | 0.99943681 | 1.026259504 |
| GO:0021889 | olfactory bulb interneuron differentiation | 0.9994368 | 1.026332433 |
| GO:0006821 | chloride transport | 0.99943545 | 1.026405373 |
| GO:0044297 | cell body | 0.99943217 | 1.026478323 |
| GO:0007600 | sensory perception | 0.99942768 | 1.026540621 |
| MP:0005445 | abnormal neurotransmitter secretion | 0.99942707 | 1.026613591 |
| MP:0005551 | abnormal eye electrophysiology | 0.99941645 | 1.026668799 |
| ENSG00000179915 | NRXN1 subnetwork | 0.99941479 | 1.026738234 |
| GO:0001937 | negative regulation of endothelial cell proliferation | 0.99940071 | 1.026782794 |
| GO:0051955 | regulation of amino acid transport | 0.99940012 | 1.026855802 |
| GO:0042813 | Wnt-activated receptor activity | 0.99938313 | 1.026911043 |
| GO:0046834 | lipid phosphorylation | 0.35183308 | 1.026937637 |
| GO:0050890 | cognition | 0.99937504 | 1.026962736 |
| REACTOME_ADHERENS_JUNCT | REACTOME_ADHERENS_JUNCTIONS_INTERACTIONS | 0.99936705 | 1.027025105 |
| GO:0051784 | negative regulation of nuclear division | 0.99936289 | 1.02708037 |
| GO:0045839 | negative regulation of mitosis | 0.99936289 | 1.027153425 |
| MP:0010404 | ostium primum atrial septal defect | 0.99935211 | 1.027219377 |
| ENSG00000164438 | TLX3 subnetwork | 0.35226343 | 1.027289013 |
| GO:0043928 | exonucleolytic nuclear-transcribed mRNA catabolic process | 0.99935147 | 1.027292452 |
| GO:0033013 | tetrapyrrole metabolic process | 0.35221376 | 1.027334262 |
| GO:0000291 | nuclear-transcribed mRNA catabolic process, exonucleolytic | 0.99935147 | 1.027365538 |
| ENSG00000117133 | RPF1 subnetwork | 0.35204608 | 1.027390438 |
| MP:0000819 | abnormal olfactory bulb morphology | 0.99934707 | 1.027431519 |
| GO:0032589 | neuron projection membrane | 0.99933581 | 1.027490394 |
| GO:0006778 | porphyrin-containing compound metabolic process | 0.35221376 | 1.027538829 |
| GO:0008608 | attachment of spindle microtubules to kinetochore | 0.99933507 | 1.027559952 |
| GO:0007626 | locomotory behavior | 0.99933322 | 1.027625961 |
| GO:0004518 | nuclease activity | 0.35219678 | 1.027683728 |
| GO:0007263 | nitric oxide mediated signal transduction | 0.99932364 | 1.027688421 |
| ENSG00000141404 | GNAL subnetwork | 0.99932081 | 1.027747331 |
| MP:0002957 | intestinal adenocarcinoma | 0.35247154 | 1.027791045 |
| ENSG00000131183 | SLC34A1 subnetwork | 0.35254295 | 1.02781536 |
| ENSG00000099341 | PSMD8 subnetwork | 0.35263316 | 1.027819773 |
| GO:0044057 | regulation of system process | 0.9993189 | 1.027820485 |
| GO:0001975 | response to amphetamine | 0.99929587 | 1.027865177 |
| ENSG00000137752 | CASP1 subnetwork | 0.35272263 | 1.027893795 |
| MP:0003123 | paternal imprinting | 0.99929505 | 1.02793835 |
| MP:0002945 | abnormal inhibitory postsynaptic currents | 0.99929074 | 1.027997295 |
| REACTOME_INCRETIN_SYNTHE | REACTOME_INCRETIN_SYNTHESIS_SECRETION_AND_INACT | 0.99929008 | 1.028070488 |
| GO:0003016 | respiratory system process | 0.99928729 | 1.028133011 |
| GO:0034704 | calcium channel complex | 0.99928241 | 1.028202663 |
| ENSG00000176697 | BDNF subnetwork | 0.99928203 | 1.028275887 |
| GO:0002076 | osteoblast development | 0.99927787 | 1.028345559 |
| GO:0050905 | neuromuscular process | 0.99927786 | 1.028418803 |
| ENSG00000170035 | UBE2E3 subnetwork | 0.35297131 | 1.028435077 |
| ENSG00000126005 | ENSG00000126005 subnetwork | 0.35309507 | 1.028463526 |
| GO:0045841 | negative regulation of mitotic metaphase/anaphase transiti | 0.99927308 | 1.028484935 |
| MP:0003996 | clonic seizures | 0.99926567 | 1.028547514 |
| ENSG00000205220 | PSMB10 subnetwork | 0.35306476 | 1.02860835 |

| | | | |
|---|---|---|---|
| MP:0006000 | abnormal corneal epithelium morphology | 0.99926435 | 1.028617226 |
| REACTOME_ACETYLCHOLINE_N | REACTOME_ACETYLCHOLINE_NEUROTRANSMITTER_RELEA | 0.99925638 | 1.028683386 |
| GO:0030665 | clathrin coated vesicle membrane | 0.99924923 | 1.028745992 |
| ENSG00000163485 | ADORA1 subnetwork | 0.99924496 | 1.028805045 |
| GO:0003002 | regionalization | 0.9992422 | 1.028871232 |
| GO:0005774 | vacuolar membrane | 0.35358837 | 1.028921763 |
| REACTOME_ENDOSOMAL_SOR | REACTOME_ENDOSOMAL_SORTING_COMPLEX_REQUIRED_ | 0.99924123 | 1.028944555 |
| GO:0008527 | taste receptor activity | 0.35337757 | 1.028958871 |
| ENSG00000105856 | HBP1 subnetwork | 0.35367008 | 1.028965654 |
| ENSG00000165458 | INPPL1 subnetwork | 0.3537281 | 1.028979754 |
| GO:0015698 | inorganic anion transport | 0.99923912 | 1.029014325 |
| MP:0000520 | absent kidney | 0.99923658 | 1.029084105 |
| ENSG00000066654 | THUMPD1 subnetwork | 0.35358558 | 1.029116187 |
| GO:0016180 | snRNA processing | 0.35336153 | 1.029133545 |
| ENSG00000156049 | GNA14 subnetwork | 0.99923495 | 1.029153896 |
| GO:0004890 | GABA-A receptor activity | 0.99923003 | 1.029216567 |
| GO:0060536 | cartilage morphogenesis | 0.99921367 | 1.029268554 |
| GO:0000794 | condensed nuclear chromosome | 0.35357738 | 1.029290822 |
| GO:0010002 | cardioblast differentiation | 0.99919593 | 1.029327677 |
| GO:0051602 | response to electrical stimulus | 0.99918265 | 1.029386809 |
| GO:0006942 | regulation of striated muscle contraction | 0.99918206 | 1.029460211 |
| GO:0008344 | adult locomotory behavior | 0.99917861 | 1.029526492 |
| GO:0030534 | adult behavior | 0.99916918 | 1.029589217 |
| GO:0021511 | spinal cord patterning | 0.99915589 | 1.029626988 |
| GO:0051890 | regulation of cardioblast differentiation | 0.99915169 | 1.029693295 |
| GO:0010659 | cardiac muscle cell apoptotic process | 0.99914813 | 1.029759612 |
| REACTOME_RNA_POLYMERASI | REACTOME_RNA_POLYMERASE_I_TRANSCRIPTION | 0.35411136 | 1.029821429 |
| MP:0002913 | abnormal PNS synaptic transmission | 0.99914736 | 1.029833072 |
| GO:0072009 | nephron epithelium development | 0.99913917 | 1.029892274 |
| MP:0000854 | abnormal cerebellum development | 0.99913399 | 1.029958619 |
| ENSG00000166866 | MYO1A subnetwork | 0.35410502 | 1.030015876 |
| GO:0030141 | secretory granule | 0.99913251 | 1.030028541 |
| GO:0030261 | chromosome condensation | 0.99912184 | 1.030080634 |
| GO:0007216 | G-protein coupled glutamate receptor signaling pathway | 0.99911859 | 1.030147006 |
| GO:0035249 | synaptic transmission, glutamatergic | 0.99911571 | 1.030216957 |
| GO:0045666 | positive regulation of neuron differentiation | 0.99911555 | 1.030290486 |
| GO:0050808 | synapse organization | 0.99911539 | 1.030364026 |
| GO:0060841 | venous blood vessel development | 0.99911114 | 1.030423299 |
| ENSG00000129514 | FOXA1 subnetwork | 0.35434334 | 1.030460226 |
| GO:0009855 | determination of bilateral symmetry | 0.99910882 | 1.03049329 |
| ENSG00000147130 | ZMYM3 subnetwork | 0.35457436 | 1.030535183 |
| GO:0072073 | kidney epithelium development | 0.99910864 | 1.030566859 |
| ENSG00000131459 | GFPT2 subnetwork | 0.3544117 | 1.030573185 |
| ENSG00000146733 | PSPH subnetwork | 0.35453142 | 1.030600714 |
| MP:0001440 | abnormal grooming behavior | 0.99910417 | 1.0306333 |
| GO:0008201 | heparin binding | 0.99909078 | 1.03069261 |
| ENSG00000100342 | APOL1 subnetwork | 0.35465509 | 1.030697582 |
| GO:0055015 | ventricular cardiac muscle cell development | 0.99909022 | 1.03076621 |
| MP:0005517 | decreased liver regeneration | 0.35452805 | 1.030795162 |
| GO:0022410 | circadian sleep/wake cycle process | 0.99908033 | 1.030825537 |
| MP:0008918 | microgliosis | 0.35479302 | 1.030853803 |
| GO:0050802 | circadian sleep/wake cycle, sleep | 0.99908033 | 1.030899157 |
| MP:0002782 | abnormal testes secretion | 0.9990791 | 1.030969216 |

| | | | |
|---|---|---|---|
| GO:0032355 | response to estradiol stimulus | 0.35477056 | 1.030988706 |
| GO:0015276 | ligand-gated ion channel activity | 0.99907746 | 1.031042857 |
| GO:0022834 | ligand-gated channel activity | 0.99907746 | 1.031116508 |
| GO:0008066 | glutamate receptor activity | 0.99906741 | 1.03117231 |
| ENSG00000136045 | PWP1 subnetwork | 0.35504637 | 1.031178218 |
| GO:0035176 | social behavior | 0.99903364 | 1.031188826 |
| ENSG00000135387 | CAPRIN1 subnetwork | 0.35498424 | 1.031204199 |
| GO:0048635 | negative regulation of muscle organ development | 0.99903334 | 1.031262504 |
| MP:0001393 | ataxia | 0.99902601 | 1.031318328 |
| GO:0016917 | GABA receptor activity | 0.99902295 | 1.031392025 |
| ENSG00000158042 | MRPL17 subnetwork | 0.35516298 | 1.03142942 |
| GO:0046530 | photoreceptor cell differentiation | 0.99902108 | 1.031458586 |
| MP:0001243 | abnormal dermal layer morphology | 0.35523701 | 1.031482581 |
| GO:0042755 | eating behavior | 0.99901927 | 1.031528731 |
| MP:0003049 | abnormal lumbar vertebrae morphology | 0.99901431 | 1.031598885 |
| MP:0003690 | abnormal glial cell physiology | 0.99900873 | 1.031669049 |
| GO:0008360 | regulation of cell shape | 0.99899606 | 1.031728501 |
| GO:0001664 | G-protein coupled receptor binding | 0.35734191 | 1.031787753 |
| GO:0048260 | positive regulation of receptor-mediated endocytosis | 0.99899553 | 1.031802259 |
| MP:0002781 | increased circulating testosterone level | 0.35586415 | 1.031824471 |
| MP:0004008 | abnormal GABA-mediated receptor currents | 0.9989861 | 1.031854579 |
| GO:0051098 | regulation of binding | 0.35752551 | 1.031863806 |
| MP:0000458 | abnormal mandible morphology | 0.99898378 | 1.031924782 |
| ENSG00000170004 | CHD3 subnetwork | 0.35543214 | 1.031961211 |
| ENSG00000085274 | MYNN subnetwork | 0.35733804 | 1.031981095 |
| GO:0060706 | cell differentiation involved in embryonic placenta develop | 0.9989725 | 1.031987844 |
| GO:0046545 | development of primary female sexual characteristics | 0.3558606 | 1.031998814 |
| KEGG_GALACTOSE_METABOLI | KEGG_GALACTOSE_METABOLISM | 0.35750901 | 1.032007874 |
| MP:0001502 | abnormal circadian rhythm | 0.35762103 | 1.032024793 |
| GO:0004221 | ubiquitin thiolesterase activity | 0.356034 | 1.032025692 |
| ENSG00000196781 | TLE1 subnetwork | 0.35767913 | 1.032038166 |
| MP:0008283 | small hippocampus | 0.99896751 | 1.032054491 |
| ENSG00000106355 | LSM5 subnetwork | 0.35554553 | 1.032063712 |
| GO:0006084 | acetyl-CoA metabolic process | 0.35580024 | 1.032094127 |
| ENSG00000149554 | CHEK1 subnetwork | 0.3572918 | 1.032105574 |
| MP:0009660 | abnormal induced retinal neovascularization | 0.35785297 | 1.032114061 |
| GO:0003084 | positive regulation of systemic arterial blood pressure | 0.99896719 | 1.032128299 |
| GO:0040017 | positive regulation of locomotion | 0.35574553 | 1.032169699 |
| ENSG00000126247 | CAPNS1 subnetwork | 0.35781208 | 1.032179386 |
| KEGG_CARDIAC_MUSCLE_CON | KEGG_CARDIAC_MUSCLE_CONTRACTION | 0.99895931 | 1.032184237 |
| MP:0005505 | increased platelet cell number | 0.35703248 | 1.032190026 |
| ENSG00000034152 | MAP2K3 subnetwork | 0.35726469 | 1.032220252 |
| GO:0048259 | regulation of receptor-mediated endocytosis | 0.99895685 | 1.032258065 |
| ENSG00000163251 | FZD5 subnetwork | 0.35718819 | 1.032285714 |
| ENSG00000170727 | BOP1 subnetwork | 0.35633944 | 1.032322734 |
| GO:0030510 | regulation of BMP signaling pathway | 0.99895234 | 1.032331903 |
| GO:0009968 | negative regulation of signal transduction | 0.35650214 | 1.0323692 |
| ENSG00000059378 | PARP12 subnetwork | 0.3570267 | 1.032373817 |
| GO:0016863 | intramolecular oxidoreductase activity, transposing C=C bo | 0.35573873 | 1.032373887 |
| ENSG00000116161 | CACYBP subnetwork | 0.3569752 | 1.032380201 |
| MP:0005458 | increased percent body fat | 0.35622946 | 1.032404663 |
| GO:0007622 | rhythmic behavior | 0.99895099 | 1.032405751 |
| ENSG00000128709 | HOXD9 subnetwork | 0.3571664 | 1.03243989 |

| | | | |
|---|---|---|---|
| MP:0004204 | absent stapes | 0.99894241 | 1.032461726 |
| MP:0000239 | absent common myeloid progenitor cells | 0.35644478 | 1.032464455 |
| ENSG00000169057 | MECP2 subnetwork | 0.35632757 | 1.032497037 |
| GO:0045880 | positive regulation of smoothened signaling pathway | 0.9989335 | 1.03252844 |
| MP:0004696 | abnormal thyroid follicle morphology | 0.35696165 | 1.032564103 |
| REACTOME_FGFR1C_LIGAND_ | REACTOME_FGFR1C_LIGAND_BINDING_AND_ACTIVATION | 0.99891534 | 1.03257012 |
| MP:0001862 | interstitial pneumonia | 0.35689472 | 1.032600118 |
| GO:0055010 | ventricular cardiac muscle tissue morphogenesis | 0.99890953 | 1.032640429 |
| ENSG00000163703 | CRELD1 subnetwork | 0.9989005 | 1.032700014 |
| MP:0005107 | abnormal stapes morphology | 0.99889292 | 1.032763186 |
| ENSG00000125731 | SH2D3A subnetwork | 0.35686679 | 1.03277427 |
| ENSG00000121807 | CCR2 subnetwork | 0.35891156 | 1.03281342 |
| REACTOME_G1S_DNA_DAMAG | REACTOME_G1S_DNA_DAMAGE_CHECKPOINTS | 0.35681757 | 1.032820209 |
| GO:0055123 | digestive system development | 0.99889087 | 1.032829946 |
| ENSG00000063438 | AHRR subnetwork | 0.3567654 | 1.032836557 |
| ENSG00000154342 | WNT3A subnetwork | 0.99888936 | 1.032900293 |
| ENSG00000130204 | TOMM40 subnetwork | 0.35878384 | 1.032904809 |
| REACTOME_G1S:SPECIFIC_TRA | REACTOME_G1S:SPECIFIC_TRANSCRIPTION | 0.99888894 | 1.03297423 |
| GO:0018214 | protein carboxylation | 0.35874576 | 1.032989792 |
| GO:0022617 | extracellular matrix disassembly | 0.35901827 | 1.033012946 |
| ENSG00000215782 | ENSG00000215782 subnetwork | 0.35891156 | 1.033016091 |
| ENSG00000072401 | UBE2D1 subnetwork | 0.99888891 | 1.033048178 |
| ENSG00000166401 | SERPINB8 subnetwork | 0.99885531 | 1.033068442 |
| ENSG00000151694 | ADAM17 subnetwork | 0.35912686 | 1.033114336 |
| GO:0045843 | negative regulation of striated muscle tissue development | 0.99884772 | 1.033117348 |
| MP:0008803 | abnormal placental labyrinth vasculature morphology | 0.35918578 | 1.033117647 |
| REACTOME_CHROMOSOME_M | REACTOME_CHROMOSOME_MAINTENANCE | 0.35842031 | 1.033120456 |
| ENSG00000169136 | ATF5 subnetwork | 0.35945009 | 1.03313737 |
| MP:0001463 | abnormal spatial learning | 0.99883792 | 1.033177001 |
| GO:0017187 | peptidyl-glutamic acid carboxylation | 0.35874576 | 1.033192617 |
| GO:0070098 | chemokine-mediated signaling pathway | 0.99880782 | 1.03320444 |
| ENSG00000096401 | CDC5L subnetwork | 0.3583119 | 1.033212109 |
| GO:0002237 | response to molecule of bacterial origin | 0.3583824 | 1.033215409 |
| MP:0000836 | abnormal substantia nigra morphology | 0.35869412 | 1.033248233 |
| GO:0090090 | negative regulation of canonical Wnt receptor signaling pat | 0.99880722 | 1.03327843 |
| MP:0011106 | partial embryonic lethality before somite formation | 0.35858059 | 1.033290766 |
| GO:0055080 | cation homeostasis | 0.35864551 | 1.033333333 |
| ENSG00000037280 | FLT4 subnetwork | 0.35944931 | 1.033339867 |
| GO:0014033 | neural crest cell differentiation | 0.99880189 | 1.033341689 |
| MP:0001701 | incomplete embryo turning | 0.35830934 | 1.033385765 |
| MP:0004275 | abnormal postnatal subventricular zone morphology | 0.99879797 | 1.033408537 |
| MP:0004144 | hypotonia | 0.99879564 | 1.033475396 |
| ENSG00000092010 | PSME1 subnetwork | 0.35941209 | 1.033483631 |
| ENSG00000100146 | SOX10 subnetwork | 0.99878871 | 1.033545845 |
| GO:0016849 | phosphorus-oxygen lyase activity | 0.9987661 | 1.033591231 |
| GO:0019934 | cGMP-mediated signaling | 0.99875322 | 1.033647371 |
| GO:0030431 | sleep | 0.99874828 | 1.033717848 |
| GO:0048246 | macrophage chemotaxis | 0.99873842 | 1.033770421 |
| MP:0001264 | increased body size | 0.99873091 | 1.033830168 |
| GO:0044319 | wound healing, spreading of cells | 0.99872976 | 1.033904257 |
| GO:0032094 | response to food | 0.99871995 | 1.033971189 |
| MP:0001395 | bidirectional circling | 0.35979206 | 1.034022335 |
| MP:0000565 | oligodactyly | 0.9987187 | 1.034041714 |

| | | | |
|---|---|---|---|
| GO:0030666 | endocytic vesicle membrane | 0.998709 | 1.03409433 |
| GO:0071548 | response to dexamethasone stimulus | 0.99870568 | 1.034168459 |
| ENSG00000187391 | MAGI2 subnetwork | 0.99868474 | 1.034203169 |
| GO:0048512 | circadian behavior | 0.99867908 | 1.034277316 |
| GO:0048565 | digestive tract development | 0.99866898 | 1.034337133 |
| MP:0004100 | abnormal spinal cord interneuron morphology | 0.99865249 | 1.03439696 |
| MP:0004215 | abnormal myocardial fiber physiology | 0.99862868 | 1.034453209 |
| ENSG00000162419 | GMEB1 subnetwork | 0.35999751 | 1.03446621 |
| GO:0033865 | nucleoside bisphosphate metabolic process | 0.99862616 | 1.034520224 |
| GO:0050953 | sensory perception of light stimulus | 0.99862411 | 1.034583662 |
| MP:0001526 | abnormal placing response | 0.99862121 | 1.034654282 |
| ENSG00000176248 | ANAPC2 subnetwork | 0.99862062 | 1.034728499 |
| GO:2000273 | positive regulation of receptor activity | 0.99861274 | 1.034795552 |
| MP:0000183 | decreased circulating LDL cholesterol level | 0.99860388 | 1.034866203 |
| GO:0071621 | granulocyte chemotaxis | 0.99860281 | 1.034933276 |
| GO:0033137 | negative regulation of peptidyl-serine phosphorylation | 0.36023662 | 1.034958872 |
| GO:0071622 | regulation of granulocyte chemotaxis | 0.99860281 | 1.035007534 |
| MP:0002243 | abnormal vomeronasal organ morphology | 0.99859892 | 1.035078215 |
| ENSG00000149930 | TAOK2 subnetwork | 0.36035892 | 1.035089093 |
| MP:0001259 | abnormal body weight | 0.99859542 | 1.035141729 |
| ENSG00000174446 | SNAPC5 subnetwork | 0.36047429 | 1.035160532 |
| GO:0070412 | R-SMAD binding | 0.36069957 | 1.035188808 |
| ENSG00000184640 | SEPT9 subnetwork | 0.3605843 | 1.035202584 |
| MP:0003194 | abnormal frequency of paradoxical sleep | 0.99859336 | 1.035216018 |
| GO:0060068 | vagina development | 0.36067184 | 1.035283757 |
| MP:0005404 | abnormal axon morphology | 0.99858702 | 1.035286729 |
| GO:0033605 | positive regulation of catecholamine secretion | 0.99856618 | 1.03532874 |
| MP:0002207 | abnormal long term potentiation | 0.99855135 | 1.035392291 |
| GO:0032421 | stereocilium bundle | 0.36138887 | 1.035400391 |
| MP:0001406 | abnormal gait | 0.99854799 | 1.035463029 |
| MP:0003722 | absent ureter | 0.99854475 | 1.035533778 |
| ENSG00000204264 | PSMB8 subnetwork | 0.36136872 | 1.035544052 |
| GO:0005104 | fibroblast growth factor receptor binding | 0.99854096 | 1.035604538 |
| ENSG00000144744 | UBA3 subnetwork | 0.36099266 | 1.035634657 |
| ENSG00000108883 | EFTUD2 subnetwork | 0.36092388 | 1.03567097 |
| ENSG00000144285 | SCN1A subnetwork | 0.99853231 | 1.035671717 |
| MP:0003703 | abnormal vestibulocochlear ganglion morphology | 0.99852854 | 1.035742496 |
| ENSG00000206234 | ENSG00000206234 subnetwork | 0.36136872 | 1.035746385 |
| GO:0051917 | regulation of fibrinolysis | 0.99852837 | 1.035816876 |
| MP:0001504 | abnormal posture | 0.99852439 | 1.035887676 |
| GO:0060402 | calcium ion transport into cytosol | 0.3611226 | 1.035901447 |
| ENSG00000128641 | MYO1B subnetwork | 0.36126335 | 1.035916732 |
| ENSG00000206298 | PSMB8 subnetwork | 0.36136872 | 1.035948798 |
| ENSG00000186979 | ENSG00000186979 subnetwork | 0.99852067 | 1.035951304 |
| MP:0003071 | decreased vascular permeability | 0.36121349 | 1.035962854 |
| MP:0000554 | abnormal carpal bone morphology | 0.99851609 | 1.036018532 |
| GO:0005545 | 1-phosphatidylinositol binding | 0.99851011 | 1.03608577 |
| GO:0019002 | GMP binding | 0.99850631 | 1.036153017 |
| MP:0002856 | abnormal vestibular ganglion morphology | 0.99849622 | 1.036202313 |
| GO:0042612 | MHC class I protein complex | 0.36166218 | 1.036262449 |
| GO:0042391 | regulation of membrane potential | 0.99849491 | 1.036273171 |
| GO:0050803 | regulation of synapse structure and activity | 0.99849397 | 1.03634404 |
| GO:0009982 | pseudouridine synthase activity | 0.36175266 | 1.036372511 |

| | | | |
|---|---|---|---|
| MP:0000276 | heart right ventricle hypertrophy | 0.99848596 | 1.036407732 |
| GO:0009950 | dorsal/ventral axis specification | 0.99846565 | 1.036453467 |
| GO:0051606 | detection of stimulus | 0.9984591 | 1.036517177 |
| MP:0003233 | prolonged QT interval | 0.99845739 | 1.036591677 |
| GO:0032982 | myosin filament | 0.99845702 | 1.036666187 |
| MP:0006033 | abnormal external auditory canal morphology | 0.99845188 | 1.036737115 |
| ENSG00000156127 | BATF subnetwork | 0.36190806 | 1.036746047 |
| GO:0016248 | channel inhibitor activity | 0.99843985 | 1.036779295 |
| GO:0008200 | ion channel inhibitor activity | 0.99843985 | 1.036853836 |
| MP:0010053 | decreased grip strength | 0.99843278 | 1.036914006 |
| ENSG00000093100 | ENSG00000093100 subnetwork | 0.99843086 | 1.036984972 |
| MP:0002739 | abnormal olfactory bulb development | 0.99842435 | 1.037052352 |
| GO:0071837 | HMG box domain binding | 0.99840637 | 1.037087379 |
| GO:0042451 | purine nucleoside biosynthetic process | 0.99839842 | 1.037143987 |
| GO:0042455 | ribonucleoside biosynthetic process | 0.99839842 | 1.037218586 |
| GO:0046129 | purine ribonucleoside biosynthetic process | 0.99839842 | 1.037293195 |
| GO:0044420 | extracellular matrix part | 0.99838315 | 1.037346234 |
| GO:0005578 | proteinaceous extracellular matrix | 0.9983753 | 1.037413669 |
| GO:0002052 | positive regulation of neuroblast proliferation | 0.99836653 | 1.037481114 |
| GO:0007368 | determination of left/right symmetry | 0.99836018 | 1.037537775 |
| MP:0008438 | abnormal cutaneous collagen fibril morphology | 0.99835503 | 1.037601641 |
| REACTOME_NEGATIVE_REGUL | REACTOME_NEGATIVE_REGULATION_OF_FGFR_SIGNALINC | 0.99833399 | 1.037654721 |
| ENSG00000089053 | ANAPC5 subnetwork | 0.99832688 | 1.037722202 |
| GO:0030672 | synaptic vesicle membrane | 0.99831905 | 1.037782496 |
| MP:0000704 | abnormal thymus development | 0.99831286 | 1.037842799 |
| GO:0048489 | synaptic vesicle transport | 0.99831083 | 1.037913907 |
| MP:0002882 | abnormal neuron morphology | 0.99831033 | 1.037977827 |
| GO:0070875 | positive regulation of glycogen metabolic process | 0.36240827 | 1.037978142 |
| GO:0017137 | Rab GTPase binding | 0.36353161 | 1.037988718 |
| REACTOME_FGFR1_LIGAND_B | REACTOME_FGFR1_LIGAND_BINDING_AND_ACTIVATION | 0.99830592 | 1.038041757 |
| GO:0003229 | ventricular cardiac muscle tissue development | 0.99829669 | 1.038102095 |
| MP:0004609 | vertebral fusion | 0.36352286 | 1.038161479 |
| GO:0051970 | negative regulation of transmission of nerve impulse | 0.99829401 | 1.038173243 |
| GO:0009266 | response to temperature stimulus | 0.99828563 | 1.0382336 |
| GO:0007584 | response to nutrient | 0.36290176 | 1.038255361 |
| ENSG00000008300 | CELSR3 subnetwork | 0.36278824 | 1.038270281 |
| GO:0007158 | neuron cell-cell adhesion | 0.99827572 | 1.038272361 |
| GO:0016578 | histone deubiquitination | 0.36343037 | 1.038273647 |
| MP:0008525 | decreased cranium height | 0.36349414 | 1.038285659 |
| ENSG00000181788 | SIAH2 subnetwork | 0.36284873 | 1.038311562 |
| REACTOME_METAL_ION_SLC_ | REACTOME_METAL_ION_SLC_TRANSPORTERS | 0.36330612 | 1.038317757 |
| ENSG00000125730 | C3 subnetwork | 0.36275737 | 1.038326507 |
| GO:0007379 | segment specification | 0.99826162 | 1.038332733 |
| GO:0048754 | branching morphogenesis of a tube | 0.36336876 | 1.038339498 |
| ENSG00000111276 | CDKN1B subnetwork | 0.36263217 | 1.038341463 |
| GO:0030857 | negative regulation of epithelial cell differentiation | 0.3637945 | 1.038343379 |
| ENSG00000125753 | VASP subnetwork | 0.36327463 | 1.038373905 |
| GO:0034763 | negative regulation of transmembrane transport | 0.36309595 | 1.038376851 |
| GO:0019098 | reproductive behavior | 0.99825815 | 1.038400317 |
| ENSG00000171681 | ATF7IP subnetwork | 0.36323603 | 1.038439813 |
| GO:0055021 | regulation of cardiac muscle tissue growth | 0.99824025 | 1.0384427 |
| MP:0001488 | increased startle reflex | 0.99822419 | 1.038470681 |
| MP:0002314 | abnormal respiratory mechanics | 0.36374629 | 1.038477246 |

| | | | |
|---|---|---|---|
| MP:0003461 | abnormal response to novel object | 0.9981852 | 1.038495065 |
| ENSG00000169813 | HNRNPF subnetwork | 0.36274704 | 1.038499805 |
| GO:0002230 | positive regulation of defense response to virus by host | 0.3632102 | 1.038544711 |
| GO:0034765 | regulation of ion transmembrane transport | 0.99816817 | 1.038548271 |
| ENSG00000196235 | SUPT5H subnetwork | 0.36309473 | 1.038559735 |
| GO:0014075 | response to amine stimulus | 0.99816228 | 1.038605087 |
| GO:0017157 | regulation of exocytosis | 0.99815762 | 1.038672719 |
| REACTOME_FGFR4_LIGAND_B | REACTOME_FGFR4_LIGAND_BINDING_AND_ACTIVATION | 0.99813169 | 1.038704331 |
| ENSG00000117399 | CDC20 subnetwork | 0.99812409 | 1.038775584 |
| MP:0003056 | abnormal hyoid bone morphology | 0.99811622 | 1.038843243 |
| MP:0003137 | abnormal impulse conducting system conduction | 0.99811384 | 1.038914516 |
| MP:0002916 | increased synaptic depression | 0.99808392 | 1.03894255 |
| ENSG00000171863 | RPS7 subnetwork | 0.36474249 | 1.03895033 |
| GO:0008146 | sulfotransferase activity | 0.99807965 | 1.039010236 |
| ENSG00000175899 | A2M subnetwork | 0.36483196 | 1.039020369 |
| ENSG00000063177 | RPL18 subnetwork | 0.36424325 | 1.03904216 |
| GO:0005834 | heterotrimeric G-protein complex | 0.99807572 | 1.039077932 |
| MP:0011090 | partial perinatal lethality | 0.36492815 | 1.039080683 |
| ENSG00000170608 | FOXA3 subnetwork | 0.36471725 | 1.039084029 |
| GO:0010522 | regulation of calcium ion transport into cytosol | 0.36422229 | 1.039127478 |
| MP:0002544 | brachydactyly | 0.99806774 | 1.039134823 |
| GO:0021700 | developmental maturation | 0.99805581 | 1.039198933 |
| GO:0030509 | BMP signaling pathway | 0.99803195 | 1.039237814 |
| GO:0003300 | cardiac muscle hypertrophy | 0.36470381 | 1.039256599 |
| GO:0032368 | regulation of lipid transport | 0.36419128 | 1.039290573 |
| GO:0032489 | regulation of Cdc42 protein signal transduction | 0.99802903 | 1.039309151 |
| ENSG00000124795 | DEK subnetwork | 0.36412497 | 1.039366252 |
| GO:0043088 | regulation of Cdc42 GTPase activity | 0.99802903 | 1.039384105 |
| MP:0001417 | decreased exploration in new environment | 0.9980239 | 1.039455463 |
| GO:0014897 | striated muscle hypertrophy | 0.36470381 | 1.039458358 |
| MP:0008814 | reduced nerve conduction velocity | 0.99802299 | 1.039530439 |
| GO:0050308 | sugar-phosphatase activity | 0.36469318 | 1.039563107 |
| GO:0010243 | response to organic nitrogen | 0.99802292 | 1.039605425 |
| MP:0002260 | abnormal thyroid cartilage morphology | 0.99799758 | 1.039640744 |
| GO:0031228 | intrinsic to Golgi membrane | 0.36456663 | 1.039656177 |
| GO:0061311 | cell surface receptor signaling pathway involved in heart de | 0.99798813 | 1.039697713 |
| GO:0007416 | synapse assembly | 0.99797851 | 1.039747475 |
| GO:0019203 | carbohydrate phosphatase activity | 0.36469318 | 1.039765003 |
| REACTOME_SHC:MEDIATED_C | REACTOME_SHC:MEDIATED_CASCADE | 0.99796694 | 1.039804459 |
| ENSG00000125084 | WNT1 subnetwork | 0.99795921 | 1.039875884 |
| MP:0010984 | abnormal metanephric mesenchyme morphology | 0.99794216 | 1.039925669 |
| MP:0003733 | abnormal retinal inner nuclear layer morphology | 0.99792325 | 1.039975462 |
| GO:0030336 | negative regulation of cell migration | 0.99792209 | 1.040043306 |
| GO:0009581 | detection of external stimulus | 0.99791828 | 1.040111159 |
| GO:0033057 | multicellular organismal reproductive behavior | 0.99791719 | 1.040182632 |
| GO:0048713 | regulation of oligodendrocyte differentiation | 0.99789837 | 1.040232457 |
| GO:0045664 | regulation of neuron differentiation | 0.99788408 | 1.0402859 |
| GO:0015812 | gamma-aminobutyric acid transport | 0.9978763 | 1.04033935 |
| ENSG00000155966 | AFF2 subnetwork | 0.36546439 | 1.040391701 |
| GO:0006112 | energy reserve metabolic process | 0.9978721 | 1.04041086 |
| ENSG00000064995 | TAF11 subnetwork | 0.36556238 | 1.040442032 |
| ENSG00000168702 | LRP1B subnetwork | 0.99786128 | 1.040457106 |
| GO:0030318 | melanocyte differentiation | 0.9978573 | 1.040528634 |

| | | | |
|---|---|---|---|
| MP:0008023 | abnormal styloid process morphology | 0.99784235 | 1.040585729 |
| GO:0050805 | negative regulation of synaptic transmission | 0.99783789 | 1.040660888 |
| ENSG00000133121 | STARD13 subnetwork | 0.36569869 | 1.040705563 |
| GO:0045601 | regulation of endothelial cell differentiation | 0.99783586 | 1.040732447 |
| KEGG_CYSTEINE_AND_METHIC | KEGG_CYSTEINE_AND_METHIONINE_METABOLISM | 0.3657982 | 1.040775194 |
| GO:0055024 | regulation of cardiac muscle tissue development | 0.99782516 | 1.040796793 |
| MP:0009538 | abnormal synapse morphology | 0.99782345 | 1.040871984 |
| GO:0006677 | glycosylceramide metabolic process | 0.99780681 | 1.040932736 |
| ENSG00000115963 | RND3 subnetwork | 0.36610923 | 1.040983924 |
| GO:0007608 | sensory perception of smell | 0.99780123 | 1.041007948 |
| ENSG00000099991 | CABIN1 subnetwork | 0.36605772 | 1.041049981 |
| GO:0007189 | adenylate cyclase-activating G-protein coupled receptor sig | 0.99778588 | 1.041065106 |
| KEGG_WNT_SIGNALING_PATH | KEGG_WNT_SIGNALING_PATHWAY | 0.36600956 | 1.041067623 |
| GO:0010579 | positive regulation of adenylate cyclase activity involved in | 0.99778588 | 1.041140338 |
| GO:0010578 | regulation of adenylate cyclase activity involved in G-protei | 0.99778588 | 1.041215581 |
| GO:0002087 | regulation of respiratory gaseous exchange by neurological | 0.9977761 | 1.041272767 |
| GO:0044065 | regulation of respiratory system process | 0.9977761 | 1.04134803 |
| MP:0001739 | abnormal adrenal gland secretion | 0.99777114 | 1.041419691 |
| MP:0001153 | small seminiferous tubules | 0.36631878 | 1.041431061 |
| GO:0022029 | telencephalon cell migration | 0.99776998 | 1.041494976 |
| GO:0006836 | neurotransmitter transport | 0.99774964 | 1.041541353 |
| ENSG00000118046 | STK11 subnetwork | 0.36646179 | 1.041550523 |
| GO:0001754 | eye photoreceptor cell differentiation | 0.99774542 | 1.041613043 |
| REACTOME_ENERGY_DEPENDI | REACTOME_ENERGY_DEPENDENT_REGULATION_OF_MTOI | 0.36659028 | 1.041668279 |
| GO:0030247 | polysaccharide binding | 0.99773779 | 1.041684743 |
| GO:0044437 | vacuolar part | 0.36644209 | 1.041694095 |
| GO:0001871 | pattern binding | 0.99773779 | 1.041760069 |
| REACTOME_ADP_SIGNALLING_ | REACTOME_ADP_SIGNALLING_THROUGH_P2Y_PURINOCEI | 0.99773135 | 1.041820943 |
| MP:0000746 | weakness | 0.99773015 | 1.041881825 |
| GO:0045879 | negative regulation of smoothened signaling pathway | 0.99772287 | 1.041942717 |
| ENSG00000175063 | UBE2C subnetwork | 0.99771226 | 1.041996383 |
| GO:0050807 | regulation of synapse organization | 0.99770919 | 1.042064525 |
| GO:0021799 | cerebral cortex radially oriented cell migration | 0.99764805 | 1.042103169 |
| GO:0045446 | endothelial cell differentiation | 0.99769537 | 1.042114592 |
| GO:0015077 | monovalent inorganic cation transmembrane transporter a | 0.99763779 | 1.042167716 |
| GO:0060759 | regulation of response to cytokine stimulus | 0.36688601 | 1.042184175 |
| ENSG00000151834 | GABRA2 subnetwork | 0.99763481 | 1.04223589 |
| MP:0002187 | abnormal fibula morphology | 0.36684759 | 1.042269737 |
| GO:0031000 | response to caffeine | 0.9976076 | 1.042289601 |
| MP:0003932 | abnormal molar crown morphology | 0.9976058 | 1.042365031 |
| MP:0003290 | intestinal hypoperistalsis | 0.99760448 | 1.042436853 |
| ENSG00000133119 | RFC3 subnetwork | 0.3675965 | 1.042448822 |
| ENSG00000145365 | TIFA subnetwork | 0.3670748 | 1.04245648 |
| ENSG00000185532 | PRKG1 subnetwork | 0.367339 | 1.042462312 |
| GO:0003231 | cardiac ventricle development | 0.9976034 | 1.042512305 |
| ENSG00000104824 | HNRNPL subnetwork | 0.36745853 | 1.042532844 |
| ENSG00000148942 | SLC5A12 subnetwork | 0.36717792 | 1.04257397 |
| MP:0001006 | abnormal retinal cone cell morphology | 0.9976002 | 1.042584148 |
| MP:0001290 | delayed eyelid opening | 0.36758009 | 1.042601893 |
| GO:0003071 | renal system process involved in regulation of systemic arte | 0.99757483 | 1.042623426 |
| MP:0005431 | decreased oocyte number | 0.36732134 | 1.0426445 |
| MP:0004363 | stria vascularis degeneration | 0.36744146 | 1.042657005 |
| ENSG00000121957 | GPSM2 subnetwork | 0.99755877 | 1.042677188 |

| | | | |
|---|---|---|---|
| GO:0003156 | regulation of organ formation | 0.99754944 | 1.042745439 |
| REACTOME_NEUROTRANSMIT | REACTOME_NEUROTRANSMITTER_RELEASE_CYCLE | 0.99754292 | 1.042802838 |
| ENSG00000187837 | HIST1H1C subnetwork | 0.36793275 | 1.04282957 |
| MP:0000292 | distended pericardium | 0.36730565 | 1.042836427 |
| ENSG00000188976 | NOC2L subnetwork | 0.36817714 | 1.042862654 |
| GO:0005921 | gap junction | 0.99753069 | 1.042863867 |
| GO:0019048 | virus-host interaction | 0.36788744 | 1.042866795 |
| GO:0042640 | anagen | 0.99751382 | 1.042932146 |
| ENSG00000035928 | RFC1 subnetwork | 0.36815417 | 1.042957746 |
| MP:0009546 | absent gastric milk in neonates | 0.9975093 | 1.042996813 |
| KEGG_GLYCOSAMINOGLYCAN_ | KEGG_GLYCOSAMINOGLYCAN_BIOSYNTHESIS_KERATAN_SI | 0.36786832 | 1.043039197 |
| GO:0001774 | microglial cell activation | 0.99749731 | 1.043061491 |
| GO:0000725 | recombinational repair | 0.36810759 | 1.043072173 |
| MP:0003216 | absence seizures | 0.99746919 | 1.043100826 |
| GO:0004016 | adenylate cyclase activity | 0.99746286 | 1.04316552 |
| GO:0016407 | acetyltransferase activity | 0.36830075 | 1.043172613 |
| MP:0001292 | abnormal lens vesicle development | 0.99745001 | 1.043222979 |
| ENSG00000135845 | PIGC subnetwork | 0.36867066 | 1.043254962 |
| REACTOME_ABC:FAMILY_PRO | REACTOME_ABC:FAMILY_PROTEINS_MEDIATED_TRANSPOI | 0.36893433 | 1.043269786 |
| MP:0004753 | abnormal miniature excitatory postsynaptic currents | 0.99743849 | 1.043276824 |
| ENSG00000131153 | GINS2 subnetwork | 0.36848688 | 1.043300559 |
| GO:0046520 | sphingoid biosynthetic process | 0.99743566 | 1.04334879 |
| MP:0001473 | reduced long term potentiation | 0.99742019 | 1.043409898 |
| ENSG00000141030 | COPS3 subnetwork | 0.3687514 | 1.043410405 |
| GO:0043596 | nuclear replication fork | 0.36846918 | 1.043434246 |
| ENSG00000168924 | LETM1 subnetwork | 0.36863254 | 1.043436777 |
| ENSG00000188170 | ENSG00000188170 subnetwork | 0.36893343 | 1.043461094 |
| GO:0014888 | striated muscle adaptation | 0.99741278 | 1.043471014 |
| MP:0004087 | abnormal muscle fiber morphology | 0.99738519 | 1.043506776 |
| ENSG00000101856 | PGRMC1 subnetwork | 0.36889247 | 1.043565787 |
| GO:0048675 | axon extension | 0.99737885 | 1.043575156 |
| ENSG00000065613 | SLK subnetwork | 0.36914885 | 1.043608009 |
| GO:0009953 | dorsal/ventral pattern formation | 0.99737049 | 1.043639922 |
| GO:0005230 | extracellular ligand-gated ion channel activity | 0.99736496 | 1.043701073 |
| GO:0035690 | cellular response to drug | 0.99735756 | 1.043776731 |
| GO:0060251 | regulation of glial cell proliferation | 0.99735457 | 1.043848775 |
| GO:0007612 | learning | 0.99734994 | 1.043917204 |
| MP:0001071 | abnormal facial nerve morphology | 0.9973401 | 1.043992894 |
| ENSG00000102781 | KATNAL1 subnetwork | 0.99731511 | 1.044054093 |
| ENSG00000139343 | SNRPF subnetwork | 0.36945794 | 1.044072363 |
| ENSG00000134697 | GNL2 subnetwork | 0.36938048 | 1.044109721 |
| GO:0003158 | endothelium development | 0.99731248 | 1.044129804 |
| GO:0044062 | regulation of excretion | 0.99731148 | 1.044205526 |
| ENSG00000101082 | SLA2 subnetwork | 0.36957852 | 1.044227439 |
| GO:0035113 | embryonic appendage morphogenesis | 0.99730725 | 1.044277633 |
| GO:0030326 | embryonic limb morphogenesis | 0.99730725 | 1.044353376 |
| MP:0003072 | abnormal metatarsal bone morphology | 0.99729775 | 1.04441825 |
| GO:0097061 | dendritic spine organization | 0.99729375 | 1.044490388 |
| GO:0060997 | dendritic spine morphogenesis | 0.99729375 | 1.044566164 |
| ENSG00000139323 | POC1B subnetwork | 0.36978264 | 1.044594075 |
| GO:0001508 | regulation of action potential | 0.99725785 | 1.044609301 |
| ENSG00000135744 | AGT subnetwork | 0.99725299 | 1.044685097 |
| GO:0005539 | glycosaminoglycan binding | 0.99725103 | 1.044760903 |

| | | | |
|---|---|---|---|
| GO:0060998 | regulation of dendritic spine development | 0.99724852 | 1.044822206 |
| ENSG00000006744 | ELAC2 subnetwork | 0.99724051 | 1.044890776 |
| ENSG00000168243 | GNG4 subnetwork | 0.99723302 | 1.044959355 |
| GO:0043195 | terminal button | 0.99719491 | 1.044995282 |
| GO:0032403 | protein complex binding | 0.36997187 | 1.045018273 |
| GO:0009583 | detection of light stimulus | 0.99718709 | 1.045063879 |
| GO:0002089 | lens morphogenesis in camera-type eye | 0.99718025 | 1.045128857 |
| MP:0009745 | abnormal behavioral response to xenobiotic | 0.99716592 | 1.045186583 |
| GO:0060008 | Sertoli cell differentiation | 0.37028911 | 1.045252739 |
| GO:0035815 | positive regulation of renal sodium excretion | 0.99715837 | 1.045255209 |
| REACTOME_OTHER_SEMAPHO | REACTOME_OTHER_SEMAPHORIN_INTERACTIONS | 0.99714247 | 1.045312954 |
| GO:0045921 | positive regulation of exocytosis | 0.99714146 | 1.045388861 |
| GO:0048545 | response to steroid hormone stimulus | 0.3702821 | 1.045405613 |
| GO:0030313 | cell envelope | 0.99713507 | 1.045457516 |
| ENSG00000158486 | DNAH3 subnetwork | 0.37041744 | 1.045493851 |
| GO:0008585 | female gonad development | 0.37114917 | 1.045521672 |
| GO:0044462 | external encapsulating structure part | 0.99713507 | 1.045533445 |
| GO:0033002 | muscle cell proliferation | 0.37026751 | 1.045577774 |
| GO:0006906 | vesicle fusion | 0.99713271 | 1.045605752 |
| ENSG00000103152 | MPG subnetwork | 0.37019754 | 1.045644231 |
| ENSG00000198569 | SLC34A3 subnetwork | 0.99712579 | 1.045681703 |
| GO:0043280 | positive regulation of cysteine-type endopeptidase activity | 0.37113983 | 1.04570305 |
| GO:0060043 | regulation of cardiac muscle cell proliferation | 0.99711778 | 1.045732239 |
| ENSG00000163347 | CLDN1 subnetwork | 0.37130274 | 1.045762224 |
| REACTOME_FGFR_LIGAND_BI | REACTOME_FGFR_LIGAND_BINDING_AND_ACTIVATION | 0.99710827 | 1.045804577 |
| MP:0005205 | abnormal eye anterior chamber morphology | 0.99709895 | 1.045873293 |
| REACTOME_SYNTHESIS_SECRE | REACTOME_SYNTHESIS_SECRETION_AND_INACTIVATION_( | 0.99705421 | 1.04589479 |
| GO:2001056 | positive regulation of cysteine-type endopeptidase activity | 0.37113983 | 1.045903684 |
| ENSG00000137203 | TFAP2A subnetwork | 0.99704445 | 1.045956256 |
| ENSG00000154229 | PRKCA subnetwork | 0.37111297 | 1.045998849 |
| MP:0011108 | partial embryonic lethality during organogenesis | 0.37147094 | 1.046021856 |
| ENSG00000070018 | LRP6 subnetwork | 0.99704135 | 1.046024998 |
| GO:0031234 | extrinsic to internal side of plasma membrane | 0.99699729 | 1.046039244 |
| ENSG00000154429 | C1orf96 subnetwork | 0.99697596 | 1.04607893 |
| ENSG00000092054 | MYH7 subnetwork | 0.99697364 | 1.04615133 |
| ENSG00000108107 | RPL28 subnetwork | 0.37110844 | 1.046190019 |
| MP:0004610 | small vertebrae | 0.99697127 | 1.046216472 |
| MP:0009845 | abnormal neural crest cell morphology | 0.99696633 | 1.046281623 |
| MP:0001683 | absent mesoderm | 0.37109089 | 1.046314072 |
| GO:0010662 | regulation of striated muscle cell apoptotic process | 0.99696284 | 1.046357688 |
| GO:0006817 | phosphate ion transport | 0.99695943 | 1.046419223 |
| ENSG00000148308 | GTF3C5 subnetwork | 0.37085908 | 1.046455331 |
| REACTOME_BASE:FREE_SUGAI | REACTOME_BASE:FREE_SUGAR:PHOSPHATE_REMOVAL_VI. | 0.37107228 | 1.046476575 |
| GO:0048278 | vesicle docking | 0.9969588 | 1.046491675 |
| GO:0005234 | extracellular-glutamate-gated ion channel activity | 0.99694902 | 1.0465605 |
| REACTOME_FGFR3_LIGAND_B | REACTOME_FGFR3_LIGAND_BINDING_AND_ACTIVATION | 0.99693899 | 1.046622064 |
| ENSG00000188739 | RBM34 subnetwork | 0.37104844 | 1.046629537 |
| MP:0008997 | increased blood osmolality | 0.37194734 | 1.046666028 |
| REACTOME_FGFR3C_LIGAND_ | REACTOME_FGFR3C_LIGAND_BINDING_AND_ACTIVATION | 0.99693899 | 1.046698182 |
| GO:0004252 | serine-type endopeptidase activity | 0.37098493 | 1.046705724 |
| GO:0060996 | dendritic spine development | 0.99686229 | 1.046726797 |
| GO:0051918 | negative regulation of fibrinolysis | 0.99692721 | 1.046759764 |
| ENSG00000133112 | TPT1 subnetwork | 0.99683237 | 1.046766567 |

| | | | |
|---|---|---|---|
| ENSG00000073921 | PICALM subnetwork | 0.37184979 | 1.046808511 |
| ENSG00000198929 | NOS1AP subnetwork | 0.99683072 | 1.046835443 |
| ENSG00000170606 | HSPA4 subnetwork | 0.37194465 | 1.046847451 |
| GO:0048934 | peripheral nervous system neuron differentiation | 0.99682611 | 1.046911604 |
| GO:0048935 | peripheral nervous system neuron development | 0.99682611 | 1.046987776 |
| MP:0009969 | abnormal cerebral cortex pyramidal cell morphology | 0.99679987 | 1.047042131 |
| GO:0021513 | spinal cord dorsal/ventral patterning | 0.99679629 | 1.047107408 |
| ENSG00000173636 | ENSG00000173636 subnetwork | 0.99678754 | 1.047169056 |
| GO:0048284 | organelle fusion | 0.99678637 | 1.047245269 |
| GO:0001505 | regulation of neurotransmitter levels | 0.99677459 | 1.047310576 |
| MP:0000743 | muscle spasm | 0.99674119 | 1.047335857 |
| ENSG00000174021 | GNG5 subnetwork | 0.99670766 | 1.047346582 |
| GO:0019206 | nucleoside kinase activity | 0.99670328 | 1.047422831 |
| ENSG00000196510 | ANAPC7 subnetwork | 0.99669432 | 1.04749909 |
| GO:0007080 | mitotic metaphase plate congression | 0.99668816 | 1.047560798 |
| GO:0031290 | retinal ganglion cell axon guidance | 0.99667789 | 1.047626156 |
| MP:0000243 | myoclonus | 0.99666866 | 1.047702447 |
| GO:0008045 | motor axon guidance | 0.99664671 | 1.0477569 |
| ENSG00000111669 | TPI1 subnetwork | 0.99664295 | 1.047825929 |
| ENSG00000122133 | PAEP subnetwork | 0.99663434 | 1.047880399 |
| GO:0060560 | developmental growth involved in morphogenesis | 0.99662195 | 1.047945804 |
| KEGG_NEUROACTIVE_LIGAND_ | KEGG_NEUROACTIVE_LIGAND_RECEPTOR_INTERACTION | 0.99661877 | 1.048014861 |
| GO:0000940 | condensed chromosome outer kinetochore | 0.9966154 | 1.048091214 |
| GO:0043101 | purine-containing compound salvage | 0.99661054 | 1.048160291 |
| GO:0006775 | fat-soluble vitamin metabolic process | 0.37280012 | 1.048162328 |
| GO:0035587 | purinergic receptor signaling pathway | 0.99659354 | 1.048225736 |
| GO:0017048 | Rho GTPase binding | 0.37277354 | 1.048257706 |
| ENSG00000197746 | PSAP subnetwork | 0.37289299 | 1.048267943 |
| GO:0035813 | regulation of renal sodium excretion | 0.99658805 | 1.048298477 |
| ENSG00000162298 | SYVN1 subnetwork | 0.37257442 | 1.048304598 |
| REACTOME_ACTIVATION_OF_( | REACTOME_ACTIVATION_OF_CHAPERONE_GENES_BY_XBF | 0.37273226 | 1.048333972 |
| GO:0035812 | renal sodium excretion | 0.99658805 | 1.048374872 |
| GO:0034508 | centromere complex assembly | 0.99656817 | 1.048425771 |
| GO:0007096 | regulation of exit from mitosis | 0.99656395 | 1.048491254 |
| GO:0042157 | lipoprotein metabolic process | 0.37272063 | 1.048496457 |
| GO:0004970 | ionotropic glutamate receptor activity | 0.99656205 | 1.048560391 |
| GO:0014013 | regulation of gliogenesis | 0.99654876 | 1.048614958 |
| REACTOME_METABOLISM_OF_ | REACTOME_METABOLISM_OF_NITRIC_OXIDE | 0.99654671 | 1.04868776 |
| REACTOME_ENOS_ACTIVATIOI | REACTOME_ENOS_ACTIVATION_AND_REGULATION | 0.99654671 | 1.048764217 |
| GO:0009948 | anterior/posterior axis specification | 0.99654404 | 1.048833394 |
| MP:0002878 | abnormal corticospinal tract morphology | 0.99653428 | 1.048891644 |
| MP:0002557 | abnormal social/conspecific interaction | 0.99651565 | 1.048957194 |
| ENSG00000090621 | PABPC4 subnetwork | 0.37331314 | 1.049005356 |
| GO:0042312 | regulation of vasodilation | 0.99650602 | 1.049030047 |
| GO:0021517 | ventral spinal cord development | 0.99650433 | 1.04910291 |
| ENSG00000140284 | SLC27A2 subnetwork | 0.37320113 | 1.049110218 |
| GO:0030224 | monocyte differentiation | 0.37328689 | 1.04912952 |
| GO:0050907 | detection of chemical stimulus involved in sensory percepti | 0.99649995 | 1.049179431 |
| ENSG00000184343 | SRPK3 subnetwork | 0.99648113 | 1.049215844 |
| GO:2000146 | negative regulation of cell motility | 0.99645997 | 1.049266851 |
| ENSG00000171867 | PRNP subnetwork | 0.9964595 | 1.049343401 |
| ENSG00000160999 | SH2B2 subnetwork | 0.37363794 | 1.049388262 |
| ENSG00000100285 | NEFH subnetwork | 0.37448319 | 1.049389662 |

| | | | |
|---|---|---|---|
| GO:0030177 | positive regulation of Wnt receptor signaling pathway | 0.99645176 | 1.049419962 |
| GO:0005796 | Golgi lumen | 0.37384091 | 1.049464934 |
| GO:0016601 | Rac protein signal transduction | 0.99643822 | 1.049485589 |
| ENSG00000158796 | DEDD subnetwork | 0.37361994 | 1.049502868 |
| GO:0005245 | voltage-gated calcium channel activity | 0.99642686 | 1.049547577 |
| GO:0044409 | entry into host | 0.3744768 | 1.049561236 |
| MP:0001157 | small seminal vesicle | 0.37379531 | 1.049569954 |
| ENSG00000121083 | DYNLL2 subnetwork | 0.99641623 | 1.049594979 |
| GO:0016579 | protein deubiquitination | 0.37359727 | 1.049607956 |
| ENSG00000077235 | GTF3C1 subnetwork | 0.37466755 | 1.049609152 |
| GO:0060828 | regulation of canonical Wnt receptor signaling pathway | 0.99641014 | 1.049667932 |
| MP:0004131 | abnormal embryonic cilium morphology | 0.37462965 | 1.049704424 |
| GO:0016339 | calcium-dependent cell-cell adhesion | 0.99640015 | 1.049740895 |
| ENSG00000173267 | SNCG subnetwork | 0.37481296 | 1.049742661 |
| MP:0005317 | increased triglyceride level | 0.37404395 | 1.049761177 |
| ENSG00000105655 | ISYNA1 subnetwork | 0.37412296 | 1.049761223 |
| GO:0052192 | movement in environment of other organism involved in sy | 0.3744768 | 1.049761496 |
| ENSG00000113282 | CLINT1 subnetwork | 0.99639733 | 1.049813869 |
| GO:2000826 | regulation of heart morphogenesis | 0.99638923 | 1.049886853 |
| ENSG00000170927 | PKHD1 subnetwork | 0.99635611 | 1.049919696 |
| GO:0051828 | entry into other organism involved in symbiotic interaction | 0.3744768 | 1.049961832 |
| MP:0005241 | abnormal retinal ganglion layer morphology | 0.99634538 | 1.049981748 |
| GO:0021987 | cerebral cortex development | 0.99633751 | 1.05005111 |
| ENSG00000125968 | ID1 subnetwork | 0.9963325 | 1.050120482 |
| GO:0051806 | entry into cell of other organism involved in symbiotic inter | 0.3744768 | 1.050162245 |
| GO:0001976 | neurological system process involved in regulation of syster | 0.99632806 | 1.050189864 |
| GO:0031683 | G-protein beta/gamma-subunit complex binding | 0.99632193 | 1.050255605 |
| GO:0050931 | pigment cell differentiation | 0.99631751 | 1.050317704 |
| GO:0007266 | Rho protein signal transduction | 0.37503641 | 1.050333524 |
| GO:0030260 | entry into host cell | 0.3744768 | 1.050362734 |
| ENSG00000100387 | RBX1 subnetwork | 0.37432802 | 1.050362872 |
| MP:0004139 | abnormal gastric parietal cell morphology | 0.37642526 | 1.05037023 |
| GO:0042311 | vasodilation | 0.9963146 | 1.050383464 |
| REACTOME_FACILITATIVE_NA: | REACTOME_FACILITATIVE_NA:INDEPENDENT_GLUCOSE_TF | 0.37621735 | 1.050389438 |
| ENSG00000154727 | GABPA subnetwork | 0.37654492 | 1.050427107 |
| GO:0007157 | heterophilic cell-cell adhesion | 0.9963103 | 1.05046019 |
| ENSG00000164587 | RPS14 subnetwork | 0.37638751 | 1.050493733 |
| ENSG00000186676 | ENSG00000186676 subnetwork | 0.37618894 | 1.050494015 |
| GO:0010658 | striated muscle cell apoptotic process | 0.99630262 | 1.050518665 |
| ENSG00000078699 | CBFA2T2 subnetwork | 0.37515359 | 1.050543064 |
| ENSG00000131236 | CAP1 subnetwork | 0.37522797 | 1.050562012 |
| GO:0052126 | movement in host environment | 0.3744768 | 1.0505633 |
| ENSG00000083896 | YTHDC1 subnetwork | 0.37634339 | 1.050569801 |
| REACTOME_SIGNALING_BY_IN | REACTOME_SIGNALING_BY_INSULIN_RECEPTOR | 0.99629236 | 1.050584454 |
| GO:0032651 | regulation of interleukin-1 beta production | 0.37601693 | 1.050608365 |
| ENSG00000108468 | CBX1 subnetwork | 0.37582133 | 1.050618223 |
| GO:0060420 | regulation of heart growth | 0.99627538 | 1.050631987 |
| MP:0004220 | abnormal peripheral nervous system regeneration | 0.3761759 | 1.050646142 |
| REACTOME_BETA_DEFENSINS | REACTOME_BETA_DEFENSINS | 0.37572742 | 1.050656518 |
| ENSG00000126756 | UXT subnetwork | 0.3759685 | 1.050665526 |
| GO:0043502 | regulation of muscle adaptation | 0.37579575 | 1.050694444 |
| MP:0000813 | abnormal hippocampus layer morphology | 0.99627181 | 1.0507051 |
| GO:0010543 | regulation of platelet activation | 0.99627104 | 1.050781878 |

| | | | |
|---|---|---|---|
| GO:0048745 | smooth muscle tissue development | 0.99622566 | 1.050803859 |
| KEGG_LONG_TERM_POTENTIA | KEGG_LONG_TERM_POTENTIATION | 0.37595068 | 1.05083682 |
| ENSG00000008128 | CDK11A subnetwork | 0.37572091 | 1.050837457 |
| GO:0006383 | transcription from RNA polymerase III promoter | 0.37617395 | 1.050845847 |
| GO:0021781 | glial cell fate commitment | 0.99620144 | 1.050862384 |
| REACTOME_ROLE_OF_SECONI | REACTOME_ROLE_OF_SECOND_MESSENGERS_IN_NETRIN: | 0.99617051 | 1.050888028 |
| ENSG00000005189 | ENSG00000005189 subnetwork | 0.37566279 | 1.050913764 |
| GO:0048708 | astrocyte differentiation | 0.99615783 | 1.050953878 |
| GO:0030539 | male genitalia development | 0.99612441 | 1.050994152 |
| ENSG00000122126 | OCRL subnetwork | 0.99612317 | 1.051070985 |
| ENSG00000082258 | CCNT2 subnetwork | 0.37564578 | 1.051085301 |
| GO:0048070 | regulation of developmental pigmentation | 0.99610929 | 1.051125896 |
| REACTOME_APOPTOTIC_CLEA | REACTOME_APOPTOTIC_CLEAVAGE_OF_CELLULAR_PROTE | 0.37552773 | 1.051161905 |
| ENSG00000114125 | RNF7 subnetwork | 0.37560058 | 1.051171205 |
| GO:0007618 | mating | 0.99610446 | 1.051195438 |
| GO:0030239 | myofibril assembly | 0.99609716 | 1.051257678 |
| GO:0007168 | receptor guanylyl cyclase signaling pathway | 0.99607393 | 1.051294333 |
| REACTOME_ADP_SIGNALLING_ | REACTOME_ADP_SIGNALLING_THROUGH_P2Y_PURINOCEI | 0.99606679 | 1.051363902 |
| REACTOME_GLYCOGEN_BREAI | REACTOME_GLYCOGEN_BREAKDOWN_GLYCOGENOLYSIS | 0.99605852 | 1.051433482 |
| ENSG00000164418 | GRIK2 subnetwork | 0.99601236 | 1.051448215 |
| ENSG00000078399 | HOXA9 subnetwork | 0.37694211 | 1.051451888 |
| GO:0050680 | negative regulation of epithelial cell proliferation | 0.99599459 | 1.051506839 |
| ENSG00000096063 | SRPK1 subnetwork | 0.99593794 | 1.051525238 |
| GO:0001825 | blastocyst formation | 0.99593371 | 1.051598508 |
| ENSG00000141552 | ANAPC11 subnetwork | 0.99591888 | 1.05166813 |
| MP:0000454 | abnormal jaw morphology | 0.99587401 | 1.051682886 |
| GO:0010470 | regulation of gastrulation | 0.99585216 | 1.051723255 |
| MP:0001052 | abnormal muscle innervation | 0.99581254 | 1.051738017 |
| GO:0021756 | striatum development | 0.99580384 | 1.05180767 |
| KEGG_HYPERTROPHIC_CARDIC | KEGG_HYPERTROPHIC_CARDIOMYOPATHY_HCM | 0.99579203 | 1.051870014 |
| GO:0003151 | outflow tract morphogenesis | 0.9957872 | 1.051947006 |
| GO:0007213 | G-protein coupled acetylcholine receptor signaling pathwa | 0.99576775 | 1.05200571 |
| GO:0021795 | cerebral cortex cell migration | 0.99575309 | 1.052075403 |
| GO:0009635 | response to herbicide | 0.99574921 | 1.052145106 |
| GO:0019201 | nucleotide kinase activity | 0.99572301 | 1.052196515 |
| GO:0070325 | lipoprotein particle receptor binding | 0.99571353 | 1.052258915 |
| MP:0004136 | abnormal tongue muscle morphology | 0.99570673 | 1.052328647 |
| GO:0030100 | regulation of endocytosis | 0.99570473 | 1.052398389 |
| ENSG00000198788 | MUC2 subnetwork | 0.99566695 | 1.052402226 |
| ENSG00000128524 | ATP6V1F subnetwork | 0.99566667 | 1.052479309 |
| ENSG00000182520 | ENSG00000182520 subnetwork | 0.99566495 | 1.05255274 |
| ENSG00000106682 | EIF4H subnetwork | 0.37736624 | 1.052571157 |
| ENSG00000171549 | ENSG00000171549 subnetwork | 0.99566495 | 1.052629844 |
| ENSG00000136238 | RAC1 subnetwork | 0.37746506 | 1.052656042 |
| MP:0005216 | abnormal pancreatic alpha cell morphology | 0.99566483 | 1.052703297 |
| MP:0005122 | increased circulating thyroid-stimulating hormone level | 0.37763099 | 1.05275934 |
| GO:0071549 | cellular response to dexamethasone stimulus | 0.99565706 | 1.052773097 |
| GO:0045214 | sarcomere organization | 0.99561857 | 1.052809936 |
| ENSG00000177542 | SLC25A22 subnetwork | 0.99559947 | 1.052868762 |
| GO:0016810 | hydrolase activity, acting on carbon-nitrogen (but not pepti | 0.37788248 | 1.052937832 |
| ENSG00000162889 | MAPKAPK2 subnetwork | 0.37761637 | 1.052940061 |
| GO:0014074 | response to purine-containing compound | 0.99559873 | 1.052942254 |
| GO:0019905 | syntaxin binding | 0.99554983 | 1.052964456 |

| | | | |
|---|---|---|---|
| GO:0007257 | activation of JUN kinase activity | 0.37775533 | 1.05301479 |
| GO:0009582 | detection of abiotic stimulus | 0.99553918 | 1.053030636 |
| ENSG00000171311 | EXOSC1 subnetwork | 0.37827457 | 1.053048665 |
| ENSG00000115750 | TAF1B subnetwork | 0.3778735 | 1.053099526 |
| ENSG00000105698 | USF2 subnetwork | 0.99553863 | 1.053107821 |
| GO:0021516 | dorsal spinal cord development | 0.99553771 | 1.053185017 |
| MP:0003964 | abnormal noradrenaline level | 0.3782668 | 1.053229167 |
| GO:0044452 | nucleolar part | 0.37812974 | 1.05323039 |
| GO:0030835 | negative regulation of actin filament depolymerization | 0.37841096 | 1.05323741 |
| GO:0015874 | norepinephrine transport | 0.99552864 | 1.053258559 |
| ENSG00000119541 | VPS4B subnetwork | 0.99551845 | 1.053306452 |
| MP:0000102 | abnormal nasal bone morphology | 0.99550732 | 1.053361683 |
| GO:0001701 | in utero embryonic development | 0.37921446 | 1.053363568 |
| ENSG00000129282 | MRM1 subnetwork | 0.37824707 | 1.053409737 |
| ENSG00000188229 | TUBB4B subnetwork | 0.37810719 | 1.053411029 |
| ENSG00000168280 | KIF5C subnetwork | 0.37917706 | 1.053430353 |
| GO:0060219 | camera-type eye photoreceptor cell differentiation | 0.9955051 | 1.053438921 |
| GO:0008343 | adult feeding behavior | 0.9954646 | 1.053475838 |
| GO:0043484 | regulation of RNA splicing | 0.99544442 | 1.05351276 |
| ENSG00000123064 | DDX54 subnetwork | 0.37913584 | 1.053544423 |
| REACTOME_REGULATION_OF_ | REACTOME_REGULATION_OF_INSULIN_SECRETION | 0.99543976 | 1.053579025 |
| ENSG00000125503 | PPP1R12C subnetwork | 0.37942064 | 1.053626747 |
| GO:0010324 | membrane invagination | 0.99543525 | 1.053652633 |
| ENSG00000100280 | AP1B1 subnetwork | 0.37938966 | 1.05371245 |
| ENSG00000011052 | NME2 subnetwork | 0.37912647 | 1.053724712 |
| GO:0006897 | endocytosis | 0.99543525 | 1.05372992 |
| MP:0004841 | abnormal small intestine crypts of Lieberkuhn morphology | 0.38027129 | 1.053788878 |
| MP:0001404 | no spontaneous movement | 0.99542212 | 1.053796215 |
| MP:0005352 | small cranium | 0.37908729 | 1.053810514 |
| ENSG00000185049 | WHSC2 subnetwork | 0.38063642 | 1.053832392 |
| ENSG00000082458 | DLG3 subnetwork | 0.99539347 | 1.053833174 |
| GO:0032981 | mitochondrial respiratory chain complex I assembly | 0.99538295 | 1.053899486 |
| GO:0032392 | DNA geometric change | 0.37890445 | 1.053907285 |
| ENSG00000152056 | AP1S3 subnetwork | 0.37904941 | 1.053943635 |
| ENSG00000082898 | XPO1 subnetwork | 0.38061732 | 1.053946129 |
| GO:0010257 | NADH dehydrogenase complex assembly | 0.99538295 | 1.053976814 |
| ENSG00000075151 | EIF4G3 subnetwork | 0.38026199 | 1.05397813 |
| ENSG00000110801 | PSMD9 subnetwork | 0.37965375 | 1.053994334 |
| GO:0061135 | endopeptidase regulator activity | 0.38013415 | 1.054026782 |
| MP:0005189 | abnormal anogenital distance | 0.38078815 | 1.054048202 |
| GO:0097031 | mitochondrial respiratory chain complex I biogenesis | 0.99538295 | 1.054054153 |
| ENSG00000147955 | SIGMAR1 subnetwork | 0.38022793 | 1.054063738 |
| GO:0044445 | cytosolic part | 0.37904059 | 1.054086266 |
| GO:0060976 | coronary vasculature development | 0.99535137 | 1.054087473 |
| ENSG00000099810 | MTAP subnetwork | 0.37976905 | 1.054087991 |
| GO:0032508 | DNA duplex unwinding | 0.37890445 | 1.054106737 |
| ENSG00000161960 | EIF4A1 subnetwork | 0.38099173 | 1.054130598 |
| ENSG00000132842 | AP3B1 subnetwork | 0.38061631 | 1.054135268 |
| GO:0052547 | regulation of peptidase activity | 0.3798613 | 1.054143855 |
| ENSG00000178053 | MLF1 subnetwork | 0.99534261 | 1.054153824 |
| MP:0000460 | mandible hypoplasia | 0.38055732 | 1.05415489 |
| ENSG00000166863 | TAC3 subnetwork | 0.38106168 | 1.054158043 |
| GO:0002011 | morphogenesis of an epithelial sheet | 0.38093087 | 1.054169019 |

| | | | |
|---|---|---|---|
| ENSG00000137936 | BCAR3 subnetwork | 0.37886402 | 1.054173765 |
| ENSG00000111364 | DDX55 subnetwork | 0.38012298 | 1.054216186 |
| ENSG00000109680 | TBC1D19 subnetwork | 0.99533389 | 1.054223853 |
| ENSG00000112237 | CCNC subnetwork | 0.38006558 | 1.054292453 |
| GO:0006911 | phagocytosis, engulfment | 0.99532569 | 1.054293893 |
| ENSG00000111641 | NOP2 subnetwork | 0.38054002 | 1.054297022 |
| MP:0001726 | abnormal allantois morphology | 0.38092534 | 1.054358057 |
| GO:0006401 | RNA catabolic process | 0.3811677 | 1.054364184 |
| GO:0010460 | positive regulation of heart rate | 0.99532567 | 1.054371284 |
| MP:0000952 | abnormal CNS glial cell morphology | 0.37999749 | 1.054397886 |
| GO:0021885 | forebrain cell migration | 0.99529337 | 1.054422992 |
| ENSG00000143537 | ADAM15 subnetwork | 0.38003545 | 1.054425363 |
| GO:0045600 | positive regulation of fat cell differentiation | 0.99527721 | 1.054471037 |
| MP:0005130 | decreased follicle stimulating hormone level | 0.38127236 | 1.054476208 |
| MP:0005236 | abnormal olfactory nerve morphology | 0.99524854 | 1.054497063 |
| ENSG00000071054 | MAP4K4 subnetwork | 0.38152101 | 1.054520677 |
| ENSG00000172794 | RAB37 subnetwork | 0.99521237 | 1.054541449 |
| GO:0006684 | sphingomyelin metabolic process | 0.3813798 | 1.054550583 |
| MP:0005498 | hyporesponsive to tactile stimuli | 0.99518529 | 1.054589514 |
| ENSG00000159788 | RGS12 subnetwork | 0.99515656 | 1.054615554 |
| GO:0000724 | double-strand break repair via homologous recombination | 0.38147753 | 1.05463433 |
| MP:0002639 | micrognathia | 0.99514976 | 1.054681992 |
| GO:0006140 | regulation of nucleotide metabolic process | 0.99513076 | 1.054748439 |
| GO:0000910 | cytokinesis | 0.99509611 | 1.054785515 |
| GO:0048593 | camera-type eye morphogenesis | 0.99507236 | 1.054818923 |
| ENSG00000156873 | PHKG2 subnetwork | 0.9950436 | 1.054878049 |
| ENSG00000066735 | KIF26A subnetwork | 0.9950403 | 1.054951877 |
| GO:0000149 | SNARE binding | 0.9950321 | 1.055018369 |
| GO:0002028 | regulation of sodium ion transport | 0.99502115 | 1.055073848 |
| MP:0003787 | abnormal imprinting | 0.99501999 | 1.055151382 |
| GO:0030148 | sphingolipid biosynthetic process | 0.99498311 | 1.055173808 |
| GO:0004112 | cyclic-nucleotide phosphodiesterase activity | 0.38192426 | 1.055232995 |
| ENSG00000163810 | TGM4 subnetwork | 0.99497464 | 1.055240335 |
| ENSG00000113319 | RASGRF2 subnetwork | 0.38314182 | 1.055263158 |
| MP:0000229 | abnormal megakaryocyte differentiation | 0.38233769 | 1.055312559 |
| GO:0032088 | negative regulation of NF-kappaB transcription factor activi | 0.38213138 | 1.055315552 |
| GO:0043174 | nucleoside salvage | 0.9949736 | 1.055317898 |
| MP:0001182 | lung hemorrhage | 0.38321178 | 1.055318352 |
| ENSG00000099995 | SF3A1 subnetwork | 0.3822112 | 1.055370892 |
| GO:0048703 | embryonic viscerocranium morphogenesis | 0.99496138 | 1.055377095 |
| ENSG00000174307 | PHLDA3 subnetwork | 0.38206314 | 1.05540109 |
| GO:0004091 | carboxylesterase activity | 0.38192203 | 1.055421913 |
| ENSG00000132142 | ACACA subnetwork | 0.38313454 | 1.05542338 |
| ENSG00000171916 | LGALS9C subnetwork | 0.38306725 | 1.055443133 |
| ENSG00000004897 | CDC27 subnetwork | 0.99495072 | 1.055443652 |
| GO:0045334 | clathrin-coated endocytic vesicle | 0.3823073 | 1.055463763 |
| GO:0051145 | smooth muscle cell differentiation | 0.9949266 | 1.055502867 |
| MP:0001539 | decreased caudal vertebrae number | 0.99491603 | 1.05554371 |
| GO:0001759 | organ induction | 0.99491516 | 1.055621324 |
| ENSG00000170298 | LGALS9B subnetwork | 0.38306725 | 1.05564093 |
| GO:0046467 | membrane lipid biosynthetic process | 0.99489727 | 1.055673211 |
| GO:0071377 | cellular response to glucagon stimulus | 0.99486366 | 1.055692014 |
| GO:0015172 | acidic amino acid transmembrane transporter activity | 0.99484755 | 1.055758623 |

| | | | |
|---|---|---|---|
| ENSG00000151617 | EDNRA subnetwork | 0.38269059 | 1.05575985 |
| GO:0022627 | cytosolic small ribosomal subunit | 0.99482664 | 1.055825243 |
| ENSG00000164220 | F2RL2 subnetwork | 0.38385122 | 1.055835048 |
| GO:0071260 | cellular response to mechanical stimulus | 0.38305908 | 1.0558388 |
| GO:0006688 | glycosphingolipid biosynthetic process | 0.994809 | 1.055880839 |
| ENSG00000105141 | CASP14 subnetwork | 0.3830186 | 1.055924259 |
| ENSG00000123349 | PFDN5 subnetwork | 0.38268522 | 1.055939201 |
| MP:0008267 | abnormal hippocampus CA3 region morphology | 0.99480394 | 1.055954833 |
| ENSG00000204394 | VARS subnetwork | 0.38383027 | 1.055957725 |
| ENSG00000163814 | CDCP1 subnetwork | 0.38283614 | 1.05596511 |
| GO:0001964 | startle response | 0.99477271 | 1.055977341 |
| ENSG00000182809 | CRIP2 subnetwork | 0.38299393 | 1.056047253 |
| GO:0001709 | cell fate determination | 0.99476896 | 1.056051354 |
| ENSG00000133265 | HSPBP1 subnetwork | 0.38267353 | 1.056109234 |
| MP:0003755 | abnormal palate morphology | 0.9947536 | 1.056110661 |
| REACTOME_ACTIVATION_OF_I | REACTOME_ACTIVATION_OF_KAINATE_RECEPTORS_UPON | 0.9947248 | 1.056151582 |
| ENSG00000096171 | VARS subnetwork | 0.38383027 | 1.056155285 |
| GO:0004745 | retinol dehydrogenase activity | 0.38405721 | 1.056170531 |
| GO:0031113 | regulation of microtubule polymerization | 0.99471289 | 1.056218265 |
| GO:0045725 | positive regulation of glycogen biosynthetic process | 0.38298964 | 1.056226557 |
| GO:0001952 | regulation of cell-matrix adhesion | 0.38381363 | 1.056287425 |
| GO:0005261 | cation channel activity | 0.9947081 | 1.056292317 |
| ENSG00000132872 | SYT4 subnetwork | 0.99467985 | 1.05634062 |
| ENSG00000173218 | VANGL1 subnetwork | 0.38420885 | 1.056365676 |
| KEGG_ARACHIDONIC_ACID_M | KEGG_ARACHIDONIC_ACID_METABOLISM | 0.99467075 | 1.056403651 |
| ENSG00000060688 | SNRNP40 subnetwork | 0.38374676 | 1.056448896 |
| GO:0005604 | basement membrane | 0.9946689 | 1.056481413 |
| ENSG00000165731 | RET subnetwork | 0.383812 | 1.056485121 |
| MP:0008415 | abnormal neurite morphology | 0.99465268 | 1.056533422 |
| MP:0010948 | abnormal double-strand DNA break repair | 0.38373036 | 1.056599888 |
| MP:0003730 | abnormal photoreceptor inner segment morphology | 0.99463871 | 1.056600162 |
| MP:0009758 | impaired behavioral response to cocaine | 0.9946175 | 1.056663231 |
| ENSG00000116984 | MTR subnetwork | 0.38454178 | 1.056717115 |
| GO:0007052 | mitotic spindle organization | 0.99461276 | 1.056733672 |
| GO:0019005 | SCF ubiquitin ligase complex | 0.99461003 | 1.056800442 |
| ENSG00000115211 | EIF2B4 subnetwork | 0.99458208 | 1.056852493 |
| ENSG00000007968 | E2F2 subnetwork | 0.38446418 | 1.056859813 |
| ENSG00000161618 | ALDH16A1 subnetwork | 0.38452628 | 1.056895907 |
| GO:0034637 | cellular carbohydrate biosynthetic process | 0.38513107 | 1.056902985 |
| MP:0000585 | kinked tail | 0.99457618 | 1.056926646 |
| GO:0060271 | cilium morphogenesis | 0.38467483 | 1.056940034 |
| GO:0019233 | sensory perception of pain | 0.99456861 | 1.05700081 |
| GO:0001935 | endothelial cell proliferation | 0.99456503 | 1.057074985 |
| GO:0019432 | triglyceride biosynthetic process | 0.38512483 | 1.057090875 |
| GO:0072089 | stem cell proliferation | 0.99456108 | 1.057149171 |
| GO:0045502 | dynein binding | 0.99451033 | 1.057175483 |
| GO:0044242 | cellular lipid catabolic process | 0.38508604 | 1.057176185 |
| KEGG_PROGESTERONE_MEDIA | KEGG_PROGESTERONE_MEDIATED_OOCYTE_MATURATION | 0.99448424 | 1.057231268 |
| GO:0001504 | neurotransmitter uptake | 0.99444356 | 1.057250221 |
| ENSG00000101182 | PSMA7 subnetwork | 0.38599449 | 1.057318436 |
| MP:0005028 | abnormal trophectoderm morphology | 0.99443695 | 1.057324442 |
| GO:0050858 | negative regulation of antigen receptor-mediated signaling | 0.38508588 | 1.05737353 |
| ENSG00000174197 | MGA subnetwork | 0.38563799 | 1.057390494 |

| | | | |
|---|---|---|---|
| ENSG00000012660 | ELOVL5 subnetwork | 0.99443266 | 1.057394989 |
| ENSG00000135624 | CCT7 subnetwork | 0.38491879 | 1.057443033 |
| GO:0072531 | pyrimidine-containing compound transmembrane transpor | 0.38559481 | 1.0574478 |
| GO:0009798 | axis specification | 0.99442839 | 1.057469231 |
| MP:0010954 | abnormal cellular respiration | 0.38599078 | 1.057496741 |
| GO:0015672 | monovalent inorganic cation transport | 0.99438969 | 1.057499263 |
| ENSG00000106462 | EZH2 subnetwork | 0.38500638 | 1.057553688 |
| GO:0050860 | negative regulation of T cell receptor signaling pathway | 0.38508588 | 1.057570948 |
| GO:0042304 | regulation of fatty acid biosynthetic process | 0.99438792 | 1.057573524 |
| MP:0000161 | scoliosis | 0.38596992 | 1.057600596 |
| ENSG00000129991 | TNNI3 subnetwork | 0.38582573 | 1.057622065 |
| MP:0009890 | cleft secondary palate | 0.99438348 | 1.05764411 |
| ENSG00000172725 | CORO1B subnetwork | 0.38559303 | 1.057644975 |
| GO:0007597 | blood coagulation, intrinsic pathway | 0.99434592 | 1.057692591 |
| GO:0042036 | negative regulation of cytokine biosynthetic process | 0.38589677 | 1.057695174 |
| ENSG00000027075 | PRKCH subnetwork | 0.38556478 | 1.057711675 |
| ENSG00000102981 | PARD6A subnetwork | 0.38548498 | 1.057713113 |
| GO:0061351 | neural precursor cell proliferation | 0.99434277 | 1.057766883 |
| MP:0001454 | abnormal cued conditioning behavior | 0.99434275 | 1.057844872 |
| GO:0007269 | neurotransmitter secretion | 0.99432086 | 1.057886005 |
| ENSG00000088930 | XRN2 subnetwork | 0.9942949 | 1.05791977 |
| MP:0005306 | abnormal phalanx morphology | 0.9942421 | 1.057924041 |
| GO:0070374 | positive regulation of ERK1 and ERK2 cascade | 0.99423605 | 1.05799469 |
| ENSG00000185008 | ROBO2 subnetwork | 0.99423515 | 1.058072725 |
| REACTOME_DEPOLARIZATION_ | REACTOME_DEPOLARIZATION_OF_THE_PRESYNAPTIC_TER | 0.99422743 | 1.058147083 |
| MP:0000061 | fragile skeleton | 0.99421555 | 1.058214075 |
| ENSG00000023171 | GRAMD1B subnetwork | 0.38633736 | 1.058220071 |
| GO:0019865 | immunoglobulin binding | 0.99419867 | 1.058284766 |
| GO:0014072 | response to isoquinoline alkaloid | 0.99419017 | 1.058351778 |
| GO:0043278 | response to morphine | 0.99419017 | 1.058429868 |
| ENSG00000211949 | ENSG00000211949 subnetwork | 0.99416733 | 1.058485832 |
| MP:0002063 | abnormal learning/memory/conditioning | 0.99416611 | 1.058563944 |
| MP:0002546 | mydriasis | 0.99410842 | 1.058631633 |
| GO:0046717 | acid secretion | 0.99415954 | 1.058638376 |
| GO:0032266 | phosphatidylinositol-3-phosphate binding | 0.99408994 | 1.058702391 |
| GO:0060048 | cardiac muscle contraction | 0.99407391 | 1.058754706 |
| REACTOME_CONVERSION_FRC | REACTOME_CONVERSION_FROM_APCCCDC20_TO_APCCCI | 0.99405674 | 1.058799646 |
| MP:0002712 | increased circulating glucagon level | 0.38662439 | 1.058870067 |
| MP:0002733 | abnormal thermal nociception | 0.99405571 | 1.058874123 |
| GO:0021514 | ventral spinal cord interneuron differentiation | 0.99405393 | 1.058952304 |
| GO:0030901 | midbrain development | 0.38671697 | 1.058980086 |
| MP:0001898 | abnormal long term depression | 0.99404912 | 1.059026804 |
| ENSG00000105649 | RAB3A subnetwork | 0.99403824 | 1.05909393 |
| GO:0016050 | vesicle organization | 0.99403288 | 1.059164759 |
| ENSG00000114019 | AMOTL2 subnetwork | 0.99403095 | 1.059235598 |
| GO:0009152 | purine ribonucleotide biosynthetic process | 0.99402189 | 1.059302755 |
| GO:0030178 | negative regulation of Wnt receptor signaling pathway | 0.99400223 | 1.059347762 |
| ENSG00000104517 | UBR5 subnetwork | 0.38718789 | 1.059352919 |
| GO:0009219 | pyrimidine deoxyribonucleotide metabolic process | 0.99396995 | 1.059381695 |
| ENSG00000149187 | CELF1 subnetwork | 0.99395843 | 1.059456265 |
| GO:0007030 | Golgi organization | 0.38715262 | 1.059475544 |
| REACTOME_ASPARAGINE_N:LI | REACTOME_ASPARAGINE_N:LINKED_GLYCOSYLATION | 0.38711057 | 1.059486607 |
| GO:0046839 | phospholipid dephosphorylation | 0.99384911 | 1.059490912 |

| | | | |
|---|---|---|---|
| GO:0032410 | negative regulation of transporter activity | 0.99395164 | 1.059519764 |
| GO:0030949 | positive regulation of vascular endothelial growth factor re | 0.99381823 | 1.059532254 |
| GO:0014061 | regulation of norepinephrine secretion | 0.99380236 | 1.059584688 |
| ENSG00000145391 | SETD7 subnetwork | 0.38707956 | 1.059637209 |
| MP:0002799 | abnormal passive avoidance behavior | 0.99380003 | 1.05965191 |
| GO:0045494 | photoreceptor cell maintenance | 0.99378635 | 1.059704361 |
| MP:0000166 | abnormal chondrocyte morphology | 0.38702906 | 1.059713435 |
| MP:0000968 | abnormal sensory neuron innervation pattern | 0.99377829 | 1.059778993 |
| GO:0001936 | regulation of endothelial cell proliferation | 0.99375694 | 1.059805588 |
| GO:0060173 | limb development | 0.99373561 | 1.059876543 |
| GO:0048736 | appendage development | 0.99373561 | 1.059954902 |
| GO:0007389 | pattern specification process | 0.99373121 | 1.060029575 |
| REACTOME_SIGNAL_AMPLIFIC | REACTOME_SIGNAL_AMPLIFICATION | 0.99372381 | 1.060096865 |
| GO:0042730 | fibrinolysis | 0.99370963 | 1.060167862 |
| GO:0045454 | cell redox homeostasis | 0.99368068 | 1.060224079 |
| GO:0005313 | L-glutamate transmembrane transporter activity | 0.99367452 | 1.060298794 |
| GO:0045109 | intermediate filament organization | 0.99355943 | 1.060329906 |
| GO:0050884 | neuromuscular process controlling posture | 0.9936304 | 1.06033284 |
| MP:0000277 | abnormal heart shape | 0.99350285 | 1.060345465 |
| GO:0030193 | regulation of blood coagulation | 0.99347613 | 1.060379522 |
| GO:0030516 | regulation of axon extension | 0.99347464 | 1.060457976 |
| MP:0001575 | cyanosis | 0.99346254 | 1.060514243 |
| GO:0033108 | mitochondrial respiratory chain complex assembly | 0.99344861 | 1.06056682 |
| ENSG00000152208 | GRID2 subnetwork | 0.99338619 | 1.060586102 |
| MP:0001716 | abnormal placenta labyrinth morphology | 0.38812102 | 1.060592276 |
| ENSG00000144182 | LIPT1 subnetwork | 0.99337844 | 1.060657194 |
| ENSG00000163736 | PPBP subnetwork | 0.38783302 | 1.060685746 |
| GO:0032373 | positive regulation of sterol transport | 0.38808704 | 1.060705664 |
| GO:0060485 | mesenchyme development | 0.9933749 | 1.060731996 |
| ENSG00000079277 | MKNK1 subnetwork | 0.38792081 | 1.060739502 |
| GO:0007409 | axonogenesis | 0.9933221 | 1.060754996 |
| ENSG00000104973 | MED25 subnetwork | 0.3885159 | 1.060767947 |
| ENSG00000113739 | STC2 subnetwork | 0.99329657 | 1.060781701 |
| ENSG00000198561 | CTNND1 subnetwork | 0.38864688 | 1.060803042 |
| GO:0046463 | acylglycerol biosynthetic process | 0.38833953 | 1.060820341 |
| GO:0006109 | regulation of carbohydrate metabolic process | 0.38773245 | 1.06082915 |
| GO:0016836 | hydro-lyase activity | 0.38800556 | 1.060830392 |
| ENSG00000174227 | PIGG subnetwork | 0.38781625 | 1.060836431 |
| KEGG_LONG_TERM_DEPRESSI | KEGG_LONG_TERM_DEPRESSION | 0.99328595 | 1.060852828 |
| GO:0061001 | regulation of dendritic spine morphogenesis | 0.99323322 | 1.060853631 |
| GO:0010596 | negative regulation of endothelial cell migration | 0.99321059 | 1.060895158 |
| GO:0032376 | positive regulation of cholesterol transport | 0.38808704 | 1.060902675 |
| GO:0050673 | epithelial cell proliferation | 0.99311673 | 1.060911582 |
| ENSG00000197879 | MYO1C subnetwork | 0.38884497 | 1.060938079 |
| ENSG00000163464 | CXCR1 subnetwork | 0.38851186 | 1.060946197 |
| ENSG00000166900 | STX3 subnetwork | 0.99320963 | 1.060966309 |
| GO:0033555 | multicellular organismal response to stress | 0.99310442 | 1.060979042 |
| GO:0015108 | chloride transmembrane transporter activity | 0.38894709 | 1.060991659 |
| GO:0046460 | neutral lipid biosynthetic process | 0.38833953 | 1.061017264 |
| REACTOME_G_BETAGAMMA_S | REACTOME_G_BETAGAMMA_SIGNALLING_THROUGH_PLC | 0.99307678 | 1.061031699 |
| GO:0006839 | mitochondrial transport | 0.38901995 | 1.061063751 |
| GO:0007004 | telomere maintenance via telomerase | 0.3891491 | 1.061078177 |
| MP:0002734 | abnormal mechanical nociception | 0.99305837 | 1.061095474 |

| | | | |
|---|---|---|---|
| MP:0003235 | abnormal alisphenoid bone morphology | 0.99302761 | 1.061133333 |
| ENSG00000113140 | SPARC subnetwork | 0.38850686 | 1.061133791 |
| GO:0000421 | autophagic vacuole membrane | 0.38884085 | 1.061134804 |
| ENSG00000213380 | COG8 subnetwork | 0.38913084 | 1.061154345 |
| GO:0006750 | glutathione biosynthetic process | 0.99301015 | 1.061204534 |
| ENSG00000125944 | HNRNPR subnetwork | 0.389317 | 1.061205779 |
| REACTOME_NUCLEOTIDE:LIKE_ | REACTOME_NUCLEOTIDE:LIKE_PURINERGIC_RECEPTORS | 0.99300735 | 1.061275745 |
| MP:0001045 | abnormal enteric ganglia morphology | 0.99300735 | 1.061354375 |
| GO:0044433 | cytoplasmic vesicle part | 0.99300498 | 1.061433017 |
| GO:0072341 | modified amino acid binding | 0.99300354 | 1.061507966 |
| ENSG00000107937 | GTPBP4 subnetwork | 0.3895881 | 1.061534901 |
| GO:0009163 | nucleoside biosynthetic process | 0.99299667 | 1.06157922 |
| ENSG00000065183 | WDR3 subnetwork | 0.38953459 | 1.061601852 |
| MP:0002842 | increased systemic arterial blood pressure | 0.99297542 | 1.061628252 |
| GO:0032105 | negative regulation of response to extracellular stimulus | 0.99297428 | 1.061699526 |
| GO:0032108 | negative regulation of response to nutrient levels | 0.99297428 | 1.061778223 |
| GO:0051592 | response to calcium ion | 0.99296405 | 1.061849518 |
| ENSG00000172757 | CFL1 subnetwork | 0.3897288 | 1.06185672 |
| MP:0001777 | abnormal body temperature homeostasis | 0.99294772 | 1.061909704 |
| GO:0004114 | 3',5'-cyclic-nucleotide phosphodiesterase activity | 0.38980288 | 1.06191005 |
| GO:0009880 | embryonic pattern specification | 0.99288488 | 1.061918001 |
| GO:0050321 | tau-protein kinase activity | 0.9928795 | 1.06199303 |
| REACTOME_ACTIVATION_OF_( | REACTOME_ACTIVATION_OF_GENES_BY_ATF4 | 0.99287111 | 1.062064363 |
| ENSG00000108587 | GOSR1 subnetwork | 0.38992578 | 1.062083642 |
| GO:2000311 | regulation of alpha-amino-3-hydroxy-5-methyl-4-isoxazole | 0.99285752 | 1.062120875 |
| MP:0009888 | palatal shelves fail to meet at midline | 0.99283324 | 1.062169979 |
| GO:0048589 | developmental growth | 0.99281842 | 1.062226507 |
| GO:0048762 | mesenchymal cell differentiation | 0.99281059 | 1.06229417 |
| MP:0005606 | increased bleeding time | 0.99277587 | 1.062343298 |
| GO:0007289 | spermatid nucleus differentiation | 0.99272591 | 1.062347923 |
| MP:0009764 | decreased sensitivity to induced morbidity/mortality | 0.99271407 | 1.062419319 |
| GO:0008188 | neuropeptide receptor activity | 0.99267385 | 1.062446209 |
| GO:0007616 | long-term memory | 0.99266395 | 1.062510203 |
| MP:0000812 | abnormal dentate gyrus morphology | 0.99264919 | 1.062570496 |
| ENSG00000155760 | FZD7 subnetwork | 0.3901874 | 1.062571693 |
| GO:0060134 | prepulse inhibition | 0.99264322 | 1.062630798 |
| REACTOME_FRS2:MEDIATED_( | REACTOME_FRS2:MEDIATED_CASCADE | 0.99263393 | 1.062705952 |
| GO:0021515 | cell differentiation in spinal cord | 0.99254693 | 1.062741241 |
| ENSG00000144021 | CIAO1 subnetwork | 0.99261393 | 1.062751429 |
| ENSG00000115254 | ENSG00000115254 subnetwork | 0.99253361 | 1.062797862 |
| ENSG00000124120 | TTPAL subnetwork | 0.99252749 | 1.062876763 |
| GO:0031623 | receptor internalization | 0.99252356 | 1.062951964 |
| GO:0035282 | segmentation | 0.99250248 | 1.062993763 |
| GO:0001649 | osteoblast differentiation | 0.99248521 | 1.063061558 |
| MP:0005584 | abnormal enzyme/coenzyme activity | 0.39041021 | 1.06308731 |
| MP:0005106 | abnormal incus morphology | 0.99246691 | 1.063114511 |
| GO:0005891 | voltage-gated calcium channel complex | 0.99246474 | 1.063186038 |
| ENSG00000120699 | EXOSC8 subnetwork | 0.3905406 | 1.063205104 |
| ENSG00000160948 | VPS28 subnetwork | 0.99245852 | 1.063253862 |
| ENSG00000131795 | RBM8A subnetwork | 0.39065437 | 1.063304364 |
| MP:0002110 | abnormal digit morphology | 0.99244663 | 1.063314269 |
| GO:0045665 | negative regulation of neuron differentiation | 0.99243031 | 1.063363542 |
| GO:0072006 | nephron development | 0.9923755 | 1.063371963 |

| | | | |
|---|---|---|---|
| MP:0004173 | abnormal intervertebral disk morphology | 0.99235498 | 1.063432392 |
| ENSG00000197969 | VPS13A subnetwork | 0.39076858 | 1.063468294 |
| GO:0090175 | regulation of establishment of planar polarity | 0.99233231 | 1.06349283 |
| GO:0060071 | Wnt receptor signaling pathway, planar cell polarity pathwa | 0.99233231 | 1.063571853 |
| MP:0003205 | testicular atrophy | 0.99232844 | 1.063643457 |
| MP:0001651 | necrosis | 0.9922586 | 1.063648187 |
| GO:0035240 | dopamine binding | 0.99223407 | 1.063690078 |
| GO:0072378 | blood coagulation, fibrin clot formation | 0.99222768 | 1.06375799 |
| GO:0055078 | sodium ion homeostasis | 0.99207583 | 1.063831685 |
| GO:0009247 | glycolipid biosynthetic process | 0.99222355 | 1.063833346 |
| MP:0001092 | abnormal trigeminal ganglion morphology | 0.99204893 | 1.063892193 |
| GO:0030514 | negative regulation of BMP signaling pathway | 0.99221179 | 1.063897562 |
| MP:0002007 | increased cellular sensitivity to gamma-irradiation | 0.39100842 | 1.063946396 |
| GO:0006369 | termination of RNA polymerase II transcription | 0.99204706 | 1.063971299 |
| MP:0002114 | abnormal axial skeleton morphology | 0.99202408 | 1.064013236 |
| GO:0051937 | catecholamine transport | 0.99201907 | 1.064092363 |
| ENSG00000159459 | UBR1 subnetwork | 0.39112652 | 1.064137867 |
| ENSG00000132639 | SNAP25 subnetwork | 0.99200821 | 1.064160345 |
| MP:0002907 | abnormal parturition | 0.99196214 | 1.064191149 |
| MP:0000298 | absent atrioventricular cushions | 0.99195135 | 1.064259149 |
| ENSG00000151623 | NR3C2 subnetwork | 0.39122851 | 1.064273836 |
| ENSG00000142798 | HSPG2 subnetwork | 0.99191799 | 1.064312281 |
| GO:0016782 | transferase activity, transferring sulfur-containing groups | 0.99190298 | 1.064376581 |
| GO:0033762 | response to glucagon stimulus | 0.99189977 | 1.06445205 |
| REACTOME_RNA_POLYMERAS | REACTOME_RNA_POLYMERASE_III_CHAIN_ELONGATION | 0.3918315 | 1.064504521 |
| GO:0043252 | sodium-independent organic anion transport | 0.99188267 | 1.064512649 |
| GO:0001676 | long-chain fatty acid metabolic process | 0.99188224 | 1.06459186 |
| REACTOME_CELL:EXTRACELLUI | REACTOME_CELL:EXTRACELLULAR_MATRIX_INTERACTIONS | 0.39163657 | 1.06463257 |
| GO:0030312 | external encapsulating structure | 0.99185113 | 1.064633874 |
| KEGG_RENIN_ANGIOTENSIN_S | KEGG_RENIN_ANGIOTENSIN_SYSTEM | 0.991814 | 1.064679616 |
| GO:0060363 | cranial suture morphogenesis | 0.9917877 | 1.06468443 |
| GO:0032984 | macromolecular complex disassembly | 0.39182971 | 1.064700997 |
| MP:0002667 | decreased circulating aldosterone level | 0.39155757 | 1.064718375 |
| GO:0097094 | craniofacial suture morphogenesis | 0.9917877 | 1.064763677 |
| ENSG00000134769 | DTNA subnetwork | 0.99176613 | 1.064813161 |
| ENSG00000069869 | NEDD4 subnetwork | 0.39152806 | 1.064831917 |
| GO:0016627 | oxidoreductase activity, acting on the CH-CH group of dono | 0.39182403 | 1.064879084 |
| ENSG00000044446 | PHKA2 subnetwork | 0.99176535 | 1.064892429 |
| ENSG00000139970 | RTN1 subnetwork | 0.99176311 | 1.064971709 |
| ENSG00000168286 | THAP11 subnetwork | 0.3914977 | 1.064991687 |
| ENSG00000148965 | SAA4 subnetwork | 0.99171723 | 1.06499516 |
| GO:0048483 | autonomic nervous system development | 0.99170988 | 1.065067014 |
| MP:0002696 | decreased circulating glucagon level | 0.99169648 | 1.065127709 |
| MP:0005642 | decreased mean corpuscular hemoglobin concentration | 0.99168986 | 1.065203307 |
| GO:0007617 | mating behavior | 0.99167669 | 1.065275192 |
| GO:0007631 | feeding behavior | 0.99166535 | 1.065347088 |
| GO:2000177 | regulation of neural precursor cell proliferation | 0.99165997 | 1.065426443 |
| MP:0002689 | abnormal molar morphology | 0.99165341 | 1.065498361 |
| GO:0009988 | cell-cell recognition | 0.39262669 | 1.06556682 |
| GO:0010453 | regulation of cell fate commitment | 0.99165227 | 1.06557774 |
| ENSG00000184708 | EIF4ENIF1 subnetwork | 0.39237852 | 1.065596753 |
| ENSG00000114503 | NCBP2 subnetwork | 0.39249441 | 1.065600221 |
| GO:0004435 | phosphatidylinositol phospholipase C activity | 0.99161341 | 1.065604977 |

| | | | |
|---|---|---|---|
| MP:0008026 | abnormal brain white matter morphology | 0.39233189 | 1.065627306 |
| GO:0031901 | early endosome membrane | 0.99159192 | 1.065654571 |
| GO:0042982 | amyloid precursor protein metabolic process | 0.3925984 | 1.065661873 |
| REACTOME_SYNTHESIS_OF_BI | REACTOME_SYNTHESIS_OF_BILE_ACIDS_AND_BILE_SALTS_ | 0.39273052 | 1.06569296 |
| GO:0045685 | regulation of glial cell differentiation | 0.99159057 | 1.065733979 |
| ENSG00000131503 | ANKHD1 subnetwork | 0.39249277 | 1.065787532 |
| MP:0004113 | abnormal aortic arch morphology | 0.99156788 | 1.065805947 |
| GO:0051952 | regulation of amine transport | 0.9915668 | 1.065885378 |
| GO:0007602 | phototransduction | 0.99156476 | 1.065964821 |
| GO:0019359 | nicotinamide nucleotide biosynthetic process | 0.99155757 | 1.066033095 |
| MP:0005558 | decreased creatinine clearance | 0.99153527 | 1.066090198 |
| GO:0061326 | renal tubule development | 0.99152291 | 1.066136126 |
| ENSG00000107186 | MPDZ subnetwork | 0.99150544 | 1.066182062 |
| GO:0043269 | regulation of ion transport | 0.99150535 | 1.066261557 |
| ENSG00000167711 | SERPINF2 subnetwork | 0.99150184 | 1.066329878 |
| GO:0051271 | negative regulation of cellular component movement | 0.99144085 | 1.06634601 |
| MP:0000757 | herniated abdominal wall | 0.39311356 | 1.066390271 |
| MP:0003460 | decreased fear-related response | 0.99143563 | 1.066414349 |
| GO:0045596 | negative regulation of cell differentiation | 0.39433412 | 1.066458486 |
| GO:0060401 | cytosolic calcium ion transport | 0.39428929 | 1.066479882 |
| GO:0021545 | cranial nerve development | 0.99142746 | 1.066482697 |
| ENSG00000168438 | CDC40 subnetwork | 0.39401567 | 1.066492002 |
| GO:0030594 | neurotransmitter receptor activity | 0.9914026 | 1.06652495 |
| ENSG00000134184 | GSTM1 subnetwork | 0.39408368 | 1.066534926 |
| GO:0045351 | type I interferon biosynthetic process | 0.99140061 | 1.066600776 |
| ENSG00000206268 | RDBP subnetwork | 0.39384742 | 1.066629875 |
| ENSG00000120899 | PTK2B subnetwork | 0.39397618 | 1.066632953 |
| ENSG00000147133 | TAF1 subnetwork | 0.39420793 | 1.066651351 |
| MP:0004485 | increased response of heart to induced stress | 0.99137397 | 1.066672883 |
| GO:0032846 | positive regulation of homeostatic process | 0.39428516 | 1.066675854 |
| GO:0061387 | regulation of extent of cell growth | 0.99137027 | 1.066741271 |
| GO:0032039 | integrator complex | 0.39395679 | 1.066746367 |
| GO:0015030 | Cajal body | 0.39356475 | 1.066792488 |
| ENSG00000111664 | GNB3 subnetwork | 0.99134988 | 1.066798478 |
| ENSG00000206357 | RDBP subnetwork | 0.39384742 | 1.066826127 |
| GO:0032965 | regulation of collagen biosynthetic process | 0.99132113 | 1.066855693 |
| GO:0019882 | antigen processing and presentation | 0.39351447 | 1.066878453 |
| GO:0010761 | fibroblast migration | 0.39368878 | 1.066918262 |
| GO:0003197 | endocardial cushion development | 0.99131794 | 1.066931572 |
| GO:0051926 | negative regulation of calcium ion transport | 0.99118293 | 1.0669341 |
| MP:0003960 | increased lean body mass | 0.99127022 | 1.06694403 |
| GO:0021954 | central nervous system neuron development | 0.9911751 | 1.067013733 |
| ENSG00000204356 | RDBP subnetwork | 0.39384742 | 1.067022451 |
| ENSG00000096433 | ITPR3 subnetwork | 0.3934919 | 1.067028919 |
| MP:0001289 | persistence of hyaloid vascular system | 0.39473436 | 1.06705526 |
| ENSG00000169679 | BUB1 subnetwork | 0.99116922 | 1.067070986 |
| GO:0017119 | Golgi transport complex | 0.39378982 | 1.067071599 |
| KEGG_PROTEIN_EXPORT | KEGG_PROTEIN_EXPORT | 0.39468754 | 1.067122659 |
| ENSG00000105290 | APLP1 subnetwork | 0.99116476 | 1.06714691 |
| MP:0003043 | hypoalgesia | 0.99103726 | 1.067164402 |
| KEGG_SELENOAMINO_ACID_M | KEGG_SELENOAMINO_ACID_METABOLISM | 0.39347463 | 1.06717944 |
| GO:0022890 | inorganic cation transmembrane transporter activity | 0.99115124 | 1.067204181 |
| MP:0006007 | abnormal basal ganglion morphology | 0.99103386 | 1.067244083 |

| | | | |
|---|---|---|---|
| GO:0015145 | monosaccharide transmembrane transporter activity | 0.39465452 | 1.067245179 |
| REACTOME_RECRUITMENT_OF | REACTOME_RECRUITMENT_OF_NUMA_TO_MITOTIC_CENT | 0.99102035 | 1.067305108 |
| ENSG00000100479 | POLE2 subnetwork | 0.39486993 | 1.067336637 |
| ENSG00000206466 | GABBR1 subnetwork | 0.99098886 | 1.06735494 |
| ENSG00000204681 | GABBR1 subnetwork | 0.99098886 | 1.067434653 |
| MP:0008263 | abnormal hippocampus CA1 region morphology | 0.99086255 | 1.067440992 |
| GO:0001573 | ganglioside metabolic process | 0.99085127 | 1.067505789 |
| ENSG00000206511 | GABBR1 subnetwork | 0.99098886 | 1.067514377 |
| MP:0004249 | abnormal crista ampullaris morphology | 0.99084967 | 1.067585537 |
| GO:0000236 | mitotic prometaphase | 0.99082252 | 1.067642884 |
| ENSG00000148180 | GSN subnetwork | 0.3950863 | 1.067700496 |
| MP:0002184 | abnormal innervation | 0.99082168 | 1.067722654 |
| ENSG00000173598 | NUDT4 subnetwork | 0.99079831 | 1.067768811 |
| MP:0004423 | abnormal squamosal bone morphology | 0.99079511 | 1.067848603 |
| ENSG00000119888 | EPCAM subnetwork | 0.99064584 | 1.067916137 |
| MP:0002651 | abnormal sciatic nerve morphology | 0.99078988 | 1.067928406 |
| MP:0002765 | short fibula | 0.99075055 | 1.067967115 |
| GO:0007420 | brain development | 0.99063705 | 1.067981014 |
| MP:0004608 | abnormal cervical axis morphology | 0.99063205 | 1.068053375 |
| GO:0005416 | cation:amino acid symporter activity | 0.99061814 | 1.068118272 |
| MP:0009009 | absent estrous cycle | 0.39534998 | 1.068165138 |
| GO:0051233 | spindle midzone | 0.99061116 | 1.068186916 |
| GO:0044236 | multicellular organismal metabolic process | 0.99060356 | 1.068248093 |
| ENSG00000213611 | ENSG00000213611 subnetwork | 0.99054322 | 1.068283108 |
| MP:0004418 | small parietal bone | 0.99052757 | 1.068336823 |
| MP:0003727 | abnormal retinal layer morphology | 0.99048279 | 1.068375589 |
| GO:0050854 | regulation of antigen receptor-mediated signaling pathway | 0.39551324 | 1.068400294 |
| MP:0003634 | abnormal glial cell morphology | 0.39560265 | 1.068442773 |
| MP:0002064 | seizures | 0.99047406 | 1.068444278 |
| MP:0004263 | abnormal limb posture | 0.99045274 | 1.068501758 |
| GO:0072080 | nephron tubule development | 0.9904126 | 1.068533064 |
| ENSG00000164930 | FZD6 subnetwork | 0.39710168 | 1.068537477 |
| ENSG00000129965 | INS-IGF2 subnetwork | 0.39808113 | 1.068553975 |
| ENSG00000177283 | FZD8 subnetwork | 0.39724129 | 1.068576389 |
| MP:0004022 | abnormal cone electrophysiology | 0.99038498 | 1.068579337 |
| ENSG00000130779 | CLIP1 subnetwork | 0.39732429 | 1.068609538 |
| ENSG00000118971 | CCND2 subnetwork | 0.39719368 | 1.068616341 |
| GO:0032098 | regulation of appetite | 0.99037854 | 1.068655544 |
| ENSG00000069275 | NUCKS1 subnetwork | 0.39806235 | 1.068685026 |
| MP:0005545 | abnormal lens development | 0.99034639 | 1.068686869 |
| GO:0045840 | positive regulation of mitosis | 0.39800277 | 1.068715797 |
| ENSG00000111432 | FZD10 subnetwork | 0.39710168 | 1.068732858 |
| MP:0001435 | no suckling reflex | 0.99033361 | 1.068755612 |
| ENSG00000125651 | GTF2F1 subnetwork | 0.39744826 | 1.06878882 |
| GO:0021543 | pallium development | 0.99030842 | 1.068798174 |
| ENSG00000106571 | GLI3 subnetwork | 0.39750829 | 1.068812785 |
| GO:0005680 | anaphase-promoting complex | 0.99027772 | 1.068863194 |
| GO:0090022 | regulation of neutrophil chemotaxis | 0.39588012 | 1.068879516 |
| ENSG00000147854 | UHRF2 subnetwork | 0.39793354 | 1.068886861 |
| ENSG00000206427 | PRRC2A subnetwork | 0.39785262 | 1.06890856 |
| GO:0051785 | positive regulation of nuclear division | 0.39800277 | 1.068910783 |
| GO:0009303 | rRNA transcription | 0.39708913 | 1.068919166 |
| REACTOME_PRESYNAPTIC_FUI | REACTOME_PRESYNAPTIC_FUNCTION_OF_KAINATE_RECEI | 0.99026369 | 1.068931966 |

| | | | |
|---|---|---|---|
| ENSG00000184371 | CSF1 subnetwork | 0.39834921 | 1.068957346 |
| GO:0042288 | MHC class I protein binding | 0.39608688 | 1.068991751 |
| MP:0006069 | abnormal retinal neuronal layer morphology | 0.99025794 | 1.069008234 |
| REACTOME_DCC_MEDIATED_A | REACTOME_DCC_MEDIATED_ATTRACTIVE_SIGNALING | 0.39704241 | 1.06902323 |
| ENSG00000162616 | DNAJB4 subnetwork | 0.39828401 | 1.069024613 |
| MP:0005330 | cardiomyopathy | 0.99025203 | 1.069084512 |
| ENSG00000206318 | ENSG00000206318 subnetwork | 0.39785262 | 1.069103687 |
| ENSG00000198959 | TGM2 subnetwork | 0.39768284 | 1.069119795 |
| ENSG00000005513 | SOX8 subnetwork | 0.99022579 | 1.06914583 |
| GO:0043034 | costamere | 0.39607326 | 1.069169417 |
| ENSG00000151224 | MAT1A subnetwork | 0.39675328 | 1.069174446 |
| ENSG00000180138 | CSNK1A1L subnetwork | 0.39647001 | 1.069179337 |
| ENSG00000148229 | POLE3 subnetwork | 0.39702438 | 1.069200512 |
| GO:0043271 | negative regulation of ion transport | 0.9902141 | 1.069222131 |
| ENSG00000166595 | FAM96B subnetwork | 0.39781999 | 1.069225854 |
| GO:0010675 | regulation of cellular carbohydrate metabolic process | 0.39640404 | 1.069246977 |
| MP:0005006 | abnormal osteoblast physiology | 0.39694477 | 1.069249771 |
| REACTOME_CRMPS_IN_SEMA3 | REACTOME_CRMPS_IN_SEMA3A_SIGNALING | 0.99019376 | 1.069279724 |
| REACTOME_INTERFERON_ALPI | REACTOME_INTERFERON_ALPHABETA_SIGNALING | 0.39689484 | 1.069299048 |
| REACTOME_P75NTR_RECRUITS | REACTOME_P75NTR_RECRUITS_SIGNALLING_COMPLEXES | 0.3963379 | 1.069314642 |
| ENSG00000136869 | TLR4 subnetwork | 0.39674535 | 1.069351886 |
| GO:0003203 | endocardial cushion morphogenesis | 0.99018963 | 1.06935979 |
| MP:0000784 | forebrain hypoplasia | 0.39627784 | 1.069364003 |
| GO:0046486 | glycerolipid metabolic process | 0.39664355 | 1.069413919 |
| GO:0030246 | carbohydrate binding | 0.99016421 | 1.069428636 |
| ENSG00000214655 | KIAA0913 subnetwork | 0.39672279 | 1.069492767 |
| MP:0001325 | abnormal retina morphology | 0.9901463 | 1.069501236 |
| REACTOME_REGULATION_OF_ | REACTOME_REGULATION_OF_SIGNALING_BY_CBL | 0.99013711 | 1.069573847 |
| MP:0006089 | abnormal vestibular saccule morphology | 0.99009091 | 1.069590293 |
| ENSG00000100503 | NIN subnetwork | 0.39865434 | 1.0696191 |
| MP:0000807 | abnormal hippocampus morphology | 0.99008312 | 1.069655431 |
| GO:0003007 | heart morphogenesis | 0.99006983 | 1.06972807 |
| MP:0008873 | increased physiological sensitivity to xenobiotic | 0.39884948 | 1.06973037 |
| MP:0008518 | retinal outer nuclear layer degeneration | 0.99002818 | 1.069748277 |
| ENSG00000168291 | PDHB subnetwork | 0.39877109 | 1.069761297 |
| GO:0016504 | peptidase activator activity | 0.99001559 | 1.069820934 |
| GO:0035107 | appendage morphogenesis | 0.99000316 | 1.069893601 |
| GO:0035108 | limb morphogenesis | 0.99000316 | 1.069973773 |
| GO:0007224 | smoothened signaling pathway | 0.98999567 | 1.070042716 |
| MP:0002798 | abnormal active avoidance behavior | 0.98998738 | 1.070104174 |
| MP:0005145 | increased circulating VLDL cholesterol level | 0.98997367 | 1.07016939 |
| GO:0071391 | cellular response to estrogen stimulus | 0.39909799 | 1.070191257 |
| GO:0007411 | axon guidance | 0.98996877 | 1.070234615 |
| ENSG00000106628 | POLD2 subnetwork | 0.39920236 | 1.070242215 |
| MP:0001402 | hypoactivity | 0.98995692 | 1.07029985 |
| REACTOME_CLEAVAGE_OF_GF | REACTOME_CLEAVAGE_OF_GROWING_TRANSCRIPT_IN_TH | 0.98995655 | 1.070380088 |
| REACTOME_RNA_POLYMERAS | REACTOME_RNA_POLYMERASE_II_TRANSCRIPTION_TERMI | 0.98995655 | 1.070460339 |
| ENSG00000101138 | CSTF1 subnetwork | 0.39937087 | 1.070502549 |
| GO:0001077 | RNA polymerase II core promoter proximal region sequence | 0.39958256 | 1.070518653 |
| REACTOME_POST:ELONGATIOI | REACTOME_POST:ELONGATION_PROCESSING_OF_THE_TR/ | 0.98995655 | 1.070540601 |
| KEGG_MELANOMA | KEGG_MELANOMA | 0.98992464 | 1.070572136 |
| MP:0002818 | abnormal dentin morphology | 0.39953604 | 1.070604296 |
| GO:0045932 | negative regulation of muscle contraction | 0.98990079 | 1.070607424 |

| | | | |
|---|---|---|---|
| MP:0010519 | atrioventricular block | 0.98988788 | 1.070668967 |
| GO:0042597 | periplasmic space | 0.98988204 | 1.070745519 |
| GO:0047485 | protein N-terminus binding | 0.39952614 | 1.070753687 |
| GO:0030288 | outer membrane-bounded periplasmic space | 0.98988204 | 1.070825833 |
| MP:0004966 | abnormal inner cell mass proliferation | 0.98986281 | 1.070868652 |
| GO:0005689 | U12-type spliceosomal complex | 0.39979283 | 1.070897016 |
| ENSG00000182010 | RTKN2 subnetwork | 0.98984831 | 1.070930233 |
| GO:0030111 | regulation of Wnt receptor signaling pathway | 0.98981845 | 1.070958061 |
| GO:0002088 | lens development in camera-type eye | 0.98979496 | 1.0710009 |
| GO:0050432 | catecholamine secretion | 0.98979359 | 1.071081264 |
| GO:0061097 | regulation of protein tyrosine kinase activity | 0.3999391 | 1.071111515 |
| KEGG_SPLICEOSOME | KEGG_SPLICEOSOME | 0.40014011 | 1.071118182 |
| MP:0005032 | abnormal ectoplacental cone morphology | 0.40007066 | 1.071131115 |
| GO:0031960 | response to corticosteroid stimulus | 0.98978373 | 1.071157887 |
| ENSG00000113327 | GABRG2 subnetwork | 0.98974988 | 1.071196998 |
| MP:0004830 | short incisors | 0.98974536 | 1.071273642 |
| GO:0042554 | superoxide anion generation | 0.40005983 | 1.071307748 |
| MP:0000964 | small dorsal root ganglion | 0.9897233 | 1.071335285 |
| ENSG00000183765 | CHEK2 subnetwork | 0.40032608 | 1.071337695 |
| GO:0042063 | gliogenesis | 0.98971988 | 1.071415703 |
| ENSG00000133226 | SRRM1 subnetwork | 0.40028642 | 1.071459735 |
| MP:0008143 | abnormal dendrite morphology | 0.98971204 | 1.07149238 |
| GO:0031902 | late endosome membrane | 0.98969542 | 1.071554054 |
| ENSG00000125378 | BMP4 subnetwork | 0.98964917 | 1.071593213 |
| MP:0002066 | abnormal motor capabilities/coordination/movement | 0.98961503 | 1.071632377 |
| MP:0001545 | abnormal hematopoietic system physiology | 0.40078099 | 1.071645179 |
| ENSG00000134365 | CFHR4 subnetwork | 0.40051556 | 1.071660912 |
| GO:0001832 | blastocyst growth | 0.40084344 | 1.07167756 |
| ENSG00000103994 | ZFP106 subnetwork | 0.40066362 | 1.071698456 |
| REACTOME_P2Y_RECEPTORS | REACTOME_P2Y_RECEPTORS | 0.98960933 | 1.071709094 |
| GO:0050662 | coenzyme binding | 0.40060841 | 1.071720567 |
| GO:0006898 | receptor-mediated endocytosis | 0.98959252 | 1.071770802 |
| ENSG00000127481 | UBR4 subnetwork | 0.40076 | 1.071803487 |
| MP:0003063 | increased coping response | 0.98958372 | 1.071843785 |
| ENSG00000025770 | NCAPH2 subnetwork | 0.98956258 | 1.071890491 |
| REACTOME_SYNTHESIS_SECRE | REACTOME_SYNTHESIS_SECRETION_AND_DEACYLATION_C | 0.98954704 | 1.071929693 |
| MP:0002797 | increased thigmotaxis | 0.98953923 | 1.071995192 |
| ENSG00000077942 | FBLN1 subnetwork | 0.98953267 | 1.072075727 |
| MP:0000528 | delayed kidney development | 0.98952965 | 1.072141247 |
| GO:0005865 | striated muscle thin filament | 0.98948086 | 1.072165452 |
| ENSG00000011485 | PPP5C subnetwork | 0.98946932 | 1.072234746 |
| GO:0002027 | regulation of heart rate | 0.98944912 | 1.072289021 |
| MP:0001510 | abnormal coat appearance | 0.40110073 | 1.072290797 |
| MP:0001053 | abnormal neuromuscular synapse morphology | 0.98943532 | 1.072350819 |
| MP:0000811 | hippocampal neuron degeneration | 0.98942859 | 1.072412627 |
| GO:0060284 | regulation of cell development | 0.98941036 | 1.072463169 |
| MP:0008840 | abnormal spike wave discharge | 0.98940681 | 1.072540029 |
| ENSG00000073969 | NSF subnetwork | 0.98938761 | 1.072586829 |
| GO:0031201 | SNARE complex | 0.98938598 | 1.072663709 |
| GO:0051781 | positive regulation of cell division | 0.98937838 | 1.072744361 |
| MP:0004091 | abnormal Z lines | 0.98931813 | 1.072746071 |
| GO:0034706 | sodium channel complex | 0.98931658 | 1.072822981 |
| GO:0045577 | regulation of B cell differentiation | 0.4013458 | 1.072831216 |

| | | | |
|---|---|---|---|
| MP:0008042 | abnormal NK T cell physiology | 0.98921484 | 1.07287154 |
| ENSG00000173674 | EIF1AX subnetwork | 0.98929582 | 1.072873581 |
| ENSG00000204967 | PCDHA4 subnetwork | 0.98918907 | 1.072937194 |
| MP:0004754 | abnormal kidney collecting duct morphology | 0.98917858 | 1.073010381 |
| REACTOME_VOLTAGE_GATED_ | REACTOME_VOLTAGE_GATED_POTASSIUM_CHANNELS | 0.98913437 | 1.073053487 |
| GO:0022412 | cellular process involved in reproduction in multicellular or | 0.98912226 | 1.073111646 |
| ENSG00000078401 | EDN1 subnetwork | 0.98909225 | 1.073151004 |
| MP:0005193 | abnormal anterior eye segment morphology | 0.98908636 | 1.07320918 |
| MP:0001663 | abnormal digestive system physiology | 0.98907555 | 1.073271126 |
| MP:0011024 | abnormal branching involved in lung morphogenesis | 0.98907048 | 1.073344371 |
| GO:0031112 | positive regulation of microtubule polymerization or depoly | 0.98902341 | 1.073368706 |
| GO:0030135 | coated vesicle | 0.40168964 | 1.07337627 |
| MP:0001314 | corneal opacity | 0.98902078 | 1.073445732 |
| GO:0009744 | response to sucrose stimulus | 0.98901864 | 1.073526534 |
| MP:0002636 | delayed vaginal opening | 0.40168692 | 1.07357104 |
| GO:0034285 | response to disaccharide stimulus | 0.98901864 | 1.073607347 |
| GO:0060042 | retina morphogenesis in camera-type eye | 0.98901131 | 1.073680644 |
| ENSG00000078369 | GNB1 subnetwork | 0.98900459 | 1.073753953 |
| ENSG00000160145 | KALRN subnetwork | 0.98895429 | 1.073759506 |
| ENSG00000127554 | GFER subnetwork | 0.98893249 | 1.073829066 |
| GO:0046326 | positive regulation of glucose import | 0.98892917 | 1.073906168 |
| ENSG00000143382 | ADAMTSL4 subnetwork | 0.98892069 | 1.073968218 |
| GO:0016500 | protein-hormone receptor activity | 0.98892065 | 1.074049107 |
| GO:2000179 | positive regulation of neural precursor cell proliferation | 0.98880019 | 1.074056497 |
| ENSG00000197279 | ZNF165 subnetwork | 0.98874246 | 1.074062076 |
| GO:0055002 | striated muscle cell development | 0.98869148 | 1.074094025 |
| GO:0044306 | neuron projection terminus | 0.98889819 | 1.074114944 |
| MP:0003862 | decreased aggression towards males | 0.98867872 | 1.074159885 |
| GO:0050750 | low-density lipoprotein particle receptor binding | 0.98867758 | 1.074237058 |
| GO:0021602 | cranial nerve morphogenesis | 0.98867405 | 1.074306707 |
| GO:0010833 | telomere maintenance via telomere lengthening | 0.40209358 | 1.074342463 |
| GO:0030201 | heparan sulfate proteoglycan metabolic process | 0.98867005 | 1.074380134 |
| MP:0001524 | impaired limb coordination | 0.98864696 | 1.074438499 |
| ENSG00000186111 | PIP5K1C subnetwork | 0.40222184 | 1.074446863 |
| GO:0045296 | cadherin binding | 0.98863958 | 1.074511947 |
| MP:0003828 | pulmonary edema | 0.98863346 | 1.074589175 |
| ENSG00000125740 | FOSB subnetwork | 0.40239505 | 1.074623753 |
| KEGG_DILATED_CARDIOMYOP | KEGG_DILATED_CARDIOMYOPATHY | 0.98862086 | 1.074643799 |
| GO:0048665 | neuron fate specification | 0.98861112 | 1.07471728 |
| GO:0048645 | organ formation | 0.98856586 | 1.074737993 |
| GO:0030195 | negative regulation of blood coagulation | 0.98853878 | 1.07477756 |
| GO:0002360 | T cell lineage commitment | 0.40256146 | 1.074845903 |
| MP:0005170 | cleft lip | 0.40261411 | 1.074850462 |
| GO:0009142 | nucleoside triphosphate biosynthetic process | 0.9885378 | 1.074858608 |
| MP:0004568 | fusion of glossopharyngeal and vagus nerve | 0.98851803 | 1.074894419 |
| GO:0030858 | positive regulation of epithelial cell differentiation | 0.98848872 | 1.074952862 |
| ENSG00000175826 | CTDNEP1 subnetwork | 0.40269941 | 1.074981877 |
| GO:0000272 | polysaccharide catabolic process | 0.98847031 | 1.075022628 |
| MP:0005324 | ascites | 0.98846535 | 1.075103719 |
| ENSG00000001497 | LAS1L subnetwork | 0.40297782 | 1.07512226 |
| ENSG00000163440 | PDCL2 subnetwork | 0.40280556 | 1.075131364 |
| MP:0005630 | increased lung weight | 0.98843653 | 1.075154647 |
| MP:0001195 | flaky skin | 0.4028907 | 1.075172101 |

| | | | |
|---|---|---|---|
| ENSG00000167414 | GNG8 subnetwork | 0.98843232 | 1.07523576 |
| MP:0002753 | dilated heart left ventricle | 0.98840407 | 1.075290478 |
| ENSG00000162188 | GNG3 subnetwork | 0.9883717 | 1.075337659 |
| ENSG00000059769 | DNAJC25 subnetwork | 0.98835847 | 1.07539994 |
| ENSG00000143153 | ATP1B1 subnetwork | 0.98833867 | 1.075454683 |
| ENSG00000133275 | CSNK1G2 subnetwork | 0.9882747 | 1.075456604 |
| GO:0033267 | axon part | 0.98825907 | 1.075522681 |
| GO:0019898 | extrinsic to membrane | 0.98822157 | 1.075558575 |
| GO:0031116 | positive regulation of microtubule polymerization | 0.98820519 | 1.075632219 |
| MP:0008908 | increased total fat pad weight | 0.98816386 | 1.075671901 |
| GO:0051705 | behavioral interaction between organisms | 0.98815002 | 1.075749339 |
| GO:0008589 | regulation of smoothened signaling pathway | 0.98814205 | 1.075826789 |
| MP:0010123 | increased bone mineral content | 0.98812385 | 1.075881598 |
| MP:0000230 | abnormal systemic arterial blood pressure | 0.98811253 | 1.075932639 |
| GO:0055008 | cardiac muscle tissue morphogenesis | 0.98809022 | 1.075991239 |
| REACTOME_L1CAM_INTERACT | REACTOME_L1CAM_INTERACTIONS | 0.98808321 | 1.076061178 |
| ENSG00000167461 | RAB8A subnetwork | 0.4037183 | 1.076140065 |
| ENSG00000107187 | LHX3 subnetwork | 0.98808316 | 1.076142458 |
| GO:0035510 | DNA dealkylation | 0.40359133 | 1.076185735 |
| GO:0006754 | ATP biosynthetic process | 0.98807506 | 1.076201088 |
| GO:0010828 | positive regulation of glucose transport | 0.98802908 | 1.076229508 |
| MP:0005159 | azoospermia | 0.40367309 | 1.076244344 |
| MP:0002804 | abnormal motor learning | 0.98802669 | 1.076310819 |
| MP:0000428 | abnormal craniofacial morphology | 0.40357656 | 1.076344378 |
| GO:0031252 | cell leading edge | 0.40348014 | 1.076367258 |
| GO:0021537 | telencephalon development | 0.98801262 | 1.076369475 |
| ENSG00000179036 | ENSG00000179036 subnetwork | 0.98799727 | 1.076431918 |
| GO:0006073 | cellular glucan metabolic process | 0.98799117 | 1.076509484 |
| GO:0044042 | glucan metabolic process | 0.98799117 | 1.07659084 |
| MP:0009289 | decreased epididymal fat pad weight | 0.40472295 | 1.076665463 |
| ENSG00000143344 | RGL1 subnetwork | 0.98798774 | 1.07666843 |
| ENSG00000206353 | SKIV2L subnetwork | 0.40454621 | 1.076688945 |
| ENSG00000138594 | TMOD3 subnetwork | 0.40460436 | 1.076693155 |
| ENSG00000143256 | PFDN2 subnetwork | 0.40403542 | 1.076700434 |
| GO:0090263 | positive regulation of canonical Wnt receptor signaling pat | 0.98794225 | 1.07670068 |
| ENSG00000171132 | PRKCE subnetwork | 0.98791927 | 1.076759392 |
| ENSG00000144713 | RPL32 subnetwork | 0.4046806 | 1.076769592 |
| REACTOME_THE_NLRP3_INFLA | REACTOME_THE_NLRP3_INFLAMMASOME | 0.98787819 | 1.076795434 |
| GO:0055029 | nuclear DNA-directed RNA polymerase complex | 0.40451754 | 1.076820235 |
| ENSG00000114209 | PDCD10 subnetwork | 0.40499682 | 1.076822447 |
| GO:0006904 | vesicle docking involved in exocytosis | 0.98784129 | 1.076839041 |
| REACTOME_RECYCLING_OF_BI | REACTOME_RECYCLING_OF_BILE_ACIDS_AND_SALTS | 0.40402352 | 1.076840963 |
| GO:0034440 | lipid oxidation | 0.40429181 | 1.076893871 |
| GO:0003205 | cardiac chamber development | 0.98781123 | 1.076893997 |
| MP:0000759 | abnormal skeletal muscle morphology | 0.98778572 | 1.076941399 |
| ENSG00000213024 | NUP62 subnetwork | 0.40436575 | 1.076979393 |
| GO:0033598 | mammary gland epithelial cell proliferation | 0.40498094 | 1.07700776 |
| GO:0000428 | DNA-directed RNA polymerase complex | 0.40451754 | 1.077014817 |
| ENSG00000106089 | STX1A subnetwork | 0.98777656 | 1.077019056 |
| ENSG00000060558 | GNA15 subnetwork | 0.98773959 | 1.07705135 |
| GO:0043256 | laminin complex | 0.40427941 | 1.077052441 |
| GO:0031047 | gene silencing by RNA | 0.4044574 | 1.077091993 |
| GO:0016775 | phosphotransferase activity, nitrogenous group as acceptor | 0.98772182 | 1.077113901 |

| | | | |
|---|---|---|---|
| REACTOME_PURINE_SALVAGE | REACTOME_PURINE_SALVAGE | 0.98766836 | 1.077146207 |
| ENSG00000118520 | ARG1 subnetwork | 0.40497328 | 1.07717509 |
| ENSG00000111880 | RNGTT subnetwork | 0.40425875 | 1.077202026 |
| GO:0050684 | regulation of mRNA processing | 0.98765397 | 1.077204992 |
| MP:0003918 | decreased kidney weight | 0.98763438 | 1.077256222 |
| GO:0008277 | regulation of G-protein coupled receptor protein signaling p | 0.98762107 | 1.077330156 |
| MP:0000755 | hindlimb paralysis | 0.98761927 | 1.077411667 |
| ENSG00000173702 | MUC13 subnetwork | 0.98761752 | 1.077489407 |
| GO:0008227 | G-protein coupled amine receptor activity | 0.98745363 | 1.077489784 |
| ENSG00000172057 | ORMDL3 subnetwork | 0.98760835 | 1.077555808 |
| MP:0005503 | abnormal tendon morphology | 0.98745137 | 1.077571331 |
| REACTOME_INTEGRATION_OF | REACTOME_INTEGRATION_OF_ENERGY_METABOLISM | 0.98745021 | 1.077652891 |
| GO:0061005 | cell differentiation involved in kidney development | 0.40562219 | 1.07767358 |
| ENSG00000117592 | PRDX6 subnetwork | 0.98741906 | 1.077689047 |
| ENSG00000109111 | SUPT6H subnetwork | 0.40619276 | 1.077714749 |
| ENSG00000157344 | ENSG00000157344 subnetwork | 0.98734371 | 1.077768945 |
| ENSG00000108100 | CCNY subnetwork | 0.98741329 | 1.077770628 |
| GO:0016125 | sterol metabolic process | 0.4055186 | 1.077791809 |
| GO:0055003 | cardiac myofibril assembly | 0.98730268 | 1.077808904 |
| ENSG00000178177 | LCORL subnetwork | 0.40561403 | 1.077849928 |
| GO:0018200 | peptidyl-glutamic acid modification | 0.40617861 | 1.077863833 |
| GO:0022411 | cellular component disassembly | 0.40592445 | 1.077865898 |
| GO:0051489 | regulation of filopodium assembly | 0.40609911 | 1.077868852 |
| MP:0005192 | increased motor neuron number | 0.98728546 | 1.077871583 |
| GO:0022839 | ion gated channel activity | 0.98724674 | 1.077919128 |
| MP:0003845 | abnormal decidualization | 0.40579404 | 1.077921024 |
| ENSG00000061987 | MON2 subnetwork | 0.40587516 | 1.07796106 |
| GO:0010524 | positive regulation of calcium ion transport into cytosol | 0.40607473 | 1.077963964 |
| ENSG00000111481 | COPZ1 subnetwork | 0.98723169 | 1.077993184 |
| ENSG00000141985 | SH3GL1 subnetwork | 0.98722356 | 1.078071039 |
| ENSG00000164331 | ANKRA2 subnetwork | 0.40605837 | 1.078113174 |
| GO:0044246 | regulation of multicellular organismal metabolic process | 0.98722257 | 1.078152693 |
| GO:0044259 | multicellular organismal macromolecule metabolic process | 0.98721966 | 1.078234358 |
| KEGG_GLYCOSPHINGOLIPID_BI | KEGG_GLYCOSPHINGOLIPID_BIOSYNTHESIS_GANGLIO_SER | 0.40645507 | 1.078267915 |
| GO:0051149 | positive regulation of muscle cell differentiation | 0.98721822 | 1.078316037 |
| GO:0050679 | positive regulation of epithelial cell proliferation | 0.98720522 | 1.078382576 |
| GO:0016460 | myosin II complex | 0.98713993 | 1.07842855 |
| GO:0010765 | positive regulation of sodium ion transport | 0.98720348 | 1.078460489 |
| ENSG00000066427 | ATXN3 subnetwork | 0.9871255 | 1.078506479 |
| GO:0051588 | regulation of neurotransmitter transport | 0.98704435 | 1.078567639 |
| GO:0050678 | regulation of epithelial cell proliferation | 0.98711249 | 1.07858063 |
| MP:0004395 | increased cochlear inner hair cell number | 0.98702298 | 1.078645596 |
| GO:0090184 | positive regulation of kidney development | 0.98701303 | 1.078712196 |
| GO:0003254 | regulation of membrane depolarization | 0.98700804 | 1.078793966 |
| REACTOME_G_ALPHA_S_SIGN | REACTOME_G_ALPHA_S_SIGNALLING_EVENTS | 0.98692355 | 1.078862775 |
| MP:0008456 | abnormal retinal rod cell outer segment morphology | 0.98700287 | 1.078868168 |
| ENSG00000100714 | MTHFD1 subnetwork | 0.40674374 | 1.078883888 |
| GO:0061333 | renal tubule morphogenesis | 0.98691675 | 1.078929411 |
| MP:0000550 | abnormal forelimb morphology | 0.98687183 | 1.078965726 |
| GO:0009262 | deoxyribonucleotide metabolic process | 0.98683396 | 1.078994464 |
| GO:0031163 | metallo-sulfur cluster assembly | 0.40724828 | 1.078996583 |
| MP:0009453 | enhanced contextual conditioning behavior | 0.98678821 | 1.079038374 |
| GO:0000159 | protein phosphatase type 2A complex | 0.40778929 | 1.079076868 |

| | | | |
|---|---|---|---|
| REACTOME_INTRINSIC_PATHW | REACTOME_INTRINSIC_PATHWAY | 0.98678244 | 1.079112628 |
| ENSG00000112685 | EXOC2 subnetwork | 0.40840435 | 1.079128564 |
| GO:0017025 | TBP-class protein binding | 0.4083356 | 1.079133788 |
| ENSG00000183814 | LIN9 subnetwork | 0.40690291 | 1.079139669 |
| GO:0006302 | double-strand break repair | 0.4082999 | 1.079174888 |
| GO:0048243 | norepinephrine secretion | 0.98677225 | 1.079179308 |
| GO:0016226 | iron-sulfur cluster assembly | 0.40724828 | 1.079190647 |
| MP:0002843 | decreased systemic arterial blood pressure | 0.40710559 | 1.079201151 |
| ENSG00000175595 | ERCC4 subnetwork | 0.40776954 | 1.079216813 |
| GO:0072078 | nephron tubule morphogenesis | 0.98677086 | 1.079257377 |
| ENSG00000143368 | SF3B4 subnetwork | 0.40748388 | 1.079264785 |
| GO:0048037 | cofactor binding | 0.40804008 | 1.079267636 |
| MP:0009640 | abnormal renal tubule epithelium morphology | 0.40853181 | 1.07928469 |
| ENSG00000172534 | HCFC1 subnetwork | 0.40772324 | 1.079311894 |
| ENSG00000108819 | ENSG00000108819 subnetwork | 0.98675664 | 1.079320285 |
| ENSG00000130255 | RPL36 subnetwork | 0.40723833 | 1.079339809 |
| ENSG00000213699 | C2orf18 subnetwork | 0.40707232 | 1.079341371 |
| ENSG00000168530 | MYL1 subnetwork | 0.40829554 | 1.079359526 |
| GO:0009712 | catechol-containing compound metabolic process | 0.98675557 | 1.07940217 |
| KEGG_TRYPTOPHAN_METABO | KEGG_TRYPTOPHAN_METABOLISM | 0.40746959 | 1.07941388 |
| MP:0002020 | increased tumor incidence | 0.40824008 | 1.079427597 |
| MP:0004543 | abnormal sperm physiology | 0.40863667 | 1.079431798 |
| ENSG00000198300 | ZIM2 subnetwork | 0.40803798 | 1.0794614 |
| GO:0006584 | catecholamine metabolic process | 0.98675557 | 1.079484067 |
| GO:0008239 | dipeptidyl-peptidase activity | 0.40771606 | 1.079496855 |
| KEGG_BUTANOATE_METABOL | KEGG_BUTANOATE_METABOLISM | 0.408013 | 1.079556473 |
| GO:0034311 | diol metabolic process | 0.98675557 | 1.079565976 |
| REACTOME_GENERIC_TRANSC | REACTOME_GENERIC_TRANSCRIPTION_PATHWAY | 0.40823493 | 1.079603374 |
| ENSG00000186852 | ENSG00000186852 subnetwork | 0.40767869 | 1.079609993 |
| ENSG00000124688 | MAD2L1BP subnetwork | 0.98674825 | 1.07964031 |
| ENSG00000125166 | GOT2 subnetwork | 0.98671473 | 1.079661531 |
| GO:0009260 | ribonucleotide biosynthetic process | 0.98671399 | 1.079743473 |
| MP:0009305 | decreased retroperitoneal fat pad weight | 0.98671386 | 1.079825427 |
| ENSG00000172915 | NBEA subnetwork | 0.40883257 | 1.079829749 |
| ENSG00000154473 | BUB3 subnetwork | 0.98670065 | 1.079892212 |
| GO:0001963 | synaptic transmission, dopaminergic | 0.98666488 | 1.079936233 |
| GO:0055038 | recycling endosome membrane | 0.98665935 | 1.080014425 |
| GO:0060191 | regulation of lipase activity | 0.98661273 | 1.080058462 |
| GO:0000086 | G2/M transition of mitotic cell cycle | 0.98660751 | 1.080132878 |
| GO:0015949 | nucleobase-containing small molecule interconversion | 0.98659057 | 1.080207305 |
| ENSG00000111450 | STX2 subnetwork | 0.98657948 | 1.080258961 |
| GO:0032607 | interferon-alpha production | 0.98656499 | 1.080322017 |
| ENSG00000095261 | PSMD5 subnetwork | 0.40948403 | 1.080374083 |
| GO:0032647 | regulation of interferon-alpha production | 0.98656499 | 1.080404071 |
| MP:0010831 | partial lethality | 0.98655275 | 1.080467148 |
| GO:0048592 | eye morphogenesis | 0.98650862 | 1.080480857 |
| GO:0021549 | cerebellum development | 0.4090717 | 1.080487368 |
| ENSG00000164346 | NSA2 subnetwork | 0.40947866 | 1.080549588 |
| GO:0016079 | synaptic vesicle exocytosis | 0.98650137 | 1.080562942 |
| ENSG00000176273 | SLC35G1 subnetwork | 0.4092025 | 1.080580437 |
| GO:0021895 | cerebral cortex neuron differentiation | 0.98645372 | 1.080591855 |
| ENSG00000125484 | GTF3C4 subnetwork | 0.40936977 | 1.080623209 |
| GO:0045920 | negative regulation of exocytosis | 0.98641531 | 1.080624573 |

| | | | |
|---|---|---|---|
| ENSG00000183395 | PMCH subnetwork | 0.9864136 | 1.080695289 |
| ENSG00000024422 | EHD2 subnetwork | 0.40946954 | 1.080716204 |
| ENSG00000132824 | SERINC3 subnetwork | 0.40990878 | 1.080727956 |
| GO:0045923 | positive regulation of fatty acid metabolic process | 0.98641324 | 1.080773615 |
| ENSG00000142684 | ZNF593 subnetwork | 0.40935493 | 1.080789898 |
| GO:0006732 | coenzyme metabolic process | 0.40978428 | 1.080819467 |
| ENSG00000156052 | GNAQ subnetwork | 0.98639404 | 1.080821553 |
| GO:0035239 | tube morphogenesis | 0.40987779 | 1.080867621 |
| GO:0010656 | negative regulation of muscle cell apoptotic process | 0.98637945 | 1.0808885 |
| MP:0001384 | abnormal pup retrieval | 0.98637301 | 1.080959258 |
| MP:0003542 | abnormal vascular endothelial cell development | 0.40978102 | 1.081012885 |
| GO:0050974 | detection of mechanical stimulus involved in sensory perce | 0.98636523 | 1.081033827 |
| ENSG00000177301 | KCNA2 subnetwork | 0.98628476 | 1.081043789 |
| ENSG00000095380 | NANS subnetwork | 0.41028463 | 1.081108132 |
| GO:0060193 | positive regulation of lipase activity | 0.98628119 | 1.081125979 |
| GO:0030120 | vesicle coat | 0.41016615 | 1.081128196 |
| ENSG00000153395 | LPCAT1 subnetwork | 0.41038308 | 1.081129378 |
| ENSG00000162409 | PRKAA2 subnetwork | 0.41060213 | 1.081130559 |
| GO:0006506 | GPI anchor biosynthetic process | 0.41054922 | 1.081189711 |
| ENSG00000159200 | RCAN1 subnetwork | 0.98626859 | 1.081192974 |
| MP:0000153 | rib bifurcation | 0.41078319 | 1.081208713 |
| ENSG00000104067 | TJP1 subnetwork | 0.41025097 | 1.081212013 |
| GO:0050920 | regulation of chemotaxis | 0.98623011 | 1.081237168 |
| GO:0001840 | neural plate development | 0.41049923 | 1.081284617 |
| MP:0004101 | abnormal brain interneuron morphology | 0.98621791 | 1.08130038 |
| ENSG00000015171 | ZMYND11 subnetwork | 0.41016526 | 1.081312589 |
| ENSG00000010017 | RANBP9 subnetwork | 0.41075017 | 1.081330357 |
| GO:0009593 | detection of chemical stimulus | 0.98619344 | 1.081363602 |
| MP:0011092 | complete embryonic lethality | 0.4109583 | 1.081381649 |
| GO:0009408 | response to heat | 0.98618937 | 1.081426833 |
| MP:0009936 | abnormal dendritic spine morphology | 0.98618842 | 1.08150909 |
| GO:0032838 | cell projection cytoplasm | 0.98608256 | 1.081589958 |
| ENSG00000068078 | FGFR3 subnetwork | 0.9861758 | 1.081591359 |
| GO:0009952 | anterior/posterior pattern specification | 0.98607358 | 1.081664638 |
| GO:0048662 | negative regulation of smooth muscle cell proliferation | 0.41120499 | 1.081664882 |
| REACTOME_GAP_JUNCTION_D | REACTOME_GAP_JUNCTION_DEGRADATION | 0.98600152 | 1.08167846 |
| GO:0045723 | positive regulation of fatty acid biosynthetic process | 0.98599388 | 1.081756962 |
| GO:0005248 | voltage-gated sodium channel activity | 0.98588391 | 1.081792237 |
| ENSG00000119048 | UBE2B subnetwork | 0.41117374 | 1.081804391 |
| ENSG00000213199 | ACCN3 subnetwork | 0.98599319 | 1.081839282 |
| GO:0008509 | anion transmembrane transporter activity | 0.98586877 | 1.081855545 |
| ENSG00000181827 | RFX7 subnetwork | 0.98585035 | 1.081907444 |
| GO:0051004 | regulation of lipoprotein lipase activity | 0.98583519 | 1.08197077 |
| MP:0003484 | abnormal channel response | 0.98581786 | 1.082034105 |
| MP:0002102 | abnormal ear morphology | 0.9858062 | 1.08209745 |
| GO:0009132 | nucleoside diphosphate metabolic process | 0.98578788 | 1.082164611 |
| ENSG00000197448 | GSTK1 subnetwork | 0.4126667 | 1.082171439 |
| KEGG_DRUG_METABOLISM_O | KEGG_DRUG_METABOLISM_OTHER_ENZYMES | 0.98575063 | 1.082197518 |
| GO:0050755 | chemokine metabolic process | 0.41263358 | 1.082257204 |
| ENSG00000152601 | MBNL1 subnetwork | 0.98575054 | 1.082279927 |
| ENSG00000109107 | ALDOC subnetwork | 0.98574352 | 1.082358541 |
| GO:0000209 | protein polyubiquitination | 0.41260799 | 1.082387476 |
| GO:0051384 | response to glucocorticoid stimulus | 0.98573144 | 1.082425743 |

| | | | |
|---|---|---|---|
| ENSG00000104897 | SF3A2 subnetwork | 0.4128575 | 1.082441323 |
| ENSG00000112818 | MEP1A subnetwork | 0.9856826 | 1.082458679 |
| ENSG00000181061 | HIGD1A subnetwork | 0.98563739 | 1.082514473 |
| ENSG00000183751 | TBL3 subnetwork | 0.4124288 | 1.08252937 |
| REACTOME_ACTIVATED_AMPK | REACTOME_ACTIVATED_AMPK_STIMULATES_FATTY:ACID_ | 0.41260582 | 1.082562278 |
| GO:0009310 | amine catabolic process | 0.41250357 | 1.082568073 |
| GO:0021846 | cell proliferation in forebrain | 0.98563146 | 1.082581702 |
| REACTOME_RNA_POLYMERASI | REACTOME_RNA_POLYMERASE_II_PRE:TRANSCRIPTION_E\ | 0.41163658 | 1.082586976 |
| GO:0060317 | cardiac epithelial to mesenchymal transition | 0.98561455 | 1.082633704 |
| GO:0030520 | intracellular estrogen receptor signaling pathway | 0.41215395 | 1.082638518 |
| GO:0050433 | regulation of catecholamine secretion | 0.98556617 | 1.082655238 |
| ENSG00000135333 | EPHA7 subnetwork | 0.41172292 | 1.082670353 |
| GO:0010977 | negative regulation of neuron projection development | 0.98552236 | 1.082680585 |
| ENSG00000124214 | STAU1 subnetwork | 0.41242323 | 1.082704291 |
| GO:0051258 | protein polymerization | 0.41229045 | 1.082742654 |
| GO:0043473 | pigmentation | 0.98545835 | 1.082754153 |
| ENSG00000092621 | PHGDH subnetwork | 0.41182933 | 1.082756776 |
| MP:0009746 | enhanced behavioral response to xenobiotic | 0.98552231 | 1.082763088 |
| MP:0000270 | abnormal heart tube morphology | 0.41191722 | 1.082804421 |
| ENSG00000215612 | HMX1 subnetwork | 0.41240578 | 1.082808048 |
| REACTOME_CDT1_ASSOCIATIC | REACTOME_CDT1_ASSOCIATION_WITH_THE_CDC6ORCORI | 0.41214351 | 1.082813614 |
| REACTOME_GAP_JUNCTION_A | REACTOME_GAP_JUNCTION_ASSEMBLY | 0.98544563 | 1.082829053 |
| REACTOME_RNA_POLYMERASI | REACTOME_RNA_POLYMERASE_I_PROMOTER_ESCAPE | 0.41199437 | 1.08285205 |
| GO:0046873 | metal ion transmembrane transporter activity | 0.98540163 | 1.082862043 |
| GO:0005740 | mitochondrial envelope | 0.41228216 | 1.082899893 |
| ENSG00000140553 | UNC45A subnetwork | 0.41208897 | 1.082926395 |
| MP:0011102 | partial embryonic lethality | 0.98539066 | 1.082929339 |
| ENSG00000002834 | LASP1 subnetwork | 0.98519487 | 1.082936871 |
| GO:0050810 | regulation of steroid biosynthetic process | 0.41182081 | 1.082940967 |
| ENSG00000101421 | CHMP4B subnetwork | 0.98536304 | 1.082977588 |
| GO:0014031 | mesenchymal cell development | 0.98517131 | 1.082985132 |
| GO:0072528 | pyrimidine-containing compound biosynthetic process | 0.98531989 | 1.083018221 |
| GO:0043584 | nose development | 0.98512352 | 1.083025774 |
| GO:0043679 | axon terminus | 0.9851115 | 1.083096927 |
| MP:0010392 | prolonged QRS complex duration | 0.98508997 | 1.083152837 |
| ENSG00000178999 | AURKB subnetwork | 0.98504615 | 1.083166806 |
| GO:0006892 | post-Golgi vesicle-mediated transport | 0.98497995 | 1.083199847 |
| GO:0031146 | SCF-dependent proteasomal ubiquitin-dependent protein c | 0.98496378 | 1.083274849 |
| ENSG00000143702 | CEP170 subnetwork | 0.98490274 | 1.083285017 |
| GO:0009206 | purine ribonucleoside triphosphate biosynthetic process | 0.98490159 | 1.083367666 |
| GO:2000736 | regulation of stem cell differentiation | 0.98489914 | 1.083446513 |
| REACTOME_INHIBITION_OF_IN | REACTOME_INHIBITION_OF_INSULIN_SECRETION_BY_ADR | 0.98488835 | 1.08350248 |
| ENSG00000119318 | RAD23B subnetwork | 0.41353293 | 1.0835614 |
| GO:0035412 | regulation of catenin import into nucleus | 0.98487184 | 1.083562271 |
| GO:0051414 | response to cortisol stimulus | 0.98484964 | 1.08359536 |
| ENSG00000165632 | TAF3 subnetwork | 0.41348075 | 1.08362069 |
| GO:0050829 | defense response to Gram-negative bacterium | 0.98480804 | 1.083639902 |
| GO:0060349 | bone morphogenesis | 0.98475328 | 1.083665369 |
| MP:0002069 | abnormal eating/drinking behavior | 0.98471611 | 1.083687023 |
| GO:0001570 | vasculogenesis | 0.98463823 | 1.083697229 |
| MP:0010067 | increased red blood cell distribution width | 0.41368408 | 1.083715352 |
| ENSG00000134308 | YWHAQ subnetwork | 0.41344391 | 1.083742222 |
| ENSG00000155111 | CDK19 subnetwork | 0.98460091 | 1.08374561 |

| | | | |
|---|---|---|---|
| ENSG00000138433 | CIR1 subnetwork | 0.41382004 | 1.083789305 |
| GO:0048640 | negative regulation of developmental growth | 0.9845942 | 1.08382454 |
| GO:0050664 | oxidoreductase activity, acting on NADH or NADPH, oxygen | 0.98459158 | 1.083899664 |
| GO:0043176 | amine binding | 0.98459077 | 1.083982436 |
| MP:0006280 | abnormal digit development | 0.98454863 | 1.08401558 |
| GO:0034483 | heparan sulfate sulfotransferase activity | 0.98453351 | 1.084086917 |
| ENSG00000070785 | EIF2B3 subnetwork | 0.98449344 | 1.084104797 |
| GO:0050773 | regulation of dendrite development | 0.98448104 | 1.084160874 |
| ENSG00000064692 | SNCAIP subnetwork | 0.98446545 | 1.084228419 |
| GO:0009201 | ribonucleoside triphosphate biosynthetic process | 0.98446158 | 1.084303614 |
| ENSG00000163531 | NFASC subnetwork | 0.98445752 | 1.084386461 |
| GO:0048469 | cell maturation | 0.98428814 | 1.084424914 |
| ENSG00000164818 | HEATR2 subnetwork | 0.41416937 | 1.084431616 |
| MP:0001431 | abnormal eating behavior | 0.98442711 | 1.084434935 |
| GO:0019228 | regulation of action potential in neuron | 0.98427593 | 1.084481046 |
| GO:0008306 | associative learning | 0.98441532 | 1.084491059 |
| MP:0004981 | decreased neuronal precursor cell number | 0.98427385 | 1.084563938 |
| ENSG00000156795 | WDYHV1 subnetwork | 0.98427126 | 1.084643021 |
| GO:0002080 | acrosomal membrane | 0.98425245 | 1.084706827 |
| ENSG00000130733 | YIPF2 subnetwork | 0.41434513 | 1.084780678 |
| GO:0004012 | phospholipid-translocating ATPase activity | 0.98424922 | 1.084789755 |
| GO:0032781 | positive regulation of ATPase activity | 0.98422234 | 1.084845936 |
| ENSG00000075618 | FSCN1 subnetwork | 0.98421942 | 1.084925065 |
| GO:0042398 | cellular modified amino acid biosynthetic process | 0.98417964 | 1.084962147 |
| GO:0051445 | regulation of meiotic cell cycle | 0.4145094 | 1.084996449 |
| GO:0060216 | definitive hemopoiesis | 0.41479533 | 1.085007097 |
| MP:0005121 | decreased circulating prolactin level | 0.98415837 | 1.085026002 |
| MP:0009402 | decreased skeletal muscle fiber diameter | 0.41469303 | 1.085063898 |
| ENSG00000031544 | ENSG00000031544 subnetwork | 0.41475464 | 1.085066548 |
| MP:0004098 | abnormal cerebellar granule cell morphology | 0.98413541 | 1.085086042 |
| MP:0003396 | abnormal embryonic hematopoiesis | 0.41464114 | 1.08512338 |
| GO:0003001 | generation of a signal involved in cell-cell signaling | 0.98413471 | 1.085169038 |
| GO:0023061 | signal release | 0.98413471 | 1.085252046 |
| ENSG00000004939 | SLC4A1 subnetwork | 0.9841304 | 1.085323592 |
| ENSG00000095066 | HOOK2 subnetwork | 0.41499051 | 1.085364556 |
| GO:0048488 | synaptic vesicle endocytosis | 0.98409597 | 1.085376023 |
| MP:0002191 | abnormal artery morphology | 0.98408164 | 1.085451415 |
| MP:0002731 | megacolon | 0.98407855 | 1.085534471 |
| GO:0000090 | mitotic anaphase | 0.98405459 | 1.085575451 |
| GO:0009145 | purine nucleoside triphosphate biosynthetic process | 0.98403552 | 1.085635571 |
| ENSG00000144191 | CNGA3 subnetwork | 0.98365908 | 1.08568147 |
| GO:0015837 | amine transport | 0.983817 | 1.085683663 |
| ENSG00000072415 | MPP5 subnetwork | 0.9835921 | 1.085688031 |
| GO:0035235 | ionotropic glutamate receptor signaling pathway | 0.98403118 | 1.085707179 |
| ENSG00000122545 | SEPT7 subnetwork | 0.98378361 | 1.085736161 |
| GO:0048255 | mRNA stabilization | 0.98398624 | 1.085744355 |
| ENSG00000164707 | SLC13A4 subnetwork | 0.98357642 | 1.085744371 |
| GO:0030662 | coated vesicle membrane | 0.9838903 | 1.085765138 |
| GO:0043489 | RNA stabilization | 0.98398624 | 1.085827465 |
| ENSG00000081800 | SLC13A1 subnetwork | 0.98357642 | 1.085827525 |
| REACTOME_CDO_IN_MYOGEN | REACTOME_CDO_IN_MYOGENESIS | 0.98351334 | 1.085857077 |
| ENSG00000108592 | FTSJ3 subnetwork | 0.41531943 | 1.085934729 |
| REACTOME_MYOGENESIS | REACTOME_MYOGENESIS | 0.98351334 | 1.085940253 |

| | | | |
|---|---|---|---|
| GO:0051183 | vitamin transporter activity | 0.98342382 | 1.085995557 |
| ENSG00000033627 | ATP6V0A1 subnetwork | 0.98350704 | 1.08601195 |
| GO:0044272 | sulfur compound biosynthetic process | 0.9834046 | 1.086051946 |
| MP:0001924 | infertility | 0.98339043 | 1.086123669 |
| GO:0007423 | sensory organ development | 0.98336345 | 1.086183908 |
| MP:0000538 | abnormal urinary bladder morphology | 0.98335637 | 1.086263315 |
| GO:0016538 | cyclin-dependent protein kinase regulator activity | 0.98334492 | 1.086342735 |
| ENSG00000151276 | MAGI1 subnetwork | 0.41595037 | 1.08638377 |
| GO:0042692 | muscle cell differentiation | 0.98333254 | 1.086422166 |
| ENSG00000011600 | TYROBP subnetwork | 0.41561252 | 1.086460365 |
| ENSG00000186469 | GNG2 subnetwork | 0.98328465 | 1.086486279 |
| ENSG00000143498 | TAF1A subnetwork | 0.41589436 | 1.086487684 |
| GO:0010800 | positive regulation of peptidyl-threonine phosphorylation | 0.98328169 | 1.086565734 |
| GO:0001726 | ruffle | 0.41586282 | 1.086591634 |
| GO:0048715 | negative regulation of oligodendrocyte differentiation | 0.98327755 | 1.086649034 |
| ENSG00000183454 | GRIN2A subnetwork | 0.98313449 | 1.086673823 |
| GO:0005977 | glycogen metabolic process | 0.98324769 | 1.086701679 |
| GO:0043094 | cellular metabolic compound salvage | 0.98310821 | 1.086749482 |
| ENSG00000111540 | RAB5B subnetwork | 0.41586003 | 1.086784258 |
| MP:0000588 | thick tail | 0.98310598 | 1.086828988 |
| ENSG00000062822 | POLD1 subnetwork | 0.41581557 | 1.086835106 |
| GO:0032956 | regulation of actin cytoskeleton organization | 0.41624395 | 1.08683791 |
| GO:0032465 | regulation of cytokinesis | 0.98309519 | 1.086904671 |
| ENSG00000080986 | NDC80 subnetwork | 0.98306086 | 1.086957355 |
| ENSG00000173660 | UQCRH subnetwork | 0.98305733 | 1.08704073 |
| GO:0031645 | negative regulation of neurological system process | 0.9830238 | 1.087081927 |
| GO:0045777 | positive regulation of blood pressure | 0.98297589 | 1.087111623 |
| ENSG00000119938 | PPP1R3C subnetwork | 0.9829053 | 1.087125978 |
| GO:0003014 | renal system process | 0.98289042 | 1.087205555 |
| ENSG00000145423 | SFRP2 subnetwork | 0.98288027 | 1.087281308 |
| GO:0030496 | midbody | 0.98278713 | 1.087352264 |
| MP:0000034 | abnormal vestibule morphology | 0.9828787 | 1.087364746 |
| MP:0002001 | blindness | 0.9827676 | 1.08740502 |
| MP:0001208 | blistering | 0.98276314 | 1.087473135 |
| GO:0012510 | trans-Golgi network transport vesicle membrane | 0.41679267 | 1.087475659 |
| GO:0006298 | mismatch repair | 0.41663817 | 1.087497786 |
| MP:0000781 | decreased corpus callosum size | 0.98263679 | 1.087547025 |
| REACTOME_TRAFFICKING_OF_ | REACTOME_TRAFFICKING_OF_GLUR2:CONTAINING_AMPA | 0.98276111 | 1.087552775 |
| MP:0001129 | impaired ovarian folliculogenesis | 0.41661224 | 1.087566419 |
| MP:0004310 | small otic vesicle | 0.98262475 | 1.087630528 |
| ENSG00000069966 | GNB5 subnetwork | 0.98275698 | 1.087632427 |
| ENSG00000141543 | EIF4A3 subnetwork | 0.41679207 | 1.087668201 |
| ENSG00000147246 | HTR2C subnetwork | 0.98261972 | 1.087710205 |
| GO:0010712 | regulation of collagen metabolic process | 0.98260954 | 1.087786054 |
| GO:0061041 | regulation of wound healing | 0.98233865 | 1.087805346 |
| GO:0045995 | regulation of embryonic development | 0.98259632 | 1.087835036 |
| GO:0043647 | inositol phosphate metabolic process | 0.98233843 | 1.087888914 |
| GO:0035567 | non-canonical Wnt receptor signaling pathway | 0.9825774 | 1.087895545 |
| ENSG00000169925 | BRD3 subnetwork | 0.41695789 | 1.087946903 |
| GO:0005922 | connexon complex | 0.98254073 | 1.087952224 |
| GO:0004864 | protein phosphatase inhibitor activity | 0.98232538 | 1.087960971 |
| ENSG00000182255 | KCNA4 subnetwork | 0.417048 | 1.087966732 |
| GO:0016073 | snRNA metabolic process | 0.41713985 | 1.0879954 |

| | | | |
|---|---|---|---|
| GO:0045745 | positive regulation of G-protein coupled receptor protein si | 0.98224969 | 1.088035961 |
| ENSG00000110318 | KIAA1377 subnetwork | 0.98218536 | 1.088038884 |
| GO:0061053 | somite development | 0.98232359 | 1.088040722 |
| GO:0033116 | endoplasmic reticulum-Golgi intermediate compartment m | 0.98216036 | 1.088080234 |
| ENSG00000134287 | ARF3 subnetwork | 0.98215294 | 1.088163861 |
| GO:0048066 | developmental pigmentation | 0.98213336 | 1.088228286 |
| MP:0009400 | decreased skeletal muscle fiber size | 0.98211543 | 1.088273503 |
| ENSG00000100823 | APEX1 subnetwork | 0.41924151 | 1.088318662 |
| ENSG00000159131 | GART subnetwork | 0.41898261 | 1.088319239 |
| MP:0005112 | abnormal spinal cord ventral horn morphology | 0.9821019 | 1.088349477 |
| GO:0009063 | cellular amino acid catabolic process | 0.41986992 | 1.088427717 |
| ENSG00000148468 | FAM171A1 subnetwork | 0.98210139 | 1.088433151 |
| ENSG00000134490 | TMEM241 subnetwork | 0.41915252 | 1.08843783 |
| GO:0030414 | peptidase inhibitor activity | 0.41897084 | 1.088449339 |
| GO:0050996 | positive regulation of lipid catabolic process | 0.98205512 | 1.088459173 |
| MP:0003026 | decreased vasoconstriction | 0.41981941 | 1.088469657 |
| ENSG00000102468 | HTR2A subnetwork | 0.41848694 | 1.088488003 |
| GO:0005798 | Golgi-associated vesicle | 0.41941143 | 1.088505545 |
| ENSG00000185024 | BRF1 subnetwork | 0.41923672 | 1.088510301 |
| MP:0001544 | abnormal cardiovascular system physiology | 0.41773915 | 1.088511842 |
| GO:0005903 | brush border | 0.41888698 | 1.0885178 |
| GO:0030669 | clathrin-coated endocytic vesicle membrane | 0.98204406 | 1.088542868 |
| MP:0002404 | increased intestinal adenoma incidence | 0.41767725 | 1.088545165 |
| GO:0019430 | removal of superoxide radicals | 0.41763463 | 1.088578501 |
| GO:0007405 | neuroblast proliferation | 0.98200602 | 1.088580437 |
| REACTOME_ACTIVATION_OF_I | REACTOME_ACTIVATION_OF_BH3:ONLY_PROTEINS | 0.41914877 | 1.088629558 |
| GO:0007179 | transforming growth factor beta receptor signaling pathwa | 0.41785804 | 1.088637568 |
| GO:0050482 | arachidonic acid secretion | 0.98198614 | 1.088641083 |
| MP:0001914 | hemorrhage | 0.41981486 | 1.088652357 |
| GO:2000758 | positive regulation of peptidyl-lysine acetylation | 0.4184795 | 1.088653609 |
| KEGG_ENDOCYTOSIS | KEGG_ENDOCYTOSIS | 0.41885867 | 1.088674423 |
| GO:0043407 | negative regulation of MAP kinase activity | 0.41961683 | 1.088674762 |
| GO:0014821 | phasic smooth muscle contraction | 0.9819582 | 1.08868251 |
| ENSG00000160967 | ENSG00000160967 subnetwork | 0.41975842 | 1.088755939 |
| GO:0043526 | neuroprotection | 0.98194991 | 1.088758557 |
| GO:0071450 | cellular response to oxygen radical | 0.41763463 | 1.088770999 |
| GO:0032411 | positive regulation of transporter activity | 0.42002739 | 1.088772639 |
| MP:0000571 | interdigital webbing | 0.98175798 | 1.08880597 |
| ENSG00000140463 | BBS4 subnetwork | 0.42010157 | 1.088818565 |
| GO:0034623 | cellular macromolecular complex disassembly | 0.41847609 | 1.088828097 |
| ENSG00000127526 | SLC35E1 subnetwork | 0.41825941 | 1.088831008 |
| GO:0045648 | positive regulation of erythrocyte differentiation | 0.4188526 | 1.088839915 |
| MP:0001304 | cataracts | 0.98194827 | 1.088842308 |
| MP:0000467 | abnormal esophagus morphology | 0.98187703 | 1.088845296 |
| ENSG00000152582 | SPEF2 subnetwork | 0.98172636 | 1.088866662 |
| ENSG00000128408 | RIBC2 subnetwork | 0.41842127 | 1.08890556 |
| MP:0003122 | maternal imprinting | 0.41753848 | 1.088908544 |
| ENSG00000158792 | SPATA2L subnetwork | 0.41882506 | 1.088934932 |
| ENSG00000127588 | GNG13 subnetwork | 0.98172218 | 1.088935057 |
| GO:0071451 | cellular response to superoxide | 0.41763463 | 1.088963566 |
| MP:0005459 | decreased percent body fat | 0.41818013 | 1.088994877 |
| GO:0045182 | translation regulator activity | 0.41824107 | 1.088996821 |
| ENSG00000120860 | CCDC53 subnetwork | 0.98170315 | 1.089007311 |

| | | | |
|---|---|---|---|
| ENSG00000087008 | ACOX3 subnetwork | 0.41840309 | 1.089018362 |
| ENSG00000196083 | IL1RAP subnetwork | 0.41812632 | 1.08905477 |
| REACTOME_APOPTOTIC_CLEA | REACTOME_APOPTOTIC_CLEAVAGE_OF_CELL_ADHESION_ | 0.98167482 | 1.089068031 |
| GO:0031365 | N-terminal protein amino acid modification | 0.4188094 | 1.089074074 |
| GO:0030017 | sarcomere | 0.98164578 | 1.089109521 |
| MP:0003050 | abnormal sacral vertebrae morphology | 0.4206617 | 1.089128908 |
| GO:0006413 | translational initiation | 0.42047532 | 1.089140749 |
| REACTOME_INTEGRIN_ALPHAI | REACTOME_INTEGRIN_ALPHAIIB_BETA3_SIGNALING | 0.42032052 | 1.08914572 |
| GO:0030864 | cortical actin cytoskeleton | 0.418755 | 1.089151526 |
| GO:0016776 | phosphotransferase activity, phosphate group as acceptor | 0.9816376 | 1.089185653 |
| ENSG00000215719 | ENSG00000215719 subnetwork | 0.4207463 | 1.089209833 |
| GO:0048487 | beta-tubulin binding | 0.42080288 | 1.089211728 |
| ENSG00000073910 | FRY subnetwork | 0.42043079 | 1.089217926 |
| MP:0005225 | abnormal vertebrae development | 0.98161182 | 1.089254099 |
| ENSG00000171557 | FGG subnetwork | 0.4210567 | 1.089261274 |
| MP:0008146 | asymmetric rib-sternum attachment | 0.42064482 | 1.089285087 |
| GO:0042742 | defense response to bacterium | 0.42099172 | 1.089294489 |
| REACTOME_DESTABILIZATION_ | REACTOME_DESTABILIZATION_OF_MRNA_BY_BUTYRATE_I | 0.42090928 | 1.08931894 |
| ENSG00000170142 | UBE2E1 subnetwork | 0.9815863 | 1.089326405 |
| GO:0031398 | positive regulation of protein ubiquitination | 0.98155533 | 1.089379475 |
| GO:0001947 | heart looping | 0.98152504 | 1.089428703 |
| MP:0005168 | abnormal female meiosis | 0.42130156 | 1.08945799 |
| REACTOME_ANTIGEN_PROCES | REACTOME_ANTIGEN_PROCESSING_UBIQUITINATION__PR | 0.42064451 | 1.089476458 |
| ENSG00000169100 | SLC25A6 subnetwork | 0.4212555 | 1.089491228 |
| GO:0061371 | determination of heart left/right asymmetry | 0.98152504 | 1.08951259 |
| GO:0045070 | positive regulation of viral genome replication | 0.42187053 | 1.089523476 |
| GO:0000782 | telomere cap complex | 0.42179064 | 1.089539162 |
| GO:0005227 | calcium activated cation channel activity | 0.98151106 | 1.089581087 |
| GO:0042976 | activation of Janus kinase activity | 0.42142823 | 1.089643985 |
| GO:0048634 | regulation of muscle organ development | 0.98150466 | 1.089657297 |
| GO:0034764 | positive regulation of transmembrane transport | 0.98149059 | 1.089729667 |
| GO:0000783 | nuclear telomere cap complex | 0.42179064 | 1.089730109 |
| ENSG00000131149 | KIAA0182 subnetwork | 0.42162755 | 1.089787868 |
| ENSG00000081479 | LRP2 subnetwork | 0.98146778 | 1.089794346 |
| MP:0001093 | small trigeminal ganglion | 0.98144103 | 1.089847481 |
| GO:0071901 | negative regulation of protein serine/threonine kinase activ | 0.4217528 | 1.089868536 |
| ENSG00000145332 | KLHL8 subnetwork | 0.42159882 | 1.089891285 |
| GO:0007350 | blastoderm segmentation | 0.98143806 | 1.089931438 |
| MP:0003492 | abnormal involuntary movement | 0.42210803 | 1.089936942 |
| ENSG00000112448 | ENSG00000112448 subnetwork | 0.98143426 | 1.090007704 |
| ENSG00000013364 | MVP subnetwork | 0.42228956 | 1.090063036 |
| ENSG00000215641 | TRIM27 subnetwork | 0.98143426 | 1.090091687 |
| ENSG00000204713 | TRIM27 subnetwork | 0.98143426 | 1.090175682 |
| GO:0010863 | positive regulation of phospholipase C activity | 0.9812135 | 1.090177264 |
| ENSG00000133958 | UNC79 subnetwork | 0.98117575 | 1.090191922 |
| ENSG00000188763 | FZD9 subnetwork | 0.42227663 | 1.090210158 |
| GO:0002040 | sprouting angiogenesis | 0.98138723 | 1.090213455 |
| ENSG00000186340 | THBS2 subnetwork | 0.42241179 | 1.090222339 |
| GO:0016055 | Wnt receptor signaling pathway | 0.9811636 | 1.090272104 |
| MP:0005140 | decreased cardiac muscle contractility | 0.98138432 | 1.090293619 |
| GO:0051084 | 'de novo' posttranslational protein folding | 0.42252702 | 1.090320322 |
| MP:0009940 | abnormal hippocampus pyramidal cell morphology | 0.98113958 | 1.090333025 |
| MP:0003871 | abnormal myelin sheath morphology | 0.98111289 | 1.090386246 |

| | | | |
|---|---|---|---|
| REACTOME_MEMBRANE_BINC | REACTOME_MEMBRANE_BINDING_AND_TARGETTING_OF_ | 0.98109003 | 1.090435621 |
| GO:0060415 | muscle tissue morphogenesis | 0.98102644 | 1.090450305 |
| GO:0060174 | limb bud formation | 0.98099077 | 1.090488125 |
| GO:0048477 | oogenesis | 0.9809542 | 1.09054523 |
| GO:0035411 | catenin import into nucleus | 0.98093362 | 1.090598488 |
| GO:0001078 | RNA polymerase II core promoter proximal region sequence | 0.98092852 | 1.09067875 |
| GO:0035019 | somatic stem cell maintenance | 0.98080162 | 1.090704312 |
| ENSG00000112096 | SOD2 subnetwork | 0.98088544 | 1.090720457 |
| ENSG00000172531 | PPP1CA subnetwork | 0.42318346 | 1.090723903 |
| MP:0008789 | abnormal olfactory epithelium morphology | 0.98078539 | 1.090765314 |
| ENSG00000138741 | TRPC3 subnetwork | 0.42280413 | 1.09079454 |
| GO:0043470 | regulation of carbohydrate catabolic process | 0.42343133 | 1.09080741 |
| MP:0000492 | abnormal rectum morphology | 0.98077351 | 1.090834041 |
| ENSG00000101557 | USP14 subnetwork | 0.42317425 | 1.090879678 |
| GO:0008656 | cysteine-type endopeptidase activator activity involved in a | 0.98074834 | 1.090883488 |
| ENSG00000132963 | POMP subnetwork | 0.42309709 | 1.090886829 |
| ENSG00000108691 | CCL2 subnetwork | 0.98074082 | 1.090967667 |
| GO:0043471 | regulation of cellular carbohydrate catabolic process | 0.42343133 | 1.090998077 |
| ENSG00000174622 | ENSG00000174622 subnetwork | 0.98069911 | 1.091005556 |
| MP:0001762 | polyuria | 0.42463751 | 1.091049329 |
| GO:0032459 | regulation of protein oligomerization | 0.42306945 | 1.091051435 |
| MP:0001386 | abnormal maternal nurturing | 0.98067294 | 1.091055028 |
| GO:0071375 | cellular response to peptide hormone stimulus | 0.42365831 | 1.091055206 |
| ENSG00000138592 | USP8 subnetwork | 0.42360643 | 1.091079853 |
| GO:0032271 | regulation of protein polymerization | 0.42387715 | 1.091086083 |
| GO:0016763 | transferase activity, transferring pentosyl groups | 0.42338005 | 1.09111014 |
| GO:0008212 | mineralocorticoid metabolic process | 0.98067233 | 1.091139241 |
| ENSG00000095564 | BTAF1 subnetwork | 0.42303565 | 1.091181102 |
| ENSG00000138071 | ACTR2 subnetwork | 0.42463072 | 1.091213389 |
| ENSG00000184357 | HIST1H1B subnetwork | 0.98067214 | 1.091223466 |
| ENSG00000146535 | GNA12 subnetwork | 0.4237901 | 1.091240175 |
| ENSG00000185627 | PSMD13 subnetwork | 0.42386598 | 1.091241705 |
| ENSG00000137218 | FRS3 subnetwork | 0.98063176 | 1.091245947 |
| MP:0005650 | abnormal limb bud morphology | 0.98059169 | 1.091303173 |
| ENSG00000120053 | GOT1 subnetwork | 0.98058363 | 1.091375849 |
| KEGG_ENDOMETRIAL_CANCER | KEGG_ENDOMETRIAL_CANCER | 0.42462746 | 1.091403662 |
| MP:0003356 | impaired luteinization | 0.42457762 | 1.091437042 |
| ENSG00000145386 | CCNA2 subnetwork | 0.98057239 | 1.091448537 |
| MP:0000788 | abnormal cerebral cortex morphology | 0.98056647 | 1.091525097 |
| MP:0004957 | abnormal blastocyst morphology | 0.42456138 | 1.091575092 |
| MP:0004890 | decreased energy expenditure | 0.42423068 | 1.091577937 |
| GO:0009584 | detection of visible light | 0.98055356 | 1.0915785 |
| ENSG00000167110 | GOLGA2 subnetwork | 0.42442363 | 1.091607049 |
| GO:0060341 | regulation of cellular localization | 0.42415716 | 1.091620112 |
| GO:0045930 | negative regulation of mitotic cell cycle | 0.42436729 | 1.091640489 |
| GO:0003417 | growth plate cartilage development | 0.42450293 | 1.091643405 |
| ENSG00000136250 | AOAH subnetwork | 0.98049913 | 1.091650575 |
| GO:0006091 | generation of precursor metabolites and energy | 0.98054435 | 1.091655082 |
| GO:0043499 | eukaryotic cell surface binding | 0.42528974 | 1.091684082 |
| ENSG00000008311 | AASS subnetwork | 0.98048342 | 1.09171945 |
| GO:0048741 | skeletal muscle fiber development | 0.98036222 | 1.091783838 |
| REACTOME_TETRAHYDROBIOP | REACTOME_TETRAHYDROBIOPTERIN_BH4_SYNTHESIS_REC | 0.98048153 | 1.091803785 |
| ENSG00000108061 | SHOC2 subnetwork | 0.980314 | 1.091825697 |

| | | | |
|---|---|---|---|
| GO:0008408 | 3'-5' exonuclease activity | 0.42504792 | 1.091861276 |
| ENSG00000172572 | PDE3A subnetwork | 0.4252794 | 1.091865529 |
| GO:0055067 | monovalent inorganic cation homeostasis | 0.98030733 | 1.09189847 |
| ENSG00000077264 | PAK3 subnetwork | 0.42520167 | 1.091907666 |
| MP:0000633 | abnormal pituitary gland morphology | 0.98025481 | 1.09192489 |
| GO:2001020 | regulation of response to DNA damage stimulus | 0.98019871 | 1.091931994 |
| GO:0003995 | acyl-CoA dehydrogenase activity | 0.42514494 | 1.091949817 |
| GO:0048013 | ephrin receptor signaling pathway | 0.98018455 | 1.091989335 |
| GO:0060026 | convergent extension | 0.9801534 | 1.092031226 |
| GO:0060198 | clathrin sculpted vesicle | 0.98013107 | 1.092092448 |
| ENSG00000117394 | SLC2A1 subnetwork | 0.98008336 | 1.092145949 |
| ENSG00000074266 | EED subnetwork | 0.42554786 | 1.092207905 |
| REACTOME_SIGNALLING_TO_F | REACTOME_SIGNALLING_TO_P38_VIA_RIT_AND_RIN | 0.98007084 | 1.092218786 |
| ENSG00000196218 | RYR1 subnetwork | 0.42569402 | 1.09227154 |
| ENSG00000087586 | AURKA subnetwork | 0.98006261 | 1.092291634 |
| ENSG00000092969 | TGFB2 subnetwork | 0.42564011 | 1.092322423 |
| GO:0048546 | digestive tract morphogenesis | 0.98005598 | 1.092372226 |
| GO:0008250 | oligosaccharyltransferase complex | 0.98003387 | 1.092433498 |
| ENSG00000099331 | MYO9B subnetwork | 0.98000853 | 1.092510247 |
| ENSG00000102678 | FGF9 subnetwork | 0.97997238 | 1.092559938 |
| ENSG00000128739 | SNRPN subnetwork | 0.42595239 | 1.09260355 |
| MP:0003209 | abnormal pulmonary elastic fiber morphology | 0.97993838 | 1.09260577 |
| GO:0050880 | regulation of blood vessel size | 0.97990423 | 1.092655476 |
| GO:0030917 | midbrain-hindbrain boundary development | 0.42608014 | 1.092691839 |
| MP:0006020 | decreased tympanic ring size | 0.9798826 | 1.092716794 |
| REACTOME_AMINE_LIGAND:BI | REACTOME_AMINE_LIGAND:BINDING_RECEPTORS | 0.97985727 | 1.092785858 |
| ENSG00000141759 | TXNL4A subnetwork | 0.4261999 | 1.092788796 |
| MP:0002944 | increased lactate dehydrogenase level | 0.9798519 | 1.092858801 |
| ENSG00000133083 | DCLK1 subnetwork | 0.9798461 | 1.092935624 |
| GO:0043462 | regulation of ATPase activity | 0.97979327 | 1.092981506 |
| MP:0004274 | abnormal embryonic/fetal subventricular zone morphology | 0.97977086 | 1.093015787 |
| MP:0000864 | abnormal cerebellum vermis morphology | 0.97976699 | 1.09309651 |
| ENSG00000164885 | CDK5 subnetwork | 0.97955171 | 1.093145224 |
| GO:0005523 | tropomyosin binding | 0.97974225 | 1.093157895 |
| GO:0044058 | regulation of digestive system process | 0.97951242 | 1.093191143 |
| MP:0003924 | herniated diaphragm | 0.97969507 | 1.093199938 |
| ENSG00000094880 | CDC23 subnetwork | 0.97945394 | 1.09323707 |
| MP:0001491 | unresponsive to tactile stimuli | 0.97945223 | 1.093321719 |
| ENSG00000159189 | C1QC subnetwork | 0.42694144 | 1.093327541 |
| GO:0004629 | phospholipase C activity | 0.97944713 | 1.093402509 |
| ENSG00000185722 | ANKFY1 subnetwork | 0.4268926 | 1.093456726 |
| ENSG00000113578 | FGF1 subnetwork | 0.97944653 | 1.093487183 |
| MP:0003038 | decreased infarction size | 0.42682339 | 1.093490353 |
| GO:0090102 | cochlea development | 0.97942972 | 1.093552509 |
| MP:0004401 | increased cochlear outer hair cell number | 0.97940896 | 1.093621718 |
| GO:0016746 | transferase activity, transferring acyl groups | 0.42682015 | 1.093680459 |
| GO:0000578 | embryonic axis specification | 0.97939277 | 1.093698683 |
| ENSG00000113272 | THG1L subnetwork | 0.42896828 | 1.093772704 |
| GO:0007202 | activation of phospholipase C activity | 0.97939042 | 1.093783407 |
| ENSG00000115756 | HPCAL1 subnetwork | 0.42890347 | 1.09383218 |
| ENSG00000140403 | DNAJA4 subnetwork | 0.9793883 | 1.093860397 |
| ENSG00000156508 | EEF1A1 subnetwork | 0.42681638 | 1.093861937 |
| ENSG00000006747 | SCIN subnetwork | 0.4288617 | 1.093874373 |

| | | | |
|---|---|---|---|
| GO:0046886 | positive regulation of hormone biosynthetic process | 0.42720793 | 1.093910702 |
| GO:0016860 | intramolecular oxidoreductase activity | 0.42671461 | 1.093911985 |
| GO:0007029 | endoplasmic reticulum organization | 0.97937851 | 1.093937398 |
| GO:0006275 | regulation of DNA replication | 0.42679674 | 1.093982609 |
| GO:0014003 | oligodendrocyte development | 0.97937841 | 1.09402216 |
| GO:0005605 | basal lamina | 0.42884776 | 1.094029076 |
| ENSG00000116141 | MARK1 subnetwork | 0.42916784 | 1.094033207 |
| ENSG00000125676 | THOC2 subnetwork | 0.42879752 | 1.094088627 |
| ENSG00000149131 | SERPING1 subnetwork | 0.97936915 | 1.094091437 |
| ENSG00000170458 | CD14 subnetwork | 0.97930311 | 1.094137022 |
| ENSG00000076321 | KLHL20 subnetwork | 0.97935547 | 1.094152976 |
| REACTOME_SIGNALLING_TO_F | REACTOME_SIGNALLING_TO_RAS | 0.42876202 | 1.094182825 |
| ENSG00000172380 | GNG12 subnetwork | 0.9792859 | 1.094202449 |
| ENSG00000180871 | CXCR2 subnetwork | 0.42871573 | 1.09425974 |
| ENSG00000183336 | BOLA2 subnetwork | 0.42832312 | 1.094263432 |
| MP:0002574 | increased vertical activity | 0.97928146 | 1.094275638 |
| REACTOME_COMPLEMENT_CA | REACTOME_COMPLEMENT_CASCADE | 0.42857044 | 1.094283735 |
| ENSG00000160224 | AIRE subnetwork | 0.42838883 | 1.094290418 |
| MP:0000936 | small telencephalic vesicles | 0.42769402 | 1.094297865 |
| ENSG00000103507 | BCKDK subnetwork | 0.42810902 | 1.094312467 |
| MP:0005297 | spina bifida occulta | 0.4286543 | 1.094319363 |
| ENSG00000104267 | CA2 subnetwork | 0.42798868 | 1.09432784 |
| GO:0002793 | positive regulation of peptide secretion | 0.9792699 | 1.094348837 |
| ENSG00000197459 | HIST1H2BH subnetwork | 0.4280499 | 1.094354839 |
| ENSG00000158828 | PINK1 subnetwork | 0.42851895 | 1.094360707 |
| GO:0006586 | indolalkylamine metabolic process | 0.97922938 | 1.094371657 |
| ENSG00000169627 | BOLA2B subnetwork | 0.42832312 | 1.094453111 |
| GO:0042430 | indole-containing compound metabolic process | 0.97922938 | 1.094456505 |
| ENSG00000108306 | FBXL20 subnetwork | 0.42824402 | 1.094460818 |
| ENSG00000149136 | SSRP1 subnetwork | 0.4276874 | 1.094461806 |
| GO:0060740 | prostate gland epithelium morphogenesis | 0.43198769 | 1.09448264 |
| ENSG00000071909 | MYO3B subnetwork | 0.42797591 | 1.094509022 |
| ENSG00000204218 | ENSG00000204218 subnetwork | 0.97920617 | 1.094510351 |
| MP:0010107 | abnormal renal reabsorbtion | 0.43189668 | 1.094516074 |
| GO:0031128 | developmental induction | 0.97918733 | 1.09454482 |
| GO:0030659 | cytoplasmic vesicle membrane | 0.97914725 | 1.094587049 |
| REACTOME_REGULATION_OF_ | REACTOME_REGULATION_OF_GENE_EXPRESSION_IN_BET/ | 0.43185539 | 1.0946011 |
| ENSG00000009335 | UBE3C subnetwork | 0.97900256 | 1.094601722 |
| ENSG00000107485 | GATA3 subnetwork | 0.42795713 | 1.094620857 |
| ENSG00000121152 | NCAPH subnetwork | 0.97909437 | 1.094621529 |
| ENSG00000177106 | EPS8L2 subnetwork | 0.43165255 | 1.094624118 |
| ENSG00000175220 | ARHGAP1 subnetwork | 0.43174578 | 1.094633643 |
| REACTOME_SMOOTH_MUSCLI | REACTOME_SMOOTH_MUSCLE_CONTRACTION | 0.4276808 | 1.094634485 |
| ENSG00000188342 | GTF2F2 subnetwork | 0.42788512 | 1.094637279 |
| REACTOME_REGULATION_OF_ | REACTOME_REGULATION_OF_WATER_BALANCE_BY_RENA | 0.97899046 | 1.094682749 |
| MP:0004025 | polyploidy | 0.42763799 | 1.094703022 |
| GO:0001894 | tissue homeostasis | 0.42945992 | 1.094708629 |
| ENSG00000091409 | ITGA6 subnetwork | 0.43162881 | 1.094726428 |
| GO:0010389 | regulation of G2/M transition of mitotic cell cycle | 0.97897783 | 1.094736638 |
| ENSG00000173156 | RHOD subnetwork | 0.42758226 | 1.094745527 |
| ENSG00000160200 | CBS subnetwork | 0.4318492 | 1.094772141 |
| GO:0035150 | regulation of tube size | 0.97896242 | 1.094806051 |
| ENSG00000188985 | ENSG00000188985 subnetwork | 0.43157589 | 1.094811564 |

| | | | |
|---|---|---|---|
| GO:0005283 | sodium:amino acid symporter activity | 0.97895591 | 1.094890992 |
| GO:0030173 | integral to Golgi membrane | 0.43154379 | 1.094905336 |
| ENSG00000163902 | RPN1 subnetwork | 0.42973581 | 1.094953336 |
| GO:0006970 | response to osmotic stress | 0.4323574 | 1.094957045 |
| GO:0012506 | vesicle membrane | 0.97895474 | 1.094964308 |
| ENSG00000115514 | TXNDC9 subnetwork | 0.43082125 | 1.094982759 |
| ENSG00000166582 | CENPV subnetwork | 0.4322953 | 1.094990548 |
| GO:0016202 | regulation of striated muscle tissue development | 0.97894068 | 1.095033755 |
| ENSG00000104368 | PLAT subnetwork | 0.42970836 | 1.095082109 |
| ENSG00000126945 | HNRNPH2 subnetwork | 0.43146586 | 1.095092975 |
| GO:0052689 | carboxylic ester hydrolase activity | 0.43154315 | 1.09509382 |
| MP:0003887 | increased hepatocyte apoptosis | 0.43247113 | 1.095095344 |
| ENSG00000163283 | ALPP subnetwork | 0.43072659 | 1.095101759 |
| GO:0008542 | visual learning | 0.97892971 | 1.095107093 |
| GO:0010458 | exit from mitosis | 0.97887978 | 1.095114474 |
| GO:0042254 | ribosome biogenesis | 0.43141848 | 1.095126571 |
| ENSG00000112049 | ENSG00000112049 subnetwork | 0.43080415 | 1.09512847 |
| ENSG00000104980 | TIMM44 subnetwork | 0.43104384 | 1.095139607 |
| MP:0000479 | abnormal enterocyte morphology | 0.42967371 | 1.095167704 |
| GO:0006081 | cellular aldehyde metabolic process | 0.97887681 | 1.09518783 |
| ENSG00000182901 | RGS7 subnetwork | 0.43058997 | 1.095220842 |
| GO:0043406 | positive regulation of MAP kinase activity | 0.43070286 | 1.095238917 |
| GO:0000155 | two-component sensor activity | 0.97885907 | 1.095253435 |
| ENSG00000075651 | PLD1 subnetwork | 0.4313889 | 1.09526352 |
| ENSG00000107862 | GBF1 subnetwork | 0.43051379 | 1.095271786 |
| ENSG00000168827 | GFM1 subnetwork | 0.43043188 | 1.095296859 |
| GO:0005088 | Ras guanyl-nucleotide exchange factor activity | 0.4310308 | 1.095302534 |
| REACTOME_CHAPERONIN:MEI | REACTOME_CHAPERONIN:MEDIATED_PROTEIN_FOLDING | 0.43125968 | 1.095330806 |
| GO:0004673 | protein histidine kinase activity | 0.97885907 | 1.095338457 |
| REACTOME_SLC:MEDIATED_TF | REACTOME_SLC:MEDIATED_TRANSMEMBRANE_TRANSPOI | 0.4303727 | 1.095356465 |
| GO:0006749 | glutathione metabolic process | 0.97883336 | 1.095376912 |
| ENSG00000039650 | PNKP subnetwork | 0.43119775 | 1.095398932 |
| ENSG00000183791 | TCEB3C subnetwork | 0.43136722 | 1.095417743 |
| GO:0034369 | plasma lipoprotein particle remodeling | 0.97881203 | 1.095427019 |
| MP:0003566 | abnormal cell adhesion | 0.43017861 | 1.095466321 |
| MP:0011093 | complete embryonic lethality at implantation | 0.4302656 | 1.095475738 |
| ENSG00000101158 | TH1L subnetwork | 0.43034137 | 1.095476519 |
| GO:0034367 | macromolecular complex remodeling | 0.97881203 | 1.095512074 |
| GO:0034368 | protein-lipid complex remodeling | 0.97881203 | 1.095597142 |
| MP:0009450 | abnormal axon fasiculation | 0.97876624 | 1.095627864 |
| REACTOME_ACTIVATION_OF_( | REACTOME_ACTIVATION_OF_CHAPERONES_BY_IRE1ALPHA | 0.43017362 | 1.095646917 |
| GO:0001885 | endothelial cell development | 0.97862539 | 1.095673786 |
| MP:0004929 | decreased epididymis weight | 0.97874741 | 1.095705188 |
| ENSG00000070193 | FGF10 subnetwork | 0.97862378 | 1.095758894 |
| ENSG00000076944 | STXBP2 subnetwork | 0.43014881 | 1.095775743 |
| MP:0002199 | abnormal brain commissure morphology | 0.97859639 | 1.095824594 |
| GO:0016010 | dystrophin-associated glycoprotein complex | 0.97858692 | 1.095898073 |
| MP:0003229 | abnormal vitelline vasculature morphology | 0.43292384 | 1.095921346 |
| ENSG00000100764 | PSMC1 subnetwork | 0.43013695 | 1.095930534 |
| ENSG00000144283 | PKP4 subnetwork | 0.97846759 | 1.095951826 |
| GO:0031461 | cullin-RING ubiquitin ligase complex | 0.9785584 | 1.095975449 |
| GO:0015295 | solute:hydrogen symporter activity | 0.43287231 | 1.095989351 |
| MP:0003008 | enhanced long term potentiation | 0.97843035 | 1.096021447 |

| | | | |
|---|---|---|---|
| GO:0006576 | cellular biogenic amine metabolic process | 0.97840851 | 1.096067765 |
| GO:0045078 | positive regulation of interferon-gamma biosynthetic proce | 0.97838549 | 1.096129634 |
| GO:0051147 | regulation of muscle cell differentiation | 0.9783803 | 1.09621483 |
| MP:0006009 | abnormal neuronal migration | 0.97824498 | 1.096283915 |
| GO:0003924 | GTPase activity | 0.97836912 | 1.096288379 |
| GO:0004129 | cytochrome-c oxidase activity | 0.97821848 | 1.0963225 |
| GO:0007605 | sensory perception of sound | 0.97835663 | 1.096365827 |
| GO:0016676 | oxidoreductase activity, acting on a heme group of donors, | 0.97821848 | 1.096407744 |
| GO:0015002 | heme-copper terminal oxidase activity | 0.97821848 | 1.096493002 |
| GO:0048841 | regulation of axon extension involved in axon guidance | 0.97819032 | 1.096547165 |
| ENSG00000178409 | BEND3 subnetwork | 0.43327189 | 1.096557349 |
| GO:0000381 | regulation of alternative nuclear mRNA splicing, via spliceos | 0.97807517 | 1.096581629 |
| GO:0010959 | regulation of metal ion transport | 0.97816662 | 1.096605226 |
| MP:0000877 | abnormal Purkinje cell morphology | 0.97803204 | 1.096643591 |
| GO:0051168 | nuclear export | 0.43344312 | 1.096644353 |
| GO:0006692 | prostanoid metabolic process | 0.97802886 | 1.09672112 |
| ENSG00000113595 | TRIM23 subnetwork | 0.43342404 | 1.096772532 |
| ENSG00000041982 | TNC subnetwork | 0.97801701 | 1.096786992 |
| MP:0003672 | abnormal ureter development | 0.97797883 | 1.096848985 |
| REACTOME_TRANSCRIPTION_( | REACTOME_TRANSCRIPTION_OF_THE_HIV_GENOME | 0.43365856 | 1.096902351 |
| GO:0060079 | regulation of excitatory postsynaptic membrane potential | 0.9779535 | 1.096903206 |
| GO:0032413 | negative regulation of ion transmembrane transporter activ | 0.97794746 | 1.09698467 |
| KEGG_CYTOSOLIC_DNA_SENSI | KEGG_CYTOSOLIC_DNA_SENSING_PATHWAY | 0.4337969 | 1.097040151 |
| MP:0002752 | abnormal somatic nervous system morphology | 0.97793463 | 1.097054475 |
| GO:0009743 | response to carbohydrate stimulus | 0.97791021 | 1.097116507 |
| ENSG00000072315 | TRPC5 subnetwork | 0.97790617 | 1.097198007 |
| GO:0033124 | regulation of GTP catabolic process | 0.4339546 | 1.097212215 |
| GO:0007076 | mitotic chromosome condensation | 0.9778746 | 1.097244493 |
| GO:0060350 | endochondral bone morphogenesis | 0.97783008 | 1.097314339 |
| GO:0045165 | cell fate commitment | 0.9778294 | 1.097399766 |
| MP:0002561 | abnormal circadian phase | 0.97777948 | 1.097438493 |
| ENSG00000099365 | STX1B subnetwork | 0.97766757 | 1.097461455 |
| ENSG00000138180 | CEP55 subnetwork | 0.97763664 | 1.097504088 |
| GO:0001838 | embryonic epithelial tube formation | 0.97777924 | 1.097523943 |
| REACTOME_MRNA_3:END_PR( | REACTOME_MRNA_3:END_PROCESSING | 0.97752299 | 1.09753096 |
| ENSG00000142186 | SCYL1 subnetwork | 0.97759298 | 1.097562305 |
| ENSG00000137309 | HMGA1 subnetwork | 0.43411892 | 1.097564322 |
| REACTOME_EXTENSION_OF_T | REACTOME_EXTENSION_OF_TELOMERES | 0.4341848 | 1.097573315 |
| REACTOME_POST:ELONGATIOI | REACTOME_POST:ELONGATION_PROCESSING_OF_INTRON | 0.97752299 | 1.097616451 |
| ENSG00000078018 | MAP2 subnetwork | 0.97751617 | 1.097686375 |
| GO:0005003 | ephrin receptor activity | 0.97737952 | 1.09768991 |
| ENSG00000108821 | COL1A1 subnetwork | 0.97748352 | 1.097721253 |
| GO:0014829 | vascular smooth muscle contraction | 0.97735391 | 1.097748169 |
| GO:0021983 | pituitary gland development | 0.97732939 | 1.097806437 |
| GO:0031145 | anaphase-promoting complex-dependent proteasomal ubic | 0.97732878 | 1.097891989 |
| MP:0003044 | impaired basement membrane formation | 0.97732365 | 1.097969761 |
| GO:0045687 | positive regulation of glial cell differentiation | 0.43473926 | 1.097969848 |
| ENSG00000124614 | RPS10 subnetwork | 0.43448574 | 1.097977027 |
| GO:0007281 | germ cell development | 0.97729238 | 1.098012471 |
| GO:0006833 | water transport | 0.97724303 | 1.098027906 |
| ENSG00000118579 | MED28 subnetwork | 0.43506205 | 1.098031159 |
| KEGG_ADHERENS_JUNCTION | KEGG_ADHERENS_JUNCTION | 0.4346313 | 1.098046272 |
| MP:0000279 | ventricular hypoplasia | 0.43468971 | 1.098055175 |

| | | | |
|---|---|---|---|
| GO:0004033 | aldo-keto reductase (NADP) activity | 0.43495516 | 1.098081863 |
| GO:0007173 | epidermal growth factor receptor signaling pathway | 0.43488324 | 1.098098664 |
| ENSG00000116044 | NFE2L2 subnetwork | 0.43516954 | 1.098099966 |
| GO:0048846 | axon extension involved in axon guidance | 0.97723694 | 1.098101809 |
| MP:0001712 | abnormal placenta development | 0.4345911 | 1.098131642 |
| ENSG00000169564 | PCBP1 subnetwork | 0.4344657 | 1.098139575 |
| GO:0030900 | forebrain development | 0.97723529 | 1.098187417 |
| GO:0070410 | co-SMAD binding | 0.43506059 | 1.098219178 |
| MP:0004000 | impaired passive avoidance behavior | 0.97723031 | 1.098273039 |
| REACTOME_ADENYLATE_CYCL | REACTOME_ADENYLATE_CYCLASE_ACTIVATING_PATHWAY | 0.97719974 | 1.098315789 |
| GO:0060037 | pharyngeal system development | 0.97718052 | 1.098374142 |
| GO:0048709 | oligodendrocyte differentiation | 0.97715136 | 1.098413008 |
| GO:0030513 | positive regulation of BMP signaling pathway | 0.97715003 | 1.098486976 |
| GO:0019363 | pyridine nucleotide biosynthetic process | 0.97714137 | 1.098564855 |
| GO:0072525 | pyridine-containing compound biosynthetic process | 0.97714137 | 1.098650546 |
| ENSG00000157152 | ENSG00000157152 subnetwork | 0.97712749 | 1.098712848 |
| ENSG00000157500 | APPL1 subnetwork | 0.97710306 | 1.098782961 |
| MP:0000160 | kyphosis | 0.97708182 | 1.098825778 |
| MP:0003728 | abnormal retinal photoreceptor layer morphology | 0.97696136 | 1.0988373 |
| ENSG00000115884 | SDC1 subnetwork | 0.97692719 | 1.098880131 |
| GO:0006901 | vesicle coating | 0.97708173 | 1.098911517 |
| ENSG00000071564 | TCF3 subnetwork | 0.97691306 | 1.098958089 |
| GO:0034035 | purine ribonucleoside bisphosphate metabolic process | 0.97690982 | 1.099039963 |
| GO:0050427 | 3'-phosphoadenosine 5'-phosphosulfate metabolic process | 0.97690982 | 1.099125751 |
| ENSG00000165556 | CDX2 subnetwork | 0.43563743 | 1.099144275 |
| GO:0034032 | purine nucleoside bisphosphate metabolic process | 0.97690982 | 1.099211553 |
| GO:0033875 | ribonucleoside bisphosphate metabolic process | 0.97690982 | 1.099297369 |
| GO:0032561 | guanyl ribonucleotide binding | 0.9769083 | 1.099379294 |
| GO:0019001 | guanyl nucleotide binding | 0.9769083 | 1.099465136 |
| GO:0045168 | cell-cell signaling involved in cell fate commitment | 0.97687069 | 1.099511948 |
| GO:0015838 | betaine transport | 0.97685189 | 1.099554861 |
| GO:0015879 | carnitine transport | 0.97685189 | 1.099640737 |
| GO:0070169 | positive regulation of biomineral tissue development | 0.97666258 | 1.099644559 |
| GO:0006944 | cellular membrane fusion | 0.97679687 | 1.099644615 |
| GO:0090207 | regulation of triglyceride metabolic process | 0.43608922 | 1.099666439 |
| MP:0004359 | short ulna | 0.97675387 | 1.099691454 |
| MP:0002133 | abnormal respiratory system physiology | 0.97665261 | 1.099730469 |
| REACTOME_REGULATION_OF_ | REACTOME_REGULATION_OF_APOPTOSIS | 0.43596474 | 1.099760438 |
| ENSG00000168490 | PHYHIP subnetwork | 0.97660638 | 1.099765607 |
| ENSG00000148396 | SEC16A subnetwork | 0.43604333 | 1.099786142 |
| ENSG00000118690 | ARMC2 subnetwork | 0.97659965 | 1.099851539 |
| GO:0001829 | trophectodermal cell differentiation | 0.97657886 | 1.099914042 |
| ENSG00000107789 | MINPP1 subnetwork | 0.97651325 | 1.09995311 |
| GO:0006888 | ER to Golgi vesicle-mediated transport | 0.97650183 | 1.100027354 |
| ENSG00000105926 | MPP6 subnetwork | 0.97648898 | 1.100105518 |
| ENSG00000213555 | ENSG00000213555 subnetwork | 0.43640405 | 1.100145349 |
| ENSG00000130164 | LDLR subnetwork | 0.97646871 | 1.100168061 |
| KEGG_ARRHYTHMOGENIC_RIG | KEGG_ARRHYTHMOGENIC_RIGHT_VENTRICULAR_CARDION | 0.97644865 | 1.100226704 |
| ENSG00000172500 | FIBP subnetwork | 0.9764177 | 1.100281448 |
| MP:0008025 | brain vacuoles | 0.43638042 | 1.100282196 |
| ENSG00000116544 | DLGAP3 subnetwork | 0.43651675 | 1.100307745 |
| MP:0000350 | abnormal cell proliferation | 0.97641262 | 1.100363565 |
| GO:0050819 | negative regulation of coagulation | 0.97635236 | 1.100379232 |

| | | | |
|---|---|---|---|
| GO:0050768 | negative regulation of neurogenesis | 0.97634744 | 1.10045355 |
| ENSG00000114739 | ACVR2B subnetwork | 0.43664808 | 1.100521368 |
| MP:0006092 | abnormal olfactory neuron morphology | 0.97634222 | 1.10053179 |
| GO:0051597 | response to methylmercury | 0.97626873 | 1.100531832 |
| GO:0021953 | central nervous system neuron differentiation | 0.97624764 | 1.100582714 |
| ENSG00000155329 | ZCCHC10 subnetwork | 0.97617966 | 1.100590582 |
| GO:0033003 | regulation of mast cell activation | 0.97613605 | 1.1006493 |
| MP:0000534 | abnormal ureter morphology | 0.97612648 | 1.100723674 |
| ENSG00000183873 | SCN5A subnetwork | 0.97612228 | 1.100801972 |
| MP:0001516 | abnormal motor coordination/ balance | 0.97610457 | 1.100884194 |
| GO:0022406 | membrane docking | 0.97608394 | 1.100954691 |
| ENSG00000198947 | DMD subnetwork | 0.97600373 | 1.100958679 |
| GO:0001658 | branching involved in ureteric bud morphogenesis | 0.97599756 | 1.10103702 |
| GO:0051898 | negative regulation of protein kinase B signaling cascade | 0.97598473 | 1.101107545 |
| GO:0046513 | ceramide biosynthetic process | 0.97598217 | 1.101181996 |
| ENSG00000127184 | COX7C subnetwork | 0.97591743 | 1.101209488 |
| ENSG00000172466 | ZNF24 subnetwork | 0.97582182 | 1.101287974 |
| ENSG00000127928 | GNGT1 subnetwork | 0.97589954 | 1.101291787 |
| ENSG00000108797 | CNTNAP1 subnetwork | 0.97574934 | 1.101354738 |
| GO:0051443 | positive regulation of ubiquitin-protein ligase activity | 0.97582176 | 1.101374207 |
| GO:0001518 | voltage-gated sodium channel complex | 0.97574602 | 1.10144099 |
| ENSG00000084674 | APOB subnetwork | 0.9755916 | 1.101456881 |
| REACTOME_CYTOSOLIC_SULFC | REACTOME_CYTOSOLIC_SULFONATION_OF_SMALL_MOLE( | 0.97569681 | 1.101480263 |
| GO:0005272 | sodium channel activity | 0.97556846 | 1.101519662 |
| GO:0006641 | triglyceride metabolic process | 0.43752765 | 1.101536623 |
| GO:0090009 | primitive streak formation | 0.97536912 | 1.101543524 |
| REACTOME_RHO_GTPASE_CYC | REACTOME_RHO_GTPASE_CYCLE | 0.43746513 | 1.1015625 |
| MP:0000516 | abnormal renal/urinary system morphology | 0.97544614 | 1.101566907 |
| ENSG00000078900 | TP73 subnetwork | 0.43763385 | 1.101570502 |
| GO:0050780 | dopamine receptor binding | 0.97553267 | 1.101570701 |
| ENSG00000175279 | APITD1 subnetwork | 0.97534578 | 1.101602413 |
| MP:0003459 | increased fear-related response | 0.43773979 | 1.101629971 |
| ENSG00000079459 | FDFT1 subnetwork | 0.4378288 | 1.101672355 |
| MP:0008947 | increased neuron number | 0.97534142 | 1.101688739 |
| GO:0031362 | anchored to external side of plasma membrane | 0.9753204 | 1.101735893 |
| REACTOME_SIGNALING_BY_RI | REACTOME_SIGNALING_BY_RHO_GTPASES | 0.43746513 | 1.10175064 |
| ENSG00000173692 | PSMD1 subnetwork | 0.43732234 | 1.101768324 |
| GO:0060078 | regulation of postsynaptic membrane potential | 0.975245 | 1.10180671 |
| GO:0003206 | cardiac chamber morphogenesis | 0.97531791 | 1.101822243 |
| ENSG00000120149 | MSX2 subnetwork | 0.9752405 | 1.101885239 |
| GO:0006664 | glycolipid metabolic process | 0.97519161 | 1.101908906 |
| ENSG00000137818 | RPLP1 subnetwork | 0.43746422 | 1.101930304 |
| ENSG00000132139 | GAS2L2 subnetwork | 0.43731771 | 1.101956596 |
| GO:0006687 | glycosphingolipid metabolic process | 0.97517337 | 1.101979616 |
| GO:0003401 | axis elongation | 0.97515548 | 1.102054257 |
| GO:0048705 | skeletal system morphogenesis | 0.97509738 | 1.10206226 |
| REACTOME_MEIOTIC_SYNAPSI | REACTOME_MEIOTIC_SYNAPSIS | 0.43841039 | 1.102088305 |
| ENSG00000101003 | GINS1 subnetwork | 0.43727588 | 1.102093659 |
| GO:0060840 | artery development | 0.97506463 | 1.102113394 |
| ENSG00000143761 | ARF1 subnetwork | 0.43816159 | 1.102132378 |
| GO:0042417 | dopamine metabolic process | 0.97506327 | 1.102195906 |
| ENSG00000078061 | ARAF subnetwork | 0.43838221 | 1.102199488 |
| GO:0034332 | adherens junction organization | 0.97504606 | 1.102262745 |

| | | | |
|---|---|---|---|
| ENSG00000147162 | OGT subnetwork | 0.4381544 | 1.10229483 |
| ENSG00000068793 | CYFIP1 subnetwork | 0.97501969 | 1.102325673 |
| ENSG00000171862 | PTEN subnetwork | 0.43834915 | 1.102344816 |
| REACTOME_SYNTHESIS_OF_DI | REACTOME_SYNTHESIS_OF_DNA | 0.4382815 | 1.102353744 |
| ENSG00000163132 | MSX1 subnetwork | 0.97500303 | 1.102392532 |
| MP:0002812 | spherocytosis | 0.97496312 | 1.102447635 |
| ENSG00000092964 | DPYSL2 subnetwork | 0.9749133 | 1.102471364 |
| GO:0051196 | regulation of coenzyme metabolic process | 0.97487335 | 1.102518635 |
| MP:0000273 | overriding aorta | 0.97477659 | 1.10258181 |
| GO:0051193 | regulation of cofactor metabolic process | 0.97487335 | 1.102605148 |
| GO:0050954 | sensory perception of mechanical stimulus | 0.97476788 | 1.102660493 |
| MP:0003148 | decreased cochlear coiling | 0.97475734 | 1.10273134 |
| MP:0001433 | polyphagia | 0.97475441 | 1.102813972 |
| ENSG00000120549 | KIAA1217 subnetwork | 0.97469943 | 1.102837742 |
| GO:0035964 | COPI-coated vesicle budding | 0.97465456 | 1.102881143 |
| GO:0048200 | Golgi transport vesicle coating | 0.97465456 | 1.102967732 |
| GO:0048205 | COPI coating of Golgi vesicle | 0.97465456 | 1.103054334 |
| GO:0044460 | flagellum part | 0.9746112 | 1.103085984 |
| GO:0044442 | microtubule-based flagellum part | 0.9746112 | 1.103172609 |
| GO:0048853 | forebrain morphogenesis | 0.97459876 | 1.10324354 |
| REACTOME_AQUAPORIN:MED | REACTOME_AQUAPORIN:MEDIATED_TRANSPORT | 0.97455322 | 1.103286993 |
| GO:0009395 | phospholipid catabolic process | 0.9745523 | 1.103373655 |
| GO:0016874 | ligase activity | 0.43907616 | 1.103459441 |
| MP:0002082 | postnatal lethality | 0.97455181 | 1.10346033 |
| GO:0046885 | regulation of hormone biosynthetic process | 0.43901545 | 1.103502642 |
| GO:0002016 | regulation of blood volume by renin-angiotensin | 0.97450463 | 1.103511666 |
| GO:0019318 | hexose metabolic process | 0.43927303 | 1.103534923 |
| ENSG00000170558 | CDH2 subnetwork | 0.9744429 | 1.103590791 |
| ENSG00000116711 | PLA2G4A subnetwork | 0.97437543 | 1.103591073 |
| MP:0000572 | abnormal autopod morphology | 0.97450407 | 1.103598366 |
| GO:0030291 | protein serine/threonine kinase inhibitor activity | 0.97436281 | 1.103669941 |
| GO:0006639 | acylglycerol metabolic process | 0.43926826 | 1.103697393 |
| ENSG00000162645 | GBP2 subnetwork | 0.97432676 | 1.103717384 |
| GO:0001967 | suckling behavior | 0.97422354 | 1.103780852 |
| MP:0000231 | hypertension | 0.43976573 | 1.10378659 |
| ENSG00000160867 | FGFR4 subnetwork | 0.97432067 | 1.103800204 |
| MP:0008572 | abnormal Purkinje cell dendrite morphology | 0.97416991 | 1.103828315 |
| ENSG00000088305 | DNMT3B subnetwork | 0.43973274 | 1.103838298 |
| REACTOME_INHIBITION_OF_A | REACTOME_INHIBITION_OF_ADENYLATE_CYCLASE_PATHW | 0.97416865 | 1.103911164 |
| GO:0010042 | response to manganese ion | 0.43993491 | 1.103973116 |
| REACTOME_INTERACTIONS_OI | REACTOME_INTERACTIONS_OF_REV_WITH_HOST_CELLULA | 0.4397134 | 1.103975145 |
| ENSG00000009844 | VTA1 subnetwork | 0.43966288 | 1.103992849 |
| MP:0009254 | disorganized pancreatic islets | 0.97408465 | 1.103994339 |
| REACTOME_ADENYLATE_CYCL | REACTOME_ADENYLATE_CYCLASE_INHIBITORY_PATHWAY | 0.97416865 | 1.103997956 |
| REACTOME_SCF:BETA:TRCP_M | REACTOME_SCF:BETA:TRCP_MEDIATED_DEGRADATION_O | 0.43955594 | 1.104019758 |
| GO:0005546 | phosphatidylinositol-4,5-bisphosphate binding | 0.97404776 | 1.104022175 |
| ENSG00000173366 | ENSG00000173366 subnetwork | 0.97399019 | 1.104053948 |
| GO:0021904 | dorsal/ventral neural tube patterning | 0.97394401 | 1.104073928 |
| ENSG00000164494 | PDSS2 subnetwork | 0.97389995 | 1.10410571 |
| ENSG00000151247 | EIF4E subnetwork | 0.43964103 | 1.104112738 |
| GO:0007210 | serotonin receptor signaling pathway | 0.9738938 | 1.104192559 |
| ENSG00000176732 | PFN4 subnetwork | 0.97384889 | 1.104224355 |
| GO:0030199 | collagen fibril organization | 0.97378961 | 1.104236488 |

| | | | |
|---|---|---|---|
| GO:0061178 | regulation of insulin secretion involved in cellular response | 0.97376924 | 1.104307632 |
| ENSG00000105486 | LIG1 subnetwork | 0.44015016 | 1.104355223 |
| ENSG00000161217 | PCYT1A subnetwork | 0.44034247 | 1.104362245 |
| GO:0035773 | insulin secretion involved in cellular response to glucose sti | 0.97376924 | 1.104394524 |
| MP:0003073 | abnormal metacarpal bone morphology | 0.97374984 | 1.104453887 |
| ENSG00000062038 | CDH3 subnetwork | 0.44030254 | 1.10445654 |
| MP:0001442 | decreased grooming behavior | 0.97367559 | 1.104493586 |
| GO:0090109 | regulation of cell-substrate junction assembly | 0.97364895 | 1.104556902 |
| GO:0051893 | regulation of focal adhesion assembly | 0.97364895 | 1.104643841 |
| ENSG00000009830 | POMT2 subnetwork | 0.44052502 | 1.10465057 |
| MP:0000955 | abnormal spinal cord morphology | 0.97358668 | 1.1046875 |
| ENSG00000187672 | ERC2 subnetwork | 0.97356068 | 1.104750846 |
| GO:0010821 | regulation of mitochondrion organization | 0.44061234 | 1.104768786 |
| ENSG00000138030 | KHK subnetwork | 0.97351553 | 1.104802393 |
| REACTOME_RIBOSOMAL_SCAN | REACTOME_RIBOSOMAL_SCANNING_AND_START_CODON | 0.97350956 | 1.104889379 |
| GO:0016675 | oxidoreductase activity, acting on a heme group of donors | 0.9735092 | 1.104976378 |
| ENSG00000198055 | GRK6 subnetwork | 0.97346723 | 1.105012206 |
| ENSG00000126267 | COX6B1 subnetwork | 0.97341633 | 1.105036226 |
| GO:0048747 | muscle fiber development | 0.97340908 | 1.105123257 |
| GO:0034381 | plasma lipoprotein particle clearance | 0.97339513 | 1.105198488 |
| MP:0001362 | abnormal anxiety-related response | 0.97336606 | 1.105257976 |
| MP:0003419 | delayed endochondral bone ossification | 0.97330736 | 1.105270206 |
| MP:0000531 | right pulmonary isomerism | 0.9730853 | 1.105291151 |
| GO:0070979 | protein K11-linked ubiquitination | 0.97315756 | 1.105302553 |
| GO:0045909 | positive regulation of vasodilation | 0.973262 | 1.105310013 |
| MP:0003271 | abnormal duodenum morphology | 0.97297031 | 1.105362913 |
| GO:0042069 | regulation of catecholamine metabolic process | 0.97308055 | 1.10537431 |
| GO:0051491 | positive regulation of filopodium assembly | 0.44086054 | 1.105388407 |
| MP:0003014 | abnormal kidney medulla morphology | 0.97294327 | 1.105438209 |
| GO:0019783 | small conjugating protein-specific protease activity | 0.44106695 | 1.105470608 |
| GO:0007620 | copulation | 0.97293461 | 1.105513518 |
| ENSG00000108001 | EBF3 subnetwork | 0.44099937 | 1.105582937 |
| ENSG00000115561 | CHMP3 subnetwork | 0.972932 | 1.105596721 |
| GO:0006956 | complement activation | 0.44104497 | 1.105607477 |
| MP:0003243 | abnormal dopaminergic neuron morphology | 0.97290783 | 1.105660229 |
| GO:0030119 | AP-type membrane coat adaptor complex | 0.44123035 | 1.105715984 |
| ENSG00000161835 | GRASP subnetwork | 0.97249049 | 1.105733891 |
| ENSG00000108963 | DPH1 subnetwork | 0.97290769 | 1.105747398 |
| GO:0017085 | response to insecticide | 0.97276998 | 1.105799558 |
| ENSG00000013455 | ENSG00000013455 subnetwork | 0.44134048 | 1.105799932 |
| ENSG00000130203 | APOE subnetwork | 0.97248606 | 1.10581322 |
| MP:0004835 | abnormal miniature endplate potential | 0.97290164 | 1.105830639 |
| GO:0048588 | developmental cell growth | 0.9723859 | 1.105849637 |
| ENSG00000164776 | PHKG1 subnetwork | 0.97274615 | 1.105867045 |
| ENSG00000003436 | TFPI subnetwork | 0.97245885 | 1.105868896 |
| ENSG00000157601 | MX1 subnetwork | 0.9723402 | 1.105881657 |
| GO:0048562 | embryonic organ morphogenesis | 0.97270638 | 1.105899054 |
| GO:0051082 | unfolded protein binding | 0.44147162 | 1.105926303 |
| GO:0060537 | muscle tissue development | 0.97233774 | 1.105961023 |
| GO:0000087 | M phase of mitotic cell cycle | 0.97231835 | 1.106016728 |
| ENSG00000007402 | CACNA2D2 subnetwork | 0.97231414 | 1.106104009 |
| ENSG00000109911 | ELP4 subnetwork | 0.44167435 | 1.106127992 |
| ENSG00000105357 | MYH14 subnetwork | 0.44184696 | 1.106168335 |

| | | | |
|---|---|---|---|
| ENSG00000137462 | TLR2 subnetwork | 0.97227848 | 1.106175519 |
| GO:0006693 | prostaglandin metabolic process | 0.97224735 | 1.106219416 |
| GO:0035809 | regulation of urine volume | 0.9721859 | 1.106231747 |
| ENSG00000123643 | SLC36A1 subnetwork | 0.44181544 | 1.106237271 |
| ENSG00000147889 | CDKN2A subnetwork | 0.44165021 | 1.106273345 |
| ENSG00000012211 | PRICKLE3 subnetwork | 0.97218451 | 1.106319072 |
| ENSG00000169282 | KCNAB1 subnetwork | 0.97217741 | 1.106402463 |
| ENSG00000167460 | TPM4 subnetwork | 0.97213445 | 1.106446392 |
| MP:0002761 | abnormal hippocampal mossy fiber morphology | 0.97212605 | 1.106529807 |
| GO:0042383 | sarcolemma | 0.97179411 | 1.106547666 |
| GO:0015909 | long-chain fatty acid transport | 0.97173813 | 1.106563981 |
| GO:0055001 | muscle cell development | 0.97189697 | 1.106570842 |
| MP:0003934 | abnormal pancreas development | 0.97209139 | 1.106577701 |
| GO:0043666 | regulation of phosphoprotein phosphatase activity | 0.44211932 | 1.106582966 |
| GO:0003073 | regulation of systemic arterial blood pressure | 0.97169951 | 1.106600047 |
| ENSG00000125266 | EFNB2 subnetwork | 0.97204358 | 1.106625602 |
| ENSG00000119041 | GTF3C3 subnetwork | 0.44219496 | 1.106675148 |
| ENSG00000049540 | ELN subnetwork | 0.97169069 | 1.10667957 |
| ENSG00000122877 | EGR2 subnetwork | 0.97168531 | 1.106763056 |
| GO:0001750 | photoreceptor outer segment | 0.9716627 | 1.106830752 |
| ENSG00000039560 | RAI14 subnetwork | 0.44231972 | 1.106843623 |
| MP:0002950 | abnormal neural crest cell migration | 0.97162447 | 1.106866851 |
| GO:0001562 | response to protozoan | 0.97151555 | 1.106919308 |
| GO:0045667 | regulation of osteoblast differentiation | 0.97162192 | 1.10694642 |
| GO:0031532 | actin cytoskeleton reorganization | 0.9714931 | 1.106979134 |
| GO:0051439 | regulation of ubiquitin-protein ligase activity involved in mi | 0.97145478 | 1.107031065 |
| ENSG00000143549 | TPM3 subnetwork | 0.97141263 | 1.107083004 |
| GO:0032412 | regulation of ion transmembrane transporter activity | 0.97141031 | 1.107170527 |
| ENSG00000163875 | MEAF6 subnetwork | 0.97140404 | 1.107246205 |
| REACTOME_PROTEIN_FOLDIN( | REACTOME_PROTEIN_FOLDING | 0.44277519 | 1.107271186 |
| GO:0042348 | NF-kappaB import into nucleus | 0.44260466 | 1.107290607 |
| GO:0045055 | regulated secretory pathway | 0.97138715 | 1.107317941 |
| GO:0033275 | actin-myosin filament sliding | 0.97137849 | 1.107385735 |
| ENSG00000165059 | PRKACG subnetwork | 0.44275051 | 1.107399559 |
| GO:0030049 | muscle filament sliding | 0.97137849 | 1.10747331 |
| GO:0042345 | regulation of NF-kappaB import into nucleus | 0.44260466 | 1.107478379 |
| ENSG00000077782 | FGFR1 subnetwork | 0.9713644 | 1.107537172 |
| GO:0060572 | morphogenesis of an epithelial bud | 0.97134366 | 1.107624773 |
| ENSG00000117601 | SERPINC1 subnetwork | 0.97134095 | 1.107708432 |
| ENSG00000171431 | KRT20 subnetwork | 0.97133142 | 1.10778815 |
| ENSG00000166930 | MS4A5 subnetwork | 0.97130553 | 1.107828323 |
| GO:0014009 | glial cell proliferation | 0.97126825 | 1.107888282 |
| ENSG00000069248 | NUP133 subnetwork | 0.97126608 | 1.107975946 |
| GO:0070252 | actin-mediated cell contraction | 0.97122648 | 1.1080201 |
| ENSG00000066136 | NFYC subnetwork | 0.97120989 | 1.108091959 |
| GO:0050982 | detection of mechanical stimulus | 0.97118411 | 1.108155916 |
| REACTOME_MEMBRANE_TRAI | REACTOME_MEMBRANE_TRAFFICKING | 0.97117542 | 1.10822384 |
| GO:0055117 | regulation of cardiac muscle contraction | 0.97115771 | 1.108275944 |
| ENSG00000116171 | SCP2 subnetwork | 0.44329749 | 1.108286731 |
| GO:0050879 | multicellular organismal movement | 0.44359763 | 1.108298052 |
| GO:0007088 | regulation of mitosis | 0.97110859 | 1.108316181 |
| GO:0046688 | response to copper ion | 0.44384736 | 1.108334744 |
| GO:0051783 | regulation of nuclear division | 0.97110859 | 1.108403927 |

| | | | |
|---|---|---|---|
| ENSG00000146587 | RBAK subnetwork | 0.44380789 | 1.108437712 |
| GO:0034361 | very-low-density lipoprotein particle | 0.97108439 | 1.108467933 |
| ENSG00000141720 | PIP4K2B subnetwork | 0.44422295 | 1.108479878 |
| GO:0050881 | musculoskeletal movement | 0.44359763 | 1.108485772 |
| ENSG00000133104 | SPG20 subnetwork | 0.44345973 | 1.108488648 |
| GO:0034385 | triglyceride-rich lipoprotein particle | 0.97108439 | 1.108555705 |
| ENSG00000156304 | SCAF4 subnetwork | 0.4451159 | 1.108563955 |
| ENSG00000128052 | KDR subnetwork | 0.44380542 | 1.108608431 |
| ENSG00000171858 | RPS21 subnetwork | 0.97107137 | 1.108627653 |
| ENSG00000162290 | ENSG00000162290 subnetwork | 0.44357811 | 1.108648145 |
| ENSG00000185129 | PURA subnetwork | 0.44421708 | 1.108658887 |
| ENSG00000146276 | GABRR1 subnetwork | 0.44377662 | 1.10866915 |
| ENSG00000198478 | SH3BGRL2 subnetwork | 0.9710544 | 1.108695652 |
| ENSG00000128708 | HAT1 subnetwork | 0.44413065 | 1.108704111 |
| GO:0007183 | SMAD protein complex assembly | 0.44510849 | 1.108708861 |
| GO:0001756 | somitogenesis | 0.97102065 | 1.108739902 |
| MP:0000939 | decreased motor neuron number | 0.44526062 | 1.108756538 |
| MP:0002978 | absent otoliths | 0.44420449 | 1.108804127 |
| MP:0005669 | increased circulating leptin level | 0.4450591 | 1.108811614 |
| GO:0010517 | regulation of phospholipase activity | 0.97101963 | 1.108827723 |
| GO:2001251 | negative regulation of chromosome organization | 0.44411519 | 1.108866328 |
| ENSG00000149294 | NCAM1 subnetwork | 0.97097992 | 1.10887199 |
| ENSG00000198301 | SDAD1 subnetwork | 0.44501604 | 1.108872193 |
| GO:0044283 | small molecule biosynthetic process | 0.44443577 | 1.108909552 |
| GO:2000108 | positive regulation of leukocyte apoptotic process | 0.44497847 | 1.108932793 |
| GO:0001725 | stress fiber | 0.44540857 | 1.108949055 |
| ENSG00000005249 | PRKAR2B subnetwork | 0.97097611 | 1.108959835 |
| MP:0002067 | abnormal sensory capabilities/reflexes/nociception | 0.97097373 | 1.109043733 |
| ENSG00000011304 | PTBP1 subnetwork | 0.4449548 | 1.109052525 |
| REACTOME_PROSTACYCLIN_SI | REACTOME_PROSTACYCLIN_SIGNALLING_THROUGH_PROS | 0.97096809 | 1.109115759 |
| ENSG00000104131 | EIF3J subnetwork | 0.97092284 | 1.109148177 |
| MP:0002332 | abnormal exercise endurance | 0.97091508 | 1.109228148 |
| REACTOME_MRNA_SPLICING_ | REACTOME_MRNA_SPLICING_:_MINOR_PATHWAY | 0.44495269 | 1.109239865 |
| ENSG00000188612 | SUMO2 subnetwork | 0.44470838 | 1.109253 |
| GO:0031076 | embryonic camera-type eye development | 0.97091173 | 1.109308131 |
| ENSG00000198898 | CAPZA2 subnetwork | 0.44468823 | 1.10938979 |
| GO:0005501 | retinoid binding | 0.97091041 | 1.10939209 |
| ENSG00000196943 | C14orf21 subnetwork | 0.44492626 | 1.109401926 |
| GO:0060070 | canonical Wnt receptor signaling pathway | 0.97086174 | 1.109420577 |
| GO:0044060 | regulation of endocrine process | 0.97080228 | 1.109429251 |
| GO:0006029 | proteoglycan metabolic process | 0.97075864 | 1.109469637 |
| MP:0001260 | increased body weight | 0.4448957 | 1.109513349 |
| GO:0051351 | positive regulation of ligase activity | 0.97074551 | 1.109545707 |
| ENSG00000157766 | ACAN subnetwork | 0.97068249 | 1.109598002 |
| ENSG00000140105 | WARS subnetwork | 0.9705621 | 1.109674861 |
| MP:0004833 | ovary atrophy | 0.97068216 | 1.109685988 |
| ENSG00000102898 | NUTF2 subnetwork | 0.97055204 | 1.109747006 |
| ENSG00000156970 | BUB1B subnetwork | 0.97048264 | 1.109763642 |
| MP:0001963 | abnormal hearing physiology | 0.97045978 | 1.109819941 |
| MP:0001044 | abnormal enteric nervous system morphology | 0.97036976 | 1.109873066 |
| MP:0002578 | impaired ability to fire action potentials | 0.97044437 | 1.109888149 |
| GO:0045773 | positive regulation of axon extension | 0.97033097 | 1.109921454 |
| ENSG00000110876 | SELPLG subnetwork | 0.97028703 | 1.109965881 |

| | | | |
|---|---|---|---|
| ENSG00000100596 | SPTLC2 subnetwork | 0.44592016 | 1.110016863 |
| ENSG00000075856 | SART3 subnetwork | 0.44585994 | 1.110035419 |
| ENSG00000109332 | UBE2D3 subnetwork | 0.44602688 | 1.110048896 |
| MP:0001529 | abnormal vocalization | 0.97028526 | 1.11005396 |
| GO:0002444 | myeloid leukocyte mediated immunity | 0.97027118 | 1.110130148 |
| ENSG00000175166 | PSMD2 subnetwork | 0.44629754 | 1.110163492 |
| MP:0002080 | prenatal lethality | 0.44621498 | 1.110182063 |
| GO:0072372 | primary cilium | 0.97025719 | 1.110202381 |
| GO:0016765 | transferase activity, transferring alkyl or aryl (other than me | 0.97025233 | 1.110286531 |
| MP:0002884 | abnormal branchial arch morphology | 0.9702014 | 1.110323067 |
| ENSG00000111907 | TPD52L1 subnetwork | 0.97007149 | 1.110380279 |
| GO:0090101 | negative regulation of transmembrane receptor protein ser | 0.97020036 | 1.110403271 |
| ENSG00000087338 | GMCL1 subnetwork | 0.44644663 | 1.110431412 |
| ENSG00000185883 | ATP6V0C subnetwork | 0.97005491 | 1.1104605 |
| MP:0004792 | abnormal synaptic vesicle number | 0.97004595 | 1.110536764 |
| GO:0022898 | regulation of transmembrane transporter activity | 0.97003145 | 1.110609069 |
| MP:0010090 | increased circulating creatine kinase level | 0.96995962 | 1.110629765 |
| ENSG00000135250 | SRPK2 subnetwork | 0.96991468 | 1.110678262 |
| MP:0001921 | reduced fertility | 0.96988885 | 1.11073471 |
| MP:0001765 | abnormal ion homeostasis | 0.96981347 | 1.110739535 |
| GO:0030048 | actin filament-based movement | 0.96980503 | 1.110819828 |
| MP:0003974 | abnormal endocardium morphology | 0.96975731 | 1.110848494 |
| ENSG00000080845 | DLGAP4 subnetwork | 0.44680913 | 1.110865903 |
| REACTOME_FORMATION_OF_I | REACTOME_FORMATION_OF_FIBRIN_CLOT_CLOTTING_CAS | 0.96964252 | 1.110909813 |
| GO:0003085 | negative regulation of systemic arterial blood pressure | 0.969751 | 1.110932782 |
| MP:0002699 | abnormal vitreous body morphology | 0.96949532 | 1.110960102 |
| GO:0048306 | calcium-dependent protein binding | 0.96963157 | 1.110974253 |
| GO:0042278 | purine nucleoside metabolic process | 0.96942883 | 1.110980844 |
| MP:0005272 | abnormal temporal bone morphology | 0.9695853 | 1.110994993 |
| MP:0000150 | abnormal rib morphology | 0.96937357 | 1.111021463 |
| GO:0051881 | regulation of mitochondrial membrane potential | 0.44692791 | 1.111024086 |
| GO:0001541 | ovarian follicle development | 0.44680076 | 1.11104465 |
| MP:0004272 | abnormal basement membrane morphology | 0.96936676 | 1.111097862 |
| GO:0000779 | condensed chromosome, centromeric region | 0.96932786 | 1.111150421 |
| GO:0045844 | positive regulation of striated muscle tissue development | 0.96932325 | 1.111230818 |
| GO:0046519 | sphingoid metabolic process | 0.96920866 | 1.11126839 |
| GO:0048636 | positive regulation of muscle organ development | 0.96932325 | 1.111319179 |
| ENSG00000197818 | SLC9A8 subnetwork | 0.96918745 | 1.111328933 |
| GO:0044089 | positive regulation of cellular component biogenesis | 0.96917391 | 1.111397439 |
| MP:0001935 | decreased litter size | 0.44719932 | 1.111458158 |
| GO:0072175 | epithelial tube formation | 0.96915993 | 1.111465956 |
| ENSG00000111790 | FGFR1OP2 subnetwork | 0.96911467 | 1.111490733 |
| MP:0008547 | abnormal neocortex morphology | 0.96910344 | 1.11155529 |
| GO:0042787 | protein ubiquitination involved in ubiquitin-dependent prot | 0.44727099 | 1.111557239 |
| MP:0005264 | glomerulosclerosis | 0.44717623 | 1.111594813 |
| ENSG00000068781 | STON1-GTF2A1L subnetwork | 0.96907689 | 1.111627814 |
| GO:0032892 | positive regulation of organic acid transport | 0.9690009 | 1.111668523 |
| MP:0002463 | abnormal neutrophil physiology | 0.96900032 | 1.111756983 |
| GO:0030501 | positive regulation of bone mineralization | 0.96899619 | 1.111841477 |
| ENSG00000013441 | CLK1 subnetwork | 0.96896197 | 1.111882212 |
| GO:0090277 | positive regulation of peptide hormone secretion | 0.96892352 | 1.111914995 |
| ENSG00000117245 | KIF17 subnetwork | 0.44756542 | 1.111957253 |
| ENSG00000117408 | IPO13 subnetwork | 0.96888601 | 1.111967683 |

| | | | |
|---|---|---|---|
| GO:0015116 | sulfate transmembrane transporter activity | 0.44753236 | 1.111984514 |
| GO:0070403 | NAD+ binding | 0.44902328 | 1.11203222 |
| GO:0021544 | subpallium development | 0.9688762 | 1.11204426 |
| ENSG00000100749 | VRK1 subnetwork | 0.96882812 | 1.112081045 |
| ENSG00000163806 | SPDYA subnetwork | 0.44912283 | 1.112114094 |
| ENSG00000100038 | TOP3B subnetwork | 0.44897928 | 1.112126553 |
| MP:0001096 | abnormal glossopharyngeal ganglion morphology | 0.96881613 | 1.112165605 |
| GO:0060438 | trachea development | 0.44894395 | 1.112212523 |
| ENSG00000105373 | GLTSCR2 subnetwork | 0.96879271 | 1.112242217 |
| REACTOME_FANCONI_ANEMI/ | REACTOME_FANCONI_ANEMIA_PATHWAY | 0.44890143 | 1.112315312 |
| MP:0000745 | tremors | 0.96877353 | 1.112322822 |
| GO:0004867 | serine-type endopeptidase inhibitor activity | 0.44841925 | 1.112369748 |
| GO:0048486 | parasympathetic nervous system development | 0.9687571 | 1.112395477 |
| GO:0032799 | low-density lipoprotein receptor particle metabolic process | 0.44804888 | 1.112396972 |
| MP:0000926 | absent floor plate | 0.4483702 | 1.112397042 |
| ENSG00000169018 | FEM1B subnetwork | 0.44812883 | 1.112403296 |
| GO:0048285 | organelle fission | 0.96869385 | 1.112428321 |
| MP:0003651 | abnormal axon outgrowth | 0.44928436 | 1.112455964 |
| ENSG00000189308 | LIN54 subnetwork | 0.44826328 | 1.112468471 |
| GO:0010631 | epithelial cell migration | 0.44888449 | 1.112468514 |
| ENSG00000161542 | PRPSAP1 subnetwork | 0.44791356 | 1.112476864 |
| ENSG00000132692 | BCAN subnetwork | 0.4498551 | 1.112487437 |
| GO:0001841 | neural tube formation | 0.96868028 | 1.112489048 |
| GO:0051437 | positive regulation of ubiquitin-protein ligase activity involv | 0.9685599 | 1.112514937 |
| ENSG00000111859 | NEDD9 subnetwork | 0.4486364 | 1.112525202 |
| GO:0030131 | clathrin adaptor complex | 0.44802011 | 1.112525236 |
| ENSG00000164611 | PTTG1 subnetwork | 0.96865239 | 1.112529871 |
| GO:0005811 | lipid particle | 0.44935052 | 1.112537739 |
| MP:0003572 | abnormal uterus development | 0.44834876 | 1.112550437 |
| ENSG00000063176 | SPHK2 subnetwork | 0.9685386 | 1.112571702 |
| REACTOME_TRAF3:DEPENDEN | REACTOME_TRAF3:DEPENDENT_IRF_ACTIVATION_PATHW/ | 0.44876691 | 1.112632286 |
| MP:0005599 | increased cardiac muscle contractility | 0.96853076 | 1.112648395 |
| GO:0090132 | epithelium migration | 0.44888449 | 1.112655358 |
| ENSG00000151348 | EXT2 subnetwork | 0.44984417 | 1.112665438 |
| GO:0006378 | mRNA polyadenylation | 0.44962411 | 1.112690696 |
| ENSG00000034713 | GABARAPL2 subnetwork | 0.44863018 | 1.112703747 |
| GO:0001502 | cartilage condensation | 0.96852886 | 1.112737052 |
| MP:0009304 | increased retroperitoneal fat pad weight | 0.9684849 | 1.112781895 |
| ENSG00000092199 | HNRNPC subnetwork | 0.4495539 | 1.112785044 |
| ENSG00000113456 | RAD1 subnetwork | 0.44983749 | 1.112818365 |
| GO:0031966 | mitochondrial membrane | 0.45046201 | 1.112832525 |
| ENSG00000135821 | GLUL subnetwork | 0.96844308 | 1.112850653 |
| ENSG00000165119 | HNRNPK subnetwork | 0.45038245 | 1.112868139 |
| ENSG00000136986 | DERL1 subnetwork | 0.44952357 | 1.112896193 |
| MP:0002065 | abnormal fear/anxiety-related behavior | 0.9684289 | 1.112927393 |
| ENSG00000141867 | BRD4 subnetwork | 0.45028599 | 1.112964513 |
| GO:0007219 | Notch signaling pathway | 0.45036144 | 1.112970711 |
| GO:0006488 | dolichol-linked oligosaccharide biosynthetic process | 0.4501232 | 1.1129794 |
| GO:0070536 | protein K63-linked deubiquitination | 0.44982937 | 1.112996481 |
| MP:0006382 | abnormal lung epithelium morphology | 0.96842734 | 1.11300813 |
| ENSG00000175203 | DCTN2 subnetwork | 0.9682659 | 1.113086981 |
| ENSG00000125775 | SDCBP2 subnetwork | 0.96841976 | 1.113092866 |
| ENSG00000167549 | CORO6 subnetwork | 0.45027754 | 1.113142474 |

| | | | |
|---|---|---|---|
| GO:0060512 | prostate gland morphogenesis | 0.45021004 | 1.11316142 |
| GO:0042307 | positive regulation of protein import into nucleus | 0.96824852 | 1.113167756 |
| KEGG_PROXIMAL_TUBULE_BIC | KEGG_PROXIMAL_TUBULE_BICARBONATE_RECLAMATION | 0.96841846 | 1.113181601 |
| ENSG00000180340 | FZD2 subnetwork | 0.44982545 | 1.113183037 |
| GO:0014706 | striated muscle tissue development | 0.96824136 | 1.113244558 |
| GO:0004180 | carboxypeptidase activity | 0.96819629 | 1.113277512 |
| ENSG00000138834 | MAPK8IP3 subnetwork | 0.4506924 | 1.113282034 |
| KEGG_GLYCOSAMINOGLYCAN_ | KEGG_GLYCOSAMINOGLYCAN_BIOSYNTHESIS_HEPARAN_S | 0.96819414 | 1.11336231 |
| ENSG00000066468 | FGFR2 subnetwork | 0.96817573 | 1.113435157 |
| GO:0048679 | regulation of axon regeneration | 0.96816761 | 1.113504028 |
| GO:0070570 | regulation of neuron projection regeneration | 0.96816761 | 1.113592853 |
| ENSG00000136044 | APPL2 subnetwork | 0.96815989 | 1.113677702 |
| REACTOME_N:GLYCAN_ANTEN | REACTOME_N:GLYCAN_ANTENNAE_ELONGATION_IN_THE_ | 0.45092477 | 1.113681218 |
| ENSG00000068028 | RASSF1 subnetwork | 0.96805373 | 1.113739727 |
| GO:0018345 | protein palmitoylation | 0.96815373 | 1.113762566 |
| ENSG00000117152 | RGS4 subnetwork | 0.96804853 | 1.113828599 |
| GO:0003018 | vascular process in circulatory system | 0.96802384 | 1.113873593 |
| GO:0007519 | skeletal muscle tissue development | 0.96800348 | 1.113950519 |
| GO:0006801 | superoxide metabolic process | 0.45115517 | 1.113977596 |
| ENSG00000212664 | ENSG00000212664 subnetwork | 0.96798239 | 1.114023466 |
| MP:0006304 | abnormal seminiferous epithelium morphology | 0.96795879 | 1.114088442 |
| GO:0050654 | chondroitin sulfate proteoglycan metabolic process | 0.96790976 | 1.114133472 |
| ENSG00000105085 | MED26 subnetwork | 0.45115288 | 1.114155518 |
| ENSG00000138363 | ATIC subnetwork | 0.45137375 | 1.114209295 |
| REACTOME_FORMATION_OF_ | REACTOME_FORMATION_OF_THE_TERNARY_COMPLEX_AI | 0.96787766 | 1.114210442 |
| ENSG00000131462 | TUBG1 subnetwork | 0.96781519 | 1.114235529 |
| ENSG00000173914 | RBM4B subnetwork | 0.96780262 | 1.11431252 |
| REACTOME_FATTY_ACYL:COA_ | REACTOME_FATTY_ACYL:COA_BIOSYNTHESIS | 0.45159338 | 1.114346591 |
| GO:0032420 | stereocilium | 0.45148624 | 1.114365703 |
| MP:0002543 | brachyphalangia | 0.96769422 | 1.114366715 |
| ENSG00000176903 | PNMA1 subnetwork | 0.96777305 | 1.11436956 |
| MP:0001724 | abnormal extraembryonic endoderm formation | 0.9676426 | 1.114403802 |
| GO:0030658 | transport vesicle membrane | 0.4519182 | 1.114403808 |
| ENSG00000165702 | GFI1B subnetwork | 0.45178716 | 1.114433679 |
| GO:0051260 | protein homooligomerization | 0.45186213 | 1.114447971 |
| ENSG00000206282 | RGL2 subnetwork | 0.96678088 | 1.114456435 |
| GO:0009409 | response to cold | 0.96762111 | 1.11446885 |
| GO:0018958 | phenol-containing compound metabolic process | 0.96709353 | 1.114496923 |
| GO:0072132 | mesenchyme morphogenesis | 0.96756085 | 1.114509945 |
| MP:0001183 | overexpanded pulmonary alveoli | 0.96704354 | 1.114538043 |
| ENSG00000206210 | ENSG00000206210 subnetwork | 0.96678088 | 1.114545527 |
| ENSG00000083642 | PDS5B subnetwork | 0.9672482 | 1.114583666 |
| ENSG00000189285 | ENSG00000189285 subnetwork | 0.96740216 | 1.114585331 |
| REACTOME_SYNTHESIS_AND_I | REACTOME_SYNTHESIS_AND_INTERCONVERSION_OF_NUC | 0.96754355 | 1.114586995 |
| REACTOME_ACTIVATION_OF_ | REACTOME_ACTIVATION_OF_THE_MRNA_UPON_BINDING | 0.96731854 | 1.114590491 |
| GO:0007507 | heart development | 0.96701101 | 1.114599153 |
| MP:0004068 | dilated dorsal aorta | 0.96675042 | 1.114610649 |
| MP:0001622 | abnormal vasculogenesis | 0.45177158 | 1.114611529 |
| GO:0051146 | striated muscle cell differentiation | 0.96750367 | 1.114636095 |
| MP:0008221 | abnormal hippocampal commissure morphology | 0.96671095 | 1.114659791 |
| GO:0060081 | membrane hyperpolarization | 0.96670913 | 1.114748921 |
| GO:0021879 | forebrain neuron differentiation | 0.96670099 | 1.114830068 |
| GO:0032401 | establishment of melanosome localization | 0.96666045 | 1.114863244 |

| | | | |
|---|---|---|---|
| GO:0000280 | nuclear division | 0.96663911 | 1.114912421 |
| GO:0007067 | mitosis | 0.96663911 | 1.1150016 |
| ENSG00000162552 | WNT4 subnetwork | 0.96663386 | 1.115082793 |
| MP:0006144 | increased systemic arterial systolic blood pressure | 0.96640084 | 1.115159638 |
| GO:0060606 | tube closure | 0.96663016 | 1.115172 |
| GO:0003143 | embryonic heart tube morphogenesis | 0.96647421 | 1.115178429 |
| GO:0045103 | intermediate filament-based process | 0.96659007 | 1.115225218 |
| GO:0001843 | neural tube closure | 0.96638201 | 1.115236876 |
| ENSG00000153140 | CETN3 subnetwork | 0.96589012 | 1.115240192 |
| ENSG00000164162 | ANAPC10 subnetwork | 0.96622872 | 1.115255323 |
| ENSG00000163637 | PRICKLE2 subnetwork | 0.96587323 | 1.115305469 |
| GO:0044253 | positive regulation of multicellular organismal metabolic pr | 0.96636868 | 1.115322129 |
| GO:0034284 | response to monosaccharide stimulus | 0.96622428 | 1.115332586 |
| GO:0031513 | nonmotile primary cilium | 0.96615066 | 1.115373839 |
| GO:0010827 | regulation of glucose transport | 0.96586423 | 1.115390775 |
| ENSG00000065054 | SLC9A3R2 subnetwork | 0.96613983 | 1.115463133 |
| GO:0045616 | regulation of keratinocyte differentiation | 0.96585238 | 1.115468087 |
| ENSG00000138092 | CENPO subnetwork | 0.96580363 | 1.11550937 |
| ENSG00000067900 | ROCK1 subnetwork | 0.45251409 | 1.115539977 |
| GO:0034661 | ncRNA catabolic process | 0.96574106 | 1.115550661 |
| GO:0019840 | isoprenoid binding | 0.96566669 | 1.115563922 |
| GO:0016830 | carbon-carbon lyase activity | 0.45247852 | 1.115567613 |
| ENSG00000125835 | SNRPB subnetwork | 0.45260387 | 1.115570761 |
| GO:0060348 | bone development | 0.96558886 | 1.115577185 |
| ENSG00000185130 | HIST1H2BL subnetwork | 0.45270901 | 1.115626564 |
| MP:0000953 | abnormal oligodendrocyte morphology | 0.96557587 | 1.115654543 |
| ENSG00000154839 | SKA1 subnetwork | 0.96552385 | 1.115691852 |
| MP:0006355 | abnormal sixth branchial arch artery morphology | 0.45246817 | 1.115728836 |
| GO:0046785 | microtubule polymerization | 0.96533722 | 1.115735695 |
| GO:0071705 | nitrogen compound transport | 0.96549373 | 1.115765224 |
| ENSG00000115507 | OTX1 subnetwork | 0.96533052 | 1.115817103 |
| ENSG00000168135 | KCNJ4 subnetwork | 0.96549093 | 1.115850629 |
| MP:0000857 | abnormal cerebellar foliation | 0.9653013 | 1.115882494 |
| GO:0007567 | parturition | 0.96528674 | 1.115971944 |
| GO:0035255 | ionotropic glutamate receptor binding | 0.9652276 | 1.115977233 |
| ENSG00000206557 | TRIM71 subnetwork | 0.45293262 | 1.116007674 |
| GO:2001022 | positive regulation of response to DNA damage stimulus | 0.96521164 | 1.116054678 |
| MP:0008809 | increased spleen iron level | 0.45303661 | 1.116113428 |
| ENSG00000001630 | CYP51A1 subnetwork | 0.45333608 | 1.116136023 |
| REACTOME_ASSEMBLY_OF_HI | REACTOME_ASSEMBLY_OF_HIV_VIRION | 0.96521062 | 1.116144163 |
| GO:0042552 | myelination | 0.96520948 | 1.116233662 |
| GO:0006691 | leukotriene metabolic process | 0.45331078 | 1.116272091 |
| MP:0011085 | complete postnatal lethality | 0.96520158 | 1.116307137 |
| ENSG00000002822 | MAD1L1 subnetwork | 0.96518326 | 1.116380624 |
| GO:0043449 | cellular alkene metabolic process | 0.45331078 | 1.116458229 |
| MP:0004740 | sensorineural hearing loss | 0.45322977 | 1.116460974 |
| MP:0009142 | decreased prepulse inhibition | 0.96518043 | 1.116470164 |
| GO:0030203 | glycosaminoglycan metabolic process | 0.9651519 | 1.116519612 |
| ENSG00000128731 | HERC2 subnetwork | 0.96511534 | 1.116557035 |
| MP:0002127 | abnormal cardiovascular system morphology | 0.96506708 | 1.116598476 |
| GO:0031032 | actomyosin structure organization | 0.9650503 | 1.116651958 |
| GO:0007632 | visual behavior | 0.96502655 | 1.116717484 |
| GO:0004620 | phospholipase activity | 0.96500768 | 1.11678302 |

| | | | |
|---|---|---|---|
| MP:0005619 | increased urine potassium level | 0.45372808 | 1.116808333 |
| MP:0009293 | decreased inguinal fat pad weight | 0.96499247 | 1.116864618 |
| MP:0004936 | impaired branching involved in ureteric bud morphogenesis | 0.96498026 | 1.116930177 |
| GO:0002275 | myeloid cell activation involved in immune response | 0.96451514 | 1.116931663 |
| MP:0001073 | abnormal glossopharyngeal nerve morphology | 0.96478908 | 1.116954323 |
| MP:0005146 | decreased circulating VLDL cholesterol level | 0.96448596 | 1.116985223 |
| GO:0070371 | ERK1 and ERK2 cascade | 0.96497697 | 1.117003772 |
| ENSG00000138396 | ENSG00000138396 subnetwork | 0.96475416 | 1.11701991 |
| ENSG00000136002 | ARHGEF4 subnetwork | 0.9643881 | 1.117032129 |
| MP:0004484 | altered response of heart to induced stress | 0.96446959 | 1.117050839 |
| GO:0033500 | carbohydrate homeostasis | 0.453991 | 1.117052649 |
| ENSG00000132612 | VPS4A subnetwork | 0.964976 | 1.117093434 |
| GO:0002446 | neutrophil mediated immunity | 0.96474893 | 1.117101566 |
| REACTOME_PHASE_II_CONJUG | REACTOME_PHASE_II_CONJUGATION | 0.96438166 | 1.117117841 |
| ENSG00000130222 | GADD45G subnetwork | 0.96472234 | 1.117167175 |
| ENSG00000131069 | ACSS2 subnetwork | 0.96435827 | 1.117183483 |
| GO:0043586 | tongue development | 0.96430112 | 1.117221017 |
| GO:0042593 | glucose homeostasis | 0.453991 | 1.117238794 |
| ENSG00000108010 | GLRX3 subnetwork | 0.45416132 | 1.117258038 |
| REACTOME_GLUTAMATE_NEU | REACTOME_GLUTAMATE_NEUROTRANSMITTER_RELEASE_ | 0.96429871 | 1.117302748 |
| MP:0001364 | decreased anxiety-related response | 0.96423535 | 1.117320209 |
| MP:0000427 | abnormal hair cycle | 0.45447134 | 1.117357642 |
| GO:0007585 | respiratory gaseous exchange | 0.96423435 | 1.117409997 |
| GO:0032272 | negative regulation of protein polymerization | 0.45460999 | 1.117437989 |
| GO:0032467 | positive regulation of cytokinesis | 0.96420664 | 1.117483726 |
| MP:0008329 | decreased somatotroph cell number | 0.45446673 | 1.117535387 |
| GO:0032963 | collagen metabolic process | 0.96407331 | 1.117542802 |
| ENSG00000100985 | MMP9 subnetwork | 0.45471371 | 1.117551598 |
| ENSG00000074201 | CLNS1A subnetwork | 0.45477346 | 1.117556998 |
| MP:0001429 | dehydration | 0.96419116 | 1.117573541 |
| MP:0002925 | abnormal cardiovascular development | 0.96407106 | 1.117628617 |
| GO:0071825 | protein-lipid complex subunit organization | 0.96397781 | 1.117642093 |
| ENSG00000173567 | GPR113 subnetwork | 0.45496433 | 1.117675927 |
| ENSG00000163909 | HEYL subnetwork | 0.45445738 | 1.117696536 |
| GO:0071827 | plasma lipoprotein particle organization | 0.96397781 | 1.11773195 |
| MP:0000937 | abnormal motor neuron morphology | 0.96395784 | 1.117777599 |
| GO:0008395 | steroid hydroxylase activity | 0.45494628 | 1.117787022 |
| MP:0004154 | renal tubular necrosis | 0.96384965 | 1.11783273 |
| ENSG00000100325 | ASCC2 subnetwork | 0.96370466 | 1.117859728 |
| GO:0000146 | microfilament motor activity | 0.96395311 | 1.117867482 |
| MP:0003140 | dilated heart atrium | 0.96366588 | 1.117897362 |
| GO:0010518 | positive regulation of phospholipase activity | 0.96382573 | 1.117902525 |
| ENSG00000196628 | TCF4 subnetwork | 0.96353286 | 1.117924377 |
| GO:0006282 | regulation of DNA repair | 0.96362473 | 1.117930979 |
| GO:0006909 | phagocytosis | 0.96346659 | 1.117937887 |
| KEGG_SNARE_INTERACTIONS_ | KEGG_SNARE_INTERACTIONS_IN_VESICULAR_TRANSPORT | 0.96343686 | 1.118003701 |
| MP:0001784 | abnormal fluid regulation | 0.96342084 | 1.118065503 |
| ENSG00000104388 | RAB2A subnetwork | 0.96340459 | 1.118127314 |
| GO:0090092 | regulation of transmembrane receptor protein serine/threo | 0.96340223 | 1.118217304 |
| GO:0055006 | cardiac cell development | 0.96334834 | 1.118238892 |
| ENSG00000170017 | ALCAM subnetwork | 0.45603356 | 1.11829653 |
| MP:0004355 | short radius | 0.96326655 | 1.118302206 |
| GO:0055013 | cardiac muscle cell development | 0.96334834 | 1.118328906 |

| | | | |
|---|---|---|---|
| REACTOME_TRANSLATION_INI | REACTOME_TRANSLATION_INITIATION_COMPLEX_FORMA | 0.9632175 | 1.118351985 |
| REACTOME_PI:3K_CASCADE | REACTOME_PI:3K_CASCADE | 0.45599885 | 1.118399203 |
| GO:0009435 | NAD biosynthetic process | 0.96320796 | 1.118442029 |
| GO:0019843 | rRNA binding | 0.45554709 | 1.11847049 |
| GO:0046328 | regulation of JNK cascade | 0.45671126 | 1.118509615 |
| KEGG_GLUTATHIONE_METABO | KEGG_GLUTATHIONE_METABOLISM | 0.96319059 | 1.118511957 |
| ENSG00000184886 | PIGW subnetwork | 0.45599851 | 1.118584953 |
| REACTOME_GLUCAGON_SIGN/ | REACTOME_GLUCAGON_SIGNALING_IN_METABOLIC_REGU | 0.96318614 | 1.118598003 |
| GO:0021695 | cerebellar cortex development | 0.45566501 | 1.11860871 |
| GO:0070304 | positive regulation of stress-activated protein kinase signali | 0.45539693 | 1.118612774 |
| REACTOME_ACTIVATION_OF_I | REACTOME_ACTIVATION_OF_DNA_FRAGMENTATION_FAC | 0.4558073 | 1.118627451 |
| ENSG00000144895 | EIF2A subnetwork | 0.45552619 | 1.118631526 |
| ENSG00000204227 | RING1 subnetwork | 0.45670604 | 1.118653623 |
| GO:0031672 | A band | 0.9631659 | 1.118655875 |
| MP:0006090 | abnormal utricle morphology | 0.9630635 | 1.118715264 |
| KEGG_GLYCOSPHINGOLIPID_BI | KEGG_GLYCOSPHINGOLIPID_BIOSYNTHESIS_GLOBO_SERIES | 0.96313872 | 1.118721811 |
| GO:0048020 | CCR chemokine receptor binding | 0.4559792 | 1.118729236 |
| ENSG00000100911 | PSME2 subnetwork | 0.45549942 | 1.118775985 |
| ENSG00000124171 | PARD6B subnetwork | 0.96305737 | 1.118801353 |
| REACTOME_APOPTOSIS_INDU | REACTOME_APOPTOSIS_INDUCED_DNA_FRAGMENTATION | 0.4558073 | 1.118813362 |
| ENSG00000206287 | RING1 subnetwork | 0.45670604 | 1.118839138 |
| REACTOME_SYNTHESIS_SECRE | REACTOME_SYNTHESIS_SECRETION_AND_INACTIVATION_( | 0.96300481 | 1.118843148 |
| GO:0008037 | cell recognition | 0.96296009 | 1.11886078 |
| ENSG00000147869 | CER1 subnetwork | 0.45693475 | 1.118904359 |
| GO:0032970 | regulation of actin filament-based process | 0.45597832 | 1.118915102 |
| GO:0016337 | cell-cell adhesion | 0.96294697 | 1.118934816 |
| GO:0015851 | nucleobase transport | 0.96293378 | 1.118996777 |
| ENSG00000206215 | ENSG00000206215 subnetwork | 0.45670604 | 1.119024714 |
| GO:0051241 | negative regulation of multicellular organismal process | 0.4563813 | 1.119048805 |
| GO:0010660 | regulation of muscle cell apoptotic process | 0.96290812 | 1.119062777 |
| ENSG00000080802 | CNOT4 subnetwork | 0.45666664 | 1.119102522 |
| ENSG00000120057 | SFRP5 subnetwork | 0.96287437 | 1.119116699 |
| ENSG00000106483 | SFRP4 subnetwork | 0.96287437 | 1.119206899 |
| ENSG00000077454 | LRCH4 subnetwork | 0.45664687 | 1.119213539 |
| ENSG00000104332 | SFRP1 subnetwork | 0.96287437 | 1.119297114 |
| ENSG00000117758 | STX12 subnetwork | 0.45655424 | 1.1193361 |
| KEGG_CALCIUM_SIGNALING_P | KEGG_CALCIUM_SIGNALING_PATHWAY | 0.96284962 | 1.119355099 |
| MP:0000036 | absent semicircular canals | 0.96277875 | 1.119368752 |
| ENSG00000205307 | SAP25 subnetwork | 0.45664687 | 1.11939927 |
| ENSG00000135604 | STX11 subnetwork | 0.96273886 | 1.119426752 |
| GO:0071845 | cellular component disassembly at cellular level | 0.45747289 | 1.119496439 |
| REACTOME_G:PROTEIN_BETA( | REACTOME_G:PROTEIN_BETAGAMMA_SIGNALLING | 0.96272398 | 1.119500887 |
| ENSG00000126067 | PSMB2 subnetwork | 0.45725664 | 1.119572423 |
| ENSG00000178035 | IMPDH2 subnetwork | 0.4574438 | 1.119582505 |
| REACTOME_SEROTONIN_RECE | REACTOME_SEROTONIN_RECEPTORS | 0.96272001 | 1.119591162 |
| GO:0071299 | cellular response to vitamin A | 0.96270031 | 1.119673387 |
| MP:0003892 | abnormal gastric gland morphology | 0.45906091 | 1.119757266 |
| GO:0071300 | cellular response to retinoic acid | 0.96270031 | 1.119763691 |
| GO:0006505 | GPI anchor metabolic process | 0.45743812 | 1.11976802 |
| MP:0003157 | impaired muscle relaxation | 0.45915625 | 1.119778768 |
| KEGG_VALINE_LEUCINE_AND_ | KEGG_VALINE_LEUCINE_AND_ISOLEUCINE_BIOSYNTHESIS | 0.4586825 | 1.119826446 |
| GO:0048639 | positive regulation of developmental growth | 0.96268871 | 1.119849976 |
| GO:0021527 | spinal cord association neuron differentiation | 0.96268592 | 1.119936275 |

| | | | |
|---|---|---|---|
| MP:0002192 | hydrops fetalis | 0.45904875 | 1.119942197 |
| ENSG00000137575 | SDCBP subnetwork | 0.96255755 | 1.119975797 |
| ENSG00000104722 | NEFM subnetwork | 0.96265162 | 1.119990319 |
| ENSG00000020633 | RUNX3 subnetwork | 0.45776247 | 1.119998344 |
| ENSG00000080839 | RBL1 subnetwork | 0.45867252 | 1.120003306 |
| GO:0030133 | transport vesicle | 0.45860986 | 1.120039683 |
| ENSG00000155959 | VBP1 subnetwork | 0.45890299 | 1.120051223 |
| ENSG00000157227 | MMP14 subnetwork | 0.45939597 | 1.120052814 |
| MP:0003998 | decreased thermal nociceptive threshold | 0.96254187 | 1.120058093 |
| ENSG00000066777 | ARFGEF1 subnetwork | 0.45935157 | 1.120072631 |
| MP:0002908 | delayed wound healing | 0.45884689 | 1.120087589 |
| GO:0004869 | cysteine-type endopeptidase inhibitor activity | 0.45904273 | 1.120102412 |
| GO:0015020 | glucuronosyltransferase activity | 0.96250685 | 1.120104091 |
| ENSG00000000419 | DPM1 subnetwork | 0.45899905 | 1.120147035 |
| GO:0070888 | E-box binding | 0.96248309 | 1.120150097 |
| GO:0032321 | positive regulation of Rho GTPase activity | 0.45962161 | 1.12017486 |
| ENSG00000091106 | NLRC4 subnetwork | 0.96238006 | 1.120181598 |
| REACTOME_SWITCHING_OF_C | REACTOME_SWITCHING_OF_ORIGINS_TO_A_POST:REPLIC/ | 0.45859851 | 1.120200099 |
| GO:0001678 | cellular glucose homeostasis | 0.96247718 | 1.120236462 |
| ENSG00000005007 | UPF1 subnetwork | 0.45956096 | 1.120252434 |
| MP:0001693 | failure of primitive streak formation | 0.96237502 | 1.12026798 |
| ENSG00000125870 | SNRPB2 subnetwork | 0.45844973 | 1.120281224 |
| ENSG00000138442 | WDR12 subnetwork | 0.4595221 | 1.120305281 |
| GO:0000777 | condensed chromosome kinetochore | 0.96236803 | 1.120350339 |
| GO:0032432 | actin filament bundle | 0.45841652 | 1.120350761 |
| REACTOME_ORC1_REMOVAL_ | REACTOME_ORC1_REMOVAL_FROM_CHROMATIN | 0.45859851 | 1.120385379 |
| ENSG00000137843 | PAK6 subnetwork | 0.45978979 | 1.120410688 |
| GO:0032291 | axon ensheathment in central nervous system | 0.96234744 | 1.120416566 |
| GO:0046890 | regulation of lipid biosynthetic process | 0.45840004 | 1.120494787 |
| GO:0022010 | central nervous system myelination | 0.96234744 | 1.120507024 |
| GO:0019897 | extrinsic to plasma membrane | 0.96227608 | 1.120516754 |
| REACTOME_UNWINDING_OF_ | REACTOME_UNWINDING_OF_DNA | 0.45808913 | 1.12054148 |
| ENSG00000104969 | SGTA subnetwork | 0.96223358 | 1.12056686 |
| MP:0004157 | interrupted aortic arch | 0.96211612 | 1.120650945 |
| ENSG00000164056 | SPRY1 subnetwork | 0.9622253 | 1.120653315 |
| GO:0046677 | response to antibiotic | 0.45836921 | 1.120663688 |
| GO:0008366 | axon ensheathment | 0.96209517 | 1.120709151 |
| ENSG00000161533 | ACOX1 subnetwork | 0.45833436 | 1.120774706 |
| GO:0007272 | ensheathment of neurons | 0.96209517 | 1.120799677 |
| GO:0005231 | excitatory extracellular ligand-gated ion channel activity | 0.96207761 | 1.120874061 |
| GO:0030258 | lipid modification | 0.45830129 | 1.120885762 |
| GO:0043601 | nuclear replisome | 0.46102406 | 1.120947836 |
| GO:0051963 | regulation of synapse assembly | 0.96206832 | 1.120952496 |
| GO:0030132 | clathrin coat of coated pit | 0.96164927 | 1.120973087 |
| GO:0006221 | pyrimidine nucleotide biosynthetic process | 0.96192775 | 1.120984163 |
| MP:0003237 | abnormal lens epithelium morphology | 0.96203573 | 1.121014785 |
| GO:0060442 | branching involved in prostate gland morphogenesis | 0.96162009 | 1.121043485 |
| ENSG00000114450 | GNB4 subnetwork | 0.961791 | 1.121048166 |
| ENSG00000174442 | ZWILCH subnetwork | 0.96190775 | 1.121066667 |
| ENSG00000177951 | BET1L subnetwork | 0.96094467 | 1.121100955 |
| REACTOME_PERK_REGULATED | REACTOME_PERK_REGULATED_GENE_EXPRESSION | 0.96160256 | 1.121109854 |
| GO:0030894 | replisome | 0.46102406 | 1.121132324 |
| GO:0072506 | trivalent inorganic anion homeostasis | 0.96146676 | 1.121133479 |

| | | | |
|---|---|---|---|
| MP:0005403 | abnormal nerve conduction | 0.96156808 | 1.121135812 |
| REACTOME_FGFR2C_LIGAND_I | REACTOME_FGFR2C_LIGAND_BINDING_AND_ACTIVATION | 0.96119447 | 1.121172665 |
| GO:0030166 | proteoglycan biosynthetic process | 0.96133756 | 1.121173284 |
| GO:0045778 | positive regulation of ossification | 0.96093353 | 1.121179516 |
| GO:0006376 | mRNA splice site selection | 0.96073416 | 1.121200842 |
| ENSG00000186871 | ERCC6L subnetwork | 0.96109325 | 1.121212489 |
| GO:0055062 | phosphate ion homeostasis | 0.96146676 | 1.121224127 |
| ENSG00000110107 | PRPF19 subnetwork | 0.46092586 | 1.121229832 |
| MP:0000474 | abnormal foregut morphology | 0.46070387 | 1.121240323 |
| ENSG00000168807 | SNTB2 subnetwork | 0.96118097 | 1.121251213 |
| GO:0015269 | calcium-activated potassium channel activity | 0.96086177 | 1.121255765 |
| ENSG00000136810 | TXN subnetwork | 0.96133451 | 1.121255863 |
| ENSG00000122679 | RAMP3 subnetwork | 0.96090979 | 1.121258091 |
| GO:0051294 | establishment of spindle orientation | 0.96050131 | 1.121272462 |
| GO:0015914 | phospholipid transport | 0.96064116 | 1.121273066 |
| KEGG_OLFACTORY_TRANSDUC | KEGG_OLFACTORY_TRANSDUCTION | 0.96072523 | 1.121279437 |
| MP:0002016 | ovary cysts | 0.46101942 | 1.121283951 |
| MP:0004814 | reduced linear vestibular evoked potential | 0.46087278 | 1.12129096 |
| MP:0001513 | limb grasping | 0.96061401 | 1.121327398 |
| GO:0000786 | nucleosome | 0.46024385 | 1.121355541 |
| GO:0000132 | establishment of mitotic spindle orientation | 0.96050131 | 1.121363232 |
| GO:0060674 | placenta blood vessel development | 0.96044213 | 1.121369009 |
| MP:0002163 | abnormal gland morphology | 0.46030812 | 1.121401484 |
| GO:0030282 | bone mineralization | 0.96040463 | 1.121419318 |
| GO:0030307 | positive regulation of cell growth | 0.46070369 | 1.121425041 |
| GO:0034660 | ncRNA metabolic process | 0.46131156 | 1.121446199 |
| GO:0071577 | zinc ion transmembrane transport | 0.46086815 | 1.121475626 |
| MP:0009172 | small pancreatic islets | 0.96039541 | 1.121497976 |
| ENSG00000196072 | BLOC1S2 subnetwork | 0.46067529 | 1.121560389 |
| ENSG00000120088 | CRHR1 subnetwork | 0.96038612 | 1.121576646 |
| GO:0060538 | skeletal muscle organ development | 0.96037847 | 1.121663427 |
| ENSG00000149182 | ARFGAP2 subnetwork | 0.46056162 | 1.121674633 |
| MP:0004252 | abnormal direction of heart looping | 0.46064382 | 1.121687541 |
| GO:0007517 | muscle organ development | 0.96034944 | 1.121717826 |
| GO:0010181 | FMN binding | 0.46050757 | 1.121727662 |
| REACTOME_NCAM1_INTERACT | REACTOME_NCAM1_INTERACTIONS | 0.96033877 | 1.121792483 |
| GO:0048813 | dendrite morphogenesis | 0.96028553 | 1.12182665 |
| GO:0033198 | response to ATP | 0.9602267 | 1.12184057 |
| ENSG00000155438 | MKI67IP subnetwork | 0.46159099 | 1.121883224 |
| ENSG00000114745 | GORASP1 subnetwork | 0.96010846 | 1.121884622 |
| GO:0008021 | synaptic vesicle | 0.96004149 | 1.121914756 |
| KEGG_PORPHYRIN_AND_CHLO | KEGG_PORPHYRIN_AND_CHLOROPHYLL_METABOLISM | 0.96020691 | 1.121923357 |
| ENSG00000120251 | GRIA2 subnetwork | 0.95987311 | 1.121930464 |
| ENSG00000102901 | CENPT subnetwork | 0.9598345 | 1.121964662 |
| GO:0030850 | prostate gland development | 0.46155337 | 1.121969074 |
| GO:0035148 | tube formation | 0.95976942 | 1.121970495 |
| MP:0005533 | increased body temperature | 0.9600402 | 1.122005673 |
| ENSG00000173230 | GOLGB1 subnetwork | 0.95972433 | 1.122029021 |
| GO:0055102 | lipase inhibitor activity | 0.95970092 | 1.122091609 |
| MP:0002825 | abnormal notochord morphology | 0.95960992 | 1.122097454 |
| ENSG00000166046 | TCP11L2 subnetwork | 0.4618639 | 1.122114436 |
| GO:0045111 | intermediate filament cytoskeleton | 0.95960959 | 1.122188438 |
| ENSG00000134313 | KIDINS220 subnetwork | 0.95958978 | 1.122259163 |

| | | | |
|---|---|---|---|
| ENSG00000151725 | MLF1IP subnetwork | 0.95954346 | 1.122277188 |
| GO:0008483 | transaminase activity | 0.46185863 | 1.122282519 |
| GO:0021782 | glial cell development | 0.95951525 | 1.122315491 |
| MP:0011087 | complete neonatal lethality | 0.9593381 | 1.122327223 |
| GO:0060675 | ureteric bud morphogenesis | 0.95921532 | 1.122387636 |
| ENSG00000134363 | FST subnetwork | 0.9595035 | 1.122402466 |
| ENSG00000171723 | GPHN subnetwork | 0.95933249 | 1.122418269 |
| ENSG00000089159 | PXN subnetwork | 0.46205704 | 1.122423146 |
| MP:0004028 | chromosome breakage | 0.46221187 | 1.122440427 |
| KEGG_MISMATCH_REPAIR | KEGG_MISMATCH_REPAIR | 0.46229058 | 1.122444956 |
| ENSG00000196226 | HIST1H2BB subnetwork | 0.46215294 | 1.122468771 |
| GO:0000097 | sulfur amino acid biosynthetic process | 0.95921312 | 1.122474645 |
| MP:0003078 | aphakia | 0.95920838 | 1.122565725 |
| MP:0005278 | abnormal cholesterol homeostasis | 0.95920604 | 1.122656821 |
| GO:0019083 | viral transcription | 0.46431614 | 1.122696776 |
| GO:0030228 | lipoprotein particle receptor activity | 0.95903799 | 1.122706981 |
| ENSG00000136152 | COG3 subnetwork | 0.46438311 | 1.122742147 |
| GO:0051057 | positive regulation of small GTPase mediated signal transdu | 0.95920499 | 1.122747931 |
| ENSG00000101189 | C20orf20 subnetwork | 0.95901432 | 1.122773764 |
| GO:0071941 | nitrogen cycle metabolic process | 0.95919128 | 1.122818765 |
| GO:0015939 | pantothenate metabolic process | 0.95898753 | 1.122840559 |
| MP:0004148 | increased compact bone thickness | 0.46275901 | 1.122873563 |
| GO:0019080 | viral genome expression | 0.46431614 | 1.122880524 |
| MP:0001126 | abnormal ovary morphology | 0.46257139 | 1.122881078 |
| MP:0001415 | increased exploration in new environment | 0.95890293 | 1.122909224 |
| ENSG00000131828 | PDHA1 subnetwork | 0.9589723 | 1.122923602 |
| GO:0033043 | regulation of organelle organization | 0.4640001 | 1.122923833 |
| ENSG00000104637 | ENSG00000104637 subnetwork | 0.4642724 | 1.122933377 |
| MP:0001326 | retinal degeneration | 0.9588402 | 1.122947625 |
| GO:0048663 | neuron fate commitment | 0.95876535 | 1.122949488 |
| KEGG_AMINO_SUGAR_AND_N | KEGG_AMINO_SUGAR_AND_NUCLEOTIDE_SUGAR_METAB | 0.46252092 | 1.12295055 |
| GO:0007286 | spermatid development | 0.95875097 | 1.123004142 |
| ENSG00000186908 | ZDHHC17 subnetwork | 0.9586872 | 1.123026316 |
| ENSG00000138443 | ABI2 subnetwork | 0.46275007 | 1.123049762 |
| MP:0004221 | abnormal iridocorneal angle | 0.46419741 | 1.123063697 |
| ENSG00000143499 | SMYD2 subnetwork | 0.46397501 | 1.123075033 |
| MP:0001560 | abnormal circulating insulin level | 0.4642696 | 1.123100851 |
| GO:0072224 | metanephric glomerulus development | 0.9586699 | 1.123109414 |
| ENSG00000132703 | APCS subnetwork | 0.46316729 | 1.123190547 |
| ENSG00000013375 | PGM3 subnetwork | 0.95866028 | 1.123196588 |
| ENSG00000101161 | PRPF6 subnetwork | 0.463371 | 1.123215751 |
| ENSG00000075426 | FOSL2 subnetwork | 0.46327313 | 1.12321956 |
| GO:0009651 | response to salt stress | 0.46396436 | 1.123242668 |
| ENSG00000100994 | PYGB subnetwork | 0.4641955 | 1.123247625 |
| MP:0008148 | abnormal rib-sternum attachment | 0.95865454 | 1.123287838 |
| GO:0051962 | positive regulation of nervous system development | 0.95856953 | 1.123301917 |
| ENSG00000138768 | USO1 subnetwork | 0.4630782 | 1.123313085 |
| ENSG00000163918 | RFC4 subnetwork | 0.46315663 | 1.123317466 |
| GO:0016813 | hydrolase activity, acting on carbon-nitrogen (but not pepti | 0.46465274 | 1.123319156 |
| REACTOME_REV:MEDIATED_N | REACTOME_REV:MEDIATED_NUCLEAR_EXPORT_OF_HIV:1_ | 0.46394776 | 1.123344805 |
| GO:0006349 | regulation of gene expression by genetic imprinting | 0.46367381 | 1.123368317 |
| GO:0040020 | regulation of meiosis | 0.46361962 | 1.12337215 |
| MP:0003141 | cardiac fibrosis | 0.4637645 | 1.123380882 |

| | | | |
|---|---|---|---|
| GO:0051965 | positive regulation of synapse assembly | 0.95856953 | 1.123393191 |
| GO:0010950 | positive regulation of endopeptidase activity | 0.46354442 | 1.123416995 |
| ENSG00000136160 | EDNRB subnetwork | 0.46391749 | 1.123446976 |
| ENSG00000105281 | SLC1A5 subnetwork | 0.46387289 | 1.123467213 |
| GO:0030947 | regulation of vascular endothelial growth factor receptor si | 0.95855031 | 1.123476353 |
| ENSG00000189367 | KIAA0408 subnetwork | 0.46491062 | 1.123499591 |
| GO:0000977 | RNA polymerase II regulatory region sequence-specific DNA | 0.46480026 | 1.123503435 |
| GO:0050872 | white fat cell differentiation | 0.95851983 | 1.123539212 |
| ENSG00000170876 | TMEM43 subnetwork | 0.9585152 | 1.123630527 |
| ENSG00000167244 | IGF2 subnetwork | 0.9584808 | 1.12368528 |
| GO:0015980 | energy derivation by oxidation of organic compounds | 0.95847331 | 1.123768493 |
| GO:0048806 | genitalia development | 0.95833983 | 1.123784553 |
| ENSG00000196839 | ADA subnetwork | 0.95846826 | 1.123855784 |
| ENSG00000171533 | MAP6 subnetwork | 0.95833725 | 1.123875925 |
| REACTOME_DESTABILIZATION_ | REACTOME_DESTABILIZATION_OF_MRNA_BY_KSRP | 0.95774141 | 1.123919941 |
| MP:0003896 | prolonged PR interval | 0.95831851 | 1.123938852 |
| GO:0044003 | modification by symbiont of host morphology or physiology | 0.95796715 | 1.123942574 |
| ENSG00000184845 | DRD1 subnetwork | 0.95768882 | 1.123946298 |
| MP:0003161 | absent lateral semicircular canal | 0.9575665 | 1.123962402 |
| ENSG00000138778 | CENPE subnetwork | 0.95784625 | 1.12396274 |
| GO:0042136 | neurotransmitter biosynthetic process | 0.95814729 | 1.123967144 |
| GO:0030308 | negative regulation of cell growth | 0.95826649 | 1.123969261 |
| GO:0006022 | aminoglycan metabolic process | 0.95808587 | 1.12397316 |
| ENSG00000167863 | ATP5H subnetwork | 0.95794547 | 1.124001464 |
| MP:0000297 | abnormal atrioventricular cushion morphology | 0.9576737 | 1.124025551 |
| ENSG00000101365 | IDH3B subnetwork | 0.95755853 | 1.124053878 |
| GO:0010975 | regulation of neuron projection development | 0.95754566 | 1.124137229 |
| GO:0045177 | apical part of cell | 0.95754178 | 1.124228734 |
| GO:0021522 | spinal cord motor neuron differentiation | 0.95754136 | 1.124320254 |
| ENSG00000105329 | TGFB1 subnetwork | 0.46626175 | 1.124322781 |
| ENSG00000137561 | TTPA subnetwork | 0.46617112 | 1.124343072 |
| ENSG00000198899 | MT-ATP6 subnetwork | 0.46593931 | 1.12439582 |
| REACTOME_PLC_BETA_MEDIA | REACTOME_PLC_BETA_MEDIATED_EVENTS | 0.46610737 | 1.124404179 |
| GO:0043044 | ATP-dependent chromatin remodeling | 0.46587974 | 1.12440797 |
| GO:0015844 | monoamine transport | 0.95753518 | 1.124411789 |
| GO:0072088 | nephron epithelium morphogenesis | 0.95748877 | 1.124466699 |
| ENSG00000122786 | CALD1 subnetwork | 0.95740537 | 1.124468691 |
| GO:0019199 | transmembrane receptor protein kinase activity | 0.46606166 | 1.124473469 |
| MP:0004261 | abnormal embryonic neuroepithelium morphology | 0.46908964 | 1.124505191 |
| ENSG00000120875 | DUSP4 subnetwork | 0.95736652 | 1.124539902 |
| ENSG00000108094 | CUL2 subnetwork | 0.4669309 | 1.124551679 |
| GO:0034470 | ncRNA processing | 0.46586029 | 1.124567135 |
| ENSG00000110721 | CHKA subnetwork | 0.46687578 | 1.124612751 |
| ENSG00000206489 | PPP1R10 subnetwork | 0.47208339 | 1.124621212 |
| ENSG00000093217 | XYLB subnetwork | 0.9573614 | 1.124623341 |
| GO:0004521 | endoribonuclease activity | 0.46682025 | 1.124641226 |
| ENSG00000102900 | NUP93 subnetwork | 0.46907196 | 1.124663313 |
| MP:0000005 | increased brown adipose tissue amount | 0.46672083 | 1.124669711 |
| ENSG00000164815 | ORC5 subnetwork | 0.95735408 | 1.124706793 |
| GO:0008047 | enzyme activator activity | 0.46578946 | 1.124722222 |
| ENSG00000118785 | SPP1 subnetwork | 0.46584743 | 1.124726352 |
| GO:0006278 | RNA-dependent DNA replication | 0.46542863 | 1.124746566 |
| ENSG00000023191 | RNH1 subnetwork | 0.9573173 | 1.124765822 |

| | | | |
|---|---|---|---|
| ENSG00000204569 | PPP1R10 subnetwork | 0.47208339 | 1.124802515 |
| GO:0031023 | microtubule organizing center organization | 0.46554907 | 1.124807912 |
| ENSG00000163468 | CCT3 subnetwork | 0.46671221 | 1.124812398 |
| ENSG00000196331 | HIST1H2BO subnetwork | 0.46906406 | 1.124821487 |
| GO:0002548 | monocyte chemotaxis | 0.95730177 | 1.124849299 |
| GO:0043496 | regulation of protein homodimerization activity | 0.46577812 | 1.124881517 |
| MP:0005587 | abnormal Meckel's cartilage morphology | 0.95728359 | 1.124916497 |
| ENSG00000125743 | SNRPD2 subnetwork | 0.46956951 | 1.124963527 |
| MP:0004787 | abnormal dorsal aorta morphology | 0.46669201 | 1.124979605 |
| ENSG00000206407 | ENSG00000206407 subnetwork | 0.47208339 | 1.124983876 |
| GO:0009225 | nucleotide-sugar metabolic process | 0.46573982 | 1.124991827 |
| GO:0010921 | regulation of phosphatase activity | 0.46905607 | 1.124995942 |
| MP:0002582 | disorganized extraembryonic tissue | 0.95727716 | 1.125 |
| MP:0011088 | partial neonatal lethality | 0.95724347 | 1.125042777 |
| GO:0060968 | regulation of gene silencing | 0.46953467 | 1.125072957 |
| ENSG00000197429 | IPP subnetwork | 0.95720273 | 1.125101858 |
| ENSG00000033122 | LRRC7 subnetwork | 0.46745336 | 1.125138482 |
| ENSG00000140829 | DHX38 subnetwork | 0.47206362 | 1.125149169 |
| ENSG00000101966 | XIAP subnetwork | 0.46904571 | 1.125154221 |
| ENSG00000000938 | FGR subnetwork | 0.46721811 | 1.125158924 |
| GO:0001727 | lipid kinase activity | 0.47246455 | 1.125177248 |
| ENSG00000173349 | SFT2D3 subnetwork | 0.95720001 | 1.125193546 |
| ENSG00000115128 | ENSG00000115128 subnetwork | 0.46739247 | 1.125207756 |
| ENSG00000117748 | RPA2 subnetwork | 0.4695167 | 1.125214853 |
| ENSG00000188488 | SERPINA5 subnetwork | 0.95712534 | 1.125220049 |
| ENSG00000112559 | MDFI subnetwork | 0.47394722 | 1.125220884 |
| ENSG00000070808 | CAMK2A subnetwork | 0.95690602 | 1.12523235 |
| MP:0002132 | abnormal respiratory system morphology | 0.46733702 | 1.125252608 |
| GO:0061025 | membrane fusion | 0.95707207 | 1.125258782 |
| ENSG00000104529 | EEF1D subnetwork | 0.46948083 | 1.125259488 |
| MP:0001258 | decreased body length | 0.95696546 | 1.1252629 |
| ENSG00000134070 | IRAK2 subnetwork | 0.46899805 | 1.12527196 |
| GO:0030880 | RNA polymerase complex | 0.46894552 | 1.125284183 |
| ENSG00000100284 | TOM1 subnetwork | 0.95681041 | 1.125285388 |
| REACTOME_P38MAPK_EVENTS | REACTOME_P38MAPK_EVENTS | 0.47389367 | 1.125297237 |
| ENSG00000136982 | DSCC1 subnetwork | 0.47204511 | 1.125306452 |
| GO:0018198 | peptidyl-cysteine modification | 0.9568971 | 1.125307786 |
| GO:0060038 | cardiac muscle cell proliferation | 0.95702674 | 1.1253179 |
| GO:0090130 | tissue migration | 0.47244223 | 1.12532635 |
| GO:0001159 | core promoter proximal region DNA binding | 0.95676631 | 1.125328223 |
| REACTOME_PPARA_ACTIVATES | REACTOME_PPARA_ACTIVATES_GENE_EXPRESSION | 0.47199316 | 1.125342797 |
| GO:0038024 | cargo receptor activity | 0.46831798 | 1.125361847 |
| GO:0033044 | regulation of chromosome organization | 0.46981523 | 1.125364668 |
| ENSG00000134086 | VHL subnetwork | 0.4676124 | 1.125386871 |
| ENSG00000131242 | RAB11FIP4 subnetwork | 0.95675834 | 1.125419997 |
| GO:0071453 | cellular response to oxygen levels | 0.46947419 | 1.125433901 |
| ENSG00000141738 | GRB7 subnetwork | 0.47388678 | 1.125437892 |
| GO:0042641 | actomyosin | 0.47383212 | 1.125466088 |
| ENSG00000136286 | MYO1G subnetwork | 0.46894097 | 1.125466948 |
| ENSG00000113575 | PPP2CA subnetwork | 0.47265851 | 1.125471242 |
| ENSG00000148943 | LIN7C subnetwork | 0.95672822 | 1.125479162 |
| ENSG00000078674 | PCM1 subnetwork | 0.4718954 | 1.125480071 |
| GO:0032393 | MHC class I receptor activity | 0.4729135 | 1.125483092 |

| | | | |
|---|---|---|---|
| GO:0051865 | protein autoubiquitination | 0.47198331 | 1.125492094 |
| ENSG00000167306 | MYO5B subnetwork | 0.47315805 | 1.12549493 |
| GO:0016624 | oxidoreductase activity, acting on the aldehyde or oxo grou | 0.46867135 | 1.125507882 |
| MP:0009358 | environmentally induced seizures | 0.95644385 | 1.125516032 |
| ENSG00000118194 | TNNT2 subnetwork | 0.46830868 | 1.125520494 |
| MP:0005039 | hypoxia | 0.47276709 | 1.125523518 |
| ENSG00000196353 | CPNE4 subnetwork | 0.47364626 | 1.125526612 |
| ENSG00000149968 | MMP3 subnetwork | 0.47286767 | 1.12552746 |
| ENSG00000089199 | CHGB subnetwork | 0.46890324 | 1.125544185 |
| GO:0015807 | L-amino acid transport | 0.95669941 | 1.125546493 |
| ENSG00000203852 | HIST2H3A subnetwork | 0.46882793 | 1.125548335 |
| ENSG00000116350 | SRSF4 subnetwork | 0.47184032 | 1.125548741 |
| REACTOME_VITAMIN_B5_PAN | REACTOME_VITAMIN_B5_PANTOTHENATE_METABOLISM | 0.95662064 | 1.125560812 |
| ENSG00000124074 | C16orf48 subnetwork | 0.47328917 | 1.125579337 |
| ENSG00000164032 | H2AFZ subnetwork | 0.47379474 | 1.125590741 |
| ENSG00000181817 | LSM10 subnetwork | 0.95642889 | 1.125591547 |
| ENSG00000106992 | AK1 subnetwork | 0.47305156 | 1.125591692 |
| GO:0035196 | production of miRNAs involved in gene silencing by miRNA | 0.9565722 | 1.125599608 |
| ENSG00000118705 | RPN2 subnetwork | 0.47360265 | 1.12561917 |
| GO:0097006 | regulation of plasma lipoprotein particle levels | 0.95636857 | 1.125626275 |
| ENSG00000165672 | PRDX3 subnetwork | 0.46828301 | 1.125630389 |
| ENSG00000167965 | MLST8 subnetwork | 0.46865971 | 1.125642068 |
| GO:0006368 | transcription elongation from RNA polymerase II promoter | 0.46880483 | 1.125658109 |
| ENSG00000131982 | ENSG00000131982 subnetwork | 0.47314884 | 1.125668062 |
| ENSG00000186895 | FGF3 subnetwork | 0.95630792 | 1.125669169 |
| MP:0001704 | abnormal dorsal-ventral axis patterning | 0.47375731 | 1.12568328 |
| ENSG00000122180 | MYOG subnetwork | 0.46861114 | 1.125695009 |
| ENSG00000074054 | CLASP1 subnetwork | 0.4685182 | 1.125707317 |
| MP:0000753 | paralysis | 0.95581325 | 1.125720585 |
| ENSG00000113569 | NUP155 subnetwork | 0.4718393 | 1.125722357 |
| ENSG00000023287 | RB1CC1 subnetwork | 0.46812958 | 1.125732422 |
| ENSG00000145912 | NHP2 subnetwork | 0.473589 | 1.125743928 |
| GO:0042573 | retinoic acid metabolic process | 0.95629938 | 1.125752877 |
| MP:0006054 | spinal hemorrhage | 0.46807403 | 1.125752889 |
| GO:0008286 | insulin receptor signaling pathway | 0.95593283 | 1.12576339 |
| ENSG00000049759 | NEDD4L subnetwork | 0.46819601 | 1.125777055 |
| ENSG00000118898 | PPL subnetwork | 0.46786081 | 1.125781759 |
| GO:0051493 | regulation of cytoskeleton organization | 0.47350697 | 1.125788288 |
| MP:0004615 | cervical vertebral transformation | 0.46827732 | 1.125797267 |
| GO:0048641 | regulation of skeletal muscle tissue development | 0.9558058 | 1.125804344 |
| ENSG00000109501 | WFS1 subnetwork | 0.95574451 | 1.125810535 |
| ENSG00000128266 | GNAZ subnetwork | 0.95605615 | 1.125814352 |
| MP:0005226 | abnormal vertebral arch development | 0.95628263 | 1.125824355 |
| GO:0005072 | transforming growth factor beta receptor, cytoplasmic mec | 0.4734472 | 1.125824618 |
| GO:0023019 | signal transduction involved in regulation of gene expressio | 0.95623481 | 1.125842788 |
| GO:0005942 | phosphatidylinositol 3-kinase complex | 0.47181183 | 1.125847594 |
| GO:0006900 | membrane budding | 0.95574034 | 1.125898399 |
| GO:0043516 | regulation of DNA damage response, signal transduction by | 0.9562266 | 1.125922449 |
| MP:0003036 | vertebral transformation | 0.46806603 | 1.125928036 |
| ENSG00000173867 | ENSG00000173867 subnetwork | 0.47430379 | 1.12595567 |
| ENSG00000135404 | CD63 subnetwork | 0.46799285 | 1.125964827 |
| GO:0050839 | cell adhesion molecule binding | 0.95572139 | 1.125982194 |
| REACTOME_REGULATION_OF_ | REACTOME_REGULATION_OF_AMPK_ACTIVITY_VIA_LKB1 | 0.47178717 | 1.12598902 |

| | | | |
|---|---|---|---|
| ENSG00000188191 | PRKAR1B subnetwork | 0.47172915 | 1.125993217 |
| GO:0015149 | hexose transmembrane transporter activity | 0.47169207 | 1.126037797 |
| GO:0005859 | muscle myosin complex | 0.95571768 | 1.126070087 |
| REACTOME_SEMAPHORIN_INT | REACTOME_SEMAPHORIN_INTERACTIONS | 0.47063344 | 1.126125324 |
| GO:0006656 | phosphatidylcholine biosynthetic process | 0.47041187 | 1.126129921 |
| GO:0006672 | ceramide metabolic process | 0.95570449 | 1.126149824 |
| GO:0031267 | small GTPase binding | 0.47168961 | 1.126203554 |
| ENSG00000121058 | COIL subnetwork | 0.47445366 | 1.126208447 |
| ENSG00000131475 | VPS25 subnetwork | 0.95570371 | 1.12624183 |
| GO:0001944 | vasculature development | 0.95555991 | 1.126258376 |
| GO:0043467 | regulation of generation of precursor metabolites and ener | 0.47097599 | 1.126262136 |
| GO:0050850 | positive regulation of calcium-mediated signaling | 0.47039354 | 1.126279974 |
| GO:0004860 | protein kinase inhibitor activity | 0.47061484 | 1.126283401 |
| MP:0004773 | abnormal bile composition | 0.47085241 | 1.126294917 |
| ENSG00000143398 | PIP5K1A subnetwork | 0.47080689 | 1.126323458 |
| ENSG00000180210 | F2 subnetwork | 0.95569071 | 1.12632568 |
| GO:0031674 | I band | 0.95553913 | 1.126325897 |
| REACTOME_LIPID_DIGESTION_ | REACTOME_LIPID_DIGESTION_MOBILIZATION_AND_TRANS | 0.47106893 | 1.126354959 |
| ENSG00000065150 | IPO5 subnetwork | 0.47167806 | 1.126369365 |
| MP:0002893 | ketoaciduria | 0.47033483 | 1.126381462 |
| GO:0019212 | phosphatase inhibitor activity | 0.95549411 | 1.126385257 |
| GO:0034695 | response to prostaglandin E stimulus | 0.47094992 | 1.126395857 |
| MP:0001719 | absent vitelline blood vessels | 0.47059619 | 1.126425332 |
| MP:0005171 | absent coat pigmentation | 0.95548671 | 1.126477319 |
| ENSG00000152455 | SUV39H2 subnetwork | 0.47166228 | 1.126510989 |
| MP:0008006 | increased stomach pH | 0.47123258 | 1.126528632 |
| ENSG00000129255 | MPDU1 subnetwork | 0.47472085 | 1.126537165 |
| ENSG00000100083 | GGA1 subnetwork | 0.47467088 | 1.126549454 |
| GO:0014002 | astrocyte development | 0.95547032 | 1.12656531 |
| GO:0021680 | cerebellar Purkinje cell layer development | 0.47163289 | 1.126620333 |
| GO:0035326 | enhancer binding | 0.47158709 | 1.126624636 |
| MP:0001780 | decreased brown adipose tissue amount | 0.47137373 | 1.126629468 |
| MP:0001570 | abnormal circulating enzyme level | 0.4714412 | 1.126641332 |
| GO:0030517 | negative regulation of axon extension | 0.9554534 | 1.126649227 |
| MP:0010379 | decreased respiratory quotient | 0.47486499 | 1.126693419 |
| ENSG00000136270 | TBRG4 subnetwork | 0.95544799 | 1.126737247 |
| MP:0002135 | abnormal kidney morphology | 0.95539643 | 1.126772136 |
| ENSG00000164086 | DUSP7 subnetwork | 0.4715807 | 1.126798707 |
| GO:0090192 | regulation of glomerulus development | 0.95538302 | 1.126843827 |
| GO:0043218 | compact myelin | 0.95534076 | 1.126903263 |
| MP:0003729 | abnormal photoreceptor outer segment morphology | 0.95510919 | 1.126926223 |
| GO:0051923 | sulfation | 0.95531734 | 1.126970886 |
| GO:0005791 | rough endoplasmic reticulum | 0.95510318 | 1.127006135 |
| GO:0004993 | serotonin receptor activity | 0.95530345 | 1.127050789 |
| MP:0003698 | abnormal male reproductive system physiology | 0.95506273 | 1.127053338 |
| MP:0000623 | decreased salivation | 0.95502372 | 1.12711282 |
| REACTOME_G_BETAGAMMA_S | REACTOME_G_BETAGAMMA_SIGNALLING_THROUGH_PI3K | 0.95498266 | 1.127160039 |
| ENSG00000105088 | OLFM2 subnetwork | 0.95497758 | 1.127252271 |
| GO:0051899 | membrane depolarization | 0.95492241 | 1.127287234 |
| GO:0009746 | response to hexose stimulus | 0.95490377 | 1.127346755 |
| ENSG00000175137 | SH3BP5L subnetwork | 0.95471222 | 1.12740668 |
| ENSG00000130560 | UBAC1 subnetwork | 0.95488768 | 1.12743084 |
| ENSG00000067842 | ATP2B3 subnetwork | 0.95469063 | 1.12747851 |

| | | | |
|---|---|---|---|
| GO:0032331 | negative regulation of chondrocyte differentiation | 0.95487612 | 1.127510846 |
| GO:0005681 | spliceosomal complex | 0.47532469 | 1.127519255 |
| GO:0045598 | regulation of fat cell differentiation | 0.95460126 | 1.127552608 |
| ENSG00000071655 | MBD3 subnetwork | 0.47526792 | 1.12755577 |
| GO:0001669 | acrosomal vesicle | 0.95468501 | 1.127566727 |
| GO:0032365 | intracellular lipid transport | 0.95455681 | 1.12760809 |
| ENSG00000159346 | ADIPOR1 subnetwork | 0.4756813 | 1.127621873 |
| ENSG00000063761 | ADCK1 subnetwork | 0.47561905 | 1.127698476 |
| ENSG00000099937 | SERPIND1 subnetwork | 0.95455563 | 1.127700434 |
| GO:0016925 | protein sumoylation | 0.95433993 | 1.127756389 |
| GO:0010559 | regulation of glycoprotein biosynthetic process | 0.47656207 | 1.127757324 |
| ENSG00000077943 | ITGA8 subnetwork | 0.47720498 | 1.12776623 |
| ENSG00000215021 | PHB2 subnetwork | 0.47580062 | 1.127769761 |
| GO:0070328 | triglyceride homeostasis | 0.95454628 | 1.127772318 |
| MP:0009549 | decreased platelet aggregation | 0.95444655 | 1.127782783 |
| GO:0010574 | regulation of vascular endothelial growth factor production | 0.47558835 | 1.127791145 |
| GO:0005782 | peroxisomal matrix | 0.47599142 | 1.127816958 |
| MP:0001405 | impaired coordination | 0.95432031 | 1.127824199 |
| ENSG00000100612 | DHRS7 subnetwork | 0.47670348 | 1.127864917 |
| ENSG00000105204 | DYRK1B subnetwork | 0.47653489 | 1.127873839 |
| REACTOME_N:GLYCAN_ANTEN | REACTOME_N:GLYCAN_ANTENNAE_ELONGATION | 0.4760965 | 1.127892628 |
| GO:0050908 | detection of light stimulus involved in visual perception | 0.95429704 | 1.127896117 |
| ENSG00000143476 | DTL subnetwork | 0.47679912 | 1.127900464 |
| KEGG_INOSITOL_PHOSPHATE_ | KEGG_INOSITOL_PHOSPHATE_METABOLISM | 0.47719208 | 1.127938589 |
| ENSG00000079435 | LIPE subnetwork | 0.47698598 | 1.12793953 |
| ENSG00000100650 | SRSF5 subnetwork | 0.47709145 | 1.127959053 |
| ENSG00000178363 | CALML3 subnetwork | 0.47647597 | 1.127966373 |
| GO:0030126 | COPI vesicle coat | 0.47641454 | 1.127970852 |
| GO:0010573 | vascular endothelial growth factor production | 0.47558835 | 1.127972084 |
| GO:0050962 | detection of light stimulus involved in sensory perception | 0.95429704 | 1.127988529 |
| GO:0031907 | microbody lumen | 0.47599142 | 1.127997756 |
| MP:0000269 | abnormal heart looping | 0.47637576 | 1.128031395 |
| GO:0004806 | triglyceride lipase activity | 0.47695539 | 1.128032 |
| MP:0003720 | abnormal neural tube closure | 0.4761916 | 1.128032367 |
| ENSG00000164168 | TMEM184C subnetwork | 0.95428806 | 1.128080957 |
| ENSG00000128881 | TTBK2 subnetwork | 0.4763269 | 1.128107978 |
| ENSG00000077522 | ACTN2 subnetwork | 0.95426935 | 1.128165205 |
| ENSG00000133101 | CCNA1 subnetwork | 0.47774368 | 1.128199393 |
| GO:0090257 | regulation of muscle system process | 0.9542511 | 1.128233077 |
| ENSG00000132780 | NASP subnetwork | 0.47789721 | 1.128262258 |
| ENSG00000213044 | ENSG00000213044 subnetwork | 0.9542141 | 1.128296861 |
| MP:0008225 | abnormal anterior commissure morphology | 0.47755974 | 1.128300831 |
| ENSG00000176986 | SEC24C subnetwork | 0.47771493 | 1.128315756 |
| MP:0002237 | abnormal nasal cavity morphology | 0.95420068 | 1.128372951 |
| ENSG00000008018 | PSMB1 subnetwork | 0.47752652 | 1.128385292 |
| MP:0003331 | hepatocellular carcinoma | 0.47801209 | 1.1283855 |
| ENSG00000131773 | KHDRBS3 subnetwork | 0.95415 | 1.128412165 |
| ENSG00000142507 | PSMB6 subnetwork | 0.4778865 | 1.128442492 |
| ENSG00000197249 | SERPINA1 subnetwork | 0.95406934 | 1.128447286 |
| ENSG00000008869 | HEATR5B subnetwork | 0.47769218 | 1.128456129 |
| GO:0016805 | dipeptidase activity | 0.95401569 | 1.128474215 |
| GO:0006661 | phosphatidylinositol biosynthetic process | 0.47811657 | 1.128476768 |
| ENSG00000166887 | VPS39 subnetwork | 0.95391972 | 1.128488849 |

| | | | |
|---|---|---|---|
| REACTOME_TRANSLATION | REACTOME_TRANSLATION | 0.95386966 | 1.128507585 |
| REACTOME_SPRY_REGULATIOI | REACTOME_SPRY_REGULATION_OF_FGF_SIGNALING | 0.95385655 | 1.12858783 |
| MP:0000010 | abnormal abdominal fat pad morphology | 0.47824221 | 1.128623883 |
| GO:0048678 | response to axon injury | 0.95383918 | 1.128672189 |
| MP:0002650 | abnormal ameloblast morphology | 0.95382028 | 1.12874836 |
| ENSG00000184979 | USP18 subnetwork | 0.47844566 | 1.128782317 |
| ENSG00000101654 | RNMT subnetwork | 0.4783683 | 1.128794892 |
| ENSG00000108852 | MPP2 subnetwork | 0.95380587 | 1.128820441 |
| GO:0015850 | organic alcohol transport | 0.95378769 | 1.128888433 |
| GO:0008375 | acetylglucosaminyltransferase activity | 0.47975502 | 1.12892391 |
| ENSG00000100591 | AHSA1 subnetwork | 0.95365949 | 1.128965291 |
| MP:0003732 | abnormal retinal outer plexiform layer morphology | 0.95378202 | 1.128981048 |
| MP:0009743 | preaxial polydactyly | 0.47960619 | 1.128996815 |
| GO:0051537 | 2 iron, 2 sulfur cluster binding | 0.47968853 | 1.12901608 |
| GO:0016505 | apoptotic protease activator activity | 0.95377169 | 1.129044962 |
| GO:0014855 | striated muscle cell proliferation | 0.9536516 | 1.129053832 |
| GO:0070242 | thymocyte apoptotic process | 0.47956129 | 1.129065138 |
| ENSG00000198938 | MT-CO3 subnetwork | 0.95363398 | 1.129105458 |
| ENSG00000169217 | CD2BP2 subnetwork | 0.47951517 | 1.129125518 |
| REACTOME_RNA_POLYMERASI | REACTOME_RNA_POLYMERASE_III_TRANSCRIPTION_INITIA | 0.47893633 | 1.129134109 |
| ENSG00000102362 | SYTL4 subnetwork | 0.95360787 | 1.129185817 |
| MP:0003817 | abnormal pituitary diverticulum morphology | 0.47905727 | 1.129201212 |
| ENSG00000164944 | KIAA1429 subnetwork | 0.47993154 | 1.129205793 |
| ENSG00000168067 | MAP4K2 subnetwork | 0.47947602 | 1.129209814 |
| ENSG00000206383 | HSPA1L subnetwork | 0.47941815 | 1.129214468 |
| REACTOME_LATE_PHASE_OF_I | REACTOME_LATE_PHASE_OF_HIV_LIFE_CYCLE | 0.4786834 | 1.129248444 |
| GO:0071805 | potassium ion transmembrane transport | 0.95359218 | 1.129262087 |
| MP:0010301 | increased stomach tumor incidence | 0.48005344 | 1.129296626 |
| ENSG00000122566 | HNRNPA2B1 subnetwork | 0.4789336 | 1.12930622 |
| GO:0071804 | cellular potassium ion transport | 0.95359218 | 1.129354786 |
| GO:0043242 | negative regulation of protein complex disassembly | 0.48016981 | 1.129371519 |
| ENSG00000206274 | ENSG00000206274 subnetwork | 0.47941815 | 1.129394422 |
| GO:0006184 | GTP catabolic process | 0.95346029 | 1.129400657 |
| ENSG00000197561 | ELANE subnetwork | 0.95341957 | 1.129423598 |
| REACTOME_E2F_MEDIATED_R | REACTOME_E2F_MEDIATED_REGULATION_OF_DNA_REPLI | 0.95357414 | 1.129431081 |
| ENSG00000117153 | KLHL12 subnetwork | 0.47891965 | 1.129454458 |
| MP:0008451 | retinal rod cell degeneration | 0.47885108 | 1.12950702 |
| MP:0005536 | Leydig cell hypoplasia | 0.47939229 | 1.129510679 |
| GO:0010043 | response to zinc ion | 0.95341706 | 1.129512235 |
| MP:0003638 | abnormal response/metabolism to endogenous compound | 0.95335407 | 1.129526977 |
| ENSG00000114742 | WDR48 subnetwork | 0.95330738 | 1.129586892 |
| GO:0051436 | negative regulation of ubiquitin-protein ligase activity invol | 0.9532355 | 1.129609856 |
| REACTOME_ASSEMBLY_OF_TH | REACTOME_ASSEMBLY_OF_THE_PRE:REPLICATIVE_COMPL | 0.47937038 | 1.129634943 |
| ENSG00000215104 | ENSG00000215104 subnetwork | 0.95321306 | 1.129682109 |
| ENSG00000158301 | GPRASP2 subnetwork | 0.95321037 | 1.129774912 |
| MP:0008028 | pregnancy-related premature death | 0.95320023 | 1.129855406 |
| ENSG00000103187 | COTL1 subnetwork | 0.95316341 | 1.129911264 |
| GO:0006937 | regulation of muscle contraction | 0.95299714 | 1.12991618 |
| GO:0071277 | cellular response to calcium ion | 0.95297266 | 1.129951512 |
| GO:0032890 | regulation of organic acid transport | 0.95311616 | 1.129958915 |
| GO:0034220 | ion transmembrane transport | 0.95296086 | 1.130044382 |
| GO:0072203 | cell proliferation involved in metanephros development | 0.95290958 | 1.130104389 |
| MP:0004046 | abnormal mitosis | 0.95284551 | 1.130106864 |

| | | | |
|---|---|---|---|
| ENSG00000107623 | GDF10 subnetwork | 0.95282631 | 1.130183328 |
| GO:0001085 | RNA polymerase II transcription factor binding | 0.95277845 | 1.130202253 |
| MP:0005104 | abnormal tarsal bone morphology | 0.9527719 | 1.130291071 |
| ENSG00000135597 | REPS1 subnetwork | 0.95270654 | 1.130310007 |
| MP:0001175 | abnormal lung morphology | 0.48060481 | 1.130313395 |
| MP:0008948 | decreased neuron number | 0.95268938 | 1.130378289 |
| GO:0046415 | urate metabolic process | 0.95257458 | 1.130407962 |
| GO:0009109 | coenzyme catabolic process | 0.48071896 | 1.130419914 |
| ENSG00000148688 | RPP30 subnetwork | 0.95267032 | 1.130438358 |
| GO:0030002 | cellular anion homeostasis | 0.95255162 | 1.130480382 |
| ENSG00000179950 | PUF60 subnetwork | 0.48081856 | 1.130510496 |
| GO:0042053 | regulation of dopamine metabolic process | 0.9525333 | 1.130556927 |
| MP:0000438 | abnormal cranium morphology | 0.95249366 | 1.130604689 |
| GO:0090287 | regulation of cellular response to growth factor stimulus | 0.95248294 | 1.130689485 |
| GO:0048863 | stem cell differentiation | 0.95245903 | 1.130766066 |
| MP:0005182 | increased circulating estradiol level | 0.95235177 | 1.130789171 |
| ENSG00000172137 | CALB2 subnetwork | 0.95235067 | 1.130882232 |
| ENSG00000155980 | KIF5A subnetwork | 0.48110109 | 1.130919065 |
| ENSG00000189369 | GSPT2 subnetwork | 0.95232924 | 1.130967078 |
| ENSG00000100162 | CENPM subnetwork | 0.95208077 | 1.130987075 |
| GO:0010657 | muscle cell apoptotic process | 0.95159377 | 1.131010625 |
| GO:0030878 | thyroid gland development | 0.95197903 | 1.131041581 |
| MP:0003054 | spina bifida | 0.95232343 | 1.13106017 |
| MP:0000752 | dystrophic muscle | 0.95156399 | 1.131062603 |
| ENSG00000142515 | KLK3 subnetwork | 0.95207096 | 1.131063725 |
| GO:0009749 | response to glucose stimulus | 0.95186973 | 1.131079634 |
| GO:0051438 | regulation of ubiquitin-protein ligase activity | 0.95195032 | 1.131089427 |
| ENSG00000143850 | PLEKHA6 subnetwork | 0.9522627 | 1.131091538 |
| MP:0010403 | atrial septal defect | 0.9515243 | 1.131118708 |
| ENSG00000089685 | BIRC5 subnetwork | 0.95133363 | 1.131119717 |
| GO:0007338 | single fertilization | 0.95184539 | 1.131156317 |
| MP:0005253 | abnormal eye physiology | 0.95148093 | 1.131162465 |
| GO:0010001 | glial cell differentiation | 0.95130917 | 1.13120056 |
| ENSG00000107537 | PHYH subnetwork | 0.95127069 | 1.131273177 |
| ENSG00000164109 | MAD2L1 subnetwork | 0.95119987 | 1.131275754 |
| ENSG00000184445 | KNTC1 subnetwork | 0.95116569 | 1.131340147 |
| ENSG00000100138 | NHP2L1 subnetwork | 0.48143214 | 1.131370211 |
| GO:0051702 | interaction with symbiont | 0.48273582 | 1.13139369 |
| ENSG00000089818 | NECAP1 subnetwork | 0.95114144 | 1.131412793 |
| ENSG00000165304 | MELK subnetwork | 0.48137889 | 1.131422893 |
| MP:0009814 | increased prostaglandin level | 0.48245367 | 1.131453276 |
| ENSG00000106399 | RPA3 subnetwork | 0.48233747 | 1.131466201 |
| ENSG00000166033 | HTRA1 subnetwork | 0.95113489 | 1.131501937 |
| ENSG00000187514 | PTMA subnetwork | 0.4822064 | 1.131571429 |
| ENSG00000084092 | NOA1 subnetwork | 0.48273578 | 1.131573105 |
| REACTOME_REMOVAL_OF_LIC | REACTOME_REMOVAL_OF_LICENSING_FACTORS_FROM_O | 0.48229962 | 1.131590224 |
| ENSG00000113658 | SMAD5 subnetwork | 0.95113472 | 1.131595218 |
| ENSG00000151422 | FER subnetwork | 0.48290558 | 1.131610653 |
| GO:0034374 | low-density lipoprotein particle remodeling | 0.95050071 | 1.131611945 |
| GO:0031663 | lipopolysaccharide-mediated signaling pathway | 0.48298874 | 1.131613568 |
| GO:0043524 | negative regulation of neuron apoptotic process | 0.95108658 | 1.131614313 |
| GO:0043300 | regulation of leukocyte degranulation | 0.95069269 | 1.131668591 |
| ENSG00000108669 | CYTH1 subnetwork | 0.95104509 | 1.13167876 |

| | | | |
|---|---|---|---|
| GO:0005881 | cytoplasmic microtubule | 0.48266402 | 1.131686231 |
| MP:0002151 | abnormal neural tube morphology/development | 0.48270991 | 1.131689136 |
| ENSG00000160075 | SSU72 subnetwork | 0.48218772 | 1.131695507 |
| ENSG00000186051 | TAL2 subnetwork | 0.95064691 | 1.131700074 |
| GO:0008236 | serine-type peptidase activity | 0.4821034 | 1.13170054 |
| ENSG00000135338 | LCA5 subnetwork | 0.95049637 | 1.13170118 |
| MP:0001282 | short vibrissae | 0.48196601 | 1.131718551 |
| GO:0050769 | positive regulation of neurogenesis | 0.48203268 | 1.131721455 |
| ENSG00000187323 | DCC subnetwork | 0.95091922 | 1.131729342 |
| MP:0004384 | small interparietal bone | 0.95101362 | 1.131743218 |
| GO:0003012 | muscle system process | 0.95087513 | 1.131756701 |
| GO:0007528 | neuromuscular junction development | 0.95047924 | 1.131773927 |
| GO:0009070 | serine family amino acid biosynthetic process | 0.94980397 | 1.131807299 |
| GO:0032728 | positive regulation of interferon-beta production | 0.95043688 | 1.131817807 |
| GO:0033028 | myeloid cell apoptotic process | 0.48192908 | 1.131850675 |
| ENSG00000136938 | ANP32B subnetwork | 0.48325355 | 1.13187292 |
| MP:0011089 | complete perinatal lethality | 0.94993214 | 1.131874845 |
| GO:0070167 | regulation of biomineral tissue development | 0.94977118 | 1.131875981 |
| ENSG00000171566 | PLRG1 subnetwork | 0.48320031 | 1.131893819 |
| ENSG00000114353 | GNAI2 subnetwork | 0.95042563 | 1.131902954 |
| KEGG_PENTOSE_AND_GLUCUI | KEGG_PENTOSE_AND_GLUCURONATE_INTERCONVERSION | 0.94974377 | 1.131940545 |
| MP:0002275 | abnormal type II pneumocyte morphology | 0.95027249 | 1.131945362 |
| REACTOME_INHIBITION_OF_R | REACTOME_INHIBITION_OF_REPLICATION_INITIATION_OF_ | 0.48188283 | 1.131951065 |
| GO:0042165 | neurotransmitter binding | 0.95038597 | 1.131963357 |
| REACTOME_SRP:DEPENDENT_( | REACTOME_SRP:DEPENDENT_COTRANSLATIONAL_PROTEII | 0.9502178 | 1.131985142 |
| MP:0003131 | increased erythrocyte cell number | 0.48183526 | 1.132011759 |
| GO:0006865 | amino acid transport | 0.9497328 | 1.132029895 |
| GO:0060571 | morphogenesis of an epithelial fold | 0.95014941 | 1.13204144 |
| ENSG00000140650 | PMM2 subnetwork | 0.48177158 | 1.132096313 |
| GO:0042220 | response to cocaine | 0.94971045 | 1.13211513 |
| GO:0014073 | response to tropane | 0.94971045 | 1.13220864 |
| GO:0045604 | regulation of epidermal cell differentiation | 0.94957934 | 1.132263527 |
| ENSG00000090273 | NUDC subnetwork | 0.94967961 | 1.132293904 |
| MP:0001300 | ocular hypertelorism | 0.94957513 | 1.132357072 |
| MP:0000886 | abnormal cerebellar granule layer | 0.94953845 | 1.132392795 |
| GO:0061061 | muscle structure development | 0.94952351 | 1.132457445 |
| GO:0043178 | alcohol binding | 0.94950691 | 1.132534501 |
| ENSG00000140941 | MAP1LC3B subnetwork | 0.94949628 | 1.132619835 |
| ENSG00000099940 | SNAP29 subnetwork | 0.48385763 | 1.132684086 |
| ENSG00000197043 | ANXA6 subnetwork | 0.48367358 | 1.132691698 |
| ENSG00000169021 | UQCRFS1 subnetwork | 0.94948048 | 1.13270105 |
| GO:0014020 | primary neural tube formation | 0.94942612 | 1.132716151 |
| GO:0048038 | quinone binding | 0.48383282 | 1.132792208 |
| ENSG00000168090 | COPS6 subnetwork | 0.94941692 | 1.132805654 |
| GO:0030016 | myofibril | 0.94925537 | 1.132823481 |
| GO:0045104 | intermediate filament cytoskeleton organization | 0.94917357 | 1.132851 |
| ENSG00000106305 | AIMP2 subnetwork | 0.94913577 | 1.132870256 |
| GO:0019229 | regulation of vasoconstriction | 0.94940241 | 1.132891038 |
| MP:0004084 | abnormal cardiac muscle relaxation | 0.94908709 | 1.132914324 |
| ENSG00000142657 | PGD subnetwork | 0.48382311 | 1.132947885 |
| ENSG00000206456 | ENSG00000206456 subnetwork | 0.94908202 | 1.133003887 |
| ENSG00000204655 | MOG subnetwork | 0.94908202 | 1.133097601 |
| GO:0006790 | sulfur compound metabolic process | 0.94884389 | 1.13311409 |

| | | | |
|---|---|---|---|
| ENSG00000137345 | MOG subnetwork | 0.94908202 | 1.133191331 |
| MP:0008428 | abnormal spatial working memory | 0.94883465 | 1.13319957 |
| ENSG00000068796 | KIF2A subnetwork | 0.94902966 | 1.133223031 |
| GO:0006820 | anion transport | 0.94879259 | 1.133247828 |
| GO:0070997 | neuron death | 0.94872728 | 1.133283681 |
| MP:0002754 | dilated heart right ventricle | 0.94867932 | 1.133302988 |
| GO:0046426 | negative regulation of JAK-STAT cascade | 0.48505307 | 1.133325431 |
| MP:0000749 | muscle degeneration | 0.94867543 | 1.133396789 |
| ENSG00000182185 | RAD51B subnetwork | 0.48502823 | 1.133449257 |
| ENSG00000186879 | ENSG00000186879 subnetwork | 0.48520112 | 1.133462389 |
| ENSG00000215467 | ENSG00000215467 subnetwork | 0.94867253 | 1.133490605 |
| ENSG00000142192 | APP subnetwork | 0.94865688 | 1.133563742 |
| ENSG00000171942 | OR10H2 subnetwork | 0.48501125 | 1.133573123 |
| ENSG00000092841 | MYL6 subnetwork | 0.48430849 | 1.133644712 |
| GO:0003407 | neural retina development | 0.94865583 | 1.133657588 |
| MP:0000031 | abnormal cochlea morphology | 0.9485998 | 1.133668654 |
| GO:0090199 | regulation of release of cytochrome c from mitochondria | 0.48476284 | 1.133736751 |
| GO:0006289 | nucleotide-excision repair | 0.48500802 | 1.133744466 |
| MP:0006309 | decreased retinal ganglion cell number | 0.94858793 | 1.133750104 |
| ENSG00000154415 | PPP1R3A subnetwork | 0.48468512 | 1.133773734 |
| GO:0031652 | positive regulation of heat generation | 0.48495685 | 1.133781433 |
| GO:0010226 | response to lithium ion | 0.94858136 | 1.133831567 |
| GO:0060419 | heart growth | 0.9485213 | 1.133846791 |
| ENSG00000214133 | ENSG00000214133 subnetwork | 0.94839752 | 1.133852398 |
| GO:0050900 | leukocyte migration | 0.48456625 | 1.133855651 |
| ENSG00000107295 | SH3GL2 subnetwork | 0.48465387 | 1.133866118 |
| MP:0003888 | liver hemorrhage | 0.48448666 | 1.133884755 |
| ENSG00000198722 | UNC13B subnetwork | 0.9485141 | 1.133936558 |
| ENSG00000158623 | COPG2 subnetwork | 0.94839752 | 1.133946322 |
| GO:0031650 | regulation of heat generation | 0.48495685 | 1.133960772 |
| ENSG00000072864 | NDE1 subnetwork | 0.94838423 | 1.134027835 |
| ENSG00000198000 | NOL8 subnetwork | 0.94827849 | 1.134079045 |
| ENSG00000174125 | TLR1 subnetwork | 0.94835876 | 1.134080365 |
| REACTOME_COMMON_PATHV | REACTOME_COMMON_PATHWAY | 0.94809142 | 1.134149677 |
| ENSG00000198728 | LDB1 subnetwork | 0.94801497 | 1.134156651 |
| REACTOME_IRON_UPTAKE_AN | REACTOME_IRON_UPTAKE_AND_TRANSPORT | 0.94826493 | 1.13416059 |
| GO:0030500 | regulation of bone mineralization | 0.94824806 | 1.134225574 |
| MP:0005574 | decreased pulmonary respiratory rate | 0.94799183 | 1.134225796 |
| ENSG00000143520 | FLG2 subnetwork | 0.94789929 | 1.134249358 |
| GO:0030073 | insulin secretion | 0.94774665 | 1.134255037 |
| ENSG00000083093 | PALB2 subnetwork | 0.94772079 | 1.134311774 |
| MP:0000162 | lordosis | 0.9474752 | 1.134316165 |
| GO:0046039 | GTP metabolic process | 0.94789743 | 1.134343392 |
| GO:0008210 | estrogen metabolic process | 0.94766002 | 1.13434779 |
| GO:0031080 | Nup107-160 complex | 0.94757377 | 1.134350639 |
| GO:0016597 | amino acid binding | 0.94746469 | 1.134401958 |
| GO:0072001 | renal system development | 0.94746308 | 1.13449606 |
| GO:0032095 | regulation of response to food | 0.94744205 | 1.134561142 |
| GO:0050818 | regulation of coagulation | 0.947403 | 1.134622086 |
| GO:0051216 | cartilage development | 0.94736914 | 1.134674743 |
| ENSG00000161888 | SPC24 subnetwork | 0.94728376 | 1.13473029 |
| ENSG00000123838 | C4BPA subnetwork | 0.48584107 | 1.134747235 |
| GO:0005882 | intermediate filament | 0.94734978 | 1.134752303 |

| | | | |
|---|---|---|---|
| MP:0008825 | abnormal cardiac epithelial to mesenchymal transition | 0.94724234 | 1.134753921 |
| ENSG00000133710 | SPINK5 subnetwork | 0.94720244 | 1.134806607 |
| GO:0031424 | keratinization | 0.48577857 | 1.134808027 |
| ENSG00000135446 | CDK4 subnetwork | 0.48593394 | 1.134836519 |
| MP:0001004 | abnormal retinal photoreceptor morphology | 0.94718703 | 1.134863451 |
| ENSG00000127884 | ECHS1 subnetwork | 0.48611842 | 1.134920259 |
| GO:0043576 | regulation of respiratory gaseous exchange | 0.94718171 | 1.134957662 |
| REACTOME_MRNA_PROCESSIN | REACTOME_MRNA_PROCESSING | 0.48608329 | 1.135020531 |
| REACTOME_RECYCLING_PATH | REACTOME_RECYCLING_PATHWAY_OF_L1 | 0.94717287 | 1.135043587 |
| REACTOME_THROMBIN_SIGNA | REACTOME_THROMBIN_SIGNALLING_THROUGH_PROTEIN | 0.94717065 | 1.135137828 |
| ENSG00000031691 | CENPQ subnetwork | 0.94714566 | 1.135207174 |
| ENSG00000111716 | LDHB subnetwork | 0.94712129 | 1.135251619 |
| ENSG00000143995 | MEIS1 subnetwork | 0.48640053 | 1.135280189 |
| MP:0008450 | retinal photoreceptor degeneration | 0.94711361 | 1.135329292 |
| GO:0008430 | selenium binding | 0.48634006 | 1.135348911 |
| ENSG00000189091 | SF3B3 subnetwork | 0.48648892 | 1.135353535 |
| GO:0034505 | tooth mineralization | 0.94699971 | 1.13536008 |
| GO:0001736 | establishment of planar polarity | 0.9470905 | 1.135361296 |
| GO:0051340 | regulation of ligase activity | 0.9469289 | 1.135363017 |
| GO:0040001 | establishment of mitotic spindle localization | 0.94691316 | 1.135449032 |
| ENSG00000119408 | NEK6 subnetwork | 0.48668988 | 1.135468602 |
| GO:0042375 | quinone cofactor metabolic process | 0.48713095 | 1.135482346 |
| GO:0055017 | cardiac muscle tissue growth | 0.94679516 | 1.135492314 |
| ENSG00000182492 | BGN subnetwork | 0.94686646 | 1.135501828 |
| MP:0004229 | abnormal embryonic erythropoiesis | 0.48693971 | 1.135538559 |
| GO:0051188 | cofactor biosynthetic process | 0.48664931 | 1.135584662 |
| GO:0015012 | heparan sulfate proteoglycan biosynthetic process | 0.94678746 | 1.135586671 |
| ENSG00000100034 | PPM1F subnetwork | 0.48711762 | 1.13560618 |
| MP:0009355 | increased liver triglyceride level | 0.4869112 | 1.135615142 |
| GO:0030163 | protein catabolic process | 0.48685368 | 1.135628648 |
| ENSG00000047457 | CP subnetwork | 0.94677567 | 1.135668578 |
| ENSG00000179051 | RCC2 subnetwork | 0.94673216 | 1.135700632 |
| REACTOME_HEMOSTASIS | REACTOME_HEMOSTASIS | 0.48708672 | 1.135737938 |
| GO:0046716 | muscle cell homeostasis | 0.94672128 | 1.135782562 |
| GO:0009185 | ribonucleoside diphosphate metabolic process | 0.94656408 | 1.135796824 |
| MP:0005590 | increased vasodilation | 0.94668311 | 1.135852037 |
| MP:0001674 | abnormal triploblastic development | 0.94609671 | 1.135860434 |
| ENSG00000178127 | NDUFV2 subnetwork | 0.94653938 | 1.135870469 |
| GO:0003338 | metanephros morphogenesis | 0.94640813 | 1.135909696 |
| ENSG00000011275 | RNF216 subnetwork | 0.94606928 | 1.135917485 |
| ENSG00000007168 | PAFAH1B1 subnetwork | 0.9465385 | 1.135960755 |
| MP:0002267 | abnormal bronchiole morphology | 0.94605 | 1.135991182 |
| MP:0001522 | impaired swimming | 0.946397 | 1.135991684 |
| GO:0016459 | myosin complex | 0.94597762 | 1.136014975 |
| ENSG00000088986 | DYNLL1 subnetwork | 0.94635999 | 1.136048736 |
| GO:0043198 | dendritic shaft | 0.94596668 | 1.136097013 |
| ENSG00000159210 | SNF8 subnetwork | 0.94594994 | 1.136187386 |
| ENSG00000155097 | ATP6V1C1 subnetwork | 0.94591663 | 1.13626113 |
| GO:0060004 | reflex | 0.94590608 | 1.136351531 |
| ENSG00000077157 | PPP1R12B subnetwork | 0.48756225 | 1.136359338 |
| GO:0051322 | anaphase | 0.94587778 | 1.136416979 |
| ENSG00000104313 | EYA1 subnetwork | 0.94583669 | 1.13646579 |
| GO:0000096 | sulfur amino acid metabolic process | 0.94574013 | 1.136468825 |

| | | | |
|---|---|---|---|
| KEGG_ETHER_LIPID_METABOL | KEGG_ETHER_LIPID_METABOLISM | 0.94565655 | 1.136484349 |
| ENSG00000151914 | DST subnetwork | 0.94564762 | 1.136566481 |
| ENSG00000165409 | TSHR subnetwork | 0.48774426 | 1.136582099 |
| GO:0001822 | kidney development | 0.9456401 | 1.136661116 |
| MP:0005633 | increased circulating sodium level | 0.94557179 | 1.136664169 |
| ENSG00000166147 | FBN1 subnetwork | 0.94556657 | 1.136758827 |
| ENSG00000051128 | HOMER3 subnetwork | 0.94554073 | 1.136828517 |
| ENSG00000142156 | COL6A1 subnetwork | 0.94548852 | 1.136860736 |
| ENSG00000120334 | CENPL subnetwork | 0.9454751 | 1.13695127 |
| ENSG00000091704 | CPA1 subnetwork | 0.94545359 | 1.137004332 |
| GO:0032400 | melanosome localization | 0.94542293 | 1.137069899 |
| ENSG00000033050 | ABCF2 subnetwork | 0.94529803 | 1.137121907 |
| ENSG00000171362 | ENSG00000171362 subnetwork | 0.94539566 | 1.13712298 |
| ENSG00000134690 | CDCA8 subnetwork | 0.94527358 | 1.137191667 |
| GO:0017171 | serine hydrolase activity | 0.48869885 | 1.137244256 |
| GO:0046356 | acetyl-CoA catabolic process | 0.48825634 | 1.137257836 |
| ENSG00000081019 | RSBN1 subnetwork | 0.48863849 | 1.137257988 |
| ENSG00000103168 | TAF1C subnetwork | 0.48876805 | 1.137285602 |
| ENSG00000188312 | CENPP subnetwork | 0.94527301 | 1.137286441 |
| GO:0030137 | COPI-coated vesicle | 0.48819299 | 1.137326717 |
| ENSG00000125351 | UPF3B subnetwork | 0.48857117 | 1.137334698 |
| ENSG00000075388 | FGF4 subnetwork | 0.9452526 | 1.137352059 |
| GO:0006929 | substrate-dependent cell migration | 0.48839453 | 1.137370079 |
| ENSG00000102024 | PLS3 subnetwork | 0.48989913 | 1.137417582 |
| GO:0005525 | GTP binding | 0.94522617 | 1.137430191 |
| MP:0004398 | cochlear inner hair cell degeneration | 0.48853465 | 1.137450795 |
| MP:0009397 | increased trophoblast giant cell number | 0.4897737 | 1.137468593 |
| GO:0005085 | guanyl-nucleotide exchange factor activity | 0.48963157 | 1.137496073 |
| ENSG00000215440 | NPEPL1 subnetwork | 0.48819089 | 1.137498031 |
| GO:0000070 | mitotic sister chromatid segregation | 0.94522458 | 1.13752084 |
| GO:0008028 | monocarboxylic acid transmembrane transporter activity | 0.48988118 | 1.137549066 |
| GO:0051259 | protein oligomerization | 0.48973159 | 1.13758442 |
| ENSG00000165588 | OTX2 subnetwork | 0.94521777 | 1.137611505 |
| ENSG00000148303 | RPL7A subnetwork | 0.4896245 | 1.137659073 |
| ENSG00000116337 | AMPD2 subnetwork | 0.49013182 | 1.137664783 |
| GO:0030834 | regulation of actin filament depolymerization | 0.49007473 | 1.137678543 |
| GO:0009125 | nucleoside monophosphate catabolic process | 0.94520653 | 1.137693847 |
| GO:0005543 | phospholipid binding | 0.49172338 | 1.137695557 |
| ENSG00000074370 | ATP2A3 subnetwork | 0.94510774 | 1.137713666 |
| ENSG00000120071 | KIAA1267 subnetwork | 0.49165961 | 1.13775622 |
| GO:0005100 | Rho GTPase activator activity | 0.48904349 | 1.137783197 |
| GO:0055081 | anion homeostasis | 0.94499157 | 1.137799183 |
| ENSG00000177105 | RHOG subnetwork | 0.49028354 | 1.137800094 |
| GO:0050911 | detection of chemical stimulus involved in sensory percepti | 0.9451067 | 1.13780437 |
| MP:0000250 | abnormal vasoconstriction | 0.48960802 | 1.137806411 |
| ENSG00000175895 | PLEKHF2 subnetwork | 0.49158356 | 1.137832551 |
| GO:0016409 | palmitoyltransferase activity | 0.94495336 | 1.137848207 |
| ENSG00000213416 | KRTAP4-12 subnetwork | 0.48947749 | 1.137857592 |
| GO:0045746 | negative regulation of Notch signaling pathway | 0.94477838 | 1.137862863 |
| GO:0042059 | negative regulation of epidermal growth factor receptor sig | 0.489346 | 1.137869497 |
| MP:0005215 | abnormal pancreatic islet morphology | 0.94486302 | 1.137872216 |
| MP:0006254 | thin cerebral cortex | 0.49150568 | 1.137893254 |
| GO:0043568 | positive regulation of insulin-like growth factor receptor sig | 0.48957941 | 1.137914506 |

| | | | |
|---|---|---|---|
| ENSG00000105656 | ELL subnetwork | 0.48916957 | 1.137926695 |
| MP:0000921 | demyelination | 0.48929634 | 1.137938355 |
| GO:0009394 | 2'-deoxyribonucleotide metabolic process | 0.94477169 | 1.137949445 |
| ENSG00000188223 | LIN37 subnetwork | 0.49091053 | 1.137956433 |
| ENSG00000105705 | SUGP1 subnetwork | 0.49055305 | 1.137962673 |
| ENSG00000197343 | ZNF655 subnetwork | 0.49098278 | 1.137966155 |
| GO:0005109 | frizzled binding | 0.49134778 | 1.138005011 |
| GO:0042277 | peptide binding | 0.49148776 | 1.138016594 |
| ENSG00000166477 | LEO1 subnetwork | 0.49085649 | 1.138017241 |
| ENSG00000212908 | ENSG00000212908 subnetwork | 0.48947749 | 1.138036472 |
| ENSG00000145362 | ANK2 subnetwork | 0.94476652 | 1.138044385 |
| MP:0004772 | abnormal bile secretion | 0.49044853 | 1.138060872 |
| ENSG00000151702 | FLI1 subnetwork | 0.4905309 | 1.138086275 |
| MP:0004937 | dilated heart | 0.94473071 | 1.138097622 |
| GO:0006816 | calcium ion transport | 0.49145046 | 1.138108658 |
| GO:0043236 | laminin binding | 0.48928899 | 1.138109468 |
| GO:0033599 | regulation of mammary gland epithelial cell proliferation | 0.49080944 | 1.138125098 |
| GO:0050873 | brown fat cell differentiation | 0.49133321 | 1.138128426 |
| GO:0060688 | regulation of morphogenesis of a branching structure | 0.94470961 | 1.138163385 |
| GO:0006829 | zinc ion transport | 0.49124945 | 1.138189223 |
| GO:0046854 | phosphatidylinositol phosphorylation | 0.49120002 | 1.138195206 |
| MP:0002452 | abnormal antigen presenting cell physiology | 0.490698 | 1.138215462 |
| ENSG00000128908 | INO80 subnetwork | 0.49077748 | 1.138232988 |
| REACTOME_FGFR2_LIGAND_B | REACTOME_FGFR2_LIGAND_BINDING_AND_ACTIVATION | 0.94469596 | 1.138241676 |
| ENSG00000211662 | ENSG00000211662 subnetwork | 0.94466744 | 1.138299115 |
| REACTOME_BOTULINUM_NEU | REACTOME_BOTULINUM_NEUROTOXICITY | 0.94455248 | 1.138338898 |
| ENSG00000102384 | CENPI subnetwork | 0.94464516 | 1.138356565 |
| ENSG00000112739 | PRPF4B subnetwork | 0.49202641 | 1.138362271 |
| GO:0000930 | gamma-tubulin complex | 0.94452837 | 1.138379664 |
| ENSG00000085978 | ATG16L1 subnetwork | 0.94443604 | 1.138382869 |
| ENSG00000129757 | CDKN1C subnetwork | 0.9441469 | 1.13839666 |
| GO:0048854 | brain morphogenesis | 0.94408657 | 1.138424921 |
| ENSG00000198918 | RPL39 subnetwork | 0.94443569 | 1.138477916 |
| ENSG00000130193 | C8orf55 subnetwork | 0.49259183 | 1.138512035 |
| ENSG00000058866 | DGKG subnetwork | 0.94408177 | 1.138520003 |
| ENSG00000005884 | ITGA3 subnetwork | 0.49312491 | 1.13852459 |
| ENSG00000198356 | ASNA1 subnetwork | 0.94440939 | 1.138527054 |
| ENSG00000198612 | COPS8 subnetwork | 0.4930691 | 1.138569644 |
| MP:0009417 | skeletal muscle atrophy | 0.49320791 | 1.138573213 |
| REACTOME_CELL:CELL_COMM | REACTOME_CELL:CELL_COMMUNICATION | 0.49285711 | 1.138603343 |
| ENSG00000074071 | MRPS34 subnetwork | 0.94395763 | 1.138605797 |
| ENSG00000038358 | EDC4 subnetwork | 0.4925522 | 1.138611849 |
| ENSG00000160783 | PMF1 subnetwork | 0.94407775 | 1.138615102 |
| ENSG00000184381 | PLA2G6 subnetwork | 0.49281362 | 1.138632813 |
| MP:0001685 | abnormal endoderm development | 0.94382873 | 1.138641491 |
| MP:0000088 | short mandible | 0.94392022 | 1.138650794 |
| ENSG00000188843 | ENSG00000188843 subnetwork | 0.49294854 | 1.138651984 |
| GO:0016328 | lateral plasma membrane | 0.49302079 | 1.138661565 |
| GO:0045940 | positive regulation of steroid metabolic process | 0.4941037 | 1.138701886 |
| REACTOME_RNA_POLYMERAS | REACTOME_RNA_POLYMERASE_I_CHAIN_ELONGATION | 0.49402474 | 1.138707918 |
| ENSG00000122952 | ZWINT subnetwork | 0.94382548 | 1.138728275 |
| GO:0042698 | ovulation cycle | 0.49276473 | 1.138748242 |
| ENSG00000135503 | ACVR1B subnetwork | 0.49242079 | 1.138749023 |

| | | | |
|---|---|---|---|
| REACTOME_INITIAL_TRIGGERII | REACTOME_INITIAL_TRIGGERING_OF_COMPLEMENT | 0.49398174 | 1.138760717 |
| MP:0003224 | neuron degeneration | 0.49253666 | 1.138774234 |
| ENSG00000198730 | CTR9 subnetwork | 0.49373392 | 1.138802246 |
| GO:0051320 | S phase | 0.49421786 | 1.138804924 |
| GO:0042056 | chemoattractant activity | 0.94382402 | 1.138823431 |
| ENSG00000126698 | DNAJC8 subnetwork | 0.49348262 | 1.138826467 |
| GO:0015992 | proton transport | 0.49367709 | 1.138831696 |
| GO:0071407 | cellular response to organic cyclic compound | 0.49239416 | 1.13887238 |
| KEGG_ECM_RECEPTOR_INTER/ | KEGG_ECM_RECEPTOR_INTERACTION | 0.49395295 | 1.138899283 |
| GO:0004843 | ubiquitin-specific protease activity | 0.49343434 | 1.138910567 |
| REACTOME_INSULIN_RECEPTC | REACTOME_INSULIN_RECEPTOR_SIGNALLING_CASCADE | 0.94382302 | 1.138918603 |
| ENSG00000129048 | CCRL1 subnetwork | 0.49391941 | 1.138983315 |
| GO:0032011 | ARF protein signal transduction | 0.94381249 | 1.139001254 |
| GO:0006521 | regulation of cellular amino acid metabolic process | 0.49361975 | 1.139007645 |
| ENSG00000113196 | HAND1 subnetwork | 0.4936724 | 1.13900936 |
| REACTOME_EUKARYOTIC_TRA | REACTOME_EUKARYOTIC_TRANSLATION_TERMINATION | 0.9437847 | 1.139092277 |
| ENSG00000030066 | NUP160 subnetwork | 0.94370713 | 1.139099724 |
| GO:0007093 | mitotic cell cycle checkpoint | 0.94369337 | 1.139165691 |
| GO:0032225 | regulation of synaptic transmission, dopaminergic | 0.94359719 | 1.13923913 |
| GO:0072283 | metanephric renal vesicle morphogenesis | 0.94368376 | 1.13924421 |
| GO:0060119 | inner ear receptor cell development | 0.94358177 | 1.139313488 |
| MP:0003694 | failure to hatch from the zona pellucida | 0.94345198 | 1.139328427 |
| GO:0051378 | serotonin binding | 0.94353445 | 1.139354407 |
| ENSG00000166579 | NDEL1 subnetwork | 0.94341499 | 1.139419538 |
| MP:0003384 | abnormal ventral body wall morphology | 0.94324944 | 1.139442864 |
| ENSG00000125885 | MCM8 subnetwork | 0.94335317 | 1.139468841 |
| ENSG00000205022 | PABPN1L subnetwork | 0.49463316 | 1.139493769 |
| GO:0046128 | purine ribonucleoside metabolic process | 0.94324938 | 1.139538191 |
| ENSG00000134809 | TIMM10 subnetwork | 0.49459551 | 1.139546658 |
| GO:0048368 | lateral mesoderm development | 0.94324899 | 1.139633534 |
| GO:0051924 | regulation of calcium ion transport | 0.94322763 | 1.139707974 |
| GO:0051155 | positive regulation of striated muscle cell differentiation | 0.94322011 | 1.139799163 |
| ENSG00000056678 | ENSG00000056678 subnetwork | 0.49520942 | 1.13980862 |
| ENSG00000115138 | POMC subnetwork | 0.49478862 | 1.139845818 |
| MP:0002887 | decreased susceptibility to pharmacologically induced seizu | 0.94307436 | 1.139856043 |
| ENSG00000153113 | CAST subnetwork | 0.94321282 | 1.139881998 |
| GO:0032835 | glomerulus development | 0.94293914 | 1.139892014 |
| GO:0016208 | AMP binding | 0.94305634 | 1.139926341 |
| MP:0000786 | abnormal embryonic neuroepithelial layer differentiation | 0.49533383 | 1.139942439 |
| GO:0006936 | muscle contraction | 0.94291456 | 1.139979071 |
| ENSG00000204197 | KIFC1 subnetwork | 0.49520942 | 1.139985994 |
| MP:0005262 | coloboma | 0.94291455 | 1.140074514 |
| MP:0004770 | abnormal synaptic vesicle recycling | 0.94284764 | 1.140107176 |
| ENSG00000136813 | KIAA0368 subnetwork | 0.49518958 | 1.140108949 |
| ENSG00000077721 | UBE2A subnetwork | 0.49544719 | 1.140130658 |
| ENSG00000163535 | SGOL2 subnetwork | 0.94274074 | 1.140180889 |
| GO:0060021 | palate development | 0.94283525 | 1.140190085 |
| GO:0043087 | regulation of GTPase activity | 0.49516406 | 1.140231943 |
| GO:0042517 | positive regulation of tyrosine phosphorylation of Stat3 pro | 0.49500479 | 1.140260044 |
| GO:0010799 | regulation of peptidyl-threonine phosphorylation | 0.94274067 | 1.140276382 |
| ENSG00000176444 | CLK2 subnetwork | 0.4956042 | 1.14029549 |
| KEGG_PENTOSE_PHOSPHATE_ | KEGG_PENTOSE_PHOSPHATE_PATHWAY | 0.94271756 | 1.140346763 |
| ENSG00000130640 | TUBGCP2 subnetwork | 0.94265646 | 1.140383649 |

| | | | |
|---|---|---|---|
| ENSG00000106541 | AGR2 subnetwork | 0.49515732 | 1.140393897 |
| GO:0010714 | positive regulation of collagen metabolic process | 0.94250687 | 1.140398794 |
| GO:0032481 | positive regulation of type I interferon production | 0.94259097 | 1.140407975 |
| GO:0032967 | positive regulation of collagen biosynthetic process | 0.94250687 | 1.140494344 |
| GO:0090276 | regulation of peptide hormone secretion | 0.94246899 | 1.140552204 |
| MP:0011110 | partial preweaning lethality | 0.94227408 | 1.140554811 |
| ENSG00000211619 | ENSG00000211619 subnetwork | 0.94241722 | 1.140597503 |
| ENSG00000120437 | ACAT2 subnetwork | 0.9422339 | 1.140600117 |
| REACTOME_ION_TRANSPORT_ | REACTOME_ION_TRANSPORT_BY_P:TYPE_ATPASES | 0.94223197 | 1.140695725 |
| GO:0003044 | regulation of systemic arterial blood pressure mediated by | 0.94222193 | 1.140778774 |
| GO:0030897 | HOPS complex | 0.49589347 | 1.140779039 |
| GO:0009434 | microtubule-based flagellum | 0.94221414 | 1.140857646 |
| ENSG00000176788 | BASP1 subnetwork | 0.49661659 | 1.140922503 |
| REACTOME_THROMBOXANE_S | REACTOME_THROMBOXANE_SIGNALLING_THROUGH_TP_I | 0.94220936 | 1.140953299 |
| REACTOME_RNA_POLYMERASI | REACTOME_RNA_POLYMERASE_I_RNA_POLYMERASE_III_A | 0.49654757 | 1.140983225 |
| MP:0011094 | complete embryonic lethality before implantation | 0.94215438 | 1.140990273 |
| ENSG00000130638 | ATXN10 subnetwork | 0.49671788 | 1.141001553 |
| MP:0001196 | shiny skin | 0.49683125 | 1.141034001 |
| ENSG00000173534 | ENSG00000173534 subnetwork | 0.94210316 | 1.141060797 |
| ENSG00000124575 | HIST1H1D subnetwork | 0.49652968 | 1.141129408 |
| ENSG00000170847 | ENSG00000170847 subnetwork | 0.94210316 | 1.141156491 |
| GO:0021988 | olfactory lobe development | 0.94203222 | 1.141176717 |
| MP:0001729 | impaired embryo implantation | 0.49696677 | 1.141237193 |
| MP:0009886 | failure of palatal shelf elevation | 0.94186539 | 1.141245805 |
| ENSG00000173482 | PTPRM subnetwork | 0.94197867 | 1.141271705 |
| GO:0021772 | olfactory bulb development | 0.94203222 | 1.141272438 |
| MP:0002981 | increased liver weight | 0.49644375 | 1.141282051 |
| MP:0003048 | abnormal cervical vertebrae morphology | 0.94183482 | 1.141282826 |
| GO:0007369 | gastrulation | 0.49652885 | 1.141306712 |
| ENSG00000181191 | PJA1 subnetwork | 0.49636785 | 1.141311781 |
| GO:0051180 | vitamin transport | 0.94182588 | 1.141374392 |
| ENSG00000170043 | TRAPPC1 subnetwork | 0.49629671 | 1.141380382 |
| GO:0060992 | response to fungicide | 0.94177409 | 1.141403038 |
| ENSG00000171793 | CTPS subnetwork | 0.94171218 | 1.141427492 |
| GO:0072215 | regulation of metanephros development | 0.49625475 | 1.141464552 |
| MP:0000852 | small cerebellum | 0.94170053 | 1.141514897 |
| ENSG00000042753 | AP2S1 subnetwork | 0.49714892 | 1.141525687 |
| ENSG00000088832 | FKBP1A subnetwork | 0.94169123 | 1.14161071 |
| GO:0004576 | oligosaccharyl transferase activity | 0.94168919 | 1.141698145 |
| ENSG00000085733 | CTTN subnetwork | 0.94165377 | 1.141773002 |
| REACTOME_RNA_POLYMERASI | REACTOME_RNA_POLYMERASE_III_TRANSCRIPTION_INITIA | 0.49736091 | 1.141783054 |
| KEGG_GAP_JUNCTION | KEGG_GAP_JUNCTION | 0.94164934 | 1.141860465 |
| GO:0005768 | endosome | 0.49817289 | 1.141933984 |
| GO:0034375 | high-density lipoprotein particle remodeling | 0.94164882 | 1.141956339 |
| ENSG00000204133 | ENSG00000204133 subnetwork | 0.94159154 | 1.141972458 |
| ENSG00000111875 | ASF1A subnetwork | 0.49814013 | 1.142025728 |
| ENSG00000143373 | ZNF687 subnetwork | 0.4980652 | 1.142039994 |
| ENSG00000167977 | KCTD5 subnetwork | 0.49761378 | 1.142049333 |
| GO:0010463 | mesenchymal cell proliferation | 0.94158874 | 1.142068357 |
| GO:0016755 | transferase activity, transferring amino-acyl groups | 0.94151646 | 1.14207189 |
| GO:0090200 | positive regulation of release of cytochrome c from mitoch | 0.49793049 | 1.14209955 |
| GO:0071715 | icosanoid transport | 0.94147314 | 1.142125819 |
| MP:0004067 | abnormal trabecula carnea morphology | 0.49803467 | 1.142155039 |

| | | | |
|---|---|---|---|
| GO:0001938 | positive regulation of endothelial cell proliferation | 0.94143766 | 1.142171357 |
| ENSG00000126217 | MCF2L subnetwork | 0.49787606 | 1.142206886 |
| ENSG00000167751 | KLK2 subnetwork | 0.49759746 | 1.142211016 |
| MP:0005534 | decreased body temperature | 0.94141869 | 1.142246304 |
| ENSG00000023608 | SNAPC1 subnetwork | 0.49782904 | 1.142267721 |
| GO:0033572 | transferrin transport | 0.94141249 | 1.142338066 |
| GO:0015682 | ferric iron transport | 0.94141249 | 1.142434045 |
| ENSG00000168028 | RPSA subnetwork | 0.49876472 | 1.142434567 |
| GO:0006397 | mRNA processing | 0.49901998 | 1.14245356 |
| ENSG00000105447 | GRWD1 subnetwork | 0.49908242 | 1.142462467 |
| GO:0009068 | aspartate family amino acid catabolic process | 0.49999676 | 1.142483004 |
| ENSG00000149636 | DSN1 subnetwork | 0.94137986 | 1.14250063 |
| GO:0006638 | neutral lipid metabolic process | 0.49863484 | 1.142556158 |
| ENSG00000090539 | CHRD subnetwork | 0.49891499 | 1.142575101 |
| ENSG00000121989 | ACVR2A subnetwork | 0.49899437 | 1.14257625 |
| GO:0051225 | spindle assembly | 0.49873616 | 1.142580545 |
| ENSG00000167842 | MIS12 subnetwork | 0.94137986 | 1.142596639 |
| GO:0006312 | mitotic recombination | 0.49928202 | 1.142634999 |
| MP:0001680 | abnormal mesoderm development | 0.49923723 | 1.142641597 |
| ENSG00000168522 | FNTA subnetwork | 0.49999215 | 1.142651831 |
| GO:0035270 | endocrine system development | 0.94137098 | 1.142680057 |
| GO:0070742 | C2H2 zinc finger domain binding | 0.49859452 | 1.142686706 |
| ENSG00000108671 | PSMD11 subnetwork | 0.49991384 | 1.142689335 |
| GO:0014911 | positive regulation of smooth muscle cell migration | 0.94124802 | 1.142733462 |
| GO:0007005 | mitochondrion organization | 0.94134305 | 1.14274668 |
| GO:0044304 | main axon | 0.94120805 | 1.142795898 |
| ENSG00000166451 | CENPN subnetwork | 0.94113836 | 1.142807902 |
| MP:0000733 | abnormal muscle development | 0.94099249 | 1.142836122 |
| GO:0031396 | regulation of protein ubiquitination | 0.94082593 | 1.142843327 |
| ENSG00000181852 | RNF41 subnetwork | 0.49980331 | 1.142849412 |
| ENSG00000117594 | HSD11B1 subnetwork | 0.49989211 | 1.142850518 |
| GO:0001540 | beta-amyloid binding | 0.94108215 | 1.14285354 |
| MP:0003446 | renal hypoplasia | 0.94096761 | 1.142898587 |
| GO:0006940 | regulation of smooth muscle contraction | 0.94077588 | 1.142901598 |
| ENSG00000174903 | RAB1B subnetwork | 0.49972491 | 1.142910159 |
| MP:0010027 | increased liver cholesterol level | 0.94074431 | 1.14296829 |
| GO:2000379 | positive regulation of reactive oxygen species metabolic pr | 0.94006523 | 1.142993014 |
| GO:0006835 | dicarboxylic acid transport | 0.94042969 | 1.142995372 |
| ENSG00000159377 | PSMB4 subnetwork | 0.50029711 | 1.143001699 |
| ENSG00000076248 | UNG subnetwork | 0.94072783 | 1.143047611 |
| ENSG00000146731 | CCT6A subnetwork | 0.49969076 | 1.143055985 |
| ENSG00000185737 | NRG3 subnetwork | 0.94005385 | 1.143076599 |
| ENSG00000131269 | ABCB7 subnetwork | 0.94026044 | 1.143077765 |
| ENSG00000184185 | KCNJ12 subnetwork | 0.94042286 | 1.143083137 |
| ENSG00000164692 | COL1A2 subnetwork | 0.94059825 | 1.143101127 |
| ENSG00000170178 | HOXD12 subnetwork | 0.49960226 | 1.143101315 |
| ENSG00000121440 | PDZRN3 subnetwork | 0.94072777 | 1.143143771 |
| ENSG00000138413 | IDH1 subnetwork | 0.94041023 | 1.143154086 |
| GO:0070372 | regulation of ERK1 and ERK2 cascade | 0.94004769 | 1.143168617 |
| GO:0048199 | vesicle targeting, to, from or within Golgi | 0.94002155 | 1.143214346 |
| ENSG00000145723 | GIN1 subnetwork | 0.49958105 | 1.143216275 |
| ENSG00000172680 | MOS subnetwork | 0.93995248 | 1.143272712 |
| ENSG00000106799 | TGFBR1 subnetwork | 0.93993038 | 1.143335298 |

| | | | |
|---|---|---|---|
| MP:0005044 | sepsis | 0.93989477 | 1.143397895 |
| GO:0071599 | otic vesicle development | 0.93976205 | 1.14342205 |
| GO:0072595 | maintenance of protein localization to organelle | 0.93964731 | 1.143454637 |
| ENSG00000169306 | IL1RAPL1 subnetwork | 0.93972817 | 1.143463612 |
| MP:0003425 | abnormal optic vesicle formation | 0.93988736 | 1.143485767 |
| ENSG00000161800 | RACGAP1 subnetwork | 0.93964724 | 1.143550969 |
| GO:0021872 | forebrain generation of neurons | 0.93962434 | 1.143622041 |
| GO:0031233 | intrinsic to external side of plasma membrane | 0.93956155 | 1.143646781 |
| MP:0003675 | kidney cysts | 0.93950641 | 1.143696806 |
| REACTOME_RETROGRADE_NEI | REACTOME_RETROGRADE_NEUROTROPHIN_SIGNALLING | 0.93949755 | 1.143788977 |
| GO:0051983 | regulation of chromosome segregation | 0.93947979 | 1.143864307 |
| MP:0000410 | waved hair | 0.93937092 | 1.143939138 |
| ENSG00000016082 | ISL1 subnetwork | 0.93946803 | 1.143943864 |
| GO:0043043 | peptide biosynthetic process | 0.93932999 | 1.143993424 |
| GO:0002009 | morphogenesis of an epithelium | 0.50102105 | 1.14403181 |
| GO:0055088 | lipid homeostasis | 0.93928351 | 1.144039288 |
| MP:0009431 | decreased fetal weight | 0.50107615 | 1.144040451 |
| REACTOME_ISG15_ANTIVIRAL_ | REACTOME_ISG15_ANTIVIRAL_MECHANISM | 0.50095297 | 1.144054054 |
| KEGG_PPAR_SIGNALING_PATH | KEGG_PPAR_SIGNALING_PATHWAY | 0.9392099 | 1.144135256 |
| ENSG00000170486 | KRT72 subnetwork | 0.9392764 | 1.14413575 |
| GO:0060713 | labyrinthine layer morphogenesis | 0.93919812 | 1.144227526 |
| REACTOME_ANTIVIRAL_MECH | REACTOME_ANTIVIRAL_MECHANISM_BY_IFN:STIMULATED | 0.50095297 | 1.144230769 |
| GO:0046928 | regulation of neurotransmitter secretion | 0.93919182 | 1.144319811 |
| ENSG00000153944 | MSI2 subnetwork | 0.93917958 | 1.144407895 |
| GO:0014044 | Schwann cell development | 0.9391692 | 1.14448334 |
| MP:0004892 | increased adiponectin level | 0.93915519 | 1.144563017 |
| MP:0009749 | enhanced behavioral response to addictive substance | 0.93914935 | 1.144651143 |
| GO:0090087 | regulation of peptide transport | 0.93914596 | 1.144747722 |
| GO:0007271 | synaptic transmission, cholinergic | 0.93904235 | 1.144827004 |
| GO:0070301 | cellular response to hydrogen peroxide | 0.93838094 | 1.14483574 |
| GO:0002791 | regulation of peptide secretion | 0.93914596 | 1.144844317 |
| GO:0006541 | glutamine metabolic process | 0.93883643 | 1.144859458 |
| GO:0002053 | positive regulation of mesenchymal cell proliferation | 0.93890483 | 1.144859892 |
| REACTOME_M_PHASE | REACTOME_M_PHASE | 0.93897411 | 1.144864546 |
| GO:0019208 | phosphatase regulator activity | 0.93830015 | 1.144864865 |
| GO:0051150 | regulation of smooth muscle cell differentiation | 0.93819665 | 1.1449358 |
| ENSG00000179715 | FAM113B subnetwork | 0.93876256 | 1.144938793 |
| GO:0050997 | quaternary ammonium group binding | 0.93852241 | 1.144941733 |
| GO:0015697 | quaternary ammonium group transport | 0.93883007 | 1.144951882 |
| ENSG00000196290 | NIF3L1 subnetwork | 0.93829903 | 1.144961568 |
| GO:0043168 | anion binding | 0.93873254 | 1.14500591 |
| GO:0033205 | cell cycle cytokinesis | 0.93818708 | 1.145024077 |
| GO:0060711 | labyrinthine layer development | 0.93871124 | 1.145056151 |
| ENSG00000060237 | WNK1 subnetwork | 0.50152905 | 1.145075641 |
| ENSG00000182132 | KCNIP1 subnetwork | 0.93817872 | 1.145099696 |
| ENSG00000104164 | PLDN subnetwork | 0.93810602 | 1.14513308 |
| ENSG00000089154 | GCN1L1 subnetwork | 0.50178706 | 1.145139639 |
| GO:0030219 | megakaryocyte differentiation | 0.50164287 | 1.145184442 |
| MP:0002428 | abnormal semicircular canal morphology | 0.93809321 | 1.145204496 |
| GO:0046902 | regulation of mitochondrial membrane permeability | 0.50172199 | 1.145208333 |
| ENSG00000077080 | ACTL6B subnetwork | 0.50260571 | 1.145216454 |
| ENSG00000176658 | MYO1D subnetwork | 0.50271681 | 1.145263401 |
| GO:0042953 | lipoprotein transport | 0.93808493 | 1.1452886 |

| | | | |
|---|---|---|---|
| GO:0071813 | lipoprotein particle binding | 0.9377045 | 1.145320426 |
| ENSG00000105997 | HOXA3 subnetwork | 0.50258796 | 1.145331279 |
| MP:0003068 | enlarged kidney | 0.50225357 | 1.145351526 |
| ENSG00000130707 | ASS1 subnetwork | 0.93807057 | 1.145355815 |
| ENSG00000167978 | SRRM2 subnetwork | 0.50281165 | 1.145356538 |
| GO:0043687 | post-translational protein modification | 0.50217237 | 1.14536623 |
| ENSG00000118094 | TREH subnetwork | 0.50364796 | 1.145379766 |
| MP:0001973 | increased thermal nociceptive threshold | 0.93795791 | 1.145388842 |
| ENSG00000123219 | CENPK subnetwork | 0.93801778 | 1.145406136 |
| GO:0032371 | regulation of sterol transport | 0.503529 | 1.145409105 |
| GO:0071814 | protein-lipid complex binding | 0.9377045 | 1.145417266 |
| GO:0000288 | nuclear-transcribed mRNA catabolic process, deadenylatior | 0.50213838 | 1.145427205 |
| ENSG00000126522 | ASL subnetwork | 0.50316151 | 1.145444051 |
| GO:0045933 | positive regulation of muscle contraction | 0.93793233 | 1.145464536 |
| ENSG00000137764 | MAP2K5 subnetwork | 0.50294408 | 1.145465045 |
| REACTOME_PROSTANOID_ME | REACTOME_PROSTANOID_METABOLISM | 0.5025702 | 1.145469256 |
| GO:0004930 | G-protein coupled receptor activity | 0.93766354 | 1.14547607 |
| GO:0060768 | regulation of epithelial cell proliferation involved in prostat | 0.93761283 | 1.145522199 |
| ENSG00000107242 | PIP5K1B subnetwork | 0.50364452 | 1.145555897 |
| GO:0045682 | regulation of epidermis development | 0.50379465 | 1.145580323 |
| GO:0032374 | regulation of cholesterol transport | 0.503529 | 1.145585295 |
| ENSG00000116455 | WDR77 subnetwork | 0.50315017 | 1.145589594 |
| ENSG00000164751 | PEX2 subnetwork | 0.50212327 | 1.145596175 |
| GO:0060324 | face development | 0.93760245 | 1.145606394 |
| REACTOME_SIGNALING_BY_C | REACTOME_SIGNALING_BY_CONSTITUTIVELY_ACTIVE_EGF | 0.50309213 | 1.145619707 |
| ENSG00000105514 | RAB3D subnetwork | 0.50332352 | 1.14562173 |
| ENSG00000146143 | ENSG00000146143 subnetwork | 0.50204441 | 1.145634064 |
| ENSG00000184678 | HIST2H2BE subnetwork | 0.50255158 | 1.145638101 |
| MP:0005543 | corneal thinning | 0.93713481 | 1.145642241 |
| ENSG00000112159 | MDN1 subnetwork | 0.50442248 | 1.145647167 |
| ENSG00000105429 | MEGF8 subnetwork | 0.5034779 | 1.145684615 |
| GO:0015749 | monosaccharide transport | 0.9375888 | 1.145694832 |
| ENSG00000197275 | RAD54B subnetwork | 0.50342016 | 1.145699338 |
| KEGG_TASTE_TRANSDUCTION | KEGG_TASTE_TRANSDUCTION | 0.93712939 | 1.145734958 |
| GO:0046661 | male sex differentiation | 0.50252519 | 1.145737629 |
| MP:0002953 | thick ventricular wall | 0.50430975 | 1.145745661 |
| GO:0019827 | stem cell maintenance | 0.93739068 | 1.145769882 |
| MP:0000441 | increased cranium width | 0.93636573 | 1.145773694 |
| GO:0007588 | excretion | 0.93758114 | 1.145787515 |
| REACTOME_SEROTONIN_NEUI | REACTOME_SEROTONIN_NEUROTRANSMITTER_RELEASE_C | 0.93679042 | 1.14580088 |
| MP:0008279 | arrest of spermiogenesis | 0.93644258 | 1.145807927 |
| GO:0009954 | proximal/distal pattern formation | 0.93705508 | 1.145814642 |
| GO:0030128 | clathrin coat of endocytic vesicle | 0.93712549 | 1.145814997 |
| GO:0051905 | establishment of pigment granule localization | 0.93734267 | 1.145816059 |
| REACTOME_PROCESSING_OF_ | REACTOME_PROCESSING_OF_CAPPED_INTRON:CONTAINI | 0.50441959 | 1.145823096 |
| GO:0060602 | branch elongation of an epithelium | 0.93753894 | 1.145837916 |
| REACTOME_CYTOCHROME_P4 | REACTOME_CYTOCHROME_P450_:_ARRANGED_BY_SUBST | 0.50462277 | 1.14583973 |
| GO:0008584 | male gonad development | 0.50426271 | 1.145844854 |
| ENSG00000130772 | MED18 subnetwork | 0.50402221 | 1.145850622 |
| GO:0005868 | cytoplasmic dynein complex | 0.93700212 | 1.145852379 |
| ENSG00000165775 | FUNDC2 subnetwork | 0.93658214 | 1.145854856 |
| GO:0008242 | omega peptidase activity | 0.93635691 | 1.145862273 |
| REACTOME_DOPAMINE_NEUR | REACTOME_DOPAMINE_NEUROTRANSMITTER_RELEASE_C | 0.93679042 | 1.145897892 |

| | | | |
|---|---|---|---|
| MP:0004021 | abnormal rod electrophysiology | 0.93697631 | 1.145923982 |
| GO:0030315 | T-tubule | 0.93632871 | 1.145925455 |
| GO:0071222 | cellular response to lipopolysaccharide | 0.50397245 | 1.145926837 |
| ENSG00000136108 | CKAP2 subnetwork | 0.93676333 | 1.145965284 |
| ENSG00000175084 | DES subnetwork | 0.93631311 | 1.146009827 |
| ENSG00000119487 | MAPKAP1 subnetwork | 0.50425516 | 1.146013212 |
| ENSG00000171885 | AQP4 subnetwork | 0.50421468 | 1.146074063 |
| MP:0002098 | abnormal vibrissa morphology | 0.93629277 | 1.14609845 |
| ENSG00000090470 | PDCD7 subnetwork | 0.93626691 | 1.146178614 |
| GO:0090004 | positive regulation of establishment of protein localization | 0.93510767 | 1.1461868 |
| ENSG00000117697 | NSL1 subnetwork | 0.93528549 | 1.146187447 |
| MP:0001392 | abnormal locomotor behavior | 0.93619034 | 1.146191001 |
| MP:0002912 | abnormal excitatory postsynaptic potential | 0.93464024 | 1.146248515 |
| GO:0006261 | DNA-dependent DNA replication | 0.50487786 | 1.146254797 |
| GO:0072028 | nephron morphogenesis | 0.93526321 | 1.146254983 |
| GO:0002062 | chondrocyte differentiation | 0.93449006 | 1.146256367 |
| MP:0001714 | absent trophoblast giant cells | 0.93618559 | 1.146279661 |
| GO:0042401 | cellular biogenic amine biosynthetic process | 0.93509873 | 1.1462798 |
| ENSG00000197858 | GPAA1 subnetwork | 0.93456102 | 1.146282149 |
| ENSG00000162368 | CMPK1 subnetwork | 0.93440971 | 1.146294252 |
| GO:0030673 | axolemma | 0.93613916 | 1.146313247 |
| ENSG00000070371 | CLTCL1 subnetwork | 0.93478989 | 1.146316727 |
| GO:0043200 | response to amino acid stimulus | 0.93589582 | 1.146320787 |
| GO:0016197 | endosomal transport | 0.93508803 | 1.146351604 |
| ENSG00000134602 | ENSG00000134602 subnetwork | 0.93439941 | 1.146374597 |
| ENSG00000150672 | DLG2 subnetwork | 0.93610691 | 1.146376504 |
| GO:0019321 | pentose metabolic process | 0.93586035 | 1.146384061 |
| GO:0015114 | phosphate ion transmembrane transporter activity | 0.93496864 | 1.146389172 |
| REACTOME_TRANSPORT_OF_C | REACTOME_TRANSPORT_OF_ORGANIC_ANIONS | 0.93558563 | 1.14642524 |
| ENSG00000184486 | POU3F2 subnetwork | 0.93568833 | 1.146425543 |
| GO:0071436 | sodium ion export | 0.93581226 | 1.146438867 |
| GO:0031102 | neuron projection regeneration | 0.9350782 | 1.14644039 |
| ENSG00000119929 | CUTC subnetwork | 0.93438043 | 1.146454955 |
| MP:0009832 | abnormal sperm mitochondrial sheath morphology | 0.93609661 | 1.146456726 |
| GO:0022626 | cytosolic ribosome | 0.934318 | 1.146484375 |
| GO:0019888 | protein phosphatase regulator activity | 0.93577499 | 1.146485203 |
| GO:0008202 | steroid metabolic process | 0.50521975 | 1.146548021 |
| ENSG00000172201 | ID4 subnetwork | 0.93413905 | 1.146559925 |
| MP:0002641 | anisopoikilocytosis | 0.93431724 | 1.146581741 |
| ENSG00000134109 | EDEM1 subnetwork | 0.93409768 | 1.146614849 |
| MP:0004132 | absent embryonic cilia | 0.50510687 | 1.146623696 |
| GO:0035051 | cardiac cell differentiation | 0.93406072 | 1.146661286 |
| ENSG00000168487 | BMP1 subnetwork | 0.50547466 | 1.146671779 |
| GO:0032309 | icosanoid secretion | 0.93431267 | 1.146679123 |
| GO:0051457 | maintenance of protein location in nucleus | 0.9340371 | 1.146703483 |
| MP:0003864 | abnormal midbrain development | 0.50521063 | 1.146708608 |
| GO:0019748 | secondary metabolic process | 0.93394364 | 1.146715949 |
| GO:0070918 | production of small RNA involved in gene silencing by RNA | 0.93381867 | 1.146749384 |
| ENSG00000153044 | CENPH subnetwork | 0.93368803 | 1.146770081 |
| GO:0000049 | tRNA binding | 0.5054491 | 1.146778647 |
| ENSG00000154310 | TNIK subnetwork | 0.93362258 | 1.146808058 |
| ENSG00000008277 | ADAM22 subnetwork | 0.93393894 | 1.146809143 |
| GO:0031050 | dsRNA fragmentation | 0.93381867 | 1.146846847 |

| | | | |
|---|---|---|---|
| GO:0010008 | endosome membrane | 0.93360322 | 1.146892799 |
| GO:0051310 | metaphase plate congression | 0.93351748 | 1.146896786 |
| ENSG00000141696 | LEPREL4 subnetwork | 0.50578906 | 1.146941122 |
| ENSG00000100151 | PICK1 subnetwork | 0.93349284 | 1.146977298 |
| ENSG00000142627 | EPHA2 subnetwork | 0.50591062 | 1.14698038 |
| GO:0052742 | phosphatidylinositol kinase activity | 0.50619709 | 1.147027731 |
| GO:0051428 | peptide hormone receptor binding | 0.93328343 | 1.147031808 |
| ENSG00000173171 | MTX1 subnetwork | 0.50603699 | 1.147034483 |
| GO:0042301 | phosphate ion binding | 0.51105636 | 1.14704142 |
| GO:0046883 | regulation of hormone secretion | 0.93347194 | 1.147045068 |
| ENSG00000196154 | S100A4 subnetwork | 0.93323773 | 1.147065578 |
| ENSG00000196236 | XPNPEP3 subnetwork | 0.50614516 | 1.147065584 |
| GO:0030811 | regulation of nucleotide catabolic process | 0.51089995 | 1.14708561 |
| GO:0031984 | organelle subcompartment | 0.50578668 | 1.147109339 |
| ENSG00000152214 | RIT2 subnetwork | 0.93344375 | 1.147117102 |
| ENSG00000183431 | SF3A3 subnetwork | 0.51103127 | 1.147132018 |
| GO:0021697 | cerebellar cortex formation | 0.50590789 | 1.147156216 |
| ENSG00000160271 | RALGDS subnetwork | 0.93323042 | 1.147163151 |
| GO:0033121 | regulation of purine nucleotide catabolic process | 0.51089995 | 1.147259754 |
| REACTOME_SPHINGOLIPID_MI | REACTOME_SPHINGOLIPID_METABOLISM | 0.93304064 | 1.147260274 |
| MP:0010465 | aberrant origin of the right subclavian artery | 0.93321503 | 1.14726074 |
| ENSG00000197903 | HIST1H2BK subnetwork | 0.51102474 | 1.147268174 |
| MP:0000846 | abnormal medulla oblongata morphology | 0.93315055 | 1.147290284 |
| ENSG00000152253 | SPC25 subnetwork | 0.93300042 | 1.147302587 |
| MP:0008114 | abnormal Kupffer cell morphology | 0.50643183 | 1.147342218 |
| ENSG00000127946 | HIP1 subnetwork | 0.93297643 | 1.147378946 |
| ENSG00000172766 | NAA16 subnetwork | 0.50708964 | 1.147383721 |
| GO:0019239 | deaminase activity | 0.50748021 | 1.147393365 |
| ENSG00000179348 | GATA2 subnetwork | 0.5108821 | 1.147403583 |
| MP:0010263 | total cataracts | 0.93291731 | 1.147408511 |
| GO:0007431 | salivary gland development | 0.5108423 | 1.147418375 |
| ENSG00000138083 | SIX3 subnetwork | 0.93287851 | 1.14746787 |
| ENSG00000136153 | LMO7 subnetwork | 0.50744628 | 1.147477064 |
| ENSG00000116251 | RPL22 subnetwork | 0.50676631 | 1.147488899 |
| ENSG00000130294 | KIF1A subnetwork | 0.50701038 | 1.147513009 |
| GO:0046849 | bone remodeling | 0.50672432 | 1.147534456 |
| GO:0031581 | hemidesmosome assembly | 0.50721011 | 1.147537097 |
| ENSG00000123737 | EXOSC9 subnetwork | 0.50684827 | 1.147550521 |
| REACTOME_SYNTHESIS_OF_VE | REACTOME_SYNTHESIS_OF_VERY_LONG:CHAIN_FATTY_AC | 0.51034783 | 1.147552448 |
| GO:0034121 | regulation of toll-like receptor signaling pathway | 0.93285412 | 1.147557031 |
| GO:0006766 | vitamin metabolic process | 0.5070866 | 1.147559296 |
| MP:0000035 | abnormal membranous labyrinth morphology | 0.51083315 | 1.147577461 |
| REACTOME_PEROXISOMAL_LI | REACTOME_PEROXISOMAL_LIPID_METABOLISM | 0.50739812 | 1.147591375 |
| ENSG00000161547 | SRSF2 subnetwork | 0.50668022 | 1.147618318 |
| MP:0003830 | abnormal testis development | 0.51027296 | 1.147620496 |
| MP:0003868 | abnormal feces composition | 0.93274333 | 1.147624723 |
| REACTOME_BILE_ACID_AND_E | REACTOME_BILE_ACID_AND_BILE_SALT_METABOLISM | 0.510774 | 1.14764545 |
| ENSG00000111052 | LIN7A subnetwork | 0.93285274 | 1.14765472 |
| ENSG00000115275 | MOGS subnetwork | 0.93269519 | 1.147658578 |
| ENSG00000163631 | ALB subnetwork | 0.51014086 | 1.147665399 |
| ENSG00000103089 | FA2H subnetwork | 0.5069858 | 1.147665697 |
| GO:0022602 | ovulation cycle process | 0.51160637 | 1.147679709 |
| ENSG00000172340 | SUCLG2 subnetwork | 0.51048854 | 1.147697218 |

| | | | |
|---|---|---|---|
| GO:0042454 | ribonucleoside catabolic process | 0.50767843 | 1.147714766 |
| ENSG00000136146 | MED4 subnetwork | 0.51024294 | 1.147718978 |
| REACTOME_MRNA_DECAY_BY | REACTOME_MRNA_DECAY_BY_3_TO_5_EXORIBONUCLEAS | 0.93259413 | 1.147730563 |
| MP:0003702 | abnormal chromosome morphology | 0.51073898 | 1.14773625 |
| GO:0072657 | protein localization in membrane | 0.93268212 | 1.147739271 |
| GO:0043015 | gamma-tubulin binding | 0.93249716 | 1.147747402 |
| ENSG00000185736 | ADARB2 subnetwork | 0.51059326 | 1.14775076 |
| GO:0032092 | positive regulation of protein binding | 0.50739655 | 1.147759254 |
| ENSG00000107447 | DNTT subnetwork | 0.51068946 | 1.147804285 |
| GO:0010951 | negative regulation of endopeptidase activity | 0.51013753 | 1.147824764 |
| ENSG00000180228 | PRKRA subnetwork | 0.51159103 | 1.147831033 |
| MP:0008439 | abnormal cortical plate morphology | 0.93248264 | 1.147845158 |
| MP:0005464 | abnormal platelet physiology | 0.50843952 | 1.147893451 |
| ENSG00000105176 | URI1 subnetwork | 0.5078318 | 1.147906159 |
| ENSG00000157077 | ZFYVE9 subnetwork | 0.5078922 | 1.147906479 |
| MP:0004321 | short sternum | 0.51151645 | 1.147906553 |
| GO:0019319 | hexose biosynthetic process | 0.50810097 | 1.147914757 |
| MP:0005030 | absent amnion | 0.93246993 | 1.147925894 |
| ENSG00000169976 | SF3B5 subnetwork | 0.50801253 | 1.147937357 |
| MP:0000929 | open neural tube | 0.51011497 | 1.147938536 |
| ENSG00000136271 | DDX56 subnetwork | 0.50854882 | 1.147977717 |
| GO:0005179 | hormone activity | 0.93245044 | 1.148010904 |
| ENSG00000106829 | TLE4 subnetwork | 0.93238867 | 1.148036292 |
| MP:0002584 | small ectoplacental cone | 0.50894961 | 1.148040262 |
| ENSG00000124222 | STX16 subnetwork | 0.51008177 | 1.148044735 |
| ENSG00000127922 | SHFM1 subnetwork | 0.50843137 | 1.148053435 |
| REACTOME_POST:TRANSLATIC | REACTOME_POST:TRANSLATIONAL_MODIFICATION_SYNTH | 0.51252407 | 1.14805421 |
| ENSG00000111987 | ENSG00000111987 subnetwork | 0.50953819 | 1.148073115 |
| GO:0006613 | cotranslational protein targeting to membrane | 0.93235228 | 1.148112806 |
| ENSG00000160307 | S100B subnetwork | 0.51247948 | 1.148122066 |
| ENSG00000150938 | CRIM1 subnetwork | 0.50891554 | 1.148123856 |
| GO:0008105 | asymmetric protein localization | 0.51240187 | 1.148174796 |
| ENSG00000105323 | HNRNPUL1 subnetwork | 0.50871096 | 1.148176408 |
| REACTOME_G1_PHASE | REACTOME_G1_PHASE | 0.51007008 | 1.148181403 |
| GO:0007043 | cell-cell junction assembly | 0.50887375 | 1.148207475 |
| MP:0006346 | small branchial arch | 0.93235172 | 1.148210634 |
| GO:0032934 | sterol binding | 0.50842595 | 1.148213468 |
| ENSG00000169249 | ZRSR2 subnetwork | 0.50827645 | 1.148220559 |
| ENSG00000112081 | SRSF3 subnetwork | 0.51230477 | 1.148227541 |
| GO:0000245 | spliceosomal complex assembly | 0.51271986 | 1.148228615 |
| ENSG00000104765 | BNIP3L subnetwork | 0.93211804 | 1.148244268 |
| MP:0011095 | complete embryonic lethality between implantation and pl | 0.51303965 | 1.148244818 |
| ENSG00000172850 | LSM2 subnetwork | 0.50953819 | 1.14824802 |
| MP:0008584 | photoreceptor outer segment degeneration | 0.93130321 | 1.148255715 |
| GO:0002532 | production of molecular mediator involved in inflammatory | 0.51339351 | 1.148261264 |
| ENSG00000150093 | ITGB1 subnetwork | 0.51333073 | 1.148268562 |
| ENSG00000136169 | SETDB2 subnetwork | 0.93231038 | 1.148270132 |
| GO:0043623 | cellular protein complex assembly | 0.50834146 | 1.148274282 |
| MP:0001554 | increased circulating free fatty acid level | 0.51319742 | 1.148283164 |
| ENSG00000163828 | ENSG00000163828 subnetwork | 0.51327148 | 1.148283424 |
| GO:0032107 | regulation of response to nutrient levels | 0.93191511 | 1.148303495 |
| MP:0009247 | meteorism | 0.93199405 | 1.148312164 |
| MP:0010025 | decreased total body fat amount | 0.51314031 | 1.148313162 |

| | | | |
|---|---|---|---|
| ENSG00000043355 | ZIC2 subnetwork | 0.93209441 | 1.148320832 |
| ENSG00000115840 | SLC25A12 subnetwork | 0.93129441 | 1.148345133 |
| GO:0005581 | collagen | 0.93229391 | 1.148346685 |
| REACTOME_CYCLIN_D_ASSOCI | REACTOME_CYCLIN_D_ASSOCIATED_EVENTS_IN_G1 | 0.51007008 | 1.148356164 |
| MP:0009937 | abnormal neuron differentiation | 0.93120739 | 1.148357789 |
| ENSG00000185313 | SCN10A subnetwork | 0.50886225 | 1.14835978 |
| GO:0045444 | fat cell differentiation | 0.51302821 | 1.148388317 |
| ENSG00000101442 | ACTR5 subnetwork | 0.50944258 | 1.148392258 |
| ENSG00000196975 | ANXA4 subnetwork | 0.50915853 | 1.148398902 |
| GO:0032104 | regulation of response to extracellular stimulus | 0.93191511 | 1.148401398 |
| MP:0002764 | short tibia | 0.51229981 | 1.148401515 |
| ENSG00000141252 | VPS53 subnetwork | 0.5100218 | 1.148401583 |
| MP:0002780 | decreased circulating testosterone level | 0.51225508 | 1.14840885 |
| ENSG00000120256 | LRP11 subnetwork | 0.51197462 | 1.148415466 |
| ENSG00000204392 | LSM2 subnetwork | 0.50953819 | 1.148422977 |
| GO:0034698 | response to gonadotropin stimulus | 0.5129162 | 1.148425674 |
| GO:0010464 | regulation of mesenchymal cell proliferation | 0.93158605 | 1.148434968 |
| MP:0005358 | abnormal incisor morphology | 0.93188227 | 1.148448158 |
| ENSG00000109472 | CPE subnetwork | 0.93120452 | 1.148455763 |
| GO:0032642 | regulation of chemokine production | 0.51298441 | 1.148463751 |
| GO:0043525 | positive regulation of neuron apoptotic process | 0.51205792 | 1.14848393 |
| GO:0005952 | cAMP-dependent protein kinase complex | 0.50998618 | 1.148492692 |
| ENSG00000162624 | LHX8 subnetwork | 0.50941403 | 1.148498704 |
| ENSG00000169155 | ZBTB43 subnetwork | 0.93185334 | 1.148503454 |
| GO:0050000 | chromosome localization | 0.93116492 | 1.148511092 |
| MP:0002674 | abnormal sperm motility | 0.51358715 | 1.148526077 |
| GO:0070491 | repressing transcription factor binding | 0.51216847 | 1.148544793 |
| ENSG00000177425 | PAWR subnetwork | 0.50996558 | 1.148553373 |
| REACTOME_PEPTIDE_LIGAND: | REACTOME_PEPTIDE_LIGAND:BINDING_RECEPTORS | 0.5122275 | 1.148567748 |
| GO:0006826 | iron ion transport | 0.93184365 | 1.148584342 |
| ENSG00000160201 | U2AF1 subnetwork | 0.51368707 | 1.148594317 |
| GO:0051402 | neuron apoptotic process | 0.93105399 | 1.148596177 |
| GO:0051303 | establishment of chromosome localization | 0.93116492 | 1.148609096 |
| ENSG00000165733 | BMS1 subnetwork | 0.50938027 | 1.148620427 |
| ENSG00000134138 | MEIS2 subnetwork | 0.93103887 | 1.148677136 |
| GO:0030036 | actin cytoskeleton organization | 0.50932964 | 1.148681201 |
| GO:0007160 | cell-matrix adhesion | 0.50996489 | 1.148720682 |
| GO:0046134 | pyrimidine nucleoside biosynthetic process | 0.93103782 | 1.148775179 |
| GO:0015758 | glucose transport | 0.93096162 | 1.148796415 |
| GO:0001657 | ureteric bud development | 0.93082974 | 1.148830359 |
| GO:0070717 | poly-purine tract binding | 0.51508459 | 1.148876828 |
| GO:0022604 | regulation of cell morphogenesis | 0.93079594 | 1.148885758 |
| GO:0008645 | hexose transport | 0.93096162 | 1.148894485 |
| ENSG00000136531 | SCN2A subnetwork | 0.93025103 | 1.148936261 |
| GO:0030072 | peptide hormone secretion | 0.93030649 | 1.148944895 |
| MP:0001436 | abnormal suckling behavior | 0.93078499 | 1.148966783 |
| ENSG00000137486 | ARRB1 subnetwork | 0.51505198 | 1.148982207 |
| GO:0009250 | glucan biosynthetic process | 0.93021149 | 1.148995984 |
| GO:2000243 | positive regulation of reproductive process | 0.51487127 | 1.149034545 |
| MP:0001852 | conjunctivitis | 0.5150184 | 1.149034836 |
| MP:0003606 | kidney failure | 0.51435088 | 1.149041075 |
| MP:0002563 | shortened circadian period | 0.93078076 | 1.149052092 |
| REACTOME_DEADENYLATION:I | REACTOME_DEADENYLATION:DEPENDENT_MRNA_DECAY | 0.51443786 | 1.149056319 |

| | | | |
|---|---|---|---|
| ENSG00000101452 | DHX35 subnetwork | 0.93013684 | 1.149077002 |
| GO:0005978 | glycogen biosynthetic process | 0.93021149 | 1.149094172 |
| GO:0050660 | flavin adenine dinucleotide binding | 0.51452262 | 1.149094203 |
| ENSG00000125991 | ERGIC3 subnetwork | 0.51498581 | 1.149117647 |
| MP:0001501 | abnormal sleep pattern | 0.93053054 | 1.149124381 |
| GO:0050770 | regulation of axonogenesis | 0.93077126 | 1.149145956 |
| GO:0040012 | regulation of locomotion | 0.93000093 | 1.1491495 |
| GO:0006220 | pyrimidine nucleotide metabolic process | 0.93070163 | 1.149154424 |
| ENSG00000136875 | PRPF4 subnetwork | 0.51403885 | 1.149161251 |
| GO:0018202 | peptidyl-histidine modification | 0.93012938 | 1.14917094 |
| GO:0043508 | negative regulation of JUN kinase activity | 0.93063584 | 1.149175707 |
| MP:0004852 | decreased testis weight | 0.51476069 | 1.149185152 |
| GO:0005840 | ribosome | 0.51485628 | 1.149185275 |
| ENSG00000198467 | TPM2 subnetwork | 0.51433655 | 1.149191965 |
| MP:0002176 | increased brain weight | 0.9299817 | 1.149239186 |
| GO:0051051 | negative regulation of transport | 0.51466746 | 1.14925283 |
| MP:0001958 | emphysema | 0.51473724 | 1.149268035 |
| GO:0042033 | chemokine biosynthetic process | 0.51431266 | 1.14929003 |
| GO:0002448 | mast cell mediated immunity | 0.92994858 | 1.149294691 |
| ENSG00000176406 | RIMS2 subnetwork | 0.92979078 | 1.149298846 |
| REACTOME_STRIATED_MUSCL | REACTOME_STRIATED_MUSCLE_CONTRACTION | 0.92962575 | 1.149307278 |
| GO:0061098 | positive regulation of protein tyrosine kinase activity | 0.92987835 | 1.149311731 |
| MP:0002841 | impaired skeletal muscle contractility | 0.51425868 | 1.149357909 |
| ENSG00000133935 | C14orf1 subnetwork | 0.92976633 | 1.149367197 |
| GO:0002438 | acute inflammatory response to antigenic stimulus | 0.51539874 | 1.149374435 |
| REACTOME_IONOTROPIC_ACT | REACTOME_IONOTROPIC_ACTIVITY_OF_KAINATE_RECEPTC | 0.92960412 | 1.149384194 |
| ENSG00000120129 | DUSP1 subnetwork | 0.5142195 | 1.149388033 |
| REACTOME_ACTIVATION_OF_( | REACTOME_ACTIVATION_OF_CA:PERMEABLE_KAINATE_RE | 0.92960412 | 1.149482508 |
| GO:0046324 | regulation of glucose import | 0.92957331 | 1.149546621 |
| MP:0004184 | abnormal baroreceptor physiology | 0.92954212 | 1.149606468 |
| GO:0071359 | cellular response to dsRNA | 0.92949441 | 1.149636379 |
| GO:0005529 | GO:0005529 | 0.92926697 | 1.149644844 |
| MP:0011104 | partial embryonic lethality before implantation | 0.92941505 | 1.149644905 |
| ENSG00000138835 | RGS3 subnetwork | 0.92931844 | 1.149649153 |
| ENSG00000117395 | EBNA1BP2 subnetwork | 0.51559254 | 1.149653353 |
| GO:0048706 | embryonic skeletal system development | 0.92920365 | 1.149696166 |
| ENSG00000086065 | CHMP5 subnetwork | 0.92886893 | 1.149708904 |
| ENSG00000172354 | GNB2 subnetwork | 0.92916914 | 1.149738937 |
| GO:0016540 | protein autoprocessing | 0.92912186 | 1.149781715 |
| ENSG00000085840 | ORC1 subnetwork | 0.9288516 | 1.149794503 |
| GO:0030259 | lipid glycosylation | 0.92882671 | 1.149858709 |
| ENSG00000107404 | DVL1 subnetwork | 0.92910036 | 1.149875867 |
| GO:0016126 | sterol biosynthetic process | 0.92879922 | 1.149931489 |
| ENSG00000167513 | CDT1 subnetwork | 0.92875482 | 1.149974306 |
| ENSG00000154162 | CDH12 subnetwork | 0.92872906 | 1.150034261 |
| MP:0003031 | acidosis | 0.92870022 | 1.150115642 |
| GO:0015872 | dopamine transport | 0.92849384 | 1.150171365 |
| GO:0055012 | ventricular cardiac muscle cell differentiation | 0.92867761 | 1.150184186 |
| ENSG00000127948 | POR subnetwork | 0.92862061 | 1.150227039 |
| REACTOME_PROCESSING_OF_ | REACTOME_PROCESSING_OF_CAPPED_INTRONLESS_PRE:M | 0.92847367 | 1.150235647 |
| GO:0048820 | hair follicle maturation | 0.92835508 | 1.15027854 |
| REACTOME_POST:ELONGATIOI | REACTOME_POST:ELONGATION_PROCESSING_OF_INTRON | 0.92847367 | 1.150334219 |
| ENSG00000116954 | RRAGC subnetwork | 0.9283197 | 1.150338562 |

| | | | |
|---|---|---|---|
| GO:0050766 | positive regulation of phagocytosis | 0.92826535 | 1.150390022 |
| ENSG00000122484 | RPAP2 subnetwork | 0.51686837 | 1.150436353 |
| ENSG00000146425 | DYNLT1 subnetwork | 0.92787959 | 1.150463082 |
| ENSG00000047579 | DTNBP1 subnetwork | 0.51661083 | 1.150466657 |
| GO:0044440 | endosomal part | 0.92826147 | 1.150480069 |
| MP:0010736 | abnormal extraembryonic ectoderm morphology | 0.92781884 | 1.150480274 |
| ENSG00000114812 | VIPR1 subnetwork | 0.92804695 | 1.150488767 |
| GO:0006818 | hydrogen transport | 0.5168103 | 1.150511663 |
| GO:0021696 | cerebellar cortex morphogenesis | 0.51614294 | 1.15051228 |
| GO:0002886 | regulation of myeloid leukocyte mediated immunity | 0.92822127 | 1.150527263 |
| MP:0003562 | abnormal pancreatic beta cell physiology | 0.92816142 | 1.150535883 |
| ENSG00000162236 | STX5 subnetwork | 0.51624645 | 1.150564929 |
| GO:0006776 | vitamin A metabolic process | 0.92781391 | 1.150578952 |
| MP:0006303 | abnormal retinal nerve fiber layer morphology | 0.51679217 | 1.150602047 |
| KEGG_FC_GAMMA_R_MEDIAT | KEGG_FC_GAMMA_R_MEDIATED_PHAGOCYTOSIS | 0.5166082 | 1.150624812 |
| GO:0070613 | regulation of protein processing | 0.9277943 | 1.150639046 |
| GO:0071230 | cellular response to amino acid stimulus | 0.51612111 | 1.150640446 |
| GO:0046456 | icosanoid biosynthetic process | 0.51712324 | 1.150699564 |
| ENSG00000101843 | PSMD10 subnetwork | 0.51655264 | 1.150700196 |
| GO:0035137 | hindlimb morphogenesis | 0.92779259 | 1.150737754 |
| GO:0035250 | UDP-galactosyltransferase activity | 0.92771369 | 1.150746397 |
| MP:0000167 | decreased chondrocyte cell number | 0.92763955 | 1.150763621 |
| GO:0005540 | hyaluronic acid binding | 0.92738529 | 1.150776691 |
| MP:0004620 | cervical vertebral fusion | 0.92758209 | 1.15080659 |
| GO:0005251 | delayed rectifier potassium channel activity | 0.92753995 | 1.150849567 |
| GO:0006406 | mRNA export from nucleus | 0.9273757 | 1.150854004 |
| KEGG_OOCYTE_MEIOSIS | KEGG_OOCYTE_MEIOSIS | 0.51648683 | 1.150858563 |
| MP:0001131 | abnormal ovarian follicle morphology | 0.51655151 | 1.150865964 |
| MP:0000965 | abnormal sensory neuron morphology | 0.92732637 | 1.150901288 |
| ENSG00000141503 | MINK1 subnetwork | 0.92727083 | 1.150935703 |
| REACTOME_TRANSMEMBRANI | REACTOME_TRANSMEMBRANE_TRANSPORT_OF_SMALL_M | 0.92723532 | 1.151000172 |
| ENSG00000079462 | PAFAH1B3 subnetwork | 0.92720328 | 1.151086117 |
| ENSG00000108231 | LGI1 subnetwork | 0.92718981 | 1.151159196 |
| GO:0030863 | cortical cytoskeleton | 0.51745334 | 1.151203369 |
| GO:0007512 | adult heart development | 0.9271512 | 1.15121082 |
| REACTOME_REGULATION_OF_ | REACTOME_REGULATION_OF_BETA:CELL_DEVELOPMENT | 0.51774726 | 1.15122538 |
| KEGG_GLYCOSAMINOGLYCAN_ | KEGG_GLYCOSAMINOGLYCAN_BIOSYNTHESIS_CHONDROIT | 0.9270781 | 1.151232394 |
| ENSG00000142875 | PRKACB subnetwork | 0.5176447 | 1.151233083 |
| REACTOME_REGULATION_OF_ | REACTOME_REGULATION_OF_DNA_REPLICATION | 0.51758739 | 1.151293428 |
| ENSG00000178028 | DMAP1 subnetwork | 0.92707619 | 1.151331272 |
| ENSG00000034677 | RNF19A subnetwork | 0.51795268 | 1.151352773 |
| GO:0050995 | negative regulation of lipid catabolic process | 0.92702721 | 1.15137004 |
| MP:0000851 | cerebellum hypoplasia | 0.92702639 | 1.151464651 |
| GO:0016831 | carboxy-lyase activity | 0.51791648 | 1.151465725 |
| ENSG00000176108 | CHMP6 subnetwork | 0.92694972 | 1.151477663 |
| GO:0035725 | sodium ion transmembrane transport | 0.92689949 | 1.151516453 |
| ENSG00000211677 | ENSG00000211677 subnetwork | 0.92689639 | 1.151611102 |
| ENSG00000211679 | ENSG00000211679 subnetwork | 0.92689639 | 1.151710063 |
| REACTOME_ACTIVATION_OF_( | REACTOME_ACTIVATION_OF_CHAPERONES_BY_ATF6:ALPH | 0.92684779 | 1.151731695 |
| MP:0004471 | short nasal bone | 0.92684059 | 1.151813494 |
| ENSG00000105509 | HAS1 subnetwork | 0.92679505 | 1.15186952 |
| GO:0010390 | histone monoubiquitination | 0.92677884 | 1.151955643 |
| ENSG00000181085 | MAPK15 subnetwork | 0.92620662 | 1.151986926 |

| | | | |
|---|---|---|---|
| GO:0021766 | hippocampus development | 0.92613737 | 1.152021505 |
| GO:0016072 | rRNA metabolic process | 0.51836788 | 1.152028855 |
| GO:0006665 | sphingolipid metabolic process | 0.92677175 | 1.15204608 |
| GO:0002576 | platelet degranulation | 0.92611509 | 1.152099105 |
| ENSG00000100554 | ATP6V1D subnetwork | 0.92673722 | 1.15210644 |
| GO:0033006 | regulation of mast cell activation involved in immune respo | 0.92644927 | 1.152128483 |
| GO:0005905 | coated pit | 0.92607149 | 1.152138002 |
| ENSG00000090372 | STRN4 subnetwork | 0.92637948 | 1.152154468 |
| GO:0046622 | positive regulation of organ growth | 0.92600608 | 1.15218551 |
| ENSG00000137812 | CASC5 subnetwork | 0.92671829 | 1.152192605 |
| ENSG00000153207 | AHCTF1 subnetwork | 0.92593808 | 1.152220119 |
| GO:0070307 | lens fiber cell development | 0.9257541 | 1.152224804 |
| ENSG00000100949 | RABGGTA subnetwork | 0.92667784 | 1.152252988 |
| GO:0031103 | axon regeneration | 0.92589155 | 1.152267642 |
| ENSG00000163950 | SLBP subnetwork | 0.92572365 | 1.152298158 |
| GO:0002063 | chondrocyte development | 0.92566042 | 1.152350004 |
| ENSG00000130803 | ZNF317 subnetwork | 0.51858351 | 1.152366642 |
| GO:0005788 | endoplasmic reticulum lumen | 0.92565172 | 1.152444904 |
| GO:0051000 | positive regulation of nitric-oxide synthase activity | 0.51881354 | 1.152508261 |
| ENSG00000145335 | SNCA subnetwork | 0.92562393 | 1.152509686 |
| ENSG00000122884 | P4HA1 subnetwork | 0.51889429 | 1.152522901 |
| ENSG00000072778 | ACADVL subnetwork | 0.51876122 | 1.15253117 |
| GO:0072111 | cell proliferation involved in kidney development | 0.92561887 | 1.15260892 |
| ENSG00000198336 | MYL4 subnetwork | 0.92559316 | 1.152678033 |
| GO:0009311 | oligosaccharide metabolic process | 0.92551076 | 1.15268257 |
| MP:0006117 | aortic valve stenosis | 0.51875665 | 1.152689303 |
| ENSG00000005882 | PDK2 subnetwork | 0.92550105 | 1.152768926 |
| REACTOME_SHC:MEDIATED_SI | REACTOME_SHC:MEDIATED_SIGNALLING | 0.92534201 | 1.152803859 |
| MP:0005479 | decreased circulating triiodothyronine level | 0.92522089 | 1.152812958 |
| GO:0051640 | organelle localization | 0.92530668 | 1.152842867 |
| GO:0042310 | vasoconstriction | 0.92548275 | 1.152859604 |
| ENSG00000100412 | ACO2 subnetwork | 0.92521902 | 1.152912287 |
| GO:0071600 | otic vesicle morphogenesis | 0.92514079 | 1.152929772 |
| GO:0032839 | dendrite cytoplasm | 0.92509569 | 1.152964495 |
| ENSG00000001626 | CFTR subnetwork | 0.92505911 | 1.153029389 |
| GO:0006643 | membrane lipid metabolic process | 0.92503963 | 1.153098604 |
| ENSG00000115540 | MOB4 subnetwork | 0.92497413 | 1.153111801 |
| ENSG00000135828 | RNASEL subnetwork | 0.92478983 | 1.153160028 |
| GO:0030194 | positive regulation of blood coagulation | 0.92474341 | 1.153203415 |
| ENSG00000103479 | RBL2 subnetwork | 0.92497147 | 1.153211207 |
| ENSG00000101444 | AHCY subnetwork | 0.92492533 | 1.153276144 |
| MP:0002910 | abnormal excitatory postsynaptic currents | 0.92473916 | 1.153294239 |
| GO:0043547 | positive regulation of GTPase activity | 0.52015883 | 1.153297856 |
| GO:0032760 | positive regulation of tumor necrosis factor production | 0.92471707 | 1.153350582 |
| ENSG00000197697 | HIST1H2BE subnetwork | 0.52009472 | 1.153433283 |
| GO:0060351 | cartilage development involved in endochondral bone mor | 0.51940725 | 1.153445429 |
| GO:0023058 | adaptation of signaling pathway | 0.92471337 | 1.153445748 |
| ENSG00000129214 | SHBG subnetwork | 0.9240933 | 1.153543375 |
| GO:0002029 | desensitization of G-protein coupled receptor protein signa | 0.92471337 | 1.153545243 |
| ENSG00000120837 | NFYB subnetwork | 0.5203591 | 1.153559652 |
| GO:0031571 | mitotic cell cycle G1/S transition DNA damage checkpoint | 0.51938464 | 1.153573574 |
| MP:0003827 | abnormal Wolffian duct morphology | 0.52008994 | 1.15359874 |
| GO:0043299 | leukocyte degranulation | 0.92406371 | 1.153612742 |

| | | | |
|---|---|---|---|
| MP:0002183 | gliosis | 0.51979128 | 1.153623406 |
| KEGG_THYROID_CANCER | KEGG_THYROID_CANCER | 0.52051521 | 1.153633503 |
| GO:0022401 | negative adaptation of signaling pathway | 0.92471337 | 1.153644755 |
| ENSG00000070367 | EXOC5 subnetwork | 0.92404683 | 1.15369507 |
| MP:0008844 | decreased subcutaneous adipose tissue amount | 0.52006621 | 1.153719256 |
| MP:0008788 | abnormal fetal cardiomyocyte morphology | 0.92396739 | 1.153725609 |
| ENSG00000105880 | DLX5 subnetwork | 0.92469915 | 1.153731343 |
| ENSG00000165417 | GTF2A1 subnetwork | 0.52047265 | 1.153731455 |
| REACTOME_RAFMAP_KINASE_ | REACTOME_RAFMAP_KINASE_CASCADE | 0.92381997 | 1.153752159 |
| GO:0002478 | antigen processing and presentation of exogenous peptide | 0.51976477 | 1.153759004 |
| MP:0001344 | blepharoptosis | 0.52073203 | 1.153759736 |
| ENSG00000115590 | IL1R2 subnetwork | 0.92444664 | 1.153767153 |
| MP:0008585 | absent photoreceptor outer segment | 0.52130412 | 1.153785725 |
| ENSG00000160789 | LMNA subnetwork | 0.52122725 | 1.153786292 |
| GO:0009416 | response to light stimulus | 0.92466902 | 1.153787748 |
| GO:0007020 | microtubule nucleation | 0.92393759 | 1.153795009 |
| ENSG00000136930 | PSMB7 subnetwork | 0.5213861 | 1.15380012 |
| GO:0048009 | insulin-like growth factor receptor signaling pathway | 0.52093739 | 1.153803534 |
| ENSG00000096696 | DSP subnetwork | 0.52102207 | 1.153817937 |
| ENSG00000139637 | C12orf10 subnetwork | 0.52088068 | 1.153834057 |
| ENSG00000117425 | PTCH2 subnetwork | 0.92379233 | 1.153834528 |
| MP:0000278 | abnormal myocardial fiber morphology | 0.52110445 | 1.15383982 |
| ENSG00000167768 | KRT1 subnetwork | 0.92372472 | 1.153852133 |
| REACTOME_ARMS:MEDIATED_ | REACTOME_ARMS:MEDIATED_ACTIVATION | 0.92444526 | 1.153858105 |
| GO:0048844 | artery morphogenesis | 0.92465332 | 1.15386142 |
| GO:0030552 | cAMP binding | 0.92363024 | 1.153874061 |
| MP:0000135 | decreased compact bone thickness | 0.51964994 | 1.153880216 |
| ENSG00000164091 | WDR82 subnetwork | 0.52153201 | 1.153881825 |
| ENSG00000206313 | ENSG00000206313 subnetwork | 0.52303092 | 1.15388574 |
| ENSG00000160087 | UBE2J2 subnetwork | 0.51974392 | 1.153887138 |
| MP:0002686 | globozoospermia | 0.52005962 | 1.153892305 |
| ENSG00000213463 | SYNJ2BP subnetwork | 0.52182057 | 1.153894454 |
| ENSG00000196497 | IPO4 subnetwork | 0.52071964 | 1.153917603 |
| ENSG00000134202 | GSTM3 subnetwork | 0.52001514 | 1.153930393 |
| GO:0030903 | notochord development | 0.52611956 | 1.153936249 |
| ENSG00000076053 | RBM7 subnetwork | 0.52621593 | 1.153943077 |
| MP:0011294 | renal glomerulus hypertrophy | 0.5212191 | 1.15394402 |
| GO:0015929 | hexosaminidase activity | 0.9246422 | 1.15394805 |
| ENSG00000084207 | GSTP1 subnetwork | 0.52195249 | 1.153961136 |
| GO:0021984 | adenohypophysis development | 0.92362698 | 1.1539651 |
| GO:0048384 | retinoic acid receptor signaling pathway | 0.521644 | 1.153978462 |
| ENSG00000105700 | KXD1 subnetwork | 0.52633982 | 1.153986957 |
| REACTOME_CLASS_C3_METAB | REACTOME_CLASS_C3_METABOTROPIC_GLUTAMATEPHER | 0.92354489 | 1.153987041 |
| GO:0010259 | multicellular organismal aging | 0.92313847 | 1.154019015 |
| ENSG00000172399 | MYOZ2 subnetwork | 0.92347161 | 1.154021946 |
| ENSG00000141026 | MED9 subnetwork | 0.52178625 | 1.154029605 |
| ENSG00000204463 | BAG6 subnetwork | 0.52303092 | 1.154057885 |
| MP:0009232 | abnormal sperm nucleus morphology | 0.52174677 | 1.154067594 |
| MP:0001155 | arrest of spermatogenesis | 0.52646265 | 1.154067872 |
| GO:0008603 | cAMP-dependent protein kinase regulator activity | 0.92309804 | 1.154084191 |
| GO:0002790 | peptide secretion | 0.92299892 | 1.154084544 |
| ENSG00000144867 | SRPRB subnetwork | 0.92344339 | 1.154087099 |
| GO:0071363 | cellular response to growth factor stimulus | 0.52578152 | 1.154088144 |

| | | | |
|---|---|---|---|
| ENSG00000160695 | ENSG00000160695 subnetwork | 0.52661632 | 1.154088889 |
| ENSG00000149257 | SERPINH1 subnetwork | 0.52611123 | 1.154099941 |
| MP:0009434 | paraparesis | 0.52318755 | 1.154123788 |
| MP:0002762 | ectopic cerebellar granule cells | 0.922654 | 1.154133518 |
| GO:0031954 | positive regulation of protein autophosphorylation | 0.92331189 | 1.154143981 |
| MP:0000740 | impaired smooth muscle contractility | 0.92341046 | 1.154147943 |
| ENSG00000197283 | SYNGAP1 subnetwork | 0.52573013 | 1.154170377 |
| GO:0002042 | cell migration involved in sprouting angiogenesis | 0.5265777 | 1.154170988 |
| GO:0009101 | glycoprotein biosynthetic process | 0.52328875 | 1.154175365 |
| GO:0006120 | mitochondrial electron transport, NADH to ubiquinone | 0.92299563 | 1.154179995 |
| GO:0030198 | extracellular matrix organization | 0.92291509 | 1.154193325 |
| REACTOME_DNA_REPLICATION | REACTOME_DNA_REPLICATION_PRE:INITIATION | 0.52609949 | 1.15420436 |
| ENSG00000187990 | HIST1H2BG subnetwork | 0.52542395 | 1.154217404 |
| REACTOME_MITOTIC_PROMET | REACTOME_MITOTIC_PROMETAPHASE | 0.92264672 | 1.154224682 |
| ENSG00000096155 | BAG6 subnetwork | 0.52303092 | 1.154230081 |
| GO:0001784 | phosphotyrosine binding | 0.52555291 | 1.154231626 |
| MP:0008332 | decreased lactotroph cell number | 0.52240268 | 1.154235136 |
| ENSG00000140990 | NDUFB10 subnetwork | 0.9226044 | 1.154242346 |
| GO:0050927 | positive regulation of positive chemotaxis | 0.52677577 | 1.154266035 |
| ENSG00000196517 | SLC6A9 subnetwork | 0.52251955 | 1.154271845 |
| MP:0011368 | increased kidney apoptosis | 0.52487689 | 1.154275093 |
| MP:0001146 | abnormal testis morphology | 0.9225659 | 1.154290286 |
| GO:0043062 | extracellular structure organization | 0.92291509 | 1.154293126 |
| ENSG00000175333 | ENSG00000175333 subnetwork | 0.92249188 | 1.154299308 |
| MP:0002970 | abnormal white adipose tissue morphology | 0.52683996 | 1.154302429 |
| GO:0071305 | cellular response to vitamin D | 0.52222583 | 1.154319235 |
| GO:0005773 | vacuole | 0.52572092 | 1.154326852 |
| MP:0000473 | abnormal stomach glandular epithelium morphology | 0.52300468 | 1.154327712 |
| MP:0000889 | abnormal cerebellar molecular layer | 0.92230426 | 1.154343312 |
| ENSG00000139352 | ASCL1 subnetwork | 0.92242496 | 1.154347262 |
| ENSG00000129559 | NEDD8 subnetwork | 0.52602725 | 1.154353953 |
| ENSG00000186141 | POLR3C subnetwork | 0.52484282 | 1.154357525 |
| GO:0007044 | cell-substrate junction assembly | 0.52237473 | 1.154362767 |
| REACTOME_MG1_TRANSITION | REACTOME_MG1_TRANSITION | 0.52609949 | 1.154375556 |
| ENSG00000080819 | CPOX subnetwork | 0.52507066 | 1.15437788 |
| ENSG00000116641 | DOCK7 subnetwork | 0.52378962 | 1.154380867 |
| KEGG_PYRIMIDINE_METABOLI | KEGG_PYRIMIDINE_METABOLISM | 0.52295804 | 1.15438806 |
| ENSG00000180596 | HIST1H2BC subnetwork | 0.52542395 | 1.154388831 |
| GO:0016411 | acylglycerol O-acyltransferase activity | 0.52282896 | 1.1544043 |
| GO:0042354 | L-fucose metabolic process | 0.5227463 | 1.154404957 |
| ENSG00000169251 | NMD3 subnetwork | 0.52232876 | 1.15441572 |
| ENSG00000073792 | IGF2BP2 subnetwork | 0.52289745 | 1.154426034 |
| ENSG00000204842 | ATXN2 subnetwork | 0.52372548 | 1.15442623 |
| GO:0050817 | coagulation | 0.52399068 | 1.1544317 |
| GO:0005496 | steroid binding | 0.52500295 | 1.154438002 |
| GO:0034605 | cellular response to heat | 0.92230415 | 1.154443195 |
| ENSG00000068400 | GRIPAP1 subnetwork | 0.52480711 | 1.154454856 |
| ENSG00000141956 | PRDM15 subnetwork | 0.52599329 | 1.154465875 |
| KEGG_BASAL_TRANSCRIPTION | KEGG_BASAL_TRANSCRIPTION_FACTORS | 0.922241 | 1.154478193 |
| ENSG00000145414 | NAF1 subnetwork | 0.52525413 | 1.154479941 |
| MP:0003406 | failure of zygotic cell division | 0.52513188 | 1.154481272 |
| GO:0032652 | regulation of interleukin-1 production | 0.52571508 | 1.154490796 |
| GO:0003743 | translation initiation factor activity | 0.52519805 | 1.154502898 |

| | | | |
|---|---|---|---|
| REACTOME_TANDEM_PORE_D | REACTOME_TANDEM_PORE_DOMAIN_POTASSIUM_CHAN | 0.5245926 | 1.154516369 |
| GO:0046330 | positive regulation of JNK cascade | 0.52396635 | 1.154529201 |
| ENSG00000174748 | RPL15 subnetwork | 0.52273414 | 1.154547491 |
| ENSG00000197846 | HIST1H2BF subnetwork | 0.52542395 | 1.154560309 |
| GO:0070848 | response to growth factor stimulus | 0.52419456 | 1.154564408 |
| ENSG00000042832 | TG subnetwork | 0.52702553 | 1.15456834 |
| MP:0003911 | increased drinking behavior | 0.92223452 | 1.154578105 |
| ENSG00000142599 | RERE subnetwork | 0.52413249 | 1.154587429 |
| REACTOME_BETA:CATENIN_PH | REACTOME_BETA:CATENIN_PHOSPHORYLATION_CASCADE | 0.52371449 | 1.154590848 |
| ENSG00000085276 | MECOM subnetwork | 0.52477863 | 1.154596846 |
| MP:0000163 | abnormal cartilage morphology | 0.92217231 | 1.154600138 |
| GO:0030279 | negative regulation of ossification | 0.92200124 | 1.154609591 |
| ENSG00000197102 | DYNC1H1 subnetwork | 0.52470574 | 1.154627288 |
| ENSG00000076864 | RAP1GAP subnetwork | 0.92212218 | 1.154639488 |
| GO:0008354 | germ cell migration | 0.92186117 | 1.15465368 |
| ENSG00000100304 | TTLL12 subnetwork | 0.52457383 | 1.154658431 |
| GO:0051293 | establishment of spindle localization | 0.9218129 | 1.15467573 |
| GO:0018149 | peptide cross-linking | 0.92198609 | 1.154700892 |
| ENSG00000168242 | HIST1H2BI subnetwork | 0.52542395 | 1.154731838 |
| REACTOME_METABOLISM_OF_ | REACTOME_METABOLISM_OF_POLYAMINES | 0.52370419 | 1.154755516 |
| GO:0033522 | histone H2A ubiquitination | 0.52360285 | 1.15476368 |
| GO:0051653 | spindle localization | 0.9218129 | 1.154775719 |
| ENSG00000115875 | SRSF7 subnetwork | 0.52454687 | 1.154778208 |
| MP:0000042 | abnormal organ of Corti morphology | 0.52440874 | 1.1548243 |
| ENSG00000175216 | CKAP5 subnetwork | 0.92177623 | 1.154828094 |
| GO:0007178 | transmembrane receptor protein serine/threonine kinase s | 0.92173268 | 1.154884809 |
| MP:0003453 | abnormal keratinocyte physiology | 0.52723797 | 1.1549008 |
| MP:0008587 | short photoreceptor outer segment | 0.52452797 | 1.154912908 |
| GO:0006023 | aminoglycan biosynthetic process | 0.92170186 | 1.154958857 |
| MP:0002718 | abnormal inner cell mass morphology | 0.92166287 | 1.155037249 |
| GO:0045661 | regulation of myoblast differentiation | 0.92162637 | 1.155089665 |
| ENSG00000134640 | MTNR1B subnetwork | 0.92160079 | 1.15516375 |
| GO:0051875 | pigment granule localization | 0.92153632 | 1.155198856 |
| ENSG00000137710 | RDX subnetwork | 0.52750833 | 1.155277572 |
| REACTOME_PEPTIDE_CHAIN_E | REACTOME_PEPTIDE_CHAIN_ELONGATION | 0.92153506 | 1.15529896 |
| GO:0016918 | retinal binding | 0.92144437 | 1.155373548 |
| GO:0016331 | morphogenesis of embryonic epithelium | 0.92152681 | 1.155390415 |
| REACTOME_SHC:RELATED_EVE | REACTOME_SHC:RELATED_EVENTS | 0.92139761 | 1.155434688 |
| GO:0048194 | Golgi vesicle budding | 0.92139643 | 1.155530513 |
| GO:0008238 | exopeptidase activity | 0.92137584 | 1.155591678 |
| REACTOME_AMINE:DERIVED_H | REACTOME_AMINE:DERIVED_HORMONES | 0.92132568 | 1.155600832 |
| ENSG00000160678 | S100A1 subnetwork | 0.9212887 | 1.155649007 |
| REACTOME_NACL:_DEPENDEN | REACTOME_NACL:_DEPENDENT_NEUROTRANSMITTER_TR | 0.92123086 | 1.155714533 |
| GO:0008017 | microtubule binding | 0.92118393 | 1.155745382 |
| ENSG00000074696 | PTPLAD1 subnetwork | 0.52792277 | 1.15576354 |
| GO:0046824 | positive regulation of nucleocytoplasmic transport | 0.92115934 | 1.155828274 |
| ENSG00000055609 | MLL3 subnetwork | 0.52788392 | 1.155860589 |
| GO:0004089 | carbonate dehydratase activity | 0.92115134 | 1.155924191 |
| ENSG00000182149 | IST1 subnetwork | 0.92093396 | 1.155947423 |
| GO:0004693 | cyclin-dependent protein kinase activity | 0.91940938 | 1.155974624 |
| REACTOME_MRNA_DECAY_BY | REACTOME_MRNA_DECAY_BY_5_TO_3_EXORIBONUCLEAS | 0.92111312 | 1.155998439 |
| ENSG00000138430 | OLA1 subnetwork | 0.92081353 | 1.156013537 |
| ENSG00000066248 | NGEF subnetwork | 0.52787632 | 1.156016874 |

| | | | |
|---|---|---|---|
| GO:0045744 | negative regulation of G-protein coupled receptor protein s | 0.91927716 | 1.156023468 |
| ENSG00000137845 | ADAM10 subnetwork | 0.91937127 | 1.156031636 |
| GO:0021532 | neural tube patterning | 0.92092893 | 1.156043384 |
| ENSG00000134072 | CAMK1 subnetwork | 0.91921708 | 1.156054416 |
| ENSG00000141200 | KIF2B subnetwork | 0.92108331 | 1.156064024 |
| MP:0005300 | abnormal corneal stroma morphology | 0.91987099 | 1.156094171 |
| GO:0016485 | protein processing | 0.92079369 | 1.156100842 |
| GO:0019205 | nucleobase-containing compound kinase activity | 0.92040065 | 1.156112172 |
| ENSG00000168397 | ATG4B subnetwork | 0.52899029 | 1.156114311 |
| GO:0007606 | sensory perception of chemical stimulus | 0.91920323 | 1.156137529 |
| ENSG00000049167 | ERCC8 subnetwork | 0.92030483 | 1.156143626 |
| GO:0050886 | endocrine process | 0.9203554 | 1.156147434 |
| GO:0006939 | smooth muscle contraction | 0.92009294 | 1.15617997 |
| MP:0004351 | short humerus | 0.91986628 | 1.156185925 |
| GO:0006612 | protein targeting to membrane | 0.92078443 | 1.156192501 |
| ENSG00000137726 | FXYD6 subnetwork | 0.92005295 | 1.15621091 |
| ENSG00000178741 | COX5A subnetwork | 0.92028493 | 1.156213634 |
| GO:0015935 | small ribosomal subunit | 0.92057046 | 1.156215817 |
| ENSG00000122778 | KIAA1549 subnetwork | 0.91918905 | 1.15621631 |
| GO:0090066 | regulation of anatomical structure size | 0.91981643 | 1.156229907 |
| GO:0046879 | hormone secretion | 0.92023902 | 1.156244572 |
| MP:0002736 | abnormal nociception after inflammation | 0.91973802 | 1.156256517 |
| MP:0009661 | abnormal pregnancy | 0.92075784 | 1.156258137 |
| ENSG00000215697 | ENSG00000215697 subnetwork | 0.52899029 | 1.156285081 |
| ENSG00000122692 | SMU1 subnetwork | 0.52841514 | 1.156285123 |
| GO:0005875 | microtubule associated complex | 0.5284618 | 1.15629898 |
| REACTOME_CYTOSOLIC_TRNA | REACTOME_CYTOSOLIC_TRNA_AMINOACYLATION | 0.91918369 | 1.156299452 |
| MP:0001954 | respiratory distress | 0.91908645 | 1.1563 |
| ENSG00000171735 | CAMTA1 subnetwork | 0.91901644 | 1.156300548 |
| GO:0051882 | mitochondrial depolarization | 0.920708 | 1.156306424 |
| GO:0019079 | viral genome replication | 0.52834877 | 1.156315634 |
| ENSG00000206380 | C6orf48 subnetwork | 0.52896064 | 1.156345103 |
| GO:0060479 | lung cell differentiation | 0.91875044 | 1.156350035 |
| GO:0016581 | NuRD complex | 0.52831968 | 1.156368343 |
| ENSG00000182923 | CEP63 subnetwork | 0.52857285 | 1.156379361 |
| MP:0000106 | abnormal basisphenoid bone morphology | 0.91899363 | 1.15637937 |
| GO:0008329 | pattern recognition receptor activity | 0.9187447 | 1.156446281 |
| GO:0090100 | positive regulation of transmembrane receptor protein seri | 0.91897713 | 1.156466904 |
| ENSG00000198001 | IRAK4 subnetwork | 0.91869477 | 1.156481643 |
| ENSG00000204387 | C6orf48 subnetwork | 0.52896064 | 1.156515957 |
| MP:0001694 | failure to form egg cylinders | 0.52830912 | 1.156517236 |
| ENSG00000214528 | ENSG00000214528 subnetwork | 0.52871849 | 1.15654102 |
| GO:0006582 | melanin metabolic process | 0.91869178 | 1.156569216 |
| REACTOME_PROLONGED_ERK | REACTOME_PROLONGED_ERK_ACTIVATION_EVENTS | 0.91866358 | 1.156617647 |
| GO:0042303 | molting cycle | 0.52945334 | 1.156635666 |
| ENSG00000121068 | TBX2 subnetwork | 0.52960042 | 1.156663223 |
| ENSG00000206271 | ENSG00000206271 subnetwork | 0.52896064 | 1.156686863 |
| ENSG00000128578 | FAM40B subnetwork | 0.91853179 | 1.156688425 |
| GO:0008514 | organic anion transmembrane transporter activity | 0.52929208 | 1.156689309 |
| ENSG00000105607 | GCDH subnetwork | 0.91863276 | 1.156692194 |
| GO:0051928 | positive regulation of calcium ion transport | 0.52980377 | 1.156698141 |
| ENSG00000106588 | PSMA2 subnetwork | 0.52954845 | 1.156708487 |
| ENSG00000136205 | TNS3 subnetwork | 0.91848752 | 1.156732527 |

| | | | |
|---|---|---|---|
| MP:0002745 | abnormal atrioventricular valve morphology | 0.9184277 | 1.156733113 |
| ENSG00000179151 | EDC3 subnetwork | 0.52989127 | 1.156734032 |
| ENSG00000214517 | PPME1 subnetwork | 0.91834502 | 1.156759815 |
| MP:0002690 | akinesia | 0.52977377 | 1.15680242 |
| GO:0042633 | hair cycle | 0.52945334 | 1.156806437 |
| GO:0051495 | positive regulation of cytoskeleton organization | 0.52894396 | 1.156820869 |
| MP:0003339 | decreased pancreatic beta cell number | 0.91834359 | 1.156860526 |
| ENSG00000008056 | SYN1 subnetwork | 0.91834128 | 1.156961254 |
| ENSG00000198648 | STK39 subnetwork | 0.91821751 | 1.157032134 |
| ENSG00000196540 | ENSG00000196540 subnetwork | 0.91832816 | 1.157048938 |
| ENSG00000106554 | CHCHD3 subnetwork | 0.5308412 | 1.157108132 |
| GO:0006471 | protein ADP-ribosylation | 0.91803821 | 1.157125436 |
| ENSG00000198835 | GJC2 subnetwork | 0.9182108 | 1.157132904 |
| GO:0006720 | isoprenoid metabolic process | 0.91798942 | 1.157187037 |
| GO:0008308 | voltage-gated anion channel activity | 0.91819726 | 1.157220625 |
| ENSG00000196611 | MMP1 subnetwork | 0.53082336 | 1.157234419 |
| MP:0001984 | abnormal olfaction | 0.53053528 | 1.157237618 |
| GO:0032314 | regulation of Rac GTPase activity | 0.91796488 | 1.157244293 |
| ENSG00000123159 | GIPC1 subnetwork | 0.53060967 | 1.157266028 |
| MP:0000681 | abnormal thyroid gland morphology | 0.5307252 | 1.157272325 |
| ENSG00000152464 | RPP38 subnetwork | 0.91792706 | 1.157305916 |
| GO:0034199 | activation of protein kinase A activity | 0.91786642 | 1.15732398 |
| ENSG00000169252 | ADRB2 subnetwork | 0.91773723 | 1.157351403 |
| ENSG00000143228 | NUF2 subnetwork | 0.91782023 | 1.157363834 |
| GO:0007163 | establishment or maintenance of cell polarity | 0.53050376 | 1.157363998 |
| ENSG00000116747 | TROVE2 subnetwork | 0.91769358 | 1.157413057 |
| REACTOME_FORMATION_OF_T | REACTOME_FORMATION_OF_THE_EARLY_ELONGATION_C | 0.5311528 | 1.157437408 |
| ENSG00000169032 | MAP2K1 subnetwork | 0.53046341 | 1.157446181 |
| MP:0002188 | small heart | 0.91764927 | 1.157452929 |
| GO:0030865 | cortical cytoskeleton organization | 0.53040585 | 1.1574694 |
| GO:0006555 | methionine metabolic process | 0.91764396 | 1.157553831 |
| ENSG00000013297 | CLDN11 subnetwork | 0.53038313 | 1.157566372 |
| GO:0031256 | leading edge membrane | 0.91758621 | 1.157589364 |
| REACTOME_FORMATION_OF_T | REACTOME_FORMATION_OF_THE_HIV:1_EARLY_ELONGAT | 0.5311528 | 1.157607895 |
| ENSG00000144935 | TRPC1 subnetwork | 0.91749121 | 1.157616183 |
| GO:0060993 | kidney morphogenesis | 0.91744243 | 1.157647367 |
| MP:0003360 | abnormal depression-related behavior | 0.91742054 | 1.15772652 |
| ENSG00000145147 | SLIT2 subnetwork | 0.91741859 | 1.15782749 |
| GO:0009116 | nucleoside metabolic process | 0.91737116 | 1.1578587 |
| MP:0004042 | decreased susceptibility to kidney reperfusion injury | 0.9173503 | 1.157946615 |
| MP:0010019 | liver vascular congestion | 0.53151194 | 1.15795053 |
| GO:0014910 | regulation of smooth muscle cell migration | 0.91721618 | 1.157965451 |
| GO:0000819 | sister chromatid segregation | 0.91731134 | 1.157969118 |
| ENSG00000123240 | OPTN subnetwork | 0.5314512 | 1.157973789 |
| REACTOME_G:PROTEIN_MEDI | REACTOME_G:PROTEIN_MEDIATED_EVENTS | 0.53186099 | 1.158027962 |
| REACTOME_S_PHASE | REACTOME_S_PHASE | 0.53194017 | 1.158034138 |
| MP:0004409 | abnormal crista ampullaris neuroepithelium morphology | 0.91534368 | 1.158047032 |
| GO:0010469 | regulation of receptor activity | 0.91719184 | 1.158049036 |
| ENSG00000213782 | DDX47 subnetwork | 0.91527793 | 1.158073964 |
| MP:0010024 | increased total body fat amount | 0.53180829 | 1.158088019 |
| ENSG00000090989 | EXOC1 subnetwork | 0.53170558 | 1.158089209 |
| ENSG00000121621 | KIF18A subnetwork | 0.91511379 | 1.158114725 |
| GO:0009914 | hormone transport | 0.91393272 | 1.158119583 |

| | | | |
|---|---|---|---|
| GO:0015936 | coenzyme A metabolic process | 0.91412249 | 1.158140044 |
| MP:0004838 | abnormal neural fold elevation formation | 0.91717888 | 1.158141361 |
| GO:0031016 | pancreas development | 0.91523398 | 1.15814899 |
| GO:0042133 | neurotransmitter metabolic process | 0.91507243 | 1.158167906 |
| GO:0048515 | spermatid differentiation | 0.9148724 | 1.158173708 |
| ENSG00000109061 | MYH1 subnetwork | 0.91551221 | 1.158177448 |
| GO:0001945 | lymph vessel development | 0.91424509 | 1.158183091 |
| ENSG00000197263 | OR8D2 subnetwork | 0.91606392 | 1.158190634 |
| GO:0001523 | retinoid metabolic process | 0.91407682 | 1.158193277 |
| MP:0001751 | increased circulating luteinizing hormone level | 0.91672156 | 1.158198009 |
| GO:0045216 | cell-cell junction organization | 0.91584471 | 1.158201521 |
| REACTOME_ACTIVATION_OF_I | REACTOME_ACTIVATION_OF_NMDA_RECEPTOR_UPON_GI | 0.91499935 | 1.158203603 |
| GO:0005793 | endoplasmic reticulum-Golgi intermediate compartment | 0.91391939 | 1.158207845 |
| MP:0002626 | increased heart rate | 0.91699399 | 1.158222048 |
| ENSG00000102893 | PHKB subnetwork | 0.91385073 | 1.158230453 |
| ENSG00000108578 | BLMH subnetwork | 0.91668954 | 1.158233651 |
| ENSG00000125845 | BMP2 subnetwork | 0.91717059 | 1.158233703 |
| KEGG_PARKINSONS_DISEASE | KEGG_PARKINSONS_DISEASE | 0.91600624 | 1.158235037 |
| ENSG00000105409 | ATP1A3 subnetwork | 0.91684762 | 1.158245308 |
| ENSG00000135480 | KRT7 subnetwork | 0.91580256 | 1.158259046 |
| ENSG00000128050 | PAICS subnetwork | 0.91594435 | 1.158261971 |
| GO:0072210 | metanephric nephron development | 0.91486349 | 1.158275017 |
| ENSG00000099250 | NRP1 subnetwork | 0.91663917 | 1.15827803 |
| GO:0042537 | benzene-containing compound metabolic process | 0.91710754 | 1.158278059 |
| GO:0045669 | positive regulation of osteoblast differentiation | 0.91627257 | 1.158280922 |
| MP:0003087 | absent allantois | 0.91572526 | 1.158281619 |
| ENSG00000172315 | TP53RK subnetwork | 0.91618576 | 1.158290382 |
| GO:0030169 | low-density lipoprotein particle binding | 0.91659578 | 1.158313684 |
| MP:0002861 | abnormal tail bud morphology | 0.9169813 | 1.15831442 |
| GO:0007164 | establishment of tissue polarity | 0.91384059 | 1.158327496 |
| GO:0008556 | potassium-transporting ATPase activity | 0.91651649 | 1.158331878 |
| ENSG00000115163 | CENPA subnetwork | 0.91484252 | 1.158358849 |
| GO:0032438 | melanosome organization | 0.91380574 | 1.158385148 |
| MP:0003637 | cochlear ganglion hypoplasia | 0.91647115 | 1.158393746 |
| ENSG00000101473 | ACOT8 subnetwork | 0.91369409 | 1.158426031 |
| MP:0000430 | absent maxillary shelf | 0.91378383 | 1.158438431 |
| ENSG00000115233 | PSMD14 subnetwork | 0.53219458 | 1.158444902 |
| GO:0046579 | positive regulation of Ras protein signal transduction | 0.91483651 | 1.158451444 |
| ENSG00000140986 | RPL3L subnetwork | 0.91474385 | 1.158474057 |
| REACTOME_G_ALPHA_Q_SIGN | REACTOME_G_ALPHA_Q_SIGNALLING_EVENTS | 0.91346851 | 1.158511477 |
| GO:0048568 | embryonic organ development | 0.91366604 | 1.158514366 |
| ENSG00000103496 | STX4 subnetwork | 0.9146997 | 1.158527301 |
| GO:0043498 | cell surface binding | 0.53236644 | 1.158530666 |
| ENSG00000161202 | DVL3 subnetwork | 0.91363747 | 1.158602716 |
| GO:0032204 | regulation of telomere maintenance | 0.91338025 | 1.158604977 |
| ENSG00000113645 | WWC1 subnetwork | 0.91346469 | 1.158608604 |
| MP:0010018 | pulmonary vascular congestion | 0.91469595 | 1.158624311 |
| ENSG00000108262 | GIT1 subnetwork | 0.53234123 | 1.158627538 |
| ENSG00000008196 | TFAP2B subnetwork | 0.91330825 | 1.158645167 |
| ENSG00000123405 | NFE2 subnetwork | 0.53265618 | 1.158651867 |
| ENSG00000108854 | SMURF2 subnetwork | 0.53257674 | 1.158653139 |
| GO:0030118 | clathrin coat | 0.53250823 | 1.158654412 |
| MP:0005201 | abnormal retinal pigment epithelium morphology | 0.91325467 | 1.158667835 |

| | | | |
|---|---|---|---|
| GO:0090177 | establishment of planar polarity involved in neural tube clo | 0.9128738 | 1.158706708 |
| ENSG00000198104 | OR2T6 subnetwork | 0.91300577 | 1.158754164 |
| REACTOME_REGULATION_OF_ | REACTOME_REGULATION_OF_INSULIN:LIKE_GROWTH_FAC | 0.91323375 | 1.158756245 |
| GO:0042562 | hormone binding | 0.913169 | 1.158774544 |
| ENSG00000181031 | RPH3AL subnetwork | 0.53278619 | 1.15877554 |
| ENSG00000166851 | PLK1 subnetwork | 0.91286694 | 1.158803928 |
| MP:0001385 | pup cannibalization | 0.91312558 | 1.158819146 |
| ENSG00000176534 | ENSG00000176534 subnetwork | 0.91263144 | 1.158867643 |
| GO:0000083 | regulation of transcription involved in G1/S phase of mitoti | 0.91274965 | 1.158880021 |
| ENSG00000185245 | GP1BA subnetwork | 0.91285851 | 1.158896782 |
| ENSG00000198637 | ENSG00000198637 subnetwork | 0.91263144 | 1.158969298 |
| ENSG00000196681 | ENSG00000196681 subnetwork | 0.91263144 | 1.159070971 |
| MP:0011506 | glomerular crescent | 0.53361388 | 1.159101585 |
| ENSG00000105939 | ZC3HAV1 subnetwork | 0.53355524 | 1.159124945 |
| GO:0008158 | hedgehog receptor activity | 0.912595 | 1.159137568 |
| ENSG00000188687 | SLC4A5 subnetwork | 0.53318105 | 1.159219806 |
| GO:0042737 | drug catabolic process | 0.91259287 | 1.159239273 |
| ENSG00000132357 | CARD6 subnetwork | 0.53311758 | 1.159243204 |
| ENSG00000214021 | TTLL3 subnetwork | 0.53326736 | 1.159247833 |
| ENSG00000105223 | PLD3 subnetwork | 0.53353959 | 1.15928047 |
| ENSG00000124164 | VAPB subnetwork | 0.91220343 | 1.159295997 |
| GO:0001764 | neuron migration | 0.91236859 | 1.159316307 |
| GO:0042228 | interleukin-8 biosynthetic process | 0.91257712 | 1.159332222 |
| GO:0030595 | leukocyte chemotaxis | 0.53308397 | 1.159347443 |
| ENSG00000105993 | DNAJB6 subnetwork | 0.91232465 | 1.159361011 |
| ENSG00000175445 | LPL subnetwork | 0.91219098 | 1.159384602 |
| GO:0003725 | double-stranded RNA binding | 0.53350227 | 1.159384638 |
| MP:0005322 | abnormal serotonin level | 0.91253983 | 1.159390083 |
| GO:0019674 | NAD metabolic process | 0.91210781 | 1.159416155 |
| GO:0046847 | filopodium assembly | 0.91206692 | 1.159452103 |
| GO:0043408 | regulation of MAPK cascade | 0.53349192 | 1.159525558 |
| GO:0015802 | basic amino acid transport | 0.91204973 | 1.159545135 |
| GO:0032024 | positive regulation of insulin secretion | 0.91198475 | 1.159589883 |
| MP:0008284 | abnormal hippocampus pyramidal cell layer | 0.91187396 | 1.159648661 |
| GO:0004181 | metallocarboxypeptidase activity | 0.91196576 | 1.15966977 |
| GO:0016298 | lipase activity | 0.9118175 | 1.159697822 |
| GO:0007041 | lysosomal transport | 0.91159959 | 1.159735524 |
| ENSG00000144596 | ENSG00000144596 subnetwork | 0.91176492 | 1.159738206 |
| ENSG00000156427 | FGF18 subnetwork | 0.9115791 | 1.159806678 |
| GO:0090278 | negative regulation of peptide hormone secretion | 0.9117422 | 1.159840098 |
| ENSG00000107831 | FGF8 subnetwork | 0.9115791 | 1.159908604 |
| GO:0043014 | alpha-tubulin binding | 0.53421593 | 1.159992663 |
| ENSG00000111241 | FGF6 subnetwork | 0.9115791 | 1.160010547 |
| ENSG00000106028 | SSBP1 subnetwork | 0.53415581 | 1.160023481 |
| GO:2000027 | regulation of organ morphogenesis | 0.53441006 | 1.160032268 |
| MP:0003662 | abnormal long bone epiphyseal plate proliferative zone | 0.53451404 | 1.160067459 |
| GO:0046605 | regulation of centrosome cycle | 0.53437618 | 1.160085081 |
| ENSG00000070388 | FGF22 subnetwork | 0.9115791 | 1.160112508 |
| ENSG00000104915 | STX10 subnetwork | 0.53461584 | 1.160124633 |
| ENSG00000163636 | PSMD6 subnetwork | 0.53415133 | 1.160171731 |
| ENSG00000171759 | PAH subnetwork | 0.91128185 | 1.160204889 |
| ENSG00000158815 | FGF17 subnetwork | 0.9115791 | 1.160214487 |
| GO:2001014 | regulation of skeletal muscle cell differentiation | 0.91118534 | 1.160214581 |

| | | | |
|---|---|---|---|
| MP:0002656 | abnormal keratinocyte differentiation | 0.53437288 | 1.160247946 |
| ENSG00000005194 | CIAPIN1 subnetwork | 0.53483194 | 1.160275579 |
| ENSG00000185324 | CDK10 subnetwork | 0.91103687 | 1.160282347 |
| GO:0016628 | oxidoreductase activity, acting on the CH-CH group of dono | 0.91149737 | 1.160291015 |
| ENSG00000116584 | ARHGEF2 subnetwork | 0.53476946 | 1.160291746 |
| GO:0071482 | cellular response to light stimulus | 0.53492959 | 1.160296057 |
| GO:0060986 | endocrine hormone secretion | 0.9111773 | 1.160312225 |
| ENSG00000162344 | FGF19 subnetwork | 0.9115791 | 1.160316484 |
| GO:0051318 | G1 phase | 0.9114743 | 1.160362261 |
| GO:0072273 | metanephric nephron morphogenesis | 0.91099347 | 1.160362421 |
| MP:0002090 | abnormal vision | 0.91079794 | 1.160400352 |
| ENSG00000115942 | ORC2 subnetwork | 0.91096088 | 1.160416117 |
| MP:0006086 | decreased body mass index | 0.91089808 | 1.16043463 |
| ENSG00000140678 | ITGAX subnetwork | 0.91065429 | 1.160454985 |
| ENSG00000197223 | C1D subnetwork | 0.91074918 | 1.160467265 |
| ENSG00000018408 | WWTR1 subnetwork | 0.91056893 | 1.160473508 |
| ENSG00000108298 | RPL19 subnetwork | 0.91056099 | 1.160571253 |
| GO:0060117 | auditory receptor cell development | 0.91051842 | 1.160616197 |
| GO:0000186 | activation of MAPKK activity | 0.53515292 | 1.160631594 |
| ENSG00000188157 | AGRN subnetwork | 0.53546653 | 1.16066198 |
| ENSG00000198755 | RPL10A subnetwork | 0.53522247 | 1.160673993 |
| KEGG_LYSOSOME | KEGG_LYSOSOME | 0.53531144 | 1.160701729 |
| MP:0005048 | thrombosis | 0.91050577 | 1.160713971 |
| GO:0033613 | activating transcription factor binding | 0.53543067 | 1.160758752 |
| ENSG00000076003 | MCM6 subnetwork | 0.9104728 | 1.160789752 |
| ENSG00000139182 | CLSTN3 subnetwork | 0.91037666 | 1.160790702 |
| GO:2000241 | regulation of reproductive process | 0.53586315 | 1.160831382 |
| MP:0000875 | abnormal cerebellar Purkinje cell layer | 0.53570362 | 1.160849195 |
| ENSG00000182117 | NOP10 subnetwork | 0.91034731 | 1.160862099 |
| MP:0002073 | abnormal hair growth | 0.53564356 | 1.160887392 |
| ENSG00000137699 | TRIM29 subnetwork | 0.53632516 | 1.160896592 |
| ENSG00000168003 | SLC3A2 subnetwork | 0.53621844 | 1.160898186 |
| GO:0032409 | regulation of transporter activity | 0.91034186 | 1.160955526 |
| MP:0004736 | abnormal distortion product otoacoustic emission | 0.91029722 | 1.161000528 |
| GO:0045069 | regulation of viral genome replication | 0.53585882 | 1.161001318 |
| GO:0032886 | regulation of microtubule-based process | 0.91012353 | 1.161024489 |
| REACTOME_CLASSICAL_ANTIB | REACTOME_CLASSICAL_ANTIBODY:MEDIATED_COMPLEME | 0.53620555 | 1.161046086 |
| REACTOME_SPHINGOLIPID_DE | REACTOME_SPHINGOLIPID_DE_NOVO_BIOSYNTHESIS | 0.91007889 | 1.161073914 |
| GO:0046323 | glucose import | 0.91028396 | 1.161098388 |
| ENSG00000100931 | ENSG00000100931 subnetwork | 0.91002843 | 1.161123348 |
| ENSG00000143013 | LMO4 subnetwork | 0.53608164 | 1.161144446 |
| ENSG00000168078 | PBK subnetwork | 0.53618859 | 1.161150132 |
| ENSG00000073756 | PTGS2 subnetwork | 0.53719344 | 1.161180079 |
| GO:0046889 | positive regulation of lipid biosynthetic process | 0.53654102 | 1.161187482 |
| MP:0000267 | abnormal heart development | 0.91002704 | 1.161221253 |
| MP:0008236 | decreased susceptibility to neuronal excitotoxicity | 0.90998378 | 1.161275115 |
| MP:0003657 | abnormal erythrocyte osmotic lysis | 0.53735737 | 1.161280666 |
| GO:0000271 | polysaccharide biosynthetic process | 0.53682647 | 1.161292209 |
| ENSG00000188529 | SRSF10 subnetwork | 0.90880693 | 1.161320921 |
| MP:0004158 | right aortic arch | 0.90970556 | 1.161323166 |
| MP:0002725 | abnormal vein morphology | 0.90993845 | 1.161328986 |
| GO:0051020 | GTPase binding | 0.53718191 | 1.16134239 |
| ENSG00000120253 | NUP43 subnetwork | 0.90985512 | 1.161343205 |

| | | | |
|---|---|---|---|
| GO:0042773 | ATP synthesis coupled electron transport | 0.90962763 | 1.161346205 |
| GO:0015175 | neutral amino acid transmembrane transporter activity | 0.90979983 | 1.161366241 |
| MP:0001664 | abnormal digestion | 0.53677257 | 1.161366959 |
| MP:0004883 | abnormal vascular wound healing | 0.53711713 | 1.161395179 |
| MP:0003084 | abnormal skeletal muscle fiber morphology | 0.53767408 | 1.161414392 |
| REACTOME_PHASE_1_:_FUNC | REACTOME_PHASE_1_:_FUNCTIONALIZATION_OF_COMPO | 0.53672601 | 1.161419798 |
| GO:0010038 | response to metal ion | 0.90880168 | 1.161423403 |
| ENSG00000180818 | HOXC10 subnetwork | 0.90895384 | 1.16143021 |
| MP:0005631 | decreased lung weight | 0.53788423 | 1.161438576 |
| MP:0001634 | internal hemorrhage | 0.53708648 | 1.161447984 |
| GO:0042775 | mitochondrial ATP synthesis coupled electron transport | 0.90962763 | 1.161448598 |
| GO:0008417 | fucosyltransferase activity | 0.53799554 | 1.161480671 |
| ENSG00000163681 | SLMAP subnetwork | 0.90877884 | 1.161512664 |
| ENSG00000153071 | DAB2 subnetwork | 0.90962084 | 1.161537783 |
| ENSG00000172301 | C17orf79 subnetwork | 0.53785992 | 1.161549686 |
| GO:0090003 | regulation of establishment of protein localization in plasm | 0.90930311 | 1.161554066 |
| MP:0001065 | abnormal trigeminal nerve morphology | 0.90918247 | 1.161556104 |
| ENSG00000185236 | RAB11B subnetwork | 0.53767037 | 1.161569343 |
| GO:0008083 | growth factor activity | 0.53707373 | 1.161595791 |
| ENSG00000132182 | NUP210 subnetwork | 0.90876984 | 1.161597529 |
| ENSG00000197860 | SGTB subnetwork | 0.90956869 | 1.161600529 |
| GO:0048738 | cardiac muscle tissue development | 0.90947867 | 1.1616236 |
| GO:0016998 | cell wall macromolecule catabolic process | 0.90916222 | 1.161649757 |
| MP:0005102 | abnormal iris pigmentation | 0.90929997 | 1.161652113 |
| ENSG00000058404 | CAMK2B subnetwork | 0.53783616 | 1.161653532 |
| GO:0033540 | fatty acid beta-oxidation using acyl-CoA oxidase | 0.53703258 | 1.161655949 |
| GO:0035136 | forelimb morphogenesis | 0.90876586 | 1.161691235 |
| ENSG00000174111 | SOCS7 subnetwork | 0.53765129 | 1.161702438 |
| GO:0047496 | vesicle transport along microtubule | 0.90872556 | 1.161749647 |
| ENSG00000136854 | STXBP1 subnetwork | 0.90841464 | 1.16183432 |
| REACTOME_IRS:RELATED_EVEI | REACTOME_IRS:RELATED_EVENTS | 0.90872263 | 1.161847797 |
| ENSG00000112493 | TAPBP subnetwork | 0.54216808 | 1.161891657 |
| ENSG00000115844 | DLX2 subnetwork | 0.90839549 | 1.161923688 |
| GO:0071158 | positive regulation of cell cycle arrest | 0.54233108 | 1.161931654 |
| GO:0010770 | positive regulation of cell morphogenesis involved in differe | 0.55298581 | 1.161937225 |
| REACTOME_IRS:MEDIATED_SI | REACTOME_IRS:MEDIATED_SIGNALLING | 0.90872263 | 1.16195038 |
| REACTOME_TELOMERE_MAIN | REACTOME_TELOMERE_MAINTENANCE | 0.55112036 | 1.161954973 |
| ENSG00000105325 | FZR1 subnetwork | 0.90836707 | 1.161973324 |
| GO:0090342 | regulation of cell aging | 0.55398636 | 1.161982416 |
| MP:0003641 | small lung | 0.55345896 | 1.161999716 |
| REACTOME_DIABETES_PATHW | REACTOME_DIABETES_PATHWAYS | 0.90870389 | 1.16202649 |
| GO:0051153 | regulation of striated muscle cell differentiation | 0.90865044 | 1.162027552 |
| ENSG00000107854 | TNKS2 subnetwork | 0.54230128 | 1.16204924 |
| GO:0002279 | mast cell activation involved in immune response | 0.90834439 | 1.16204947 |
| ENSG00000123975 | CKS2 subnetwork | 0.55296061 | 1.162052557 |
| ENSG00000206281 | TAPBP subnetwork | 0.54216808 | 1.162059974 |
| ENSG00000166716 | ZNF592 subnetwork | 0.55394462 | 1.162083392 |
| ENSG00000123685 | BATF3 subnetwork | 0.5511166 | 1.162099188 |
| ENSG00000111087 | GLI1 subnetwork | 0.53833685 | 1.162106184 |
| ENSG00000197111 | PCBP2 subnetwork | 0.55328298 | 1.162125515 |
| ENSG00000107816 | LZTS2 subnetwork | 0.90833773 | 1.162143299 |
| GO:0090305 | nucleic acid phosphodiester bond hydrolysis | 0.55104397 | 1.162143672 |
| GO:0006364 | rRNA processing | 0.5534562 | 1.162164656 |

| | | | |
|---|---|---|---|
| GO:0060736 | prostate gland growth | 0.53886195 | 1.162168464 |
| ENSG00000139269 | INHBE subnetwork | 0.55154013 | 1.162176018 |
| GO:0000323 | lytic vacuole | 0.55294822 | 1.162189231 |
| ENSG00000111961 | SASH1 subnetwork | 0.55208311 | 1.162192346 |
| GO:0045445 | myoblast differentiation | 0.90830797 | 1.162201802 |
| ENSG00000115616 | SLC9A2 subnetwork | 0.55099035 | 1.162202423 |
| MP:0003058 | increased insulin secretion | 0.55201631 | 1.16220831 |
| MP:0008670 | decreased interleukin-12b secretion | 0.55340198 | 1.162208972 |
| MP:0003232 | abnormal forebrain development | 0.53860588 | 1.162210235 |
| ENSG00000206208 | TAPBP subnetwork | 0.54216808 | 1.16222834 |
| ENSG00000159479 | MED8 subnetwork | 0.55089159 | 1.162232678 |
| ENSG00000166441 | RPL27A subnetwork | 0.55279888 | 1.162235328 |
| GO:0003729 | mRNA binding | 0.55393755 | 1.162241135 |
| GO:0006884 | cell volume homeostasis | 0.5427187 | 1.162252135 |
| ENSG00000122490 | PQLC1 subnetwork | 0.53882554 | 1.162264976 |
| GO:0010632 | regulation of epithelial cell migration | 0.54266862 | 1.162268384 |
| ENSG00000114698 | PLSCR4 subnetwork | 0.90829171 | 1.162269153 |
| ENSG00000103502 | CDIPT subnetwork | 0.55327378 | 1.162269242 |
| GO:0072401 | signal transduction involved in DNA integrity checkpoint | 0.5485438 | 1.162294143 |
| MP:0001967 | deafness | 0.55150666 | 1.162305939 |
| ENSG00000160957 | RECQL4 subnetwork | 0.90825945 | 1.162318841 |
| GO:0043277 | apoptotic cell clearance | 0.54262062 | 1.162320834 |
| GO:0045017 | glycerolipid biosynthetic process | 0.53905118 | 1.162326971 |
| KEGG_PHENYLALANINE_META | KEGG_PHENYLALANINE_METABOLISM | 0.54212451 | 1.162331546 |
| ENSG00000109072 | SEBOX subnetwork | 0.9081477 | 1.162333186 |
| GO:0050706 | regulation of interleukin-1 beta secretion | 0.55200193 | 1.16234524 |
| MP:0001970 | abnormal pain threshold | 0.55438309 | 1.162352941 |
| GO:0005764 | lysosome | 0.55294822 | 1.162354362 |
| REACTOME_POLYMERASE_SW | REACTOME_POLYMERASE_SWITCHING_ON_THE_C:STRANI | 0.55087908 | 1.162355625 |
| ENSG00000184481 | FOXO4 subnetwork | 0.53859065 | 1.16235783 |
| ENSG00000169957 | ZNF768 subnetwork | 0.55278116 | 1.162372086 |
| GO:0035085 | cilium axoneme | 0.55391509 | 1.162377642 |
| GO:0051238 | sequestering of metal ion | 0.53879857 | 1.162383382 |
| MP:0000527 | abnormal kidney development | 0.90794369 | 1.162385078 |
| MP:0001556 | increased circulating HDL cholesterol level | 0.90812567 | 1.162404985 |
| ENSG00000124172 | ATP5E subnetwork | 0.55252979 | 1.162412911 |
| ENSG00000068323 | TFE3 subnetwork | 0.55148263 | 1.16241453 |
| ENSG00000171403 | KRT9 subnetwork | 0.55449358 | 1.162429138 |
| GO:0060326 | cell chemotaxis | 0.55228126 | 1.162432432 |
| GO:0007435 | salivary gland morphogenesis | 0.55174068 | 1.162437705 |
| MP:0008974 | proportional dwarf | 0.53855718 | 1.162447134 |
| GO:0072413 | signal transduction involved in mitotic cell cycle checkpoint | 0.5485438 | 1.162460613 |
| ENSG00000184313 | HEATR8 subnetwork | 0.54211174 | 1.162463768 |
| GO:0015103 | inorganic anion transmembrane transporter activity | 0.55143428 | 1.162466163 |
| ENSG00000130787 | HIP1R subnetwork | 0.55378477 | 1.162466298 |
| GO:0006006 | glucose metabolic process | 0.55388677 | 1.162471623 |
| GO:0003081 | regulation of systemic arterial blood pressure by renin-angi | 0.90791835 | 1.162483423 |
| GO:0046148 | pigment biosynthetic process | 0.54203781 | 1.162494564 |
| MP:0002021 | increased incidence of induced tumors | 0.55239611 | 1.162501778 |
| MP:0005309 | increased circulating ammonia level | 0.90811944 | 1.162503315 |
| GO:0006520 | cellular amino acid metabolic process | 0.55437236 | 1.162503544 |
| GO:0048008 | platelet-derived growth factor receptor signaling pathway | 0.55276907 | 1.162508884 |
| GO:0050704 | regulation of interleukin-1 secretion | 0.55200193 | 1.162510675 |

| | | | |
|---|---|---|---|
| ENSG00000018699 | TTC27 subnetwork | 0.55250356 | 1.162521331 |
| REACTOME_LEADING_STRAND | REACTOME_LEADING_STRAND_SYNTHESIS | 0.55087908 | 1.162521392 |
| MP:0005637 | abnormal iron homeostasis | 0.90755328 | 1.162542013 |
| GO:2000191 | regulation of fatty acid transport | 0.55431752 | 1.162547852 |
| MP:0000849 | abnormal cerebellum morphology | 0.55194063 | 1.162548043 |
| GO:0072529 | pyrimidine-containing compound catabolic process | 0.55186837 | 1.162556948 |
| GO:0045987 | positive regulation of smooth muscle contraction | 0.9073161 | 1.162558613 |
| MP:0008770 | decreased survivor rate | 0.90791075 | 1.162572944 |
| GO:0032435 | negative regulation of proteasomal ubiquitin-dependent pr | 0.90717968 | 1.162572996 |
| ENSG00000198053 | SIRPA subnetwork | 0.55270632 | 1.162581746 |
| MP:0004783 | abnormal cardinal vein morphology | 0.54174522 | 1.162603336 |
| ENSG00000173372 | C1QA subnetwork | 0.90785406 | 1.162605005 |
| GO:0051900 | regulation of mitochondrial depolarization | 0.90751574 | 1.162605042 |
| MP:0003861 | abnormal nervous system development | 0.54199382 | 1.162605103 |
| GO:0043304 | regulation of mast cell degranulation | 0.90711818 | 1.162609504 |
| MP:0008531 | increased chemical nociceptive threshold | 0.54294005 | 1.162626628 |
| GO:0072422 | signal transduction involved in DNA damage checkpoint | 0.5485438 | 1.162627131 |
| ENSG00000123124 | WWP1 subnetwork | 0.54900886 | 1.162659224 |
| GO:0050796 | regulation of insulin secretion | 0.90780982 | 1.162668023 |
| GO:0010506 | regulation of autophagy | 0.54169004 | 1.162670438 |
| REACTOME_POLYMERASE_SW | REACTOME_POLYMERASE_SWITCHING | 0.55087908 | 1.162687206 |
| MP:0010879 | decreased trabecular bone volume | 0.90776081 | 1.162691253 |
| GO:0000002 | mitochondrial genome maintenance | 0.90749916 | 1.162694621 |
| MP:0004097 | abnormal cerebellar cortex morphology | 0.90710881 | 1.16270354 |
| ENSG00000065328 | MCM10 subnetwork | 0.53930467 | 1.1627331 |
| ENSG00000110841 | PPFIBP1 subnetwork | 0.9070686 | 1.162762191 |
| ENSG00000087365 | SF3B2 subnetwork | 0.54996706 | 1.162766109 |
| ENSG00000140694 | PARN subnetwork | 0.54199208 | 1.16276642 |
| MP:0003207 | decreased cellular sensitivity to gamma-irradiation | 0.5415894 | 1.162775682 |
| GO:0072431 | signal transduction involved in mitotic cell cycle G1/S transi | 0.5485438 | 1.162793696 |
| GO:0046504 | glycerol ether biosynthetic process | 0.55085945 | 1.162817404 |
| GO:0033180 | proton-transporting V-type ATPase, V1 domain | 0.5490016 | 1.162818494 |
| GO:0045073 | regulation of chemokine biosynthetic process | 0.54168885 | 1.162831858 |
| GO:0051452 | intracellular pH reduction | 0.90688404 | 1.162831976 |
| GO:0030125 | clathrin vesicle coat | 0.55558224 | 1.162832484 |
| MP:0002075 | abnormal coat/hair pigmentation | 0.54980026 | 1.162835906 |
| GO:0045786 | negative regulation of cell cycle | 0.554757 | 1.162838317 |
| ENSG00000181790 | BAI1 subnetwork | 0.55025108 | 1.162839189 |
| GO:0043154 | negative regulation of cysteine-type endopeptidase activity | 0.54196501 | 1.162862529 |
| ENSG00000160803 | UBQLN4 subnetwork | 0.9070685 | 1.162865109 |
| GO:0042594 | response to starvation | 0.90683205 | 1.162872953 |
| ENSG00000115919 | KYNU subnetwork | 0.55063605 | 1.162879977 |
| ENSG00000158987 | RAPGEF6 subnetwork | 0.54993937 | 1.162882252 |
| GO:0007250 | activation of NF-kappaB-inducing kinase activity | 0.55080511 | 1.162883436 |
| ENSG00000148660 | CAMK2G subnetwork | 0.55073058 | 1.162892409 |
| ENSG00000136942 | RPL35 subnetwork | 0.55488209 | 1.162893171 |
| GO:0006903 | vesicle targeting | 0.907014 | 1.162897229 |
| GO:0006707 | cholesterol catabolic process | 0.55551619 | 1.162897977 |
| MP:0002230 | abnormal primitive streak formation | 0.54975683 | 1.162902073 |
| GO:0060428 | lung epithelium development | 0.90670139 | 1.162906225 |
| GO:0043394 | proteoglycan binding | 0.9067742 | 1.162913937 |
| GO:0030117 | membrane coat | 0.55581666 | 1.162918965 |
| GO:0061035 | regulation of cartilage development | 0.54928918 | 1.162920303 |

| | | | |
|---|---|---|---|
| REACTOME_PEPTIDE_HORMOI | REACTOME_PEPTIDE_HORMONE_BIOSYNTHESIS | 0.54157822 | 1.162922653 |
| ENSG00000142949 | PTPRF subnetwork | 0.90654377 | 1.162935081 |
| ENSG00000149557 | FEZ1 subnetwork | 0.54921129 | 1.162936463 |
| GO:0072474 | signal transduction involved in mitotic cell cycle G1/S check | 0.5485438 | 1.162960309 |
| ENSG00000004948 | CALCR subnetwork | 0.55627726 | 1.162966365 |
| GO:0008191 | metalloendopeptidase inhibitor activity | 0.54899911 | 1.162970651 |
| ENSG00000153234 | NR4A2 subnetwork | 0.90667955 | 1.162982643 |
| ENSG00000100410 | PHF5A subnetwork | 0.55023947 | 1.162991001 |
| GO:0032006 | regulation of TOR signaling cascade | 0.54321852 | 1.162993778 |
| ENSG00000153208 | MERTK subnetwork | 0.54971465 | 1.162996854 |
| GO:0010565 | regulation of cellular ketone metabolic process | 0.54153677 | 1.163004354 |
| ENSG00000124193 | SRSF6 subnetwork | 0.53953969 | 1.163006117 |
| ENSG00000198554 | WDHD1 subnetwork | 0.55060919 | 1.163010277 |
| REACTOME_DNA_STRAND_ELC | REACTOME_DNA_STRAND_ELONGATION | 0.54816553 | 1.163021655 |
| ENSG00000185624 | P4HB subnetwork | 0.53994764 | 1.16302576 |
| ENSG00000107263 | RAPGEF1 subnetwork | 0.54788798 | 1.16302726 |
| ENSG00000099882 | ENSG00000099882 subnetwork | 0.54784282 | 1.163036304 |
| MP:0010418 | perimembraneous ventricular septal defect | 0.90654045 | 1.163038087 |
| GO:0019400 | alditol metabolic process | 0.55670914 | 1.163041943 |
| GO:0004540 | ribonuclease activity | 0.55020108 | 1.163042857 |
| GO:0042575 | DNA polymerase complex | 0.5499366 | 1.163048449 |
| GO:0045668 | negative regulation of osteoblast differentiation | 0.55534904 | 1.163052095 |
| GO:0016127 | sterol catabolic process | 0.55551619 | 1.163062553 |
| MP:0008235 | increased susceptibility to neuronal excitotoxicity | 0.90648954 | 1.163065816 |
| MP:0004502 | decreased incidence of chemically-induced tumors | 0.5413376 | 1.163068099 |
| GO:0050702 | interleukin-1 beta secretion | 0.54835682 | 1.163073394 |
| ENSG00000003096 | KLHL13 subnetwork | 0.53950637 | 1.163080845 |
| GO:0048475 | coated membrane | 0.55581666 | 1.163083451 |
| MP:0001730 | embryonic growth arrest | 0.54342605 | 1.163084045 |
| ENSG00000154096 | THY1 subnetwork | 0.55626967 | 1.163088339 |
| ENSG00000154710 | RABGEF1 subnetwork | 0.5480242 | 1.163097117 |
| ENSG00000140795 | MYLK3 subnetwork | 0.90642127 | 1.16309798 |
| GO:0006977 | DNA damage response, signal transduction by p53 class me | 0.5485438 | 1.16312697 |
| ENSG00000168538 | TRAPPC11 subnetwork | 0.54968741 | 1.163127413 |
| GO:0071216 | cellular response to biotic stimulus | 0.54128517 | 1.163135347 |
| GO:0048551 | metalloenzyme inhibitor activity | 0.54899911 | 1.163137171 |
| ENSG00000006451 | RALA subnetwork | 0.54147359 | 1.163138792 |
| REACTOME_GLOBAL_GENOMI | REACTOME_GLOBAL_GENOMIC_NER_GG:NER | 0.55059767 | 1.163147752 |
| ENSG00000111752 | PHC1 subnetwork | 0.55577204 | 1.16314896 |
| ENSG00000184083 | FAM120C subnetwork | 0.54337006 | 1.163151042 |
| GO:0016879 | ligase activity, forming carbon-nitrogen bonds | 0.54814627 | 1.16315261 |
| ENSG00000162961 | DPY30 subnetwork | 0.55045217 | 1.163172926 |
| MP:0002801 | abnormal long term object recognition memory | 0.54153275 | 1.163173175 |
| REACTOME_VIRAL_MESSENGE | REACTOME_VIRAL_MESSENGER_RNA_SYNTHESIS | 0.53993458 | 1.163173217 |
| REACTOME_NUCLEOTIDE_EXC | REACTOME_NUCLEOTIDE_EXCISION_REPAIR | 0.55549152 | 1.163177636 |
| ENSG00000115207 | GTF3C2 subnetwork | 0.90641433 | 1.163183308 |
| GO:0034080 | CenH3-containing nucleosome assembly at centromere | 0.55670151 | 1.163185028 |
| REACTOME_FRS2:MEDIATED_A | REACTOME_FRS2:MEDIATED_ACTIVATION | 0.90634534 | 1.163193337 |
| GO:0009066 | aspartate family amino acid metabolic process | 0.54783732 | 1.163203215 |
| MP:0000627 | abnormal mammary gland morphology | 0.54827769 | 1.163206194 |
| ENSG00000136653 | RASSF5 subnetwork | 0.55534604 | 1.163209684 |
| GO:0009612 | response to mechanical stimulus | 0.5562379 | 1.163210348 |
| ENSG00000136156 | ITM2B subnetwork | 0.54851263 | 1.163214849 |

| | | | |
|---|---|---|---|
| ENSG00000109062 | SLC9A3R1 subnetwork | 0.55508608 | 1.16321717 |
| ENSG00000197958 | RPL12 subnetwork | 0.54026377 | 1.163238289 |
| KEGG_VIBRIO_CHOLERAE_INFE | KEGG_VIBRIO_CHOLERAE_INFECTION | 0.541264 | 1.163238925 |
| ENSG00000175482 | POLD4 subnetwork | 0.5483537 | 1.163240143 |
| ENSG00000156475 | PPP2R2B subnetwork | 0.53988769 | 1.163240646 |
| GO:0004984 | olfactory receptor activity | 0.5505439 | 1.163249572 |
| GO:0051289 | protein homotetramerization | 0.54966968 | 1.163250858 |
| ENSG00000174243 | DDX23 subnetwork | 0.54118642 | 1.163255375 |
| MP:0002835 | abnormal cranial suture morphology | 0.90330613 | 1.163258687 |
| ENSG00000137992 | DBT subnetwork | 0.55614744 | 1.163261699 |
| MP:0009288 | increased epididymal fat pad weight | 0.53982842 | 1.163264415 |
| GO:0090178 | regulation of establishment of planar polarity involved in ne | 0.90632504 | 1.163265397 |
| ENSG00000108828 | VAT1 subnetwork | 0.54961602 | 1.16327421 |
| MP:0001330 | abnormal optic nerve morphology | 0.904814 | 1.163284231 |
| ENSG00000183386 | FHL3 subnetwork | 0.55607796 | 1.163291855 |
| GO:0050891 | multicellular organismal water homeostasis | 0.90445799 | 1.163293387 |
| GO:0006323 | DNA packaging | 0.9034064 | 1.163297494 |
| MP:0001906 | increased dopamine level | 0.90576622 | 1.163303484 |
| MP:0004110 | transposition of great arteries | 0.54955118 | 1.163304721 |
| ENSG00000196136 | SERPINA3 subnetwork | 0.55532314 | 1.163317757 |
| ENSG00000108272 | DHRS11 subnetwork | 0.90458328 | 1.163327712 |
| MP:0001723 | disorganized yolk sac vascular plexus | 0.90496331 | 1.163340728 |
| ENSG00000063245 | EPN1 subnetwork | 0.90329062 | 1.163344294 |
| MP:0001242 | hyperkeratosis | 0.55527915 | 1.163347968 |
| GO:0034724 | DNA replication-independent nucleosome organization | 0.55670151 | 1.163349343 |
| GO:0014909 | smooth muscle cell migration | 0.90560091 | 1.163350182 |
| GO:0050701 | interleukin-1 secretion | 0.55992826 | 1.163355346 |
| GO:0045739 | positive regulation of DNA repair | 0.90316973 | 1.163355556 |
| GO:0048407 | platelet-derived growth factor binding | 0.53978708 | 1.163361002 |
| ENSG00000178982 | EIF3K subnetwork | 0.90324082 | 1.163367701 |
| GO:0090179 | planar cell polarity pathway involved in neural tube closure | 0.90632504 | 1.163368486 |
| MP:0003633 | abnormal nervous system physiology | 0.5478366 | 1.163370174 |
| ENSG00000007237 | GAS7 subnetwork | 0.56015691 | 1.163370787 |
| GO:0007254 | JNK cascade | 0.5402343 | 1.163371163 |
| GO:0031100 | organ regeneration | 0.55815112 | 1.163371847 |
| ENSG00000180198 | RCC1 subnetwork | 0.90524114 | 1.16337266 |
| GO:0006027 | glycosaminoglycan catabolic process | 0.90615822 | 1.163375288 |
| GO:0032446 | protein modification by small protein conjugation | 0.9041737 | 1.16337803 |
| ENSG00000150867 | PIP4K2A subnetwork | 0.55988624 | 1.163378302 |
| GO:0072077 | renal vesicle morphogenesis | 0.90369578 | 1.163379531 |
| ENSG00000136842 | TMOD1 subnetwork | 0.90388897 | 1.163381595 |
| GO:0071824 | protein-DNA complex subunit organization | 0.54370025 | 1.163383948 |
| MP:0005195 | abnormal posterior eye segment morphology | 0.90481278 | 1.163387469 |
| ENSG00000124333 | VAMP7 subnetwork | 0.90437095 | 1.163388973 |
| GO:0051412 | response to corticosterone stimulus | 0.90444647 | 1.163392223 |
| MP:0004859 | abnormal synaptic plasticity | 0.90362425 | 1.163394047 |
| MP:0005307 | head tossing | 0.90575697 | 1.163397766 |
| REACTOME_TELOMERE_C:STR | REACTOME_TELOMERE_C:STRAND_LAGGING_STRAND_SYI | 0.56026815 | 1.163411038 |
| GO:0031514 | motile cilium | 0.9055364 | 1.163413444 |
| ENSG00000013503 | POLR3B subnetwork | 0.54541051 | 1.163413579 |
| GO:0008194 | UDP-glycosyltransferase activity | 0.90626467 | 1.163422849 |
| MP:0003055 | abnormal long bone epiphyseal plate morphology | 0.54118319 | 1.163424379 |
| GO:0030042 | actin filament depolymerization | 0.5438369 | 1.16342539 |

| | | | |
|---|---|---|---|
| GO:0045742 | positive regulation of epidermal growth factor receptor sig | 0.90431994 | 1.163425679 |
| MP:0005075 | abnormal melanosome morphology | 0.56051643 | 1.163426446 |
| ENSG00000030582 | GRN subnetwork | 0.55524071 | 1.163427762 |
| ENSG00000164919 | COX6C subnetwork | 0.90612045 | 1.16342966 |
| GO:0014704 | intercalated disc | 0.9031606 | 1.163432305 |
| ENSG00000147883 | CDKN2B subnetwork | 0.54110063 | 1.163433595 |
| ENSG00000164061 | BSN subnetwork | 0.90519837 | 1.163435947 |
| GO:0000460 | maturation of 5.8S rRNA | 0.56033993 | 1.163437237 |
| MP:0003814 | vascular smooth muscle cell hypoplasia | 0.90476935 | 1.163437472 |
| ENSG00000047621 | C12orf4 subnetwork | 0.90384747 | 1.163440526 |
| MP:0004624 | abnormal thoracic cage morphology | 0.56058053 | 1.163445614 |
| MP:0001154 | seminiferous tubule degeneration | 0.90510765 | 1.163446012 |
| ENSG00000174292 | TNK1 subnetwork | 0.54365211 | 1.163450969 |
| ENSG00000138107 | ACTR1A subnetwork | 0.54778874 | 1.163451048 |
| ENSG00000097033 | SH3GLB1 subnetwork | 0.55705116 | 1.163468869 |
| GO:0071702 | organic substance transport | 0.90416801 | 1.163472469 |
| ENSG00000076924 | XAB2 subnetwork | 0.56046935 | 1.163477467 |
| ENSG00000102755 | FLT1 subnetwork | 0.5566065 | 1.163480288 |
| REACTOME_SHC1_EVENTS_IN_ | REACTOME_SHC1_EVENTS_IN_ERBB2_SIGNALING | 0.55983599 | 1.163485594 |
| GO:0031345 | negative regulation of cell projection organization | 0.90408466 | 1.163504752 |
| MP:0009399 | increased skeletal muscle fiber size | 0.9055235 | 1.163512195 |
| GO:0006336 | DNA replication-independent nucleosome assembly | 0.55670151 | 1.163513704 |
| ENSG00000136110 | LECT1 subnetwork | 0.5477488 | 1.163517588 |
| ENSG00000063244 | U2AF2 subnetwork | 0.54021847 | 1.163518626 |
| ENSG00000120500 | ARR3 subnetwork | 0.90610226 | 1.163519504 |
| GO:0051567 | histone H3-K9 methylation | 0.54758215 | 1.163521471 |
| GO:0014896 | muscle hypertrophy | 0.54530157 | 1.163525595 |
| ENSG00000076554 | TPD52 subnetwork | 0.56014269 | 1.163527181 |
| GO:0014823 | response to activity | 0.55814873 | 1.163528749 |
| MP:0005564 | increased hemoglobin content | 0.5476821 | 1.163533889 |
| GO:0050999 | regulation of nitric-oxide synthase activity | 0.90316037 | 1.16353574 |
| GO:0006094 | gluconeogenesis | 0.54750247 | 1.163537777 |
| GO:0006626 | protein targeting to mitochondrion | 0.54558973 | 1.163541366 |
| ENSG00000166233 | ARIH1 subnetwork | 0.55700385 | 1.163548433 |
| REACTOME_DSCAM_INTERACT | REACTOME_DSCAM_INTERACTIONS | 0.5410746 | 1.163551809 |
| GO:0060338 | regulation of type I interferon-mediated signaling pathway | 0.55808574 | 1.163565891 |
| ENSG00000197586 | ENTPD6 subnetwork | 0.54540951 | 1.163581315 |
| GO:0010822 | positive regulation of mitochondrion organization | 0.56009617 | 1.163585277 |
| GO:0090103 | cochlea morphogenesis | 0.90550027 | 1.163588788 |
| GO:0018195 | peptidyl-arginine modification | 0.56164932 | 1.163600056 |
| GO:0046887 | positive regulation of hormone secretion | 0.9030213 | 1.163604837 |
| GO:0048365 | Rac GTPase binding | 0.54511941 | 1.163610791 |
| GO:0005537 | mannose binding | 0.54102653 | 1.163611919 |
| ENSG00000013583 | HEBP1 subnetwork | 0.54570189 | 1.163618677 |
| ENSG00000204310 | AGPAT1 subnetwork | 0.55891148 | 1.163626126 |
| MP:0001144 | vagina atresia | 0.54527497 | 1.163628497 |
| ENSG00000139116 | KIF21A subnetwork | 0.56156217 | 1.163629993 |
| ENSG00000100519 | PSMC6 subnetwork | 0.54747232 | 1.163633099 |
| REACTOME_VIRAL_MRNA_TRA | REACTOME_VIRAL_MRNA_TRANSLATION | 0.90314643 | 1.163634747 |
| ENSG00000167657 | DAPK3 subnetwork | 0.54083775 | 1.163644955 |
| ENSG00000151320 | AKAP6 subnetwork | 0.55982307 | 1.163649143 |
| GO:0033993 | response to lipid | 0.55791857 | 1.163649182 |
| ENSG00000177731 | FLII subnetwork | 0.5579926 | 1.163661356 |

| | | | |
|---|---|---|---|
| GO:0016709 | oxidoreductase activity, acting on paired donors, with incor | 0.55735372 | 1.163669725 |
| GO:0003779 | actin binding | 0.55783202 | 1.163672261 |
| GO:0035036 | sperm-egg recognition | 0.55758013 | 1.163678047 |
| ENSG00000085365 | ENSG00000085365 subnetwork | 0.540961 | 1.163679314 |
| ENSG00000171444 | MCC subnetwork | 0.55767575 | 1.163683171 |
| GO:0032434 | regulation of proteasomal ubiquitin-dependent protein cat | 0.54475823 | 1.163701992 |
| ENSG00000107581 | EIF3A subnetwork | 0.54494298 | 1.163703276 |
| ENSG00000179071 | CCDC89 subnetwork | 0.90301661 | 1.163703868 |
| GO:0035295 | tube development | 0.55912368 | 1.163713763 |
| ENSG00000111667 | USP5 subnetwork | 0.55808249 | 1.163715816 |
| REACTOME_SYNTHESIS_OF_GL | REACTOME_SYNTHESIS_OF_GLYCOSYLPHOSPHATIDYLINOS | 0.55751091 | 1.163722308 |
| ENSG00000152818 | UTRN subnetwork | 0.54522904 | 1.163731429 |
| MP:0002085 | abnormal embryonic tissue morphology | 0.54743192 | 1.163742816 |
| REACTOME_REPAIR_SYNTHESI | REACTOME_REPAIR_SYNTHESIS_OF_PATCH_27:30_BASES_ | 0.55976745 | 1.163749473 |
| ENSG00000079950 | STX7 subnetwork | 0.54510989 | 1.16374982 |
| KEGG_STEROID_BIOSYNTHESIS | KEGG_STEROID_BIOSYNTHESIS | 0.55904697 | 1.16375088 |
| GO:0032925 | regulation of activin receptor signaling pathway | 0.55960202 | 1.16375334 |
| ENSG00000003393 | ALS2 subnetwork | 0.54490458 | 1.163762991 |
| GO:0043240 | Fanconi anaemia nuclear complex | 0.54473222 | 1.163768953 |
| ENSG00000127337 | YEATS4 subnetwork | 0.56099735 | 1.163769641 |
| ENSG00000160741 | CRTC2 subnetwork | 0.561556 | 1.163772077 |
| ENSG00000206255 | ENSG00000206255 subnetwork | 0.55891148 | 1.163789948 |
| GO:0030029 | actin filament-based process | 0.54407839 | 1.163792106 |
| GO:0034104 | negative regulation of tissue remodeling | 0.56094348 | 1.163799635 |
| GO:0009881 | photoreceptor activity | 0.5450479 | 1.163802309 |
| GO:0016567 | protein ubiquitination | 0.90300758 | 1.163802917 |
| GO:0005201 | extracellular matrix structural constituent | 0.5573308 | 1.163805759 |
| ENSG00000170734 | POLH subnetwork | 0.54083287 | 1.163814163 |
| MP:0010375 | increased kidney iron level | 0.55781907 | 1.163822285 |
| MP:0005156 | bradykinesia | 0.54485452 | 1.163822723 |
| GO:0001948 | glycoprotein binding | 0.54071688 | 1.163823444 |
| GO:0090218 | positive regulation of lipid kinase activity | 0.54464541 | 1.163837932 |
| ENSG00000164258 | NDUFS4 subnetwork | 0.5445675 | 1.163839931 |
| ENSG00000170515 | PA2G4 subnetwork | 0.54613079 | 1.16384848 |
| GO:0061077 | chaperone-mediated protein folding | 0.54470529 | 1.163857597 |
| ENSG00000100968 | NFATC4 subnetwork | 0.54741333 | 1.16385975 |
| ENSG00000108296 | CWC25 subnetwork | 0.55956606 | 1.163860759 |
| GO:0035112 | genitalia morphogenesis | 0.55750657 | 1.163872424 |
| ENSG00000132603 | NIP7 subnetwork | 0.56180988 | 1.16387838 |
| MP:0005656 | decreased aggression | 0.90284417 | 1.163891113 |
| GO:0001568 | blood vessel development | 0.90299739 | 1.163897536 |
| GO:0051208 | sequestering of calcium ion | 0.54067313 | 1.163898182 |
| MP:0004613 | fusion of vertebral arches | 0.55851086 | 1.163905325 |
| REACTOME_REPAIR_SYNTHESI | REACTOME_REPAIR_SYNTHESIS_FOR_GAP:FILLING_BY_DN | 0.55976745 | 1.163913105 |
| ENSG00000117906 | RCN2 subnetwork | 0.56193058 | 1.163925469 |
| GO:0005761 | mitochondrial ribosome | 0.56153186 | 1.163928221 |
| GO:0071219 | cellular response to molecule of bacterial origin | 0.56092326 | 1.163934886 |
| ENSG00000131721 | RHOXF2 subnetwork | 0.55951593 | 1.163940076 |
| GO:0009925 | basal plasma membrane | 0.54738247 | 1.163940788 |
| ENSG00000138162 | TACC2 subnetwork | 0.55933269 | 1.163943999 |
| ENSG00000198838 | RYR3 subnetwork | 0.54441136 | 1.163945087 |
| MP:0001458 | abnormal object recognition memory | 0.90295168 | 1.163952144 |
| ENSG00000206324 | AGPAT1 subnetwork | 0.55891148 | 1.163953816 |

| | | | |
|---|---|---|---|
| ENSG00000203813 | HIST1H3H subnetwork | 0.55870717 | 1.163957746 |
| KEGG_TOLL_LIKE_RECEPTOR_S | KEGG_TOLL_LIKE_RECEPTOR_SIGNALING_PATHWAY | 0.55881124 | 1.163962822 |
| ENSG00000100347 | SAMM50 subnetwork | 0.55862963 | 1.163966756 |
| ENSG00000003756 | RBM5 subnetwork | 0.54611783 | 1.163987324 |
| GO:0071326 | cellular response to monosaccharide stimulus | 0.90284365 | 1.163994662 |
| REACTOME_AMINO_ACID_TRA | REACTOME_AMINO_ACID_TRANSPORT_ACROSS_THE_PLA | 0.55945284 | 1.163998312 |
| ENSG00000011451 | WIZ subnetwork | 0.5445562 | 1.164008091 |
| ENSG00000115310 | RTN4 subnetwork | 0.54601655 | 1.164027378 |
| ENSG00000100029 | PES1 subnetwork | 0.54736436 | 1.16404341 |
| MP:0004086 | absent heartbeat | 0.54437384 | 1.164055499 |
| GO:0051297 | centrosome organization | 0.54607416 | 1.164061374 |
| GO:0008093 | cytoskeletal adaptor activity | 0.5471432 | 1.164071038 |
| ENSG00000160551 | TAOK1 subnetwork | 0.54729447 | 1.164081369 |
| GO:0000313 | organellar ribosome | 0.56153186 | 1.164091419 |
| GO:0071333 | cellular response to glucose stimulus | 0.90284365 | 1.164098229 |
| GO:0005792 | microsome | 0.56145261 | 1.164100407 |
| ENSG00000082781 | ITGB5 subnetwork | 0.54661812 | 1.164106809 |
| ENSG00000169727 | GPS1 subnetwork | 0.54685707 | 1.164107914 |
| REACTOME_TRANSPORT_OF_F | REACTOME_TRANSPORT_OF_RIBONUCLEOPROTEINS_INTO | 0.56134388 | 1.164109397 |
| ENSG00000105220 | GPI subnetwork | 0.54678651 | 1.16413153 |
| ENSG00000132825 | PPP1R3D subnetwork | 0.56127953 | 1.16413943 |
| ENSG00000131508 | UBE2D2 subnetwork | 0.54431782 | 1.164144261 |
| GO:0071108 | protein K48-linked deubiquitination | 0.54725555 | 1.164162473 |
| GO:0071331 | cellular response to hexose stimulus | 0.90284365 | 1.164201815 |
| GO:0032319 | regulation of Rho GTPase activity | 0.90273646 | 1.164207529 |
| GO:0015036 | disulfide oxidoreductase activity | 0.90267702 | 1.164217693 |
| GO:0035066 | positive regulation of histone acetylation | 0.54713422 | 1.164224076 |
| GO:0051010 | microtubule plus-end binding | 0.54676657 | 1.164241508 |
| GO:0016798 | hydrolase activity, acting on glycosyl bonds | 0.54659954 | 1.164267204 |
| MP:0006319 | abnormal epididymal fat pad morphology | 0.90265234 | 1.164272363 |
| GO:0015711 | organic anion transport | 0.54707542 | 1.164276467 |
| ENSG00000163362 | C1orf106 subnetwork | 0.54703391 | 1.16436484 |
| GO:0048598 | embryonic morphogenesis | 0.9023415 | 1.16437539 |
| MP:0005296 | abnormal humerus morphology | 0.9026447 | 1.164376001 |
| GO:0007141 | male meiosis I | 0.54658794 | 1.164406048 |
| ENSG00000196914 | ARHGEF12 subnetwork | 0.54651603 | 1.164408122 |
| GO:0002685 | regulation of leukocyte migration | 0.9025962 | 1.164412891 |
| ENSG00000075891 | PAX2 subnetwork | 0.90231036 | 1.164430098 |
| MP:0008033 | impaired lipolysis | 0.90248828 | 1.164436432 |
| GO:0010976 | positive regulation of neuron projection development | 0.90229515 | 1.164515985 |
| GO:0004690 | cyclic nucleotide-dependent protein kinase activity | 0.90224668 | 1.16456181 |
| ENSG00000196584 | XRCC2 subnetwork | 0.90224578 | 1.164665538 |
| GO:0048247 | lymphocyte chemotaxis | 0.56314084 | 1.164694363 |
| GO:0033059 | cellular pigmentation | 0.90220656 | 1.1647292 |
| ENSG00000060339 | CCAR1 subnetwork | 0.56360086 | 1.164746995 |
| ENSG00000102312 | PORCN subnetwork | 0.563543 | 1.164763036 |
| GO:0046851 | negative regulation of bone remodeling | 0.56309827 | 1.164794348 |
| ENSG00000142871 | CYR61 subnetwork | 0.90219152 | 1.16481069 |
| MP:0010386 | abnormal urinary bladder physiology | 0.56307775 | 1.164852386 |
| GO:0006575 | cellular modified amino acid metabolic process | 0.563748 | 1.16487072 |
| ENSG00000142731 | PLK4 subnetwork | 0.56348306 | 1.164876957 |
| GO:0030204 | chondroitin sulfate metabolic process | 0.90216739 | 1.16489665 |
| ENSG00000139514 | SLC7A1 subnetwork | 0.56342208 | 1.164913998 |

| | | | |
|---|---|---|---|
| ENSG00000121892 | PDS5A subnetwork | 0.56306708 | 1.164994402 |
| MP:0003656 | abnormal erythrocyte physiology | 0.90216525 | 1.16499599 |
| ENSG00000197299 | BLM subnetwork | 0.56339414 | 1.165 |
| ENSG00000138675 | FGF5 subnetwork | 0.90165325 | 1.165021842 |
| GO:0048643 | positive regulation of skeletal muscle tissue development | 0.90210555 | 1.16502406 |
| GO:0009161 | ribonucleoside monophosphate metabolic process | 0.56302121 | 1.165031491 |
| GO:0004859 | phospholipase inhibitor activity | 0.90200884 | 1.165061046 |
| GO:0070534 | protein K63-linked ubiquitination | 0.5640455 | 1.165090122 |
| MP:0006143 | increased systemic arterial diastolic blood pressure | 0.90140249 | 1.165094087 |
| MP:0010099 | abnormal thoracic cage shape | 0.90162006 | 1.165094508 |
| ENSG00000105968 | H2AFV subnetwork | 0.56412531 | 1.165094999 |
| REACTOME_PI3K_CASCADE | REACTOME_PI3K_CASCADE | 0.90198634 | 1.165106952 |
| ENSG00000177791 | MYOZ1 subnetwork | 0.90134312 | 1.165113271 |
| ENSG00000203814 | HIST2H2BF subnetwork | 0.56256933 | 1.165114162 |
| ENSG00000169371 | SNUPN subnetwork | 0.56299167 | 1.165152576 |
| GO:0003382 | epithelial cell morphogenesis | 0.90157804 | 1.165153812 |
| GO:0043631 | RNA polyadenylation | 0.56433576 | 1.165167598 |
| GO:0008156 | negative regulation of DNA replication | 0.90153219 | 1.165177457 |
| REACTOME_CHYLOMICRON:M | REACTOME_CHYLOMICRON:MEDIATED_LIPID_TRANSPORT | 0.90122473 | 1.165182872 |
| MP:0004924 | abnormal behavior | 0.90196693 | 1.165188519 |
| MP:0005409 | darkened coat color | 0.90132721 | 1.165199358 |
| GO:0045178 | basal part of cell | 0.56272676 | 1.165210084 |
| GO:0051050 | positive regulation of transport | 0.56295652 | 1.165238695 |
| MP:0006359 | absent startle reflex | 0.56404256 | 1.16523896 |
| ENSG00000107949 | BCCIP subnetwork | 0.90191868 | 1.165247816 |
| MP:0001005 | abnormal retinal rod cell morphology | 0.90110693 | 1.165252498 |
| ENSG00000198681 | MAGEA1 subnetwork | 0.56431394 | 1.165253527 |
| MP:0000547 | short limbs | 0.90117781 | 1.165260059 |
| ENSG00000158161 | EYA3 subnetwork | 0.90105756 | 1.165267244 |
| GO:0006704 | glucocorticoid biosynthetic process | 0.90103178 | 1.16534892 |
| GO:0005614 | interstitial matrix | 0.56287721 | 1.165354992 |
| ENSG00000090054 | SPTLC1 subnetwork | 0.56293426 | 1.165373845 |
| GO:0060325 | face morphogenesis | 0.90094783 | 1.165385988 |
| ENSG00000151743 | AMN1 subnetwork | 0.90087134 | 1.165387362 |
| MP:0009887 | abnormal palatal shelf fusion at midline | 0.9008703 | 1.165491386 |
| ENSG00000183495 | EP400 subnetwork | 0.9007725 | 1.165561111 |
| ENSG00000111275 | ALDH2 subnetwork | 0.56458425 | 1.165563469 |
| GO:0001533 | cornified envelope | 0.90086102 | 1.165586502 |
| ENSG00000182754 | ENSG00000182754 subnetwork | 0.90017823 | 1.165588708 |
| MP:0000372 | irregular coat pigmentation | 0.56467551 | 1.165603183 |
| GO:0014066 | regulation of phosphatidylinositol 3-kinase cascade | 0.90062745 | 1.165613001 |
| MP:0010029 | abnormal basicranium morphology | 0.90051693 | 1.165618861 |
| GO:0051650 | establishment of vesicle localization | 0.90073892 | 1.165638393 |
| ENSG00000118523 | CTGF subnetwork | 0.89995361 | 1.165664373 |
| GO:0072087 | renal vesicle development | 0.90034027 | 1.165672175 |
| ENSG00000169139 | UBE2V2 subnetwork | 0.90049867 | 1.165691703 |
| ENSG00000163682 | RPL9 subnetwork | 0.90017823 | 1.165692844 |
| MP:0002948 | abnormal neuron specification | 0.89993408 | 1.165737265 |
| MP:0002115 | abnormal limb bone morphology | 0.9004516 | 1.165746695 |
| ENSG00000120708 | TGFBI subnetwork | 0.89983087 | 1.165747609 |
| GO:0009069 | serine family amino acid metabolic process | 0.90012605 | 1.165747856 |
| GO:0030139 | endocytic vesicle | 0.8997642 | 1.165762424 |
| ENSG00000108590 | MED31 subnetwork | 0.56499089 | 1.165792045 |

| | | | |
|---|---|---|---|
| GO:0017075 | syntaxin-1 binding | 0.89947869 | 1.165799356 |
| ENSG00000146047 | HIST1H2BA subnetwork | 0.8987934 | 1.165855404 |
| REACTOME_INTERACTION_BET | REACTOME_INTERACTION_BETWEEN_L1_AND_ANKYRINS | 0.89976198 | 1.165857692 |
| ENSG00000018236 | CNTN1 subnetwork | 0.89896974 | 1.165861514 |
| GO:0050912 | detection of chemical stimulus involved in sensory percepti | 0.89927977 | 1.165870673 |
| GO:0019861 | flagellum | 0.89917757 | 1.165876565 |
| GO:0030238 | male sex determination | 0.89944927 | 1.165876777 |
| MP:0003130 | anal atresia | 0.89910908 | 1.165882458 |
| GO:0006650 | glycerophospholipid metabolic process | 0.56495526 | 1.165905918 |
| REACTOME_INSULIN_RECEPTC | REACTOME_INSULIN_RECEPTOR_RECYCLING | 0.89863747 | 1.165907464 |
| ENSG00000135249 | RINT1 subnetwork | 0.8996391 | 1.165914171 |
| GO:0045026 | plasma membrane fusion | 0.89895194 | 1.165934508 |
| ENSG00000104419 | NDRG1 subnetwork | 0.89876933 | 1.16593736 |
| ENSG00000074590 | NUAK1 subnetwork | 0.89975586 | 1.165939567 |
| ENSG00000100632 | ERH subnetwork | 0.8994195 | 1.165940798 |
| GO:0031648 | protein destabilization | 0.89858897 | 1.165962588 |
| MP:0010182 | decreased susceptibility to weight gain | 0.56551596 | 1.165997211 |
| ENSG00000071082 | RPL31 subnetwork | 0.56492348 | 1.165998883 |
| GO:0006721 | terpenoid metabolic process | 0.89857586 | 1.166058002 |
| ENSG00000164171 | ITGA2 subnetwork | 0.89850966 | 1.166081819 |
| MP:0001303 | abnormal lens morphology | 0.89844583 | 1.166092211 |
| ENSG00000183963 | SMTN subnetwork | 0.56549991 | 1.166118008 |
| MP:0005191 | head tilt | 0.56565229 | 1.16613443 |
| GO:0005484 | SNAP receptor activity | 0.89838189 | 1.166142896 |
| ENSG00000120265 | PCMT1 subnetwork | 0.56527294 | 1.16619453 |
| ENSG00000116329 | OPRD1 subnetwork | 0.565342 | 1.166206223 |
| GO:0044349 | DNA excision | 0.8982005 | 1.166217426 |
| REACTOME_GRB2_EVENTS_IN | REACTOME_GRB2_EVENTS_IN_ERBB2_SIGNALING | 0.56547559 | 1.166224888 |
| GO:0019841 | retinol binding | 0.8983616 | 1.166229405 |
| GO:0000718 | nucleotide-excision repair, DNA damage removal | 0.8982005 | 1.16632187 |
| MP:0000750 | abnormal muscle regeneration | 0.5658575 | 1.166362242 |
| MP:0008128 | abnormal brain internal capsule morphology | 0.89810758 | 1.166391974 |
| GO:0022900 | electron transport chain | 0.89819893 | 1.166426332 |
| GO:0030057 | desmosome | 0.89806577 | 1.166447192 |
| GO:0016471 | vacuolar proton-transporting V-type ATPase complex | 0.56645044 | 1.166515743 |
| ENSG00000067533 | RRP15 subnetwork | 0.89805973 | 1.166547214 |
| REACTOME_GAP:FILLING_DNA | REACTOME_GAP:FILLING_DNA_REPAIR_SYNTHESIS_AND_L | 0.56642751 | 1.166629511 |
| ENSG00000166598 | HSP90B1 subnetwork | 0.56608667 | 1.166631814 |
| ENSG00000112038 | OPRM1 subnetwork | 0.89804322 | 1.166642774 |
| ENSG00000108559 | NUP88 subnetwork | 0.56620678 | 1.166713131 |
| MP:0001056 | abnormal cranial nerve morphology | 0.8980262 | 1.166747312 |
| ENSG00000138175 | ARL3 subnetwork | 0.56713224 | 1.166773385 |
| REACTOME_GAP:FILLING_DNA | REACTOME_GAP:FILLING_DNA_REPAIR_SYNTHESIS_AND_L | 0.56642751 | 1.166792085 |
| ENSG00000110237 | ARHGEF17 subnetwork | 0.56696284 | 1.166812865 |
| GO:0050771 | negative regulation of axonogenesis | 0.89801718 | 1.166833946 |
| REACTOME_NCAM_SIGNALING | REACTOME_NCAM_SIGNALING_FOR_NEURITE_OUT:GROW | 0.89757688 | 1.166837009 |
| ENSG00000147416 | ATP6V1B2 subnetwork | 0.89769824 | 1.16687584 |
| MP:0003849 | greasy coat | 0.5671091 | 1.166894055 |
| GO:0034405 | response to fluid shear stress | 0.89798833 | 1.166907152 |
| MP:0001081 | abnormal cranial ganglia morphology | 0.89722181 | 1.166911831 |
| GO:0045137 | development of primary sexual characteristics | 0.89781264 | 1.166919147 |
| ENSG00000167526 | RPL13 subnetwork | 0.56683695 | 1.166928969 |
| ENSG00000100299 | ARSA subnetwork | 0.56642003 | 1.166940767 |

| | | | |
|---|---|---|---|
| GO:0000978 | RNA polymerase II core promoter proximal region sequenc | 0.89757612 | 1.16694163 |
| GO:0070528 | protein kinase C signaling cascade | 0.89792704 | 1.166944519 |
| ENSG00000116750 | UCHL5 subnetwork | 0.56692294 | 1.1669475 |
| ENSG00000078053 | AMPH subnetwork | 0.89748947 | 1.166947633 |
| ENSG00000211614 | ENSG00000211614 subnetwork | 0.89738513 | 1.166962604 |
| MP:0009593 | absent chorion | 0.56679571 | 1.167000975 |
| GO:0051817 | modification of morphology or physiology of other organisr | 0.89720078 | 1.16700305 |
| ENSG00000165410 | CFL2 subnetwork | 0.56731499 | 1.167007655 |
| ENSG00000165688 | PMPCA subnetwork | 0.89735132 | 1.16703139 |
| ENSG00000117385 | LEPRE1 subnetwork | 0.8964679 | 1.167048209 |
| ENSG00000038382 | TRIO subnetwork | 0.89637391 | 1.167063207 |
| ENSG00000172062 | SMN1 subnetwork | 0.89621341 | 1.167066272 |
| GO:0035821 | modification of morphology or physiology of other organisr | 0.89720078 | 1.167107742 |
| GO:0051444 | negative regulation of ubiquitin-protein ligase activity | 0.89685741 | 1.167113883 |
| MP:0009146 | abnormal pancreatic acinar cell morphology | 0.89693294 | 1.167116834 |
| ENSG00000128683 | GAD1 subnetwork | 0.89632183 | 1.167123103 |
| MP:0001905 | abnormal dopamine level | 0.89703144 | 1.16713773 |
| ENSG00000137124 | ALDH1B1 subnetwork | 0.89711929 | 1.16714965 |
| ENSG00000205571 | SMN2 subnetwork | 0.89621341 | 1.167171082 |
| GO:0051352 | negative regulation of ligase activity | 0.89685741 | 1.167218632 |
| GO:0010721 | negative regulation of cell development | 0.89681402 | 1.167265057 |
| ENSG00000159228 | CBR1 subnetwork | 0.89620271 | 1.167271421 |
| MP:0000097 | short maxilla | 0.8960107 | 1.167283507 |
| MP:0004007 | abnormal lung vasculature morphology | 0.89674563 | 1.16728456 |
| GO:0006760 | folic acid-containing compound metabolic process | 0.89613434 | 1.167313393 |
| ENSG00000144908 | ALDH1L1 subnetwork | 0.56796736 | 1.167352614 |
| MP:0000751 | myopathy | 0.89593079 | 1.167380952 |
| ENSG00000158169 | FANCC subnetwork | 0.89600606 | 1.167383883 |
| GO:0015301 | anion:anion antiporter activity | 0.56770924 | 1.167404007 |
| REACTOME_G_ALPHA_I_SIGNA | REACTOME_G_ALPHA_I_SIGNALLING_EVENTS | 0.56793599 | 1.167417605 |
| GO:0045931 | positive regulation of mitotic cell cycle | 0.89583267 | 1.16746046 |
| ENSG00000183785 | TUBA8 subnetwork | 0.56813717 | 1.167461421 |
| ENSG00000184895 | SRY subnetwork | 0.89592445 | 1.167476862 |
| GO:0010564 | regulation of cell cycle process | 0.5676831 | 1.167489912 |
| ENSG00000145321 | GC subnetwork | 0.89580058 | 1.167497978 |
| GO:0009119 | ribonucleoside metabolic process | 0.89566691 | 1.167546067 |
| ENSG00000169213 | RAB3B subnetwork | 0.56791678 | 1.16755911 |
| GO:0006367 | transcription initiation from RNA polymerase II promoter | 0.89559009 | 1.167561129 |
| MP:0008392 | decreased primordial germ cell number | 0.89579004 | 1.167598418 |
| MP:0000729 | abnormal myogenesis | 0.56764377 | 1.167603674 |
| ENSG00000088179 | PTPN4 subnetwork | 0.56786007 | 1.167617193 |
| GO:0008353 | RNA polymerase II carboxy-terminal domain kinase activity | 0.89558045 | 1.167652612 |
| ENSG00000214717 | ZBED1 subnetwork | 0.89551325 | 1.167676677 |
| GO:0017046 | peptide hormone binding | 0.89545999 | 1.167727722 |
| MP:0001447 | abnormal nest building behavior | 0.89527241 | 1.167768484 |
| ENSG00000166483 | WEE1 subnetwork | 0.89538196 | 1.167798363 |
| GO:0032845 | negative regulation of homeostatic process | 0.8954496 | 1.167805755 |
| ENSG00000111711 | GOLT1B subnetwork | 0.89526136 | 1.167860034 |
| GO:0019217 | regulation of fatty acid metabolic process | 0.89521847 | 1.167920115 |
| MP:0001548 | hyperlipidemia | 0.8951801 | 1.16797121 |
| GO:0008195 | phosphatidate phosphatase activity | 0.89501926 | 1.167983443 |
| ENSG00000137975 | CLCA2 subnetwork | 0.89512542 | 1.168008818 |
| GO:0044441 | cilium part | 0.56913032 | 1.168015829 |

| | | | |
|---|---|---|---|
| MP:0000556 | abnormal hindlimb morphology | 0.89428588 | 1.168052053 |
| GO:0071855 | neuropeptide receptor binding | 0.89501076 | 1.168075054 |
| MP:0000418 | focal hair loss | 0.89494043 | 1.168108181 |
| GO:0070303 | negative regulation of stress-activated protein kinase signal | 0.56859721 | 1.168116748 |
| ENSG00000169783 | LINGO1 subnetwork | 0.89467097 | 1.168122074 |
| ENSG00000143106 | PSMA5 subnetwork | 0.56911263 | 1.168143313 |
| MP:0011423 | kidney cortex atrophy | 0.89428268 | 1.168148248 |
| ENSG00000139190 | VAMP1 subnetwork | 0.89478175 | 1.168160951 |
| MP:0001706 | abnormal left-right axis patterning | 0.5685405 | 1.168181818 |
| GO:0033344 | cholesterol efflux | 0.89462678 | 1.168182227 |
| ENSG00000136888 | ATP6V1G1 subnetwork | 0.89490585 | 1.168186319 |
| ENSG00000163520 | FBLN2 subnetwork | 0.56945598 | 1.168202637 |
| ENSG00000143379 | SETDB1 subnetwork | 0.894266 | 1.168235453 |
| GO:0019866 | organelle inner membrane | 0.5717987 | 1.168249689 |
| MP:0001179 | thick pulmonary interalveolar septum | 0.56908248 | 1.168256944 |
| MP:0001731 | abnormal postnatal growth | 0.56900976 | 1.16825948 |
| ENSG00000127564 | PKMYT1 subnetwork | 0.8946077 | 1.168269404 |
| ENSG00000185825 | BCAP31 subnetwork | 0.57169546 | 1.16828931 |
| MP:0009655 | abnormal secondary palate development | 0.56941577 | 1.168295391 |
| GO:0006071 | glycerol metabolic process | 0.56887243 | 1.168313186 |
| REACTOME_PYRUVATE_METAI | REACTOME_PYRUVATE_METABOLISM | 0.56877336 | 1.168315731 |
| ENSG00000173406 | DAB1 subnetwork | 0.89455833 | 1.168316074 |
| GO:0072404 | signal transduction involved in G1/S transition checkpoint | 0.57141524 | 1.168320188 |
| GO:0016101 | diterpenoid metabolic process | 0.89425268 | 1.168327178 |
| REACTOME_MRNA_SPLICING_ | REACTOME_MRNA_SPLICING_:_MAJOR_PATHWAY | 0.57208008 | 1.168338861 |
| ENSG00000119392 | GLE1 subnetwork | 0.57165112 | 1.168347165 |
| REACTOME_NUCLEAR_IMPOR | REACTOME_NUCLEAR_IMPORT_OF_REV_PROTEIN | 0.57156347 | 1.168349703 |
| REACTOME_ANDROGEN_BIOS | REACTOME_ANDROGEN_BIOSYNTHESIS | 0.56896607 | 1.168373159 |
| GO:0032480 | negative regulation of type I interferon production | 0.571954 | 1.168392314 |
| GO:0044449 | contractile fiber part | 0.89423488 | 1.168396396 |
| MP:0004374 | bowed radius | 0.57178987 | 1.1683974 |
| GO:0016591 | DNA-directed RNA polymerase II, holoenzyme | 0.57007121 | 1.168409375 |
| ENSG00000177084 | POLE subnetwork | 0.56970984 | 1.168412654 |
| ENSG00000144028 | SNRNP200 subnetwork | 0.5715164 | 1.168428334 |
| MP:0001785 | edema | 0.89414888 | 1.168429588 |
| GO:0034976 | response to endoplasmic reticulum stress | 0.56941201 | 1.168443704 |
| ENSG00000137403 | HLA-F subnetwork | 0.57027678 | 1.168459725 |
| MP:0000764 | abnormal tongue epithelium morphology | 0.57001148 | 1.168474341 |
| GO:0072395 | signal transduction involved in cell cycle checkpoint | 0.57141524 | 1.168481871 |
| GO:0030521 | androgen receptor signaling pathway | 0.56967073 | 1.168484596 |
| MP:0002837 | dystrophic cardiac calcinosis | 0.89411722 | 1.168485313 |
| REACTOME_MRNA_SPLICING | REACTOME_MRNA_SPLICING | 0.57208008 | 1.168500346 |
| ENSG00000085415 | SEH1L subnetwork | 0.89405816 | 1.168532036 |
| MP:0011083 | complete lethality at weaning | 0.57137574 | 1.168574394 |
| GO:0006270 | DNA-dependent DNA replication initiation | 0.57120888 | 1.16858646 |
| GO:0019842 | vitamin binding | 0.57067363 | 1.168601912 |
| GO:0016042 | lipid catabolic process | 0.57026676 | 1.168607876 |
| ENSG00000148334 | PTGES2 subnetwork | 0.8940266 | 1.16861031 |
| GO:0007339 | binding of sperm to zona pellucida | 0.56999942 | 1.168629491 |
| GO:0007006 | mitochondrial membrane organization | 0.56993356 | 1.168659822 |
| GO:0042776 | mitochondrial ATP synthesis coupled proton transport | 0.89402114 | 1.168711131 |
| ENSG00000075624 | ACTB subnetwork | 0.57118709 | 1.168713653 |
| ENSG00000119772 | DNMT3A subnetwork | 0.57135691 | 1.168722315 |

| | | | |
|---|---|---|---|
| ENSG00000185420 | SMYD3 subnetwork | 0.57066583 | 1.168729213 |
| MP:0000084 | abnormal fontanelle morphology | 0.89400812 | 1.168789436 |
| ENSG00000133316 | WDR74 subnetwork | 0.57104492 | 1.168795014 |
| MP:0004522 | abnormal orientation of cochlear hair cell stereociliary bun | 0.57115797 | 1.16880626 |
| GO:0042119 | neutrophil activation | 0.89395429 | 1.168822681 |
| ENSG00000128692 | ENSG00000128692 subnetwork | 0.57093535 | 1.168839174 |
| GO:0010677 | negative regulation of cellular carbohydrate metabolic proc | 0.89389973 | 1.168846917 |
| GO:0060122 | inner ear receptor stereocilium organization | 0.57065302 | 1.168870409 |
| GO:0045912 | negative regulation of carbohydrate metabolic process | 0.89389973 | 1.168952304 |
| ENSG00000171357 | C1orf190 subnetwork | 0.57090621 | 1.1689734 |
| GO:0031640 | killing of cells of other organism | 0.57063206 | 1.16898392 |
| ENSG00000067369 | TP53BP1 subnetwork | 0.57269891 | 1.169046961 |
| REACTOME_PLATELET_HOMEC | REACTOME_PLATELET_HOMEOSTASIS | 0.89389261 | 1.169053201 |
| MP:0004567 | decreased myocardial fiber number | 0.89381074 | 1.169054919 |
| ENSG00000186847 | KRT14 subnetwork | 0.57253071 | 1.169093672 |
| MP:0009413 | skeletal muscle fiber atrophy | 0.89378037 | 1.169133297 |
| GO:0045309 | protein phosphorylated amino acid binding | 0.5726386 | 1.169139384 |
| GO:0004065 | arylsulfatase activity | 0.57321372 | 1.169169197 |
| ENSG00000122966 | CIT subnetwork | 0.57351523 | 1.169202649 |
| ENSG00000110436 | SLC1A2 subnetwork | 0.89375883 | 1.169216199 |
| ENSG00000077380 | DYNC1I2 subnetwork | 0.57251148 | 1.169220672 |
| ENSG00000133398 | MED10 subnetwork | 0.57342402 | 1.16923979 |
| GO:0016408 | C-acyltransferase activity | 0.5733705 | 1.169256244 |
| GO:0043330 | response to exogenous dsRNA | 0.57365038 | 1.169303448 |
| MP:0004777 | abnormal phospholipid level | 0.89373295 | 1.169308136 |
| ENSG00000163159 | VPS72 subnetwork | 0.57320183 | 1.169330573 |
| MP:0000552 | abnormal radius morphology | 0.89372121 | 1.169413622 |
| ENSG00000174123 | TLR10 subnetwork | 0.89316482 | 1.169434916 |
| ENSG00000187558 | ENSG00000187558 subnetwork | 0.89306615 | 1.169441184 |
| ENSG00000167645 | YIF1B subnetwork | 0.57380978 | 1.169459385 |
| MP:0001666 | abnormal intestinal absorption | 0.89360699 | 1.169484797 |
| ENSG00000114480 | GBE1 subnetwork | 0.57319276 | 1.169485091 |
| ENSG00000151150 | ANK3 subnetwork | 0.89371069 | 1.169505594 |
| ENSG00000184203 | PPP1R2 subnetwork | 0.89306615 | 1.169546768 |
| ENSG00000182054 | IDH2 subnetwork | 0.89358408 | 1.169572279 |
| GO:0032769 | negative regulation of monooxygenase activity | 0.89274286 | 1.169580925 |
| GO:0008206 | bile acid metabolic process | 0.89350856 | 1.169587582 |
| ENSG00000158773 | USF1 subnetwork | 0.57318126 | 1.169625846 |
| ENSG00000056345 | ENSG00000056345 subnetwork | 0.89346103 | 1.169634477 |
| ENSG00000129810 | SGOL1 subnetwork | 0.8926908 | 1.169636889 |
| ENSG00000114850 | SSR3 subnetwork | 0.89305582 | 1.169647856 |
| ENSG00000132507 | EIF5A subnetwork | 0.89341238 | 1.169672353 |
| MP:0001353 | increased aggression towards mice | 0.89299136 | 1.16967672 |
| GO:0048753 | pigment granule organization | 0.89290901 | 1.169683013 |
| KEGG_ASCORBATE_AND_ALDA | KEGG_ASCORBATE_AND_ALDARATE_METABOLISM | 0.89266231 | 1.169706414 |
| ENSG00000156076 | WIF1 subnetwork | 0.57414649 | 1.169720154 |
| MP:0003355 | decreased ovulation rate | 0.57314576 | 1.169725214 |
| ENSG00000119638 | NEK9 subnetwork | 0.57420937 | 1.169738112 |
| ENSG00000126432 | PRDX5 subnetwork | 0.57308412 | 1.169762464 |
| ENSG00000162992 | NEUROD1 subnetwork | 0.89264211 | 1.169789502 |
| ENSG00000181029 | TRAPPC5 subnetwork | 0.57411038 | 1.169812491 |
| ENSG00000172845 | SP3 subnetwork | 0.89262212 | 1.169886158 |
| ENSG00000143418 | CERS2 subnetwork | 0.89225516 | 1.169917744 |

| | | | |
|---|---|---|---|
| GO:0033138 | positive regulation of peptidyl-serine phosphorylation | 0.57409129 | 1.169925538 |
| ENSG00000197535 | MYO5A subnetwork | 0.57699319 | 1.169947867 |
| ENSG00000197976 | AKAP17A subnetwork | 0.89258694 | 1.169951206 |
| GO:0005743 | mitochondrial inner membrane | 0.5770475 | 1.169951989 |
| GO:0001667 | ameboidal cell migration | 0.89243191 | 1.169981925 |
| ENSG00000107438 | PDLIM1 subnetwork | 0.89239886 | 1.170006327 |
| MP:0001286 | abnormal eye development | 0.8922501 | 1.170009944 |
| ENSG00000112306 | RPS12 subnetwork | 0.89255586 | 1.170025303 |
| ENSG00000183943 | PRKX subnetwork | 0.57719438 | 1.170031546 |
| ENSG00000115252 | PDE1A subnetwork | 0.5769896 | 1.170101537 |
| KEGG_RIBOSOME | KEGG_RIBOSOME | 0.89223091 | 1.170106681 |
| GO:0006119 | oxidative phosphorylation | 0.89219852 | 1.170180832 |
| GO:0071418 | cellular response to amine stimulus | 0.57461788 | 1.170208075 |
| GO:0003170 | heart valve development | 0.57731304 | 1.170234504 |
| ENSG00000158691 | ZSCAN12 subnetwork | 0.57587396 | 1.170246116 |
| ENSG00000162244 | RPL29 subnetwork | 0.57697544 | 1.170248388 |
| ENSG00000148798 | INA subnetwork | 0.89219802 | 1.170286644 |
| ENSG00000119401 | TRIM32 subnetwork | 0.57567924 | 1.170288858 |
| GO:0042598 | vesicular fraction | 0.5757714 | 1.170292945 |
| GO:0018410 | C-terminal protein amino acid modification | 0.57458868 | 1.170321114 |
| REACTOME_PLATELET_SENSITI | REACTOME_PLATELET_SENSITIZATION_BY_LDL | 0.57694803 | 1.170326654 |
| ENSG00000131981 | LGALS3 subnetwork | 0.89218425 | 1.170383433 |
| ENSG00000131469 | RPL27 subnetwork | 0.57689175 | 1.170384351 |
| GO:0045335 | phagocytic vesicle | 0.57586864 | 1.170393289 |
| ENSG00000075239 | ACAT1 subnetwork | 0.57764238 | 1.170404387 |
| MP:0000445 | short snout | 0.57567626 | 1.170449856 |
| GO:0006099 | tricarboxylic acid cycle | 0.57481659 | 1.170453293 |
| MP:0000159 | abnormal xiphoid process morphology | 0.57684208 | 1.170462658 |
| REACTOME_GRB2SOS_PROVID | REACTOME_GRB2SOS_PROVIDES_LINKAGE_TO_MAPK_SIG | 0.577485 | 1.170471685 |
| KEGG_VASCULAR_SMOOTH_M | KEGG_VASCULAR_SMOOTH_MUSCLE_CONTRACTION | 0.57758327 | 1.170475733 |
| GO:0061138 | morphogenesis of a branching epithelium | 0.57777973 | 1.170476974 |
| ENSG00000099624 | ATP5D subnetwork | 0.892184 | 1.170489283 |
| ENSG00000075188 | NUP37 subnetwork | 0.89214226 | 1.17053636 |
| ENSG00000165023 | DIRAS2 subnetwork | 0.57521923 | 1.170542476 |
| GO:0060347 | heart trabecula formation | 0.57508295 | 1.170575678 |
| GO:0048729 | tissue morphogenesis | 0.57791198 | 1.170590654 |
| ENSG00000181856 | SLC2A4 subnetwork | 0.57682226 | 1.170602774 |
| MP:0006396 | decreased long bone epiphyseal plate size | 0.57567507 | 1.170610897 |
| ENSG00000069702 | TGFBR3 subnetwork | 0.57516668 | 1.170627926 |
| GO:0060612 | adipose tissue development | 0.89213638 | 1.170628675 |
| REACTOME_TRANSPORT_OF_M | REACTOME_TRANSPORT_OF_MATURE_MRNA_DERIVED_FI | 0.57865865 | 1.170633726 |
| GO:0048041 | focal adhesion assembly | 0.5755868 | 1.170641255 |
| GO:0008320 | protein transmembrane transporter activity | 0.89208065 | 1.170648634 |
| ENSG00000106397 | PLOD3 subnetwork | 0.89155919 | 1.170661718 |
| MP:0003303 | peritoneal inflammation | 0.57550013 | 1.170671621 |
| REACTOME_TRANSFERRIN_EN | REACTOME_TRANSFERRIN_ENDOCYTOSIS_AND_RECYCLINC | 0.89147676 | 1.170677168 |
| KEGG_RENAL_CELL_CARCINON | KEGG_RENAL_CELL_CARCINOMA | 0.57506322 | 1.170716253 |
| REACTOME_MITOCHONDRIAL_ | REACTOME_MITOCHONDRIAL_TRNA_AMINOACYLATION | 0.57863775 | 1.170732375 |
| ENSG00000100288 | CHKB subnetwork | 0.57500548 | 1.170732883 |
| GO:0022884 | macromolecule transmembrane transporter activity | 0.89208065 | 1.170754546 |
| GO:0048566 | embryonic digestive tract development | 0.8916792 | 1.170754888 |
| ENSG00000189229 | ENSG00000189229 subnetwork | 0.57681147 | 1.17075666 |
| ENSG00000110321 | EIF4G2 subnetwork | 0.89199633 | 1.170765472 |

| | | | |
|---|---|---|---|
| GO:0080008 | CUL4 RING ubiquitin ligase complex | 0.57547398 | 1.170770819 |
| ENSG00000162385 | MAGOH subnetwork | 0.57816623 | 1.170776819 |
| ENSG00000106617 | PRKAG2 subnetwork | 0.89183979 | 1.170778281 |
| ENSG00000196531 | NACA subnetwork | 0.89147305 | 1.17078316 |
| GO:0050840 | extracellular matrix binding | 0.57542835 | 1.170801211 |
| ENSG00000156113 | KCNMA1 subnetwork | 0.89141753 | 1.170807678 |
| ENSG00000037965 | HOXC8 subnetwork | 0.89195525 | 1.170817121 |
| MP:0002823 | abnormal rib development | 0.57845094 | 1.17082991 |
| GO:0002792 | negative regulation of peptide secretion | 0.89179928 | 1.170829939 |
| GO:0072511 | divalent inorganic cation transport | 0.57828114 | 1.170842466 |
| GO:0050830 | defense response to Gram-positive bacterium | 0.5766056 | 1.170881989 |
| ENSG00000106803 | SEC61B subnetwork | 0.57655902 | 1.170884858 |
| ENSG00000161647 | MPP3 subnetwork | 0.89124048 | 1.170885789 |
| GO:0008340 | determination of adult lifespan | 0.89139402 | 1.170891062 |
| ENSG00000105464 | GRIN2D subnetwork | 0.5786354 | 1.170892662 |
| GO:0043492 | ATPase activity, coupled to movement of substances | 0.57679136 | 1.170903722 |
| ENSG00000197170 | PSMD12 subnetwork | 0.57814871 | 1.170909838 |
| GO:0045671 | negative regulation of osteoclast differentiation | 0.89132392 | 1.170933708 |
| REACTOME_HDL:MEDIATED_LI | REACTOME_HDL:MEDIATED_LIPID_TRANSPORT | 0.57840824 | 1.170935488 |
| GO:0045833 | negative regulation of lipid metabolic process | 0.57674264 | 1.170975275 |
| GO:0031253 | cell projection membrane | 0.89123747 | 1.170991848 |
| ENSG00000151923 | TIAL1 subnetwork | 0.57639034 | 1.171003436 |
| REACTOME_SIGNALING_BY_RC | REACTOME_SIGNALING_BY_ROBO_RECEPTOR | 0.57909761 | 1.171004379 |
| ENSG00000197930 | ERO1L subnetwork | 0.57862141 | 1.171025606 |
| ENSG00000126351 | THRA subnetwork | 0.57655067 | 1.171032019 |
| GO:0060562 | epithelial tube morphogenesis | 0.57633589 | 1.171033819 |
| REACTOME_PLATELET_ADHESI | REACTOME_PLATELET_ADHESION_TO_EXPOSED_COLLAGE | 0.89123182 | 1.171093396 |
| MP:0005123 | increased circulating growth hormone level | 0.57969781 | 1.171114149 |
| GO:0048266 | behavioral response to pain | 0.5790859 | 1.171137266 |
| ENSG00000156931 | VPS8 subnetwork | 0.89089558 | 1.17113729 |
| GO:0043523 | regulation of neuron apoptotic process | 0.89121599 | 1.171172314 |
| ENSG00000127920 | GNG11 subnetwork | 0.89056237 | 1.171190282 |
| GO:0033631 | cell-cell adhesion mediated by integrin | 0.57654973 | 1.171192963 |
| GO:0051385 | response to mineralocorticoid stimulus | 0.89047974 | 1.171196736 |
| GO:0046888 | negative regulation of hormone secretion | 0.89087941 | 1.171211709 |
| REACTOME_GLUTATHIONE_CC | REACTOME_GLUTATHIONE_CONJUGATION | 0.8911501 | 1.171219534 |
| GO:0006400 | tRNA modification | 0.57969512 | 1.171260596 |
| REACTOME_SIGNAL_REGULAT | REACTOME_SIGNAL_REGULATORY_PROTEIN_SIRP_FAMILY | 0.89083704 | 1.171286142 |
| GO:0001542 | ovulation from ovarian follicle | 0.89047007 | 1.171289328 |
| MP:0004769 | abnormal synaptic vesicle morphology | 0.89110915 | 1.171289416 |
| ENSG00000171241 | SHCBP1 subnetwork | 0.57932897 | 1.171336708 |
| REACTOME_MITOTIC_G2:G2M | REACTOME_MITOTIC_G2:G2M_PHASES | 0.89080691 | 1.171360587 |
| GO:0008217 | regulation of blood pressure | 0.89045584 | 1.171391005 |
| GO:0048010 | vascular endothelial growth factor receptor signaling pathw | 0.89037291 | 1.171402013 |
| REACTOME_CLASS_A1_RHODC | REACTOME_CLASS_A1_RHODOPSIN:LIKE_RECEPTORS | 0.57968593 | 1.17141392 |
| MP:0002663 | failure to form blastocele | 0.58017663 | 1.171474447 |
| ENSG00000136026 | CKAP4 subnetwork | 0.58024774 | 1.171492007 |
| ENSG00000091140 | DLD subnetwork | 0.8900833 | 1.171493377 |
| ENSG00000091129 | NRCAM subnetwork | 0.89036229 | 1.171494649 |
| GO:0021952 | central nervous system projection neuron axonogenesis | 0.89000549 | 1.171527085 |
| GO:0060395 | SMAD protein signal transduction | 0.57966543 | 1.171539934 |
| GO:0016254 | preassembly of GPI anchor in ER membrane | 0.58035695 | 1.171557377 |
| ENSG00000159217 | IGF2BP1 subnetwork | 0.89024864 | 1.171580189 |

| | | | |
|---|---|---|---|
| ENSG00000084733 | RAB10 subnetwork | 0.89035575 | 1.171591837 |
| ENSG00000198523 | PLN subnetwork | 0.58014104 | 1.171600383 |
| GO:0009086 | methionine biosynthetic process | 0.88997976 | 1.171601633 |
| ENSG00000172809 | RPL38 subnetwork | 0.89022061 | 1.171650186 |
| ENSG00000171564 | FGB subnetwork | 0.57965288 | 1.171700178 |
| GO:0014046 | dopamine secretion | 0.88997964 | 1.171707959 |
| MP:0004402 | decreased cochlear outer hair cell number | 0.58012848 | 1.171740022 |
| GO:0005149 | interleukin-1 receptor binding | 0.57959196 | 1.171744186 |
| GO:0014059 | regulation of dopamine secretion | 0.88997964 | 1.171814304 |
| MP:0002693 | abnormal pancreas physiology | 0.88978747 | 1.171856559 |
| MP:0005435 | hemoperitoneum | 0.88995714 | 1.171870745 |
| ENSG00000138398 | PPIG subnetwork | 0.88991701 | 1.171931736 |
| REACTOME_REGULATION_OF_ | REACTOME_REGULATION_OF_MITOTIC_CELL_CYCLE | 0.88977691 | 1.171949337 |
| ENSG00000012963 | UBR7 subnetwork | 0.58068284 | 1.172052998 |
| REACTOME_APCC:MEDIATED_ | REACTOME_APCC:MEDIATED_DEGRADATION_OF_CELL_CY | 0.88977691 | 1.172055752 |
| GO:0006949 | syncytium formation | 0.88962585 | 1.172082463 |
| GO:0010498 | proteasomal protein catabolic process | 0.88970171 | 1.172084998 |
| GO:0006103 | 2-oxoglutarate metabolic process | 0.58076774 | 1.17213876 |
| GO:0031497 | chromatin assembly | 0.889597 | 1.172148047 |
| GO:0035115 | embryonic forelimb morphogenesis | 0.88950908 | 1.172150059 |
| GO:0008252 | nucleotidase activity | 0.88950853 | 1.172251999 |
| GO:0051453 | regulation of intracellular pH | 0.88946384 | 1.172276733 |
| ENSG00000175224 | ATG13 subnetwork | 0.58090957 | 1.172299604 |
| ENSG00000174780 | SRP72 subnetwork | 0.88942891 | 1.172342359 |
| ENSG00000160752 | FDPS subnetwork | 0.88926567 | 1.172369138 |
| MP:0005172 | reduced eye pigmentation | 0.889118 | 1.172391383 |
| GO:0030728 | ovulation | 0.88939834 | 1.17239891 |
| ENSG00000155363 | MOV10 subnetwork | 0.88905813 | 1.172425234 |
| MP:0009750 | impaired behavioral response to addictive substance | 0.88923763 | 1.172439335 |
| GO:0038032 | termination of G-protein coupled receptor signaling pathwa | 0.8889927 | 1.172468182 |
| GO:0021915 | neural tube development | 0.88891927 | 1.172488408 |
| REACTOME_G2M_TRANSITION | REACTOME_G2M_TRANSITION | 0.88891262 | 1.172585925 |
| GO:0030705 | cytoskeleton-dependent intracellular transport | 0.58127556 | 1.172634812 |
| MP:0003993 | abnormal ventral spinal root morphology | 0.88888514 | 1.172678912 |
| ENSG00000138101 | DTNB subnetwork | 0.58125302 | 1.17275396 |
| REACTOME_EUKARYOTIC_TRA | REACTOME_EUKARYOTIC_TRANSLATION_ELONGATION | 0.88887494 | 1.172781011 |
| MP:0003797 | abnormal compact bone morphology | 0.58144257 | 1.172822823 |
| ENSG00000136824 | SMC2 subnetwork | 0.88874583 | 1.172830635 |
| ENSG00000140416 | TPM1 subnetwork | 0.88886751 | 1.172855844 |
| MP:0002989 | small kidney | 0.88869813 | 1.172873647 |
| MP:0003047 | abnormal thoracic vertebrae morphology | 0.88863623 | 1.172893923 |
| GO:0016854 | racemase and epimerase activity | 0.8878215 | 1.172937534 |
| GO:0043303 | mast cell degranulation | 0.8879859 | 1.172969774 |
| ENSG00000132693 | CRP subnetwork | 0.88861493 | 1.172973342 |
| GO:0050650 | chondroitin sulfate proteoglycan biosynthetic process | 0.88794047 | 1.173003733 |
| GO:0006893 | Golgi to plasma membrane transport | 0.88780575 | 1.173026136 |
| ENSG00000132485 | ZRANB2 subnetwork | 0.58165506 | 1.173038078 |
| MP:0002058 | neonatal lethality | 0.88858491 | 1.173039126 |
| ENSG00000145348 | TBCK subnetwork | 0.88842706 | 1.17304332 |
| ENSG00000076356 | PLXNA2 subnetwork | 0.88836363 | 1.173081824 |
| GO:0000987 | core promoter proximal region sequence-specific DNA bind | 0.88765499 | 1.173094089 |
| GO:0032897 | negative regulation of viral transcription | 0.88777644 | 1.173114754 |
| MP:0001312 | abnormal cornea morphology | 0.88833397 | 1.173124886 |

| | | | |
|---|---|---|---|
| GO:0016651 | oxidoreductase activity, acting on NADH or NADPH | 0.88856203 | 1.173132223 |
| ENSG00000143006 | DMRTB1 subnetwork | 0.88755645 | 1.173148401 |
| ENSG00000137267 | TUBB2A subnetwork | 0.88763518 | 1.173159956 |
| GO:0071229 | cellular response to acid | 0.58186114 | 1.173168236 |
| ENSG00000091136 | LAMB1 subnetwork | 0.58181959 | 1.173219159 |
| ENSG00000183049 | CAMK1D subnetwork | 0.88832662 | 1.173227128 |
| GO:0015662 | ATPase activity, coupled to transmembrane movement of i | 0.88753989 | 1.173241618 |
| ENSG00000158373 | HIST1H2BD subnetwork | 0.58215819 | 1.173267867 |
| ENSG00000127329 | PTPRB subnetwork | 0.88685425 | 1.173276805 |
| MP:0008533 | abnormal anterior visceral endoderm morphology | 0.88752626 | 1.17332574 |
| GO:0043046 | DNA methylation involved in gamete generation | 0.58240801 | 1.173336515 |
| ENSG00000144837 | PLA1A subnetwork | 0.58211343 | 1.173352885 |
| ENSG00000172936 | MYD88 subnetwork | 0.58204396 | 1.173356071 |
| GO:0070469 | respiratory chain | 0.88684108 | 1.173365551 |
| GO:0030278 | regulation of ossification | 0.88734408 | 1.173366445 |
| ENSG00000113312 | TTC1 subnetwork | 0.88744592 | 1.173382541 |
| GO:0046850 | regulation of bone remodeling | 0.58233899 | 1.173394245 |
| MP:0008545 | absent sperm flagellum | 0.88709674 | 1.173395624 |
| MP:0000778 | abnormal nervous system tract morphology | 0.5825117 | 1.173408316 |
| GO:0033005 | positive regulation of mast cell activation | 0.88682624 | 1.173436075 |
| REACTOME_NONSENSE_MEDI | REACTOME_NONSENSE_MEDIATED_DECAY_INDEPENDENT | 0.88732616 | 1.173459716 |
| MP:0008406 | increased cellular sensitivity to hydrogen peroxide | 0.88724748 | 1.173484641 |
| GO:0051085 | chaperone mediated protein folding requiring cofactor | 0.88709296 | 1.17349804 |
| ENSG00000101265 | RASSF2 subnetwork | 0.88630794 | 1.173528607 |
| REACTOME_REGULATION_OF_ | REACTOME_REGULATION_OF_GLUCOKINASE_BY_GLUCOKI | 0.58272209 | 1.173531416 |
| MP:0002279 | abnormal diaphragm morphology | 0.88681246 | 1.173533972 |
| MP:0004933 | abnormal epididymis epithelium morphology | 0.5829175 | 1.173565881 |
| MP:0011346 | renal tubule atrophy | 0.58299994 | 1.173569482 |
| GO:0015491 | cation:cation antiporter activity | 0.88627957 | 1.173599197 |
| ENSG00000126461 | SCAF1 subnetwork | 0.88668882 | 1.173602116 |
| GO:0016862 | intramolecular oxidoreductase activity, interconverting ket | 0.88678892 | 1.173613645 |
| ENSG00000138495 | COX17 subnetwork | 0.88647617 | 1.173626825 |
| KEGG_ALDOSTERONE_REGULA | KEGG_ALDOSTERONE_REGULATED_SODIUM_REABSORPTI | 0.58267903 | 1.173630044 |
| ENSG00000159086 | GCFC1 subnetwork | 0.88622289 | 1.17364242 |
| GO:0050764 | regulation of phagocytosis | 0.88600566 | 1.173646737 |
| GO:0007603 | phototransduction, visible light | 0.88664513 | 1.173649881 |
| GO:0030511 | positive regulation of transforming growth factor beta rece | 0.88658995 | 1.173688532 |
| MP:0009404 | centrally nucleated skeletal muscle fibers | 0.88618982 | 1.173699343 |
| MP:0001156 | abnormal spermatogenesis | 0.58291448 | 1.173718997 |
| ENSG00000163539 | CLASP2 subnetwork | 0.88541166 | 1.173739496 |
| ENSG00000065427 | KARS subnetwork | 0.58380014 | 1.173744727 |
| KEGG_STARCH_AND_SUCROSE | KEGG_STARCH_AND_SUCROSE_METABOLISM | 0.88600156 | 1.17375388 |
| ENSG00000162105 | SHANK2 subnetwork | 0.88525818 | 1.173775809 |
| GO:0009113 | purine base biosynthetic process | 0.88591848 | 1.173783438 |
| GO:0044291 | cell-cell contact zone | 0.88538317 | 1.173823879 |
| MP:0002750 | exophthalmos | 0.88585298 | 1.173840394 |
| ENSG00000135365 | PHF21A subnetwork | 0.88524114 | 1.173846505 |
| MP:0003119 | abnormal digestive system development | 0.88515003 | 1.17386239 |
| GO:0031985 | Golgi cisterna | 0.58376678 | 1.173863636 |
| MP:0004057 | thin myocardium compact layer | 0.58371225 | 1.173894106 |
| GO:0000387 | spliceosomal snRNP assembly | 0.58346361 | 1.173910675 |
| MP:0002766 | situs inversus | 0.58361939 | 1.173924585 |
| REACTOME_INSULIN_SYNTHES | REACTOME_INSULIN_SYNTHESIS_AND_PROCESSING | 0.88512611 | 1.173937677 |

| | | | |
|---|---|---|---|
| GO:0060322 | head development | 0.88584439 | 1.173938453 |
| GO:0042166 | acetylcholine binding | 0.88581713 | 1.173995434 |
| ENSG00000116701 | NCF2 subnetwork | 0.88223891 | 1.174000733 |
| GO:0032580 | Golgi cisterna membrane | 0.58344666 | 1.174029688 |
| GO:0006024 | glycosaminoglycan biosynthetic process | 0.88512057 | 1.174040395 |
| GO:0042274 | ribosomal small subunit biogenesis | 0.58336594 | 1.174046581 |
| ENSG00000083312 | TNPO1 subnetwork | 0.58360734 | 1.174050374 |
| ENSG00000162511 | LAPTM5 subnetwork | 0.88422987 | 1.174060013 |
| GO:0031114 | regulation of microtubule depolymerization | 0.58330387 | 1.174063479 |
| ENSG00000184672 | RALYL subnetwork | 0.88495607 | 1.174072212 |
| REACTOME_PLATELET_DEGRAI | REACTOME_PLATELET_DEGRANULATION | 0.88479223 | 1.174081185 |
| GO:0010948 | negative regulation of cell cycle process | 0.88580082 | 1.174088958 |
| GO:0071248 | cellular response to metal ion | 0.88473748 | 1.174097102 |
| GO:0045907 | positive regulation of vasoconstriction | 0.88223819 | 1.174103787 |
| GO:0000175 | 3'-5'-exoribonuclease activity | 0.88434192 | 1.174108123 |
| GO:0006525 | arginine metabolic process | 0.88411335 | 1.174128466 |
| GO:0043487 | regulation of RNA stability | 0.88420692 | 1.174135407 |
| GO:0032332 | positive regulation of chondrocyte differentiation | 0.88470081 | 1.174140454 |
| REACTOME_CALCITONIN:LIKE_ | REACTOME_CALCITONIN:LIKE_LIGAND_RECEPTORS | 0.88511978 | 1.174147701 |
| ENSG00000100813 | ACIN1 subnetwork | 0.88464712 | 1.174170096 |
| MP:0000761 | thin diaphragm muscle | 0.88405674 | 1.174171852 |
| ENSG00000065135 | GNAI3 subnetwork | 0.88495531 | 1.174179541 |
| GO:0015986 | ATP synthesis coupled proton transport | 0.88398257 | 1.174183216 |
| GO:0009220 | pyrimidine ribonucleotide biosynthetic process | 0.88222231 | 1.174183935 |
| MP:0008883 | abnormal enterocyte proliferation | 0.88260656 | 1.174186601 |
| ENSG00000163527 | STT3B subnetwork | 0.88457013 | 1.174190598 |
| MP:0008875 | abnormal xenobiotic pharmacokinetics | 0.58420855 | 1.174193987 |
| MP:0005323 | dystonia | 0.88254434 | 1.174197984 |
| ENSG00000147684 | NDUFB9 subnetwork | 0.88364672 | 1.174221754 |
| MP:0006354 | abnormal fourth branchial arch artery morphology | 0.58415866 | 1.17422449 |
| GO:0007032 | endosome organization | 0.88247501 | 1.174227702 |
| ENSG00000133116 | KL subnetwork | 0.88218277 | 1.174236589 |
| REACTOME_G_ALPHA_Z_SIGN | REACTOME_G_ALPHA_Z_SIGNALLING_EVENTS | 0.88454273 | 1.17424769 |
| ENSG00000145191 | EIF2B5 subnetwork | 0.88377528 | 1.174274467 |
| REACTOME_COPI_MEDIATED_ | REACTOME_COPI_MEDIATED_TRANSPORT | 0.88388609 | 1.174279176 |
| GO:0015985 | energy coupled proton transport, down electrochemical gra | 0.88398257 | 1.174290683 |
| ENSG00000157927 | RADIL subnetwork | 0.58520456 | 1.174297161 |
| MP:0005120 | decreased circulating growth hormone level | 0.88354413 | 1.174299451 |
| ENSG00000118985 | ELL2 subnetwork | 0.58529634 | 1.174300652 |
| GO:0043616 | keratinocyte proliferation | 0.88363674 | 1.174324696 |
| GO:0010510 | regulation of acetyl-CoA biosynthetic process from pyruvat | 0.88191809 | 1.174328043 |
| ENSG00000087152 | ATXN7L3 subnetwork | 0.88217011 | 1.174339692 |
| GO:0005372 | water transmembrane transporter activity | 0.88351756 | 1.174384101 |
| REACTOME_GOLGI_TO_ER_RE | REACTOME_GOLGI_TO_ER_RETROGRADE_TRANSPORT | 0.88388609 | 1.174386672 |
| GO:0005746 | mitochondrial respiratory chain | 0.88287886 | 1.174399743 |
| GO:0032757 | positive regulation of interleukin-8 production | 0.88212575 | 1.174419884 |
| MP:0000078 | abnormal supraoccipital bone morphology | 0.880065 | 1.174430147 |
| GO:0006086 | acetyl-CoA biosynthetic process from pyruvate | 0.88191809 | 1.17443578 |
| ENSG00000115806 | GORASP2 subnetwork | 0.8816727 | 1.174442507 |
| ENSG00000101413 | RPRD1B subnetwork | 0.58519512 | 1.174443086 |
| ENSG00000135932 | CAB39 subnetwork | 0.88333587 | 1.174464089 |
| ENSG00000117360 | PRPF3 subnetwork | 0.58556847 | 1.17447054 |
| ENSG00000130741 | EIF2S3 subnetwork | 0.88351045 | 1.174477926 |

| | | | |
|---|---|---|---|
| GO:0016820 | hydrolase activity, acting on acid anhydrides, catalyzing tra | 0.58563708 | 1.17448758 |
| ENSG00000072134 | EPN2 subnetwork | 0.88004621 | 1.174510525 |
| GO:0004716 | receptor signaling protein tyrosine kinase activity | 0.88211763 | 1.174513851 |
| ENSG00000125352 | RNF113A subnetwork | 0.585493 | 1.174514596 |
| MP:0010956 | abnormal mitochondrial ATP synthesis coupled electron tra | 0.88189803 | 1.174520598 |
| GO:0032535 | regulation of cellular component size | 0.58580341 | 1.174521645 |
| ENSG00000110245 | APOC3 subnetwork | 0.8832887 | 1.174525882 |
| ENSG00000184363 | PKP3 subnetwork | 0.88183683 | 1.174532024 |
| GO:0004708 | MAP kinase kinase activity | 0.58595411 | 1.174535341 |
| ENSG00000069974 | RAB27A subnetwork | 0.87996336 | 1.17453576 |
| GO:0031069 | hair follicle morphogenesis | 0.8816559 | 1.174536527 |
| MP:0004181 | abnormal carotid artery morphology | 0.88348967 | 1.174539709 |
| MP:0002988 | decreased urine osmolality | 0.88156039 | 1.174543369 |
| MP:0000018 | small ears | 0.87988816 | 1.174561 |
| ENSG00000108433 | GOSR2 subnetwork | 0.88023689 | 1.174561162 |
| ENSG00000165868 | HSPA12A subnetwork | 0.58470859 | 1.174588715 |
| ENSG00000162664 | ZNF326 subnetwork | 0.8804119 | 1.174588808 |
| ENSG00000181991 | MRPS11 subnetwork | 0.58590727 | 1.174592944 |
| ENSG00000009307 | CSDE1 subnetwork | 0.58519117 | 1.174595843 |
| GO:0004861 | cyclin-dependent protein kinase inhibitor activity | 0.88034079 | 1.174614042 |
| GO:0051261 | protein depolymerization | 0.58578642 | 1.174626764 |
| GO:0007274 | neuromuscular synaptic transmission | 0.87985895 | 1.17462762 |
| ENSG00000215755 | ENSG00000215755 subnetwork | 0.8832887 | 1.174633498 |
| GO:0031225 | anchored to membrane | 0.8815364 | 1.174637415 |
| ENSG00000164167 | LSM6 subnetwork | 0.58514826 | 1.174653533 |
| GO:0001990 | regulation of systemic arterial blood pressure by hormone | 0.88145293 | 1.174662627 |
| GO:0043292 | contractile fiber | 0.8797049 | 1.174668935 |
| GO:0006739 | NADP metabolic process | 0.88322151 | 1.174695318 |
| GO:0007059 | chromosome segregation | 0.88090423 | 1.174699183 |
| ENSG00000114416 | FXR1 subnetwork | 0.58876749 | 1.17470628 |
| MP:0000194 | hypercalcemia | 0.87982841 | 1.174708046 |
| ENSG00000124406 | ATP8A1 subnetwork | 0.58883983 | 1.174709695 |
| ENSG00000139618 | BRCA2 subnetwork | 0.58470247 | 1.17472124 |
| ENSG00000171345 | KRT19 subnetwork | 0.58707515 | 1.174729144 |
| GO:0001101 | response to acid | 0.88133214 | 1.174736021 |
| ENSG00000152822 | GRM1 subnetwork | 0.58465604 | 1.174751802 |
| MP:0003988 | disorganized embryonic tissue | 0.88127645 | 1.174752066 |
| GO:0045780 | positive regulation of bone resorption | 0.5865763 | 1.174756031 |
| MP:0005595 | abnormal vascular smooth muscle physiology | 0.87968767 | 1.174758576 |
| ENSG00000198807 | PAX9 subnetwork | 0.88115002 | 1.174758931 |
| ENSG00000145555 | MYO10 subnetwork | 0.58612651 | 1.174762615 |
| MP:0002092 | abnormal eye morphology | 0.58512609 | 1.174765593 |
| MP:0000966 | decreased sensory neuron number | 0.88144589 | 1.174765883 |
| GO:0042809 | vitamin D receptor binding | 0.58700693 | 1.174773127 |
| GO:0060487 | lung epithelial cell differentiation | 0.88087147 | 1.174784126 |
| GO:0032611 | interleukin-1 beta production | 0.58685877 | 1.174786614 |
| ENSG00000160563 | MED27 subnetwork | 0.58673825 | 1.174789973 |
| GO:0000084 | S phase of mitotic cell cycle | 0.58728483 | 1.174790144 |
| GO:0070507 | regulation of microtubule cytoskeleton organization | 0.87951411 | 1.174790728 |
| ENSG00000182580 | EPHB3 subnetwork | 0.58459161 | 1.174802775 |
| REACTOME_TRYPTOPHAN_CAT | REACTOME_TRYPTOPHAN_CATABOLISM | 0.58485743 | 1.174809679 |
| ENSG00000137801 | THBS1 subnetwork | 0.58694962 | 1.174810349 |
| ENSG00000166963 | MAP1A subnetwork | 0.87963727 | 1.174811442 |

| | | | |
|---|---|---|---|
| ENSG00000213023 | SYT3 subnetwork | 0.87941819 | 1.174816007 |
| GO:0004177 | aminopeptidase activity | 0.58994789 | 1.174818059 |
| MP:0003169 | abnormal scala media morphology | 0.58639986 | 1.174827119 |
| GO:0007596 | blood coagulation | 0.58646494 | 1.17483731 |
| GO:0046135 | pyrimidine nucleoside catabolic process | 0.58875781 | 1.174837925 |
| ENSG00000134046 | MBD2 subnetwork | 0.58895816 | 1.174841366 |
| GO:0009100 | glycoprotein metabolic process | 0.58497807 | 1.174847084 |
| GO:0001953 | negative regulation of cell-matrix adhesion | 0.88112633 | 1.174848457 |
| ENSG00000127688 | GAN subnetwork | 0.59025027 | 1.174868651 |
| ENSG00000164695 | CHMP4C subnetwork | 0.87931465 | 1.174871181 |
| GO:0042095 | interferon-gamma biosynthetic process | 0.88085552 | 1.174873679 |
| MP:0004200 | decreased fetal size | 0.5874144 | 1.17487478 |
| ENSG00000105613 | MAST1 subnetwork | 0.58724791 | 1.174881517 |
| ENSG00000106723 | SPIN1 subnetwork | 0.58987872 | 1.17488206 |
| ENSG00000138750 | NUP54 subnetwork | 0.59010097 | 1.174888829 |
| ENSG00000126858 | RHOT1 subnetwork | 0.58635321 | 1.174891511 |
| MP:0009237 | kinked sperm flagellum | 0.87939551 | 1.174896495 |
| GO:0042445 | hormone metabolic process | 0.88080596 | 1.174908122 |
| GO:0046852 | positive regulation of bone remodeling | 0.5865763 | 1.174915277 |
| ENSG00000164683 | HEY1 subnetwork | 0.87924134 | 1.174924082 |
| MP:0002270 | abnormal pulmonary alveolus morphology | 0.58512583 | 1.174925251 |
| ENSG00000014641 | MDH1 subnetwork | 0.58672972 | 1.174928852 |
| GO:0004115 | 3',5'-cyclic-AMP phosphodiesterase activity | 0.58628667 | 1.174935576 |
| ENSG00000163032 | VSNL1 subnetwork | 0.87918244 | 1.174967789 |
| ENSG00000204469 | PRRC2A subnetwork | 0.58940868 | 1.174986508 |
| ENSG00000161057 | PSMC2 subnetwork | 0.58836774 | 1.174993241 |
| GO:0001076 | RNA polymerase II transcription factor binding transcriptior | 0.58875261 | 1.174996623 |
| MP:0006050 | pulmonary fibrosis | 0.59022915 | 1.175 |
| GO:0070838 | divalent metal ion transport | 0.5893597 | 1.175003373 |
| MP:0003793 | abnormal submandibular gland morphology | 0.58986831 | 1.17500674 |
| GO:0031983 | vesicle lumen | 0.87912597 | 1.175006903 |
| ENSG00000126583 | PRKCG subnetwork | 0.58976019 | 1.175023594 |
| ENSG00000205420 | KRT6A subnetwork | 0.58853171 | 1.175060811 |
| ENSG00000153006 | SREK1IP1 subnetwork | 0.58929385 | 1.175067476 |
| MP:0009754 | enhanced behavioral response to cocaine | 0.87886903 | 1.175069048 |
| ENSG00000146674 | IGFBP3 subnetwork | 0.58970357 | 1.175087648 |
| REACTOME_THE_CITRIC_ACID_ | REACTOME_THE_CITRIC_ACID_TCA_CYCLE_AND_RESPIRAT | 0.58873746 | 1.175094569 |
| MP:0006126 | abnormal outflow tract development | 0.8790976 | 1.175101252 |
| ENSG00000143553 | SNAPIN subnetwork | 0.58866115 | 1.175111471 |
| ENSG00000213741 | RPS29 subnetwork | 0.58917939 | 1.175114741 |
| ENSG00000175592 | FOSL1 subnetwork | 0.58925587 | 1.175145094 |
| ENSG00000067191 | CACNB1 subnetwork | 0.87882183 | 1.175149618 |
| MP:0008029 | abnormal paraxial mesoderm morphology | 0.5883651 | 1.175152089 |
| ENSG00000171786 | NHLH1 subnetwork | 0.8790591 | 1.175177207 |
| GO:0032148 | activation of protein kinase B activity | 0.58952904 | 1.175185485 |
| ENSG00000093009 | CDC45 subnetwork | 0.58850823 | 1.175185836 |
| ENSG00000177879 | AP3S1 subnetwork | 0.58966391 | 1.175198921 |
| GO:0019884 | antigen processing and presentation of exogenous antigen | 0.58819406 | 1.175243441 |
| GO:2000377 | regulation of reactive oxygen species metabolic process | 0.87880783 | 1.175253223 |
| ENSG00000116016 | EPAS1 subnetwork | 0.58962824 | 1.17526976 |
| ENSG00000025772 | TOMM34 subnetwork | 0.58834196 | 1.175270416 |
| ENSG00000187098 | MITF subnetwork | 0.58785779 | 1.175321424 |
| ENSG00000106459 | NRF1 subnetwork | 0.87880537 | 1.175356847 |

| | | | |
|---|---|---|---|
| GO:0048339 | paraxial mesoderm development | 0.58801347 | 1.175382222 |
| MP:0000536 | hydroureter | 0.58832084 | 1.175388776 |
| MP:0004077 | abnormal striatum morphology | 0.87874505 | 1.175396021 |
| GO:0000187 | activation of MAPK activity | 0.58810361 | 1.17539908 |
| ENSG00000143801 | PSEN2 subnetwork | 0.58817881 | 1.175402408 |
| ENSG00000166501 | PRKCB subnetwork | 0.58795688 | 1.175419486 |
| ENSG00000043591 | ADRB1 subnetwork | 0.87868249 | 1.175430598 |
| ENSG00000047410 | TPR subnetwork | 0.58784265 | 1.17544667 |
| GO:0048710 | regulation of astrocyte differentiation | 0.87860932 | 1.175488209 |
| MP:0001850 | increased susceptibility to otitis media | 0.87859711 | 1.175568862 |
| MP:0009703 | decreased birth body size | 0.5913788 | 1.175639128 |
| MP:0011084 | partial lethality at weaning | 0.87855604 | 1.175644924 |
| GO:0023021 | termination of signal transduction | 0.87789608 | 1.175668449 |
| GO:0072498 | embryonic skeletal joint development | 0.878159 | 1.175670569 |
| ENSG00000101224 | CDC25B subnetwork | 0.59071976 | 1.175693696 |
| GO:0000780 | condensed nuclear chromosome, centromeric region | 0.8777345 | 1.175696238 |
| ENSG00000206419 | ENSG00000206419 subnetwork | 0.87670821 | 1.175713231 |
| MP:0000652 | enlarged sebaceous gland | 0.59123634 | 1.175713324 |
| GO:0001659 | temperature homeostasis | 0.87828528 | 1.175714286 |
| ENSG00000215425 | DDX39B subnetwork | 0.8785211 | 1.175720999 |
| ENSG00000117410 | ATP6V0B subnetwork | 0.87784528 | 1.175735362 |
| ENSG00000089022 | MAPKAPK5 subnetwork | 0.59135583 | 1.175750235 |
| GO:0045730 | respiratory burst | 0.87769933 | 1.175763165 |
| ENSG00000166206 | GABRB3 subnetwork | 0.87815268 | 1.175774336 |
| ENSG00000151164 | RAD9B subnetwork | 0.87763455 | 1.175807047 |
| REACTOME_PROTEOLYTIC_CLE | REACTOME_PROTEOLYTIC_CLEAVAGE_OF_SNARE_COMPLE | 0.8771542 | 1.175812108 |
| MP:0005108 | abnormal ulna morphology | 0.87683116 | 1.175817024 |
| ENSG00000123080 | CDKN2C subnetwork | 0.59120344 | 1.175817741 |
| ENSG00000206495 | TRIM39 subnetwork | 0.87670821 | 1.175821791 |
| ENSG00000215412 | ENSG00000215412 subnetwork | 0.8785211 | 1.17582934 |
| REACTOME_GLYCOSPHINGOLII | REACTOME_GLYCOSPHINGOLIPID_METABOLISM | 0.87759156 | 1.175864773 |
| GO:0046488 | phosphatidylinositol metabolic process | 0.59084599 | 1.17586532 |
| REACTOME_EUKARYOTIC_TRA | REACTOME_EUKARYOTIC_TRANSLATION_INITIATION | 0.87747148 | 1.175876384 |
| GO:0007034 | vacuolar transport | 0.87814946 | 1.175882733 |
| MP:0001940 | testis hypoplasia | 0.87714418 | 1.175906784 |
| ENSG00000065609 | SNAP91 subnetwork | 0.59115496 | 1.175922186 |
| ENSG00000204599 | TRIM39 subnetwork | 0.87670821 | 1.175930372 |
| GO:0051148 | negative regulation of muscle cell differentiation | 0.87661758 | 1.175932767 |
| ENSG00000130307 | USHBP1 subnetwork | 0.87730946 | 1.175934299 |
| REACTOME_CALNEXINCALRETI | REACTOME_CALNEXINCALRETICULIN_CYCLE | 0.87645417 | 1.175937558 |
| ENSG00000198563 | DDX39B subnetwork | 0.8785211 | 1.175937702 |
| MP:0001922 | reduced male fertility | 0.87735685 | 1.175941133 |
| GO:0035335 | peptidyl-tyrosine dephosphorylation | 0.87655485 | 1.175981343 |
| REACTOME_CAP:DEPENDENT_ | REACTOME_CAP:DEPENDENT_TRANSLATION_INITIATION | 0.87747148 | 1.175984869 |
| GO:0004437 | inositol or phosphatidylinositol phosphatase activity | 0.59109678 | 1.175986266 |
| MP:0001511 | disheveled coat | 0.87639476 | 1.175990762 |
| GO:0019835 | cytolysis | 0.59097562 | 1.176003232 |
| GO:0072163 | mesonephric epithelium development | 0.87713141 | 1.176006092 |
| ENSG00000151532 | VTI1A subnetwork | 0.87638988 | 1.17609017 |
| GO:0072164 | mesonephric tubule development | 0.87713141 | 1.17611465 |
| GO:0042753 | positive regulation of circadian rhythm | 0.87627286 | 1.176173535 |
| GO:0006486 | protein glycosylation | 0.59225171 | 1.176182796 |
| ENSG00000170871 | KIAA0232 subnetwork | 0.87636789 | 1.176194216 |

| | | | |
|---|---|---|---|
| ENSG00000164045 | CDC25A subnetwork | 0.59199623 | 1.176206804 |
| ENSG00000197756 | RPL37A subnetwork | 0.8761548 | 1.176224584 |
| GO:0006405 | RNA export from nucleus | 0.87625081 | 1.176249884 |
| REACTOME_NONSENSE:MEDIA | REACTOME_NONSENSE:MEDIATED_DECAY | 0.5919574 | 1.176277569 |
| MP:0011091 | complete prenatal lethality | 0.59238609 | 1.176286789 |
| ENSG00000104613 | INTS10 subnetwork | 0.87609967 | 1.176296331 |
| ENSG00000148143 | ZNF462 subnetwork | 0.59215813 | 1.176337725 |
| GO:0043413 | macromolecule glycosylation | 0.59225171 | 1.176340906 |
| MP:0008511 | thin retinal inner nuclear layer | 0.87522694 | 1.176355477 |
| ENSG00000184897 | H1FX subnetwork | 0.87575529 | 1.176359349 |
| GO:0055072 | iron ion homeostasis | 0.87539344 | 1.176369103 |
| ENSG00000176177 | ENTHD1 subnetwork | 0.59253875 | 1.176370599 |
| ENSG00000164080 | RAD54L2 subnetwork | 0.87599702 | 1.176379773 |
| GO:0016525 | negative regulation of angiogenesis | 0.87609298 | 1.176381956 |
| GO:0030004 | cellular monovalent inorganic cation homeostasis | 0.87586743 | 1.176403144 |
| ENSG00000198399 | ITSN2 subnetwork | 0.87520148 | 1.176408809 |
| REACTOME_NONSENSE_MEDI | REACTOME_NONSENSE_MEDIATED_DECAY_ENHANCED_B | 0.5919574 | 1.176435777 |
| GO:0008593 | regulation of Notch signaling pathway | 0.87572897 | 1.176440396 |
| GO:0045576 | mast cell activation | 0.87504899 | 1.17644609 |
| GO:0042346 | positive regulation of NF-kappaB import into nucleus | 0.87538238 | 1.176459432 |
| GO:0031406 | carboxylic acid binding | 0.87557661 | 1.176468412 |
| ENSG00000004779 | NDUFAB1 subnetwork | 0.87598192 | 1.17647929 |
| GO:0005487 | nucleocytoplasmic transporter activity | 0.87516697 | 1.176499167 |
| ENSG00000164758 | MED30 subnetwork | 0.59190925 | 1.176499865 |
| GO:0015695 | organic cation transport | 0.59183031 | 1.176503431 |
| REACTOME_CELL:CELL_JUNCTI | REACTOME_CELL:CELL_JUNCTION_ORGANIZATION | 0.87569477 | 1.176516833 |
| GO:0031122 | cytoplasmic microtubule organization | 0.87504321 | 1.176550352 |
| MP:0006113 | abnormal heart septum morphology | 0.8749024 | 1.176601555 |
| GO:0007530 | sex determination | 0.87483636 | 1.176636423 |
| GO:0043691 | reverse cholesterol transport | 0.8750365 | 1.176654633 |
| ENSG00000135506 | OS9 subnetwork | 0.5929236 | 1.176668905 |
| KEGG_OXIDATIVE_PHOSPHOR | KEGG_OXIDATIVE_PHOSPHORYLATION | 0.87478516 | 1.176694444 |
| MP:0000434 | megacephaly | 0.59285401 | 1.176699355 |
| GO:0042249 | establishment of planar polarity of embryonic epithelium | 0.87450409 | 1.176704335 |
| MP:0001566 | hyperphosphatemia | 0.87466612 | 1.176717911 |
| GO:0010811 | positive regulation of cell-substrate adhesion | 0.87461687 | 1.176766694 |
| ENSG00000197780 | TAF13 subnetwork | 0.59279572 | 1.176790273 |
| ENSG00000152104 | PTPN14 subnetwork | 0.59327392 | 1.176792427 |
| ENSG00000126768 | TIMM17B subnetwork | 0.59401344 | 1.176793617 |
| ENSG00000131941 | RHPN2 subnetwork | 0.59409211 | 1.176796728 |
| ENSG00000137825 | ITPKA subnetwork | 0.87478119 | 1.176803408 |
| ENSG00000013374 | NUB1 subnetwork | 0.87449157 | 1.17681334 |
| KEGG_MATURITY_ONSET_DIA | KEGG_MATURITY_ONSET_DIABETES_OF_THE_YOUNG | 0.87442902 | 1.17687141 |
| GO:0042177 | negative regulation of protein catabolic process | 0.59369619 | 1.17689521 |
| ENSG00000104375 | STK3 subnetwork | 0.59338743 | 1.176929789 |
| MP:0001851 | eye inflammation | 0.59400613 | 1.176938036 |
| GO:0072075 | metanephric mesenchyme development | 0.59327325 | 1.17695045 |
| GO:0003215 | cardiac right ventricle morphogenesis | 0.87441261 | 1.176971185 |
| GO:0035023 | regulation of Rho protein signal transduction | 0.59394962 | 1.177002012 |
| GO:0031109 | microtubule polymerization or depolymerization | 0.87438782 | 1.17704318 |
| ENSG00000100346 | CACNA1I subnetwork | 0.59367689 | 1.17704643 |
| GO:0010952 | positive regulation of peptidase activity | 0.59392004 | 1.17707942 |
| ENSG00000137876 | RSL24D1 subnetwork | 0.59325015 | 1.17708837 |

| | | | |
|---|---|---|---|
| GO:0016757 | transferase activity, transferring glycosyl groups | 0.87437138 | 1.17714299 |
| GO:0003735 | structural constituent of ribosome | 0.59366209 | 1.177184271 |
| GO:0002347 | response to tumor cell | 0.59361018 | 1.177201342 |
| ENSG00000112941 | PAPD7 subnetwork | 0.87435463 | 1.177242817 |
| ENSG00000136999 | NOV subnetwork | 0.87401693 | 1.177245759 |
| GO:0005876 | spindle microtubule | 0.87387166 | 1.1772879 |
| GO:0046034 | ATP metabolic process | 0.87434531 | 1.177338029 |
| GO:0016758 | transferase activity, transferring hexosyl groups | 0.87401195 | 1.177350269 |
| ENSG00000021574 | SPAST subnetwork | 0.87364801 | 1.177351141 |
| GO:0005178 | integrin binding | 0.87425271 | 1.177359103 |
| GO:0048704 | embryonic skeletal system morphogenesis | 0.87384954 | 1.177364614 |
| GO:0046496 | nicotinamide nucleotide metabolic process | 0.87379366 | 1.1773857 |
| MP:0001394 | circling | 0.8736129 | 1.177427882 |
| ENSG00000152684 | PELO subnetwork | 0.87356086 | 1.177462894 |
| REACTOME_EXPORT_OF_VIRA | REACTOME_EXPORT_OF_VIRAL_RIBONUCLEOPROTEINS_FF | 0.59681635 | 1.177474289 |
| MP:0004003 | abnormal vascular endothelial cell physiology | 0.87346548 | 1.177546855 |
| GO:0060767 | epithelial cell proliferation involved in prostate gland devel | 0.8735571 | 1.177572131 |
| ENSG00000146463 | ZMYM4 subnetwork | 0.59769474 | 1.177587357 |
| GO:0016829 | lyase activity | 0.59764033 | 1.177604375 |
| KEGG_COMPLEMENT_AND_CC | KEGG_COMPLEMENT_AND_COAGULATION_CASCADES | 0.59681116 | 1.177631579 |
| GO:0072012 | glomerulus vasculature development | 0.87345585 | 1.17765148 |
| ENSG00000097046 | CDC7 subnetwork | 0.59784539 | 1.177693333 |
| MP:0005592 | abnormal vascular smooth muscle morphology | 0.59793298 | 1.177709639 |
| ENSG00000179801 | ENSG00000179801 subnetwork | 0.87344476 | 1.177732925 |
| GO:0016303 | 1-phosphatidylinositol-3-kinase activity | 0.59763646 | 1.177754803 |
| ENSG00000173113 | TRMT112 subnetwork | 0.59678304 | 1.177762191 |
| ENSG00000163104 | SMARCAD1 subnetwork | 0.5978327 | 1.177783704 |
| GO:0033574 | response to testosterone stimulus | 0.87340833 | 1.177814385 |
| ENSG00000197498 | RPF2 subnetwork | 0.59655279 | 1.177877289 |
| ENSG00000142892 | PIGK subnetwork | 0.59467907 | 1.177899182 |
| GO:0006702 | androgen biosynthetic process | 0.59676925 | 1.177899519 |
| GO:0033189 | response to vitamin A | 0.87339319 | 1.177905142 |
| GO:0035004 | phosphatidylinositol 3-kinase activity | 0.59763646 | 1.177911941 |
| ENSG00000185615 | PDIA2 subnetwork | 0.59504443 | 1.177924427 |
| ENSG00000101146 | RAE1 subnetwork | 0.59898221 | 1.17793824 |
| ENSG00000068903 | SIRT2 subnetwork | 0.596496 | 1.177941176 |
| REACTOME_RNA_POLYMERAS | REACTOME_RNA_POLYMERASE_III_TRANSCRIPTION | 0.5986757 | 1.177959782 |
| GO:2000021 | regulation of ion homeostasis | 0.59673343 | 1.177963384 |
| ENSG00000174233 | ADCY6 subnetwork | 0.59751831 | 1.177972775 |
| ENSG00000168476 | REEP4 subnetwork | 0.59760307 | 1.177975714 |
| GO:0001942 | hair follicle development | 0.5961138 | 1.177986622 |
| ENSG00000136695 | IL36RN subnetwork | 0.59480179 | 1.177989276 |
| GO:0016896 | exoribonuclease activity, producing 5'-phosphomonoesters | 0.87336212 | 1.177991274 |
| ENSG00000139180 | NDUFA9 subnetwork | 0.59833752 | 1.17799467 |
| ENSG00000163191 | S100A11 subnetwork | 0.59669436 | 1.178020583 |
| ENSG00000129515 | SNX6 subnetwork | 0.59893088 | 1.178035144 |
| GO:0006501 | C-terminal protein lipidation | 0.59621614 | 1.178036383 |
| GO:0045295 | gamma-catenin binding | 0.59572414 | 1.178038822 |
| KEGG_ARGININE_AND_PROLIN | KEGG_ARGININE_AND_PROLINE_METABOLISM | 0.59501538 | 1.17804878 |
| ENSG00000103043 | VAC14 subnetwork | 0.59563642 | 1.17804927 |
| GO:0070279 | vitamin B6 binding | 0.59934744 | 1.178066791 |
| MP:0000455 | abnormal maxilla morphology | 0.87333276 | 1.17806814 |
| ENSG00000180190 | C8orf42 subnetwork | 0.59579795 | 1.178068532 |

| | | | |
|---|---|---|---|
| ENSG00000122641 | INHBA subnetwork | 0.59880799 | 1.178069241 |
| GO:0004385 | guanylate kinase activity | 0.59747761 | 1.178069941 |
| ENSG00000068438 | FTSJ1 subnetwork | 0.59961564 | 1.178082192 |
| REACTOME_DESTABILIZATION_ | REACTOME_DESTABILIZATION_OF_MRNA_BY_TRISTETRAPI | 0.5984588 | 1.178084199 |
| GO:0032101 | regulation of response to external stimulus | 0.59721297 | 1.178098291 |
| GO:0006040 | amino sugar metabolic process | 0.59830855 | 1.178098348 |
| ENSG00000198242 | RPL23A subnetwork | 0.59649187 | 1.178098676 |
| ENSG00000171824 | EXOSC10 subnetwork | 0.59557942 | 1.178099893 |
| ENSG00000100242 | SUN2 subnetwork | 0.87328349 | 1.17810324 |
| REACTOME_RNA_POLYMERASI | REACTOME_RNA_POLYMERASE_III_ABORTIVE_AND_RETRA | 0.5986757 | 1.178116676 |
| GO:0048536 | spleen development | 0.59495181 | 1.178132958 |
| GO:0043536 | positive regulation of blood vessel endothelial cell migratio | 0.59524335 | 1.178135048 |
| ENSG00000099864 | PALM subnetwork | 0.59889832 | 1.17813873 |
| GO:0022404 | molting cycle process | 0.5961138 | 1.178144233 |
| GO:0034185 | apolipoprotein binding | 0.59744654 | 1.178160459 |
| GO:0050918 | positive chemotaxis | 0.59732886 | 1.17816798 |
| GO:0006303 | double-strand break repair via nonhomologous end joining | 0.59543141 | 1.178174391 |
| ENSG00000168412 | MTNR1A subnetwork | 0.59552604 | 1.178177314 |
| ENSG00000130402 | ACTN4 subnetwork | 0.59592922 | 1.178178533 |
| ENSG00000120063 | GNA13 subnetwork | 0.59827535 | 1.178188725 |
| ENSG00000158864 | NDUFS2 subnetwork | 0.87325657 | 1.178189415 |
| GO:0005355 | glucose transmembrane transporter activity | 0.59972436 | 1.178198138 |
| GO:0004222 | metalloendopeptidase activity | 0.59634239 | 1.178213187 |
| ENSG00000107201 | DDX58 subnetwork | 0.598648 | 1.178213667 |
| GO:0009886 | post-embryonic morphogenesis | 0.59739912 | 1.178217623 |
| GO:0006516 | glycoprotein catabolic process | 0.59644519 | 1.178222787 |
| GO:0030170 | pyridoxal phosphate binding | 0.59934744 | 1.178223553 |
| REACTOME_KINESINS | REACTOME_KINESINS | 0.59960611 | 1.178232243 |
| ENSG00000137757 | CASP5 subnetwork | 0.60701739 | 1.178256013 |
| MP:0002273 | abnormal pulmonary alveolus epithelial cell morphology | 0.59539391 | 1.17825854 |
| GO:0070243 | regulation of thymocyte apoptotic process | 0.59822649 | 1.178259131 |
| MP:0005023 | abnormal wound healing | 0.60695854 | 1.178272871 |
| GO:0048514 | blood vessel morphogenesis | 0.87277537 | 1.17827945 |
| GO:0000080 | G1 phase of mitotic cell cycle | 0.87258749 | 1.178289351 |
| ENSG00000134259 | NGF subnetwork | 0.87325537 | 1.178298821 |
| GO:0022405 | hair cycle process | 0.5961138 | 1.178301887 |
| GO:0003279 | cardiac septum development | 0.87314289 | 1.178306092 |
| GO:0042626 | ATPase activity, coupled to transmembrane movement of s | 0.59953528 | 1.178315817 |
| ENSG00000196313 | POM121 subnetwork | 0.5993386 | 1.178320468 |
| GO:0042805 | actinin binding | 0.87273234 | 1.178333178 |
| GO:0032868 | response to insulin stimulus | 0.87253979 | 1.178333798 |
| ENSG00000066032 | CTNNA2 subnetwork | 0.5998881 | 1.178340646 |
| ENSG00000107614 | TRDMT1 subnetwork | 0.87248381 | 1.178359665 |
| ENSG00000149925 | ALDOA subnetwork | 0.87311241 | 1.17839231 |
| ENSG00000130653 | PNPLA7 subnetwork | 0.87291212 | 1.178406874 |
| MP:0004542 | impaired acrosome reaction | 0.87302225 | 1.178413524 |
| GO:0019433 | triglyceride catabolic process | 0.60695572 | 1.178414618 |
| MP:0011107 | partial embryonic lethality before turning of embryo | 0.6071958 | 1.178423127 |
| MP:0002792 | abnormal retinal vasculature morphology | 0.87247435 | 1.178459894 |
| ENSG00000163605 | PPP4R2 subnetwork | 0.6067292 | 1.178491583 |
| GO:0008361 | regulation of cell size | 0.87244626 | 1.178513664 |
| GO:0042168 | heme metabolic process | 0.60695469 | 1.17856955 |
| GO:0070588 | calcium ion transmembrane transport | 0.87235417 | 1.178584046 |

| | | | |
|---|---|---|---|
| GO:0045072 | regulation of interferon-gamma biosynthetic process | 0.87243931 | 1.178590685 |
| ENSG00000118007 | STAG1 subnetwork | 0.60612964 | 1.178591178 |
| GO:0051101 | regulation of DNA binding | 0.60661847 | 1.178624046 |
| ENSG00000179218 | CALR subnetwork | 0.60671728 | 1.178626858 |
| ENSG00000079785 | DDX1 subnetwork | 0.60139362 | 1.178634916 |
| MP:0002795 | dilated cardiomyopathy | 0.87211633 | 1.178666419 |
| ENSG00000181610 | MRPS23 subnetwork | 0.6054369 | 1.178667457 |
| ENSG00000120705 | ETF1 subnetwork | 0.60607853 | 1.178673953 |
| MP:0006344 | small second branchial arch | 0.60692439 | 1.178678501 |
| GO:0007351 | tripartite regional subdivision | 0.87234681 | 1.178688982 |
| GO:0010595 | positive regulation of endothelial cell migration | 0.60536806 | 1.178697601 |
| GO:0048103 | somatic stem cell division | 0.60135428 | 1.178698421 |
| GO:0003755 | peptidyl-prolyl cis-trans isomerase activity | 0.60750717 | 1.178711245 |
| ENSG00000181019 | NQO1 subnetwork | 0.60776148 | 1.178732764 |
| GO:0034446 | substrate adhesion-dependent cell spreading | 0.60659666 | 1.178733061 |
| GO:0005913 | cell-cell adherens junction | 0.87209146 | 1.178734189 |
| ENSG00000115738 | ID2 subnetwork | 0.60129196 | 1.178735403 |
| GO:0080111 | DNA demethylation | 0.60108133 | 1.178743032 |
| GO:0032273 | positive regulation of protein polymerization | 0.60605635 | 1.17875675 |
| ENSG00000091073 | ENSG00000091073 subnetwork | 0.60568829 | 1.178778495 |
| ENSG00000159164 | SV2A subnetwork | 0.60579022 | 1.178781291 |
| GO:0045749 | negative regulation of S phase of mitotic cell cycle | 0.87201918 | 1.17878802 |
| GO:0008595 | anterior/posterior axis specification, embryo | 0.87234681 | 1.178798587 |
| ENSG00000171700 | RGS19 subnetwork | 0.60656831 | 1.178822368 |
| ENSG00000108813 | DLX4 subnetwork | 0.60535262 | 1.178826632 |
| GO:0000038 | very long-chain fatty acid metabolic process | 0.87197771 | 1.178827907 |
| GO:0032606 | type I interferon production | 0.60749798 | 1.178846407 |
| ENSG00000044524 | EPHA3 subnetwork | 0.60035883 | 1.178854333 |
| ENSG00000181690 | PLAG1 subnetwork | 0.60602964 | 1.178859326 |
| GO:0051181 | cofactor transport | 0.60564698 | 1.17886136 |
| GO:0051270 | regulation of cellular component movement | 0.60636966 | 1.178873239 |
| ENSG00000151332 | MBIP subnetwork | 0.6077542 | 1.178874442 |
| ENSG00000089234 | BRAP subnetwork | 0.60128402 | 1.178878567 |
| GO:0043648 | dicarboxylic acid metabolic process | 0.60045721 | 1.178883721 |
| ENSG00000104964 | AES subnetwork | 0.60107348 | 1.178892871 |
| GO:0000726 | non-recombinational repair | 0.60019999 | 1.178895241 |
| MP:0002836 | abnormal chorion morphology | 0.60830651 | 1.178923885 |
| ENSG00000111676 | ATN1 subnetwork | 0.87196234 | 1.178928272 |
| REACTOME_POST_NMDA_REC | REACTOME_POST_NMDA_RECEPTOR_ACTIVATION_EVENT | 0.60633698 | 1.1789297 |
| ENSG00000144648 | CCBP2 subnetwork | 0.60031451 | 1.178937924 |
| ENSG00000122122 | SASH3 subnetwork | 0.60656272 | 1.178938018 |
| GO:0051055 | negative regulation of lipid biosynthetic process | 0.60595963 | 1.178942168 |
| ENSG00000068305 | MEF2A subnetwork | 0.60771132 | 1.178950479 |
| GO:0015718 | monocarboxylic acid transport | 0.60824357 | 1.178967056 |
| ENSG00000170276 | ENSG00000170276 subnetwork | 0.60057205 | 1.178972894 |
| REACTOME_GLYCOLYSIS | REACTOME_GLYCOLYSIS | 0.60534846 | 1.178975475 |
| GO:0033144 | negative regulation of intracellular steroid hormone recept | 0.60483721 | 1.178987993 |
| REACTOME_GLUCONEOGENES | REACTOME_GLUCONEOGENESIS | 0.60506091 | 1.178993536 |
| MP:0005598 | decreased ventricle muscle contractility | 0.87194987 | 1.179005396 |
| GO:2000045 | regulation of G1/S transition of mitotic cell cycle | 0.60651867 | 1.179014214 |
| ENSG00000103942 | HOMER2 subnetwork | 0.60105922 | 1.179016198 |
| GO:0001522 | pseudouridine synthesis | 0.60495787 | 1.179023747 |
| ENSG00000204271 | SPIN3 subnetwork | 0.604355 | 1.179027998 |

| | | | |
|---|---|---|---|
| ENSG00000135409 | AMHR2 subnetwork | 0.60191544 | 1.179041241 |
| ENSG00000185046 | ANKS1B subnetwork | 0.87192084 | 1.179049967 |
| ENSG00000112531 | QKI subnetwork | 0.60100307 | 1.179073164 |
| GO:0005665 | DNA-directed RNA polymerase II, core complex | 0.60460787 | 1.179075908 |
| ENSG00000161920 | MED11 subnetwork | 0.60528872 | 1.179078201 |
| ENSG00000123360 | PDE1B subnetwork | 0.60201921 | 1.179083797 |
| MP:0002591 | decreased mean corpuscular volume | 0.60089754 | 1.179087528 |
| ENSG00000126778 | SIX1 subnetwork | 0.60446134 | 1.179103394 |
| MP:0002026 | leukemia | 0.60482434 | 1.179110583 |
| ENSG00000183570 | PCBP3 subnetwork | 0.60824214 | 1.179121817 |
| MP:0004901 | decreased male germ cell number | 0.60095562 | 1.179136786 |
| ENSG00000185920 | PTCH1 subnetwork | 0.60302254 | 1.179150119 |
| GO:0046658 | anchored to plasma membrane | 0.87190652 | 1.179155034 |
| ENSG00000215639 | ENSG00000215639 subnetwork | 0.60181529 | 1.179168325 |
| GO:0042542 | response to hydrogen peroxide | 0.60328027 | 1.179171629 |
| ENSG00000130414 | NDUFA10 subnetwork | 0.60273658 | 1.179172185 |
| GO:0048599 | oocyte development | 0.60317563 | 1.17917549 |
| ENSG00000130340 | SNX9 subnetwork | 0.6008524 | 1.179177736 |
| MP:0000639 | abnormal adrenal gland morphology | 0.60456457 | 1.179178769 |
| ENSG00000072682 | P4HA2 subnetwork | 0.871832 | 1.179181014 |
| ENSG00000186787 | SPIN2B subnetwork | 0.604355 | 1.179183727 |
| GO:0004527 | exonuclease activity | 0.60347749 | 1.179190369 |
| REACTOME_DEVELOPMENTAL_ | REACTOME_DEVELOPMENTAL_BIOLOGY | 0.60879725 | 1.179193443 |
| GO:0035304 | regulation of protein dephosphorylation | 0.60190846 | 1.179197613 |
| ENSG00000127824 | TUBA4A subnetwork | 0.60526809 | 1.179200739 |
| MP:0003111 | abnormal cell nucleus morphology | 0.60339533 | 1.179207462 |
| GO:0070585 | protein localization in mitochondrion | 0.60079446 | 1.179214827 |
| ENSG00000184937 | WT1 subnetwork | 0.60415971 | 1.179215116 |
| GO:0009411 | response to UV | 0.60313204 | 1.17921906 |
| ENSG00000131910 | NR0B2 subnetwork | 0.60298238 | 1.179220177 |
| ENSG00000102218 | RP2 subnetwork | 0.60290494 | 1.179230667 |
| ENSG00000160094 | ZNF362 subnetwork | 0.60821436 | 1.179230668 |
| ENSG00000090061 | CCNK subnetwork | 0.6025043 | 1.179253909 |
| ENSG00000168546 | GFRA2 subnetwork | 0.60402605 | 1.179255882 |
| GO:0070647 | protein modification by small protein conjugation or remov | 0.87161745 | 1.179258983 |
| ENSG00000164402 | SEPT8 subnetwork | 0.60482345 | 1.179259601 |
| GO:0046394 | carboxylic acid biosynthetic process | 0.60389056 | 1.179263617 |
| ENSG00000166889 | PATL1 subnetwork | 0.60431051 | 1.179266843 |
| GO:0006636 | unsaturated fatty acid biosynthetic process | 0.60424996 | 1.179270709 |
| ENSG00000071242 | RPS6KA2 subnetwork | 0.60360426 | 1.179272487 |
| MP:0004566 | myocardial fiber degeneration | 0.60815785 | 1.179273897 |
| GO:0060644 | mammary gland epithelial cell differentiation | 0.60369367 | 1.179275228 |
| ENSG00000074047 | GLI2 subnetwork | 0.60877348 | 1.179275971 |
| ENSG00000132670 | PTPRA subnetwork | 0.60270955 | 1.179282024 |
| ENSG00000168539 | CHRM1 subnetwork | 0.8718084 | 1.179290767 |
| MP:0001475 | reduced long term depression | 0.60871857 | 1.179319166 |
| ENSG00000008988 | RPS20 subnetwork | 0.60287556 | 1.17932062 |
| GO:0007098 | centrosome cycle | 0.60396205 | 1.179325843 |
| MP:0002961 | abnormal axon guidance | 0.87159124 | 1.179326878 |
| ENSG00000162923 | WDR26 subnetwork | 0.87173806 | 1.179335381 |
| GO:0006493 | protein O-linked glycosylation | 0.60246624 | 1.179337309 |
| GO:0051046 | regulation of secretion | 0.6041356 | 1.17935113 |
| MP:0002081 | perinatal lethality | 0.60859201 | 1.179353103 |

| | | | |
|---|---|---|---|
| ENSG00000165659 | DACH1 subnetwork | 0.60260459 | 1.179356036 |
| GO:0018208 | peptidyl-proline modification | 0.60380556 | 1.179363925 |
| ENSG00000164742 | ADCY1 subnetwork | 0.60228608 | 1.17938486 |
| GO:0017127 | cholesterol transporter activity | 0.60239679 | 1.179387593 |
| GO:0090030 | regulation of steroid hormone biosynthetic process | 0.87087469 | 1.179390664 |
| GO:0051093 | negative regulation of developmental process | 0.60897556 | 1.17940598 |
| MP:0004779 | abnormal production of surfactant | 0.60480869 | 1.179408659 |
| GO:0042744 | hydrogen peroxide catabolic process | 0.87155459 | 1.179408752 |
| GO:0016053 | organic acid biosynthetic process | 0.60389056 | 1.179419543 |
| ENSG00000099622 | CIRBP subnetwork | 0.60270469 | 1.179438262 |
| GO:0006361 | transcription initiation from RNA polymerase I promoter | 0.60871637 | 1.179473891 |
| MP:0002177 | abnormal outer ear morphology | 0.87086955 | 1.179500559 |
| ENSG00000123374 | CDK2 subnetwork | 0.87113879 | 1.179515603 |
| ENSG00000150787 | PTS subnetwork | 0.87155285 | 1.179518577 |
| GO:0050832 | defense response to fungus | 0.8714743 | 1.179553921 |
| ENSG00000154928 | EPHB1 subnetwork | 0.60923673 | 1.179555585 |
| MP:0009435 | abnormal miniature inhibitory postsynaptic currents | 0.87082268 | 1.179559221 |
| ENSG00000136861 | CDK5RAP2 subnetwork | 0.87126663 | 1.179559426 |
| GO:0051904 | pigment granule transport | 0.87053951 | 1.179584227 |
| ENSG00000087263 | OGFOD1 subnetwork | 0.87143053 | 1.179603241 |
| MP:0001525 | impaired balance | 0.87079727 | 1.179622554 |
| MP:0002920 | decreased paired-pulse facilitation | 0.87031426 | 1.17962514 |
| GO:0000922 | spindle pole | 0.87113447 | 1.179625489 |
| GO:0030301 | cholesterol transport | 0.87064 | 1.179632737 |
| ENSG00000171346 | KRT15 subnetwork | 0.87072789 | 1.179648616 |
| GO:0001503 | ossification | 0.87052866 | 1.179675555 |
| GO:0006805 | xenobiotic metabolic process | 0.87030596 | 1.179707172 |
| MP:0001158 | abnormal prostate gland morphology | 0.60922556 | 1.17971024 |
| ENSG00000164022 | AIMP1 subnetwork | 0.87049203 | 1.179738928 |
| REACTOME_REGULATION_OF_ | REACTOME_REGULATION_OF_APCC_ACTIVATORS_BETWEI | 0.87029457 | 1.179793882 |
| KEGG_SPHINGOLIPID_METABC | KEGG_SPHINGOLIPID_METABOLISM | 0.87019199 | 1.179801325 |
| GO:0030324 | lung development | 0.8701859 | 1.179902052 |
| ENSG00000145782 | ATG12 subnetwork | 0.87013096 | 1.179979476 |
| GO:0045926 | negative regulation of growth | 0.61067049 | 1.179994766 |
| ENSG00000179041 | RRS1 subnetwork | 0.87012463 | 1.180070909 |
| MP:0003670 | dilated renal glomerular capsule | 0.60959203 | 1.180076026 |
| ENSG00000111262 | KCNA1 subnetwork | 0.61226047 | 1.180090055 |
| ENSG00000172006 | ZNF554 subnetwork | 0.61064181 | 1.180116462 |
| MP:0001191 | abnormal skin condition | 0.61246316 | 1.180140919 |
| MP:0009414 | skeletal muscle fiber necrosis | 0.61220292 | 1.180152722 |
| REACTOME_3_:UTR:MEDIATED | REACTOME_3_:UTR:MEDIATED_TRANSLATIONAL_REGULAT | 0.87011549 | 1.180181021 |
| ENSG00000196890 | HIST3H2BB subnetwork | 0.61049046 | 1.180189791 |
| GO:0033146 | regulation of intracellular estrogen receptor signaling pathv | 0.61061389 | 1.180198927 |
| ENSG00000102144 | PGK1 subnetwork | 0.61241375 | 1.18022315 |
| GO:0008081 | phosphoric diester hydrolase activity | 0.86934371 | 1.180223218 |
| REACTOME_PURINE_METABOI | REACTOME_PURINE_METABOLISM | 0.61201791 | 1.180229825 |
| ENSG00000132698 | RAB25 subnetwork | 0.61039714 | 1.180236973 |
| GO:0048814 | regulation of dendrite morphogenesis | 0.86959734 | 1.180238095 |
| ENSG00000100505 | TRIM9 subnetwork | 0.86945124 | 1.180239074 |
| ENSG00000057294 | PKP2 subnetwork | 0.61024654 | 1.180257988 |
| ENSG00000087302 | C14orf166 subnetwork | 0.61133086 | 1.180271931 |
| ENSG00000169862 | CTNND2 subnetwork | 0.61218539 | 1.180274151 |
| GO:0034762 | regulation of transmembrane transport | 0.86931879 | 1.180286755 |

| | | | |
|---|---|---|---|
| REACTOME_L13A:MEDIATED_T | REACTOME_L13A:MEDIATED_TRANSLATIONAL_SILENCING_ | 0.87011549 | 1.180291153 |
| MP:0000792 | abnormal cortical marginal zone morphology | 0.86957207 | 1.180292278 |
| GO:0032862 | activation of Rho GTPase activity | 0.61260674 | 1.180306588 |
| GO:0006700 | C21-steroid hormone biosynthetic process | 0.61158064 | 1.180329369 |
| MP:0005164 | abnormal response to injury | 0.61020497 | 1.180333988 |
| ENSG00000012061 | ERCC1 subnetwork | 0.61048386 | 1.180337741 |
| MP:0000934 | abnormal telencephalon development | 0.86926585 | 1.180340962 |
| ENSG00000115524 | SF3B1 subnetwork | 0.6103815 | 1.180345685 |
| ENSG00000168497 | SDPR subnetwork | 0.61199998 | 1.180357842 |
| ENSG00000104064 | GABPB1 subnetwork | 0.6110632 | 1.180366252 |
| ENSG00000184588 | PDE4B subnetwork | 0.61195831 | 1.1803814 |
| ENSG00000065717 | TLE2 subnetwork | 0.61099778 | 1.180383307 |
| GO:0045124 | regulation of bone resorption | 0.61130626 | 1.180387029 |
| ENSG00000134686 | PHC2 subnetwork | 0.61217402 | 1.180389085 |
| GO:0006098 | pentose-phosphate shunt | 0.87010659 | 1.180391974 |
| ENSG00000108688 | CCL7 subnetwork | 0.61188205 | 1.180398432 |
| ENSG00000065548 | ZC3H15 subnetwork | 0.61154817 | 1.180405229 |
| GO:0015800 | acidic amino acid transport | 0.86923568 | 1.180423206 |
| GO:0033197 | response to vitamin E | 0.8690993 | 1.18042422 |
| ENSG00000071994 | PDCD2 subnetwork | 0.6101619 | 1.180436206 |
| MP:0001134 | absent corpus luteum | 0.86995942 | 1.180439653 |
| MP:0000872 | abnormal cerebellum external granule cell layer morpholog | 0.86917227 | 1.180454078 |
| ENSG00000124610 | HIST1H1A subnetwork | 0.87008781 | 1.180474146 |
| ENSG00000105894 | PTN subnetwork | 0.8690672 | 1.18047846 |
| GO:0006090 | pyruvate metabolic process | 0.61126883 | 1.180495619 |
| ENSG00000154978 | VOPP1 subnetwork | 0.61119153 | 1.180499608 |
| MP:0000519 | hydronephrosis | 0.86994138 | 1.180503174 |
| ENSG00000128591 | FLNC subnetwork | 0.61010878 | 1.180505699 |
| GO:0043243 | positive regulation of protein complex disassembly | 0.61171957 | 1.180508364 |
| ENSG00000077348 | EXOSC5 subnetwork | 0.61186548 | 1.18051999 |
| ENSG00000079739 | PGM1 subnetwork | 0.86991419 | 1.180566707 |
| ENSG00000073111 | MCM2 subnetwork | 0.60999358 | 1.180579216 |
| GO:0061082 | myeloid leukocyte cytokine production | 0.86906597 | 1.180588785 |
| ENSG00000153201 | RANBP2 subnetwork | 0.86898386 | 1.180610337 |
| MP:0000074 | abnormal neurocranium morphology | 0.61008509 | 1.180627621 |
| MP:0004678 | split xiphoid process | 0.61301789 | 1.180646844 |
| GO:0001917 | photoreceptor inner segment | 0.61186128 | 1.180661179 |
| MP:0010856 | dilated respiratory conducting tubes | 0.86897545 | 1.180692653 |
| GO:0004712 | protein serine/threonine/tyrosine kinase activity | 0.60997367 | 1.180694626 |
| ENSG00000205609 | EIF3CL subnetwork | 0.61297556 | 1.180716056 |
| REACTOME_TRANSPORT_OF_T | REACTOME_TRANSPORT_OF_THE_SLBP_INDEPENDENT_M | 0.61311437 | 1.180721085 |
| GO:0008635 | activation of cysteine-type endopeptidase activity involved | 0.86893934 | 1.180751613 |
| ENSG00000111786 | SRSF9 subnetwork | 0.61293423 | 1.180752674 |
| GO:0021903 | rostrocaudal neural tube patterning | 0.86714062 | 1.180810304 |
| GO:0009218 | pyrimidine ribonucleotide metabolic process | 0.86745032 | 1.18081281 |
| GO:0043968 | histone H2A acetylation | 0.86739895 | 1.180825061 |
| GO:0060393 | regulation of pathway-restricted SMAD protein phosphoryl | 0.8670874 | 1.180845981 |
| GO:0006418 | tRNA aminoacylation for protein translation | 0.86893002 | 1.180847981 |
| REACTOME_METABOLISM_OF_ | REACTOME_METABOLISM_OF_CARBOHYDRATES | 0.86733031 | 1.180851363 |
| GO:0032008 | positive regulation of TOR signaling cascade | 0.86727071 | 1.180872986 |
| REACTOME_GABA_SYNTHESIS_ | REACTOME_GABA_SYNTHESIS_RELEASE_REUPTAKE_AND_I | 0.86830568 | 1.180899139 |
| GO:0007016 | cytoskeletal anchoring at plasma membrane | 0.86880017 | 1.180914532 |
| ENSG00000112029 | FBXO5 subnetwork | 0.86888192 | 1.180930341 |

| | | | |
|---|---|---|---|
| ENSG00000133019 | CHRM3 subnetwork | 0.86846271 | 1.180935454 |
| ENSG00000115268 | RPS15 subnetwork | 0.86707529 | 1.18094725 |
| GO:0031110 | regulation of microtubule polymerization or depolymerizati | 0.86862161 | 1.180948373 |
| ENSG00000102225 | CDK16 subnetwork | 0.86856636 | 1.180969975 |
| GO:0051656 | establishment of organelle localization | 0.8684115 | 1.180975769 |
| GO:0001525 | angiogenesis | 0.86703626 | 1.180987631 |
| ENSG00000011465 | DCN subnetwork | 0.86876995 | 1.180992238 |
| GO:0048485 | sympathetic nervous system development | 0.86830399 | 1.181009638 |
| GO:0007623 | circadian rhythm | 0.86784254 | 1.181050463 |
| GO:0016486 | peptide hormone processing | 0.86775102 | 1.181076779 |
| MP:0003052 | omphalocele | 0.86701303 | 1.181079561 |
| GO:0007276 | gamete generation | 0.86828132 | 1.181096762 |
| ENSG00000142945 | KIF2C subnetwork | 0.86692644 | 1.181174431 |
| ENSG00000205726 | ITSN1 subnetwork | 0.86700822 | 1.181185567 |
| GO:0030641 | regulation of cellular pH | 0.868271 | 1.181193262 |
| ENSG00000110717 | NDUFS8 subnetwork | 0.86675651 | 1.181194338 |
| GO:0043488 | regulation of mRNA stability | 0.86802494 | 1.181197341 |
| ENSG00000065268 | WDR18 subnetwork | 0.86686945 | 1.181228909 |
| ENSG00000214869 | ENSG00000214869 subnetwork | 0.86820785 | 1.18122894 |
| MP:0001178 | pulmonary hypoplasia | 0.86619789 | 1.181252345 |
| GO:0034312 | diol biosynthetic process | 0.86612267 | 1.181259968 |
| GO:0006878 | cellular copper ion homeostasis | 0.86815014 | 1.181264626 |
| MP:0003915 | increased left ventricle weight | 0.86674014 | 1.181281643 |
| MP:0009907 | decreased tongue size | 0.86631413 | 1.181286934 |
| ENSG00000175324 | LSM1 subnetwork | 0.86588359 | 1.181329767 |
| ENSG00000115361 | ACADL subnetwork | 0.6136122 | 1.181338808 |
| MP:0001745 | increased circulating corticosterone level | 0.86584877 | 1.181370249 |
| GO:0009713 | catechol-containing compound biosynthetic process | 0.86612267 | 1.181370801 |
| ENSG00000025796 | SEC63 subnetwork | 0.86673424 | 1.181383029 |
| ENSG00000163430 | FSTL1 subnetwork | 0.61372741 | 1.181419447 |
| ENSG00000197905 | TEAD4 subnetwork | 0.8657026 | 1.181427767 |
| ENSG00000188419 | CHM subnetwork | 0.8657922 | 1.18142951 |
| ENSG00000105701 | FKBP8 subnetwork | 0.61357654 | 1.181447197 |
| GO:0005243 | gap junction channel activity | 0.86565103 | 1.181468269 |
| GO:0006536 | glutamate metabolic process | 0.8666994 | 1.181470368 |
| GO:0042423 | catecholamine biosynthetic process | 0.86612267 | 1.181481655 |
| MP:0001106 | abnormal Schwann cell morphology | 0.8665518 | 1.181518477 |
| ENSG00000142528 | ZNF473 subnetwork | 0.8656049 | 1.18153225 |
| GO:0071295 | cellular response to vitamin | 0.86669012 | 1.18157179 |
| GO:0048742 | regulation of skeletal muscle fiber development | 0.86521042 | 1.181584633 |
| ENSG00000180902 | D2HGDH subnetwork | 0.86558319 | 1.181615023 |
| ENSG00000147082 | CCNB3 subnetwork | 0.86508395 | 1.181628147 |
| GO:0000380 | alternative nuclear mRNA splicing, via spliceosome | 0.86517257 | 1.181643964 |
| GO:0043542 | endothelial cell migration | 0.86540191 | 1.181689678 |
| ENSG00000160299 | PCNT subnetwork | 0.86504922 | 1.181701588 |
| ENSG00000215692 | ENSG00000215692 subnetwork | 0.86558319 | 1.181725984 |
| MP:0000048 | abnormal stria vascularis morphology | 0.61397464 | 1.181734654 |
| GO:0031344 | regulation of cell projection organization | 0.86501502 | 1.181742154 |
| GO:0004549 | tRNA-specific ribonuclease activity | 0.86555238 | 1.18180879 |
| GO:0005790 | smooth endoplasmic reticulum | 0.86498156 | 1.181815619 |
| GO:0030325 | adrenal gland development | 0.8649738 | 1.181907895 |
| GO:0034109 | homotypic cell-cell adhesion | 0.86153137 | 1.181940383 |
| ENSG00000125965 | GDF5 subnetwork | 0.86150664 | 1.181995283 |

| | | | |
|---|---|---|---|
| GO:0015171 | amino acid transmembrane transporter activity | 0.86496946 | 1.182018987 |
| ENSG00000137767 | SQRDL subnetwork | 0.86478585 | 1.182034408 |
| GO:0005902 | microvillus | 0.8614859 | 1.182059628 |
| MP:0000477 | abnormal intestine morphology | 0.86183907 | 1.182061681 |
| GO:0030299 | intestinal cholesterol absorption | 0.86232913 | 1.1820624 |
| GO:0015701 | bicarbonate transport | 0.86172725 | 1.182064705 |
| ENSG00000112640 | PPP2R5D subnetwork | 0.86081303 | 1.182076095 |
| ENSG00000100227 | POLDIP3 subnetwork | 0.86140343 | 1.182076807 |
| ENSG00000114346 | ECT2 subnetwork | 0.8607062 | 1.182079124 |
| GO:0030018 | Z disc | 0.86134786 | 1.182112862 |
| GO:0032288 | myelin assembly | 0.86477392 | 1.182122038 |
| ENSG00000171848 | RRM2 subnetwork | 0.86496398 | 1.1821254 |
| MP:0008877 | abnormal DNA methylation | 0.86229888 | 1.182126697 |
| GO:0048520 | positive regulation of behavior | 0.86064995 | 1.182129367 |
| MP:0001968 | abnormal touch/ nociception | 0.86125472 | 1.182134768 |
| ENSG00000136450 | SRSF1 subnetwork | 0.61425066 | 1.182167058 |
| ENSG00000125810 | CD93 subnetwork | 0.86215802 | 1.182175184 |
| ENSG00000139668 | WDFY2 subnetwork | 0.8605997 | 1.18217962 |
| ENSG00000168542 | COL3A1 subnetwork | 0.86365667 | 1.182197326 |
| GO:0009410 | response to xenobiotic stimulus | 0.86474307 | 1.182204984 |
| ENSG00000108848 | LUC7L3 subnetwork | 0.86201443 | 1.182214259 |
| ENSG00000154188 | ANGPT1 subnetwork | 0.86101906 | 1.18221467 |
| GO:0051219 | phosphoprotein binding | 0.86209305 | 1.182215936 |
| ENSG00000170275 | CRTAP subnetwork | 0.86258775 | 1.182224317 |
| ENSG00000158290 | CUL4B subnetwork | 0.86124663 | 1.182232185 |
| ENSG00000164442 | CITED2 subnetwork | 0.86229833 | 1.182238145 |
| MP:0010454 | abnormal truncus arteriosus septation | 0.86434078 | 1.18224365 |
| GO:0031268 | pseudopodium organization | 0.86115469 | 1.182244667 |
| GO:0030667 | secretory granule membrane | 0.86273686 | 1.182263689 |
| GO:0001706 | endoderm formation | 0.86459913 | 1.182267469 |
| GO:0048525 | negative regulation of viral reproduction | 0.86058032 | 1.182277106 |
| GO:0034435 | cholesterol esterification | 0.86363824 | 1.182280388 |
| MP:0008271 | abnormal bone ossification | 0.86290209 | 1.182295298 |
| GO:0071616 | acyl-CoA biosynthetic process | 0.86328279 | 1.182306678 |
| ENSG00000121552 | CSTA subnetwork | 0.86428967 | 1.182307837 |
| GO:0043552 | positive regulation of phosphatidylinositol 3-kinase activity | 0.61442602 | 1.182312704 |
| GO:0071466 | cellular response to xenobiotic stimulus | 0.86474307 | 1.182316156 |
| MP:0004921 | decreased placenta weight | 0.86421386 | 1.182320286 |
| ENSG00000104408 | EIF3E subnetwork | 0.86283996 | 1.182331323 |
| GO:0015833 | peptide transport | 0.86415085 | 1.182337442 |
| MP:0003910 | decreased eating behavior | 0.86410211 | 1.182359307 |
| GO:0007566 | embryo implantation | 0.86459513 | 1.182359857 |
| MP:0009331 | absent primitive node | 0.61485632 | 1.182372087 |
| MP:0004180 | failure of initiation of embryo turning | 0.86454184 | 1.182381714 |
| ENSG00000104290 | FZD3 subnetwork | 0.61480069 | 1.182382813 |
| GO:0045071 | negative regulation of viral genome replication | 0.86058032 | 1.182388779 |
| GO:0034433 | steroid esterification | 0.86363824 | 1.182391714 |
| GO:0002026 | regulation of the force of heart contraction | 0.85862295 | 1.1823961 |
| MP:0001409 | increased stereotypic behavior | 0.86052414 | 1.182415454 |
| GO:0035384 | thioester biosynthetic process | 0.86328279 | 1.182418048 |
| ENSG00000182934 | SRPR subnetwork | 0.85856277 | 1.182422837 |
| MP:0010819 | primary atelectasis | 0.86407675 | 1.182442353 |
| ENSG00000185518 | SV2B subnetwork | 0.86399726 | 1.182450113 |

| | | | |
|---|---|---|---|
| GO:0009074 | aromatic amino acid family catabolic process | 0.86321945 | 1.182458785 |
| MP:0000131 | abnormal long bone epiphysis morphology | 0.85873728 | 1.182459296 |
| GO:0000737 | DNA catabolic process, endonucleolytic | 0.86009576 | 1.182462193 |
| REACTOME_PASSIVE_TRANSPO | REACTOME_PASSIVE_TRANSPORT_BY_AQUAPORINS | 0.86392703 | 1.182462581 |
| MP:0002216 | abnormal seminiferous tubule morphology | 0.86351755 | 1.182473159 |
| GO:0040036 | regulation of fibroblast growth factor receptor signaling pat | 0.86050563 | 1.182484648 |
| REACTOME_GTP_HYDROLYSIS_ | REACTOME_GTP_HYDROLYSIS_AND_JOINING_OF_THE_60S | 0.85941321 | 1.182494561 |
| GO:0050926 | regulation of positive chemotaxis | 0.61477959 | 1.182497721 |
| MP:0010867 | abnormal bone trabecula morphology | 0.86314024 | 1.182499529 |
| MP:0004738 | abnormal brainstem auditory evoked potential | 0.86041577 | 1.18250189 |
| GO:0034434 | sterol esterification | 0.86363824 | 1.182503061 |
| MP:0001302 | eyelids open at birth | 0.858541 | 1.182506391 |
| ENSG00000187741 | FANCA subnetwork | 0.85933525 | 1.182507096 |
| ENSG00000084623 | EIF3I subnetwork | 0.85887239 | 1.182508282 |
| ENSG00000140988 | RPS2 subnetwork | 0.8592226 | 1.182519633 |
| GO:0050994 | regulation of lipid catabolic process | 0.85916279 | 1.182527441 |
| GO:0010594 | regulation of endothelial cell migration | 0.85898313 | 1.182533598 |
| GO:0001763 | morphogenesis of a branching structure | 0.61504614 | 1.182543608 |
| GO:0006363 | termination of RNA polymerase I transcription | 0.61472001 | 1.182554051 |
| GO:0006309 | apoptotic DNA fragmentation | 0.86009576 | 1.182573967 |
| GO:0046527 | glucosyltransferase activity | 0.86039591 | 1.182594727 |
| ENSG00000078295 | ADCY2 subnetwork | 0.85842907 | 1.182607254 |
| GO:0006595 | polyamine metabolic process | 0.8585236 | 1.182608902 |
| ENSG00000171314 | PGAM1 subnetwork | 0.85954678 | 1.182628642 |
| ENSG00000148248 | SURF4 subnetwork | 0.85916093 | 1.182634617 |
| GO:0006740 | NADPH regeneration | 0.85972344 | 1.182646113 |
| GO:0017145 | stem cell division | 0.85841109 | 1.182667172 |
| KEGG_MELANOGENESIS | KEGG_MELANOGENESIS | 0.8596552 | 1.182672846 |
| GO:0048864 | stem cell development | 0.86009219 | 1.182685763 |
| GO:0021533 | cell differentiation in hindbrain | 0.61462566 | 1.182692809 |
| ENSG00000139835 | GRTP1 subnetwork | 0.61470188 | 1.182695063 |
| ENSG00000198400 | NTRK1 subnetwork | 0.86039529 | 1.182706483 |
| REACTOME_SYNTHESIS_OF_BI | REACTOME_SYNTHESIS_OF_BILE_ACIDS_AND_BILE_SALTS | 0.6152722 | 1.182743363 |
| GO:0009452 | RNA capping | 0.85838817 | 1.182760254 |
| REACTOME_RAS_ACTIVATION_ | REACTOME_RAS_ACTIVATION_UOPN_CA2_INFUX_THROUG | 0.86008273 | 1.182788125 |
| ENSG00000114841 | DNAH1 subnetwork | 0.86036911 | 1.182789906 |
| ENSG00000167792 | NDUFV1 subnetwork | 0.85833511 | 1.182810724 |
| ENSG00000130208 | APOC1 subnetwork | 0.86005486 | 1.182852685 |
| MP:0010209 | abnormal circulating chemokine level | 0.61526596 | 1.182877782 |
| GO:0046434 | organophosphate catabolic process | 0.85830692 | 1.182903837 |
| GO:0005041 | low-density lipoprotein receptor activity | 0.86002217 | 1.182926714 |
| GO:0022011 | myelination in peripheral nervous system | 0.85825254 | 1.18295433 |
| ENSG00000151748 | SAV1 subnetwork | 0.61617075 | 1.182969319 |
| ENSG00000126215 | XRCC3 subnetwork | 0.61624811 | 1.18300403 |
| GO:0006890 | retrograde vesicle-mediated transport, Golgi to ER | 0.6163608 | 1.183006239 |
| ENSG00000174791 | RIN1 subnetwork | 0.61575988 | 1.183055809 |
| GO:0032292 | peripheral nervous system axon ensheathment | 0.85825254 | 1.183066427 |
| MP:0009171 | enlarged pancreatic islets | 0.61615231 | 1.18311663 |
| GO:0001569 | patterning of blood vessels | 0.61662889 | 1.183116799 |
| MP:0002703 | abnormal renal tubule morphology | 0.85824235 | 1.183169067 |
| MP:0003560 | osteoarthritis | 0.61573462 | 1.1831707 |
| GO:0034394 | protein localization at cell surface | 0.85791767 | 1.183214827 |
| GO:0006213 | pyrimidine nucleoside metabolic process | 0.61662148 | 1.183257536 |

| | | | |
|---|---|---|---|
| ENSG00000167136 | ENDOG subnetwork | 0.61596276 | 1.183266129 |
| GO:0032855 | positive regulation of Rac GTPase activity | 0.61614504 | 1.183270481 |
| ENSG00000119421 | NDUFA8 subnetwork | 0.85823063 | 1.183276467 |
| ENSG00000144554 | FANCD2 subnetwork | 0.61571655 | 1.18330514 |
| ENSG00000180098 | TRNAU1AP subnetwork | 0.85791581 | 1.183322272 |
| GO:0015631 | tubulin binding | 0.85811989 | 1.183353872 |
| ENSG00000169189 | NSMCE1 subnetwork | 0.85821192 | 1.183364929 |
| ENSG00000198056 | PRIM1 subnetwork | 0.61659609 | 1.183365822 |
| GO:0046164 | alcohol catabolic process | 0.61609727 | 1.183378853 |
| ENSG00000140262 | TCF12 subnetwork | 0.85787708 | 1.183420254 |
| GO:0048265 | response to pain | 0.85779296 | 1.18344239 |
| GO:0030168 | platelet activation | 0.61688598 | 1.183456742 |
| ENSG00000122705 | CLTA subnetwork | 0.85775481 | 1.183521434 |
| ENSG00000189319 | FAM53B subnetwork | 0.61704615 | 1.183549812 |
| ENSG00000130176 | CNN1 subnetwork | 0.85741234 | 1.183622735 |
| ENSG00000030304 | MUSK subnetwork | 0.85775295 | 1.183633691 |
| REACTOME_LYSOSOME_VESIC | REACTOME_LYSOSOME_VESICLE_BIOGENESIS | 0.85732906 | 1.183640159 |
| ENSG00000087470 | DNM1L subnetwork | 0.61769749 | 1.183642616 |
| ENSG00000145241 | CENPC1 subnetwork | 0.85717978 | 1.183670273 |
| ENSG00000157916 | RER1 subnetwork | 0.61777105 | 1.183670689 |
| ENSG00000215754 | ENSG00000215754 subnetwork | 0.85769003 | 1.183674825 |
| GO:0071900 | regulation of protein serine/threonine kinase activity | 0.61748248 | 1.183707646 |
| GO:0030276 | clathrin binding | 0.8575417 | 1.183709677 |
| ENSG00000161681 | SHANK1 subnetwork | 0.85712896 | 1.18372093 |
| MP:0003212 | increased susceptibility to age related obesity | 0.8573157 | 1.18373351 |
| MP:0004970 | kidney atrophy | 0.85700295 | 1.183736827 |
| MP:0000288 | abnormal pericardium morphology | 0.61766434 | 1.183737833 |
| ENSG00000163513 | TGFBR2 subnetwork | 0.61741208 | 1.183750974 |
| GO:0033143 | regulation of intracellular steroid hormone receptor signali | 0.61757404 | 1.183755192 |
| MP:0003545 | increased alcohol consumption | 0.85707016 | 1.183762104 |
| ENSG00000117118 | SDHB subnetwork | 0.6172559 | 1.183766234 |
| MP:0001658 | increased mortality induced by gamma-irradiation | 0.61733296 | 1.183774834 |
| GO:0006879 | cellular iron ion homeostasis | 0.85767825 | 1.18377763 |
| GO:0000165 | MAPK cascade | 0.6178886 | 1.183796056 |
| ENSG00000109917 | ZNF259 subnetwork | 0.85699334 | 1.183839727 |
| GO:0007599 | hemostasis | 0.61801169 | 1.183856531 |
| ENSG00000100316 | RPL3 subnetwork | 0.61817465 | 1.183886655 |
| GO:0043161 | proteasomal ubiquitin-dependent protein catabolic process | 0.85688819 | 1.183931624 |
| ENSG00000169118 | CSNK1G1 subnetwork | 0.85697776 | 1.183937898 |
| ENSG00000171401 | KRT13 subnetwork | 0.85683879 | 1.183987083 |
| GO:0000722 | telomere maintenance via recombination | 0.61817387 | 1.184040208 |
| ENSG00000166225 | FRS2 subnetwork | 0.85682203 | 1.184080547 |
| ENSG00000126456 | IRF3 subnetwork | 0.85678671 | 1.184145531 |
| GO:0016209 | antioxidant activity | 0.61847049 | 1.184195514 |
| GO:0042149 | cellular response to glucose starvation | 0.85677687 | 1.184258028 |
| GO:0031670 | cellular response to nutrient | 0.85670146 | 1.184299287 |
| GO:0045785 | positive regulation of cell adhesion | 0.61862009 | 1.184307752 |
| ENSG00000185345 | PARK2 subnetwork | 0.61845706 | 1.184323133 |
| GO:0015035 | protein disulfide oxidoreductase activity | 0.85642932 | 1.184340842 |
| GO:0042470 | melanosome | 0.85666972 | 1.184354808 |
| MP:0003105 | abnormal heart atrium morphology | 0.85637499 | 1.184386882 |
| ENSG00000132464 | ENAM subnetwork | 0.85622551 | 1.184388667 |
| ENSG00000158022 | TRIM63 subnetwork | 0.85630726 | 1.184409164 |

| | | | |
|---|---|---|---|
| GO:0014812 | muscle cell migration | 0.85618504 | 1.184434725 |
| GO:0048770 | pigment granule | 0.85666972 | 1.184467357 |
| GO:0070206 | protein trimerization | 0.61978101 | 1.184487445 |
| REACTOME_DEPOSITION_OF_I | REACTOME_DEPOSITION_OF_NEW_CENPA:CONTAINING_N | 0.61928007 | 1.184529206 |
| ENSG00000132688 | NES subnetwork | 0.85617789 | 1.184542602 |
| GO:0015669 | gas transport | 0.85664549 | 1.184551416 |
| GO:0051209 | release of sequestered calcium ion into cytosol | 0.61974397 | 1.184582524 |
| ENSG00000163754 | GYG1 subnetwork | 0.85617215 | 1.184645744 |
| ENSG00000101367 | MAPRE1 subnetwork | 0.61895787 | 1.184655262 |
| REACTOME_NUCLEOSOME_AS | REACTOME_NUCLEOSOME_ASSEMBLY | 0.61928007 | 1.184682642 |
| GO:0015294 | solute:cation symporter activity | 0.61951688 | 1.184693085 |
| ENSG00000204217 | BMPR2 subnetwork | 0.6192058 | 1.184726001 |
| GO:0051282 | regulation of sequestering of calcium ion | 0.61974397 | 1.184735888 |
| GO:0001892 | embryonic placenta development | 0.61891474 | 1.184737524 |
| REACTOME_DUAL_INCISION_R | REACTOME_DUAL_INCISION_REACTION_IN_TC:NER | 0.85616886 | 1.184753662 |
| MP:0003691 | abnormal microglial cell physiology | 0.8560532 | 1.184817352 |
| GO:0003785 | actin monomer binding | 0.6191814 | 1.184821197 |
| REACTOME_FORMATION_OF_T | REACTOME_FORMATION_OF_TRANSCRIPTION:COUPLED_N | 0.85616886 | 1.184866356 |
| MP:0005618 | decreased urine potassium level | 0.6191195 | 1.184877543 |
| GO:0051283 | negative regulation of sequestering of calcium ion | 0.61974397 | 1.184889292 |
| KEGG_REGULATION_OF_AUTO | KEGG_REGULATION_OF_AUTOPHAGY | 0.85603439 | 1.184896775 |
| GO:0000152 | nuclear ubiquitin ligase complex | 0.85599103 | 1.184957184 |
| ENSG00000120498 | TEX11 subnetwork | 0.62032831 | 1.184974127 |
| ENSG00000170743 | SYT9 subnetwork | 0.85594931 | 1.185022362 |
| ENSG00000130119 | GNL3L subnetwork | 0.62090585 | 1.185031024 |
| ENSG00000111142 | METAP2 subnetwork | 0.62031345 | 1.185101566 |
| ENSG00000036257 | CUL3 subnetwork | 0.8550585 | 1.185108106 |
| MP:0002777 | absent ovarian follicles | 0.85593013 | 1.185111344 |
| GO:0042752 | regulation of circadian rhythm | 0.85514949 | 1.185119048 |
| MP:0010825 | abnormal lung saccule morphology | 0.85470282 | 1.185140543 |
| ENSG00000115307 | AUP1 subnetwork | 0.85481369 | 1.185146723 |
| MP:0009050 | dilated proximal convoluted tubules | 0.62018023 | 1.185149476 |
| ENSG00000057663 | ATG5 subnetwork | 0.85536237 | 1.185150448 |
| GO:0070085 | glycosylation | 0.62106704 | 1.185155745 |
| MP:0001728 | failure of embryo implantation | 0.62088366 | 1.185158371 |
| ENSG00000068354 | TBC1D25 subnetwork | 0.85490589 | 1.185167191 |
| ENSG00000134333 | LDHA subnetwork | 0.85546625 | 1.185185185 |
| ENSG00000174851 | YIF1A subnetwork | 0.6207952 | 1.185195242 |
| ENSG00000130724 | CHMP2A subnetwork | 0.85503484 | 1.18519718 |
| GO:0010737 | protein kinase A signaling cascade | 0.85440499 | 1.185211133 |
| ENSG00000133773 | CCDC59 subnetwork | 0.8559173 | 1.185219378 |
| GO:0045132 | meiotic chromosome segregation | 0.62029754 | 1.185229037 |
| ENSG00000171703 | TCEA2 subnetwork | 0.85469353 | 1.18523442 |
| ENSG00000111845 | PAK1IP1 subnetwork | 0.85566014 | 1.185253237 |
| ENSG00000171497 | PPID subnetwork | 0.85534744 | 1.185253785 |
| GO:0009595 | detection of biotic stimulus | 0.85451695 | 1.185255433 |
| ENSG00000198804 | MT-CO1 subnetwork | 0.85583736 | 1.185270322 |
| ENSG00000166478 | ZNF143 subnetwork | 0.62066665 | 1.185281945 |
| ENSG00000125977 | EIF2S2 subnetwork | 0.85439985 | 1.185324118 |
| GO:0009913 | epidermal cell differentiation | 0.85430864 | 1.185332253 |
| GO:0009268 | response to pH | 0.62077797 | 1.185335575 |
| ENSG00000136573 | BLK subnetwork | 0.85469312 | 1.185347374 |
| GO:0045095 | keratin filament | 0.62061646 | 1.185351184 |

| | | | |
|---|---|---|---|
| ENSG00000212875 | ENSG00000212875 subnetwork | 0.85583736 | 1.185383151 |
| GO:0046466 | membrane lipid catabolic process | 0.85430577 | 1.185440503 |
| GO:0051015 | actin filament binding | 0.62129511 | 1.185493668 |
| ENSG00000150086 | GRIN2B subnetwork | 0.85420351 | 1.185523555 |
| GO:0030149 | sphingolipid catabolic process | 0.85430577 | 1.185553542 |
| ENSG00000122218 | COPA subnetwork | 0.85410233 | 1.185573254 |
| ENSG00000108469 | RECQL5 subnetwork | 0.62507133 | 1.185627088 |
| ENSG00000100934 | SEC23A subnetwork | 0.8541965 | 1.185631855 |
| GO:0043500 | muscle adaptation | 0.85408686 | 1.185657732 |
| ENSG00000073536 | NLE1 subnetwork | 0.62517493 | 1.18566748 |
| ENSG00000106392 | C1GALT1 subnetwork | 0.85402645 | 1.185694524 |
| MP:0000242 | impaired fertilization | 0.8507916 | 1.185698554 |
| ENSG00000173991 | TCAP subnetwork | 0.62502801 | 1.185715204 |
| ENSG00000150995 | ITPR1 subnetwork | 0.85087588 | 1.185733435 |
| ENSG00000214078 | CPNE1 subnetwork | 0.62530202 | 1.185739979 |
| REACTOME_GLUTATHIONE_SY | REACTOME_GLUTATHIONE_SYNTHESIS_AND_RECYCLING | 0.8540013 | 1.185774258 |
| MP:0001176 | abnormal lung development | 0.85078065 | 1.185792952 |
| ENSG00000197548 | ATG7 subnetwork | 0.62498287 | 1.185822622 |
| ENSG00000120896 | SORBS3 subnetwork | 0.85390001 | 1.185866972 |
| GO:0044243 | multicellular organismal catabolic process | 0.85040578 | 1.185877168 |
| ENSG00000188153 | COL4A5 subnetwork | 0.85399629 | 1.185882634 |
| GO:0016051 | carbohydrate biosynthetic process | 0.85076206 | 1.185887367 |
| GO:0043279 | response to alkaloid | 0.85067987 | 1.185895594 |
| GO:0009167 | purine ribonucleoside monophosphate metabolic process | 0.62555009 | 1.185897765 |
| GO:0072079 | nephron tubule formation | 0.85383684 | 1.185913342 |
| GO:0006200 | ATP catabolic process | 0.85062656 | 1.18594214 |
| GO:0007548 | sex differentiation | 0.85126142 | 1.18595425 |
| REACTOME_GPCR_LIGAND_BI | REACTOME_GPCR_LIGAND_BINDING | 0.85380321 | 1.185959721 |
| GO:0019438 | aromatic compound biosynthetic process | 0.85054214 | 1.185959954 |
| ENSG00000145692 | BHMT subnetwork | 0.62333267 | 1.185961861 |
| GO:0034067 | protein localization in Golgi apparatus | 0.62345506 | 1.185963669 |
| ENSG00000182944 | EWSR1 subnetwork | 0.85108499 | 1.18597415 |
| ENSG00000145375 | SPATA5 subnetwork | 0.62498263 | 1.185975061 |
| MP:0002633 | persistent truncus arteriosis | 0.85037379 | 1.185976428 |
| REACTOME_TRANS:GOLGI_NE | REACTOME_TRANS:GOLGI_NETWORK_VESICLE_BUDDING | 0.62327714 | 1.185992268 |
| GO:0005507 | copper ion binding | 0.85196103 | 1.18599847 |
| GO:0009065 | glutamine family amino acid catabolic process | 0.84288663 | 1.186 |
| GO:0014015 | positive regulation of gliogenesis | 0.62201546 | 1.186027893 |
| GO:0004364 | glutathione transferase activity | 0.85125235 | 1.186039054 |
| ENSG00000111361 | EIF2B1 subnetwork | 0.85032549 | 1.186046957 |
| GO:0009126 | purine nucleoside monophosphate metabolic process | 0.62555009 | 1.186050096 |
| ENSG00000092208 | GEMIN2 subnetwork | 0.62495366 | 1.186063255 |
| ENSG00000142541 | RPL13A subnetwork | 0.853797 | 1.186063383 |
| GO:0072655 | establishment of protein localization in mitochondrion | 0.62196986 | 1.186077748 |
| MP:0000592 | short tail | 0.85192867 | 1.186078431 |
| MP:0008260 | abnormal autophagy | 0.85120504 | 1.186080796 |
| ENSG00000109220 | CHIC2 subnetwork | 0.84303242 | 1.186097962 |
| ENSG00000137693 | YAP1 subnetwork | 0.85029544 | 1.186103124 |
| GO:0010810 | regulation of cell-substrate adhesion | 0.84287425 | 1.186104938 |
| GO:0030323 | respiratory tube development | 0.84277138 | 1.186113259 |
| KEGG_FRUCTOSE_AND_MANN | KEGG_FRUCTOSE_AND_MANNOSE_METABOLISM | 0.62319601 | 1.186136891 |
| GO:0052312 | modulation of transcription in other organism involved in s | 0.62491655 | 1.186138614 |
| REACTOME_CLATHRIN_DERIVE | REACTOME_CLATHRIN_DERIVED_VESICLE_BUDDING | 0.62327714 | 1.186145122 |

| | | | |
|---|---|---|---|
| GO:0051701 | interaction with host | 0.85378106 | 1.186162291 |
| MP:0001944 | abnormal pancreas morphology | 0.85189823 | 1.186163191 |
| GO:0031099 | regeneration | 0.6219317 | 1.186179282 |
| MP:0003806 | abnormal nucleotide metabolism | 0.85154118 | 1.186180496 |
| GO:0009064 | glutamine family amino acid metabolic process | 0.84237126 | 1.186188727 |
| ENSG00000211653 | ENSG00000211653 subnetwork | 0.62467008 | 1.186197582 |
| MP:0002175 | decreased brain weight | 0.84274253 | 1.186198898 |
| REACTOME_ASSOCIATION_OF_ | REACTOME_ASSOCIATION_OF_TRICCCT_WITH_TARGET_PF | 0.84247298 | 1.186209397 |
| ENSG00000112851 | ERBB2IP subnetwork | 0.85029382 | 1.186216812 |
| REACTOME_LOSS_OF_NLP_FR( | REACTOME_LOSS_OF_NLP_FROM_MITOTIC_CENTROSOME | 0.62439202 | 1.18621799 |
| GO:0010972 | negative regulation of G2/M transition of mitotic cell cycle | 0.84268001 | 1.186221728 |
| GO:0071371 | cellular response to gonadotropin stimulus | 0.62315364 | 1.186225345 |
| ENSG00000048540 | LMO3 subnetwork | 0.85368298 | 1.186226487 |
| ENSG00000113812 | ACTR8 subnetwork | 0.62488445 | 1.186226852 |
| GO:0014068 | positive regulation of phosphatidylinositol 3-kinase cascade | 0.85188131 | 1.186233617 |
| GO:0031269 | pseudopodium assembly | 0.85361753 | 1.186249045 |
| GO:0051593 | response to folic acid | 0.8517037 | 1.18625012 |
| GO:0016712 | oxidoreductase activity, acting on paired donors, with incor | 0.62477893 | 1.186257235 |
| ENSG00000213397 | HAUS7 subnetwork | 0.85182387 | 1.186261003 |
| ENSG00000104879 | CKM subnetwork | 0.85376854 | 1.186265992 |
| MP:0001938 | delayed sexual maturation | 0.62290737 | 1.186271602 |
| GO:0046939 | nucleotide phosphorylation | 0.84235102 | 1.186274415 |
| KEGG_PURINE_METABOLISM | KEGG_PURINE_METABOLISM | 0.62451939 | 1.186277663 |
| ENSG00000130592 | LSP1 subnetwork | 0.84263543 | 1.186292895 |
| REACTOME_TRANSCRIPTION | REACTOME_TRANSCRIPTION | 0.62285363 | 1.186295627 |
| GO:0000266 | mitochondrial fission | 0.85024958 | 1.186301764 |
| ENSG00000137642 | SORL1 subnetwork | 0.84970844 | 1.186313063 |
| GO:0000041 | transition metal ion transport | 0.85244824 | 1.186318004 |
| MP:0008657 | increased interleukin-1 beta secretion | 0.62191836 | 1.186319597 |
| ENSG00000106258 | CYP3A5 subnetwork | 0.62276274 | 1.186319659 |
| ENSG00000124789 | NUP153 subnetwork | 0.62230926 | 1.186321973 |
| MP:0000774 | decreased brain size | 0.8432725 | 1.186331144 |
| MP:0011495 | abnormal head shape | 0.62312942 | 1.186333161 |
| ENSG00000078668 | VDAC3 subnetwork | 0.85013913 | 1.186347076 |
| ENSG00000140525 | FANCI subnetwork | 0.62173669 | 1.186348365 |
| ENSG00000103351 | CLUAP1 subnetwork | 0.85331454 | 1.186348873 |
| GO:0009620 | response to fungus | 0.85169959 | 1.186349282 |
| ENSG00000211660 | ENSG00000211660 subnetwork | 0.62467008 | 1.186350187 |
| MP:0004145 | abnormal muscle electrophysiology | 0.84231602 | 1.18635045 |
| GO:0015721 | bile acid and bile salt transport | 0.85361514 | 1.186352784 |
| REACTOME_CELL_JUNCTION_C | REACTOME_CELL_JUNCTION_ORGANIZATION | 0.62385221 | 1.186360124 |
| ENSG00000168172 | HOOK3 subnetwork | 0.62378189 | 1.186364807 |
| ENSG00000176170 | SPHK1 subnetwork | 0.8502346 | 1.186367558 |
| ENSG00000184117 | NIPSNAP1 subnetwork | 0.84225713 | 1.186368472 |
| GO:0060053 | neurofilament cytoskeleton | 0.85344266 | 1.186369281 |
| REACTOME_LOSS_OF_PROTEIN | REACTOME_LOSS_OF_PROTEINS_REQUIRED_FOR_INTERPH | 0.62439202 | 1.186370656 |
| ENSG00000129824 | RPS4Y1 subnetwork | 0.84984046 | 1.186371919 |
| GO:0060205 | cytoplasmic membrane-bounded vesicle lumen | 0.84967287 | 1.186378897 |
| GO:0045599 | negative regulation of fat cell differentiation | 0.62431325 | 1.186381774 |
| ENSG00000184983 | NDUFA6 subnetwork | 0.85009892 | 1.186398504 |
| MP:0001011 | abnormal superior cervical ganglion morphology | 0.62307041 | 1.186402321 |
| ENSG00000106400 | ZNHIT1 subnetwork | 0.85256075 | 1.186414914 |
| GO:0015248 | sterol transporter activity | 0.8524276 | 1.186417097 |

| | | | |
|---|---|---|---|
| ENSG00000115866 | DARS subnetwork | 0.8535867 | 1.186427889 |
| ENSG00000138698 | RAP1GDS1 subnetwork | 0.85330244 | 1.186433553 |
| ENSG00000133216 | EPHB2 subnetwork | 0.85002659 | 1.186435558 |
| ENSG00000138308 | PLA2G12B subnetwork | 0.62229966 | 1.186436411 |
| ENSG00000123384 | LRP1 subnetwork | 0.84962405 | 1.18644954 |
| MP:0008807 | increased liver iron level | 0.62428962 | 1.186450824 |
| ENSG00000167996 | FTH1 subnetwork | 0.62191046 | 1.186453488 |
| GO:0010922 | positive regulation of phosphatase activity | 0.85322394 | 1.186470476 |
| ENSG00000021461 | CYP3A43 subnetwork | 0.62276274 | 1.186472713 |
| GO:0006144 | purine base metabolic process | 0.62422077 | 1.186474829 |
| ENSG00000185010 | F8 subnetwork | 0.8422401 | 1.186478383 |
| REACTOME_HEXOSE_TRANSPC | REACTOME_HEXOSE_TRANSPORT | 0.62266424 | 1.186483871 |
| ENSG00000169744 | LDB2 subnetwork | 0.84956826 | 1.186491413 |
| GO:0001539 | ciliary or flagellar motility | 0.85274068 | 1.186507026 |
| GO:0005769 | early endosome | 0.85314082 | 1.186507406 |
| ENSG00000115266 | APC2 subnetwork | 0.62254867 | 1.186512648 |
| GO:0032648 | regulation of interferon-beta production | 0.85240888 | 1.186516209 |
| MP:0010377 | abnormal gut flora balance | 0.62261692 | 1.186533746 |
| ENSG00000124535 | WRNIP1 subnetwork | 0.6224797 | 1.186536724 |
| GO:0000407 | pre-autophagosomal structure | 0.84419643 | 1.1865457 |
| GO:0035121 | tail morphogenesis | 0.84817265 | 1.186560638 |
| MP:0004182 | abnormal spermiation | 0.8486671 | 1.186573185 |
| ENSG00000037241 | RPL26L1 subnetwork | 0.85300965 | 1.186581286 |
| ENSG00000139433 | GLTP subnetwork | 0.62414716 | 1.186582539 |
| GO:0070936 | protein K48-linked ubiquitination | 0.85310962 | 1.186582569 |
| GO:0030216 | keratinocyte differentiation | 0.84223014 | 1.186588315 |
| ENSG00000101199 | ARFGAP1 subnetwork | 0.84443925 | 1.186596545 |
| ENSG00000105829 | BET1 subnetwork | 0.84956269 | 1.186600461 |
| ENSG00000170310 | STX8 subnetwork | 0.84435824 | 1.186614553 |
| ENSG00000143632 | ACTA1 subnetwork | 0.62408732 | 1.186619446 |
| REACTOME_G0_AND_EARLY_C | REACTOME_G0_AND_EARLY_G1 | 0.84948723 | 1.186623165 |
| REACTOME_ASSOCIATION_OF_ | REACTOME_ASSOCIATION_OF_LICENSING_FACTORS_WITH | 0.84838747 | 1.186625673 |
| ENSG00000160062 | ZBTB8A subnetwork | 0.84938854 | 1.186626679 |
| ENSG00000167880 | EVPL subnetwork | 0.8441922 | 1.186650579 |
| ENSG00000115947 | ORC4 subnetwork | 0.848329 | 1.186653214 |
| GO:0060389 | pathway-restricted SMAD protein phosphorylation | 0.85299232 | 1.186666029 |
| ENSG00000197728 | RPS26 subnetwork | 0.84817163 | 1.186674676 |
| ENSG00000010256 | UQCRC1 subnetwork | 0.84858031 | 1.186681076 |
| MP:0005423 | abnormal somatic nervous system physiology | 0.84866542 | 1.186687158 |
| ENSG00000156110 | ADK subnetwork | 0.84935251 | 1.186687782 |
| ENSG00000086827 | ZW10 subnetwork | 0.84221444 | 1.186698268 |
| ENSG00000116106 | EPHA4 subnetwork | 0.84917271 | 1.186731951 |
| GO:0008211 | glucocorticoid metabolic process | 0.84925272 | 1.186733225 |
| MP:0001297 | microphthalmia | 0.84460917 | 1.18674257 |
| GO:0051648 | vesicle localization | 0.84416311 | 1.186755478 |
| ENSG00000130396 | MLLT4 subnetwork | 0.84216245 | 1.186774381 |
| GO:0006415 | translational termination | 0.84158422 | 1.186775099 |
| REACTOME_REGULATION_OF_ | REACTOME_REGULATION_OF_INSULIN_SECRETION_BY_GL | 0.84480953 | 1.186783716 |
| ENSG00000196656 | ENSG00000196656 subnetwork | 0.84817163 | 1.186788735 |
| GO:0008209 | androgen metabolic process | 0.84150568 | 1.186793184 |
| GO:0034502 | protein localization to chromosome | 0.84857952 | 1.186795081 |
| ENSG00000100461 | RBM23 subnetwork | 0.84894503 | 1.186800154 |
| GO:0005930 | axoneme | 0.84740076 | 1.186801347 |

| | | | |
|---|---|---|---|
| GO:0071285 | cellular response to lithium ion | 0.8493525 | 1.186801689 |
| ENSG00000014138 | POLA2 subnetwork | 0.84373464 | 1.186805757 |
| ENSG00000188428 | MUTED subnetwork | 0.84395983 | 1.186814407 |
| GO:0015918 | sterol transport | 0.84810191 | 1.186816303 |
| MP:0003632 | abnormal nervous system morphology | 0.84389976 | 1.18682762 |
| REACTOME_FORMATION_OF_ | REACTOME_FORMATION_OF_A_POOL_OF_FREE_40S_SUB | 0.84803405 | 1.186829456 |
| ENSG00000089169 | RPH3A subnetwork | 0.84915471 | 1.186836294 |
| GO:0002577 | regulation of antigen processing and presentation | 0.84792983 | 1.186842611 |
| ENSG00000066933 | MYO9A subnetwork | 0.84413891 | 1.186845916 |
| ENSG00000107290 | SETX subnetwork | 0.84906812 | 1.186849433 |
| ENSG00000118402 | ELOVL4 subnetwork | 0.84384608 | 1.186860151 |
| ENSG00000154723 | ATP5J subnetwork | 0.84704534 | 1.186863632 |
| ENSG00000106366 | SERPINE1 subnetwork | 0.84181289 | 1.186864776 |
| ENSG00000171560 | FGA subnetwork | 0.84214782 | 1.186865022 |
| ENSG00000172638 | EFEMP2 subnetwork | 0.84758791 | 1.18688564 |
| ENSG00000137996 | RTCD1 subnetwork | 0.84480766 | 1.186888567 |
| GO:0008334 | histone mRNA metabolic process | 0.84698809 | 1.186891242 |
| GO:0042246 | tissue regeneration | 0.84147363 | 1.18689358 |
| ENSG00000168477 | TNXB subnetwork | 0.84140415 | 1.186906837 |
| GO:0055070 | copper ion homeostasis | 0.84739551 | 1.186910718 |
| GO:0009072 | aromatic amino acid family metabolic process | 0.84694334 | 1.186933295 |
| MP:0005217 | abnormal pancreatic beta cell morphology | 0.84202733 | 1.186935062 |
| GO:0002064 | epithelial cell development | 0.842119 | 1.186936327 |
| ENSG00000149806 | FAU subnetwork | 0.84412339 | 1.186936372 |
| ENSG00000181104 | F2R subnetwork | 0.84542688 | 1.186940802 |
| ENSG00000062725 | APPBP2 subnetwork | 0.84791753 | 1.186942308 |
| ENSG00000153767 | GTF2E1 subnetwork | 0.6262341 | 1.186946192 |
| ENSG00000087303 | NID2 subnetwork | 0.84724571 | 1.186956313 |
| ENSG00000115241 | PPM1G subnetwork | 0.84733564 | 1.186957568 |
| ENSG00000181072 | CHRM2 subnetwork | 0.84787477 | 1.186960285 |
| KEGG_DRUG_METABOLISM_C | KEGG_DRUG_METABOLISM_CYTOCHROME_P450 | 0.84195799 | 1.186962834 |
| GO:0034364 | high-density lipoprotein particle | 0.62636663 | 1.186967129 |
| REACTOME_PROCESSING_OF_ | REACTOME_PROCESSING_OF_INTRONLESS_PRE:MRNAS | 0.84519953 | 1.186970778 |
| KEGG_NITROGEN_METABOLISI | KEGG_NITROGEN_METABOLISM | 0.84180665 | 1.186974831 |
| MP:0010878 | increased trabecular bone volume | 0.84778062 | 1.186983074 |
| GO:0043028 | cysteine-type endopeptidase regulator activity involved in a | 0.84758612 | 1.186994998 |
| GO:0070498 | interleukin-1-mediated signaling pathway | 0.84690092 | 1.186999422 |
| GO:0008378 | galactosyltransferase activity | 0.84677745 | 1.187007798 |
| MP:0003938 | abnormal ear development | 0.84572457 | 1.187021687 |
| MP:0002625 | heart left ventricle hypertrophy | 0.84140229 | 1.187021792 |
| GO:0008207 | C21-steroid hormone metabolic process | 0.62646742 | 1.187026576 |
| ENSG00000069329 | VPS35 subnetwork | 0.845327 | 1.187029894 |
| GO:0045333 | cellular respiration | 0.84516427 | 1.187037037 |
| MP:0003354 | astrocytosis | 0.84556957 | 1.187038465 |
| ENSG00000163288 | GABRB1 subnetwork | 0.84541076 | 1.187045608 |
| ENSG00000143627 | PKLR subnetwork | 0.84673102 | 1.187049875 |
| GO:0002495 | antigen processing and presentation of peptide antigen via | 0.84055052 | 1.187055173 |
| GO:0042074 | cell migration involved in gastrulation | 0.84581033 | 1.187056669 |
| GO:0006869 | lipid transport | 0.84048073 | 1.187068464 |
| ENSG00000198910 | L1CAM subnetwork | 0.84567723 | 1.187083092 |
| MP:0009115 | abnormal fat cell morphology | 0.84668279 | 1.187116033 |
| ENSG00000102391 | ENSG00000102391 subnetwork | 0.84044933 | 1.187120551 |
| ENSG00000147044 | CASK subnetwork | 0.84139759 | 1.187131926 |

| | | | |
|---|---|---|---|
| ENSG00000109390 | NDUFC1 subnetwork | 0.8463614 | 1.187139967 |
| GO:0048029 | monosaccharide binding | 0.845151 | 1.187141893 |
| GO:0047555 | 3',5'-cyclic-GMP phosphodiesterase activity | 0.84040437 | 1.1871484 |
| MP:0006027 | impaired lung alveolus development | 0.84603609 | 1.187149465 |
| MP:0002886 | abnormal glutamate-mediated receptor currents | 0.84663627 | 1.187158128 |
| REACTOME_TRANSPORT_OF_M | REACTOME_TRANSPORT_OF_MATURE_MRNAS_DERIVED_ | 0.62665173 | 1.18716303 |
| GO:0060716 | labyrinthine layer blood vessel development | 0.84135277 | 1.187169427 |
| MP:0000832 | abnormal thalamus morphology | 0.84620979 | 1.187176029 |
| ENSG00000211893 | ENSG00000211893 subnetwork | 0.84630831 | 1.187206166 |
| ENSG00000053918 | KCNQ1 subnetwork | 0.84660917 | 1.187214678 |
| ENSG00000171724 | VAT1L subnetwork | 0.62688125 | 1.187219299 |
| ENSG00000160285 | LSS subnetwork | 0.84133103 | 1.187240845 |
| MP:0005029 | abnormal amnion morphology | 0.84616291 | 1.187247061 |
| ENSG00000118137 | APOA1 subnetwork | 0.84038908 | 1.187249006 |
| MP:0011097 | complete embryonic lethality before turning of embryo | 0.84076204 | 1.18726973 |
| GO:0015300 | solute:solute antiporter activity | 0.84654378 | 1.187271239 |
| GO:0043486 | histone exchange | 0.62677408 | 1.187280195 |
| ENSG00000103549 | RNF40 subnetwork | 0.62685114 | 1.187333162 |
| GO:0032069 | regulation of nuclease activity | 0.84133096 | 1.187355876 |
| ENSG00000138081 | FBXO11 subnetwork | 0.84124123 | 1.187359496 |
| ENSG00000215756 | ENSG00000215756 subnetwork | 0.84038908 | 1.187364183 |
| MP:0000522 | kidney cortex cysts | 0.84110786 | 1.187384899 |
| ENSG00000107779 | BMPR1A subnetwork | 0.62971229 | 1.18740736 |
| ENSG00000178184 | PARD6G subnetwork | 0.63288444 | 1.187407831 |
| ENSG00000206340 | C4A subnetwork | 0.63053844 | 1.18741705 |
| GO:0022904 | respiratory electron transport chain | 0.84105955 | 1.187422451 |
| ENSG00000138771 | SHROOM3 subnetwork | 0.62966003 | 1.187444089 |
| MP:0000433 | microcephaly | 0.62981047 | 1.187447298 |
| GO:0008299 | isoprenoid biosynthetic process | 0.83975848 | 1.187456311 |
| ENSG00000170445 | HARS subnetwork | 0.84036796 | 1.187459979 |
| GO:0009127 | purine nucleoside monophosphate biosynthetic process | 0.84123572 | 1.187464871 |
| REACTOME_REDUCTION_OF_C | REACTOME_REDUCTION_OF_CYTOSOLIC_CA_LEVELS | 0.6274397 | 1.18748397 |
| MP:0003935 | abnormal craniofacial development | 0.6272 | 1.187491982 |
| ENSG00000065618 | COL17A1 subnetwork | 0.62960813 | 1.187512781 |
| ENSG00000112936 | C7 subnetwork | 0.63286705 | 1.187520661 |
| ENSG00000163207 | IVL subnetwork | 0.84105514 | 1.187532719 |
| REACTOME_ADVANCED_GLYC | REACTOME_ADVANCED_GLYCOSYLATION_ENDPRODUCT_F | 0.84035297 | 1.18754609 |
| GO:0006637 | acyl-CoA metabolic process | 0.63052786 | 1.187549458 |
| ENSG00000160194 | NDUFV3 subnetwork | 0.83975063 | 1.18755219 |
| GO:0016859 | cis-trans isomerase activity | 0.62731664 | 1.187557722 |
| ENSG00000127831 | VIL1 subnetwork | 0.63279878 | 1.187563581 |
| GO:0009168 | purine ribonucleoside monophosphate biosynthetic proces | 0.84123572 | 1.187579957 |
| GO:0007019 | microtubule depolymerization | 0.63035691 | 1.187584578 |
| REACTOME_LAGGING_STRAND | REACTOME_LAGGING_STRAND_SYNTHESIS | 0.62719079 | 1.187605851 |
| ENSG00000105298 | C19orf29 subnetwork | 0.62742231 | 1.187610619 |
| GO:0070566 | adenylyltransferase activity | 0.83969767 | 1.187618955 |
| GO:0015804 | neutral amino acid transport | 0.84032417 | 1.187637069 |
| MP:0008108 | abnormal small intestinal villus morphology | 0.62960573 | 1.187664579 |
| ENSG00000139626 | ITGB7 subnetwork | 0.83964958 | 1.187680878 |
| MP:0005399 | increased susceptibility to fungal infection | 0.63033766 | 1.187697906 |
| GO:0035383 | thioester metabolic process | 0.63052786 | 1.187701047 |
| GO:0043921 | modulation by host of viral transcription | 0.63278897 | 1.187714613 |
| GO:0006694 | steroid biosynthetic process | 0.6315889 | 1.187727794 |

| | | | |
|---|---|---|---|
| MP:0004989 | decreased osteoblast cell number | 0.8402959 | 1.187737772 |
| ENSG00000106263 | EIF3B subnetwork | 0.63152559 | 1.187751721 |
| GO:0033630 | positive regulation of cell adhesion mediated by integrin | 0.63028349 | 1.187753799 |
| MP:0000933 | abnormal rhombomere morphology | 0.63000518 | 1.18776188 |
| GO:0060425 | lung morphogenesis | 0.63082839 | 1.187775935 |
| GO:0045271 | respiratory chain complex I | 0.83963903 | 1.187781663 |
| GO:0045684 | positive regulation of epidermis development | 0.63009556 | 1.187782603 |
| GO:0042770 | signal transduction in response to DNA damage | 0.62959001 | 1.187784454 |
| REACTOME_CELL_CYCLE | REACTOME_CELL_CYCLE | 0.62765758 | 1.187786896 |
| GO:0005852 | eukaryotic translation initiation factor 3 complex | 0.63320789 | 1.187847973 |
| GO:0051635 | bacterial cell surface binding | 0.84028764 | 1.1878482 |
| GO:0048002 | antigen processing and presentation of peptide antigen | 0.63024876 | 1.187860792 |
| GO:0017153 | sodium:dicarboxylate symporter activity | 0.8401532 | 1.187865256 |
| GO:0052472 | modulation by host of symbiont transcription | 0.63278897 | 1.187865683 |
| GO:0051354 | negative regulation of oxidoreductase activity | 0.62957663 | 1.187891574 |
| GO:0001614 | purinergic nucleotide receptor activity | 0.63150667 | 1.18789675 |
| GO:0030964 | NADH dehydrogenase complex | 0.83963903 | 1.187897037 |
| ENSG00000114982 | KANSL3 subnetwork | 0.63121012 | 1.187909705 |
| MP:0004763 | absent brainstem auditory evoked potential | 0.62870888 | 1.187912932 |
| ENSG00000130811 | EIF3G subnetwork | 0.84026352 | 1.187919821 |
| GO:0006997 | nucleus organization | 0.63109027 | 1.187957648 |
| REACTOME_CHOLESTEROL_BIO | REACTOME_CHOLESTEROL_BIOSYNTHESIS | 0.63136085 | 1.187962255 |
| ENSG00000096467 | ENSG00000096467 subnetwork | 0.62953994 | 1.18797954 |
| ENSG00000121741 | ZMYM2 subnetwork | 0.62865425 | 1.187994622 |
| ENSG00000137474 | MYO7A subnetwork | 0.63117555 | 1.187997449 |
| MP:0001899 | absent long term depression | 0.63277845 | 1.188004071 |
| GO:0005343 | organic acid:sodium symporter activity | 0.83955837 | 1.188006412 |
| GO:0005747 | mitochondrial respiratory chain complex I | 0.83963903 | 1.188012434 |
| ENSG00000130147 | SH3BP4 subnetwork | 0.63102807 | 1.188019903 |
| ENSG00000164270 | HTR4 subnetwork | 0.62796273 | 1.188027176 |
| GO:0048569 | post-embryonic organ development | 0.62803824 | 1.188035119 |
| GO:0016502 | nucleotide receptor activity | 0.63150667 | 1.18804819 |
| ENSG00000149743 | TRPT1 subnetwork | 0.62811533 | 1.188075099 |
| ENSG00000100796 | SMEK1 subnetwork | 0.63405344 | 1.18807619 |
| MP:0000284 | double outlet heart right ventricle | 0.63397193 | 1.188093726 |
| ENSG00000070814 | TCOF1 subnetwork | 0.63273442 | 1.188097964 |
| MP:0004632 | abnormal cochlear OHC efferent innervation pattern | 0.63146542 | 1.188104042 |
| ENSG00000135940 | COX5B subnetwork | 0.62861378 | 1.18810835 |
| ENSG00000125538 | IL1B subnetwork | 0.62790483 | 1.188115385 |
| ENSG00000184408 | KCND2 subnetwork | 0.63388027 | 1.188117617 |
| ENSG00000120907 | ADRA1A subnetwork | 0.83955771 | 1.188121842 |
| ENSG00000204427 | ABHD16A subnetwork | 0.62953994 | 1.188131475 |
| GO:0042058 | regulation of epidermal growth factor receptor signaling pa | 0.63345183 | 1.18814184 |
| MP:0005202 | lethargy | 0.63378803 | 1.188154217 |
| ENSG00000106804 | C5 subnetwork | 0.63364301 | 1.18815756 |
| ENSG00000197597 | ENSG00000197597 subnetwork | 0.63372806 | 1.188159065 |
| ENSG00000124702 | KLHDC3 subnetwork | 0.62857691 | 1.188170872 |
| ENSG00000130702 | LAMA5 subnetwork | 0.63430767 | 1.188180779 |
| MP:0008720 | impaired neutrophil chemotaxis | 0.83951191 | 1.188188709 |
| GO:0008144 | drug binding | 0.62850063 | 1.188201384 |
| ENSG00000120868 | APAF1 subnetwork | 0.6327205 | 1.188223693 |
| GO:0048511 | rhythmic process | 0.63442522 | 1.188239401 |
| ENSG00000126803 | HSPA2 subnetwork | 0.63361762 | 1.188245012 |

| | | | |
|---|---|---|---|
| GO:0050821 | protein stabilization | 0.63268598 | 1.188254009 |
| MP:0004214 | abnormal long bone diaphysis morphology | 0.63426265 | 1.188261808 |
| ENSG00000206403 | ABHD16A subnetwork | 0.62953994 | 1.188283448 |
| MP:0004556 | enlarged allantois | 0.83950264 | 1.188289602 |
| GO:2000117 | negative regulation of cysteine-type endopeptidase activity | 0.62844752 | 1.188308776 |
| GO:0022804 | active transmembrane transporter activity | 0.634546 | 1.188336083 |
| REACTOME_REMOVAL_OF_TH | REACTOME_REMOVAL_OF_THE_FLAP_INTERMEDIATE | 0.63266161 | 1.188341606 |
| GO:0004835 | tubulin-tyrosine ligase activity | 0.62908552 | 1.188351254 |
| ENSG00000106348 | IMPDH1 subnetwork | 0.63251117 | 1.188383195 |
| GO:0009792 | embryo development ending in birth or egg hatching | 0.63467008 | 1.188388325 |
| ENSG00000132424 | PNISR subnetwork | 0.62951634 | 1.188390687 |
| GO:0060441 | epithelial tube branching involved in lung morphogenesis | 0.83947518 | 1.188395374 |
| ENSG00000197785 | ATAD3A subnetwork | 0.62842845 | 1.188429011 |
| GO:0033178 | proton-transporting two-sector ATPase complex, catalytic c | 0.63246713 | 1.188439012 |
| GO:0034728 | nucleosome organization | 0.62902668 | 1.188445782 |
| REACTOME_MITOTIC_G1:G1S_ | REACTOME_MITOTIC_G1:G1S_PHASES | 0.62919616 | 1.188448739 |
| ENSG00000148175 | STOM subnetwork | 0.63479581 | 1.188453242 |
| KEGG_REGULATION_OF_ACTIN | KEGG_REGULATION_OF_ACTIN_CYTOSKELETON | 0.62936494 | 1.188470889 |
| ENSG00000163634 | THOC7 subnetwork | 0.63765336 | 1.188488754 |
| ENSG00000211592 | ENSG00000211592 subnetwork | 0.62947032 | 1.188491556 |
| ENSG00000111245 | MYL2 subnetwork | 0.63265965 | 1.188492872 |
| ENSG00000141564 | RPTOR subnetwork | 0.83945326 | 1.188501166 |
| ENSG00000128951 | DUT subnetwork | 0.6324328 | 1.188520311 |
| MP:0008034 | enhanced lipolysis | 0.62931655 | 1.188520604 |
| ENSG00000105664 | COMP subnetwork | 0.6377486 | 1.188521794 |
| GO:0006487 | protein N-linked glycosylation | 0.83937393 | 1.188524351 |
| GO:0009164 | nucleoside catabolic process | 0.63500317 | 1.18854497 |
| KEGG_FOLATE_BIOSYNTHESIS | KEGG_FOLATE_BIOSYNTHESIS | 0.63508119 | 1.188559107 |
| GO:0008601 | protein phosphatase type 2A regulator activity | 0.63517098 | 1.188566899 |
| GO:0019213 | deacetylase activity | 0.63492753 | 1.188581578 |
| ENSG00000182636 | NDN subnetwork | 0.6378434 | 1.188592724 |
| MP:0003921 | abnormal heart left ventricle morphology | 0.8384339 | 1.188623978 |
| GO:0006873 | cellular ion homeostasis | 0.63764686 | 1.188626311 |
| MP:0005547 | abnormal Muller cell morphology | 0.83936146 | 1.188630177 |
| ENSG00000114391 | RPL24 subnetwork | 0.63668849 | 1.18864988 |
| ENSG00000006740 | ARHGAP44 subnetwork | 0.63241963 | 1.188652573 |
| ENSG00000038002 | AGA subnetwork | 0.6321251 | 1.188659531 |
| ENSG00000158528 | PPP1R9A subnetwork | 0.63924063 | 1.188662717 |
| MP:0009454 | impaired contextual conditioning behavior | 0.63220275 | 1.188667346 |
| GO:0045834 | positive regulation of lipid metabolic process | 0.63845383 | 1.18867365 |
| MP:0003890 | abnormal embryonic-extraembryonic boundary morpholog | 0.8384002 | 1.188690998 |
| GO:0032391 | photoreceptor connecting cilium | 0.63679582 | 1.188695597 |
| ENSG00000115414 | FN1 subnetwork | 0.83894439 | 1.188707324 |
| GO:0031529 | ruffle organization | 0.83882714 | 1.188709991 |
| MP:0000606 | decreased hepatocyte number | 0.63530547 | 1.188733198 |
| GO:0016655 | oxidoreductase activity, acting on NADH or NADPH, quinon | 0.83935644 | 1.188736023 |
| ENSG00000099860 | GADD45B subnetwork | 0.63856446 | 1.18873817 |
| MP:0005179 | decreased circulating cholesterol level | 0.63763117 | 1.188738625 |
| GO:0001702 | gastrulation with mouth forming second | 0.63237337 | 1.188740288 |
| GO:0009566 | fertilization | 0.63541191 | 1.188747306 |
| MP:0005405 | axon degeneration | 0.63918868 | 1.188749527 |
| ENSG00000058262 | SEC61A1 subnetwork | 0.63910861 | 1.188754413 |
| GO:0048557 | embryonic digestive tract morphogenesis | 0.63660506 | 1.188754588 |

| | | | |
|---|---|---|---|
| GO:0046906 | tetrapyrrole binding | 0.63666259 | 1.188756011 |
| ENSG00000005961 | ITGA2B subnetwork | 0.63756889 | 1.188768803 |
| GO:0019953 | sexual reproduction | 0.83891279 | 1.188769455 |
| ENSG00000107611 | CUBN subnetwork | 0.8383656 | 1.188782363 |
| GO:0005916 | fascia adherens | 0.8387805 | 1.188786729 |
| GO:0006891 | intra-Golgi vesicle-mediated transport | 0.63716269 | 1.188801062 |
| MP:0005244 | hemopericardium | 0.63844609 | 1.188804746 |
| GO:0010970 | microtubule-based transport | 0.63698553 | 1.188823529 |
| GO:0006544 | glycine metabolic process | 0.6374862 | 1.188843236 |
| GO:0010717 | regulation of epithelial to mesenchymal transition | 0.83935548 | 1.188851614 |
| ENSG00000179364 | PACS2 subnetwork | 0.63819265 | 1.188855916 |
| ENSG00000155561 | NUP205 subnetwork | 0.83834551 | 1.188864012 |
| MP:0002914 | abnormal endplate potential | 0.6383273 | 1.188871355 |
| ENSG00000083750 | RRAGB subnetwork | 0.63659886 | 1.188879747 |
| ENSG00000145649 | GZMA subnetwork | 0.83874237 | 1.188882942 |
| ENSG00000064601 | CTSA subnetwork | 0.63811761 | 1.188886082 |
| ENSG00000116833 | NR5A2 subnetwork | 0.63237144 | 1.18889172 |
| ENSG00000186230 | ZNF749 subnetwork | 0.83931136 | 1.188894292 |
| ENSG00000165476 | REEP3 subnetwork | 0.63910361 | 1.188897995 |
| REACTOME_HORMONE:SENSIT | REACTOME_HORMONE:SENSITIVE_LIPASE_HSL:MEDIATED_ | 0.63558431 | 1.18891354 |
| ENSG00000137672 | TRPC6 subnetwork | 0.63742154 | 1.188924011 |
| REACTOME_SIGNALLING_TO_E | REACTOME_SIGNALLING_TO_ERKS | 0.63949387 | 1.188928796 |
| ENSG00000171873 | ADRA1D subnetwork | 0.63715518 | 1.188938781 |
| ENSG00000179841 | AKAP5 subnetwork | 0.83830794 | 1.188945678 |
| ENSG00000198951 | NAGA subnetwork | 0.63844137 | 1.188948498 |
| MP:0008874 | decreased physiological sensitivity to xenobiotic | 0.83925254 | 1.188956429 |
| GO:0005901 | caveola | 0.83821596 | 1.188959206 |
| ENSG00000035862 | TIMP2 subnetwork | 0.63905088 | 1.188984868 |
| GO:2000242 | negative regulation of reproductive process | 0.83816694 | 1.18899221 |
| GO:0003179 | heart valve morphogenesis | 0.63651269 | 1.188997214 |
| ENSG00000127586 | CHTF18 subnetwork | 0.63657974 | 1.188998607 |
| ENSG00000007171 | NOS2 subnetwork | 0.6389987 | 1.189002396 |
| MP:0001306 | small lens | 0.63891113 | 1.189007316 |
| GO:0070207 | protein homotrimerization | 0.63832622 | 1.189008838 |
| ENSG00000146007 | ZMAT2 subnetwork | 0.6363567 | 1.189019757 |
| KEGG_GLYCOSAMINOGLYCAN_ | KEGG_GLYCOSAMINOGLYCAN_DEGRADATION | 0.63810425 | 1.189029936 |
| REACTOME_PROCESSIVE_SYNT | REACTOME_PROCESSIVE_SYNTHESIS_ON_THE_LAGGING_S | 0.63739462 | 1.189030096 |
| ENSG00000182400 | TRAPPC6B subnetwork | 0.64036051 | 1.18905601 |
| MP:0001925 | male infertility | 0.63644027 | 1.189065468 |
| ENSG00000049283 | EPN3 subnetwork | 0.63887732 | 1.189069005 |
| ENSG00000114302 | PRKAR2A subnetwork | 0.63881948 | 1.189073934 |
| GO:0032526 | response to retinoic acid | 0.8381621 | 1.189103126 |
| ENSG00000063322 | MED29 subnetwork | 0.63623539 | 1.189111984 |
| MP:0004910 | decreased seminal vesicle weight | 0.63578783 | 1.189117759 |
| ENSG00000115484 | CCT4 subnetwork | 0.63970829 | 1.189157006 |
| GO:0016634 | oxidoreductase activity, acting on the CH-CH group of dono | 0.63634315 | 1.189157695 |
| ENSG00000031823 | RANBP3 subnetwork | 0.83812547 | 1.189160499 |
| GO:0006921 | cellular component disassembly involved in apoptotic proce | 0.83669416 | 1.189186421 |
| MP:0003393 | decreased cardiac output | 0.64034009 | 1.189186808 |
| ENSG00000133030 | MPRIP subnetwork | 0.83666665 | 1.189229268 |
| ENSG00000071243 | ING3 subnetwork | 0.63622559 | 1.189262638 |
| ENSG00000061337 | LZTS1 subnetwork | 0.83811957 | 1.189271452 |
| MP:0004704 | short vertebral column | 0.83662289 | 1.189277003 |

| | | | |
|---|---|---|---|
| ENSG00000168907 | PLA2G4F subnetwork | 0.83653319 | 1.189280835 |
| ENSG00000163931 | TKT subnetwork | 0.83684704 | 1.189299649 |
| ENSG00000175189 | INHBC subnetwork | 0.83698954 | 1.189306612 |
| ENSG00000165029 | ABCA1 subnetwork | 0.64032249 | 1.189317638 |
| ENSG00000047056 | WDR37 subnetwork | 0.83809171 | 1.189358075 |
| MP:0002258 | abnormal cricoid cartilage morphology | 0.8371003 | 1.189361287 |
| ENSG00000118181 | RPS25 subnetwork | 0.83696028 | 1.189378718 |
| GO:0030968 | endoplasmic reticulum unfolded protein response | 0.64010632 | 1.189382872 |
| GO:0072234 | metanephric nephron tubule development | 0.83757276 | 1.189385965 |
| MP:0009038 | decreased inferior colliculus size | 0.83652889 | 1.189392017 |
| REACTOME_SCFSKP2:MEDIATE | REACTOME_SCFSKP2:MEDIATED_DEGRADATION_OF_P27P | 0.64158553 | 1.189392987 |
| ENSG00000105289 | TJP3 subnetwork | 0.83732559 | 1.189397485 |
| MP:0001008 | abnormal sympathetic ganglion morphology | 0.83804093 | 1.189405748 |
| ENSG00000099800 | TIMM13 subnetwork | 0.63622257 | 1.189406994 |
| GO:0015085 | calcium ion transmembrane transporter activity | 0.64019743 | 1.189409394 |
| MP:0001636 | irregular heartbeat | 0.63991288 | 1.189435555 |
| GO:0006885 | regulation of pH | 0.83647157 | 1.189449541 |
| ENSG00000044115 | CTNNA1 subnetwork | 0.64031588 | 1.189461093 |
| REACTOME_TIE2_SIGNALING | REACTOME_TIE2_SIGNALING | 0.83746201 | 1.189466758 |
| ENSG00000197530 | MIB2 subnetwork | 0.64172154 | 1.189482282 |
| GO:0005275 | amine transmembrane transporter activity | 0.83730865 | 1.18948908 |
| GO:0072243 | metanephric nephron epithelium development | 0.83757276 | 1.189501901 |
| GO:0046825 | regulation of protein export from nucleus | 0.64183443 | 1.189515014 |
| GO:0006895 | Golgi to endosome transport | 0.83802204 | 1.189516758 |
| GO:0060039 | pericardium development | 0.63621135 | 1.189519706 |
| GO:0010466 | negative regulation of peptidase activity | 0.64158141 | 1.18952363 |
| ENSG00000114854 | TNNC1 subnetwork | 0.83642366 | 1.189526598 |
| GO:0034620 | cellular response to unfolded protein | 0.64010632 | 1.189532687 |
| REACTOME_CDC6_ASSOCIATIC | REACTOME_CDC6_ASSOCIATION_WITH_THE_ORCORIGIN_ | 0.64140425 | 1.189533568 |
| MP:0000149 | abnormal scapula morphology | 0.6413633 | 1.189601408 |
| REACTOME_PYRIMIDINE_CATA | REACTOME_PYRIMIDINE_CATABOLISM | 0.83640131 | 1.18960367 |
| GO:0008528 | G-protein coupled peptide receptor activity | 0.83799963 | 1.189608302 |
| GO:0048873 | homeostasis of number of cells within a tissue | 0.6419534 | 1.189610553 |
| ENSG00000129084 | PSMA1 subnetwork | 0.63617555 | 1.189626109 |
| MP:0002427 | disproportionate dwarf | 0.64008035 | 1.189644747 |
| ENSG00000100241 | SBF1 subnetwork | 0.64154737 | 1.18964802 |
| ENSG00000153933 | DGKE subnetwork | 0.64125134 | 1.189655389 |
| GO:0007033 | vacuole organization | 0.64650452 | 1.189659261 |
| GO:0000976 | transcription regulatory region sequence-specific DNA bind | 0.64643987 | 1.189664212 |
| MP:0002280 | abnormal intercostal muscle morphology | 0.64556676 | 1.18967629 |
| ENSG00000144218 | AFF3 subnetwork | 0.64245793 | 1.189686127 |
| GO:0008272 | sulfate transport | 0.64119305 | 1.189691824 |
| ENSG00000165629 | ATP5C1 subnetwork | 0.64659753 | 1.189697991 |
| ENSG00000154518 | ATP5G3 subnetwork | 0.64133755 | 1.189700704 |
| ENSG00000131495 | NDUFA2 subnetwork | 0.83798924 | 1.189704736 |
| ENSG00000175334 | BANF1 subnetwork | 0.64220941 | 1.18971364 |
| GO:0048538 | thymus development | 0.83639781 | 1.189719809 |
| ENSG00000105438 | KDELR1 subnetwork | 0.64111252 | 1.189721978 |
| ENSG00000135631 | RAB11FIP5 subnetwork | 0.64553898 | 1.18973125 |
| GO:0019722 | calcium-mediated signaling | 0.64604911 | 1.1897327 |
| ENSG00000100364 | KIAA0930 subnetwork | 0.64640965 | 1.189750312 |
| GO:0033261 | regulation of S phase | 0.6421619 | 1.189781434 |
| ENSG00000081014 | AP4E1 subnetwork | 0.83796396 | 1.189806062 |

| | | | |
|---|---|---|---|
| ENSG00000102572 | STK24 subnetwork | 0.64600581 | 1.189806371 |
| ENSG00000140326 | CDAN1 subnetwork | 0.64244279 | 1.189810397 |
| ENSG00000101160 | CTSZ subnetwork | 0.83637843 | 1.18981156 |
| GO:0002827 | positive regulation of T-helper 1 type immune response | 0.83621501 | 1.189814453 |
| KEGG_NUCLEOTIDE_EXCISION_ | KEGG_NUCLEOTIDE_EXCISION_REPAIR | 0.64106241 | 1.18983392 |
| ENSG00000077063 | CTTNBP2 subnetwork | 0.6458605 | 1.189835062 |
| MP:0004722 | abnormal platelet dense granule number | 0.64549485 | 1.18983623 |
| ENSG00000183625 | CCR3 subnetwork | 0.6435716 | 1.189839539 |
| REACTOME_SEMA3A:PLEXIN_F | REACTOME_SEMA3A:PLEXIN_REPULSION_SIGNALING_BY_I | 0.64594644 | 1.189848826 |
| ENSG00000105991 | HOXA1 subnetwork | 0.836327 | 1.189854506 |
| REACTOME_ABCA_TRANSPORT | REACTOME_ABCA_TRANSPORTERS_IN_LIPID_HOMEOSTAS | 0.64090592 | 1.189856532 |
| ENSG00000183283 | DAZAP2 subnetwork | 0.64324018 | 1.189859526 |
| REACTOME_PROCESSIVE_SYNT | REACTOME_PROCESSIVE_SYNTHESIS_ON_THE_C:STRAND_ | 0.64674287 | 1.189861492 |
| GO:0016894 | endonuclease activity, active with either ribo- or deoxyribo | 0.64496008 | 1.189864865 |
| ENSG00000162402 | USP24 subnetwork | 0.64260397 | 1.189869445 |
| ENSG00000131473 | ACLY subnetwork | 0.64619103 | 1.189883852 |
| GO:0006957 | complement activation, alternative pathway | 0.64639613 | 1.189886378 |
| MP:0000484 | abnormal pulmonary artery morphology | 0.64340501 | 1.189899687 |
| ENSG00000131023 | LATS1 subnetwork | 0.64101166 | 1.18990185 |
| ENSG00000135999 | EPC2 subnetwork | 0.64488871 | 1.189907396 |
| GO:0015813 | L-glutamate transport | 0.83595383 | 1.189909153 |
| GO:0046364 | monosaccharide biosynthetic process | 0.6450538 | 1.189909921 |
| GO:0021575 | hindbrain morphogenesis | 0.64471987 | 1.189917386 |
| ENSG00000164076 | CAMKV subnetwork | 0.64522175 | 1.189918699 |
| ENSG00000104549 | SQLE subnetwork | 0.83620765 | 1.189925774 |
| ENSG00000105669 | COPE subnetwork | 0.64354307 | 1.189944835 |
| GO:0032869 | cellular response to insulin stimulus | 0.83582751 | 1.189946263 |
| ENSG00000119969 | HELLS subnetwork | 0.64689371 | 1.189956332 |
| ENSG00000112379 | KIAA1244 subnetwork | 0.64244081 | 1.189959814 |
| ENSG00000109519 | GRPEL1 subnetwork | 0.83611219 | 1.18996386 |
| ENSG00000135097 | MSI1 subnetwork | 0.64585235 | 1.189977506 |
| ENSG00000160613 | PCSK7 subnetwork | 0.64517302 | 1.189979985 |
| GO:0010817 | regulation of hormone levels | 0.83591979 | 1.189981438 |
| MP:0002947 | hemangioma | 0.64548734 | 1.189984996 |
| GO:0010869 | regulation of receptor biosynthetic process | 0.64337232 | 1.189986205 |
| GO:0070873 | regulation of glycogen metabolic process | 0.64321202 | 1.189989965 |
| MP:0003178 | left pulmonary isomerism | 0.64539196 | 1.190002501 |
| ENSG00000120697 | ALG5 subnetwork | 0.6453418 | 1.190013757 |
| ENSG00000101558 | VAPA subnetwork | 0.8357083 | 1.190022476 |
| ENSG00000147383 | NSDHL subnetwork | 0.64486121 | 1.190025031 |
| GO:0060337 | type I interferon-mediated signaling pathway | 0.83564489 | 1.190026388 |
| ENSG00000070010 | UFD1L subnetwork | 0.64469549 | 1.190028793 |
| MP:0003659 | abnormal lymph circulation | 0.64376876 | 1.190028829 |
| MP:0000248 | macrocytosis | 0.64638284 | 1.190034965 |
| ENSG00000183648 | NDUFB1 subnetwork | 0.83581396 | 1.190038108 |
| ENSG00000124802 | EEF1E1 subnetwork | 0.64407055 | 1.190045107 |
| MP:0003409 | decreased width of hypertrophic chondrocyte zone | 0.64435707 | 1.190061373 |
| KEGG_LINOLEIC_ACID_METAB | KEGG_LINOLEIC_ACID_METABOLISM | 0.83555372 | 1.190092864 |
| MP:0001078 | abnormal phrenic nerve morphology | 0.64465411 | 1.190096407 |
| ENSG00000130312 | MRPL34 subnetwork | 0.64420766 | 1.190108995 |
| MP:0001672 | abnormal embryogenesis/ development | 0.64428531 | 1.190116498 |
| ENSG00000212868 | ENSG00000212868 subnetwork | 0.83550554 | 1.190126112 |
| REACTOME_NEPNS2_INTERAC | REACTOME_NEPNS2_INTERACTS_WITH_THE_CELLULAR_E | 0.64402877 | 1.190137845 |

| | | | |
|---|---|---|---|
| GO:0032881 | regulation of polysaccharide metabolic process | 0.64321202 | 1.190139255 |
| GO:0071357 | cellular response to type I interferon | 0.83564489 | 1.190142704 |
| GO:0005874 | microtubule | 0.64707041 | 1.190150948 |
| GO:2000602 | regulation of interphase of mitotic cell cycle | 0.64318242 | 1.190181932 |
| ENSG00000131143 | COX4I1 subnetwork | 0.64462382 | 1.19018282 |
| ENSG00000177733 | HNRNPA0 subnetwork | 0.64736279 | 1.19022322 |
| MP:0004734 | small thoracic cavity | 0.83539908 | 1.19023174 |
| ENSG00000198727 | MT-CYB subnetwork | 0.83550554 | 1.190242472 |
| GO:0003416 | endochondral bone growth | 0.64401348 | 1.190268204 |
| ENSG00000050405 | LIMA1 subnetwork | 0.64316383 | 1.190287364 |
| GO:0060412 | ventricular septum morphogenesis | 0.64747677 | 1.190299252 |
| ENSG00000187079 | TEAD1 subnetwork | 0.64732366 | 1.190328012 |
| ENSG00000039319 | ZFYVE16 subnetwork | 0.64462242 | 1.190331872 |
| GO:0001707 | mesoderm formation | 0.83538815 | 1.190333464 |
| KEGG_BIOSYNTHESIS_OF_UNS | KEGG_BIOSYNTHESIS_OF_UNSATURATED_FATTY_ACIDS | 0.83531946 | 1.190356968 |
| MP:0000313 | abnormal cell death | 0.64313728 | 1.190405371 |
| GO:0006699 | bile acid biosynthetic process | 0.83528052 | 1.19040982 |
| ENSG00000110713 | NUP98 subnetwork | 0.64730118 | 1.19043283 |
| ENSG00000206211 | ENSG00000206211 subnetwork | 0.64857746 | 1.190506723 |
| GO:0042475 | odontogenesis of dentin-containing tooth | 0.83526952 | 1.190516482 |
| ENSG00000151239 | TWF1 subnetwork | 0.6478063 | 1.19051982 |
| ENSG00000169220 | RGS14 subnetwork | 0.64312954 | 1.190529685 |
| GO:0032637 | interleukin-8 production | 0.64824113 | 1.190533134 |
| GO:0009267 | cellular response to starvation | 0.83448636 | 1.190547288 |
| MP:0002631 | abnormal epididymis morphology | 0.83514078 | 1.19054887 |
| MP:0005298 | abnormal clavicle morphology | 0.8352256 | 1.190549795 |
| ENSG00000167881 | SRP68 subnetwork | 0.83405934 | 1.190557351 |
| GO:0010830 | regulation of myotube differentiation | 0.83505241 | 1.190562622 |
| GO:0016592 | mediator complex | 0.64820541 | 1.1905631 |
| ENSG00000087274 | ADD1 subnetwork | 0.83484243 | 1.190565668 |
| ENSG00000078269 | SYNJ2 subnetwork | 0.8344123 | 1.190565945 |
| ENSG00000132694 | ARHGEF11 subnetwork | 0.83500474 | 1.190586163 |
| ENSG00000213672 | NCKIPSD subnetwork | 0.83476215 | 1.190594108 |
| MP:0004179 | transmission ratio distortion | 0.83388937 | 1.190599589 |
| MP:0008943 | increased sensitivity to induced cell death | 0.64775769 | 1.190599676 |
| GO:0046320 | regulation of fatty acid oxidation | 0.8342579 | 1.190603271 |
| GO:0060123 | regulation of growth hormone secretion | 0.83470179 | 1.190612764 |
| GO:0016796 | exonuclease activity, active with either ribo- or deoxyribonu | 0.83436188 | 1.190623776 |
| GO:0045453 | bone resorption | 0.64815841 | 1.190624221 |
| GO:0015849 | organic acid transport | 0.83422205 | 1.190641528 |
| ENSG00000140022 | STON2 subnetwork | 0.83402348 | 1.190654389 |
| ENSG00000206283 | PFDN6 subnetwork | 0.64857746 | 1.190654962 |
| GO:0006013 | mannose metabolic process | 0.83368 | 1.190660525 |
| ENSG00000151746 | BICD1 subnetwork | 0.83387294 | 1.19069175 |
| ENSG00000100401 | RANGAP1 subnetwork | 0.64843657 | 1.190696226 |
| ENSG00000174996 | KLC2 subnetwork | 0.83467901 | 1.190699951 |
| ENSG00000172409 | CLP1 subnetwork | 0.64812286 | 1.190722741 |
| REACTOME_NOREPINEPHRINE | REACTOME_NOREPINEPHRINE_NEUROTRANSMITTER_RELE | 0.83363229 | 1.190728217 |
| ENSG00000144736 | SHQ1 subnetwork | 0.83386431 | 1.190798628 |
| ENSG00000204220 | PFDN6 subnetwork | 0.64857746 | 1.190803238 |
| GO:0001556 | oocyte maturation | 0.8336289 | 1.190830229 |
| MP:0005076 | abnormal cell differentiation | 0.64812269 | 1.190864905 |
| GO:0048608 | reproductive structure development | 0.64891914 | 1.190887589 |

| | | | |
|---|---|---|---|
| MP:0011448 | decreased dopaminergic neuron number | 0.83359688 | 1.19089305 |
| ENSG00000071127 | WDR1 subnetwork | 0.83321941 | 1.190957238 |
| ENSG00000212872 | ENSG00000212872 subnetwork | 0.83313618 | 1.19096616 |
| GO:0001824 | blastocyst development | 0.83358089 | 1.190990196 |
| ENSG00000137177 | KIF13A subnetwork | 0.64809667 | 1.19099464 |
| GO:0051028 | mRNA transport | 0.83333162 | 1.191036579 |
| ENSG00000198888 | MT-ND1 subnetwork | 0.83344857 | 1.19105707 |
| GO:0043392 | negative regulation of DNA binding | 0.83354793 | 1.191082459 |
| ENSG00000212871 | ENSG00000212871 subnetwork | 0.83313618 | 1.19108299 |
| MP:0003886 | abnormal embryonic epiblast morphology | 0.64913817 | 1.191106547 |
| ENSG00000054356 | PTPRN subnetwork | 0.64919211 | 1.1911201 |
| ENSG00000198840 | MT-ND3 subnetwork | 0.83313618 | 1.191199843 |
| ENSG00000198868 | ENSG00000198868 subnetwork | 0.83313618 | 1.191316719 |
| GO:0001653 | peptide receptor activity | 0.83305497 | 1.191345305 |
| MP:0001559 | hyperglycemia | 0.83304894 | 1.191447498 |
| GO:0035050 | embryonic heart tube development | 0.8328889 | 1.191475265 |
| ENSG00000196501 | ENSG00000196501 subnetwork | 0.64944708 | 1.191506969 |
| GO:0001190 | RNA polymerase II transcription factor binding transcriptior | 0.83284578 | 1.191518602 |
| ENSG00000113240 | CLK4 subnetwork | 0.8330429 | 1.191559525 |
| GO:0001105 | RNA polymerase II transcription coactivator activity | 0.83284578 | 1.191635578 |
| REACTOME_BASIGIN_INTERAC | REACTOME_BASIGIN_INTERACTIONS | 0.8327953 | 1.191698576 |
| GO:0031528 | microvillus membrane | 0.64990528 | 1.191753731 |
| MP:0009767 | decreased sensitivity to xenobiotic induced morbidity/mort | 0.83166032 | 1.191784661 |
| MP:0000539 | distended urinary bladder | 0.83247235 | 1.191787819 |
| ENSG00000101057 | MYBL2 subnetwork | 0.64974718 | 1.191789002 |
| MP:0004259 | small placenta | 0.83278562 | 1.191795954 |
| GO:0000076 | DNA replication checkpoint | 0.83272338 | 1.191804969 |
| GO:0043009 | chordate embryonic development | 0.64986478 | 1.191821122 |
| ENSG00000170421 | KRT8 subnetwork | 0.83153439 | 1.191823188 |
| ENSG00000111581 | NUP107 subnetwork | 0.83266884 | 1.191833628 |
| MP:0001382 | abnormal nursing | 0.83231747 | 1.191850069 |
| ENSG00000161270 | NPHS1 subnetwork | 0.83224095 | 1.191864007 |
| MP:0005176 | eyelids fail to open | 0.83244353 | 1.191885254 |
| ENSG00000131381 | ZFYVE20 subnetwork | 0.83198685 | 1.191905043 |
| ENSG00000126218 | F10 subnetwork | 0.64973567 | 1.191906184 |
| ENSG00000094796 | KRT31 subnetwork | 0.83261862 | 1.191906492 |
| MP:0000841 | abnormal hindbrain morphology | 0.83152598 | 1.191910897 |
| KEGG_AMINOACYL_TRNA_BIO | KEGG_AMINOACYL_TRNA_BIOSYNTHESIS | 0.83207118 | 1.191930411 |
| ENSG00000152556 | PFKM subnetwork | 0.83223074 | 1.191966392 |
| ENSG00000151491 | EPS8 subnetwork | 0.83196943 | 1.192007471 |
| GO:0051646 | mitochondrion localization | 0.83143198 | 1.192017509 |
| GO:0031018 | endocrine pancreas development | 0.83151662 | 1.192018294 |
| REACTOME_INFLUENZA_INFEC | REACTOME_INFLUENZA_INFECTION | 0.83191777 | 1.192065677 |
| MP:0002864 | abnormal ocular fundus morphology | 0.83221898 | 1.192068796 |
| ENSG00000128656 | CHN1 subnetwork | 0.83139527 | 1.192105263 |
| ENSG00000109929 | SC5DL subnetwork | 0.65068567 | 1.19210886 |
| GO:0044106 | cellular amine metabolic process | 0.6506187 | 1.192145165 |
| MP:0010402 | ventricular septal defect | 0.65019785 | 1.192190026 |
| GO:0046457 | prostanoid biosynthetic process | 0.83137568 | 1.192207792 |
| ENSG00000139549 | DHH subnetwork | 0.65048617 | 1.19223645 |
| ENSG00000134444 | KIAA1468 subnetwork | 0.65057386 | 1.192262275 |
| ENSG00000140481 | CCDC33 subnetwork | 0.65043743 | 1.192279 |
| ENSG00000177963 | RIC8A subnetwork | 0.65139266 | 1.192290503 |

| | | | |
|---|---|---|---|
| GO:0001516 | prostaglandin biosynthetic process | 0.83137568 | 1.192325101 |
| REACTOME_GOLGI_ASSOCIATE | REACTOME_GOLGI_ASSOCIATED_VESICLE_BIOGENESIS | 0.65035819 | 1.192346431 |
| MP:0003227 | abnormal vascular branching morphogenesis | 0.65135196 | 1.192357835 |
| ENSG00000131187 | F12 subnetwork | 0.83134557 | 1.19240307 |
| ENSG00000167325 | RRM1 subnetwork | 0.65164941 | 1.192404121 |
| MP:0001916 | intracerebral hemorrhage | 0.65092247 | 1.192432903 |
| ENSG00000124782 | RREB1 subnetwork | 0.65132531 | 1.192462436 |
| MP:0001625 | cardiac hypertrophy | 0.65098713 | 1.192464902 |
| GO:0002579 | positive regulation of antigen processing and presentation | 0.65106455 | 1.192465839 |
| GO:0005095 | GTPase inhibitor activity | 0.65177987 | 1.192467113 |
| MP:0000967 | abnormal sensory neuron projections | 0.83129684 | 1.192471213 |
| ENSG00000108515 | ENO3 subnetwork | 0.65158896 | 1.19247145 |
| MP:0003085 | abnormal egg cylinder morphology | 0.65116273 | 1.192510247 |
| GO:0019829 | cation-transporting ATPase activity | 0.83066252 | 1.192515265 |
| ENSG00000136521 | NDUFB5 subnetwork | 0.83049562 | 1.192518716 |
| ENSG00000128609 | NDUFA5 subnetwork | 0.83041296 | 1.19252783 |
| ENSG00000173786 | CNP subnetwork | 0.83118655 | 1.19257801 |
| ENSG00000205531 | NAP1L4 subnetwork | 0.83126983 | 1.19257874 |
| ENSG00000120616 | EPC1 subnetwork | 0.83064801 | 1.192603171 |
| GO:0070330 | aromatase activity | 0.65130276 | 1.192604322 |
| ENSG00000168653 | NDUFS5 subnetwork | 0.83039764 | 1.192615764 |
| GO:0031143 | pseudopodium | 0.83079954 | 1.192619399 |
| MP:0009283 | decreased gonadal fat pad weight | 0.83111924 | 1.192621579 |
| ENSG00000185721 | DRG1 subnetwork | 0.6520112 | 1.192666584 |
| ENSG00000086475 | SEPHS1 subnetwork | 0.65207621 | 1.192667494 |
| GO:0043255 | regulation of carbohydrate biosynthetic process | 0.83106946 | 1.192694693 |
| ENSG00000213920 | MDP1 subnetwork | 0.8303762 | 1.192713568 |
| ENSG00000140285 | FGF7 subnetwork | 0.83022267 | 1.192761407 |
| GO:0003337 | mesenchymal to epithelial transition involved in metaneph | 0.83102007 | 1.192762899 |
| GO:0042493 | response to drug | 0.65319135 | 1.192791677 |
| ENSG00000164252 | AGGF1 subnetwork | 0.83036501 | 1.192816318 |
| GO:0022600 | digestive system process | 0.65311579 | 1.192834138 |
| ENSG00000091536 | MYO15A subnetwork | 0.8298354 | 1.192846579 |
| ENSG00000198042 | MAK16 subnetwork | 0.83021263 | 1.192859255 |
| ENSG00000007372 | PAX6 subnetwork | 0.83012798 | 1.19286348 |
| GO:0015926 | glucosidase activity | 0.65306069 | 1.192882805 |
| GO:0009898 | internal side of plasma membrane | 0.65613651 | 1.192890615 |
| MP:0002100 | abnormal tooth morphology | 0.82981452 | 1.19291983 |
| MP:0001152 | Leydig cell hyperplasia | 0.65343215 | 1.192935859 |
| GO:0031647 | regulation of protein stability | 0.65601846 | 1.192938202 |
| MP:0002276 | abnormal lung interstitium morphology | 0.65609528 | 1.192939073 |
| MP:0008277 | abnormal sternum ossification | 0.653645 | 1.192943798 |
| ENSG00000143556 | S100A7 subnetwork | 0.65237526 | 1.192954602 |
| REACTOME_AUTODEGRADATI | REACTOME_AUTODEGRADATION_OF_CDH1_BY_CDH1APC | 0.65289965 | 1.192961586 |
| REACTOME_CYCLIN_ACDK2:AS | REACTOME_CYCLIN_ACDK2:ASSOCIATED_EVENTS_AT_S_PH | 0.65358277 | 1.192973876 |
| GO:0034340 | response to type I interferon | 0.83011359 | 1.192976144 |
| GO:0002474 | antigen processing and presentation of peptide antigen via | 0.65304913 | 1.193024408 |
| ENSG00000175575 | PAAF1 subnetwork | 0.65257221 | 1.193030754 |
| GO:0070972 | protein localization in endoplasmic reticulum | 0.82981327 | 1.193037475 |
| ENSG00000169992 | NLGN2 subnetwork | 0.83005388 | 1.193039535 |
| GO:0044264 | cellular polysaccharide metabolic process | 0.65545862 | 1.19304321 |
| ENSG00000145041 | VPRBP subnetwork | 0.65342505 | 1.193052632 |
| MP:0001236 | abnormal epidermis stratum spinosum morphology | 0.65234402 | 1.193052971 |

| | | | |
|---|---|---|---|
| ENSG00000105185 | PDCD5 subnetwork | 0.65249798 | 1.193054694 |
| GO:0001104 | RNA polymerase II transcription cofactor activity | 0.65270372 | 1.193057277 |
| GO:0015629 | actin cytoskeleton | 0.65599511 | 1.193060696 |
| ENSG00000166407 | LMO1 subnetwork | 0.82501947 | 1.193104303 |
| MP:0001177 | atelectasis | 0.65289895 | 1.193109431 |
| ENSG00000172594 | SMPDL3A subnetwork | 0.82979276 | 1.19311076 |
| ENSG00000100614 | PPM1A subnetwork | 0.65543046 | 1.193134955 |
| ENSG00000164327 | RICTOR subnetwork | 0.65285756 | 1.193158156 |
| GO:0043073 | germ cell nucleus | 0.82438129 | 1.193168287 |
| ENSG00000135903 | PAX3 subnetwork | 0.65642288 | 1.193175092 |
| ENSG00000171219 | CDC42BPG subnetwork | 0.6558941 | 1.193182379 |
| ENSG00000088367 | EPB41L1 subnetwork | 0.65598529 | 1.193195558 |
| GO:0010039 | response to iron ion | 0.65269809 | 1.193199008 |
| GO:0006353 | transcription termination, DNA-dependent | 0.82976693 | 1.193203788 |
| ENSG00000163162 | RNF149 subnetwork | 0.65280168 | 1.193206892 |
| GO:0042533 | tumor necrosis factor biosynthetic process | 0.82434575 | 1.193212266 |
| ENSG00000135336 | ORC3 subnetwork | 0.82500266 | 1.193212692 |
| MP:0005332 | abnormal amino acid level | 0.65562284 | 1.193223059 |
| ENSG00000113558 | SKP1 subnetwork | 0.82951454 | 1.193226443 |
| MP:0001438 | aphagia | 0.82971569 | 1.193232712 |
| GO:0072207 | metanephric epithelium development | 0.82935162 | 1.193249778 |
| MP:0006030 | abnormal otic vesicle development | 0.8233014 | 1.19325385 |
| MP:0003620 | oliguria | 0.82382887 | 1.193257869 |
| GO:0051931 | regulation of sensory perception | 0.82927063 | 1.193268851 |
| MP:0002786 | abnormal Leydig cell morphology | 0.65541803 | 1.193269943 |
| ENSG00000166862 | CACNG2 subnetwork | 0.82484369 | 1.193270852 |
| MP:0004247 | small pancreas | 0.82356223 | 1.193280691 |
| REACTOME_OPIOID_SIGNALLI | REACTOME_OPIOID_SIGNALLING | 0.65533527 | 1.193281462 |
| MP:0001633 | poor circulation | 0.82495117 | 1.193291353 |
| MP:0002727 | decreased circulating insulin level | 0.82378601 | 1.193301887 |
| MP:0006325 | impaired hearing | 0.65527749 | 1.193305336 |
| GO:0046942 | carboxylic acid transport | 0.82948673 | 1.193309651 |
| GO:0031576 | G2/M transition checkpoint | 0.65587705 | 1.193311119 |
| ENSG00000119729 | RHOQ subnetwork | 0.82341853 | 1.193314127 |
| ENSG00000135862 | LAMC1 subnetwork | 0.82350646 | 1.193314791 |
| GO:0042534 | regulation of tumor necrosis factor biosynthetic process | 0.82434575 | 1.193330687 |
| ENSG00000160801 | PTH1R subnetwork | 0.82968814 | 1.193335635 |
| GO:0035904 | aorta development | 0.82908505 | 1.193335966 |
| ENSG00000212876 | ENSG00000212876 subnetwork | 0.82407163 | 1.193353519 |
| ENSG00000080345 | RIF1 subnetwork | 0.65661385 | 1.193354703 |
| GO:0016705 | oxidoreductase activity, acting on paired donors, with incor | 0.65582861 | 1.193359664 |
| ENSG00000160868 | CYP3A4 subnetwork | 0.82329041 | 1.193367448 |
| ENSG00000113810 | SMC4 subnetwork | 0.82321493 | 1.193371758 |
| ENSG00000188846 | RPL14 subnetwork | 0.6540442 | 1.193372525 |
| MP:0003666 | impaired sperm capacitation | 0.82302113 | 1.19337541 |
| MP:0001951 | abnormal breathing pattern | 0.82483625 | 1.193384249 |
| GO:0042771 | DNA damage response, signal transduction by p53 class me | 0.82919295 | 1.193385982 |
| GO:0051930 | regulation of sensory perception of pain | 0.82927063 | 1.193386635 |
| GO:0031397 | negative regulation of protein ubiquitination | 0.82420441 | 1.193403812 |
| GO:0046379 | extracellular polysaccharide metabolic process | 0.82478892 | 1.193408392 |
| GO:0032874 | positive regulation of stress-activated MAPK cascade | 0.65759276 | 1.193419109 |
| MP:0001293 | anophthalmia | 0.82297351 | 1.193419483 |
| MP:0001923 | reduced female fertility | 0.82378518 | 1.193420399 |

| | | | |
|---|---|---|---|
| MP:0001244 | thin dermal layer | 0.82463636 | 1.193421966 |
| ENSG00000101144 | BMP7 subnetwork | 0.65424673 | 1.193423658 |
| ENSG00000104142 | VPS18 subnetwork | 0.65525278 | 1.193428042 |
| ENSG00000113407 | TARS subnetwork | 0.82433024 | 1.193444169 |
| GO:0035909 | aorta morphogenesis | 0.82908505 | 1.193453791 |
| ENSG00000161638 | ITGA5 subnetwork | 0.65771381 | 1.193469162 |
| GO:0021587 | cerebellum morphogenesis | 0.65401104 | 1.193470727 |
| ENSG00000198763 | MT-ND2 subnetwork | 0.82407163 | 1.193472002 |
| MP:0003089 | decreased skin tensile strength | 0.82291335 | 1.193473506 |
| ENSG00000149782 | PLCB3 subnetwork | 0.82540375 | 1.193476752 |
| MP:0000091 | short premaxilla | 0.82283843 | 1.1934828 |
| REACTOME_METABOLISM_OF_ | REACTOME_METABOLISM_OF_NUCLEOTIDES | 0.82215044 | 1.193483235 |
| ENSG00000127603 | MACF1 subnetwork | 0.82320981 | 1.193485391 |
| ENSG00000143393 | PI4KB subnetwork | 0.82556849 | 1.193507137 |
| GO:0031575 | mitotic cell cycle G1/S transition checkpoint | 0.65523148 | 1.193526069 |
| GO:0045226 | extracellular polysaccharide biosynthetic process | 0.82478892 | 1.193526786 |
| MP:0009862 | abnormal aorta elastic tissue morphology | 0.82278806 | 1.193541812 |
| ENSG00000004975 | DVL2 subnetwork | 0.82905912 | 1.193542016 |
| ENSG00000104081 | BMF subnetwork | 0.65423629 | 1.193546591 |
| ENSG00000104976 | SNAPC2 subnetwork | 0.65758786 | 1.193547593 |
| GO:0016620 | oxidoreductase activity, acting on the aldehyde or oxo grou | 0.82212696 | 1.193552239 |
| ENSG00000157020 | SEC13 subnetwork | 0.82238496 | 1.193554163 |
| ENSG00000125998 | FAM83C subnetwork | 0.82567711 | 1.19355734 |
| ENSG00000166925 | TSC22D4 subnetwork | 0.82273214 | 1.193580947 |
| GO:0007229 | integrin-mediated signaling pathway | 0.82263345 | 1.193585281 |
| MP:0006267 | abnormal intercalated disc morphology | 0.65729274 | 1.193606012 |
| ENSG00000196712 | NF1 subnetwork | 0.65520432 | 1.193630298 |
| GO:0019751 | polyol metabolic process | 0.65754677 | 1.193639163 |
| GO:0031123 | RNA 3'-end processing | 0.82904903 | 1.19365001 |
| ENSG00000141198 | TOM1L1 subnetwork | 0.82237423 | 1.193657979 |
| GO:0044275 | cellular carbohydrate catabolic process | 0.82212311 | 1.193666036 |
| ENSG00000165527 | ARF6 subnetwork | 0.65741021 | 1.193668391 |
| ENSG00000132849 | INADL subnetwork | 0.82173218 | 1.19367284 |
| ENSG00000185359 | HGS subnetwork | 0.8258908 | 1.193681863 |
| ENSG00000142864 | SERBP1 subnetwork | 0.82262181 | 1.193694052 |
| ENSG00000214114 | MYCBP subnetwork | 0.65875209 | 1.193699287 |
| GO:0000151 | ubiquitin ligase complex | 0.6580193 | 1.193716923 |
| REACTOME_VPR:MEDIATED_N | REACTOME_VPR:MEDIATED_NUCLEAR_IMPORT_OF_PICS | 0.65837235 | 1.193732316 |
| GO:0031668 | cellular response to extracellular stimulus | 0.82639303 | 1.193734522 |
| ENSG00000101997 | CCDC22 subnetwork | 0.6572751 | 1.193740759 |
| ENSG00000158417 | EIF5B subnetwork | 0.6587142 | 1.193741547 |
| GO:0035265 | organ growth | 0.65795394 | 1.193753077 |
| ENSG00000144048 | DUSP11 subnetwork | 0.82903913 | 1.193753086 |
| GO:0010720 | positive regulation of cell development | 0.6575256 | 1.193755389 |
| ENSG00000117154 | IGSF21 subnetwork | 0.82654194 | 1.193764857 |
| ENSG00000143575 | HAX1 subnetwork | 0.65519575 | 1.193765447 |
| GO:0045851 | pH reduction | 0.82211358 | 1.193769904 |
| ENSG00000124155 | PIGT subnetwork | 0.82608345 | 1.193771678 |
| GO:0005542 | folic acid binding | 0.65692168 | 1.193774655 |
| MP:0002233 | abnormal nose morphology | 0.82172176 | 1.193781739 |
| GO:0008641 | small protein activating enzyme activity | 0.82205294 | 1.193789191 |
| KEGG_PANTOTHENATE_AND_( | KEGG_PANTOTHENATE_AND_COA_BIOSYNTHESIS | 0.65814535 | 1.193797686 |
| MP:0005402 | abnormal action potential | 0.8289951 | 1.193806796 |

| | | | |
|---|---|---|---|
| GO:0010288 | response to lead ion | 0.82636855 | 1.193808203 |
| GO:0000307 | cyclin-dependent protein kinase holoenzyme complex | 0.82132202 | 1.193808528 |
| ENSG00000153162 | BMP6 subnetwork | 0.82198191 | 1.193823412 |
| ENSG00000169188 | APEX2 subnetwork | 0.82158287 | 1.193830296 |
| ENSG00000136717 | BIN1 subnetwork | 0.82169091 | 1.193835889 |
| MP:0010412 | atrioventricular septal defect | 0.82667562 | 1.193844706 |
| ENSG00000139998 | RAB15 subnetwork | 0.65517842 | 1.193851193 |
| ENSG00000215699 | ENSG00000215699 subnetwork | 0.65868721 | 1.1938576 |
| REACTOME_PACKAGING_OF_T | REACTOME_PACKAGING_OF_TELOMERE_ENDS | 0.82190184 | 1.193867596 |
| ENSG00000180104 | EXOC3 subnetwork | 0.82623778 | 1.193871383 |
| GO:0004497 | monooxygenase activity | 0.65836072 | 1.193873031 |
| ENSG00000128322 | IGLL1 subnetwork | 0.82680715 | 1.193875025 |
| ENSG00000183691 | NOG subnetwork | 0.82130055 | 1.193882634 |
| MP:0010420 | muscular ventricular septal defect | 0.82633353 | 1.193886852 |
| REACTOME_PKA:MEDIATED_P | REACTOME_PKA:MEDIATED_PHOSPHORYLATION_OF_CREE | 0.65727364 | 1.193887862 |
| GO:0048019 | receptor antagonist activity | 0.65991657 | 1.193892708 |
| ENSG00000125249 | RAP2A subnetwork | 0.65862483 | 1.19389374 |
| MP:0003076 | increased susceptibility to ischemic brain injury | 0.82897568 | 1.19389509 |
| GO:0032456 | endocytic recycling | 0.82154529 | 1.193904382 |
| GO:0090136 | epithelial cell-cell adhesion | 0.65923533 | 1.19391128 |
| GO:0045747 | positive regulation of Notch signaling pathway | 0.65711731 | 1.19391717 |
| GO:0016049 | cell growth | 0.65915837 | 1.193935111 |
| ENSG00000122026 | RPL21 subnetwork | 0.82049731 | 1.193936372 |
| GO:0051281 | positive regulation of release of sequestered calcium ion in | 0.65721598 | 1.193936406 |
| GO:0006998 | nuclear envelope organization | 0.65964794 | 1.193938836 |
| ENSG00000168593 | ENSG00000168593 subnetwork | 0.81858402 | 1.193943028 |
| REACTOME_UNBLOCKING_OF_ | REACTOME_UNBLOCKING_OF_NMDA_RECEPTOR_GLUTAM | 0.65833413 | 1.19398302 |
| MP:0004163 | abnormal adenohypophysis morphology | 0.82894797 | 1.193983402 |
| GO:0006457 | protein folding | 0.65517535 | 1.193986403 |
| ENSG00000151552 | QDPR subnetwork | 0.65903458 | 1.193995083 |
| ENSG00000104812 | GYS1 subnetwork | 0.82059273 | 1.193996809 |
| GO:0000279 | M phase | 0.65938015 | 1.193998034 |
| GO:0016846 | carbon-sulfur lyase activity | 0.82153498 | 1.193998406 |
| ENSG00000090104 | RGS1 subnetwork | 0.82128655 | 1.194001594 |
| MP:0000885 | ectopic Purkinje cell | 0.82888174 | 1.194002569 |
| MP:0002746 | abnormal semilunar valve morphology | 0.82095062 | 1.194004187 |
| ENSG00000101150 | TPD52L2 subnetwork | 0.65858719 | 1.19400984 |
| ENSG00000075142 | SRI subnetwork | 0.65463597 | 1.194012124 |
| ENSG00000166285 | ENSG00000166285 subnetwork | 0.82048382 | 1.194020547 |
| REACTOME_RNA_POLYMERASI | REACTOME_RNA_POLYMERASE_III_TRANSCRIPTION_INITIA | 0.66006926 | 1.19402234 |
| GO:0061384 | heart trabecula morphogenesis | 0.65511973 | 1.194022747 |
| GO:0002407 | dendritic cell chemotaxis | 0.65959324 | 1.194030217 |
| ENSG00000103742 | IGDCC4 subnetwork | 0.82090067 | 1.194038481 |
| GO:0030547 | receptor inhibitor activity | 0.65991657 | 1.194039288 |
| ENSG00000125954 | CHURC1-FNTB subnetwork | 0.82115003 | 1.194045246 |
| ENSG00000089280 | FUS subnetwork | 0.8212323 | 1.19404584 |
| REACTOME_AXON_GUIDANCE | REACTOME_AXON_GUIDANCE | 0.82884056 | 1.194046443 |
| GO:0014902 | myotube differentiation | 0.65977847 | 1.194050104 |
| MP:0000644 | dextrocardia | 0.82876724 | 1.194055737 |
| ENSG00000206440 | NFKBIL1 subnetwork | 0.81858402 | 1.194062375 |
| ENSG00000115306 | SPTBN1 subnetwork | 0.66434132 | 1.194071002 |
| ENSG00000152520 | PAN3 subnetwork | 0.65915728 | 1.194081858 |
| GO:0001654 | eye development | 0.6644381 | 1.194090022 |

| | | | |
|---|---|---|---|
| ENSG00000175305 | CCNE2 subnetwork | 0.65987186 | 1.194118369 |
| ENSG00000032514 | ENSG00000032514 subnetwork | 0.82856145 | 1.194133057 |
| GO:0030855 | epithelial cell differentiation | 0.8211228 | 1.19413934 |
| ENSG00000204359 | CFB subnetwork | 0.82048382 | 1.194139651 |
| GO:0016574 | histone ubiquitination | 0.82874364 | 1.194149041 |
| MP:0004938 | dilated vasculature | 0.65957743 | 1.194152334 |
| ENSG00000085832 | EPS15 subnetwork | 0.8208871 | 1.194152542 |
| ENSG00000128595 | CALU subnetwork | 0.82822413 | 1.194155459 |
| REACTOME_XENOBIOTICS | REACTOME_XENOBIOTICS | 0.81857217 | 1.194156753 |
| MP:0002640 | reticulocytosis | 0.66430879 | 1.194161786 |
| MP:0008519 | thin retinal outer plexiform layer | 0.65511913 | 1.194170376 |
| REACTOME_INFLUENZA_VIRAL | REACTOME_INFLUENZA_VIRAL_RNA_TRANSCRIPTION_AND | 0.82034304 | 1.19417839 |
| ENSG00000107863 | ARHGAP21 subnetwork | 0.65496951 | 1.194187485 |
| ENSG00000138039 | LHCGR subnetwork | 0.82870955 | 1.194192943 |
| GO:0035924 | cellular response to vascular endothelial growth factor stim | 0.82817425 | 1.194204332 |
| GO:0046329 | negative regulation of JNK cascade | 0.82084765 | 1.194211786 |
| GO:0002690 | positive regulation of leukocyte chemotaxis | 0.65505156 | 1.194219117 |
| ENSG00000133812 | SBF2 subnetwork | 0.65480876 | 1.194223157 |
| GO:0017144 | drug metabolic process | 0.82047021 | 1.194223863 |
| REACTOME_INFLAMMASOMES | REACTOME_INFLAMMASOMES | 0.82855879 | 1.194241226 |
| GO:0051329 | interphase of mitotic cell cycle | 0.81854713 | 1.194246151 |
| ENSG00000140600 | SH3GL3 subnetwork | 0.65490636 | 1.194248609 |
| ENSG00000013573 | DDX11 subnetwork | 0.81849207 | 1.194265573 |
| GO:0003006 | developmental process involved in reproduction | 0.82725572 | 1.194267327 |
| MP:0005449 | abnormal food intake | 0.66427546 | 1.194270897 |
| GO:0005212 | structural constituent of eye lens | 0.82031597 | 1.1942726 |
| MP:0002551 | abnormal blood coagulation | 0.82779451 | 1.194285573 |
| ENSG00000135390 | ATP5G2 subnetwork | 0.82842562 | 1.194289528 |
| MP:0001274 | curly vibrissae | 0.81889868 | 1.194293424 |
| ENSG00000198785 | GRIN3A subnetwork | 0.82816552 | 1.194312562 |
| GO:0050930 | induction of positive chemotaxis | 0.82853477 | 1.194319755 |
| ENSG00000197555 | SIPA1L1 subnetwork | 0.66031999 | 1.194329897 |
| GO:0030262 | apoptotic nuclear change | 0.82720271 | 1.194331122 |
| REACTOME_EGFR_DOWNREGU | REACTOME_EGFR_DOWNREGULATION | 0.82791673 | 1.19435045 |
| ENSG00000162613 | FUBP1 subnetwork | 0.82801251 | 1.194351009 |
| GO:0005669 | transcription factor TFIID complex | 0.82028342 | 1.194351861 |
| ENSG00000141279 | NPEPPS subnetwork | 0.81847601 | 1.194355 |
| ENSG00000162302 | RPS6KA4 subnetwork | 0.82776916 | 1.194369124 |
| ENSG00000153914 | SREK1 subnetwork | 0.8276939 | 1.194373515 |
| ENSG00000138041 | SMEK2 subnetwork | 0.66405424 | 1.194378662 |
| GO:0070723 | response to cholesterol | 0.66424272 | 1.194380034 |
| ENSG00000129351 | ILF3 subnetwork | 0.8281508 | 1.194410921 |
| ENSG00000005810 | MYCBP2 subnetwork | 0.66485926 | 1.194420732 |
| GO:0044455 | mitochondrial membrane part | 0.82026298 | 1.194441118 |
| MP:0001675 | abnormal ectoderm development | 0.66494223 | 1.194445799 |
| ENSG00000168447 | SCNN1B subnetwork | 0.82765235 | 1.194452143 |
| ENSG00000174483 | BBS1 subnetwork | 0.66418755 | 1.194458684 |
| GO:0006569 | tryptophan catabolic process | 0.81846413 | 1.194464446 |
| GO:0021871 | forebrain regionalization | 0.81931835 | 1.194464982 |
| ENSG00000163082 | SGPP2 subnetwork | 0.66162729 | 1.194468945 |
| GO:0090316 | positive regulation of intracellular protein transport | 0.66504116 | 1.194470861 |
| MP:0011100 | complete preweaning lethality | 0.82010916 | 1.194479936 |
| GO:0006518 | peptide metabolic process | 0.81996735 | 1.194503794 |

| | | | |
|---|---|---|---|
| ENSG00000145220 | LYAR subnetwork | 0.82024152 | 1.19451043 |
| REACTOME_METABOLISM_OF_ | REACTOME_METABOLISM_OF_PORPHYRINS | 0.81967657 | 1.194517128 |
| ENSG00000125814 | NAPB subnetwork | 0.66218445 | 1.194522644 |
| ENSG00000166228 | PCBD1 subnetwork | 0.66405289 | 1.194524478 |
| MP:0011086 | partial postnatal lethality | 0.66058788 | 1.194527607 |
| GO:0072659 | protein localization in plasma membrane | 0.66482408 | 1.194529821 |
| ENSG00000135486 | HNRNPA1 subnetwork | 0.66366438 | 1.194534017 |
| ENSG00000006634 | DBF4 subnetwork | 0.66159612 | 1.194535653 |
| GO:0048193 | Golgi vesicle transport | 0.82752792 | 1.194540145 |
| GO:0005979 | regulation of glycogen biosynthetic process | 0.66209274 | 1.194540335 |
| ENSG00000206412 | GNL1 subnetwork | 0.66146982 | 1.194546569 |
| ENSG00000168309 | FAM107A subnetwork | 0.82763736 | 1.194550584 |
| GO:0005310 | dicarboxylic acid transmembrane transporter activity | 0.8195747 | 1.194550994 |
| GO:0032354 | response to follicle-stimulating hormone stimulus | 0.66051046 | 1.194557614 |
| MP:0001074 | abnormal vagus nerve morphology | 0.82007815 | 1.194559249 |
| GO:0071417 | cellular response to organic nitrogen | 0.66386949 | 1.194559775 |
| MP:0001327 | decreased retinal photoreceptor cell number | 0.66236825 | 1.194560695 |
| MP:0000272 | abnormal aorta morphology | 0.81984392 | 1.194567605 |
| MP:0001125 | abnormal oocyte morphology | 0.66375366 | 1.194571324 |
| MP:0006108 | abnormal hindbrain development | 0.8199374 | 1.194578133 |
| GO:0046218 | indolalkylamine catabolic process | 0.81846413 | 1.194583917 |
| GO:0032732 | positive regulation of interleukin-1 production | 0.81931419 | 1.194584333 |
| ENSG00000108829 | LRRC59 subnetwork | 0.66175792 | 1.194585987 |
| GO:0045176 | apical protein localization | 0.6622937 | 1.194590625 |
| GO:0032755 | positive regulation of interleukin-6 production | 0.6631953 | 1.194591787 |
| ENSG00000139132 | FGD4 subnetwork | 0.81965683 | 1.194596484 |
| MP:0001388 | abnormal stationary movement | 0.66155945 | 1.194602377 |
| ENSG00000139496 | NUPL1 subnetwork | 0.66076918 | 1.194608024 |
| GO:0016840 | carbon-nitrogen lyase activity | 0.81923577 | 1.194608774 |
| ENSG00000106100 | NOD1 subnetwork | 0.6639781 | 1.19460928 |
| REACTOME_CYCLIN_E_ASSOCI | REACTOME_CYCLIN_E_ASSOCIATED_EVENTS_DURING_G1S | 0.66311855 | 1.194621684 |
| ENSG00000104325 | DECR1 subnetwork | 0.81956806 | 1.19466034 |
| GO:0007586 | digestion | 0.66364205 | 1.194661617 |
| GO:0010962 | regulation of glucan biosynthetic process | 0.66209274 | 1.194686582 |
| ENSG00000206492 | GNL1 subnetwork | 0.66146982 | 1.194692977 |
| GO:0042436 | indole-containing compound catabolic process | 0.81846413 | 1.194703411 |
| ENSG00000143546 | S100A8 subnetwork | 0.81839671 | 1.194747899 |
| MP:0004016 | decreased bone mass | 0.6629367 | 1.194754219 |
| ENSG00000141446 | ESCO1 subnetwork | 0.6635855 | 1.194758705 |
| MP:0008528 | polycystic kidney | 0.66311468 | 1.194767726 |
| GO:0061134 | peptidase regulator activity | 0.66275147 | 1.194782875 |
| GO:0017091 | AU-rich element binding | 0.66260421 | 1.194806069 |
| GO:0016052 | carbohydrate catabolic process | 0.81833683 | 1.194812406 |
| GO:0032102 | negative regulation of response to external stimulus | 0.66271099 | 1.194818938 |
| GO:0072331 | signal transduction by p53 class mediator | 0.66344368 | 1.194824636 |
| GO:0032885 | regulation of polysaccharide biosynthetic process | 0.66209274 | 1.194832864 |
| ENSG00000204590 | GNL1 subnetwork | 0.66146982 | 1.194839421 |
| ENSG00000129682 | FGF13 subnetwork | 0.66309428 | 1.194852671 |
| GO:0032856 | activation of Ras GTPase activity | 0.66292134 | 1.194869757 |
| ENSG00000119718 | EIF2B2 subnetwork | 0.66357877 | 1.194886364 |
| ENSG00000212802 | ENSG00000212802 subnetwork | 0.8183234 | 1.19491695 |
| GO:0030295 | protein kinase activator activity | 0.66142888 | 1.194930734 |
| ENSG00000170917 | NUDT6 subnetwork | 0.66136203 | 1.194948504 |

| | | | |
|---|---|---|---|
| REACTOME_GLUCOSE_TRANSF | REACTOME_GLUCOSE_TRANSPORT | 0.66208502 | 1.194948567 |
| ENSG00000116095 | PLEKHA3 subnetwork | 0.6620385 | 1.194984691 |
| ENSG00000148848 | ADAM12 subnetwork | 0.66291355 | 1.194991438 |
| ENSG00000145592 | RPL37 subnetwork | 0.66555639 | 1.195033516 |
| ENSG00000124357 | NAGK subnetwork | 0.66131124 | 1.195033722 |
| ENSG00000174766 | ENSG00000174766 subnetwork | 0.8183234 | 1.195036526 |
| MP:0009456 | impaired cued conditioning behavior | 0.66125028 | 1.195100564 |
| ENSG00000109193 | SULT1E1 subnetwork | 0.81829014 | 1.195136109 |
| GO:0072530 | purine-containing compound transmembrane transport | 0.66554898 | 1.195154803 |
| GO:0051184 | cofactor transporter activity | 0.81809585 | 1.195159676 |
| KEGG_OTHER_GLYCAN_DEGRA | KEGG_OTHER_GLYCAN_DEGRADATION | 0.66121821 | 1.195173556 |
| ENSG00000086589 | RBM22 subnetwork | 0.81825237 | 1.195185667 |
| MP:0000192 | abnormal mineral level | 0.81819643 | 1.195225225 |
| GO:0061383 | trabecula morphogenesis | 0.81804037 | 1.195229275 |
| GO:0035914 | skeletal muscle cell differentiation | 0.6612002 | 1.195277233 |
| GO:0008484 | sulfuric ester hydrolase activity | 0.66554103 | 1.1953005 |
| MP:0001676 | abnormal apical ectodermal ridge morphology | 0.81791854 | 1.195323453 |
| ENSG00000169714 | CNBP subnetwork | 0.818003 | 1.195323921 |
| ENSG00000135655 | USP15 subnetwork | 0.66735595 | 1.195330739 |
| ENSG00000101977 | MCF2 subnetwork | 0.81787175 | 1.195358037 |
| GO:0042559 | pteridine-containing compound biosynthetic process | 0.66608827 | 1.195370934 |
| ENSG00000144848 | ATG3 subnetwork | 0.66659931 | 1.195404747 |
| GO:0071496 | cellular response to external stimulus | 0.66689869 | 1.195412509 |
| ENSG00000183474 | GTF2H2C subnetwork | 0.81783849 | 1.195417668 |
| GO:0010878 | cholesterol storage | 0.66761213 | 1.195466148 |
| GO:0008373 | sialyltransferase activity | 0.66734934 | 1.195476104 |
| ENSG00000140307 | GTF2A2 subnetwork | 0.66606861 | 1.195486111 |
| ENSG00000206315 | PBX2 subnetwork | 0.66784704 | 1.195504253 |
| MP:0005282 | decreased fatty acid level | 0.81783362 | 1.195527397 |
| GO:0032201 | telomere maintenance via semi-conservative replication | 0.66658704 | 1.195532019 |
| GO:0015291 | secondary active transmembrane transporter activity | 0.66794211 | 1.195541247 |
| ENSG00000100722 | ZC3H14 subnetwork | 0.66689021 | 1.19554582 |
| ENSG00000150687 | PRSS23 subnetwork | 0.66597158 | 1.195552035 |
| REACTOME_RNA_POLYMERASI | REACTOME_RNA_POLYMERASE_I_PROMOTER_OPENING | 0.66758965 | 1.195556771 |
| MP:0001957 | apnea | 0.66731956 | 1.195566772 |
| ENSG00000163453 | IGFBP7 subnetwork | 0.66681332 | 1.195593963 |
| GO:0009994 | oocyte differentiation | 0.66605489 | 1.195595224 |
| ENSG00000124635 | HIST1H2BJ subnetwork | 0.66640339 | 1.195597369 |
| ENSG00000135218 | CD36 subnetwork | 0.66754208 | 1.195598784 |
| ENSG00000131037 | EPS8L1 subnetwork | 0.66840586 | 1.195604662 |
| ENSG00000147677 | EIF3H subnetwork | 0.81779838 | 1.195607093 |
| REACTOME_TRANSPORT_OF_T | REACTOME_TRANSPORT_OF_THE_SLBP_DEPENDANT_MAT | 0.66708289 | 1.195613822 |
| ENSG00000206247 | ENSG00000206247 subnetwork | 0.66784704 | 1.195649532 |
| GO:0006986 | response to unfolded protein | 0.6665684 | 1.195653233 |
| GO:0030730 | sequestering of triglyceride | 0.66650086 | 1.195670969 |
| GO:0008137 | NADH dehydrogenase (ubiquinone) activity | 0.81776108 | 1.195681795 |
| ENSG00000164118 | CEP44 subnetwork | 0.66730474 | 1.195693955 |
| ENSG00000111344 | RASAL1 subnetwork | 0.66724714 | 1.19573601 |
| ENSG00000181789 | COPG subnetwork | 0.6663959 | 1.195736906 |
| ENSG00000143870 | PDIA6 subnetwork | 0.66840105 | 1.195749848 |
| MP:0002971 | abnormal brown adipose tissue morphology | 0.6715834 | 1.195769882 |
| ENSG00000204304 | PBX2 subnetwork | 0.66784704 | 1.195794847 |
| ENSG00000196776 | CD47 subnetwork | 0.66819785 | 1.19579689 |

| | | | |
|---|---|---|---|
| GO:0003954 | NADH dehydrogenase activity | 0.81776108 | 1.195801603 |
| ENSG00000144566 | RAB5A subnetwork | 0.671205 | 1.195809651 |
| MP:0011405 | tubulointerstitial nephritis | 0.6685849 | 1.195823722 |
| ENSG00000141480 | ARRB2 subnetwork | 0.67498088 | 1.195838345 |
| ENSG00000182957 | SPATA13 subnetwork | 0.66868846 | 1.195860646 |
| GO:0061136 | regulation of proteasomal protein catabolic process | 0.67157029 | 1.195884202 |
| ENSG00000138031 | ADCY3 subnetwork | 0.66838836 | 1.195888997 |
| ENSG00000120885 | CLU subnetwork | 0.6749409 | 1.195897991 |
| ENSG00000173369 | C1QB subnetwork | 0.67134173 | 1.195918984 |
| GO:0050136 | NADH dehydrogenase (quinone) activity | 0.81776108 | 1.195921435 |
| ENSG00000124762 | CDKN1A subnetwork | 0.67119943 | 1.195948234 |
| MP:0000462 | abnormal digestive system morphology | 0.67153273 | 1.195950193 |
| GO:0008629 | induction of apoptosis by intracellular signals | 0.66836664 | 1.195973521 |
| ENSG00000183048 | SLC25A10 subnetwork | 0.8177126 | 1.195981159 |
| GO:0043567 | regulation of insulin-like growth factor receptor signaling pa | 0.67178984 | 1.196006042 |
| ENSG00000100201 | DDX17 subnetwork | 0.66927158 | 1.196032998 |
| MP:0005238 | increased brain size | 0.67493978 | 1.196041867 |
| ENSG00000035403 | VCL subnetwork | 0.67473348 | 1.196052473 |
| REACTOME_E2F:ENABLED_INH | REACTOME_E2F:ENABLED_INHIBITION_OF_PRE:REPLICATIC | 0.81768263 | 1.196075975 |
| MP:0002810 | microcytic anemia | 0.67480669 | 1.196077016 |
| ENSG00000106683 | LIMK1 subnetwork | 0.67152015 | 1.196082699 |
| MP:0001547 | abnormal lipid level | 0.67519085 | 1.196085388 |
| GO:0042558 | pteridine-containing compound metabolic process | 0.67119693 | 1.196086851 |
| ENSG00000155868 | MED7 subnetwork | 0.67488924 | 1.196101552 |
| ENSG00000065000 | AP3D1 subnetwork | 0.66922958 | 1.196105314 |
| ENSG00000170604 | IRF2BP1 subnetwork | 0.6689868 | 1.196109965 |
| GO:0015297 | antiporter activity | 0.66914236 | 1.196116976 |
| ENSG00000106976 | DNM1 subnetwork | 0.67469111 | 1.196124218 |
| MP:0005178 | increased circulating cholesterol level | 0.66909875 | 1.196195388 |
| GO:0009636 | response to toxin | 0.81767862 | 1.19619587 |
| ENSG00000100292 | HMOX1 subnetwork | 0.67118657 | 1.196219453 |
| ENSG00000069345 | DNAJA2 subnetwork | 0.67561044 | 1.196231971 |
| GO:0090181 | regulation of cholesterol metabolic process | 0.6710235 | 1.196236689 |
| GO:0016684 | oxidoreductase activity, acting on peroxide as acceptor | 0.81762464 | 1.196240602 |
| GO:0030275 | LRR domain binding | 0.67468058 | 1.196268208 |
| ENSG00000154380 | ENAH subnetwork | 0.67212308 | 1.196278845 |
| MP:0010300 | increased skin tumor incidence | 0.6711294 | 1.196285541 |
| MP:0004701 | decreased circulating insulin-like growth factor I level | 0.81749288 | 1.196289983 |
| GO:0046943 | carboxylic acid transmembrane transporter activity | 0.67098519 | 1.196290693 |
| MP:0000754 | paresis | 0.67544502 | 1.196308765 |
| GO:0070633 | transepithelial transport | 0.81467972 | 1.196322568 |
| GO:0031526 | brush border membrane | 0.67357231 | 1.196334258 |
| ENSG00000106290 | TAF6 subnetwork | 0.67560006 | 1.196351725 |
| GO:0002673 | regulation of acute inflammatory response | 0.67339056 | 1.196357496 |
| GO:0050848 | regulation of calcium-mediated signaling | 0.81747093 | 1.196359807 |
| GO:0004601 | peroxidase activity | 0.81762464 | 1.196360537 |
| GO:0051345 | positive regulation of hydrolase activity | 0.67586363 | 1.196365056 |
| GO:0018904 | organic ether metabolic process | 0.67210287 | 1.19637506 |
| GO:0001837 | epithelial to mesenchymal transition | 0.81478802 | 1.1963833 |
| REACTOME_LIPOPROTEIN_ME | REACTOME_LIPOPROTEIN_METABOLISM | 0.67466975 | 1.196388153 |
| GO:0031111 | negative regulation of microtubule polymerization or depol | 0.67420026 | 1.196391566 |
| GO:0043241 | protein complex disassembly | 0.67351851 | 1.196400145 |
| GO:0010876 | lipid localization | 0.67097898 | 1.196417332 |

| | | | |
|---|---|---|---|
| ENSG00000095637 | SORBS1 subnetwork | 0.67333461 | 1.19641737 |
| ENSG00000079805 | DNM2 subnetwork | 0.67580215 | 1.1964187 |
| GO:0034774 | secretory granule lumen | 0.81465986 | 1.196427853 |
| ENSG00000160746 | ANO10 subnetwork | 0.67249943 | 1.19643159 |
| MP:0004703 | abnormal vertebral column morphology | 0.81700032 | 1.19643323 |
| GO:0045022 | early endosome to late endosome transport | 0.6741549 | 1.19643933 |
| ENSG00000010438 | PRSS3 subnetwork | 0.67543815 | 1.196440596 |
| GO:0030546 | receptor activator activity | 0.67311044 | 1.196446241 |
| ENSG00000139842 | CUL4A subnetwork | 0.67079971 | 1.196446731 |
| ENSG00000100075 | SLC25A1 subnetwork | 0.67091341 | 1.196447161 |
| MP:0005478 | decreased circulating thyroxine level | 0.81458464 | 1.19644762 |
| GO:0035966 | response to topologically incorrect protein | 0.67263456 | 1.19645617 |
| ENSG00000151366 | NDUFC2 subnetwork | 0.81694476 | 1.196457957 |
| GO:0032994 | protein-lipid complex | 0.81450475 | 1.196462359 |
| GO:0030136 | clathrin-coated vesicle | 0.67559203 | 1.196471508 |
| ENSG00000087258 | GNAO1 subnetwork | 0.81746132 | 1.196474777 |
| GO:0031105 | septin complex | 0.66972317 | 1.196483143 |
| ENSG00000125170 | DOK4 subnetwork | 0.67449572 | 1.196483199 |
| MP:0004190 | abnormal direction of embryo turning | 0.67287527 | 1.196487204 |
| MP:0008544 | impaired olfaction | 0.67246126 | 1.196491546 |
| GO:0002687 | positive regulation of leukocyte migration | 0.6740865 | 1.196511208 |
| ENSG00000157087 | ATP2B2 subnetwork | 0.67329516 | 1.196513452 |
| REACTOME_REGULATION_OF_ | REACTOME_REGULATION_OF_INSULIN_SECRETION_BY_AC | 0.67300482 | 1.196523838 |
| MP:0004607 | abnormal cervical atlas morphology | 0.67307625 | 1.196524258 |
| MP:0006058 | decreased cerebral infarction size | 0.8173718 | 1.196524574 |
| GO:0048871 | multicellular organismal homeostasis | 0.67459089 | 1.196525771 |
| GO:0034614 | cellular response to reactive oxygen species | 0.67466793 | 1.196526189 |
| MP:0005274 | abnormal viscerocranium morphology | 0.67013603 | 1.196533753 |
| ENSG00000171621 | SPSB1 subnetwork | 0.67320759 | 1.196537162 |
| ENSG00000067829 | IDH3G subnetwork | 0.67866482 | 1.196546565 |
| GO:0005342 | organic acid transmembrane transporter activity | 0.67750732 | 1.196552758 |
| GO:0004714 | transmembrane receptor protein tyrosine kinase activity | 0.677695 | 1.196553584 |
| ENSG00000129245 | FXR2 subnetwork | 0.81726935 | 1.196554318 |
| ENSG00000138193 | PLCE1 subnetwork | 0.67043312 | 1.196559661 |
| ENSG00000170348 | TMED10 subnetwork | 0.67077693 | 1.196561327 |
| GO:0005319 | lipid transporter activity | 0.67242273 | 1.196569634 |
| MP:0001688 | abnormal somite development | 0.67402511 | 1.19657105 |
| ENSG00000198695 | MT-ND6 subnetwork | 0.81694206 | 1.196578023 |
| GO:0034358 | plasma lipoprotein particle | 0.81450475 | 1.196582788 |
| ENSG00000137878 | GCOM1 subnetwork | 0.81605805 | 1.196584288 |
| KEGG_GLYCINE_SERINE_AND_ | KEGG_GLYCINE_SERINE_AND_THREONINE_METABOLISM | 0.67790393 | 1.196584781 |
| GO:0046961 | proton-transporting ATPase activity, rotational mechanism | 0.6785032 | 1.196587644 |
| ENSG00000152583 | SPARCL1 subnetwork | 0.67741396 | 1.196594316 |
| GO:0044036 | cell wall macromolecule metabolic process | 0.81598756 | 1.196599015 |
| ENSG00000131746 | TNS4 subnetwork | 0.67285581 | 1.196607509 |
| MP:0002685 | abnormal spermatogonia proliferation | 0.81723004 | 1.196609149 |
| MP:0004411 | decreased endocochlear potential | 0.81617224 | 1.196609744 |
| ENSG00000127993 | RBM48 subnetwork | 0.81502374 | 1.196609999 |
| ENSG00000058668 | ATP2B4 subnetwork | 0.67732712 | 1.196611897 |
| ENSG00000215727 | ENSG00000215727 subnetwork | 0.6738638 | 1.196612417 |
| GO:0004842 | ubiquitin-protein ligase activity | 0.67763346 | 1.196613116 |
| GO:0035967 | cellular response to topologically incorrect protein | 0.67039974 | 1.196619821 |
| ENSG00000143858 | SYT2 subnetwork | 0.67449032 | 1.196621296 |

| | | | |
|---|---|---|---|
| GO:0034593 | phosphatidylinositol bisphosphate phosphatase activity | 0.67234539 | 1.196623581 |
| GO:0032156 | septin cytoskeleton | 0.66972317 | 1.19662826 |
| MP:0008563 | decreased interferon-alpha secretion | 0.67864418 | 1.196641925 |
| ENSG00000131263 | RLIM subnetwork | 0.67058744 | 1.196644864 |
| GO:0016236 | macroautophagy | 0.67074174 | 1.196645677 |
| GO:0048596 | embryonic camera-type eye morphogenesis | 0.81561407 | 1.196647567 |
| ENSG00000122367 | LDB3 subnetwork | 0.67445283 | 1.196657029 |
| ENSG00000105372 | RPS19 subnetwork | 0.67012416 | 1.196660606 |
| GO:0006283 | transcription-coupled nucleotide-excision repair | 0.81418747 | 1.196667002 |
| MP:0005087 | decreased acute inflammation | 0.67397823 | 1.196667068 |
| GO:0048048 | embryonic eye morphogenesis | 0.67788592 | 1.196668265 |
| MP:0000920 | abnormal myelination | 0.81513588 | 1.196685778 |
| KEGG_PYRUVATE_METABOLISI | KEGG_PYRUVATE_METABOLISM | 0.81557237 | 1.196687443 |
| MP:0001798 | impaired macrophage phagocytosis | 0.81449011 | 1.196688142 |
| GO:0042439 | ethanolamine-containing compound metabolic process | 0.81685814 | 1.196692763 |
| ENSG00000212869 | ENSG00000212869 subnetwork | 0.81694206 | 1.196698113 |
| ENSG00000102309 | PIN4 subnetwork | 0.67036239 | 1.196704229 |
| ENSG00000055732 | MCOLN3 subnetwork | 0.66968963 | 1.196718826 |
| GO:0071554 | cell wall organization or biogenesis | 0.81598756 | 1.196719252 |
| GO:0043114 | regulation of vascular permeability | 0.67848928 | 1.196724943 |
| GO:0031432 | titin binding | 0.67732035 | 1.196737436 |
| MP:0004811 | abnormal neuron physiology | 0.81575784 | 1.196738366 |
| MP:0006032 | abnormal ureteric bud morphology | 0.67030701 | 1.196746243 |
| ENSG00000067836 | ROGDI subnetwork | 0.67838398 | 1.196748503 |
| ENSG00000065518 | NDUFB4 subnetwork | 0.6738638 | 1.196756692 |
| GO:0072170 | metanephric tubule development | 0.8165562 | 1.196761398 |
| GO:0060047 | heart contraction | 0.81684644 | 1.196762698 |
| GO:0046686 | response to cadmium ion | 0.81667594 | 1.196767068 |
| ENSG00000155511 | GRIA1 subnetwork | 0.68367049 | 1.196767293 |
| MP:0000189 | hypoglycemia | 0.81417734 | 1.196767372 |
| GO:0001893 | maternal placenta development | 0.81647702 | 1.196776137 |
| GO:0006568 | tryptophan metabolic process | 0.81547643 | 1.196782303 |
| ENSG00000079819 | EPB41L2 subnetwork | 0.81539148 | 1.196787007 |
| GO:0051654 | establishment of mitochondrion localization | 0.81588806 | 1.196788945 |
| GO:0045776 | negative regulation of blood pressure | 0.67072618 | 1.196790602 |
| GO:0030252 | growth hormone secretion | 0.67012162 | 1.196793551 |
| GO:0045806 | negative regulation of endocytosis | 0.67833099 | 1.196796023 |
| ENSG00000172164 | SNTB1 subnetwork | 0.67726358 | 1.196797025 |
| ENSG00000188021 | UBQLN2 subnetwork | 0.68376691 | 1.196797386 |
| MP:0011101 | partial prenatal lethality | 0.67787243 | 1.196799712 |
| MP:0001689 | incomplete somite formation | 0.81410287 | 1.196802296 |
| ENSG00000089009 | RPL6 subnetwork | 0.81557144 | 1.196802735 |
| MP:0000107 | abnormal frontal bone morphology | 0.81448677 | 1.196803584 |
| ENSG00000023228 | NDUFS1 subnetwork | 0.81393677 | 1.196806689 |
| ENSG00000173542 | MOB1B subnetwork | 0.81386753 | 1.196811404 |
| GO:0008380 | RNA splicing | 0.81665193 | 1.196811929 |
| GO:0000377 | RNA splicing, via transesterification reactions with bulged a | 0.67003895 | 1.19681741 |
| GO:0004857 | enzyme inhibitor activity | 0.68363992 | 1.196832283 |
| MP:0008227 | absent anterior commissure | 0.81598093 | 1.196839514 |
| MP:0008642 | decreased circulating interleukin-1 beta level | 0.81441647 | 1.19684857 |
| ENSG00000170906 | NDUFA3 subnetwork | 0.81681282 | 1.196852726 |
| ENSG00000102189 | EEA1 subnetwork | 0.81644221 | 1.196861189 |
| GO:0043410 | positive regulation of MAPK cascade | 0.81370495 | 1.196865867 |

| | | | |
|---|---|---|---|
| ENSG00000123562 | MORF4L2 subnetwork | 0.67829442 | 1.196873503 |
| GO:0015405 | P-P-bond-hydrolysis-driven transmembrane transporter act | 0.67822652 | 1.196879118 |
| GO:0030867 | rough endoplasmic reticulum membrane | 0.81535925 | 1.196882229 |
| ENSG00000125818 | PSMF1 subnetwork | 0.67678726 | 1.196890756 |
| ENSG00000112769 | LAMA4 subnetwork | 0.81379279 | 1.196891374 |
| GO:0006695 | cholesterol biosynthetic process | 0.81384957 | 1.196891688 |
| ENSG00000204983 | PRSS1 subnetwork | 0.81408417 | 1.196902699 |
| GO:0046620 | regulation of organ growth | 0.67708677 | 1.196909876 |
| GO:0002244 | hemopoietic progenitor cell differentiation | 0.67726238 | 1.196934613 |
| ENSG00000183092 | BEGAIN subnetwork | 0.67917185 | 1.196948666 |
| MP:0009866 | abnormal aorta wall morphology | 0.67674674 | 1.196950414 |
| GO:0050820 | positive regulation of coagulation | 0.68362506 | 1.196950785 |
| MP:0008272 | abnormal endochondral bone ossification | 0.67720496 | 1.196952244 |
| GO:0000398 | nuclear mRNA splicing, via spliceosome | 0.67003895 | 1.196962532 |
| ENSG00000147123 | NDUFB11 subnetwork | 0.81369348 | 1.196971377 |
| KEGG_RNA_DEGRADATION | KEGG_RNA_DEGRADATION | 0.68357465 | 1.197009868 |
| REACTOME_APCCCDC20_MED | REACTOME_APCCCDC20_MEDIATED_DEGRADATION_OF_S | 0.67707131 | 1.197017523 |
| GO:0015399 | primary active transmembrane transporter activity | 0.67822652 | 1.197022526 |
| ENSG00000104835 | FBXO17 subnetwork | 0.81330547 | 1.197030651 |
| MP:0000876 | Purkinje cell degeneration | 0.6767291 | 1.197040106 |
| REACTOME_GRB2_EVENTS_IN | REACTOME_GRB2_EVENTS_IN_EGFR_SIGNALING | 0.67695637 | 1.197047173 |
| ENSG00000137076 | TLN1 subnetwork | 0.67667382 | 1.197057764 |
| ENSG00000134216 | CHIA subnetwork | 0.81367349 | 1.197071868 |
| ENSG00000104435 | STMN2 subnetwork | 0.67915409 | 1.197073959 |
| ENSG00000150768 | DLAT subnetwork | 0.67659351 | 1.197075426 |
| MP:0011290 | decreased nephron number | 0.67629907 | 1.19708038 |
| ENSG00000152795 | HNRPDL subnetwork | 0.68351446 | 1.197080856 |
| ENSG00000085563 | ABCB1 subnetwork | 0.68345249 | 1.197104293 |
| GO:0000315 | organellar large ribosomal subunit | 0.81330422 | 1.197151356 |
| ENSG00000004864 | SLC25A13 subnetwork | 0.81366444 | 1.19718246 |
| GO:0042446 | hormone biosynthetic process | 0.67658644 | 1.197195195 |
| ENSG00000198780 | FAM169A subnetwork | 0.68410822 | 1.197201759 |
| GO:0005770 | late endosome | 0.68003152 | 1.197202964 |
| GO:0072594 | establishment of protein localization to organelle | 0.68089643 | 1.197206637 |
| ENSG00000103740 | ACSBG1 subnetwork | 0.67914853 | 1.197217235 |
| ENSG00000160973 | FOXH1 subnetwork | 0.67995859 | 1.197220562 |
| ENSG00000204308 | RNF5 subnetwork | 0.6834396 | 1.197222883 |
| ENSG00000197956 | S100A6 subnetwork | 0.68296993 | 1.197233131 |
| GO:0007292 | female gamete generation | 0.81358204 | 1.197237625 |
| GO:0005762 | mitochondrial large ribosomal subunit | 0.81330422 | 1.197272086 |
| ENSG00000198692 | EIF1AY subnetwork | 0.67654105 | 1.197284959 |
| GO:0051279 | regulation of release of sequestered calcium ion into cytosc | 0.6831265 | 1.197316754 |
| MP:0003070 | increased vascular permeability | 0.68555054 | 1.197325664 |
| MP:0002679 | abnormal corpus luteum morphology | 0.6798425 | 1.197339471 |
| GO:0009312 | oligosaccharide biosynthetic process | 0.68018888 | 1.197340743 |
| ENSG00000129990 | SYT5 subnetwork | 0.68089278 | 1.197343601 |
| ENSG00000196954 | CASP4 subnetwork | 0.68503554 | 1.197347496 |
| MP:0000521 | abnormal kidney cortex morphology | 0.68294888 | 1.197351821 |
| GO:0072376 | protein activation cascade | 0.68543769 | 1.197354686 |
| ENSG00000169020 | ATP5I subnetwork | 0.67995243 | 1.197363702 |
| ENSG00000183574 | RNF5 subnetwork | 0.6834396 | 1.197365291 |
| ENSG00000112312 | GMNN subnetwork | 0.68551662 | 1.197372791 |
| ENSG00000188994 | ZNF292 subnetwork | 0.81330131 | 1.197392839 |

| | | | |
|---|---|---|---|
| GO:0090307 | spindle assembly involved in mitosis | 0.68536393 | 1.197401827 |
| MP:0009264 | failure of eyelid fusion | 0.68648949 | 1.197406135 |
| ENSG00000090615 | GOLGA3 subnetwork | 0.68489958 | 1.19740622 |
| MP:0001211 | wrinkled skin | 0.68431787 | 1.197415944 |
| GO:0005544 | calcium-dependent phospholipid binding | 0.682169 | 1.197420162 |
| ENSG00000136011 | STAB2 subnetwork | 0.67954252 | 1.197421632 |
| REACTOME_RESPIRATORY_ELE | REACTOME_RESPIRATORY_ELECTRON_TRANSPORT_ATP_S' | 0.68274476 | 1.197440171 |
| GO:0019003 | GDP binding | 0.68208904 | 1.19744369 |
| GO:0045263 | proton-transporting ATP synthase complex, coupling factor | 0.68478134 | 1.197447162 |
| ENSG00000100167 | SEPT3 subnetwork | 0.68644234 | 1.197447287 |
| GO:0033238 | regulation of cellular amine metabolic process | 0.68267749 | 1.197451774 |
| GO:0032731 | positive regulation of interleukin-1 beta production | 0.68638279 | 1.197458832 |
| GO:0034644 | cellular response to UV | 0.68629616 | 1.197470379 |
| ENSG00000196470 | SIAH1 subnetwork | 0.67978007 | 1.197470398 |
| MP:0001496 | audiogenic seizures | 0.67983714 | 1.197470701 |
| GO:0006041 | glucosamine metabolic process | 0.68088674 | 1.197474627 |
| KEGG_AXON_GUIDANCE | KEGG_AXON_GUIDANCE | 0.68262557 | 1.197475289 |
| GO:0030010 | establishment of cell polarity | 0.68285084 | 1.19747619 |
| ENSG00000147601 | TERF1 subnetwork | 0.68579755 | 1.197480436 |
| ENSG00000099725 | ENSG00000099725 subnetwork | 0.68590076 | 1.197480735 |
| GO:0048471 | perinuclear region of cytoplasm | 0.68293257 | 1.197482443 |
| ENSG00000120805 | ARL1 subnetwork | 0.68487057 | 1.197489018 |
| ENSG00000167283 | ATP5L subnetwork | 0.68503388 | 1.197489614 |
| GO:0046131 | pyrimidine ribonucleoside metabolic process | 0.67963314 | 1.197499701 |
| GO:0015931 | nucleobase-containing compound transport | 0.67970976 | 1.1975 |
| GO:0043555 | regulation of translation in response to stress | 0.68473028 | 1.197500297 |
| ENSG00000065665 | SEC61A2 subnetwork | 0.81328912 | 1.19750353 |
| ENSG00000206254 | ENSG00000206254 subnetwork | 0.6834396 | 1.197507733 |
| ENSG00000170312 | CDK1 subnetwork | 0.68533661 | 1.197508306 |
| ENSG00000170248 | PDCD6IP subnetwork | 0.68113224 | 1.197523275 |
| GO:0051187 | cofactor catabolic process | 0.68465379 | 1.197523753 |
| GO:0045005 | maintenance of fidelity involved in DNA-dependent DNA re | 0.68448915 | 1.197535044 |
| ENSG00000119917 | IFIT3 subnetwork | 0.68178997 | 1.197537563 |
| GO:0009112 | nucleobase metabolic process | 0.68038066 | 1.197538241 |
| ENSG00000105048 | TNNT1 subnetwork | 0.81324227 | 1.19754363 |
| ENSG00000135424 | ITGA7 subnetwork | 0.68207748 | 1.197544696 |
| ENSG00000143333 | RGS16 subnetwork | 0.68608916 | 1.197558374 |
| GO:0005753 | mitochondrial proton-transporting ATP synthase complex | 0.68195524 | 1.197561993 |
| GO:0008305 | integrin complex | 0.68172157 | 1.197567084 |
| GO:0008033 | tRNA processing | 0.68577138 | 1.197569074 |
| GO:0032479 | regulation of type I interferon production | 0.68162967 | 1.197578721 |
| ENSG00000078967 | UBE2D4 subnetwork | 0.68526717 | 1.19757921 |
| GO:0030670 | phagocytic vesicle membrane | 0.68668727 | 1.197584083 |
| GO:0043550 | regulation of lipid kinase activity | 0.68460759 | 1.197588787 |
| ENSG00000111816 | FRK subnetwork | 0.68058318 | 1.197592593 |
| GO:0016645 | oxidoreductase activity, acting on the CH-NH group of donc | 0.68261347 | 1.197594092 |
| GO:0045540 | regulation of cholesterol biosynthetic process | 0.68627477 | 1.197594502 |
| GO:0050909 | sensory perception of taste | 0.68203987 | 1.197604005 |
| GO:0016893 | endonuclease activity, active with either ribo- or deoxyribo | 0.68341916 | 1.197608566 |
| GO:0006044 | N-acetylglucosamine metabolic process | 0.68088674 | 1.197617626 |
| ENSG00000145242 | EPHA5 subnetwork | 0.68141115 | 1.197625582 |
| ENSG00000164344 | KLKB1 subnetwork | 0.68052764 | 1.197628152 |
| GO:0040037 | negative regulation of fibroblast growth factor receptor sig | 0.68604178 | 1.197641062 |

| | | | |
|---|---|---|---|
| GO:0004691 | cAMP-dependent protein kinase activity | 0.68148202 | 1.19764376 |
| GO:0001619 | lysosphingolipid and lysophosphatidic acid receptor activity | 0.8132149 | 1.19764427 |
| ENSG00000109814 | UGDH subnetwork | 0.68714468 | 1.197650331 |
| MP:0005620 | abnormal muscle contractility | 0.68067143 | 1.197664556 |
| GO:0005795 | Golgi stack | 0.68192461 | 1.197669012 |
| GO:0009055 | electron carrier activity | 0.68084804 | 1.197671086 |
| ENSG00000197579 | TOPORS subnetwork | 0.68623686 | 1.1976831 |
| ENSG00000116903 | EXOC8 subnetwork | 0.68159103 | 1.197685793 |
| MP:0004599 | abnormal vertebral arch morphology | 0.68258646 | 1.197695057 |
| GO:0051117 | ATPase binding | 0.68138504 | 1.197720764 |
| MP:0004322 | abnormal sternebra morphology | 0.68698706 | 1.197732655 |
| ENSG00000100664 | EIF5 subnetwork | 0.68740202 | 1.197739645 |
| REACTOME_P130CAS_LINKAGI | REACTOME_P130CAS_LINKAGE_TO_MAPK_SIGNALING_FO | 0.81319822 | 1.197749975 |
| GO:0006825 | copper ion transport | 0.68729466 | 1.197751213 |
| ENSG00000101004 | NINL subnetwork | 0.68712334 | 1.1977566 |
| GO:0001578 | microtubule bundle formation | 0.68079032 | 1.197766364 |
| ENSG00000186432 | KPNA4 subnetwork | 0.68249824 | 1.197783868 |
| ENSG00000175213 | ZNF408 subnetwork | 0.81314527 | 1.197785066 |
| GO:0030675 | Rac GTPase activator activity | 0.68691709 | 1.197785672 |
| MP:0000748 | progressive muscle weakness | 0.81306406 | 1.197789888 |
| ENSG00000115677 | HDLBP subnetwork | 0.68136008 | 1.197798067 |
| GO:0015924 | mannosyl-oligosaccharide mannosidase activity | 0.68257845 | 1.197831785 |
| ENSG00000206376 | EHMT2 subnetwork | 0.81306191 | 1.19789564 |
| ENSG00000007047 | MARK4 subnetwork | 0.68756725 | 1.19791149 |
| MP:0002211 | abnormal primary sex determination | 0.68771741 | 1.197970894 |
| ENSG00000137324 | ENSG00000137324 subnetwork | 0.81306191 | 1.198016554 |
| ENSG00000198886 | MT-ND4 subnetwork | 0.81257517 | 1.198091102 |
| GO:0005123 | death receptor binding | 0.81253146 | 1.198126263 |
| ENSG00000198018 | ENTPD7 subnetwork | 0.81296168 | 1.198132256 |
| ENSG00000204371 | EHMT2 subnetwork | 0.81306191 | 1.198137492 |
| GO:0044070 | regulation of anion transport | 0.68803612 | 1.198160634 |
| ENSG00000092108 | SCFD1 subnetwork | 0.68815544 | 1.19819042 |
| GO:0051048 | negative regulation of secretion | 0.81293362 | 1.198192649 |
| GO:0031998 | regulation of fatty acid beta-oxidation | 0.81249963 | 1.198216992 |
| GO:0033177 | proton-transporting two-sector ATPase complex, proton-tra | 0.68798354 | 1.198225482 |
| MP:0008843 | absent subcutaneous adipose tissue | 0.68845408 | 1.198267912 |
| MP:0000562 | polydactyly | 0.81292852 | 1.198303544 |
| ENSG00000134057 | CCNB1 subnetwork | 0.81247992 | 1.198307739 |
| ENSG00000173545 | ZNF622 subnetwork | 0.68829721 | 1.198308893 |
| MP:0001255 | decreased body height | 0.81284102 | 1.198318522 |
| ENSG00000055957 | ITIH1 subnetwork | 0.81243291 | 1.19836314 |
| MP:0000281 | abnormal interventricular septum morphology | 0.68843794 | 1.198397777 |
| GO:0032592 | integral to mitochondrial membrane | 0.81239156 | 1.198408448 |
| ENSG00000118271 | TTR subnetwork | 0.81235505 | 1.198499242 |
| GO:0031091 | platelet alpha granule | 0.81227998 | 1.198529412 |
| REACTOME_MUSCLE_CONTRA | REACTOME_MUSCLE_CONTRACTION | 0.68921826 | 1.198582398 |
| GO:0007184 | SMAD protein import into nucleus | 0.69282242 | 1.198589231 |
| GO:0019825 | oxygen binding | 0.81222734 | 1.198589912 |
| GO:0001660 | fever generation | 0.69247996 | 1.198600329 |
| GO:0031124 | mRNA 3'-end processing | 0.68874094 | 1.198616858 |
| ENSG00000136574 | GATA4 subnetwork | 0.68908497 | 1.19862342 |
| GO:0000216 | M/G1 transition of mitotic cell cycle | 0.6926261 | 1.198629895 |
| ENSG00000132773 | TOE1 subnetwork | 0.68995522 | 1.198642748 |

| | | | |
|---|---|---|---|
| MP:0003912 | decreased drinking behavior | 0.68916597 | 1.198647212 |
| ENSG00000196872 | C2orf55 subnetwork | 0.68991706 | 1.198666195 |
| ENSG00000163737 | PF4 subnetwork | 0.68944788 | 1.198671312 |
| MP:0001313 | increased incidence of corneal inflammation | 0.69293591 | 1.198683437 |
| ENSG00000138756 | BMP2K subnetwork | 0.68985825 | 1.198683745 |
| GO:0005516 | calmodulin binding | 0.81222073 | 1.198695916 |
| GO:0030427 | site of polarized growth | 0.68905278 | 1.198700071 |
| GO:0018298 | protein-chromophore linkage | 0.69246998 | 1.198729561 |
| ENSG00000008853 | RHOBTB2 subnetwork | 0.69281583 | 1.198730159 |
| ENSG00000120254 | MTHFD1L subnetwork | 0.69011781 | 1.198731414 |
| ENSG00000165156 | ZHX1 subnetwork | 0.68940211 | 1.198736121 |
| ENSG00000148297 | MED22 subnetwork | 0.69275642 | 1.198741769 |
| GO:0046365 | monosaccharide catabolic process | 0.68958466 | 1.198742324 |
| MP:0003139 | patent ductus arteriosus | 0.6923384 | 1.198758677 |
| GO:0002070 | epithelial cell maturation | 0.81217622 | 1.1987615 |
| MP:0004491 | abnormal orientation of outer hair cell stereociliary bundles | 0.69240347 | 1.198764706 |
| ENSG00000163235 | TGFA subnetwork | 0.81210765 | 1.198776542 |
| ENSG00000115594 | IL1R1 subnetwork | 0.69306956 | 1.198777621 |
| ENSG00000105726 | ATP13A1 subnetwork | 0.68889431 | 1.198788416 |
| ENSG00000147905 | ZCCHC7 subnetwork | 0.68902763 | 1.198794469 |
| GO:0048730 | epidermis morphogenesis | 0.68983843 | 1.198801653 |
| GO:0065005 | protein-lipid complex assembly | 0.81201784 | 1.198811811 |
| ENSG00000188536 | HBA2 subnetwork | 0.6920552 | 1.19881709 |
| GO:0045922 | negative regulation of fatty acid metabolic process | 0.69031605 | 1.198837895 |
| MP:0002621 | delayed neural tube closure | 0.69326471 | 1.198848414 |
| ENSG00000211973 | ENSG00000211973 subnetwork | 0.69192512 | 1.198858017 |
| ENSG00000114784 | EIF1B subnetwork | 0.69026252 | 1.198861357 |
| REACTOME_RNA_POLYMERAS | REACTOME_RNA_POLYMERASE_III_TRANSCRIPTION_INITIA | 0.69321122 | 1.198877659 |
| REACTOME_SHC1_EVENTS_IN_ | REACTOME_SHC1_EVENTS_IN_EGFR_SIGNALING | 0.69233498 | 1.198893857 |
| GO:0034377 | plasma lipoprotein particle assembly | 0.81201784 | 1.19893305 |
| GO:0042572 | retinol metabolic process | 0.69228885 | 1.198934918 |
| GO:0015464 | acetylcholine receptor activity | 0.68983169 | 1.198937301 |
| ENSG00000173726 | TOMM20 subnetwork | 0.69345265 | 1.198954417 |
| ENSG00000206172 | HBA1 subnetwork | 0.6920552 | 1.198958211 |
| GO:0034329 | cell junction assembly | 0.81195405 | 1.198968342 |
| GO:0032026 | response to magnesium ion | 0.81149959 | 1.198982999 |
| ENSG00000211979 | ENSG00000211979 subnetwork | 0.69192512 | 1.198999176 |
| ENSG00000213512 | GBP7 subnetwork | 0.81172395 | 1.199023675 |
| ENSG00000138642 | HERC6 subnetwork | 0.69095527 | 1.199027352 |
| GO:0001833 | inner cell mass cell proliferation | 0.69077508 | 1.199038915 |
| ENSG00000111725 | PRKAB1 subnetwork | 0.6934332 | 1.199042416 |
| GO:0015238 | drug transmembrane transporter activity | 0.69357732 | 1.199048514 |
| ENSG00000138439 | FAM117B subnetwork | 0.81166947 | 1.199069109 |
| MP:0008658 | decreased interleukin-1 beta secretion | 0.69188488 | 1.199069713 |
| GO:0060323 | head morphogenesis | 0.81146229 | 1.199079041 |
| ENSG00000173540 | GMPPB subnetwork | 0.8119426 | 1.199079506 |
| GO:0015934 | large ribosomal subunit | 0.69128466 | 1.199080731 |
| ENSG00000136243 | NUPL2 subnetwork | 0.69541575 | 1.199086116 |
| ENSG00000140451 | PIF1 subnetwork | 0.69120907 | 1.199098303 |
| ENSG00000101400 | SNTA1 subnetwork | 0.81189404 | 1.199124937 |
| GO:0042632 | cholesterol homeostasis | 0.81143372 | 1.199144737 |
| ENSG00000196586 | MYO6 subnetwork | 0.69481492 | 1.199155623 |
| ENSG00000152804 | HHEX subnetwork | 0.69537915 | 1.199162175 |

| | | | |
|---|---|---|---|
| ENSG00000090006 | LTBP4 subnetwork | 0.6909546 | 1.19916873 |
| ENSG00000047249 | ATP6V1H subnetwork | 0.69474788 | 1.199178982 |
| REACTOME_SEMA3A_PAK_DEI | REACTOME_SEMA3A_PAK_DEPENDENT_AXON_REPULSION | 0.69077342 | 1.199180328 |
| MP:0002014 | increased papilloma incidence | 0.69187933 | 1.199181486 |
| MP:0009674 | decreased birth weight | 0.69151638 | 1.199192883 |
| ENSG00000156453 | PCDH1 subnetwork | 0.69115672 | 1.199198397 |
| GO:0015450 | P-P-bond-hydrolysis-driven protein transmembrane transpo | 0.8109699 | 1.199205063 |
| GO:0060041 | retina development in camera-type eye | 0.6950081 | 1.199208582 |
| ENSG00000087250 | MT3 subnetwork | 0.69142513 | 1.199210464 |
| ENSG00000213619 | NDUFS3 subnetwork | 0.79089301 | 1.199212027 |
| REACTOME_SIGNALING_BY_BI | REACTOME_SIGNALING_BY_BMP | 0.79100947 | 1.199212109 |
| ENSG00000119013 | NDUFB3 subnetwork | 0.81037267 | 1.1992197 |
| ENSG00000198925 | ATG9A subnetwork | 0.69578385 | 1.199226985 |
| ENSG00000168005 | C11orf84 subnetwork | 0.81082233 | 1.199240352 |
| REACTOME_PKA_ACTIVATION | REACTOME_PKA_ACTIVATION | 0.69492289 | 1.199243668 |
| ENSG00000143079 | CTTNBP2NL subnetwork | 0.69072367 | 1.199245105 |
| ENSG00000108826 | MRPL27 subnetwork | 0.69425757 | 1.199248738 |
| MP:0009780 | abnormal chondrocyte physiology | 0.69571858 | 1.199250322 |
| GO:0055093 | response to hyperoxia | 0.69165212 | 1.199251885 |
| GO:0001558 | regulation of cell growth | 0.69182476 | 1.199252061 |
| MP:0004073 | caudal body truncation | 0.81069824 | 1.19925547 |
| ENSG00000108179 | PPIF subnetwork | 0.69382335 | 1.199260042 |
| GO:0003230 | cardiac atrium development | 0.81091545 | 1.199260685 |
| ENSG00000116852 | KIF21B subnetwork | 0.69173177 | 1.199263753 |
| GO:0055092 | sterol homeostasis | 0.81143372 | 1.19926612 |
| ENSG00000107371 | EXOSC3 subnetwork | 0.69565035 | 1.199273664 |
| ENSG00000164687 | FABP5 subnetwork | 0.790562 | 1.199294679 |
| ENSG00000145494 | NDUFS6 subnetwork | 0.81122748 | 1.199296345 |
| ENSG00000014216 | CAPN1 subnetwork | 0.69537125 | 1.199296848 |
| GO:0071396 | cellular response to lipid | 0.69473613 | 1.199302053 |
| ENSG00000171603 | CLSTN1 subnetwork | 0.81034138 | 1.199305767 |
| ENSG00000090266 | NDUFB2 subnetwork | 0.81115435 | 1.199306399 |
| ENSG00000133392 | MYH11 subnetwork | 0.69392518 | 1.199307105 |
| GO:0021761 | limbic system development | 0.79087984 | 1.199310452 |
| MP:0004765 | decreased brainstem auditory evoked potential | 0.78828296 | 1.199313573 |
| GO:0050772 | positive regulation of axonogenesis | 0.8105863 | 1.199316109 |
| ENSG00000213949 | ITGA1 subnetwork | 0.79248496 | 1.199316912 |
| GO:0001960 | negative regulation of cytokine-mediated signaling pathwa | 0.78771652 | 1.19932348 |
| GO:0016045 | detection of bacterium | 0.69465647 | 1.199325434 |
| GO:0031952 | regulation of protein autophosphorylation | 0.78745632 | 1.199328475 |
| GO:0007346 | regulation of mitotic cell cycle | 0.79066048 | 1.199331052 |
| ENSG00000113889 | KNG1 subnetwork | 0.69069994 | 1.199339389 |
| MP:0001982 | decreased chemically-elicited antinociception | 0.7871935 | 1.199343887 |
| ENSG00000198700 | IPO9 subnetwork | 0.81068091 | 1.199351636 |
| GO:0009309 | amine biosynthetic process | 0.78728611 | 1.199354368 |
| ENSG00000172432 | GTPBP2 subnetwork | 0.78839589 | 1.199365641 |
| ENSG00000180817 | PPA1 subnetwork | 0.8105473 | 1.199376837 |
| ENSG00000037749 | MFAP3 subnetwork | 0.78739038 | 1.199380466 |
| ENSG00000125485 | DDX31 subnetwork | 0.78822102 | 1.199381111 |
| ENSG00000113368 | LMNB1 subnetwork | 0.81142149 | 1.199382466 |
| GO:0031011 | Ino80 complex | 0.78643079 | 1.199384968 |
| MP:0010299 | increased mammary gland tumor incidence | 0.69425703 | 1.199389528 |
| GO:0005518 | collagen binding | 0.7871295 | 1.199390688 |

| | | | |
|---|---|---|---|
| MP:0003345 | decreased rib number | 0.69534308 | 1.19939639 |
| ENSG00000109846 | CRYAB subnetwork | 0.69610425 | 1.199397026 |
| GO:0016324 | apical plasma membrane | 0.78767635 | 1.199411887 |
| GO:0005976 | polysaccharide metabolic process | 0.79084719 | 1.199414083 |
| ENSG00000138685 | FGF2 subnetwork | 0.78817574 | 1.199417456 |
| REACTOME_TRAF6_MEDIATED | REACTOME_TRAF6_MEDIATED_IRF7_ACTIVATION | 0.79055822 | 1.199419087 |
| GO:0034362 | low-density lipoprotein particle | 0.79264381 | 1.19942047 |
| ENSG00000165309 | ARMC3 subnetwork | 0.78997159 | 1.199423915 |
| GO:0051129 | negative regulation of cellular component organization | 0.81033965 | 1.199427326 |
| GO:0005506 | iron ion binding | 0.79247504 | 1.199430701 |
| GO:0035091 | phosphatidylinositol binding | 0.69411507 | 1.199442226 |
| ENSG00000123700 | KCNJ2 subnetwork | 0.69457103 | 1.199448486 |
| MP:0000530 | abnormal kidney blood vessel morphology | 0.69465138 | 1.199448551 |
| ENSG00000164404 | GDF9 subnetwork | 0.7871115 | 1.19946875 |
| GO:0001738 | morphogenesis of a polarized epithelium | 0.69627684 | 1.199473191 |
| ENSG00000167491 | GATAD2A subnetwork | 0.69606948 | 1.199478923 |
| GO:0010576 | metalloenzyme regulator activity | 0.8102902 | 1.199483021 |
| ENSG00000157349 | DDX19B subnetwork | 0.69422137 | 1.199483386 |
| GO:0003281 | ventricular septum development | 0.79050313 | 1.199486461 |
| GO:0070168 | negative regulation of biomineral tissue development | 0.7928576 | 1.199487843 |
| GO:0019787 | small conjugating protein ligase activity | 0.78995503 | 1.199506903 |
| GO:0031093 | platelet alpha granule lumen | 0.81017871 | 1.199508263 |
| GO:0033202 | DNA helicase complex | 0.78643079 | 1.199510008 |
| ENSG00000127388 | ENSG00000127388 subnetwork | 0.69532548 | 1.199513539 |
| MP:0005319 | abnormal enzyme/ coenzyme level | 0.79311153 | 1.199519032 |
| ENSG00000167900 | TK1 subnetwork | 0.78767129 | 1.199521133 |
| ENSG00000105127 | AKAP8 subnetwork | 0.79304658 | 1.199524154 |
| MP:0008546 | abnormal vesicle-mediated transport | 0.80452548 | 1.199530564 |
| ENSG00000164107 | HAND2 subnetwork | 0.69454375 | 1.199530572 |
| ENSG00000133318 | RTN3 subnetwork | 0.78977592 | 1.19953795 |
| ENSG00000112983 | BRD8 subnetwork | 0.78817328 | 1.199542239 |
| ENSG00000115274 | INO80B subnetwork | 0.78987627 | 1.199543189 |
| MP:0009885 | abnormal palatal shelf elevation | 0.69602143 | 1.199549128 |
| GO:0007220 | Notch receptor processing | 0.79246494 | 1.199549689 |
| GO:0034383 | low-density lipoprotein particle clearance | 0.80335813 | 1.199550378 |
| ENSG00000152268 | ENSG00000152268 subnetwork | 0.78662813 | 1.199551803 |
| ENSG00000164164 | OTUD4 subnetwork | 0.80355089 | 1.199555578 |
| GO:0001836 | release of cytochrome c from mitochondria | 0.78809591 | 1.199557798 |
| ENSG00000151576 | QTRTD1 subnetwork | 0.7868891 | 1.199562363 |
| ENSG00000159082 | SYNJ1 subnetwork | 0.81027872 | 1.199564071 |
| GO:0007492 | endoderm development | 0.79280752 | 1.199565397 |
| GO:0005154 | epidermal growth factor receptor binding | 0.7870875 | 1.199567663 |
| GO:0031970 | organelle envelope lumen | 0.80445443 | 1.199571341 |
| GO:0003009 | skeletal muscle contraction | 0.78700398 | 1.199572828 |
| GO:0001158 | enhancer sequence-specific DNA binding | 0.7904725 | 1.199579788 |
| ENSG00000092531 | SNAP23 subnetwork | 0.79237443 | 1.199580702 |
| MP:0010909 | pulmonary alveolar hemorrhage | 0.7863883 | 1.199588156 |
| GO:0003013 | circulatory system process | 0.80978622 | 1.199619598 |
| MP:0002954 | abnormal aerobic energy metabolism | 0.79303755 | 1.199627561 |
| GO:0046933 | hydrogen ion transporting ATP synthase activity, rotational | 0.81017479 | 1.199629893 |
| ENSG00000081052 | COL4A4 subnetwork | 0.78972272 | 1.19963136 |
| ENSG00000183856 | IQGAP3 subnetwork | 0.79137312 | 1.19963201 |
| GO:0007162 | negative regulation of cell adhesion | 0.69452753 | 1.199642019 |

| | | | |
|---|---|---|---|
| REACTOME_CGMP_EFFECTS | REACTOME_CGMP_EFFECTS | 0.78797466 | 1.199651369 |
| MP:0001408 | stereotypic behavior | 0.78808748 | 1.199651405 |
| ENSG00000197558 | ENSG00000197558 subnetwork | 0.69532548 | 1.199654162 |
| GO:0042993 | positive regulation of transcription factor import into nucle | 0.78686385 | 1.199656107 |
| ENSG00000175602 | CCDC85B subnetwork | 0.80335095 | 1.199657639 |
| MP:0008321 | small adenohypophysis | 0.79211522 | 1.199658208 |
| ENSG00000153707 | PTPRD subnetwork | 0.8044158 | 1.199663162 |
| GO:0006972 | hyperosmotic response | 0.80354152 | 1.199667927 |
| ENSG00000095139 | ARCN1 subnetwork | 0.79045817 | 1.199667946 |
| ENSG00000117500 | TMED5 subnetwork | 0.79218107 | 1.199673778 |
| MP:0010124 | decreased bone mineral content | 0.79027884 | 1.199678256 |
| GO:0000775 | chromosome, centromeric region | 0.78679996 | 1.199682126 |
| GO:0004532 | exoribonuclease activity | 0.78864488 | 1.199682853 |
| GO:0033032 | regulation of myeloid cell apoptotic process | 0.79035743 | 1.199683479 |
| GO:0030916 | otic vesicle formation | 0.79235282 | 1.1996842 |
| MP:0005221 | abnormal rostral-caudal axis patterning | 0.81011468 | 1.199690701 |
| ENSG00000135547 | HEY2 subnetwork | 0.78637835 | 1.199708029 |
| MP:0009409 | abnormal skeletal muscle fiber type ratio | 0.79338218 | 1.199720757 |
| ENSG00000112305 | SMAP1 subnetwork | 0.78967852 | 1.19972479 |
| ENSG00000054116 | TRAPPC3 subnetwork | 0.80978328 | 1.199731156 |
| GO:0051851 | modification by host of symbiont morphology or physiology | 0.79379514 | 1.199736407 |
| ENSG00000184916 | JAG2 subnetwork | 0.80491776 | 1.199739849 |
| ENSG00000159186 | ENSG00000159186 subnetwork | 0.79206777 | 1.19974104 |
| ENSG00000160208 | RRP1B subnetwork | 0.79372713 | 1.199741549 |
| GO:0032091 | negative regulation of protein binding | 0.80334085 | 1.199759812 |
| ENSG00000169347 | GP2 subnetwork | 0.80382221 | 1.199759935 |
| GO:0033280 | response to vitamin D | 0.80955969 | 1.199761518 |
| MP:0000039 | abnormal otic capsule morphology | 0.80439701 | 1.19976521 |
| ENSG00000198010 | DLGAP2 subnetwork | 0.79197919 | 1.199766912 |
| ENSG00000049449 | RCN1 subnetwork | 0.81001285 | 1.199771782 |
| GO:0060761 | negative regulation of response to cytokine stimulus | 0.80327003 | 1.19977512 |
| ENSG00000162374 | ELAVL4 subnetwork | 0.78964269 | 1.199781886 |
| REACTOME_ACTIVATION_OF_A | REACTOME_ACTIVATION_OF_APCC_AND_APCCDC20_ME | 0.79349658 | 1.199782834 |
| GO:0043001 | Golgi to plasma membrane protein transport | 0.79369738 | 1.199782878 |
| GO:0072332 | signal transduction by p53 class mediator resulting in induc | 0.79234114 | 1.199792896 |
| ENSG00000169031 | COL4A3 subnetwork | 0.80488161 | 1.199801041 |
| GO:0030330 | DNA damage response, signal transduction by p53 class me | 0.6968527 | 1.199801077 |
| ENSG00000168765 | GSTM4 subnetwork | 0.78885587 | 1.199802474 |
| MP:0005421 | loose skin | 0.80973635 | 1.199812297 |
| ENSG00000134684 | YARS subnetwork | 0.8101134 | 1.199812373 |
| MP:0002885 | abnormal AMPA-mediated synaptic currents | 0.80543287 | 1.199816476 |
| ENSG00000196415 | PRTN3 subnetwork | 0.78637251 | 1.199822714 |
| ENSG00000088926 | F11 subnetwork | 0.785661 | 1.199838205 |
| ENSG00000074319 | TSG101 subnetwork | 0.78526234 | 1.199843342 |
| GO:0051953 | negative regulation of amine transport | 0.78881296 | 1.199844042 |
| ENSG00000196220 | SRGAP3 subnetwork | 0.80953298 | 1.199847762 |
| GO:0006004 | fucose metabolic process | 0.78632749 | 1.199848769 |
| MP:0000435 | shortened head | 0.79185341 | 1.199854937 |
| GO:0009991 | response to extracellular stimulus | 0.80539872 | 1.199857245 |
| ENSG00000089041 | P2RX7 subnetwork | 0.80968089 | 1.19985794 |
| ENSG00000181929 | PRKAG1 subnetwork | 0.80324871 | 1.199861991 |
| ENSG00000197959 | DNM3 subnetwork | 0.8067757 | 1.199862553 |
| MP:0000371 | diluted coat color | 0.80438141 | 1.199867279 |

| | | | |
|---|---|---|---|
| GO:0005758 | mitochondrial intermembrane space | 0.79365032 | 1.199870748 |
| ENSG00000156976 | EIF4A2 subnetwork | 0.78555098 | 1.199879933 |
| MP:0001515 | abnormal grip strength | 0.79197144 | 1.199880854 |
| GO:0031941 | filamentous actin | 0.7895099 | 1.199885726 |
| GO:0071156 | regulation of cell cycle arrest | 0.80305637 | 1.199887526 |
| GO:0002675 | positive regulation of acute inflammatory response | 0.69662315 | 1.199888798 |
| REACTOME_PLATELET_AGGRE | REACTOME_PLATELET_AGGREGATION_PLUG_FORMATION | 0.69683454 | 1.199888824 |
| ENSG00000111049 | MYF5 subnetwork | 0.785465 | 1.199890362 |
| GO:0051100 | negative regulation of binding | 0.78962923 | 1.199901319 |
| ENSG00000154277 | UCHL1 subnetwork | 0.79180045 | 1.199901554 |
| GO:0003015 | heart process | 0.8051018 | 1.199903091 |
| GO:0001965 | G-protein alpha-subunit binding | 0.78519764 | 1.199905995 |
| MP:0010254 | nuclear cataracts | 0.7862518 | 1.199906123 |
| ENSG00000125356 | NDUFA1 subnetwork | 0.80318868 | 1.199913097 |
| ENSG00000114942 | EEF1B2 subnetwork | 0.8048585 | 1.199913265 |
| GO:0003727 | single-stranded RNA binding | 0.80672018 | 1.199913451 |
| GO:0010894 | negative regulation of steroid biosynthetic process | 0.78616802 | 1.199916545 |
| GO:0016229 | steroid dehydrogenase activity | 0.80534756 | 1.199918417 |
| ENSG00000101084 | C20orf24 subnetwork | 0.78902094 | 1.199927235 |
| GO:0001704 | formation of primary germ layer | 0.78911119 | 1.199937636 |
| GO:0000959 | mitochondrial RNA metabolic process | 0.80566538 | 1.199938838 |
| REACTOME_G2M_CHECKPOIN | REACTOME_G2M_CHECKPOINTS | 0.80603786 | 1.199938863 |
| REACTOME_SOS:MEDIATED_SI | REACTOME_SOS:MEDIATED_SIGNALLING | 0.80302046 | 1.199943757 |
| GO:0005328 | neurotransmitter:sodium symporter activity | 0.79401305 | 1.19994832 |
| GO:0005548 | phospholipid transporter activity | 0.78564401 | 1.199953022 |
| ENSG00000084234 | APLP2 subnetwork | 0.78947947 | 1.199953247 |
| GO:0001501 | skeletal system development | 0.80410448 | 1.199959146 |
| MP:0009278 | abnormal bone marrow cell physiology | 0.80952441 | 1.199959399 |
| GO:0008643 | carbohydrate transport | 0.78516701 | 1.199979108 |
| ENSG00000091513 | TF subnetwork | 0.80435837 | 1.199979579 |
| GO:0035065 | regulation of histone acetylation | 0.80945774 | 1.199979697 |
| GO:0001655 | urogenital system development | 0.80428814 | 1.199984683 |
| GO:0008015 | blood circulation | 0.8066599 | 1.199984725 |
| MP:0000925 | abnormal floor plate morphology | 0.80938474 | 1.199984772 |
| ENSG00000156973 | PDE6D subnetwork | 0.80526903 | 1.1999898 |
| GO:0060669 | embryonic placenta morphogenesis | 0.8053246 | 1.199989801 |
| MP:0000913 | abnormal brain development | 0.78941383 | 1.199994805 |
| MP:0006072 | abnormal retinal apoptosis | 0.78923444 | 1.2 |
| GO:0010862 | positive regulation of pathway-restricted SMAD protein ph | 0.78545573 | 1.200010443 |
| MP:0005293 | impaired glucose tolerance | 0.80922479 | 1.200015232 |
| GO:0051262 | protein tetramerization | 0.69681891 | 1.200017556 |
| GO:0043270 | positive regulation of ion transport | 0.80407036 | 1.200020429 |
| ENSG00000136273 | HUS1 subnetwork | 0.7917951 | 1.200020728 |
| GO:0033687 | osteoblast proliferation | 0.80298198 | 1.200025568 |
| GO:0060590 | ATPase regulator activity | 0.80697613 | 1.200030541 |
| ENSG00000049245 | VAMP3 subnetwork | 0.80602643 | 1.200030572 |
| GO:0055007 | cardiac muscle cell differentiation | 0.80565256 | 1.200035682 |
| GO:0000045 | autophagic vacuole assembly | 0.80178413 | 1.200035846 |
| REACTOME_SYNTHESIS_OF_SU | REACTOME_SYNTHESIS_OF_SUBSTRATES_IN_N:GLYCAN_BI | 0.78609394 | 1.200036519 |
| KEGG_TERPENOID_BACKBONE | KEGG_TERPENOID_BACKBONE_BIOSYNTHESIS | 0.80906412 | 1.200040626 |
| GO:0045939 | negative regulation of steroid metabolic process | 0.78616802 | 1.200041732 |
| MP:0003400 | kinked neural tube | 0.80934394 | 1.20004569 |
| MP:0005136 | decreased growth hormone level | 0.80593281 | 1.200045862 |

| | | | |
|---|---|---|---|
| ENSG00000110786 | PTPN5 subnetwork | 0.78505591 | 1.200047017 |
| GO:0009214 | cyclic nucleotide catabolic process | 0.80916257 | 1.200055855 |
| GO:0000226 | microtubule cytoskeleton organization | 0.78514111 | 1.200057459 |
| GO:0015078 | hydrogen ion transmembrane transporter activity | 0.80899423 | 1.200060945 |
| MP:0003311 | aminoaciduria | 0.80218861 | 1.200066537 |
| GO:0034330 | cell junction organization | 0.80714079 | 1.200071247 |
| ENSG00000186081 | KRT5 subnetwork | 0.80663058 | 1.20007129 |
| GO:0043086 | negative regulation of catalytic activity | 0.80294216 | 1.200076711 |
| MP:0001407 | short stride length | 0.80426486 | 1.200081699 |
| ENSG00000152413 | HOMER1 subnetwork | 0.80188122 | 1.200081925 |
| REACTOME_CDC20PHOSPHO:A | REACTOME_CDC20PHOSPHO:APCC_MEDIATED_DEGRADAT | 0.80894733 | 1.200086347 |
| REACTOME_CELL_SURFACE_IN | REACTOME_CELL_SURFACE_INTERACTIONS_AT_THE_VASC | 0.80585828 | 1.200086637 |
| MP:0000024 | lowered ear position | 0.79429793 | 1.200098161 |
| ENSG00000133805 | AMPD3 subnetwork | 0.78939432 | 1.200103918 |
| MP:0002784 | abnormal Sertoli cell morphology | 0.69719552 | 1.200105275 |
| ENSG00000130066 | SAT1 subnetwork | 0.80709182 | 1.20011706 |
| ENSG00000157985 | AGAP1 subnetwork | 0.801767 | 1.200117792 |
| GO:0001106 | RNA polymerase II transcription corepressor activity | 0.80815972 | 1.200122013 |
| ENSG00000179091 | CYC1 subnetwork | 0.80199208 | 1.200122875 |
| ENSG00000197303 | ENSG00000197303 subnetwork | 0.78608254 | 1.200125222 |
| MP:0002111 | abnormal tail morphology | 0.79179091 | 1.200134743 |
| GO:0045123 | cellular extravasation | 0.80291513 | 1.200153437 |
| ENSG00000175416 | CLTB subnetwork | 0.80168346 | 1.200153657 |
| GO:0003854 | 3-beta-hydroxy-delta5-steroid dehydrogenase activity | 0.8088995 | 1.200157472 |
| GO:0061036 | positive regulation of cartilage development | 0.79899882 | 1.200164406 |
| ENSG00000104725 | ENSG00000104725 subnetwork | 0.79420121 | 1.200165358 |
| GO:0043038 | amino acid activation | 0.80861224 | 1.200167683 |
| GO:0015074 | DNA integration | 0.78505538 | 1.200172414 |
| MP:0006036 | abnormal mitochondrial physiology | 0.80632175 | 1.200173204 |
| GO:0072524 | pyridine-containing compound metabolic process | 0.80218345 | 1.200174038 |
| GO:0051603 | proteolysis involved in cellular protein catabolic process | 0.7989329 | 1.200174699 |
| GO:2001021 | negative regulation of response to DNA damage stimulus | 0.79427561 | 1.200180841 |
| ENSG00000032742 | IFT88 subnetwork | 0.80239037 | 1.200184237 |
| ENSG00000061676 | NCKAP1 subnetwork | 0.80662434 | 1.200193522 |
| GO:0015485 | cholesterol binding | 0.8028667 | 1.200194373 |
| ENSG00000143322 | ABL2 subnetwork | 0.80783629 | 1.200198352 |
| ENSG00000136709 | WDR33 subnetwork | 0.78605796 | 1.200213943 |
| MP:0009873 | abnormal aorta tunica media morphology | 0.80163247 | 1.200220264 |
| ENSG00000169896 | ITGAM subnetwork | 0.69718999 | 1.200228124 |
| GO:0019902 | phosphatase binding | 0.76809041 | 1.200234767 |
| ENSG00000164251 | F2RL1 subnetwork | 0.80141217 | 1.20023568 |
| GO:0001191 | RNA polymerase II transcription factor binding transcriptior | 0.80815972 | 1.200244051 |
| GO:0009147 | pyrimidine nucleoside triphosphate metabolic process | 0.76787681 | 1.200245517 |
| GO:0006690 | icosanoid metabolic process | 0.69733294 | 1.20025731 |
| ENSG00000146457 | WTAP subnetwork | 0.80736424 | 1.200259516 |
| ENSG00000161970 | RPL26 subnetwork | 0.78502623 | 1.20026126 |
| MP:0005132 | decreased luteinizing hormone level | 0.78473037 | 1.20026137 |
| GO:0010927 | cellular component assembly involved in morphogenesis | 0.76798264 | 1.200261501 |
| ENSG00000102119 | EMD subnetwork | 0.80887544 | 1.200264174 |
| GO:0042147 | retrograde transport, endosome to Golgi | 0.78463789 | 1.200271853 |
| MP:0001340 | abnormal eyelid morphology | 0.80878099 | 1.200274362 |
| ENSG00000173281 | PPP1R3B subnetwork | 0.80660128 | 1.200275033 |
| GO:0043039 | tRNA aminoacylation | 0.80861224 | 1.200289664 |

| | | | |
|---|---|---|---|
| ENSG00000206509 | HLA-F subnetwork | 0.80129675 | 1.200292098 |
| ENSG00000183155 | RABIF subnetwork | 0.80780816 | 1.200295015 |
| GO:0019362 | pyridine nucleotide metabolic process | 0.80218345 | 1.200296918 |
| ENSG00000172660 | TAF15 subnetwork | 0.78602845 | 1.200297464 |
| ENSG00000107281 | NPDC1 subnetwork | 0.79893257 | 1.200298047 |
| GO:0045767 | regulation of anti-apoptosis | 0.80138479 | 1.200302316 |
| GO:0003309 | type B pancreatic cell differentiation | 0.80285082 | 1.200312052 |
| ENSG00000077514 | POLD3 subnetwork | 0.80268589 | 1.200317233 |
| ENSG00000141052 | MYOCD subnetwork | 0.79848269 | 1.200318799 |
| GO:0004602 | glutathione peroxidase activity | 0.80652539 | 1.200320905 |
| ENSG00000198742 | SMURF1 subnetwork | 0.7680695 | 1.200325507 |
| MP:0008976 | delayed female fertility | 0.80773444 | 1.200335741 |
| GO:0043331 | response to dsRNA | 0.76824034 | 1.200336108 |
| ENSG00000171747 | LGALS4 subnetwork | 0.80163085 | 1.200343238 |
| MP:0011096 | complete embryonic lethality before somite formation | 0.6978127 | 1.200344828 |
| MP:0005269 | abnormal occipital bone morphology | 0.76786966 | 1.200346963 |
| ENSG00000129562 | DAD1 subnetwork | 0.784997 | 1.200355351 |
| GO:0042625 | ATPase activity, coupled to transmembrane movement of i | 0.80855209 | 1.200355763 |
| GO:0010171 | body morphogenesis | 0.80814854 | 1.200355944 |
| GO:0032494 | response to peptidoglycan | 0.69717915 | 1.20035685 |
| ENSG00000100852 | ARHGAP5 subnetwork | 0.79888907 | 1.200359749 |
| GO:0008016 | regulation of heart contraction | 0.78490508 | 1.200360615 |
| MP:0004324 | vestibular hair cell degeneration | 0.80840226 | 1.200371086 |
| ENSG00000138668 | HNRNPD subnetwork | 0.78443616 | 1.2003713 |
| ENSG00000111652 | COPS7A subnetwork | 0.8075556 | 1.200371426 |
| GO:0032369 | negative regulation of lipid transport | 0.80766251 | 1.20038665 |
| MP:0005658 | increased susceptibility to diet-induced obesity | 0.76782394 | 1.200389707 |
| ENSG00000166136 | NDUFB8 subnetwork | 0.80850526 | 1.200391379 |
| MP:0000837 | abnormal hypothalamus morphology | 0.80127739 | 1.200394629 |
| ENSG00000125450 | NUP85 subnetwork | 0.7848478 | 1.20039724 |
| ENSG00000115232 | ITGA4 subnetwork | 0.78463029 | 1.200397365 |
| ENSG00000122585 | NPY subnetwork | 0.80082227 | 1.200410214 |
| MP:0003961 | decreased lean body mass | 0.76775659 | 1.200411105 |
| GO:0072384 | organelle transport along microtubule | 0.79845972 | 1.200411396 |
| ENSG00000134025 | ENSG00000134025 subnetwork | 0.79461529 | 1.200413266 |
| GO:0046982 | protein heterodimerization activity | 0.8028404 | 1.200414407 |
| ENSG00000204175 | GPRIN2 subnetwork | 0.79861631 | 1.200416452 |
| MP:0001953 | respiratory failure | 0.80120443 | 1.200420297 |
| GO:0033688 | regulation of osteoblast proliferation | 0.80091136 | 1.200420427 |
| ENSG00000196655 | TRAPPC4 subnetwork | 0.80267679 | 1.200434961 |
| REACTOME_TRANSPORT_OF_M | REACTOME_TRANSPORT_OF_MATURE_MRNA_DERIVED_FI | 0.76767693 | 1.200448526 |
| GO:0004303 | estradiol 17-beta-dehydrogenase activity | 0.78457993 | 1.200449697 |
| GO:0060541 | respiratory system development | 0.80813213 | 1.200457689 |
| GO:0022829 | wide pore channel activity | 0.76761359 | 1.200464595 |
| GO:0042044 | fluid transport | 0.78441637 | 1.200475941 |
| ENSG00000110244 | APOA4 subnetwork | 0.80105779 | 1.200476776 |
| ENSG00000170542 | SERPINB9 subnetwork | 0.69779562 | 1.200479308 |
| MP:0002106 | abnormal muscle physiology | 0.79888716 | 1.200483141 |
| GO:0001608 | G-protein coupled nucleotide receptor activity | 0.69772277 | 1.20048521 |
| GO:0035254 | glutamate receptor binding | 0.80117306 | 1.200492106 |
| KEGG_CELL_CYCLE | KEGG_CELL_CYCLE | 0.80079781 | 1.200497436 |
| GO:0042476 | odontogenesis | 0.76754191 | 1.20050737 |
| MP:0005103 | abnormal retinal pigmentation | 0.79844863 | 1.20051944 |

| | | | |
|---|---|---|---|
| ENSG00000114978 | MOB1A subnetwork | 0.7670569 | 1.200529072 |
| ENSG00000169592 | INO80E subnetwork | 0.7948602 | 1.200537135 |
| ENSG00000149084 | HSD17B12 subnetwork | 0.76713513 | 1.200539703 |
| MP:0006279 | abnormal limb development | 0.79479633 | 1.200557851 |
| GO:0000793 | condensed chromosome | 0.79886511 | 1.200560296 |
| ENSG00000150347 | ARID5B subnetwork | 0.69957726 | 1.20056573 |
| ENSG00000173581 | CCDC106 subnetwork | 0.76894112 | 1.200575754 |
| MP:0002062 | abnormal associative learning | 0.76921703 | 1.2005809 |
| ENSG00000204531 | POU5F1 subnetwork | 0.79838099 | 1.200581216 |
| MP:0000233 | abnormal blood flow velocity | 0.76846377 | 1.200581457 |
| ENSG00000121691 | CAT subnetwork | 0.6996752 | 1.200583158 |
| ENSG00000118680 | MYL12B subnetwork | 0.80078332 | 1.200589804 |
| GO:0016814 | hydrolase activity, acting on carbon-nitrogen (but not pepti | 0.76743116 | 1.200592949 |
| ENSG00000170296 | GABARAP subnetwork | 0.76660622 | 1.200593519 |
| ENSG00000164867 | NOS3 subnetwork | 0.78439991 | 1.200596297 |
| MP:0006362 | abnormal male germ cell morphology | 0.76751232 | 1.200598227 |
| MP:0000780 | abnormal corpus callosum morphology | 0.7693982 | 1.200602089 |
| ENSG00000105568 | PPP2R1A subnetwork | 0.76871862 | 1.200602602 |
| ENSG00000163083 | INHBB subnetwork | 0.76681315 | 1.200604084 |
| GO:0032608 | interferon-beta production | 0.76732848 | 1.200614382 |
| GO:0043551 | regulation of phosphatidylinositol 3-kinase activity | 0.79883758 | 1.200622044 |
| ENSG00000184702 | SEPT5 subnetwork | 0.79498216 | 1.200624871 |
| GO:0045028 | G-protein coupled purinergic nucleotide receptor activity | 0.69772277 | 1.200625585 |
| ENSG00000183020 | AP2A2 subnetwork | 0.79750013 | 1.200628218 |
| ENSG00000187498 | COL4A1 subnetwork | 0.76956922 | 1.200628596 |
| GO:0014037 | Schwann cell differentiation | 0.7666971 | 1.200630881 |
| REACTOME_INFLUENZA_LIFE_( | REACTOME_INFLUENZA_LIFE_CYCLE | 0.80072541 | 1.200636028 |
| MP:0004448 | abnormal presphenoid bone morphology | 0.76948075 | 1.200644646 |
| GO:0060076 | excitatory synapse | 0.76704606 | 1.200646713 |
| ENSG00000104960 | PTOV1 subnetwork | 0.69953015 | 1.200647457 |
| MP:0002269 | muscular atrophy | 0.76916369 | 1.20065558 |
| ENSG00000198786 | MT-ND5 subnetwork | 0.7961142 | 1.200660202 |
| ENSG00000161011 | SQSTM1 subnetwork | 0.76934348 | 1.200666098 |
| ENSG00000151577 | DRD3 subnetwork | 0.79631005 | 1.20067038 |
| KEGG_ALZHEIMERS_DISEASE | KEGG_ALZHEIMERS_DISEASE | 0.76891242 | 1.200671785 |
| REACTOME_RNA_POLYMERASI | REACTOME_RNA_POLYMERASE_II_TRANSCRIPTION | 0.7962181 | 1.200675606 |
| ENSG00000104497 | SNX16 subnetwork | 0.69945896 | 1.200682534 |
| ENSG00000127527 | EPS15L1 subnetwork | 0.78437792 | 1.20068529 |
| ENSG00000206349 | ENSG00000206349 subnetwork | 0.79838099 | 1.200704733 |
| MP:0000182 | increased circulating LDL cholesterol level | 0.79792292 | 1.200705168 |
| MP:0001328 | disorganized retinal layers | 0.79746301 | 1.200705531 |
| GO:0015093 | ferrous iron transmembrane transporter activity | 0.76658863 | 1.200705882 |
| REACTOME_PLATELET_CALCIU | REACTOME_PLATELET_CALCIUM_HOMEOSTASIS | 0.76870778 | 1.200709333 |
| ENSG00000136527 | TRA2B subnetwork | 0.80046568 | 1.200713259 |
| ENSG00000115234 | SNX17 subnetwork | 0.69768181 | 1.200713367 |
| ENSG00000102580 | DNAJC3 subnetwork | 0.76698112 | 1.200716271 |
| MP:0004500 | increased incidence of ionizing radiation-induced tumors | 0.76731671 | 1.200721308 |
| ENSG00000213496 | ENSG00000213496 subnetwork | 0.79642102 | 1.200721873 |
| GO:0008652 | cellular amino acid biosynthetic process | 0.80069756 | 1.200723299 |
| ENSG00000123992 | DNPEP subnetwork | 0.79597846 | 1.200727404 |
| GO:0033273 | response to vitamin | 0.76913705 | 1.200735608 |
| ENSG00000072832 | CRMP1 subnetwork | 0.79785213 | 1.200741275 |
| GO:0045766 | positive regulation of angiogenesis | 0.69814275 | 1.200742169 |

| | | | |
|---|---|---|---|
| MP:0006055 | abnormal vascular endothelial cell morphology | 0.80062648 | 1.200743895 |
| GO:0009084 | glutamine family amino acid biosynthetic process | 0.69834836 | 1.200747838 |
| ENSG00000184432 | COPB2 subnetwork | 0.76653211 | 1.200764788 |
| MP:0006035 | abnormal mitochondrial morphology | 0.79562232 | 1.200768993 |
| ENSG00000166971 | AKTIP subnetwork | 0.76887641 | 1.200773168 |
| MP:0009114 | decreased pancreatic beta cell mass | 0.79573423 | 1.200774074 |
| ENSG00000212870 | ENSG00000212870 subnetwork | 0.7961142 | 1.200784071 |
| GO:0018022 | peptidyl-lysine methylation | 0.80043172 | 1.200785179 |
| MP:0008515 | thin retinal outer nuclear layer | 0.80033775 | 1.20078526 |
| MP:0003324 | increased liver adenoma incidence | 0.69827648 | 1.200788828 |
| GO:0071241 | cellular response to inorganic substance | 0.79743786 | 1.20079316 |
| GO:0033764 | steroid dehydrogenase activity, acting on the CH-OH group | 0.79654664 | 1.200793978 |
| GO:0007018 | microtubule-based movement | 0.69845992 | 1.200800327 |
| REACTOME_RESPONSE_TO_EL | REACTOME_RESPONSE_TO_ELEVATED_PLATELET_CYTOSOI | 0.80059925 | 1.20080041 |
| MP:0008965 | increased basal metabolism | 0.7843738 | 1.200810924 |
| ENSG00000214826 | ENSG00000214826 subnetwork | 0.6994505 | 1.200810968 |
| ENSG00000165264 | NDUFB6 subnetwork | 0.79971267 | 1.200816641 |
| ENSG00000131791 | PRKAB2 subnetwork | 0.79595452 | 1.200820349 |
| ENSG00000149428 | HYOU1 subnetwork | 0.79545688 | 1.200820772 |
| MP:0002576 | abnormal enamel morphology | 0.79962255 | 1.200821862 |
| REACTOME_SIGNALING_BY_VE | REACTOME_SIGNALING_BY_VEGF | 0.79831607 | 1.200823215 |
| REACTOME_NITRIC_OXIDE_STI | REACTOME_NITRIC_OXIDE_STIMULATES_GUANYLATE_CYC | 0.79782691 | 1.200823723 |
| MP:0002769 | abnormal vas deferens morphology | 0.7625831 | 1.200827779 |
| ENSG00000206454 | POU5F1 subnetwork | 0.79838099 | 1.200828275 |
| REACTOME_FACTORS_INVOLV | REACTOME_FACTORS_INVOLVED_IN_MEGAKARYOCYTE_DI | 0.79807881 | 1.200828616 |
| GO:0051721 | protein phosphatase 2A binding | 0.76870379 | 1.200832089 |
| ENSG00000137955 | RABGGTB subnetwork | 0.76650351 | 1.200845101 |
| ENSG00000061938 | TNK2 subnetwork | 0.79958047 | 1.200863043 |
| MP:0003723 | abnormal long bone morphology | 0.79997208 | 1.200878094 |
| ENSG00000205560 | CPT1B subnetwork | 0.80032478 | 1.200887999 |
| GO:0015684 | ferrous iron transport | 0.79742401 | 1.20089111 |
| GO:0032677 | regulation of interleukin-8 production | 0.79561753 | 1.200892949 |
| MP:0003786 | premature aging | 0.76609716 | 1.20090442 |
| MP:0006356 | abnormal third branchial arch artery morphology | 0.76529022 | 1.200910747 |
| ENSG00000212789 | ENSG00000212789 subnetwork | 0.79780621 | 1.200911338 |
| GO:0030502 | negative regulation of bone mineralization | 0.79704127 | 1.200917242 |
| GO:0071322 | cellular response to carbohydrate stimulus | 0.79696276 | 1.200917337 |
| GO:0033559 | unsaturated fatty acid metabolic process | 0.76582972 | 1.200920869 |
| ENSG00000157483 | MYO1E subnetwork | 0.78436449 | 1.200920887 |
| ENSG00000143622 | RIT1 subnetwork | 0.77159278 | 1.200924647 |
| KEGG_GLYCOSPHINGOLIPID_BI | KEGG_GLYCOSPHINGOLIPID_BIOSYNTHESIS_LACTO_AND_N | 0.76519337 | 1.200926918 |
| GO:0043588 | skin development | 0.76511064 | 1.200927017 |
| GO:0006767 | water-soluble vitamin metabolic process | 0.77088203 | 1.20093095 |
| ENSG00000173207 | CKS1B subnetwork | 0.79594979 | 1.200939112 |
| GO:0006096 | glycolysis | 0.79545237 | 1.200939597 |
| GO:0016529 | sarcoplasmic reticulum | 0.76648112 | 1.200941479 |
| ENSG00000020577 | SAMD4A subnetwork | 0.79992781 | 1.200944947 |
| MP:0004001 | decreased hepatocyte proliferation | 0.77153564 | 1.200946003 |
| REACTOME_VEGF_LIGAND:REC | REACTOME_VEGF_LIGAND:RECEPTOR_INTERACTIONS | 0.79831607 | 1.200946794 |
| GO:0030433 | ER-associated protein catabolic process | 0.79531611 | 1.200950119 |
| ENSG00000111788 | ENSG00000111788 subnetwork | 0.6994505 | 1.200951103 |
| ENSG00000114354 | TFG subnetwork | 0.76258162 | 1.200956886 |
| MP:0001783 | decreased white adipose tissue amount | 0.76542511 | 1.20095886 |

| | | | |
|---|---|---|---|
| GO:0035116 | embryonic hindlimb morphogenesis | 0.7953706 | 1.200960347 |
| ENSG00000072110 | ACTN1 subnetwork | 0.79719586 | 1.200973825 |
| ENSG00000136231 | IGF2BP3 subnetwork | 0.76606444 | 1.200974095 |
| ENSG00000118491 | C6orf94 subnetwork | 0.80029834 | 1.200975359 |
| GO:0018196 | peptidyl-asparagine modification | 0.77132862 | 1.200983519 |
| REACTOME_CENTROSOME_M/ | REACTOME_CENTROSOME_MATURATION | 0.76643223 | 1.200984378 |
| ENSG00000103490 | PYCARD subnetwork | 0.6987712 | 1.200987034 |
| GO:0016725 | oxidoreductase activity, acting on CH or CH2 groups | 0.77099369 | 1.200989362 |
| GO:0006733 | oxidoreduction coenzyme metabolic process | 0.70021363 | 1.200991023 |
| REACTOME_INTERACTIONS_OI | REACTOME_INTERACTIONS_OF_VPR_WITH_HOST_CELLUL/ | 0.79740751 | 1.20099423 |
| GO:0006914 | autophagy | 0.79827009 | 1.200998353 |
| GO:0017002 | activin-activated receptor activity | 0.6986996 | 1.200998832 |
| KEGG_PRIMARY_BILE_ACID_BI | KEGG_PRIMARY_BILE_ACID_BIOSYNTHESIS | 0.77105343 | 1.201005212 |
| ENSG00000134001 | EIF2S1 subnetwork | 0.76579135 | 1.201011994 |
| GO:0033293 | monocarboxylic acid binding | 0.70012189 | 1.201014459 |
| GO:0006333 | chromatin assembly or disassembly | 0.69924408 | 1.201015643 |
| MP:0005114 | premature hair loss | 0.80019807 | 1.20102177 |
| ENSG00000163220 | S100A9 subnetwork | 0.77183207 | 1.201025396 |
| MP:0001713 | decreased trophoblast giant cell number | 0.77084636 | 1.201026814 |
| GO:0015923 | mannosidase activity | 0.79696097 | 1.201030822 |
| REACTOME_GLUCOSE_METAB | REACTOME_GLUCOSE_METABOLISM | 0.78385947 | 1.201036649 |
| GO:0043632 | modification-dependent macromolecule catabolic process | 0.78435856 | 1.20104134 |
| ENSG00000179222 | MAGED1 subnetwork | 0.76629599 | 1.20104345 |
| MP:0006065 | abnormal heart position or orientation | 0.78378405 | 1.20104723 |
| REACTOME_APCCDH1_MEDI/ | REACTOME_APCCDH1_MEDIATED_DEGRADATION_OF_CI | 0.76556753 | 1.201049813 |
| ENSG00000131238 | PPT1 subnetwork | 0.76510379 | 1.201055734 |
| MP:0010869 | decreased bone trabecula number | 0.69941475 | 1.201056256 |
| GO:0006308 | DNA catabolic process | 0.7707984 | 1.201058849 |
| GO:0010269 | response to selenium ion | 0.8002693 | 1.201062737 |
| GO:0044447 | axoneme part | 0.76256028 | 1.201064516 |
| GO:0005819 | spindle | 0.78396409 | 1.201067951 |
| ENSG00000060140 | STYK1 subnetwork | 0.7660513 | 1.201070549 |
| ENSG00000133107 | TRPC4 subnetwork | 0.7841018 | 1.201073074 |
| ENSG00000154262 | ABCA6 subnetwork | 0.78373221 | 1.201073523 |
| ENSG00000165684 | SNAPC4 subnetwork | 0.77153421 | 1.201073669 |
| REACTOME_ROLE_OF_DCC_IN | REACTOME_ROLE_OF_DCC_IN_REGULATING_APOPTOSIS | 0.69921313 | 1.201074139 |
| ENSG00000185633 | NDUFA4L2 subnetwork | 0.77178439 | 1.20107864 |
| ENSG00000171843 | MLLT3 subnetwork | 0.70008455 | 1.201078717 |
| ENSG00000189043 | NDUFA4 subnetwork | 0.7657505 | 1.201081718 |
| GO:0009629 | response to gravity | 0.79690259 | 1.201082474 |
| ENSG00000104805 | NUCB1 subnetwork | 0.76297028 | 1.201085555 |
| ENSG00000173566 | NUDT18 subnetwork | 0.76567819 | 1.201087189 |
| GO:0030574 | collagen catabolic process | 0.79683394 | 1.201098051 |
| ENSG00000198873 | GRK5 subnetwork | 0.76459762 | 1.201104676 |
| GO:0055037 | recycling endosome | 0.69891528 | 1.201109554 |
| GO:0018279 | protein N-linked glycosylation via asparagine | 0.77132862 | 1.201111229 |
| REACTOME_RECRUITMENT_OI | REACTOME_RECRUITMENT_OF_MITOTIC_CENTROSOME_P | 0.76643223 | 1.201112895 |
| ENSG00000063601 | MTMR1 subnetwork | 0.70048202 | 1.201113183 |
| ENSG00000152661 | GJA1 subnetwork | 0.78430037 | 1.201114716 |
| GO:0001656 | metanephros development | 0.7974016 | 1.20111798 |
| ENSG00000136158 | SPRY2 subnetwork | 0.76507373 | 1.201136242 |
| GO:0030104 | water homeostasis | 0.77150544 | 1.201148203 |
| MP:0000787 | abnormal telencephalon morphology | 0.6990369 | 1.201156137 |

| | | | |
|---|---|---|---|
| ENSG00000100767 | PAPLN subnetwork | 0.77121292 | 1.201159328 |
| ENSG00000148835 | TAF5 subnetwork | 0.69915081 | 1.20116184 |
| MP:0004819 | decreased skeletal muscle mass | 0.70043602 | 1.201165773 |
| ENSG00000101213 | PTK6 subnetwork | 0.76255177 | 1.201166792 |
| ENSG00000067057 | PFKP subnetwork | 0.78424733 | 1.201167173 |
| ENSG00000109534 | GAR1 subnetwork | 0.7712823 | 1.201169839 |
| ENSG00000164093 | PITX2 subnetwork | 0.69939489 | 1.201173106 |
| ENSG00000104863 | LIN7B subnetwork | 0.7632566 | 1.201176534 |
| GO:0043425 | bHLH transcription factor binding | 0.77079514 | 1.201186675 |
| ENSG00000109272 | PF4V1 subnetwork | 0.78372207 | 1.201194092 |
| GO:0007398 | ectoderm development | 0.7645811 | 1.201195967 |
| ENSG00000125508 | SRMS subnetwork | 0.7660513 | 1.201199143 |
| MP:0001722 | pale yolk sac | 0.77066544 | 1.201208218 |
| MP:0003990 | decreased neurotransmitter release | 0.76336051 | 1.201208638 |
| GO:0000139 | Golgi membrane | 0.76296226 | 1.201214662 |
| GO:0015296 | anion:cation symporter activity | 0.77434321 | 1.201218349 |
| GO:0046718 | viral entry into host cell | 0.77074508 | 1.201224055 |
| ENSG00000138411 | HECW2 subnetwork | 0.76493176 | 1.201227619 |
| REACTOME_CELL_CYCLE_CHEC | REACTOME_CELL_CYCLE_CHECKPOINTS | 0.77446438 | 1.201244703 |
| ENSG00000169180 | XPO6 subnetwork | 0.70088228 | 1.201258301 |
| MP:0003809 | abnormal hair shaft morphology | 0.76507252 | 1.201259648 |
| ENSG00000107341 | UBE2R2 subnetwork | 0.76324019 | 1.201273372 |
| GO:0016780 | phosphotransferase activity, for other substituted phospha | 0.70071334 | 1.201276075 |
| ENSG00000065978 | YBX1 subnetwork | 0.762546 | 1.2012906 |
| GO:0005884 | actin filament | 0.70107209 | 1.201304601 |
| ENSG00000205813 | ENSG00000205813 subnetwork | 0.78372207 | 1.201319925 |
| GO:0006725 | cellular aromatic compound metabolic process | 0.76457946 | 1.201324823 |
| GO:0008544 | epidermis development | 0.77065561 | 1.201325455 |
| MP:0001700 | abnormal embryo turning | 0.70101162 | 1.201328052 |
| ENSG00000146963 | LUC7L2 subnetwork | 0.70084873 | 1.201328362 |
| MP:0002196 | absent corpus callosum | 0.77432864 | 1.201329731 |
| ENSG00000072201 | LNX1 subnetwork | 0.77425705 | 1.201340468 |
| ENSG00000169131 | ZNF354A subnetwork | 0.77013431 | 1.201352935 |
| ENSG00000174718 | C12orf35 subnetwork | 0.7649306 | 1.201356423 |
| REACTOME_CELL_CYCLE_MITC | REACTOME_CELL_CYCLE_MITOTIC | 0.76485344 | 1.201356568 |
| MP:0006379 | abnormal spermatocyte morphology | 0.70067041 | 1.201363636 |
| GO:0006399 | tRNA metabolic process | 0.76358588 | 1.201364125 |
| GO:0043535 | regulation of blood vessel endothelial cell migration | 0.76321924 | 1.201380978 |
| ENSG00000102081 | FMR1 subnetwork | 0.76445509 | 1.20139485 |
| REACTOME_APCCCDC20_MED | REACTOME_APCCCDC20_MEDIATED_DEGRADATION_OF_N | 0.77042894 | 1.201395101 |
| ENSG00000124194 | GDAP1L1 subnetwork | 0.77051501 | 1.201400277 |
| ENSG00000167774 | NDUFA7 subnetwork | 0.76239461 | 1.201403981 |
| ENSG00000206480 | FLOT1 subnetwork | 0.77354533 | 1.201405239 |
| GO:0005732 | small nucleolar ribonucleoprotein complex | 0.76245449 | 1.201414587 |
| ENSG00000165996 | PTPLA subnetwork | 0.76355638 | 1.201417983 |
| GO:0051236 | establishment of RNA localization | 0.78369985 | 1.201419591 |
| GO:0006513 | protein monoubiquitination | 0.76254337 | 1.201419813 |
| GO:0034754 | cellular hormone metabolic process | 0.70144405 | 1.201432231 |
| ENSG00000037042 | TUBG2 subnetwork | 0.76456512 | 1.20143225 |
| MP:0009838 | abnormal sperm axoneme morphology | 0.77384492 | 1.2014419 |
| GO:0042743 | hydrogen peroxide metabolic process | 0.77365128 | 1.201442206 |
| GO:0072074 | kidney mesenchyme development | 0.77393998 | 1.201447048 |
| MP:0005627 | increased circulating potassium level | 0.77065294 | 1.201448041 |

| | | | |
|---|---|---|---|
| GO:0046461 | neutral lipid catabolic process | 0.70697828 | 1.20146209 |
| ENSG00000115760 | BIRC6 subnetwork | 0.77425614 | 1.201467783 |
| ENSG00000163462 | TRIM46 subnetwork | 0.70139037 | 1.20147898 |
| ENSG00000143033 | MTF2 subnetwork | 0.76441802 | 1.201480846 |
| ENSG00000168872 | DDX19A subnetwork | 0.77041263 | 1.201491107 |
| ENSG00000078403 | MLLT10 subnetwork | 0.70181633 | 1.201507216 |
| ENSG00000101349 | PAK7 subnetwork | 0.762391 | 1.201527867 |
| GO:0071320 | cellular response to cAMP | 0.76436177 | 1.201529298 |
| REACTOME_UNFOLDED_PROT | REACTOME_UNFOLDED_PROTEIN_RESPONSE | 0.77420034 | 1.201531532 |
| ENSG00000206379 | FLOT1 subnetwork | 0.77354533 | 1.201532669 |
| GO:0050658 | RNA transport | 0.78369985 | 1.201545474 |
| ENSG00000104738 | MCM4 subnetwork | 0.70731867 | 1.201548238 |
| ENSG00000198846 | TOX subnetwork | 0.71543929 | 1.201548394 |
| GO:0032388 | positive regulation of intracellular transport | 0.7071242 | 1.201548596 |
| GO:0032924 | activin receptor signaling pathway | 0.76396978 | 1.201562332 |
| ENSG00000091651 | ORC6 subnetwork | 0.77383772 | 1.201569293 |
| ENSG00000114554 | PLXNA1 subnetwork | 0.70135512 | 1.20157815 |
| GO:0006706 | steroid catabolic process | 0.70724587 | 1.201583083 |
| ENSG00000140740 | UQCRC2 subnetwork | 0.77038914 | 1.201587133 |
| ENSG00000135698 | MPHOSPH6 subnetwork | 0.70178426 | 1.201588872 |
| MP:0000432 | abnormal head morphology | 0.70170533 | 1.201594878 |
| GO:0015370 | solute:sodium symporter activity | 0.77417334 | 1.201600594 |
| GO:0044269 | glycerol ether catabolic process | 0.70697828 | 1.201600971 |
| GO:0007498 | mesoderm development | 0.76432997 | 1.201615327 |
| ENSG00000101439 | CST3 subnetwork | 0.76234486 | 1.201619499 |
| ENSG00000137500 | CCDC90B subnetwork | 0.76384277 | 1.201621738 |
| GO:0060231 | mesenchymal to epithelial transition | 0.70165537 | 1.201629992 |
| MP:0002286 | cryptorchism | 0.70580259 | 1.201643899 |
| MP:0004875 | increased mean systemic arterial blood pressure | 0.70593405 | 1.201655284 |
| ENSG00000137312 | FLOT1 subnetwork | 0.77354533 | 1.201660125 |
| MP:0009243 | hairpin sperm flagellum | 0.76396076 | 1.201669888 |
| ENSG00000109805 | NCAPG subnetwork | 0.78173478 | 1.201669993 |
| GO:0050657 | nucleic acid transport | 0.78369985 | 1.201671382 |
| GO:0048332 | mesoderm morphogenesis | 0.71656368 | 1.201677508 |
| ENSG00000124097 | ENSG00000124097 subnetwork | 0.71543929 | 1.201685714 |
| GO:0006007 | glucose catabolic process | 0.78305823 | 1.201693582 |
| GO:0019637 | organophosphate metabolic process | 0.76420981 | 1.201696189 |
| ENSG00000130762 | ARHGEF16 subnetwork | 0.76431419 | 1.201717475 |
| ENSG00000147509 | RGS20 subnetwork | 0.7616808 | 1.201717824 |
| GO:0035336 | long-chain fatty-acyl-CoA metabolic process | 0.76233174 | 1.201721911 |
| GO:0016667 | oxidoreductase activity, acting on a sulfur group of donors | 0.78319631 | 1.201735347 |
| GO:0046464 | acylglycerol catabolic process | 0.70697828 | 1.201739884 |
| GO:0016866 | intramolecular transferase activity | 0.78171389 | 1.201743697 |
| MP:0002855 | abnormal cochlear ganglion morphology | 0.7830179 | 1.201746198 |
| ENSG00000049323 | LTBP1 subnetwork | 0.76415254 | 1.20176079 |
| ENSG00000171421 | MRPL36 subnetwork | 0.76163101 | 1.20176648 |
| GO:0017022 | myosin binding | 0.78367984 | 1.201781597 |
| ENSG00000180370 | PAK2 subnetwork | 0.77353505 | 1.201782304 |
| ENSG00000168646 | AXIN2 subnetwork | 0.70580067 | 1.201783027 |
| ENSG00000178209 | PLEC subnetwork | 0.7159314 | 1.201793261 |
| KEGG_METABOLISM_OF_XENO | KEGG_METABOLISM_OF_XENOBIOTICS_BY_CYTOCHROME_ | 0.71655415 | 1.201803241 |
| ENSG00000130332 | LSM7 subnetwork | 0.78298441 | 1.201814558 |
| ENSG00000123728 | RAP2C subnetwork | 0.70558462 | 1.201818392 |

| | | | |
|---|---|---|---|
| GO:0051018 | protein kinase A binding | 0.77347482 | 1.201819629 |
| ENSG00000103460 | TOX3 subnetwork | 0.71543929 | 1.201823065 |
| MP:0009757 | impaired behavioral response to morphine | 0.70670623 | 1.201827435 |
| GO:0006511 | ubiquitin-dependent protein catabolic process | 0.77308857 | 1.20183121 |
| GO:0045736 | negative regulation of cyclin-dependent protein kinase acti | 0.70574025 | 1.20183534 |
| MP:0000060 | delayed bone ossification | 0.7175058 | 1.201840875 |
| GO:0030851 | granulocyte differentiation | 0.77326046 | 1.201841435 |
| GO:0071384 | cellular response to corticosteroid stimulus | 0.7054779 | 1.20184177 |
| GO:0004553 | hydrolase activity, hydrolyzing O-glycosyl compounds | 0.77486483 | 1.201843025 |
| GO:0009264 | deoxyribonucleotide catabolic process | 0.70650283 | 1.201845211 |
| GO:0019887 | protein kinase regulator activity | 0.71536506 | 1.201846136 |
| GO:0035338 | long-chain fatty-acyl-CoA biosynthetic process | 0.76233174 | 1.201851254 |
| GO:0005161 | platelet-derived growth factor receptor binding | 0.78168858 | 1.201854186 |
| MP:0004090 | abnormal sarcomere morphology | 0.71689538 | 1.201859457 |
| ENSG00000121931 | LRIF1 subnetwork | 0.70696763 | 1.201861487 |
| ENSG00000128513 | POT1 subnetwork | 0.71604711 | 1.201861581 |
| MP:0004174 | abnormal spine curvature | 0.77342723 | 1.201862267 |
| MP:0000790 | abnormal stratification in cerebral cortex | 0.78290967 | 1.201867198 |
| GO:0004659 | prenyltransferase activity | 0.77337629 | 1.201873077 |
| GO:0008654 | phospholipid biosynthetic process | 0.71590048 | 1.201873429 |
| ENSG00000121542 | SEC22A subnetwork | 0.76161309 | 1.201874394 |
| GO:0046165 | alcohol biosynthetic process | 0.71709469 | 1.201876141 |
| MP:0002113 | abnormal skeleton development | 0.76226052 | 1.201883746 |
| ENSG00000023318 | ERP44 subnetwork | 0.77250574 | 1.20188569 |
| GO:0072527 | pyrimidine-containing compound metabolic process | 0.71744702 | 1.201886685 |
| ENSG00000125798 | FOXA2 subnetwork | 0.70665257 | 1.201891267 |
| GO:0032933 | SREBP-mediated signaling pathway | 0.75908421 | 1.201896682 |
| ENSG00000105972 | ENSG00000105972 subnetwork | 0.7732117 | 1.201900011 |
| ENSG00000078579 | FGF20 subnetwork | 0.78367604 | 1.201902316 |
| GO:0034694 | response to prostaglandin stimulus | 0.75884699 | 1.201902703 |
| GO:0090329 | regulation of DNA-dependent DNA replication | 0.78197494 | 1.201906112 |
| ENSG00000163435 | ELF3 subnetwork | 0.77273175 | 1.20190633 |
| GO:0043534 | blood vessel endothelial cell migration | 0.70644384 | 1.201909059 |
| ENSG00000111530 | CAND1 subnetwork | 0.70525055 | 1.201911935 |
| ENSG00000163993 | S100P subnetwork | 0.77244441 | 1.201912452 |
| GO:0032414 | positive regulation of ion transmembrane transporter activi | 0.75891889 | 1.201913307 |
| GO:0048286 | lung alveolus development | 0.70856694 | 1.20191509 |
| ENSG00000091592 | NLRP1 subnetwork | 0.77301456 | 1.201916339 |
| ENSG00000100842 | EFS subnetwork | 0.78162822 | 1.20191742 |
| ENSG00000163002 | NUP35 subnetwork | 0.71720456 | 1.201921542 |
| GO:0032722 | positive regulation of chemokine production | 0.71655046 | 1.201923296 |
| GO:0016903 | oxidoreductase activity, acting on the aldehyde or oxo grou | 0.77285232 | 1.201927365 |
| ENSG00000139239 | ENSG00000139239 subnetwork | 0.70769338 | 1.201929075 |
| GO:0000768 | syncytium formation by plasma membrane fusion | 0.72472522 | 1.201930894 |
| ENSG00000052802 | MSMO1 subnetwork | 0.70572732 | 1.20193978 |
| ENSG00000152700 | SAR1B subnetwork | 0.71628182 | 1.201941082 |
| MP:0002813 | microcytosis | 0.78348534 | 1.201944648 |
| ENSG00000162231 | NXF1 subnetwork | 0.75920721 | 1.201945105 |
| GO:0007440 | foregut morphogenesis | 0.78286468 | 1.201946076 |
| GO:0007520 | myoblast fusion | 0.78341004 | 1.201950094 |
| ENSG00000198805 | PNP subnetwork | 0.77294627 | 1.201953706 |
| ENSG00000116962 | NID1 subnetwork | 0.78154543 | 1.201954397 |
| ENSG00000170144 | HNRNPA3 subnetwork | 0.7023348 | 1.201954625 |

| | | | |
|---|---|---|---|
| ENSG00000182319 | SGK223 subnetwork | 0.7174085 | 1.201955307 |
| ENSG00000159199 | ATP5G1 subnetwork | 0.71686775 | 1.201956646 |
| MP:0000523 | cortical renal glomerulopathies | 0.78222111 | 1.201958005 |
| MP:0005455 | increased susceptibility to weight gain | 0.71128088 | 1.20195977 |
| ENSG00000131558 | EXOC4 subnetwork | 0.70694568 | 1.201959991 |
| REACTOME_G_ALPHA_1213_S | REACTOME_G_ALPHA_1213_SIGNALLING_EVENTS | 0.76157342 | 1.201960784 |
| MP:0004405 | absent cochlear hair cells | 0.75905843 | 1.201961738 |
| GO:0002320 | lymphoid progenitor cell differentiation | 0.71706816 | 1.201961903 |
| GO:0010639 | negative regulation of organelle organization | 0.77269756 | 1.20196495 |
| ENSG00000175390 | EIF3F subnetwork | 0.70621336 | 1.201967593 |
| MP:0005058 | abnormal lysosome morphology | 0.71535215 | 1.201972105 |
| GO:0042481 | regulation of odontogenesis | 0.70816719 | 1.20197414 |
| GO:0048617 | embryonic foregut morphogenesis | 0.76222324 | 1.201975455 |
| GO:0071385 | cellular response to glucocorticoid stimulus | 0.7054779 | 1.201981001 |
| ENSG00000047932 | GOPC subnetwork | 0.78363859 | 1.201981132 |
| GO:0007026 | negative regulation of microtubule depolymerization | 0.71166761 | 1.201981847 |
| ENSG00000135723 | FHOD1 subnetwork | 0.71147526 | 1.201982303 |
| GO:0051604 | protein maturation | 0.70784319 | 1.201986602 |
| MP:0001721 | absent visceral yolk sac blood islands | 0.70328647 | 1.201986986 |
| KEGG_NICOTINATE_AND_NICC | KEGG_NICOTINATE_AND_NICOTINAMIDE_METABOLISM | 0.72467912 | 1.201987578 |
| GO:0042440 | pigment metabolic process | 0.71589641 | 1.20198789 |
| GO:0010769 | regulation of cell morphogenesis involved in differentiation | 0.70261669 | 1.201988835 |
| ENSG00000171634 | BPTF subnetwork | 0.70520943 | 1.201993278 |
| GO:0046875 | ephrin receptor binding | 0.7114004 | 1.201994024 |
| ENSG00000069011 | PITX1 subnetwork | 0.70688639 | 1.201994912 |
| ENSG00000165525 | NEMF subnetwork | 0.70244293 | 1.201995114 |
| GO:0060343 | trabecula formation | 0.77263188 | 1.201997026 |
| GO:0051668 | localization within membrane | 0.70540878 | 1.20199861 |
| MP:0004965 | inner cell mass degeneration | 0.71120509 | 1.20200023 |
| GO:0007009 | plasma membrane organization | 0.78282801 | 1.202009233 |
| ENSG00000135052 | GOLM1 subnetwork | 0.70766788 | 1.202010166 |
| ENSG00000140374 | ETFA subnetwork | 0.70853974 | 1.202019153 |
| ENSG00000146677 | ENSG00000146677 subnetwork | 0.78244566 | 1.202020573 |
| MP:0005643 | decreased dopamine level | 0.70219645 | 1.202024904 |
| MP:0000747 | muscle weakness | 0.75884363 | 1.202027246 |
| GO:0007143 | female meiosis | 0.76154135 | 1.202036418 |
| ENSG00000128534 | NAA38 subnetwork | 0.70643225 | 1.202036566 |
| ENSG00000075643 | MOCOS subnetwork | 0.78217798 | 1.202042209 |
| ENSG00000166855 | CLPX subnetwork | 0.71653379 | 1.202049087 |
| GO:0008307 | structural constituent of muscle | 0.71626648 | 1.202049789 |
| GO:0014070 | response to organic cyclic compound | 0.70347096 | 1.202050656 |
| GO:0005262 | calcium channel activity | 0.71160797 | 1.202051017 |
| ENSG00000131711 | MAP1B subnetwork | 0.71739122 | 1.202058153 |
| GO:0030663 | COPI coated vesicle membrane | 0.70229675 | 1.202059576 |
| GO:0045652 | regulation of megakaryocyte differentiation | 0.78153426 | 1.202059689 |
| ENSG00000163879 | DNALI1 subnetwork | 0.70411744 | 1.20206036 |
| ENSG00000105819 | PMPCB subnetwork | 0.71685582 | 1.202065267 |
| GO:0070373 | negative regulation of ERK1 and ERK2 cascade | 0.70848334 | 1.202065544 |
| ENSG00000005469 | CROT subnetwork | 0.7621918 | 1.202067183 |
| GO:0065004 | protein-DNA complex assembly | 0.70798467 | 1.202067213 |
| ENSG00000115694 | STK25 subnetwork | 0.71585714 | 1.202068099 |
| GO:0016441 | posttranscriptional gene silencing | 0.70882928 | 1.202076125 |
| ENSG00000162702 | ZNF281 subnetwork | 0.7225838 | 1.202078143 |

| | | | |
|---|---|---|---|
| ENSG00000112742 | TTK subnetwork | 0.76148162 | 1.202079741 |
| GO:0015908 | fatty acid transport | 0.70517581 | 1.202086231 |
| ENSG00000168264 | IRF2BP2 subnetwork | 0.70837512 | 1.202089104 |
| KEGG_BLADDER_CANCER | KEGG_BLADDER_CANCER | 0.7025928 | 1.202093754 |
| ENSG00000148925 | BTBD10 subnetwork | 0.70815554 | 1.202095601 |
| GO:0016876 | ligase activity, forming aminoacyl-tRNA and related compou | 0.71534708 | 1.202098102 |
| MP:0003564 | abnormal insulin secretion | 0.78104694 | 1.202103049 |
| ENSG00000123066 | MED13L subnetwork | 0.70639465 | 1.20211781 |
| ENSG00000158874 | APOA2 subnetwork | 0.70810776 | 1.202118938 |
| MP:0008395 | abnormal osteoblast differentiation | 0.75882472 | 1.202119377 |
| MP:0010900 | abnormal pulmonary interalveolar septum morphology | 0.70327871 | 1.20212086 |
| GO:0016469 | proton-transporting two-sector ATPase complex | 0.72467884 | 1.202123334 |
| GO:0006085 | acetyl-CoA biosynthetic process | 0.70499052 | 1.20212729 |
| MP:0006386 | absent somites | 0.78281857 | 1.202130115 |
| REACTOME_RNA_POLYMERASI | REACTOME_RNA_POLYMERASE_II_TRANSCRIPTION_PRE:IN | 0.75874003 | 1.202130421 |
| GO:0006198 | cAMP catabolic process | 0.78241064 | 1.20213101 |
| MP:0002840 | abnormal lens fiber morphology | 0.71651829 | 1.202134947 |
| GO:0031418 | L-ascorbic acid binding | 0.71120306 | 1.202138423 |
| ENSG00000204086 | RPA4 subnetwork | 0.71022922 | 1.202141377 |
| GO:0002065 | columnar/cuboidal epithelial cell differentiation | 0.7614396 | 1.202144628 |
| MP:0004813 | absent linear vestibular evoked potential | 0.70385039 | 1.202148415 |
| GO:0004197 | cysteine-type endopeptidase activity | 0.72461473 | 1.202151813 |
| ENSG00000067177 | PHKA1 subnetwork | 0.71012606 | 1.202153138 |
| ENSG00000180914 | OXTR subnetwork | 0.71006651 | 1.202153386 |
| ENSG00000169271 | HSPB3 subnetwork | 0.76206558 | 1.20215378 |
| GO:0015081 | sodium ion transmembrane transporter activity | 0.70493545 | 1.202156522 |
| GO:0070059 | intrinsic apoptotic signaling pathway in response to endopl | 0.76216499 | 1.202158932 |
| MP:0009356 | decreased liver triglyceride level | 0.76137815 | 1.202161026 |
| GO:0008630 | DNA damage response, signal transduction resulting in indu | 0.70512191 | 1.202161818 |
| ENSG00000154889 | MPPE1 subnetwork | 0.78216942 | 1.202163184 |
| ENSG00000182899 | RPL35A subnetwork | 0.72415111 | 1.202164576 |
| ENSG00000177200 | CHD9 subnetwork | 0.70846466 | 1.202175418 |
| REACTOME_TRAFFICKING_OF_ | REACTOME_TRAFFICKING_OF_AMPA_RECEPTORS | 0.78152143 | 1.202175512 |
| ENSG00000129083 | COPB1 subnetwork | 0.70410698 | 1.202176689 |
| ENSG00000100253 | MIOX subnetwork | 0.70361429 | 1.202178206 |
| GO:0046689 | response to mercury ion | 0.76082183 | 1.202178837 |
| ENSG00000159593 | NAE1 subnetwork | 0.72501456 | 1.202179067 |
| ENSG00000124641 | MED20 subnetwork | 0.7607231 | 1.202179072 |
| KEGG_HUNTINGTONS_DISEASI | KEGG_HUNTINGTONS_DISEASE | 0.71185733 | 1.202182654 |
| MP:0000069 | kyphoscoliosis | 0.71107968 | 1.202190662 |
| ENSG00000138696 | BMPR1B subnetwork | 0.72256756 | 1.202191641 |
| REACTOME_AMINO_ACID_ANI | REACTOME_AMINO_ACID_AND_OLIGOPEPTIDE_SLC_TRAN | 0.70836479 | 1.202199007 |
| ENSG00000169509 | CRCT1 subnetwork | 0.71100048 | 1.202202415 |
| REACTOME_METABOLISM_OF_ | REACTOME_METABOLISM_OF_WATER:SOLUBLE_VITAMINS | 0.71090807 | 1.202202669 |
| GO:0009378 | four-way junction helicase activity | 0.70489357 | 1.202203154 |
| REACTOME_TRANSPORT_OF_I | REACTOME_TRANSPORT_OF_INORGANIC_CATIONSANIONS | 0.72454607 | 1.20220854 |
| GO:0035194 | posttranscriptional gene silencing by RNA | 0.70882928 | 1.202214788 |
| ENSG00000088038 | CNOT3 subnetwork | 0.72519782 | 1.202218083 |
| GO:0030317 | sperm motility | 0.7810421 | 1.20221895 |
| GO:2000756 | regulation of peptidyl-lysine acetylation | 0.72393418 | 1.202221845 |
| ENSG00000095319 | NUP188 subnetwork | 0.72248401 | 1.202225872 |
| ENSG00000161040 | FBXL13 subnetwork | 0.76131825 | 1.202225935 |
| REACTOME_FORMATION_OF_ | REACTOME_FORMATION_OF_ATP_BY_CHEMIOSMOTIC_CO | 0.71001413 | 1.202228492 |

| | | | |
|---|---|---|---|
| GO:0006814 | sodium ion transport | 0.78281053 | 1.202235282 |
| GO:0016875 | ligase activity, forming carbon-oxygen bonds | 0.71534708 | 1.202235563 |
| GO:0022625 | cytosolic large ribosomal subunit | 0.71118141 | 1.202236403 |
| ENSG00000136149 | ENSG00000136149 subnetwork | 0.70326731 | 1.202237331 |
| REACTOME_BIOLOGICAL_OXID | REACTOME_BIOLOGICAL_OXIDATIONS | 0.78094689 | 1.202240219 |
| MP:0006085 | myocardial necrosis | 0.76068096 | 1.202244039 |
| REACTOME_RNA_POLYMERASI | REACTOME_RNA_POLYMERASE_II_HIV:1_PROMOTER_ESC/ | 0.75874003 | 1.202260437 |
| GO:0005771 | multivesicular body | 0.71201503 | 1.202262807 |
| ENSG00000103154 | NECAB2 subnetwork | 0.70383782 | 1.202270616 |
| MP:0000111 | cleft palate | 0.72452163 | 1.202276579 |
| GO:0000287 | magnesium ion binding | 0.70439958 | 1.202280376 |
| ENSG00000196150 | ZNF250 subnetwork | 0.70408268 | 1.202281435 |
| ENSG00000038274 | MAT2B subnetwork | 0.70400128 | 1.202293312 |
| MP:0001606 | impaired hematopoiesis | 0.70449237 | 1.202297517 |
| GO:0010718 | positive regulation of epithelial to mesenchymal transition | 0.72414951 | 1.202300475 |
| REACTOME_GLUTAMATE_BIN | REACTOME_GLUTAMATE_BINDING_ACTIVATION_OF_AMP | 0.78152143 | 1.202301871 |
| KEGG_VASOPRESSIN_REGULAT | KEGG_VASOPRESSIN_REGULATED_WATER_REABSORPTION | 0.7827635 | 1.202303736 |
| GO:0007051 | spindle organization | 0.7759539 | 1.202312169 |
| ENSG00000135047 | CTSL1 subnetwork | 0.76130023 | 1.202312419 |
| ENSG00000179776 | CDH5 subnetwork | 0.70989275 | 1.202315401 |
| GO:0000082 | G1/S transition of mitotic cell cycle | 0.72373105 | 1.202318742 |
| ENSG00000180616 | SSTR2 subnetwork | 0.72408672 | 1.202323347 |
| ENSG00000132561 | MATN2 subnetwork | 0.714761 | 1.202323452 |
| ENSG00000093000 | NUP50 subnetwork | 0.71467823 | 1.202323718 |
| GO:0007264 | small GTPase mediated signal transduction | 0.78140416 | 1.202328638 |
| GO:0046697 | decidualization | 0.72246242 | 1.202339413 |
| ENSG00000064999 | ANKS1A subnetwork | 0.72392152 | 1.202340835 |
| REACTOME_METABOLISM_OF_ | REACTOME_METABOLISM_OF_VITAMINS_AND_COFACTOF | 0.71090807 | 1.202340964 |
| MP:0003992 | increased mortality induced by ionizing radiation | 0.725444 | 1.202341722 |
| ENSG00000139567 | ACVRL1 subnetwork | 0.70488366 | 1.202342572 |
| ENSG00000038427 | VCAN subnetwork | 0.70999809 | 1.20234393 |
| GO:2000142 | regulation of transcription initiation, DNA-dependent | 0.71067651 | 1.202347526 |
| ENSG00000107282 | APBA1 subnetwork | 0.72519152 | 1.20234816 |
| GO:0008333 | endosome to lysosome transport | 0.72449343 | 1.202350282 |
| ENSG00000196374 | HIST1H2BM subnetwork | 0.70436571 | 1.202356082 |
| ENSG00000173744 | AGFG1 subnetwork | 0.76067033 | 1.202362969 |
| GO:0006370 | mRNA capping | 0.78093513 | 1.202366677 |
| GO:0043624 | cellular protein complex disassembly | 0.71462986 | 1.202369777 |
| GO:0008237 | metallopeptidase activity | 0.72282765 | 1.202372325 |
| GO:0004812 | aminoacyl-tRNA ligase activity | 0.71534708 | 1.202373056 |
| MP:0009406 | decreased skeletal muscle fiber number | 0.71085399 | 1.202375748 |
| ENSG00000047936 | ROS1 subnetwork | 0.71077044 | 1.202376021 |
| GO:0007017 | microtubule-based process | 0.70326694 | 1.202377078 |
| ENSG00000130810 | PPAN subnetwork | 0.70317953 | 1.202377354 |
| ENSG00000155974 | GRIP1 subnetwork | 0.7048372 | 1.202377639 |
| ENSG00000123143 | PKN1 subnetwork | 0.77592174 | 1.202381204 |
| ENSG00000185637 | ENSG00000185637 subnetwork | 0.75998443 | 1.20238121 |
| MP:0005410 | abnormal fertilization | 0.72292355 | 1.202383379 |
| GO:0031214 | biomineral tissue development | 0.76125959 | 1.20238814 |
| REACTOME_RNA_POLYMERASI | REACTOME_RNA_POLYMERASE_II_PROMOTER_ESCAPE | 0.75874003 | 1.202390481 |
| REACTOME_RESPIRATORY_ELE | REACTOME_RESPIRATORY_ELECTRON_TRANSPORT | 0.78136602 | 1.202391967 |
| GO:0010885 | regulation of cholesterol storage | 0.70382527 | 1.202392845 |
| ENSG00000151208 | DLG5 subnetwork | 0.77616218 | 1.202396318 |

| | | | |
|---|---|---|---|
| KEGG_DNA_REPLICATION | KEGG_DNA_REPLICATION | 0.7098453 | 1.202402074 |
| REACTOME_PKA_ACTIVATION_ | REACTOME_PKA_ACTIVATION_IN_GLUCAGON_SIGNALLINC | 0.71218481 | 1.20240611 |
| ENSG00000187778 | MCRS1 subnetwork | 0.7599264 | 1.202408467 |
| ENSG00000117707 | PROX1 subnetwork | 0.75984451 | 1.202408728 |
| ENSG00000089250 | NOS1 subnetwork | 0.78088882 | 1.202409005 |
| ENSG00000100504 | PYGL subnetwork | 0.77635087 | 1.202411678 |
| ENSG00000100941 | PNN subnetwork | 0.78150621 | 1.202412488 |
| GO:0006352 | transcription initiation, DNA-dependent | 0.70307241 | 1.202412791 |
| ENSG00000112773 | FAM46A subnetwork | 0.7254157 | 1.202420993 |
| ENSG00000125354 | SEPT6 subnetwork | 0.77673321 | 1.202421231 |
| ENSG00000105737 | GRIK5 subnetwork | 0.7231523 | 1.202428119 |
| ENSG00000048828 | FAM120A subnetwork | 0.7605296 | 1.202428232 |
| GO:0015298 | solute:cation antiporter activity | 0.70297763 | 1.202430515 |
| ENSG00000107625 | DDX50 subnetwork | 0.76061629 | 1.202433366 |
| GO:0006026 | aminoglycan catabolic process | 0.77657904 | 1.202442893 |
| GO:0008278 | cohesin complex | 0.70957178 | 1.202443522 |
| MP:0000137 | abnormal vertebrae morphology | 0.76107626 | 1.202448231 |
| REACTOME_SIGNAL_TRANSDU | REACTOME_SIGNAL_TRANSDUCTION_BY_L1 | 0.7236437 | 1.202449372 |
| GO:0016891 | endoribonuclease activity, producing 5'-phosphomonoestel | 0.76044586 | 1.202450081 |
| ENSG00000129993 | CBFA2T3 subnetwork | 0.70915977 | 1.202450698 |
| MP:0003866 | abnormal defecation | 0.72446926 | 1.202452254 |
| GO:0015293 | symporter activity | 0.72373049 | 1.202454751 |
| MP:0008535 | enlarged lateral ventricles | 0.75976026 | 1.202463001 |
| MP:0003917 | increased kidney weight | 0.72245202 | 1.20246431 |
| GO:0007050 | cell cycle arrest | 0.72390192 | 1.202465506 |
| MP:0001602 | impaired myelopoiesis | 0.75961158 | 1.202468936 |
| GO:0001673 | male germ cell nucleus | 0.71332076 | 1.202471614 |
| GO:0006984 | ER-nucleus signaling pathway | 0.71447331 | 1.20247366 |
| GO:0071103 | DNA conformation change | 0.77631779 | 1.202475405 |
| ENSG00000107130 | NCS1 subnetwork | 0.71532213 | 1.202476267 |
| ENSG00000197616 | MYH6 subnetwork | 0.70316328 | 1.202476456 |
| MP:0000690 | absent spleen | 0.71524898 | 1.20247655 |
| GO:0005001 | transmembrane receptor protein tyrosine phosphatase acti | 0.77589081 | 1.202476715 |
| MP:0003878 | abnormal ear physiology | 0.71453285 | 1.202484828 |
| ENSG00000140332 | TLE3 subnetwork | 0.70926346 | 1.202485009 |
| GO:0060260 | regulation of transcription initiation from RNA polymerase | 0.71067651 | 1.202485902 |
| ENSG00000071626 | DAZAP1 subnetwork | 0.70482779 | 1.20248811 |
| ENSG00000149970 | CNKSR2 subnetwork | 0.77685906 | 1.202489692 |
| GO:0019903 | protein phosphatase binding | 0.71460548 | 1.202490268 |
| GO:0052745 | inositol phosphate phosphatase activity | 0.76124652 | 1.202490835 |
| ENSG00000142856 | ITGB3BP subnetwork | 0.77667711 | 1.202495506 |
| GO:2000104 | negative regulation of DNA-dependent DNA replication | 0.77693983 | 1.2025 |
| GO:0043403 | skeletal muscle tissue regeneration | 0.77613026 | 1.202502381 |
| REACTOME_SIGNAL_ATTENUA | REACTOME_SIGNAL_ATTENUATION | 0.7150243 | 1.202506008 |
| GO:0009067 | aspartate family amino acid biosynthetic process | 0.72311977 | 1.202507642 |
| ENSG00000133313 | CNDP2 subnetwork | 0.78087568 | 1.202509206 |
| GO:0060765 | regulation of androgen receptor signaling pathway | 0.76041272 | 1.202509715 |
| ENSG00000212874 | ENSG00000212874 subnetwork | 0.70477803 | 1.202511601 |
| REACTOME_DNA_REPLICATION | REACTOME_DNA_REPLICATION | 0.71053258 | 1.202515253 |
| MP:0000109 | abnormal parietal bone morphology | 0.71344104 | 1.202517202 |
| REACTOME_HIV:1_TRANSCRIP | REACTOME_HIV:1_TRANSCRIPTION_INITIATION | 0.75874003 | 1.202520554 |
| REACTOME_ACTIVATION_OF_T | REACTOME_ACTIVATION_OF_THE_PRE:REPLICATIVE_COMI | 0.70954191 | 1.202536023 |
| ENSG00000100353 | EIF3D subnetwork | 0.70984489 | 1.202540615 |

| | | | |
|---|---|---|---|
| MP:0002239 | abnormal nasal septum morphology | 0.77571259 | 1.202541027 |
| GO:0044257 | cellular protein catabolic process | 0.76019434 | 1.202542922 |
| ENSG00000164708 | PGAM2 subnetwork | 0.72333861 | 1.202546689 |
| ENSG00000154174 | TOMM70A subnetwork | 0.76034705 | 1.202547771 |
| ENSG00000132196 | HSD17B7 subnetwork | 0.77656858 | 1.202548916 |
| GO:0000375 | RNA splicing, via transesterification reactions | 0.7152188 | 1.202551196 |
| ENSG00000074800 | ENO1 subnetwork | 0.77846712 | 1.202553551 |
| MP:0004111 | abnormal coronary artery morphology | 0.71254021 | 1.202554535 |
| GO:0043434 | response to peptide hormone stimulus | 0.72569788 | 1.202555568 |
| GO:0051972 | regulation of telomerase activity | 0.77579474 | 1.202556638 |
| ENSG00000088320 | REM1 subnetwork | 0.71804016 | 1.202558696 |
| MP:0003883 | enlarged stomach | 0.72243189 | 1.202560907 |
| ENSG00000169891 | REPS2 subnetwork | 0.7597502 | 1.202565903 |
| ENSG00000165917 | RAPSN subnetwork | 0.72363776 | 1.202568454 |
| KEGG_SULFUR_METABOLISM | KEGG_SULFUR_METABOLISM | 0.7244567 | 1.202582505 |
| ENSG00000133059 | DSTYK subnetwork | 0.71497794 | 1.202586404 |
| MP:0000063 | decreased bone mineral density | 0.76123686 | 1.202588159 |
| GO:0019320 | hexose catabolic process | 0.71064797 | 1.202589779 |
| REACTOME_RNA_POL_II_CTD_ | REACTOME_RNA_POL_II_CTD_PHOSPHORYLATION_AND_II | 0.71330565 | 1.202598073 |
| ENSG00000145794 | MEGF10 subnetwork | 0.77877626 | 1.202600211 |
| GO:0030660 | Golgi-associated vesicle membrane | 0.72358407 | 1.202602693 |
| GO:0019198 | transmembrane receptor protein phosphatase activity | 0.77589081 | 1.202604001 |
| ENSG00000176601 | YSK4 subnetwork | 0.70947769 | 1.202605488 |
| ENSG00000177156 | TALDO1 subnetwork | 0.72235701 | 1.202606528 |
| ENSG00000168398 | BDKRB2 subnetwork | 0.72563998 | 1.202606635 |
| ENSG00000105327 | BBC3 subnetwork | 0.7144649 | 1.202611385 |
| GO:0006662 | glycerol ether metabolic process | 0.7143855 | 1.202617411 |
| ENSG00000167840 | ZNF232 subnetwork | 0.77545304 | 1.202621267 |
| ENSG00000078747 | ITCH subnetwork | 0.71250992 | 1.202629464 |
| MP:0003982 | increased cholesterol level | 0.78087077 | 1.202630471 |
| GO:0007320 | insemination | 0.77843292 | 1.202638244 |
| ENSG00000164342 | TLR3 subnetwork | 0.76032378 | 1.202639819 |
| ENSG00000196549 | MME subnetwork | 0.71358605 | 1.202648779 |
| GO:0042403 | thyroid hormone metabolic process | 0.77831577 | 1.202649356 |
| REACTOME_RNA_POLYMERAS | REACTOME_RNA_POLYMERASE_II_TRANSCRIPTION_INITIA | 0.75874003 | 1.202650655 |
| ENSG00000198712 | MT-CO2 subnetwork | 0.70477803 | 1.20265112 |
| ENSG00000067082 | KLF6 subnetwork | 0.77837521 | 1.202654354 |
| ENSG00000103051 | COG4 subnetwork | 0.71520289 | 1.202660183 |
| ENSG00000135213 | POM121C subnetwork | 0.77570871 | 1.202663066 |
| GO:0000301 | retrograde transport, vesicle recycling within Golgi | 0.72352429 | 1.202665233 |
| GO:0019439 | aromatic compound catabolic process | 0.70983596 | 1.202673427 |
| MP:0003313 | abnormal locomotor activation | 0.77734229 | 1.202673571 |
| GO:0021536 | diencephalon development | 0.77873054 | 1.202674333 |
| GO:0050892 | intestinal absorption | 0.78079107 | 1.202678102 |
| ENSG00000105695 | MAG subnetwork | 0.72631176 | 1.202700722 |
| GO:0002688 | regulation of leukocyte chemotaxis | 0.70945339 | 1.202703793 |
| ENSG00000164733 | CTSB subnetwork | 0.78063536 | 1.202704978 |
| GO:0070306 | lens fiber cell differentiation | 0.77717804 | 1.202705845 |
| GO:0021955 | central nervous system neuron axonogenesis | 0.7132723 | 1.202707353 |
| GO:0006379 | mRNA cleavage | 0.71370156 | 1.202717267 |
| GO:0008235 | metalloexopeptidase activity | 0.77898354 | 1.202721232 |
| ENSG00000100522 | GNPNAT1 subnetwork | 0.77561808 | 1.202721593 |
| ENSG00000173546 | CSPG4 subnetwork | 0.78028945 | 1.202727177 |

| | | | |
|---|---|---|---|
| GO:0000075 | cell cycle checkpoint | 0.77917936 | 1.202731203 |
| ENSG00000107819 | SFXN3 subnetwork | 0.71247435 | 1.202733119 |
| ENSG00000176749 | CDK5R1 subnetwork | 0.77726279 | 1.202737265 |
| ENSG00000179588 | ZFPM1 subnetwork | 0.72234929 | 1.202742831 |
| GO:0019941 | modification-dependent protein catabolic process | 0.78075424 | 1.20274679 |
| GO:0031572 | G2/M transition DNA damage checkpoint | 0.77908579 | 1.202747311 |
| GO:0007176 | regulation of epidermal growth factor-activated receptor a | 0.78056046 | 1.202747368 |
| GO:0051346 | negative regulation of hydrolase activity | 0.75857419 | 1.202748918 |
| ENSG00000160844 | GATS subnetwork | 0.71438334 | 1.202749456 |
| GO:0010035 | response to inorganic substance | 0.78039225 | 1.20276374 |
| ENSG00000174175 | SELP subnetwork | 0.70981502 | 1.202765933 |
| ENSG00000168061 | SAC3D1 subnetwork | 0.72625231 | 1.202768693 |
| MP:0000079 | abnormal basioccipital bone morphology | 0.77830807 | 1.202771033 |
| ENSG00000165966 | PDZRN4 subnetwork | 0.71405666 | 1.202773321 |
| GO:0007040 | lysosome organization | 0.78047114 | 1.20277924 |
| REACTOME_RNA_POLYMERASI | REACTOME_RNA_POLYMERASE_II_TRANSCRIPTION_INITIA | 0.75874003 | 1.202780783 |
| GO:0005247 | voltage-gated chloride channel activity | 0.77751377 | 1.202784235 |
| ENSG00000127334 | DYRK2 subnetwork | 0.77871796 | 1.202795949 |
| ENSG00000157191 | NECAP2 subnetwork | 0.71323298 | 1.202799449 |
| MP:0004505 | decreased renal glomerulus number | 0.71312204 | 1.202799771 |
| MP:0002608 | increased hematocrit | 0.714215 | 1.202813109 |
| MP:0005480 | increased circulating triiodothyronine level | 0.72599791 | 1.202826038 |
| GO:0000776 | kinetochore | 0.78028345 | 1.202832772 |
| ENSG00000114573 | ATP6V1A subnetwork | 0.71305128 | 1.202834519 |
| ENSG00000110169 | HPX subnetwork | 0.77827957 | 1.202834671 |
| GO:0044241 | lipid digestion | 0.75855655 | 1.202835805 |
| ENSG00000109475 | RPL34 subnetwork | 0.71297063 | 1.202840583 |
| ENSG00000186834 | HEXIM1 subnetwork | 0.78013791 | 1.202843901 |
| GO:0090398 | cellular senescence | 0.75562093 | 1.202851401 |
| ENSG00000058600 | POLR3E subnetwork | 0.71286172 | 1.202852388 |
| GO:0042402 | cellular biogenic amine catabolic process | 0.77797406 | 1.20285669 |
| GO:0060429 | epithelium development | 0.72650627 | 1.20285827 |
| GO:0046459 | short-chain fatty acid metabolic process | 0.75870636 | 1.202862244 |
| GO:0010812 | negative regulation of cell-substrate adhesion | 0.77790315 | 1.202862273 |
| GO:0000413 | protein peptidyl-prolyl isomerization | 0.72622144 | 1.202870517 |
| REACTOME_TRANSPORT_OF_M | REACTOME_TRANSPORT_OF_MATURE_TRANSCRIPT_TO_C | 0.75462731 | 1.202876876 |
| GO:0030545 | receptor regulator activity | 0.77821123 | 1.202877204 |
| MP:0010551 | abnormal coronary vessel morphology | 0.72234875 | 1.202879166 |
| GO:0003777 | microtubule motor activity | 0.71396994 | 1.202882852 |
| KEGG_STEROID_HORMONE_BI | KEGG_STEROID_HORMONE_BIOSYNTHESIS | 0.75412318 | 1.202884197 |
| MP:0010763 | abnormal hematopoietic stem cell physiology | 0.72674388 | 1.202885808 |
| MP:0003308 | abnormal cochlear sensory epithelium morphology | 0.72663775 | 1.202886133 |
| ENSG00000126883 | NUP214 subnetwork | 0.7143817 | 1.202887259 |
| GO:0001823 | mesonephros development | 0.77809416 | 1.202888068 |
| GO:0032570 | response to progesterone stimulus | 0.77938835 | 1.202889076 |
| GO:0006297 | nucleotide-excision repair, DNA gap filling | 0.71404521 | 1.202893983 |
| ENSG00000173145 | NOC3L subnetwork | 0.71389063 | 1.202894646 |
| ENSG00000130706 | ADRM1 subnetwork | 0.77783966 | 1.202899546 |
| MP:0004725 | decreased platelet serotonin level | 0.718361 | 1.202911349 |
| ENSG00000136944 | LMX1B subnetwork | 0.75555984 | 1.202911461 |
| ENSG00000159720 | ATP6V0D1 subnetwork | 0.72066787 | 1.20291411 |
| ENSG00000130041 | ENSG00000130041 subnetwork | 0.78009978 | 1.202923207 |
| MP:0000880 | decreased Purkinje cell number | 0.71281236 | 1.202927333 |

| | | | |
|---|---|---|---|
| ENSG00000179889 | PDXDC1 subnetwork | 0.72783275 | 1.202937866 |
| ENSG00000178585 | CTNNBIP1 subnetwork | 0.7777786 | 1.202942109 |
| GO:0003333 | amino acid transmembrane transport | 0.78027292 | 1.202943655 |
| MP:0008582 | short photoreceptor inner segment | 0.72616566 | 1.202949803 |
| GO:0032330 | regulation of chondrocyte differentiation | 0.72194668 | 1.20295452 |
| GO:0060065 | uterus development | 0.72776598 | 1.202960711 |
| GO:0008543 | fibroblast growth factor receptor signaling pathway | 0.7796972 | 1.202961948 |
| GO:0071696 | ectodermal placode development | 0.75855619 | 1.20296601 |
| MP:0010810 | increased type II pneumocyte number | 0.75452001 | 1.202975413 |
| GO:0071779 | G1/S transition checkpoint | 0.72081082 | 1.202976258 |
| GO:0016881 | acid-amino acid ligase activity | 0.77953037 | 1.202978387 |
| ENSG00000133706 | LARS subnetwork | 0.75513463 | 1.202978585 |
| ENSG00000155657 | TTN subnetwork | 0.75506543 | 1.202984344 |
| ENSG00000127955 | GNAI1 subnetwork | 0.75461967 | 1.202985968 |
| ENSG00000187239 | FNBP1 subnetwork | 0.72233141 | 1.20298719 |
| GO:0006386 | termination of RNA polymerase III transcription | 0.75531358 | 1.202988806 |
| ENSG00000113068 | PFDN1 subnetwork | 0.71832419 | 1.202997151 |
| GO:0060896 | neural plate pattern specification | 0.77996229 | 1.202997893 |
| ENSG00000139726 | DENR subnetwork | 0.75537099 | 1.202999348 |
| GO:0035337 | fatty-acyl-CoA metabolic process | 0.75411532 | 1.203009688 |
| GO:0045861 | negative regulation of proteolysis | 0.75437732 | 1.203014146 |
| ENSG00000115008 | IL1A subnetwork | 0.77774789 | 1.203016376 |
| KEGG_HEDGEHOG_SIGNALING | KEGG_HEDGEHOG_SIGNALING_PATHWAY | 0.75554218 | 1.203020426 |
| KEGG_RETINOL_METABOLISM | KEGG_RETINOL_METABOLISM | 0.7579963 | 1.203022097 |
| MP:0000013 | abnormal adipose tissue distribution | 0.77981208 | 1.203024874 |
| GO:0071774 | response to fibroblast growth factor stimulus | 0.75500936 | 1.203028161 |
| MP:0000285 | abnormal heart valve morphology | 0.72093976 | 1.203032712 |
| ENSG00000108504 | ENSG00000108504 subnetwork | 0.75445233 | 1.203035578 |
| GO:0002504 | antigen processing and presentation of peptide or polysacc | 0.72064845 | 1.203039427 |
| ENSG00000128245 | YWHAH subnetwork | 0.72749903 | 1.203046514 |
| MP:0001486 | abnormal startle reflex | 0.75431667 | 1.203047122 |
| GO:0031055 | chromatin remodeling at centromere | 0.75795925 | 1.203049507 |
| ENSG00000177954 | RPS27 subnetwork | 0.78009978 | 1.203049937 |
| REACTOME_G1S_TRANSITION | REACTOME_G1S_TRANSITION | 0.78006165 | 1.203050258 |
| ENSG00000113555 | PCDH12 subnetwork | 0.77993023 | 1.203050901 |
| GO:0000178 | exosome (RNase complex) | 0.72717555 | 1.203053521 |
| GO:0032612 | interleukin-1 production | 0.72106211 | 1.203060761 |
| GO:0034599 | cellular response to oxidative stress | 0.7548512 | 1.203061446 |
| GO:0005504 | fatty acid binding | 0.77968886 | 1.203078221 |
| MP:0008898 | abnormal acrosome morphology | 0.72191507 | 1.203079628 |
| MP:0009748 | abnormal behavioral response to addictive substance | 0.72775341 | 1.203084891 |
| GO:0060788 | ectodermal placode formation | 0.75855619 | 1.203096243 |
| MP:0001410 | head bobbing | 0.72231926 | 1.203100907 |
| ENSG00000070182 | SPTB subnetwork | 0.75552183 | 1.203102249 |
| ENSG00000064490 | RFXANK subnetwork | 0.72815214 | 1.20310566 |
| GO:0006385 | transcription elongation from RNA polymerase III promoter | 0.75531358 | 1.203119565 |
| ENSG00000106638 | TBL2 subnetwork | 0.75780222 | 1.203120936 |
| GO:0031369 | translation initiation factor binding | 0.72769101 | 1.203124648 |
| MP:0006358 | absent pinna reflex | 0.75340405 | 1.203127043 |
| GO:0022603 | regulation of anatomical structure morphogenesis | 0.75791807 | 1.203131094 |
| ENSG00000100380 | ST13 subnetwork | 0.71862599 | 1.203138886 |
| GO:0060600 | dichotomous subdivision of an epithelial terminal unit | 0.72116874 | 1.203139905 |
| GO:0046949 | fatty-acyl-CoA biosynthetic process | 0.75411532 | 1.203140649 |

| | | | |
|---|---|---|---|
| ENSG00000147274 | RBMX subnetwork | 0.72746843 | 1.2031426 |
| ENSG00000162688 | AGL subnetwork | 0.72802612 | 1.203145751 |
| ENSG00000103326 | SOLH subnetwork | 0.7281039 | 1.203151024 |
| GO:0022616 | DNA strand elongation | 0.71974526 | 1.203151308 |
| ENSG00000101152 | DNAJC5 subnetwork | 0.72762729 | 1.203153153 |
| GO:0070509 | calcium ion import | 0.72163004 | 1.203154789 |
| GO:0044344 | cellular response to fibroblast growth factor stimulus | 0.75500936 | 1.203158982 |
| ENSG00000206181 | TCEB3B subnetwork | 0.75787018 | 1.20316394 |
| ENSG00000104177 | MYEF2 subnetwork | 0.7221802 | 1.203163983 |
| GO:0050661 | NADP binding | 0.72734745 | 1.203171474 |
| GO:0072509 | divalent inorganic cation transmembrane transporter activi | 0.72064816 | 1.203176136 |
| GO:2000178 | negative regulation of neural precursor cell proliferation | 0.72717315 | 1.203183457 |
| MP:0002282 | abnormal trachea morphology | 0.75258196 | 1.203184991 |
| GO:0006000 | fructose metabolic process | 0.7222775 | 1.203197641 |
| REACTOME_MRNA_CAPPING | REACTOME_MRNA_CAPPING | 0.75236893 | 1.2032024 |
| GO:0010719 | negative regulation of epithelial to mesenchymal transition | 0.72190788 | 1.203204765 |
| ENSG00000130288 | ENSG00000130288 subnetwork | 0.71969048 | 1.203208556 |
| GO:0071697 | ectodermal placode morphogenesis | 0.75855619 | 1.203226505 |
| ENSG00000090520 | DNAJB11 subnetwork | 0.75407982 | 1.203228089 |
| ENSG00000068394 | GPKOW subnetwork | 0.72153795 | 1.203229285 |
| ENSG00000159166 | LAD1 subnetwork | 0.72056119 | 1.203233322 |
| ENSG00000091428 | RAPGEF4 subnetwork | 0.75777922 | 1.203235071 |
| MP:0005100 | abnormal choroid pigmentation | 0.75339191 | 1.203236352 |
| ENSG00000033011 | ALG1 subnetwork | 0.72713849 | 1.203245802 |
| GO:0048232 | male gamete generation | 0.75769559 | 1.203246261 |
| ENSG00000143614 | GATAD2B subnetwork | 0.7216125 | 1.203251617 |
| MP:0001324 | abnormal eye pigmentation | 0.72745435 | 1.203255604 |
| ENSG00000135916 | ITM2C subnetwork | 0.72708554 | 1.203263075 |
| GO:0050716 | positive regulation of interleukin-1 secretion | 0.75401809 | 1.203266551 |
| ENSG00000115286 | NDUFS7 subnetwork | 0.75222028 | 1.203274037 |
| ENSG00000161016 | RPL8 subnetwork | 0.72188616 | 1.20329022 |
| ENSG00000130725 | UBE2M subnetwork | 0.72028452 | 1.203291643 |
| ENSG00000059573 | ALDH18A1 subnetwork | 0.71879343 | 1.203292322 |
| GO:0000982 | RNA polymerase II core promoter proximal region sequenc | 0.75234054 | 1.203295504 |
| ENSG00000149503 | INCENP subnetwork | 0.7189485 | 1.203297267 |
| ENSG00000075292 | ZNF638 subnetwork | 0.72133715 | 1.20330419 |
| ENSG00000100568 | VTI1B subnetwork | 0.75624526 | 1.203306189 |
| ENSG00000173402 | DAG1 subnetwork | 0.71992996 | 1.203310204 |
| ENSG00000016490 | CLCA1 subnetwork | 0.75258179 | 1.203316243 |
| ENSG00000099795 | NDUFB7 subnetwork | 0.71924558 | 1.203318912 |
| ENSG00000102007 | PLP2 subnetwork | 0.72150644 | 1.203320468 |
| ENSG00000143401 | ANP32E subnetwork | 0.75251597 | 1.20332206 |
| GO:0090002 | establishment of protein localization in plasma membrane | 0.71967364 | 1.203322713 |
| GO:0005911 | cell-cell junction | 0.75288106 | 1.203326063 |
| MP:0001391 | abnormal tail movements | 0.75833744 | 1.203330445 |
| MP:0002666 | increased circulating aldosterone level | 0.75853618 | 1.203340552 |
| GO:0030530 | heterogeneous nuclear ribonucleoprotein complex | 0.71909126 | 1.203342444 |
| MP:0006395 | abnormal epiphyseal plate morphology | 0.75843881 | 1.203346329 |
| MP:0010103 | small thoracic cage | 0.75612586 | 1.203350348 |
| REACTOME_TRANSCRIPTION:C | REACTOME_TRANSCRIPTION:COUPLED_NER_TC:NER | 0.71940576 | 1.203352305 |
| ENSG00000105426 | PTPRS subnetwork | 0.72185717 | 1.203353001 |
| ENSG00000198625 | MDM4 subnetwork | 0.72055987 | 1.203364401 |
| GO:0008376 | acetylgalactosaminyltransferase activity | 0.75339064 | 1.20336748 |

| | | | |
|---|---|---|---|
| GO:0007283 | spermatogenesis | 0.75769559 | 1.203376694 |
| MP:0002116 | abnormal craniofacial bone morphology | 0.75283444 | 1.203380958 |
| ENSG00000152256 | PDK1 subnetwork | 0.72145267 | 1.203383288 |
| GO:0045495 | pole plasm | 0.75221313 | 1.203383541 |
| GO:0050718 | positive regulation of interleukin-1 beta secretion | 0.75401809 | 1.203397582 |
| ENSG00000179603 | GRM8 subnetwork | 0.72891415 | 1.203406791 |
| GO:0043531 | ADP binding | 0.719208 | 1.203410385 |
| GO:0009148 | pyrimidine nucleoside triphosphate biosynthetic process | 0.7576444 | 1.203420425 |
| ENSG00000100883 | SRP54 subnetwork | 0.72027069 | 1.203428474 |
| MP:0001695 | abnormal gastrulation | 0.71894395 | 1.203428637 |
| GO:0006633 | fatty acid biosynthetic process | 0.7562375 | 1.203431426 |
| ENSG00000174989 | FBXW8 subnetwork | 0.7566626 | 1.20343499 |
| ENSG00000213588 | ZBTB9 subnetwork | 0.71966891 | 1.203448276 |
| ENSG00000164403 | SHROOM1 subnetwork | 0.75164558 | 1.20345675 |
| ENSG00000135823 | STX6 subnetwork | 0.71937435 | 1.20346653 |
| MP:0000120 | malocclusion | 0.75611524 | 1.203470186 |
| GO:0008637 | apoptotic mitochondrial changes | 0.75314535 | 1.203477976 |
| ENSG00000176124 | DLEU1 subnetwork | 0.75338341 | 1.203482289 |
| GO:0060411 | cardiac septum morphogenesis | 0.72054353 | 1.203484142 |
| ENSG00000102109 | PCSK1N subnetwork | 0.75758135 | 1.203485851 |
| ENSG00000155897 | ADCY8 subnetwork | 0.72888181 | 1.203485888 |
| GO:0090150 | establishment of protein localization in membrane | 0.75399549 | 1.203512307 |
| GO:0043186 | P granule | 0.75221313 | 1.2035149 |
| ENSG00000086102 | NFX1 subnetwork | 0.7196329 | 1.20352265 |
| REACTOME_FORMATION_OF_I | REACTOME_FORMATION_OF_INCISION_COMPLEX_IN_GG: | 0.72872669 | 1.203526038 |
| ENSG00000122194 | PLG subnetwork | 0.75662896 | 1.203527624 |
| GO:0035195 | gene silencing by miRNA | 0.75310699 | 1.203543779 |
| ENSG00000178252 | WDR6 subnetwork | 0.75162875 | 1.203555434 |
| ENSG00000142168 | SOD1 subnetwork | 0.72027002 | 1.203565336 |
| GO:0007090 | regulation of S phase of mitotic cell cycle | 0.75752929 | 1.203578399 |
| ENSG00000093167 | LRRFIP2 subnetwork | 0.75649922 | 1.203582673 |
| ENSG00000152578 | GRIA4 subnetwork | 0.72885015 | 1.203593117 |
| ENSG00000168385 | SEPT2 subnetwork | 0.75396069 | 1.203599826 |
| GO:0016853 | isomerase activity | 0.75387483 | 1.203600218 |
| ENSG00000213905 | ENSG00000213905 subnetwork | 0.75378275 | 1.20360061 |
| GO:0017134 | fibroblast growth factor binding | 0.75337206 | 1.203602572 |
| GO:0031589 | cell-substrate adhesion | 0.72053151 | 1.203603911 |
| ENSG00000198822 | GRM3 subnetwork | 0.75195929 | 1.203614326 |
| MP:0002730 | head shaking | 0.72024252 | 1.203616924 |
| ENSG00000100297 | MCM5 subnetwork | 0.75659032 | 1.203625706 |
| ENSG00000176476 | ENSG00000176476 | 0.75185797 | 1.203631102 |
| GO:0060293 | germ plasm | 0.75221313 | 1.203646288 |
| GO:0030286 | dynein complex | 0.75206391 | 1.203657605 |
| ENSG00000083857 | FAT1 subnetwork | 0.75731716 | 1.203660918 |
| REACTOME_DUAL_INCISION_R | REACTOME_DUAL_INCISION_REACTION_IN_GG:NER | 0.72872669 | 1.203661417 |
| MP:0005608 | cardiac interstitial fibrosis | 0.72857967 | 1.203684743 |
| GO:0030334 | regulation of cell migration | 0.7516253 | 1.203686913 |
| ENSG00000123612 | ACVR1C subnetwork | 0.75749406 | 1.203687236 |
| ENSG00000148516 | ZEB1 subnetwork | 0.75723225 | 1.20369386 |
| ENSG00000164077 | MON1A subnetwork | 0.7286682 | 1.203723703 |
| MP:0008719 | impaired neutrophil recruitment | 0.75336936 | 1.203733784 |
| GO:0005086 | ARF guanyl-nucleotide exchange factor activity | 0.75720629 | 1.203753933 |
| ENSG00000091483 | FH subnetwork | 0.75745666 | 1.203774403 |

| | | | |
|---|---|---|---|
| GO:0060601 | lateral sprouting from an epithelium | 0.75161817 | 1.203812958 |
| ENSG00000197153 | HIST1H3J subnetwork | 0.75108002 | 1.203836904 |
| ENSG00000167552 | TUBA1A subnetwork | 0.7511887 | 1.20384195 |
| ENSG00000127914 | AKAP9 subnetwork | 0.75718238 | 1.203846571 |
| ENSG00000164163 | ABCE1 subnetwork | 0.7515265 | 1.203851617 |
| REACTOME_CREB_PHOSPHOR | REACTOME_CREB_PHOSPHORYLATION_THROUGH_THE_AC | 0.7292945 | 1.203901068 |
| GO:0009060 | aerobic respiration | 0.75714363 | 1.203933804 |
| MP:0005167 | abnormal blood-brain barrier function | 0.75149595 | 1.203933996 |
| MP:0000762 | abnormal tongue morphology | 0.75139333 | 1.20395082 |
| ENSG00000196532 | HIST1H3C subnetwork | 0.75108002 | 1.203968514 |
| ENSG00000138448 | ITGAV subnetwork | 0.7295384 | 1.204068787 |
| ENSG00000182572 | HIST1H3I subnetwork | 0.75108002 | 1.204100153 |
| ENSG00000103415 | HMOX2 subnetwork | 0.72948981 | 1.204102968 |
| ENSG00000112727 | ENSG00000112727 subnetwork | 0.75108002 | 1.204231821 |
| ENSG00000022840 | RNF10 subnetwork | 0.74560592 | 1.204310725 |
| ENSG00000196966 | HIST1H3E subnetwork | 0.75108002 | 1.204363517 |
| MP:0001299 | abnormal eye distance/ position | 0.74558733 | 1.204399295 |
| GO:0015179 | L-amino acid transmembrane transporter activity | 0.74535433 | 1.204422293 |
| MP:0000383 | abnormal hair follicle orientation | 0.74530736 | 1.204439304 |
| ENSG00000197409 | HIST1H3D subnetwork | 0.75108002 | 1.204495242 |
| GO:0001968 | fibronectin binding | 0.74556657 | 1.204498899 |
| GO:0020037 | heme binding | 0.72998791 | 1.204506631 |
| ENSG00000095485 | CWF19L1 subnetwork | 0.74492046 | 1.204535435 |
| GO:0005326 | neurotransmitter transporter activity | 0.7451299 | 1.204561983 |
| ENSG00000127022 | CANX subnetwork | 0.74530006 | 1.204566487 |
| GO:0051325 | interphase | 0.74485926 | 1.204574515 |
| ENSG00000110148 | CCKBR subnetwork | 0.74753476 | 1.204580907 |
| GO:0008088 | axon cargo transport | 0.74524364 | 1.204589026 |
| GO:0014065 | phosphatidylinositol 3-kinase cascade | 0.73011882 | 1.204590403 |
| ENSG00000122034 | GTF3A subnetwork | 0.74736676 | 1.204626374 |
| ENSG00000198366 | HIST1H3A subnetwork | 0.75108002 | 1.204626996 |
| GO:0043395 | heparan sulfate proteoglycan binding | 0.74727404 | 1.204632377 |
| GO:0042588 | zymogen granule | 0.74507999 | 1.204634119 |
| GO:0009314 | response to radiation | 0.74952671 | 1.204636125 |
| GO:0001974 | blood vessel remodeling | 0.74653822 | 1.204641954 |
| GO:0001786 | phosphatidylserine binding | 0.73030889 | 1.20465678 |
| GO:0006414 | translational elongation | 0.74751701 | 1.204658317 |
| ENSG00000168454 | TXNDC2 subnetwork | 0.75010851 | 1.204682366 |
| GO:0071695 | anatomical structure maturation | 0.74484991 | 1.204690773 |
| GO:0033176 | proton-transporting V-type ATPase complex | 0.73132687 | 1.204695389 |
| GO:0006644 | phospholipid metabolic process | 0.74948602 | 1.204702401 |
| GO:0006206 | pyrimidine base metabolic process | 0.74723455 | 1.204715322 |
| ENSG00000198744 | ENSG00000198744 subnetwork | 0.73143605 | 1.204717299 |
| ENSG00000168374 | ARF4 subnetwork | 0.74747676 | 1.204719262 |
| GO:0015893 | drug transport | 0.74970169 | 1.204728767 |
| KEGG_BASAL_CELL_CARCINOM | KEGG_BASAL_CELL_CARCINOMA | 0.74940672 | 1.204730322 |
| GO:0015991 | ATP hydrolysis coupled proton transport | 0.74996715 | 1.204732691 |
| MP:0002622 | abnormal cochlear hair cell morphology | 0.746501 | 1.204741474 |
| ENSG00000126821 | SGPP1 subnetwork | 0.74148714 | 1.204750831 |
| GO:0046112 | nucleobase biosynthetic process | 0.75007424 | 1.20475408 |
| ENSG00000178458 | ENSG00000178458 subnetwork | 0.75108002 | 1.204758779 |
| ENSG00000087086 | FTL subnetwork | 0.74603153 | 1.204761118 |
| GO:0017069 | snRNA binding | 0.73163977 | 1.204766712 |

| | | | |
|---|---|---|---|
| GO:0045765 | regulation of angiogenesis | 0.74982154 | 1.204783037 |
| GO:0046546 | development of primary male sexual characteristics | 0.73030852 | 1.204786517 |
| ENSG00000011243 | AKAP8L subnetwork | 0.73159741 | 1.20478968 |
| ENSG00000135441 | BLOC1S1 subnetwork | 0.7446613 | 1.204791575 |
| ENSG00000164329 | PAPD4 subnetwork | 0.74482982 | 1.204801544 |
| REACTOME_AMINE_COMPOUI | REACTOME_AMINE_COMPOUND_SLC_TRANSPORTERS | 0.74643169 | 1.204802509 |
| GO:0045737 | positive regulation of cyclin-dependent protein kinase activ | 0.73175453 | 1.204805428 |
| GO:0002762 | negative regulation of myeloid leukocyte differentiation | 0.7459847 | 1.204805681 |
| GO:0016528 | sarcoplasm | 0.7307257 | 1.204817518 |
| ENSG00000205572 | SERF1B subnetwork | 0.74926431 | 1.204819079 |
| ENSG00000125675 | GRIA3 subnetwork | 0.7472181 | 1.20482027 |
| ENSG00000114054 | PCCB subnetwork | 0.73802291 | 1.204822024 |
| GO:0006403 | RNA localization | 0.731325 | 1.204824955 |
| GO:0030512 | negative regulation of transforming growth factor beta rece | 0.74939204 | 1.204840478 |
| MP:0005294 | abnormal heart ventricle morphology | 0.74714348 | 1.204848285 |
| ENSG00000124006 | OBSL1 subnetwork | 0.74701417 | 1.204849351 |
| GO:0090183 | regulation of kidney development | 0.73090414 | 1.204850118 |
| GO:0046474 | glycerophospholipid biosynthetic process | 0.7306874 | 1.204857367 |
| GO:0015988 | energy coupled proton transport, against electrochemical g | 0.74996715 | 1.204864687 |
| REACTOME_AMYLOIDS | REACTOME_AMYLOIDS | 0.75081243 | 1.204864835 |
| MP:0003953 | abnormal hormone level | 0.74691096 | 1.204871879 |
| MP:0006107 | abnormal fetal atrioventricular canal morphology | 0.73086216 | 1.204873119 |
| GO:0051287 | NAD binding | 0.74161554 | 1.204877644 |
| GO:0009108 | coenzyme biosynthetic process | 0.73188092 | 1.204877775 |
| ENSG00000173805 | HAP1 subnetwork | 0.74148313 | 1.204884262 |
| ENSG00000124693 | HIST1H3B subnetwork | 0.75108002 | 1.204890591 |
| GO:0008406 | gonad development | 0.75092689 | 1.204891661 |
| ENSG00000131100 | ATP6V1E1 subnetwork | 0.74465052 | 1.204902393 |
| ENSG00000205542 | TMSB4X subnetwork | 0.7312897 | 1.204904051 |
| REACTOME_PYRIMIDINE_MET/ | REACTOME_PYRIMIDINE_METABOLISM | 0.74915896 | 1.204907875 |
| ENSG00000136631 | VPS45 subnetwork | 0.75032662 | 1.204911839 |
| REACTOME_SHC1_EVENTS_IN_ | REACTOME_SHC1_EVENTS_IN_ERBB4_SIGNALING | 0.74711968 | 1.204925783 |
| ENSG00000148498 | PARD3 subnetwork | 0.74642341 | 1.204929577 |
| ENSG00000131931 | THAP1 subnetwork | 0.74907452 | 1.20493035 |
| GO:0009156 | ribonucleoside monophosphate biosynthetic process | 0.74482943 | 1.204934392 |
| ENSG00000108387 | SEPT4 subnetwork | 0.75046124 | 1.204938136 |
| ENSG00000103343 | ZNF174 subnetwork | 0.73124815 | 1.204949495 |
| ENSG00000108518 | PFN1 subnetwork | 0.73801488 | 1.204950495 |
| ENSG00000172058 | SERF1A subnetwork | 0.74926431 | 1.204951201 |
| ENSG00000106636 | YKT6 subnetwork | 0.74637519 | 1.204952129 |
| GO:0051591 | response to cAMP | 0.73106139 | 1.204956219 |
| MP:0000961 | abnormal dorsal root ganglion morphology | 0.74787456 | 1.204964851 |
| GO:0008198 | ferrous iron binding | 0.74144424 | 1.204967878 |
| ENSG00000182199 | SHMT2 subnetwork | 0.73067627 | 1.204970235 |
| MP:0004358 | bowed tibia | 0.74133521 | 1.204979506 |
| GO:0031649 | heat generation | 0.74456452 | 1.204980695 |
| GO:0051647 | nucleus localization | 0.75080424 | 1.204996716 |
| REACTOME_DOWNREGULATIC | REACTOME_DOWNREGULATION_OF_ERRB2ERBB3_SIGNAL | 0.74690258 | 1.2049989 |
| MP:0002059 | abnormal seminal vesicle morphology | 0.73797062 | 1.205006676 |
| ENSG00000006638 | TBXA2R subnetwork | 0.74463473 | 1.205007721 |
| REACTOME_CREATION_OF_C4 | REACTOME_CREATION_OF_C4_AND_C2_ACTIVATORS | 0.73119286 | 1.205017398 |
| MP:0009292 | increased inguinal fat pad weight | 0.74375379 | 1.205019881 |
| ENSG00000177189 | RPS6KA3 subnetwork | 0.75107507 | 1.205022431 |

| | | | |
|---|---|---|---|
| ENSG00000104626 | ERI1 subnetwork | 0.74819797 | 1.205023608 |
| GO:0031272 | regulation of pseudopodium assembly | 0.74904822 | 1.205040588 |
| ENSG00000186832 | KRT16 subnetwork | 0.7504443 | 1.205042707 |
| REACTOME_MITOTIC_M:MG1_ | REACTOME_MITOTIC_M:MG1_PHASES | 0.74857848 | 1.205043354 |
| ENSG00000094804 | CDC6 subnetwork | 0.73232618 | 1.205043712 |
| GO:0045259 | proton-transporting ATP synthase complex | 0.74636242 | 1.205051728 |
| ENSG00000126581 | BECN1 subnetwork | 0.74352837 | 1.20505469 |
| MP:0003674 | oxidative stress | 0.73253457 | 1.205064993 |
| ENSG00000082397 | EPB41L3 subnetwork | 0.73244069 | 1.205065561 |
| ENSG00000134871 | COL4A2 subnetwork | 0.74295112 | 1.20507022 |
| GO:0046685 | response to arsenic-containing substance | 0.75069763 | 1.205074447 |
| REACTOME_TRNA_AMINOACY | REACTOME_TRNA_AMINOACYLATION | 0.74402649 | 1.205078944 |
| KEGG_GLYCOLYSIS_GLUCONEC | KEGG_GLYCOLYSIS_GLUCONEOGENESIS | 0.74368806 | 1.205081189 |
| GO:0072593 | reactive oxygen species metabolic process | 0.74898786 | 1.205085025 |
| MP:0009712 | impaired conditioned place preference behavior | 0.7430484 | 1.205091774 |
| ENSG00000184110 | EIF3C subnetwork | 0.74087402 | 1.20509367 |
| MP:0000296 | absent trabeculae carneae | 0.73065482 | 1.205094361 |
| GO:0006334 | nucleosome assembly | 0.74456077 | 1.205097087 |
| MP:0000293 | absent myocardial trabeculae | 0.74814084 | 1.205106523 |
| GO:0048644 | muscle organ morphogenesis | 0.75078921 | 1.205106732 |
| GO:0032436 | positive regulation of proteasomal ubiquitin-dependent prc | 0.74183423 | 1.20510961 |
| GO:2000145 | regulation of cell motility | 0.74834997 | 1.205110892 |
| MP:0002796 | impaired skin barrier function | 0.74322596 | 1.205112192 |
| ENSG00000089597 | GANAB subnetwork | 0.74133267 | 1.205113007 |
| MP:0000343 | altered response to myocardial infarction | 0.7321895 | 1.205118287 |
| REACTOME_REGULATION_OF_ | REACTOME_REGULATION_OF_PYRUVATE_DEHYDROGENAS | 0.74124197 | 1.205119114 |
| ENSG00000178951 | ZBTB7A subnetwork | 0.74113741 | 1.205119681 |
| ENSG00000167565 | SERTAD3 subnetwork | 0.74436673 | 1.205120848 |
| ENSG00000159063 | ALG8 subnetwork | 0.73773055 | 1.205125779 |
| ENSG00000197766 | CFD subnetwork | 0.74414408 | 1.205128064 |
| ENSG00000105971 | CAV2 subnetwork | 0.74317732 | 1.205134866 |
| MP:0004564 | enlarged myocardial fiber | 0.73766389 | 1.205137482 |
| MP:0005450 | abnormal energy expenditure | 0.74234357 | 1.20513998 |
| MP:0003719 | abnormal pericyte morphology | 0.73225036 | 1.205140135 |
| GO:0060525 | prostate glandular acinus development | 0.73797061 | 1.205140759 |
| MP:0003843 | abnormal sagittal suture morphology | 0.74081554 | 1.205144124 |
| MP:0003503 | decreased activity of thyroid | 0.73781603 | 1.205147468 |
| ENSG00000198841 | KTI12 subnetwork | 0.73231591 | 1.205150768 |
| ENSG00000184270 | HIST2H2AB subnetwork | 0.74225761 | 1.205151616 |
| GO:0001530 | lipopolysaccharide binding | 0.74452475 | 1.205152819 |
| ENSG00000184752 | NDUFA12 subnetwork | 0.74447043 | 1.205153388 |
| MP:0003731 | abnormal retinal outer nuclear layer morphology | 0.74107382 | 1.205153497 |
| MP:0009238 | coiled sperm flagellum | 0.74431984 | 1.205154525 |
| ENSG00000154134 | ROBO3 subnetwork | 0.74400144 | 1.205162323 |
| GO:0016646 | oxidoreductase activity, acting on the CH-NH group of donc | 0.74313459 | 1.205163074 |
| ENSG00000151148 | UBE3B subnetwork | 0.74015065 | 1.205165335 |
| MP:0000164 | abnormal cartilage development | 0.74856483 | 1.205170143 |
| ENSG00000197321 | SVIL subnetwork | 0.7434856 | 1.205171271 |
| ENSG00000186298 | PPP1CC subnetwork | 0.7463527 | 1.205173363 |
| ENSG00000106665 | CLIP2 subnetwork | 0.73788868 | 1.205174716 |
| GO:0050921 | positive regulation of chemotaxis | 0.7433344 | 1.20517794 |
| ENSG00000204843 | DCTN1 subnetwork | 0.74248796 | 1.205178137 |
| GO:0017015 | regulation of transforming growth factor beta receptor sign | 0.74292835 | 1.205181376 |

| | | | |
|---|---|---|---|
| GO:0051291 | protein heterooligomerization | 0.74809991 | 1.205183965 |
| ENSG00000182606 | TRAK1 subnetwork | 0.74894766 | 1.205184332 |
| ENSG00000166128 | RAB8B subnetwork | 0.73300668 | 1.205190951 |
| MP:0002204 | abnormal neurotransmitter level | 0.74207493 | 1.205191499 |
| GO:0070542 | response to fatty acid | 0.74198901 | 1.205197609 |
| ENSG00000163743 | RCHY1 subnetwork | 0.74368411 | 1.205208794 |
| ENSG00000105402 | NAPA subnetwork | 0.74343273 | 1.205221571 |
| ENSG00000094914 | AAAS subnetwork | 0.7422025 | 1.205235196 |
| ENSG00000140750 | ARHGAP17 subnetwork | 0.73765409 | 1.205238254 |
| ENSG00000164975 | SNAPC3 subnetwork | 0.73428158 | 1.205243153 |
| GO:0031669 | cellular response to nutrient levels | 0.7410569 | 1.205248282 |
| ENSG00000159176 | CSRP1 subnetwork | 0.74880049 | 1.205251317 |
| MP:0002834 | decreased heart weight | 0.74287746 | 1.205253844 |
| ENSG00000179562 | GCC1 subnetwork | 0.74012806 | 1.205254689 |
| MP:0002109 | abnormal limb morphology | 0.74888659 | 1.205256227 |
| ENSG00000206258 | TNXB subnetwork | 0.73439592 | 1.205259334 |
| GO:0009071 | serine family amino acid catabolic process | 0.73310906 | 1.205274356 |
| MP:0010413 | complete atrioventricular septal defect | 0.73298349 | 1.205275538 |
| ENSG00000211895 | ENSG00000211895 subnetwork | 0.74430759 | 1.205276521 |
| GO:0032587 | ruffle membrane | 0.74081191 | 1.205277747 |
| MP:0009858 | abnormal cellular extravasation | 0.74855394 | 1.205285981 |
| MP:0003985 | renal fibrosis | 0.74400019 | 1.205295417 |
| MP:0000480 | increased rib number | 0.74280851 | 1.205298673 |
| ENSG00000215693 | ENSG00000215693 subnetwork | 0.73947217 | 1.205309341 |
| GO:0005929 | cilium | 0.73295506 | 1.205326537 |
| ENSG00000137822 | TUBGCP4 subnetwork | 0.73280349 | 1.205338936 |
| ENSG00000116285 | ERRFI1 subnetwork | 0.73426123 | 1.205349955 |
| MP:0005318 | decreased triglyceride level | 0.73764297 | 1.205350184 |
| MP:0005602 | decreased angiogenesis | 0.74009994 | 1.20536626 |
| ENSG00000174469 | CNTNAP2 subnetwork | 0.73845474 | 1.205372039 |
| GO:0035586 | purinergic receptor activity | 0.7427688 | 1.205382233 |
| MP:0002980 | abnormal postural reflex | 0.73753029 | 1.205401492 |
| ENSG00000173599 | PC subnetwork | 0.74004389 | 1.205405705 |
| GO:0055069 | zinc ion homeostasis | 0.74080677 | 1.205411399 |
| GO:0010634 | positive regulation of epithelial cell migration | 0.73404101 | 1.205413265 |
| ENSG00000144597 | EAF1 subnetwork | 0.73759458 | 1.205423163 |
| ENSG00000170579 | DLGAP1 subnetwork | 0.73422229 | 1.205428827 |
| GO:0010165 | response to X-ray | 0.73294279 | 1.205433565 |
| KEGG_ALPHA_LINOLENIC_ACID | KEGG_ALPHA_LINOLENIC_ACID_METABOLISM | 0.73902041 | 1.205440702 |
| ENSG00000106278 | PTPRZ1 subnetwork | 0.73978867 | 1.205440817 |
| ENSG00000168395 | ING5 subnetwork | 0.73947217 | 1.205443235 |
| ENSG00000010818 | HIVEP2 subnetwork | 0.73988591 | 1.205451316 |
| GO:0005381 | iron ion transmembrane transporter activity | 0.73746289 | 1.205457786 |
| MP:0005424 | jerky movement | 0.73931418 | 1.205466667 |
| GO:0060766 | negative regulation of androgen receptor signaling pathway | 0.7339826 | 1.205486577 |
| GO:0005200 | structural constituent of cytoskeleton | 0.74059642 | 1.205490849 |
| ENSG00000213123 | TCTEX1D2 subnetwork | 0.74050628 | 1.205497005 |
| REACTOME_N:GLYCAN_TRIMM | REACTOME_N:GLYCAN_TRIMMING_IN_THE_ER_AND_CALI | 0.73975321 | 1.205508051 |
| GO:0005801 | cis-Golgi network | 0.74003674 | 1.205522869 |
| ENSG00000185479 | KRT6B subnetwork | 0.73741957 | 1.205525231 |
| ENSG00000100109 | TFIP11 subnetwork | 0.73900194 | 1.205530236 |
| ENSG00000144642 | RBMS3 subnetwork | 0.73691571 | 1.205539456 |
| ENSG00000111445 | RFC5 subnetwork | 0.73420454 | 1.205541266 |

| | | | |
|---|---|---|---|
| GO:0006882 | cellular zinc ion homeostasis | 0.74080677 | 1.205545082 |
| ENSG00000100170 | SLC5A1 subnetwork | 0.73944729 | 1.205549383 |
| ENSG00000150527 | CTAGE5 subnetwork | 0.74072209 | 1.205556788 |
| ENSG00000171914 | TLN2 subnetwork | 0.7339492 | 1.205571093 |
| REACTOME_AMINO_ACID_SYN | REACTOME_AMINO_ACID_SYNTHESIS_AND_INTERCONVER | 0.73930956 | 1.20558951 |
| ENSG00000168961 | LGALS9 subnetwork | 0.73880526 | 1.205593239 |
| ENSG00000136603 | SKIL subnetwork | 0.73705956 | 1.205605706 |
| GO:0043010 | camera-type eye development | 0.73378363 | 1.205605908 |
| ENSG00000182752 | PAPPA subnetwork | 0.73337788 | 1.205615273 |
| MP:0003954 | abnormal Reichert's membrane morphology | 0.73873039 | 1.205616103 |
| GO:0003774 | motor activity | 0.7405005 | 1.205625208 |
| MP:0002759 | abnormal caudal vertebrae morphology | 0.73390251 | 1.205633251 |
| MP:0000600 | liver hypoplasia | 0.73974428 | 1.205641937 |
| GO:0034453 | microtubule anchoring | 0.73899101 | 1.205642023 |
| MP:0000443 | abnormal snout morphology | 0.73740696 | 1.205642825 |
| GO:0006362 | transcription elongation from RNA polymerase I promoter | 0.73373971 | 1.205645703 |
| GO:0006271 | DNA strand elongation involved in DNA replication | 0.73926138 | 1.205651256 |
| ENSG00000118972 | FGF23 subnetwork | 0.73689352 | 1.205668264 |
| ENSG00000115461 | IGFBP5 subnetwork | 0.73723715 | 1.205705371 |
| ENSG00000111237 | VPS29 subnetwork | 0.73371556 | 1.20570789 |
| REACTOME_OLFACTORY_SIGN | REACTOME_OLFACTORY_SIGNALING_PATHWAY | 0.73523468 | 1.205741734 |
| ENSG00000197747 | S100A10 subnetwork | 0.736579 | 1.205743281 |
| GO:0030866 | cortical actin cytoskeleton organization | 0.73578792 | 1.205759571 |
| GO:0043274 | phospholipase binding | 0.73898846 | 1.205764954 |
| MP:0001879 | abnormal lymphatic vessel morphology | 0.73352234 | 1.205765786 |
| ENSG00000171365 | CLCN5 subnetwork | 0.73685983 | 1.205769231 |
| ENSG00000132334 | PTPRE subnetwork | 0.73739843 | 1.205771588 |
| MP:0001915 | intracranial hemorrhage | 0.73533433 | 1.205780185 |
| GO:0046503 | glycerolipid catabolic process | 0.73679474 | 1.205803323 |
| ENSG00000039068 | CDH1 subnetwork | 0.73588105 | 1.205803571 |
| REACTOME_ACTIVATION_OF_A | REACTOME_ACTIVATION_OF_ATR_IN_RESPONSE_TO_REPL | 0.73368803 | 1.205803671 |
| GO:0031333 | negative regulation of protein complex assembly | 0.73360632 | 1.205815516 |
| ENSG00000129170 | CSRP3 subnetwork | 0.73576255 | 1.205838357 |
| ENSG00000134853 | PDGFRA subnetwork | 0.73566465 | 1.205861338 |
| MP:0009403 | increased variability of skeletal muscle fiber size | 0.73612397 | 1.205869226 |
| MP:0002657 | chondrodystrophy | 0.73522201 | 1.205870852 |
| ENSG00000067225 | PKM2 subnetwork | 0.73514249 | 1.205871508 |
| ENSG00000087245 | MMP2 subnetwork | 0.73657497 | 1.205872184 |
| MP:0003858 | enhanced coordination | 0.73509007 | 1.205922449 |
| MP:0000026 | abnormal inner ear morphology | 0.73609405 | 1.205931258 |
| GO:0046676 | negative regulation of insulin secretion | 0.73679404 | 1.205937779 |
| GO:0031667 | response to nutrient levels | 0.73656062 | 1.205984384 |
| GO:0033327 | Leydig cell differentiation | 0.73565512 | 1.205990397 |
| GO:0030426 | growth cone | 0.73507001 | 1.206006929 |
| GO:0015643 | toxin binding | 0.73647352 | 1.206012941 |
| GO:0045768 | positive regulation of anti-apoptosis | 0.73639549 | 1.206024768 |
| ENSG00000101680 | LAMA1 subnetwork | 0.7356371 | 1.206041318 |
| GO:0003209 | cardiac atrium morphogenesis | 0.73502257 | 1.20608025 |
| ENSG00000178896 | EXOSC4 subnetwork | 0.7356206 | 1.206136922 |

## Enrichment analyses for the Genome wide significant loci from largest GWAS of autoimmune diseases performed in Caucasian individuals

| Disease | Publication [PMID] | No. hits* | Fraction of loci associated to allergy [P<0.05] | Fraction in same direction | Enrichment OR** | 95%CI | | P |
|---|---|---|---|---|---|---|---|---|
| Crohn's disease | 21102463 | 68 | 0.28 | 0.63 | 6.9 | 3.8 | 12.0 | 1.6E-09 |
| Multiple sclerosis | 21833088 | 52 | 0.23 | 0.50 | 5.3 | 2.6 | 10.4 | 1.4E-05 |
| Ulcerative colitis | 21297633 | 39 | 0.28 | 0.36 | 7.0 | 3.1 | 14.5 | 4.0E-06 |
| Celiac disease | 20190752 | 27 | 0.30 | 0.50 | 7.5 | 2.8 | 18.0 | 5.7E-05 |
| Primary biliary cirrhosis | 21399635 | 20 | 0.40 | 0.38 | 11.9 | 4.2 | 31.6 | 4.5E-06 |

*Able for lookup within the allergy dataset

**Enrichment of loci associated to allergy as compared to number of significant [P<0.05] independent loci within the allergy meta-analysis

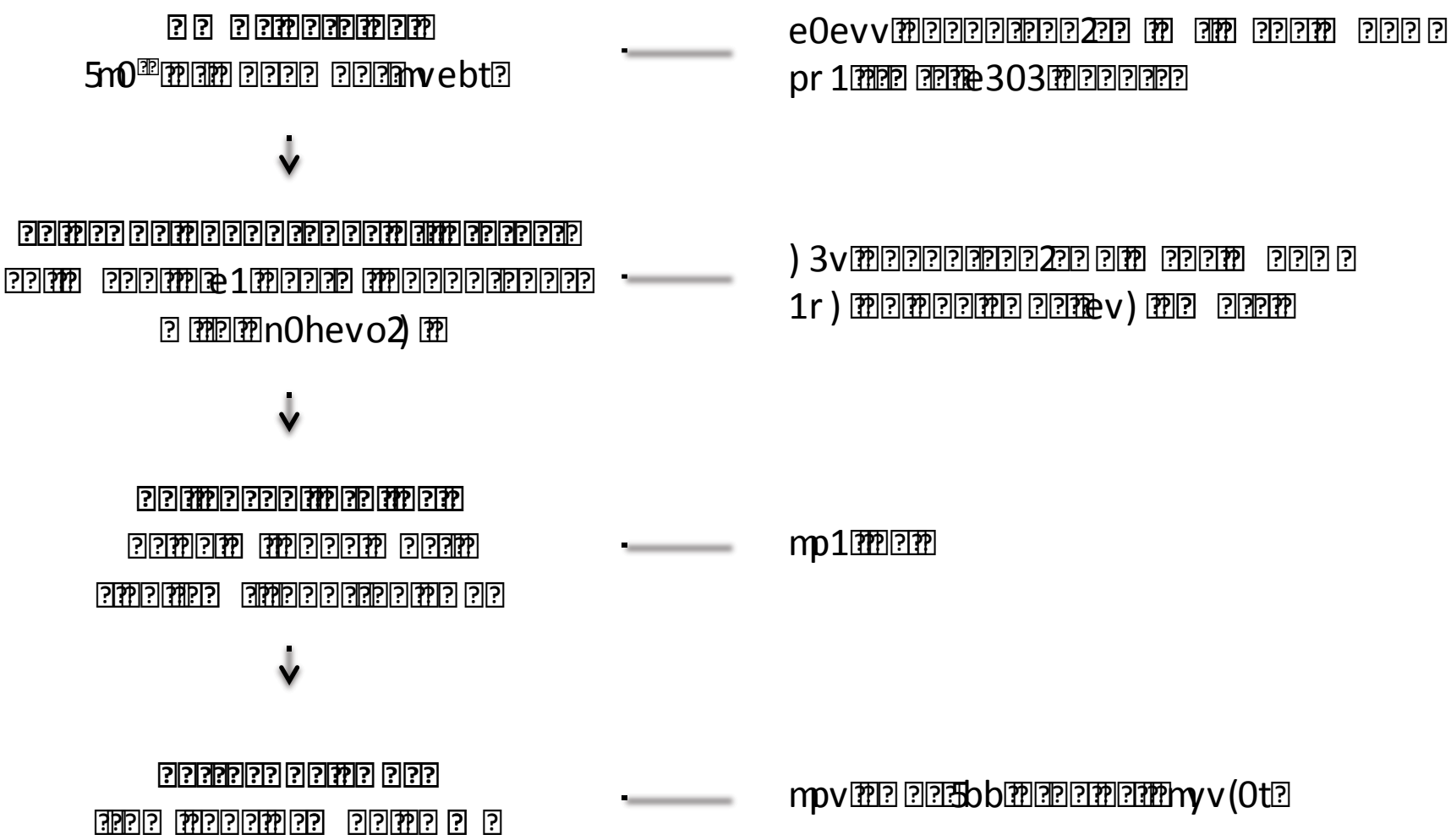

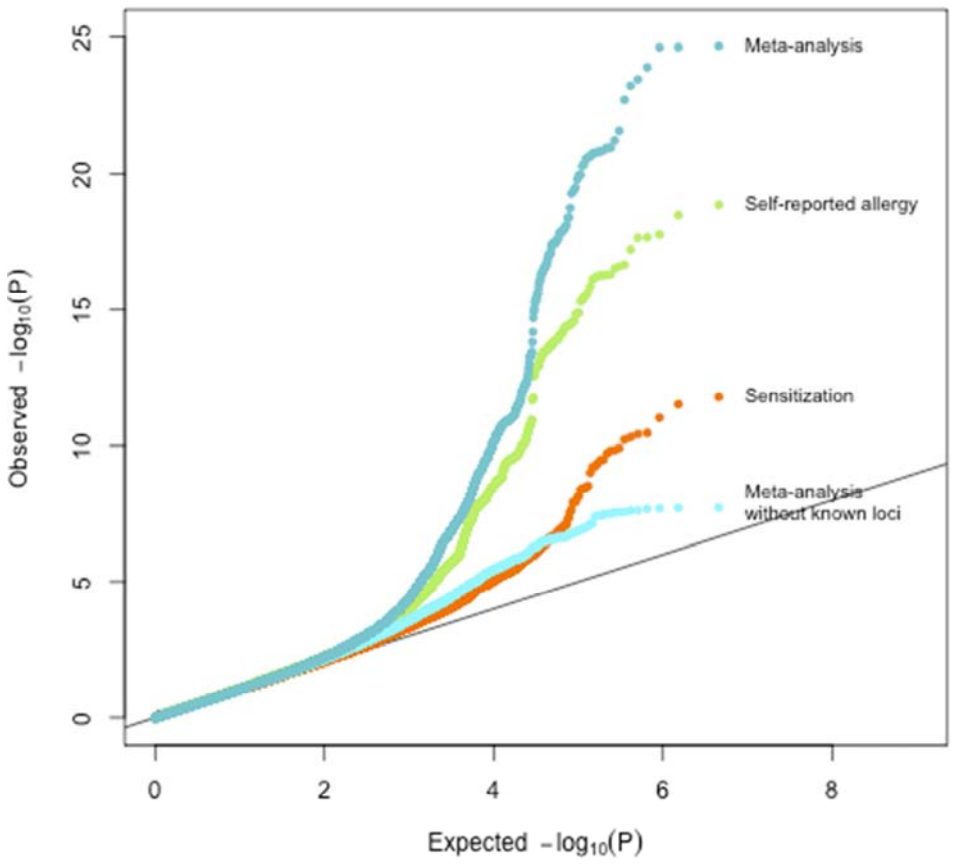

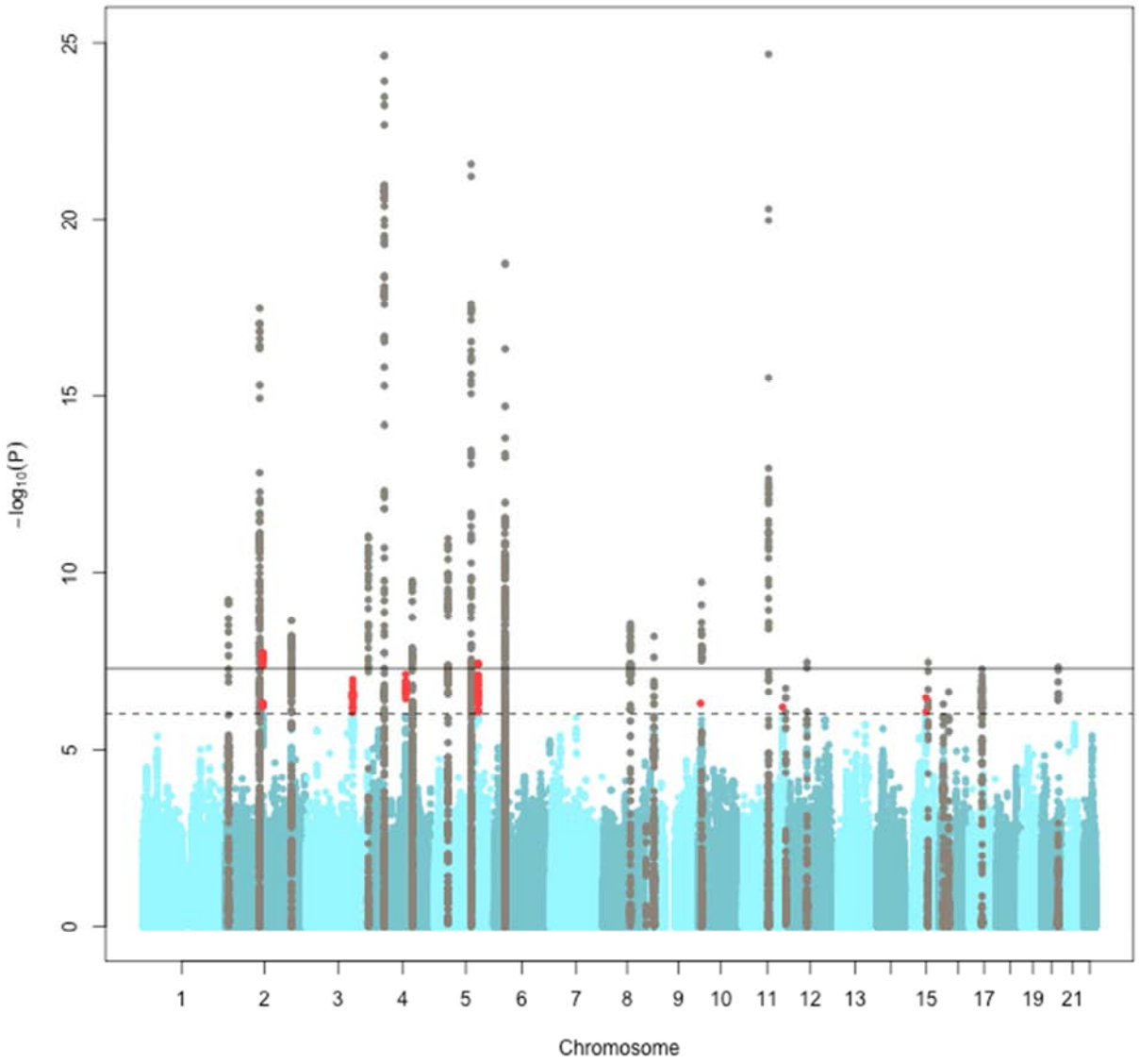
25
20
15
10
5
0
$-\log_{10}(P)$
1
2
3
4
5
6
7
8
9
10
11
12
13
15
17
19
21
Chromosome

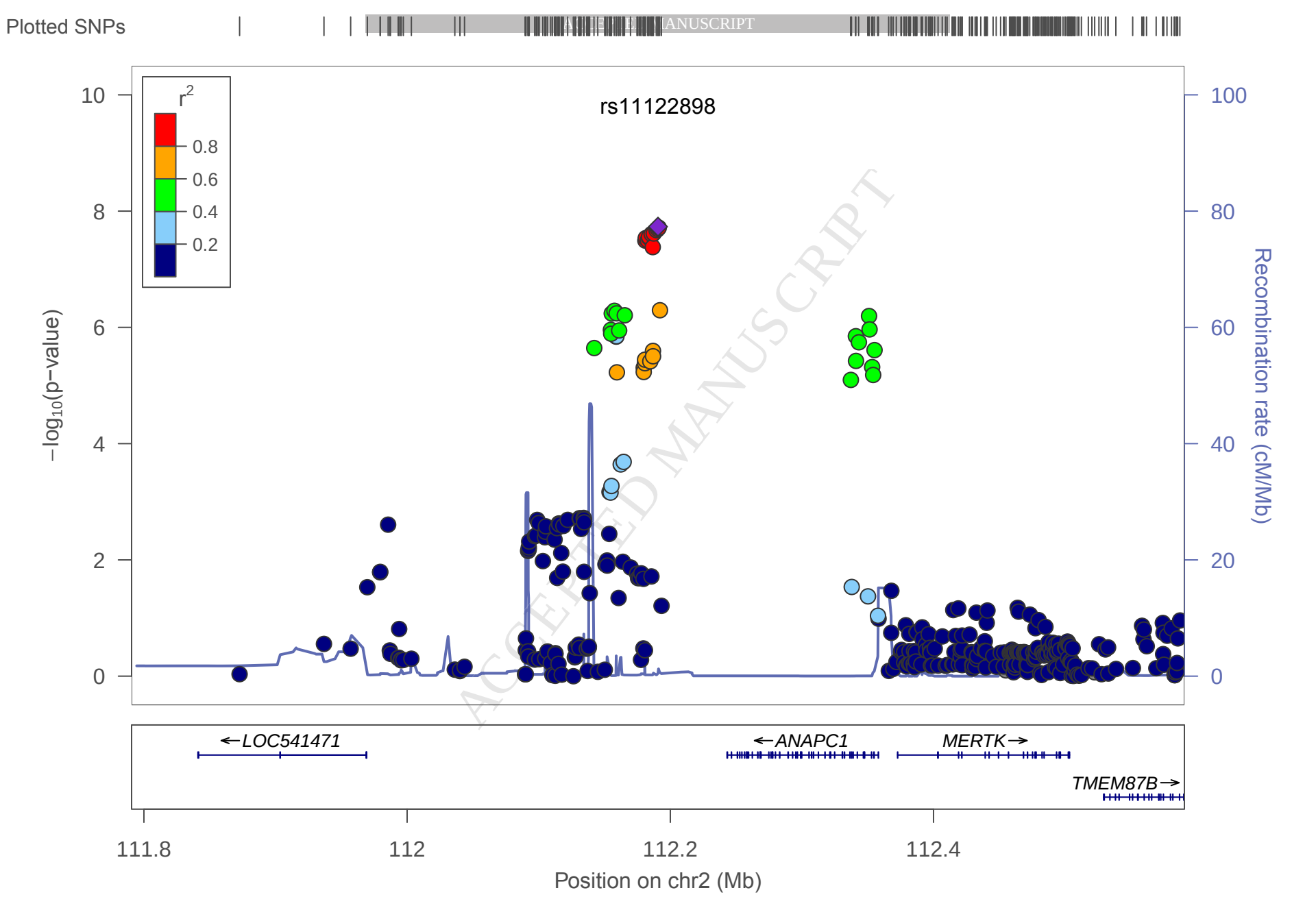
Plotted SNPs
rs11122898
r2
0.8
0.6
0.4
0.2
−log10(p−value)
Recombination rate (cM/Mb)
LOC541471
ANAPC1
MERTK
TMEM87B
111.8
112
112.2
112.4
Position on chr2 (Mb)

| | |
|---|---|
| date: | Mon Dec 23 05:36:52 2013 |
| build: | hg18 |
| display range: | chr2:111790645−112590645 [111790645−112590645] |
| hilite range: | 0 − 0 [ 0 − 0 ] |
| reference SNP: | chr2:112190645 |
| number of SNPs plotted: | 348 |
| max P.value: | 1.85E−8 [chr2:112190645] |
| min P.value: | 9.97E−1 [chr2:112126313] |

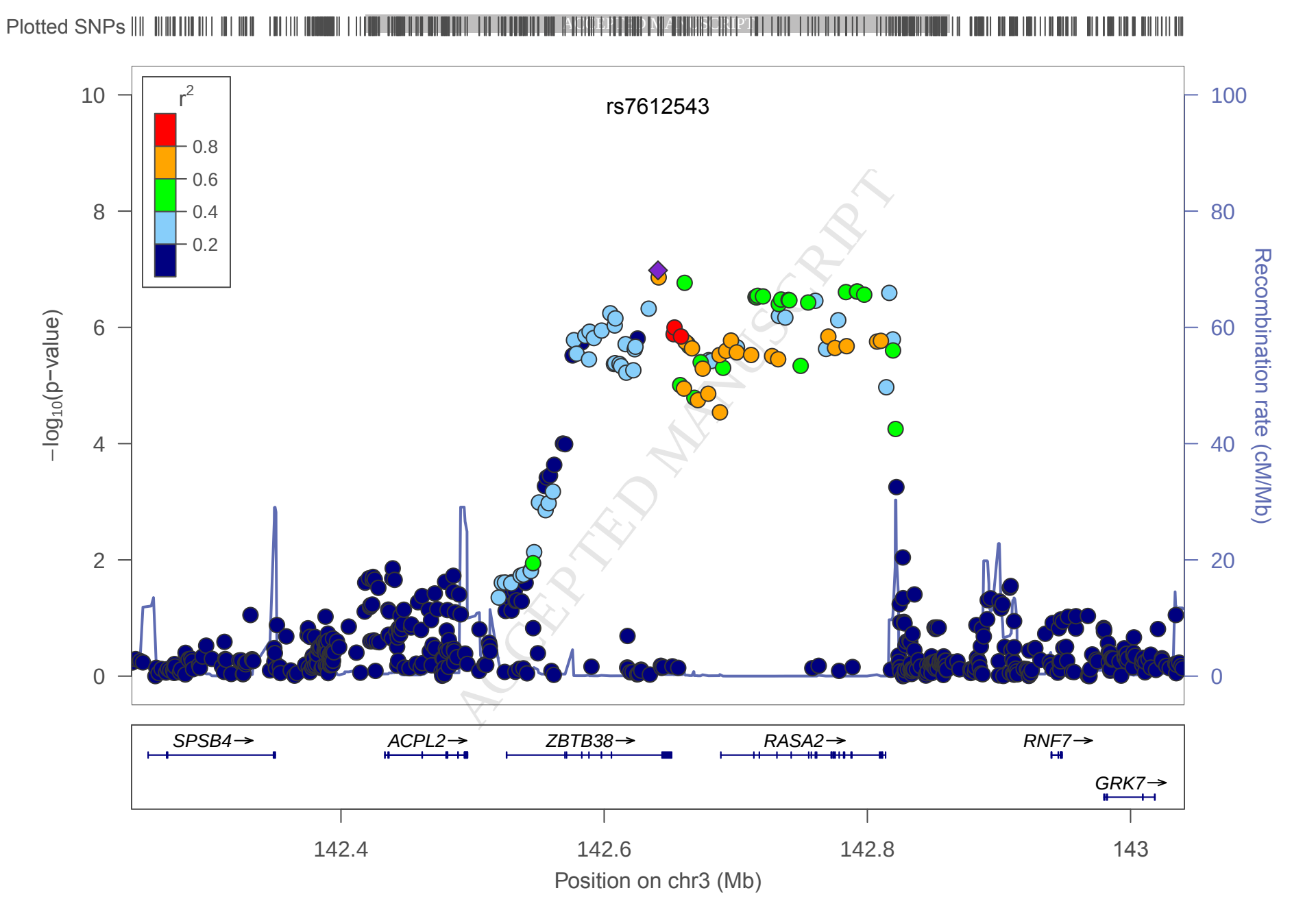

| | |
|---|---|
| date: | Mon Dec 23 05:39:26 2013 |
| build: | hg18 |
| display range: | chr3:142240902−143040902 [142240902−143040902] |
| hilite range: | 0 − 0 [ 0 − 0 ] |
| reference SNP: | chr3:142640902 |
| number of SNPs plotted: | 561 |
| max P.value: | 1.05E−7 [chr3:142640902] |
| min P.value: | 9.95E−1 [chr3:142827041] |

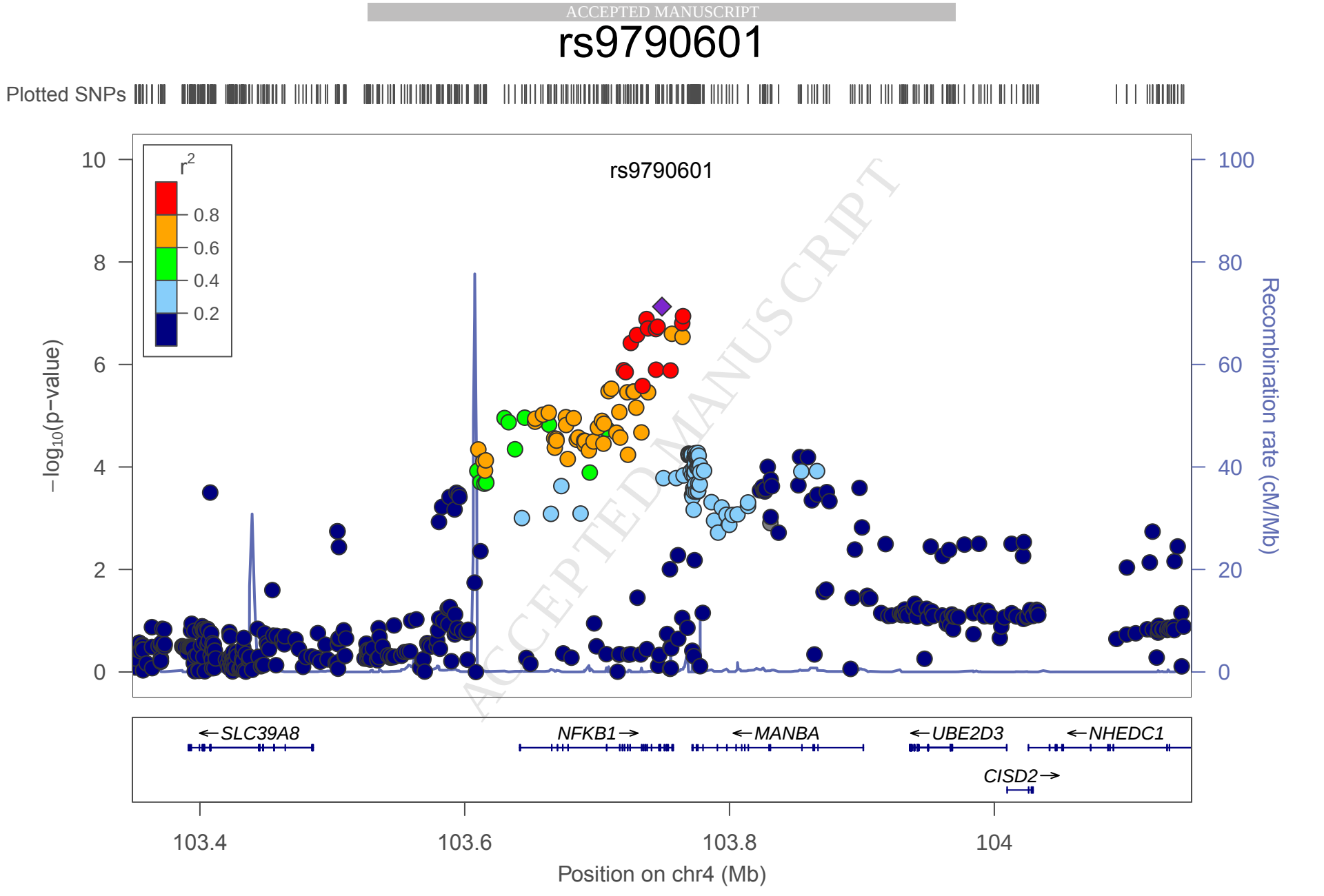

| | |
|---|---|
| date: | Mon Mar 31 15:03:02 2014 |
| build: | hg18 |
| display range: | chr4:103349001−104149001 [103349001−104149001] |
| hilite range: | 0 − 0 [ 0 − 0 ] |
| reference SNP: | chr4:103749001 |
| number of SNPs plotted: | 514 |
| max P.value: | 7.44E−8 [chr4:103749001] |
| min P.value: | 9.91E−1 [chr4:103608433] |

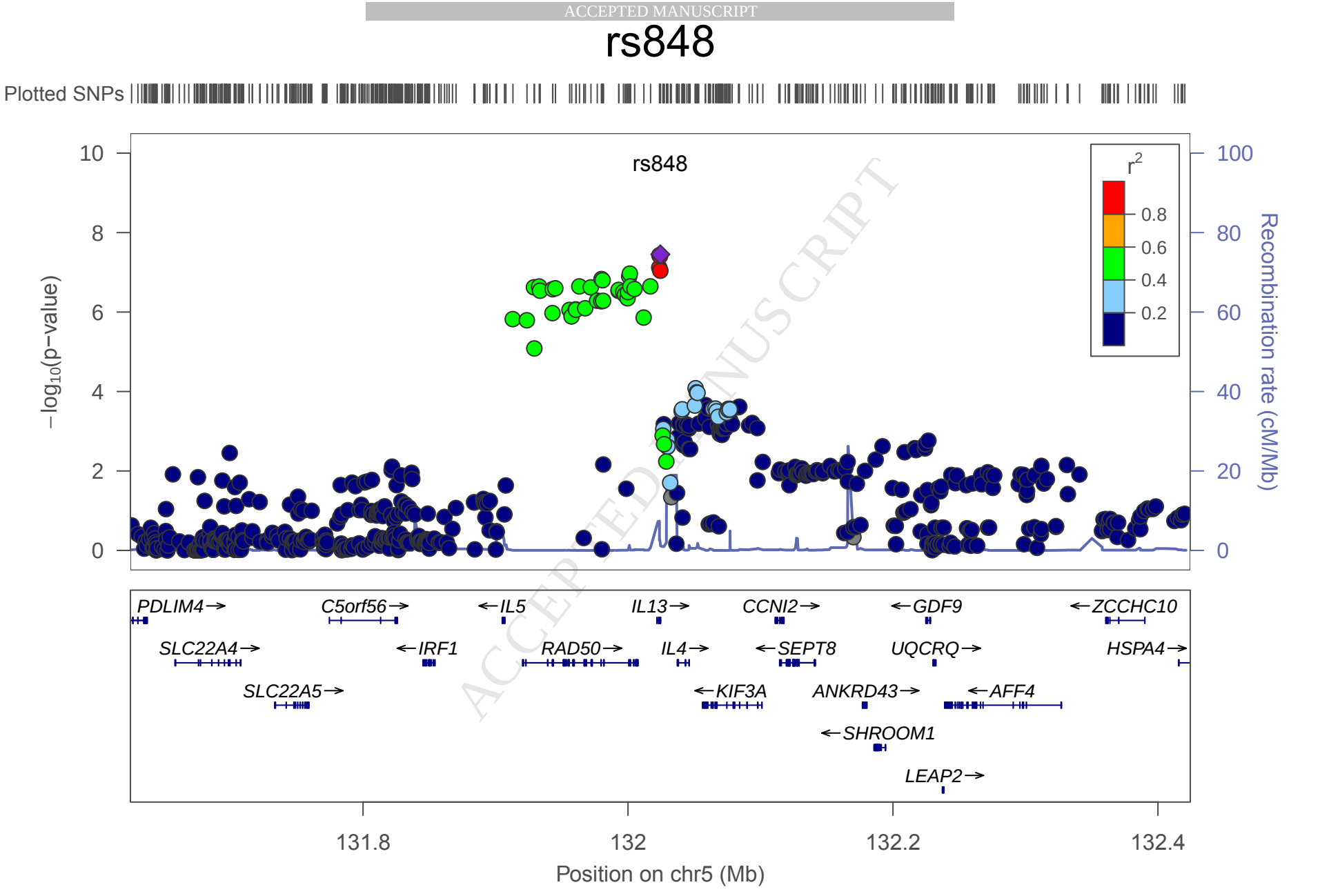

| | |
|---|---|
| date: | Mon Mar 31 15:06:39 2014 |
| build: | hg18 |
| display range: | chr5:131624399−132424399 [131624399−132424399] |
| hilite range: | 0 − 0 [ 0 − 0 ] |
| reference SNP: | chr5:132024399 |
| number of SNPs plotted: | 560 |
| max P.value: | 3.54E−8 [chr5:132024399] |
| min P.value: | 9.97E−1 [chr5:131652285] |

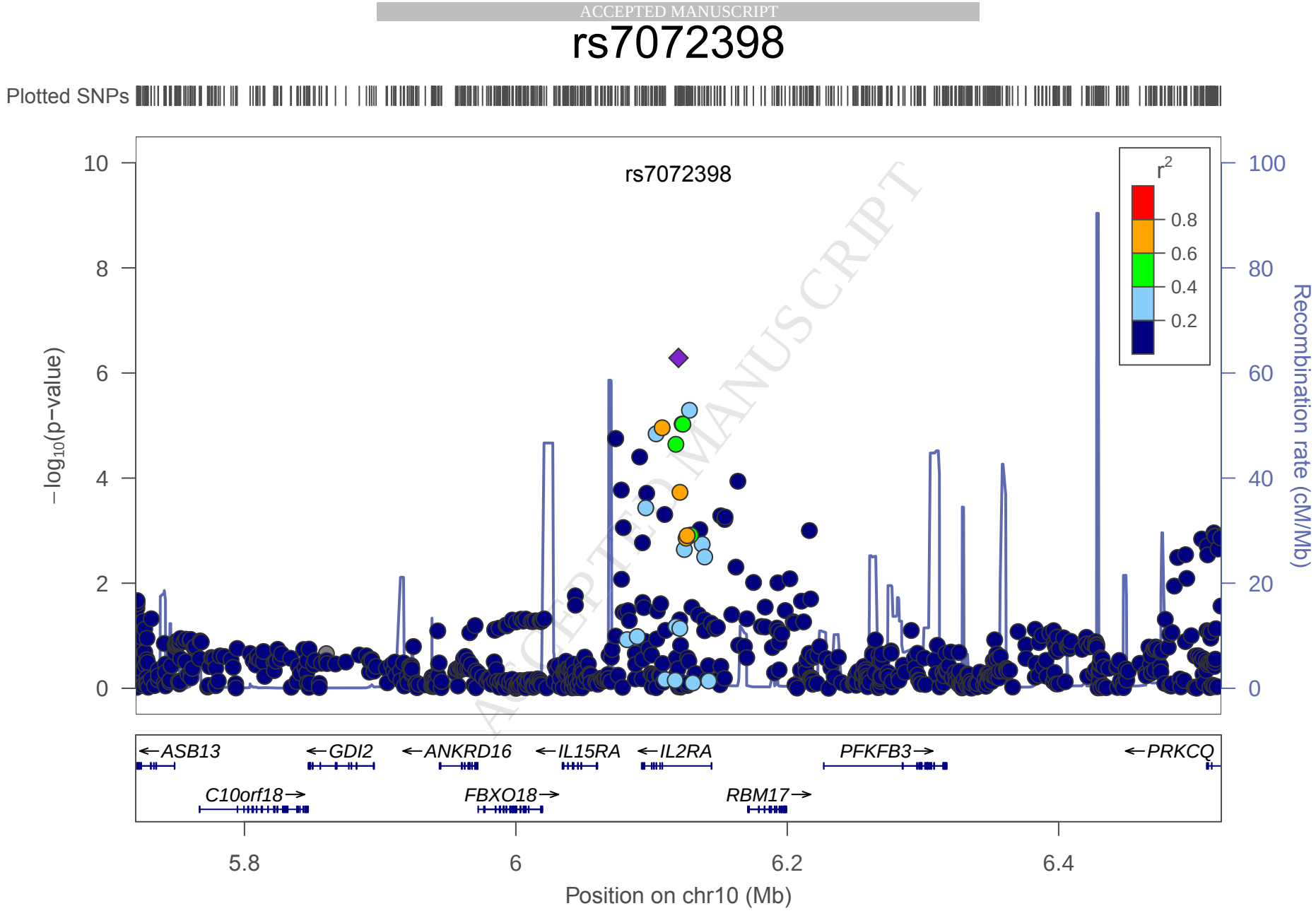

| | |
|---|---|
| date: | Mon Mar 31 15:15:04 2014 |
| build: | hg18 |
| display range: | chr10:5719852−6519852 [5719852−6519852] |
| hilite range: | 0 − 0 [ 0 − 0 ] |
| reference SNP: | chr10:6119852 |
| number of SNPs plotted: | 793 |
| max P.value: | 5.17E−7 [chr10:6119852] |
| min P.value: | 9.96E−1 [chr10:6000215] |

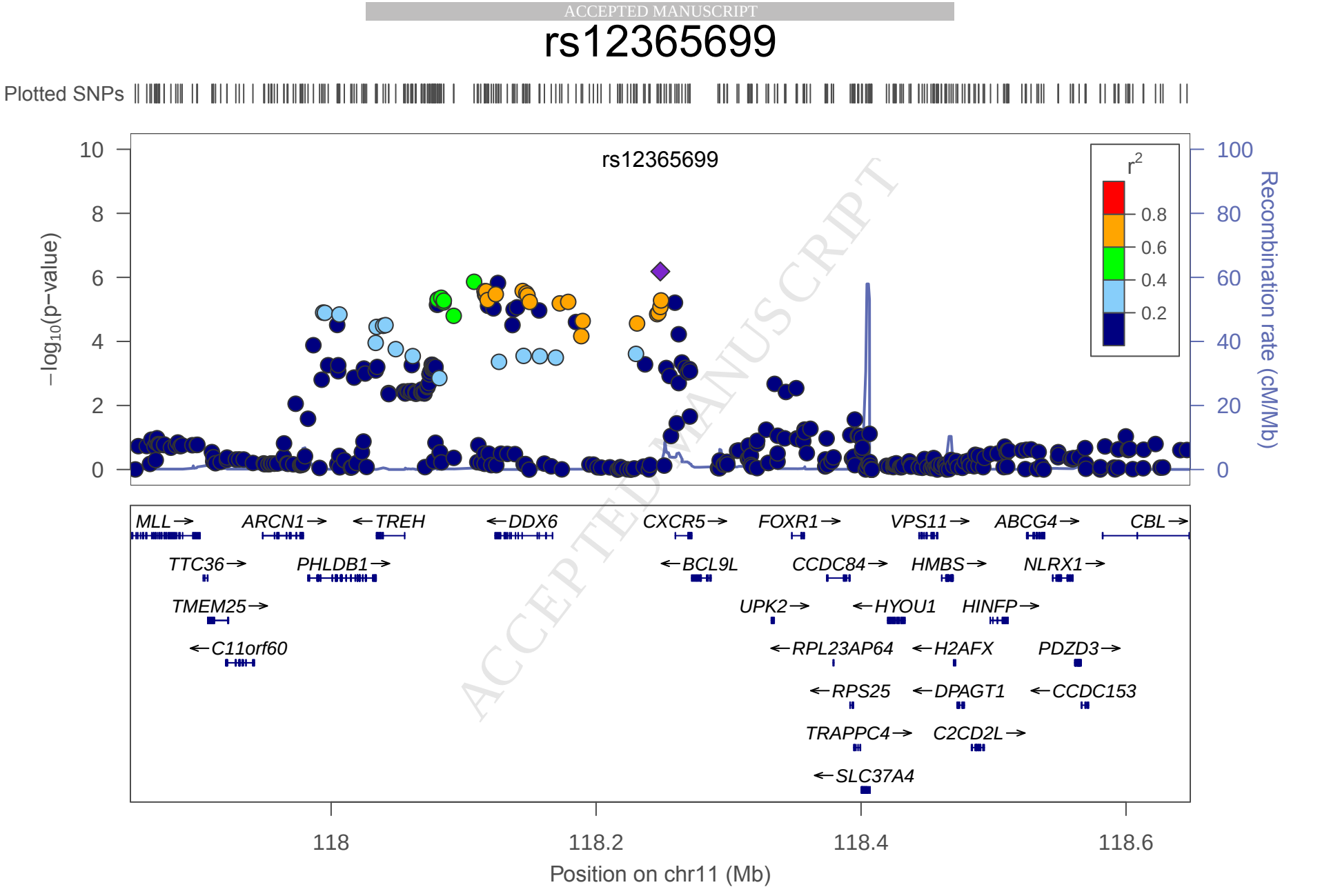

| | |
|---|---|
| date: | Mon Mar 31 15:19:15 2014 |
| build: | hg18 |
| display range: | chr11:117848496−118648496 [117848496−118648496] |
| hilite range: | 0 − 0 [ 0 − 0 ] |
| reference SNP: | chr11:118248496 |
| number of SNPs plotted: | 374 |
| max P.value: | 6.54E−7 [chr11:118248496] |
| min P.value: | 9.96E−1 [chr11:118407819] |

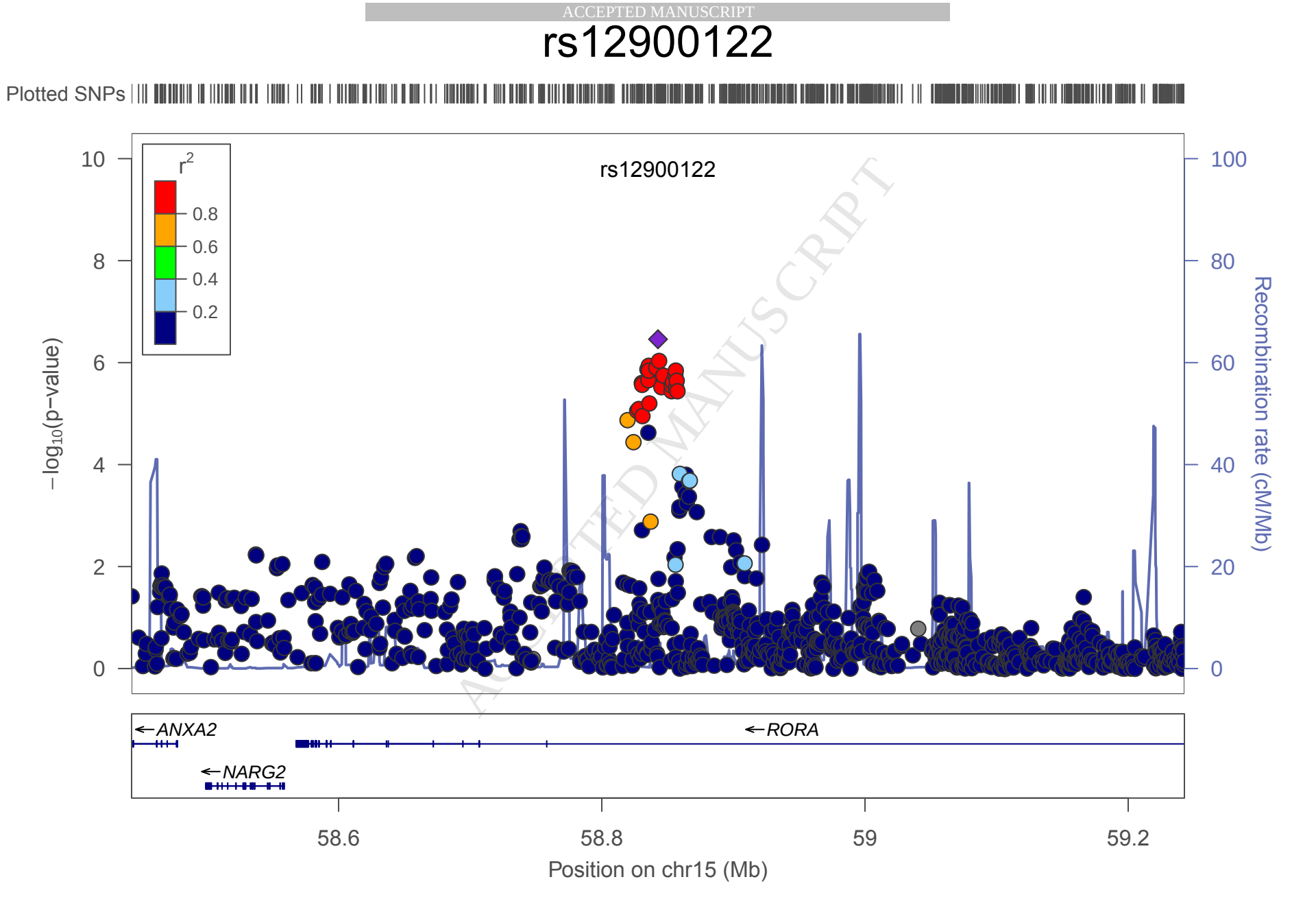

| | |
|---|---|
| date: | Mon Mar 31 15:23:06 2014 |
| build: | hg18 |
| display range: | chr15:58442703−59242703 [58442703−59242703] |
| hilite range: | 0 − 0 [ 0 − 0 ] |
| reference SNP: | chr15:58842703 |
| number of SNPs plotted: | 944 |
| max P.value: | 3.48E−7 [chr15:58842703] |
| min P.value: | 9.99E−1 [chr15:58711195] |

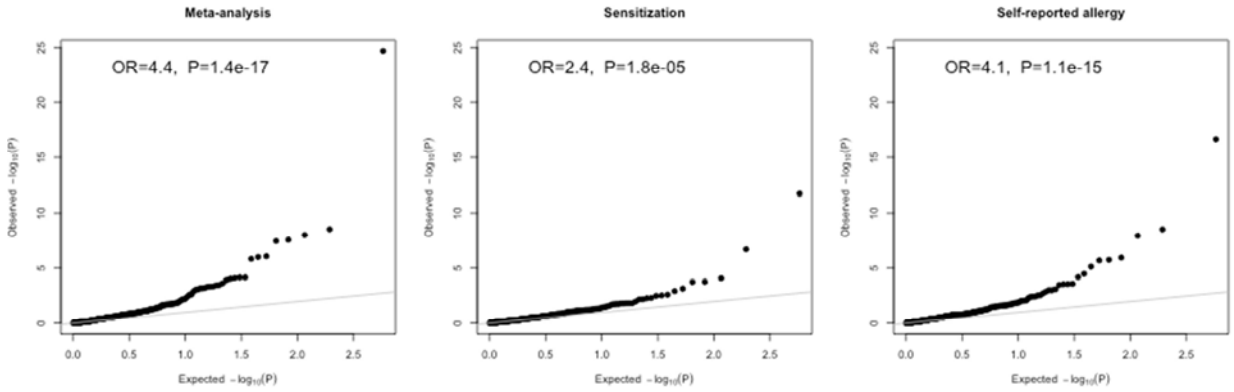

# ANKYLOSING SPONDYLITITS META−ANALYSIS

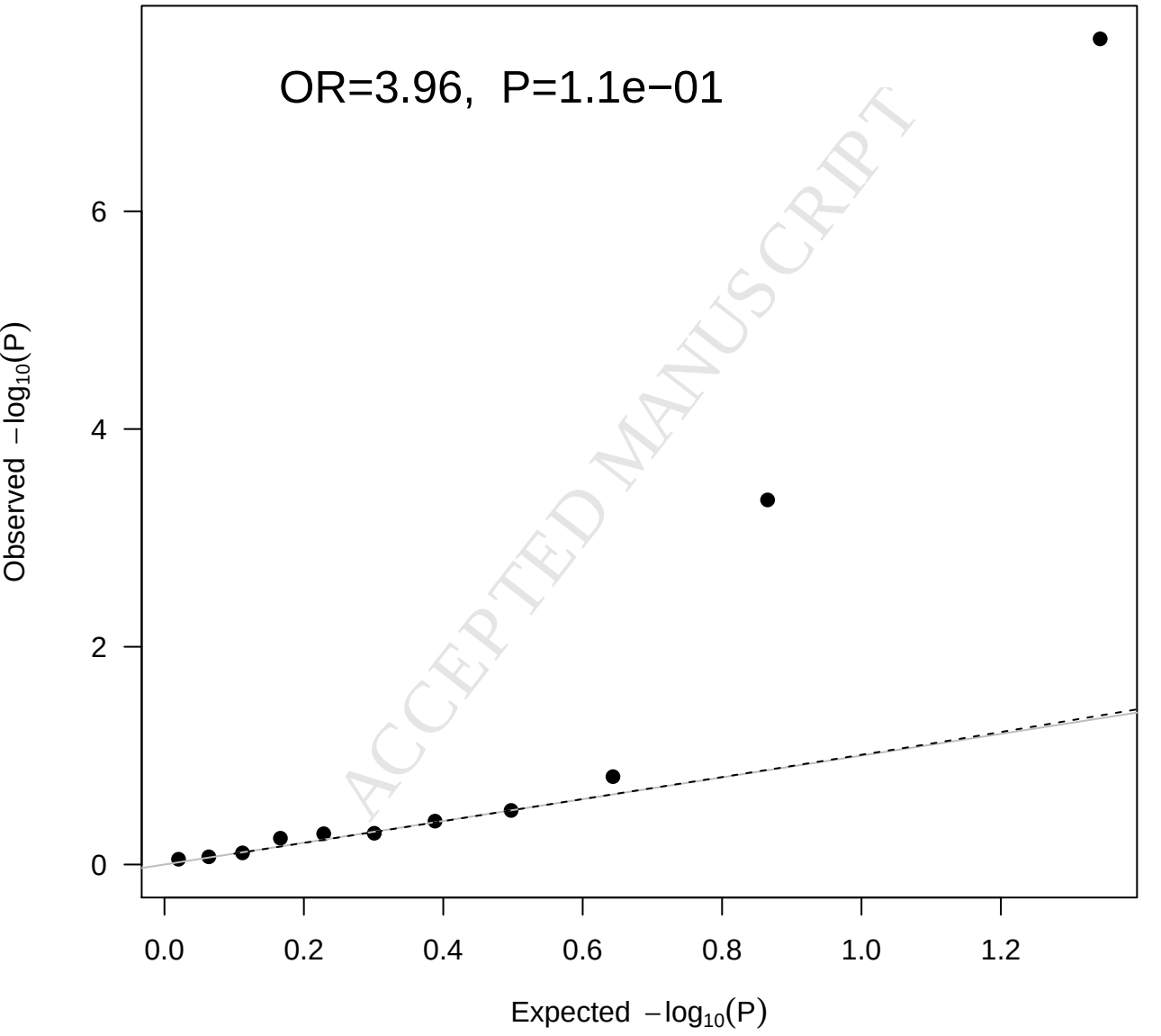

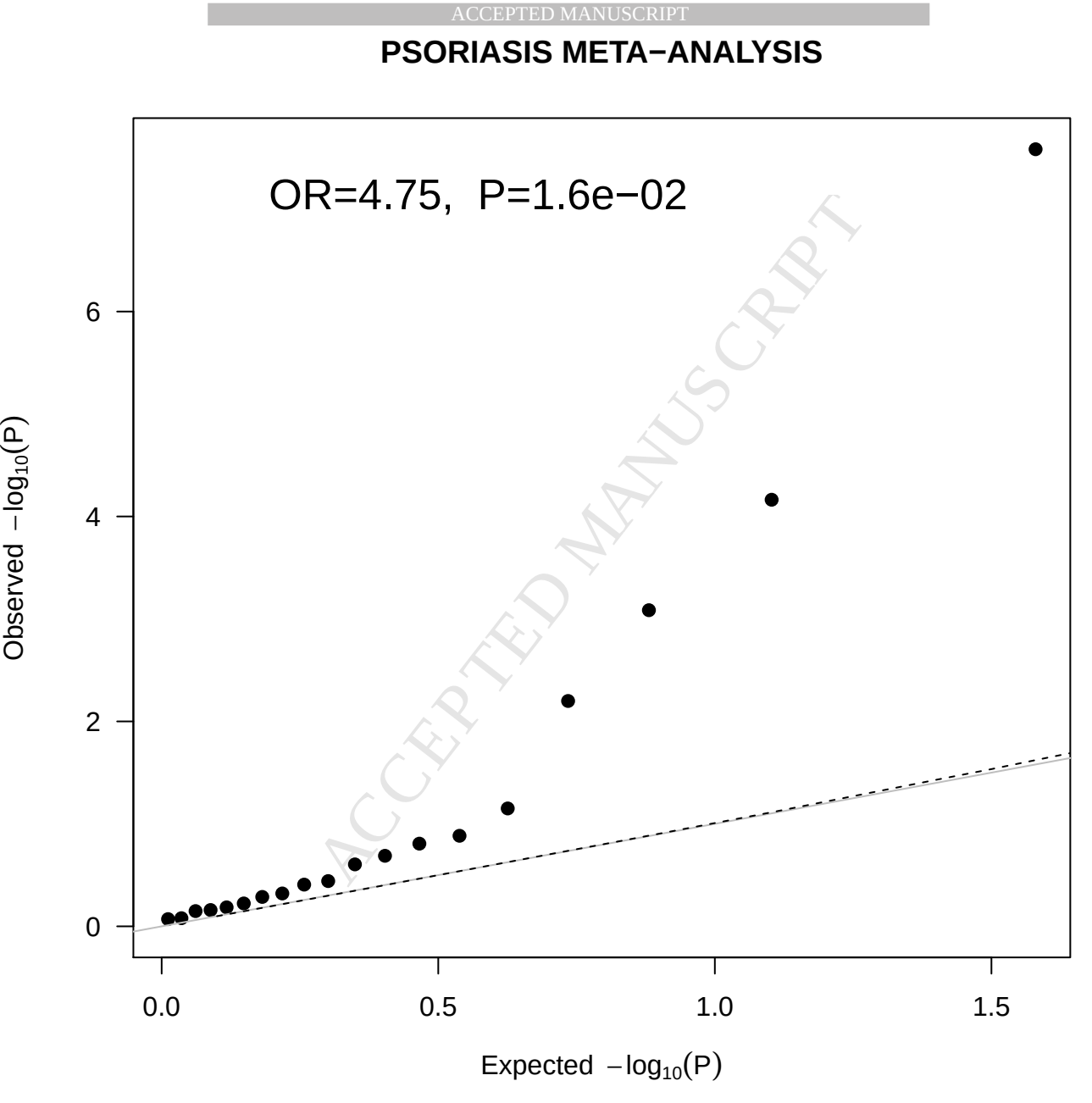

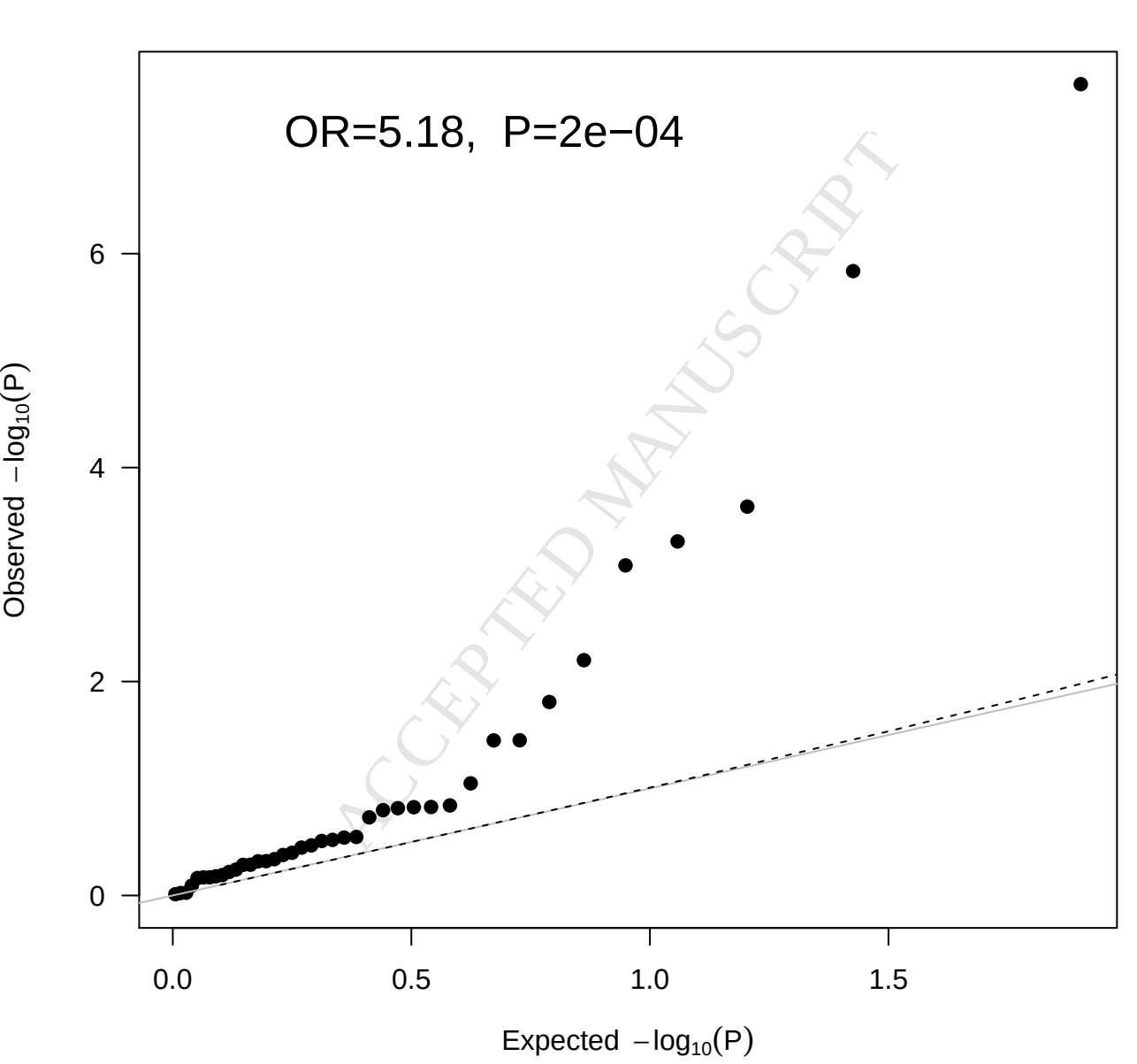

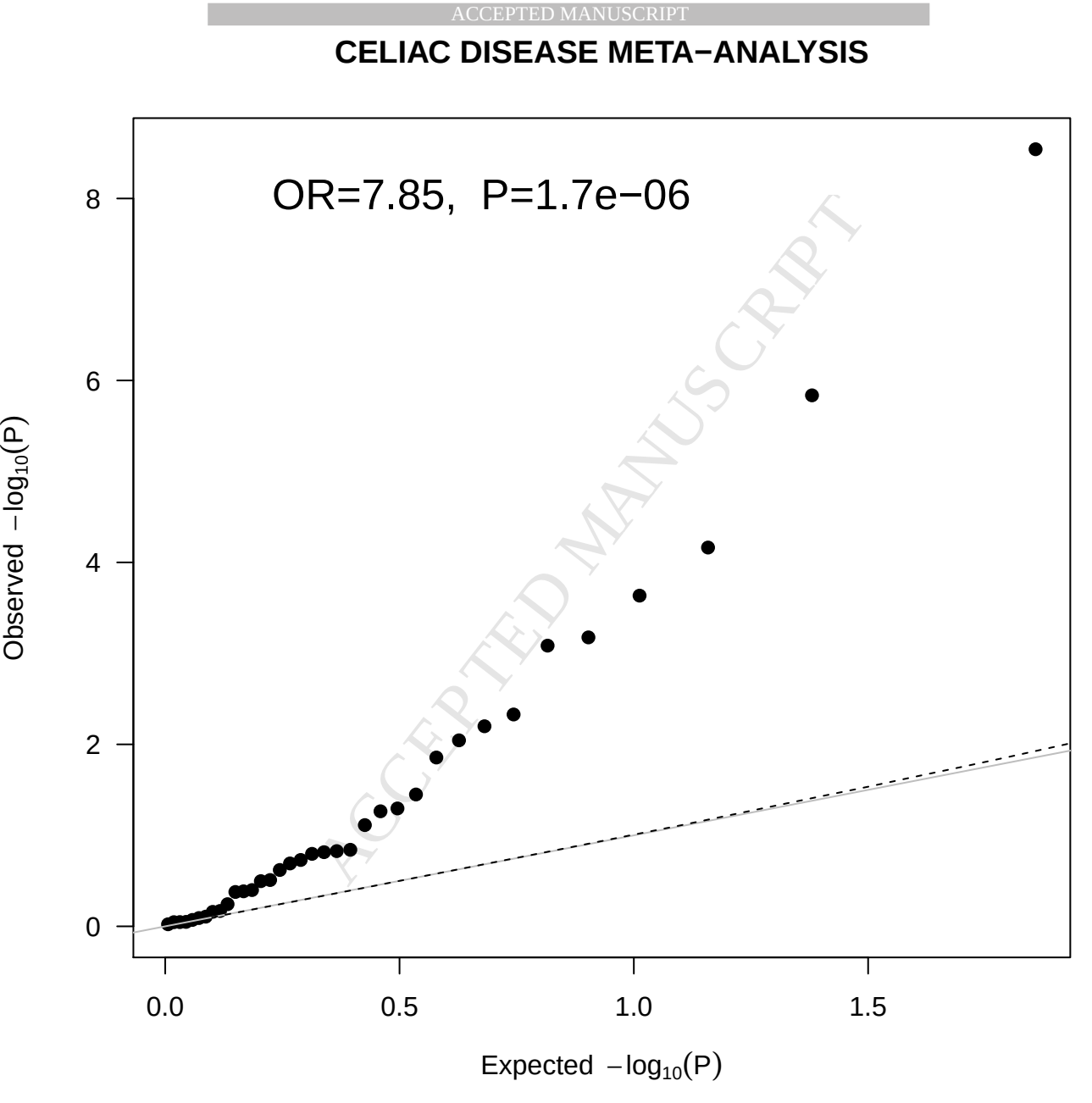

# PRIMARY BILIARY CIRROSIS META−ANALYSIS

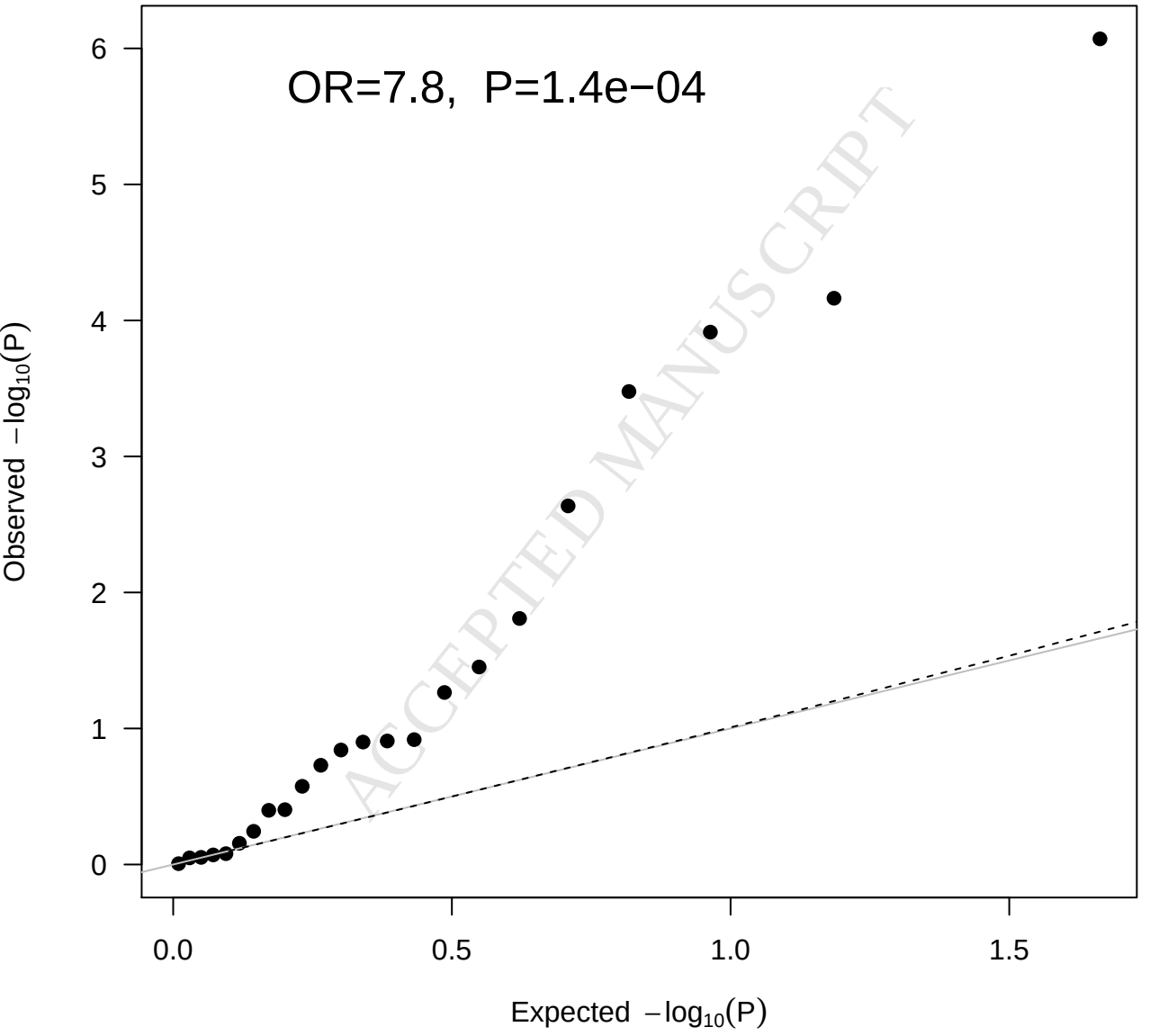

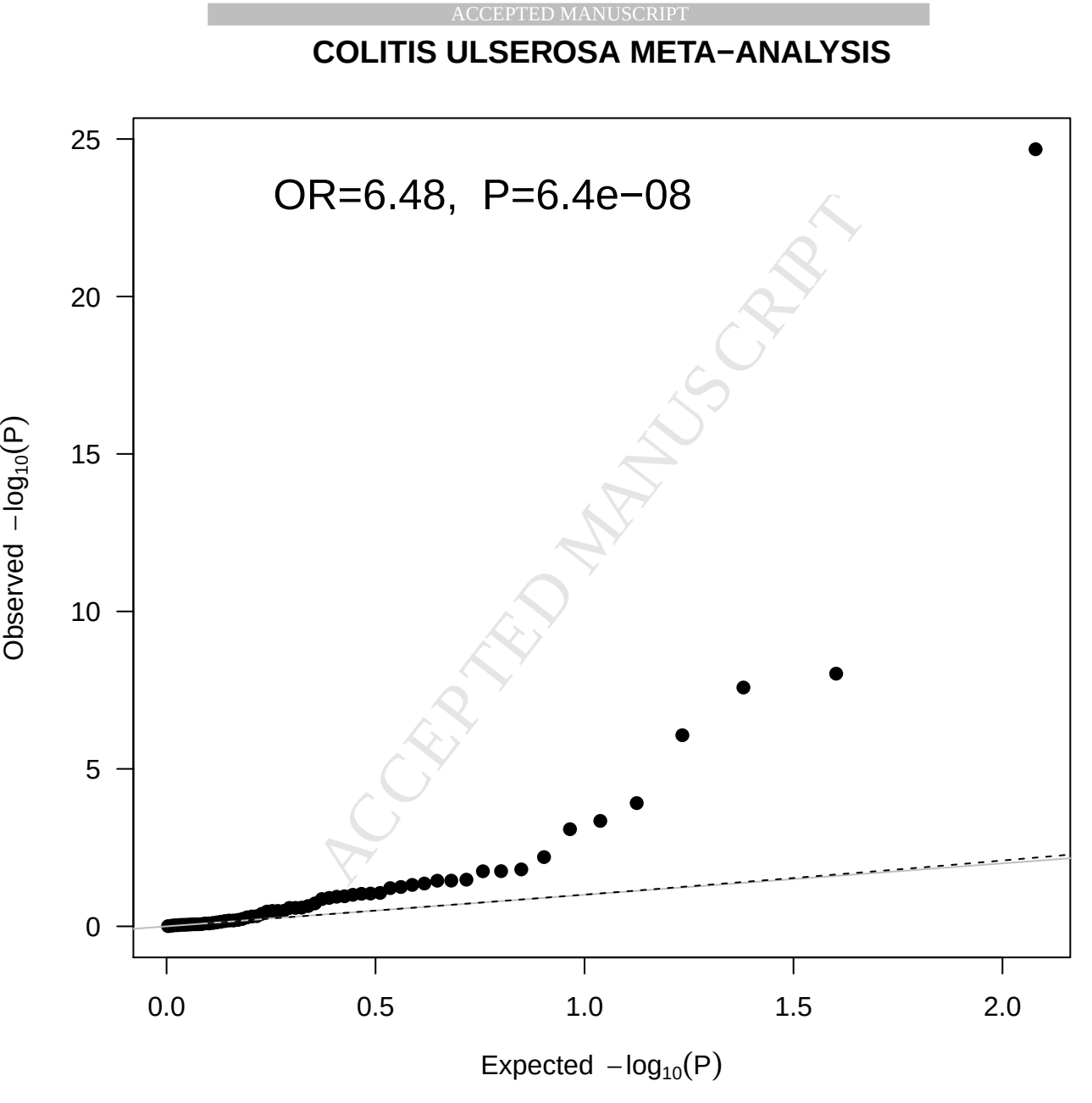

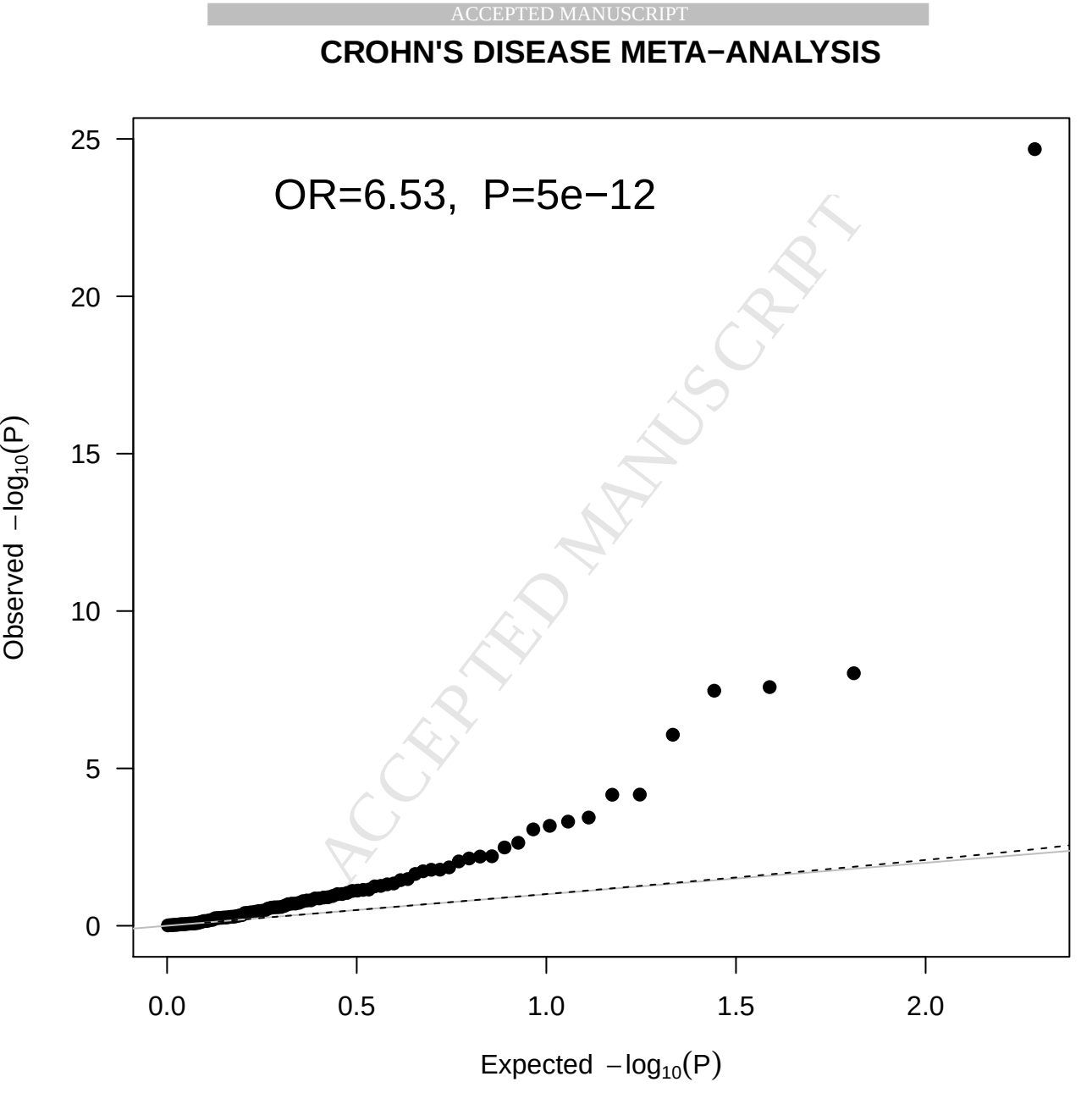

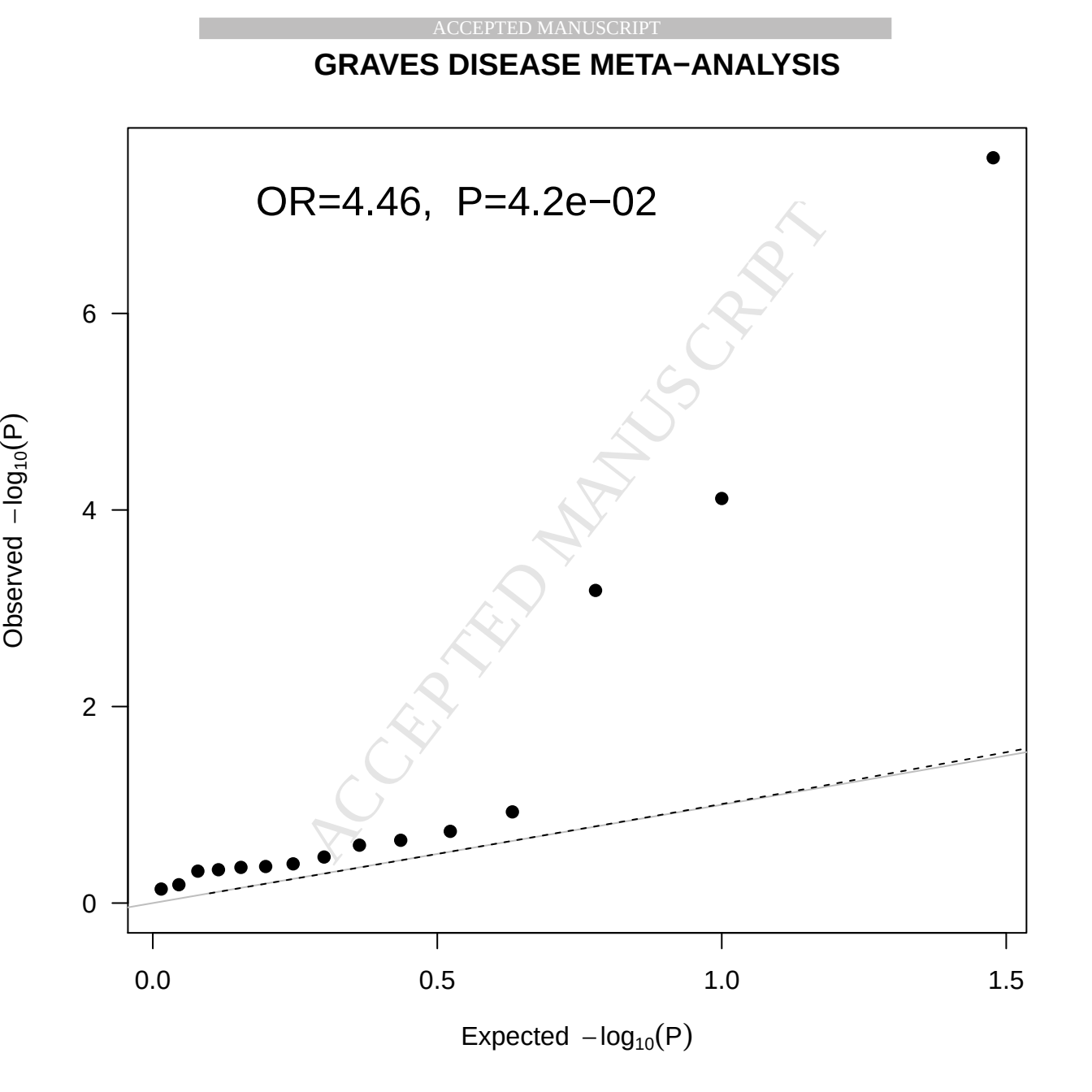

# INFLAMMATORY BOWEL DISEASE META−ANALYSIS

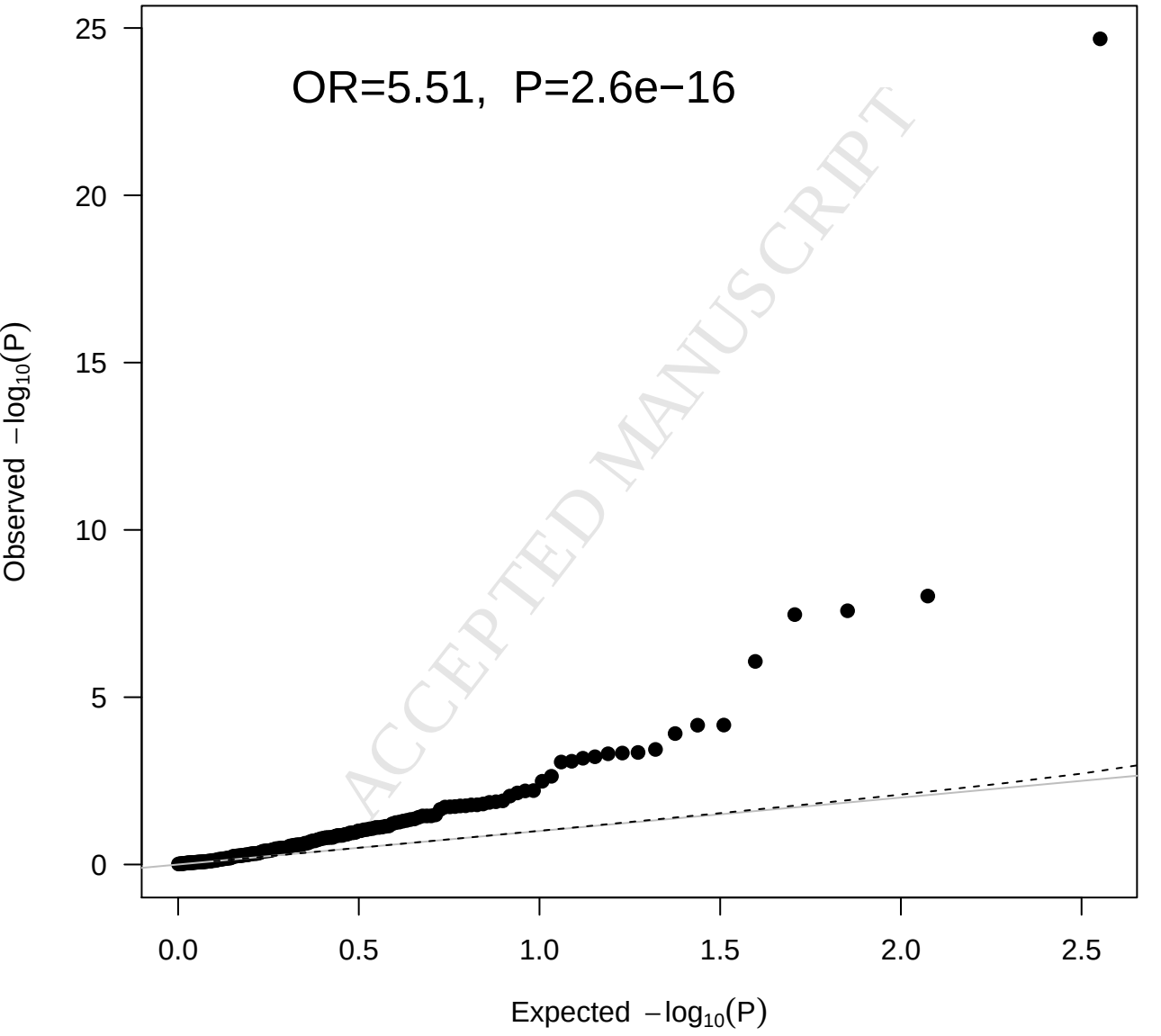

# SYSTEMIC LUPUS ERYTHEMATOSUS META−ANALYSIS

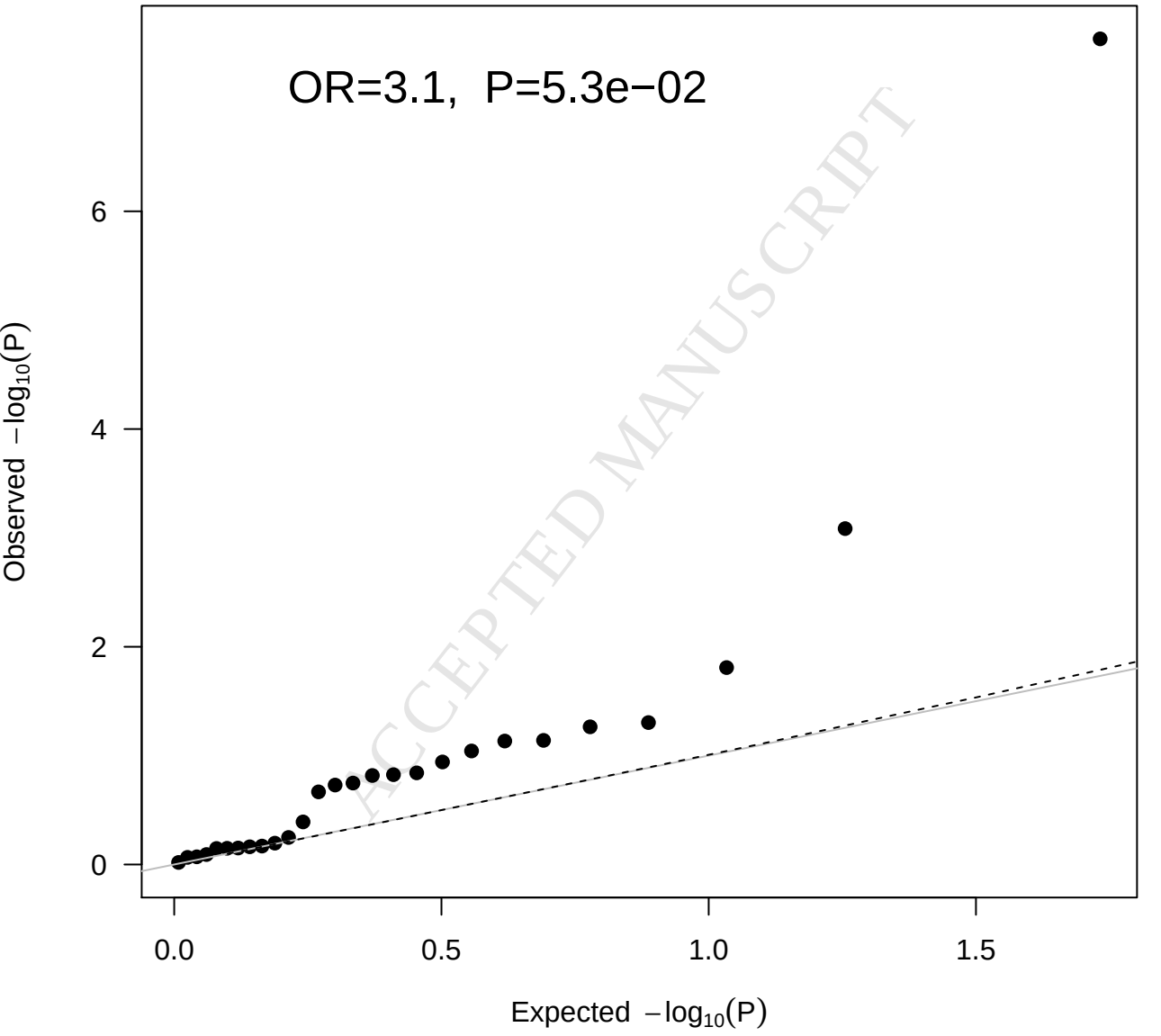

# MULTIPLE SCLEROSIS META−ANALYSIS

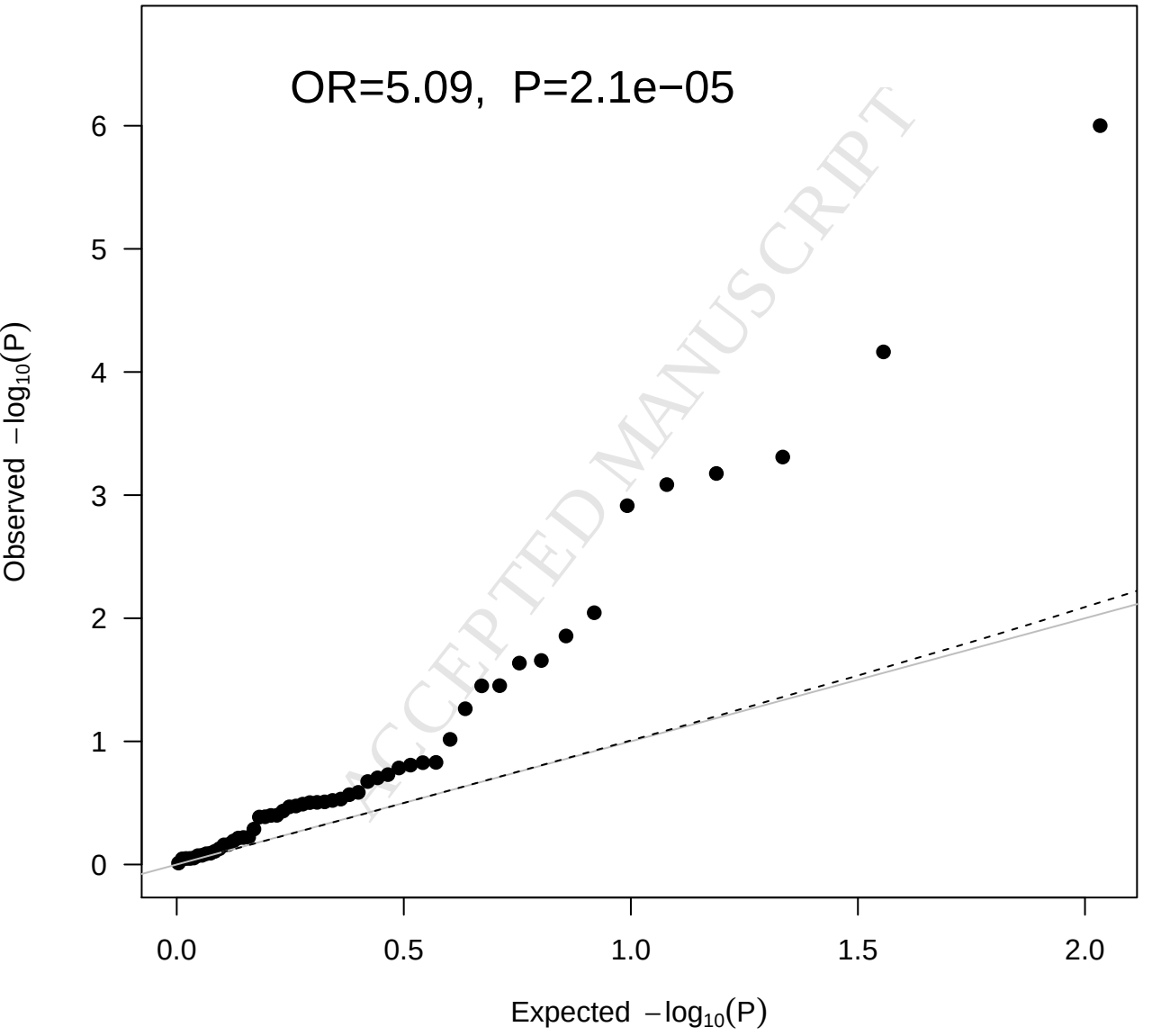

# TYPE 1 DIABETES META−ANALYSIS

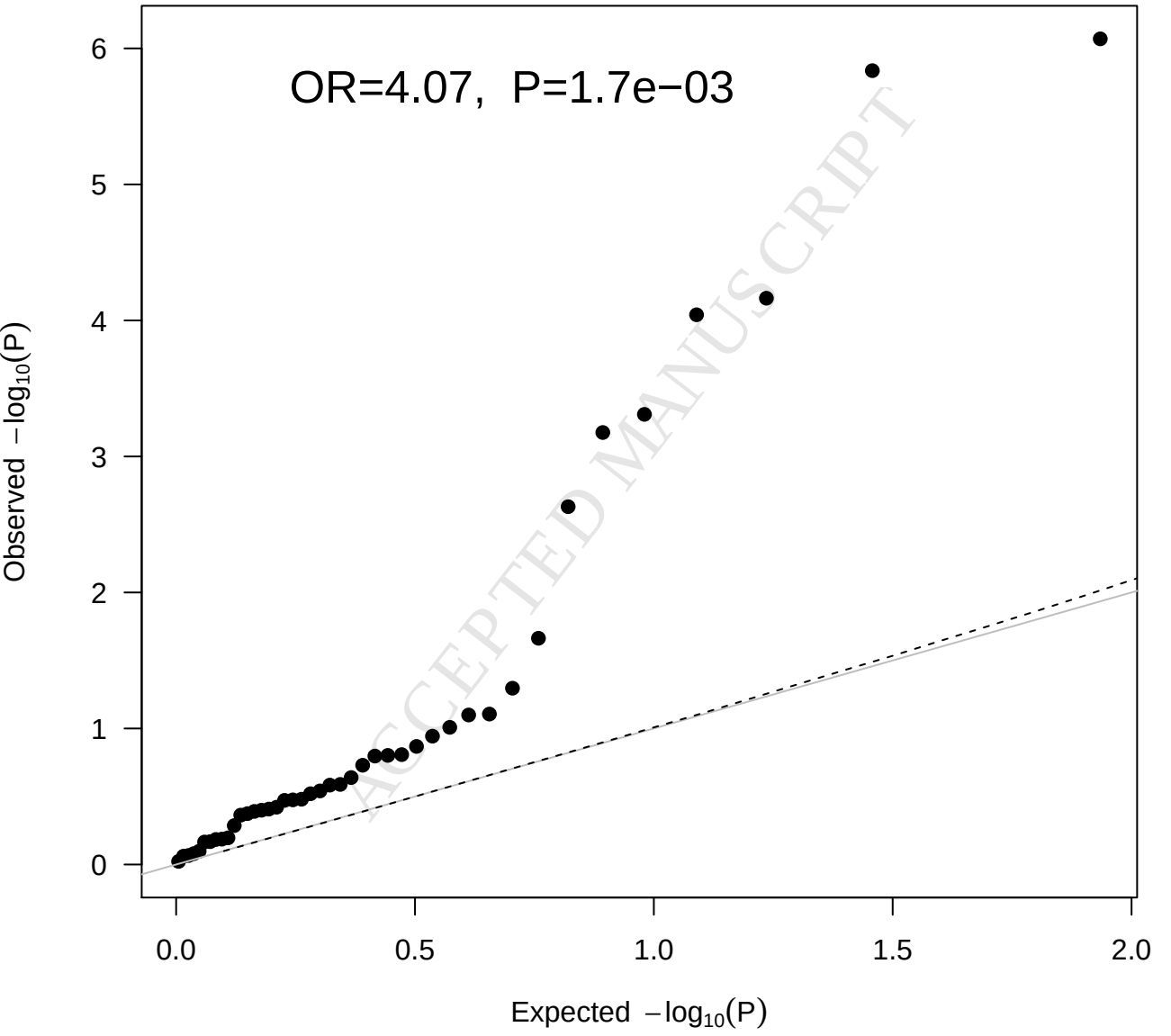

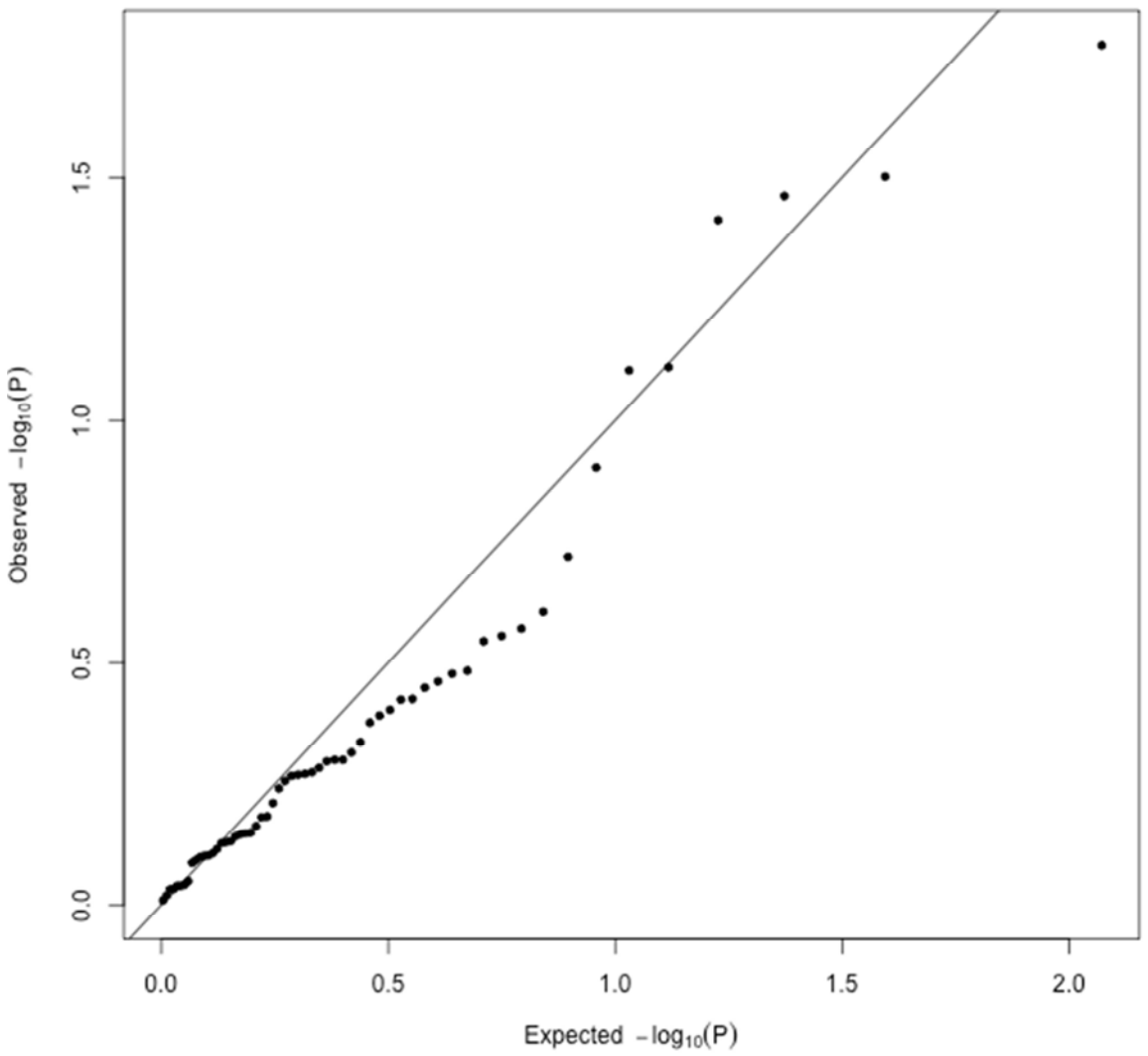

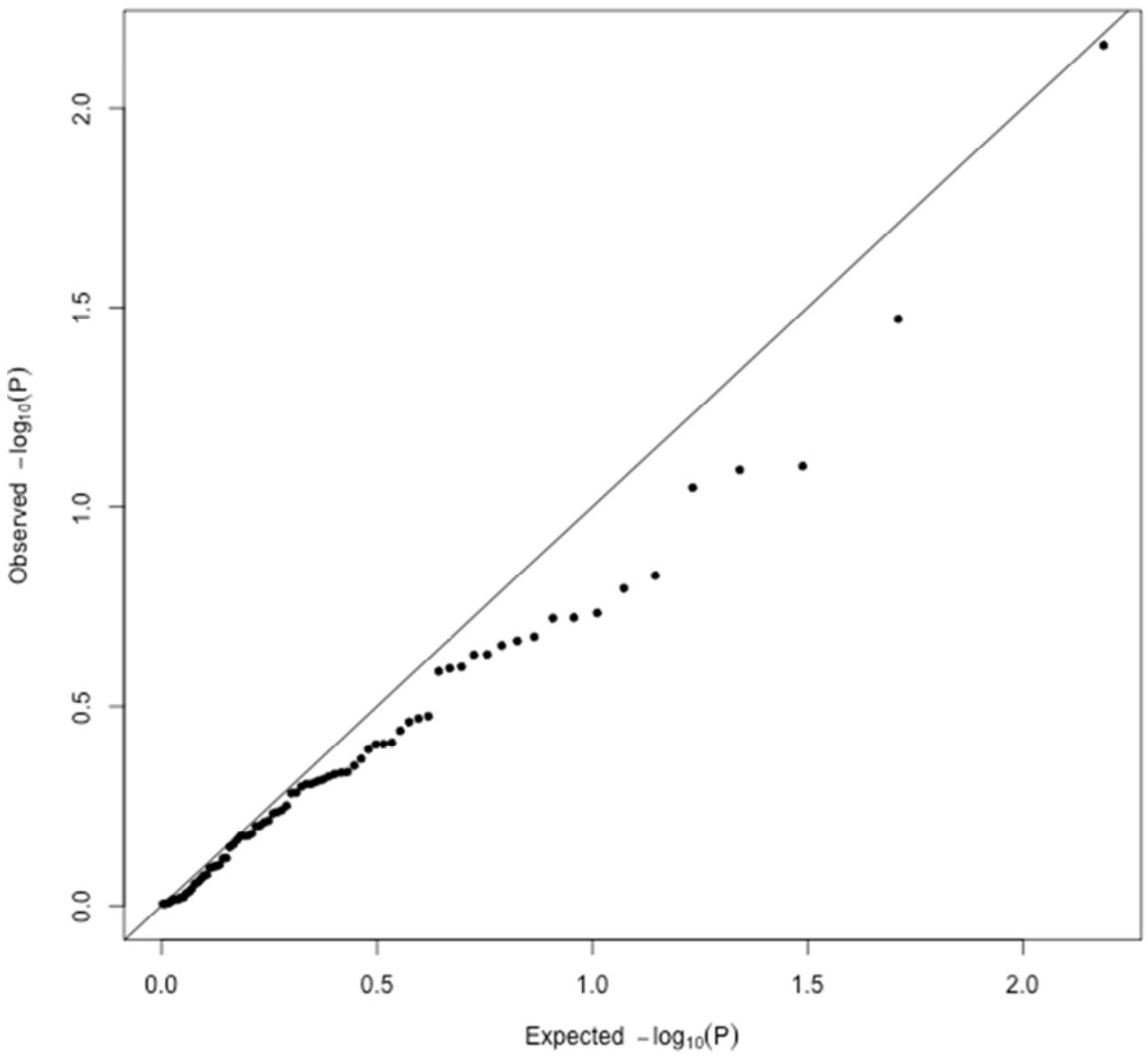

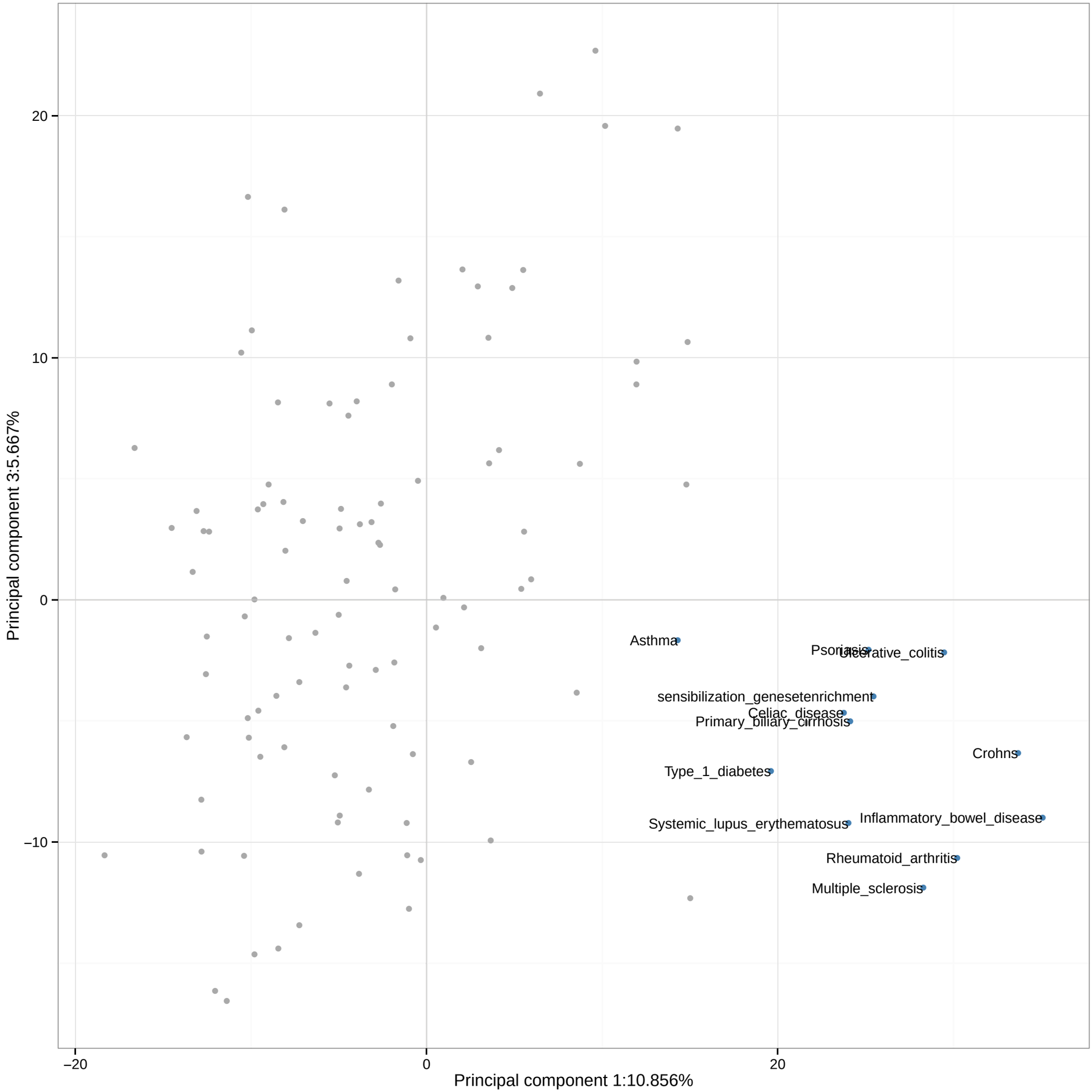
Asthma
Psoriasis
Ulcerative_colitis
sensibilization_genesetenrichment
Celiac_disease
Primary_biliary_cirrhosis
Crohns
Type_1_diabetes
Systemic_lupus_erythematosus
Inflammatory_bowel_disease
Rheumatoid_arthritis
Multiple_sclerosis
20
10
0
−10
−20
0
20
Principal component 3:5.667%
Principal component 1:10.856%

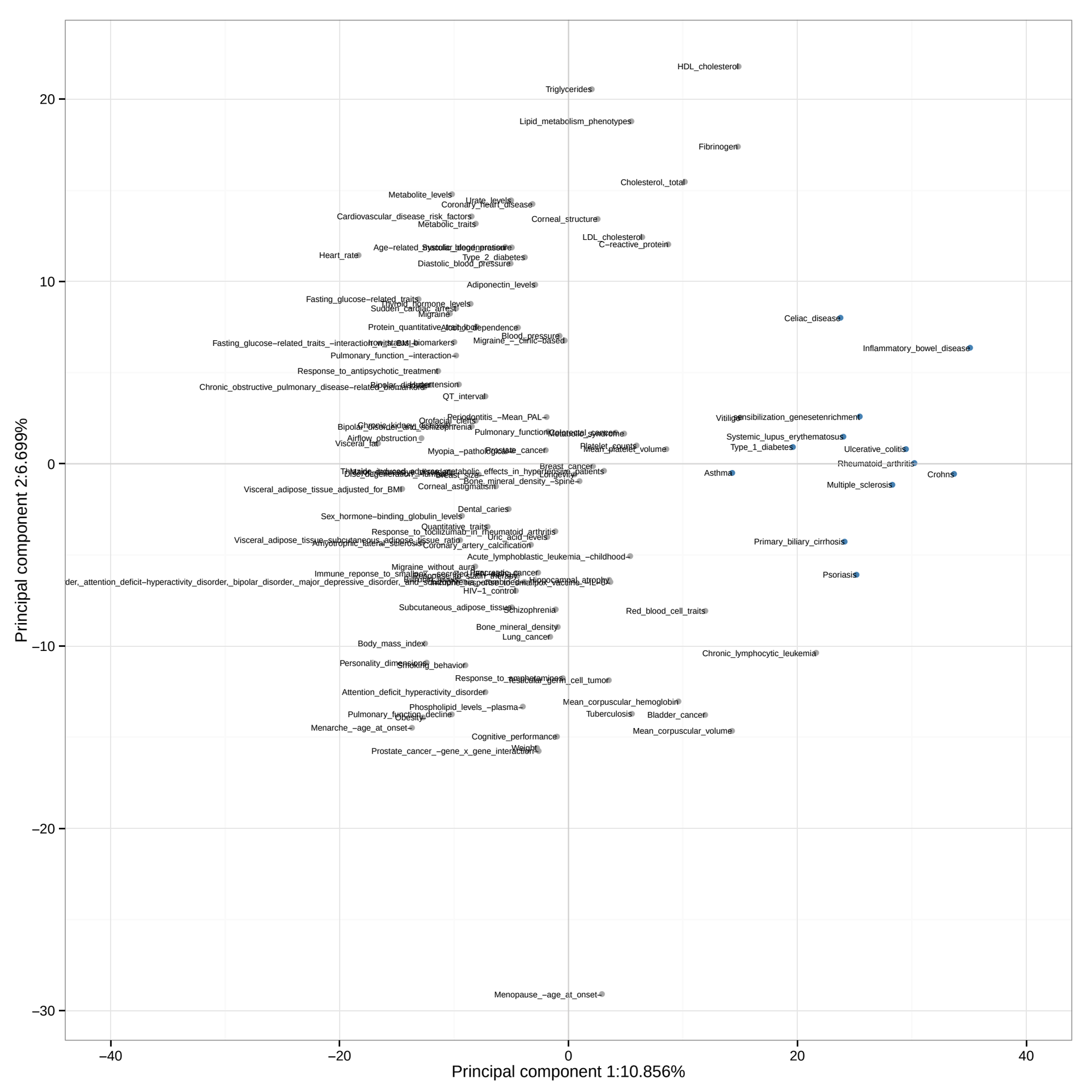
HDL_cholesterol
Triglycerides
Lipid_metabolism_phenotypes
Fibrinogen
Cholesterol,_total
Metabolite_levels
Urate_levels
Coronary_heart_disease
Cardiovascular_disease_risk_factors
Corneal_structure
Metabolic_traits
LDL_cholesterol
C−reactive_protein
Heart_rate
Type_2_diabetes
Diastolic_blood_pressure
Adiponectin_levels
Fasting_glucose−related_traits
Thyroid_hormone_levels
Sudden_cardiac_arrest
Migraine
Celiac_disease
Protein_quantitative_trait_loci
Alcohol_dependence
Blood_pressure
Migraine_−_clinic−based
Inflammatory_bowel_disease
Pulmonary_function_−interaction−
Response_to_antipsychotic_treatment
QT_interval
Periodontitis_−Mean_PAL−
Vitiligo
Sensibilization_genesetenrichment
Orofacial_clefts
Pulmonary_function
Metabolic_syndrome
Systemic_lupus_erythematosus
Airflow_obstruction
Visceral_fat
Platelet_counts
Mean_platelet_volume
Type_1_diabetes
Ulcerative_colitis
Myopia_−pathological−
Prostate_cancer
Rheumatoid_arthritis
Breast_cancer
Asthma
Crohns
Breast_size
Longevity
Bone_mineral_density_−spine−
Multiple_sclerosis
Corneal_astigmatism
Visceral_adipose_tissue_adjusted_for_BMI
Dental_caries
Sex_hormone−binding_globulin_levels
Quantitative_traits
Response_to_tocilizumab_in_rheumatoid_arthritis
Uric_acid_levels
Visceral_adipose_tissue_subcutaneous_adipose_tissue_ratio
Coronary_artery_calcification
Primary_biliary_cirrhosis
Acute_lymphoblastic_leukemia_−childhood−
Migraine_without_aura
Psoriasis
HIV−1_control
Subcutaneous_adipose_tissue
Schizophrenia
Red_blood_cell_traits
Bone_mineral_density
Lung_cancer
Body_mass_index
Chronic_lymphocytic_leukemia
Smoking_behavior
Response_to_amphetamines
Testicular_germ_cell_tumor
Attention_deficit_hyperactivity_disorder
Mean_corpuscular_hemoglobin
Phospholipid_levels_−plasma−
Pulmonary_function_decline
Tuberculosis
Bladder_cancer
Obesity
Menarche_−age_at_onset−
Mean_corpuscular_volume
Cognitive_performance
Weight
Prostate_cancer_−gene_x_gene_interaction−
Menopause_−age_at_onset−
20
10
0
−10
−20
−30
−40
−20
0
20
40
Principal component 2:6.699%
Principal component 1:10.856%

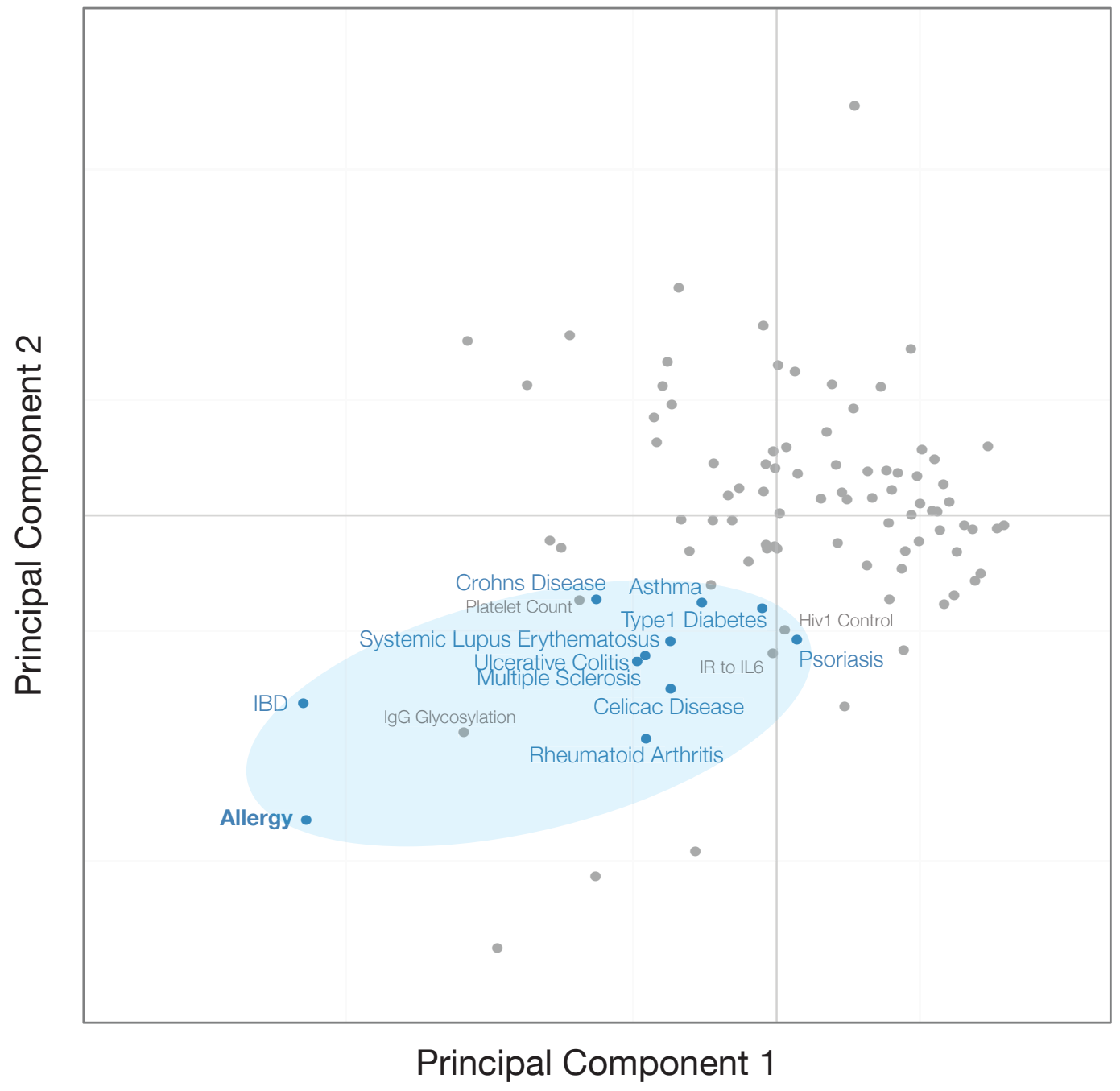
Principal Component 2
Principal Component 1
Crohns Disease
Platelet Count
Asthma
Type1 Diabetes
Hiv1 Control
Systemic Lupus Erythematosus
Ulcerative Colitis
IR to IL6
Psoriasis
Multiple Sclerosis
IBD
IgG Glycosylation
Celicac Disease
Rheumatoid Arthritis
Allergy

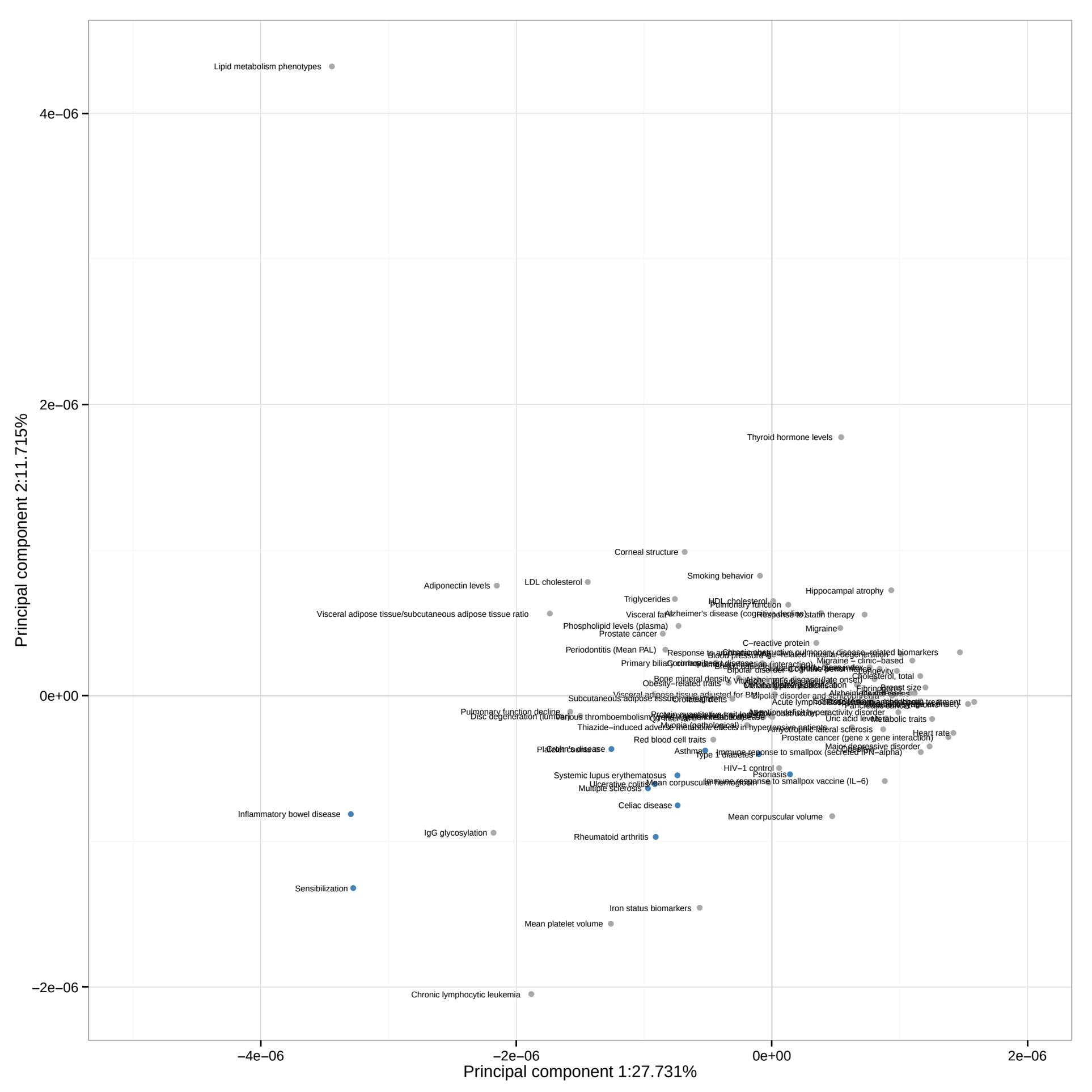
Lipid metabolism phenotypes
Thyroid hormone levels
Corneal structure
Smoking behavior
Adiponectin levels
LDL cholesterol
Hippocampal atrophy
Triglycerides
HDL cholesterol
Pulmonary function
Visceral adipose tissue/subcutaneous adipose tissue ratio
Alzheimer's disease (cognitive decline)
Response to statin therapy
Phospholipid levels (plasma)
Migraine
Prostate cancer
C−reactive protein
Periodontitis (Mean PAL)
Migraine − clinic−based
Cholesterol, total
Bone mineral density
Obesity−related traits
Breast size
Pulmonary function decline
Uric acid levels
Metabolic traits
Thiazide−induced adverse metabolic effects in hypertensive patients
Heart rate
Red blood cell traits
Prostate cancer (gene x gene interaction)
Asthma
Type 1 diabetes
Major depressive disorder
HIV−1 control
Systemic lupus erythematosus
Psoriasis
Ulcerative colitis
Multiple sclerosis
Immune response to smallpox vaccine (IL−6)
Celiac disease
Inflammatory bowel disease
Mean corpuscular volume
IgG glycosylation
Rheumatoid arthritis
Sensibilization
Iron status biomarkers
Mean platelet volume
Chronic lymphocytic leukemia
4e−06
2e−06
0e+00
−2e−06
−4e−06
−2e−06
0e+00
2e−06
Principal component 2:11.715%
Principal component 1:27.731%

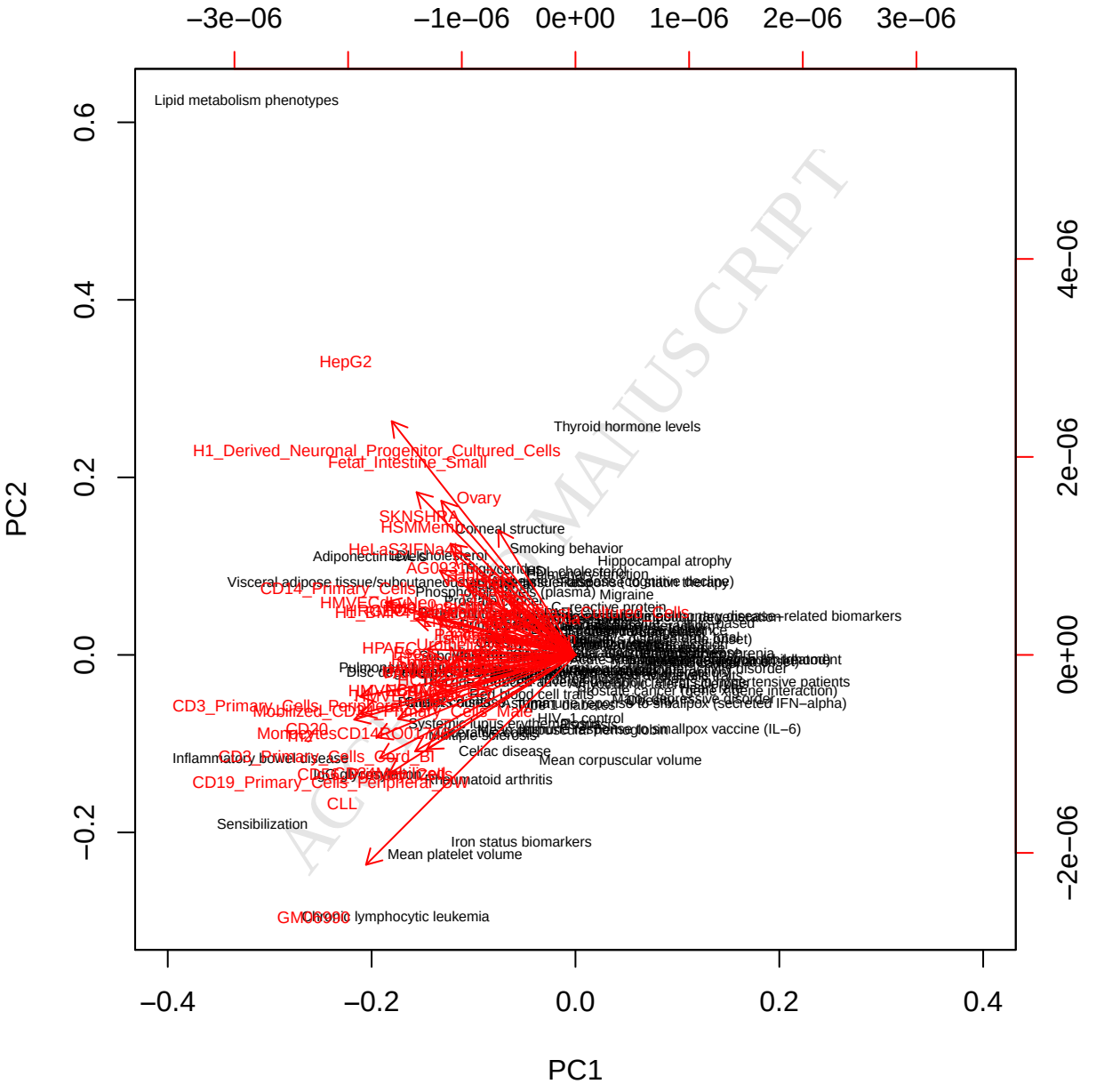

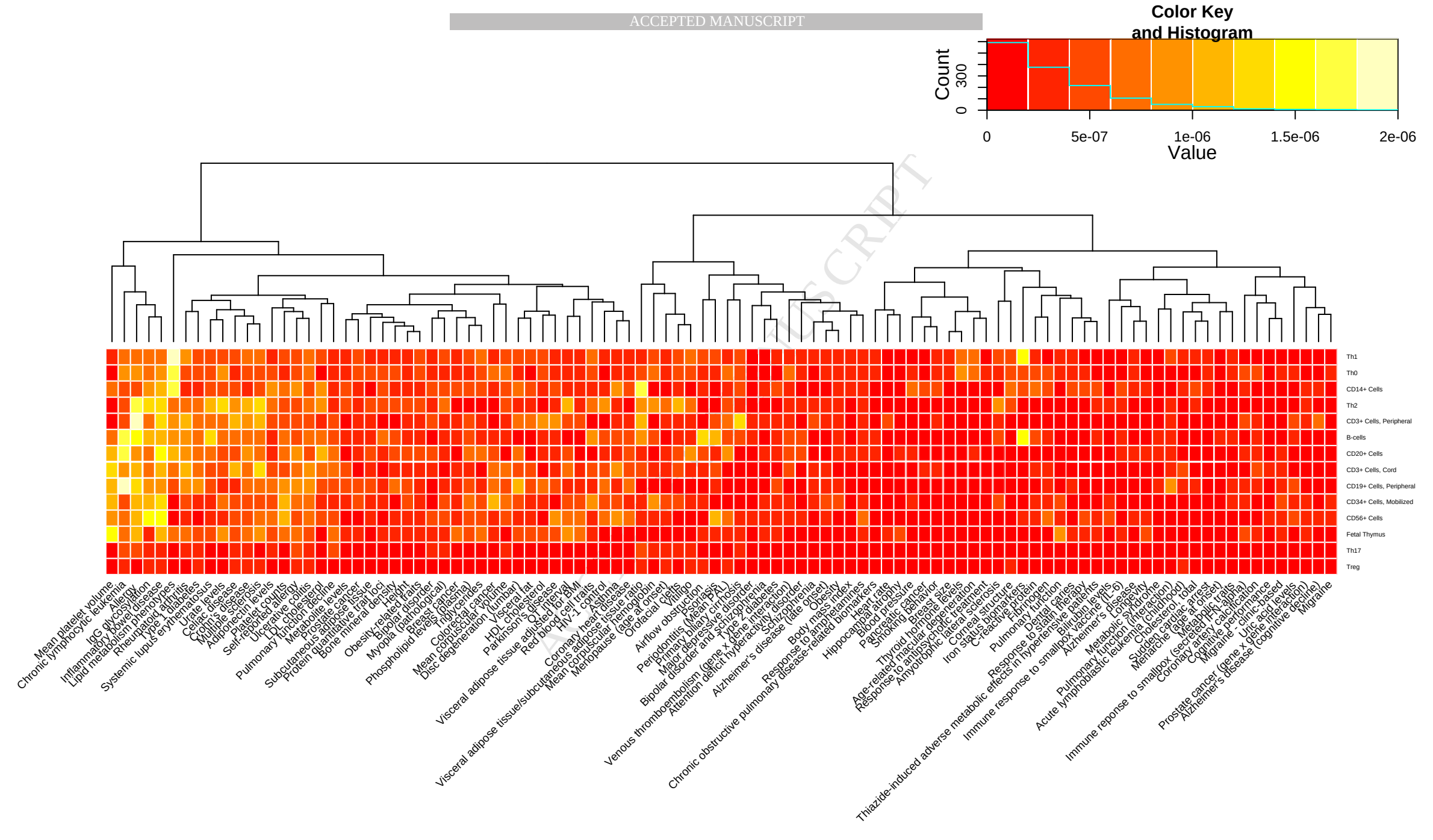

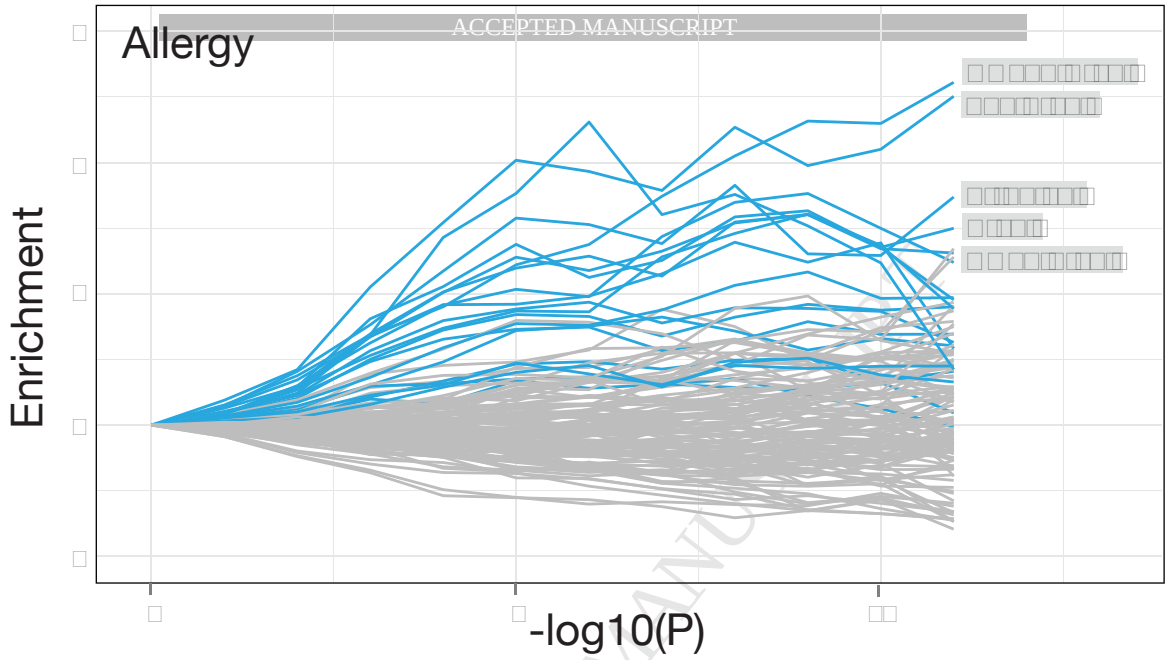


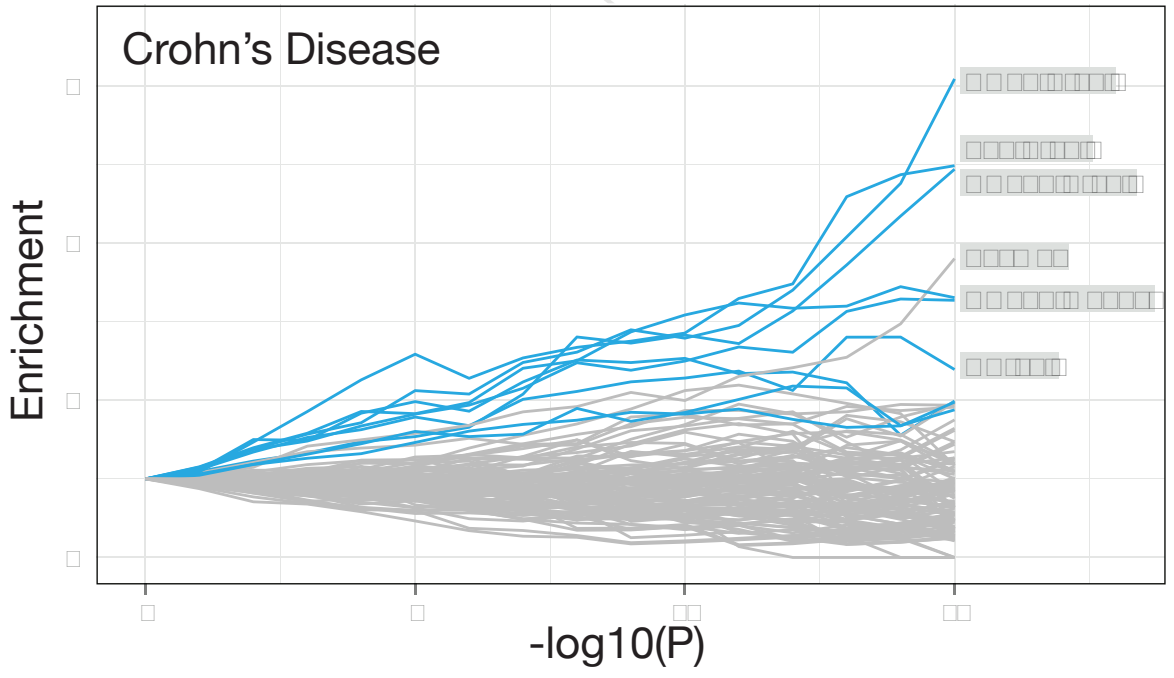

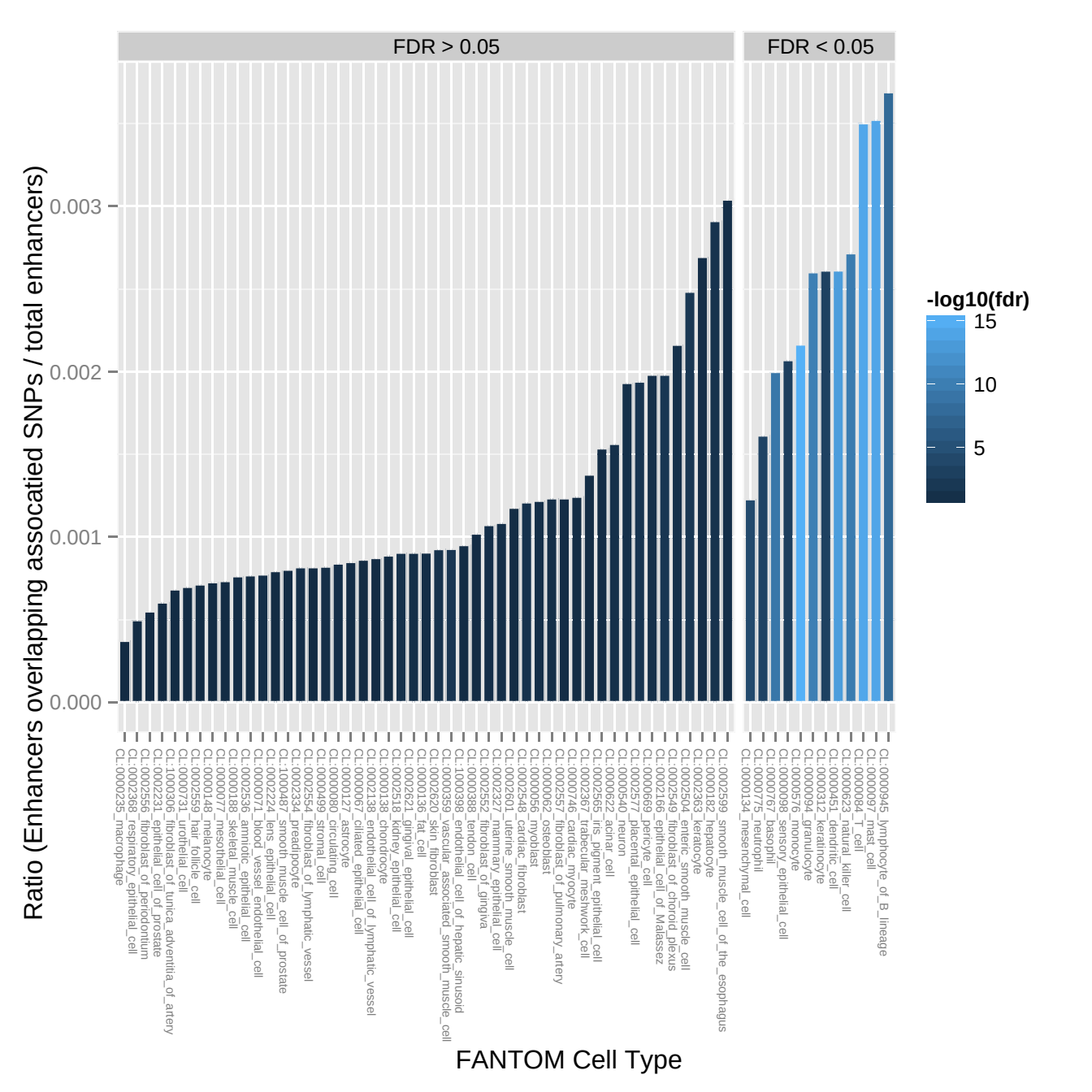
FDR > 0.05
FDR < 0.05
Ratio (Enhancers overlapping associatied SNPs / total enhancers)
0.000
0.001
0.002
0.003
-log10(fdr)
15
10
5
FANTOM Cell Type
CL:0000235_macrophage
CL:0002368_respiratory_epithelial_cell
CL:0002556_fibroblast_of_periodontium
CL:0002231_epithelial_cell_of_prostate
CL:1000306_fibroblast_of_tunica_adventitia_of_artery
CL:0000731_urothelial_cell
CL:0002559_hair_follicle_cell
CL:0000148_melanocyte
CL:0000077_mesothelial_cell
CL:0000188_skeletal_muscle_cell
CL:0002536_amniotic_epithelial_cell
CL:0000071_blood_vessel_endothelial_cell
CL:0002224_lens_epithelial_cell
CL:1000487_smooth_muscle_cell_of_prostate
CL:0002334_preadipocyte
CL:0002554_fibroblast_of_lymphatic_vessel
CL:0000499_stromal_cell
CL:0000080_circulating_cell
CL:0000127_astrocyte
CL:0002138_endothelial_cell_of_lymphatic_vessel
CL:0000067_ciliated_epithelial_cell
CL:0000138_chondrocyte
CL:0002518_kidney_epithelial_cell
CL:0002621_gingival_epithelial_cell
CL:0000136_fat_cell
CL:0002620_skin_fibroblast
CL:1000359_vascular_associated_smooth_muscle_cell
CL:1000398_endothelial_cell_of_hepatic_sinusoid
CL:0000388_tendon_cell
CL:0002552_fibroblast_of_gingiva
CL:0002327_mammary_epithelial_cell
CL:0002601_uterine_smooth_muscle_cell
CL:0002548_cardiac_fibroblast
CL:0000056_myoblast
CL:0000062_osteoblast
CL:0002557_fibroblast_of_pulmonary_artery
CL:0000746_cardiac_myocyte
CL:0002367_trabecular_meshwork_cell
CL:0002565_iris_pigment_epithelial_cell
CL:0000622_acinar_cell
CL:0000540_neuron
CL:0002577_placental_epithelial_cell
CL:0000669_pericyte_cell
CL:0002166_epithelial_cell_of_Malassez
CL:0002549_fibroblast_of_choroid_plexus
CL:0002504_enteric_smooth_muscle_cell
CL:0002363_keratinocyte
CL:0000182_hepatocyte
CL:0002599_smooth_muscle_cell_of_the_esophagus
CL:0000134_mesenchymal_cell
CL:0000775_neutrophil
CL:0000767_basophil
CL:0000098_sensory_epithelial_cell
CL:0000576_monocyte
CL:0000094_granulocyte
CL:0000312_keratinocyte
CL:0000623_natural_killer_cell
CL:0000451_dendritic_cell
CL:0000084_T_cell
CL:0000097_mast_cell
CL:0000945_lymphocyte_of_B_lineage

somatic recombination of immunoglobulin genes involved in immune response
somatic diversification of immunoglobulins involved in immune response
immunoglobulin production involved in immunoglobulin mediated immune response
isotype switching
positive regulation of T cell proliferation
B cell activation involved in immune response
somatic recombination of immunoglobulin gene segments
positive regulation of lymphocyte proliferation
regulation of immunoglobulin production
somatic diversification of immunoglobulins
positive regulation of mononuclear cell proliferation
regulation of lymphocyte mediated immunity
regulation of isotype switching
regulation of DNA recombination
positive regulation of leukocyte proliferation
immunoglobulin production
somatic diversification of immune receptors
regulation of mononuclear cell proliferation
regulation of interleukin−10 production
activated T cell proliferation
interleukin−10 production
increased susceptibility to autoimmune diabetes
regulation of leukocyte mediated immunity
regulation of immunoglobulin secretion
tumor necrosis factor receptor binding
regulation of leukocyte proliferation
positive regulation of B cell activation
regulation of lymphocyte activation
regulation of T cell activation
T cell proliferation
lymphocyte activation involved in immune response
positive regulation of lymphocyte activation
lymphocyte proliferation
regulation of interleukin−2 production
positive regulation of production of molecular mediator of immune response
abnormal CD4−positive T cell physiology
positive regulation of leukocyte activation
leukocyte proliferation
positive regulation of immune effector process
negative regulation of lymphocyte apoptotic process
regulation of leukocyte activation
tumor necrosis factor receptor superfamily binding
positive regulation of T cell activation
regulation of immune effector process
interleukin−4 production
negative regulation of alpha−beta T cell activation
decreased spleen germinal center number
alpha−beta T cell activation
abnormal cytotoxic T cell physiology
abnormal T−helper 1 cell differentiation
T cell activation involved in immune response
lymphocyte apoptotic process
T cell differentiation
decreased susceptibility to autoimmune diabetes
myeloid dendritic cell activation
T cell activation
decreased interleukin−4 secretion
increased activated T cell number
alpha−beta T cell differentiation
tolerance induction
immune effector process
membrane protein ectodomain proteolysis
CD4−positive, alpha−beta T cell differentiation
decreased interferon−gamma secretion
abnormal CD4−positive T cell morphology
decreased IgG level
increased T cell apoptosis
lymphocyte differentiation
lymphocyte homeostasis
regulation of cytokine production
decreased regulatory T cell number
leukocyte homeostasis
intestinal ulcer
lymphocyte activation
decreased immunoglobulin level
cytokine production
abnormal T−helper 2 physiology
leukocyte activation
T cell differentiation in thymus
membrane protein proteolysis
abnormal immunoglobulin level
increased IgG1 level
positive regulation of immune system process
positive regulation of immune response
abnormal lymphocyte cell number
abnormal interleukin level
stomach inflammation
heart inflammation
regulation of protein transport
abnormal lymphocyte physiology
abnormal lymphocyte morphology
regulation of establishment of protein localization
decreased T cell proliferation
decreased IgM level
increased T cell number
abnormal spleen red pulp morphology
hemopoiesis
homeostasis of number of cells
negative regulation of protein phosphorylation
REACTOME_INTERLEUKIN.2_SIGNALING
abnormal immune system physiology
increased IgA level
hemopoietic or lymphoid organ development
increased single−positive T cell number
induction of apoptosis by extracellular signals
abnormal cytokine secretion
decreased NK T cell number
decreased double−positive T cell number
lymph node hyperplasia
intestinal inflammation
induction of programmed cell death
abnormal cochlear inner hair cell morphology
absent spleen germinal center
mixed cellular infiltration to dermis
induction of apoptosis
abnormal spleen morphology
increased eosinophil cell number
increased follicular B cell number
thymus cortex hypoplasia
decreased megakaryocyte cell number
increased double−positive T cell number
abnormal lymphopoiesis
increased spleen red pulp amount
spleen atrophy
abnormal Peyer's patch germinal center morphology
abnormal Peyer's patch follicle morphology
myeloid cell differentiation
NF−kappaB binding
abnormal spleen B cell follicle morphology
decreased thymocyte number
abnormal lymph node B cell domain morphology
abnormal mesenteric lymph node morphology
decreased leukocyte cell number
retinoic acid receptor binding
abnormal mammary gland development
dermatitis
abnormal Peyer's patch morphology
abnormal T cell number
REACTOME_BMAL1CLOCKNPAS2_ACTIVATES_GENE_EXPRESSION
increased granulocyte number
increased leukocyte cell number
REACTOME_TRAF6_MEDIATED_NF.KB_ACTIVATION
nuclear hormone receptor binding
hormone receptor binding
REACTOME_MYD88_CASCADE_INITIATED_ON_PLASMA_MEMBRANE
protein kinase binding
kinase binding
REACTOME_TOLL_LIKE_RECEPTOR_5_TLR5_CASCADE
REACTOME_TOLL_LIKE_RECEPTOR_10_TLR10_CASCADE
50
0
−50
−100
−100
−50
0
50
100
Principal component 1:11.74%
Principal component 1:87.66%

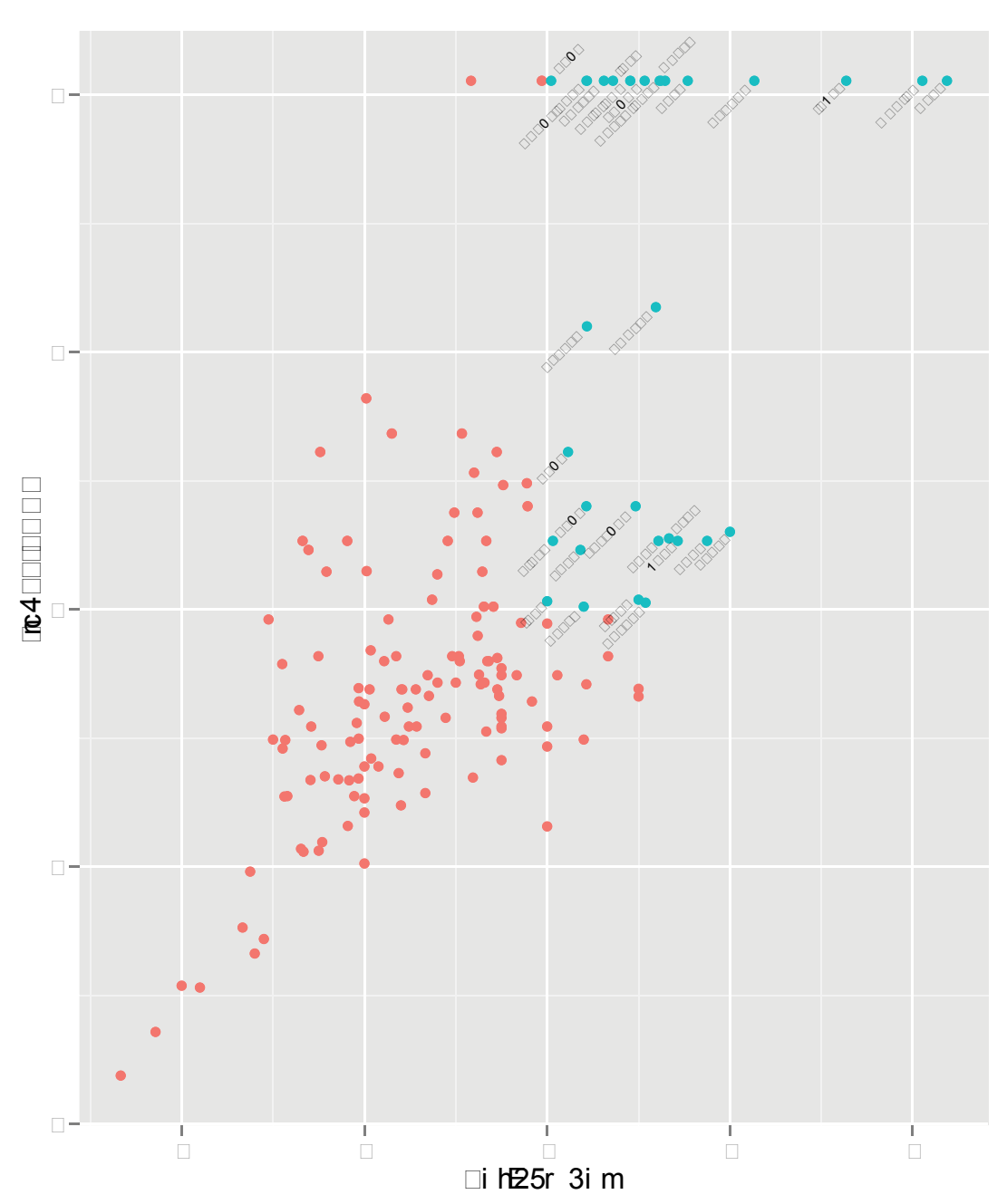

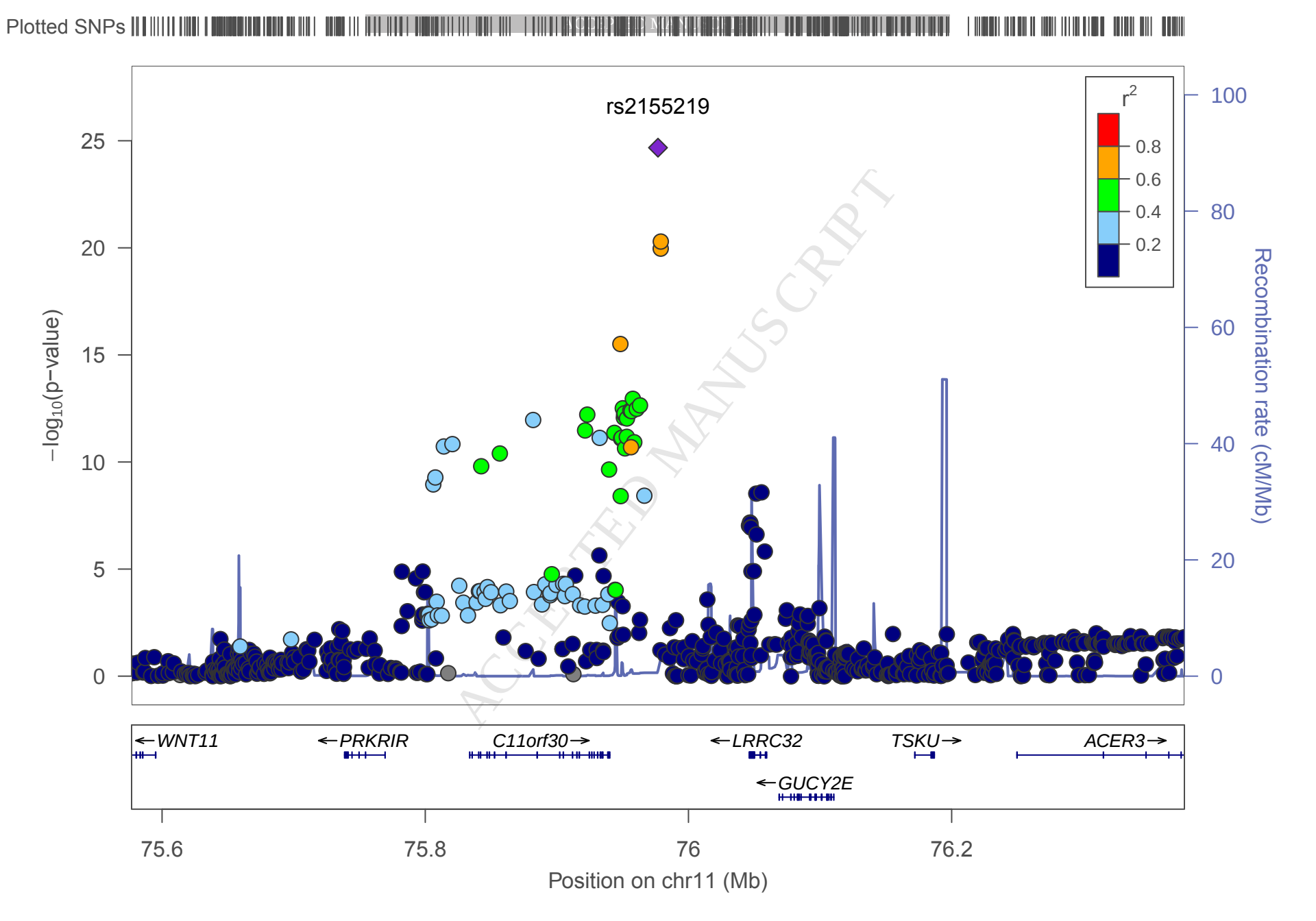

| | |
|---|---|
| date: | Tue Jun 24 05:24:41 2014 |
| build: | hg18 |
| display range: | chr11:75576842−76376842 [75576842−76376842] |
| hilite range: | 0 − 0 [ 0 − 0 ] |
| reference SNP: | chr11:75976842 |
| number of SNPs plotted: | 664 |
| max P.value: | 2.11E−25 [chr11:75976842] |
| min P.value: | 10E−1 [chr11:76077902] |

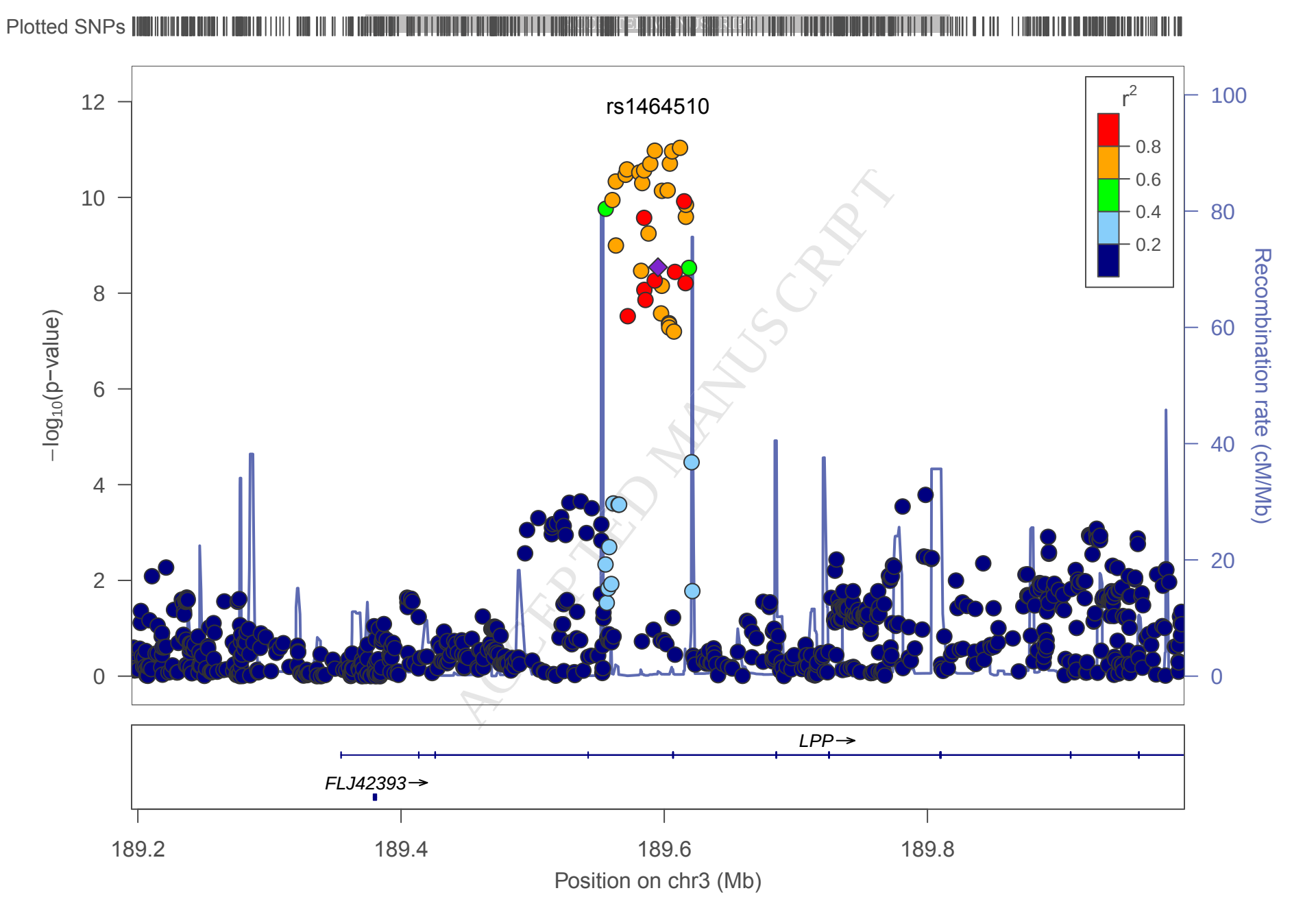

| | |
|---|---|
| date: | Tue Jun 24 05:29:23 2014 |
| build: | hg18 |
| display range: | chr3:189195248−189995248 [189195248−189995248] |
| hilite range: | 0 − 0 [ 0 − 0 ] |
| reference SNP: | chr3:189595248 |
| number of SNPs plotted: | 782 |
| max P.value: | 9.15E−12 [chr3:189611673] |
| min P.value: | 9.98E−1 [chr3:189370256] |

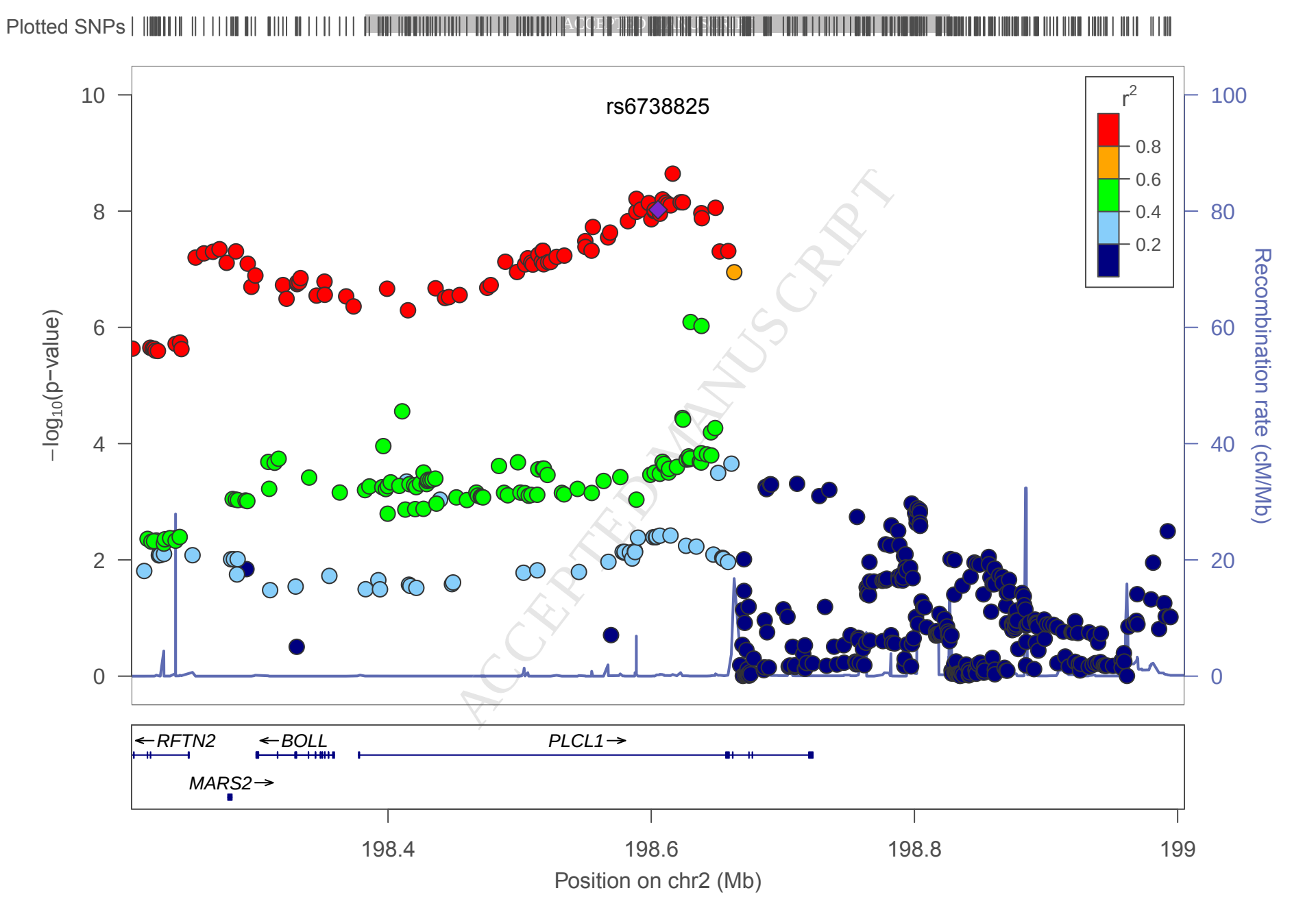

| | |
|---|---|
| date: | Tue Jun 24 05:33:00 2014 |
| build: | hg18 |
| display range: | chr2:198205140−199005140 [198205140−199005140] |
| hilite range: | 0 − 0 [ 0 − 0 ] |
| reference SNP: | chr2:198605140 |
| number of SNPs plotted: | 506 |
| max P.value: | 2.25E−9 [chr2:198616285] |
| min P.value: | 9.82E−1 [chr2:198669634] |

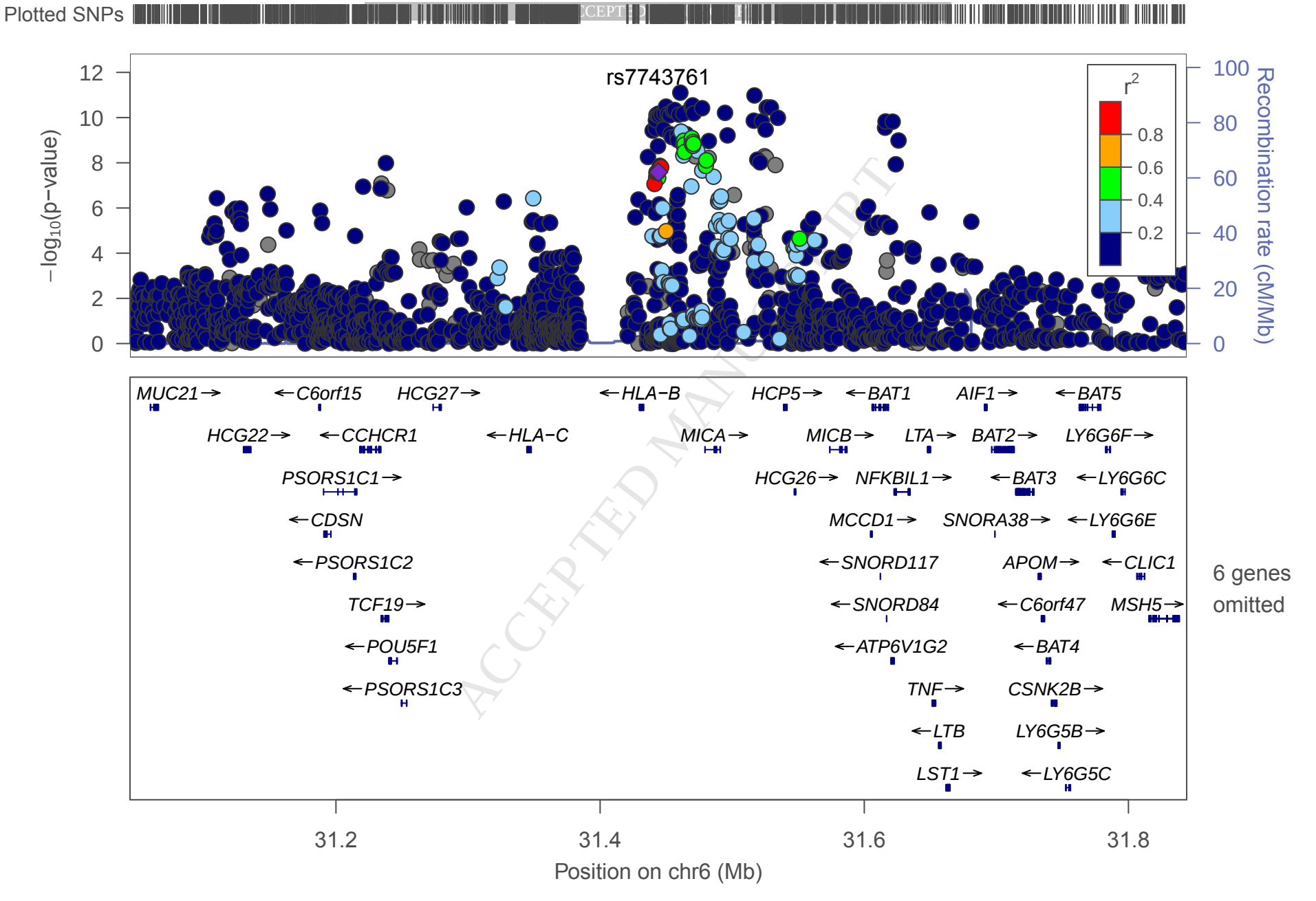

| | |
|---|---|
| date: | Tue Jun 24 05:36:47 2014 |
| build: | hg18 |
| display range: | chr6:31044079−31844079 [31044079−31844079] |
| hilite range: | 0 − 0 [ 0 − 0 ] |
| reference SNP: | chr6:31444079 |
| number of SNPs plotted: | 2001 |
| max P.value: | 7.8E−12 [chr6:31460092] |
| min P.value: | 9.99E−1 [chr6:31240064] |
| omitted Genes: | NCR3, LY6G6D, C6orf25 |
| omitted Genes: | DDAH2, C6orf26, C6orf27 |

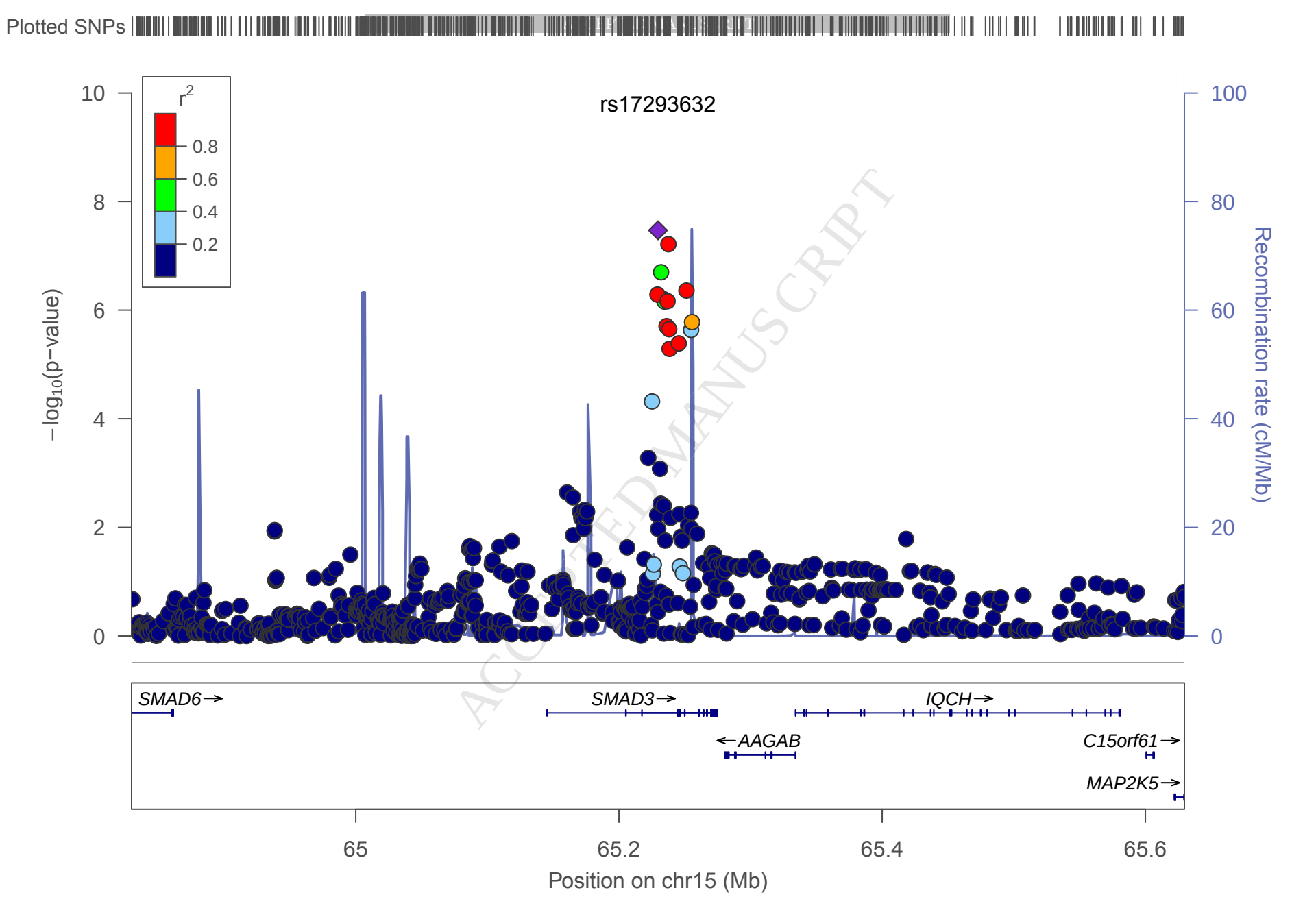

| | |
|---|---|
| date: | Tue Jun 24 05:39:41 2014 |
| build: | hg18 |
| display range: | chr15:64829650−65629650 [64829650−65629650] |
| hilite range: | 0 − 0 [ 0 − 0 ] |
| reference SNP: | chr15:65229650 |
| number of SNPs plotted: | 737 |
| max P.value: | 3.39E−8 [chr15:65229650] |
| min P.value: | 9.98E−1 [chr15:64917040] |

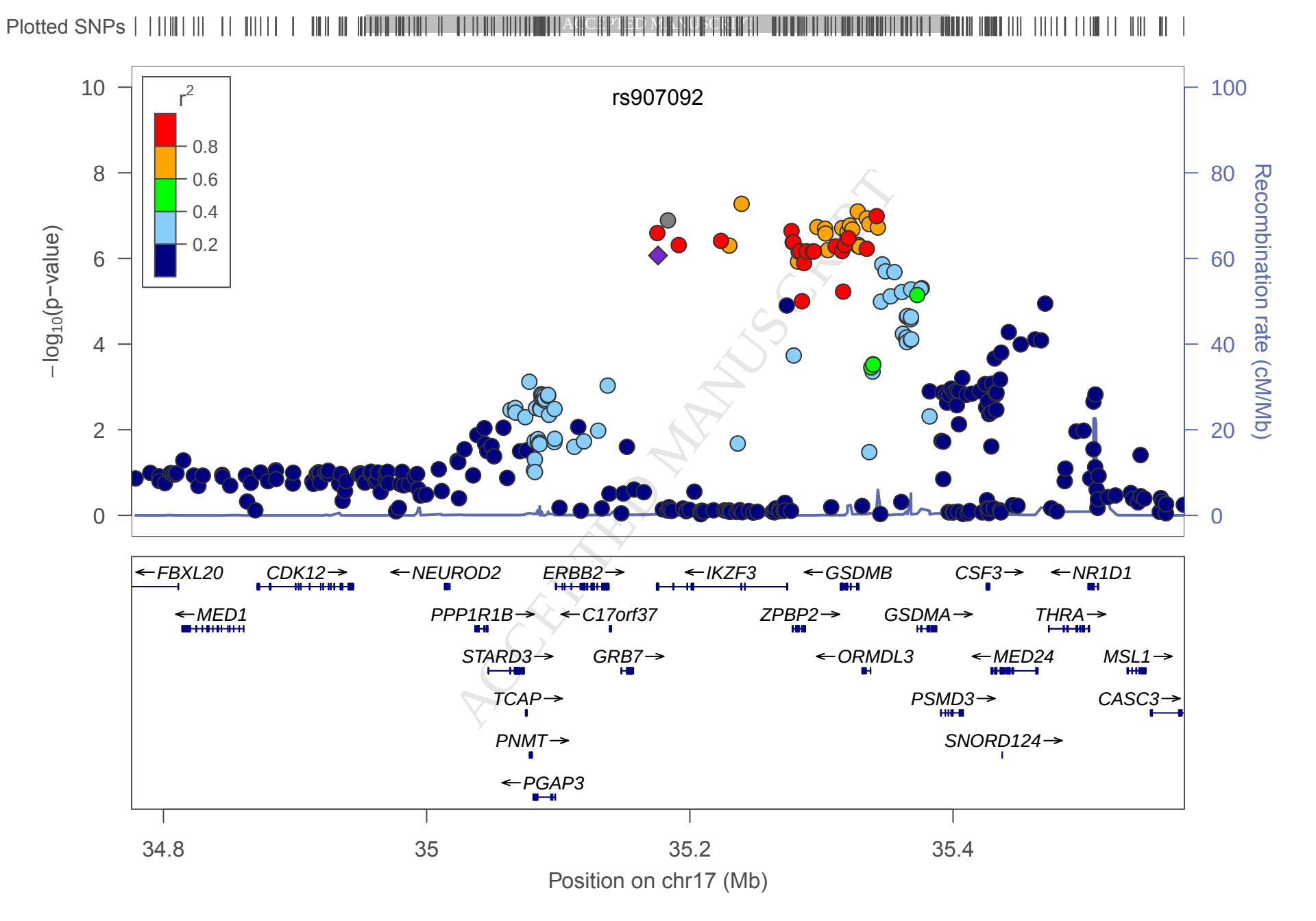

| | |
|---|---|
| date: | Tue Jun 24 05:42:52 2014 |
| build: | hg18 |
| display range: | chr17:34775785−35575785 [34775785−35575785] |
| hilite range: | 0 − 0 [ 0 − 0 ] |
| reference SNP: | chr17:35175785 |
| number of SNPs plotted: | 326 |
| max P.value: | 5.3E−8 [chr17:35239327] |
| min P.value: | 9.32E−1 [chr17:35208284] |

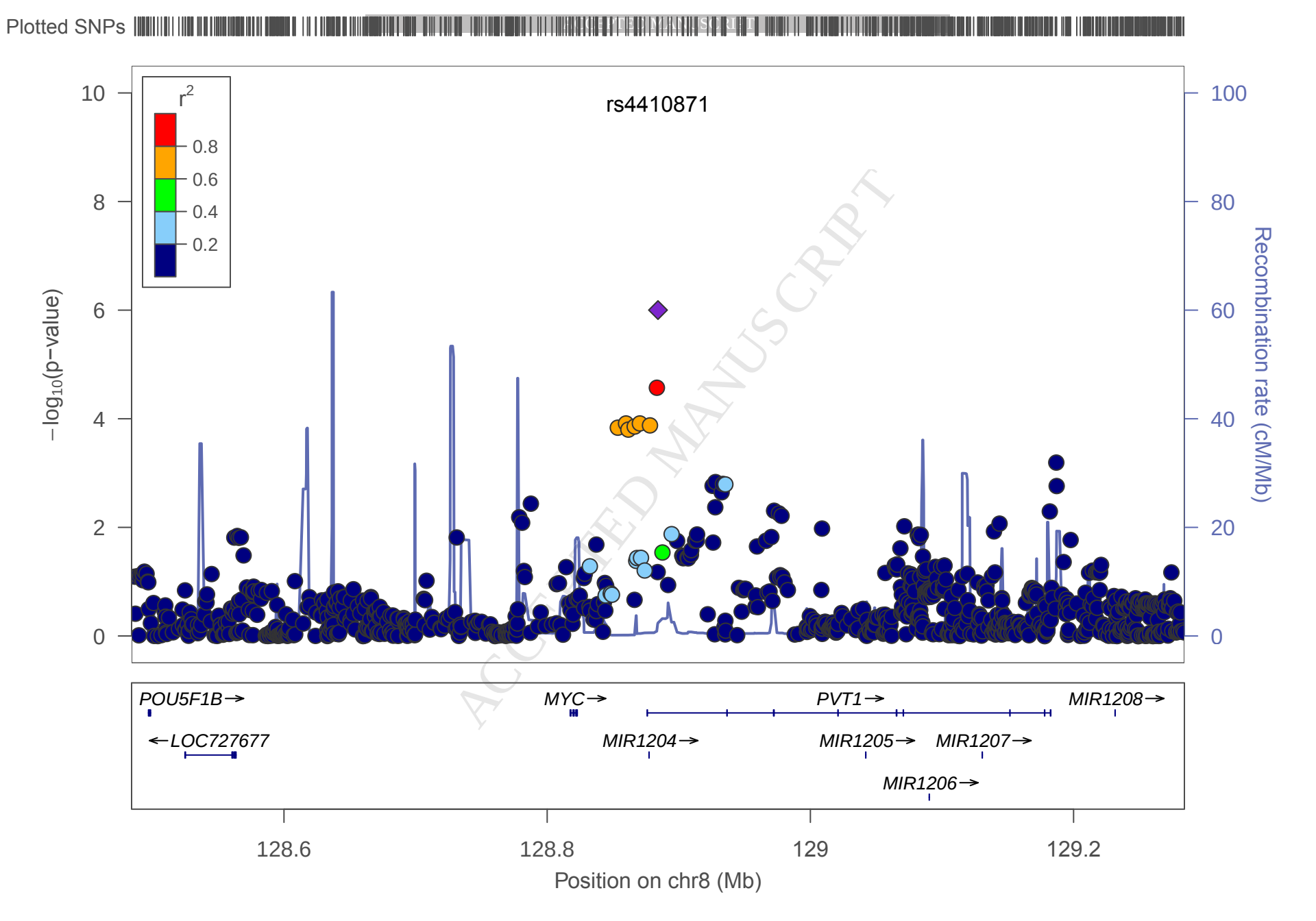

| | |
|---|---|
| date: | Tue Jun 24 06:24:05 2014 |
| build: | hg18 |
| display range: | chr8:128484211−129284211 [128484211−129284211] |
| hilite range: | 0 − 0 [ 0 − 0 ] |
| reference SNP: | chr8:128884211 |
| number of SNPs plotted: | 922 |
| max P.value: | 9.97E−7 [chr8:128884211] |
| min P.value: | 10E−1 [chr8:128660128] |

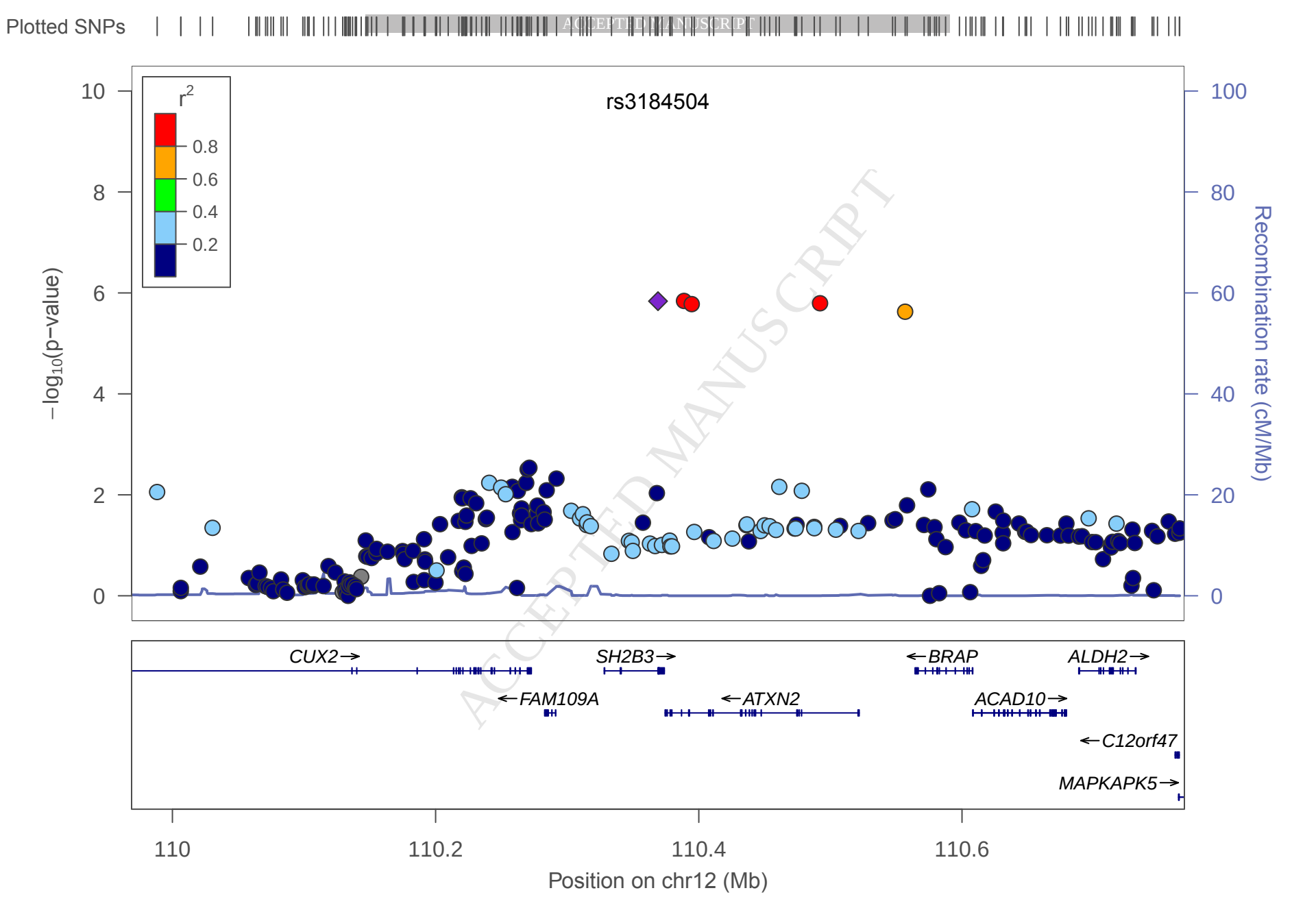
Plotted SNPs
ACCEPTED MANUSCRIPT
rs3184504
r2
0.8
0.6
0.4
0.2
−log10(p−value)
Recombination rate (cM/Mb)
CUX2
SH2B3
BRAP
ALDH2
FAM109A
ATXN2
ACAD10
C12orf47
MAPKAPK5
Position on chr12 (Mb)

| | |
|---|---|
| date: | Tue Jun 24 06:25:11 2014 |
| build: | hg18 |
| display range: | chr12:109968991−110768991 [109968991−110768991] |
| hilite range: | 0 − 0 [ 0 − 0 ] |
| reference SNP: | chr12:110368991 |
| number of SNPs plotted: | 194 |
| max P.value: | 1.44E−6 [chr12:110388754] |
| min P.value: | 9.97E−1 [chr12:110575739] |

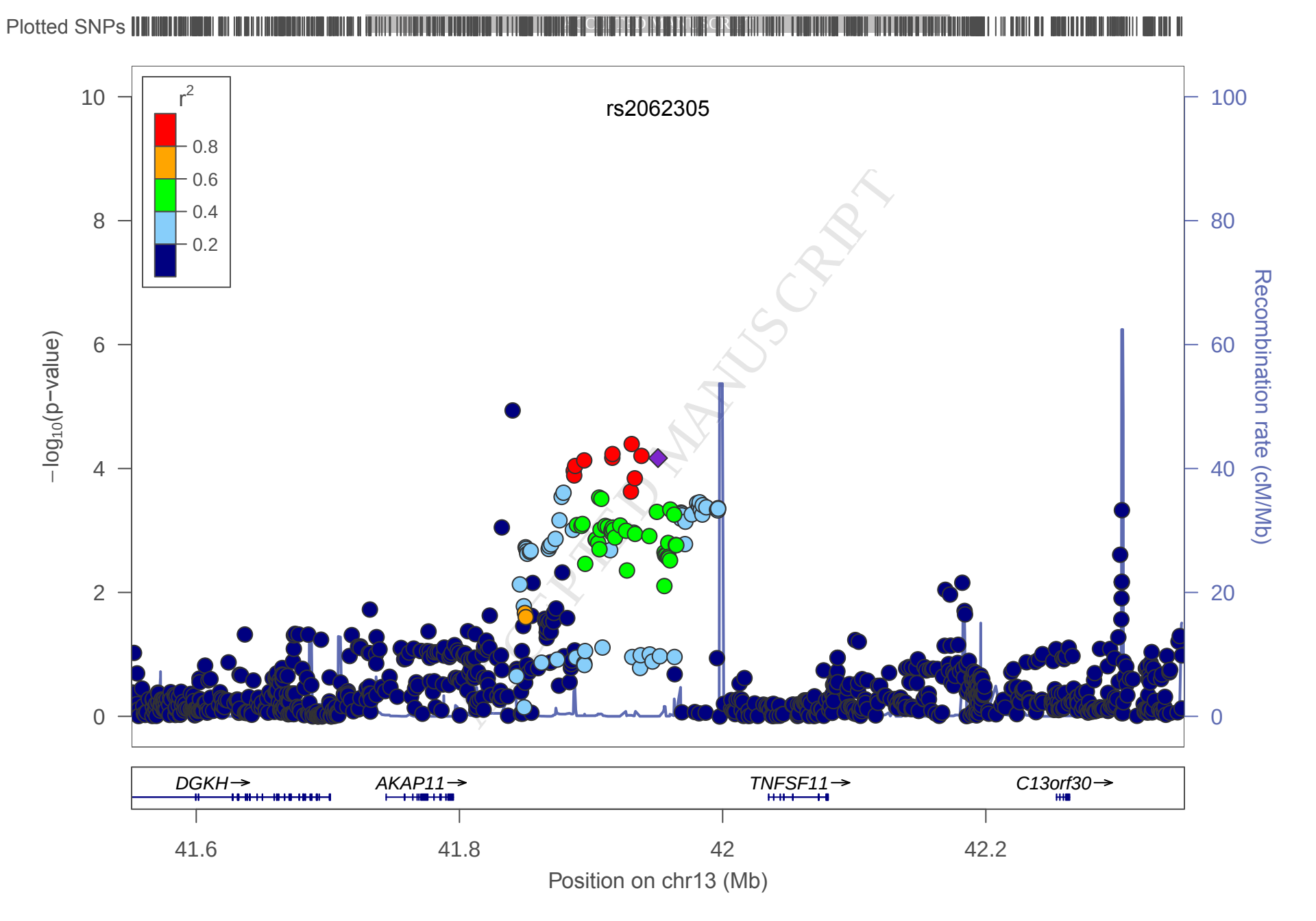
Plotted SNPs
rs2062305
r2
0.8
0.6
0.4
0.2
−log10(p−value)
Recombination rate (cM/Mb)
DGKH
AKAP11
TNFSF11
C13orf30
Position on chr13 (Mb)
41.6
41.8
42
42.2

| | |
|---|---|
| date: | Tue Jun 24 06:26:25 2014 |
| build: | hg18 |
| display range: | chr13:41550880−42350880 [41550880−42350880] |
| hilite range: | 0 − 0 [ 0 − 0 ] |
| reference SNP: | chr13:41950880 |
| number of SNPs plotted: | 959 |
| max P.value: | 1.15E−5 [chr13:41840263] |
| min P.value: | 9.98E−1 [chr13:41997648] |

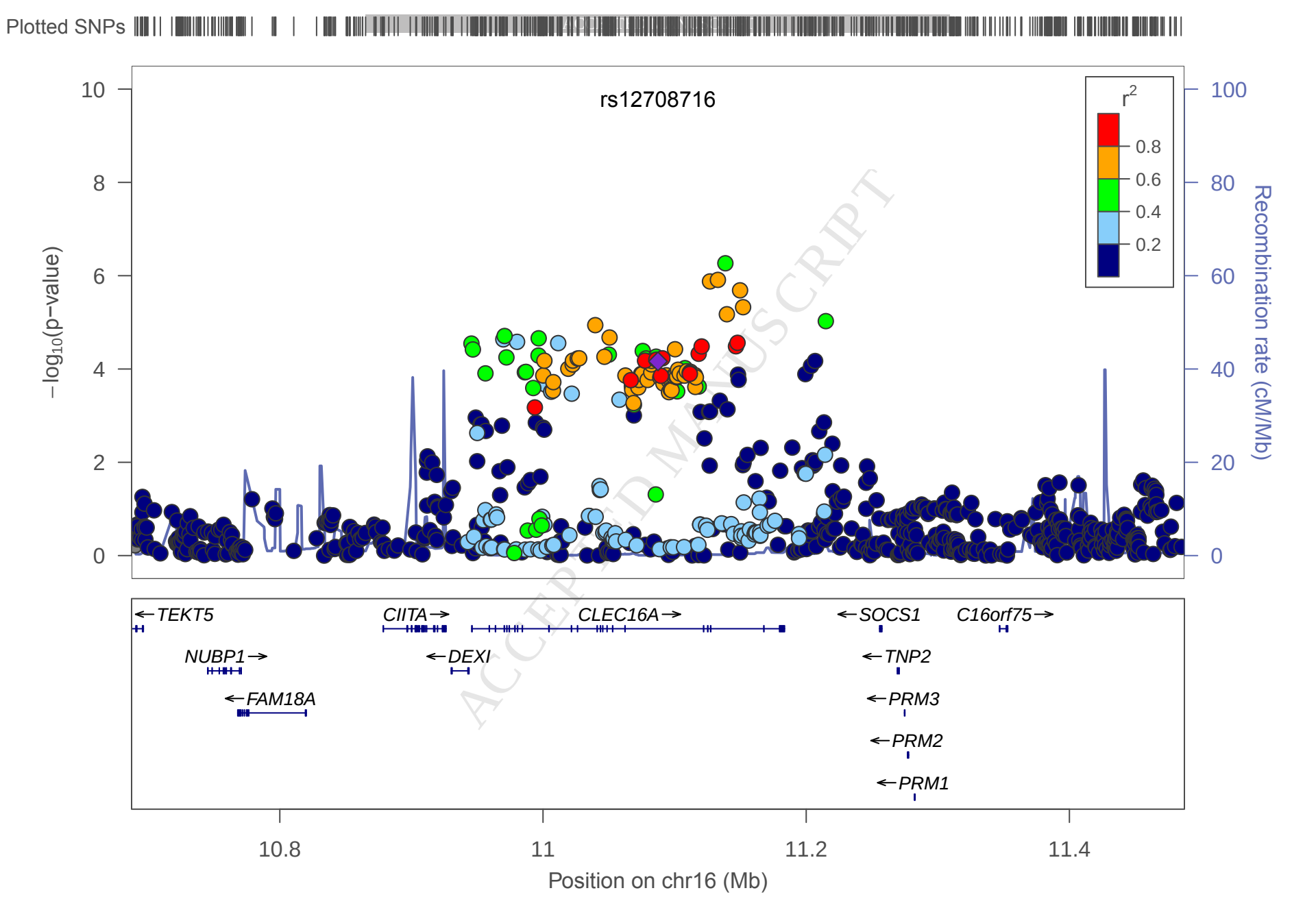

| | |
|---|---|
| date: | Tue Jun 24 06:27:25 2014 |
| build: | hg18 |
| display range: | chr16:10687374−11487374 [10687374−11487374] |
| hilite range: | 0 − 0 [ 0 − 0 ] |
| reference SNP: | chr16:11087374 |
| number of SNPs plotted: | 755 |
| max P.value: | 5.41E−7 [chr16:11138204] |
| min P.value: | 9.98E−1 [chr16:10833635] |

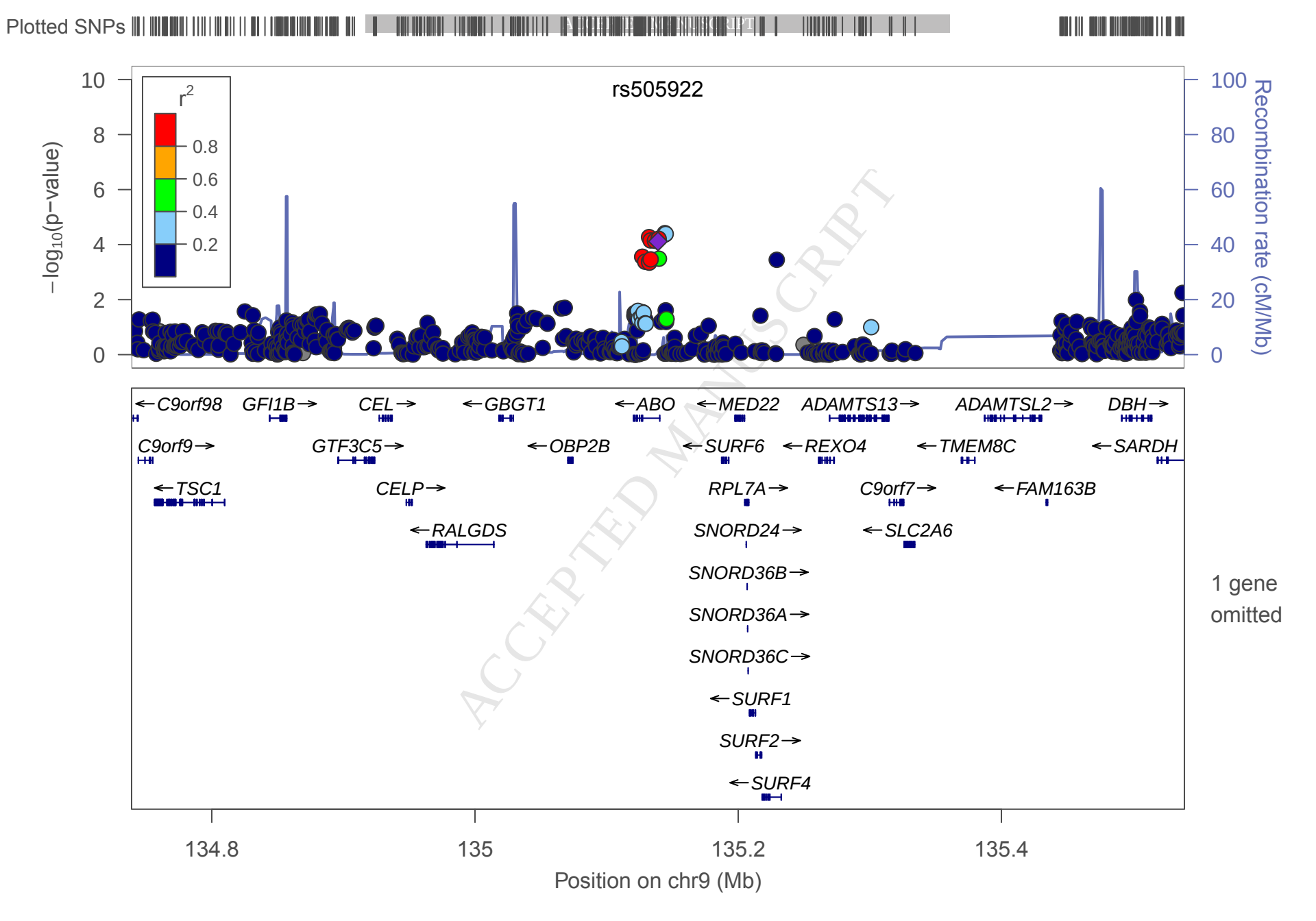

| | |
|---|---|
| date: | Tue Jun 24 06:28:30 2014 |
| build: | hg18 |
| display range: | chr9:134739050−135539050 [134739050−135539050] |
| hilite range: | 0 − 0 [ 0 − 0 ] |
| reference SNP: | chr9:135139050 |
| number of SNPs plotted: | 583 |
| max P.value: | 3.85E−5 [chr9:135144125] |
| min P.value: | 10E−1 [chr9:135121136] |
| omitted Genes: | C9orf96 |

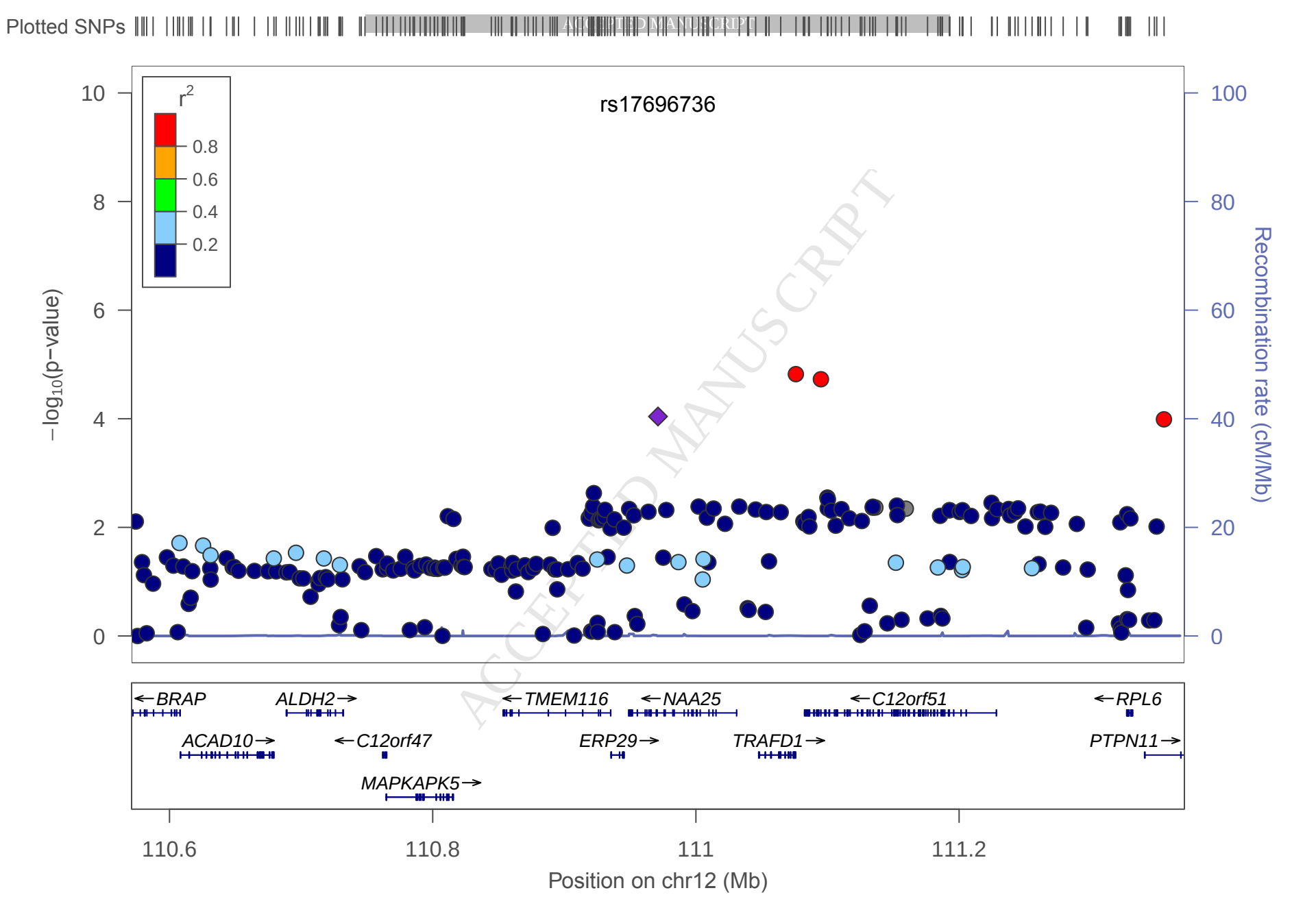

| | |
|---|---|
| date: | Tue Jun 24 06:29:26 2014 |
| build: | hg18 |
| display range: | chr12:110571201−111371201 [110571201−111371201] |
| hilite range: | 0 − 0 [ 0 − 0 ] |
| reference SNP: | chr12:110971201 |
| number of SNPs plotted: | 214 |
| max P.value: | 1.5E−5 [chr12:111076069] |
| min P.value: | 9.97E−1 [chr12:110575739] |

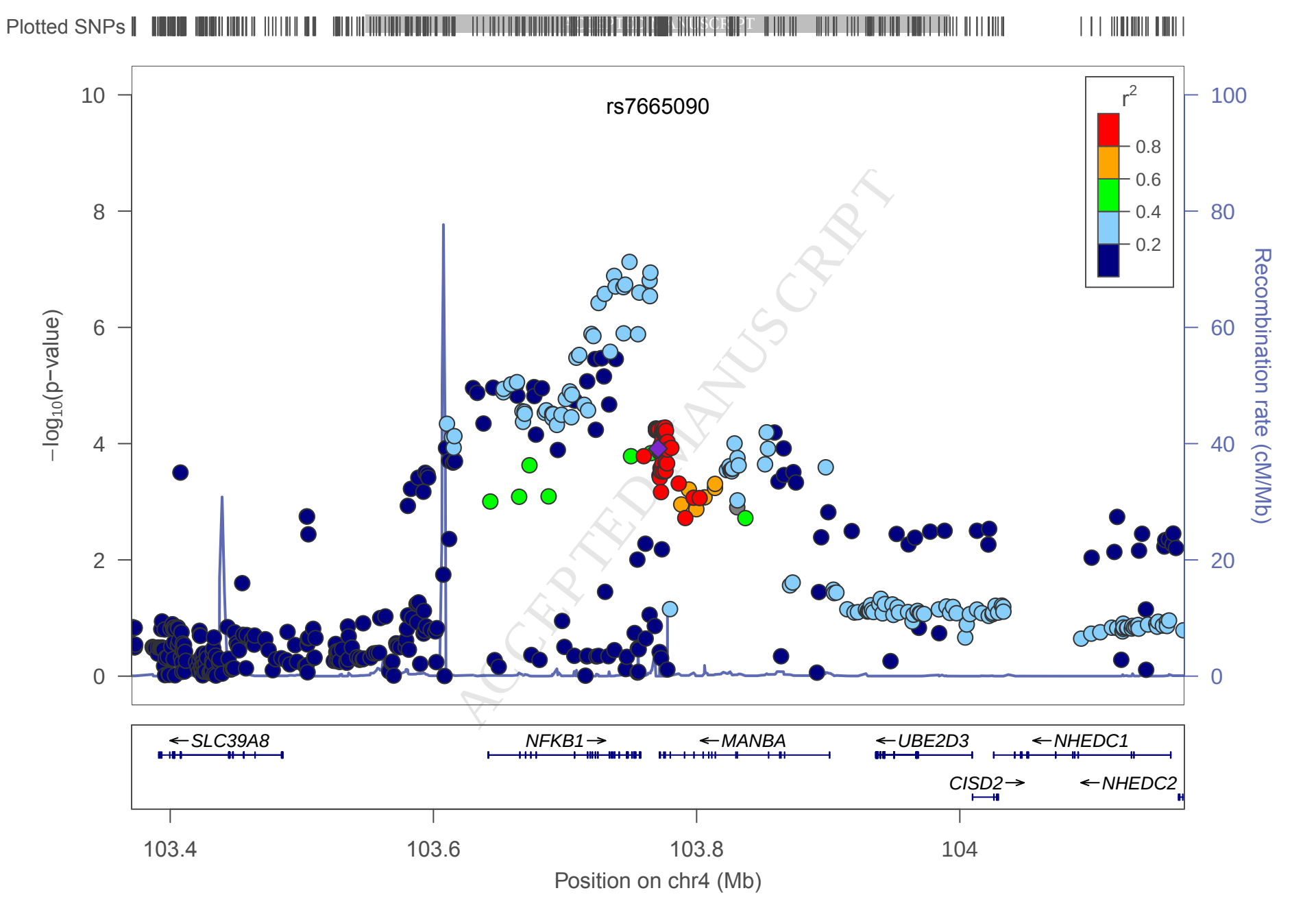
Plotted SNPs
rs7665090
r2
0.8
0.6
0.4
0.2
−log10(p−value)
Recombination rate (cM/Mb)
SLC39A8
NFKB1
MANBA
UBE2D3
NHEDC1
CISD2
NHEDC2
Position on chr4 (Mb)

| | |
|---|---|
| date: | Tue Jun 24 06:31:23 2014 |
| build: | hg18 |
| display range: | chr4:103370651−104170651 [103370651−104170651] |
| hilite range: | 0 − 0 [ 0 − 0 ] |
| reference SNP: | chr4:103770651 |
| number of SNPs plotted: | 506 |
| max P.value: | 7.44E−8 [chr4:103749001] |
| min P.value: | 9.91E−1 [chr4:103608433] |

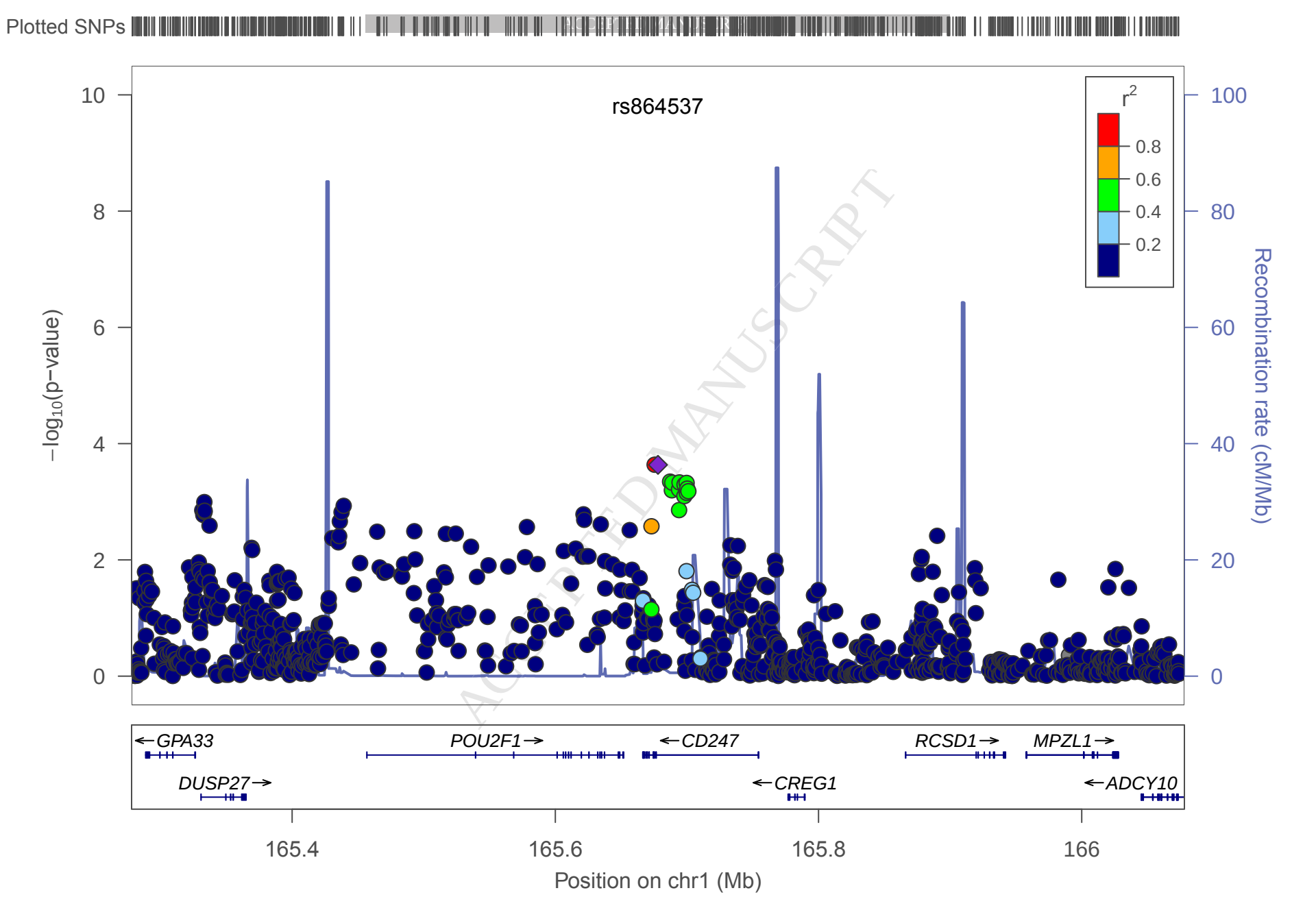

| | |
|---|---|
| date: | Tue Jun 24 06:33:41 2014 |
| build: | hg18 |
| display range: | chr1:165278008−166078008 [165278008−166078008] |
| hilite range: | 0 − 0 [ 0 − 0 ] |
| reference SNP: | chr1:165678008 |
| number of SNPs plotted: | 874 |
| max P.value: | 2.31E−4 [chr1:165675294] |
| min P.value: | 10E−1 [chr1:166056582] |

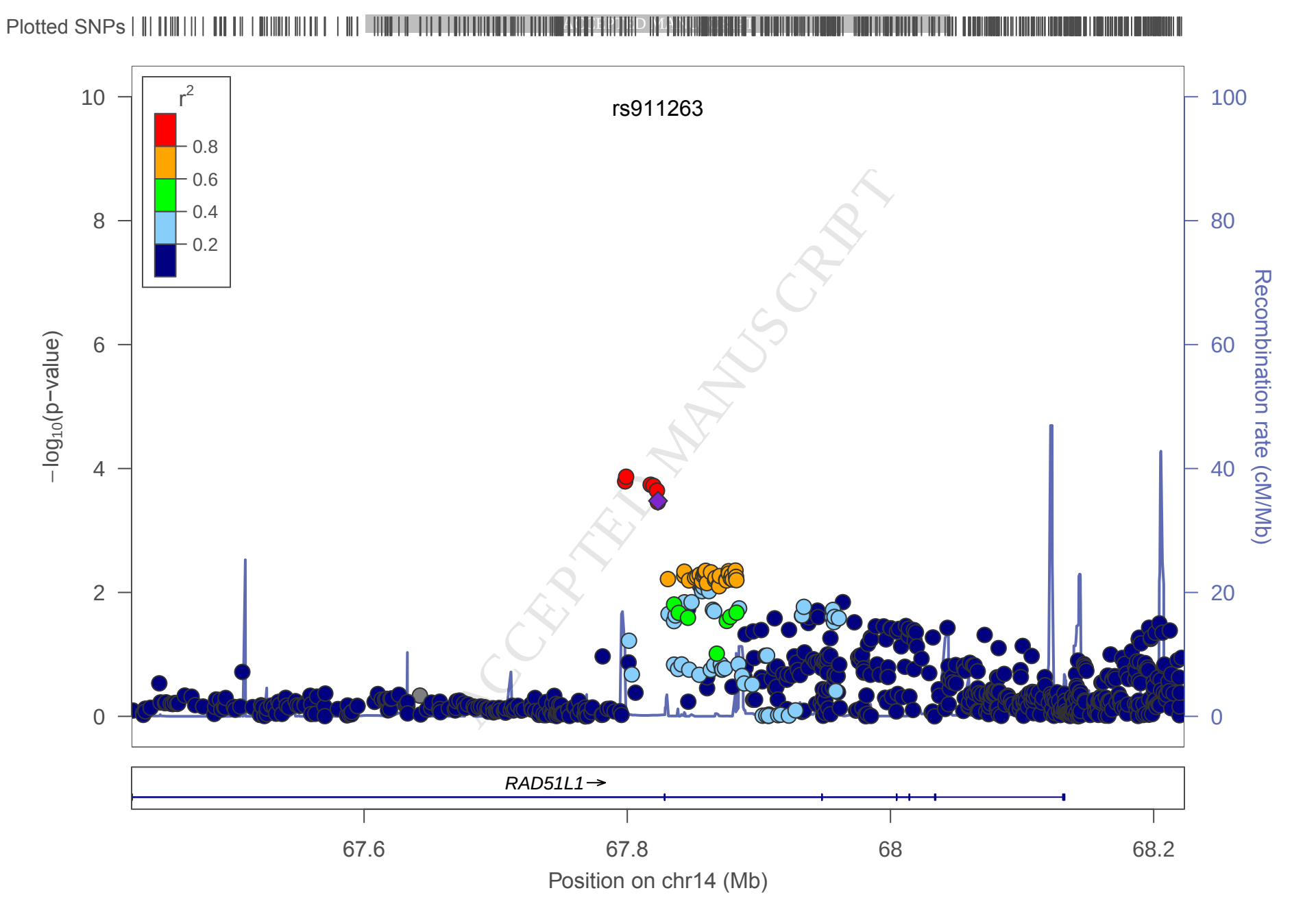
Plotted SNPs
rs911263
r2
0.8
0.6
0.4
0.2
−log10(p−value)
Recombination rate (cM/Mb)
RAD51L1
Position on chr14 (Mb)
67.6
67.8
68
68.2
ACCEPTED MANUSCRIPT

| | |
|---|---|
| date: | Tue Jun 24 06:35:39 2014 |
| build: | hg18 |
| display range: | chr14:67423346−68223346 [67423346−68223346] |
| hilite range: | 0 − 0 [ 0 − 0 ] |
| reference SNP: | chr14:67823346 |
| number of SNPs plotted: | 713 |
| max P.value: | 1.36E−4 [chr14:67798977] |
| min P.value: | 9.98E−1 [chr14:67768225] |

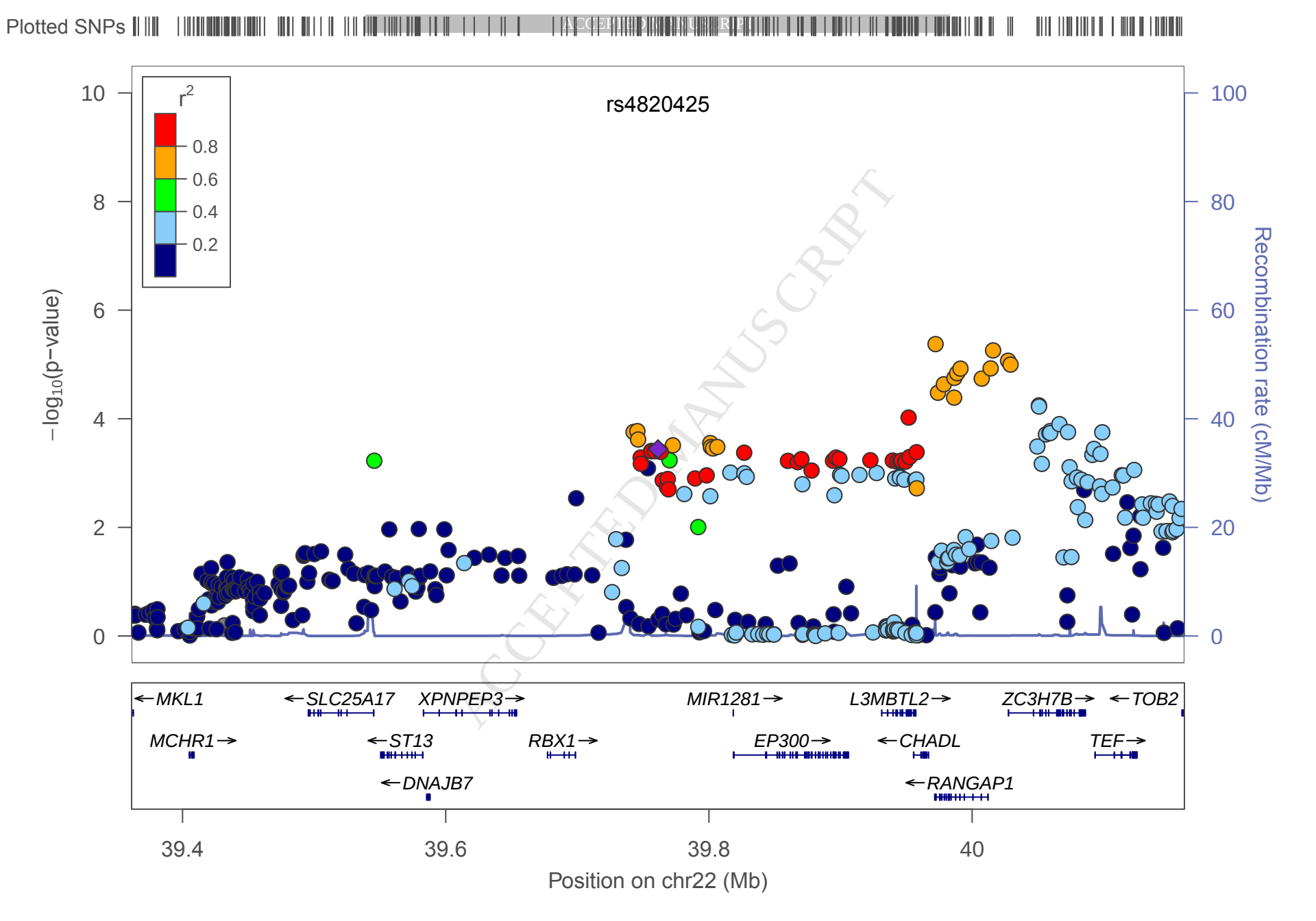
Plotted SNPs
rs4820425
r2
0.8
0.6
0.4
0.2
−log10(p−value)
Recombination rate (cM/Mb)
MKL1
SLC25A17
XPNPEP3
MIR1281
L3MBTL2
ZC3H7B
TOB2
MCHR1
ST13
RBX1
EP300
CHADL
TEF
DNAJB7
RANGAP1
Position on chr22 (Mb)

| | |
|---|---|
| date: | Tue Jun 24 06:39:27 2014 |
| build: | hg18 |
| display range: | chr22:39361288−40161288 [39361288−40161288] |
| hilite range: | 0 − 0 [ 0 − 0 ] |
| reference SNP: | chr22:39761288 |
| number of SNPs plotted: | 389 |
| max P.value: | 4.18E−6 [chr22:39972158] |
| min P.value: | 9.93E−1 [chr22:39880985] |

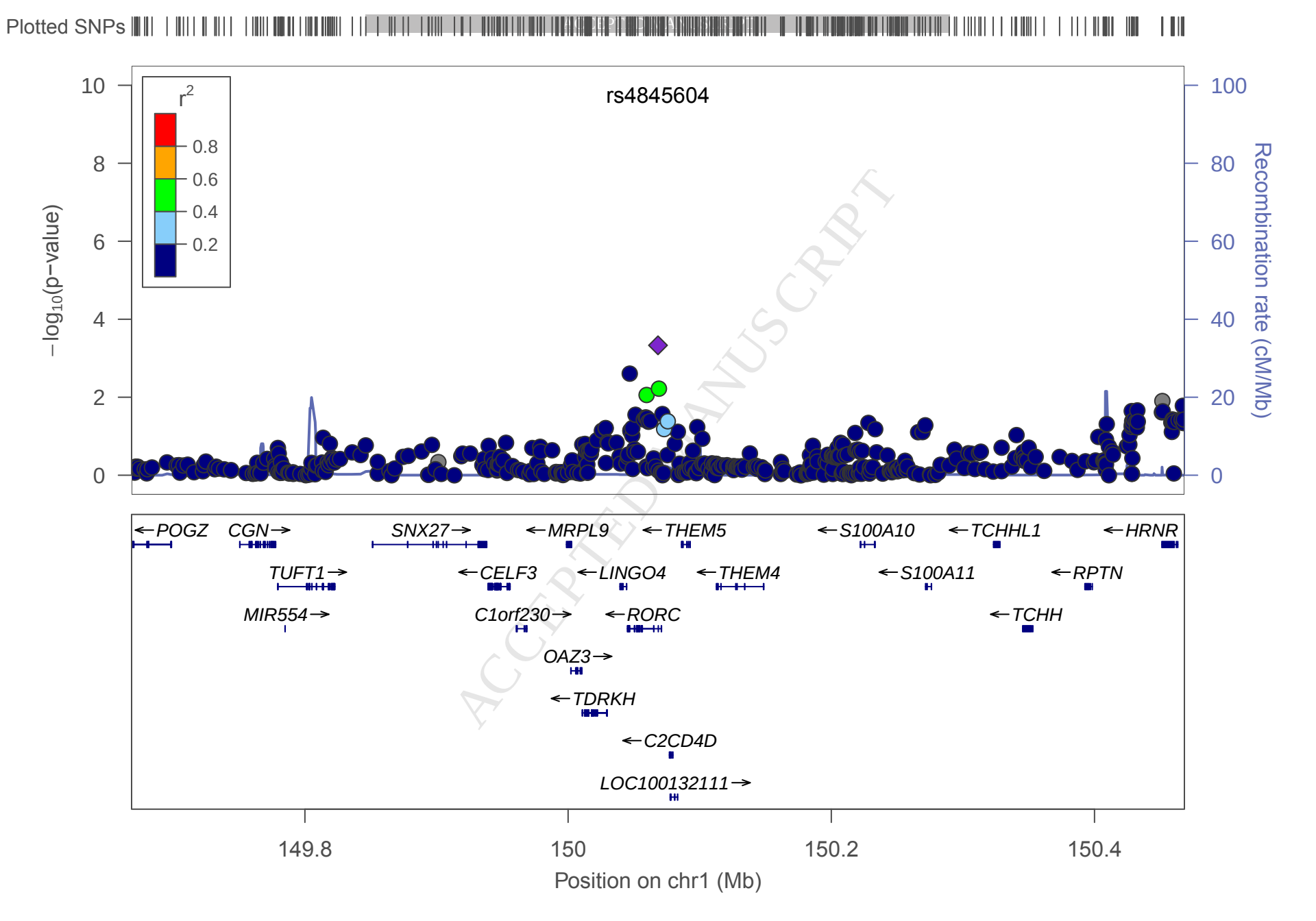

| | |
|---|---|
| date: | Tue Jun 24 06:41:09 2014 |
| build: | hg18 |
| display range: | chr1:149668304−150468304 [149668304−150468304] |
| hilite range: | 0 − 0 [ 0 − 0 ] |
| reference SNP: | chr1:150068304 |
| number of SNPs plotted: | 446 |
| max P.value: | 4.67E−4 [chr1:150068304] |
| min P.value: | 9.99E−1 [chr1:150176878] |

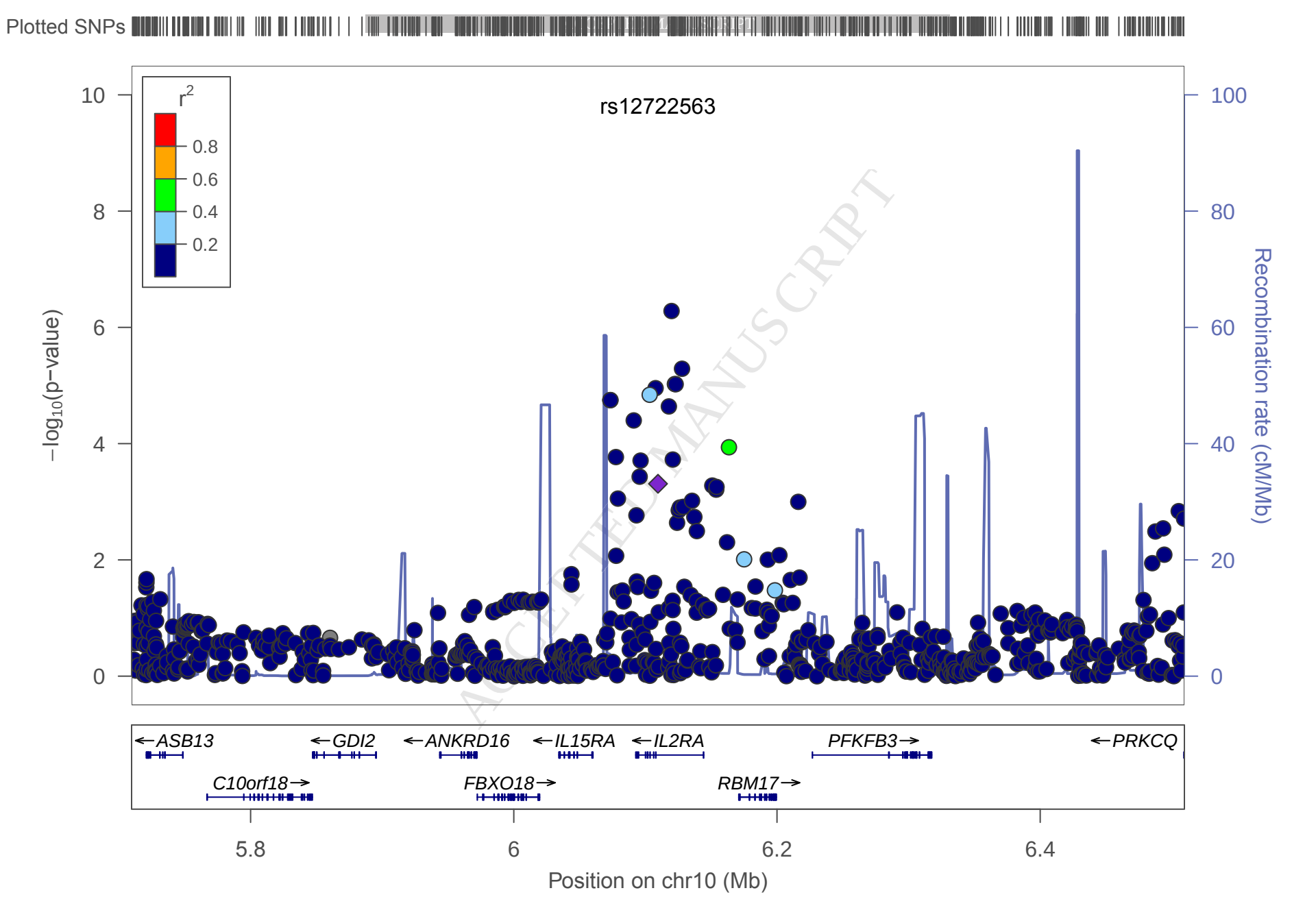

| | |
|---|---|
| date: | Tue Jun 24 06:42:40 2014 |
| build: | hg18 |
| display range: | chr10:5709567−6509567 [5709567−6509567] |
| hilite range: | 0 − 0 [ 0 − 0 ] |
| reference SNP: | chr10:6109567 |
| number of SNPs plotted: | 788 |
| max P.value: | 5.17E−7 [chr10:6119852] |
| min P.value: | 9.96E−1 [chr10:6000215] |

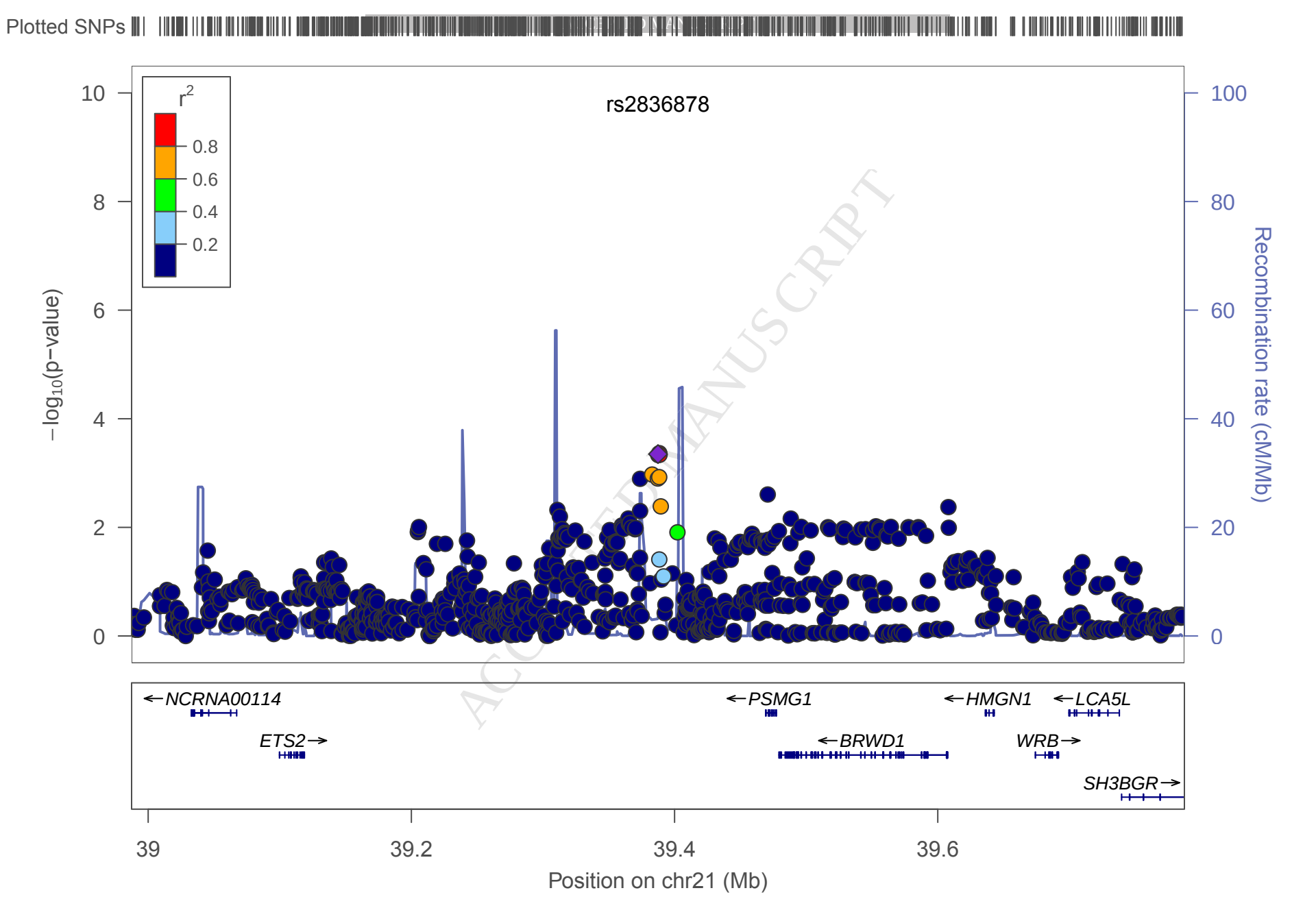
Plotted SNPs
rs2836878
r2
0.8
0.6
0.4
0.2
−log10(p−value)
Recombination rate (cM/Mb)
NCRNA00114
ETS2
PSMG1
BRWD1
HMGN1
LCA5L
WRB
SH3BGR
Position on chr21 (Mb)

| | |
|---|---|
| date: | Tue Jun 24 06:43:59 2014 |
| build: | hg18 |
| display range: | chr21:38987404−39787404 [38987404−39787404] |
| hilite range: | 0 − 0 [ 0 − 0 ] |
| reference SNP: | chr21:39387404 |
| number of SNPs plotted: | 885 |
| max P.value: | 4.31E−4 [chr21:39388169] |
| min P.value: | 9.97E−1 [chr21:39213972] |

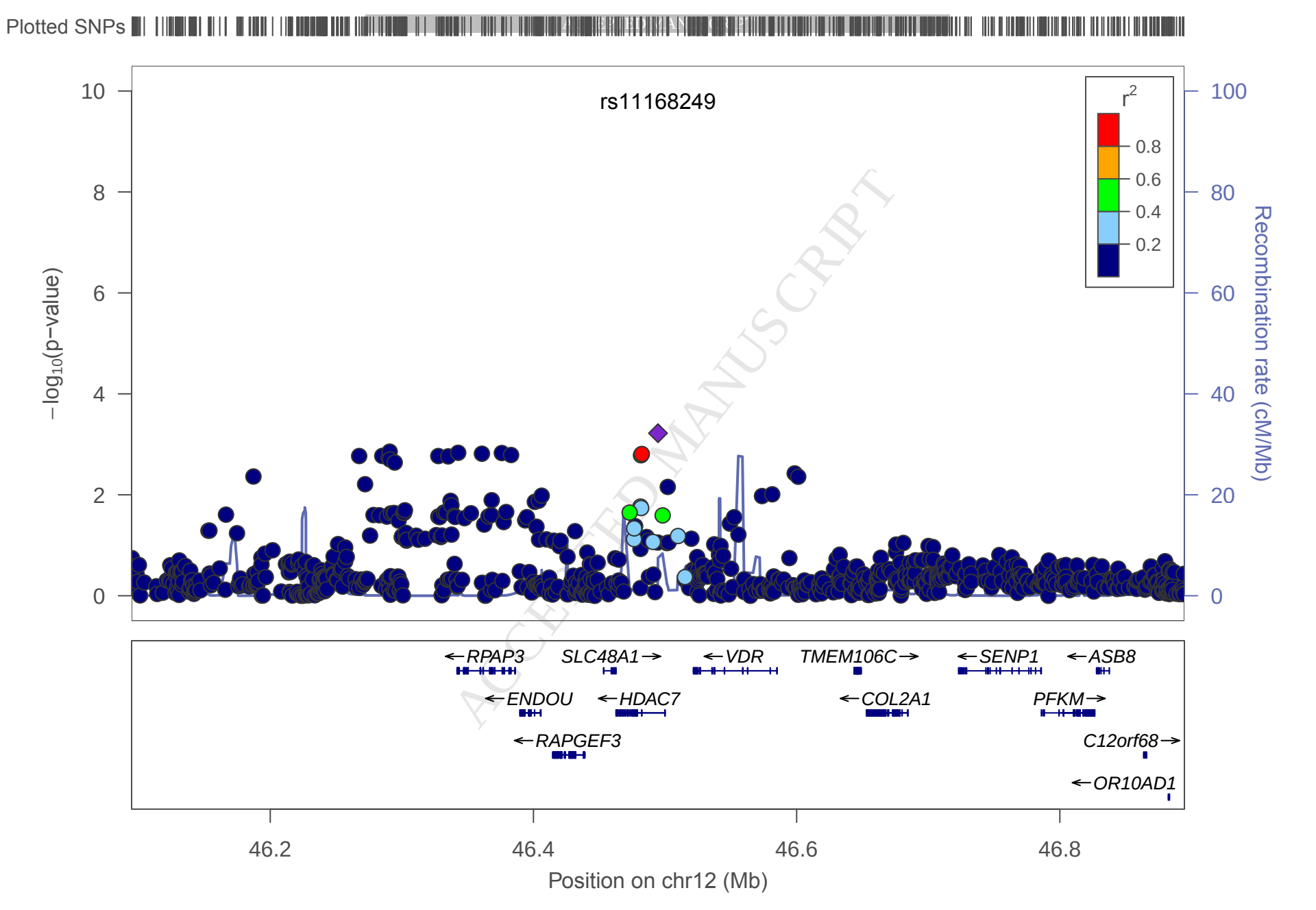

| | |
|---|---|
| date: | Tue Jun 24 06:45:10 2014 |
| build: | hg18 |
| display range: | chr12:46094635−46894635 [46094635−46894635] |
| hilite range: | 0 − 0 [ 0 − 0 ] |
| reference SNP: | chr12:46494635 |
| number of SNPs plotted: | 795 |
| max P.value: | 6.01E−4 [chr12:46494635] |
| min P.value: | 9.96E−1 [chr12:46446588] |

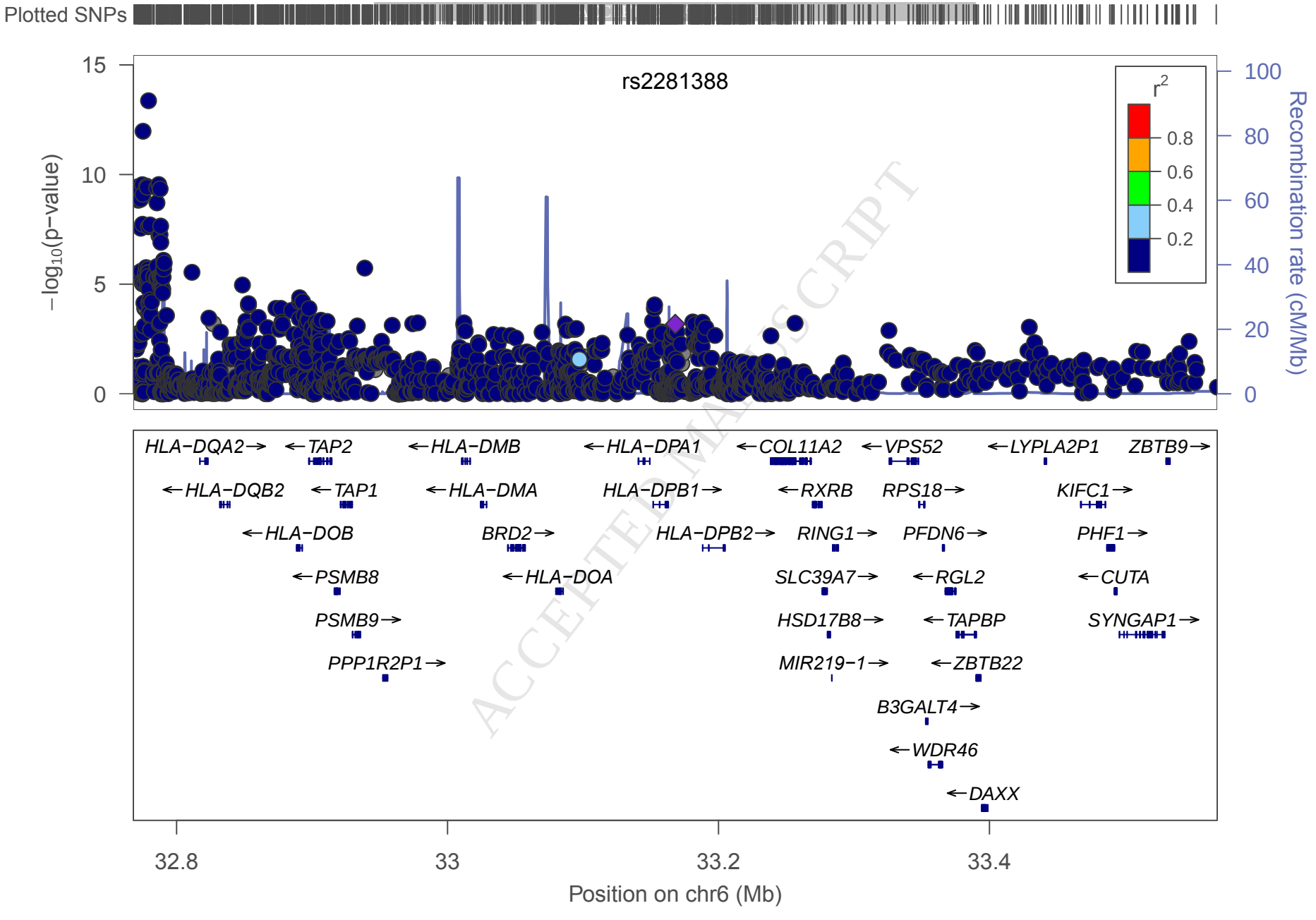

| | |
|---|---|
| date: | Tue Jun 24 06:47:02 2014 |
| build: | hg18 |
| display range: | chr6:32768096−33568096 [32768096−33568096] |
| hilite range: | 0 − 0 [ 0 − 0 ] |
| reference SNP: | chr6:33168096 |
| number of SNPs plotted: | 1723 |
| max P.value: | 4.2E−14 [chr6:32779226] |
| min P.value: | 10E−1 [chr6:32774800] |

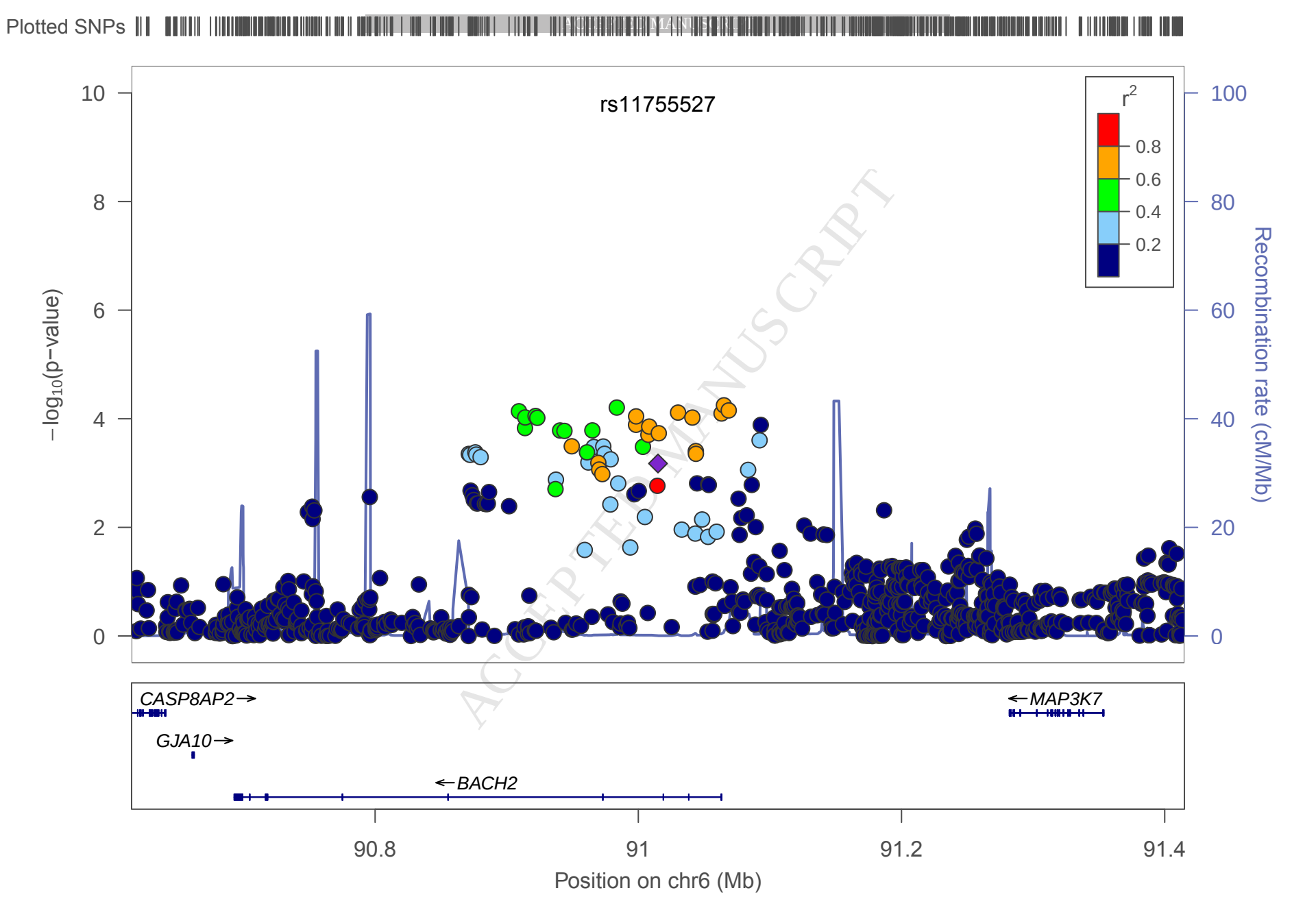

| | |
|---|---|
| date: | Tue Jun 24 06:48:44 2014 |
| build: | hg18 |
| display range: | chr6:90614952−91414952 [90614952−91414952] |
| hilite range: | 0 − 0 [ 0 − 0 ] |
| reference SNP: | chr6:91014952 |
| number of SNPs plotted: | 805 |
| max P.value: | 5.61E−5 [chr6:91064748] |
| min P.value: | 9.99E−1 [chr6:90691633] |

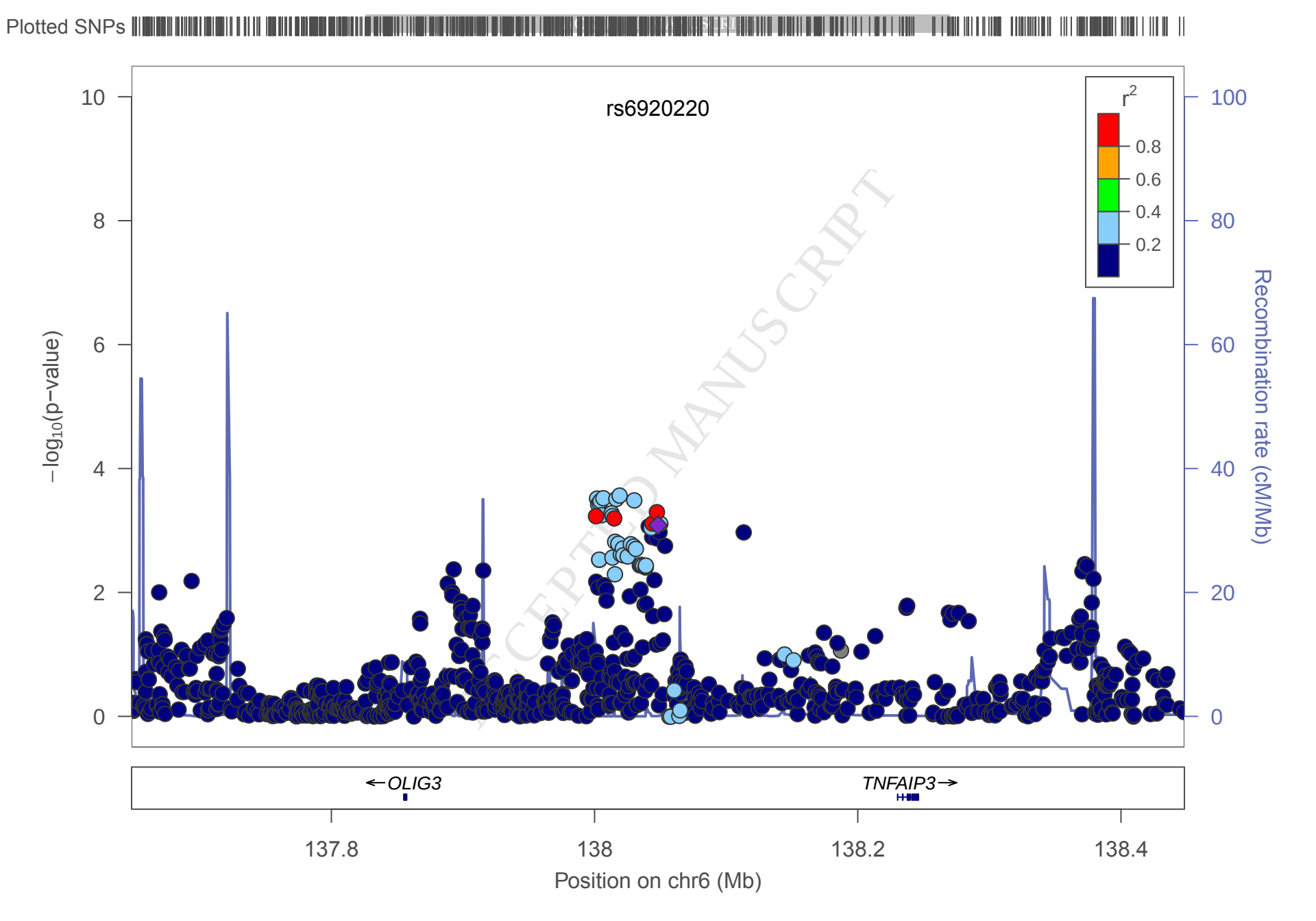

| | |
|---|---|
| date: | Tue Jun 24 06:50:52 2014 |
| build: | hg18 |
| display range: | chr6:137648197−138448197 [137648197−138448197] |
| hilite range: | 0 − 0 [ 0 − 0 ] |
| reference SNP: | chr6:138048197 |
| number of SNPs plotted: | 864 |
| max P.value: | 2.7E−4 [chr6:138018860] |
| min P.value: | 10E−1 [chr6:138057818] |

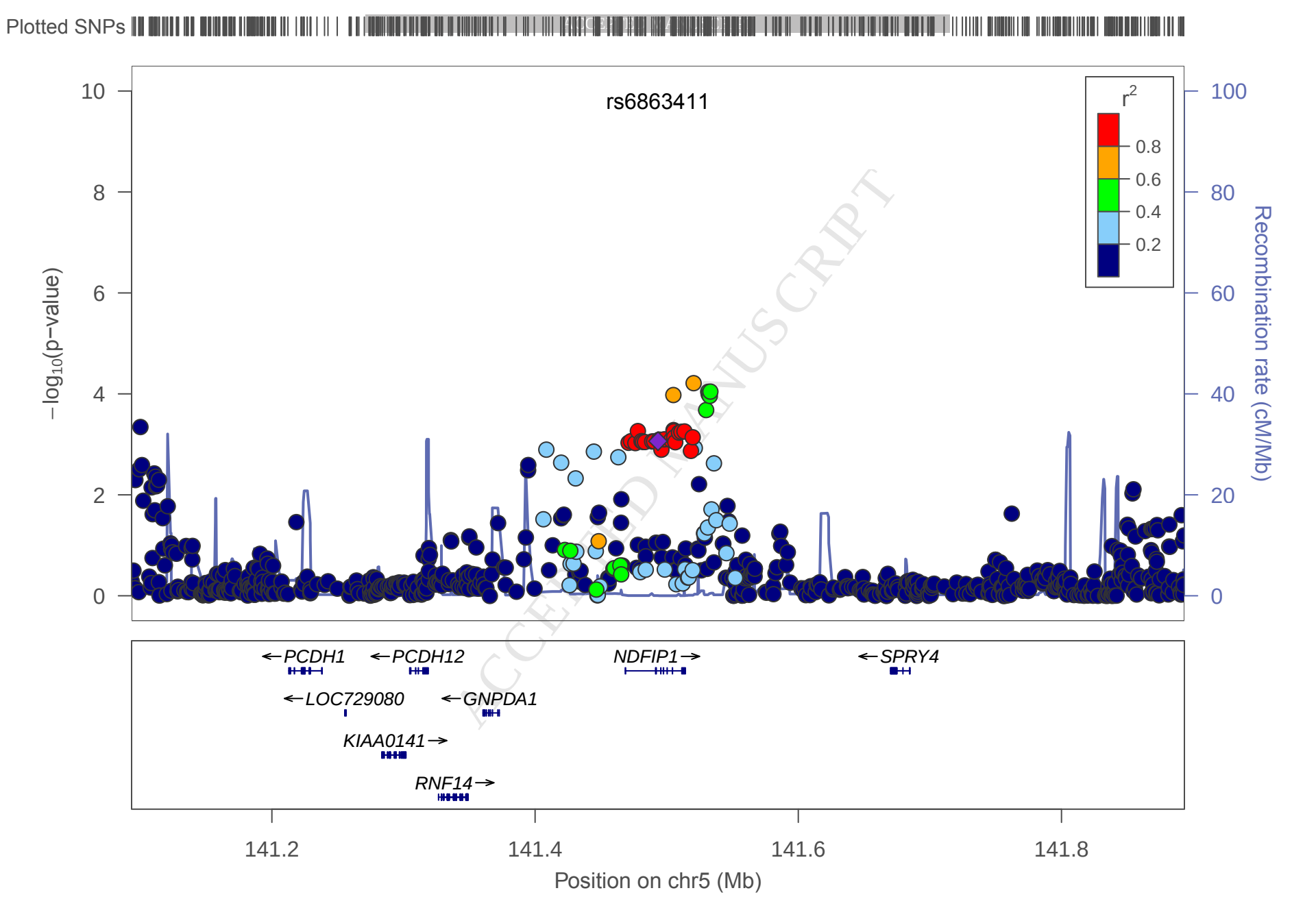

| | |
|---|---|
| date: | Tue Jun 24 07:22:37 2014 |
| build: | hg18 |
| display range: | chr5:141093388−141893388 [141093388−141893388] |
| hilite range: | 0 − 0 [ 0 − 0 ] |
| reference SNP: | chr5:141493388 |
| number of SNPs plotted: | 716 |
| max P.value: | 6.06E−5 [chr5:141520201] |
| min P.value: | 10E−1 [chr5:141756052] |

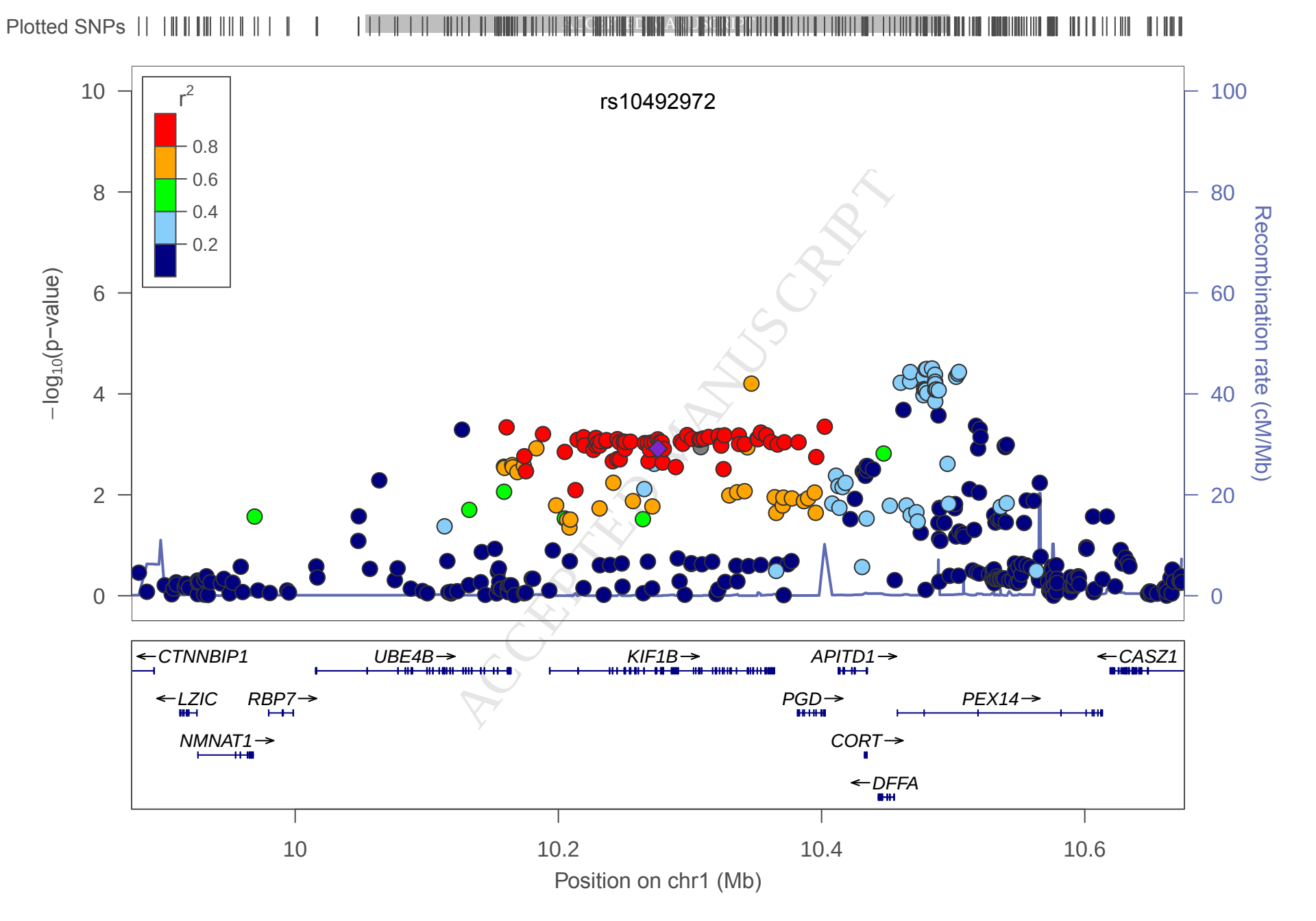
Plotted SNPs
rs10492972
r2
0.8
0.6
0.4
0.2
−log10(p−value)
Recombination rate (cM/Mb)
CTNNBIP1
UBE4B
KIF1B
APITD1
CASZ1
LZIC
RBP7
PGD
PEX14
NMNAT1
CORT
DFFA
Position on chr1 (Mb)
ACCEPTED MANUSCRIPT

| | |
|---|---|
| date: | Tue Jun 24 07:30:17 2014 |
| build: | hg18 |
| display range: | chr1:9875699−10675699 [9875699−10675699] |
| hilite range: | 0 − 0 [ 0 − 0 ] |
| reference SNP: | chr1:10275699 |
| number of SNPs plotted: | 391 |
| max P.value: | 3.13E−5 [chr1:10483869] |
| min P.value: | 9.91E−1 [chr1:10576209] |

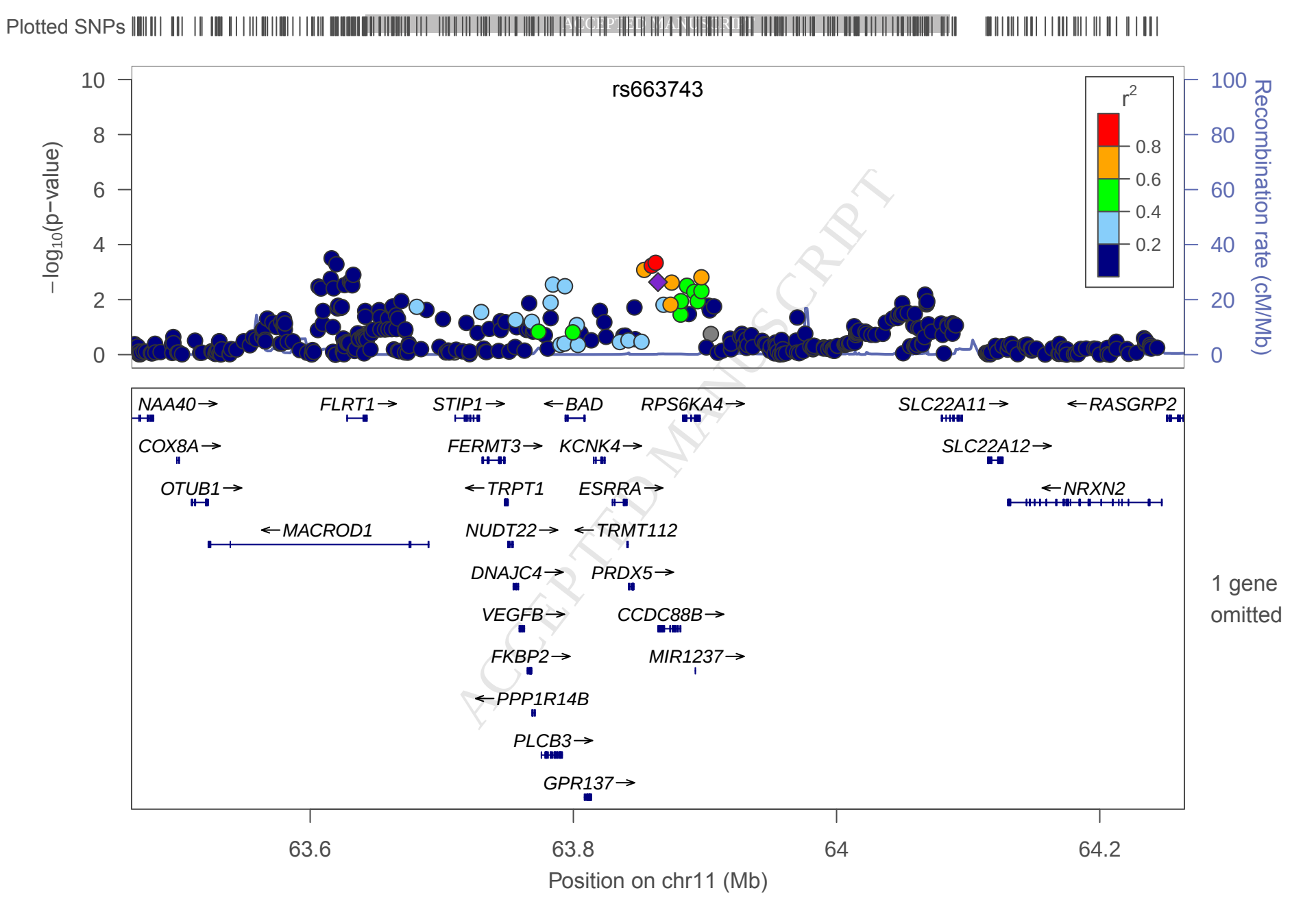
Plotted SNPs
rs663743
r²
0.8
0.6
0.4
0.2
−log10(p−value)
Recombination rate (cM/Mb)
NAA40
FLRT1
STIP1
BAD
RPS6KA4
SLC22A11
RASGRP2
COX8A
FERMT3
KCNK4
SLC22A12
OTUB1
TRPT1
ESRRA
NRXN2
MACROD1
NUDT22
TRMT112
DNAJC4
PRDX5
VEGFB
CCDC88B
FKBP2
MIR1237
PPP1R14B
PLCB3
GPR137
1 gene omitted
Position on chr11 (Mb)

| | |
|---|---|
| date: | Tue Jun 24 07:33:32 2014 |
| build: | hg18 |
| display range: | chr11:63464311−64264311 [63464311−64264311] |
| hilite range: | 0 − 0 [ 0 − 0 ] |
| reference SNP: | chr11:63864311 |
| number of SNPs plotted: | 387 |
| max P.value: | 3.13E−4 [chr11:63616327] |
| min P.value: | 10E−1 [chr11:64207857] |
| omitted Genes: | C11orf20 |

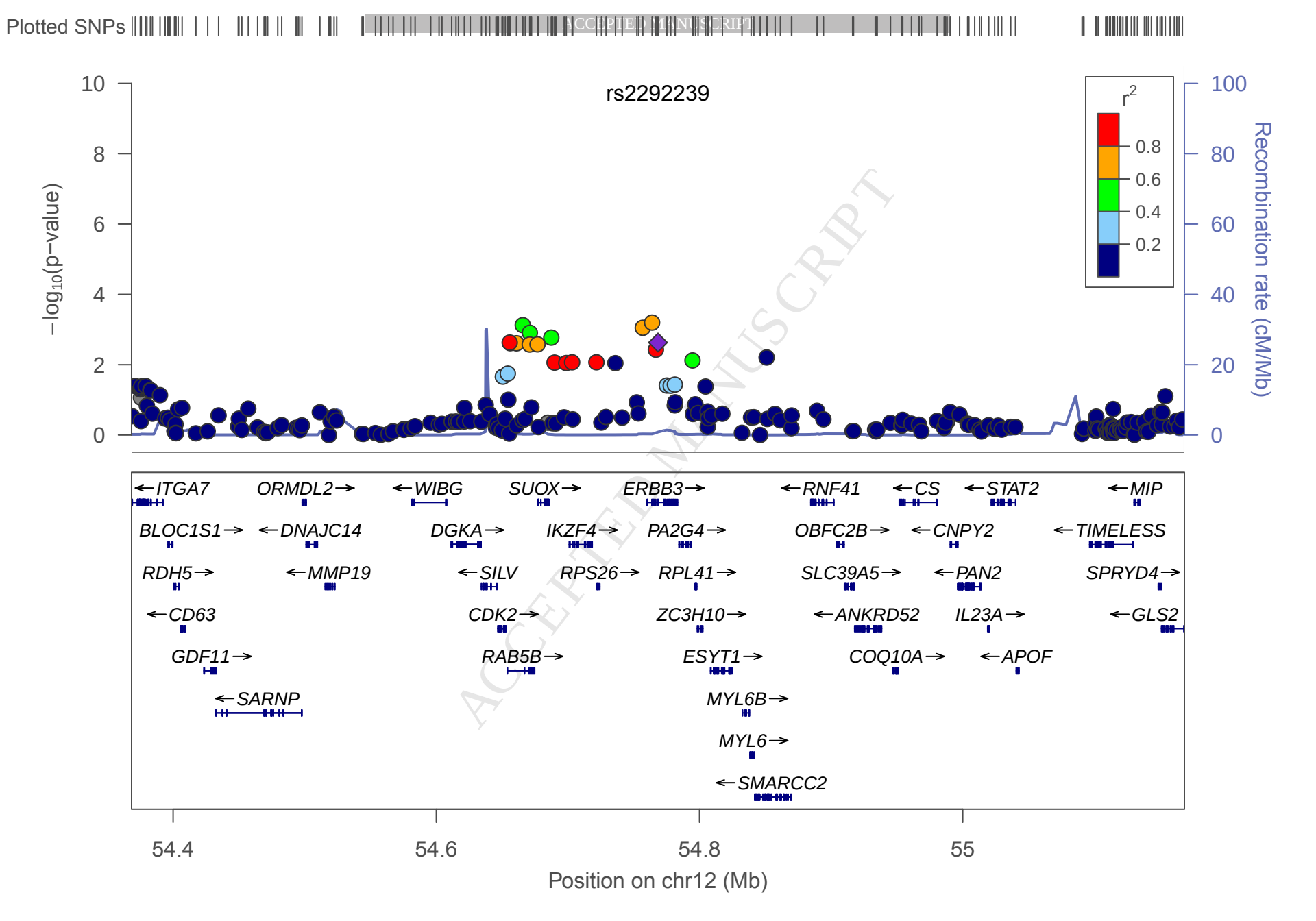

| | |
|---|---|
| date: | Tue Jun 24 07:37:53 2014 |
| build: | hg18 |
| display range: | chr12:54368447−55168447 [54368447−55168447] |
| hilite range: | 0 − 0 [ 0 − 0 ] |
| reference SNP: | chr12:54768447 |
| number of SNPs plotted: | 217 |
| max P.value: | 6.27E−4 [chr12:54763961] |
| min P.value: | 9.91E−1 [chr12:54518443] |

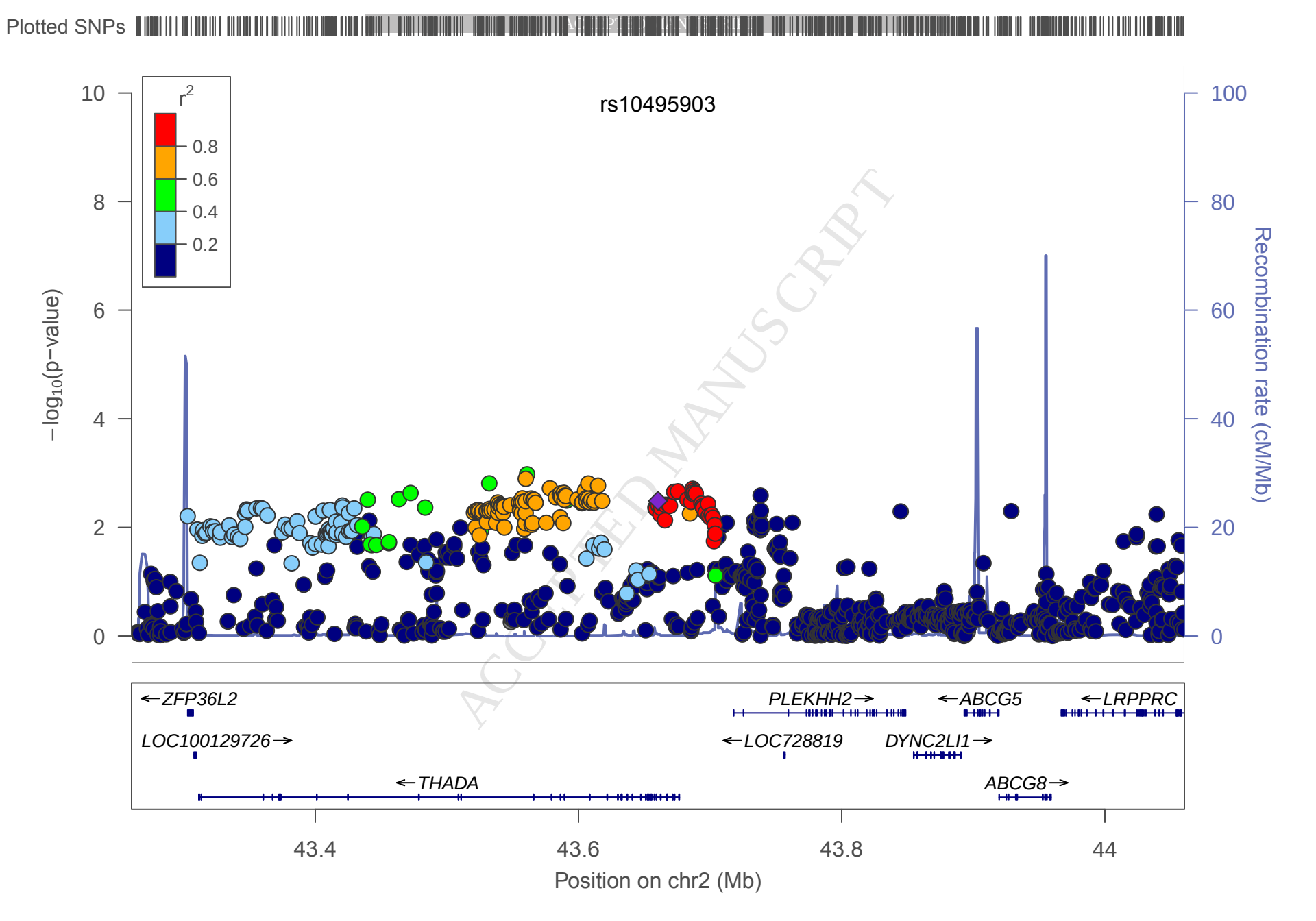

| | |
|---|---|
| date: | Tue Jun 24 07:41:08 2014 |
| build: | hg18 |
| display range: | chr2:43260422−44060422 [43260422−44060422] |
| hilite range: | 0 − 0 [ 0 − 0 ] |
| reference SNP: | chr2:43660422 |
| number of SNPs plotted: | 856 |
| max P.value: | 1.05E−3 [chr2:43560889] |
| min P.value: | 9.97E−1 [chr2:43892797] |

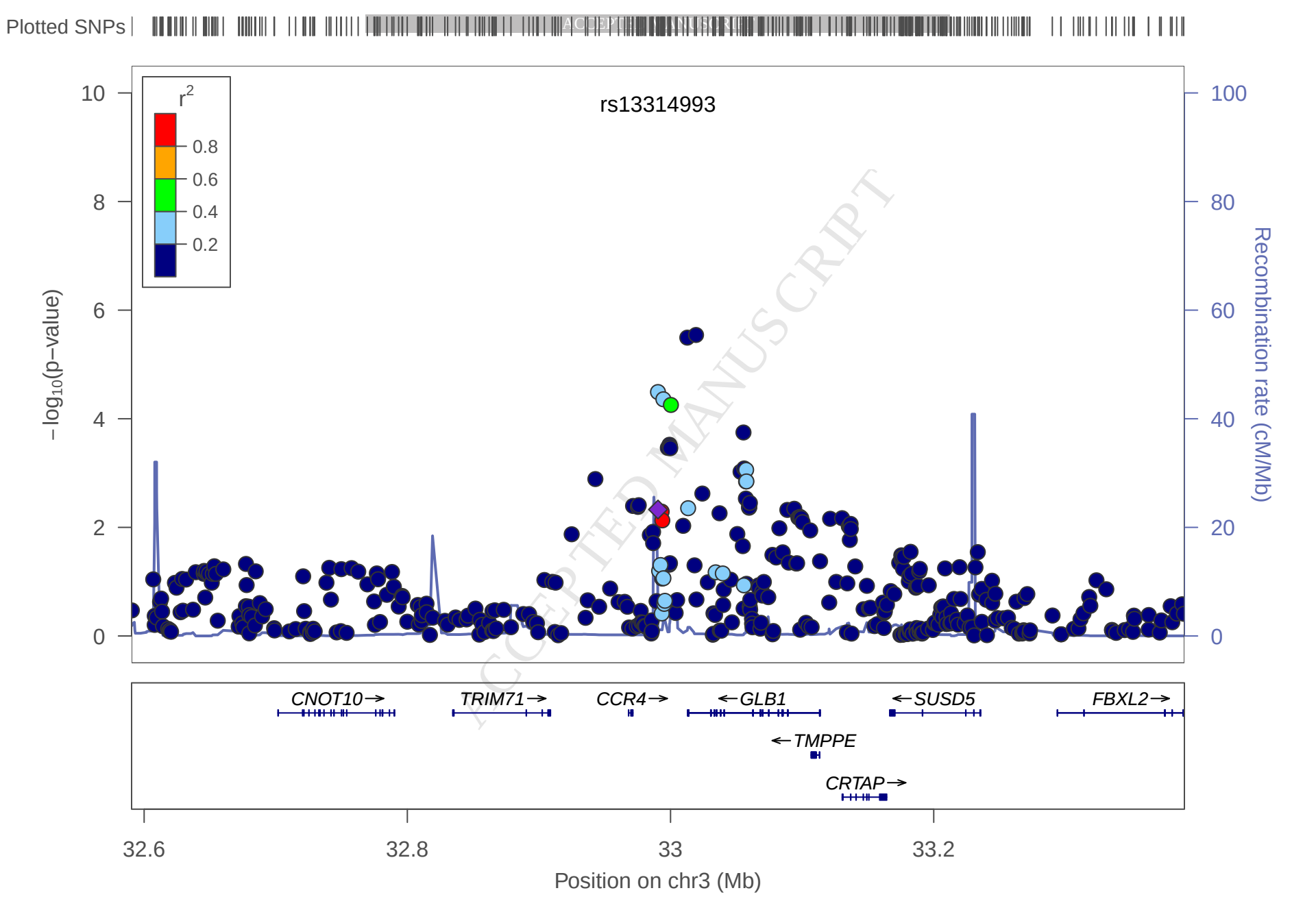

| | |
|---|---|
| date: | Tue Jun 24 07:53:54 2014 |
| build: | hg18 |
| display range: | chr3:32590473–33390473 [32590473–33390473] |
| hilite range: | 0 – 0 [ 0 – 0 ] |
| reference SNP: | chr3:32990473 |
| number of SNPs plotted: | 391 |
| max P.value: | 2.86E–6 [chr3:33019343] |
| min P.value: | 9.74E–1 [chr3:33230596] |

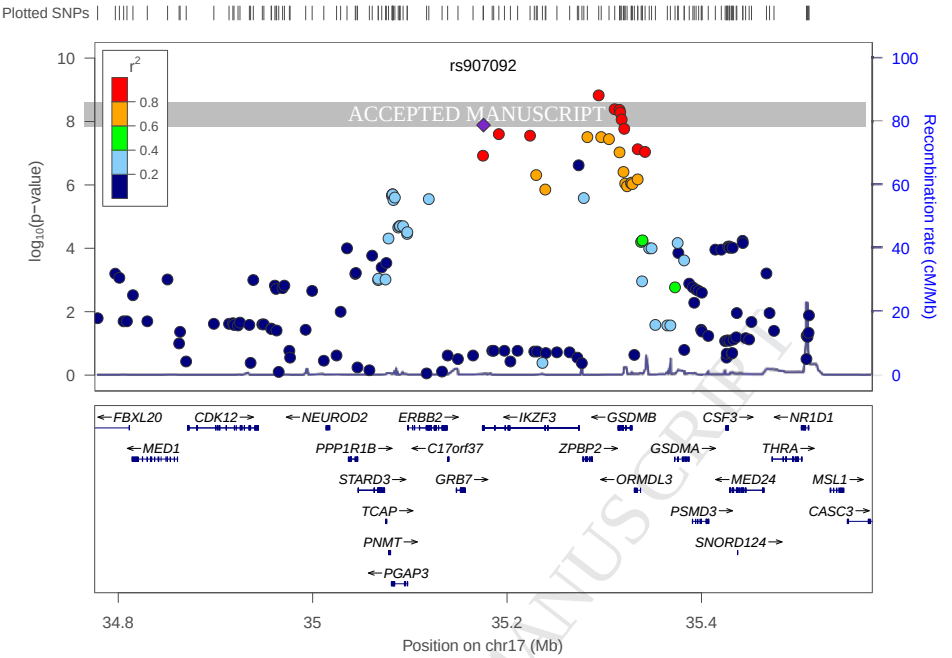




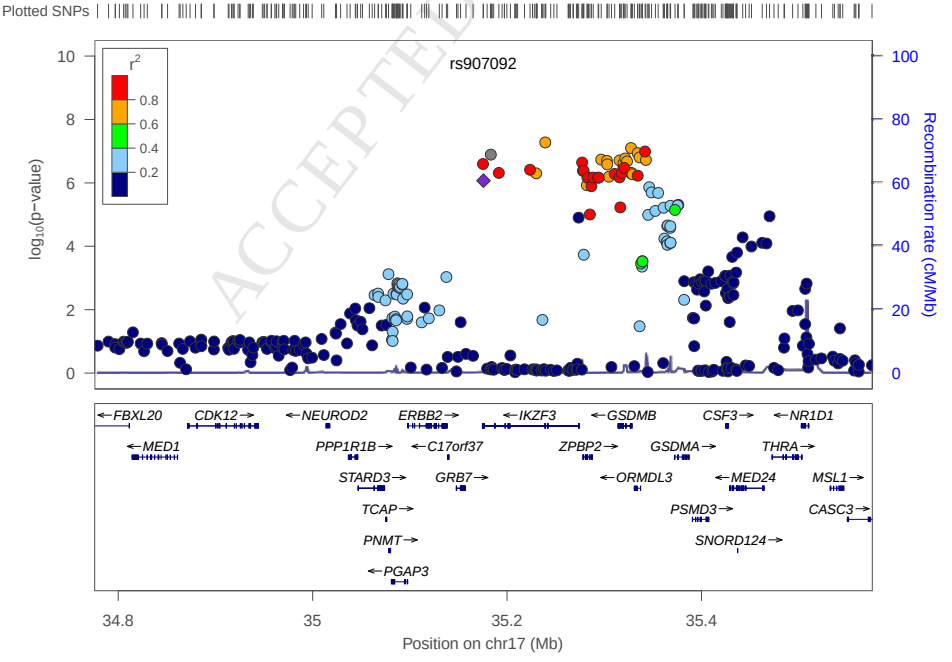

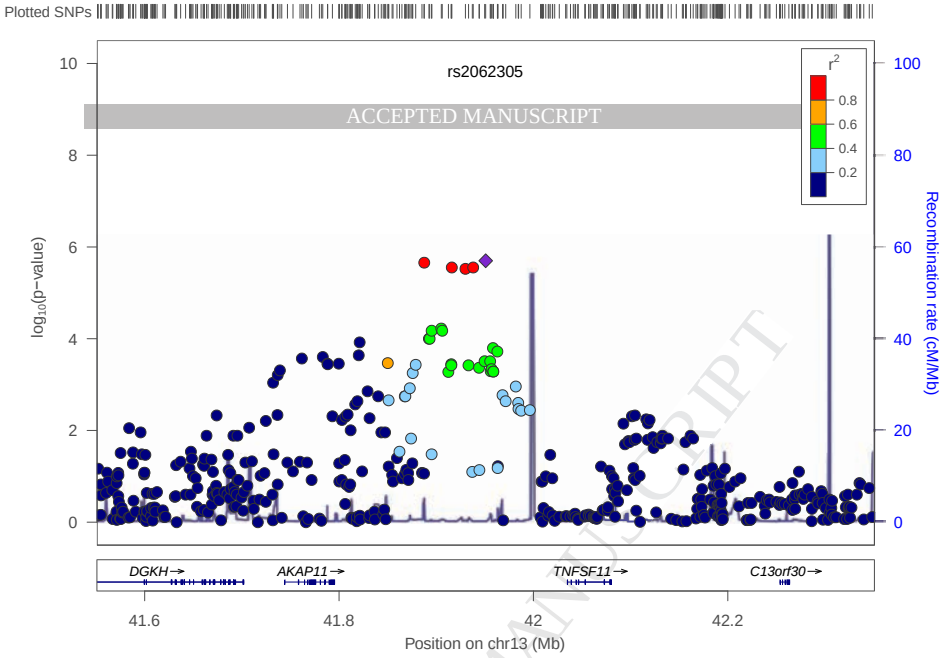




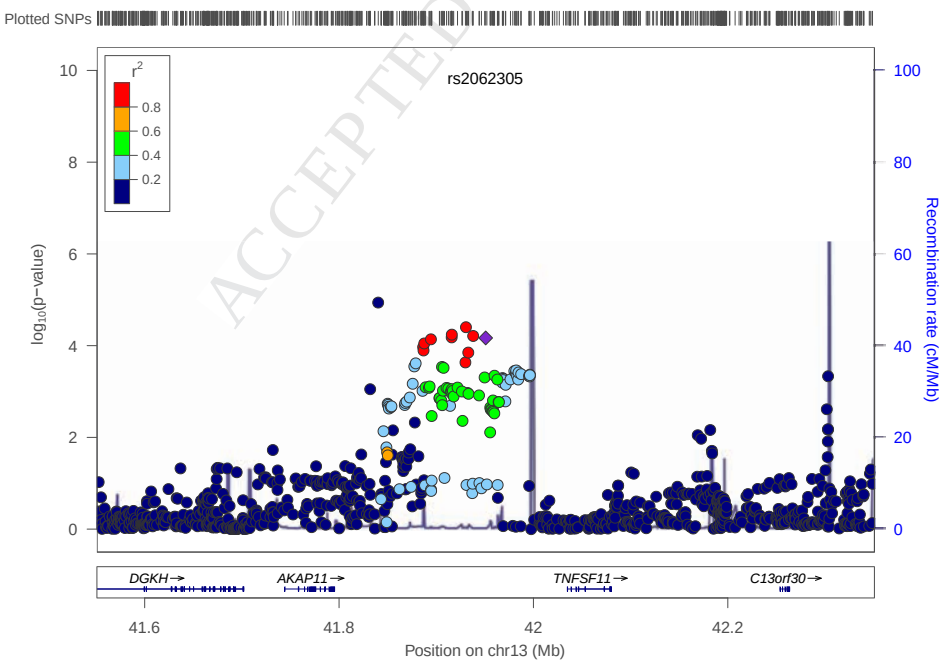

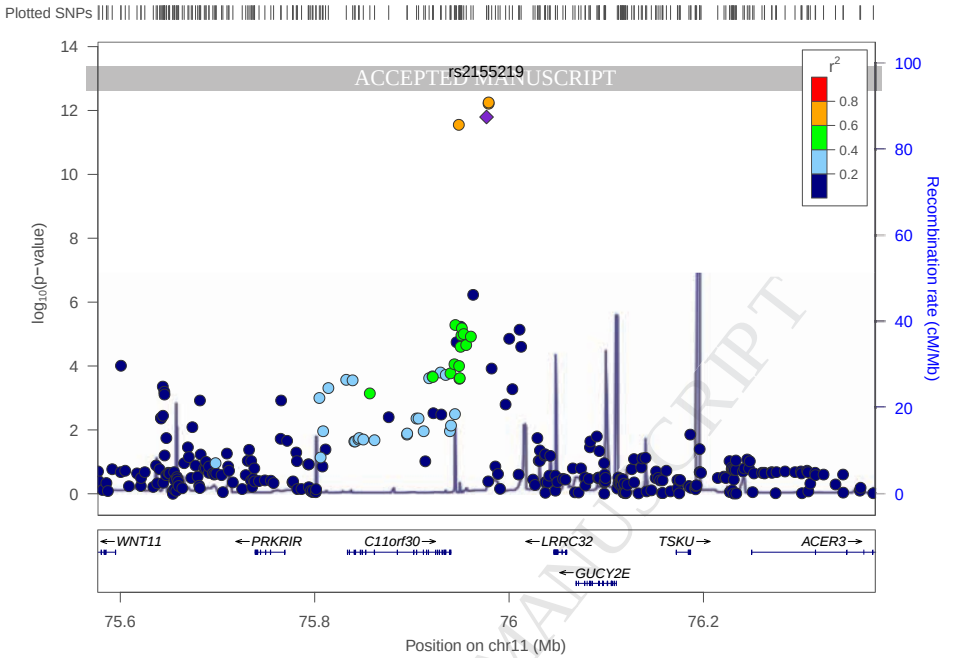


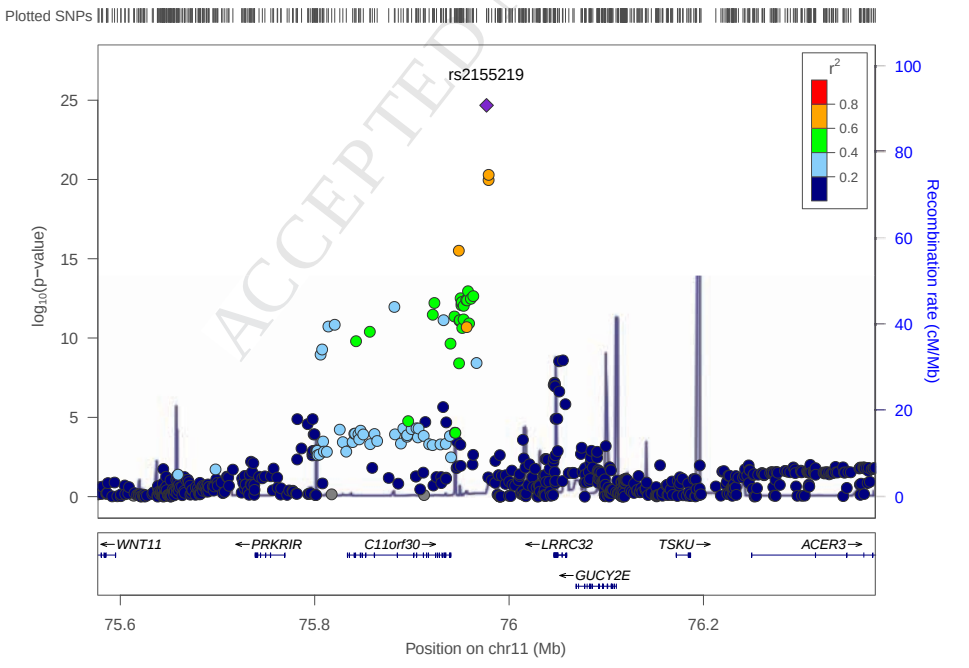

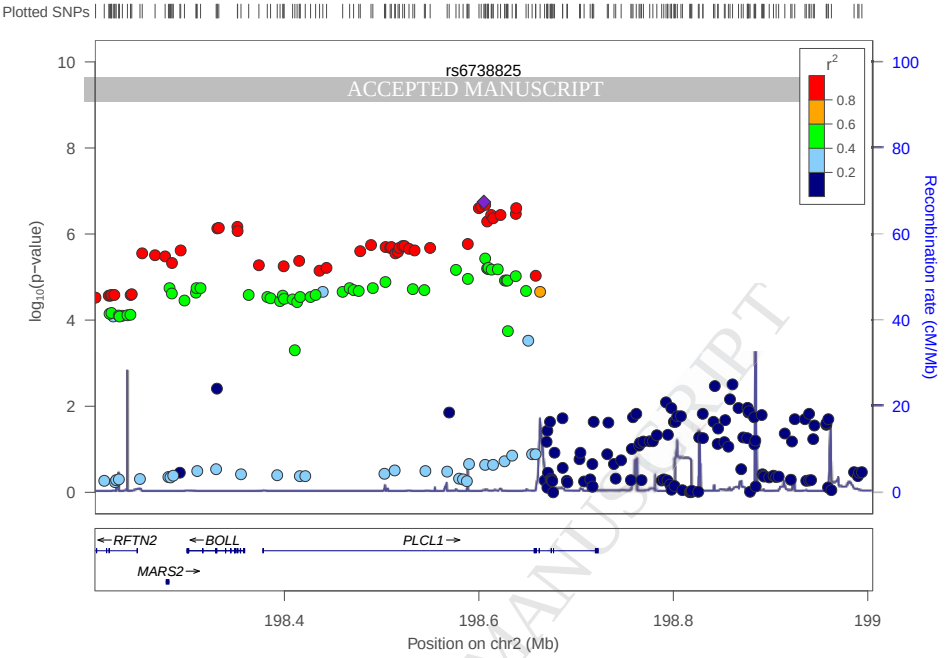




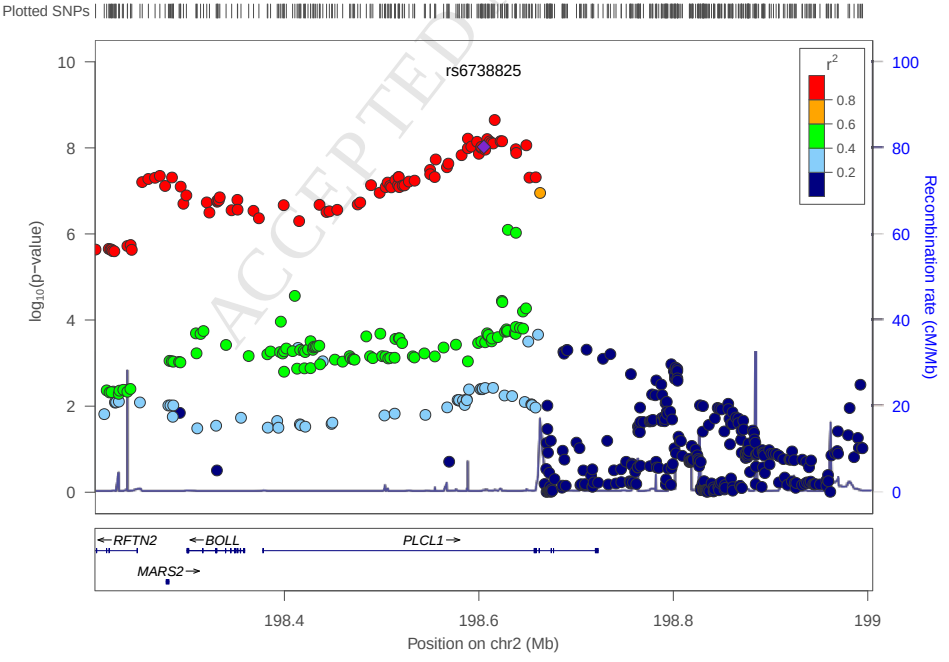


ACCEPTED MANUSCRIPT

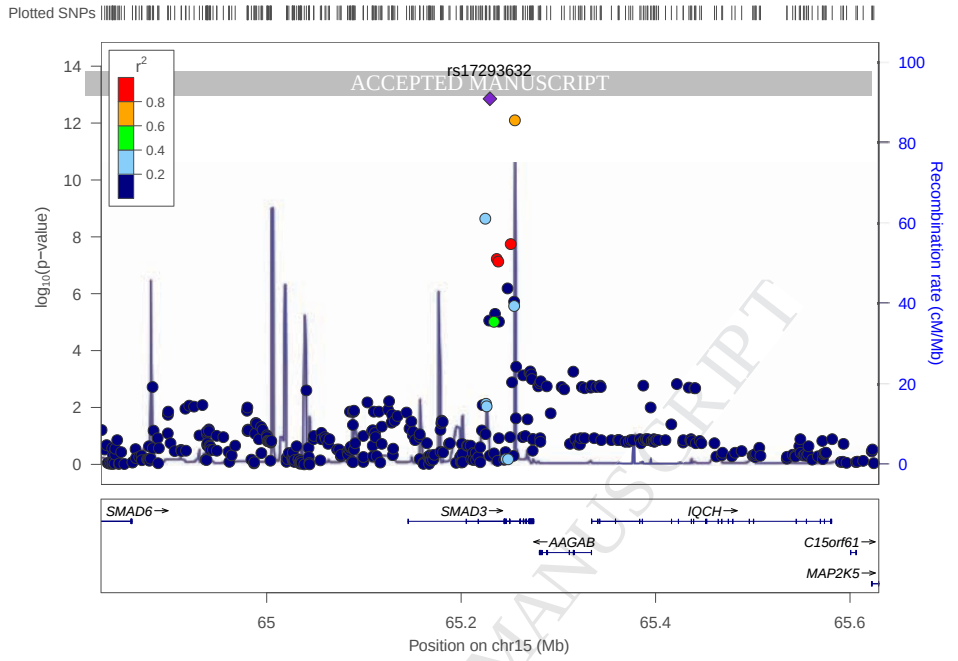


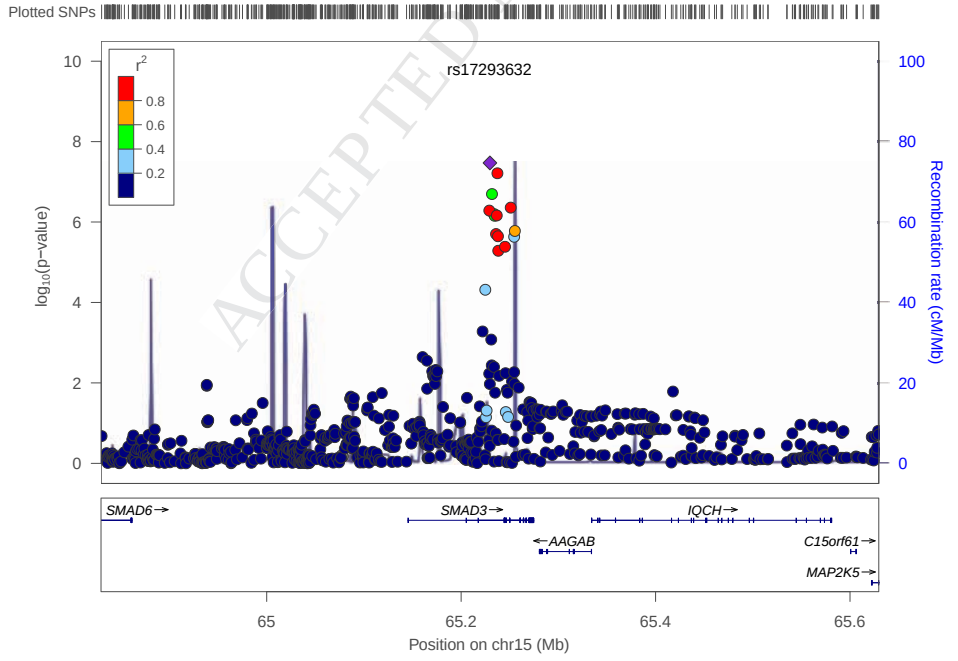

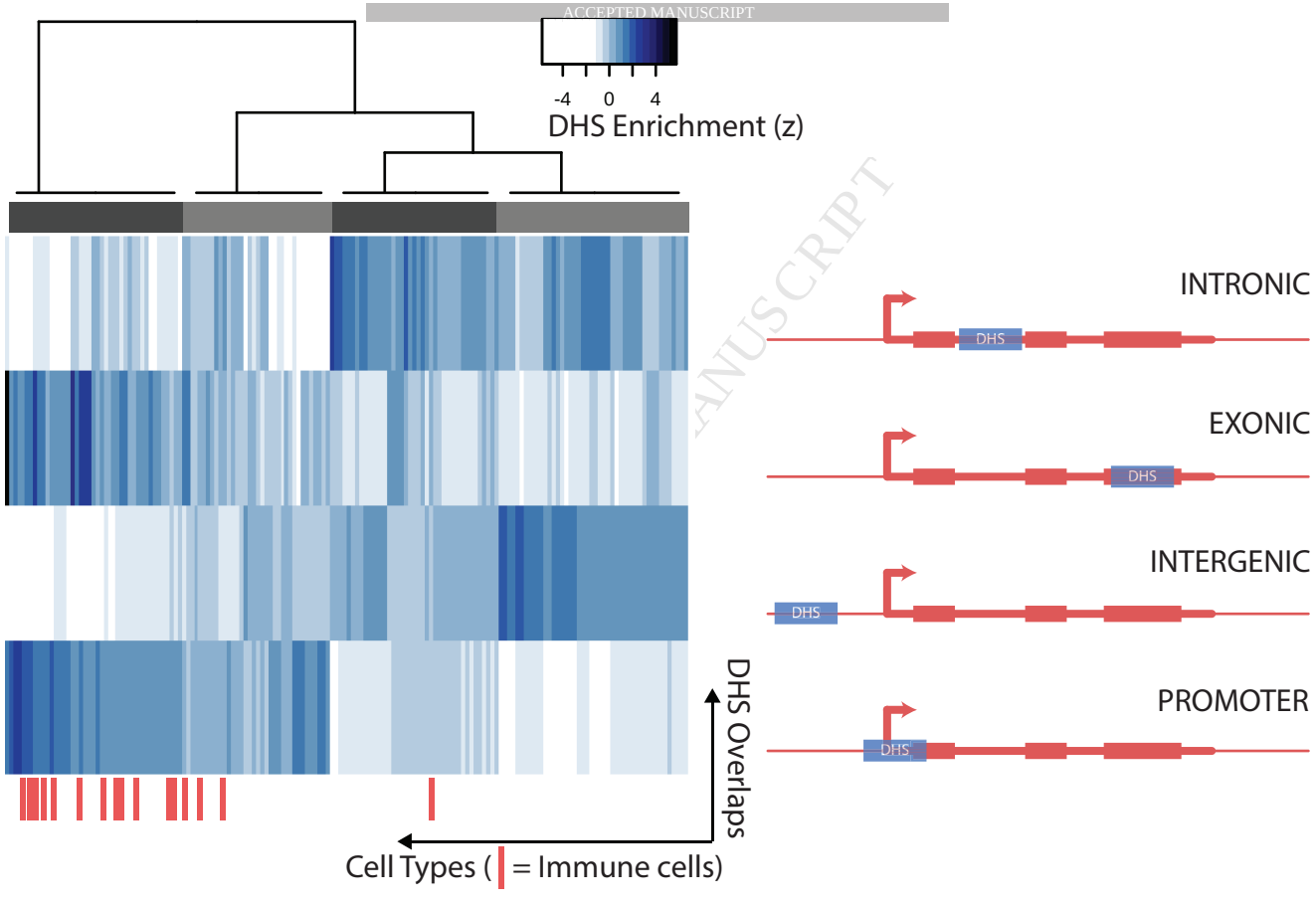

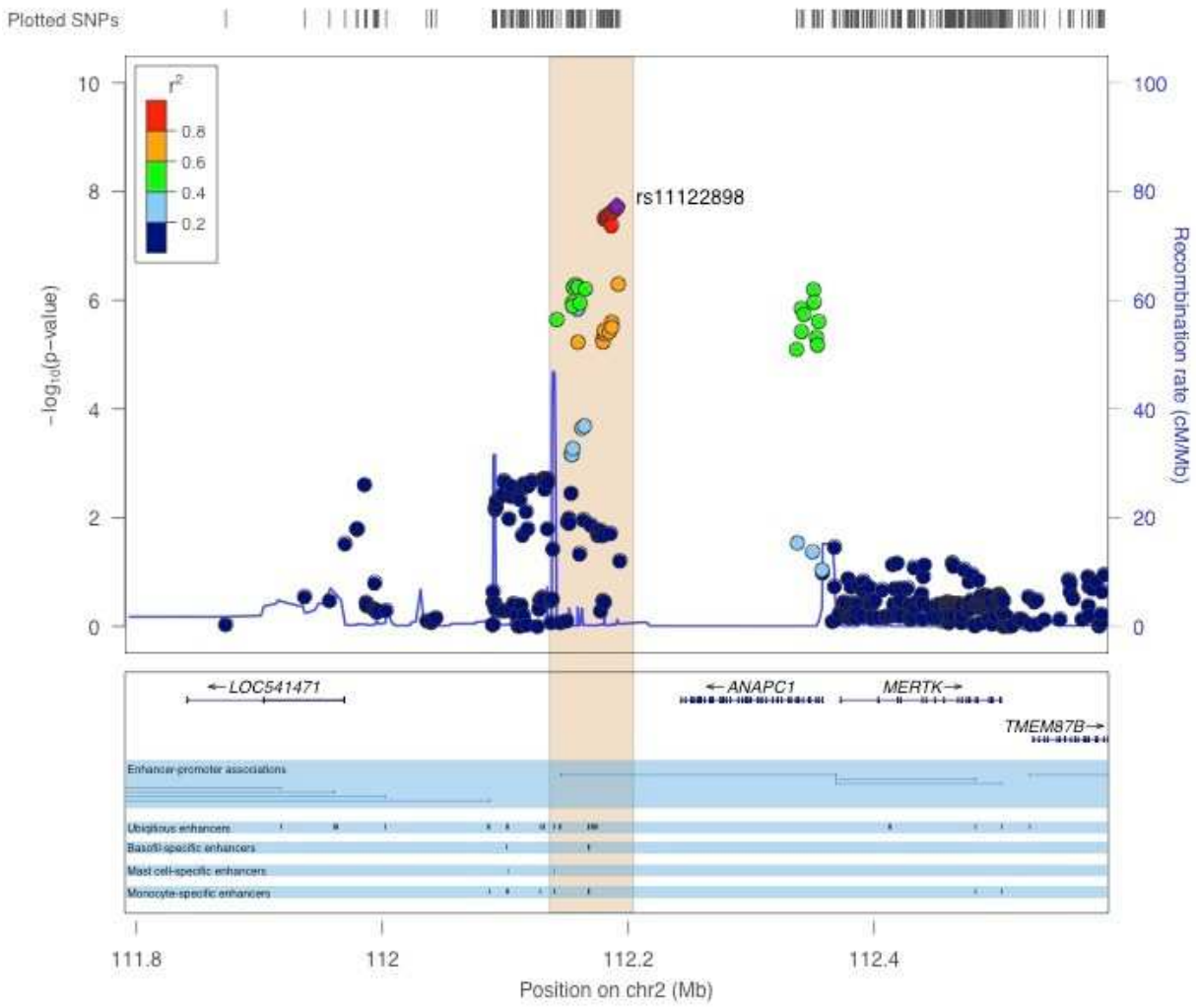
Plotted SNPs
r²
0.8
0.6
0.4
0.2
rs11122898
−log10(p−value)
Recombination rate (cM/Mb)
LOC541471
ANAPC1
MERTK
TMEM87B
Enhancer-promoter associations
Ubiquitous enhancers
Basofil-specific enhancers
Mast cell-specific enhancers
Monocyte-specific enhancers
111.8
112
112.2
112.4
Position on chr2 (Mb)